ACTA CHEMICA SCANDINAVICA 27 (1973) 1004–1018

Multicomponent Polyanions

IV. The Molecular and Crystal Structure of $Na_6Mo_5P_2O_{23}(H_2O)_{13}$, a Compound Containing Sodium-coordinated Pentamolybdodiphosphate Anions

ROLF STRANDBERG

Department of Inorganic Chemistry, University of Umeå, S-901 87 Umeå, Sweden

The crystal structure of $Na_6Mo_5P_2O_{23}(H_2O)_{13}$ has been determined from three-dimensional X-ray data, collected by the equi-inclination Weissenberg method using Cu$K\alpha$-radiation. There are four formula units in the orthorhombic unit cell, and the cell dimensions are $a = 15.423$ Å, $b = 16.896$ Å, and $c = 12.394$ Å. The space group is *Pbcn*. The structure is built up of sodium coordinated $Mo_5P_2O_{23}^{6-}$-groups. These groups are coupled together through bonds O – Na – O and O – Na – H_2O – Na – O. Final refinement by least squares analysis with isotropic temperature factors, using 2681 (visually estimated) independent reflections, resulted in an R-value of 9.4 %.

In a recent emf-investigation [1] aqueous equilibria

$$p\mathrm{H}^+ + q\mathrm{MoO_4}^{2-} + r\mathrm{HPO_4}^{2-} \rightleftharpoons (\mathrm{H}^+)_p(\mathrm{MoO_4}^{2-})_q(\mathrm{HPO_4}^{2-})_r$$

were studied at 25°C in a 3.0 M $NaClO_4$-medium. It was found that with excess phosphate ions the main complexes were: $(H^+)_8(MoO_4^{2-})_5(HPO_4^{2-})_2^{6-}$, $(H^+)_9(MoO_4^{2-})_5(HPO_4^{2-})_2^{5-}$, and $(H^+)_{10}(MoO_4^{2-})_5(HPO_4^{2-})_2^{4-}$ (removal of five water gives, respectively, $Mo_5P_2O_{23}^{6-}$, $HMo_5P_2O_{23}^{5-}$, and $H_2Mo_5P_2O_{23}^{4-}$), with the formation constants log $\beta_{8,5,2} = 61.97$, log $\beta_{9,5,2} = 67.07$, and log $\beta_{10,5,2} = 70.86$. In close connection with this equilibrium investigation, attempts were made to obtain crystals, which could contain the complexes. The crystallization experiments were carried out by slow evaporation of equilibrium solutions of known compositions at 25°C. Hitherto the phases given in Table 1 have been prepared and characterized.

Complete structure determination has been carried out for the phases (1) and (4). The phase (4) investigation will be published in a forthcoming paper and structure (1) is the topic of the present report. Intensity data are being collected for phases (2) and (3).

Table 1. Crystal data for sodium-pentamolybdo-diphosphates under investigation.

Formula	System	Cell-dimensions	Space group	Density (g/cm³)	Z
(1) $Na_6Mo_5P_2O_{23}(H_2O)_{13}$	Orthorhombic	$a=15.423$ $b=16.896$ $c=12.394$	*Pbcn*	2.62	4
(2) $Na_6Mo_5P_2O_{23}(H_2O)_x$	»	$a=10.7$ $b=15.8$ $c=19.9$	$P2_12_12_1$	2.63	4
(3) $Na_5HMo_5P_2O_{23}(H_2O)_{7-9}$	Triclinic	$a=10.45$ $b=18.65$ $c=8.32$ $\alpha=89.8$ $\beta=108.7$ $\gamma=101.3$		2.66	2
(4) $Na_4H_2Mo_5P_2O_{23}(H_2O)_{10}$	Monoclinic	$a=26.388$ $b=13.661$ $c=8.041$ $\beta=91.37°$	$P2_1/n$	2.71	4

EXPERIMENTAL

In a typical preparation of the crystals a solution with the composition $[MoO_4^{2-}]_{tot}=2.04$ M, $[H_2PO_4^-]_{tot}=0.82$ M, and $[HClO_4]_{tot}=2.442$ M was placed for crystallization at room temperature. After a few days (sometimes weeks) colourless ball-shaped crystals were obtained. Sometimes the crystals grew to a radius of about 0.4 cm. They are not stable in air, and during the X-ray exposures they were enclosed together with part of the mother liquid in a sealed glass capillary.

The contents of Na, P, and Mo in the crystals were determined by analysis (carried out at the Department of Analytical Chemistry, Umeå University). (Found: Na 10.8; P 4.7; Mo 38.0. Calc. for $Na_6Mo_5P_2O_{23}(H_2O)_{13}$: Na 10.8; P 4.8; Mo 37.4.) Water analysis was performed with the Karl-Fisher method and gave 18.0 % H_2O (calc. 18.3). In some experiments we also measured the loss of water in a thermo-balance analysis. The results found were in very good agreement with those mentioned above. Here we also observed that the loss of water occurred in three steps at the following temperatures: 95°C (loss of 7 H_2O); 143°C (another 4), and 330°C (the last 2).

From rotation photographs (around [001], [010], and [100]) and the corresponding Weissenberg photographs (zero, first and second layer lines) taken with Cu$K\alpha$-radiation it was concluded that the crystals are orthorhombic. The dimensions were refined from powder data. Systematic extinctions gave the unique space group *Pbcn*. Precession photographs were taken to confirm the space group.

Equi-inclination Weissenberg films, $hk0-hk11$, were taken with Cu$K\alpha$-radiation. The intensities of 2681 independent reflections were estimated visually with the multiple film technique. No correction was applied for absorption as the crystal was spherical with a radius of 0.06 mm.

The computer programs used were the same as those given in Ref. 2.

CRYSTAL DATA

$Na_6Mo_5P_2O_{23}(H_2O)_{13}$ F.W. = 1281.8
Orthorhombic *Pbcn* $Z=4$
$a=15.423$ (1) Å
$b=16.896$ (1) Å $d_{calc}=2.64$ g/cm³
$c=12.394$ (1) Å $d_{exp}=2.62$ g/cm³ (flotation method)
$V=3229.7$ Å³

STRUCTURE DETERMINATION AND REFINEMENT

From a three-dimensional Patterson synthesis the approximate coordinates for the Mo-atoms were readily found. With 20 Mo in the unit cell at least one must be in a special four-fold position and this provided a starting point.

The remaining Mo-atoms were found to be in two general eightfold positions. A refinement at this stage gave an R-value of 37 %.

A three-dimensional Fourier synthesis was performed with the known Mo-atoms. This gave the coordinates of P and oxygens bound to P and Mo. The R-value decreased to 28 %.

In a second electron density calculation the remaining atoms, Na and water oxygens, appeared.

By using the least squares method with block-diagonal matrix approximation, the various atomic parameters were refined and the resulting R-value was 9.4 %

$$R = \sum ||F_o| - |F_c|| / \sum |F_o|$$

The scattering factors for Mo^+, P, O^-, and Na^+ were used [3] and account was taken of the real part of the dispersion correction. The weighting scheme used was that proposed by Cruickshank: $w = 1/(a + |F_o| + c|F_o|^2 + d|F_o|^3)$ with the values for the constants $a = 20$, $c = 0.004$, and $d = 0.0001$.

Final atomic coordinates, vibrational parameters, and corresponding standard deviations are given in Table 2, and a comparison between the observed and calculated structure factors is reported in Table 3.

Table 2. Fractional atomic coordinates and isotropic thermal parameters. The standard deviations in parentheses are for the last decimal place given. For the oxygen atoms indexed O(ij) or OP(ij) the (ij) means that the atom is bonded to the molybdenum atoms i and j. When the oxygen atoms are denoted Aq(ij) they are water oxygens and (ij) means that the atom is bonded to the sodium atoms i and j.

	x	y	z	B
Mo1	0.50000(0)	0.55505(8)	0.25000(0)	0.69(2)
Mo2	0.54308(6)	0.67007(6)	0.03499(8)	0.76(1)
Mo3	0.54863(6)	0.85956(6)	0.11588(9)	1.00(2)
P	0.6195 (2)	0.7243 (2)	0.2909 (2)	0.76(4)
O(1)	0.5880 (6)	0.4931 (6)	0.2355 (8)	1.6 (2)
O1(2)	0.6360 (6)	0.6195 (6)	−0.0029 (8)	1.7 (2)
O2(2)	0.4818 (7)	0.6740 (6)	−0.0809 (9)	1.8 (2)
O1(3)	0.6261 (7)	0.9307 (6)	0.0935 (9)	2.2 (2)
O2(3)	0.4682 (7)	0.8898 (7)	0.0283 (9)	2.2 (2)
O(12)	0.4776 (6)	0.5866 (5)	0.1023 (7)	1.2 (1)
O(23)	0.5930 (6)	0.7735 (6)	0.0294 (8)	1.5 (1)
O(33′)	0.5000 (0)	0.8916 (8)	0.2500 (0)	1.5 (2)
OP	0.6956 (6)	0.6951 (5)	0.3540 (7)	1.3 (1)
OP(3)	0.6398 (5)	0.7993 (5)	0.2276 (7)	1.1 (1)
OP(12)	0.5909 (5)	0.6579 (5)	0.2119 (7)	0.9 (1)
OP(23)	0.4582 (5)	0.7447 (5)	0.1322 (7)	1.0 (1)
Aq(2)	0.3842 (8)	0.0317 (8)	0.131 (1)	2.9 (2)
Aq1(12)	0.3310 (7)	0.4544 (6)	0.4977 (9)	2.0 (2)
Aq2(12)	0.2498 (7)	0.4107 (6)	0.1860 (8)	1.9 (2)
Aq1(13)	0.2861 (7)	0.2675 (6)	0.4355 (9)	2.3 (2)
Aq2(13)	0.3572 (7)	0.2519 (7)	0.2166 (9)	2.3 (2)
Aq(23)	0.2879 (7)	0.0801 (6)	0.3608 (9)	2.2 (2)
Aq(33′)	0.0000 (0)	0.624 (1)	0.2500 (0)	2.8 (3)
Na1	0.3469 (4)	0.3732 (4)	0.3335 (5)	2.6 (1)
Na2	0.2362 (5)	0.0582 (4)	0.1790 (5)	3.0 (1)
Na3	0.3971 (4)	0.1828 (4)	0.3766 (5)	2.3 (1)

Table 3. Observed and calculated structure factors.

0 K 0			9 K 0			16 55 -50			17 37 -39			12 K 1			12 184 177		
4 226 -316			19 34 25			15 39 -34			15 52 32			17 28 -24			8 36 -35		
6 87 104			17 99 -82			14 51 45			14 52 46			16 57 -52			6 241 268		
8 77 -88			15 197 187			13 184 175			13 35 30			14 141 135			4 208 -237		
10 287 -312			13 92 90			12 133 123			12 75 66			12 122 124					
12 66 66			11 287 -311			11 155 149			11 129 -140			8 126 -128			1 K 2		
14 49 25			9 77 69			10 142 -145			9 104 100			6 42 36			21 131 -122		
16 77 62			5 108 -99			9 81 -72			7 219 240			5 102 103			20 26 -23		
18 97 99			3 40 38			8 20 7			6 42 -42			4 80 -83			19 61 -50		
20 48 -47			1 74 69			7 46 -40			5 350 -435			3 37 -36			18 40 -25		
						6 120 -124			4 165 -168			2 87 -87			16 29 22		
1 K 0			10 K 0			4 49 -58			3 34 -20			1 107 -108			15 163 -148		
21 158 -148			18 108 91			3 136 -147			2 20 -3						14 55 44		
19 153 127			12 93 -82			2 46 -43			1 150 164			13 K 1			13 55 -47		
17 301 279			10 141 134									16 95 96			12 28 21		
15 245 -242			8 154 -152			2 K 1			7 K 1			15 86 88			11 264 253		
13 48 46			6 206 -203			21 30 -23			20 124 143			14 38 -41			10 52 -47		
11 194 179			4 270 302			20 86 -74			19 66 -57			13 28 26			9 143 -144		
9 258 -276			2 147 152			19 33 31			18 63 54			12 74 -66			8 53 54		
7 161 -177			0 201 -225			16 161 147			17 73 66			11 30 17			7 133 145		
5 219 271						15 55 44			16 228 -200			10 76 80			6 103 106		
			11 K 0			11 105 -94			15 42 31			9 85 80			5 78 80		
2 K 0			17 154 -159			10 95 86			14 132 124			7 89 -97			4 179 -191		
18 92 94			15 265 261			9 101 103			13 39 40			6 68 -69			3 256 -304		
12 104 100			11 221 -209			8 49 46			12 82 80			5 120 -138			2 73 -68		
10 245 -243			7 64 64			7 55 61			11 29 -8			4 35 -13					
8 28 20			5 139 -137			6 128 -150			10 138 -151			3 102 -102			2 K 2		
6 274 373			3 117 117			5 177 -196			9 144 150			1 117 127			21 93 -85		
4 245 -351			1 118 121			4 101 -104			8 25 17						20 133 -118		
2 132 -160						3 70 77			7 52 -54			14 K 1			19 64 53		
			12 K 0			1 157 164			6 137 136			14 80 71			17 79 60		
3 K 0			16 69 67						5 235 -252			12 74 77			16 76 -68		
21 95 -88			12 119 -113			3 K 1			4 81 -74			11 75 77			15 118 -103		
19 96 79			10 73 63			21 30 -31			3 59 -46			9 56 -59			14 95 -90		
17 155 138			8 81 -72			20 135 115			2 22 -16			8 53 -44			13 84 -68		
15 140 -128			6 174 -186			19 39 31			1 62 58			7 93 -86			12 194 190		
11 264 279			4 141 141			18 62 49						5 148 165			11 90 76		
9 328 -392			2 261 280			17 35 -29			8 K 1			4 173 -131			10 62 59		
7 230 -252			0 243 -273			16 223 -201			19 45 51			3 110 -121			8 70 -67		
5 176 209						15 80 76			14 75 69			2 35 -31			7 85 88		
3 106 114			13 K 0			14 39 37			13 43 46			1 140 -159			6 188 195		
1 55 45			15 190 204			13 69 50			12 194 204						4 188 -197		
			13 45 -38			12 176 169			11 121 -122			15 K 1			3 163 169		
4 K 0			11 191 -193			11 129 127			10 109 -111			14 72 -78			2 214 -235		
20 85 60			7 66 55			10 190 -216			8 88 -90			13 64 71			1 110 -94		
18 53 47			5 167 -178			9 159 -169			7 160 166			12 105 -102			0 192 178		
16 60 47			3 142 139			8 76 79			6 55 -60			10 137 144					
14 38 -31			1 130 136			7 39 36			5 219 -228			9 47 38			3 K 2		
12 106 99						6 86 94			4 101 -94			7 96 -53			21 110 -108		
10 155 -156			14 K 0			5 34 -29			3 22 -8			6 81 -77			19 83 -67		
8 165 -178			14 43 43			4 169 -193			2 124 -129			5 65 -74			18 65 -47		
6 47 -32			12 123 -123			3 216 -268			1 191 202			4 85 80			16 53 41		
4 240 -293			6 160 -176			1 174 -180						3 34 -34			15 148 -143		
2 155 179			4 92 87						9 K 1						14 105 82		
0 175 178			2 130 135			4 K 1			19 89 -86			16 K 1			13 102 97		
			0 125 -134			21 74 -71			17 110 99			12 61 61			11 164 155		
5 K 0						20 77 -66			16 134 -126			11 83 94			10 123 -116		
17 101 87			15 K 0			19 25 33			15 82 69			10 54 -53			8 69 -66		
13 86 -80			13 44 -39			18 38 29			14 58 53			9 33 -40			7 124 127		
9 252 -271			11 109 -107			15 48 40			13 86 79			7 101 -100			6 263 293		
7 203 -213			9 60 51			14 164 160			12 79 78			6 89 -96			5 116 122		
5 153 156			7 65 -63			12 50 45			10 54 -54			5 172 192			4 305 -340		
3 24 -20			3 65 63			11 155 -150			9 79 79			4 48 -50			3 255 -278		
1 174 190						10 105 103			6 32 28			3 34 -41			2 83 -70		
			16 K 0			9 128 130			5 244 -258			1 148 -162			1 86 -67		
6 K 0			12 96 -110			8 36 -33			4 109 -111						0 340 392		
20 53 47			10 44 -42			7 194 205			3 39 -41			17 K 1					
18 65 53			8 36 -36			6 124 -121			2 42 33			10 152 179			4 K 2		
16 97 90			6 91 -94			5 218 -252			1 53 49			9 48 -46			20 100 -94		
14 81 -71			2 69 72			4 218 -256						8 37 -39			19 91 79		
12 123 -115						3 69 66			10 K 1			6 83 -89			17 127 109		
10 38 -30			17 K 0			2 73 -66			18 31 29			5 81 -77			16 110 -96		
8 70 -61			7 158 -173			1 297 390			16 87 -76			4 91 94			15 155 -132		
6 130 -126			3 93 90						14 110 109			3 46 -55			14 34 -30		
4 57 -50						5 K 1			12 136 135			2 45 -39			13 72 -65		
2 98 89			18 K 0			20 138 135			10 63 -58			1 79 -81			12 143 139		
0 43 40			4 34 -40			19 27 22			9 30 24						11 241 246		
			0 126 129			18 50 41			8 58 -56			18 K 1			10 81 77		
7 K 0						17 38 -26			7 99 107			8 30 32			9 118 -114		
15 117 96			19 K 0			16 221 -215			5 76 -76			7 94 -103			8 98 99		
11 211 -219			5 49 43			15 138 130			3 52 43			6 103 -121			7 187 -185		
5 169 -178			3 63 67			14 105 106			2 243 -270			5 129 137			6 218 226		
1 140 141						13 34 25						4 58 -63			5 133 133		
			0 K 1			12 165 162			11 K 1			1 129 -138			4 67 61		
8 K 0			20 128 -104			10 226 -233			17 71 61						3 146 138		
18 141 117			16 231 210			8 52 55			15 89 88			19 K 1			2 335 -366		
16 48 39			12 48 37			7 150 -149			9 60 62			4 57 59			1 67 -65		
12 105 -103			10 181 187			6 162 170			8 76 68			3 53 -60			0 84 77		
10 70 67			8 327 -430			5 108 -118			6 63 -57			2 68 -71					
8 135 -133			4 112 -120			4 75 -72			5 155 -168			1 41 -44			5 K 2		
6 291 -328						3 159 -168			3 44 -41						19 61 -52		
4 176 179			1 K 1			2 69 65			2 55 56			0 K 2			18 63 -41		
2 170 170			21 27 -22						1 116 116			20 149 -139			16 60 -51		
0 97 88			20 53 46			6 K 1						16 82 -70			15 118 -115		
			17 48 48			19 45 49						14 172 -164			14 98 91		

Table 3. Continued.

13 128 120	11 41 37	6 96 -101
11 49 45	10 107 110	4 119 130
10 171 -165	9 33 -29	2 57 54
9 124 122	8 129 128	1 52 -53
8 86 88	7 68 66	0 169 -190
7 67 63	6 164 -162	
6 293 310	5 64 65	18 K 2
5 143 140	4 111 107	8 22 25
4 165 -165	3 27 -20	7 54 61
3 164 -152	2 41 -39	6 71 72
2 178 -172	1 57 -53	5 31 -32
1 22 18	0 263 -268	2 49 -43
0 229 225		0 31 -36
	11 K 2	
6 K 2	17 121 -123	19 K 2
20 34 -31	16 25 19	4 50 56
19 76 63	15 76 70	3 47 -49
18 49 -37	14 40 -42	2 26 31
17 205 170	12 72 71	1 21 -28
16 71 -68	11 76 -70	0 85 -94
15 193 -181	9 173 190	
13 53 -29	8 84 -94	0 K 3
12 86 79	5 137 -141	20 63 -50
11 194 192	3 117 121	18 38 -29
10 76 73	1 136 -145	16 93 77
9 50 -47	0 34 -33	14 146 -135
8 41 35		12 348 -376
7 179 -182	12 K 2	10 214 238
6 90 83	16 58 -55	8 62 59
5 173 196	15 47 41	6 89 -88
4 24 -20	14 85 76	4 112 127
3 25 22	12 105 -103	
2 81 71	11 77 -76	1 K 3
1 163 -163	10 152 100	21 78 76
0 58 -51	9 31 -37	20 22 21
	8 109 111	19 57 46
7 K 2	7 77 85	18 41 33
20 32 -31	6 130 -133	17 113 -90
19 38 -35	5 44 -39	15 130 -109
18 31 -11	4 142 156	14 65 -59
17 104 -93	2 56 -55	13 82 -74
16 51 -45	1 45 43	12 42 -34
15 40 35	0 236 -277	11 97 87
14 109 96		10 79 75
13 34 -33	13 K 2	9 162 -163
12 53 -40	15 47 44	8 62 63
11 63 61	14 100 -90	7 118 118
10 161 -169	11 64 -57	6 33 -30
9 129 127	10 78 69	5 267 315
8 92 84	9 233 234	4 105 -102
7 106 99	8 47 -49	3 62 -59
6 160 162	7 31 -29	2 153 163
4 193 -204	5 53 -51	
3 37 -34	4 123 137	2 K 3
2 21 11	3 47 41	21 53 -55
1 24 -27	2 35 -34	20 68 -53
0 237 242	1 123 -129	19 150 135
	0 127 -140	18 64 -47
8 K 2		17 53 -47
19 37 24	14 K 2	16 127 114
18 133 -127	14 64 64	15 49 -49
17 131 118	13 51 46	14 179 -173
15 91 -80	12 36 -38	13 82 73
13 77 -69	11 126 -133	12 195 -186
11 136 146	10 83 85	10 116 114
10 124 127	9 44 43	9 100 -109
9 72 -75	8 123 120	8 89 85
8 135 131	7 98 105	7 17 -7
7 110 -102	6 76 -79	6 66 -72
5 108 82	5 29 -33	5 66 -59
4 26 -22	4 50 50	4 109 108
3 45 -45	3 104 -123	3 103 -104
2 48 34	1 68 72	2 189 200
0 325 -364	0 192 -209	1 190 207
9 K 2	15 K 2	3 K 3
19 73 -79	10 87 93	20 33 -17
18 21 -13	9 138 157	19 28 19
17 147 -132	8 38 -36	18 28 21
16 28 25	7 34 42	17 34 -18
15 88 81	6 126 -121	15 126 -124
14 36 25	4 47 158	14 89 93
13 44 -47	1 64 -69	13 64 -58
12 39 -37	0 83 -91	12 40 -33
11 34 25		10 36 29
10 52 -41	16 K 2	9 79 -71
9 196 208	11 135 -142	8 59 63
7 115 112	10 48 49	7 45 43
6 176 181	9 28 31	6 134 -140
5 145 -145	8 77 81	5 234 267
4 124 -130	7 92 96	4 65 -69
3 39 35	6 41 43	3 55 63
2 57 -50	5 42 -41	2 281 299
1 170 -172	4 28 -23	1 252 -246
0 32 31	3 69 -75	
	1 54 54	4 K 3
10 K 2	0 155 -155	20 24 -14
18 144 -157		19 137 126
15 43 -43	17 K 2	17 131 -115
14 62 55	10 56 59	16 27 26
13 51 -48	9 49 55	15 78 -81
12 64 -61	7 89 91	14 192 -181

13 213 210	5 84 -78	18 K 3
12 49 -39	4 97 -96	7 73 -83
11 103 -98	3 80 80	6 25 23
10 48 41	2 229 248	5 40 39
9 99 -95	1 305 340	4 39 37
8 140 141		3 25 20
7 147 155	10 K 3	2 84 91
6 70 67	18 30 27	1 46 -44
5 108 108	17 56 -51	
4 48 46	16 207 -204	19 K 3
3 224 -225	14 34 30	3 29 34
2 88 75	13 33 25	2 73 -88
1 61 47	11 69 -64	1 45 -52
	10 118 -136	
5 K 3	7 60 53	0 K 4
19 24 18	6 191 211	20 39 -38
16 60 -55	1 96 94	18 359 336
15 81 -71		14 184 -172
14 43 47	11 K 3	12 48 42
13 97 -84	16 42 -41	10 44 33
12 61 -59	15 50 -53	8 159 -155
11 69 -70	14 51 48	6 23 -29
10 135 -141	13 43 -35	4 204 212
9 26 18	11 163 -182	
8 228 257	9 98 107	1 K 4
6 25 -7	8 40 -37	20 33 -32
5 193 202	7 117 127	18 53 43
4 133 -133	6 67 67	17 50 50
3 122 117	5 136 -148	16 30 -22
2 208 204	3 144 156	15 68 50
1 54 -50	1 206 233	13 104 97
		12 58 51
6 K 3	12 K 3	11 176 -155
20 53 51	16 144 -159	10 64 -60
19 80 74	15 42 38	9 293 -305
18 39 29	12 72 61	8 67 -72
17 69 -55	10 171 -186	7 199 199
16 89 -76	8 75 76	6 108 -103
15 87 -82	6 129 151	5 112 112
14 81 -79	3 79 -84	4 116 117
13 207 221	2 32 23	3 176 -196
11 128 -139	1 54 51	2 98 -98
10 76 -76		
9 155 -160	13 K 3	2 K 4
8 65 67	15 59 -55	20 42 -38
7 218 228	13 45 -38	18 269 239
6 115 115	12 38 36	17 73 59
5 76 71	11 118 -126	16 45 38
4 126 120	9 37 35	15 101 -100
3 53 -52	8 68 -67	14 143 -134
2 31 28	7 105 113	12 67 60
1 44 34	5 78 -85	11 59 68
	4 103 108	10 58 52
7 K 3	3 125 142	9 35 -26
18 37 29	2 125 -144	8 251 -255
17 30 -26	1 136 157	7 106 -111
15 38 -31		6 29 -26
14 74 69	14 K 3	5 168 157
13 110 -112	13 97 -101	4 59 62
12 32 25	10 118 -117	3 89 -91
11 30 -18	9 72 73	2 116 110
10 112 -118	8 57 66	1 35 -34
9 59 56	7 56 -61	0 132 125
8 118 126	6 92 101	
7 141 143	4 32 31	3 K 4
6 155 -150	3 69 82	20 88 -88
5 54 -48	2 51 58	19 45 42
4 263 -279	1 36 -33	18 64 61
3 73 74		17 39 19
2 276 309	15 K 3	16 44 -36
1 150 146	13 26 -25	15 100 93
	12 70 76	14 27 -27
8 K 3	11 46 -47	13 28 25
19 89 93	8 81 -87	12 71 66
18 63 51	7 47 50	11 115 -107
17 67 -61	5 36 35	10 64 -62
16 186 -173	4 128 129	9 182 -202
15 61 -51	3 51 52	8 22 -19
13 141 143	2 129 -141	7 112 110
12 28 -30	1 79 86	6 124 126
11 62 -61		5 107 101
10 108 -116	16 K 3	3 185 -184
7 62 63	11 68 67	2 186 -186
6 206 219	10 31 -31	1 64 65
5 125 -126	9 63 74	0 101 92
4 72 74	8 29 31	
3 43 -33	7 82 -85	4 K 4
1 26 19	6 61 69	18 145 120
	4 29 39	17 118 97
9 K 3	3 84 85	16 68 68
18 40 38	2 79 88	15 113 -111
17 30 -32	1 62 -56	14 119 -113
16 72 -70		13 34 -26
15 23 -24	17 K 3	11 113 111
14 43 37	10 45 48	10 55 -45
13 73 -74	9 20 -26	9 98 -107
12 56 -52	8 94 -109	8 193 -202
11 121 -133	6 57 63	7 66 70
9 121 118	5 117 132	6 50 51
8 68 72	4 81 87	5 43 40
7 119 124	2 99 -115	4 46 -49
6 25 -26		3 133 -124

Table 3. Continued.

2	179	172		10 K 4		6	89	-96	10	88	94		10 K 5		5	90	-106
1	16	11	17	59	62	4	40	40	9	156	-155	17	18	20	4	89	95
0	26	-12	16	47	41	3	21	-21	8	143	-146	15	47	-49	2	79	-90
			15	77	-71	2	57	56	7	137	145	14	125	122			
	5 K 4		14	198	201	1	84	94	6	122	-129	13	83	74		18 K 5	
20	39	-48	13	37	43	0	93	-88	5	89	88	12	62	58	5	50	-60
19	65	62	12	141	-153				4	29	19	10	47	-49	3	58	67
18	39	44	10	168	-195		18 K 4		3	58	-56	9	29	-24	2	77	-89
17	50	40	8	161	180	6	59	-71	2	149	-136	8	92	102	1	46	-42
15	34	28	7	28	-22	5	25	-28	1	22	-10	7	37	34			
14	57	-55	6	85	-80	4	64	70				6	102	-109		0 K 6	
12	75	77	5	92	93	3	46	45		5 K 5		5	58	-52	20	80	-77
11	110	-103	4	74	-80	2	49	52	19	40	-36	4	239	-256	16	34	-39
10	81	-77	3	104	-111	1	19	-15	18	24	-15	2	175	197	14	103	-95
9	136	-144	2	103	104				17	44	34				12	23	14
8	92	-91	1	73	69		19 K 4		16	56	37		11 K 5		10	84	77
7	91	-85	0	118	131	1	90	123	15	65	56	16	20	-18	8	38	24
6	181	195				0	36	-47	14	58	59	14	31	-24	6	22	6
5	56	-65		11 K 4					13	42	32	13	185	196	4	41	-49
4	178	-181	17	59	63		0 K 5		12	104	-97	12	55	47	2	34	-39
3	129	120	15	26	24	20	45	-56	11	69	70	10	52	-53			
2	80	-72	13	101	-90	16	95	91	10	47	37	9	100	-115		1 K 6	
1	40	-28	11	37	28	14	24	3	8	126	119	8	41	39	19	74	-68
0	266	289	7	173	-208	12	147	148	7	29	-26	7	95	100	18	45	38
			6	40	42	10	101	97	6	115	-117	5	152	-157	17	82	-57
	6 K 4		5	28	23	8	278	-288	5	55	-51	4	61	64	14	82	-76
18	35	21	4	55	42	6	168	160	4	214	-218	3	75	-78	12	43	32
17	128	113	3	262	293	4	83	90	3	213	-202	1	37	21	10	37	27
16	77	74	2	104	-101	2	205	-231	2	342	338				9	54	53
15	100	-100	1	70	-59				1	89	80		12 K 5		8	68	-46
12	105	-105	0	76	71		1 K 5					15	35	27	7	152	153
11	136	139				20	18	-18		6 K 5		14	122	126	6	111	114
10	125	-127		12 K 4		19	175	-172	19	145	149	13	34	-33	5	39	-36
9	179	-184	16	59	65	17	188	162	18	36	-31	12	33	29	4	62	63
8	90	-92	14	139	142	16	53	37	17	124	-117	11	45	-41	3	163	-204
7	37	36	12	118	-116	15	137	130	16	62	53	10	54	-54	2	29	-31
6	54	-55	10	132	-148	14	50	33	15	33	-21	9	28	25	1	18	-14
5	70	59	9	32	35	13	95	-87	14	90	84	8	105	113	0	39	-56
4	56	-51	8	60	63	11	95	87	13	149	160	7	37	29			
3	148	-141	7	35	37	10	43	-31	12	78	76	6	69	-81		2 K 6	
2	105	94	6	68	-70	9	147	144	11	47	-43	5	75	-86	19	27	-20
1	143	142	4	31	-33	8	67	59	9	156	-158	4	185	-225	18	79	-68
0	200	193	3	36	-38	7	238	-249	8	37	-33	3	71	74	15	38	21
			2	124	136	6	161	-167	7	66	66	2	79	84	14	78	-69
	7 K 4		0	145	170	5	22	-20	6	111	-112	1	54	53	13	39	28
19	72	70				4	15	-12	5	171	172				12	93	86
18	30	30		13 K 4		3	97	-107	4	146	-140		13 K 5		11	94	90
17	105	100	15	37	43	2	78	80	3	117	-113	14	34	39	10	103	91
14	79	-84	13	64	-62	1	195	-202	2	64	-57	13	161	178	9	193	-198
13	60	-58	12	40	-35				1	17	-11	12	61	64	8	96	91
12	117	124	10	40	45		2 K 5					11	34	-29	7	210	214
11	76	-74	7	127	-150	20	37	-40		7 K 5		10	43	-44	6	71	70
10	79	-72	6	45	-42	19	40	30	19	34	36	9	53	-57	5	27	-20
9	49	-48	5	39	-42	18	28	-20	18	36	36	8	92	-96	4	104	103
8	67	-66	3	197	231	17	35	-17	17	23	-24	7	73	81	3	217	-249
7	192	-219	2	49	46	16	78	73	15	47	39	6	50	54	2	165	-196
6	270	297	1	51	-50	15	102	-95	14	51	48	5	91	-98	1	127	170
4	112	-100	0	82	-80	14	41	31	13	154	167	4	33	37	0	241	-321
3	207	223				13	180	171	12	97	-97	3	71	-78			
2	118	-115		14 K 4		12	159	139	11	27	-25	2	80	-93		3 K 6	
1	40	-37	14	49	55	11	31	-31	10	23	18	1	42	35	19	59	-57
0	68	58	13	34	-35	10	146	146	9	65	-64				18	137	126
			12	99	-98	9	136	-129	8	72	66		14 K 5		17	84	-66
	8 K 4		11	38	-29	8	196	-201	6	40	-31	13	85	-91	16	37	-29
19	34	37	10	75	-69	7	54	51	5	112	-107	12	43	41	15	73	-64
18	51	-48	9	59	-59	6	120	-120	4	204	-215	11	22	-20	14	170	-158
17	73	65	5	75	-80	5	49	-50	3	102	-106	10	50	-56	13	91	81
16	66	60	3	73	85	4	69	64	2	242	244	9	79	78	12	184	190
15	120	-112	2	49	54	3	146	-144	1	76	-77	8	35	33	11	61	53
14	139	143	1	24	-21	2	261	-312				7	46	-46	10	36	31
12	151	-162	0	89	96	1	38	36		8 K 5		6	53	-53	9	83	86
11	122	127							17	56	-48	5	59	-56	8	167	-172
10	115	-122		15 K 4			3 K 5		15	60	-48	4	139	-162	7	139	138
9	112	-122	12	49	-45	20	21	-21	14	93	86	2	53	56	6	60	48
8	116	111	11	78	-86	19	104	-103	13	116	125	1	100	103	5	41	41
7	59	59	10	34	26	17	131	113	12	45	51				4	70	66
6	80	-86	8	37	27	16	64	52	11	29	-25		15 K 5		3	67	-59
5	125	132	7	89	-90	15	120	124	10	43	-43	12	34	38	2	60	64
4	85	-81	6	68	-68	14	29	-22	9	101	-108	9	25	-21	1	162	-187
3	123	-122	5	83	-84	13	72	-67	8	101	114	8	107	-119	0	43	37
2	38	-32	4	63	70	12	95	-92	7	40	41	7	28	25			
1	32	19	3	99	114	11	117	110	6	106	-106	6	92	105		4 K 6	
0	208	217	2	49	50	10	58	-50	5	98	101	5	121	-140	19	25	-18
			1	26	25	9	91	89	4	174	-178	4	45	42	18	52	-46
	9 K 4		0	145	-185	8	223	236	3	76	-71	3	73	-76	16	47	-44
18	59	62				7	171	-174	2	103	93	2	112	-126	13	76	78
17	106	89		16 K 4		6	168	-173	1	23	-24	1	55	51	12	110	106
16	30	-24	11	40	-48	5	80	-83							10	99	89
14	34	-28	9	60	65	3	40	-35		9 K 5			16 K 5		9	171	-184
13	61	-61	8	36	-41	2	254	270	17	49	-46	10	30	-31	8	40	-32
12	112	119	6	92	-94	1	57	-52	14	35	32	9	85	94	7	239	273
11	36	21	5	45	-48				13	170	175	8	29	30	6	34	23
10	74	-81	4	25	28		4 K 5		10	47	-47	7	51	-58	5	41	40
8	74	-74	3	57	56	20	26	-33	9	70	-70	6	58	-59	4	77	76
7	227	-258	2	48	43	19	121	110	8	42	43	4	77	-90	3	333	-363
6	83	82	1	50	-44	17	111	-102	7	53	46	3	46	57	2	55	-42
5	26	25	0	28	32	16	64	50	6	70	-73	1	77	80	1	234	239
4	38	-24				15	108	-96	5	136	-148				0	134	-126
3	245	246		17 K 4		14	41	40	3	95	-95		17 K 5				
2	39	-30	9	28	-34	13	167	169	2	149	154	8	72	-91		5 K 6	
1	30	-25	8	31	32	12	42	28	1	73	-12	7	30	-31	19	35	-33
0	165	164	7	50	-44	11	52	-53				6	49	53	18	218	207

Table 3. Continued.

17	53	-47	0	143	-155	2	166	-207	4	132	131	8	132	141	16	28	23
16	38	-28							3	40	34	7	23	16	15	69	-60
15	37	-22		11 K 6			1 K 7		2	135	132	6	27	22	14	93	79
14	202	-210	15	49	-49	19	174	-192	1	31	23	5	35	34	13	49	34
12	211	231	13	28	-23	18	34	33				4	44	-43	12	75	-66
11	41	39	12	32	27	17	153	132		7 K 7		2	133	153	11	58	57
10	32	25	11	73	70	16	28	-21	17	59	-63	1	56	-61	10	108	-110
9	96	96	10	44	-43	15	64	54	16	26	-22				9	142	-139
8	158	-153	9	102	105	14	50	36	15	109	-99		15 K 7		8	44	35
7	115	106	8	37	37	13	300	-325	14	35	24	9	34	-36	7	81	70
6	42	40	5	26	-5	9	174	165	12	66	65	8	37	42	6	79	-72
5	67	62	4	45	-47	8	101	-104	11	48	-50	7	99	118	5	57	37
4	178	180	3	47	42	7	160	-169	10	77	-74	6	39	-38	4	51	-39
3	34	-25	2	27	26	6	45	46	9	97	-101	3	47	52	3	209	-209
2	193	-182	1	147	-161	5	102	105	8	29	23	2	40	39	2	28	21
1	79	-70	0	27	29	4	29	-23	7	111	109	1	90	100	1	126	124
0	69	49				3	165	238	6	22	-26				0	68	57
				12 K 6		1	29	-33	5	130	131		16 K 7				
	6 K 6		14	56	54				4	58	54	8	54	65		5 K 8	
18	68	-63	13	59	-56		2 K 7		3	97	92	6	47	62	17	39	34
16	33	-26	11	95	94	19	43	48	2	82	-74	4	33	31	16	27	-26
15	77	-74	8	75	79	18	29	-22	1	68	62	2	33	27	14	131	-123
13	121	128	7	62	-59	17	39	-41				1	43	-49	13	36	-32
11	88	-86	3	45	35	16	54	-32		8 K 7					12	161	156
10	62	61	2	44	-44	15	70	69	17	20	13		17 K 7		11	63	-60
9	55	-56	1	24	-17	14	150	-148	15	30	25	3	53	63	10	49	44
8	150	152	0	59	-56	13	61	-46	12	81	-84	2	36	43	9	98	-98
7	110	119				12	26	-16	11	34	-30	1	45	54	8	190	-218
6	110	111		13 K 6		11	45	40	10	47	-47				7	101	-101
5	105	95	14	103	120	10	37	32	9	37	-33		0 K 8		6	124	133
4	28	-20	13	28	-26	9	79	74	8	165	175	18	87	-87	5	58	55
3	379	-379	12	48	-48	8	184	-186	7	67	58	16	108	93	4	19	-10
2	67	-58	11	29	29	7	62	-58	6	50	-47	14	95	84	3	33	27
1	260	266	10	73	-73	6	198	214	5	131	-134	12	118	-120	2	47	-35
0	118	-109	9	104	102	4	274	342	4	61	-52	10	135	-130	1	79	68
			8	103	112	2	149	-197	3	81	75	8	55	45	0	30	21
	7 K 6		6	28	-21	1	19	-19	2	242	253	6	56	54			
18	155	165	5	41	-39							4	106	-117		6 K 8	
17	31	-29	4	47	-52		3 K 7			9 K 7		2	89	94	17	35	38
16	25	-13	3	26	10	19	105	-117	16	27	-22				16	29	23
14	186	-179	1	71	-72	18	76	23	15	131	-123		1 K 8		15	92	-83
12	176	185	0	53	64	17	56	55	13	135	129	18	66	57	14	26	-15
11	46	42				16	49	-40	11	84	-88	17	105	98	13	48	34
10	60	65		14 K 6		15	45	33	9	134	-152	16	30	-31	12	47	-45
9	151	168	11	23	27	13	191	-201	7	133	148	14	47	-33	11	71	78
8	212	-233	10	54	51	12	62	63	6	43	44	13	68	-59	10	58	-59
7	60	55	9	96	101	11	27	-22	5	97	100	12	41	38	9	153	-165
6	40	27	8	81	92	10	31	-19	4	65	-53	11	57	42	8	109	-113
5	26	-22	7	113	-127	9	96	91	2	47	37	10	23	-17	7	175	197
4	104	100	6	34	32	8	91	-88	1	27	-24	9	40	-34	6	123	-132
3	35	-34	4	42	-44	7	53	-54				8	43	33	5	22	7
2	157	-151	3	126	148	6	84	89		10 K 7		7	202	-205	4	30	26
1	51	-45	2	39	-34	5	150	164	13	23	-20	6	43	-30	3	197	-188
0	130	122	1	76	-82	4	45	-38	12	136	-136	5	34	-24	2	119	107
			0	99	-109	3	119	117	10	88	-91	4	25	19	1	111	91
	8 K 6					2	19	-19	9	29	30	3	191	307	0	116	100
17	34	32		15 K 6		1	24	-17	8	176	217	2	56	-71			
16	60	-45	11	52	56				6	34	34	1	48	-58		7 K 8	
15	65	-65	10	35	-35		4 K 7		4	127	-123	0	21	28	17	23	21
14	50	41	9	96	106	18	33	-32	3	24	-21				15	55	55
13	71	68	8	113	125	17	40	33	2	263	298		2 K 8		14	121	-117
11	54	-51	7	37	36	15	37	32	1	75	66	18	38	-32	13	29	26
10	38	36	6	44	-43	14	60	-59				17	32	31	12	153	163
9	82	-82	4	38	-43	13	69	-61		11 K 7		16	76	63	11	106	-114
8	135	152	3	39	-39	12	46	-38	15	117	-140	15	37	-33	9	105	-120
7	106	112	1	56	-60	11	31	16	14	38	33	14	119	104	8	140	-152
6	49	35	0	68	72	9	33	21	13	125	136	13	37	28	6	179	140
4	55	-54				8	136	-136	12	56	-50	12	93	-84	5	58	-63
3	203	-192		16 K 6		7	35	33	11	95	-102	11	36	-32	4	72	-65
2	31	-28	9	102	115	6	104	98	9	123	-137	10	161	-163	3	27	-19
1	145	130	8	44	45	5	34	-32	8	41	-38	9	43	-33	2	35	27
0	111	-109	7	131	-148	4	229	233	7	158	181	8	77	61	1	149	142
			6	20	27	3	70	70	6	24	17	7	21	14	0	95	78
	9 K 6		5	33	-33	2	82	-78	5	77	84	6	78	-73			
17	37	-41	3	168	205	1	79	74	4	24	-19	5	32	24		8 K 8	
15	25	-18	2	39	-40				3	37	31	4	79	-85	16	49	49
14	120	-115	1	85	-99		5 K 7		2	74	72	3	136	-164	15	65	-50
12	93	102	0	78	-83	16	61	-46	1	24	16	2	56	70	14	108	-96
11	90	91				15	38	-26				1	79	110	13	57	47
10	26	26		17 K 6		13	82	-73		12 K 7		0	191	308	11	51	45
9	98	97	7	35	42	12	75	72	13	23	14				10	25	22
8	118	-137	6	30	-29	10	61	-57	12	116	-117		3 K 8		9	81	-92
6	91	91	4	48	-56	9	25	20	10	82	-81	18	118	123	8	119	-124
4	24	-10	3	23	-23	8	30	19	8	148	168	17	83	77	7	82	82
3	43	45	2	50	51	6	50	37	5	58	59	16	39	-38	6	43	-37
1	147	-147	0	33	-28	5	136	135	4	102	-112	14	110	-93	5	45	38
0	26	-31				4	75	70	3	37	-32	13	28	-5	4	60	63
				18 K 6		3	42	38	2	231	285	12	83	80	3	203	-201
	10 K 6		3	137	179	2	81	-68				9	55	-37	2	91	81
16	64	-51	2	22	-28	1	70	57		13 K 7		8	100	-99	1	172	170
15	28	-28	1	85	-110				13	81	95	7	191	-205	0	40	-42
14	64	59	0	62	-73		6 K 7		11	64	-59	6	32	24			
11	73	78				17	55	47	9	91	-88	5	34	30		9 K 8	
10	54	50		0 K 7		14	105	-92	8	41	47	4	69	62	15	98	105
9	69	-79	18	25	-21	13	26	-17	7	134	150	3	148	153	14	64	-59
8	75	76	16	60	-40	12	109	-111	6	39	-42	2	123	-134	13	32	27
7	52	46	14	128	-116	11	48	-53	4	32	-24	1	18	12	12	100	99
6	45	44	12	67	56	9	41	35	1	89	92	0	66	80	11	107	-109
5	45	-40	10	95	87	8	96	92							10	26	-14
3	76	-71	8	248	-264	7	49	44		14 K 7			4 K 8		9	89	-90
2	95	-97	6	119	120	6	21	8	10	56	-66	18	23	22	8	44	-41
1	44	34	4	248	332	5	117	-121	9	61	-67	17	22	30	7	107	116

Table 3. Continued.

6 93 95	1 K 9	1 78 64	6 26 -32	8 26 19	5 48 -41
5 69 -71	17 58 62		5 60 64	7 61 63	2 69 -80
3 69 -69	16 40 -28	7 K 9	4 115 -136	6 156 155	1 22 28
2 72 -66	15 135 112	16 34 -31	3 76 -73	5 74 -66	0 65 -61
1 103 102	14 43 -31	15 63 58	2 20 19	4 166 -172	
0 95 95	13 54 -43	13 67 57	1 24 -26	3 46 33	13 K 10
	12 44 35	12 70 60		2 70 -54	9 41 -39
10 K 8	11 133 143	11 31 21	15 K 9	1 67 -54	7 97 112
15 51 -53	10 29 -16	10 40 41	6 55 -67	0 264 298	6 68 -80
14 89 -95	9 23 -22	8 127 -158	5 77 -92		5 22 19
13 57 50	8 21 -14	7 40 -33	4 76 -84	6 K 10	4 88 100
12 39 30	7 144 -144	6 90 93	3 53 -58	15 120 -137	3 110 -129
10 58 53	6 24 -20	5 98 -102	2 122 147	14 30 -29	0 56 -60
8 161 -189	5 90 86	4 84 77	1 41 41	13 35 -33	
7 31 -23	4 15 18	3 110 -102		12 56 53	14 K 10
6 51 -62	3 41 -48	2 185 -191	16 K 9	11 137 141	6 60 79
5 60 60	2 19 -23	1 52 48	3 63 -76	10 74 69	5 40 -41
4 75 82	1 159 -218		1 23 10	9 73 -63	2 56 -67
3 89 -91		8 K 9		8 68 46	1 31 32
2 102 111	2 K 9	15 35 34	0 K 10	7 78 -87	0 48 -62
1 74 71	17 87 85	14 105 103	16 81 -72	6 30 23	
0 75 21	16 172 168	13 107 -105	14 142 120	5 113 118	15 K 10
	15 31 20	12 70 64	12 67 -54	4 45 39	3 56 -76
11 K 8	14 25 17	11 57 52	8 148 150	3 79 -63	2 33 39
14 37 33	13 118 -96	10 27 -21	6 57 -51	2 38 -30	1 31 -35
13 45 49	12 40 24	9 90 87	4 52 -52	0 104 -107	0 90 -130
12 27 20	10 165 158	8 40 -37	2 32 -34		
11 139 -138	9 115 110	7 61 -65		7 K 10	0 K 11
9 95 -97	8 166 -168	5 82 -79	1 K 10	15 29 -35	14 163 -175
7 39 37	7 79 -69	4 154 -162	15 59 -47	14 35 32	12 165 -147
6 23 -11	6 136 -138	3 75 20	14 25 19	13 28 20	10 107 103
3 54 -52	5 102 -108	2 22 -11	13 30 -16	12 31 27	8 62 56
2 31 -29	4 57 48	1 60 52	12 46 34	11 31 23	6 92 -88
1 149 172	3 87 95		11 50 39	10 106 -104	4 138 169
0 43 42	2 85 -97	9 K 9	9 184 188	9 87 89	2 40 54
	1 53 71	14 39 -43	8 73 -70	7 87 83	
12 K 8		13 104 106	7 87 -76	6 141 149	1 K 11
9 26 25	3 K 9	12 40 35	6 83 75	5 52 43	15 110 -121
8 114 -125	17 71 75	11 46 -42	5 38 -29	4 112 -111	13 36 -29
7 47 -53	16 58 -49	10 30 29	4 61 -68	3 130 -121	12 25 15
6 48 -48	15 93 71	8 26 -23	3 68 78	2 71 -63	11 65 53
5 40 -36	14 21 -20	7 38 39	2 15 15	1 19 -12	10 77 69
4 109 125	13 125 118	6 20 -11	1 97 -134	0 130 126	9 110 -118
3 71 72	12 122 128	5 129 -144	0 62 91		8 57 -52
2 49 48	11 58 -57	4 85 92		8 K 10	7 23 17
1 28 -25	9 71 -65	3 56 -51	2 K 10	14 52 -47	6 17 -6
	7 135 -136	2 104 -102	16 43 -41	12 88 95	5 225 262
13 K 8	6 31 16	1 136 143	15 88 -80	11 104 112	4 24 -20
12 54 -67	5 28 3		14 114 99	10 105 101	3 18 17
11 82 -91	4 70 61	10 K 9	13 71 -13	9 62 -58	2 34 -35
9 67 -75	3 115 -108	14 124 160	12 39 -32	7 70 -73	1 191 -237
8 38 46	2 140 -158	13 28 -30	11 118 121	6 22 6	
7 23 25	1 149 -199	12 65 70	10 53 53	5 82 78	2 K 11
6 42 -45		10 75 -65	9 99 -102	4 43 46	15 15 8
5 25 14	4 K 9	9 25 23	8 130 129	3 50 -42	14 121 -128
4 24 -14	17 50 52	8 23 14	7 22 15	2 112 -115	13 27 -29
3 44 -42	16 107 104	6 40 -30	5 23 13	1 20 -24	12 173 -166
2 28 22	15 93 82	5 26 21	4 56 -50		11 38 36
1 108 115	14 36 -24	4 138 -153	3 83 98	9 K 10	10 146 144
0 31 -21	13 160 -141	3 40 40	2 54 -61	13 67 69	9 29 -23
	12 84 71	1 26 -27	1 22 -18	12 24 20	8 38 33
14 K 8	11 23 -14		0 68 -87	10 39 -32	7 77 -71
9 57 58	10 57 48	11 K 9		9 44 46	6 66 -58
8 82 -91	9 144 144	13 111 149	3 K 10	8 62 -62	5 60 55
7 47 -44	8 29 -23	12 18 11	14 32 23	7 105 113	4 109 108
6 48 -49	7 37 -30	11 45 -53	13 62 -31	6 85 88	2 65 69
5 78 -77	6 131 -113	9 29 30	12 57 49	5 32 29	1 62 -57
3 119 123	5 114 -103	8 43 40	11 109 103	4 77 -74	
2 63 65	4 69 51	7 56 60	10 71 -68	3 164 -191	3 K 11
1 72 -79	3 107 96	6 22 -18	9 121 123	1 38 24	15 42 -43
0 36 39	2 115 -112	5 189 -215	8 198 227	0 50 45	14 61 -46
	1 16 -5	4 28 -15	5 49 -42		13 94 -84
15 K 8		3 53 -63	4 128 -123	10 K 10	12 54 -52
8 68 84	5 K 9	1 98 107	3 56 44	12 94 110	11 45 29
7 24 -19	16 71 -65		2 106 -114	11 37 37	10 126 119
6 79 -88	15 74 70	12 K 9	1 113 -129	10 68 64	9 41 -38
4 31 -31	13 23 20	12 70 89	0 140 170	9 56 -57	8 59 -52
3 21 -13	12 74 63	10 108 -112		8 37 -23	7 41 -39
2 76 72	11 49 42	9 45 -46	4 K 10	7 22 20	5 204 217
1 68 74	10 37 -27	8 70 65	16 34 -28	6 75 76	4 102 99
0 56 -56	8 139 -139	7 37 30	15 123 -123	5 25 -15	2 69 -61
	7 109 -117	6 23 -6	14 31 27	4 28 21	1 83 -92
16 K 8	6 200 215	5 27 29	13 25 -23	2 94 -100	
5 60 -68	5 44 -37	4 143 -140	12 24 15	1 29 17	4 K 11
4 24 -30	4 117 103	3 34 -30	11 167 161	0 88 -89	15 12 -10
3 126 149	3 40 -36	2 47 38	10 79 76		14 79 -80
2 38 39	2 218 -222	1 108 -102	9 69 -65	11 K 10	13 68 -61
1 77 -80	1 141 -137		8 87 86	11 32 31	12 114 -113
0 54 63		13 K 9	7 48 -41	9 47 -36	11 63 63
	6 K 9	8 69 72	6 55 47	8 20 -20	10 89 77
17 K 8	16 35 33	7 58 53	5 87 77	7 123 139	9 36 39
0 63 -79	15 97 93	6 37 -40	4 57 -45	6 35 27	7 83 -85
	14 64 60	5 159 -178	3 16 -9	5 29 17	6 44 38
0 K 9	13 165 -154	4 84 -88	2 29 17	3 159 -163	5 117 119
16 144 146	12 102 101	3 31 -34	0 153 -169	0 59 -51	4 70 60
14 22 -2	9 113 122	2 99 97			3 21 -13
12 52 -53	8 51 -48	1 81 76	5 K 10	12 K 10	2 94 97
10 249 257	7 52 -47		14 54 45	10 51 55	1 100 -95
8 166 -151	6 92 -88	14 K 9	12 54 51	9 30 25	
6 134 -139	5 67 -59	9 52 -66	11 103 93	8 54 -53	5 K 11
4 53 44	4 57 -68	8 55 49	10 127 -138	7 60 56	14 48 -43
2 105 -149	2 65 -56	7 22 21	9 46 53	6 83 83	13 95 -96

Table 3. Continued.

12	49	-45	9	24	15	6	26	-29	1	101	-107	9	22	20	12	K	11		
11	25	-18	8	26	26	4	68	61				7	58	-61	8	21	-24		
10	108	98	7	97	-99	3	80	81		9	K 11	6	122	140	7	22	17		
8	60	-53	6	93	105	2	85	-82	11	73	-90	5	47	42	6	145	175		
7	22	20	5	104	114	1	87	90	10	61	67	4	47	46	5	21	-18		
6	50	-45	4	54	51				9	75	80	3	25	-25	2	19	4		
5	121	117	3	53	-37		8 K 11		8	51	-49	1	34	-20	1	34	32		
4	116	104	2	21	14	13	45	-59	7	99	105								
3	25	22	1	92	-95	12	45	44	6	21	-20		11 K 11		13	K	11		
2	102	-90				11	44	40	5	132	-128	10	38	52	5	25	-24		
1	27	26		7 K 11		10	116	-130	4	46	37	9	55	69	3	62	52		
			13	54	-58	9	38	35	3	136	150	7	84	85	1	123	152		
	6 K 11		12	40	-40	8	39	33	2	55	-45	6	22	21					
14	37	-43	11	90	-87	7	89	-91	1	122	131	5	89	-93	14	K	11		
13	57	-53	10	70	57	6	94	99				3	91	93	2	35	43		
12	26	-22	9	85	74	5	80	80		10 K 11		2	30	-30					
11	78	75	8	51	-40	4	99	93	11	17	17	1	168	188					
10	49	-44	7	59	58	2	28	-34	10	100	-125								

Finally a difference Fourier synthesis was calculated in which no abnormalities could be detected. No attempt was made to locate hydrogen atoms.

DESCRIPTION AND DISCUSSION OF THE STRUCTURE

The structure is built up of $Mo_5P_2O_{23}^{6-}$-groups linked together by sodium-oxygen octahedra. The $Mo_5P_2O_{23}^{6-}$ groups are oriented with their pentagon of Mo-atoms approximately parallel to the *yz*-plane and connected through Na^+-ions (O – Na1 – O) forming two symmetry related zig-zag chains directed along the *c*-axis (see Fig. 1).

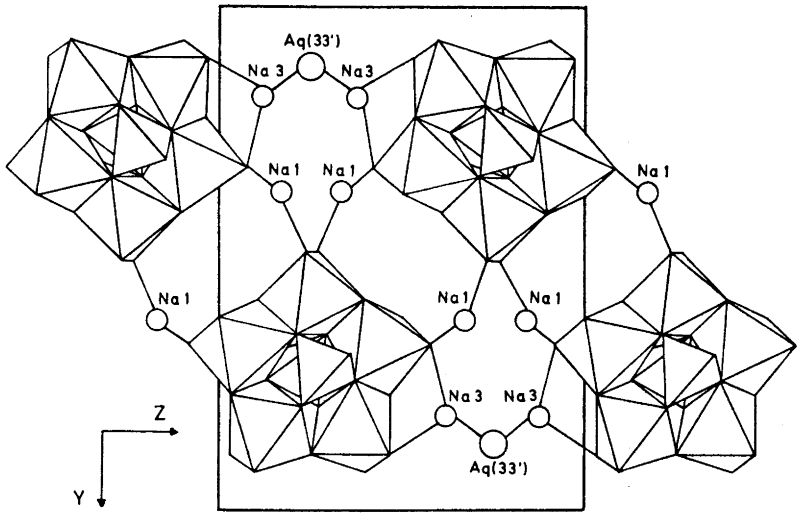

Fig. 1. The zig-zag arrangement of $Mo_5P_2O_{23}^{6-}$-groups in the *yz*-plane and the two types of Na^+-linking between the groups.

The connection within the chains is strengthened by bridges O – Na3 – H_2O – Na3 – O. The symmetry related chains are then coupled together through bridges O – Na2 – H_2O – Na3 – O as shown in Fig. 2.

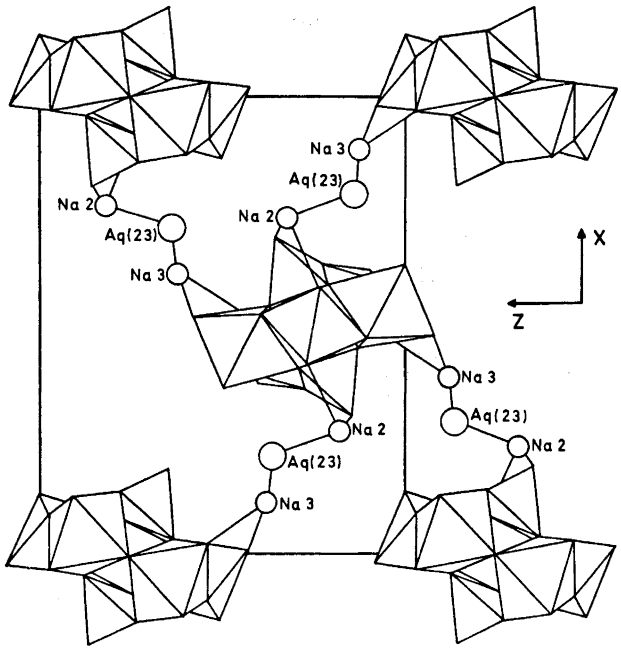

Fig. 2. The Na^+-coupling between symmetry related zig-zag chains.

The $Mo_5P_2O_{23}^{6-}$-group. In this group, five MoO_6-octahedra are coupled together forming a ring. The octahedra are joined together by sharing edges except for in one contact where only a corner is shared. Two PO_4-tetrahedra are attached to the ring, one above and the other below, each having three oxygen atoms in common with the ring. This configuration implies that each MoO_6-octahedron has four shared and two unshared oxygens and each PO_4-tetrahedron has one oxygen unshared. In this way the group becomes ball-shaped with the twelve unshared oxygen atoms protruding from the ball. The symmetry in the group is a twofold rotation axis. The arrangement in the group is shown in Fig. 3.

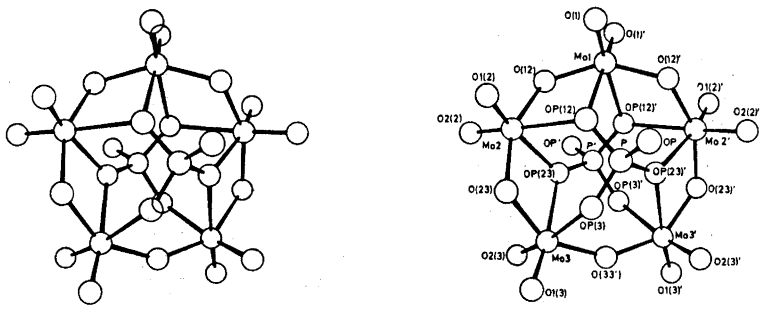

Fig. 3. Stereoscopic view of the $Mo_5P_2O_{23}^{6-}$-group.

Table 4. Distances (Å) and angles (degrees) within the $Mo_5P_2O_{23}^{6-}$-group. The numbering of the atoms is in accordance with that shown in Table 2, with primes indicating atoms in a symmetry related position. The estimated standard deviations are given in parentheses and refer to the last decimal place given.

		Mo, P	
Mo1 – Mo2	3.364(1)	P – Mo1	3.439(3)
Mo2 – Mo3	3.356(1)	P – Mo2	3.505(3)
Mo3 – Mo3′	3.647(2)	P – Mo3	3.335(3)
Mo1 – Mo3	5.459(2)	P – Mo2′	3.432(3)
Mo2 – Mo2′	5.493(2)	P – Mo3′	3.644(3)
Mo2 – Mo3′	5.566(1)	P – P′	3.822(6)
Mo2′ – Mo1 – Mo2	109.44(5)		
Mo1 – Mo2 – Mo3	108.63(4)		
Mo2 – Mo3 – Mo3′	105.18(3)		
		MoO_6-octahedra	
Mo1 – O(1)	1.72(1)	O(1) – Mo1 – O(12)	102.0(4)
Mo1 – O(12)	1.937(9)	O(1) – Mo1 – OP(12)	87.5(4)
Mo1 – OP(12)	2.281(8)	O(1) – Mo1 – O(1)′	105.2(5)
O(1) – O(1)′	2.74(2)	O(1) – Mo1 – O(12)′	97.2(4)
O(1) – O(12)	2.85(1)	O(12) – Mo1 – OP(12)	72.8(3)
O(1) – O(12)′	2.75(1)	O(12) – Mo1 – OP(12)′	82.9(3)
O(1) – OP(12)	2.80(1)	OP(12) – Mo1 – OP(12)′	80.8(3)
OP(12) – O(12)	2.52(1)		
OP(12) – O(12)′	2.81(1)		
OP(12) – OP(12)′	2.96(2)		
Mo2 – O(23)	1.91(1)	O(23) – Mo2 – O1(2)	96.2(4)
Mo2 – O(12)	1.925(9)	O(23) – Mo2 – O2(2)	99.0(4)
Mo2 – O1(2)	1.73(1)	O(23) – Mo2 – OP(23)	74.5(4)
Mo2 – O2(2)	1.72(1)	O(23) – Mo2 – OP(12)	89.3(3)
Mo2 – OP(23)	2.181(9)	O(12) – Mo2 – O1(2)	101.0(4)
Mo2 – OP(12)	2.322(9)	O(12) – Mo2 – O2(2)	95.9(4)
O(23) – O1(2)	2.72(1)	O(12) – Mo2 – OP(23)	82.5(4)
O(23) – O2(2)	2.76(1)	O(12) – Mo2 – OP(12)	72.1(3)
O(23) – OP(23)	2.49(1)	O1(2) – Mo2 – O2(2)	104.3(5)
O(23) – OP(12)	2.99(1)	O1(2) – Mo2 – OP(12)	87.1(4)
O(12) – O1(2)	2.83(1)	O2(2) – Mo2 – OP(23)	96.2(4)
O(12) – O2(2)	2.71(1)	OP(23) – Mo2 – OP(12)	73.8(3)
O(12) – OP(23)	2.72(1)		
O(12) – OP(12)	2.52(1)		
O1(2) – O2(2)	2.73(1)		
O1(2) – OP(12)	2.83(1)		
OP(23) – O2(2)	2.92(1)		
OP(23) – OP(12)	2.71(1)		
Mo3 – O2(3)	1.73 (1)	O2(3) – Mo3 – O(23)	97.4(5)
Mo3 – O(23)	1.932(9)	O2(3) – Mo3 – O(33′)	100.5(4)
Mo3 – O(33′)	1.902(4)	O2(3) – Mo3 – O1(3)	101.0(5)
Mo3 – O1(3)	1.72 (1)	O2(3) – Mo3 – OP(23)	82.8(4)
Mo3 – OP(23)	2.398(9)	O(23) – Mo3 – O1(3)	101.0(5)
Mo3 – OP(3)	2.220(9)	O(23) – Mo3 – OP(23)	69.1(3)
O2(3) – O(23)	2.75(2)	O(23) – Mo3 – OP(3)	77.1(4)
O2(3) – O(33′)	2.79(1)	O(33′) – Mo3 – O1(3)	102.5(5)
O2(3) – O1(3)	2.66(2)	O(33′) – Mo3 – OP(23)	85.8(4)
O2(3) – OP(23)	2.77(1)	O(33′) – Mo3 – OP(3)	80.5(3)
OP(3) – O(23)	2.60(1)	O1(3) – Mo3 – OP(3)	88.9(4)
OP(3) – O(33′)	2.67(1)	OP(23) – Mo3 – OP(3)	86.8(3)

Table 4. Continued.

OP(3) – O1(3)	2.78(1)		
OP(3) – OP(23)	3.18(1)		
O(23) – O1(3)	2.82(1)		
O(23) – OP(23)	2.49(1)		
O(33′) – O1(3)	2.83(1)		
O(33′) – OP(23)	2.95(2)		
		PO_4-tetrahedron	
P – OP	1.495(9)	OP(23) – P – OP	110.8(5)
P – OP(3)	1.524(9)	OP(23) – P – OP(3)	106.6(5)
P – OP(12)	1.553(9)	OP(23) – P – OP(12)	109.0(5)
P – OP(23)	1.570(9)	OP – P – OP(3)	112.5(5)
OP(23) – OP	2.52(1)	OP – P – OP(12)	108.3(5)
OP(23) – OP(3)	2.48(1)	OP(3) – P – OP(12)	109.6(5)
OP(23) – OP(12)	2.54(1)		
OP – OP(3)	2.51(1)		
OP – OP(12)	2.47(1)		
OP(3) – OP(12)	2.51(1)		

Distances and angles between the Mo-atoms in the group are collected in Table 4. It can be seen that when the MoO_6-octahedra share edges the Mo – Mo distances are 3.364 Å (Mo1 – Mo2) and 3.356 Å (Mo2 – Mo3) and when the octahedra only share a corner the distance increases to 3.647 Å (Mo3 – Mo3′). These distances are quite normal. For comparison it may be mentioned that the Mo – Mo distances when octahedra share edges in the structures $Na_3(CrMo_6O_{24}H_6).8H_2O$ [4] and $(NH_4)_6Mo_7O_{24}.4H_2O$ [5] are 3.309 – 3.351 Å and 3.20 – 3.44 Å, respectively. Cross distances within the ring are 5.459, 5.493, and 5.566 Å. These cross distances would be of particular interest as characteristic fingerprints in, for instance, solution X-ray studies.

The sodium coordination around the $Mo_5P_2O_{23}^{6-}$-groups. As mentioned above the $Mo_5P_2O_{23}^{6-}$-group has twelve unshared oxygens. To eight of these, Na^+-ions are coordinated (see Fig. 4). There are three kinds of crystallographically

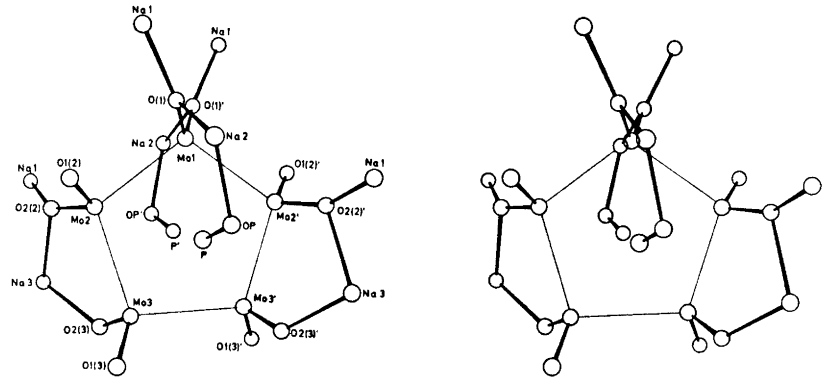

Fig. 4. Stereoscopic view of the sodium coordination to the $Mo_5P_2O_{23}^{6-}$-group (for clarity only the twelve unshared oxygens in the group have been drawn).

different sodium atoms, Na1, Na2, and Na3. Each of these atoms is always coordinated to two $Mo_5P_2O_{23}^{6-}$-oxygens, Na1 to oxygens (the Mo-oxygens O(1) and O2(2)) in two different groups, Na2 and Na3 to oxygens in one and the same group. Na2 binds to one Mo- and one P-oxygen (O(1) and OP) and Na3 to the two Mo-oxygens O2(2) and O2(3). The fact that the sodium ion Na1 is directly bound to oxygens in adjacent $Mo_5P_2O_{23}^{6-}$-groups gives rise to a chain-formation where Na1 acts as a link between the groups. Owing to the symmetry each link consists of a double O – Na1 – O bond (see Fig. 1).

It may be worth mentioning that there are, on average, six Na^+ coordinated per $Mo_5P_2O_{23}^{6-}$, and thus the charge of the group actually has been completely neutralized by the Na^+-ions. If this behaviour is extrapolated to the conditions in aqueous solution one may propose, that also aqueous $Mo_5P_2O_{23}^{6-}$-ions may be thought of as uncharged $Mo_5P_2O_{23}^{6-}$ $(Na^+)_6(H_2O)_x$-molecules, more or less coupled together through the Na^+-ions.

The coupling of the sodium-oxygen octahedra. Besides binding to two $Mo_5P_2O_{23}^{6-}$-oxygens, every sodium also binds to four water oxygens thus forming an octahedral oxygen configuration around each Na^+-ion. The different octahedra [$NaO_6(1)$, $NaO_6(2)$, and $NaO_6(3)$] are more or less coupled together. $NaO_6(1)$ has a surface in common with $NaO_6(3)$ [through the oxygens Aq1(13), Aq2(13), and O2(2)] and an edge in common with $NaO_6(2)$ [through the oxygens Aq2(12) and O(1)]. The remaining oxygen around Na1(Aq1(12)) is shared with a corner of a $NaO_6(2)$ octahedron. $NaO_6(2)$ and $NaO_6(3)$ share a corner through the water oxygen Aq(23). The fourth water-oxygen around Na3, (Aq(33')), is shared with a symmetry-related $NaO_6(3)$ octahedron. This sharing of oxygens between different octahedra binds the $Mo_5P_2O_{23}^{6-}$-groups together forming a three-dimensional network. The smallest unit of coupled NaO_6-octahedra in this network is shown in Fig. 5.

The MoO_6-octahedra. The octahedra are somewhat distorted and the Mo – O distances range from 1.72 Å to 2.40 Å depending on the oxygen coordination. The shortest distances, 1.72 Å, are to oxygens coordinated to only one Mo-atom and the longest, on average 2.30 Å, are to oxygens coordinated

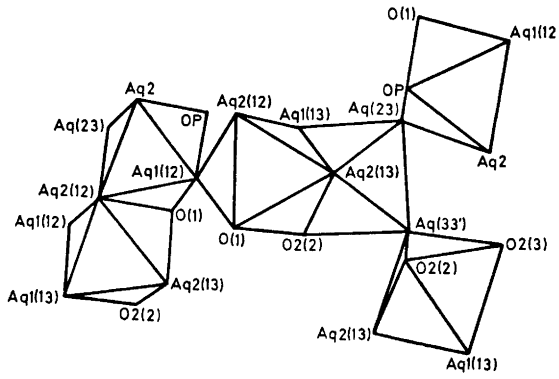

Fig. 5. The smallest unit of coupled NaO_6-octahedra (for clarity the octahedra are idealized).

to one P- and two Mo-atoms. This trend of increasing distances by increasing coordination numbers has been found also in other heteropolyanions containing molybdenum, and a comparison is made in Table 5.

Table 5. Distances (average) Mo—O in relation to the bond number of the oxygen. A comparison with other structures.

Bond number of oxygen	Distances Mo—O (Å)				Coordinating atoms
	$Mo_5P_2O_{23}^{6-}$	$CrMo_6O_{24}H_6^{3-}$	$TeMo_6O_{24}^{6-}$	$CeMo_{12}O_{42}^{8-}$	
1	1.72	1.707	1.714	1.68	Mo
2	1.92	1.939	1.943	1.98	Mo, Mo
3	2.30	2.292	2.299	2.28	Mo, Mo and, respectively, P, Cr, Te or Ce

Table 6. Distances within the NaO_6-octahedra (Å).

Na1 – O2(2)	2.47(1)	O(1) – O2(2)	3.58(1)
Na1 – O(1)	2.42(1)	O(1) – Aq1(12)	3.22(2)
Na1 – Aq1(13)	2.38(1)	O(1) – Aq2(12)	3.02(1)
Na1 – Aq2(13)	2.51(1)	O(1) – Aq2(13)	4.20(2)
Na1 – Aq1(12)	2.47(1)	Aq1(13) – O2(2)	3.18(2)
Na1 – Aq2(12)	2.45(1)	Aq1(13) – Aq1(12)	3.32(2)
		Aq1(13) – Aq2(12)	3.97(1)
		Aq1(13) – Aq2(13)	2.94(2)
		Aq2(13) – O2(2)	3.40(2)
		Aq2(13) – Aq2(12)	3.17(2)
		Aq1(12) – O2(2)	3.33(2)
		Aq1(12) – Aq2(12)	4.13(1)
Na2 – OP	2.43(1)	OP – O(1)	4.07(1)
Na2 – O(1)	2.75(1)	OP – Aq(23)	3.59(1)
Na2 – Aq(23)	2.42(1)	OP – Aq1(12)	3.15(1)
Na2 – Aq1(12)	2.48(1)	OP – Aq(2)	4.01(2)
Na2 – Aq2(12)	2.50(1)	Aq2(12) – O(1)	3.02(1)
Na2 – Aq(2)	2.40(1)	Aq2(12) – Aq(23)	3.64(2)
		Aq2(12) – Aq1(12)	3.49(1)
		Aq2(12) – Aq(2)	2.99(2)
		O(1) – Aq(23)	3.62(1)
		O(1) – Aq1(12)	3.64(2)
		Aq(2) – Aq(23)	3.31(2)
		Aq(2) – Aq1(12)	3.72(2)
Na3 – O2(3)	2.50(1)	O2(3) – Aq(23)	3.51(2)
Na3 – O2(2)	2.80(1)	O2(3) – Aq(33′)	3.49(1)
Na3 – Aq(23)	2.43(1)	O2(3) – O2(2)	3.89(2)
Na3 – Aq1(13)	2.35(1)	O2(3) – Aq1(13)	4.03(2)
Na3 – Aq2(13)	2.38(1)	Aq2(13) – Aq(23)	3.57(2)
Na3 – Aq(33′)	2.44(1)	Aq2(13) – Aq(33′)	3.11(2)
		Aq2(13) – O2(2)	3.40(2)
		Aq2(13) – Aq1(13)	2.94(2)
		O2(2) – Aq(33′)	4.01(2)
		O2(2) – Aq1(13)	3.18(2)
		Aq(23) – Aq(33′)	3.63(1)
		Aq(23) – Aq1(13)	3.30(2)

The NaO_6-octahedra. Distances are collected in Table 6. The distances Na – O range between 2.35 Å and 2.80 Å. There is no significant difference between the distances regardless of whether the oxygens arise from water or from the $Mo_5P_2O_{23}^{6-}$-groups, but two distances are considerably long. These distances are Na2 – O(1) = 2.75 Å and Na3 – O2(2) = 2.80 Å, no other Na – O distance being longer than 2.51 Å. The cause of these long distances is probably that O(1) and O2(2) are in contact also with Na1.

The configuration with four water-oxygens and two "oxide"-oxygens, which characterized the $Na^+ - O$ coordination in the present structure, has also been reported for other structures, for instance in $NaNH_4CrO_4(H_2O)_2$[6] and $Na_3CrMo_6O_{24}H_6(H_2O)_8$.[4] Concerning the distortion of the octahedra it is difficult to find any systematic effects and the octahedra are all far from regular.

The PO_4-tetrahedron. Distances and angles within the group are collected in Table 4. The distances P – O range between 1.50 Å and 1.57 Å and agree well with distances found in other compounds containing phosphate groups. One of the oxygens (OP) in the group is not shared with any Mo-atom and this gives rise to a short distance P – OP (1.50 Å). The O – O distances are 2.47 – 2.54 Å and these are also in agreement with those found in other structures. As can be seen from the distances and angles this group is almost regular.

Acknowledgements. I thank Professor Nils Ingri for much valuable advice, for his great interest, and for all the facilities placed at my disposal. The English of the paper has been corrected by Dr. Michael Sharp. The work forms part of a program supported by *Statens Naturvetenskapliga Forskningsråd.*

REFERENCES

1. Pettersson, L. *Acta Chem. Scand.* **25** (1971) 1959.
2. Strandberg, R. and Lundberg, B. K. S. *Acta Chem. Scand.* **25** (1971) 1767.
3. *International Tables for X-Ray Crystallography*, Kynoch Press, Birmingham 1962, Vol. III.
4. Perloff, A. *Inorg. Chem.* **9** (1970) 2228.
5. Evans, Jr., H. T. *J. Am. Chem. Soc.* **90** (1968) 3275.
6. Khan, A. A. and Baur, W. H. *Acta Cryst.* **B 28** (1972) 683.

Received October 11, 1972.

ACTA CHEMICA SCANDINAVICA 27 (1973) 1019–1028

Multicomponent Polyanions

V. A Potentiometric and Polarimetric Study of Borate-Mannitol Equilibria in 3.0 M $Na(ClO_4)$ Medium

LAGE PETTERSSON and INGEGÄRD ANDERSSON

Department of Inorganic Chemistry, University of Umeå, S-901 87 Umeå, Sweden

Equilibria between H^+, $B(OH)_3$, and D-mannitol ($C_6H_{14}O_6$) have been studied in 3.0 M $Na(ClO_4)$ medium at 25°C by means of potentiometric (glass electrode) and polarimetric measurements. The pH-range 2 – 9 has been covered. All data could be explained with the ternary complexes $(H)_{-1}(B(OH)_3)(C_6H_{14}O_6)^-$, $(H_{-1})(B(OH)_3)(C_6H_{14}O_6)_2^-$, $(H)_{-2}(B(OH)_3)_2(C_6H_{14}O_6)^{2-}$, and $(H)_{-2}(B(OH)_3)_2(C_6H_{14}O_6)_2^{2-}$ and a binary uncharged complex $(B(OH)_3)(C_6H_{14}O_6)$. The existence of the last complex has been established mainly from polarimetric measurements.

Data have been analysed using the least squares computer program LETAGROPVRID. "Best" equilibrium constants obtained from the potentiometric and polarimetric measurements are collected in Tables 2 and 3, respectively. "Best" molar rotations are given in Table 4.

Complex formation between borate ions and mannitol has long been known. Most frequently proposed complexes are $(B(OH)_4)(C_6H_{14}O_6)^-$ and $(B(OH)_4)(C_6H_{14}O_6)_2^-$. For the experimental methods used and equilibrium constants obtained in these previous investigations we refer to Stability Constants [1] (covered up to the end of 1968). The investigations can be divided into two groups, one assuming solely $(B(OH)_4)(C_6H_{14}O_6)_2^-$ and another both $(B(OH)_4)(C_6H_{14}O_6)^-$ and $(B(OH)_4)(C_4H_{14}O_6)_2^-$.

In a recent investigation Knoeck and Taylor [2] have shown that both a 1 : 1 and 1 : 2 borate-mannitol complex exist together. They have also discussed and reevaluated data of previous workers and thereby obtained results consistent with their own.

Although the existence of 1 : 1 and 1 : 2 borate-mannitol complexes, both with the charge −1, seems to be well established there are no thorough investigations covering wide concentration ranges and consequently the models proposed are restricted to rather narrow concentration ranges. Furthermore, the existence of possible uncharged and/or polynuclear complexes has not yet been thoroughly tested.

The need for a thorough study of the borate-mannitol euqilibria has been expressed (so *e.g.* in a critical review by Magnusson [3]). In order to undertake a complicated equilibrium study such as the borate-mannitol system presents, it is necessary to take the following general points into special consideration:

(i) that the system must be considered as a three component system with equilibria $pA+qB+rC \rightleftharpoons A_pB_qC_r$, where A, B, and C stand for H^+, $B(OH)_3$, and mannitol, respectively;

(ii) that the binary equilibria must be determined in separate experiments before one can obtain the ternary complexes;

(iii) that data must be collected over as wide concentration ranges as possible; and

(iv) that the experimental data can be adequately mathematically analysed. Graphical methods and hand calculations are of little use and it is necessary to use least squares computer methods. It is important that the finally proposed model can be tested directly against the measured quantities to assess how well or how poorly the proposed model fits the data.

The aim of the present study is to collect suitable data and try to analyse them in order to obtain a more exact equilibrium model of the system. We will thereby use experimental and computational methods especially suited for treating complicated three component equilibria.[15]

EXPERIMENTAL

The present study has been carried out in close connection with Parts II [4] and III [5] in this series.

Chemicals and analyses. Solutions of $NaClO_4$, $HClO_4$, and NaOH were prepared and analysed as described by Sjöberg [6] and D-mannitol as in Part II.[4] Boric acid solutions were prepared by dissolving known amount of recrystallized $B(OH)_3$ (Merck *p.a*).

Coulometric OH^--addition. In titrations with low B concentrations (10 and 20 mM), OH^- was added by using a coulometer with the following cell-arrangement:

$$-\text{Pt-gauze} \;\Big|\; \begin{matrix}\text{equilibrium}\\ \text{solutions}\end{matrix} \;\Big\|\; 3.0\ \text{M}\ NaClO_4 \;\Big\|\; 3.0\ \text{M NaCl} \;\Big|\; \text{Ag}+$$

cathode reaction: $H^+ + e^- \rightleftharpoons 1/2\ H_2(g)$
anode reaction: $Ag(s) + Cl^- \rightleftharpoons AgCl(s) + e^-$

The coulometer used was either a Metrohm type E 211 or a Leeds and Northrup coulometric analyzer (catalogue No. 7960).

Methods and apparatus in the emf measurements were essentially the same as described earlier.[6,7] The measurements were carried out as a series of potentiometric titrations in 3.0 M $Na(ClO_4)$ medium. In every titration the total boron concentration, B, and the total mannitol concentration, C, were kept constant. The free hydrogen ion concentration, h, was varied by addition of OH^- or H^+. The equilibrium concentration of $H^+ = h$ was determined by measuring emf of the cell

$$\text{Ag, AgCl} \;\Big|\; \begin{matrix}3.000\ \text{M}\ Na^+\\ 2.990\ \text{M}\ ClO_4^-\\ 0.010\ \text{M}\ Cl^-\end{matrix} \;\Big\|\; \begin{matrix}3.000\ \text{M}\ Na^+\\ 3.000\ \text{M}\ ClO_4^-\end{matrix} \;\Big\|\; \begin{matrix}\text{equilibrium}\\ \text{solutions}\end{matrix} \;\Big|\; \begin{matrix}\text{glass}\\ \text{electrode}\end{matrix}$$

Assuming the activity coefficients to be constant the following expression is valid for the measured emf:

$$E = E_0 + 59.157 \log h + E_j \qquad (1)$$

Table 1. Experimental data $H(\log h)_{BC}$. For each point the quantities H (in mM), $\log h$, and Δ are given. The quantity Δ is the residual $(Z_{calc} - Z) \times 1000$.

SATS 1
B = 0.010 C = 0.0025

H	log h	Δ
.43	-3.355	.74
.23	-3.628	.23
.03	-4.498	-0.26
-0.07	-6.010	2.66
-0.27	-6.777	4.00
-1.07	-7.533	7.17
-1.87	-7.900	7.13
-2.67	-8.155	9.24
-3.47	-8.361	11.73
-4.47	-8.589	11.56
-5.47	-8.787	16.13
-6.07	-8.904	18.59

SATS 2
B = 0.010 C = 0.005

H	log h	Δ
.32	-3.492	.18
.12	-3.912	.21
.02	-4.487	1.04
-0.08	-5.834	2.77
-0.48	-6.819	2.16
-0.88	-7.156	1.04
-1.48	-7.477	-0.88
-2.48	-7.844	-1.76
-3.48	-8.123	.73
-4.48	-8.368	2.28
-5.48	-8.594	3.97
-6.48	-8.812	7.88

SATS 3
B = 0.010 C = 0.010

H	log h	Δ
.42	-3.376	.08
.22	-3.656	-0.01
.02	-4.365	1.91
-0.08	-5.421	3.49
-0.28	-6.148	3.30
-0.78	-6.703	1.17
-1.58	-7.129	-2.83
-2.28	-7.382	-5.16
-2.98	-7.594	-6.65
-4.28	-7.937	-9.14
-5.48	-8.228	-9.42
-6.38	-8.449	-9.94
-7.38	-8.699	-4.66

SATS 4
B = 0.010 C = 0.020

H	log h	Δ
.42	-3.376	-0.15
.22	-3.655	-0.27
.02	-4.314	1.60
-0.29	-5.721	3.17
-0.88	-6.297	2.89
-1.98	-6.769	3.66
-2.98	-7.059	4.02
-3.78	-7.256	5.78
-4.98	-7.538	4.47
-6.49	-7.891	3.96
-7.58	-8.165	8.35
-8.48	-8.427	15.97

SATS 5
B = 0.010 C = 0.040

H	log h	Δ
.43	-3.369	-0.20
.23	-3.648	-0.81
-0.07	-4.698	1.44
-0.67	-5.648	3.16
-1.07	-5.888	3.33
-2.07	-6.258	5.22
-2.87	-6.473	6.23
-3.67	-6.662	5.21
-4.47	-6.830	7.64
-5.67	-7.081	7.65
-6.87	-7.345	8.51
-8.27	-7.712	13.07
-9.67	-8.385	18.95

SATS 6
B = 0.010 C = 0.080

H	log h	Δ
.46	-3.328	.19
.22	-3.602	.63
-0.08	-4.324	1.18
-0.58	-5.038	3.36
-1.09	-5.360	.80
-1.80	-5.638	-2.48
-2.60	-5.856	-2.85
-3.40	-6.033	-1.64
-4.60	-6.277	-2.78
-5.21	-6.378	4.80
-6.01	-6.540	2.01

SATS 7
B = 0.010 C = 0.160

H	log h	Δ
1.39	-2.857	-1.52
.79	-3.101	-2.13
-0.01	-3.886	-0.72
-0.81	-4.677	-0.71
-1.41	-4.954	-3.83
-2.61	-5.287	-2.53
-3.41	-5.459	-2.74
-4.41	-5.650	-2.31
-5.41	-5.826	1.96
-6.41	-6.014	2.99
-7.41	-6.215	8.23
-8.81	-6.617	10.86
-9.61	-7.059	13.13

SATS 8
B = 0.020 C = 0.0025

H	log h	Δ
.09	-4.025	.14
-0.11	-6.114	.27
-0.51	-6.843	.52
-1.31	-7.355	.22
-2.11	-7.634	2.13
-3.71	-8.013	3.40
-5.71	-8.322	7.01
-7.31	-8.512	10.96
-9.11	-8.694	16.34

SATS 9
B = 0.020 C = 0.005

H	log h	Δ
.68	-3.168	-0.02
.27	-3.567	-0.05
-0.32	-6.324	.43
-1.52	-7.154	-0.40
-3.12	-7.624	2.15
-5.12	-8.038	-1.30
-7.12	-8.324	2.83
-9.12	-8.564	5.26
-11.12	-8.774	10.25
-13.12	-8.978	14.98

SATS 10
B = 0.020 C = 0.020

H	log h	Δ
.69	-3.159	.09
.19	-3.721	-0.25
-0.31	-5.499	.28
-1.41	-6.245	-0.21
-3.31	-6.765	-0.83
-5.11	-7.098	-0.07
-6.71	-7.370	-5.77
-9.11	-7.734	-12.21
-11.11	-8.016	-15.07
-13.11	-8.277	-8.93
-15.61	-8.648	-6.10
-18.01	-9.090	5.77

SATS 11
B = 0.020 C = 0.040

H	log h	Δ
.26	-3.589	-0.62
-0.04	-4.392	.21
-0.64	-5.322	1.16
-1.84	-5.846	2.39
-3.84	-6.285	3.23
-6.34	-6.674	.44
-8.34	-6.943	-2.35

SATS 12
B = 0.020 C = 0.320

H	log h	Δ
2.55	-2.591	-1.81
1.45	-2.838	-4.45
-1.25	-4.089	-9.15
-3.65	-4.569	-10.88
-5.25	-4.776	-13.30
-6.65	-4.918	-10.37
-9.15	-5.151	-8.16
-11.75	-5.401	-13.68

SATS 13
B = 0.050 C = 0.005

H	log h	Δ
9.33	-2.028	1.06
4.81	-2.323	-1.25
1.88	-2.726	-0.06
-0.20	-5.699	.21
-0.89	-6.395	.82
-3.63	-7.267	-0.84
-8.61	-7.913	-1.78
-15.53	-8.378	2.75
-19.79	-8.588	5.41
-27.44	-8.916	7.41

SATS 14
B = 0.050 C = 0.010

H	log h	Δ
9.25	-2.031	1.18
4.81	-2.316	.42
1.97	-2.711	-0.57
-0.14	-5.229	-0.22
-2.09	-6.515	.39
-5.97	-7.281	-2.45
-10.72	-7.827	-5.94
-15.18	-8.162	-4.31
-23.29	-8.603	-0.59
-28.77	-8.853	.76

SATS 15
B = 0.050 C = 0.020

H	log h	Δ
9.09	-2.040	.70
4.70	-2.328	-0.07
1.86	-2.731	-0.11
-0.28	-5.005	.91
-2.20	-6.067	.78
-6.02	-6.740	1.75
-10.82	-7.323	-4.89
-15.32	-7.744	-11.08
-19.52	-8.053	-12.18
-27.17	-8.503	-9.12
-33.91	-8.853	-5.89

SATS 16
B = 0.050 C = 0.040

H	log h	Δ
9.14	-2.041	-0.90
4.71	-2.323	.75
1.89	-2.723	-0.10
-0.77	-5.036	-0.17
-3.46	-5.783	1.11
-8.42	-6.385	3.47
-15.18	-7.004	-3.25
-19.38	-7.343	-9.89
-26.93	-7.893	-20.90
-33.71	-8.334	-22.48
-39.58	-8.728	-18.50

SATS 17
B = 0.050 C = 0.080

H	log h	Δ
7.67	-2.114	.13
4.74	-2.323	.20
1.91	-2.725	-0.75
-0.14	-4.023	-0.75
-2.16	-4.946	2.32
-5.92	-5.516	-0.42
-13.02	-6.084	-1.38
-17.37	-6.358	.13
-21.38	-6.600	1.14
-28.74	-7.058	-2.45
-32.10	-7.277	-5.29
-36.77	-7.604	-9.17
-41.15	-7.957	-12.87
-45.14	-8.359	-10.13

SATS 18
B = 0.100 C = 0.040

H	log h	Δ
10.16	-1.987	1.50
6.79	-2.167	.13
3.08	-2.510	.05
-0.11	-4.197	-0.60
-2.05	-5.229	-0.51
-9.87	-6.196	.46
-18.37	-6.828	-2.50
-27.71	-7.372	-7.98
-38.68	-7.857	-9.39
-50.76	-8.275	-5.09
-59.18	-8.532	-2.63
-70.39	-8.846	2.98

SATS 19
B = 0.100 C = 0.080

H	log h	Δ
10.21	-1.989	.54
6.81	-2.165	.17
3.06	-2.518	-0.46
-0.32	-4.030	-1.12
-3.48	-4.938	-1.11
-11.81	-5.638	2.84
-21.81	-6.180	4.76
-32.94	-6.677	5.66
-44.20	-7.201	1.66
-55.63	-7.654	-2.97
-67.44	-8.079	-2.79
-77.58	-8.435	1.87
-86.36	-8.777	7.83

SATS 20
B = 0.100 C = 0.160

H	log h	Δ
9.53	-2.014	1.29
5.06	-2.296	-0.38
2.87	-2.540	-0.45
-0.13	-3.499	-0.99
-4.49	-4.485	-1.42
-15.16	-5.151	.70
-25.57	-5.550	2.07
-36.51	-5.907	5.34
-47.61	-6.263	7.68
-58.58	-6.625	10.66
-68.27	-6.970	11.28
-79.59	-7.418	9.72
-90.82	-7.999	5.06

SATS 21
B = 0.200 C = 0.040

H	log h	Δ
9.34	-2.026	.38
6.94	-2.159	-0.00
4.54	-2.338	.23
2.18	-2.665	-0.15
-0.96	-4.608	-0.28
-3.30	-5.185	-0.09
-8.96	-5.786	.54
-19.12	-6.420	1.27
-33.67	-7.059	-3.32
-54.87	-7.678	-3.99
-78.53	-8.179	2.50
-107.42	-8.669	10.50

SATS 22
B = 0.200 C = 0.080

H	log h	Δ
43.16	-1.363	.74
33.11	-1.481	-0.42
17.99	-1.747	-0.44
2.22	-2.620	.69
-1.11	-4.073	.89
-4.39	-4.763	.55
-16.97	-5.627	1.40
-34.36	-6.357	2.54
-50.18	-6.909	-1.78
-69.18	-7.446	-9.23
-82.07	-7.745	-10.02
-101.38	-8.130	-6.16
-121.53	-8.486	-0.92
-139.02	-8.774	3.13
-149.45	-8.944	5.19

SATS 23
B = 0.200 C = 0.160

H	log h	Δ
9.53	-2.016	.40
7.00	-2.152	.02
2.38	-2.601	.01
-0.41	-3.416	-0.07
-5.59	-4.309	.27
-16.87	-4.929	.19
-38.06	-5.575	4.20
-69.04	-6.371	11.53
-92.57	-6.946	10.94
-117.60	-7.492	6.24
-135.29	-7.849	5.01
-156.77	-8.263	10.89
-173.44	-8.615	16.15

SATS 24
B = 0.200 C = 0.320

H	log h	Δ
39.10	-1.404	1.41
23.55	-1.629	-0.64
16.20	-1.795	-1.19
2.26	-2.619	-1.63
-4.35	-3.709	-3.97
-16.92	-4.347	-8.57
-37.03	-4.833	-11.35
-57.48	-5.196	-9.89
-71.31	-5.421	-6.88
-84.02	-5.625	-3.35
-95.75	-5.817	.60
-110.03	-6.058	5.96
-136.14	-6.541	14.87
-151.77	-6.867	17.35
-171.86	-7.353	15.10
-188.77	-7.930	9.74
-198.63	-8.737	6.22

SATS 25
B = 0.400 C = 0.040

H	log h	Δ
9.06	-2.040	.17
4.29	-2.365	.02
1.11	-2.958	-0.14
-0.87	-4.216	.18
-8.96	-5.350	1.58
-33.79	-6.353	-0.80
-69.62	-7.137	-7.34
-107.70	-7.759	-9.97
-151.63	-8.315	-5.64
-192.61	-8.762	-4.45

where E_0 is a constant and E_j the liquid junction potential. E_0 was determined in every titration in the acid range where complex formation with H^+ can be neglected.

For the liquid junction potential we have used $E_j = -16.3\ h + 8.0\ K_w h^{-1}$ (mV), where $K_w = 6.17 \times 10^{-15}$ M^2 (the ionic product of water in 3.0 M $NaClO_4$).[8] From h, calculated by using eqn. (1), and from H, the excess concentration of hydrogen ions over the zero level $B(OH)_3$, mannitol and H_2O one can calculate Z, the average number of H^+ bound per B, using the relation:

$$Z = \frac{H - h + K_w h^{-1}}{B} \qquad (2)$$

Methods and apparatus in the polarimetric measurements were the same as described in Part II in this series.[4] The angle of optical rotation, α, was measured at points with known H, B, and C, at the five wavelengths: λ_1 = Na 589 nm, λ_2 = Hg 578 nm, λ_3 = Hg 546 nm, λ_4 = Hg 436 nm, and λ_5 = Hg 365 nm. We had no difficulties in obtaining stable α-values at these wavelengths.

Data treatment. The mathematical analysis of data was made using the least squares program LETAGROPVRID.[9] For the emf data the version ETITR [10] and for the polarimetric data the version SPEFO [11] have been used. On treating the emf and the polarimetric data the error squares sums $U = \sum(Z_{calc} - Z)^2$ and $U = \sum(\alpha_{calc} - \alpha)^2$ have been minimized, respectively. The standard deviations are defined and calculated according to Sillén.[12,13] The computation has been performed both on CD 3600 (Uppsala) and on CD 3200 (Umeå) computors.

DATA, CALCULATIONS AND RESULTS

Emf data. Data $Z(\log h)_{BC}$ have been collected covering the concentrations 10 mM $\leq B \leq$ 400 mM, 2.5 mM $\leq C \leq$ 360 mM; $-\log h$ has been varied from $\approx$1.5 to 9.0. All experimental data used in the calculations are collected in Table 1.

Accurate equilibrium data for $H^+ - B(OH)_3$ (25°C and 3.0 M $Na(ClO_4)$) has already been presented by Ingri.[14] He reports the following species and formation constants:

$B(OH)_4^-$ ($\log \beta_{-1,1} = -8.94$); $B_3O_3(OH)_4^-$ ($\log \beta_{-1,3} = -6.80$);
$B_3O_3(OH)_5^{2-}$ ($\log \beta_{-2,3} = -16.75$); $B_4O_5(OH)_4^{2-}$ ($\log \beta_{-2,4} = -14.89$);
$B_5O_6(OH)_4^-$ ($\log \beta_{-1,5} = -6.79$).

Note that the values of the constants given by Ingri are calculated with OH^- as component and they have been recalculated with H^+ as component using the ionic product of water in 3.0 M $Na(ClO_4)$ medium ($\log K_w = -14.21$).[8]

We have assumed these species and constants to be correct and in the search for complexes no attempts were made to introduce new species or to refine the constants.

The LETAGROP calculations were started with data for low B-values (B = 10 and 20 mM; 2.5 $\leq C \leq$ 320 mM) and gave clear indications for simultaneous existence of the two complexes $A_{-1}B\ C$ and $A_{-1}B\ C_2$ (see Table 2). The complex $A_pB_qC_r$ will often be referred to as the (p,q,r) species or complex.

We then extended the data range to include higher total concentration of B and tested this model. However, in this case it was impossible to explain the data solely with the complexes $(-1,1,1)$ and $(-1,1,2)$. We found deviations which indicated the possibility of complexes, polynuclear in boron. In order to find the composition of these additional complexes we made a *pqr*-analysis [16]

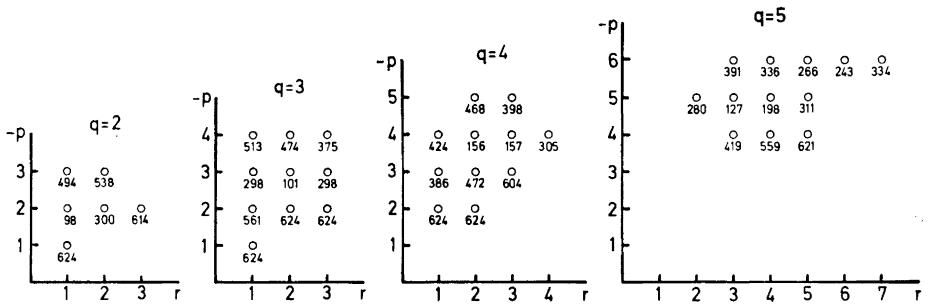

Fig. 1. Results of a *pqr*-analysis using data with $B = 200$ and 400 mM. Lowest error squares sums are plotted as a function of various *pr*-sets for $q = 2$, 3, 4, and 5.

using data for $B = 200$ and 400 mM. The result of the analysis is given in Fig. 1. We see that the lowest error squares sums are obtained for $(-2,2,1)$, $(-3,3,2)$, $(-4,4,2)$, $(-4,4,3)$, and $(-5,5,3)$. However, the magnitude of the sums are approximately the same and it is impossible to distinguish between them. We may however notice that in all these "possible" complexes $p/q = -1$ and q/r always are greater than one.

In the next step in our calculations the data range was extended to include $B = 50$, 100, 200, and 400 mM and the *pqr*-search was continued. It was then found that of the possible complexes, $(-2,2,1)$ gave the lowest error squares sum and the other complexes could be more or less excluded.

However, the residuals obtained in the calculations still showed systematic deviations especially at high total boron-mannitol concentrations. The deviations appeared both in the acidic and the alkaline regions. These observations would indicate the existence of both an uncharged $B(OH)_3$-mannitol complex and an additional three component complex polynuclear in boron.

In order to test the possibility of an uncharged complex we made a series of polarimetric measurements in acidic $B(OH)_3$-mannitol solutions, with $Z = 0$. We thereby found an optical activity, much higher than would be expected due to the mannitol alone. An equilibrium analysis of a set of optical data (see below) indicated the existence of an uncharged complex (0,1,1) with $\log \beta_{0,1,1} = -0.14$.

By introducing this (0,1,1) complex together with the polynuclear $(-2,2,2)$ complex into a LETAGROP calculation the observed systematic deviations disappeared and we could obtain a good explanation of all data assuming the complexes (0,1,1) $(-1,1,1)$, $(-1,1,2)$, $(-2,2,1)$, and $(-2,2,2)$. "Best" constants and standard deviations obtained in the calculations are collected in Table 2.

Polarimetric data. The only one of the three components possessing optical activity is mannitol. The molar rotation of mannitol at the wavelengths 589, 578, 546, 436, and 365 nm had earlier been determined (see Part II in this series [4]) and the values are given in Table 4.

Table 2. Results from LETAGROP calculations on potentiometric data minimizing $U = \sum(Z_{calc} - Z)^2$. In all the calculations the binary $H^+ - B(OH)_3$ species were given the values found by Ingri. However, in calculations No. 6 $\log \beta_{-1,1,0}$ was varied. In the calculations 4, 5, and 6 the complex (0,1,1) with $\log \beta = -0.14$ (found from polarimetric data) was added.

No.	B (mM)	$U \times 10^4$	$\sigma(Z)$	$\log (\beta_{-1,1,0} \pm 3\sigma)$	$\log (\beta_{-1,1,1} \pm 3\sigma)$	$\log (\beta_{-1,1,2} \pm 3\sigma)$	$\log (\beta_{-2,2,1} \pm 3\sigma)$	$\log (\beta_{-2,2,2} \pm 3\sigma)$
1	$10 \leq B \leq 20$ (132 points)	133	0.0101	−8.94	-5.92 ± 0.02	-4.17 ± 0.02	–	–
2	$10 \leq B \leq 400$ (293 points)	961	0.0182	−8.94	-5.84 ± 0.03	-4.21 ± 0.03	–	–
3	»	329	0.0107	−8.94	-5.91 ± 0.02	-4.18 ± 0.02	-13.50 ± 0.07	–
4	»	300	0.0102	−8.94	-5.91 ± 0.02	-4.11 ± 0.02	-13.45 ± 0.07	–
5	»	114	0.0063	−8.94	-6.00 ± 0.02	-4.10 ± 0.01	-13.53 ± 0.05	-10.79 ± 0.08
6	»	102	0.0060	-8.92 ± 0.01	-6.01 ± 0.02	-4.10 ± 0.01	-13.61 ± 0.08	-10.76 ± 0.07

Table 3. Results from LETAGROP calculations on polarimetric data minimizing $U=\sum(\alpha_{calc}-\alpha)^2$. In calculations 2 and 3 the binary species were given the values found by Ingri. When no 3σ is given, the formation constant has not been varied.

No.	Z	$U\times 10^2$	$\sigma(\alpha)°$	$\log(\beta_{0,1,1}\pm 3\sigma)$	$\log(\beta_{-1,1,1}\pm 3\sigma)$	$\log\beta_{-1,1,2}$	$\log(\beta_{-2,2,1}\pm 3\sigma)$	$\log(\beta_{-2,2,2}\pm 3\sigma)$
1	$Z=0$ (21 solutions)	0.11	0.003	-0.14 ± 0.03	–	–	–	–
2	$-1\leq Z\leq 0$ (86 solutions)	9.1	0.018	-0.14	-6.00	-4.10	-13.53	-10.79
3	»	6.9	0.013	-0.14	-5.78 ± 0.13	-4.10	-13.09 ± 0.11	-10.78 ± 0.22

Table 4. Molar rotations $\phi(\lambda)\pm\sigma$ of the optically active species, results from LETAGROP calculations. The molar rotations of mannitol were obtained in a separate determination and (0,1,1) in calculation No. 1. The molar rotations of (−1,1,1), (−1,1,2), (−2,2,1), and (−2,2,2) were obtained in calculation No. 3. The corresponding formation constants are given in Table 3.

λ (nm)	$\phi_{0,0,1}\pm\sigma$ (deg dm^{-1} M^{-1})	$\phi_{0,1,1}\pm\sigma$ (deg dm^{-1} M^{-1})	$\phi_{-1,1,1}\pm\sigma$ (deg dm^{-1} M^{-1})	$\phi_{-1,1,2}\pm\sigma$ (deg dm^{-1} M^{-1})	$\phi_{-2,2,1}\pm\sigma$ (deg dm^{-1} M^{-1})	$\phi_{-2,2,2}\pm\sigma$ (deg dm^{-1} M^{-1}
589	-0.109 ± 0.003	6.43 ± 0.02	6.02 ± 0.11	4.71 ± 0.03	5.37 ± 0.08	7.81 ± 0.19
578	-0.119 ± 0.003	6.71 ± 0.02	6.25 ± 0.10	4.90 ± 0.03	5.60 ± 0.07	8.15 ± 0.17
546	-0.142 ± 0.003	7.58 ± 0.02	6.96 ± 0.11	5.50 ± 0.03	6.36 ± 0.08	9.35 ± 0.20
436	-0.329 ± 0.004	12.42 ± 0.04	11.31 ± 0.19	8.54 ± 0.05	10.52 ± 0.13	15.20 ± 0.33
365	-0.750 ± 0.007	18.58 ± 0.05	16.69 ± 0.26	11.71 ± 0.07	15.96 ± 0.19	22.65 ± 0.46

In order to test the possibility of the existence of uncharged complexes ($p = 0$) the present optical data collecting was started with a series of measurements on acidic $B(OH)_3$-mannitol solutions ($40 \leq B \leq 400$ and $40 \leq C \leq 400$ mM) with $Z = 0$. The data clearly indicated that at least one uncharged complex must be formed and in a LETAGROP calculation we found that the complex (0,1,1) with $\log \beta = -0.14$ could well explain the data ($\sigma(\alpha) = 0.003°$). Calculations assuming the complex (0,2,2) could not explain data ($\sigma(\alpha) = 0.015°$).

The polarimetric measurements were then extended to the more alkaline region ($-1 \leq Z \leq 0$), and the following $B(C)$ concentrations (in mM) were studied: 50 (50,100,400); 200 (100,200,400); 400 (100, 200, 400). The B-concentrations were intentionally kept rather high in the hope of obtaining a distinct answer to the question of which was the predominant three component complex polynuclear in boron. The analysis of these data was started by testing the emf models where only one complex polynuclear in boron is present together with (−1,1,1), (−1,1,2), and (0,1,1). We found that none of these emf models could explain the optical data. However, a combination of the two polynuclear complexes (−2,2,1) and (−2,2,2) gave an acceptable explanation of the data (see Table 3).

In a final calculation the formation constants of (−1,1,1), (−2,2,2), and (−2,2,1) were varied together with the molar rotations for the optical active species. The "best" values of equilibrium constants and molar rotations obtained are collected in Table 3 and 4, respectively.

CONCLUSIONS

The present investigation has strongly established the existence of the complexes (0,1,1), (−1,1,1), and (−1,1,2). The data also clearly indicate that polynuclear (in boron) three component complexes must be formed and that these polynuclear complexes most certainly have the p/q ratio −1.

Since the mononuclear complexes (−1,1,1) and (−1,1,2) also have this ratio it was found very difficult, especially from emf data, to make a choice between different models containing polynuclear complexes with this ratio. However, in this situation the polarimetric data have been of great value. It was possible to discard a great number of possibilities and it was found that the most probable polynuclear complexes are (−2,2,1) and (−2,2,2). Another great advantage with the polarimetric data was that it became possible to detect the uncharged complex (0,1,1) and to determine its formation constant. From emf data alone, this determination would certainly have been impossible.

Strengths and concentrations of species in the present system in the pH-range 3 − 9 are well illustrated at some B, C concentrations by the distribution diagrams given in Fig. 2, a − c. When the B to C ratio is 1 and $B = 20$ mM (see Fig. 2a) the main ternary complex is (−1,1,1) but there are also small amounts of the complexes (−2,2,2), (−1,1,2), and (−2,2,1) present. At the same $B = 20$ mM but with great mannitol excess $C = 160$ mM (see Fig. 2b), the (−1,1,2) complex is quite predominating. One may, however, note that about 20 % of B is bound in the complex (0,1,1) in the acid range. For rather high total concentrations of B and C and with a small mannitol excess, as

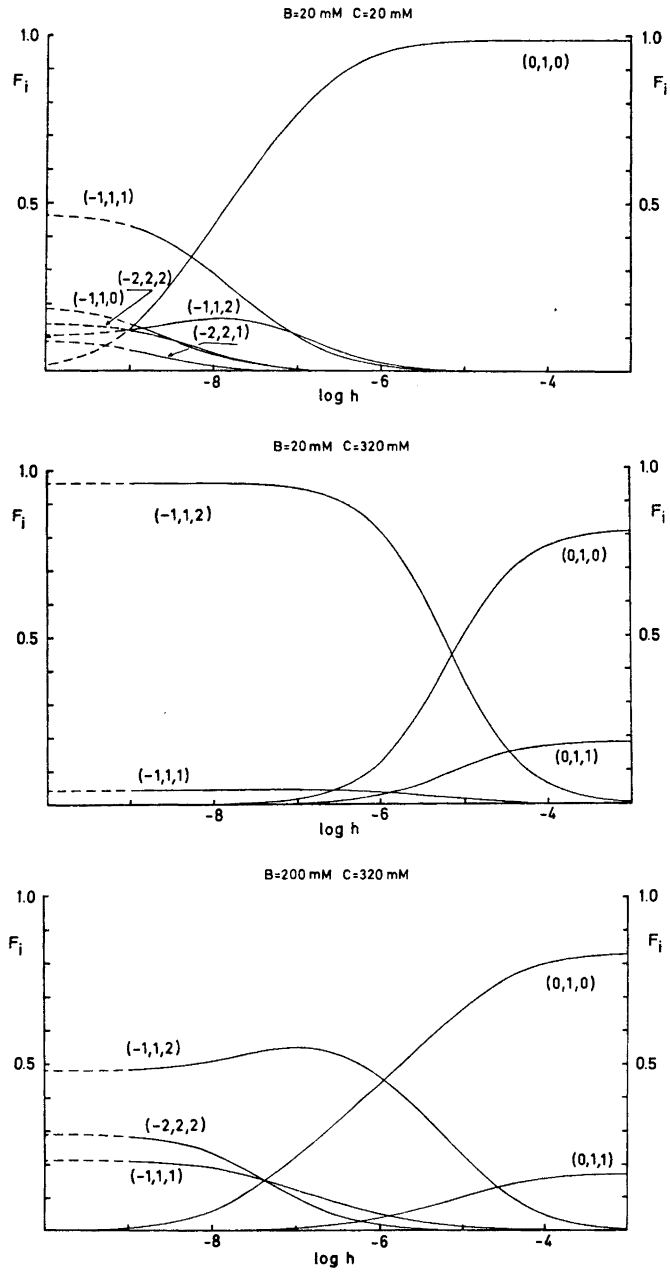

Fig. 2. Distribution diagrams F_i (log $h)_{BC}$. The quantity F_i is defined as the ratio between boron in a species to total boron. The computer program HALTAFALL [16] was used for the calculation with the constants in Table 2, calculation No. 5.

illustrated in Fig. 2c, the $(-1,1,2)$, $(-2,2,2)$, and $(-1,1,1)$ complexes are all present in considerable amounts.

In Part III of this series [5] we have made a potentiometric study of germanate-mannitol equilibria in 0.5 M Na(Cl) medium. In this system the three ternary complexes $(-1,1,1)$, $(-1,1,2)$, and $(-2,2,2)$ were found with $\log \beta_{-1,1,1} = -6.46$, $\log \beta_{-1,1,2} = -3.94$, and $\log \beta_{-2,2,2} = -10.68$. Complexes with these compositions have also been found as main species in the present investigation. The equilibria in the two systems thus show many similarities and the reason that the complexes $(0,1,1)$ and $(-2,2,1)$ were not found in the germanate-mannitol system may simply be that only low total concentrations of germanium was studied because of the low solubility of $Ge(OH)_4$.

A comparison of the formation constants for species with the same *pqr*-values in the two systems shows that they are of the same magnitude. A direct comparison cannot, however, be made since the ionic media were not the same in the two investigations.

Acknowledgements. We thank Professor Nils Ingri for much valuable advice, for his great interest, and for all the facilities placed at our disposal. The English of the present paper has been corrected by Dr. Michael Sharp. The work forms part of a program, financially supported by the *Swedish Natural Science Research Council.*

REFERENCES

1. Sillén, L. G. and Martell, A. E. (compilers). *Stability Constants Suppl. No. 1. Chem. Soc. Spec. Publ. No. 25* (1971) 425.
2. Knoeck, J. and Taylor, J. K. *Anal. Chem.* **41** (1969) 1730.
3. Magnusson, L. B. *J. Inorg. Nucl. Chem.* **33** (1971) 3602.
4. Pettersson, L. *Acta Chem. Scand.* **26** (1972) 4067.
5. Pettersson, L. and Andersson, I. *Acta Chem. Scand.* **27** (1973) 977.
6. Sjöberg, S. *Acta Chem. Scand.* **25** (1971) 2149.
7. Pettersson, L. *Acta Chem. Scand.* **25** (1971) 1959.
8. Boström, L. and Ingri, N. *Private communications.*
9. Ingri, N. and Sillén, L. G. *Arkiv Kemi* **23** (1964) 97.
10. Arnek, R., Sillén, L. G. and Wahlberg, O. *Arkiv Kemi* **31** (1969) 353; Brauner, P., Sillén, L. G. and Whiteker, R. *Arkiv Kemi* **31** (1969) 365.
11. Sillén, L. G. and Warnqvist, B. *Arkiv Kemi* **31** (1969) 377.
12. Sillén, L. G. *Acta Chem. Scand.* **16** (1962) 159.
13. Sillén, L. G. and Warnqvist, B. *Arkiv Kemi* **31** (1969) 341.
14. Ingri, N. *Acta Chem. Scand.* **17** (1963) 581.
15. Pettersson, L., Andersson, I., Lyhamn, L. and Ingri, N. *Trans. Roy. Inst. Technol., Stockholm 1972*, No. 256.
16. Ingri, N., Kakolowicz, W., Sillén, L. G. and Warnqvist, B. *Talanta* **14** (1967) 1261.

Received October 11, 1972.

ACTA CHEMICA SCANDINAVICA 27 (1973) 1029–1033

Diphenic Acid and 2-Phenylbenzoic Acid from Decarboxylation of Copper Phthalate

JADWIGA CHODOWSKA-PALICKA and MARTIN NILSSON*

Department of Organic Chemistry, Royal Institute of Technology, S-100 44 Stockholm 70, Sweden

Copper(I) phthalate when heated in quinoline above *ca.* 120° is decarboxylated giving mainly diphenic and 2-phenylbenzoic acids. Depending on the conditions varying amounts of benzoic acid, salicylic acid, phenyl benzoate, and biphenyl are also formed, though generally in smaller amounts.

Decarboxylation of copper(I) 2-nitrobenzoates in quinoline may give 2,2'-dinitrobiphenyls.[1–4] In the presence of iodoarenes decarboxylative coupling to unsymmetric 2-nitrobiphenyls is the major reaction.[1,2,4–6] An *ortho* nitro group accelerates copper-catalysed decarboxylation and also reactions of halogenobenzenes with organocopper compounds. This apparent paradox has analogies also for the carboxyl group. The facile decarboxylation of phthalic acid has been utilised for industrial production of benzoic acid.[7] 2-Iodobenzoic acid reacts very rapidly with copper acetylides and 2-bromobenzoic acids react readily with several nucleophiles in the copper-catalysed Hurtley reaction.[8,9]

We have studied the decarboxylation of copper(I) phthalate in quinoline at temperatures between 120 and 160°. The reactions were interrupted when one mol of carbon dioxide had been evolved per mol of phthalate.

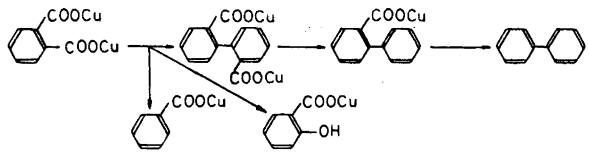

The acids were converted to methyl esters and yields were determined after chromatographic separation or in some cases by gas chromatography.

* Present address: Department of Organic Chemistry, Chalmers University of Technology and University of Göteborg, Fack, S-402 20 Göteborg 5, Sweden.

As shown in the scheme and in Table 1 formation of diphenic acid is a major reaction, which may be followed by further decarboxylation to 2-phenylbenzoic acid and eventually to biphenyl. The formation of biphenyl derivatives seems to be favoured by high concentration, at which formation of benzoic acid is less marked (at 120° and 0.8 M gross concentration the reaction mixture is heterogeneous). In most reactions metallic copper precipitated, indicating the stoichiometry of the reaction.

Table 1. Products (yields in per cent) from decarboxylation of copper(I) phthalate in quinoline. The reactions were interrupted after evolution of one mol of carbon dioxide per mol of phthalate. Products isolated, the acids as methyl esters (exceptions starred with yields determined by gas chromatography). Concentrations refer to initial approximate gross concentrations.

	120° 0.4 M 360 min	120° 0.8 M 280 min	130° 0.4 M 200 min	130° 0.8 M 360 min	160° 0.4 M 160 min
Diphenic acid	18	27	36	57	0
2-Phenylbenzoic acid	10	28	50	15	60 *
Benzoic acid	27	21	5	8	14 *
Salicylic acid	16	5	4	6	–
Biphenyl					10
Phenyl benzoate					4
Unreacted phthalic acid	10	10	< 1	< 1	
Total	81	91	95	86	88

Decarboxylation of copper(I) diphenate was investigated separately (Table 2). The diphenate decarboxylates considerably slower than phthalate, but more rapidly than 2-phenylbenzoate. Thus, it seems possible to direct the reaction towards diphenic acid or to 2-phenylbenzoic acid.

The formation of salicylic acid from copper phthalate is surprising since the reactions were performed under nitrogen. When oxygen was bubbled through the reaction mixture (at 140 – 160°) the carbon dioxide evolution was slower than usual and less biphenyl derivatives were formed. After evolu-

Table 2. Decarboxylation of copper(I) diphenate, initial gross concentration *ca.* 0.4 M in quinoline. Reactions were interrupted after evolution of one mol of carbon dioxide per mol of diphenate. Product yields in per cent determined by gas chromatography of the methyl esters, the biphenyl determined on the neutral fraction.

	140°, 370 min	160°, 290 min
4-Phenylbenzoic acid	40	80
D iphenic acid, unreacted	40	5
Biphenyl	–	*ca.* 10

tion of 0.25 mol of carbon dioxide per mol phthalate a 13 % yield of salicylic acid (based on copper phthalate) could be isolated.

Preliminary experiments on the decarboxylation of copper(I) 3- and 4-nitrophthalates have shown the formation of dinitrobiphenyl derivatives as well as formation of nitrosalicylic acids.

DISCUSSION

There are several indications that copper-promoted decarboxylation of aromatic acids proceeds *via* the copper(I) salts to give arylcopper compounds, which usually undergo further reactions [1–6,10] but under certain conditions may accumulate in the reaction mixture.[2,10] For phthalic acid analogies are provided by the formation of stable organomercury compounds (1) from mercury(II) phthalates,[11,12] and by the formation of arylcobalt derivatives (*e.g.* 2) from phthalic anhydride and octacarbonyldicobalt or tetracarbonylcobalt hydride.[13,14]

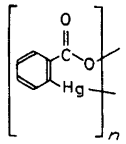

1

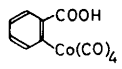

2

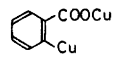

3

It is tempting to assume an analogous organocopper intermediate (*e.g.* 3) to account for the results of the present investigation. Such an intermediate could be expected to give copper(I) diphenate and metallic copper. Alternatively it could react with protons to give benzoic acid or be oxidised to salicylic acid. A similar intermediate is possible also in the reaction between 2-bromobenzoic acid and metallic copper which gives diphenic acid in aqueous alkaline solution.[9]

The formation of benzoic acid and 2-phenylbenzoic acid in the aprotic medium indicates abstraction of protons from the solvent or other compounds present, and is analogous to but less marked than the formation of nitrobenzenes from copper(I) nitrobenzoates.[1–5]

The formation of salicylic acid during decarboxylation of copper(I) phthalate reminds of the copper-catalysed, "oxidative decarboxylation" of benzoic acid to phenol *via* salicylic acid derivatives,[14] a reaction which forms the basis of the Dow phenol process.[15] The mechanism is not well known. However, a rapid exchange of the *ortho* hydrogens in copper(II) benzoate in heavy water has been observed.[17] The latter reaction might be interpreted in terms of "cupriation", a reaction, which has been also suspected in the thiophene series.[18–20] From these considerations it seems possible that the decarboxylation of copper(I) phthalates and the Dow process may have a common intermediate, possibly of the general type indicated in formula 3. If this were true several new transformations of both phthalic and benzoic acids would be possible.

The copper-promoted reactions of copper(I) phthalate should also be compared with thermal reactions of silver phthalates, which may give for example biphenylenes, presumably *via* benzynes.[21]

The present results raise several new problems. The kinetics of phthalic acid decarboxylation is probably not quite analogous to that for 2-nitrobenzoic acid. The factors governing the formation of salicylic acids are not yet defined and should be investigated further. The interactions between the phthalic acids and the quinoline seem to be important and are now being investigated.

EXPERIMENTAL

Copper(I) salts. Phthalic acid (0.2 mol) and copper(I) oxide (0.2 mol) were boiled in xylene (*ca.* 300 ml) for 20 h with continuous removal of water (3.4 ml) from the azeotrope. The yellow-grey *copper(I) phthalate* was filtered off, washed with hot xylene and dried in vacuum; yield 90 %. For analysis the product was treated with nitric acid and titrated with EDTA at pH 7 to 8 against murexide. (Found: Cu 43.3. Calc. for $C_8H_4O_4Cu_2$: Cu 43.6.) Similarly diphenic acid and copper(I) oxide in boiling xylene gave *copper(I) diphenate.* (Found: Cu 34.2. Calc. for $C_{14}H_8O_4Cu_2$: Cu 34.6.)

Decarboxylations. The appropriate copper salt (generally 0.01 mol) was suspended in quinoline (25 ml, in some experiments 12.5 ml) in a three-necked flask equipped with a nitrogen inlet tube (*ca.* 8 ml nitrogen/sec), a powerful magnetic stirrer and a reflux condenser. The outlet gases were passed through a U-tube with activated charcoal and some magnesium perchlorate *via* a three-way valve to U-tubes for carbon dioxide absorption (Ascarite and magnesium perchlorate). The reaction flask was immersed in a thermostated oil bath, a vigorous stirring maintained (important) and the carbon dioxide evolved was determined from the weight increase for the Ascarite tubes. When 0.01 mol of carbon dioxide had evolved the reaction mixtures were allowed to cool and diluted with *ca.* 200 ml ether. An excess 2 M hydrochloric acid was added to dissolve the quinoline and the mixture filtered. The solid phase was apparently mainly metallic copper. The ether phase of the filtrate was separated, washed with hydrochloric acid and with water and then extracted with sodium hydrogen carbonate solution. Acidic and neutral fractions were recovered in the usual way. The basic fraction, which was mainly quinoline, was not investigated. Alternatively, the reaction mixture was treated directly with aqueous alkali and acids recovered from solids and alkaline extract.

The acid fractions were screened by thin-layer chromatography on silica gel using ethanol : water : aqueous ammonia (25 %) (35 : 13 : 2 volumes) containing thymol blue (3 mg/100 ml).[22] This system separated benzoic, salicylic, and diphenic acids, but 2-phenylbenzoic acid was not well separated from diphenic acid.

The acids were methylated with diazomethane in ether/methanol. The mixtures of methyl esters were investigated by gas chromatography (5 % SE 30 on Chromosorb W) or thin-layer chromatography (20 % toluene in light petroleum or 20 % toluene and 20 % di-isopropyl ether in light petroleum). Generally, the ester mixtures were separated on silica gel columns using similar solvent systems.

The isolated esters were identified by m.p., infrared spectra and sometimes mass spectra, or after hydrolysis as the acids. 2-Phenylbenzoic acid was also characterised by its conversion with sulphuric acid into fluorenone.

Acknowledgements. The work has been supported by the *Swedish Board for Technical Development.* The spectra were recorded by Miss G. Hammarberg. The English was checked by Dr. L. Henderson.

REFERENCES

1. Chodowska-Palicka, J. and Nilsson, M. *Acta Chem. Scand.* **24** (1970) 3353.
2. Cairncross, A., Roland, I. R., Henderson, R. M. and Sheppard, W. A. *J. Am. Chem. Soc.* **92** (1970) 3187.

3. Cohen, T. and Shambach, R. A. *J. Am. Chem. Soc.* **92** (1970) 3189.
4. Chodowska-Palicka, J. and Nilsson, M. *Acta Chem. Scand.* **25** (1971) 3451.
5. Nilsson, M. *Acta Chem. Scand.* **20** (1966) 423.
6. Björklund, C. and Nilsson, M. *Acta Chem. Scand.* **22** (1968) 2585.
7. Kirk-Otmer, *Encyclopedia of Chemical Technology*, John Wiley, New York 1964, Vol. 3, p. 424.
8. Castro, C. E., Havlin, R., Honwad, V. K., Malte, A. and Mojé, S. *J. Am. Chem. Soc.* **91** (1969) 6464.
9. Hurtley, W. R. H. *J. Chem. Soc.* **1929** 1870.
10. Nilsson, M. and Ullenius, C. *Acta Chem. Scand.* **25** (1971) 2428.
11. Deacon, G. B. *Organometal. Chem. Rev.* **A 5** (1970) 355.
12. Sartori, P. and Golloch, A. *Chem. Ber.* **101** (1968) 2004.
13. Wender, I., Friedman, S., Steiner, W. A. and Anderson, R. B. *Chem. Ind. (London)* **1958** 1694.
14. Bird, C. W. *Transition Metal Intermediates in Organic Synthesis*, Logos Press, London 1967, p. 246.
15. Kaeding, W. W. and Collins, G. R. *J. Org. Chem.* **30** (1965) 3750.
16. Kirk-Otmer, *Encyclopedia of Chemical Technology*, John Wiley, New York 1964, Vol. 15, p. 155.
17. Schoo, W., Veenland, J. U., de Boer, T. J. and Sixma, F. L. J. *Rec. Trav. Chim.* **82** (1963) 172.
18. Nilsson, M. *Tetrahedron Letters* **1966** 679.
19. Nilsson, M. and Ullenius, C. *Acta Chem. Scand.* **22** (1968) 1998.
20. Gjøs, N. and Gronowitz, S. *Acta Chem. Scand.* **25** (1971) 2596.
21. Sartori, P. and Golloch, A. *Chem. Ber.* **102** (1969) 1765.
22. Hartley, R. D. and Lawson, G. J. *J. Chromatog.* **7** (1962) 69.

Received October 12, 1972.

ACTA CHEMICA SCANDINAVICA 27 (1973) 1034–1038

A Proton Magnetic Resonance Study of $SbCl_5.H_2O$ and $SbCl_5.2H_2O$ Adducts in Solution

LARS BERNANDER and GERD OLOFSSON

Thermochemistry Laboratory, Chemical Center, University of Lund, S-220 07 Lund, Sweden

The interaction between H_2O and the Lewis acid $SbCl_5$ has been studied in CH_2Cl_2 solution with varying H_2O:$SbCl_5$ molar ratios by PMR at temperatures between -100 and $+40$°C. In solutions with H_2O:$SbCl_5 \leq 1$ the monomeric adduct $SbCl_5.H_2O$ is quantitatively formed. If $1 < H_2O$:$SbCl_5 \leq 2$ a second water molecule is added forming a stable, probably hydrogen bonded complex $SbCl_5.2H_2O$.

It is well known that a number of metal halides, MeX_n, form stable complexes with water, which function as catalysts in a number of Friedel-Crafts reactions.[1] The only NMR spectroscopic study on such systems in non-aqueous solutions that to our knowledge has been reported concerns BF_3-H_2O in acetone solution.[2] As the $MeX_n.H_2O$ complexes are considered to behave as strong Brønsted acids a basic solvent like acetone might be expected to interact quite strongly with the complexes. It seemed therefore to be of interest to carry out a study in the weakly interacting solvent CH_2Cl_2. Due to the high solubility of $SbCl_5-H_2O$ complexes in halogenated hydrocarbons this system was studied instead of the less soluble BF_3-H_2O system.

EXPERIMENTAL

Materials. $SbCl_5$ (Merck, chromatographic grade) was used without further treatment. CH_2Cl_2 (Fisher Certified Reagent) was distilled shortly before use and stored over dust free beads of 4A molecular sieves. No impurities were detected by analytical GLC using dinonyl phthalate as stationary phase. The water content was checked by GSC[3] and found to be less than 10 ppm.

Samples. Stock solutions of $SbCl_5$ in CH_2Cl_2 were prepared by mixing weighed amounts of the components. Known amounts of solution were transferred to the NMR tubes and water was added from a calibrated Hamilton syringe. Whenever judged necessary the samples were prepared in a glove bag in an atmosphere of dry N_2. The composition of the samples was checked by determination of peak areas in the NMR spectra using the ^{13}C-satellites of the solvent as an internal standard. The sample composition is considered to be known to within a few per cent. The samples were stable and could be kept at room temperature for days without showing changes in the NMR spectra.

Apparatus and measurements. NMR spectra were recorded on a Varian A-60 A spectrometer equipped with a V-6040 temperature controller. Temperature calibration was carried out using sample substitution with a Varian methanol sample and is estimated to be accurate to within ± 1°C.

Chemical shift values of $SbCl_5-H_2O$ in CH_2Cl_2 were determined either directly relative to the low field ^{13}C-satellite of the solvent or relative to the solvent bulk peak with side band technique using an HP 200 CD Audio Oscillator and an HP Electronic Frequency Counter. The chemical shift values were recalculated to δ values relative to internal TMS using a value of δ 5.36 for the CH_2Cl_2 peak and a value of δ 6.84 for the low field ^{13}C-satellite at 60 MHz. The reproducibility of the chemical shift values is estimated to be better than 0.01 ppm.

The spectra of $SbCl_5.H_2O$ in $C_2H_4Cl_2$ and CCl_4 and of $BF_3.H_2O$ in $C_2H_4Cl_2$ were recorded at the working temperature of the spectrometer, about 40°C. The shift values were measured relative to that of $C_2H_4Cl_2$ (a small amount of $C_2H_4Cl_2$ had been added to the CCl_4 sample) and recalculated to δ in ppm relative to internal TMS using a value of δ 3.76 for neat $C_2H_4Cl_2$ and of δ 3.69 for $C_2H_4Cl_2$ in CCl_4.

RESULTS

PMR spectra of samples containing $SbCl_5$ and H_2O in CH_2Cl_2 solution were recorded at temperatures ranging from −100 to +40°C and with varying $SbCl_5$:H_2O concentration ratios. Only one narrow peak was observed from the water protons in all cases indicating fast proton and/or water exchange between different species. The concentration of $SbCl_5$ was kept constant, 0.56 *m*.* In samples with water concentration below 0.56 *m* a proton chemical shift of δ 6.62 at 41°C was observed which is ascribed to the $SbCl_5.H_2O$ adduct. The differences observed at constant temperature between proton shifts of samples containing $SbCl_5.H_2O$ concentrations from 0.05 *m* to 0.56 *m* were less than 0.02 ppm (*cf.* below). This indicates that $SbCl_5.H_2O$ is not associated in solution.

In NMR spectra recorded at 41°C of samples with water concentration between 0.56 to 1.03 *m*, *i.e.* molar ratios H_2O:$SbCl_5$ between 1.0 and 1.8, a steady change of the proton chemical shift to lower field with increasing water concentration was observed. Assuming quantitative formation of a 1:2 complex $SbCl_5.H_2O + H_2O \rightarrow SbCl_5.2H_2O$, the following eqn. (1) between the observed chemical shift δ and the concentrations of the reactants should be applicable:

$$\delta = [2\, m(SbCl_5)\, (\delta_1 - \delta_2)/m(H_2O)] - \delta_1 + 2\, \delta_2 \qquad (1)$$

where δ_1 and δ_2 denote the proton chemical shifts of the 1:1 and 1:2 complexes, respectively. A plot of observed chemical shift values against $SbCl_5$:H_2O concentration ratios is shown in Fig. 1 and as can be seen a linear relationship is observed. It can be concluded that the variation of δ can be ascribed to quantitative association of water with the 1:1 complex to form a 1:2 complex. Least squares fitting gives the values 6.61 and 7.02 for δ_1 and δ_2, respectively. The value of δ_1 is in good agreement with the chemical shift of the 1:1 complex observed in samples with $SbCl_5$ in excess.

Samples with H_2O:$SbCl_5$ molar ratios larger than 2 have not been studied.

The temperature dependence of the proton chemical shift was studied for four samples of $SbCl_5$ concentration 0.56 *m* and water concentration of 0.10 *m* (a), 0.31 *m* (b), 0.83 *m* (c), and 1.00 *m* (d), respectively. Samples (a) and (b)

* Concentrations are expressed in mol/kg solvent and denoted by *m*.

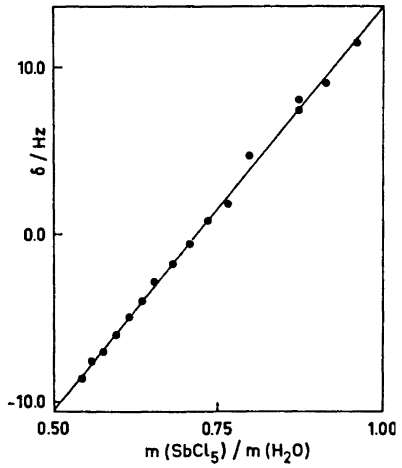

Fig. 1. Chemical shift of water protons against $SbCl_5$:H_2O molar ratio at 41°C. The chemical shifts are relative to that of the low field solvent ^{13}C-satellite.

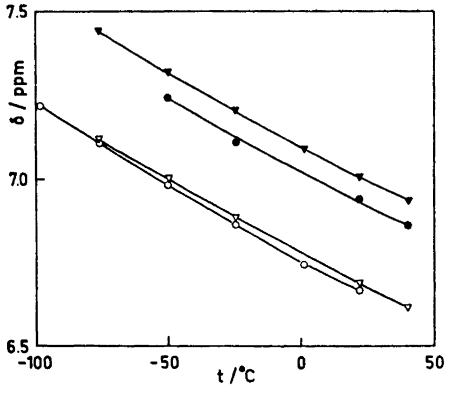

Fig. 2. Water proton chemical shifts of samples (a) – (d) against temperature. (a) ○, (b) ▽, (c) ●, (d) ▼. Chemical shifts are given in ppm relative to internal TMS.

thus contain the 1:1 complex while in samples (c) and (d) the two complexes are present in different proportions. The results are shown in Fig. 2 where the observed δ values are plotted against temperature. The results obtained with sample (a) differ slightly from those of (b), the differences being less than 0.02 ppm. The points obtained with samples (c) and (d) are equidistantly shifted to lower field from those of (a) and (b), the shift change being 0.25 ppm for sample (c) and 0.33 ppm for (d). The observed chemical shifts vary almost linearly with temperature and give an average temperature coefficient $\Delta\delta/\Delta T$ of -4.1×10^{-3} ppm/°C. Thus samples containing mixtures of the 1:1 and 1:2 complexes give the same temperature coefficient as samples containing only the 1:1 complex.

The chemical shift of water dissolved in CH_2Cl_2 was observed to be δ 1.59 in a 6.5×10^{-3} *m* solution and δ 1.62 in a 39×10^{-3} *m* solution at 20°C.

The proton chemical shift of $SbCl_5.H_2O$ in the presence of excess $SbCl_5$ was observed to be δ 7.0 in $C_2H_4Cl_2$ solution and δ 6.4 in CCl_4 solution at 40°C.

$BF_3 - H_2O$. A signal from the water protons was observed at δ 8.2 in a sample containing BF_3 and H_2O in $C_2H_4Cl_2$. The sample was prepared by introducing BF_3 into a solution containing 0.10 % by weight of water. The solution was turbid at room temperature but became clear at 40°C. Further addition of BF_3 did not affect the proton resonance signal which is ascribed to the protons in the $BF_3.H_2O$ adduct. Due to the low solubility in CH_2Cl_2 and $C_2H_4Cl_2$ the $BF_3 - H_2O$ system was not further studied.

DISCUSSION

The complexes $SbCl_5.H_2O$ and $BF_3.H_2O$ are considered to exist in weakly interacting solvents as molecular electron-pair donor-acceptor adducts. The

vibrational spectrum of (solid?) $SbCl_5.H_2O$ has been observed to be closely similar to that of $SbCl_5.HOCN(CH_3)_2$ in the range for the vibrational motions of the Cl_5SbO moiety.[4] The latter complex is known from an X-ray crystallographic study to exist as a donor-acceptor adduct.[5]

The donor strength of water towards $SbCl_5$ is about the same as that of alkyl ethers and alkyl ketones as judged from the enthalpies of formation of the adducts in $C_2H_4Cl_2$ solution.[6-8]* Adduct formation will increase the acidity of the water protons and thus make the adducts apt to interact with basic molecules either through protonation or through hydrogen bond formation.

Preliminary calorimetric experiments indicate that the association of the second water molecule to give the $SbCl_5.2H_2O$ complex is less exothermic than the formation of the 1:1 adduct.[9] The high solubility of both the 1:1 and 1:2 complexes in inert solvents like CH_2Cl_2 and $C_2H_4Cl_2$ indicates non-ionic structures for both complexes. The 1:2 complex may be described as a hydrogen bonded complex in which the second water molecule is held by hydrogen bonding to the 1:1 adduct.

The temperature coefficient of -4.1×10^{-3} ppm/°C of the water proton chemical shift in both the 1:1 and 1:2 complexes is larger than those usually observed for non-associated species; see *e.g.* Ref. 10. However, it does not seem likely that the shift changes are caused by changes in association equilibria within the $SbCl_5-H_2O$ system. Solute-solvent interaction might be the reason for the large temperature coefficients. It is also possible that low frequency motions of the adduct molecules could give rise to the observed effect. Muller and Reiter[10] have pointed out that in the case of hydrogen bonded species large temperature coefficients may arise from causes other than changes in association equilibria. They have shown that the chemical shift of hydrogen bonded protons depend quite strongly on the degree of excitation of the hydrogen bond stretching vibrational mode and that a large $\Delta\delta/\Delta T$ value would result from changes in population of excited states of this low frequency motion. Their discussion would be applicable to other types of low frequency motions that could affect the electrostatic field at the protons studied.

The large difference between the proton chemical shift of the $BF_3.H_2O$ adduct in acetone, δ 12.46,[2] and in $C_2H_4Cl_2$, δ 8.2, indicates solute-solvent interaction in acetone solution. $SbCl_5.H_2O$ has been found to interact with weak bases like ethers and ketones in $C_2H_4Cl_2$ solution to give stable ternary complexes of 1:1:1 composition.[9] The water proton chemical shifts are observed at lower field in the ternary complexes than in $SbCl_5-H_2O$. It is likely that the primary interaction between $BF_3.H_2O$ and acetone is the formation of an analogous ternary complex and that therefore Gillespie and Hartman[2] in their NMR study observed the behaviour of the ternary complex $BF_3.H_2O.OC(CH_3)_2$ instead of the binary adduct $BF_3.H_2O$ as hitherto thought. Their statement that "...acetone is much inferior to water as an electron pair donor to BF_3" is not corroborated by comparison of donor strengths towards $SbCl_5$. The ex-

* The enthalpy value for the formation of the $SbCl_5.H_2O$ adduct referred to in Ref. 8 has been found to be in error. Later experiments have confirmed the value of -18.0 kcal mol^{-1} given in Ref. 6.[9]

change between acetone bound in the ternary complex and bulk acetone is expected to be rapid on the NMR time scale in accordance with observations on ternary complexes of $SbCl_5.H_2O$ [9] and the complexation of acetone will therefore not be revealed by NMR.

Acknowledgement. The authors are grateful to professor S. Forsén, Div. of Physical Chemistry, Lund Institute of Technology, for putting the NMR spectrometer at our disposal. A grant from the *Swedish Natural Science Research Council* is gratefully acknowledged.

REFERENCES

1. Olah, G. A. *Friedel-Crafts and Related Reactions*, Interscience, New York 1963, Vol.1.
2. Gillespie, R. J. and Hartman, J. S. *Can. J. Chem.* **45** (1967) 859.
3. Sellers, P. *Acta Chem. Scand.* **25** (1971) 2295.
4. Burgard, M., Kaufman, G. and Rohmer, R. *C. R. H. Acad. Sci. Ser. C* **267** (1968) 689.
5. Brun, L. and Brändén, C.-I. *Acta Cryst.* **20** (1966) 749.
6. Gutman, V. and Mayer, U. *Monatsh.* **98** (1967) 294.
7. Olofsson, G. *Acta Chem. Scand.* **22** (1968) 377.
8. Olofsson, G. *Acta Chem. Scand.* **22** (1968) 1352.
9. Olofsson, G. and Olofsson, I. *To be published.*
10. Muller, N. and Reiter, R. C. *J. Chem. Phys.* **42** (1965) 3265.

Received October 21, 1972.

ACTA CHEMICA SCANDINAVICA 27 (1973) 1039–1052

Sur les Alcaloïdes de *Knightia deplanchei* Vieill. ex Brongn. et Gris (Protéacées)*,**

CHRISTIANE KAN-FAN et MAURI LOUNASMAA***

Institut de Chimie des Substances Naturelles, CNRS, 91-Gif-sur-Yvette, France

La composition alcaloïdique de *Knightia deplanchei* Vieill. ex Brongn. et Gris (Protéacées) a été étudiée. Quatre alcaloïdes nouveaux ont été isolés et leurs structures planes (I à IV) ont été déterminées principalement par spectrométrie de masse. Il s'agit des benzyl-2 tropanes qui forment un nouveau groupe d'alcaloïdes tropaniques.

Le genre *Knightia* (Protéacées) comprend trois espèces, dont deux sont endémiques en Nouvelle-Calédonie (*K. deplanchei* et *K. strobilina*)[1] et l'une en Nouvelle-Zélande (*K. excelsa*).[2] Parmi ces plantes, nous avons étudié *K. deplanchei* Vieill. ex Brongn. et Gris, à partir des feuilles duquel nous avons isolé plusieurs produits alcaloïdiques, dont quatre font l'objet du présent mémoire. Excepté un cas récent,[3] concernant la bellendine (et deux autres bases, pas encore caractérisées†), isolés de *Bellendena montana*, c'est la première fois que des alcaloïdes sont isolés d'une plante appartenant à la famille Protéacées.

Pour les quatre produits, nommés provisoirement par les lettres A, B, C et D, nous proposons, en nous basant principalement sur les donnés des spectres de masse, les structures planes suivantes (I à IV).

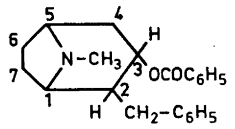

Produit A

I

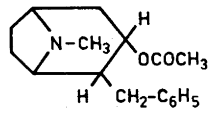

Produit B

II

* Plantes de Nouvelle-Calédonie. Partie XXIV. Pour partie XXIII, voir M. Païs, R. Sarfati, F. X. Jarreau et R. Goutarel, *Tetrahedron* **29** (1973) 1001.

** Le présent mémoire a fait l'objet d'une communication le 13 septembre 1972 aux Journées de Chimie Organique d'Orsay, organisées par la Société Chimique de France.

*** Adresse actuelle: Centre National de la Recherche Technique (VTT), Laboratoire Chimico-Technique, SF-02150 Otaniemi, Finlande.

† *Note ajoutée à l'épreuve:* Dans une lettre datée du 17 janvier 1973 le Professeur Bick nous a indiqué que l'une de ces deux bases a été caractérisée comme une méthylbellendine.

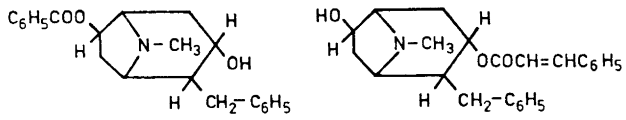

Produit C
III*

Produit D
IV*

La fragmentation des alcaloïdes tropaniques en spectrométrie de masse est bien connue,[4,5] et peut être présentée de la façon suivante (Schéma 1):

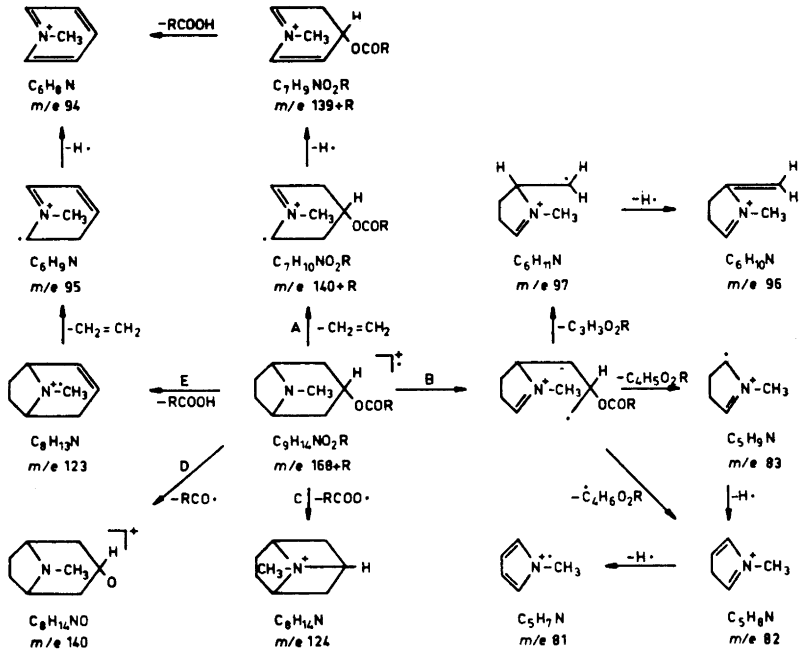

Schéma 1.

Les spectres de masse des produits A, B, C et D (Fig. 1, 2, 3 et 4), ainsi que ceux de leurs dérivés d'hydrolyse (Fig. 5 et 6 (identiques), 7 et 8) montrent une fragmentation analogue, qui rend compte des structures proposées (I à IV).

Pour le spectre de masse du produit A (Fig. 1) nous proposons l'interprétation suivante (Schéma 2). Les transitions marquées par un m^* s'appuient sur l'examen des pics métastables présents dans le spectre.

Le pic moléculaire à m/e 335 correspond à la formule $C_{22}H_{25}NO_2$ conformément à la structure proposée (I). La supposition que le produit A contient un groupement acyle en position 3, est en accord avec le fait qu'on ne décèle qu'un pic très faible, dû à la perte d'éthylène à partir de l'ion moléculaire ($M^+ - 28$) (Voie A). Cette conclusion est également en accord avec les résultats antérieurs.[4,5]

* Le groupement fonctionnel, placé arbitrairement en position 6, peut se trouver également en position 7 (*cf.* plus loin).

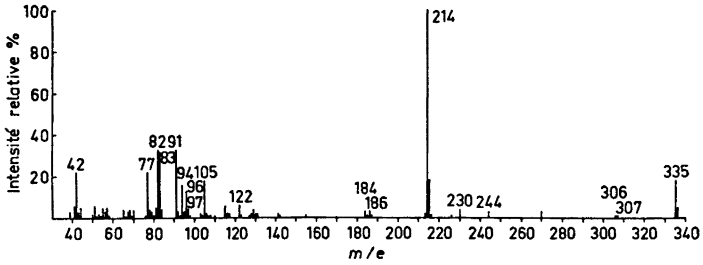

Fig. 1. Spectre de masse du produit A.

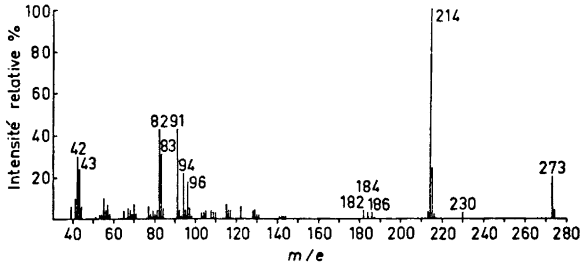

Fig. 2. Spectre de masse du produit B.

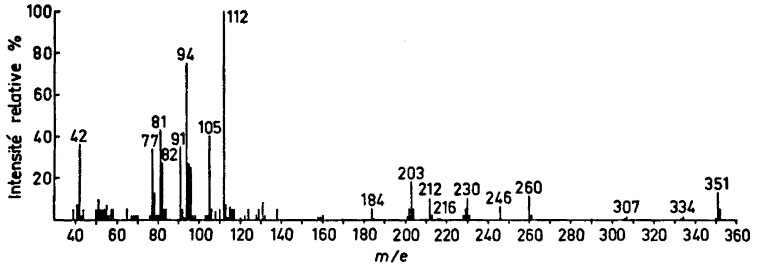

Fig. 3. Spectre de masse du produit C.

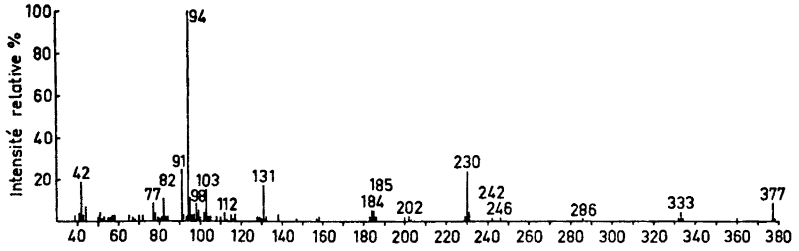

Fig. 4. Spectre de masse du produit D.

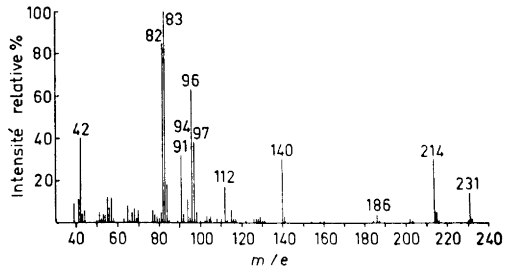

Fig. 5 (*et 6*). Spectre de masse du produit d'hydrolyse de A (et de B).

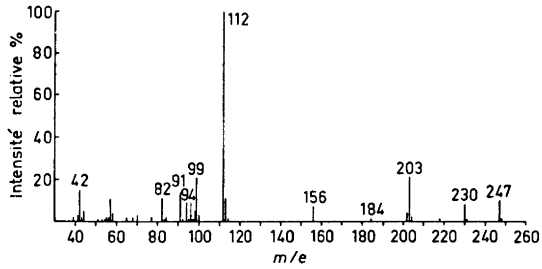

Fig. 7. Spectre de masse du produit d'hydrolyse de C.

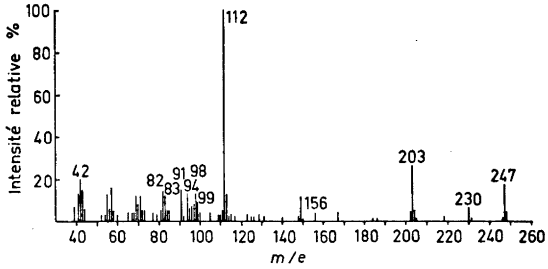

Fig. 8. Spectre de masse du produit d'hydrolyse de D.

Les pics à *m/e* 97, 96, 83, 82 et 81 peuvent être expliqués par les clivages selon la Voie B_1 où la rupture initiale du cycle pipéridinique a eu lieu en 1 – 2. Ces clivages, importants dans les spectres des tropanols acylés en position 3,[4,5] sont vérifiés grâce à la présence des pics métastables (Schéma 2), et sont bien en accord avec la structure proposée (I). La rupture initiale du cycle pipéridinique en 4 – 5 (Voie B_2), moins favorable que la rupture en 1 – 2, conduit aux ions *m/e* 187, 186, 83, 82 et 81.

Le pic de base à *m/e* 214 est attribuable à l'ion $(M-121)^+$ provenant de la perte du groupement benzoyloxy sous forme de $C_6H_5-COO\cdot$ (Voie C). Le fait que ce pic correspond bien à l'ion $(M-121)^+$ est confirmé par la présence d'un pic métastable à *m/e* 137.

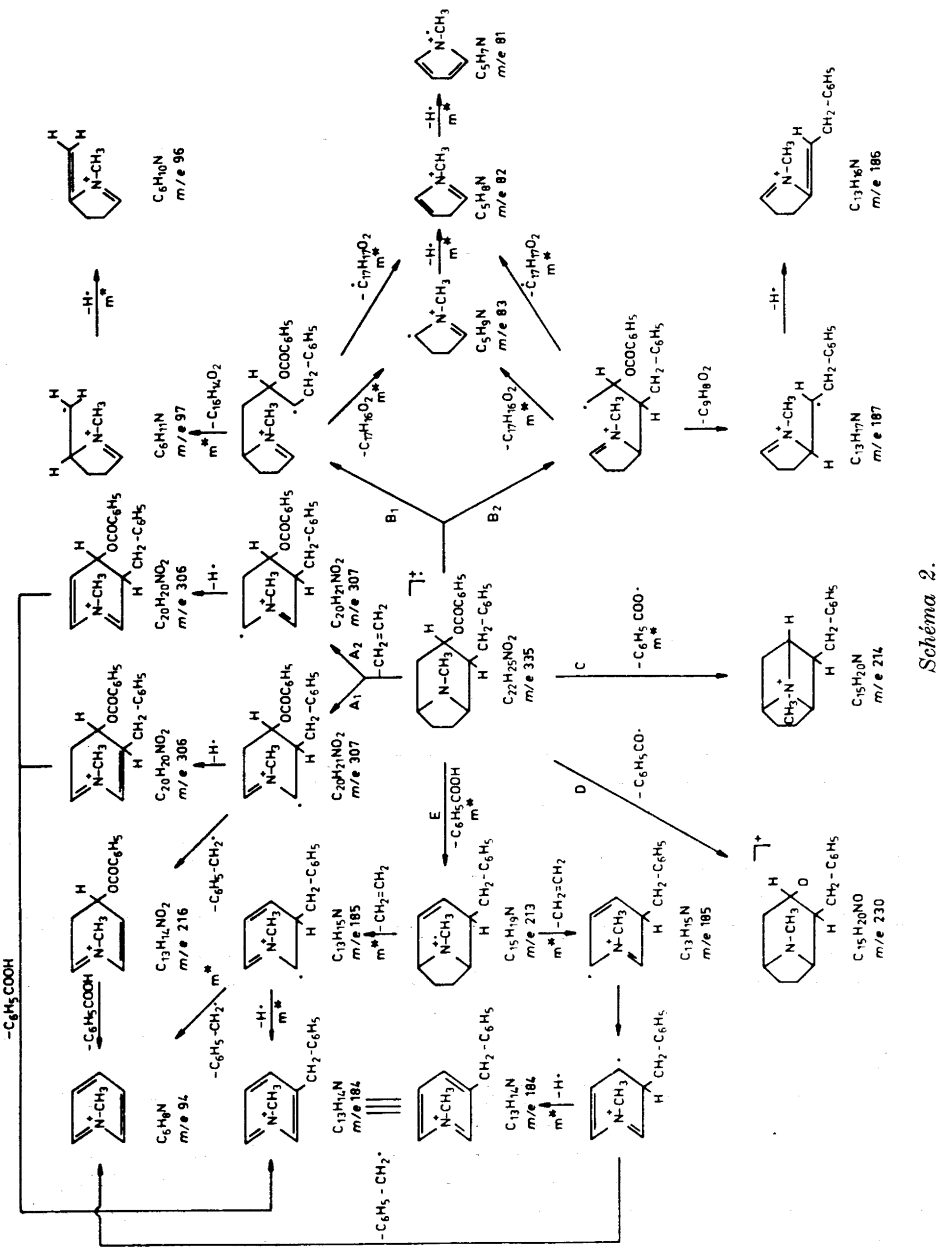

Schéma 2.

Le pic à *m/e* 230 peut être rapporté au clivage de $C_6H_5-CO\cdot$ à partir de l'ion moléculaire (Voie D).

La fragmentation selon la Voie E, importante dans les cas des tropanols acylés en position 3,[4,5] conduit à l'ion *m/e* 213. La perte d'une molécule d'éthylène amène la formation de l'ion *m/e* 185 qui peut, à son tour, perdre soit un atome d'hydrogène conduisant à l'ion *m/e* 184, soit un radical benzylique conduisant à l'ion *m/e* 94. Les pics métastables indiqués dans le Schéma 2 viennent à l'appui de cette interprétation.

La présence du groupement benzylique ressort également de la présence d'un pic intense à *m/e* 91, dû à l'ion $C_7H_7^+$, apparemment présent sous forme de l'ion tropylium. Cet ion, ainsi que l'ion correspondant à $(M-91)^+$, sont présents dans tous les spectres examinés. Le pic à *m/e* 42, également omniprésent dans les spectres des composés étudiés, peut être représenté, selon Djerassi,[4] par $CH_3-\overset{+}{N}\equiv CH$. Les pics à *m/e* 122, 105 et 77 sont en accord avec le fait que le produit A est un ester benzoïque.

Le spectre de RMN ($CDCl_3$) du produit A montre deux multiplets à τ 1,8 – 2,0 (2H) et à τ 2,3 – 2,65 (3H), qui présentent toutes les caractéristiques d'un groupement benzoyloxy,[6] un multiplet étroit, centré à τ 2,83 (5H), qui peut être attribué aux protons aromatiques du groupement benzylique et un groupe de raies mal définies entre τ 6,8 et τ 8,2 (14H), dont la seule raie bien définie, attribuable aux protons de $>N-CH_3$, se trouve à τ 7,72 (3H). De plus, le spectre montre une raie de résonance d'un proton à τ 4,81, qui a l'allure d'un triplet (étalé sur 12 cps).

Le spectre IR du produit A confirme la présence d'une fonction ester; ν C=O à 1705 cm^{-1}.

Le spectre de masse du produit d'hydrolyse de A (Fig. 5) montre un pic moléculaire à *m/e* 231 correspondant à la formule $C_{15}H_{21}NO$. Ce fait, ainsi que la fragmentation très similaire à celle du produit A, est en accord avec la structure proposée. Il est à noter que, dans ce cas, la fragmentation selon la Voie A est plus nette que dans le cas précédent, ce qui est en accord avec les résultats antérieurs.[4,5]

Le spectre de RMN ($CDCl_3$) du produit d'hydrolyse de A montre un groupe de raies mal définies entre τ 6,8 et 8,6 (15H), dont la seule raie identifiée est à τ 7,80 (3H) ($>N-CH_3$). De plus, le spectre montre un multiplet étroit, centré à τ 2,80 (5H) (protons aromatiques du groupement benzylique) et une raie de résonance d'un proton à τ 6,29, qui a l'allure d'un triplet (étalé sur 13 cps) (proton en position 3).

Le produit B, pour lequel nous proposons la structure plane (II), se présente sous forme d'une huile visqueuse. Le spectre de masse (Fig. 2) montre un pic moléculaire à *m/e* 273, qui correspond à la formule $C_{17}H_{23}NO_2$. Le pic de base à *m/e* 214, qui résulte du clivage du groupement acétyloxy sous forme de $CH_3-COO\cdot$, ainsi que les autres pics, montrent une fragmentation analogue à celle du produit A (*cf.* plus haut) en accord avec la structure proposée (II). La présence du groupement acétyloxy est également indiquée par un pic à *m/e* 43 dû à l'ion CH_3CO^+.

Le spectre de RMN ($CDCl_3$) du produit B montre un groupe de raies mal définies entre τ 6,8 et 8,3 (17H). Les seules raies identifiées sont à τ 7,78 (3H)

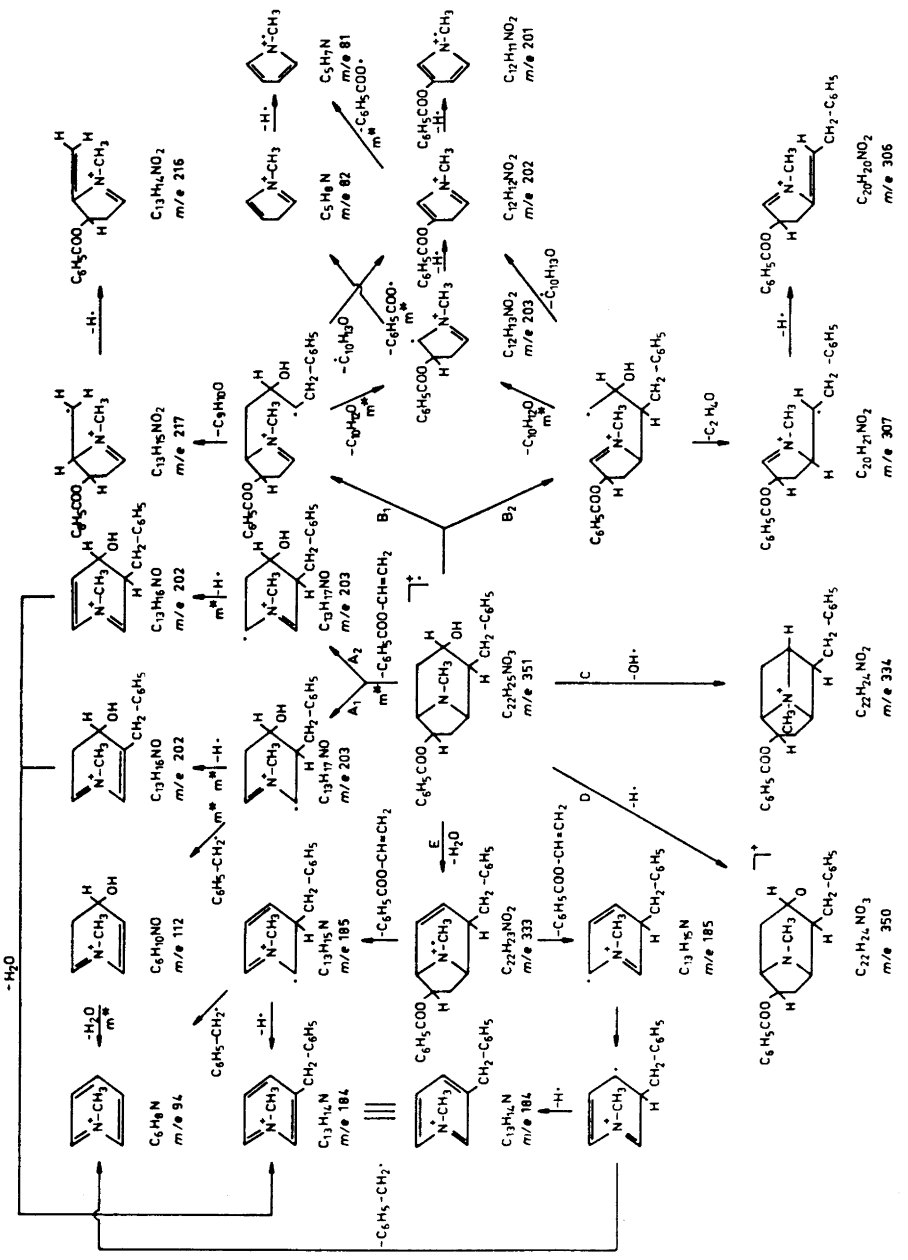

Schéma 3.

($\gtrless N-CH_3$) et à τ 7,93 (3H) ($-O-CO-CH_3$). De plus, le spectre montre un multiplet étroit, centré à τ 2,81 (protons aromatiques du groupement benzylique) et une raie de résonance d'un proton à τ 5,12, qui a l'allure d'un triplet (étalé sur 13 cps) (proton en position 3).

Le spectre IR du produit B indique la présence d'une fonction ester: ν C=O à 1740 cm^{-1}.

Le fait que les produits A et B conduisent, par hydrolyse, à un dérivé commun apparait en faveur de ce que les produits A et B ne diffèrent que par la nature de l'acide qui les estérifie et, qu'en particulier, ils ont la même stéréochimie.

Le produit C, pour lequel nous proposons la structure plane (III), fond, après deux cristallisations dans le benzène, à 168 – 170°C. Par analogie avec la fragmentation générale des alcaloïdes tropaniques,[4,5] on peut présenter le Schéma 3 pour un produit ayant la structure (III).

Le spectre de masse obtenu (Fig. 3) correspond bien, en effet, à la structure supposée (III). Ainsi le spectre montre-t-il un pic moléculaire à *m/e* 351 correspondant à la formule $C_{22}H_{25}NO_3$. Le pic de base à *m/e* 112 est formé principalement par la perte de $C_6H_5-CH_2\cdot$ à partir de l'ion *m/e* 203 $(C_{13}H_{17}NO)^{+\cdot}$ (Voie A_1). Un fort pic métastable à *m/e* 61,9 vient à l'appui de cette interprétation. Quant au pic à *m/e* 203 $(C_{13}H_{17}NO)^{+\cdot}$, il résulte du clivage de $C_6H_5COO-CH=CH_2$ à partir de l'ion moléculaire et indique que le groupement benzoyloxy se situe soit en position 6 soit en position 7. La perte d'un atome d'hydrogène à partir de l'ion *m/e* 203 $(C_{13}H_{17}NO)^{+\cdot}$ conduit à l'ion *m/e* 202 $(C_{13}H_{16}NO)^{+}$, lequel peut subir une deshydratation en donnant naissance à l'ion *N*-méthyl-benzylpyridinium (*m/e* 184), stabilisé par résonance. Une deshydratation de l'ion *m/e* 112 conduit à l'ion *m/e* 94, également stabilisé par résonance.

L'existence des pics à *m/e* 203 $(C_{12}H_{13}NO_2)^{+\cdot}$, 202 $(C_{12}H_{12}NO_2)^{+}$, 82 et 81 peut s'expliquer par les clivages selon la Voie B, où la rupture initiale du cycle pipéridinique a eu lieu soit en 1 – 2 (Voie B_1) soit en 4 – 5 (Voie B_2), et confirme ainsi la présence du groupement benzoyloxy dans le cycle pyrrolidinique. Considérant le cas théorique où la rupture initiale a eu lieu en 1 – 2 et le groupement benzoyloxy se trouve en position 7, on constate que ce mode de fragmentation ne conduit pas à l'ion *m/e* 82. La même chose est valable dans le cas où la rupture initiale a eu lieu en 4 – 5 et le groupement benzoyloxy se trouve en position 6. Pourtant les résultats disponibles ne permettent pas de déterminer avec certitude la position exacte du groupement benzoyloxy; il est à noter, en particulier, que les pics à *m/e* 307, 306, 217 et 216 sont à peine visibles.

Le pic à *m/e* 334 résulte du clivage de OH· à partir de l'ion moléculaire (Voie C).

La fragmentation du produit C, qui possède un groupement hydroxyle en position 3, semble suivre très légèrement les Voies D et E. Ce comportement est bien en accord avec les résultats antérieurs.[4,5]

Le spectre de masse du produit C montre, en plus, plusieurs pics, non représentés sur le Schéma 3. Les pics à *m/e* 246, 230 et 229 peuvent être attribués à la perte de la fonction ester sous formes de $C_6H_5-CO\cdot$, $C_6H_5-COO\cdot$ et C_6H_5-COOH, respectivement. Le pic à *m/e* 229 peut aussi se former partielle-

ment par perte d'un atome d'hydrogène à partir de l'ion *m/e* 230. La présence des pics à *m/e* M − 91, 91 et 42, dans tous les spectres des composés étudiés, à déjà été commentée.

Le spectre de RMN ($CDCl_3$) du produit C montre deux multiplets à τ 1,95 − 2,15 (2H) et 2,5 − 2,75 (3H), qui présentent toutes les caractéristiques d'un groupement benzoyloxy.[6] En plus le spectre montre un singulet à τ 2,84 (5H), attribuable aux protons aromatiques du groupement benzylique, un groupe de raies mal définies entre τ 6,7 et 8,15 (13H), dont la seule raie identifiée est à τ 7,49 (3H) ($>N-CH_3$), ainsi qu'un quadruplet à τ 4,19 (1H) ($J_1 = 8$ cps; $J_2 = 3$ cps), attribuable au proton géminé au groupement ester (soit en 6 soit en 7), et un massif d'un proton, centré à τ 6,21 (étalé sur 15 cps), dû au proton en position 3.

La présence d'une fonction ester est confirmée par le spectre IR: ν C=O à 1715 cm^{-1}.

Le spectre de masse du produit d'hydrolyse de C (Fig. 7) montre un pic moléculaire à *m/e* 247 correspondant à la formule $C_{15}H_{21}NO_2$. Le pic de base à *m/e* 112, ainsi que les autres pics, montrent une fragmentation analogue à celle du produit C et sont en accord avec la structure proposée.

Le spectre de RMN ($(CD_3)_2SO$) du produit d'hydrolyse de C montre un groupe de raies mal définies entre τ 5,3 et 8,7 (16H), dont la seule raie identifiée est à τ 7,66 (3H) ($>N-CH_3$). De plus, le spectre montre un multiplet étroit, centré à τ 2,80 (5H) (protons aromatiques du groupement benzylique).

Le produit D, pour lequel nous proposons la structure plane (IV), se présente sous forme de cristaux blancs, qui, après deux cristallisations dans un mélange de benzène et d'héxane, fondent à 174 − 175°C.

Le spectre de masse montre un pic moléculaire à *m/e* 377 répondant à la formule $C_{24}H_{27}NO_3$. Dans ce cas également la fragmentation semble typique de celle des alcaloïdes tropaniques et peut être représentée de la façon suivante (Schéma 4).

La rupture du cycle pyrrolidinique en 5 − 6, suivie du clivage en 1 − 7, conduit après perte d'une molécule de $HO-CH=CH_2$, à l'ion *m/e* 333 ($C_{22}H_{23}NO_2$) (Voie A_1). Un processus analogue, commençant par la rupture du cycle pyrrolidinique en 1 − 7, conduit également à un ion de même formule brute (Voie A_2). Ces ions, qui indiquent la présence du groupement hydroxyle dans le cycle pyrrolidinique, peuvent donner naissance aux ions *m/e* 332, 242, 184 et 94 selon de Schéma 4.

La rupture initiale du cycle pipéridinique en 1 − 2 peut conduire aux ions *m/e* 113, 112, 99, 98, 97, 82 et 81 (Voie B_1) et la rupture du cycle pipéridinique en 4 − 5 (Voie B_2) aux ions *m/e* 203, 202, 99, 98, 97, 82 et 81. L'existence de ces pics est en accord avec la présence du groupement hydroxyle dans le cycle pyrrolidinique. Par analogie avec le produit C, il est à noter que le cas théorique ou la rupture initiale a eu lieu en 1 − 2 et où le groupement hydroxyle se trouve en position 7, ne conduit pas, selon le mode de fragmentation présenté (Voie B), aux ions *m/e* 98 et 82. Ceci est également valable dans le cas où la rupture initiale a eu lieu en 4 − 5 et où le groupement hydroxyle se trouve en position 6. Pourtant, les résultats disponibles ne permettent, non plus dans ce cas, de choisir entre les positions 6 ou 7 comme emplacement du groupement hydroxyle.

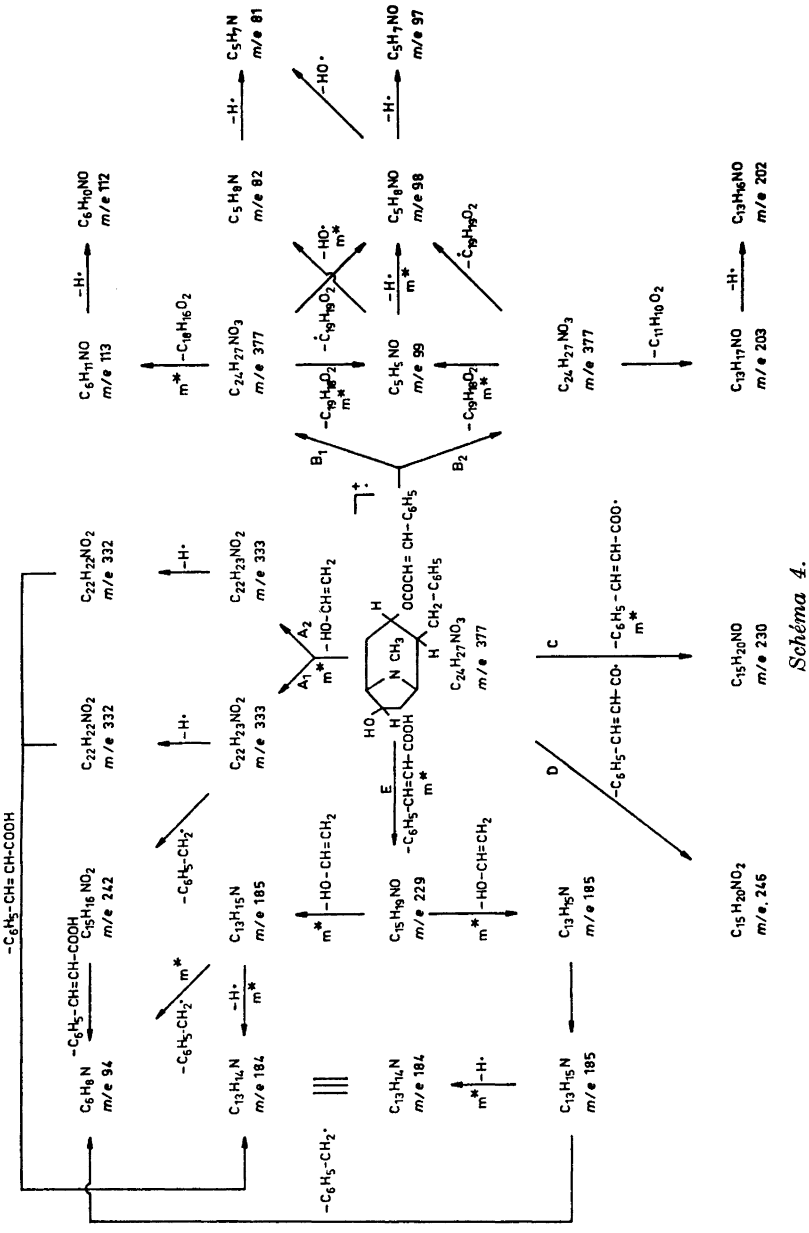

Schéma 4.

Le pic à *m/e* 230 résulte du clivage de $C_6H_5CH=CH-COO\cdot$ et celui à *m/e* 246 du clivage $C_6H_5CH=CH-CO\cdot$ à partir de l'ion moléculaire (Voies C et D).

La fragmentation selon la Voie E, bien visible, conduit à l'ion *m/e* 229, qui, par perte d'une molécule de $HO-CH=CH_2$, conduit à la formation de l'ion *m/e* 185. Celui-ci peut, à son tour, perdre soit un atome d'hydrogène, donnant la naissance à l'ion *m/e* 184, soit un radical benzylique conduisant à l'ion *m/e* 94.

L'existence des pics à *m/e* M − 91, 91 et 42 a déjà été interprétée et la présence des pics à *m/e* 131 et 103 confirme que le produit D est un ester d'acide cinnamique.

Le spectre de RMN ($CDCl_3$) du produit D montre un multiplet à τ 2,5 − 2,85 (5H), attribuable aux protons aromatiques du groupement cinnamoyloxy, un multiplet étroit, centré à τ 2,90 (5H), dû aux protons aromatiques du groupement benzylique et deux doublets d'un proton à τ 2,36 ($J = 16$ cps) et à τ 3,61 ($J = 16$ cps), qui sont en accord avec le fait que le produit D est un ester de l'acide *trans*-cinnamique. De plus, le spectre montre un multiplet de deux protons entre τ 4,95 et τ 5,25, attribuable au proton attaché au même atome de carbone que le groupement hydroxyle (soit en 6 soit en 7) et au proton en position 3. Dans le spectre il se trouve un groupe de raies mal définies entre τ 6,6 et τ 8,7 (13H), dont la seule raie identifiée est à τ 7,52 (3H) ($>N-CH_3$).

La fonction ester du produit D est également indiquée par le spectre IR: ν C=O à 1705 cm^{-1}.

Le spectre de masse du produit d'hydrolyse de D (Fig. 8) est bien en accord avec les prévisions montrant un pic moléculaire à *m/e* 247 ($C_{15}H_{21}NO_2$). Le pic de base se trouve à *m/e* 112 et la fragmentation suit un schéma analogue à ceux que nous venons de présenter.

Le spectre de RMN ($CDCl_3$) du produit d'hydrolyse de D montre un groupe de raies entre τ 6,6 et τ 8,8 (14H), dont la seule raie identifiée est à τ 7,49 (3H) ($>N-CH_3$). Le multiplet étroit, centré à τ 2,73 (5H), peut être attribué aux protons aromatiques du groupement benzylique. De plus, le spectre montre deux multiplets d'un proton, centrés à τ 5,12 et à τ 6,24, dont celui-là a l'allure d'un quadruplet (étalé sur 12 cps) et celui-ci l'allure d'un triplet (étalé sur 16 cps). Ces multiplets sont attribuables aux protons attachés aux même atomes de carbones que les groupements hydroxyles.

Il est à noter, en particulier, que les produits C et D ne donnent pas le même produit d'hydrolyse.

Dans les cas des produits A, C et D, les acides libérés par l'hydrolyse furent identifiés par la spectrométrie de masse ainsi que par la chromatographie gaz-liquide (sous forme d'esters méthyliques).

Le fait que les produits décrits ne montrent pas d'activité optique apparait en faveur de ce que les produits existent sous forme des mélanges *d,l*. Pourtant une racémisation ne peut pas être totalement exclue. Une étude plus détaillée de la stéréochimie des produits décrits est en progrès.

PARTIE EXPÉRIMENTALE

Les spectres IR ont été enregistrés sur appareil Perkin-Elmer Infracord type 137 E, les spectres UV en solution éthanolique sur appareil Perkin-Elmer 137 UV et les pouvoirs rotatoires, en solution chloroformique, à l'aide d'un polarimètre Perkin-Elmer 141.

Les spectres de RMN ont été obtenus avec un appareil Varian A 60 en utilisant le tétraméthylsilane comme référence interne. Les spectres de masse ont été mesurés sur spectromètre AEI MS 9.

Les points de fusion pris en tube capillaire ne sont pas corrigés.

Les analyses élémentaires ont été effectuées dans le service du Docteur A. Bernhardt, Laboratoire de Microanalyse, Elbach-sur-Engelskirchen, République Fédérale Allemande.

Extraction des alcaloïdes

8 kg de feuilles sèches pulvérisées de *Knightia deplanchei* Vieill. ex Brongn. et Gris* sont humectées par une solution aqueuse ammoniacale (6 – 7 %), puis épuisées par de l'éther dans un appareil de percolation jusqu' à réaction de Meyer négative. La solution éthérée est extraite par une solution aqueuse d'acide chlorhydrique (2 %), qui est ensuite alcalinisée par de l'ammoniaque. Les alcaloïdes sont enfin extraits par de l'éther. Les solutions éthérées sont lavées par de l'eau, séchées sur sulfate de sodium et évaporées sous vide. On obtient ainsi 59,8 g d'alcaloïdes totaux.

Séparation des alcaloïdes

Les alcaloïdes bruts sont chromatographiés sur 1,5 kg d'alumine (Merck; activité II – III). La composition des fractions (Tableau 1) est suivie par chromatographie sur couche mince.

Tableau 1.

Fraction	Eluant	Poids	Composition
1	Benzène	29,3 g	Mélange contenant prod. A (en majorité), prod. B et autres produits alcaloïdiques.
2	Ether	11,4 g	Mélange contenant prod. A (un peu), prod. B (un peu) et prod. C (en majorité).
3	Chloroforme	13,6 g	Mélange contenant prod. C (un peu), prod. D et autres produits alcaloïdiques.
4	Chloroforme/ méthanol; 90/10	5,4 g	Mélange contenant prod. D et autres produits alcaloïdiques.

Les produits A et B sont isolés d'une partie de la fraction 1 par chromatographie sur couches préparatives de silice alcaline (chloroforme/méthanol; 90/10). Le produit C est isolé de la fraction 2 par deux cristallisation successives dans le benzène et le produit D de la fraction 3 par deux cristallisation successives dans un mélange de benzène et héxane.

Produit A. Huile visqueuse, qui présente les constantes suivantes: Analyse $C_{22}H_{25}NO_2$. Calculé C 78,77; H 7,51; N 4,18. Trouvé C 79,01; H 7,71; N 4,10. $[\alpha]_D \pm 0°$. Spectre UV: λ_{max} 205 nm ($\varepsilon = 26\,000$), 275 nm ($\varepsilon = 24\,500$). Spectre IR (film): $\nu C{=}O$ 1705 cm^{-1}. Spectre de RMN ($CDCl_3$): voir partie théorique. Spectre de masse: voir partie théorique.

Saponification du produit A. 150 mg de produit A chauffés à reflux pendant 24 heures dans une solution diluée de KOH, contenant un peu de méthanol, donnent 100 mg de produit d'hydrolyse de A et 40 mg d'acide, isolés à la manière habituelle.

* Echantillon d'herbier; Sévenet 161 S.

Produit d'hydrolyse de A. Cristaux blancs, qui, après une recristallisation dans l'acétone, présentent les constantes suivantes: Analyse $C_{15}H_{21}NO$. Calculé C 77,88; H 9,15; N 6,05. Trouvé C 77,48; H 9,03; N 6,19. F. 123 – 124°. $[\alpha]_D \pm 0°$. Spectre UV: λ_{max} 211 nm ($\varepsilon = 21\,500$). Spectre IR (KBr): ν OH 3160 cm^{-1}. Spectre de RMN ($CDCl_3$): voir partie théorique. Spectre de masse: voir partie théorique.

Acide benzoïque. Identifié par la spectrométrie de masse, ainsi que par la chromatographie gaz-liquide (sous forme d'ester méthylique).

Produit B. Huile visqueuse, qui présente les constantes suivantes: Analyse $C_{17}H_{23}NO_2$. Calculé C 74,69; H 8,48; N 5,12. Trouvé C 74,69; H 8,39; N 5,08. $[\alpha]_D \pm 0°$. Spectre UV: λ_{max} 208 nm ($\varepsilon = 11\,450$). Spectre IR (film): ν C=O 1740 cm^{-1}. Spectre de RMN ($CDCl_3$): voir partie théorique. Spectre de masse: voir partie théorique.

Saponification du produit B. 80 mg de produit B chauffés à reflux pendant 6 heures dans une solution diluée de KOH, contenant un peu de méthanol, donnent 60 mg de produit d'hydrolyse de B, isolés à la manière habituelle. Cristaux blancs, qui sont identiques au produit d'hydrolyse de A.

Produit C. Cristaux blancs, qui, après deux recristallisations dans le benzène, présentent les constantes suivantes: Analyse $C_{22}H_{25}NO_3$. Calculé C 75,18; H 7,17; N 3,99. Trouvé C 75,15; H 7,16; N 4,05. F. 168 – 170°. $[\alpha]_D \pm 0°$. Spectre UV: λ_{max} 207 nm ($\varepsilon = 12\,500$), 217 nm ($\varepsilon = 11\,600$), 229 nm ($\varepsilon = 12\,200$), 268 nm ($\varepsilon = 2600$), 273 nm ($\varepsilon = 2680$), 280 nm ($\varepsilon = 2550$). Spectre IR ($CHCl_3$): ν C=O 1715 cm^{-1}. Spectre de RMN ($CDCl_3$): voir partie théorique. Spectre de masse: voir partie théorique.

Saponification du produit C. 400 mg de produit C chauffés à reflux pendant 3 heures dans une solution diluée de KOH, contenant un peu de méthanol, donnent 290 mg de produit d'hydrolyse de C et 90 mg d'acide, isolés à la manière habituelle.

Produit d'hydrolyse de C. Cristaux blancs, qui, après une recristallisation dans l'acétone, présentent les constantes suivantes: Analyse $C_{15}H_{21}NO_2$. Calculé C 72,84; H 8,56; N 5,66. Trouvé C 72,43; H 8,75; N 5,56. F. 170 – 172°. $[\alpha]_D \pm 0°$. Spectre UV: λ_{max} 211 nm ($\varepsilon = 23\,700$). Spectre IR (KBr): ν OH 3330 cm^{-1}, 3080 (épaulement) cm^{-1}. Spectre de RMN ($(CD_3)_2SO$): voir partie théorique. Spectre de masse: voir partie théorique.

Acide benzoïque. Identifié par la spectrométrie de masse, ainsi que par la chromatographie gaz-liquide (sous forme d'ester méthylique).

Produit D. Cristaux blancs, qui, après deux recristallisations dans un mélange benzène/héxane, présentent les constantes suivantes: Analyse $C_{24}H_{27}NO_3$. Calculé C 76,36; H 7,21; N 3,71. Trouvé C 75,83; H 7,07; N 3,82. F. 174 – 175°. $[\alpha]_D \pm 0°$. Spectre UV: λ_{max} 208 nm ($\varepsilon = 19\,600$), 216 nm ($\varepsilon = 19\,800$), 222 nm ($\varepsilon = 14\,150$), 279 nm ($\varepsilon = 23\,550$). Spectre IR ($CHCl_3$): ν C=O 1705 cm^{-1}. Spectre de RMN ($CDCl_3$): voir partie théorique. Spectre de masse: voir partie théorique.

Saponification du produit D. 50 mg de produit D chauffés à reflux pendant 3 heures dans une solution diluée de KOH, contenant un peu de méthanol, donnent 30 mg de produit d'hydrolyse de D et 15 mg d'acide, isolés à la manière habituelle.

Produit d'hydrolyse de D. Cristaux blancs, qui, après une recristallisation dans l'acétone, présentes les constantes suivantes: Analyse $C_{15}H_{21}NO_2$. Calculé C 72,84; H 8,56; N 5,66. Trouvé C 72,61; H 8,83; N 5,44. F. 192 – 195°. $[\alpha]_D \pm 0°$. Spectre UV: λ_{max} 211 nm ($\varepsilon = 19\,500$). Spectre IR (KBr): ν OH 3280 cm^{-1}. Spectre de RMN ($CDCl_3$): voir partie théorique. Spectre de masse: voir partie théorique.

Acide cinnamique. Identifié par la spectrométrie de masse, ainsi que par la chromatographie gaz-liquide (sous forme d'ester méthylique).

Nous remercions vivement MM. les Docteurs P. Potier et B. C. Das de toute leur aide amicale au long de la réalisation du présent travail.

Nos remerciements vont également à M. T. Sévenet pour la récolte de la matière première, effectuée en Nouvelle-Calédonie (Plateau de Thio) en mars 1968, ainsi qu'à toute l'équipe du Docteur Potier à l'Institut de Chimie des Substances Naturelles du CNRS à Gif-sur-Yvette.

BIBLIOGRAPHIE

1. Guillaumin, A. *Flore analytique et synoptique de la Nouvelle Calédonie*, Phanérogames, Office de la Recherche Scientifique Coloniale, Paris 1948, p. 105.
2. Cheeseman, T. F. *Manual of the New Zealand Flora*, John Mackay, Wellington 1906, p. 606.
3. Motherwell, W. D. S., Isaacs, N. W., Kennard, O., Bick, I. R. C., Bremner, J. B. et Gillard, J. *Chem. Commun.* **1971** 133; voir aussi, Bick, I. R. C., Bremner, J. B. et Gillard, J. W. *Phytochemistry* **10** (1971) 475.
4. Blossey, E. C., Budzikiewicz, H., Ohashi, M., Fodor, G. et Djerassi, C. *Tetrahedron* **20** (1964) 585.
5. Parello, J., Longevialle, P., Vetter, W. et McCloskey, J. A. *Bull. Soc. Chim. France* **1963** 2787.
6. *Varian Catalog Vol. 2.*, Spectrum No. 627, Varian Associates, Palo Alto 1963.

Reçu le 9 octobre 1972.

ACTA CHEMICA SCANDINAVICA 27 (1973) 1053–1058

Lipids in Carrot Roots

I. The Purification of Crude Lipids and the Composition of the Neutral Lipids

JUHANI SOIMAJÄRVI* and REINO R. LINKO

Department of Biochemistry, University of Turku, SF-20500 Turku 50, Finland

Filtration through a Sephadex LH-20 gel column was found to be an effective method for the removal of contaminating sugars, phosphorus compounds and amino acids from lipids extracted from carrot root.

At the end of the growth season, the lipids in carrot root amount on average to 0.23 % of the fresh weight, and 1.8 % of the dry weight. Neutral lipids represent 63 %, glycolipids 21 %, and phospholipids 16 % of total lipids.

When the neutral lipids were fractionated by chromatography on a silicic acid column, the largest fractions consisted of triglycerides, sterol esters, sterol, and free fatty acids which amounted to 36, 31, 10, and 6 %, respectively, of the neutral lipids, and 23, 20, 6, and 4 % of the total lipids.

Most non-photosynthetic plant tissues contain very little lipids.[1] Despite their low contents, the lipids are important in many respects. As is well known, they are precursors of numerous aroma compounds and their oxidation may shorten the shelf-life of many food products.[2,3] Plants like the carrot which contain very little lipids, but much water pose great analytical problems. Especially when their lipids are extracted, abundant non-lipid components accompany the lipids.[4] Promising results in the purification of plant extracts have been obtained by gel filtration.[5] For this reason we undertook to study whether filtration through Sephadex LH-20 gel can be used to purify lipids extracted from carrots.

Lipids extracted from carrot roots were resolved into neutral lipid, glycolipid, and phospholipid fractions by chromatography on a silicic acid column and the neutral lipids were separated into subclasses. Before fractionation of the purified lipids on the silicic acid column, they were passed through a column of a chelating resin in the sodium form to ensure a definite chromatographic elution sequence of the anionic phospholipids and glycolipids.[6]

* Present address: Department of Biology, University of Jyväskylä, Jyväskylä 10, Finland.

EXPERIMENTAL

Materials. Carrots (*Daucus carota*), variety Feonia AH, were obtained from a farm in Köyliö, South-western Finland. The carrots were harvested in October, 1970. They were washed with water, the tips and short green upper sections of the roots were removed, and the roots were cut into small cubes.

The reagents and solvents were of analytical grade. The solvents were dried and distilled before use.

Extraction of lipids. One hundred grams of the freshly cut carrot cubes were extracted with 600 ml of a 2 : 1 (v/v) chloroform-methanol mixture at 7°C for 2 min in a Serval Omni-Mixer rotating at 5000 r.p.m. The solids remaining after filtration of the homogenate were extracted again with 100 ml of the same solvent mixture. The final residue was washed with four 50 ml portions of chloroform on a Büchner funnel. The water that separated from the combined extract and wash mixture was washed with chloroform, which was then added to the organic phase. The extracts were dried with a mixture of anhydrous sodium sulphate and sodium bicarbonate and the solvents were removed in a rotating evaporator at 25°C. The crude lipids that remained were weighed and dissolved in chloroform and the solution in chloroform was stored at −20°C.

Column chromatography on Sephadex LH-20 gel. The crude lipids were purified by eluting them through a column of Sephadex LH-20 gel (AB Pharmacia, Uppsala, Sweden) as proposed by Maxwell and Williams.[5] The Sephadex LH-20 gel had been washed with water but dried with acetone instead of air. The loading was 5 – 50 mg of crude lipids per gram of dry Sephadex LH-20. The total bed volume of the column was about 14 ml. The lipids were eluted first with a 3 : 1 (v/v) chloroform-methanol mixture and then with a 1 : 1 (v/v) methanol-water mixture. To determine how the lipid and non-lipid sugars and phosphorus compounds migrated during the fractionation, 27 eluate fractions with the volumes given in Figs. 1 and 2 were collected during the elution of a sample of the crude lipids. In routine Sephadex gel chromatography of the crude lipids, the following fractions were collected on elution of the column with the chloroform-methanol mixture: a 7 ml forerun, fraction A, which preceded a pigment band, a 9 ml lipid fraction B containing coloured matter, and a 32 ml fraction C. A 32 ml fraction D was collected on elution of the column with the methanol-water mixture.

Ion-exchange column chromatography was used to replace calcium and magnesium of the lipids by sodium. The resin (Chelex, 100, 100 – 200 mesh, sodium form, Bio-Rad Laboratories, Richmond, California) was prepared and the aqueous solvent was replaced by the used solvent mixture as described by Carter and Weber [6] with the exception that the pH of the resin slurry was 7 – 7.5 as proposed by Renkonen.[7] The bed volume of the resin in a chromatography column 15 cm long and 1.6 cm in diameter was 30 ml. The loading was at most 10 mg of lipids per ml of bed volume. The lipids were eluted as one fraction from the column with six bed volumes of a 5 : 4 : 1 (v/v/v) chloroform-methanol-water mixture.

Chromatography on a silicic acid column was employed to fractionate the lipids after the ion-exchange chromatography into neutral lipids, glycolipids, and phospholipids. Silicic acid (100 mesh, AR, Mallincrodt Chemical Works, St. Louis, Missouri) was activated by heating at 115°C for 20 h. The column and the eluting solvents and their volumes were identical with those used by Rouser *et al.*[8] The loading was 10 – 60 mg of lipids per gram of silicic acid.

Column chromatography on silicic acid was used also to resolve the neutral lipids into subclasses. 15 g of silicic acid was added to a glass tube, 1.6 cm in inside diameter, whereupon a column, 15 cm long, resulted. The loading was 10 – 15 mg of lipids per gram of silicic acid. The lipids were eluted with the same solvents as Barron and Hanahan [9] employed to resolve neutral lipids from rat liver, but the volumes of the solvents were only one fourth of those used by Barron and Hanahan. Ninety 15 ml samples were collected during the fractionation.

Thin-layer chromatography. Glass plates covered with a layer of silica gel G (for thin-layer chromatography, E. Merck AG), 0.25 mm thick, were heated at 110°C for 60 min to activate the gel. The chromatograms were developed by one-dimensional chromatography in glass jars lined with filter paper using a 65 : 25 : 4 (v/v/v) chloroform-methanol-water mixture for glyco- and phospholipids, and a 90 : 10 : 1 (v/v/v) hexane-diethyl ether-glacial acetic acid mixture for neutral lipids. In two-dimensional chromatography, the

plates were developed in the first run with the mentioned chloroform-methanol-water mixture and in the second run with a 80 : 50 : 10 (v/v/v) di-isobutyl ketone-glacial acetic acid-water mixture. The spots containing components were rendered visible by exposing the plates to iodine vapour, by spraying the plates with a solution of ninhydrin in butyl alcohol, Dragendorff's reagent,[10] or periodate-Schiff[11] reagent, or by spraying the plates with 30 % sulfuric acid and heating them at about 120°C.

Analysis of eluted fractions. All the fractions collected by column chromatography were weighed after evaporation of the solvent. In addition, the contents of total sugars, water-soluble sugars, and total phosphorus in the effluent fractions collected during gel filtration were determined. The sugars were determined with the anthrone reagent[12] as described by Maxwell and Williams.[5] The sugar contents of the lipid fractions were obtained by subtracting the water-soluble sugar contents from the total sugar contents. Total phosphorus was determined by the method of Chen *et al.*[13] except that the residues remaining after the samples had been heated with perchloric acid were neutralized by adding first 6 N potassium hydroxide and then dilute aqueous potassium carbonate solution. During the column chromatography of neutral lipids on silicic acid, the Liebermann-Burchard reaction was used to follow the elution of sterol esters and sterols. The free fatty acids were determined by titration of the samples in ethanol with 0.01 N methanolic sodium hydroxide.

RESULTS AND DISCUSSION

The contents of crude lipids found in different extractions of carrot roots varied slightly, from 250 to 300 mg/100 g of fresh plant tissue. The results are in satisfactory agreement with those of Dalgarno and Birt.[1]

Preliminary experiments show that a significant proportion of the impurities in crude lipids extracted from carrot roots are sugars and phosphates. A

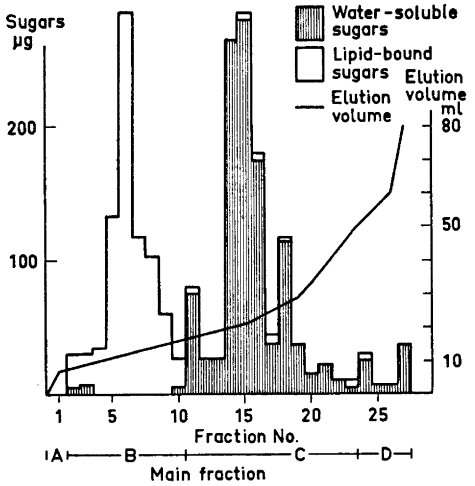

Fig. 1. Distribution of lipid-bound sugars and water-soluble sugars in eluate fractions when crude lipids extracted from carrot root were eluted from a Sephadex LH-20 column. Fractions 1 – 23 were eluted with a 3 : 1 chloroform-methanol mixture and fractions 24 – 27 with a 1 : 1 methanol-water mixture. The main fractions A – D are described in Methods.

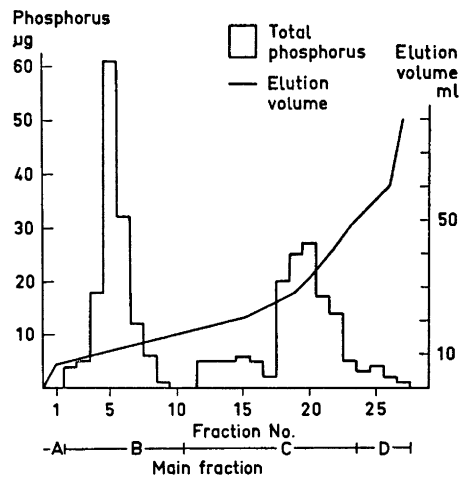

Fig. 2. Distribution of total phosphorus in eluate fractions when crude lipids extracted from carrot root were eluted from a Sephadex LH-20 column. Fractions 1 – 23 were eluted with a 3 : 1 chloroform-methanol mixture and fractions 24 – 27 with a 1 : 1 methanol-water mixture. The main fractions A – D are described in Methods.

detailed picture of the elution of sugars when crude lipids were purified by gel filtration is provided by the sugar contents of 27 eluate fractions that are plotted in Fig. 1. The results show that the lipid-bound sugars were eluted first in a rather narrow band (fractions 2 – 10) followed by the non-lipid sugars in a much wider band (fractions 11 – 27). The separation of lipid and non-lipid sugars was effective although the weight of crude lipids taken varied from 4 to 80 mg/g of Sephadex LH-20.

In the elution pattern of total phosphorus presented in Fig. 2, there was a narrow band in nearly the same position as that of lipid-bound sugars. Another broader phosphorus band emerged in the fractions 12 – 27; about half of the total phosphorus was eluted with this band. Thus phosphorus was eluted in two separate zones. Thin-layer chromatographic analyses revealed that the first narrow band contained phospholipids whereas the latter broad band, where the phosphorus was also in bound form, did not contain phospholipids. It was not possible to detect in the fractions 12 – 27 degradation products of phosphatides other than orthophosphate by the hydrolysis and alcoholysis series of Dawson.[14]

When the fractionation on the Sephadex LH-20 column was followed by thin-layer chromatography, all the lipids were found to be eluted in fractions 2 – 10. The thin-layer chromatographic analyses revealed also that amino acids were eluted with fractions 11 – 20 with a peak in the fractions 15 – 16 and were well separated from lipid components. Pigments were visible in lipid fractions 2 – 10.

On the basis of the results presented above, the elution program described in Methods was chosen for the purification of the crude lipids of carrot roots routinely. Four main fractions A – D were collected, of which fraction B contained the lipids (fractions 2 – 10 in Figs. 1 and 2).

When the crude lipids were purified by gel filtration, the weights of recovered lipids (fraction B) varied from 213 to 259 mg, average 232 mg, per 100 g of fresh carrot roots. This corresponds on average to 1.8 % of the dry weight of roots. The weights of solids in the fraction C was on average 27 mg, and the weights of solids in the fraction D was on average 3 mg/100 g of fresh carrot tissue. The forerun fraction A contained no solids. The recovery of total solids in the fractionation was 99.2 %. The crude lipids of carrot root contained from 8 to 14 %, average 12 %, non-lipid compounds; comparable data are not available in the literature. This shows that careful purification of extracted lipids is necessary before any attempt is made to determine the composition of the lipids.

The recovery of carrot root lipids after passage through the column of Chelex ion-exchange resin in the sodium form was on average 99.8 %. The fractionation of the lipids so treated on a silicic acid column showed that they contained 63 % neutral lipids, 21 % glycolipids, and 16 % phospholipids, the total recovery being about 98 %. One hundred grams of fresh carrot roots contained 143 mg of neutral lipids, 40 mg of glycolipids, and 35 mg of phospholipids. The respective percentages on a dry weight basis were 1.15, 0.38, and 0.28. When the course of the fractionation was followed by weighing the eluted solutes and by thin-layer chromatography employing specific colour reagents, the lipid classes were found to be eluted in the order stated by Rouser *et al.*[8]

Table 1. Composition of neutral lipids of carrot root determined by silicic acid column chromatography.

Lipid fraction in order of elution	% of neutral lipids	% of total lipids	mg per 100 g of fresh roots	mg per 100 g of dry roots
Hydrocarbons and pigments	5.1	3.3	7.4	59
Sterol esters	30.9	19.5	45.1	362
Triglycerides and free fatty acids	41.8	26.3	61.1	489
Free fatty acids [a]	5.9	3.7	8.6	69
Sterols	9.7	6.1	14.1	113
Diglycerides	3.0	1.9	4.3	34
Unidentified	2.3	1.5	3.4	27
Monoglycerides	3.0	1.9	4.4	35
Other unidentified components	6.5	4.1	9.6	75
Total	100.0	63.0	145.8	1167

[a] Determined by titration assuming a mean molecular weight of 280.

and that the employed volumes of solvents were appropriate for the fractionation of carrot root lipids.

The results presented for the fractions in Table 1 in the order of elution were obtained when the carrot root neutral lipids were separated into subclasses by silicic acid column chromatography. It was confirmed by thin-layer chromatography and using special reagents that the lipid classes were separated as presented in the elution scheme of Barron and Hanahan.[9] The main components of the neutral lipids were triglycerides, which represented about 36 %, and sterol esters, which represented about 31 % of the neutral lipids. Sterols amounted to about 10 % and free fatty acids, which were present in the triglyceride fraction, to about 6 % of the neutral lipids. These four fractions together amounted to 83 % of the neutral lipids.

Comparatively little information is available on the compositions of the lipids of plants and especially their nonphotosynthetic tissues.[15] Carrot root lipids contain as much glycolipids as potato lipids but relatively more neutral lipids and relatively less phospholipids.[16] Particularly high, 26 %, is the proportion of steroids in carrot root lipids; in potato lipids the percentage is about 9. Also the percentage of triglycerides is higher in carrot roots (over 20 % of the lipids) than in potatotes (15 % of the lipids).

Further investigation on the composition of glycolipids and phospholipids is in progress.

REFERENCES

1. Dalgarno, L. and Birt, L. M. *Biochem. J.* **87** (1963) 586.
2. Fricker, A. *Z. Lebensm. Unters. Forsch.* **142** (1970) 24.
3. Johnson, A. E., Nursten, H. E. and Williams, A. A. *Chem. Ind. (London)* **1971** 556, 1212.

4. Hanahan, D. J. and Chaikoff, I. L. *J. Biol. Chem.* **168** (1947) 233.
5. Maxwell, M. A. B. and Williams, J. P. *J. Chromatog.* **31** (1967) 62.
6. Carter, H. E. and Weber, E. J. *Lipids* **1** (1966) 16.
7. Renkonen, O. *Biochim. Biophys. Acta* **152** (1968) 114.
8. Rouser, G., Kritchevsky, G. and Yamamoto, A. In Marinetti, G. V., Ed., *Lipid Chromatographic Analysis*, Marcel Dekker, New York 1967, Vol. 1, p. 118.
9. Barron, E. J. and Hanahan, D. J. *J. Biol. Chem.* **231** (1958) 493.
10. Gregoff, H. M., Roberts, E. and Delwiche, C. C. *J. Biol. Chem.* **205** (1953) 565.
11. Baddiley, J., Buchanan, J., Handschumacher, R. E. and Prescott, J. F. *J. Chem. Soc.* **1956** 2818.
12. Scott, T. A. and Melvin, E. H. *Anal. Chem.* **25** (1953) 1656.
13. Chen, P. S., Jr., Toribara, T. Y. and Warner, H. *Anal. Chem.* **28** (1956) 1756.
14. Dawson, R. M. C. In Marinetti, G. V., Ed., *Lipid Chromatographic Analysis*, Marcel Dekker, New York 1967, Vol. 1, p. 163.
15. Kates, M. *Advan. Lipid. Res.* **10** (1970) 225.
16. Galliard, T. *Phytochemistry* **7** (1968) 1907.

Received September 15, 1972.

ACTA CHEMICA SCANDINAVICA 27 (1973) 1059–1066

N-Quaternary Compounds

Part XXX.[1] Synthesis and Configurational Assignments of Chiral Pyridine Derivatives

KJELL UNDHEIM and GUNNAR ARNFINN ULSAKER

Department of Chemistry University of Oslo, Oslo 3, Norway

A synthesis of 9-hydroxy-6-methyldihydro[1,3]thiazino[3,2-a] pyridinium-4-carboxylate is described. An intermediate *S*-α-pyridyl-homocysteine was optically resolved, the isolated enantiomer α-brominated and cyclised. Configurational correlations using circular dichroism show that the cyclisation goes with configurational inversion. Modes of racemisation and optical stability have been investigated.

Configurational inversion on the chiral carbon takes place in the Menschutkin reaction between 3-hydroxypyridine and α-bromo-carboxylic acids except when the alkylating agent is branched at the β-carbon.[2] Depending on relative position, sulphur present in the alkylating agent may affect the stereochemical course of the reaction by neighbouring group participation.[2] In this work the sulphur in the alkylating agent is present in a thioether with pyridine in the α-position in which case the Menschutkin reaction leads to cyclisation. The α-pyridyl thioether from 2-bromo-4-mercaptobutyric acid thus yields the corresponding dihydro[1,3]thiazino[3,2 – a]pyridinium-4-carboxylate illustrated by I. The latter is a homologue of 8-hydroxy-5-methyldihydrothiazolo[3,2-a]pyridinium-3-carboxylate (II) whose absolute configuration has been established by synthesis.[3] The chiroptical properties of II have been determined[4] and are thus available for comparative purposes. The synthesis of I was achieved as shown in Scheme 1.

The S-pyridyl homocysteine (X) is the key substance in the synthetic scheme. Its racemic modification was first synthesized and then optically resolved for the stereochemical cyclisation studies. The synthesis of X was originally attempted by the reaction of the sodium salt of 3-hydroxy-6-methylpyrid-2-thione (VII) with 2-amino-4-butyrolactone in the same way as methione is synthesized by means of sodium methiolate.[5] The latter reaction involves nucleophilic attack by the sulphur on the sp^3-carbon of the lactone group. The reaction between the butyrolactone and VII failed to yield pre-

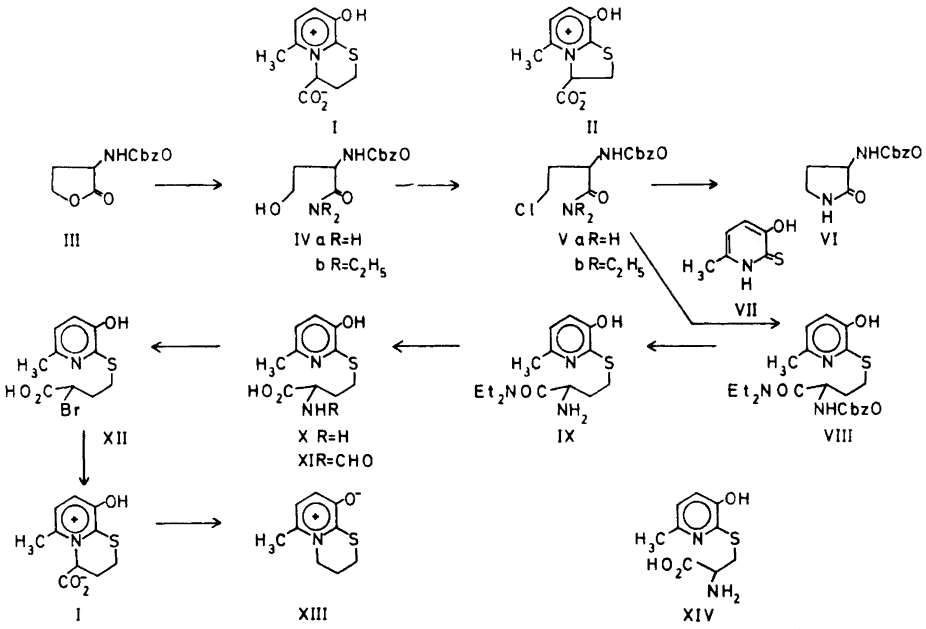

paratively useful yields of the *S*-pyridyl homocysteine X. The latter was therefore synthesized over several steps. For this purpose *N*-carbobenzoxy-2-amino-4-butyrolactone (III) was prepared.[6,7] Ammonia will attack the sp^2-carbon of the lactone (III) under formation of the hydroxy-amide IVa.[8] The latter was converted to the 4-chloro compound Va with thionyl chloride. Treatment of Va with the sodium salt of the thione VII resulted in selective cyclisation of Va with formation of a pyrrolidone (VI). Intramolecular reaction such as in Va was prevented by removal of the acidic amido hydrogens. The same series of reactions from III using diethylamine was therefore repeated and yielded Vb. The latter was successfully reacted with the thione (VII) using potassium carbonate as base. The carbobenzoxy group in VIII was removed using HBr in cold acetic acid. Stereospecific replacement of the amino group by bromine by means of diazotisation requires the holding effect of an α-carboxyl group. The amide IX was therefore further hydrolyzed to the acid (X). The reaction was run in 6N HCl at 100°C. Direct hydrolysis of the carbobenzoxy derivative (VIII) to X was also possible. For optical resolution the amino acid was formylated (XI) and resolved as brucine salt by fractional crystallisation from dilute methanol. The *N*-formyl acid (XI), isolated after ammonia decomposition of the brucine salt, had specific rotation $[\alpha]_D^{25} = +11.5°$ (N HCl). The formyl group was removed by acid hydrolysis; $[\alpha]_D^{25} = -18.0°$ (N HCl).

Optically active 2-bromocarboxylic acids are most conveniently prepared from the corresponding amino acids by diazotisation in the precence of bromide ions.[9] The reaction goes with retention of configuration and the optical purity is of the order of 90 % somewhat dependent on the nature of the substituents.[9] The diazotisation of X was carried out with nitrosyl bromide generated *in situ*

to yield the bromo derivative XII, specific rotation $[\alpha]_D^{25} = +17.5°$ (N HCl). Cyclisation of XII, by heating in an organic solvent such as acetontrile with and without added organic base, led largely to decarboxylation (XIII) of the cyclisation product (I) due to the activating effect of the α-pyridinium nitrogen. Decarboxylation was avoided by cyclisation at 60°C in aqueous solution. The reaction required several hours for completion. The relatively low reactivity of XII is in marked contrast to the high reactivity of simple 3-α-pyridylthio-2-bromopropionic acids.[10] The latter can only be isolated with difficulty as HBr salt and are cyclised immediately to dihydrothiazolo[3,2-a]-pyridinium derivatives (II) on neutralisation.[10] Besides the normally higher rate of 5- rather than 6-ring formation, sulphur group participation is invoked in the 5-ring formation to explain the relatively large rate difference.

The cyclisation reaction of the optically active bromo acid (XII) was stopped when the reaction was only partially completed due to increasing racemisation with time as discussed below. The product which crystallized from the reaction solution was racemic. Optically active acid I was isolated by phenol extraction of the filtrate after removal of the precipitated racemate, $[\alpha]_D^{25} = +73.6°$ (H_2O). From the CD curves, as discussed below, the amino and bromo compounds have the (R)-configuration. The bicyclic product I has the (*S*)-configuration in agreement with net inversion of configuration in the cyclisation step. The optical rotation observed, however, cannot be used as a measure of the stereochemical homogeneity of the cyclisation due to extensive racemisations occurring which do not involve the actual cyclisation step. Thus optically inactive bromo compound (XII) was isolated from the reaction solution after the reaction had been stopped. Previously we have also found that it is racemisation by bromine interchange in the alkylating agent which is mainly responsible for the low optical yield in reactions which requires a long time for completion.[2] Racemisation caused by proton abstraction from the activated chiral carbon in I was excluded since the racemic acid I from reactions in deuterium oxide showed no deuterium incorporation. This also follows from the optical stability studies below. Thus the quaternary acid I in acid solution is optically quite stable. Information on the stability in alkaline solution was obtained by studies in 0.4 N NaOD at 40°C. NMR was used to study the deuterium incorporation on the chiral carbon while the racemisation was followed by means of the sodium D-line rotation. Fifty percent deuteriation was observed in I after 60 min and in the case of the thiazolo analogue (II) after 30 min. The optical rotation for either compound was practically the same after 2.5 h at which time compound I was fully deuteriated.

The chemical shifts in trifluoroacetic acid for the methine protons are at 4.0 and 3.7 τ for I and II, respectively, and in 0.4 N NaOD at 4.7 and 4.3 τ. The chemical shift thus reflects the relative acidity as measured by the rate of deuteriation. The explanation advanced[11] for the optical stability of II is equally applicable to I. Since proton exchange occurs rapidly, while the optical rotation remains virtually constant, the intermediate pyramidal carbanion must recapture a proton from the solvent faster than inversion can occur. The increased energy barrier to inversion arises because of non-bonded interaction between the 4-carboxyl group and the 6-methyl group in a planar or nearly planar inversion intermediate.

For configurational correlations the CD curves of the optically active compounds have been recorded. α-Amino acids of the L-series in acid solution have a strong positive Cotton effect in the 210-220 nm region.[12,13] For aliphatic amino acids this has been ascribed to $n \rightarrow \pi^*$ transitions of the carboxyl group.[12,14] In neutral or alkaline solution a weaker band with opposite sign is seen in the 230 – 245 nm region ascribed to the same optical transition but due to a

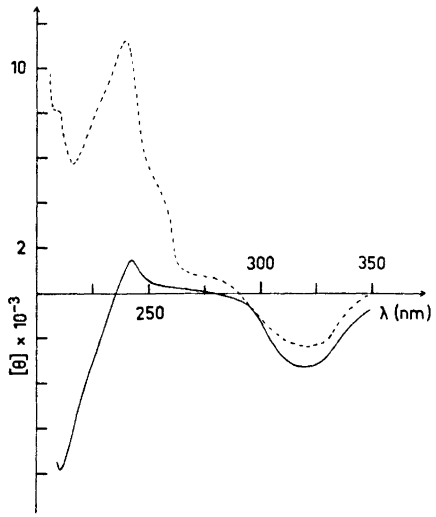

Fig. 1. CD curves recorded in 1 N HCl for (*R*)-X (———) and (*R*)-XIV (– – –).

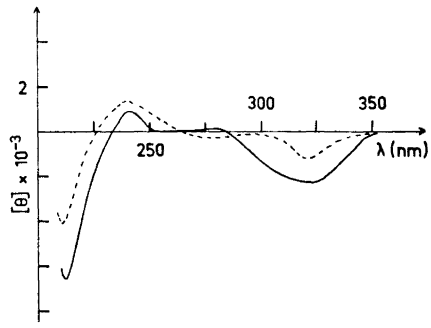

Fig. 2. CD curves recorded in 1 N HCl for (*R*)-XI (———) and (*R*)-XII (– – –).

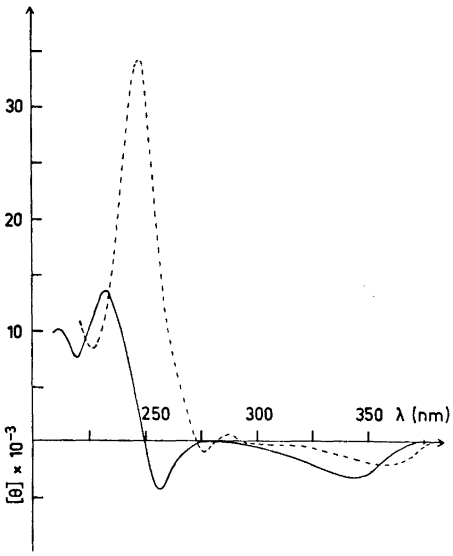

Fig. 3. CD curves for (*S*)-I recorded in 1 N HCl (———) and in 1 N NaOH (– – –).

different rotamer.[12,14] In the aromatic amino acids the observed Cotton effect is near 220 nm but the assignment of the 220 nm band is difficult due to the proximity of the $n\rightarrow\pi^*$ transition of the carboxyl group and the ^1L_a transition of the aromatic ring. Otherwise a weak Cotton effect, with considerable fine structure, is observed at 260 – 280 nm due to weak ^1L_b transitions of the aromatic chromophore.[13]

Table 1. UV absorption maxima in N HCl.

Compound:	X		XIV		XI		XII		I		I in N NaOH	
λ nm, log ε	321	3.96	318	3.97	323	3.83	322	3.96	342	4.06	360	4.07
λ nm, log ε	237	3.59	237	3.59	238	3.47	238	3.61	239	3.70	247	3.94
λ nm, log ε									211	4.00		

The pyridyl chromophore gives rise to intense dichroic absorption near and below 220 nm [15] which corresponds to the region for the $n\rightarrow\pi^*$ transition of the carboxyl group. The observed dichroic absorption in the low wavelength region therefore results from superposition of group dichroic bands. The isolated enantiomer of the amino acid X has a strong negative CD band at 211 nm in acid solution (Fig. 1). In accordance with the dichroic absorption of aromatic amino acids, the enantiomer of X is assigned the (*R*)-configuration. Support for this assignment follows from the CD absorption of the cysteine derived amino acid XIV, a lower homologue of X. The acid XIV has the (*R*)-configuration [10] and shows positive dichroic absorption near 210 nm (Fig. 1). In this connection it is pointed out that (*R*)-X belongs to the amino acid D-series while (*R*)-XIV belongs to the L-series. The formylated derivative XI has closely similar dichroic absorption to that of the amino acid X (Fig. 2). Further support for the (*R*)-configurational assignment is found in the spectrum of the bromo acid XII (Fig. 2), which is prepared from X with configurational retention as discussed above. Thus α-bromo acids of the (*S*)-configuration have been reported [16] to have a positive Cotton effect at 205 – 220 nm and a negative Cotton effect at 235 – 263 nm. The strong negative band at 210 nm for XII is in accordance with (*R*)-configurational assignment. The dichroic bands at higher wavelengths (Figs. 1 and 2) correspond well to the respective UV-maxima (Table 1). The pyridyl absorption near 240 nm will interfere with the otherwise observed $n\rightarrow\pi^*$ transition from the carboxyl group in alternative conformational rotamers. In all cases the highest wavelength dichroic bands near 320 nm, due to the pyridyl chromophore, are negative even for the configurationally opposite cysteine derived amino acid XIV.

Fig. 3 shows CD curves for the quaternary acid I in acid and alkaline solution. The spectrum in acid solution has positive bands at 212 and 233 nm and negative bands at 257 and 345 nm with observed UV maxima at 342, 239 and 211 nm. At least the former two bands are associated with the aromatic chromophore. In alkaline solution a bathochromic shift has occurred because

of dissociation of the phenolic group. Positive dichroic absorption is indicated below 220 nm but the maximum was not reached because of strong absorption. UV maxima at 360 and 247 nm correspond to the negative CD maximum at 360 nm and the positive maximum at 247 nm. The CD curves in Fig. 3, both in acid and alkaline solution, have closely similar positional maxima and signs for the dichroic bands as reported[4] for the dihydrothiazolo analogue II of the (*R*)-configuration. The dihydro[1,3]thiazino acid I is therefore assigned the (*S*)-configuration. Since the dichroic absorption requires assignment of the (*R*)-configuration to the (+)-amino acid enantiomer X and the derived (+)-bromo acid, but (*S*)-configuration to the quaternary acid I, the intramolecular Menschutkin reaction must proceed by inversion of the configuration.

EXPERIMENTAL

The CD and UV spectra were recorded on a Jasco model J – 10 spectropolarimeter. The cell length was 1 mm and the temperature 27°C. NMR data were recorded on a Varian A – 60A instrument.

2-Carbobenzoxyamino-4-hydroxy-N,N-*diethylbutyramide (IVb)*. A solution of 2-carbobenzoxyamino-4-butyrolactone[6,7] (105 g, 0.52 mol) and diethylamine (300 ml) in benzene (600 ml) was kept at 45°C for 4 days before evaporation. The residual oil crystallized on drying. The product appeared homogeneous on chromatography and was used as such in the next step. The yield was 131 g (95 %). The analytical sample in benzene was filtered through a short column of aluminium oxide and recrystallized from carbon tetrachloride, m.p. 73°C. (Found: C 62.69; H.7.88; N 9.15. Calc. for $C_{16}H_{24}N_2O_4$: C 62.31; H 7.85; N 9.09.) NMR in $CDCl_3$: 8.8 – 8.9 and 6.3 – 6.8 τ (*N* – Et); 8.2 τ ($2H^3$); 7.2 τ ($2H^4$); 5.2 τ (H^2); 4.9 τ (benzyl-CH_2) and 2.7 τ (benzyl-C_6H_5).

2-Carbobenzoxyamino-4-chloro-N,N-*diethylbutyramide (Vb)*. 2-Carbobenzoxyamino-4-hydroxy-*N*,*N*-diethylbutyramide (131 g, 0.43 mol) was added gradually with stirring to ice-cold thionyl chloride (300 ml). To minimize loss of the carbobenzoxy group the volatile acids liberated were removed as formed at reduced pressure. The excess thionyl chloride was evaporated at reduced pressure after 2 ½ h and the residual oil triturated with water before crystallisation from dilute ethanol. Recrystallisation from benzene/carbon tetrachloride gave the white title compound in 72 % yield (100 g); m.p. 86°C. (Found: C 58.97; H 6.79; N 8.29. Calc. for $C_{16}H_{23}ClN_2O_3$: C 58.77; H 7.07; N 8.57.) NMR in $CDCl_3$: 8.8 – 8.9 and 6.3 – 6.9 τ (*N* – Et); 8.0 τ ($2H^3$); 6.3 – 6.9 τ ($2H^4$); 5.2 τ (H^2); 4.9 τ (benzyl-CH_2) and 2.7 τ (benzyl-C_6H_5).

2-Carbobenzoxyamino-4-chlorobutyramide (Va). This compound was prepared and crystallized as Vb; yield 70 %, m.p. 121°C. (Found: C 53.38; H 5.52; N 10.17. Calc. for $C_{12}H_{15}ClN_2O_3$: C 53.19; H 5.58; N 10.34.)

3-Carbobenzoxyamino-2-pyrrolidinone (VI). The title compound was formed when 2-carbobenzoxyamino-4-chlorobutyramide was heated for 1 h in methanolic sodium methylate. The product was isolated by evaporation of the solution, trituration with water followed by crystallisation from ethyl acetate/ethanol; m.p. 168°C. An attempt to carry out *S*-alkylation of 3-hydroxy-6-methylpyrid-2-thione (VII) using Va gave only the title compound. (Found: C 61.34; H 5.70; N 11.73. Calc. for $C_{12}H_{14}N_2O_3$: C 61.52; H 6.00; N 11.96.) NMR in TFA: 7.5 τ ($2H^4$); 6.4 τ ($2H^5$); 5.2 τ (H^3); 4.7 τ (benzyl-CH_2); 2.6 τ (benzyl-C_6H_5).

2-Carbobenzoxyamino-4-(3-hydroxy-6-methyl-2-pyridylthio)-N,N-*diethylbutyramide (VIII)*. 2-Carbobenzoxyamino-4-chloro-*N*,*N*-diethylbutyramide (100 g, 0.30 mol), anhydrous potassium carbonate (45.6 g, 0.33 mol), and 3-hydroxy-6-methylpyrid-2-thione (42.3 g, 0.30 mol) in dimethylformamide (600 ml) were stirred for 4 days at 40°C. The reaction mixture was then diluted with water, pH adjusted to 5 and the solution extracted with chloroform. The chloroform extract was dried, decolorized with charcoal, the solution evaporated and the residual material crystallized from carbon tetrachloride; yield 77 g (60 %). The analytical sample was recrystallized once from carbon tetrachloride/benzene; m.p. 140°C. (Found: C 61.32; H 6.72; N 9.81. Calc. for $C_{22}H_{29}N_3O_4S$: C 61.24;

H 6.77; N 9.74.) NMR in $CDCl_3$: 8.8 – 9.1 and 6.4 – 7.2 τ (*N*-Et); 8.0 τ ($2H^3$); 7.6 τ (pyridyl-CH_3); 6.4 – 7.2 τ ($2H^4$); 5.3 τ (H^2); 4.9 τ (benzyl-CH_2); 2.7 τ (benzyl-C_6H_5); 3.0 and 3.2 τ (pyridyl-H^4, H^5).

2-Amino-4-(3-hydroxy-6-methyl-2-pyridylthio)-N,N-*diethyl-butyramide (IX).* A solution of 2-carbobenzoxyamino-4-(3-hydroxy-6-methyl-2-pyridylthio)-*N*,*N*-diethylbutyramide (4.3 g, 0.01 mol) in 40 % HBr in acetic acid (40 ml) was left in the cold for 2 h, excess ether added, the supernatant solution decanted from the oily precipitate, the residue dissolved in water, the aqueous solution washed with ether to remove any residual benzyl bromide before the solution was neutralized with sodium bicarbonate. The precipitated title compound was recrystallized from dilute ethanol; yield 2.1 g (71 %), m.p. 170°C. (Found: C 56.61; H 7.44; N 14.18. Calc. for $C_{14}H_{23}N_3O_2S$: C 56.55; H 7.80; N 14.13.) NMR in TFA: 8.4 – 8.9 and 6.0 – 6.7 τ (*N*-Et); 7.4 τ ($2H^3$); 7.1 τ (pyridyl-CH_3); 6.0 – 6.7 τ ($2H^4$); 1.9 and 2.3 τ (pyridyl-H^4, H^5.)

2-Amino-4-(3-hydroxy-6-methyl-2-pyridylthio)butyric acid (X). 2-Amino-4-(3-hydroxy-6-methyl-2-pyridylthio)-*N*,*N*-diethylbutyramide or 2-carbobenzoxyamino-4-(3-hydroxy-6-methyl-2-pyridylthio)-*N*,*N*-diethylbutyramide were hydrolyzed to the title compound by heating in 6 N HCl at 100°C for 12 days. The cold solution was then extracted with ethyl acetate, the aqueous solution evaporated, the residual oil redissolved in water, the aqueous solution treated with a little charcoal and filtered before the pH was adjusted to 5. The solid precipitate was recrystallized from dilute ethanol; yield 60 – 65 %, m.p. 265°C (decomp.). (Found: C 49.21; H 6.04; N 11.48. Calc. for $C_{10}H_{14}N_2O_3S$: C 49.47; H 5.83; N 11.57.) NMR in TFA: 7.4 τ ($2H^3$); 7.2 τ (pyridyl-CH_3); 6.4 τ ($2H^4$); 5.3 τ (H^2); 2.0 and 2.3 τ (pyridyl-H^4, H^5).

2-Formylamino-4-(3-hydroxy-6-methyl-2-pyridylthio)butyric acid (XI). Acetic anhydride (21 ml) was added dropwise with stirring to an ice-cold solution of 2-amino-4-(3-hydroxy-6-methyl-2-pyridylthio) butyric acid (7.26 g, 0.3 mol) in formic acid (100 ml). The resultant solution was left at room temperature overnight, evaporated at reduced pressure, redissolved in boiling ethanol and treated with charcoal. A hygroscopic solid was obtained which was recrystallized from ethanol; yield 7.0 g (86 %), m.p. *ca.* 98°C. The molecular ion ($C_{11}H_{14}N_2O_4S$) on mass spectrometry corresponds to the title compound. The hygroscopic nature of the substance made elementary analyses difficult but chromatography shows a homogeneous product. NMR in TFA: 7.6 τ ($2H^3$); 7.2 τ (pyridyl-CH_3); 6.5 τ ($2H^4$); 4.9 τ (H^2); 2.0 and 2.3 τ (pyridyl-H^4, H^5).

Optical resolution of the 2-formylamino derivative (XI). XI (8.1 g, 0.03 mol) was dissolved in methanol (20 ml) and added to a solution of brucine. $4H_2O$ (14.0 g, 0.03 mol) in methanol (30 ml) containing water (3 ml). On cooling the warm solution, 14.3 g of salt was precipitated, $[\alpha]_D^{25} = -15.4°$. The specific sodium D-line rotation for the racemic salt was $-18°$. All the rotations were measured as 1 % solution in N HCl at 25°C. The salt was redissolved in methanol (50 ml) and water (9.5 ml) by heating. Two well defined crystal modifications were formed which were separated mechanically. The major part consisted of fine needles (7.3 g), $[\alpha]_D^{25} = -14.3°$. The cubic crystals (1.8 g) had $[\alpha]_D = -21.5°$. The major product was recrystallized from methanol (65 ml) and water (15 ml) which gave $[\alpha]_D^{25} = -12.8°$. Two more recrystallisations hardly changed the rotation which was $-12.7°$; final yield 4.4 g. This salt was dissolved in 1 N ammonia (130 ml), the brucine extracted into chloroform, and the solution evaporated to yield 2.0 g of the title compound shown to be homogeneous by chromatography; $[\alpha]_D^{25} = +11.5°$ ($c = 1$ in N HCl).

(R)-*2-Amino-4-(3-hydroxy-6-methyl-2-pyridylthio)butyric acid (X).* The *N*-formyl derivative (XI) (2.0 g) was heated in 1 N HCl for 2 h and the pH of the cold solution adjusted to 5.5 with sodium bicarbonate. The title compound was slowly precipitated; yield 1.3 g (73 %), $[\alpha]_D^{25} = -18.0°$ ($c = 1$ in N HCl).

(R)-*2-Bromo-4-(3-hydroxy-6-methyl-2-pyridylthio)butyric acid (XII) as HBr salt.* Sodium nitrite (1.60 g, 0.02 mol) in water (10 ml) was added over 1 h to an ice-cold solution of the *(R)*-amino acid (X) (1.08 g, 0.0045 mol) in 5 N HBr (70 ml). The resultant solution was left at 5°C overnight, evaporated at reduced pressure, the hygroscopic solid redissolved in water and the pH brought to 2.5. The bromo compound was extracted into ethyl acetate, the solution washed, dried and a few drops of HBr added before the solution was evaporated. A crystalline product was obtained in this way; yield 1.36 g, (79 %), m.p. 175°C, $[\alpha]_D^{25} = 17.5$ ($c = 1$ in N HCl). (Found: C 31.10; H 3.40; N 3.83. Calc. for $C_{10}H_{12}BrNO_3S$. HBr: C 31.04; H 3.39; N 3.62.) NMR in TFA: 7.6 τ ($2H^3$); 7.2 τ (pyridyl-CH_3); 6.5 τ ($2H^4$); 5.3 τ (H^2); 2.0 and 2.3 τ (pyridyl-H^4, H^5).

9-Hydroxy-6-methyldihydro[1,3]thiazino[3,2-a]pyridinium-4-carboxylate (I). 2-Bromo-4-(3-hydroxy-6-methyl-2-pyridylthio)butyric acid HBr salt (1.0 g, 0.0033 mol) was dissolved in water (60 ml), the pH adjusted to 4.5 with sodium bicarbonate, the solution heated at 60°C for 12 h, concentrated to a small volume and left in the cold. The title compound was slowly precipitated and was recrystallized from water; yield 0.45 g (78 %), m.p. 177° (decomp.). (Found: C 53.09; H 5.27; N 6.06. Calc. for $C_{10}H_{11}NO_3S$: C 53.33; H 4.92; N 6.22.) NMR in TFA: 7.2 τ (6-CH_3); 6.4 – 6.8 τ ($2H^2$, H^3); 7.2 – 7.7 τ (H^3); 4.0 τ (H^4); 2.3 and 2.6 τ (H^7, H^8).

(S)-*9-Hydroxy-6-methyldihydro[1,3]thiazino[3,2-a]pyridinium-4-carboxylate (I).* The (*R*)-bromo compound (XII) as hydrobromide (0.75 g) was dissolved in a small volume of water, the pH adjusted to 2.5 and the bromo compound extracted into ethyl acetate to remove the bromide ions. The ethyl acetate was evaporated and the bromo compound dissolved in water (40 ml) which gave pH 4.5. The solution was then heated at 60°C for 4 h, and the pH readjusted to 4.5 before concentration to a small volume. The zwitterion precipitated (0.2 g) was optically inactive. The filtrate was brought to pH 2.5 and unreacted bromo acid (XII) extracted into ethyl acetate. XII was optically inactive. The aqueous solution was extracted with aqueous phenol (90 %, 3 × 10 ml), the phenol extract washed with water (10 ml), ether (150 ml) added to the phenol, the separated water layer collected, the phenol/ether phase extracted with water (4 × 10 ml), the combined aqueous solutions washed with ether (2 × 10 ml) and the aqueous phase acidified with HCl before evaporation. The residue was the hydrochloride of the title compound which after trituration with acetone and ethyl acetate was a white solid (39 mg), $[\alpha]_D^{25} = +73.6°$ (c = 0.7 in H_2O).

6-Methyldihydro[1,3]thiazino[3,2-a]pyridinium-9-oxide (XIII). 2-Bromo-4-(3-hydroxy-6-methyl-2-pyridylthio)butyric acid hydrobromide (1.0 g, 0.0033 mol) was dissolved in acetonitrile (50 ml) containing triethylamine (1 ml). The resultant solution was heated at 80°C overnight, evaporated, the residue triturated with a little water and recrystallized from ethanol; yield 0.3 g (50 %). M.p. 167°C (decomp.). The product had spectral properties as previously described.[17]

REFERENCES

1. Part XXIX. Undheim, K. and Fjeldstad, P. E. *J. Chem. Soc. Perkin Trans. 1* **1973** 829.
2. Undheim, K. and Grönneberg, T. *Acta Chem Scand.* **25** (1971) 18.
3. Undheim, K., Røe, J. and Greibrokk, T. *Acta Chem. Scand.* **23** (1969) 2501.
4. Greibrokk, T. and Undheim, K. *Tetrahedron* **28** (1972) 1223.
5. Plieninger, H. *Chem. Ber.* **83** (1950) 265.
6. Hillmann, B. *Z. Naturforsch.* **1** (1946) 682.
7. Knobler, Y. and Frankel, M. *J. Chem. Soc.* **1958** 1629.
8. Sheradsky, T., Knobler, Y. and Frankel, M. *J. Org. Chem.* **26** (1961) 1482.
9. Greenstein, J. P. and Winitz, M. *Chemistry of the Amino Acids*, Wiley, 1961, Vol. 1, p. 165, and references given therein.
10. Undheim, K. and Ulsaker, G. A. *To be published.*
11. Undheim, K. and Greibrokk, T. *Acta Chem. Scand.* **23** (1969) 2505.
12. Craig, J. C. and Pereira, W. E. *Tetrahedron* **26** (1970) 3457.
13. Klyne, W., Scopes, P. M., Thomas, R. N. and Dahn, H. *Helv. Chim. Acta* **54** (1971) 2420.
14. Toniolo, C. *J. Phys. Chem.* **74** (1970) 1390.
15. Gacek, M. and Undheim, K. *Acta Chem. Scand.* **26** (1972) 2655.
16. Gaffield, W. and Galetto, W. G. *Tetrahedron* **27** (1971) 915.
17. Undheim, K. and Reistad, K. R. *Acta Chem. Scand.* **24** (1970) 2949.

Received September 8, 1972.

ACTA CHEMICA SCANDINAVICA 27 (1973) 1067–1072

Relationship between the Energy of Activation and the Overall Free Energy of Bridge-assisted Electron Transfer Reactions in Polar Media

JENS ULSTRUP

Chemistry Department A, Building 207, The Technical University of Denmark, DK-2800 Lyngby, Denmark

Experimental kinetic data for the bridge-catalyzed oxidation of $[Cr(bipy)_3]^{2+}$ by some closely related Co(III) complexes have been analyzed on the basis of a newly developed quantum mechanical theory for coupled electron transfer reactions in polar media. The relation between the energy of activation and the overall Gibbs free energy of the reaction is found to agree with that predicted by the theory, and conclusions can be drawn as to the mechanism of the reaction and the relative positions of the electronic terms of the initial, intermediate, and final states.

Several cases of homogeneous catalysis of outer sphere electron transfer reactions have been reported.[1–4] In a systematic study of such reactions the influence of γ,γ'-bipyridyl on the kinetics of the electron transfer reaction between $[Cr(bipy)_3]^{2+}$ and some closely related Co(III) complexes was investigated recently.[5,6] The observed strong catalysis was interpreted in terms of the formation of a γ,γ'-bipyridyl complex of chromium(II), in which an electron was first transferred from Cr^{2+} to coordinated γ,γ'-bipyridyl (brigde), and then by a second transfer from this ligand to Co(III). In such a series of electron transfer reactions between a common reducing ion and a series of closely related oxidizing ions the energy of reorganization of ligand and solvent spheres as well as electrostatic interactions between the reacting ions can be considered approximately constant, so that variation in the energy of activation E_a may be attributed solely to variation in the Gibbs free energy of the overall reaction, $\Delta G°$.

The theory for a mechanism consisting of two coupled electron transfer reactions applicable to homogeneous as well as electrode reactions in polar media was developed recently.[7–10] The probability per unit time of an overall electron transfer from one ionic species to another or to an electrode, *via* a third species (a "bridge") was calculated under the assumption that the electronic state corresponding to the localization of the electron on the bridge is

a (quantum mechanical) virtual state. This corresponds to the "double" exchange mechanism suggested previously for inner sphere electron transfer reactions as opposed to a "chemical" mechanism which consists of two consecutive one-electron transfer steps involving a temporary oxidation or reduction of the electron-mediating species.[11] The theoretical results showed that for suitable relative positions of the electronic terms of the various states, a decrease in E_a (a catalysis) could be expected for the bridge-assisted path as compared with the direct electron transfer from the initial to the final state. The overall probability of electron transfer *via* the intermediate state was calculated from second order quantum mechanical perturbation theory,[12] under the assumption of a weak interaction between the reacting ions and the bridge. This assumption appears justified for the Co(III)-γ,γ'-bipyridyl outer sphere interaction. Cr^{2+} is bound to γ,γ'-bipyridyl by a covalent chemical bond which, however, from thermodynamic data is found to be weak.[5] The perturbation treatment for the interaction between Cr^{2+} and coordinated γ,γ'-bipyridyl is therefore a first approximation, but it is emphasized that the arguments presented below concerning the distinction between direct and bridge-assisted electron transfer are also valid for stronger interactions between the reacting ions and the bridge.

The present work is an analysis of the kinetic data obtained previously in the light of the newly developed theory of bridge electron transfer reactions. In order to extend the ΔG° range they have been supplemented by new data for the reactions between $[Co(bn)_3]^{3+}$, where bn stands for optically active $(-)_D$-2,3-butanediammine, and the two chromium(II) complexes.

EXPERIMENTAL

The materials were purified, and the two chromium(II) complexes synthesized as described previously.[5,6] $[Co(bn)_3]Cl_3$ was prepared as described in Ref. 13. All kinetic measurements were carried out in a nitrogen atmosphere and in an ionic medium 0.1 M in NaCl under pseudofirst order conditions in chromium(II);[6] the reactions between $[Co(bn)_3]^{3+}$ and both chromium(II) complexes were found to proceed by the same mechanisms as described earlier.

RESULTS AND DISCUSSION

The determined rate constants and activation parameters for the direct (1) and bridge-assisted path (2) are given in Table 1. Here only the bridge-assisted path is considered (the reaction of the γ,γ'-bipyridyl complex of chromium(II)). Provided that the energy of reorganization of the ligand sphere and the interaction between the ions and the bridge can be neglected or

Table 1. Kinetic data for the reactions between the two chromium(II) complexes and $[Co(bn)_3]^{3+}$

k_1 l/mol sec	k_2 l/mol sec	$\Delta H_1^{\ddagger}$ kcal/mol	$\Delta H_2^{\ddagger}$ kcal/mol	$\Delta S_1^{\ddagger}$ cal/K mol	$\Delta S_2^{\ddagger}$ cal/K mol
9.8	206	12.8	7.8	−11.3	−36

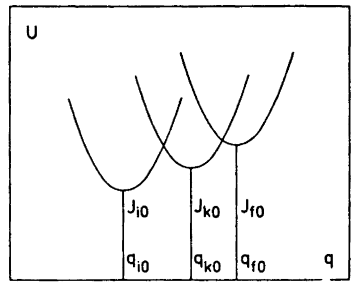

Fig. 1. Electronic terms of the various states. The q_0's are the equilibrium values of the solvent coordinate, and the J_0's the equilibrium energies of the various states. U is the total potential energy of the system.

considered constant, the electronic terms of the initial (i), intermediate (k) and final state (f) can be plotted as in Fig. 1. q is a generalized solvent coordinate, and the harmonic approximation is adopted for the solvent librations in all the states.[14] It was shown previously,[7] that the overall energy of activation is then determined by the highest intersections point between the intermediate and either the initial or final term, whereas the energy of activation for the direct electron transfer corresponds to the intersection point between the initial and final term. As observed,[6] the energy of activation is always smaller for the bridge-assisted reaction, and q_{k0} must therefore be situated between q_{i0} and q_{f0}.

In the harmonic approximation for the solvent coordinate [14–16] the energy of activation for an elementary electron transfer, *e.g.* from the electron donating ion to the bridge, is given by the expression

$$E_a = \frac{[E_s^{ki} + \Delta J^{ki}]^2}{4E_s^{ki}} = \frac{[E_s^{ki} + \Delta J^{fi} - \Delta J^{fk}]^2}{4E_s^{ki}} \quad (1)$$

where E_s is the energy of reorganization of the solvent (*e.g.* $E_s^{ki} = \frac{1}{2}\hbar\omega(q_{k0} - q_{i0})^2$; ω is the characteristic solvent frequency), and ΔJ the heat of reaction. In the theory of Levich and Dogonadze,[14] whoose symbols we shall use here, ΔJ is strictly speaking the internal energy of the reaction (ΔU). For reactions in solution this quantity can, however, with sufficient accuracy be put equal to the heat of reaction (ΔH). If the left hand intersection point is the higher, the overall energy of activation is thus given by an expression of the form of eqn. (1), whereas if the right hand intersection point is the higher, the energy of activation is given by

$$E_a = \frac{[E_s^{fk} + \Delta J^{fk}]^2}{4_s E^{fk}} + \Delta J^{ki} = \frac{[E_s^{fk} + \Delta J^{fi} - \Delta J^{ki}]^2}{4E_s^{fk}} + \Delta J^{ki} \quad (2)$$

where the superscripts refer to the states between which the transitions occur.

The variation of E_a for the different Co(III) complexes is mainly due to the change in the overall free energy of reaction ΔG°, other contributions to E_a being approximately constant. Provided that the entropy part of ΔG° is constant, which seems to be a reasonable assumption, considering that the same charge is found on all the ions except the acetatopentammine, ΔJ^{fi} in eqns. (1) and (2) can be replaced by ΔG° (including formally the entropy part of ΔG° in the constant E_s). The dependence of E_a on ΔG° thus adopts the same form as the dependence on ΔJ^{fi}.

A priori it is necessary to consider the push-pull as well as the pull-push double exchange mechanism as defined in Ref. 8. Superexchange mechanisms [11,17] involving higher vacant and lower occupied orbitals of γ,γ'-bipyridyl might be considered, but as the difference between the energies of these orbitals is high (several electron volts [5]) such mechanisms would involve very high energies of activation. We therefore only consider the lowest empty bridge orbital in the push-pull mechanism and the highest filled bridge orbital in the pull-push mechanism.

Values of the overall ΔG° were calculated from the standard oxidation potentials of the Co(III)/Co(II) complexes,[13,18-22], the formation constant of the γ,γ'-bipyridyl complex,[5] and from the half-wave potential of the Cr(III)/Cr(II) couple,[23] since the equilibrium potential of the latter is not available. The possible error thus introduced is small and does not interfere with the trend of the results observed.

The push-pull mechanism. For this mechanism, within a series of related electron receiving Co(III) complexes, the final state electronic term is shifted vertically with respect to the initial and intermediate term, while the relative position of the latter two terms remains fixed.[8] Thus when ΔJ^{fi} (ΔG°) increases, the final term is shifted upwards with respect to the initial and intermediate terms. If at a given ΔJ^{fi} the left hand intersection point is the higher, E_a is determined by this point *i.e.* by the energy of activation of the electron transfer from the donating ion to the bridge. Thus E_a should not depend upon the nature of the electron receiving ion (ΔJ^{ki} is a constant). When the right hand intersection point becomes the higher, E_a suddenly (*i.e.* within a few multiples of kT) begins to increase with increasing ΔJ^{fi}, and the slope α of the plot of E_a against ΔJ^{fi} will be $0<\alpha\lesssim 1$, corresponding to a "normal" ($\alpha\approx 0.5$) and/or a "barrierless" region,[24] whereas an "activationless" region ($\alpha\approx 0$) does not exist.

The pull-push mechanism. In this case, when the electron receiving ion changes, the initial term changes with respect to the intermediate and final term, while the relative position of the latter terms does not change. If the left hand intersection point is the higher, a "normal" and an "activationless" range should be observed, corresponding to $\alpha\approx 0.5$ and $\alpha\approx 0$, respectively, and with smooth transitions (*i.e.* within about $E_s\approx 30$ kcal/mol) between the regions. If the right hand intersection ponts is the higher, E_a is given by eqn. (2), where ΔJ^{fk} is now a constant (*i.e.* the heat of reaction for the electron transfer from Cr^{2+} to γ,γ'-bipyridyl).

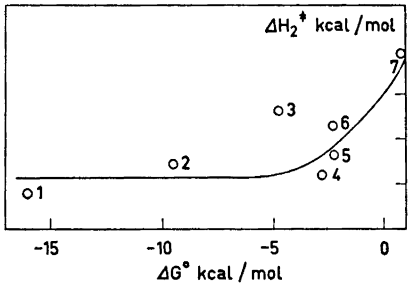

Fig. 2. $\Delta H_2^{\ddagger}$(kcal/mol) plotted against ΔG^0 for the bridge-assisted reaction. The numbers refer to the following Co(III) complexes: 1, acetatopentaammine; 2; hexammine; 3, tris-meso-butanediammine; 4, bis-diethylenetriammine; 5, tris-ethylenediammine; 6, tris-(racemic)-propanediammine; 7, tris-(−)-butanediammine.

The experimental values of ΔH_2^+ are plotted against the overall ΔG° (ΔJ^{fi}) in Fig. 2. The dependence changes rather suddenly (*i.e.* within a few multiples of kT) from a region of very weak dependence to a region where α is somewhere between 0.5 and 1. The Co(III) complex of *meso*-butanediammine does not fit the otherwise smooth correlation, and possible reasons for this were discussed previously.[6]

The experimental plot can be interpreted on the basis of the push-pull mechanism, as changing from a region where the left hand intersection point is the higher to a region, where the right hand one is the higher, for increasing ΔG° (ΔJ^{fi}). The experimental points indicate that $\alpha > 0.5$, when the right hand point becomes the higher, corresponding to a "normal" and a "barrierless" region, and therefore $|\Delta J^{fk}| \lesssim E_s^{fk}$.

An alternative interpretation could be made on the basis of the pull-push mechanism. The horizontal part of the curve in Fig. 2 would then correspond to an "activationless" region, where either intersection point may be the higher. When ΔG° increases, the initial term is shifted downwards with respect to the other two terms. If the left hand intersection point is the higher, a smooth change of α (*i.e.* within a change in ΔG° of the order $E_s^{ki} \approx 30$ kcal/mol) from 0 to 1 is observed, while if the right hand intersection point during this shift becomes the higher, an abrupt (*i.e.* within a few multiples of kT) change to unity is observed. Although this second interpretation cannot be rejected, it seems less probable, because of the large "activationless" range and because of the apparent shift from $\alpha = 0$ to $\alpha > 0.5$ within an extremely narrow range of ΔG°.

The experimental results show that meaningful correlations between E_a and ΔG° can be made for bridge-assisted electron transfer reactions, in analogy with what has been reported for direct electron transfer reactions. In principle the correlations allow a distinction between the push-pull and the pull-push mechanism, and they justify conclusions as to the relative positions of the terms of the various states.

The $[Cr(bipy)_3]^{2+}$-γ,γ'-bipyridyl-Co(III) system is not the one best suited for an experimental test of the correlations predicted by the theory, since it is not of strictly outer sphere nature; but it seems to be the only one, where a systematic study has been made on the relation between kinetic and thermodynamic parameters for a bridge electron transfer reaction. However, the arguments presented above are also qualitatively valid, when there is a somewhat stronger interaction between the bridge and the reacting ions than in general for outer sphere electron transfer reactions.

Acknowledgement. The author expresses his thanks to Dr. Yu. I. Kharkats, the Institute of Electrochemistry of the Academy of Sciences of the USSR, for helpful discussions.

REFERENCES

1. Gjertsen, L. and Wahl, A. C. *J. Am. Chem. Soc.* **81** (1959) 1572.
2. Campion, R. J., Deck, C. F., King, Jr., P. and Wahl, A. C. *Inorg. Chem.* **6** (1967) 672.
3. Ulstrup, J. *Acta Chem. Scand.* **23** (1969) 3091.
4. Jansen, P. H. and Ulstrup, J. *Acta Chem. Scand.* **23** (1969) 1822.
5. Ulstrup, J. *Acta Chem. Scand.* **25** (1971) 3397.

6. Ulstrup, J. *Trans. Faraday Soc.* **67** (1971) 2645.
7. Volkenstein, M. V., Dogonadze, R. R., Madumarov, A. K. and Kharkats, Yu. I. *Dokl. Akad. Nauk SSSR, Ser. Phys. Chem.* **199** (1971) 124.
8. Dogonadze, R. R., Ulstrup, J. and Kharkats, Yu. I. *J. Theoret. Biol. In press.*
9. Dogonadze, R. R., Ulstrup, J. and Kharkats, Yu. I. *J. Electroanal. Chem. Interfacial Electrochem.* **39** (1972) 47.
10. Dogonadze, R. R., Ulstrup, J. and Kharkats, Yu. I. *J. Electroanal. Chem. Interfacial Electrochem. In press.*
11. George, P. and Griffith, J. S. *Enzymes* **1** (1959) 347.
12. Landau, L. D. and Lifshitz, E. M. *Quantum Mechanics*, Pergamon, Oxford 1965.
13. Woldbye, F. *Studier over Optisk Aktivitet*, Polyteknisk Forlag, København 1968.
14. Levich, V. G. and Dogonadze, R. R. *Collect. Czech. Chem. Commun.* **26** (1961) 193.
15. Marcus, R. A. *J. Chem. Phys.* **24** (1965) 966.
16. Marcus, R. A. *J. Chem. Phys.* **43** (1965) 679.
17. Gould, E. S. and Taube, H. *Accounts Chem. Res.* **2** (1969) 321.
18. Bjerrum, J. *Metal Ammine Formation in Aqueous Solution*, 2nd Ed., P. Haase and Son, Copenhagen 1957.
19. Bartelt, H. and Skilandat, H. *J. Electroanal. Chem.* **23** (1969) 407.
20. Bartelt, H. and Skilandat, H. *J. Electroanal. Chem.* **24** (1970) 207.
21. Bartelt, H. and Prügel, M. *Electrochim. Acta* **16** (1971) 1815.
22. Basolo, F. and Pearson, R. G. *Mechanisms of Inorganic Reactions*, 2nd Ed., Wiley, New York, London and Sidney 1967.
23. Vlcek, A. A. *Nature* **189** (1961) 393.
24. Dogonadze, R. R. and Kuznetsov, A. M. *Itogi Nauki Elektrokhim. 1967*, Akademiya Nauk, SSSR 1969.

Received October 3, 1972.

ACTA CHEMICA SCANDINAVICA 27 (1973) 1073–1082

Constituents of *Solidago* Species

III.[1] The Constitution and Stereochemistry of Diterpenoids from *Solidago missouriensis* Nutt.

THORLEIF ANTHONSEN and GUDRUN BERGLAND

Organic Chemistry Laboratories, Norway Institute of Technology, University of Trondheim, Trondheim, Norway

The constitution and stereochemistry of several diterpenoids isolated from root extracts of *Solidago missouriensis* Nutt. are deduced from their spectroscopic and chemical properties. Two of them are *ent*-13-epimanoyl oxide and its 3-oxo derivative; the remaining ones are non-acidic members of the abietane group.

Investigations of the genus *Solidago* belonging to the Compositae family have shown that plants in this genus have an extraordinary ability to produce diterpenoids. The first species to be examined in this respect was the very common Canadian goldenrod *S. canadensis* L.[2] which gives solidagenone (*1*) in very high yield. Since then, *S. serotina* Ait.,[3] *S. altissima* L.,[4] *S. elongata* Nutt.,[5] *S. Shortii* Torr. & Gray [6], and now *S. missouriensis* Nutt. have been investigated and the total number of diterpenoids isolated is not far from thirty. They all belong to the labdane (*2*) or clerodane [7] (*3*) group except for some of the diterpenoids now reported from *S. missouriensis* Nutt. which are abietanes (*4*).

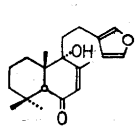

1

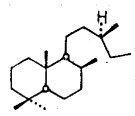

2

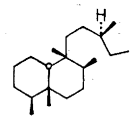

3

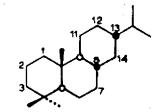

4

The majority of abietanes found in nature are either resin acids from conifers or diterpenoids with an aromatized ring A or C as found in conifers and labiates.[8,9] In a previous communication [10] we have reported that the abietanes from *S. missouriensis* Nutt. are 7,13-abietadienes. However, we did not exclude the possibility that they were artefacts formed during our work up. We now verify that our assumption was right and that the naturally occurring com-

pounds are indeed 8(14)-abieten-13-ols and as such fit very neatly into the commonly accepted biosynthetic scheme. The abietanes are believed to arise from a rearrangement of pimaradiene (*5*) to the carbonium ion *6* (Scheme 1).[11]

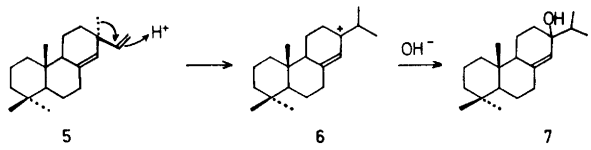

5 6 7

Scheme 1.

Hydroxylation of this ion leads directly to the 13-hydroxy-8(14)-abietenes (*7*) which are enantiomers of the abietenes found in *S. missouriensis* Nutt. In the following they will be designated missourienols.

The characteristic features of the allylic alcohol system are firstly that the missourienols do not show a molecular ion peak in their mass spectra, but $M-H_2O$ and $M-C_3H_7$. Secondly, their NMR spectra exhibit the resonance of only one olefinic proton as a rather narrow ($W_{1/2}$ 5 Hz) peak around τ 4.5. The hydroxy group is detected by its absorption in the IR (3440 cm^{-1}) and by a concentration dependent signal around τ 8.7 in the NMR spectrum, which disappears when the solution is shaken with D_2O.

Dehydration of the missourienols under mild acidic conditions furnishes dienes, more precisely heteroannular dienes as indicated by their UV spectra λ_{max} (EtOH) 234 (21 000), 241 (22 800), 249 (15 000) nm.[12] Their NMR spectra have resonances due to two olefinic protons, one narrow ($W_{1/2}$ 4 Hz) at τ 4.2 and one fairly broad ($W_{1/2}$ 9 Hz) at 4.5. The narrow signal is due to H-14 being only allylically coupled whereas H-7, which is vicinally coupled, gives rise to the broader peak. The 7,13-abietadienes were also isolated from the natural material in various amounts.

Missourienol A, $C_{20}H_{32}O_2$, m.p. 82–84°C, which is the major diterpenoid of *Solidago missouriensis*, is a ketone (ν_{max} 1705 cm^{-1}). It has been identified as *ent*-13-hydroxy-8(14)-abieten-3-one (*8*). The NMR spectrum contains, in addition to the peaks due to the allylic alcohol system already mentioned, resonances of three tertiary (τ 8.91, 8.93 and 8.99) and two secondary (9.06, 9.11 $J=7$ Hz) methyl groups. The dehydration product, a heteroannular diene (*9*), $C_{20}H_{30}O$ (*vide supra*), is still an unconjugated six ring ketone (ν_{max} 1712 cm^{-1}). Its NMR spectrum in addition to the resonances due to the olefinic protons H-7 and H-14 shows three tertiary (τ 8.86, 8.91, 8.97) and two secondary (8.97 $J=7$ Hz) methyl groups. The isopropyl methyl groups show chemical shift equivalence in all the dienes while they are non-equivalent in all the missourienols. This ketone yields on Wolff-Kishner reduction a hydro-

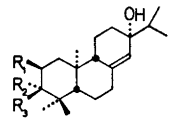

8 R_1=H, R_2R_3=O
14 R_1=R_2=H, R_3=OH
15 R_1=OAc, R_2=R_3=H
11 R_1=R_2=R_3=H

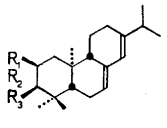

9 R_1=H, R_2R_3=O
12 R_1=R_2=H, R_3=OH
16 R_1=OAc, R_2=R_3=H
17 R_1=OH, R_2=R_3=H
10 R_1=R_2=R_3=H

carbon $C_{20}H_{32}$ (*10*) which is identical with a compound also isolated from the plant material and also has spectroscopic and chromatographic properties similar to a synthetic sample of 7,13-abietadiene. However, its optical rotation $[\alpha]_D^{24} + 127°$ suggests that it belongs to the *enantio* series. The reported value of 7,13-abietadiene isolated from *Pinus sibirica* is $[\alpha]_D^{20} - 75°$ [13] and synthetic $[\alpha]_D^{21} - 86°$.[14] We consider the naturally occurring *ent*-7,13-abietadiene (*10*) to be an artefact. However, we were unable to isolate the corresponding missourienol (*11*).

The position of the keto function in missourienol A (*8*) and the corresponding diene (*9*) was deduced as follows. Since the dienone (*9*) was not a conjugated ketone, only positions 1, 2, 3, and 11 were possible. LAH reduction of the dienone yields the alcohol (*12*). The NMR spectrum of this compound exhibits the carbinyl proton at τ 6.76 as a doublet of doublets ($J = 8.5$ and 6.0 Hz) thus revealing its axial nature and in turn the equatorial nature of the hydroxy function. Moreover, it shows that it is flanked by only two protons and consequently C-1 and C-3 are the two remaining positions for the keto function. Benzene induced solvent shifts lead to a choice of the latter. The Δ-values $\Delta = \tau(\text{benzene}) - \tau(CDCl_3)$ for the methyl group resonances in the NMR spectrum of missourienol A, -0.07 and -0.02 (isopropyl methyl groups), $+0.28$ (C-10 Me), $+0.19$ (C-4 axial Me), and -0.03 ppm (C-4 equatorial Me) accord only with a C-3 keto function.[15,16]

Treatment of the dieneol (*12*) with PCl_5 [17] yielded a dehydration product which is a triene $C_{20}H_{30}$. Its NMR spectrum showed resonances due to two secondary (τ 8.98), one tertiary (9.37) and two olefinic (8.29, 8.39) methyl groups and no additional olefinic hydrogen. This hydrocarbon, therefore, must be the rearrangement product (*13*) and thus is the conclusive evidence for the hydroxy group being at C-3 and equatorial. The remarkable upfield shift of the tertiary C-10 methyl group must be due to the disappearance of the 1,3 diaxial collision with the axial C-4 methyl group.

Missourienol B (*14*), $C_{20}H_{34}O_2$, m.p. 155–156°C is a secondary alcohol. Its dehydration product (*12*) is identical with the reduction product of the dienone (*9*).

The last of the 8(14)-abietenes in *Solidago missouriensis* Nutt. is an oily secondary acetate, missourienol C (*15*), $C_{22}H_{36}O_3$ (IR 1739 cm^{-1}, NMR τ 8.05 3 H *s*). The carbinyl proton in the NMR spectrum (Fig. 1) resonates at τ 5.12 as a triplet of triplets ($J = 12$ and 4 Hz) thus indicating that it is axial and consequently that the acetoxy group has equatorial stereochemistry. Furthermore, the multiplicity of this peak demonstrates that it is flanked by two methylene groups. Consequently, on the basis of a 8(14)-abietene skeleton, the only possible position of attachment is at C-2.

Its dehydration product the dieneacetate (*16*) yielded on hydrolysis an oily dieneol (*17*) $C_{20}H_{32}O$. In its NMR spectrum the methine proton gives resonance at τ 6.07 (*t,t*) and is thus moved upfield by nearly one ppm compared with the corresponding proton of the dieneacetate (τ 5.08).

Hydrogenation of missourienol A (*8*) furnished a hydrogenolysis product $C_{20}H_{32}O$ (*18*). The mass spectrum of this ketone exhibits a prominent molecular ion peak (81 %) in contrast to the mass spectra of the missourienols (*vide supra*). The NMR spectrum contains a peak due to the olefinic proton (H-14)

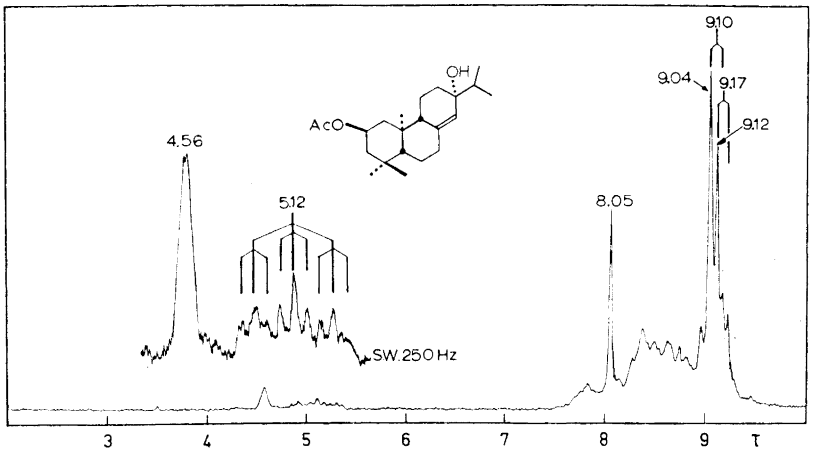

Fig. 1. The 60 MHz spectrum of Missourienol C in CCl_4 solution.

at τ 4.50 slightly broadened ($W_1/_2$ 7 Hz) in comparison with the corresponding peak in the NMR spectrum of the 8(14)-en-13-ols.

The final point to be settled concerning the missourienols is the stereochemistry at C-13. We have not been able to solve this problem on the basis of the data so far presented. However, the $Eu(DPM)_3$ shift in the NMR spectrum of missourienol A (*8*) suggested an axial (α) hydroxy group. The shift values observed for the methyl groups at the molar ratio substrate/complex 0.5 are: 2.94, 2.66 (isopropyl methyls), 2.54, 1.63 and 1.39 ppm.

The two isopropyl methyl groups and one tertiary methyl group show considerably larger downfield shifts than the two remaining methyl groups. Assuming that the complexing takes place preferentially at the hydroxy group,[18,19] it seems reasonable that the methyl group at C-10 will suffer a relatively larger shift than the geminal methyls at C-4 when the C-13 hydroxyl is axial (α) than when it is equatorial. An equatorial hydroxy group would probably cause a more similar shift in all the three tertiary methyl groups. We consider, however, this final question of stereochemistry not to be satisfactorily answered.

The two remaining diterpenoids in *S. missouriensis* are labdanes, more specifically manoyl oxides. Previously four not further oxygenated manoyl oxides have been described, one of them in both the normal and the enantiomeric form. Their melting points and optical rotations are given in Table 1.

The not further oxygenated manoyl oxide we have isolated had $[\alpha]_D^{24} - 31°$ and melted at 97 – 98°C. It is thus *ent*-13-epimanoyl oxide (*19*) or more precisely [7] *ent*-8,13β-epoxy-14-labdene. The NMR spectrum exhibits, beside resonances due to five tertiary methyl groups (8.86, 8.97, 9.16, 9.24 and 9.30), the characteristic ABC pattern of a vinyl group τ_A 4.03, τ_B 5.08, τ_C 5.14, $J_{AB} = 18.0$, $J_{AC} = 10.5$ and $J_{BC} = 1.3$ Hz). According to Wenkert *et al.*[24] there exists a characteristic difference between the appearance of this ABC pattern in the NMR spectra of manoyl and 13-epimanoyl oxide. This difference is

Table 1. Melting points and optical rotations of the known manoyl oxides.

	M.p.	$[\alpha]_D$	Ref.
Manoyl oxide	24.5 – 26°	+23°	20
13-Epimanoyl oxide	100.5 – 101.5°	+35.3°	21
ent-13-Epimanoyl oxide	99°	−35.8°	22
8-Epimanoyl oxide	44 – 45°	−9.5°	23
8,13-Diepimanoyl oxide	79 – 84°	+23.4	23

mainly due to the chemical shift difference between H_B and H_C which is 0.21 ppm in manoyl oxide and 0.06 ppm in 13-epimanoyl oxide. The corresponding value of our oxide is 0.06 and the ABC part of our NMR spectrum is superimposable with that of 13-epimanoyl oxide [24] (see Fig. 2).

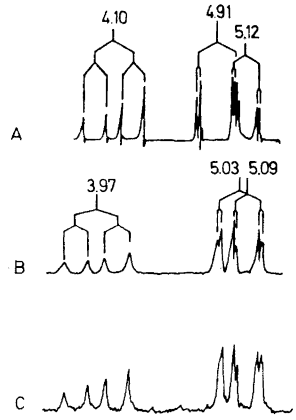

Fig. 2. The characteristic vinyl ABC pattern in the 60 MHz NMR spectra of manoyl oxide (A) and 13-epimanoyl oxide (B) redrawn after Wenkert *et al.*[24] compared with the corresponding ABC pattern in the NMR spectrum of 13-epimanoyl oxide (C) isolated from *S. Missouriensis*. The spectra are redrawn here due to earlier obscurities [21,24] and analyzed according to ABX rules.

The further oxygenated manoyl oxide ($C_{20}H_{32}O_2$, m.p. 94 – 95°C, $[\alpha]_D^{23}$ −53°) is a ketone (IR 1705 cm^{-1}). It was converted to *ent*-13-epimanoyl oxide (*19*) on Wolff-Kishner reduction. The strong peaks in the mass spectrum at *m/e* 206 and *m/e* 191 arising from cleavage of bond C-9, C-11, and the C-8 oxide bond indicate that the keto group is in ring A or B.

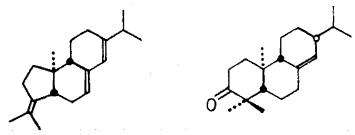

13 18

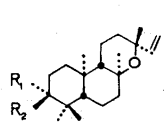

19 $R_1=R_2=H$
20 $R_1R_2=O$
21 $R_1=OH, R_2=H$

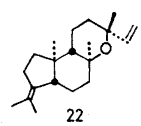

22

The values obtained from the benzene induced solvent shifts in the NMR spectrum accord only with *ent*-8,13β-epoxy-14-labden-3-one (*20*).[15] τ(benzene) $-\tau(CDCl_3)$ – +0.25 (C-10 Me), +0.03 (C-8 Me), +0.04 (C-13 Me), +0.08 (C-4 axial Me) and −0.17 ppm (C-4 equatorial Me).

Furthermore, on LAH reduction an alcohol (*21*) was produced. The NMR spectrum revealed that its hydroxy group is equatorial (τ 6.78 1H *dd*, $J = 6$ and 9 Hz). Consequently, treatment with PCl_5 yielded the rearranged product *22*. The NMR spectrum of this dienoxide also showed the remarkable upfield shift for the C-10 methyl group (τ 9.50) as observed for compound *1*.

The C-13 epimer of this oxide in the normal series, 8,13-epoxy-14-labden-3-one, has previously been isolated from *Xylia dolabriformis*.[17]

The mass spectra

In the discussion of the mass spectra the present diterpenoids are preferably divided into three groups, the 8,13-oxides, the 8(14)-abieten-13-ols, and the 7,13-abietadienes. The spectra of the diterpenoids in the first group which comprises *19*, *20*, *21*, and *22* are thoroughly discussed in the review by Enzell and Ryhage.[25] The fragmentation patterns in our spectra are easily explainable on the basis of the principles of Enzell and Ryhage. However, the base peak in their spectrum of 3-ketomanoyl oxide (*m/e* 81, $C_6H_9^{+\cdot}$) is of minor importance in our spectrum of the 13-epimer. In the spectrum of the rearrangement product with exocyclic double bond (*22*), loss of a C_3H_7 radical is important. A prominent peak at *m/e* 245 may be explained as ion *A* (Scheme 2).

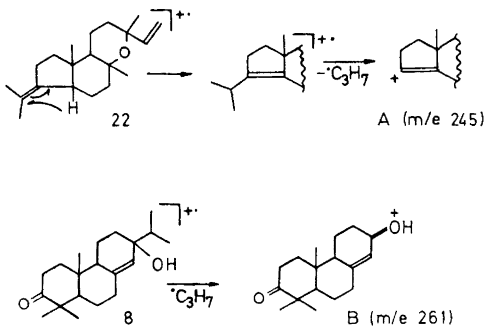

Scheme 2.

As previously mentioned the dominating feature in the mass spectral behaviour of the missourienols (*8*), (*14*), and (*15*) is their immediate loss of $\cdot C_3H_7$ or water, thus missing the molecular ion peak. The result is ions like *B* (Scheme 2) and simply the corresponding 7,13-dienes ($M - H_2O$). Consequently the remaining spectra after loss of water are almost identical with the spectra of the dienes.

In contrast to the missourienols the abietadienes show remarkably abundant molecular ion peaks in their mass spectra. Apart from this the spectra are

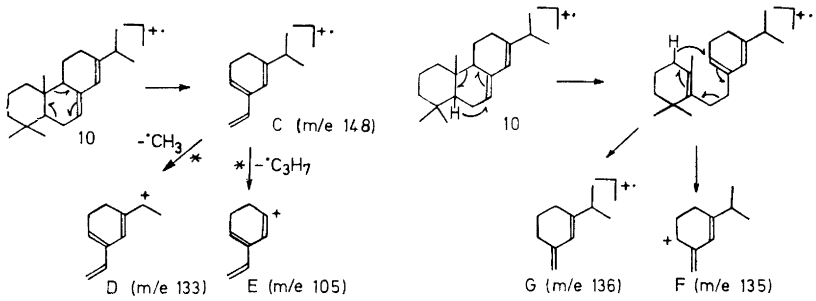

Scheme 3.

characterized by peaks due to ions such as $C-G$ (Scheme 3). Ions due to loss of an isopropyl radical are also visible in the spectra. Particularly abundant is this ion in the spectrum of the rearrangement product (*13*) similar to the corresponding oxide (*22*) (see Scheme 2).

The ketone (*18*) lacking the C-13 hydroxy group exhibits a fragmentation pattern markedly different from the missourienols. As in the latter spectra the base peak of *18* is due to loss of an isopropyl radical. However, the molecular ion is now of high abundance (70 %). Peaks of importance in the spectrum

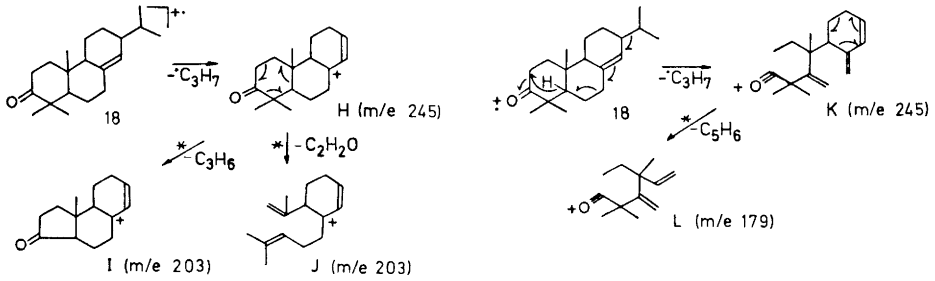

Scheme 4.

may be accounted for by ions $H-L$ (Scheme 4). Ion L seems to be of particular significance (45 %). Most reactions leading to these ions are accompanied by metastable transitions (marked by an asterisk).

EXPERIMENTAL

NMR spectra were recorded on a Varian A-60A spectrometer in CCl_4 or $CDCl_3$ solutions with TMS as internal standard. UV spectra were recorded on a Hitachi 124 spectrophotometer in 96 % ethanol unless otherwise stated. IR spectra were recorded on a Perkin-Elmer 257 spectrophotometer. Mass spectra were run on an AEI MS 902 equipped with a PDP 8 computer using direct inlet probe, ion source temperature 150 – 180°C and electron bombardment energy 70 eV. Optical rotations were measured on a Zeiss circular polarimeter in $CHCl_3$ solutions. Solvents for spectroscopy were *p.a.* grade. For GLC was used Perkin-Elmer F-11 and Aerograph Hy-Fi 600 instruments. Melting points are uncorrected. TLC plates were prepared from silica gel G (Merck) and silica gel $PF_{254+366}$ (Merck). Silica gel 70 – 325 mesh (Merck) and neutral alumina grade III (Woelm) was used for column chromatography. Solvents were either analytical grade or distilled. (% e-lp) refers to % ether in light petroleum.

Isolation of diterpenoids

Roots of *S. missouriensis* Nutt. were collected at Bergianska Trädgården, Stockholm. The material was washed, dried, ground and Soxhlet extracted for 5 h with dry, peroxide-free, distilled ether. Evaporation of the solvent yielded a pale yellow oil (9.3 g) which was separated into 12 crude fractions by chromatography on alumina. Fractions 1 – 8 (0 – 50 % e-lp) yielded diterpenoids, fractions 9 – 12 (0 – 50 % methanol in ether) yielded no terpenoids on methylation and acetylation.

ent-*7,13-Abietadiene* (*10*) was isolated as an oil (200 mg) from the first 3 fractions (0 – 10 % e-lp). Rechromatography on TLC (light petroleum) yielded an oil which was pure on GLC. $[\alpha]_D^{24}$ +127° (*c* 2.05), λ_{max} (hexane) 234 (21 000), 241 (22 800), and 249 (15 600) nm. NMR signals (CCl_4) at τ 4.32 (*m*, 1H; H-14), 4.68 (*m*, 1H; H-7), 9.01 (*d*, $J = 7$ Hz, 6H; isopropyl methyls, 9.10, 9.13 and 9.23 (all, *s*, 3H; 3 tertiary methyls). M^+ 272.2498, calc. for $C_{20}H_{32}$ 272.2504.

ent-*13-Epimanoyloxide* (ent-*8,13β-epoxy-14-labdene*) (*19*) was isolated from the already mentioned TLC plates as an oil (54 mg) which was pure on GLC. Crystallization twice from methanol yielded white plates, m.p. 97 – 98°C, $[\alpha]_D^{24}$ −31° (*c* 1.95), ν_{max} (KBr) 1100 (ether), 990 and 920 cm^{-1} (vinyl). NMR signals (CCl_4) at τ 4.03, 5.08, 5.14 (ABC, $J_{AB} = 18.0$, $J_{AC} = 10.5$, and $J_{BC} = 1.3$ Hz, 3H; vinyl), 8.86, 8.97, 9.16, 9.24 and 9.30 (all, *s*, 3H; 5 tertiary methyls). M^+ 290.2631, calc. for $C_{20}H_{34}O$ 290.2610.

ent-*8,13β-Epoxy-14-labden-3-one* (*20*) was isolated from fraction *3* after recromatography on alumina (0 – 30 % e-lp) and TLC (30 % e-lp) as an oil (254 mg). Two crystallizations from methanol gave long white needles, m.p. 94 – 95°,C $[\alpha]_D^{23}$ −53° (*c* 2.47), ν_{max} (KBr) 1705 (ketone), 990 and 920 cm^{-1} (vinyl). NMR signals (CCl_4) at τ 4.02, 5.06, 5.12 (ABC, 3H; vinyl), 8.79, 8.84, 8.87, 9.04 and 9.18 (all, *s*, 3H; 5 tertiary methyls). M^+ 304.2410, calc. for $C_{20}H_{32}O_2$ 304.2402.

ent-*7,13-Abietadien-2α-ol acetate* (*16*) was isolated from fractions 2 – 4 (5 – 20 % e-lp) after further purifications on TLC (30 % e-lp) as a colourless oil (280 mg). $[\alpha]_D^{27}$ +111° (*c* 6.1), λ_{max} 234 (18 600), 240 (19 400) and 248 (13 200) nm, ν_{max} (neat) 1740 and 1712 cm^{-1} (ester). NMR signals (CCl_4) at τ 4.30 (*m*, 1H; H-14), 4.65 (*m*, 1H; H-7), 5.08 (*tt*, $J_{2\beta,1\alpha} = J_{2\beta 3\alpha} = 12$ Hz and $J_{2\beta 1\beta} = J_{2\beta 3\beta} = 4$ Hz, 1H; H-2β), 8.06 (*s*, 3H; acetoxy CH_3), 8.97, 9.07, 9.12 (all, *s*, 3H; 3 tertiary methyls) and 9.00 (*d*, $J = 7$ Hz, 6H; isopropyl methyls). M^+ 330.2576, calc. for $C_{22}H_{34}O_2$ 330.2559.

ent-*7,13-Abietadien-3-one* (*9*) was isolated from fractions 2 – 4 after further purifications on TLC (30 % e-lp) as an oil (470 mg). $[\alpha]_D^{27}$ +100° (*c* 13.3), λ_{max} 234 (16 400), 240 (17 600), and 248 (12 400) nm, ν_{max} (neat) 1712 cm^{-1} (ketone). NMR signals (CCl_4) at τ 4.24 (*m*, 1H; H-14), 4.62 (*m*, 1H; H-7), 7.5 (*m*, 2H; 2 H-2), 8.93, 9.00, 9.00 (all, *s*, 3H; 3 tertiary methyls) and 8.98 (*d*, $J = 7$ Hz, 6H; isopropyl methyls). M^+ 286.2299, calc. for $C_{20}H_{30}O$ 286.2297.

ent-*7,13-Abietadien-3β-ol* (*12*) was isolated as a colourless oil (48 mg) from fraction 6 (40 % e-lp) after further purifications on TLC (30 % e-lp). $[\alpha]_D^{25}$ +108° (*c* 2.3), ν_{max} (neat) 3400 cm^{-1} (bonded OH). NMR signals ($CDCl_3$) at τ 4.19 (*m*, 1H; H-14), 4.57 (*m*, 1H; H-7), 6.76 (*d d*, $J_{3\alpha 2\beta} = 8.5$ and $J_{3\alpha 2\alpha} = 6.0$ Hz, 1H; $H_{3\alpha}$), 9.00 (*d*, $J = 7$Hz, 6H: isopropyl methyls), 9.04, 9.12 and 9.21 (all, *s*, 3H; 3 tertiary methyls). M^+ 288.2457, calc. for $C_{20}H_{32}O$ 288.2453.

Missourienol C (ent-*2α-acetoxy-8(14)-abieten-13-ol)* (*15*) was iaolated from fractions 4 and 5 (20 – 30 % e-lp) by rechromatography on alumina. Fractions eluted with 30 % ether in light petroleum yielded a colourless oil (90 mg), pure on TLC, $[\alpha]_D^{26}$ +7° (*c* 1.67), ν_{max} (CCl_4) 3620 (free OH), 3450 (bonded OH), 1735, 1245 (ester) and 1660 cm^{-1} (trisubstituted double bond). NMR signals at τ 4.56 (*m*, 1H; H-14) 5.12 (*t t*, $J_{2\beta 3\alpha} = J_{2\beta 1\alpha} = 12$ and $J_{2\beta 3\beta} = J_{2\beta 1\beta} = 4$ Hz, 1H; H-2β), 8.05 (*s*, 3H; acetoxy CH_3), 8.70 (D_2O exchangeable, hydroxyl H), 9.04, 9.04, 9.12 (all, *s*, 3H; 3 tertiary methyls), 9.10 and 9.17 (both, *d*, $J = 7$ Hz, 3H; isopropyl methyls). $(M-18)^+$ 330.2570, calc. for $C_{22}H_{34}O_2$ 330.2559, $(M-43)^+$ 305.2115, calc. for $C_{19}H_{29}O_3$ 305.2117.

Missourienol A (ent-*13-hydroxy-8(14)abieten-3-one)* (*8*) crystallized from fraction 4. Two recrystallizations from 50 % ether in CCl_4 yielded white crystals (700 mg), m.p. 80 – 84°C, $[\alpha]_D^{25}$ −3° (*c* 2.25), ν_{max} ($CHCl_3$) 3610 (free OH), 3470 (bonded OH), 1705 (ketone) and 1660 cm^{-1} (trisubstituted double bond). NMR signals ($CDCl_3$) at τ 4.50 (*m*, 1H; H-14), 7.39 (*m*, 2H; 2 H-2), 8.70 (D_2O exchangeable, hydroxyl H), 8.92, 8.9,2 8.99 (all, *s*, 3H; 3 tertiary methyls), 9.06 and 9.11 (both, *d*, $J = 7$ Hz, 3H; isopropyl

methyls). $(M-18)^{+\cdot}$ 286.2296, calc. for $C_{20}H_{30}O$ 286.2297, $(M-43)^{+}$ 261.1847, calc. for $C_{17}H_{25}O_2$ 261.1854. Workup of fractions 6–8 yielded more missourienol A (1110 mg total).

Missourienol B (ent-*8(14)-abietene-3β,13-diol)* (*14*) crystallized from fraction 7 (50 % e-lp). White crystals (60 mg) recrystallized from ether, m.p. 155–156°C, $[\alpha]_D^{26}$ −47° (*c* 1.65), ν_{max} (KBr) 3400 (bonded OH) and 1670 cm^{-1} (trisubstituted double bond). NMR signals ($CDCl_3$) at τ 4.53 (*m*, 1H, H-14), 6.72 (*d d*, $J_{2\beta 3\alpha}=12$ and $J_{2\alpha 3\alpha}=4$ Hz, 1H; H-3α), 8.63 (D_2O exchangeable, hydroxyl H), 8.99, 9.18, 9.21 (all, *s*, 3H; 3 tertiary methyls), 9.09 and 9.13 (both, *d*, $J=7$ Hz, 3H; isopropyl methyls). $(M-18)^{+\cdot}$ 288.2452, calc. for $C_{20}H_{32}O$ 288.2453, $(M-43)^{+}$ 263.2032, calc. for $C_{17}H_{27}O_2$ 263.2011.

Dehydration of missourienols. The missourienols A, B and C were dehydrated by chromatography over silica (e-lp), yielding the abietadienes (*9*), (*12*), and (*16*), respectively. Missourienol A (45 mg) was refluxed with 1 % *p*-toluenesulphonic acid in methanol (7 ml) for 4 h, yielding abietadien-3-one (*9*) (36 mg) after workup and purification on TLC. The identity of the dehydration products to the abietadienes from the plant was established by IR, UV, NMR, MS, and mixed TLC.

Wolff-Kishner reduction of ent-*7,13-abietadien-3-one* (*9*). The ketone (65 mg) and 80 % hydrazine hydrate (400 mg) were heated in refluxing diethylene glycol (2 ml) for 5 h, and the temperature raised to 220°C during 6 h. After cooling, KOH (500 mg) was added, and refluxing was continued for 3 h. After cooling, dilution with water and extraction with ether, the crude product was purified on TLC, yielding abietadiene (31 mg). $M^{+\cdot}$ 272.2503, calc. for $C_{20}H_{32}$ 272.2504.

Abietadiene from abietinol. A sample of abietinol prepared from abietic acid was purified by chromatography. Pure abietinol (272 mg) in pyridine (1 ml) was added to a solution of CrO_3 (275 mg) in pyridine (6 ml), dropwise with stirring. The reaction mixture was left for 24 h at 20°C, water was added and the crude aldehyde extracted with ether. The aldehyde (154 mg) was pure on TLC and showed an aldehyde proton at 0.72 τ. It yielded abietadiene (111 mg) on Wolff-Kishner reduction as above. The NMR spectrum was identical with that of the abietadiene from the plant. $M^{+\cdot}$ 272.2488, calc. for $C_{20}H_{32}$ 272.2504.

The two synthetic abietadienes and the abietadiene from the plant material exhibited identical properties on mixed TLC on ordinary and $AgNO_3$ treated plates.

Reduction of ent-*7,13-abietadien-3-one* (*9*). The ketone (72 mg) and excess LAH in anhydrous ether (15 ml) were refluxed for 2 h. Aqueous ether and then water were added, the product was extracted with ether and purified on TLC (40 % e-lp), yielding *ent*-7,13-abietadien-3β-ol (57 mg), identical with that from the plant by NMR, MS and TLC. $M^{+\cdot}$ 288.2453, calc. for $C_{20}H_{32}O$ 288.2453.

Retropinacol rearrangement. ent-7,13-Abietadien-3β-ol (*12*) (57 mg) in light petroleum (10 ml) was shaken with PCl_5 (87 mg) for 10 min at 20°C. The solution was filtered, washed with aqueous 2 N NaOH and then water, dried and purified on TLC (10 % e-lp), yielding the triene *13* (28 mg). $[\alpha]_D^{25}$ +136° (*c*. 0.93), NMR signals (CCl_4) at τ 4.22 (*m*, 1H; H-14), 4.68 (*m*, 1H; H-7), 8.28, 8.39 (both, *m*, 3H; isopropylidene methyls), 8.97 (*d*, $J=7$ Hz, 6H; isopropyl methyls) and 9.37 (*s*, 3H; C-10 CH_3). $M^{+\cdot}$ 270.2352, calc. for $C_{20}H_{30}$ 270.2347.

Hydrolysis of ent-*7,13-abietadien-2α-ol acetate* (*16*). The acetate (97 mg) was heated in refluxing 1.5 N methanolic KOH (5 ml) for 2 h. The mixture, after standing for 12 h at 20°C, was concentrated, diluted with water, extracted with ether, and purified on TLC (50 % e-lp), yielding *ent*-7,13-abietadien-2α-ol (*17*) as an oil (57 mg), pure on TLC. ν_{max} (CCl_4) 3610 (free OH) and 3300 cm^{-1} (bonded OH). NMR signals ($CDCl_3$) at τ 4.18 (*m*, 1H; H-14), 4.53 (*m*, 1H; H-7), 6.07 (*t t*, $J_{2\beta 1\alpha}=J_{2\beta 3\alpha}=12$ and $J_{2\beta 1\beta}=J_{2\beta 3\beta}=4$ Hz, 1H; H-2β), 8.98 (*d*, $J=7$ Hz, 6H; isopropyl methyls), 9.05, 9.05 and 9.16 (all, *s*, 3H; 3 tertiary methyls). M^{+} 288.2450, calc. for $C_{20}H_{32}O$ 288.2453.

Hydrogenation of missourienol A. The ketone (21 mg) in ethanol (5 ml) was hydrogenated with 10 % Pd on alumina as catalyst. Filtration, evaporation of the solvent, extraction with ether and purification on TLC (30 % e-lp) yielded *ent*-8(14)-abieten-3-one (*18*) (14 mg), $M^{+\cdot}$ 288.2457, calc. for $C_{20}H_{32}O$ 288.2453.

Reduction and retropinacol rearrangement of ent-*8,13β-epoxy-14-labden-3-one* (*20*). The ketone (72 mg) was reduced with LAH and worked up as above, yielding the alcohol *21* (69 mg). NMR signals ($CDCl_3$) at τ 3.92, 5.03, 5.07 (ABC, 3H; vinyl), 6.77 (*d d*, $J_{3\alpha 2\beta}=9$ and $J_{3\alpha 2\beta}=6$ Hz, 1H; H-3α), 8.77, 8.87, 9.02, 9.24 and 9.24 (all, *s*, 3H; 5 tertiary methyls).

$M^{+\cdot}$ 306.2545, calc. for $C_{20}H_{34}O_2$ 306.2559. The alcohol (69 mg) was heated with PCl_5 (99 mg) in light petroleum (10 ml) and worked up as above, yielding the ether *22* (43 mg), pure on TLC (10 % e-lp). $[\alpha]_D^{25}$ −13° (*c* 1.00), ν_{max} (CCl_4) 1080 (ether), 970 and 915 cm^{-1} (vinyl). NMR signals (CCl_4) at τ 3.97, 5.08, 5.13 (ABC, 3H; vinyl), 8.30, 8.43 (both, *m*, 3H; isopropylidene methyls) 8.81, 8.93 (both, *s*, 3H; 2 tertiary methyls) and 9.50 (*s*, 3H; C-10 CH_3). $M^{+\cdot}$ 288.2475, calc. for $C_{20}H_{32}O$ 288.2453.

Wolff-Kishner reduction of ent-*8,13β-epoxy-14-labden-3-one* (*20*). The ketone (55 mg) was reduced and worked up as above, yielding an oil (52 mg) pure on TLC (10 % e-lp). The product was identical with *ent*-13-epimanoyloxide (*19*) isolated from the plant (TLC, GLC). $M^{+\cdot}$ 290.2612, calc. for $C_{20}H_{34}O$ 290.2610.

Acknowledgements. We are grateful to the University of Trondheim, Norwegian Institute of Technology, for a fellowship to G. B. and for a grant from *Norges Tekniske Høgskole's fond* to T. A. Curator Jan Tengner, Bergianska Trädgården, Stockholm, is warmly thanked for providing the plant material. We are also grateful to Professor N. A. Sørensen for inspiring discussions and his never failing interest in our work.

REFERENCES

1. Anthonsen, T., McCabe, P. H., McCrindle, R., Murray, R. D. H. and Young, G. A. R. *Tetrahedron* **26** (1970) 3091.
2. Anthonsen, T., McCabe, P. H., McCrindle, R. and Murray, R. D. H. *Tetrahedron* **25** (1969) 2233.
3. Anthonsen, T., Henderson, M. S., Martin A., McCrindle, R. and Murray, R. D. H. *Acta Chem. Scand.* **22** (1968) 351.
4. Kusumoto, S., Okazaki, T., Ohsuka, A. and Kotake, M. *Bull. Chem. Soc. Japan* **42** (1969) 812.
5. Anthonsen, T. and McCrindle, R. *Acta Chem. Scand.* **23** (1969) 1068.
6. Anthonsen, T. and Bergland, G. *Acta Chem. Scand.* **25** (1971) 1924.
7. Rowe, J. W. *The Common and Systematic Nomenclature of Cyclic Diterpenes*, Third Revision, October 1968, with *addenda* and *corrigenda*, Madison, Wisconsin, February 1969.
8. McCrindle, R. and Overton, K. H. *Rodd's Chemistry of Carbon Compounds*, 2nd Ed., Elsevier, Amsterdam 1969, Vol. II C, p. 369.
9. Geissman, T. A. and Crout, D. H. G. *Organic Chemistry of Secondary Plant Metabolism*, Freeman, Cooper and Co., San Francisco 1969, p. 308.
10. Anthonsen, T. and Bergland, G. *Acta Chem. Scand.* **24** (1970) 1860.
11. *Cf., e.g.*, Ref. 8, p. 298.
12. Tabacik, C. and Poisson, C. *Bull. Soc. Chim. France* **1969** 3264.
13. Mayr, R., Pentegova, V. A. and Kashtanova, N. K. *Khim. Prir. Soedin.* **1965** 223.
14. Briggs, L. H., Cain, B. F. and Cambie, R. D. *Tetrahedron Letters* **1959** 17.
15. Williams, D. H. and Bhacca, N. S. *Tetrahedron* **21** (1965) 2021.
16. Bhacca, N. S. and Williams, D. H. *Application of NMR Spectroscopy in Organic Chemistry*, Holden Day, San Francisco 1964, p. 165.
17. Laidlaw, R. A. and Morgan, J. W. W. *J. Chem. Soc.* **1963** 644.
18. Hart, H. and Love, G. M. *Tetrahedron Letters* **1971** 625.
19. Flemming, I., Hanson, S. W. and Sanders, J. K. M. *Tetrahedron Letters* **1971** 3733.
20. Hodges, R. and Reed, R. I. *Tetrahedron* **10** (1960) 71.
21. Giles, J. A., Schumacher, J. N., Mims, S. S. and Bernasek, E. *Tetrahedron* **18** (1962) 169.
22. Ohloff, G. *Ann.* **617** (1958) 134.
23. Cheng, Y. S. and von Rudloff, E. *Tetrahedron Letters* **1970** 1131.
24. Wenkert, E., Beak, P. and Grant, P. K. *Chem. Ind. (London)* **1961** 1574.
25. Enzell, C. R. and Ryhage, R. *Arkiv Kemi* **23** (1965) 367.

Received October 12, 1972.

ACTA CHEMICA SCANDINAVICA 27 (1973) 1083–1113

Short Communications

A Method for Studying the Liberation of a Radioprotective Agent (AET) Bound to Proteins as a Mixed Disulfide

MAGDOLNA HORVÁTH* and BENGT MANNERVIK

Department of Biochemistry, University of Stockholm, Box 6409, S-113 82 Stockholm, Sweden

It has been found that many proteins are able to bind low molecular weight thiols to sulfhydryl groups.[1,2] The possible importance of such mixed disulfide formation for modulation of enzyme activity, radioprotection, *etc.* is presently unclear.[3] The study of these presumptive functions require adequate methods for determination and release of the low molecular weight thiols. In the present communication we describe a method, based on the use of ion exchangers in small columns, for studying the release of the radioprotective agent *S*-2-aminoethylisothiouronium bromide (AET) bound (as an isomer 2-mercaptoethylguanidine, MEG) *via* a disulfide linkage to proteins.

Materials and methods. The mixed disulfide, which is formed between serum albumin and AET (in the form of MEG), was used as a model compound.[4] Bovine albumin (10 μmol) was dissolved in 18 ml of 0.2 M phosphate buffer pH 7.5, 35 μmol of [^{14}C]-AET in 2 ml of the same buffer were added, and the mixture incubated at room temperature for 24 h. Unbound AET was removed by dialysis against several changes of 20 to 25 volumes of 10 mM phosphate buffer of a pH required in subsequent experiments.

The protein content of the incubation mixture was determined spectrophotometrically at 278 nm or by the Lowry method.[5] Radioactivity was measured in a Beckman LS-100 liquid scintillation counter. Generally a ratio of about 0.7 mol AET/mol albumin was found.

The mixed disulfide compounds of equine hemoglobin and bovine insulin were prepared in a similar manner. For details see Horváth *et al.*[4] The AET content was 2 – 3 mol/mol Hb or insulin.

Incubations for studying the release of radioactivity upon treatment with thiols were carried out at 30° in 200 μl incubation mixtures containing buffer, labeled protein, and thiol. After incubation, a 100 μl aliquot was transferred to an ion exchange column (5 × 40 mm), which was packed in a Pasteur pipette, and washed into the bed with 0.5 ml of 10 mM sodium phosphate pH 6.5. In pilot experiments 1 ml fractions were collected during the subsequent elution, but in routine experiments a single 5 ml fraction was taken. The radioactivity in the effluent was measured after mixing 1 ml of effluent with 10 ml of toluene-Triton X-100 (2:1) scintillation fluid.[6]

Results. It was assumed that a suitable separation between the negatively charged albumin and liberated MEG, which is positively charged, could be made on DEAE-cellulose columns. Accordingly, it should be possible to measure the release of radioactive MEG from labeled albumin simply by determination of radioactivity in the effluent from a DEAE-cellulose column. It was found that the principle of the measurement worked, but a complication arose due to slow release of radioactivity from the albumin bound to the ion-exchanger. The adsorbed protein was retained as shown by lack of absorbance at 280 nm in the effluent, and, as it had previously been demonstrated that MEG is bound covalently by means of a disulfide bond to albumin,[4] we conclude that the radioactive group is split off due to microenvironmental effects in the ion-

* Present address: "Frédéric Joliot-Curie" National Research Institute for Radiobiology and Radiohygiene, Budapest 22, Hungary.

exchange matrix. The nature of this reaction was not established, but it was found that the sulfhydryl reagents *N*-ethylmaleimide and $HgCl_2$ did not prevent the decomposition. However, only a minor portion of the total radioactivity was released in the first 5 ml of effluent, which contained the radioactive MEG liberated from labeled albumin by treatment with thiols. This portion could be accounted for in the measurement by control experiments, and the accuracy was therefore sufficient to allow quantitative determinations of the liberation of MEG.

To demonstrate the utility of the technique the reaction of thiols and albumin labeled with [^{14}C]-AET was studied. Treatment of 0.075 μmol labeled albumin with 0.2 μmol of unlabeled AET (which isomerizes to MEG at pH-values > 7) at pH 7.5, liberated 75 % of the radioactivity within the shortest possible time of measurement. To investigate the possibility to follow the kinetics, the splitting reaction was run at lower pH values. In these experiments penicillamine, mercaptoethylamine, or glutathione were used. Fig. 1

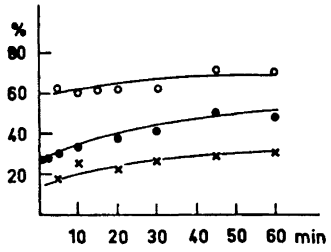

Fig. 1. Release of radioactivity (per cent of total activity) from [^{14}C]-AET-labeled albumin by treatment with mercaptoethylamine or glutathione at pH 5 for different periods of time. ○, 0.063 μmol albumin and 0.2 μmol GSH; ●, 0.063 μmol albumin and 0.2 μmol MEA; ×, 0.063 μmol albumin and 0.066 μmol MEA.

demonstrates that even at pH 5 a substantial amount of radioactivity is released almost instantaneously, and that glutathione is about twice as active as mercaptoethylamine. It should also be noted that in no case more than 85 % of the radioactivity was released from albumin. Whether this means that part of the label is inaccessible to the reagents used or that the label is bound covalently not exclusively by disulfide linkage has not been established.

Similar experiments have been carried out with [^{14}C]-labeled insulin and hemoglobin. In the latter case CM-Sephadex was substituted for DEAE-cellulose in the chromatographic columns. It was found that the radioactivity was much less easily removed from hemoglobin than from albumin by treatment with glutathione.

Acknowledgement. This work has been supported by grants from the *Swedish Natural Science Research Council* and the *Swedish Cancer Society*.

1. Jocelyn, P. C. *Biochemistry of the SH Group*, Academic, New York and London 1972, p. 123.
2. Modig, H. G., Edgren, M. and Révész, L. *Int. J. Radiat. Biol.* **22** (1971) 257.
3. Sanner, T. and Pihl, A. *Scand. J. Clin. Lab. Invest. Suppl.* **106** (1969) 53.
4. Horváth, M., Fóris, G., Cságoly, E., Sztanyik, L. and Dalos, B. *Int. J. Radiat. Biol.* **21** (1972) 263.
5. Lowry, O. H., Rosebrough, N. J., Farr, A. L. and Randall, R. J. *J. Biol. Chem.* **193** (1951) 265.
6. Patterson, M. S. and Greene, R. C. *Anal. Chem.* **37** (1965) 854.

Received February 17, 1973.

Asymmetric Synthesis of (+)-Diethyl Citramalate

SVANTE BRANDÄNGE, STAFFAN JOSEPHSON and STAFFAN VALLÉN

Department of Organic Chemistry, University of Stockholm, Sandåsgatan 2, S-113 27 Stockholm, Sweden

Two hydroxyacids, 2-isobutylmalic acid [1] and 2-benzylmalic acid,[2] have been found in optically active forms as components in *Orchidaceae* alkaloids. (+)-2-Methylmalic acid, (+)-citramalic acid, is known to have the (*S*)-configuration.[3] Asymmetric syn-

exchange matrix. The nature of this reaction was not established, but it was found that the sulfhydryl reagents *N*-ethylmaleimide and $HgCl_2$ did not prevent the decomposition. However, only a minor portion of the total radioactivity was released in the first 5 ml of effluent, which contained the radioactive MEG liberated from labeled albumin by treatment with thiols. This portion could be accounted for in the measurement by control experiments, and the accuracy was therefore sufficient to allow quantitative determinations of the liberation of MEG.

To demonstrate the utility of the technique the reaction of thiols and albumin labeled with [^{14}C]-AET was studied. Treatment of 0.075 μmol labeled albumin with 0.2 μmol of unlabeled AET (which isomerizes to MEG at pH-values > 7) at pH 7.5, liberated 75 % of the radioactivity within the shortest possible time of measurement. To investigate the possibility to follow the kinetics, the splitting reaction was run at lower pH values. In these experiments penicillamine, mercaptoethylamine, or glutathione were used. Fig. 1

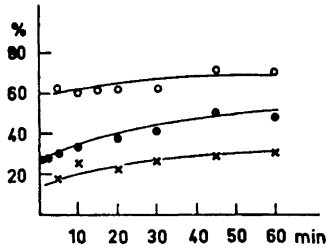

Fig. 1. Release of radioactivity (per cent of total activity) from [^{14}C]-AET-labeled albumin by treatment with mercaptoethylamine or glutathione at pH 5 for different periods of time. ○, 0.063 μmol albumin and 0.2 μmol GSH; ●, 0.063 μmol albumin and 0.2 μmol MEA; ×, 0.063 μmol albumin and 0.066 μmol MEA.

demonstrates that even at pH 5 a substantial amount of radioactivity is released almost instantaneously, and that glutathione is about twice as active as mercaptoethylamine. It should also be noted that in no case more than 85 % of the radioactivity was released from albumin. Whether this means that part of the label is inaccessible to the reagents used or that the label is bound covalently not exclusively by disulfide linkage has not been established.

Similar experiments have been carried out with [^{14}C]-labeled insulin and hemoglobin. In the latter case CM-Sephadex was substituted for DEAE-cellulose in the chromatographic columns. It was found that the radioactivity was much less easily removed from hemoglobin than from albumin by treatment with glutathione.

Acknowledgement. This work has been supported by grants from the *Swedish Natural Science Research Council* and the *Swedish Cancer Society*.

1. Jocelyn, P. C. *Biochemistry of the SH Group*, Academic, New York and London 1972, p. 123.
2. Modig, H. G., Edgren, M. and Révész, L. *Int. J. Radiat. Biol.* **22** (1971) 257.
3. Sanner, T. and Pihl, A. *Scand. J. Clin. Lab. Invest. Suppl.* **106** (1969) 53.
4. Horváth, M., Fóris, G., Cságoly, E., Sztanyik, L. and Dalos, B. *Int. J. Radiat. Biol.* **21** (1972) 263.
5. Lowry, O. H., Rosebrough, N. J., Farr, A. L. and Randall, R. J. *J. Biol. Chem.* **193** (1951) 265.
6. Patterson, M. S. and Greene, R. C. *Anal. Chem.* **37** (1965) 854.

Received February 17, 1973.

Asymmetric Synthesis of (+)-Diethyl Citramalate

SVANTE BRANDÄNGE, STAFFAN JOSEPHSON and STAFFAN VALLÉN

Department of Organic Chemistry, University of Stockholm, Sandåsgatan 2, S-113 27 Stockholm, Sweden

Two hydroxyacids, 2-isobutylmalic acid [1] and 2-benzylmalic acid,[2] have been found in optically active forms as components in *Orchidaceae* alkaloids. (+)-2-Methylmalic acid, (+)-citramalic acid, is known to have the (*S*)-configuration.[3] Asymmetric syn-

thesis of diethyl citramalate has therefore been investigated in order to determine its steric course and find suitable conditions for similar syntheses of the two new acids.

In a high optical yield (93 %) synthesis of (*S*)-(+)-3-hydroxy-3-phenylbutyric acid a solution of diethylaminomagnesium bromide was added to a mixture of acetophenone and (−)-menthyl acetate.[4,5] We synthesised ethyl (−)-menthyl citramalate (I) from ethyl pyruvate, (−)-menthyl acetate and diethylaminomagnesium bromide, using an addition order different from that above. The product I was then converted into diethyl citramalate (II). As the yield and optical yield in this synthesis were moderate, other bases were tested, including lithium bis(trimethylsilyl)-amide [6] and lithium diisopropylamide.[7] The yields, estimated by NMR and GLC, and the optical yields, calculated from the optical rotations of II and of authentic (*S*)-(+)-diethyl citramalate, are given in Table 1. When diisopropylaminomagnesium bromide or isopropylmagnesium chloride [8] were used as bases the yields of I were negligible and poor (2 %), respectively.

Table 1. Yields and optical yields in asymmetric syntheses of diethyl citramalate.

Base	Yield of I %	$[\alpha]_D$ of I	$[\alpha]_D$ of II	Optical yield %
Et_2NMgBr	20	−56°	+3.7°	19
$(Me_3Si)_2NLi$	60	−48°	+4.7°	24
$(Me_2CH\text{-})_2NLi$	75	−48°	+5.1°	26

The reaction between ethyl pyruvate and the Grignard reagent from (−)-menthyl bromoacetate (THF, 20°, 15 h) gave a low yield of I (10 %), and also a low optical yield (10 %) of (+)-II. Similar reactions, using the organozinc compound, have previously been used in asymmetric synthesis of hydroxyacids.[9,10]

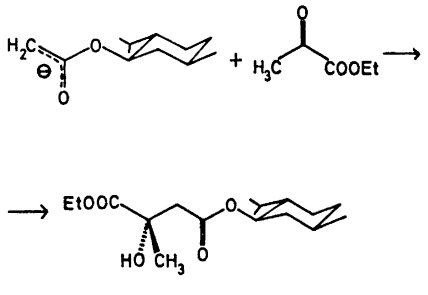

I, predominant stereoisomer

Experimental. Analytical GLC was carried out on a JXR column (3 % on Gas-Chrom Q, 100−120 mesh, 0.2×180 cm) using a Perkin-Elmer 900 chromatograph. Preparative GLC was carried out on an SE-52 column (15 % on Chromosorb AW DMCS, 60−80 mesh, 0.8×155 cm) at 180° for compound I and at 100° for compound II. These separations were performed on an Aerograph A-90-P instrument. Yields of I are estimated from GLC and NMR spectra of crude reaction mixtures. Optical rotations were measured on a Perkin-Elmer 141 polarimeter.

(S)-(+)-*Diethyl citramalate* was prepared by refluxing an ethanol solution of the acid [11] and conc. sulphuric acid for 30 h. The ester, after purification by preparative GLC, showed $[\alpha]_D^{24}$ +19.4° (*c* 2.2, chloroform).

Asymmetric synthesis of I. (a) To a solution of diethylaminomagnesium bromide (prepared from 63 mmol of starting materials) in ether (50 ml), kept at 0°, was first added a solution of (−)-menthyl acetate (4.0 g, 21 mmol) in toluene (15 ml), followed by a solution of ethyl pyruvate (2.4 g, 21 mmol) in toluene (10 ml). The reaction mixture was stirred at 0° for 2 h, and was then poured into cold dilute sulphuric acid. The organic layer was dried (Na_2SO_4), volatile components distilled off (1 mm, 100°), and the product I was isolated by preparative GLC.

(b) A solution of butyllithium in ether (5 ml, 1.5 M) was added under stirring (N_2) to a solution of hexamethyldisilazan (1.25 g, 7.6 mmol) in tetrahydrofuran (20 ml). After reflux (30 min) the solution was kept cool (−70° to −80°) during the addition of a solution of (−)-menthyl acetate (1.40 g, 7.35 mmol) in tetrahydrofuran (10 ml). After stirring for 30 min, a solution of ethyl pyruvate (1.0 g, 8.6 mmol) in tetrahydrofuran (5 ml) was added, and the temperature was then allowed to reach 0°. The reaction mixture was worked up as above yielding I. (Found: C 65.1; H 9.73; O 25.3. Calc. for $C_{17}H_{30}O_5$: C 64.9; H 9.62; O 25.4.)

(c) To a solution of lithium diisopropylamide [7] (30 mmol) in ether (20 ml) and tetrahydrofuran (30 ml), kept cooled (−60° to −70°), was added a solution of (−)-menthyl acetate (4.9 g, 26 mmol) in tetrahydrofuran (20 ml). After 1.5 h, ethyl pyruvate (4.0 g, 34 mmol) was added, and after further 40 min

the temperature was allowed to reach 0° and the reaction mixture was worked up as above.

Diethyl citramalate (II) was obtained from crude I by treatment with ethanol and conc. sulphuric acid (reflux for 3 weeks), followed by preparative GLC. Another method, giving similar results, was also used. The crude reaction product was hydrolysed by treatment with potassium hydroxide (2 M) in ethanol (reflux overnight). Water was added, and the mixture was washed several times with ether. The aqueous layer was acidified, the solvent evaporated, and the residue was treated with ethanol and conc. sulphuric acid (reflux 3 days).

Acknowledgements. We thank Dr. Björn Lüning for his interest and the *Swedish Natural Science Research Council* for support.

1. Brandänge, S., Lüning, B., Moberg, C. and Sjöstrand, E. *Acta Chem. Scand.* **25** (1971) 349.
2. Brandänge, S. and Lüning, B. *Acta Chem. Scand.* **23** (1969) 1151.
3. Weber, H. *Diss.*, Eidgenössische Technische Hochschule, Zürich 1965.
4. Mitsui, S. and Kudo, Y. *Tetrahedron* **23** (1967) 4271.
5. Kudo, Y., Iwasawa, M., Kobayashi, M., Senda, Y. and Mitsui, S. *Tetrahedron Letters* **1972** 2125.
6. Rathke, M. W. *J. Am. Chem. Soc.* **92** (1970) 3222.
7. Reiffers, S., Wynberg, H. and Strating, J. *Tetrahedron Letters* **1971** 3001.
8. Dubois, J.-E. and Fellous, R. *Bull. Soc. Chim. France* **1963** 786.
9. Palmer, M. H. and Reid, J. A. *J. Chem. Soc.* **1960** 931.
10. Palmer, M. H. and Reid, J. A. *J. Chem. Soc.* **1962** 1762.
11. Barker, H. A. *Biochem. Prep.* **9** (1962) 25.

Received March 3, 1973.

An X-Ray Single Crystal Study of $K_2HgCl_4.H_2O$

KARIN AURIVILLIUS and CLAES STÅLHANDSKE

Divisions of Inorganic Chemistry 1,2, Chemical Center, University of Lund, Box 740, S-220 07 Lund 7, Sweden

In connection with studies on the crystal chemistry of inorganic compounds of mercury(II) in different environments, the present X-ray single crystal investigation of $K_2HgCl_4.H_2O$ was performed. The compound has earlier been the object of X-ray diffraction studies.[1,2] The position of all non-hydrogen atoms were derived from intensity data and geometrical considerations in the study in 1938.[1] In the next work on the structure in 1955,[2] the positions of the mercury, potassium, and chlorine atoms were determined from two-dimensional Fourier projections.[2] The positions of the oxygen and hydrogen atoms were not found, however.

Considering the state of the experimental X-ray technique and of the numerical calculation methods at the time for the earlier investigations, the accuracy in the determination of the positions of the light atoms could not be particularly high because of the presence of the heavy mercury atoms. Our aim was to redetermine the positions of the light atoms in order to discuss the coordination of the mercury atoms. The compound $K_2HgCl_4.H_2O$ crystallizes in the orthorhombic space group *Pbam* (No. 55) with four formula units in a unit cell with the dimensions $a = 8.258$ Å, $b = 11.662$ Å, $c = 8.925$ Å, and $V = 860$ Å^3. X-Ray single crystal diffractometer data (PAILRED) were collected using MoK-radiation and a graphite monochromator. A suitable needle-shaped crystal was rotated along [001] and the recorded data resulted in 843 independent reflections with intensities larger than $3\sigma_I$. The intensities were corrected for absorption; the linear absorption coefficient was 203 cm^{-1}. The positions of the mercury atoms were obtained from three-dimensional Patterson functions and the positions of the chlorine, potassium and oxygen atoms from difference Fourier syntheses. A least-squares refinement of the positional parameters of all non-hydrogen atoms including one scale factor was at first performed with isotropic tem-

the temperature was allowed to reach 0° and the reaction mixture was worked up as above.

Diethyl citramalate (II) was obtained from crude I by treatment with ethanol and conc. sulphuric acid (reflux for 3 weeks), followed by preparative GLC. Another method, giving similar results, was also used. The crude reaction product was hydrolysed by treatment with potassium hydroxide (2 M) in ethanol (reflux overnight). Water was added, and the mixture was washed several times with ether. The aqueous layer was acidified, the solvent evaporated, and the residue was treated with ethanol and conc. sulphuric acid (reflux 3 days).

Acknowledgements. We thank Dr. Björn Lüning for his interest and the *Swedish Natural Science Research Council* for support.

1. Brandänge, S., Lüning, B., Moberg, C. and Sjöstrand, E. *Acta Chem. Scand.* **25** (1971) 349.
2. Brandänge, S. and Lüning, B. *Acta Chem. Scand.* **23** (1969) 1151.
3. Weber, H. *Diss.*, Eidgenössische Technische Hochschule, Zürich 1965.
4. Mitsui, S. and Kudo, Y. *Tetrahedron* **23** (1967) 4271.
5. Kudo, Y., Iwasawa, M., Kobayashi, M., Senda, Y. and Mitsui, S. *Tetrahedron Letters* **1972** 2125.
6. Rathke, M. W. *J. Am. Chem. Soc.* **92** (1970) 3222.
7. Reiffers, S., Wynberg, H. and Strating, J. *Tetrahedron Letters* **1971** 3001.
8. Dubois, J.-E. and Fellous, R. *Bull. Soc. Chim. France* **1963** 786.
9. Palmer, M. H. and Reid, J. A. *J. Chem. Soc.* **1960** 931.
10. Palmer, M. H. and Reid, J. A. *J. Chem. Soc.* **1962** 1762.
11. Barker, H. A. *Biochem. Prep.* **9** (1962) 25.

Received March 3, 1973.

An X-Ray Single Crystal Study of $K_2HgCl_4.H_2O$

KARIN AURIVILLIUS and CLAES STÅLHANDSKE

Divisions of Inorganic Chemistry 1,2, Chemical Center, University of Lund, Box 740, S-220 07 Lund 7, Sweden

In connection with studies on the crystal chemistry of inorganic compounds of mercury(II) in different environments, the present X-ray single crystal investigation of $K_2HgCl_4.H_2O$ was performed. The compound has earlier been the object of X-ray diffraction studies.[1,2] The position of all non-hydrogen atoms were derived from intensity data and geometrical considerations in the study in 1938.[1] In the next work on the structure in 1955,[2] the positions of the mercury, potassium, and chlorine atoms were determined from two-dimensional Fourier projections.[2] The positions of the oxygen and hydrogen atoms were not found, however.

Considering the state of the experimental X-ray technique and of the numerical calculation methods at the time for the earlier investigations, the accuracy in the determination of the positions of the light atoms could not be particularly high because of the presence of the heavy mercury atoms. Our aim was to redetermine the positions of the light atoms in order to discuss the coordination of the mercury atoms. The compound $K_2HgCl_4.H_2O$ crystallizes in the orthorhombic space group *Pbam* (No. 55) with four formula units in a unit cell with the dimensions $a = 8.258$ Å, $b = 11.662$ Å, $c = 8.925$ Å, and $V = 860$ Å^3. X-Ray single crystal diffractometer data (PAILRED) were collected using MoK-radiation and a graphite monochromator. A suitable needle-shaped crystal was rotated along [001] and the recorded data resulted in 843 independent reflections with intensities larger than $3\sigma_I$. The intensities were corrected for absorption; the linear absorption coefficient was 203 cm^{-1}. The positions of the mercury atoms were obtained from three-dimensional Patterson functions and the positions of the chlorine, potassium and oxygen atoms from difference Fourier syntheses. A least-squares refinement of the positional parameters of all non-hydrogen atoms including one scale factor was at first performed with isotropic tem-

'able 1. Final positional and thermal parameters with standard deviations for the non-hydrogen atoms in $K_2HgCl_4.H_2O$ 'he point positions of the atoms are: 4 Hg in 4(*e*), 4 K1, 4 Cl1 in 4(*g*), 4 K2, 4 Cl2 in 4(*h*), 8 Cl3 in 8(*i*), 4 O in 4(*f* *bam*). The expression for the anisotropic temperature factors is exp $-(\beta_{11}h^2+\beta_{22}k^2+\beta_{33}l^2+2\beta_{12}hk+2\beta_{13}hl+2\beta_{23}kl)$ where $\beta_{13}=\beta_{23}=0$ for the fourfold point positions.

tom	*x*	*y*	*z*	β_{11}/B	β_{22}	β_{33}	β_{12}	β_{13}	β_{23}
g	0	0	0.22925(8)	0.01204(10)	0.00302(4)	0.01636(10)	0.00203(4)	0	0
1	0.0819(3)	0.3410(2)	0	0.00833(39)	0.00297(17)	0.00787(29)	0.00048(20)	0	0
2	0.1047(3)	0.3047(2)	½	0.00759(35)	0.00339(17)	0.01036(35)	0.00024(21)	0	0
l1	0.2042(3)	0.0763(2)	0	0.00617(35)	0.00338(18)	0.00803(31)	0.00030(21)	0	0
l2	0.2489(4)	0.0601(2)	½	0.00882(40)	0.00268(18)	0.01018(36)	0.00077(22)	0	0
l3	−0.1169(2)	0.1860(2)	0.2520(3)	0.00827(27)	0.00290(12)	0.00823(22)	0.00072(15)	0.00070(22)	−0.00022(13
	0	½	0.2312(12)	3.6(2)					

perature factors introduced for the atoms. The resulting *R*-factor was 12.5 %. Anisotropic temperature factors were then inserted for the mercury, chlorine, and potassium atoms and a new refinement ended in an *R*-value of 4.5 % (818 reflections). Out of the 843 reflections, 25 at low angles ($\sin\theta/\lambda < 0.30$) had much too low observed intensities, probably depending on extinction effects, and they were omitted in the last refinement.

The final atomic parameters of all non-hydrogen atoms with standard deviations are presented in Table 1 and the *R.M.S.* components of the mercury, chlorine, and potassium atoms in Table 2.

Table 2. The R.M.S.-components, R_i (Å), of thermal vibrations of the atoms.

Atom	*R*1	*R*2	*R*3
Hg	0.257(1)	0.130(1)	0.214(1)
K1	0.178(3)	0.141(4)	0.171(4)
K2	0.204(4)	0.151(4)	0.163(4)
Cl1	0.180(4)	0.143(4)	0.155(4)
Cl2	0.203(4)	0.132(5)	0.178(4)
Cl3	0.185(3)	0.136(3)	0.170(3)

The parameters of all atoms are in good agreement with the values given by Mac Gillavry *et al.*,[1] including also the then geometrically derived value for the oxygen atom. The position of this atom has shifted only 0.17 Å. In connection with a nuclear magnetic resonance experiment on a single crystal of $K_2HgCl_4.H_2O$, performed by Itoh *et al.*,[3] the *z* parameter of the oxygen atom was calculated. The obtained value of $z=0.23$ is in excellent agreement with the value 0.231 found in the present X-ray diffraction study.

Selected interatomic distances and angles in the structure are given in Table 3 and a projection of the structure on the *xy*-plane is presented in Fig. 1.

The nearest neighbours of the divalent mercury atom are only chlorine atoms. The shortest distances Hg−2 Cl are 2.383(2) Å and the corresponding angle Cl−Hg−Cl 170.2(2)°, indicating the presence of nearly linear molecules $HgCl_2$ as

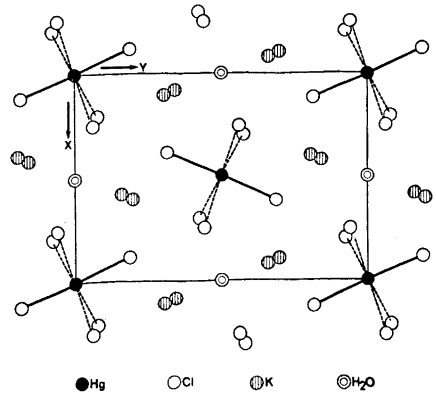

Fig. 1. Projection of the structure of $K_2HgCl_4.H_2O$ on the *xy*-plane, showing the octahedral environments of the mercury atoms. The heavy lines show the shortest mercury to chlorine contacts and the dotted lines the longer distances between mercury and chlorine. One unit cell is marked in the drawing.

Table 3. Selected interatomic distances (Å) and angles (°) in the structure of $K_2HgCl_4.H_2O$.

Hg – 2 Cl3	2.383(2)	∠Cl3 – Hg – Cl3	170.2(2)		
– 2 Cl1	2.797(2)	∠Cl1 – Hg – Cl1	86.0(1)		
– 2 Cl2	3.249(2)	∠Cl2 – Hg – Cl2	83.9(1)		
K1 – 2 O	2.856(8)			K2 – 2 O	3.419(8)
– 3 Cl1	3.249(4), 3.263(4), 3.265(4)			– Cl2	3.091(4)
– 4 Cl3	3.320(3), 3.369(3)			– 4 Cl3	3.187(4), 3.193(3)
				– 2 Cl2	3.215(4), 3.334(4)
O – 2 Cl2	3.247(8)	∠Cl2 – O – Cl2	84.8(3)		
– 2 Cl1	3.319(7)	∠Cl1 – O – Cl1	103.1(3)		

compared to the values reported for $HgCl_2$ [4] (Hg – 2 Cl 2.25 Å, ∠Cl – Hg – Cl 180°). Similar values are also given for the distances Hg – Cl in, *e.g.*, the structures of $CsHgCl_3$ [2] and NH_4HgCl_3 [5] (Hg – 2 Cl 2.29 Å, 2.34 Å, respectively). In the compound Hg_3OCl_4 [6] the mercury atom forms two nearly collinear bonds to one oxygen and one chlorine atom. The distance Hg – Cl is 2.32(2) Å and the angle O – Hg – Cl 175.8(8)°. In the present compound, the next nearest distances mercury to chlorine are considerably longer (Hg – 2 Cl 2.797(2) Å, 3.249(2) Å) indicating that these chlorine atoms probably occur as chloride ions. The distances mercury to chloride ions in NH_4HgCl_3 (2.99 Å) and in Hg_3OCl_4 (2.99(2) Å) are given as a comparison.

From a *geometrical* point of view, the coordination polyhedron around mercury is a distorted octahedron with two distances mercury to chlorine much shorter than the others. Fundamental building elements of the structure are then chains of deformed octahedra, sharing edges; a description that is in accordance with that given in Ref. 1.

The potassium atoms K1 and K2 (notations of the atoms, *cf.* Table 1) are each surrounded in an irregular way by seven chlorine and two oxygen atoms at distances varying from 2.86 to 3.37 Å and from 3.09 to 3.42 Å, respectively. These distances are in agreement with data available in the literature [7] on the coordination K – Cl and K – O.

Each water molecule has four neighbouring chloride ions at distances O – 2 Cl2 3.247(8) Å and O – 2 Cl1 3.319(8) Å with corresponding angles Cl – O – Cl of 84.8(3)° and 103.1(3)°. The distances and angles seem to indicate hydrogen bonds between the water molecules and the chloride ions. No effort has been made to determine the positions of the hydrogen atoms from the X-ray data available.

According to our opinion, the best way to describe $K_2HgCl_4.H_2O$ is that the structure is built up of molecules $HgCl_2$, ions K^+ and Cl^- and water molecules.

Neutron single crystal diffractometer data have been collected for the compound in order to determine the positions of the hydrogen atoms. The results of this investigation will be published elsewhere. Lists of observed and calculated structure factors are available by request to the authors.

These studies form part of a research program on mercury(II)salts financially supported by the *Swedish Natural Science Research Council.*

1. Mac Gillavry, C. H., de Wilde, J. H. and Bijvoet, J. M. *Z. Krist.* **100** (1938) 212.
2. Zvonkova, Z. V., Samodurova, V. V. and Vorontsova, L. G. *Dokl. Akad. Nauk SSSR* **102** (1955) 1115.
3. Itoh, J., Kusada, R., Yamagata, Y., Kiriyama, R. and Ibamsto, H. *J. Phys. Soc.* **8** (1953) 293.
4. Brackken, H. and Scholten, W. *Z. Krist.* **89** (1934) 448.
5. Harmsen, E. J. *Z. Krist.* **100** (1938) 208.
6. Aurivillius, K. *Arkiv Kemi* **22** (1964) 517.
7. *International Tables for X-Ray Crystallography*, Kynoch Press, Birmingham 1962, Vol. III, p. 258 f.

Received February 1, 1973.

The Crystal Structure of Monoclinic *trans*-Tetrachlorobis-(tetramethylthiourea)tellurium (IV)

STEINAR ESPERÅS, JOHN W. GEORGE,* STEINAR HUSEBYE and ØYVIND MIKALSEN

Chemical Institute, University of Bergen, N-5000 Bergen, Norway

Dark red, prism-shaped crystals of *trans*-tetrachlorobis(tetramethylthiourea)tellurium(IV), $[TeCl_4(C_5H_{12}N_2S)_2]$, are obtained by recrystallization from methanol.[1] In a fresh sample the crystals belong to the orthorhombic crystal system, but upon standing they become monoclinic.[2] The structure of the orthorhombic crystals have earlier been determined by Husebye and George [2] by means of three-dimensional X-ray methods, using the multiple-film technique. The present investigation is concerned with monoclinic crystals belonging to a five-year-old sample. The following unit cell parameters were found: $a = 14.009(3)$ Å, $b = 14.708(3)$ Å, $c = 10.053(2)$ Å, $\beta = 90.37(2)°$ and $Z = 4$. The measured and calculated densities are 1.70 and 1.71 g/cm^3, respectively, and the space group is $P2_1/n$. For comparison, the cell dimensions in the orthorhombic structure with space group *Pbca* are: $a = 14.74(3)$ Å, $b = 13.87(3)$ Å, $c = 10.06(2)$ Å, and $Z = 4$, *i.e.*, only one axis is significantly different.

The intensity data of 4028 reflections greater than background were recorded by means of a Siemens AED-1 single-crystal diffractometer using Mo$K\alpha$-radiation. The structure has been solved by Patterson and Fourier methods and refined by a full-matrix least squares program using the three-dimensional diffractometer data. The intensities were corrected for absorption. The R-value is 0.08 at the present stage of refinement.

Some bond lengths and angles for both the orthorhombic and monoclinic form of *trans*-tetrachlorobis(tetramethylthiourea) tellurium(IV) are given in Table 1, while the coordination around the tellurium atom in the monoclinic crystals is shown in Fig. 1. In the orthorhombic structure, where the tellurium atoms lie in centers of symmetry, the octahedral configuration around the tel-

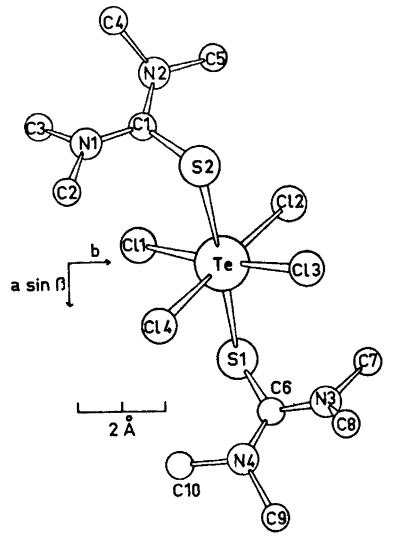

Fig. 1. The *trans*-tetrachlorobis(tetramethylthiourea)tellurium(IV) molecule seen along the *c*-axis.

Table 1. Some bond lengths (in Å) and bond angles (in degrees) found for the monoclinic structure (I) compared to the corresponding values for the centrosymmetric structure (II).

	I	II
Te–Cl1	2.457(3)	2.520(8)
Te–Cl2	2.528(3)	2.536(8)
Te–Cl3	2.598(3)	2.520(8)
Te–Cl4	2.542(3)	2.536(8)
Te–S1	2.725(3)	2.699(8)
Te–S2	2.649(3)	2.699(8)
S1–C6	1.745(9)	1.75(2)
S2–C1	1.740(9)	1.75(2)
∠Cl1–Te–Cl2	89.6(1)	89.1(2)
Cl1–Te–Cl3	172.0(1)	180.0
Cl1–Te–Cl4	91.3(1)	90.9(2)
Cl2–Te–Cl3	90.4(1)	90.9(2)
Cl2–Te–Cl4	177.2(1)	180.0
Cl3–Te–Cl4	89.1(1)	89.1(2)
Cl1–Te–S1	81.9(1)	81.5(2)
Cl1–Te–S2	92.3(1)	98.5(2)
Cl2–Te–S1	88.8(1)	91.1(2)
Cl2–Te–S2	89.7(1)	88.9(2)
Cl3–Te–S1	106.1(1)	98.5(2)
Cl3–Te–S2	79.8(1)	81.5(2)
Cl4–Te–S1	88.7(1)	88.9(2)
Cl4–Te–S2	92.9(1)	91.1(2)
S1–Te–S2	174.0(1)	180.0

* Present address: Dept. of Chemistry, University of Massachusetts, Amherst, USA.

lurium atom is slightly distorted.[2] In the present, not centrosymmetric structure, the distortion is found to be larger (Table 1). It is not clear if this can be interpreted as resulting from lattice-packing effects or from a stereochemical activity of the lone pair of electrons. However, the lone pair is not stereochemically active in the sense that it occupies a position in the coordination polyhedron.

The tellurium-chlorine bond lengths are ranging from 2.457(3) Å to 2.598(3) Å, while the tellurium-sulphur distances are found to be 2.649(3) Å and 2.725(3) Å. These values show a much greater variation than the corresponding ones in the orthorhombic structure; however, the average Te–Cl and Te–S bond lengths of 2.53 Å and 2.69 Å found here are in good agreement with the corresponding values of 2.53 Å and 2.70 Å found for the orthorhombic form. The average Te–Cl distance is further in good agreement with reported bond lengths in hexachlorotellurate species,[3,4] *i.e.*, equal to the sum of the octahedral radius of Te(IV) [5] and the covalent radius of Cl, while the average Te–S distance is significantly larger than the sum of the octahedral radius of Te(IV) and the covalent radius of S, 2.59 Å. Similar Te–S bond lengths or even greater ones are found in other tellurium(IV) complexes.[6,7] An explanation of why the Te–Cl bond lengths are normal while the Te–S ones are so large can at present not be given.

The S–C bond lengths of 1.745(9) Å and 1.740(9) Å are in good agreement with the corresponding values found for the orthorhombic structure and for tetramethylthiourea complexes of tellurium(II).

1. Foss, O. and Johannessen, W. *Acta Chem. Scand.* **15** (1961) 1939.
2. Husebye, S. and George, J. W. *Inorg. Chem.* **8** (1969) 313.
3. Aynsley, E. E. and Hazell, A. C. *Chem. Ind. (London)* **1963** 611.
4. Hazell, A. C. *Acta Chem. Scand.* **20** (1966) 165.
5. Foss, O. In *Selected Topics in Structure Chemistry*, Universitetsforlaget, Oslo 1967, p. 145.
6. Esperås, S., Husebye, S. and Sværen, S. E. *Acta Chem. Scand.* **25** (1971) 3539.
7. Esperås, S. and Husebye, S. *Acta Chem. Scand.* **27** (1973) 706.

Received February 21, 1973.

Synthesis of Tritium-labelled Tetrahydrocannabinol and Cannabidiol

STIG AGURELL,[a] BERTIL GUSTAFSSON,[a] TAMAS GOSZTONYI,[b] KAJ HEDMAN[c] and KURT LEANDER[c]

[a] *Central Military Pharmacy, Karolinska Hospital, S-104 01 Stockholm 60,* [b] *Research Laboratories, AB Astra Läkemedel, S-151 85 Södertälje and* [c] *Department of Organic Chemistry, University of Stockholm, Sandåsgatan 2, S-113 27 Stockholm, Sweden*

Several syntheses of ^{3}H-[1-5] and ^{14}C-labelled [1,6-8] tetrahydrocannabinols (THC's) have been reported. In distribution studies using autoradiography it is necessary to use compounds of high specific activity. For this purpose [9] tritium-labelled Δ^{1}-THC of specific activity 1.6 Ci/mmol has been prepared. This synthesis together with the preparation of tritium-labelled cannabidiol is here reported.

1-(3,5-Dimethoxyphenyl)-1-pentanone, synthesised according to the method of Baeckström and Sundström,[10] was reduced with sodium borohydride. The resulting alcohol,[4] dissolved in methanol, was tritiated with tritium gas over palladium supported on carbon. The reduction was then completed with hydrogen. The labelled dimethylolivetol was demethylated by heating with hydriodic acid.[11] The resulting olivetol was reacted with (+)-*trans*-*p*-menthadien-2,8-ol-1 to give (−)$\Delta^{1,6}$-THC,[12] which after purification on silica gel, was isomerised to (−)Δ^{1}-THC.[12]

1-(3,5-Dimethoxyphenyl)-1-pentanone could also be tritiated with tritium gas using the same condition as described above. The reduction was, however, slower than that of the corresponding alcohol and the exchange of tritium with the hydrogen atoms in the solvent occurred to such an extent that the resulting labelled dimethylolivetol had a specific activity only half of that obtained by tritiation of the alcohol.

The synthesis of tritium-labelled cannabidiol was achieved by a different route.

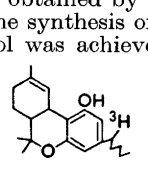

Δ¹-TETRAHYDROCANNABINOL

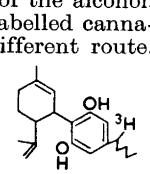

CANNABIDIOL

lurium atom is slightly distorted.[2] In the present, not centrosymmetric structure, the distortion is found to be larger (Table 1). It is not clear if this can be interpreted as resulting from lattice-packing effects or from a stereochemical activity of the lone pair of electrons. However, the lone pair is not stereochemically active in the sense that it occupies a position in the coordination polyhedron.

The tellurium-chlorine bond lengths are ranging from 2.457(3) Å to 2.598(3) Å, while the tellurium-sulphur distances are found to be 2.649(3) Å and 2.725(3) Å. These values show a much greater variation than the corresponding ones in the orthorhombic structure; however, the average Te–Cl and Te–S bond lengths of 2.53 Å and 2.69 Å found here are in good agreement with the corresponding values of 2.53 Å and 2.70 Å found for the orthorhombic form. The average Te–Cl distance is further in good agreement with reported bond lengths in hexachlorotellurate species,[3,4] *i.e.*, equal to the sum of the octahedral radius of Te(IV) [5] and the covalent radius of Cl, while the average Te–S distance is significantly larger than the sum of the octahedral radius of Te(IV) and the covalent radius of S, 2.59 Å. Similar Te–S bond lengths or even greater ones are found in other tellurium(IV) complexes.[6,7] An explanation of why the Te–Cl bond lengths are normal while the Te–S ones are so large can at present not be given.

The S–C bond lengths of 1.745(9) Å and 1.740(9) Å are in good agreement with the corresponding values found for the orthorhombic structure and for tetramethylthiourea complexes of tellurium(II).

1. Foss, O. and Johannessen, W. *Acta Chem. Scand.* **15** (1961) 1939.
2. Husebye, S. and George, J. W. *Inorg. Chem.* **8** (1969) 313.
3. Aynsley, E. E. and Hazell, A. C. *Chem. Ind. (London)* **1963** 611.
4. Hazell, A. C. *Acta Chem. Scand.* **20** (1966) 165.
5. Foss, O. In *Selected Topics in Structure Chemistry*, Universitetsforlaget, Oslo 1967, p. 145.
6. Esperås, S., Husebye, S. and Sværen, S. E. *Acta Chem. Scand.* **25** (1971) 3539.
7. Esperås, S. and Husebye, S. *Acta Chem. Scand.* **27** (1973) 706.

Received February 21, 1973.

Synthesis of Tritium-labelled Tetrahydrocannabinol and Cannabidiol

STIG AGURELL,[a] BERTIL GUSTAFSSON,[a] TAMAS GOSZTONYI,[b] KAJ HEDMAN[c] and KURT LEANDER[c]

[a] *Central Military Pharmacy, Karolinska Hospital, S-104 01 Stockholm 60,* [b] *Research Laboratories, AB Astra Läkemedel, S-151 85 Södertälje and* [c] *Department of Organic Chemistry, University of Stockholm, Sandåsgatan 2, S-113 27 Stockholm, Sweden*

Several syntheses of ^{3}H-[1-5] and ^{14}C-labelled [1,6-8] tetrahydrocannabinols (THC's) have been reported. In distribution studies using autoradiography it is necessary to use compounds of high specific activity. For this purpose [9] tritium-labelled Δ^{1}-THC of specific activity 1.6 Ci/mmol has been prepared. This synthesis together with the preparation of tritium-labelled cannabidiol is here reported.

1-(3,5-Dimethoxyphenyl)-1-pentanone, synthesised according to the method of Baeckström and Sundström,[10] was reduced with sodium borohydride. The resulting alcohol,[4] dissolved in methanol, was tritiated with tritium gas over palladium supported on carbon. The reduction was then completed with hydrogen. The labelled dimethylolivetol was demethylated by heating with hydriodic acid.[11] The resulting olivetol was reacted with (+)-*trans*-*p*-menthadien-2,8-ol-1 to give (−)$\Delta^{1,6}$-THC,[12] which after purification on silica gel, was isomerised to (−)Δ^{1}-THC.[12]

1-(3,5-Dimethoxyphenyl)-1-pentanone could also be tritiated with tritium gas using the same condition as described above. The reduction was, however, slower than that of the corresponding alcohol and the exchange of tritium with the hydrogen atoms in the solvent occurred to such an extent that the resulting labelled dimethylolivetol had a specific activity only half of that obtained by tritiation of the alcohol.

The synthesis of tritium-labelled cannabidiol was achieved by a different route.

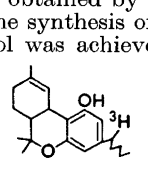

Δ¹-TETRAHYDROCANNABINOL

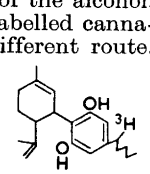

CANNABIDIOL

1-(3,5-Dimethoxyphenyl)-1-pentanone was reduced with lithium aluminium hydride-^{3}H. The alcohol obtained was further reduced with hydrogen to dimethylolivetol, which was demethylated as described above. The resulting labelled olivetol was reacted with (+)-*trans*-*p*-menthadien-2,8-ol-1 in the presence of *N*,*N*-dimethylformamide dineopentylacetal giving (−)-cannabidiol.[12]

The latter procedure using lithium aluminium hydride-^{3}H or sodium borohydride-^{3}H would, in general, be a suitable procedure for labelling cannabinoids of low or intermediate specific activity, since the pentanone derivative, an intermediate in the preparation of olivetol,[10] is readily available. Further, no special laboratory facilities are needed, and the hydride-^{3}H is efficiently utilized in the synthesis. In contrast to tritium-labelled cannabinoids prepared by exchange methods,[1,3,5] the stability of the label in the benzylic position in the side chain is satisfactory during both metabolic experiments [9] and isolation procedures.

Experimental. Δ^1-Tetrahydrocannabinol-^{3}H. A solution of 1-(3,5-dimethoxyphenyl)-1-pentanol (122 mg) in methanol (2 ml) was tritiated with tritium gas (19 Ci tritium) over palladium supported on carbon (10 %, 22 mg) at room temperature and atmospheric pressure. After 70 min the reduction was continued with hydrogen for 3 h, after which the catalyst was filtered off and the solvent evaporated. Any exchangeable tritium was removed by repeatedly dissolving the residue in methanol and evaporating the solvent. The crude dimethylolivetol and hydriodic acid (57 %, 4 ml) were stirred for 3 h at 110° under nitrogen. The mixture was poured into ice water and extracted with chloroform. The extract was subjected to preparative thin layer chromatography (silica gel, chloroform:methanol, 19:1) giving olivetol (70 mg) of specific activity 1.6 Ci/mmol. The labelled Δ^1-THC was then synthesised as previously described,[12] and purified by preparative thin layer chromatography (silica gel, ether:light petroleum, 1:9). The plates were developed three times.

Cannabidiol-^{3}H. To a solution of 1-(3,5-dimethoxyphenyl)-1-pentanone (424 mg) in ether (20 ml), lithium aluminium hydride-^{3}H (5 mg, 25 mCi) was added. The mixture was refluxed for 15 h, after which an excess of inactive lithium aluminium hydride was added. Refluxing was then continued for 5 h. The resulting alcohol (420 mg) was dissolved in methanol (5 ml) and hydrogenated over palladium (from 20 % palladium hydroxide[13] on carbon, 50 mg) at room temperature and atmospheric pressure. After 4 h one molar equivalent of hydrogen had been consumed. The catalyst was filtered off and the solvent evaporated. The crude dimethylolivetol was demethylated and purified as described above, giving olivetol (235 mg) with specific activity 11 mCi/mmol. Dilution with inactive olivetol (2.0 g) and condensation with (+)-*trans*-*p*-menthadien-2,8-ol-1 in the presence of *N*,*N*-dimethylformamide dineopentylacetal afforded (−)cannabidiol of specific activity 0.9 mCi/mmol.

Acknowledgements. We are indebted to the *Swedish Medical Research Council* and *Försvarsmedicinska Forskningsdelegationen* for support.

1. Nilsson, J. L. G., Nilsson, I. M. and Agurell, S. *Acta Chem. Scand.* **23** (1969) 2209.
2. Burstein, S. and Mechoulam, R. *J. Am. Chem. Soc.* **90** (1968) 2420.
3. Timmons, M. L., Pitt, L. G. and Wall, M. E. *Tetrahedron Letters* **1969** 3129.
4. Gill, E. W. and Jones, G. *J. Label. Compounds* **8** (1972) 237.
5. Idänpään-Heikkilä, J., Fritchie, G. E., Englert, L. F., Ho, B. T. and McIsaac, W. M. *N. Engl. J. Med.* **281** (1969) 330.
6. Liebman, A. A., Malarek, D. H., Dorsky, A. M. and Kaegi, H. H. *J. Label. Compounds* **7** (1971) 241.
7. Gau, W., Bieniek, D. and Korte, F. *Tetrahedron Letters* **1972** 2507.
8. Miras, C. J. In Wolstenholme, G. E. W. and Knight, J., Eds., *Hashish: Its Chemistry and Pharmacology*, Churchill, London 1965.
9. Ryrfeldt, Å., Ramsay, C. H., Nilsson, I. M., Widman, M. and Agurell, S. *Acta Pharm. Suecica* **10** (1973). *In press.*
10. Baeckström, P. and Sundström, G. *Acta Chem. Scand.* **24** (1970) 716.
11. Asahina, Y. *Ber.* **69** (1936) 1643.
12. Petrzilka, T., Haefliger, W. and Sikemeier, C. *Helv. Chim. Acta* **52** (1969) 1102.
13. Pearlmann, W. M. *Tetrahedron Letters* **1967** 1663.

Received March 2, 1973.

4-Butyl-1,2-diphenylpyrazolidine and Its Conformation Based on NMR Spectrometry

K. BERG-NIELSEN

Kjemisk Institutt, Universitetet i Oslo, Oslo 3, Norway

The ring inversion of a five-membered ring is usually much faster than the pyramidal nitrogen inversion.[1] In 1,2,4,4-tetramethylpyrazolidine the inversion about the two nitrogen atoms has been studied by NMR spectroscopy.[1] At low temperature the protons at 3 and 5 position appeared as two identical AB quartets. The coalescence temperature was found to be -45°C in dichloromethane and the inversion barrier $\Delta G^{\ddagger} = 11.1$ kcal/mol.

Inversion of pyramidal nitrogen passes through a planar transition state.[2] The conjugation of the lone pair with a phenyl substituent is expected to give the nitrogen sites a more planar shape and to decrease the inversion barrier. This decrease may be calculated by the empirical equation [3]

$$\Delta G^{\ddagger}_1 = XZ = \Delta G^{\ddagger}_{CH_3} Z_1$$

where Z_1 represents the substituent and X the rest of the molecule. Choosing methyl as unity ($Z_{CH_3} = 1$) gives $\Delta G^{\ddagger}_{C_6H_5} = \Delta G^{\ddagger}_{CH_3} Z_{C_6H_5}$, where $Z_{C_6H_5}$ is found to be 0.59.[6] The barrier to nitrogen inversion in 4,4-dimethyl-1,2-diphenylpyrazolidine may thus be calculated as $11.1 \times 0.59 \sim 6.55$ kcal/mol.

Pyrazolidine-3-ones can be reduced by lithium aluminium hydride in a suitable solvent to the corresponding pyrazolidines.[4-6]

In continuation of our work with lithium aluminium hydride reduction of acyl hydrazobenzenes [7] also 4-butyl-1,2-diphenylpyrazolidine-3,5-dione has now been reduced to 4-butyl-1,2-diphenylpyrazolidine (I).

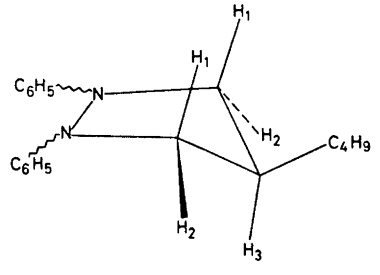

(I)

The NMR shifts for H_1 and H_2 are temperature dependent. The difference between them, $\Delta\nu$, in Freon 21 is 0.93 ppm at -90°C and 0.84 ppm at 0°C. In carbon tetrachloride $\Delta\nu$ is 0.80 ppm at 0°C, 0.77 ppm at 29°C, and 0.72 ppm at 73°C, the coupling picture being the same.

Thus the nitrogen inversion is, as expected, too fast to give a low-temperature spectrum at -90°C, which should correspond to a barrier lower than *ca.* 8.5 kcal/mol.

Since corresponding protons at C_3 and C_5 are identical at all temperatures, the rapid inversion must produce a plane of symmetry in the molecule perpendicular to and through the middle of the N–N bond.

The difference in chemical shifts for H_1 and H_2, 0.77 ppm, is too large to be caused by the butyl group only; it must be due to shielding and deshielding effects of the benzene rings. The NMR spectra therefore indicate that the energy minimum of the ring corresponds to C_s symmetry with the butyl group in "equatorial" position at the tip of the envelope.

Because of the butyl group all other conformations have higher energy. Their population must increase somewhat with temperature to explain the decrease in $\Delta\nu$ between H_1 and H_2. Possibly some kind of solvent interaction is also involved.

1,2-Diphenylpyrazolidine has no substituents at C_4 providing energy difference of this kind. In its NMR spectrum the H_1 and H_2 protons therefore appear as a triplet at δ 3.43, $J = 6.5$ Hz showing that they are equal. The protons at C_4 appear as a quintet at δ 1.94.

Models of 4-butyl-1,2-diphenylpyrazolidine (II and III) suggest a difference in shielding and deshielding effects at H_1 and H_2 in good agreement with the found values (Fig. 1). When the adjacent phenyl group is *trans* to H_2(II), this proton will be very near to the plane of the benzene ring and therefore in the deshielding zone. At the same time H_1 will be in the shielding zone. The other phenyl group is more remote and gives a smaller effect, only a slight shielding effect at H_2. When the adjacent phenyl group is *trans* to H_1, (III), the distance from the ring to H_1 is greater and the deshielding effect will be reduced. H_2 in (III) will be less shielded than H_1 in (II). The other phenyl group gives only a slight shielding effect at H_1.

An inspection of a model of this molecule

Table 1. The NMR spectrum of (I) in carbon tetrachloride at 29°C in δ values.

C_6H_5	H_1	H_2	H_3	C_4H_9
8.25–6.64 10 H	2.93t 2H	3.70d 2H	~2.3c 1H	0.86t 3H 1.31c 6H

t=triplet, d=2 doublets, c=complex; $J_{1,2}=9.8$ Hz, $J_{1,3}\approx 9.4$ Hz, $J_{2,3}=7.0$ Hz.

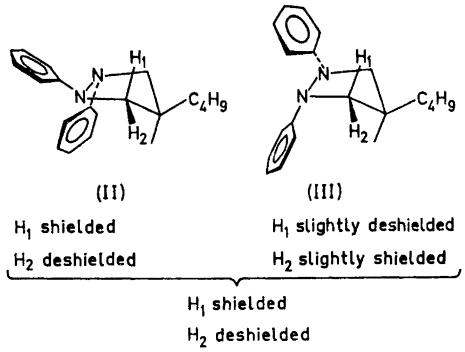

Fig. 1. Models of 4-butyl-1,2-diphenylpyrazolidine showing shielding and deshielding effects of the benzene rings at H_1 and H_2.

also shows that the dihedral angle between H_1 and H_3, $\theta_{1,3}$, is closer to 180° than the dihedral angle between H_2 and H_3, $\theta_{2,3}$, is close to zero. The observed coupling constants $J_{1,3}=9.4$ Hz $> J_{2,3}=7.0$ Hz are therefore in agreement with values predicted from the Karplus equation.

Experimental. Melting points were determined on a micro hot-stage. NMR spectra were recorded on Varian A-60 A and HA 100 Spectrometers with tetramethylsilane as internal reference, mass spectra on an AEI/EC MS 902 instrument, and infrared spectra on a Perkin-Elmer 457 Grating Infrared Spectrophotometer. Thin layer chromatography was used with toluene as eluent and iodine vapour as staining reagent.

4-Butyl-1,2-diphenylpyrazolidine (I). To a solution of 4-butyl-1,2-diphenylpyrazolidine-3,5-dione (6.2 g, 20 mmol) in dry ether (40 ml) was added a suspension of lithium aluminium hydride (2.7 g, 70 mmol) in dry ether (40 ml), and the mixture was refluxed for 2 h. After cooling, water (5 ml) was added cautiously and then 2 N sodium hydroxide (2 ml). After 30 min the solid material was filtered off and the solution dried with calcium chloride. The ether was removed at low pressure and the product purified by column chromatography on aluminium oxide with toluene as eluent. The yield was 1.8 g (31 %) of a liquid which was not further purified. It was kept at −10°C to avoid darkening. The IR spectra showed no absorption due to carbonyl. The mass spectrum showed $m/e=280$.

1,2-Diphenylpyrazolidine. A dispersion of hydrazobenzene (6.3 g, 33 mmol), 1,3-diiodopropane (9.7 g, 33 mmol), and sodium hydrogen carbonate (5.7 g, 66 mmol) in ethanol (200 ml) was refluxed with stirring under nitrogen for 22 h. Undissolved sodium iodide (2.4 g) was filtered off and the solvent removed at low pressure, leaving a solid residue (13 g). This was extracted with toluene (3×15 ml) giving more undissolved sodium iodide (3.2 g). The toluene was evaporated *in vacuo*, and the solid residue was extracted thoroughly with petrol ether, b.p. 60–80°C (4×15 ml), leaving hydrazobenzene undissolved (4.8 g). The petrol ether was removed at low pressure, and the residue solidified on cooling. It was then washed with some petrol ether (3×4 ml) leaving 0.9 g (13 %) of a white product, m.p. 99.5–100.5°C after crystallization from ethanol. (Lit. 96–98°C [9] and 98.5–99°C [10].) The mass spectrum showed $m/e=224$.

1. Lehn, J. M. *Fortschr. Chem. Forsch.* **15** (1970) 311.
2. Kessler, H. *Angew. Chem.* **82** (1970) 244.
3. Kessler, H. and Leibfritz, D. *Tetrahedron Letters* **1970** 4297.
4. Bouchet, P., Elguero, J. and Jacquier, R. *Tetrahedron* **22** (1966) 2461.
5. Dittli, C., Elguero, J. and Jacquier, R. *Bull. Soc. Chim. France* **1969** 4469.
6. Elguero, J., Jacquier, R. and Tizané, D. *Bull. Soc. Chim. France* **1970** 1936.
7. Berg-Nielsen, K. and Bernatek, E. *Acta Chem. Scand.* **26** (1972) 4130.
8. Eliel, E. L., Allinger, N. L., Angyal, S. J. and Morrison, G. A. *Conformational Analysis*, Interscience, New York 1966, p. 60.
9. Wittig, G., Joos, W. and Rathfelder, P. *Ann.* **610** (1957) 180.
10. Daniels, R. and Martin, B. D. *J. Org. Chem.* **27** (1962) 178.

Received February 6, 1973.

Hydrolysis of Periodate Oxidized-reduced Glycosides

BERTIL ERBING, OLLE LARM, BENGT LINDBERG and SIGFRID SVENSSON

Institutionen för organisk kemi, Stockholms Universitet, Sandåsgatan 2, S-113 27 Stockholm, Sweden

The Smith degradation of polysaccharides,[1] which is a sequence of reactions comprising oxidation, borohydride reduction and hydrolysis of the resulting polyalcohol under mild conditions, has become an important tool in polysaccharide chemistry.

The conditions of the hydrolysis are critical, and Smith and VanCleve [2] studied the rate of hydrolysis of the mixed acetal I, prepared from methyl-α-D-glucopyranoside. No other model substances seem to have been studied. Dutton and Gibney [3] have, however, recently showed how the hydrolysis of the polyalcohol could be monitored by GLC of the products.

We now report hydrolysis studies on I, II, and III, the two latter prepared from methyl 2- and 4-*O*-methyl-α-D-glucopyranoside, respectively.

These glycosides, which are known substances, were prepared by conventional methods. After oxidation with periodate in aqueous methanol, they were reduced with borohydride and the products purified by distillation or preparative TLC. The products which were amorphous, were chromatographically pure (TLC).

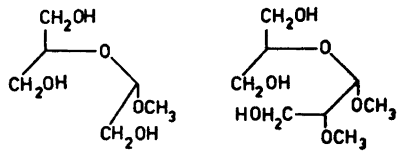

I

II

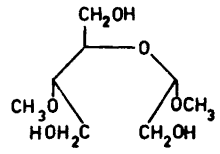

III

The acetate derivatives were also pure (GLC) and their NMR and mass spectra were in agreement with the postulated structures. The origin of some primary fragments on MS are indicated in the formulae below.

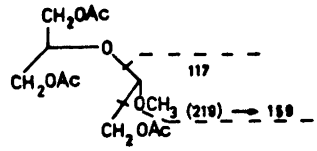

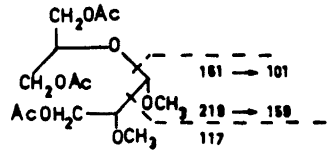

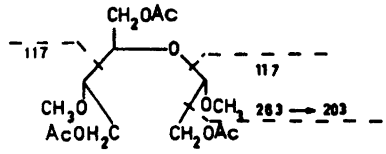

The hydrolyses of I, II, and III, each at three different temperatures, were followed polarimetrically. Inactive products should be formed from I, but II and III should give optically active products, in accordance with the experimental finding. Because of the rather low change in optical rotation during the hydrolysis, the rate constants and activation energies (Table 1) may be subject to rather large errors. Whilst I and III are hydrolysed at about the same rate, II reacts about ten times slower. This is attributed to the presence in II of electron attracting groups in both the α- and β-positions to the acetal carbon atom. The corresponding values for methyl α-D-glucopyranoside at 40°, extrapolated from published values,[4] are also given in Table 1. The differences in rate of hydrolysis for the acyclic acetals and the glucoside are considerable and it should be possible to hydrolyse the former completely without affecting the latter. The activation energy is higher for the glucoside, and the difference in rate is consequently enhanced at low temperatures. Smith and his coworkers [1] also used comparatively strong

Table 1. Rate constants and activation energies for the acid hydrolysis of the mixed acetals I, II, and III.

Compound	Temperature	$k \times 10^4$ sec^{-1}	E kcal/mol
	20	0.89	
I	30	3.62	23.5
	40	11.30	
	40	0.94	
II	50	2.40	19.6
	60	5.89	
	20	1.04	
III	30	3.49	23.3
	40	12.90	
Methyl α-D-glucopyranoside	40	0.00005	35.1

acid and low temperature for the hydrolysis of polyalcohols.

It is, however, often observed that the yields in a Smith degradation are not as high as expected from the other structural information available. Further much stronger hydrolytic conditions have to be applied than those recommended [1] and indicated in the present study. A possible reason for this discrepancy is that acetal migration, with formation of more stable cyclic acetals, competes with the hydrolysis. The formation of a cyclic acetal during a Smith degradation has been reported.[1] This complication could easily be avoided if the hydroxyl groups in the polyalcohol were protected, *e.g.* by methylation, before the hydrolysis step.

Experimental. Concentrations were performed under reduced pressure at a bath temperature below 40°. Precoated plates with Silica Gel F 254 (Merck) were used for TLC and silicic acid (230 mesh, Merck) for column chromatography. NMR spectra were recorded with a Varian A60 A instrument and chemical shifts are given as τ-values. MS were recorded with a Perkin-Elmer 270 instrument and optical rotations with a Perkin-Elmer 141 polarimeter. GLC was performed with a Perkin-Elmer model 900 instrument using a column packed with ECNSS-M 3 % on Gas-Chrom Q.

Methyl 2-O-methyl-α-D-glucopyranoside. Methyl iodide (3.8 g) was added over 2 h to a stirred mixture of methyl 4,6-*O*-benzylidene-α-D-glucopyranoside (7.6 g) and silver oxide (6.4 g) in dimethylformamide (60 ml), kept below 4° by external cooling. The mixture was allowed to reach room temperature and stirring was continued overnight. The mixture was filtered, concentrated and fractionated on a silicic acid column (6 × 50 cm), using toluene-ethyl acetate (1:1) as irrigant. The eluate was monitored polarimetrically and by TLC. The third component eluted (1.8 g) was pure methyl 4,6-*O*-benzylidene 2-*O*-methyl-α-D-glucopyranoside, which after crystallization showed m.p. 169–170° and $[\alpha]_D^{24}$ +97° (*c* 0.8, chloroform), in good agreement with published values.[5] This substance was hydrogenated (H_2/Pd) and the product crystallized from ethyl acetate, giving the title compound (0.7 g), m.p. 147–148°, $[\alpha]_D^{24}$ +158° (*c* 1.0, water), in good agreement with published values.[6]

Methyl 4-O-methyl-α-D-glucopyranoside was prepared essentially as described by Whistler and coworkers [7] and showed m.p. 95–96°, $[\alpha]_D^{24}$ +172° (*c* 0.8, water).

Preparation of the mixed acetals I, II, and III. Sodium metaperiodate (22 g) in water (150 ml) was added to a solution of methyl α-D-glucopyranoside (10 g) in methanol (700 ml). The mixture was kept in the dark at room temperature for 15 h, filtered and concentrated. The resulting syrup and sodium borohydride (15 g) in water (200 ml) was kept for 12 h at room temperature, excess borohydride was decomposed with acetic acid and the solution concentrated. Boric acid was removed by codistillations with methanol and the product extracted with ethanol, concentrated and distilled at 200–210°/0.2 mm. The resulting syrup (3.0 g), $[\alpha]_{578}^{24}$ −13° (*c* 2.45, water), consisted of chromatographically pure I (TLC, chloroform-ethanol, 7:3). The acetate, which gave a single peak on GLC, showed the following peaks on NMR: 5.19 (t, 1H) proton at C-1 of the original glucoside, 5.70–5.95 (m, 7H) protons at C-2, C-4, C-5 and C-6, 6.55 (s, 3H) OCH_3, 7.92 (s, 9H) $OOCCH_3$. It gave the following ions on MS (relative intensities in brackets): 43(100), 45(4), 99(2), 103(2), 117(19), 145(1), 159(12).

The mixed acetals II and III were prepared analogously, except that half of the molar amount of periodate was used and the products were not distilled, but purified by TLC (chloroform-ethanol 7:3). They were both obtained as chromatographically pure syrups and their acetates gave single peaks on GLC.

II, $[\alpha]_{578}^{24}$ +13° (*c* 2.8, water). NMR of the acetate: 5.40 (d, 1H) proton at C-1, 5.65–5.90 (m, 8H) protons at C-2, C-3, C-4, C-5 and C-6, 6.52 (s, 3H) and 6.53 (s, 3H) two OCH_3, 7.92 (s, 9H) $OOCCH_3$. MS of acetate: 43(100), 99(9),

101(23), 103(5), 117(5), 129(1), 145(3), 159(60), 161(5) and 219(3).

III, $[\alpha]_{578}^{24}$ −11.5° (*c* 2.2, water). NMR of acetate: 5.13 (t, 1H) proton at C-1, 5.55–5.98 (m, 8H) protons at C-2, C-3, C-4, C-5 and C-6, 6.53 (s, 3H) and 6.55 (s, 3H) two OCH_3, 7.81 (s, 9.11) $OOCCH_3$. MS of acetate: 43(100), 69(7), 71(5), 87(4), 101(6), 117(55), 129(1), 143(5), 161(1), 203(8) and 263(1).

Acid hydrolysis of I, II and III. The mixed acetal (approximately 0.2 M) in 0.125 M sulphuric acid (2 ml) was transferred to a jacketed polarimeter tube (10 cm), maintained at the required temperature, and the optical rotation was determined at intervals. The observed changes in rotation were approximately: I, −0.105°→0°. II, +0.155°→0.075°. III, −0.315°→0.040°. Duplicate experiments gave results in good agreement with those given in Table 1.

Acknowledgements. The skilled technical assistance of Miss Birthe Abrahamsson and Miss Birgitta Sundberg is acknowledged. This work was supported by a grant from *Statens Naturvetenskapliga Forskningsråd.*

1. Goldstein, I. J., Hay, G. W., Lewis, B. A. and Smith, F. *Methods Carbohyd. Chem.* **5** (1965) 361.
2. Smith, F. and VanCleve, J. W. *J. Am. Chem. Soc.* **77** (1955) 3091.
3. Dutton, G. G. S. and Gibney, K. B. *Carbohyd. Res.* **25** (1972) 99.
4. Timell, T. E. *Can. J. Chem.* **42** (1964) 1456.
5. Bourne, E. J., Stacey, M., Tatlow, C. E. M. and Tatlow, J. C. *J. Chem. Soc.* **1951** 826.
6. Haworth, W. N., Hirst, E. L. and Teece, E. G. *J. Chem. Soc.* **1931** 2858.
7. Whistler, R. L., Linke, E. G. and Kazeniac, S. *J. Am. Chem. Soc.* **78** (1956) 4704.

Received March 10, 1973.

Studies on Orchidaceae Alkaloids

XXXVI.* Alkaloids from Some *Vanda* and *Vandopsis* Species

SVANTE BRANDÄNGE and INGRID GRANELLI

Department of Organic Chemistry, University of Stockholm, Sandåsgatan 2, S-113 27 Stockholm, Sweden

Esters of 1-hydroxymethylpyrrolizidine have previously been isolated from orchid extracts. Laburnine acetate (I) has been isolated from *Vanda cristata* Lindl.[1] and more complex esters from *Phalaenopsis*[2] and *Liparidinæ*[3–6] species. We now report similar studies on some other *Vanda* and closely related *Vandopsis* species.

From *Vandopsis lissochiloides* Pfitz. the alcohols laburnine (III) and lindelofidine (IV) were isolated, together with the corresponding acetates I and II,[1] in the *exo/endo* ratios 1/3. From *Vandopsis gigantea* Pfitz. the same alcohols and acetates were isolated in the *exo/endo* ratios 10/1. Laburnine acetate (I) has been isolated

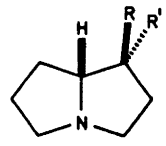

I: $R = CH_2OAc$, $R' = H$

II: $R = H$, $R' = CH_2OAc$

III: $R = CH_2OH$, $R' = H$

IV: $R = H$, $R' = CH_2OH$

from *Vanda hindsii* Lindl., and I and III from *Vanda helvola* Bl. An extract of *Vanda luzonica* Loher contained either I or its enantiomer (GLC-MS). A small amount of hygrine was detected (GLC-MS) in an extract of *Vandopsis parishii* Schltr.

In some of the above investigations a modified reineckate procedure was used to purify and quantify small amounts of

* For number XXXV in this series, see Ref. 6.

101(23), 103(5), 117(5), 129(1), 145(3), 159(60), 161(5) and 219(3).

III, $[\alpha]_{578}^{24}$ −11.5° (*c* 2.2, water). NMR of acetate: 5.13 (t, 1H) proton at C-1, 5.55–5.98 (m, 8H) protons at C-2, C-3, C-4, C-5 and C-6, 6.53 (s, 3H) and 6.55 (s, 3H) two OCH_3, 7.81 (s, 9.11) $OOCCH_3$. MS of acetate: 43(100), 69(7), 71(5), 87(4), 101(6), 117(55), 129(1), 143(5), 161(1), 203(8) and 263(1).

Acid hydrolysis of I, II and III. The mixed acetal (approximately 0.2 M) in 0.125 M sulphuric acid (2 ml) was transferred to a jacketed polarimeter tube (10 cm), maintained at the required temperature, and the optical rotation was determined at intervals. The observed changes in rotation were approximately: I, −0.105°→0°. II, +0.155°→0.075°. III, −0.315°→0.040°. Duplicate experiments gave results in good agreement with those given in Table 1.

Acknowledgements. The skilled technical assistance of Miss Birthe Abrahamsson and Miss Birgitta Sundberg is acknowledged. This work was supported by a grant from *Statens Naturvetenskapliga Forskningsråd.*

1. Goldstein, I. J., Hay, G. W., Lewis, B. A. and Smith, F. *Methods Carbohyd. Chem.* **5** (1965) 361.
2. Smith, F. and VanCleve, J. W. *J. Am. Chem. Soc.* **77** (1955) 3091.
3. Dutton, G. G. S. and Gibney, K. B. *Carbohyd. Res.* **25** (1972) 99.
4. Timell, T. E. *Can. J. Chem.* **42** (1964) 1456.
5. Bourne, E. J., Stacey, M., Tatlow, C. E. M. and Tatlow, J. C. *J. Chem. Soc.* **1951** 826.
6. Haworth, W. N., Hirst, E. L. and Teece, E. G. *J. Chem. Soc.* **1931** 2858.
7. Whistler, R. L., Linke, E. G. and Kazeniac, S. *J. Am. Chem. Soc.* **78** (1956) 4704.

Received March 10, 1973.

Studies on Orchidaceae Alkaloids

XXXVI.* Alkaloids from Some *Vanda* and *Vandopsis* Species

SVANTE BRANDÄNGE and INGRID GRANELLI

Department of Organic Chemistry, University of Stockholm, Sandåsgatan 2, S-113 27 Stockholm, Sweden

Esters of 1-hydroxymethylpyrrolizidine have previously been isolated from orchid extracts. Laburnine acetate (I) has been isolated from *Vanda cristata* Lindl.[1] and more complex esters from *Phalaenopsis*[2] and *Liparidinæ*[3–6] species. We now report similar studies on some other *Vanda* and closely related *Vandopsis* species.

From *Vandopsis lissochiloides* Pfitz. the alcohols laburnine (III) and lindelofidine (IV) were isolated, together with the corresponding acetates I and II,[1] in the *exo/endo* ratios 1/3. From *Vandopsis gigantea* Pfitz. the same alcohols and acetates were isolated in the *exo/endo* ratios 10/1. Laburnine acetate (I) has been isolated

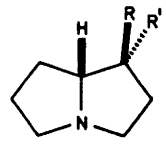

I: $R = CH_2OAc$, $R' = H$

II: $R = H$, $R' = CH_2OAc$

III: $R = CH_2OH$, $R' = H$

IV: $R = H$, $R' = CH_2OH$

from *Vanda hindsii* Lindl., and I and III from *Vanda helvola* Bl. An extract of *Vanda luzonica* Loher contained either I or its enantiomer (GLC-MS). A small amount of hygrine was detected (GLC-MS) in an extract of *Vandopsis parishii* Schltr.

In some of the above investigations a modified reineckate procedure was used to purify and quantify small amounts of

* For number XXXV in this series, see Ref. 6.

alkaloids. In order to regenerate an alkaloid (alk) from the reineckate precipitate, $alkH^+ Cr(NH_3)_2(SCN)_4^-$, the latter has hitherto been treated successively with silver sulphate, hydrogen sulphide and barium hydroxide.[7] Instead, the reineckate has here been converted to the hydrochloride by passing a solution of it, in acetone-methanol, through an ion exchange column in chloride form. This procedure has also been used in isolations of some hydrophilic alkaloids.[4-6]

Experimental. Preparative GLC was carried out on a 20 % SE-52 on Chromosorb AW DMCS column (0.8 × 290 cm, 60 – 80 mesh) in an Aerograph A-90-P chromatograph, and analytical GLC on a 20 % SE-52 on Chromosorb AW DMCS column (0.2 × 180 cm, 80 – 100 mesh) using a Perkin-Elmer 900 instrument. On the latter column the retention times (155°, 35 ml/min) for compounds I – IV were 7.4, 8.4, 4.8, and 5.2 min, respectively. Optical rotations were measured on a Perkin-Elmer 141 polarimeter.

General procedure for separation and identification of the pyrrolizidine alkaloids I – IV. The plant extract (methanol) was concentrated, dilute hydrochloric acid was added, and the resulting solution was washed with carbon tetrachloride. The aqueous layer was made alkaline (pH 9) and the acetates I and II were extracted with carbon tetrachloride. The last traces of I and II and some III and IV were then extracted with chloroform. A final extraction with chloroform-ethanol (3:2) yielded the alcohols III and IV. The acetates were separated by repeated preparative GLC at 155°. The *exo*-acetate from *Vandopsis gigantea* showed $[\alpha]_D^{24}$ + 12° (*c* 5.1, ethanol) lit.[1] value for I: + 13°, and the *endo*-acetate $[\alpha]_D^{24}$ + 66° (*c* 0.82, ethanol), value [8] for II: + 65°. Owing to the poor recovery of the alcohols on preparative GLC these were either acetylated with ketene followed by preparative GLC, or precipitated as reineckates (see below). Acetylation of the amino alcohols from *Vandopsis gigantea* gave acetates showing $[\alpha]_D^{24}$ + 15° (*c* 3.3, ethanol) and $[\alpha]_D^{24}$ + 64° (*c* 1.26, ethanol). An increased *exo*/*endo* ratio and a decreased yield of acetates were obtained if prolonged reaction times were used in the reactions with ketene.

Reineckate precipitation procedure. Commercial ammonium reineckate was recrystallised from water, and a freshly prepared, concentrated and filtered solution in water was added dropwise with shaking to a slightly acidic aqueous solution of the alkaloids in a weighed test tube. When the precipitation was complete (red mother liquor) the mixture was centrifuged and the mother liquor removed with a pipette, water was then added, the suspension shaken, and the new mother liquor removed. This washing procedure was repeated a few times and the precipitate was then dried in vacuum and weighed. The reineckate was dissolved in acetone and an equal amount of methanol added, and the reineckate anion was then replaced by chloride ion by passage through a column of Dowex 1-X4 (Cl^-) with methanol (if necessary mixed with acetone) as solvent. The solvent was evaporated and the residue dissolved in ethanol. One drop of sodium hydroxide solution was then added and the solution filtered. After this treatment the reineckate (103 mg) of the alcohol from *Vanda helvola* gave an alcohol showing $[\alpha]_D^{23}$ + 15° (*c* 3.2, ethanol), lit.[9] value for III + 15.45°. The reineckate (41.4 mg) of the acetate from the same species gave an acetate (I) with $[\alpha]_D^{22}$ + 18° (*c* 1.3, ethanol).

Acknowledgements. We thank Dr. Björn Lüning for valuable discussions and the *Swedish Natural Science Research Council* for support.

1. Lindström, B. and Lüning, B. *Acta Chem. Scand.* **23** (1969) 3352.
2. Brandänge, S., Lüning, B., Moberg, C. and Sjöstrand, E. *Acta Chem. Scand.* **26** (1972) 2558.
3. Leander, K. and Lüning, B. *Tetrahedron Letters* **1967** 3477.
4. Lindström, B. and Lüning, B. *Acta Chem. Scand.* **25** (1971) 895.
5. Lindström, B., Lüning, B. and Siirala-Hansén, K. *Acta Chem. Scand.* **25** (1971) 1900.
6. Lindström, B. and Lüning, B. *Acta Chem. Scand.* **26** (1972) 2963.
7. Werle, E. In Paech, K. and Tracey, M. V., Eds., *Moderne Methoden der Pflanzenanalyse*. Vol. IV, Berlin 1955.
8. Lindström, B. and Lüning, B. *Unpublished.*
9. Galinovsky, F., Goldberger, H. and Pöhm, M. *Monatsh.* **80** (1949) 550.

Received March 10, 1973.

Stereoselective Cyclopropane Ring Opening Reactions of Nortricyclene Hydrocarbons in Formic Acid. II. Reactions of Cyclofenchene and α-Fenchene

JAAKKO PAASIVIRTA [a] and PEKKA HIRSJÄRVI [b]

[a] *Department of Chemistry, University of Jyväskylä, Jyväskylä, Finland, and*
[b] *Department of Chemistry, University of Helsinki, Helsinki, Finland*

Addition of formic acid to nortricyclene or tricyclene produced only one formate in both cases, exo-2-norbornyl or isobornyl formate.[1] We have studied the analogous treatment of cyclofenchene (I), and found it to lead to a very complicated mixture of initial, intermediate and final products. α-Fenchene (II) was the most important early intermediate of the reaction of I. A closer study was made of the rates and product ratios at different temperatures of the reactions of I and II in a formic acid-methylene chloride 1:1 mixture. The initial hydrocarbons I and II were purified by preparative gas chromatography. Gas chromatography, IR, mass and NMR-spectrometry were used for product analysis All products except one formate X were identified by comparing the spectra with the authentic samples of the Department of Chemistry, University of Helsinki.

The kinetic measurements were done from the start until 50 % of the initial hydrocarbon had reacted. The consumption of I and II during the reactions followed first order kinetics. The experimental rate constants and Arrhenius parameters together with the values of apparent entropy and free energy of activation at 25 and 105°C are collected in Table 1. The free energy difference of cyclofenchene (I) and α-fenchene (II) was determined at 105°C by equilibrating the mixture without formic acid using silica gel as catalyst. Other fenchenes appeared in the mixture,[2] but the molar ratio II:I approached 17.5:1. Thus $\Delta G^\circ = -RT \ln K = -2.15$ kcal/mol; α-fenchene (II) being thermodynamically more stable than cyclofenchene (I). From the apparent free energies of activation at 105° (Table 1), the calculated free energy of the apparent transition state for the reaction of cyclofenchene (I) is 3 kcal/mol higher than for the reaction of α-fenchene (II). This indicates different mechanisms for the reactions of I and II. The Arrhenius parameters and apparent entropies of activation (Table 1) also show differences in the reaction mechanisms: the reaction of α-

Table 1. The first order rate constants (k), Arrhenius parameters and the apparent values of the entropies and free energies of activation of the reactions of cyclofenchene (I) and α-fenchene (II) in a formic acid-methylene chloride 1:1 mixture.

Compound	Temp. °C	$k \times 10^5$ sec^{-1}	E kcal/mol	log A	Corr. factor	ΔS^{*} [a] cal/degr. mol	ΔG^{*} [a] kcal/mol
I	0.	0.294					
	13.8	2.975					
	26.2	16.54	23.18 ± 1.62	13.06 ± 1.22	−0.9952		
	32.0	23.24					
	25.0	13.7 [b]				−0.726	22.81
	105					−1.20	22.88
II	0.	2.107					
	15.4	12.31	17.27 ± 0.58	9.15 ± 0.44	−0.9995		
	25.4	31.01					
	25.0	30.2 [b]				−18.62	22.23
	105					−19.10	23.74

[a] Calculated from E and log A according to the theory of absolute reaction rates.
[b] Interpolated from the experimental values at different temperatures.

fenchene (II) is electronically favored over the reaction of cyclofenchene (I), as is demonstrated by the lower energy of activation of II.[3] From the apparent entropies of activation it could be concluded that the transition state of the reaction of II has a definite structure, while conversely, the reaction of I proceeds *via* random collisions of protonated-I with surrounding (mainly solvent) molecules.

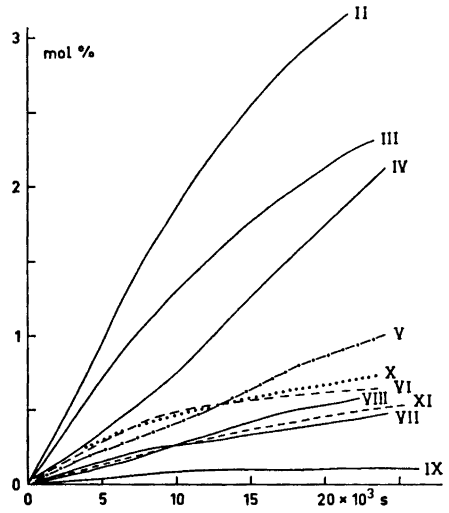

Fig. 1. Product composition (mol % of the sum I + products) in the reaction of cyclofenchene (I) in a formic acid-methylene chloride 1:1 mixture at 0°C. Notation as in the text.

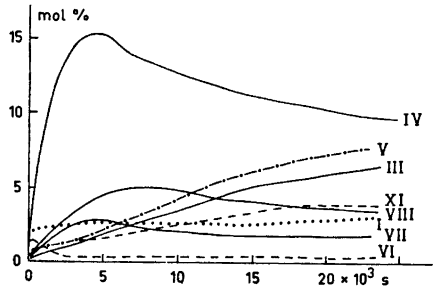

Fig. 2. Product composition (mol % of the sum II + products) in the reaction of α-fenchene (II) in a formic acid-methylene chloride 1:1 mixture at 0°C. Notation as in the text.

The product ratios (see Figs. 1 and 2) also show differences in the reactions of I and II. Exo-α-fenchene hydrate formate (IV) seems to be the only first intermediate product formed from α-fenchene (II). Cyclofenchene (I), however, appears to react *via* three main routes: α-fenchene (II), exo-β-fenchene hydrate formate (III) and exo-α-fenchene hydrate formate (IV) all appear to be direct reaction products from I. Tertiary endo-isomers of III and IV, endo-β-fenchene hydrate formate (VII) and endo-α-fenchene hydrate formate (VIII), appeared as the next intermediates, and the secondary exo-formates α-isofenchyl formate (V) and β-fenchyl formate (VI) as the final products on the main reaction routes. α-Fenchyl formate (IX), ε-fenchene (XI), β-fenchene (XII), and an unknown formate X appeared as minor side products of the reaction of cyclofenchene (I). Only ε-fenchene (XI) and cyclofenchene (I), however, were observed as side products in the reaction of α-fenchene (II) (see Fig. 2). The progress of the reactions of I and II can be presented as follows (most reverse reactions are unmarked; the main reactions are shown by solid arrows): Scheme 1.

The results of the product analysis show that no Wagner-Meerwein rearrangement occurs in the additions of formic acid to cyclofenchene (I) or α-fenchene (II) with the conditions employed. Such rearrangements are, however, involved in the formation of the final products V and VI from the adducts III and IV or their (Walden inversion products) epimers VII and VIII. This behavior is completely different from the reaction of nortricyclene, norbornene, and tricyclene under corresponding conditions, in which only secondary exo-products were formed.[1] In the present reactions, the final product ratio V:VI was 4:1, quite the same as the corresponding ratio of the final product acetates from the reaction of cyclofenchene (I) in Bertram-Walbaum solution (acetic acid containing a little 50 % sulfuric acid).[2,4,5]

Both kinetic and product ratio data indicate different reaction mechanims for the consumption of I and II, with no Wagner-Meerwein rearrangement occurring in the first phases. Thus, intermediate cation structures, if any, other than "asymmetrically bridged" (see Ref. 1), following the protonation of I or II, should be considered. The opening of the cyclopropane ring of cyclofenchene (I) to give III and IV can be considered as normal Markowni-

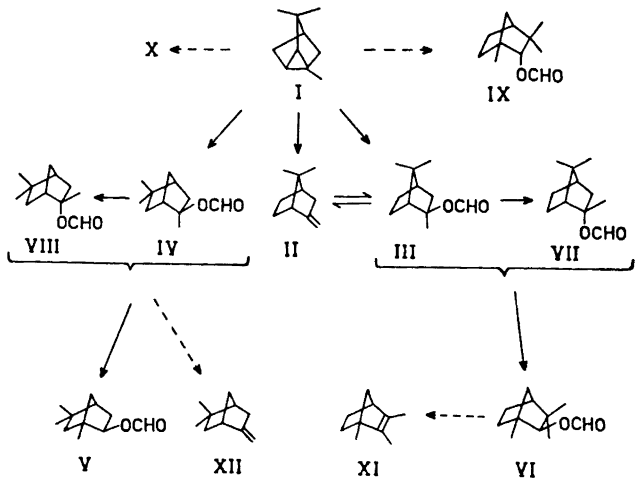

Scheme 1.

kov-addition reactions. Reasonable first structures formed from I might be the edge-protonated cyclopropanes,[6] "C-cyclofenchonium ions",[7] XIII and XIV. These ions closely resemble intermediate (S_N1 type) structures, which form the products II, III, and IV by random collisions with formic acid molecules through "disorganized transition states". Addition of formic acid to α-fenchene (II) seems to be more synchronous; perhaps an ion-pair transition state with a fixed structure is formed. The considerable exo-preference of the product (IV as sole or major product) gives some justification for a partially σ-bond-delocalised structure XV as the cation part of the transition state. This structure is analogous to the partially delocalised 2-methylnorbornonium ion (XVI), experimentally deduced by Paasivirta [8] and by Olah et al.[7,9,10]

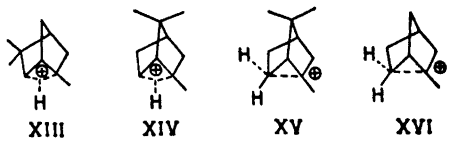

Acknowledgement. The authors are gratefu to Mrs. Tellervo Laasonen and Mr. Reijo Kauppinen for their skilful assistance with the experimental work which was financially supported by the *National Research Council for Sciences (Valtion Luonnontieteellinen Toimikunta).*

1. Paasivirta, J. *Acta Chem. Scand.* **27** (1973) 374.
2. Pulkkinen, E. *Ann. Acad. Sci. Fennicae Ser. A II* (1956) No. 72.
3. Laidler, K. J. *Chemical Kinetics*, McGraw, New York 1965, p. 238.
4. Toivonen, N. J. *Suomen Kemistilehti* **B 24** (1951) 62.
5. Hirsjärvi, P. and Hesso, A. *Unpublished results.*
6. Collins, C. J. *Chem. Rev.* **69** (1969) 543.
7. Olah, G. A. *J. Am. Chem. Soc.* **94** (1972) 808.
8. Paasivirta, J. *Ann.* **686** (1965) 1.
9. Olah, G. A., DeMember, J. R., Lui, C. Y. and White, A. M. *J. Am. Chem. Soc.* **91** (1969) 3958.
10. Olah, G. A. and White, A. M. *J. Am. Chem. Soc.* **91** (1969) 5801.

Received February 20, 1973.

Molecular Structure of Gaseous Succinic Anhydride Studied by Gas Electron Diffraction

K. BRENDHAUGEN, M. KOLDERUP FIKKE and H. M. SEIP

Department of Chemistry, University of Oslo, Oslo 3, Norway

Succinic anhydride has been shown by Ehrenberg[1] to have an essentially planar heavy atom skeleton in the crystal. We have now shown by electron diffraction that the same is probably true in the gas phase.

Diffraction diagrams of succinic anhydride were recorded with Balzers Eldigraph KDG2.[2,3] Four plates recorded with a nozzle-to-plate distance of 49.88 cm and five plates with a distance of 24.89 cm were used. The electron wavelength was in both cases 0.04941 Å and the nozzle temperature about 140°C. The data were treated in the usual way.[4] Intensity values covering the s-range 1.50 – 36.0 Å^{-1} were obtained, but the quality of the outer data was not satisfactory, and the final refinements were carried out with a composite intensity curve in the s-range 1.5 – 28.0 Å^{-1}.

Results and discussion. The parameters (r_a distances[5]) obtained by least-squares refinement using a diagonal weight matrix are given in Table 1. The Bastiansen-Morino shrinkage effect[5,6] was neglected and all the asymmetry constants assumed to be zero.[4,7] Because of many nearly equally long distances, it was difficult to refine all the bond distances in the ring, and C3 – C4 (*cf.* Fig. 1) was assumed to be

Table 1. Distances, angles and mean amplitudes of vibration obtained for succinic anhydride. Standard deviations applied to the last decimal place are given in parentheses. Mean amplitudes calculated from spectroscopic data and the results found by X-ray diffraction are also given.

	r_a (Å)	u (Å)	u_{calc} (Å)	X-ray results (Å)
C=O	1.190 (2)	0.035 (3)	0.039	1.19, 1.19 (1)
C–O	1.389 (3)	0.040	0.051	1.38, 1.37 (1)
C2–C3	1.510 (4)	0.043 (5)[d]	0.050	1.47, 1.48 (1)
C3–C4	1.535 [c]	0.043	0.050	1.51 (1)
C–H	1.118 (9)	0.077 [c]	0.078	
C2···C5	2.274 (7)	0.065	0.054	
O1···C3	2.383 (6)	0.067	0.056	
O1···O6	2.259 (5)	0.066 (4)[d]	0.057	
C2···C4	2.396 (3)	0.068	0.057	
C3···O7	2.425 (7)	0.071	0.060	
C3···O6	3.556 (5)	0.072 (6)[d]	0.062	
C2···O6	3.401 (5)	0.068	0.058	
O6···O7	4.467 (4)	0.086 (8)	0.063	
	Angles (degrees)			Angles (degrees)
∠C5O1C2	109.9 (5)			110.1
∠O1C2C3	110.5 (4)			110.2, 110.4
∠C2C3C4	103.8 (5)			105.2, 104.1
∠O1C2O7	122.1 (4)			119.6, 119.2
∠C3C2O7	127.8 (4)			130.3, 130.4
∠HCH	110.0 [c]			
α [a]	52.3 [e]			
ϕ [b]	4.1 (20)			

[a] Angle between the intersection of the planes through C2C3C4 and HCH and the C2 – C3 bond. [b] Torsional angle C5O1C2C3. [c] Assumed value. [d] The differences between the u values were assumed. [e] The parameter was not refined with the other parameters.

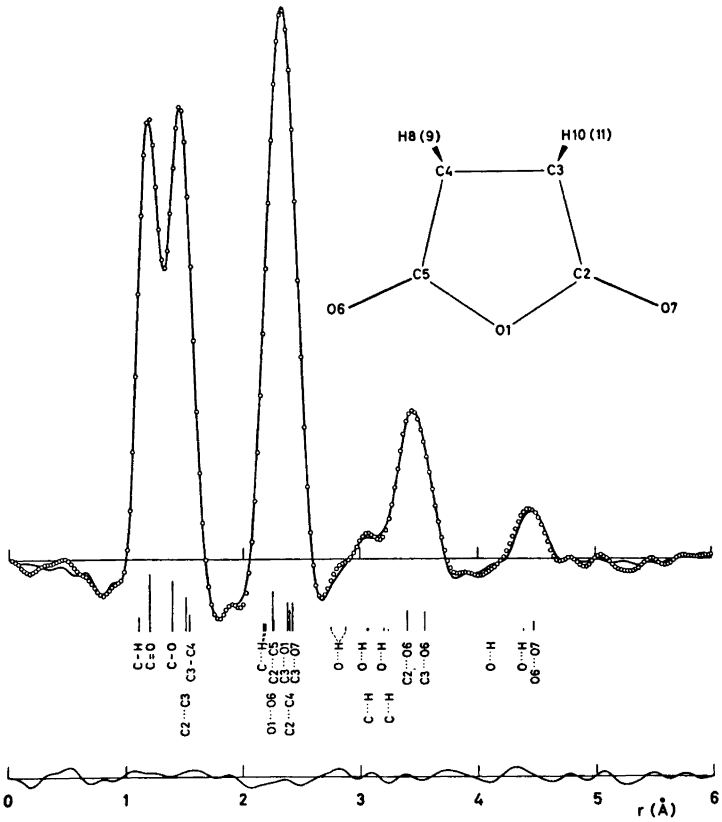

Fig. 1. Experimental (circles) and theoretical (full line) radial distribution curves calculated with an artificial damping constant $k = 0.002$ Å^2.[2] The differences between experimental and theoretical values are also shown. The positions and approximate areas of the peaks corresponding to all interatomic distances, except H···H, are indicated.

1.535 Å. The value found in the X-ray investigation, 1.51 Å, seems unreasonably small. The uncertainty (standard deviation of 0.01 Å) in this assumed value,[7] as well as the effect of correlation between the data,[8] has been estimated and included in the standard deviations in Table 1. Further assumptions made in the refinement are given in Table 1. The experimental and theoretical radial distribution curves [4] are compared in Fig. 1.

The deviation from planarity in the skeleton is given by the torsional angle, ϕ, about the O1 – C2 bond. This parameter refines to about 4°, but the standard deviation is so large (2.0°) that the value can only be regarded as a slight indication of a small distortion, or, more probable, of fairly large out-of-plane vibrations. It should be remembered that the shrinkage effect has been neglected since the force constants for out-of-plane motions are not known. This may lead to a small apparent deviation from planarity.

Table 1 shows that the bond distances found in the present investigation are somewhat longer than those obtained in the X-ray investigation except for the C = O bond, where the agreement is exact. The agreement in the bond angles is fairly good.

The mean amplitudes of vibration [6] (u), calculated by the method described by Stølevik *et al.*[9] using the force constants in Ref. 10, are included in Table 1. Because

of the rather limited s-range used in this investigation and the large number of nearly equal distances, the u-values are not very well determined by this electron-diffraction study. The conclusion drawn about the skeleton structure does not depend critically on the u-values as shown by carrying out a refinement keeping the mean amplitudes for all distances C2···C5 to C2···O6 in Table 1 equal to the values calculated from spectroscopic data (u_{calc}). The torsional angle refined then to $\phi = 4.8°$.

1. Ehrenberg, M. *Acta Cryst.* **19** (1966) 698.
2. Zeil, W., Haase, J. and Wegmann, L. *Z. Instrumentenk.* **74** (1966) 84.
3. Bastiansen, O., Graber, R. and Wegmann, L. *Balzers High Vacuum Report*, 1969, 1.
4. Andersen, B., Seip, H. M., Strand, T. G. and Stølevik, R. *Acta Chem. Scand.* **23** (1969) 3224.
5. Kuchitsu, K. and Cyvin, S. J. In Cyvin, S. J., Ed., *Molecular Structures and Vibrations*, Elsevier, Amsterdam 1972, Chapter 12.
6. Cyvin, S. J. *Molecular Vibrations and Mean Square Amplitudes*, Universitetsforlaget, Oslo, and Elsevier, Amsterdam 1968.
7. Seip, H. M. In Sim, G. A. and Sutton, L. E., Eds., *Molecular Structure by Diffraction Methods* (Specialist Periodical Reports), The Chemical Society, London 1973, Vol. 1, Part 1, Chapter 1.
8. Seip, H. M. and Stølevik, R. In Cyvin, S. J., Ed., *Molecular Structures and Vibrations*, Elsevier, Amsterdam 1972, Chapter 11.
9. Stølevik, R., Seip, H. M. and Cyvin, S. J. *Chem. Phys. Lett.* **15** (1972) 263.
10. diLauro, C., Califano, S. and Adembri, G. *J. Mol. Struct.* **2** (1968) 173.

Received February 13, 1973.

PMR Analysis of the *cis* and *trans* Isomers of 2-Chloro-4-methyl- and 2-Phenyl-4-methyl-1,3,2-dithiaphospholanes

KNUT BERGESEN and MALVIN BJORØY

Chemical Institute, University of Bergen, N-5000 Bergen, Norway

In the last two years the ring conformation of 1,3,2-dithiaphospholanes and 1,3,2-oxathiophospholanes have received some attention. The PMR spectra of 2-phenyl-[1,2] and 2-fluoro-1,3,2-dithiaphospholanes [3] have been completely analysed. The spin-system confirms the existence of pseudorotation with a pseudo-axial phenyl or fluor group. The PMR analysis of 2-chloro-, 2-phenyl-, and 2-phenoxy-1,3,2-oxathiaphospholanes [4] have shown that the five-membered oxathiaphospholane ring exists mainly in an equilibrium between two envelope conformations, with the carbon atom 5 out of the ring plane. This paper reports the PMR analysis of the *cis* and *trans* isomers of 2-chloro- and 2-phenyl-4-methyl-1,3,2-dithiaphospholanes, I and II.

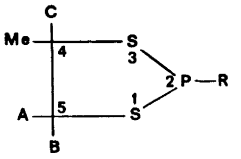

I: R = Cl.
II: R = Ph.

The PMR spectra of I and II show that there are two kinds of methyl groups in magnetically different environments in the ratio approx. 1:3. The reasonable interpretation of the spectra is that the two kinds of methyl groups are *cis* and *trans* to the substituent attached to the phosphorus atom.

The 100 MHz spectrum of I (Fig. 1) consists of three main regions ($\delta = 4.7$ to 4.3, 4.2 to 3.9, and 3.8 to 2.8). The low field band is due to the methine proton at carbon 4 of the *cis* and *trans* isomers and the band in the region 4.2 to 3.9 is assigned to one of the protons at carbon 5 of the *cis* isomer. The complex high field region

of the rather limited s-range used in this investigation and the large number of nearly equal distances, the u-values are not very well determined by this electron-diffraction study. The conclusion drawn about the skeleton structure does not depend critically on the u-values as shown by carrying out a refinement keeping the mean amplitudes for all distances C2···C5 to C2···O6 in Table 1 equal to the values calculated from spectroscopic data (u_{calc}). The torsional angle refined then to $\phi = 4.8°$.

1. Ehrenberg, M. *Acta Cryst.* **19** (1966) 698.
2. Zeil, W., Haase, J. and Wegmann, L. *Z. Instrumentenk.* **74** (1966) 84.
3. Bastiansen, O., Graber, R. and Wegmann, L. *Balzers High Vacuum Report*, 1969, 1.
4. Andersen, B., Seip, H. M., Strand, T. G. and Stølevik, R. *Acta Chem. Scand.* **23** (1969) 3224.
5. Kuchitsu, K. and Cyvin, S. J. In Cyvin, S. J., Ed., *Molecular Structures and Vibrations*, Elsevier, Amsterdam 1972, Chapter 12.
6. Cyvin, S. J. *Molecular Vibrations and Mean Square Amplitudes*, Universitetsforlaget, Oslo, and Elsevier, Amsterdam 1968.
7. Seip, H. M. In Sim, G. A. and Sutton, L. E., Eds., *Molecular Structure by Diffraction Methods* (Specialist Periodical Reports), The Chemical Society, London 1973, Vol. 1, Part 1, Chapter 1.
8. Seip, H. M. and Stølevik, R. In Cyvin, S. J., Ed., *Molecular Structures and Vibrations*, Elsevier, Amsterdam 1972, Chapter 11.
9. Stølevik, R., Seip, H. M. and Cyvin, S. J. *Chem. Phys. Lett.* **15** (1972) 263.
10. diLauro, C., Califano, S. and Adembri, G. *J. Mol. Struct.* **2** (1968) 173.

Received February 13, 1973.

PMR Analysis of the *cis* and *trans* Isomers of 2-Chloro-4-methyl- and 2-Phenyl-4-methyl-1,3,2-dithiaphospholanes

KNUT BERGESEN and MALVIN BJORØY

Chemical Institute, University of Bergen, N-5000 Bergen, Norway

In the last two years the ring conformation of 1,3,2-dithiaphospholanes and 1,3,2-oxathiophospholanes have received some attention. The PMR spectra of 2-phenyl-[1,2] and 2-fluoro-1,3,2-dithiaphospholanes [3] have been completely analysed. The spin-system confirms the existence of pseudorotation with a pseudo-axial phenyl or fluor group. The PMR analysis of 2-chloro-, 2-phenyl-, and 2-phenoxy-1,3,2-oxathiaphospholanes [4] have shown that the five-membered oxathiaphospholane ring exists mainly in an equilibrium between two envelope conformations, with the carbon atom 5 out of the ring plane. This paper reports the PMR analysis of the *cis* and *trans* isomers of 2-chloro- and 2-phenyl-4-methyl-1,3,2-dithiaphospholanes, I and II.

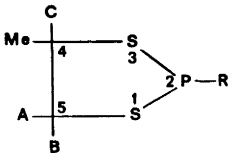

I: R = Cl.
II: R = Ph.

The PMR spectra of I and II show that there are two kinds of methyl groups in magnetically different environments in the ratio approx. 1:3. The reasonable interpretation of the spectra is that the two kinds of methyl groups are *cis* and *trans* to the substituent attached to the phosphorus atom.

The 100 MHz spectrum of I (Fig. 1) consists of three main regions ($\delta = 4.7$ to 4.3, 4.2 to 3.9, and 3.8 to 2.8). The low field band is due to the methine proton at carbon 4 of the *cis* and *trans* isomers and the band in the region 4.2 to 3.9 is assigned to one of the protons at carbon 5 of the *cis* isomer. The complex high field region

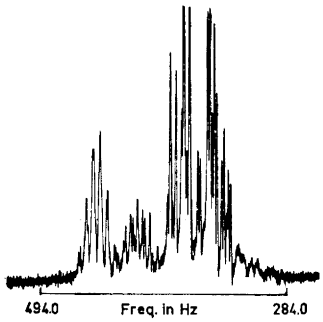

Fig. 1. 100 MHz PMR spectrum of 2-chloro-4-methyl-1,3,2-dithiaphospholane. The methyl group is not recorded.

of the spectrum is due to the two protons at carbon 5 of the *trans* isomer and one of the protons at carbon 5 of the *cis* isomer.

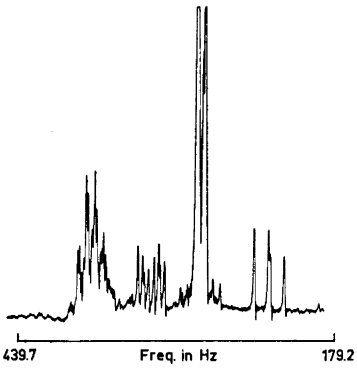

Fig. 2. 100 MHz PMR spectrum of 2-phenyl-4-methyl-1,3,2-dithiaphospholane. The phenyl group is not recorded.

The 100 MHz spectrum of II (Fig. 2) consists of four main regions ($\delta = 4.0$ to 3.5, 3.5 to 3.0, 2.8 to 2.6, and 2.4 to 2.1). The low field band is assigned to the methine proton at carbon 4 of the two isomers. One of the protons at carbon 5 of the *cis* isomer is found to resonance in the region 3.5 to 3.0, while the two protons at carbon 5 of the *trans* isomer resonance in the region 2.8 to 2.6. The high field band of the spectrum is due to one of the protons at carbon 5 of the *cis* isomer.

The detailed spectral analysis of the $CH_2-CH-CH_3$ protons was carried out successfully on the basis of an $ABCX_3P$ spin system for the *cis* and *trans* isomers of I and II, using the iterative computer program UEAITR.[5] The spectral parameters are listed in Table 1. The experimental and calculated spectra of some of the protons of the *cis* and *trans* isomers of II are shown in Figs. 3 and 4.

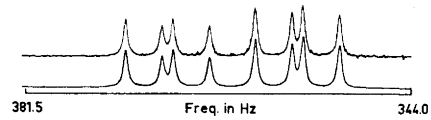

Fig. 3. 100 MHz PMR spectrum of the A proton in the *cis* isomer of 2-phenyl-4-methyl-1,3,2-dithiaphospholane. Upper: Observed spectrum. Lower: Calculated spectrum.

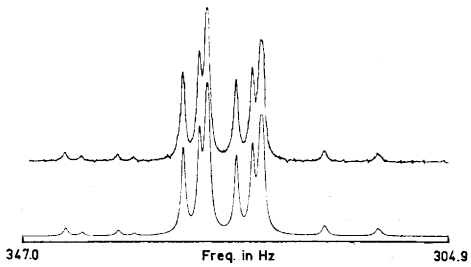

Fig. 4. 100 MHz PMR spectrum of the A and B protons in the *trans* isomer of 2-phenyl-4-methyl-1,3,2-dithiaphospholane. Upper: Observed spectrum. Lower: Calculated spectrum.

The succession of the chemical shifts for the methyl groups in the *cis* and *trans* isomers of I and II was found to be the reverse of that for the corresponding methine proton. It is believed that this effect must arise from the pseudo-axial position of the substituent attached to the phosphorus atom. The proton at carbon 5 which is *cis* to the methyl group, exhibits the same shielding as the axial protons at carbon 4 and 6 in 2-chloro-1,3,2-dioxaphosphorinane,[6] which are always found in the lower field as compared to the equatorial protons.

The magnitude of the geminal coupling constants in the isomers of I and II are in the expected range[1-3] (-11.0 to -12.5 Hz). These coupling constants are smaller (more negative) than those found in the 1,3,2-dioxaphospholanes.[7-8] This is ap-

Table 1. Chemical shifts and coupling constants for the *cis* and *trans* isomers of I and II.

Compound	Isomer	δCH_3	δA	δB	δC	Coupling constants, Hz							
						J_{AB}	J_{AC}	J_{AP}	J_{BC}	J_{BP}	J_{CP}	J_{CH_3-C-H}	$J_{P-S-C-CH_3}$
I	*cis*	1.66	4.07	3.44	4.45	−12.07	4.40	6.50	10.44	−1.94	1.00	6.73	0.00
	trans	1.43	3.69	3.39	4.41	−11.82	5.05	0.15	5.64	2.30	1.36	6.58	0.00
II	*cis*	1.35	3.17	2.26	3.63	−12.48	3.52	4.59	11.11	−0.77	0.99	6.52	0.00
	trans	1.19	2.83	2.76	3.65	−11.61	5.47	2.34	5.03	−0.49	1.74	6.71	0.00

parently due to a combination of (a) a reduced H−C−H angle and (b) a smaller electron withdrawal effect of sulfur as compared to oxygen. The *cis* and *trans* coupling constants in the *trans* isomer of I and II are very similar in magnitude (Table 1), which probably implies that pseudo-rotation interconverts the non-polar forms at rates that are large on the PMR time scale, but that inversion at phosphorus is slow. Dreiding stereomodels of the *trans* isomer of I and II indicate that the ring exists mainly in an equilibrium between envelope conformations A and B with carbon atom 4 out of the ring plane.

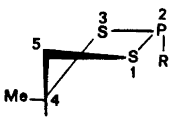

A

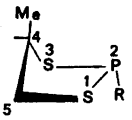

B

The large difference in the coupling constants between the *trans* and *cis* coupling in the *cis* isomer of I and II (Table 1) is probably due to a fixed conformation, C, with the carbon in position 4 out of the ring plane and with an equatorial position of both the methyl group and the substituent attached to the phosphorus atom.

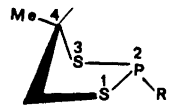

C

This is also in agreement with that found from Dreiding models. Further detailed studies and analysis of proton magnetic resonance of other ring-substituted 1,3,2-dithiaphospholanes are in progress in this laboratory.

Experimental. *2-Chloro-4-methyl-1,3,2-dithiaphospholane (I)* was prepared from 1,2-propandithiol and phosphorus trichloride in benzene solution using triethylamine as base, b.p.$_1$ 104°C.

2-Phenyl-4-methyl-1,3,2-dithiaphospholane (II) was prepared from 1,2-propandithiol and dichlorophenylphosphine in benzene solution using triethylamine as base, b.p.$_{0.2}$ 118°C.

The PMR spectra of I and II were measured as 50 % solution in $CDCl_3$. The spectra were recorded on a 60 MHz JEOL, C-60 H and a 100 MHz Varian HA-100 spectrometer. The samples were degassed by the usual freezing and thawing procedure using a vacuum line, and the tubes were sealed in vacuum. Line positions were taken by averaging the data from five spectra using a frequency counter. The counter is accurate to 0.1 Hz for a 10 sec count. The computations were carried out on an IBM 360/50 computer and the graphical output was obtained using a Calcomp Plotter. The final error observed was 0.1 when all parameters were allowed to vary. The probable errors in the coupling constants are 0.02−0.03 Hz.

1. Peake, S. C., Field, M., Smutzler, R., Harris, R. K., Nichols, J. M. and Rees, R. G. *J. Chem. Soc. Perkin Trans. 2* **1972** 380.
2. Bergesen, K., Bjorøy, M. and Gramstad, T. *Acta Chem. Scand.* **26** (1972) 3037.
3. Albrand, J. P., Cogne, A., Gagnaire, D., Martin, J., Robert, J. B. and Venier, J. *Org. Magn. Resonance* **3** (1971) 75.
4. Bergesen, K., Bjorøy, M. and Gramstad, T. *Acta Chem. Scand.* **26** (1972) 2532.
5. Johannessen, R. B., Ferretti, J. A. and Harris, R. K. *J. Magn. Resonance* **3** (1970) 84.
6. Bergesen, K. and Albriktsen, P. *Acta Chem. Scand.* **25** (1971) 2257.
7. Bergesen, K. and Vikane, T. *Acta Chem. Scand.* **26** (1972) 2153.
8. Haake, P., McNeal, J. P. and Goldsmith, E. S. *J. Am. Chem. Soc.* **90** (1968) 715.

Received January 19, 1973.

Pseudomonas Cytochrome *c* Peroxidase

IX. Molecular Weight of the Enzyme in Dodecyl Sulfate-Polyacrylamide Gel Electrophoresis

RITVA SOININEN, NILS ELLFOLK and NISSE KALKKINEN

Department of Biochemistry, University of Helsinki, SF-00170 Helsinki 17, Finland

Cytochrome *c* peroxidase has been purified from *Pseudomonas aeruginosa* in a homogeneous form.[1,2] Minimum molecular weights of 21 600 and 24 400 were calculated for the enzyme from its iron and heme *c* content, respectively.[3] A molecular weight of 53 500 was obtained on the basis of the sedimentation and diffusion coefficients determined on the analytical ultracentrifuge and the experimentally measured partial specific volume.[3] This value indicates that the enzyme contains two heme groups per molecule. The molecular weights calculated for two iron atoms and two heme groups are 43 200 and 48 800, respectively. Further studies were necessary to establish the molecular weight of the enzyme and to clarify whether it consists of one or two polypeptide chains. The enzyme was therefore studied by electrophoresis in polyacrylamide gel in the presence of the ionic detergent sodium dodecyl sulfate (SDS) which dissociates oligomeric proteins to protomers. Under these conditions, the electrophoretic mobilities of proteins are related to the molecular weight of the protomer polypeptide chain.[4]

Experimental. Pseudomonas cytochrome *c* peroxidase (PsCCP) was prepared from the acetone-dried cells of *P. aeruginosa* as previously described.[1,2] The preparation was homogeneous in disc electrophoresis (performed according to Maurer,[5] pH 8.6, 7 % gel; staining according to Weber and Osborne [4]). SDS-polyacrylamide gel electrophoresis was carried out in 10 % gel as described by Weber and Osborne.[4] When preparing the samples for SDS-electrophoresis, the protein solutions were heated at 100°C for 5 min before incubation and dialysis to prevent possible proteolysis during these steps.[6] Bovine serum albumin (Fraction V, Armour), ovalbumin (Grade V, Sigma), pepsine (crystallized, Sigma) and horse

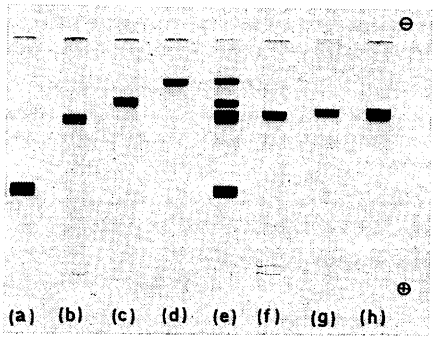

Fig. 1. SDS-polyacrylamide gel electrophoresis of *Pseudomonas* cytochrome *c* peroxidase and the molecular weight marker proteins in 10 % gel, according to Weber and Osborne.[4] (a) Horse heart cytochrome *c*, M.W. 12 400; (b) pepsin, M.W. 35 000; (c) ovalbumin, M.W. 45 000; (d) serum albumin, M.W. 67 000 (the marker proteins were treated with 1 % SDS and 1 % β-mercaptoethanol); (e) marker proteins *plus* PsCCP, treated with 1 % SDS and 1 % β-mercaptoethanol; (f) PsCCP, treated with 1 % SDS and 1 % β-mercaptoethanol; (g) PsCCP, treated with 1 % SDS; and (h) succinylated PsCCP, treated with 1 % SDS and 1 % β-mercaptoethanol.

1. Peake, S. C., Field, M., Smutzler, R., Harris, R. K., Nichols, J. M. and Rees, R. G. *J. Chem. Soc. Perkin Trans. 2* **1972** 380.
2. Bergesen, K., Bjorøy, M. and Gramstad, T. *Acta Chem. Scand.* **26** (1972) 3037.
3. Albrand, J. P., Cogne, A., Gagnaire, D., Martin, J., Robert, J. B. and Venier, J. *Org. Magn. Resonance* **3** (1971) 75.
4. Bergesen, K., Bjorøy, M. and Gramstad, T. *Acta Chem. Scand.* **26** (1972) 2532.
5. Johannessen, R. B., Ferretti, J. A. and Harris, R. K. *J. Magn. Resonance* **3** (1970) 84.
6. Bergesen, K. and Albriktsen, P. *Acta Chem. Scand.* **25** (1971) 2257.
7. Bergesen, K. and Vikane, T. *Acta Chem. Scand.* **26** (1972) 2153.
8. Haake, P., McNeal, J. P. and Goldsmith, E. S. *J. Am. Chem. Soc.* **90** (1968) 715.

Received January 19, 1973.

Pseudomonas Cytochrome *c* Peroxidase

IX. Molecular Weight of the Enzyme in Dodecyl Sulfate-Polyacrylamide Gel Electrophoresis

RITVA SOININEN, NILS ELLFOLK and NISSE KALKKINEN

Department of Biochemistry, University of Helsinki, SF-00170 Helsinki 17, Finland

Cytochrome *c* peroxidase has been purified from *Pseudomonas aeruginosa* in a homogeneous form.[1,2] Minimum molecular weights of 21 600 and 24 400 were calculated for the enzyme from its iron and heme *c* content, respectively.[3] A molecular weight of 53 500 was obtained on the basis of the sedimentation and diffusion coefficients determined on the analytical ultracentrifuge and the experimentally measured partial specific volume.[3] This value indicates that the enzyme contains two heme groups per molecule. The molecular weights calculated for two iron atoms and two heme groups are 43 200 and 48 800, respectively. Further studies were necessary to establish the molecular weight of the enzyme and to clarify whether it consists of one or two polypeptide chains. The enzyme was therefore studied by electrophoresis in polyacrylamide gel in the presence of the ionic detergent sodium dodecyl sulfate (SDS) which dissociates oligomeric proteins to protomers. Under these conditions, the electrophoretic mobilities of proteins are related to the molecular weight of the protomer polypeptide chain.[4]

Experimental. Pseudomonas cytochrome *c* peroxidase (PsCCP) was prepared from the acetone-dried cells of *P. aeruginosa* as previously described.[1,2] The preparation was homogeneous in disc electrophoresis (performed according to Maurer,[5] pH 8.6, 7 % gel; staining according to Weber and Osborne [4]). SDS-polyacrylamide gel electrophoresis was carried out in 10 % gel as described by Weber and Osborne.[4] When preparing the samples for SDS-electrophoresis, the protein solutions were heated at 100°C for 5 min before incubation and dialysis to prevent possible proteolysis during these steps.[6] Bovine serum albumin (Fraction V, Armour), ovalbumin (Grade V, Sigma), pepsine (crystallized, Sigma) and horse

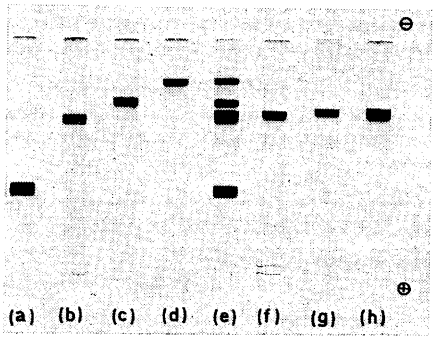

Fig. 1. SDS-polyacrylamide gel electrophoresis of *Pseudomonas* cytochrome *c* peroxidase and the molecular weight marker proteins in 10 % gel, according to Weber and Osborne.[4] (a) Horse heart cytochrome *c*, M.W. 12 400; (b) pepsin, M.W. 35 000; (c) ovalbumin, M.W. 45 000; (d) serum albumin, M.W. 67 000 (the marker proteins were treated with 1 % SDS and 1 % β-mercaptoethanol); (e) marker proteins *plus* PsCCP, treated with 1 % SDS and 1 % β-mercaptoethanol; (f) PsCCP, treated with 1 % SDS and 1 % β-mercaptoethanol; (g) PsCCP, treated with 1 % SDS; and (h) succinylated PsCCP, treated with 1 % SDS and 1 % β-mercaptoethanol.

heart cytochrome *c* (Type III, Sigma) were used as molecular weight markers. The gels were photographed according to the instructions of Oliver and Chalkley.[7] Succinylation of PsCCP with succinic anhydride was performed as described by Hass.[8]

Results and discussion. PsCCP was treated with SDS in the absence and presence of β-mercaptoethanol and studied by SDS-electrophoresis (Fig. 1). The relative mobility of PsCCP was found to be independent of the presence of β-mercaptoethanol, so indicating the protomer nature of PsCCP. Additional evidence for this was obtained by succinylation of PsCCP, another technique used for the dissociation of oligomeric proteins into their subunits.[8] Fig. 2 shows the quantitative succinylation

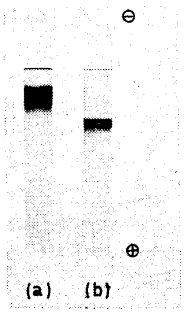

Fig. 2. Disc electrophoresis of (a) *Pseudomonas* cytochrome *c* peroxidase; and (b) succinylated *Pseudomonas* cytochrome *c* peroxidase in 7 % gel, pH 8.6, according to Maurer.[5] The gels were equal in length and diameter.

of PsCCP as studied by disc electrophoresis. The succinylated PsCCP was treated with SDS and β-mercaptoethanol and analyzed in SDS-electrophoresis (Fig. 1). It moved as a single band with an insignificantly lower relative mobility than the PsCCP of the previous experiments. An apparent mean molecular weight of 40 000 ± 1 500 for the polypeptide chain was obtained on the basis of its relative mobility and a standard curve drawn by plotting the logarithm of the known protomer weights of the marker proteins as a function of their respective relative mobilities (Fig. 3). The protomer molecular weight of PsCCP obtained by SDS-electrophoresis agrees

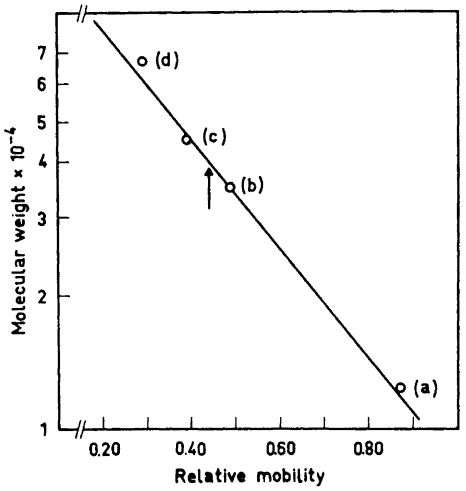

Fig. 3. Determination of the molecular weight of *Pseudomonas* cytochrome *c* peroxidase in SDS-electrophoresis according to Weber and Osborne.[4] The markers are the same as in Fig. 1. The arrow indicates the relative mobility of PsCCP. The extrapolated value for PsCCP is 40 000.

well with those calculated from the chemical analyses assuming the presence of two heme groups per molecule. This shows that the two heme groups are linked to a single polypeptide chain.

1. Ellfolk, N. and Soininen, R. *Acta Chem. Scand.* **24** (1970) 2126.
2. Soininen, R. *Acta Chem. Scand.* **26** (1972) 2535.
3. Ellfolk, N. and Soininen, R. *Acta Chem. Scand.* **25** (1971) 1535.
4. Weber, K. and Osborne, M. *J. Biol. Chem.* **244** (1969) 4406.
5. Maurer, H. R. *Disk-Elektrophorese*, Walter de Gruyter, Berlin 1968.
6. Pringle, J. R. *Biochem. Biophys. Res. Commun.* **39** (1970) 46.
7. Oliver, D. and Chalkley, R. *Anal. Biochem.* **44** (1971) 540.
8. Hass, L. F. *Biochemistry* **3** (1964) 535.

Received February 28, 1973.

Radiation Degradation of Crystalline D-Fructose and α-Lactose Monohydrate

TORBJÖRN GEJVALL and GÖRAN LÖFROTH

Radiobiology Department, University of Stockholm, Wallenberg Laboratory, S-104 05 Stockholm 50, Sweden

Crystalline D-fructose and α-lactose monohydrate are considerably more sensitive towards ionizing radiations than other studied carbohydrates.[1,2] Initial G-values of about 40 for D-fructose [1] and about 50 – 55 for α-lactose monohydrate [1,2] have been recorded. The method employed in the determination of the degradation includes, however, dissolution of the irradiated solid sample in water as a primary step, followed by isotope dilution and synthesis of a suitable derivative.[1,2] Hence, the measured breakdown may also comprise possible degradative reactions during the dissolution in water in addition to the effects already present in the solid state. We have now measured the degradation of D-fructose and α-lactose monohydrate irradiated in the solid state by a technique which may exclude dissolution in water.

Experimental. Pyridine was added to a weighed amount of the irradiated (or unirradiated) sample and to a weighed amount of a suitable internal standard (mannitol for fructose and trehalose for lactose). The trimethylsilyl derivatives were then prepared as described by Sweeley *et al.*[3] The pyridine solution of the derivatives was analyzed by gas chromatography on a Perkin Elmer F 11 with FID detection and a 1.4 m × 2.2 mm glass column packed with 2 % SE 30 on Chromosorb W 60 – 80 mesh. The column temperature was 165°C for the monosaccharide and 230°C for the disaccharide analysis. The amount of fructose and lactose in relation to the internal standards was determined by planimetry of the chromatograms.

This technique has certain limitations. The derivative synthesis and the gas chromatographic analysis introduce experimental errors of one or a few per cent, and these errors become amplified in the final result as the measured degradation is a difference between two large values. In the present case, it seems to us that the analyses of fructose were less variable than those of lactose; this might be due to the fact that fructose readily dissolves in the pyridine whereas lactose does not dissolve until after the silylating reagents have been added. Also, the possibility exists that some silyl derivative(s) of the degradation products may chromatograph within the fructose and lactose peaks, which would result in a degradation yield lower than the true value.

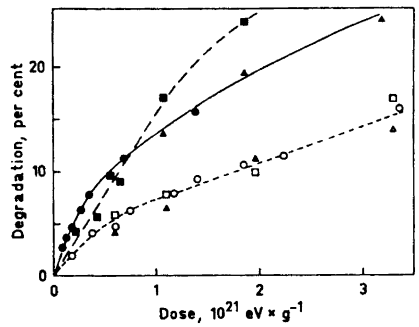

Fig. 1. γ-Radiation induced degradation yield *vs.* dose for crystalline D-fructose (open symbols) and α-lactose monohydrate (filled symbols): ○, ●, determined by ^{14}C-isotope dilution after dissolution in water (Ref. 1); △, ▲, determined by gas chromatography of the trimethylsilyl derivative prepared after dissolution in water and subsequent freeze-drying; □, ■, determined by gas chromatography of the trimethylsilyl derivative with pyridine as the only solvent for the samples.

In Fig. 1 the radiation induced degradation of D-fructose and α-lactose monohydrate, as determined by gas chromatography of the trimethylsilyl derivatives, is compared with the previously reported degradation, as determined by ^{14}C-isotope dilution. The gas chromatographic determination has been applied to samples directly after the irradiation as well as to samples which were first dissolved in water after the irradiation and then freeze-dried. The results for D-fructose show that the degradation is independent of the mode of dissolution and method of analysis. For α-lactose monohydrate the results are similar, although it is indicated that the degradation might be more linearly dependent on the dose when pyridine is the solvent than when water is the solvent. A

G-value of about 26 can be calculated from the assumed linear part of the degradation curve for pyridine as solvent. This is not significantly different from the average slope of the degradation curve for dissolution in water within the same dose interval, *i.e.* $0.3 \times 10^{21} - 10^{21}$ eV g^{-1}.

It therefore seems most likely that the dissolution in water is not a reason for the high radiation induced degradation of these crystalline carbohydrates but that the major part or all of the degradation is present already in the solid state. Ahmed *et al.*[2] have inferred a similar conclusion indirectly by means of spectroscopic studies of irradiated lactose samples.

Acknowledgement. This investigation has been supported by grants from the *Swedish Atomic Research Council* and by a stipend (to T.G.) from the *Hierta-Retzius Foundation.*

1. Löfroth, G. *Intern. J. Radiation Phys. Chem.* **4** (1972) 277.
2. Ahmed, N. U., Baugh, P. J. and Phillips, G. O. *J. Chem. Soc. Perkin Trans. 2* **1972** 1305.
3. Sweeley, C. C., Bentley, R., Makita, M. and Wells, W. W. *J. Am. Chem. Soc.* **85** (1963) 2497.

Received February 21, 1973.

Polychlorinated Biphenyls

IV.* Synthesis of 2,2′,3,3′,4,4′,5,6′-Octachlorobiphenyl-^{14}C from 3-Nitro-2,2′,3′,4,4′,5,6′-heptachlorobiphenyl-^{14}C and Tetrachloromethane**

GÖRAN SUNDSTRÖM

Wallenberglaboratoriet, Stockholms Universitet, Lilla Frescati, S-104 05 Stockholm, Sweden

As a part of an investigation concerning the distribution and metabolism in mice and quails of the industrial chemical and environmental pollutant PCB (polychlorinated biphenyls) [1-3] we recently reported the syntheses of some ^{14}C-labelled tetra- and hexachlorobiphenyls.[4,5] The simple syntheses of some unlabelled tetra- and pentachlorobiphenyls were also reported.[6]

The present paper describes the synthesis of 2,2′,3,3′,4,4′,5,6′-octachlorobiphenyl-^{14}C (II) labelled in the 2,3,4,6-substituted ring. Acetylation of aniline-^{14}C hydrogen sulphate followed by chlorination [5] gave 2,4,6-trichloroacetanilide-^{14}C [5] which was nitrated to give 3-nitro-2,4,6-trichloroacetanilide-^{14}C.[7] Hydrolysis of the anilide gave 3-nitro-2,4,6-trichloroaniline-^{14}C, which was coupled with 1,2,3,4-tetrachlorobenzene by the method of Cadogan [8] (*cf.* Refs. 5, 6) to yield 3-nitro-2,2′,3′,4,4′,5′,6-heptachlorobiphenyl-^{14}C (I). The nitroheptachlorobiphenyl I on treatment with tetrachloromethane at 280 – 290° for 70 min gave 2,2′,3,3′,4,4′,5,6′-octachlorobiphenyl-^{14}C (II) (isotope yield from I, 72 %).

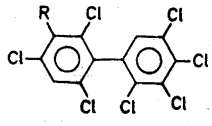

I: R = NO_2
II: R = Cl

The labelled compound was chromatographically identical (TLC, GLC) with 2,2′,3,3′,4,4′,5,6′-octachlorobiphenyl as

* Part III, Ref. 5.

** Presented in part at the PCB Conference II, Stockholm, Dec. 14, 1972.

G-value of about 26 can be calculated from the assumed linear part of the degradation curve for pyridine as solvent. This is not significantly different from the average slope of the degradation curve for dissolution in water within the same dose interval, *i.e.* $0.3 \times 10^{21} - 10^{21}$ eV g^{-1}.

It therefore seems most likely that the dissolution in water is not a reason for the high radiation induced degradation of these crystalline carbohydrates but that the major part or all of the degradation is present already in the solid state. Ahmed *et al.*[2] have inferred a similar conclusion indirectly by means of spectroscopic studies of irradiated lactose samples.

Acknowledgement. This investigation has been supported by grants from the *Swedish Atomic Research Council* and by a stipend (to T.G.) from the *Hierta-Retzius Foundation.*

1. Löfroth, G. *Intern. J. Radiation Phys. Chem.* **4** (1972) 277.
2. Ahmed, N. U., Baugh, P. J. and Phillips, G. O. *J. Chem. Soc. Perkin Trans. 2* **1972** 1305.
3. Sweeley, C. C., Bentley, R., Makita, M. and Wells, W. W. *J. Am. Chem. Soc.* **85** (1963) 2497.

Received February 21, 1973.

Polychlorinated Biphenyls

IV.* Synthesis of 2,2′,3,3′,4,4′,5,6′-Octachlorobiphenyl-^{14}C from 3-Nitro-2,2′,3′,4,4′,5,6′-heptachlorobiphenyl-^{14}C and Tetrachloromethane**

GÖRAN SUNDSTRÖM

Wallenberglaboratoriet, Stockholms Universitet, Lilla Frescati, S-104 05 Stockholm, Sweden

As a part of an investigation concerning the distribution and metabolism in mice and quails of the industrial chemical and environmental pollutant PCB (polychlorinated biphenyls) [1-3] we recently reported the syntheses of some ^{14}C-labelled tetra- and hexachlorobiphenyls.[4,5] The simple syntheses of some unlabelled tetra- and pentachlorobiphenyls were also reported.[6]

The present paper describes the synthesis of 2,2′,3,3′,4,4′,5,6′-octachlorobiphenyl-^{14}C (II) labelled in the 2,3,4,6-substituted ring. Acetylation of aniline-^{14}C hydrogen sulphate followed by chlorination [5] gave 2,4,6-trichloroacetanilide-^{14}C [5] which was nitrated to give 3-nitro-2,4,6-trichloroacetanilide-^{14}C.[7] Hydrolysis of the anilide gave 3-nitro-2,4,6-trichloroaniline-^{14}C, which was coupled with 1,2,3,4-tetrachlorobenzene by the method of Cadogan [8] (*cf.* Refs. 5, 6) to yield 3-nitro-2,2′,3′,4,4′,5′,6-heptachlorobiphenyl-^{14}C (I). The nitroheptachlorobiphenyl I on treatment with tetrachloromethane at 280 – 290° for 70 min gave 2,2′,3,3′,4,4′,5,6′-octachlorobiphenyl-^{14}C (II) (isotope yield from I, 72 %).

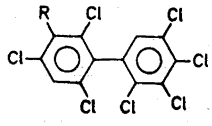

I: R = NO_2
II: R = Cl

The labelled compound was chromatographically identical (TLC, GLC) with 2,2′,3,3′,4,4′,5,6′-octachlorobiphenyl as

* Part III, Ref. 5.

** Presented in part at the PCB Conference II, Stockholm, Dec. 14, 1972.

prepared (a) from 2,3,4,6-tetrachloroaniline by a coupling with 1,2,3,4-tetrachlorobenzene according to Cadogan,[8] and (b) from 3-nitro-2,4,6-trichloroaniline by the above method. This compound is reported as a minor component of Aroclor 1260.[9]

The substitution of the nitro group of I for chlorine was achieved through the use of a reaction first described by Ponomarenko.[10–13] The reaction involves treatment of an aromatic nitro compound with a suitable aliphatic chlorine compound, *e.g.* tetrachloromethane, at temperatures around 250 – 300°. Hereby, substitution of nitro groups for chlorine occurs rapidly and in high yields, most probably through a radical displacement reaction.

This type of reaction constitutes a convenient alternative being used as a route to polychlorinated biphenyls of defined structure. The substitution of nitro groups for chlorine is usually carried out by reduction and a subsequent Sandmeyer reaction on the amine. However, yields are moderate, side reactions are often disturbing,[14] and moreover the Sandmeyer reaction is not easily handled on a micro scale.

The Ponomarenko reaction requires well defined conditions (time, temp.) to certify satisfactory yields. In the present case polymerisation reactions sometimes occurred. However, the use of a large excess of tetrachloromethane – in contrast to the molar ratio 1:1 as originally recommended – reduced the effects of these side reactions. Further chlorination of the expected product was also observed when too long reaction times were used.

Experimental. Conditions and equipment were those earlier described.[4–6]

Gas chromatography. The products were characterised by GLC using a Hewlett-Packard 7620A instrument fitted with an EC detector. Glass columns (0.20 × 160 cm) containing 4 % (w/w) SF 96 on Chromosorb W A/W DMCS (100 – 120 mesh) at 200° were used. The gas flow (nitrogen) was about 25 ml/min.

Thin layer chromatography. The reactions were followed by TLC on 0.1 mm layers of silica gel (Kieselgel HF_{254}, Merck) using chloroform, hexane-ethyl acetate (9:1), or hexane as solvent. Preparative TLC was performed on *ca.* 1 mm layers of the same adsorbent.

3-Nitro-2,4,6-trichloroacetanilide-^{14}C. 2,4,6-Trichloroacetanilide-^{14}C synthesised as described in Ref. 5 (2.05 mCi, 25 Ci/mol) was dissolved in sulphuric acid (95 – 97 %, 0.5 ml) at 0° and potassium nitrate (11.1 mg, 0.10 mmol) was added. The mixture was stirred for 1 h at 0°, diluted with ice water (5 ml) and extracted with chloroform (5 × 2 ml). The extracts were filtered through a column (0.8 × 2.5 cm) of magnesium sulphate. After evaporation of solvent the product was used in the next step without purification.

3-Nitro-2,4,6-trichloroaniline-^{14}C. To the above 3-nitro-2,4,6-trichloroacetanilide-^{14}C was added hydrochloric acid (12 M, 1 ml) and acetic acid (0.5 ml) and the mixture was stirred for 3 h at 100°. The acids were evaporated in a vacuum desiccator over sodium hydroxide and silica gel to give crude 3-nitro-2,4,6-trichloroaniline-^{14}C which was used in the following reaction.

3-Nitro-2,2′,3′,4,4′,5′,6-heptachlorobiphenyl-^{14}C. 1,2,3,4-Tetrachlorobenzene (Fluka, m.p. 47° (EtOH), 1.5 g) was added to the 3-nitro-2,4,6-trichloroaniline-^{14}C and the mixture was heated to 70°. Isoamyl nitrite (Riedel-de Haën, pure DAB. 6., 0.1 ml) was added with stirring which was continued for 1 h at 70°. The temperature was then raised to 100° and another portion of isoamyl nitrite (0.05 ml) was added. After 1.5 h at 100° excess tetrachlorobenzene was evaporated *in vacuo* and collected in a cold trap (*cf.* Ref. 5). Activity measurements indicated the presence of a low boiling by-product (0.93 mCi) in the trap, probably 2,4,6-trichloronitrobenzene-^{14}C (TLC). The residue, containing some tetrachlorobenzene, was dissolved in a small amount of chloroform-hexane (1:1) and added to a column (0.8 × 1 cm) of neutral alumina (Merck, activity grade I) which was irrigated with hexane-ethyl acetate (9:1). The eluate was collected on preparative TLC plates (20 × 20 cm) which were eluted twice with hexane-ethyl acetate (9:1). The desired zones were collected and eluted with chloroform. Evaporation of solvent gave 3-nitro-2,2′,3′,4,4′,5′,6-heptachlorobiphenyl-^{14}C, 0.32 mCi, 16 %, as crystals free from 2,4,6-trichloronitrobenzene-^{14}C (TLC).

2,2′,3,3′,4,4′,5,6′-Octachlorobiphenyl-^{14}C. The nitrobiphenyl was transferred to an ampoule (Pyrex glass, volume 2.3 ml) with the aid of carbon tetrachloride (Riedel-de Haën, A.R.). The amount of carbon tetrachloride was adjusted to *ca.* 0.5 ml and the ampoule, placed in a steel autoclave, was heated at 280 – 290° for 70 min in an electric oven. After cooling the solvent was evaporated and the residue dissolved in hexane and added to a column of neutral alumina (0.5 × 1 cm). Elution with 10 ml hexane and evaporation of solvent gave 2,2′,3,3′,4,4′,5,6′-octachlorobiphenyl-^{14}C, 0.23 mCi, as a slowly crystallising oil, overall yield from acetanilide-^{14}C 7.5 %.

Elution of the column with hexane-ethyl acetate (4:1, 10 ml) gave some starting material, 0.02 mCi.

2,3,4,6-Tetrachloroaniline. *m*-Chloroaniline, dissolved in carbon tetrachloride, was chlorinated at *ca.* −30° as described for the synthesis of pentachloroaniline.[15] Yield *ca.* 35 %, m.p. 88−90° (aq. EtOH) (m.p. lit.[16] 88°).

3-Nitro-2,2′,3′,4,4′,5′,6-heptachlorobiphenyl. 3-Nitro-2,4,6-trichloroaniline [7] (*cf.* above) (0.72 g, 3 mmol) and 1,2,3,4-tetrachlorobenzene (5 g) were heated to 70° and isoamyl nitrite (0.6 ml) was added with stirring. After 1 h the temperature was raised to *ca.* 100° and another portion of isoamyl nitrite (0.25 ml) was added. Stirring was continued for 1.5 h whereafter excess tetrachlorobenzene was removed *in vacuo*. The residue was dissolved in chloroform-hexane (1:1, 4 ml) and filtered through a column (2 × 15 cm) of neutral alumina (*cf.* above) which was eluted with hexane-ethyl acetate (9:1). Crystallisation from ethanol gave 3-nitro-2,2′,3′,4,4′,5′,6-heptachlorobiphenyl (0.2 g), m.p. 160−161° (Found: C 32.9; H 0.6; N 3.3; M^+ 437 (7 Cl). $C_{12}H_2Cl_7NO_2$ (440.3) requires C 32.7; H 0.5; N 3.2). λ_{max} (EtOH) 285 nm (ε=1,120), 294 nm (ε=1,100).

GLC as described above showed a retention time of 16.1 min for this compound.

2,2′,3,3′,4,4′,5,6′-Octachlorobiphenyl. (a) The compound was synthesised from 2,3,4,6-tetrachloroaniline and 1,2,3,4-tetrachlorobenzene by the same procedure as the above nitrobiphenyl. Purification on an alumina column which was eluted with hexane, crystallisation from ethanol and sublimation *in vacuo* gave 2,2′,3,3′,4,4′,5,6′-octachlorobiphenyl (0.12 g), m.p. 126−128° (Found: C 33.6; H 0.6; M^+ 426 (8 Cl). $C_{12}H_2Cl_8$ (429.8) requires C 33.5; H 0.5). λ_{max} (EtOH) 285 nm (ε=960), 294 nm (ε=930).

GLC as above showed a retention time of 12.8 min for the octachlorobiphenyl.

(b) The octachlorobiphenyl was also synthesised by the same route as the labelled compound. 3-Nitro-2,2′,3′,4,4′,5′,6-heptachlorobiphenyl (30 mg) and carbon tetrachloride (0.5 ml) were heated in an ampoule (Pyrex glass, volume 2.2 ml) at 280−290° for 80 min. Purification of product was performed as described for the labelled compound and gave 2,2′,3,3′,4,4′,5,6′-octachlorobiphenyl (28 mg), indistinguishable from the biphenyl synthesised by the method (a) above (GLC, TLC, m.p., mixed m.p.).

Acknowledgement. I am indebted to Dr. C. A. Wachtmeister for his interest and advice. The skilful assistance of Fil.kand. Maria Moron is gratefully acknowledged. Financial support was given by the *Research Committee of the Swedish Environmental Protection Board.*

1. Melvås, B. and Brandt, J. *PCB Conference II, National Swedish Environmental Protection Board Publications, 1972:* 17 E, p. 87.
2. Arrhenius, E. and Beije, B. *To be published.*
3. Berlin, M. and Gage, J. C. *To be published.*
4. Moron, M., Sundström, G. and Wachtmeister, C. A. *Acta Chem. Scand.* **26** (1972) 830.
5. Sundström, G. and Wachtmeister, C. A. *Acta Chem. Scand.* **26** (1972) 3816.
6. Sundström, G. *Acta Chem. Scand.* **27** (1973) 600.
7. Berckmanns, V. S. F. and Holleman, A. F. *Rec. Trav. Chim.* **44** (1925) 851.
8. Cadogan, J. I. G. *J. Chem. Soc.* **1962** 4257.
9. Sissons, D. and Welti, D. *J. Chromatog.* **60** (1971) 15.
10. Ponomarenko, A. A. *Zh. Obshch. Khim.* **32** (1962) 4029. (*Chem. Abstr.* **58** (1963) 13744d.)
11. Ponomarenko, A. A. *Zh. Obshch. Khim.* **32** (1962) 4035. (*Chem. Abstr.* **58** (1963) 13744g.)
12. Ponomarenko, A. A. and Tsybina, N. A. *Zh. Obshch. Khim.* **32** (1962) 4038. (*Chem. Abstr.* **58** (1963) 13774g.)
13. Ponomarenko, A. A. *Dopov. Akad. Nauk Ukr. RSR* **1963** 787. (*Chem. Abstr.* **59** (1963) 12665h.)
14. Ayres, D. C. *Nature* **240** (1972) 161.
15. Goldschmidt, S. and Strohmenzer, L. *Ber.* **55** (1922) 2450.
16. Beilstein, F. and Kurbatow, A. *Ann.* **196** (1879) 214.

Received March 13, 1973.

A Synthesis of the Indano-[1,2-b]aziridine System

PER EGIL HANSEN and
KJELL UNDHEIM

Department of Chemistry, University of Oslo, Oslo 3, Norway

Recently we have reported a synthesis of 1-benzyl-indano[1,2-b]aziridin-6-one (*4b*) for comparison of properties with those of its valence isomeric isoquinolinium-4-oxide.[1] For further studies we required a more convenient synthetic approach to the indano[1,2-b]aziridin-6-one system and a such synthesis is reported in this paper. The key intermediate in the synthesis is an indano[2,1-d]triazoline such as (3) in the scheme below as it is well established that Δ^2-1,2,3-triazolines can be converted photochemically or pyrolytically to aziridines.[2]

This approach requires easy access to indenone (*2*). The older syntheses were deemed less suitable [3-5] while the recent synthesis [6] by reductive acetylation of indane-1,3-dione followed by sodium carbonate treatment proved difficult in larger scale preparations. Slight modifications [1] in the reported [7] procedure for free radical bromination of indanone, however, made 3-bromoindanone (*1*) readily available and therefore suitable as a starting material. HBr elimination from (*1*) was achieved by means of trimethylamine. The use of a tertiary amine prevents Michael addition to the indenone formed, and the relatively low basicity does not initiate polymerisation of the highly reactive indenone molecule. By this procedure (*2*) was obtained in 55 % overall yield from indanone.

Formation of the indano[2,1-d]triazoline (*3*) was thought difficult because of the polymerisation tendency of the indenone molecule. Running the reaction between (*2*) and phenylazide at 0°C in the dark for 3 days, however, gave preparatively a homogeneous product (TLC) with expected spectral properties. Aryl azides react with dipolarophiles according to a concerted 1,3-dipolar cycloaddition mechanism [2,8,9] and a *cis*-adduct is therefore formed from indenone. With unsymmetrically substituted electrophilic double bonds the cycloaddition is regioselective giving a product in agreement with the orientation based on electronic effects [8,10] but a *gem*-substituent to the electron withdrawing group might upset the regioselectivity.[8,11] In the absence of a such *gem*-substituent addition of aryl azides to simple α,β-unsaturated carbonyl compounds and nitriles gives a Δ^2-1,2,3-triazoline which carries the electron withdrawing group in the 4-position.[8,10,11] By analogy the product from indenone is assigned structure (*3*). Triazolines containing an electron withdrawing group in the 4-position are frequently unstable or exist in an equilibrium with the isomeric amino-azo compound.[8,10,11] No such difficulties were experienced from the indenone adduct.

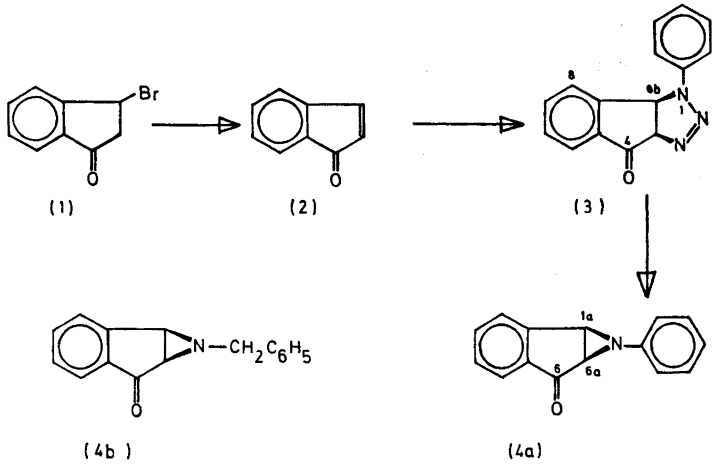

Scheme 1.

Photolysis of (*3*) gave preparatively a homogeneous product with spectral properties in accordance with the desired aziridine. For the photochemical transformation the cold reaction flask was externally illuminated by a 300 watt lamp. Pyrolysis of (*3*) in boiling xylene gave a more heterogeneous product.

The mass spectrum shows characteristic features as reported for (*4b*). The alicyclic indanyl protons in NMR ($CDCl_3$) appear as doublets at 6.62 and 6.09 τ ($J = 3.5$ Hz), the values being similar to those of (*4b*). The lower field signal is a broadened doublet which means that this proton is involved in long-range interannular coupling ($J < 0.5$ Hz) with an aromatic indanyl proton.[12] In the triazoline (*3*) a corresponding broadened doublet is seen at 4.28 τ, the other methine doublet being at 4.54 τ ($J = 9.7$ Hz). The broadened doublets are therefore ascribed to the alicyclic indanyl protons in β-position to the carbonyl group. Since the triazoline (*3*) is thermally unstable its mass spectrum was found to be similar to that of (*4a*).

Experimental. The NMR spectra were recorded on a Varian A-60A spectrophotometer.

Indenone (2). Indanone (10.6 g, 0.08 mol) was brominated by means of *N*-bromosuccinimide as previously described[1] and the crude product dissolved in ether (100 ml). Trimethylamine (11.8 g, 0.20 mol) was added dropwise to the stirred ethereal bromoindanone solution at 0°C. After about 2 h at 0°C the precipitated salt was filtered off, the filtrate evaporated and the residual oil distilled; yield 5.7 g (55 %), b.p. 40–42°C/0.1 mmHg. (Lit.[6] b.p. 61–63°C/0.9 mmHg.)

1-Phenylindano[2,1-d]triazolin-4-one (3). Indenone (2.6 g, 0.02 mol) and phenylazide[13] (2.4 g, 0.02 mol) were mixed and left at 0°C in the dark for 3 days. The original liquid solution had then solidified. The solid was crystallized from chloroform; yield 3.5 g (70 %), m.p. 132°C (decomp.). (Found: C 72.51; H 4.80. Calc. for $C_{15}H_{11}N_3O$: C 72.13; H 4.44.) NMR ($CDCl_3$): 4.54 τ ($H^{3a}(H\alpha)$, d., $J = 9.7$ Hz), 4.28 τ ($H^{3b}(H\beta)$, broadened d.), 2.1–2.8 τ (H-arom., m.). IR (KBr) 1725 cm^{-1} (CO).

1-Phenylindano[1,2-b]aziridin-6-one (4a). *Photolysis:* The triazoline (*3*) (0.9 g, 0.0036 mol) was dissolved in benzene (50 ml) and the solution water-cooled by means of a "cold-finger" immersed in the solution during the illumination. The light source was a 300 watt Philips HP 3202 UV lamp which was placed about 10 cm away from the reaction flask. The illumination was stopped when the evolution of nitrogen had almost ceased (3/4–1 h). The solution was then evaporated at reduced pressure without heating. The residual oil was crystallized from hexane; yield 0.5 g (65 %), m.p. 92°C. (Found: C 81.65; H 5.02. Calc. for $C_{15}H_{11}NO$: C 81.43; H 5.01.) NMR ($CDCl_3$): 6.62 τ ($H^{6a}(H\alpha)$, d, $J = 3.5$ Hz), 6.09 τ ($H^{1a}(H\beta)$, broadened d.), 2.4–3.4 τ (H-arom., m.). IR (Br) 1725 cm^{-1} (CO).

Pyrolysis: Pyrolysis of (*3*) in refluxing xylene gave a heterogeneous product from which (*4a*) was isolated after silica gel column chromatography. The title compound was eluated with hexane:EtOAc (2:1).

1. Undheim, K. and Hansen, P. E. *Chemica Scripta* **3** (1973) 113.
2. Scheiner, P. In Thyagarajan, B. S., Ed., *Selective Organic Transformations*, Wiley-Interscience, New York 1970, Vol. 1, p. 327.
3. Stoermer, R. and Asbrand, E. *Ber.* **64** (1931) 2796.
4. Hock, H. and Ernst, F. *Chem. Ber.* **92** (1959) 2723.
5. Marvel, C. S. and Hinman, C. W. *J. Am. Chem. Soc.* **76** (1954) 5435.
6. Lacy, P. H. and Smith, D. C. C. *J. Chem. Soc.* **1971** 41.
7. Treibs, W. and Schroth, W. *Ann.* **639** (1961) 204.
8. Huisgen, R., Szeimies, G. and Möbius, L. *Chem. Ber.* **99** (1966) 475.
9. Huisgen, R. *J. Org. Chem.* **93** (1968) 2291.
10. Texier, F. and Carrié, R. *Bull. Soc. Chim. France* **1971** 4119.
11. Broeckx, W., Overbergh, N., Samyn, C., Smets, G. and L'abbé, G. *Tetrahedron* **27** (1971) 3527.
12. Lustig, E. and Ragelis, E. P. *J. Org. Chem.* **32** (1967) 1398.
13. Lindsay, R. O. and Allen, C. F. H. *Org. Syn. Coll. Vol.* **3** (1955) 710.

Received February 16, 1973.

ACTA CHEMICA SCANDINAVICA 27 (1973) 1115–1129

Exploratory Calculations of Medium and Large Rings

Part 1. Conformational Minima of Cycloalkanes

JOHANNES DALE

Kjemisk Institutt, Universitetet i Oslo, Oslo 3, Norway

A novel approach to the semiquantitative calculation of the conformational energy of C_9-C_{16} cycloalkanes is based on simple summation of the energy in all CC-bonds, as read off from their dihedral angles on the complete potential curve for internal rotation about the central bond in butane. All 1,2-, 1,3- and 1,4-hydrogen interactions are thereby included. Valency angles are kept constant and such strain neglected. The selection of conformations is based on a scheme for joining together three, four, or five straight-chain side-units; even-membered rings have quadrangular conformations, odd-membered the more strained triangular and quinquangular conformations.

Computer calculations of cycloalkane conformations by minimization of both valency-angle strain, torsional strain and non-bonded interactions have been carried out systematically only for rings up to and including cyclononane.[1–4] For ten-, eleven-, and twelve-membered rings a few sporadic calculations [1–4] have been reported. For higher cycloalkanes no attempts seem to have been made, but a qualitative analysis [5] led to the conclusion that for C_{14} as well as for C_{16} a single strainfree diamond-lattice conformation is possible, whereas odd-membered rings have none. However, nothing at all is known about which conformations odd-membered rings above C_9 adopt, or what is the nature of the other conformations of cyclohexadecane known [6] to be present above its solid-solid transition temperature.

The methods used to calculate conformations of normal and medium rings have the general limitation of increasing complexity as ring size increases, and no satisfactory systematic method for selecting the types of conformations to be tested has been proposed. Thus, only conformations with symmetry elements are handled by Hendrickson's method,[1] and in the steepest-descent method of Wiberg [2] and of Bixon and Lifson [3] further and lower minima may not be detected and false minima may appear.

In the same way as variation of bond length is energetically expensive and produces small geometric changes and therefore has been neglected in those calculations, it seemed justified in large rings to neglect also valency-

angle deformation, since this is more expensive and produces much smaller changes than variation of torsional angles. Furthermore, if instead of using the ethane torsional potential, the complete potential curve for internal rotation about the central bond in butane is applied, this will automatically take care also of non-bonded interactions between hydrogens in 1,2-, 1,3-, and 1,4-relationship. (Of course, such a procedure cannot be used for normal rings where the 1- and 4-carbon atoms are not repelled at short distances, but linked by one or a few bonds.) Other hydrogen interactions (1,5- and higher) can usually be avoided by adjusting the conformation so that these hydrogen distances are kept above a minimum value. This limit was chosen as short as 1.8 Å since the Fieser-Dreiding molecular models [7] used to construct the conformations and obtain dihedral angles, have tetrahedral valency angles instead of a more realistic value of 112°. Conformations which cannot be physically constructed without shorter H – H distances are rejected, except in medium rings; their calculated energies are therefore obviously too low. It should be noted that computer calculations on medium rings, especially those of Bixon and Lifson,[3] reveal that a substantial part of the strain is in fact torsional strain, and that similar total energies and geometries result from rather different distributions of the strain on valency-angle strain, torsional strain and non-bonded interaction. This suggests that a considerable part of the non-bonded interactions can be traded into torsional strain by small adjustments of dihedral angles and justifies the simplified procedure used here for the larger rings.

CONSTRUCTION OF POTENTIAL CURVE FOR BUTANE

The enthalpy difference between *anti* and *gauche* butane has been determined by several experimental methods, and the chosen value of 0.8 kcal/mol is also in agreement with theoretical values.[8,9] The dihedral angle for the *gauche* minimum was placed at 65°, close to the electron-diffraction value [10] of 67.5°, while theoretical values [8,9] are around 70°. Good experimental values for the barriers have only recently become available. Ultrasonic relaxation of butane [11] gives a barrier height between *anti* and *gauche* of 3.8 kcal/mol in enthalpy terms, and a relaxation value for methylbutane,[11] involving the passage of two methyl groups past each other, allows the adoption of an enthalpy value of 6.9 kcal/mol for the *syn*-barrier in butane. Both values are in surprisingly good agreement with recent *ab initio* calculations.[8,9]

These points are then connected with sine-shaped curves (Fig. 1). For the present exploratory calculations on mechanical models, with dihedral angles manually adjusted to minimize the energy, it was considered unrealistic to read off angles to an accuracy better than a couple of degrees. Only values for every five degrees were therefore taken from this curve and tabulated for ready use in the calculation.

SELECTION OF CONFORMATIONAL CANDIDATES

In large rings there is sufficient freedom of choice that the best conformations have only relatively staggered bonds, and as many as possible are *anti*. For rings to be formed, a certain number of *gauche* bonds must be accepted,

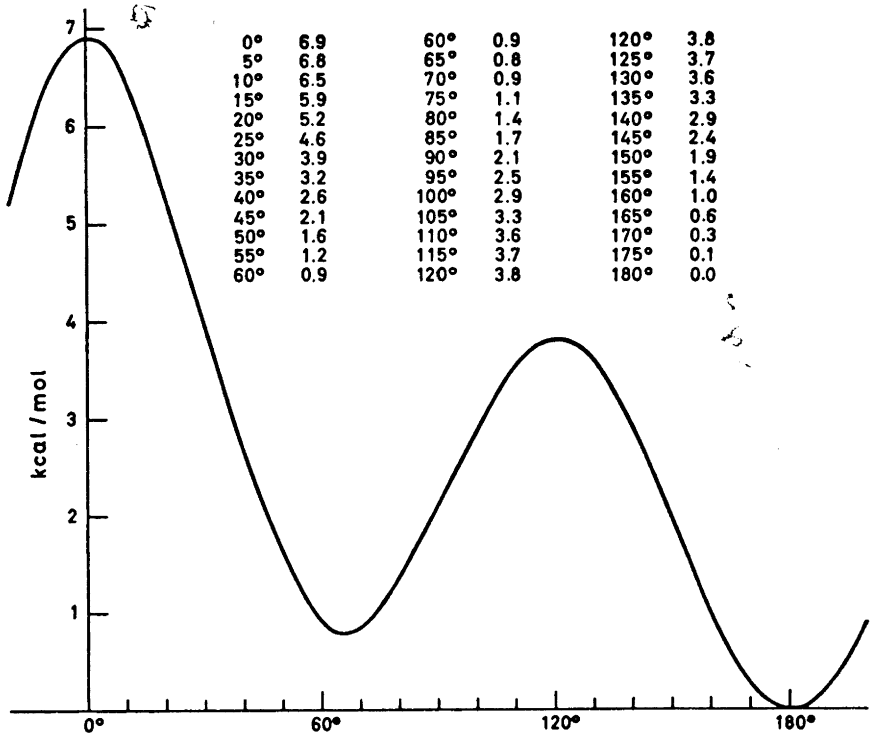

Fig. 1. Potential energy curve for butane.

and the problem is to find the smallest possible number and the best distribution as regards relative position and sign of their dihedral angles.* In Fig. 2 are shown the various possibilities when one or a sequence of *gauche* bonds are in an *anti* environment. A "wedge" representation of the CC-bond is introduced already here, since it had to be used for top-view perspective drawings of the larger rings; such drawings were found much more convenient than the familiar side-view perspective drawings. As an illustration, top-view representations of the diamond-lattice conformations of C_6-, C_8-, and C_{10}-rings are included in Fig. 2, a-c.

An isolated *gauche* bond (Fig. 2d) is defined as "allowed", since it has only the strain of one *gauche*-butane interaction. This arrangement is not very efficient for chain bending and becomes of interest only for rings larger than the 16-membered; it can in fact be used six times with alternating sign to produce one of the diamond-lattice conformations of cyclooctadecane.[5]

A sequence of two *gauche* bonds of the same sign (Fig. 2e) is also allowed; in fact, the two sets of 1,4-hydrogen interactions are essentially unperturbed

* Looking along the axis of a bond, a + sign means clockwise rotation of the rear ring-bond away from the front ring-bond, a − sign counterclockwise.

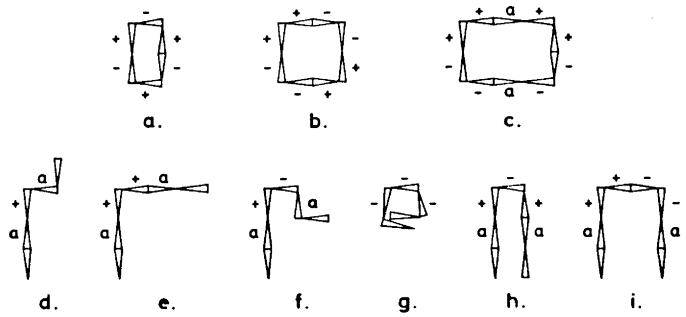

Fig. 2. "Wedge" representation for the CC-bond in some carbon ring skeletons (a – c) and some folded open chains (d – i). a = *anti*, + = + *gauche*, – = – *gauche*.

by one another.[12] This sequence is efficient for chain bending and is used four times in unstrained diamond-lattice conformations of large rings as well as in the established conformation of cyclododecane.

A sequence of two *gauche* bonds of opposite sign (Fig. 2f) is excluded by a prohibitively large steric interaction in open chains [12] (the so-called 1,5-pentane interaction). It is little efficient for ring formation and therefore not even encountered in medium rings.

A sequence of three (or more) *gauche* bonds of equal sign (Fig. 2g) is allowed, as there will be no interactions more serious than 1,4-*gauche*; however, only a helix-structure will result.

A sequence of three *gauche* bonds of alternating sign (Fig. 2h) leads in principle to a formidable steric conflict (1,6-hexane interaction). A systematic deviation from 60° dihedral angles may nevertheless relieve the interaction sufficiently to allow the acceptance of this element in the inherently strained medium rings and odd-membered large rings, since this double chain-bend is particularly efficient for ring formation.

A sequence of four *gauche* bonds is of interest only when two equal signs are followed by two equal opposite signs (Fig. 2i). This is actually nothing else than a combination of two chain bends of the allowed type (e), but involves a considerable strain (1,5- and 1,7-interactions). Again, a systematic deviation from 60° dihedral angles may relieve much strain so that this element may become of interest even for odd-membered larger rings; for medium rings it is an indispensable element.

It is easy to show that the best chain-bend element (+ *gauche*, + *gauche* or – *gauche*, – *gauche*) is perfectly suited to join together, at right angles in a projection on the main molecular plane, four side-units, each consisting of straight all-*anti*-chains, to give diamond-lattice conformations of rectangular or square shape. Also less regular conformations can be formed in this way, but only for even-membered rings. This general type of conformation will here be called "quadrangular". If the ring is to remain even-membered, there can be only four types of quadrangular conformations (Fig. 3): all four sides contain an odd number of bonds; two adjacent or opposite sides are odd and the others even; or all sides are even.

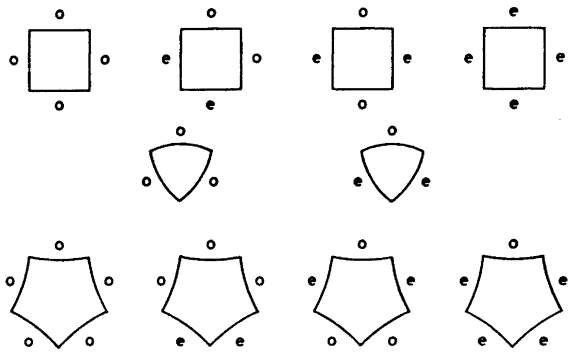

Fig. 3. Allowed combinations of ring "sides" having an odd or even number of bonds.

For odd-membered rings it can be similarly shown that it is impossible to fit together four sides so as to form the above type of "corners". Either three- or five-corner conformations will be the best alternatives and give least deformation at the corners, ideally at right angles in the ring projection. The former type will be called "triangular" and must have one or more "convex" sides (Fig. 3). The latter type will be called "quinquangular" and must have one or more "concave" sides (Fig. 3). Being odd-membered, these rings will have only two types of triangular conformations (Fig. 3): all three sides contain an odd number of bonds; or two sides are even and one odd. Similarly, there are four types of quinquangular conformations (Fig. 3): all sides contain an odd number of bonds; two adjacent or next-to-adjacent are even and the other three odd; or one is odd and four even.

It may be noted that the present scheme for selecting conformations will include conformations of odd-membered rings having a two-fold axis of symmetry, and their isoclinal position [1] is in fact nothing else than a + +(or − −)*gauche*, *gauche* corner. On the other hand, the corresponding [1] conformations having a plane of symmetry are all left out. This is entirely logical, since a C_s-conformation must have one *syn*-bond and so be on a potential maximum rather than in a minimum. It is therefore not classified as a conformation, but as a symmetric barrier separating two equivalent unsymmetric conformations (see Part 2).

Before setting up the formally possible conformations according to the present scheme, which by the way is independent of symmetry, the restriction was placed on 14-membered and higher rings that one- and two-bond sides be used not more than twice, so as to avoid the handling of an excessive number of non-competitive conformations.

STRAIN CALCULATION ON MOLECULAR MODELS

About half of the formally derived conformations could be eliminated in the model-building step, since they could not be made without prohibitively short hydrogen-hydrogen distances. The remaining possibilities were then

constructed with commercial Fieser-Dreiding models,[7] which had their bond rotation sufficiently braked by putting thin paper strips between tubes and sticks so as to allow the "freezing" of any chosen conformation. The energy minimization was carried out manually by trying to improve the most eclipsed bonds without creating worse problems elsewhere, in particular by keeping all 1,5- and higher hydrogen interactions above 1.8 Å, or as little below this value as possible in medium rings. It was encouraging that this procedure gave the

Table 1. Calculated conformational strain enthalpies of cycloalkanes.

	Conf.	$\sum H$	H_0	ΔH		Conf.	$\sum H$	H_0	ΔH
C_9:	[234]	18.5	11.3	1.4	C_{10}:	[1243]	25.4	18.2	12.2
	[333]	17.1	9.9	0		[1324]	17.9	10.7	4.7
	[12222]	19.9	12.7	2.8		[1333]	14.6	7.4	1.4
						[1414]	14.0	6.8	0.8
						[2233]	14.6	7.4	1.4
						[2323]	13.2	6.0	0
C_{11}:	[155]	22.5	15.3	6.1	C_{12}:	[1335]	19.0	11.8	9.4
	[227]	27.8	20.6	11.4		[1344]	17.1	9.9	7.5
	[245]	18.7	11.5	2.3		[1434]	21.3	14.1	11.7
	[335]	16.6	9.4	0.2		[2235]	21.7	14.5	12.1
	[344]	16.4	9.2	0		[2325]	21.3	14.1	11.7
	[12323]	16.1	9.5	0.3		[2334]	14.1	6.8	4.4
	[13223]	17.0	9.8	0.6		[2343]	14.0	6.8	4.4
						[2424]	17.2	10.0	7.6
						[3333]	9.6	2.4	0
C_{13}:	[247]	26.9	19.7	13.0	C_{14}:	[2345]	20.7	13.5	13.5
	[256]	23.7	16.5	9.8		[2435]	15.2	8.0	8.0
	[337]	21.7	14.5	7.8		[2444]	14.4	7.2	7.2
	[346]	18.3	11.1	4.4		[2525]	20.4	13.2	13.2
	[355]	16.1	8.9	2.2		[3335]	13.0	5.8	5.8
	[445]	15.6	8.4	1.7		[3344]	9.8	2.6	2.6
	[12433]	13.9	6.7	0		[3434]	7.2	0	0
	[13333]	15.0	7.8	1.1					
C_{15}:	[357]	16.1	8.9	4.6	C_{16}:	[2446]	17.2	10.0	10.0
	[366]	15.8	8.6	4.3		[2455]	20.9	13.7	13.7
	[447]	15.8	8.6	4.3		[2464]	16.2	9.0	9.0
	[456]	15.1	7.9	3.6		[2536]	13.8	6.6	6.6
	[555]	15.0	7.8	3.5		[2545]	10.8	3.6	3.6
	[12534]	14.1	6.9	2.6		[3346]	16.0	8.8	8.8
	[13344]	19.3	12.1	7.8		[3355]	13.8	6.6	6.6
	[13353]	14.0	6.8	2.5		[3436]	13.6	6.4	6.4
	[13434]	14.2	7.0	2.7		[3445]	10.4	3.2	3.2
	[13443]	13.0	5.8	1.5		[3454]	10.6	3.4	3.4
	[14334]	12.7	5.5	1.2		[3535]	8.4	1.2	1.2
	[23334]	15.9	8.7	4.4		[4444]	7.2	0	0
	[23343]	17.7	10.5	6.2					
	[33333]	11.5	4.3	0					

$\sum H$ = total calculated strain enthalpy (kcal/mol).
H_0 = strain enthalpy relative to best conf. of cyclotetradecane.
ΔH = strain enthalpy relative to best conf. of the same cycloalkane.

same results when repeated from different starting points. All dihedral angles were then read off to the nearest 5° value, again with no problem of reproducibility, and the total conformational enthalpy calculated from the tables in Fig. 1.

This procedure cannot of course give numerical values reliable to more than ± 1 kcal/mol. Nevertheless, the results are given in Table 1 with one decimal, and for the only reason that these represent the lowest values actually obtained for each conformation.

A shorthand notation for conformational type is used in Table 1, consisting of a series of numbers within brackets, each giving the number of bonds in one "side", starting with the shortest. The direction around the ring is so chosen that the following number is smallest possible. A triangular conformation is thus uniquely defined by three numbers, a quadrangular by four, and a quinquangular by five; the sum gives the ring size.

In Table 1 the conformational enthalpies are compared with that of the lowest conformation of the least strained ring, taken to be the diamond-lattice conformation of cyclotetradecane. In addition, all conformers of each ring are compared with the one among them which is of lowest enthalpy. Finally, the actual geometries with dihedral angles indicated are shown in Figs. 4 – 11 for all conformers calculated to be less than 6 kcal/mol higher than the best conformer of each set, except in the case of cyclopentadecane where only the six lowest out of twelve are given. It may be noted that the sign of the dihedral angle alternates along all convex sides, whereas in a concave portion a near-*anti* bond gets the same sign as neighboring bonds.

GENERAL DISCUSSION OF RESULTS

The listing order of tested conformations in Table 1 follows the shorthand notation and therefore implies that the most regular conformations come last. It is immediately seen, and might have been intuitively expected, that these are of lowest enthalpy in even-membered rings and among the triangular conformations in odd-membered rings. For quinquangular conformations, however, this is true only in the case of the largest ring considered, cyclopentadecane. The best of all cyclotridecane conformations is in fact a completely irregular quinquangular one having one single-bond side, and several conformations of this type are of lower enthalpy than any of triangular type also in cyclopentadecane, and of equal energy in cycloundecane. In general, the potential minimum is not well-defined in such cases, and the enthalpy may vary smoothly from that of a very irregular triangular conformation [*abc*], where c is much larger than a and b, to that of a quinquangular conformation [*1xaby*], where $1+x+y=c$. This is formally acceptable, since dihedral angle signs are alternating in the same way along a convex side of c bonds as through the two corners adjoining a one-bond side. It is also energetically acceptable, since in both forms many of the bonds in question will have to be very high up on either sides of the 120° barrier, and it is merely a question of continuous redistribution of strain on these bonds. Sometimes there is even a problem of classification, since a definition based on whether the ring projection "looks" triangular or quinquangular, and a definition based on whether the relevant dihedral angles are above or below 120°, may lead to different results.

If the dihedral angles of the outer two bonds are considerably above 120° in sufficiently large rings, the strained *+gauche, −gauche, +gauche* sequence will effectively degenerate to a strain-free *anti,gauche,anti* system (Fig. 2d).

It is interesting to note that a given quinquangular conformation having one single-bond side is closely related to a quadrangular conformation of the even-membered ring immediately below and immediately above its ring size, and it can be derived from these by insertion of one bond at a corner "ring expansion") or by cutting off a corner ring-atom ("ring contraction"), respectively. Thus, in cases where such quinquangular conformations have lower energies than their triangular partners, it is clearly more favourable to keep the main part of the ring skeleton diamond-lattice-like and concentrate the inherent strain at a few bonds, rather than to distribute the strain over many bonds in a more symmetric fashion.

A comparison of the calculated lowest enthalpies for the different ring sizes is shown graphically in Fig. 12, where also experimental strain energies from combustion calorimetry [13,14] are given. The deviation of calculated from experimental values is clearly systematic and larger than the reproducibility of the method. First of all, the calculated values are too low for all medium rings, and this is obviously due to the necessity of accepting too short 1,5- and 1,6-hydrogen interactions (marked in Figs. 4 – 7). Secondly, the odd-even alternation is too strong, which may be due to the use of fixed tetrahedral valency angles. If the experimentally established value close to 112° for the CCC-angle had been used, clearly this would have led to less favourable dihedral angles in the near-diamond-lattice conformations of even-membered rings and raised their enthalpy, whereas the inherent bond-eclipsing in odd-membered rings would be reduced and their enthalpy lowered (compare Hendrickson's calculations [1] of normal rings with tetrahedral and 112° angles as "normal" value).* On the other hand, the enthalpy order among individual conformations within those medium rings for which more rigorous calculations have been made, comes out the same, and the lowest-enthalpy conformations of larger rings are those found experimentally wherever information is available.

It is interesting to note in Fig. 12 that the enthalpy of the lowest conformation of each type (triangular, quadrangular or quinquangular) decreases very regularly with increasing ring size.

The number of low-enthalpy conformations of the types considered here increases very much in the 15- and 16-membered rings (Table 1), and the increase must be expected to continue exponentially in higher rings. For this reason, and because other conformational types having also isolated *gauche* bonds will start to be competitive in the 17- and 18-membered ring, the number of conformations with low and close-lying enthalpies would be so large that this type of exploratory calculation is hardly worthwhile.

* A further systematic error is introduced by the energy summation procedure, since each 1,3-interaction in the ring is actually counted twice (1,2- and 1,4-interactions are correctly counted once). This is, however, only of importance at the 120° barrier, where a double 1,3-interaction in butane contributes 0.8 kcal/mol, the barrier in propane and ethane being 3.4 and 3.0 kcal/mol, respectively. This again will tend to accent the alternation, since odd-membered rings have more dihedral angles approaching 120° and come out too strained from the calculation.

DISCUSSION OF INDIVIDUAL RINGS

Cyclononane (Fig. 4). The lowest-enthalpy conformation is of triangular type [333] and identical with the D_3 conformation found by more rigorous methods,[1–3] and also established experimentally [15] by low-temperature ^{13}C

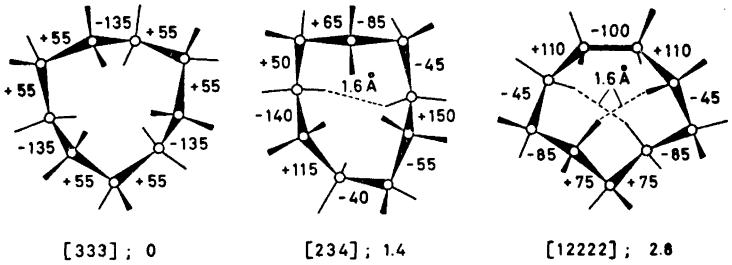

Fig. 4. Lowest minima for cyclononane.

NMR. It is of particular interest that an asymmetric triangular conformation [234], never considered before, is found to be only 1.5 kcal/mol less stable; it may be thought of as being formed by ring contraction of the diamond-lattice conformation [2323] of cyclodecane. The third may be defined both as quinquangular [12222] and as triangular [225], and can be derived by ring expansion of the diamond-lattice conformation [2222] of cyclooctane (Fig. 2b). It is identical with the ring conformation found for crystalline cyclononyl ammonium bromide,[13] and its relative enthalpy is calculated by Hendrickson [1] to be 2.2, by Bixon and Lifson [3] 3.9, while the present value of 2.8 kcal/mol is intermediate.

Cyclodecane (Fig. 5). The lowest conformation is as expected the "rectangular" diamond-lattice [2323] established for a number of derivatives.[13] Only 1.4 kcal/mol higher are two conformations [2233] and [1333], identical with the two found as a mixture in the crystal of 4,4,8,8-tetramethylcyclodecanecarboxylic acid and then calculated to have relative enthalpies of 2.1 and 3.1 kcal/mol, respectively.[13] Unexpectedly, the very low relative enthalpy of 0.8 kcal/mol was obtained for the *trans*-decalin-like conformation [1414], which can also be considered as a deformed crown conformation. Another type of deformation, the stretched crown, has sometimes been discussed,[1] but would be classified as a barrier in the present scheme and is of much higher enthalpy (see Part 2). The [1414] conformation has already been proposed [16] for the solution conformation of cyclodecane-1,6-dione.

Cycloundecane (Fig. 6). For this ring as many as four conformations have about equally low enthalpies, the two most regular triangular, [344] and [335], and two irregular quinquangular, [12323] and [13223]. The [344] conformation comes out lowest also in the calculations by Bixon and Lifson.[3] The [335] conformation is an example of a set where a clear triangular type is of much lower enthalpy than the corresponding quinquangular [12332]; both can be thought of as being formed by ring contraction from the [3333] cyclododecane conformation. The opposite situation is represented by [13223] which is clearly

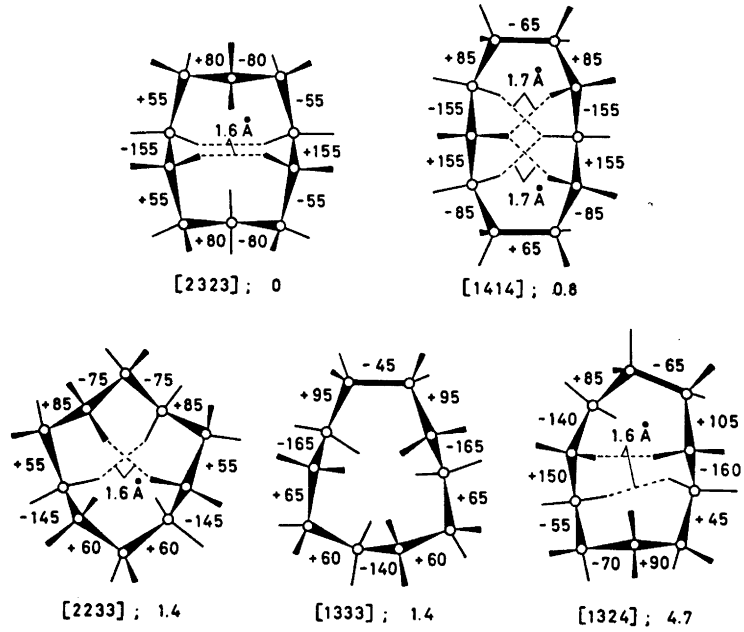

Fig. 5. Lowest minima for cyclodecane.

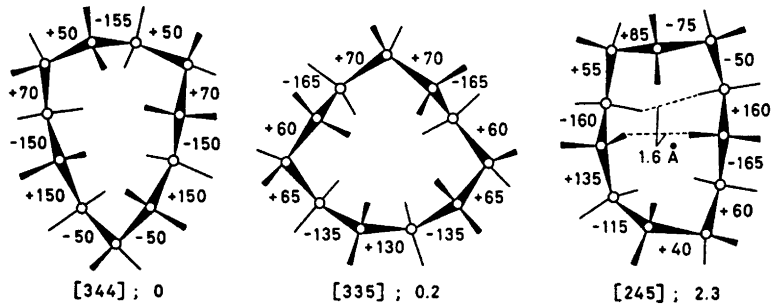

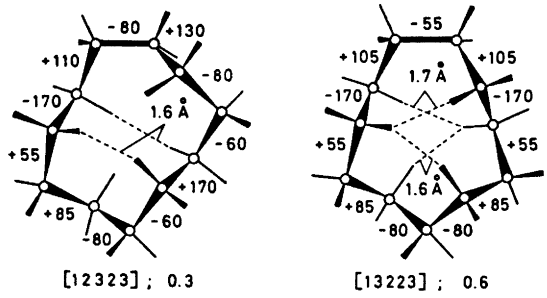

Fig. 6. Lowest minima for cycloundecane.

quinquangular of type and of much lower enthalpy than is triangular partner [227]; these can both be derived by ring expansion from the [2233] cyclodecane conformation. The ill-defined conformation marked [12323] is intermediate of character since it results on attempts to minimize both a quinquangular and a triangular type [236]; it is derivable by ring expansion from the [2323] cyclodecane conformation.

Somewhat higher in enthalpy is the unsymmetric triangular conformation [245].

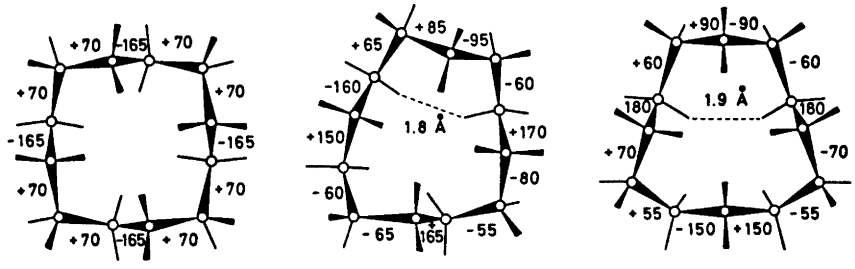

Fig. 7. Lowest minima for cyclododecane.

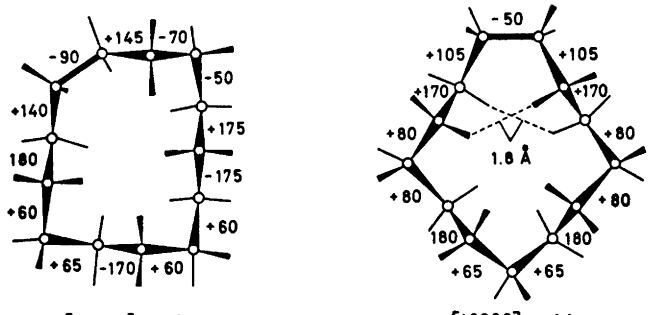

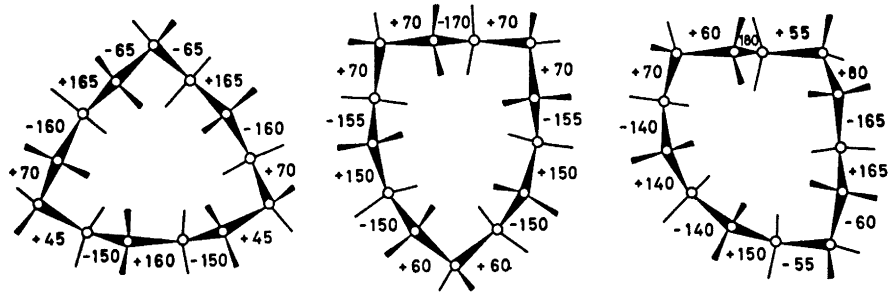

Fig. 8. Lowest minima for cyclotridecane.

Cyclododecane (Fig. 7). This is the conformationally most homogeneous ring of all studied, although its favoured "square" [3333] conformation is not of diamond-lattice type. It is identical with the one found experimentally in the crystalline state,[13] and is also the one calculated to be of lowest enthalpy by Wiberg [2] and by Bixon and Lifson.[3] The two next lowest, [2334] and [2343], are of so much higher enthalpy (4.4 kcal/mol) as to be unobservable in the equilibrium.

Cyclotridecane (Fig. 8). Both lowest conformations are here of quinquangular type. This is the only ring for which the most stable conformation, [12433], is asymmetric; it may be derived by ring contraction from the diamond-lattice conformation [3434] of cyclotetradecane and has a triangular partner [346] which is 4.4 kcal/mol higher. The next lowest conformation [13333] is at 1.1 kcal/mol and should therefore be quite important in the equilibrium; it is derivable from the [3333] conformation of cyclododecane by ring expansion, and has a much less stable triangular partner [337] at 7.8 kcal/mol. The two most regular triangular conformations [445] and [355] are of sufficiently low enthalpies (1.7 and 2.2 kcal/mol) so that they should also be detectable in the equilibrium.

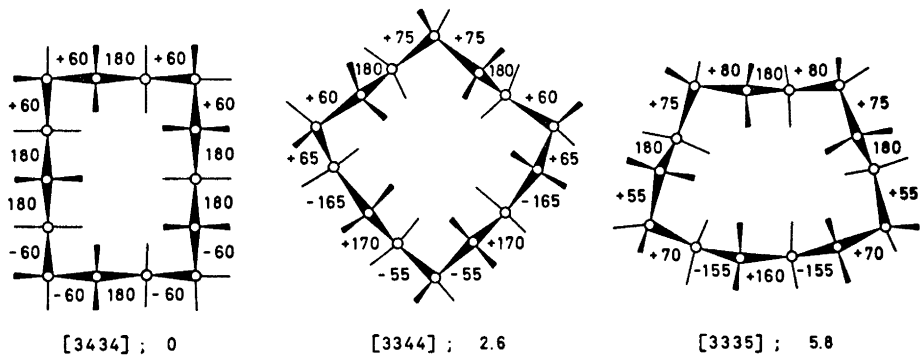

Fig. 9. Lowest minima for cyclotetradecane.

Cyclotetradecane (Fig. 9). As expected, this ring is conformationally very homogeneous with the "rectangular" diamond-lattice conformation [3434] favoured. This is also the observed conformation in the crystal,[17] liquid and solution.[6] The [3344] conformation is calculated to be 2.6 kcal/mol higher, corresponding to 1 % in the equilibrium, and none else is below 5.8 kcal/mol.

Cyclopentadecane (Fig. 10). This odd-membered ring turned out to have one clearly enthalpy-preferred, highly symmetric and regular quinquangular conformation [33333], a kind of homologue of the preferred C_9 and C_{12} conformations. The next five lowest conformations are also quinquangular, but of the type having a very irregular triangular partner of higher enthalpy. Thus, [14334] at 1.2 kcal/mol and [13434] at 2.7 kcal/mol, the latter derivable by ring expansion from the [3434] conformation of cyclotetradecane, have the very strained triangular counterparts [339] and [348], while [13443] at 1.5

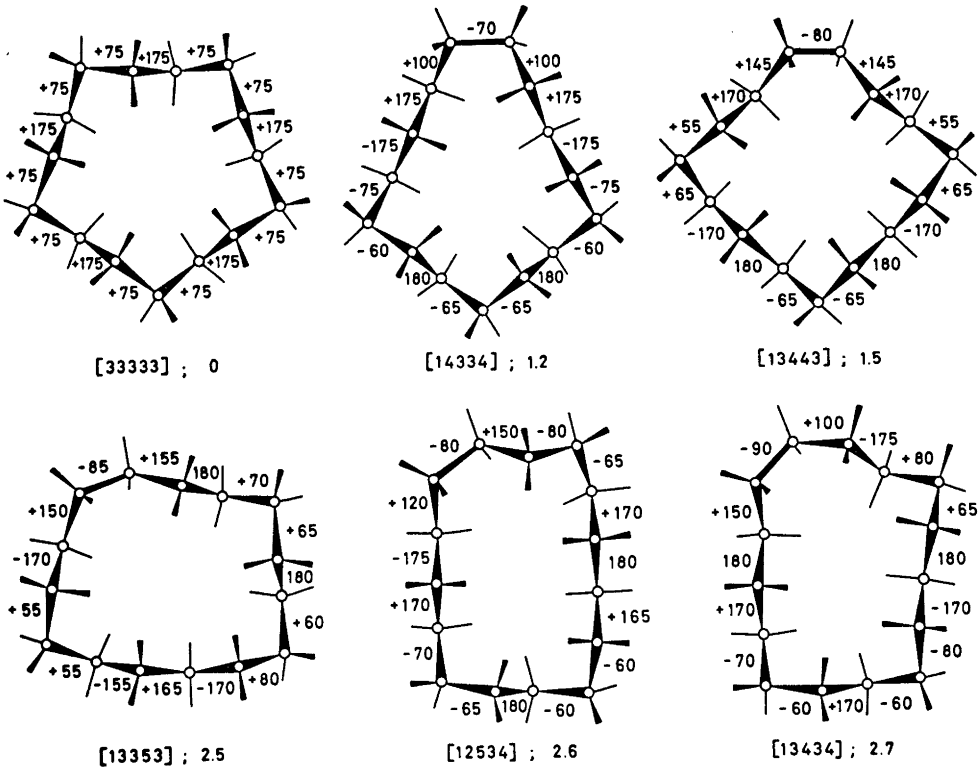

Fig. 10. Lowest minima for cyclopentadecane.

kcal/mol, derivable by ring contraction from the [4444] conformation of cyclohexadecane, is related to [447] at 4.3 kcal/mol, and [13353] as well as [12534], both at 2.5 kcal/mol, are related to [357] at 4.6 kcal/mol. The lowest triangular conformations are the regular [555] and next-most regular [456], both at 3.5 kcal/mol.

A consideration of entropy terms due to symmetry, so that free-energy differences might be used to estimate more accurate equilibria, seemed in most cases unjustified because such terms would be smaller than expected errors in the present enthalpy calculation. However, the lowest cyclopentadecane conformations have so very different symmetries, that the symmetry number of 10 for [33333], compared to only 2 for [14334] and [13443] (all are *d,l-pairs*), gives an entropy term at 300 K of 1.0 kcal/mol favouring the two latter. Their free energies are therefore only 0.2 and 0.5 kcal/mol higher, and conformational homogeneity is not to be expected.

Cyclohexadecane (Fig. 11). The "square" [4444] conformation, being of diamond-lattice type, has the lowest enthalpy. This is also the one indicated by infrared spectroscopy of the low-temperature crystal.[6] The next-lowest is the compact "rectangular" [3535] envisaged earlier.[5] Since it is

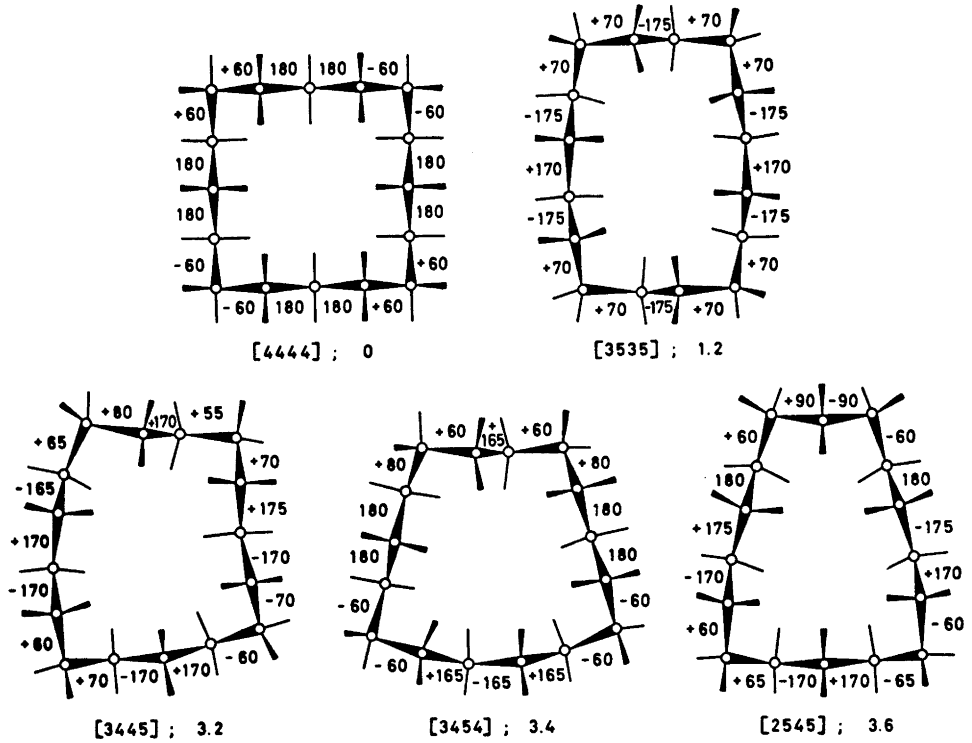

Fig. 11. Lowest minima for cyclohexadecane.

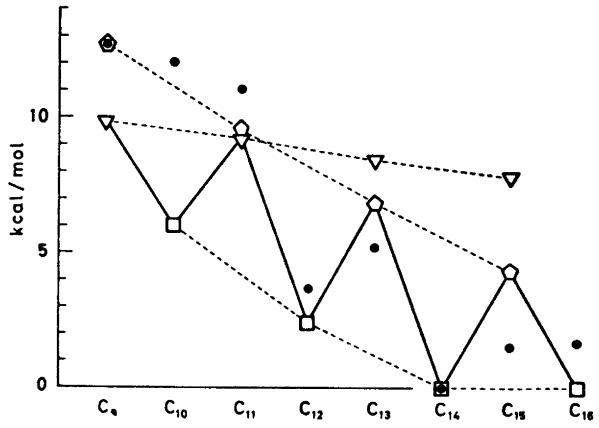

Fig. 12. Calculated enthalpy of the best conformation for each cycloalkane relative to that of cyclotetradecane.
□ = quadrangular type, △ = triangular type, ⬠ = quinquangular type,
● = experimental heat of combustion values.

only 1.2 kcal/mol higher, entropy terms must also be considered. The symmetry number is 4 for both, but only [3535] is a *d,l*-pair, thus giving an entropy term at 300° K of 0.4 kcal/mol in its favour. With a resulting free-energy difference of only 0.8 kcal/mol, it becomes understandable that the liquid is conformationally heterogeneous.[6]

Three other less symmetric conformations [3445], [3454], and [2545] are as high as 3.2 – 3.6 kcal/mol in enthalpy, and symmetry-determined entropy contributions could hardly make them important in the equilibrium. On the other hand, vibrational entropy terms might perhaps modify this picture, but cannot be considered here.

A NOTE ON CYCLOOCTANE

Obviously, the present method cannot be used for numerical calculation of cyclooctane conformations, since the very serious transannular interactions [1] are not taken properly into account; their neglect would therefore strongly favour the only diamond-lattice conformation [2222]. Nevertheless, it seemed of interest to try the present scheme for selection of conformational candidates, accepting that "non-*gauche*" bonds might in reality be very far away from *anti;* in fact quite close to the 120° barrier.[1,13] This leads to only four conformational minima: [2222], which corresponds to the boat-boat (saddle), including the twist-boat; [1223], which is a deformed boat-chair; [1232], which corresponds to the twist-boat-chair; and [1313], which is the twist-chair-chair, the lowest member of the crown family.[1] Thus, all the energetically impossible forms included in Hendrickson's symmetry-based selection scheme [1] are here automatically eliminated.

It is of particular interest that the symmetrical boat-chair, which in all numerical calculations [1–4] has the lowest energy, is not classified as a minimum in the present scheme, but as a barrier (Part 2) separating two enantiomeric [1223] conformers.

REFERENCES

1. Hendrickson, J. B. *J. Am. Chem. Soc.* **83** (1961) 4537; **86** (1964) 4854; **89** (1967) 7036.
2. Wiberg, K. B. *J. Am. Chem. Soc.* **97** (1965) 1070.
3. Bixon, M. and Lifson, S. *Tetrahedron* **23** (1967) 769.
4. Allinger, N. L., Tribble, M. T., Miller, M. A. and Wertz, D. H. *J. Am. Chem. Soc.* **93** (1971) 1637.
5. Dale, J. *J. Chem. Soc.* **1963** 93.
6. Borgen, G. and Dale, J. *Chem. Commun.* **1970** 1340.
7. Fieser, L. F. *J. Chem. Educ.* **40** (1963) 457.
8. Hoyland, J. R. *J. Chem. Phys.* **49** (1968) 2563.
9. Radom, L. and Pople, J. A. *J. Am. Chem. Soc.* **92** (1970) 4786.
10. Kuchitsu, K. *Bull. Chem. Soc. Japan* **32** (1959) 748.
11. Piercy, J. E. and Rao, M. G. S. *J. Chem. Phys.* **46** (1967) 3951.
12. Abe, A., Jernigan, R. L. and Flory, P. J. *J. Am. Chem. Soc.* **88** (1966) 631.
13. For a review see: Dunitz, J. D. *Perspectives in Structural Chemistry* **2** (1968) 1.
14. Coops, J., van Kamp, H., Lambregts, W. A., Visser, B. J. and Dekker, H. *Rec. Trav. Chim.* **79** (1960) 1226.
15. Anet, F. A. L. and Wagner, J. J. *J. Am. Chem. Soc.* **93** (1971) 5266.
16. Alvik, T., Borgen, G. and Dale, J. *Acta Chem. Scand.* **26** (1972) 1805.
17. Newman, B. A. (Bristol). *Unpublished.*

Received October 9, 1972.

ACTA CHEMICA SCANDINAVICA 27 (1973) 1130–1148

Exploratory Calculations of Medium and Large Rings

Part 2. Conformational Interconversions in Cycloalkanes

JOHANNES DALE

Kjemisk Institutt, Universitetet i Oslo, Oslo 3, Norway

The mechanistic steps in conformational interconversions have been analysed and the enthalpy of the barriers calculated. These come out relatively low for the medium rings, but surprisingly high for cyclododecane and the largest rings studied ($C_{14}-C_{16}$). The critical step in all these rings is the passage of one ring bond through a torsional *syn* barrier. An alternative mechanism involving the passage of only 120° barriers becomes almost competitive in cycohexadecane; larger rings should therefore have lower barriers.

Computer calculation of conformational barriers should be as straightforward as of conformational minima when the nature of the barrier can be geometrically defined *a priori*. A search for the lowest interconversion barriers by the method of steepest descent would on the other hand seem difficult, since one is not looking for an absolute minimum. The type of approach used in Part 1 to find the geometries and calculate the enthalpies of potential minima seems therefore even more appropriate in a search for barriers, provided the various mechanistic possibilities can be satisfactorily analysed.

INTERCONVERSION MECHANISMS

The common distinction between ring inversion and pseudorotation in normal rings seems arbitrary and misleading if the mechanisms involved are implied. Thus, the observation of the exchange of non-identical axial and equatorial substituent positions on all identical ring positions in cyclohexane has given rise to the term inversion, although the mechanism is of course passage to the boat-forms and back again in two distinctly separate steps.[1] Strictly, the only cycloalkane for which inversion through total ring flattening must occur, is cyclobutane. The real barrier in cyclohexane involves the geometrical feature of a flattened four-carbon atom system,[1] but this is also the case for the pseudorotational barrier (the envelope form) of cyclopentane.[2] Energetically, the two situations are of course very different; in cyclohexane the four-

carbon flattening induces strain also in the rest of the ring, while in cyclopentane it relieves about the same amount of strain elsewhere in the ring.

In medium and large rings the conformations are generally of such high symmetry that it is inconceivable that the nearest barrier is also symmetric, since this would imply a synchronous change in two or more parts of the ring, hence the added energy of several changes. It is more likely that the least expensive conformational changes may be rather localized. In fact "elementary processes" can be devised involving the movement of a "corner" by one or two steps, which when repeated will produce any desired effect: the passage to other conformational minima and return to an equivalent conformation with exchange of ring-atom sites and/or substituent sites. These elementary processes are equivalent to the migration of *gauche* bonds in *anti* surroundings

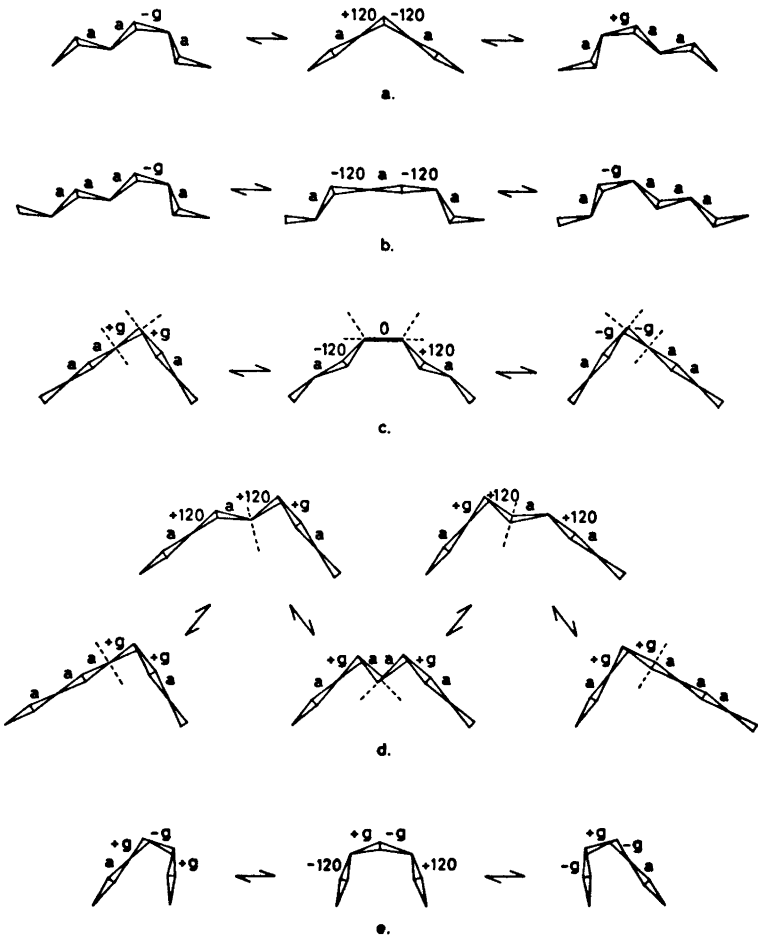

Fig. 1. Different types of barriers to the movement of *gauche* bonds or "corners".

along a chain. In an open chain, or infinitely large ring, the ends of the chain are unrelated to each other, and a *gauche* bond can be "moved" by turning it to *anti* and then the neighbouring or any other *anti* bond to *gauche*. In medium and moderately large rings the constraints of the ring may lead to partial eclipsing also in other bonds than the one just passing through a barrier. Extreme situations, obtained when a bent chain preserves as much as possible its overall shape during the whole process, are illustrated in Fig. 1.

An isolated *gauche*-bond can move by one step (Fig. 1a), changing sign, through a transition state with two adjacent bonds passing over the lower butane barrier (120°); in actual rings the eclipsing need not be totally synchronous. An isolated *gauche*-bond can move also by two steps (Fig. 1b), with unchanged sign, through a transition state having now two non-adjacent bonds on the lower butane barrier; again the two barriers must not necessarily be passed synchronously. These two mechanisms will be needed only in rings larger than C_{16} where conformations having isolated *gauche*-bonds play a role.

The more common corner element, two adjacent *gauche*-bonds of the same sign, can be moved by one step (Fig. 1c), with both signs changed, through a transition state having one bond passing the higher (*syn*) and two adjacent bonds passing the lower (120°) butane barrier; in most actual rings the three bonds may of course become eclipsed considerably out of phase. This process is particularly attractive for medium rings, since "inner" substituents will become "outer" in the transition state and transannular interactions thereby relieved. The same element can also be moved by two steps with unchanged sign (Fig. 1d), but the process involves then an intermediate conformation of low stability in the rings considered here, as well as higher-energy transition states, since "outer" substituents have to become "inner"; a methylene group is actually rotating "through" the ring. This mechanism should become of interest in rings larger than cyclohexadecane, because the transition state requires the eclipsing of only two bonds, both in low-barrier positions, and the eclipsing may not even need to be synchronous.

SEARCH FOR LOWEST BARRIERS

The procedure adopted was to define a transition state as being the situation the moment the bond between the old and the new corner atom becomes exactly eclipsed on the high-energy *syn*-barrier, as in Fig. 1c. The adjacent bonds, however, were generally hardly more than half-eclipsed (on the slopes of the low-energy 120° barrier), since these bonds, as well as the remainder of the bonds, were adjusted manually to minimize the strain in the same way as in the calculation of conformational minima (Part 1). It turned out in most cases to be energetically advantageous to keep one of these two dihedral angles above 120° (the one having the shortest adjoining side) and the other below 120° (the one having the longest adjoining side). Thus, the eclipsing rolls like a wave through the three contiguous bonds (from right to left as the models are oriented in the figures).

The notation introduced for the minima in Part 1 can be used also for the barriers if the *syn*-eclipsed bond is defined as a one-bond side; it is marked in italics. As an example, the conversion of [333] to [234], and *vice*

versa, proceeds over a barrier defined as [*1*233]. In general, triangular conformations have quadrangular barriers, and quadrangular conformations have quinquangular barriers. The quinquangular conformations may have both sexangular and quadrangular barriers, the latter *via* triangular partners.

A particular type of barrier is encountered when two corners are adjacent, since they cannot then be changed independently; passage over this barrier will shift a *+gauche, −gauche, +gauche* sequence by one step with all signs changed (Fig. 1e). The transition state has two eclipsed bonds of low-torsional-barrier type and looks like a conformation with a "forbidden" type of corner; such conformations were neglected in the search for minima (Part 1). Quad-

Table 1. Calculated strain enthalpies of conformational barriers of cycloalkanes.

	Notation	$\sum H$	H_0	ΔH		Notation	$\sum H$	H_0	ΔH
C_9	[*1*224]	26.3	19.1	9.2	C_{10}	[*1*2133]	27.4	20.2	14.2
	[*1*233]	25.7	18.5	8.6		[*1*2232]	21.1	13.9	7.9
	[*1*242]	26.1	18.9	9.0		[*244*]	19.8	12.6	6.6
	[*1*323]	22.7	15.5	5.6		[*334*]	19.4	12.2	6.2
						[**55**]	23.2	16.4	10.0
C_{11}	[*1*22312]	28.3	21.1	11.9	C_{12}	[*1*2333]	23.6	16.4	14.0
	[*1*235]	26.9	19.7	10.5		[*1*2342]	21.7	14.5	12.1
	[*1*244]	28.2	21.0	11.8		[*1*2423]	26.0	18.8	16.4
	[*1*253]	30.8	23.6	14.4		[*1*3233]	23.2	16.0	13.6
	[*1*334]	19.9	12.7	3.5		[*444*]	18.2	11.0	8.6
	[*1*343]	22.1	14.9	5.7					
	[*1*424]	27.7	20.5	11.3					
C_{13}	[*1*21333]	26.5	19.3	12.6	C_{14}	[*1*2443]	24.3	17.1	17.1
	[*1*336]	24.9	17.7	11.0		[*1*3334]	20.2	13.0	13.0
	[*1*345]	23.0	15.8	9.1		[*1*3343]	21.0	13.8	13.8
	[*1*354]	26.4	19.2	12.5					
	[*1*363]	30.0	22.8	16.1					
	[*1*435]	21.6	14.4	7.7					
	[*1*444]	21.1	13.9	7.2					
C_{15}	[*1*23333]	24.9	17.7	13.4	C_{16}	[*1*3444]	19.8	12.6	12.6
	[*1*23342]	21.8	14.6	10.3		[*1*3453]	22.7	15.5	15.5
	[*1*23432]	18.7	11.5	7.2		[*1*3534]	20.7	13.5	13.5
	[*1*31343]	28.7	21.5	17.2		[*1*4344]	19.2	12.0	12.0
	[*1*31433]	28.0	20.8	16.5		[*1*3264]	23.7	16.5	16.5
	[*1*347]	31.1	23.9	19.6		[*1*3246]	23.2	16.0	16.0
	[*1*356]	21.6	14.4	10.1		[*1*3444]	16.5	9.3	9.3
	[*1*365]	26.8	19.6	15.3		[*2*3344]	21.6	14.4	14.4
	[*1*437]	26.6	19.4	15.1		[*2*3344]	23.8	16.6	16.6
	[*1*446]	21.9	14.7	10.4		[*2*4334]	24.9	17.7	17.7
	[*1*455]	23.7	16.5	12.2					
	[*1*464]	24.6	17.4	13.1					
	[*1*536]	24.2	17.0	12.7					
	[*1*545]	21.2	14.0	9.7					

$\sum H$ = total calculated strain enthalpy (kcal/mol).
H_0 = strain enthalpy relative to best conf. of cyclotetradecane.
ΔH = strain enthalpy relative to best conf. of the same cycloalkane.

rangular conformations having a one-bond side therefore get triangular transition states, quinquangular get quadrangular. The two sides which meet at such a corner with opposite dihedral angle signs become italicized in the notation (underlined in the figures). As an example, the conversion of [1333] to [1234], and *vice versa*, proceeds over a barrier defined as [3*34*].*

Only barriers between the lowest conformational minima and those less stable minima which serve as intermediate conformations on low-energy interconversion paths have been calculated. The results are listed in Table 1 and the geometries and dihedral angles are given for the most important ones in Figs. 2 – 9.

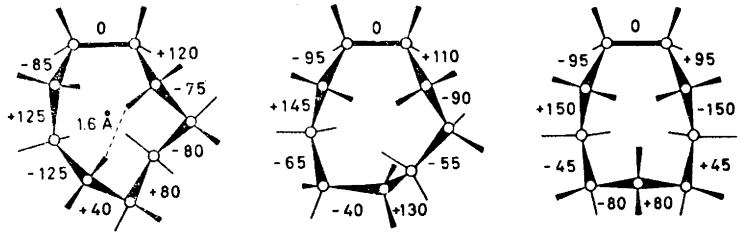

Fig. 2. Barriers for cyclononane.

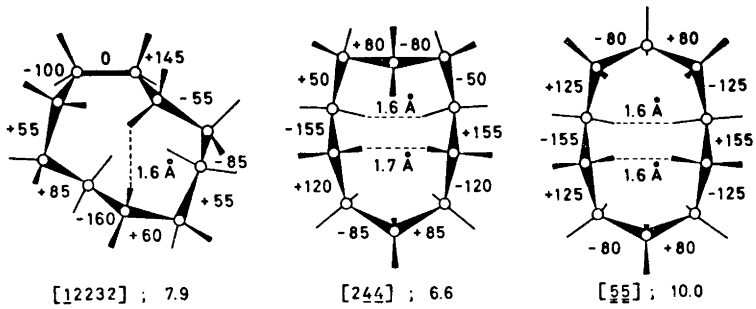

Fig. 3. Barriers for cyclodecane.

GENERAL DISCUSSION OF RESULTS

One general comment to make is that the spread in enthalpy is smaller for the barriers than for the minima. This may be related to the fact that all barriers must be strained by definition, whereas some minima are unstrained, others strained. It would, however, seem without interest to compare lowest

* The distinction between the triangular barrier [3*34*] and the quadrangular conformations [1333] or [1234], and even their biangular partner [37], becomes rather vague, in the same way as the distinction between triangular and quinquangular conformation partners and their intervening barrier (Part 1).

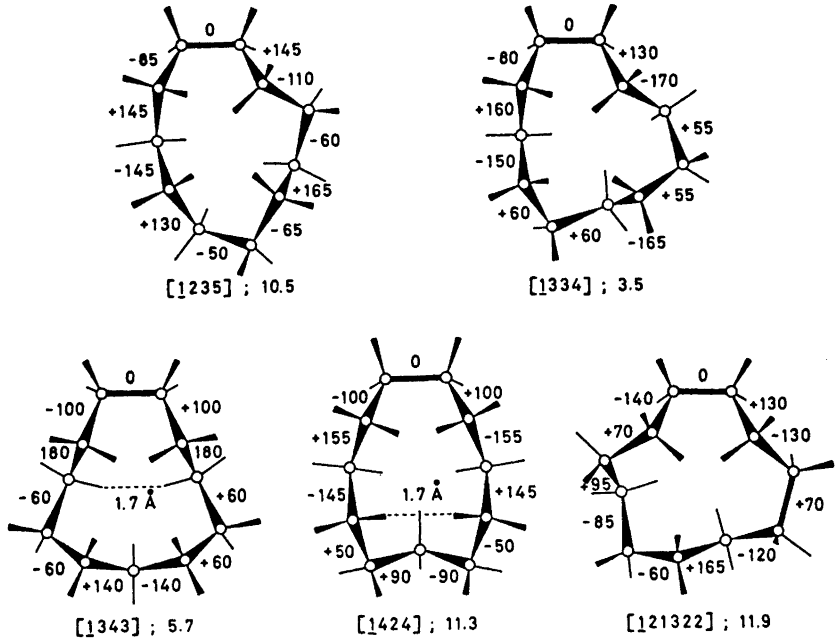

Fig. 4. Barriers for cycloundecane.

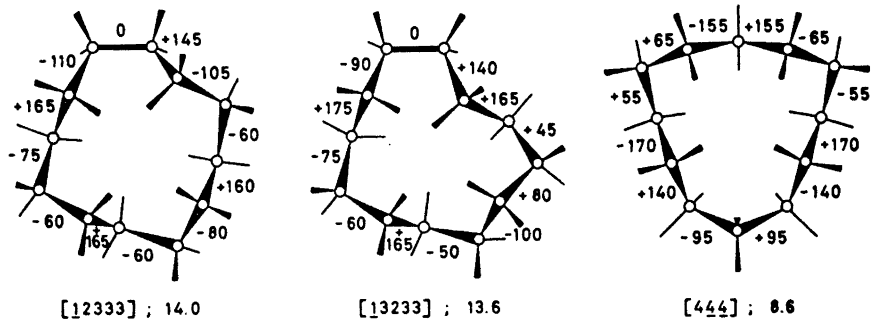

Fig. 5. Barriers for cyclododecane.

absolute values of barriers for different ring sizes, as they have meaning only in relation to the minima they connect. The barriers will therefore be discussed only in connection with the interconversion processes for each individual ring.

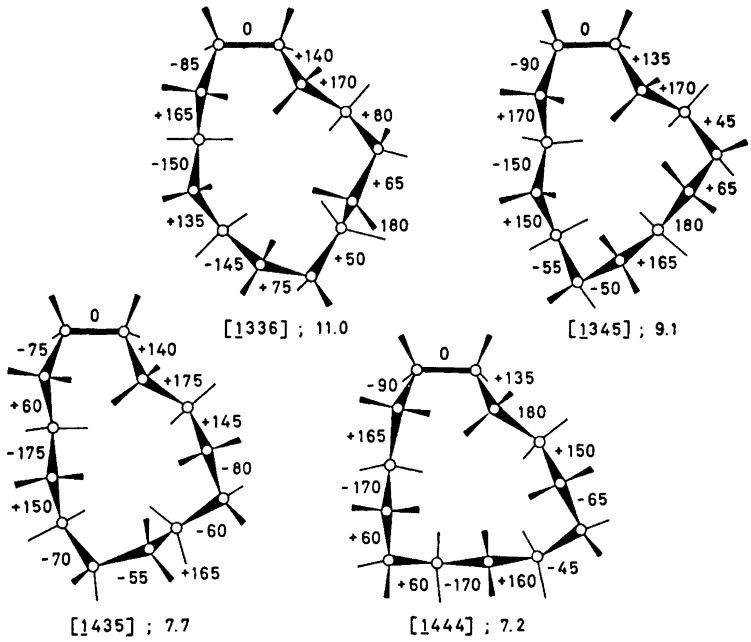

Fig. 6. Barriers for cyclotridecane.

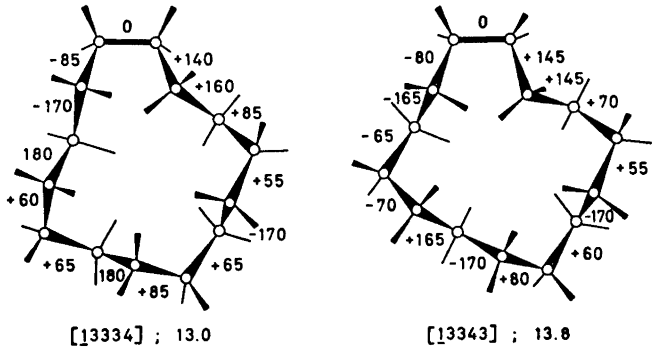

Fig. 7. Barriers for cyclotetradecane.

As to the possible systematic errors in the calculation, they will most likely produce too high barriers, and the more so the larger the rings. There are three reasons for this:

1. The search for the lowest enthalpy value of stable conformations is more easy because these represent absolute minima and have a relatively well-defined symmetry. The barriers, on the other hand, are generally less symmetric and may conceivably be further minimized by better timing of the

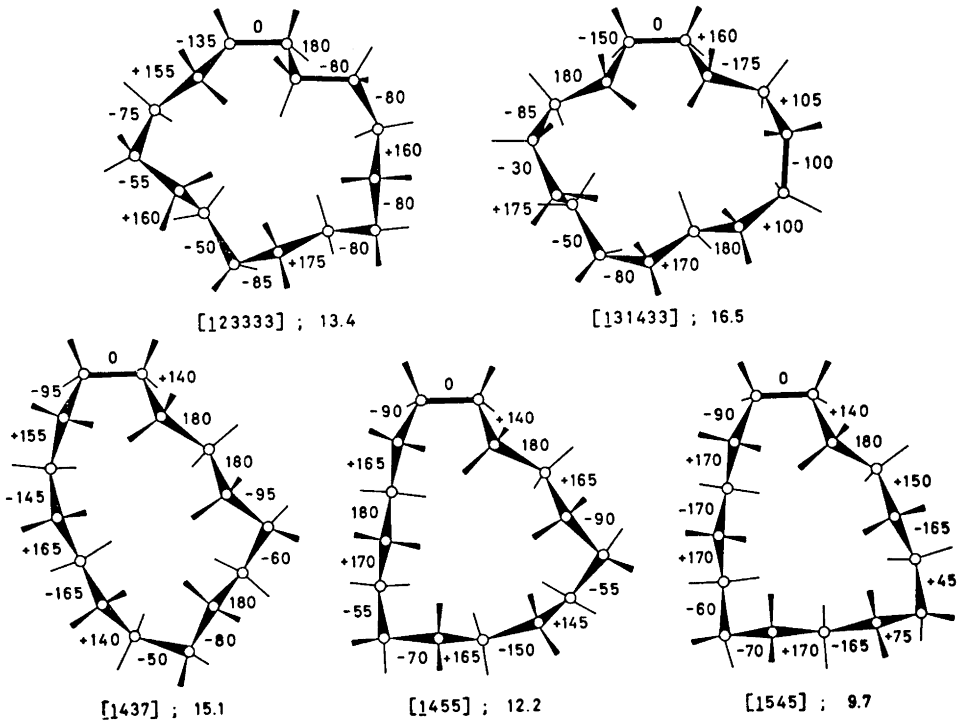

Fig. 8. Barriers for cyclopentadecane.

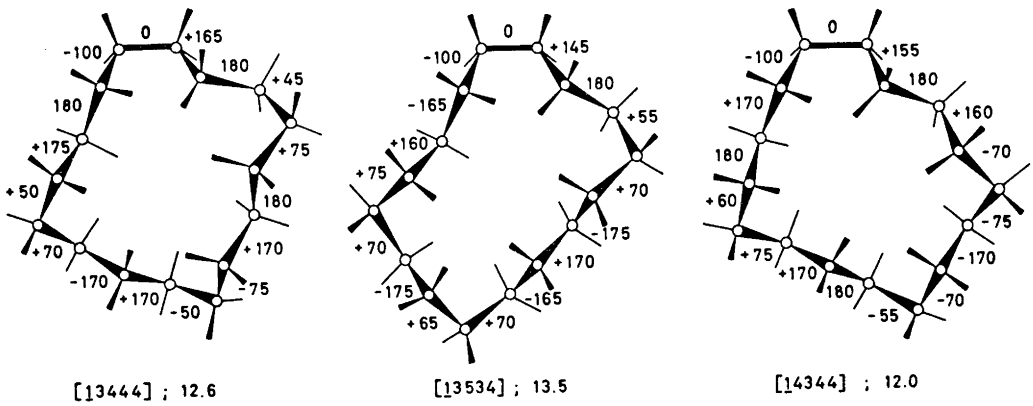

Fig. 9. Barriers for cyclohexadecane.

"eclipsing wave" through the three bonds and by better adjustment of the dihedral angles in the remainder of the ring. Of course, an asymmetric minimum may well have nearest barriers that are more symmetric, but these cases are relatively rare.

2. If the tetrahedral CCC-angle of the models were replaced by a more realistic 112°, the calculated enthalpy of the diamond-lattice-like conformational minima of the larger rings would be raised (*cf.* Fig. 12 of Part 1), whereas the enthalpy of the barriers would probably be lowered considerably because of relieved interactions in the flattened part of the ring.

3. The double weight of the 1,3-interactions inherent in the calculation procedure (see Part 1) leads to overemphasis of strain in bonds having dihedral angles near 120°, and the barriers have generally more such bonds than the minima.

Within each ring the error in relative barrier heights is likely to be small, and therefore the use of the calculated barriers to clarify the qualitative nature of the lowest-energy interconversion paths becomes the most important feature of the present work, not the absolute numerical values of the barriers.

DISCUSSION OF INDIVIDUAL RINGS

Cyclononane. The first step in any interconversion of the [333] conformation, and decisive in the site exchange process, is its passage to the [234] conformation; the relevant barrier [*1*233] is asymmetric (Fig. 2) and calculated at 8.6 kcal/mol, which value is to be compared with the free-energy value of $\approx$ 6 kcal/mol observed by ^{13}C resonance.[3] Before being able to return to an alternative [333] conformation, the [234] conformation must change to its mirror image by passing one of the symmetrical barriers [*1*242] or [*1*323]. Of these, the latter is by far the lowest and seen to be identical with the boat-chair of Hendrickson, classified by him as a conformation.[1,4] After the last passage over the [*1*233] barrier, the [333] conformation produced is not only the mirror image of the starting conformation, but all ring atoms have moved by one step around the ring. The complete cycle is illustrated in Fig. 10. Repetitions of this cycle will lead to interchange of all ring-atom sites so that the result will appear like a pseudorotation, although mechanistically it is not. Focusing the attention on outer and inner substituents of a "side" carbon-atom, these remain outer and inner until the ring-atom arrives at a corner position, where they become identical (iso-clinal),[4] then exchange roles on the next side. The result will thus appear like a ring inversion, although the mechanism is the same.

Finally, it should be noted that also the [12222] (=[225]) conformation, if it had been the stable one, might have had its sites exchanged by passing to the same [234] conformation over a similar barrier [*1*224].

Cyclodecane. The lowest conformation [2323] of this ring must go through several steps to exchange all ring-atom and substituent sites. The first step is the passage over the [*1*2232] barrier (Fig. 3) leading to the intermediate conformation [2233] (the other conceivable barrier [*1*1323] is extremely high having two adjacent one-bond sides). Repetition of this process at the diametrically opposite corner leads over the same barrier to the starting con-

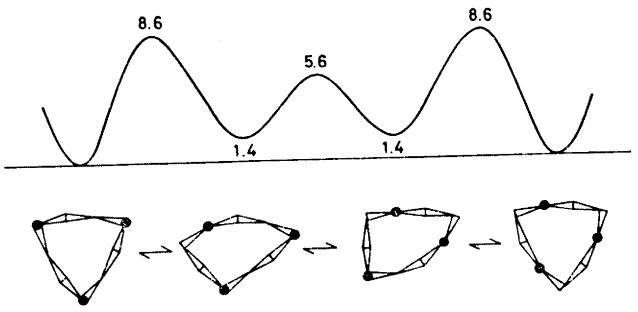

Fig. 10. Interconversion cycle for cyclononane.

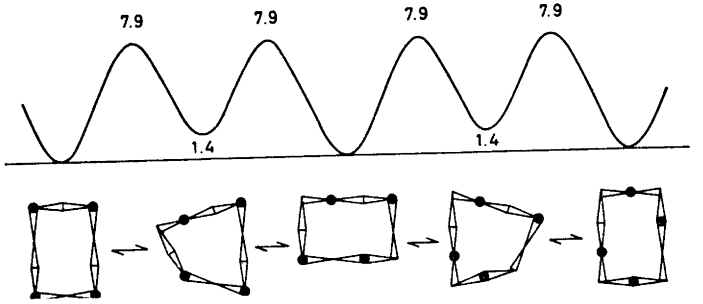

Fig. 11. Double interconversion cycle for cyclodecane.

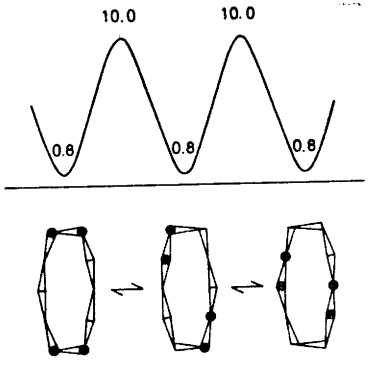

Fig. 12. Two interconversion steps for cyclodecane.

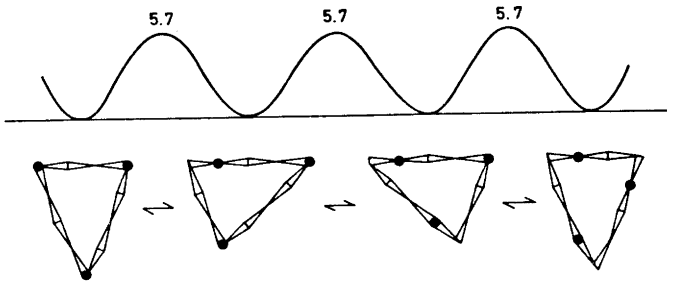

Fig. 13. Triple interconversion cycle for cycloundecane.

formation, but the ring atoms at the remaining two corners are unchanged (Fig. 11). However, if attention is focused on the substituents on each of these, they have undergone site exchange, so that the result has already the appearance of a ring inversion. The calculated value for the two identical barriers is 7.9 kcal/mole, in good agreement with the activation enthalpy value of 6.7 kcal/mol observed [5] by ^{19}F resonance for fluorine site exchange in 1,1-difluorocyclodecane (activation free energy 5.7 kcal/mol at $-135°$).

In order to get a result with the aspect of pseudorotation, the process must be repeated at the remaining corners so that all ring atoms are moved by one step. Exchange of all substituents is obtained by repetitions of the complete cycle; outer substituents become inner, and *vice versa*, each time a corner is passed (Fig. 11). The same exchanges might in principle have been effected by passing through an alternative [1333] intermediate in the middle of each complete cycle, but the necessary [*I*1332] barrier turned out to be forbiddingly high.

It may be of interest to note that the asymmetric [1324] conformation at 4.7 kcal/mol can be converted to its mirror image by passing over the symmetric [*244*] barrier at only 6.6 kcal/mol (Fig. 3), identical with the chair-chair-boat classified by Hendrickson [4] as a conformation. The enthalpy difference is so small (1.9 kcal/mol) that if the NMR-spectrum of this pair of conformers could be observed, it would reflect the symmetry of the barrier.

The other low-enthalpy conformation [1414] is seen from the regular alternation of dihedral angle sign to belong to the crown family and can best undergo ring-atom exchange (Fig. 12) over a particular [**55**] double barrier (Fig. 3) identical with Hendrickson's chair-chair-chair [4] or "stretched crown". Mechanistically, this resembles a pseudorotation, since only one barrier and one minimum are involved, but not energetically, the enthalpy difference being as high as 9.2 kcal/mol. All ring sites become exchanged, but on each carbon one substituent remains inner or "axial", the other outer or "equatorial". To exchange also these, the ring has to pass into some of the other conformations, although a barrier of the type [1*I*314] must be exceedingly high.

Cycloundecane. Of the four low-enthalpy conformations of this ring the two of triangular type interconvert particularly easily. In fact, the lowest conformation [344] can pass over the symmetric [*I*343] barrier at 5.7 kcal/mol (Fig. 4) to its own mirror image, and after three such passages all atoms will have moved by one step around the ring (Fig. 13). After further repetitions, all substituent sites will be exchanged. Mechanistically, this comes closest to a pseudorotation process. However, an even lower barrier [*I*334] at 3.5 kcal/mol (Fig. 4) separates [344] from the [335] conformation, and by switching systematically three times back and forth over only this low barrier, all ring atoms will have moved by two steps around the ring (Fig. 14). After a number of repetitions, all sites will be exchanged.

The interconversion of the two low-lying quinquangular conformations is much more difficult. They can be transformed one to the other over the [*I*21322] barrier at 11.9 kcal/mol, but this will not lead to full exchange of all sites. The [12323] conformation can, however, change slightly uphill to its triangular partner [236], which communicates over the [*I*235] barrier at 10.5 kcal/mol with the [335] conformation; from this point full exchange can be effected through the scheme given in Fig. 14 before return occurs by the same route.

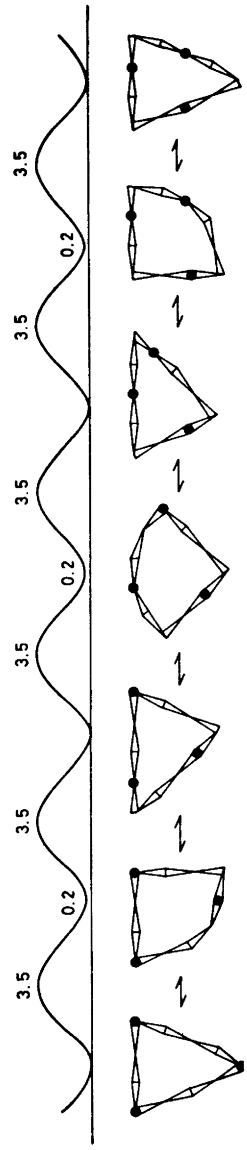

Fig. 14. Complex triple interconversion cycle for cycloundecane.

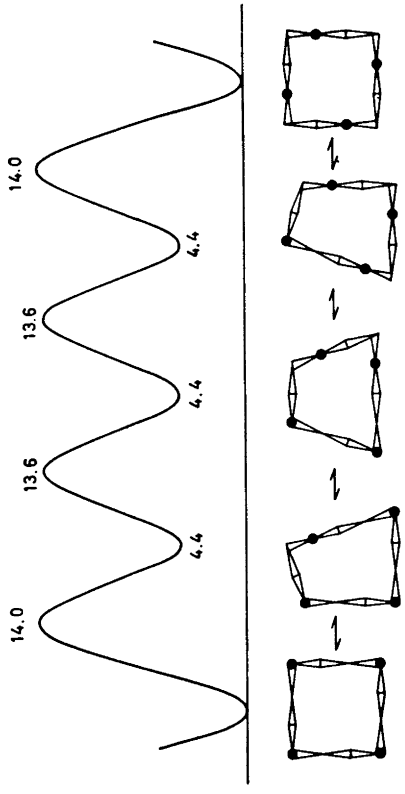

Fig. 15. Interconversion cycle for cyclododecane.

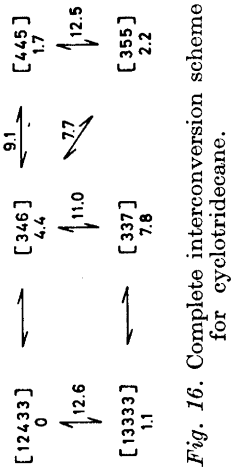

Fig. 16. Complete interconversion scheme for cyclotridecane.

The asymmetric triangular conformation [245] at 2.3 kcal/mol is also isolated by relatively high barriers, both from [344] and [335] by barriers at 11.8 and 14.4 kcal/mol, respectively (Table 1), and from its own mirror image by the symmetric [*1*424] barrier at 11.3 kcal/mol (Fig. 4).

Cyclododecane. The first barrier to pass on any route from the most stable [3333] conformation is [*1*2333], which lies as high as 14.0 kcal/mol (Fig. 5). The most economical route for effecting complete exchange of all sites, is to continue from the resulting [2334] conformation over a slightly lower [*1*3233] barrier to [2343] and then in a reversed fashion, operating at the remaining corners (Fig. 15). An alternative "central" intermediate might have been [2424], but the barrier [*1*2423] which must then be passed is much higher (16.4 kcal/mol).

The lowest calculated barrier [*44*4] at 8.6 kcal/mol (Fig. 5) is of symmetric type and can only serve to interconvert the enantiomers of the asymmetric [1344] conformation, which is nearly as high in enthalpy (7.5 kcal/mol).

Cyclotridecane. The two lowest quinquangular conformations of this ring can interconvert directly over a [*1*21333] barrier at 12.6 kcal/mol. A better path is available if both go smoothly uphill to their triangular partners, [12433] to [346] and [13333] to [337], which communicate over a lower [*1*336] barrier at 11.0 kcal/mol (Fig. 6).

The [346] conformation, although at 4.4 kcal/mol, plays a central role in the dynamics of this ring (Fig. 16), since it is not only the direct partner of the lowest-enthalpy conformation, but is also separated by a single barrier from the other three lowest conformations, notably by the [*1*345] barrier at 9.1 kcal/mol from the most regular triangular conformation [445] needed for complete site exchange. In fact, [445] can be converted to its own mirror image by passing the lowest calculated barrier ([*1*444] at 7.2 kcal/mol) in this ring, and repetition of this process therefore comes closest to a pseudorotation mechanistically. Fig. 17 shows how the lowest conformation [12433] transforms to [445], which then pseudorotates and goes back again to the mirror image with all ring atoms moved by one step.

Also the [355] conformation needs to transform to [346] over a [*1*435] barrier at 7.7 kcal/mol, and further to [445], to effect complete site exchange. The critical barrier will therefore be 9.1 kcal/mol also here, while [13333] has its critical barrier in the earlier step at 11.0 kcal/mol (Fig. 16).

It is important to note that the [*1*444] barrier (Fig. 6), as well as the [*1*363] barrier, which notation-wise are both symmetric, had to be made asymmetric to lower their energy.

Cyclotetradecane. Conversion of the favoured diamond-lattice conformation [3434] to [3344] goes over the rather high [*1*3343] barrier at 13.8 kcal/mol (Fig. 7). Systematic passage over the same barrier three more times (Fig. 18) gives one complete cycle for moving the ring atoms around the ring, and repetitions lead to complete site exchange, exactly as for cyclodecane. Also as for cyclodecane, only half a cycle is needed for substituent site exchange at the two untouched corners. In contrast, however, there is now an alternative and competitive path for the middle part of each cycle over a slightly lower [*1*3334] barrier to a less stable intermediate conformation [3335] and back again (Fig. 18). It may be noted that if this were the only path, it would have led to

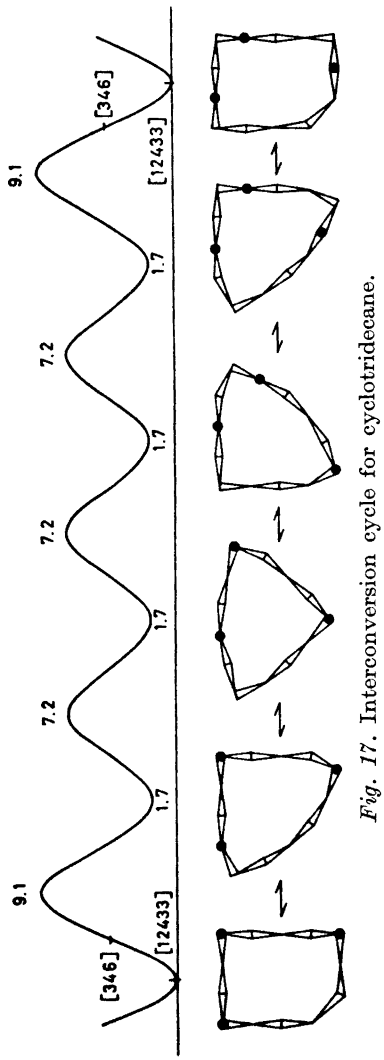

Fig. 17. Interconversion cycle for cyclotridecane.

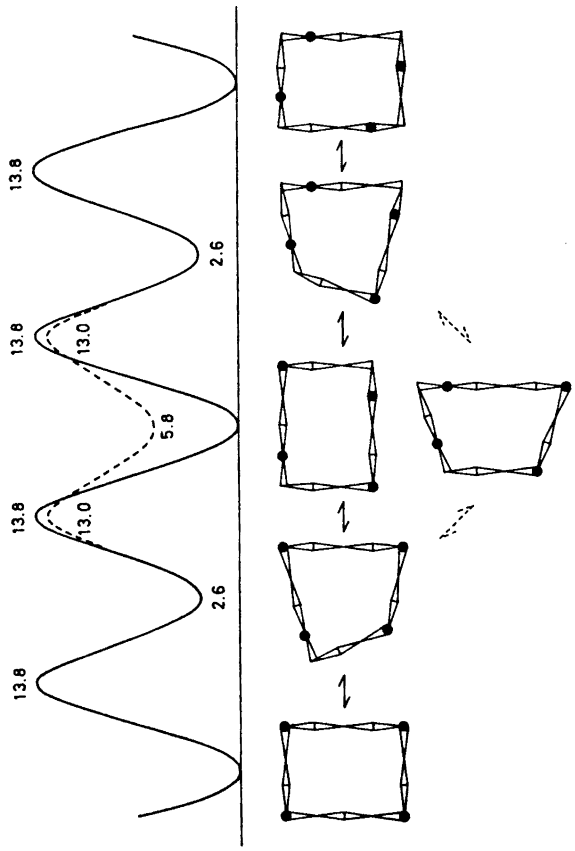

Fig. 18. Double and single interconversion cycles for cyclotetradecane.

exchange of all ring sites, but not to exchange of geminal substituents on each ring atom; outer substituents on long sides would become inner on short sides, and *vice versa*.

Cyclopentadecane. In this ring the lowest-enthalpy conformation [33333] cannot interconvert over any reasonably low and calculable barriers with the other five lowest conformations, which are all of one-bond-side quinquangular type, nor with the triangular counterparts of these latter. Higher-lying conformations [23334] and [23343] must therefore serve as intermediates, and the barriers [*1*23333] (Fig. 8), [*1*23342] and [*1*23432] must be passed to effect inter-

change of all sites. It is noteworthy (Fig. 19) that the decisive barrier, as high as 13.4 kcal/mol, is closest to the stable conformation, and that the highest minimum is surrounded by the lowest barriers.

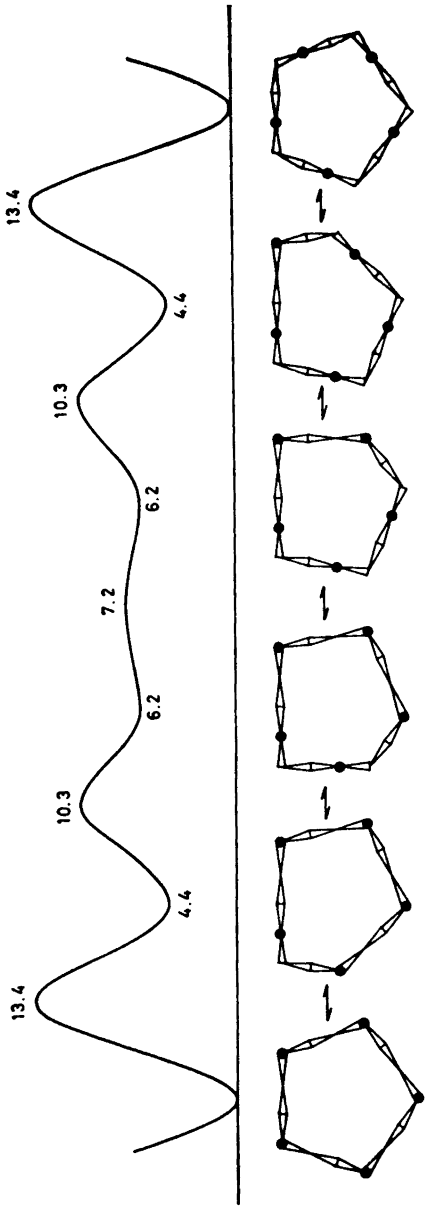

Fig. 19. Interconversion cycle for cyclopentadecane.

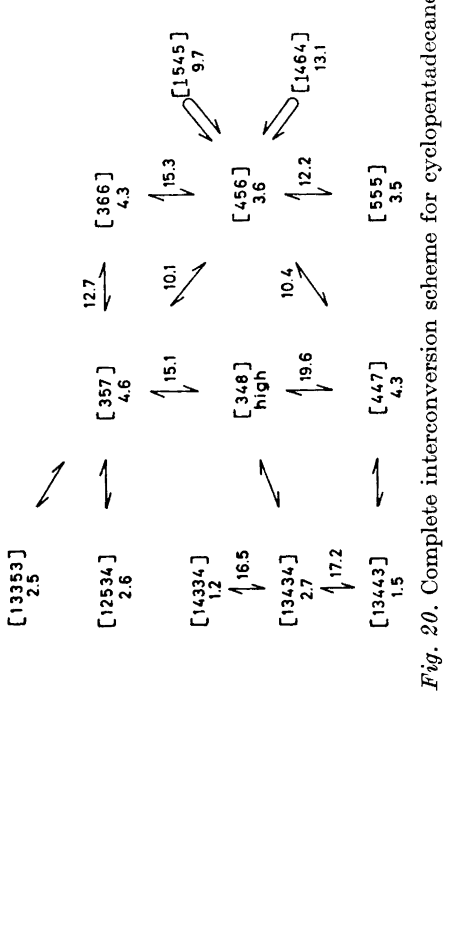

Fig. 20. Complete interconversion scheme for cyclopentadecane.

The direct interconversion of the five next-lowest conformations *via* sexangular barriers is either impossible or requires barriers higher than 16 kcal/mol. Much easier paths are available for four of them *via* their triangular partners and over the corresponding quadrangular barriers, as best clarified in the complete interconversion scheme in Fig. 20. For the dynamics of this ring, the [456] conformation, although itself high in enthalpy, plays a central

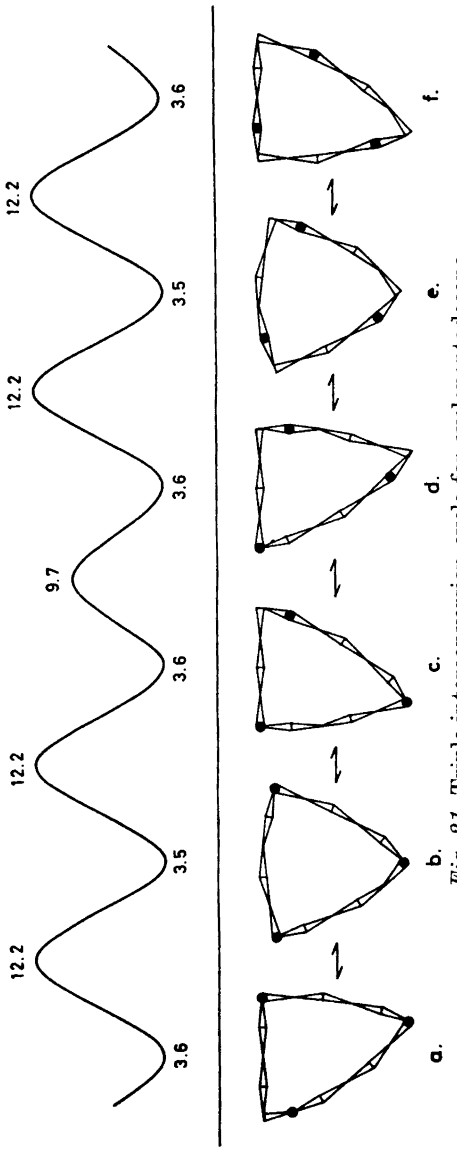

Fig. 21. Triple interconversion cycle for cyclopentadecane.

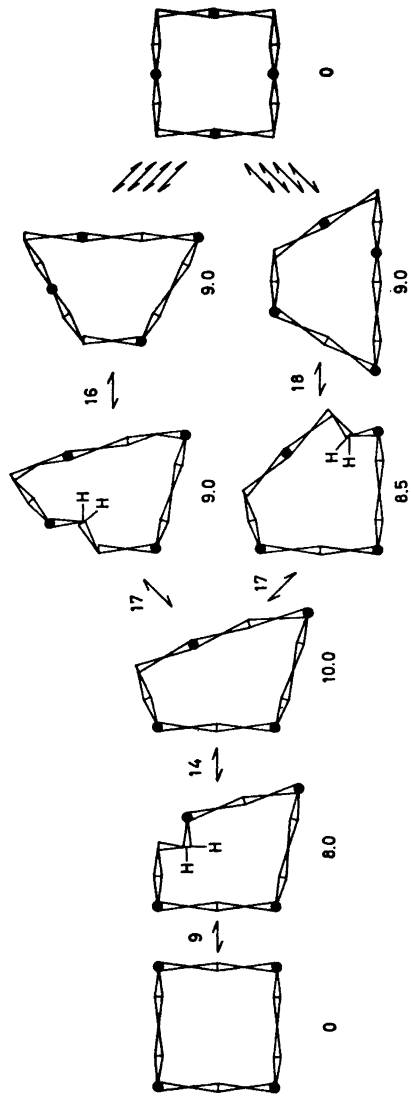

Fig. 23. Complex interconversion cycle for cyclohexadecane (numbers give enthalpies of minima and barriers).

role, as full site exchange must go through it. In fact, passage over either of two notation-wise symmetric, but in reality unsymmetric barriers, the higher [*1*464] or the lower [*1*545], converts this asymmetric conformation to its own mirror image. This is, however, not sufficient, and for full exchange also the [555] conformation is needed as an intermediate. The lowest path is shown in Fig. 21 (a – d or c – f), which also shows the lowest interconversion path for the [555] conformer as such (b-e); the decisive barrier is in both cases [*1*455] at 12.2 kcal/mol. From Fig. 20 it can be concluded that this is also the highest of the barriers in the complete site exchange process for the three conformations [13353], [12534] and [13443], whereas [14334] and [13434] have first to pass the [*1*437] barrier at 15.1 kcal/mol. The lowest of these two, as well as of this whole group of conformations, [14334], must pass even a higher sexangular barrier [*1*31433] at 16.5 kcal/mol (Fig. 20).

Cyclohexadecane. The dynamic situation in this ring is much easier to survey than the foregoing, especially since the intermediate conformations needed on the simplest route to effect complete site exchange of the lowest-enthalpy diamond-lattice conformation [4444] are exactly the three next-lowest conformations (Fig. 22). The [*1*3444] barrier at 12.6 kcal/mol (Fig.

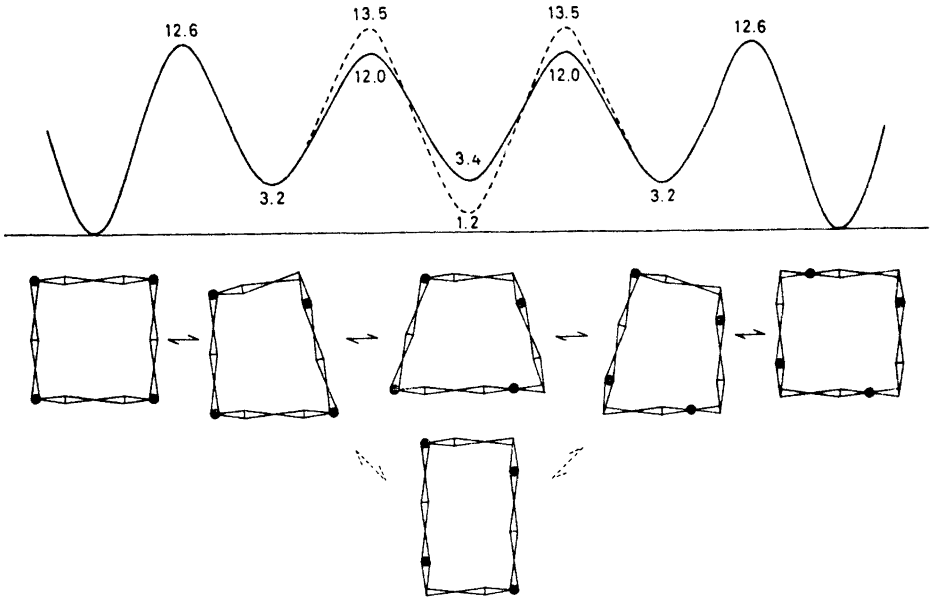

Fig. 22. Two interconversion cycles for cyclohexadecane.

9) is the only possible one for the first step, whereas two paths are available for the second step (Fig. 22). Again, it is a situation where the higher barrier [*1*3534] leads to the lower minimum [3535], and the lower barrier [*1*4344] to the higher minimum [3454].

For this largest ring studied, the elementary conformational process consisting in the rotation of a CH_2-group "through" the ring (Fig. 1d) had to be examined and was found to be a possible mechanism, although requiring the passage of somewhat higher barriers than in the classic "outwards flattening" mechanism (Fig. 1c) considered so far. The transition states are here much more difficult to define, and for simplicity have been assumed to have two synchronously eclipsed bonds. The strained sequence of three bonds at 120°, 180°, and 120° is defined as a "side" and underlined in the notation (Table 1). The calculated enthalpies are thus maximum values and may well be several kcal/mol too high. A complete cycle is now much more complex and includes not only two intermediate quadrangular conformations of high enthalpy, but requires in addition two intermediate conformations of a novel type having isolated *gauche* bonds (Fig. 23) which are also quite high in enthalpy. A most interesting aspect of this particular mechanism in this particular ring is that, if it had been of lowest overall activation enthalpy, only corner positions and central side positions would have been exchanged, while ring atoms next to corner positions would be left unaffected.

A NOTE ON PSEUDOROTATION

Free pseudorotation as defined by Pitzer for cyclopentane [2] is strictly a description of a particular thermodynamic situation rather than of a particular process. This situation is caused by the accidental, and not inherent, absence of an energy barrier between the two non-planar forms of defined symmetry (the envelope and the twist-envelope (half-chair)), and manifested by an increased entropy. Pseudorotation in cyclopentane is also intimately connected with degeneracy; in fact, the two symmetry-defined conformers correspond exactly to the deformations produced by the two symmetry-defined components of the doubly degenerate normal vibration perpendicular to a planar five-membered ring.[6]

An extended definition of pseudorotation was introduced by Hendrickson,[1] based on the analysis of various *mechanistic schemes* for conformational interconversions, and applied even for processes involving rather high barriers. A somewhat different meaning of the word is implied by Anet [7] in his distinction between pseudorotation and inversion in connection with the observation by dynamic NMR spectroscopy of a low-barrier and a high-barrier process in cyclooctane and derivatives. Strictly, this use relates to *the observed result*, the exchange of ring atom positions and geminal substituents respectively, and is independent of the actual mechanisms involved.* As shown earlier in this paper, both types of exchange may in higher cycloalkanes often result from one and the same mechanism.

* The formalism and the type of barriers used in this paper permit deduction of interconversion paths also for cyclooctane, which, although only qualitative, are in perfect correspondence with those proposed by Anet.[7] Thus, the [1223] conformer (boat-chair) may pass over a low barrier to [1232] (twist-boat-chair) and back again to exchange ring sites only, and over a medium barrier to [2222] (boat-boat) and back again to exchange also geminal substituents. The [1313] conformer (twist-chair-chair) meets very low barriers going to a symmetric crown and back again to effect ring-site exchange, but must pass a high barrier to [1223] and further to [2222] and back again to exchange also geminal substituents.

The objections to the use of the term "pseudorotation" to describe the mechanism of ring-atom site exchange (topomerization) in larger rings may therefore be several:

1. The ring is very far from planar.
2. The barriers are not negligible, so that the criterion of high entropy is not met.
3. The ring conformation is not close enough to a regular polygon.
4. The dynamic process is not a simple one with one type of minimum and one type of barrier.

Of the rings examined here, two have a conformation against which only the first two objections can be raised. These are the [344] conformation of the 11-membered ring and the [445] conformation of the 13-membered ring. Both are characterized by being closest possible to regular and by having two equal sides and the third side one bond shorter or longer. This allows a single corner-movement-step of relatively low activation enthalpy to transform it into itself. A similar situation would next arise in the [566] conformation of the 17-membered and the [667] conformation of the 19-membered ring.

It is interesting to note that when the present notation is stretched to include smaller rings, the only formally similar cases would be the [122] conformation of the 5-membered and the [223] conformation of the 7-membered ring. These are easily identified with the two most perfect examples of pseudorotation, both formally and energetically, namely the twist-envelope of cyclopentane,[2] with the symmetrical barrier [1*1*12] corresponding to the envelope, and the twist-boat of cycloheptane,[1] with the symmetrical barrier [*1*222] corresponding to the boat.

Also quinquangular conformations provide examples of possible genuine pseudorotation, at least formally: the [12222] conformation of cyclononane and the [22223] conformation of cycloundecane; the relevant barriers are [1*1*1222] and [*1*22222].

REFERENCES

1. Hendrickson, J. B. *J. Am. Chem. Soc.* **89** (1967) 7047.
2. Pitzer, K. S. and Donath, W. E. *J. Am. Chem. Soc.* **81** (1959) 3213.
3. Anet, F. A. L. and Wagner, J. J. *J. Am. Chem. Soc.* **93** (1971) 5266.
4. Hendrickson, J. B. *J. Am. Chem. Soc.* **86** (1964) 4854.
5. Noe, E. A. and Roberts, J. D. *J. Am. Chem. Soc.* **94** (1972) 2020.
6. Dale, J. *Spectrochim. Acta* **19** (1963) 521.
7. Anet, F. A. L. In Chiurdoglu, G., Ed., *Conformational Analysis*, Academic, New York 1971, p. 15.

Received October 9, 1972.

ACTA CHEMICA SCANDINAVICA 27 (1973) 1149–1158

Exploratory Calculations of Medium and Large Rings

Part 3. Mono- and Bis(*gem*-dimethyl)cycloalkanes

JOHANNES DALE

Kjemisk Institutt, Universitetet i Oslo, Oslo 3, Norway

A conformational analysis of *gem*-dimethyl substituted cycloalkanes has been carried out based on calculated data for conformational minima and barriers of unsubstituted cycloalkanes. 1,2- and 1,3-Bis-substitution must always perturb any ring conformation; 1,4- and more distant relative substitution will perturb only some of the ring conformations.

Complete exchange of ring-atom and substituent sites to give a time-averaged higher symmetry will always require passage over increased barriers, whereas partial site exchange should in some cases be possible over unchanged barriers.

The introduction of a single substituent, such as a methyl group, into medium- and large-ring cycloalkanes is not expected to change the stability order of the possible ring conformations, since there will always be on each of these a number of unhindered positions for the substituent. It should, however, lead to a complex mixture of conformers differing only in the choice of methyl group position on the lowest-enthalpy ring conformation(s).

When two ring atoms are singly substituted, some restrictions are introduced both for the *cis*- and *trans*-isomer, but there will in general still be too many possibilities to warrant a detailed discussion.

A *gem*-dimethyl substituted carbon, on the other hand, is always restricted to corner positions in rings of the sizes discussed here ($C_9 - C_{16}$) on a simple steric hindrance argument. There is also an additional factor which favours the corner positions even in rings large enough to accommodate an internal methyl group in certain non-corner positions, such as the middle positions on "long sides" in the [3636] conformation of cyclooctadecane. Since no energy difference between *gauche* and *anti* (with respect to the ring skeleton) is expected in the ring bond adjacent to the substituted atom (methyl is equivalent to methylene), a ring corner can be built around this atom without the expenditure of two extra *gauche*-butane interactions. The total economy of the ring is thereby improved. The number of conformers on each of the ring confor-

mations (in unchanged stability order) will therefore become rather small and surveyable. The most interesting consequence is, however, that the conformational interconversion paths derived in Part 2 will become partially or completely blocked because intermediate conformations and their adjoining barriers will be higher in energy.

When two ring carbon atoms are *gem*-dimethyl substituted, the number of possible conformers on each ring conformation becomes severely limited, because their relative position must fit the relative position of two corner atoms. This also means of course that in certain cases the lowest-enthalpy conformation for the unsubstituted ring may be excluded and a higher one become the preferred. The argument implies that corner occupation by methyl substituents does not perturb the ring conformation. Obviously, this cannot be true when the *gem*-dimethyl groups are 1,2- and 1,3-related. Thus, in the 1,2-case only conformations having a one-bond "side" can have both substituted carbons at corners, and since there is then always considerable eclipsing both in this bond and in adjacent ring bonds (Part 1), the strongly increased torsional barriers due to the crowding of methyl groups will raise the energy. Similarly, in the 1,3-case only conformations with a two-bond "side" can have both substituted carbons at corners, but although there must be some increased torsional strain due to the (less severe) methyl crowding in adjacent partially eclipsed ring bonds (Part 1), it is the 1,3-diaxial-like methyl-methyl interaction which is certainly the most serious. Due to transannular repulsion between 1,5-related methylene groups (Part 1), the "axial" methyl groups become squeezed together much more than those in the familiar cyclohexane case.

For such reasons the discussion of bis(*gem*-dimethyl)cycloalkanes will be limited to those isomers which have the substituted carbon atoms separated by two or more methylene groups. The best conformation will be predicted for each isomer and the possible partial interconversion paths over unchanged barriers deduced. No attempt will, however, be made to estimate the heights of barriers which are increased by extra methyl-ring or methyl-methyl interactions and which must be passed to effect full site exchange.

A fundamental assumption in the procedure is that *gem*-dimethyl substitution does not raise the energy of interconversion barriers as long as substituted atoms remain in corner positions and do not form part of the flattened four-carbon system common to most barriers (Part 2), nor in the critical portions of other barrier types.

SUBSTITUTED CYCLONONANES

1,1-Dimethyl. There is one possible conformer on the lowest [333] ring conformation (Fig. 1). Like unsubstituted cyclononane, it may pass the unchanged [*1*233] barrier to [234], then continue over the unchanged [*1*323] barrier to a [234] conformer having the *gem*-dimethyl group on a different corner, but the last [*1*233] barrier in this cycle, as well as the resulting [333] conformer with a *gem*-dimethyl group at a non-corner position, must be of increased energy. Return to the initial conformer over only unchanged barriers will produce

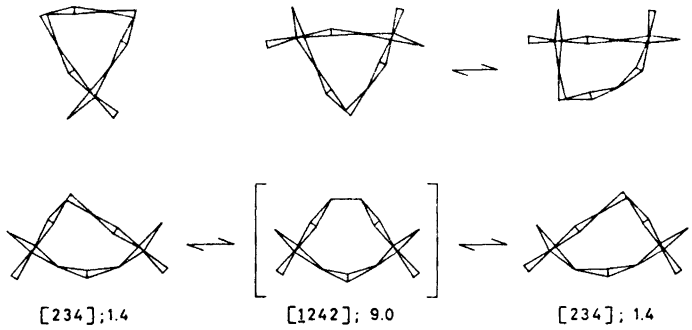

Fig. 1. Lowest conformations for substituted cyclononanes.

no partial averaging. The second of the three cycles needed to bring about full site exchange, involves barriers whose energies are now all increased, but differently, by the *gem*-dimethyl group. Once these are passed, the third cycle is identical with the first. The decisive barrier in this over-all process has been determined [1] as ~ 9 kcal/mol (free energy) by ^{13}C and ^{1}H spectroscopy, and is to be compared with the experimental value of ~ 6 kcal/mol for cyclononane itself.[1]

1,1,4,4-Tetramethyl. There is only one possible conformer on the lowest [333] as well as on the next-lowest [234] ring conformations (Fig. 1). The former may pass over the unchanged [*1*233] barrier to the latter and back again unchanged, but all further steps on the full-exchange path must go over increased [*1*323] and [*1*233] barriers, and *via* high-energy intermediate conformers, most of which involve very serious transannular methyl-methyl interactions. One would therefore expect more than a simple additive effect of the methyl groups on the barrier height, in agreement with the observed ^{1}H spectroscopic value of ~ 20 kcal/mol.[2]

1,1,5,5-Tetramethyl. The [333] conformation is now excluded and [234] becomes the lowest with [12222] next; on each of these latter ring conformations there is only one possible conformer. A time-averaging process (Fig. 1) over an unchanged [*1*242] barrier, actually identical with Hendrickson's chair-boat,[3] will give to the [234] conformer the apparent symmetry of this barrier; its calculated net barrier height is 7.6 kcal/mol. Full exchange requires the passage also over [*1*233] barriers to intermediate [333] conformers, all of considerably increased energies.

SUBSTITUTED CYCLODECANES

1,1-Dimethyl. There is only one possible conformer on the lowest [2323] ring conformation. Two passages over [*1*2232] barriers of unchanged energy *via* either of two intermediate [2233] conformations (Fig. 2, R = Me, R′ = H or R = H, R′ = Me) will produce time-averaging so that the apparent symmetry corresponds to that of the intermediates. This means that all ring atoms as

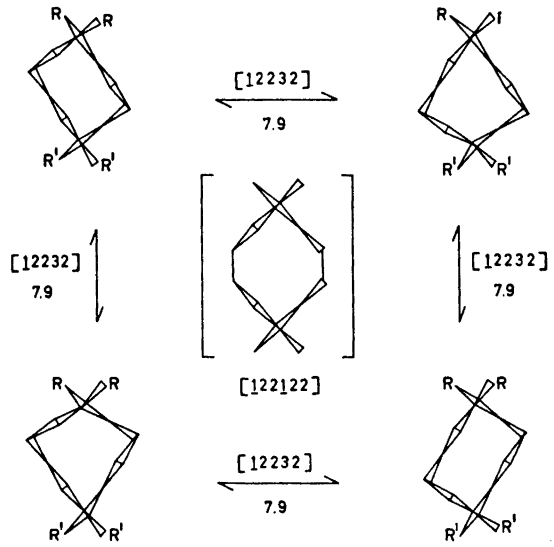

Fig. 2. Partial interconversion of 1,1- or 1,1,6,6-substituted cyclodecanes.

well as the 1-methyls and 6-hydrogens obtain the constitutional symmetry, whereas the hydrogens on all other ring atoms will be geminally non-equivalent. For full site exchange, [*1*2232] barriers of increased energy must be passed in subsequent cycles.

1,1,4,4-Tetramethyl. The only conformer possible on the lowest [2323] ring conformation (Fig. 3) can be converted over the unchanged [*1*2232] barrier to the only conformer possible on the [2233] conformation (Fig. 3), but it can only return by the same route. Any type of site exchange must therefore take place over increased barriers.

1,1,5,5-Tetramethyl. The lowest [2323] ring conformation is now excluded. The [1414] conformation is the lowest one that can accommodate the *gem-*

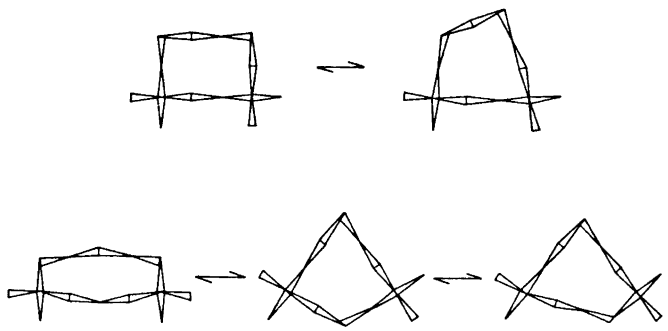

Fig. 3. Lowest conformations for substituted cyclodecanes.

dimethyl groups, and this in a single manner (Fig. 3), and it can only undergo pseudorotation-like exchange over [**55**] barriers and through intermediate conformations of increased energy. Also the two next-lowest [2233] and [1333] conformations can accept this substitution pattern, each in only one way (Fig. 3), and these are the conformers actually found in the crystal lattice of 4,4,8,8-tetramethyl-cyclodecane-carboxylic acid.[4]

1,1,6,6-Tetramethyl. A single conformer is possible on the lowest [2323] ring conformation (Fig. 2, R = R′ = Me). Exactly as for 1,1-dimethylcyclodecane, the unchanged [*I*2232] barrier can be passed twice to effect partial exchange. Since the two intermediate [2233] conformers (of unchanged energy) are now identical, again the ring atoms and the methyl groups acquire by time-averaging the constitutional symmetry corresponding to an imaginary superposition of both barriers (center of Fig. 2). The methylene hydrogens remain geminally non-equivalent. Full site exchange requires passage over further [*I*2232] barriers of much increased energy. Also the next lowest [1414] ring conformation can accept this substitution pattern.

SUBSTITUTED CYCLOUNDECANES

1,1-Dimethyl. The four lowest ring conformations are very close in energy, and as each has two or more types of corner positions able to accommodate the *gem*-dimethyl group, no clear preference for any of these can be recognized. Thus, the two triangular ring conformations, [344] and [335], will have two types of such corners, and the two quinquangular ones, [12323] and [13223], will have three and two types, respectively, and even more if corners at one-bond "sides" are also included. Partial interconversion within each, and between some of them, will be possible over unchanged barriers, but will be too complex to warrant a consideration in the necessary detail.

1,1,4,4-Tetramethyl. If again corner positions at one-bond "sides" are excluded, there will be one possible conformer for each of the [344], [335] and [12323] ring conformations, but none for [13223]. The [344] conformer (Fig. 4) cannot pass any unchanged "pseudorotation barrier" [*I*343] at all and passage over the unchanged [*I*334] barrier leads to no averaging process; therefore increased barriers must be passed to effect any site exchange. The [335] conformer, on the other hand, can go twice over the unchanged and low [*I*334] barrier to its mirror image *via* the [344] conformer, whose apparent symmetry it acquires by such time-averaging (Fig. 4). Full exchange requires the passage over increased barriers.

1,1,5,5-Tetramethyl. One conformer is possible on each of the [344] and [13223] ring conformations, but none on [335] and [12323]. The [344] conformer can pass to its mirror image over the unchanged [*I*343] barrier and acquire its symmetry by time-averaging (Fig. 4). Full exchange requires passage over increased barriers. The [13223] conformer (Fig. 4) cannot acquire higher symmetry by averaging over unchanged barriers, and must pass increased barriers for any site exchange.

1,1,6,6-Tetramethyl. The situation is here reversed from the preceding case, with one possible conformer on each of the [335] and [12323] ring conformations,

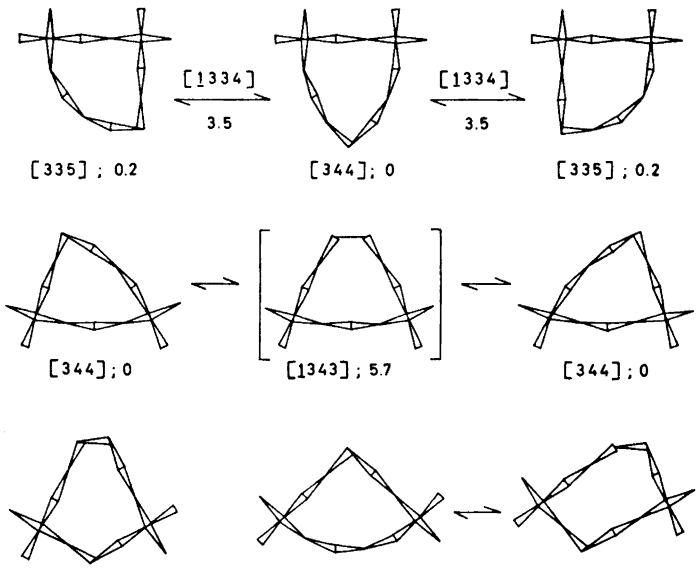

Fig. 4. Lowest conformations for substituted cycloundecanes.

but none on [344] and [13223]. The [335] conformer (Fig. 4) must pass increased barriers to produce any kind of site exchange, whereas the [12323] conformer (Fig. 4) could conceivably pass *via* its triangular partner [236] over an unchanged [*1*262] barrier, which however turned out to be forbiddingly high even in cycloundecane itself, to the enantiomeric [236] conformer and further to the enantiomeric [12323] conformer, whereby averaged constitutional symmetry would be obtained for the ring atoms.

SUBSTITUTED CYCLODODECANES

1,1-Dimethyl. One conformer (Fig. 5) is possible on the lowest [3333] ring conformation, and although it can pass unchanged barriers in the three first steps of the first cycle (Part 2, Fig. 15), the subsequent barriers which have to be passed to effect any type of site exchange, are of increased energy.

1,1,4,4-Tetramethyl. Again there is only one possible conformer on the lowest [3333] ring conformation (Fig. 5), and again no site exchange can occur over unchanged barriers.

1,1,5,5-Tetramethyl. The lowest [3333] ring conformation is now excluded, but the two next lowest, [2334] and [2343], can accommodate the substituents each in one way. The former is asymmetric and can pass twice over the unchanged [*1*2342] barrier through the latter conformation as an intermediate so as to acquire its symmetry by time-averaging (Fig. 5). The calculated net barrier is 7.7 kcal/mol. Full site exchange requires the passage over increased barriers.

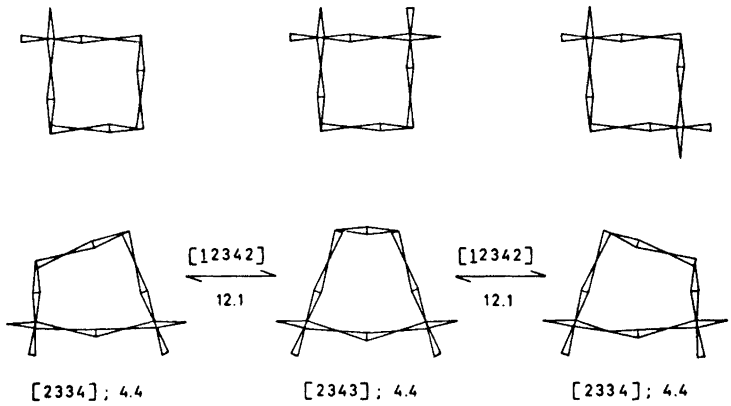

Fig. 5. Lowest conformations for substituted cyclododecanes.

1,1,6,6-Tetramethyl. The lowest [3333] ring conformation is excluded also for this isomer, and again both [2334] and [2343] can accommodate the methyl groups, each in one manner. These two conformers (Fig. 6) can transform one to the other either over the unchanged [*12*342] barrier (calculated net height 7.7 kcal/mol) or over the slightly higher unchanged [*13*233] barrier (calculated net height 9.2 kcal/mol). Successive passage over both barriers will convert either conformer to its mirror image so as to produce an apparent averaged symmetry corresponding to the imaginary superposition of both barriers (center, Fig. 6). The constitutional symmetry is thus attained for the ring atoms,

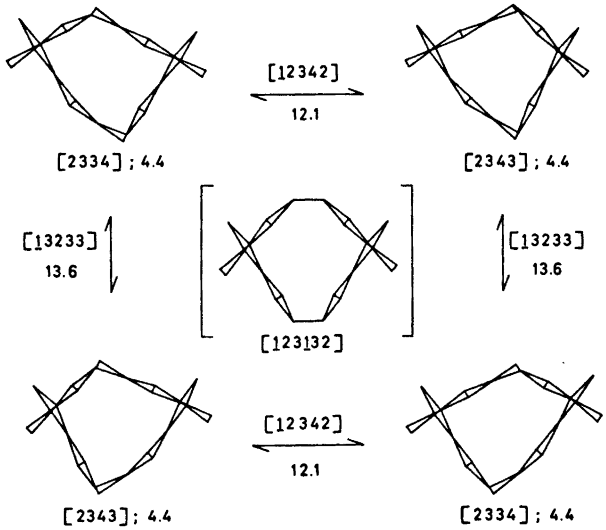

Fig. 6. Partial interconversion of 1,1,6,6-substituted cyclododecane.

but to average also geminal hydrogens and methyls, increased barriers must be passed.

1,1,7,7-Tetramethyl. There is only one possible conformer on the lowest [3333] ring conformation (Fig. 5). No site exchange can occur without passage over increased barriers.

SUBSTITUTED CYCLOTRIDECANES

For this and the larger rings only the most stable conformations will be deduced. The possible partial interconversion processes over unchanged barriers, which lead to time-averaged higher apparent symmetry, can be derived along the same lines as given in detail in the preceding discussions of the medium rings.

1,1-Dimethyl. Excluding *gem*-dimethyl groups at one-bond "sides", there still remain three possible equienergetic conformers on the lowest [12433] ring conformation. Partial averaging paths are available for all.

1,1,4,4-Tetramethyl. Only one conformer is possible on the lowest [12433] ring conformation. Partial averaging can occur.

1,1,5,5-Tetramethyl. There is again only one conformer on the lowest ring conformation [12433], and partial averaging is possible.

1,1,6,6-Tetramethyl. Both lowest ring conformations [12433] and [13333] are now excluded, but one conformer is possible on each of the two next lowest [445] and [355]. Only the latter can undergo partial averaging.

1,1,7,7-Tetramethyl. One conformer is possible on the lowest [12433] ring conformation, and it can be partially averaged.

SUBSTITUTED CYCLOTETRADECANES

1,1-Dimethyl. There is only one conformer on the lowest [3434] ring conformation, and it can undergo partial averaging of the same type as shown in Fig. 2 for 1,1-dimethylcyclodecane.

1,1,4,4-Tetramethyl. Only one conformer is possible on the lowest [3434] ring conformation. No partial averaging can take place.

1,1,5,5-Tetramethyl. Again only one conformer is possible on the lowest [3434] ring conformation, and again no partial averaging can take place.

1,1,6,6-Tetramethyl. Both lowest ring conformations [3434] and [3344] are excluded. One conformer is possible on the next lowest [3335] ring conformation, and it has no partial averaging process.

1,1,7,7-Tetramethyl. The lowest ring conformation [3434] is excluded, but one conformer is possible on the next lowest [3344]. No partial averaging can occur.

1,1,8,8-Tetramethyl. Only one conformer is possible on the lowest [3434] ring conformation; it can undergo partial averaging of the same type as shown in Fig. 2 for 1,1,6,6-tetramethylcyclodecane.

SUBSTITUTED CYCLOPENTADECANES

1,1-Dimethyl. There is only one conformer on the lowest [33333] ring conformation, and it cannot undergo partial averaging.

1,1,4,4-Tetramethyl. Only one conformer is possible on the lowest [33333] ring conformation, and it has no partial averaging path.

1,1,5,5-Tetramethyl. Both lowest ring conformations [33333] and [14334] are excluded. One conformer only is possible on the next-lowest ring conformation [13443], and partial averaging can occur.

1,1,6,6-Tetramethyl. All three lowest ring conformations [33333], [14334], and [13443] are excluded. One conformer is possible on each of the next-lowest [13353] and [12534], and both can undergo partial averaging.

1,1,7,7-Tetramethyl. There is one conformer on the lowest [33333] ring conformation and it has a partial averaging process.

1,1,8,8-Tetramethyl. Both lowest ring conformations [33333] and [14334] are excluded. One conformer only is possible on the next-lowest [13443], and no partial averaging path is available.

SUBSTITUTED CYCLOHEXADECANES

1,1-Dimethyl. One conformer is possible on the lowest [4444] ring conformation. It can undergo no partial averaging.

1,1,4,4-Tetramethyl. The lowest ring conformation [4444] is excluded. One conformer is possible on the next-lowest [3535]; it can undergo no partial averaging.

1,1,5,5-Tetramethyl. There is one conformer on the lowest ring conformation [4444]; no partial averaging can occur.

1,1,6,6-Tetramethyl. The lowest ring conformation [4444] is excluded. On the next-lowest [3535] one conformer is possible; it can undergo no partial averaging.

1,1,7,7-Tetramethyl. All five lowest ring conformations (Part 1, Fig. 11) are excluded, but the three next-lowest [3436], [3355] and [2536] can have one conformer each. The two former have no partial averaging processes, whereas the latter has.

1,1,8,8-Tetramethyl. Both lowest ring conformations [4444] and [3535] are excluded. The two next-lowest [3445] and [3454] can have one conformer each, and both can convert to each other by passage over two different unchanged barriers in the same way as demonstrated in Fig. 6 for 1,1,6,6-tetramethylcyclododecane. Also the [2545] ring conformation fits 1,1,8,8-substitution if one substituted atom occupies a corner next to a two-bond "side", but this is assumed to raise somewhat its energy.

1,1,9,9-Tetramethyl. One conformer is possible on the lowest [4444] ring conformation. No partial averaging path is available.

Acknowledgements. The work presented in this and the preceding two papers was carried out during my visits to Brandeis University, Waltham, Mass., and the University of California, Los Angeles, Calif. I thank Professors F. A. L. Anet, E. Grunwald, and J. B. Hendrickson, as well as Dr. J. D. Schofield, for their interest and helpful criticism, and *Norges Teknisk-Naturvitenskapelige Forskningsråd* for a grant.

REFERENCES

1. Anet, F. A. L. and Wagner, J. J. *J. Am. Chem. Soc.* **93** (1971) 5266.
2. Borgen, G., Dale, J. and Schaug, J. *Acta Chem. Scand.* **26** (1972) 1073.
3. Hendrickson, J. B. *J. Am. Chem. Soc.* **86** (1964) 4854.
4. Dunitz, J. D. *Perspectives in Structural Chemistry* **2** (1968) 1.

Received October 9, 1972.

ACTA CHEMICA SCANDINAVICA 27 (1973) 1159–1161

Studies on the Kolbe Electrolysis

X.[1] Generation of Optically Active Radicals from Monoethyl (+)-Ethylmethylmalonate and Their Fate in a Mixed Coupling Reaction

L. EBERSON* and G. RYDE-PETTERSON

Division of Organic Chemistry 1, Chemical Center, University of Lund, P.O. Box 740, S-220 07 Lund, Sweden

The mixed Kolbe coupling of monoethyl (+)-ethylmethylmalonate and isovaleric acid at a platinum anode in methanol has been found to give a product which is racemized to an extent of at least 99.98 %.

The problem of free *vs.* adsorbed radicals, R·, as intermediates in the Kolbe electrochemical oxidation of carboxylates, $RCOO^-$, has been under lively discussion during recent years.[2–5] The overwhelming part of the evidence from electrochemical studies seems to indicate that formation of the coupling product, R–R, takes place *via* adsorbed radicals;[5] on the other hand, there is no real need for this postulate in order to account for the product distributions observed.[4,6,7] In particular, it has been suggested [4] that the formation of racemized coupling products from the anodic oxidation of optically active carboxylates having an asymmetric α carbon atom [8,9] must be due to the intervention of free radicals, since a mechanism involving adsorbed radicals would be expected to give coupling products with at least partial retention of configuration. On the other hand, it has been claimed that the microscopic roughness of the anode surface might as well provide the necessary racemization mechanism.[5]

While the nature of the racemization step must still be a matter for speculation, the stereochemical studies referred to above [8,9] are not entirely satisfactory for the distinction between different mechanisms. Even a small degree of retention of configuration in the coupling product would constitute significant evidence in favor of the postulate of adsorbed radicals as intermediates, and hence it is important to know the exact extent of racemization. The two studies reported [8,9] do not give exact data on this point, and we there-

* To whom inquiries should be addressed.

fore decided to undertake a study of a more suitable system. This paper is a report of the stereochemistry of the mixed Kolbe coupling of a mixture of monoethyl (+)-ethylmethylmalonate and isovaleric acid. The mixed coupling product, ethyl ethylisobutylmethylacetate, is racemic to an extent of 99.98 %.

RESULTS AND DISCUSSION

The system studied, mixed coupling between monoethyl ethylmethylmalonate and isovaleric acid (eqn. 1), was chosen because of the relatively good yields of coupling product that are obtained in mixed couplings of

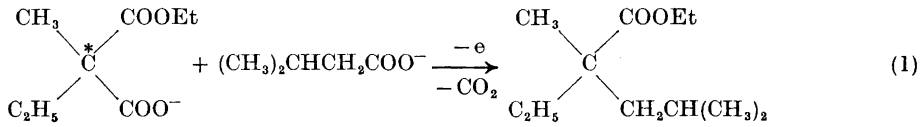

(1)

substituted malonates and alkanoic acids [10] and the fact that the optical properties of the product are well known.[11] It is especially important to note that ethylisobutylmethylacetic acid has a relatively high specific rotation allowing for a high precision in measuring the degree of racemization. For the same reason, a mixed coupling process was preferred in order to avoid dilution by the *meso* isomer that always accompanies the *dl* isomer in a symmetrical coupling process.[12,13]

Monoethyl ethylmethylmalonate was completely resolved,[14] and then electrolyzed together with isovaleric acid in a 1 : 3 ratio in methanolic solution at a platinum anode, the acid mixture being neutralized with potassium hydroxide to an extent of 1 %. The reaction mixture was worked up as described previously,[10] giving 99 % pure (GLC) ethyl ethylisobutylmethylacetate in 23 % yield. After preparative GLC to remove the last traces of impurities, $[\alpha]_{589}^{25}$ of a neat sample was $0.004 = 0.002°$, showing that racemization had taken place to an extent of at least 99.98 %. A sample of ethyl ethylisobutylmethylacetate of 62.7 % optical activity ($[\alpha]_{589}^{25} \pm 13.44°$; neat) was prepared from the optically active acid [12] by treatment of its chloride with ethanol and used as a reference compound.

Thus, in the above coupling process racemization takes place to a very high extent, indicating that a very efficient racemization step must be included in the mechanism. At present, we do not wish to discuss the nature of this step in any length, but it is obvious that a mechanism involving discharge of adsorbed carboxylate ions with formation of free radicals, as previously suggested,[2,4] provides a satisfactory racemization process. This is, however, in conflict with results from electrochemical studies [5] showing that adsorbed radicals must be involved. Recent studies [15] on the competition between 2e-(acetamidation) and 1e-oxidation (coupling) of carboxylates at the carbon anode in acetonitrile as a function of the chain-length of the carboxylate indicate that readsorption of initially formed free radicals might play an important role. For short-chain carboxylates, readsorption of radicals is favored (and leads to further oxidation to carbonium ions in the particular case of carbon anodes), whereas for long-chain radicals a stacking or layering effect prevents

the radicals from diffusing toward the anode surface, coupling thus becoming the favored process. Similar conclusions were reached in a study of the competition between 2e- (methoxylation) and 1e-oxidation (coupling) in the electrolysis of phenylacetate ions.[16]

EXPERIMENTAL

Resolution of monoethyl ethylmethylmalonate. This resolution was made according to the procedure described by Kenyon and Ross,[14] $[\alpha]_{589}^{22}$ (Perkin-Elmer 141 polarimeter) for the completely resolved compound being $+3.38°$ ($c = 9.3$, chloroform); reported [14] $[\alpha]_{589}^{18} = 3.38°$ ($c = 15.0$, chloroform).

(+)-*Ethylisobutylmethylacetic acid.* The acid was prepared as described previously [10] and was partially resolved by recrystallization of its brucine salt.[11] The distilled optically active acid had $[\alpha]_{589}^{24} = +13.44°$ ($c = 9.5$, 95 % ethanol), corresponding to a degree of resolution of 62.7 %.[11]

Ethyl (+)-*ethylisobutylmethylacetate.* Optically active ethylisobutylmethylacetic acid (2.0 g) from above was treated with thionyl chloride (5 ml) in ether (5 ml) overnight at room temperature and then the solution was refluxed for 3 h. After evaporation of the volatile components, the residue was refluxed with absolute ethanol (5 ml) for 48 h, whereafter the ethanol was distilled off. Distillation then gave the ethyl ester (2.0 g), b.p. 75–76°/11 mm. The last traces of impurities were removed by preparative GLC on a 9 mm × 4 m Apiezon L column at 150° (Autoprep gas chromatograph), $[\alpha]_{589}^{25} = 13.44°$ (neat).

Mixed coupling of monoethyl (+)-*ethylmethylmalonate and isovaleric acid.* This reaction was carried out as described previously,[10,12] with fully resolved monoethyl (+)-ethylmethylmalonate (12.0 g) and isovaleric acid (21.3 g), partly neutralized with potassium hydroxide (0.16 g), in methanol (200 ml). The product was distilled and a fraction (3.5 g) with b.p. 79–80°/15 mm was collected. After preparative GLC on the same column as above the sample showed $[\alpha]_{589}^{25} = 0.004 \pm 0.002°$ (neat).

Acknowledgements. Financial support from the *Swedish Natural Science Research Council* (to L. E.) and the *Faculty of Science*, University of Lund, (to G. R.-P.) is gratefully acknowledged.

REFERENCES

1. Paper IX: Eberson, L., Gränse, S. and Olofsson, B. *Acta Chem. Scand.* **22** (1968) 2462.
2. Eberson, L. *Acta Chem. Scand.* **17** (1963) 2004.
3. Conway, B. E. and Vijh, A. K. *Electrochim. Acta* **12** (1967) 102.
4. Eberson, L. *Electrochim. Acta* **12** (1967) 1473.
5. Vijh, A. K. and Conway, B. E. *Chem. Rev.* **76** (1967) 623.
6. Eberson, L. In Baizer, M. M., Ed., *Organic Electrochemistry*, Dekker, New York 1973, Chapter 13.
7. Eberson, L. In Patai, S., Ed., *Chemistry of Carboxylic Acids and Esters*, Interscience, London 1970, Chapter 2.
8. Kharasch, M. S., Kuderna, J. G. and Urry, W. H., cited from Wheland, G. *Advanced Organic Chemistry*, 2nd Ed., Wiley, New York 1949, p. 714.
9. Wallis, E. S. and Adams, F. H. *J. Am. Chem. Soc.* **55** (1933) 3838.
10. Eberson, L. *J. Org. Chem.* **27** (1962) 3706.
11. Doering, W. von E. and Wiberg, K. *J. Am. Chem. Soc.* **72** (1950) 2608.
12. Eberson, L. *Acta Chem. Scand.* **13** (1959) 40.
13. Eberson, L. *Acta Chem. Scand.* **14** (1960) 641.
14. Kenyon, J. and Ross, W. A. *J. Chem. Soc.* **1951** 3407.
15. Muck, D. L. and Wilson, E. R. *J. Electrochem. Soc.* **117** (1970) 1358.
16. Coleman, J. P., Utley, J. H. P. and Weedon, B. C. L. *Chem. Commun.* **1971** 438.

Received November 11, 1972.

ACTA CHEMICA SCANDINAVICA 27 (1973) 1162–1174

Palladium(II) Catalyzed Aromatic Acetoxylation

I. Factors Influencing the Nuclear Acetoxylation of *p*-Xylene

LENNART EBERSON* and LUIS GOMEZ-GONZALEZ

Division of Organic Chemistry 1, Chemical Center, University of Lund, P.O. Box 740, S-220 07 Lund, Sweden

The reaction between Pd(II) acetate and *p*-xylene in acetic acid has been studied with the intention of developing an efficient process for preparing the nuclear acetoxylation product, 2,5-dimethylphenyl acetate. This compound can actually be obtained as the main product when *p*-xylene is treated with Pd(II) acetate in refluxing acetic acid in the presence of oxygen; the reaction is catalytic in Pd(II) but is unfortunately too slow for practical use. Addition of alkali metal acetates, *e.g.* sodium acetate, favors the formation of the α acetoxylation product, *p*-methylbenzyl acetate, at the expense of the nuclear acetate. The nature of the alkali metal cation strongly affects the rate of formation of *p*-methylbenzyl acetate. This is probably due to the intervention of binuclear complexes between Pd(II) acetate and the alkali metal acetate as the oxidizing species (as supported by kinetic studies).

Palladium compounds play an important role in organic synthesis,[1–3] especially in connection with the chemistry of olefinic compounds. The Wacker process, air oxidation of ethylene in the presence of catalytic amounts of palladium(II) chloride, is a prominent example of such reactions on an industrial scale, whereas Heck's work [3] beautifully demonstrates the synthetic applications in the laboratory.

Aromatics can also function as substrates for oxidation by Pd(II) complexes. The most important reaction types hitherto observed are coupling to form biaryls [4–12] or sometimes diphenylmethane derivatives,[8] and oxidative substitution by nucleophiles – in most cases acetate ion – in the aromatic nucleus or in the α position of the side-chain of alkylaromatics.[5,6,8,10,13–16] These reactions are normally effected by stoichiometric amounts of the Pd(II) salt (most often added as the acetate, but sometimes as the chloride,[4] nitrate [10] or chloride-olefin complex [11]), but can also be made catalytic in Pd(II) by adding reagents that favor reoxidation of Pd(0) to Pd(II).[12,14] The

* To whom inquiries should be addressed.

solvent employed is in most cases acetic acid, but it was recently found advantageous in the biaryl coupling reaction to avoid this solvent.[12] The use of acetic acid as solvent also means that the most commonly encountered oxidative substitution process – if observed at all – is acetoxylation, *i.e.* formation of aryl or benzyl acetates. Other oxidative substitutions become possible in acetic acid, however, if other nucleophiles are added.[16]

It is at present difficult to make a consistent summary of the influence of experimental conditions on the occurrence of each of these reactions, mainly due to the fact that knowledge about the nature of the oxidizing species is very limited. It is, however, rather well established that biaryl coupling is favored by the addition of perchloric acid, [5,7,10] by the presence of ligands, *e.g.* chloride ion, that favor formation of binuclear complexes,[4,11] and by the presence of water,[10] silver nitrate,[11] or iron(III).[11] Acetoxylation seems to be favored by the presence of acetate ion in large excess over Pd(II),[5,6,10,14] the use of $Pd(NO_3)_2$ as a source of Pd(II),[10] and the addition of a co-oxidant such as dichromate ion.[16] Nuclear acetoxylation, but not biaryl coupling [12] or α acetoxylation,[13,14] is almost suppressed if the reaction is conducted under oxygen pressure.[6,8]

In connection with earlier studies on anodic [17,20] and Mn(III) acetate [18] acetoxylation processes, we became interested in the possibility of effecting *nuclear* acetoxylation of aromatic substrates *via* a Pd(II) catalyzed reaction. This paper is a report [21] of an investigation of the Pd(II) mediated acetoxylation of *p*-xylene, considered to be a suitable substrate because of its known tendency [10] to undergo both α and nuclear substitution (in the reported [10] ratio of about 1 : 3). Hence this compound represents a challenge for increasing the relative yield of nuclear acetate. Moreover, only one isomer each of α and nuclear monosubstitution product is possible from *p*-xylene, which simplifies the analytical work. Finally, *p*-xylene undergoes biaryl coupling with difficulty even under the most favorable conditions,[12] presumably for steric reasons,[4,12] so that this side-reaction would hopefully interfere only to a small extent.

RESULTS

Structure of palladium(II) acetate in solution. In order to be able to discuss the reaction mechanism of aromatic acetoxylation *via* Pd(II) acetate, it is necessary to know something about the structure and composition of the Pd(II) complex present under the actual reaction conditions (acetic acid as solvent, in many cases with acetate ion added). In the solid, the structure of Pd(II) acetate has been shown to be a trimeric cluster [23] of the type I. It is trimeric in benzene at 37° but breaks up [23] to the monomer (II) at 80°.

We now postulate that Pd(II) acetate exists as the trimer (I) also in glacial acetic acid at or slightly above room temperature. Support for this assumption stems from the fact that the NMR spectrum of Pd(II) acetate in $CDCl_3$ displays a singlet at $\delta = 2.22$ ppm, and in CD_3COOD a singlet at $\delta = 2.07$ ppm. If a small amount of water is added, the $CDCl_3$ spectrum consists of four signals [24] with intensities in the ratio 1 : 2 : 2 : 1. A probable structure for this species is III, formed by breaking one Pd-acetate bond in I by a water molecule.

This shows that Pd(II) acetate exists as a trimer also in the absence of water. The similarity between the NMR spectrum of Pd(II) acetate in $CDCl_3$ and in CD_3COOD, respectively, suggests that also in the latter solvent a trimer exists at room temperature, presumably with structure (I) which would give a one-singlet NMR spectrum.

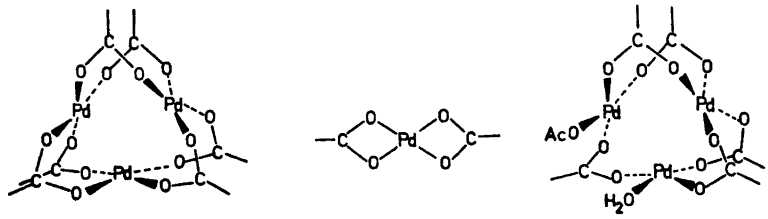

(I) (II) (III)

Further support was obtained by investigating the effect of adding NaOAc to Pd(II) acetate in acetic acid. It is known that oligomeric or polymeric acetates, *e.g.* the Co(III) acetate trimer [25] and Cu(II) acetate dimer, [26] break down to monomeric species upon the addition of sodium acetate. Acetates of bivalent metals, such as barium and calcium acetate, react with Pd(II) acetate in acetic acid with the formation of binuclear, isolable, Pd-metal-acetate complexes [27] of the general formula $MPd(OAc)_4.nHOAc$. For univalent metal acetates, such as KOAc, it was claimed that virtually no reaction was observed.

We now have studied the reaction between Pd(II) acetate and acetates of mono- and divalent metals by UV spectrophotometry and found that all systems behave in an essentially identical manner: A fast decrease in the intensity of the original maximum due to Pd(II) acetate at 397 nm and a shift of the maximum toward shorter wave-lengths with the formation of a new maximum of higher intensity around 360 nm, with two isosbestic points (Table 1). After the fast reaction has subsided, the new maximum grows slowly in

Table 1. Changes in the UV spectrum of Pd(II) acetate in acetic acid observed upon addition of different alkali metal salts.

Salt present [a]	Position of isosbestic points, nm		Position of new[b] λ_{max}, nm
	1	2	
LiOAc	381	322	364
KOAc	397	322	368
NaOAc	403	322	368
RbOAc	393	325	
CsOAc	397	324	
$Ca(OAc)_2$	397	322	352
$Ba(OAc)_2$	388	316	356

[a] Added as carbonates, except for the K, Na, and Ba salt.
[b] Position of λ_{max} for Pd(II) acetate = 389 nm.

intensity with no isosbestic point, probably due to polymerization of the new complex. The kinetics of two of these reactions (with sodium and barium acetate) were also measured at several temperatures (Table 2) and found to be first order in both Pd(II) acetate and added metal acetate. From these results

Table 2. Rate constants and activation energies [a] for the reaction between Pd(II) acetate and $Ba(OAc)_2$ or NaOAc.

Temperature, °C	Metal	[Metal acetate]$_0$, M	k, m^{-1}	k', m^{-1} M^{-1}
20.1	Ba	0.0521	0.0151	0.290
20.1	Ba	0.1042	0.0324	0.311
20.1	Ba	0.1563	0.0524	0.336
25.7	Ba	0.2084	0.1010	0.484
30.9	Ba	0.2084	0.1320	0.633
35.6	Ba	0.2084	0.1580	0.758
35.6	Ba	0.1563	0.1210	0.774
35.6	Ba	0.1042	0.0798	0.766
35.6	Ba	0.0521	0.0361	0.693
20.1	Na	0.1102	0.0117	0.106
20.1	Na	0.2204	0.0246	0.112
25.7	Na	0.2204	0.0338	0.153
30.9	Na	0.2204	0.0422	0.192
35.6	Na	0.2204	0.0610	0.277
44.7	Na	0.2204	0.10	0.45
60.9	Na	0.2204	0.24	1.1

[a] Ba salt, $E_a = 12.3$ kcal/mol; Na salt, $E_a = 11.3$ kcal/mol.

and the derived activation parameters it is obvious that the sodium acetate reaction is of the same type as that taking place with barium acetate. We formulate the processes occurring in these systems at or slightly above room temperature as shown in Scheme 1. The reaction is assumed to be reversible, which would account for the fact that the binuclear complex cannot be isolated in cases of unfavorable solubility relationships.[27]

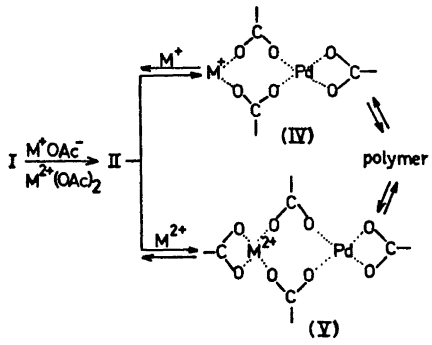

Scheme 1.

As shown in Table 2, the reaction between sodium acetate and Pd(II) acetate is fast even at fairly low temperatures. Around 100°, where most reactions to be described in this paper have been performed, the Pd(II) species prevailing in the presence of sodium acetate should therefore be IV, and II in the absence of sodium acetate. The trimer is not stable above 35° in glacial acetic acid.[24]

In certain reactions triphenylphosphine was present, and then a complex of structure VI is formed.[23]

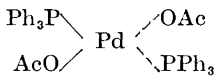

(VI)

Palladium(II) acetate oxidation of p-*xylene in acetic acid with added acetate ion.* At this stage of the investigation, we were mainly interested in determining the dependence of the product distribution upon certain experimental factors, such as solvent, atmosphere, additives, *etc.*, always with the goal in view of maximizing the yield of the nuclear acetoxylation product, 2,4-dimethylphenyl acetate (VIII). Hence the results to be described below have been obtained from runs on the semi-micro or micro scale, using a large excess of *p*-xylene over Pd(II) acetate and analyzing at fairly low conversions in order to avoid further oxidation of primary products as much as possible.

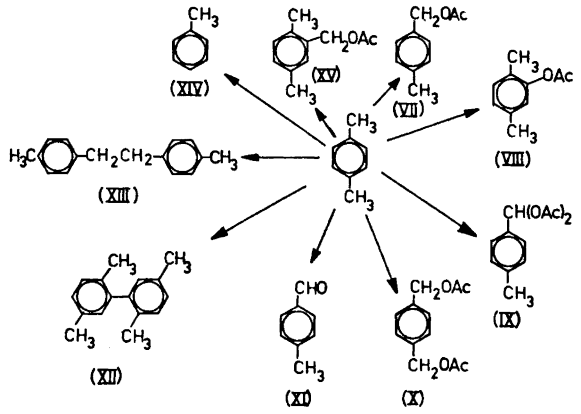

Scheme 2.

The complexity of the problem at hand is amply demonstrated by Scheme 2 which shows the considerable number of products that may be formed – very rarely alone – in the Pd(II) acetate oxidation of *p*-xylene.

Among these products, the acetates VII, VIII, and X, all three together or in pairs, are almost always predominant, and the other compounds either appear in minor amounts (< 5 %) or can be made major components of the

product mixtures only under rather special conditions. We shall here first describe how experimental conditions affect the product distribution in the experiments where acetate products are predominant, and then briefly comment on the side-products. It is only fair to state from the beginning that in very few experiments is it possible to obtain high selectivity in the formation of any single product.

Fig. 1 shows the rate at which VII and VIII form in an argon atmosphere as a function of the [NaOAc]/[Pd(II)] ratio (in the following to be abbreviated

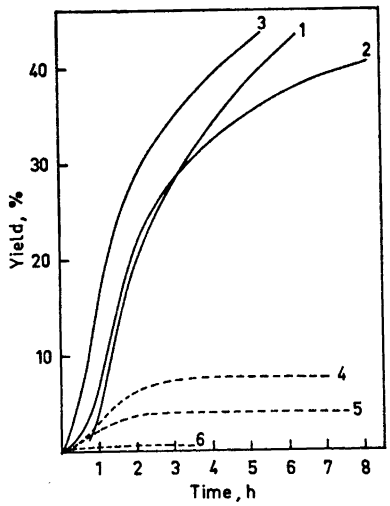

Fig. 1. Yield of VII (solid lines) and of VIII (broken lines) *vs.* time in the oxidation of *p*-xylene with Pd(II) acetate in acetic acid at 111°C (Ar atmosphere). [*p*-Xylene]/[Pd(II)] ≈ 50; [NaOAc]/[Pd(II)]: curves 1 and 4, 0; 2 and 5, 2.1; 3 and 6, 27.7. At the highest ratio, 57, no VIII was detectable.

Na/Pd). The yields given are absolute ones. At a low Na/Pd ratio there is an induction period for the formation of VII, which is diminished at higher ratios. The nuclear acetate (VIII) disappears completely at very high ratios. This behavior is more clearly demonstrated in Fig. 2, which shows the yields of VII and VIII after 20 h as a function of the Na/Pd ratio. Under argon, the yield of VII passes through a maximum at moderate Na/Pd ratios (between 10 and 20).

In an oxygen atmosphere, the over-all behavior with respect to formation of VII and VIII upon varying the Na/Pd ratio is similar, although other major products now appear. These are *p*-methylbenzaldehyde (XI) and *p*-xylylenediol

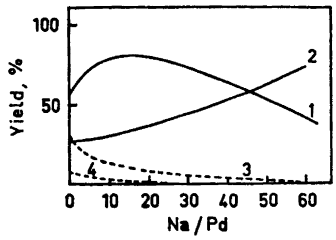

Fig. 2. Yield of VII (solid lines) and of VIII (broken lines) *vs.* the Na/Pd ratio in the oxidation of *p*-xylene with Pd(II) acetate in glacial acetic acid (as analyzed after 20 h). Temperature, 111°C; curves 1 and 4 in Ar atmosphere; curves 2 and 3 in O_2 atmosphere.

acetate (X). The former compound is present in all product mixtures from experiments conducted under oxygen. The induction period for the formation of VII is still apparent and perhaps even somewhat longer; it gets shorter with higher Na/Pd ratios, and the formation of VIII is strongly suppressed at a high Na/Pd ratio (see Fig. 3). The rate of formation of the aldehyde (XI)

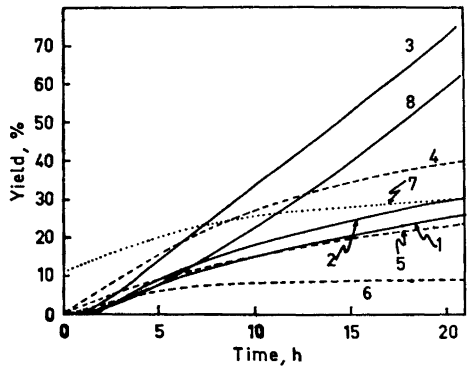

Fig. 3. Yield of VII (solid lines), VIII (broken lines), and XI (dotted lines) *vs.* time in the oxidation of *p*-xylene with Pd(II) acetate in acetic acid at 111°C (O_2 atmosphere). Na/Pd: curves 1 and 4, 0; curves 2, 5, and 7, 1.9; curves 6 and 8, 13; curve 3, 61 (no VIII is formed at this ratio).

is shown for one ratio (Na/Pd = 1.9); after an initial period of fast formation, the rate is approximately constant. *p*-Xylylenediol diacetate (X) is always formed as a minor product (< 10 % under argon), but becomes a major product when both oxygen and sodium acetate are present. Fig. 4 shows the ratio between the yields of VII and X, plotted *vs.* time for different Na/Pd ratios. Interestingly enough (*cf.* Ref. 14), X appears in large amounts also at the beginning of the reaction in cases where it is the predominant product (see Fig. 4, curve 4), suggesting that it is formed *via* a separate reaction path directly from *p*-xylene, and not *via* further oxidation of initially formed VII.

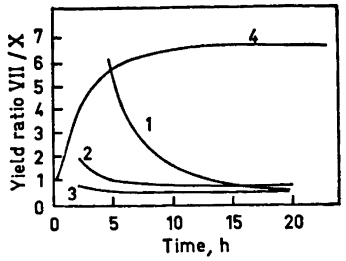

Fig. 4. Variation in the yield ratio of VII to X with time during oxidation of *p*-xylene with Pd(II) acetate in acetic acid at 110° in oxygen (curves 1, 2, and 3) or argon atmosphere (curve 4). Na/Pd: curve 1, 1.9; curve 2, 13; curve 3, 61; curve 4, 27.

The quotient between the yields of nuclear (VIII) and side-chain (VII + X) acetates has been plotted *vs.* time at different Na/Pd ratios in Fig. 5. This does not only again serve to emphasize the fact that the formation of VIII is strongly suppressed at high Na/Pd ratios (*cf.* Figs. 1 and 2) but furthermore shows that VIII is the major product at very low conversions, *i.e.* before the induction period for the formation of VII and X has elapsed. The end of the induction

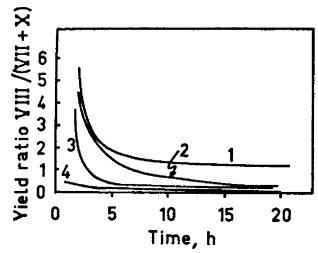

Fig. 5. Variation in the yield ratio VIII/(VII + X) with time during oxidation of *p*-xylene with Pd(II) acetate in acetic acid at 110° in oxygen (curves 1 – 3) or argon atmosphere (curve 4). Na/Pd: curve 1, 0; curve 2, 1.9; curve 3, 13; curve 4, 0.

period in many cases seems to coincide with the precipitation of black Pd(0) from the solution.

The possibility that binuclear complexes of the type IV might be the kinetically active species in the oxidation process prompted us to study the effect of adding alkali metal acetates other than sodium acetate. These experiments are represented in Figs. 6 – 8 in the form of yield of VII *vs.* time curves

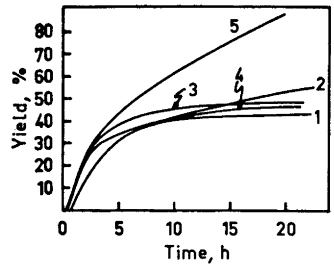

Fig. 6. Variation in the yield of VII with time during oxidation of *p*-xylene with Pd(II) acetate in acetic acid at 111° with different alkali metal acetates added. Curve 1, Li/Pd = 2.5; curve 2, Na/Pd = 2.1; curve 3, K/Pd 2.2; curve 4, Rb/Pd 2.9; curve 5, Cs/Pd 2.0. Argon atmosphere.

for different alkali metal ions at a low (Fig. 6) and high (Fig. 7) metal/Pd ratio. All these reactions were run under argon. Fig. 8 is a more informative representation of some of the results in Figs. 6 and 7. The strong dependence of the rate of formation of VII upon the nature of the cation supports the assumption that binuclear complexes (IV) are the kinetically active species.

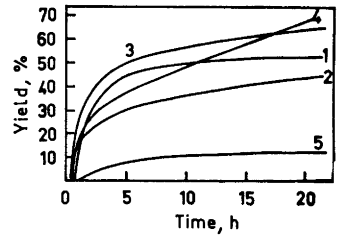

Fig. 7. Variation of the yield of VII with time during oxidation of *p*-xylene with Pd(II) acetate in acetic acid at 111° with different alkali metal acetates added. Curve 1, Li/Pd = 115; curve 2, Na/Pd = 56.7; curve 3, K/Pd = 49: curve 4, Rb/Pd = 48; curve 5, Cs/Pd = 55. Argon atmosphere.

In the experiments with added alkali metal acetates other than sodium acetate, the yield of VIII was always low (about 5 %) at low to moderately high metal/Pd ratios (2 – 20). At high such ratios, VIII is not formed at all except in the presence of Cs(I) ion where a 1 % yield was obtained. The yield

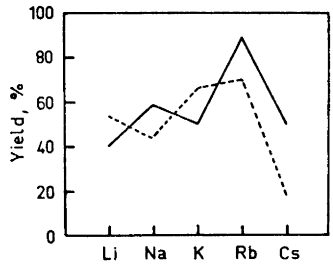

Fig. 8. Schematic representation of the variation of the yield of VII with the nature of the added ion (*cf.* Figs. 6 and 7) in the oxidation of *p*-xylene with Pd(II) acetate in acetic acid at 111° under argon atmosphere. Solid line, metal/Pd ≈ 2; broken line, metal/Pd ≈ 50. Analyses were performed after 22 h.

of *p*-xylylenediol diacetate (X) is fairly low (3 – 12 %) and does not change significantly with the nature of the added cation.

Among the minor products, *p*-methylbenzylidene diacetate (IX) is of special interest as a possible precursor for the aldehyde (XI). IX is formed only in small amounts under the conditions of the experiments summarized in Figs. 1 – 7. It is of interest to note that IX is also formed under argon where the aldehyde is not formed. This indicates that the aldehyde is not formed *via* hydrolysis of the diacetate, as previously suggested.[15] Under certain conditions [oxidation with Pd(II) acetate/Cu(II) acetate in a ratio 1 : 10 under oxygen at reflux], IX can be made the major product.

The hydrocarbons in Scheme 2, toluene (XIV) and the two dimers, 2,5,2′,5′-tetramethylbiphenyl (XII) and 4,4′-dimethylbibenzyl (XIII), are formed in small amounts (< 1 % each) in many experiments. Traces of acetoxylation products of toluene have also been detected. The bibenzyl (XIII) has not been observed before in this type of reactions and commands special interest, since it must be formed *via* coupling of two 4-methylbenzyl radicals. Characteristically, XIII is not formed under oxygen, since then the benzylic radical is trapped efficiently by oxygen and diverted to the aldehyde according to the usual autoxidation mechanism.[28] It thus appears probable that benzylic radicals are formed as intermediates in at least one reaction taking place between Pd(II) acetate and *p*-xylene.

Palladium(II) acetate oxidation of p-*xylene in the presence of various additives.* In order to change the nature of the oxidizing species one can in principle add either a Lewis base, which would be expected to lower the oxidation potential of the Pd(II) complex by coordination of its free electron pair with Pd(II), or a Lewis acid which would be expected to increase the oxidizing power by virtue of coordination to Pd(II) and partial electron withdrawal from the metal.

Triphenylphosphine was chosen as a representative Lewis base, since it is known that the prevalent complex will then be of the type VI. This additive causes certain complications in the analytical procedure, though, since it is oxidized itself during the reaction. This results in the formation of triphenylphosphine oxide and products from cleavage of the C – P bond, *viz.*, phenyl acetate, biphenyl, phenol, and diacetoxybenzenes. The formation of biphenyl and phenol indicates that phenyl radicals may be intermediates, an assumption that is supported by the formation of small amounts of a product of phenyl radical attack on *p*-xylene, 2,5-dimethylbiphenyl. The main products from the

Table 3. Changes in the product distribution from the oxidation of *p*-xylene with Pd(II) acetate in acetic acid at 115° at different [triphenylphosphine]/[Pd(II)] ratios; [Pd(II) acetate] = 0.01 – 0.04 M; O_2 atmosphere.

$[PPh_3]/[Pd(II)]$	[VIII]/([VII]+[X]) after		[VII]/[X] after	
	30 min	4 h	30 min	4 h
0	∞	5.0	∞	∞
1	0.025	0.12	0.64	1.1
2	0.028	0.23	1.16	2.0
10	–	0.063	–	2.5

oxidation of *p*-xylene in the presence of triphenylphosphine in an oxygen atmosphere are XI, VII, VIII, and X. In addition, small amounts of toluene are formed together with traces of two isomers corresponding to the formula XV. Table 3 shows the main changes that take place upon addition of triphenylphosphine: α acetoxylation is favored over nuclear, and the formation of X is favored.

The addition of aluminium chloride to a solution of Pd(II) acetate, *p*-xylene, and glacial acetic acid precipitates a red solid, whose IR spectrum differs from that of Pd(II) acetate. The compound is probably a mixed complex between Pd(II) acetate and aluminium chloride. The main effects of conducting the oxidation in the presence of aluminium chloride are demonstrated in Table 4:

Table 4. Changes in the product distribution from the oxidation of *p*-xylene with Pd(II) acetate in acetic acid at 115° at different $[AlCl_3]/[Pd(II)]$ ratios;[a] [Pd(II) acetate] about 0.02 M; O_2 atmosphere.

$[AlCl_3]/[Pd(II)]$	[VIII]/[VII]	[VIII]/[XII]
0	5.0	> 10
1	0.47	0.59
2	0.55	0.62
10	0.37	1.0

[a] Analyzed after a reaction period of 4 h.

α acetoxylation increases, and the yield of biaryl (XII) goes up drastically. The finding that biaryl formation is favored upon addition of a Lewis acid is analogous to the effect of adding a strong protonic acid such as perchloric acid [5,7,10] which also strongly favors biaryl formation.

The addition of water has no particular influence on the oxidation of *p*-xylene with Pd(II) acetate in glacial acetic acid under conditions of argon atmosphere and high Na/Pd ratio (as already shown, the α acetate (VII) is the major product under these conditions). Table 5 summarizes these experiments. Neither aldehyde (XI) nor nuclear acetate (VIII) is formed.

Table 5. Yield of (VII) after oxidation of *p*-xylene with Pd(II) acetate in acetic acid [a] at different $[H_2O]/[Pd(II)]$ ratios at 111°; Na/Pd = 54; Ar atmosphere; [Pd(II)] about 0.01 M.

$[H_2O]/[Pd(II)]$	Yield, %
0	34
1.2	32
2.5	34
63.2	35

[a] Reaction period 5.5 h.

p-Methylbenzoic acid (XVI) was isolated under special conditions only: oxidation in acetic acid at reflux temperature with Pd(II) acetate in the presence of a large excess of sodium nitrite. Furthermore, trace amounts of VII and VIII (3 : 1) were detected. It should be noted that no nitro product was detectable, although these conditions have been known to favor the formation of nitro compounds in other systems.[10,16]

Tetraalkylammonium acetates occupy a special position among the possible acetate salts, since binuclear complexes cannot form from Pd(II) and a tetraalkylammonium ion. Hence addition of, *e.g.*, tetrabutylammonium acetate (TBA) to the oxidation mixture should cause the monomer (II) to be the oxidizing species.

Table 6. Changes in the product distribution from the oxidation of *p*-xylene with Pd(II) acetate in acetic acid at 115° at different [TBA]/[Pd(II)] ratios; [Pd(II)] 0.02 M; O_2 atmosphere.

[TBA]/[Pd(II)]	[VIII]/([VII]+[X]) after		[VII]/[X] after	
	30 min	4 h	30 min	4 h
0	∞	5.0	∞	∞
1	1.8	0.13	3.0	0.77
2	2.4[a]	0.32		0.63[b]
10		3.1		

[a] Value at the same ratio with sodium acetate = 1.4.
[b] Value at the same ratio with NaOAc = 5.4.

Table 6 shows the effect of the addition of TBA in the oxidation of *p*-xylene with Pd(II) acetate at different ratios of TBA/Pd in an oxygen atmosphere. The ratio of VIII/(VII+X) goes through a minimum with a change in the TBA/Pd ratio from 1 to 10. The ratio VII/X is smaller at small TBA/Pd ratios than at small Na/Pd ratios, showing that the addition of acetate favors formation of the α,α′-diacetate (X) as long as it is not coordinated as a ligand to Pd(II).

Preparative oxidations. Some preparative runs have also been performed in order to establish the usefulness of Pd(II) acetate oxidation for nuclear aromatic acetoxylation (no excess acetate, O_2). Thus Pd(II) acetate (10 mmol) in *p*-xylene and acetic acid (100 ml) was kept at 110° with a slow stream of oxygen bubbling through for 150 h, resulting in an isolated yield of 450 % of VII + VIII in a 30 : 70 ratio. A similar result was obtained from an experiment identical to the one above except that triphenylphosphine (10 mmol) was also added. A 480 % yield of VII + VIII (ratio 46 : 56) was isolated. In both cases the solutions were still catalytically active at the discontinuation of the experiment. From these experiments it is obvious that the sluggishness of the reaction seriously hampers its preparative use. We are presently working on the problem of speeding it up to useful rates.

The discussion of the results described in this paper is deferred to Part III of this series.[29]

EXPERIMENTAL PART

Materials. The following starting or reference chemicals were purchased in the highest quality available: *p*-Xylene (Schuchardt AG, München, Germany, 99.85 % purity), XI (Fluka AG, Buchs, Switzerland), triphenylphosphine (Merck AG, Darmstadt, Germany), and palladium(II) acetate (Engelhard, also prepared according to a literature method [23]). Solvents and inorganic reagents were of analytical grade quality. The following reference compounds were synthesized according to well-known methods: VII,[30] VIII[31], IX,[32] X,[33] XII,[34] and XIII.[35] The identity and purity of all compounds used were checked by mass, IR, and NMR spectral analysis as well as by gas chromatography. Retention times (min) for the reference compounds (4 m × 0.3 cm 5 % neopentylglycolsuccinate on Chromosorb W, temperature programming between 120 and 210° at a rate of 2°/min, Perkin-Elmer 880 gas chromatograph equipped with a disc or electronic integrator) were: XI (15.6), VIII (20.8), VII (23.2), *m-t*-butylphenyl acetate [17] (used as internal standard; 25.6), XII (33.0), IX (43.2), XIII (46.4), and X (57.2 min).

Kinetic procedure. Stock solutions of accurately known concentrations of Na, Ba, and Pd acetate in acetic acid were made up and mixed to give kinetic samples of appropriate concentrations (see Table 2). Solutions of the same concentrations in Na or Ba acetate were used in the reference cell. The kinetics were followed by recording (Unicam SP 800B UV spectrophotometer) the change in extinction at 356 nm. First-order rate constants were evaluated *via* Guggenheim plots.[36]

Analytical oxidation experiments. The oxidation experiments were performed according to one of the following methods:

A. Solutions of Pd(II) acetate (0.02 M) and substrate (40 – 80 times in excess over Pd(II) acetate) in acetic acid, together with additive if applicable, were filled (2 ml) into 5 ml ampoules, through which a slow stream of either argon or oxygen was passed for 30 min at room temperature. The ampoules were sealed and kept in a thermostated bath at the appropriate temperature. Analyses were then performed after approximately 30 min, 1, 2, 4, 8, and 20 h.

B. The reaction mixture (50 – 100 ml) was kept in a jacketed reaction vessel which could be kept at a suitable temperature by circulating triethylene glycol from an ultrathermostat. Argon or oxygen was slowly passed through the solution *via* a glass frit inlet tube. An efficient condenser was attached to the vessel which was also provided with an opening covered by a rubber septum. Analytical samples were withdrawn by use of a hypodermic syringe.

The samples obtained either from method A or B were neutralized with saturated sodium bicarbonate solution. The organic components were extracted by ether and the extracts washed with water. After the addition of an internal standard (*m-t*-butylphenyl acetate), the product composition and yield were determined by gas chromatographic analysis (see above). In doubtful cases the combination gas chromatography/mass spectrometry (LKB 9000 system) was used for checking the identity of the components.

Preparative oxidations. See text.

Acknowledgements. We wish to gratefully acknowledge the generous financial support we have obtained from the *Swedish Board for Technical Development* (L. E.) and the *Faculty of Science, University of Lund* (L. G.).

REFERENCES

1. Maitlis, P. M. *The Organic Chemistry of Palladium*, Vols. 1 and 2, Academic, New York 1971.
2. Hüttel, R. *Synthesis* **1970** 225.
3. Heck, R. F. *Fortschr. Chem. Forsch.* **16** (1970/71) 221.
4. Van Helden, R. and Verberg, G. *Rec. Trav. Chim.* **84** (1965) 1263.
5. Davidson, J. M. and Triggs, C. *Chem. Ind. (London)* **1966** 457.
6. Davidson, J. M. and Triggs, C. *Chem. Ind. (London)* **1967** 1361.
7. Davidson, J. M. and Triggs, C. *J. Chem. Soc.* **A 1968** 1324.
8. Davidson, J. M. and Triggs, C. *J. Chem. Soc.* **A 1968** 1331.
9. Unger, M. O. and Fouty, R. A. *J. Org. Chem.* **34** (1969) 18.
10. Ichikawa, K., Uemura, S. and Okada, T. *Nippon Kagaku Zasshi* **90** (1969) 212; Tisue, T. and Downs, W. J. *Chem. Commun.* **1969** 410.
11. Fujiwara, Y., Moritani, I., Ikegami, K., Tanaka, R. and Teranishi, S. *Bull. Chem. Soc. Japan* **43** (1970) 863.
12. Itatani, H. and Yoshimoto, H. *Chem. Ind. (London)* **1971** 674.
13. Bryant, D. R., McKeon, J. E. and Ream, B. C. *Tetrahedron Letters* **1968** 3371.
14. Bryant, D. R., McKeon, J. E. and Ream, B. C. *J. Org. Chem.* **33** (1968) 4123.
15. Bushweller, C. H. *Tetrahedron Letters* **1968** 6123.
16. Henry, P. M. *J. Org. Chem.* **36** (1971) 1886.
17. Eberson, L. *J. Am. Chem. Soc.* **89** (1967) 4669.
18. Eberson, L. and Nyberg, K. *J. Am. Chem. Soc.* **88** (1966) 1686.
19. Bernhardson, E., Eberson, L., Nyberg, K. and Rietz, B. *Acta Chem. Scand.* **25** (1971) 1224.
20. a. Eberson, L. and Sternerup, H. *Acta Chem. Scand.* **26** (1972) 1431; b. Dirlam, J. P. and Eberson, L. *Acta Chem. Scand.* **26** (1972) 1454; c. Dirlam, J. P., Eberson, L. and Sternerup, H. *Chem. Ingr. Tech.* **44** (1972) 178; Eberson, L. and Wilkinson, R. G. *Acta Chem. Scand.* **26** (1972) 1671.
21. A preliminary account of this work has been published; Eberson, L. and Gomez-Gonzalez, L. *Chem. Commun.* **1971** 263.
22. Skapski, A. C. and Smart, M. L. *Chem. Commun.* **1970** 658.
23. Stephenson, T. A., Morehouse, S. M., Powell, A. R., Heffer, J. P. and Wilkinson, G. *J. Chem. Soc.* **1965** 3632.
24. Campbell, P. G. C. and Wolfe, S. *Private communication.*
25. Lande, S. S. and Kochi, J. K. *J. Am. Chem. Soc.* **90** (1968) 5196.
26. Kochi, J. K. and Subramanian, R. V. *Inorg. Chem.* **4** (1965) 1527.
27. Brandon, P. W. and Claridge, D. V. *Chem. Commun.* **1968** 677.
28. See, for example, Morimoto, T. and Ogata, Y. *J. Chem. Soc.* **B 1967** 62.
29. Eberson, L. and Gomez-Gonzalez, L. *Acta Chem. Scand.* **27** (1973) 1255.
30. Carill, G. W. K. and Solomon, D. H. *J. Chem. Soc.* **1954** 3943.
31. von Auwers, K., Bundesmann, H. and Wieners, F. *Ann.* **447** (1926) 162.
32. Claussner, P. *Ber.* **38** (1905) 2860.
33. Murray, R. W. and Tazzolo, A. M. *J. Org. Chem.* **29** (1964) 1268.
34. Ullmann, F. *Ann.* **332** (1904) 47.
35. Farthing, A. C. *J. Chem. Soc.* **1953** 3261.
36. Guggenheim, E. A. *Phil. Mag.* **2** (1920) 538.

Received October 25, 1972.

ACTA CHEMICA SCANDINAVICA 27 (1973) 1175–1182

The Crystal and Molecular Structure of *p*-Dioxanyl Hydroperoxide

ANDERS G. NORD and BÖRJE LINDBERG

Institute of Inorganic and Physical Chemistry, University of Stockholm, Box 6801, S-113 86 Stockholm, Sweden

The crystal structure of *p*-dioxanyl hydroperoxide has been determined and refined from three-dimensional X-ray photographic data. The unit cell is monoclinic with the cell constants $a = 12.222$, $b = 4.636$, $c = 18.971$ Å, $\beta = 100.85°$. The space group is $C2/c$; there are 8 molecules of *p*-dioxanyl hydroperoxide ($C_4H_8O_4$) in the unit cell. All atoms occupy 8-fold positions. This investigation has confirmed the general features of the molecule determined from IR and NMR spectra by Gierer and Pettersson.

Crystals of *p*-dioxanyl hydroperoxide have been prepared by Gierer and Pettersson.[1] The compound was analysed and characterized by means of IR, NMR, mass spectra, and also by reductive degradation. These investigations indicated a chair-formed molecule with its hydroperoxy group axially oriented. In order to check this an X-ray structure determination was suggested.

EXPERIMENTAL

Colourless needle-shaped crystals, suitable for X-ray diffraction studies, were kindly supplied by Dr. J. Gierer. The melting point was determined to 56°C. The sample decomposed slowly, even when kept below 0°C, producing a colourless liquid. At room temperature the crystals could stand X-rays less than half an hour before they changed into a yellowish drop. Therefore it was necessary to cool the crystals down during the radiation.

A powder photograph was taken in a Guinier-Hägg focusing camera with strictly monochromatized Cu$K\alpha_1$ radiation ($\lambda = 1.54050$ Å) and with KCl ($a = 6.29228$ Å) as an internal standard. All high angle reflections were very diffuse, but from 25 low angle ($\theta < 20°$) powder reflections the unit cell dimensions could be refined with the least-squares program POWDER.[3] The cell constants are shown in Table 1 together with some crystallographic data.

Preliminary Weissenberg and rotation photographs indicated monoclinic symmetry. Systematic absences occurred for hkl with $h + k$ odd, and in addition for $h0l$ with l odd, which is characteristic of the space group Cc (No. 9) and its centrosymmetric equivalence $C2/c$ (No. 15). $C2/c$ was chosen as being the most probable (see below).

Table 1. Crystal data of *p*-dioxanyl hydroperoxide. The estimated standard deviations are given in parentheses and refer to the last decimal place of the respective value.

Cell constants	$a = 12.222(2)$ Å $b = 4.636(1)$ Å $c = 18.971(2)$ Å $\beta = 100.85(2)°$
Cell volume	$V = 1056$ Å^3
Density (X-ray)	$D = 1.51$ g/cm^3
Molecules per unit cell	$Z = 8$
Space group	$C2/c$

All atoms occupy general equivalent positions 8(*f*): $\pm(x,y,z)$; $\pm(\frac{1}{2}+x,\frac{1}{2}+y,z)$; $\pm(\bar{x},y,\frac{1}{2}-z)$; $\pm(\frac{1}{2}-x,\frac{1}{2}+y,\frac{1}{2}-z)$.

Since the crystals dissolved instantaneously in water and in most organic liquids it was not possible to determine the density of the crystals experimentally. However, it seems most likely to assume 8 molecules in the unit cell which gives a density of 1.51 g/cm^3.

For the Weissenberg equi-inclination exposures ($h0l - h2l$) a needleshaped crystal with the dimensions 0.40 mm (in the direction of the *b* axis) × 0.06 mm × 0.08 mm was enclosed in a thin-walled capillary and mounted along the *b* axis. During the exposures it was cooled down to −40°C by a stream of dry air. The reflections were recorded with the multiple film technique. The intensities of the reflections were estimated visually by comparing with an intensity scale obtained by photographing a reflection with different exposure times. A total of 250 independent reflections were measured. It should be emphasized that the $h2l$ reflections were rather diffuse and only a minor part of these reflections were used henceforth. The net intensities were corrected for Lorentz and polarization effects but not for absorption. However, μ is very low ($\mu = 3.7$ cm^{-1}) and the crystal was rotated about the needle axis.

The programs for the IBM 360/75 of the Stockholm Data Centre used in all calculations involved in the present work are described in a paper by Brandt and Nord.[4]

STRUCTURE DETERMINATION AND REFINEMENT

An ordinary Wilson plot [5] and some tests for centric distribution from intensity statistics were performed with the programs WILP and ZTEST, written by one of the authors (A.G. N.). From the Wilson plot an approximate scale factor and an overall temperature factor were calculated. With the program FAME (Dewar & Stone, Chicago, USA) normalized structure factors, $|E|$, were calculated and rescaled to set the average of $|E|^2$ equal to 1. The

Table 2. Statistical averages and distributions of the normalized structure factors.

	Experimental	Theoretical values	
		Centric	Acentric
$\langle\|E\|\rangle$	0.81	0.798	0.886
$\langle\|E\|^2 - 1\rangle$	0.94	0.968	0.736
$\langle\|E\|\rangle^2$	1.00	1.000	1.000
$\|E\| > 1$	35 %	32 %	37 %
$\|E\| > 2$	3.5 %	5.0 %	1.8 %
$\|E\| > 3$	0.47 %	0.30 %	0.01 %

distribution of the $|E|'$ s after rescaling is given in Table 2. The result of the $N(z)$ test [6] is shown in Fig. 1. This test and the results presented in Table 2 indicate a centric distribution. For this reason the space group $C2/c$ (No. 15) was chosen as being the most probable.

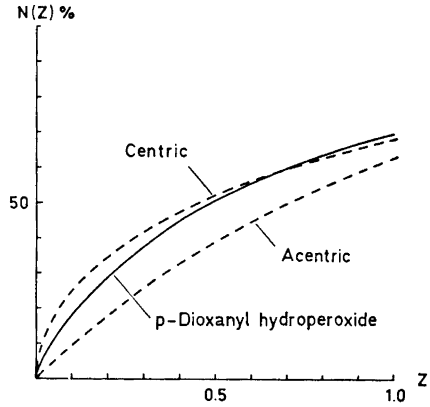

Fig. 1. $N(z)$ test. Distribution for *p*-dioxanyl hydroperoxide compared with theoretical curves for centric and acentric distribution.

The 45 highest $|E|$ values ($|E| > 1.27$) were used to generate 57 triple relations. The reflections 519 ($E = +2.59$) and $71\bar{6}$ ($E = +1.72$) were used to specify the origin of the unit cell. The signs of 44 $|E|$ values could then be determined by symbolic addition of the triple-product sign relationships.[7] 42 of these signs proved to be correct. The E map calculated for this solution (44 E values) clearly revealed the positions of all the eight non-hydrogen atoms in the asymmetric unit.

The structure was refined by a combination of full-matrix least-squares (program LALS) and Fourier methods. Isotropic temperature factors were always used. The scattering factor curves applied were those given by McMaster *et al.*[8] corrected for the real part of the anomalous dispersion coefficient. Hughes' weighting function [9] with $h=4$ and $F_{o,min}=7.5$ was applied. After 3 cycles of refinement a three-dimensional difference Fourier synthesis was calculated. The interpretation of the Fourier maps was hampered by the presence of spurious maxima. Of the eight hydrogen atoms in the asymmetric unit it was only possible to locate four (H1, H2, H3, H5). However, the calculated C–H bond distances were rather unreliable, nor was it possible to refine the hydrogen atom positions. Therefore the seven hydrogen atoms H1 – H7 were introduced geometrically assuming a C–H bond distance of 1.10 Å, tetrahedral angles, and a temperature factor of 1.50 Å^2. The eight non-hydrogen atoms were further refined improving the R value ($R=\sum||F_{obs}| - |F_{calc}||/\sum|F_{obs}|$) to 11 %. From the subsequent difference Fourier maps it was now possible to determine the position of the last hydrogen atom, H8.

The weighting scheme obtained in the final cycle of refinement is shown in Table 3. Zero weight was given to 10 reflections with $|F_{obs}|/|F_{calc}|$ less than 0.5 or greater than 2. A list of the observed and calculated structure factors is presented in Table 4. Owing to its somewhat uncertain position the

Table 3. Weight analysis obtained in the final cycle of the least-squares refinement. w = weighting factor, $\Delta = ||F_{obs}| - |F_{calc}||$. Zero weight was given to 10 reflections.

Interval $\|F_{obs}\|$	$\overline{w\Delta^2}$	Number of independent reflections	Interval sin θ	$\overline{w\Delta^2}$	Number of independent reflections
0 – 10	0.57	23	0.00 – 0.37	1.20	55
10 – 14	0.94	20	0.37 – 0.47	1.08	51
14 – 18	1.24	22	0.47 – 0.54	0.92	48
18 – 22	1.17	25	0.54 – 0.59	1.11	21
22 – 26	1.05	25	0.59 – 0.64	0.60	26
26 – 31	1.19	26	0.64 – 0.68	1.18	16
31 – 39	1.18	24	0.68 – 0.71	0.31	6
39 – 48	1.20	25	0.71 – 0.74	0.61	8
48 – 67	0.76	25	0.74 – 0.77	1.68	6
67 – 140	0.67	25	0.77 – 0.80	0.40	3

Table 4. Observed and calculated structure factors. Reflections marked with an asterisk were assigned zero weight in the final cycles of least-squares refinement.

H	K	L	$\|F_o\|$	F_c	H	K	L	$\|F_o\|$	F_c	H	K	L	$\|F_o\|$	F_c	H	K	L	$\|F_o\|$	F_c	H	K	L	$\|F_o\|$	F_c	H	K	L	$\|F_o\|$	F_c
2	0	0	40	-46	0	0	16	16	19	1	1	2	57	-55	7	1	6	38	-35	-5	1	5	34	-34	2	2	3	22	30
2	0	2	51	-45	0	0	18	26	-21	1	1	3	12	18	9	1	0	21	-22	-5	1	6	30	-29	2	2	4	54	48
2	0	4	14	-11	-2	0	2	82	82	1	1	4	6	-4	9	1	1	28	25	-5	1	7	15	11	2	2	5	33	-36
2	0	6	118	-125	-2	0	4	113	111	1	1	5	63	-60	9	1	2	12	-9	-5	1	9	85	92	2	2	6	13	12
2	0	8	103	-98	-2	0	6	29	26	1	1	6	27	-28	9	1	3	41	-45	-5	1	10	21	18	2	2	7	36	33
2	0	10	81	85	-2	0	8	38	32	1	1	7	44	-41	11	1	0	22	18	-5	1	11	18	-13	2	2	8	46	52
2	0	12	23	18	-2	0	10	14	-13	1	1	8	42	-33	-1	1	1	74	81	-5	1	12	17	-10	2	2	9	20	-25
2	0	14	29	-31	-2	0	12	52	45	1	1	9	9	6	-1	1	2	42	54	-5	1	13	12	9	-2	2	1	57	59
4	0	0	67	-69	-2	0	14	5	-4	1	1	10	19	24	-1	1	3	139	-158	-5	1	15	21	-21	-2	2	2	6	10
4	0	2	7	-2*	-2	0	16	103	-98	1	1	11	45	40	-1	1	4	16	19	-5	1	16	29	32	-2	2	3	36	-49
4	0	4	81	-81	-4	0	2	54	53	1	1	12	18	-14	-1	1	5	6	1*	-5	1	17	25	-26	-2	2	4	72	-57
4	0	6	28	28	-4	0	4	39	-33	3	1	0	89	-93	-1	1	6	28	25	-7	1	1	13	-15	-2	2	5	19	18
4	0	8	41	38	-4	0	6	135	-137	3	1	1	85	-89	-1	1	7	21	-13	-7	1	2	13	6*	-2	2	7	10	10
4	0	10	39	-33	-4	0	8	111	119	3	1	2	62	55	-1	1	9	18	-13	-7	1	3	25	-21	-2	2	8	5	4
4	0	12	40	38	-4	0	10	58	57	3	1	3	27	-27	-1	1	10	9	-6	-7	1	4	16	-14	-2	2	9	10	-14
6	0	0	8	5	-4	0	14	62	58	3	1	4	20	-21	-1	1	11	10	0*	-7	1	5	39	-42	4	2	0	47	48
6	0	2	9	8	-4	0	16	12	-3*	3	1	5	41	-36	-1	1	12	20	-18	-7	1	6	51	58	4	2	1	11	14
6	0	4	9	-7	-4	0	18	28	-29	3	1	6	13	-10	-1	1	13	68	-70	-7	1	7	33	30	4	2	2	67	69
6	0	6	36	-37	-6	0	2	8	-8	3	1	7	89	91	-1	1	14	24	-21	-7	1	8	18	-17	4	2	3	69	-52
6	0	8	31	33	-6	0	4	50	-47	3	1	8	49	49	-1	1	15	20	19	-7	1	9	30	31	4	2	4	39	42
6	0	10	31	32	-6	0	8	70	-69	3	1	9	21	19	-1	1	16	13	14	-7	1	10	35	-39	4	2	5	26	22
8	0	0	19	-13	-6	0	10	10	-8	3	1	10	11	0*	-1	1	17	21	21	-7	1	11	12	6	4	2	6	19	21
8	0	2	11	-7	-6	0	12	41	37	3	1	11	16	-17	-3	1	1	25	27	-7	1	12	24	22	4	2	7	20	22
8	0	4	41	45	-6	0	16	47	49	3	1	12	12	7	-3	1	2	44	-45	-7	1	13	25	21	4	2	8	21	17
8	0	6	25	-20	-8	0	2	23	25	3	1	13	36	36	-3	1	3	52	-47	-9	1	1	6	-6	4	2	9	22	-24
8	0	8	39	44	-8	0	4	10	-11	5	1	0	50	48	-3	1	4	35	38	-9	1	2	19	17	-4	2	1	67	-52
8	0	10	25	24	-8	0	6	11	8	5	1	1	8	-9	-3	1	5	77	83	-9	1	3	12	-13	-4	2	2	62	-65
8	0	12	19	-21	-8	0	8	42	-48	5	1	2	8	8	-3	1	6	14	-9	-9	1	4	12	-10	-4	2	3	62	54
10	0	0	38	38	-8	0	10	18	-15	5	1	3	33	36	-3	1	7	16	9	-9	1	5	25	-28	-4	2	4	14	-13
10	0	2	6	3	-8	0	12	19	17	5	1	4	20	-26	-3	1	8	29	29	-9	1	6	25	-28	-4	2	5	10	7
10	0	4	12	-13	-8	0	14	20	-21	5	1	5	16	15	-3	1	9	32	-29	-9	1	7	12	-12	-4	2	6	31	23
10	0	6	34	39	-10	0	2	12	2*	5	1	6	48	50	-3	1	11	6	1*	-9	1	8	30	33	-4	2	7	24	-20
12	0	0	27	33	-10	0	4	27	29	5	1	7	17	16	-3	1	12	19	16	-9	1	9	25	-26	-4	2	8	36	-33
12	0	2	12	-12	-10	0	6	25	-26	5	1	8	18	-15	-3	1	14	17	5*	-9	1	10	23	18	6	2	0	36	34
12	0	4	26	-34	-10	0	8	31	-21	5	1	9	51	62	-3	1	15	50	-47	-9	1	11	29	29	6	2	1	37	-33
0	0	2	18	-12	-10	0	10	24	22	5	1	10	39	-43	-3	1	16	36	-36	0	2	4	6	4	6	2	3	31	34
0	0	4	98	-97	-10	0	12	22	-26	5	1	11	20	-19	-3	1	17	29	-27	0	2	5	6	-9	6	2	4	10	13
0	0	6	63	64	-12	0	2	16	-10	7	1	0	10	7	-3	1	19	27	25	0	2	7	10	-11	-6	2	1	17	-18
0	0	8	72	-80	-12	0	4	21	20	7	1	2	21	-19	-5	1	1	8	-4	2	2	0	61	-61	-6	2	2	13	13
0	0	10	22	-17	-12	0	6	46	47	7	1	3	17	16	-5	1	2	8	-2*	2	2	1	6	7	-6	2	3	26	19
0	0	12	48	-45	1	1	0	35	37	7	1	4	18	14	-5	1	3	54	60	2	2	2	37	-36	-6	2	4	62	55
0	0	14	11	-7	1	1	1	114	-123	7	1	5	43	39	-5	1	4	19	-16										

H8 atom was not included in the calculation of the structure factors, nor was it included in the final cycles of least-squares refinement. The atomic parameters and temperature factors are given in Table 5. Note that no hydrogen atoms were refined. (The atoms H1 – H7 were introduced geometrically, and H8 had been located from the last ΔF synthesis.) The parameters in Table 5 were also used to calculate the structure factors for the unobserved reflec-

Table 5. Fractional atomic coordinates and thermal parameters. The estimated standard deviations are given in parentheses and refer to the last decimal places of the respective values. Note that the hydrogen atoms were not refined.

Atom	*x*	*y*	*z*	*B*
O1	0.1037(5)	0.2422(21)	0.0404(3)	1.60(10)
O2	0.1692(5)	0.0937(24)	0.1848(4)	1.23(9)
O3	0.3131(6)	0.3061(23)	0.1331(4)	1.69(10)
O4	0.3963(6)	0.3019(24)	0.2008(4)	2.45(11)
C1	0.1776(8)	0.0076(36)	0.0587(6)	1.26(13)
C2	0.2445(9)	0.0682(40)	0.1353(6)	2.01(14)
C3	0.0906(8)	0.3320(38)	0.1655(5)	0.96(13)
C4	0.0273(8)	0.2645(36)	0.0910(6)	1.94(14)
H1	0.2345	−0.0084	0.0203	1.50
H2	0.1304	−0.1946	0.0582	1.50
H3	−0.0170	0.0585	0.0920	1.50
H4	−0.0332	0.4375	0.0734	1.50
H5	0.0330	0.3451	0.2035	1.50
H6	0.1356	0.5374	0.1656	1.50
H7	0.2983	−0.1194	0.1517	1.50
H8	0.3260	0.4780	0.2130	1.50

tions. This revealed no $|F_{calc}|$ value greater than 10. Furthermore, the ΔF Fourier synthesis showed no peak or hole greater than 0.5 eÅ^{-3}. These facts, together with the statistical tests and the reasonable molecular dimensions presented below, enable the authors to assume, with a high degree of probability, that the crystal possesses the centric space-group symmetry $C2/c$.

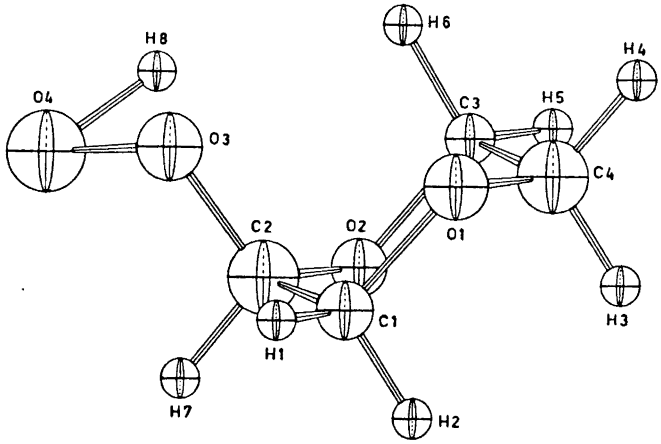

Fig. 2. Three-dimensional model of a molecule of *p*-dioxanyl hydroperoxide.

DESCRIPTION AND DISCUSSION OF THE CRYSTAL STRUCTURE

According to the present X-ray structure investigation, the configuration of the *p*-dioxanyl hydroperoxide molecule is in good agreement with the results by Gierer and Pettersson.[1] The molecule has a pronounced chair form with the hydroperoxy group axially oriented. Fig. 2 shows a three-dimensional model of one molecule with all hydrogen atoms (H1 – H8). It has been produced by the plot program ORTEP [10] and its graphic display version.[11] Fig. 3 shows the contents of a unit cell with eight molecules. Only the oxygen and carbon atoms are drawn.

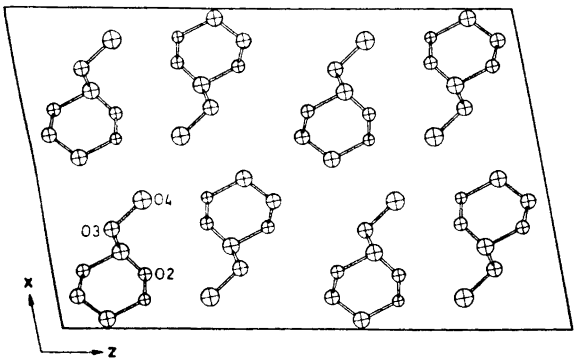

Fig. 3. The contents of one unit cell projected along the *b* axis. Only oxygen and carbon atoms are drawn.

Table 6. Interatomic distances (Å) with standard deviations ($\pm\sigma$ in Å) and some angles in *p*-dioxanyl hydroperoxide. The e.s.d. of the angles are $\pm 1°$ or less. For comparison the corresponding average values in 1,4-dioxane (Ref. 2) are within parentheses and marked by an asterisk.

Intramolecular distances and angles					
C1 – C2	1.55(2)		C1 – O1 – C4	110.5°	
C3 – C4	1.51(2)		C2 – O2 – C3	111.7°	
Average:	1.53	(1.523)*	Average:	111.1°	(112.5°)*
C1 – O1	1.41(2)		O1 – C1 – C2	106.9°	
C2 – O2	1.44(1)		O2 – C2 – C1	109.7°	
C2 – O3	1.39(2)		O2 – C3 – C4	105.9°	
C3 – O2	1.46(2)		O1 – C4 – C3	110.6°	
C4 – O1	1.46(1)		O3 – C2 – C1	109.2°	
Average:	1.43	(1.423)*	Average:	108.5°	(109.2°)*
O3 – O4	1.48(1)		O4 – O3 – C2	106.5°	
			O2 – C2 – O3	114.7°	

Some interatomic distances and angles concerning the hydrogen bond. Atom denotations used: (x,y,z) without subscript; subscript (ii) denotes $(\frac{1}{2}-x,\frac{1}{2}+y,\frac{1}{2}-z)$.

O4 – O2	2.90(1)	O4 – O2(ii)	2.80(1)
O3 – O4 – O2	55.0°	O3 – O4 – O2(ii)	115.6°

Table 6 contains some interatomic bond distances with estimated standard deviations (σ) and a few interesting angles. The C–C and C–O bond distances are all among the usual covalent bond length distances in the literature.[12] The average interatomic distances and two kinds of angles (C–O–C and O–C–C) are also compared in Table 6 with the corresponding values obtained from electron diffraction studies of 1,4-dioxane.[2] The agreements between all averaged values are always within the standard deviations. The O–O distance of the hydroperoxy group (1.48 Å) is also in good agreement with earlier results, *i.e.* from the crystal structure analysis (X-ray) of hydrogen peroxide [13] with a reported O–O distance of 1.49 Å.

The hydrogen atom H8 is likely to form a weak hydrogen bond in connection with two oxygen atoms. This hydrogen bond would involve the atoms O4 and H8 from one molecule, and one O2 atom. Looking at the pertinent O2 – O4 distances and the O3 – O4 – O2 angles in Table 6, an intermolecular hydrogen bond seems to be far more likely than an intramolecular one as suggested by Gierer and Pettersson.[1] Intramolecular hydrogen bonds are relatively rare, and the present hydrogen bond dimensions assuming an intermolecular bond would be more within the range of ordinary O–H–O hydrogen bonds.[14] As a matter of fact, Abrahams *et al.* also reported an O–O hydrogen bond distance of 2.78 Å in hydrogen peroxide.[13] The sharp bending of the present hydrogen bond (about 125° for the intermolecular O–H–O hydrogen bond angle) might well be caused by the uncertainty of the H8 hydrogen atom position. If its position was well established, the hydrogen bond could almost be regarded to be bifurcated.

All other interatomic distances between atoms in neighbouring molecules are long enough to allow only van der Waals bondings between the molecules. Compared with the melting point and density of ordinary 1,4-dioxane (12°C resp. 1.03 g/cm^3), the corresponding values for *p*-dioxanyl hydroperoxide (56°C resp. 1.51 g/cm^3) indicate a slightly higher degree of stability which could be caused by weak intermolecular hydrogen bonds.

Acknowledgements. The authors are indebted to Professors Peder Kierkegaard and Arne Magnéli for their active and stimulating interest in this work and for all facilities placed at their disposal. The authors also wish to thank Dr. Josef Gierer for suggesting the problem and for the supply of crystals. Thanks are also due to Dr. B. G. Gäfvert for his correction of the English of this paper. This investiation has been performed with financial support from the *Tri-Centennial Fund of the Bank of Sweden* and from the *Swedish Natural Science Research Council.*

REFERENCES

1. Gierer, J. and Pettersson, I. *Acta Chem. Scand.* **22** (1968) 3183.
2. Davis, M. and Hassel, O. *Acta Chem. Scand.* **17** (1963) 1181.
3. Lindqvist, O. and Wengelin, F. *Arkiv Kemi* **28** (1967) 179.
4. Brandt, B. G. and Nord, A. G. *Chem. Commun. Univ. Stockholm 1970*, No. 5.
5. Wilson, A. J. C. *Nature* **150** (1942) 152.
6. Howells, F. R., Phillips, D. C. and Rogers, O. *Acta Cryst.* **3** (1950) 210.
7. Hauptman, H. and Karle, J. *Solution of the Phase Problem. 1. The Centrosymmetric Crystal, A. C. A. Monograph No. 3*, Polycrystal Book Service, Pittsburg 1953.
8. McMaster, W. H. *et al. UCRL-50174*, Sec. II, Rev. 1, UCLA, Calif. 1970.

9. Hughes, E. W. *J. Am. Chem. Soc.* **63** (1941) 1737.
10. Johnson, C. K. *AEC Accession No. 33516*, ORNL-3794, Oak Ridge National Laboratory, Tenn. 1965.
11. Nord, A. G. *J. Appl. Cryst.* **4** (1971) 196.
12. *Interatomic Distances*, The Chemical Society, London 1958.
13. Abrahams, S. C., Collin, R. L. and Lipscomb, W. N. *Acta Cryst.* **4** (1951) 15.
14. Hamilton, W. C. and Ibers, J. A. *Hydrogen Bonding in Solids*, Benjamin, New York 1968.

Received November 3, 1972.

ACTA CHEMICA SCANDINAVICA 27 (1973) 1183–1191

Studies of Polarized Ethylenes

Part VI.* Internal Rotations, Dipole Moments, and Ultraviolet Spectra of Nitroethylenes. Experimental Results and PPP Calculations

GUNILLA ISAKSSON and JAN SANDSTRÖM

Division of Organic Chemistry 1, Chemical Center, University of Lund, P.O. Box 740, S-220 07 Lund, Sweden

The barrier to rotation around the C=C bond in 1-methylthio-1-benzylthio-2-nitroethylene has been found to be *ca.* 28 kcal/mol by stereomutation. Considerably lower barriers to rotations around C=C and C–N bonds in the 1-methylthio-1-dimethylamino- and 1,1-bis-dimethylamino analogs have been determined by the NMR lineshape technique. Dipole moments and UV spectra have been measured and correlated with charge distributions and transition energies calculated by the PPP method.

The ^{1}H NMR spectrum of 1,1-bis-methylthio-2-nitroethylene (Ia) has been described by three groups of workers.[1–3] While Gompper and Schaefer[1] and Jensen *et al.*[2] observed a singlet for the *S*-methyl protons at ambient temperature, a doublet was observed below 0°C in deuteriochloroform ($\Delta\nu = 1.4$ Hz) and below −5°C in pyridine ($\Delta\nu = 2.3$ Hz, both at 60 MHz).[3] This observation was interpreted as the result of a hindered rotation around the C=C bond with $\Delta G^{\ddagger} = 14.8$ kcal/mol (from the coalescence temperature). However, later investigations showed that Ia gave a doublet at ambient temperature in benzene solution, which persisted when the temperature was raised. Furthermore, the benzyl analog Ib gave a doublet for the benzylic methylene protons also in deuteriochloroform solution,[2] and in *o*-dichlorobenzene solution this doublet persisted without exchange broadening to +180°C. It was therefore concluded that the barrier reported for Ia in Ref. 3 was questionable, and new attempts were made to determine this and analogous barriers. It has been observed that the barriers to rotation around the C=C bond in polarized ethylenes depend to a great extent on the character of the electron-donating groups, and for this reason the study has been extended to compounds III, IV, and V. The UV spectra have been recorded for compounds Ia, III, IV, and V, and the dipole

* Part V. Wennerbeck, I. *Acta Chem. Scand.* **27** (1973) 258.

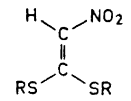

I, a. R = CH_3

b. R = CH_2Ph

moments have been measured for Ia, IV, and V. These data have been correlated with the results of MO calculations by the Pariser-Parr-Pople (PPP) method.

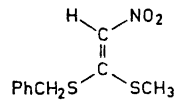

IIa

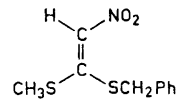

IIb

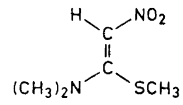

III

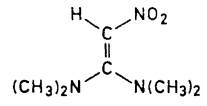

IV

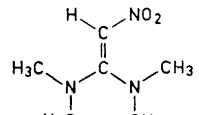

V

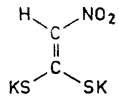

VI

EXPERIMENTAL

Preparative part. The starting material, *d potassium 2-nitroethylene-1,1-dithiolate* (VI) was prepared according to Freund [4] from nitromethane, carbon disulphide, and potassium hydroxide in ethanolic solution. The dry crystals are labile and have detonated at room temperature on several occasions.

1,1-Bis-methylthio-2-nitroethylene (Ia) was prepared as described by Gompper and Schaefer [1] and gave the same physical data as reported by these authors.

1,1-Bis-benzylthio-2-nitroethylene (Ib) was prepared as described by Jensen *et al.*[2]

1-Methylthio-1-benzylthio-2-nitroethylene (II) was formed in two diastereomeric forms, here referred to as A and B. Methyl iodide (1.23 ml, 0.02 mol) in ethanol (20 ml) was added to a solution of VI (4.26 g, 0.02 mol) in water (20 ml). After 30 min a precipitate of Ia was removed by filtration, and benzyl chloride (2.3 ml, 0.03 mol) in ethanol (60 ml) was added. On the following day a precipitate of pale yellow crystals had formed, consisting according to the NMR spectrum of a mixture of A and B in the ratio 1:1. Variation of solvent ratios and order of addition of the alkylating agents gave different proportions of A and B. This result was in some cases observed even in parallel experiments under apparently identical conditions. In one experiment even a sample of pure isomer B was obtained, but this could never be repeated.

The separation of isomers A and B was most advantageously performed in the following way. Glass rods were placed in a hot, dilute solution of the isomer mixture in cyclohexane. After several days isomer A had formed long needles on the rods, projecting into the solution, whereas isomer B formed plates, firmly adhering to the surface of the rods. The crystals could be separated manually, and the needles were recrystallized until the pure isomer A was obtained. The melting points are 120 – 123° (A) and 114 – 115.5° (B). (Found: C 49.0; H 4.58; N 5.64; S 26.3. $C_{10}H_{11}NO_2S_2$ (241.34) requires C 49.8; H 4.59; N 5.80; S 26.6.)

1-Dimethylamino-1-methylthio-2-nitroethylene (II). Ia (4.95 g, 0.03 mol) was added to a solution of dimethylamine (0.031 mol) in benzene (40 ml), and the solution was refluxed for 25 min. According to TLC on silica a mixture of Ia, III, and IV had resulted. Chromatography on silica gel and repeated recrystallizations from ethyl acetate gave pure III

(0.3 g, 6 % yield) as orange prisms, m.p. 59°C. (Found: C 37.2; H 6.28; N 17.2; S 19.7. $C_5H_{10}N_2O_2S$ (162.22) requires C 37.0; H 6.21; N 17.3; S 19.8.) The time of refluxing is critical, since on prolonged reaction time only Ia and IV are observed.

1,1-Bis-dimethylamino-2-nitroethylene (IV). Ia (4.95 g, 0.03 mol) was dissolved with dimethylamine (0.12 mol) in benzene (90 ml), and the mixture was allowed to stand for 24 h at room temperature. Evaporation and recrystallization twice from acetone gave pale yellow prisms (2.4 g, 50 % yield), m.p. 118°. (Found: C 45.1; H 8.25; N 26.3; O 20.3. $C_6H_{13}N_3O_2$ (159.19) requires C 45.3; H 8.23; N 26.4; O 20.1.)

1,3-Dimethyl-2-(nitromethylene)imidazolidine (V). *N,N'*-Dimethylethylenediamine (8.8 g, 0.1 mol) was added to a solution of Ia (16.5 g, 0.1 mol) in ethanol (300 ml), and the solution was refluxed for 2 h. Evaporation and repeated recrystallization from toluene gave light yellow prisms (4.2 g, 27 % yield), m.p. 120 – 121°. (Found: C 45.7; H 7.10; N 26.4; O 20.7. $C_6H_{11}N_3O_2$ (157.18) requires C 45.8; H 7.05; N 26.7; O 20.4.)

NMR Spectra were recorded on Varian A 60, HA-100, and/or XL-100 instruments, equipped with variable temperature probes and V-6040 temperature controllers.

Temperature measurements. In the majority of the isomerization experiments, the temperature was measured with the aid of an internal ethylene glycol capillary, previously calibrated against a copper-constantan thermocouple. In the other cases, the temperatures were recorded by the substitution technique, employing a precalibrated methanol or ethylene glycol sample. In the former case, the temperature readings are probably accurate to $\pm 0.3°$, in the latter to $\pm 2°$.

Isomerization experiments. The kinetics of the isomerization A $\rightleftharpoons$ B (IIa $\rightleftharpoons$ IIb) was studied by integration of the methyl and methylene signals of samples in *o*-dichlorobenzene solution (60 mg of substance in 0.5 ml of solvent) at different temperatures in the range 84 – 109°. The equilibrium ratio was 1:1 within the experimental accuracy in this temperature range. The evaluation of the rate constants was performed as described in Ref. 5, and the results are presented in Table 1.

Table 1. Rate constants and thermodynamic parameters for the isomerization IIa $\rightleftharpoons$ IIb.

Isomer	T°C	$k \times 10^{-3}$ sec^{-1}	$\Delta G^{\ddagger}$ kcal/mol
A	92.0	0.40	27.7
A	102.0	0.71	28.0
B	84.9	0.066	28.4
B	90.0	0.122	28.5
B	91.4	0.182	28.2
B	95.0	0.230	28.3
B	97.5	0.268	28.4
B	109.0	0.63	28.7

$\Delta H^{\ddagger} = 24.0 \pm 2.7$ kcal/mol.
$\Delta S^{\ddagger} = -12 \pm 7$ e.u.

Lineshape determination of rotational barriers. The barrier to rotation around the C–N bond in III (see Results and discussion) was determined at the coalescence temperature by employing the approximate formula 1, obtained from the Eyring equation and the expression for the mean lifetime at coalescence.[6] In IV, one of the two barriers to rotation

$$\Delta G^{\ddagger} = 0.004573\ T_c\left(9.972 + \log \frac{T_c}{\Delta \nu_0}\right) \quad (1)$$

around C–N bonds and the one to rotation around the C=C bond were determined by a line-fitting procedure. Theoretical spectra were generated by a four-sites exchange program, utilizing the exchange scheme in Fig. 1 and the Bloch equations with exchange

terms as described in Ref. 7, and the chemical shifts and rate constants were varied to give the best visual fit between theoretical and experimental spectra. The results are presented in the discussion.

Dipole moment measurements were performed with a Dipolmeter Type DM 01 from WTW, Weilheim, D.B.R. The standardization was made with benzene (Merck, zur Analyse) and dibutyl ether (freshly distilled). The measurements were performed in benzene solution in a cell thermostated to 25.0°C, and the dipole moments were evaluated using the method of Hedestrand.[8] The slopes of the plots of dielectric constants and indexes of refraction *versus* weight fractions (a_ε and a_n) were obtained by the method of least squares. The results are given in Table 2.

Table 2. Dipole moment data.

Compound	Weight fraction range × 10^2	a_ε	a_n	μD
Ia	0.921 – 2.89	21.46	0.41	5.64 ± 0.02
IV	0.139 – 2.00	38.60	0.44	7.64 ± 0.01
V	0.0486 ± 0.491	38.39	0.38	7.39 ± 0.01

Compound V is rather slightly soluble in benzene and had to be measured in the weight fraction range $(0.5-5)\times10^{-3}$. However, measurements on IV in this range and in the range $(0.14-2.0)\times10^{-2}$ gave nearly the same result, and the value for V can be regarded as reliable.

Molecular orbital calculations were carried out with the SCF–MO–CI method according to Pariser and Parr [9,10] and Pople [11] with the parametrization developed by Roos *et al.*[12,13] Configuration interaction was performed between all singly excited states. The geometry

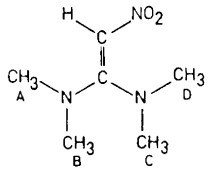

Fig. 1. Exchange diagram for rotation around the C=C and both C–N bonds in IV.

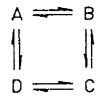

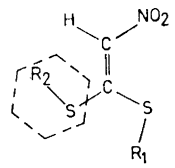

Fig. 2. Assumed time-average orientation of 1,1-bis-alkylthio-2-nitroethylene and benzene molecules.

of the nitroethylene part of the molecule was taken from the microwave study of Hess *et al.*[14] The geometry around carbon atom 1 was taken from an X-ray crystallographic investigation by Abrahamsson *et al.*[15] on 1,1-bis-methylthio-2-cyano-2-*p*-bromobenzoylethylene and 1,3-dimethyl-2-(cyano-*p*-bromobenzoylmethylene)imidazolidine.

RESULTS AND DISCUSSION

NMR Spectra and barriers. The NMR spectrum of Ia shows a doublet for the *S*-methyl protons in benzene up to 70°C, and in *o*-dichlorobenzene solution a sharp doublet persists up to 170°C. The behaviour in deuteriochloroform and in pyridine solution previously interpreted as a coalescence due to exchange [3] is instead due to a temperature-dependent chemical shift difference. This is demonstrated by the fact that the singlet splits into a doublet above +59°

in deuteriochloroform solution. In pyridine a similar behaviour is observed, with $\Delta\nu = 1.6$ Hz at $+98°C$ (60 MHz). This shows that great care must be exercised when barriers are obtained from exchange broadened doublets with small non-exchanging internal chemical shifts.

Evidently, the normal lineshape method is not suited for measuring the barriers in Ia and Ib. Instead, the stereomutation of an unsymmetrical analog was investigated by the integration technique. As described in the experimental part, two diastereomers, A and B, of the general structure II could be prepared. The assignment of structures IIa and IIb to these diastereomers could be made with the aid of the shifts induced by aromatic solvents (ASIS). It is generally conceded that dipolar solute molecules and aromatic solvent molecules form loose collision complexes, in which the aromatic molecules are oriented on the time-average as far away from the negative ends of the solute dipoles as possible.[16] In the case of compounds II, the time-average orientation should be as in Fig. 2. The benzylic methylene protons in IIa should show a larger upfield shift than those in IIb on going from deuteriochloroform to benzene solution or on increasing the dilution in a pure benzene solution. In the same way, the *S*-methyl proton signal in the spectrum of IIb should show larger upfield shifts than that in the spectrum of IIa under the same conditions.

Table 3. Chemical shifts of methyl and benzylic methylene protons in A and B at large dilution.

Compound	Group	ν_{CDCl_3} Hz	$\nu_{C_6H_6}$ Hz	$\Delta\nu$ [a] Hz
A	CH_3	149	105	44
B	CH_3	149	79	70
A	CH_2Ph	248	190	58
B	CH_2Ph	255	230	25

[a] $\Delta\nu = \nu_{CDCl_3} - \nu_{C_6H_6}$

The shift values listed in Table 3 show that, provided the above assumptions are correct, compound A has structure IIa and compound B structure IIb.

The negative activation entropy is in qualitative agreement with the negative entropies observed for 1-benzylthio-1-methylthio-2-carbomethoxy-2-cyanoethylene ($\Delta S^{\ddagger} = -24.0 \pm 2.9$ e.u.) and 1,1-bis-methylthio-2-benzoyl-2-cyanoethylene ($\Delta S^{\ddagger} = -16.5 \pm 1.6$ e.u.).[17] For these compounds, as well as for compounds I and II, a polar transition state is assumed for the rotation around the C=C bond. The negative $\Delta S^{\ddagger}$ values indicate that this transition state is also more strongly solvated than the initial state. Unfortunately, the uncertainty in $\Delta S^{\ddagger}$ in the present case precludes a more detailed analysis of this effect.

The barrier measured for II is considerably lower than for simple ethylenes, but it is higher than for the majority of ethylenes with push-pull substituents studied in Ref. 17. In these, two electron-attracting groups contribute to the stabilization of the negative charge in the polar transition state, whereas in II there is only one, although a rather efficient one. The σ_R-value for the

nitro group, 0.64, is less than the sum of those for, *e.g.*, the cyano and carbomethoxy groups (+0.77),[18] which may be qualitatively correlated with the $\Delta H^{\ddagger}$ values for the rotation in II (24.0 kcal/mol) and in 1-methylthio-1-benzylthio-2-carbomethoxy-2-cyanoethylene (14.7 and 15.0 kcal/mol for forward and reverse reactions).

At ambient temperature, the NMR spectrum of III in deuteriochloroform consists of singlets for the methylthio, dimethylamino, and vinyl protons at δ=2.58, 3.33 and 6.80 ppm, respectively.

The same general appearance is observed in dichlorofluoromethane solution, but at −99°C the dimethylamino signal splits into a symmetrical doublet ($\Delta\nu_0$=12.2 Hz). Since neither the *S*-methyl nor the vinyl proton signals show broadening or doubling indicative of exchange down to *ca.* −115°C, it is evident that the doubling of the dimethylamino signal is due to a slow rotation around the C–N bond. For this rotation, $\Delta G^{\ddagger}$ = 8.9 kcal/mol at the coalescence temperature is calculated by formula (1). The rotation around the C=C bond may be fast at −115°, but the absence of exchange broadening of the vinyl and *S*-methyl proton signals at this temperature may also be due to the existence of one strongly preferred conformation with respect to the C=C bond. If this is the reason, steric factors indicate the *Z* conformation as the most likely one (nitro and *S*-methyl groups on the same side of the double bond).[19]

The low temperature NMR spectrum of IV in dichlorofluoromethane showed splittings indicative of slow exchange, but a detailed analysis was precluded by the small internal chemical shifts. In a 1:1 (v/v) mixture of fluorobenzene and dichloromethane a singlet was observed at ambient temperature, but this broadened from *ca.* −40° and split at −53° into a doublet with the intensity ratio 3:1 (Fig. 3). At −63° the low field signal split into a 2:1 doublet, and from

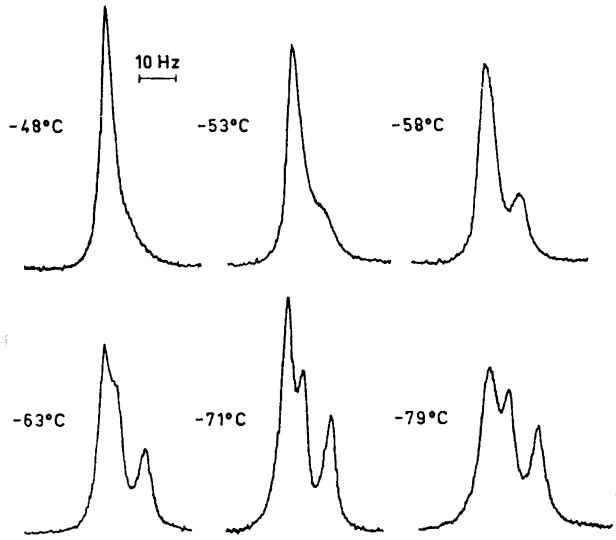

Fig. 3. 60 MHz ^{1}H NMR spectra of the dimethylamino groups in IV in a solution in fluorobenzene and dichloromethane (1:1, v/v).

about $-80°$ the low field component of this was further broadened, but at still lower temperatures crystallization of the solute precluded further measurements. An analysis as described in the experimental part shows that the upfield doublet below $-63°$ is due to one dimethylamino group and the downfield singlet to the other. At $-71°$ $\Delta G^{\ddagger}$ for rotation around the C=C bond is found to be 10.7 kcal/mol, and for rotation around one of the C–N$(CH_3)_2$ bonds 11.8 kcal/mol. The barrier for the other C–N$(CH_3)_2$ bond is probably lower than 10 kcal/mol. The NMR spectrum of V in dichlorofluoromethane shows singlets for the *N*-methyl protons and the ring protons down to $-125°$.

Dipole moments. The dipole moments have been recorded for Ia, IV, and V in order to get an idea of the π-electron distribution in these molecules. The dipole moments have been treated as vector sums of π and σ moments, and the σ moments have been taken from Ref. 20, with the exception of that for the nitro group. The σ moment for this group was obtained from nitromethane. A PPP calculation on the nitro group gave a π moment of 2.9 D, which was subtracted together with the methyl group moment (0.4 D) from the nitromethane gas phase value of 3.46 D [21] to give a σ moment for the nitro group of 0.2 D, directed from the nitrogen towards the oxygen atoms along the symmetry axis.

In Ia, the methyl groups are assumed to be oriented as in Fig. 2 to avoid steric interferences. The group moment for the SCH_3 group, 1.4 D,[20] is assumed to bisect the  angle and to be directed as indicated by the arrow. In IV, the CN bond moments in the dimethylamino group are assumed to cancel, which is an approximation, since the carbon atoms have different states of hybridization.

The PPP calculations gave a π-electron moment of 3.74 D for Ia and 6.18 D for IV. Vector addition of the σ moments gave a total moment of 4.15 D for Ia and 6.75 D for IV. The calculated moments are 1.5 D and 0.7 D too low, which is not discouraging in view of the uncertainties in the σ moments. The calculated π-electron distributions in the ground and first excited states and the π bond orders in the ground state are shown in Fig. 4.

The close similarity of the moments of IV and V is surprising in view of the large differences in barriers to rotation around the C=C bond observed for analogs of IV and V with the same set of electron-attracting substituents.[7,22] Since the analogs of V have the lowest barriers, they would be expected to show the largest initial state polarizations. An explanation may be found in different degrees of twisting around C-amino and C-nitro bonds. However, a detailed discussion of this effect will have to await the results of a more extensive investigation of dipole moments of polarized ethylenes, which is at present underway.

The π-electron densities on C_2 in Ia (0.83), III (0.96), and IV (1.03) show a rough correlation with the chemical shifts of the vinyl protons, 7.12, 6.80, and 6.38 ppm, respectively, in deuteriochloroform solution. In this case, however, the anisotropy effects of the neighbouring groups must also be taken into account.

Ultraviolet spectra have been recorded for compounds Ia, III, IV, and V

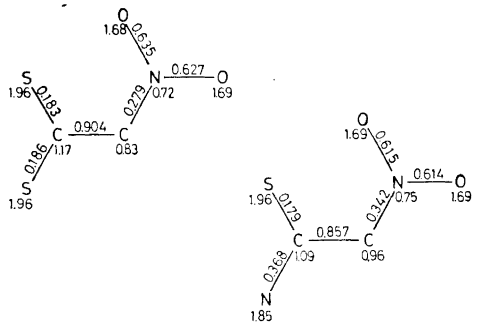

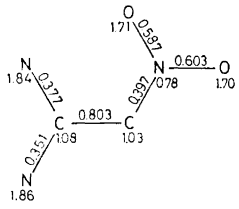

Fig. 4a. Calculated charge distributions and bond orders in the ground states of Ia, III, and IV.

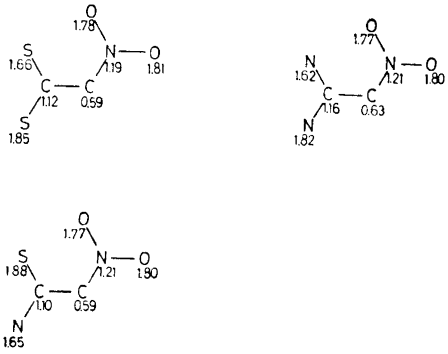

Fig. 4b. Calculated charge distributions in the first excited states of Ia, III, and IV.

in heptane (with 0.3 % dichloromethane for solubility reasons) and absolute ethanol solutions. The experimental and theoretical λ_{max} values, experimental log ε values, and experimental and theoretical oscillator strengths (f) are found in Table 4. Since λ_{max} for nitroethylene is 203 nm with a shoulder at 242 nm,[23] the electron-donating substituents have considerable bathochromic effects. The strongest bathochromic effect is observed in III with one dimethylamino and one methylthio group, whereas the other three compounds have rather similar spectra in heptane solution. This effect is not reproduced by the PPP calculations, which give λ_{max} values increasing in the series I, III, and IV.

Table 4. Experimental and theoretical ultraviolet spectra.

Compound	Experimental					Theoretical	
	Ethanol		Heptane				
	λ_{max} nm	log ε	λ_{max} nm	log ε	f	λ_{max}	f
I	291	3.78					
	355	4.17	335	4.12	0.221	298.1	0.318
III	370	4.28	348	4.09	0.232	308.0 [a]	0.484
IV	345	4.33	333.5	4.21	0.296	328.3	0.459
V	333.5	4.22	332 [b]	4.19 [b]	—	—	—

[a] *Z* conformation.
[b] In heptane with 0.6 % dichloromethane.

The calculated oscillator strengths are 1.5 – 2 times as large as the experimental ones, but this is a general feature of the PPP method.

Changing the solvent from heptane to ethanol causes considerable bathochromic shifts for Ia, III, and IV, but only a small one for V. Such large shifts are generally interpreted as consequences of increased polarization during the electronic transition. The charge distribution in the first excited state of compounds I, III, and IV (taking configuration interaction into account) is given in Fig. 4. The excited state dipole moments are 11.5 D, 10.6 D, and 11.6 D, respectively, nearly parallel with the ground state dipole moments. Evidently, the excitation causes strong increases in the dipole moments in the same direction as that of the ground state moments, and this is in very satisfactory agreement with the observed solvent shifts.

Acknowledgements. We are grateful to the *Swedish Natural Science Research Council* for valuable financial support, to Ing. Eva Ericsson and Ing. Jan Glans for experimental assistance, and to Dr. Torbjörn Drakenberg for giving us access to his four-site lineshape program.

REFERENCES

1. Gompper, R. and Schaefer, H. *Chem. Ber.* **100** (1967) 591.
2. Jensen, K. A., Buchardt, O. and Lohse, C. *Acta Chem. Scand.* **21** (1967) 2797.
3. Isaksson, G., Sandström, J. and Wennerbeck, I. *Tetrahedron Letters* **1967** 2233.
4. Freund, E. *Ber.* **52** (1919) 542.
5. Frost, A. A. and Pearson, R. G. *Kinetics and Mechanism*, Wiley, New York 1953, p. 172.
6. Gutowsky, H. S. and Holm, C. H. *J. Chem. Phys.* **25** (1956) 1228.
7. Wennerbeck, I. and Sandström, J. *Org. Magn. Resonance* **4** (1972) 78.
8. Hedestrand, G. *Z. phys. Chem.* **B 2** (1969) 428.
9. Pariser, R. and Parr, R. G. *J. Chem. Phys.* **21** (1953) 466.
10. Pariser, R. and Parr, R. G. *J. Chem. Phys.* **21** (1953) 767.
11. Pople, J. A. *Trans. Faraday Soc.* **49** (1953) 1375.
12. Roos, B. and Skancke, P. N. *Acta Chem. Scand.* **21** (1967) 233.
13. Sundbom, M. *Acta Chem. Scand.* **25** (1971) 487, where earlier references to the same series are found.
14. Hess, H. D., Bander, A. and Günthard, H. H. *J. Mol. Spectry.* **22** (1967) 208.
15. Abrahamsson, S., Rehnberg, G., Liljefors, T. and Sandström, J. *To be published.*
16. Laszlo, P. *Progr. Nucl. Magn. Resonance Spectrosc.* **3** (1967) 231.
17. Sandström, J. and Wennerbeck, I. *Acta Chem. Scand.* **24** (1970) 1191.
18. Taft, Jr. R. W. *J. Am. Chem. Soc.* **79** (1957) 1045.
19. Blackwood, J. E., Gladys, C. L., Loening, K. L., Petrarca, A. E. and Rush, J. E. *J. Am. Chem. Soc.* **90** (1968) 509.
20. Smyth, C. P. *Dielectric Behaviour and Structure*, McGraw, New York 1955, p. 253.
21. Le Fèvre, R. J. W. and Rao, D. A. A. S. N. *Austr. J. Chem.* **7** (1954) 135.
22. Sandström, J. and Wennerbeck, I. *Chem. Commun.* **1971** 1088.
23. Loos, K. R., Wild, V. P. and Günthard, H. H. *Spectrochim. Acta* **25** (1969) 275.

Received November 1, 1972.

ACTA CHEMICA SCANDINAVICA 27 (1973) 1192–1202

The Crystal Structure and Spectra of $Na_4[Ni(NH_3)_4][Ag(S_2O_3)_2]_2 \cdot NH_3$

ROLF STOMBERG,[a] ING-BRITT SVENSSON[a] and A. A. G. TOMLINSON[b]*

[a] *Department of Inorganic Chemistry, Chalmers University of Technology and University of Göteborg, P.O.Box, S-402 20 Göteborg 5, Sweden and* [b] *Institute of General and Inorganic Chemistry, University of Perugia, Italy*

A Ni^{II} compound previously formulated as a tetraammine has been found to contain an extra ammonia molecule. The crystal structure of this compound, $Na_4[Ni(NH_3)_4][Ag(S_2O_3)_2]_2 \cdot NH_3$, has been determined from visually estimated X-ray data collected with an integrating camera. The crystals are tetragonal, space group $I4/m$, with $a = 14.025(2)$ Å, $c = 5.761(1)$ Å, $V = 1133.09(3)$ Å^3 and $Z = 2$. Least-squares refinement based on 513 observed reflexions yielded an R value of 0.079. Difference syntheses showed that the fifth ammonia molecule is statistically distributed between (0;0;0.40) and (0;0;0.60). The in-plane Ni – N distances of 2.01 Å are intermediate between those found in square planar complexes and those in octahedral ones. In agreement with this the visible and infra-red spectra, and magnetic moment show that both $Ni(NH_3)_4^{2+}$ and $Ni(NH_3)_6^{2+}$ are present instantaneously.

In 1952, Ferrari *et al.* reported the synthesis of $Na_4[Ni(NH_3)_4][Ag(S_2O_3)_2]_2$ and $Na_4[Cu(NH_3)_4][Cu(S_2O_3)_2]_2$.[1,2] In 1966 the structure of the latter was solved by Ferrari *et al.*,[3] who concluded that copper(II) is surrounded by four ammonia molecules in a square planar arrangement. The preliminary analysis of the corresponding nickel complex indicated the formula $Na_4[Ni(NH_3)_4][Ag(S_2O_3)_2]_2$. If the nickel complex were isostructural with the copper complex this would be a rare case of a square planar nickel-ammonia complex. In fact both compounds are tetragonal with very similar unit cell dimensions.[1,2]

EXPERIMENTAL

Preparation. The compound was prepared by a diffusion method, similar to the original one.[1] A solution of silver nitrate (8.5 g, 0.05 mol) and freshly-prepared nickel tetraammine sulphate dihydrate (6.5 g, 0.025 mol), in 30 ml water, was allowed to diffuse

* Present address: C.N.R. Laboratory for Electronic Structure of Coordination Compounds, c/o Istituto di Chimica Generale, Città Universitaria, 00185 Rome, Italy.

through a collodion membrane into a solution of sodium thiosulphate pentahydrate (21.7 g, 0.0875 mol) in 25 ml water. After nine days at room temperature, clusters of yellow needles had formed, on which there also formed some easily separated purple needles (presumably a hexaammine). Intermixed were several particles, presumably metallic silver, which were accurately separated mechanically.

Attempts to change experimental conditions slightly, so as to obtain other derivatives such as the monohydrate given by the analogous $Cu^{II}Cu^{I}$ complex,[4] were unsuccessful. Analyses, crystal structure and physical methods were all performed on the same sample although no evidence of other products was ever obtained. (Found: NH_3 9.5; Ni 6.7, S 28.9. Calc. for $N_5H_{15}O_{12}Na_4NiAg_2S_8$: NH_3 9.46; Ni 6.50; S 28.5.) These analyses were carried out by A. Bernhardt, W. Germany, and numerous other analyses, such as the volumetric determination of NH_3, Ni as dimethyl glyoximate, and $S_2O_3^{2-}$ as barium sulphate, after oxidation with bromine, are in agreement.

A thermogravimetric analysis was carried out to confirm the presence of the fifth ammonia molecule. With a heating rate of 1 K min^{-1} there was a slow weight loss of about 2.5 % up to 175°C, corresponding to approximately one ammonia group. Above this temperature the weight loss rate increased more than tenfold.

Attempts to eliminate the fifth ammonia molecule were not successful. Constant weight and good analyses were not obtained on heating *in vacuo* at 100°C for 5 h. The fifth ammonia was not removed on storage over P_2O_5 *in vacuo* for a week.

Physical methods. Magnetic measurements were carried out on a Gouy balance, calibrated with $[Nien_3](S_2O_3)$.[5] Reflectance spectra were run on a Beckmann DK 1A spectrophotometer and IR on a Perkin-Elmer 521 equipped with a cold tip.

X-Ray methods. The cell dimensions were obtained from X-ray powder photographs obtained by the Guinier-Hägg method, using $CuK\alpha_1$ radiation and $Pb(NO_3)_2$ ($a = 7.8566$ Å at 21°C) as an internal standard.

Multiple film (6 films) equi-inclination Weissenberg photographs were taken on a Nonius integrating camera with the crystal rotating about [001] (layer lines $0-5$) using $CuK\alpha$ radiation. 513 independent reflexions were registered. The intensities were corrected for Lorentz, polarization, and absorption but not for extinction.

Computing methods. The computational work was performed at Göteborg Universities' Computing Centre using an IBM 360/65 computer and a set of crystallographic programs in use at Göteborg.[6,7]

The atomic scattering factors used in the calculation of the structure factors were taken from Cromer and Waber. [8]

RESULTS

Unit cell and space group. The unit cell dimensions were obtained from the measured $\sin^2\theta$ values by a least-squares procedure using 63 observed lines. The dimensions of the tetragonal cell thus determined, $a = b = 14.025(2)$ Å, $c = 5.761(1)$ Å, $V = 1133.09(3)$ Å^3, were in close agreement with those reported by Ferrari *et al.*, *i.e.* $a = b = 14.00(1)$ Å and $c = 5.75(3)$ Å. From the observed density $Z = 2$ was found.[1] Observed and calculated $\sin^2\theta$ values are given in Table 1. The Laue symmetry is $4/m$. Since the only missing reflexions were of the type $h+k+l = 2n+1$, possible space groups are thus $I4/m$ (No. 87), $I\bar{4}$ (No. 83), and $I4$ (No. 79). The structure can be described according to space group $I4/m$ as was also found for $Na_4[Cu(NH_3)_4][Cu(S_2O_3)_2]_2$.

Structure determination and refinement. The structure analysis was performed in the usual way by solving the Patterson function for the heavy atoms, introducing these into structure factor calculations to obtain the signs of the Fourier coefficients and thereafter making Fourier summations alternating with new structure factor calculations as more atomic positions were revealed. Thus, no assumption was made about possible isomorphism with $Na_4[Cu(NH_3)_4][Cu(S_2O_3)_2]_2$.

Table 1. Observed lines in the powder photograph of $Na_4[Ni(NH_3)_4][Ag(S_2O_3)_2]_2.NH_3$ at 21°C (Guinier focusing camera). $\lambda(CuK\alpha_1) = 1.54051$ Å. Internal standard: $Pb(NO_3)_2$ ($a = 7.8566$ Å at 21°C). $d_{hkl} = d_{khl}$, $F_{hkl} \neq F_{khl}$.

$h\ k\ l$ $k\ h\ l$	$10^5 \times \sin^2\theta_{obs}$	$10^5 \times \sin^2\theta_{calc}$	d_{calc}	I_{obs}	F_{hkl}	F_{khl}
1 1 0	608	603	9.917	m	161	161
2 0 0	1210	1206	7.013	m−	132	132
2 2 0	2417	2413	4.959	m−	180	180
3 1 0	3021	3016	4.435	m−	161	30
2 1 1	3308	3296	4.243	m+	211	44
3 0 1	4505	4502	3.630	vvw	60	60
4 0 0	4827	4826	3.506	w−	175	175
3 3 0	5435	5429	3.306	vw	153	153
3 2 1	5716	5709	3.224	vvw	29	59
4 2 0	6040	6032	3.136	m	234	275
4 1 1	6927	6915	2.929	m	38	174
0 0 2	7174	7152	2.880	vvw	150	150
1 1 2	7766	7755	2.766	vvw	142	142
5 1 0	7857	7842	2.751	vvw	53	131
2 0 2	8380	8358	2.664	vw	93	93
5 0 1	9340	9328	2.522	vvw	69	69
2 2 2	9579	9564	2.491	m−	161	161
4 4 0	9671	9652	2.479	vw	130	130
3 1 2	10169	10168	2.416	m+	248	222
5 3 0	10271	10255	2.405	m−	29	194
6 0 0	10883	10858	2.337	vvw	92	92
4 0 2	11986	11977	2.226	vw	107	107
6 2 0	12072	12065	2.218	vw	157	81
3 3 2	12619	12581	2.172	vvw	68	68
6 1 1	12954	12948	2.141	w+	50	171
4 2 2	13203	13184	2.121	vw	76	104
5 4 1	14171	14154	2.047	vvw	57	7
5 1 2	15006	14994	1.9892	w+	142	187
6 4 0	15683	15684	1.9449	w+	148	294
5 3 2	17422	17407	1.8462	w	242	51
7 2 1	17789	17774	1.8270	w	159	69
6 0 2	18020	18010	1.8150	vw	138	138
6 2 2	19199	19216	1.7571	vw	113	62
8 0 0	19322	19304	1.7531	vw	234	234
3 2 3	20004	20012	1.7218	vvw	9	98
6 5 1	20189	20187	1.7144	vvw	0	14
8 2 0	20542	20510	1.7008	vw	153	161
4 1 3	21214	21218	1.6722	vvw	42	90
8 1 1 7 4 1	21398	21393	1.6653	vw	37 81	83 72
6 6 0	21728	21717	1.6529	vw	147	147
5 5 2	22257	22232	1.6336	m−	100	100
6 4 2	22853	22836	1.6118	vvw	79	32
5 0 3	23668	23632	1.5845	vvw	69	69
8 4 0	24154	24130	1.5680	vw−	182	60
7 3 2 9 1 0	24697	24646 24733	1.5488	vw	45 81	135 103
7 6 1 9 2 1	27422	27426	1.4708	vvw	19 14	70 37
8 5 1	28681	28632	1.4395	vvw	47	49
7 5 2 7 7 0	29523	29559	1.4176	vvw	120 74	53 74

Table 1. Continued.

10 0 0 8 6 0	30199	30162	1.4025	vvw	121 21	121 113
10 2 0	31372	31368	1.3753	vvw	108	20
3 3 4	34068	34035	1.3203	vvw	99	99
9 3 2	34305	34297	1.3152	vvw	78	186
10 3 1	34668	34664	1.3082	vvw	88	12
8 1 3 7 4 3	35702	35696	1.2892	vvw	46 97	97 85
7 7 2	36749	36710	1.2713	vvw	120	120
10 0 2 8 6 2	37299	37314	1.2610	vvw	5 155	5 24
10 2 2	38502	38520	1.2410	vvw	88	114
5 3 4	38868	38861	1.2356	vvw	15	116
9 5 2	39179	39123	1.2314	vvw	169	117
10 5 1 11 2 1	39522	39490	1.2257	vvw	28 44	13 51
11 1 2	43959	43949	1.1619	vvw	45	119
6 4 4	44257	44290	1.1574	vvw	73	135
2 1 5	46226	46205	1.1332	vvw	91	21

The electron density function with Fourier signs based on Ag, Ni, and S showed the positions of all the light atoms. In particular a peak approximately half the height of a nitrogen peak appeared at (0;0;0.41) and at the symmetry-related position (0;0;0.59). The distance between these positions, 1.0 Å, is, however, too short to be an intermolecular distance between ammonia groups (or water molecules). A difference synthesis with all atoms introduced, except the fifth nitrogen atom, N(2), also showed a peak at (0;0;0.40). Obviously, both the analytical data and the structure analysis indicated the presence of a fifth ammonia group not expected at the start of the investigation.

Due to the troublesome distance 1.0 Å, alternative assumptions about space group and occupancy were tried. A difference synthesis with N(2) at $(0;0;\frac{1}{2})$ showed a large hole at $(0;0;\frac{1}{2})$ and a peak at (0;0;0.40). Space group $I4$ was tried in a difference synthesis with all atoms except N(2); this gave peaks at (0;0;0.385) and (0;0;0.620) with peak heights approximately half those due to nitrogen peaks.

The structure was refined by the structure factor least-squares method using a full matrix program and 513 observed, independent reflexions. A separate scale factor for each layer, atomic coordinates, and anisotropic temperature parameters for N and O were refined. The structure factors were weighted according to Cruickshank,[9] $w=(a+|F_o|+c|F_o|^2+d|F_o|^3)^{-1}$, with $a=30$, $c=0.005$, and $d=0$.

The least-squares refinement was applied to the several alternatives. Both refinement according to space group $I4/m$ and I4 converged to a final R-value of 0.079 for the 513 observed reflexions indicating approximately half a nitrogen atom at (0;0;0.40) and (0;0;0.60). We have, therefore, chosen to describe the structure according to space group $I4/m$. The parameters, together with their standard deviations, are given in Table 2, the weight analysis in Table 3, and observed and calculated structure factors in Table 4. The contributions to the structure factors from the hydrogen atoms have not been taken into consideration. The final difference synthesis showed no anomalies.

Table 2a. Atomic coordinates, expressed as fractions of the cell edges, for $Na_4[Ni(NH_3)_4][Ag(S_2O_3)_2]_2.NH_3$. Space group $I4/m$, $Z=2$. The numbers in parentheses are the standard deviations of the last significant figures. The temperature factor $=\exp(-B\sin^2\theta/\lambda^2)$.

Atom	Position	x	y	z	B
Ni	2*a*	0	0	0	
Ag	4*d*	0	½	¼	
S(1)	8*h*	0.0936(2)	0.2642(2)	½	
S(2)	8*h*	0.1217(3)	0.4067(2)	½	
Na	8*h*	0.2927(4)	0.1669(4)	½	0.7(1)
O(1)	8*h*	−0.0080(7)	0.2445(7)	½	2.3(2)
O(2)	16*i*	0.1403(5)	0.2258(6)	0.2945(17)	2.9(1)
N(1)	8*h*	0.3619(9)	0.4618(9)	½	2.3(2)
N(2)	4*e*	0	0	0.3929(69)	1.3(5)

Table 2b. Anisotropic temperature parameters β_{ij} and their standard deviations. The expression used is $\exp-(\beta_{11}h^2+\beta_{22}k^2+\beta_{33}l^2+\beta_{12}hk+\beta_{13}hl+\beta_{23}kl)$.

Atom	β_{11}	β_{22}	β_{33}	β_{12}	β_{13}	β_{23}
Ni	0.0034(2)	0.0034(2)	0.0219(17)	0	0	0
Ag	0.0042(1)	0.0042(1)	0.0146(9)	0	0	0
S(1)	0.0015(1)	0.0016(1)	0.0102(11)	0.0001(2)	0	0
S(2)	0.0020(2)	0.0017(2)	0.0278(15)	−0.0003(3)	0	0

Table 3. Weight analysis for $Na_4[Ni(NH_3)_4][Ag(S_2O_3)_2]_2.NH_3$.

$\lvert F_o\rvert$-interval	$w\Delta^2$	Number of reflexions
0.0 – 16.2	1.11	51
16.2 – 21.8	1.09	51
21.8 – 27.2	1.10	51
27.2 – 34.5	0.94	52
34.5 – 39.9	0.90	51
39.9 – 51.0	0.83	51
51.0 – 65.2	0.86	52
65.2 – 82.2	0.97	51
82.2 – 115.6	0.91	51
115.6 – 264.3	1.29	52

DISCUSSION

During the structure investigation it became apparent that the structure of $Na_4[Ni(NH_3)_4][Ag(S_2O_3)_2]_2.NH_3$ was very similar to that reported for $Na_4[Cu(NH_3)_4][Cu(S_2O_3)_2]_2$, the only difference being the presence of a fifth ammonia group. Curiously enough, the analytical results obtained by Ferrari

Table 4. Observed and calculated structure factors for $Na[Ni(NH_3)_4][Ag(S_2O_3)_2]_2.NH_3$. The columns are successively h, $|F_o|$ and $|F_c|$.

	H 0 0		4	92	99	11	35	-33		H 17 1		4	21	-19	8	19	-20		H 2 4	
2	130	132	6	105	102	13	-	-10	2	-	1	6	64	-59	10	-	1	2	86	81
4	162	175	8	108	89	15	68	65	4	28	30	8	25	14	12	75	70	4	122	118
6	99	92	10	27	28	17	20	26		H 0 2		10	53	-53	14	-	0	6	80	76
8	229	234	12	44	46		H 5 1		2	97	-93	12	27	-24		H 6 3		8	96	103
10	120	121	14	26	30	2	32	31	4	109	-107		H 11 2		1	83	85	10	49	44
12	107	98				4	-	7	6	138	-138	1	116	119	3	19	19	12	43	41
14	51	47		H 11 0		6	-	0	8	40	-23	3	86	88	5	-	4	14	-	-3
16	16	17	1	27	-27	8	57	-47	10	-	-5	5	45	45	7	-	10		H 3 4	
	H 1 0		3	25	18	10	-	27	12	-	-3	7	35	33	9	34	28	1	14	-13
1	127	-161	5	73	-69	12	79	69	14	61	-58	9	-	6	11	31	29	3	108	-59
3	156	-161	7	83	-59	14	-	-2	16	28	-34	11	73	77	13	-	6	5	18	-15
5	67	53	9	93	-89	16	27	-27				13	52	59	15	10	14	7	118	-105
7	20	-19	11	54	46					H 1 2								9	56	-49
9	86	-81	13	10	7		H 6 1		1	125	142		H 12 2			H 7 3		11	35	-32
11	59	-91				1	169	171	3	220	248	2	91	-83	2	55	-54	13	17	9
13	13	6		H 12 0		3	-	2	5	143	142	4	-	-16	4	82	85			
15	-	-8	2	47	49	5	18	-14	7	193	201	6	51	-52	6	33	30		H 4 4	
17	33	-36	4	96	90	7	20	19	9	85	86	8	24	18	8	72	70	2	121	121
			6	13	12	9	39	37	11	45	45	10	-	-10	10	21	-23	4	78	77
	H 2 0		8	124	119	11	36	29	13	68	66	12	21	-30	12	-	-5	6	79	73
2	159	180	10	53	53	13	-	-4	15	64	60				14	-	-5	8	89	95
4	224	234	12	19	21	15	29	27	17	18	21		H 13 2					10	54	45
6	156	157										1	29	30		H 8 3		12	72	73
8	139	153		H 13 0			H 7 1			H 2 2		3	26	24	1	96	97	14	24	22
10	105	108	1	67	-60	2	62	-67	2	154	-161	5	86	89	3	-	8			
12	65	64	3	67	-63	4	77	72	4	84	-76	7	47	45	5	43	46		H 5 4	
14	-	-5	5	-	-1	6	63	70	6	121	-113	9	34	40	7	40	-39	1	71	-68
16	80	82	7	-	-8	8	83	79	8	35	35	11	20	22	9	14	15	3	119	-116
			9	-	-9	10	43	-40	10	84	-88				11	29	24	5	75	-73
	H 3 0		11	33	-38	12	-	-7	12	40	-40		H 14 2		13	-	10	7	-	-12
1	25	30				14	-	-3	14	75	-77	2	45	39				9	15	6
3	160	-153		H 14 0		16	24	28	16	32	29	4	-	-4		H 9 3		11	56	-56
5	33	-29	2	105	96							6	37	-37	2	38	35	13	33	-34
7	163	-150	4	89	87		H 8 1			H 3 2		8	50	-54	4	-	-1			
9	73	-65	6	35	31				1	158	222				6	57	52		H 6 4	
11	25	-27	8	-	4	1	85	83	3	62	68		H 15 2		8	-	-9	2	74	69
13	12	10	10	-	2	3	19	23	5	238	242	1	66	63	10	-	-9	4	127	135
15	-	1				5	51	49	7	47	45	3	-	11	12	15	11	6	92	97
17	39	-43		H 15 0		7	40	-43	9	77	78	5	26	26				8	25	-17
			1	-	-4	9	-	-4	11	62	58	7	32	32		H 10 3		10	32	31
	H 4 0		3	64	-61	11	51	42	13	127	124				1	-	2	12	36	36
2	242	275	5	-	-9	13	-	11	15	45	45		H 16 2		3	-	2			
4	125	130	7	33	-33	15	-	-14				2	-	-11	5	21	20		H 7 4	
6	150	148	9	25	26					H 4 2		4	14	-15	7	-	7	1	58	-56
8	177	182					H 9 1		2	115	-104	6	13	-18	9	54	59	3	23	-23
10	63	66		H 16 0		2	32	37	4	36	-31				11	17	13	5	78	-76
12	113	114	2	62	60	4	23	21	6	88	-79		H 17 2					7	48	-44
14	45	37	4	39	40	6	46	45	8	37	-37	1	14	18		H 11 9		9	39	-36
16	38	37	6	27	29	8	-	-9	10	53	-47				2	49	51	11	25	-28
						10	-	-17	12	-	12		H 0 3		4	17	-14	13	13	-14
	H 5 0			H 17 0		12	-	17	14	34	-36	1	24	29	6	46	46			
1	134	-131	1	14	-13	14	27	29	16	31	-33	3	10	8	8	-	-11		H 8 4	
3	189	-194	3	-	-5							5	70	69	10	36	38	2	81	86
5	131	-128	5	-	-5		H 10 1			H 5 2		7	31	-24				4	32	30
7	33	26				1	-	3	1	188	187	9	38	37		H 12 3		6	70	69
9	15	8		H 0 1		3	18	12	3	52	51	11	33	-32	1	36	-33	8	74	63
11	73	-71	1	10	-6	5	19	13	5	100	100	13	37	34	3	32	27	10	65	64
13	40	-37	3	56	60	7	-	0	7	121	120	15	-	4	5	51	47	12	32	30
15	32	-33	5	73	69	9	91	84	9	170	169				7	-	6			
17	21	20	7	52	-46	11	-	7	11	38	35		H 1 3		9	25	-28		H 9 4	
			9	28	24	13	24	22	13	23	25	2	87	95	11	10	-10	1	88	-91
	H 6 0		11	19	-10				15	24	27	4	49	42				3	-	-7
2	71	81	13	27	26		H 11 1					6	68	65		H 13 3		5	-	-11
4	262	294	15	-	-1	2	55	51		H 6 2		8	47	-46	2	56	53	7	20	-19
6	149	147	17	-	-7	4	31	-25	2	81	-62	10	33	26	4	26	-27	9	37	-40
8	37	-21				6	56	51	4	35	-32	12	-	-5	6	33	-34	11	12	-13
10	43	41		H 1 1		8	-	-7	6	15	-11	14	40	44	8	-	8			
12	82	78	2	177	211	10	47	41	8	151	-155	16	-	0	10	29	38		H 10 4	
14	58	89	4	41	38	12	-	-13	10	60	-54							2	16	12
16	28	31	6	47	50				12	51	-44		H 2 3			H 14 3		4	69	70
			8	43	-37		H 12 1		14	31	27	1	40	43	1	-	-9	6	55	50
	H 7 0		10	23	27	1	39	-42				3	16	-9	3	14	16	8	55	58
1	90	-82	12	-	-11	3	-	3		H 7 2		5	25	29	5	-	3	10	16	13
3	18	-14	14	31	39	5	82	75	1	126	124	7	93	91	7	28	33			
5	111	-100	16	-	11	7	-	3	3	139	135	9	-	11					H 11 4	
7	81	-74				9	37	-39	5	56	53	11	52	54		H 15 3		1	13	-14
9	26	-23		H 2 1		11	-	-17	7	121	120	13	-	12	2	25	-25	3	11	-7
11	44	-38	1	40	44				9	54	51	15	-	-10	4	40	46	5	48	-53
13	24	-21	3	46	-29		H 13 1		11	64	57				6	26	28	7	38	-42
15	59	-58	5	-	2	2	71	68	13	46	46		H 3 3					9	53	-60
			7	166	159	4	36	-36	15	-	6	2	92	98		H 16 3				
	H 8 0		9	-	14	6	35	-39				4	-	-9	1	29	36		H 12 4	
2	149	161	11	50	44	8	-	-5		H 8 2		6	22	22				2	22	18
4	52	60	13	25	20	10	50	54	2	50	-49	8	18	13		H 0 4		4	50	55
6	106	113	15	-	-11				4	58	-91	10	85	87	2	75	76	6	13	8
8	111	112	17	-	-4		H 14 1		6	20	-24	12	-	-15	4	89	88	8	64	73
10	115	105				1	-	-9	8	36	-29	14	30	29	6	39	41			
12	46	44		H 3 1		3	28	26	10	-	-15				8	111	116		H 13 4	
14	58	57	2	51	59	5	-	-4	12	-	-9		H 4 3		10	75	77	1	39	-46
			4	-	12	7	24	37	14	-	-15	1	91	-90	12	67	66	3	40	-48
	H 9 0		6	22	24	9	-	-10		H 9 2		3	55	50	14	21	23	5	-	0
1	113	-103	8	16	19				1	-	5	5	15	10				7	-	-16
3	23	-13	10	84	88		H 15 1		3	181	186	7	98	97		H 1 4				
5	21	11	12	19	-6	2	20	-23	5	115	117	9	37	-34	1	80	-93		H 14 4	
7	25	-19	14	38	37	4	47	45	7	80	79	11	20	-22	3	81	-76	2	54	68
9	56	-52	16	24	-29	6	30	31	9	49	45	13	14	-13	5	33	-25	4	48	56
11	14	-13				8	-	2	11	77	69	15	54	62	7	19	-15			
13	41	-46		H 4 1					13	-	10		H 5 3		9	50	-52		H 0 5	
15	20	16	1	170	-174		H 16 1					11	60	-62	13	-	-15	1	7	-7
			3	32	39	1	34	34		H 10 2		2	11	9				3	44	37
	H 10 0		5	60	57	3	23	24	2	107	-114	4	17	15				5	40	39
2	21	20	7	75	81	5	19	-26				6	11	8				7	18	-15
			9	37	-37	7	-	10												

Table 1. Continued.

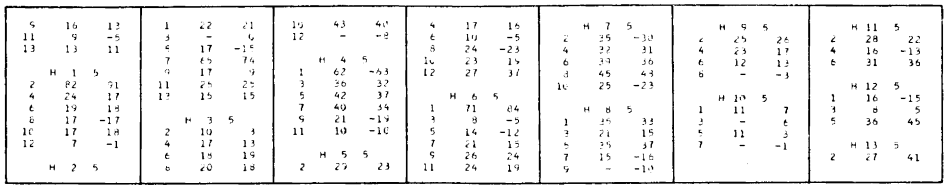

et al. for the copper compound, 10.7 % NH_3 on the average,[2] is more consistent with the formulation $Na_4[Cu(NH_3)_5][Cu(S_2O_3)_2]_2$ (theoretical amount 10.43 % NH_3) than with $Na_4[Cu(NH_3)_4][Cu(S_2O_3)_2]_2$ (theoretical amount 8.55 % NH_3). At the final stage of this structure determination the structure investigation performed by Ferrari *et al.* was doubted. Refinement of the original X-ray data [4,10] as well as a new structure investigation by Hathaway *et al.*[4] have shown that the formulation $Na_4[Cu(NH_3)_4][Cu(S_2O_3)_2]_2$ is incorrect. There exist, in fact, both a monoaquo- and a mono-ammonia-adduct, which they formulate $Na_4[Cu(NH_3)_4][Cu(S_2O_3)_2]_2L$ ($L = H_2O$ or NH_3).

The present investigation of $Na_4[Ni(NH_3)_4][Ag(S_2O_3)_2]_2.NH_3$ has shown a similar situation, the only difference being that while Morosin *et al.* on the one hand and Hathaway *et al.* on the other both report the adduct ammonia molecule at (0;0;$\frac{1}{2}$) our data are more consistent with describing the adduct molecule statistically at (0;0;0.39) and (0;0;0.61). Despite this difference there can be no doubt that there is a fifth ammonia molecule between the two nickel atoms. A further indication that the nickel atom is coordinated to more than four ligands is the in-plane Ni – N distance of 2.01 Å, which is significantly longer than those, 1.82 – 1.92 Å, found in square planar complexes (see Table 8 in Ref. 11). This distance is shorter than Ni – N distances, 2.04 – 2.15 Å, observed in octahedral complexes of nickel(II).[11]

Bond distances are given in Table 5 and packing distances in Table 6. Apart from the fifth ammonia molecule, the structural description given by Ferrari *et al.*[3] for the copper complex applies.

Table 5. Bond distances and angles with their standard deviations in $Na_4[Ni(NH_3)_4][Ag(S_2O_3)_2]_2.NH_3$.

	Distance (Å)		Angle (°)
Ni – N(1)	2.010(13)	S(2) – Ag – S(2) ($\bar{x}$, 1 – y, z)	112.38(9)
– N(2)	2.263(40)	S(2) – Ag – S(2) ($\frac{1}{2}-y$, $\frac{1}{2}+x$, $\frac{1}{2}-z$)	108.04(5)
Ag – S(2)	2.588(3)	S(2) – S(1) – O(1)	112.1(4)
S(1) – O(1)	1.451(10)	S(2) – S(1) – O(2)	106.0(4)
– O(2)	1.456(9)	O(1) – S(1) – O(2)	111.8(4)
– S(2)	2.037(4)	O(2) – S(1) – O(2) (x, y, 1 – z)	108.8(7)
		Ag – S(2) – Ag (x, y, 1 – z)	67.62(9)
		Ag – S(2) – S(1)	111.62(16)

Table 6. Interatomic distances other than bond distances in $Na_4[Ni(NH_3)_4][Ag(S_2O_3)_2]_2.NH_3$. Distances less than 4.0 Å are included.

Ni	$-N(2)$ $(x, y, 1-z)$	3.50 Å	Na	$-O(1)$ $(y, \bar{x}, z)$	2.33 Å
Ag	$-Ag$ $(x, y, \bar{z})$	2.88		$-O(2)$ $(\frac{1}{2}-x, \frac{1}{2}-y, \frac{1}{2}+z)$	2.46
	$-S(1)$	3.84		$-O(2)$ $(x, y, 1-z)$	2.58
	$-O(1)$	3.86	O(1)	$-O(2)$	2.41
S(1)	$-Na$	3.11		$-N(1)$ $(-\frac{1}{2}+y, \frac{1}{2}-x, \frac{1}{2}+z)$	3.27
	$-Na$ $(\frac{1}{2}-x, \frac{1}{2}-y, \frac{1}{2}-z)$	3.43		$-N(2)$	3.49
	$-Na$ $(\bar{y}, x, z)$	3.68		$-O(2)$ $(\bar{y}, x, z)$	3.59
	$-N(1)$ $(y-\frac{1}{2}, \frac{1}{2}-x, \frac{1}{2}-z)$	3.85	O(2)	$-O(2)$ $(x, y, 1-z)$	2.37
	$-N(2)$	3.98		$-N(1)$ $(\frac{1}{2}-x, \frac{1}{2}-y, \frac{1}{2}-z)$	3.13
S(2)	$-O(2)$	2.81		$-O(2)$ $(\frac{1}{2}-x, \frac{1}{2}-y, \frac{1}{2}-z)$	3.19
	$-O(1)$	2.91		$-N(1)$ $(y-\frac{1}{2}, \frac{1}{2}-x, \frac{1}{2}-z)$	3.26
	$-Na$ $(\frac{1}{2}-x, \frac{1}{2}-y, \frac{1}{2}-z)$	3.29		$-O(2)$ $(x, y, \bar{z})$	3.39
	$-N(1)$	3.46		$-N(2)$	3.77
	$-O(1)$ $(\frac{1}{2}-y, \frac{1}{2}+x, \frac{1}{2}-z)$	3.64	N(1)	$-N(1)$ $(y, 1-x, z)$	2.84
				$-N(2)$ $(\frac{1}{2}-x, \frac{1}{2}-y, \frac{1}{2}-z)$	3.03

There are several possible structures for the complex as a result of the presence of the fifth ammonia molecule. These are:

(a) this ammonia molecule undergoes free rotation, and N(2) lies at $(0;0;\frac{1}{2})$;

(b) as well as rotating, the ammonia molecule inverts in a 'synchronised' fashion, along the *c* axis, giving instantaneously a five-coordinate structure;

(c) the ammonia molecule inverts in a 'non-synchronised' fashion, giving instantaneously one six-coordinated and one square planar nickel;

(d) the 'fifth ammonia' molecules are situated at (0;0;0.39) in a given row of unit cells in the *c*-direction and at (0;0;0.61) in a neighbouring, parallel, row of unit cells. This means on OD-structure with alternating octahedral and square planar nickel complexes in static coordination. There were, however, no visible signs that the structure was an OD-structure. The possibility cannot, however, be excluded since the difference between the contributions from nitrogen to the structure factors in cases (a) – (d) is so small that it is highly unlikely to be observable (the rotation photograph about [001] ought in case (d) to have shown extra streaks between the layer lines.

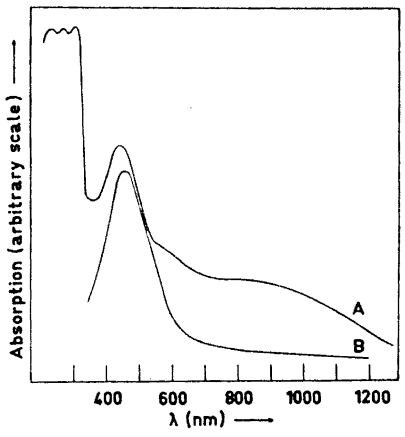

Fig. 1. Reflectance spectra. A. $Na_4[Ni(NH_3)]_4[Ag(S_2O_3)_2]_2.NH_3$ B. $[Ni(en)_2][AgBr_2]_2$.

If (a) were the case, either diamagnetic square planar or strongly tetragonal octahedral (since Ni–N(2) = 2.88 Å) structures would be present. According to Ballhausen and Liehr [12] the latter may be either diamagnetic or paramagnetic. The reflectance spectrum (Fig. 1) shows two ill-resolved bands at *ca.* 11 000 cm^{-1} and *ca.* 17 000 cm^{-1}, followed by a more intense band at 22 500 cm^{-1}. This type of spectrum is not in agreement with the strongly tetragonal paramagnetic possibility, which should give only very weak bands in the visible region since all transitions would be spin-forbidden in character.[12] The compound is not diamagnetic and the reflectance spectrum is different from that of $[Ni(en)_2][AgBr_2]_2$ (see Fig. 1). Since the latter compound is strictly square planar in structure,[11] then all possibilities under (a) may be eliminated.

Possibility (b) may also be discounted, both on the grounds of the spectrum being very different from that expected for a high spin five-coordinate structure [13] and also because such a structure should give a magnetic moment of *ca.* 3.2 BM.[14] Instead, the magnetic moment is *ca.* 2.2 BM.

The results are consistently interpreted assuming the presence of both octahedral and square planar nickel complexes. Thus, the peak at 22 500 cm^{-1} in the electronic spectrum arises from the spin-allowed transitions $^1A_{1g} \rightarrow {}^1A_{2g}$, *etc.* of $Ni(NH_3)_4^{2+}$, which are, in fact, very close to those in $Ni(en)_2^{2+}$. The $Ni(NH_3)_6^{2+}$ ion gives a spectrum with bands at 10 750, 17 500 and 27 200 cm^{-1},[15] which is in reasonable agreement with Fig. 1 if it is assumed that the

Table 7. Magnetic properties of the compound.

T/K	$10^6\chi_{corr}$/c.g.s.u.	$\mu_{eff.}$/BM
112	4717	2.07
116	4924	2.14
121	4606	2.12
126	4358	2.10
130	4257	2.11
133	4187	2.12
138	4046	2.12
143	4035	2.16
153	3783	2.16
156	3720	2.16
160	3620	2.16
167	3554	2.19
175	3317	2.16
188	3135	2.18
196	2561	2.01
215	2376	2.03
223	2305	2.03
240	2316	2.12
302	2005	2.21
314	1946	2.22
318	1916	2.22
295	2028	2.20

Diamagnetic correction = -338.4×10^{-6} c.g.s.u. (from Selwood, P. W. *Magnetochemistry*, Wiley, New York 1956).

highest energy band is covered by the onset of c.t. transitions at 27 000 cm^{-1}. The broadening at lower energy could be caused by the 'tail' of the more intense 22 500 cm^{-1} band, and also by some splitting of the $^3T_{1g}$ and $^3T_{2g}$ (F) energy levels of $Ni(NH_3)_6^{2+}$ (since Ni – N(2) = 2.26 Å represents sensible tetragonal character).[16]

Strong evidence for the presence of both octahedral and square planar nickel complexes is provided by the magnetic properties. At room temperature the magnetic moment is 2.2 BM decreasing to 2.07 BM at 112 K. In this range the susceptibility obeys the Curie-Weiss law with θ (extrapolated) *ca.* 5 K (Table 7). Almost identical magnetic moments have been found in other cases of simultaneous presence of diamagnetic and paramagnetic octahedral chromophores of Ni^{2+} in the unit cell.[17] The corrected magnetic moments then become 2.99 (r.t.) and 2.87 (112 K) BM, assuming 50 % diamagnetic and 50 % paramagnetic (2 electrons). Hexaammine nickel(II) complexes typically show magnetic moments between 3.04 and 3.11 BM.[18]

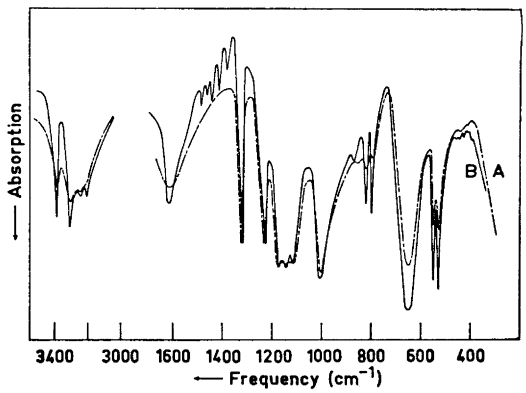

Fig. 2. IR spectra of $Na_4[Ni(NH_3)_4][Ag(S_2O_3)_2]_2.NH_3$. A. Room temperature. B. 100 K.

The IR spectrum of the compound is also in agreement with this interpretation. The split bands at 1180, 1145, 1120 and 530, 550 cm^{-1} are ascribed to $\nu_4(S_2O_3)^{2-}$ and $\nu_5(S-O)$, respectively, and the strong, broad bands at 650 and 1010 cm^{-1} to $\nu_2(S-O)$ and $\nu_1(S-O)$, respectively.[19] There is no absorption due to water molecules at *ca.* 3600 cm^{-1}, and the remaining strong bands are presumably due solely to NH_3 vibrations. It is immediately seen that there are two symmetric deformation modes, $\delta_{sym}(NH_3)$, at 1330 and 1235 cm^{-1}. The latter may be assigned to that arising from the $Ni(NH_3)_6^{2+}$ part (although at rather higher frequency than in many hexaamminenickel(II) complexes, possibly due to the tetragonal chromophore present [20]) and the former to $Ni(NH_3)_4^{2+}$. A further NH_3 symmetric deformation mode expected to arise from $Ni(NH_3)_6^{2+}$ may be hidden under $\nu_4(S_2O_3)^{2-}$. Also, there is clearly more than one $\varrho(NH_3)$ mode, at 862, 834, and 800 cm^{-1}, all of which are considerably more intense at *ca.* 100 K.

Apart from better resolution, there is almost no significant change in the other IR bands at 100 K, apart from the appearance of many weak-medium bands between 1385 and 1480 cm^{-1}. These may be combination bands between

$\nu_1(S-O)$ at 1010 cm^{-1} and several very weak bands at 410, 420, 438, 460, and 470 cm^{-1}, the origin of which is unclear, but which may include S – S stretching vibrations. The lack of a sensible temperature effect on the NH_3 vibrations favours the interpretation according to (d).

It is interesting to note that the analogous $Cu^{II}Cu^{I}$ compound has electronic properties which are not consistent with a $CuN_4 - CuN_6$ formulation [4] and shows only one band in the IR ascribable to $\delta_{sym}(NH_3)$. (The 1180 cm^{-1} band previously assigned to δ_{sym}('NH_3') is more reasonably attributed to one of the components of $\nu_4(S_2O_3)$,$^{2-}$ and that assigned to $\varrho(NH_3)$ at 655 cm^{-1} is probably due to $\nu_2(S-O)$). These differences indicate that the difference in position of the fifth ammonia molecule in these two compounds as found in the difference syntheses is, in fact, real.

To date we have no reasonable explanation to account for the differences between the $Ni^{II}Ag^{I}$ and $Cu^{II}Cu^{I}$ compounds.

Acknowledgement. A grant from the *Swedish Natural Science Research Council* is gratefully acknowledged.

REFERENCES

1 Ferrari, A., Cavalca, L. and Coghi, L. *Gazz. Chim. Ital.* **82** (1952) 703.
2. Ferrari, A., Cavalca, L. and Coghi, L. *Gazz. Chim. Ital.* **82** (1952) 385.
3. Ferrari, A., Braibanti, A. and Tiripicchio, A. *Acta Cryst.* **21** (1966) 605.
4. Hathaway, B. J. and Stephens, F. *J. Chem. Soc.* **A 1970** 884.
5. Curtis, N. F. *J. Chem. Soc.* **1961** 3147.
6. Lindqvist, O. and Wengelin, F. *Arkiv Kemi* **28** (1967) 179.
7. Lindgren, O. *To be published.*
8. Cromer, D. T. and Waber, J. T. *Acta Cryst.* **18** (1965) 104.
9. Cruickshank, D. W. J. *The Equations of Structure Refinements*, Glasgow 1964.
10 Morosin, B. and Larson, A. C. *Acta Cryst.* **B 25** (1969) 1417.
11. Stomberg, R. *Acta Chem. Scand.* **23** (1969) 3498.
12. Ballhausen, C. J. and Liehr, A. D. *J. Chem. Soc.* **81** (1959) 538.
13. Sacconi, L. In Carlin, R. L., Ed., *Transition Metal Chemistry*, Interscience, New York 1968, Vol. 4, p. 199.
14. Sacconi, L. *J. Chem. Soc.* **A 1970** 248.
15. Jorgensen, C. K. *Absorption Spectra and Chemical Bonding in Complexes*, Pergamon, London 1962, p. 297.
16. Chiang, A. L. and Drago, R. S. *Inorg. Chem.* **10** (1971) 453.
17. Barefield, R. K., Busch, D. H. and Nelson, S. M. *Quart. Rev. Chem. Soc.* **22** (1968) 457.
18. Figgis, B. N. and Lewis, J. *Progr. Inorg. Chem.* **6** (1964) 200.
19. Newman, G. A. *J. Mol. Struct.* **5** (1970) 61.
20. Sacconi, L., Sabatini, A. and Gans, P. *Inorg. Chem.* **3** (1964) 1772.

Received October 18, 1972.

ACTA CHEMICA SCANDINAVICA 27 (1973) 1203–1209

The Crystal and Molecular Structure of 2,6-*cis*-Diphenylhexamethylcyclotetrasiloxane

D. CARLSTRÖM and G. FALKENBERG

Department of Medical Physics, Karolinska Institutet, S-104 01 Stockholm, Sweden

The crystal structure of 2,6-*cis*-diphenylhexamethylcyclotetrasiloxane, $C_{18}H_{28}O_4Si_4$, has been determined and refined using three-dimensional X-ray diffractometer data. The unit cell is monoclinic, space group $C2/c$ with the constants $a = 15.155$, $b = 8.829$, $c = 18.020$ Å, $\beta = 93.44°$. There is half a formula unit in the asymmetric unit. The structure was solved by direct methods and refined by least-squares procedures. The final R-value was 0.048 for 2144 symmetry independent observed reflexions.

The eight-membered siloxane ring has a "boat form" and differs thereby from configurations earlier reported for cyclotetrasiloxanes. The intra- and intermolecular distances are discussed.

The material for the X-ray crystallographic analysis was synthesized by Dow-Corning, USA, and was, in the form of large colourless transparent crystals, placed at our disposal by AB Kabi, Stockholm. The substance has a very marked estrogen-like activity especially on the male sexual organs of the mouse, rat, rabbit, dog, and monkey (Åberg, B., personal communication).

EXPERIMENTAL

Preliminary rotation and Weissenberg diagrams showed that the crystals were monoclinic and the systematic absences indicated either of the two C-centered space groups Cc or $C2/c$. While the former is non-centrosymmetric with 4 general positions, the latter is centrosymmetric with 8 general positions. A rough determination of the density of the crystals showed that there were 4 molecules in the unit cell.

For the recording of the reflexion intensities an optically perfect crystal was trimmed to an almost spherical shape (diameter = 0.3 mm). The crystal was mounted about its b axis and was sealed within a capillary of Lindemann glass as it had been observed that crystals kept in open air slowly evaporated. Three-dimensional intensity data were collected with a Philips linear automatic diffractometer (PAILRED). The Mo$K\alpha$-radiation was monochromatized with a graphite crystal. Unit cell parameters: $a = 15.155 \pm 0.006$, $b = 8.829 \pm 0.004$, $c = 18.020 \pm 0.008$ Å, $\beta = 93.44 \pm 0.09°$. Integrated intensities were collected with the ω-scanning technique within $\sin\theta/\lambda < 0.66$ corresponding to the Cu-sphere. A scanning speed of 2.5° min^{-1} was employed and the scanning range was varied

between 1.6° and 2.5°. For reflexions giving less than 10 000 counts during one scan, the scan was repeated up to 3 times. Background was measured for one minute at the beginning and the end of each scan. As a check on the stability of the crystal and the instrument, standard reflexions were measured twice a day during the recording period. Excluding systematic absences, 2834 symmetry independent reflexions of the layers $h0l$ through $h11l$ were recorded. Out of these, 690 did not differ significantly from the background intensity. The integrated intensities were corrected for Lorentz and polarization factors but no corrections were made for extinction or absorption. The latter could be neglected altogether because of the spherical shape of the crystal and the low linear absorption coefficient of the material ($\mu = 2.63$ cm^{-1} for Mo$K\alpha$ radiation, $\lambda = 0.7107$ Å). The corrected structure amplitudes were placed on an approximately absolute scale by Wilson statistics. The Wilson plot gave a correlation coefficient for the K-curve of -0.994 and the over all temperature factor, $B = 4.4$ Å^2, showed that the molecules had a high thermal mobility which was in accordance with the low melting point (+43°C) of the crystals. The normalized structure factors, $|E|$'s, were computed and the $|E|$ value distribution (Table 1) indicated the centrosymmetric space group ($C2/c$).

Table 1. Statistical averages and distribution of normalized structure factors.

	Experimental	Theoretical for centrosymmetric	Theoretical for non-centrosymmetric
$\langle\|E\|\rangle$	0.790	0.798	0.886
$\langle\|E\|^2-1\rangle$	0.912	0.968	0.736
$\langle\|E\|^2\rangle$	0.960	1.000	1.000
$\|E\|>1$	31.3 %	32.0 %	37.0 %
$\|E\|>2$	4.3 %	5.0 %	1.8 %
$\|E\|>3$	0.1 %	0.3 %	0.01 %

DETERMINATION AND REFINEMENT OF THE STRUCTURE

Since 2,6-*cis*-diphenylhexamethyltetrasiloxane does not contain atoms with atomic numbers higher than 14 it was evident that the "heavy atom technique" probably would be difficult as the silicon atoms could not be located with certainty in the three-dimensional Patterson maps. However, the strong accumulation of vector maxima in $x0z$ was a further indication that the structure was centrosymmetric and it was decided to determine the structure by the symbolic addition procedure (*cf.* Karle and Karle [1]). Several attempts to solve the structure by this method failed, probably depending on the low $|E|$ values with $l = n + 1$. Through the courtesy of Dr. R. Norrestam, Stockholm University, a new attempt was made with his programme for direct methods (Norrestam [2]). The signs of the reflexions $\bar{7}$ 3 13 and 4 4 1 were used for the specification of origin. In addition the reflexions $\bar{9}$ 1 2, $\bar{10}$ 0 2 and $\bar{7}$ 1 14 were used as the basic set for solving the triple relations calculated for the 200 strongest $|E|$ values. The phases 0 or π in all combinations were assigned to the latter three reflexions. In the subsequent generation of eight different solutions of the sign relations, one solution was found to be superior to the other ones. In this solution all triple relations were utilized resulting in signs for 123 $|E|$ values. In the three-dimensional E-maps, based on these signs, four strong maxima were found separated by distances acceptable for Si – O bonds. These maxima fitted well half an eight-membered

Table 2. Fractional atomic coordinates($\times 10^5$) for non-hydrogen atoms and ($\times 10^4$) for hydrogen atoms. Anisotropic temperature parameters ($\times 10^5$) for non-hydrogen atoms and isotropic temperature factors for hydrogen atoms. Standard deviations in parentheses. β_{ij} are the coefficients in the expression: exp $[-(\beta_{11}h^2+\beta_{22}k^2+\beta_{33}l^2+\beta_{12}hk+\beta_{13}hl+\beta_{23}kl)]$.

Atom	x	y	z	β_{11}	β_{22}	β_{33}	β_{12}	β_{13}	β_{23}
Si(1)	38084 (4)	7538 (8)	18140 (4)	372 (3)	1551 (11)	298 (2)	194 (8)	−4 (4)	37 (7)
Si(2)	42510 (4)	575 (8)	34920 (4)	426 (3)	1568 (11)	266 (2)	−132 (8)	91 (4)	68 (7)
O(1)	46750 (11)	−1097 (21)	15262 (11)	427 (8)	1668 (27)	385 (6)	271 (22)	12 (11)	−147 (19)
O(2)	38677 (13)	8303 (25)	27193 (10)	561 (9)	2269 (34)	310 (6)	356 (28)	131 (11)	303 (22)
C(1)	38044 (16)	27408 (30)	14693 (14)	455 (11)	1639 (34)	300 (7)	356 (30)	61 (14)	27 (25)
C(2)	36983 (28)	30419 (43)	7112 (16)	1055 (25)	2028 (52)	312 (9)	593 (56)	−40 (23)	82 (34)
C(3)	37551 (34)	44969 (49)	4336 (22)	1116 (30)	2400 (59)	389 (13)	883 (69)	90 (30)	579 (45)
C(4)	38894 (37)	56915 (48)	9103 (27)	1322 (34)	1865 (63)	599 (17)	548 (74)	281 (37)	564 (52)
C(5)	39831 (47)	54373 (52)	16515 (29)	1913 (53)	1685 (51)	561 (19)	−66 (82)	183 (49)	−269 (52)
C(6)	39300 (32)	39622 (41)	19336 (20)	1183 (29)	1815 (49)	349 (11)	126 (56)	97 (28)	−132 (35)
C(7)	28203 (20)	−3328 (42)	14660 (23)	474 (12)	2112 (48)	640 (16)	16 (41)	−169 (22)	−134 (45)
C(8)	38021 (25)	−18641 (41)	35773 (21)	695 (18)	2078 (50)	534 (14)	−838 (50)	107 (25)	353 (42)
C(9)	39570 (29)	12994 (50)	42667 (19)	875 (22)	2817 (69)	397 (11)	491 (66)	197 (24)	−471 (46)

Atom	x	y	z	B	Atom	x	y	z	B
H(2)	3619 (27)	2211 (44)	350 (24)	6.5	H(7C)	2237 (24)	152 (38)	1660 (21)	5.5
H(3)	3630 (29)	4693 (52)	−108 (24)	7.0	H(8A)	3929 (24)	−2540 (39)	3080 (20)	5.5
H(4)	3867 (29)	6841 (50)	685 (25)	7.5	H(8B)	3158 (24)	−1886 (39)	3597 (19)	5.5
H(5)	4082 (27)	6487 (51)	2037 (23)	7.0	H(8C)	4122 (24)	−2401 (38)	3930 (20)	5.5
H(6)	4025 (26)	3716 (47)	2501 (23)	6.5	H(9A)	4208 (23)	2424 (41)	4200 (19)	5.5
H(7A)	2918 (23)	−1360 (43)	1610 (19)	5.5	H(9B)	3284 (23)	1325 (44)	4367 (20)	5.5
H(7B)	2754 (24)	−233 (41)	894 (20)	5.5	H(9C)	4218 (24)	994 (39)	4750 (21)	5.5

ring having a rotation diad through its centre. Phased by the four atomic positions of the *E*-maps, three-dimensional electron density maps were calculated from the 957 strongest structure amplitudes observed. It was now easy to locate all the 13 non-hydrogen atoms of the asymmetric unit. The positional coordinates were refined by the full-matrix least-squares method. Atomic scattering factors were taken from International Tables for X-Ray Crystallography.[3] After two cycles of refinement using individual isotropic temperature factors the descrepancy index R ($R = \sum||F_o| - |F_c||/\sum|F_o|$) dropped from an initial value of 0.32 to 0.10. One cycle of refinement with anisotropic temperature factors lowered the R-value to 0.065. A difference Fourier synthesis prepared at this stage revealed the positions of the 14 hydrogen atoms. Two further cycles of refinement of the positional and thermal parameters of the non-hydrogen atoms and the positional coordinates of the hydrogen atoms gave a final R-index of 0.048. The hydrogen atoms were assigned isotropic temperature factors of the same magnitudes as those of the atoms to which they were bound. The atomic scattering factors for the hydrogen atoms were taken from the data of Stewart *et al.*[4] and the weighting scheme was that of Hughes.[5] The positional and thermal parameters for the final structure are given in Table 2. On request, a list of the final observed and calculated structure factors may be obtained from the authors.

DESCRIPTION AND DISCUSSION OF THE STRUCTURE

Intramolecular bond distances and bond angles uncorrected for thermal motion are given in Table 3 and Fig. 1 which also shows the numbering system of the atoms. The average Si–O and Si–C distances are 1.631 and 1.851 Å, respectively. The angles around the silicon atoms are all close to the expected tetrahedral value and the mean Si–O–Si angle is 144.2°. These values may be compared with those reported for octamethylcyclotetrasiloxane by Steinfink *et al.*[6] who found the following average interatomic distances and angles: Si–O = 1.65 Å, Si–C = 1.92 Å, O–Si–O = 109.0°, C–Si–C = 106.0°, and Si–O–Si = 142.5°. The benzene ring attached to Si(1) is slightly distorted. The bonds around C(4) are thus considerably shorter than the standard aromatic C–C value (1.395 Å)[3] and the planarity of the ring is not very good; some of the carbon atoms deviate as much as 0.01 Å from the least-squares plane through the ring. The pronounced thermal movements of the atoms, especially of C(3), C(4), and C(5), strongly influencing the accuracy of their positional parameters may cause the descrepancies observed. All the C–H distances agree, within experimental errors, with accepted values and the angles involving hydrogen atoms are likewise quite normal.

The eight-membered siloxane ring has a twofold rotation symmetry with the rotation diad passing through the centre of the ring. The wide Si–O–Si angles make the ring relatively planar (the largest deviation from the plane for Si and O atoms is 0.4 Å) and prevents collision between phenyl and methyl groups. The two phenyl rings of the molecule are nearly parallel to each other and to the rotation diad which means that they are almost perpendicular to the plane of the siloxane ring. The overall configuration of the molecule can

Table 3. Interatomic distances and angles with estimated standard deviations in parentheses. Atoms with the superscript ′ belong to the symmetry related $(1-x, y, 0.5-z)$ half of the molecule.

Si(1) – O(1)	1.630 (2) Å	C(2) – H(2)	0.98 (4) Å
Si(1) – O(2)	1.630 (2)	C(3) – H(3)	1.00 (4)
Si(2) – O(2)	1.626 (2)	C(4) – H(4)	1.09 (5)
Si(2) – O(1′)	1.637 (2)	C(5) – H(5)	1.16 (4)
Si(1) – C(1)	1.861 (3)	C(6) – H(6)	1.05 (4)
Si(1) – C(7)	1.856 (3)	C(7) – H(7A)	0.95 (4)
Si(2) – C(8)	1.838 (4)	C(7) – H(7B)	1.03 (4)
Si(2) – C(9)	1.850 (4)	C(7) – H(7C)	1.06 (4)
C(1) – C(2)	1.392 (4)	C(8) – H(8A)	1.10 (4)
C(2) – C(3)	1.383 (6)	C(8) – H(8B)	0.98 (3)
C(3) – C(4)	1.368 (6)	C(8) – H(8C)	0.91 (4)
C(4) – C(5)	1.353 (7)	C(9) – H(9A)	1.07 (4)
C(5) – C(6)	1.402 (6)	C(9) – H(9B)	1.05 (3)
C(6) – C(1)	1.371 (4)	C(9) – H(9C)	0.97 (4)
O(1) – Si(1) – O(2)	109.9 (1)°	C(8) – Si(2) – C(9)	112.1 (2)°
O(1) – Si(1) – C(1)	108.7 (1)	Si(1) – O(2) – Si(2)	146.6 (2)
O(1) – Si(1) – C(7)	107.5 (2)	Si(2) – O(1′) – Si(1′)	141.7 (2)
O(2) – Si(1) – C(1)	107.1 (1)	Si(1) – C(1) – C(2)	120.4 (2)
O(2) – Si(1) – C(7)	110.8 (2)	Si(1) – C(1) – C(6)	122.7 (3)
C(1) – Si(1) – C(7)	112.8 (2)	C(1) – C(2) – C(3)	121.8 (4)
O(2) – Si(2) – O(1′)	109.0 (1)	C(2) – C(3) – C(4)	119.9 (4)
O(2) – Si(2) – C(8)	110.1 (1)	C(3) – C(4) – C(5)	119.7 (5)
O(2) – Si(2) – C(9)	107.9 (2)	C(4) – C(5) – C(6)	120.5 (6)
O(1′) – Si(2) – C(8)	107.0 (1)	C(5) – C(6) – C(1)	121.2 (4)
O(1′) – Si(2) – C(9)	110.7 (2)	C(6) – C(1) – C(2)	116.9 (3)

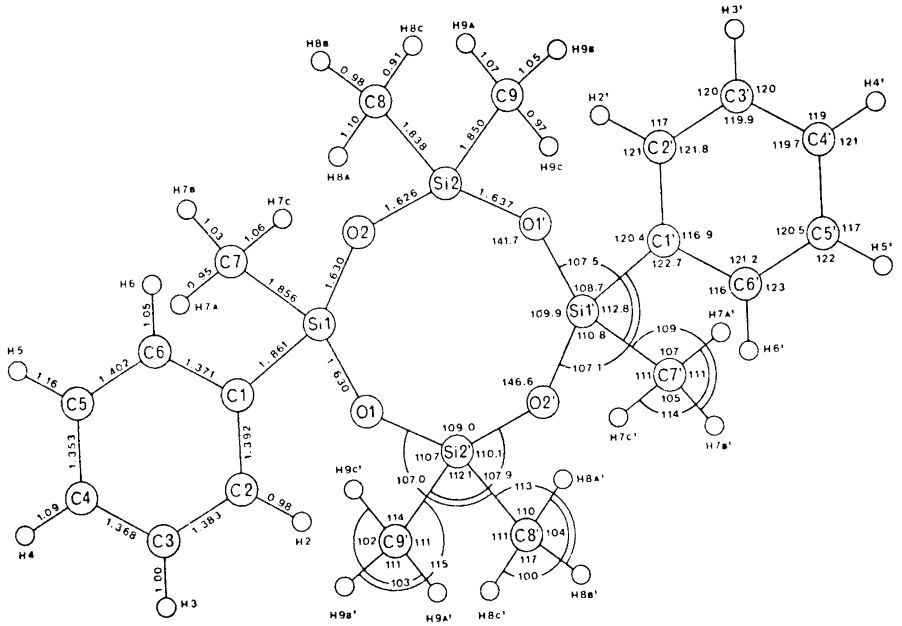

Fig. 1. The numbering of the atoms and bond distances and bond angles in the 2,6-*cis*-diphenylhexamethylcyclotetrasiloxane molecule.

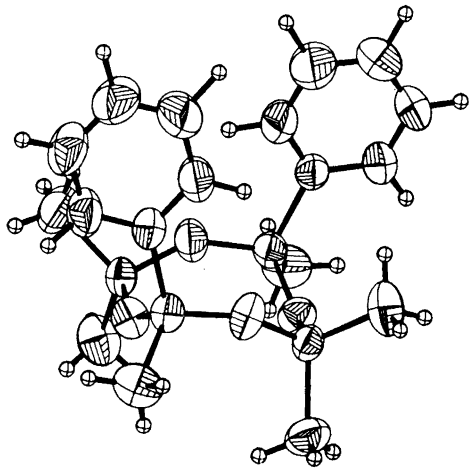

Fig. 2. The configuration of the 2,6-*cis*-diphenylhexamethylcyclotetrasiloxane molecule. The thermal ellipsoids for the non-hydrogen atoms are scaled to 50 % probability. Hydrogen atoms are shown as equally large spheres. The drawing is made with the plotting programme ORTEP by Johnson.[9]

be seen in Fig. 2 which also depicts the ellipsoids of thermal motion scaled to 50 % probability. The cyclotetrasiloxane ring of the present structure can best be described as having a "boat form" which is quite different from the "cradle form" with a twofold rotation symmetry predicted by Yokoi [7] from electron diffraction on octamethylcyclotetrasiloxane in the gas phase. In the crystal structure determination of octamethylcyclotetrasiloxane already mentioned [6] the siloxane ring was found to possess a centre of symmetry and it

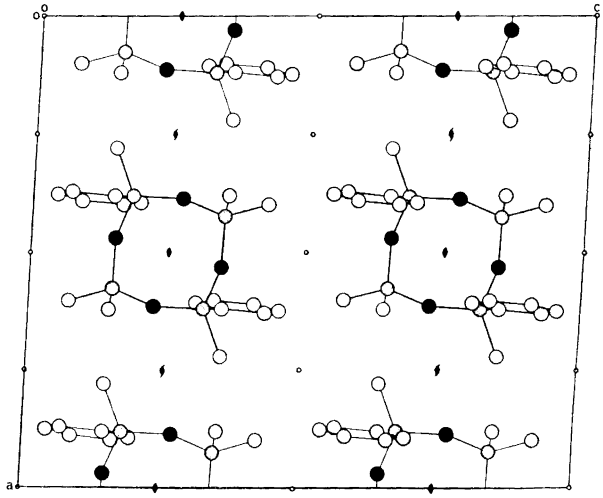

Fig. 3. Projection along *b* of the crystal structure of 2,6-*cis*-diphenylhexamethylcyclotetrasiloxane. The atoms are represented by filled circles (oxygen atoms), dotted circles (silicon atoms), and open circles (carbon atoms). The unit cell contains four molecules each of which having a rotation diad through its center.

had accordingly a "chair form" configuration. It seems plausible that the large Si – O – Si angles contribute to a conformational instability in the eight-membered ring system and that the energy barriers between different conformations are small.

The packing of the molecules in the diphenylhexamethylcyclotetrasiloxane structure is shown in Fig. 3 which is a projection along the *b* axis. There are no intermolecular distances between non-hydrogen atoms less than 3.80 Å and the closest carbon-hydrogen approach is 2.99 Å which is well above the sum of the van der Waals radii. The rather loose packing of the structure is in accordance with the low density 1.16 g cm^{-3} of the compound.

Acknowledgements. We are very much indebted to Dr. Rolf Norrestam, Institute of Inorganic and Physical Chemistry, University of Stockholm, for his kindness and valuable help. All calculations except for the phasing procedure were carried out with the programme system by Bergin [8] on an IBM 360/75 and we want to thank Dr. Rolf Bergin for his help and interest in this study. We also want to thank AB Kabi for generous financial support during this investigation.

REFERENCES

1. Karle, J. and Karle, I. L. *Acta Cryst.* **21** (1966) 849.
2. Norrestam, R. *Acta Chem. Scand.* **25** (1971) 1040.
3. *International Tables for X-Ray Crystallography*, Kynoch Press, Birmingham 1959.
4. Stewart, R. F., Davidson, E. R. and Simpson, W. T. *J. Chem. Phys.* **42** (1965)3175.
5. Hughes, E. W. *J. Am. Chem. Soc.* **63** (1941) 1737.
6. Steinfink, H., Post, B. and Fankuchen, I. *Acta Cryst.* **8** (1955) 420.
7. Yokoi, M. *Bull. Chem. Soc. Japan* **30** (1957) 100.
8. Bergin, R. *X-Ray Crystallographic Programs for IBM 360/75*, Internal Report I/71 (1971), Department of Medical Physics, Karolinska Institutet, Stockholm.
9. Johnson, C. K. ORTEP, Report ORNL-3794, (1965), Oak Ridge National Laboratory, Oak Ridge, Tennessee.

Received October 30, 1972.

ACTA CHEMICA SCANDINAVICA 27 (1973) 1210–1218

The Crystal and Molecular Structure of Tetramethylammonium 3,3′-Commo-bis[1,2-dicarba-3-nickela-closo-dodecaborate](1-)

F. V. HANSEN†, R. G. HAZELL,[a] C. HYATT[b] and G. D. STUCKY[b]

[a] *Department of Inorganic Chemistry, Aarhus University, DK-8000 Aarhus C, Denmark, and* [b] *Department of Chemistry and Chemical Engineering and Materials Research Laboratory, University of Illinois, Urbana, Illinois 61801, USA*

The crystal and molecular structure of tetramethyl-ammonium 3,3′-commo-bis[undecahydro-1,2-dicarba-3-nickela-closo-dodecaborate] (1−), $(CH_3)_4NNi^{III}(B_9C_2H_{11})_2$, has been determined from three-dimensional single crystal X-ray data. The orthorhombic cell (space group *Ccmm*) with $a = 10.328$ Å, $b = 9.841$ Å, $c = 21.86$ Å contains four formula units. The structure was initially solved by Patterson and Fourier methods from a three-dimensional set of visually estimated intensities, but to solve space group ambiguities a set of diffractometer data had to be collected. Positional and anisotropic thermal parameters for Ni, N, C, and B and positional parameters for H were refined from 716 observed reflections by the method of least squares. The final R-value is 0.054.

The structure of the $Ni(C_2B_9H_{11})_2$ anion is of a symmetrical π-sandwich type (point group 2/m) with the two dicarbollyl icosahedra joined at the Ni apex. The carbon atoms in the dicarbollyl cage are adjacent to each other in the two CCBBB pentagons coordinated to nickel, and they are ordered in the structure.

Several transition metal compounds containing the dicarbollyl ion $C_2B_9H_{11}^{2-}$ have been subject to structural studies. It has been shown [1] that in $(\phi_3PCH_3)Cu(III)(C_2B_9H_{11})_2$ (d^8 configuration), isomorphous with $[\phi_3PCH_3][Au(III)(C_2B_9H_{11})_2]$ (d^8), and in $(Et_4N)_2Cu(II)(C_2B_9H_{11})_2$ (d^9), isomorphous with $(Et_4N)_2$ $Ni(II)(C_2B_9H_{11})_2$ (d^8), the $M(C_2B_9H_{11})_2$-entity (M=transition metal) suffers a distortion from the symmetrical π-sandwich structure found in corresponding compounds with six or less d-electrons. The distortion takes place by an antiparallel slippage of the two cages, making metal-carbon distances longer than the metal-boron distances.

In view of this the d^7-configuration found in the $Ni(III)(C_2B_9H_{11})_2^-$ ion has considerable interest, for which reason we undertook this study of $(CH_3)_4NNi(C_2B_9H_{11})_2$.

† Deceased.

EXPERIMENTAL

The dark red crystals of $(CH_3)_4NNi(C_2B_9H_{11})_2$ were kindly supplied by L. F. Warren and F. Hawthorne. Weissenberg and precession exposures taken with Mo$K\alpha$ radiation showed the crystal system to be orthorhombic with systematic absences: hkl, $h+k=2n+1$; $0kl$, $l=2n+1$. These are consistent with the space groups: $Ccmm$ (centric), $Cc2m$ (acentric), and $Ccm2_1$ (acentric): the first one was shown to be correct in the final refinements of the structure. The unit cell dimensions as determined with Mo$K\alpha_1$ radiation ($\lambda=.70926$ Å) by the method of least squares from angular settings of fourteen non-axial high order reflections on a four circle Picker diffractometer are: $a=10.328\pm.003$ Å, $b=9.841\pm.003$ Å, $c=21.862\pm.006$ Å (measured at room temperature). No density was measured. Assuming $Z=4$, later confirmed by structure analysis, a density of 1.20 g/cm³ is calculated, close to that of 1.304 g/cm³ found by us for Ni(IV) $(C_2B_9H_{11})_2$.

Two sets of data were collected for the solution of the structure. The structure was roughly solved with a visually measured data set. However, space group ambiguities could not be solved from this set of data, so when a four circle diffractometer became available, a new set of intensities was measured and the structure refined with these.

The diffractometer data were collected with a manual four circle Picker diffractometer using Mo$K\alpha$ radiation in connection with a scintillation counter mounted 21 cm from the crystal. The take off angle was 0.8°. A crystal showing very good extinctions in a polarizing microscope and approximately in the form of a box with dimensions $0.35\times0.35\times0.19$ mm³ was mounted with the b-axis parallel to the ϕ-axis of the instrument. One independent set of reflections, totalling approximately 1570 were measured using the $\theta-2\theta$ scan technique with a scan rate of 2° min^{-1}. Data were collected out to $2\theta=60°$ for l even and to 2θ max $=45°$ for l odd, the latter because of a pronounced weakness of these intensities. The scan range was from 0.8° below to 1.2° degrees above the Mo$K\alpha_1$ peak for $2\theta<45°$ and from 0.8° below to 1.53° above for $2\theta>45°$.

Stationary background counts for 10 sec were recorded at the beginning and end of each scan. The diffracted beam was filtered through a 0.0005 inch Zr-foil. The 24 strongest reflections were attenuated with a 0.05 mm Ni foil (attenuation factor 8.1) assuring the intensity to be within the linear response range of the detector. The attenuation factor was only approximately known and accordingly introduced as a parameter in the refinements. Standard reflections were recorded before every layer line but indicated no decomposition.

The intensities were reduced to relative structure factors with the program ACAC.[3] No correction for extinction, anomalous dispersion or absorption was made, the relative absorption effect being not more than about 3 % ($\mu_{MoK\alpha}=8.6$ cm^{-1}). Intensities for which $I<3\sigma(I)$ were taken as unobserved, leaving 721 reflections for refinement of the structure. Of these, five were later discarded as improperly measured, three of them very strong low angle reflections in which incompletely attenuated β-peaks had been measured in the first background.

SOLUTION AND REFINEMENT OF THE STRUCTURE

The structure was solved roughly from the visual data set. Patterson and successive Fourier syntheses revealed the approximate positions of all atoms except hydrogen. The symmetry restrictions to be imposed on the molecule in each of the possible space groups are:

1. $Ccm2_1$ (acentric):

Ni $(C_2B_9H_{11})_2^-$ and $(CH_3)_4N^+$ have m-symmetry, the mirror-plane in $Ni(C_2B_9H_{11})_2^-$ going through the nickel atom and the two apical (B7 and B7′) boron atoms.

2. $Cc2m$ (acentric):

$(CH_3)_4N^+$ has m-symmetry. $Ni(C_{12}B_9H_{11})_2^-$ has 2-fold symmetry, the 2-fold axis lying parallel to the faces of the coordinating pentagons of the two cages.

3. *Ccmm* (centric):

$(CH_3)_4N^+$ has *mm*-symmetry. $Ni(C_2B_9H_{11})_2^-$ has $2/m$ symmetry, the symmetry being a combination of that in the two other space groups.

In the acentric space groups the Ni atoms have a centre of symmetry, making it impossible to distinguish the centric from the acentric space groups from a breakdown of Friedel's law.

With all cage atoms put in as boron, isotropic and anisotropic refinement (Ni and $(CH_3)_4N^+$ anisotropic) was carried out in all three space groups choosing the origin in the acentric space groups at the Ni atom. However, the results were inconclusive with respect to which space group was the correct one. In trying to locate the carbon atoms in the cage, we used the distances found by Zalkin *et. al.*[3] in $CsC_2B_9H_{11}Re(CO)_3$: C–C = 1.61 Å, C–B = 1.72 Å, B–B = 1.78 Å. The distances showed the carbon atoms probably to be placed in the pentagons coordinated to nickel. However, no models, including some with disorder of the carbon atoms in the pentagons or presence of dicarbollyl isomers, could be set up, accounting for the distances found in the cages. Therefore, refinement with these data was given up and diffractometer data collected.

In the space groups *Ccmm* and *Cc2m* the Ni atoms give no contribution to reflections with $l=2n+1$. Of a total of 721 significant observations only 135 have l odd and these have an average intensity much lower than that for reflections with l even.

To distinguish between the possible space groups a statistical test was run with the 135 reflections to which the Ni atoms do not contribute. This favoured strongly an acentric space group and refinement was initiated in *Cc2m*. Starting with coordinates determined from the visual data set, three cycles of full matrix least squares refinement with the program ORFLS,[4] refining Ni and the tetramethylammonium ion anisotropically and all cage atoms isotropically, lowered the conventional R-value to $R_1 = \sum||F_o| - |F_c||/\sum F_o = 0.083$, $R_2 = (\sum W(F_o - F_c)^2/\sum WF_o^2)^{\frac{1}{2}} = 0.099$.

A difference synthesis was computed and revealed as the 11 highest peaks all hydrogen atoms in the cage. Two atoms adjacent to each other in the pentagons coordinated to Ni had temperature factors of 2.11 and 2.20 Å^2, the other ones ranging from 2.80 to 2.85 Å^2. Furthermore, the distance 1.60 Å between these was the lowest found in the cage, the others being 1.63 – 1.89 Å. Accordingly, these two atoms were taken to be carbon atoms (later proved to be correct), and anisotropic thermal vibrations of the cage atoms were introduced in the refinement. Because of the large number of variables involved, the two pentagons in the cage were refined independent of each other in successive cycles. Two cycles lowered the R-values to $R_1 = 0.074$, $R_2 = 0.085$, but temperature factors of two adjacent cage atoms became non-positive definite and many distances unsatisfactory (ranging from 1.54 Å to 1.99 Å). At this stage a version of ORFLS modified in this department for the IBM 360/75 computer by G. Sproul became available. This version is able to refine 300 variables among 500 parameters. One final cycle was run in the space group *Cc2m* with this program to take into account the correlation between atoms in different pentagons but no improvement in distances was found.

Finally, refinement was carried out in the space group *Ccmm* with the IBM 369/75 version of ORFLS. Starting again with all cage atoms put in as

boron, two cycles gave $R_1 = 7.7$ %. The distances now became chemically very acceptable for an ordered structure with the two carbon atoms in the cage adjacent to each other in the pentagon coordinated to Ni. A difference synthesis was computed and now revealed all the hydrogen atoms in the tetramethylammonium ion except one, supposedly in the mirror plane.

No indication of disorder of this ion was found. Four more cycles gave the final R-values $R_1 = 0.058$, $R_2 = 0.077$ with all hydrogen atoms included.

Table 1. Final atomic coordinates in fractions. Standard deviations $\times 10^4$ in parentheses. For hydrogen atoms isotropic B-values with standard deviations are included.

	x	y	z	B(Å²)
Ni	0.0000 (0)	0.0000 (0)	0.0000 (0)	
C2	0.1809 (5)	0.0807 (5)	0.0317 (3)	
B3	0.0458 (6)	0.1426 (7)	0.0686 (3)	
B5	−0.0395 (8)	0.0000 (0)	0.0970 (4)	
B7	0.2927 (10)	0.0000 (0)	0.0797 (5)	
B8	0.2036 (7)	0.1453 (8)	0.1029 (3)	
B9	0.0673 (6)	0.0894 (8)	0.1463 (3)	
B12	0.2150 (10)	0.0000 (0)	0.1516 (5)	
N	0.1624 (10)	0.5000 (0)	0.2500 (0)	
C1N	0.0813 (11)	0.5000 (0)	0.1927 (6)	
C2N	0.2464 (8)	0.3751 (10)	0.2500 (0)	
H1	0.2156 (47)	0.1271 (50)	−0.0039 (23)	1.12 (0.92)
H2	0.0272 (42)	0.2436 (55)	0.0527 (22)	0.80 (0.99)
H3	−0.1446 (59)	0.0000 (0)	0.1040 (30)	−0.15 (1.25)
H4	0.4029 (106)	0.0000 (0)	0.0672 (56)	6.26 (3.09)
H5	0.2584 (74)	0.2226 (77)	0.1185 (45)	6.58 (2.22)
H6	0.0388 (48)	0.1638 (55)	0.1834 (26)	1.63 (1.12)
H7	0.2751 (99)	0.0000 (0)	0.1925 (46)	2.82 (2.39)
H8	0.3182 (68)	0.3748 (80)	0.2095 (31)	4.70 (1.88)
H9	0.0168 (62)	0.5735 (76)	0.2003 (33)	5.09 (1.94)
H10	0.1321 (112)	0.5000 (0)	0.1570 (68)	7.13 (3.78)
H11	0.1743 (81)	0.2957 (87)	0.2500 (0)	−2.28 (1.93)

Table 2. Mean square vibration amplitudes, u_{ij}, in Å² $\times 10^{-4}$, with standard deviations.

	u_{11}	σu_{11}	u_{22}	σu_{22}	u_{33}	σu_{33}	u_{12}	σu_{12}	u_{13}	σu_{13}	u_{23}	σu_{23}
Ni	344	5	308	5	287	5	0	0	38	4	0	0
C2	451	28	449	28	414	26	−50	24	86	22	−19	22
B3	485	29	426	31	390	28	20	30	60	28	−35	26
B5	405	43	500	49	406	44	0	0	51	44	0	0
B7	476	51	922	82	422	53	0	0	3	43	0	0
B8	510	36	717	45	444	34	−124	35	71	29	−207	34
B9	448	34	674	43	393	30	−59	31	85	26	−81	32
B12	464	54	1005	88	442	51	0	0	−37	46	0	0
N	401	51	592	60	610	63	0	0	0	0	0	0
C1N	677	71	1096	95	1021	88	0	0	−504	66	0	0
C2N	525	47	634	55	634	53	224	45	0	0	0	0

Table 3. Observed and calculated structure factors on 1.97 × absolute scale.

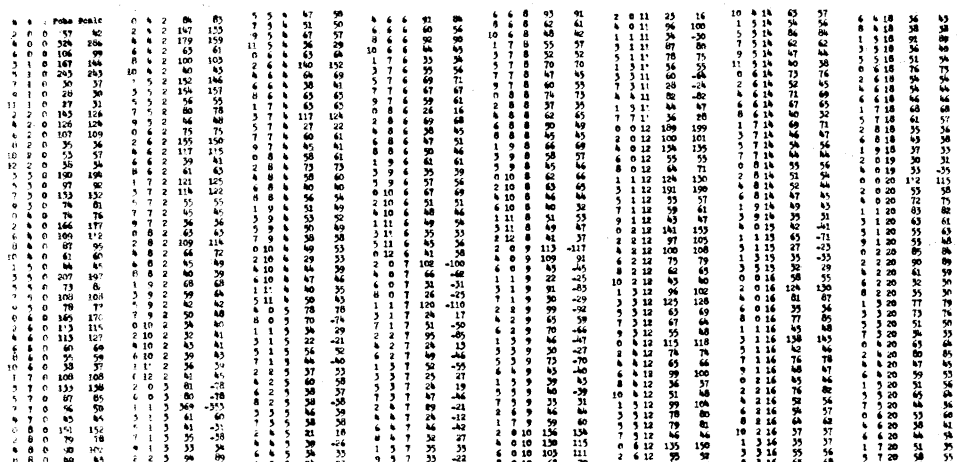

The weights used in the first cycles were $W = 1/\sigma^2(F)$ with

$$\sigma(|F|) = \frac{|F|}{2I}[\mathrm{CN} + (\mathrm{TC}/\mathrm{TB})^2\ (\mathrm{B}_1 + \mathrm{B}_2) + (k \times I)^2]^{1/2}\ \text{(Ref. 5)}$$

CN is the intensity integrated in a scantime of TC, B_1 and B_2 are the backgrounds counted in a time TB. The systematic "error" factor k was taken to 0.03.

In the final cycles these weights seemed not to account for all errors and a weighting scheme $W = 1/(\mu F)^2$ with

$$\mu F = (\sigma(F_o^2) + (k + 1)\ F_o^2)^{1/2} - F_o$$

was used. The factor k was systematically varied to give a $W\Delta^2$ nearly independent of the size of F_o. All scattering factors were taken from *International*

Tables for X-Ray Crystallography, Vol. III, pp. 202 – 207. In the final cycle the shift/standard deviation was less than one, except for H3, H6, and H7 (up to 3.2).

DISCUSSION

The details of the chemistry of bis[π-(3)-1,2-dicarbollyl]metalates of nickel and palladium have been discussed previously.[5] Singly crystal studies of Ni(II) [1,6] and Ni(IV) [7,8] bis[π-dicarbollyl] metalates have also been reported. The structure of tetramethylammonium 3,3′-commo-bis[1,2-dicarba-3-nickela-closo-dodecaborate](1 –) is of particular interest in that it completes the series of Ni(II) (d^6), Ni(III) (d^7), and Ni(IV) (d^8) dicarbollides which have been studied by single crystal X-ray analysis. The "slipped sandwich" structure observed for the Cu(III), Au(III), Cu(II), and Ni(II) dicarbollides results in the metal-carbon distances being longer than the metal-boron distances. This geometry was originally suggested to be the result of electronic factors;[1] however, the nearly symmetrical π sandwich configuration obtained with the bis-(3)-1,7-dicarbollylnickelate(II) dianion,[6] the distortions observed in the molecular structure of the racemic (3,4′)[$(CH_3)_2B_9C_2H_9$]$_2$Ni(IV),[8] and in the [$Co(B_9C_2H_8Br_3)_2^-$] anion [9] have led to the more recent conclusion that ligand symmetry and inter-cage non-bonded repulsions are probably responsible for observed differences in the geometries of the bis[π-dicarbollyl] metalates.[6]

In particular, in the structure of (3,4′)[$(CH_3)_2B_9C_2H_9$]$_2$Ni(IV),[8] the average Ni – C distance is 2.194 Å (± 0.031) and the average Ni – B distance is 2.109 Å (± 0.050). The structure of this compound strongly implies that inter-cage non-bonded repulsions are important. It is significant that the non-planarity of the two facial pentagonal planes apparently occurs at the expense of the metal-ring carbon bonds.

The nickel-cage interatomic distances given in Table 4 are slightly larger than those obtained for the corresponding Ni(IV) complex, $Ni(B_9C_2H_{11})_2$. In the nickel(IV) compound the average Ni – C distance is 2.071 Å within a range of ± 0.006 Å, while the average Ni – B distance is 2.103 Å within a range of ± 0.018 Å. The corresponding values for the nickel(III) compound are 2.146 Å and 2.134 (± 0.026) Å. The details of the Ni(II) 1,2-dicarbollide must be inferred from the structure of the isomorphous Cu(II) compound.[2] However, the corresponding values for the 1,7-dicarbollylnickelate(II) dianion are 2.25 (± 0.14) Å and 2.14 (± 0.04) Å.

In fact, however, a comparison of the metal-ring atom distances is complicated by the three different configurations observed for the bis(3)-1,2-dicarbollides of nickel. The Ni(II) derivative has the "slipped" sandwich structure with the nickel atom 0.6 Å from the centre of the five face atoms of the cage.[1] The Ni(IV) compound has the carbon atoms in opposite cages nearly *cis* to each other, with staggered five membered rings. In the present structure, the carbon atoms in the two facial five membered rings which form the sandwich are *trans* to each other, and the nickel atom is only 0.05 Å from the (unweighted) centre of the ring (Fig. 1). If inter-cage proton-proton repulsion forces are alone responsible for the differences in these structures,

Table 4. Bond lengths and selected angles. Standard deviations in terms of the last digit.

Bond	Å	Bond	Å
Ni – C2	2.146 (5)	B9 – B9′	1.759 (14)
Ni – B3	2.108 (6)	B9 – B12	1.764 (11)
Ni – B5	2.160 (9)	C2 – H1	0.97 (5)
C2 – C2′	1.589 (10)	B3 – H2	1.07 (5)
C2 – B3	1.724 (8)	B5 – H3	1.10 (6)
C2 – B7	1.750 (10)	B7 – H4	1.17 (11)
C2 – B8	1.698 (9)	B8 – H5	1.01 (8)
B3 – B5	1.769 (8)	B9 – H6	1.13 (6)
B3 – B8	1.795 (9)	B12 – H7	1.09 (10)
B3 – B9	1.791 (9)	N – C1N	1.506 (14)
B5 – B9	1.775 (10)	N – C2N	1.505 (11)
B7 – B8	1.775 (10)	C1N – H9	1.00 (7)
B7 – B12	1.767 (15)	C1N – H10	0.94 (14)
B8 – B9	1.784 (10)	C2N – H8	1.16 (7)
B8 – B12	1.787 (10)	C2N – H11	1.08 (9)

Angle	Degrees	In cage:	Degrees
C1N – N – C1N′	112.4 (9)	C2 – Ni – C2′	43.5 (2)
C1N – N – C2N	108.7 (3)	C2 – Ni – B3	47.8 (2)
C2N – N – C2N′	109.6 (8)	B3 – Ni – B5	49.0 (2)
		C2 – Ni – B3	79.7 (2)
		C2 – Ni – B5	81.2 (3)
		B3 – Ni – B3′	83.5 (2)

Between cages:	Degrees
C2 – Ni – B3	100.3 (2)
C2 – Ni – B5	98.8 (3)
B3 – Ni – B3″	96.6 (2)

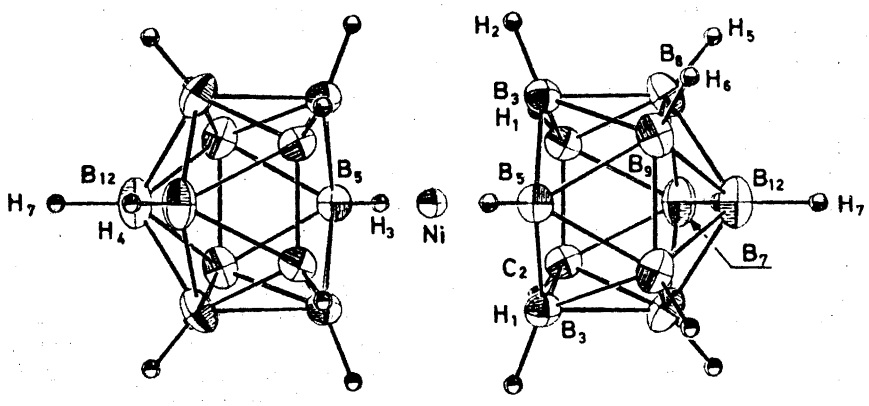

Fig. 1. Perspective drawing of the complex anion showing 50 % probability ellipsoids for the heavier atoms, and small, arbitrary size spheres for hydrogen atoms, made by means of program ORTEP2.[10]

it is difficult to understand why the *trans* structure is possible for the smaller d^7 (Ni(III)) but not for the larger d^8 (Ni(II)).

One is struck by the result that in all of the nickel dicarbollide structures, the average nickel-boron atom distances are within ± 0.04 Å of each other while the average nickel-carbon distances vary from 2.07 to 2.25 Å. In the three unsubstituted compounds, the average nickel-carbon bond lengths are 0.03 Å shorter, 0.01 Å longer and 0.11 Å longer than the nickel-boron bond lengths for Ni(IV), Ni(III), and Ni(II), respectively. Although the last figure must be taken with some reservation since the two nickel carbon distances to the 2,7-dicarbollide anion differ greatly and the distances for the Ni(II) 1,2 dicarbollide are not precisely known, it would appear that the different gross geometries in the unsubstituted nickel series may be the result of relatively constant nickel-boron bond properties but different nickel-carbon bond requirements for Ni(II), Ni(III), and Ni(IV). The observed electron deficiency of the carbon atoms [5] in the Ni(IV) compound would be expected to result in their readily accepting charge in the Ni(II) and Ni(III) complexes, with accordingly larger values for the electron-electron repulsion integrals associated with the metal-carbon interaction. The importance of the inter-cage nonbonded interactions is not lessened by this interpretation, and undoubtedly also must be considered in dicarbollide stereochemistry.

Table 5. Distances from best planes. Plane I through C2, B3, B5, B3′, C2′. Plane II through B7, B8, B9, B9′, B8′.

Atom	Distance from I (Å)	Distance from II (Å)
C2	−0.012	1.468
B3	0.031	1.539
B5	−0.037	1.490
B7	−1.510	−0.037
B8	−1.462	0.030
B9	−1.532	−0.011
B12	−2.430	−0.931
Ni	1.557	3.058

The angle between I and II: 1.0°.

Table 6. Distances between atoms in adjacent cages.

	Å		Å		Å
C2 – B3	3.266	B3 – H1	3.052	H1 – H2	2.956
C2 – B5	3.269	B3 – H2	2.931	H1 – H3	2.625
B3 – B3	3.146	B5 – H1	3.003	H2 – H2	2.370
		C2 – H3	3.094		

The relative planarities of the rings C2′ – C2 – B3 – B5 – B3′, and B7 – B8 – B9 – B9′ – B8′ and the dihedral angle between the above planes are given in Table 5. Selected nonbonded distances are given in Table 6.

Acknowledgement. The generous support of the *Advanced Projects Agency* under Contract HC 15 – 67 CO221 is gratefully acknowledged. Special tribute is due to the late Dr. F. V. Hansen for this role in this work.

REFERENCES

1. Wing, R. M. *J. Am. Chem. Soc.* **90** (1968) 4828.
2. Guggenberger, L. J. and Prewitt, C. Program ACAC, E. I. duPont de Nemours and Co., Wilmington, Del. 1966.
3. Zalkin, A., Hopkins, T. E. and Templeton, D. H. *Inorg. Chem.* **5** (1966) 1189.
4. Busing, W. R., Martin, K. O. and Levy, H. A. *ORFLS.* Oak Ridge National Laboratory, Oak Ridge, Tenn. 1962.
5. Warren, Jr., L. F. and Hawthorne, M. F. *J. Am. Chem. Soc.* **92** (1970) 1157.
6. Wing, R. M. *J. Am. Chem. Soc.* **92** (1970) 1187.
7. St. Clair, D., Zalkin, A. and Templeton, D. H. *J. Am. Chem. Soc.* **92** (1970) 1173.
8. Churchill, M. R. and Gold, K. *J. Am. Chem. Soc.* **92** (1970) 1180.
9. DeBoer, B. G., Zalkin, A. and Templeton, D. H. *Inorg. Chem.* **7** (1968) 2289.
10. Johnson, C. K. *ORTEP2.* Oak Ridge National Laboratory, Oak Ridge, Tenn. 1971.

Received November 3, 1972.

ACTA CHEMICA SCANDINAVICA 27 (1973) 1219–1225

Reactions between Furfurylidenemalonic Esters and Grignard Reagents II. 1,4-, 1,6-, and 1,8-Additions of *t*-Butylmagnesium Chloride to Diethyl Furfurylidenemalonate

GUST.-AD. HOLMBERG, MARIANNE OLLI, ULLA STRAND, and HARRY JALONEN

Institutionen för organisk kemi, Åbo Akademi, SF-20500 Åbo 50, Finland

When the primary reaction products formed when *t*-butylmagnesium chloride reacts with diethyl furfurylidenemalonate are decomposed with dilute hydrochloric acid, a reduction product (diethyl furfurylmalonate) and 1,6- and 1,8-addition products (dihydrofuran derivatives) are formed besides the 1,4-addition product (diethyl 1-(2-furyl)-propylmalonate). However, the 1,8-addition product immediately rearranges prototropically to diethyl 5-*t*-butylfurfurylmalonate. The 1,6-addition products are more stable, but they also rearrange to diethyl 3-*t*-butylfurfurylmalonate on standing in an acid ether solution.

It has previously been demonstrated that 1,4-addition products and, in some cases, reduction products are formed when diethyl furfurylidenemalonate (I) reacts with simple aliphatic Grignard reagents.[1] When benzylmagnesium chloride is employed, both a 1,4-addition product and a 1,8-addition product are primarily formed. However, the latter, a 2,5-dihydrofuran derivative, immediately rearranges prototropically to diethyl 5-benzylfurfurylmalonate when the magnesium-containing reaction products are decomposed in dilute aqueous acid.

The present paper deals with the reactions between *t*-butylmagnesium chloride and diethyl furfurylidenemalonate (I). Gas chromatographic analysis of the products of the reactions on a column containing OV-17 as the stationary phase showed that five compounds had formed. Attempts to separate them by classical methods or by adsorption chromatography on bentonite and aluminium oxide were not successful. They were therefore identified by comparing their mass spectra obtained with a combined gas chromatograph/mass spectrometer with each other and with mass spectra of known or synthetized compounds.

The compound with the shortest retention time (compound A) proved to be diethyl furfurylmalonate (II) because the mass spectra and retention times of these compounds were identical.

The compound with the next shortest retention time (compound B) was identified as diethyl 2,2-dimethyl-1-(2-furyl)-propylmalonate (III) by comparison of its mass spectrum with the spectra of homologous compounds (see the interpretation in the experimental part). The conclusion is supported

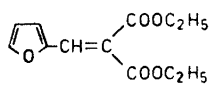

I

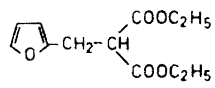

II

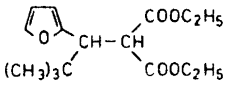

III

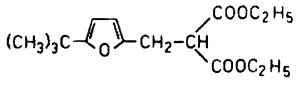

IV

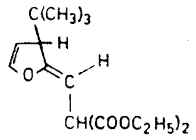

V

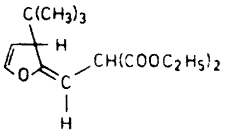

VI

by the fact that diethyl malonate and the chloride obtained from 2,2-dimethyl-1-(2-furyl)propanol-1 and thionyl chloride react to give a compound with a mass spectrum identical with that of compound B. This compound is accordingly a 1,4-addition product of *t*-butylmagnesium chloride to diethyl furfurylidenemalonate.

The third compound (C) had the same retention time as diethyl 5-*t*-butylfurfurylmalonate (IV). The identity of these compounds was further confirmed by their identical mass spectra. Compound C is accordingly formed by a 1,8-addition of the Grignard reagent to the unsaturated ester followed by a prototropical rearrangement of the primary reaction product. The reaction mechanisms are, of course, analogous to those which lead to the formation of diethyl 5-benzylfurfurylmalonate from benzylmagnesium chloride and diethyl furfurylidenemalonate.[1]

The mass spectra of the two remaining compounds (D and E) were practically identical. When an ether solution of the reaction products to which a small quantity of sulphuric acid had been added was stored for some time, the gas chromatogram showed that the two not yet identified compounds had disappeared and a new compound (F) had formed. The mass spectra of the three compounds showed that their molecular ions have equal masses. Further, the mass spectrum of compound F and that of diethyl 5-*t*-butylfurfurylmalonate (IV) were not identical, although clearly of the same type. Because a 1,6-addition is possible besides 1,4- and 1,8-additions, the best explanation of these facts is that compounds D and E are geometrical isomers with the structures V and VI. These compounds were transformed by the action of

hydrogen ions into diethyl 3-*t*-butylfurfurylmalonate (VII). The reaction mechanism of this prototropical rearrangement is analogous to that of the formation of the 5-butyl isomer above.

The molar ratios of the compounds A, B, C, D, and E in the reaction mixture calculated from the peak areas in the gas chromatograms and the structures of the compounds are 8 : 48 : 21 : 11 : 12. After the rearrangement of compounds D and E, the ratios of the compounds A, B, C, and F were 7 : 49 : 23 : 21. These data clearly show that compounds D and E are transformed into compound F. Further the ratios of the reduction product and the 1,4-, 1,6-, and 1,8-addition products are about 4 : 24 : 11 : 11.

EXPERIMENTAL

The reactions between t-*butylmagnesium chloride and diethyl furfurylidenemalonate.* The experiments were performed on a semimicro scale exactly according to the previously described method.[1-3] The reaction products were analysed by gas chromatography (column 1/8″ × 1.8 m, stationary phase 1 % OV-17, nitrogen flow rate 28 ml/min, initial temperature 100°, linear programming 10°/min). Five peaks with the relative retention times 1.00 (compound A), 1.21 (compound B), 1.26 (compound C), 1.42 (compound D), and 1.46 (compound E) were obtained. The compounds in the reaction mixture were stable. A gas chromatogram of a reaction mixture that had been stored for one month was identical with that first obtained. The mass spectra of the compounds were taken on a combined gas chromatograph/mass spectrometer (LKB 9000). The most important ions in these spectra are collected in Table 1.

The reaction products from one experiment were dissolved in about 30 ml of ether and a small quantity of sulphuric acid was added. After one week, the ether solution was shaken first with water and then with an aqueous solution of sodium hydrogen carbonate. The gas chromatogram showed now four peaks with the retention times (relative to that of compound A) 1.00 (compound A′), 1.21 (compound B′), 1.26 (compound C′), and 1.33 (compound F). The mass spectra of the compounds and the retention times revealed that the compounds A, B, and C were identical with the compounds A′, B′, and C′, respectively. The most important ions in the mass spectrum of compound F are listed in Table 1.

*Diethyl 5-*t*-butylfurfurylmalonate* (IV). Methyl 5-*t*-butylfuroate was reduced to 5-*t*-butylfurfuryl alcohol, which was transformed into the corresponding chloride. This chloride was used to introduce the 5-*t*-butylfurfuryl group into diethyl malonate.

Methyl 5-*t*-butylfuroate, b.p. 105 – 106°/12 mmHg, was prepared from methyl furoate and *t*-butyl chloride according to Gilman and Calloway.[4] The ester was reduced with lithium aluminium hydride in the usual way.[5] However, in all experiments, before all the ester had been added, a semi-solid doughy substance, probably an aluminium or lithium alcoholate, precipitated. This apparently prevented the reaction from proceeding to completion and the product was consequently heavily contaminated by unreduced ester. This ester was removed by alkaline hydrolysis and the butylfurfuryl alcohol extracted with ether. From 39.8 g of methyl 5-*t*-butylfuroate and 12.9 g of lithium aluminium hydride, 11.6 g (34 %) of 5-*t*-butylfurfuryl alcohol, b.p. 89 – 90°/8 mmHg, was obtained after a reduction time of 10 h. NMR spectrum: two furan protons gave an AB system at τ 3.98 and 4.20, $J = 3.3$ Hz; two methylene protons a doublet at τ 5.62 coupled to the hydroxy proton, $J = 4$ Hz; one hydroxy proton a very ill-defined triplet at τ 6.80; nine methyl protons a singlet at τ 8.77. On irradiation at the frequency of the hydroxy proton, the methylene signal was transferred into a singlet.

5-*t*-Butylfurfuryl alcohol was transformed into 5-*t*-butylfurfuryl chloride by the method which Kirner [6] used for the preparation of furfuryl chloride from furfuryl alcohol. The yield of pure substance, b.p. 75°10 mmHg, was 37 %.

This chloride (6.61 g), diethyl malonate (5.85 g), sodium (0.88 h), and dry ethanol (30 ml) were used in a malonic ester synthesis performed in the usual way.[7] The gas chromatographic analysis of the reaction products showed that three compounds were present.

Table 1. Abundances of important ions in the mass spectra of the compounds B, C, D, E, and F.

m/e	Abundance in the spectrum of compound					Type of ion
	B	C	D	E	F	
297	1	4	–	–	5	$(M+1)^+$
296	4	24	1	1	27	$M^{+\cdot}$
282	–	15	–	–	–	
281	1	87	1	1	14	$(M-CH_3)^+$
251	4	6	–	–	–	$(M-OC_2H_5)^+$
241	6	–	3	3	–	
240	41	2	21	20	1	$(M-C_4H_8)^{+\cdot}$
239	2	–	2	1	–	$(M-C_4H_9)^+$
223	–	5	–	–	16	$(M-73)^+$ X[a]
222	1	20	1	1	85	$(M-74)^+$ XI
208	–	12	–	–	6	
207	–	81	1	2	42	
187	2	–	2	2	3	
188	–	–	–	–	24	
180	–	3	–	–	1	
179	1	12	1	–	6	
167	27	3	41	37	12	
166	100	7	100	100	4	$(M-130)^{+\cdot}$, *e.g.* XII
139	11	5	15	13	6	
138	19	12	20	19	12	
137	31	100	3	4	100	$(M-159)^+$, *e.g.* VIII, IX
122	7	13	5	5	17	
121	48	54	51	47	78	$(Furyl\text{-}CH=CH-CO)^+$
95	6	9	2	3	11	
94	10	3	13	14	3	
82	2	2	2	2	2	
81	11	5	8	8	6	$(Furyl\text{-}CH_2)^+$
58	2	1	3	6	1	
57	37	19	51	51	28	$t\text{-}C_4H_9^+$

[a] The abundances of these ions decrease to 2 % for compound C and 4 % for compound F, if the abundances of the ^{13}C isomers of the ions at *m/e* 222 are observed.

The product with the shortest retention time was 5-*t*-butylfurtyryl ethyl ether. Mass spectrum: $M^{+\cdot}$ at *m/e* 182, calc. 182, rel. abund. 30.5 %; $(M+1)^+$ at *m/e* 183, rel. abund. 3.8 %, calc. 3.7 %; $(M-CH_3)^+$ at *m/e* 167, base peak; $(M-OC_2H_5)^+$ at *m/e* 137, rel. abund. 38 %; readily identified ions with high abundances at *m/e* 57, 45, 43, and 29.

The compound with the longest retention time was apparently diethyl di(5-*t*-butylfurfuryl)malonate. Mass spectrum: $M^{+\cdot}$ at *m/e* 432, calc. 432, rel. abund. 14.8 %; $(M+1)^+$ at *m/e* 433, rel. abund. 4.3 %, calc. 4.0 %; $(M-CH_3)^+$ at *m/e* 417, rel. abund. 3.0 %; $(M-COOC_2H_5)^+$ at *m/e* 359, rel. abund. 5.8 %; $(M-5\text{-}t\text{-butylfurfuryl})^+$ at *m/e* 295, rel. abund. 7.9 %; unknown ion at *m/e* 245, rel. abund. 94 %; $(5\text{-}t\text{-butylfurfuryl})^+$ at *m/e* 137, base peak; readily identified ions with high abundances at *m/e* 45, 29, 28, and 15.

The main product, which had a retention time between those of the above products, was isolated by repeated distillation under reduced pressure, finally in a Todd distillation assembly. The pure substance, diethyl 5-*t*-butylfurfurylmalonate (IV), came over a 107°/1 mmHg. (Found: C 64.93; H 8.20. Calc. for $C_{16}H_{24}O_5$: C 64.84; H 8.16.) The NMR spectrum (*cf.* Table 2) confirms the structure.

Table 2. Chemical shifts (τ) and coupling constants (J) in the NMR spectrum of diethyl 5-*t*-butylfurfurylmalonate.

Proton(s)	τ	Spin system	J in Hz
a	6.44	AB_2	7.9
b	6.87		
c and d	4.20, 4.28	AB	3.3
e	8.77	–	–
f	5.88	AX	7.1
g	8.77		

Diethyl 2,2-dimethyl-1-(2-furyl)propylmalonate (III). An attempt was made to prepare this ester by the method used to prepare diethyl 5-*t*-butylfurfurylmalonate by substituting 2,2-dimethyl-1-(2-furyl)propanol-1[8] for 5-*t*-butylfurfuryl alcohol. Gas chromatography revealed that the reaction products consisted of three compounds. The mass spectrum of the third compound ($M^{+\cdot}$ at m/e 296) is discussed below. Attempts to isolate this compound in the pure state were not successful.

Identification of the products of the reaction between t-butylmagnesium chloride and diethyl furfurylidenemalonate. Compound A and diethyl furfurylmalonate (II) had the same retention time and identical mass spectra. Compound A was thus a reduction product.

Compound C was identified as diethyl 5-*t*-butylfurfurylmalonate (IV) because both compounds had the same retention times and identical mass spectra. Substance C was thus a prototropically rearranged 1,8-addition product.

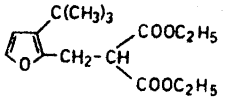

VII

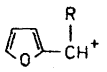

VIII

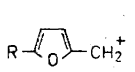

IX

It is necessary to discuss the mass spectra of diethyl 5-*t*-butylfurfurylmalonate and the substituted malonates presented in Part I[1] before the compounds B and F can be identified.

In Part I it was established that the ions $(M-159)^+$ are important fission products of the molecular ions of furyl substituted malonates. These ions consist of the substituent attached to the central carbon atom of the malonate. It was also pointed out that the relative abundances of these ions decrease with increasing size of the group R if the ions are of the type VIII ($R \neq H$).

Diethyl furfurylmalonate, diethyl 5-benzylfurfurylmalonate, and diethyl 5-*t*-butylfurfurylmalonate give ions of type IX ($R = H$, $C_6H_5CH_2$, and $(CH_3)_3C$, respectively) in the corresponding fission reactions. The abundances of these ions are 100 %.

In Part I it was also showed that another series of fragmentation reactions of the molecular ions leads to the formation of ions of type X, which are not stable, but decompose either by reaction *a* to ions of type XI, *i.e.* $(M-74)^{+\cdot}$, and hydrogen atoms or by reaction *b* to the ion XII (m/e 166) and alkyl radicals. In both cases the fragmentation does not come to a stop but proceeds with loss of ethoxy radicals. If R is methyl or ethyl, reaction *a* predominates, but with increasing size of the substituent R, reaction *a* is suppressed and reaction *b* gains in importance.

Diethyl furfurylmalonate and its 5-benzyl and 5-*t*-butyl substituted derivatives undergo the fragmentation reaction *a*. Reaction *b* cannot occur when the substituent is attached to the furan nucleus.

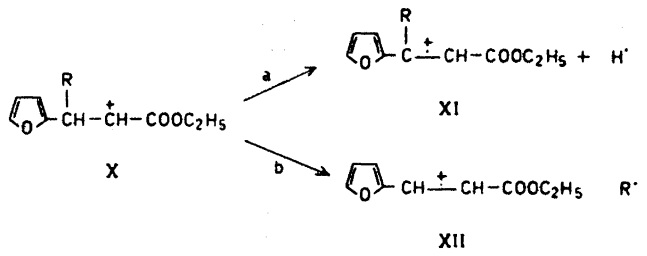

Against this background, the abundances of some ions in the mass spectrum of diethyl 2,2-dimethyl-1-(2-furyl)propylmalonate (III) can easily be predicted. Thus, the ion $(M-159)^+$ should have a relatively low, but not extremely low abundance. Further, the ions formed in the fragmentation reaction *b* should be very abundant, whereas those formed in reaction *a* should have low abundances.

When the question which of the compounds B, D, E, and F is diethyl 2,2-dimethyl-1-(2-furyl)propylmalonate (III) is to be answered, the compounds D and E must first be excluded because they undergo a prototropic rearrangement which diethyl 2,2-dimethyl-1-(2-furyl)propylmalonate cannot be expected to do. The remaining compounds, B and F, have very different mass spectra and it is easily established that only the mass spectrum of compound B complies with the above predictions. This implies that compound B is diethyl 2,2-dimethyl-1-(2-furyl)-propylmalonate (III). This conclusion is strongly supported by the fact that compound B and the unisolated compound from the attempt to prepare diethyl 2,2-dimethyl-1-(2-furyl)propylmalonate have the same retention times and identical mass spectra.

The only fact that might contradict this result is the presence of the abundant ion at *m/e* 240 because this was not detected in the spectra of the malonic esters in Part I. The ion in question had apparently been formed by loss of the *t*-butyl group of the molecular ion as an isobutylene molecule. It is quite understandable that such a reaction occurs more easily than, for example, the formation of a propylene molecule from a compound with an isopropyl substituent.

The spectrum of compound F resembles, but is not identical with the spectrum of diethyl 5-*t*-butylfurfurylmalonate. This fact implies that the *t*-butyl group of compound F is bound to the furan nucleus. Because the only possible isomer is that with the substituent in position 3, compound F seems to be diethyl 3-*t*-butylfurfurylmalonate (VII).

The two remaining compounds, D and E, rearrange to diethyl 3-*t*-butylfurfurylmalonate. Their mass spectra are almost identical. These facts and their formation in the reaction between *t*-butylmagnesium chloride and furfurylidenemalonic ester suggest that they have the structures V and VI.

The mass spectra of the compounds D and E are very similar to the spectrum of diethyl 2,2-dimethyl-1-(2-furyl)propylmalonate (compound B). The most important differences are found in the abundances of the ions at *m/e* 137. The very low abundances of these ions in the spectra of the compounds D and E show that the *t*-butyl group must be bound otherwise than in compound B.

The formation of the ions at *m/e* 166 in the spectra of the compounds D and E is easily explained by the fragmentation of the ion XIII according to reaction c. The ion XIII originates in the molecular ion which first loses an ethoxy radical and then a carbon

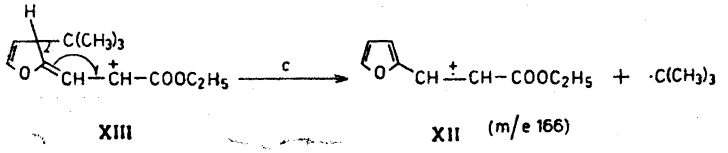

monoxide molecule. The formation of the ions at *m/e* 240 from the molecular ion of the compounds D and E by loss of an isobutylene molecule is understandable.

The elemental analysis was performed by Mr. F. Sels, Janssen Pharmaceutica, Beerse, Belgium. *Statens Naturvetenskapliga Kommission* (Finland) has supported the work.

REFERENCES

1. Holmberg, G.-A., Karlsson, M., Ulfstedt, O. and Olli, M. *Acta Chem. Scand.* **26** (1972) 3483.
2. Holmberg, G.-A. and Lundell, R. *Acta Acad. Aboensis, Ser. B.* **26** (1967) No. 12.
3. Holmberg, G.-A., Virtanen, E. and Bäckström, T. *Acta Chem. Scand.* **23** (1969) 1304.
4. Gilman, H. and Calloway, N. O. *J. Am. Chem. Soc.* **55** (1933) 4197.
5. Brown, W. G. *Org. Reactions* **6** (1951) 469.
6. Kirner, W. R. *J. Am. Chem. Soc.* **50** (1928) 1955.
7. *E.g.* Adams, R. and Kamm, R. H. *Org. Syn. Coll. Vol.* **1** (1967) 250.
8. Ushakov, M. I. and Kucherow, V. F. *J. Gen. Chem. (USSR)* **14** (1944) 1073.

Received November 7, 1972.

ACTA CHEMICA SCANDINAVICA 27 (1973) 1226–1232

Crystal Structure of Arginine Diethyl Phosphate

S. FURBERG and J. SOLBAKK

Department of Chemistry, University of Oslo, Oslo 3, Norway

The crystal structure of the arginine salt of diethyl phosphoric acid has been derived by X-ray analysis based on 568 observed reflections measured on a photometer. The space group is $P3_121$, with $a = 9.25$ Å and $c = 34.25$ Å. The accuracy is low, with $R = 0.09$ and standard deviations of 0.02 – 0.09 Å in bonds between non-hydrogen atoms. The conformation of the diethyl phosphate ion is *gauche* about both P – O ester bonds. The protonated arginine zwitterions are linked together by two pairs of N–H···O hydrogen bonds to form ring-shaped dimers. The crystal consists of layers (001) of hydrogen-bonded ions.

In order to obtain information on the stereochemistry of the interaction between nucleic acids and basic proteins we have investigated the crystal structures of a number of salts between diethyl phosphoric acid and compounds related to arginine and lysine. The structures of the propylguanidinium [1] and putrescinium [2] salts have been reported and in this paper the arginine complex is described. The purpose of the work is to study the mode of bonding and the relative orientation of the two ions, not to derive accurate bond lengths and angles.

EXPERIMENTAL. CRYSTAL DATA

The compound was prepared by mixing equivalent amounts of arginine and diethyl phosphoric acid (prepared as previously described [1]) in aqueous solution. The solution was placed in a closed system containing some ethanol and crystals of the salt gradually precipitated. They had the shape of trigonal pyramids and cleaved very easily perpendicular to the three-fold axis.

Weissenberg photographs showed the crystals to be trigonal with Laue symmetry $\bar{3}m$. The $00l$ reflections are present only for $l = 3n$ and the space group was assumed to be $P3_121$. The cell dimensions were measured on a manual Picker diffractometer and found to be $a = 9.251(3)$ Å and $c = 34.25(2)$ Å. Flotation in mixtures of bromobenzene and *m*-xylene gave a density of 1.30 g/cm^3. There are six (calc. 6.05) formula units $(C_2H_5O)_2PO(OH).HOOC.CH(NH_2)(CH_2)_3.NH.C(NH)NH_2$ in the unit cell.

The reflections from a crystal of dimensions 0.2 – 0.4 mm were recorded on integrated Weissenberg photographs $h0l - h3l$ using Cu$K\alpha$ radiation. Their

Table 1. Positional and thermal parameters with estimated standard deviations. All values except those of B are multiplied by 10^4. The temperature factor is given by $\exp -(B_{11}h^2+B_{22}k^2+B_{33}l^2+B_{12}hk+B_{13}hl+B_{23}kl)$.

Atom	x	y	z	B_{11}(B)	B_{22}	B_{33}	B_{12}	B_{13}	B_{23}
P	2811	0498	2479	111	128	10	138	15	11
	7	7	2	11	11	1	20	5	5
O1	2256	1743	2316	93	213	19	150	54	78
	16	18	4	29	36	2	60	13	14
O2	3469	−0035	2111	273	423	18	406	−8	−32
	24	25	5	42	52	2	81	16	19
O3	4340	1343	2718	136	177	17	121	−14	−17
	17	18	4	31	32	2	54	12	13
O4	1323	−0836	2656	220	251	19	342	12	32
	19	20	5	35	39	2	65	15	15
C1	3458	3152	2127	232	256	12	216	−9	39
	32	32	6	60	59	3	101	21	22
C2	2944	3757	1863	610	998	44	433	9	346
	58	76	14	149	229	8	310	62	79
C3	2276	−0957	1834	980	737	55	627	9	−238
	83	73	17	245	190	11	383	86	80
C4	2315	−2469	1741	218	1035	44	413	46	−75
	47	80	14	86	214	8	234	45	68
O5	5512	5371	2903	6.2					
	19	19	4	.4					
O6	3548	6092	2978	5.3					
	19	19	4	.4					
N1	7608	8893	4189	5.2					
	23	23	5	.4					
N2	9519	11581	4062	4.7					
	21	21	5	.4					
N3	6745	10670	4004	6.0					
	24	25	5	.5					
N4	4259	2906	3423	3.8					
	20	20	4	.4					
C5	7970	10370	4079	5.4					
	30	29	6	.6					
C6	5958	7421	4190	5.5					
	31	29	6	.5					

Table 1. Continued.

C7	5663	6550	3826	5.0
	27	27	6	.5
C8	3846	5056	3786	4.3
	27	27	5	.5
C9	3510	4043	3419	3.3
	24	24	5	.4
C10	4194	5155	3076	5.2
	29	28	6	.5

intensities were measured on a photometer. The layers were scaled by equivalent reflections. The fall-off in intensity was rapid and only 568 independent reflections had measurable intensities. Corrections for absorption and secondary extinction were not applied. All programs used are described in Ref. 3.

Table 2. Distances (Å) and angles (°). E.s.d. in parenthesis.

P–O1	1.58(1)	O1–P–O2	105(1)
P–O2	1.58(2)	O1–P–O3	113(1)
P–O3	1.48(2)	O1–P–O4	105(1)
P–O4	1.44(2)	O2–P–O3	101(1)
O1–C1	1.38(3)	O2–P–O4	115(1)
C1–C2	1.27(4)	O3–P–O4	118(1)
O2–C3	1.38(6)	P–O1–C1	117(1)
C3–C4	1.45(9)	O1–C1–C2	116(3)
O5–C10	1.28(3)	P–O2–C3	115(3)
O6–C10	1.32(3)	O2–C3–C4	110(5)
C9–C10	1.48(3)	O5–C10–O6	119(2)
C9–N4	1.52(3)	O5–C10–C9	121(2)
C9–C8	1.51(3)	O6–C10–C9	119(2)
C8–C7	1.56(3)	N4–C9–C10	108(2)
C7–C6	1.43(3)	C8–C9–C10	110(2)
C6–N1	1.45(3)	N4–C9–C8	113(2)
N1–C5	1.29(3)	C9–C8–C6	114(2)
C5–N2	1.31(3)	C8–C7–C7	113(2)
C5–N3	1.32(3)	C7–C6–N1	110(2)
		C6–N1–C5	126(2)
Hydrogen bonds		N1–C5–N3	119(2)
N1···O1′	3.08	N1–C5–N2	121(2)
N2···O4′	2.86	N2–C5–N3	120(2)
N2···O5′	2.78		
N3···O3′	3.01		
N3···O6′	2.93		
N4···O4′	2.79		
N4···O6′	2.77		
N4···O3	2.84		

Prime denotes an atom in any neighbouring ion.

Table 3. Observed and calculated structure factors.

h k	l	Fo	Fc
0 0	3	100	94
0 0	6	154	185
0 0	9	106	113
0 0	12	68	72
0 0	15	30	28
0 0	18	27	28
0 0	21	17	10
0 0	24	45	53
1 0	29	14	22
1 0	28	21	22
1 0	27	12	10
1 0	26	13	15
1 0	25	17	21
1 0	24	13	17
1 0	22	13	14
1 0	21	14	15
1 0	18	14	13
1 0	17	28	26
1 0	16	27	26
1 0	15	33	38
1 0	14	42	50
1 0	13	24	22
1 0	12	91	100
1 0	11	12	11
1 0	10	43	35
1 0	9	84	79
1 0	8	72	63
1 0	7	35	37
1 0	6	107	110
1 0	5	45	43
1 0	4	116	120
1 0	3	68	72
1 0	2	66	67
1 0	1	73	72
1 0	0	33	28
1 0	-2	20	14
1 0	-3	46	38
1 0	-5	122	120
1 0	-6	114	117
1 0	-7	159	177
1 0	-8	16	16
1 0	-9	48	50
1 0	-10	16	14
1 0	-11	58	55
1 0	-12	70	71
1 0	-13	42	48
1 0	-14	61	61
1 0	-16	11	9
1 0	-18	21	23
1 0	-19	48	53
1 0	-20	23	26
1 0	-22	31	39
1 0	-23	18	19
1 0	-24	15	14
1 0	-29	16	14
2 0	24	15	15
2 0	23	17	16
2 0	21	28	28
2 0	20	25	30
2 0	19	18	17
2 0	18	55	57
2 0	17	19	19
2 0	16	21	19
2 0	15	14	15
2 0	14	30	26
2 0	13	14	12
2 0	12	105	112
2 0	11	46	42
2 0	10	17	15
2 0	8	27	20
2 0	7	107	114
2 0	6	25	25
2 0	5	14	12
2 0	4	63	56
2 0	3	11	4
2 0	2	63	61
2 0	1	52	48
2 0	-0	43	39
2 0	-1	138	143
2 0	-2	64	66
2 0	-3	110	115
2 0	-4	73	67
2 0	-6	52	48
2 0	-7	47	44
2 0	-8	45	45
2 0	-9	46	42
2 0	-11	28	30
2 0	-12	28	25
2 0	-13	53	56
2 0	-14	22	26
2 0	-16	14	14
2 0	-19	41	45
2 0	-21	23	23
2 0	-22	21	17
2 0	-25	28	31
h 0	-22	31	35
h 0	-20	22	21
h 0	-18	32	31
h 0	-16	22	22
h 0	-15	30	36
h 0	-12	39	41
h 0	-11	21	16
h 0	-10	14	13
h 0	-9	17	16
h 0	-8	16	15
h 0	-7	52	47
h 0	-6	34	30
h 0	-5	33	24
h 0	-4	94	87
h 0	-3	22	20
h 0	-2	21	21
h 0	2	30	31
h 0	3	26	26
h 0	6	30	27
h 0	7	26	22
h 0	8	26	26
h 0	9	21	17
h 0	12	16	13
h 0	13	39	40
h 0	20	28	29
5 0	-25	20	22
5 0	-19	21	24
5 0	-16	27	28
5 0	-11	24	25
5 0	-10	34	32
5 0	-6	15	14
5 0	-5	40	41
5 0	-4	37	38
5 0	-2	48	39
5 0	1	17	11
5 0	2	18	16
5 0	5	22	21
5 0	6	44	46
5 0	9	18	14
5 0	10	22	21
5 0	11	17	13
5 0	14	34	34
5 0	15	18	17
5 0	16	26	25
5 0	20	28	31
6 0	-15	25	26
6 0	-14	19	17
6 0	-12	21	22
6 0	-6	22	19
6 0	-4	31	27
6 0	0	31	27
6 0	1	21	22
6 0	2	17	13
6 0	3	34	33
6 0	6	16	15
6 0	8	18	16
6 0	12	29	30
6 0	13	40	39
7 0	4	19	22
7 0	7	23	24
7 0	10	19	19
7 0	14	18	17
1 1	0	131	128
1 1	1	93	97
1 1	2	76	69
1 1	3	34	32
1 1	4	37	30
1 1	5	79	67
1 1	6	91	84
1 1	7	74	71
1 1	8	35	35
1 1	9	43	45
1 1	10	28	24
1 1	11	47	44
1 1	12	35	34
1 1	13	44	42
1 1	14	29	34
1 1	15	35	34
1 1	16	18	17
1 1	17	38	45
1 1	18	26	24
1 1	19	10	10
1 1	20	16	19
1 1	22	17	20
1 1	23	20	21
1 1	24	23	24
1 1	25	13	15
1 1	27	14	13
1 1	29	13	11
1 1	30	15	19
2 1	26	15	15
2 1	25	14	14
2 1	24	15	13
2 1	23	13	14
2 1	20	13	12
2 1	19	14	16
2 1	18	30	24
2 1	17	10	10
2 1	16	17	12
2 1	14	16	16
2 1	13	34	35
2 1	12	63	68
2 1	11	27	21
2 1	10	12	14
2 1	9	36	31
2 1	8	44	45
2 1	5	15	10
2 1	6	106	102
2 1	5	81	79
2 1	4	46	46
2 1	3	89	83
2 1	2	26	22
2 1	1	15	10
2 1	-0	49	46
2 1	-1	30	29
2 1	-2	9	8
2 1	-3	82	74
2 1	-4	36	34
2 1	-5	35	34
2 1	-6	33	33
2 1	-7	26	25
2 1	-8	28	27
2 1	-9	23	20
2 1	-10	50	50
2 1	-11	33	33
2 1	-12	32	31
2 1	-13	41	41
2 1	-14	17	16
2 1	-15	49	44
2 1	-16	19	19
2 1	-17	20	8
2 1	-18	20	23
2 1	-19	17	15
2 1	-20	12	6
2 1	-23	14	11
2 1	-24	14	12
2 1	-25	15	15
h 1	-22	16	11
h 1	-21	21	23
h 1	-19	18	21
h 1	-17	17	15
h 1	-16	39	46
h 1	-15	14	13
h 1	-14	20	20
h 1	-13	11	8
h 1	-12	15	11
h 1	-11	11	5
h 1	-10	32	33
h 1	-9	17	16
h 1	-8	21	20
h 1	-7	18	16
h 1	-6	29	27
h 1	-5	25	23
h 1	-3	29	26
h 1	-1	47	44
h 1	0	41	41
h 1	1	22	24
h 1	2	36	31
h 1	3	36	36
h 1	4	24	22
h 1	5	35	33
h 1	6	23	27
h 1	7	16	17
h 1	8	37	36
h 1	9	19	20
h 1	10	17	18
h 1	11	24	21
h 1	12	26	25
h 1	13	10	7
h 1	14	18	20
h 1	15	11	12
h 1	16	18	22
h 1	17	16	17
5 1	-19	18	18
5 1	-18	17	14
5 1	-15	17	19
5 1	-14	22	19
5 1	-13	13	10
5 1	-12	21	24
5 1	-11	18	21
5 1	-8	20	18
5 1	-7	16	11
5 1	-6	19	21
5 1	-5	15	14
5 1	-3	18	12
5 1	-2	18	18
5 1	-1	13	7
5 1	0	22	23
5 1	2	30	31
5 1	3	20	23
h 2	4	17	17
h 2	9	29	31
h 2	11	21	19
h 2	12	19	18
h 2	13	19	15
h 2	15	21	22
h 2	16	16	16
h 2	17	16	14
h 2	19	25	25
h 2	20	20	20
5 2	-9	20	20
5 2	-7	23	21
5 2	-4	37	34
5 2	-3	29	32
5 2	-1	16	14
5 2	0	15	13
5 2	1	16	18
5 2	2	24	23
5 2	3	23	22
5 2	4	17	19
5 2	8	28	31
5 2	11	23	20
5 2	12	18	19
5 2	14	23	22
6 2	0	14	14
6 2	1	19	15
6 2	2	22	27
6 2	6	17	15
6 2	7	20	23
6 2	8	20	23
0 3	25	13	8
0 3	24	32	34
0 3	23	17	12
0 3	22	24	27
0 3	20	24	22
0 3	18	23	20
0 3	17	34	31
0 3	16	22	23
0 3	14	25	23
0 3	13	31	32
0 3	10	10	9
0 3	9	27	28
0 3	8	16	17
0 3	7	23	19
0 3	6	18	22
0 3	3	17	19
0 3	2	61	52
0 3	1	25	24
0 3	-0	27	27
0 3	-1	14	13
0 3	-2	13	14
0 3	-3	13	13
0 3	-4	64	71
0 3	-5	51	46
0 3	-6	57	49
0 3	-7	74	71
0 3	-8	10	9
0 3	-9	27	25
0 3	-10	26	26
0 3	-11	56	58
0 3	-12	51	57
0 3	-13	13	11
0 3	-14	28	28
0 3	-15	18	13
0 3	-17	33	28
0 3	-18	39	37
1 3	23	20	20
1 3	21	16	14
1 3	19	20	20
1 3	18	27	29
1 3	17	23	26
1 3	16	15	17
1 3	15	27	29
1 3	14	12	10
1 3	13	42	43
1 3	12	36	36
1 3	11	30	30
1 3	10	39	39
1 3	9	44	39
1 3	8	16	13
1 3	7	31	26
1 3	6	30	27
1 3	5	52	49
1 3	4	38	38
1 3	3	36	34
1 3	2	30	30
1 3	1	23	19
1 3	-0	24	18
1 3	-1	26	27
1 3	-2	14	12
1 3	-4	22	19
1 3	-5	23	20
1 3	-6	17	17
1 3	-7	20	15
1 3	-8	41	45
1 3	-9	20	21
1 3	-10	33	31
1 3	-12	17	16
1 3	-13	26	25
1 3	-14	22	23
1 3	-15	19	19
1 3	-16	29	27
1 3	-17	11	10
1 3	-18	11	11
1 3	-19	25	29
1 3	-21	17	17
1 3	-22	16	17
1 3	-23	14	14
1 3	-24	13	9
1 3	-25	16	19
2 3	23	16	4
2 3	22	14	16
2 3	21	17	19
2 3	19	24	27
2 3	18	13	9
2 3	17	15	15
2 3	16	17	19
2 3	15	15	13
2 3	14	20	23
2 3	13	26	28
2 3	12	12	10
2 3	10	37	36
2 3	9	19	18
2 3	8	30	30
2 3	7	50	47
2 3	6	19	19
2 3	5	17	13
2 3	4	19	20
2 3	3	13	17
2 3	2	37	35
2 3	1	32	29
2 3	-0	14	12
2 3	-1	30	33
2 3	-2	34	32
2 3	-3	15	13
2 3	-4	16	17
2 3	-5	11	8
2 3	-6	17	14
2 3	-7	48	49
2 3	-8	29	32
2 3	-9	21	18
2 3	-10	31	27
2 3	-11	18	20
2 3	-12	32	33
2 3	-13	12	11
2 3	-14	15	19
2 3	-15	23	22
2 3	-16	20	20
2 3	-17	28	27
2 3	-18	21	22
2 3	-19	21	22
2 3	-20	13	9
2 3	-22	16	9
2 3	-23	14	16
3 3	0	18	13
3 3	1	21	21
3 3	2	31	29
3 3	3	19	18
3 3	4	44	40
3 3	5	13	12
3 3	7	16	15
3 3	8	18	18
3 3	9	16	18
3 3	10	22	19
3 3	11	12	13
3 3	17	19	20
3 3	19	19	19
3 3	21	22	16
3 3	22	17	19
h 3	-18	17	13
h 3	-17	17	17
h 3	-15	18	17
h 3	-14	14	14
h 3	-13	23	22
h 3	-11	26	24
h 3	-10	21	18
h 3	-9	20	24
h 3	-8	22	19
h 3	-4	18	15
h 3	-3	18	18
h 3	-1	18	17
h 3	0	14	12
h 3	1	13	12
h 3	2	18	19
h 3	3	15	17
h 3	5	13	14
h 3	6	15	16
h 3	7	21	21
h 3	8	19	19
h 3	9	26	26
h 3	10	16	17
h 3	11	16	16
h 3	13	19	23
h 3	14	19	17
h 3	17	17	19
5 3	-5	24	25
5 3	-4	18	20
5 3	-3	22	22
5 3	-2	18	14
5 3	-1	17	11
5 3	1	22	22
5 3	2	16	9
5 3	3	28	27
5 3	5	15	13
5 3	6	16	12
5 3	7	22	24
5 3	8	18	14
5 3	9	17	15
5 3	10	14	11
5 3	12	15	12
5 3	14	13	9

STRUCTURE ANALYSIS

The position of the phosphorus atom was derived from a sharpened Patterson map and repeated weighted Fourier syntheses eventually led to the correct structure. It was refined by block diagonal least squares calculations. In view of the small number of reflections, anisotropic temperature factors were applied only to the atoms of the diethyl phosphate ion. The atoms of the arginine ion were given individual isotropic temperature factors. A common isotropic temperature factor was assigned to the 25 hydrogen atoms, which were included in fixed calculated positions. It refined to $B = 6.6$ Å^2. The final value of R is 0.09, of R_w 0.12. The structure factors were given weights $(a + F + cF^2)^{-1/2}$, with $a = 2F_{min}$ and $c = 2/F_{max}$.

The atomic parameters are given in Table 1 and observed and calculated structure factors in Table 3. The atomic scattering factors used were those of Hanson *et al.*[4] for non-hydrogen atoms and of Stewart *et al.*[5] for hydrogen atoms.

RESULTS AND DISCUSSION

The bond lengths and angles are given in Table 2 and Fig. 1. They are all normal within the limits of error. The accuracy is low because of the small number of reflections and the large thermal vibrations of the ethyl groups, and only the general features of the molecular and crystal structure will be discussed.

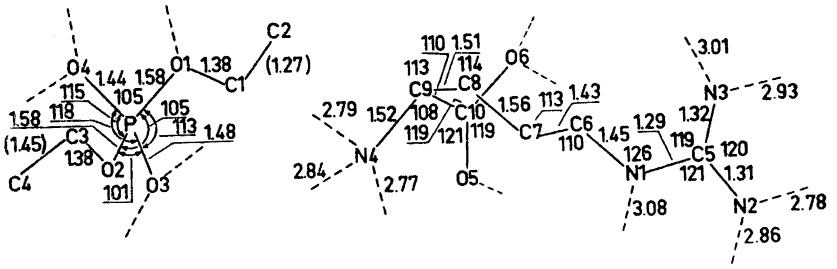

Fig. 1. Bond lengths (Å) and angles (°).

The diethyl phosphate ion. The structure of this ion is essentially the same as found in the propylguanidinium salt,[1] the conformation being *gauche* about both P – O ester bonds (dihedral angles O2 – P – O1 – C1 and O1 – P – O2 – C3 are 58.4° (1.8°) and 66.0° (3.5°), respectively). However, the positions of the terminal methyl groups deviate much from the expected *anti* conformation, the dihedral angles about bonds C3 – O2 and C1 – O1 being 151° and 128°, respectively. These deviations are probably due to crystal forces. They bring the methyl hydrogen atoms closer to layers (001) of the ethyl hydrogen atoms in the structure. The ethyl groups vibrate strongly the mean B-values for C1, C2, C3, and C4 being 6.5, 18.8, 17.3, and 21.3 Å^2, respectively, whereas they lie in the range 3.3 – 7.3 Å^2 for the other atoms.

The arginine ion. The arginine molecule occurs in the crystal as a protonated zwitterion (-OOC).CH(NH_3^+)(CH_2)$_3$(NH)C(NH_2)$_2^+$, as found in other salts of arginine.[6,7] This is indicated mainly by the scheme of hydrogen bonding, the α-amino group taking part in three such bonds, the guanidyl group in five.

The conformation of the arginine molecule in four different crystals has been discussed by Ramachandran *et al.*[6] In all structures nearly planar guanidyl and carboxylate groups are linked together by a chain of coplanar carbon atoms, but the dihedral angles about $C_\alpha - C_\beta$ and C_δ – N vary and the molecules have different conformations in the crystals. In the present structure the atoms of the carboxylate group (C9, C10, O6, and O5) are coplanar to within 0.04 Å, those of the guanidyl group (N1, C5, N2, and N3) to within 0.02 Å, whereas the maximum deviation of atoms C9, C8, C7, C6, and N1 from their best plane is 0.05 Å. The angles between the latter plane and those of the carboxylate and guanidyl groups are 89° and 82°, respectively. Atom N4 of the NH_3^+ group is 0.31 Å away from the carboxylate plane, and C6 0.13 Å from the guanidyl plane. The dihedral angle C7 – C8 – C9 – N4 is 75° (C9 – H *anti* to C7 – C8) and the one about C6 – N1 (C_δ – N) is 91°. Each of these values is

similar to what is found in structures previously investigated.[6] However, in none of these this particular combination of the two dihedral angles occurs and the present structure appears to represent an arginine conformation previously not observed. Its main characteristics is that the carboxylate and guanidyl groups point to the same side of the C9 – C8 – C7 – C6 – N1 chain, with C – O and C – N bonds very roughly parallel. This conformation would appear stereochemically favourable for the formation of cyclic dimers through pairs of N – H···O hydrogen bonds, as found in the present structure.

The crystal structure. The crystal consists of layers (001) of thickness $c/3$ (11.4 Å) related by the 3_1 axis. One layer is shown in Fig. 2. The layers have

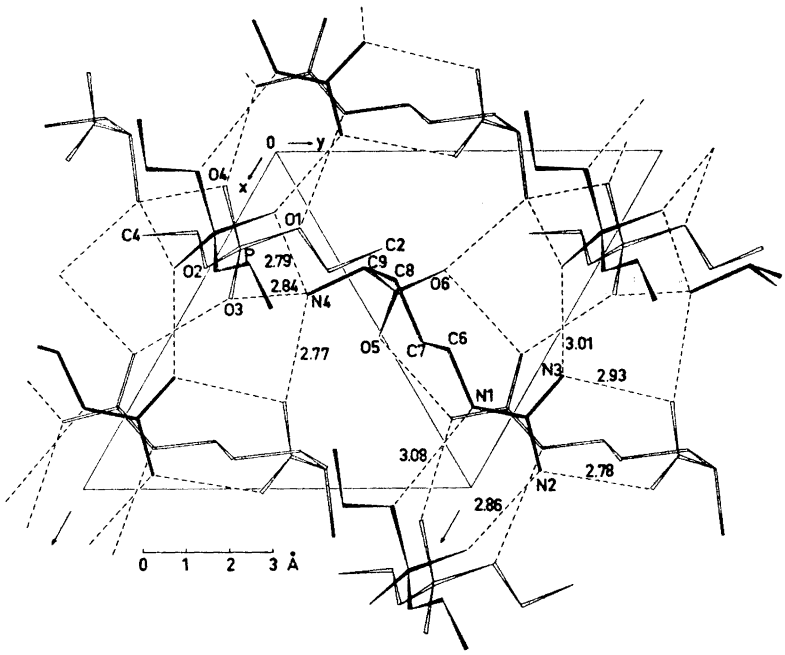

Fig. 2. One layer of the structure viewed along the 3_1 axis.

twofold axes of symmetry and the ethyl groups of adjacent layers interlock so as to give corrugated sheets of ethyl groups at roughly van der Waals distances from each other. Between these sheets are the phosphate and arginine ions which are held together by an extensive system of N – H···O hydrogen bonds, one for each hydrogen atom bonded to nitrogen. The main structural unit in a layer is a dimer of arginine ions related by a twofold axis of symmetry and held together by two pairs of hydrogen bonds (lengths 2.78 Å and 2.93 Å) between the guanidyl group in one molecule and the carboxylate group in the other, forming an 18-membered ring system. Two of the hydrogen bonds between a dimer and neighbouring diethyl phosphate ions, N1 – H···O1 (length 3.08 Å) and N2 – H···O4 (length 2.86 Å), are nearly parallel and link

the guanidyl group to two oxygen atoms in the same diethyl phosphate ion. Ester oxygen atoms like O1 are in general not involved in hydrogen bond formation, but in the present structure the distance H···O1 of 2.04 Å is considerably smaller than van der Waals contact and it seems reasonable to consider it a weak hydrogen bond. A similar bond (3.09 Å) occurs also in the propylguanidinium salt.[1]

The guanidyl group takes part in five hydrogen bonds, all of which are approximately linear and roughly lying in the guanidyl plane. The NH_3^+ group forms three hydrogen bonds (lengths 2.78 Å, 2.84 Å, and 2.81 Å) in nearly tetrahedral arrangement, two to different diethyl phosphate groups and the third to O6 in a neighbouring dimer.

There are no hydrogen bonds between the layers. This explains the good (001) cleavage of the crystals.

REFERENCES

1. Furberg, S. and Solbakk, J. *Acta Chem. Scand.* **26** (1972) 2855.
2. Furberg, S. and Solbakk, J. *Acta Chem. Scand.* **26** (1972) 3699.
3. Dahl, T., Gram., F., Groth, P., Klewe, B. and Rømming, C. *Acta Chem. Scand.* **24** (1970) 2232.
4. Hanson, H. P., Herman, F., Lea, J. D. and Skillman, L. *Acta Cryst.* **17** (1964) 1040.
5. Stewart, R. F., Davidson, E. and Simpson, W. *J. Chem. Phys.* **42** (1965) 3175.
6. Ramachandran, G. N., Mazumdar, S. K., Venkatesan, K. and Lakshminarayanan, A. V. *J. Mol. Biol.* **15** (1966) 232.
7. Aoki, K., Nagano, K. and Iitaka, Y. *Acta Cryst.* **B 27** (1971) 11.

Received November 16, 1972.

ACTA CHEMICA SCANDINAVICA 27 (1973) 1233–1239

Tetrazole Analogues of Benzilic Acid Esters and Substituted Glycolic Acid Esters. II

ERIK BALIEU and ERIK BJARNOV *

Danish Civil Defence Analytical-Chemical Laboratory, Universitetsparken 2, DK-2100 Copenhagen, Denmark

A number of 1,5- and 2,5-disubstituted tetrazolylmethanols have been synthesized as potential anticholinergic compounds. The presence of an intramolecular hydrogen bond in the 1,5-isomers is shown by IR-spectroscopy, and the ^{1}H NMR-spectra are discussed.

In a previous paper [1] the syntheses of a number of new 1,5- and 2,5-disubstituted tetrazoles (I–II) were given. The assignment of structure to the isomers was based on their ^{1}H NMR-spectra, and confirmed by synthesis.

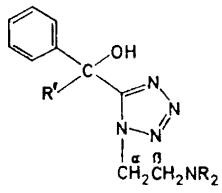

I

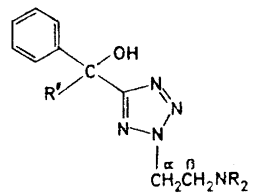

II

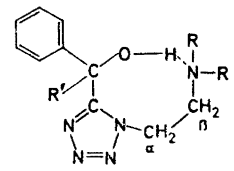

I'

An unexpected splitting pattern in the ^{1}H NMR-spectra of the 1,5-disubstituted tetrazoles led us to assume the presence of an intramolecular hydrogen bond in these isomers (I'). In the present paper this assumption is confirmed by IR-spectroscopy. The syntheses of an additional number of tetrazoles (Scheme 1; I a–e, II a–e) of the corresponding structure are given.

These tetrazoles have been selected for synthesis after a preliminary test [2] for anticholinergic activity was carried out on the earlier prepared compounds.[1] The presence of a cycloalkane ring is a common feature of the tetrazolyl-

* Present address: Chemistry Department V, H. C. Ørsted Institute, University of Copenhagen, DK-2100 Copenhagen, Denmark.

Table 1. 1,5-Disubstituted tetrazoles (I a – e).

Compound	Yield, %	Melting point °C	Eluent for PLC	Crystallized from	Formula	Analyses (C, H, N, Cl)	Chemical shifts (ppm)[a] δH_α	δH_β
Ia	11	Oil	Benzene-abs. ethanol 8:2	–	$C_{17}H_{25}N_5O$		4.35 (m)	2.73 (m)
Ia, HCl	–	119–124	–	Abs. ethanol	$C_{17}H_{26}N_5ClO$	Found: 57.35 7.40 19.58 10.32 Calc.: 58.04 7.45 19.91 10.08	–	–
Ib	7	77– 79	Benzene-acetone 8:2	Ethanol-water	$C_{19}H_{29}N_5O$	Found: 66.60 8.79 20.48 Calc.: 66.43 8.51 20.39	4.21 (m)	2.77 (m)
Ic	2	116–118	Benzene-acetone 8:2	Ether	$C_{20}H_{29}N_5O$	Found: 67.50 8.29 19.57 Calc.: 67.57 8.22 19.71	4.26 (m)	2.68 (m)
Id	9	126–128	Benzene-acetone 9:1	Abs. ethanol	$C_{20}H_{31}N_5O$	Found: 67.30 8.75 19.61 Calc.: 67.19 8.74 19.59	4.34 (m)	2.83 (m)
Ie	8	119–121	Benzene-acetone 9:1	Cyclohexane	$C_{21}H_{31}N_5O$	Found: 68.10 8.52 18.73 Calc.: 68.27 8.46 18.95	4.36 (m)	2.68 (m)

[a] (m) = multiplet.

Table 2. 2,5-Disubstituted tetrazoles (II a – e).

Compound	Yield, %	Melting point, °C	Eluent for PLC	Crystallized from	Formula	Analyses (C, H, N)	Chemical shifts (ppm)[a] δH_α	δH_β
IIa	3	103 – 104	Benzene-abs. ethanol 8:2	Abs. ethanol	$C_{17}H_{25}N_5O$	Found: 64.55 8.11 22.26 Calc.: 64.76 7.99 22.21	4.69 (t)	2.90 (t)
IIb	4	67 – 69	Benzene-acetone 8:2	Ether	$C_{19}H_{29}N_5O$	Found: 66.25 8.60 20.23 Calc.: 66.43 8.51 20.39	4.63 (t)	3.01 (t)
IIc	8	77 – 80	Benzene-acetone 8:2	Ether-petroleum ether	$C_{20}H_{29}N_5O$	Found: 67.35 8.24 19.78 Calc.: 67.57 8.22 19.71	4.70 (t)	2.92 (t)
IId	12	78 – 80	Benzene-acetone 9:1	Ethanol-water	$C_{10}H_{31}N_5O$	Found: 66.90 8.92 19.08 Calc.: 67.19 8.74 19.59	4.66 (t)	3.05 (t)
IIe	9	82 – 84	Benzene-acetone 9:1	Cyclohexane	$C_{21}H_{31}N_5O$	Found: 68.40 8.52 18.98 Calc.: 68.27 8.46 18.95	4.70 (t)	2.93 (t)

[a] $J_{\alpha\beta}$ = 7 Hz; (t) = triplet.

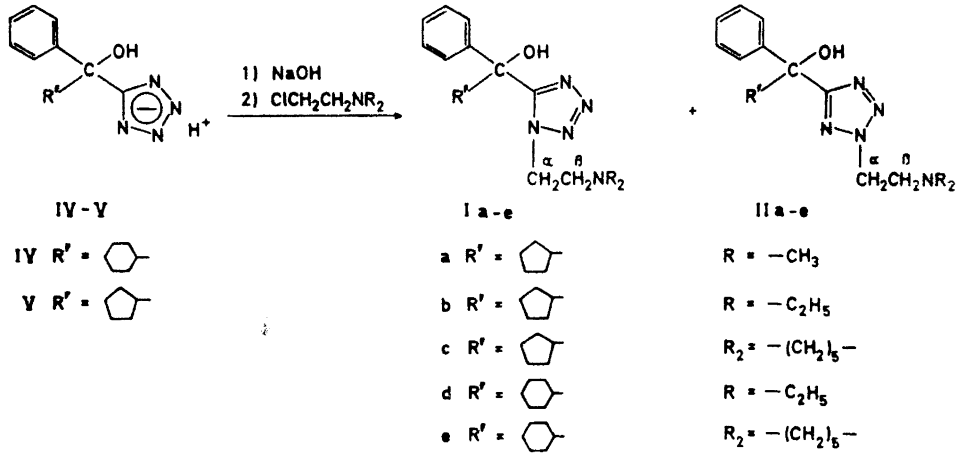

Scheme 1.

methanols I a–e and II a–e. Some special features of the ^{1}H NMR-spectra of this type of compounds are discussed.

Synthesis. The procedure for synthesizing I a–e and II a–e was identical to that presented earlier [1,3,4a] (Scheme 1).

^{1}H NMR-spectra. The chemical shifts of the α- and β-protons (I – II) of the new 1,5- and 2,5-disubstituted tetrazoles are given in Tables 1 and 2. Of each isomer pair, the compound in which the α-protons appeared at a lower δ-value was assigned the 1,5-isomeric structure according to previous findings.[1] The ^{1}H NMR-spectra of all the 1,5-tetrazoles showed multiplet signals from the α- and β-protons whereas the corresponding signals from the 2,5-isomers were triplets.

Table 3. Chemical shifts of phenyl protons of tetrazoles with structures I and II (δ-values in ppm; solvent: deuteriochloroform). I and II f, g and h were published in Ref. 1.

Compound	δH_o, $\delta H_{m,p}$	Compound	δH_o	$\delta H_{m,p}$	$\Delta = \delta H_o - \delta H_{m,p}$
Ia	7.40	IIa	7.69	7.29	0.40
Ib	7.33	IIb	7.71	7.30	0.41
Ic	7.39	IIc	7.68	7.29	0.39
Id	7.43	IId	7.69	7.31	0.38
Ie	7.41	IIe	7.71	7.33	0.38
If[a]	7.37	IIf[a]	7.33		–
Ig[b]	7.33	IIg[b]	7.63	7.26	0.37
Ih[c]	7.39	IIh[c]	7.41		–

[a] R′ = C_6H_5–; R = C_2H_5–

[b] R′ = 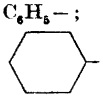 ; R = CH_3–

[c] R′ = H–; R = C_2H_5–

The chemical shifts of the benzene protons of I a–e and II a–e are given in Table 3. In the tetrazoles I a–e all the benzene protons give rise to one multiplet, whereas in II a–e there is a marked difference between the chemical shifts of the *ortho*-protons and those of the *meta*- and *para*-protons. We have only observed this effect in compounds of type II in which R′ is a cycloalkyl group. If, *e.g.*, R′ = C_6H_5-(II f) or R′ = H-(II h), the benzene protons only give rise to one multiplet signal. The difference ($\Delta = \delta H_o - \delta H_{m,p}$) between the chemical shifts of the *ortho*-protons and the *meta*- and *para*-protons is rather constant, about 0.4 ppm.

Tentative calculations of the benzene part of the spectrum of II c gave good agreement with the observed spectrum when the chemical shifts relative to benzene of the *ortho*-, *meta*-, and *para*-protons were 0.39, 0.00, and −0.083 ppm, respectively. The calculations were performed for an AA′BB′C system using the coupling constants of trichloromethylbenzene given by Hayamizu and Yamamoto.[4b]

Similar observations have been reported for 2-methyl-5-phenyltetrazole when compared to 1-methyl-5-phenyltetrazole [5] and in 2-(5-phenyltetrazolyl)-acetic- or propionic acids when compared to the 1-substituted compounds.[6]

In these compounds a substituent in the tetrazole ring affects the chemical shifts of the protons of a benzene ring attached directly to the tetrazole nucleus.[5] In our case, however, a carbon atom is inserted between the benzene- and tetrazole rings.

IR-spectra. The intramolecular hydrogen bond in the 1,5-isomers. In order to show the presence of the intramolecular hydrogen bond in compounds of type I, the infrared spectra of diphenyl-5-[1-(diethylaminoethyl)tetrazolyl]methanol (I f) (R′ = C_6H_5−, R = C_2H_5−) and diphenyl-5-[2-(diethylaminoethyl)tetrazolyl]methanol (II f) (R′ = C_6H_5−, R = C_2H_5−) in tetrachloromethane were recorded (Fig. 1).

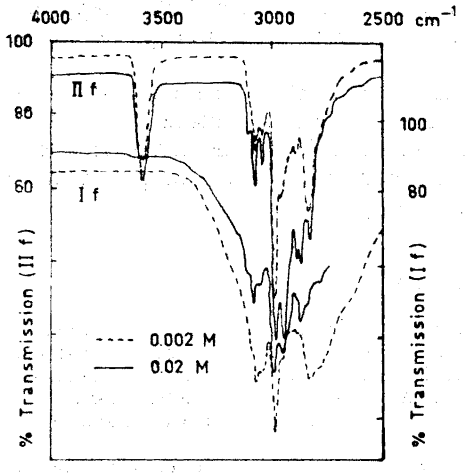

Fig. 1. IR-spectra of I f and II f. Cell path: 1 mm for 0.02 M solutions and 10 mm for 0.002 M solutions. Solvent: CCl_4.

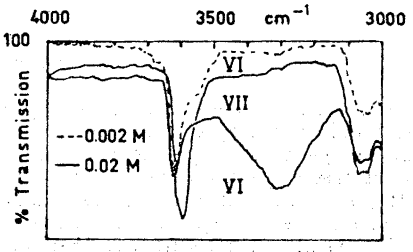

Fig. 2. IR-spectra of VI and VII. Cell path: 1 mm for 0.02 M solutions and 10 mm for 0.002 M solutions. Solvent: CCl_4.

The spectrum of II f in 0.02 M solution showed absorption at 3590 cm^{-1} arising from non-bonded OH and weak broad absorption at 3450 cm^{-1} arising from bonded OH, while the spectrum of I f (0.02 M solution) showed a broad absorption in the region 2500 – 3300 cm^{-1} indicating a strongly bonded OH group. At tenfold dilution combined with a corresponding increase in cell path the spectrum of I f showed no changes while the broad band from bonded OH in the spectrum of II f had disappeared (Fig. 1).

These spectra fully support the assumption that in the compound I f the hydrogen atom of the alcohol group is internally bound to the amino group (I') whereas this is not the case for the compound II f in which the two interacting groups are too far from each other.[1]

The tetrazole ring has been reported to possess base properties.[7] In order to show that the above-mentioned intramolecular hydrogen bond is not established between the alcohol group and the tetrazole ring itself, the IR-spectra of the model compounds VI and VII (Scheme 2) were recorded (Fig. 2).

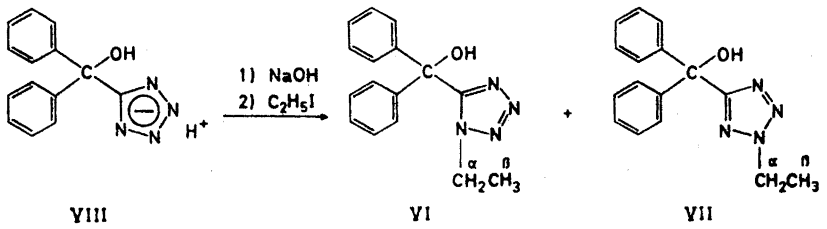

Scheme 2.

The spectra of VI show the presence of bonded and non-bonded OH in 0.02 M solution; on tenfold dilution the absorption from bonded OH disappears. In the spectra of I f no absorption from non-bonded OH was present even in 0.002 M solution. (Fig 1).

The ^1H NMR-spectra of VI and VII in deuteriochloroform showed triplet signals from the β-protons and quartet signals from the α-protons.

From the similar multiplet pattern of the α- and β-protons in the ^1H NMR-spectra of all the tetrazoles I a–e it is concluded that the amino group in all cases is internally bound to the tertiary alcohol group.

EXPERIMENTAL

Microanalysis were carried out by Preben Hansen, Microanalytical Department of Chemical Laboratory II, University of Copenhagen. Melting points were determined with a hot stage microscope, (Mikroskop-Heiztisch 350, Ernst Leitz G.m.b.H., Wetzlar). The ^1H NMR-spectra were recorded on a Varian A 60 NMR-spectrometer operating at 60 Mc. All values of δ (ppm) are relative to TMS = 0. The IR-spectra were recorded on a Perkin-Elmer 337 spectrophotometer.

Cyclopentyl-phenyl-5-tetrazolylmethanol (V) was prepared from cyclopentylmagnesium bromide and 5-benzoyltetrazole [3] (III) as described for IV.[1] It could not be obtained in a crystalline, analytically pure form and was used without further purification as its structure was proved by its ^1H NMR-spectrum.

1,5- and 2,5-Disubstituted tetrazoles (I a–e, II a–e). The procedure outlined in Ref. 1 was used except that the reagents were stirred for 2 h. After isolation of the isomer mixtures (as oils) separation of the 1,5- and 2,5-disubstituted tetrazoles was performed by PLC on 20 × 100 cm plates with a 2 mm layer of silica gel (Merck PF_{254}), with a suitable eluent. After separation the compounds were crystallized. In one case (II a) the hydrochloride was prepared, as the free amine could not be obtained in a crystalline state.

Eluents, solvents of crystallization, yields and analytical data are given in Tables 1 and 2.

Diphenyl-5-[(1- or 2-ethyl)tetrazolyl]methanol (VI, VII). 0.01 mol of VIII,[4] 0.01 mol of sodium hydroxide, and 0.01 mol of ethyl bromide were dissolved in 0.5 ml of water and 5 ml of acetone. The mixture was kept at 40°C for 3 h, and then extracted with two 25 ml portions of ether. The etheral solution was dried with anhydrous magnesium sulphate, filtered and evaporated to an oily mixture of the isomers.

This residue was chromatographed on silica gel (Merck PF_{254}) using benzene-acetone 9:1 as an eluent. The isomers were identified by means of ^1H NMR-spectroscopy. Yields: VI 2 %; VII 9 %. Melting points: VI oil; VII 115.5–117.0°C. (Analysis, VII. Found: C 68.50; H 5.81; N 19.92. Calc. for $C_{16}H_{16}N_4O$: C 68.58; H 5.76; N 19.99.)

Acknowledgement. J. P. Jacobsen and H. K. Bildsø, Chem. Dept. V, H. C. Ørsted Institute, are acknowledged for their help in calculating the ^1H NMR-spectra.

REFERENCES

1. Balieu, E. and Klitgaard, N. A. *Acta Chem. Scand.* **26** (1972) 2951.
2. Fjalland, B. *Unpublished results.*
3. Yates, P. and Farnum, D. G. *J. Am. Chem. Soc.* **85** (1963) 2967.
4. a. Fischer, B. E., Tomson, A. J. and Horwitz, J. P. *J. Org. Chem.* **25** (1959) 1650; b. Hayamizu, K. and Yamamoto, O. *J. Mol. Spectry.* **25** (1968) 422.
5. Fraser, R. R. and Haque, K. E. *Can. J. Chem.* **46** (1968) 2855.
6. Sørensen, A. K. and Klitgaard, N. A. *Acta Chem. Scand.* **26** (1972) 541.
7. Lykkeberg, J. and Klitgaard, N. A. *Acta Chem. Scand.* **26** (1972) 266.

Received November 23, 1972.

ACTA CHEMICA SCANDINAVICA 27 (1973) 1240–1248

Transformation of Steroids by Cell-free Preparations of *Penicillium lilacinum* NRRL 895
II. Hydrolysis of Steroid Esters

KJELL CARLSTRÖM and KARL KROOK

Division of Applied Microbiology, Royal Institute of Technology and the Department of Obstetrics and Gynaecology, Sabbatsberg Hospital, Karolinska Institutet, Stockholm, Sweden*

Supernatants obtained after centrifugation at 100 000 g of homogenates of *Penicillium lilacinum* NRRL 895 were shown to contain inducible steroid esterase activity. Acetoxyl groups in positions 3α, 3β, 3(phenolic)17α(*sec*), 17β(*sec*), 20α, and 21 were hydrolyzed to the corresponding alcohols. The 6β, 11α, 17α(*tert*) and 20β-acetates were resistant to hydrolysis. Testosterone propionate was partially hydrolyzed, whereas testosterone oenanthate, benzoate, and hemisuccinate were unaffected. The influence of pH, of metals and of inhibitors was studied.

Hydrolysis of steroid esters is brought about by several organisms and was one of the first microbial steroid transformations to be reported.[1] Few systematic studies have, however, been carried out in cell-free systems. Partially purified steroid esterases from *Nocardia restrictus* and *Cylindrocarpon radicicola* have been studied by Sih and co-workers.[2–4] They found interesting differences in substrate specificity and stability properties of these two enzymes. Steroid lactonase and esterase activities in cell-free preparations of *Cephalosporium acremonium* were investigated by Holmlund and Blank, who claimed two different enzymes as being responsible for these activities.[5] They also prepared cellfree extracts of *Streptomyces roseochromogenes* and *Flavobacterium dehydrogenans var. hydrolyticus*, having steroid inducible esterase activity. However they did not pursue their study of the steroid esterase activity in these organisms. More recently, Lestrovaya *et al.* described the preparation of cell-free extracts from *Mycobacterium album*, containing inducible steroid esterase activity.[6,7]

The steroid transforming capacity of the fungus *Penicillium lilacinum* is well documented.[1] Hydrolysis of testololactone to testolic acid has been demonstrated by Prairie and Talalay in soluble and partially purified enzyme

* Present address.

preparations from this microbe.[8] During a study of the side chain cleavage of some progesterone derivatives in cell-free preparations of the fungus at this laboratory, it was observed that the 21-acetoxyl group of desoxycorticosterone acetate was easily hydrolyzed. It is well known that the hydrolysis of steroid esters and lactones will play an important role in the breakdown of steroids by several microorganisms.[1] This has led us to investigate the steroid esterase activity of *P. lilacinum* in somewhat greater detail.

Abbreviations and trivial names. DFP: diisopropyl fluorophosphate; GLC: gas liquid chromatography; GC-MS: gas chromatography-mass spectrometry; t_R: retention time relative to 5α-cholestane; Silyl: trimethylsilyl; TLC: thin layer chromatography; UV: ultraviolet. Androsterone: 3α-hydroxy-5α-androstane-17-one; Desoxycorticosterone: 21-hydroxy-4-pregnene-3,20-dione; Dehydroepiandrosterone: 3β-hydroxy-5-androsten-17-one; Epiandrosterone: 3β-hydroxy-5α-androstane-17-one; Epitestosterone: 17α-hydroxy-4-androsten-3-one; Oestrone: 3-hydroxy-1,3,5(10)-oestratriene-17-one; Progesterone: 4-pregnene-3,20-dione; Testololactone: 17a-oxa-4-androsten-3,17-dione; Testolic acid: 13-hydroxy-3-oxo-13,17-*seco*-4-androsten-17-oic acid; Testosterone: 17β-hydroxy-4-androsten-3-one.

MATERIALS AND METHODS

Steroids. All steroids were checked for purity by GLC and/or TLC. Steroid ester substrate solutions in ethanol were prepared immediately before use.

Androsterone and its acetate, 5α-cholestane, desoxycorticosterone acetate, dehydroepiandrosterone and its acetate, epiandrosterone and its acetate, oestrone, progesterone, 11α-hydroxyprogesterone and its acetate, 17α-hydroxyprogesterone, testosterone and its acetate, benzoate, oeanthate, and propionate were obtained from Sigma Chemical Company, St. Louis, Mo. Desoxycorticosterone, 20α- and β-hydroxy-4-pregnene-3-one were obtained from Ikapharm Ltd., Ramat-Gan, Israel. Epitestosterone and its acetate, 20α- and β-acetoxy-4-pregnene-3-one, oestrone acetate, 6β-hydroxyprogesterone, 17α-acetoxyprogesterone and testosterone hemisuccinate were obtained from Steraloids Inc., Pawling, N.Y.

6β-Acetoxy progesterone was prepared from the corresponding alcohol by acetylation with acetic anhydride in pyridine. The homogeneity of the acetylation product was checked by TLC and by hydrolysis to the parent alcohol.

Other chemicals. Solvents were of reagent grade and with the exception of the ethanol they were redistilled before use. The water used in the enzyme experiments was deionized and distilled in an all glass apparatus. All other chemicals were of reagent grade and were used without further purification. DFP was obtained from the Research Institute of National Defence (FOA), Ursvik, Sweden. Sodium phosphate buffer 0.06 M pH 7.2 was used throughout the investigation except in the stability test and occasionally in the washing of the cells where 0.06 M Tris-HCl pH 7.2 was used. The type of buffer does not affect the enzyme activity or the stability in frozen state.

Growth of organism and preparations of cell-free extracts. P. lilacinum NRRL 895 was grown on Czapek-Dox medium, induced, washed and frozen as described previously.[9] Testosterone acetate was used as inducer (70 mg in 2 ml of dimethylformamide per 300 ml culture). Cell-free extracts were prepared by grinding with sand as described previously but before the final centrifugation at 100 000 *g* the homogenates were frozen at −22° for at least 24 h. Before the 100 000 *g* centrifugation they were thawed and centrifuged at 6000 rpm for 15 min. A considerable amount of inactive precipitate is removed in this way. The supernatant was centrifuged in a Beckman-Spinco Model L ultracentrifuge at 100 000 *g* for 60 min. Phosphate buffer was added to the supernatant to give a fourfold dilution of the original homogenate. This diluted extract was immediately used in the enzyme experiments.

Transformation of steroid substrate. To 1 ml of diluted 100 000 *g* supernatant in a centrifuge tube, 0.3 μmol of steroid ester substrate in 10 μl of ethanol was added. After

Table 1. t_R- and R_F-values for the TLC and GLC systems described in the text.

Compound	t_R, OV-17 (1,2,3,4)	t_R, XE-60 (5)	t_R, SE-30 (6)	Internal standard in quantitative GLC	R_F-value
Cholestane	1.00	1.00	1.00		
Oestrone	1.47 (1)		0.51	Cholestane	0.52
Oestrone acetate	1.76 (1)			»	0.58
Testosterone	1.39 (2)			»	0.20
Testosterone acetate	1.70 (2)			»	0.47
Testosterone propionate	2.23 (2)			»	0.48
Testosterone oenanthate					0.55
Testosterone benzoate					0.54
Testosterone hemisuccinate					0.00
Testosterone silyl ether	0.95 (4)	2.17	0.67		
Epitestosterone	1.36 (1)			Cholestane	0.21
Epitestosterone acetate	1.61 (1)			»	0.44
Epitestosterone silyl ether	0.81 (4)	1.74	0.60		
Androsterone	0.87 (1)			Progesterone	0.26
Androsterone acetate	1.05 (1)			»	0.63
Androsterone silyl ether		0.87	0.46		
Epiandrosterone	0.93 (1)			Progesterone	0.27
Epiandrosterone acetate	1.24 (1)			»	0.66
Epiandrosterone silyl ether		1.27	0.56		
Dehydroepiandrosterone	0.89 (1)			Progesterone	0.24
Dehydroepiandrosterone acetate	1.18 (1)			»	0.58
Dehydroepiandrosterone silyl ether		1.20	0.51		
20α-Hydroxy-4-pregnene-3-one	2.22 (2)			Cholestane	0.23
20α-Acetoxy-4-pregnene-3-one	2.79 (2)			»	0.46
20α-Trimethylsilyloxy-4-pregnene-3-one	1.78 (4)	4.10	1.21		
20β-Hydroxy-4-pregnene-3-one	2.00 (2)			Cholestane	0.25
20β-Acetoxy-4-pregnene-3-one	2.63 (2)			»	0.48
Progesterone	2.15 (1)				
6β-Hydroxyprogesterone					0.17
6β-Acetoxyprogesterone					0.41
11α-Hydroxyprogesterone					0.05
11α-Acetoxyprogesterone					0.25
17α-Hydroxyprogesterone	3.27 (3)			Cholestane	0.31
17α-Acetoxyprogesterone	4.60, 2.27, 2.00 (3)			»	0.34
Desoxycorticosterone					0.20
Desoxycorticosterone acetate					0.40
Desoxycorticosterone silyl ether			1.87		

Indications	Column temp.	Carrier gas inlet pressure	Retention time for cholestane, min
(1)	237°	2.7 kp/cm²	16.2
(2)	247°	2.7 kp/cm²	11.5
(3)	257°	2.7 kp/cm²	8.2
(4)	250°	2.7 kp/cm²	9.8
(5)	228°	2.4 kp/cm²	7.35
(6)	240°	Gas flow 35 ml/min	8.35

mixing on a Vortex mixer for 5 sec, incubation took place on a shaking table at +26°. All incubations were run as duplicates. After the desired incubation time, the reaction was terminated in two ways, depending upon the type of steroid ester substrate. For esters of C_{18} and C_{19} steroids, 0.1 ml of 1 M HCl was added and the steroids were extracted with 4 ml of chloroform. The chloroform layer was dried over Na_2SO_4 and subjected to analysis. For esters of C_{21} steroids, 4 ml of acetone was added and the tube was shaken thoroughly. After cooling under running tap water for 30 min, the precipitate was removed by centrifugation and the supernatant was subjected to analysis. This latter procedure was used because of the water solubility of certain hydroxylated progesterone derivatives, *e.g.* desoxycorticosterone. Blanks without steroid substrate added were prepared and treated similarly. At the dilution of the extract used in these incubations, no interfering compounds from the inducer or the fungus could be detected. Unless otherwise stated, this procedure was used throughout the study and is referred to as the standard procedure.

Assay techniques. Before quantitative analysis, the samples were subjected to a qualitative TLC on Silica gel GF_{254} plates (100 × 200 mm) with ethyl acetate:benzene:hexane 5:4:4 as solvent (single run). Δ^4-3-ketosteroids were visualized in 254 nm UV light, other steroids with 10 % $SbCl_5$ in chloroform. In the alcohol/ester pairs oestrone/oestrone acetate and 17α-hydroxyprogesterone/17α-acetoxyprogesterone, the ester and the alcohol were poorly separated, and in these cases qualitative GLC on OV-17 was performed. The R_F-values in the TLC system are given in Table 1.

Samples showing formation of hydroxysteroids were quantitatively analyzed by GLC. A Perkin-Elmer F-11 MK II gas chromatograph with flame ionization detection was used. The column was a 2 m × 3 mm i.d. glass column, packed with 2.5 % OV-17 on AW-DMCS Chromosorb W, 80-100 mesh. t_R values are given in Table 1. The mean recovery in the whole analytical procedure, including the chloroform extraction was ≥ 95 % for testosterone and ≥ 95 % for testosterone acetate. The variation between the individual samples in the duplicate incubations for testosterone and testosterone acetate is given in Table 2.

Desoxycorticosterone and its acetate were quantitated by measurement of absorbance at 240 nm in a Beckman DB UV-VIS spectrophotometer. The ester and the alcohol were separated by TLC before the quantitation.

Protein assays were made by the biuret method.[10]

Identifications. Hydroxy steroids formed by enzymatic hydrolysis were identified on the basis of the following criteria:

(1) R_F-values in the TLC.

(2) t_R as free alcohols on 2.5 % OV-17, and as silyl ethers on 2.5 % XE-60 and on 1.5 % SE-30. Prior to the formation of the silyl esters, the hydroxysteroids were isolated by TLC.

(3) GC-MS analysis of the silyl ether derivatives in an LKB 9000 gas chromatograph-mass spectrometer. The conditions were the same as those previously described, except that the column temperature was 240° and the spectra were recorded in the *m/e* range 0 – 800.[9]

Table 2. Variation in duplicate incubations for testosterone and testosterone acetate. Single analysis of each sample. N = number of duplicate incubations. S.D. = $\sqrt{\sum d^2/2N}$.

Expressed in μmol steroid per tube	μmol steroid/tube	S.D.	N
Testosterone	0.157 (0.028 – 0.246)	±0.017	10
Testosterone acetate	0.182 (0.041 – 0.281)	±0.014	13
Expressed in mol % steroid	**Mol % steroid**	**S.D.**	**N**
Testosterone	62.3 (9.6 – 85.4)	±2.3	16
Testosterone acetate	37.7 (14.6 – 90.4)	±2.3	16

RESULTS

Effect of different steps in the preparation of the cell free extracts. The treatment of the culture with inducer steroids is an essential step for obtaining esterase active cell free extracts. To one of two 100 ml aliquots from the same 6 day culture, 35 mg of testosterone acetate in 1 ml dimethylformamide was added and to the other aliquot the dimethylformamide only. After 14 h of incubation, cell-free extracts were prepared and incubated with testosterone acetate for 15 min according to the standard procedure. With the extract from the steroid treated cells, 70.0 % of the substrate was hydrolyzed whereas the non induced cells yielded a completely inactive extract. Progesterone as well as testosterone acetate may be used as inducer.

Grinding the cells with sand yielded the most active cell free extracts and proved far more effective than treatment of the cells in an Elvehjem-Potter homogenizer or by sonication.

The crude homogenate obtained after the first 6000 rpm centrifugation is fairly stable at $-22°$, losing about 50 % of its activity in the course of three weeks. The stability of this preparation at three different temperatures is given in Fig. 1.

The freezing and thawing procedure removes a considerable amount of inactive protein. In one experiment the specific activity, expressed in μmoles testosterone acetate hydrolyzed by 1 mg protein in 15 min, increased from 0.78 to 1.24. The precipitate contained no esterase activity. This has previously been observed by Rahim and Sih for the steroid esterase of *C. radicicola*.[4] Attempts to purify the extracts by treatment with freeze cold CH_2Cl_2 according to Sih *et al.*[2] proved unsuccessful, despite extensive purification of the solvent. The CH_2Cl_2 treatment caused a 95 % inhibition of the activity.

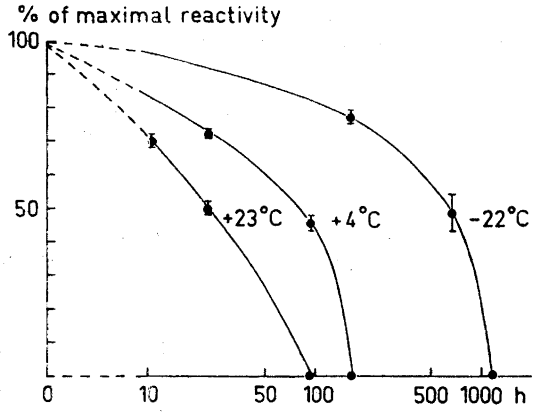

Fig. 1. Stability of crude cell free esterase preparations of *P. lilacinum* at three different temperatures.

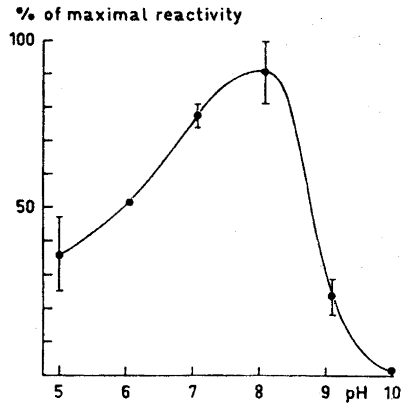

Fig. 2. pH-activity relationship for the hydrolysis of testosterone acetate by 100 000 *g* cell-free supernatants of *P. lilacinum*. Incubation time 2 min. Maximal hydrolysis of testosterone acetate = 15.9 %.

Enzymatic nature of the reaction. Influence of pH. Boiled extracts (100° for 5 min) were completely inactive, thereby demonstrating the enzymatic nature of the reaction. Hydrolysis of testosterone acetate was optimal at pH 8.1 (Fig. 2). The pH profile is similar to that obtained by Sih and co-workers for the steroid esterase of *N. restrictus*.[3]

Effect of inhibitors. Aliquots (1.0 ml) of the cell-free extract were preincubated with enzyme inhibitors at 1×10^{-3} M concentration for 15 min at 26°, The inhibitors were added in 0.1 ml phosphate buffer solution. Incubation with testosterone acetate was subsequently carried out for 2 min according to the standard procedure. In the controls without inhibitors 18.0 % of the substrate was hydrolyzed. $HgCl_2$ caused an inhibition of 100 %, and *p*-hydroxymercuri benzoate and NaF of 89 and 65 %, respectively. KCN, EDTA, 8-hydroxyquinoline, and NaN_3 were without significant effect.

The inhibition caused by the organophosphorus compound DFP is strongly dependent upon the concentrations of enzyme and inhibitor and of the preincubation time. The DFP was added as a freshly prepared 10 % (v/v) solution in ethanol. To the controls only ethanol was added. The results are given in Table 3. In concentrated extracts high concentrations of DFP are necessary for obtaining inhibition.

Table 3. Effect of DFP on the hydrolysis of testosterone acetate by 100 000 *g* cell-free supernatants from *P. lilacinum*. Preparation 1 is diluted with buffer according to the standard procedure, preparations 2 and 3 are undiluted.

Preparation	Protein mg/ml	DFP added	Preincubation time, min.	% hydrolysis	% inhibition
1	0.120	None		76.7	–
1	0.120	1×10^{-3}M	20	70.3	8.3
1	0.120	1×10^{-3}M	40	53.9	29.8
1	0.120	1×10^{-2}M	40	0	100
2	0.520	None		85.4	–
2	0.520	1×10^{-2}M	20	81.5	4.6
2	0.520	1×10^{-2}M	40	31.2	63.5
3	1.370	None		100	–
3	1.370	1×10^{-2}M	30	100	–

Effect of metal ions. 1×10^{-3} M concentrations of $MgCl_2$, $CaCl_2$, $MnCl_2$, $ZnCl_2$, $CuCl_2$, $NiCl_2$, and $CoCl_2$ had no significant effect upon the enzyme activity (incubation with testosterone acetate for 15 min according to the standard procedure, in the controls 40.4 % of the substrate was hydrolyzed). The type of buffer medium did not influence the effect of metals.

Substrate specificity. Different steroid esters were incubated with the enzyme preparation for 15 min following the standard procedure. The incubations were run in two series: Testosterone acetate plus esters of C_{18} and C_{19} steroids, and testosterone acetate plus esters of C_{21} steroids. In the two series,

Table 4. Substrate specificity of the steroid esterase activity in 100 000 *g* cell-free supernatants from *P. lilacinum*.

Steroid ester substrate	Position	% relative hydrolysis (testosterone acetate = 100 %)
Testosterone acetate	17β(sec)	100.0
Testosterone propionate	17β(sec)	16.9
Testosterone oenanthate	17β(sec)	0
Testosterone benzoate	17β(sec)	0
Testosterone hemisuccinate	17β(sec)	0
Epitestosterone acetate	17α(sec)	96.3
Androsterone acetate	3α	28.8
Epiandrosterone acetate	3β	92.8
Dehydroepiandrosterone acetate	3β	99.3
Oestrone acetate	3 (phenolic)	98.8
20α-Acetoxy-4-pregnene-3-one	20α	86.5
20β-Acetoxy-4-pregnene-3-one	20β	0
6β-Acetoxyprogesterone	6β	0
11α-Acetoxyprogesterone	11α	0
17α-Acetoxyprogesterone	17α (tert)	0
Desoxycorticosterone acetate	21	85.0

testosterone acetate was hydrolyzed to 80.3 % and 83.8 %, respectively. The hydroxy steroids formed were identified as described in Identifications. In all cases, TLC, GLC and mass-spectrometric properties were identical to those of the authentic reference compounds. The results are given in Table 4. A check was made to ensure that incubation with buffer only did not cause any hydrolysis of the steroid esters studied.

Testosterone acetate was readily hydrolyzed and testosterone propionate to a lesser degree. Testosterone oenanthate, benzoate, and hemisuccinate were unaffected. Acetoxyl groups at position 3α, 3β, 3 (phenolic), 17α (sec), 17β (sec), 20α and 21 were hydrolyzed whereas 6β, 11α, 17α (tert) and 20 β-acetates were resistant to hydrolysis.

DISCUSSION

Most of the properties shown by the steroid esterase activity of *P. lilacinum* resemble those reported for other microbial enzymes of this kind.[2–7] However when making such comparisons, the state of purification of the different esterase preparations must be taken into consideration. It is well known that such preparations usually contain more than one esterase and that substrate specificity as well as sensitivity to inhibitors may vary considerably for the individual esterases in one preparation.

A system for the classification of esterases into A-, B-, and C esterases on the basis of their sensitivity to organophosphorus inhibitors was introduced by Aldridge.[11] The steroid esterase activity in *P. lilacinum* is relatively insensitive to DFP but a definite classification is not possible with the crude preparation used. The insensitivity might be due to real insensitivity of the esterase or

to a rapid hydrolysis of the DFP by the esterase itself or by more specific DFP-hydrolyzing enzymes ("DFP-ase, Sarinase"). This might also explain the relative inertness towards organophosphorus inhibitors shown by the steroid esterase activity in *Septomyxa affinis* and of acetyl esterase preparations of fungal and plant origin.[12-14] DFP-hydrolyzing enzymes have previously been demonstrated in microorganisms.[15]

Like other microbial steroid esterases, this enzyme is sensitive to SH-reacting inhibitors such as *p*-hydroxymercuri benzoate.[2-5] However, during the preliminary experiments it was difficult to obtain reproducible results with this inhibitor for different cell-free preparations. The degree of inhibition reported for other enzymes of this kind also varies considerably.[2-5] It has been shown for the acetyl esterase in wheat germ that the inhibition caused by SH-reacting inhibitors strongly depends upon the type of substrate used and it was concluded that a typical SH-enzyme nature of this enzyme seemed doubtful.[13] This might also be valid for the microbial steroid esterases. With the exception of Hg^{2+}, metal ions and metal complexing and chelating agents had no significant influence upon the esterase activity. Fluoride exerted a strong inhibitory effect (65 % at 1×10^{-3} M) and the degree of inhibition was not dependent upon the type of buffer used (phosphate or Tris-HCl). The inhibition caused by fluoride is probably not due to any interaction with metals. It is well known that liver esterase and other hydrolytic enzymes not depending upon metals are strongly inhibited by fluoride.[16]

The substrate specificity roughly resembles that reported for the steroid esterases in *N. restrictus* and *C. radicicola*.[2-4] The differences shown might be of quantitative rather than qualitative character. As expected, all three preparations failed to hydrolyze the tertiary acetoxyl group in 17α-acetoxyprogesterone. However, a few cases of microbial hydrolysis of tertiary 17α-acetyl esters have been reported.[1,17] Of the epimeric 20-hydroxy-4-pregnene-3-ones, the 20α-epimer was easily hydrolyzed whereas the 20β-epimer resisted enzymatic hydrolysis. The inertness of the 20β-ester might be explained by steric hindrance from the C_{18} and C_{21} methyl groups and from the 12α-hydrogen. Similar selectivity in the hydrolysis of epimeric 20-acetates has previously been demonstrated in *Aspergillus ochracaeus*.[18] Hydrolysis of 20β-acetates has, however, been reported for *Flavobacterium dehydrogenans* and for the steroid esterase from *N. restrictus*.[1,2]

Acknowledgement. The GC-MS analysis was carried out at the Department of Chemistry 1, Karolinska Institutet, Stockholm, Sweden.

REFERENCES

1. Charney, W. and Herzog, H. L. *Microbial Transformations of Steroids. A Handbook*, Academic, New York and London 1967.
2. Sih, C. J., Laval, J. and Rahim, M. A. *J. Biol. Chem.* **238** (1963) 566.
3. Rahim, M. A. and Sih, C. J. *J. Biol. Chem.* **241** (1966) 3615.
4. Rahim, M. A. and Sih, C. J. *Microbial Steroid Esterases.* In Colowick, S. P. and Kaplan, N. O., Eds., *Methods of Enzymology*, Academic, New York and London 1969, Vol. 15, p. 675.
5. Holmlund, C. E. and Blank, R. H. *Arch. Biochem. Biophys.* **109** (1965) 29.

6. Lestrovaya, N. N., Koshchenko, K. A. and Ksandopulo, G. B. *Izv. Akad. Nauk SSSR, Ser. Biol.* **5** (1969) 773; *Chem. Abstr.* **72** (1970) 62907.
7. Lestrovaya, N. N., Ksandopulo, G. B. and Karasevich, Zh. G. *Mikrobiologiya* **40** (1971) 461; Chem. Abstr. **75** (1971) 85547.
8. Prairie, R. L. and Talalay, P. *Biochemistry* **2** (1963) 203.
9. Carlström, K. *Acta Chem. Scand.* **26** (1972) 1718.
10. Lowry, O. H., Rosebrough, N. J., Farr. A. L. and Randall, R. J. *J. Biol. Chem.* **193** (1951) 265.
11. Aldridge, W. N. *Biochem. J.* **53** (1953) 110.
12. Miller, T. L. *Biochim. Biophys. Acta* **270** (1972) 167.
13. Oosterbaan, R. A. and Jansz, H. S. *Cholinesterases, Esterases and Lipases (Review)*. In Florkin, M. and Stotz, E. H., Eds., *Comprehensive Biochemistry*, Elsevier, Amsterdam, London and New York 1965, Vol. 16.
14. Krisch, K. *Carboxylic Ester Hydrolases (Review)*. In Boyer, P. D., Ed., *The Enzymes*, 3rd Ed. Academic, New York and London 1971, Vol. V, p. 43.
15. Mounter, L. A., Baxter, R. F. and Chanutin, A. *J. Biol. Chem.* **215** (1955) 699.
16. Wiseman, A. *Effect of Inorganic Fluoride on Enzymes (Review)*. In Smith, F. A., Ed., *Handbuch der experimentellen Pharmakologie*, Springer-Verlag, Berlin, Heidelberg and New York 1970, p. 48.
17. Noguchi, S., Otsuka, H. and Takahashi, T. *Japan. Pat.* 71 16. 149, May 1, 1971; Chem. Abstr. **75** (1971) 74910.
18. Lewbart, M. L. and Schneider, J. J. *J. Org. Chem.* **29** (1964) 2559.

Received November 7, 1972.

ACTA CHEMICA SCANDINAVICA 27 (1973) 1249–1254

Palladium(II) Catalyzed Aromatic Acetoxylation

II. Nuclear Acetoxylation of Aromatic Compounds: A Reversal of the Usual Isomer Distribution Pattern in Aromatic Substitution

LENNART EBERSON* and LUIS GOMEZ-GONZALEZ

Division of Organic Chemistry 1, Chemical Center, University of Lund, P.O. Box 740, S-220 07 Lund, Sweden

The reaction between monosubstituted aromatics and Pd(II) acetate in acetic acid in an oxygen atmosphere has been investigated. The monoacetoxylation products from compounds containing *o,p*-directing substituents were found to consist of predominantly *meta* isomer, whereas one compound with a *meta*-orienting substituent was found to give mainly *o,p*-acetoxylation. Thus the isomer distributions observed are reversed with respect to ordinary electrophilic aromatic substitutions. Polymethylsubstituted benzenes were found to give side-chain acetoxylation products.

The first paper in this series [1] reported a study of the oxidation of *p*-xylene with Pd(II) acetate in acetic acid. The objective of this study was to optimize the reaction parameters for formation of the *nuclear* acetoxylation product, 2,4-dimethylphenyl acetate (I), in competition with primarily the α acetates II–IV and other compounds, such as biaryl V.

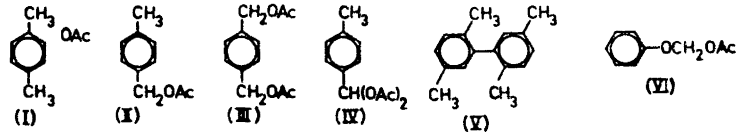

The best relative yields of I were realized when the oxidation was carried out in the presence of oxygen at reflux temperature with only Pd(II) acetate present. Addition of alkali metal acetates strongly favors side-chain acetoxylation. Under these conditions a I/II ratio of 70:30 was obtained, and the reaction was catalytic in the Pd(II) species, although it had the disadvantage

* To whom inquiries should be addressed.

of being very slow. Nevertheless, we felt it would be of considerable interest to elucidate the characteristics of this direct nuclear acetoxylation process. This paper is a report [2] of the Pd(II) acetate oxidation of a series of aromatic compounds with the goal of determining the isomer distribution of the monoacetoxy derivatives. The results obtained reveal an unusual and interesting effect, in that predominant *meta* substitution is observed in the acetoxylation of compounds with substituents which behave as *ortho,para*-directing in normal electrophilic aromatic substitutions.

RESULTS

The compounds listed in Table 1 were chosen so as to make only nuclear substitution possible, and were oxidized with Pd(II) acetate in glacial acetic acid at 115° in an oxygen atmosphere. Product distributions were determined at low conversion, the [Pd(II)]/[substrate] ratio being kept at about 0.1 in order to favor the acetoxylation process. Lower ratios tend to produce more of the biaryl products (see below).

Table 1. Isomer distributions in Pd(II) acetate acetoxylation,[a] anodic acetoxylation,[b] and diisopropyl peroxydicarbonate-cupric chloride oxygenation[c] of aromatic compounds.

Compound	Pd(II) acetate acetoxylation			Anodic acetoxylation			$(i\text{-PrOCO}_2)_2$-$CuCl_2$ oxygenation[d]		
	o(α)	*m*(β)	*p*	*o*(α)	*m*(β)	*p*	*o*(α)	*m*(β)	*p*
t-Butylbenzene	–	95	5	35	22	43			
Anisole	1	97	2	67	4	29	63	1	36
Biphenyl	2	98	–	31	1	68	47	4	49
Chlorobenzene	3	88	9	37	6	58	54	13	33
Bromobenzene	5	81	14	30	3	67			
Iodobenzene	25	69	6	17	4	79			
Methyl benzoate	44	35	21	No reaction					
Toluene[e]	19	62	19	43	11	46	57	15	28
Naphthalene	56	44		94	4		92	8	

[a] [Pd(II)]/[substrate]≈0.1, temp. 115°, oxygen atmosphere, reaction period 4 h. [b] In HOAc/0.5 M NaOAc at 25°, Pt anode. [c] For experimental conditions, see Ref. 4. [d] Aryl isopropyl carbonates are formed. [e] Henry [5] reported this distribution under conditions differing from those employed here; potassium dichromate was present as a co-oxidant in a strongly acidic medium (CH_3SO_3H in HOAc).

Table 1 shows the isomer distributions of the acetates formed. A strong preponderance of *meta* substitution is observed for compounds with *o,p*-directing substituents. In line with this behavior, the proportion of β isomer from naphthalene is unusually high, although it is not the major product. If a *meta*-orienting substituent is present, as in methyl benzoate, the isomer distribution is in favor of the *ortho* and *para* isomers, again a reversal of the normal substitution pattern in aromatic substitution. For comparison, isomer distributions from two other direct aromatic oxygenation reactions, anodic

acetoxylation [3] and oxygenation with diisopropyl peroxydicarbonate-cupric chloride,[4] are included in Table 1. Both of these processes show isomer distributions characteristic of electrophilic aromatic substitutions. For certain substrates, side-reactions occurred with formation of products other than acetoxy derivatives. From naphthalene, two binaphthyls (ratio of 1,1′- to 1,2′-binaphthyl 22 : 78) were detectable in a yield corresponding to 1 % of the two acetoxynaphthalenes. In the *t*-butylbenzene reaction, small amounts of toluene and phenol were observed. In the oxidation of anisole, the nuclear acetates were not the main products. Instead, cleavage of the CH_3-O bond to give phenol and attack on the methyl group to give acetoxymethyl phenyl ether (VI) are important side-reactions, the distribution of phenol, VI, and nuclear acetates being 63, 17, and 17 %. In addition, 1 % of dimethoxybiphenyls (three isomers) was detected together with small amounts of three unidentified products.

Chloro- and bromobenzene gave in addition to the acetates traces of phenol and phenyl acetate. Iodobenzene gave only 12 % iodophenyl acetates, the remaining part of the product mixture consisting of phenyl acetate (23 %), biphenyl (31 %), and two isomers of diiodobenzene (together 34 %).

Phenyl acetate did not undergo acetoxylation under the conditions specified,[5] phenol and diacetoxybiphenyls (at least four isomers) being the only products found.

For three substrates, naphthalene, *t*-butylbenzene, and methyl benzoate, we also studied the influence of adding aluminium chloride (a Lewis acid), triphenylphosphine (a Lewis base) and tetrabutylammonium acetate (TBA). The possible mode of action of these additives was described in Part I.[1] The results are shown in Tables 2 (naphthalene) and 3 (*t*-butylbenzene). For methyl benzoate it suffices to say that all three additives completely suppressed the acetoxylation process, biaryl coupling being the favored process in the presence of aluminium chloride and triphenylphosphine.

Table 2. Effect of additives on the Pd(II) acetate acetoxylation of naphthalene in acetic acid at 115° in an oxygen atmosphere; reaction period 4 h; [Pd(II)]/[naphthalene] = 0.1.

[Additive]/[Pd(II)]	Nuclear acetoxylation		Binaphthyls			Ratio acetoxy/biaryl
	α	β	1,1′	1,2′	2,2′	
– –	56	44	22	78	–	100
$[AlCl_3]/[Pd(II)] = 1$	89	11	15	67	18	1
$[PPh_3]/[Pd(II)] = 1$	58	42	18	72	–	100
[TBA]/[Pd(II)] = 10	73	27	26	74	–	100

In the naphthalene experiments (Table 2) aluminium chloride changed the isomer distribution for acetoxylation toward a more normal 89 : 11 ratio between α and β isomer, whereas triphenylphosphine left it unchanged. TBA had a small effect toward increasing the amount of α isomer. As in the case of *p*-xylene,[1] aluminium chloride strongly increased the proportion of biaryl

Table 3. Effect of additives on the Pd(II) acetate acetoxylation of *t*-butylbenzene in acetic acid at 115° in an oxygen atmosphere; reaction period 4 h; [Pd(II)]/[*t*-butylbenzene] = 0.1.

[Additive]/[Pd(II)]	Nuclear acetoxylation			Biaryl coupling products
	o	*m*	*p*	
–	–	95	5	–
$[AlCl_3]/[Pd(II)] = 1$	–	–	–	Main product
$[PPh_3]/[Pd(II)] = 1$	–	92	8	Traces
[TBA]/[Pd(II)] = 10	–	95	15	Traces

product. The results with *t*-butylbenzene (Table 3) were similar to those with naphthalene: Aluminium chloride strongly favored biaryl coupling, triphenylphosphine had little effect, and TBA changed the isomer distribution of acetoxy derivatives toward a more "normal" one.

A number of different polymethylbenzenes were also oxidized under identical conditions in order to study the competition between nuclear and side-chain acetoxylation. As demonstrated in Table 4, only *p*-xylene gave a nuclear

Table 4. Product distributions in the Pd(II) acetate acetoxylation of methylsubstituted aromatic hydrocarbons in acetic acid at 115° in an oxygen atmosphere; reaction period 4 h; [Pd(II)]/[substrate] = 0.1.

Ar in Ar–CH_3	ArCHO	$Ar'(CHO)_2$[a]	$ArCH_2OH$	$ArCH_2OAc$	Ar'' < CH_2OH[b] / CH_2OAc	Nuclear acetate
4-$CH_3C_6H_4$	56			7		37
3,5-$(CH_3)_2C_6H_3$	82		7	11		–
2,4,5-$(CH_3)_3C_6H_2$	63	8	7	21		–
3,4,5-$(CH_3)_3C_6H_2$	48[c]	11		10	30[d]	–
2,3,4,5-$(CH_3)_4C_6H$	18[e]	3[f]		28[g]	50[i]	–
				trace[h]		

[a] No attempt was made to establish the exact structure of the dialdehydes. [b] Denotes a compound derived from the substrate by substitution with one hydroxy and one acetoxy group. No attempt was made to establish the exact structure of these compounds; mass spectral data indicate that both substituents appear in the methyl groups. [c] Three isomers in the proportions 20 : 36 : 44. [d] Four isomers (1 : 2 : 19 : 78). [e] Three isomers (8 : 14 : 78). [f] Four isomers (6 : 7 : 29 : 58). [g] 2,3,5,6-Isomer. [h] 2,3,4,5-Isomer. [i] Two isomers (9 : 91).

acetate, whereas the higher polymethylbenzenes studied gave side-chain acetates. At very low conversion, mesitylene also gives a trace of nuclear acetate. In most cases a large proportion of aldehyde and dialdehyde(s) was present in the product mixture, which is characteristic for reactions carried out under oxygen.[1] From isodurene and pentamethylbenzene, products derived from substitution by one hydroxyl and one acetoxy group were obtained in relatively large amounts.

The acetoxylation of one heteroaromatic compound, thiophene, was attempted, but failed consistently. Incidentally, anodic acetoxylation also fails in this case.[6] Only bithienyls were formed under the conditions employed (see Table 5).

Table 5. Isomer distribution in the biaryl coupling of thiophene in acetic acid.

Reaction conditions	Bithienyls 2,2′	2,3′	3,3′
$PdCl_2$/NaOAc, reflux	56	44	Traces
$Pd(OAc)_2/O_2$/111° (3 h)	93	7	–
$Pd(OAc)_2$/Ar/NaOAc (3 h)	83	15	–

Some preparative experiments were run with naphthalene as substrate, and were conducted under conditions known to make the process catalytic in Pd(II) species: Pd(II) acetate in acetic acid, reflux temperature, oxygen bubbling, no additive, [Pd(II)]/[substrate]≈0.01). Table 6 summarizes the

Table 6. Yields and product distribution in the oxidation of naphthalene (3.3 M) with Pd(II) acetate (0.03 M) in acetic acid at reflux temperature after 400 h.

	Naphthyl acetates α+β	Binaphthyls 1,1′	1,2′	2,2′	Oligomers[a]
Yield, g	0.75	15.3	17.8	3.9	33.8
Yield, mmol	4.03	60.2	70.8	15.2	89.0[b]
Yield, %	45	670	790	170	1490[b]

[a] Mixture of trimer (15 %), tetramer (65 %), pentamer (19 %), and hexamer (1 %). [b] Calculated on the basis that the whole mixture consists of trimer.

distribution and yields of products after a reaction period of 400 h; at the low [Pd(II)]/[substrate] ratio employed, the biaryl coupling process is seen to be strongly favored, binaphthyls and higher oligomers being by far the major products. Apparently the successful application of the acetoxylation reaction among other things demands conditions at which [Pd(II)]/[substrate] can be kept at a much higher value, *e.g.*, by continuously adding the substrate as the reaction progresses. The conclusion arrived at in Part I[1] with regard to preparative applications still appears to be valid: Nuclear acetoxylation mediated by Pd(II) acetate is an impractically slow process. It is, however, synthetically interesting due to its unusual tendency toward *meta* substitution. We are at present working on the problem of speeding up the reaction while retaining the anomalous features with respect to orientation.

The discussion of the results will be deferred to Part III[7] of this series.

EXPERIMENTAL PART

Materials. Substrates and other chemicals used were purchased in the highest quality available and further purified by recrystallization, distillation, or preparative gas chromatography, if deemed necessary. Reference compounds (acetoxy compounds,[3] aldehydes, biaryls, *etc.*) were synthesized according to well known procedures. The identity and purity of all compounds were checked by mass, IR, and NMR spectral analysis as well as by gas chromatography. Retention times (Perkin-Elmer Model 880 gas chromatograph, equipped with an electronic integrator) for nuclear acetates are given in Table 7.

Table 7. Retention times[a] for nuclear acetates.

Substrate	Retention times, nuclear acetates			Column temperature
	o(α)	*m*(β)	*p*	
Naphthalene	44	49		200
t-Butylbenzene	39.0	41.3	50.5	155
Anisole	25.3	34.4	37.2	155
Phenyl acetate	27.6	38.5	40.0	170
Biphenyl	13.9	31.8	35.1	200
Chlorobenzene	25.1	30.8	31.9	150
Bromobenzene	35.7	45.5	47.5	155
Iodobenzene	34.2	44.2	46.5	180
Methyl benzoate	13.8	29.8	41.6	190

[a] Analyses were performed on a 4 m × 0.3 cm 10 % Apiezon L on Chromosorb W column, except for the biphenyl products, where a 3 m × 0.3 cm 5 % neopentylglycol succinate on Chromosorb W column was used.

For side-chain acetates the following values were found on a 3 m × 0.3 cm 5 % neopentylglycol succinate on Chromosorb W column (temperature of column and retention time in min given in parentheses): 2,4,6-trimethylphenyl (165°, 9.5), 2,4-dimethylbenzyl (165°, 12.0), 2,3,5,6-tetramethylphenyl (165°, 19.6), 2,4,5-trimethylbenzyl (165°, 22.3), 2,4,6-trimethylbenzyl (165°, 19.5), 2,3,5,6-tetramethylbenzyl (180°, 26.7), 2,3,4,6-tetramethylbenzyl (180°, 27.4), and 2,3,4,5-tetramethylbenzyl acetate (180°, 32.9).

Oxidation experiments were performed according to either of the two methods described in Part I.[1] Identification of compounds was based on mass spectral analysis alone, or mass spectral/gas chromatographic comparison with authentic samples (LKB 9000 system).

Acknowledgements. We wish to gratefully acknowledge the generous financial support we have obtained from the *Swedish Board for Technical Development* (L. E.) and the *Faculty of Science, University of Lund* (L. G.).

REFERENCES

1. Eberson, L. and Gomez-Gonzalez, L. *Acta Chem. Scand.* **27** (1973) 1162.
2. A preliminary report has been published; Eberson, L. and Gomez-Gonzalez, L. *Chem. Commun.* **1971** 263.
3. Eberson, L. *J. Am. Chem. Soc.* **89** (1967) 4669.
4. Kovacic, P., Reid, G. and Kurz, M. E. *J. Org. Chem.* **34** (1969) 3302; Kurz, M. E., Kovacic, P., Bose, A. K. and Kugajevsky, I. *J. Am. Chem. Soc.* **90** (1968) 1818.
5. The formation of traces of diacetoxybenzenes has been reported under significantly different conditions; Henry P. M. *J. Org. Chem.* **36** (1886) 1971.
6. Eberson, L. and Nyberg, K. *Unpublished observations.*
7. Eberson, L. and Gomez-Gonzalez, L. *Acta Chem. Scand.* **27** (1973) 1255.

Received October 25, 1972.

ACTA CHEMICA SCANDINAVICA 27 (1973) 1255–1267

Palladium(II) Catalyzed Aromatic Acetoxylation

III. Reaction between Pd(II) Complexes and Organic Electron Transfer Reductants

LENNART EBERSON* and LUIS GOMEZ-GONZALEZ

Division of Organic Chemistry 1, Chemical Center, University of Lund, P.O. Box 740, S-220 07 Lund, Sweden

Two compounds, 9,10-diphenylanthracene and tetra-*p*-anisylethylene, known to undergo facile electron transfer oxidation, have been allowed to interact with $Pd(CH_3CN)_2(BF_4)_2$ in acetonitrile. For the former substrate no reaction was observed, whereas the latter gave a blue complex, presumably of the π-type. Treatment of this complex with 3,5-lutidine caused an intramolecular coupling process to occur (formation of a phenanthrene derivative), whereas addition of water regenerated the parent compound in a ligand displacement reaction. Thus, it appears improbable that the initial process in the oxidation by Pd(II) complexes is an electron transfer to give a cation radical.

The mechanism of the reaction between Pd(II) complexes and aromatics is discussed. It is proposed that a π-complex between Pd(II) and the aromatic substrate is first formed, followed by (1) attack of a nucleophile at a ring position to give an arylpalladium adduct, (2) attack of a base at an α hydrogen, if available, to form a benzylpalladium adduct, and/or (3) direct collapse to give a Wheland-type intermediate. These three possibilities appear to give a reasonably satisfactory picture of the reaction.

The first two papers of this series [1,2] have dealt with attempts to establish optimal reaction conditions for the Pd(II) catalyzed nuclear acetoxylation of the model compound, *p*-xylene,[1] and the application of these findings to other aromatic substrates.[2] It was shown that under the most favorable conditions nuclear acetoxylation is a fairly general reaction, albeit an impractically slow one, and that the isomer distribution of acetoxy products is *reversed* as compared to ordinary electrophilic substitutions. Part I also dealt in some detail with the problem of defining the oxidizing species present in the reaction mixture, and it was concluded that the Pd(II) acetate monomer (I) is the oxidizing species above 35° in acetic acid in the presence of tetra-

* To whom inquiries should be addressed.

butylammonium acetate or in the absence of excess acetate with a metal as the counterion, whereas in the presence of an alkali metal acetate Pd(II) is bound as a binuclear complex (II). We now wish to report some additional

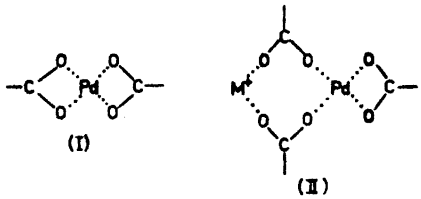

(I) (II)

results with a bearing on the possible mechanism of Pd(II) oxidation of aromatics. The results from the two preceding papers [1,2] will be discussed in this context.

RESULTS

Our approach in this paper has been to subject compounds which are known to undergo *facile oxidation* via *electron transfer* to give either cation radicals or dications to oxidation by Pd(II) complexes in order to be able to compare the observed behavior with that of known processes. Two compounds were especially attractive from this point of view: 9,10-Diphenylanthracene (DPA) and tetra-*p*-anisylethylene (TAE), since their behavior upon electron transfer is well known from electrochemical investigations. Thus, DPA is oxidized anodically in $CH_3CN/LiClO_4$,[3] CH_2Cl_2/Bu_4NClO_4,[4] and $C_6H_5NO_2/Pr_4NClO_4$ [5] to form stable solutions of its cation radical ($DPA^{+\cdot}$), whereas TAE gives a reasonably stable solution of the corresponding dication, TAE^{2+}, in equilibrium with a low concentration of the cation radical in $CH_3CN/LiClO_4$.[6,7]

Given these characteristic reactions, it was of interest to use DPA and TAE as diagnostic tools for finding out whether Pd(II) complexes can act as electron transfer oxidants with the formation of radical cations or dications. Since both $DPA^{+\cdot}$ and TAE^{2+} are sensitive toward nucleophiles, such as acetate ion, it was necessary to find a Pd(II) complex with less nucleophilic ligands. An accompanying favorable feature of such a complex would be its higher oxidation potential. A complex of this type is $Pd(CH_3CN)_2(BF_4)_2$ (III), reported a few years ago by Schramm and Wayland.[8] Acetonitrile is a very weak nucleophile and fluoroborate ion is virtually inert in this respect.

Treatment of DPA with complex III in CH_3CN solution gave no reaction, and the introduction of oxygen produced no change either. Thus no electron transfer from DPA to Pd(II) takes place. Oxidation of DPA with Pd(II) acetate in acetic acid at 115° under oxygen gave no 9,10-diacetoxy-9,10-dihydro-9,10-diphenylanthracene, the normal product from electron transfer oxidation of DPA in the presence of acetate ion.[9] Also here electron transfer from DPA to Pd(II) apparently does not take place.

Interaction of TAE with III in acetonitrile at 20° under argon resulted in the slow appearance of a blue colour (λ_{max} at 568 and 300 nm, compared to

those of TAE and III alone, 315 and 280 nm) which is slowly converted to a yellow one (λ_{max} 482 nm). TAE^{2+} is known to possess a characteristic blue colour with λ_{max} at 575 nm in ethylene chloride,[10,11] but that the blue colour is not due to the dication in the Pd(II) case is shown by cyclic voltammetry of the blue solution produced from TAE and III. The cyclic voltammogram in $CH_3CN/LiClO_4$ has the appearance shown in Fig. 1, which clearly indicates

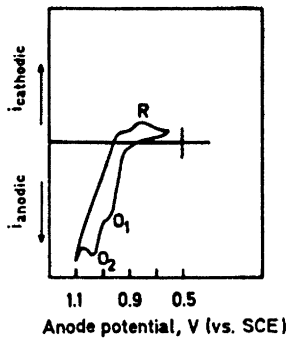

Fig. 1. Cyclic voltammogram of the TAE–Pd(II) complex in $CH_3CN/LiClO_4$ at a Pt button anode.

that a species different from TAE^{2+} must be present. The TAE/TAE^{2+} system displays an almost perfectly reversible single-step cyclic voltammogram under the same conditions. Instead we interpret the voltammogram as being due to a complex between Pd(II) andTAE, for simplicity referred to as IV in the following. This complex undergoes two oxidation steps at O_1 and O_2 and a reduction step at R, the latter presumably being due to reduction of a compound formed at O_1 or O_2. We do not wish to speculate further about the nature of these redox processes, since for the purpose at hand it is sufficient to establish that TAE^{2+} is not present.

In line with the assumption that IV is formed from III and TAE in acetonitrile solution, addition of water caused the blue colour to disappear immediately and TAE to precipitate. This must be due to a displacement of TAE in IV by water. Also by addition of 3,5-lutidine the colour disappeared, but in this case TAE was not recovered unchanged. Instead the phenanthrene derivative V could be isolated, together with unchanged starting material.

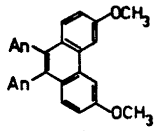

(V)

An = *p*-anisyl

This type of behavior is known from the anodic oxidation of TAE in CH_3CN/Et_4NClO_4.[12] Apparently proton abstraction by lutidine from IV or a similar complex can cause intramolecular coupling in a way at least formally resembling that proposed earlier[13] for intermolecular coupling of aromatics by Pd(II) chloride in the presence of acetate ion (see also Discussion).

Oxygen had an interesting effect upon the formation of the blue complex and its conversion into the yellow one, in that the reactions were speeded up considerably. Thus the blue colour appeared after a few minutes (in argon after 6 h), turned blue-greenish after 3 h, and yellow after standing overnight. In argon the blue colour persists for several days. Attempts to study these transformations quantitatively by UV spectrophotometry failed due to side-reactions between III and acetonitrile.

Finally, *p*-xylene, as a representative of a compound that is much more oxidation-resistent than DPA or TAE, was refluxed with III with no solvent, whereupon a small amount of *N*-(*p*-methylbenzyl)acetamide, together with 2,5,4′-triphenyldiphenylmethane as the major product, was isolated. This reaction is formally analogous to a similar electrode process, anodic oxidation of *p*-xylene in $CH_3CN/NaClO_4$, in which the same compounds are formed and postulated to originate *via* a mechanism involving a sequence of electron transfer and chemical steps.[14,15]

DISCUSSION

Previous mechanistic proposals. It is appropriate to start the discussion of the results described in this series of papers (in the following to be referred to as Parts I, II, and III) by bringing to mind Maitlis' general statement [16] about organic reactions catalyzed by transition metals:

"A curious feature of reactions catalyzed by transition metals is the relative lack of evidence for the typical reactive intermediates of organic chemistry, carbanions and carbonium ions. This probably arises from the metal acting both as a source and a sink of electrons and making such ionic intermediates energetically unfavorable. Although organic free radical intermediates have been postulated as intermediates in metal-catalyzed reactions, there is again little evidence for them. Most reactions should, therefore, on present evidence, be regarded as occurring largely within the coordination sphere of the metal."

Such a generalization, based as it is upon a scrutiny of hundreds of mechanistic suggestions for transition metal mediated reactions,[17] should carry great weight in any discussion of Pd(II) catalyzed processes, and it is therefore a suitable starting point to review previous mechanistic proposals for reactions between Pd(II) complexes and aromatics with this statement in mind.

Van Helden and Verberg [13] studied the biaryl coupling reaction that takes place when aromatics are treated with sodium acetate and Pd(II) chloride (ratio 5:1, no reaction was observed in the absence of acetate) in acetic acid at 90°. The reaction was found to be first order in benzene and in Pd(II) chloride, and independent of [NaOAc]. The isomer distribution of biaryls was that characteristic for an electrophilic process, and electron-withdrawing substituents had a weak rate-decreasing effect, whereas the opposite was true for electron-donating substituents. Sterically demanding substituents had an adverse effect upon the yield of biaryl(s). A mechanism involving a rate-determining electrophilic attack of Pd(II) chloride on the aromatic ring to form a σ-complex (VI), as exemplified in eqn. (1) for benzene, was proposed. VI would then react with acetate ion in a fast reaction to form a π-cyclo-

hexadienyl complex (VII), which dimerizes rapidly to binuclear complex VIII. Breakdown of VIII gives the products shown in eqn. (2).

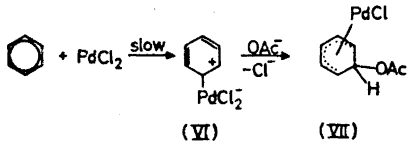

(VI) (VII) (1)

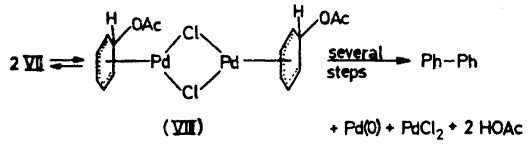

(VIII) + Pd(0) + $PdCl_2$ + 2 HOAc (2)

In the oxidation of toluene, an increase in the [NaOAc]/[Pd(II)] ratio (Na/Pd ratio) from 5 to a value between 10 and 15, under otherwise identical conditions, changes the nature of the product, in that side-chain (α) acetoxylation becomes the predominant process.[18,19] Use of Pd(II) acetate instead of the chloride in this reaction gives acetoxylation also at *low* Na/Pd ratios and in the absence of added acetate.[20] It was suggested [19] that the coupling reaction requires an aggregate of two or more palladium ions connected by a bridging ligand. Such polynuclear complexes should be easily broken down by acetate ion in the case of Pd(II) acetate but less easily so when chloride ion, a more effective bridging ligand, is present. However, this mechanism does not account for the necessity [13] of having a moderate amount of NaOAc present in order to obtain biaryls. On the contrary, if only the good bridging ligand, chloride ion, is necessary, optimal yields of biaryls would be expected without NaOAc. Moreover, it is difficult to explain the strong favorable effect of perchloric acid upon biaryl coupling [19,23] *via* Pd(II) acetate, since no good bridging ligand is present in this case (see below).

In this context it is important to note that two stable benzylpalladium complexes (IX and X) have been isolated and characterized.[21] Both compounds on treatment with KOAc in HOAc at 100° give benzyl acetate, whereas with AgOAc under identical conditions benzyl acetate and benzylidene acetate are formed.

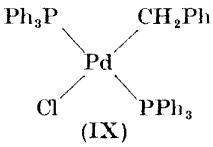

(IX)

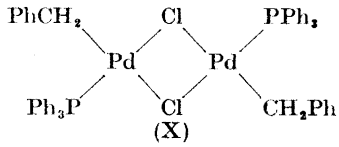

(X)

Oxygen strongly influences the ratio between acetoxylation and biaryl coupling. Under 100 atmospheres of oxygen, a reaction mixture containing toluene as substrate, which would normally give essentially only acetoxyla-

tion product, gave almost exclusively biaryl coupling, apparently by suppression of acetoxylation and a slight acceleration of coupling.[19] Complete absence of solvents like acetic acid and a high oxygen pressure in the Pd(II) acetate catalyzed oxidation of aromatics has actually turned out to be the best conditions hitherto found to effect biaryl coupling.[22] Nuclear acetoxylation is also almost completely suppressed at high oxygen pressure,[19] the biaryl coupling being again slightly accelerated.

Davidsson and Triggs [19,23] noted a strong accelerating effect by perchloric acid upon biaryl coupling by Pd(II) acetate in acetic acid. Kinetic studies [23] with benzene as the substrate showed the reaction to be first order in monomeric Pd(II) and first order in benzene. For hexadeuteriobenzene, a large primary isotope effect, $k_H/k_D = 5.0$, was determined in analogy to that found in the mercuration of benzene. At 100° Pd metal is the product of reduction, whereas at temperatures below 60°, Pd(I) is formed. The results for the acid-catalyzed reaction were interpreted in terms of a rate-determining electrophilic palladation reaction to form an arylpalladium complex (eqn. (3)), followed by a fast, bimolecular concerted recombination step, giving biaryl and Pd(0) or Pd(I) complex (eqn. 4).[23] The role of perchloric acid would then presumably

$$Ar-H + Pd^{2+} \rightarrow Ar-Pd^{+} + H^{+} \quad (3)$$

$$2\ Ar-Pd^{+} \rightarrow Ar-Ar + 2\ Pd^{+} \quad (4)$$

be to increase the electrophilicity of Pd(II), although it was not stated how this would take place in molecular terms. Since the strongly acidic conditions mean that no acetate ion can be present, the only remaining ligands are HOAc and perchlorate ion. Formation of $Pd(ClO_4)_2$ was actually suggested later.[24]

More support for the formation of arylpalladium intermediates stems from the fact that aromatic organometallics, *e.g.* organomercury compounds [24] and arylboronic acids [23] undergo biaryl coupling upon treatment with Pd(II) acetate. Substitution of the metal by Pd(II) to form Ar–Pd(II) species is a well-established mechanism [17] in palladium chemistry.

Even more complicated systems have been shown to give good yields of biaryls. Thus, complexes of the type olefin-Pd(II) chloride gave biaryls from aromatics when treated with silver nitrate in acetic acid.[25] If no silver nitrate was present, biaryl coupling was not observed. The olefins used were ethylene, styrene, and cyclohexene, and the yields of biphenyl from benzene were 99, 68, and 3 %, respectively; with no olefinic ligand present, the yield was 40 %. Incidentally, this experiment seems to contradict the necessity for the presence of sodium acetate.[13] This sequence of yields is consistent with the order of stability of the three complexes, and it was therefore suggested that the reactivity is dependent upon the rate at which the olefin ligand exchanges with benzene. The role of silver nitrate was presumably that of an oxidant, since nitrogen dioxide was evolved in the reaction. A mechanism involving σ-arylpalladium complexes was again invoked.

Using Pd(II) nitrate as an oxidant, it was established [26] that in acetic acid, benzene is converted primarily to phenyl acetate, with nitrobenzene [27] and biphenyl as by-products. Certain additives, such as perchloric acid or water, made the biaryl become the major product. Chloride ion inhibited

both processes completely. It was concluded that acetoxylation takes place *via* a mononuclear π-complex between Pd(II) salts and aromatics (eqn. (5)), whereas biaryl coupling occurs *via* a binuclear complex (as in eqns. (1) and (2)). Nitration was also assumed to proceed through an arene π-complex (eqn. (6)), since the product distribution was very much different from that of ordinary nitration processes (*meta* orientation!).

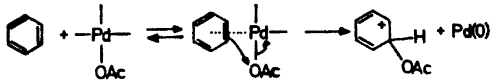

(5)

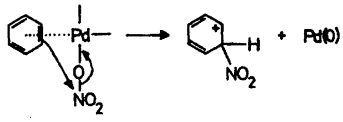

(6)

This acetoxylation mechanism is, however, not the only one suggested. Davidson and Triggs,[19] referring to the fact that Pd(II) acetate acetoxylation is inhibited by oxygen in a way similar to lead tetraacetate oxidation processes, proposed a radical chain mechanism in which initially a univalent Pd(OAc) species is formed in a concerted reaction from Pd(II) acetate. The Pd(I) species would then act as an electron transfer oxidant toward the aromatic compound, giving a radical cation as an intermediate. Loss of a proton from the radical cation would give a neutral aryl radical which would be further oxidized by Pd(II) acetate to give an aryl cation and a new Pd(I)OAc species, *etc.* (eqns. (7) – (9)).

$$Pd(OAc) + Ar-H \rightarrow ArH^{+\cdot} + AcO^- + Pd(0) \quad (7)$$

$$ArH^{+\cdot} \rightarrow Ar^{\cdot} + H^+ \quad (8)$$

$$Ar^{\cdot} + Pd(OAc)_2 \rightarrow Ar^+ + AcO^- + Pd(OAc) \quad (9)$$

While this mechanism would in principle be feasible for α acetoxylation of *easily* oxidizable methylaromatic substrates ($ArCH_2$ instead of Ar in eqns. (7) – (9)), we think it rather improbable in the case of nuclear acetoxylation, since such high-energy species as aryl cations [28] are postulated as intermediates. Moreover, the inhibition by oxygen is not complete even under 50 atmospheres of oxygen; hence the similarity with the radical chain mechanism proposed for lead tetraacetate oxidation is only superficial, since here inhibition is complete even with traces of oxygen.[29] Our own results regarding acetoxylation under oxygen (Parts I and II) fully confirm that oxygen does not perceptibly inhibit acetoxylation at atmospheric pressure. The Pd-catalyzed air oxidation of methylbenzenes to give benzyl acetates [30] is another demonstration that oxygen is not deleterious to acetoxylation. For the latter process it was proposed that a mononuclear Pd(II) species is the reagent responsible for α acetoxylation.

Finally, Henry [31] has made a very interesting study of the nuclear acetoxylation of benzene and benzene derivatives with Pd(II) acetate in acetic acid in the presence of a co-oxidant. The best one was found to be potassium dichromate, but $Pb(OAc)_4$, $KMnO_4$, CrO_3, and $KClO_3$ also worked reasonably well. In the absence of co-oxidant, biphenyl was the major product from benzene. Both benzene and phenylmercury acetate worked well as substrates, and for the latter a number of other oxidative nucleophilic substitutions became possible, *e.g.* chlorination in the presence of Cl^- and cyanation in the presence of CN^-. Similar halogenations [32] and cyanations [33] have been reported also with nonmetallic oxidants. Toluene gave predominantly nuclear acetate in this reaction, in contrast to most of the acetoxylation reactions already mentioned above, and with methanesulphonic acid present, the isomer distribution of cresyl acetates was $o:m:p = 19:62:19$, the same striking preponderance of *meta* substitution as found for other aromatics in Part II. The mechanism of nuclear acetoxylation under these conditions was proposed to involve attack by either a Pd(IV) species, formed by oxidation of Pd(II) by the co-oxidant (eqn. (10)), or a Pd(II) species to form an arylpalladium intermediate (eqn. (1)). The role of the co-oxidant would then be to substitute the -PdX moiety oxidatively by the nucleophile, since control experiments showed that the nucleophile will not attack the arylpalladium compound in the absence of co-oxidant. The latter type of mechanism was deemed the more likely one for various reasons.

$$PdX_2 + \text{oxidant} \xrightarrow{2\,X^-} PdX_4 \xrightarrow{Ar-H} Ar-X + PdX_2 + X^- \qquad (10)$$

$$Ar-H + PdX_2 \rightarrow ArPdX \xrightarrow[X^-]{\text{oxidant}} Ar-X \qquad (11)$$

Nature of the product-forming intermediate. Transient arylpalladium complexes have frequently been postulated as intermediates in Pd(II) mediated reactions.[18,34] As can be seen from the review given above, most proposals concerning biaryl coupling and nuclear acetoxylation also involve this kind of intermediate. The high reactivity of arylmercury [23,24,31] and arylboron [23] compounds toward Pd(II) complexes as compared to the parent aromatics, and the similarity in the product distribution from both types of starting material, supports this postulate in a very convincing way. In the following discussion, we shall assume the intervention of C–Pd bonded intermediates both for reactions on the ring (arylpalladium species) and at the α position (benzylpalladium species). In the latter case the finding that isolatable benzylpalladium complexes can be converted into benzyl acetate [21] carries strong weight as evidence for this assumption. Thus, a crude mechanistic picture for these processes would appear as in eqns. (12) and (13):

$$Ar-H \xrightarrow{PdL_4} [Ar'PdL_3] \begin{matrix} \nearrow ArOAc \\ \searrow Ar-Ar \end{matrix} \qquad (12)$$

$$ArCH_3 \xrightarrow{PdL_4} [ArCH_2PdL_3] \rightarrow ArCH_2OAc \qquad (13)$$

L = unspecified ligand

The remaining and by far most difficult task in outlining a detailed mechanism is now to try to understand how the nature of L influences (a) the mode of formation of organopalladium complexes, and (b) the further reactions of $Ar'PdL_3$ and $ArCH_2PdL_3$.

Nature of the initial step. Certain metal ion oxidations with ions of high oxidizing power (*e.g.*, Mn(III),[35] Co(III),[36] and Pb(IV)[37]) in acetic acid produce acetoxylation products from aromatics *via* an initial one-electron transfer from the substrate to the metal ion to produce a radical cation as the product-forming intermediate. Such a mechanism has also been proposed for Pd(II) mediated reactions[23] (see above), but appears less likely in view of the weak oxidizing power of Pd(II) and/or Pd(I) compounds as compared to the ions mentioned. In fact, as shown in Part III, compounds that easily undergo electron transfer oxidation (DPA, TAE) show no signs of reacting with Pd(II) (as III) to give products characteristic of such a process. For DPA no reaction is observed, and with TAE a complex is formed (IV, below formulated as a π-complex). Likewise, in the reaction between Pd(II) acetate and DPA, none of the products to be expected from electron transfer oxidation is obtained.

Thus we can see no compelling reason for assuming that Pd(II) oxidation of aromatics occurs *via* an initial electron transfer to give a radical cation, which would then react to form products in subsequent chemical and/or electron transfer steps. Instead, the results referred to above and those reported in Part III are in agreement with the assumption that electron transfer takes place *within* the coordination sphere of the metal ion, presumably with assistance of a base/nucleophile within or outside the coordination sphere (as exemplified in eqns. (5) and (6)). A very striking illustration of this behavior is afforded by IV, which on attack by a weak nucleophile/base, such as water, gives back the π-donor (TAE), whereas with the stronger base, lutidine, electron transfer within the complex takes place and an oxidation product is formed. This is formulated as in eqn. (14), in which IV is shown as the usual type of π-donor-acceptor resonance hybride, although with only one of the resonance forms given. Assuming that an intramolecular attack between two rings occurs in a fast reversible step, the removal of the proton by a base would then be rate-determining and eventually lead to the phenanthrene derivative V and Pd(0). Similar additions across a double bond of the donor of a purely organic charge-transfer complex have been reported.[38]

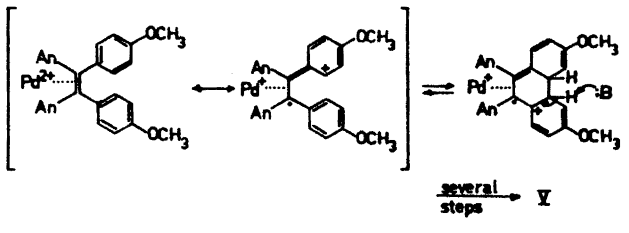

(14)

An = p-anisyl

We now postulate that the first step in the reaction between aromatics and Pd(II) complexes is the formation of a π-complex (XI), which according to its structure and the prevailing reaction conditions can undergo: (1) nucleophilic attack at the ring to form an arylpalladium *adduct* [39] (XII), (2) attack of a base at an α hydrogen, if available, to form a benzylpalladium *substitution* intermediate (XIII), or (3) direct collapse to a Wheland-type intermediate (XIV, see eqn. (15)).

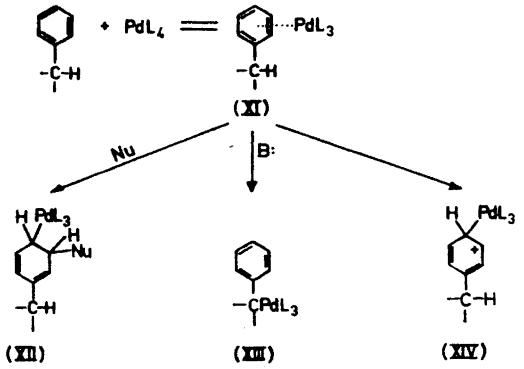

(15)

As shown in Part I and pointed out at the beginning of Part III, nuclear acetoxylation of *p*-xylene presumably takes place *via* Pd(II) acetate monomer (I), whereas binuclear species II is the active complex under conditions leading to α acetoxylation.[40] Since the nature of the alkali metal acetate added has a strong effect on the rate of formation of the α acetoxylation product from *p*-xylene (Part I, Figs. 7 and 8), we find it reasonable to assume that the corresponding π-complexes (XI) also have different structures and that this is the reason that the reaction takes a different course in the two cases. To suggest a definite structure for either of the two types of complexes is at present only a matter of speculation; it may be that the complex leading to α acetoxylation is less susceptible to attack on the ring by an external nucleophile for reasons of steric hindrance, or that, if the attacking nucleophile is bound to the π-complex (XI) as a ligand, the structure of a given complex is such as to favor only one of the two processes. The fact that added triphenylphosphine favors α acetoxylation (Part I) might be cited as supporting the former assumption, since triphenylphosphine would act both as a bulky ligand and as an aid in the removal of acetate ligand from Pd(II). Similarly, only α acetoxylation is observed in the case of the sterically hindered higher methylbenzenes (Part II).

Given conditions that lead to nuclear acetoxylation, the intervention of arylpalladium adduct (XII), affords a satisfactory explanation for the observation of the inverse isomer distribution pattern reported in Part II. Then Pd(II) will simply become attached to ring positions susceptible to electrophilic attack, and removal of PdHX from the adduct will lead to the "wrong" isomer.

The induction period observed at low Na/Pd ratios for α acetoxylation (Part I, Figs. 1 and 3) is difficult to reconcile with the mechanism given above

(eqn. (15)). The end of the induction period appears to coincide with the appearance of Pd metal, but since the induction period disappears at high Na/Pd ratios, we believe this to be fortuitous. This is supported by the fact that added triphenylphosphine, which keeps Pd(0) in solution as a complex, actually favors α acetoxylation, showing that a heterogeneous step involving Pd metal is not required for this reaction to occur. The possibility that a radical chain mechanism is responsible for α acetoxylation is excluded by the fact that the induction period is observed both under argon and oxygen.

The effect of oxygen on Pd(II) mediated reactions presents several puzzling problems, as discussed above. It appears to increase the rate of biaryl coupling and decrease the rate of acetoxylation; in our own investigation we have also noted that aldehydes are among the major products from methylbenzenes when oxygen is present (Parts I and II). We have no consistent explanation for this behavior, but would like to suggest that dioxygen complexes of Pd(II) [41] and/or Pd(0) [42] play an important role in the phenomena observed. Dioxygen complexes of Pd(II) are known to cause peroxidation reactions,[41] which might be the reason that aldehydes are formed from methylbenzenes under oxygen. The role of dioxygen complexes in these reactions merits further attention.

Nature of the follow-up reactions of organopalladium species. Having postulated the general mechanism shown in eqn. (15) to account for the formation of organopalladium intermediates it now remains to explain how the arylpalladium species are diverted between biaryl coupling and nuclear acetoxylation, assuming that α acetoxylation occurs *via* benzylpalladium complex XIII. As discussed earlier, the presence of a good bridging ligand, such as chloride ion, has often been considered a prerequisite for biaryl formation. However, this is really not necessary, since Pd(II) acetate in the presence of perchloric acid [19,23] effects biaryl coupling in a fast, reasonably efficient process.

Returning to eqn. (15), adduct XII is assumed to be formed in the slow step from the π-complex (XI). As mentioned above, removal of PdHX from the adduct gives the nuclear acetate; since a co-oxidant strongly favors this mode of reaction, it appears reasonable to assume that the oxidant operates in assisting this stage of the reaction. Under our conditions for favoring nuclear acetoxylation, Pd(II) acetate alone in acetic acid under oxygen, oxygen probably plays this oxidative role in the removal of PdHX. However, under strongly acidic conditions ($HClO_4$ present), two additional factors are introduced. In the first place, acetate ion will be removed from the solution, giving a much less strongly coordinated Pd(II) complex with a concomitant increase in electrophilic reactivity. This appears to be the case also for the addition of the strong Lewis acid, $AlCl_3$; see Part I. Hence an arylpalladium species (XV) may be formed directly from the π-complex (eqn. (16)) in an ordinary electrophilic mechanism with the same high k_H/k_D ratio as observed for mercuration. In the second place, any adduct (XII) formed would immediately solvolyze under acidic conditions to produce the arylpalladium substitution product (XV) *via* XIV.

$$\mathrm{Ar-H + Pd^{2+}} \rightleftharpoons [\mathrm{Ar-H\cdots Pd^{2+}}] \rightarrow \left[\mathrm{Ar}\begin{matrix}\diagup \mathrm{H} \\ \diagdown \mathrm{Pd}\end{matrix}\right]^{2+} \xrightarrow{-\mathrm{H^+}} \underset{\text{(XV)}}{\mathrm{ArPd^+}} \qquad (16)$$

This reasoning leads to the assumption that an arylpalladium substitution product (XV) is the critical intermediate in biaryl coupling, at least under acidic conditions, but probably also under others. The problem of how the coupling reaction takes place is not easy to solve, but we suggest that a mixed arene-arylpalladium complex is involved (eqn. (17)).

$$[Ar-Pd^{+}\cdots ArH] \rightarrow Ar-Ar+H^{+}+Pd(0) \qquad (17)$$

EXPERIMENTAL

Materials. Solvents and inorganic chemicals used were of reagent grade quality. $Pd(CH_3CN)_2(BF_4)_2$ (III) was prepared according to the procedure given by Schramm and Wayland,[8] DPA was a recrystallized specimen of commercial origin (Aldrich), and TAE was obtained through the courtesy of Dr. Klas Nyberg.[6]

Attempted reaction between DPA and Pd(II) complexes. (a) DPA (0.091 mmol) was dissolved in acetonitrile (5 ml) and III (0.094 mmol) dissolved in acetonitrile (0.2 ml) was added. No reaction took place, the starting material being recovered unchanged after standing overnight. In a similar experiment, bubbling with oxygen had no effect.

(b) DPA (2.1 mmol) was dissolved in acetic acid (50 ml). The solution was thermostated at 115° and oxygen was bubbled through it. After 30 min Pd(II) acetate (1.0 mmol) was added and the solution kept at 115° under oxygen for 4 h. The usual work-up [1] gave a crystalline material which lacked the characteristic IR spectral bands of 9,10-diacetoxy-9,10-dihydro-9,10-diphenylanthracene [43] (1760, 1255, 770, 760, 750, and 710 cm^{-1}). Most of this sample was unchanged starting material.

Reaction between TAE and III. (a) To prepare solutions of the blue complex no special precautions were taken to avoid contact with oxygen from the air. Thus, TAE (0.066 mmol) was dissolved in acetonitrile (5 ml) and III (0.094 mmol in 0.2 ml of acetonitrile) was added. After 1 h the solution was strongly blue-colored, and its UV spectrum exhibited λ_{max} at 300 and 568 nm. After standing for several days, the solution attained a yellow colour (λ_{max} 482 nm).

(b) To demonstrate the effect of oxygen, solutions 1 mM in TAE and containing 0.188 mmol of III were shaken in stoppered flasks under either oxygen or argon. The following colour changes were noticeable:

Time lapse	Under O_2	Under Ar
10 min	Blue colour appears	No change
3 h	Blue-greenish	No change
6 h	Blue-greenish	Blue colour appears
7 h	Green	Blue
20 h	Yellow	Blue

Thus, oxygen appears to catalyze the changes that take place in solutions of TAE and III. Attempts to follow the kinetics of these processes failed due to side-reactions, probably between acetonitrile and III.

(c) Cyclic voltammograms (Heath EUW 19 A operational amplifier with polarography module EUA-19-2 and a Moseley 7035 B x,y-recorder) were determined at a Beckman platinum button electrode (No. 39273), using a solution made up according to the procedure given under (a) above.

Acknowledgements. We gratefully acknowledge the generous financial support we have obtained from the *Swedish Board for Technical Development* (L.E.) and the *Faculty of Science, University of Lund* (L.G.).

REFERENCES

1. Eberson, L. and Gomez-Gonzalez, L. *Acta Chem. Scand.* **27** (1973) 1162.
2. Eberson, L. and Gomez-Gonzalez, L. *Acta Chem. Scand.* **27** (1973) 1249.
3. Sioda, R. E. *J. Phys. Chem.* **72** (1968) 2322; Peover, M. E. and White, B. S. *J. Electroanal. Chem.* **13** (1967) 93.
4. Phelps, J., Santhaman, K. S. V. and Bard, A. J. *J. Am. Chem. Soc.* **89** (1967) 1752.
5. Marcoux, L. S., Fritsch, J. M. and Adams, R. N. *J. Am. Chem. Soc.* **89** (1967) 5766.
6. Parker, V. D., Nyberg, K. and Eberson, L. *J. Electroanal. Chem.* **22** (1969) 150.
7. Phelps, J. and Bard, A. J. *J. Electroanal. Chem.* **25** (1970) App. 2 – 5.
8. Schramm, R. F. and Wayland, B. B. *Chem. Commun.* **1968** 1898.
9. Parker, V. D. *Acta Chem. Scand.* **24** (1970) 3151.
10. Baenziger, N. C., Buckles, R. E. and Simpson, T. D. *J. Am. Chem. Soc.* **89** (1967) 3405.
11. Buckles, R. E. and Womer, W. D. *J. Am. Chem. Soc.* **80** (1958) 5055.
12. Stuart, J. D. and Ohnesorge, W. E. *J. Electroanal. Chem.* **30** (1971) App. 11 – 13; *cf.* also *J. Am. Chem. Soc.* **93** (1971) 4531.
13. Van Helden, R. and Verberg, G. *Rec. Trav. Chim.* **84** (1965) 1263.
14. Eberson, L. and Olofsson, B. *Acta Chem. Scand.* **23** (1969) 2355.
15. Parker, V. D. and Adams, R. N. *Tetrahedron Letters* **1969** 1721.
16. See Ref. 17b, p. 2.
17. a. Maitlis, P. M. *The Organic Chemistry of Palladium, Vol. 1, Metal Complexes*, Academic, New York 1971; b. *The Organic Chemistry of Palladium, Vol. 2, Catalytic Reactions*, Academic, New York 1971.
18. Bryant, D. R., McKeon, J. E. and Ream, B. C. *Tetrahedron Letters.* **1968** 3371.
19. Davidsson, J. H. and Triggs, C. *J. Chem. Soc.* **A 1968** 1331.
20. Bushweller, H. *Tetrahedron Letters* **1968** 6123.
21. Fitton, P., McKeon, J. E. and Ream, B. C. *Chem. Commun.* **1969** 370.
22. Itatani, H. and Yoshimoto, H. *Chem. Ind. (London)* **1971** 674.
23. Davidson, J. H. and Triggs, C. *J. Chem. Soc.* **A 1968** 1324.
24. Unger, M. F. and Fouty, R. C. *J. Org. Chem.* **34** (1969) 18.
25. Fujiwara, Y., Moritani, I., Ikegami, K., Tanaka, R. and Teranishi, S. *Bull. Chem. Soc. Japan* **43** (1970) 863.
26. Ichikawa, K., Uemura, S. and Okada, T. *Nippon Kagaku Zasshi* **90** (1969) 212.
27. Tisue, T. and Downs, W. J. *Chem. Commun.* **1969** 410.
28. Richey, H. G. and Richey, J. In Olah, G. A. and von R. Schleyer, P., Eds., *Carbonium Ions*, Wiley-Interscience, New York 1970, Vol. II, p. 922.
29. See, for example; Kochi, J. K. *J. Am. Chem. Soc.* **87** (1965) 3609; *J. Org. Chem.* **30** (1965) 3265.
30. Bryant, D. R., McKeon, J. E. and Ream, B. C. *J. Org. Chem.* **33** (1968) 4123.
31. Henry, P. M. *J. Org. Chem.* **36** (1971) 1886.
32. Wilk, M. and Hoppe, U. *Ann.* **727** (1969) 81.
33. Whitaker, K. E., Galbraith, B. E. and Snyder, H. R. *J. Org. Chem.* **34** (1969) 1411.
34. Heck, R. F. *Fortschr. Chem. Forsch.* **16** (1970/71) 221.
35. Andrulis, P. J., Dewar, M. J. S., Dietz, R. and Hunt, R. L. *J. Am. Chem. Soc.* **88** (1966) 5473.
36. Heiba, E. I., Dessau, R. M. and Koehl, W. J. *J. Am. Chem. Soc.* **91** (1969) 6830, and references cited therein.
37. McClelland, R. A., Norman, R. O. C. and Thomas, C. B. *J. Chem. Soc. Perkin 1* **1972** 562.
38. Becker, H.-D. *J. Org. Chem.* **34** (1969) 1203.
39. Analogous mechanisms have been proposed for the vinylic and allylic acetoxylation of olefins by Pd(II) acetate: Kitching, W., Rappoport, Z., Winstein, S. and Young, W. G. *J. Am. Chem. Soc.* **88** (1966) 2054.
40. Similar suggestions have been made by Pandey, R. N. and Henry, P. M. *Abstracts of Papers, 164th American Chemical Society National Meeting, New York City, N.Y., September 1972*, Abstract No. 29.
41. Otsuka, S., Nakamura, A., Tatsano, Y. and Miki, M. *J. Am. Chem. Soc.* **94** (1972) 3761.
42. Wilke, G., Schott, H. and Heimback, P. *Angew. Chem.* **79** (1967) 62.
43. Pinazzi, C. *Ann. Chim. Rome* **7** (1962) 397.

Received October 25, 1972.

ACTA CHEMICA SCANDINAVICA 27 (1973) 1268–1276

The Anomalous Periodate Oxidation Limit of Guaran

MONA FAHMY ISHAK* and TERENCE PAINTER

Institute for Marine Biochemistry, N-7034 Trondheim-NTH, Norway

Guaran, containing residues of D-galactose and D-mannose in the ratio 36:64, was oxidised in 12.5 mM sodium metaperiodate at 20°, and the consumption of oxidant and the liberation of formic acid were measured until constant values were obtained. At intervals during the reaction, samples of substrate were isolated and reduced with borohydride; they were then re-oxidised, with measurement of the consumption of additional periodate and of the formaldehyde liberated.

From these data, curves were obtained showing, separately, the consumption of periodate and the liberation of formic acid by the galactose residues, and the consumption of periodate by the mannan backbone. The galactose residues behaved similarly to methyl α-D-galactopyranoside, oxidised under the same conditions, and ultimately consumed 2 mol of periodate with liberation of 1 mol of formic acid.

Only 58 % of the mannose residues in the main chain were directly oxidisable. The remainder resisted oxidation, even in 60 mM periodate. They became freely oxidisable, however, after the 58 % oxidised chain had been reduced with borohydride.

From these and other data, it was concluded that, when a mannose residue carrying a galactose residue at position 6 is oxidised, the liberated aldehyde groups immediately form stable hemiacetals with the closest hydroxyl groups on the two adjacent mannose residues, thus preventing their subsequent oxidation.

The anomalous periodate-oxidation limit of sodium alginate (0.44 mol of periodate per non-terminal hexuronic-acid residue) has been traced to the formation of stable, six-membered hemiacetal rings between the aldehyde groups of oxidised hexuronic-acid residues and the closest hydroxyl groups on adjacent, unoxidised hexuronic-acid residues in the 1,4′-linked polyuronide chains.[1] The methyl ester of alginic acid behaved similarly, and therefore the extreme stability of these inter-unit hemiacetal rings could not be attributed to some special property of the carboxyl groups.[1]

It was therefore suggested that the stability arose mainly because of the absence of a primary hydroxyl group at position 6 of the oxidised residues. Such a group, if present, could be expected to give rise to intra-residue

* On leave of absence from the Chemical Department of Cairo, Ministry of Industry, Cairo, Egypt.

hemiacetals,[2] formed competitively with the inter-residue forms, thus shifting the position of the equilibrium away from the latter.

To test this idea, it was necessary to find a β-1,4′-linked mannan in which the hydroxyl groups at C(6) were blocked or replaced by some group other than a carboxyl group. However, native mannans are so insoluble that it seemed an impossible task to modify them chemically in a systematic manner, to yield a suitable, water-soluble derivative.

This difficulty prompted the present re-investigation of the periodate oxidation of guaran. Although only about 50 % of the mannose residues in the main chain of guaran are substituted at position 6 with α-D-galactopyranosyl groups, a clearly anomalous periodate-oxidation limit should still be demonstrable if the reasoning just described is correct. The galactose side-groups also consume periodate, but a way was found to correct for this, and to study the oxidation of the mannan chain separately.

Although standard text-books [3,4] state that guaran, containing residues of galactose and mannose in the usual ratio of 1:2, shows the expected, Malapradian oxidation-limit of 1.33 mol of periodate per hexose residue, they do not record the full historical facts. Before the correct structure of guaran had been established by methylation [5,6] and partial hydrolysis,[7,8] its oxidation by periodate had been studied by two groups of workers.[9,10] Both reported oxidation-limits close to 1.0 mol of periodate per hexose residue, and from this result, they inevitably drew erroneous conclusions about the structure of guaran.[9,10]

The results reported here are in good agreement with those of the early workers,[9,10] and it is not understood why later workers [5,6] were able to report the theoretical oxidation-limit.

EXPERIMENTAL

Materials. The sample of guaran was Meypro rein Guarin, supplied by Meyhall Chemical AG, Kreuzlingen, Switzerland. It contained 10.1 % moisture and 1.2 % ash, which were corrected for in subsequent analyses, and 0.2 % nitrogen (Kjeldahl). By hydrolysis and gas-liquid chromatography of the derived alditol acetates,[11] it was found to contain residues of galactose and mannose in the ratio 36:64.

The methyl α-D-galactopyranoside was purchased from Koch-Light Laboratories, Colnbrook, England, as its monohydrate, having m.p. 110° and $[\alpha]_D^{20} = +178°$ (*c*, 1.0 in water). Meso-inositol, m.p. 224 – 226°, was purchased from the same company. The other reagents were of Merck analytical grade.

Analytical oxidations. Reference is made to earlier papers [1,12,13] for detailed information concerning procedure and accuracy. Guaran (600 mg) was oxidised in unbuffered, 12.5 mM sodium metaperiodate (800 ml) at 20° in the dark. The consumption of periodate was followed by withdrawing portions (10 ml), adding them to an ice-cold mixture of 0.5 M sodium phosphate buffer (pH 7.0; 20 ml) and aqueous potassium iodide (30 % w/v; 3 ml), and titrating the liberated iodine with 0.01 M sodium thiosulphate. The liberation of formic acid was followed by pipetting portions (10 ml) of reaction mixture into aqueous ethanediol (50 % v/v; 3 ml), waiting 10 min, and titrating with 0.005 N sodium hydroxide, with methyl red as the indicator. A blank solution was prepared and used to correct the titres in the usual way.

In another experiment, guaran (150 mg) was oxidised in 60 mM periodate (200 ml). In this case, portions (10 ml) of reaction mixture were added to 50 ml of the ice-cold buffer-potassium iodide mixture, and the sodium thiosulphate solution used for titration was 0.05 M.

Methyl α-D-galactopyranoside monohydrate (58 mg) was oxidised in 11.25 mM periodate (200 ml). The conditions and methods of measurement were otherwise identical with those used for oxidation of guaran in 12.5 mM periodate.

Preparative oxidations. Eleven portions of guaran (750 mg each) were dissolved separately in water (950 ml). The solutions were brought to 20°, and oxidation was started by adding 0.25 M sodium metaperiodate (50 ml) to each. The solutions were kept in the dark at 20°, and after chosen times (35 min, 1.5 h, 3.5 h, 5 h, 7 h, 9 h, 11 h, 13.5 h, 20 h, 24 h, and 30 h, respectively), reaction was stopped by adding ethanediol (50 ml). The resultant solutions were concentrated separately in the rotary evaporator at 30° to 100 ml, and then dialysed against distilled water until the dialysates gave no colour with an acidified mixture of starch and potassium iodide. They were then concentrated again to 50 ml, and sodium borohydride (1 g) was dissolved in each. After 12 h, they were brought to pH 6 with glacial acetic acid, and dialysed thoroughly against distilled water. They were then centrifuged for 1 h at 40 000 *g*, and freeze-dried. The yields were almost quantitative. The conditions of dialysis required to give ash-free products were ascertained by carrying out ash determinations on several samples. The samples were stored in a desiccator.

Re-oxidation of the partially oxidised and reduced samples of guaran. These experiments were carried out on 150 mg samples in 200 ml of reaction mixture at 20° in the dark. The initial concentration of periodate was adjusted in each case so as to correspond as closely as possible to the concentration of periodate remaining in the reaction mixture at the time when the first part of the oxidation was stopped. This was done by pipetting the following volumes (given in ml) of 0.25 M periodate into the eleven reaction mixtures, respectively, before diluting them up to 200 ml: 7.81, 7.47, 7.22, 7.13, 7.05, 6.98, 6.92, 6.84, 6.63, 6.56, and 6.51. Blank solutions containing the same amounts of periodate were also prepared and titrated. The consumption of periodate was followed by withdrawing 10 ml samples and titrating them as before.

After the titres became constant, the amount of formaldehyde that had been liberated was measured as follows. A portion (25 ml) of the reaction mixture was treated with a solution of meso-inositol (250 mg) in water (10 ml). After 1 h, aqueous sodium sulphite (26 % w/v; 1.25 ml) was added, and the solution was diluted to 50 ml with water. As a standard, erythritol (27 mg) was oxidised in 12.5 mM periodate (200 ml) at 20° for 45 min, after which titration of a portion indicated liberation of a theoretical yield of formic acid. A portion (25 ml) was then withdrawn and treated in the same way as the test samples. As a blank, 12.5 mM periodate (25 ml) was treated similarly. Portions (0.5 ml) were then taken in triplicate from each solution for the assay of formaldehyde by the chromotropic acid method.[14]

RESULTS

Figs. 1 and 2 show the consumption of periodate (P) and the liberation of formic acid (F) by guaran in 12.5 mM periodate at 20°. Because of the very slow rate of the terminal phase of the oxidation, the full range of the reaction is shown by plotting the results on different time-scales in the two figures. The final consumption of periodate is 1.10 mol per hexose residue, and the final yield of formic acid is 0.36 mol. Also shown is a curve, calculated from the two others, according to the formula, $P-2F$. This is clearly the fraction of hexose residues that have suffered a single oxidative attack at any time. As expected, it rises to a maximum, and then decreases again, as the singly oxidised galactose residues are replaced by doubly oxidised galactose residues.

The final value of $P-2F$ is 0.38. At that time, all the galactose residues had been attacked twice, as is shown by the liberation of a theoretical yield of formic acid. The singly oxidised residues that remained must therefore have been mannose residues. However, the fraction of mannose residues in the guaran was 0.64, and hence only 0.38/0.64, or 59 % of them, were oxidisable under the conditions of the experiment.

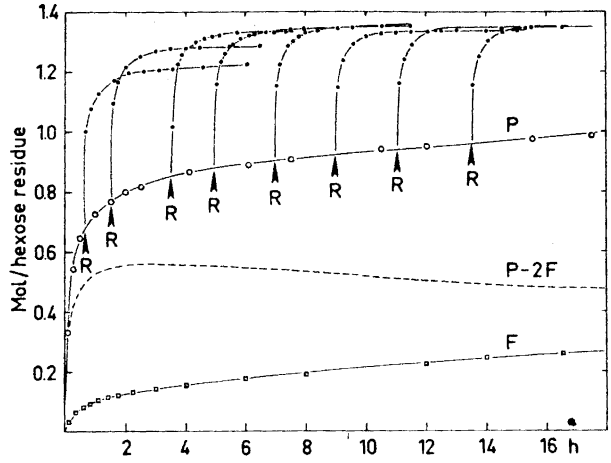

Fig. 1. Oxidation of guaran in 12.5 mM periodate at 20°. The concentration of substrate was 4 mM with respect to hexose residues. P is the periodate consumed and F is the formic acid liberated. The broken curve is calculated from $P-2F$, and shows the fraction of singly oxidised hexose residues present at any time. At the points marked R, samples of substrate were reduced with borohydride, and re-oxidised, with measurement of the additional periodate consumed, as shown.

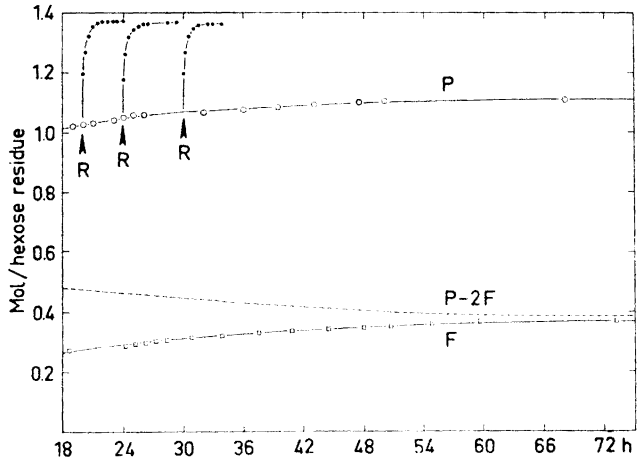

Fig. 2. Continuation of the experiment shown in Fig. 1. The time-scale is shortened to one-third of that in Fig. 1.

The effect of reduction of the substrate with borohydride at different times is also shown in the figures. The conditions were chosen such that the curves give an accurate impression of what would have happened, had it been possible to reduce the substrate instantaneously during the original oxidation,

without interrupting the reaction. Apart from the first two samples, and possibly also the third, which can be expected still to contain contiguous, unoxidised mannose residues and hence to give rise to a second, anomalous oxidation-limit, it is seen that in every case, the theoretical, Malapradian oxidation-limit of 1.36 mol of periodate per hexose residue is quickly reached.

The measurement of formaldehyde in the samples that were reduced and re-oxidised was undertaken, since this would give a direct measure of the fraction of singly oxidised galactose residues present at any time. If subtracted from $P-2F$, this would then give the fraction of singly oxidised mannose residues present at any time, thus permitting construction of a curve, showing the oxidation of the mannan chain alone.

Table 1 shows the yields of formaldehyde (A) from the eleven samples, the corresponding values of $P-2F$, the differences ($P-2F-A$), and the differences expressed as percentages of the total mannan. The limits of error

Table 1. Calculation of the degree of oxidation of the mannan chain in guaran after different times of oxidation in 12.5 mM periodate at 20°. P is the periodate consumed by the whole guaran, F is the formic acid liberated from the galactose residues, and A is the formaldehyde liberated after reduction of the substrate with borohydride, and re-oxidation with periodate. All yields are given in moles per hexose residue. The guaran contained 64 % mannose.

Time	A	$P-2F$	$P-2F-A$	$(P-2F-A)/0.64$ %
35 min	0.258	0.480	0.222	34.6
1.5 h	0.255	0.539	0.284	44.3
3.5 h	0.192	0.555	0.363	56.6
5.0 h	0.190	0.550	0.360	56.2
7.0 h	0.176	0.537	0.361	56.3
9.0 h	0.141	0.520	0.379	59.1
11.0 h	0.117	0.507	0.390	60.8
13.5 h	0.112	0.488	0.376	58.7
20.0 h	0.103	0.475	0.372	58.0
24.0 h	0.071	0.471	0.400	62.4
30.0 h	0.071	0.449	0.378	59.0

in this last column are such that the degree of oxidation of the mannan chain should be regarded as reaching a constant value of 58 ± 2 % from 3.5 h onwards.

In an attempt to determine whether the use of more-concentrated periodate would increase the oxidation limit, guaran was oxidised in five times the concentration of periodate (60 mM). The molar excess of periodate in the system was then about 12-fold. The results are shown in Table 2. The limiting consumption in this case was 1.02 mol, which was substantially lower than that (1.10 mol) in 12.5 mM periodate.

An experiment was next carried out to investigate the possibility that the anomalous oxidation limit of the mannan could be due to the formation of hemiacetals between the aldehyde groups of singly oxidised galactose residues

Table 2. Oxidation of guaran in 60 mM periodate at 20°. The concentration of substrate was 4 mM with respect to hexose residues.

Time (h)	Periodate consumed (mol/hexose unit)
0.25	0.594
1.00	0.715
2.00	0.795
3.00	0.850
5.00	0.895
17.0	0.968
25.0	0.986
29.0	1.02
100	1.02

and the hydroxyl groups of unoxidised mannose residues. It was reasoned that, if this happened, the kinetics of the oxidation of the galactose residues in guaran should be different from those of the oxidation of methyl α-D-galactopyranoside under the same conditions.

Methyl α-D-galactopyranoside was therefore oxidised in a solution that was equimolar, in galactose residues, with the solution of guaran studied earlier. To correct as far as possible for the amount of periodate consumed by the mannan chain, the initial concentration of periodate in this experiment was 11.25 mM. This introduced a maximum possible error of 10 % into the measured consumption of periodate at any time.

Fig. 3 shows the consumption of periodate (P') and the liberation of formic acid (F') by the methyl galactoside, with the data for the release of formic acid by guaran included for comparison. In this figure, all the quantities are expressed as moles per galactose residue.

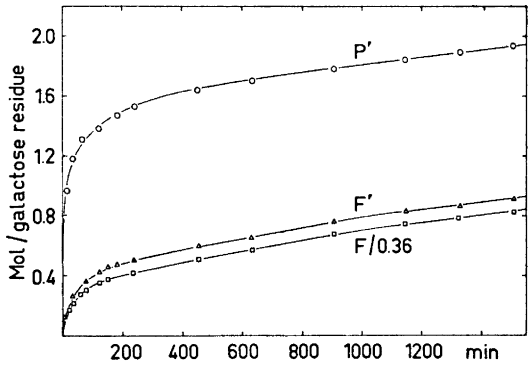

Fig. 3. Oxidation of methyl α-D-galactopyranoside (1.4 mM) in 11.25 mM periodate at 20°. P' is the periodate consumed, and F' is the formic acid liberated. For comparison with F', values of F for guaran, taken from Fig. 1, are plotted as $F/0.36$.

In Fig. 4, the points are values of $(P-2F-A)$, taken from Table 1. The curve in the figure, however, was drawn from calculated values of $P-0.36P'$, where P is expressed in moles per hexose residue, and P' is expressed in moles per galactose residue.

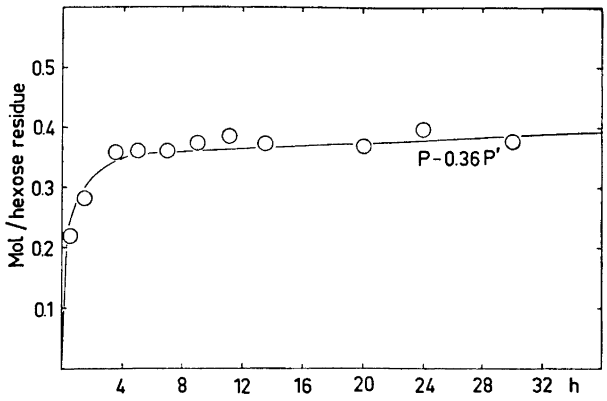

Fig. 4. The open circles are values of $P-2F-A$, taken from Table 1, and show the oxidation of the mannan chain when guaran is oxidised in 12.5 mM periodate at 20°. The curve is drawn from calculated values of $P-0.36P'$, where P is taken from Fig. 1, and P' from Fig. 3.

The possibility that mannose residues could be protected from oxidation by forming hemiacetals with the aldehyde groups of doubly oxidised galactose residues was discounted, because the yield of formic acid after 3.5 h (Fig. 1) showed that only about one-third of the galactose residues had been doubly oxidised, whereas the mannan chain had been fully oxidised to its anomalous limit of 58 % after that time (Table 1 and Fig. 4).

DISCUSSION

Insofar as the consumption of periodate by guaran becomes immeasurably slow before the theoretical, Malapradian oxidation-limit is reached, the oxidation of this polysaccharide is just as anomalous as that of alginate.[1] Indeed, the anomaly is more easily demonstrable with guaran, because the attachment of galactose residues to position 6 of mannose residues in the main chain prevents overoxidation.

An increase in the concentration of periodate in the system (from 12.5 mM to 60 mM) does not increase the oxidation-limit, but lowers it. This result is startling, but a similar effect has been observed with other polysaccharides, and is now under investigation. It appears that, at concentrations above 25 mM, the periodate ion is able to stabilise the inter-residue hemiacetals, thus inhibiting its own action. The effect of increasing the concentration of periodate still further has not been investigated, but any increase in con-

sumption resulting from this would be more likely to arise from non-specific oxidation than from Malapradian oxidation.

There is little doubt that the anomalous oxidation limit is a fundamental property of the β-1,4′-linked mannan chain itself, and that it does not arise from any direct chemical interaction between the galactose and mannose residues. The galactose residues and the mannan chain appear to oxidise independently of one another (Figs. 3 and 4). This is to be expected, since the smallest hemiacetal ring that could be formed between an aldehyde group in an oxidised galactose residue and a hydroxyl group in an unoxidised mannose residue would be eight-membered. It is very unlikely that a stable structure of this kind would be formed, in competition with the six-membered, intra-residue hemiacetals that could be formed in both singly [15] and doubly [2] oxidised galactose residues.[16]

In the light of earlier work,[1,12,13,16] the effect of borohydride reduction in permitting the rapid completion of Malapradian oxidation is here accepted as adequate evidence that the anomaly is due to the formation of highly stable, six-membered hemiacetal rings between the aldehyde groups of oxidised mannose residues and the closest hydroxyl groups on adjacent, unoxidised mannose residues in the main chain.

The question remains as to which kind of mannose residues are involved in these stable hemiacetal structures. The early work of Moe *et al.*[9] is helpful in this respect. These workers not only oxidised guaran, with results very similar to those reported here, but they also examined Honey locust (*Gleditschia tricanthos*, L.) gum, which contained only 18 % of galactose, and locust-bean (*Ceratonia siliqua*, L.) gum, which contained only 20 – 25 % of galactose. These other galactomannans showed oxidation limits of 1.04 and 1.06 mol of periodate per hexose residue, respectively, from which it may be calculated that their mannan chains contained only 20 – 25 % of periodate-resistant residues. The oxidation-limit of the mannan chain therefore increases as the galactose content of the galactomannan decreases, and hence unsubstituted mannose residues cannot, when oxidised, completely protect other unsubstituted mannose residues from oxidation. A similar conclusion was reached in an earlier study of partially carboxyl-reduced alginates.[1]

Finally, it may be noticed that, in all three galactomannans, the percentage of periodate-resistant mannose residues is about the same as the percentage of galactose-bearing mannose residues. Because of the statistical pattern of the attack of periodate on the chains, this could only come about if the substituted mannose residues, when oxidised, are able to protect both their nearest neighbours from oxidation, regardless of whether or not these neighbours are themselves substituted.

One of the authors (M. F. I.) is indebted to the *Norwegian Agency for International Development* (N.O.R.A.D.) for financial assistance. Both authors thank Prof. N. A. Sørensen for his kind interest and encouragement.

REFERENCES

1. Painter, T. J. and Larsen, B. *Acta Chem. Scand.* **24** (1970) 813.
2. Guthrie, R. D. *Advan. Carbohydrate Chem.* **16** (1961) 105.

3. Whistler, R. L. and Smart, C. L. *Polysaccharide Chemistry*, Academic, New York 1953.
4. Smith, F. and Montgomery, R. *The Chemistry of Plant Gums and Mucilages*, Reinhold, New York 1959.
5. Ahmed, Z. F. and Whistler, R. L. *J. Am. Chem. Soc.* **72** (1950) 2524.
6. Rafique, C. M. and Smith, F. *J. Am. Chem. Soc.* **72** (1960) 4634.
7. Whistler, R. L. and Durso, D. F. *J. Am. Chem. Soc.* **73** (1951) 4189.
8. Whistler, R. L. and Durso, D. F. *J. Am. Chem. Soc.* **74** (1952) 5140.
9. Moe, O. A., Miller, S. E. and Iwen, M. H. *J. Am. Chem. Soc.* **69** (1947) 2621.
10. Whistler, R. L., Li, T. K. and Dvonch, W. *J. Am. Chem. Soc.* **70** (1948) 3144.
11. Gunner, S. W., Jones, J. K. N. and Perry, M. B. *Can. J. Chem.* **39** (1961) 1892.
12. Painter, T. J. and Larsen, B. *Acta Chem. Scand.* **24** (1970) 2366.
13. Painter, T. J. and Larsen, B. *Acta Chem. Scand.* **24** (1970) 2724.
14. Frisell, W. R., Meech, L. A. and Mackensie, C. G. *J. Biol. Chem.* **207** (1954) 709.
15. Yu, R. J. and Bishop, C. T. *Can. J. Chem.* **45** (1967) 2195.
16. Fahmy Ishak, M. and Painter, T. J. *Acta Chem. Scand.* **25** (1971) 3875.

Received November 20, 1972.

ACTA CHEMICA SCANDINAVICA 27 (1973) 1277–1289

Solvent Extraction Studies on Complex Formation between Methylmercury(II) and Chloride Ions

OMORTAG BUDEVSKY*, FOLKE INGMAN** and DJIET HAY LIEM

Department of Inorganic Chemistry, Royal Institute of Technology, S-100 44 Stockholm 70, Sweden

Complex formation between $CH_3Hg(II)$ and Cl^- ions in the two-phase system *o*-xylene/1 M $(Na,H)(ClO_4,Cl)$ has been studied by measuring the distribution of methylmercury(II) as a function of chloride concentration. The distribution of $CH_3Hg(II)$ between the two phases has been studied by a radiometric method using Hg-203 labelled $CH_3Hg(II)$ and also by a spectrophotometric titration method for the analysis of non-radioactive methylmercury(II). The distribution data have been analyzed with the computer program LETAGROP-DISTR.[1–5] The results of the analysis give evidence to the formation of the complex CH_3HgCl in both the aqueous and organic phases with the following equilibrium constants:

$CH_3Hg^+(aq) + Cl^- \rightleftharpoons CH_3HgCl(aq)$; $\log (K \pm 3\sigma) = 5.32 \pm 0.09$
$CH_3Hg^+(aq) + Cl^- \rightleftharpoons CH_3HgCl(org)$; $\log (K \pm 3\sigma) = 6.39 \pm 0.09$

No extraction of CH_3HgClO_4 into *o*-xylene was found. The extracted CH_3HgCl was found predominantly as undissociated species.

Organic mercury compounds, *e.g.* methylmercury salts, being effective pesticides, have been widely used for seed disinfection [6–10]. Great interest has arisen in the solution chemistry of such organomercurial compounds during the past few years because of their polluting effects in natural water. Microbiological processes are believed to lead to the formation of methylmercury(II) from industrial waste containing inorganic mercury [11–13]. Numerous studies have also been devoted to the clarification of their metabolism, since the organomercurials were found to be a hazard to the health of man and animals.[14–20].

Organomercurials are normally found in natural waters in tracer concentrations only. Studies of their chemical state at low concentration levels are

* Present address: Faculty of Pharmacy, High Medical Institute, Ehz. Josiph No. 15, Sofia, Bulgaria.

** Present address: Department of Analytical Chemistry, Royal Institute of Technology, S-100 44 Stockholm 70, Sweden.

therefore of importance for the understanding of their distribution in nature. Solvent extraction using radiometric techniques is quite appropiate for this purpose, since it has proven to be a fruitful method for the study of chemical equilibria at very low concentration levels.[21]

In this paper we report solvent extraction studies of complex formation between methylmercury(II) and chloride ions in the two-phase systems $CH_3Hg(II) - 1$ M (Na,H) (ClO_4,Cl)/*o*-xylene. The present work is part of a larger project in this laboratory concerned with studies of the solution chemistry of methylmercury(II) in particular and other heavy metal ions in general, primarily at the low concentration levels as found in natural waters.

The knowledge of the extraction properties of methylmercury(II)-chloride complexes has subsequently been used in studies of the complex equilibria between methylmercury(II) and other ligands.[22] This work also illustrates the possibility and advantages of using solvent extraction techniques for accurate studies of complex equilibria. The preliminary results have been reported elsewhere.[23] The present studies were initiated by one of us (O.B.) who did the preliminary work using spectrophotometric and titration methods. The work has been continued and extended by F. I. and D. H. L. who applied both radiometric and spectrophotometric methods to the distribution studies.

Previous work. The distribution of methylmercuric chloride between toluene and water has previously been studied by Simpson [24] who reported the following value for the distribution constant $K_D = [CH_3HgCl]_{org}[CH_3HgCl]^{-1} = 11$. However, this result may not be taken as conclusive since for the calculation of K_D the author has only a single experimental point available and thus gives no evidences as to the CH_3HgCl species assumed to be formed.

Solubility studies as well as potentiometric studies on the formation of CH_3HgCl have previously been reported by Waugh *et al.*[25] However, their results are open to question, since these authors did not use a defined ionic medium in their studies and thus did not control the activity factors of the species studied. Results of potentiometric studies on the formation of CH_3HgCl in 0.1 M KCl medium have also been reported by Schwarzenbach and Schellenberg [26-28] and in 0.1 M KNO_3 by Zanella *et al.*[29] These authors [25-29] all found evidence for the formation of CH_3HgCl species in the aqueous solution. However, the values given for the formation constant for CH_3HgCl varied between $\log K = 4.90$ and 6.60 for the various media studied. Moreover no detailed studies on the possible formation of polynuclear methylmercuric species in two-phase systems have been reported. Thus further studies in the solution chemistry of $CH_3Hg(II)$ species are well motivated.

Barbieri and Bjerrum,[30] using a polarographical method, studied the solubility of organomonohalogeno and organomonothiocyanato mercury(II) complexes in 1 M salt solution ($NaX + NaClO_4$) or in a 50 vol % methanol-water solvent. They found evidence for the formation of distinct negatively charged complexes $RHgX_n^{1-n}$ ($R = C_2H_5$ and 2-butyl; $n = 1, 2, 3$) only in the thiocyanate and iodide systems. Rizzardi *et al.*[31] by ion-exchange studies found indications of the formation of C_2H_5HgCl and probably also $C_2H_5HgCl_2^-$ and $C_2H_5HgCl_3^{2-}$ in aqueous solutions at high ligand concentrations. Eigen *et al.*[32] studied the kinetics of the formation of CH_3HgX^{1-n} from CH_3HgOH for $X^{n-} = Cl^-$, Br^-, I^-, SCN^-, and SO_3^{2-}.

Symbols and equilibrium constants

$[\ ]$ = equilibrium concentration in the aqueous phase.
$[\ ]_{org}$ = equilibrium concentration in the organic phase.

C_{Cl} = initial total concentration of chloride ion in the aqueous and organic phase.

C_{MeHg} = initial total concentration of methylmercury(II) ion in the organic phase.

$K_{pqr,org}$ = $[(H^+)_p(MeHg^+)_q(Cl^-)_r]_{org}[H^+]^{-p}[MeHg^+]^{-q}[Cl^-]^{-r}$, formation constant of the complex $(H^+)_p(MeHg^+)_q(Cl^-)_r$ in the organic phase.

$K_{klm,aq}$ = $[(H^+)_k(MeHg^+)_l(Cl^-)_m][H^+]^{-k}[MeHg^+]^{-l}[Cl^-]^{-m}$, formation constant of the complex $(H^+)_k(MeHg^+)_l(Cl^-)_m$ in the aqueous phase.

I_{aq}, I_{org} = gamma-activity of $Me^{203}Hg$ in the aqueous and organic phase, cpm for equal volumes of samples.

N_{aq}, N_{org} = number of moles of MeHg(II) in equal volumes of equilibrated aqueous and organic phases analyzed by spectrophotometric titration.

D = $\frac{\sum[MeHg]_{org}}{\sum[MeHg]} = I_{org}/I_{aq}$ or N_{org}/N_{aq}, net distribution ratio of $CH_3Hg(II)$.

MeHg = CH_3Hg, methylmercury(II).

$\sigma(y)$ = standard deviation in y (*cf.* Ref. 3, eqn. 17).

EXPERIMENTAL

Reagents. $HClO_4$ (*p.a.* Merck, Darmstadt) was used without further purification. $NaClO_4$ was prepared from Na_2CO_3 (*p.a.* Merck, Darmstadt) and $HClO_4$ (*p.a.*) as described in Ref. 34. *o*-Xylene (*puriss.*, Kebo) was purified by washing it with dilute NaOH solution, distilled water, dilute mineral acid (*e.g.* $HClO_4$) solution and finally several times with distilled water. Benzene (*p.a.* Merck, Darmstadt) was purified in the same way as *o*-xylene. Chloroform (*p.a.* Merck, Darmstadt) was purified by washing it several times with an equal volume of distilled water to remove any traces of ethanol. Dithizone (*p.a.* Merck, Darmstadt) was purified according to a procedure described by Irving and Cox [35] and the stock solution so prepared was stored under a layer of dilute sulfuric acid and kept in a refrigerator.[36]

Non-radioactive methylmercuric hydroxide solution was prepared by shaking an aqueous suspension of methylmercuric bromide with freshly prepared $Ag_2O(s)$ at about pH 12 for 10 – 12 h, centrifuging the mixture and pipetting the clear CH_3HgOH solution. The CH_3HgBr used was prepared from commercial methylmercuric bromide (Casco) which had been recrystallized twice from absolute alcohol.

Radioactive $CH_3{}^{203}Hg(II)$ was purchased from the Radiochemical Centre, Amersham, England, in the form of $(CH_3{}^{203}Hg)_2O$ and from the Swedish Atomic Energy Company, Studsvik, as $CH_3{}^{203}HgNO_3$ in aqueous solution. The $Me^{203}Hg(II)$ was purified from the small amount of inorganic $^{203}Hg(II)$ present by the following procedure which is a somewhat improved modification of the method described by Östlund:[20] The radioactive $Me^{203}Hg(II)$ was first converted into $Me^{203}HgCl$ by the addition of an excess of HCl and the solution obtained then evaporated nearly to dryness in order to decompose any HNO_3 present. The residual solution was finally adjusted to 0.5 M with respect to HCl and was shaken several times with equal volumes of benzene, which extracted MeHgCl into the organic phase. Afterwards the benzene phase was shaken several times with 0.5 M HCl solution to remove any coextracted $HgCl_2$. The MeHgCl benzene solution obtained was found to be free from inorganic Hg(II) as shown by the thin-layer chromatographic analysis method described by Östlund.[20] The purified MeHg(II) in the benzene phase

was used as the stock solution for the distribution experiments. In those experiments in which radioactive $Me^{203}HgCl$ was used, $C_{Me^*HgCl} = 8.2 \times 10^{-6}$ M, the *o*-xylene solvent contained 0.1 vol. % benzene. By comparison with the experiments in which pure *o*-xylene was used this small percentage of benzene was found not to affect the distribution of MeHg(II).

Analysis of methylmercury(II). Non-radioactive methylmercury(II) was analyzed using a spectrophotometric titration method developed for this purpose by Ingman.[37]

Distribution experiments. Equal volumes of aqueous and organic phases were equilibrated for at least 2 h in glass-stoppered centrifuge tubes using a rotating shaker. The two phases were afterwards separated from each other by centrifugation at approximately 3500 rpm. Samples of the solutions were pipetted out and the γ-radioactivity of the ^{203}Hg measured in a Tracerlab SC-57 low background well scintillation counter with a Tl-activitated NaI crystal in conjunction with a Tracerlab SC-70 Compu/Matic V scaler. In the case of non-radioactive methylmercury(II) the amounts of MeHg(II) in the two phases were analyzed as described by Ingman.[37] All experiments were carried out in rooms thermostated at 25 ± 0.3°C.

CHEMICAL MODEL

The methylmercury(II) species in the aqueous phase will be represented by the general formula:

$$(H^+)_k(MeHg^+)_l(Cl^-)_m$$

in which complex formation with other ions and molecules present in the ionic medium, such as ClO_4^-, Na^+, and H_2O has been disregarded. For example the species $CH_3HgCl(aq)$ and $CH_3HgOH(aq)$ will be denoted as the (0,1,1) and (−1,1,0) species in the aqueous phase. Similarly the general formula $(H^+)_p(MeHg^+)_q(Cl^-)_r$ will be used to represent the extractable $CH_3Hg(II)$ species in the organic phase, *e.g.* (0,1,1) species in the organic phase for $CH_3HgCl(org)$. As usual we make the assumption that only uncharged $CH_3Hg(II)$ species are extractable into the organic phase. The calculated distribution ratio for $CH_3Hg(II)$ in the two-phase system may be expressed by the following relationship:

$$D_{calc} = \frac{\sum q[(H^+)_p(MeHg^+)_q(Cl^-)_r]_{org}}{\sum l[(H^+)_k(MeHg^+)_l(Cl^-)_m]} = \frac{\sum qK_{pqr,\,org}[H^+]^p[MeHg^+]^q[Cl^-]^r}{\sum lK_{klm,\,aq}[H^+]^k[MeHg^+]^l[Cl^-]^m} \quad (1)$$

For low values of C_{MeHg} ($< 9.5 \times 10^{-4}$ M) we may make the reasonable assumption that only mononuclear MeHg(II) species are formed in both the organic and aqueous phases, *i.e.* q and l may only have the values 0 or 1. As will be shown later, some experimental evidence seems to support this assumption for the extraction conditions used. Assuming the formation of only mononuclear methylmercury(II) species, D will be independent of $[MeHg^+]$ and (1) may be written in the form:

$$D_{calc} = \frac{\sum K_{pqr,\,org}[H^+]^p[Cl^-]^r}{\sum K_{klm,\,aq}[H^+]^k[Cl^-]^m} \quad (2)$$

The mass balances for $CH_3Hg(II)$ and Cl^- are given by the following equations:

$$C_{MeHg} = \sum qK_{pqr,\,org}[H^+]^p[MeHg^+]^q[Cl^-]^r + \sum lK_{klm,\,aq}[H^+]^k[MeHg^+]^l[Cl^-]^m \quad (3)$$

$$C_{Cl} = \sum rK_{pqr,\,org}[H^+]^p[MeHg^+]^q[Cl^-]^r + \sum mK_{klm,\,aq}[H^+]^k[MeHg^+]^l[Cl^-]^m \quad (4)$$

Given the values of C_{MeHg}, C_{Cl}, $[H^+]$ for each point and the equilibrium constants $K_{pqr,\,org}$, $K_{klm,\,aq}$ for the formation of the $CH_3Hg(II)$ species in the organic and aqueous phase, we may calculate $[CH_3Hg^+]$ and $[Cl^-]$ from (3) and (4) and D_{calc} from (1) or (2).

ANALYSIS OF THE DATA

The distribution data given in Table 1 were analyzed using the computer program LETAGROP-DISTR,[1-5] which is a version of LETAGROP (=pit-mapping) for the analysis of distribution data. This program is used to find from the data the "best" set of constants K_1, $K_2 \ldots K_N$ for the formation of the species $(H^+)_p(MeHg^+)_q(Cl^-)_r$ in both phases by, *e.g.*, minimizing the error-square sum $U = \sum_1^{Np} (\log D_{calc} - \log D_{exp})^2$, where Np represents the number of experimental points available. The program also allows the choice of minimizing the error-squares sums of other types of errors. *i.e.* $Fel[2] = (D_{exp}D_{calc}^{-1} - 1)$ or $Fel[3] = (D_{calc}D_{exp}^{-1} - 1)$, $(Fel = \text{error})$. The results of the computer analysis of the data in this work, assuming the same chemical model but minimizing different types of error-squares sums, are given in Table 3. Their comparison will be discussed further below. The input data for the computer are: (1) I_{aq}, I_{org} or N_{aq}, N_{org} (2) C_{MeHg} in mol/l; (3) C_{Cl} in mol/l, and (4) $\log [H^+]$.

Table 1. The distribution of $CH_3Hg(II)$ between 1 M $(Na,H)(ClO_4,Cl)$ and *o*-xylene at 25°C. Data given as C_{Cl} M, $\log D_{exp}$, $\log[Cl^-]$ and $\log (D_{calc}D_{exp}^{-1})$. $-\log [H^+] = 1.699$.

$C_{MeHg(II)} = 2.358 \times 10^{-4}$ M[a]

6.916×10^{-5}, −0.407, −6.809, −0.025; 1.089×10^{-4}, −0.038, −6.495, −0.094; 1.333×10^{-4}, 0.101, −6.315, −0.068; 1.582×10^{-4}, 0.244, −6.123, −0.039; 1.831×10^{-4}, 0.434, −5.898, −0.044; 2.089×10^{-4}, 0.667, −5.581, −0.047; 2.363×10^{-4}, 0.891, −5.023, 0.002; 2.588×10^{-4}, 0.982, −4.580, 0.017; 3.107×10^{-4}, 1.039, −4.119, 0.006; 3.627×10^{-4}, 1.053, −3.894, 0.002; 4.627×10^{-4}, 1.080, −3.643, −0.018; 7.547×10^{-4}, 1.055, −3.285, 0.012; 1.282×10^{-3}, 1.064, −2.980, 0.005; 6.356×10^{-3}, 1.102, −2.213, −0.031; 1.000, 1.082, −0.000, −0.010.

$C_{MeHg(II)} = 5.900 \times 10^{-4}$ M[a]

1.333×10^{-4}, −0.578, −6.961, −0.003.

$C_{MeHg(II)} = 9.432 \times 10^{-4}$ M[b]

5.638×10^{-5}, −1.212, −7.623, −0.022; 1.589×10^{-4}, −0.699, −7.119, −0.037; 2.596×10^{-4}, −0.437, −6.847, −0.032; 3.589×10^{-4}, −0.282, −6.638, 0.014; 4.836×10^{-4}, −0.061, −6.404, 0.012; 5.635×10^{-4}, 0.087, −6.255, 0.000; 6.656×10^{-4}, 0.250, −6.048, 0.018; 7.685×10^{-4}, 0.474, −5.787, 0.002; 8.704×10^{-4}, 0.734, −5.375, 0.008; 1.016×10^{-3}, 1.013, −4.112, 0.033; 1.524×10^{-3}, 1.018, −3.236, 0.049.

[a] Distribution of $CH_3Hg(II)$ measured by a radiometric method. Initial total concentration of radioactive $CH_3{}^{203}HgCl$ in the organic phase was 8.2×10^{-6} M.

[b] Distribution of $CH_3Hg(II)$ measured by a spectrophotometric method.

RESULTS

The data given in Table 1 are represented as log D *versus* log C_{Cl} in Fig. 1. The distribution curve obtained shows clearly the following characteristics for the extraction system studied. The levelling of the curve to a limiting value of log D ($\approx +1.06$) with increasing total concentration of chloride indicates the formation of MeHg(II) species with the same chloride composition in both the aqueous and the organic phase for $C_{Cl} > 3.107 \times 10^{-4}$ M.

The results of the Letagrop analysis of the data ($Np = 27$ points) are summarized in Table 2. Assuming the formation of only mononuclear

Table 2. Equilibrium constants [a] log β_{pqr} for the formation of $(H^+)_p(MeHg^+)_q(Cl^-)_r$ species in the system MeHg(II) – 1 M (Na,H)(ClO_4,Cl)/*o*-xylene for various assumptions of chemical models which minimize the error-square sum $U = \sum_1^{27} (\log D_{calc} - \log D_{exp})^2$.

Model	$(H^+)_p(MeHg^+)_q(Cl^-)_r$(aq)	$(H^+)_p(MeHg^+)_q(Cl^-)_r$(org)	U_{min}	σ(log D)
I		(0,1,1) 4.18, max. 4.58	13.672	0.725
II [b]	(0,1,1) 5.32, max. 5.65	(0,1,1) 6.39, max. 6.71	0.029	0.034
III	(0,1,2) 3.64, max. 4.19	(0,1,1) 4.54, max. 4.80	2.953	0.344
IV	(0,1,1) 5.32, max. 5.66; (0,1,2) $\beta = 0$, max. 4.58	(0,1,1) 6.39, max. 6.72	0.029	0.034
V	(0,2,2) 14.17, max. 14.66	(0,1,1) 6.02, max. 6.29	0.443	0.133
VI	(0,1,1) 5.32, max. 5.51	(0,1,1) 6.39, max. 6.61; (0,2,2) $\beta = 0$, max. 14.72	0.029	0.033
VII	(0,1,1) 5.26, max. 5.56; (0,2,2) 13.67, max. 14.19	(0,1,1) 6.37, max. 6.65	0.024	0.031
VIII	(0,1,1) $\beta = 0$, max. 5.40; (0,2,2) 15.99, $\sigma(\beta)$ undetd.	(0,1,1) 5.80, max. 6.05; (0,2,2) 15.94, $\sigma(\beta)$ undetd.	0.021	0.030

[a] The equilibrium constant $\beta_{pqr} = [(H^+)_p(MeHg^+)_q(Cl^-)_r]_t[H^+]^{-p}[MeHg^+]^{-q}[Cl^-]^{-r}$, where the lower index t indicates the phase referred to in the reaction. The limits given (= max.) correspond approximately to log $(\beta + 3\sigma(\beta))$.
[b] The "best" model assumed.

$CH_3Hg(II)$ species in both the aqueous and organic phase and minimizing the square-sum of the error $Fel[1] = \log (D_{calc} D_{exp}^{-1})$, model II clearly gives the lowest value for the minimized error-square sum U ($U_{min} = 0.029$ and $\sigma(\log D) = 0.034$) compared with the other chemical models tried. A slight improvement of U_{min} and $\sigma(\log D)$ is obtained when additional dimeric $CH_3Hg(II)$ species in the aqueous phase or in both phases are assumed to be formed (*cf.* models VII and VIII). However, for these latter models the standard deviations found for the formation constant β are greater than those

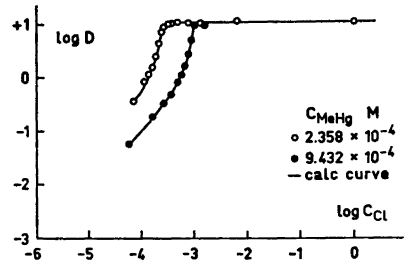

Fig. 1. Distribution of MeHg(II) between *o*-xylene and 1 M (Na,H)(ClO_4,Cl) aqueous solutions as a function of the initial total concentration of chloride, C_{Cl} M, for $-\log [H^+] = 1.699$ and different constant values of initial total concentration of MeHg(II), $C_{MeHg} = 2.358 \times 10^{-4}$ (○) and 9.432×10^{-4} M (●). The full-drawn lines have been calculated using the equilibrium constants given in model II (Tables 2 and 3) for the formation of the $(H^+)_p(MeHg^+)_r(Cl^-)_s$ species: $MeHg^+$(aq), MeHgCl(aq) and MeHgCl(org). The data are given in Table 1.

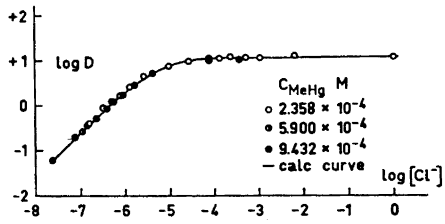

Fig. 2. The distribution of MeHg(II) in the system 1 M (Na,H) (ClO_4,Cl)/*o*-xylene as a function of the equilibrium concentration of chloride ions in the aqueous phase, $[Cl^-]$ M, for $-\log [H^+] = 1.699$ and different constant values of initial total concentration of MeHg(II), $C_{MeHg} = 2.358 \times 10^{-4}$ (○); 5.900×10^{-4} (◑) and 9.432×10^{-4} M (●). The full-drawn line has been calculated assuming the set of MeHg(II) – Cl^- species and the equilibrium constants given in model II (Tables 2 and 3). The data are given in Table 1.

Table 3. Comparison of equilibrium constants[a] log β_{pqr} for the formation of $(H^+)_p(MeHg^+)_q(Cl^-)_r$ species in the two-phase system MeHg(II) – 1.0 M (Na,H)(ClO_4,Cl)/*o*-xylene which minimize the error-square sum $U = \sum_1^{27} Fel[i]^2$, where $Fel[1] = \log(D_{calc}D_{exp}^{-1})$; $Fel[2] = (D_{exp}D_{calc}^{-1} - 1)$ and $Fel[3] = (D_{calc}D_{exp}^{-1} - 1)$.

Model (*cf.* Table 2)	$(H^+)_p(MeHg^+)_q(Cl^-)_r$(aq)	$(H^+)_p(MeHg^+)_q(Cl^-)_r$(org)	Choice of error *Fel*[i]	U_{min}	$\sigma(y)$
II	(0,1,1) 5.32, max. 5.65	(0,1,1) 6.39, max. 6.71	*Fel* [1]	0.029	0.034
	(0,1,1) 5.32 ± 0.09	(0,1,1) 6.40 ± 0.09	*Fel* [2]	0.171	0.083
	(0,1,1) 5.32 ± 0.09	(0,1,1) 6.39 ± 0.09	*Fel* [3]	0.138	0.074
IV	(0,1,1) 5.32, max. 5.66; (0,1,2) $\beta = 0$, max. 4.58	(0,1,1) 6.39, max. 6.72	*Fel* [1]	0.029	0.034
	(0,1,1) 5.33, max. 5.66; (0,1,2) $\beta = 0$, max. 4.72	(0,1,1) 6.40, max. 6.73	*Fel* [2]	0.171	0.084
	(0,1,1) 5.32, max. 5.69; (0,1,2) $\beta = 0$, max. 4.81	(0,1,1) 6.39, max. 6.75	*Fel* [3]	0.138	0.076

The equilibrium constant $\beta_{pqr} = [(H^+)_p(MeHg^+)_q(Cl^-)_r]_l[H^+]^{-p}[MeHg^+]^{-q}[Cl^-]^{-r}$, where the lowerindex indicates the phase referred to in the reaction. The limits given correspond approximately to log $(\beta \pm 3\,\sigma(\beta))$ nd if $\sigma(\beta) > 0.2\beta$, the maximum value log $(\beta + 3\sigma(\beta))$ is given.

found for model II. Within the experimental accuracy these three models all give a satisfactory description of the available data. Since in these experiments the total concentration of MeHg(II) was always kept rather low ($C_{MeHg} < 9.432 \times 10^{-4}$ M), it seems reasonable to assume the formation of only mononuclear MeHg(II) species in both phases. This assumption is supported by the fact that the experimental points describing the extraction of MeHg(II) for different initial total concentrations of methylmercury ($C_{MeHg} = 2.358 \times 10^{-4} - 9.432 \times 10^{-4}$ M) as a function of [Cl^-] (*cf.* Fig. 2) practically all fall on the same line. From Table 3 it can be seen that practically the same values for the formation constant of β_{pqr} are found for the set of $(H^+)_p(MeHg^+)_q(Cl^-)_r$ species in model II and model IV even if other types of error square sums are minimized, *i.e.* the square sums of the errors $Fel[2] = (D_{exp}D_{calc}^{-1} - 1)$ or $Fel[3] = (D_{calc}D_{exp}^{-1} - 1)$. This indicates that for the set of data available, the assumption made in the data analysis that equal weight may be given to the different experimental points, *i.e.* weight factor = 1, is not unreasonable.

In Fig. 3 are illustrated some data from Ref. 22, which show the distribution of MeHg(II) at $C_{Cl} = 1.27 \times 10^{-3}$ M with varying values of [H^+] (pH = = 1.26 – 2.55). The practically constant value of log D as a function of log [H^+] indicates that the hydrolysis of MeHg(II) is negligible in the pH range studied. This agrees with the results reported by Schwarzenbach and Schellenberg.[26–28]

TEST FOR THE EXTRACTION OF METHYLMERCURIC PERCHLORATE

To test whether $MeHgClO_4$ species may also be extractable in *o*-xylene the following two sets of experiments were performed:

(a) The distribution of MeHg(II) was studied at constant values of $C_{MeHg} = 5.90 \times 10^{-4}$ M and log [H^+] = -1.699, while varying the concentration of the perchlorate ions ($C_{ClO_4} = 2.5$, 1.0 and 0.5 M). Within this series of experiments the distribution of MeHg(II) increased with increasing [ClO_4^-] (*cf.* Fig. 4). This effect may be interpreted as being due to the extraction of either $MeHgClO_4$ or of MeHgCl complex due to the presence of chloride ion impurities in the $NaClO_4$ medium used.

(b) Five solutions, each containing 1 M (Na,H)ClO_4 and 1.18×10^{-4} M, 2.36×10^{-4} M, 4.72×10^{-4} M, 5.90×10^{-4} M, and 9.34×10^{-4} M CH_3Hg(II) (added as non-radioactive CH_3HgOH), respectively, were equilibrated with equal volumes of *o*-xylene. The organic phases were then analyzed for CH_3Hg(II) using the photometric titration method. In all cases, the organic phase was found to contain the same concentration of methylmercury(II), namely $C_{MeHg(org)} = 4.70 \times 10^{-6}$ M.

Table 4. The distribution of methylmercury(II) between $NaClO_4$ solutions and *o*-xylene at 25°C. $-\log [H^+] = 1.699$.

(a) $C_{MeHg(II)} = 5.895 \times 10^{-4}$ M

C_{ClO_4} M (log D): 0.50 (-2.407); 1.00 (-2.095); 2.0 (-1.690).

(b) $C_{ClO_4} = 1.0$ M.

$C_{MeHg(II)}$ M (log D): 1.18×10^{-4} (-1.381); 2.36×10^{-4} (-1.691); 4.72×10^{-4} (-1.998); 5.90×10^{-4} (-2.095); 9.43×10^{-4} (-2.300).

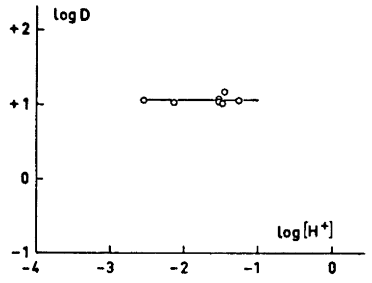

Fig. 3. The distribution of MeHg(II) in the system MeHg(II) – 1 M (Na,H)(Cl,ClO_4)/*o*-xylene as a function of $[H^+]$ for $C_{Cl} = 1.27 \times 10^{-3}$ M and $C_{MeHg(II)} = 4.15 \times 10^{-5} - 5.349 \times 10^{-4}$ M. The full-drawn line has been calculated assuming the formation of the species $MeHg^+$(aq), MeHgCl(aq) and MeHgCl(org) with equilibrium constants given in Table 2 (model II). The data are taken from Ref. 25.

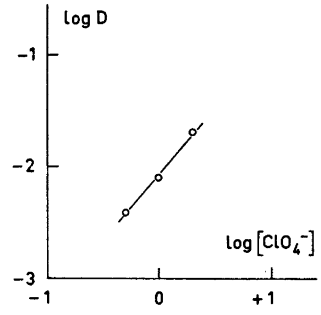

Fig. 4. The distribution of CH_3Hg(II) between (Na,H)ClO_4 solutions ($-\log[H^+] = 1.699$) and *o*-xylene as a function of $[ClO_4^-]$ M. The initial total concentration of MeHg(II), $C_{MeHg} = 5.895 \times 10^{-5}$ M. The data are given in Table 4.

Assuming the extraction of both MeHgCl and $MeHgClO_4$ in *o*-xylene we may write the following expression for the distribution ratio D:

$$D = \frac{[MeHgClO_4]_{org} + [MeHgCl]_{org}}{[MeHg^+] + [MeHgCl]} =$$

$$= \frac{{}^*K_{011,org}[ClO_4^-] + K_{011,org}[Cl^-]}{1 + K_{011,aq}[Cl^-]} =$$

$$\simeq {}^*K_{011,org}[ClO_4^-] + K_{011,org}[Cl^-] \quad (5)$$

since for the low concentration range of $[Cl^-] < 10^{-7}$ M, $K_{011,aq}[Cl^-] \ll 1$.

From the equation for the mass balance of Cl^- we find the following expression for $[Cl^-]$:

$$C_{Cl} = [Cl^-] + [MeHgCl] + [MeHgCl]_{org} \simeq [MeHgCl] + [MeHgCl]_{org} = (K_{011,aq} + K_{011,org})[MeHg^+][Cl^-], \text{ and thus } [Cl^-] = C_{Cl}(K_{011,aq} + K_{011,org})^{-1}[MeHg^+]^{-1} \approx C_{Cl}(K_{011,aq} + K_{011,org})^{-1} C_{MeHg(aq)}^{-1} \quad (6)$$

Substituting (6) and the value $[ClO_4^-] = 1$ M into (5) gives the following relationship:

$$D = {}^*K_{011,org} + K_{011,org}(K_{011,aq} + K_{011,org})^{-1} C_{Cl} C_{MeHg(aq)}^{-1} \quad (7)$$

According to (7) the plot log D *versus* log $C_{MeHq(aq)}^{-1}$ will give two straight lines with limiting slopes equal 0 and +1 in the case when both $MeHgClO_4$ and MeHgCl species are extracted. As seen in Fig. 5 this plot gives only one straight line with a slope of +1, indicating that for the concentration of

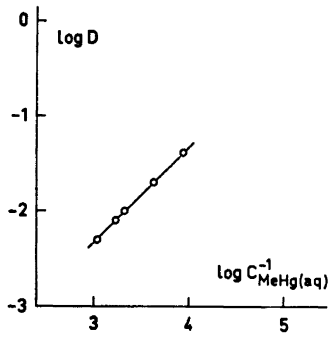

Fig. 5. The distribution of $CH_3Hg(II)$ between 1.0 M $(Na,H)ClO_4$ solutions ($-\log [H^+] = 1.699$) and *o*-xylene as a function of the total concentration of $CH_3Hg(II)$ in the aqueous phase, $C_{MeHg(aq)}$ M. The data are given in Table 4.

ClO_4^- studied ($C_{ClO_4} = 1.0$ M) no detectable extraction of $MeHgClO_4$ in *o*-xylene occurred. Goggin and Woodward [38] from Raman spectra studies found no evidence for the formation of a $MeHgClO_4$ complex in aqueous solution, which is not surprising in view of the present results.

Using the values found for D, $K_{011,aq} = 10^{5.32}$ M^{-1}, $K_{011,org} = 10^{6.39}$ M^{-1}, $^*K_{011,org} = 0$ for the formation of $MeHgClO_4$ (org), and the given values of C_{MeHg}, the background concentration of Cl^- for the 1.0 M $NaClO_4$ medium used was calculated to be $C_{Cl} = 5.1 \times 10^{-6}$ M. The values of C_{Cl} given in Table 1 have been corrected for with this background chloride concentration.

Conclusion. We thus conclude that the simplest chemical model which gives a satisfactory description of the available data is the assumption of the formation of $CH_3HgCl(aq)$ and $CH_3HgCl(org)$ with the following equilibrium constants:

$$CH_3Hg^+ + Cl^- \rightleftharpoons CH_3HgCl(aq);\ \log (K \pm 3\sigma) = 5.32 \pm 0.09 \quad (8)$$

$$CH_3Hg^+ + Cl^- \rightleftharpoons CH_3HgCl(org);\ \log (K \pm 3\sigma) = 6.39 \pm 0.09 \quad (9)$$

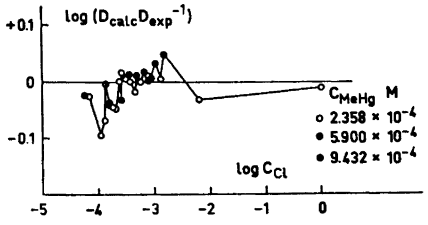

Fig. 6. The error $\log (D_{calc}D_{exp}^{-1})$ as a function of $\log C_{Cl}$ for the two-phase system MeHg(II) – 1.0 M $(Na,H)(ClO_4,Cl)$/*o*-xylene, assuming the $(H^+)_p(MeHg^+)_q(Cl^-)_r$ species and equilibrium constants given in model II (Tables 2 and 3). The distribution data are given in Table 1.

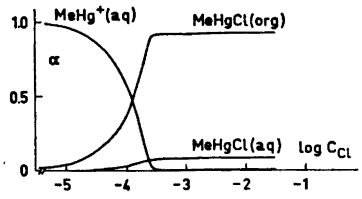

Fig. 7. The mol fraction of different MeHg(II) species in the two-phase system MeHg(II) – 1.0 M $(Na,H)(ClO_4,Cl)$ as a function of C_{Cl} for $C_{MeHg} = 2.36 \times 10^{-4}$ M and $-\log [H^+] = 1.699$. The curves have been calculated assuming the formation of MeHg(II) – Cl^- species with the equilibrium constants given in model II (Tables 2 and 3).

and from (8) and (9) one finds for the distribution equilibrium of CH_3HgCl:

$$CH_3HgCl(aq) \rightleftharpoons CH_3HgCl(org); \quad \log (K_D \pm 3\sigma) = 1.07 \pm 0.13.$$

In Fig. 6 the error, $\log (D_{calc} D_{exp}^{-1})$, found for the different experimental points when model II is assumed has been plotted as a function of $\log C_{Cl}$. Fig. 7 shows the mol fraction of the different MeHg(II) species as a function of C_{Cl} for $C_{MeHg} = 2.36 \times 10^{-4}$ M, calculated using the HALTAFALL program [39] and the values of the constants for model II.

The results of the present work have been used in studies of the complex formation of $CH_3Hg(II)$ with other inorganic ligands,[22] *e.g.* OH^- and HPO_4^{2-}. These have been carried out by studying the extraction of $CH_3Hg(II)$ as a function of the concentration of the ligand in question at different constant values of chloride concentration.

DISCUSSION

The value found for the formation constant of $CH_3HgCl(aq)$ is comparable with that reported by Waugh *et al.*[25] ($\log K = 5.38 - 6.06$, proposed mean value 5.45) in chloride medium and by Schwarzenbach and Schellenberg [26–28] at ionic strength $I = 0.1$ ($\log K = 5.25$). This latter value was found by potentiometric titration of $CH_3Hg(II)$ solution with HCl solution and thus the chloride and the hydrogen ion concentration of the solution varied. ($C_{Cl} = = 0.1005 - 0.1019$ M and $-\log [H^+] = 9.35 - 8.17$.) Since the titration was performed for only one value of the total concentration of methylmercury ($C_{MeHg} = 2.34 \times 10^{-3}$ M) Schwarzenbach and Schellenberg's data cannot be used to test the possibility of the formation of polynuclear $CH_3Hg(II)$-Cl species. Zanella *et al.*[29] reported the value $K = 10^{4.90}$ M^{-1} for the formation of MeHgCl in 0.1 M KNO_3 solution. Compared with the results found by the other authors this value is definitely too low, especially since no complex formation between CH_3Hg^+ and NO_3^- is expected.[38] In Table 5 we summarise

Table 5. Distribution constant K_D and equilibrium constant [a] K_{011} for formation of CH_3HgCl complex in various systems.

System	log K_D	log K_{011}	Experimental method	Ref.
Water/toluene	1.04		Distr.	Simpson [24]
0 – 7 mM Cl^-		5.45	EMF	Waugh *et al.*[25]
0.1 M KCl		5.25	EMF	Schwarzenbach and Schellenberg [26–28]
0.1 M KNO_3		4.90	EMF	Zanella *et al.*[29]
1.0 M (Na,H)ClO_4/ *o*-xylene	1.07 ± 0.13	5.32 ± 0.09	Distr.	This work

[a] The distribution constant $K_D = [CH_3HgCl]_{org}[CH_3HgCl]^{-1}$ and equilibrium constant $K_{011} = [CH_3HgCl][CH_3Hg^+]^{-1}[Cl^-]^{-1}$. The limits given correspond approximately to log $(K \pm 3\sigma(K))$.

the results of work on the distribution and formation of CH_3HgCl species in various systems reported previously.

Test for the dissociation of CH_3HgCl in o-xylene. An interesting question which may be raised is whether or not the available data can indicate the formation of dissociated CH_3HgCl species in the organic phase. Assuming this to be the case the following additional equilibrium reaction must be taken into account:

$$CH_3HgCl(org) \rightleftharpoons CH_3Hg^+(org) + Cl^-(org); \quad K_{dis,\,org} \tag{10}$$

The condition for electroneutrality in the organic phase requires that $[CH_3Hg^+]_{org} = [Cl^-]_{org}$, assuming that no other charged species are extracted.

From (9) and (10) the following relationship may be obtained:

$$[CH_3Hg^+]_{org} = (K_{dis,\,org} K_{011,\,aq} [CH_3Hg^+][Cl^-])^{\frac{1}{2}} \tag{11}$$

The distribution ratio D for $CH_3Hg(II)$ may now be expressed as follows:

$$D = \frac{[MeHgCl]_{org} + [MeHg^+]_{org}}{[MeHg^+] + [MeHgCl]} = \frac{K_{011,\,org}[MeHg^+][Cl^-] + (K_{dis,\,org} K_{011,aq}[MeHg^+][Cl^-])^{\frac{1}{2}}}{K_{011,\,aq}[MeHg^+][Cl^-] + [MeHg^+]} \tag{12}$$

From (12) we now may derive the expression for D for the following two limiting cases when $[Cl^-]$ is varied:

$$\log D_{[Cl^-]\to 0} = \log (K_{011,\,org}[Cl^-] + (K_{dis,\,org} K_{011,\,aq} C_{MeHg}^{-1})^{\frac{1}{2}}[Cl^-]^{\frac{1}{2}} \tag{13}$$

$$\log D_{[Cl^-]\to \infty} = \log (K_{011,\,org} K_{011,aq}^{-1} + K_{dis,\,org}^{\frac{1}{2}} K_{011,\,aq}^{-\frac{1}{2}} ([MeHg^+][Cl^-])^{-\frac{1}{2}} \tag{14}$$

From eqn. (13) it follows that a plot of log D *versus* log $[Cl^-]$ will give a straight line with a limiting slope of $+1$ in the region where undissociated CH_3HgCl predominates and the limiting slope $+\frac{1}{2}$ in case dissociated species of MeHg(II) predominate. Furthermore from eqn. (14) we will expect a limiting value of $-\frac{1}{2}$ with increasing value of $[Cl^-]$ for the extraction at a constant value of MeHg(II) concentration. The distribution data available, as seen in Fig. 2 where log D is plotted as a function of log $[Cl^-]$ indicates only a limiting slope of $+1$ with decreasing $[Cl^-]$ and a limiting slope of 0 with increasing $[Cl^-]$. This gives evidence that under the condition of experiments the extracted MeHgCl species are predominantly in the undissociated form. This fact is not surprising considering the low value found for the dissociation constant in the aqueous solution $K_{dis,\,aq} = K_{011,\,aq}^{-1} = 10^{-5.32}$ M. The formation of dissociated MeHgCl in nonaqueous solvent thus may only be expected in rather polar solvents.

Acknowledgements. The authors are obliged for the interest shown by the late Professor Lars Gunnar Sillén during the course of the work. The financial support given by the *Statens Naturvårdsverk* (*The Swedish National Environment Protection Board*) and the *Swedish Natural Science Research Council* is gratefully acknowledged. Dr. Derek Lewis has kindly revised the English of the manuscript.

REFERENCES

1. Liem, D. H. *Acta Chem. Scand.* **25** (1971) 1521.
2. Ingri, N. and Sillén, L. G. *Arkiv Kemi* **23** (1964) 97.
3. Sillén, L. G. and Warnqvist, B. *Arkiv Kemi* **31** (1969) 315.
4. Sillén, L. G. and Warnqvist, B. *Arkiv Kemi* **31** (1969) 341.
5. Arnek, R., Sillén, L. G. and Wahlberg, O. *Arkiv Kemi* **31** (1969) 353.
6. a. Lindström, O. *Trans. Royal Inst. Technol. Stockholm* **1968** 185; b. Ulfvarson, U. *Svensk Kem. Tidskr.* **73** (1961) 553.
7. Torgeson, D. C. *Fungicides*, Academic, New York 1967, Vol. I.
8. Grewal, J. S. and Vir, D. *Indian Phytopathol.* **14** (1961) 213; *Chem. Abstr.* **62** (1968) 3339c.
9. Schmutterer, H. Z. *Pflanzenkrankh. Pflanzenschutz* **68** (1961) 479; *Chem. Abstr.* **56** (1962) 738b.
10. Schuhmann, G. *Nachrbl. Deut. Pflanzenschutzdienstes (Brunswick)* **15** (1963) 37; *Chem. Abstr.* **59** (1965) 10707e.
11. Jensen, S. and Jernelöv, A. *Biocidinformation* **10** (1967) 4.
12. Jensen, S. and Jernelöv, A. *Biocidinformation* **14** (1968) 3.
13. Wood, J. M., Kennedy, F. S. and Rosén, C. G. *Nature* **220** (1968) 173.
14. Borg, K., Wanntorp, H., Erne, K. and Hanko, E. *Viltrevy (Swedish Wildlife)* **6** (1969) 301; *J. Appl. Ecol.* **3** (1966) 171.
15. Borg, K. *Proc. VIII Nord. Veterinärmötet*, Helsingfors 1968, p. 394.
16. Westöö, G. *Acta Chem. Scand.* **20** (1966) 2131; **21** (1967) 1790.
17. Westöö, G. and Rydälv, M. *Vår Föda* **7–8** (1971) 1; *Report on Mercury in Foods*, by the Joint FAO/WHO Expert Committee on Food Additives, 1970.
18. Norén, K. and Westöö, G. *Vår Föda* **19** (1967) 13.
19. a. Boetius, J. *Medd. Komm. Danmarks Fiskeri Havundersøgelser* **3** (4) (1960) 93; *Chem. Abstr.* **61** (1967) 6311b; b. *FAO Fisheries Reports*, No. 99, Rome 1971.
20. Östlund, K. *Acta Pharmacol. Toxicol.* **27** (1969) 1.
21. a. Rydberg, J. *Svensk Kem. Tidskr.* **67** (1955) 499; b. Dyrssen, D. *Svensk Kem. Tidskr.* **68** (1956) 212; c. Liem, D. H. *Inaugural Dissertation*, Royal Institute of Technology, Stockholm 1971 (available on request).
22. Liem, D. H. and Ingman, F. *To be published; Proc. 15th Int. Conf. Coord. Chem.*, Moscow 1973.
23. Budevsky, O., Ingman, F. and Liem, D. H. *Proc. 14th Nordic Chem. Conf.*, Umeå 1971.
24. Simpson, R. B. *J. Am. Chem. Soc.* **83** (1961) 4711.
25. Waugh, T. D., Harold, F. W. and Laswick, J. A. *J. Phys. Chem.* **59** (1955) 395.
26. Schellenberg, M. *Diss.* ETH, Zürich 1963.
27. Schellenberg, M. and Schwarzenbach, G. *Proc. 7th Int. Conf. Coord. Chem.*, Stockholm 1962, p. 157.
28. Schwarzenbach, G. and Schellenberg, M. *Helv. Chim. Acta* **48** (1965) 28.
29. Zanella, P., Plazzogna, G. and Tagliavini, G. *Inorg. Chim. Acta* **2** (3) (1960) 340.
30. Barbieri, R. and Bjerrum, J. *Acta Chem. Scand.* **19** (1965) 469.
31. Rizzardi, G., Pietropaolo, R. and Barbieri, R. *Gazz Chim. Ital.* **96** (1965) 1371.
32. Eigen, M., Geier, G. and Kruse, W. *Experientia* **9** (1964) 164.
33. Sillén, L. G. *Acta Chem. Scand.* **16** (1962) 159.
34. Some laboratory methods in current use at the Department of Inorganic Chemistry, Royal Institute of Technology, Stockholm, Mimeograph 1959.
35. Irving, H. M. N. H. and Cox, J. J. *J. Chem. Soc.* **1961** 1470.
36. Irving, H. M. N. H. and Kiwan, A. M. *Anal. Chim. Acta* **45** (1969) 243.
37. Ingman, F. *Talanta* **18** (1971) 744.
38. Goggin, P. L. and Woodward, L. A. *Trans. Faraday Soc.* **58** (1962) 1495.
39. Ingri, N., Kakolowicz, W., Sillén, L. G. and Warnqvist, B. *Talanta* **14** (1967) 1261.

Received October 16, 1972.

ACTA CHEMICA SCANDINAVICA 27 (1973) 1290–1298

On the Properties of the Zirconium and Hafnium Dichalcogenides

LEIF BRATTÅS and ARNE KJEKSHUS

Kjemisk Institutt, Universitetet i Oslo, Blindern, Oslo 3, Norway

The dichalcogenide phases of zirconium and hafnium have been studied by means of X-ray diffraction and diffuse reflectance measurements. The results show that these phases have the general formula $T_{1+t}X_2$ where T and X denote the metal and chalcogen components, respectively, and $t \geq 0$. The $Zr_{1+t}Se_2$, $Zr_{1+t}Te_2$, $Hf_{1+t}Se_2$, and $Hf_{1+t}Te_2$ phases exhibit appreciable ranges of homogeneity, whereas $Zr_{1+t}S_2$ and $Hf_{1+t}S_2$ exist only for $t \approx 0.00$. Single crystals of all phases have been prepared by chemical transport reactions. The $Zr_{1+t}S_2$, $Zr_{1+t}Se_2$, $Hf_{1+t}S_2$, and $Hf_{1+t}Se_2$ phases are intrinsic semiconductors, whereas no conclusion could be drawn as to the type of electrical conduction of $Zr_{1+t}Te_2$ and $Hf_{1+t}Te_2$ from their diffuse reflectance spectra.

Three features emerge on considering the occurrence of the $Cd(OH)_2$ type structure among transition metal compounds (*cf.*, *e.g.*, Refs. 1–3):

(i) This structure type occurs exclusively with a chalcogen (S, Se, or Te) as the non-metal component.

(ii) The metal component of these phases belongs to the beginning and end of the transition periods.

(iii) The $Cd(OH)_2$ phases in which the metal comes from an earlier group of the transition series generally exhibit broad ranges of homogeneity in contrast with those (except for the $NiTe_2$ phase) in which the metal belongs to a later group.

Reasons for these trends are not clearly understood as yet and more extensive investigations are necessary in order to clarify the situation.

The present paper concerns the dichalcogenides of zirconium and hafnium, which, despite several previous studies,[4–28] have not hitherto been fully explored.

EXPERIMENTAL

The experimental details concerning the purity of the elements, sample preparation (see also the results section), X-ray diffraction, and diffuse reflectance measurements have been presented in a previous communication.[29]

RESULTS AND DISCUSSION

(i) *Polycrystalline samples.* Polycrystalline samples of $Zr_{1+t}S_2$, $Zr_{1+t}Se_2$, $Zr_{1+t}Te_2$, $Hf_{1+t}S_2$, $Hf_{1+t}Se_2$, and $Hf_{1+t}Te_2$ are easily synthesized by direct reactions between the elements at 800°C. Guinier data show, in addition to confirming the identity with earlier investigations, that the di-phases are isostructural with $Cd(OH)_2$. When $t > 0$, *i.e.* with an excess of metal,[12,18] the structure is modified to an intermediate between the $Cd(OH)_2$ and NiAs types.[1] The largest deviations from the $Cd(OH)_2$ type structure are found for the $Zr_{1+t}Te_2$ and $Hf_{1+t}Te_2$ phases, in which cases the maximum values of t are 0.33 and 0.43, respectively.

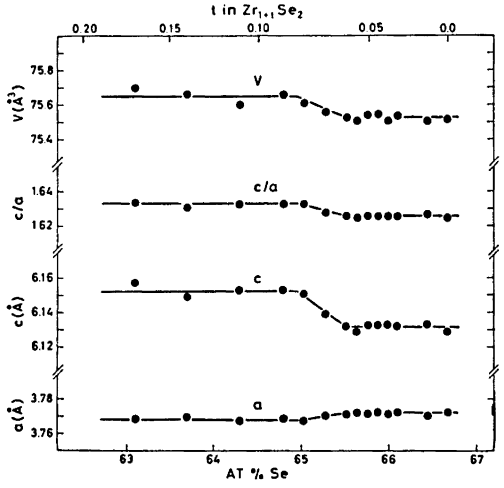

(a)

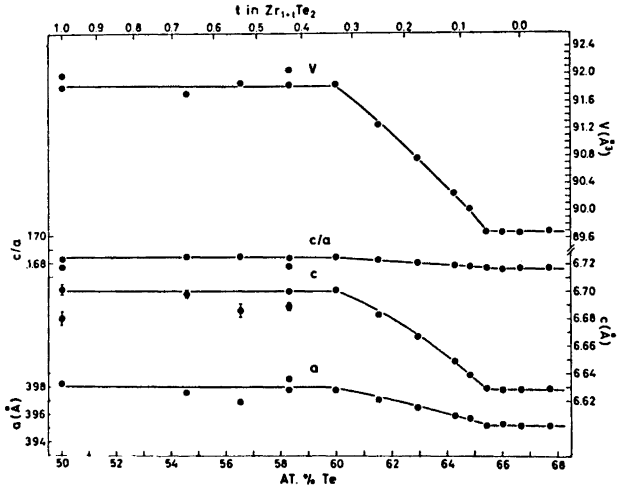

(b)

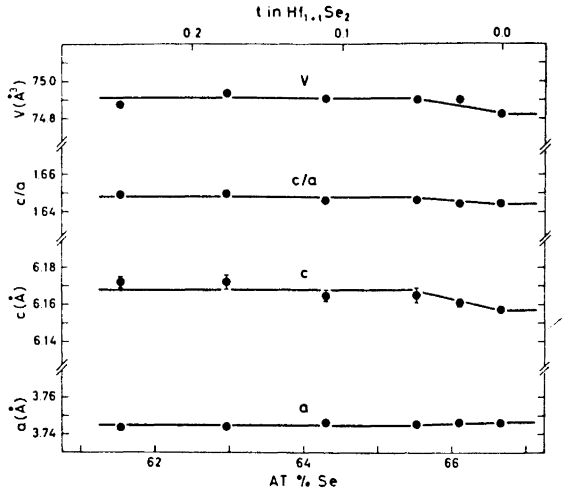

Fig. 1. Unit cell dimensions *versus* composition for the (a) $Zr_{1+t}Se_2$, (b) $Zr_{1+t}Te_2$, and (c) $Hf_{1+t}Se_2$ phases. Vertical bars show calculated error limits (twice the standard deviations) where these exceed the size of the symbols.

The Guinier photographs of the $Zr_{1+t}Te_2$ phase show additional reflections for samples with $t > 0.3$ which cannot be indexed on the basis of the $Cd(OH)_2$/NiAs type unit cell. These reflections could, on the other hand, be indexed by doubling the c axis in accordance with the findings of Gleizes and Jeannin.[27] A determination of this structure is not attempted since only powder data are at hand, but it is assumed that the $Cd(OH)_2$/NiAs type structure is modified by the spiral dislocations which are induced during the crystal growth, the problem being apparently analogous to that encountered for CdI_2 (*cf.* Ref. 31).

The variation of the unit cell dimensions with composition (Fig. 1) shows that there is an appreciable region of homogeneity for the $Zr_{1+t}Se_2$, $Zr_{1+t}Te_2$, and $Hf_{1+t}Se_2$ phases. The corresponding data for the $Hf_{1+t}Te_2$ phase are given in a previous communication.[30] The present data show that the homogeneity range of $Zr_{1+t}Se_2$ extends from 65.5 ± 0.2 to 64.9 ± 0.1 atomic % Se ($0.05 \pm 0.01 \leq t \leq 0.08 \pm 0.01$); for $Zr_{1+t}Te_2$ from 65.5 ± 0.1 to 60.0 ± 0.5 atomic % Te ($0.05 \pm 0.01 \leq t \leq 0.33 \pm 0.03$); and for $Hf_{1+t}Se_2$ from 66.6 ± 0.1 to 65.5 ± 0.5 atomic % Se ($0.00 \pm 0.01 \leq t \leq 0.05 \pm 0.02$). The $Zr_{1+t}S_2$ and $Hf_{1+t}S_2$ phases exhibit no variations beyond the standard deviations in the unit cell dimensions ($a = 3.6617(6)$ Å, $c = 5.8275(11)$ Å for $Zr_{1+t}S_2$ and $a = 3.6318(8)$ Å, $c = 5.8517(12)$ Å for $Hf_{1+t}S_2$), and it is assumed that their homogeneity ranges are extremely narrow.

In some cases, contaminations from the phases TOS [32,33] and/or TSiX [34–37] were noted in the samples. The oxide impurity TOS was only detected for the sulphides. As a matter of fact, HfOS ($a = 5.6659(14)$ Å) has only briefly been mentioned in a recent, independent report [33] on hafnium sulphides. As a

consequence of the disturbing presence of these impurities it proved in some cases difficult to establish the correct sample composition. However, the results obtained on samples with appreciable amounts of impurities are not included in this paper.

In connection with the above phase-analytical data we also report a continuous range of solid solubility between hafnium disulphide and hafnium diselenide. In terms of the formula $HfS_{2-x}Se_x$ this implies that possible values of x cover the entire range $0.00 \leq x \leq 2.00$. The unit cell dimension a of $HfS_{2-x}Se_x$ exhibits (Fig. 2) a linear dependence with x, the c axis, however, does not show such a linear behaviour.

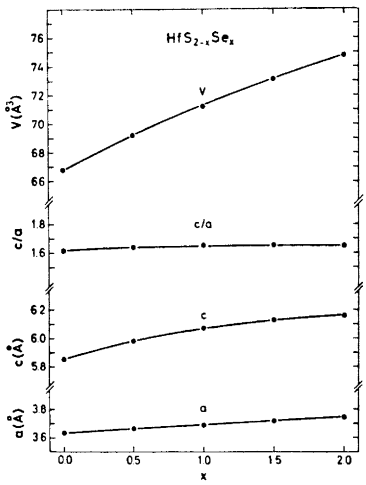

Fig. 2. Unit cell dimensions of the $HfS_{2-x}Se_x$ phase as a function of composition. The calculated error limits do not exceed the size of the symbols.

(ii) *Single crystals.* A systematic search for the suitable thermal conditions necessary for large single crystal growth employing chemical transport reactions was performed. Table 1 shows the optimum thermal conditions required for the binary phases. The transport and/or growth rates of the crystals vary considerably from one phase to the other, ranging from ~10 h for the production of large amounts of $Zr_{1+t}S_2$ crystals to ~100 h in the case of $Hf_{1+t}Se_2$.

Table 1. Suitable thermal conditions for chemical transport reactions.

Phase	t_1 (°C)	t_2 (°C)	$\Delta t/l$(°C/mm)
$Zr_{1+t}S_2$	900	770	0.9
$Zr_{1+t}Se_2$	900	780	0.8
$Zr_{1+t}Te_2$	1100	850	1.7
$Hf_{1+t}S_2$	900	810	0.6
$Hf_{1+t}Se_2$	900	775	0.8
$Hf_{1+t}Te_2$	1025	850	1.2

The transport conditions for the individual phases are, on the other hand, somewhat insensitive to the choice of hot and cold zone temperatures t_1 and t_2, respectively, of the reaction vessel. A homogeneous sample of $Zr_{1+t}Te_2$ is required in order to obtain this phase by means of transport reaction, otherwise crystals of $ZrTe_3$ are invariably obtained.

Flaky single crystals of up to 2 mm thickness and 100 mm^2 cross section were obtained in accordance with the typical layer structure of the phases. Although the colours of the various crystals are thickness dependent, in general, the sulphides are red, the selenides range from green to black, and the tellurides possess a bronze-like appearance. These observations agree with earlier findings.[12,16–20,26]

The unit cell dimensions, obtained from Guinier data of the crushed crystals (Table 2), gave constant values for each phase, showing the crystals to be of constant composition. A comparison of the values listed in Table 2

Table 2. Estimated compositions and unit cell dimensions for zirconium and hafnium dichalcogenides prepared by chemical transport reactions.

Phase	Estimated composition		Unit cell dimensions		
	Atomic % X	t	a (Å)	c (Å)	c/a
$Zr_{1+t}S_2$	66.7	0.00	3.6617(6)	5.8275(11)	1.5915(5)
$Zr_{1+t}Se_2$	65.5	0.05	3.7706(12)	6.133(3)	1.627(2)
$Zr_{1+t}Te_2$	65.5	0.05	3.9524(9)	6.625(2)	1.676(1)
$Hf_{1+t}S_2$	66.7	0.00	3.6320(9)	5.8500(14)	1.6107(8)
$Hf_{1+t}Se_2$	66.7	0.00	3.7440(7)	6.155(2)	1.644(1)
$Hf_{1+t}Te_2$	61.5	0.25	3.9509(9)	6.651(3)	1.683(2)

with the corresponding data for the polycrystalline samples provided a means of estimating crystal composition. These estimated compositions show, as expected, that the crystals belong to the non-metal rich phase-limit in all cases. Further confirmation as to the average compositions was provided by electron microprobe analyses on single crystals. However, in addition the latter analyses suggested concentration gradients of ≤ 2 atomic % X. Such a result conflicts with the Guinier data and the most probable explanation is that the electron microprobe results are reflecting local inhomogeneities at or near the crystal surfaces. The electron microprobe technique did, however, indicate the absence of detectable amounts of iodine.

The most suitable transport conditions according to the present study (Table 1) differ to some extent from the data already recorded in the literature.[19,20,26] There are in particular considerable differences between the values for t_1 and t_2 listed in Table 1 and the corresponding data recently published by Rimmington *et al.*[26] The less favourable transport conditions used by the latter authors are clearly reflected in the longer reaction periods employed in their study.

(iii) *Diffuse reflectance.* Fig. 3 shows the diffuse reflectance spectra of $HfS_{2-x}Se_x$ for different x, which are also representative for $Zr_{1+t}S_2$ and

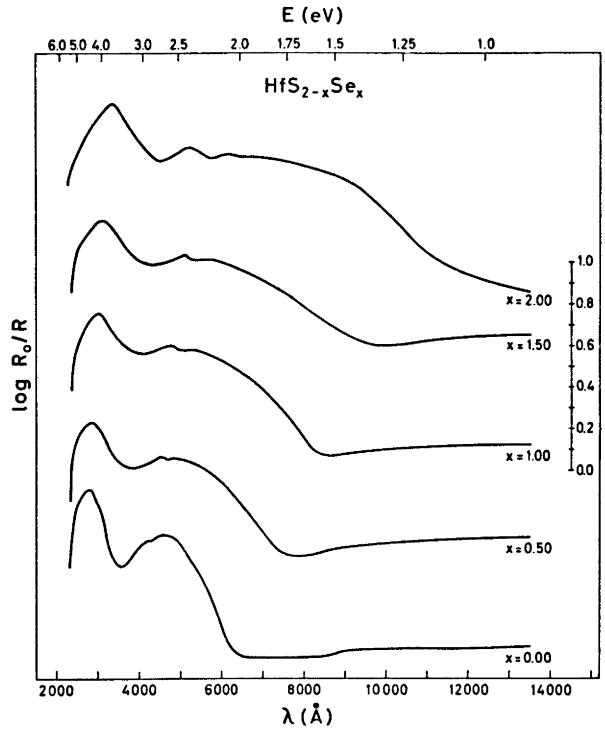

Fig. 3. Diffuse reflectance spectra of various samples of the $HfS_{2-x}Se_x$ phase.

$Zr_{1+t}Se_2$. In the corresponding spectra of $Zr_{1+t}Te_2$ and $Hf_{1+t}Te_2$ there is a characterless, rather uniform increase in log R_0/R between 2000 and 19 000 Å. Repeated measurements on different samples show that the results are well reproducible.

The evaluation of the band gap (ΔE) from diffuse reflectance spectra depends on the determination of the location of the absorption edge. By employing the extrapolation method [38] for determining the band gap, ΔE values of 1.72 ± 0.02 and 1.97 ± 0.03 eV were obtained for ZrS_2 and HfS_2, respectively. The band gaps for the corresponding selenides increase with t for both $Zr_{1+t}Se_2$ and $Hf_{1+t}Se_2$. The compositional dependence of the band gap is more substantial for the case of $Zr_{1+t}Se_2$ (0.87 ± 0.02 eV at $t = 0.05$; 1.61 ± 0.02 eV at $t = 0.08$) than for $Hf_{1+t}Se_2$ (1.08 ± 0.02 eV for $t = 0.00$; 1.14 ± 0.02 eV for $t = 0.05$). The present values for the sulphides are reasonably consistent with those previously reported.[19,20,22,25] For the selenides, on the other hand, the agreement is less satisfactory. The reported $\Delta E = 1.13$ eV for $Hf_{1+t}Se_2$ ($t = 0$) by Greenaway and Nitsche [19] is in close agreement with the present finding whereas the value 1.31 eV given by Murray *et al.*[25] is incompatible. On taking into account the variation of ΔE with t, the values

reported by Lee *et al.*[22] and Murray *et al.*[25] for the $Zr_{1+t}Se_2$ phase become consistent. The inconsistency apparently arises in the latter case because of the assumption of stoichiometric $ZrSe_2$.

Murray *et al.*[25] have presented semiempiric, tight binding calculated band structures for $Zr_{1+t}S_2$, $Zr_{1+t}Se_2$, $Hf_{1+t}S_2$, and $Hf_{1+t}Se_2$ ($t=0$). The calculated band gaps are in good agreement with the experimental values reported here for ZrS_2 and HfS_2, whereas the discrepancy increases in the order $HfSe_2$ and $ZrSe_2$, and becomes quite large for the latter compound. These calculations, however, are based on an idealized model and on slightly incorrect experimental parameters. In this connection it is relevant to note that there is a substantial difference between the calculated reduction parameters for $ZrSe_2$ and those for ZrS_2, HfS_2, and $HfSe_2$.

Since ΔE decreases with x in an approximately linear manner (Fig. 4), it is assumed that a similar relationship holds for the ΔE values for $Zr_{1+t}S_2$

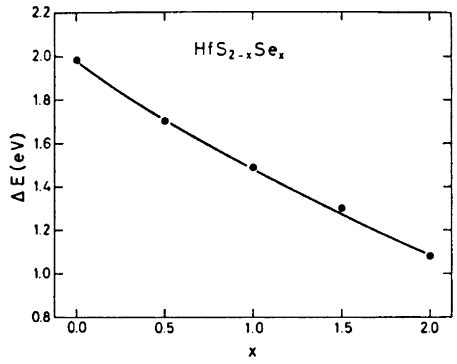

Fig. 4. Band gap (ΔE) *versus* x in $HfS_{2-x}Se_x$.

and $Zr_{1+t}Se_2$; $Hf_{1+t}S_2$ and $Hf_{1+t}Se_2$ to $Zr_{1+t}Te_2$ and $Hf_{1+t}Te_2$, respectively. This procedure yields $\Delta E \approx 0.2$ eV for both cases.

For all permitted values of t the $Zr_{1+t}Se_2$ and $Hf_{1+t}Se_2$ phases exhibit semiconductivity, which is tentatively explained in terms of the generalized (8 − N) rule (*cf.*, *e.g.*, Ref. 39). The correct mathematical formulation of the rule is in this case $n+P-Q=8a$, where, per formula unit, n is the total number of electrons involved in bonding, P and Q are the number of electrons in $X-X$ and $T-T$ bonds, respectively, and a is the number of X atoms. In accordance with previous experience and the observed diamagnetism for the compounds, each T atom is assumed to contribute 4 electrons, and each X atom 6 electrons to n ($=16$), *i.e.* the valence states of the constituent atoms correspond to their group number of the Periodic Table. For $t=0$, the crystal structure unequivocally requires that $P=Q=0$. The semiconducting nature of the dichalcogenides are consistent with this result. For $t\neq 0$ the interpretation of Q from the structure becomes less certain. The shortest metal-metal distance along [001] for $t\neq 0$ corresponds to $c/2$ which amounts to:

3.077 – 3.065 Å for $Zr_{1+t}Se_2$,
3.350 – 3.314 Å for $Zr_{1+t}Te_2$,
2.929 – 2.925 Å for $Hf_{1+t}S_2$,
3.085 – 3.078 Å for $Hf_{1+t}Se_2$, and
3.325 – 3.316 Å for $Hf_{1+t}Te_2$.

Although these distances appear to be somewhat longer than those expected for Zr – Zr or Hf – Hf single bonds (~ 3.0 Å) they may possibly be interpreted as such. Thus, assuming that each additional T atom incorporated in the lattice for $t > 0$ is bonded to two neighbouring T atoms and that two electrons are involved in these bonds, $Q = 4t$. The total number of valence electrons $n = 4(1+t) + 2 \times 6 = 16 + 4t$ when a metal valence of 4 is maintained. With $n = 16 + 4t$, $P = 0$, $Q = 4t$, and $a = 2$ the generalized (8 – N) rule is satisfied for all values of t. This appears to provide an explanation for the observed semiconducting properties of $Zr_{1+t}Se_2$ and $Hf_{1+t}Se_2$ for $t > 0$.

REFERENCES

1. Kjekshus, A. and Pearson, W. B. *Progr. Solid State Chem.* **1** (1964) 82.
2. Hulliger, F. *Struct. Bonding (Berlin)* **4** (1968) 83.
3. Wilson, J. A. and Yoffe, A. D. *Advan. Phys.* **18** (1969) 193.
4. van Arkel, A. E. *Physica (Eindhoven)* **4** (1924) 286.
5. Strotzer, E. F., Biltz, W. and Meisel, K. *Z. anorg. allgem. Chem.* **242** (1939) 249.
6. Zhuze, V. P. and Ryvkin, S. M. *Dokl. Akad. Nauk SSSR* **62** (1948) 55; Ryvkin, S. M. *Zh. Tekhn. Fiz.* **18** (1948) 1521.
7. Hägg, G. and Schönberg, N. *Arkiv Kemi* **7** (1954) 371.
8. Hahn, H., Harder, B., Mutschke, U. and Ness, P. *Z. anorg. allgem. Chem.* **292** (1957) 82.
9. Bracuti, A. J. J. *Dissertation Abstr.* **19** (1958) 1217.
10. Clearfield, A. *J. Am. Chem. Soc.* **80** (1958) 6511.
11. Hamann, S. D. *Australian J. Chem.* **11** (1958) 391.
12. McTaggart, F. K. and Wadsley, A. D. *Australian J. Chem.* **11** (1958) 445.
13. Bear, J. and McTaggart, F. K. *Australian J. Chem.* **11** (1958) 458.
14. McTaggart, F. K. *Australian J. Chem.* **11** (1958) 471.
15. McTaggart, F. K. and Moore, A. *Australian J. Chem.* **11** (1958) 481.
16. Hahn, H. and Ness, P. *Z. anorg. allgem. Chem.* **302** (1959) 37.
17. Hahn, H. and Ness, P. *Z. anorg. allgem. Chem.* **302** (1959) 136.
18. Jellinek, F. *Arkiv Kemi* **20** (1963) 447.
19. Greenaway, D. L. and Nitsche, R. *J. Phys. Chem. Solids* **26** (1965) 1445.
20. Park, K. C. *Thesis*, University of Minnesota 1967; Park, K. C. *Dissertation Abstr.* **B 28** (1967) 3208; Conroy, L. E. and Park, K. C. *Inorg. Chem.* **7** (1968) 459.
21. Lee, P. A., Said, G. and Davis, R. *Solid State Commun.* **7** (1969) 1359.
22. Lee, P. A., Said, G., Davis, R. and Lim, T. H. *J. Phys. Chem. Solids* **30** (1969) 2719.
23. Gleizes, A. and Jeannin, Y. *J. Solid State Chem.* **1** (1970) 180.
24. Wieting, T. J. *J. Phys. Chem. Solids* **31** (1970) 2148.
25. Murray, R. B., Bromley, R. A. and Yoffe, A. D. *J. Phys.* **C 5** (1972) 746.
26. Rimmington, H. P. B., Balchin, A. A. and Tanner, B. K. *J. Cryst. Growth* **15** (1972) 51.
27. Gleizes, A. and Jeannin, Y. *J. Solid State Chem.* **5** (1972) 42.
28. Smeggil, J. G. and Bartram, S. *J. Solid State Chem.* **5** (1972) 391.
29. Brattås, L. and Kjekshus, A. *Acta Chem. Scand.* **27** (1973) 3441.
30. Brattås, L. and Kjekshus, A. *Acta Chem. Scand.* **25** (1971) 2783.
31. Mitchell, R. S. *Z. Krist.* **108** (1956) 296, 341.
32. McCullough, J. D., Brewer, L. and Bromley, L. A. *Acta Cryst.* **1** (1948) 287.

33. Stocks, K., Eulenberger, G. and Hahn, H. *Naturwiss.* **58** (1971) 54.
34. Jellinek, F. and Hahn, H. *Naturwiss.* **49** (1962) 103.
35. Onken, H., Vierheilig, K. and Hahn, H. *Z. anorg. allgem. Chem.* **333** (1964) 267.
36. Haneveld, A. J. K. and Jellinek, F. *Rec. Trav. Chim.* **83** (1964) 776.
37. Jeannin, Y. and Mosset, A. *J. Less-Common Metals* **27** (1972) 237.
38. Tandon, S. P. and Gupta, J. P. *Phys. Status Solidi* **38** (1970) 363.
39. Kjekshus, A. *Acta Chem. Scand.* **18** (1964) 2379.

Received November 6, 1972.

ACTA CHEMICA SCANDINAVICA 27 (1973) 1299–1306

Equilibrium Studies in the Systems K_3AlF_6-Na_3AlF_6 and K_3AlF_6-Rb_3AlF_6

KAI GRJOTHEIM, JAN LÜTZOW HOLM and SHAHEER AZIZ MIKHAIEL*

Institute of Inorganic Chemistry, The Technical University of Norway, Trondheim, Norway

The binary systems K_3AlF_6-Na_3AlF_6 and K_3AlF_6-Rb_3AlF_6 have been investigated and the phase diagrams constructed, using ordinary thermal analysis (TA), differential thermal analysis (DTA), low- and high-temperature X-ray diffraction studies. In the system K_3AlF_6-Na_3AlF_6 an intermediate compound with the composition $2K_3AlF_6.Na_3AlF_6$, corresponding to the mineral elpasolite, K_2NaAlF_6, which melts congruently at 954°C, was detected. The compound was found to be cubic, with $a = 8.095 \pm 0.02$ Å, and has no polymorphic transformations. In the system K_3AlF_6-Rb_3AlF_6, a continuous solid solution was detected.

There has been a great interest in the structure and behaviour of the alkali-metal hexafluoroaluminates in recent years. The results reported in the literature, however, are often in disagreement. The present work is a part of an extensive study on the hexafluoroaluminates of Li, Na, K, Rb, and Cs. In a previous paper,[1] the phase diagrams of the binary systems Li_3AlF_6-K_3AlF_6 and Li_3AlF_6-Rb_3AlF_6 were presented. In this work, the phase diagrams of the systems K_3AlF_6-Na_3AlF_6 and K_3AlF_6-Rb_3AlF_6 have been determined.

EXPERIMENTAL

(a) *Thermal analysis (TA).* The equipments and technique used for the determination of cooling curves were similar to those used by Grjotheim.[2] An ordinary vertical tube furnace, with Kanthal A wire as the heating element, was used. The samples were melted in a crucible made of pure graphite (from Skandinaviska Grafitindustri AB with a minimum carbon content of 99.79 %. The temperature was measured with a Pt-Pt 10 % Rh thermocouple (calibrated at the melting point of silver) connected to a precision potentiometer (W. G. Pye, Cambridge, England), with a mirror galvanometer (Multiflex-Galvanometer, type MGO, Berlin, Germany). The end of the alumina

* Present address: National Research Centre, Dokki, Cairo, United Arab Republic.

jacket containing the hot junction of the thermocouple was sealed off with alundum cement. The temperature could be measured with an accuracy of ± 0.1°C, and was recorded at half minute intervals.

The runs were carried out in a purified nitrogen atmosphere. Before cooling, the temperature of the furnace was kept 10°C above the expected crystallization temperature for about 15 min. The cooling rate was 1 – 1.5°C per minute. Supercooling of the melt was prevented by continuous stirring as well as seeding with small crystals of one of the cryolites. For each experiment, about 80 g of the sample were used.

(b) *Differential thermal analysis (DTA), low- and high-temperature X-ray measurements.* The procedure was the same as in the previous paper.[1]

(c) *Materials.* Na_3AlF_6: Handpicked natural cryolite from Ivigtut, Greenland, of the same type as used by Holm.[3] AlF_3: Prepared at the Slovak Academy of Sciences, Bratislava, Czechoslovakia, purified by sublimation. Analysis: AlF_3 99.2 – 99.5 %, Al_2O_3 0.5 – 0.8 % as reported by Matiasovsky and Malinovsky.[4] KF: Anhydrous KF, laboratory reagent (B.D.H., Poole, England). Dried at 400°C under vacuum for 3 h in a Pt-crucible. RbF: Rubidium fluoride for laboratory use (Koch-Light Laboratories, Colnbrook, Bucks, England, min. 99.8 %), as well as El. quality (Merck, Darmstadt, Germany) was used. The fluoride was melted in a Pt-crucible under pure nitrogen atmosphere, and pure crystals were selected from the sample. KF and RbF were always handled inside a dry box.

For the preparation of K_3AlF_6 and Rb_3AlF_6, stoichiometric amounts of the alkali fluoride and aluminium fluoride were melted together in a Pt-crucible in a purified nitrogen atmosphere. The composition of each of the cryolites was carefully adjusted by adding aluminium fluoride until no eutectic reaction could be observed by DTA.

RESULTS AND DISCUSSION

(a) *The system K_3AlF_6-Na_3AlF_6.* The binary system K_3AlF_6-Na_3AlF_6 has been studied by several authors,[5–13] but their results are not in agreement. Neither the solidus line nor the change in the polymorphic transformation temperature with composition has been clearly determined in any of these works.

Belyaev and Studentsov,[5] Baimakov and Bataschev,[6] as well as Lundina [7] reported that a continuous solid solution exists between Na_3AlF_6 and K_3AlF_6, and that the liquidus line has a minimum at 940°C and about 50 mol % K_3AlF_6. Bukhalova *et al.*[8] indicated the minimum to be at 927°C and about 26 mol % K_3AlF_6. Naray-Szabo and Sigmond [9] reported the existence of six intermediate compounds as follows: $5K_3AlF_6.2Na_3AlF_6$, $2K_3AlF_6.Na_3AlF_6$ (elpasolite), $5K_3AlF_6.3Na_3AlF_6$, $K_3AlF_6.Na_3AlF_6$, $3K_3AlF_6.5Na_3AlF_6$ and $K_3AlF_6.2Na_3AlF_6$. Only the compound $2K_3AlF_6.Na_3AlF_6$ was reported to be stable at room temperature. Edoyan *et al.*[10] confirmed the existence of the same compounds.

Bukhalova and Mal'tsev [11] reported the presence of the following compounds: $3K_3AlF_6.Na_3AlF_6$, formed in the solid phase at 796°C and decomposed at 715°C; $K_3AlF_6.Na_3AlF_6$, formed in the solid phase at 832°C and decomposed at 736°C; and $2K_3AlF_6.Na_3AlF_6$ which does not decompose when cooled to room temperature. Chin and Hollingshead [12] reported that with the addition of increasing amounts of K_3AlF_6, the primary freezing point of Na_3AlF_6 decreases to 945°C at 40 mol % K_3AlF_6 and then rises to 955°C at 60 – 70 mol % K_3AlF_6. They also confirmed the presence of the compound K_2NaAlF_6. Yoshioka and Koroda [13] determined the liquidus line and their results were in fair agreement with those of Chin and Hollingshead.[12]

Table 1. DTA and TA data for the system Na_3AlF_6-K_3AlF_6.

Mol % Na_3AlF_6	Mol % K_3AlF_6	Experimental, °C DTA T_1	DTA T_2	TA T_1
100.00	0.00	1010	560.0	–
97.50	2.50	999.0	545.0	–
95.90	4.10	995.0	542.0	995.6
91.71	8.29	983.0	–	–
87.46	12.54	–	–	974.0
83.11	16.89	963.5	498.0	964.0
81.35	18.65	956.8	–	–
78.68	21.32	953.0	–	952.2
74.16	25.84	945.0	482.0	945.6
71.41	28.59	941.0	–	–
69.55	30.45	–	–	938.0
66.74	33.26	940.0	–	–
64.85	35.15	940.0	420.0	940.4
62.40	37.60	941.7	–	–
60.05	39.95	941.2	–	941.5
57.13	42.87	943.0	–	–
55.16	44.84	943.7	390.0	944.0
52.17	47.83	947.6	–	–
50.16	49.84	947.0	–	947.2
47.11	52.89	950.6	354.0	–
45.06	54.94	950.3	350.0	–
39.84	60.16	951.0	338.0	–
34.52	65.48	954.0	–	–
33.33	66.67	954.0	–	–
29.08	70.92	951.0	–	–
23.52	76.48	956.4	340.0	–
17.84	82.16	966.0	–	–
12.02	87.98	974.9	–	–
6.08	93.92	983.0	–	–
3.65	96.35	987.0	–	–
0.00	100.00	995.0	310.0	–

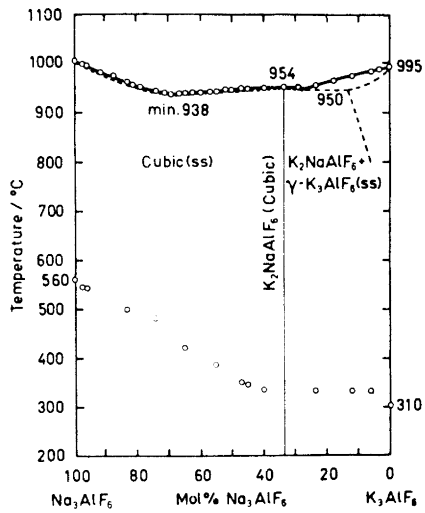

Fig. 1. The phase diagram of the system Na_3AlF_6-K_3AlF_6 according to the TA and DTA results (cooling curves).

The results obtained in the present work for the system K_3AlF_6-Na_3AlF_6 are shown in Table 1, and the corresponding phase diagram in Fig. 1. The results obtained by thermal analysis are in good agreement with those obtained by differential thermal analysis. The melting points and the solid transformation temperatures of the pure compounds K_3AlF_6 and Na_3AlF_6 were determined as 995, 310, 134°C (K_3AlF_6), and 1010 and 560°C (Na_3AlF_6).

Representative samples were examined by X-ray powder diffraction at different temperatures as follows:

Pure Na_3AlF_6 at room temp. 492, 605, 700°C
87.46 mol % Na_3AlF_6 at room temp. 437, 498, 590, 695, 812, 906°C
66.74 mol % Na_3AlF_6 at room temp. 430, 817, 884°C
55.16 mol % Na_3AlF_6 at room temp. 500, 599, 685°C
34.52 mol % Na_3AlF_6 at room temp. 592, 646, 690°C
23.52 mol % Na_3AlF_6 at room temp. 622, 752, 822°C
12.02 mol % Na_3AlF_6 at room temp. 594, 649, 693, 710, 770°C
Pure K_3AlF_6 at room temp. 510, 620, 710°C

The liquidus line is relatively flat throughout the whole diagram, especially in the middle region. No solidus line was detected, even by using low cooling rates (less than 0.5°C per minute in the case of the differential thermal analysis). An intermediate compound with the composition $2K_3AlF_6.Na_3AlF_6$, which melts congruently at 954°C, was the only compound detected. The X-ray data of this compound (Table 2) are in good agreement with those reported by Frondel [14] for the mineral elpasolite. The results indicate that the compound has a cubic structure with a lattice constant $a = 8.095 \pm 0.02$ Å at 20°C. No solid transformation of this compound was observed. From the obtained results

Table 2. X-Ray data for K_2NaAlF_6 (20°C); cubic: $a = 8.095 \pm 0.02$ Å.

h k l	Int.	$\sin^2 \theta_{obs} \times 10^4$	$\sin^2 \theta_{calc} \times 10^4$	d_{obs} This work	d_{obs} Frondel [14]
1 1 1	vw	272	272	4.667	4.673
2 0 0	vw	364	363	4.037	4.047
2 2 0	vs	718	726	2.873	2.862
2 2 2	vs	1085	1088	2.339	2.336
					2.244
4 0 0	vs	1440	1451	2.030	2.023
3 3 1	vw	1720	1723	1.857	1.852
4 2 2	m	2168	2177	1.654	1.652
					1.587
5 1 1	w	2448	2449	1.557	1.558
4 4 0	m	2892	2902	1.433	1.431
5 3 1	vw	3173	3175	1.368	1.368
6 2 0	w	3622	3628	1.280	1.280
6 2 2	vw	3978	3991	1.220	1.220
4 4 4	w	4339	4354	1.169	1.168
5 5 1	vw	4616	4626	1.134	1.133

it seems more convenient to describe the system as two separate systems, namely Na_3AlF_6-K_2NaAlF_6 and K_2NaAlF_6-K_3AlF_6.

In the first system, Na_3AlF_6-K_2NaAlF_6, it is observed that the polymorphic transformation temperature of pure Na_3AlF_6 (560°C) decreases with the addition of increasing amounts of the compound K_2NaAlF_6. Near the composition of pure K_2NaAlF_6, the transformation temperature was found to be about 340°C. Guinier X-ray patterns at room temperature showed the presence of a mechanical mixture of Na_3AlF_6 and K_2NaAlF_6 in this region. From the high-temperature X-ray diffraction experiments, a mechanical mixture was also found to exist in the area just below the transformation line. The area above the transformation line, however, was found to contain a solid solution of K_2NaAlF_6 and the cubic high-temperature modification of Na_3AlF_6. These results suggest that the solidus line is very close to the liquidus, enclosing an area where the liquid phase is present in equilibrium with the solid solution, with a minimum at about 938°C and 69.5 mol % Na_3AlF_6, as shown in the diagram.

The system K_2NaAlF_6-K_3AlF_6 on the other hand is a binary system with a eutectic point. The eutectic point was determined at 950°C and 27 mol % Na_3AlF_6. The solid transformation temperature of K_3AlF_6 (310°C) shows a small increase very near to pure K_3AlF_6 and is then almost constant at all other compositions. The transformation line was determined at 340°C. The area below this line and down to room temperature was found to contain a mechanical mixture of K_3AlF_6 and K_2NaAlF_6. Above this line, a mechanical mixture of the high temperature modification of K_3AlF_6 and K_2NaAlF_6 was determined. However, the high-temperature X-ray diffraction method is inefficient for detecting as little as 3 – 4 % of one compound in a mixture, and the change in the solid transformation temperature of K_3AlF_6 indicates that there is a narrow area of solid solution on the K_3AlF_6 side of the diagram.

(b) *The system K_3AlF_6-Rb_3AlF_6.* The only work published on the system K_3AlF_6-Rb_3AlF_6 was carried out by Mal'tsev and Bukhalova,[15] using visual observation and thermal analysis. They indicated the presence of a continuous solid solution of K_3AlF_6 and Rb_3AlF_6 which decomposes at low temperatures. The melting points of the pure compounds K_3AlF_6 and Rb_3AlF_6 were found to be 986 and 914°C, and the polymorphic transformation temperatures 310 and 340°C, respectively. A minimum was found at 900°C and 20 mol % Rb_3AlF_6 by visual observation, and at 906°C and the same composition by thermal analysis.

In the present work, the system K_3AlF_6-Rb_3AlF_6 was studied by DTA. The results are presented in Table 3 and the corresponding phase diagram is shown in Fig. 2. The melting points of the pure compounds K_3AlF_6 and Rb_3AlF_6 were found to be 995 and 924°C, respectively, and polymorphic transformations were found at 310 and 134°C for K_3AlF_6 and 356°C for Rb_3AlF_6. A continuous solid solution of K_3AlF_6 and Rb_3AlF_6 was detected. The solidus points were recorded as small breaks in the DTA cooling/heating curve when the cooling (or heating) rate was sufficiently low (T_2). The system seems to contain a very narrow field where liquid exists in equilibrium with solid solution. The temperature difference between the liquidus and the solidus line does not exceed 6°C at any composition.

Table 3. DTA data for the system K_3AlF_6-Rb_3AlF_6.

Mol %		Experimental, °C		
K_3AlF_6	Rb_3AlF_6	T_1	T_2	T_3
100.00	0.00	995.0	–	310.0
92.90	7.10	985.0	–	296.0
89.71	10.29	982.0	979.0	282.0
85.22	14.78	978.2	974.2	280.0
82.20	17.80	975.0	970.5	254.0
78.21	21.79	969.4	965.0	–
72.08	25.92	966.0	961.5	212.0
69.77	30.23	960.4	954.2	–
65.29	34.71	957.0	–	–
60.61	39.39	953.0	–	–
55.73	44.27	949.5	–	–
50.64	49.36	946.2	942.0	–
45.31	54.69	942.0	939.2	–
39.74	60.26	940.0	937.5	–
34.12	65.88	936.5	933.0	–
27.78	72.22	934.0	930.0	–
21.36	78.64	930.0	927.0	–
14.60	85.40	928.2	926.0	–
7.49	92.51	926.0	923.0	–
3.79	96.21	925.0	–	292.0
0.00	100.00	924.0	–	356.0

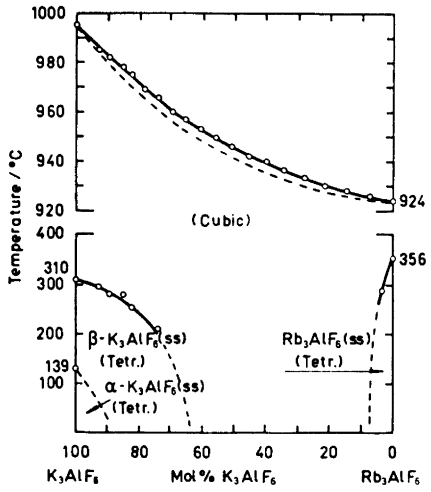

Fig. 2. The phase diagram of the system K_3AlF_6-Rb_3AlF_6 according to the DTA results (cooling curves).

Guinier X-ray studies were made of the following samples at room temperature: Pure Rb_3AlF_6, 3.79, 7.49, 14.6, 21.36, 34.12, 50.64, 55.73, 60.61, 65.29, 69.77, 74.08, 78.21, 82.20, 85.22, 89.71, 92.90 mol % K_3AlF_6, and pure K_3AlF_6. The results show that at room temperature, a tetragonal solid

solution is present in the region between pure Rb_3AlF_6 and 7.5 ± 2.5 mol % K_3AlF_6. In the region between 7.5 ± 2.5 and 62 ± 2.5 mol % K_3AlF_6, a cubic solid solution was detected, which indicates that the high-temperature modifications of K_3AlF_6 and Rb_3AlF_6 can be preserved even at room temperature in that region. The change in the lattice constant with composition in

Table 4. The lattice constant a, as a function of composition in the system K_3AlF_6-Rb_3AlF_6 at room temperature.

K_3AlF_6 mol %	a Å
21.36	8.692
34.12	8.665
50.60	8.602
60.61	8.555

this region is given in Table 4. Between 62 ± 2.5 mol % and 87 ± 2.5 mol %, and between 87 ± 2.5 mol % and pure K_3AlF_6, two regions of tetragonal [16] solid solutions, β-K_3AlF_6(ss) and α-K_3AlF_6(ss), were detected.

Acknowledgement. The experimental work was sponsored by the *Royal Norwegian Council for Scientific and Industrial Research* and the *Norwegian Agency for International Development*, whose support is gratefully acknowledged.

REFERENCES

1. Grjotheim, K., Holm, J. L., Malinovsky, M. and Mikhaiel, S. A. *Acta Chem. Scand.* **25** (1971) 1695.
2. Grjotheim, K. *Kgl. Norske Videnskab. Selskabs, Skrifter* **1956** No. 5.
3. Holm, J. L. *Undersøkelser av struktur og faseforhold for en del systemer med tilknytning til aluminium elektrolysen*, Institute of Inorganic Chemistry, the Technical Yniversity of Norway, Trondheim 1963.
4. Matiasovsky, K. and Malinovsky, M. *Internal Report*, the Academy of Sciences, Bratislava 1968.
5. Belyaev, A. I. and Studentsov, A. E. *Legk. Metal.* **3** (1936) 15.
6. Baimakov, J. W. and Batashev, P. P. In Belyaev, Rapoport and Firsanova, Eds., *Metallurgie des Aluminiums*, VEB Verlag Technik, Berlin 1956, Vol. 1, p. 81.
7. Lundina, S. F. In Belyaev, Rapoport and Firsanova, Eds., *Metallurgie des Aluminiums*, VEB Verlag Technik, Berlin 1956, Vol. 1, p. 61.
8. Bukhalova, G. A., Maslennikova, G. N. and Rabkin, D. M. *Zh. Neorgan. Khim.* **7** (1962) 1640.
9. Naray-Szabo, S. V. and Sigmond, G. *Neues Jahrb. Mineral. Geol. Palaeontol. Ref.* **1** (1942) 112.
10. Edoyan, R. S., Manvelyan, M. G. and Babayan, G. G. *Izv. Akad. Nauk Arm. SSR, Khim. Nauki* **18** (1965) 10.
11. Bukhalova, G. A. and Mal'tsev, V. T. *Izv. Akad. Nauk SSSR, Neorg. Mater.* **2** (1966) 721.
12. Chin, D. A. and Hollingshead, E. A. *J. Electrochem. Soc.* **113** (1966) 736.
13. Yoshioka, T. and Kuroda, T. *Denki Kagaku* (*J. Electrochem. Japan*) **36** (1968) 797.
14. Frondel, K. *Amer. Mineral.* **33** (1948) 84.
15. Mal'tsev, V. T. and Bukhalova, G. A. *Izv. Vysshikh Uchebn. Zavedenii. Khim. i Khim. Tekhnol.* **9** (1966) 151.

16. Jenssen, B. *Fase- og strukturforhold for noen komplekse alkalialuminiumfluorider, Lic. Thesis*, Institute of Inorganic Chemistry, the Technical University of Norway, Trondheim 1969.

Received November 1, 1972.

ACTA CHEMICA SCANDINAVICA 27 (1973) 1307–1314

Compounds with the Skutterudite Type Crystal Structure

I. On Oftedal's Relation

A. KJEKSHUS, D. G. NICHOLSON and T. RAKKE

Kjemisk Institutt, Universitetet i Oslo, Blindern, Oslo 3, Norway

The $CoAs_3$ (skutterudite) type crystal structure is examined and anisotropic interactions arising from the non-metal (X) sublattice are suggested as the principal cause of the rectangular distortion of the X_4 groups.

Cobalt triarsenide constitutes the prototype of an interesting class of transition metal pnictides. The most striking feature of the $CoAs_3$ type structure (in which the transition metal (T) and pnigogen (X) atoms are, respectively, octahedrally and tetrahedrally coordinated) is the collection of the pnigogens into planar X_4 groups.

The original crystal structure determination [1] of the mineral skutterudite ($CoAs_3$ with variable amounts of Fe and/or Ni substituted for Co; *cf.*, *e.g.*, Ref. 2) was based on the assumption of a postulated relation ($y+z=1/2$) between the variable parameters for the X atoms. Such a constraint, which has been termed "Oftedal's relation", implies that the X_4 groups are strictly square. Oftedal's relation was also assumed in subsequent determinations [3,4] of the isostructural compounds $CoSb_3$, $RhSb_3$, and $IrSb_3$ and in a redetermination [5] of skutterudite itself. The validity of this postulate was first explicitly questioned during X-ray powder studies [6,7] of RhP_3, $IrAs_3$, and $IrSb_3$. More recently, accurate structure determinations,[8] on CoP_3, RhP_3, IrP_3, and NiP_3 using X-ray powder diffraction methods and a single crystal study [9] on skutterudite show unequivocally that there are small, but significant deviations from Oftedal's relation, implying that the X_4 groups are rectangular rather than square. Rundqvist and Ersson [8] proposed a possible explanation as to the physical cause of this observation, an interpretation which has been accepted by Mandel and Donohue.[9]

We present here an alternative model which we believe provides a more realistic explanation for the rectangular arrangement of the X_4 groups.

ATOMIC ARRANGEMENT

In the $CoAs_3$ type structure the T atoms occupy the fixed coordinate position 8(e) and the X atoms the general position 24(g) of space group $Im3$. Hence, the atomic arrangement is completely specified by the two positional parameters y and z and the unit cell edge a. Given the composition TX_3 then, without any loss of generality, the positional parameters are assumed to be within the intervals

$$1/4 \leqq y < 1/2, \quad 0 < z \leqq 1/4 \tag{1}$$

It is evident, however, that this neglects the finite size of the atoms and their mutual interactions which further restrict these permitted intervals for y and z (*vide infra*). It should also be noted that the combination

$$y = z = 1/4 \tag{2}$$

converts the $CoAs_3$ type structure into the ReO_3 type structure (space group $Pm3m$ with only one TX_3 group per unit cell).

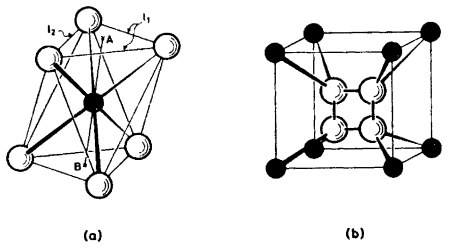

Fig. 1. Coordinations in the $CoAs_3$ type structure: (a) 6X atoms about T, and (b) 2X and 2T atoms about X.

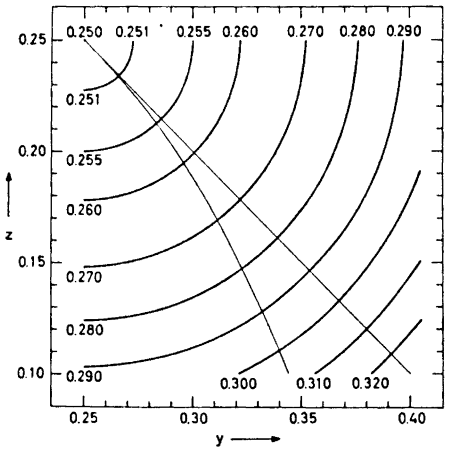

Fig. 2. Normalized $T-X$ distance (d/a) as functions of y and z. Oftedal's relation (eqn. 9) and the condition for perfect octahedral symmetry about T (eqn. 6) are shown by the thin lines.

The trigonal antiprismatic environment of the T atoms (Fig. 1a) is such that a straight line through T and the centres A and B of a pair of congruent, equilateral triangles intersects their planes at right angles. With this coordination symmetry the six $T-X$ distances d are equal

$$d = a[(1/4)^2 + (y - 1/4)^2 + (1/4 - z)^2]^{\frac{1}{2}} \tag{3}$$

The dependence of the normalized $T-X$ distance d/a on y and z is, as shown in Fig. 2, a set of concentric circles around $y=z=1/4$. The dimensions l_1 and l_2 of the triangle are given by

$$l_1 = a[(1/2 - y)^2 + (1/2 - z)^2 + (1/2 - y - z)^2]^{\frac{1}{2}} \quad (4)$$

$$l_2 = a[y^2 + z^2 + (y - z)^2]^{\frac{1}{2}} \quad (5)$$

Equating l_1 and l_2 places the restraint

$$2y(1/2 - z) = 3/8 - z \quad (6)$$

on the positional parameters and produces in this case perfect octahedral symmetry. The only permissible distortion from perfect octahedral symmetry within the $CoAs_3$ type structure follows from the condition $l_1 \neq l_2$ which gives rise to two sets (6 + 6) of mutually supplementary $X-T-X$ angles. Fig. 3 shows the dependence of one of these sets on y and z.

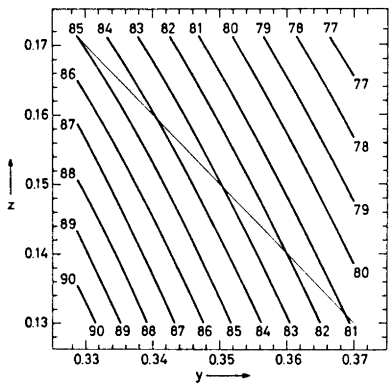

Fig. 3. $X-T-X$ bond angle *versus* y and z, the thin line showing Oftedal's relation.

Each X atom is surrounded by two X and two T atoms at the corners of a tetrahedron which is more severely distorted than the octahedron. The $X-X-X$ angle (within the planar X_4 groups, *cf.* Fig. 1b) is fixed at 90°,

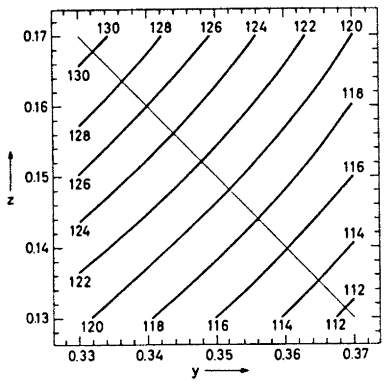

Fig. 4. Variation of $T-X-T'$ bond angle with y and z, Oftedal's relation being shown by the thin line.

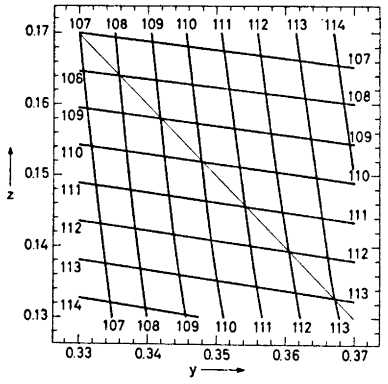

Fig. 5. $X-X-T$ bond angles *versus* y and z, Oftedal's relation being indicated.

whereas the $T-X-T$ and $X-X-T$ angles depend on the positional parameters as shown in Figs. 4 and 5, respectively. The interatomic distances

$$d_1 = 2az \tag{7}$$

$$d_2 = 2a(1/2 - y) \tag{8}$$

within the rectangular X_4 group reflect strong covalent interactions. The dependence of the ratio d_2/d_1 on y and z is shown in Fig. 6, Oftedal's relation

$$y+z=1/2 \tag{9}$$

being obtained for $d_1=d_2$.

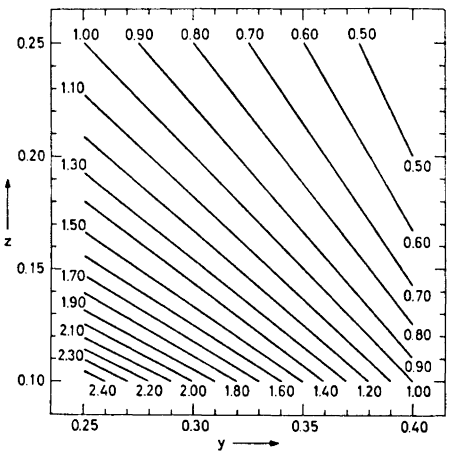

Fig. 6. Ratio of $X-X$ bond lengths (d_2/d_1) as functions of y and z.

Rundqvist and Ersson [8] have suggested that the distortion of the X_4 groups from square to rectangular is a compromise imposed by the competing tendency for T to attain regular octahedral coordination. The simultaneous fulfilment of eqns. 6 and 9 results in a reversion to the ReO_3 type structure with $d=a/4$ and $d_1=d_2=a/2$, the latter distance being too long for $X-X$ bonding. Hence, the following three features are together mutually incompatible:

(i) Regular octahedral symmetry around T (eqn. 6).
(ii) Square X_4 groups, *i.e.* $d_1=d_2$ (Oftedal's relation, eqn. 9).
(iii) $X-X$ distances (*i.e.* d_1 and/or d_2) within the range for bonding.

There are, however, no objections as far as the space group is concerned as to the compatibility of any two of these requirements. The supposition that point (iii) is essential * for the $CoAs_3$ type structure thus naturally raises the question of whether point (i) or (ii) is the most important factor in determining the structural stability. A quantitative criterion for judgements of this type is unfortunately not available.

* This severely limits the permitted parameter ranges for y and z, and it is consistently observed [8,9] that $0.3431 \leqq y \leqq 0.3547$ and $0.1393 \leqq z \leqq 0.1503$.

As a specific example the data for the skutterudite mineral [9] give $d_1 = 2.464$ Å, $d_2 = 2.572$ Å, and $X-T-X = 84.6°$. It is possible to imagine a hypothetical $CoAs_3$ structure with $d_1' = d_2' = d_1$ giving an $X-T-X$ angle of 83.0°. Thus, the difference between the actual and hypothetical structure amounts to 1.6° in $X-T-X$ bond angle and 0.108 Å in $X-X$ bond length. It seems unlikely that the energy gain resulting from such a small variation in bond angle should be comparable to that involved in making d_1 and d_2 unequal by as much as 0.108 Å. On this basis it appears that the principal cause of the deviation from Oftedal's relation is not the competition between points (i) and (ii), but is to be sought elsewhere.

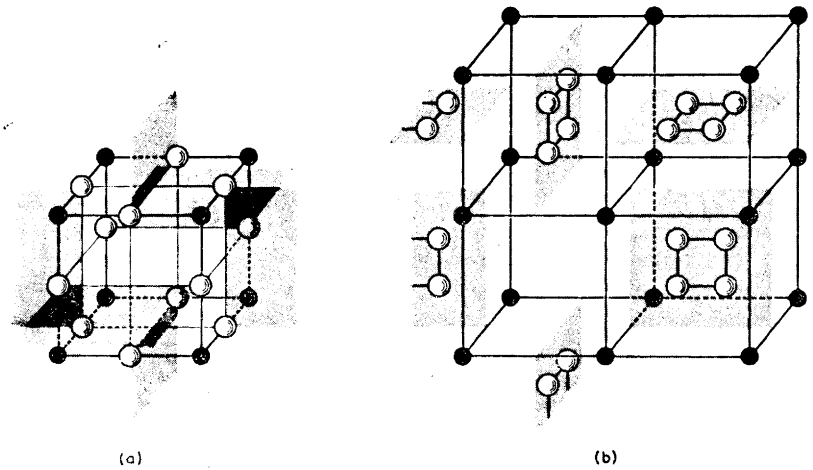

Fig. 7. Relationship between the ReO_3 (a; one unit cell) and $CoAs_3$ (b; half a unit cell in which the origin is shifted to 1/4,1/4,1/4) type structures. The shading emphasizes the planes through the X_4 groups.

At this stage it is useful to take advantage of the similarities and differences between the $CoAs_3$ and ReO_3 type structures, which are brought out in Fig. 7. In a hypothetical transformation from the more symmetric ReO_3 type structure to the $CoAs_3$ type, the formerly square X_4 groups are drawn together by covalent $X-X$ interactions, thus leaving two cavities per $CoAs_3$ unit cell symmetrically arranged on opposite sides of the X_4 groups. It is to be noted that these cavities are consistently arranged with respect to the $X-X$ bond distance d_2, and it is accordingly suggested that the consequent anisotropic environment of the X_4 groups is primarily responsible for the observed inequality $d_1 < d_2$.

ATOMIC INTERACTIONS

Since the properties of these macromolecular TX_3 compounds strongly suggest [10] a high degree of covalency the subsequent description of the interatomic interactions may be divided into two parts. Firstly, there is the major

effect due to covalent bonding between nearest neighbour atoms and secondly the perturbation from the remainder of the lattice. The lattice contribution arises as a consequence of the electronic distribution within the $T-X$ bonds. This effect should not be neglected, because, although individual contributions decrease with increasing distance R from any given atom, the number of atoms contained in a volume shell dR is proportional to R^2. The overall interaction experienced by a given atom is treated as follows.

The equilibrium distance (r_0) between two covalently bound atoms is due to a balance between shorter range internuclear and electronic core repulsions (**R**) and the attractive force (**A**) resulting from the interactions of their valence shells, *i.e.* $\mathbf{R}(r_0)+\mathbf{A}(r_0)=\mathbf{0}$ for an isolated, diatomic molecule. In a crystal structure, however, the lattice influences the interatomic distance (r) such that $\mathbf{R}(r)+\mathbf{A}(r)=\mathbf{G}(r)\neq\mathbf{0}$, and the net force (**F**) resulting from the lattice is defined by

$$\mathbf{G}(r)+\mathbf{F}=\mathbf{0} \tag{10}$$

Consideration of the immediate environment about the X atoms in the $CoAs_3$ type structure (Fig. 1b) yields

$$\mathbf{G}=\mathbf{G}_1(d_1)+\mathbf{G}_2(d_2)+\mathbf{G}_3(d)+\mathbf{G}_4(d) \tag{11}$$

where the subscripts 1 and 2 refer to the two $X-X$ bonds and 3 and 4 to the two $X-T$ bonds. The components of the vector **G** in the three crystallographic directions a, b, and c are

$$\begin{aligned} G_a &= 0 \\ G_b &= -G_2(d_2)+\frac{2a(y-1/4)}{d}G_3(d) \\ G_c &= G_1(d_1)-\frac{2a(1/4-z)}{d}G_3(d) \end{aligned} \tag{12}$$

where $|\mathbf{G}_3(d)|=|\mathbf{G}_4(d)|$ because the two $X-T$ bond lengths are equal.

The lattice interactions as defined by **F** (eqn. 10) are conveniently described in terms of the X and T atom sublattices, *i.e.* $\mathbf{F}=\mathbf{F}(X)+\mathbf{F}(T)$. The effective charges on the T and X atoms are denoted $3q$ and $-q$, respectively, although the sign and magnitude of q is unimportant for the present considerations.

Within a given unit cell $\mathbf{r}_n[0,0,0]$ represents the vector from atom X_n to the X atom with coordinates $1/2,1/2-y,1/2-z$, which is numbered as X_7 in Table 1 and arbitrarily chosen as the origin. The vector from atom X_n in another unit cell, specified by the integers i,j,k, to the origin is given by

$$\mathbf{r}_n[i,j,k]:(1/2-u_n-i,1/2-y-v_n-j,1/2-z-w_n-k) \tag{13}$$

$$-\infty<i,j,k<\infty \tag{14}$$

The interaction of the X sublattice on $X_7[0,0,0]$ is expressed as

$$\mathbf{F}(X)=\left[\frac{q}{a}\right]^2\sum_n\sum_{i,j,k}\mathbf{f}_n[i,j,k] \tag{15}$$

where $\mathbf{f}_n$ is the normalized contribution to the total Coulomb force from a general $X_n[i,j,k]$ acting on $X_7[0,0,0]$ and is given by

$$\mathbf{f}_n = \frac{\mathbf{r}[i,j,k]}{(r[i,j,k])^3} \tag{16}$$

Similarly, the influence of the T sublattice on $X_7[0,0,0]$ is

$$\mathbf{F}(T) = 3\left[\frac{q}{a}\right]^2 \sum_m \sum_{i,j,k} \mathbf{f}_m[i,j,k] \tag{17}$$

Table 1. Numbering of non-metal (X_n) and metal (T_m) atoms within the unit cell of the $CoAs_3$ type structure.

n	u_n	v_n	w_n	n	u_n	v_n	w_n
1	x	0	y	13	$1/2-x$	1/2	$1/2-y$
2	$\bar{x}$	0	y	14	$1/2+x$	1/2	$1/2-y$
3	x	0	$\bar{y}$	15	$1/2-x$	1/2	$1/2+y$
4	$\bar{x}$	0	$\bar{y}$	16	$1/2+x$	1/2	$1/2+y$
5	y	x	0	17	0	$\bar{y}$	x
6	$\bar{y}$	x	0	18	$1/2-y$	$1/2+x$	1/2
7	1/2	$1/2-y$	$1/2-x$	19	$1/2+y$	$1/2+x$	1/2
8	1/2	$1/2-y$	$1/2+x$	20	0	$\bar{y}$	$\bar{x}$
9	0	y	x	21	y	$\bar{x}$	0
10	$1/2-y$	$1/2-x$	1/2	22	$\bar{y}$	$\bar{x}$	0
11	$1/2+y$	$1/2-x$	1/2	23	1/2	$1/2+y$	$1/2-x$
12	0	y	$\bar{x}$	24	1/2	$1/2+y$	$1/2+x$

m	u_m	v_m	w_m	m	u_m	v_m	w_m
1	1/4	1/4	1/4	5	1/4	3/4	1/4
2	3/4	1/4	1/4	6	3/4	3/4	1/4
3	1/4	1/4	3/4	7	1/4	3/4	3/4
4	3/4	1/4	3/4	8	3/4	3/4	3/4

The components of $\mathbf{F}(X)$ and $\mathbf{F}(T)$ in the a direction fulfil the condition

$$F_a(X) \equiv F_a(T) \equiv 0 \tag{18}$$

whereas in the b and c directions this is generally not the case and the components must satisfy the conditions

$$G_b(X,T) + F_b(X) + F_b(T) = 0 \tag{19}$$

$$G_c(X,T) + F_c(X) + F_c(T) = 0 \tag{20}$$

Only the difference between the overall forces acting in the b and c directions is relevant to the discussion and this may be obtained by combination of eqns. 19 and 20. The assumption of Oftedal's relation (eqn. 9) considerably simplifies the resulting expression since both $X-X$ bonds are then equivalent and hence

$$G_b(X,T) + G_c(X,T) = 0 \tag{21}$$

Summing over those parts of the T sublattice with a fixed value for the summation index m (see Table 1) gives eight terms each in the b and c directions, which on substituting Oftedal's relation and rearranging yields

$$\sum_m \left\{ \sum_{i,j,k} f_m[i,j,k] \right\}_b + \sum_m \left\{ \sum_{i,j,k} f_m[i,j,k] \right\}_c = 0 \tag{22}$$

and therefore

$$F_b(T) + F_c(T) = 0 \tag{23}$$

Thus, it is seen that the total interaction of the T sublattice is equal in the two $X-X$ bond directions.

Repeating essentially the same procedure for the X sublattice interaction the twenty-four terms which are thereby obtained for the components in the b and c directions may be considerably simplified so that only those corresponding to the positions numbered $n=1$, 3, 5, 10, 13, 15, 18, and 21 in Table 1 need to be considered. Numerical computations based on Oftedal's relation show that

$$F_b(X) + F_c(X) \neq 0 \tag{24}$$

unless

$$y = z = 1/4 \text{ or } q = 0$$

The former condition gives rise to the ReO_3 type structure (*vide supra*) whereas the latter requirement would imply a non-existent lattice interaction.

The conclusion is accordingly that the assumption of Oftedal's relation is not consistent with the $CoAs_3$ type structure, and that the principal cause of the rectangular deviation lies in the X sublattice interactions and is not attributable to differences in covalency between the $T-X$ and $X-X$ bonds or to the T sublattice.

REFERENCES

1. Oftedal, I. *Z. Krist.* **A 66** (1928) 517.
2. Roseboom, E. H. *Am. Mineralogist* **47** (1962) 310.
3. Rosenqvist, T. *Acta Met.* **1** (1953) 761; *N. T. H.-Trykk*, Trondheim 1953.
4. Zhuravlev, N. N. and Zhdanov, G. S. *Kristallografiya* **1** (1956) 509.
5. Ventriglia, U. *Periodico Mineral (Rome)* **26** (1957) 345.
6. Rundqvist, S. and Hede, A. *Acta Chem. Scand.* **14** (1960) 893.
7. Kjekshus, A. and Pedersen, G. *Acta Cryst.* **14** (1961) 1065.
8. Rundqvist, S. and Ersson, N.-O. *Arkiv Kemi* **30** (1968) 103.
9. Mandel, N. and Donohue, J. *Acta Cryst.* **B 27** (1971) 2288.
10. Kjekshus, A., Nicholson, D. G. and Rakke, T. *Acta Chem. Scand.* **27** (1973) 1315.

Received November 15, 1972.

ACTA CHEMICA SCANDINAVICA 27 (1973) 1315–1320

Compounds with the Skutterudite Type Crystal Structure

II. The ^{121}Sb Mössbauer Effect in $CoSb_3$, $Fe_{0.5}Ni_{0.5}Sb_3$, $RhSb_3$, and $IrSb_3$

A. KJEKSHUS, D. G. NICHOLSON and T. RAKKE

Kjemisk Institutt, Universitetet i Oslo, Blindern, Oslo 3, Norway

^{121}Sb Mössbauer spectra of $CoSb_3$, $Fe_{0.5}Ni_{0.5}Sb_3$, $RhSb_3$, and $IrSb_3$ have been obtained at 4.2 K and are discussed in relation to their $CoAs_3$ type structure. The data provide additional evidence in support of the bonding being predominantly of a covalent nature in these compounds.

The application of ^{121}Sb Mössbauer spectroscopy has, in recent years, stimulated studies on the bonding properties of antimony compounds. Of particular interest in this connection are a number of binary antimonides whose accurately determined crystal structures facilitate the interpretation and permit semi-quantitative comparisons between the crystallographic and electronic environments of antimony. As an example of such an investigation reference [1] is made to a recent discussion on the ^{121}Sb Mössbauer parameters for a series of diantimonides with the pyrite, marcasite, or arsenopyrite type crystal structures. We report here corresponding data for $CoSb_3$, $Fe_{0.5}Ni_{0.5}Sb_3$, $RhSb_3$, and $IrSb_3$ with the $CoAs_3$ (skutterudite) type crystal structure.

EXPERIMENTAL

The compounds were prepared by heating stoichiometric quantities of the elements (in the form of turnings from Fe, Co, and Ni rods and Rh, Ir, and Sb powders all from Johnson, Matthey & Co; spectroscopically standardized and of purity better than 99.99 %) in evacuated, sealed quartz tubes. The binary samples were maintained for one week at 750 ($CoSb_3$) or 850°C ($RhSb_3$ and $IrSb_3$), crushed, reannealed for a further week at the same temperature, and finally cooled to room temperature over a period of three days. The ternary sample $Fe_{0.5}Ni_{0.5}Sb_3$ was prepared similarly at 650°C, crushed and subjected to three further annealings at 600°C with intermediate crushings.

The experimental details concerning the X-ray diffraction and ^{57}Fe and ^{121}Sb Mössbauer measurements have been presented in previous communications.[1,2]

RESULTS AND DISCUSSION

The identity and homogeneity of the compounds were ascertained from Guinier photographs, which gave the unit cell dimensions $a = 9.0347(6)$, 9.2322(6), 9.2533(5), and 9.0904(5) Å for $CoSb_3$, $RhSb_3$, $IrSb_3$, and $Fe_{0.5}Ni_{0.5}Sb_3$, respectively, in good agreement with earlier findings.[3–9]

The room temperature ^{57}Fe Mössbauer spectrum for $Fe_{0.5}Ni_{0.5}Sb_3$ consists of a single absorption peak of line-width $\Gamma = 0.64$ mm/s which is positioned at a chemical shift value of $\delta = 0.29 \pm 0.01$ mm/s relative to metallic iron.

The magnitude of δ is consistent with the Fe atoms attaining a formal low-spin $3d^6$ electron configuration (*vide infra*). In compounds with the $CoAs_3$ type structure the metal (T) atoms are octahedrally coordinated to six non-metal (X) atoms, the T site being only slightly distorted from O_h symmetry (*cf.*, *e.g.*, Refs. 10 – 12). The lack of a resolvable quadrupole interaction reflects this high crystallographic symmetry at the Fe site since for low-spin Fe(II) there is no contribution arising from the non-bonding d electrons.

Fig. 1 shows the ^{121}Sb Mössbauer spectra of $Fe_{0.5}Ni_{0.5}Sb_3$, $CoSb_3$, $RhSb_3$, and $IrSb_3$ taken at 4.2 K.

The Mössbauer transitions in ^{121}Sb occur between the nuclear spin states $7/2 \rightarrow 5/2$. The presence of an electric field gradient at the antimony nucleus will remove some of the degeneracies of these transitions although the short half-life of the excited state usually results in unresolved quadrupole split spectra. The relative line positions are determined by the eigenvalues of the ground and excited state Hamiltonians which involve the ratio ($R = 1.38$ [13]) of the excited and ground state quadrupole coupling constants and the asymmetry parameter η. For $\eta = 0$ the selection rules restrict the number of possible transitions to eight.

Using the same procedure as that outlined previously,[1] the observed spectra were initially least squares computer fitted to eight Lorentzians on a parabolic base line with $\eta = 0$. This resulted, however, in unsatisfactory fits for all the compounds. When η was allowed to vary in the least squares fitting procedure, the values listed in the diagram were obtained.

The spectral line shapes are broad and symmetrical for all compounds. There are a number of reasons to which line broadening can be attributed, *e.g.*, non-homogeneity, non-stoichiometry, more than one crystallographic Sb environment, and/or an internal magnetic field induced at the Sb site by the metal atoms. None of these factors, however, is relevant for these particular samples. Thus an explanation as to the line broadening must be sought elsewhere.

Inspection of the atomic arrangement of the $CoAs_3$ type structure [12] reveals that η must differ from zero since the immediate environment of the Sb atoms is of lower symmetry than C_{2v}. In fact, for a site of symmetry C_{2v}, in which all the bond angles attain the ideal tetrahedral value, η is expected to approach unity. For finite values of η all twelve possible Mössbauer transitions become allowed and the ratios of the individual peak intensities are modified. As an example of this effect we refer to Nichols *et al.*[14] who studied the influence of the asymmetry parameter on unresolved quadrupole splittings of the $7/2 \rightarrow 5/2$ Mössbauer transitions in ^{151}Eu showing that $\eta > 0.5$ causes significant spectral

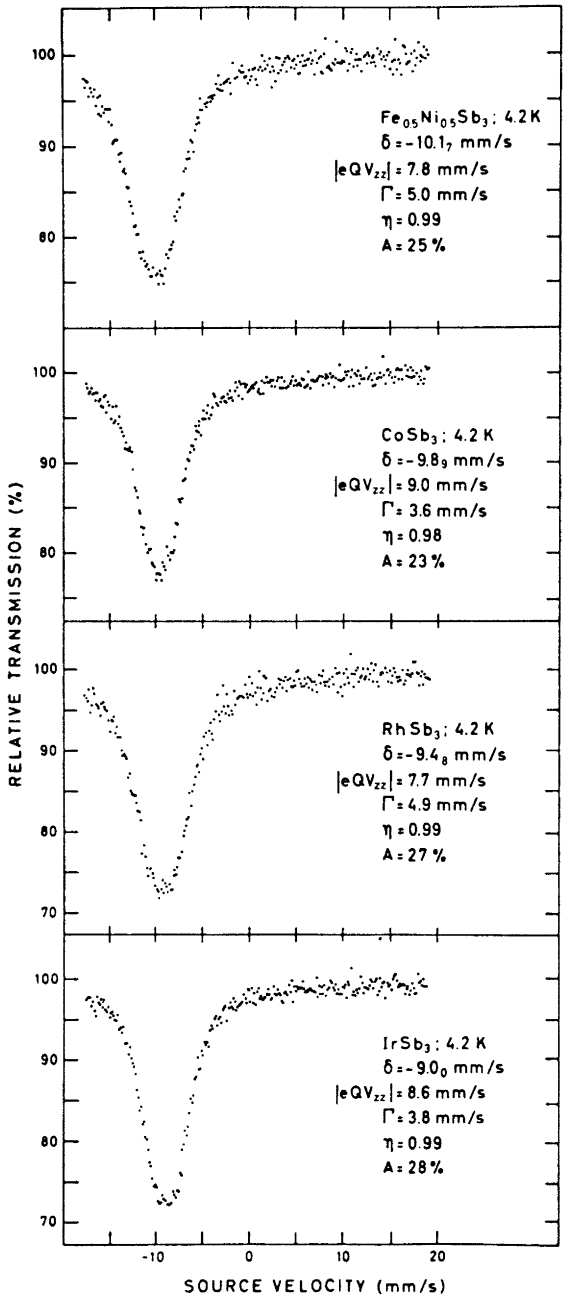

Fig. 1. ^{121}Sb Mössbauer spectra of $Fe_{0.5}Ni_{0.5}Sb_3$, $CoSb_3$, $RhSb_3$, and $IrSb_3$ at 4.2 K.

broadening. It is thus apparent that the fitting to eight Lorentzians for the present ^{121}Sb Mössbauer spectra is not a reasonable approximation.

In view of the time required to prepare a programme dealing with the considerably more complex general case for $\eta > 0.5$ it was decided to evaluate the computer data already at hand. In this situation the chemical shift values are taken to be meaningful because of the symmetric line shapes. Moreover, since the compounds are closely related the line widths of the individual transitions are assumed to be similar and the overall values for Γ provide at least an order for the magnitudes of the quadrupole interactions $|eQV_{zz}|$. There is of course a sign uncertainty in V_{zz} as a result of $\eta = 1$, because then $V_{yy} = -V_{zz}$.

The ^{121}Sb chemical shift values listed on Fig. 1 confirm the bonding to be of a predominantly covalent nature in the TSb$_3$ compounds. These δ values are more negative than that for the reference InSb (-8.9_3 mm/s at 4.2 K) implying higher total s electron densities at the Sb nuclei in the present compounds. The chemical shifts for CoSb$_3$, RhSb$_3$, and IrSb$_3$ are similar to, and show the same trend as, the corresponding compounds CoSb$_2$, RhSb$_2$, and IrSb$_2$ with the arsenopyrite type crystal structure.[1] The latter compounds have distorted tetrahedral environments around the Sb atoms in common with the TSb$_3$ compounds. Whilst the Sb atoms in the TSb$_2$ compounds are coordinated to one Sb and three T the Sb atoms in the TSb$_3$ compounds are coordinated to two Sb and two T. The observed variations in δ for the different chemical and crystallographic environments result from changes in population of the valence orbitals, the p and/or d orbitals affecting the overall s electron density at the Mössbauer nucleus by virtue of their shielding properties. The fact that substitution of a T by a Sb atom on going from the TSb$_2$ to the TSb$_3$ series does not cause large variations in δ lends support to the already inferred covalent nature of the bonding.

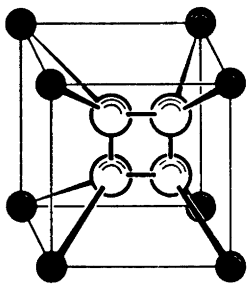

Fig. 2. Model showing a rectangular Sb$_4$ group bonded to two T atoms at each corner.

As illustrated in Fig. 2 the most striking feature of the CoAs$_3$ type structure is the collection of the non-metal atoms into planar X_4 groups. There is a rectangular distortion from an ideal square arrangement of these X_4 groups which is of the order of 5 %. This rectangular distortion is imposed by the crystal structure and is attributed to anisotropic interactions arising from the non-metal sublattice and not to any differences in covalency between the Sb–T and Sb–Sb bonds or to the T sublattice.[12]

The Sb and T atomic wave functions of the molecular fragment SbT_2Sb_2 (Fig. 2) transform to a first approximation as described by the irreducible representations of point group C_{2v}. The bonding orbitals are envisaged as linear combinations taken over a Sb and its surrounding two Sb and two T atoms using s, p, and d atomic wave functions for T and s and p atomic wave functions for Sb. The magnitude of the $T-Sb-T$ bond angle reflects the mixing of the $5p_z$ and $5s$ contributions. The fact that the $Sb-Sb-Sb$ bond angle is fixed at 90° implies that the contribution to the $Sb-Sb$ bonds comes from the $5p_x$ and $5p_y$ orbitals only.

The rectangular distortion of the Sb_4 groups which causes two different $Sb-Sb$ bond lengths is not insignificant.[15] The effect of this is to decrease orbital overlap in the longer $Sb-Sb$ bond with respect to the shorter. However, these bond differences do not vary significantly within the TSb_3 series and this suggests that the rectangular distortion is not the major cause of the variation in δ values. Thus, within this series of compounds the changes in δ, which parallel those found for the corresponding TSb_2 compounds, mainly reflect the different bonding characteristics of the T atoms, notably the differences in the principal quantum number which causes significant variations in $Sb-T$ orbital overlaps.

In a previous paper [1] it is shown that a measure of the angular part of the distortion from cubic (T_d) symmetry is given by the average deviation (ξ) of the bond angles from the tetrahedral value of 109.47°. For the TSb_2 compounds the values of ξ (ranging between 8.3 and 13.6°) have been found to correlate well with the ^{121}Sb Mössbauer quadrupole coupling constants. Largely because of the restrained $Sb-Sb-Sb$ bond angle (90°) ξ is virtually constant for compounds with the $CoAs_3$ type structure. Hence, a corresponding relationship is unobservable for the TSb_3 series and any variation in $|eQV_{zz}|$ is attributable to dissimilar electron imbalances in the Sb $5p_z$ orbital.

It is characteristic for compounds with the $CoAs_3$ type structure that the T atoms attain a formal low-spin d^6 (t_{2g}^6) configuration. The apparent exception provided by NiP_3,[10] in which the Ni atoms are formally d^7, is explained by the seventh electron being delocalized over the macromolecule. The ternary series [16-18] produced by substituting Co by Fe or Ni are additional pieces of the "jigsaw puzzle" which fall into position. The limit to which the apparently incompatible Ni atoms are tolerated by the $CoAs_3$ type structure without destroying its basic stability decreases in the sequence CoP_3, $CoAs_3$, and $CoSb_3$. The opposite trend is evident on substitution of Co by Fe.

As for the non-metal atoms the $CoAs_3$ type structure appears to be limited to pnictides and there are no reports concerning the existence of corresponding compounds with Group IVB or VIB elements. Regarding the t_{2g}^6 configuration of T as being a significant feature of the skutterudites, then the hypothetical chalcogenides would be restricted to Cr, Mo, or W in a formally zero valence state. Because of the large diffuse d orbitals on the non-metal atoms [19] π back-bonding is presumably ineffective and hence, such low valence states on T would be unstable. On the other hand, hypothetical Group IVB skutterudites would require an unusually high valence state of T (*e.g.* Zn(VI), Cd(VI), or Hg(VI)).

REFERENCES

1. Donaldson, J. D., Kjekshus, A., Nicholson, D. G. and Tricker, M. J. *Acta Chem. Scand.* **26** (1972) 3215.

2. Kjekshus, A., Nicholson, D. G. and Mukherjee, A. D. *Acta Chem. Scand.* **26** (1972) 1105.
3. Rosenqvist, T. *Acta Met.* **1** (1953) 761; *N.T.H.-Trykk*, Trondheim 1953.
4. Zhuravlev, N. N. and Zhdanov, G. S. *Kristallografiya* **1** (1956) 509.
5. Dudkin, L. D. and Abrikosov, N. Kh. *Zh. Neorgan. Khim.* **1** (1956) 2096.
6. Hulliger, F. *Helv. Phys. Acta* **34** (1961) 782.
7. Kjekshus, A. and Pedersen, G. *Acta Cryst.* **14** (1961) 1065.
8. Kuz'min, R. N. and Snovidov, V. M. In Sirota, N. N., Ed., *Chemical Bonds in Semiconductors and Solids*, Consultants Bureau, New York 1967, p. 257.
9. Bjerkelund, E. and Kjekshus, A. *Acta Chem. Scand.* **24** (1970) 3317.
10. Rundqvist, S. and Ersson, N.-O. *Arkiv Kemi* **30** (1968) 103.
11. Mandel, N. and Donohue, J. *Acta Cryst.* **B 27** (1971) 2288.
12. Kjekshus, A., Nicholson, D. G. and Rakke, T. *Acta Chem. Scand.* **27** (1973) 1307.
13. Ruby, S. L., Kalvius, G. M., Snyder, R. E. and Beard, G. B. *Phys. Rev.* **148** (1966) 176.
14. Nichols, A. L., Large, N. R. and Lang, G. *Chem. Phys. Letters* **15** (1972) 598.
15. Kjekshus, A., and Rakke, T. *To be published.*
16. Roseboom, E. H. *Am. Mineralogist* **47** (1962) 310.
17. Pleass, C. M. and Heyding, R. D. *Can. J. Chem.* **40** (1962) 590.
18. Kuz'min, R. N. In Sirota, N. N., Ed., *Chemical Bonds in Semiconductors and Solids*, Consultants Bureau, New York 1967, p. 265.
19. Craig, D. P., Maccoll, A., Nyholm, R. S., Orgel, L. E. and Sutton, L. E. *J. Chem. Soc.* **1954** 332.

Received November 21, 1972.

ACTA CHEMICA SCANDINAVICA 27 (1973) 1321–1327

Inter-residue Lactones Formed by Treatment of Periodate-oxidised Polysaccharides with Aqueous Bromine

MONA FAHMY ISHAK* and TERENCE PAINTER

Institute for Marine Biochemistry, N-7034 Trondheim (NTH), Norway

When amylose was oxidised with periodate until 64 % of the glucose residues had been converted into "dialdehyde" units, and then treated at 20° with aqueous bromine buffered at pH 4.6, a product was isolated in which 60 % of the aldehyde groups had been converted into free carboxylic acid, and 40 % into lactones.

The remaining 36 % of intact glucose residues in the product were resistant to oxidation by periodate, but after hydrolysis of the lactones with mild alkali, they became freely oxidisable. After hydrolysis with alkali, treatment with aqueous acid or bromine did not regenerate the lactones. Sodium alginate and a xylan also contained lactones after partial oxidation with periodate and treatment with aqueous bromine.

The lactones must have arisen by direct oxidation, in their closed-ring form, of hemiacetals formed between the aldehyde groups of periodate-oxidised sugar residues and the secondary hydroxyl groups of intact sugar residues in the same molecular chain.

In connection with studies [1–5] of the hemiacetals that occur in polysaccharides after partial oxidation with periodate, a better method was needed to identify the aldehyde and hydroxyl groups involved. It was thought that, if the hemiacetals could be converted directly into lactones by oxidation with aqueous bromine, the required information might be provided by circular-dichroism spectroscopy of the products. A study of conditions was therefore undertaken, and the present paper describes results that appear promising.

EXPERIMENTAL

Materials. The preparation of 64 % periodate-oxidised amylose has been described elsewhere,[3] as also has the preparation of 44 % periodate-oxidised sodium alginate.[1] The sample of xylan was prepared from the red seaweed, *Rhodymenia palmata*,[6] by Dr. Arne Jensen, and kindly donated by him. It was water-soluble, of high intrinsic viscosity, and contained 78 % of 1,4-linked xylose residues, as indicated by its periodate-oxidation

* On leave of absence from the Chemical Department of Cairo, Ministry of Industry, Cairo, Egypt.

limit.[5] A portion of the xylan was oxidised in 25 mM periodate to the extent of 40 %, essentially as described elsewhere for a sample of maize-cob xylan.[2]

Kinetics of oxidation of 64 % periodate-oxidised amylose with aqueous bromine. A 0.5 M sodium acetate-acetic acid buffer of pH 5.0 was almost saturated with bromine at room temperature. A portion (10 ml) was added to a mixture of aqueous potassium iodide (30 % w/v; 10 ml) and 2 N hydrochloric acid (2 ml), and titrated with 0.1 M sodium thiosulphate. A bromine content of 0.176 g atom l^{-1} was thus found. A volume (150 ml) of this solution, and a solution of 64 % periodate oxidised amylose (0.5 g) in water (100 ml) were brought separately to 20°, and then mixed. At intervals, portions (10 ml) were withdrawn and titrated as just described. To correct for bromine lost by evaporation, a parallel experiment was done on 150 ml of the bromine-containing buffer, diluted to 250 ml with water. The pH of both the test and control solutions remained constant at 4.6 throughout.

Isolation of 64 % periodate-oxidised amylose after complete oxidation with bromine. A portion (1 g) of the 64 % periodate-oxidised amylose was oxidised for 48 h under the analytical conditions just described. Residual bromine was removed by addition of an excess of formic acid, and the solution was dialysed against water. It was concentrated in the rotary evaporator to 100 ml, and dialysed for 6 h against 0.01 N hydrochloric acid at 4°, with hourly replacement of the dialysate. It was then dialysed against water, and freeze-dried. The product (yield, 850 mg) had an equivalent weight, determined by titration with 0.02 N sodium hydroxide to a faint pink end-point with phenolphthalein, of 215. Another sample of the same product was isolated, as its sodium salt, by dialysis, first against 0.1 M sodium acetate, and then against water. Its equivalent weight, determined by titration with cetylpyridinium chloride,[7] was 283.

Kinetics of saponification of the lactones in the amylose derivative. A portion (100 mg) of the product (free acid), in water (20 ml), was titrated with 0.02 N sodium hydroxide in the presence of phenolphthalein (0.1 %; 2 ml) to a faint pink end-point. This solution, at 20°, was mixed with 0.02 N sodium hydroxide (50 ml), and then quickly diluted to 100 ml with water, and kept at 20°. As a control, phenolphthalein (0.1 % w/v; 2 ml), in water (20 ml), was titrated to a faint pink end-point, after which 0.02 N sodium hydroxide (50 ml) was added, followed by water to give 100 ml. At intervals, portions (10 ml) were withdrawn and back-titrated with 0.01 N oxalic acid.

Analytical oxidation of the saponified amylose derivative with periodate. A portion (100 mg) of the unsaponified amylose derivative (sodium salt), in water (50 ml), was mixed with 0.02 N sodium hydroxide (50 ml) and kept at 20° for 5 h. Acetic acid (1.0 N; 4.0 ml) was then added, followed by water (90 ml), and the solution was cooled to 2° in an ice-bath. Its pH was 4. Sodium metaperiodate (0.25 M; 4.0 ml) was then added, and the solution was quickly diluted to 200 ml with water. It was kept in the dark at 2°, and at intervals, portions (10 ml) were pipetted into an ice-cold mixture of 0.5 M sodium phosphate buffer (pH 7.0; 20 ml) and aqueous potassium iodide (30 % w/v; 3 ml), and the liberated iodine was titrated with 0.01 M sodium thiosulphate. A control solution, containing everything but the substrate, was also prepared and titrated.

Analytical oxidation of the unsaponified amylose derivative with periodate. To a mixture of 0.02 N sodium hydroxide (50 ml) and 1.0 N acetic acid (4.0 ml) was added a solution of the unsaponified amylose derivative (sodium salt) (100 mg) in water. The remainder of the procedure was as described above.

Preparative oxidation of the saponified and unsaponified amylose derivative, and analysis of the products for glucose. The conditions of oxidation were the same as in the analytical procedures, except that 2.5 times the quantities were used. After oxidation for 6 h, ethanediol (10 ml) was added to each reaction mixture. The solutions were then evaporated to 100 ml, dialysed thoroughly against water, and freeze-dried. A portion (10 mg) of each product was heated for 5.5 h in a sealed ampoule with 0.5 N hydrochloric acid (2.5 ml). The solutions were then neutralised with 0.2 M sodium acetate (3 ml) and 0.5 N sodium hydroxide (2.5 ml). A blank was also prepared, and, as a control, a sample of the original amylose derivative containing the lactones, but not subsequently treated with periodate, was treated similarly. Triplicate portions (0.06 ml) of each solution, and of an external glucose standard, were measured with an Agla micrometer syringe, and analysed for glucose by the glucose-oxidase procedure.[8]

Position of the equilibrium between the lactones and the corresponding free acids. A portion (100 mg) of the amylose derivative, in water (20 ml), was mixed with phenolphthalein

(0.1 %; 2 ml) and 0.02 N sodium hydroxide (50 ml), and kept 1 h at 20°. Oxalic acid (0.1 N; 30 ml) was then added, and the solution was diluted to 100 ml with water, and kept at 20°. Portions (10 ml) were withdrawn at intervals and titrated with 0.02 N sodium hydroxide. The titres were constant over a period of 50 h. In another experiment, the amylose derivative (100 mg) was kept at 20° in 0.033 N oxalic acid (100 ml; pH 1.5), and the change in the acidity of the system was followed by titrating portions (10 ml) with 0.02 N sodium hydroxide. The acidity increased, indicating hydrolysis of the lactones with a time of half change of approximately 48 h.

Oxidation of 40 % periodate-oxidised xylan with aqueous bromine. The kinetics were followed in the same way as, and were closely similar to, those of the periodate-oxidised amylose. After oxidation for 8 h, a sample was isolated as its sodium salt. It had an equivalent weight, determined by titration with cetylpyridinium chloride,[7] of 223. After saponification, this decreased to 207.5 (theory, assuming complete oxidation, requires 203).

Oxidation of 44 % periodate-oxidised alginate with aqueous bromine. An amount of bromine corresponding to the oxidation of one-half of the aldehyde groups was consumed very rapidly, after which further consumption was very slow. The half-oxidised material was isolated as its sodium salt, and its equivalent weight, determined by titration with cetylpyridinium chloride,[7] was 227. The kinetics of saponification were studied in the same way as for the amylose derivative, but the reaction mixture was made 2 M with respect to sodium chloride, to minimise the Donnan effect. The consumption of alkali became constant after 20 h, and indicated a final equivalent weight of 153 (theory, assuming 50 % oxidation, requires 167).

RESULTS

In the first series of experiments, the partially periodate-oxidised polysaccharides were treated with unbuffered, aqueous bromine. Under these conditions, there was an initial, rapid consumption of bromine, but the reaction then became very slow, as the pH dropped to about 1.5 because of the formation of hydrogen bromide. Isolation and examination of the partly oxidised materials revealed the presence of lactones as well as free carboxylic acid, but as the materials were successively given further treatments with bromine water in an attempt to complete the oxidation, the proportion of lactones decreased. With the partially periodate-oxidised amylose and xylan, products were finally obtained which contained no remaining aldehydic functions, as judged by a lack of reactivity with aqueous phenylhydrazine hydrochloride, but they also contained no lactones.

The kinetics of the oxidation with bromine were next studied under buffered conditions. A pH range of 4 – 5 was chosen, in the expectation that the rate of hydrolysis of the lactones would be minimal in this region. Fig. 1 shows the consumption of bromine by the 64 % periodate-oxidised amylose at pH 4.6. After oxidation for 48 h under these conditions, a product was obtained whose equivalent weight depended upon the conditions of isolation. When the free acid was isolated, after dialysis in the refrigerator against hydrochloric acid at pH 2, it had an equivalent weight of 215, as determined by direct titration with alkali. The corresponding theoretical value, assuming that all the carboxyl functions were present as free acid, was 142. This implies that about one-third of the carboxyl functions were present as lactones.

When the oxidised amylose derivative was isolated after dialysis against sodium acetate at pH 6, its sodium salt had an equivalent weight, determined by titration with cetylpyridinium chloride,[7] of 283. This compares with a

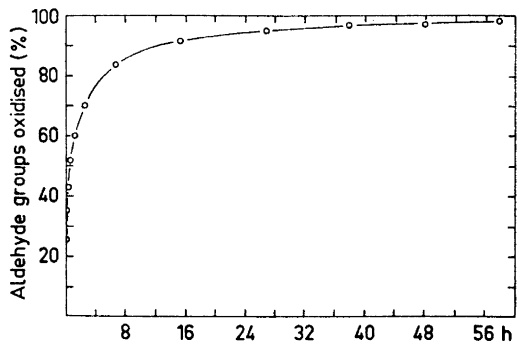

Fig. 1. Oxidation of 64 % periodate-oxidised amylose in aqueous bromine at pH 4.6 and 20°. The initial concentrations of bromine and aldehydic groups (free and combined) were 94 and 27 mequiv. l^{-1}, respectively.

theoretical figure for the sodium salt of 164, and implies the presence of 42 % of lactones. This figure is probably the more accurate of the two, since some hydrolysis of lactones would be expected to occur during isolation of the free acid.

Fig. 2 illustrates the saponification of the amylose derivative at pH 12 and 20°, and shows how the equivalent weight, calculated on a basis of the free acid, decreased to approximately the theoretical value of 142. Further experimentation as described in the experimental section showed that acidification of the reaction mixture did not cause the lactones to re-form. On the contrary, acid merely hydrolysed the lactones in the unsaponified material, as was already indicated by the oxidations carried out in unbuffered bromine water. No attempt was made to measure the exact position of the equilibrium between the free-acid and lactone forms in aqueous solution, but the results are sufficient to indicate that this must lie very far on the side of the free acid. Freeze-drying of the fully hydrolysed material in its free-acid form did not

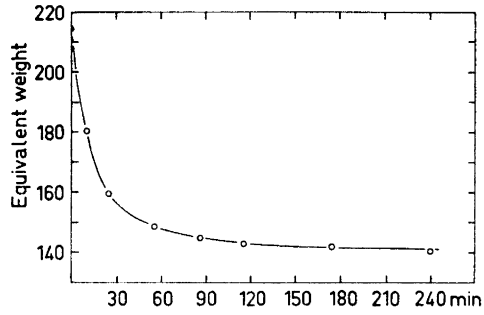

Fig. 2. Saponification of the lactones in 64 % periodate-oxidised amylose after complete oxidation with aqueous bromine. The initial concentration of sodium hydroxide was 0.01 N, and it was present in a molar excess of 4:1. The temperature was 20°.

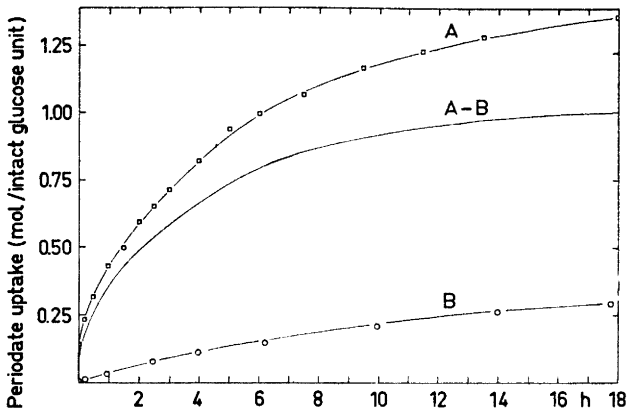

Fig. 3. Oxidation at 2° in 5 mM sodium metaperiodate of 64 % periodate-oxidised amylose after complete oxidation with aqueous bromine. Curve A: after saponification for 5 h under the conditions shown in Fig. 2. Curve B: without prior saponification. The pH of the reaction mixture was 4 in both experiments.

regenerate any lactones. It is possible that lactones would have been formed by heating the material in a vacuum, but this was not investigated.

Similar oxidations and assays of the free acid and lactones in the products were carried out on 40 % periodate-oxidised xylan and 44 % periodate-oxidised sodium alginate, as described in the experimental section. The xylan derivative was readily oxidised to completion, but the product contained only about 10 % of its carboxyl groups as lactones. The alginate consumed only about half the theoretical amount of bromine, without any decrease in equivalent weight at all; the aldehyde groups concerned were converted quantitatively into lactones.

An experiment was next carried out to determine whether any of the lactones in the amylose derivative involved the secondary hydroxyl groups of the intact glucose residues remaining in the material. Fig. 3 shows the consumption of periodate by the saponified and unsaponified material. Both consumed periodate, but when the curve for the unsaponified material was subtracted from that for the saponified material as shown, a limiting difference in consumption corresponding almost exactly to the Malapradian oxidation of the glucose residues in the latter material was indicated.

The consumption of periodate in excess of 1 mol per intact glucose residue in the saponified material must have been due to non-Malapradian oxidation, and it seemed likely that the parallel consumption by the unsaponified material was also due to this alone. To confirm this, the two substrates were isolated after oxidation for 6 h, and analysed for intact glucose residues by acid-hydrolysis and application of the glucose-oxidase method of analysis. Whereas the unsaponified material still contained 28 % of glucose residues after the treatment with periodate, the saponified material contained only 4 %.

DISCUSSION

The present investigation was prompted by the classical work of Isbell and his associates,[9–12] who first showed that glucose, and other aldohexoses and aldopentoses, are directly oxidised by aqueous bromine in their cyclic, hemiacetal forms, to give δ-lactones as the initial products. The delta-lactones formed in this kinetically-controlled reaction are unstable, and they spontaneously undergo hydrolysis in water to give mainly the free aldonic acid. In unbuffered solutions, this reaction is autocatalytic.[10] If the free aldonic acids are kept in aqueous solution for a relatively long time, they spontaneously and partially re-lactonise, but the lactones formed in this way are the thermodynamically more stable γ-lactones.[9,10] It was therefore impossible for the δ-lactones to have been formed as secondary products from the free acids, and the pyranose-ring structure of the parent sugars in solution was thereby established.

Apart from the possible presence of D-erythrofuranose rings in the periodate-oxidised amylose,[13] all the hemiacetals in the materials examined in the present work were expected to be derivatives of dioxan.[1–5] The lactones derived from them were therefore expected to resemble the aldonic δ-lactones in properties, even though some differences in stability could be expected to arise from the presence of two hetero-atoms in the rings, and the presence of any inter-residue lactones as parts of fused-ring systems.

Initial attempts to carry out the oxidation with unbuffered bromine quickly confirmed that the lactones were unstable in acid, and could not have been formed as secondary products from previously oxidised aldehyde groups. By carrying out the oxidation at pH 4.6, hydrolysis of the lactones was kept to a minimum, and any lactonisation of previously formed carboxyl groups would have been virtually precluded. It was also hoped that any trans-lactonisation (intramolecular trans-esterification) would be kept to a minimum at this pH, but the possibility of this reaction unfortunately cannot be excluded.

The yield of a particular lactone is unfortunately no indication of the relative amount of its parent hemiacetal in the starting-material. In the case of the xylan derivative, for example, it was known from earlier work [2] that the position of the equilibrium between the aldehydic and hemiacetal forms lay about 85 % on the side of the latter, and yet only 10 % of them were recovered as lactones. In contrast, half the hemiacetals in the periodate-oxidised alginate were quantitatively converted into lactones, while the remainder were very resistant to oxidation.

There are clearly two reasons for this. The first is that every lactone is subject to spontaneous hydrolysis from the moment of its formation, and the rate of hydrolysis will depend upon its stereochemistry.[10,14] The second is that the yield of a lactone is determined not only by the position of the equilibrium between its parent hemiacetal and the corresponding open-chain aldehydic form, but also by the relative rates of oxidation of these. The rate of oxidation of a cyclic hemiacetal is known [11,12,15] to be highly dependent upon the stereochemistry of the ring.

It may not always be useful to attempt complete oxidation with bromine,

as was done in the present work, because during the period of time required for this, extensive hydrolysis of the less-stable lactones could occur. Fig. 1 shows that half the aldehyde groups in the periodate-oxidised amylose were oxidised in a few minutes, while it took many hours to complete the last 10 % of the oxidation. It should be noted that this kinetic behaviour is certainly due in part to the fact [16,17] that the tribromide ion, Br_3^-, does not oxidise hemiacetals.

In conclusion, there is a strong element of unpredictability in the use of bromine-oxidation to study this kind of hemiacetal, but possibilities exist for overcoming the problems encountered, and the results appear to be generally encouraging.

One of the authors (M.F.I.) is indebted to the *Norwegian Agency for International Development* (N.O.R.A.D.) for financial assistance.

REFERENCES

1. Painter, T. J. and Larsen, B. *Acta Chem. Scand.* **24** (1970) 813.
2. Painter, T. J. and Larsen, B. *Acta Chem. Scand.* **24** (1970) 2366.
3. Painter, T. J. and Larsen, B. *Acta Chem. Scand.* **24** (1970) 2724.
4. Smidsrød, O., Larsen, B. and Painter, T. J. *Acta Chem. Scand.* **24** (1970) 3201.
5. Fahmy Ishak, M. and Painter, T. J. *Acta Chem. Scand.* **25** (1971) 3875.
6. Percival, E. and McDowell, R. H. *Chemistry and Enzymology of Marine Algal Polysaccharides*, Academic, London and New York 1967, p. 88.
7. Scott, J. E. *Methods Biochem. Analy.* **8** (1960) 163.
8. Richterich, R. *Klinische Chemie, Theorie und Praxis*, S. Karger, Basel 1965, p. 191.
9. Isbell, H. S. and Hudson, C. S. *J. Res. Natl. Bur. Std.* **8** (1932) 327.
10. Isbell, H. S. *J. Res. Natl. Bur. Std.* **8** (1932) 615.
11. Isbell, H. S. and Pigman, W. *J. Res. Natl. Bur. Std.* **10** (1933) 337.
12. Isbell, H. S. and Pigman, W. *J. Res. Natl. Bur. Std.* **18** (1937) 141.
13. Guthrie, R. D. *Advan. Carbohydrate Chem.* **16** (1961) 105.
14. Haworth, W. N. *The Constitution of Sugars*, Edward Arnold, London 1929, p. 24.
15. Barker, I. R. L., Overend, W. G. and Rees, C. W. *J. Chem. Soc.* **1964** 3254.
16. Bunzel, H. H. and Mathews, A. P. *J. Am. Chem. Soc.* **31** (1909) 464.
17. Perlmutter-Hayman, B. and Persky, A. *J. Am. Chem. Soc.* **82** (1960) 276.

Received November 21, 1972.

ACTA CHEMICA SCANDINAVICA 27 (1973) 1328–1336

Chlorinated Long-chain Fatty Acids. Their Properties and Reactions. V. Alkaline Dehydrochlorination of Sodium *threo*- and *erythro*-9(10)-Chloro-10(9)-hydroxyoctadecanoates

MARTTI KETOLA

Department of Chemistry, University of Turku, SF-20500 Turku 50, Finland

The base-catalyzed dehydrochlorination of *threo*- and *erythro*-9(10)-chloro-10(9)-hydroxyoctadecanoic acids in water and in ethylene glycol-water mixtures has been studied. The reactions followed apparent second-order kinetics and *threo*- and *erythro*-isomers formed *cis*- and *trans*-9,10-epoxyoctadecanoic acids, respectively. In water solutions the contribution of the water reaction was very significant besides the hydroxide ion catalysis but no catalytic effect of solvent was found in aqueous ethylene glycol mixtures, which contained 16.6 mol % of water. The rate ratios of *threo*- and *erythro*-chlorohydroxyoctadecanoic acids determined for the base catalysis, for the water reaction, and for the reaction in aqueous ethylene glycol at 25°C were 0.45, 0.50, and 0.35, respectively.

The alkaline dehydrochlorination of sodium *threo*-9,10-dichlorooctadecanoate (I) (chlorinated oleic acid [1a]) may take place by a bimolecular elimination (E2) or a substitution (S_N2) mechanism. Earlier results [1b,1c] showed, however, that the alkaline dehydrochlorination of I very likely proceeds by the E2 mechanism in water and ethylene glycol-water mixtures. However, the occurrence of the substitution reaction could not be fully excluded.[1b,1c] To solve this problem, *threo*-9(10)-chloro-10(9)-hydroxyoctadecanoic acid (II), the product of the alkaline S_N2-type dehydrochlorination of I,[1c] was prepared and the rate of its alkaline dehydrochlorination was determined and compared with the rate of removal of the second chlorine atom from I.

EXPERIMENTAL

The NMR-spectra were taken for 10 – 15 % solutions of the samples in carbon tetrachloride using a 60 MHz Perkin Elmer R-10 spectrometer. The chemical shifts are given in ppm downfield from tetramethylsilane (TMS) which was used as internal reference.

The chlorine contents and melting points were determined as reported earlier.[1a]

Synthesis. threo-9(10)-Chloro-10(9)-hydroxyoctadecanoic acid (II) and *erythro*-9(10)-chloro-10(9)-hydroxyoctadecanoic acid (III) were synthesized according to Swern *et al.*[2,3] Oleic acid (25 g) (Fluka AG, 96 % by GLC) and elaidic acid (12 g) were oxidized with peracetic acid to *cis*- (22.2 g) and *trans*-9,10-epoxyoctadecanoic acids (13.7 g), respectively. Ring opening (with HCl) of these epoxides yielded 11.8 g (45 %) of II and 7.3 g (51 %) of III after three crystallizations from hexane (1 g of acid in 4 ml of solvent). The *threo* compound II melted at 37 – 39°C (lit.[3-5] 39°; 38 – 41°; 35 – 41°C) and its chlorine content based on six determinations was 10.54 ± 0.09 % (calc. 10.59 %). The *erythro* compound III melted at 53 – 54°C (lit.[3-5] 58.0 – 58.8°; 52 – 57°; 53 – 58°C) and its chlorine content was 10.25 ± 0.13 % (calc. 10.59 %). The wide melting ranges are due to the fact that both stereoisomers were mixtures of two isomeric acids (9,10 and 10,9) that have different melting points.[6]

Elaidic acid (m.p. 42.5°C, lit.[7] 43 – 44°C) was prepared from oleic acid.[7]

Kinetic measurements. The alkaline dehydrochlorinations of II and III were carried out in water and ethylene glycol-water mixtures as described earlier [1b,1c] except that only single samples were taken at intervals (Tables 1 and 2). The effects of base concentration and the ethylene glycol content of the solvent on the reaction rate were also studied (Fig. 1; Table 1). The substrate concentrations in the reaction mixtures varied from 0.020 to 0.021 mmol/g of solvent.

Table 1. Rate coefficients of the alkaline dehydrochlorination of sodium *threo*- and *erythro*-9(10)-chloro-10(9)-hydroxyoctadecanoates in aqueous ethylene glycol mixtures.

Temp.[a] °C	10^2 [OH^-] mol kg^{-1}	Water content mol fraction	wt. %	10^3 k_{OH} kg mol^{-1} s^{-1}
threo-*9(10)-Chloro-10(9)-hydroxyoctadecanoate*				
30	8.24	0.536	25.1	17.6 ± 0.1[b]
	8.39	0.737	44.9	16.2 ± 0.1
	8.21	0.837	59.8	14.1 ± 0.1
	8.39	0.888	69.8	13.9 ± 0.1
	8.41	0.950	84.8	18.1 ± 0.1
20	16.2	0.165	5.4	2.27 ± 0.03
25	16.5			4.71 ± 0.03
30	16.9			8.63 ± 0.04
35	16.4			15.8 ± 0.1
30	5.33	0.165	5.4	8.17 ± 0.05
	7.94			7.90 ± 0.06
	10.3			8.20 ± 0.05
	20.1			8.00 ± 0.07
erythro-*9(10)-Chloro-10(9)-hydroxyoctadecanoate*				
20	5.82	0.165	5.4	7.49 ± 0.05
25	6.00			14.1 ± 0.2
30	6.09			24.6 ± 0.4
35	6.09			41.9 ± 0.5
25	3.34	0.165	5.4	3.93 ± 0.03
	9.95			14.3 ± 0.1
	12.5			14.4 ± 0.2

[a] ± 0.1°C. [b] Standard error.

Table 2. Rate coefficients of the alkaline dehydrochlorination of sodium *threo-* and *erythro-*9(10)-chloro-10(9)-hydroxyoctadecanoates in water.

Temp.[a] °C	10^2 [OH^-] mol kg^{-1}	10^2 k_{app} kg mol^{-1} s^{-1}	kg mol^{-1} s^{-1}
threo-*9(10)-Chloro-10(9)-hydroxyoctadecanoate*			
	3.94	0.953 ± 0.01[b]	$10^6k_{H_2O}$ = 3.96 ± 1.57
15	8.39	0.727 ± 0.008	10^3k_{OH} = 4.20 ± 1.11
	9.89	0.613 ± 0.006	
	2.06	2.40 ± 0.03	$10^6k_{H_2O}$ = 6.04 ± 0.51
20	4.04	1.50 ± 0.04	10^3k_{OH} = 7.11 ± 0.52
	8.24	1.13 ± 0.01	
	2.17	3.09 ± 0.05	$10^6k_{H_2O}$ = 6.52 ± 0.33
25	4.04	2.25 ± 0.04	10^3k_{OH} = 13.8 ± 0.4
	8.20	1.83 ± 0.02	
	3.83	3.75 ± 0.04	$10^6k_{H_2O}$ = 9.28 ± 1.04
30	5.90	3.35 ± 0.03	10^3k_{OH} = 24.3 ± 0.9
	8.23	3.05 ± 0.04	
35	8.20	4.24 ± 0.05	
erythro-*9(10)-Chloro-10(9)-hydroxyoctadecanoate*			
	1.99	3.15 ± 0.02	$10^6k_{H_2O}$ = 7.91 ± 1.73
15	3.95	2.37 ± 0.03	10^3k_{OH} = 11.1 ± 2.1
	6.81	1.72 ± 0.03	
	2.03	4.51 ± 0.06	
	2.13	4.34 ± 0.09	$10^6k_{H_2O}$ = 10.1 ± 0.6
20	3.75	3.07 ± 0.06	
	5.98	2.72 ± 0.10	
	7.52	2.42 ± 0.04	10^3k_{OH} = 17.0 ± 0.5
	9.93	2.26 ± 0.06	
	2.03	6.68 ± 0.06	
25	2.94	5.47 ± 0.05	$10^6k_{H_2O}$ = 15.2 ± 0.2
	5.92	4.00 ± 0.13	10^3k_{OH} = 25.7 ± 1.8
	7.81	3.65 ± 0.05	
	2.08	10.1 ± 0.1	$10^6k_{H_2O}$ = 18.6 ± 0.5
30	3.11	8.24 ± 0.08	10^3k_{OH} = 49.6 ± 0.8
	4.43	7.30 ± 0.10	

[a] ± 0.1°C. [b] Standard error for 10 – 15 individual values.

Calculation of rate coefficients. The alkaline dehydrochlorinations of the studied *threo* (II) and *erythro* (III) compound follow apparently second-order kinetics.[8] The rate equation is

$$k_{app} = \frac{1}{t(a-b)} \ln \frac{b(a-x)}{a(b-x)} \quad (1)$$

where $a = v_\infty - v_0$ (mequiv./g), $b = [OH^-] - v_0$ (mequiv./g), $[OH^-]$ is the initial hydroxide ion concentration after correction for salt formation with the chlorohydroxy acid, and v_0 is the initial and v_∞ the final consumption of the titrant. The rate coefficients were calculated from the equation

$$k_{app} = \frac{1}{(v_\infty - [OH^-])(t - t_0)} \ln \frac{([OH^-] - v_0)(v_\infty - v_t)}{(v_\infty - v_0)([OH^-] - v_t)} \quad (2)$$

where t_0 is the time of removal of the first sample and v_t the consumption of the titrant (mequiv./g) at time t.

The second-order rate coefficients (k_{OH}) for the dehydrochlorinations in aqueous ethylene glycol mixtures were obtained directly from eqn. (2), but only apparent second-order rate coefficients of the reactions in water were obtained from this equation. The following expression may be written for the rates of the reactions in alkaline water solutions:[9]

$$k_{app}[OH^-][S] = (k_0 + k_{OH}[OH^-])[S] \quad (3)$$

k_{app} is the observed second-order rate coefficient (eqn. (2)), [S] the substrate concentration, and k_0 the rate coefficient of the reaction catalyzed by water. The apparent second-

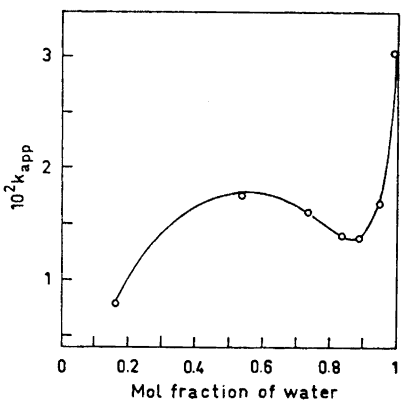

Fig.1. Dependence of the observed second-order rate coefficient (k_{app}) of the alkaline dehydrochlorination of sodium *threo*-9(10)-chloro-10(9)-hydroxyoctadecanoate on water content in aqueous ethylene glycol mixtures at 30°C.

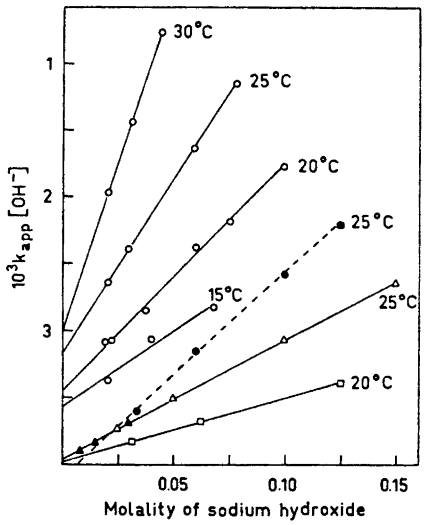

Fig. 2. First-order rate coefficient $k_{app}[OH^-]$ of dehydrochlorination of sodium *erythro*-9(10)-chloro-10(9)-hydroxyoctadecanoate (A) and ethylene chlorohydrin (B) as a function of hydroxide ion concentration in water at different temperatures. A. ○, this work. ●, this work: aqueous ethylene glycol mixture ($x_{H_2O} = 0.165$). B. ▲, values of Smith.[20] △, values of Ballinger and Long.[22] □, values of Porret.[21]

order kinetics of the neutral reaction is due to the fact that each released mol of hydrogen chloride consumes one mol of sodium hydroxide. Consequently, the relation

$$k_{app}[OH^-] = k_0 + k_{OH}[OH^-] \quad (4)$$

represents a straight line whose slope is equal to k_{OH} and intercept to k_0. The values of these quantities were determined by the method of least squares (Fig. 2 and Tables 2 and 3).

Table 3. Values of thermodynamic functions of activation at 25°C for the alkaline dehydrochlorination of sodium *threo-* and *erythro*-9(10)-chloro-10(9)-hydroxyoctadecanoates in water and in an aqueous ethylene glycol mixture ($x_{H_2O} = 0.165$).

Compound [a]		$\Delta H^{\ddagger}$ kJ mol^{-1}	$\Delta S^{\ddagger}$ J deg^{-1} mol^{-1}	$\Delta G^{\ddagger}$ kJ mol^{-1}	Ref.
In water					
I[b]	A	78.0 ± 3.9[c]	−19.5 ± 13.1[c]	83.8 ± 0.09[c]	This work
I[b]	B	35.8 ± 6.5	−223.6 ± 21.9	102.4 ± 0.14	This work
II	A	68.6 ± 6.7	−44.4 ± 22.5	81.8 ± 0.14	This work
II	B	40.7 ± 3.9	−201.2 ± 13.2	100.7 ± 0.09	This work
III[d]		90.8 ± 0.9	+20.5 ± 2.1	84.5 ± 0.05	(21)
III[d]		81.6 ± 3.4	−9.6 ± 10.0	84.5 ± 0.13	(10)
III[d]		95.0 ± 0.5	+35.2 ± 1.3	84.5 ± 0.02	(25)
III[d,e]		103.8 ± 3.8	−102.1 ± 10.9	134.3 ± 0.54	(24)
III	A[f]	88.3	+12.1	84.7	(20,21,22)
III	B[f]	71.4	−123.8	108.4	(20,21,22)
In aqueous ethylene glycol					
I		94.2 ± 2.4	+26.1 ± 8.0	86.4 ± 0.05	This work
II		83.5 ± 1.6	−0.4 ± 5.3	83.6 ± 0.04	This work

[a] I, sodium *threo*-9(10)-chloro-10(9)-hydroxyoctadecanoate; II, sodium *erythro*-9(10)-chloro-10(9)-hydroxyoctadecanoate; III, ethylene chlorohydrin. [b] A, base catalyzed reaction; B, water reaction. [c] Standard deviation. [d] Over-all reaction. [e] Neutral hydrolysis. [f] Recalculated from literature values.

RESULTS AND DISCUSSION

Solvent effects. The rates of the dehydrochlorination of the *threo* and *erythro* compounds depend greatly on the composition of the ethylene glycol-water mixture (see Fig. 1 and Tables 1, 2, and 3). Stevens *et al.*[8] investigated the alkaline dehydrochlorination of ethylene chlorohydrin in alcohol-water and dioxane-water mixtures. Their results are not, however, directly comparable with the results obtained in this work owing to the different solvent mixtures. The solvent effects on alkaline dehydrochlorination reaction were extensively discussed in an earlier paper.[1c]

Mechanism of dehydrochlorination. After the study of Evans [10] in the year 1891 the kinetics and mechanism of the reaction between hydroxide ion and ethylene chlorohydrin have been the subjects of several investigations.[11–13] This reaction is subject to specific rather than to general base catalysis.[13]

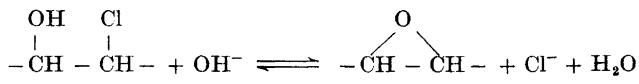

(5)

The reverse reaction does not play any significant role [14] and the effect of ionic strength on the reaction rate is very small except when the ionic strength is high.[15] The main product in alkaline media is the epoxide.[8] Reactions of various halogenohydroxyoactadecanoates in alkaline media have also been described by many authors,[3–5] but the kinetics and mechanisms of the reactions have not been clarified.

According to Winstein and Lucas [11] the reaction mechanism is the following:

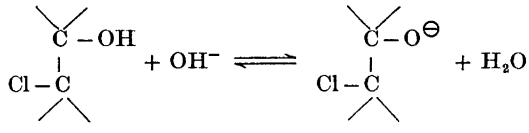

(6)

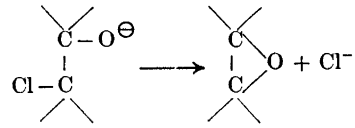

(7)

The reaction involves a pre-equilibrium stage (eqn. (6)) followed by the rate-determining release of the chloride ions (eqn. (7)). This mechanism was later confirmed by the experiments of Swain *et al.*[12]

The mechanisms of the alkaline dehydrochlorination reactions of II and III in water and in aqueous ethylene glycol mixtures were in agreement with NMR analyses of the reaction products. The *threo*- and *erythro*-9(10)-chloro-10(9)-hydroxyoctadecanoic acids give characteristic signals at 3.40 – 3.95 ppm and 3.59 – 4.04 ppm, respectively, from TMS that indicate the presence of the secondary –C*H*OH– grouping (lit. 3.4 – 3.6 ppm;[16,17] 3.3 – 3.7 ppm [18]) and the –C*H*Cl– grouping (lit. 3.8 – 4.3 ppm;[18] 4.0 – 4.3 ppm [19]). After treatment of the acids with alkali in water and in aqueous ethylene glycol, the above signals were replaced by new ones at 2.81 ppm (II) and 2.46 ppm (III). The ring protons of *cis*-9,10-epoxy- and *trans*-9,10-epoxyoctadecanoic acids resonate at 2.80 and 2.46 ppm, respectively, in close agreement with the above values.[17] The fact that the presence of a secondary –CHOH– grouping could not be verified supports the conclusion that the main products are epoxy acids. These observations are in good agreement with the results obtained with ethylene chlorohydrin by Stevens *et al.*[8] The present results confirm the alkaline dehydrochlorination of II and III to occur by the same mechanism as that of ethylene chlorohydrin (eqns. (5) – (7)).

Water reaction. There are many contradictory observations on the alkaline dehydrochlorination of ethylene chlorohydrin, *e.g.*, on the dependence of the reaction rate on the initial concentrations of the reactants.[20–22] According to Winstrom and Warner,[15] this may be due to the effect of carbon dioxide on the alkaline reagent. Ballinger and Long [22] assumed that the dependence is mainly due to a primary salt effect, although, according to earlier reports, the primary salt effect is negligible.[15,20] Our results showed that the second-order rate coefficients increase with decreasing base concentration and that the first-order rate coefficients ($k_{app}[OH^-]$) of II and III vary linearly as the concentration of the base in aqueous ethylene glycol mixtures and in water (Fig.

2; Tables 1 and 2). Only the base catalysis could be detected in the mixtures, whereas in water the neutral reaction contributes appreciably to the rate as seen in Fig. 2 and Table 2. The reaction of ethylene chlorohydrin with water has earlier been found to be very slow [15] and has consequently been disregarded in examinations of the rates of dehydrochlorination of this compound. The present results led, however, to the conclusion that the contribution of the water reaction in alkaline water solution is significant and may even be augmented by substitution. The *threo* and *erythro* acids II and III may be considered disubstituted ethylene chlorohydrins. The great increase in reaction rate with increasing water content of the solvent (Fig. 1) seems to be due to a significant contribution of the water reaction. Using literature values [20–22] for ethylene chlorohydrin in alkaline water solution and plotting $k_{app}[OH^-]$ as a function of base concentration (Fig. 2), it was possible to estimate the second-order rate coefficient of the water reaction (k_{H_2O}) of this compound. Values of the rate coefficient $k_0/55.5 = k_{H_2O}$ (M^{-1} s^{-1}) calculated in the way are 6.5×10^{-7} at 25° and 2.2×10^{-7} at 20°C and values of the rate coefficient of the base-catalyzed reaction k_{OH} (M^{-1} s^{-1}) 8.9×10^{-3} at 25° and 4.8×10^{-3} at 20°C.[20–22] These values are very reasonable when compared with those for II and III (Table 2). The values of k_{H_2O} and k_{OH} for ethylene chlorohydrin, II and III show that alkyl-substitution increases the over-all reaction rate as reported earlier [13,23] and increases the rate of the water reaction appreciably more than that of the reaction catalyzed by hydroxide ion.

The activation enthalpy is greater for the water reaction than for the base-catalyzed reaction (Table 3). The ratio $k_{H_2O}/k^0_{H_2O}$, where k_{H_2O} is the second-order rate coefficient of the water reaction in alkaline water [20,22] and $k^0_{H_2O}$ the second-order rate coefficient of the neutral hydrolysis,[24] is of the order of 10^4 for ethylene chlorohydrin at 25°C. We can see from Table 3 that the value of the free energy of activation for the latter reaction of ethylene chlorohydrin is markedly larger than that for the water reaction, 134 and 108 kJ per mol, respectively, These values led us to conclude that the mechanism of the water reaction in alkaline media differs somewhat from that of the neutral hydrolysis in water. The results of analyses of the reaction products of II and III are in agreement with this conclusion. According to Cowan *et al.*,[24] glycol is the main product in the neutral hydrolysis of ethylene chlorohydrin in water. In this work no alkoxy or hydroxyl groups were detected in the products formed in alkaline aqueous ethylene glycol or in water, whereas epoxide formation was observed in both cases. The water-catalyzed reaction of ethylene chlorohydrin in water containing hydroxide ions requires, however, more detailed supplementary studies because the contribution of the reaction to the over-all rate of dehydrochlorination is very much smaller than in the case of the salts of long-chain chlorohydroxy acids studies in the present work.

Final choice between the possible routes of the alkaline dehydrochlorination of sodium threo-*9,10-dichloro-octadecanoate.* As reported earlier,[1b,1c] the alkaline dehydrochlorination of sodium *threo*-9,10-dichlorooctadecanoate (I) may occur by bimolecular substitution or elimination:

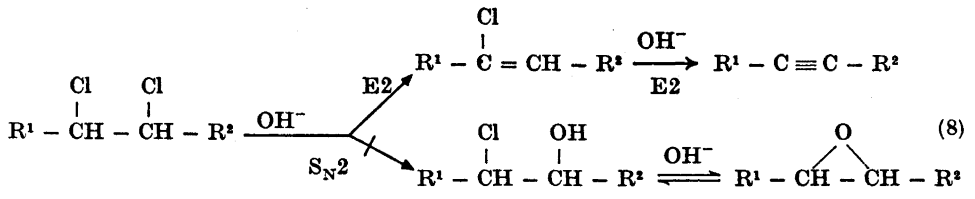

$R^1 = CH_3(CH_2)_7-$
$R^2 = -(CH_2)_7COONa$

The relative rates of the first and second stages of dehydrochlorination of I and the relative rate of dehydrochlorination of II in aqueous ethylene glycol ($x_{H_2O} = 0.165$) at 90°C are 1, 0.003, and 15 000, respectively. The very high rate of reaction of II in comparison with that of the second stage of dehydrochlorination of I supports the view that substitution occurs to only a negligible extent. The same situation prevails also in the alkaline dehydrochlorination of sodium *threo,threo*-9,10,12,13-tetrachlorooctadecanoate.[1d] Almost equal amounts of chlorine were observed to be removed in both stages of dehydrochlorination of I. Consequently, the above and earlier results [1b,1c] show that the S_N2 mechanism (eqn. (8)) may be disregarded in the alkaline dehydrochlorination of I in aqueous ethylene glycol mixtures.

Acknowledgments. The author thanks Miss Maija-Liisa Mäki for her skillful assistance and the *Suomen Kulttuurirahasto* for financial aid.

REFERENCES

1. a. Pihlaja, K. and Ketola, M. *Suomen Kemistilehti* **B 43** (1970) 21; b. Ketola, M. and Pihlaja, K. *Ibid.* **B 43** (1970) 289; c. Ketola, M. and Pihlaja, K. *J. Am. Oil Chemists' Soc.* **48** (1971) 462; d. Ketola, M. *Tetrahedron In press.*
2. Findley, T. W., Swern, D. and Scanlan, J. T. *J. Am. Chem. Soc.* **67** (1945) 412.
3. Swern, D. *J. Am. Chem. Soc.* **70** (1948) 1235.
4. King, G. *J. Chem. Soc.* **1949** 1817.
5. McGhie, J. F., Ross, W. A., Rao, B. L., Cramp, W. A. and Thornton, C. B. *J. Chem. Soc.* **1962** 3108.
6. Jungermann, E. and Spoerri, P. E. *J. Am. Chem. Soc.* **75** (1953) 4704.
7. Teeter, H. M., Gast, L. E., Raleigh, D. and Woods, L. C. *J. Am. Chem. Soc.* **73** (1951) 2302.
8. Stevens, J. E., McCabe, C. L. and Warner, J. C. *J. Am. Chem. Soc.* **70** (1948) 2449.
9. Bender, M. L. *Mechanisms of Homogeneous Catalysis from Protons to Proteins*, Wiley-Interscience, New York – London – Sydney – Toronto 1971, p. 73.
10. Evans, W. P. *Z. physik. Chem.* **7** (1891) 337.
11. Winstein, S. and Lucas, H. J. *J. Am. Chem. Soc.* **61** (1939) 1576.
12. Swain, C. G., Ketley, A. D. and Bader, R. F. *J. Am. Chem. Soc.* **81** (1959) 2353.
13. Frost, A. A. and Pearson, R. G. *Kinetics and Mechanism*, 2nd Ed., Wiley, New York – London 1961, pp. 289 – 306.
14. Brönstedt, J. N., Kilpatrick, M. and Kilpatrick, M. *J. Am. Chem. Soc.* **51** (1929) 428.
15. Winstrom, L. O. and Warner, J. C. *J. Am. Chem. Soc.* **61** (1939) 1205.
16. Tulloch, A. P. *J. Am. Oil Chemists' Soc.* **43** (1966) 670.
17. Hopkins, C. Y. *J. Am. Oil Chemists' Soc.* **38** (1961) 664.
18. Ewart, H. W. and Hergert, H. L. *Tappi 5th International Pulp Bleaching Conference*, May 17 – 21, 1970, Atlanta, Georgia, p. 227.
19. Mohacsi, E. *J. Chem. Educ.* **41** (1964) 38.
20. Smith, L. *Z. physik. Chem.* **A 152** (1931) 153; **81** (1912) 339.

21. Porret, D. *Helv. Chim. Acta* **24** (1941) 80E; **27** (1944) 1321.
22. Ballinger, P. and Long, F. A. *J. Am. Chem. Soc.* **81** (1959) 2347.
23. Nilsson, H. and Smith, L. *Z. physik. Chem.* **A 166** (1933) 136.
24. Cowan, H. D., McCabe, C. L. and Warner, J. C. *J. Am. Chem. Soc.* **72** (1950) 1194.
25. McCabe, C. L. and Warner, J. C. *J. Am. Chem. Soc.* **70** (1948) 4031.

Received November 6, 1972.

ACTA CHEMICA SCANDINAVICA 27 (1973) 1337–1344

NMR Studies on Cyclic Arsenites

Spectral Analysis and Conformational Studies of Some Arsolanes.

DAGFINN W. AKSNES and OLAV VIKANE

Chemical Institute, University of Bergen N-5000 Bergen, Norway

The 60 MHz NMR data of five arsolanes are reported and discussed. The NMR spectra of 2-chloro-1,3,2-oxathiarsolane and two dithiarsolanes recorded at 30°C, have been fully analyzed on basis of an AA'BB' system. The low-temperature spectrum of the former compound, however, is of the ABCD type. The examined rings appear to exist in slightly distorted envelope conformations with the ring carbon adjacent to oxygen (sulfur in the dithiarsolanes) at the apex of the "flap". Rapid pseudo-rotation seems to be present in these systems.

Several NMR studies on five-membered heterocycles have been reported in recent years.[1] However, the application of NMR spectroscopy to the determination of the conformations and configurations of five-membered rings presents considerable difficulties owing to facile interconversions between nearly equi-energy conformers. It is generally believed that the five-membered ring exists in highly flexible puckered conformations. The puckering is not fixed but moves freely about the ring (pseudo-rotation).

Although the NMR spectra of some 1,3,2-dithiaphospholanes [2,3] and 1,3,2-oxathiaphospholanes [4] have been analyzed no NMR data of the analogous cyclic arsenites are available.

This paper reports preparation and NMR studies of the following five-membered arsenites:

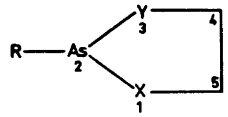

I; R = Ph, X = Y = O
II; R = Cl, X = Y = O
III; R = Ph, X = Y = S
IV; R = Cl, X = Y = S
V; R = Cl, X = O, Y = S

The preparation of several 1,3,2-dithiarsolanes and 1,3,2-oxathiarsolanes, including III – V, has been reported by Sommer and Becke-Goehring in a recent paper.[30] The following two substances of particular relevance to this work, have also been prepared and their NMR spectra recorded:[5]

VI; R = Me, X = Y = O
VII; R = Me, X = Y = S

Our studies on the present arsolanes were undertaken in order to (1) analyze these spin systems, (2) determine if any dominant conformations existed and (3) examine whether rapid chlorine exchange and pseudo-rotation were occurring on the NMR time scale.

EXPERIMENTAL

Phenyl dichloroarsine was prepared from diphenyl mercury and trichloroarsine according to a procedure of Blicke and Smith.[6] Compounds I, II, and III were synthesized by the method of Kamai and Chadaeva.[7] To illustrate the method a detailed procedure for the synthesis of 2-phenyl-1,3,2-dithiarsolane (III) is given: A solution of 9.4 g ethane dithiol and 15.8 g pyridine in 100 ml sodium dried diethyl ether was added dropwise, while stirring, to a solution of 22.3 g phenyl dichloroarsine in 100 ml dried diethyl ether at room temperature. The mixture was held at refluxing temperature for 30 min. After cooling the reaction mixture to room temperature, the pyridine hydrochloride was filtered off. The diethyl ether was removed by rotary evaporation. The oily residue was distilled at reduced pressure, and the distillate fractionated on a Vigreux column at 2 mmHg pressure.

Compounds IV and V were prepared according to a method of Ruggeberg *et al.*[8] The preparation of 2-chloro-1,3,2-dithiarsolane (IV) is described below as an example of these syntheses: To a solution of 36.2 g trichloroarsine in 100 ml carbon tetrachloride was added dropwise, while stirring, 18.8 g of ethane dithiol. The liberation of HCl during the reaction caused self-cooling of the reaction mixture. After stirring the mixture overnight to assure the complete liberation of HCl, the volume was reduced to *ca.* 50 ml by rotary evaporation and cooled in a refrigerator. The white crystalline precipitate was recrystallized from carbon tetrachloride.

The boiling or melting points of the prepared compounds are as follows: $B.p._{10}$ 132 – 134°C, $b.p._{12}$ 78 – 80°C, $b.p._{2}$ 154 – 156°C, and $b.p._{1}$ 76 – 78°C for I, II, III, and V, respectively. M.p. 38 – 39°C (lit. 37.5 – 39°C)[8,30] for IV.

The NMR spectra of the five compounds at ambient probe temperature (*ca.* 30°C) were examined in benzene solutions (*ca.* 50 % v/v for the liquid compounds). The low-temperature spectrum of V was studied in toluene solution. After adding a small amount of TMS to the samples they were degassed and sealed under vacuum.

The spectra were run on a JEOL-C-60H spectrometer. Line positions were obtained by averaging the results of four frequency-calibrated spectra at 54 Hz sweep width.

The AA'BB' and ABCD spin systems were analyzed by means of the computer programs LACX [9] and LAOCN3,[10] respectively. Stick and line-shape plots were generated by means of the sub-routine KOMBIP used in conjunction with LAOCN3 and LACX.

Computations were performed on an IBM/50H computer. The graphical output was obtained using a Calcomp Plotter.

RESULTS AND DISCUSSION

The 60 MHz spectra of the methylene protons of freshly distilled samples of I and II in acetone, carbon tetrachloride, chloroform, benzene, and toluene yielded singlets at 30°C. The singlet of II did not split up but broadened slightly at −60°C.

Owing to the large anisotropy effect of the phenyl and chlorine groups the methylene protons in I and II were expected to produce a complex spectrum of the AA'BB' type. However, oxygen containing arsolanes with unsubstituted ring carbons are rather unstable due to the weak ring As–O bond. We therefore believe that the observed singlets are caused by dimerization of the examined solutes. A similar polymerization is also reported to occur for VI.[5] Compounds VI, VII, and 2,4,4,5,5-pentamethyl-1,3,2-dioxarsolane also give singlets [5] for the ring protons or methyl protons at carbons 4 and 5. The observed singlets have probably resulted from insufficient anisotropy generated by the methyl substituent at arsenic [12] rather than polymerization of the examined samples. The effect of the reported dimerization of VI would therefore not appear in its NMR spectrum.

The detailed spectral analyses of III and IV were carried out successfully on the basis of an AA'BB' system. The spectral parameters are listed in Table 1. The experimental and calculated spectrum of III is shown in Fig. 1. The

Table 1. Chemical shifts in Hz from TMS and coupling constants (Hz) obtained at 60 MHz.

Compound:	III	IV	V [a]	
Solvent:	Benzene	Benzene	Benzene	Toluene
Temp., °C:	30	30	30 [b]	−35
Assigned lines:	24	20	20	27
Root-mean-square dev.:	0.078	0.072	0.060	0.136
ν_1	176.65	189.70	263.88	249.06
ν_2			182.68	170.38
ν_3	166.01	178.55	182.68	156.38
ν_4			263.88	254.23
$^2J_{14}$	−11.77	−11.99	−9.7 [c]	−9.64
$^2J_{23}$			−11.26	−11.48
$^3J_{12}$	4.30	4.06	4.96	4.14
$^3J_{34}$	4.30	4.06	4.96	4.37
$^3J_{13}$	7.13	7.57	6.86	9.01
$^3J_{24}$				6.11

[a] The protons at carbon 5 (adjacent oxygen) are labelled 1 and 4. [b] Rapid chlorine exchange. [c] Only the difference $|^2J_{14}-{}^2J_{23}|$ is obtained from the analysis.

spectrum of IV has a very similar appearance. On basis of the small differences in the coupling constants it may be confidently concluded that the molecular conformations are very similar.

The type of spin system found for III and IV implies that pseudo-rotation interconverts the non-planar forms at rates that are large on the NMR time scale but that inversion at arsenic is slow. Similar observations have been made in analogous dioxaphospholanes,[13] dithiaphospholanes,[2,3] and ring-substituted dioxarsolanes.[14,15] These results are also consistent with the pyramidal stability reported for arsines and phosphines.[12,16]

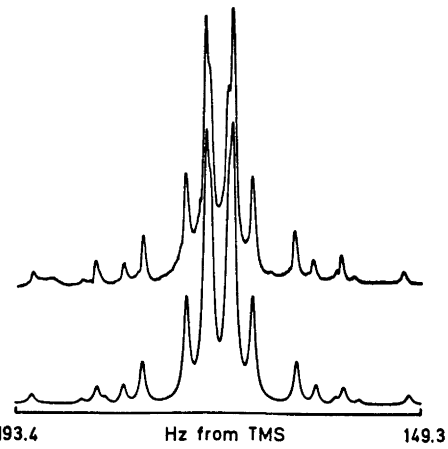

Fig. 1. Experimental (upper trace) and calculated (lower trace) 60 MHz spectrum at 30°C of the methylene protons in compound III in benzene solution.

The internal shift difference, $\Delta\nu$, is remarkably similar for III and IV. This indicates that the stereospecific effect of the phenyl and chlorine substituents is comparable in these compounds. In accordance with previous assignments,[4,13–15] we believe that the resonances at lower and higher field arise from the nuclei that are *cis* and *trans* to the substituent at arsenic, respectively.

The magnitude of the geminal coupling constants in III and IV are in the expected ranges. The equality of $^3J_{12}$ and $^3J_{34}$, within the accuracy of the experiment, is in contrast to the reported situation in 2-phenyl-1,3,2-dithiaphospholane.[2] The observed *cis* coupling constants in ethylene sulfite [13] and several dioxaphospholanes,[13,17,18] however, are mutually equal within experimental error.

The *trans* coupling constants in III and IV are appreciably greater than the *cis* coupling constant. The same observation has been made for 1,3,2-dithiaphospholanes [2,3] and 1,3-dithiolanes.[19] The reverse is, however, true for the analogous dioxaphospholanes,[13,17,18] dioxolanes,[20] and ethylene sulfite.[13]

The S–C–C–S torsional angle in III and IV can be calculated from the vicinal coupling constants of the $CH_2.CH_2$ moiety using the R-value method due to Lambert [21] and Buys.[22] The calculated R-values are 1.66 and 1.86 corresponding to torsional angles of approximately 54° and 56° for III and IV, respectively. Similar calculations based on the reported NMR data for 1,3,2-dithiaphospholanes,[2] 1,3-dithiolanes,[19] 1,3-dioxolanes,[19] and 1,3,2-dioxaphospholanes [13] give torsional angles of approximately 48°, 49°, 42°, and 42°, respectively. Haake *et al.*[13] have calculated O–C–C–O torsional angles of *ca.* 30° in dioxaphospholanes from the vicinal coupling constants using a different approach. We believe, however, that they have underestimated the torsional angle.

The increased ring puckering of the sulfur hetero rings, as compared to their oxygen counterparts, is consistent with the greater degree of flexibility conferred by the presence of sulfur rather than oxygen in the ring.[2]

Dreiding stereomodels of III and IV indicate that the most stable forms are two mutually equivalent pairs of slightly distorted, envelope conformations with one of the ring carbons at the apex of the "flap". The other ring carbon is situated slightly out of the plane defined by SAsS on the opposite side. The pair of conformations possessing carbon 5 at the "tip" of the envelope is shown below.

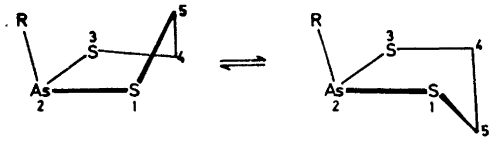

The Dreiding model also indicates a torsional angle slightly less than 60°, that is, close to the calculated average torsional angle (*ca.* 55°) for these rings. The NMR data are therefore consistent with predominance of the above pseudo-rotamers.

The NMR spectra of V recorded at 30°C and −35°C were analyzed as AA'BB' and ABCD systems, respectively. The experimental spectra together with the corresponding calculated spectra are displayed in Figs. 2–4.

The observed type of spectrum at 30°C implies that a rapid chlorine-exchange process results in inversion at arsenic. Similar observations have been made for 2-chloro-4,5-dimethyl-1,3,2-dioxarsolane [14] and several 2-chloro-substituted dioxaphospholanes.[13,17] The observed concentration

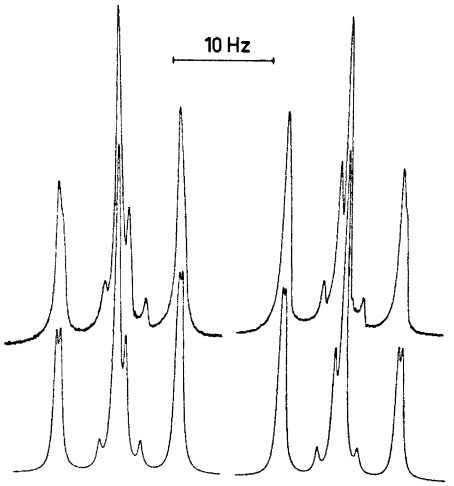

Fig. 2. Experimental (upper traces) and calculated (lower trace) 60 MHz spectrum at 30°C of the methylene protons in compound V in benzene solution. The symmetrical spectrum is a result of rapid chlorine exchange.

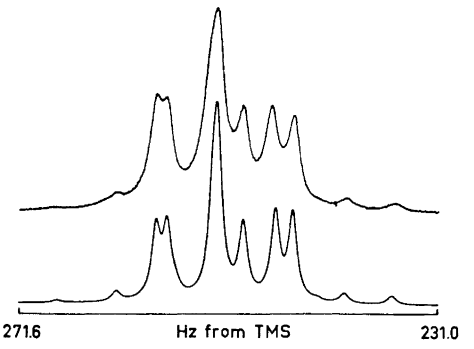

Fig. 3. Experimental (upper trace) and calculated (lower trace) 60 MHz spectrum at −35°C of the $-O-CH_2-$ protons in compound V in toluene solution.

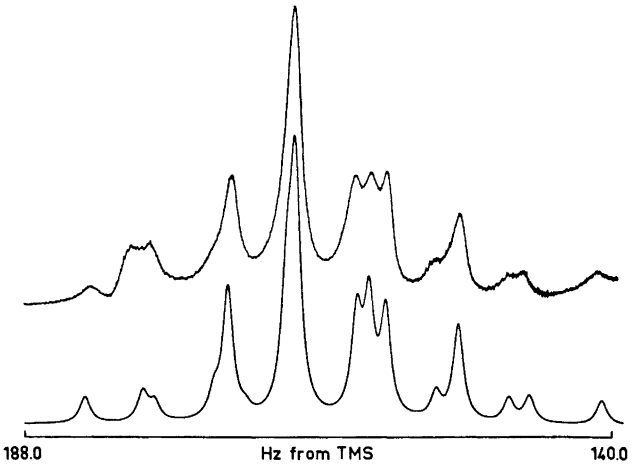

Fig. 4. Experimental (upper trace) and calculated (lower trace) 60 MHz spectrum at −35°C of the $-S-CH_2-$ protons in compound V in toluene solution.

dependence suggests that the exchange occurs by a bimolecular process.[23] The spectrum recorded at −35° is of the expected asymmetrical type thus indicating that chlorine exchange is slow. The observed temperature effect is not expected to arise from freezing out the pseudo-rotation process since the barriers are relatively low.[24]

The internal shift difference, $\Delta\nu$, of the protons at carbons 4 and 5 is 14.0 Hz and 5.2 Hz, respectively. These $\Delta\nu$ values are comparable to the corresponding differences observed for 2-chloro-1,3,2-oxathiaphospholane [4] (10.8 Hz and 7.2 Hz, respectively). It is seen that the $-S-CH_2-$ protons have larger $\Delta\nu$ values than the $-O-CH_2-$ protons. The reverse order is, however, observed for 2-chloro-1,3,2-dithiaphospholane [3] and 2-chloro-1,3,2-dioxaphospholane [13] measured at 60 MHz (7.8 Hz and 23.2 Hz, respectively).

The Dreiding model indicates that the oxathiarsolane ring should exist predominantly as two very slightly distorted envelope conformations with carbon 5 (adjacent to oxygen) at the apex of the "flap". The O–C–C–S torsional angle is seen to be about 47° in these models.

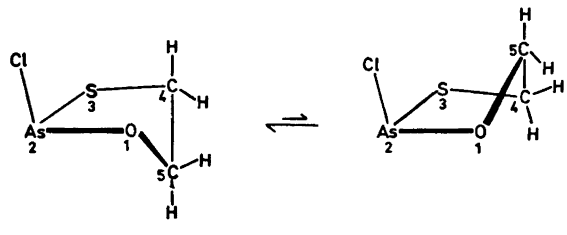

Va **Vb**

In pseudo-rotamer Va the pseudo-axial hydrogen at carbon 4 will suffer a considerable anisotropy shift whereas the pseudo-equatorial hydrogen will be much less affected. The net effect would probably be a significant internal shift displacement $\Delta\nu$. The protons at carbon 5, however, would be more equally affected by the anisotropy of the As–Cl bond. Predominance of Va is thus expected on basis of the chemical shift data. This conclusion is consistent with the expected decrease in syn-axial repulsions in Va as compared to Vb.

Comparable contributions of the Va and Vb forms would result in similar values of $^3J_{13}$ and $^3J_{24}$. However, since the observed coupling constants are quite different it follows that one conformation predominates. A similar conclusion concerning 2-substituted 1,3-oxathiolanes was reached by Wilson and co-workers [24] upon interpretation of NMR data.

Application of the *R*-value method to the vicinal coupling constants obtained at 30°C and −35°C, gives 51° and 55° for the O–C–C–S torsional angle, respectively. A part of this discrepancy results from experimental errors in the measured parameters, in particular at −35°C. A certain deviation is, however, expected due to changes with solvent and temperature in the distribution of populated pseudo-rotameric forms.

It can be anticipated from the Dreiding model of V and the Karplus relationship [25] that the largest vicinal coupling constant (9.01 Hz) involves the pseudo-axial protons. From this assumption it follows that the chemical shifts of the pseudo-axial protons appear at higher field than the geminal pseudo-equatorial protons. However, the uncertainty about the contributing conformations makes this a tentative conclusion. Upfield shift of the axial proton at carbon 6 relative to the equatorial proton in 2-phenyl-1,3-oxathiane has been observed.[26] The reverse assignment has, however, been made for six-membered phosphites [27] and 2-chloro-1,3,2-dithiarsenane.[28]

The NMR spectrum of V was also examined at intermediate rates of chlorine exchange. It was noted that the "coalescence" of the $-S-CH_2-$ region of the spectrum occurred at a higher temperature than in the $-O-CH_2-$ region, that is, at a higher rate of exchange. This observation reflects the fact that the $-S-CH_2-$ protons suffer larger internal anisotropy shifts, $\Delta\nu$, than the $-O-CH_2-$ protons in the absence of exchange.

The final conclusion is that each of the 1,3,2-dithiarsolane and 1,3,2-oxathiarsolane rings mainly exists in two rapidly interconverting envelope conformations. However, since pseudo-libration is expected to occur in these systems,[29] each of the pseudo-rotamers represents the average of a range of conformations of similar energies.

REFERENCES

1. For a recent review, see Thomas, W. A. *Annu. Rep. NMR spectrosc.* **3** (1970) 91.
2. Peake, S. C., Fild, M., Schmutzler, R., Harris, R. K., Nichols, J. M. and Rees, R. G. *J. Chem. Soc. Perkin Trans 2* **1972** 380.
3. Bergesen, K., Bjorøy, M. and Gramstad, T. *Acta Chem. Scand.* **26** (1972) 3037.
4. Bergesen, K., Bjorøy, M. and Gramstad, T. *Acta Chem. Scand.* **26** (1972) 2156.
5. Wieber, M. and Werther, H. U. *Monatsh. Chem.* **99** (1968) 1159.
6. Blicke, F. F. and Smith, F. D. *J. Am. Chem. Soc.* **51** (1929) 3479.

7. Kamai, G. and Chadaeva, N. A. *Chem. Abstr.* **47** (1953) 3792 c–f, 10470 c–h.
8. Ruggeberg, W. H. C., Grinsburg, A. and Cook, W. A. *J. Am. Chem. Soc.* **68** (1946) 1860.
9. Haigh, C. W. *LACX*, Department of Chemistry, University College, Swansea, England.
10. Bothner-By, A. A. and Castellano, S. *LAOCN3*, Mellon Institute, Pittsburgh, Penn., U.S.A.
11. Aksnes, D. W. *KOMBIP*, Quantum Chemistry Program Exchange, Indiana University, Chemistry Department, Indiana, U.S.A.
12. Casey, J. P. and Mislow, K. *Chem. Commun.* **1970** 999.
13. Haake, P., McNeal, J. P. and Goldsmith, E. J. *J. Am. Chem. Soc.* **90** (1968) 715.
14. Aksnes, D. W. and Vikane, O. *Acta Chem. Scand.* **26** (1972) 835.
15. Aksnes, D. W. and Vikane, O. *Acta Chem. Scand.* **26** (1972) 2532.
16. Senkler, G. H., Jr. and Mislow, K. *J. Am. Chem. Soc.* **94** (1972) 291.
17. Gagnaire, R. D., Robert, J.-B., Verrier, J. and Wolf, R. *Bull. Soc. Chim. France* **1966** 3719.
18. Kainosho, M. and Nakamura, A. *Tetrahedron* **25** (1969) 4071.
19. Sternson, L. A., Coviello, D. A. and Egan, R. S. *J. Am. Chem. Soc.* **93** (1971) 6529.
20. See, for example, Booth, H. *Progr. Nucl. Magn. Resonance Spectrosc.* **5** (1969) 149.
21. Lambert, J. B. *Accounts Chem. Res.* **4** (1971) 87.
22. Buys, H. R. *Rec. Trav. Chim.* **88** (1969) 1003.
23. Fontal, B. and Goldwhite, H. *Tetrahedron* **22** (1966) 3275.
24. Wilson, G. E., Jr., Huang, M. G. and Bovey, F. A. *J. Am. Chem. Soc.* **92** (1970) 5907.
25. Karplus, M. *J. Chem. Phys.* **30** (1959) 11.
26. Buys, H. R. *Rec. Trav. Chim.* **89** (1970) 1244.
27. Bergesen, K. and Albriktsen, P. *Acta Chem. Scand.* **26** (1972) 1680, and references therein.
28. Aksnes, D. W. and Vikane, O. *Acta Chem. Scand.* **26** (1972) 4170.
29. Altona, C., Buys, H. R. and Havinga, E. *Rec. Trav. Chim.* **85** (1966) 973.
30. Sommer, K. and Becke-Goehring, M. *Z. anorg. allgem. Chem.* **355** (1967) 182.

Received November 9, 1972.

ACTA CHEMICA SCANDINAVICA 27 (1973) 1345–1350

The Molecular Structure of 2,4,6-Trimethyl-trioxan (Paraldehyde)

E. E. ASTRUP

Department of Chemistry, University of Oslo, Oslo 3, Norway

The molecular structure of 2,4,6-trimethyl-trioxan in the gas phase has been investigated by electron diffraction. The ring is found to have a chair conformation, and the three methyl groups are in equatorial positions. The most important molecular parameters are as follows: r(C–O) = 1.410 (0.004) Å, r(C–C) = 1.494 (0.009) Å, r(C–H) = 1.104 (0.007) Å, ∠COC = 112.3 (0.8)°, ∠OCO = 110.7 (0.7)°, $\angle O_1C_1C_2$ = 109.2 (1.0)°, $\angle C_3C_4H_6$ = 110.7 (1.3)°; the dihedral angle of the ring, δ(OCOC), is found to be 54.6 (1.2)°.

The structure investigation of 2,4,6-trimethyl-trioxan has been carried out as part of a study on cyclic and acyclic ethers.

The structure of 2,4,6-trimethyl-trioxan has earlier been studied by electron diffraction by Ackermann and Mayer [1] in 1936, by Carpenter and Brockway [2]

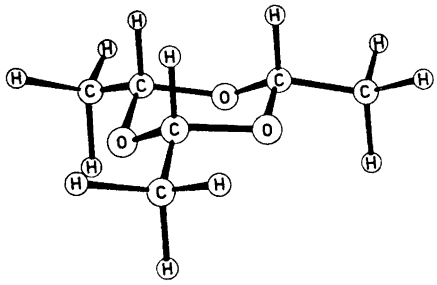

Fig. 1. 2,4,6-Trimethyl-trioxan.

in 1936, and by Aoki [3] in 1953. These investigations were all based on visually estimated intensity data and the authors express doubt as to whether the compound contained a pure *e,e,e* conformation or a mixture of two isomers.

The sample of 2,4,6-trimethyl-trioxan used in the experiment was kindly supplied by J. Krane.[4] The synthesis gives a mixture of the *e,e,e* and the *e,e,a* isomers and the two have been separated on a preparative gas chromatograph. The purity of the separated *e,e,e* sample was checked in the NMR spectrum

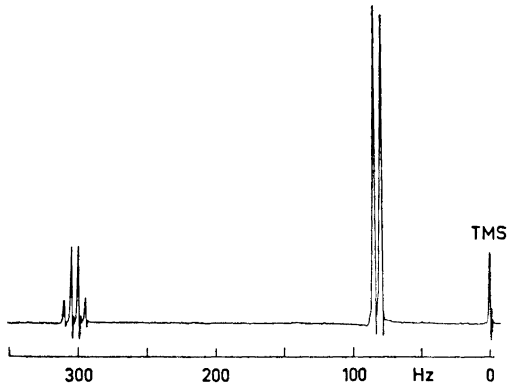

Fig. 2. NMR spectrum of 2,4,6-trimethyl-trioxan, showing the presence of a pure *e,e,e* conformation.

(Fig. 2). The spectrum shows one quartet due to the C–H protons and one doublet caused by the CH_3 protons. The spectrum shows no change with decreasing temperature. The chemical shift relative to TMS is 83 Hz for the CH_3 protons and 302 Hz for the C–H protons.

EXPERIMENTAL

Electron diffraction diagrams were taken on a Balzers Eldigraph KDG2. The nozzle temperature was about 23°C, and the electron wave length 0.05847 Å. The nozzle-to-plate distances were 50 and 25 cm. The pressure in the apparatus during exposure was 3×10^{-6} mmHg. Five selected plates were used for each distance. The intensity was recorded on a photometer for each 0.25 mm on the photographic plate. The plates were oscillated about the centre of each plate and the data integrated over the arc. The data were treated the usual way.[5] The experimental background was subtracted on each plate before averaging the intensity data. The molecular intensity curves from the 50 cm plates and the 25 cm plates were scaled, and the mean values were used in the overlap region. The final intensity curve, shown in Fig. 3, extends from $s = 1.75$ Å^{-1} to $s = 29.25$ Å^{-1}.

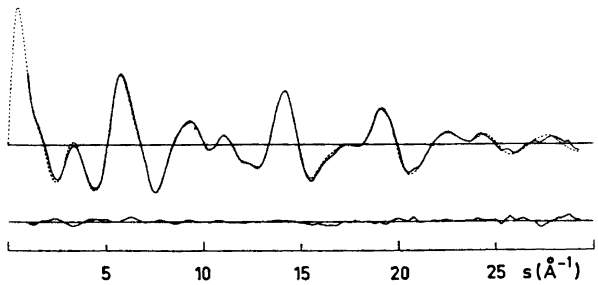

Fig. 3. 2,4,6-Trimethyl-trioxan. Experimental (solid line), theoretical (dotted line), and difference molecular intensity curve.

The modified molecular intensity may be expressed by the equation

$$I(s) = \text{const.} \sum_{i \neq j} \sum g_{ij/mn}(s) \exp(-\tfrac{1}{2} u_{ij}^2 s^2)[(\sin r_{ij}s)/r_{ij}]$$

where

$$g_{ij/mn}(s) = \frac{|f_i||f_j|}{|f_m||f_n|} \cos(\Delta n_{ij})$$

In this case f_m was put equal to the complex scattering factor for carbon and f_n equal to the oxygen scattering factor to obtain a Gaussian shape of the carbon-oxygen peaks in the RD (radial distribution) curve.

The distances and u-values (vibrational amplitudes) estimated from the RD curve were refined by a least squares procedure. The numerical calculations have been carried out on a CDC 3300 computer.[6]

STRUCTURE ANALYSIS AND RESULTS

Approximate values for the molecular parameters, which were used in the least squares analysis of the structure, were determined from the experimental RD curve (Fig. 4).

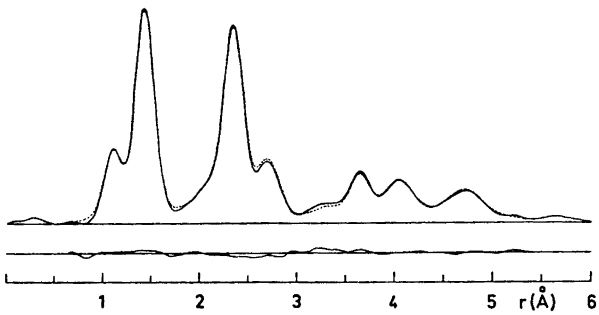

Fig. 4. 2,4,6-Trimethyl-trioxan. Experimental (solid line), theoretical (dotted line), and difference radial distribution curve. The damping constant is equal to 0.002 Å^2.

There is no indication from the RD curve that a contribution from the *a,a,a* conformation is present. This is as expected since the energy of this conformation must be much higher than for the *e,e,e* conformation because of the methyl-methyl interaction in axial positions.

The bond distances in the molecule are found in the two first peaks in the RD curve. At about 1.1 Å is the peak corresponding to the C–H bond distances, and the C–O and the C–C bond distances contribute to the peak at 1.3 – 1.6 Å. The C–O bond lengths are determined to be about 1.41 Å, as found in other ethers,[7,8] and the C–C bond length 1.49 Å, which is slightly shorter than expected. The peak at 2.3 Å is composed of C···O distances from the ring oxygen atoms to the nearest methyl carbon atoms and O···O and C···C distances in the ring. The main contribution to the peak at 2.7 Å is from the C···O distances in the ring. The C···C distances from the carbon atoms in the ring to the methyl carbon atoms must be expected to occur at 3.6 Å, the long C···O distances from the oxygen atoms to the methyl carbon at 4.0 Å, and the C···C distances

between the methyl carbon atoms at 4.7 Å, which explains the three well resolved outer peaks on the RD curve.

The C–H axial bond distances are assumed to be parallel to the threefold axis. This assumption may not be quite correct and may be responsible for some minor discrepancies between the experimental and the theoretical curves. But because of the insignificant contribution of the distances containing these hydrogen atoms to the RD curve, their exact positions are difficult to determine. An attempt was made to determine a possible difference between the C–H bond distances in the methyl groups and the axial C–H bond distances in the ring, but no difference could be determined.

The position and the shape of the peak at 2.7 Å is sensitive to a twist of the methyl groups about the C–C bonds. A twist angle, $\tau(CH_3)$, of approximately $10-11°$ from an ideal staggered position of the methyl hydrogen atoms with respect to the axial C–H bonds gives a better fit between the experimental and the theoretical RD curve for this peak than is obtained for an ideal staggered conformation, but less good for the peak at 2.3 Å and 3.6 Å. The lowest sum of square residuals in the least squares refinement is obtained for the exact staggered conformation.

The following independent molecular parameters were simultaneously refined (Fig. 5): C–O, C–C, C–H, α (the angle between the $O_1C_1C_5$ plane and

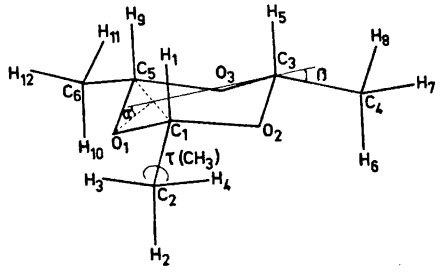

Fig. 5. The symbols and numbering system used for the 2,4,6-trimethyl-trioxan model.

the plane through $C_1C_3C_5$), β (the angle between the plane $C_1C_3C_5$ and C_3–C_4), $\angle C_3C_4H_6$, and the vibrational amplitudes for the bond distances C–O and C–H and for the non-bonded distances O···C and the C···C between the methyl carbon atoms. The remaining u-values were grouped according to distance type and length. The values for the remaining non-bonded O···H and C···H distances were obtained from separate cycles of refinement, while the amplitudes for the non-bonded H···H distances were fixed at reasonable values.

The least squares refinement converges to the results listed in Table 1. The u-values found for the C–H bond distances are smaller than what is usually found for C–H bonds. From the correlation matrix (Table 2) it is seen that the C–H amplitude of vibration is only slightly correlated with the other parameters, and consequently this amplitude will hardly influence the overall result.

In Table 3 is shown a comparison of the ring angles OCO and COC in 2,4,6-trimethyl-trioxan and in different investigations of 1,3,5-trioxan. In the

Table 1. Structure parameters for 2,4,6-trimethyl-trioxan obtained by least squares refinement on the intensity data. Distances (r_a-values) and mean amplitudes of vibration (u-values) are given in Å, angles in degrees. The standard deviations given in parentheses have been corrected to take into account data correlation. The uncertainty arising from error in the electron wavelength is included. (For numbering system of atoms, see Fig. 5.)

Distances	r		u	
C_1-O_1	1.410	(0.004)	0.057	(0.005)
C_1-C_2	1.494	(0.009)	0.052	(0.005)
C–H	1.104	(0.007)	0.051	(0.009)
$O_1\cdots O_2$	2.319	(0.012)	0.067	(0.006)
$C_2\cdots O_1$	2.366	(0.008)	0.065	(0.009)
$C_3\cdots O_1$	2.723	(0.008)	0.081	(0.014)
$C_4\cdots O_1$	4.067	(0.009)	0.108	(0.025)
$C_1\cdots C_5$	2.341	(0.015)	0.076	(0.007)
$C_1\cdots C_4$	3.644	(0.005)	0.087	(0.010)
$C_2\cdots C_4$	4.719	(0.014)	0.101	(0.040)
$C_3\cdots H_6$	2.146	(0.018)	0.109	
$C_3\cdots H_1$	2.587	(0.012)	0.140	
$C_2\cdots H_1$	2.175	(0.015)	0.074	
Angles				
$\angle C_5O_1C_1$	112.3	(0.8)		
$\angle O_1C_1O_2$	110.7	(0.7)		
α	32.4	(1.0)		
β	23.1	(1.6)		
$\tau(CH_3)$	0.0			
δ(OCOC)	54.6	(1.2)		
$\angle O_1C_1C_2$	109.2	(1.0)		
$\angle C_2C_1H_1$	113.1			
$\angle O_2C_1H_1$	107.4			
$\angle C_3C_4H_6$	110.7	(1.3)		

Table 2. Correlation matrix (× 100) for the parameters. (The coefficients having absolute values less than 20 are not given.)

	Parameters	1	2	3	4	5	6	7	8	9	10	11	12	13	14
1	r(C–O)	100													
2	$r(C_1\cdots C_5)$		100												
3	r(C–C)	−40	−39	100											
4	r(C–H)			29	100										
5	α	38	−20			100									
6	β	−20	51	41		−69	100								
7	$\angle C_3C_4H_6$							100							
8	u_{C-O}	32	36	−89	−32		−37		100						
9	u_{C-H}			35					−44	100					
10	$u_{O_1\cdots C_2}$					−61	30				100				
11	$u_{O_1\cdots C_4}$							30				100			
12	$u_{C_2\cdots C_4}$												100		
13	$u_{O_1\cdots C_3}$							38			−22			100	
14	Scale								25		20				100

Table 3. Comparison of the ring angles and the bond distance C–O in 2,4,6-trimethyl-trioxan and in 1,3,5-trioxan.

		r(C–O) Å		∠OCO°		∠COC°	
2,4,6-Trimethyl-trioxan (this work)	Electron diff.	1.410	(0.004)	110.7	(0.7)	112.3	(0.8)
1,3,5-Trioxan	X-Ray diff.[10]	1.421	(0.006)	109.6	(0.3)	110.4	(0.3)
	X-Ray diff.[11]	1.429	(0.004)	107.8	(0.2)	108.0	(0.2)
	Electron diff.[7]	1.411	(0.002)	111.0	(0.7)	109.2	(1.0)
	Micro-wave [12]	1.411	(0.01)	111.2	(1.0)	108.2	(1.0)
	Micro-wave [13]	1.403	(0.002)	112.0	(0.3)	110.4	(0.3)

electron diffraction and microwave investigation of 1,3,5-trioxan the agreement between the results is very good, and in these investigations the ∠OCO is found to be greater than the ∠COC. In the X-ray diffraction investigations of 1,3,5-trioxan and in this investigation of 2,4,6-trimethyl-trioxan, however, the ∠COC is found to be the greater. It is also seen from Table 3 that the ring angles are somewhat greater in 2,4,6-trimethyl-trioxan and consequently the ring is less puckered, as expected from the effect of the larger equatorial groups. A recent article [9] on the structure of 1,3,5-trioxan suggests on the basis of potential energy calculations that the order of the two angles is in agreement with that found for 2,4,6-trimethyl-trioxan.

REFERENCES

1. Ackermann, P. G. and Mayer, J. E. *J. Chem. Phys.* **4** (1936) 377.
2. Carpenter, P. C. and Brockway, L. O. *J. Am. Chem. Soc.* **58** (1936) 1270.
3. Aoki, K. *Nippon Kagaku Zasshi* **74** (1953) 110.
4. Krane, J. *Private communication.*
5. Bastiansen, O. and Skancke, P. N. *Advan. Chem. Phys.* **3** (1960) 323.
6. Andersen, B., Seip, H. M., Strand, T. G. and Stølevik, R. *Acta Chem. Scand.* **23** (1969) 3224.
7. Clark, A. H. and Hewitt, T. G. *J. Mol. Struct.* **9** (1971) 33.
8. Blukis, U., Kasai, P. H. and Myers, R. J. *J. Chem. Phys.* **38** (1963) 2753.
9. Pickett, H. M. and Strauss, H. L. *J. Chem. Phys.* **53** (1970) 376.
10. Busetti, V., Del Pra, A. and Mammi, M. *Acta Cryst.* **B 25** (1969) 1191.
11. Busetti, V., Mammi, M. and Carazzolo, G. *Z. Krist.* **119** (1963) 310.
12. Oka, T., Tsuchiya, K., Iwata, S. and Morino, Y. *Bull. Chem. Soc. Japan* **37** (1964) 4.
13. Colmont, J. M. and Depannemaecker, J. C. *Second European Microwave Spectroscopy Conference, 1972.*

Received November 6, 1972.

ACTA CHEMICA SCANDINAVICA 27 (1973) 1351–1354

The Hydrolysis of Methyl Hydrogen Orthophthalate in Water

LAURI PEKKARINEN

Central Laboratory of OTK, Helsinki 50, Finland

The hydrolysis of methyl hydrogen orthophthalate in water has been studied over a pH range of −0.05 to 6.97 at 90°C. The pH was adjusted with hydrochloric acid or a citrate-phosphate buffer solution. In the acid range two reactions take place concurrently, one (intermolecular catalysis) at a rate proportional to the concentration of added hydronium ion and the other (intramolecular catalysis) at a rate independent of this concentration. The reaction mechanisms are discussed.

In a study of the hydrolysis of ethyl hydrogen maleate and ethyl hydrogen citraconate in the acidic range,[1] it was found that the rates of the reactions in water are independent of the concentration of added hydronium ion, at least when this is low (intramolecular catalysis). The rates were found to be proportional to the concentration of the undissociated ester. When acetone was added to the solution, the contribution of intramolecular catalysis decreased rapidly and the influence of the strong acid added (intermolecular catalysis) became clearly evident. The study was later extended to the hydrolysis of acid esters of *o*-phthalic and maleic acids in the acidic range in water and water-dioxane and water-acetone mixtures.[2] The hydrolysis of the monomethyl, monoethyl, and monopropyl esters of orthophthalic acid in water was found to be subject to strong intramolecular catalysis, the rate being proportional to the concentration of the undissociated ester acid. Organic solvents such as acetone and dioxane strongly suppress intramolecular catalysis, and with a high proportion of an organic component in the solvent intermolecular catalysis became clearly evident. Ethanol was not found to exert any specific effect. A discussion of the mechanism of the intramolecularly catalysed reaction led to the conclusion that two or three molecules of water take part in the rate-determining stage of the reaction. The reaction was considered to take place by normal acyl-oxygen fission with the undissociated carboxyl group acting as the intramolecular catalyst.

The formation of an anhydride as an intermediate is suggested by the acceleration of the reaction on introduction of a methyl group into maleic ester acid to give citraconic ester acid. However, other observations, such as the rate of formation of the anhydride from the ester acid, the usual solvent

effect of ethanol on the hydrolysis of ethyl hydrogen maleate, and inability to detect the anhydride with aniline, did not support the view that the anhydride is formed as an intermediate in the hydrolysis of monoalkyl esters. The mechanisms of the two hydrolytic reactions were concluded to be otherwise similar except that the hydrogen ion is transferred to the ester group from the solvent in the intermolecularly catalysed reaction, but from the adjacent carboxyl group in the intramolecularly catalysed reaction.

Bender and his co-workers[3] studied the hydrolysis of monomethyl orthophthalate at pH values from 0.8 to 2.3 adjusted with hydrochloric acid and from 2.6 to 7.0 adjusted with citrate-phosphate buffer solutions. However, their results deviate from those presented above and the mechanism proposed differs accordingly. The data of these workers suggest that the carboxylate ion functions as a nucleophilic catalyst and that phthalic anhydride is formed as an intermediate. The data in question have been discussed by Ågren *et al.*,[4] Eberson,[5] and Thanassi and Bruice.[6] It has been suggested that the components of the citrate-phosphate buffers may exert specific effects on the hydrolysis of monomethyl orthophthalate. Thanassi and Bruice in a study of monomethyl orthophthalate and Eberson in a study of monomethyl 3,6-dimethylphthalate concluded that the rate of hydrolysis is proportional to the concentration of the undissociated ester acid, thus confirming earlier results.[1,2] In the mechanism proposed by Eberson, the formation of the anhydride is the rate-determining stage. Thanassi and Bruice did not propose any detailed mechanism but only several possible models. The mechanism has been discussed recently by Killian,[7] Hurst and Bender,[8] and Capon,[9] who all consider that anhydride formation is a possible intermediate in the reaction. The data of Ågren *et al.*[4] suggest that the hydrolysis of monoethyl orthophthalate in water is also catalysed intermolecularly at high mineral acid concentrations (at very low pH values).

The aim of the work described below was to clarify the mechanism of hydrolysis of monomethyl orthophthalate in the acid range. The first problem was to determine whether the components of citrate-phosphate buffer exert specific effects on the hydrolysis. The rate of the intermolecularly catalysed acid hydrolysis of methyl hydrogen orthophthalate in water was then measured and compared with the previously reported rates of the same reaction in mixtures of water and organic solvents.[2]

EXPERIMENTAL

Procedure. The kinetic experiments were run in water solution, the pH of which was varied from −0.05 to 1.20 with hydrochloric acid and from 2.83 to 6.97 by adding citrate-phosphate buffer solutions composed of 0.2 M citric acid and 0.4 M dipotassium hydrogen phosphate in various ratios. The initial concentration of the ester in the experiments was about 3×10^{-3} M and the temperature 90.0°C. The ester solution containing hydrochloric acid or buffer solution was transferred with a pipette in 5 or 10 ml amounts to Pyrex ampoules, which were sealed by fusion before immersion in a water bath at 90°C. After a suitable interval, an ampoule was removed from the water bath and cooled in an ice bath. The reaction mixture was then diluted with 1 M potassium phosphate solution of pH about 7. The absorbance of the resulting solution at 279 nm was measured with a Beckman DU spectrophotometer. The rate constants were calculated from the equation

$$k = \frac{2.303}{t} \log \frac{A_0 - A_\infty}{A_t - A_\infty}$$

where A_0 is the initial absorbance, A_∞ the final absorbance, and A_t the absorbance at time t.

Chemicals. Monomethyl orthophthalate was prepared by the method of Eliel and Burgstahler.[10] The melting point of this ester was 83°C. The other chemicals were guaranteed reagents from E. Merck. The water used had been distilled twice.

Results. The results are presented in Table 1.

Table 1. The rates of hydrolysis of monomethyl orthophthalate in aqueous solutions of various pH values at 90°C.

pH	−0.05	0.31	0.66	0.66[a]	0.66[b]	0.92	0.92[c]	1.20	2.83	3.17	4.74	6.97
$k \times 10^4$ min^{-1}	138	105	91.2	92.4	93.7	83.6	83.9	82.4	81.2	66.5	7.44	2.56

[a] 0.32 M KCl. [b] 0.96 M KCl. [c] 0.16 M KCl.

DISCUSSION

The rate constant of the hydrolysis of monomethyl orthophthalate in 0.02 M hydrochloric acid at 90°C was earlier [2] found to be $12\,000 \times 10^{-8}$ s^{-1} or 72×10^{-4} min^{-1}. This value is about 15 % smaller than the value obtained in the present study. The rate constant of the reaction in an acetate buffer solution of pH 2.83, found in the present study, is likewise 15 % lower than the rate constant of the reaction in a citrate-phosphate buffer of the same pH (Table 1). Thanassi and Bruice [6] obtained the value 85×10^{-4} min^{-1} for the rate constant in a potassium phosphate buffer of pH 2.00 at 91.3°C. This is in good agreement with the values obtained in the present study. The buffer, as Thanassi and Bruice had also noted, has a certain effect on the rate of hydrolysis of monomethyl phthalate. In the light of the results of the present study, however, it is seen that the citrate-phosphate buffer does not essentially alter the course of the hydrolysis.

The data in Table 1 further show that hydrochloric acid has a significantly greater effect than potassium chloride on the rate of hydrolysis of monomethyl orthophthalate. Hence in water monomethyl phthalate also undergoes a normal intermolecularly catalysed acid hydrolysis with a rate constant of 8×10^{-5} M^{-1} s^{-1}. This is about twice the value 4.2×10^{-5} M^{-1} s^{-1}, which is the rate constant of the acid-catalysed hydrolysis in a 90 % acetone-water mixture at the same temperature.[2] The changes in the rate constants of the hydrolysis of monoethyl succinate and monoethyl fumarate when the solvent is changed from water to a 90 % acetone-water mixture are of the same order as in the case of monomethyl orthophthalate, although the rate constant of the hydrolysis of the last mentioned ester is significantly lower in value than those of the first two.[1] In addition it may be mentioned that the rate constants

for the hydrochloric acid-catalysed hydrolysis of ethyl hydrogen *p*-phthalate and ethyl hydrogen *m*-phthalate in a 50 % acetone-water mixture at 95°C are 91×10^{-6} and 69×10^{-6} $M^{-1} s^{-1}$, respectively.[2] The corresponding rate constant for ethyl hydrogen *o*-phthalate in the same conditions was found to be 60×10^{-6} $M^{-1}s^{-1}$. According to the results presented above, it seems unlikely that the mechanism of the intermolecularly catalysed hydrolysis of methyl hydrogen orthophthalate differs from the $A_{AC}2$ mechanism, as Hurst an Bender have claimed.[8]

The rate of the intramolecularly catalysed hydrolysis of monomethyl orthophthalate falls steeply, as the proportion of organic solvent in the reaction medium is increased.[2] In this respect monomethyl phthalate behaves differently from monophenyl orthophthalate, for instance, the hydrolysis of which in dioxan-water mixtures accelerates slightly with increasing dioxan content.[11] In the case of the phenyl ester the mechanism of the reaction has been shown to be nucleophilic intramolecular catalysis by the ionized carboxyl group, with the anhydride as an intermediate.[6] The observation that intramolecular catalysis of methyl orthophthalate occurs only after hydration makes an anhydride intermediate less probable. The higher rate of the intramolecularly catalysed hydrolysis of ethyl hydrogen citraconate as compared with ethyl hydrogen maleate [1] can be explained by assuming that the methyl substituent facilitates the transfer of hydrogen ion from the carboxyl group to the ester group. One would expect that the hydration of the carboxyl group would make it possible for the carboxyl group to function as an intramolecular catalyst, *i.e.* to promote the transfer of the proton to the ester group. The intermolecularly and intramolecularly catalysed reactions can both be considered to be acid catalyses. The water is probably added to the protonated ester group in both cases.

REFERENCES

1. Pekkarinen, L. *Ann. Acad. Sci Fennicae Ser. A II* **62** (1954).
2. Pekkarinen, L. *Ann. Acad. Sci Fennicae Ser. A II* **85** (1957).
3. Bender, M. L., Chloupek, F. and Neveu, M. C. *J. Am. Chem. Soc.* **80** (1958) 5384.
4. Ågren, A., Hedsten, U. and Jonsson, B. *Acta Chem. Scand.* **15** (1961) 1532.
5. Eberson, L. *Acta Chem. Scand.* **18** (1964) 2015.
6. Thanassi, J. W. and Bruice, T. C. *J. Am. Chem. Soc.* **88** (1966) 747.
7. Killian, F. L. *Intramolecular Catalysis in the Hydrolysis of Esters*, Diss., Northwestern University, Illinois 1967, p. 91.
8. Hurst, G. H. and Bender, M. L. *J. Am. Chem. Soc.* **93** (1971) 704.
9. Capon, B. In Bradley, J. N., Gillard, R. D. and Hudson, R. F., Eds., *Essays in Chemistry*, Academic, London 1972, Vol. 3, p. 142.
10. Eliel, E. L. and Burgstahler, A. W. *J. Am. Chem. Soc.* **71** (1949) 2251.
11. Bruice, T. C. and Turner, A. *J. Am. Chem. Soc.* **92** (1970) 3422.

Received November 11, 1972.

ACTA CHEMICA SCANDINAVICA 27 (1973) 1355–1368

Zum alkalischen Abbau von Arylglycerin-β-(2,6-dimethoxy-4-alkylaryl)-ätherstrukturen*

GERHARD E. MIKSCHE

Institutionen för organisk kemi, Chalmers Tekniska Högskola och Göteborgs Universitet, Fack, S-402 20 Göteborg 5, Schweden

Die β-Alkyl-arylätherbindung in Ligninmodellverbindungen für *p*-Hydroxyarylglycerin-β-(2,6-dimethoxy-4-alkylaryl)-ätherstrukturen mit freier (Typ *1*) und verätherter (Typ *2*) phenolischer Hydroxylgruppe wurde beim Erhitzen in Natronlauge gespaltet; der Mechanismus der Spaltungsreaktionen wird diskutiert. Die Ergebnisse dieser Modellversuche tragen zur Kenntnis des Verhaltens von Laub- und Nadelholzligninen unter den Bedingungen der technischen Soda- und Sulfatcelluloseprozesse bei.

Die Lignine vieler Laubhölzer sind zu etwa gleichen Teilen aus Guajacylpropaneinheiten und Syringylpropaneinheiten aufgebaut. Wie am Lignin der Warzenbirke (*Betula verrucosa*) – einem typischen Laubholzlignin – gezeigt wurde, liegen die Syringylpropaneinheiten zum Grossteil als Aroxylreste in Arylglycerin-β-(2,6-dimethoxy-4-alkylaryl)-ätherstrukturen mit freier (*1*) oder verätherter (*2*) phenolischer Hydroxylgruppe vor.[1a] Die Kenntnis des Verhaltens dieser Strukturen beim Erhitzen unter alkalischen Bedingungen ist daher eine der Voraussetzungen für das Verständnis des Abbaus von Laubholzligninen beim technischen Soda- und Sulfatcelluloseprozess (Erhitzen des

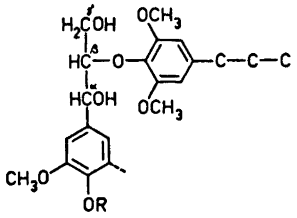

1 R = H
2 R = C

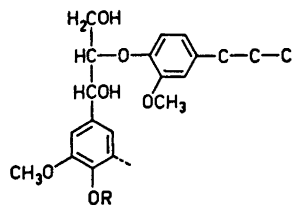

3 R = H
4 R = C

* IX. Mitteilung in der Reihe: Über das Verhalten des Lignins bei der Alkalikochung. VIII. Mitt. siehe Lit. 6b.

Holzes mit Natronlauge bzw. natriumsulfidhaltiger Natronlauge). Die den Gegenstand dieser Arbeit bildenden Abbauversuche an Modellen der Strukturtypen *1* und *2* sollen hierzu einen Beitrag liefern.

Abbau von p-*Hydroxyarylglycerin-β-(2,6-dimethoxy-4-alkylaryl)-ätherstrukturen (1).* Der Verlauf des alkalischen Abbaus der *p*-Hydroxyarylglycerin-*β*-(2-methoxy-4-alkylaryl)-ätherstrukturen (*3*) des Nadelholzlignins ist aufgrund von Modellversuchen bekannt; Strukturen vom Typ *3* sind in geringerer Frequenz auch in Laubholzligninen enthalten.[1a] Beim Erhitzen mit Natronlauge gab die Verbindung *5* (ein Modell für den Strukturtyp *3*; das Fehlen des 4-Alkylsubstituenten am Aroxylrest von *5* ist ohne wesentlichen Einfluss auf den Reaktionsverlauf, vergl. Lit. 2) als Hauptprodukt (*ca.* 70 % d. Th.) den Styryl-aryläther *7*.[3,4]

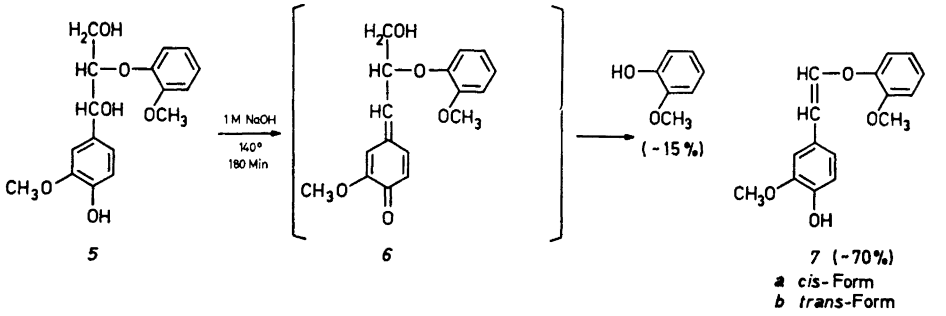

Ein dem Modell *5* entsprechendes Verhalten konnte beim alkalischen Abbau des 4-Hydroxy-3,5-dimethoxy-phenylglycerin-*β*-(2,6-dimethoxy-4-methyl-phenyl)-äthers (*8*), einem Modell für den Strukturtyp *1*, erwartet werden. Die *erythro-* (*8a*) und die *threo-* (*8b*) Form dieses Modells gaben jedoch beim Erhitzen in 1 M NaOH auf 140° nur geringe Mengen (~5 %) der *cis-* (*11a*) und der *trans-* (*11b*) Form des erwarteten Styryl-aryläthers. Der Abbau von *8* verlief überwiegend unter Spaltung der Alkyl-arylätherbindung, wobei als Hauptprodukt (*ca.* 75 % d. Th.) 2,6-Dimethoxy-4-methyl-phenol (*10*) entstand.

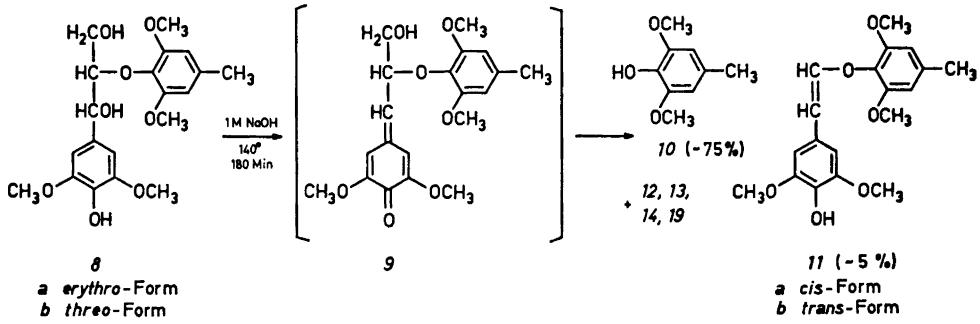

Weiters wurden geringe Mengen der Phenole *12*, *13*, *14* und *19* aufgefunden; aus der Arylpropan-Einheit in *8* waren vorwiegend höhermolekulare Abbauprodukte gebildet worden.

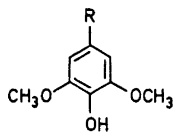

12 R = H
13 R = CHO
14 R = $COCH_3$
15 R = CH_2OH
16 R = $CHOHCH_3$
17 R = CH_2CHO
18 R = $CH{=}CH_2$

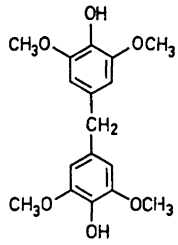

19

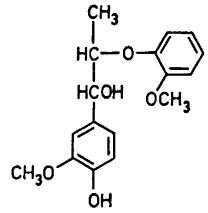

20
a erythro-Form
b threo-Form

Das beim Abbau von *8b* gebildete 2,6-Dimethoxy-4-methylphenol (*10*) wurde gaschromatographisch gemessen (Tab. 1). Die für eine Reaktion erster Ordnung inbezug auf Substrat berechneten Geschwindigkeitskonstanten fallen mit der Reaktionsdauer nur wenig ab. Sie zeigen auch, dass die Geschwindigkeit des Abbaus von *8b* unabhängig von der Hydroxidionenkonzentration ist. Dies stimmt mit experimentellen Befunden zur Kinetik des alkalischen Abbaus des Modells *5* überein; der geschwindigkeitsbestimmende Schritt beim Abbau von *5* (*threo-* oder *erythro*-Form) ist die Bildung des Chinonmethids *6*.[5] Da der Abbau von *8b* überdies mit etwa derselben Geschwindigkeit wie der von *threo-5* [5] verläuft, kann die Bildung des Chinonmethids *9* im langsamen Schritt des Abbaus von *8b* (oder *8a*) als gesichert angesehen werden. Auch die Isomerisierung von *threo-* und *erythro-20* in verdünnter Natronlauge verläuft über ein Chinonmethid; die etwa das zweifache der Isomerisierungsgeschwindigkeit von *20b* ($T = 119{,}4°$; $k \simeq 2 \times 10^{-3}$ Min^{-1}) [6b] betragende Bildungsgeschwindigkeit des Chinonmethids von *20* kommt der Abbaugeschwindigkeit des Phenols *8b* ($T = 120{,}0°$; $k \simeq 3.5 \times 10^{-3}$ Min^{-1}) nahe.

Bei der Sulfatkochung wurde *8b* mit fast der gleichen Geschwindigkeit abgebaut wie bei der Sodakochung (Tab. 1). Die bei der Sodakochung gebildeten Nebenprodukte *12*, *13*, *14*, und *19* fehlten jedoch fast vollständig. Auch hier ist Bildung des Chinonmethids *9* geschwindigkeitsbestimmend; entsprechendes wurde für die Sulfatkochung der beiden Formen von *5* und *20* gefunden.[5]

Für den Abbau des Modells *8* waren zunächst zwei mögliche Abbauwege inbetracht zu ziehen, die zu einer hydrolytischen Spaltung der Alkyl-aryläther-bindung führen; sie sollen anschliessend diskutiert werden.

Es ist bekannt, dass beim alkalischen Abbau des Modells *20* grössere Mengen Guajakol gebildet werden; die Bildung des Guajakols erfolgt allerdings langsam, verglichen mit der über das Chinonmethid von *20* verlaufenden Isomerisierung von *20a* bzw. *20b*.[6] Für die Bildung von Guajakol aus *20* wurde eine intramolekulare nucleophile Substitution des Phenoxylrestes durch das Alkoxidion der benzylalkoholischen Hydroxylgruppe vorgeschlagen.[6a] Eine entsprechende Reaktion des Methyläthers von *20* ist bekannt;[3] sie folgt dem Gesetz erster Ordnung inbezug auf Substrat und Hydroxidion.[7] Da die Ge-

schwindigkeit der Bildung von *10* beim alkalischen Abbau von *8b* von der Hydroxidionenkonzentration unabhängig ist (Tab. 1), kann dieser Weg für die Öffnung der Alkyl-arylätherbindung in *8* ausgeschlossen werden; vergl. auch die Geschwindigkeiten der Bildung von *10* aus *8b* und aus *37b* (s.u.).

Weiters war als Abbauweg von *8* eine mögliche nucleophile Substitution des Aroxylrestes im Chinonmethid *9* durch Hydroxidion inbetracht zu ziehen. Das hierbei zu erwartende Chinonmethid *22* gibt, wie durch Sodakochung von *erythro*-4-Hydroxy-3,5-dimethoxy-phenylglycerin (*21*) gezeigt wurde, ein vorwiegend aus höhermolekularen Phenolen bestehendes Substanzgemisch. Letzteres ist wahrscheinlich durch *retro*-Aldolkondensation von *22* zu 4-Hydroxy-3,5-dimethoxy-phenylacetaldehyd (*17*) und Formaldehyd, gefolgt von Selbstkondensation von *17*, entstanden (vergl. Lit. 6a).

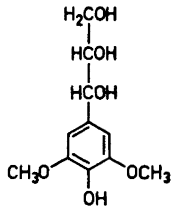

21

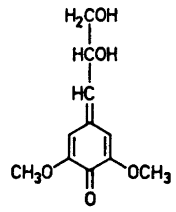

22

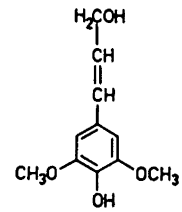

23

Tab. 1. Bildung von 2,6-Dimethoxy-4-methylphenol (*10*) aus *threo*-3,5-Dimethoxy-4-hydroxyphenylglycerin-*β*-(2,6-dimethoxy-4-methylphenyl)-äther (*8b*) beim Erhitzen in alkalischer Lösung auf 120°.

c_{NaOH} (Mol/l)	Reaktionszeit (Min)	gebildetes *10* (% d. Th.)	$k \times 10^{-3}$ (Min^{-1})
1	60	23,2 [a]	4,4
	68	23,3	3,9
	120	33,9 [a]	3,5
	120	32,4 [a]	3,3
	120	32,6	3,3
	123	35,8	3,6
	180	44,4 [a]	3,3
	180	42,7 [a]	3,1
	180	43,5 [a]	3,2
	189	42,1	2,9
0,3	112	36,4	4,0
	180	47,6	3,6
	285	60,5	3,3
	362	67,0	3,1
0,2 + 1 M Na_2S	65	24,3	4,3
	136	41,2	3,9
	207	53,3	3,7

[a] Bestimmt als Acetat.

Die Zusammensetzung des beim Abbau von *8* erhaltenen Reaktionsgemisches sprach also weder für, noch gegen die Spaltung der Alkyl-aryläther-bindung durch nucleophile Substitution des Chinonmethids *9*. Um eine Entscheidung bezüglich dieses möglichen Abbauwegs zu treffen, wurde das Modell *24* dargestellt und alkalisch abgebaut. Da in *24* die Hydroxymethylgruppe des Modells *8* durch eine Methylgruppe ersetzt ist, war bei einer Substitution von OAr durch OH im Chinonmethid *25* die Bildung des relativ alkalistabilen Guajacylacetons (*29*) zu erwarten, das – im Gegensatz zur etwaigen Bildung von *17* beim Abbau von *8* – nachweisbar sein sollte (vergl. Lit. 6a).

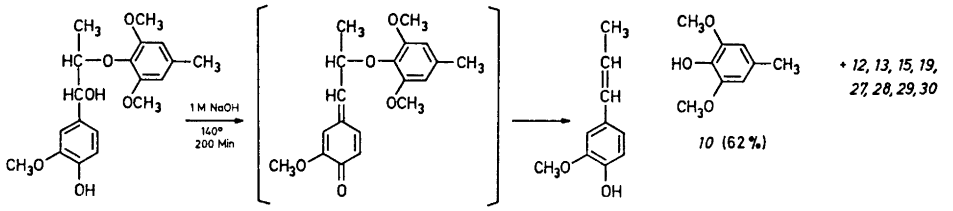

24
a erythro-Form
b threo-Form

25

26
a cis-Form (Spuren)
b trans-Form (43 %)

Unter den Produkten der Sodakochung von *24* wurde Guajacylaceton (*29*) nur in Spuren aufgefunden. Als Hauptprodukte entstanden *10* und *trans*-Isoeugenol (*26b*). In geringeren Mengen wurden weiters die Phenole *12*, *13*, *15*, *19*, *26a*, *27*, *28*, *29* und *30* nachgewiesen. Auf den Nachweis des etwa gebildeten Vinyl-aryläthers *31* wurde hier verzichtet; die gaschromatographische Untersuchung des acetylierten Reaktionsgemisches zeigte, dass schwerer flüchtige, zweikernige Reaktionsprodukte in jeweils nur geringen Mengen entstanden waren.

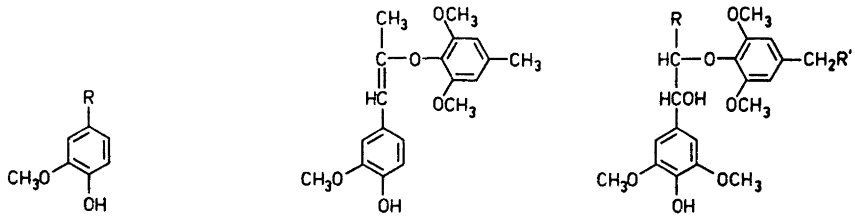

27 R = CHO
28 R = $COCH_2CH_3$
29 R = CH_2COCH_3
30 R = $CHOHCH_2CH_3$

31

32 R, R' = H
33 R = H, R' = OH
34 R = CH_2OH, R' = OH
a erythro-Form
b threo-Form

Das ebenfalls dargestellte Modell *32*, in dem die Hydroxymethylgruppe der Verbindung *8* durch H ersetzt ist, gab bei der Sodakochung neben dem Haupt-

produkt *10* (75 %) 10 – 20 % d. Th. von jedem der folgenden Phenole: *13*, *14*, *16* und *18*, weiters die beiden Formen des Styryl-aryläthers *11* und Spuren der Phenole *12*, *15* und *19*.

Die beim Abbau der Verbindungen *24* und *32* erhaltenen Ergebnisse schliessen für diese Verbindungen – und auch für das Modell *8* – einen hydrolytischen Abbauweg, wie etwa die nucleophile Substitution von OAr durch OH^- in den entsprechenden Chinonmethiden, als Hauptreaktion aus. Die Spaltung der Alkyl-arylätherbindung in den Modellen vom Typ *1* ist vielmehr eine intramolekulare und, wie die Produktzusammensetzung aus dem Abbau von *24* zeigt, auch in gewissem Masse eine intermolekulare Redoxreaktion. Diese Ergebnisse ermöglichen jedoch nicht die detaillierte Angabe des Reaktionswegs; über letzteren können nur Vermutungen angestellt werden.

Alle bekannten Reaktionen von Chinonmethiden, die in alkalischer Lösung aus *p*-Hydroxybenzylalkoholen entstehen, führen unter Wiederausbildung des aromatischen Systems zu Phenolatanionen. Die Rearomatisierung erfolgt entweder durch Anlagerung von Nucleophilen an den Methid-Kohlenstoff des Chinonmethidsystems (Reaktionsweg A; vergl. z.B. Lit. 6a, 8, 9, 10) oder durch Heterolyse einer der von allylischen Kohlenstoffatom des Chinonmethids ausgehenden Bindungen (Reaktionsweg B; vergl. z.B. Lit, 2, 3, 4, 6a, 9, 10, 11) nach dem Schema:

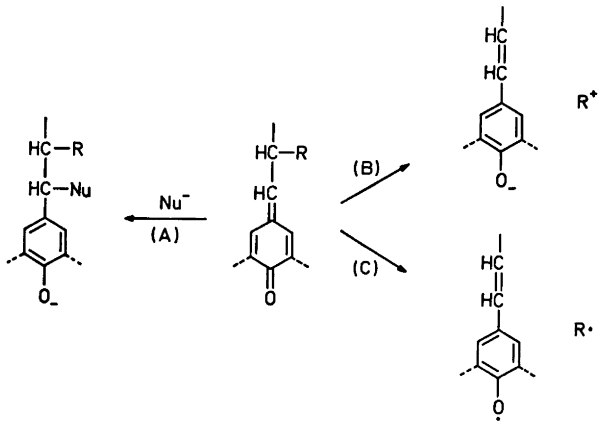

Für die Spaltung der Alkyl-arylätherbindung ist also auch eine Heterolyse der allylischen C-OAr-Bindung in den Chinonmethiden der Modelle *8*, *24* und *32* inbetracht zu ziehen (Reaktionsweg B; R = 2,6-Dimethoxy-4-methylphenoxy). Sie führt zu den Phenolatanionen der *p*-Hydroxystyrole *23*, *26* und *18* sowie zum Phenoniumion von *10*. Die Verbindungen *26* und *18* wurden tatsächlich als mengenmässig bedeutende Produkte des Abbaus der Modelle *24* und *32* aufgefunden, der aus *8* zu erwartende Sinapylalkohol (*23*) ist dagegen unter den Bedingungen der Sodakochung instabil und konnte daher nicht als Abbauprodukt von *8* nachgewiesen werden. Das Phenol *10* sollte dann durch Reduktion des entsprechenden Phenoniumions beim Abbau jedes der drei Modelle (*8*, *24* und *32*) entstehen. Die gleichzeitig gebildeten Oxydations-

produkte stammen, wie insbesonders die Produktzusammensetzung aus dem Abbau von *24* zeigt, sowohl aus der Arylpropaneinheit als auch aus dem β-Aroxylrest. Die überraschend leichte Spaltbarkeit der C-OAr-Bindung in Chinonmethiden vom Typ der Verbindung *9* muss auf die *o,o*-Disubstitution des Phenoxylrestes zurückzuführen sein. Bei entsprechenden *o*-monosubstituierten Chinonmethiden ist eine analog verlaufende Spaltung der Alkyl-arylätherbindung bestenfalls eine Nebenreaktion (vergl. den Nachweis der Bildung geringer Mengen von *26* bei der Sodakochung von *20*).[6a, 10a]

Die heterolytische Spaltung der allylischen C-S Bindung in den bei der Sulfatkochung von *5* und *20* intermediär gebildeten Chinonmethiden *35* und *36* ist ebenfalls bekannt und als intramolekulare Redox-reaktion aufzufassen.[10]

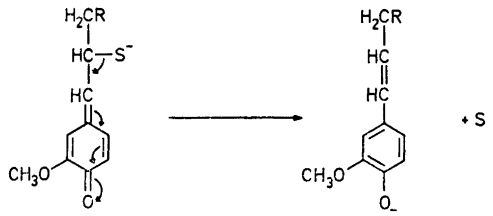

35 R=H
36 R=CH_2OH *26* R=H

Neben einer Heterolyse der Alkyl-arylätherbindung in Chinonmethiden vom Typ der Verbindung *9*, die durch den polaren Charakter des Lösungsmittels begünstigt werden sollte, kann eine Homolyse nicht ausgeschlossen werden (Abbauweg C). Es bestehen hier Analogien zum Verhalten von *p*-Chinoläthern. 4-Aryloxy-2,5-cyclohexadienone zerfallen in aprotischen Lösungsmitteln reversibel in die entsprechenden Phenoxylradikale.[12] Im Phenoxylrest 2,6-disubstituierte Chinoläther sind um etwa 5 kcal/Mol energiereicher als die in diesen Positionen unsubstituierten Verbindungen; diese Destabilisierung wurde auf sterische Einflüsse zurückgeführt.[13] Im Aroxylrest 2,6-disubstituierte Chinonmethide vom Typ der Verbindung *9* sind vinyloge *p*-Chinoläther, was ihren spontanen Zerfall verständlich erscheinen lässt.

Vielleicht ist auch die Bildung[14] von Dihydro-dehydro-diconiferylalkohol beim Erhitzen einer wässrigen Lösung von Guajacylglycerin-β-dihydroconiferyläther auf eine homolytische oder heterolytische Spaltung der Alkyl-arylätherbindung des entsprechenden Chinonmethids zurückzuführen.

Der für die Modelle vom Strukturtyp *1* gefundene Abbauweg sollte auch für andere, im Phenoxylrest *o,o*-disubstituierte *p*-Hydroxyarylglycerin-β-aryläther gelten, so beispielsweise für die in Alkyl-arylätherstrukturen verätherten phenolischen Kerne der 6,6'-Dihydroxy-5,5'-dimethoxy-biarylstrukturen und der 2-Hydroxy-3-methoxy-diarylätherstrukturen der Laubholz- und Nadelholzlignine.

Abbau von p-*Alkoxyarylglycerin-β-(2,6-dimethoxy-4-alkylaryl)-ätherstrukturen (2).* *p*-Alkoxyarylglycerin-β-arylätherstrukturen, in denen der Aroxylrest

ein 2-Methoxy-4-alkyl-aroxylrest ist (Typ *4*), werden durch Erhitzen mit Alkali über Epoxide zu den entsprechenden *p*-Alkoxyarylglycerinen und 2-Methoxy-4-alkylphenolen abgebaut.[3,15] Die Verbindung *37b*, ein Modell für die *p*-Alkoxyarylglycerin-*β*-arylätherstrukturen vom Typ *2* mit, gegenüber *4*, einem zusätzlichen *o*-Methoxylsubstituenten im Aroxylrest, verhielt sich auf gleiche Weise. Die Spaltungsgeschwindigkeit, bestimmt durch gaschromatographische Messung von *10*, war etwa gleich gross ($T = 139{,}4°$, $k = 1{,}2 \times 10^{-3}$ Min^{-1}) wie die des Methyläthers von *5b* ($T = 139{,}4°$, $k = 1{,}5 \times 10^{-3}$ Min^{-1}).[7] Neben *10* entstand als Hauptprodukt das als Acetat nachgewiesene Arylglycerin *38* (vermutlich *erythro*-Form, siehe exp. Teil).

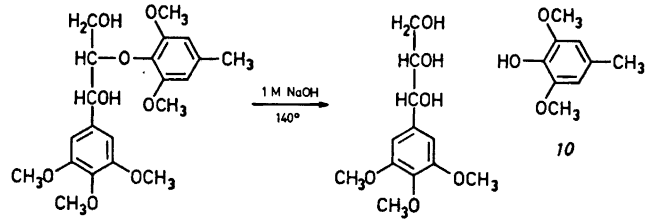

37
a *erythro*-Form
b *threo*-Form

38
a *erythro*-Form
b *threo*-Form

10

Wie die Abbauversuche mit *8b* und *37b* zeigen, ist die Spaltungsgeschwindigkeit der Strukturen des Typs *2*, verglichen mit der des Typs *1*, gering. Beim alkalischen Abbau des Lignins wird also ein bedeutender Teil der Strukturen vom Typ *2* (R = das *β*-C-Atom einer Propanseitenkette) in Strukturen vom Typ *1* umgewandelt und in Form der letzteren weiter abgebaut. Es verhält sich somit ein grösserer Teil der Arylglycerin-*β*-(2,6-dimethoxy-4-alkylaryl)-ätherstrukturen beim Abbau wie der Strukturtyp *1*, als es aufgrund der Frequenz dieses Strukturtyps zu erwarten ist.

Darstellung der Modellverbindungen 8, 24 *und* 32. Die Synthese dieser Modelle lehnt sich an die von Adler und Eriksoo beschriebene Darstellung [16] des Modells *5* an; die Verbindungen *39*–*48* wurden als Zwischenstufen dargestellt.

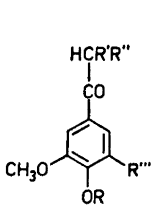

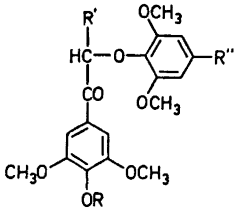

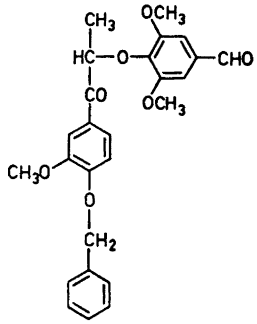

48

39 R = $COCH_3$, R',R'' = H, R''' = OCH_3
40 R = $COCH_3$, R' = Br, R'' = H, R''' = OCH_3
41 R = $CH_2C_6H_5$, R', R'' = H, R''' = OCH_3
42 R,R' = H, R'' = Br, R''' = OCH_3
43 R = $CH_2C_6H_5$, R' = Br, R'' = CH_3, R''' = H
44 R = $COCH_3$, R' = H, R'' = CHO
45 R = $COCH_3$, R' = CH_2OH, R'' = CHO
46 R = H, R' = CH_2OH, R'' = CHO
47 R = $COCH_3$, R' = H, R'' = CH_3

Über die sterische Zuordnung der beiden Formen von *8* zur *erythro-* bzw. *threo*-Reihe mit Hilfe der Protonenresonanzspektren der Triacetate wurde bereits berichtet;[17] die Zuordnung der beiden Formen von *24* erfolgte auf gleiche Weise.

EXPERIMENTELLER TEIL

Abbauversuche

Arbeitsweise bei Abbauversuchen, die eine Identifizierung der Reaktionsprodukte zum Ziel hatten. Etwa 20 mg der Modellverbindung in 2 ml 1 M NaOH (*37b* in 1 M NaOH in 20-proz. Dioxan) wurden unter N_2 in einem Autoklaven mit Teflonauskleidung auf 140° erhitzt. Nach Sättigen mit CO_2 wurde 3 × mit $CHCl_3$ ausgezogen. Der mit Acetanhydrid-Pyridin 1:1 acetylierte Verdampfungsrückstand wurde zur gaschromatographischen Untersuchung verwendet.

Durch Ansäuern der bicarbonatalkalischen wässrigen Phase mit H_3PO_4 auf pH 1 – 2 und Extrahieren mit $CHCl_3$ wurden die sauren Reaktionsprodukte isoliert, die aber nicht weiter untersucht wurden.

Bei jedem Versuch wurde angegeben: eingesetztes Modell (mg), Reaktionsdauer (Min), Neutralprodukte (mg), saure Produkte (mg).

Abbau von 8b (23,1; 180; 19,9; 2,2). Als Acetate wurden nachgewiesen: *10* (73 %), *11a* und *11b* (Ausbeute insgesamt ~5 % d. Th.), *12* (Spuren), *13* (~5 %), *14* (~10 %), *19* (Spuren). Die Zuordnung der *cis*-Form für *11a* und der *trans*-Form für *11b* erfolgte durch Vergleich des gaschromatographischen Verhaltens mit dem des *cis-* und des *trans*-Acetats von *7*; das *cis*-Acetat von *7* (stereochemische Zuordnung aufgrund des Protonenresonanzspektrums) besitzt die kürzere Retentionszeit (stationäre Phase SE-30) von beiden.[9] Die *erythro*-Form *8a* gab die gleichen Abbauprodukte wie *8b*.

Abbau von 21 (15,2; 60; 14,2; nicht bestimmt). Als Abbauprodukte wurden nachgewiesen: *13* und *14*. Der grösste Teil des Reaktionsprodukts wanderte nicht im Dünnschichtchromatogramm (Kieselgel G; Aceton-Hexan 2:1, Sprühreagens H_2SO_4-Formalin 9:1).

Die hier verwendete höherschmelzende Form der Verbindung *21* (Schmp. 127°)[18] besitzt, wie bereits früher angenommen,[18] *erythro*-Konfiguration. Dies zeigt der Vergleich des Protonenresonanzspektrums des Tetraacetats der höherschmelzenden Form von *21* (Schmp. 88 – 89° aus Essigester-Hexan) mit dem von *erythro*-Guajacylglycerin-tetraacetat.[9] NMR (10 %): 2,00 (3) s, C–OCOCH$_3$; 2,05 (3) s, C–OCOCH$_3$; 2,14 (3) s, C–OCOCH$_3$; 2,32 (3) s, Ar – OCOCH$_3$; 3,85 (6) s, 2 OCH$_3$; 4,28 (2) d, H$_\gamma$; 5,42 (1) dt, H$_\beta$;6,02 (1) d, H$_\alpha$; 7,14 (2) s, H_{ar}. $J_{\alpha\beta} = 5{,}1$ Hz; $J_{\beta\gamma} = 5{,}7$ Hz.

Abbau von 24 (90 % *erythro-*, 10 % *threo*-Form. (22,1; 180; 19,8; 2,6). Als Acetate wurden nachgewiesen: *10* und *26b* (Hauptprodukte), weiters *12*, *13*, *15*, *19*, *26a*, *27*, *28*, *29* und *30*.

Nach einem gesonderten Abbauversuch (200 Min) wurden *10* und *26b* als Acetate gaschromatographisch bestimmt (auf einer 2 m langen, 3 Gew.-% des Trägermaterials an SE-30 enthaltenden Trennsäule; innerer Standard Anissäure-methylester, Retentionszeit (160°) 2,4 Min; Bedingungen für die Gaschromatographie siehe unten). Die Ausbeute an *10* betrug 62 %, die an *26b* 43 % d. Th.

Abbau von 32 (23,4; 120; 20,8; 3,1). Aufgefunden wurden: *10* (Hauptprodukt) *11a*, *11b*, *12* (Spuren), *13*, *14*, *15* (Spuren), *16*, *18* und *19* (Spuren).

Abbau von 37b (23,7; 1200; nicht best.; nicht best.). Die Lösung der Abbauprodukte wurde mit Essigsäure neutralisiert und zur Trockene gebracht. Nach zweimaligem Abdampfen des Rückstands mit Pyridin im Vakuum wurden 5 ml eines Gemisches von Acetanhydrid-Pyridin (1:1) zugegeben und die Suspension wurde 2 Stunden auf 85° erhitzt. Dann wurde ein Überschuss an Methanol zugesetzt und nach 30 Min das Lösungsmittelgemisch im Vakuum vertrieben. Die gaschromatographische Untersuchung des Verdampfungsrückstands zeigte, dass *10* und *38* (stereochemische Zuordnung unsicher, vergl. Lit. 15; das Massenspektrum des Triacetates zeigte mit dem eines Vergleichspräparates mit *erythro*-Konfiguration gute Übereinstimmung) als Hauptprodukte gebildet worden waren. Dünnschichtchromatographie des acetylierten Reaktionsproduktes

(Kieselgel G, Merck, Aceton-Hexan 1:2) zeigte keine langsamer als die Acetate von *37* und *38* laufende Verbindungen an und schliesst daher die Gegenwart von höhermolekularen Abbauprodukten aus.

Vergleichssubstanzen. Die Literaturangaben beziehen sich auf die Schmelzpunkts- oder Siedepunktsangaben der Acetate. Letztere wurden, mit Ausnahme des Acetats von *29*, aus den entsprechenden Phenolen bzw. Alkoholen mit Acetanhydrid-Pyridin dargestellt. Die Acetate sämtlicher Vergleichssubstanzen lieferten mit den angegebenen Strukturen im Einklang stehende Massenspektren. Literaturangaben (Acetate): 2,6-Dimethoxyphenol (*12*),[19] Syringaaldehyd (*13*),[20] 4-Hydroxy-3,5-dimethoxy-acetophenon (*14*),[21] 4-Hydroxy-3,5-dimethoxy-benzylalkohol (*15*),[22] 4,4′-Dihydroxy-3,3′,5,5′-tetramethoxy-diphenylmethan (*19*),[23] *cis*-Isoeugenol (*26a*),[24] *trans*-Isoeugenol (*26b*),[24] Vanillin (*27*),[25] 4-Hydroxy-3-methoxy-propiophenon (*28*),[26] 1-(4-Hydroxy-3-methoxyphenyl)-2-propanon (*29*),[27] 1-(4-Hydroxy-3-methoxyphenyl)-1-propanol (*30*).[28] Die Acetate der Verbindungen *10*, *16*, *18* und *33* waren bisher nicht beschrieben worden.

Acetat von 10. Aus 2,6-Dimethoxy-4-methyl-phenol (*10*) [20] mit Pyridin-Acetanhydrid. Farblose Nadeln vom Schmp. 77 – 78° aus Äther-Pentan.

Diacetat von 16. Aus 1-(4-Hydroxy-3,5-dimethoxyphenyl)-1-äthanol (*16*) [29] mit Acetanhydrid-Pyridin. Farbloses Öl, Kp. 100 – 110°/0,01 Torr.

Acetat von 18. Das 4-Hydroxy-3,5-dimethoxy-styrol (*18*) ist bekannt.[30] Ein Vergleichspräparat für das Acetat von *18* wurde durch Decarboxylierung von Acetylsinapinsäure [31] nach dem für die Darstellung von 4-Acetoxy-3-methoxy-styrol beschriebenen Verfahren [26] dargestellt. Gelbes Öl, Kp. 90 – 95°/0,005 Torr. Das Acetat von *18* konnte präparativ nicht vollkommen von Begleitsubstanzen befreit werden; das Vergleichsspektrum wurde mit einer geringen Menge von gaschromatographisch gereinigter Substanz aufgenommen.

Triacetat von erythro-38. Aus *erythro-21* [18] mit Dimethylsulfat-KOH in wässrigem Methanol. Das so erhaltene farblose Harz gab mit Acetanhydrid-Pyridin ein gaschromatographisch einheitliches, öliges Triacetat. Für das Molekülion des Triacetats von *erythro-38* wurde eine Masse von 384,1407 gefunden (ber. für $C_{18}H_{24}O_9$: M = 384,1420).

Gaschromatographie. Gerät: Perkin-Elmer Modell 900. *Trennsäule:* aus nichtrostendem Stahl, 2 m lang, äusserer Durchmesser 0,3 cm. *Trägermaterial:* Chromosorb G, gewaschen mit Säure, behandelt mit Dimethyldichlorsilan. *Stationäre Phase:* Silikonelastomer SE-30, 3 Gew.- % des Trägermaterials. *Arbeitstemperaturen:* Injektor 250°, Trennsäule 160 – 255°, 5° per Min oder 160° bzw. 240° isotherm. *Trägergas:* N_2, Strömungsgeschw. 25 ml per Min. *Retentionszeiten der Acetate:* (Min). $T = 160°$: *10*, 5,5; *12*, 3,6; *13*, 10,0; *14*,14,3; *15*, 21,3; *16*, 22,1; *18*, 8,3; *26a*, 6,8; *26b*, 5,5; *27*, 4,6; *28*, 10,3; *29*, 9,1; *30*, 14,3. $T = 240°$: *8b*, 38,9; *11a*, 18,7; *11b*, 24,2; *19*, 17,9; *21*, 7,6; *24b*, 17,2; *32*, 24,3; *37b*, 29,1; *38*, 4,3.

Identifizierung der Abbauprodukte. Mikrogrammengen der acetylierten Abbauprodukte wurden nach der gaschromatographischen Trennung in Kapillaren aufgefangen. Die Bedingungen der Gaschromatographie entsprechen den oben angegebenen, es wurde aber ein Perkin-Elmer Modell 880 Gerät mit einer 2 m langen Trennsäule (äusserer Durchmesser 6 mm) verwendet. Die mit einem AEI MS 20 Massenspektrometer (Elektronenstossionenquelle, Elektronenenergie 70 eV) aufgenommenen Massenspektren dieser Fraktionen wurden mit den mit dem gleichen Gerät aufgenommenen Spektren der synthetisch erhaltenen Verbindungen verglichen; im Falle des Acetats von *11* genügte der Vergleich mit dem Acetat von *7*.

Massenspektren von 11a und 11b. Aufgenommen mit einem AEI MS 902 Massenspektrometer. *Elektronenenergie:* 70 eV. *Ionenquellentemperatur:* 120°.

Teilmassenspektrum von *11a*. Nur Ionen mit einer Massenzahl von ≥ 100 und einer relativen Intensität von ≥ 10 wurden beachtet. *m/e, rel. Int.*: 388,35; 346, 100; 345, 11; 318, 48; 286, 13; 179, 17; 168, 16; 167, 18; 165, 12; 121, 13.

Teilmassenspektrum von *11b*. Intensitätsgrenzen und Massenbereich wie bei *11a*. *m/e, rel. Int.*: 388, 48; 346, 100; 345, 13; 318, 34; 286, 12; 179, 16; 168, 16; 167, 18; 165, 10; 121, 11. Die Masse des Molekülions wurde zu 388,1482 bestimmt (ber. für $C_{21}H_{24}O_7$: 388,1522). Die erheblich stärkere Fragmentierung des Molekülions der *cis*-Form *11a* ist bemerkenswert.

Kinetische Messungen. siehe Best. von Guajakol;[7] nur abweichende Bedingungen sind angegeben: Abbau in 1 M NaOH oder 1 M NaOH, enthaltend 1 Mol Na_2S/l, von *37b* in 1 M NaOH in Dioxan-H_2O 1:4. Autoklav mit Tefloneinsatz. Ansäuern auf pH 5,5 – 6.

Bestimmung von *10* als Acetat. Der Rückstand des $CHCl_3$-Auszugs der neutralisierten Kochlauge wurde mit 0,2 ml Pyridin-Acetanhydrid 1:1 acetyliert (48 Stunden, 25°). Dann wurde Methanol (2 ml) zugegeben und nach 30 Min bei 50°/1 – 2 Torr eingeengt. Rückstand gelöst in 1 ml $CHCl_3$, davon 1 µl zur gaschromatographischen Best.

Gaschromatographie. Siehe oben; davon abweichend: *Stationäre Phase:* Silikonelastomer XE-60, 5 Gew.-% des Trägermaterials. *Arbeitstemperaturen:* Trennsäule 170° (Best. von *10*) oder 200° (Best. von *10* als Acetat). *Retentionszeiten* (Min) $T = 170°$: 2,4,5-Trimethylphenol (innerer Standard) 4,2; *10*, 8,6. $T = 200°$: 2,4,5-Trimethylphenol-acetat, 1,5; Acetat von *10*, 4,6. Berechnung über Standardkurven.

Die Ergebnisse des Abbaus von *8b* sind in Tab. 1 angegeben. Für *37b* wurde gefunden (Reaktionstemperature 139,4° ±0,1°; Reaktionszeit 120 Min): 14,3 % und 14,8 % *10* $k = 1{,}19$ und $1{,}24 \times 10^{-3}$ Min^{-1}.

Synthesen

4-Acetoxy-3,5-dimethoxy-α-brom-acetophenon (40). Zu einer Lösung von 10 g 4-Acetoxy-3,5-dimethoxy-acetophenon [21] in 150 ml $CHCl_3$ wurden 6,7 g Br_2 in 50 ml $CHCl_3$ getropft. Die Reaktionslösung wurde mit wässr. Na-dithionit, $NaHCO_3$ und H_2O gewaschen. Farblose Kristalle (10,6 g) vom Schmp. 127 – 128° (Lit.[21] Schmp. 122 – 125°). (Gef.: C 45,54; H 4,37. Ber. für $C_{12}H_{13}O_5Br$ (317,14): C 45,44; H 4,13.)

4-Hydroxy-3,5-dimethoxy-α-brom-acetophenon (42). Eine $CHCl_3$-Lösung von 18 g *14* [32] in 150 mg $CHCl_3$ wurde, wie oben beschrieben, bromiert. Aus Äthanol kristallisierten 6,7 g schwach gefärbte Kristalle vom Schmp. 118 – 120°. (Gef.: C 44,00; H 4,25; Br 28,24. Ber. für $C_{10}H_{11}O_4Br$ (275,12): C 43,66; H 4,03; Br 29,05. NMR (10 %): 3,94 (6) s, 2 OCH_3; 4,38 (2) s, CH_2; 7,25 (2) s, H_{ar}.

4-Acetoxy-3,5-dimethoxy-α-(4-formyl-2,6-dimethoxy-phenoxy)-acetophenon (44). Ein Gemisch, bestehend aus 29 g *40*, 20 g *13*, 20 g K_2CO_3 und 10 g KJ in 250 ml Aceton wurde zwei Stunden am Rückfluss erhitzt. Aus wässr. Essigsäure kristallisierten 22,5 g *44* vom Schmp. 165 – 167°. (Gef:. C 59,88; H 5,45. Ber. für $C_{21}H_{22}O_9$ (418,41): C 60,28; H 5,30.)

4-Acetoxy-3,5-dimethoxy-α-(2,6-dimethoxy-4-methyl-phenoxy)-acetophenon (47). Ein Gemisch, bestehend aus 1,0 g *40*, 600 mg *10* und 200 mg KJ in 10 ml Aceton wurde, wie vorangehend beschrieben, umgesetzt. Farblose Kristalle (560 mg) vom Schmp. 112 – 114° (Äthanol). (Gef.: C 62,01; H 6,05. Ber. für $C_{21}H_{24}O_8$ (404,42): C 62,37; G 5,98.)

1-(4-Acetoxy-3,5-dimethoxyphenyl)-2-(4-formyl-2,6-dimethoxy-phenoxy)-3-hydroxy-1-pronanon (45). Zu einer Lösung von 22,5 g *44* in 80 ml Dimethylsulfoxid wurden 2,5 g K_2CO_3 und 1,7 g Paraformaldehyd (mittlerer Polymerisationsgrad 40) gegeben. Die Lösung wurde über Nacht unter N_2 geschüttelt. Farblose Kristalle (13,5 g) vom Schmp; 148 – 149° (Essigester). (Gef.: C 58,79; H 5,53. Ber. für $C_{22}H_{24}O_{10}$ (448,43): C 58,93. H 5,39.)

2-(4-Formyl-2,6-dimethoxy-phenoxy)-3-hydroxy-1-(4-hydroxy-3,5-dimethoxyphenyl)-1-propanon (46). Eine Lösung von 8 g *45* und 3 g Piperidin in 100 ml Äthanol wurde eine Stunde am Rückfluss erhitzt. Farblose Kristalle (5,1 g) vom Schmp. 158 – 161° (Essigester). (Gef.: C 59,30; H 5,68. Ber. für $C_{20}H_{22}O_9$ (406,40): C 59,11; H 5,46.)

1-(4-Hydroxy-3,5-dimethoxyphenyl)-2-(4-hydroxymethyl-2,6-dimethoxyphenoxy)-1,3-propandiol (34). Die Verbindung *45* (12 g) wurde in Tetrahydrofuran bei 50° mit $LiAlH_4$ (5 g) reduziert (4 Stunden). Das ölige Reaktionsprodukt kristallisierte zum Teil aus Essigester-Hexan; Schmp. (*threo-Form 34b*) nach zweimaligem Umkristallisieren aus dem gleichen Lösungsmittelgemisch 154 – 155°. (Gef.: C 58,33; H 6,43. Ber. für $C_{20}H_{26}O_9$ (410,43): C 58,53; H 6,39.)

Tetraacetat von 34b. Prismen vom Schmp. 104 – 105° aus Essigester-Hexan. (Gef.: C 57,95; H 5,90. Ber. für $C_{28}H_{34}O_{13}$ (578,58): C 58,13; H 5,92.) NMR (15 %): 1,91 (3) s, α- oder γ-$OCOCH_3$; 1,94 (3) s, α- oder γ-$OCOCH_3$; 2,03 (3) s, α′-$OCOCH_3$; 2,24 (3) s, Ar-$OCOCH_3$; 3,72 (6) s, 2 OCH_3; 3,75 (6) s, 2 OCH_3; *ca.* 4,18 (2) m, H_γ; *ca.* 4,48 (1) m, H_β; 4,97 (2) s, H_α′; 6,08 (1) d, H_α; 6,53 (2) s, H_{ar} am Phenoxylrest; 6,67 (2) s, H_{ar} am Phenylrest. $J_{\alpha\beta} = 6{,}0$ Hz.

Die Mutterlauge von *34b* wurde nach Abdampfen des Lösungsmittels auf einer Kieselgelsäule (Silicic acid, Mallinckrodt; Benzol-Essigester 1:2) chromatographiert. Dabei trennten die Diastereomeren teilweise auf, und zwar in schneller laufendes *threo-34* und langsamer laufendes *erythro-34*. Nach wiederholtem Umkristallisieren aus wässr.

Äthanol wurden insgesamt 1,9 g *34a* und 0,55 g *34b* erhalten. Die *erythro*-Form *34a* schmilzt bei 178 – 180° (Äthanol-H_2O). (Gef.: C 58,50; H 6,52. Ber. für $C_{20}H_{26}O_9$ (410,43): C 58,53; H 6,39.)

Tetraacetat von 34a. Farblose, kugelförmige Drusen vom Schmp. 86 – 87° (wässr. Äthanol). (Gef.: C 57,88; H 5,85. Ber. für $C_{28}H_{34}O_{13}$ (578,58): C 58,13; H 5,92.) NMR (15 %): 1,92 (3) s, γ-$OCOCH_3$; 2,05 (3) s, α'-$OCOCH_3$; 2,09 (3) s, α-$OCOCH_3$; 2,25 (3) s, 4-$OCOCH_3$; 3,71 (6) s, 2 OCH_3; 3,75 (6) s, 2 OCH_3; *ca.* 4,32 (2) m, H; *ca.* 4,57 (1) m, H; 4,96 (2) s, H; 6,03 (1) d, H; 6,50 (2) s, H_{ar} am Phenoxylrest; 6,61 (2) s, H_{ar} am Phenylrest. $J_{\alpha\beta} = 4{,}9$ Hz.

erythro-*1-(4-Hydroxy-3,5-dimethoxyphenyl)-2-(2,6-dimethoxy-4-methyl-phenoxy)-1,3-propandiol* (8a). Eine Suspension von 100 mg *34a* in 5 ml Essigester-Äthanol 3:2 wurde nach Zusatz von 50 mg 10 % Pd/C hydriert. Aus Essigester-Hexan kristallisierten 54 mg *8a* in Form farbloser Nadeln vom Schmp. 147 – 149° (Umwandlung bei 105°). (Gef.: C 60,78; H 6,64. Ber. für $C_{20}H_{26}O_8$ (394,43): C 60,90; H 6,64.)

Tetraacetat von 8a. Rhomboedrische Stäbchen vom Schmp. 154,5 – 155° aus Äthanol. (Gef.: C 59,87; H 6,41. Ber. für $C_{26}H_{32}O_{11}$ (520,55): C 59,99; H 6,20.)

threo-*1-(4-Hydroxy-3,5-dimethoxyphenyl)-2-(2,6-dimethoxy-4-methyl-phenoxy)-1,3-propandiol* (8b). Eine Suspension von 3,0 g *34b* und 100 mg 10 % Pd/C in 40 ml Äthylenglykol-monomethyläther wurde hydriert. Aus Essigester-Hexan kristallisierten 2,45 g *8b* in Form farbloser Nadeln vom Schmp. 147 – 149°. Ein Gemisch von *8a* und *8b* zeigte Schmelzpunktsdepression. (Gef.: C 60,76; H 6,63. Ber. für $C_{20}H_{26}O_8$ (394,43): C 60,90; H 6,64.)

Tetraacetat von 8b. Farblose Nadeln vom Schmp. 141,5° aus Essigester-Hexan. (Gef.: C 59,89; H 6,32. Ber. für $C_{26}H_{32}O_{11}$ (520,55): C 59,99; H 6,20.)

threo-*1-(3,4,5-Trimethoxyphenyl)-2-(2,6-dimethoxy-4-methyl-phenoxy)-1,3-propandiol* (37b). Aus *8b* mit Dimethylsulfat-KOH.[33] Farblose Kristalle vom Schmp. 79 – 81° aus Essigester-Hexan.

Triacetat von 37b. Farblose Prismen vom Schmp. 122° (Essigester-Hexan).

Hydrierung von 46 (in Äthanol mit 10 % Pd/C). Führte zu einem vorwiegend aus *8b* und *34b* bestehenden Gemisch.

1-(4-Benzyloxy-3-methoxyphenyl)-2-(4-formyl-2,6-dimethoxy-phenoxy)-1-propanon (48). Zu einer Lösung von 2,0 g *13* und 1,2 g K-*tert.*-butanolat in 10 ml Dimethylsulfoxid wurden 3,5 g 1-(4-Benzyloxy-3-methoxyphenyl)-2-brom-1-propanon (*43*, wurde auch in einer isomorphen Form vom Schmp. 96 – 97°, feine Nadeln aus Essigester-Hexan, erhalten; für die andere Form war ein Schmp. von 86 – 87° gefunden worden [33]) gegeben. Das Gemisch wurde 30 Min unter Schütteln auf 80° erwärmt. Das Keton *48* kristallisierte aus wässrigem Methylglykol und wurde 2 × aus Essigester-Hexan umgelöst. Feine, farblose Nadeln (1,22 g) vom Schmp. 101 – 102°. (Gef.: C 69,30; H 5,92. Ber. für $C_{26}H_{26}O_7$ (450,47): C 69,32; H 5,82.)

1-(4-Hydroxy-3-methoxyphenyl)-2-(2,6-dimethoxy-4-methyl-phenoxy)-1-propanol (24). Eine Lösung von 0,90 g *48* in 50 ml Essigester (3:7) wurde in Gegenwart von 0,35 g 10 % Pd/C hydriert. Das Reaktionsprodukt wurde durch präparative Dünnschichtchromatographie gereinigt (Kieselgel HF 254, Merck; Aceton-Hexan 1:1). Isomerengemisch, 626 mg, *ca.* 65 % *threo*- und 35 % *erythro*-Form.

Ein Teil des Reaktionsproduktes wurde auf analytischen Dünnschichtplatten (Kieselgel HF 254, Aceton-Hexan 1:2, 4 × entwickelt) in langsamer laufende *threo*-Form und in schneller laufende *erythro*-Form getrennt. Beide Formen sind gaschromatographisch (Acetate) einheitliche, zähe farblose Öle; sie wurden durch die Diacetate charakterisiert.

Diacetat von 24a. Zähes, farbloses Öl. NMR (5 %): 1,29 (3) d, H_γ; 2,17 (3) s, C–$OCOCH_3$; 2,28 (3) s, Ar–$OCOCH_3$; 2,30 (3) s, Ar–CH_3; 3,76 (6) s, 2 OCH_3; 3,80 (3) s, OCH_3; 4,41 (1) dqu, H_β; 5,90 (1) d, H_α; 6,35 (2) H_{ar} am Phenoxylrest; *ca.* 6,90 (3) m, H_{ar} am Phenylrest. $J_{\alpha\beta} = 3{,}6$ Hz; $J_{\beta\gamma} = 6{,}5$ Hz.

Diacetat von 24b. Farblose Prismen vom Schmp. 104 – 105° aus Essigester-Hexan (Exakte Massenbestimmung am Molekülion. Gef.: M = 432,1765. Ber. für $C_{23}H_{28}O_8$: M = 432,1784.)NMR (3 %): 1,13 (3) d, H_γ; 1,95 (3) s, C – $OCOCH_3$; 2,28 (6) s, Ar – CH_3 und Ar – $OCOCH_3$; 3,78 (6) s, 2 OCH_3; 3,81 (3) s, OCH_3; 4,42 (1) dqu, $H\beta$; 5,94 (1) d, H_α; 6,38 (2) s, H_{ar} am Phenoxylrest; *ca.* 7,01 (3) m, H_{ar} am Phenylrest. $J_{\alpha\beta} = 6{,}6$ Hz, $J_{\beta\gamma} = 6{,}5$ Hz. Für die Protonen des α-Acetoxylrests von 1-(4-Acetoxy-3,5-dimethoxyphenyl)-2-(2,6-dimethoxy-4-*trans*-propenylphenoxy)-propanol wurden δ-Werte von 1,28 (*erythro*-

Form) bzw. 1,13 (*threo*-Form) beobachtet.[34]

1-(4-Hydroxy-3,5-dimethoxyphenyl)-2-(4-hydroxymethyl-2,6-dimethoxyphenoxy)-1-äthanol (33). Aus *44* (567 mg) mit $LiAlH_4$ (0,8 g) in THF (1 Stunde Rückfluss). Farblose Kristalle (396 mg) vom Schmp. 132–133° (Essigester-Hexan). (Gef.: C 59,86; H 6,41. Ber. für $C_{19}H_{24}O_8$ (380,38): C 60,00; H 6,36.)

1-(4-Hydroxy-3,5-dimethoxyphenyl)-2-(2,6-dimethoxy-4-methyl-phenoxy)-1-äthanol (32). Aus 215 mg *33*, suspendiert in 50 ml Äthanol, wurden durch Hydrierung unter Zusatz von 40 mg 10 % Pd/C 122,5 mg *32* in Form feiner, farbloser Nadeln vom Schmp. 97–98° (Essigester-Hexan) erhalten. (Gef.: C 62,81; H 6,61. Ber. für $C_{19}H_{24}O_7$ (364,38): C 62,62; H 6,64.)

Diacetat von 32. Rhomben vom Schmp. 127–128° (Essigester-Hexan). NMR (5 %): 2,09 (3) s, $C-OCOCH_3$; 2,30 (6) s, $Ar-CH_3$ und $Ar-OCOCH_3$; 3,69 (12) s, 4 OCH_3; 4,20 (2) d, H_β; 6,00 (1) t, H_α; 6,36 (2) s, H_{ar} am Phenoxylrest; 6,59 (2) s, H_{ar} am Phenylrest. $J = 6{,}0$ Hz.

Die Verbindung *32* wurde auch durch Reduktion von *47* mit $LiAlH_4$ in THF in 70-proz. Ausbeute erhalten.

Protonenresonanzspektren: 60 MHz; Tetramethylsilan als innerer Standard; in $CDCl_3$; δ-Werte.

Die Elementaranalysen wurden unter Leitung von Herrn Dr. J. Zak am Mikroanalytischen Laboratorium am Inst. f. physik. Chemie der Univ. Wien ausgeführt.

Herrn Prof. Dr. E. Adler sei für wertvolle Diskussionen, Herrn Dipl. Ing. J. Bäckström, Frl. Ing. G. Karlsson und Herrn Ing. H. Gaber für experimentelle Mitarbeit gedankt. Diese Arbeit wurde von der Westvaco Corp., New York, sowie durch ein Stipendium von *Cellulosaindustriens stiftelse för skoglig forskning samt utbildning* unterstützt.

LITERATUR

1. a. Larsson, S. und Miksche, G. E. *Acta Chem. Scand.* **25** (1971) 647; b. Erickson, M., Larsson, S. und Miksche, G. E. *Ibid.* **27** (1973) 127.
2. Nimz, H. *Chem. Ber.* **99** (1966) 2638.
3. Gierer, J. und Norén, I. *Acta Chem. Scand.* **16** (1962) 1713.
4. Adler, E., Falkehag, I., Marton, J. und Halvarson, H. *Acta Chem. Scand.* **18** (1964) 1313.
5. Miksche, G. E. *et al. In Vorbereitung.*
6. a. Johansson, B. und Miksche, G. E. *Acta Chem. Scand.* **23** (1969) 924; b. Miksche, G. E. *Acta Chem. Scand.* **26** (1972) 4137.
7. Miksche, G. E. *Acta Chem. Scand.* **26** (1972) 3275.
8. Hästbacka, K. *Soc. Sci. Fennica Commentationes Phys.-Math.* **26** (1961).
9. Johansson, B. und Miksche, G. E. *Acta Chem. Scand.* **26** (1972) 289.
10. a. Brunow, G. und Miksche, G. E. *Acta Chem. Scand.* **23** (1969) 1444; b. *Ibid.* **26** (1972) 1123.
11. Adler, E., Marton, J. und Falkehag, I. *Acta Chem. Scand.* **18** (1964) 1311.
12. Becker, H. D. *J. Org. Chem.* **30** (1965) 982. Cooper, C. D., Blanchard, H. S. und Finkbeiner, G. F. *J. Am. Chem. Soc.* **87** (1965) 3996.
13. Mahoney, L. R. und DaRooge, M. A. *J. Am. Chem. Soc.* **92** (1970) 890.
14. Nimz, H. *Angew. Chem.* **78** (1966) 821.
15. Gierer, J. und Norén, I. *Acta Chem. Scand.* **16** (1962) 1976.
16. Adler, E. und Eriksoo, E. *Acta Chem. Scand.* **9** (1955) 341.
17. Erickson, M. und Miksche, G. E. *Acta Chem. Scand.* **26** (1972) 3085.
18. Nimz, H. *Chem. Ber.* **98** (1965) 315.
19. Graebe, C. und Hess, H. *Ann. Chem.* **340** (1905) 232.
20. Freudenberg, K. und Hübner, H. H. *Chem. Ber.* **85** (1952) 1181.
21. Brit. Pat. 1.188.480 (Zambeletti, Dr. L., S.p.A.); citiert in *Chem. Abstr.* **73** (1970) 3660.
22. Lounasmaa, M. *Acta Chem. Scand.* **22** (1968) 70.
23. Richtzenhain, H. *Ber.* **77** (1944) 409.
24. Boedecker, F. und Volk, H. *Ber.* **64** (1931) 61.

25. Tiemann, F. und Nagai, N. *Ber.* **11** (1878) 647.
26. Riegel, B. und Witcoff, H. *J. Am. Chem. Soc.* **68** (1946) 1913.
27. von Wacek, A. *Ber.* **77** (1944) 85.
28. Roberti, P. C., York, R. F. und MacGregor, W. S. *J. Am. Chem. Soc.* **72** (1950) 5760.
29. Arlt, H. G., Gross, S. K. und Schuerch, C. *Tappi* **41** (1958) 64.
30. Lustre, A. O. und Issenberg, P. *J. Agr. Food Chem.* **17** (1969) 1387.
31. Gadamer, J. *Ber.* **30** (1897) 2330.
32. Bradley, W. und Robinson, R. *J. Chem. Soc.* **1928** 1541.
33. Adler, E., Delin, S. und Miksche, G. E. *Acta Chem. Scand.* **20** (1966) 1035.
34. Wallis, A. F. A. *Austr. J. Chem. Im Druck.*

Eingegangen am 2. November 1972.

ACTA CHEMICA SCANDINAVICA 27 (1973) 1369–1384

The Hydrolysis of Zr^{4+} and Hf^{4+}

BERTIL NORÉN

Inorganic Chemistry 1, Chemical Center, University of Lund, P.O. Box 740, S-220 07 Lund 7, Sweden

The hydrolysis of Zr^{4+} and Hf^{4+} has been investigated by means of potentiometric and solvent extraction measurements. In the potentiometric investigations, a fluoride membrane electrode has been used for the determination of the stability constants, $*K_n$ for the complex equilibria

$$MF_{n-1} + HF \rightleftharpoons MF_n + H^+$$

where $M = Zr^{4+}$ or Hf^{4+}. From the variation of the conditional constant, $*K_1^{calc}$, with the acidity of the solutions, the equilibrium constant, $*\gamma_1$, has been calculated for the reaction

$$M + H_2O \rightleftharpoons MOH + H^+$$

In the solvent extraction measurements, the distribution of the metal ions between xylene solutions of thenoyltrifluoroacetone and aqueous solutions containing various concentrations of perchloric acid has been studied.

All the measurements have been performed in a medium having a constant concentration of 4 M of perchlorate ions. The composition of the medium has been changed from 4 M $HClO_4$ to 0.5 M $HClO_4$ + 3.5 M $NaClO_4$. Th^{4+}, which is not hydrolysed in the hydrogen ion concentration range studied, has been used as a model ion for the determination of the activity changes caused by this variation of the medium. In the solvent extraction and in the potentiometric investigations, the temperature was 20°C and 25°C, respectively.

The limits of error given for the values of the constants calculated in the present paper correspond to 99 % confidence limits if not otherwise stated.

Four valent metal ions are known to be extensively hydrolysed in aqueous solution. Even in the most acid solutions some of them exist exclusively as yl-ions, *e.g.* TiO^{2+}, VO^{2+}. No simple hydrated ions with a charge of +4 are formed. For Zr(IV) and Hf(IV), it has long been discussed whether or not these too form yl-ions in solid salts and in aqueous solutions. Recently performed measurements of the infra-red spectra of hydrated and deuterated nitrates and chlorides of zirconium(IV)[1] show, however, no evidence of the existence of the zirconyl group (Zr=O) in these compounds. In aqueous solutions, zirconium(IV) and hafnium(IV) are both known to be involved in

complicated hydrolysis equilibria. The large amount of experimental results of the solution chemistry of these metal ions has been reviewed by Solovkin and Tsvetkova,[2] Caletka,[3] Hala [4] and recently by Larsen.[5] They concluded [2] that in aqueous solution there is no justification for the zirconyl theory. However, without doubt, both metal ions form, besides mononuclear species, also polynuclear hydrolysis products. Presumably, trimeric and tetrameric species of the type $M_3(OH)_4^{8+}$ and $M_4(OH)_8^{8+}$ are formed.[6-9] Even in rather acid solutions (2 M) the polynuclear species exist at low total metal ion concentrations (10^{-4} M).

For the mononuclear hydrolysis of Zr^{4+}, disparate values of the stability constants for the formation of the various hydroxo complexes have been reported in the literature.[10-12] Only one set of values of the corresponding stability constants for Hf^{4+} has been given.[13] Solvent extraction utilizing different organic acids as competing ligands is the only experimental method that has been used in Refs. 10 – 13. The values of the constants obtained in Ref. 10 for the hydrolysis of Zr^{4+} were calculated from the measurements of Connick and McVey.[14] With the exception of Ref. 14, the highest hydrogen ion concentration used was about 1 M. At this acidity only low concentrations of M^{4+} exist (17 % Zr^{4+}, 29 % Hf^{4+}). Hence, the calculated value of the first hydrolysis constant might be fairly uncertain. It therefore seems desirable to extend the study of the hydrolysis of Zr^{4+} and Hf^{4+} to more acid solutions and to try another method of investigation than the mentioned solvent extraction.

Since polynuclear hydrolysis products are formed, the experimental method chosen must give accurate results even at low total metal ion concentrations. Preferably a potentiometric method should be used, as such measurements are known to give results of high precision. However, due to the low metal ion concentrations (usually 10^{-4} M), direct measurements of the hydrogen ions set free in the hydrolysis reactions are not possible in strongly acid solutions. Obviously, the investigation has to be performed by means of some indirect method. Recently, a fluoride membrane (FME-)electrode was used by the present author to study the fluoride complexes of Th^{4+} and U^{4+}; *cf.* Ref. 15. This electrode was proved to be of great value for investigations of fluoride complex systems. From accurate determinations of the conditional equilibrium constant of

$$M^{4+} + HF \rightleftharpoons MF^{3+} + H^+$$

at different hydrogen ion concentrations, it is possible to obtain the hydrolysis constants of the metal ion in question, *vide infra* p. 1372. Hence, the fluoride complexes of Zr^{4+} and Hf^{4+} were investigated, using a fluoride membrane electrode, in 4.000 M $HClO_4$, 1.000 M $HClO_4$ + 3.000 M $NaClO_4$, and 0.500 M $HClO_4$ + 3.500 M $NaClO_4$. The composition of these ionic media varies considerably. Thus, it is likely that the values of the stability constants cannot be directly compared and that a correction for the change of the medium has to be applied. Th^{4+}, which is not hydrolysed [16,17] in the solutions investigated, was used as a model ion for a quantitative determination of this medium effect.

Some years ago, solvent extraction measurements were performed by the present author to elucidate the hydrolysis of Zr^{4+} and Hf^{4+}. The metal ions

were distributed between an acid aqueous phase and a xylene phase containing thenoyltrifluoroacetone as a competing ligand. The study was part of an investigation of the complexes formed by four valent cations with ligands of various donating properties. Values of the stability constants were collected at a temperature of 20°C. Thus, the solvent extraction experiments referred to were carried out at this temperature. The results, not yet published, are included in this paper for a comparison with the results of the potentiometric measurements performed at 25°C.

EXPERIMENTAL

Stock solutions were prepared and analysed in the same way as described in Refs. 15 and 18 – 20. These references should be consulted for experimental details of the procedure of the solvent extraction and potentiometric measurements.

To avoid errors in the emf measurements due to diffusion potentials between the reference half-cell and the FME half-cell, the composition of their solutions as well as that of the salt bridge was always the same except for the fairly small contents of metal ion and hydrofluoric acid in the FME half-cell.

SYMBOLS

$^*\gamma_m$ = $[M(OH)_m][H^+]^m/[M]$.
$^*\beta_n$ = $[MF_n][H^+]^n/[M][HF]^n$.
β_{nH} = $^*\beta_n/[H^+]^n$.
β_{nH}^{calc} = $\beta_{nH}/1 + \sum_{m=1}^{M} {}^*\gamma_m[H^+]^{-m}$.
$^*K_n$ = $[MF_n][H^+]/[MF_{n-1}][HF]$; $^*K_1 = {}^*\beta_1$.
$^*K_n^{calc}$ = $\beta_{nH}^{calc}\,[H^+]/\beta_{(n-1)H}^{calc}$; $^*K_1^{calc} = \beta_{1H}^{calc}\,[H^+]$.
HA = thenoyltrifluoroacetone.
[ ] = equilibrium concentration in the aqueous phase.
[ ]$_{org}$ = equilibrium concentration in the xylene phase.
C_{HA}' = initial total concentration of HA in the xylene phase.
K_a = $[H^+][A^-]/[HA]$.
K_{dHA} = $[HA]_{org}/[HA]$.
K_{dMA_4} = $[MA_4]_{org}/[MA_4]$.
β_n = $[MA_n]/[M][A^-]^n$.

CALCULATIONS AND RESULTS OF THE EMF MEASUREMENTS

According to Farrer and Rossotti,[21] F^-, HF and HF_2^- exist in hydrofluoric acid solutions. However, from the results reported one obtains for the hydrogen ion concentrations used in the present investigation that $[F^-] < 10^{-3}$ [HF] and $[HF_2^-] < 5 \times 10^{-5}$ [HF]. Thus, the concentrations of F^- and HF_2^- are negligible and can be excluded in the following derivations. If only mononuclear fluoride and hydroxo complexes are taken into consideration and mixed complexes containing these ligands are neglected, the total concentrations of hydrofluoric acid and metal ion can be written:

$$C_{HF} = [HF] + [M] \sum_{n=1}^{N} n\beta_{nH}[HF]^n \qquad (1)$$

$$C_M = [M]\left(1 + \sum_{m=1}^{M} {}^*\gamma_m [H^+]^{-m} + \sum_{n=1}^{N} \beta_{nH} [HF]^n\right) \quad (2)$$

Since the hydrogen ion concentration is kept constant in each titration series, $\bar{n} = (C_{HF} - [HF])/C_M$ is a function of [HF] only given by:

$$\bar{n} = \frac{\sum_{n=1}^{N} n\, \beta_{nH}{}^{calc} [HF]^n}{1 + \sum_{n=1}^{N} \beta_{nH}{}^{calc} [HF]^n} \quad (3)$$

The free ligand concentration, [HF], is obtained from the measured emf's, E_F, using:

$$E_F = E_C - RTF^{-1} \ln [HF] \quad (4)$$

A numerical method for calculation of stability constants described by Sandell in Ref. 22, p. 2611, is easily verified to be applicable here and is used for the calculations of $\beta_{nH}{}^{calc}$. From corresponding values of $\beta_{nH}{}^{calc}$ and $[H^+]$, the constants ${}^*K_n{}^{calc}$ are obtained. Of these constants, all except ${}^*K_1{}^{calc}$ are independent of the hydrogen ion concentration whether the investigated metal ions are hydrolysed or not. For ${}^*K_1{}^{calc}$, the following expression is valid:

$$\frac{1}{{}^*K_1{}^{calc}} = \frac{1}{{}^*K_1}\left(1 + \sum_{m=1}^{M} {}^*\gamma_m [H^+]^{-m}\right) \quad (5)$$

Evidently it is only for such metal ions which are not hydrolysed that ${}^*K_1{}^{calc}$ is a true constant. In the present investigation the stability constants have been determined in solutions with three different hydrogen ion concentrations. From the variation of ${}^*K_1{}^{calc}$ with $[H^+]$, after a correction for medium changes has been introduced for the calculations in ${}^*K_1{}^{calc}$, the hydrolysis constants, ${}^*\gamma_m$, were obtained graphically according to eqn. (5).

The thorium system. The experimentally obtained results are given in Table 1. Different total concentrations of Th^{4+} within the range $0.18\ mM \leq C_{Th} \leq 4.48\ mM$ were used. No variation of $\bar{n}$ with C_{Th} could be observed, confirming that only mononuclear complexes are formed. The maximum value of C_{HF} was about 10 mM, which is negligible compared to the total ionic strength of 4 M. The variation of the composition of the medium may therefore be neglected within the titration series having the same constant value of C_H. Using the numerical method of Sandell,[22] the following values for the constants were calculated:

$[H^+]$/M	$\beta_{1H}{}^{calc} \times 10^{-4}/M^{-1}$	$\beta_{2H}{}^{calc} \times 10^{-6}/M^{-2}$	$\beta_{3H}{}^{calc} \times 10^{-8}/M^{-3}$
4.000	1.043 ± 0.005	1.67 ± 0.06	0.4 ± 0.1
1.000	3.54 ± 0.02	17.6 ± 0.7	6 ± 5
0.500	6.53 ± 0.02	62 ± 1	32 ± 9

where the given errors are standard deviations. The constants determined for $C_H = 4.000$ M agree quite well with those earlier reported in Ref. 15, valid

Table 1. Corresponding values of C_{HF} mM and E_F mV obtained in the various titration series for thorium.

4.000 M $HClO_4$

$C_{Th} = 0.4482$ mM, $E_C = -24.6$ mV: 0.1430, 241.6; 0.2759, 219.8; 0.2759, 219.1; 0.5189, 193.6; 0.7316, 179.0; 0.9840, 167.0.
$C_{Th} = 1.810$ mM, $E_C = -23.7$ mV: 0.3557, 252.3; 0.4548, 244.4; 0.5429, 238.5; 0.6810, 230.9; 0.6948, 229.7; 0.8187, 223.4; 0.9560, 216.9; 1.022, 214.7; 2.011, 176.1; 3.276, 147.2; 4.483, 132.4; 5.634, 123.3; 7.817, 111.4.
$C_{Th} = 1.810$ mM, $E_C = -24.1$ mV: 1.391, 197.6; 1.999, 175.6; 2.591, 159.5; 3.554, 143.1; 3.739, 140.3; 4.837, 129.2; 5.889, 121.4; 8.603, 108.5.
$C_{Th} = 4.482$ mM, $E_C = -24.5$ mV: 0.4786, 268.9; 0.6932, 257.9; 1.056, 244.7; 1.345, 236.5; 1.582, 230.6; 1.844, 224.6; 3.885, 184.1; 2.573, 209.4; 3.872, 184.4; 5.109, 162.4; 6.287, 146.8; 7.410, 135.9; 9.538, 122.2.

1.000 M $HClO_4$ and 3.000 M $NaClO_4$

$C_{Th} = 0.8980$ mM, $E_C = -68.4$ mV: 0.1378, 245.4; 0.2687, 224.1; 0.3931, 209.8; 0.5116, 197.9; 0.6244, 187.1; 0.7321, 177.3; 0.8349, 168.3; 0.9333, 160.2; 1.027, 153.0; 1.117, 146.9; 1.204, 141.7.
$C_{Th} = 0.8980$ mM, $E_C = -70.4$ mV: 0.0992, 255.7; 0.1378, 245.1; 0.1947, 235.8; 0.2868, 222.2.
$C_{Th} = 0.8980$ mM, $E_C = -69.1$ mV: 0.0992, 255.1; 0.1378, 244.8; 0.1947, 235.0; 0.2868, 222.1; 0.3757, 212.0; 0.4615, 203.3; 0.5443, 195.3; 0.6243, 187.9; 0.7000, 180.9; 0.7748, 174,1; 0.8471, 167.9.
$C_{Th} = 0.8980$ mM, $E_C = -81.5$ mV: 0.9416, 147.0; 1.370, 120.9; 1.385, 120.3; 1.519, 114.5; 1.820, 104.7; 2.082, 98.3; 2.286, 94.0; 2.631, 88.0; 2.742, 86.3; 2.770, 85.8; 2.955, 83.2; 3.041, 82.2; 3.167, 80.5; 3.336, 78.6.
$C_{Th} = 1.796$ mM, $E_C = -68.2$ mV: 0.2353, 249.1; 0.4372, 229.8; 0.4660, 228.3; 0.6176, 217.7; 0.7797, 208.3; 1.058, 193.8; 1.290, 182.1; 1.486, 172.0; 1.654, 163.4.
$C_{Th} = 1.796$ mM, $E_C = -69.1$ mV: 0.7901, 208.6; 0.9305, 201.3; 1.091, 192.1; 1.324, 181.3; 1.705, 161.8; 2.073, 144.5; 2.428, 131.4.
$C_{Th} = 1.796$ mM, $E_C = -67.5$ mV: 0.3347, 239.9; 0.6156, 219.2; 0.8546, 206.0; 1.060, 195.3; 1.489, 173.6; 1.903, 152.6; 2.301, 136.2.

0.500 M $HClO_4$ and 3.500 M $NaClO_4$

$C_{Th} = 0.1796$ mM, $E_C = -84.7$ mV: 0.00923, 276.0; 0.01800, 258.7; 0.02632, 248.1, 0.03423, 240.4; 0.04177, 234.4; 0.05580, 225.1; 0.06861, 218.1; 0.09583, 205.1; 0.1219, 194.4; 0.1709, 177.1; 0.2161, 164.1; 0.2579, 154.8; 0.2968, 147.7; 0.3330, 142.3; 0.4103; 133.4; 0.5387, 122.8.
$C_{Th} = 0.3592$ mM, $E_C = -84.8$ mV: 0.03548, 258.0; 0.06914, 239.0; 0.1011, 226.8; 0.1315, 217.5; 0.1605, 209.8; 0.1881, 202.9; 0.2145, 196.7; 0.2637, 185.6; 0.3088, 176.0; 0.3503, 167.7; 0.3886, 160.5; 0.4240, 154.8; 0.4824, 146.3; 0.6115, 132.6; 0.8535, 116.4; 1.094, 106.2.
$C_{Th} = 0.5388$ mM, $E_C = -84.7$ mV: 0.05810, 255.3; 0.1114, 236.0; 0.1605, 223.8; 0.2058, 214.8; 0.2478, 207.0; 0.2868, 200.3; 0.3231, 194.3; 0.3571, 188.9; 0.3888, 183.9; 0.4465, 174.8; 0.4976, 167.0; 0.5433, 160.3; 0.6150, 150.8; 0.6750, 144.0; 1.338, 105.6; 1.667, 96.2.
$C_{Th} = 0.8980$ mM, $E_C = -84.1$ mV: 0.06986, 264.9; 0.1989, 234.2; 0.2588, 225.2; 0.3158, 218.1; 0.3702, 211.9; 0.4221, 206.2; 0.4718, 201.1; 0.5192, 196.3; 0.5647, 191.7; 0.6498, 183.2; 0.7283, 175.2; 0.8008, 167.9; 0.9200, 155.9; 1.025, 146.9; 1.118, 139.4.
$C_{Th} = 0.8980$ mM, $E_C = -84.4$ mV: 0.1021, 254.2; 0.1667, 239.8; 0.2282, 229.7; 0.2867, 221.8; 0.3954, 209.1; 0.4946, 198.9; 0.5854, 189.6; 0.6689, 181.1; 0.8050, 167.1; 0.9236, 155.2; 1.028, 145.9; 1.120, 138.8; 1.580, 115.0; 2.036, 100.9.
$C_{Th} = 0.8980$ mM, $E_C = -98.7$ mV: 0.7085, 163.4; 0.9241, 141.6; 1.118, 124.8; 1.293, 113.4; 1.452, 105.3; 1.555, 100.9; 1.597, 99.3; 1.730, 94.7; 1.852, 90.8; 1.964, 87.7; 2.069, 85.0; 2.165, 82.7; 2.223, 81.4; 2.255, 80.7; 2.339, 79.0; 2.477, 76.3.

in the same medium but at a temperature of 20.00°C. From corresponding values of $\beta_{n\mathrm{H}}^{\mathrm{calc}}$ and $[\mathrm{H}^+]$ one obtains:

$[\mathrm{H}^+]$/M	$*K_1^{\mathrm{calc}} \times 10^{-4}$	$*K_2^{\mathrm{calc}} \times 10^{-3}$
4.000	4.17 ± 0.05	6.4 ± 0.6
1.000	3.54 ± 0.06	5.0 ± 0.5
0.500	3.27 ± 0.03	4.7 ± 0.2

where $*K_3^{\mathrm{calc}}$ is omitted because of the large errors in the determined values of $\beta_{3\mathrm{H}}^{\mathrm{calc}}$. This will not influence the conclusions drawn regarding the hydrolysis of Zr^{4+} and Hf^{4+}.

For the reason given on p. 1372, it is expected that $*K_1^{\mathrm{calc}}$ and $*K_2^{\mathrm{calc}}$ will have the same value for the three hydrogen ion concentrations used. Obviously there is a significant difference between the results obtained in the media used. The most probable explanation of this fact is that the values of the activity coefficients of the species involved in the different equlibria are not the same in the various media. Hence, the following correction factors have to be applied to relate the results of the zirconium and hafnium measurements to 4 M $HClO_4$ as a reference medium.

Medium	f_1	f_2
1 M $HClO_4$ + 3 M $NaClO_4$	1.18 ± 0.02	1.3 ± 0.2
0.5 M $HClO_4$ + 3.5 M $NaClO_4$	1.28 ± 0.02	1.4 ± 0.1

f_1 and f_2 are calculated by dividing the value of $*K_n^{\mathrm{calc}}$ valid in 4 M $HClO_4$ with the value of the same constant obtained in the medium in question. Recently, the stability constants for the fluoride complexes of U^{4+} have been determined in 0.6 M $HClO_4$ and 3.4 M $NaClO_4$ at a temperature of 25°C by Grenthe and Varfeldt.[23] Using the values for these constants obtained in 4 M $HClO_4$ and 20°C [15] (no values at 25°C are available) f_1 and f_2 are calculated to be 1.5 and 1.8, respectively. Considering that the complex formation reactions probably are exothermic, the agreement with the results obtained in the present paper for Th^{4+} in almost the same medium is fairly good, thus supporting the method used for the medium corrections to Zr^{4+} and Hf^{4+}.

The zirconium system. To investigate whether polynuclear species were formed or not, titration series having different values of C_{Zr} were performed. For all the hydrogen ion concentrations used, $\bar{n}$ was found to be a function of both [HF] and C_{Zr}, showing polynuclear species to exist in the solutions. However, when [HF] or $[\mathrm{H}^+]$ increased, $\bar{n}$ became more and more independent of C_{Zr}. For low enough values of C_{Zr}, $\bar{n}$ could be obtained as a function of the free ligand concentration only. Therefore, efforts were made to keep C_{Zr} within a concentration range where $\bar{n}$ was unaffected by the metal ion concentrations used. This was not the case at the lowest values of [HF] where $\bar{n}$ varied with C_{Zr}. In such solutions, $\bar{n}$ was obtained by extrapolations to $C_{\mathrm{Zr}} = 0$. Since the computer program cannot use data series having $C_{\mathrm{M}} = 0$, corresponding values of E_{F} and C_{HF} valid for the extrapolated data were calculated from arbitrarily chosen values of C_{Zr} (within the metal concentration range used) and E_{C}. In the calculations of the stability constants, few extrapolated values were used. The values of the stability constants obtained were only slightly influenced by these.

Table 2. Corresponding values of $C_{HF} \times 10^5$ M and E_F mV obtained in the various titration series for zirconium.

4.000 M $HClO_4$

$C_{Zr} = 0.5000$ mM, $E_C = -25.0$ mV (extrapolated): 4.900, 347.8; 9.200, 330.3; 12.98, 319.5; 16.10, 312.2; 18.75, 306.4; 21.00, 301.7; 22.75, 297.8.
$C_{Zr} = 0.2420$ mM, $E_C = -23.8$ mV: 15.39, 283.1; 21.22, 262.8; 22.92, 257.0; 24.60, 251.3; 27.91, 241.2; 33.24, 227.8; 38.37, 217.7; 43.30, 209.8; 48.05, 203.4.
$C_{Zr} = 0.2420$ mM, $E_C = -24.6$ mV: 11.90, 295.1; 14.52, 285.7; 16.97, 277.1; 22.08, 259.3; 27.00, 243.5; 31.75, 230.7; 36.34, 220.9; 40.78, 213.1; 45.06, 206.9; 49.21, 201.7.
$C_{Zr} = 0.5035$ mM, $E_C = -24.9$ mV: 27.09, 290.5; 32.46, 281.0; 37.61, 271.9; 42.57, 262.9; 47.34, 254.3; 51.94, 246.1; 56.38, 238.6.
$C_{Zr} = 1.009$ mM, $E_C = -24.5$ mV: 51.55, 292.3; 72.86, 273.3; 91.67, 255.8; 177.3; 193.1; 243.3, 167.7.
$C_{Zr} = 2.523$ mM, $E_C = -25.7$ mV: 152.3, 281.8; 192.9, 267.0; 230.1, 252.6; 264.3, 239.1; 295.8, 227.2; 324.8, 217.4; 351.8, 209.0.
$C_{Zr} = 5.045$ mM, $E_C = -25.1$ mV: 297.5, 283.0; 344.3, 274.9; 408.3, 263.0; 461.6, 256.6; 575.1, 230.3; 684.9, 211.3.

1.000 M $HClO_4$ and 3.000 M $NaClO_4$

$C_{Zr} = 0.1000$ mM, $E_C = -66.0$ mV (extrapolated): 2.850, 302.1; 3.206, 298.1; 3.520, 294.7; 3.834, 291.7; 4.120, 289.0; 4.345, 286.5; 4.620, 284.3.
$C_{Zr} = 0.1009$ mM, $E_C = -67.5$ mV: 5.187, 276.9; 6.088, 269.5; 6.747, 263.9; 7.179, 260.6; 8.233, 251.8; 8.233, 252.1; 9.252, 243.9; 10.24, 236.2; 11.19, 229.1; 12.11, 222.9; 13.01, 217.5.
$C_{Zr} = 0.1017$ mM, $E_C = -66.2$ mV: 5.562, 276.8; 6.049, 273.0; 7.108, 264.5; 8.119, 256.4; 9.084, 248.6; 10.01, 241.4; 10.89, 234.6; 11.74, 228.6; 12.55, 223.2; 14.77, 210.6; 16.90, 200.9; 18.95, 193.2.
$C_{Zr} = 0.1017$ mM, $E_C = -66.0$ mV: 5.020, 280.3; 6.130, 271.0; 7.180, 262.5; 8.190, 254.3; 10.07, 239.4; 11.79, 226.8; 13.38, 216.7; 14.84, 208.8.
$C_{Zr} = 0.2518$ mM, $E_C = -66.0$ mV: 13.22, 276.2; 15.81, 267.7; 18.28, 259.4; 20.64, 251.3; 24.59, 237.7; 26.68, 230.3; 31.01, 216.6; 35.16, 204.9.
$C_{Zr} = 0.2518$ mM, $E_C = -65.9$ mV: 12.07, 280.3; 17.66, 261.7; 22.97, 243. 4; 25.35, 235.1; 27.63, 227.2; 29.80, 220.3; 34.37, 207.3; 38.74, 196.7; 42.93, 187.8.
$C_{Zr} = 0.5035$ mM, $E_C = -66.9$ mV: 37.45, 255.1; 41.85, 247.8; 46.06, 240.8; 53.93, 226.9; 61.18, 214.9; 67.87, 204.8; 74.06, 196.2.
$C_{Zr} = 1.009$ mM, $E_C = -67.5$ mV: 92.81, 237.3.
$C_{Zr} = 2.523$ mM, $E_C = -66.6$ mV: 256.8, 226.2.

0.500 M $HClO_4$ and 3.500 M $NaClO_4$

$C_{Zr} = 0.02500$ mM, $E_C = -85.0$ mV (extrapolated): 1.155, 279.1; 1.296, 274.1.
$C_{Zr} = 0.02523$ mM, $E_C = -84.4$ mV: 1.482, 268.7; 1.980, 253.9; 2.434, 241.5; 2.851, 231.3; 3.234, 223.4; 3.588, 217.2; 4.168, 208.7; 5.514, 193.7; 6.769, 184.0.
$C_{Zr} = 0.05045$ mM, $E_C = -84.5$ mV: 2.891, 267.8; 3.764, 254.3; 4.599, 241.4; 5.400, 229.7; 6.167, 219.8; 6.905, 211.3; 7.613, 204.7; 8.294, 199.0; 9.577, 189.7.
$C_{Zr} = 0.05045$ mM, $E_C = -83.0$ mV: 3.077, 265.0; 3.956, 251.6; 4.797, 238.7; 5.603, 227.0; 6.375, 217.2; 7.117, 209.2; 8.510, 196.9.
$C_{Zr} = 0.1017$ mM, $E_C = -84.7$ mV: 5.607, 266.0; 7.195, 254.3; 8.655, 243.7; 11.03, 225.4; 12.20, 217.1; 14.12, 204.7; 18.75, 182.4.
$C_{Zr} = 0.1017$ mM, $E_C = -84.3$ mV: 4.576, 274.1; 6.282, 261.1; 7.842, 250.0; 9.276, 239.3; 10.46, 230.3; 11.56, 222.1; 12.13, 218.1; 13.56, 208.7; 17.18, 189.5.
$C_{Zr} = 0.2518$ mM, $E_C = -84.3$ mV: 25.10, 228.0; 26.72, 223.1; 28.27, 218.5.
$C_{Zr} = 0.2518$ mM, $E_C = -84.1$ mV: 22.31, 237.1; 31.20, 210.2; 39.74, 187.1.

The results obtained in the various titration series are collected in Table 2. For all the given values (except those pointed out as extrapolated), having the same [HF], the variation of $\bar{n}$ with C_{Zr} was within a random experimental error of ± 2 %. The following values were obtained for the constants β_{nH}^{calc}:

$[H^+]$/M	$\beta_{1H}^{calc} \times 10^{-5}/M^{-1}$	$\beta_{2H}^{calc} \times 10^{-9}/M^{-2}$	$\beta_{3H}^{calc} \times 10^{-11}/M^{-3}$
4.000	2.20 ± 0.02	1.15 ± 0.02	2.6 ± 0.6
1.000	6.24 ± 0.06	11.8 ± 0.2	140 ± 50
0.500	9.46 ± 0.16	33 ± 1	600 ± 260

The errors quoted are standard deviations. The values valid in 4 M $HClO_4$ are in accordance with those given in Refs. 19, 20, and 24. The values of $*K_n^{calc}$ $(1 \leq n \leq 2)$ calculated using the medium correction factors obtained in the thorium measurements are as follows:

$[H^+]$/M	$*K_1^{calc} \times 10^{-5}$	$*K_2^{calc} \times 10^{-4}$
4.000	8.8 ± 0.2	2.1 ± 0.1
1.000	7.4 ± 0.2	2.5 ± 0.4
0.500	6.1 ± 0.3	2.5 ± 0.3

Evidently there is still a significant decrease (the limits of error correspond to a confidence limit of 99 %) of $*K_1^{calc}$ as the hydrogen ion concentration decreases. It may therefore be concluded that Zr^{4+} is hydrolysed even in these fairly acid solutions.

Fig. 1 shows $(*K_1^{calc})^{-1}$ as a function of $[H^+]^{-1}$. A straight line can be drawn through the points indicating that predominantly the first hydroxo complex is formed. Using eqn. (5), the value of the stability constant, $*\gamma_1$, is calculated to be 0.28, with graphically estimated maximum limits of error of ± 0.05, As predicted, $*K_2^{calc}$ is independent of the hydrogen ion concentration. Furthermore, almost the same value is found as previously determined from results obtained using other methods of investigation.[19,20] As an average value of $*K_1$ for the equilibrium $Zr^{4+} + HF \rightleftharpoons ZrF^{3+} + H^+$ one obtains 9.4×10^5 (valid in a reference medium of 4 M $HClO_4$) using $*\gamma_1 = 0.28$. The three different media give values within a fairly small interval ($\pm 0.05 \times 10^5$).

The hafnium system. For hafnium as well, $\bar{n}$ was found to depend both on [HF] and C_{Hf}. However, the variation of $\bar{n}$ values corresponding to the same free ligand concentration with C_{Hf} was smaller than the C_M variation in the zirconium system. As for zirconium, titration series having quite low metal ion concentrations were performed in order to prevent formation of polynuclear complexes. The results given in Table 3 are from measurements made in solutions which meet this condition. Only a few values had to be obtained from extrapolations to $C_M = 0$. From the numerical calculation method the following stability constants were determined:

$[H^+]$/M	$\beta_{1H}^{calc} \times 10^{-5}/M^{-1}$	$\beta_{2H}^{calc} \times 10^{-8}/M^{-2}$	$\beta_{3H}^{calc} \times 10^{-11}/M^{-3}$
4.000	0.778 ± 0.003	2.06 ± 0.04	0.4 ± 0.2
1.000	2.43 ± 0.06	19.0 ± 0.9	19 ± 6
0.500	4.30 ± 0.05	61 ± 2	170 ± 30

Table 3. Corresponding values of $C_{HF} \times 10^4$ M and E_F mV obtained in the various titration series for hafnium.

4.000 M $HClO_4$

$C_{Hf} = 0.6152$ mM, $E_C = -24.4$ mV: 0.6489, 320.0; 0.9386, 310.2; 1.208, 302.4; 1.696, 292.5; 1.696, 291.6; 2.577, 276.5; 3.405, 264.5; 5.108, 242.3; 6.756, 222.6; 7.415, 215.7; 8.955, 202.1; 10.45, 191.8.
$C_{Hf} = 1.538$ mM, $E_C = -25.1$ mV: 1.649, 319.0; 2.228, 310.5; 2.407, 308.5; 2.783, 303.9; 3.732, 294,7; 4.455, 289.6; 4.616, 287.6; 5.443, 281.7; 7.242, 270.2; 8.978, 260.3; 10.65, 251.0; 12.27, 242.1; 13.84, 233.5; 15.35, 225.3; 16.82, 217.7; 18.24, 210.8.
$C_{Hf} = 1.538$ mM, $E_C = -23.8$ mV: 1.223, 327.7; 2.146, 312.0; 2.922, 304.2; 5.977, 278.4; 8.837, 261.2; 9.564, 257.2; 11.11, 248,6; 12.93, 238.7; 13.28, 236.8; 15.37, 225.4.
$C_{Hf} = 3.076$ mM, $E_C = -24.8$ mV: 3.668, 316.0; 4.643, 309.0; 6.232, 300.2; 8.766, 289.8; 10.03, 284.2; 13.58, 272.5; 16.90, 262.7; 20.02, 253.8; 22.95, 245.5; 25.72, 237.7; 28.33, 230.3; 30.79, 223.3; 33.13, 216.9; 35.34, 211.0; 37.45, 205.8; 40.99, 197.5.

1.000 M $HClO_4$ and 3.000 M $NaClO_4$

$C_{Hf} = 0.5000$ mM, $E_C = -66.0$ mV (extrapolated): 0.5750, 306.8; 1.065, 289.0; 1.493; 278.5; 1.850, 271.2; 2.113, 265.4; 2.355, 263.7; 2.572, 256.8; 2.760, 253.3; 2.970, 250.3; 3.100, 247.6.
$C_{Hf} = 0.4614$ mM, $E_C = -67.6$ mV: 2.787, 240.9; 3.193, 233.7; 3.882, 221.3; 4.519, 209.9.
$C_{Hf} = 0.4614$ mM, $E_C = -67.3$ mV: 2.866, 239.6; 3.269, 233.0; 3.654, 226.2; 4.023, 219.4; 4.650, 208.2; 5.231, 198.4; 5.773, 190.1; 6.278, 183.0; 6.750, 177.1; 7.192, 172.0; 7.607, 167.6.
$C_{Hf} = 0.4614$ mM, $E_C = -66.4$ mV: 2.802, 246.1; 3.284, 237.3; 3.744, 229.0; 4.184, 221.1; 4.604, 213.6; 5.007, 206.8; 5.762, 195.0; 6.457, 185.6; 7.101, 177.8.
$C_{Hf} = 0.4614$ mM, $E_C = -66.6$ mV: 3.036, 241.8; 3.507, 233.3; 3.957, 225.1; 4.388, 217.5; 4.800, 210.4; 5.571, 198.2; 6.281, 188.3; 6.938, 180.2; 7.546, 173.4.
$C_{Hf} = 0.9228$ mM, $E_C = -67.3$ mV: 5.782, 242.2; 6.287, 237.9; 6.758, 233.7; 8.216, 220.4; 9.586, 208.1; 10.87, 197.1; 12.09, 187.8; 13.23, 179.7.
$C_{Hf} = 0.9228$ mM, $E_C = -66.9$ mV: 5.566, 243.9; 7.240, 229.1; 8.834, 209.5; 10.35, 200.8; 11.80, 188.8; 13.19, 178.8; 14.51, 170.2; 15.78, 162.8.
$C_{Hf} = 2.307$ mM, $E_C = -67.5$ mV: 20.35, 218.9; 22.38, 212.0; 24.26, 205.4; 26.01, 199.3; 27.64, 193.7; 31.56, 181.0; 35.36, 170.0.
$C_{Hf} = 4.614$ mM, $E_C = -66.9$ mV: 46.72, 205.9; 51.41, 198.5; 55.91, 191.2; 60.22, 184.2; 64.35, 177.8; 72.12, 166.2.

0.500 M $HClO_4$ and 3.500 M $NaClO_4$

$C_{Hf} = 0.03000$ mM, $E_C = -85.0$ mV (extrapolated): 0.05960, 287.8; 0.08243, 277.3; 0.1033, 270.0; 0.1224, 264.2; 0.1392, 259.5; 0.1535, 255.6; 0.1652, 252.2.
$C_{Hf} = 0.03076$ mM, $E_C = -84.7$ mV: 0.1978, 247.2; 0.2433, 237.3; 0.3167, 223.6; 0.3802, 213.8; 0.4355, 206.6.
$C_{Hf} = 0.03076$ mM, $E_C = -84.8$ mV: 0.2032, 244.0; 0.2224, 239.8; 0.2697, 230.1; 0.3490, 216.3; 0.4253, 205.9; 0.5563, 192.6; 0.7294, 180.5; 1.027, 166.8.
$C_{Hf} = 0.06200$ mM, $E_C = -82.8$ mV: 0.3439, 250.7; 0.3989, 243.7; 0.4476, 237.8; 0.4910, 232.6; 0.5591, 224.9; 0.6159, 218.9; 0.6640, 214.1; 0.8105, 201.3; 0.9456, 191.8.
$C_{Hf} = 0.06200$ mM, $E_C = -83.8$ mV: 0.3589, 247.6; 0.4515, 236.2; 0.5265, 227.4; 0.5886, 220.7; 0.7566, 204.8; 0.9101, 193.4; 1.051, 185.1; 1.279, 174.5.
$C_{Hf} = 0.1538$ mM, $E_C = -82.4$ mV: 0.8407, 249.2; 1.011, 240.4; 1.162, 232.8; 1.394, 221.2; 1.584, 212.0; 1.743, 204.8; 1.877, 199.1; 1.993, 194.5; 2.050, 192.4.
$C_{Hf} = 0.4614$ mM, $E_C = -84.0$ mV: 3.887, 220.8; 4.464, 211.7; 4.975, 203.2; 5.772, 190.3; 6.788, 176.2; 7.709, 165.0.
$C_{Hf} = 1.538$ mM, $E_C = -84.6$ mV: 16.19, 199.7; 23.42, 169.0.

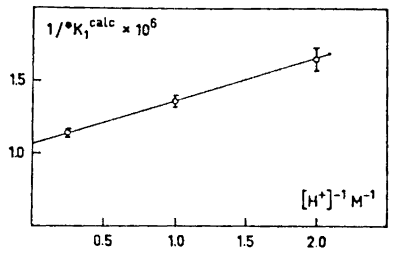

Fig. 1. The variation of $1/{}^*K_1^{calc}$ with $1/[H^+]$ for zirconium(IV). The straight line has been calculated from the values ${}^*K_1 = 9.43 \times 10^5$ and ${}^*\gamma_1 = 0.28$ M.

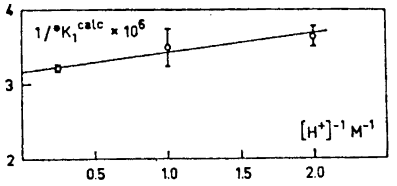

Fig. 2. The variation of $1/{}^*K_1^{calc}$ with $1/[H^+]$ for hafnium(IV). The straight line has been calculated from the values ${}^*K_1 = 3.15 \times 10^5$ and ${}^*\gamma_1 = 0.08$ M.

The errors given for the constants are standard deviations. In Refs. 18 and 25, the fluoride complexes of hafnium were investigated by means of quite different methods. The measurements were performed (particularly in the solvent extraction experiments) with very low hafnium ion concentrations (10^{-6} M). The values of the stability constants agree very well with those obtained in the present investigation. Hence it may be concluded that no systematic errors emerge from formation of polynuclear species in the present measurements.

By application of the correction factors f_1 and f_2 on the values of the stability constants obtained, the following values of ${}^*K_1^{calc}$ and ${}^*K_2^{calc}$ are calculated:

$[H^+]$/M	${}^*K_1^{calc} \times 10^{-5}$	${}^*K_2^{calc} \times 10^{-4}$
4.000	3.11 ± 0.03	1.06 ± 0.06
1.000	2.9 ± 0.2	1.0 ± 0.2
0.500	2.8 ± 0.1	1.0 ± 0.1

The values of ${}^*K_1^{calc}$ indicate that Hf^{4+} is only slightly hydrolysed in the solutions investigated. As for Zr^{4+}, the results indicate that only the first hydroxo complex is formed, *cf.* Fig. 2. ${}^*\gamma_1 = 0.08 \pm 0.03$ is graphically obtained from Fig. 2 giving a value of the stability constant, ${}^*K_1$, equal to 3.2×10^5. The concordant values of ${}^*K_2^{calc}$ justify the applied medium corrections.

CALCULATIONS AND RESULTS OF THE SOLVENT EXTRACTION MEASUREMENTS

The calculation of the hydrolysis constants is based upon the assumption that MA_4 is the only metal containing species in the xylene phase. If, moreover, the formation of mixed complexes in the aqueous phase between M, A, and OH is neglected, the following expressions are valid for the total concentrations of the metal ion in the two different phases:

$$C_{MO} = [MA_4]_{org} \tag{6}$$

$$C_M = [M]\left(1 + \sum_{m=1}^{M} {}^*\gamma_m [H^+]^{-m} + \sum_{n=1}^{N} \beta_n [A]^n\right) \tag{7}$$

In Ref. 18 it is shown that under the present conditions,

$$[HA]_{org} = k\, C_{HA}' \tag{8}$$

where k is a constant (≈ 1). Thus it follows that the distribution ratio, q, can be expressed as:

$$q = \frac{K_{dMA_4}\, \beta_4\, (k\, K_a/K_{dHA})^4\, (C_{HA}')^4}{[H^+]^4 \left\{1 + \sum_{m=1}^{M} {}^*\gamma_m [H^+]^{-m} + \sum_{n=1}^{N} \beta_n (k\, K_a\, C_{HA}'/K_{dHA}[H^+])^n\right\}} \tag{9}$$

Previously it was found for Zr(IV) [20] and Hf(IV) [18] that at a constant hydrogen ion concentration of 4.00 M:

$$q = \text{const.}\ (C_{HA}')^4 \tag{10}$$

The same result is also found for Th(IV) in the present investigation; *cf.* Fig. 3. (In these calculations, f_{HA}, the activity factor of HA in the xylene phase, is used to correct for the activity variation of HA and MA_4 in the xylene phase; *cf.* Ref. 18.) It may therefore be concluded that the last term in the denominator of eqn. (9) is negligible, *i.e.* within the experimental errors no formation of complexes between M and A in the aqueous phase could be detected at a hydrogen ion concentration of 4.00 M. If this is true in the entire hydrogen ion concentration range investigated ($1.50\ M \leq [H^+] \leq 4.00\ M$), eqn. (9) could be transformed to

$$Q([H^+]) \equiv \frac{1}{q\,[H^+]^4} = \frac{1}{K} + \sum_{m=1}^{M} \frac{{}^*\gamma_m}{K} [H^+]^{-m} \tag{11}$$

where K is constant as long as C_{HA}' is the same in all the measurements. From corresponding values of q and $[H^+]$ the hydrolysis constants are obtained by plotting $Q([H^+])$ as a function of $[H^+]^{-1}$, using graphical extrapolation methods.

Table 4. Corresponding values of $[H^+]$ and q obtained in the distribution measurements made for thorium. $Q([H^+])$ corrected to a 4 M $HClO_4$ reference medium using eqn. (12) on p. 1380, is given in the fourth column.

$[H^+]$ / M	q	$Q([H^+]) \times 10^2$ / M^{-4}	$Q([H^+])\ F([H^+]) \times 10^2$ / M^{-4}
1.540	4.962	3.583	2.69
1.794	2.779	3.474	2.69
2.107	1.522	3.334	2.68
2.310	1.066	3.295	2.72
2.490	0.8117	3.205	2.70
2.724	0.5870	3.094	2.67
2.958	0.4175	3.129	2.78
3.264	0.2996	2.941	2.70
3.570	0.2162	2.848	2.70
4.000	0.1439	2.698	2.67

The thorium system. Table 4 shows the results obtained for the thorium system. The measurements were performed at a constant concentration of $C_{HA}' = 1.485$ M. The hydrogen ion concentration varied from 1.540 M to 4.000 M. Within this acidity range the hydrolysis of Th^{4+} could be completely neglected.[16,17] Thus, one should expect $Q([H^+])$ to be independent of $[H^+]$. As Table 4 shows, this is not true. Probably, the activity coefficients of the

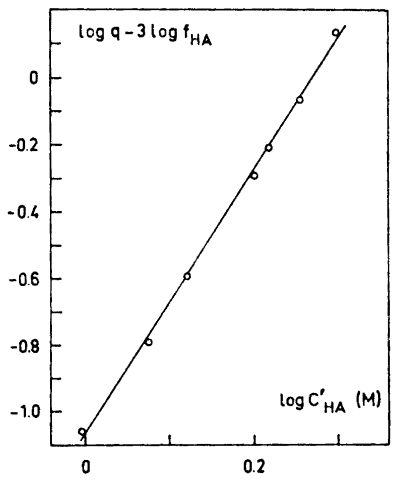

Fig. 3. $\log q - 3 \log f_{HA}$ as a function of $\log C_{HA}'$ for thorium. $C_{Th} = 4 \times 10^{-5}$ M. Aqueous phase 4.00 M $HClO_4$. The straight line drawn has a slope of 3.95.

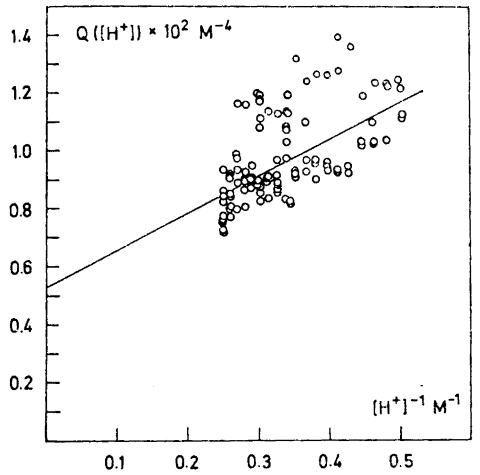

Fig. 4. $Q([H^+])$ as a function of $[H^+]^{-1}$ for zirconium. $C_{HA}' = 18.2$ mM; $C_{Zr} = 5 \times 10^{-6}$ M. The line was calculated using the constants $K^{-1} = 5.24 \times 10^{-3}$ M^{-4} and ${}^*\gamma_1 K^{-1} = 1.27 \times 10^{-2}$ M^{-3}.

species involved in the different equilibria are influenced by the medium change taking place in going from pure 4 M $HClO_4$ to a solution of 1.5 M $HClO_4$ and 2.5 M $NaClO_4$. If all the activity coefficients in question are collected in a common function, $F([H^+])$, an exact thermodynamic derivation gives $Q([H^+])\ F([H^+])$ to be a constant. Thus, by chosing 4 M $HClO_4$ as reference medium, $F([H^+])$ can be calculated from $Q(4)/Q([H^+])$. From the results given in Table 4, $F([H^+])$ was found to increase linearly with $[H^+]$ according to the following relationship:

$$F([H^+]) = 0.60 + 0.097\ [H^+] \qquad (12)$$

The zirconium and hafnium systems. The chemical properties of Zr^{4+} and Hf^{4+} are in many respects similar to Th^{4+}. Therefore, it seems reasonable to assume that the distribution of Zr^{4+} and Hf^{4+} is influenced by the medium changes to the same extent as Th^{4+}. Accordingly, the distribution ratios obtained for Zr^{4+} and Hf^{4+} are corrected to a 4 M $HClO_4$ reference medium by the use of $F([H^+])$ calculated from eqn. (12). The values of $Q([H^+])$ so obtained are given in Figs. 4 and 5 for Zr^{4+} and Hf^{4+}, respectively.

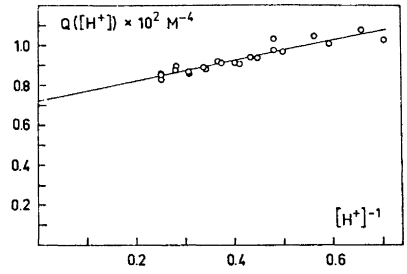

Fig. 5. $Q([H^+])$ as a function of $[H^+]^{-1}$ for hafnium. $C_{HA}' = 39.6$ mM; $C_{Hf} = 3 \times 10^{-5}$ M. The line was calculated using the constants $K^{-1} = 7.25 \times 10^{-3}$ M^{-4} and $^*\gamma_1 K^{-1} = 4.97 \times 10^{-3}$ M^{-3}.

To avoid errors due to incomplete separation of the two phases, such values of C_{HA}' were chosen as to give distribution ratios within the range $0.1 < q < 10$. For hafnium as well as for thorium the q values could be determined with random errors of about 3 %. This is of a magnitude which is usually found in distribution experiments. However, the distribution ratios for zirconium were obtained with unexpectedly large random errors. Different preparations of zirconium stock solutions and of sodium perchlorate were used to find out the reason for this. Unfortunately, the cause of this poor reproducibility could not be traced. It may be due to some unknown impurity present in the chemicals used or introduced during the measurements. Another possibility is the formation of polynuclear hydroxo compounds in the preparation of the zirconium stock solutions. Polynuclear species of this type are notorious for their slow reactions. Hence, no definite conclusions may be drawn from the results obtained in the zirconium measurements.

According to eqn. (11), $Q([H^+])$ as a function of $[H^+]^{-1}$ will give a straight line if a metal ion forms only the first hydroxo complex. Within the experimental random errors, $Q([H^+])$ for both zirconium and hafnium can be described having such a linear relationship to $[H^+]^{-1}$. The best lines fitting the data are drawn in Figs. 4 and 5. These lines were calculated using the principle of least squares. From these results, the following stability constants were obtained for the formation of the first hydroxo complexes:

$$Zr^{4+} \quad ^*\gamma_1 = 2 \pm 1 \quad (M)$$
$$Hf^{4+} \quad ^*\gamma_1 = 0.7 \pm 0.2 \quad (M)$$

DISCUSSION

The values of the stability constants, computed from the results of the present investigation, for the formation of the first hydroxo complex of Zr^{4+}

Table 5. Calculated values of $^*\gamma_1/M$ obtained from the two different methods used.

Method	Temp. °C	Zr^{4+}	Hf^{4+}
Solvent extraction	20.00	2 ± 1	0.7 ± 0.2
FME-electrode	25.00	0.28 ± 0.05	0.08 ± 0.03

and Hf^{4+} are given in Table 5. At both temperatures zirconium(IV) is more strongly hydrolysed than hafnium(IV). This fact is in accordance with the theoretical prediction made from the values of the ionic radius of the two ions and also with the experimental results earlier found. The results of the two methods can be compared since the difference in the temperatures is fairly small. There is such a large difference between the values of the hydrolysis constant for both metal ions that a systematic error must be present in one of the investigations.

The calculations of the hydrolysis constant from the solvent extraction measurements are based upon the assumption that complexes between the metal ion and the anion of thenoyltrifluoroacetone are absent in the aqueous phase (a fact proved by the fourth power dependence of the distribution ratio on the concentration of thenoyltrifluoroacetone). These measurements were performed at only one acidity (4 M $HClO_4$). In the aqueous phase the concentration of the anion of thenoyltrifluoroacetone increases when the hydrogen ion concentration decreases. Thus, an appreciable complex formation might occur at lower acidities. To make sure that this is not the case, measurements of the dependence of the distribution ratio on the concentration of thenoyltrifluoroacetone have to be performed also at the lowest hydrogen ion concentrations used. It is evident from eqn. (9) that only maximum values of the hydrolysis constants are obtained from the solvent extraction measurements.

The calculations of the various equilibrium constants from the fluoride membrane measurements require fewer assumptions than from the solvent extraction measurements. Furthermore, the emf results are obtained with a high degree of accuracy. Hence, the values of the first hydrolysis constant for Zr^{4+} and Hf^{4+} obtained from the present potentiometric measurements are considered as the most reliable, as can be seen in Table 6 where values of

Table 6. $^*K_1 \times 10^{-5}$ of the zirconium(IV) and hafnium(IV) fluoride systems computed from the potentiometric results of this work and from values of the hydrolysis constants previously published.

	Temp °C	Medium, I/M and inert salt	$[H^+]$/M 4.000	1.000	0.500
Zr^{4+}					
This work	25	4(Na,H)ClO_4	9.4	9.4	9.4
Refs. 10/14	25	2(Li,H)ClO_4	10	13	17
Ref. 11	25	1(Na,H)ClO_4	15	44	134
Hf^{4+}					
This work	25	4(Na,H)ClO_4	3.2	3.1	3.2
Ref. 13	25	1(Na,H)ClO_4	4	10	29

$^*K_1$ are calculated using previously determined hydrolysis constants. The comparison is complicated by the fact that the different investigations were not performed in the same medium. However, when the values given in Refs.

11 and 13 are used, the variation of $*K_1$ with the hydrogen ion concentration is so pronounced that these values of the hydrolysis constants must be too high. Recently, Nazarenko and Mandzhgaladze,[26] using a spectrophotometric method, obtained results of the hydrolysis of zirconium(IV) in conformity with those of Ref, 11. However, the results of Ref. 26 are no independent confirmation of the results of Ref. 11. Their calculations assume that $Zr(OH)_2(HL)_2^{2-}$ (H_3L = 3,4-dihydroxyazobenzene-4′-sulphonic acid) or $Zr(OH)_2(H_3K)_2$ (H_4K = 9-*o*-hydroxyphenyl-2,3,7-trihydroxy-6-fluorone) are the light absorbing species in the solutions investigated. To prove this, Nazarenko and Mandzhgaladze [27] have to rely on the hydrolysis constants determined in Ref. 11. Consequently, concordant results should be obtained provided that the reproducibility of the spectrophotometric measurements is good enough.

An objection to the results of the present potentiometric measurements might be that mixed complexes are neglected in the calculations. Since the acid dissociation constant is very much larger for hydrofluoric acid than for water, it is much easier to split off a proton from HF than from H_2O. Thus, despite the larger concentration of H_2O than of HF, the concentrations of mixed complexes are probably much smaller than those of the pure fluoride complexes.

Finally, it may be concluded from the results of the present potentiometric measurements that within the acidity range $0.5 \leq [H^+] \leq 4$ M both zirconium(IV) and hafnium(IV) form only one hydroxo complex, presumably MOH^{3+}. At these hydrogen ion concentrations the predominant species are Zr^{4+} and Hf^{4+}, respectively. The hydrolysis of these ions is not at all so extensive as previously believed. If corrections are made for the hydrolysis, the value of the stability constant, $*K_1$, for the formation of the first fluoride complex is calculated to be 9.4×10^5 for zirconium(IV) and 3.2×10^5 for hafnium(IV). Hydroxide and fluoride ions are considered to be bonded to zirconium(IV) and hafnium(IV) mainly by electrostatic forces. Thus one should expect the ratio between $*K_1$(Zr) and $*K_1$(Hf) to be the same as that between $*\gamma_1$(Zr) and $*\gamma_1$(Hf). Almost the same ratios (≈ 3) are obtained using the values of the present investigation, while $*\gamma_1(Zr)/*\gamma_1(Hf)$ from Refs. 11 and 13 is found to be 1.6, which supports the conclusions drawn in the present work. These are further supported by the fact that the predicted independence of $*K_2$ (after the plausible correction for the medium changes) with the hydrogen ion concentration is confirmed both for Zr(IV) and Hf(IV).

Acknowledgements. My sincere thanks are due to Professor Sture Fronæus and Dr. Ingmar Grenthe for valuable discussions and comments during the course of this work. I also thank Dr. Arvid Sandell for his help with the computer calculations and Dr. Peter Sellers for the linguistic corrections of the manuscript.

REFERENCES

1. Hardy, C. J., Field, B. O. and Scargill, D. *J. Inorg. Nucl. Chem.* **28** (1966) 2408.
2. Solovkin, A. S. and Tsvetkova, S. V. *Russ. Chem. Rev. (English Transl.)* **31** (1962) 655.
3. Caletka, R. *Chem. Listy* **58** (1964) 349.
4. Hala, J. *U.S. At. Energy Comm., Accession No. 35508 Rept. No. UJV – 1066/64.*

5. Larsen, E. M. *Advan. Inorg. Chem. Radiochem.* **13** (1970) 1.
6. Zielen, A. J. and Connick, R. E. *J. Am. Chem. Soc.* **78** (1956) 5785.
7. Johnson, J. S. and Kraus, K. A. *J. Am. Chem. Soc.* **78** (1956) 3937.
8. Castor, W. S., Jr. and Basalo, F. *J. Am. Chem. Soc.* **75** (1953) 4804.
9. Muha, G. and Vaughan, P. *J. Chem. Phys.* **33** (1960) 194.
10. Solovkin, A. S. *Russ. J. Inorg. Chem. (English Transl.)* **2** (1957) 216.
11. Peshkova, V. M., Mel'chakova, N. V. and Zhemchuzhin, S. G. *Russ. J. Inorg. Chem. (English Transl.)* **6** (1961) 630.
12. Solovkin, A. S. and Ivantsov, A. I. *Russ. J. Inorg. Chem. (English Transl.)* **11** (1966) 1013.
13. Peshkova, V. M. and P'eng Ang. *Russ. J. Inorg. Chem. (English Transl.)* **7** (1962) 1091.
14. Connick, R. E. and McVey, W. H. *J. Am. Chem. Soc.* **71** (1949) 3182.
15. Norén, B. *Acta Chem. Scand.* **23** (1969) 931.
16. Baes, C. F., Jr., Meyer, N. J. and Roberts, C. E. *Inorg. Chem.* **4** (1965) 518.
17. Hietanen, S. and Sillén, L. G. *Acta Chem. Scand.* **22** (1968) 265.
18. Norén, B. *Acta Chem. Scand.* **21** (1967) 2435.
19. Norén, B. *Acta Chem. Scand.* **21** (1967) 2457.
20. Norén, B. *Acta Chem. Scand.* **23** (1969) 379.
21. Farrer, H. N. and Rossotti, F. J. C. *J. Inorg. Nucl. Chem.* **26** (1964) 1959.
22. Sandell, A. *Acta Chem. Scand.* **25** (1971) 2609.
23. Grenthe, I. and Varfeldt, J. *Acta Chem. Scand.* **23** (1969) 988.
24. Ahrland, S., Karipides, D. and Norén, B. *Acta Chem. Scand.* **17** (1963) 411.
25. Norén, B. *Acta Chem. Scand.* **21** (1967) 2449.
26. Nazarenko, V. A. and Mandzhgaladze, O. V. *Russ. J. Inorg. Chem. (English Transl.)* **14** (1969) 639.
27. Nazarenko, V. A. and Mandzhgaladze, O. V. *Russ. J. Inorg. Chem. (English Transl.)* **13** (1968) 396.

Received November 6, 1972.

ACTA CHEMICA SCANDINAVICA 27 (1973) 1385–1389

Pyrylium Salts

I. Studies of 2,6-Dimethoxycarbonyl Derivatives

KJELL UNDHEIM and EILIF TERJE ØSTENSEN*

Department of Chemistry, University of Oslo, Oslo 3, Norway

2,6-Dimethoxycarbonylpyrylium perchlorate and its 4-methyl derivative have been synthesised from the respective 4H-pyrans. With amines the 4-methylpyrylium salt gives the anhydro-base while the desmethyl analogue suffers ring opening. Initial α-adduct formation was shown by NMR to take place by water addition at low temperature, and the product was rearranged to an acyclic compound on temperature increase. Alcohols are oxidised to the corresponding carbonyl compound with concurrent formation of the 4H-pyran.

Substituted pyrylium cations have been shown to be versatile synthetic intermediates.[1,2] Depending on the nature of the α- and γ-substituents the pyrylium cation will add nucleophiles in either of these positions. Most pyrylium salts carry substituents in both α- and γ-positions and often the substituents are aryl groups. Without the stabilising aryl groups the pyrylium ion can only exist in the presence of a weak nucleophilic anion such as perchlorate or fluoroborate.

Pyrylium salts without α-substituents are highly reactive towards weak nucleophiles.[3–7] We were interested in synthetically readily available pyrylium salts carrying activating substituents in the α-positions. This report deals with studies of 2,6-dicarboxylic esters which were synthesised according to Scheme 1. The choice of synthetic pathway to V was directed by the reported preparation of 2,6-dicarboxy-4H-pyran (III). Diethyl oxaloacetate was condensed with the respective aldehyde,[8,9] the condensation product (II) hydrolysed and β-decarboxylated in dilute sulphuric acid and finally cyclised to III in cold concentrated sulphuric acid.[10] The methyl ester IV was prepared by methanolysis of the acid chloride available by phosphorus pentachloride treatment of the acid. Pyrylium formation with hydride abstraction was achieved using triphenylmethyl perchlorate [11] in liquid sulphur dioxide.

* Present address: Organic Chemistry Laboratories, The Norwegian Institute of Technology, University of Trondheim, N-7034 Trondheim-NTH, Norway.

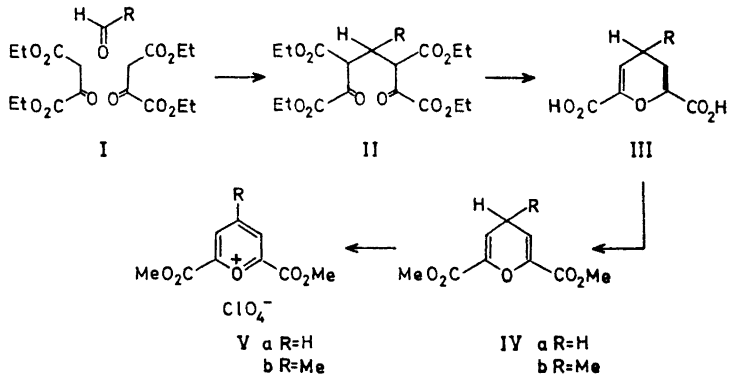

Scheme 1.

The NMR spectra of the pyrylium salts, recorded in trifluoroacetic acid (TFA), show clearly a highly electron deficient aromatic system. The methyl ester protons in V (5.7 τ) are at lower field than in the 4H-pyrans (6.0 τ). The three pyrylium protons in Va give rise to an AB_2-system (7-lines) with the γ-proton at 0.15 τ and the β-protons at 0.75 τ. The β-protons in Vb are at higher field (1.04 τ) which demonstrates the inductive contribution from the methyl group into the electron deficient nucleus which on the other side results in activation of the methyl group (6.82 τ). The 2,4,6-trimethylpyrylium cation has been reported to react with primary amines to form pyridinium derivatives.[12] In contrast, treatment of Vb with benzylamine led to anhydro-base (VI) formation. Pyridine was also a proton abstractor from Vb.

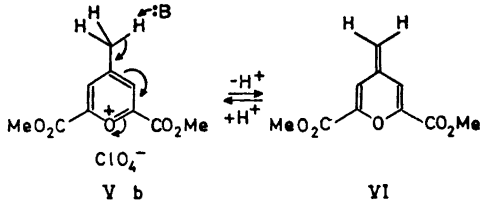

Scheme 2.

The chemical shifts in deuteriochloroform for the anhydro-base methyl ester (6.14 τ) and pyranyl (3.24 τ) protons correspond closely to those in the 4H-pyrans discussed above. Deuteriation of the 4-methyl group in Vb, as discussed below, has confirmed that the singlet at 5.20 τ is due to the terminal vinyl protons. Being an anhydro-base, VI is readily reprotonated to Vb. Thus the NMR spectrum of the latter was obtained on dissolution of the anhydro-base in TFA.

Since the 2,4,6-trimethylpyrylium cation reacts differently from Vb with primary amines it was prepared for comparative purposes. In its perchlorate salt in deuterium oxide the γ-methyl protons are exchanged rapidly, the

α-methyl protons more slowly.[13] For comparison of the rate of deuterium incorporation in the γ-methyl groups, NMR spectra of an equimolecular mixture of the trimethylpyrylium salt and Vb in partly deuteriated TFA were recorded after 10 and 100 min. No detectable deuteriation was seen in the trimethyl cation while the deuteriation figures for Vb were 30 and 60 % respectively, the integration standard being the non-exchangeable methyl ester protons. The signals from the β-protons and from the 4-methyl-protons in Vb are at lower field ($\Delta\nu_{4\text{-}CH_3} = 25$ cps, $\Delta\nu_{\beta\text{-}H} = 75$ cps) than in the trimethylpyrylium salt. The exchange of the α-methyl groups in the trimethylpyrylium cation with methoxycarbonyl groups (Vb) has changed the behaviour towards primary amines from that of a Lewis acid to that of a Brønsted acid.

Attempts to isolate methylene pyrans like VI have been reported unsuccessful.[13] The instability of VI was readily seen by NMR. A spectrum of VI in $CDCl_3$ recorded after 48 h at 25°C showed only polymeric product. Storage of the isolated solid also led to decomposition. The ready polymerisation is understandable in terms of the polarisability as indicated by resonance forms in Scheme 3.

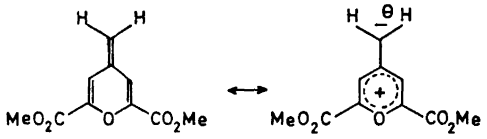

Scheme 3.

Compound Va, which does not contain the acidic 4-methyl protons, reacts immediately and exothermally with primary amines. The highly coloured reaction mixture suggests ring-opening. Recyclisation to pyridinium derivatives was not achieved. With ammonium carbonate, however, pyridine-2,6-dicarboxylic acid was detected chromatographically [14] after hydrolysis. Evidence for preferential α-attack was more convincingly achieved with water as nucleophile. α-Aryl substituted pyrylium salts are relatively stable towards water while Va reacts immediately. The NMR spectrum after addition of three equivalents of water to a solution of Va in acetonitrile-d_3 at −40°C showed the methyl ester protons as two closely spaced singlets at 6.15 − 6.18 τ. The nonequivalence of the methyl groups and the ABC pattern (3.25 − 4.14 τ) for the pyranyl protons only satisfy α-substitution to a 2H-pyran. Addition of deuterium oxide instead of water gave the same spectrum. Both solutions on reaching room temperature gave the same spectrum. This spectrum was different from that at low temperature and was not changed on recooling. Addition of water to a solution of Va in acetonitrile-d_3 at room temperature gave the same spectrum. The spectrum in this case has the methyl ester protons as a singlet at 6.15 τ. The signals (7 lines) from the vinyl protons (1.97 − 3.59 τ) are interpreted to be of the AB_2 type with $\delta\nu/J_{A,B} = 5.1$ which requires the β-protons to be equivalent. In an acyclic structure this could be explained by a very rapid proton exchange between two equivalent tautomeric forms or simply due to equivalence through strong intermolecular hydrogen bonding (Scheme 4).

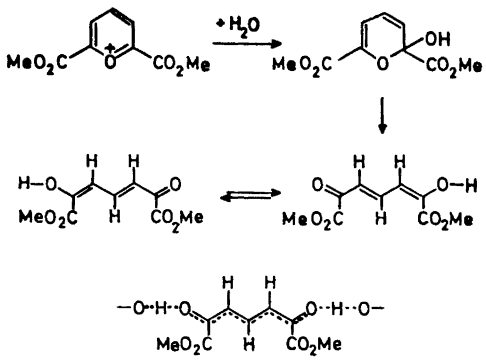

Scheme 4.

Calculations for the chemical shift of the protons in the AB_2 system give the value 3.42 τ and 2.22 τ for the β- and γ-protons, respectively, with $J_{\beta,\gamma} = 14$ cps. The coupling constant is in agreement with the *trans* arrangement of protons shown in Scheme 4.

In UV the highest wavelength-band in acetonitrile is at 335 nm (log $\varepsilon = 4.17$) which is changed to 455 nm on addition of base. The bathochromic shift is attributed to the resonance stabilised (equivalent structures) oxenol-anion.

The pyrylium salt Va is less reactive towards alcohols than towards water. The NMR spectrum of the reaction product, after heating Va in methanol for 30 min followed by evaporation, showed that 50 % of the pyrylium salt had been reduced to the 4H-pyran (IVa) with no ring-opened derivative present. For the purpose of isolation of the carbonyl compound in the reaction, IVa was heated with diphenylcarbinol in nitromethane for 30 min. Benzophenone and the 4H-pyran (IVa) were formed quantitatively. Little is known about the mechanism of this reaction. Direct hydride abstraction into the γ-pyrylium position would seem reasonable. Since water attacks in the α-

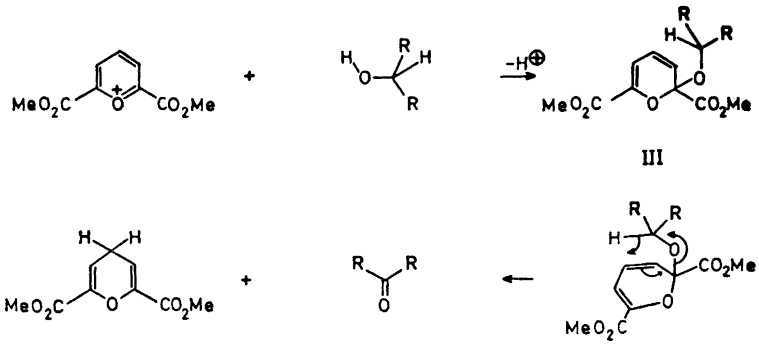

III

Scheme 5.

position, however, α-adduct formation also in this case cannot be excluded (Scheme 5). The adduct can be regarded as an allyl ether and as such could undergo a Claisen type rearrangement as indicated in Scheme 5.

EXPERIMENTAL

NMR spectra were recorded on a Varian A-60A spectrophotometer.

2,6-Dimethoxycarbonyl-4H-pyran (IVa). NMR in TFA: 6.89 τ (triplet, $2H^4$, $J_{3,4}=4.0$ cps), 3.75 τ (triplet, H^3H^5), 6.03 τ (singlet OCH_3).

2,6-Dimethoxycarbonyl-4-methyl-4H-pyran (IVb). NMR in TFA: 8.68 τ (doublet, 4-CH_3, $J_{4,CH_3}=7.0$ cps), 6.68 τ (multiplet, H^4), 3.78 τ (doublet, H^3H^5), 6.00 τ (singlet, OCH_3).

2,6-Dimethoxycarbonylpyrylium perchlorate (Va). 2,6-Dimethoxycarbonyl-4H-pyran (6.93 g, 0.035 mol) was dissolved in dry, liquid sulphur dioxide (100 ml) at −30°C and triphenylmethyl perchlorate (11.65 g, 0.034 mol) added with stirring under anhydrous conditions. The reaction mixture was then left by itself until the sulphur dioxide had evaporated. The residue was triturated with anhydrous ether (250 ml) under stirring for about 10 min and most of the ether sucked out. The process was repeated three times more with fresh ether before the solid was isolated by filtration. The product is very hygroscopic and is decomposed by the moisture in the atmosphere and should be kept in a tight bottle in a refrigerator; yield 9.00 g (90 %), m.p. 146 – 148°C (decomp.). (Found: C 36.34; H 3.18; Cl 11.84. Calc. for $C_9H_9ClO_5$: C 36.42; H 3.03; Cl 11.95.) NMR in TFA: 5.69 (singlet, OCH_3). The pyrylium protons give a 7 line spectrum. Calculated for $AB_2(\delta\nu/J_{AB}=4.4)$ gave: 0.75 τ (H^3H^5), 0.15 τ (H^4, $J_{3,4}=8.1$ cps).

2,6-Dimethoxycarbonyl-4-methylpyrylium perchlorate (Vb) was prepared as above from 2,6-dimethoxycarbonyl-4-methyl-4H-pyran in 78 % yield, m.p. 135°C (decomp.). (Found: C 39.61; H 4.36; Cl 10.85. Calc. for $C_{10}H_{11}ClO_5$: C 38.65; H 3.54; Cl 11.4.) NMR in TFA: 6.82 τ (singlet, 4-CH_3), 1.04 τ (singlet, H^3H^5) 5.71 τ (singlet, OCH_3).

2,6-Dimethoxycarbonyl-4-methylenepyran (VI). 2,6-Dimethoxycarbonyl-4-methylpyrylium perchlorate (1.55 g, 0.005 mol) was suspended in anhydrous ether (300 ml) and a solution of pyridine (0.39 g, 0.005 mol) in ether (25 ml) was added dropwise with vigorous stirring. The reaction was stirred in the cold overnight, the pyridinium salt removed by filtration and the filtrate evaporated; yield 0.8 g (76 %). The compound is unstable and did not have a sharp melting point. Molecular weight determined by mass spectrometry: 210.0533. Calc. for $C_{10}H_{10}O_5$: 210.0528. NMR in $CDCl_3$: 5.20 τ (singlet, 4-CH_2), 3.24 τ (singlet, H^3H^5), 6.14 τ (singlet, OCH_3).

REFERENCES

1. Dimroth, K. and Wolf, K. H. *Newer Methods of Preparative Organic Chemistry*, Academic, New York 1964, Vol. 3, p. 357.
2. Balaban, A. T., Schroth, W. and Fischer, G. *Advan. Heterocycl. Chem.* **10** (1969) 241.
3. Købrich, G. *Annalen* **648** (1961) 114.
4. Degani, I. and Vincenzi, C. *Boll. Sci. Fac. Chim. Ind. Bologna* **25** (1967) 51.
5. Klages, F. and Träger, H. *Chem. Ber.* **86** (1953) 1327.
6. Balaban, A. T. and Nenitzescu, C. D. *Izv. Akad. Nauk. SSSR* **11** (1960) 2064.
7. Degani, I., Fochi, R. and Vincenzi, G. *Gazz. Chim. Ital.* **94** (1964) 203.
8. Cope, A. and Fournier, A. *J. Am. Chem. Soc.* **79** (1957) 3896.
9. Gault, H. *Bull. Soc. Chim. France* **1907** 21, 40.
10. Blaise, E. E. and Gault, H. *Bull. Soc. Chim. France* **1907** 129.
11. Dauben, H. I. and Honnen, L. *J. Org. Chem.* **25** (1960) 1442.
12. Toma, C. and Balaban, A. T. *Tetrahedron Suppl.* **7** (1966) 9.
13. Gârd, E., Stanoiu, I. and Balaban, A. T. *Rev. Roum. Chim.* **14** (1969) 247.
14. Tallent, W. H. and Horning, E. C. *J. Am. Chem. Soc.* **78** (1956) 4467.

Received November 23, 1972.

ACTA CHEMICA SCANDINAVICA 27 (1973) 1390–1394

N-Quaternary Compounds

Part XXXI. Sulphur Participation in the Cyclisation of a 2-Bromo-3-α-pyridylthiopropionic Acid

KJELL UNDHEIM and GUNNAR ARNFINN ULSAKER

Department of Chemistry, University of Oslo, Oslo 3, Norway

(*R*)-2-Bromo-3-(3-hydroxy-6-methyl-2-pyridylthio)propionic acid has been synthesised from (*R*)-cysteine. Cyclisation of the bromo acid gives 8-hydroxy-5-methyldihydrothiazolo[3,2-a]pyridinium-3- and -2-carboxylates with configurational inversion. The isomeric mixture is formed by sulphur participation in the reaction and the isomer ratio varies with experimental conditions.

Pyrid-2-thiones add to 2-bromo-2,3-unsaturated carbonyl compounds.[2,3] The initial Michael adduct is rapidly cyclised over the pyridyl nitrogen and the compound isolated from the reaction mixture is a dihydrothiazolo[3,2-a]pyridinium derivative.[2,3] As part of a project to establish the stereochemical course for the overall reaction this paper deals with studies of the cyclisation step. For this purpose an optically active 2-bromo-3-α-pyridylthiopropionic acid of known absolute configuration was required since the chiroptical properties of 8-hydroxy-5-methyldihydrothiazolo[3,2-a]pyridinium-3-carboxylate (I) have already been correlated to its absolute stereochemistry.[4–6] 2-Bromo-3-(3-hydroxy-6-methyl-2-pyridylthio)propionic acid (IV) is very easily cyclised and must be obtained under mild experimental conditions. A successful synthesis from L-cysteine is shown in Scheme 1. The thiol group

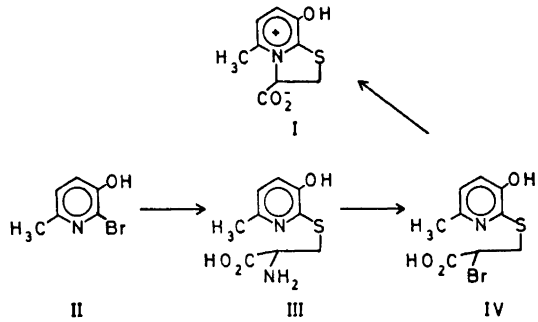

Scheme 1.

in cysteine can be arylated on treatment with diazotised anilines in the presence of copper(I) salts.[7,8] A similar reaction using diazotised 2-amino-3-hydroxy-6-methylpyridine gave III in very low yield. Attention was therefore turned to the reaction of the 2-bromopyridine II with cysteine. The 2-pyridyl bromine is deactivated towards nucleophilic substitution by the other nuclear substituents in II and its displacement requires vigorous conditions.[9] In its reaction with cysteine in the presence of potassium carbonate only partial

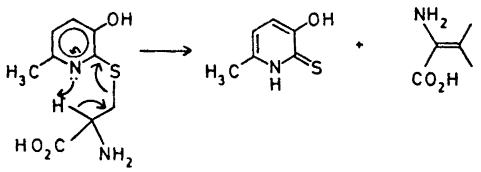

III V VI

Scheme 2.

conversion to III was achieved due to decomposition reactions. Among the products on forcing the reaction, was the pyrid-2-thione V (Scheme 2). The latter must be formed from III through elimination, presumably in an intramolecular process. The amino acid III was isolated from the reaction mixture in 7 % yield, $[\alpha]_D^{25} = +129.0°$ (N HCl). Racemisation of III under the conditions for its formation was excluded by subjecting III to simulated reaction conditions in deuterium oxide. Despite the failure to incorporate deuterium at the chiral carbon the pyrid-2-thione V was formed. Any proton abstraction thus leads preferably to elimination in good agreement with the mechanism suggested in Scheme 2. As cysteine is expected to be optically stable under the reaction conditions, the product (III) is assumed optically pure.

Bromination of optically active α-amino acids by means of diazotisation in the presence of bromide ions goes with retention of the configuration. The optical purity is of the order of 90 % depending to some degree on the nature of the substituents.[10] The same stereochemical course has been claimed for the sulphur containing amino acids *S*-benzylcysteine[11] and methionine.[12] The bromo compound IV obtained by this diazotisation reaction from III has by analogy retained the (*R*)-configuration.

The bromo compound IV is highly reactive. At pH 2.5 it could be extracted from the diazonium solution into ethyl acetate but was rapidly cyclised to I at higher pH value. The cyclisation also takes place in ethyl acetate on standing. Due to its high reactivity IV is best distinguished from the hydrobromide of the cyclic product I by its spectroscopic properties. In acid solution both the amino acid III and the diazotised product have UV maxima at about 235 and 320 nm to be compared with 240 and 340 nm for the bicyclic product (I). The NMR shifts for the methylene and methine protons in trifluoroacetic acid are also different, the shifts being 6.1 and 5.3 τ for IV compared to 5.8 and 3.7 τ for I.

The optical purity of IV is uncertain. In view of previous findings [1,13] partial racemisation is expected to have taken place by nucleophilic bromide ion interchange in the bromo acid IV. On the other hand the bicyclic product (I) is optically stable.[14] The specific rotation shows the product to be of 65 % optical purity. Taking into account some racemisation of IV, the cyclisation must be highly stereospecific. The sign of the sodium D-line rotation shows the product to have the (*S*)-configuration.[4] The cyclisation therefore proceeds by configurational inversion. The same stereochemical course was observed in the cyclisation of 2-bromo-4-(3-hydroxy-6-methyl-2-pyridylthio)butyric acid.[1] The latter differs from IV in having an additional methylene group between the sulphur and the α-carbon. This higher homologue of IV requires heating for some time to effect cyclisation. It is well established that 5-membered rings are formed faster than 6-membered rings. The observed large reactivity difference in this case, however, leads to the additional invokement of sulphur participation in the cyclisation of IV (Scheme 3). Back-side displacement of the bromine results in configurational inversion (VIIa). In the next step, however, the pyridine nitrogen must add *cis* to the sulphur. A such steric course seems acceptable if the sulphur from some distance holds the positive charge and thereby the configuration. The suggested mechanism bears some resemblance to the accepted S_Ni mechanism in halogenations of alcohols which go with configurational retention.

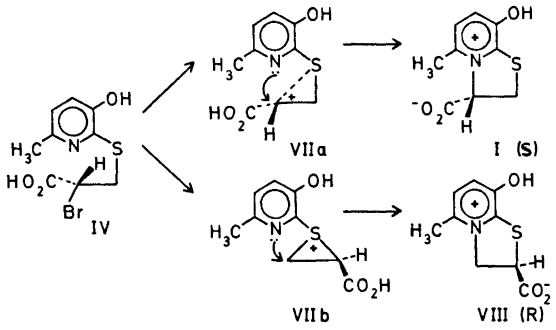

Scheme 3.

Furthermore, in an episulphonium intermediate the nitrogen attack can occur on either the methine carbon (VIIa) or on the methylene carbon (VIIb) with the formation of the isomers I and VIII, respectively. Although I and VIII have very similar physico-chemical properties,[9] the chemical shifts in NMR of the dihydrothiazolo ring protons are different, and they can be distinguished chromatographically. In fact careful chromatography of the crude reaction product showed a small amount of VIII present. The conditions for cyclisation were then varied. The highest yield of VIII was obtained by sodium carbonate addition when the product was found to consist of I and VIII in the ratio 3:2 as estimated by NMR integration. The isomers were separated by chromatography. The specific rotation for I, $[\alpha]_D^{25} = +99°$

(0.1 N NaOH), corresponds to 65 % optical purity. The specific rotation for VIII was $[\alpha]_D^{25} = -19°$ (0.1 N NaOH). Its configuration is not known but the mechanism suggested for its formation in Scheme 3 leads to the assignment of (*R*)-configuration.

EXPERIMENTAL

(R)-*2-Amino-3-(3-hydroxy-6-methyl-2-pyridylthio)propionic acid (III).* A solution of 2-bromo-3-hydroxy-6-methylpyridine (11.3 g, 0.06 mol), (*R*)-cysteine hydrochloride (9.4 g, 0.06 mol), and potassium carbonate (24.8 g, 0.18 mol) in water (180 ml) was heated at 65°C for 3 days. The pH of the cold solution was then adjusted to 3.5, the solution extracted with 90 % phenol (3 × 30 ml), the phenolic solution washed with water (30 ml), ether (200 ml) added to the phenol solution, the separated water layer collected, the ether-phenol layer washed with water (4 × 30 ml), the combined water phases washed with a little ether and the aqueous solution concentrated to a small volume. The title compound was slowly precipitated on standing and was recrystallised from water to which had been added a little sodium bisulphite. The white crystalline material thus obtained had m.p. 221°C (decomp.); yield 1.0 g (7 %). (Found: C 47.36; H 5.11; N 11.99. Calc. for $C_9H_{12}N_2O_3S$: C 47.37; H 5.30; N 12.28). $[\alpha]_D^{25} = +129.0°$ ($c = 1$ in N HCl).

NMR in TFA: 7.20 τ (CH_3), 6.0 τ (CH_2), 5.3 τ (CH), 1.87 τ and 2.22 τ (pyridyl H^4 and H^5). UV in 0.1 N HCl: 318 nm (log ε 3.97) and 237 nm (3.59). 0.1 N NaOH: 326 nm (log ε 4.00) and 248 nm (3.90).

(R)-*2-Bromo-3-(3-hydroxy-6-methyl-2-pyridylthio)propionic acid (IV).* A solution of sodium nitrite (1.6 g, 0.02 mol) in water (10 ml) was added dropwise over 1 h with stirring to an ice-cold solution of (*R*)-2-amino-3-(3-hydroxy-6-methyl-2-pyridylthio)propionic acid (1.0 g, 0.0045 mol) in 5 N HBr (70 ml). The reaction mixture was then left at 0°C overnight before evaporation at reduced pressure.

NMR in TFA: 7.22 τ (CH_3), 6.12 τ (CH_2), 5.33 τ (CH), 1.92 τ and 2.32 τ (pyridyl H^4 and H^5). UV in 0.1 N HCl: Maxima at 320 nm and 235 nm. The absorption is variable due to the strong tendency for cyclisation to I.

(S)-*8-Hydroxy-5-methyldihydrothiazolo[3,2-a]pyridinium-3-carboxylate (I) and* (R)-*8-hydroxy-5-methyldihydrothiazolo[3,2-a]pyridinium-2-carboxylate (VIII).* An aqueous solution of the crude 2-bromopropionic acid (IV)hydrobromide on neutralisation was rapidly cyclised to I. The amount of the isomer VIII present in the product under these conditions was very small according to chromatography. Excess sodium carbonate addition led to increasing amounts of VIII reaching a maximum on saturation.

The product in either case was extracted into 90 % phenol solution from the aqueous solution at pH 3.5 as described for III, and the product isolated by freeze-drying of the final aqueous concentrate. NMR integration in TFA of the dihydrothiazolo protons for I (H^3 at 3.7 τ, $2H^2$ at 5.7 τ) and for VIII (H^2 and $2H^3$ in the region 4.2 – 5.1 τ) [9] shows the I/VIII ratio to be 3/2 after saturation of the reaction solution with sodium carbonate.

Compounds I and VIII were separated by TLC on silica gel plates using the system BuOH:AcOH:H_2O (100:22:50). Compound I has the higher R_F value. The separated bands were scraped off, extracted with methanol, the methanol solutions filtered through a short silica gel column and the filtered solutions concentrated to small volumes when the title compounds were precipitated.

Optical rotation for I $[\alpha]_D^{25} = +99°$ ($c = 0.6$ in 0.1 N NaOH); for VIII $[\alpha]_D = -19°$ ($c = 0.5$ in 0.1 N NaOH).

Physical data are otherwise as previously described.[9]

REFERENCES

1. Part XXX. Undheim, K. and Ulsaker, G. A. *Acta Chem. Scand.* **27** (1973) 1059.
2. Undheim, K. and Borka, L. *Acta Chem. Scand.* **23** (1969) 1715.
3. Undheim, K. and Lie, R. *Acta Chem. Scand. In press.*
4. Undheim, K., Røe, J. and Greibrokk, T. *Acta Chem. Scand.* **23** (1969) 2501.

5. Greibrokk, T. and Undheim, K. *Tetrahedron* **27** (1972) 1223.
6. Grønneberg, T. and Undheim, K. *Acta Chem. Scand.* **26** (1972) 2267.
7. du Vigneaud, V., Wood, J. L. and Binkley, F. J. *J. Biol. Chem.* **138** (1941) 369.
8. Goodman, L., Ross, L. O. and Baker, B. R. *J. Org. Chem.* **23** (1958) 1251.
9. Undheim, K., Nordal, V. and Tjønneland, K. *Acta Chem. Scand.* **23** (1969) 1704.
10. Fu, S. C. J., Birnbaum, S. M. and Greenstein, J. P. *J. Am. Chem. Soc.* **76** (1954) 6054.
11. Izumiya, N. *J. Chem. Soc. Japan* **72** (1951) 1050.
12. Izumiya, N. *J. Chem. Soc. Japan* **72** (1951) 149.
13. Undheim, K. and Grønneberg, T. *Acta Chem. Soc.* **25** (1971) 18.
14. Undheim, K. and Greibrokk, T. *Acta Chem. Soc.* **23** (1969) 2505.

Received September 15, 1972.

ACTA CHEMICA SCANDINAVICA 27 (1973) 1395–1400

The Chemistry of Dibenzo[d,f][1,3]diazepines

2.[1] Mass Spectrometric Studies of 6-Methyl- and 6-Ethyl-5,7-dihydroxy-6,7-dihydro-5*H*-dibenzo[d,f][1,3]diazepine

JAN BECHER[a] and JØRGEN MØLLER[b]

[a] *Department of Chemistry, University of Odense, DK-5000, Odense, Denmark,* [b] *Physical Laboratory II, University of Copenhagen, The H. C. Ørsted Institute, DK-2100 Copenhagen, Denmark*

The mass spectra of 6-methyl- and 6-ethyl-5,7-dihydroxy-6,7-dihydro-5*H*-dibenzo[d,f][1,3]diazepine are given. The main fragmentation pathways are suggested from the use of deuterium labelling, high resolution mass measurements and the metastable defocusing technique. Characteristic features are the loss of an oxygen atom and a molecule of water from the molecular ion and the formation of several abundant odd-electron fragments which may be ascribed to various heterocyclic structures derived from 2,2′-substituted biphenyles.

Continuing the investigation[1] on 5,7-dihydroxy-6,7-dihydro-5*H*-dibenzo-[d,f][1,3]diazepines * we have examined the electron impact induced fragmentation of 6-methyl- and 6-ethyl-5,7-dihydroxy-6,7-dihydro-5*H*-dibenzo[d,f][1,3]diazepines (I and II).

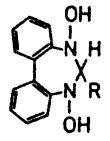

I: R=CH_3
II: R=C_2H_5

Only little knowledge of the chemical behaviour of these compounds is available at present. I and II were found to decompose by melting and upon oxidation to give rise to a mixture of unstable radicals. Probably the oxidized form, *i.e.* the α-nitronyl nitroxide, is unstable because of the enforced planarity

* The syntheses, properties and spectroscopic data of a number of other dibenzo[d,f][1,3]-diazepines will be published.

of the non-aromatic 1,3-diazepine ring. Reduced 1,3-diazepines in general display the lability of diaminomethane derivatives, and the oxidized form of some dibenzo[d,f][1,3]diazepines are easily cleaved upon methylation or acetylation.[2]

The ring system of I and II can be regarded as a 2,2′-disubstituted biphenyl. Therefore, either ring rupture or ring contraction might give rise to stable heterocyclic products.[3] It cannot be excluded that such processes may also be reflected in the electron-impact induced fragmentation of these compounds.

DISCUSSION

On account of the thermal instability of these compounds it could be expected that thermal decomposition would take place prior to the ionization process. However, mass spectra recorded at ion source temperatures well below the melting points of the compounds were reproducible, and low energy spectra did not indicate any contribution of other molecular ions. Raising the temperature caused a drastic change in the appearance of the spectra. The fragmentation was increased considerably and especially the abundances of *m/e* 196, 167, 152, 140, and 139 (in the mass spectrum of I) were augmented.

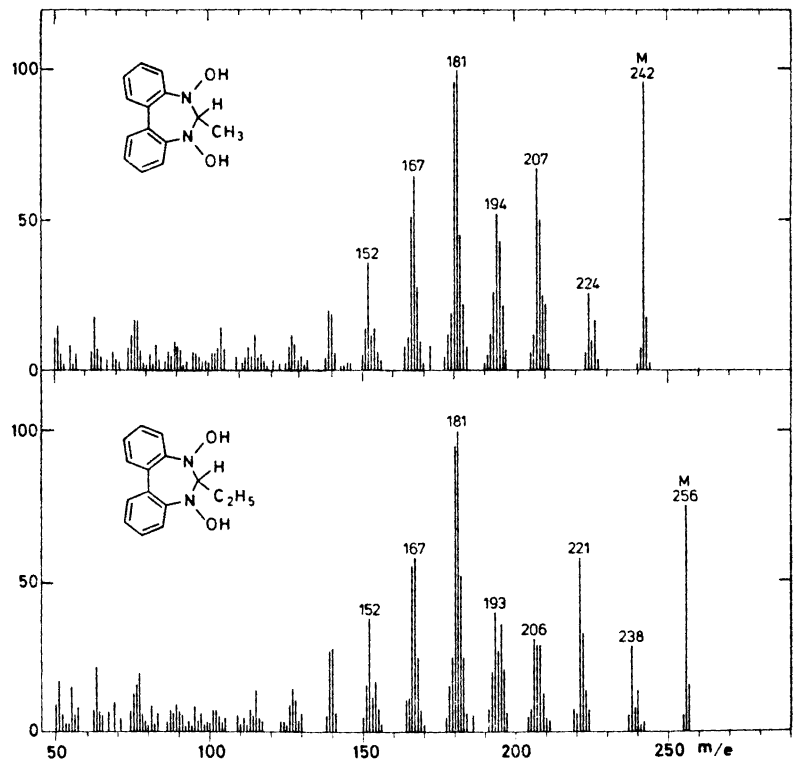

Fig. 1. The mass spectra of I and II.

The mass spectra are shown in Fig. 1, where particular attention should be drawn to the abundant molecular ion peaks and to the considerable number of intense peaks in the higher mass range corresponding to even as well as odd-electron ions. The lower mass range exhibits peaks of low intensities at nearly every mass number.

A noteworthy feature in the mass spectra of I and II is the loss of an oxygen atom from the molecular ions. Such M-16 peaks are also important in the mass spectra of alicyclic and aromatic ketoximes [4] in which cases strong M − OH peaks are exhibited. The mass spectra of cyclic hydroxamic acids show direct loss of O or ·OH from the molecular ion.[5] The elimination of an OH-radical from the molecular ions of I and II is also observed but the loss of H_2O seems to be much more favoured. The odd-electron $M-H_2O$ ion is a progenitor of several abundant fragments (shown in Scheme 1 for I) and is twice as abundant as the even-electron M − OH ion. The mass spectrum of 5,7-dideuteriooxy-6-methyl-6,7-dihydro-5*H*-dibenzo[d,f][1,3]diazepine showed that both hydrogen atoms involved in the H_2O loss preferentially originated from the OH-groups. Inspection of Dreiding models has indicated, that in one of the conformations the two OH-groups could easily approach each other closely. The rather complex decomposition pattern observed for the $M-H_2O$ ion involves the elimination of the following neutral species: O, NO·, $CHCH_3$, CH_3CHO, $\cdot C_2H_3O$, and C_2H_2O, and may suggest the fragmentation to proceed through a number of intermediates (*a-d*) as visualized in Scheme 1.

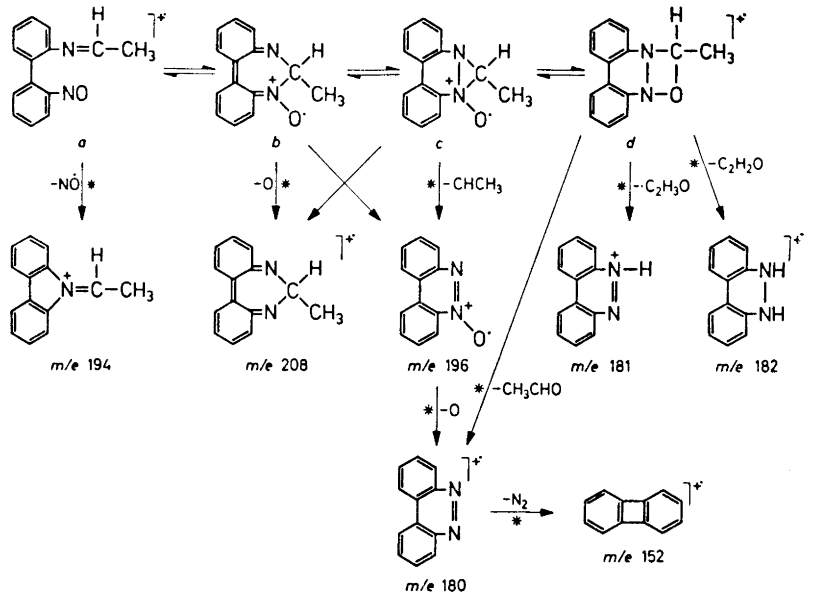

Scheme 1.

Due to some hydrogen/deuterium exchange taking place in the ion source when the mass spectrum of the deuterium labelled compound was recorded it cannot be excluded that *e* to some extent contributes to the $M-H_2O$ ion:

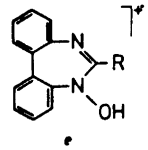

e

Ion *e* may readily eliminate ·OH and thus be a precursor for the abundant M-35 ion (*f*). Also *b* or *c* are possible progenitors for *f*, implying that a hydrogen rearrangement takes place. In addition *f* is formed directly from the molecular ion, probably by a concerted loss of H_2O and ·OH. Ion *f* is decomposed to form the *m/e* 180 ion and it is the main progenitor for the *m/e* 167 ion, *g*, by elimination of C_2H_2N·.

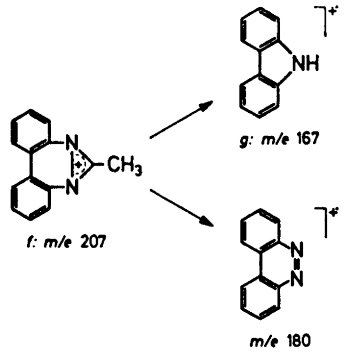

The molecular ion and the $M-H_2O$ ion are also found to be precursors for *g*.

It has recently been claimed [6] that the loss of an oxygen atom from the molecular ions of quinoline *N*-oxide and isoquinoline *N*-oxide is due to thermal, rather than electron-impact fragmentation. The M – O ions in the mass spectra of I and II may also be due to a thermal degradation prior to ionization as their abundances are increased when the ion source temperature is raised. However, application of the metastable defocusing technique revealed that the molecular ion is precursor for the M – O ion, thus clearly demonstrating the electron-impact induced origin of the M – O ion. This mechanistically interesting process may be depicted by the transformation M→*h*,

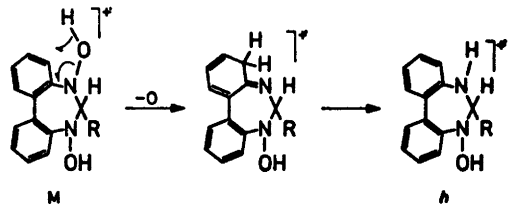

M *h*

Ion *h* is further decomposed by loss of ·OH to yield the M – 33 ion.

Loss of an oxygen atom is also found to take place both from the $M-H_2O$ ion and from the *m/e* 196 ion yielding *m/e* 208 and 180, respectively (mass spectrum of I). The *m/e* 180 ion is believed to possess the benzo[c]cinnoline structure, since N_2 is further expelled yielding the *m/e* 152 ion in parallel to the predominant electron-impact fragmentation of benzo[c]cinnoline.[7,8] Assuming the possibility of a fragment ion with an *N*-oxide structure to undergo further decomposition by elimination of the oxygen atom from the *N*-oxide function, the structure of the *m/e* 196 ion may correspond to that of benzo[c]cinnoline-*N*-oxide. The mass spectrum of this compound is reported [9] to exhibit an M – O ion. The precursor for the *m/e* 196 ion may also possess an *N*-oxide structure, as shown by *b* and *c* in Scheme 1. The oxygen loss observed to take place from the $M-H_2O$ ion may then similarly be interpreted as an elimination of the oxygen atom from the *N*-oxide function.

The *m/e* 180 ion is also generated directly from the $M-H_2O$ ion, by elimination of CH_3CHO (Scheme 1). This may suggest a formulation of the $M-H_2O$ ion as *d*. Also losses of C_2H_2O and $\cdot C_2H_3O$ from the $M-H_2O$ ion (*d*) are important processes yielding the abundant ions at m/*e* 182 and 181, respectively.

In low voltage spectra the abundance of *m/e* 180 and 182 decrease more rapidly than that of *m/e* 181, and a metastable peak indicates that the process M→*m/e* 181 takes place. At 70 eV this decomposition also occurs, but it is to some extent overshadowed by the competing process now taking place.

CONCLUSION

The electron impact induced fragmentations of the two diazepines give rise to similar, but rather complex mass spectra. A number of fragment ions are formed in several decomposition processes as shown in Scheme 2, where

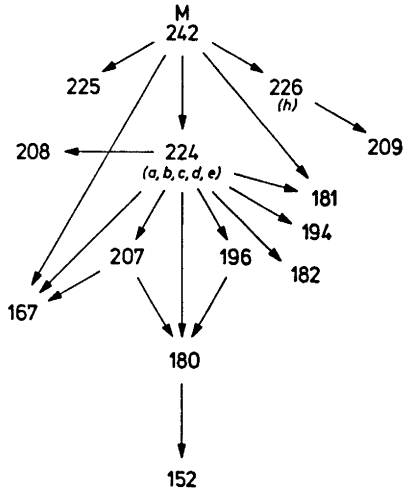

Scheme 2. Main decomposition of I.

the main decomposition mode for I is given. The major degradation proceeds *via* the $M-H_2O$ ions, *a-e*, and is to a great extent conducted by the biphenyl function. A number of abundant odd-electron fragment ions are formed which are ascribed to ions corresponding to well known stable heterocyclic compounds such as:

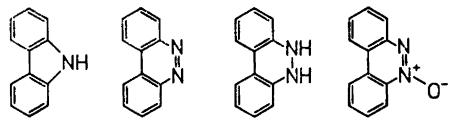

MW 167 MW 180 MW 182 MW 196

The formation of these ions may be a natural consequence of the stability of the biphenyl system together with the easy interaction of the 2,2′-substituents.

EXPERIMENTAL

Mass spectra were obtained on an MS902 mass spectrometer using the direct sample insertion system (ion source temperature: 130°C). Unless otherwise stated, 70 eV electrons were used. All transitions given are verified by metastable defocusing, and the elemental compositions are substantiated by high resolution mass measurements (± 5 ppm). Peaks corresponding to double charged ions appearing at half masses and peaks of lower abundance than 2 % are omitted.

Microanalyses were carried out in the Microanalytical Department of the University of Copenhagen by Mr. Preben Hansen. Melting points (uncorrected) were determined on a Büchi melting point apparatus. Infrared spectra were recorded on a Perkin Elmer Model 137 infrared spectrophotometer. Compounds I and II were prepared as described previously.[1]

*5,7-Dideuteriooxy-6-methyl-6,7-dihydro-5*H*-dibenzo[d,f][1,3]diazepine.* 5,7-Dihydroxy-6-methyl-6,7-dihydro-5*H*-dibenzo[d,f][1,3]diazepine (40 mg) was dissolved in CD_3OD (1 ml) and D_2O (0.2 ml) was added. The precipitated crystals were collected, redissolved in CD_3OD (1 ml) and D_2O (0.5 ml) was added. The precipitated pale yellow crystals of 5,7-dideuteriooxy-6-methyl-6,7-dihydro-5*H*-dibenzo[d,f][1,3]diazepine (11 mg) had m.p. 158–160°d. (Found: C 68.80; H+D 5.74; N 11.46. Calc. for $C_{14}H_{12}D_2N_2O_2$: C 68.60; H+D 5.77; N 11.37.) IR: ν_{max}(nujol) 2400 cm^{-1}, (OD).

REFERENCES

1. Becher, J. *Acta Chem. Scand.* **26** (1972) 1659. (Part 1 in this series.)
2. Elderfield, R. C., Ed., *Heterocyclic Compounds*, Wiley, New York 1967, Vol. 9.
3. Buntrock, R. E. and Taylor, E. C. *Chem. Rev.* **68** (1968) 209.
4. Goldsmith, D., Becher, D., Sample, S. and Djerassi, C. *Tetrahedron, Suppl.* **7** (1966) 145.
5. Bapat, J. B., Black, D., St. C. and Brown, R. F. C. give a review of the mass spectra of cyclic hydroxamic acids in the chapter: Cyclic Hydroxamic Acids, *Advan. Heterocycl. Chem.* **10** (1969) 199.
6. Duffield, A. M. and Buchardt, O. *Acta Chem. Scand.* **26** (1972) 2423.
7. Eland, J. H. D. and Danly, C. J. *J. Chem. Soc.* **1965** 5935.
8. Bowie, J. H., Lewis, G. E. and Reiss, J. A. *Australian J. Chem.* **21** (1968) 1233.
9. Bowie, J. H., Cooks, R. G., Jamieson, N. C. and Lewis, G. E. *Australian J. Chem.* **20** (1967) 2545.

Received November 9, 1972.

ACTA CHEMICA SCANDINAVICA 27 (1973) 1401–1409

Animal Carotenoids

8.* Synthesis of β,γ-Carotene and γ,γ-Carotene

A. G. ANDREWES and S. LIAAEN-JENSEN

Organic Chemistry Laboratories, Norwegian Institute of Technology, University of Trondheim, Trondheim, Norway

The detailed synthesis of racemic β,γ-carotene (*12*) and optically inactive γ,γ-carotene (*10*) is reported. Both carotenes were synthesized by routes which, in principle, have been used for other carotenoids. Physical properties of intermediates and products and comparative studies with naturally occurring compounds are reported.

In an earlier communication[1] we briefly outlined the approach to the synthesis of β,γ-carotene (*12*, 5,18-didehydro-5,6-dihydro-β,β-carotene by the proposed IUPAC nomenclature[2,3]) and γ,γ-carotene (*10*, 5,18,5′,18′-tetradehydro-5,6,5′,6′-tetrahydro-β,β-carotene). The full details are now reported.

The synthesis was prompted by the finding of β,γ-carotene (*12*) by Arpin *et al.*[4] in the fungus *Caloscypha fulgens* (Pers.) Boud. and of both β,γ-carotene (*12*) and α,α-carotene (*10*) in the aphid *Macrosiphum liriodendri* Monell.[5,6] These are to date the only sources of carotenes with an exocyclic terminal methylene group.

RESULTS AND DISCUSSION

The synthesis of both carotenes (*10* and *12*) followed the $C_{15}+C_{10}+C_{15}$ approach used by a number of workers for the preparation of cyclic and acyclic carotenoids[7,8] (Scheme 1). Construction of the phosphonium salts containing the γ- and β-end groups (*8* and *4*) was followed by selective condensation of the γ-C_{15} phosphoran of *8* with C_{10}-dial (*9*) to yield γ,γ-carotene (*10*) and the intermediate γ-C_{25}-al (*11*). The β-C_{15} phosphoran of *4* was then reacted with the γ-C_{25}-al (*11*) to give β,γ-carotene (*12*).

β-Ionone (*1*) was condensed in a Horner reaction with ethyl diethylphosphonoacetate[9] in the presence of sodium methoxide to give methyl β-

* No. 7. *Acta Chem. Scand.* **25** (1971) 3878.

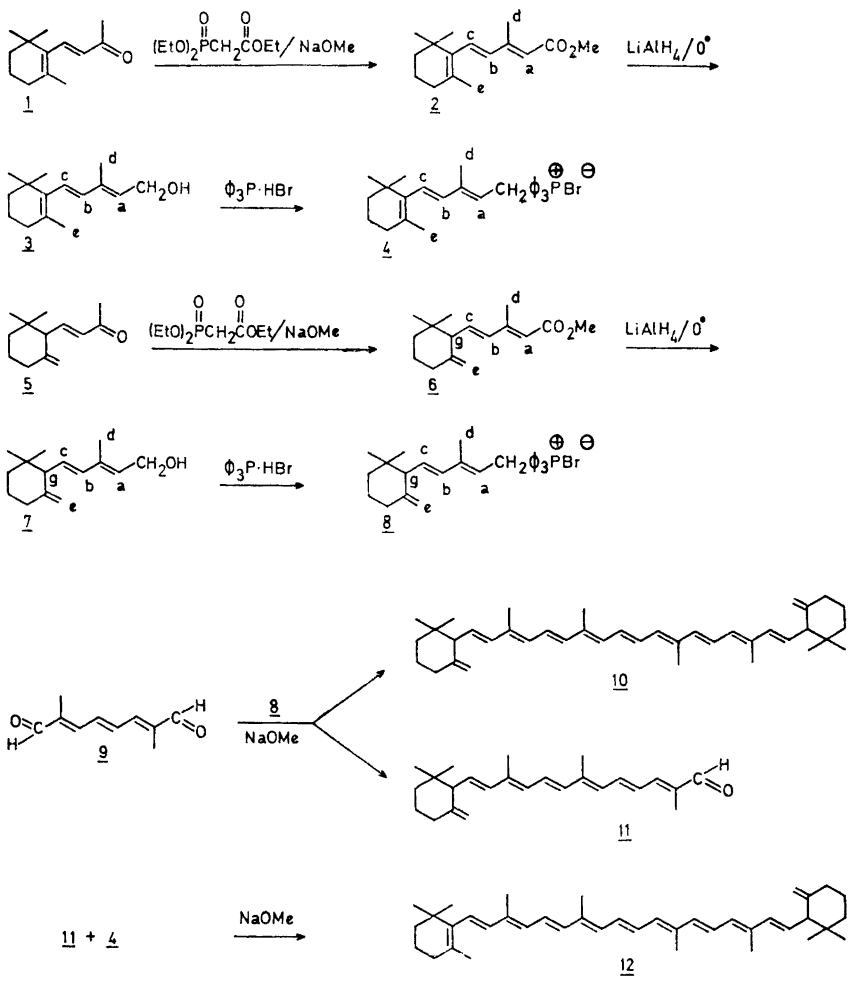

Scheme 1.

ionylideneacetate (*2*) in 90 % yield. During the reaction ester interchange occurred. The product consisted of 65 % *trans* and 35 % *cis* isomers (around the new double bond). Reduction with lithium aluminium hydride gave *β*-ionylidene-ethanol (*3*) which when reacted with triphenylphosphine hydrobromide gave the corresponding phosphonium salt (*4*).

Synthetic, racemic *γ*-ionone (*5*) when reacted with ethyl diethylphosphonoacetate gave *γ*-ionylideneacetate (*6*) in 90 % yield (*cis* and *trans* as in *2* above). During the reaction *ca.* 10 % isomerization [10] to the *β*-analogue (*2*) was observed. Lithium aluminium hydride reduction followed by reaction with triphenylphosphine hydrobromide gave the phosphonium salt *8* in 70 % yield.

C_{10}-dial (*9*) was prepared by selective hydrogenation of the acetylenic analogue with central triple bond.[11] Reaction of the γ-C_{15}-phosphoran of *8* with C_{10}-dial (*9*) gave γ,γ-carotene (*10*; 20 % yield) as the double condensation product and the γ-C_{25}-al (*11*; 50 % yield) as the monocondensation product. The latter was purified and used in a second Wittig reaction with the phosphoran of *4* to give β,γ-carotene (*12*; 15 % yield).

In the above Wittig reactions the phosphorans were generated externally with sodium methoxide and added to a methanolic solution of the appropriate aldehyde (*11* or *9*). The reactions were monitored by thin layer chromatography and in each case excess amounts of phosphorans were required.

The chromatographic properties of the synthetic (*10* and *12*) and natural carotenes were identical on direct comparison. R_F values are given in Table 1.

Sufficient β,γ-carotene of natural origin was available for mixed melting point determination with the synthetic compound (*12*). No depression was observed.

The electronic absorption data of synthetic β,γ-carotene (*12*) and γ,γ-carotene (*10*; spectrum not published elsewhere) are given in Fig. 1 and in Experimental. These are identical in every respect with those of the corresponding carotenes from natural sources.

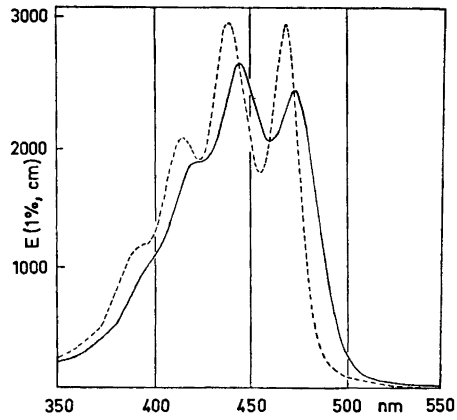

Fig. 1. Absorption spectrum in visible light of synthetic, *trans* β,γ-carotene (*12*, ——) and synthetic, *trans* γ,γ-carotene (*10*, – –) in petroleum ether.

Infrared spectra (KBr) of natural [4] and synthetic β,γ-carotene (*12*, Fig. 2) showed good agreement. Fig. 2 also includes the IR spectrum of γ,γ-carotene (*10*) not reported elsewhere; the 889 cm^{-2} absorption ascribed to $R_1R_2C=CH_2$ being of diagnostic value.

The proton magnetic resonance spectrum of synthetic β,γ-carotene (*12*) was fully consistent with that reported for natural β,γ-carotene.[4] That of synthetic γ,γ-carotene (*10*; spectrum not available elsewhere) is reproduced in Fig. 3 including signal assignments.

The upper mass region of the mass spectra of β,γ-carotene (*12*) and γ,γ-carotene (*10*) are given in Fig. 4. Both carotenes showed the common M – 92, M – 106, and M – 158 losses on electron impact.[12,13] The M – 92/M – 106 in-

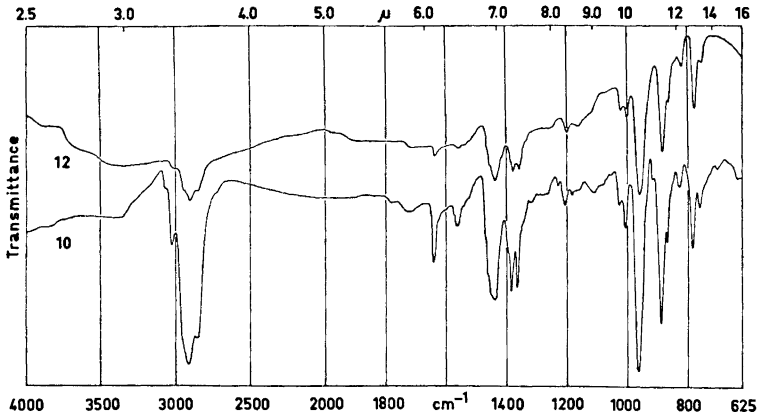

Fig. 2. Infrared spectra (KBr) of synthetic β,γ-carotene (*12*) and synthetic γ,γ-carotene (*10*).

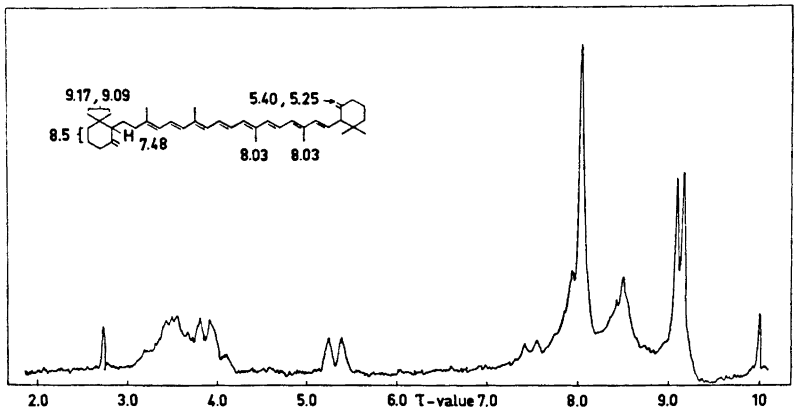

Fig. 3. Proton magnetic resonance spectrum (in $CDCl_3$) of synthetic γ,γ-carotene (*10*).

tensity ratio (1.62 for *12* and 1.57 for *10*) was within the expected range for bicyclic carotenoids with nine conjugated double bonds in the central acyclic chain.[14] Fragment ions of low intensity consistent with in-chain cleavages, some of which require hydrogen transfer, are indicated in Fig. 4. M − 123 ions compatible with cleavage of the C(6) − C(7) single bond of the γ-end were observed for both *10* and *12* and may be of diagnostic value. This same ion is observed in cleavages of the C(6) − C(7) bond of an α-end group but in this latter case an M − 56 ion which arises from a formal *retro*-Diels-Alder reaction is also noted.[12,15] An M − 137 ion, previously connected with carotenoids containing unsubstituted β-rings and ascribed to cleavage of the C(7) − C(8) double bond with hydrogen transfer to the smaller fragment,[12] was observed for β,γ-carotene (*12*) and not for γ,γ-carotene (*10*). Doubly charged molecular

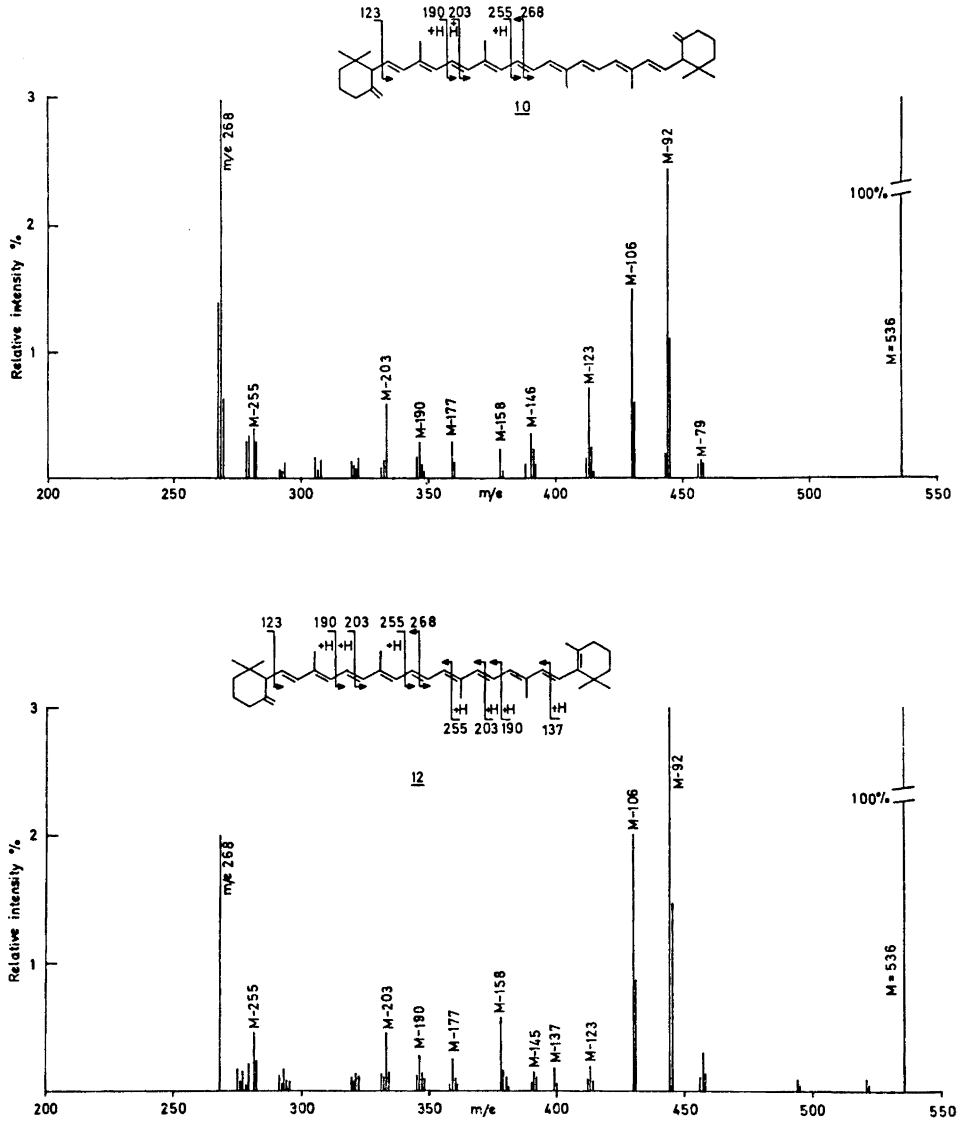

Fig. 4. Mass spectra of synthetic β,γ-carotene (*12*) and of synthetic γ,γ-carotene (*10*).

ions or ions due to cleavage of the central double bond (*m/e* 268) were abundant in both cases. M − 190, M − 203, and M − 255 peaks attributed to in-chain cleavages were also noted for both *10* and *12*.

Certain minor differences in the M − 92/M − 106 ratio and the low-intensity fragment ions of the previously published [4] mass spectrum of natural β,γ-carotene (*12*) and that of synthetic *12* given in Fig. 4 are ascribed to different

recording conditions. Thus natural *12* gave a mass spectrum essentially identical with the one presented for synthetic *12*, when recorded under similar conditions. The differences observed are accounted for by some variation in the hydrogen transfer pattern of certain in-chain cleavages; the present M − 123 contra the previously discussed [4] M − 135 ion may be explained by alternative processes of electron impact and thermal character.

β,γ-Carotene (*12*) has an asymmetric carbon atom at C − 6′ and the natural compound is, as expected, optically active.[16] It is not yet known whether the absolute configuration is 6′*R* (as in natural β,ε-carotene [3]) or 6′*S*.

Provided optically active γ-ionone was available the synthesis of natural β,γ-carotene or its enantiomer by the scheme outlined here should be feasible, assuming no extensive racemization of the conjugated ketone *5* occurred during the Horner reaction. However, conversion of γ-ionone (*5*) to γ-ionol followed by condensation of the γ-ionol-derived phosphonium salt with the appropriate β-C_{27}-aldehyde may be a preferred route to the optically active carotene *12*.

EXPERIMENTAL

General. Solvents were of reagent grade and were purified by distillation before use.

Preparative chromatography was carried out on silica gel G plates and thin layer chromatography on silica gel HF_{254} plates. Mixtures of petroleum ether (b.p. 40 − 65°) and acetone were used for development. Woelm Al_2O_3 (deactivated with 2 % water) was used for column chromatography. For comparative chromatography of synthetic and natural carotenes, Schleicher & Schüll paper No. 288 (Al_2O_3) was used after heat activation at 90° for 2 h. Mixtures of petroleum ether and diethyl ether were used to develop the paper chromatograms.

Melting points were determined on an Electrothermal melting point apparatus in sealed, evacuated tubes and are uncorrected.

Electronic absorption spectra were recorded on a Coleman Hitachi 124 spectrometer and IR spectra on a Perkin-Elmer 257 spectrometer using potassium bromide disks or liquid films. PMR spectra were obtained on a Varian A-60 A instrument using deuteriochloroform solutions with tetramethylsilane as internal standard. An AEI MS902 instrument was used for recording the mass spectra; the electron bombardment energy was 70 eV and the accelerating voltage 8 kV. Carotenes were recorded at 200°.

Gas chromatography involved the use of a Perkin-Elmer F11 Flame Ionization Instrument equipped with a 180 × 0.6 cm column packed with 10 % Silicon OV-17 (methyl-50 % phenylsilicon, Serva, Heidelberg) on Chromosorb W.

Methyl β-ionylideneacetate (2). Sodium methoxide in methanol was added dropwise to a stirred solution of β-ionone (*1*, 15 g) and ethyl diethylphosphonoacetate (18 g) in dry benzene (40 ml). The mixture was stirred at 40° for 10 h; the reaction being monitored by TLC on silica HF_{254} plates. The reaction mixture was poured over ice, extracted with ether and the organic layer washed with water until the aqueous extract was neutral to phenolphthalein. The ether solution was dried over sodium chloride and the solvent removed under vacuum. The residue consisted of 17.3 g (90 %) of *2*. Analyses by GLC showed 65 % *trans*- and 35 % *cis*-isomers. *2* had b.p. 118 − 120°/0.3 torr; λ_{max} (methanol) 260, 295 nm; ν_{max} (liq.) 3020 − 2820 (CH), 1715 (C=O), 1610 (conj. C=C), 1235 (C−O), 1135 (C−O) cm^{-1}; τ ($CDCl_3$; *trans*-isomer, signal assignments with reference to *2*, Scheme 1) 8.98 (6H, *gem.* dimethyl), 8.30 (3H, CH_3-*e*), 7.65 (CH_3-*d*), 6.28 (3H, OCH_3), 4.23 (1H, H-*a*), 3.92 d (1H, J = 16 Hz, H-*b*), 3.48 d (1H, J = 16 Hz, H-*c*); *m/e* 248 (M), 233 (M − 15), 217 (M − 31) and 189 (M − 59).

β-Ionylidene-ethanol (3). A solution of *2* (10 g) in ethyl ether (40 ml) was added to a suspension of lithium aluminium hydride (1.7 g) in ether (30 ml) at 0 − 5° over a period of 30 min. Stirring was continued for 1 h during which time the reaction was followed by TLC (disappearance of the starting material). The complex was decomposed by the

addition of wet methanol followed by a 10 % aqueous solution of ammonium chloride. The ether solution was washed with water and the solvent evaporated under vacuum to yield 8.5 g (90 %) of *3*; b.p. 140–145°/0.3 torr; λ_{max} (methanol) 237, 265 nm; ν_{max} (liq.) 3320 (OH), 3020–2820 (CH), 1010 (CH_2OH), 970 (*trans* CH=CH) cm^{-1}; τ ($CDCl_3$; with reference to *3*, Scheme 1) 8.98 (6H, *gem.* dimethyl), 8.30 (3H, CH_3-*e*), 8.14 (3H, CH_3-*d*), 5.71 d (2H, J=7 Hz, CH_2OH), 4.27 t (1H, J=7 Hz, H-*a*), 3.91 (2H, olefinic H-*b*,*c*); *m/e* 220 (M).

β-Ionylidene-ethyltriphenylphosphonium bromide (4). A solution of *3* (5 g) and triphenylphosphonium bromide (9 g) in methanol-chloroform (40 ml, 1:1) was stirred at 20° for 48 h. The solution was washed with water, the organic layer dried with sodium sulfate and the solvents removed under vacuum. The residue was triturated with ethyl acetate to give 9.2 g (75 %) of *4*. After recrystallization from methylene chloride-ethyl acetate *4* melted at 123°; τ ($CDCl_3$; see Scheme 1) 9.03 (6H, *gem.* dimethyl), 8.53 (3H, CH_3-*d*), 8.37 (3H, CH_3-*e*), 5.25 dd (2H, J_{H-P}=15. Hz, J_{H-H}=8 Hz, CH_2P), 4.70 (1H, complex coupling, H-*a*), 4.00 (2H, olefinic H-*b*,*c*) and 2.4–1.9 (aromatic H).

Methyl γ-ionylideneacetate (6). Sodium methoxide in methanol was added to a solution of γ-ionone (*5*, 2 g) and ethyl diethylphosphonoacetate (2.4 g) in a manner analogous to that described for the preparation of *2*. After work-up, GLC analysis showed a mixture of 52 % *trans-6*, 38 % *cis-6*, and 10 % *2*. The oily product was purified by column chromatography on Al_2O_3 to give 2.32 g (90 %) *6*; λ_{max} (methanol) 260 nm; ν_{max} (liq.) 3080–2840 (CH), 1718 (C=O), 1610 (conj. C=C), 892 ($R_1R_2C=CH_2$) cm^{-1}; τ ($CDCl_3$; see Scheme 1) 9.17, 9.08 (6H, *gem.* dimethyl), 7.68 (3H, CH_3-*d*), 7.45 d (1H, J=7 Hz, H-*g*), 6.28 (3H, OCH_3), 5.28, 5.40 (2H, $=CH_2$-*e*), 5.76 (1H, H-*a*), 4.03–3.70 (2H, olefinic H-*b*,*c*); *m/e* 248 (M), 233 (M–15), 217 (M–31), 205 (M–43), 201 (M–47), 192 (M–56), 189 (M–59) and 177 (M–71).

γ-Ionylidene-ethanol (7). *6* (2.2 g) was reduced with lithium aluminium hydride (0.4 g) as described for the preparation of *3*. After work-up, *7* (2 g, 90 %) was obtained; λ_{max} (methanol) 238 nm; ν_{max} (liq.) 3350 (OH), 3020–2860 (CH), 1640 (C=C), 1035 (CH_2OH), 893 ($R_1R_2C=CH_2$) cm^{-1}; τ ($CDCl_3$; see Scheme 1) 9.18, 9.10 (6H, *gem.* dimethyl), 8.25 (CH_3-*d*), 7.80 d (1H, J=6 Hz, H-*g*), 5.72 d (2H, J=6 Hz, CH_2OH), 5.30, 5.40 (2H, $=CH_2$-*e*), 4.5–3.7 (3H, olefinic H-*a*,*b*,*c*); *m/e* 220 (M), 205 (M–15), 194 (M–26), 179 (M–41), 176 (M–44), 161 (M–59) and 136 (M–84).

γ-Ionylidene-ethyltriphenylphosphonium bromide (8). *8* was prepared from *7* (2 g) and triphenylphosphonium bromide (3.7 g) in a manner identical to that described for the preparation of *4*. The phosphonium salt could not be crystallized and was dried to an amorphous powder under vacuum and used without further purification; τ ($CDCl_3$; see Scheme 1) 9.24, 9.31 (6H, *gem.* dimethyl), 8.60 (3H, CH_3-*d*), 7.60 d (1H, J=8 Hz, H-*g*), 5.53, 5.30 (2H, $=CH_2$-*e*), 5.25 dd (2H, J_{H-P}=16 Hz, J_{H-H}=8 Hz, CH_2-P), 4.70 (complex coupling, 1H, H-*a*), and 4.3–3.7 (2H, olefinic H-*b*,*c*).

γ,γ-Carotene (10) and *γ-apo-12′-carotenal (11).* Sodium methoxide was slowly added to a stirred solution of *8* (250 mg) in dry methanol (5 ml) until the phosphonium salt was completely converted to the deep red phosphoran. A solution of 2,7-dimethyl-2,4,6-trienedial (*9*, 75 mg, prepared from the acetylenic analogue [11]) was added and the mixture stirred. The progress of the reaction was monitored by TLC and additional phosphoran, generated externally, was added until analysis showed no starting dial (*9*). Water was added and the crude product extracted with ether, the ether extract dried over sodium sulfate and the solvent removed under vacuum. Preparative thick layer chromatography afforded *10* (49 mg, 20 % based on starting dial, mixture of *cis-* and *trans*-isomers) and *11* (80 mg, 50 % based on starting dial, mixture of *cis-* and *trans*-isomers). Both *10* and *11* were purified by re-chromatography. After repeated crystallizations from benzene-methanol all *trans-10* was isolated, m.p. 183°; λ_{max} (petroleum ether) 414, 438 E(1 %, 1 cm)=2960, 468 nm, (acetone) 416, 440 E(1 %, 1 cm)=2870, 469 nm, (ether) 415, 439, 469 nm, see Fig. 1; ν_{max} (KBr) 889 ($R_1R_2C=CH_2$), 963 cm^{-1} (*trans*-disubstituted double bonds), see Fig. 2; τ ($CDCl_3$) see Fig. 3 with assignments; *m/e* 536 (M), 457 (M–79), 444 (M–92), 430 (M–106), 413 (M–123), 378 (M–158), 346 (M–190), 333 (M–203), and 268, see Fig. 4. For *11*, λ_{max} (petroleum ether) 386, 405, 428 nm, ($CHCl_3$) 425 nm, (acetone) 413 nm; τ ($CDCl_3$) 9.16, 9.08 (6H, *gem.* dimethyl), 8.12 (3H, CH_3-*a*), 8.02, 7.97 (6H, CH_3-*b*,*c*), 7.49 d (1H, J=7 Hz, H-*d*), 5.43, 5.25 (2H, $=CH_2$-*e*), 4.1–3.0 (9H, olefinic), 0.53 (1H, H-*f*); *m/e* 350 (M), 335 (M–15), 322 (M–28), 307 (M–28–15), 227 (M–123), and 201 (M–149).

Co-chromatography of synthetic *10* and *10 ex Macrosiphum liriodendri* gave no separation, see Table 1.

Table 1. Chromatographic properties of natural and synthetic γ,γ-carotene (*10*) and β,γ-carotene (*12*).

Compound	R_F value S & S 288 paper		Al_2O_3 plates
10 (natural)	0.16[a]	0.28[b]	0.23[c]
10 (synthetic)	0.16[a]	0.28[b]	0.23[c]
12 (natural)	0.20[a]	0.40[b]	0.33[c]
12 (synthetic)	0.20[a]	0.40[b]	0.33[c]

[a] Petroleum ether. [b] 1 % ether in petroleum ether. [c] 5 % ether in petroleum ether.

β,γ-Carotene (12). Sodium methoxide was added dropwise to a stirred solution of *4* (100 mg) in dry methanol (5 ml). *11* (50 mg) in dry methanol was added to the red phosphoran solution. The reaction mixture was stirred at room temperature and the progress followed by TLC. Additional phosphoran was added until no starting aldehyde (*11*) remained. The solution was worked up as described for *10* and β,γ-carotene (*12*) isolated by preparative thick layer chromatography (11.5 mg, 15 % based on starting aldehyde *11*). After purification by plate chromatography and repeated crystallizations from benzene-methanol solution *trans*-β,γ-carotene (*12*) melted at 174°; λ_{max} (petroleum ether) 421, 444 E(1 %, 1 cm)=2600, 472 nm, (acetone) 425, 447.5, 475 nm, (ether) 422, 444, 473 nm, see Fig. 1; τ ($CDCl_3$, τ-values previously [1,4] reported were for CCl_4solution and not $CDCl_3$) 9.17, 9.09 (6H, *gem.*-dimethyl on γ-ring), 8.96 (6H, *gem.*-dimethyl on β-ring), 8.50 mult. (8H, non-allylic methylene), 8.28 (3H, end-of-chain methyl in β-ring), 8.03 (12H, in-chain methyl), 7.9 mult. (4H, allylic methylene), 7.49 d (1H, J=8 Hz, methine at C-6′), 5.25, 5.43 (2H, $=CH_2$), 4.1–3.1 (14H, olefinic); *m/e* 536 (M), 457 (M–79), 444 (M–92), 430 (M–106), 413 (M–123), 399 (M–137), 378 (M–158), 359 (M–177), 346 (M–190), 333 (M–203), and 268, see Fig. 4.

Mixed melting point determination with natural β,γ-carotene (m.p. 176°) gave no depression. Co-chromatography of synthetic *12* with natural material from two sources gave no separation, see Table 1. Comparison of the visible light absorption spectra of synthetic and natural β,γ-carotene showed compatibility in every detail.

Acknowledgements. Synthetic γ-ionone was a gift from Dr. J. Becker through Dr. A. F. Thomas, Research Department, Firmenich & Cie, Geneva. 2,7-Dimethyl-2,6-dien-4-yne-1,8-dial was a gift from Dr. O. Isler, Hoffmann-La Roche, Basel.

A.G.A. was the recipient of a postdoctorate fellowship through the auspices of the *Royal Norwegian Council for Industrial and Scientific Research.*

REFERENCES

1. Andrewes, A. G. and Liaaen-Jensen, S. *Acta Chem. Scand.* **25** (1971) 1922.
2. IUPAC. Tentative Rules of Carotenoid Nomenclature. *Biochemistry. In press.*
3. Straub, O. In Isler, O., Ed., *Carotenoids*, Appendix, Birkhäuser, Basel 1971.
4. Arpin, N., Fiasson, J.-L., Bouchez-Dangye-Caye, M. P., Francis, G. W. and Liaaen-Jensen, S. *Phytochemistry* **10** (1971) 1595.
5. Andrewes, A. G., Kjøsen, H., Liaaen-Jensen, S., Weisgraber, K. H., Lousberg, R. J. J. C. and Weiss, U. *Acta Chem. Scand.* **25** (1971) 3878.
6. Weisgraber, K. H., Lousberg, R. J. J. C. and Weiss, U. *Experientia* **27** (1971) 1017.
7. Mayer, H. and Isler, O. In Isler, O., Ed., *Carotenoids*, Birkhäuser, Basel 1971, Chapter 6.

8. Manchand, P. S., Rüegg, R., Schwieter, U., Siddons, P. T. and Weedon, B. C. L. *J. Chem. Soc.* **1965** 2019.
9. Wadsworth, W. S. and Emmons, W. D. *J. Am. Chem. Soc.* **83** (1961) 1733.
10. Willhalm, B., Steiner, U. and Schinz, H. *Helv. Chim. Acta* **41** (1958) 1359.
11. Surmatis, J. and Ofner, A. *J. Org. Chem.* **28** (1963) 2735.
12. Vetter, W., Englert, G., Rigassi, N. and Schwieter, U. In Isler, O., Ed., *Carotenoids*, Birkhäuser, Basel 1971, Chapter 4.
13. Enzell, C. R., Francis, G. W. and Liaaen-Jensen, S. *Acta Chem. Scand.* **23** (1969) 727.
14. Enzell, C. R., Francis, G. W. and Liaaen-Jensen, S. *Acta Chem. Scand.* **22** (1968). 1054.
15. Svec, W. A., Harkness, A. L., Strain, H. H. and Katz, J. J. *Org. Mass Spectrom.* **6** (1972) 843.
16. Borch, G., Andrewes, A. G. and Liaaen-Jensen, S. *Unpublished results.*

Received November 22, 1972.

ACTA CHEMICA SCANDINAVICA 27 (1973) 1410–1416

The Lattice Energy and Thermochemical Properties of the Compound $NaAlF_4$, Sodium Tetrafluoroaluminate

JAN LÜTZOW HOLM

Institute of Physical Chemistry, The University of Trondheim, N-7034 Trondheim, Norway

The author's earlier phase investigations show that $NaAlF_4$ does not exist as a stable compound in the solid phase in the system NaF-AlF_3. Lattice energy calculations of the hypothetical compound $NaAlF_4$, sodium tetrafluoroaluminate, with a tetrahedral AlF_4^- ion have been carried out. On the basis of these calculations some recommended enthalpies of reaction between compounds in the system sodium fluoride-aluminium fluoride at 298 and 1300 K in the solid, liquid, and gaseous state are given.

The phase diagram of the system NaF-AlF_3 has been investigated by a number of workers throughout the last 50 years, with different conclusions. Even recent investigations of the phase diagram of this system are in disagreement.[1–6]

The present author [2] was not able to detect any stable phase which could correspond to $NaAlF_4$. He therefore revised Grjotheim's [1] diagram and presented a phase diagram [2,3] which is shown in Fig. 1. In the course of this work [2] samples of the composition 50 mol % NaF + 50 mol % AlF_3 were examined both by X-ray and microscopy. All samples examined contained very well-formed crystals of chiolite, $Na_5Al_3F_{14}$, which could easily be detected under a microscope. In addition, two other phases were observed, one phase corresponding to the eutectic mixture and another to a so-called "corroded" phase. This phase consisted of powder which had not melted. It was possible to pick out some very tiny crystals from this phase. These crystals were identified in the microscope as AlF_3. The 50:50 composition was examined by DTA, and only one exothermic peak was observed on cooling, at 695°C, corresponding to the eutectic temperature in the system $Na_5Al_3F_{14} - AlF_3$. It was confirmed that the $NaAlF_4$ compound could be obtained as a *metastable* phase by quenching the vapour, in agreement with Howard's [4] results.

It was shown by DTA and X-ray studies [2] of the quenched metastable $NaAlF_4$ that it disproportionates to chiolite, $Na_5Al_3F_{14}$, and aluminium fluoride upon heating. This dissociation will take place slowly even at room temperature. *E.g.*, a sample quenched by Howard [4] and shown to be $NaAlF_4$,

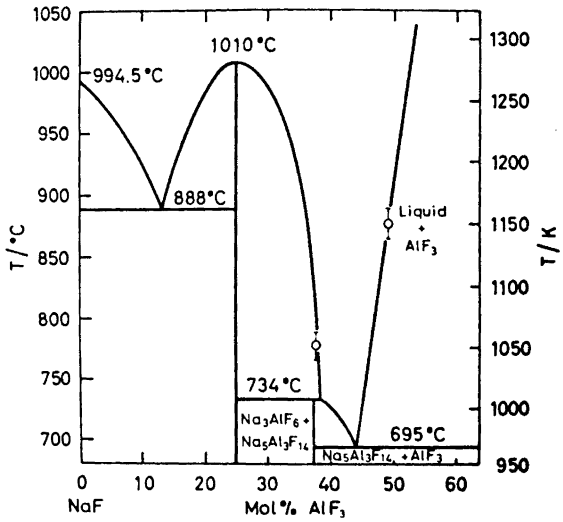

Fig. 1. The revised phase diagram of the system NaF-AlF_3. Circles with vertical bars denote points determined for $Na_5Al_3F_{14}$ and $NaAlF_4$ by drop calorimetry.[8]

was contained by the present author in a desiccator for 2 – 3 years. After this period, new X-ray examinations showed that only $Na_5Al_3F_{14}$ and AlF_3 were present.

Ginsberg and Wefers [5] in a more recent work claim that the compound $NaAlF_4$ is stable in a very narrow temperature range, 680 – 710°C. They were, however, not able to prove the existence of this compound by phase studies by high-temperature X-ray diffraction or other methods.

Foster [6] reexamined the AlF_3-side of the system by DTA and quenching, and reached the same conclusion as the present author and also Phillips *et al.*[7] did, namely that there is no sign of any stability range for $NaAlF_4$ in the system NaF-AlF_3 at any temperature and at normal pressure.

Some new examinations carried out by the present author [8] on the heat content of both the solid and molten mixtures of the composition 50 mol % NaF + 50 mol % AlF_3 show that the liquidus point for this composition is at 880 ± 5°C (1150 K). This strongly indicates that the phase diagram presented in Fig. 1 is the correct one.

Attempts to discuss the stability or the thermodynamic properties of solid $NaAlF_4$ in relation to the other fluoroaluminates were made by Sidorov *et al.*[9–11] and later also by Grjotheim *et al.*[12] The main reason why the stability of sodium tetrafluoroaluminate has been of particular interest is the fact that the dissociation scheme

$$Na_3AlF_{6(l)} = 2NaF_{(l)} + NaAlF_{4(l)}$$

for some time has been suggested as the most probable one for molten cryolite.

This reaction scheme has been suggested on the basis of thermodynamic calculations and also from spectroscopic examinations.[13] The results from the latter are, however, doubtful. It should also be pointed out that the approaches to the problem of dissociation of the cryolite anion based on phase diagram calculations have been built on assumptions like the ideality of the molten mixture. It has been shown by the present author,[14] who measured enthalpies of mixing in the system Na_3AlF_6-NaF, that this assumption is not valid.

In the following, the stability of the compound $NaAlF_4$, both as a tetrahedral compound with isolated AlF_4^- ions and as an octahedral compound, will be calculated by use of enthalpy cycles and thermodynamic data available in the literature.

CALCULATIONS

(a) *Lattice energy calculations.* The fluoride affinity, $Y(AlF_4^-)$, of gaseous aluminium trifluoride is given by the reaction

$$AlF_{3(g)} + F_{(g)}^- = AlF_{4(g)}^-$$

The value of this affinity can be calculated from the following enthalpy cycle (cycle 1):

$$\begin{array}{ccccc} NaF_{(g)} & + & AlF_{3(g)} & \xrightarrow{\Delta H_3} & NaAlF_{4(g)} \\ \downarrow \Delta H_1 & & \downarrow \Delta H_2 & & \uparrow \Delta H_4 \\ Na_{(g)}^+ + F_{(g)}^- & + & AlF_{3(g)} & \xrightarrow{Y(AlF_4^-)} & Na_{(g)}^+ + AlF_{4(g)}^- \end{array}$$

which gives

$$Y(AlF_4^-) = \Delta H_3 - \Delta H_1 - \Delta H_2 - \Delta H_4$$

Here $\Delta H_1 = 152$ kcal (Chao [15])

$\Delta H_2 = 0$

$\Delta H_3 = -76$ kcal (Sidorov *et al.*[9-11] and Grjotheim *et al.*[12]).

The enthalpy change, ΔH_4, has to be calculated. The Coulomb energy is given by

$$\Delta H_4 = -U = -\frac{Z_1 Z_2 e^2}{d_{NaAlF_4}}(1 - \varrho/\varrho_0) \qquad (1)$$

By using an interatomic distance, $d = 3.10$ Å, in the gas molecule $NaAlF_4$, one finds from eqn. (1): $\Delta H_4 = -97$ kcal mol^{-1}. The fluoride affinity of gaseous aluminium trifluoride is

$$Y(AlF_4^-) = -76 - 152 + 97 = -131 \text{ kcal}$$

This value should be compared with the fluoride affinity of $BF_{3(g)}$, which is -76 kcal mol^{-1}.[16] Hence, gaseous aluminium trifluoride has a higher affinity for fluoride ions than boron trifluoride.

The lattice energy of $NaAlF_4$, sodium tetrafluoroaluminate, a hypothetical compound with isolated tetrahedral AlF_4^- ions, which is isomorphous with $NaBF_4$, can be calculated from the well-known Kapustinskii [17] equation

$$U_L = 287.2 \frac{vZ_1Z_2}{r_+ + r_-}\left(1 - \frac{0.345}{r_+ + r_-}\right) \text{kcal mol}^{-2} \quad (2)$$

where v is the number of ions (here 2), $r_+ = 0.98$ Å, and $r_- = 2.60$ Å. The last value is the estimated thermochemical radius of the tetrahedral AlF_4^- ion. This value is reasonable when compared with the thermochemical radius of the BF_4^- ion, which is 2.28 Å.[16] Using these values one obtains a lattice energy of $NaAlF_4$ at 0 K of $U_L = 146$ kcal mol^{-1}. At 298.15 K, this value should be corrected to 145 kcal mol^{-1}.

(b) *The enthalpy of formation of $NaAlF_4$.* When both the lattice energy and the fluoride affinity are known, the enthalpy of formation of the hypothetical compound $NaAlF_4$ can be calculated at 298.15 K, from the following enthalpy cycle (cycle 2):

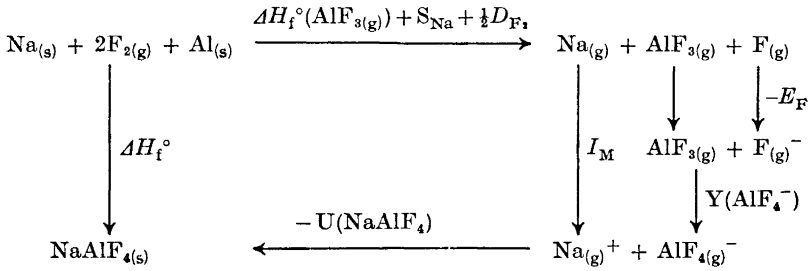

$$\Delta H_{f\,298.15}^\circ = \Delta H_f^\circ(AlF_{3(g)}) + S_{Na} + \tfrac{1}{2}D_{F_2} + I_{Na} - E_{F^-} - Y(AlF_4^-) - U(NaAlF_4)$$

After inserting the values given in Table 1, one optains for the enthalpy of formation of $NaAlF_{4(s)}$

$$\Delta H_{f\,298.15}^\circ = -290 + 26 + 18 + 118 - 80 - 131 - 145 = -482 \text{ kcal mol}^{-1}.$$

Table 1. Some lattice energy and enthalpy data in kcal mol^{-1} for $NaBF_4$ and $NaAlF_4$. (From Waddington,[16] JANAF,[18] and this work.)

Comp.	$Na_{(s)} \rightarrow Na_{(g)}$	$M_{(s)} + \frac{3}{2}F_{2(g)} \rightarrow MF_{3(g)}$	$\frac{1}{2}F_{2(g)} \rightarrow F_{(g)}$	$F_{(g)} + e^- = F_{(g)}^-$ [a]	$MF_{3(g)} + F_{(g)}^- = MF_{(g)}^-$	$Na_{(g)} = Na_{(g)}^+ + e^-$	$-U_{NaMF_4}$	$\Delta H_{f\,(NaMF_4)}^\circ$
$NaBF_4$	26	−271	18	−80	−76	118	−160	−425
$NaAlF_4$	26	−290	18	−80	−131	118	−145	−482

[a] From Ladd, M. F. C. and Lee, W. H. *Progr. Solid State Chem.* **1** (1963) 37 and **2** (1965) 378.

In Table 1 the values for $NaAlF_4$ are compared with the corresponding enthalpy data for sodium tetrafluoroberyllate. $NaBeF_4$, which is a stable compound in the solid state. The data are the same as those given in the review by Waddington.[16]

Table 2. Enthalpies of formation, ΔH_f, in kcal mol^{-1} for some important compounds in the system NaF-AlF_3 at 298.15 and 1300 K. (From JANAF [18] and this work [a]).

Phase	Temp/K	NaF	AlF_3	Na_3AlF_6	$NaAlF_4$ tetrahedral	$NaAlF_4$ octahedral
Solid	298.15	−137.5	−361	−793	−482 [a]	−498 [a]
	1300	−159.1	−360	−851.5	−509 [a]	−523 [a]
Liquid	298.15	−130.5	−353 [a]	−774 [a]	−478 [a]	
	1300	−151.1	−349 [a]	−824 [a]	−502 [a, b]	
Gas	298.15	−69.4	−289		−435	
	1300	−95.6	−293		−464	

[a] Estimated uncertainties for the new values 1−2 kcal.
[b] See Ref. 22.

It is now possible to calculate more accurate enthalpies of reaction for the compounds in the binary system NaF-AlF_3, by use of the new values. These results are summarized in Table 2. The enthalpy of fusion of AlF_3 at 1300 K, $\Delta H_f = 11$ kcal, is a hypothetical value which has been determined by the author.[14] This value has been added to the enthalpy of formation of solid AlF_3 to give the enthalpy of formation of liquid AlF_3.

The enthalpy values given for solid $NaAlF_4$ with octahedral coordination at 298.15 and 1300 K are taken as the most probable ones, giving the enthalpy of the reaction

$$NaF_{(s)} + AlF_{3(s)} = NaAlF_{4(s)}(\text{oct.})$$

as follows:

$$\Delta H^\circ = +1 \text{ kcal at } 298.15 \text{ K}$$

and

$$\Delta H^\circ = -4 \text{ kcal at } 1300 \text{ K}.$$

Hence one gets for the solid state reaction

$$NaAlF_4(\text{tetr.}) \rightarrow NaAlF_4(\text{oct.})$$

$\Delta H_{298.15} = -16$ kcal showing a strong preference for octahedral co-ordination of aluminium with respect to fluorine.

From the enthalpies given in Table 1 it is possible to calculate the enthalpy for the reaction

$$3NaAlF_{4(s)} = Na_3AlF_{6(s)} + 2AlF_{3(s)}$$

At 298.15 K one obtains $\Delta H = -21$ kcal. This result clearly shows the unstability of $NaAlF_4$ with respect to Na_3AlF_6 and AlF_3, in complete agreement with the phase diagram investigations.

The enthalpy of fusion of the hypothetical compound $NaAlF_4$ with tetrahedral AlF_4^- ions was taken as 7 kcal mol^{-1} at 1300 K and 5 kcal mol^{-1} at 298.15 K. These values should be of the same magnitude as the enthalpy of fusion of the compound $NaBF_4$, which is 5 kcal mol^{-1} according to Dworkin and Bredig.[19] The enthalpy of fusion of $NaAlF_4$ with octahedral structure was taken as 19 kcal mol^{-1}, the value which has been determined by the author [8] for a mixture of $\frac{1}{3}Na_3AlF_6$ and $\frac{2}{3}AlF_3$.

The enthalpy of fusion of cryolite, Na_3AlF_6, was taken as $\Delta H_f = 27.5$ kcal mol^{-1}, a value which was obtained by the present author [14] in good agreement with the value given by O'Brien and Kelley,[20] 27.64, kcal mol^{-1}. From these values one can calculate enthalpies of reaction in the liquid state. Here the following three reactions are of particular interest:

$$\text{(I)}\quad Na_3AlF_{6(l)} = 3NaF_{(l)} + AlF_{3(l)}, \qquad \Delta H = 22 \pm 1 \text{ kcal}$$

$$\text{(II)}\quad Na_3AlF_{6(l)} = 2NaF_{(l)} + NaAlF_{4(l)}, \qquad \Delta H = 18 \pm 1 \text{ kcal}$$

$$\text{(III)}\quad 3NaAlF_{4(l)} = Na_3AlF_{6(l)} + 2AlF_{3(l)}, \qquad \Delta H = -12 \pm 1 \text{ kcal}$$

The enthalpies given for the three reactions are those calculated at 1300 K from the data in Table 1. These results give new and important information about the *thermodynamically* most probable dissociation scheme for molten cryolite in the system NaF-Na_3AlF_6 [21] as well as about the stability of the AlF_4^- ion in the system Na_3AlF_6-AlF_3.[8,12]

In the gas phase the enthalpy for the reaction

$$NaF_{(g)} + AlF_{3(g)} = NaAlF_{4(g)} \qquad \Delta H = -74 \text{ kcal}$$

given by Sidorov *et al.*[9-11] and also by Grjotheim *et al.*[12] has been adopted as the most probable value. It has been shown by Kvande [23] that this value is nearly temperature independent.

REFERENCES

1. Grjotheim, K. *Contribution to the Theory of the Aluminium Electrolysis, Kgl. Norske Videnskap. Selskaps, Skrifter* **1956** No. 5.
2. Holm, J. L. *Undersøkelser av struktur og faseforhold for en del systemer med tilknytning til aluminiumelektrolysen*, Lic. thesis, Institute of Inorganic Chemistry, NTH, Trondheim 1963.
3. Brynestad, J., Grjotheim, K. and Holm, J. L. *Bul. Inst. Politeh. Bucuresti* **15** (1963) 57.
4. Howard, E. H. *J. Am. Chem. Soc.* **76** (1954) 2041.
5. Ginsberg, H. and Wefers, K. *Z. Erzbergbau Metallhüttenw.* **20** (1967) 156.
6. Foster, P. A., Jr. *J. Am. Ceram. Soc.* **53** (1970) 598.
7. Phillips, N. W. F., Singleton, R. H. and Hollingshead, E. A. *J. Electrochem. Soc.* **102** (1955) 690.
8. Holm, J. L. *High Temp. Science. In press.*
9. Sidorov, L. N., Erokhin, E. V., Akishin, P. A. and Kolosov, E. N. *Dokl. Akad. Nauk SSSR* **73** (1967) 370.
10. Sidorov, L. N. and Kolosov, E. N. *Zh. Fiz. Khim.* **42** (1968) 2617; *Russ. J. Phys. Chem.* **42** (1968) 1382.

11. Sidorov, L. N., Kolosov, E. N. and Shol'ts, V. B. *Zh. Fiz. Khim.* **42** (1968) 2620; *Russ. J. Phys. Chem.* **42** (1968) 1384.
12. Grjotheim, K., Motzfeldt, K. and Rao, D. B. In Edgeworth, T. G., Ed., *Light Metals* 1971, Proceedings of Symposia at the 100th AIME Annual Meeting, New York 1971, p. 223.
13. Solomons, C., Clarke, J. H. R. and Bockris, J. O'M. *J. Chem. Phys.* **49** (1968) 445.
14. Holm, J. L. *Thermodynamic Properties of Molten Cryolite and other Fluoride Mixtures*, Dr. thesis, The University of Trondheim, NTH, Norway, Nov. 1971.
15. Chao, J. *Thermochim. Acta* **1** (1970) 71.
16. Waddington, T. C. *Advan. Inorg. Chem. Radiochem.* **1** (1959) 157.
17. Kapustinskii, A. F. *Quart. Rev. (London)* **10** (1956) 283.
18. *JANAF Thermochemical Tables*, Clearinghouse, Springfield, Va. 1971.
19. Dworkin, A. S. and Bredig, M. A. *J. Chem. Eng. Data* **15** (1970) 505.
20. O'Brien, C. J. and Kelley, K. K. *J. Am. Chem. Soc.* **79** (1957) 5616.
21. Holm, J. L. *Inorg. Chem. In press.*
22. Holm, J. L. *Acta Chem. Scand.* **27** (1973) 371.
23. Kvande, H. *Kryolitt-aluminiumoksyd-blandingers termodynamikk studert ved damptrykkmålinger*, Lic. thesis, Institute of Inorganic Chemistry, NTH, Trondheim 1972.

Received November 7, 1972.

ACTA CHEMICA SCANDINAVICA 27 (1973) 1417–1420

The Synthesis of [Dihalo(*N*,*N*-pentamethylenecarbamoyl)-methyl]phenylmercury Compounds and Their Thermal Decomposition to Halo-β-lactams*

NILS GUNNAR JOHANSSON

Department of Organic Chemistry, Royal Institute of Technology, S-100 44 Stockholm 70, Sweden

The base catalyzed condensation between phenylmercuric chloride and the *N*-(dihaloacetyl)piperidines *4a* and *4b* has been investigated. The yields are strongly influenced by the temperature and the state of the base. The thermal generation of β-lactam from the condensation product *1a* was quite facile whereas the compound *1b* reacted very sluggishly.

A novel synthesis of bromo-β-lactams has recently been described.[1] In this synthesis [dibromo(*N*,*N*-pentamethylenecarbamoyl)methyl]phenylmercury (*1a*) was decomposed in refluxing bromobenzene to yield a mixture of the two isomeric bromo-β-lactams *2a* and *3a*. The reaction is an extension of the mercury induced dihalocarbene synthesis introduced by Seyferth and his coworkers.[2]

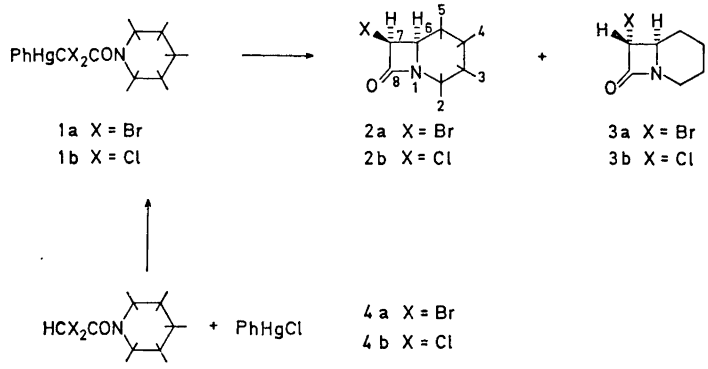

Mercury compound *1a* was synthesized in 50 % yield by stirring a benzene solution of *N*-(dibromoacetyl)piperidine (*4a*), potassium *t*-butoxide (*t*-BuOK)

* Synthesis of Strained Heterocyclic Compounds, 4. Part 3. Johansson, N. G. and Åkermark, B. *Tetrahedron Letters* **1971** 4785.

and phenylmercuric chloride with a high-speed stirrer at 5 – 10°.[1,3] The yield can be increased to 70 – 80 % (*cf.* Ref. 4) by the use of tetrahydrofuran (THF) in place of benzene. Two different *t*-BuOK preparations have been used, the solid 1/1 complex *t*-BuOK/*t*-BuOH[5] (referred to as complexed *t*-BuOK) and noncomplexed *t*-BuOK made from equimolar amounts of potassium metal and *t*-BuOH in THF.

The yields of the mercury compounds *1a* and *1b* obtained at different reaction conditions are listed in Table 1. The yields are highest when noncomplexed

Table 1. Yields of [dihalo(*N*,*N*-pentamethylenecarbamoyl)methyl]phenylmercury (*1a*, *1b*) from *N*-(dihaloacetyl)piperidine (*4a*, *4b*), phenylmercuric chloride, and *t*-BuOK for variations of the condensation method.

Method	Solvent	Base	Temp. °C	Yield *1a*	Yield *1b*
A. High-speed stirring [1,3]	Benzene	1/1 complex *t*-BuOK/*t*-BuOH[5]	5 – 10	50	35
B. Base added to a mixture of PhHgCl and *4*	THF	1/1 complex *t*-BuOK/*t*-BuOH	– 20 to – 30	75	60
C. Base added to a mixture of PhHgCl and *4*	THF	1/1 complex *t*-BuOK/BuOH	– 70 to – 75	~10	–
D. Base added to a mixture of PhHgCl and *4*	THF	Noncomplexed *t*-BuOK (see text)	– 20 to – 30	80	60
E. Base added to a mixture of PhHgCl and *4*	THF	Noncomplexed *t*-BuOK	– 70 to – 75	50	–
F. *4* and PhHgCl consecutively added to the base		Noncomplexed *t*-BuOK	– 70 to – 75	70	60

t-BuOK is used at – 25° or – 75° (methods D and F) and when complexed *t*-BuOK is used at – 25° (method B). The order in which the reagents are added is also important (*cf.* Experimental, methods E and F). It is noteworthy that the dichloro compound *1b* is obtained in 10 – 20 % lower yield than the dibromo compound *1a*. Since the THF solution of noncomplexed *t*-BuOK is easier to make and handle than the 1/1 complex, method D appears to be the most convenient.

These findings are contrary to the results of Seyferth and Lambert concerning the condensation between phenylmercuric chloride and haloforms in THF.[4] They found that complexed *t*-BuOK gave high yields of phenyl(trihalomethyl)mercury compounds at – 25° as well as at – 75° whereas the noncomplexed commercial *t*-BuOK they used was not very effective at these temperatures. The reason for these discrepancies may be the different nature of the dihaloacetylpiperidines and the haloforms. Also the noncomplexed commercial product may be less pure than that freshly prepared from *t*-butyl alcohol and potassium.

[Dichloro(*N*,*N*-pentamethylenecarbamoyl)methyl]phenylmercury (*1b*) was decomposed by refluxing a solution in bromobenzene for a 22 h period. Phenylmercuric chloride and two isomeric chloro-β-lactams were obtained. The IR, NMR, and mass spectra of these were quite analogous to those of the *cis*- and *trans*-bromo-β-lactams *2a* and *3a*.[1] Consequently the chloro-β-lactams are assigned the *cis*- and *trans*-structures *2b* and *3b*, respectively. Some *N*-(dichloroacetyl)piperidine (*4b*) was also isolated.

Dichloro compound *1b* is considerably more stable than dibromo compound *1a*. This is shown by the fact that heating in refluxing bromobenzene for 22 h was required to decompose compound *1b* while only 1.7 h was required for compound *1a*. This is analogous to the findings of Seyferth *et al.* that the dihalocarbene is formed much more rapidly from phenyl(tribromomethyl)-mercury than from phenyl(trichloromethyl)mercury.[6]

A synthesis of the diiodo- and bromochloroanalogues of [dibromo(*N*,*N*-pentamethylenecarbamoyl)methyl]phenylmercury is under way.

EXPERIMENTAL

Melting points were determined on a micro hot stage and are uncorrected. Elemental analyses were carried out by A. Bernhardt, Elbach über Engelskirchen, West Germany. Infrared spectra were recorded on a Perkin Elmer No. 421, nuclear magnetic resonance spectra on a Varian A-60, and mass spectra on an LKB 2000 spectrometer. All THF used was freshly distilled from potassium metal under a nitrogen atmosphere.

Noncomplexed t-BuOK. *t*-BuOH (60.0 g, 0.81 mol), freshly distilled from sodium metal, and potassium metal (31.3 g, 0.80 mol) were heated in refluxing THF (700 ml) under an atmosphere of purified nitrogen until the reaction was complete (approximately 3 days). The solution was stored under nitrogen in the refrigerator. The concentration of *t*-BuOK was determined by titration of an aliquot of the solution; samples were removed with a pipette under nitrogen flushing.

[Dibromo(N,N-pentamethylenecarbamoyl)methyl]phenylmercury (1a). The apparatus was dried in an oven prior to use and was assembled and flushed with nitrogen while still hot.

The compositions of the crude reaction products were determined by quantitative IR spectroscopy and TLC.

Method A, see Refs. 1 and 3.

Method B (*cf.* Ref. 4). A magnetically stirred solution of *N*-(dibromoacetyl)piperidine (2.8 g, 10 mmol) and phenylmercuric chloride (3.1 g, 10 mmol) in THF was maintained at −30° to −20° by the use of an acetone bath to which dry ice was added as needed. A suspension of complexed *t*-BuOK [5] (1.9 g, 10 mmol) in THF (100 ml) was added to the reaction mixture over a 15 min period from a pressure equalizing addition funnel equipped with a magnetic stirrer. When the addition was complete the reaction mixture was stirred an additional 30 min at about −25°. The temperature was quickly raised to +10°, the solution was then transferred to a one-necked flask and the solvent evaporated on a rotary evaporator at room temperature. The residue was dissolved in benzene (250 ml), washed with distilled water (40 ml) and dried ($MgSO_4$).

Crystallization from dry diethyl ether gave [dibromo(*N*,*N*-pentamethylenecarbamoyl)methyl]phenylmercury [1] (*1a*) (4.1 g, 75 %), m.p. 126–128°.

Method C. As method B but performed at −75°. IR analysis of the crude product indicated that the yield of *1a* was *ca.* 10 %.

Method D. As method B except that the 1/1 *t*-BuOK/*t*-BuOH complex was replaced with noncomplexed *t*-BuOK (10 mmol in 50 ml of THF). Yield 4.4 g (80 %), m.p. 126–128°.

Method E. As method D but performed at −75°. Yield 50 % (from IR).

Method F. A magnetically stirred solution of noncomplexed *t*-BuOK (10 mmol) in THF (100 ml) was cooled to −75°. To this was added *N*-(dibromoacetyl)piperidine (2.8 g,

10 mmol) in THF (50 ml) over a 10 min period, immediately followed by a solution of phenylmercuric chloride (3.1 g, 10 mmol) in THF (50 ml), also over a 10 min period. The solution was stirred at −75° an additional 30 min. The reaction mixture was worked up as usual. Yield 70 % (from IR).

N-(*Dichloroacetyl*)*piperidine* (4b). The title compound was synthesized like the dibromo analogue,[1] m.p. 61−62°. (Found: C 44.1; H 5.9; Cl 35.1. Calc. for $C_7H_{11}NOCl_2$: C 42.9; H 5.7; Cl 36.1.) NMR ($CDCl_3$, δ units relative to TMS as internal standard): 1.65 (s, CH_2), 3.60 (s, $N-CH_2$), 6.2−6.5 (s, $CHCl_2$. δ depended on concentration). IR: (KBr) CO 1645 cm^{-1}.

[*Dichloro*(N,N-*pentamethylenecarbamoyl*)*methyl*]*phenylmercury* (1b). The yields of the different synthetic variations are listed in Table 1. M.p. 103−104°. (Found: C 33.1; H 3.1; Cl 14.9; Hg 42.7. Calc. for $C_{13}H_{15}NOCl_2Hg$: C 33.0; H 3.2; Cl 15.0; Hg 42.4.) NMR: 1.65 (s, CH_2), 3.70 (s, $N-CH_2$), 7.25 (s, aromatic protons). IR: (KBr) CO 1625 cm^{-1}.

Thermal decomposition of [*dichloro*(N,N-*pentamethylenecarbamoyl*)*methyl*]*phenylmercury* (1b). A solution of *1b* (18.5 g, 0.039 mol) in freshly distilled bromobenzene was refluxed for 22 h. The solvent was removed *in vacuo*, ether was added and the insoluble phenylmercuric chloride (10.3 g, 0.033 mol, 85 %) was filtered off. Separation of the ether soluble products was accomplished by chromatography on a short column of thin layer grade silica gel.[7] Elution with increasing amounts of diethyl ether in light petrol ether afforded *cis*-7-chloro-8-oxo-1-azabicyclo[4.2.0]octane(*2b*) (0.5 g, 8 %) and *trans*-7-chloro-8-oxo-1-azabicyclo[4.2.0]octane (*3b*), (2.7 g, 45 %). *cis*-7-Chloro-8-oxo-1-azabicyclo[4.2.0]octane (*2b*). (Found: C 52.5; H 6.3; Cl 22.0. Calc. for $C_7H_{10}ClNO$: C 52.7; H 6.3; Cl 22.2.) NMR: 1.1−2.1 (m, H-3, H-4 and H-5), 2.5−4.0 (m, H-2, H-6), 4.95 (two d, J 1.4 and 4.4 cps, H-7). IR (KBr) CO 1760 cm^{-1}. MS: 161, 159 (M, 14), 124 (M−Cl, 100). *trans*-7-Chloro-8-oxo-1-azabicyclo[4.2.0]octane (*3b*), m.p. 58−60°. (Found: C 52.3; H 6.5; Cl 22.1. Calc. for $C_7H_{10}ClNO$: C 52.7; H 6.3; Cl 22.2.) NMR: 1.1−2.2 (m, H-3, H-4 and H-5), 2.5−4.0 (m, H-2, H-6), 4.30 (d, J 1.3 cps, H-7). IR (KBr): CO 1760 cm^{-1}. MS: 161, 159 (M, 30) 124 (M−Cl, 100).

Acknowledgements. I thank Drs. B. Åkermark and B. Sjöberg for their interest and for stimulating discussions. The work has been supported by the *Swedish Board for Technical Development* and *AB Astra*. Miss G. Hammarberg recorded the spectra.

REFERENCES

1. Johansson, N. G. and Åkermark, B. *Acta Chem. Scand.* **25** (1971) 1927.
2. Seyferth, D., Burlitch, J. M., Minasz, R. J., Yick-Pui Mui, J., Simmars, Jr., H. D Treiber, A. J. and Dowd, S. R. *J. Am. Chem. Soc.* **87** (1965) 4259.
3. Seyferth, D. and Burlitch, J. M. *J. Organometal. Chem.* **4** (1965) 127.
4. Seyferth, D. and Lambert, Jr., R. L. *J. Organometal. Chem.* **16** (1969) 21.
5. Speziale, A. J. and Ratts, K. W. *J. Am. Chem. Soc.* **84** (1962) 854.
6. Seyferth, D., Burlitch, J. M. and Heeren, J. K. *J. Org. Chem.* **27** (1962) 1491.
7. Hunt, B. J. and Rigby, W. *Chem. Ind. (London)* **1967** 1868.

Received November 17, 1972.

ACTA CHEMICA SCANDINAVICA 27 (1973) 1421–1426

Oxidation of Phenyl-substituted Allenes with Peracids

TYGE GREIBROKK and LARS SKATTEBØL

Department of Chemistry, University of Oslo, Oslo 3, Norway

Oxidation of phenyl-substituted allenes with performic acid or *m*-chloroperbenzoic acid has been investigated. Phenylallene (*1a*) and 1,3-diphenylallene (*1b*) gave benzaldehyde and the respective acyloin ester *3* as products. Triphenylallene (*1c*) underwent acid-catalyzed dimerization to the indene *4* while tetraphenylallene (*1d*) oxidized to the indanone *5*. The respective allene oxide is clearly an intermediate in the oxidation reactions; moreover, the formation of *5* is best explained *via* the spiro dioxide *8*. Peracid oxidation of tetraphenylbutatriene (*2*) gave the tetralindione *12*.

Peracid oxidation of alkyl-substituted allenes has been reported.[1–5] The isolation of allene oxides was successfully achieved from reactions of both 1,3-di-*t*-butylallene[3] and 1,1,3-tri-*t*-butylallene[4] with *m*-chloroperbenzoic acid. Furthermore a buffered peracetic acid oxidation of *t*-butyl-1,1-dimethylallene resulted in the formation of a spirodioxide.[5] On the other hand, from tetramethylallene no allene oxides were isolated, although some of the products could be rationalized as resulting from both allene oxide and spirodioxide intermediates.[2]

We want to report the peracid oxidation of some phenyl-substituted allenes, *viz.* phenylallene (*1a*), 1,3-diphenylallene (*1b*), 1,1,3-triphenylallene (*1c*), and tetraphenylallene (*1d*). * We have also oxidized the cumulene tetraphenylbutatriene (*2*)under similar conditions. As oxidizing agents we employed both performic acid (PFA) and *m*-chloroperbenzoic acid (MCPBA).

Reaction of phenylallene (*1a*) with one equivalent of MCPBA resulted in recovery of almost half the amount of starting material. Using two equivalents of peracid, most of the allene reacted, and benzaldehyde was obtained in 50 % yield as the main product. From the residue the benzoate *3a* ($R^4 = m\text{-}ClC_6H_4CO$-) was isolated in 9 % yield. Oxidation of *1a* with PFA gave a small yield of benzaldehyde besides almost equal amounts (30 %) of 1-hydroxy-1-phenyl-2-propanone (*3a*, $R^4 = H$) and its formate (*3a*, $R = HCO-$). Similar results were obtained from the oxidation of 1,3-diphenylallene (*1b*); in this case benzaldehyde and the benzoate (*3b*, $R = m\text{-}ClC_6H_4CO-$) were obtained in 20 and 40 % yields, respectively, using MCPBA as oxidizing

* *Note added in proof.* After this paper was submitted for publication the peracid oxidation of *1d* to the hydroxyindanone *5* was reported by Oku *et al.* [*Bull. Chem. Soc., Japan* **46** (1973) 275].

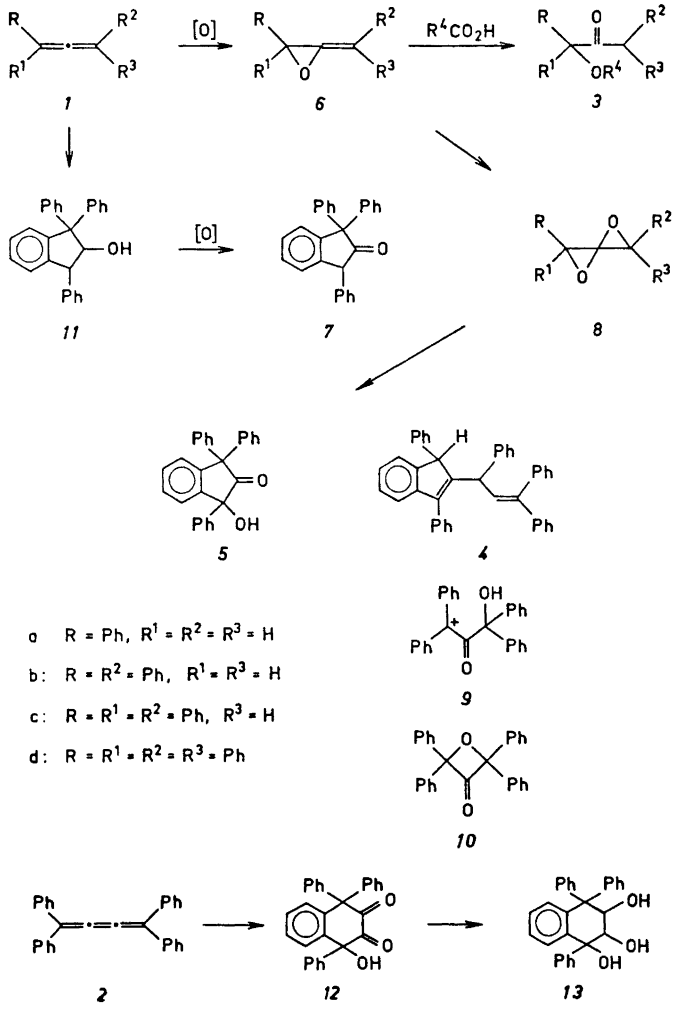

Scheme 1.

agent. With PFA the allene *1b* was oxidized to the formate 3b ($R^4 = HCO-$) and a small amount of benzaldehyde.

The reaction of triphenylallene with PFA took another course; the allene is extremely sensitive to acids which cause dimerization to 1,3-diphenyl-2-[1,3,3-triphenylallyl]indene *4*.[6] This compound was also one of the products using MCPBA together with a mixture of several compounds including acyloin esters which we could not separate.

So far neutral compounds have been described, but acidic compounds were also products from these reactions. They were removed with the alkaline washings and thus provide an explanation for the poor material balances.

However, attempts to obtain pure compounds from these mixtures were unsuccessful.

The oxidation of tetraphenylallene (*1d*) with either PFA or MCPBA proceeded slowly and was complete after the consumption of two equivalents of peracid. A single product was obtained in 83 % yield and identified as 1-hydroxy-1,3,3-triphenyl-2-indanone (*5*) on the basis of spectral data. The structure was subsequently proven by comparison with an independently synthesized authentic sample.[7]

There is ample evidence in the literature supporting the view that the formation of allene oxide *6* is the first step in the peracid oxidation of allenes. The fact that all our reactions followed approximately second order kinetics indicates that this must also be the rate-determining step. This oxide could rearrange to the corresponding cyclopropanone or react with the available carboxylic acid to the ring-opened product *3*. In our examples the latter reaction took place while no evidence for the presence of the cyclopropanone was obtained. If the ketone *3* is enolizable,* we have shown that it is further oxidized to benzaldehyde at a rate faster than that of the initial oxirane formation.[8] However, the corresponding compound from tetraphenylallene would not be enolizable and rearrangement *via* the carbonium ion to the indanone *7* could take place; further oxidation could then possibly lead to the observed product *5*. Another possibility available would be further oxidation of the allene oxide to the spiro dioxide *8* which in analogy with compound *6* could form the ketone *9*. Acid-catalyzed rearrangements to an oxetanone *10* or to the observed hydroxyindanone *5* are also possible reactions of the spiro dioxide. In order to distinguish between these alternative routes to 5 we synthesized the indanone *7* starting from tetraphenylallene. Acid-catalyzed rearrangement gave the corresponding indene. Hydroboration lead to 1,1,3-triphenylindan-2-ol (*11*) which by oxidation with Jones reagent afforded the indanone *7*. Treatment of this with MCPBA under conditions similar to those employed with tetraphenylallene gave no reaction. Hence we must conclude that the spiro dioxide is formed as a transient intermediate in the oxidation of *1d* to *5*. All attempts to isolate or to obtain evidence for the presence of the spiro oxide in the reaction mixture were unsuccessful. This is perhaps not surprising considering the strained structure and the observations by Crandall *et al.*[2,5] that compounds of this class are very sensitive to acids. The rearrangement of *8* to *5* would involve the carbonium ion *9* which also is the origin of tetraphenyl-oxetanone[9] (*10*). The latter is stable under the reaction conditions but we could not detect its presence in the reaction mixture. In this connection it is interesting that the oxetane *10* is formed by autooxidation of tetraphenylallene.[9]

It was of interest to see whether the cumulene tetraphenylbutatriene would behave in a similar way. The reaction with MCPBA gave besides a number of unidentified products a 40 % yield of a yellow compound, $C_{28}H_{20}O_3$. The NMR spectrum exhibited aromatic absorption and a broad singlet which disappeared on treatment with deuterium oxide. The presence

* At least one non-enolizable compound of structure *3* has been shown to react with peracid, while others have been resistant.[2]

of carbonyl and hydroxyl groups was evident from the infrared spectrum. As expected, the carbonyl absorption disappeared on reduction of the compound with sodium borohydride. The mass spectrum showed the molecular ion M (*m/e* 404) and the M − CO as well as M − 2 CO fragments corresponding to aryl-substituted α-diketones. The data are in agreement with the structure 1-hydroxy-1,4,4-triphenyltetralindione (*12*). The formation of this dione is quite analogous to the formation of *5* from *1d*. Several routes leading to *12* can be depicted including one *via* a spirotrioxide; however, without more information, further speculation is unwarranted.

Some simple kinetic measurements were carried out by following the consumption of peracid. For the first 50 % reaction, fairly good second order plots were obtained for compounds *1a*, *1b*, and *1d*; the rate constants were 0.7×10^{-3}, 0.7×10^{-3}, and 0.2×10^{-3} l mol^{-1} sec^{-1}, respectively. For comparison, the rate of oxidation of 3-methyl-1,2-butadiene was measured to 4.5×10^{-3} l mol^{-1} sec^{-1} which shows that phenyl-substitution does result in a significant rate decrease, as expected.

EXPERIMENTAL

General. NMR spectra were recorded on Varian Associates A60A and HA 100-15D spectrometers. Mass spectral data were obtained using an A.E.I. MS 902 mass spectrometer, and a Perkin Elmer model 457 spectrophotometer was used for obtaining infrared spectra. Elemental analyses were carried out by Ilse Beetz Microanalytical Laboratory, 8640 Kronach, Germany.

Oxidation of phenylallene (1a). (a) *With* m-*chloroperbenzoic acid.* To a solution of the allene *1a*[10] (3.5 g, 30 mmol) in 100 ml dichloromethane was added 2.9 g of 70 % MCPBA (60 mmol) and the reaction mixture left with stirring at 0° overnight. The solution was washed with aqueous Na_2CO_3 and dried (Na_2CO_3). Evaporation gave 3.6 g of a liquid which by distillation gave 1.5 g (50 %) of benzaldehyde. The residue was chromatographed on silica gel and 0.75 g (9 %) of the viscous liquid *3a* ($R^4 = ClC_6H_4COO-$) was isolated. (Found: C 66.27; H 4.48. Calc. for $C_{16}H_{13}O_3Cl$: C 66.50; H 4.51.) NMR ($CDCl_3$) CH_3 δ 2.2 (s), CH δ 6.3 (s), arom. H δ 7.2 − 8.1 in a ratio of 3:1:9. IR (CCl_4) 1720 and 1730 cm^{-1}. The mass spectrum exhibited a small molecular ion, but fragments corresponding to α-fission to carbonyl groups were all present.

(b) *With performic acid.* Phenylallene (3.5 g, 0.03 mol) was added to a solution of 30 % H_2O_2 (0.03 mol) in 90 % formic acid (30 ml) at room temperature. The mixture was stirred overnight, concentrated at reduced pressure and the residue dissolved in ether. The ether solution was washed with aqueous Na_2CO_3 and the ether evaporated. The NMR spectrum of the residue (3.0 g) revealed a mixture of 5 % yield of benzaldehyde, 30 % of 1-hydroxy-1-phenyl-2-propanone (*3a*, $R^4 = H$), and 30 % of its formate (*3a*, $R^4 = HCO-$). Further treatment with aqueous Na_2CO_3 solution, followed by distillation, gave 1.6 g (36 %) of *3a* ($R^4 = H$), b.p. 70° (0.05 mm),[11] the *semicarbazone* was formed, m.p. 193 − 194° (lit.[12] m.p. 194°).

Oxidation of 1,3-diphenylallene (1b). (a) *With* m-*chloroperbenzoic acid.* A solution of 1,3-diphenylallene[13] (1.92 g, 10 mmol) in dichloromethane was treated with MCPBA as described for *1a*. Reaction time was 3 days at 0°. The product was worked up in the usual way and analyzed by NMR. This revealed that benzaldehyde was formed in 20 % yield and the benzoate ester 3b ($R^4 = ClC_6H_4COO-$) in 40 % yield. A pure sample of the latter was obtained as a viscous liquid by chromatography on silica gel. (Found: C 73.25; H 4.87. Calc. for $C_{22}H_{17}O_3Cl$: C 72.45; H 4.67.) IR (CCl_4) 1720 and 1730 cm^{-1}. NMR ($CDCl_3$) CH_2 3.8 δ(s), CH 6.3 δ(s), arom. H 7.1 − 8.1 δ. The expected α-fission fragment of the carbonyl group was observed in the mass spectrum.

(b) *With performic acid.* 1,3-Diphenylallene (1.92 g, 10 mmol) was treated with performic acid as described under *1a*. After 24 h at room temperature and the usual work-up a liquid, 1.5 g (68 %), was obtained which consisted of a small amount of benzaldehyde

and the formate ester of *3b* ($R^4 = HCO-$). Hydrolysis of this with aqueous Na_2CO_3 gave pure 1,3-diphenyl-1-hydroxy-2-propanone (*3b*, $R^4 = H$), m.p. 115–116°, undepressed on admixture with an authentic sample.[14]

Oxidation of triphenylallene (1c). (a) *With* m-*chloroperbenzoic acid.* Triphenylallene [6] (2.68 g, 10 mmol) was treated with MCPBA as described under *1a*. After 3 days at 0° and the usual work-up, 0.7 g of a mixture of compounds was obtained.

Chromatography on neutral alumina (activity II) gave starting material (0.15 g), mixture of acyloin esters (0.25 g) and 1,3-diphenyl-2-[1,3,3-triphenylallyl]indene (*4*, 0.1 g), m.p. 211–213° from cyclohexane-hexane, undepressed on admixture with an authentic sample,[15] m.p. 214–215°.

(b) *With performic acid.* Reaction of triphenylallene (2.68 g, 10 mmol) with performic acid as described under *1a* gave as the only isolable product the indene *4* in 56 % yield.

1-Hydroxy-1,3,3-triphenyl-2-indanone (5). A cold (0°C) solution of 70 % *m*-chloroperbenzoic acid (3.65 g, 15 mmol) in dichloromethane (50 ml) was added to a solution of tetraphenylallene (1.72 g, 5 mmol) in dichloromethane (50 ml) at 0°. After 5 days at 0°, the reaction mixture was washed with aqueous sodium carbonate solution and dried (Na_2CO_3). The filtrate was evaporated giving 1.55 g (83 %) of *5* which was recrystallized from cyclohexane, m.p. 156–157°. (Found: C 85.92; H 5.45. Calc. for $C_{27}H_{20}O_2$: C 86.14; H 5.36.)

The product (II) was in all respects identical with authentic material which was synthesized according to literature;[7] m.p.157–159°.

1,3,3-Triphenyl-indan-2-ol (11). To a solution of 1,3,3-triphenylindene [16] (1.72 g, 5 mmol) in dry tetrahydrofuran (30 ml) $NaBH_4$ (0.38 g, 10 mmol) was added under nitrogen. A solution of BF_3OEt_2 (1.42 g, 0.1 mol) in THF (10 ml) was added to the cooled (0°) reaction mixture during 3 h. The mixture was stirred at room temperature overnight and treated with sodium hydroxide/hydrogen peroxide in the usual way. The ether extract was washed with water and dried. The solvent was evaporated and the residue purified by chromatography on neutral alumina (activity III).

The carbinol *11* was eluted with benzene; 0.8 g (56 %), m.p. 60–65. (Found: C 89.32; H 6.30. Calc. for $C_{22}H_{22}O$: C 89.50; H 6.08.) NMR ($CDCl_3$) OH δ 1.7 (s), CH δ 3.8 (d), CH δ 5.1 (d) ($J = 10$ cps) and arom. H δ 6.8–7.4 in a ratio of 1:1:1:19. MS: M (*m/e* 362), M–OH, M–H_2O, M–CHOH, M–CH_2OH.

1,3,3-Triphenyl-indan-2-one (7). To a solution of carbinol *11* (0.36 g, 1 mmol) in acetone (20 ml) was added Jones reagent (0.4 ml, 0.001 mol) and the mixture stirred for 2 h at room temperature. Water (25 ml) was then added, the solution extracted with ether, the organic phase washed with water and dried ($MgSO_4$). Evaporation gave 0.35 g (97 %) of the pure compound. Recrystallisation from benzene/hexane gave a final m.p. at 85–90° after rearrangements in the crystalline phase at about 50°. (Found: C 89.75; H 5.40. Calc. for $C_{27}H_{20}O$: C 90.00; H 5.56.)

NMR ($CDCl_3$) CH δ 4.3 (s) and arom. H δ 6.9–7.4 in a ratio of 1:19. MS: M–CO (*m/e* 332), M–CHO, M–CO–Ph, M–CHO–Ph.

Attempted oxidation of *7*: To a solution of *7* in dichloromethane (20 ml) was added 2 equiv. of 70 % MCPBA. No peracid was consumed, even after 6 days at 0°.

Oxidation of tetraphenylbutariene (2). A cold solution of 70 % *m*-chloroperbenzoic acid (4.80 g, 0.02 mol) in dichloromethane (100 ml) was added to a suspension of tetraphenylbutratriene *2* [17] (1.78 g, 0.005 mol) in dichloromethane (100 ml) at 0°. After one week at 0°, the reaction mixture was washed with aqueous sodium carbonate solution, dried and evaporated. The residue was chromatographed on neutral alumina (activity III). Elution with benzene/ethylacetate (4:1) gave 0.8 g (40 %) coloured *12*, m.p. 60–65° from cyclohexane. (Found: C 82.80; H 5.12. Calc. for $C_{28}H_{20}O_3$: C 83.20; H 4.96.)

NMR ($CDCl_3$) OH δ 4.7 (s) and arom. H δ 7–8 in a ratio of 1:19. IR (CCl_4) 3500 cm^{-1} OH and 1760 cm^{-1} CO.

Compound *12* (0.2 g) was treated with $NaBH_4$ (0.1 g) in ethanol (10 ml) overnight. The strong yellow colour had disappeared. The solution was worked up in the usual way with ether to give semicrystalline *13*. (Found: C 82.21; H 5.77. Calc. for $C_{28}H_{22}O_3$: C 82.75; H 5.42.) NMR ($CDCl_3$) CH δ 5.3 (m), OH δ 4.0–4.5 (m) and arom. H δ 6.8–7.5 in a ratio of 2:3:19. IR (CCl_4) 3600 cm^{-1}. MS: M (*m/e* 408), M–H, M–H_2O, M–$2H_2O$, M–H_2O–HCHO, M–Ph, M–Ph–H_2O–HCHO.

Kinetics. 0.005 mol of the allene was added to a solution of 70 % *m*-chloroperbenzoic acid (0.01 mol) in methylene chloride (75 ml) at 0°C. The solution was stirred at 0°,

aliquots were withdrawn and the amount of peracid was determined by iodometrical titration. Rate constants were calculated from a second order plot.

REFERENCES

1. Boeseken, J., van Asperen, M., Cauchy, M., Maters, M. C. and Ottenhoff, M. P. *Rec. Trav. Chim.* **54** (1935) 657.
2. Crandall, J. K. and Machleder, W. H. *J. Am. Chem. Soc.* **90** (1968) 7292.
3. Camp, R. L. and Greene, F. D. *J. Am. Chem. Soc.* **90** (1968) 7349.
4. Crandall, J. K. and Machleder, W. H. *J. Heterocycl. Chem.* **6** (1969) 777.
5. Crandall, J. K., Machleder, W. H. and Thomas, M. J. *J. Am. Chem. Soc.* **90** (1968) 7346.
6. Jacobs, T. L., Dankner, D. and Singer, S. *Tetrahedron* **20** (1964) 2177.
7. Koelsch, C. F. *J. Org. Chem.* **3** (1939) 456.
8. Greibrokk, T. *To be published.*
9. Hoey Brook, G., Dean, D. O. and Lester, C. T. *J. Am. Chem. Soc.* **77** (1955) 391.
10. Skattebøl, L. *Acta Chem. Scand.* **17** (1963) 1683.
11. Richard, G. *Compt. Rend.* **214** (1942) 673.
12. Hey, D. H. *J. Chem. Soc.* **1930** 1232.
13. Jacobs, T. L. and Dankner, D. *J. Org. Chem.* **22** (1957) 1424.
14. Laweson, S. O., Jonsson, P. R. and Taipale, J. *Arkiv Kemi* **17** (1961) 441.
15. Rewicki, D. *Chem. Ber.* **99** (1966) 392.
16. Vorländer, D. and Siebert, C. *Ber.* **39** (1906) 1024.
17. Kuhn, R. and Krauch, H. *Chem. Ber.* **88** (1955) 309.

Received November 25, 1972.

ACTA CHEMICA SCANDINAVICA 27 (1973) 1427–1462

Short Communications

The Mutarotation of D-Glucose and Its Dependence on Solvent

II. The Equilibrium Components in *N,N*-Dimethylformamide

JOHAN A. HVEDING, OVE KJØLBERG and ANDREAS REINE

Department of Chemistry, University of Oslo, Oslo 3, Norway

Investigations of D-glucose in different water-DMF mixtures have shown that at higher concentrations of DMF the mutarotation deviates significantly from the simple logarithmic law.[1] In an earlier report [2] we have described the mutarotation of D-glucose in DMF. By GLC of the HMDS-TMCS treated equilibrium solution it was found a third peak in addition to the two pyranose peaks. Evidence of furanose constituents in mutarotation equilibria of glucose using refluxing pyridine as solvent has been reported earlier.[3,4] The present communication describes the evidence for the presence of substantial quantities of D-glucofuranose in equilibria using DMF as solvent.

The mutarotation of D-glucose in DMF is extremely slow at room temperature. At 20°C several weeks are required to obtain the equilibrium. Increasing the temperature to 70°C, on the other hand, the equilibrium is obtained after a few hours. Furthermore, the third peak is about doubled in area by elevation of the temperature from 20 to 70°C. We therefore preferred to use the latter temperature for the identification of the third peak. GLC gave three distinct peaks A, B, and C with relative retention times of 0.82, 1.00, and 1.33 which accounted for 4.7, 42.5, and 52.8 %, respectively, of the total area. The peaks B and C were assigned to penta-*O*-trimethylsilyl-α- and -β-D-glucopyranose, respectively, by comparisons of their retention times with those of the TMS ethers of pure α- and β-D-glucose. The mixture was analyzed further by combined GLC-mass spectrometry. According to DeJongh *et al.*[4] fully TMS-substituted furanoses will give different mass spectra from the fully substituted pyranoses. A marked distinction between these isomers is the high intensity of *m/e* 204 ion and the low intensity of *m/e* 217 ion in the mass spectra of the pyranoses while the reverse holds true for the mass spectra of the furanoses. Another striking difference is found in the intensity of the fragment at *m/e* 319 which is known to be characteristic of the furanoses. The mass spectrum of A was found to be different from those of B and C which were nearly identical. The most important intensity data for A and C are shown in Table 1.

Table 1. Selected relative intensity data from the mass spectra of A and C.

m/e	525	319	217	205	204	191	147	129	73
A, %	0.3	13	100	7	4	19	23	5	78
C, %	0.3	2	19	21	100	50	27	8	95

A comparison of the data in Table 1 with the data given by DeJongh *et al.*[4] leads to the conclusion that peak A represents penta-*O*-trimethylsilylglucofuranose. Whether the furanose is the α- or the β-anomer or a mixture of both has not yet been established. Such investigation is, however, under progress. Nevertheless, from these experiments it can be concluded that the complex character of the mutarotation of glucose in DMF may be due to the formation of a substantial amount of the furanose isomer(s).

Experimental. The materials and the thermostat equipment were as specified earlier.[1] The equilibrated solution (1 g/100 ml) was silylated with trimethylchlorosilane and hexamethyldisilazane as described by Sweeley *et al.*[3] To secure full silylation the reaction mixture was kept at room temperature for 8 h. The precipitated salts were removed by decantation and the solution was concentrated *in vacuo*, and the TMS-ethers were extracted with hexane.

The gas chromatograph used was a Varian Aerograph, Model 80-P, equipped with a thermal conductivity detector. The chromatography was carried out isothermally (225°C) in an aluminium column (1.7 m × 6 mm) containing 20 % SE-30 on Chromosorb W (60–80 mesh). The combined GLC-mass spectrometric studies were carried out with an Atlas Varian CH7 mass spectrometer using a ionizing energy of 70 eV. Again the GLC was performed with SE-30 as the stationary phase.

Acknowledgement. We are grateful to Dr. E. Jellum at Rikshospitalet for placing the mass spectrometer at our disposal.

1. Gram, F., Hveding, J. A. and Reine, A. *Acta Chem. Scand. In press.*
2. Communicated to the 11th National Meeting of the *Norwegian Chemical Society*, June 1970, and briefly reported in *Tidsskr. Kjemi, Bergvesen Met.* **30** No. 6 (1970) 8.
3. Sweeley, C. C., Bentley, R., Makita, M. and Wells, W. W. *J. Am. Chem. Soc.* **85** (1963) 2497.
4. DeJongh, D. C., Radford, T., Hribar, J. D., Hanessian, S., Bieber, M., Dawson, G. and Sweeley, C. C. *J. Am. Chem. Soc.* **91** (1969) 1728.

Received March 16, 1973.

Sterical Orientation in Diels-Alder Dimerisation of *o*-Quinols

BENGT KARLSSON,[a] PEDER KIERKEGAARD,[a] ANNE-MARIE PILOTTI,[a] ANNE-CHARLOTTE WIEHAGER[a] and BENGT O. LINDGREN[b]

[a]*Institute of Inorganic and Physical Chemistry, University of Stockholm, S-104 05 Stockholm, and* [b]*Swedish Forest Products Research Laboratory, S-114 86 Stockholm, Sweden*

The Diels-Alder dimerisation of *o*-quinols and similar *o*-quinoid compounds gives usually only one of the conceivable stereoisomers. The reaction is considered to be governed by the *endo* rule, by the rule of the lowest dipole moment of the transition state,[1] and by steric requirements.[2,3] From these it follows that the dimer structure should be one of the types *4* – *6* (Fig. 1). For

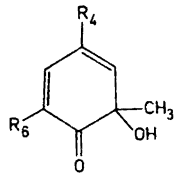

1-3

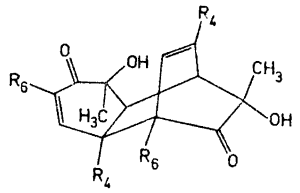

4-6

1 $R_4 = R_6 = H$ *4*
2 $R_4 = H$, $R_6 = CH_3$ *5*
3 $R_4 = CH_3$, $R_6 = H$ *6*

a discussion of this subject, see Adler *et al.* A complete structure has, however, been established only for the dimer (Fig. 1, *4*) of 2-methyl-*o*-quinol (Fig. 1, *1*) by a chemical and spectral investigation [4] and an X-ray diffraction analysis.[5]

By X-ray analysis we have now found that the dimers of 2,6-dimethyl-*o*-quinol (Fig. 1, *2*) and 2,4-dimethyl-*o*-quinol (Fig.

Experimental. The materials and the thermostat equipment were as specified earlier.[1] The equilibrated solution (1 g/100 ml) was silylated with trimethylchlorosilane and hexamethyldisilazane as described by Sweeley *et al.*[3] To secure full silylation the reaction mixture was kept at room temperature for 8 h. The precipitated salts were removed by decantation and the solution was concentrated *in vacuo*, and the TMS-ethers were extracted with hexane.

The gas chromatograph used was a Varian Aerograph, Model 80-P, equipped with a thermal conductivity detector. The chromatography was carried out isothermally (225°C) in an aluminium column (1.7 m × 6 mm) containing 20 % SE-30 on Chromosorb W (60–80 mesh). The combined GLC-mass spectrometric studies were carried out with an Atlas Varian CH7 mass spectrometer using a ionizing energy of 70 eV. Again the GLC was performed with SE-30 as the stationary phase.

Acknowledgement. We are grateful to Dr. E. Jellum at Rikshospitalet for placing the mass spectrometer at our disposal.

1. Gram, F., Hveding, J. A. and Reine, A. *Acta Chem. Scand. In press.*
2. Communicated to the 11th National Meeting of the *Norwegian Chemical Society*, June 1970, and briefly reported in *Tidsskr. Kjemi, Bergvesen Met.* **30** No. 6 (1970) 8.
3. Sweeley, C. C., Bentley, R., Makita, M. and Wells, W. W. *J. Am. Chem. Soc.* **85** (1963) 2497.
4. DeJongh, D. C., Radford, T., Hribar, J. D., Hanessian, S., Bieber, M., Dawson, G. and Sweeley, C. C. *J. Am. Chem. Soc.* **91** (1969) 1728.

Received March 16, 1973.

Sterical Orientation in Diels-Alder Dimerisation of *o*-Quinols

BENGT KARLSSON,[a] PEDER KIERKEGAARD,[a] ANNE-MARIE PILOTTI,[a] ANNE-CHARLOTTE WIEHAGER[a] and BENGT O. LINDGREN[b]

[a]*Institute of Inorganic and Physical Chemistry, University of Stockholm, S-104 05 Stockholm, and* [b]*Swedish Forest Products Research Laboratory, S-114 86 Stockholm, Sweden*

The Diels-Alder dimerisation of *o*-quinols and similar *o*-quinoid compounds gives usually only one of the conceivable stereoisomers. The reaction is considered to be governed by the *endo* rule, by the rule of the lowest dipole moment of the transition state,[1] and by steric requirements.[2,3] From these it follows that the dimer structure should be one of the types *4* – *6* (Fig. 1). For

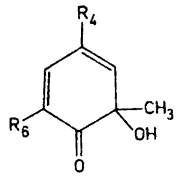

1-3

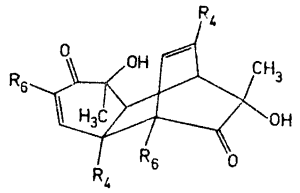

4-6

1 $R_4 = R_6 = H$ *4*
2 $R_4 = H$, $R_6 = CH_3$ *5*
3 $R_4 = CH_3$, $R_6 = H$ *6*

a discussion of this subject, see Adler *et al.* A complete structure has, however, been established only for the dimer (Fig. 1, *4*) of 2-methyl-*o*-quinol (Fig. 1, *1*) by a chemical and spectral investigation [4] and an X-ray diffraction analysis.[5]

By X-ray analysis we have now found that the dimers of 2,6-dimethyl-*o*-quinol (Fig. 1, *2*) and 2,4-dimethyl-*o*-quinol (Fig.

The present investigation has received financial support from the *Tri-Centennial Fund of the Bank of Sweden* and from the *Swedish Natural Science Research Council.*

1. Horner, L. and Dürckheimer, W. *Chem. Ber.* **95** (1962) 1219.
2. Kende, A. S. and MacGregor, P. J. *J. Am. Chem. Soc.* **83** (1961) 4197.
3. Adler, E., Brasen, S. and Miyake, H. *Acta Chem. Scand.* **25** (1971) 2055.
4. Adler, E. and Holmberg, K. *Acta Chem. Scand.* **25** (1971) 2775.
5. Vannerberg, N. G. and Brasen, S. *Acta Chem. Scand.* **24** (1970) 1894.
6. Germain, G., Main, P. and Woolfson, H. M. *Acta Cryst.* **B 26** (1970) 274.
7. Norrestam, R. *Acta Cryst.* **A 28** (1972) 303.
8. Sutton, L. E. *Tables of Interatomic Distances and Configuration in Molecules and Ions*, Supplement 1956–1959, The Chemical Society, London.
9. Karlsson, B., Pilotti, A.-M. and Wiehager, A.-C. *To be published.*

Received March 22, 1973.

Studies on the Melting Process of Polyethylene Glycol

P. TÖRMÄLÄ and A. SAVOLAINEN

Department of Wood and Polymer Chemistry, University of Helsinki, Helsinki, Finland

Polymer samples containing minute amounts of free and covalently bound nitroxyl radicals were prepared in a study of the dynamic properties of polyethylene glycol (PEG).[1] The concentration ratio of radicals to polymer repeat units was very low (1 : 20 000). It was assumed that the radicals did not affect the bulk properties of polymer (*cf.* Ref. 2). Four different rotational relaxation regions were found in these samples. Melting region thermograms of PEG in the $\overline{M}_n$ range 1 000 – 22 000 were measured by means of differential scanning calorimetry (DSC) in order to study the nature of these relaxations with respect to the melting process of PEG.

PEG is a highly crystalline polymer. The calorimetric value $\Delta H_m{}^a$ is related to $\Delta H_m{}^c$, the heat of fusion for 100 % crystalline PEG, by $\Delta H_m{}^c = \Delta H_m{}^a/a$, where a is the degree of crystallinity of the sample.

The molecular weights ($\overline{M}_n$) and the heats of fusion ($\Delta H_m{}^a$) for PEG samples are given in Table 1. The crystallinities of the samples (calculated by means of the $\Delta H_m{}^c = 51.5$ cal/g of Beaumont [3]) are given in Fig. 1. The melting points (T_m) of the samples are also shown in this figure.

Table 1. Molecular weights ($\overline{M}_n$) and the heats of fusion ($\Delta H_m{}^a$) for PEG samples containing free (A) and covalently bound (B) nitroxyl radicals.

M_n	A $\Delta H_m{}^a$(cal/g)	B $\Delta H_m{}^a$(cal/g)
1 000 ± 50	42.1	42.4
1 550 ± 100	45.1	46.5
2 050 ± 150	45.9	48.6
3 000 ± 300	49.4	47.7
4 000 ± 500	51.0	49.8
6 700 ± 700	50.1	49.4
9 500 ± 500	50.4	49.8
15 000 ± 2 000	48.2	49.3
22 000	49.4	46.8

From Fig. 1 is seen that the T_m of PEG increases rapidly until $\overline{M}_n$ 3000 – 4000 and thereafter slowly approaches its limiting value. These results are in accord with other measurements.[3–6] Evidently the differences between the T_m values of polymers containing spin probes and spin labels are caused by differences in the history of the polymers.

In the low $\overline{M}_n$ region the degree of crystallinity is directly comparable to $\overline{M}_n$, while at high $\overline{M}_n$ the crystallinities are lower than in the 4000 – 10 000 region. The decrease in crystallinity at high molecular weight is probably due to the increasing difficulty of a polymer molecule forming a crystal lattice.

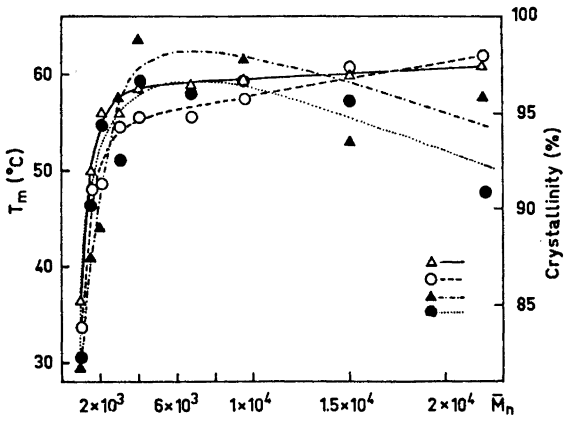

Fig. 1. T_m values and crystallinities of PEG samples as a function of $\bar{M}_n$; symbols △ and ○ express T_m values of PEG containing free and bound radicals, ▲ and ● are the crystallinities of the corresponding samples.

The melting of the polymer is located in the same temperature region where a strong change in the rotational relaxation times (τ) (sec) of nitroxyl radicals in PEG

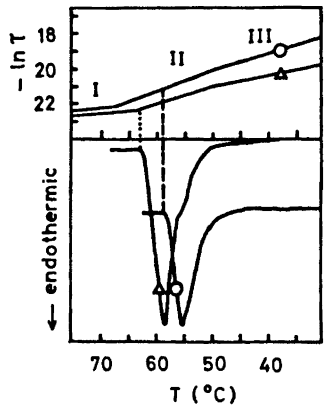

Fig. 2. DSC curves of PEG 4000 containing free △ and bound ○ radicals and their corresponding rotational relaxation Arrhenius plots.

was observed.[1] This can be seen from Fig. 2 where the DSC curves of PEG 4000 A and B and $-\ln\tau$ values of spin probe and spin label radicals in these polymers are given as a function of T. When $\bar{M}_n$ was ≥ 1000, a similar correspondence between DSC and τ measurements was also observed in other PEG samples.

It can be seen that the activation energy E_a of radicals in PEG reaches its maximum value in the temperature region (relaxation region II) corresponding to the endothermic melting process. Because segmental relaxations of surrounding polymer molecules contribute strongly to the τ of radicals, E_a^{II} shows a strong change in short range segmental motions in the transition region II.

The endothermic DSC curve of PEG with free radicals correlates well with the corresponding E_a^{II} curve. The DSC curve of PEG 4000 B, however, does not correlate exactly with its relaxation II. Although PEG 4000 B melts at a lower temperature than 4000 A according to DSC, the transition temperature from relaxation region II to I in the former is clearly higher than the initial temperature of the endothermic change. This indicates that after the melting of the polymer crystals the environment of bound radicals is not yet liquid-like. The transition to a purely liquid-like state in the micro-environment of bound radicals occurs only some degrees above the end-point of the endothermic change. Because this phenomenon is not so prominent in the case of free radicals, it can be assumed that the effect is essentially intramolecular in origin. It is known that crystalline PEG in the solid state has

a helical conformation.[7] Since the esterified radical is in intimate contact with the host polymer, the transition from helix to a random coil conformation is a reasonable explanation for the observed phenomenon. It is thus probable that the polymer molecules in the relaxation region I are in a random coil conformation. Even if the helical conformations still exist, their fluctuations are so rapid that they do not affect the spin rotational relaxation.

Because the nitroxyl radicals incorporated into PEG exhibit a transitional relaxation region (II) in the temperature range where the endothermic melting of polymer crystals occurs, it is evident that radicals are in close contact with the crystalline phase. The isotropic nature of the ESR spectra refers to the amorphous environment.[1] On the other hand, the bulky radicals would surely distort the tightly packed crystal lattice about them and exhibit an amorphous-like environment even though they were in the crystalline phase. The structural changes in the crystal phase are thus reflected in the rotating radicals as changes in the forces caused by crystalline phase in the amorphous environment of radicals. This hypothesis is supported by the observation that in the $\overline{M}_n$ region, where end group effects become negligible ($\overline{M}_n \geq 9500$), the degree of crystallinity and E_a^{II} decrease as a function of $\overline{M}_n$ (Fig. 1 in this report and Fig. 6 in Ref. 1).

Experimental. The PEG samples were of commercial origin (Fluka and Merck). Their M_n values were measured by a vapour pressure osmometer (Perkin-Elmer Modell 115) in chloroform at 32°C. The spin probe radical 3-methoxycarbonyl-2,2,5,5-tetramethyl-pyrroline-1-oxyl and the spin label radical 3-PEG-carbonyl - 2,2,5,5 - tetramethylpyrroline-1-oxyl were prepared and incorporated into PEG as reported earlier.[1] The history of the polymers was as follows: The PEG samples containing spin probes (set A) were dissolved in chloroform and the solvent was carefully evaporated in vacuum. The PEG samples containing spin labels (set B) were dissolved in chloroform precipitated with ether and dried in vacuum.[1] All these procedures were carried out at room temperature (24°C). DSC-curves were scanned at a rate of 8°C/min in an N_2-atmosphere using a Perkin Elmer DSC-1B calorimeter. T_m was measured from the maximum of the endothermic peak height.

Acknowledgements. One os us (P.T.) thanks the *National Research Council for Sciences* and the *Foundation of Neste Oy* for financial aid.

1. Törmälä, P., Lättilä, H. and Lindberg, J. J. *Polymer. In press.*
2. Gross, S. C. *J. Polym. Sci., Part A-1,* **9** (1971) 3327.
3. Beaumont, R. H., Clegg, B., Gee, G., Herbert, J. B. M., Marks, D. J., Roberts, R. C. and Sims, D. *Polymer* **7** (1966) 401.
4. Booth, C., Bruce, J. M. and Buggy, M. *Polymer* **13** (1972) 475.
5. Alfthan, E. and de Ruvo, A. *Private communication.*
6. Godovsky, Yu. K., Slonimsky, G. L. and Garbar, N. M. *J. Polym. Sci., Part C, 38* (1972) 1.
7. Tadokoro, H., Chatani, Y., Yoshihara, T., Tahara, S. and Murahashi, S. *Makromol. Chem.* **73** (1964) 109.

Received March 14, 1973.

Isolation of D-Galactaric Acid and Isocitric Acid from *Ferocactus acanthodes* Br. et R.

RANDI KRINGSTAD and ARNOLD NORDAL

Institute of Pharmacy, Department of Pharmacognosy, University of Oslo, Oslo 3, Norway

Phytochemical investigations during recent years have revealed that the predominating acids of several succulent plants are hydroxy acids, which are able to form lactones.[1-4] Some of these acids, like phorbic acid, were first isolated from a succulent.[5] The cumulation of hydroxy acids in succulent plants is undoubtedly connected with the unique form of metabolism that is so characteristic for this group of plants, and it is believed that

a helical conformation.[7] Since the esterified radical is in intimate contact with the host polymer, the transition from helix to a random coil conformation is a reasonable explanation for the observed phenomenon. It is thus probable that the polymer molecules in the relaxation region I are in a random coil conformation. Even if the helical conformations still exist, their fluctuations are so rapid that they do not affect the spin rotational relaxation.

Because the nitroxyl radicals incorporated into PEG exhibit a transitional relaxation region (II) in the temperature range where the endothermic melting of polymer crystals occurs, it is evident that radicals are in close contact with the crystalline phase. The isotropic nature of the ESR spectra refers to the amorphous environment.[1] On the other hand, the bulky radicals would surely distort the tightly packed crystal lattice about them and exhibit an amorphous-like environment even though they were in the crystalline phase. The structural changes in the crystal phase are thus reflected in the rotating radicals as changes in the forces caused by crystalline phase in the amorphous environment of radicals. This hypothesis is supported by the observation that in the $\overline{M}_n$ region, where end group effects become negligible ($\overline{M}_n \geq 9500$), the degree of crystallinity and E_a^{II} decrease as a function of $\overline{M}_n$ (Fig. 1 in this report and Fig. 6 in Ref. 1).

Experimental. The PEG samples were of commercial origin (Fluka and Merck). Their M_n values were measured by a vapour pressure osmometer (Perkin-Elmer Modell 115) in chloroform at 32°C. The spin probe radical 3-methoxycarbonyl-2,2,5,5-tetramethyl-pyrroline-1-oxyl and the spin label radical 3-PEG-carbonyl - 2,2,5,5 - tetramethylpyrroline-1-oxyl were prepared and incorporated into PEG as reported earlier.[1] The history of the polymers was as follows: The PEG samples containing spin probes (set A) were dissolved in chloroform and the solvent was carefully evaporated in vacuum. The PEG samples containing spin labels (set B) were dissolved in chloroform precipitated with ether and dried in vacuum.[1] All these procedures were carried out at room temperature (24°C). DSC-curves were scanned at a rate of 8°C/min in an N_2-atmosphere using a Perkin Elmer DSC-1B calorimeter. T_m was measured from the maximum of the endothermic peak height.

Acknowledgements. One os us (P.T.) thanks the *National Research Council for Sciences* and the *Foundation of Neste Oy* for financial aid.

1. Törmälä, P., Lättilä, H. and Lindberg, J. J. *Polymer. In press.*
2. Gross, S. C. *J. Polym. Sci., Part A-1,* **9** (1971) 3327.
3. Beaumont, R. H., Clegg, B., Gee, G., Herbert, J. B. M., Marks, D. J., Roberts, R. C. and Sims, D. *Polymer* **7** (1966) 401.
4. Booth, C., Bruce, J. M. and Buggy, M. *Polymer* **13** (1972) 475.
5. Alfthan, E. and de Ruvo, A. *Private communication.*
6. Godovsky, Yu. K., Slonimsky, G. L. and Garbar, N. M. *J. Polym. Sci., Part C, 38* (1972) 1.
7. Tadokoro, H., Chatani, Y., Yoshihara, T., Tahara, S. and Murahashi, S. *Makromol. Chem.* **73** (1964) 109.

Received March 14, 1973.

Isolation of D-Galactaric Acid and Isocitric Acid from *Ferocactus acanthodes* Br. et R.

RANDI KRINGSTAD and ARNOLD NORDAL

Institute of Pharmacy, Department of Pharmacognosy, University of Oslo, Oslo 3, Norway

Phytochemical investigations during recent years have revealed that the predominating acids of several succulent plants are hydroxy acids, which are able to form lactones.[1-4] Some of these acids, like phorbic acid, were first isolated from a succulent.[5] The cumulation of hydroxy acids in succulent plants is undoubtedly connected with the unique form of metabolism that is so characteristic for this group of plants, and it is believed that

lactone forming hydroxy acids play an important part in the succulent metabolism, *e.g.* as pH regulators.[6,7]

In a current investigation on organic acids in succulents it was observed that *Ferocactus acanthodes* contains a rare organic acid which was isolated and identified as D-galactaric acid. This acid has been found in free state in plants only once, namely in the fruits of cylon olive,[8] which belongs to a quite different group of plants. During the investigation another lactone forming acid, namely isocitric acid, was isolated and identified.

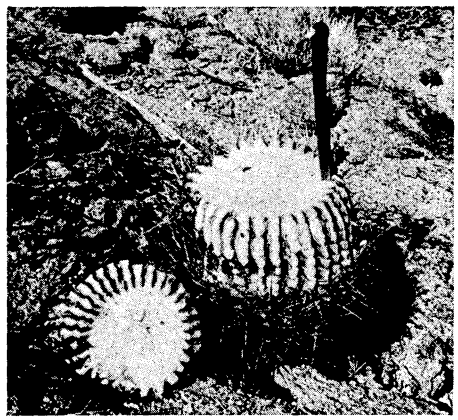

Fig. 1. Ferocactus acanthodes Br. et R.

Experimental. The plant used for the investigations (Fig. 1) was collected by one of the authors (A. N.) in the deserts of Baja California, Mexico, in 1967. The fresh plant was cut into 1 – 2 cm thick slices and dried at 60°C. The dried material, which was yellowish white, was kept in well closed containers till it was used for the following investigation.

30.0 g of freshly prepared powder was extracted for half an hour at room temperature with 400 ml of distilled water. The cations were removed from the filtrate with Dowex 50 W × 8 (H^+), and the acid extract was concentrated to about 250 ml. The extract was then treated with barium hydroxide solution till no more barium salt precipitated.

The precipitate, which mainly consisted of barium sulphate, was removed, and the filtrate (pH near to 1) was adjusted with barium hydroxide solution to pH 6. The extract was concentrated to 20 ml and put in a refrigerator for two days, during which time a white precipitate had formed. The precipitate (Substance A) was removed by centrifugation and the supernatant (in the following referred to as Solution I) was put aside for further investigation.

Substance A, which was a mixture of barium salts, was suspended in 30 ml of distilled water and deionized with Dowex 50 W × 8 (H^+). On evaporation to about 5 ml, a white microcrystalline substance (Substance B) separated. It was washed with distilled water and ethanol, and dried. Yield 12.4 mg. The mother liquor from this substance will in the following be referred to as Solution II.

Investigation of Substance B. The substance melted at about 227°C, when inserted into the micro melting point apparatus at 205°C. When mixed with D-galactaric acid no melting point depression was observed.

The melting point of the substance varied a great deal according to the conditions,[9,10] but corresponded always to the values observed with authentic D-galactaric acid under the same conditions. For the melting point determination, a Reichert micro melting point apparatus No. 250282 was used. (Found: C 34.07; H 4.99. Calc. for $C_6H_{10}O_8$: C 34.29; H 4.80.)

The IR-spectrum was identical with that of the authentic substance. The isatine test[11] and the *p*-dimethyl-aminobenzaldehyde test[12] were positive.

Thin-layer chromatography (TLC) was run on Polygram cel 300 MN. Solvent system: pyridine – ethyl acetate – acetic acid – water (5 : 5 : 1 : 3). Detecting reagents: a. Bromophenol Blue 0.1 % in methanol. b. Hydroxylamine – ferric chloride.[13]

The chromatographic behaviour of the substance was identical with that of authentic D-galactaric acid. Both acids gave two spots.

Investigation of Solution I and Solution II. Solution I was deionized with Dowex 50 W × 8 (H^+), and the acid extract passed through a column of Dowex 1 × 8 (OH^-). After washing of the column with distilled water, the acids were eluted with hydrochloric acid (2 N), the eluate was evaporated and the residue dried. TLC of the acid residue, performed under the same conditions as above, gave two purple-brown spots – one weak and one stronger – when using detecting reagent b. The spots corresponded to the two spots given by isocitric acid under the same conditions. As reference was used DL-isocitric acid lactone (No. 1 – 1377 Sigma).

To confirm the presence of isocitric acid, the acid residue was converted into the ethyl esters, and the ester mixture subjected to gas chromatography, using the ethyl ester of DL-

isocitric acid and an isocitric acid ethyl ester isolated from *Sedum acre* [14] as references.

Esterification of the acid from Solutions I and II, and of the reference sample, was performed by boiling one part of the acids with about 50 parts of anhydrous ethanol for 10 h, using 2–3 g of Dowex 50 W × 8 (H^+) as a catalyst.

The gas chromatograph used was an Aerograph Hy-Fi 600 B with a hydrogen flame ionization detector. Nitrogen served as a carrier gas. The column used was of stainless steel, 2 m × 3 mm with Gas Chrome Q, coated with 3 % DEGS. The temperature of the column chamber was kept constant at 180°C during the runs.

Under the conditions described above, isocitric acid ethyl ester gives two well separated peaks on the gas chromatogram.[15] The first peak often shows a shoulder indicating a double peak. Sometimes this double peak is fairly clear.

Both solutions were found to contain isocitric acid ethyl ester. The main part was found in Solution I.

Discussion. D-Galactaric acid might easily be overlooked during an investigation on organic acids in plants, as it in its physical and chemical properties differs much from other organic acids commonly found in plant tissues. In our case we came across the acid more or less incidentally as it was noticed that a white substance separated when a deionized solution of a calcium salt isolated from *Ferocactus acanthodes* was left for some days in the cold store. A preliminary investigation of the white precipitate pointed towards D-galactaric acid, for which reason a more thorough investigation of the problem was initiated.

In the method for isolation of D-galactaric acid described above, sulphuric acid is precipitated as barium salt under conditions where the barium salt of galactaric acid remains in solution (pH 1). After removal of the barium salts which separate at pH 1, the pH of the filtrate is adjusted to pH 6, and the solution concentrated. Under these conditions the barium salt of D-galactaric acid will separate (admixed, *e.g.*, with the barium salts of isocitric and malic acids). On deionization of the barium salt mixture and concentration of the acid solution, D-galactaric acid will first separate from the acid solution owing to its slight solubility in water.

We assume that D-galactaric acid is much more common in plants, especially in succulents, than hitherto believed, and that this might be shown when suitable methods for its detection are applied.

Acknowledgements. The authors thank Dr. A. A. Benson, Scripps Institution of Oceanography, La Jolla, California, for valuable assistance in providing material for this investigation. We also thank the *Foundation for Ocean Research*, San Diego, for financial support in connection with the plant collection expeditions to the Baja California, Mexico, in 1967.

1. Söderström, T. R. *Am. J. Botany* **49** (1962) 850.
2. Nordal, A., Krogh, A. and Ogner, G. *Acta Chem. Scand.* **19** (1963) 1705.
3. Winsnes, R. and Andrew, M. *Acta Chem. Scand.* **24** (1970) 3428.
4. Bøe, J. E., Winsnes, R., Nordal, A. and Bernatek, E. *Acta Chem. Scand.* **23** (1969) 3609.
5. Bernatek, E., Nordal, A. and Ogner, G. *Acta Chem. Scand.* **17** (1963) 2375.
6. Nordal, A. and Benson, A. A. *Plant Physiol.* **44** (1966) 78.
7. Nordal, A. *Det norske Videnskapsakademi i Oslo, Årbok 1969* p. 35.
8. Yamamoto, R., Osima, V. and Goma, T. *Sci. Papers Inst. Phys. Chem. Res. (Tokyo)* **19** (1932) 132.
9. The Merck Index 1968.
10. *Beilsteins Handbuch der organischen Chemie, Drittes Ergänzungswerk*, 4. Ed., 1962, p. 1123.
11. Rosenthaler, L. *Der Nachweis organischer Verbindungen*, Stuttgart 1914, p. 353.
12. Feigl, F. *Spottests in Organic Analysis*, Amsterdam, London and New York 1966, p. 47.
13. Abdel-Akher, M. and Smith, F. *J. Am. Chem. Soc.* **73** (1851) 5859.
14. Nordal, A. *Medd. Norsk Farm. Selskap* **7** (1943) 1.
15. McKeown, G. G. and Read, S. I. *Anal. Chem.* **37** (1965) 1780.

Received March 23, 1973.

Microwave Spectrum of 1-Fluoronaphthalene

HASSE KARLSSON*

Department of Medical Physics, University of Göteborg, S-400 33 Göteborg 33, Sweden

The microwave spectrum of 2-fluoronaphthalene was assigned earlier by Bak *et al.*,[1] and preliminary results for 1-fluoronaphthalene were obtained at the same time.[2] This work is a more detailed investigation of 1-fluoronaphthalene (AFN).

A sample of 1-fluoronaphthalene was purchased from Fluka. Its purity was checked by capillary gas chromatography and used without further purification.

The microwave spectrum was observed in the range 18.0 – 40.0 GHz on a Hewlett-Packard Model 8460 A MRR spectrometer. All measurements were made at room temperature and at Starkfields of 2000 – 3800 V/cm. The transition frequencies were measured with a sample pressure of 0.005 to 0.010 mmHg.

The 1-fluoronaphthalene molecule is quite heavy and its rotational constants are rather small. Reasonable molecular models have values of the asymmetry parameter, $\varkappa$, around −0.3. The approximate orientation of the principal inertial axes are given in Fig. 1.

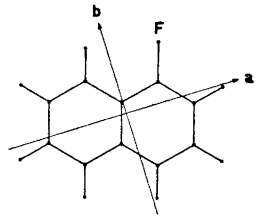

Fig. 1. Molecular model of 1-fluoronaphthalene, $C_{10}H_7F$. *a* and *b* are principal inertial axes.

Based on a vector model, the dipole moment of AFN has its main contribution along the C,F bond. This suggests that the molecular dipole moment is directed mainly along the principal *b*-axis, see Fig. 1. Consequently, the microwave spectrum is very rich and the majority of the observed lines could be assigned to be *b*-type transitions. No *a*-type transitions were assigned.

A part of the *b*-type spectrum calculated from a molecular model is given as a FORTRAT-diagram in Fig. 2. The curves in this figure connect transitions with common values of K_{-1}. It should be noted, that several lines appear as close doublets, see Fig. 2 and Table 1, although the molecule is quite asymmetric, see above.

Table 1. Selected microwave transitions (MHz) of 1-fluoronaphthalene.

Transition	Obs. frequency[a]	Obs. − calc.
$12_{0,12}-13_{1,13}$ / $12_{1,12}-13_{0,13}$	19129.09	+0.04
$12_{1,11}-13_{2,12}$	20550.66	+0.02
$12_{2,11}-13_{1,12}$	20549.46	+0.04
$13_{0,13}-14_{1,14}$ / $13_{1,13}-14_{0,14}$	20545.97	+0.04
$15_{11,4}-15_{12,3}$ / $15_{11,5}-15_{12,4}$	22328.77	0.00
$16_{11,5}-16_{12,4}$ / $16_{11,6}-16_{12,5}$	22205.83	+0.08
$19_{10,9}-19_{11,8}$	19203.05	+0.01
$19_{10,10}-19_{11,9}$	19319.09	−0.04

[a] ±0.05 MHz.

The spectrum is dominated by the intense high-*J* *Q*-branch transitions. The characteristic *R*-branch transitions, almost equidistant with differences of 2C, were however assigned first. Some of the 78 measured transitions are marked in Fig. 2. A selection of experimental frequencies are given in Table 1. The list of measured frequencies ($J \leq 20$) is available from the author or from the Microwave Data Center at the National Bureau of Standards, Washington, D.C., U.S.A., where it has been deposited.

A least-squares fit of the measured frequencies in the rigid rotor approximation (using a computer program received from Dr. Stig Ljunggren at the Royal Institute of Technology, Stockholm) was satisfactory and gave the results in Table 2.

* On leave at Chemical Laboratory V, University of Copenhagen, March – May 1973, incl.

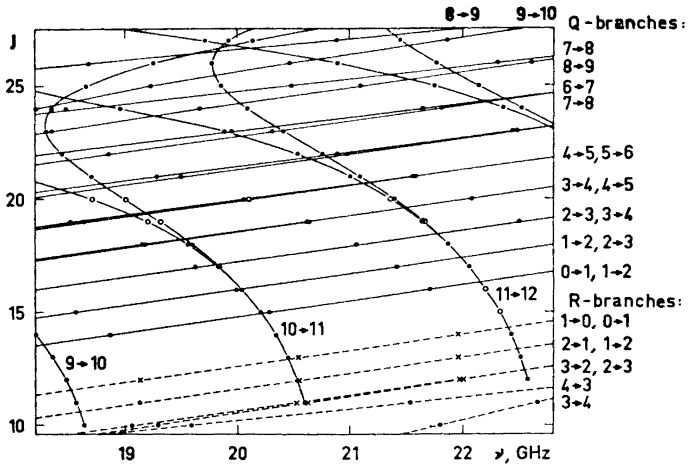

Fig. 2. FORTRAT-diagram of 1-fluoronaphthalene. ×, measured R-lines. ○, measured Q-lines. The R-branches (– – –) and Q-branches (———) are marked with the K_{-1}-values.

Table 2. Rotational constants, principal moments of inertia and inertial defect of 1-fluoronaphthalene. Conversion factor 505376 MHz × uÅ².

Maximum J		20
Number of lines		78
σ (MHz) [a]		0.069
A	(MHz)	1920.5617 ± 0.0008
B	(MHz)	1122.2318 ± 0.0010
C	(MHz)	708.4778 ± 0.0004
I_a	(uÅ²)	263.1397 ± 0.0001
I_b	(uÅ²)	450.3312 ± 0.0004
I_c	(uÅ²)	713.3265 ± 0.0004
I.D.	(uÅ²)	−0.1444 ± 0.0007

[a] $\sigma = [\sum(\nu_i(\text{obs}) - \nu_i(\text{calc}))^2/N]^{1/2}$

A fit including centrifugal distortion (using computer programs by Dr. G. O. Sørensen, Copenhagen University) resulted in a decrease of the mean deviation from 0.069 to 0.052 MHz. However, the significance of the distortion constants was doubtful, and the corrections were quite small, less than 0.4 MHz. Centrifugal distortion effects could therefore be neglected for J-values less than 20, as was expected for this rather heavy and rigid molecule. Transitions with J-values less than 40 could easily be observed (but were not measured exactly). They did not deviate seriously from frequencies calculated in the rigid rotor approximation.

The inertial defect of AFN (Table 2) is small and negative and of the same order of magnitude as was found for the 2-fluoro species, −0.132 uÅ², Ref. 1. This indicates that these molecules are planar.

Since no isotopic species were investigated, a molecular structure of AFN cannot be derived from the present results.

Acknowledgement. The author is grateful to Dr. Lise Nygaard, Copenhagen, for suggesting this investigation, and to microwave colleagues in Copenhagen, Oslo, and Stockholm for computer programs, help and discussions.

1. Bak, B., Christensen, D., Hansen-Nygaard, L. and Rastrup-Andersen, J. *Spectrochim. Acta* **18** (1962) 229.
2. Christensen, D. *Spectrochim. Acta* **15** (1959) 767.

Received April 6, 1973.

Synthesis of Methyl 3,6 Dideoxy-α-D-*ribo*-hexopyranoside

GÖRAN EKBORG and SIGFRID SVENSSON

Institutionen för organisk kemi, Stockholms Universitet, Sandåsgatan 2, S-113 27 Stockholm, Sweden

Paratose (3,6-dideoxy-D-*ribo*-hexose) is a constituent of the O-specific side chains of cell wall lipopolysaccharides from serogroup A *Salmonella* bacteria (*e.g. S. paratyphi* A).[1] The synthesis of methyl α,β-paratopyranoside and paratose *via* 3-deoxy-D-glucose (3-deoxy-D-*ribo*-hexose) has been reported by Fouquey *et al.*[2] However, the preparation of 3-deoxy-D-glucose and its conversion into paratose is laborious and the overall yield is low.

The present communication reports a two step synthesis of methyl α-paratopyranoside starting from methyl α-D-glucopyranoside.

Methyl α-D-glucopyranoside was converted into methyl 2,3,4,6-tetra-*O*-*p*-toluenesulphonyl-α-D-glucoside (I) in nearly quantitative yield. This substance, on treatment with excess lithium aluminium hydride (LAH), yielded two components which were identified as methyl α-paratopyranoside (II) and a methyl 4,6-dideoxy-hexoside, respectively. If the reaction mixture was neutralized with aqueous phosphoric acid, the methyl 4,6-dideoxy-hexopyranoside was destroyed, probably due to hydrolysis, and methyl α-paratopyranoside could be isolated in a pure state by chromatography on silicic acid in a yield of 16 %. A possible mechanism for the transformation of (I) into (II) by reduction with LAH is depicted in Scheme 1.

The primary 6-*O*-tosyl group is first reduced to a deoxy function by LAH. The 2-*O*-tosyl group of this intermediate is then cleaved, and the LAH adduct formed can serve as a hydride donor for replacement of the 3-*O*-tosyl group.[3] Finally the 4-*O*-tosyl function is cleaved in the expected manner. When the reduction was performed with lithium aluminium deuteride (LAD), the resulting methyl α-D-paratopyranoside contained one deuterium atom at C-6 and one axial deuterium atom at C-3 in agreement with the above mechanism.

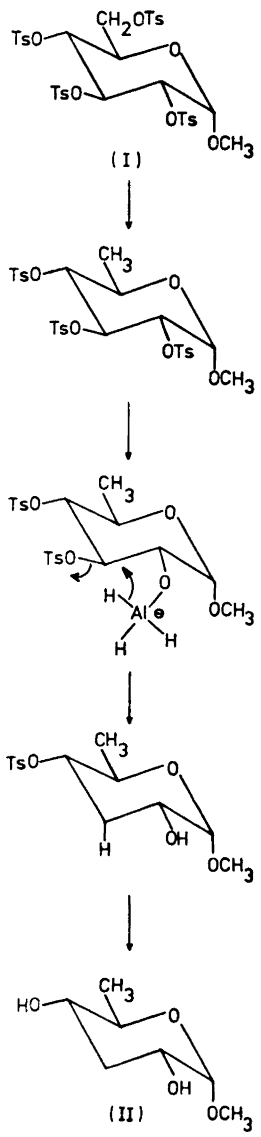

Scheme 1.

The structures of the synthesized methyl α-paratopyranoside and the deuterium labelled analogue were established by NMR and MS of the corresponding diacetates and were further corroborated

by hydrolysis and identification of paratose and paratose labelled with deuterium atoms at C-3 and C-6, as their alditol acetates by GLC[4]–MS.[5] The NMR spectra of the diacetates of (I) and its deuterated analogue could be fully interpreted with the aid of spin decoupling and a shift reagent. The position of the deuterium atom at C-6 in the deuterated compound was established through the change of a three-proton doublet at τ 8.84 into a two-proton group of protons centered at τ 8.84. Further, the splitting pattern of H-5 was simplified. An axial deuterium atom at C-3 was adduced from the disappearance of H-3a at τ 8.10 and the changes in splitting patterns of H-3e, H-2, and H-4. The MS of the diacetates of I and its deuterated analogue (Fig. 1) exhibited, as expected, few degradation pathways.

Structural elucidation of the methyl 4,6-dideoxy-hexopyranoside and the mechanism of its formation are under investigation.

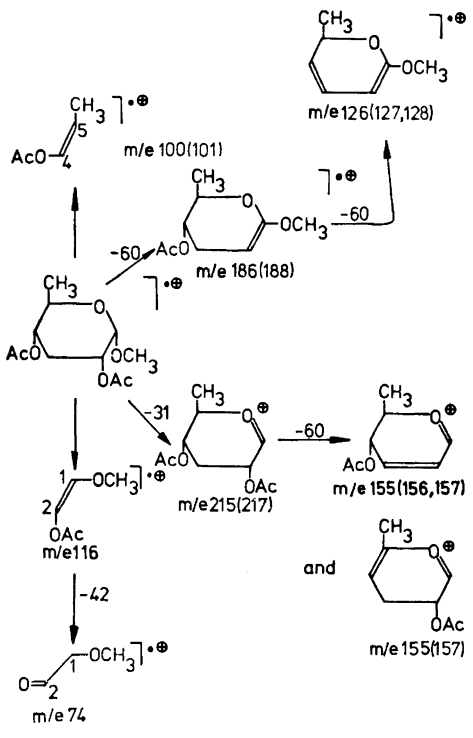

Fig. 1. Fragmentation routes for methyl 2,4-di-*O*-acetyl-α-paratoside. Values for the dideuterated analogue are given in brackets.

Experimental. Concentrations were performed at reduced pressure, at bath temperatures not exceeding 40°C. Melting points are corrected. Analytical TLC was performed on plates (20 × 20 cm) with a layer (0.25 mm) of Silica Gel F_{254} (Merck). Ethyl acetate was used as solvent. Compounds were detected by spraying with 8 % aqueous sulphuric acid and subsequent heating at 140°C. Silica Gel 60 (<0.063 mm) was used for column chromatography. GLC was carried out on OV 225 SCOT- and OS 138 SCOT-columns (15 m × 0.5 mm) at 170 and 190°C, respectively. A Perkin-Elmer 900 Gas Chromatograph was used. For GLC-MS a Perkin-Elmer 270 instrument and the above columns were used. Mass spectra were recorded at a manifold temperature of 200°C, an ionization potential of 70 eV, ionization current of 80 μA and an ion source temperature of 80°C. Optical rotations were determined with a Perkin-Elmer 141 polarimeter and 1 dm microtubes. NMR spectra were recorded on a Varian XL100 (100 MHz) or a Varian A60A (60 MHz) instrument in chloroform-*d*, using TMS as internal standard.

Methyl 2,3,4,6-tetra-O-p-*toluenesulphonyl*-α-D-*glucoside (I).* This compound was prepared essentially as previously described[6] with the exceptions that the tosyl chloride was added at −10°C and that the reaction conditions were changed to 8 days at +4°C. These modifications minimized chlorine containing by-products.

Methyl 3,6-dideoxy-α-D-ribo-*hexopyranoside (II).* I (5.0 g) was mixed with Celite (10.0 g) and placed in the thimble of a Soxhlet apparatus. LAH (10.0 g) in dry ethyl ether (500 ml) was added to the reaction vessel and the mixture was refluxed for 15 h. The excess of LAH was destroyed by the addition of ethyl acetate at 0°C with vigorous stirring. The resulting slurry was neutralized with 1.0 M aqueous phosphoric acid, filtered and concentrated to a syrup. The crude product was fractionated on a silicic acid column (60 × 4 cm), using ethyl acetate as irrigant. The separation was monitored by polarimetry and TLC. The compound with *RF* 0.33 (ethyl acetate) was isolated as a syrup (0.16 g, 16 %), $[\alpha]_{578}^{23}$ +170° (*c* 1.0, chloroform). NMR (60 MHz) showed, *inter alia:* τ 5.39, 1 proton, doublet, H-1, $J_{1,2}$ 3.5 Hz; τ 7.61–8.50, 2 protons, multiplet, H-3a and H-3e; τ 8.76, 3 protons, doublet, C–CH_3, $J_{5,6}$ 6.0 Hz. Part of the syrup (100 mg) was converted into the 2,4-di-*O*-3,5-dinitrobenzoyl derivative[7]

which was recrystallized from ethanol (300 mg, 88 %). This compound melted at 147–148°C and on further heating new crystals were formed which melted at 184–186°C, $[\alpha]_{578}^{23}$ +69° (*c* 1.7, chloroform). (Found: C 45.66; H 3.40; N 10.39. Calc. for $C_{21}H_{18}O_{14}N_4$: C 45.83; H 3.30; N 10.18.)

Another part of the syrup (4 mg) was hydrolysed with 0.25 M aqueous sulphuric acid (2 ml) at 100° for 1 h, neutralized and converted into the alditol acetate. This alditol acetate had the same retention time as an authentic sample of paratitol acetate on both the OV 225 and OS 138 columns. The MS was indistinguishable from that given by the authentic sample.

A sample of II (10 mg) was acetylated with acetic anhydride/pyridine. The diacetate was isolated in the usual manner as a chromatographically pure syrup. The MS of this compound had peaks, *inter alia*, at *m/e* (peak intensities relative to the base peak in brackets): 43(100), 44(4), 45(5), 71(12), 74(18), 83(8), 84(9), 100(25), 103(7), 113(5), 116(11), 143(1.5), 155(1.1), 186(1.1) and 215(3.3). The NMR spectrum (100 MHz) (first order analysis) gave the following results: τ 5.15, 1 proton, octet, H-2, $J_{1,2}$ 3.5 Hz, $J_{2,3e}$ 5 Hz, $J_{2,3a}$ 12 Hz; τ 5.25, 1 proton, doublet, H-1, $J_{1,2}$ 3.5 Hz; τ 5.43, 1 proton, octet, H-4, $J_{4,5}$ 10 Hz, $J_{4,3e}$ 5 Hz, $J_{4,3a}$ 11 Hz; τ 6.23, 1 proton, octet, H-5, $J_{4,5}$ 10 Hz, $J_{5,6}$ 6 Hz; τ 6.58, 3 protons, singlet, OCH_3; τ 7.78, 1 proton, sextet, H-3e, $J_{3e,3a}$ 11 Hz, $J_{3e,2}$ 5 Hz, $J_{3e,4}$ 5 Hz; τ 7.93, 3 protons, singlet, *O*-acetyl; τ 7.96, 3 protons, singlet, *O*-acetyl; τ 8.10, 1 proton, sextet, H-3a, $J_{3a,3e}$ 11 Hz, $J_{3a,2}$ 12 Hz, $J_{3a,4}$ 11 Hz; τ 8.84, 3 protons, doublet, C–CH_3, $J_{5,6}$ 6 Hz. The above analysis was made on the basis of decoupling experiments and by using $Eu(fod)_3$ as shift reagent to separate overlapping protons.

In another preparation of II the reduction was performed with LAD. The MS of the acetylated, deuterium labelled II had peaks at, *inter alia*, *m/e* (peak intensities relative to the base peaks in brackets): 43(100), 44(12), 45(8), 73(13), 75(22), 85(6), 86(5), 101(3), 102(24), 104(8), 117(11), 145(9), 157(0.9), 188(0.8), 217(2.3).

The NMR spectrum (100 MHz) was similar to that obtained for the non-deuterated diacetate with the following exceptions: The 1 proton sextet at τ 7.78 (H-3e) appeared as a triplet ($J_{3e,2}$ 5 Hz, $J_{3e,4}$ 5 Hz); the 1 proton sextet at τ 8.10 had disappeared; the 3 proton doublet at τ 8.84 was changed into a 2 proton doublet; further, the multiplets of H-2, H-4 and H-5 were altered.

When the reduction mixture was processed without neutralization, the combined yield of dideoxyglycosides was increased to 50 %. GLC–MS of the acetylated reaction product and of the derived alditol acetates established a ratio between II and a methyl 4,6-dideoxyhexoside of 3:2, reprectively.

Acknowledgements. We are indebted to *Institutionen för kemi, Avd. II, Ultuna Lantbrukshögskola*, Sweden, for placing the Varian XL 100 instrument at our disposal, to Professor Bengt Lindberg for his interest, and to the *Swedish Natural Science Research Council* for financial support.

1. Davies, D. A. L., Fromme, I., Lüderitz, O., Staub, A. M. and Westphal, O. *Nature* **181** (1958) 822.
2. Fouquey, C., Polonsky, J., Lederer, E., Westphal, O. and Lüderitz, O. *Nature* **182** (1958) 944.
3. Umezawa, S., Tsuchiya, T. and Hineno, H. *Bull. Chem. Soc. Japan* **43** (1970) 4.
4. Sawardeker, J. S., Sloneker, J. H. and Jeanes, A. R. *Anal. Chem.* **12** (1965) 1602.
5. Chizhov, O. S., Golovkina, L. S. and Wulfson, N. S. *Izv. Akad. Nauk. SSSR Otd. Khim. Nauk.* **1966** 1915.
6. Hess, K. and Stenzel, H. *Ber* **68** (1935) 981.
7. Wiley, P. F. *Methods Carbohyd. Chem.* **1** (1962) 265.

Received March 28, 1973.

Studies on Orchidaceae Alkaloids

XXXVII.* Dendrowardine, a Quaternary Alkaloid from *Dendrobium wardianum* Wr.

LARS BLOMQVIST, SVANTE BRANDÄNGE, LARS GAWELL, KURT LEANDER and BJÖRN LÜNING

Department of Organic Chemistry, University of Stockholm, Sandåsgatan 2, S-113 27 Stockholm, Sweden

The occurrence in various *Dendrobium*, species of fourteen alkaloids of the

* For number XXXVI of this series, see Ref. 1.

which was recrystallized from ethanol (300 mg, 88 %). This compound melted at 147–148°C and on further heating new crystals were formed which melted at 184–186°C, $[\alpha]_{578}^{23}$ +69° (*c* 1.7, chloroform). (Found: C 45.66; H 3.40; N 10.39. Calc. for $C_{21}H_{18}O_{14}N_4$: C 45.83; H 3.30; N 10.18.)

Another part of the syrup (4 mg) was hydrolysed with 0.25 M aqueous sulphuric acid (2 ml) at 100° for 1 h, neutralized and converted into the alditol acetate. This alditol acetate had the same retention time as an authentic sample of paratitol acetate on both the OV 225 and OS 138 columns. The MS was indistinguishable from that given by the authentic sample.

A sample of II (10 mg) was acetylated with acetic anhydride/pyridine. The diacetate was isolated in the usual manner as a chromatographically pure syrup. The MS of this compound had peaks, *inter alia*, at *m/e* (peak intensities relative to the base peak in brackets): 43(100), 44(4), 45(5), 71(12), 74(18), 83(8), 84(9), 100(25), 103(7), 113(5), 116(11), 143(1.5), 155(1.1), 186(1.1) and 215(3.3). The NMR spectrum (100 MHz) (first order analysis) gave the following results: τ 5.15, 1 proton, octet, H-2, $J_{1,2}$ 3.5 Hz, $J_{2,3e}$ 5 Hz, $J_{2,3a}$ 12 Hz; τ 5.25, 1 proton, doublet, H-1, $J_{1,2}$ 3.5 Hz; τ 5.43, 1 proton, octet, H-4, $J_{4,5}$ 10 Hz, $J_{4,3e}$ 5 Hz, $J_{4,3a}$ 11 Hz; τ 6.23, 1 proton, octet, H-5, $J_{4,5}$ 10 Hz, $J_{5,6}$ 6 Hz; τ 6.58, 3 protons, singlet, OCH_3; τ 7.78, 1 proton, sextet, H-3e, $J_{3e,3a}$ 11 Hz, $J_{3e,2}$ 5 Hz, $J_{3e,4}$ 5 Hz; τ 7.93, 3 protons, singlet, *O*-acetyl; τ 7.96, 3 protons, singlet, *O*-acetyl; τ 8.10, 1 proton, sextet, H-3a, $J_{3a,3e}$ 11 Hz, $J_{3a,2}$ 12 Hz, $J_{3a,4}$ 11 Hz; τ 8.84, 3 protons, doublet, C–CH_3, $J_{5,6}$ 6 Hz. The above analysis was made on the basis of decoupling experiments and by using $Eu(fod)_3$ as shift reagent to separate overlapping protons.

In another preparation of II the reduction was performed with LAD. The MS of the acetylated, deuterium labelled II had peaks at, *inter alia*, *m/e* (peak intensities relative to the base peaks in brackets): 43(100), 44(12), 45(8), 73(13), 75(22), 85(6), 86(5), 101(3), 102(24), 104(8), 117(11), 145(9), 157(0.9), 188(0.8), 217(2.3).

The NMR spectrum (100 MHz) was similar to that obtained for the non-deuterated diacetate with the following exceptions: The 1 proton sextet at τ 7.78 (H-3e) appeared as a triplet ($J_{3e,2}$ 5 Hz, $J_{3e,4}$ 5 Hz); the 1 proton sextet at τ 8.10 had disappeared; the 3 proton doublet at τ 8.84 was changed into a 2 proton doublet; further, the multiplets of H-2, H-4 and H-5 were altered.

When the reduction mixture was processed without neutralization, the combined yield of dideoxyglycosides was increased to 50 %. GLC–MS of the acetylated reaction product and of the derived alditol acetates established a ratio between II and a methyl 4,6-dideoxyhexoside of 3:2, reprectively.

Acknowledgements. We are indebted to *Institutionen för kemi, Avd. II, Ultuna Lantbrukshögskola*, Sweden, for placing the Varian XL 100 instrument at our disposal, to Professor Bengt Lindberg for his interest, and to the *Swedish Natural Science Research Council* for financial support.

1. Davies, D. A. L., Fromme, I., Lüderitz, O., Staub, A. M. and Westphal, O. *Nature* **181** (1958) 822.
2. Fouquey, C., Polonsky, J., Lederer, E., Westphal, O. and Lüderitz, O. *Nature* **182** (1958) 944.
3. Umezawa, S., Tsuchiya, T. and Hineno, H. *Bull. Chem. Soc. Japan* **43** (1970) 4.
4. Sawardeker, J. S., Sloneker, J. H. and Jeanes, A. R. *Anal. Chem.* **12** (1965) 1602.
5. Chizhov, O. S., Golovkina, L. S. and Wulfson, N. S. *Izv. Akad. Nauk. SSSR Otd. Khim. Nauk.* **1966** 1915.
6. Hess, K. and Stenzel, H. *Ber* **68** (1935) 981.
7. Wiley, P. F. *Methods Carbohyd. Chem.* **1** (1962) 265.

Received March 28, 1973.

Studies on Orchidaceae Alkaloids

XXXVII.* Dendrowardine, a Quaternary Alkaloid from *Dendrobium wardianum* Wr.

LARS BLOMQVIST, SVANTE BRANDÄNGE, LARS GAWELL, KURT LEANDER and BJÖRN LÜNING

Department of Organic Chemistry, University of Stockholm, Sandåsgatan 2, S-113 27 Stockholm, Sweden

The occurrence in various *Dendrobium*, species of fourteen alkaloids of the

* For number XXXVI of this series, see Ref. 1.

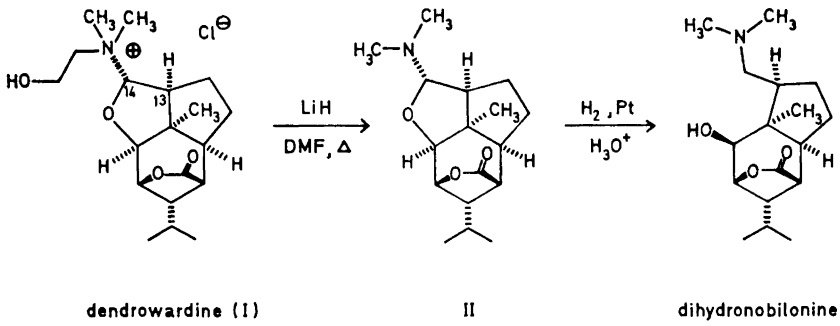

Fig. 1. Transformation of dendrowardine (I) to dihydronobilonine.

dendrobine type has previously been reported.[2,3] In this communication we report the isolation and structure determination of a quaternary alkaloid, dendrowardine (I), from *Dendrobium wardianum* Wr.

Dendrowardine was isolated as the chloride, which has the molecular formula $C_{25}H_{32}ClNO_4$. Pyrolysis of its hydroxide produced *N*,*N*-dimethylethanolamine, a small amount of a base (II), and a product of molecular weight 248 which was not further investigated. When dendrowardine was treated with lithium hydride in *N*,*N*-dimethylformamide at 100°, compound II was formed in excellent yield. Hydrogenolysis of II in aqueous hydrochloric acid over Adams catalyst gave a product indistinguishable (TLC, GLC and MS) from dihydronobilonine.[2] From the similarity between the CD curve of dendrowardine, showing a positive maximum at 228 nm, and that of dendrobine [4] it is obvious that the alkaloids have the same absolute configuration.[2] From the evidence presented above, the structure and absolute configuration of dendrowardine should be either I, or its C-14 epimer.

Information concerning the configuration at C-14 was gained from the NMR spectrum of dendrowardine. The signal from H-14 is a doublet with a coupling constant of 4.5 Hz, which is consistent with a dihedral angle between H-14 and H-13 of either 50° or 120°. The rigid structure of the dendrowardine ring system should give a dihedral angle of about 120° between H-14 and H-13 in the *exo* epimer and an angle close to 0° in the *endo* epimer. Thus, based on the Karplus equation, dendrowardine should be the *exo* epimer and possess the relative and absolute configuration depicted in Fig. 1.

Experimental. All melting points are corrected. Mass spectra were measured on an LKB 9000 spectrometer (ionization energy 70 eV), and the optical rotations on a Perkin-Elmer 141 polarimeter. The IR spectra were recorded on a Perkin-Elmer 257 instrument, the NMR spectra on a Varian A-60A spectrometer, and the CD spectra on a Cary 60 spectropolarimeter.

Isolation of dendrowardine (I). Fresh plants of *Dendrobium wardianum* Wr. (10.7 kg) were extracted with methanol (36 l). The extract was concentrated to 2 l, washed with carbon tetrachloride (5 × 0.3 l), and extracted with chloroform-ethanol (3 : 2, v/v, 11 × 0.3 l). The combined chloroform-ethanol extracts were concentrated to 100 ml, water (200 ml) was added and the solution was filtered through a column of Dowex 1-X4 (Cl^-, 2.5 × 30 cm) irrigated with water. The eluate was evaporated to dryness, and the residue was chromatographed on neutral alumina (5 × 30 cm, activity II–III) using ethanol as eluent. The first fraction contained I and the second choline together with a small amount of I.

The first fraction was evaporated to dryness. To the residue, dissolved in water (10 ml), a saturated solution of ammonium reineckate was added until no more precipitate was formed. The alkaloid reineckate was washed with ice-water (2 × 5 ml), dissolved in acetone-water (1 : 1, 3 ml) and filtered through a column of Dowex 1-X4 (Cl^-, 2 × 20 cm) irrigated with acetone-water (1 : 1). The eluate was evaporated to dryness and the residue filtered through neutral alumina (1 × 10 cm) using ethanol as eluent. The filtrate was evaporated to dryness giving crude I (0.65 g) as a glass. Crystallization from acetone gave I, m.p. 168–172° (dec.), $[\alpha]_D^{25}$ −28° (*c* 1.1, methanol), circular dichroism: $[\theta]_{228}$ +5060°.

(Found: C 60.2; H 8.69; Cl 9.87; N 3.77; O 17.6. Calc. for $C_{19}H_{32}ClNO_4$: C 61.0; H 8.63; Cl 9.48; N 3.75; O 17.1.) IR spectrum: σ_{max} (KBr) 3190 (s), 1772 (s) cm^{-1}. NMR spectrum (DMSO-d_6) τ: 4.13 (t, 1 H, $J=5.0$ Hz, exchangeable in D_2O), 4.97 (d, 1 H, $J=4.5$ Hz), 5.21 (q, 1 H, $J_1=5.0$ Hz, $J_2=3.0$ Hz), 5.68 (d, 1 H, $J=3.0$ Hz), 5.90–6.30 (m, 2 H), 6.40–7.20 (m, 3 H), 6.86 (s, 6 H), 7.60–8.45 (m, 8 H), 8.54 (s, 3 H), 9.06 (d, 6 H, $J=6.0$ Hz).

Degradation of I with lithium hydride. A mixture of I (1.5 mg) and lithium hydride (5 mg) in *N,N*-dimethylformamide (0.5 ml) was heated at 100° for 18 h, and then cooled and acidified with aqueous hydrochloric acid. The solution was washed with ether (2 × 1 ml), neutralized with sodium hydrogen carbonate and extracted with ether (2 × 1 ml). The ether solution was dried and evaporated to dryness leaving II (1.0 mg). IR spectrum: σ_{max} ($CHCl_3$) 1778 (s) cm^{-1}. Pertinent mass spectral peaks *m/e* (rel. intensity): M^+ 293 (13), 292 (9), 249 (6), 220 (6), 177 (5), 175 (4), 138 (100), 124 (9), 111 (9), 93 (11), 91 (9), 74 (24).

Hydrogenation of II. A solution of II (1.8 mg) in aqueous hydrochloric acid (2 ml, 1 %) was hydrogenated over Adams catalyst (9 mg) at room temperature and atmospheric pressure. After 20 h the catalyst was filtered off and the solution made alkaline with sodium hydrogen carbonate and extracted with ether (3 × 1 ml). The ether solution was dried and evaporated to dryness leaving a quantitative yield of dihydronobilonine, indistinguishable (TLC, GLC, MS) from an authentic sample.

Acknowledgements. We are indebted to Dr. Rolf Håkansson and Mr. Jan Glans (Kemicentrum, Lund) for measuring the circular dichroism spectra, and to Dr. Ragnar Ryhage for measuring the mass spectra. We thank the *Swedish Natural Science Research Council* for support.

1. Brandänge, S. and Granelli, I. *Acta Chem. Scand.* **27** (1973) 1096.
2. Behr, D. and Leander, K. *Acta Chem. Scand.* **26** (1972) 3196.
3. Okamoto, T., Natsume, M., Onaka, T., Uchimaru, F. and Shimizu, M. *Chem. Pharm. Bull. (Tokyo)* **20** (1972) 418.
4. Elander, M. and Leander, K. *Acta Chem. Scand.* **25** (1971) 717.

Received April 3, 1973.

On the Polarity of the Dinitrogen Ligand in a Dinitrogen Complex of Iron

BÖRJE FOLKESSON

Division of Inorganic Chemistry, Chemical Center, University of Lund, Box 740, S-220 07 Lund 7, Sweden

In a previous study,[1] infrared absorption intensities of the N–N stretching vibration in some dinitrogen complexes of rhenium and iridium were reported. It was found that the intensity of the N–N stretching vibration (A_{NN}) increases with decreasing frequency (ν_{NN}) (*cf.* Fig. 2 in Ref. 1). It was concluded that the lower the ν_{NN} and the higher the A_{NN}, the greater was the disturbance of the dinitrogen ligand. Furthermore, from ESCA measurements [2] on the above mentioned dinitrogen complexes, the charge distribution on the dinitrogen ligand was determined. The presence of two peaks in the N1*s* electron spectra shows that the dinitrogen ligand has an appreciable polarity. It has been found that both the nitrogen atoms in the complexes carry a negative charge. A connection between the magnitude of the shift in N1*s* binding energy and the N–N stretching frequency has been found, *viz.* the lower the ν_{NN}, the larger the chemical shift in binding energy. Thus, when the disturbance of the dinitrogen ligand is large, *i.e.* low ν_{NN}, the more pronounced is the charge separation on the nitrogen atoms.

In order to further substantiate these observations, both infrared intensity and ESCA measurements have been performed on a dinitrogen complex of iron, *viz.* $FeH_2N_2(PPh_3)_3$. In view of the occurrence of iron in the nitrogen-fixing enzyme [3] in biological systems, such an investigation could be of added interest. $FeH_2N_2(PPh_3)_3$ was first prepared by Sacco and Aresta [4] and later by Borod'ko *et al.*[5] The complex investigated in this work has been prepared according to the procedure given by Borod'ko *et al.*[5] The purity of the compound was checked by elemental analysis and by its IR spectrum. (Found: C 74.0; H 5.69; N 3.16. Calc. C 74.3; H 5.43; N 3.21.) The IR spectrum shows a strong band at 2075 cm^{-1} (N–N stretching vibration) and a weak broad band at 1895 cm^{-1} (Fe–H stretching

(Found: C 60.2; H 8.69; Cl 9.87; N 3.77; O 17.6. Calc. for $C_{19}H_{32}ClNO_4$: C 61.0; H 8.63; Cl 9.48; N 3.75; O 17.1.) IR spectrum: σ_{max} (KBr) 3190 (s), 1772 (s) cm^{-1}. NMR spectrum (DMSO-d_6) τ: 4.13 (t, 1 H, $J=5.0$ Hz, exchangeable in D_2O), 4.97 (d, 1 H, $J=4.5$ Hz), 5.21 (q, 1 H, $J_1=5.0$ Hz, $J_2=3.0$ Hz), 5.68 (d, 1 H, $J=3.0$ Hz), 5.90–6.30 (m, 2 H), 6.40–7.20 (m, 3 H), 6.86 (s, 6 H), 7.60–8.45 (m, 8 H), 8.54 (s, 3 H), 9.06 (d, 6 H, $J=6.0$ Hz).

Degradation of I with lithium hydride. A mixture of I (1.5 mg) and lithium hydride (5 mg) in *N,N*-dimethylformamide (0.5 ml) was heated at 100° for 18 h, and then cooled and acidified with aqueous hydrochloric acid. The solution was washed with ether (2 × 1 ml), neutralized with sodium hydrogen carbonate and extracted with ether (2 × 1 ml). The ether solution was dried and evaporated to dryness leaving II (1.0 mg). IR spectrum: σ_{max} ($CHCl_3$) 1778 (s) cm^{-1}. Pertinent mass spectral peaks *m/e* (rel. intensity): M^+ 293 (13), 292 (9), 249 (6), 220 (6), 177 (5), 175 (4), 138 (100), 124 (9), 111 (9), 93 (11), 91 (9), 74 (24).

Hydrogenation of II. A solution of II (1.8 mg) in aqueous hydrochloric acid (2 ml, 1 %) was hydrogenated over Adams catalyst (9 mg) at room temperature and atmospheric pressure. After 20 h the catalyst was filtered off and the solution made alkaline with sodium hydrogen carbonate and extracted with ether (3 × 1 ml). The ether solution was dried and evaporated to dryness leaving a quantitative yield of dihydronobilonine, indistinguishable (TLC, GLC, MS) from an authentic sample.

Acknowledgements. We are indebted to Dr. Rolf Håkansson and Mr. Jan Glans (Kemicentrum, Lund) for measuring the circular dichroism spectra, and to Dr. Ragnar Ryhage for measuring the mass spectra. We thank the *Swedish Natural Science Research Council* for support.

1. Brandänge, S. and Granelli, I. *Acta Chem. Scand.* **27** (1973) 1096.
2. Behr, D. and Leander, K. *Acta Chem. Scand.* **26** (1972) 3196.
3. Okamoto, T., Natsume, M., Onaka, T., Uchimaru, F. and Shimizu, M. *Chem. Pharm. Bull. (Tokyo)* **20** (1972) 418.
4. Elander, M. and Leander, K. *Acta Chem. Scand.* **25** (1971) 717.

Received April 3, 1973.

On the Polarity of the Dinitrogen Ligand in a Dinitrogen Complex of Iron

BÖRJE FOLKESSON

Division of Inorganic Chemistry, Chemical Center, University of Lund, Box 740, S-220 07 Lund 7, Sweden

In a previous study,[1] infrared absorption intensities of the N–N stretching vibration in some dinitrogen complexes of rhenium and iridium were reported. It was found that the intensity of the N–N stretching vibration (A_{NN}) increases with decreasing frequency (ν_{NN}) (*cf.* Fig. 2 in Ref. 1). It was concluded that the lower the ν_{NN} and the higher the A_{NN}, the greater was the disturbance of the dinitrogen ligand. Furthermore, from ESCA measurements [2] on the above mentioned dinitrogen complexes, the charge distribution on the dinitrogen ligand was determined. The presence of two peaks in the N1*s* electron spectra shows that the dinitrogen ligand has an appreciable polarity. It has been found that both the nitrogen atoms in the complexes carry a negative charge. A connection between the magnitude of the shift in N1*s* binding energy and the N–N stretching frequency has been found, *viz.* the lower the ν_{NN}, the larger the chemical shift in binding energy. Thus, when the disturbance of the dinitrogen ligand is large, *i.e.* low ν_{NN}, the more pronounced is the charge separation on the nitrogen atoms.

In order to further substantiate these observations, both infrared intensity and ESCA measurements have been performed on a dinitrogen complex of iron, *viz.* $FeH_2N_2(PPh_3)_3$. In view of the occurrence of iron in the nitrogen-fixing enzyme [3] in biological systems, such an investigation could be of added interest. $FeH_2N_2(PPh_3)_3$ was first prepared by Sacco and Aresta [4] and later by Borod'ko *et al.*[5] The complex investigated in this work has been prepared according to the procedure given by Borod'ko *et al.*[5] The purity of the compound was checked by elemental analysis and by its IR spectrum. (Found: C 74.0; H 5.69; N 3.16. Calc. C 74.3; H 5.43; N 3.21.) The IR spectrum shows a strong band at 2075 cm^{-1} (N–N stretching vibration) and a weak broad band at 1895 cm^{-1} (Fe–H stretching

vibration). The intensity measurements on the N–N stretching vibration have been performed as before [1] both in the solid state and in solution. The intensity of the N–N band in solution was found to decrease with time, indicating the instability of the complex in solution. Therefore, the measurements were performed rapidly. Three spectra were recorded successively and the intensity was extrapolated to zero time. The results are given in Table 1.

Table 1. The results of the absorption intensity measurements on $FeH_2N_2(PPh_3)_3$.

Dispersion medium	ν_{NN} cm^{-1}	ε_{NN} $M^{-1}cm^{-1}$	$A_{NN}\times 10^{-4}$ $M^{-1}cm^{-2}$
KBr	2075	950±100	4.5±0.4
$C_6H_5CH_3$	2076	800±100	4.3±0.4

The good agreement of the intensity values (A_{NN}) determined in various dispersion media shows that the intensity is not dependent on the medium. There is further a good agreement between these intensity values and the value 4.4×10^4 M^{-1} cm^{-2}, which was reported by Borod'ko *et al.*[5] (the medium unspecified). The intensity values (A_{NN}) found for the $Fe-N_2$ complex are somewhat larger than corresponding A_{NN} for $IrClN_2(PPh_3)_2$ measured before.[1] This is expected as the frequency (ν_{NN}) is somewhat lower in the $Fe-N_2$ complex than in the iridium complex (2075 cm^{-1} and 2105 cm^{-1}, respectively). Indeed, the intensity values measured for the $Fe-N_2$ complex fall on the correlation curve between intensity (A_{NN}) and frequency (ν_{NN}) presented before (*cf.* Fig. 2 in Ref. 1). As mentioned above a high intensity value of the N–N stretching vibration means a great disturbance of the dinitrogen ligand and a decrease in the N–N bond order. Consequently, this means a strong metal-dinitrogen bond. The intensity values found for the $Fe-N_2$ complex are considerably smaller than the previously [1] determined values for the rhenium dinitrogen complexes. In agreement with this, it may be noted that the Fe–N bond is not so stable to chemical attack as the metal–N bond in the rhenium dinitrogen complexes.

The ESCA measurements were performed at low temperature, since it was found that the complex decomposes with evolution of dinitrogen under vacuum at room temperature. The nitrogen 1*s* electron spectrum of the complex obtained at −50°C is given in Fig. 1. It is evident

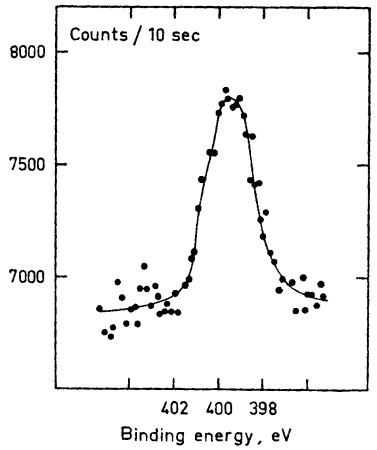

Fig. 1. Nitrogen 1*s* electron spectrum of $FeH_2N_2(PPh_3)_3$ obtained at −50°C.

that the 1*s* electrons of coordinated dinitrogen did not give rise to two separate peaks, but only one broad peak. The half-width of the peak was 2.4 eV. The half-width of a separate N1*s* electron peak has been found to be 1.4 eV for the dinitrogen complexes of rhenium. The value 2.4 eV for $FeH_2N_2(PPh_3)_3$ thus gives an indication of two N1*s* electron peaks. To get the energy difference between the two peaks, the deconvolution procedure given in Ref. 6, Appendix D, has been used. Under the assumption that the half-width of a separate N1*s* electron peak in the iron dinitrogen complex is the same as the half-width of the N1*s* electron peaks found for the dinitrogen complexes of rhenium, the energy difference becomes 1.1 eV. The maxima of the two N1*s* electron peaks are then placed on each side of the maximum of the obtained peak. The N1*s* electron binding energies of the two nitrogen atoms then become 399.0 eV and 400.1 eV. Analogous to the earlier results,[1] the smallest N1*s* binding energy is assigned to the inner nitrogen atom, which thus is the most negative one. The charges on the nitrogen atoms can now be estimated from the binding energies with the aid of the correlation diagrams presented before (Figs. 3–5 in Ref. 2). It is evident that

both the nitrogen atoms become negatively charged. The charges obtained from the correlation diagram based on CNDO calculated charges ($M-N_1-N_2$) are $q_{N_1} = -0.41$ a.u. and $q_{N_2} = -0.28$ a.u. The charge separation (0.13 a.u.) on the nitrogen atoms is thus smaller for this dinitrogen complex than the charge separation found for, *e.g.*, the dinitrogen complexes of rhenium [2] (0.23 a.u.). The N–N bond in the iron dinitrogen complex thus shows smaller polarity than the N–N bond in the dinitrogen complexes of rhenium, which also is expected from the IR results.

To get an idea about the charge on the iron atom in the dinitrogen complex some metal core electron spectra have also been recorded. Table 2 shows the Fe $2p_{3/2}$ and Fe $3p$ electron binding energies in the dinitrogen complex together with the corresponding binding energies for some other iron compounds. It is evident that the binding energies measured for the dinitrogen complex are closer to those found for Fe metal than those measured for other iron compounds of the same formal oxidation state. This indicates a low positive charge on the metal atom in the dinitrogen complex. On the other hand, it is expected that the π^*-acceptor ability of the dinitrogen ligand should cause a lower electron density around the metal atom and consequently a high binding energy and thereby a high positive charge on the metal atom. It must, however, be pointed out that the binding energy is dependent not only on the effective charge on the atom in question, but also on the potential at that atom originating from the effective charge of all the other atoms in the molecule. It is thus quite reasonable that the potential originating from the surrounding phosphines and especially the hydride ions in the dinitrogen complex causes a low binding energy at the metal atom and thereby seemingly a low positive charge. A low positive charge on the metal atom has earlier been found [2] for the dinitrogen complexes of rhenium and iridium.

Table 2. The binding energies of Fe $2p_{3/2}$ and Fe $3p$ electrons in some iron compounds.

Compound	E_b eV	
	Fe $2p_{3/2}$	Fe $3p$
Fe metal	706.5	53.2
$FeH_2N_2(PPh_3)_3$	707.1	54.2
$FeCl_2$	710.9	56.0
$FeSO_4$	711.1	55.9

The shift in N1*s* binding energy earlier found for $IrClN_2(PPh_3)_2$ was 1.4 eV. This is to be compared with the shift (1.1 eV) now obtained for $FeH_2N_2(PPh_3)_2$. The N–N stretching frequency is somewhat higher in $IrClN_2(PPh_3)_2$ than in $FeH_2N_2(PPh_3)_3$, so the shift found earlier is probably somewhat too large. It was also pointed out [2] that the intensity of the two N1*s* electron peaks in $IrClN_2(PPh_3)_2$ was small and therefore it was difficult to determine the exact position of the two peaks. The reported N1*s* binding energies for $IrClN_2(PPh_3)_2$ are consequently somewhat uncertain.

Another interesting observation is further confirmed through the measurements on the iron dinitrogen complex, *viz.* that the difference in N1*s* binding energy of the terminal nitrogen atom for various complexes (*cf.* Table 1 in Ref. 2) is not so pronounced as the difference in N1*s* binding energy of the inner nitrogen atom. Consequently, the charges on the terminal nitrogen atoms are more similar than the charges on the inner nitrogen atoms.

The financial support from the *Swedish Board for Technical Development* and the *Bank of Sweden Tercentenary Fund* is gratefully acknowledged. The author is also indebted to Dr. R. Larsson for his kind interest in this work.

1. Folkesson, B. *Acta Chem. Scand.* **27** (1973) 276.
2. Folkesson, B. *Acta Chem. Scand.* **27** (1973) 287.
3. Burns, R. C., Holsten, R. D. and Hardy, R. W. F. *Biochem. Biophys. Res. Commun.* **39** (1970) 90.
4. Sacco, A. and Aresta, M. *Chem. Commun.* **1968** 1223.
5. Borod'ko, Yu. G., Broitman, M. O., Kachapina, L. M., Shilova, A. K. and Shilov, A. E. *Zh. Strukt. Khim.* **12** (1971) 545.
6. Siegbahn, K., Nordling, C., Johansson, G., Hedman, J., Hedén, P. F., Hamrin, K., Gelius, U., Bergmark, T., Werme, L. O., Manne, R. and Baer, Y. *ESCA Applied to Free Molecules*, North-Holland, Amsterdam 1969.

Received April 7, 1973.

Comparison of Structural Effects in the Hydrolysis of Carboxylic Acid Ortho-esters

ALPO KANKAANPERÄ, MARKKU LAHTI and RIITTA ÄÄLTONEN

Department of Chemistry, University of Turku, SF-205 00 Turku 50, Finland

Structural effects in the hydrolysis of carboxylic acid ortho-esters have been discussed in only a few papers.[1,2] The effect of the alcohol component in formic and benzoic acid esters has been recently investigated,[3,4] but no systematic study has been made of the effect of the acid component. In contrast to the hydrolysis of the related acetals,[1,5] it can be inferred from the few kinetic values available[1,2,6] that the effect of the alkyl or aryl substituent at the reaction centre is relatively small. Thus, ethyl orthoacetate is hydrolyzed only 40 times faster than the corresponding orthoformate whereas, surprisingly, a similar substitution in acetals increases the rate by a factor of about $10^{3.5}$. However, it should be noted that with ethyl ortho-esters the mechanism of hydrolysis changes when the acid component is altered: ethyl orthoformate [3] and ethyl orthobenzoate [4] are hydrolyzed through a pre-equilibrium protonation (A-1 mechanism), while the hydrolysis of the orthoacetates and orthopropionates involves a rate-determining proton transfer (A-S_E2 mechanism).[6]

These complications are avoided with a series of compounds in which the hydrolysis mechanism does not change with the acid component. Diethyl 2,2,2-trichloroethyl derivatives were expected to be suitable model compounds, as it could be concluded [7,8] that the hydrolysis proceeds exclusively with trichloroethoxy as the leaving group. Furthermore, the A-S_E2 mechanism is greatly favoured here owing to the low basicity of the protonation site and the high stability of the diethoxy carbonium ion formed.

Materials. Two alternative methods were used in the preparation of the unsymmetrical ortho-esters. In most cases the ortho-ester was synthesized from the corresponding triethyl ortho-ester through acid-catalyzed transesterification. The most volatile component, ethanol, was distilled off from an equimolar mixture of the symmetrical ortho-ester and 2,2,2-trichloroethanol. A small amount of *p*-toluenesulfonic acid was present as catalyst. It has been shown previously [8] that under mild conditions only one of the ethoxy groups is replaced. Formation of more chlorinated derivatives is rendered difficult by the low stability of the dialkoxy-carbonium ions with one or two trichloroethoxy groups.

In the preparation of the monochloroacetic acid and dichloroacetic acid derivatives an alternative method was applied; a ketene acetal was alcoholyzed with trichloroethanol using *p*-toluenesulfonic acid as the catalyst. After neutralization the product was purified by distillation. Symmetrical products were not formed.

Diethyl 2,2,2-trichloroethyl orthopropionate was prepared from ethyl orthopropionate (Fluka) and 2,2,2-trichloroethanol (Fluka). After transesterification the reaction mixture was neutralized with sodium ethoxide and fractionally distilled. B.p. 106–109°C/7 torr. NMR spectrum: 3H at δ 0.96 ppm (CH_3), 6 H at δ 1.22 ppm (CH_3), 2 H at δ 1.77 ppm (CH_2), 4 H at δ 3.70 ppm (CH_2) and 2 H at δ 4.16 ppm (CH_2). Other signals were not observed.

Diethyl 2,2,2-trichloroethyl orthoacetate was synthesized from triethyl orthoacetate and trichloroethanol. B.p. 107–108°C/10 torr. NMR spectrum: 6 H at δ 1.20 ppm (CH_3), 3 H at δ 1.45 ppm (CH_3), 4 H at δ 3.65 ppm (CH_2) and 2 H at δ 4.10 ppm (CH_2).

In the preparation of diethyl 2,2,2-trichloroethyl orthoformate, triethyl orthoformate (E. Merck) and trichloroethanol were used as the substrates. B.p. 92–96°C/6 torr. NMR spectrum: 6 H at δ 1.25 ppm (CH_3), 4 H at δ 3.74 ppm (CH_2), 2 H at δ 4.20 ppm (CH_2) and 1 H at δ 5.42 ppm (CH). Other signals were not observed.

Diethyl 2,2,2-trichloroethyl orthobenzoate was prepared by transesterification from triethyl orthobenzoate (Fluka) and trichloroethanol. B.p. 154–160°C/10 torr. NMR spectrum: 6 H at δ 1.18 ppm (CH_3), 4 H at δ 3.47 ppm (CH_2), 2 H at δ 4.02 ppm (CH_2) and 5 H at δ 7.53 ppm (aromatic).

1-Chloro-2,2-diethoxyethene was prepared by refluxing 1,1-dichloro-2,2-diethoxyethane (The British Drug Houses Ltd) with potassium *t*-butoxide in *t*-butanol.[9] After the potassium chloride had been filtered off, the solvent and the ketene acetal were separated by distillation. The ketene acetal was alcoholyzed with 2,2,2-trichloroethanol and the product, diethyl 2,2,2-trichloroethyl monochloro-orthoacetate, was further purified. B.p. 113–114°C/5 torr. NMR spectrum: 6 H at δ 1.26 ppm (CH_3), 6 H at δ 3.49–3.98 ppm (CH_2) and 2 H at δ 4.33 ppm (CH_2).

1,1,1-Trichloro-2,2-diethoxyethane was prepared from trichloroacetaldehyde and ethanol

using a large excess of concentrated sulfuric acid as the catalyst.[9] B.p. 88–89°C/11 torr. The corresponding ketene acetal was prepared from this acetal by refluxing with potassium *t*-butoxide.[9] The ketene acetal obtained was alcoholyzed with trichloroethanol to give diethyl 2,2,2-trichloroethyl dichloro-orthoacetate. B.p. 94°C/10 torr. NMR spectrum: 6 H at δ 1.24 ppm (CH_3), 4 H at δ 3.75 ppm (CH_2), 2 H at δ 4.28 ppm (CH_2) and 1 H at δ 5.63 ppm (CH). Other signals were not observed.

Kinetic measurements. Most of the kinetic measurements were made in 65/35 w/w dioxane-water mixtures. Dioxane (E. Merck AG) was purified by standard methods.[10] The heavy water used was a product of Norsk Hydro-Elektrisk Kvaelstofaktieselskap. The concentration of the catalyst, perchloric acid, varied between 10^{-4} and 10^{-2} M. However, in the case of diethyl 2,2,2-trichloroethyl dichloro-orthoacetate higher acid concentrations (up to 0.2 M) were necessary owing to the slowness of the reaction. In these solutions the rate was not strictly proportional to the acid concentration, and so the results obtained at different concentrations were extrapolated to infinite dilution.

An equimolar solution of dichloroacetic acid and sodium dichloroacetate was used in the buffer experiments. A constant ionic strength was maintained with sodium chloride. In these experiments a mixture of dimethyl sulfoxide and water (2/1 v/v) was used as the solvent.

The hydrolysis of the ortho-esters was followed spectrophotometrically from the appearance of the carboxylic acid ester at wavelengths between 230 and 240 nm. In the case of the benzoic acid derivative the wavelength was 270 nm. The initial concentration of the ortho-ester was usually 0.005 to 0.01 M. In the case of the benzoic acid derivative the concentration of the substrate was less, 0.001 M. Replicate determinations were made in each case.

Table 1. The hydronium ion-catalyzed hydrolysis of unsymmetrical ortho-esters $RC(OEt)_2(OCH_2CCl_3)$ in 65/35 w/w dioxane-water mixtures. Temperature 25°C.

R	L_2O	k (M^{-1} s^{-1})	$\frac{k_{D_3O^+}}{k_{H_3O^+}}$
CH_3CH_2	H_2O	65.2	
	D_2O	75.5	1.16
CH_3	H_2O	81.8	
	D_2O	103.1	1.26
H	H_2O	10.15	
	D_2O	9.92	0.98
Phenyl	H_2O	0.343	
	D_2O	0.425	1.24
$ClCH_2$	H_2O	0.982	
	D_2O	1.058	1.08
Cl_2CH	H_2O	0.0026	
	D_2O	0.0047	1.83

Table 2. The hydrolysis of diethyl 2,2,2-trichloroethyl orthobenzoate in dichloroacetic acid-sodium dichloroacetate buffer (molar ratio 1/1) in 2/1 v/v dimethyl sulfoxide-water mixture at 25°C. The ionic strength was maintained at 0.1 M with sodium chloride.

$[Cl_2CHCOOH]$ (M)	10^3k (s^{-1})	k_{HA} (M^{-1} s^{-1})
0.100	1.741	
0.0667	1.400	
0.0333	1.032	0.0106 ± 0.0020

The kinetic data collected in Tables 1 and 2 are consistent with the A-S_E2 mechanism. Firstly, the magnitudes of the solvent deuterium isotope effects, $k_{D_3O^+}/k_{H_3O^+} = 0.98 - 1.83$, are those observed previously for this mechanism in the hydrolysis of ortho-esters.[3] In the hydrolysis of related compounds, acetals, $k_{D_3O^+}/k_{H_3O^+}$ values lower than two have also been obtained for the rate-determining proton transfer mechanism.[11]

Secondly, the general acid catalysis observed for the hydrolysis of the benzoic acid derivative (Table 2) shows directly that, at least in this case, the proton transfer is the rate-determining stage of the reaction. Unfortunately, only in the hydrolysis of this particular compound could the involvement of general acid catalysis be studied directly. The compounds were too sparingly soluble in water and thus necessitated the use of organic solvents. Dioxane-water mixtures could not, however, be used in the buffer experiments because of the specific salt effects, which are very significant in this solvent system.[12,13] These difficulties are avoided in dimethyl sulfoxide-water mixtures.[14] Unfortunately, this solvent system has an absorption maximum in the UV region and therefore only wavelengths higher than 250 nm can be used. Thus, the only hydrolysis which could be followed spectro-

photometrically was that of the benzoic acid derivative. A direct detection of general catalysis is, however, unnecessary for the hydrolysis of the remaining ortho-esters because of the structural effects. The site of protonation is the same for all the compounds studied, and thus the variation in the rates is due solely to differences in the dialkoxy-carbonium ion stabilities. Excepting the dichloroacetic acid derivative, the ortho-esters studied are more susceptible to acid-catalyzed hydrolysis than the benzoic acid derivative, and therefore the rate-determining proton transfer is even more favoured than in the hydrolysis of the orthobenzoate.

As discussed above, considerable structural variations in series of diethyl trichloroethyl ortho-esters do not effect a change in the mechanism. Direct information on the effect of the acid component

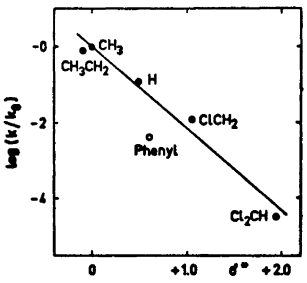

Fig. 1. Plot of log k against polar substituent constants for the hydrolysis of ortho-esters of the type $RC(OEt)_2(OCH_2CCl_3)$.

can thus be obtained. In Fig. 1 the logarithms of the rate coefficients are plotted against the polar substituent constants [15] of the atoms or groups attached to the central carbon atom. Excepting the phenyl-substituted derivative, the correlation is seen to be fairly linear. The slope of this plot (δ^*-value) is -2.2 ± 0.2. In addition to the inductive effects, the resonance effects cannot be wholly excluded. However, differences in the latter must be negligible for the substituents CH_3CH_2, CH_3, H, $ClCH_2$, and Cl_2CH. This being so, the structural effect in the hydrolysis of ortho-esters cannot be considered exceptional. The only difference from the hydrolysis of acetals is the diminished influence of structural effects. This is shown by the δ^*-value, -2.2, which is markedly less than the -3.8 observed for the hydrolysis of acetals.[16]

The rate coefficient for the hydrolysis of the benzoic acid derivative seems to be exceptionally low (Fig. 1). If only inductive polar effects were operating, a rate coefficient higher by a factor of ten would be expected. The actual rate is even more abnormal than can be seen from the plot of log k against σ^* since for this compound the resonance effects in the transition state should also be significant. Additional, more detailed information is needed before firm conclusions can be drawn.

Acknowledgement. Grants for support of this work from the *Finnish Academy, Division of Sciences*, are gratefully acknowledged.

1. Cordes, E. H. *Progr. Phys. Org. Chem.* **4** (1967) 1.
2. Cordes, E. H. In Patai, S., Ed., *The Chemistry of the Carboxylic Acids and Esters*, Interscience, London 1969, pp. 623–667.
3. Kankaanperä, A. and Lahti, M. *Suomen Kemistilehti* **B 43** (1970) 75, 101, 105.
4. Lahti, M., Kankaanperä, A. and Aaltonen, R. *Suomen Kemistilehti* **B 45** (1972) 160.
5. Ingold, C. K. *Structure and Mechanism in Organic Chemistry*, 2nd Ed., Cornell University Press, Ithaca, N.Y. 1969, pp. 447–448.
6. Brönsted, J. N. and Wynne-Jones, W. F. K. *Trans. Faraday Soc.* **25** (1929) 59.
7. Salomaa, P. *Ann. Acad. Sci. Fennicae Ser. A* **II** (1961) No. 103.
8. Kankaanperä, A. and Lahti, M. *Suomen Kemistilehti* **B 42** (1969) 406.
9. Straub, T. S., Ph. D. Thesis, Illinois Institute of Technology, Chicago 1970.
10. Vogel, A. I. *Practical Organic Chemistry*, 3rd Ed., Longmans, London 1967, p. 177.
11. a. Fife, T. H. and Jao, L. K. *J. Am. Chem. Soc.* **90** (1968) 4081; b. Kankaanperä, A. and Lahti, M. *Acta Chem. Scand.* **23** (1969) 2465, 3266; c. Anderson, E. and Capon, B. *J. Chem. Soc.* **B 1969** 1033.
12. Lahti, M. and Kankaanperä, A. *Acta Chem. Scand.* **24** (1970) 706.
13. Salomaa, P., Kankaanperä, A. and Lahti, M. *J. Am. Chem. Soc.* **93** (1971) 2084.
14. Lahti, M. and Kankaanperä, A. *Acta Chem. Scand.* **26** (1972) 2130.
15. Taft, Jr., R. W. *J. Am. Chem. Soc.* **75** (1953) 4231.
16. Kreevoy, M. M. and Taft, Jr., R. W. *J. Am. Chem. Soc.* **77** (1955) 5590.

Received March 14, 1973.

On the Crystal Structure of $Sn_3O(OH)_2SO_4$

SIV GRIMVALL

Department of Inorganic Chemistry, Chalmers University of Technology and the University of Göteborg, P. O. Box, S-402 20 Göteborg 5, Sweden

The crystal structure of $Sn_3O(OH)_2SO_4$ has been determined from X-ray diffraction data collected by Weissenberg techniques. The crystals are orthorhombic and the unit cell dimensions, determined from Guinier powder diffraction data, are: $a = 13.0203 \pm 0.0034$ Å, $b = 4.9451 \pm 0.0013$ Å, $c = 12.0783 \pm 0.0035$ Å, $V = 777.7$ Å^3.

If the a and b axes are interchanged, the cell dimensions are in good agreement with values published by Davies and Donaldson.[1] There are four formula units in the unit cell. The space group is $Pca2_1$,[2] which is the noncentrosymmetric alternative among the groups suggested previously.[1]

Patterson and electron density functions were calculated with $h0l$, $h1l$, and $h2l$ data. Atomic parameters obtained from these calculations and refined by the method of least squares yielded a preliminary R value of 13.3 %. No correction has yet been made for absorption.

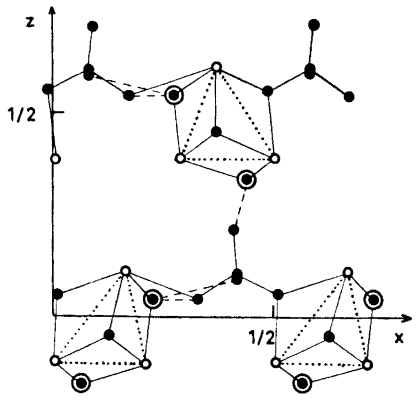

Fig. 1. Projection of the structure of $Sn_3O(OH)_2SO_4$ on the xz plane. Tin triangles are marked with dotted lines, coordinated atoms are connected by full lines and O–O distances available for hydrogen bonds are dashed. O′ corresponds to an oxygen atom in the next unit cell above or below.

A projection of the structure on the xz plane is shown in Fig. 1. Three tin atoms form a triangle with Sn-Sn distances of 3.49 Å, 3.57 Å, and 3.59 Å, respectively. One oxygen atom is coordinated to all three tin atoms, while two hydroxide ions are coordinated each to two tin atoms. On the third side of the Sn triangle there is a sulphate oxygen atom coordinated to two tin atoms. The arrangement of tin, oxygen and hydroxide ions yields the ion $Sn_3O(OH)_2^{2+}$, which is in accordance with that suggested, though not verified, by Davies and Donaldson.[1] It differs from the $Sn_3(OH)_4^{2+}$ ion proposed by Tobias [3] from emf measurements by one water molecule. The $Sn_3O(OH)_2^{2+}$ ion is, however, also coordinated to sulphate groups, so that two of the tin atoms are three-coordinated, whereas the third has four oxygen neighbours. The tin triangles form a zig-zag chain running along the b axis, connection being provided by the coordination of two tin atoms to hydroxide ions in the unit cell below (*cf.* Fig. 1).

Differential thermal analysis and thermogravimetric analysis indicated different modes of coordinations for the two hydroxide groups since the water is expelled in two steps separated by 65°. This is confirmed by the O–O distances. One of the O–H···O bonds is of the usual linear type with an O–O distance of 2.79 Å, whereas for the other there are two O–O distances of 2.61 Å and 2.68 Å, corresponding to a bifurcated hydrogen bond The O–O distances of interest are marked in Fig. 1. All the oxygen atoms in the sulphate group are coordinated to other atoms which results in a distortion of the sulphate group.

Further refinement of this structure is in progress and the results will soon be published.

This work has been supported financially by the *Swedish Natural Science Research Council*, Contract No. 2318.

1. Davies, C. G. and Donaldson, J. D. *J. Chem. Soc.* **A 1967** 1790.
2. *International Tables for X-Ray Crystallography*, 2nd Ed., Kynoch Press, Birmingham 1952, Vol. 1.
3. Tobias, R. S. *Acta Chem. Scand.* **12** (1958) 198.

Received April 17, 1973.

Redetermined Crystal Structure of FeAs

KARI SELTE and ARNE KJEKSHUS

Kjemisk Institutt, Universitetet i Oslo, Blindern, Oslo 3, Norway

The crystal structures of MnP and its isostructural compounds are commonly regarded (*cf.*, *e.g.*, Ref. 1) as belonging to space group *Pnma*. However, recent results [2-5] obtained at this institute suggest that the mirror plane perpendicular to [010] is lacking in the crystal structures of some members (*viz.* VAs, FeP, FeAs, and CoAs) of this class. As is frequently the case in science, the basis for an inference of this type is of fundamental importance. In fact, the significance of this simple fact increases the finer distinctions of the object one is examining. The inherent approximations and other limiting conditions concerning our structure determinations of VAs, FeP, FeAs, and CoAs were perhaps not emphasized strongly enough in Refs. 2 – 5. It may therefore be appropriate to recapitulate that the latter studies were based on *inter alia* the following limitations:

(i) The photographic (Weissenberg) technique was used to record the diffraction intensities, which in turn were evaluated microphotometrically (or visually in the case of the weakest reflections).

(ii) The complex polyhedral shapes of the crystals were approximated to spherical in relation to the corrections for absorption and secondary extinction.

(iii) The effect of dispersion in the scattered X-rays was not taken into account.

The above deficiencies clearly obscure our previous suggestions concerning the space group of VAs, FeP, FeAs, and CoAs, and since specific improvements in these and other respects are now conceivable, it was considered worthwhile to reexamine one of the structures very thoroughly. The structure of FeAs was arbitrarily selected for this purpose. A parallel study has been carried out on a corresponding problem regarding marcasite (FeS_2).[6]

Experimental. A single crystal of FeAs (from the same batch as that of the preceding study [2]) was ground into an almost perfect sphere of 0.32 mm diameter.

Three dimensional intensity data were recorded on a computer controlled four-circle (Syntex) diffractometer using graphite crystal monochromatized Mo$K\alpha$-radiation. The $2\theta{:}\theta$ scan technique was utilized at a variable scan speed, very weak reflections (*viz.* those with intensities less than twice their estimated standard deviations according to counting statistics) being automatically omitted. In all 817 reflections with $\sin\theta/\lambda < 1.0$ and indices of the types hkl and $hk\bar{l}$ (according to $Pna2_1$) were registered, and the intensities of 3 check reflections were measured for every 50th reflection during the data collection.

The computational work followed largely the same scheme as in the preceding study.[2] Noteworthy distinctions concern the use of the atomic scattering factors of Doyle and Turner,[7] the inclusion of the real and imaginary parts of the dispersion,[8] and the separate treatment of reflections which may be Friedel non-equivalent according to space group $Pna2_1$.

Results. A survey of various experimental and computational sources of error and other questions which enter into a study of this kind, is given by Brostigen *et al.*[6] and will not be repeated here. Essentially the same refinement models as those used earlier [2-5] were considered, including anisotropic temperature factors according to the expression $\exp[-(\beta_{11}h^2 + \beta_{22}k^2 + \beta_{33}l^2 + \beta_{12}hk + \beta_{13}hl + \beta_{23}kl)]$. In addition to the specific improvements concerning data collection, absorption correction, and dispersion factors (*vide supra*) the effect of omitting low angle reflections from the refinement procedure was examined.

Comparison of the results with different $\sin\theta/\lambda$ cuts show that the omission of low angle data has no significant consequence for the refined parameters and the relative values of R^*. The results presented in Table 1 refer to a data set with $\sin\theta/\lambda > 0.6$. Moreover, only the results obtained for the most unrestrained models according to the space groups *Pnam* and $Pna2_1$ are included in the table.

In the case of the models based on space group *Pnam*, all parameters subject to refinement are virtually unaffected by the neglect to take account of dispersion, whereas R^* varies appreciably. The opposite situation is seen on comparison of the two models specified in terms of space group $Pna2_1$, where, in particular, the parameters β_{13} and β_{23} which determine the orientation of the vibrational ellipsoids relative to the crystallographic axes, are affected on the inclusion of dispersion factors.

Table 1. Positional parameters and temperature factors with standard deviations for four refinement models of FeAs. (No. of observations, $n = 627$ with $\sin\theta/\lambda > 0.60$; only the results for $\Delta f'' > 0$ being presented.)

Refined parameters		*Pnam*		$Pna2_1$	
		Incl. disp.	Excl. disp.	Incl. disp.	Excl. disp.
Fe	x	0.00331(6)	0.00330(6)	0.00331(6)	0.00330(6)
	y	0.19919(5)	0.19918(6)	0.19918(5)	0.19921(6)
	β_{11}	0.00192(8)	0.00144(8)	0.00199(8)	0.00149(8)
	β_{22}	0.00227(7)	0.00188(7)	0.00228(6)	0.00195(6)
	β_{33}	0.0146(2)	0.0134(2)	0.0149(2)	0.0138(2)
	β_{12}	0.0000(1)	0.0000(1)	0.0001(1)	0.0000(1)
	β_{13}	—	—	−0.0052(7)	0.0001(1)
	β_{23}	—	—	0.0026(7)	0.0026(7)
As	x	0.19915(4)	0.19914(5)	0.19914(4)	0.19912(4)
	y	0.57734(4)	0.57734(4)	0.57734(4)	0.57734(4)
	z	¼	¼	0.2510(6)	0.2519(6)
	β_{11}	0.00256(7)	0.00233(7)	0.00261(7)	0.00251(8)
	β_{22}	0.00236(6)	0.00217(6)	0.00238(6)	0.00222(6)
	β_{33}	0.0087(2)	0.0080(2)	0.0088(2)	0.0085(2)
	β_{12}	0.0005(1)	0.0005(1)	0.0005(1)	0.0005(1)
	β_{13}	—	—	0.0016(6)	0.0054(5)
	β_{23}	—	—	0.0013(7)	0.0029(5)
R^*		0.0301	0.0313	0.0292	0.0293
$\sum w\Delta^2$		2382	2575	2252	2263

If judgements were based exclusively on the Hamilton [9] test, the unambiguous conclusion of the present study would be that the crystal structure of FeAs belongs to space group $Pna2_1$ (*cf.* Ref. 2). However, comparison of the difference $(z_{As} - \frac{1}{4})$ with the standard deviation in z_{As}, strongly suggests the opposite conclusion. Furthermore, the latter inference is supported by the approximately equal (within the experimental error limits) values found for structure factors which should have been Friedel non-equivalent according to space group $Pna2_1$. The possible deviation of z_{As} from ¼ is, in any case, so small that no practical significance is attached to it. The principal cause of the difference between the present and preceding [2] study appears to be associated with the absorption corrections.

In view of the present result we are forced to suspect that our structure determinations of the isostructural compounds CoAs,[3] FeP,[4] and VAs [5] are burdened with corresponding inaccuracies and that they, at least for the time being, should be described in terms of space group *Pnam*. On the other hand, as clearly demonstrated by the comparison of the present and previous results for FeAs, the x and y parameters for the metal and non-metal atoms of the above structure determinations can be regarded as correct within the error limits stated.

Acknowledgements. The authors are grateful to Universitetslektor Bernt Klewe and Dosent Christian Rømming for valuable help.

1. Pearson, W. B. *A Handbook of Lattice Spacings and Structures of Metals and Alloys*, Pergamon, Oxford – London – Edinburgh – New York – Toronto – Paris – Braunschweig 1967, Vol. II.
2. Selte, K. and Kjekshus, A. *Acta Chem. Scand.* **23** (1969) 2047.
3. Selte, K. and Kjekshus, A. *Acta Chem. Scand.* **25** (1971) 3277.
4. Selte, K. and Kjekshus, A. *Acta Chem. Scand.* **26** (1972) 1276.
5. Selte, K., Kjekshus, A. and Andresen, A. F. *Acta Chem. Scand.* **26** (1972) 4057.
6. Brostigen, G., Kjekshus, A. and Römming, C. *Acta Chem. Scand. In press.*
7. Doyle, P. A. and Turner, P. S. *Acta Cryst.* **A 24** (1968) 390.
8. Cromer, D. T. *Acta Cryst.* **18** (1965) 17.
9. Hamilton, W. C. *Acta Cryst.* **18** (1965) 502.

Received April 6, 1973.

Résonance Magnétique Nucléaire du ^{13}C. Confirmation de la Structure du Produit β-Lactonique Obtenu dans la Réaction entre la Diméthoxy-2,6 benzoquinone-1,4 et l'Anhydride Isobutyrique*

MAURI LOUNASMAA

Centre National de la Recherche Technique, Laboratoire de Chimie, SF-02150 Otaniemi, Finlande

Il y a peu de temps nous avons montré que dans une réaction entre la diméthoxy-2,6 benzoquinone-1,4 et l'anhydride isobutyrique il se forme entre autres un produit β-lactonique pour lequel nous avons proposé la structure 1.[1] Pourtant les données analytiques présentées, bien que favorisant fortement la structure 1, ne pouvaient pas totalement exclure l'autre possibilité présentée par la structure 2.

Pour choisir entre les deux possibilités la RMN du ^{13}C nous a paru d'une technique particulièrement appropriée. Dans la présente note nous exposons les résultats obtenus par cette technique.

Les déplacements chimiques des carbones et le spectre de RMN du ^{13}C du produit β-lactonique sont indiqués dans le Tableau 1 et sur la Figure 1.

Le signal à 19,6 ppm représente les carbones des deux méthyles attachés au C-7 et celui à 56,0 ppm les carbones des deux méthoxyles. Les signaux à 65,1 ppm et à 78,9 ppm sont attribués aux carbones C-7 et C-1 respectivement.

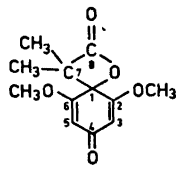

1

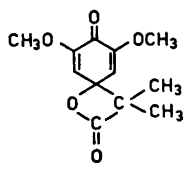

2

* Partie XI. Sur les Réactions des Quinones. Pour partie X, voir Réf. 1.

Tableau 1.

Lignes	Déplacements chimiques en ppm	Attributions
1	0,0	TMS
2	19,6	$2\times 7\text{-}CH_3$
3	56,0	$2\text{-}OCH_3$, $6\text{-}OCH_3$
4	65,1	C-7
5	78,9	C-1
6	102,9	C-3, C-5
7	167,0	C-2, C-6
8	172,2	C-8
9	185,7	C-4

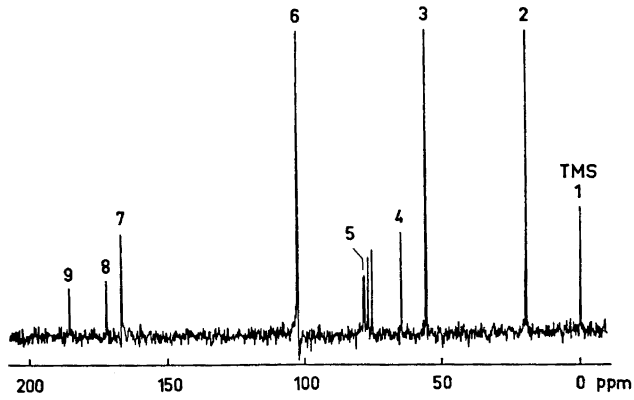

Fig. 1. Spectre de RMN du ^{13}C du produit β-lactonique ($CDCl_3$) à 22,63 MHz. Découplage par bruit.

Les deux signaux se trouvant à 172,2 ppm et à 185,7 ppm peuvent être attribués au carbone du groupement lactonique (C-8) et à celui du groupement cétonique (C-4) respectivement. La distinction entre ces signaux est basée sur les données de la littérature (*cf.* p. ex. Réf. 2 p. 119 (*β*-propiolactone; 171,2 ppm) et Réf. 3 (*p*-benzoquinone; 187,0 ppm)).

Les signaux observés à 167,0 ppm et à 102,9 ppm représentent chacun deux carbones. Leur intensité relative indique deux carbones non protonés et deux carbones protonés respectivement.

La théorie du déplacement chimique du carbone [2] permet de prévoir dans le cas des cétones α,β-éthyléniques une différence sensible entre l'α-carbone et le β-carbone, ce dernier apparaissant à champ nettement plus faible. On en déduit aisément que la structure correcte du produit β-lactonique correspond à la formule 1 puisque les α-carbones du composé étudié absorbant à 102,9 ppm se trouvent protonés.

Le spectre de RMN du ^{13}C a été mesuré en solution dans le $CDCl_3$ à 22,63 MHz sur un spectromètre Bruker Spectrospin muni d'une transformée de Fourier. Les déplacements chimiques sont donnés par rapport au tétraméthylsilane (TMS = 0).

Nous remercions vivement Monsieur le Docteur G. Lukacs, Institut de Chimie des Substances Naturelles, Gif-sur-Yvette, France, pour une discussion fructueuse.

1. Lounasmaa, M. *Acta Chem. Scand.* **27** (1973) 715.
2. Levy, G. C. et Nelson, G. L. *Carbon-13 Nuclear Magnetic Resonance for Organic Chemists*, Wiley, New York 1972.
3. Berger, St. et Rieker, A. *Tetrahedron* **28** (1972) 3123.

Reçu le 16 avril 1973.

A Convenient Method for the Preparation of Dichloromethanesulphonyl Chloride

TOMAS KEMPE and TORBJÖRN NORIN

Department of Organic Chemistry, Royal Institute of Technology, S-100 44 Stockholm 70, Sweden

Previously reported methods for the preparation of dichloromethanesulphonyl chloride (*3*) require several steps and the over-all yields are low.[1-4] During the course of a study of halosulphinic acids, a new method for the preparation of dichloromethanesulphonyl chloride (*3*) has been developed. It is known that chlorosulphonylacetic acid (2) can be prepared from thioglycolic acid (*1*) by chlorination in aqueous solution.[5] We have found that chlorination of thioglycolic acid in concentrated aqueous hydrochloric acid gives dichloromethanesulphonyl chloride (*3*) in one step without isolation of intermediates, *e.g.* chlorosulphonylacetic acid (2). The formation of the product (*3*) may proceed *via* decarboxylation of dichlorinated chlorosulphonylacetic acid as indicated in the tentative reaction scheme.

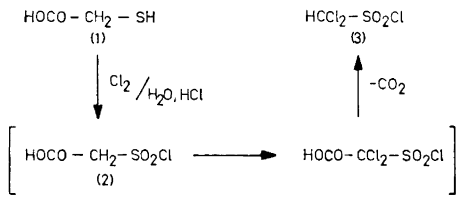

Experimental. Thioglycolic acid (92 g, 1 mol) was dissolved in 300 ml of concentrated aqueous hydrochloric acid (37 % w/v) and treated with a slow stream of chlorine during 2 days at about 10°. The dichloromethanesulphonyl chloride (*3*) separated during the reaction as a heavy oil. This oil was recovered, washed with water, dried over anhydrous sodium sulphate, and distilled under vacuum to give the pure dichloromethanesulphonyl chloride (82 g; b.p. 56°/6 mm; $n_D^{25} = 1.4954$; lit.[3] b.p. 60–62°/9 mm, n_D^{20} 1.4949) in 45 % of the theoretical yield. The product was characterized as the dichloromethanesulphonanilide, m.p. 76° (lit.[3] m.p. 76°).

Les deux signaux se trouvant à 172,2 ppm et à 185,7 ppm peuvent être attribués au carbone du groupement lactonique (C-8) et à celui du groupement cétonique (C-4) respectivement. La distinction entre ces signaux est basée sur les données de la littérature (*cf.* p. ex. Réf. 2 p. 119 (*β*-propiolactone; 171,2 ppm) et Réf. 3 (*p*-benzoquinone; 187,0 ppm)).

Les signaux observés à 167,0 ppm et à 102,9 ppm représentent chacun deux carbones. Leur intensité relative indique deux carbones non protonés et deux carbones protonés respectivement.

La théorie du déplacement chimique du carbone [2] permet de prévoir dans le cas des cétones α,β-éthyléniques une différence sensible entre l'α-carbone et le β-carbone, ce dernier apparaissant à champ nettement plus faible. On en déduit aisément que la structure correcte du produit β-lactonique correspond à la formule 1 puisque les α-carbones du composé étudié absorbant à 102,9 ppm se trouvent protonés.

Le spectre de RMN du ^{13}C a été mesuré en solution dans le $CDCl_3$ à 22,63 MHz sur un spectromètre Bruker Spectrospin muni d'une transformée de Fourier. Les déplacements chimiques sont donnés par rapport au tétraméthylsilane (TMS = 0).

Nous remercions vivement Monsieur le Docteur G. Lukacs, Institut de Chimie des Substances Naturelles, Gif-sur-Yvette, France, pour une discussion fructueuse.

1. Lounasmaa, M. *Acta Chem. Scand.* **27** (1973) 715.
2. Levy, G. C. et Nelson, G. L. *Carbon-13 Nuclear Magnetic Resonance for Organic Chemists*, Wiley, New York 1972.
3. Berger, St. et Rieker, A. *Tetrahedron* **28** (1972) 3123.

Reçu le 16 avril 1973.

A Convenient Method for the Preparation of Dichloromethanesulphonyl Chloride

TOMAS KEMPE and TORBJÖRN NORIN

Department of Organic Chemistry, Royal Institute of Technology, S-100 44 Stockholm 70, Sweden

Previously reported methods for the preparation of dichloromethanesulphonyl chloride (*3*) require several steps and the over-all yields are low.[1-4] During the course of a study of halosulphinic acids, a new method for the preparation of dichloromethanesulphonyl chloride (*3*) has been developed. It is known that chlorosulphonylacetic acid (2) can be prepared from thioglycolic acid (*1*) by chlorination in aqueous solution.[5] We have found that chlorination of thioglycolic acid in concentrated aqueous hydrochloric acid gives dichloromethanesulphonyl chloride (*3*) in one step without isolation of intermediates, *e.g.* chlorosulphonylacetic acid (2). The formation of the product (*3*) may proceed *via* decarboxylation of dichlorinated chlorosulphonylacetic acid as indicated in the tentative reaction scheme.

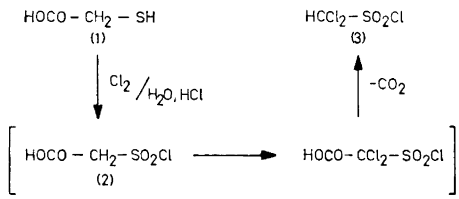

Experimental. Thioglycolic acid (92 g, 1 mol) was dissolved in 300 ml of concentrated aqueous hydrochloric acid (37 % w/v) and treated with a slow stream of chlorine during 2 days at about 10°. The dichloromethanesulphonyl chloride (*3*) separated during the reaction as a heavy oil. This oil was recovered, washed with water, dried over anhydrous sodium sulphate, and distilled under vacuum to give the pure dichloromethanesulphonyl chloride (82 g; b.p. 56°/6 mm; $n_D^{25} = 1.4954$; lit.[3] b.p. 60–62°/9 mm, n_D^{20} 1.4949) in 45 % of the theoretical yield. The product was characterized as the dichloromethanesulphonanilide, m.p. 76° (lit.[3] m.p. 76°).

1. Farrar, W. V. *J. Chem. Soc.* **1960** 3058.
2. Backer, H. J. *Rec. Trav. Chim.* **45** (1926) 830.
3. Goldwhite, H., Gibbson, M. S. and Harris, C. *Tetrahedron* **20** (1964) 1613.
4. Mc Gowan, G. *J. prakt. Chem.* **30** (1884) 280.
5. Dickey, J. B. U.S. Patent 2,466,396 Apr. 5, 1949; *cf. Chem. Abstr.* **43** (1949) 4868.

Received April 28, 1973.

Epimeric 2-[(1S)-7,7-Dimethyl-2-oxo-1-norbornanyl]-thiirane-1,1-dioxides

TOMAS KEMPE and TORBJÖRN NORIN

Department of Organic Chemistry, Royal Institute of Technology, S-100 44 Stockholm 70, Sweden

The reaction between diazomethane and the intermediate sulphene produced by treatment of (1*S*)-camphor-10-sulphonyl chloride with triethylamine has been reported to give a thiiranedioxide (m.p. 83–85°).[1,2] We have repeated this experiment. The two epimeric thiiranedioxides (*1a* and *1b*) thus formed have now been separated by thin layer and column chromatography on silica gel. The mixture of epimers as well as each of the two pure isomers decomposed when heated above their melting points yielding the known (1*S*)-7,7-dimethyl-1-vinyl-2-norbornanone (*2*).[1,2]

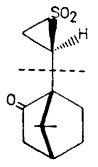

1a

1b

2

*Experimental. 2-[(1S)-7,7-dimethyl-2-oxo-1-norbornanyl]-thiirane-1,1-dioxides (*1a *and* 1b*).* The mixture of the epimeric thiiranedioxides (*1a* and *1b*) was prepared from (1*S*)-camphor-10-sulphonyl chloride (m.p. 67–68°; $[\alpha]_D^{21}$ +30°, *c* 2.0 in $CHCl_3$) according to the procedure of Opitz and Fischer.[1,2] The two compounds could be separated by TLC (Merck Silica gel HF_{254}), *e.g.* when eluted with ethyl ether, R_F values were 0.55 and 0.77. The epimers were separated on preparative scale by column chromatography (silica gel/ethyl ether) to yield a low-melting isomer (R_F 0.77; m.p. 81–86° dec.; approximate yield 70 %; $[\alpha]_D^{21}$ −5.6°, *c* 3.1 in $CHCl_3$) and a high-melting isomer (R_F 0.55; m.p. 100–106° dec.; approximate yield 15 %; $[\alpha]_D^{21}$ −58.6, *c* 0.8 in $CHCl_3$). The two isomers exhibited similar IR spectra: ν ($CHCl_3$) 1735 (C=O), 1320 and 1160 (SO_2) cm^{-1}.[2] The compounds were insufficiently stable at room temperature for meaningful elemental analysis. However, they could readily be characterized by heating to yield (1*S*)-7,7-dimethyl-1-vinyl-2-norbornanone (*2*) (m.p. 65–66°; $[\alpha]_D^{21}$ +16°, *c* 3.3 in $CHCl_3$).[1,2]

1. Opitz, G. and Fischer, K. *Angew. Chem.* **77** (1965) 41.
2. Fischer, N. and Opitz, G. *Org. Syn.* **48** (1968) 106.

Received April 28, 1973.

On the Electrical Properties of $Pd_{17}Se_{15}$, Pt_5Se_4, and PtTe

ARNE KJEKSHUS

Kjemisk Institutt, Universitetet i Oslo, Blindern, Oslo 3, Norway

Only sparse information is available on the low temperature electrical behaviours of transition metal pnictides and chalcogenides. Moreover, the few investigations hitherto have been concerned with phases having relatively simple compositions and crystal structures. Therefore, it was considered worthwhile to study a few phases which do not satisfy the above

1. Farrar, W. V. *J. Chem. Soc.* **1960** 3058.
2. Backer, H. J. *Rec. Trav. Chim.* **45** (1926) 830.
3. Goldwhite, H., Gibbson, M. S. and Harris, C. *Tetrahedron* **20** (1964) 1613.
4. Mc Gowan, G. *J. prakt. Chem.* **30** (1884) 280.
5. Dickey, J. B. U.S. Patent 2,466,396 Apr. 5, 1949; *cf. Chem. Abstr.* **43** (1949) 4868.

Received April 28, 1973.

Epimeric 2-[(1S)-7,7-Dimethyl-2-oxo-1-norbornanyl]-thiirane-1,1-dioxides

TOMAS KEMPE and TORBJÖRN NORIN

Department of Organic Chemistry, Royal Institute of Technology, S-100 44 Stockholm 70, Sweden

The reaction between diazomethane and the intermediate sulphene produced by treatment of (1*S*)-camphor-10-sulphonyl chloride with triethylamine has been reported to give a thiiranedioxide (m.p. 83–85°).[1,2] We have repeated this experiment. The two epimeric thiiranedioxides (*1a* and *1b*) thus formed have now been separated by thin layer and column chromatography on silica gel. The mixture of epimers as well as each of the two pure isomers decomposed when heated above their melting points yielding the known (1*S*)-7,7-dimethyl-1-vinyl-2-norbornanone (*2*).[1,2]

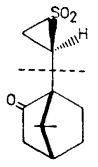

1a

1b

2

*Experimental. 2-[(1S)-7,7-dimethyl-2-oxo-1-norbornanyl]-thiirane-1,1-dioxides (*1a *and* 1b*).* The mixture of the epimeric thiiranedioxides (*1a* and *1b*) was prepared from (1*S*)-camphor-10-sulphonyl chloride (m.p. 67–68°; $[\alpha]_D^{21}$ +30°, *c* 2.0 in $CHCl_3$) according to the procedure of Opitz and Fischer.[1,2] The two compounds could be separated by TLC (Merck Silica gel HF_{254}), *e.g.* when eluted with ethyl ether, R_F values were 0.55 and 0.77. The epimers were separated on preparative scale by column chromatography (silica gel/ethyl ether) to yield a low-melting isomer (R_F 0.77; m.p. 81–86° dec.; approximate yield 70 %; $[\alpha]_D^{21}$ −5.6°, *c* 3.1 in $CHCl_3$) and a high-melting isomer (R_F 0.55; m.p. 100–106° dec.; approximate yield 15 %; $[\alpha]_D^{21}$ −58.6, *c* 0.8 in $CHCl_3$). The two isomers exhibited similar IR spectra: ν ($CHCl_3$) 1735 (C=O), 1320 and 1160 (SO_2) cm^{-1}.[2] The compounds were insufficiently stable at room temperature for meaningful elemental analysis. However, they could readily be characterized by heating to yield (1*S*)-7,7-dimethyl-1-vinyl-2-norbornanone (*2*) (m.p. 65–66°; $[\alpha]_D^{21}$ +16°, *c* 3.3 in $CHCl_3$).[1,2]

1. Opitz, G. and Fischer, K. *Angew. Chem.* **77** (1965) 41.
2. Fischer, N. and Opitz, G. *Org. Syn.* **48** (1968) 106.

Received April 28, 1973.

On the Electrical Properties of $Pd_{17}Se_{15}$, Pt_5Se_4, and PtTe

ARNE KJEKSHUS

Kjemisk Institutt, Universitetet i Oslo, Blindern, Oslo 3, Norway

Only sparse information is available on the low temperature electrical behaviours of transition metal pnictides and chalcogenides. Moreover, the few investigations hitherto have been concerned with phases having relatively simple compositions and crystal structures. Therefore, it was considered worthwhile to study a few phases which do not satisfy the above

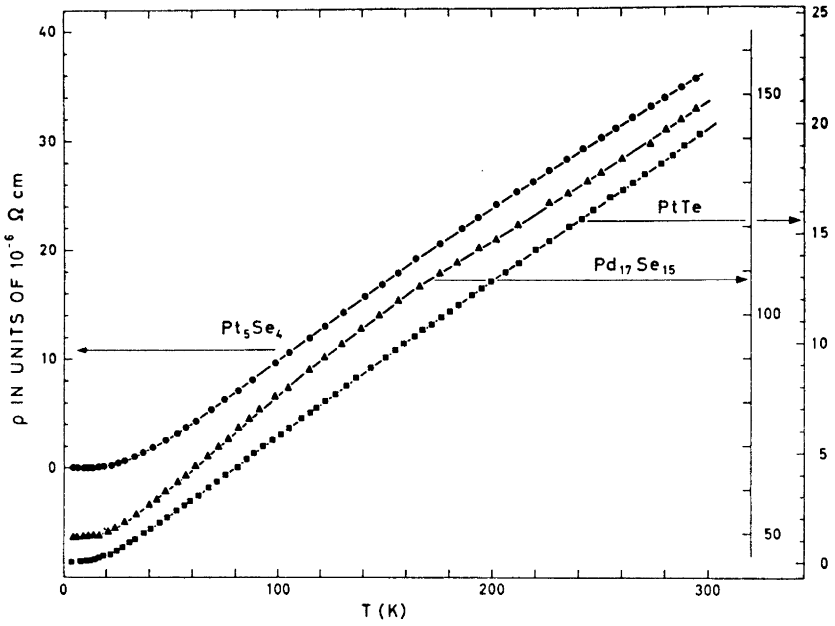

Fig. 1. Electrical resistivity of $Pd_{17}Se_{15}$, Pt_5Se_4, and PtTe as a function of temperature.

criteria. $Pd_{17}Se_{15}$, Pt_5Se_4, and PtTe were chosen as suitable candidates for examination, since as opposed to the structural [1-5] and magnetic [1,3] studies no electrical measurements have been published.

Experimental. Polycrystalline samples were made by heating weighed quantities of the elements (99.999 % Pd and Pt (Koch-Light Laboratories), 99.998 % Se (Bolidens Gruvaktiebolag), and 99.999 % Te (American Smelting and Refining Co.)) in evacuated, sealed quartz tubes. During the syntheses, the temperature was slowly increased to 600°C in the case of $Pd_{17}Se_{15}$ and 850°C for Pt_5Se_4 and PtTe, the samples were kept at these temperatures for 10 days, and then quenched in ice water.

The experimental details concerning the zone melting and crystal cutting procedures and the measurements of electrical resistance and temperature were performed as described in Ref. 6 and references therein.

Results. X-Ray and microscopical examination showed that the $Pd_{17}Se_{15}$ and Pt_5Se_4 samples consisted of a single phase, whereas globular inclusions of a second phase occurred in the PtTe sample. After some difficulties it proved possible to cut essentially single crystal specimens of the three compounds.

The temperature dependence of the electrical resistivity of $Pd_{17}Se_{15}$, Pt_5Se_4, and PtTe is shown in Fig. 1. The curves were reproducible for conditions of both decreasing and increasing temperature whenever repeated measurements were performed on the *same* sample. The results obtained for different specimens vary somewhat, the effect being most marked for PtTe, least for Pt_5Se_4. This is provisionally attributed to anisotropy in ϱ, but can equally well be due to variation in specimen homogeneity and/or crystalline perfection. Further investigations are required to clarify this point.

The residual resistance ratios $(R_{4.2}/(R_{298}-R_{4.2}))$ of the various $Pd_{17}Se_{15}$ specimens were never better than about $\frac{1}{2}$, as opposed to the ratios of approximately 6.1×10^{-3} and 2.2×10^{-3} for the measured samples of Pt_5Se_4 and PtTe, respectively. The temperature coefficients, $\alpha=(1/\varrho_{273})(d\varrho/dT)$, calculated from the linear por-

tions of the $\varrho(T)$-curves are $2.8_1 \times 10^{-3}$ °C^{-1} (30 – 150 K) and $2.2_3 \times 10^{-3}$ °C^{-1} (180 – 300 K) for $Pd_{17}Se_{15}$, $4.3_2 \times 10^{-3}$ °C^{-1} (50 – 160 K) and $3.9_3 \times 10^{-3}$ °C^{-1} (180 – 300 K) for Pt_5Se_4, and $3.9_5 \times 10^{-3}$ °C^{-1} (40 – 300 K) for PtTe. Hence, the temperature dependences of ϱ for $Pd_{17}Se_{15}$ and Pt_5Se_4 differ from that of PtTe in that the former curves are slightly concave towards the temperature axis. In line with earlier suggestions [6-10] this behaviour (which is commonly found for phases comprising palladium) is tentatively attributed to *s-d* interband scattering.

Using the procedure of Kelly and MacDonald,[10] the characteristic temperatures θ_R derived from the $\varrho(T)$-curves of Pt_5Se_4 and PtTe are approximately 190 and 230 K, respectively. The θ_R-value for PtTe is in close agreement with $\theta_D = 245$ K estimated from the heat capacity data [11] and θ_R for Pt_5Se_4 probably differ by no more than a few per cent at most from the Debye temperature (θ_D) in the region of θ itself. The $\varrho(T)$-curve for $Pd_{17}Se_{15}$ is inconsistent with a finite value of θ_R.

Although the crystal structure of Pt_5Se_4 is hitherto unknown, the atomic arrangement of $Pd_{17}Se_{15}$ [4] will almost certainly prove to be the most heterogeneous (as evident from the entirely different coordinations of its three non-equivalent Pd atoms) of these compounds. Thus, the diversity in structure is paralleled by the distinctly different electrical properties of $Pd_{17}Se_{15}$ (Fig. 1 and *vide supra*).

1. Grønvold, F. and Røst, E. *Acta Chem. Scand.* **10** (1956) 1620.
2. Kjekshus, A. *Acta Chem. Scand.* **14** (1960) 1623.
3. Grønvold, F., Haraldsen, H. and Kjekshus, A. *Acta Chem. Scand.* **14** (1960) 1879.
4. Geller, S. *Acta Cryst.* **15** (1962) 713.
5. Bhan, S., Gödecke, T. and Schubert, K. *J. Less-Common Metals* **19** (1969) 121.
6. Kjekshus, A. *Acta Chem. Scand.* **25** (1971) 3883.
7. Mott, N. F. and Stevens, K. W. H. *Phil. Mag.* **2** (1957) 1364.
8. Coles, B. R. *Advan. Phys.* **7** (1958) 40.
9. Kjekshus, A. and Pearson, W. B. *Can. J. Phys.* **43** (1965) 438.
10. Kelly, F. M. and MacDonald, D. K. C. *Can. J. Phys.* **31** (1953) 147.
11. Grønvold, F., Thurmann-Moe, T., Westrum, E. F. and Chang, E. *J. Chem. Phys.* **35** (1961) 1665.

Received April 6, 1973.

Homogeneous Chemical Kinetics at the Rotating Disk Electrode. Application to the Pyridination of Diphenylanthracene Cation Radical

ULLA SVANHOLM and VERNON D. PARKER

Department of General and Organic Chemistry, The H. C. Ørsted Institute, University of Copenhagen, Universitetsparken 5, DK-2100 Copenhagen, Denmark

The rotating disk electrode (rde) has been shown to be a versatile tool for the study of the kinetics of chemical reactions coupled to electron transfer. Pseudo first order rate constants as high as 10^3 sec^{-1} may be estimated. The rde method as well as other electrochemical methods are limited by the need to compare data to working curves obtained by calculations based on an assumed mechanism and ideal behaviour. Adams [1] has reviewed the use of the rde in studying ECE processes and cautions the practice of assigning mechanisms to reactions occurring at solid electrodes on the basis of a single electroanalytical technique. Here we report the use of the rde as an analytical device to follow the progress of a homogeneous chemical reaction.* The reaction chosen to illustrate the method is the pyridination of the 9,10-diphenylanthracene (DPA) cation radical, previously studied as a coupled chemical reaction at the rde.[2] This reaction is of particular interest in that studies using two different electroanalytical techniques, rde voltammetry [2] and chronoamperometry,[3] led to conflicting results and the assignment of different mechanisms.

Rate data for seven experiments involving the reaction of $DPA^{+\cdot}$ (initial concentration 1.3 to 6.25×10^{-6} M) with pyridine (1.0 to 5.0×10^{-5} M) are summarized in Table 1. Pseudo first order rate constants ranging from 0.38 to 2.1 sec^{-1} were observed. The second order rate constant at $11.7 \pm 0.2°$ for reaction (1) was found to be equal to $(4.5 \pm 0.9) \times 10^4$ M^{-1}

* Polarographic methods have been used extensively to follow the kinetics of homogeneous reactions; however this appears to be the first application to the study of very fast reactions.

1. Farrar, W. V. *J. Chem. Soc.* **1960** 3058.
2. Backer, H. J. *Rec. Trav. Chim.* **45** (1926) 830.
3. Goldwhite, H., Gibbson, M. S. and Harris, C. *Tetrahedron* **20** (1964) 1613.
4. Mc Gowan, G. *J. prakt. Chem.* **30** (1884) 280.
5. Dickey, J. B. U.S. Patent 2,466,396 Apr. 5, 1949; *cf. Chem. Abstr.* **43** (1949) 4868.

Received April 28, 1973.

Epimeric 2-[(1S)-7,7-Dimethyl-2-oxo-1-norbornanyl]-thiirane-1,1-dioxides

TOMAS KEMPE and TORBJÖRN NORIN

Department of Organic Chemistry, Royal Institute of Technology, S-100 44 Stockholm 70, Sweden

The reaction between diazomethane and the intermediate sulphene produced by treatment of (1*S*)-camphor-10-sulphonyl chloride with triethylamine has been reported to give a thiiranedioxide (m.p. 83–85°).[1,2] We have repeated this experiment. The two epimeric thiiranedioxides (*1a* and *1b*) thus formed have now been separated by thin layer and column chromatography on silica gel. The mixture of epimers as well as each of the two pure isomers decomposed when heated above their melting points yielding the known (1*S*)-7,7-dimethyl-1-vinyl-2-norbornanone (*2*).[1,2]

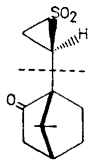

1a

1b

2

*Experimental. 2-[(1S)-7,7-dimethyl-2-oxo-1-norbornanyl]-thiirane-1,1-dioxides (*1a *and* 1b*).* The mixture of the epimeric thiiranedioxides (*1a* and *1b*) was prepared from (1*S*)-camphor-10-sulphonyl chloride (m.p. 67–68°; $[\alpha]_D^{21}$ +30°, *c* 2.0 in $CHCl_3$) according to the procedure of Opitz and Fischer.[1,2] The two compounds could be separated by TLC (Merck Silica gel HF_{254}), *e.g.* when eluted with ethyl ether, R_F values were 0.55 and 0.77. The epimers were separated on preparative scale by column chromatography (silica gel/ethyl ether) to yield a low-melting isomer (R_F 0.77; m.p. 81–86° dec.; approximate yield 70 %; $[\alpha]_D^{21}$ −5.6°, *c* 3.1 in $CHCl_3$) and a high-melting isomer (R_F 0.55; m.p. 100–106° dec.; approximate yield 15 %; $[\alpha]_D^{21}$ −58.6, *c* 0.8 in $CHCl_3$). The two isomers exhibited similar IR spectra: ν ($CHCl_3$) 1735 (C=O), 1320 and 1160 (SO_2) cm^{-1}.[2] The compounds were insufficiently stable at room temperature for meaningful elemental analysis. However, they could readily be characterized by heating to yield (1*S*)-7,7-dimethyl-1-vinyl-2-norbornanone (*2*) (m.p. 65–66°; $[\alpha]_D^{21}$ +16°, *c* 3.3 in $CHCl_3$).[1,2]

1. Opitz, G. and Fischer, K. *Angew. Chem.* **77** (1965) 41.
2. Fischer, N. and Opitz, G. *Org. Syn.* **48** (1968) 106.

Received April 28, 1973.

On the Electrical Properties of $Pd_{17}Se_{15}$, Pt_5Se_4, and PtTe

ARNE KJEKSHUS

Kjemisk Institutt, Universitetet i Oslo, Blindern, Oslo 3, Norway

Only sparse information is available on the low temperature electrical behaviours of transition metal pnictides and chalcogenides. Moreover, the few investigations hitherto have been concerned with phases having relatively simple compositions and crystal structures. Therefore, it was considered worthwhile to study a few phases which do not satisfy the above

tions of the $\varrho(T)$-curves are $2.8_1 \times 10^{-3}$ °C^{-1} (30 – 150 K) and $2.2_3 \times 10^{-3}$ °C^{-1} (180 – 300 K) for $Pd_{17}Se_{15}$, $4.3_2 \times 10^{-3}$ °C^{-1} (50 – 160 K) and $3.9_3 \times 10^{-3}$ °C^{-1} (180 – 300 K) for Pt_5Se_4, and $3.9_5 \times 10^{-3}$ °C^{-1} (40 – 300 K) for PtTe. Hence, the temperature dependences of ϱ for $Pd_{17}Se_{15}$ and Pt_5Se_4 differ from that of PtTe in that the former curves are slightly concave towards the temperature axis. In line with earlier suggestions [6-10] this behaviour (which is commonly found for phases comprising palladium) is tentatively attributed to *s-d* interband scattering.

Using the procedure of Kelly and MacDonald,[10] the characteristic temperatures θ_R derived from the $\varrho(T)$-curves of Pt_5Se_4 and PtTe are approximately 190 and 230 K, respectively. The θ_R-value for PtTe is in close agreement with $\theta_D = 245$ K estimated from the heat capacity data [11] and θ_R for Pt_5Se_4 probably differ by no more than a few per cent at most from the Debye temperature (θ_D) in the region of θ itself. The $\varrho(T)$-curve for $Pd_{17}Se_{15}$ is inconsistent with a finite value of θ_R.

Although the crystal structure of Pt_5Se_4 is hitherto unknown, the atomic arrangement of $Pd_{17}Se_{15}$ [4] will almost certainly prove to be the most heterogeneous (as evident from the entirely different coordinations of its three non-equivalent Pd atoms) of these compounds. Thus, the diversity in structure is paralleled by the distinctly different electrical properties of $Pd_{17}Se_{15}$ (Fig. 1 and *vide supra*).

1. Grønvold, F. and Røst, E. *Acta Chem. Scand.* **10** (1956) 1620.
2. Kjekshus, A. *Acta Chem. Scand.* **14** (1960) 1623.
3. Grønvold, F., Haraldsen, H. and Kjekshus, A. *Acta Chem. Scand.* **14** (1960) 1879.
4. Geller, S. *Acta Cryst.* **15** (1962) 713.
5. Bhan, S., Gödecke, T. and Schubert, K. *J. Less-Common Metals* **19** (1969) 121.
6. Kjekshus, A. *Acta Chem. Scand.* **25** (1971) 3883.
7. Mott, N. F. and Stevens, K. W. H. *Phil. Mag.* **2** (1957) 1364.
8. Coles, B. R. *Advan. Phys.* **7** (1958) 40.
9. Kjekshus, A. and Pearson, W. B. *Can. J. Phys.* **43** (1965) 438.
10. Kelly, F. M. and MacDonald, D. K. C. *Can. J. Phys.* **31** (1953) 147.
11. Grønvold, F., Thurmann-Moe, T., Westrum, E. F. and Chang, E. *J. Chem. Phys.* **35** (1961) 1665.

Received April 6, 1973.

Homogeneous Chemical Kinetics at the Rotating Disk Electrode. Application to the Pyridination of Diphenylanthracene Cation Radical

ULLA SVANHOLM and VERNON D. PARKER

Department of General and Organic Chemistry, The H. C. Ørsted Institute, University of Copenhagen, Universitetsparken 5, DK-2100 Copenhagen, Denmark

The rotating disk electrode (rde) has been shown to be a versatile tool for the study of the kinetics of chemical reactions coupled to electron transfer. Pseudo first order rate constants as high as 10^3 sec^{-1} may be estimated. The rde method as well as other electrochemical methods are limited by the need to compare data to working curves obtained by calculations based on an assumed mechanism and ideal behaviour. Adams [1] has reviewed the use of the rde in studying ECE processes and cautions the practice of assigning mechanisms to reactions occurring at solid electrodes on the basis of a single electroanalytical technique. Here we report the use of the rde as an analytical device to follow the progress of a homogeneous chemical reaction.* The reaction chosen to illustrate the method is the pyridination of the 9,10-diphenylanthracene (DPA) cation radical, previously studied as a coupled chemical reaction at the rde.[2] This reaction is of particular interest in that studies using two different electroanalytical techniques, rde voltammetry [2] and chronoamperometry,[3] led to conflicting results and the assignment of different mechanisms.

Rate data for seven experiments involving the reaction of $DPA^{+\cdot}$ (initial concentration 1.3 to 6.25×10^{-6} M) with pyridine (1.0 to 5.0×10^{-5} M) are summarized in Table 1. Pseudo first order rate constants ranging from 0.38 to 2.1 sec^{-1} were observed. The second order rate constant at $11.7 \pm 0.2°$ for reaction (1) was found to be equal to $(4.5 \pm 0.9) \times 10^4$ M^{-1}

* Polarographic methods have been used extensively to follow the kinetics of homogeneous reactions; however this appears to be the first application to the study of very fast reactions.

Table 1. Rate data for the pyridination of DPA cation radical in acetonitrile at 11.7 ± 0.2°.

Run	10^6 $(DPA^{+\cdot})_0$[a]	10^6 $(DPA^{+\cdot})$[b]	10^6 (pyr)	k_1 (sec^{-1})	10^{-4} k_2 M^{-1} sec^{-1}.
1	6.25	3.3	50.0	2.1	4.2
2	3.5	2.5	50.0	1.8	3.6
3	5.0	4.1	20.0	1.1	5.5
4	5.0	4.1	20.0	1.0	5.1
5	4.25	3.5	20.0	0.92	4.6
6	3.25	2.9	10.0	0.46	4.6
7	1.3	1.2	10.0	0.38	3.8
					ave. 4.5

[a] Concentration at time of addition of pyridine.
[b] Concentration at time that measurements were started.

sec^{-1}. Under ECE conditions at a pyridine concentration

$$DPA^{+\cdot} + Pyr \xrightarrow{k} DPA\cdot - Pyr^{+} \quad (1)$$

of 0.025 M, the pseudo first order rate constant was estimated to be about 300 sec^{-1} at 25° which translates to a second order rate constant of about 10^4 M^{-1} sec^{-1}. Thus, considering the temperature difference, it appears that the ECE estimate is about an order of magnitude lower than that found in this work.

The cation radical concentrations employed in this study by no means define the limitation of the method. We are readily able to accurately monitor cation radical concentrations lower than 10^{-8} M. Thus the limitation to the method is the rate of mixing the reactants. Since it required from 0.1 to 0.2 sec for mixing, we arbitrarily set the minimum half life to be used at about 0.3 sec (this is readily adjusted by changes in concentration of the pyridine in the present case). The latter was also about the limitation imposed by the use of pen and ink recording, it would be necessary to go to oscilloscopic recording for faster reactions. Despite the limitations described above, it is readily shown that a half life of 0.3 sec at a concentration of 10^{-8} M gives a second order rate constant of about 3×10^8 M^{-1} sec^{-1} for a reaction of the type shown in eqn. 2. Thus, the method as it was used here is capable of giving second

$$2\,A \longrightarrow B \quad (2)$$

order rate constants close to the diffusion controlled limit. In a flow system, it is possible to achieve mixing in about one millisecond. It is conceivable that the method can be adapted in a flow system and thus make it possible to measure second order rate constants of the order of 10^{10} M^{-1} sec^{-1}.

Needless to say, determining the kinetics of a reaction by following the decrease in concentration of a reactant in homogeneous solution has the distinct advantage over ECE methods in that the order of the reaction in reactants is readily determined. It has been pointed out that rde and chronoamperometric working curves for the ECE mechanism very closely resemble that for a disproportionation mechanism which gives a different kinetic order.[3] Thus, we are able to say definitively from our results that the reaction of the DPA cation radical with pyridine is first order in both the cation radical and pyridine, facts which neither of the previous studies [2,3] were able to demonstrate.

Experimental. DPA was reagent grade and used without further purification. Acetonitrile was purified by the method of Moe [4] and passed through a column of neutral alumina (Woelm V 200) directly into the reaction cell under an atmosphere of dry argon. Sodium perchlorate was reagent grade, dried and stored at 150°. Pyridine was reagent grade and used without further purification.

The apparatus and general procedure followed for electrolyses have been described.[5,6] The cell used both for the kinetic study and for the preparation of the acetonitrile solution of the DPA cation radical was a cylindrical, round bottom, water jacketed container with openings for the auxiliary electrode compartment, reference electrode, inert gas supply and thermometer. The auxiliary electrode compart-

ment was removed after preparation of the cation radical and replaced by the rde. The recording device was a Watanabe XY recorder with time base.

Preparation of DPA cation radical in acetonitrile. DPA (5.0×10^{-4} M) in acetonitrile (100 ml) containing sodium perchlorate (0.1 M) was subjected to constant current electrolysis at 12.5 mA at a platinum gauze electrode for 20 sec (theoretical cation radical concentration, 2.6×10^{-5} M). The blue cation radical color did not begin to develop until after about 5 sec. The temperature was controlled by tap water at $11.7 \pm 2°$. After removing the auxiliary electrode compartment and placing the Beckman rde in the solution, the limiting current at the rde indicated that the $DPA^{+\cdot}$ concentration was close to 10^{-5} M.

Typical kinetic experiment (Run 3). The slow decay of the limiting current for reduction of $DPA^{+\cdot}$ was followed (rde rotation rate 100 rps) until the $DPA^{+\cdot}$ concentration fell to 5.0×10^{-6} M. Pyridine (200 μl of a 10^{-2} M solution in acetonitrile) was injected into the solution with a Hamilton spring driven syringe and simultaneously the recorder was started at a chart speed of 5 cm/sec. Mixing was complete in 0.2 sec. and the smooth current time curve which quickly approached zero current was used to determine the rate constant. A plot of log limiting current *vs.* time was linear for more than one half life.

Alternatively, a stationary Beckman Platinum Button Electrode was used as the indicator electrode. In this case the electrode was carefully situated above a rapidly rotating magnetic stirrer. The current time curve in this case was not as smooth as with the rde; however the data still fit first order plots for greater than one half life.

Time of mixing. The time of mixing the pyridine solution with the cation radical solution was determined by the time required for the limiting current for the cation radical to fall to zero when 100 μl of pyridine was injected into the solution in the same manner as described above. The time to fall to zero current was variable depending upon where and how the pyridine entered the bulk solution but generally was in the range 0.1 to 0.2 sec.

1. Adams, R. N. *Electrochemistry at Solid Electrodes*, Marcel Dekker, New York 1969.
2. Manning, G., Parker, V. D. and Adams, R. N. *J. Am. Chem. Soc.* **91** (1969) 4584.
3. Marcoux, L. S. *J. Am. Chem. Soc.* **93** (1971) 537.
4. Moe, N. S. *Acta Chem. Scand.* **21** (1967) 1389.
5. Parker, V. D. *Acta Chem. Scand.* **24** (1970) 2768.
6. Hammerich, O. and Parker, V. D. *J. Chem. Soc. Perkin Trans. 1* **1972** 1718.

Received April 6. 1973.

Versuche zur Darstellung von 6-Thioacylaminopenicillansäuren

AASE WINTHER und ALEXANDER SENNING

Chemisches Institut der Universität Aarhus DK-8000 Aarhus C, Dänemark

Obwohl bereits viele tausend halbsynthetische Penicilline [1] dargestellt und auf ihre antibiotische Wirksamkeit untersucht worden sind, handelt es sich ganz überwiegend um 6-Acylaminopenicillansäuren *I*. Andere Verknüpfungsarten der Aminogruppe der 6-Aminopenicillansäure sind nur vereinzelt bearbeitet worden.

Uns interessierte in diesem Zusammenhang, wieweit 6-Thioacylaminopenicillansäuren *II* und zwar insbesondere Thioanaloge biologisch aktiver *I* antibiotische Eigenschaften besitzen. Unseres Wissens liegt als einziges Material zu dieser Frage ein britisches Patent aus dem Jahre 1964 [2] vor.

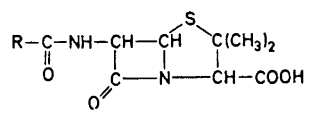

I

Von den insgesamt vier in diesem Patent beschriebenen *II* ist nur eine Verbindung ein Thioanaloges einer antibiotisch wirksamen *I*, nämlich die 6-(Phenyl-thioacetyl-

ment was removed after preparation of the cation radical and replaced by the rde. The recording device was a Watanabe XY recorder with time base.

Preparation of DPA cation radical in acetonitrile. DPA (5.0×10^{-4} M) in acetonitrile (100 ml) containing sodium perchlorate (0.1 M) was subjected to constant current electrolysis at 12.5 mA at a platinum gauze electrode for 20 sec (theoretical cation radical concentration, 2.6×10^{-5} M). The blue cation radical color did not begin to develop until after about 5 sec. The temperature was controlled by tap water at $11.7 \pm 2°$. After removing the auxiliary electrode compartment and placing the Beckman rde in the solution, the limiting current at the rde indicated that the $DPA^{+\cdot}$ concentration was close to 10^{-5} M.

Typical kinetic experiment (Run 3). The slow decay of the limiting current for reduction of $DPA^{+\cdot}$ was followed (rde rotation rate 100 rps) until the $DPA^{+\cdot}$ concentration fell to 5.0×10^{-6} M. Pyridine (200 μl of a 10^{-2} M solution in acetonitrile) was injected into the solution with a Hamilton spring driven syringe and simultaneously the recorder was started at a chart speed of 5 cm/sec. Mixing was complete in 0.2 sec. and the smooth current time curve which quickly approached zero current was used to determine the rate constant. A plot of log limiting current *vs.* time was linear for more than one half life.

Alternatively, a stationary Beckman Platinum Button Electrode was used as the indicator electrode. In this case the electrode was carefully situated above a rapidly rotating magnetic stirrer. The current time curve in this case was not as smooth as with the rde; however the data still fit first order plots for greater than one half life.

Time of mixing. The time of mixing the pyridine solution with the cation radical solution was determined by the time required for the limiting current for the cation radical to fall to zero when 100 μl of pyridine was injected into the solution in the same manner as described above. The time to fall to zero current was variable depending upon where and how the pyridine entered the bulk solution but generally was in the range 0.1 to 0.2 sec.

1. Adams, R. N. *Electrochemistry at Solid Electrodes*, Marcel Dekker, New York 1969.
2. Manning, G., Parker, V. D. and Adams, R. N. *J. Am. Chem. Soc.* **91** (1969) 4584.
3. Marcoux, L. S. *J. Am. Chem. Soc.* **93** (1971) 537.
4. Moe, N. S. *Acta Chem. Scand.* **21** (1967) 1389.
5. Parker, V. D. *Acta Chem. Scand.* **24** (1970) 2768.
6. Hammerich, O. and Parker, V. D. *J. Chem. Soc. Perkin Trans. 1* **1972** 1718.

Received April 6. 1973.

Versuche zur Darstellung von 6-Thioacylaminopenicillansäuren

AASE WINTHER und ALEXANDER SENNING

Chemisches Institut der Universität Aarhus DK-8000 Aarhus C, Dänemark

Obwohl bereits viele tausend halbsynthetische Penicilline [1] dargestellt und auf ihre antibiotische Wirksamkeit untersucht worden sind, handelt es sich ganz überwiegend um 6-Acylaminopenicillansäuren *I*. Andere Verknüpfungsarten der Aminogruppe der 6-Aminopenicillansäure sind nur vereinzelt bearbeitet worden.

Uns interessierte in diesem Zusammenhang, wieweit 6-Thioacylaminopenicillansäuren *II* und zwar insbesondere Thioanaloge biologisch aktiver *I* antibiotische Eigenschaften besitzen. Unseres Wissens liegt als einziges Material zu dieser Frage ein britisches Patent aus dem Jahre 1964 [2] vor.

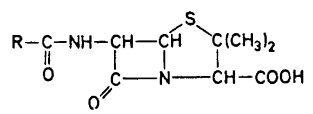

I

Von den insgesamt vier in diesem Patent beschriebenen *II* ist nur eine Verbindung ein Thioanaloges einer antibiotisch wirksamen *I*, nämlich die 6-(Phenyl-thioacetyl-

amino)-penicillansäure (»Thio-penicillin G») *II* (R = $C_6H_5CH_2$). Alle vier Verbindungen wurden nur als Rohprodukte erhalten und weder chemisch und physikalisch, noch biologisch näher charakterisiert.

Zur Entscheidung der Frage, ob *II* ganz allgemein aktive Antibiotika sind oder nicht, erschien es uns unerlässlich, einmal reine und wohlcharakterisierte Verbindungen zu untersuchen und zum anderen insbesondere Thioanaloge antibiotisch hochwirksamer *I*.

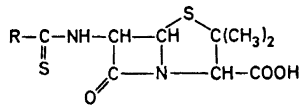

II

Im Rahmen unserer orientierenden Vorarbeiten auf diesem Gebiet gelang es uns nun, die 6-(2-Phenyl-thiobenzoylamino)-penicillansäure *II* (R = 2-$C_6H_5C_6H_4$), das Thioanaloge des Ancillins [1] durch Thioacylierung von 6-Aminopenicillansäure zu erhalten. Abgesehen von einer Aktivität gegenüber *Staphylococcus aureus* 133 und *Klebsiella* 8085 (im Mäuseversuch bei oraler Gabe), die etwa der des Oxacillins [1] entspricht, besitzt das »Thio-ancillin» keine interessanten antibiotischen Eigenschaften. Bei einer Reihe anderer Syntheseversuche stiess entweder die Darstellung der benötigten Dithioester oder die Thioacylierung der 6-Aminopenicillansäure auf Schwierigkeiten.

Wir sind der Bayer AG, Leverkusen (Deutschland) für die biologischen Untersuchungen zu Dank verpflichtet.

Carboxymethyl-(2-phenyl-dithiobenzoat). Dieses Thioacylierungsreagenz wurde nach der allgemeinen Vorschrift von Kjær [3] dargestellt. Eine aus 65,2 g (0,23 mol) 2-Joddiphenyl und 6,1 g (0,25 mol) Magnesiumspänen in 100 ml Äther hergestellte Grignardlösung wurde unter Eiskühlung zu einer Lösung von 27,2 g (0,36 mol) Schwefelkohlenstoff in 60 ml Äther zugetropft. Nach Zusatz von 135 g Eis wurde die Ätherphase verworfen und die wässrige Phase mit einer Lösung von 28,0 g (0,24 mol) Natriumchloracetat in 85 ml Wasser versetzt. Nach 48 Std. Stehens bei 5°C wurde mit 16 ml konz. Schwefelsäure angesäuert und mit Benzol ausgeschüttelt. Die Benzolphase wurde über Calciumchlorid getrocknet und der rote Dithioester mit Petroläther (Kp. 50–80°C) ausgefällt. Ausbeute 24,0 g (36 %), F: 109°C. [Gef. C 62,26; H 4,20; S 21,95. Ber. für $C_{15}H_{12}O_2S_2$ (288,4): C 62,44; H 4,20; S 22,24.]

6-(2-Phenyl-thiobenzoylamino)-penicillansäure. Nach dem Verfahren der Distillers Co.[2] wurden 8,0 g (0,028 mol) Carboxymethyl-(2-phenyl-dithiobenzoat) und 6,1 g (0,028 mol) 6-Aminopenicillansäure in 150 ml 0,1 M Phosphatpuffer (pH = 7,0) aufgeschlämmt und durch Zusatz 10-proz. Natronlauge in Lösung gebracht. Während des gesamten Versuches wurde der pH laufend mit einem pH-Meter kontrolliert und bei Bedarf durch Zusatz von 10-proz. Natronlauge wieder auf 7,0 eingestellt. Unter Rühren und Kühlen auf 0°C wurde eine Lösung von 13,90 g (0,055 mol) Jod und 9,15 g (0,055 mol) Kaliumjodid in 14 ml Wasser zugetropft und anschliessend noch 2 Std. bei Zimmertemperatur weitergerührt. Nach Filtrieren und Ausschütteln mit Äther wurden 100 ml Butylacetat zugesetzt und die wässrige Phase durch Zusatz 10-proz. Schwefelsäure auf pH = 2 gebracht. Nach Abtrennen der organischen Phase wurde nochmals mit 100 ml Butylacetat ausgeschüttelt. Die vereinigten organischen Phasen wurden mit soviel 10-proz. Kaliumbicarbonatlösung versetzt (35 ml), dass der pH der wässrigen Phase zum Schluss 7 betrug. Anschliessend wurde die organische Phase verworfen, die wässrige Phase im Vakuum zur Trockne gebracht, der Rückstand in Methanol gelöst und mit Äther ausgefällt. Man erhielt so 4,8 g (34 %) des Kaliumsalzes von *II* (R = 2-$C_6H_5C_6H_4$) als Trihydrat, Zers.-P. 195–200°C, ν_{CO} 1760–1770 cm^{-1}. [Gef. C 49,26; H 4,29; N 4,97; S 12,47. Ber. für $C_{21}H_{19}KN_2O_3S_2.3H_2O$ (504,7): C 49,98; H 4,99; N 5,55; S 12,71.]

Beide Verbindungen besitzen NMR-Spektren, die der Erwartung entsprechen.

1. Ehrhart, G. und Ruschig, H. *Arzneimittel*, 2. Aufl., Band 4, S. 237, Verlag Chemie, Weinheim 1972.
2. Distillers Co. Ltd. (Hall, R. H., Hollingworth, H. D., Young, D. P. und Sherlock, R.), Brit. Patent 952519 (1964); *Chem. Abstr.* **60** (1964) 15877.
3. Kjær, A. *Acta Chem. Scand.* **4** (1950) 1347.

Eingegangen am 13. April 1973.

A Novel Superoxide Dismutase of High Molecular Weight from Bovine Liver

STEFAN MARKLUND

Department of Chemistry, Section of Physiological Chemistry, University of Umeå, S-901 87 Umeå, Sweden

Since the discovery of the enzymic activity in 1969,[1] superoxide dismutases have been isolated from a wide variety of organisms. Eukaryotes have been found to contain enzymes containing 2 Cu and 2 Zn whereas the enzymes from prokaryotes contain 2 Mn.[2] Both types of enzymes have molecular weights in the range 30 000 – 40 000. In mammals superoxide dismutases have been isolated from several tissues, *e.g.* liver,[3] brain,[3] heart,[4] and all have been found to be identical to the enzyme found in erythrocytes:[3,4] erythrocuprein.

When hemolysates are run on polyacrylamide gel electrophoresis and stained for superoxide dismutase activity one group of bands is found, apparently representing erythrocuprein. However, many tissue homogenates show two groups of bands (Fig. 1a), one fast, apparently

Fig. 1. Electrophoresis in polyacrylamide gels at pH 8.9 with staining for superoxide dismutase activity.[10] (a) Liver homogenate; (b) High molecular weight fraction from gel chromatography, *cf.* Fig. 2; (c) Low molecular weight fraction, *cf.* Fig. 2.

given by erythrocuprein and one slow, the origin of which is so far unknown. The two groups in bovine liver homogenates are easily separated by gel chromatography, the electrophoretically slow fraction apparently having the higher molecular weight.

The present communication reports some properties of the high molecular weight component, shown to have a molecular weight of ≈73 000 and an isoelectric point around pH 7.9. Some studies on metal content were also performed.

Materials and methods. Bovine liver was obtained fresh from a local slaughterhouse and stored at −70°C. It was cut into thin slices, thoroughly washed in icecold saline and homogenized in a Turmix with 3 volumes of 5 mM Na phosphate, pH 7.4. After centrifugation of the homogenate at 30 000 *g* for 60 min, the supernatant was applied to a Sephadex G-200 column (9.2 × 70 cm) and eluted with 30 mM Na phosphate, pH 7.40 at 60 ml h^{-1}.

Bovine erythrocuprein was prepared by the method of McCord and Fridovich [5] as modified by Weser *et al.*[6]

The molecular weight was determined according to Andrews [7] on a Sephadex G-200 (preswollen >6 months) column (2.5 × 70 cm, elution rate 2 ml cm^{-2} h^{-1}) with 30 mM Na phosphate, pH 7.4+0.2 M NaCl as eluent. The column was calibrated with human gamma globulin, human transferrin, bovine serum albumin, and bovine myoglobin.

Discontinuous polyacrylamide gel electrophoresis was performed according to Maurer [8] in 7.5 % gels at pH 8.9. Isoelectric focusing was performed for 72 h at 600 V, in the LKB column 8101, 110 ml (LKB Stockholm, Sweden) with 1 % Ampholine, pH 3 – 10, according to LKB's suggestions and with a sucrose density gradient. Metal analyses were performed by atomic absorption spectroscopy in a graphite furnace.[9]

Results and discussion. Fig. 1a shows a polyacrylamide gel electrophoresis of a bovine liver homogenate stained for superoxide dismutase activity. The activity is found to be divided into two groups of bands.

The dismutase activity of a liver homogenate is also separated into two fractions upon chromatography on Sephadex

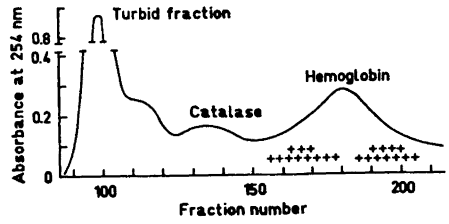

Fig. 2. Chromatography of bovine liver homogenate on Sephadex G-200. The preparation of the homogenate and the chromatography were carried out as described in Materials and Methods. Superoxide dismutase activity was detected by the nitro blue tetrazolium-photoreduction method,[10] + +.

G-200, Fig. 2. The high molecular weight component corresponds to the electrophoretically slow group and the low molecular weight component corresponds to the fast group, Fig. 1b, c. The position of the latter group in the chromatogram corresponds to a molecular weight ≈30 000 and it cannot be distinguished from bovine erythrocyte erythrocuprein on a polyacrylamide gel stained for superoxide dismutase. Hence it is probably the erythrocuprein present in liver (hepatocuprein).[3]

The yield of the high molecular weight component varies from liver to liver. The activity in the liver used in the present investigation was high and about equal to that of the low molecular weight component. It has apparently not been described before and was subjected to a number of investigations.

All assay procedures for superoxide dismutase are indirect and there is therefore a risk that components lacking true superoxide dismutase activity may give rise to positive reactions. However, three different procedures for superoxide dismutase determination gave the same result for the high molecular weight fraction; the xanthine oxidase-cytochrome C procedure,[5] the photoreduction of nitro blue tetrazolium,[10] and the reduction of nitro blue tetrazolium by NADH mediated by phenazine methosulfate.[11] Further, the fraction contained no cytochrome C oxidizing activity. However, the method employing the autooxidation of adrenalin at pH 10.2 [12] could not be used for the high molecular weight fraction which, unlike erythrocuprein, apparently loses its activity at this pH.

The activity was not affected by exposure to 10 mM EDTA at pH 6.6 at room temperature for a few hours. Neither did exposure to 4 M urea for an hour affect its activity or electrophoretic mobility.

The apparent molecular weight as determined by chromatography on a calibrated Sephadex G-200 column was = 73 000. The molecular weight is hence much higher than those of previously described copper- or manganese-containing superoxide dismutases. Isoelectric focusing (Fig. 3) revealed an isoelectric point of pH 7.9, much higher than that of bovine erythrocuprein, 4.95.[13] The zone of activity in the polyacrylamide gel (Fig. 1b) and the band in isofocusing (Fig. 3) are fairly broad. This is indicative of an inhomogeneity in the high molecular weight fraction. Whether this is due to the presence of isoenzymes or to secondary changes in the protein cannot be decided at present.

The band of superoxide dismutase activity from the electrofocusing was analyzed for Mn and Cu content by means of atomic absorption in a graphite furnace. The enzyme activity correlated with the presence of Mn but the region also contained much Cu. The active fraction is probably not pure. Some copper complexes display a superoxide dismutase activity approaching ≤7.5 % of that of erythrocuprein.[14] Irrespective of whether the active component contains all Cu or Mn or both, the activity per metal in the

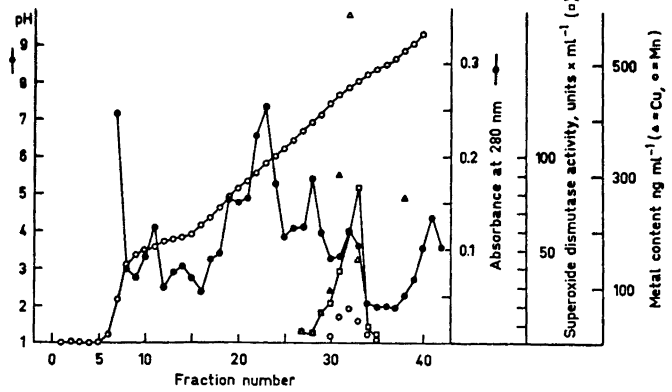

Fig. 3. Isoelectric focusing of the high molecular weight superoxide dismutase. Superoxide dismutase activity was determined according to McCord and Fridovich.[5] Metals were determined by means of atomic absorption spectroscopy [9].

most active fraction (33) is ≥ 50 % of that of Cu in erythrocuprein.[5] This, together with its resistance towards EDTA, seems to exclude that the activity is of a non-specific metal-complex type.

Some people have genetic variant forms of erythrocuprein.[15] Variants are not found in the electrophoretically slow component from placentas of such persons, which indicates different genetic control.[16] Preliminary investigations indicate that an electrophoretically slow component staining for superoxide dismutase activity from Kb cells is associated with a particulate fraction, probably mitochondria, whereas a fast component is cytoplasmatic.[16] The slow component may be related to the manganese containing superoxide dismutase recently mentioned as present in chicken liver mitochondria.[17]

Acknowledgement. I want to thank Dr. G. Lundgren for performing the atomic absorption spectroscopy.

1. McCord, J. M. and Fridovich, I. *Fed. Proc.* **28** (1969) 346.
2. Fridovich, I. *Accounts Chem. Res.* **5** (1972) 321.
3. Carrico, R. J. and Deutsch, H. F. *J. Biol. Chem.* **244** (1969) 6087.
4. Keele, B. B., McCord, J. M. and Fridovich, I. *J. Biol. Chem.* **246** (1971) 2875.
5. McCord, J. and Fridovich, I. *J. Biol. Chem.* **244** (1969) 6049.
6. Weser, U., Bunnenberg, E., Cammack, R., Djerassi, C., Flohé, L., Thomas, G. and Volter, W. *Biochim. Biophys. Acta* **243** (1971) 203.
7. Andrews, P. *Methods Biochem. Anal.* **18** (1970) 1.
8. Maurer, H. R. *Disk-Electrophorese*, Walter de Gruyter, Berlin 1968.
9. Lundgren, G. and Johansson, G. *Talanta. Submitted.*
10. Beauchamp, C. and Fridovich, I. *Anal. Biochem.* **44** (1971) 276.
11. Nishikimi, M., Rao, N. A. and Yagi, K. *Biochem. Biophys. Res. Commun.* **46** (1972) 849.
12. Misra, H. P. and Fridovich, I. *J. Biol. Chem.* **247** (1972) 3170.
13. Bannister, J., Bannister, W. and Wood, E. *Eur. J. Biochem.* **18** (1971) 178.
14. Joester, K.-E., Jung, G., Weber, U. and Weser, U. *FEBS Lett.* **25** (1972) 25.
15. Beckman, G. *Hereditas. In press 1973.*
16. Beckman, G., Lundgren, E. and Tärnvik, A. *In manuscript.*
17. Fridovich, I. *Biochem. Soc. Trans.* **1** (1973) 48.

Received March 22, 1973.

Ring Inversion in Substituted Spiro[2.5]octanes

PER KOLSAKER, HANS JOHAN STORESUND, JAN SCHAUG and GRETE WØIEN LARSEN

Department of Chemistry, University of Oslo, Blindern-Oslo 3, Norway

Some of the interest in the field of inversion of cyclohexane rings has been focused on compounds having hybridization different from sp^3 at one or more of the ring atoms. NMR spectroscopy has proven useful to evaluate rate constants for such processes provided the free energy of activation is larger than about 6 kcal/mol. By this technique 1,4-dimethylenecyclohexane (I) has been studied and a $\Delta G^{\ddagger}$ value of 7.5 kcal/mol was calculated for the inversion for which arguments are presented showing that this most likely is a chair-chair interconversion.[1] A change in the hybridization from sp^2 to sp^3 as in 1,1,4,4-tetramethylcyclohexane (II) raises the barrier to inversion to 11.6 kcal/mol.[2] An intermediate value of 10.7 kcal/mol has recently been found in dispiro[2.2.2.2]decane (III) and fits qualitatively in the picture of the ring atoms involved in substitution having a slightly higher *s*-character than in II.[3] Methylenecyclohexane (IV) has also been found to exist predominantly in a chair

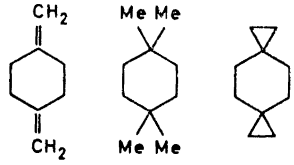

I II III

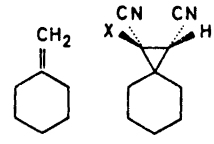

a: x = CN
b: x = COOMe

IV V

most active fraction (33) is ≥ 50 % of that of Cu in erythrocuprein.[5] This, together with its resistance towards EDTA, seems to exclude that the activity is of a non-specific metal-complex type.

Some people have genetic variant forms of erythrocuprein.[15] Variants are not found in the electrophoretically slow component from placentas of such persons, which indicates different genetic control.[16] Preliminary investigations indicate that an electrophoretically slow component staining for superoxide dismutase activity from Kb cells is associated with a particulate fraction, probably mitochondria, whereas a fast component is cytoplasmatic.[16] The slow component may be related to the manganese containing superoxide dismutase recently mentioned as present in chicken liver mitochondria.[17]

Acknowledgement. I want to thank Dr. G. Lundgren for performing the atomic absorption spectroscopy.

1. McCord, J. M. and Fridovich, I. *Fed. Proc.* **28** (1969) 346.
2. Fridovich, I. *Accounts Chem. Res.* **5** (1972) 321.
3. Carrico, R. J. and Deutsch, H. F. *J. Biol. Chem.* **244** (1969) 6087.
4. Keele, B. B., McCord, J. M. and Fridovich, I. *J. Biol. Chem.* **246** (1971) 2875.
5. McCord, J. and Fridovich, I. *J. Biol. Chem.* **244** (1969) 6049.
6. Weser, U., Bunnenberg, E., Cammack, R., Djerassi, C., Flohé, L., Thomas, G. and Volter, W. *Biochim. Biophys. Acta* **243** (1971) 203.
7. Andrews, P. *Methods Biochem. Anal.* **18** (1970) 1.
8. Maurer, H. R. *Disk-Electrophorese*, Walter de Gruyter, Berlin 1968.
9. Lundgren, G. and Johansson, G. *Talanta. Submitted.*
10. Beauchamp, C. and Fridovich, I. *Anal. Biochem.* **44** (1971) 276.
11. Nishikimi, M., Rao, N. A. and Yagi, K. *Biochem. Biophys. Res. Commun.* **46** (1972) 849.
12. Misra, H. P. and Fridovich, I. *J. Biol. Chem.* **247** (1972) 3170.
13. Bannister, J., Bannister, W. and Wood, E. *Eur. J. Biochem.* **18** (1971) 178.
14. Joester, K.-E., Jung, G., Weber, U. and Weser, U. *FEBS Lett.* **25** (1972) 25.
15. Beckman, G. *Hereditas. In press 1973.*
16. Beckman, G., Lundgren, E. and Tärnvik, A. *In manuscript.*
17. Fridovich, I. *Biochem. Soc. Trans.* **1** (1973) 48.

Received March 22, 1973.

Ring Inversion in Substituted Spiro[2.5]octanes

PER KOLSAKER, HANS JOHAN STORESUND, JAN SCHAUG and GRETE WØIEN LARSEN

Department of Chemistry, University of Oslo, Blindern-Oslo 3, Norway

Some of the interest in the field of inversion of cyclohexane rings has been focused on compounds having hybridization different from sp^3 at one or more of the ring atoms. NMR spectroscopy has proven useful to evaluate rate constants for such processes provided the free energy of activation is larger than about 6 kcal/mol. By this technique 1,4-dimethylenecyclohexane (I) has been studied and a $\Delta G^{\ddagger}$ value of 7.5 kcal/mol was calculated for the inversion for which arguments are presented showing that this most likely is a chair-chair interconversion.[1] A change in the hybridization from sp^2 to sp^3 as in 1,1,4,4-tetramethylcyclohexane (II) raises the barrier to inversion to 11.6 kcal/mol.[2] An intermediate value of 10.7 kcal/mol has recently been found in dispiro[2.2.2.2]decane (III) and fits qualitatively in the picture of the ring atoms involved in substitution having a slightly higher *s*-character than in II.[3] Methylenecyclohexane (IV) has also been found to exist predominantly in a chair

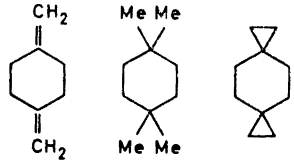

I II III

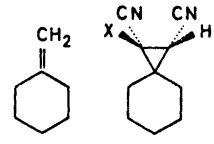

a: x = CN
b: x = COOMe

IV V

conformation with a $\Delta G^{\ddagger}$ value of 8.4 kcal/mol for the inversion process.[4]

By analogy one would expect spiro-[2.5]octane to exhibit a barrier to inversion of approximately 10.4 – 10.5 kcal/mol *i.e.* intermediate between III and cyclohexane itself ($\Delta G^{\ddagger} \approx 10.2$ kcal/mol).

The ring inversion in unsubstituted spiro[2.5]octane has hitherto not been investigated, but the easy preparation of 1,1,2-trisubstituted spiro[2.5]octanes (V) gave us in hand compounds well suited for barrier determination.[5]

The NMR spectra at room temperature of the compounds Va or Vb indicated rapid interconversion with singlets for the cyclopropyl proton at 2.37 and 2.64 ppm, respectively (downfield from Me_4Si). The cyclohexyl resonance consisted of broad non-resolvable multiplets at 1.4 – 2.0 and 1.2 – 2.0 ppm, respectively. Lowering the temperature to about −40°C some changes were observed in the cyclohexyl region. On further cooling a splitting of the cyclopropyl resonance ($\Delta\nu = 6.7$ Hz) occurred which obviously must be due to the two possible conformers of the spiro compounds. A population difference was indicated by the unequal intensities of the two peaks. The rate of interconversion at seven different temperatures ranging from about −70°C to −100°C was then calculated using a complete line-shape analysis, (Gutowsky *et al.*[6]) and the free energy of activation was calculated using the Eyring equation $\Delta G^{\ddagger} = RT \ln (kT\tau/h)$ where τ is the lifetime at temperature T (Table 1).

Table 1.[a] Interconversion barrier and free energy difference between the two conformers of 1,1,2-trisubstituted spiro[2.5]octanes V.

	$\Delta G^{\ddagger}_{A\rightarrow B}$	$\Delta G^{\ddagger}_{B\rightarrow A}$	ΔG_0	t(°C)
Va	10.5	10.3	0.2	−78
Vb	10.5	10.4	0.1	−72.5

[a] A is the conformer of lowest energy; free energy difference (ΔG) in kcal/mol.

The calculated difference in free energy of the two conformers, ΔG_0, indicates only slight difference in population while the observed intensities in the spectra (by integration) point to a preference for the lower energy state of about 0.25 kcal/mol for both Va and Vb. However, the limit of error in the calculation, 0.1 kcal/mol, may account for this discrepancy.

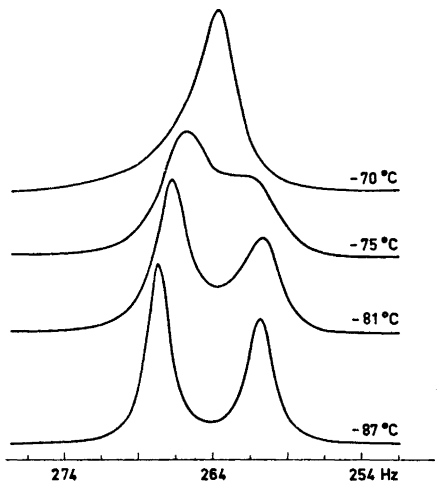

Fig. 1. The cyclopropyl region of the NMR spectrum of Vb as a function of sample temperature.

The thus observed values for the barrier to inversion, 10.3 – 10.5 kcal/mol, agree very well with those expected. It remains to be seen whether the substituents exhibit any effect on the barrier. If so, it will probably be more of electronic nature, *i.e.* an effect in the hybridization at the spiro atom. The substituents are probably too far away for the observation of a sizeable van der Waals repulsion.

Experimental. The spectra were obtained using a Varian HA 100-15D spectrometer (operating at 98 MHz) with Model V4333 variable temperature probe and Model V6040 Temperature Controller. The temperatures were calibrated using a copper-constantan thermocouple which was introduced in the sample tube before and after each run. Temperature accuracy was estimated to ±1°C.

The compounds were dissolved in dichlorofluoromethane to a concentration of about 0.2 M.

Spectra were recorded in the field sweep mode and at a sweep rate of 0.1 Hz/sec, thus approaching "slow passage" conditions. Internal lock with dichlorofluoromethane as

lock signal was used. Field homogeneity was checked for each run using the resonance signal from tetramethylsilane run at the same rate (0.1 Hz/sec).

1. St-Jacques, M. and Bernard, M. *Can. J. Chem.* **47** (1960) 2911.
2. Friebolin, H., Faisst, W., Schmid, H. G. and Kabuss, S. *Tetrahedron Letters* **1966** 1317.
3. Lambert, J. B., Gosnell, J. L., Jr., Bailey, D. S. and Greifenstein, L. G. *Chem. Commun.* **1970** 1004.
4. Gerig, J. T. and Rimmerman, R. A. *J. Am. Chem. Soc.* **92** (1970) 1220.
5. Storesund, H. J. and Kolsaker, P. *Tetrahedron Letters* **1972** 2255.
6. Gutovsky, H. S., McCall, D. W. and Schlichter, C. P. *J. Chem. Phys.* **21** (1953) 279.

Received January 11, 1973.

ACTA CHEMICA SCANDINAVICA 27 (1973) 1463–1477

Chlorophylls

I. Separation and Isolation of Chlorophylls *a* and *b* by Multiple Liquid-Liquid Partition

PAAVO H. HYNNINEN and NILS ELLFOLK

Department of Biochemistry, University of Helsinki, SF-00170 Helsinki 17, Finland

The fractionation of chloroplast pigments by means of multiple liquid-liquid partition has been studied utilizing three types of solvent system: petroleum ether-ethanol-formamide (PEF), petroleum ether-methanol-formamide (PMF), and petroleum ether-benzene-methanol-formamide (PBMF). Of these, the PBMF-system was found to be most suitable for the separation and isolation of chlorophylls. The PMF-system, although it was most selective, appeared to be unsuitable for this purpose due to the formation of a 10-methoxy-lactone derivative from chlorophyll *a* during fractionation. This allomerization reaction was sensitive to the polarity of the lower phase and did not occur when the PBMF-system was employed, provided the fractionation time did not exceed 24 h. According to the interpretation presented for this observation, the enolization reaction is the first and also the rate-limiting step in the reaction sequence of the allomerization.

In order to extract chloroplast pigments from plant material, a "two-phasic" method was developed. Conventional extraction methods invariably led to the formation of considerable amounts of 10-hydroxy-chlorophylls, these allomerization products being produced in all probability by the enzymatic oxidation of chlorophylls during the extraction. In the "two-phasic" extraction method, the pigments are loosened from the chloroplasts by the polar lower phase and transferred immediately into the nonpolar upper phase, where the chlorophylls do not undergo alteration.

In the final method developed, the pigments were extracted from frozen soybean leaves by means of the PMF-system and thereafter separated in the PBMF-system utilizing a partition apparatus of 100 tubes. By this method, chlorophyll *a* and chlorophyll *b*, each of a high degree of purity, were yielded in approximately 24 h, including the time required for the extraction of the pigments from the plant material. The ratio of the absorbance at the Soret band wavelength to the absorbance at the chlorin band wavelength (A_S/A_I) was, in diethyl ether, 1.32 for chlorophyll *a* and 2.88 for chlorophyll *b*. The isolated chlorophyll preparations have been kept frozen in cyclohexane at $-15°C$ for a period of six months and no changes have been observed in their behaviour.

During extraction and fractionation, the chlorophylls are susceptible to a number of chemical transformations which yield various alteration products or "isomers".[1] These transformations include keto-enol tautomerism, epimerization, enzymatic or nonenzymatic oxidation (allomerization), solvolysis, pheophytinization, and photochemical bleaching. Due to these transformations, the isolation of pure chlorophylls from plant material is a difficult task. When chromatographic methods [1–10] are employed for this purpose, two or three successive fractionations are generally required in order to isolate relatively pure chlorophyll *a* and chlorophyll *b*. Even such an extensive purification as this apparently does not guarantee that a chlorophyll preparation of high purity will be obtained.[11,12] It should also be emphasized in this context that *neither* the crystallinity [5,6] of, *nor* a positive Molisch phase test for a chlorophyll preparation is reliable evidence of its purity.

Liquid-liquid partition methods have, in only a few cases, been utilized for the fractionation of chlorophylls. Willstätter and co-workers [13,14] obtained partially purified chlorophyll *a* and chlorophyll *b* by successive distribution of the pigments between petroleum ether and aqueous methanol in a separating funnel. The same solvent system (or a slight modification of it) was later employed for the fractionation of chlorophylls by means of either countercurrent distribution (CCD) [15–17] or Martin-Synge distribution (MSD).[18] However, the results of these fractionations have not been very promising due to the low selectivity of the utilized solvent systems and to the great tendency of the chlorophylls to undergo transformation.

In the present investigation, the authors have undertaken a detailed study on the applicability of the partition principle to the separation and isolation of chlorophylls. As a result of this study, a method yielding both highly-purified chlorophyll *a* and highly-purified chlorophyll *b* in one fractionation can now be described.

EXPERIMENTAL

Equipment and solvents. Multiple liquid-liquid partition was performed utilizing the apparatus developed by Hietala.[19] The properties and operation of this apparatus, as well as methods for the calculation of theoretical distribution curves and partition coefficients, have been described in an earlier publication.[20] The upper phase was employed as the mobile solvent in all fractionations described in this publication. The phase ratio among the different fractionations varied from 0.21 to 0.33. A shaking frequency of 22 cycles/min, an amplitude of $\pm 45°$ and a flow rate of $1-2$ ml/min were utilized in the present study.

Three types of solvent system were employed:

(1) The PEF-system: petroleum ether(3)/ethanol(2)-formamide(1);

(2) The PMF-system: petroleum ether(4)/methanol(3)-formamide (1); and

(3) The PBMF-system: petroleum ether(8)-benzene(1)/methanol(6.75)-formamide (2.25).

The values in parentheses state the initial volume ratios of the solvent components. Occasionally, oxalic acid was added to the lower phase, since it has been proclaimed that allomerization would thereby be prevented.[13] The concentration of the oxalic acid was the same as that employed by Arn *et al.*:[18] 10 mg/l of lower phase.

The solvents required for the distribution apparatus, for the extraction of pigments from the plant material and for spectroscopy were of reagent grade purity. They were utilized as commercially supplied, with the exceptions of diethyl ether and formamide.

The latter was purified immediately before use according to the method of Verhoek,[21] except for the fractional crystallization. The final product resulted in a green to green-yellow colour upon reaction with bromthymolblue. The diethyl ether was treated with a concentrated solution of ferrous sulphate, following which the ether was washed, dried and distilled. The employed boiling point fraction of the petroleum ether was 60 – 80°C. Ethanol (99.5 %) was purchased from Alko Oy (Finland).

A Cary Spectrophotometer Model 15 was used to record the absorption spectra and a Beckman DU Spectrophotometer to measure single absorbances.

Extraction of the pigments from plant material. Frozen soybean leaves were generally utilized as a source of choloroplast pigments. Immediately after harvesting, the leaves were transferred to the dark at a temperature of −15°C and were stored under these conditions until used. For the purpose of comparison, however, fresh or dried leaf material was occasionally employed. The extraction procedures described as follows were performed rapidly and in dimmed light. Methods 1 and 2 describe the extraction of the pigments by slightly modified conventional procedures. Since the conventional procedures consistently led to the formation of considerable amounts of allomerization or other alteration products, regardless of how quickly or carefully the extraction was performed, a "two-phasic" extraction method was developed (Method 3).

Method 1. Sixty grams of frozen soybean leaves were suspended in 400 ml of a petroleum ether(3)-methanol(1) mixture. The suspension was homogenized by means of a Waring Blendor (1 min) and filtered in a Büchner funnel with the aid of suction. The residue in the funnel was re-extracted with 400 ml of the petroleum ether-methanol mixture. The two filtrates were then transferred into a dark bottle, 1 l of concentrated sodium chloride solution was added and the mixture shaken gently. After a few minutes standing, the petroleum ether containing the chloroplast pigments was collected into the upper phase. The phases were then separated by means of a separatory funnel and the lower phase was re-extracted with 100 ml of pure petroleum ether. The related petroleum ether extracts were then washed three times with distilled water (pH 5) and subsequently evaporated to a volume of 38 ml by means of a rotatory evaporator.

Method 2. Two hundred grams of frozen soybean leaves were crushed in the cold and then extracted with 1 l of 80 % (w/w) acetone. The resulting suspension was allowed to stand, with occasional stirring, for 1 h at 4°C, after which it was filtered in a Büchner funnel. The residue remaining in the funnel was re-extracted with 900 ml of 80 % acetone. Following this re-extraction, the leaf material still retained a green colouring. The two filtrates were subsequently treated as in Method 1. The final volume of the pigment-containing petroleum ether solution was 10 ml.

Method 3. One hundred grams of frozen soybean leaves were crushed in the cold and suspended, while in a separatory funnel, in a mixture of 600 ml petroleum ether + 600 ml methanol(3)-formamide(1). Argon gas was continuously bubbled throughout the phase system both before the leaves were suspended therein and also during the suspending procedure. The funnel was then tightly stoppered and the suspension vigorously shaken by hand for 20 min. After phase separation, the lower phase was allowed to drain from the funnel. The upper phase was then permitted to empty directly through a filter into a glass cylinder. The filtrate was washed three times with distilled water and subsequently evaporated to a volume of 15 ml.

Preparation of some chlorophyll derivatives. Magnesium-free chlorophyll derivatives were prepared by treating an ethyl ether solution of the chlorophyll with 13 % hydrochloric acid. The phytyl group was removed by hydrolysis of the ester in 30 % hydrochloric acid. Methyl esters of the derivatives were prepared by means of diazomethane. The ethereal solution of diazomethane was prepared from nitrosomethylurea by saponification, as described by Eistert.[22]

RESULTS

Fractionation employing the PEF-system. The results of the first fractionation experiment are presented in Fig. 1. Several components were resolved by employing the PEF-system with 70 fractionation tubes. However, many of the green components were allomerization products of chlorophylls, since they reacted negatively to phase testing.

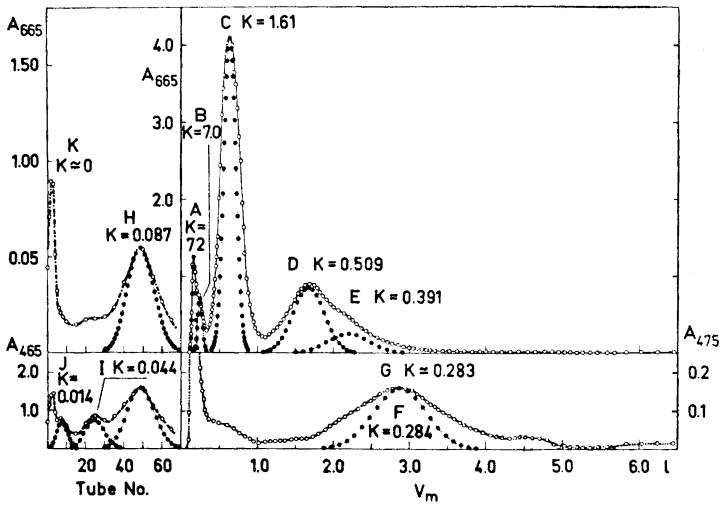

Fig. 1. Separation of chloroplast pigments employing the PEF-system. 10 ml of the extract prepared according to Method 1 were sampled into tubes r = 0,..,3. Number of fractionation tubes utilized $= N = 70$. Average volume of the mobile phase in a partition unit $= v_m = 2.31$ ml; average volume of the stationary phase in a partition unit $= v_s = 11.19$ ml. Total volume of effluent eluted from the apparatus $= V_m = 6443$ ml; flow rate = 1.5 ml/min. Theoretical (●) and experimental (○) values, the latter obtained by measuring the absorbances of the effluent fractions or of the lower phases in the tubes: — $= A_{665}$, ··· $= A_{475}$, -·- $= A_{652}$, and -- $= A_{465}$. A = β-carotene, B = pheophytin *a*, C = chlorophyll *a*, D = 10-hydroxy-chlorophyll *a*, E = chlorophyll *b*, F = lutein, G = Mg-*b*-purpurin 7-lactone-alkyl ether-methylphytyl ester, H = 10-hydroxy-chlorophyll *b*, I = Mg-unstable rhodin-methylphytyl ester, J = neoxanthin, and K = chlorophyllide.

In the effluent series, the first two components, A and B, eluted from the apparatus, were spectroscopically identified as β-carotene and pheophytin *a*, respectively. Components A and B were only partially resolved, due to their large partition coefficients ($K_A = 72.3$, $K_B = 7.0$). The blue-green component C yielded both a positive Molisch phase test and an absorption spectrum closely resembling that of pure chlorophyll *a* (Table 1; a). The green component D was identified as 10-hydroxy-chlorophyll *a* upon the basis of the following characteristics: (1) the visible absorption spectrum of D (Table 1; d) resembled that of chlorophyll *a*;[23,24] (2) the phase test was negative; and (3) the extraction of D from an ethyl ether solution into 10 % aqueous potassium hydroxide by shaking for 2 h converted the pigment into Mg-unstable chlorin-monomethyl ester and a small amount of Mg-purpurin 18.[25] These products were identified both spectroscopically and by esterification with diazomethane, which yielded a mixture of Mg-purpurin 7-trimethyl ester and Mg-purpurin 18-monomethyl ester.[25] Component D has since been found to be identical with the compound isolated by means of multiple liquid-liquid partition from an allomerization mixture of chlorophyll *a* in methanol.[26] Furthermore, it appears evident that component D is identical to the chlorophyll derivative found by Arn *et al.*[18]

Table 1. Spectroscopic properties of the chlorophylls and their derivatives.

Compound [a]	Solvent	Peak positions (nm)								Peak ratios	
		I	II	III	IV	V	VI	S	Ss1	A_S/A_I	A_S/A_{Ss1}
a. Chlorophyll *a* (1C)	Pe	661.5	615	577	532	498		429.0	412	1.31	1.33
b. Chlorophyll *a* (2C)	Ee	661.0	615	577	532	498		430.0	410	1.32	1.59
c. Chlorophyll *a* (4C)	Ee	660.0	614	576	530	497		429.0	409	1.32	1.56
d. 10-Hydroxy-chlorophyll *a* (1D)	Pe	661.5	614	575	530	499		428.0	413	1.27	1.20
e. Mg-purpurin 7-lactone-alkyl ether-methylphytyl ester (3D)	Pe	652.5	608	566	523			417.0		1.82	
f. Mg-unstable chlorin-methylphytyl ester (4I)	Pe	654.0	608	566	523			418.0		1.88	
g. Unstable chlorin(-monomethyl ester)	Ee	668.0	611	560	528	498	468	399.0		2.50	
h. Pheophytin *a*	Ee	667.0	609	560	532	503	467	408.0		2.14	
i. Pheophorbide *a*	Ee	667.0	609	560	533	504	467	408.0		2.07	
j. Chlorophyll *b* (3F)	Ee	642.0	593					453.0	430	2.89	2.64
k. Chlorophyll *b* (4D)	Ee	642.5	595					452.5	430	2.88	2.55
l. 10-Hydroxy-chlorophyll *b* (1H)	Pe	645.5	600					452.0	430	2.97	1.80
m. Mg-*b*-purpurin 7-lactone-alkyl ether-methylphytyl ester (1G)	Pe	631.5	585	536				443.0		4.42	
n. Mg-unstable rhodin-methylphytyl ester (1I)	Ee	630.0	584	535				443.0		4.58	
o. Unstable rhodin(-monomethyl ester)	Ee	653.0	598	522				427.0		6.53	
p. Pheophytin *b*	Ee	654.0	599	555	525			433.0	412	4.81	2.28
q. Pheophorbide *b*	Ee	655.0	599	555	525			433.0	412	4.83	2.04

[a] The number and letter in parentheses refer, respectively, to the figure number and to the component in that figure.
S = Soret band, Ss1 = 1st satellite of the Soret band; Ee = ethyl ether, Pe = petroleum ether.

and assumed by them to be an "artifact" produced by the action of oxalic acid.

A small amount of material yielding a positive phase test was eluted at 2250 ml (component E), although it was poorly resolved from components D and F and could not be spectroscopically identified. The similarity of its partition coefficient ($K_E = 0.391$) to that of component E in Fig. 2 ($K_E =$

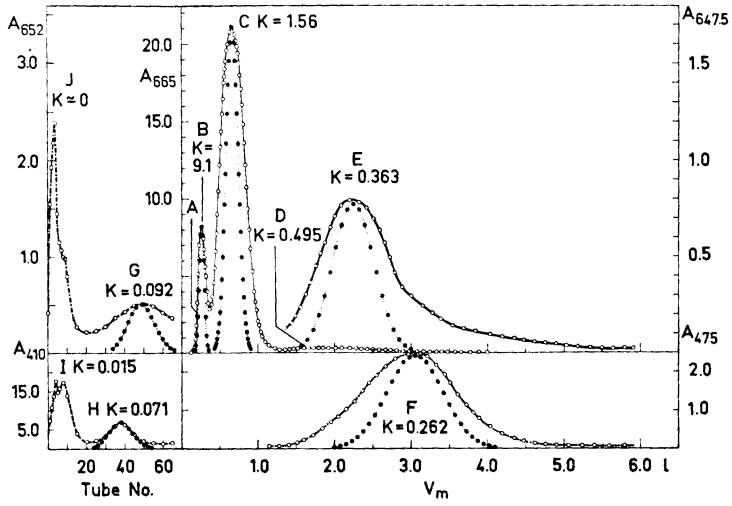

Fig. 2. Separation of chloroplast pigments employing the PEF-system. 10 ml of the extract prepared according to Method 2 were sampled into tubes r = 0,..,4. $N = 70$. $v_m =$ 2.60 ml; $v_s = 10.90$ ml. $V_m = 5910$ ml; flow rate = 1.5 ml/min. Theoretical (●) and experimental (○) values, the latter obtained by measuring the absorbances of the effluent fractions or of the lower phases in the tubes: – $= A_{665}$, — $= A_{647.5}$, ··· $= A_{475}$, -·- $= A_{652}$, and —— $= A_{410}$. A = β-carotene, B = pheophytin *a*, C = chlorophyll *a*, D = 10-hydroxy-chlorophyll *a*, E = chlorophyll *b*, F = lutein, G = 10-hydroxy-chlorophyll *b*, H = violaxanthin, I = neoxanthin, and J = chlorophyllide.

0.363) indicates, however, that component E of Fig. 1 is probably a small amount of intact chlorophyll *b*.

Component F was spectroscopically identified as xanthophyll (lutein). A slight absorption peak (632 nm) within the lutein fraction ($V_m = 3000 - 3825$ ml) revealed that this fraction was overlapped by some chlorophyll derivative. Indeed, the fractions eluted within the range $V_m = 3925 - 5000$ ml contained principally this derivative, which was purified by extracting the lutein from the petroleum ether solution by means of methanol-water. The derivative yielded a negative phase test and was spectroscopically very similar to the pigment characterized as a 10-methoxy-lactone derivative (Mg-*b*-purpurin 7-lactone-methyl ether-methylphytyl ester) by Pennington *et al.*[24] (Table 1; m). Further evidence regarding the 10-alkoxy-lactone nature of component G was given by the following properties: (1) the pigment was not extracted from an ether solution by 10 % aqueous potassium hydroxide;[25] (2) the visible absorp-

tion spectrum of the magnesium-free derivative resembled that of unstable rhodin monomethyl ester; and (3) treatment with diazomethane did not convert the pigment into Mg-*b*-purpurin 7-triester.[25] The pigment has since been found to closely resemble the primary allomerization product of chlorophyll *b* in methanol.[26]

At this stage, several pigments were still remaining in the apparatus, as shown in Fig. 1. Component H is undoubtedly 10-hydroxy-chlorophyll *b*, since it possessed properties analogous to those of 10-hydroxy-chlorophyll *a*, *viz.* (1) the visible absorption spectrum (Table 1; l) resembled that of chlorophyll *b*; (2) the phase test was negative; and (3) the agitation of an ethyl ether solution of H with 10 % aqueous potassium hydroxide for 2 h resulted in derivatives (Mg-unstable rhodin monomethyl ester and Mg-*b*-purpurin 18) which were soluble in the aqueous alkali phase. Component I was characterized as Mg-unstable rhodin methylphytyl ester. Its visible absorption spectrum (Table 1; n) closely resembled that of component G. The other components remaining in the apparatus could not be characterized with certainty, since they were only partially resolved. Fraction J appeared to contain a carotenoid (neoxanthin) as its principal component. The chlorophyllides, *etc.*, remained at the sampling end of the apparatus.

It was concluded from the results presented in Fig. 1 that oxidation of the chlorophylls had occurred primarily during extraction of the pigments from the plant material, since deviations from the theoretical values were rather small in the case of the chlorophyll *a* fraction (component C). Therefore, it was considered necessary to employ a different method of extracting the pigments from the plant material.

Fig. 2 presents the results obtained from the second fractionation. In this case, the pigments were extracted according to Method 2 and again separated by means of the partition apparatus utilizing PEF as the solvent system. The relative amount of 10-hydroxy-chlorophyll *a* (component D) separated in this instance is much smaller than that distinguishable as a result of the first fractionation (Fig. 1). More intact chlorophyll *b* (component E) was probably also obtained in this case. However, the concentration profile of chlorophyll *b* reveals a lengthy tail, thus indicating that a slow transformation of chlorophyll *b* to a 10-ethoxy-lactone derivative had probably occurred during the fractionation.

Fractionation employing the PMF-system. Since the selectivity of the PEF-system was unsatisfactory, especially in regard to chlorophyll *b* and lutein, a second solvent system was utilized. Preliminary determination of the partition coefficients for chlorophyll *a*, chlorophyll *b* and lutein indicated that the PMF-system would be considerably more selective than the PEF-system. Therefore, the former solvent system was employed in the fractionation to be described in this section. In order to avoid the occurrence of allomerization during extraction of the pigments from the plant material, a "two-phasic" extraction method (Method 3) was simultaneously introduced.

The results subsequent to these alterations in the conditions of extraction and fractionation are presented in Fig. 3, where it can be seen that the PMF-system is indeed considerably more selective than the PEF-system. Chlorophyll *b* and lutein (components F and G) are now almost completely separated

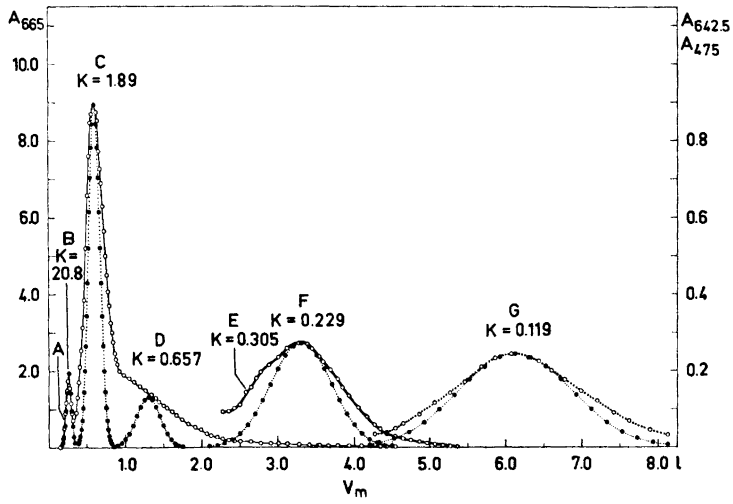

Fig. 3. Separation of chloroplast pigments employing the PMF-system. 15 ml of the extract prepared according to Method 3 were sampled into tubes r = 0,..,4. $N = 70$. $v_m = 3.27$ ml; $v_s = 10.23$ ml. $V_m = 8125$ ml; flow rate = 2 ml/min. Theoretical (●) and experimental (○) values, the latter obtained by measuring the absorbances of the effluent fractions: — $= A_{665}$, — — $= A_{642.5}$, and ··· $= A_{475}$. A = β-carotene, B = pheophytin *a*, C = chlorophyll *a*, D = Mg-purpurin 7-lactone-methyl ether-methylphytyl ester, E = 10-hydroxy-chlorophyll *a*, F = chlorophyll *b*, and G = lutein.

from each other. However, a change has occurred in the concentration profile of chlorophyll *a*, the character of which clearly indicates that chlorophyll *a* (C) has undergone a partial transformation to some derivative (D) during the fractionation. The material eluted at $V_m = 600$ ml yielded a clearly positive phase test as well as an absorption spectrum closely resembling that of pure chlorophyll *a*. The material eluted at $V_m = 1300$ ml gave, on the contrary, a negative phase test and was spectroscopically quite different from chlorophyll *a*. These facts indicated that the allomerization of chlorophyll *a* had now occurred in the apparatus. The absorption spectrum of pigment D (Table 1; e) was the same as that described by Holt [25] for Mg-purpurin 7-lactone-methyl ether-dimethyl ester and by Pennington *et al.*[24] for the 10-methoxy-lactone derivative of chlorophyll *a* (Mg-purpurin 7-lactone-methyl ether-methylphytyl ester). In a manner analogous to that of the 10-alkoxy-lactone derivative of chlorophyll *b*, component D had the following properties: (1) it was not extracted from an ethyl ether solution by 10 % aqueous potassium hydroxide; (2) the visible absorption spectrum of the magnesium-free derivative closely matched that of the unstable chlorin monomethyl ester; and (3) treatment with diazomethane did not convert the pigment into Mg-purpurin 7-triester. Component D has since been found to be identical with the primary allomerization product of chlorophyll *a* in methanol.[26]

Although chlorophyll *a* appeared to be very unstable in the PMF-system, chlorophyll *b* (component F), on the contrary, revealed practically no tailing

at all in this system, thus suggesting some difference in the allomerization behaviour of the two chlorophylls. The fractions eluted within the range $V_m = 3250 - 4000$ ml contained spectroscopically pure chlorophyll *b* (Table 1; j). The initial portion of the concentration zone, however, contained as impurity a small amount of 10-hydroxy-chlorophyll *a*, which was indicated by the measurement of the red absorption peak of the fractions eluted from 2300 to 3250 ml. This small amount of impurity was probably formed during the extraction of the pigments from the plant material, as in the previous experiments.

Fractionation employing the PMF-system was repeated with a fresh pigment extract prepared according to Method 3. The results were similar to those presented in Fig. 3. The addition of oxalic acid to the lower phases of the solvent systems utilized in the extraction and fractionation procedures was of no help in preventing the formation of the 10-methoxy-lactone derivative of chlorophyll *a*.

Since the 10-alkoxy-lactone derivative did not form from chlorophyll *a* during the first two fractionations in which the PEF-system was employed, it was concluded that the transformation was correlated with the polarity of the lower phase in the fractionation solvent system. The lower phase of the PMF-system is evidently more polar than the lower phase of the PEF-system,

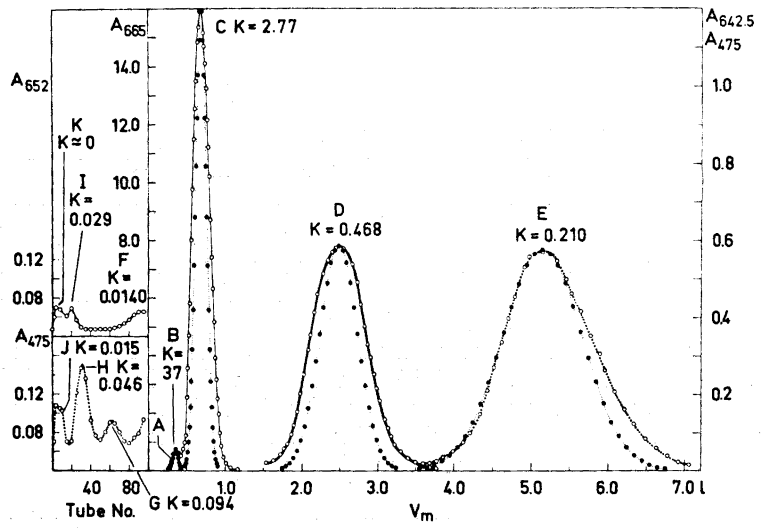

Fig. 4. Separation of chloroplast pigments employing the PBMF-system. 15 ml of the extract prepared according to Method 3 were sampled into tubes r = 0,..,4. N = 100. $v_m = 3.25$ ml; $v_s = 10.25$ ml. $V_m = 7050$ ml; flow rate = 2 ml/min. Theoretical (●) and experimental (○) values, the latter obtained by measuring the absorbances of the effluent fractions or of the lower phases in the tubes: — = A_{665}, — = $A_{642.5}$, ··· = A_{475}, and -·- = $A_{652\ nm}$. A = β-carotene, B = pheophytin *a*, C = chlorophyll *a*, D = chlorophyll *b*, E = lutein, F = 10-hydroxy-chlorophyll *b*, G = one form of violaxanthin, H = a second form of violaxanthin, I = Mg-unstable chlorin-methylphytyl ester, J = neoxanthin, and K = chlorophyllide.

since methanol is only partially miscible with petroleum ether (60 – 80°C), whereas ethanol is completely miscible with it. In order to test this hypothesis, an additional solvent component was sought which would induce greater non-polarity within the lower phase of the PMF-system without appreciably impairing the selectivity of the system as a whole. Such an additional solvent component appeared to be benzene.

Fractionation employing the PBMF-system. The results of a fractionation utilizing the PBMF-system are presented in Fig. 4. The pigments were extracted from the plant material in exactly the same manner as for the experiment presented in Fig. 3. In spite of this fact, the results of Fig. 4 differ considerably from those of Fig. 3. Firstly, the amount of pheophytin *a* fractionated was negligible with the PBMF-system, and, secondly, utilizing this solvent system, chlorophyll *a* emerged from the apparatus as a symmetrical peak with only slight deviations from theoretical values. The eluted interval between 1300 and 1500 ml was almost colourless, thus demonstrating that the resolution of chlorophyll *a* and chlorophyll *b* was practically absolute. Traces of 10-hydroxy-chlorophyll *a* could be spectroscopically detected in the initial portion of the concentration zone of chlorophyll *b*.

The resolution of chlorophyll *b* and lutein is superior in this case when compared with the result presented in Fig. 3. This is obviously due to the fact that the initial 3500 ml of the effluent was re-utilized, after evaporation of the fractions, in order to drive lutein out of the apparatus. The composition of the upper phase probably altered somewhat during the evaporation. This also explains the slight asymmetry of the concentration profile of lutein. No alkoxy-lactone derivative of chlorophyll *b* could spectroscopically be detected between chlorophyll *b* and lutein. Only traces of pigments remained in the apparatus following the complete elution of lutein. The probable character of these pigments is mentioned in the legend to Fig. 4.

The fractionation presented in Fig. 4 resulted in about 80 mg of pure chlorophyll *a* ($V_m = 513 - 918$ ml) and 8 mg of pure chlorophyll *b* ($V_m = 2327 - 3091$ ml), as estimated upon the basis of spectrophotometric concentration determinations. When the effluent solutions of chlorophyll *a* and chlorophyll *b* were cooled to 0°C and washed several times with distilled water, aggregated or "crystalline" chlorophylls were obtained. In agreement with the investigations of Jacobs *et al.*,[5,27] Anderson and Calvin,[28] and Sherman and Wang,[29] the solid chlorophyll *a* exhibited red and blue absorption maxima at 748 and at 451 nm, respectively. When a small amount of ethanol was added to an aggregated solution of chlorophyll *a* in petroleum ether, the normal spectrum of chlorophyll *a* was restored.[30]

The spectroscopic properties of the purest chlorophyll *a* and chlorophyll *b* preparations, isolated by the final method developed, appear in Table 1; c and k. Treatment of ethyl ether solutions of these chlorophyll preparations with 13 % and 30 % hydrochloric acid produced spectroscopically pure pheophytins and pheophorbides, respectively (Table 1; h, i, p and q). The isolated chlorophylls in the aggregated state have been stored in cyclohexane at −15°C for six months and no changes have been observed in their characteristics.

Selectivities of the solvent systems. The selectivities of the three solvent systems employed can easily be compared upon the basis of the partition coefficient, as presented in Table 2. For example, with regard to chlorophylls

Table 2. Partition coefficients of the chloroplast pigments and their alteration products.

Compound	PEF	PMF	PBMF
β-Carotene	72.3	156.7	∞
Pheophytin *a*	8.02[a]	20.8	42.1[a]
Chlorophyll *a*	1.59[a]	1.89	2.83[a]
Mg-purpurin 7-lactone-alkyl ether-methylphytyl ester	0.947	0.657	0.750
10-Hydroxy-chlorophyll *a*	0.502[a]	0.305	0.697[a]
Chlorophyll *b*	0.377[a]	0.229	0.482[a]
Mg-*b*-purpurin 7-lactone-alkyl ether-methylphytyl ester	0.283		0.250
Lutein	0.273[a]	0.119	0.238[a]
10-Hydroxy-chlorophyll *b*	0.091		0.140
Violaxanthin	0.071		0.094
Mg-unstable rhodin-methylphytyl ester	0.044		
Mg-unstable chlorin-methylphytyl ester			0.029
Neoxanthin	0.014		0.015
Chlorophyllides	0.000	0.000	0.000

[a] Average value of two fractionations.

a and *b*, the separation factor, $\beta = K_1/K_2$, has the values 8.2, 5.9, and 4.2, when the PMF-, PBMF-, and PEF-solvent systems, respectively, are utilized. Thus the selectivity of the PBMF-system lies approximately midway between the selectivities of the other two solvent systems.

DISCUSSION

The results presented demonstrate the possibilities of liquid-liquid partition methods regarding the fractionation of such labile compounds as the chlorophylls. They also serve as a good example of the decisive importance of selecting the proper solvent system, when applying these methods to difficult fractionation problems.

Success in the development of the final isolation method must be ascribed to the formulation of an appropriate solvent system for the fractionation, as well as to the development of an improved method for the extraction of the pigments from the plant material with minimal production of allomerization products. In the "two-phasic" extraction method, the pigments are immediately transferred into the nonpolar phase after having been detached from the chloroplasts by the polar phase. Thus, little or no transformation can occur during the extraction procedure.

The formation of alkoxy-lactone derivatives from the chlorophylls was observed to depend sensitively upon the polarity of the fractionation solvent system. This observation can be satisfactorily explained by the reaction scheme presented in Fig. 5. According to this scheme, the first step in the reaction sequence of allomerization is keto-enol tautomerism (reaction 1). Solvents such as aliphatic hydrocarbons, carbon tetrachloride, and water, which cause the chlorophylls to occur in an aggregated state,[5,27–32] preclude the possibility of enolization. In electron donor solvents (ethyl ether, acetone, pyridine, dioxane, tetrahydrofuran, alcohols, *etc.*), however, the chlorophylls occur as monomers and will therefore undergo keto-enol tautomerization. The extent to which enolization occurs in these solvents is, however, sensitive to the particular properties of the solvent concerned. Thus, in some solvents (*viz.* the ethers), the free enol form (II) is not further transformed. In this case, the chlorophylls in all probability exist predominantly as the all-keto form.[33] In solvents possessing relatively weak hydrogen bonding capabilities (pyridine, tetrahydrofuran, petroleum ether containing a small amount of propanol), the free enol can be transformed into the chelated enol (III),[34] which may then be stabilized by additional resonance (IV). In such a case, the total concentration of the enol form may be appreciable. In polar solvents

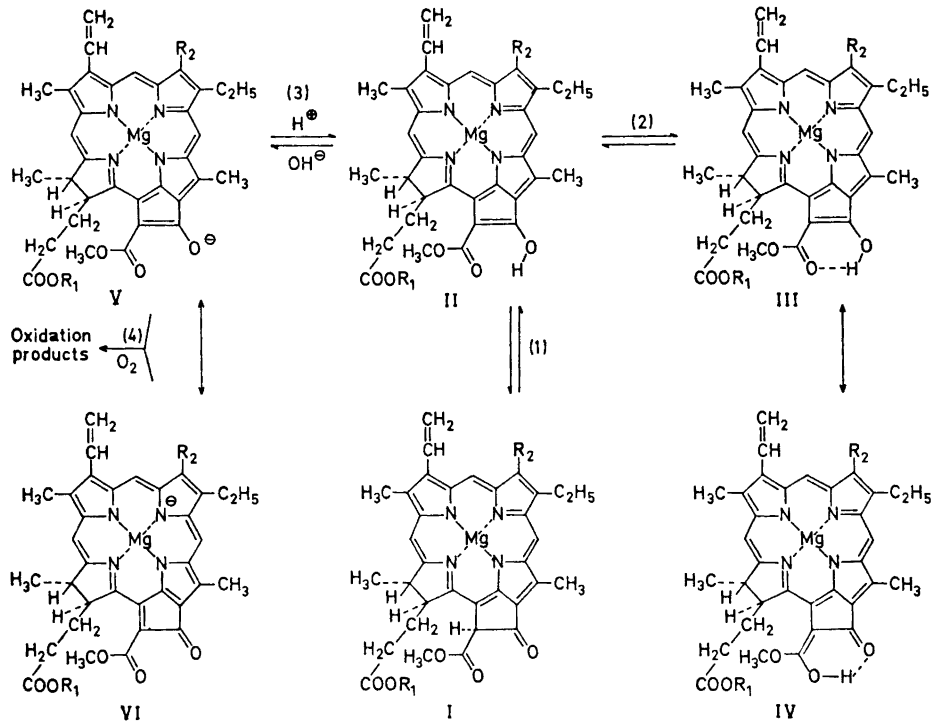

Fig. 5. Probable reactions of the chlorophylls. R_1 = phytyl; in chlorophyll *a*, R_2 = methyl, and in chlorophyll *b*, R_2 = formyl.

(Lewis bases: OH^-, OCH_3^-, *etc.*), the free enol is probably ionized to the enolate anion (V). This anion has been assumed to be the intermediate in the Molisch phase test and in the allomerization of the chlorophylls.[25,35–38] The enolate anion is unstable, being rapidly attacked by oxygen to yield various oxidation products whose nature depends upon the solvent.

The drastic colour change that occurs upon formation of the enolate anion during the phase test has been tentatively explained by assuming [39] that the negative charge becomes principally centred upon the pyrrolenine nitrogen atom, as is illustrated in Fig. 5 (VI). This assumption is based upon the research of Woodward and Scaric,[40] who observed that the pyrrolenine nitrogen atom tends to attract electrons. A second possible explanation to the change of colour upon formation of the enolate is obtained on assuming that the anion forms a diradical.[38] This alternative appears to explain satisfactorily the instability of the intermediate in the presence of oxygen. It also agrees with the fact that measured spectra of the phase test intermediate exhibit strong absorption bands at 500 – 550 nm which disappear in the presence of oxygen.[25,38]

The slow formation of the alkoxy-lactone derivative during fractionation suggests that reactions 1 and 3 are the rate-limiting steps in the reaction sequence of allomerization. This proposition is also in accord with the fact that no drastic colour change can be observed when allomerization occurs. Under conditions promoting allomerization, either reaction 1 or reaction 3 (or both) is slower than reaction 4. Thus, the unstable enolate anion is oxidized as soon as it is formed. Under the conditions prevalent during a positive phase test, however, the enolate is in all probability produced more rapidly than consumed.

Strain [23] has presented evidence to the effect that hydroxy-chlorophylls are produced enzymatically during the extraction of the pigments from leaves. The results obtained in this laboratory are in agreement with this viewpoint. The mechanism of the enzymatic allomerization may be quite different from that of the nonenzymatic.

The spectroscopic properties of the pure chlorophylls have long been a matter of much debate and controversy. An important criterion regarding the purity of a chlorophyll preparation has been the ratio of the absorbance at the Soret band wavelength to that at the chlorin band wavelength (A_S/A_I). Anderson and Calvin [10] (refer also to Aronoff [41]) obtained a ratio of 1.19 for chlorophyll *a* and claimed that the purity of this compound when isolated by chromatography on columns of powdered polyethylene was superior to that when prepared by other means. The purest chlorophyll *a* preparations obtained in this laboratory had a ratio of 1.32, which agrees very well with the generally accepted value of 1.31 – 1.32.[3,4,8,42,43] Moreover, the A_S/A_I ratio of 2.88 obtained for the purest chlorophyll *b* preparation agrees quite well with values (2.82 – 3.01) reported in the literature.[3,4,8]

The final isolation method resulted in a good yield of chlorophyll *a* (80 mg/100 g frozen soybean leaves).[1,10] The yield with regard to chlorophyll *b* (8 mg/100 g frozen soybean leaves) is low, but can easily be increased by adding water to the phase system in Method 3, before the phases are separated. A second possible way of obtaining higher yields of chlorophyll *b* is to utilize a greater number of fractionation tubes, thereby achieving better resolution of

10-hydroxy-chlorophyll *a* and chlorophyll *b*. In such a case, however, it is apparently important to increase the flow rate so that the chlorophyll *b* will be completely eluted from the apparatus within about 24 h. If this time limit is exceeded appreciably, then some lactonization of the chlorophyll *b* may occur during fractionation.

Acknowledgement. This investigation was supported by grants to one of us (N.E.) from the *Finnish National Research Council for Sciences*, which is gratefully acknowledged.

REFERENCES

1. Strain, H. H. and Svec, W. A. In Vernon, L. P. and Seely, G. R., Eds., *The Chlorophylls*, Academic, New York – London 1966, p. 21.
2. Mackinney, G. *J. Biol. Chem.* **132** (1940) 91.
3. Zeile, F. P. and Comar, C. L. *Botan. Gaz.* **102** (1941) 463.
4. Smith, J. H. C. and Benitez, A. In Paech, K. and Tracey, M. V., Eds., *Modern Methods of Plant Analysis*, Springer Berlin – Göttingen – Heidelberg 1955, Vol. IV, p. 142.
5. Jacobs, E. E., Vatter, A. E. and Holt, A. S. *Arch. Biochem. Biophys.* **53** (1954) 228.
6. Stoll, A. and Wiedemann, E. *Helv. Chim. Acta* **42** (1959) 679.
7. Strain, H. H., Thomas, M. R., Crespi, H. L., Blake, M. I. and Katz, J. J. *Ann. N. Y. Acad. Sci.* **84** (1960) 617.
8. Strain, H. H., Thomas, M. R. and Katz, J. J. *Biochim. Biophys. Acta* **75** (1963) 306.
9. Kutyurin, V. M., Ulubekova, M. V. and Artamkina, I. Yu. *Fiziol. Rast.* **9** (1962) 115.
10. Anderson, A. F. H. and Calvin, M. *Nature* **194** (1962) 285.
11. Brody, S. S. and Broyde, S. B. *Nature* **199** (1963) 1097.
12. Broyde, S. B. and Brody, S. S. *Biochem. Biophys. Res. Commun.* **19** (1965) 444.
13. Willstätter, R. and Isler, M. *Ann. Chem.* **390** (1912) 269.
14. Willstätter, R. and Stoll, A. *Untersuchungen über Chlorophyll*, Springer Berlin 1913.
15. Lancaster, C. R., Lancaster, E. B. and Dutton, H. J. *J. Am. Oil. Chemists' Soc.* **27** (1950) 386.
16. Coniglio, J. G. and Wolf, F. T. *Phyton (Buenos Aires)* **17** (1961) 189.
17. Metzner, H. and Struss, S. *Z. Naturforsch.* **B 18** (1963) 707.
18. Arn, H., Grob, E. C. and Signer, R. *Helv. Chim. Acta* **49** (1966) 851.
19. Hietala, P. *Ann. Acad. Sci. Fennicae, Ser. A II* **100** (1960).
20. Ellfolk, N., Hynninen, P. and Sievers, G. *Acta Chem. Scand.* **23** (1969) 846.
21. Verhoek, F. H. *J. Am. Chem. Soc.* **58** (1936) 2577.
22. Eistert, B. In *Newer Methods of Preparative Organic Chemistry*, Interscience, New York 1948, p. 513.
23. Strain, H. H. *Agr. Food Chem.* **2** (1954) 1222.
24. Pennington, F. C., Strain, H. H., Svec, W. A. and Katz, J. J. *J. Am. Chem. Soc.* **89** (1967) 3875.
25. Holt, A. S. *Can. J. Biochem. Physiol.* **36** (1958) 439.
26. Hynninen, P. H. and Assandri, S. *Acta Chem. Scand.* **27** (1973). *In press.*
27. Jacobs, E. E. and Holt, A. S. *J. Chem. Phys.* **22** (1954) 142.
28. Anderson, A. F. H. and Calvin, M. *Arch. Biochem. Biophys.* **107** (1964) 251.
29. Sherman, G. and Wang, S. F. *Nature* **212** (1966) 588.
30. Katz, J. J., Closs, G. L., Pennington, F. C., Thomas, M. R. and Strain, H. H. *J. Am. Chem. Soc.* **85** (1963) 3801.
31. Sauer, K., Smith, J. R. L. and Schultz, A. J. *J. Am. Chem. Soc.* **88** (1966) 2681.
32. Ballschmiter, K. and Katz, J. J. *J. Am. Chem. Soc.* **91** (1969) 2661.
33. Katz, J. J., Dougherty, R. C. and Boucher, L. J. In Vernon, L. P. and Seely, G. R., Eds., *The Chlorophylls*, Academic, New York – London 1966, p. 185.
34. Hynninen, P. H. *Acta Chem. Scand.* **27** (1973). 1487.
35. Fischer, H. and Oestreicher, A. *Ann. Chem.* **546** (1941) 49.
36. Fischer, H. and Pfeiffer, H. *Ann. Chem.* **555** (1944) 94.

37. Fischer, H. and Orth, H. *Die Chemie des Pyrrols*, Akad. Verlag, Leipzig 1940, Vol. II/2, p. 26.
38. Weller, A. *J. Am. Chem. Soc.* **76** (1954) 5819.
39. Seely, G. R. In Vernon, L. P. and Seely, G. R., Eds., *The Chlorophylls*, Academic, New York–London 1966, p. 87.
40. Woodward, R. B. and Scaric, J. *J. Am. Chem. Soc.* **83** (1961) 4676.
41. Aronoff, S. *Biochim. Biophys. Acta* **60** (1962) 193.
42. Perkins, H. J. and Roberts, D. W. A. *Biochim. Biophys. Acta* **79** (1964) 20.
43. Seely, G. R. and Jensen, R. G. *Spectrochim. Acta* **21** (1965) 1835.

Received November 28, 1972.

ACTA CHEMICA SCANDINAVICA 27 (1973) 1478–1486

Chlorophylls

II. Allomerization of Chlorophylls *a* and *b*

PAAVO H. HYNNINEN and SANDRO ASSANDRI*

Department of Biochemistry, University of Helsinki, SF-00170 Helsinki 17, Finland

Chloroplast pigments, obtained by extracting dry leaf powder with pyridine, were separated by multiple liquid-liquid partition using 70 fractionation tubes and employing petroleum ether-ethanol-formamide (PEF) as the solvent system. The longer the extraction time with pyridine, the more completely was chlorophyll *a* converted into a 10-ethoxy-lactone derivative. This observation was interpreted as supporting the concept, presented in Part I of this series, that allomerization of the chlorophylls is initiated by enolization.

The allomerization products of chlorophylls *a* and *b* in methanol were fractionated by multiple liquid-liquid partition utilizing 50 tubes and employing petroleum ether-benzene-methanol-formamide (PBMF) as the solvent system. The two chief products of chlorophyll *a* were a 10-methoxy-lactone derivative and 10-hydroxy-chlorophyll *a*. In addition to these, four minor components were detected: Mg-unstable chlorin methylphytyl ester, Mg-purpurin 7-(di)methylphytyl ester, Mg-chlorin e_6-dimethylphytyl ester and 10-methoxy-chlorophyll *a*. Evidence was presented demonstrating that chlorophyll *a* preparations isolated by means of conventional methods may be contaminated by the Mg-purpurin 7-triester. The principal allomerization product of chlorophyll *b* was a 10-methoxy-lactone derivative. The concentration profile of the fractionation revealed that this derivative was in slow equilibrium with another component, presumed to be Mg-*b*-purpurin 7-(di)methylphytyl ester. Mg-unstable rhodin methylphytyl ester was a third product of the *b*-series.

A reaction scheme for the allomerization of the chlorophylls was proposed. In addition, the formation of the 10-hydroxy- and 10-methoxy-chlorophylls, which were not included in the scheme, was briefly discussed.

In a previous investigation [1] concerning the fractionation of chlorophylls employing three different types of solvent system, the formation of the 10-alkoxy-lactone derivative from chlorophyll *a* during fractionation was observed to depend in a sensitive manner upon the polarity of the lower phase of the solvent system. When either petroleum ether-ethanol-formamide

* Present address: Via P. Finzi 15, 20126 Milan, Italy.

(PEF) or petroleum ether-benzene-methanol-formamide (PBMF) was employed as the solvent system, the alkoxy-lactone derivative did not form; in petroleum ether-methanol-formamide (PMF), however, such formation could not be avoided. This observation was interpreted as signifying that allomerization is preceded by enolization.

In the present article, further evidence will be forwarded in support of the reaction scheme previously presented by one of the authors.[1] This evidence derives from two fractionations in which pyridine was employed in the extraction of the pigments from the plant material. In addition, the allomerization products of chlorophylls *a* and *b* were separated by means of multiple liquid-liquid partition. The results of these studies will be compared with earlier investigations.[2–21]

EXPERIMENTAL

Extraction of the pigments from plant material. Extract 1. Five grams of dry powder prepared from soybean leaves were suspended in 250 ml of pyridine and the mixture was vigorously stirred manually. After 10 min, the suspension was filtered and the filtrate evaporated to dryness by means of a rotatory evaporator. The remaining residue was then dissolved in 10 ml of petroleum ether.

Extract 2. This extract was prepared in the same manner as Extract 1, except that the mixture was stirred by means of a magnetic stirrer for 1 h, rather than being stirred manually for 10 min.

Preparation of allomerized chlorophyll. Fifty milligrams of chlorophyll *a* (7 mg of chlorophyll *b*), isolated by multiple liquid-liquid partition,[1] were dissolved in 25 ml of methanol. The solution was then allowed to stand for 7 days in an Erlenmeyer flask provided with a loose glass stopper. At the conclusion of this time, the solution was evaporated to dryness and the residue dissolved in 15 ml of petroleum ether.

Preparation of some phyllin derivatives. Magnesium-free phyllin derivatives were prepared by treating a solution of the phyllin with 13 % hydrochloric acid. The phytyl group was removed by hydrolysis of the ester in 30 % hydrochloric acid. Methyl esters of the phyllins or their magnesium-free derivatives were prepared by means of diazomethane. The ethereal solution of diazomethane was prepared from nitrosomethylurea by saponification, as described by Eistert.[22] The magnesium-free derivatives were purified by partition between aqueous hydrochloric acid and diethyl ether.[3,23,24]

Equipment and solvents. Separations by multiple liquid-liquid partition were performed by means of the Hietala apparatus. Operating conditions were, in general, similar to those described previously.[1]

The PEF- and PBMF-solvent systems were prepared as earlier described.[1] The other solvents employed were of reagent grade and were used as commercially supplied.

A Cary Spectrophotometer Model 15 was utilized to record the absorption spectra and a Beckman DU Spectrophotometer to measure single absorbances.

RESULTS AND DISCUSSION

The results of the distribution experiment performed on Extract 1 are presented in Fig. 1. PEF was employed as solvent system for this fractionation. The concentration profile of chlorophyll *a* revealed that a reaction of some type had occurred during fractionation. Judging upon the basis of spectroscopic and chemical characteristics, the deeply blue-green product D appeared to be Mg-purpurin 7-lactone-ethyl ether-methylphytyl ester (a 10-ethoxy-lactone derivative of chlorophyll *a*). These properties closely resembled those of Mg-purpurin 7-lactone-methyl ether-diester, which had been previ-

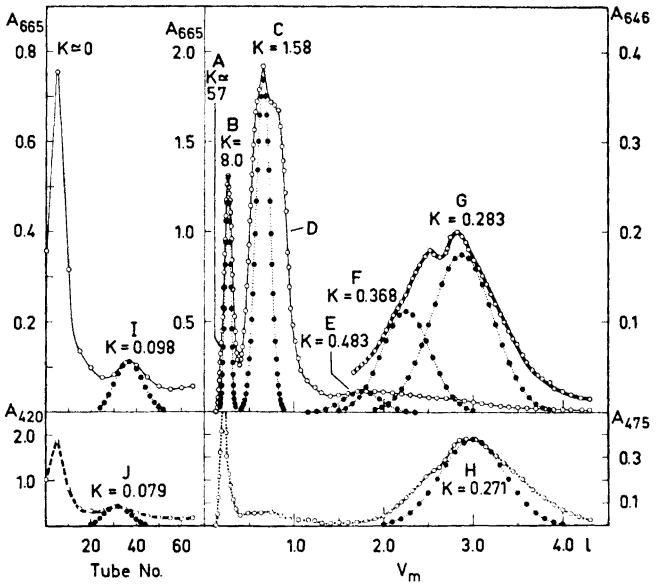

Fig. 1. Separation of chloroplast pigments employing Extract 1 and the PEF-system. The extract was sampled into tubes r = 0,..,3. Number of fractionation tubes utilized = $N = 70$. Average volume of the mobile phase in a partition unit = $v_m = 2.39$ ml; average volume of the stationary phase in a partition unit = $v_s = 11.11$ ml. Total volume of effluent eluted from the apparatus = $V_m = 4307$ ml; flow rate = 2 ml/min. Theoretical (●) and experimental (○) values, the latter obtained by measuring the absorbances of the effluent fractions or of the lower phases in the tubes: — = A_{665}, ▬ = A_{646}, ··· = A_{475}, and ▪▪ = A_{420}. A = β-carotene, B = pheophytin *a*, C = chlorophyll *a*, D = Mg-purpurin 7-lactone-ethyl ether-methylphytyl ester, E = 10-hydroxy-chlorophyll *a*, F = chlorophyll *b*, G = Mg-*b*-purpurin 7-lactone-ethyl ether-methylphytyl ester, H = lutein, I = 10-hydroxy-chlorophyll *b*, J = violaxanthin, and K = chlorophyllide, *etc.*

ously characterized as the allomerization product of chlorophyll *a* when the PMF-system was utilized.[1] The material eluted at 2200 ml yielded a positive reaction to the Molisch phase test, whereas that eluted at 3000 ml appeared to react negatively. Components F and G were characterized, respectively, as chlorophyll *b* and Mg-*b*-purpurin 7-lactone-ethyl ether-methylphytyl ester (a 10-ethoxy-lactone derivative of chlorophyll *b*). The spectroscopic and chemical properties of the latter compound closely resembled those of the 10-alkoxy-lactone derivative found previously.[1] Only relatively small amounts of the 10-hydroxy-chlorophylls (components E and I) were detectable in the present case and these probably did not form during the fractionation. It appears more likely that they arose during extraction of the pigments from the plant material or during drying of the soybean leaves.

Since the lactonization of chlorophyll *a* did not occur in the PEF-system when the pigments had been extracted from the frozen soybean leaves with either 80 % acetone or petroleum ether(3)-methanol(1),[1] it was therefore concluded that some reaction preceding lactonization had taken place in the

pyridine. In order to test the validity of this conclusion, a partition fractionation was performed on Extract 2. In this instance, the pyridine extraction was carried out for a considerably longer time than in the preparation of Extract 1. The resulting concentration profile revealed that chlorophyll *a* had now been transformed almost completely to the 10-alkoxy-lactone derivative (Fig. 2). Considering the fact that Extracts 1 and 2 both yielded clearly positive reactions to the Molisch phase test, the results described may best be interpreted by assuming that enolization proceeds with considerable velocity in pyridine and that it is this reaction which precedes the formation of the alkoxy-lactone derivative. These results appear to support strongly the reaction scheme previously presented for the allomerization.[1]

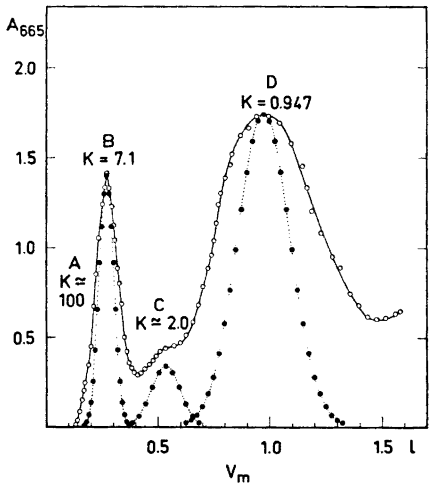

Fig. 2. Separation of chloroplast pigments employing Extract 2 and the PEF-system. The extract was sampled into tubes r = 0,..,3. $N = 70$. $v_m = 2.36$ ml; $v_s = 11.14$ ml. $V_m = 1580$ ml; flow rate = 2 ml/min. Theoretical (●) and experimental (O) values, the latter obtained by measuring A_{665} of the effluent fractions. A = β-carotene, B = pheophytin *a*, C = chlorophyll *a*, and D = Mg-purpurin 7-lactone-ethyl ether-methylphytyl ester.

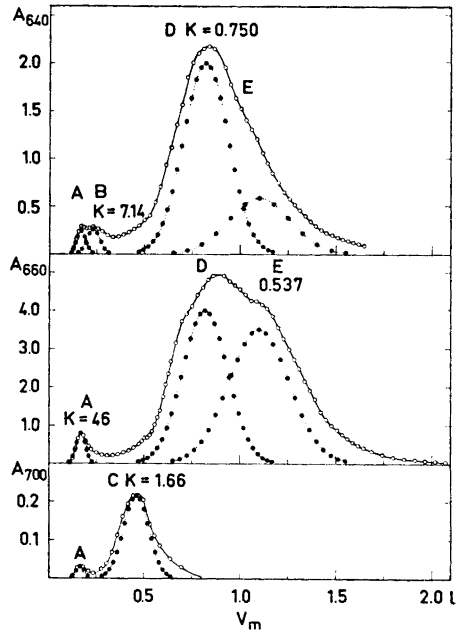

Fig. 3. Separation of the allomerization products of chlorophyll *a* employing the PBMF-system. The petroleum ether solution of the allomerization products of chlorophyll *a* was sampled into tubes r = 0,..,2. $N = 50$. $v_m = 3.14$ ml; $v_s = 10.36$ ml. $Vm = 2100$ ml; flow rate = 2 ml/min.. Theoretical (●) and experimental (O) values, the latter obtained by measuring the absorbances of the effluent fractions at three different wavelengths. A = 10-methoxy-chlorophyll *a*, B = Mg-chlorin e_6-dimethylphytyl ester, C = Mg-purpurin 7-(di)methylphytyl ester, D = Mg-purpurin 7-lactone-methyl ether-methylphytyl ester, and E = 10-hydroxy-chlorophyll *a*.

Fig. 3 presents the results obtained from the fractionation performed on the allomerization products of chlorophyll *a* in methanol. The components of the allomerization mixture were separated by means of the PBMF-system utilizing 50 fractionation tubes. This solvent system was selected in order to avoid the occurrence of further allomerization in the apparatus due to the possible presence of intact chlorophyll in the mixture. Five components were spectroscopically detected in the effluent series. The primary allomerization products of chlorophyll *a* were components D and E. Component D was spectroscopically and chemically very similar to the D of Fig. 2 and, therefore, undoubtedly represents Mg-purpurin 7-lactone-methyl ether-methylphytyl ester. Component E exhibited the properties of 10-hydroxy-chlorophyll *a*.[1]

The minor component A revealed, in diethyl ether, absorption maxima at 429 and 661 nm. When the ethereal solution of A was treated with 30 % hydrochloric acid, a product was formed which reacted negatively to the phase test, had a hydrochloric acid number greater than 15 and resembled pheophorbide *a* according to its visible absorption spectrum (maxima, in diethyl ether, at 667, 609, 560, 537, 504, and 408 nm).[25] These characteristics indicate that component A probably represents 10-methoxy-chlorophyll *a*.

The fractions eluted within the interval 200 – 300 ml exhibited an absorption peak at approximately 640 nm. This was interpreted as indicating a small amount of Mg-chlorin e_6-dimethylphytyl ester (component B).[20] The presence of this compound was ascertained by isolating the magnesium- and phytyl-free derivative from two fractions eluted at about 250 ml. This isolation was effected by first treating the ethereal solution of the pigments from the fractions with 30 % hydrochloric acid. The pigments were then transferred into fresh ether by adding water to the acid phase. The pigment that was extracted from the ether solution into 5 % hydrochloric acid closely resembled chlorin e_6 according to its visible absorption spectrum (maxima, in diethyl ether, at 666, 609, 560, 529, 499, and 400 nm).[25]

Component C was characterized as Mg-purpurin 7-(di)methylphytyl ester upon the basis of the following properties: first, the visible absorption spectrum of C was quite similar to that of Mg-purpurin 7-triester, which Holt [20] has identified as being an allomerization product of methylchlorophyllide *a* in methanol; second, the magnesium-free derivative of C exhibited absorption maxima, in diethyl ether, at 680, 635, 542, 504, and 406 nm;[26] and third, the treatment of an ethereal solution of C with 25 % potassium hydroxide in propanol resulted in the formation of Mg-unstable chlorin.[11,24]

One additional pigment was also characterized as being among the allomerization products of chlorophyll *a*. This component (F) remained at the sampling end of the apparatus ($r_{max} = 4$, not indicated in Fig. 3), had a partition coefficient (K_F) equalling 0.024 and closely resembled the 10-methoxy-lactone derivative (D) according to its visible absorption spectrum.[1] When an ethereal solution of F was treated with diazomethane, the resulting product was Mg-purpurin 7-triester.[28] Upon the basis of these properties, F was characterized as representing Mg-unstable chlorin-methylphytyl ester.

The results obtained from the fractionation performed on the allomerization products of chlorophyll *b* in methanol are presented in Fig. 4. The principal allomerization product (D) was in this case also a 10-methoxy-lactone deriva-

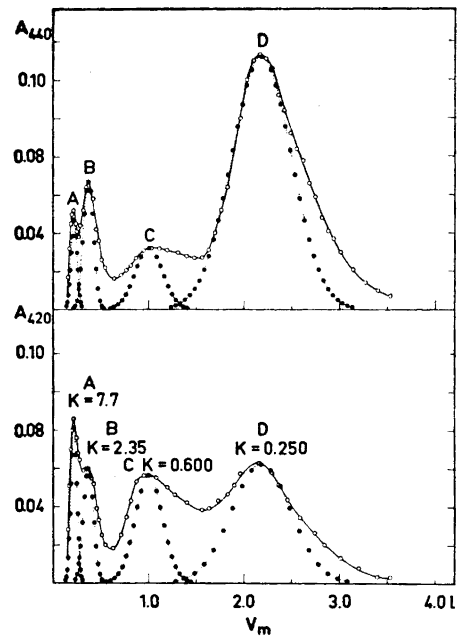

Fig. 4. Separation of the allomerization products of chlorophyll *b* employing the PBMF-system. The petroleum ether solution of the allomerization products of chlorophyll *b* was sampled into tubes r = 0,...,2. $N = 50$. $v_m = 3.14$ ml; $v_s = 10.36$ ml. $V_m = 2180$ ml; flow rate = 2 ml/min. Theoretical (●) and experimental (○) values, the latter obtained by measuring the absorbances of the effluent fractions at two different wavelengths. A and B = magnesium-free pigments, C = Mg-*b*-purpurin 7-(di)methylphytyl ester, and D = Mg-*b*-purpurin 7-lactone-methyl ether-methylphytyl ester.

tive (Mg-*b*-purpurin 7-lactone-methyl ether-methylphytyl ester), being spectroscopically and chemically very similar to the alkoxy-lactone derivative of chlorophyll *b* described earlier.[1] Component C exhibited the red band (I) at 645 nm and the Soret band (S) at 422 nm and yielded an A_S/A_I ratio of 2.96. Based upon the concentration profile presented in Fig. 4, it may be deduced that a slow equilibrium has existed between components C and D. The interchangeability of these components was also demonstrated by the fact that, upon standing in the effluent, C converted to D. These characteristics appear to indicate that fraction C consisted of Mg-*b*-purpurin 7-(di)methylphytyl ester. Components A and B, apparently magnesium-free pigments, were not further studied due to their incomplete resolution and small amounts.

One additional component (E) also remained at the sampling end of the apparatus in the fractionation performed on the allomerization products of chlorophyll *b*. This component was spectroscopically similar to Mg-*b*-purpurin 7-lactone-methyl ether-methylphytyl ester and was identified as Mg-unstable rhodin methylphytyl ester, a result analogous to that obtained in the *a*-series. No hydroxy-chlorophyll *b* was detectable in the *b*-series. Furthermore, neither Mg-rhodin g_7-triester nor 10-methoxy-chlorophyll *b* were identified among the allomerization products of chlorophyll *b*. Small amounts of these latter compounds, if present, may well have been obscured by the magnesium-free pigments.

The results of the fractionations presented in Figs. 3 and 4 reveal the utmost importance of avoiding allomerization during the extraction of the pigments from plant material. Preparations of isolated chlorophyll are other-

wise liable to become contaminated by small amounts of impurities, which have been observed as minor allomerization products in the above fractionations. For example, chlorophyll *a* may become contaminated by component C of Fig. 3. The separation of this component ($K_C = 1.66$) from chlorophyll *a*, which has a partition coefficient of 2.83 [1] in the same solvent system, would be difficult. Brody and Broyde [27,28] found small amounts of a chlorophyll derivative in chlorophyll *a* isolated by means of conventional chromatographic methods. This impurity could be separated from the chlorophyll *a* by washing with petroleum ether, since the derivative had a higher solubility in nonpolar solvents. Brody and Broyde have suggested that this pigment could be a form of chlorophyll *a* which is reactive in photosynthesis. The present authors believe, however, that this pigment is actually an allomerization product of chlorophyll. Evidence for this belief derives from the fact that the difference spectrum presented by Broyde and Brody [28] for the pigment referred to as F 698 is remarkably similar to the absorption spectrum of Mg-purpurin 7-triester (component C of Fig. 3). This similarity concerns not only the positions of the Soret band and band I (at approximately 420 and 670 nm, respectively), but extends also to the ratio of their peak heights. A ratio of 2.6 is obtained from the spectrum given by Broyde and Brody, whereas the corresponding ratio as determined by the present authors is 2.7.

Fischer and Pfeiffer [12] identified Mg-purpurin 7-lactone-ethyl ether-diester as a product of the allomerization of ethylchlorophyllide *a* in ethanol. According to the mechanism postulated by the above authors, the C-10 carbon atom is first attacked by oxygen, thus resulting in the formation of a hydroperoxide at the C-10 position. This causes the isocyclic ring to become labile, and the ring is thereafter split hydrolytically. A free carboxyl group is then introduced at C-6 and simultaneously a disproportionation of the oxygens at C-10 occurs. Subsequently, one of the newly-formed hydroxyl groups at C-10 reacts with the solvent to form the ether, while the other hydroxyl group at C-10 reacts with the C-6 carboxyl group and produces the lactone bridge.

The results obtained in this laboratory do not support the above mechanism proposed by Fischer and Pfeiffer for the formation of the lactone derivative. The present authors propose the mechanism illustrated in Fig. 5 for the formation of Mg-purpurin 7-lactone-alkyl ether-diester (V), Mg-purpurin 7-triester (X) and Mg-unstable chlorin-diester (VII). According to this reaction scheme, chlorophyll (I) is first enolized. Due to the double bond formed between C-9 and C-10, the enolate ion (II) is labile and the double bond undergoes oxygen cleavage, thus resulting in the formation of Mg-purpurin 7-monomethylphytyl ester (III). The instability of this compound arises from the activation of C-10 by the methoxycarbonyl group (the authors are not aware of compound III having been either isolated or synthesized [24]). This component is rapidly solvated by methanol to give Mg-purpurin 7-lactone-methyl ether-methylphytyl ester (V), with IV as a possible intermediate. In the presence of water or hydroxyl ions, however, compound III yields Mg-unstable chlorin-monomethylphytyl ester (VII), with VI as a possible intermediate. Purpurin 18 (IX) may be obtained from VII by hydrolysis (yielding VIII), followed by the splitting-off of formic acid. As a third possibility, compound III can be esterified, thus resulting in the formation of the Mg-purpurin 7-triester (X).

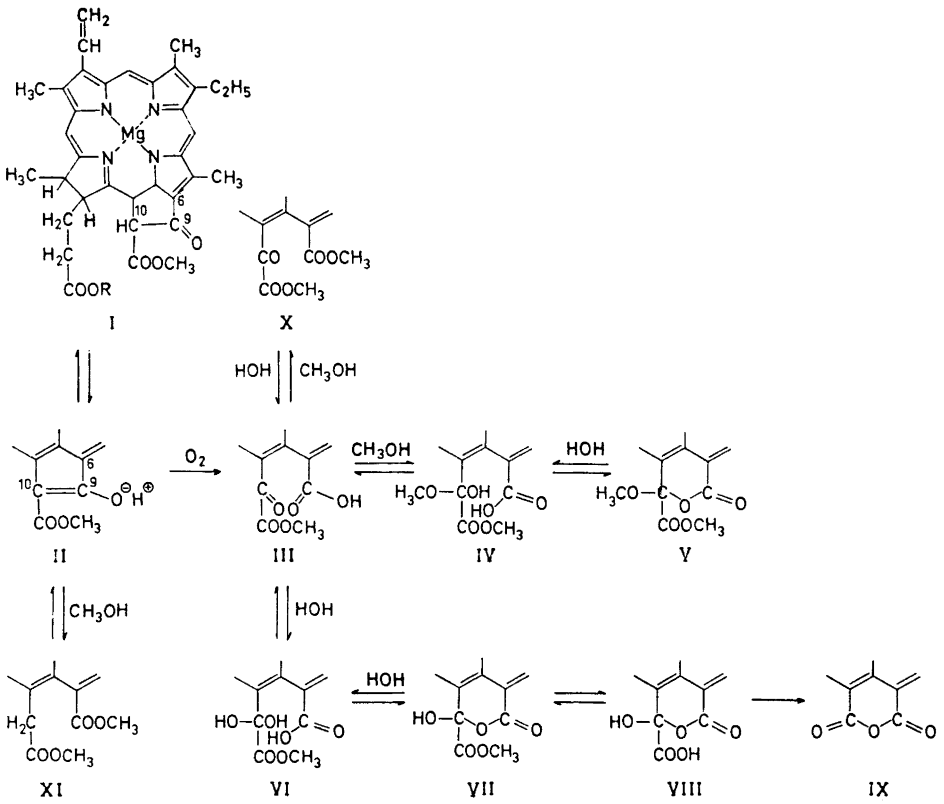

Fig. 5. Proposed mechanism for the allomerization of chlorophyll *a*. R = phytyl.

A reaction competing with the oxidation of the enolate ion (II) is that of methanolysis,[29] which yields the Mg-chlorin e_6-triester (XI). It should be noted, however, that such methanolysis is reversible, while the oxidation is irreversible.

The reaction scheme presented in Fig. 5 is in general agreement with the studies of Holt [20] and of Conant *et al.*[3,4] Holt concluded that the formation of the 10-alkoxy-lactone derivative in alcohols involves the oxidation of trace amounts of phase test intermediate, which was assumed to be the enolate anion. Conant *et al.* characterized unstable chlorin and its monomethyl ester as the allomerization products of pheophorbide *a* in the presence of hydroxide. Upon standing, these compounds were reported to yield purpurin 18 and purpurin 7-trimethyl ester. When esterified with diazomethane, both unstable chlorin and its monomethyl ester were converted into purpurin 7-trimethyl ester.

Fig. 5 does not account for the formation of the 10-hydroxy- and 10-methoxy-chlorophylls. No clear conclusions can be drawn, upon the basis of the results presented above, regarding the mechanism of the formation of these

allomerization products. However, it appears likely that, in the light of these results and of those previously reported,[1] the 10-hydroxy-chlorophylls are formed independently of the allomerization products illustrated in Fig. 5. Evidently, the formation of 10-hydroxy- or 10-methoxy-chlorophylls does not require enolization as a preliminary step. They may well arise directly through the action of hydroxyl or methoxyl ions upon the C-10 atom of chlorophyll. Earlier investigations [7,12,15,17,20] in which quinone, potassium permanganate or iodine were utilized as the oxidizing agent, rather than oxygen, suggest a second possible mechanism: The proton at C-10 is first abstracted by base (OH^-, OCH_3^-, *etc.*) to give a carbanion, which is subsequently oxidized by the oxidant (quinone, I_2, $KMnO_4$, O_2, *etc.*), thus yielding a carbonium ion. This carbonium ion thereafter reacts rapidly with either methoxyl or hydroxyl ions to produce, respectively, 10-methoxy- or 10-hydroxy-chlorophyll.

REFERENCES

1. Hynninen, P. H. and Ellfolk, N. *Acta Chem. Scand.* **27** (1973) 1463.
2. Seely, G. R. In Vernon, L. P. and Seely, G. R., Eds., *The Chlorophylls*, Academic, New York–London 1966, p. 91.
3. Conant, J. B. and Moyer, W. W. *J. Am. Chem. Soc.* **52** (1930) 3013.
4. Conant, J. B., Hyde, J. F., Moyer, W. W. and Dietz, E. M. *J. Am. Chem. Soc.* **53** (1931) 359.
5. Fischer, H. and Riedmair, J. *Ann. Chem.* **506** (1933) 107.
6. Fischer, H. and Hagert, W. *Ann. Chem.* **502** (1933) 41.
7. Fischer, H. and Heckmaier, J. *Ann. Chem.* **508** (1934) 250.
8. Fischer, H., Heckmaier, J. and Hagert, W. *Ann. Chem.* **505** (1933) 209.
9. Fischer, H. and Kahr, K. *Ann. Chem.* **531** (1937) 209.
10. Fischer, H. and Scherer, T. *Ann. Chem.* **519** (1935) 234.
11. Fischer, H., Süs, O. and Klebs, G. *Ann. Chem.* **490** (1931) 38.
12. Fischer, H. and Pfeiffer, H. *Ann. Chem.* **555** (1944) 94.
13. Fischer, H. and Spiegelberger, G. *Ann. Chem.* **510** (1934) 156.
14. Fischer, H. and Spiegelberger, G. *Ann. Chem.* **515** (1935) 130.
15. Fischer, H., Filser, L. and Plötz, E. *Ann. Chem.* **495** (1932) 1.
16. Fischer, H., Heckmaier, J. and Scherer, T. *Ann. Chem.* **510** (1934) 169.
17. Strell, M. *Ann. Chem.* **550** (1942) 50.
18. Strain, H. H. *Agr. Food Chem.* **2** (1954) 1222.
19. Johnston, L. G. and Watson, W. F. *J. Chem. Soc.* **1956** 1203.
20. Holt, A. S. *Can. J. Biochem. Physiol.* **36** (1958) 439.
21. Pennington, F. C., Strain, H. H., Svec, W. A. and Katz, J. J. *J. Am. Chem. Soc.* **89** (1967) 3875.
22. Eistert, B. In *Newer Methods of Preparative Organic Chemistry*, Interscience, New York 1948, p. 513.
23. Willstätter, R. and Mieg, W. *Ann. Chem.* **350** (1906) 1.
24. Fischer, H. and Stern, A. *Die Chemie des Pyrrols*, Akad. Verlag. Leipzig 1940, Vol. II/2.
25. Stern, A. and Wenderlein, H. *Z. physik. Chem. (Leipzig)* **A 174** (1935) 81.
26. Stern, A. and Pruckner, F. *Z. physik. Chem. (Leipzig)* **A 180** (1937) 321.
27. Brody, S. S. and Broyde, S. B. *Nature* **199** (1963) 1097.
28. Broyde, S. B. and Brody, S. S. *Biochem. Biophys. Res. Commun.* **19** (1965) 444.
29. Fischer, H. and Oestreicher, A. *Ann. Chem.* **546** (1940) 53.

Received November 28, 1972.

ACTA CHEMICA SCANDINAVICA 27 (1973) 1487–1495

Chlorophylls

III. Keto-Enol Tautomerism of Chlorophylls *a* and *b*. The Nature of Chlorophylls *a'* and *b'*

PAAVO H. HYNNINEN

Department of Biochemistry, University of Helsinki, SF-00170 Helsinki 17, Finland

Chlorophylls *a'* and *b'*, formed in pyridine solution, were separated from the principal chlorophyll zones by means of chromatography on sugar columns. Small amounts of pheophytinlike pigments, as well as various allomerization compounds, were also observed among the transformation products of the chlorophylls.

Chlorophyll *a'* was highly soluble in petroleum ether, differed distinctly from chlorophyll *a* in terms of its visible absorption spectrum and exhibited a strong tendency to form pheophytin *a*. Spectroscopically, chlorophyll *b'* differed only slightly from the primary chlorophyll *b* zone. Chlorophylls *a'* and *b'*, as well as their respective pheophytins, yielded positive reactions to the Molisch phase test and were converted into pheophorbides *a* and *b* upon treatment with 30 % hydrochloric acid.

Chlorophylls *a'* and *b'* were characterized as hydrogen chelates of the enol forms of chlorophylls *a* and *b*, respectively. In view of the evidence presented in the present article, the possibility that chlorophylls *a'* and *b'* are C-10 epimers of the chlorophylls appears unlikely. The spectroscopic differences between chlorophylls *a* and *a'* were attributed to the electron-withdrawing effect of the conjugated ring V in the enol form of chlorophyll. The fact that the visible absorption spectrum of chlorophyll *b'* differed only slightly from that of chlorophyll *b* was interpreted as being due to the electron-withdrawing effect of the formyl group, which tends to counteract the effect of ring V in the enol.

The transformation of chlorophylls *a* and *b* into, respectively, chlorophylls *a'* and *b'*, first observed by Strain and Manning,[1] has confounded chlorophyll researchers for approximately 30 years. Since chlorophylls *a* and *a'* had been found to be interconvertible as well as spectroscopically very similar and since chlorophylls *b* and *b'* had also been discovered to behave in like manner, the transformation between these paired compounds was assumed to be an isomeric reaction. Strain [2] presented the hypothesis that chlorophylls *a'* and *b'* are C-10 epimers of the ordinary chlorophylls. Katz and co-workers [3] inter-

preted their results, obtained by nuclear magnetic resonance (NMR), in favour of this hypothesis.

In previous publications [4,5] originating from the present laboratory, convincing evidence was forwarded in support of the concept that enolization is the initial step in the reaction sequence of the allomerization leading to the 10-alkoxy-lactone derivatives. Due to the fact that formation of the intermediate (enol) occurred readily in pyridine and that "isomerization" to chlorophylls *a'* and *b'* had also been reported to take place in pyridine or propanol,[1,3] it was thought that the *a'* and *b'* "isomers" could be identical with the chelated enol forms of the chlorophylls. The experimental results given in the present article strongly support this viewpoint.

EXPERIMENTAL

Preparation of chlorophylls a' and b'. Five milligrams of chlorophyll *a* (3.0 mg of chlorophyll *b*), isolated by the method previously described,[4] were dissolved in 5.0 ml of reagent grade pyridine and the solution was then allowed to stand overnight at room temperature and in the dark.

Chromatography on sugar columns. Conventional chromatographic procedures, as described by Strain and Svec,[6] were employed in separations of chlorophylls *a* and *a'* as well as *b* and *b'*. Icing sugar, containing 0.6 % calcium phosphate, was mixed with the eluent (petroleum ether, b.p. 60 – 80°C, containing 0.5 % propanol) to form a slurry, which was then poured into a glass column having an inside diameter of 3.0 cm and a height of 50 cm. The sugar particles were allowed to settle overnight. After standing, the sugar layer utilized in the separation of chlorophylls *a* and *a'* had a height of 26 cm, while that employed for separating chlorophylls *b* and *b'* was 22.5 cm.

The pyridine solution of chlorophyll, having stood overnight, was then evaporated nearly to dryness using a Thunberg tube at reduced pressure. The remaining residue was subsequently dissolved in 1.0 ml of the eluent and the resulting solution was immediately sampled into the top of the sugar column. The column was then eluted until the slower-moving principal chlorophyll zone had emerged. The absorbances of the collected fractions were measured at selected wavelengths by means of a Beckman DU spectrophotometer. The chromatographic separations were performed at a temperature of about + 4°C.

The absorption spectra of the components were determined utilizing a Cary Model 15 spectrophotometer. Measurements were performed directly upon the effluent after the components had emerged from the column as well as after they had been transferred into diethyl ether by means of a Thunberg tube at reduced pressure.

RESULTS

Fig. 1 presents the results of a typical separation of the products formed from chlorophyll *a* in pyridine. The more rapidly-moving component (B = chlorophyll *a'*) was easily separated from the principal component (C = chlorophyll *a*). The complete resolution of these components indicates the very slow equilibrium between them under the conditions prevalent during fractionation. Components B and C both yielded clearly positive reactions to the Molisch phase test, thus demonstrating that neither can be an allomerization product. The two chlorophylls differed distinctly, however, regarding their visible absorption spectra (Figs. 2 and 3; Table 1, b and c). Peak I of chlorophyll *a'* was located at a slightly longer wavelength than that of chlorophyll *a*. The primary differences, however, existed in the region of the Soret band and are clearly reflected in the values of the peak ratios as presented in Table 1. It may be

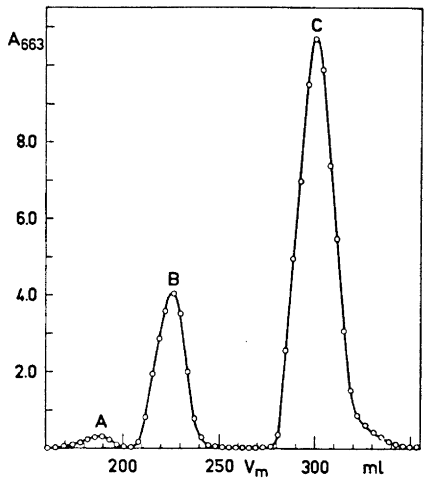

Fig. 1. Separation of chlorophylls *a* and *a'* employing chromatography on a sugar column. Experimental values (O) obtained by measuring A_{663} of the effluent fractions. *A* = pheophytin *a*, B = chlorophyll *a'*, and C = chlorophyll *a*.

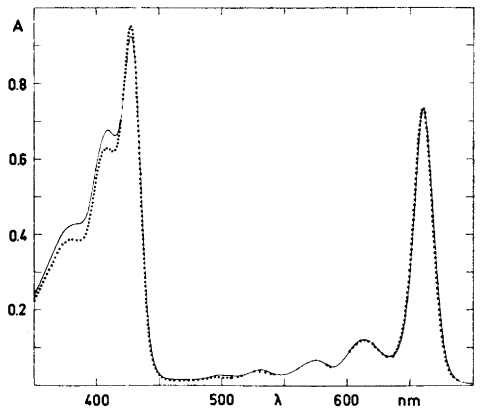

Fig. 2. Absorption spectra of chlorophylls *a'* (—) and *a* (···) in diethyl ether.

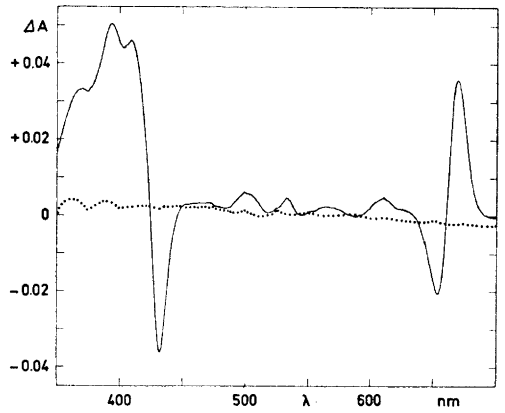

Fig. 3. Difference spectrum of chlorophylls *a'* and *a* in diethyl ether.

further observed that component C (Table 1, b) spectroscopically resembles very closely the original chlorophyll *a* (Table 1, a) utilized in the experiment. The spectroscopic differences between components B and C did not arise due to transference of the pigments from the effluent into diethyl ether, as demonstrated by the fact that similar differences had already been noticed when the spectra were recorded directly from the effluent (Table 1, d and e).

Table 1. Spectroscopic properties of the chlorophylls.

Compound	Solvent	Peak positions (nm)								Peak ratios			Halfwidths (nm)	
		I	II	III	IV	V	S	Ss1	Ss2	A_S/A_I	A_S/A_{Ss1}	A_S/A_{Ss2}	$w_{I1/2}$	$w_{S1/2}$
a. Chl. *a*[a]	Ee	660.0	614	576	530	497	428.0	409	380	1.32	1.56	2.48	17.9	39.0
b. Chl. *a* (1C)[a]	Ee	660.5	614	576	530	496	428.0	409	381	1.30	1.51	2.48	18.1	39.3
c. Chl. *a'* (1B)	Ee	661.0	614	575	532	499	428.0	409	(383)[b]	1.24	1.37	2.18	18.3	42.9
d. Chl. *a* (1C)	Pe+0.5 % PrOH	661.5	616	578	530	497	429.5	411	380	1.17	1.55	2.50	17.3	38.8
e. Chl. *a'* (1B)	Pe+0.5 % PrOH	662.5	614	576	533	502	429.0	410	(380)	1.14	1.25	(1.96)	17.8	61.0
f. Chl. *b*[a]	Ee	642.5	595				452.5	430		2.88	2.55		17.0	22.5
g. Chl. *b* (4C)	Ee	642.0	593				452.5	428		2.86	2.79		16.9	22.3
h. Chl. *b'* (4B)	Ee	642.0	592				452.5	428		2.86	2.73		17.2	21.7

[a] Number in parentheses refers to figure number and capital letter to component in that figure.
[b] Peak positions and ratios in parentheses are approximate.

S = Soret band, Ss1 = 1st satellite of Soret band, Ss2 = 2nd satellite of Soret band; Chl. = chlorophyll, Ee = diethyl ether, Pe = petroleum ether, PrOH = 1-propanol.

A small amount of yellow pigment (component A) was eluted prior to chlorophyll *a'*. This pigment exhibited a pheophytin *a*-like spectrum and yielded a positive phase test. A slight amount of pheophytin *a* was probably formed from chlorophyll *a'* in the pyridine solution, either while it was standing overnight or when it was evaporated to near dryness. This view is supported by the observation that chlorophyll *a'* is easily converted to pheophytin *a* upon standing in petroleum ether or cyclohexane, or upon washing the petroleum ether solution of the pigment with water.

Small amounts of at least three allomerization products remained in the column following the elution of component C. When the original chlorophyll *a* was fractionated under the same chromatographic conditions as the chlorophyll *a* that had been standing overnight in pyridine, no distinct chlorophyll *a'* zone separated. However, when a sugar layer of greater height (50 cm) was employed in such a fractionation, a small amount of chlorophyll *a'* was observed to separate slowly from the principal chlorophyll *a* zone. Neither allomerization products nor a pheophytin *a*-like pigment could be separated from the original chlorophyll *a* preparation.

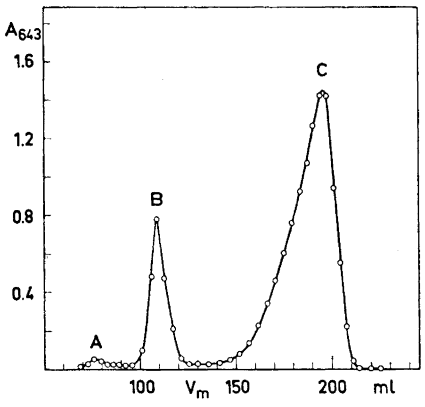

Fig. 4. Separation of chlorophylls *b* and *b'* employing chromatography on a sugar column. Experimental values (O) obtained by measuring A_{643} of the effluent fractions. A = pheophytin *b*, B = chlorophyll *b'*, and C = chlorophyll *b*.

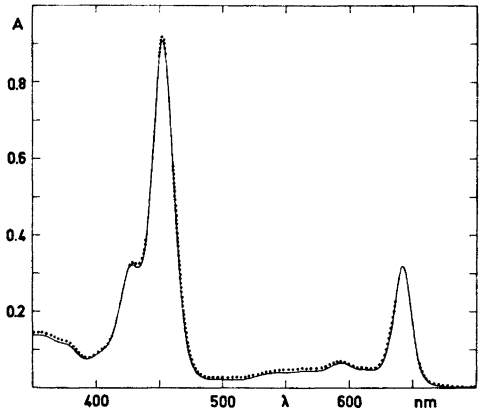

Fig. 5. Absorption spectra of chlorophylls *b'* (—) and *b* (···) in diethyl ether.

The result of a fractionation of the products formed from chlorophyll *b* in pyridine are presented in Fig. 4. The resolution of components B (chlorophyll *b'*) and C (chlorophyll *b*) was not as complete as in the chlorophyll *a* fractionation. The concentration profile reveals that slow equilibrium has probably existed between these components during fractionation. This difference, as compared to the chlorophyll *a* fractionation, is understandable, since the time required for the separation of chlorophylls *b* and *b'* was considerably longer than that needed for the separation of chlorophylls *a* and *a'*. Spectroscopically,

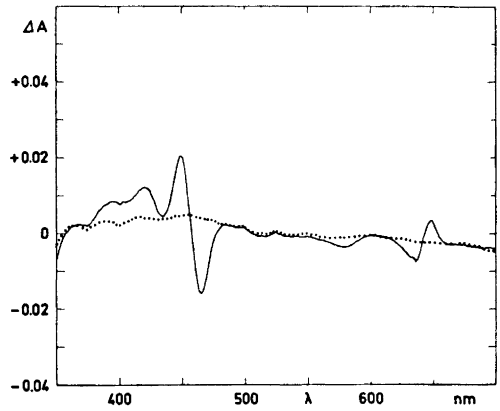

Fig. 6. Difference spectrum of chlorophylls *b'* and *b* in diethyl ether.

chlorophylls *b* and *b'* differed only slightly from each other (Figs. 5 and 6; Table 1, g and h). Chlorophyll *b'* yielded a positive phase test and was converted to normal pheophytin *b* or pheophorbide *b* upon treatment with 13 % or 30 % hydrochloric acid, respectively.

Component A consisted of a pheophytin *b*-like pigment. When components B and C were refractionated after standing overnight in pyridine, the pheophytin-containing zone was considerably smaller, thus suggesting that the original chlorophyll *b* preparation contained a slight amount of pheophytin *b*. This viewpoint is also supported by the fact that the spectra of components B and C differed slightly from that of the original chlorophyll *b* (Table 1, h, g and f, respectively).

The results described above may be satisfactorily interpreted by utilizing the reaction scheme previously presented for the chlorophylls.[4] Chlorophylls *a'* and *b'*, which are easily separated from the principal chlorophyll zones, probably represent chelated enol forms of the chlorophylls. The following evidence supports this concept and is contrary to the postulation of Strain [2] and Katz *et al.*[3] that the chlorophyll *a'* and *b'* "isomers" are merely C-10 epimers of the chlorophylls:

1. Chlorophylls *a'* and *b'* differ very significantly from chlorophylls *a* and *b* by their higher solubility in nonpolar solvents (*e.g.* petroleum ether), a phenomenon which is to be expected if it is assumed that they are chelated enol forms of the chlorophylls. Conversely, if it is assumed that chlorophylls *a'* and *b'* are merely diastereoisomers of chlorophylls *a* and *b*, then the great difference in the solubility properties of the components is not easily explained. Also, under the latter supposition, the components would probably not be so readily separable as has been experimentally observed.

2. The visible absorption spectrum of chlorophyll *a'* differs considerably from that of chlorophyll *a*. Again, this is to be expected upon the formation of the enol form of chlorophyll *a*. The conjugated double bond system of ring V will draw electrons from the tetrapyrrole system, thereby resulting in a

weakening of the bonds between the magnesium atom and the nitrogen atoms. If chlorophylls *a'* and *a* were indeed C-10 epimers, then no spectroscopic difference between them would be expected.

3. Chlorophyll *a'* was observed to exhibit a strong tendency to undergo conversion to pheophytin *a*, thus also indicating that electronic rearrangements occur upon the formation of chlorophyll *a'*.

4. The fact that chlorophyll *b* and *b'* are more similar spectroscopically than are chlorophylls *a* and *a'* may be interpreted upon the basis of the electron-withdrawing effect of the formyl group, which tends to counteract the effect of the conjugated ring V in the enol form.

5. The fact that the chlorophylls contain an exchangeable hydrogen at the C-10 position supports the concept of enolization. The presence of this hydrogen was demonstrated by Fischer and Goebel [7] upon the basis of Zerewitinoff's test and later confirmed by Dougerthy *et al.*[8] utilizing NMR.

6. The relationship between epimerization and enolization is a well-known phenomenon which may be found, for example, in sugar chemistry.

7. The probable intermediate in the formation of some chlorophyll derivatives (*e.g.* the 10-alkoxy-lactone derivatives and chlorin e_6-triester) is the enolate ion.[5] Assuming that the intermediate is a C-10 epimer, the lability of ring V towards oxygenation and solvolysis is then more difficult to comprehend.

8. Chlorophylls *a'* and *b'* have never been detected when multiple liquid-liquid partition methods have been employed for fractionation of the chlorophylls.[4] This is obviously not due to the lower selectivity of these methods compared to that of chromatography. A more plausible explanation is that the hydrogen bridge of the chelated enol is unstable in the highly-polar lower phases of the solvent systems utilized. Thus, if the enol form is originally present in the mixture to be fractionated or if it is formed during fractionation, it will rapidly be allomerized in the presence of alcohol and oxygen. This is in accord with the experimental results previously obtained.[4,5]

DISCUSSION

The formation of chelated enol forms of the chlorophylls is not a new concept, since it has already been proposed by Holt and Jacobs [9] in order to account for the IR absorption bands of chlorophyll *a* at 1640 cm^{-1} in the crystalline state and at 1652 cm^{-1} in carbon tetrachloride and carbon disulfide. This interpretation was supported by the IR studies of Russian investigators.[10–12]

A group of researchers [13] at the Argonne National Laboratory (USA) later demonstrated that the chlorophylls have a strong tendency to form aggregates in nonpolar solvents and that the absorption peak at 1652 cm^{-1} in the IR spectrum of chlorophyll *a* is an "aggregation peak". These results were confirmed by Ballschmiter and Katz.[14] However, the conclusions drawn by Katz and co-workers [8,13,15] regarding the keto-enol tautomerism of the chlorophylls have led to some controversy. The afore-mentioned investigators have stated that in solution, chlorophylls occur almost completely in the all-keto form. The present author cannot agree with this statement as long as the solvent is

insufficiently specified. According to the experience of this laboratory, the behavior of the chlorophylls is sensitive to the properties of the solvent. In completely nonpolar solvents (aliphatic hydrocarbons, carbon tetrachloride) and in water, the chlorophylls exist primarily in an aggregated state which thus precludes keto-enol tautomerism. In electron donor solvents (diethyl ether, acetone, pyridine, dioxane, tetrahydrofuran, the lower alcohols), however, the chlorophylls occur as monomers and will therefore undergo the tautomerization. The rate of enolization and the concentration of free enol are, in this case, sensitive to the particular properties of the solvent in question. Thus, in the lower alcohols (methanol, ethanol), the alcoholysis and oxidation of ring V, along with the concomitant solvation, consume the free enol form and draw the enolization reaction forward.[5] Formation of the chelated enol is probably not possible in these solvents due to their strong hydrogen-bonding capability. In the higher alcohols (propanol, butanol), the oxidation of ring V probably competes with the formation of the chelated enol. In solvents (pyridine, tetrahydrofuran, petroleum ether containing a small amount of propanol) which are polar enough to prevent aggregation but which do not possess a strong hydrogen-bonding capability, the formation of the hydrogen chelate appears to be the principal reaction that consumes the free enol. Thus, the keto-enol tautomeric equilibrium shifts towards the enol form at the expense of the all-keto form. When the reaction that consumes the free enol proceeds more rapidly than the reaction that produces it, the concentration of the free enol may be rather low. Indeed, the argument presented by Katz and co-workers may be true only in regard to relatively few solvents (diethyl ether, acetone).

Upon the basis of the slow exchange rate observed for epi-C-10-resonance, Katz *et al.*[3] have excluded the possibility that this resonance is due to an enolic hydroxyl group. It appears, however, that the afore-mentioned authors have not taken into account the possibility of the enol existing predominantly in the chelated form under the conditions prevalent during the exchange studies. The hydrogen of a chelated enol would be expected to exchange more slowly than the hydrogen of a free enol. The hydrogen chelate ring of a chelated enol may be quite stable in nonpolar solvents, since there exists the possibility of additional resonance.[4] Therefore, the present author does not consider evidence based upon the rate of hydrogen exchange strong enough to exclude the possibility that the satellite resonance peak observed by Katz *et al.*[3] is due to an enolic hydroxyl group.

REFERENCES

1. Strain, H. H. and Manning, W. M. *J. Biol. Chem.* **146** (1942) 275.
2. Strain, H. H. *Agr. Food Chem.* **2** (1954) 1222.
3. Katz, J. J., Norman, G. D., Svec, W. A. and Strain, H. H. *J. Am. Chem. Soc.* **90** (1968) 6841.
4. Hynninen, P. H. and Ellfolk, N. *Acta Chem. Scand.* **27** (1973) 1463.
5. Hynninen, P. H. and Assandri, S. *Acta Chem. Scand.* **27** (1973) 1478.
6. Strain, H. H. and Svec, W. A. In Vernon, L. P. and Seely, G. R., Eds., *The Chlorophylls*, Academic, New York–London 1966, p. 21.
7. Fischer, H. and Goebel, S. *Ann. Chem.* **522** (1936) 168.
8. Dougherty, R. C., Strain, H. H. and Katz, J. J. *J. Am. Chem. Soc.* **87** (1965) 104.

9. Holt, A. S. and Jacobs, E. E. *Plant Physiol.* **30** (1955) 553.
10. Sidorov, A. N. and Terenin, A. M. *Opt. i Spektroskopiya* **8** (1960) 259.
11. Sidorov, A. N. *Opt. i Spektroskopiya* **3** (1962) 206, 374; **14** (1963) 834.
12. Karyakin, A. J. and Chibisov, A. K. *Opt. i Spektroskopiya* **13** (1962) 379.
13. Katz, J. J., Closs, G. L., Pennington, F. C., Thomas, M. R. and Strain, H. H. *J. Am. Chem. Soc.* **85** (1963) 3801.
14. Ballschmiter, K. and Katz, J. J. *J. Am. Chem. Soc.* **91** (1969) 2661.
15. Katz, J. J., Dougherty, R. C. and Boucher, L. J. In Vernon, L. P. and Seely, G. R., Eds., *The Chlorophylls*, Academic, New York – London 1966, p. 185.

Received November 28, 1972.

ACTA CHEMICA SCANDINAVICA 27 (1973) 1496–1502

Design and Testing of a Vaporisation Calorimeter. Enthalpies of Vaporisation of Some Alkyl Cyanides

JIRI KONICEK*

Thermochemistry Laboratory, Institute of Physical Chemistry, Czechoslovak Academy of Sciences, Vinicna 7, Prague 2, Czechoslovakia, and Thermochemistry Laboratory, Chemical Center, University of Lund, S-220 07 Lund 7, Sweden

An enthalpies of vaporisation calorimeter for work at 25°C has been designed and tested. Results of test experiments indicate an accuracy of about ±0.25 %. The calorimeter has been used for a study of ΔH_v for a series of alkyl cyanides.

The enthalpy of formation data of liquid and solid substances which can be obtained from combustion measurements reflect the complexity of the condensed state. In order to study properties such as bond energies, resonance energies, *etc.*, a knowledge of enthalpies of formation in the ideal vapour state is needed. Obviously, enthalpies of vaporisation data are indispensable for such investigations.

In connection with the investigation on ΔH_c of some alkyl cyanides [1,2] it was felt necessary to build a vaporisation calorimeter for small samples.

In the present paper, a new semi-microcalorimeter for measurements of ΔH_v of liquid compounds is described. The amount of substance necessary for ΔH_v determination is in the range of 0.1 g to 1 g.

DESCRIPTION OF THE CALORIMETER

Principle. The basic principle of the present calorimeter has been used in several earlier constructions [3,4] where, however, the instruments were designed for comparatively large quantities of substance.

The present calorimeter basically consists of an inverted U-tube which contains the compound to be investigated only (in liquid and gas phases). A suitable amount of liquid substance is vaporised from one end of the tube and condensed in the other. The vaporisation end (the calorimetric vessel) is heated electrically in order to keep the temperature constant, while the other end (the condensation bulb) is suitably cooled. The heat supplied to

* Present adress: Perstorp AB, S-284 00 Perstorp, Sweden.

maintain the constant temperature of the calorimetric vessel, together with the amount of vaporised substance, is used for ΔH_v calculation.

In contrast to the earlier calorimeters of a similar type the present method is based on the complete vaporisation of the compound from the calorimetric vessel. The amount of compound necessary for measurement is, thus, considerably reduced.

Vaporisation vessel. The calorimetric vessel is made of brass and consists of several parts (Fig. 1). The cylindrical part *a* has a threaded part for connection to the vaporisation tube. The piston *b*, which is equipped with twelve vertical grooves, is pressed into the cylindrical body *a*. The calorimetric vessel is closed by means of lid *c*, which is sealed with Araldite epoxy resin. Screw *e* serves to attach the U-shaped glass tube, joined to ring *d* with epoxy resin, to the body of the calorimeter over a lead amalgam packing, *g*.

The U-tube can be joined to the vacuum system by means of tube H (Fig. 2). Through this tube the substance can be introduced into the vaporisation system and condensed in bulb I. The system can be sealed and detached in a vacuum.

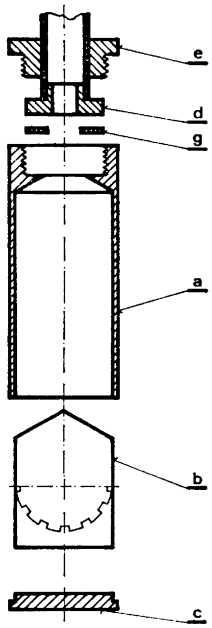

Fig. 1. Construction of the calorimetric vessel.

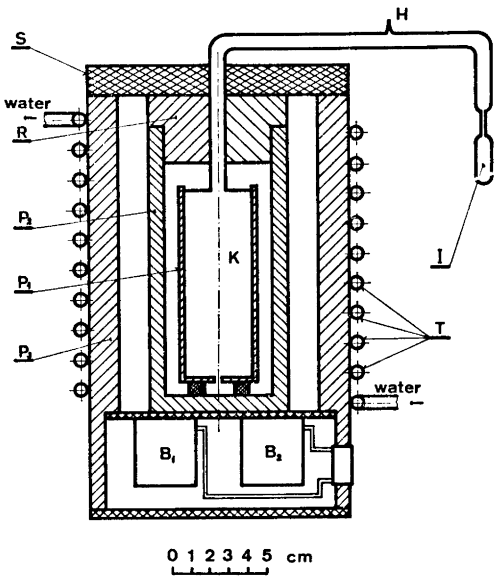

Fig. 2. Schematic view of the calorimetric assembly.

Calorimeter. The calorimeter consists of three cylinders P_1, P_2, P_3 (Fig. 2). The measuring part of the calorimeter, P_1, is made of copper. There is a copper resistance thermometer wound in a groove on the lower part and a heater in another groove on the upper part of the cylinder. The thermometer is con-

nected in a Wheatstone bridge and controls the heater by means of an electronic device. The surface is coated with a layer of heat-hardened varnish, aluminium-metalized in a vacuum.

Cylinder P_1 is located in the centre of the cylindrical brass jacket P_2. The space between the walls is 10 mm. There is a platinum resistance thermometer and a heater wound around the surface of jacket P_2. The thermometer forms part of a Wheatstone bridge and controls the function of the heater by means of proportional control system. The temperature of jacket P_2 is kept constant within $\pm 5 \times 10^{-4}$°C. In the upper part of jacket P_2 there is an opening through which the vaporisation vessel can be inserted into jacket P_1. Insert R is a two part copper ring which fits tightly around the glass tube of the vaporisation system in order to minimize uncontrolled heat exchange between the surroundings and the calorimeter.

The duraluminium cylinder P_3 is divided into two parts. In the upper part, the calorimetric jackets are placed. The lower cavity contains two boxes B_1, B_2 made of permalloy in which 2×3 calibrated manganine resistors (100 Ω) are placed. They form two Wheatstone bridges together with resistance thermometers on the measuring (P_1) and thermostating (P_2) jackets, respectively. As the bridges are supplied with alternating current they are – together with preamplifiers – enclosed in shielding boxes B_1, B_2 to avoid capacity coupling between the two bridges. The temperature of jacket P_3 must be kept about 0.3°C lower than the temperature of jacket P_2. Therefore, a copper tube T is wound around the surface, and the temperature is kept constant by circulating thermostated water.

Electronic equipment. The electronic equipment consists of two identical parts; one of them is used for the calorimetric cylinder P_1 and the other for jacket P_2. The bridges are supplied with alternating current; the voltage on the bridge is 0.2 V. The signal is used for the control of the heaters and can also be recorded. The signal from the P_2 bridge serves thus as a steering signal for the control of the heater on P_2. At the output side of the measuring part of the electronic system an electronic power relay is connected with two parallel contacts. One of the contacts connects and disconnects a lead storage battery with the calibrated heater on jacket P_1. The parallel contact serves for switching on and off an electronic stop watch (pulse counter Universal Counter Tesla BM-52).

PROCEDURE

Sample filling. The sample is introduced into the vaporisation system by the filling system shown schematically in Fig. 3. The sample is transferred into bulb B, the system is evacuated to about 10^{-1} mmHg and valve V_4 is closed. Ampoule A is filled with granulated charcoal and when cooled by liquid nitrogen, a vacuum in the order of 10^{-4} mmHg is obtained. The sample in B is cooled and heated several times in this vacuum for degassing. Finally, the sample in B is heated to room temperature, bulb I in the vaporisation system C is cooled down, and a suitable amount of the sample is condensed in I. The vaporisation system C is separated from the filling system by melting

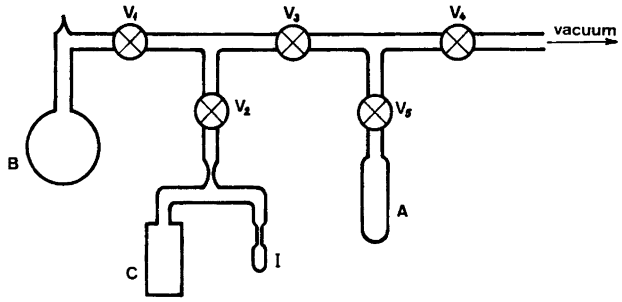

Fig. 3. The filling system.

off the connecting tube under vacuum. The sample is distilled into the calorimetric vessel by heating the glass part and by cooling the brass part.

Measurement. The calorimetric vessel is now filled with the sample. The calorimetric vessel fits into the copper cylinder P_1. Jacket P_2 is then closed by the two parts of lid R and covered by styrofoam lid, S (Fig. 2). The calorimeter is then heated to the equilibrium temperature (25°C). The temperature of the surrounding air is kept at 25.3°C to avoid a condensation of the sample in the glass tube before the beginning of the measurement. When the temperature in the calorimeter has come to the equilibrium, bulb I is cooled to a suitable pre-determined temperature. The sample is vaporised from the calorimetric vessel K and condensed in bulb I. The vaporisation in the calorimeter causes a temperature drop which is compensated by the calibrated heater. The usual on and off periods of the heater are from 2 to 5 sec during the measurements. When the last residues of the sample are being vaporised the rate of switching on of the heater slows down and the heating periods become very short, about 0.2 sec.

When the sample has condensed completely in bulb I, and when no further vaporisation takes place in the calorimeter, the total heating time is shown on the screen of the counter. The final temperature is identical with the equilibrium temperature before the experiment. The calorimetric vessel K is removed from the cylinder, and the sample is distilled back into the brass body. Using this procedure, the experiment can be repeated several times on the same sample.

After the final experiment, the sample is condensed in bulb I and thermostated at 24.5°C, while keeping the temperature of the vaporisation vessel and the U-tube approximately 0.5°C higher. Then bulb I is cut off, the hole is closed by a rubber stopper and the bulb and its content are weighed, emptied and weighed again. From the amount of the substance and from the energy supplied by the heater the enthalpy of vaporisation, ΔH_v, is calculated (eqn. 1):

$$\Delta H_v = Q/g \text{ kJ/mol} \quad (1)$$

Q is the heat supplied by the heater and g the weight of the sample.

Testing of the instrument. The calorimeter was tested by measurements on water, methanol, benzene, and carbon tetrachloride. For these compounds well established ΔH_v data at 25°C are available.

Table 1. Comparison of the ΔH_v values at 25°C for water, methanol, benzene, and carbon tetrachloride.

	ΔH_v (kJ/mol)	
	This work	Other results
Water	44.04 ± 0.10	43.99 ± 0.02 [6] 44.02 ± 0.08 [11] 43.98 ± 0.02 [5]
Benzene	33.90 ± 0.10	33.87 ± 0.05 [3]
Methanol	37.42 ± 0.10	37.70 ± 0.18 [4] 37.40 ± 0.05 [7] 37.28 ± 0.08 [9] 37.43 ± 0.02 [5]
Carbon tetrachloride	32.54 ± 0.10	32.43 ± 0.08 [11] 32.41 ± 0.02 [8]

Water redistilled in glass was used. The other test substances were of *p.a.* grade. The test compounds were dried by molecular sieves and were further purified by fractional distillation.

The results of the test experiments are summarised in Table 1. Experiments were performed on two or three independent samples. The weight of the samples varied from 93 mg to 400 mg for water, and from 250 mg to 1200 mg for the other compounds. For each sample, four experiments were performed.

Enthalpies of vaporisation of alkyl cyanides. As a part of a study on formation enthalpies of some alkyl cyanides [1,2] measurements of their ΔH_v values were made. Results are summarised in Table 2. Each value is an average of eight determinations with two independent samples.

Table 2. Enthalpies of vaporisation of some cyanides at 25°C.

Compound	ΔH_v kJ/mol
Allyl cyanide	40.01 ± 0.10
cis-1-Propenyl cyanide	38.91 ± 0.15
trans-1-Propenyl cyanide	40.04 ± 0.15
trans-2-Butenyl cyanide	44.77 ± 0.15
cis-1-Butenyl cyanide	43.22 ± 0.15
trans-1-Butenyl cyanide	44.89 ± 0.15
Cyclopentyl cyanide	43.43 ± 0.20
1-Cyclopentenyl cyanide	44.98 ± 0.20
Cyclohexyl cyanide	51.92 ± 0.25
1-Cyclohexenyl cyanide	53.55 ± 0.20

DISCUSSION

A robust construction of the vaporisation vessel, made from brass, was chosen. The vaporisation vessel serves not only as a container of the liquid to

be investigated but has an important heat distributing function. Stirring is thus not necessary and yet reasonably fast evaporation rates can be achieved. The results of the test experiments suggest that there is no significant deviation from the equilibrium condition at the given temperature. The liquid in the vaporisation vessel is in intimate contact with the bottom of the vessel. A sample of 1 cm^3 forms a layer 2 mm high if the amount which condenses on the walls and in the grooves is not considered.

The minimum amount of the substance to be investigated is limited by the precision of the temperature measurement and by the heat capacity of the calorimetric vessel. The heat capacity of the calorimeter (*i.e.* calorimetric vessel and cylinder P_1) was about 130 J/deg. With the difference between the initial and final temperature of the calorimeter of 0.001°C, the error of the measurement would be 0.1 % for a heat quantity of 130 J. This amount of energy is consumed when about 50 mg water or about 400 mg of a hydrocarbon are vaporised. Usually, larger samples were used, especially during the test experiments.

The calorimeter with the condensation vessel is a closed system containing the substance to be measured only, in liquid and vapour phase. The total volume of the system is about 25 cm^3. In order to establish the true amount of the substance vaporised from the vaporisation vessel accurately, it is necessary to keep a small temperature difference between the calorimetric vessel and the U-tube, especially for volatile compounds. For the same reason, the temperature of the condensation bulb should not be kept much lower than the equilibrium temperature when cutting it off for weighing. If this type of calorimeter is used at higher temperatures it becomes even more important to observe these conditions. The error introduced when measuring the enthalpy of vaporisation at temperature T_0 and determining the amount of substance vaporised at temperature T_1 can be expressed by the equation:

$$\% \text{ error} = \frac{(d_{T_0} - d_{T_1}) \times V}{g} \times 100 \qquad (2)$$

where d_{T_0} and d_{T_1}, are saturated vapor densities at the respective temperatures, V is the volume of the instrument, and g is the amount of the substance to be investigated in the calorimeter.

A calorimeter, which was based partly on the present design, has recently been used by Polak and Benson.[5] They used a different approach to determine the amount of substance vaporised. The amount of substance present in vapour phase at the start of vaporisation was calculated from the known liquid density, the state equation of the substance in vapour phase, and the total volume of the calorimetric system. The advantage of this procedure lies in the fact that measurements can be made at different temperatures by only once filling the calorimeter with a sample.

For proper function of the calorimeter, it is important that the heating intervals are of approximately the same duration as the intervals during which the heater is shut off. This condition can be achieved by suitable temperature choice of the condensation bulb. A proper vaporisation rate for most of the measurements reported here is about 0.5 W which corresponds to a cooling

rate of about 0.004°C/sec. At this vaporisation rate the electrical heat effect was chosen to be about 1 W. Under these conditions, the temperature of the calorimeter varies regularily ± 0.02°C around the experimental temperature.

A necessary condition for obtaining a stable vaporisation rate is that the volume of the condensation bulb be kept several times larger than the volume of the liquid which will condense in it. Otherwise, the vaporisation rate will slow down proportionally to the decrease in the cooled vapour's volume in the condensation bulb.[4]

Results of the test experiments indicate a precision of ± 0.15 %, expressed as twice the standard deviation of the mean. The standard deviation was calculated from eight experiments on two independent samples. Comparison of results from the test experiments with the literature data (Table 1) has not indicated any significant systematic error. However, an uncertainty of ± 0.1 % was added to the standard deviation to account for eventual errors.

Enthalpies of vaporisation of some alkyl cyanides were measured (Table 2). Values of CH_2 increments can be derived from ΔH_v of propenyl cyanides and butenyl cyanides. The increment is 4.31 kJ/mol for the *cis*-compounds and 4.85 kJ/mol for the *trans*-compounds. It is interesting to note that for the *trans*-compounds the increment value is close to the normal value of 4.95 kJ/mol.[10] For *cis*-cyanides, similarly as for n-alkyl cyanides,[11] the CH_2 increment is significantly lower. Enthalpies of vaporisation of the *cis*-isomers are somewhat lower than for the *trans*-isomers which probably is due to the lower dipole-dipole interactions.

Acknowledgements. The support in the years 1966 – 1968 from the *Institute of Chemical Process Fundamentals* and the *Institute of Physical Chemistry of the Czechoslovak Academy of Sciences* is gratefully acknowledged. The author thanks also for the support from the *Thermochemistry Laboratory*, University of Lund, where the work was completed.

REFERENCES

1. Konicek, J., Prochazka, M., Krestanova, V. and Smisek, M. *Collection Czech. Chem. Commun.* **34** (1969) 2249.
2. Prochazka, M., Krestanova, V., Konicek, J. and Smisek, M. *Collection Czech. Chem. Commun.* **35** (1970) 727.
3. Osborne, N. S. and Ginnings, D. C. *J. Res. Natl. Bur. Std.* **39** (1947) 453.
4. McCurdy, K. G. and Laidler, K. L. *Can. J. Chem.* **41** (1963) 1867.
5. Polak, J. and Benson, G. C. *J. Chem. Thermodyn.* **3** (1971) 235.
6. Rossini, F. D., Wagman, D. D., Ewans, W. H., Levine, S. and Jaffe, J. *Selected Values of Chemical Thermodynamic Properties, Circular of National Bureau of Standards 500*, U.S. Government Printing Office, Washington D.C. 1952.
7. Green, J. H. S. *Chem. Ind. (London)* **1960** 1215.
8. Hildebrand, D. L. and McDonald, R. A. *J. Phys. Chem.* **64** (1959) 1521.
9. Wadsö, I. *Acta Chem. Scand.* **20** (1966) 544.
10. Howard, P. B. and Wadsö, I. *Acta Chem. Scand.* **24** (1970) 145.
11. Wadsö, I. *Acta Chem. Scand.* **20** (1966) 536.

Received November 29, 1972.

ACTA CHEMICA SCANDINAVICA 27 (1973) 1503–1508

The Methanolysis of Bromo Diphenylphosphine

LEIV J. STANGELAND

Chemical Institute, University of Bergen, N-5000 Bergen, Norway

The rate of methanolysis of bromo diphenylphosphine has been examined in toluene by the spectrophotometric stopped flow technique. The rate of the reaction has been found to depend both on the square and on the cube of the methanol concentration. In the presence of various pyridines at constant methanol concentration the rate of reaction depends linearily on the concentration of the pyridines. The mechanism for these reactions has been discussed and reaction schemes are proposed.

Phosphinous halides, R_2P-X, are known to react with alcohols in the presence of a tertiary amine to form the corresponding phosphinites, R_2P-OR'.

Arbuzov and Nikonorov [1] made methyl diphenylphosphinite from chloro diphenylphosphine and methanol in the presence of pyridine. Similarly, Quin and Anderson [2] made the bisphosphinites from chloro diphenylphosphine and diols in the presence of diethylaniline. In the absence of an amine, Seel and Velleman [3] found that chloro dimethylphosphine and methanol first formed dimethyl methoxyphosphonium chloride, which decomposed at temperatures above -10°C to dimethyl phosphinoxide and methyl chloride, while the same substrate and sodium methoxide readily reacted to form methyl dimethylphosphinite. They also found that dimethyl fluorophosphine and methanol gave methyl dimethylphosphinite and dimethyl difluorophosphorane.[4]

With regard to the mechanism of the reaction between phosphinous halides and alcohols, very little is known as no kinetic studies appear to have been performed, probably due to the high rate of the reactions. We found that the methanolysis of bromo diphenylphosphine could be conveniently followed by the "stopped flow" technique.

Dimethyl methoxyphosphonium chloride can be isolated as an intermediate in reaction (I).[3]

$$Me_2PCl + MeOH \xrightarrow{1} Me_2\overset{H}{\underset{Cl}{P}}OMe \xrightarrow{2} Me_2\overset{H}{\underset{O}{P}} + MeCl \qquad (I)$$

and there should probably also be an intermediate of the same kind when bromo diphenylphosphine is the substrate.

The second step in reaction (I) should be similar to the last step in the Arbuzov reaction,[5] and is thought to be rather slow compared with the rate of the measured reaction.

The methanolysis of bromo diphenylphosphine (BDP) was studied in toluene with a concentration of methanol ranging from 0.1 to 0.9 M.

The kinetics were found to be represented by:

$$-\mathrm{d[BDP]}/\mathrm{d}t = k_3[\mathrm{BDP}][\mathrm{MeOH}]^2 + k_4[\mathrm{BDP}][\mathrm{MeOH}]^3 \quad (1)$$

As pseudo first order conditions were used, the reaction could be described by:

$$-\mathrm{d[BDP]}/\mathrm{d}t = k'[\mathrm{BDP}] \quad (2)$$

This equation was found to be followed for more than 85 % of the reaction and no autocatalysis due to liberated acid could be observed. The pseudo first order rate constants obtained are listed in Table 1. A plot of $k'[\mathrm{MeOH}]^{-2}$

Table 1. Pseudo first order rate constants for the reaction between bromo diphenylphosphine and methanol in toluene.[a]

Concn. MeOH M	$k' \times 10^3$ sec^{-1}	$k'[\mathrm{MeOH}]^{-2}$ $\mathrm{M}^{-2}\ \mathrm{sec}^{-1}$
0.116	7.7	0.57
0.255	51.0	0.78
0.379	154	1.07
0.590	490	1.40
0.898	1400	1.73
1.00	2000 [b]	

[a] Substrate concentration *ca.* 4×10^{-4} M. [b] Calculated.

as a function of the concentration of methanol, [MeOH], was found to be linear with an intercept of k_3 (0.38 $\mathrm{M}^{-2}\ \mathrm{sec}^{-1}$) and a slope of k_4 (1.63 $\mathrm{M}^{-3}\ \mathrm{sec}^{-1}$). (Fig. 1).

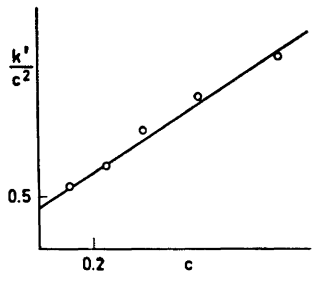

Fig. 1. Pseudo first order rate constants divided by the square of the methanol concentration as a function of the methanol concentration for the methanolysis of bromo diphenylphosphine.

Aksnes and Aksnes [6] found a third order reaction which was second order in water for the hydrolysis of tripropyl phosphite in acetonitrile and suggested a sixmembered cyclic transition state (I).

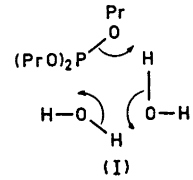

(I)

As alcohols are known to be extensively associated in nonpolar solvents,[7] intermediates like II and III may be responsible for both the third and the fourth order terms in rate eqn. (1).

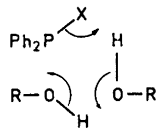

(II)

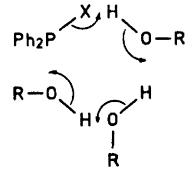

(III)

If we assume that the phosphorus-halogen bond is not completely broken in the transition state leading to the ionic intermediate, another reaction sequence may be set up:

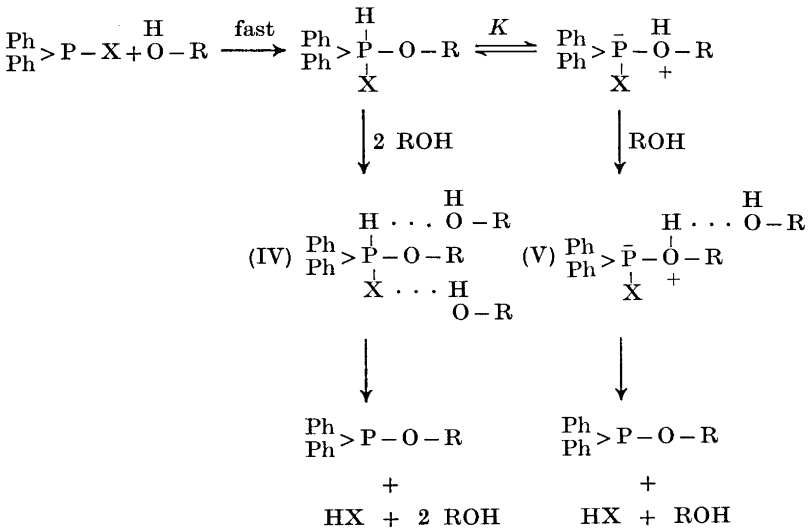

The intermediate V would carry a formal negative charge on the phosphorus atom, while intermediate IV will not. Because of this the intermediate V will not have any need for assistance to eliminate the halogen while intermediate IV will have. As a result, these two species may give rise to the two different terms in the rate equation.

THE PYRIDINE CATALYZED METHANOLYSIS

The base catalyzed methanolysis of bromo diphenylphosphine was studied in toluene at pseudo first order conditions. The concentration of methanol was kept constant at 1 M while the concentrations of the three pyridines, 4-methylpyridine, pyridine, and ethyl pyridine-3-carboxylate were varied from 3.75×10^{-2} M to 25.5×10^{-2} M. All the reactions were found to follow the following rate equation:

$$-\mathrm{d[BDP]}/\mathrm{d}t = k_2(\mathrm{BDP})\ (\mathrm{pyridine}) = k'(\mathrm{BDP}) \qquad (3)$$

When k' was plotted as a function of the pyridine concentrations, linear plots without intercepts were obtained (Fig. 2). The results are listed in Table 2.

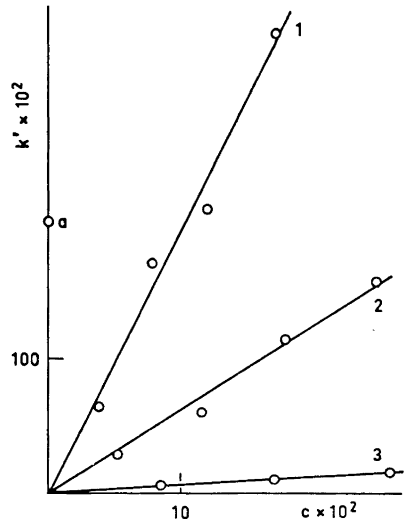

Fig. 2. Pseudo first order rate constants as a function of the pyridine concentration for the pyridine catalyzed methanolysis of bromo diphenylphosphine. (a) The uncatalyzed methanolysis. (1) 4-Methylpyridine. (2) Pyridine. (3) Ehtyl pyridine-3-carboxylate.

The presence of a tertiary amine in the alcoholysis of halogeno phosphines will give the desired product.[1,2] This might be thought to be caused by the ability of the amine to form an ammonium salt with the halo acid liberated during the reaction. If the catalysis by the amine is general base catalyzed, an increase in rate should be expected.[8] In our reaction there was a lowering in k' from the pure methanolysis for almost every pyridine concentration examined. Aksnes and Aksnes [6] also found that a small amount of pyridine

Table 2. Summary of the pseudo first order and second order rate constants for the pyridine catalyzed reaction between bromo diphenylphosphine and methanol.[a,b]

Nucleophile	Concn. of nucl. $\times 10^2$ M	$k' \times 10^2$ sec^{-1}	k_2 $M^{-1}sec^{-1}$
4-Methyl-pyridine	3.75	63	
	7.66	169	
	11.84	210	
	16.96	338	19.6
Pyridine	5.32	27.2	
	11.54	59.2	
	17.70	113.6	
	24.20	157.6	6.4
Ethyl-pyridine-3-carboxylate	8.40	5.48	
	16.87	9.76	
	25.52	15.23	0.6

[a] Methanol concentration 1 M. [b] Substrate concentration *ca.* 4×10^{-4} M.

present, retarded the rate of hydrolysis of tripropylphosphite considerably. The following mechanism is proposed for the catalyzed reaction:

$$\mathrm{Ph_2P{-}Br} + \mathrm{:N} \overset{K}{\longleftrightarrow} \mathrm{Ph_2P{\cdots}N}\ (\mathrm{Br})$$

(VI)

$$\mathrm{VI} + \mathrm{MeOH} \dashrightarrow \mathrm{Ph_2P(Br)(O{\cdots}H)(Me)}\ {\cdots}\mathrm{N} \overset{k_2}{\dashrightarrow} \mathrm{Ph_2P{-}O{-}Me} + \mathrm{HN^+}\ \mathrm{Br^-}$$

Association constants for hydrogen bonding between phenol and pyridines [9] are known to increase with increasing pK_a values of the pyridines.

A hydrogen bonded complex between methanol and pyridine may be expected to react more rapidly with both the phosphinous halide and the intermediate than the free methanol. No competition from the general base catalyzed reaction between methanol and the phosphinous halide is observed and we may conclude that K has to be large.

When log k_2 is plotted *versus* pK_a of the pyridines, a Brønsted β-coefficient of 0.5 is obtained. This Brønsted coefficient has been related to the amount of bond formation in the transition state of nucleophilic substitution reactions.[10,11] In our reaction, however, more than one bond being formed or broken in the transition state, little significance can be given this figure.

EXPERIMENTAL

Reagent grade toluene was refluxed over sodium and fractionated. Acetonitrile, reagent grade, was first distilled from phosphorus pentoxide and then refluxed and fractionated from anhydrous potassium carbonate.

The pyridines were commercial products except for ethyl pyridine-3-carboxylate. The commercial pyridines were twice distilled from potassium hydroxide pellets. The ethyl pyridine-3-carboxylate was prepared by esterification of nicotinic acid with ethanol in the presence of sulfuric acid as described by Gilman and Broadbent.[12] Dry methanol was prepared as described by Vogel.[13] Bromo diphenylphosphine was prepared as described by Kuchen and Grünewald.[14] The pale yellow liquid thus obtained solidified when placed in the refrigerator, and did not melt until the temperature had reached 23 – 24°C.

The reactions were followed at 310 nm with a Durrum stopped flow apparatus by measuring the disappearance of the halophosphine. In a typical run, the pyridine was weighed in a 25 ml volumetric flask and diluted to the mark with a previously made 2 M solution of methanol in toluene. The solution of phosphine was made by injecting about 0.1 ml of a standard solution of substrate in toluene into 5 ml of toluene. Solutions of nucleophile and substrate were then mixed in the stopped flow apparatus and the reaction measured. Dry nitrogen had been bubbled through the solutions beforehand.

Acknowledgement. Thanks are due to *Norges Teknisk-Naturvitenskapelige Forskningsråd* for a maintenance grant and to the *Instituto di Chimica Generale*, University of Pisa, Italy, where the experimental part of this work was performed, for the use of its laboratory facilities.

REFERENCES

1. Arbuzov, A. E. and Nikonorov, K. V. *Zh. Obshch. Khim.* **18** (1948) 2008; *Chem. Abstr.* **43** (1949) 3801i.
2. Quin, L. D. and Anderson, H. G. *J. Org. Chem.* **29** (1964) 1859.
3. Seel, F. and Velleman, K. D. *Chem. Ber.* **105** (1972) 406.
4. Seel, F., Gombler, W. and Velleman, K. D. *Liebigs Ann. Chem.* **756** (1972) 181.
5. Kirby, A. J. and Warren, S. G. *The Organic Chemistry of Phosphorus*, Elsevier, Amsterdam 1967, p. 37.
6. Aksnes, G. and Aksnes, D. *Acta Chem. Scand.* **18** (1964) 1623.
7. Brodskii, A. I., Pokhodenko, V. D. and Kuts, V. S. *Russ. Chem. Rev.* **39** (1970) 347.
8. Hine, J. *Physical Organic Chemistry*, McGraw, New York 1962, p. 104.
9. Gramstad, T. *Acta Chem. Scand.* **18** (1962) 807.
10. Hudson, R. F. *Chimica* **16** (1963) 173.
11. Marcus, R. A. *J. Phys. Chem.* **72** (1968) 891.
12. Gilman, H. and Broadbent, H. S. *J. Am. Chem. Soc.* **70** (1948) 2757.
13. Vogel, A. I. *Practical Organic Chemistry*, 3rd Ed., Longmans, Green and Co., London 1964.
14. Kuchen, W. and Grünewald, W. *Chem. Ber.* **98** (1965) 480.

Received November 29, 1972.

ACTA CHEMICA SCANDINAVICA 27 (1973) 1509–1518

Bi- and Tricyclic Products from Tetra- and Penta-peptides of α-Methylalanine

MOHAMMAD YUSUFF ALI, JOHANNES DALE and KIRSTEN TITLESTAD

Kjemisk Institutt, Universitetet i Oslo, Oslo 3, Norway

Tetra- and penta-peptides of α-methylalanine give with PCl_5, $SOCl_2$, *etc.*, intermediates which, with or without loss of amino acids, lead to bi- and tricyclic products containing imidazole and piperazine rings.

During attempts to prepare cyclic peptides from linear peptides of α-methylalanine (α-aminoisobutyric acid), a series of abnormal reactions have been encountered. Although there is no reason to expect that such cyclic products are particularly unstable, the higher members were never obtained and the cyclic dipeptide only with difficulty.

CYCLIZATION OF DIPEPTIDES

The 2,4,5-trichlorophenyl ester of α-methylalanyl-α-methylalanine gave no cyclic product when refluxed in methanol or in benzene for 24 h, and only a 15 % yield when heated at 100° without solvent for 48 h. The otherwise less reactive methyl ester gave under the same conditions better yields, 15 and 90 %, respectively. This general reluctance of the linear dipeptide to form a monocyclic peptide is quite surprising, considering the perfect stability of the product and the presence of two *gem*-dimethyl groups, which are generally observed [1] to promote cyclization. The anomaly is best explained by the difficulty of obtaining the *cis*-amide conformation required for cyclization (Fig. 1).

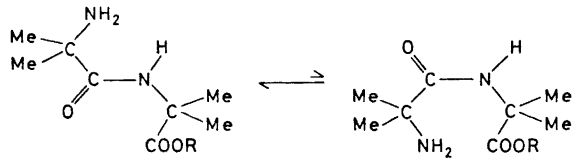

Fig. 1.

The heavy substitution is in fact comparable to that in di-*t*-butyl ethylene where the *cis*-isomer is 9.3 kcal/mol higher in energy than the *trans*-isomer.[2] Also, the bulkiness of the activated ester group explains the more facile reaction with the less "active" but smaller methyl ester group. In cases such as sarcosyl-sarcosine,[3] where *cis*-amide is as likely as *trans*, cyclic dipeptide formation is unavoidable under mild conditions.

ATTEMPTS TO CYCLIZE HIGHER PEPTIDES

Several attempts were made to cyclize the tri- and tetra-peptide of α-methylalanine activated either as the 2,4,5-trichlorophenyl ester,[4] with dicyclohexylcarbodiimide,[5] or with Woodward's reagent K.[6] At most, some polymer was obtained together with unchanged peptide. This is all in accord with the failure of other workers [7] to cyclize these peptides through oxazolone intermediates.

Under conditions used for the formation of the more reactive acid chlorides and for their subsequent cyclization in pyridine solution, two crystalline sublimable substances were obtained both from the tetra- and the penta-peptide, together with polymers and unreacted peptide. One of these, having infrared bands at 1730, 1670, and 1640 cm^{-1}, proved to have the bicyclic imidazolone structure (VI, Fig. 2), formed by loss of one, and two, respectively, amino

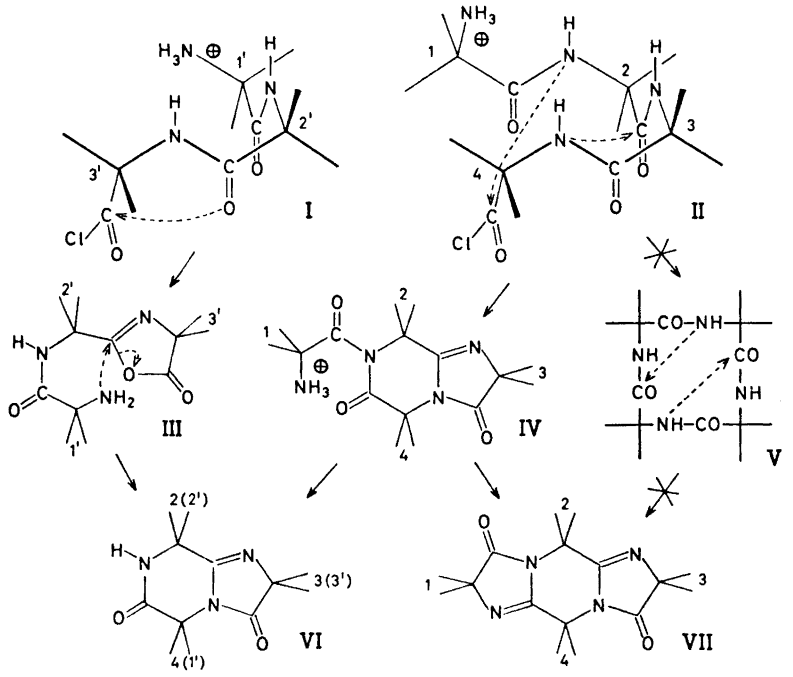

Fig. 2.

acids. It was identical with a product reported earlier by Kenner's group [8] to be formed from the tripeptide oxazolone (III). The second crystalline product had infrared bands at 1720 and 1630 cm^{-1} and was shown to possess a tricyclic bis-imidazolone structure (VII, Fig. 2); in the case of the penta-peptide it was formed by loss of one amino acid.

That the bis-imidazolone (VII) did not arise from initially formed monocyclic tetrapeptide (V) by subsequent double transannular cyclol formation [9] and dehydration was shown by the observation that replacement of one of the amino acids of the tetrapeptide by a fully methyl-deuterated amino acid did not lead to the required equal distribution of deuterium on all positions of VII, but to specific deuteration of only one (see below).

The following additional arguments point to partial ring-formation already in the chlorination step:

1. Identical products are formed from the tetra- and penta-peptide.

2. Infrared bands for the amide group at 1670 and 1525 cm^{-1} are absent in the precipitated intermediate obtained from the tetra- and penta-peptide with PCl_5 in acetyl chloride, while three new bands are present at 1790, 1730, and 1590 cm^{-1}. Of these, the 1730 cm^{-1} band may be the same as found in the product, while the 1790 cm^{-1} band must be due to the acid chloride. The intermediate obtained from the tripeptide with $SOCl_2$ has no band at 1790 cm^{-1}, but instead a band at 1820 cm^{-1} typical of all oxazolones used as intermediates in the synthesis [7,10] of the linear peptides, and so must be in fact the oxazolone.

3. The authentic oxazolone of the tetrapeptide does not give the bi- and tricyclic products on attempted cyclization.

4. The bi- and tricyclic products (VI and VII) are formed also by direct sublimation of the chlorinated intermediate at reduced pressure.

To gain insight into the mechanism of this reaction, one residue of α-methylalanine fully deuterated in both methyl groups was introduced systematically by synthesis in various positions of the tri-, tetra-, and penta-peptide, and the bi- and tricyclic products examined by NMR-spectroscopy in $CDCl_3$ (Fig. 3). Earlier ^{14}C labelling experiments by Kenner's group [8] on the tripeptide oxazolone (III) showed that the last amino acid ended up in the imidazolone ring; hence the methyl groups in this ring give rise to the line at 1.35 δ. For the tricyclic product, the lines at 1.33 and 1.89 δ are by inference assigned to the methyl groups in the five- and six-membered rings, respectively.

On the basis of these deuteration experiments a reaction mechanism II→IV→VI+VII can be proposed for the case of the tetrapeptide (Fig. 2.) The assumption is made that any intermediate chloroimine double bond, as well as the parent amide group, is exclusively in *trans*,* and that chain-folding therefore can only occur at the α-carbon to give part of a 4-helix (I and II). The amino-end being protected as the hydrochloride, the acid chloride can only be attacked by the 2-carbonyl oxygen in the tripeptide (I) to give the

* Although the figures have been drawn with amide groups in all positions, it is understood that the chloroimine ($-\overset{\overset{Cl}{|}}{C}=N-$) and the amide ($-\overset{\overset{O}{\|}}{C}-NH-$) are comparable both sterically and mechanistically, carbon having similar electrophilic and nitrogen similar nucleophilic properties in the two cases.

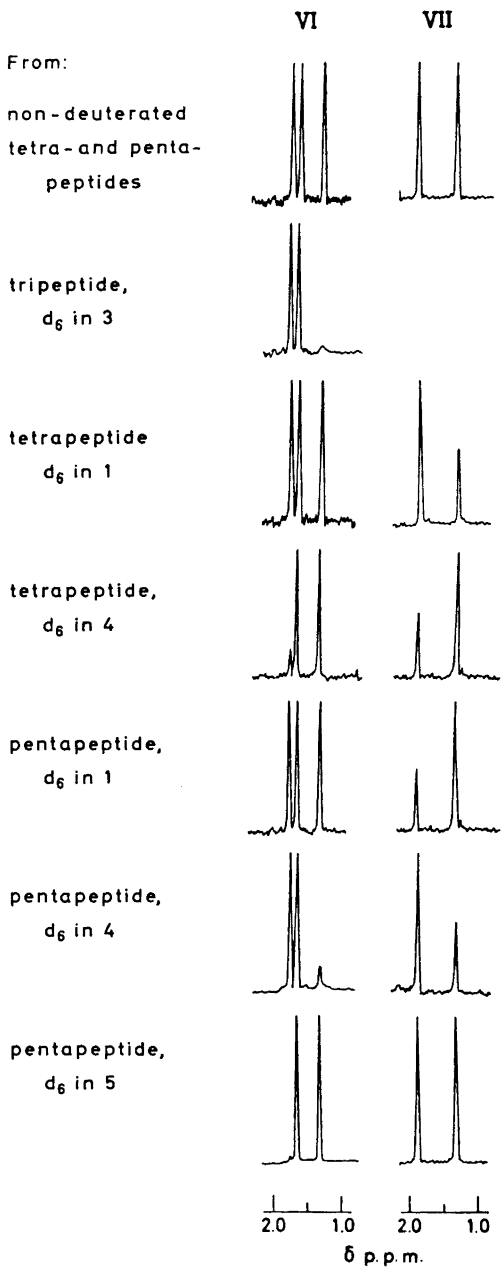

Fig. 3. NMR-spectra at 60 MHz in $CDCl_3$-solution of bicyclic imidazolone (VI) and tricyclic bis-imidazolone (VII) formed from non-deuterated peptides (top) and from various deuterated peptides (lower curves).

oxazolone (III), whereas in the tetrapeptide (II) imidazolone-formation seems likely (*cf.* hippuric amide [11] using PCl_5, and benzoyl-α-methylalanine amide [12] by simple heating) and presumably synchronized with fused piperazine formation as the acid chloride group is drawn closer to the remaining amide group. Elimination of the side-chain of the resulting intermediate (IV) gives the bicyclic imidazolone (VI), and cyclization of the side-chain when the amino group is liberated affords the tricyclic bis-imidazolone (VII).

A corresponding scheme for the pentapeptide is also in full agreement with the deuteration results (Fig. 3) for the bicyclic imidazolone assuming elimination of a dipeptide side-chain on the amino end. However, it does not explain the deuteration results for the tricyclic bis-imidazolone, which show that now the C-terminal residue is eliminated. Possibly, cyclization of the dipeptide side-

Table 1. Properties of bicyclic imidazolone (VI) and tricyclic bis-imidazolone (VII).

	VI	VII
M.p.	255°	253°
Mol. ion (mass spectrometry)	237	304
Yield from tripeptide	11 %	–
tetrapeptide	26 %	10 %
pentapeptide	33 %	15 %
Double bond abs. in IR	1730, 1670, 1640 cm^{-1}	1720, 1630 cm^{-1}
NMR shifts (ppm) in $CDCl_3$	1.78, 1.68, 1.35	1.89, 1.33

chain is now unlikely since an 8-membered ring would be formed. A different mechanism seems in this case to lead to the same bis-imidazolone in even better yield (Table 1). Initial imidazolone formation at the 2-residue might lead to this substance by final elimination of a side-chain consisting now of the 5-residue.

RING OPENING REACTIONS

Certain acylamidines of bicyclic type are known to undergo reversible conversion to mono-cyclic amides.[9] The possibility that our mono- and bis-imidazolones (VI and VII) might in alkaline medium be hydrated to cyclols, and then converted to cyclic tri- and tetrapeptides, was therefore examined. In alkaline water/methanol solution the imidazolone (VI) was slowly converted to the salt of the amidino acid (VIII, Fig. 4), whose structure was subsequently confirmed by NMR-spectroscopic comparison with the authentic substance.[8] The bis-imidazolone (VII) under the same conditions gave the salts of the mono-amidino acid (IX) and the bis-amidino acid (X). This was concluded by following the NMR-spectral changes of the solutions as well as from a study of

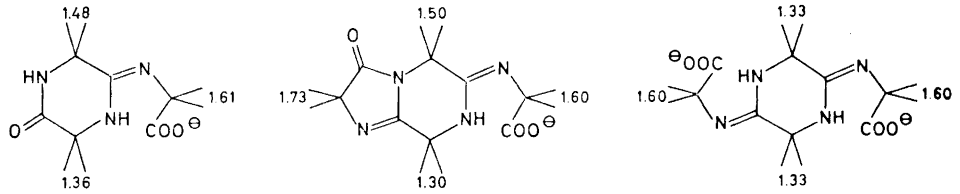

VIII IX X

Fig. 4.

partially deuterated amidino acids (VIII) which made possible the assignments of NMR-signals given in Fig. 4.

All these amidino acids reverted to the parent imidazolone (VI or VII) under acidic or even neutral conditions. No further change, apart from a low-field shift of the NMR-signals, could be observed in strongly acidic water/methanol solutions.

SYNTHETIC PATHS

The linear peptides were built up according to the methods developed by Kenner's group [7,10] using benzyloxycarbonyl protection at the amino end and *t*-butyl ester protection at the carboxyl end. Methyl ester protection could be used only for the dipeptide; thus, alkaline hydrolysis of the methyl ester of benzyloxycarbonyl dipeptide in aqueous dioxan [13] gave the acid in 85 % yield, whereas the tripeptide gave only 41 % (*cf.* Ref. 7). Oxazolone activation [7] was employed for coupling the tri- and higher peptides. This method was usefully modified to combine oligopeptide oxazolones with amino-esters containing more than one amino acid residue, although a longer reaction time (> 96 h) was needed. The individual operations necessary to prepare a penta-peptide were thus reduced by four steps (overall yield 50 %).

α-Methylalanine-d_6 was prepared from acetone-d_6 *via* the hydantoin derivative.[14,15] The isotopic purity of the labelled residue in labelled tri-, tetra-, and penta-peptides was 96 – 98 % as determined by NMR-spectroscopy.

EXPERIMENTAL

Derivatives and oligomers of α-methylalanine were prepared according to Kenner *et al.*,[7,10] except when otherwise stated. Evaporations were under reduced pressure. Neutral products were isolated by washing in ethyl acetate solution successively with 0.1 N HCl, water, 0.5 M $NaHCO_3$, water, and finally dried over $MgSO_4$ and evaporated.

Benzyloxycarbonyl-(α-methylalanyl)$_3$-α-methylalanine t-butyl ester. α-Methylalanyl-α-methylalanine *t*-butyl ester (2.2 g = 9 mmol), prepared by catalytic hydrogenation of the corresponding benzyloxycarbonyl derivative, was dissolved in dry acetonitrile (40 ml), 2-(1′-benzyloxycarbonylamino-1′-methyl)ethyl-4,4-dimethyloxazolone [10] (2.74 g = 9 mmol) added, and the solution heated under reflux for 96 h. The acetonitrile was evaporated and the neutral tetrapeptide isolated in the usual way and recrystallized from ethyl acetate-light petroleum (4.5 g = 91 %), m.p. 178°.[7]

Benzyloxycarbonyl-(α-methylalanyl)$_4$-α-methylalanine t-butyl ester. (a) A solution of 2-(1′-benzyloxycarbonyl-α-methylalanylamino-1′-methyl)ethyl 4,4-dimethyloxazolone [7] (0.98 g = 2.5 mmol) and α-methylalanyl-α-methylalanine *t*-butyl ester (0.73 g = 3 mmol) in dry acetonitrile (20 ml) was heated under reflux for 7 days. The neutral pentapeptide was isolated in the usual way and recrystallized from ethyl acetate-light petroleum or acetonitrile (1.1 g = 70 %), m.p. 236° (decomp.).[7]

(b) (α-Methylalanyl)$_2$-α-methylalanine *t*-butyl ester (0.82 g = 2.5 mmol), prepared by catalytic hydrogenation of the corresponding benzyloxycarbonyl derivative,[7] was dissolved in dry acetonitrile (15 ml), 2-(1′-benzyloxycarbonylamino-1′-methyl)ethyl-4,4-dimethyl-oxazolone [10] (0.6 g = 2 mmol) added, and the mixture heated under reflux for 7 days. The pentapeptide ester was isolated and recrystallized as above (0.8 g = 63 %), m.p. 236° (decomp.).[7]

Imidazolone VI from (α-methylalanyl)$_2$-α-methylalanine. Benzyloxycarbonyl-(α-methylalanyl)$_2$-α-methylalanine [7] (1.26 g = 3 mmol) was hydrogenated in methanol (50 ml) containing 5 % Pd-C catalyst (0.4 g) until evolution of CO_2 ceased, then filtered and evaporated. The resulting (α-methylalanyl)$_2$-α-methylalanine (0.82 g = 3 mmol) was refluxed with thionyl chloride (25 ml) for 1 h and evaporated. Traces of $SOCl_2$ were removed by evaporation with benzene. The product (0.9 g), showing ν_{max} at 1820 cm^{-1}, was dissolved in dry dimethylformamide (25 ml) and added during 1 h to dry pyridine (700 ml) at 70° with stirring. Heating and stirring was continued for 5 h. After evaporation the residue was taken into methanol (10 ml) and kept overnight at 0°. A precipitate of polymers (0.28 g) was filtered off and unreacted tripeptide (0.3 g) precipitated with ether from the filtrate. The filtered solution was evaporated, the residue dissolved in chloroform and washed with water to remove remaining traces of unreacted tripeptide and polymers. The chloroform solution was dried over $MgSO_4$ and evaporated to afford the imidazolone VI (0.075 g = 11 %), purified by sublimation (90 – 110°/0.02 mmHg), m.p. 255° (sealed tube).[8]

Imidazolone VI and bis-imidazolone VII. A. *From (α-methylalanyl)$_3$-α-methylalanine.* Benzyloxycarbonyl-(α-methylalanyl)$_3$-α-methylalanine (2.5 g = 5 mmol), m.p. 244°, prepared by hydrolysis of the corresponding *t*-butyl ester in trifluoroacetic acid,[7] was hydrogenated in methanol (100 ml) using 5 % Pd-C catalyst (0.7 g). After filtration, the solution was evaporated to afford the tetrapeptide, which was reprecipitated from acetone-ether (1.7 g = 95 %).

(a) (α-Methylalanyl)$_3$-α-methylalanine (0.72 g = 2 mmol) was refluxed with thionyl chloride (20 ml) for 1 h and evaporated. Traces of thionyl chloride were removed by repeating the evaporation with benzene. The residue (0.8 g), showing ν_{max} at 1790 cm^{-1}, was dissolved in dry dimethylformamide (25 ml) and added during 1 h to dry pyridine (700 ml) at 70° with stirring; the mixture was kept at this temperature for 4 h. The residue after evaporation was taken into methanol (10 ml) and left overnight at 0°. Some bis-imidazolone VII crystallized along with a precipitation of polymers. The crystals (0.02 g) were picked out manually and the polymers (0.2 g) filtered off. The filtrate was evaporated and the residue taken into water and extracted with chloroform. The aqueous solution contained the polymers, unreacted peptide and α-methylalanine. The chloroform solution was dried over $MgSO_4$ and evaporated, and the imidazolone VI and more bis-imidazolone VII were fractionally crystallized from methanol and further purified by sublimation. Total yields and properties were: VI (0.068 g = 14 %), subl. at 90 – 110°/0.02 mmHg, m.p. 255° (sealed tube);[8] VII (0.31 g = 5 %, subl. at 100 – 120°/0.02 mmHg, m.p. 253° (sealed tube). (Found: C 63.12; H 7.77; N 18.60. $C_{16}H_{24}N_4O_2$ requires C 63.16; H 7.95; N 18.42.)

(b) (α-Methylalanyl)$_3$-α-methylalanine (0.1 g = 0.27 mmol) was suspended in freshly distilled acetyl chloride (10 ml), cooled to 0° and PCl_5 (0.25 g) added. A clear solution was formed after 3 min, and this was stirred for 20 h at room temp., when a white precipitate formed. The solution was decanted and the precipitate washed with a little acetyl chloride. The solid showed ν_{max} (KBr) at 1790, 1730, 1590 cm^{-1}.

A portion of the precipitate, dissolved in dry dimethylformamide (25 ml), was added to pyridine (500 ml) as described above. The residue after evaporation was dissolved in chloroform and washed with water. The water layer contained polymers, unreacted peptide and α-methylalanine. Evaporation of the chloroform solution afforded a mixture of VI and VII, finally separated and purified as in the preceding experiment to give pure VI (0.017 g) and VII (0.007 g).

B. *From (α-methylalanyl)$_4$-α-methylalanine.* Hydrogenolysis of benzyloxycarbonyl-(α-methylalanyl)$_4$-α-methylalanine (1.15 g = 2 mmol) in methanol (50 ml) containing Pd-C catalyst (0.5 g) yielded (α-methylalanyl)$_4$-α-methylalanine, precipitated from acetone-ether (0.83 g = 95 %).

This pentapeptide (0.22 g = 0.5 mmol) was suspended in freshly distilled acetyl chloride (20 ml), cooled to 0° and PCl_5 (0.5 g) added. The clear solution which appeared after few minutes was stirred at room temp. for 20 h, when a white substance precipitated. Both the precipitate and the filtrate after evaporation showed absorption at ν_{max} 1790, 1730, and 1690 cm^{-1}. The combined products in dry dimethylformamide (25 ml) were added to pyridine (700 ml) as in the preceding experiment. After evaporation, the residue was dissolved in chloroform and washed with water. The imidazolone VI (0.024 g = 20 %) and bis-imidazolone VII (0.006 g = 4 %) were isolated in the usual way.

α-*Methylalanine*-d_6. Acetone-cyanohydrin-d_6 was prepared from hexadeuterioacetone (16.5 g = 0.25 mol) and converted into 5,5-dimethylhydantoin-d_6 by the method of Wagner and Simons,[14] recrystallized from water, m.p. 175 – 178°. The resulting hydantoin (13 g = 0.1 mol), $Ba(OH)_2.8H_2O$ (45 g) and water (180 ml) were placed in an autoclave and heated for ½ h at 160 – 170°. After cooling, the solution was filtered and treated with $(NH_4)_2CO_3$ to precipitate the excess of barium, heated again to expel excess of $(NH_4)_2CO_3$, and filtered. The filtrate was concentrated until crystals appeared, and crystallization was completed by addition of methanol. The α-methylalanine-d_6 (7.2 g = 66 %) sublimed [15] at 280°, *m/e* 109.

Benzyloxycarbonyl-α-methylalanine-d_6. α-Methylalanine-d_6 (10.9 g = 0.1 mol) was reacted with benzyl chloroformate,[10] and formed benzyloxycarbonyl-α-methylalanine-d_6 recrystallized from ethyl acetate-light petroleum (20.5 g = 85 %), m.p. 74 – 75°. The integrated NMR-spectrum showed that 98 % of the α-methyl protons were deuterated.

Benzyloxycarbonyl-α-methylalanyl-d_6-*α-methylalanine.* Benzyloxycarbonyl-α-methylalanine-d_6 (8.5 g = 25 mmol) and α-methylalanine methyl ester hydrochloride (3.2 g = 27 mmol) in acetonitrile (150 ml) containing triethylamine (2.5g) was cooled to 0° and dicyclohexylcarbodiimide (5.8 g = 28 mmol) added. The mixture was stirred at room temp. (24 h) and evaporated. The neutral product was isolated in the usual manner and recrystallized from ethyl acetate-light petroleum (5.1 g = 15 mmol), m.p. 110°. Hydrolysis [13] gave benzyloxycarbonyl-α-methylalanyl-d_6-α-methylalanine, recrystallized from aqueous methanol (4.1 g = 85 %), m.p. 161°.

α-*Methylalanine*-d_6 *t-butyl ester.* Benzyloxycarbonyl-α-methylalanine-d_6 *t*-butyl ester (12.7 g = 87 %), m.p. 61°, was prepared from benzyloxycarbonyl-α-methylalanine-d_6 (12.15 g = 50 mmol).[7] Hydrogenolysis of the benzyloxycarbonyl group afforded α-methylalanine-d_6 *t*-butyl ester [7] (94 %).

Deuterated imidazolone VI from (α-methylalanyl)$_2$-α-methylalanine-d_6 via *the oxazolone.* α-Methylalanine-d_6 *t*-butyl ester (0.5 g = 3 mmol) was reacted with 2-(1′-benzyloxycarbonylamino-1′-methyl)ethyl-4,4-dimethyloxazolone [10] (0.92 g = 3 mmol) to yield the protected tripeptide (0.9 g = 64 %), m.p. 167°. The *t*-butyl ester was cleaved in TFA [7] to the acid (0.75 g), m.p. 202°. Treatment of the acid with acetic anhydride gave 2-(1′-benzyloxycarbonyl-α-methylalanylamino-1′-methyl)ethyl-4,4-dideuteromethyloxazolone (0.72 g), m.p. 125°. The oxazolone derivative (0.72 g = 1.8 mmol) was hydrogenated in dry ethyl acetate and set aside for 3 days at room temp.[8] The precipitation of amidine-d_6 was collected and recrystallized from ethanol-ether (0.4 g), δ_{TMS} 1.58, 1.66 in $CDCl_3$, integration ratio 1:1. Sublimation (90 – 110°/0.02 mmHg) gave dehydration to the imidazolone VI-d_6 (0.38 g = 88 %) m.p. 255° (sealed tube), *m/e* 243 (Fig. 3).

Deuterated imidazolone VI and bis-imidazolone VII. (a) *From α-methylalanyl*-d_6-(α-*methylalanyl)$_2$-α-methylalanine.* Benzyloxycarbonyl-α-methylalanyl-d_6-α-methylalanine (2.6 g = 8 mmol) was dehydrated to the corresponding oxazolone [10] (2.3 g = 93 %), m.p. 126°. Part of it (1.1 g = 3.5 mmol) was reacted with dipeptide *t*-butyl ester (0.9 g = 3.5 mmol) to yield benzyloxycarbonyl-α-methylalanyl-d_6-(α-methylalanyl)$_2$-α-methylalanine *t*-butyl ester (1.7 g = 88 %), m.p. 178°. Cleavage of the *t*-butyl ester in TFA [7] yielded benzyloxycarbonyl-tetrapeptide (1.4 g = 93 %), m.p. 245°. Hydrogenolysis in acetic acid (200 ml) using Pd-C catalyst (0.6 g) afforded α-methylalanyl-d_6-(α-methylalanyl)$_2$-α-methylalanine (1 g = 99 %). This tetrapeptide (0.36 g = 1 mmol) was treated with PCl_5 (0.55 g) in acetyl chloride (30 ml) at 0° and stirred at room temp. for 20 h. After evaporation, the residue (showing ν_{max} 1790 cm^{-1}) was dissolved in dimethylformamide (20 ml) and added during ½ h into pyridine (500 ml) at 70° with stirring. After 4½ h at 70° the solution

was evaporated and the residue treated with chloroform-water. The cyclic compounds were isolated from chloroform and purified in the usual way; imidazolone VI (0.06 g = 25 %), *m/e* 237, bis-imidazolone VII-d_6 (0.03 g = 10 %), *m/e* 310 (Fig. 3).

(b) *From (α-methylalanyl)$_3$-α-methylalanine*-d$_6$. α-Methylalanine-d_6 *t*-butyl ester (1.5 g = 9 mmol) was reacted with 2-(1′-benzyloxycarbonyl-α-methylalanylamino-1′-methyl)-ethyl-4,4-dimethyloxazolone [7] (3.2 g = 8 mmol). The resulting protected tetrapeptide (3.4 g = 77 %), m.p. 178°, was hydrolyzed in TFA [7] to the corresponding acid (2.8 g = 93 %), m.p. 245°, and a part of it (1.5 g = 3 mmol) hydrogenated in acetic acid (300 ml) to (α-methylalanyl)$_3$-α-methylalanine-d_6 (1 g = 98 %). This tetrapeptide-d_6 (0.5 g = 1.4 mmol) was reacted with PCl_5 (1.1 g) in acetyl chloride (30 ml), and after evaporation cyclized in pyridine as described. The imidazolone VI-d_6 (0.013 g = 3.4 %), *m/e* 243, and the bis-imidazolone VII-d_6 (0.008 g = 1.8 %), *m/e* 310, were isolated (Fig. 3).

(c) *From α-methylalanyl*-d$_6$-*(α-methylalanyl)$_3$-α-methylalanine*. The oxazolone of benzyl-oxycarbonyl-α-methylalanyl-d_6-α-methylalanine (0.93 g = 3 mmol) was reacted with the tripeptide *t*-butyl ester (1 g = 3 mmol) to give the protected pentapeptide (1.7 g = 89 %), m.p. 236°. The *t*-butyl ester was hydrolyzed to the acid (1.5 g = 96 %), m.p. 256°, and hydrogenated in acetic acid (200 ml) to α-methylalanyl-d_6-(α-methylalanyl)$_3$-α-methyl-alanine (1.1 g = 97 %). This pentapeptide (0.3 g = 0.67 mmol) was reacted with PCl_5 (0.6 g) in acetyl chloride (30 ml) and cyclized in pyridine as usual. The imidazolone VI (0.048 g = 30 %), *m/e* 237, and the bis-imidazolone VII-d_6 (0.006 g = 3 %), *m/e* 310, were isolated (Fig. 3).

(d) *From (α-methylalanyl)$_3$-α-methylalanyl*-d$_6$-*α-methylalanine*. Benzyloxycarbonyl-(α-methylalanyl)$_3$-α-methylalanine-d_6 (1 g = 2 mmol) was dehydrated to the oxazolone [7] (0.95 g = 2 mmol), m.p. 158° and reacted with α-methylalanine *t*-butyl ester (0.3 g = 2 mmol) to give the protected pentapeptide [7] (1 g = 78 %), m.p. 236°. This was hydrolyzed to the acid (0.8 g = 92 %), m.p. 256°, and then hydrogenated in acetic acid (200 ml) to (α-methylalanyl)$_3$-α-methylalanyl-d_6-α-methylalanine (0.6 g = 97 %). This pentapeptide (0.3 g = 0.67 mmol) was reacted with PCl_5 (0.55 g) in acetyl chloride (15 ml), and after evaporation of solvents cyclized in pyridine to give the imidazolone VI-d_6 (0.051 g = 31 %), *m/e* 243, and the bis-imidazolone VII-d_6 (0.015 g = 7 %), *m/e* 310 (Fig. 3).

(e) *From (α-methylalanyl)$_4$-α-methylalanine*-d$_6$. α-Methylalanine-d_6 *t*-butyl ester (0.7 g = 4.2 mmol) was reacted with 2-(1′-benzyloxycarbonyl-α-methylalanyl-α-methylalanyl-amino-1′-methyl)ethyl-4,4-dimethyloxazolone [7] (1.9 g = 4 mmol) to give the protected pentapeptide (2 g = 74 %), m.p. 236°. The *t*-butyl ester was hydrolyzed to the acid (1.7 g = 98 %), m.p. 256°, and part of it (0.9 g = 1.5 mmol) hydrogenated to (α-methylalanyl)$_4$-α-methylalanine-d_6 (0.65 g = 98 %). The pentapeptide (0.2 g = 0.45 mmol) was reacted with PCl_5 (0.4 g) in acetyl chloride (20 ml), and cyclized in pyridine to give the imidazolone VI-d_6 (0.035 g = 32 %), *m/e* 243, and the bis-imidazolone VII (0.02 g = 15 %), *m/e* 304 (Fig. 3).

Ring opening reactions. These were followed directly in the NMR-tubes in a mixture of 20 % NaOD in D_2O (0.2 ml) and CD_3OD (0.5 ml). The final spectrum starting from non-deuterated imidazolone (VI) had δ 1.61, 1.48, and 1.36, while the same compound deuterated in the five-membered ring had δ 1.48 and 1.36, and in the six-membered ring δ 1.61 and 1.48.

Experiments in acid medium were conducted in a mixture of 36 % DCl in D_2O 0.1 ml) and CD_3OD (0.5 ml).

REFERENCES

1. Eliel, E. L., Allinger, N. L., Angyal, S. J. and Morrison, G. A. *Conformational Analysis*, Wiley-Interscience, New York 1965, p. 191.
2. Turner, R. B., Nettleton, D. E. and Perelman, M. *J. Am. Chem. Soc.* **80** (1958) 1430.
3. Dale, J. and Titlestad, K. *Chem. Commun.* **1969** 656.
4. Pless, J. and Boissonas, R. A. *Helv. Chim. Acta* **46** (1963) 1609.
5. Wieland, T. and Ohly, K.W . *Ann.* **605** (1957) 179.
6. Kopple, K. D., Ohnishi, M. and Go, A. *J. Am. Chem. Soc.* **91** (1969) 4264.
7. Jones, D. S., Kenner, G. W., Preston, J. and Sheppard, R. C. *J. Chem. Soc.* **1965** 6227.
8. Jones, D. S., Kenner, G. W., Preston, J. and Sheppard, R. C. *Tetrahedron* **21** (1965) 3209.

9. Shemyakin, M. M., Antonov, V. K., Shkrob, A. M., Shchelokov, V. I. and Agadzhanyan, Z. E. *Tetrahedron* **21** (1965) 3537.
10. Leplawy, M. T., Jones, D. S., Kenner, G. W. and Sheppard, R. C. *Tetrahedron* **11** (1960) 39.
11. Karrer, P. and Gränacher, C. *Helv. Chim. Acta* **7** (1924) 763.
12. Mohr, E. *J. prakt. Chem.* **81** (1910) 49.
13. Diel, J. and Young, E. A. *J. Med. Chem.* **7** (1964) 820.
14. Wagner, E. C. and Simons, J. K. *J. Chem. Educ.* **13** (1936) 265.
15. Clarke, H. T. and Bean, H. J. *Org. Syn. Coll. Vol.* **2** (1943) 29.

Received October 27, 1972.

ACTA CHEMICA SCANDINAVICA 27 (1973) 1519–1525

Eight-ring Monomeric and Sixteen-ring Dimeric Formals and Ketals

JOHANNES DALE and TERJE EKELAND

Kjemisk Institutt, Universitetet i Oslo, Oslo 3, Norway

1,3-Dioxacyclooctanes and 1,3,9,11-tetraoxacyclohexadecanes, with and without *gem*-dimethyl substituents in the 2- or 6- (and 10- or 14-) positions, have been synthesized. They are all conformationally homogeneous, and the observed low dipole moments show that the 2- (and 10-) carbon atoms must be in "corner" positions. Two of the 16-membered rings must therefore have "square" diamond-lattice conformations, while the other two may be "square" or "rectangular".

Cyclohexadecane itself is conformationally heterogeneous in solution, and its lowest-enthalpy "square" diamond-lattice conformation becomes exclusive only in the low-temperature crystal phase.[1] One might therefore have expected the conformational situation in a corresponding tetra-ether, 1,5,9,13-tetraoxacyclohexadecane, to be even more complex, since on each type of ring skeleton there should be several possible dispositions of the oxygen atoms, for example the three shown in Fig. 1 for the square ring conformation.

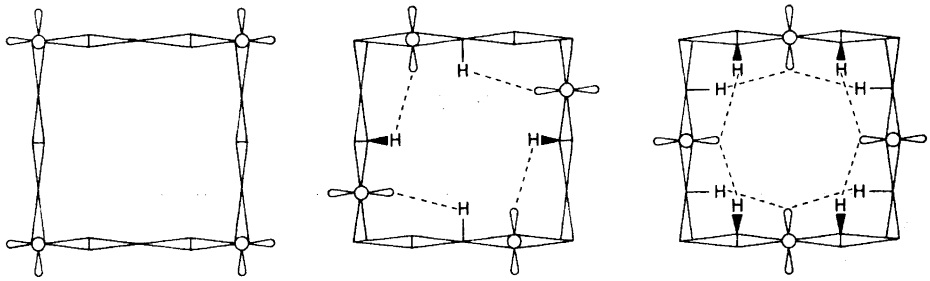

8 H-H gauche	4	0
7.2 kcal/mol	3.6	0
0 Debye	0	0
a.	b.	c.

Fig. 1.

Nevertheless, this tetraether turned out [1] to have a single conformation in solution, the same as in the crystal. The rationale of this was that when the ether oxygens are β to all corners (Fig. 1c), all eight repulsive *gauche* CH···CH interactions of the hydrocarbon, two at each corner, are changed into *gauche* CH···O interactions, which must be less repulsive and perhaps even slightly attractive. This conformation was subsequently verified by Groth for the crystal.[2] * The measured dipole moment was extremely low for this tetraether (0.3 D) and for the 3,3,7,7,11,11,15,15-octamethyl derivative (~ 0) which has this oxygen location imposed by the restriction of the substituents to corner positions; however, a zero dipole moment is also expected for the other two conformers (a and b) in Fig. 1.

For 1,3,9,11-tetraoxacyclohexadecane a stability argument in terms of number of CH···O *gauche* interactions cannot predict the best location of the oxygen atoms on the "square" ring conformation; in each of the three possible conformers (Fig. 2) only four *gauche* interactions are improved. On the other hand, the expected dipole moments are vastly different and should allow experimental identification.

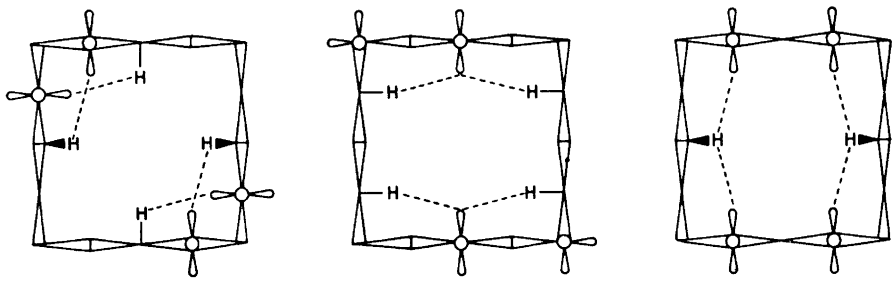

Fig. 2.

To examine this conformational problem, and at the same time study the related 1,3-dioxacyclooctanes, four pairs of compounds (I and II) were synthesized:

* It is interesting that the chemically related poly(trimethylene oxide) in the crystalline state has a helical conformation built up of the same *anti*, *anti*, +*gauche*, +*gauche* $CH_2-O-CH_2-CH_2$-repeat unit (Takokoro, H., Takahashi, Y. and Chatani, Y. Cited by Mark, J. E. *J. Polymer Sci.* **B 4** (1966) 825). Even 1,3-dibromopropane and 1,3-dichloropropane, as well as the 2,2-dimethyl derivative, show a remarkable preference (~ 60 %) for the +*gauche*, +*gauche* conformation in the gas phase, as shown by electron diffraction (Stølevik, R., unpublished).

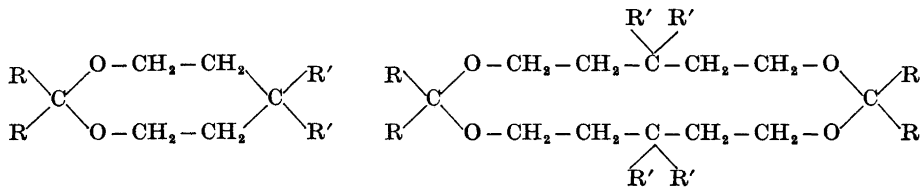

I II

	a.	b.	c.	d.
R:	H	H	Me	Me
R′:	H	Me	H	Me

Some of these carry *gem*-dimethyl substituents in order to define "corner" positions.

SYNTHETIC ASPECTS

The cyclic formals (Ia, b; IIa,b) were prepared from paraformaldehyde and pentane-1,5-diol (or 3,3-dimethylpentane-1,5-diol) in benzene solution in the presence of an acid ion-exchange resin,[3] removing formed water as an azeotrope with benzene. A relatively small yield of the crystalline dimeric cyclic formal was obtained. The main product was a polymer which could be pyrolyzed in the presence of an acid catalyst to give in good yield the liquid monomeric cyclic formal. The unsubstituted rings (Ia; IIa) have been prepared by Hill and Carothers [4] by a different method.

The cyclic ketals (Ic,d; IIc,d) were prepared from 2,2-dimethoxypropane and the same diols in benzene solution in the presence of an acid ion-exchange resin; formed methanol was removed as an azeotrope with benzene. The liquid monomeric cyclic ketal was obtained directly in 60 – 70 % yield. This could be converted in 70 – 80 % yield to the crystalline dimeric cyclic ketal by simply stirring a solution in hexane in the presence of the same acid resin. Presumably, the strain in the 8-membered ring is the driving force for its conversion to the unstrained 16-membered ring. A further reaction to still larger rings provides no additional strain relief and would even be thermodynamically disfavoured, since the entropy of the whole system must thereby decrease.

CONFORMATIONS OF THE 1,3-DIOXACYCLOOCTANES

The conformations of the 8-membered rings have already been discussed in a preliminary communication.[5] First of all, the temperature-invariant infrared spectra of these liquids on cooling suggest conformational homogeneity. Secondly, the observed low values of their molecular dipole moments (Table 1) are very close to those of the simplest aliphatic analogs, 2,2-dimethoxypropane and dimethoxymethane, and the preferred conformation of the latter has been established [6] as +*gauche*, +*gauche*. A much larger value (Table 1) is found [7] for 1,3-dioxan, where the corresponding bonds are +*gauche*, −*gauche*,

Table 1. Data for 1,3-dioxacyclooctanes.

	B.p.	Found C	Found H	Analysis Formula	Calc. C	Calc. H	Dipole moment in benzene at 25°C
Ia [4]	130–140°/760 mm			$C_6H_{12}O_2$			0.73 D[a]
Ib	164–168°/765 mm	66.83	11.49	$C_8H_{16}O_2$	66.70	11.10	1.00 D[a]
Ic	40–41°/9 mm	67.31	10.63	$C_8H_{16}O_2$	66.70	11.10	0.58 D[b]
Id	58–60°/10 mm	69.98	11.72	$C_{10}H_{20}O_2$	69.97	11.63	0.61 D[b]

[a] To be compared with 0.99 D for dimethoxymethane and 1.9 D for 1,3-dioxan.[7]
[b] To be compared with 0.61 D for 2,2-dimethoxypropane.

and still higher values are expected for *anti, gauche* and *anti, anti*. This means that the oxygen atoms must be adjoining a nearly perfect corner formed by two staggered C–O bonds, which thus limits the possibilities to the boat-boat and boat-chair (Fig. 3).

In our preliminary publication,[5] 100 MHz ^{1}H NMR-spectroscopic data were taken to indicate that the boat-chair was chosen by the two compounds lacking substituents in the diol component (Ia,c) and the boat-boat by the two that carry such substituents (Ib,d). However, more recent 251 MHz ^{1}H and 63 MHz ^{13}C data [8] suggest that all four adopt the boat-chair conformation and also confirm by an independent method that the $-O-CR_2-O-$group is straddling the perfect corner position (Fig. 3b). This is of course expected for the ketal group because of the bulk of the substituents (R = Me) but is a surprising and most important conclusion for the formal group (R = H). In this ring system, one explanation may be that transannular H–H interactions are relieved. In addition, the favourable antiparallel dipole orientation may play a role, since also open-chain systems prefer this *+gauche, +gauche* geometry. Thus, not only the already mentioned dimethoxymethane,[6] but also the oxymethylene polymer has, at least in the crystal, a helix conformation with all bonds *gauche* of the same sign.[9]

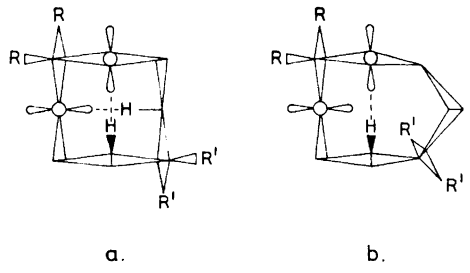

Fig. 3.

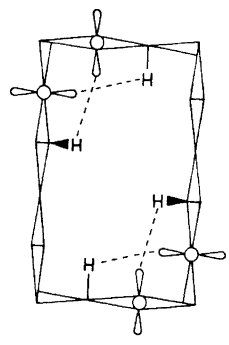

Fig. 4.

CONFORMATIONS OF THE 1,3,9,11-TETRAOXACYCLOHEXADECANES

All four sixteen-membered rings are conformationally homogeneous by the criterion that their infrared spectra have sharp bands and are practically identical in the solid and in solution. The unsubstituted ring shows a few crystal splittings suggesting a tighter packing in the crystal; this may also be concluded from its higher enthalpy (and entropy) of melting (Table 2).

Table 2. Data for 1,3,9,11-tetraoxacyclohexadecanes.

	M.p. (°C)	ΔH_m (kcal/mol)	ΔS_m (cal/deg.mol)	Found C	Found H	Analysis Formula	Calc. C	Calc. H	Dipole moment in benzene at 25°C
IIa [4]	56– 58	8.5	25.6			$C_{12}H_{24}O_4$			0.9 D
IIb	82– 85	7.1	19.8	66.55	11.19	$C_{16}H_{32}O_4$	66.70	11.10	~0
IIc	102–104	6.2	16.7	66.85	11.25	$C_{16}H_{32}O_4$	66.70	11.10	0
IId	138–140	5.9	14.5	69.08	11.39	$C_{20}H_{40}O_4$	69.97	11.63	0

Conformational homogeneity is in itself surprising when no substituents are present, since the number of *gauche* H–H interactions is the same in all three possible conformers of the square ring skeleton (Fig. 2). That we have again a preference for the conformer with both $-O-CH_2-O-$ systems across corners * is unequivocally demonstrated by the low observed dipole moment (Table 2) of this compound (as of the substituted compounds). Whether it is in fact the "square" ring skeleton (Fig. 2a) cannot be definitely decided from these data. A "rectangular" non-diamond-lattice type of ring conformation, calculated [10] to be only about 1 kcal/mol higher in enthalpy of cyclohexadecane, would also allow both $-O-CR_2-O-$ groups to be at diametric corners and have cancelled dipole moments (Fig. 4) in the two cases when there is no substituent R′ in the diol component (IIa,c). In the other cases (IIb,d) all corners are fixed, so as to impose the square ring skeleton, by the bulk of the *gem*-dimethyl groups and by the dipole-favoured orientation of the 1,3-dioxa-grouping across a corner.**

The strong conformational preference and the apparent rigidity of these four 1,3,9,11-tetraoxacyclohexadecanes, as well as of the two 1,5,9,13-tetraoxacyclohexadecanes discussed in the introduction, is very striking and in contrast both to cyclohexadecane on the one hand and to other macrocyclic oligoethers on the other hand. Thus, the hydrocarbon is a conformer mixture in solution,[1] and 15- and 18-ring homologues of ethylene oxide have broad infrared bands and dipole moments close to the statistical value calculated for

* A very recent crystal structure determination of 1,3,8,10-tetraoxacyclotetradecane reveals the same feature of corner location of both formal groups on the unique 14-ring diamond-lattice conformation (Bassi, I. W., Scordamaglia, R. and Fiore, L. *J. Chem. Soc. Perkin 2* **1972** 1726).

** Anet and Krane [8] have recently shown by 251 MHz ^1H and 63 MHz ^{13}C NMR spectroscopy that not only the latter two compounds (IIb, d) but also one of the former (IIa) are indeed square, whereas the ketal IIc is rectangular.

independently oriented ether dipoles.[11] When it is considered that the calculated value for four ether dipoles is as high as $\sqrt{4} \times 1.3$ D = 2.6 D, the observed near-zero values for our 16-membered rings force us to believe that the interaction between CH α and oxygen β to the same corner (or *vice versa*), indicated by pointed lines in Figs. 1, 2, and 4, has a certain attractive character and so acts to stiffen the whole ring. This is in contrast with the transannular CH···O interaction (Fig. 3), one step closer on the diamond lattice, which in 8-membered rings seems to be repulsive.

EXPERIMENTAL

Preparation of cyclic formals (Ia,b; IIa,b). A mixture of pentane-1,5-diol or 3,3-dimethylpentane-1,5-diol[12] (0.5 mol), paraformaldehyde (0.5 mol), benzene (150 ml), and Amberlite IR-120 cation-exchange resin (3 g) in its acid form[3] was boiled for 2 – 3 h, when the calculated quantity of formed water had been collected from the distilled azeotrope in a water separator. The catalyst was filtered off and remaining benzene evaporated *in vacuo*. Distillation of the residue at reduced pressure gave a small quantity of the dimeric formal which distilled as a liquid and crystallized partly (IIa) or sublimed directly (IIb). If necessary, the solid can be washed free of diol with water and recrystallized from water/ethanol containing a trace of KOH.

The non-distillable solid residue was mixed with a trace of sulfuric or *p*-toluenesulfonic acid and pyrolysed at 100 – 200°. The camphor-smelling liquid pyrolysate was collected over potassium carbonate, redistilled at atmospheric pressure and identified as the monomeric formal (Ia,b).

Analytical and physical data are given in Tables 1 and 2.

Preparation of cyclic ketals (Ic,d; IIc,d). A mixture of pentane-1,5-diol or 3,3-dimethylpentane-1,5-diol[12] (0.5 mol), 2,2-dimethoxypropane (0.5 mol), benzene (150 ml), and Amberlite IR-120 resin (3 g) was heated in a flask fitted with a 60 cm Vigreux column. Formed methanol started to distil as an azeotrope with benzene at 58°, and heating was continued until the b.p. was 80°. After cooling, the catalyst was filtered off and the benzene evaporated. Distillation of the residue at 10 mmHg gave the liquid monomeric ketal and left a residue which at further reduced pressure (0.1 mmHg) gave more monomer, before finally some dimeric ketal sublimed.

The monomeric ketal was dissolved in hexane or pentane and stirred for 4 h with the same Amberlite resin. The catalyst was filtered off, the solution then filtered through potassium carbonate, and the solvent evaporated. The solid residue was taken up in warm ethanol, and the dimeric ketal crystallized on cooling.

Analytical and physical data are given in Tables 1 and 2.

Calorimetric measurements. These were performed in a Perkin-Elmer Differential Scanning Calorimeter DSC-1B.

Determination of dipole moments. Dielectric constants were measured at 25° in a Weilheim Dipolmeter DM 01 on four different benzene solutions of each compound. Refractive indices were measured on the same solutions in a Brice-Phoenix Differential Refractometer. Dipole moments were calculated according to Hedestrand[13] using no correction for atomic polarization.

Infrared spectra. These were recorded in a Perkin-Elmer Grating Infrared Spectrophotometer 457 as KBr pellets and in CS_2- and CCl_4-solutions. Low-temperature spectra were obtained in an RIIC low-temperature cell cooled with methanol/dry-ice mixture.

REFERENCES

1. Borgen, G. and Dale, J. *Chem. Commun.* **1970** 1340.
2. Groth, P. *Acta Chem. Scand.* **25** (1971) 725.
3. Astle, M. J., Zaslowsky, J. A. and Lafyatis, P. G. *Ind. Eng. Chem.* **46** (1954) 787.
4. Hill, J. W. and Carothers, W. H. *J. Am. Chem. Soc.* **57** (1935) 925.
5. Dale, J., Ekeland, T. and Krane, J. *J. Am. Chem. Soc.* **95** (1972) 1389.

6. Astrup, E. E. *Acta Chem. Scand.* **25** (1971) 1494.
7. Arbousow, B. A. *Bull. Soc. Chim. France* **1960** 1311.
8. Anet, F. A. L. and Krane, J. *Unpublished.*
9. Mizushima, S. I. and Shimanouchi, T. *J. Am. Chem. Soc.* **86** (1964) 3521.
10. Dale, J. *Unpublished.*
11. Dale, J. and Kristiansen, P. O. *Chem. Commun.* **1971** 670; *Acta Chem. Scand.* **26** (1972) 1471.
12. Blomquist, A. T., Wheeler, E. S. and Chu, Y. *J. Am. Chem. Soc.* **77** (1955) 6307.
13. Hedestrand, G. *Z. physik. Chem.* **B 2** (1929) 428.

Received October 31, 1972.

ACTA CHEMICA SCANDINAVICA 27 (1973) 1526–1530

Glyoxylic Acid as Reductant in Ozonolysis. I

PER KOLSAKER*, ERLING BERNATEK**, RONNIE JOHANSON and RUTH HYTTA

Universitetets Kjemiske Institutt, Blindern-Oslo 3, Norway

The use of glyoxylic acid as a reducing agent in ozonolyses in protic solvents has been studied. When ketones are formed during the ozonolysis and subsequent reduction, the reaction is completed using equimolar amounts of glyoxylic acid. Whenever aldehydes are formed, excess of glyoxylic acid has to be used, probably due to autoxidation of the aldehydes. The presence of acid is a necessity and acetic acid is the solvent of choice.

Reduction of ozonolysis mixtures has been accomplished with a number of agents.[1] A common feature for most of them is that they leave their oxidation products as nonvolatile compounds in the mixture. The only exception to this is catalytic hydrogenation. However, if the ozonation is performed at low temperature, it is difficult to carry out the hydrogenation without increasing the temperature.

Glyoxylic acid is oxidized by hydrogen peroxide to formic acid and carbon dioxide.[2] It was therefore of interest whether the hydroperoxides formed by ozonolysis in protic solvents could oxidize glyoxylic acid to volatile products exclusively. A few disubstituted and one tetrasubstituted olefin were selected to test this reaction.

trans-Stilbene was ozonized in a mixture of acetic acid and methylene chloride. After addition of equimolar amounts of glyoxylic acid dissolved in glacial acetic acid, the decrease in active oxygen was followed iodometrically. (Fig. 1).

trans-4-Octene was ozonized in glacial acetic acid and subsequently one half, one, and two mol equivalents of glyoxylic acid, respectively, were added. (Fig. 2). Satisfactory reduction took place only when an excess of glyoxylic acid was used. The increase in the active oxygen content in the decomposition experiment, and when using semi- and equimolar proportions of glyoxylic

* To whom inquiries should be directed.
** Present address: Universitetets Farmasøytiske Institutt, Blindern/Oslo 3, Norway.

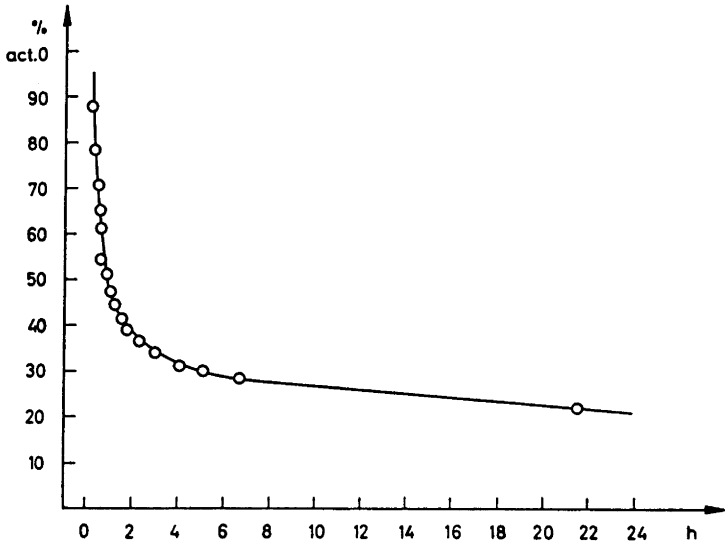

Fig. 1. Reduction of ozonized stilbene with one molar equivalent of glyoxylic acid monohydrate.

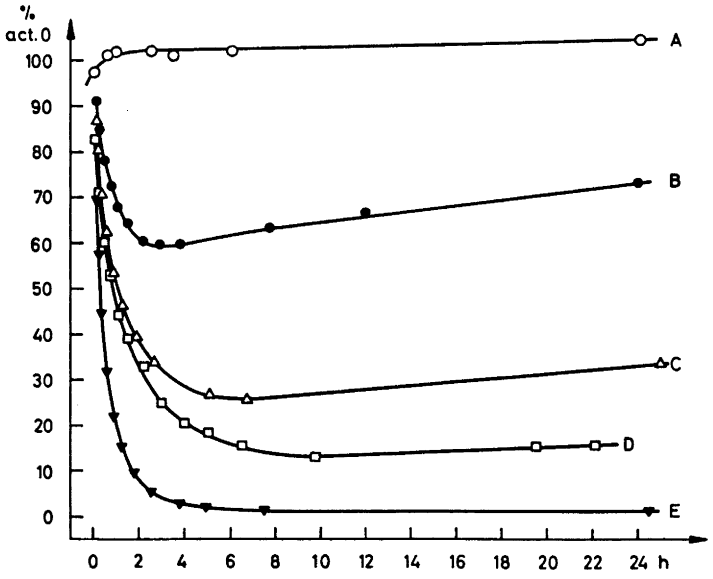

Fig. 2. Decomposition and reduction of ozonized *trans*-4-octene. A. decomposition in glacial acetic acid. B. Reduction with semimolar equivalent of glyoxylic acid monohydrate. C. Reduction with molar equivalent of glyoxylic acid monohydrate. D. As in C, but in a nitrogen atmosphere. E. Reduction with 2 mol equivalents of glyoxylic acid monohydrate.

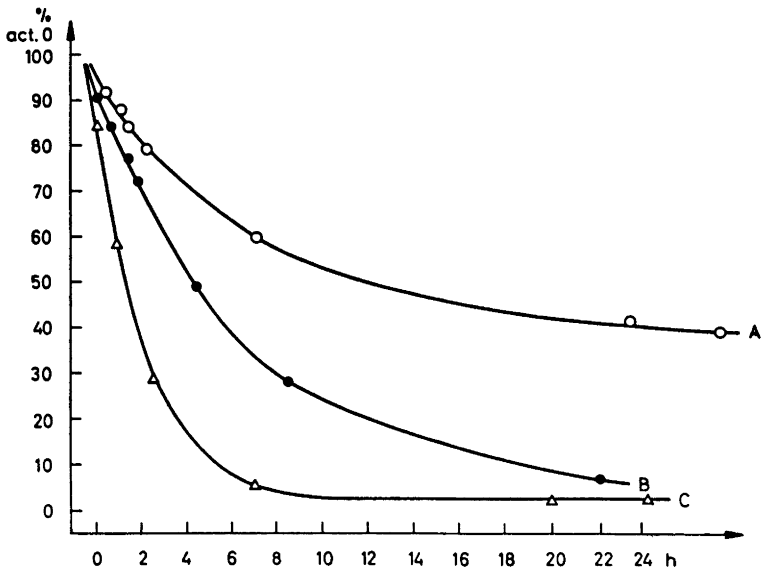

Fig. 3. Reduction of ozonized 2,3-dimethyl-2-butene with glyoxylic acid monohydrate. A. Semimolar equivalent. B. Molar equivalent. C. 2 mol equivalents.

acid, is probably due to autoxidation of the butyraldehyde formed in the ozonolysis. In fact, benzaldehyde and butyraldehyde were both shown to undergo autoxidation (probably to peracids) [3] under the prevailing conditions. Carrying out the reduction in a nitrogen atmosphere a more "normal" reduction took place. When ozonizing 2,3-dimethyl-2-butene where the reduction product is acetone, autoxidation is avoided. Reduction with semimolar proportions of glyoxylic acid goes halfway and with equimolar proportions goes approximately to completion. (Fig. 3).

The reduction of the ozonized solution of anethole (1-(4-methoxyphenyl)-1-propene) in glacial acetic acid followed the same general pattern (Fig. 4). More than one mol equivalent glyoxylic acid had to be used to ensure an approximately complete reduction in a reasonable time. Since it was shown that autoxidation of benzaldehyde or acetaldehyde did not take place in methanol, ozonolysis was carried out in this solvent. However, no reduction with glyoxylic acid was achieved, even in the presence of small amounts of trifluoroacetic acid. If, after ozonolysis in methanol, acetic acid was added in excess, reduction took place, but at a much lower rate. According to the proposed mechanism [4] protonation of glyoxylic acid (or its monohydrate) is involved. The presence of the much stronger base methanol will therefore slow down the reaction drastically.

It has been reported [5] that pyruvic acid is oxidized twelve times faster by hydrogen peroxide than glyoxylic acid. However, reduction of an ozonized acetic acid solution of anethole using two mol equivalents of pyruvic acid was

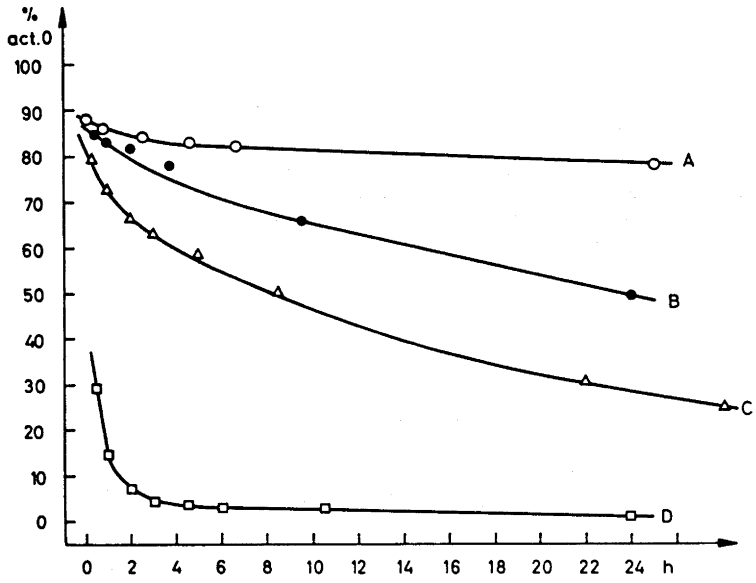

Fig. 4. Decomposition and reduction of ozonized anethole. A. Decomposition in glacial acetic acid. B. Reduction with 2 mol equivalents of glyoxylic acid monohydrate in methanol/acetic acid (3:7). C. Reduction with 2 mol equivalents of pyruvic acid. D. Reduction with 2 mol equivalents of glyoxylic acid monohydrate in acetic acid.

much slower than with glyoxylic acid (Fig. 4). This may be due to steric effects in the supposed rate-determining step, *viz.* the reaction between the protonated α-keto acid and the hydroperoxide formed during the ozonolysis.[4]

The yields of reduction products by using glyoxylic acid (or its monohydrate) are shown in Table 1.

Table 1.

Compound ozonized	Reduction product	Yields, %
2,3-Dimethyl-2-butene	Acetone	98 [a]
Anethole	Anisaldehyde	84 [a]
4,4'-Dimethoxystilbene	Anisaldehyde	90 [b]

[a] Estimation by GLC. [b] Estimation by weighing the residue after washing with aqueous sodium bicarbonate. Purity 97–98 % (GLC).

Reduction of peroxidic products normally formed in ozonation in non-protic solvents (ozonides, dimeric peroxides) with glyoxylic acid was not feasible.

EXPERIMENTAL PART

General. The ozone source was a Welsbach T 23 ozone generator which gave a concentration of 4 – 6 % ozone in oxygen.

Reduction procedure. After the ozonolysis solution was purged for 3 min with nitrogen at 25°C, it was transferred to a volumetric flask, the reducing agent was added, the solution diluted to correct volume and the flask kept at 25 ± 0.1°C. Aliquots (5 ml) were taken out and deoxygenated by adding small pieces of solid carbon dioxide. Sodium iodide in acetonitrile (5 ml of a 10 % solution) was added and the reduction vessel stoppered tightly and left in the dark for 1 h before being titrated with 0.01 N sodium thiosulphate (after dilution with large volumes of ice-water). Blanks were determined.

Gas liquid chromatography. Acetone was estimated using a Varian Aerograph Model 200 (Thermal Conductivity Detector) with a Polyethylene glycol 1000 on Chromosorb WHMDS (60/80 mesh) column. Anisaldehyde was estimated using a Varian Aerograph Model 1520 (Flame Ionisation Detector) with an Apiezon L (20 %) on Chromosorb WHMDS (60/80 mesh) column.

REFERENCES

1. Bailey, P. S. *Chem. Rev.* **58** (1958) 925.
2. Hatcher, W. H. and Holden, G. W. *Trans. Roy. Soc. Can.* (3) **19** (1925) 11.
3. Wittig, G. *Angew. Chem.* **60** (1948) 169.
4. Kolsaker, P. and Johanson, R. *To be published.*
5. Hatcher, W. H. and Hill, A. C. *Trans. Roy. Soc. Can.* (3) **22** (1928) 211.

Received July 3, 1972.

ACTA CHEMICA SCANDINAVICA 27 (1973) 1531–1540

Molecular Structure of Gaseous Cyanogen Azide and Azodicarbonitrile

ARNE ALMENNINGEN,[a] BØRGE BAK,[b] PETER JANSEN[b] and T. G. STRAND[a]

[a] *Department of Chemistry, University of Oslo, Oslo 3, Norway, and* [b] *Chemical Laboratory V, The H. C. Ørsted Institute, University of Copenhagen, DK-2100 Copenhagen, Denmark*

The molecules were studied by the gas electron diffraction method. Root mean-square amplitudes of vibration, and correction terms to transfer the electron diffraction parameters R_a to thermal average parameters R_α, were computed from available spectroscopic data. The molecules are *trans* planar about the central N=N bonds. The N≡C–N arrangements deviate slightly from linearity with the N≡C bonds *trans* to the N=N bonds. The following R_α parameters (distances in Å, angles in degrees) and standard deviations corrected for systematic errors were obtained for cyanogen azide: $R(N{\equiv}C) = 1.155(2)$, $R(C-N) = 1.355(2)$, $R(N=N) = 1.261(2)$, $R(\overset{+}{N}=\bar{N}) = 1.121(2)$, $\theta(N{\equiv}C=N) = 175.3(1.4)$, $\theta(C-N=N) = 114.5(0.2)$, and $\theta(N=\overset{+}{N}=\bar{N}) = 169.2(1.6)$, and for azodicarbonitrile (C_{2h}-symmetry): $R(N{\equiv}C) = 1.151(1)$, $R(C-N) = 1.363(2)$, $R(N=N) = 1.261(2)$, $\theta(N{\equiv}C-N) = 172.5(0.3)$, and $\theta(C-N=N) = 113.0(0.2)$. Like in chlorine azide the azide group of cyanogen azide is non-linear. This deviation from linearity as well as the non-linearity of the N≡C–N arrangement were confirmed by *ab initio* calculations.

The infrared and Raman spectra of cyanogen azide and its condensation product, azodicarbonitrile, have previously been recorded and assigned (Refs. 1 and 2). With access to these interesting compounds, an electron diffraction investigation of the molecules seemed worth-while. The results are given in the present paper.

EXPERIMENTAL

Diffraction photographs from samples synthesized in Copenhagen [1,2] were obtained on the Oslo apparatus.[3] The unstable cyanogen azide was transported solved in dimethyl phthalate and distilled into the apparatus from this solution. The nozzle temperatures were about 20°C and the accelerating voltage was about 36 kV. Five plates for each of the two camera distances of about 48 and 20 cm were used for the structure investigation of cyanogen azide. For azodicarbonitrile, six plates from each of the two distances were applied. The plates were photometered in the usual way.[4]

CALCULATION OF u- AND K-VALUES FROM THE NORMAL FREQUENCIES OF THE MOLECULES

To the approximation of small vibrations, the electron diffraction parameter R_a may be related to the equilibrium distance R_e by [5]

$$R_a = R_e + \langle \Delta z \rangle - u^2/R + K + \delta R + \ldots, \quad (1)$$

where

$$K = (\langle \Delta x^2 \rangle + \langle \Delta y^2 \rangle)/2R, \quad (2)$$

u is the root mean-square amplitude of vibration, $u = (\langle \Delta z^2 \rangle)^{\frac{1}{2}}$, and δR is a small correction for centrifugal distortion. Omitting this term, the effects of harmonic vibrations may be removed by defining the distance parameter R_α according to:[5]

$$R_e + \langle \Delta z \rangle = R_a + u^2/R - K \equiv R_\alpha \quad (3)$$

Then the R_α distances should, except for anharmonic effects, be consistent with the molecular symmetry and geometry.

Due to the closely spaced bonded distances in the molecules it was desirable to know the root-mean square amplitudes of vibration from the spectroscopic data. When the small deviations from linearity of the N≡C−N arrangements appeared during the electron diffraction investigation, knowledge of the K-values for the molecules were of interest to correct the R_a- to R_α-distances in order to compute angles based on R_α models.

Initial calculations by Cyvin [6] indicated that the second assignment for the normal frequencies of cyanogen azide [1] was correct, but that some normal frequencies for azodicarbonitrile [2] had to be reassigned to obtain reasonable force constants. Since the assignment of Ref. 2 was not final, a possible alternative is suggested (Table 2). The calculations were continued on this foundation using a modified [7] computer program by Gwinn.[8] By this program Urey-Bradley force fields were fitted to the normal frequencies by a trial and error procedure.

The normal frequencies are compared to the computed ones in Table 1 and Table 2. The force constants are given in Table 3, the computed u- and

Table 1. Observed and computed normal frequencies for cyanogen azide in cm^{-1}.

	Observed [1]	Computed
ν_1	2248	2261
ν_2	2198	2201
ν_3	1246	1226
ν_4	921	933
ν_5	666	627
ν_6	444	467
ν_7	167	167
ν_8	520	520
ν_9	444	442

Table 2. Observed and computed normal frequencies for azodicarbonitrile in cm^{-1}.

		Observed [2,6]	Computed
ν_1		2176	2188
ν_2		1422	1422
ν_3	A_g	1002	1005
ν_4		482 [a,b]	508
ν_5		282	302
ν_6	B_g	504 [a,b]	508
ν_7		2204	2191
ν_8	B_u	982	981
ν_9		596	585
ν_{10}		152 [a,b]	150
ν_{11}	A_u	574	577
ν_{12}		133	133

[a] Reassignment based on $\nu_9 = 596$; $2\nu_{10} + \nu_9 = 904$, $\nu_{10} = 152$; $\nu_4 - \nu_5 = 200$, $\nu_4 = 482$; $\nu_6 - 2\nu_{10} = 200$, $\nu_6 = 504$. [b] Not directly observed.

Table 3. Force constants for cyanogen azide and azodicarbonitrile.

	Cyanogen azide	Azodicarbonitrile
K(1,2) [a]	16.1	16.1
K(2,3) [a]	5.5	5.5
K(3,4) [a]	8.5	7.4
K(4,5) [a]	17.8	
F(2,4) [a]	1.2	0.46
H(1,2,3) [b]	0.53	0.49
H(2,3,4) [b]	0.35	0.57
H(3,4,5) [b]	0.44	
θ(1,2,3,4) [c]	0.53	0.56
θ(2,3,4,5) [c]	0.44	0.13

[a] Stretching force constants in mdyn $Å^{-1}$. [b] Bending force constants in mdyn Å rad^{-2}. [c] Out-of-plane bending force constants in mdyn Å rad^{-2}.

Table 4. u- and K-values for cyanogen azide and azodicarbonitrile in Å.

	Cyanogen azide			Azodicarbonitrile		
Distance	K [a]	u^a	u^b	K^a	u^a	u^b
1–2	0.0065	0.0352		0.0115	0.0352	
2–3	0.0034	0.0446		0.0064	0.0447	
3–4	0.0037	0.0397		0.0020	0.0416	
4–5	0.0077	0.0336				
1–3	0.0028	0.0485	0.0475(25)	0.0106	0.0490	0.0502(10)
1–4	0.0017	0.0793	0.0758(15) [c]	0.0078	0.0819	0.0803(19)
1–5	0.0003	0.1121	0.1141(41)	0.0023	0.0732	0.0754(15)
3–5	0.0033	0.0462	0.0454(26)			
2–4	0.0023	0.0609	0.0558(24)	0.0038	0.0671	0.0568(12)
2–5	0.0017	0.0757	0.0758(15) [c]	0.0016	0.0672	0.0718(46)
1–6				0.0003	0.0757	0.0823(26)

[a] Computed for the force fields of Table 3. [b] Experimental values. [c] Average value of $u(1-4)$ and $u(2-5)$.

K-values are listed in Table 4, and the numbering of the atoms are illustrated in Fig. 1.

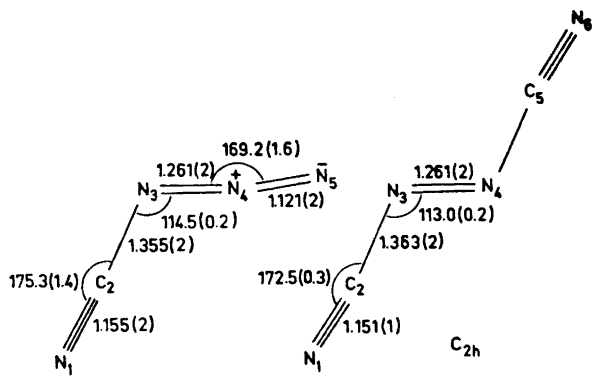

Fig. 1. Numbering of the atoms of cyanogen azide and azodicarbonitrile. Corrected R_α parameters (distances in Å and angles in degrees) and standard deviations from Table 6 are given.

THE STRUCTURE INVESTIGATION

The electron diffraction data were processed and analyzed in the usual way.[4] Partial waves scattering factors computed for 35 kV electrons [9] based upon analytical HF potentials for the atoms [10] were applied. The first backgrounds were drawn on the levelled intensity curves, and the molecular intensities obtained were modified by $s/|f_N'||f_C'|$.

The backgrounds were adjusted on the individual intensities from each plate by comparing intensities calculated for the first models of the molecules to the experimental intensities. The curves were then scaled and averaged, and the average correlation coefficients [11] and the standard deviations at each point of the intensities were computed. The correlation in the data were as usual for the Oslo apparatus, and in the final least-squares refinements p_2 and p_3 of the weight matrix [11] were -0.6 and 0.11 for the 48 cm data and -0.6 and 0.115 for the data from the 20 cm camera distance. The constants w_1, s_1, w_2, and s_2 for the diagonal part of the weight matrix [4] were for both of the molecules 4.5, 5.5, 0.06, and 10.0, and 4.5, 11.0, 0.008, and 20.0 for the 48 cm and 20 cm data, respectively. The two curves were kept separated in the final refinements and they were given the same weight. The molecular intensities are illustrated in Fig. 2.

For data and theory without systematic errors, about two thirds of the differences between the experimental and calculated intensities should be within the standard deviations of the average intensities, and only 1 per cent of the differences should be greater than 2.5 times the standard deviations. This seems to be the case for the middle part of the 20 cm camera distance data, while the differences for the middle part of the 48 cm data seem larger than indicated by the standard deviations. The large differences at small

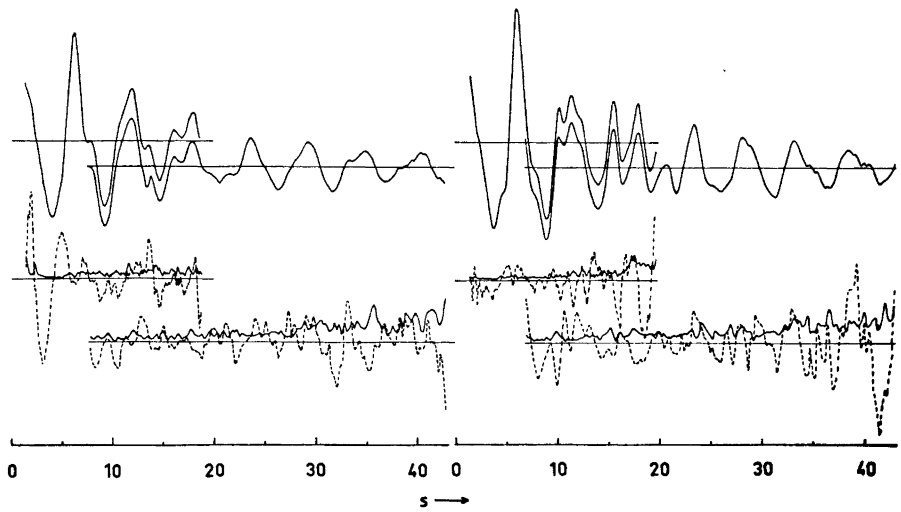

Fig. 2. Average experimental molecular intensities, standard deviations of the average intensities and differences between experimental and calculated molecular intensities (broken curves) for cyanogen azide (left) and azodicarbonitrile (right). The standard deviations and differences were multiplied by a factor of 10.

s-values of the 48 cm data for cyanogen azide could not be included in a smooth background. Corresponding differences for azodicarbonitrile were removed by an unsmooth background. The constants for the diagonal

Table 5. Distances R_a in Å and angles for cyanogen azide and azodicarbonitrile from least-squares refinements.

	Cyanogen azide		Azodicarbonitrile		
	A	B	B	C	A
$R(1,2)$	1.1569(15)	1.1591(17)	1.1605(5)	1.1604(6)	1.1585(5)
$R(2,3)$	1.3531(12)	1.3550(12)	1.3662(6)	1.3658(8)	1.3629(6)
$R(3,4)$	1.2608(12)	1.2620(11)	1.2599(12)	1.2601(12)	1.2581(12)
$R(4,5)$	1.1272(16)	1.1265(18)			
$\theta(1,2,3)$	178.23(1.09)	175.32(1.39)	172.54(0.35)		173.65(0.33)
$\theta(2,3,4)$	114.56(0.20)	114.48(0.21)	113.04(0.13)		112.96(0.14)
$\theta(3,4,5)$	167.78(1.35)	169.24(1.56)			
$R(1,3)$	2.5097(17)	2.5065(16)	2.5157(7)	2.5155(9)	2.5175(7)
$R(1,4)$	3.2557(77)	3.2689(92)	3.2735(14)	3.2702(20)	3.2687(14)
$R(1,5)$	4.2545(43)	4.2541(44)	4.5490(10)	4.5515(17)	4.5533(11)
$R(3,5)$	2.3745(18)	2.3713(17)			
$R(2,4)$	2.1995(21)	2.1982(21)	2.1883(10)	2.1876(11)	2.1857(10)
$R(2,5)$	3.2730(80)	3.2562(98)	3.4181(13)	3.4167(45)	3.4186(13)
$R(1,6)$			5.6853(15)	5.6877(32)	5.6975(15)
$\mathbf{V'PV} \times 10^{-3}$	2.88	2.95	3.57	3.49	3.99

A. The R_a distances were consistent with the molecular geometries.
B. The corresponding R_α distances were consistent with the molecular geometries.
C. All the distances were independent parameters.

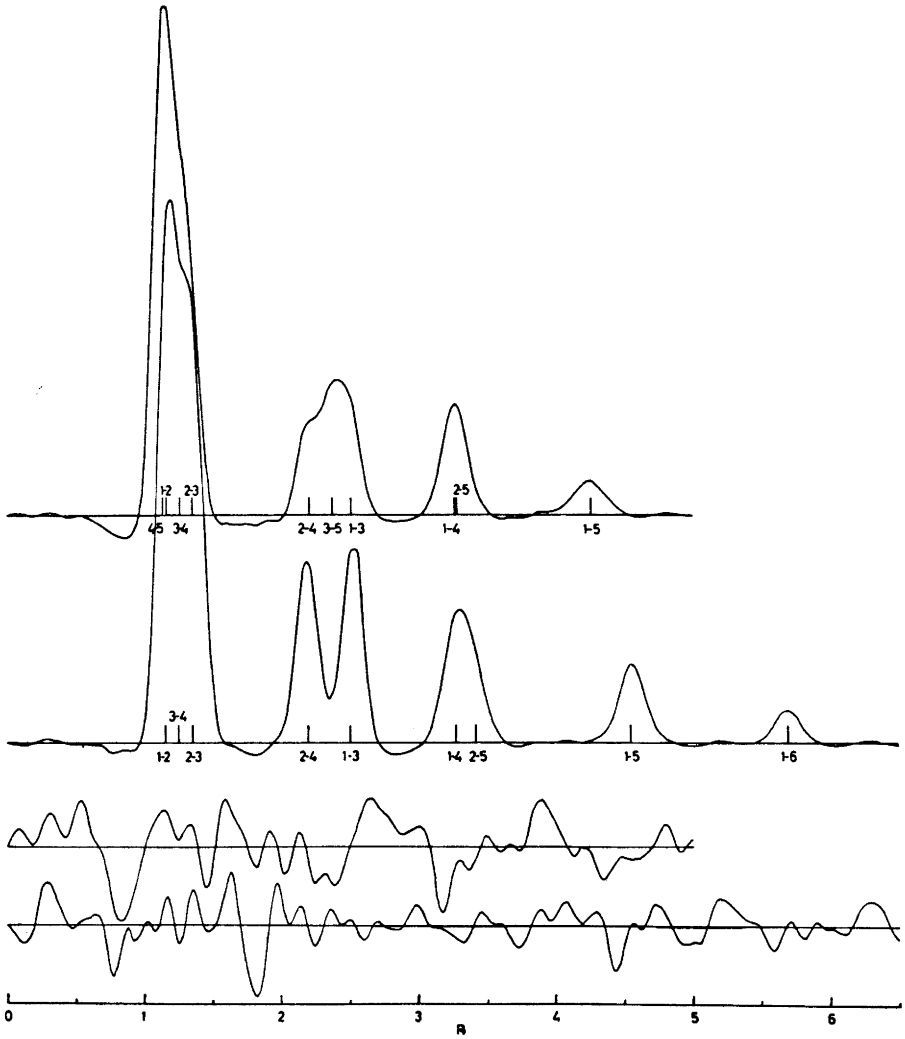

Fig. 3. Experimental radial distribution functions for cyanogen azide (top) and azodicarbonitrile, and differences between experimental and calculated functions. The differences were multiplied by a factor of 10. For the experimental functions, calculated intensities were added inside $s = 5$ Å^{-1}, and the intensities were multiplied by a damping function of exp $(-0.0018\ s^2)$ before the functions were computed.

part of the weighting matrix give for both molecules very little weight to the data inside $s = 5$ Å^{-1}, and calculated values were added to the experimental intensities inside $s = 5$ Å^{-1} before computing the radial distribution functions.

The results of different least-squares refinements are given in Table 5. Attempts to determine the u-values of all the bonded distances gave unreasonable results, and these u-values were fixed on the calculated values (Table 4). In cyanogen azide $R(1,3)$ is so close to $R(2,5)$ that reasonable u-values were not obtained independently for the two distances. These u-values were therefore started on equal values and given the same shifts in the least squares refinements. By this procedure an average value is determined. The other u-values could be obtained by least-squares calculations, and their values are included in Table 4.

The data for the two camera distances were connected applying the scale factors of the least-squares refinements and adding theoretical intensities for the inner unobserved parts. Radial distribution functions were computed from these intensities and compared to functions computed from the models of Table 5 B with u-values from Table 4, using the experimental ones whenever possible. These curves are illustrated in Fig. 3.

Distances from data of the Oslo apparatus seem presently low by about 0.1 % in comparison to an R_a(C–C) in benzene of 1.397 Å,[12] but the magnitude of this correction is uncertain. In Table 6, 0.1 % has been added to the R_α distances corresponding to the R_a distances of Table 5, B, and the standard deviations have been corrected for systematic uncertainties in the distances of 0.1 %.

Table 6. Corrected R_α distances (Å) and angles for cyanogen azide and azodicarbonitrile.

	Cyanogen azide	Azodicarbonitrile
$R(N\equiv C)$	1.155(2)	1.151(1)
$R(C-N)$	1.355(2)	1.363(2)
$R(N=N)$	1.261(2)	1.261(2)
$R(\overset{+}{N}=\overset{-}{N})$	1.121(2)	
$\theta(N\equiv C-N)$	175.3(1.4)	172.5(0.3)
$\theta(C-N=N)$	114.5(0.2)	113.0(0.2)
$\theta(N=\overset{+}{N}=\overset{-}{N})$	169.2(1.6)	

Ab initio calculations. Table 7 reports results of *ab initio* calculations of the energy of 3 configurations of cyanogen azide, consistent with the electron diffraction results. The basis set of Ref. 13 was applied.

DISCUSSION

The molecules have *trans* configurations about the central N=N bonds. The amount of any *cis* configurations present cannot be more than a few per cent. Refinements started with the N≡C bonds *cis* to the central N=N bonds converge to *trans* positions of the former bonds for both molecules. This deviation from linearity of the N≡C–N arrangement is significant for

Table 7. Results of *ab initio* calculations of the energy (in a.u.) of 3 configurations, A, B and C, of cyanogen azide. Distances in Å, angles in degrees.

	A [a]	B [b]	C [c]
Distances			
1 – 2	1.158	1.158	1.158
2 – 3	1.354	1.354	1.354
3 – 4	1.260	1.260	1.260
4 – 5	1.127	1.127	1.127
Angles			
1,2,3	180.0	180.0	178.0
2,3,4	114.4	114.4	114.4
3,4,5	180.0	168.0	168.0
Energy	−255.12984	−255.13146	−255.13176
Sum of atomic energies			−255.012

[a] Straight N≡C−N and azide groups. [b] Straight N≡C−N and bent azide groups. [c] Bent N≡C−N and azide groups.

azodicarbonitrile. For cyanogen azide the significance of the deviation may be somewhat doubtful if the effect were based on the electron diffraction result for only this molecule.

Some of the K-values necessary to transfer the R_a- to the R_α-distances are relatively large, especially in the case of azodicarbonitrile. For this molecule, distances from the refinement constrained by an R_α model agree favourably with the independently determined distances (Table 5, B, C), and the agreement is better than from the refinement constrained by an R_a model not corrected for shrinkage (Table 5, B, A). For cyanogen azide, where the number of geometric parameters are greater and the number of atoms are fewer than in azodicarbonitrile, the R_a model fits the data slightly better than the R_α model (Table 5, A, B). All the distances could not be determined independently for this molecule.

The u-values computed from the force fields agree favourably with the obtainable experimental ones (Table 4). Only the values of distance 2 – 4 of azodicarbonitrile disagree significantly in terms of the uncorrected least-squares standard deviations. The computed u-values of the non-bonded distances are more uncertain than for the bonded ones, and the least-squares standard deviations may be too small. The uncertainties of the force constants are probably large. Other sets of values might reproduce the normal frequencies just as well and give reasonable u- and K-values.

The conclusion of the electron diffraction investigation is that the molecules are *trans* planar about the central N=N bonds with small deviations from linearity of the N≡C−N arrangements with the N≡C bonds *trans* to the N=N bonds. The best estimates of the structure parameters and their standard deviations are given in Table 6.

Comparing the parameters of Table 6, the N=N distances are the same in the two molecules. The variations in R(N≡C), R(C–N) and θ(C–N=N) are consistent with a somewhat greater contribution from the linear structure $::\overset{-1}{\ddot{N}}=C=\overset{+1}{N}=\overset{+1}{N}=\overset{-1}{\ddot{N}}::$ in cyanogen azide than from $::\overset{-1}{\ddot{N}}=C=\overset{+1}{N}=\overset{+1}{N}=C=\overset{-1}{\ddot{N}}::$ in azodicarbonitrile. If R_a parameters are compared, the R(C≡N)'s do not fit into this scheme. The nonlinearity of the N≡C–N̈ arrangements could be due to the lone pair at the nitrogen atoms. The larger deviation from linearity of azodicarbonitrile as compared to cyanogen azide may be explained by an attraction of the lone pair by the formal +1 charge at N_4 in the latter molecule, thereby increasing the effect on θ(N=N=N) and decreasing the effect on θ(N≡C–N).

Ab initio calculations have been carried out for azodicarbonitrile.[13] In agreement with the present result, the possible *cis* conformer is computed to be unstable by about 20 kcal mol^{-1} in relation to the *trans* form.

The central N=N bonds may be compared to the values of 1.25 Å in azomethane [14,15] and chlorine azide.[16] For azide [17] and methyl azide [18] values of 1.24 Å are given. The terminal N=N bond of cyanogen azide should be compared to the values of 1.13 Å in chlorine azide,[16] azide,[17] and methyl azide.[18] Deviation from linearity of the –N=N=N arrangement is reported for chlorine azide [16] with 8° towards the *trans* position.

Nonlinear C–C≡N arrangements are known. For tetracyanoethylene oxide [19] the effect is explained by delocalization of the oxygen lone pair into antibonding π orbitals of the cyano group. The deviation is about 4° or about half the size of the N̈–C≡N deviation in azodicarbonitrile where the lone pair is situated at the atom next to the cyano group. Due to the charge distribution in cyanogen azide,[20] a lone pair delocalization to the cyano group might be less than in azodicarbonitrile.

Whereas to the best of our knowledge no other structure determination of azodicarbonitrile has been carried out, microwave investigators [20,21] have studied cyanogen azide. In Ref. 21 a structure was derived, building on 2

Table 8. Comparison of the structure of cyanogen azide as formed by microwave technique (MW) and by electron diffraction (ED). Distances in Å, angles in degrees.

	MW	ED
Distances		
1–2	1.164(5)	1.155(2)
2–3	1.312(20)	1.355(2)
3–4	1.252(10)	1.261(2)
4–5	1.133(10)	1.121(2)
Angles		
1,2,3	176.0(2.0)	175.3(1.4)
2,3,4	120.2(1.0)	114.5(0.2)
3,4,5	180 (assumed)	169.2(1.6)

Table 9. Microwave rotational constants A, B, and C, of cyanogen azide from Ref. 21 compared to rotational constants (in MHz) from the electron diffraction model of Table 6.

	MW	ED
A	38066.8 ± 0.15	38108.7
B	3185.15 ± 0.025	3185.8
C	2933.30 ± 0.025	2940.0

isotopic substitutions ($^{15}N{\equiv}C-N_3$ and $N{\equiv}^{13}C-N_3$) and an assumed linear azide group. By necessity this structure is in disagreement with ours (Table 8). In Table 9 the rotational constants corresponding to the ED model of Table 8 are confronted with the experimental ones.[20,21] The agreement is quite satisfactory.

Acknowledgements. The authors wish to thank Professor S. J. Cyvin for his initial calculations of the molecular force fields and for helpful discussions. As to the *ab initio* calculations the help of Helge Johansen, Chemical Laboratory IV, the H. C. Ørsted Institute. is gratefully acknowledged.

REFERENCES

1. Bak, B., Bang, O., Nicolaisen, F. and Rump, O. *Spectrochim. Acta* **A27** (1971) 1865.
2. Bak, B. and Jansen, P. *J. Mol. Struct.* **11** (1972) 25.
3. Bastiansen, O., Hassel, O. and Risberg, F. *Acta Chem. Scand.* **9** (1955) 232.
4. Andersen, B., Seip, H. M., Strand, T. G. and Stølevik, R. *Acta Chem. Scand.* **23** (1969) 3224.
5. Morino, Y., Kuchitsu, K. and Oka, T. *J. Chem. Phys.* **36** (1962) 1108.
6. Cyvin, B. and Cyvin, S. *Private communication.*
7. Stølevik, R., Seip, H. M. and Cyvin, S. *Chem. Phys. Lett.* **15** (1972) 263.
8. Gwinn, W. D. *J. Chem. Phys.* **55** (1971) 477.
9. Peacher, J. and Wills, J. C. *J. Chem. Phys.* **46** (1967) 4809.
10. Strand, T. G. and Bonham, R. A. *J. Chem. Phys.* **40** (1964) 1686.
11. Seip, H. M., Strand, T. G. and Stølevik, R. *Chem. Phys. Lett.* **3** (1969) 617.
12. Seip, H. M. *Private communication.*
13. Bak, B. and Jansen, P. *J. Mol. Struct.* **12** (1972) 167.
14. Almenningen, A., Anfinsen, I. M. and Haaland, A. *Acta Chem. Scand.* **24** (1970) 1230.
15. Chang, C. H., Porter, R. F. and Bauer, S. H. *J. Am. Chem. Soc.* **92** (1970) 5313.
16. Cook, R. L. and Gerry, M. C. L. *J. Chem. Phys.* **53** (1970) 2525.
17. Cook, R. L. and Winnewisser, M. *J. Chem. Phys.* **41** (1964) 999.
18. Salathiel, W. M. and Curl, R. F. *J. Chem. Phys.* **44** (1966) 1288.
19. Matthews, D. A., Swanson, J., Mueller, M. H. and Stucky, G. D. *J. Am. Chem. Soc.* **93** (1971) 5945.
20. Bolton, K., Brown, R. D. and Burden, F. R. *Chem. Phys. Lett.* **15** (1972) 79.
21. Costain, C. C. and Kroto, H. W. *Can. J. Phys.* **50** (1972) 1453.

Received November 25, 1972.

ACTA CHEMICA SCANDINAVICA 27 (1973) 1541–1551

The Crystal Structure of $ZnSO_3.2\frac{1}{2}H_2O$

BIRGIT NYBERG

Division of Inorganic Chemistry 2, Chemical Center, Box 740, S-220 07 Lund 7, Sweden

The crystal structure of $ZnSO_3.2\frac{1}{2}H_2O$ has been determined from three-dimensional X-ray diffractometer data. The unit cell is triclinic, space group $P\bar{1}$, with the following dimensions: $a = 7.651(2)$, $b = 7.549(2)$, $c = 9.094(2)$ Å, $\alpha = 90.06(2)$, $\beta = 88.53(2)$, $\gamma = 93.75(3)°$. There are four formula units in the cell. The structure was refined by full-matrix least-squares calculations to an R value of 0.059 for 1855 observed reflections. Pyramidal sulfite groups link the structure together, which may be described as built up of ZnO_4 tetrahedra (mean distance Zn – O 1.99 Å) and ZnO_6 octahedra (mean distance Zn – O 2.10 Å). The average dimensions of the sulfite group are: S–O distance 1.525 Å, O–O distance 2.403 Å, and ∠O–S–O 103.8°.

A preliminary crystal structure determination of $ZnSO_3.2\frac{1}{2}H_2O$ has been published earlier.[1] Later a structure determination of the compound $ZnSO_3.2H_2O$ was reported by Quinones and Baggio.[2] The cell dimensions, cell content and atomic positions of all atoms, besides one half water molecule, the lattice water, make it possible that the very same compound has been investigated in both cases. Independent solution and refinement have, however, been made with diffractometer data in the hope of obtaining a more accurate structure determination.

EXPERIMENTAL

The sample of zinc sulfite hydrate was prepared according to Pannetier *et al.*[3] The analyses confirm the formula $ZnSO_3.2\frac{1}{2}H_2O$. The amount of zinc was determined by titration with EDTA and the amount of sulfur was determined gravimetrically as $BaSO_4$. The water content was determined at 390°C by controlled potential coulometry according to Karlsson and Karrman.[4] The analyses gave: 34.4(1) % Zn, 16.7(2) % S and 23.6(1) % H_2O; calculated for $ZnSO_3.2\frac{1}{2}H_2O$: 34.32 % Zn, 16.83 % S and 23.65 % H_2O.

Values for the cell dimensions were calculated from an indexed Guinier-Hägg powder photogram. Least-squares refinement of the cell parameters gave $a = 7.651(2)$ Å, $b = 7.549(2)$ Å, $c = 9.094(2)$ Å, $\alpha = 90.06(2)°$, $\beta = 88.53(2)°$, $\gamma = 93.75(3)°$ and $V = 524.0$ Å^3. Observed and calculated $\sin^2\theta$ values are listed together with calculated structure factors in Table 1.

The cell is not reduced according to Delaunay [5] because of the pseudotetragonal character of the selected unit cell. In Table 2 the dimensions of the reduced cell are given.

The observed density, 2.43 g cm^{-3}, found from the apparent loss of weight in benzene, gives four formula units in the cell (calculated density 2.41 g cm^{-3}).

Table 1. Guinier-Hägg powder photogram of $ZnSO_3.2\frac{1}{2}H_2O$. Cu$K\alpha_1$ radiation. KCl was used as an internal standard. $a_{KCl} = 6.2923$ Å at 25°C.

hkl	$10^5 \times \sin^2 \theta_{obs}$	$10^5 \times \sin^2 \theta_{calc}$	$\|F\|_{calc}$	I_{obs}
001	–	718	1	
100	1017	1019	101	vst
010	1044	1045	97	st
101	1689	1693	51	m
011		1762	51	
$0\bar{1}1$	1757	1764	54	st
$\bar{1}01$		1780	55	
$\bar{1}10$	–	1929	9	
110	–	2199	2	
$1\bar{1}1$	2603	2604	28	w
$\bar{1}11$	2682	2689	54	m
002	2873	2871	55	
111		2873	50	vst
$\bar{1}\bar{1}1$	2959	2962	37	vw
102	3806	3803	27	vw
012	3934	3915	31	vw
$0\bar{1}2$		3919	11	
$\bar{1}02$	–	3977	5	
200	4074	4074	87	st
020	4196	4182	79	vst
201	4707	4705	51	st
$1\bar{1}2$		4715	78	
$\bar{2}10$	–	4850	10	
$\bar{2}01$	4892	4879	55	vst
$\bar{1}12$		4885	99	
021		4898	30	
$0\bar{2}1$		4902	51	
$\bar{1}20$	–	4930	33	
112	4995	4981	102	w
$\bar{1}\bar{1}2$	5163	5160	98	vst
210	–	5390	38	
120	–	5471	25	
$2\bar{1}1$	–	5481	19	
$1\bar{2}1$	5612	5606	113	m
$\bar{2}11$	–	5653	10	
$\bar{1}21$	5699	5690	127	st
211	5995	6020	147	st
121	–	6143	24	
$\bar{2}\bar{1}1$	6202	6196	79	w
$\bar{1}\bar{2}1$	–	6234	9	
003	–	6460	7	
202	6785	6771	46	vw
022	7052	7049	80	m
$0\bar{2}2$		7057	67	
$\bar{2}02$	7123	7120	57	vw
103	–	7348	9	
013	–	7503	19	
$0\bar{1}3$	7504	7509	71	st
$2\bar{1}2$		7548	76	
$\bar{1}03$	7620	7610	74	w
$\bar{2}20$	7720	7716	78	m
$1\bar{2}2$	–	7722	22	
$\bar{1}22$	7884	7885	52	m
$\bar{2}12$		7893	90	

Table 1. Continued.

212	–	8095	45	
122	8259	8251	62	
1$\bar{1}$3		8261	42	w
2$\bar{2}$1	–	8348	34	
1$\bar{2}$2	8425	8433	80	w
2$\bar{1}$2	–	8438	27	
$\bar{1}$13	–	8517	17	
$\bar{2}$21	–	8519	9	
113	–	8526	33	
1$\bar{1}$3	–	8793	22	
220	8791	8797	59	vw
300	–	9167	5	
030	–	9409	4	
221	–	9426	3	
2$\bar{2}$1	–	9604	3	
301	9760	9754	52	vw
3$\bar{1}$0	–	9870	11	
3$\bar{0}$1	–	10016	14	
$\bar{1}$30	–	10022	10	
031	10123	10124	45	vw
0$\bar{3}$1		10130	34	
203	–	10273	11	
3$\bar{1}$1	–	10395	16	
2$\bar{2}$2	–	10416	19	
310	–	10618	5	
023	10642	10636	17	vvw
0$\bar{2}$3		10648	29	
3$\bar{1}$1	–	10655	3	
1$\bar{3}$1	–	10700	21	
2$\bar{2}$2	–	10757	14	
$\bar{1}$31	10778	10781	40	vw
2$\bar{0}$3		10796	35	
130	–	10834	12	
2$\bar{1}$3		11051		
311		11204		
3$\bar{1}$1	–	11486	1	
004	11471	11485	117	st
222	–	11490	11	
131	–	11505	3	
$\bar{1}$23	–	11515	40	
2$\bar{1}$3	–	11568	22	
213	–	11586	44	
$\bar{1}$31	–	11598	12	
302	–	11777	43	
123	–	11794	6	
2$\bar{2}$2	–	11847	35	
2$\bar{1}$3	12117	12115	74	vw
032	–	12275	21	
0$\bar{3}$2	12289	12287	66	w
3$\bar{0}$2	–	12300	7	
104	–	12329	11	
3$\bar{1}$2	12421	12419	103	w
014	–	12526	2	
0$\bar{1}$4	12561	12534	65	vw
3$\bar{2}$0	–	12538	21	
2$\bar{3}$0	–	12673	50	
$\bar{1}$04	–	12678	34	
1$\bar{3}$2	12824	12812	105	w

The powder was completely indexed to $\sin^2\theta = 0.16$.

Table 2. The reduced unit cell according to Delaunay.

$a = 11.734$ Å	$\alpha = 90.06°$
$b = 7.549$ Å	$\beta = 139.32°$
$c = 9.094$ Å	$\gamma = 92.40°$
	$V = 524.0$ Å^3

The methods of data collection and of structure determination used in the preliminary structure investigation have already been reported.[1] In Table 3 the statistical averages and distribution of the $|E|$ values from the first study are compared with the theoretical values expected for centrosymmetric and non-centrosymmetric structures according to Karle and Karle.[6] These values support the choice of the space group $P\bar{1}$.

Table 3. Statistical averages and distribution of normalized structure factors.

	Observed	Theoretical	
		Centric	Non-centric
Average $\|E\|$	0.72	0.798	0.886
Average $\|E\|^2$	1.0	1.0	1.0
Average $\|E^2-1\|$	1.018	0.968	0.736
$\|E\| > 1$	31.15 %	31.73 %	36.79 %
$\|E\| > 2$	4.82 %	4.55 %	1.83 %
$\|E\| > 3$	0.34 %	0.27 %	0.01 %

In order to collect further X-ray data a crystal with the volume 8.74×10^{-4} mm^3 was mounted along its c axis. The dimension in the b axis direction was 0.0258 mm and in the a axis direction 0.0450 mm. The intensities were recorded at room temperature using a CAD-4 four-circle diffractometer with Cu$K\alpha$ radiation. The collection of data was based on the application of the $\omega - 2\theta$ scan method with an upper limit of $2\theta = 70°$ and a scan range of $(1° + 0.15° \tan\theta)$. Reflections with $I < 3\sigma(I)$, where $\sigma(I)$ is based on counting statistics, were considered to be insignificantly different from the background. The 040 and $1\bar{2}1$ reflections were used as standards and one of them was remeasured after every 20 reflections. The structure factors were derived by means of a data reduction program which performed Lorentz and polarization corrections and absorption corrections ($\mu = 99$ cm^{-1}). Many dependent intensities were recorded, and after averaging the equivalent ones the data set consisted of 1855 reflections. A list of the programs used in the calculations is given in Table 4.

Table 4. Computer programs used for the crystallographic calculations.

Program name and function	Authors
CELSIUS. Refinement of direct cell dimensions by the method of least-squares.	J. Tegenfeldt, Uppsala, Sweden.
CELL. Calculation of direct and reciprocal cell parameters and the constants in the quadratic formula. Transformation of the unit cell to the reduced cell according to Delaunay.	G. Malmros, B. Nyberg and C. Svensson, Lund, Sweden.

Table 4. Continued.

CADDY. Reads CAD-4 reflection data and decodes them to card images.	C. Särnstrand and C. Svensson, Lund, Sweden.
DATAPC. Processes data obtained with CAD-4. Performs corrections for Lorentz, polarization and absorption. Calculates extinction components for the program LINUS.	Originally written by P. Coppens; modified by W. C. Hamilton, New York, USA. (DATAPH). Modified by C. Svensson, Lund, Sweden.
SORTA. Sorting and averaging of equivalent reflections.	J.-O. Lundgren, Uppsala, Sweden.
LINUS. Full-matrix least-squares refinement of atomic parameters with extinction refinement.	P. Coppens and W. C. Hamilton. Modification of the program ORFLS originally written by W. R. Busing, K. O. Martin and H. A. Levy, Tennessee, USA. Further modified by P.-G. Jönsson, Uppsala, Sweden.
DISTAN. Calculation of interatomic distances, angles and their standard deviations.	A. Zalkin, Berkeley, USA.
DRF. Data reduction and Fourier calculations.	A. Zalkin, Berkeley, USA.
SACTA. Prints structure factor tables for publication.	J. Albertsson, Lund, Sweden.

STRUCTURE DETERMINATION AND REFINEMENT

The parameters for Zn, S, and O from the preliminary structure determination were used in a full-matrix least-squares refinement with isotropic temperature factors for the water oxygen atoms and anisotropic ones for the other atoms. This resulted in a discrepancy factor $R = 0.075$.

A new refinement with anisotropic temperature factors for all the non-hydrogen atoms and an isotropic extinction parameter, g, according to Coppens and Hamilton,[7] gave an R-value of 0.059 and a g-value of $1.2(1) \times 10^{-4}$.

From a three-dimensional difference map small residual maxima not above 15 % of the heights of the oxygen peaks in an F_o synthesis were found. Some of these could indicate hydrogen atoms as well as background peaks.

A weighting scheme with $w^{-1} = \sigma^2(F_o) + 0.005\ F_o^2$ was used. Atomic scattering factors for neutral atoms were applied.[8]

In Table 5 the final values of the atomic parameters and their standard deviations are presented. The observed and calculated structure factors are listed in Table 6.

DESCRIPTION AND DISCUSSION OF THE STRUCTURE

A schematic drawing of the structure of $ZnSO_3.2\frac{1}{2}H_2O$ is shown in Fig. 1. The interatomic distances and angles are listed in Table 7.

The structure may be described in terms of pyramidal sulfite groups, ZnO_4 tetrahedra, and ZnO_6 octahedra. The tetrahedral coordination around half the zinc atoms is provided by four oxygen atoms belonging to four different sulfite groups. The mean Zn – O distance (1.99 Å) is in good agreement with

Table 5. Final atomic parameters and their standard deviations. The anisotropic temperature factors are of the form $\exp[-(\beta_{11}h^2+\beta_{22}k^2+\beta_{33}l^2+2\beta_{12}hk+2\beta_{13}hl+2\beta_{23}kl)]$.

Atom	x	y	z	β_{11}	β_{22}	β_{33}	β_{12}	β_{13}	β_{23}
Zn1	0	½	0	0.0061(2)	0.0103(2)	0.0045(2)	−0.0000(2)	−0.0002(1)	0.0003(1)
Zn2	½	0	½	0.0096(2)	0.0071(2)	0.0041(2)	0.0021(2)	−0.0004(1)	0.0003(1)
Zn3	0.48793(8)	0.49657(8)	0.25042(7)	0.0075(2)	0.0083(2)	0.0047(1)	0.0005(1)	0.0006(1)	−0.0002(1)
S1	0.62763(15)	0.25797(14)	0.98344(12)	0.0042(2)	0.0047(2)	0.0018(2)	0.0016(2)	−0.0001(1)	0.0002(1)
S2	0.73830(14)	0.65656(15)	0.50643(12)	0.0037(3)	0.0046(2)	0.0019(2)	−0.0002(2)	−0.0002(1)	0.0007(1)
O1	0.2534(5)	0.5792(5)	0.0465(5)	0.0045(6)	0.0106(7)	0.0061(5)	−0.0009(5)	−0.0019(4)	0.0030(5)
O2	0.5221(5)	0.7171(5)	0.1225(4)	0.0069(6)	0.0064(6)	0.0029(4)	−0.0010(5)	−0.0019(4)	−0.0006(4)
O3	0.5448(5)	0.2865(5)	0.1343(4)	0.0121(8)	0.0068(6)	0.0022(4)	0.0018(5)	0.0019(4)	0.0001(4)
O4	0.7010(5)	0.5534(5)	0.3638(4)	0.0050(6)	0.0119(7)	0.0025(4)	0.0007(5)	−0.0013(4)	−0.0006(4)
O5	0.2693(4)	0.4889(4)	0.3731(3)	0.0042(6)	0.0083(7)	0.0014(4)	0.0011(5)	−0.0004(4)	0.0016(4)
O6	0.4256(5)	0.2497(5)	0.4570(5)	0.0090(7)	0.0066(7)	0.0067(5)	0.0034(5)	0.0019(5)	0.0016(5)
O7	0.8911(5)	0.7549(6)	0.0396(5)	0.0060(7)	0.0107(8)	0.0077(6)	0.0003(5)	−0.0001(5)	−0.0014(5)
O8	0.2615(5)	0.8694(6)	0.4205(6)	0.0087(8)	0.0092(8)	0.0111(7)	0.0009(6)	−0.0043(6)	0.0001(6)
O9	0.9709(5)	0.4176(5)	0.2169(4)	0.0064(6)	0.0109(7)	0.0028(4)	0.0000(5)	0.0004(4)	0.0006(4)
O10	0.6214(5)	0.0018(5)	0.2918(4)	0.0095(7)	0.0070(6)	0.0049(5)	0.0015(5)	0.0002(5)	0.0006(4)
O11	0.0080(6)	0.0100(6)	0.2431(6)	0.0129(11)	0.0131(10)	0.0110(8)	0.0009(8)	−0.0031(7)	0.0004(7)

Table 6. Observed and calculated structure factors of $ZnSO_3.2\frac{1}{2}H_2O$. The reflections are sorted in groups. In each group k and l have constant values. 10 $|F_o|$ and 10 $|F_c|$ are given after the running index h.

Table 6. Continued.

Table 6. Continued.

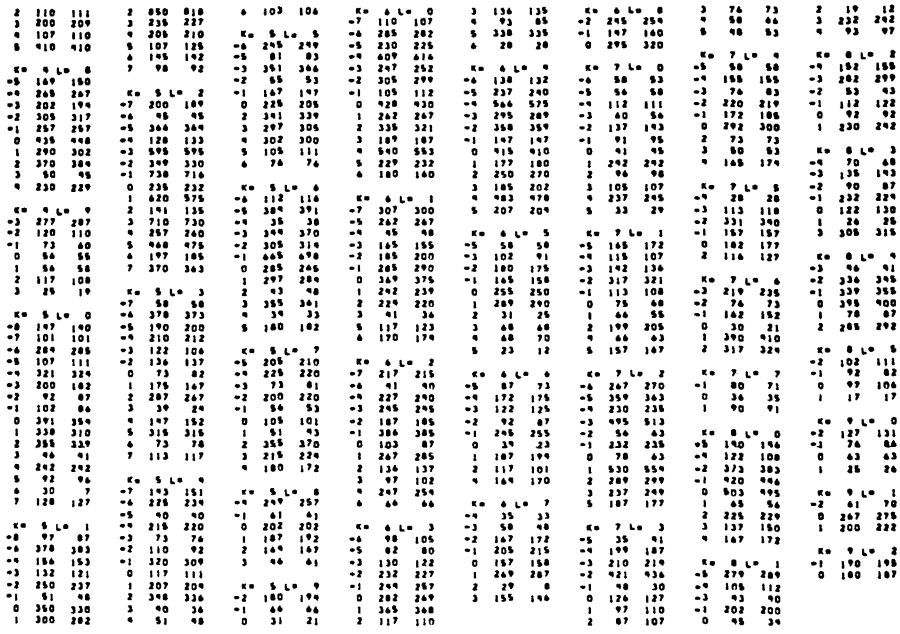

Table 7. Interatomic distances (Å) and angles (°) with standard deviations. The distances are not corrected for thermal motion.

Metal-oxygen distances			
Zn1 – O1	2.045(4)	Zn2 – O6	2.045(4)
– O9	2.071(4)	– O10	2.087(4)
– O7	2.172(4)	– O8	2.157(4)
Zn3 – O3	1.970(4)		
– O5	1.975(4)		
– O4	1.984(3)		
– O2	2.031(4)		
Sulfite groups			
S1 – O1	1.502(4)	S2 – O6	1.509(4)
– O3	1.518(4)	– O4	1.535(4)
– O2	1.537(4)	– O5	1.549(3)
O1 – O2	2.362(5)	O4 – O6	2.430(6)
O1 – O3	2.405(6)	O4 – O5	2.432(5)
O2 – O3	2.404(5)	O5 – O6	2.367(5)
O1 – S1 – O2	102.0(2)	O6 – S2 – O4	105.9(2)
O1 – S1 – O3	105.6(2)	O6 – S2 – O5	101.4(2)
O2 – S1 – O3	103.8(2)	O4 – S2 – O5	104.1(2)
Short O–O distances indicating possible hydrogen bonds			
O11 – O7	2.791(6)	O4 – O9	2.689(5)
O11 – O8	2.815(7)	O5 – O9	2.744(5)
O2 – O10	2.721(5)	O5 – O8	2.909(6)
O2 – O7	2.899(5)		
O3 – O10	2.689(5)		

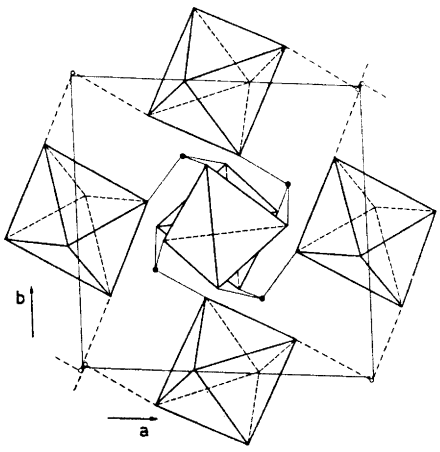

Fig. 1. The structure of $ZnSO_3.2\frac{1}{2}H_2O$. Schematic drawing showing the ZnO_4 tetrahedra and the ZnO_6 octahedra. The structure is viewed along the *c* axis. Filled circles denote sulfur atoms and unfilled circles oxygen atoms from the lattice water molecules. Possible hydrogen bonds between the lattice water and the other oxygen atoms are indicated by dotted lines.

the sum of the effective ionic radii (1.98 Å) according to Shannon and Prewitt [9] for four-coordinated zinc. The octahedral coordination around the rest of the zinc atoms is provided by two oxygen atoms from two different sulfite groups and four oxygen atoms belonging to water molecules. The two ZnO_6 groups in the structure are independent. The mean distance calculated for both groups is 2.10 Å in agreement with a greater distance for six-coordinated zinc. The value from the work of Shannon and Prewitt is 2.14 Å.

The zinc polyhedra have no corner in common, and the structure is held together by linking the sulfite groups to the polyhedra (Fig. 1). Possible O–H···O distances are given in Table 7. The assumed linking of the lattice water molecule to the polyhedra is illustrated in Fig. 1.

The dimensions of the sulfite group are consistent with a structure in which this group is coordinated through oxygen.[10] Two independent sulfite groups exist, but their oxygen atoms have similar surroundings. A sulfite group is connected to two different zinc tetrahedra and to one zinc octahedron.

The oxygen atoms O2 and O5, from two sulfite groups, are bonded to four-coordinated zinc and also probably have two hydrogen bonds to the water molecules. They have the longest S–O distance in each group (S1–O2 1.537 Å and S2–O5 1.549 Å).

The oxygen atoms in the sulfite groups with the shortest S–O distances are O1 and O4 (S1–O1 1.502 Å and S2–O6 1.509 Å). These oxygen atoms are bonded only to six-coordinated zinc and the S–O distances are not significantly different from the distance of 1.504 found in Na_2SO_3 [11] for the free anion.

O3 and O4 are both bonded to four-coordinated zinc and probably to one water molecule. They have S–O bonds between the values for the other two distances in the group (S1–O3 1.518 Å and S2–O4 1.535 Å).

The differences in lengths between the longest and shortest S–O bond in the groups are 0.035 Å (S1) and 0.040 Å (S2), corresponding to differences of

8σ and 10σ in the bond lengths. Similar variations of individual S – O bonds, because of coordination effects on oxygen, have been observed in $(NH_4)_9[Fe(SO_3)_6]$ [12] and $Tl_2[Cu(SO_3)_2]$.[13]

The average S – O distance (1.525 Å) in the sulfite groups is approximately the same as in other sulfites with oxygen engaged in metal bonding and/or hydrogen bonding. In $(NH_4)_2SO_3.H_2O$ [14] the same distance is 1.524 Å and in $(NH_4)_9[Fe(SO_3)_6]$ 1.517 Å.

Acknowledgement. The author expresses her sincere gratitude to Professor Bengt Aurivillius for his encouraging interest in this work and for invaluable advice. Her thanks are due also to Mr. Christer Särnstrand and Mr. Christer Svensson for their valuable help during the data collecting with CAD-4. The skilful technical assistance of Miss Kerstin Renhult is gratefully acknowledged. The author thanks Dr. Karin Aurivillius for critically reading the manuscript.

The investigation has received financial support from the *Swedish Natural Science Research Council.*

REFERENCES

1. Nyberg, B. *Acta Chem. Scand.* **26** (1972) 857.
2. Quinones, H. and Baggio, S. *J. Inorg. Nucl. Chem.* **34** (1972) 2153.
3. Pannetier, G., Djega-Madriadassou, G. and Bregault, J. M. *Bull. Soc. Chim. France* **1964** 1749.
4. Karlsson, R. and Karrman, K. J. *Talanta* **18** (1971) 459.
5. *International Tables for X-Ray Crystallography*, Kynoch Press, Birmingham 1962, Vol. I, p. 550.
6. Karle, J. and Karle, I. L. *Acta Cryst.* **21** (1966) 849.
7. Coppens, P. and Hamilton, W. C. *Acta Cryst.* **A 26** (1970) 71.
8. Doyle, P. A. and Turner, P. S. *Acta Cryst.* **A 24** (1968) 390.
9. Shannon, R. D. and Prewitt, C. T. *Acta Cryst.* **B 25** (1969) 925.
10. Kierkegaard, P., Larsson, L. O. and Nyberg, B. *Acta Chem. Scand.* **26** (1972) 218.
11. Larsson, L. O. and Kierkegaard, P. *Acta Chem. Scand.* **23** (1969) 2253.
12. Larsson, L. O. and Niinistö, L. *Acta Chem. Scand.* **27** (1973) 859.
13. Hjertén, I. and Nyberg, B. *Acta Chem. Scand.* **27** (1973) 345.
14. Battle, L. F. and Trueblood, K. N. *Acta Cryst.* **19** (1965) 531.

Received November 17, 1972.

ACTA CHEMICA SCANDINAVICA 27 (1973) 1552–1556

Mechanism of the Grignard Addition Reaction

X. Kinetics and Deuterium Isotope Effects in the Reaction of Isobutylmagnesium Bromide with Benzophenone

TORKIL HOLM

Department of Organic Chemistry, Technical University of Denmark, DK-2800 Lyngby, Denmark

Direct rate measurements and product distribution data have been obtained for the reaction of isobutylmagnesium bromide and β-deuterioisobutylmagnesium bromide with benzophenone in diethyl ether. Interpretation of the results requires separation of a rate determining step and a product determining step if Grignard reagent is in excess, but a one step mechanism is indicated when benzophenone is in excess.

The separation of a rate determining and a product determining step in the reaction of benzophenone with *tert*-butylmagnesium chloride has been demonstrated by kinetic means.[1] Intervention of radical species in this type of reaction has been shown by product analysis [2] and by ESR spectroscopy.[3] The reaction most probably takes place in accordance with the general scheme by Blicke and Powers.[4] Thus the rate limiting initial step is the transfer of a single electron (SET) from the Grignard reagent to benzophenone. Since the majority of the reaction seems to occur *via* the dialkylmagnesium of the Schlenk equilibrium,[5] the SET step may be written:

$$R{:}Mg{:}R + (C_6H_5)_2CO \rightarrow R{\cdot}Mg{:}R^+ + (C_6H_5)_2C-O^- \quad (1)$$

The various reaction products are produced in rapidly succeeding steps in which the radial ion pairs combine or disproportionate. A SET rate determining step was well documented [1] for the case of R = *tert*-butyl and evidence has been presented in favor of the operation of SET also with secondary and primary Grignard reagents.[6] With these reagents some reduction to benzhydrol occurs by transfer of a β-hydrogen to the ketone. As suggested by Whitmore [7] the reduction process has been assumed to occur *via* a synchronous shift of electrons in a cyclic arrangement of a complex of the reactants as shown in Fig 1 (I). This concerted one step mechanism requires a primary deuterium isotope effect, if the β-hydrogen is substituted with deuterium.

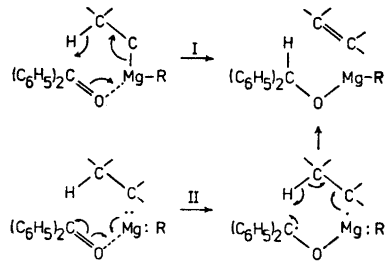

Fig. 1. I. Cyclic one step mechanism for the reduction of benzophenone with isobutylmagnesium bromide. II. Two step SET mechanism for the same process.

A SET mechanism would show only a secondary isotope effect in the rate limiting electron transfer step.

With isobutylmagnesium bromide the reaction with benzophenone yields more than 90 % benzhydrol. The β-deuteriated reagent was found to react almost as fast as the non-deuteriated, when the rate was measured directly,[6] while a rather large isotope effect was observed in a competition experiment between deuterio and non-deuterio reagent.[6,8] The results were explained by assuming a two step mechanism initiated by SET. The present work has included a repetition of the rate measurements with isobutylmagnesium bromide and benzophenone and measurements have been made at several concentrations and at various ratios of Grignard reagent to substrate. The reaction mixtures have been analysed to obtain the product distributions shown in Table 2.

The present work indicates that the earlier measurements with isobutylmagnesium bromide were somewhat in error. This was probably due to the formation of small amounts of *tert*-butyl bromide in the isobutyl bromide and the deuterioisobutyl bromide used. With the best obtainable reagents the deuterium isotope effect for β-deuterioisobutylmagnesium bromide reacting with pseudo first order concentrations of benzophenone is in the present work found to be $k_H/k_D = 1.46$. If this value is compared with the isotope effects obtained with other Grignard reagents shown in Table 1, it follows that there is a clear correlation between the amount of benzhydrol formed in the reaction and the deuterium isotope effect for the over all reaction. $k_H/k_D = 1.0$ for *tert*-butyl and ethyl Grignards. These derivatives yield none and very little

Table 1. Yield of benzhydrol in the reaction of non-deuteriated Grignard reagents with 0.02 M benzophenone at 20° in diethyl ether and kinetic isotope effect of the total reaction by β-deuteriation of the Grignard reagent to the extent shown.

	$\frac{k_H}{k_D}$	Benzhydrol %	$\frac{\beta\text{-D}}{\beta\text{-(H+D)}}$ %
0.50 M C_2H_5MgBr	1.01	6	95
0.20 M C_4H_9MgBr	1.28	55	97
0.50 M $(CH_3)_2CHMgBr$	1.16	20	92
0.25 M iso-C_4H_9MgBr	1.46	91	95
0.26 M *t*-C_4H_9MgCl	1.0	0	64

reduction product. $k_H/k_D=1.28$ for butyl and isobutyl compounds which produce 55 % and 92 % reduction product, respectively.

This observed correlation would in itself indicate a primary isotope effect which is associated with the reduction and not the addition reaction. The value 1.46 should therefore be compared with the change in the ratio between reduction product and addition product observed by the introduction of β-deuterium in isobutylmagnesium bromide. This ratio changes by a factor of 2.4 (Table 2). Competition between equal amounts of deuterio and non deuterio

Table 2. Ratio between the amount of reduction product and addition product in the reaction of isobutylmagnesium bromide with benzophenone at 20° in diethyl ether at various concentrations of the reagents.

	red/add
0.25 M $(CH_3)_2CHCH_2MgBr$ + 0.01 M benzophenone	10.8
0.50 M » + 0.05 M »	10.6
1.00 M » + 0.05 M »	10.6
1.50 M » + 0.05 M »	6.1
0.50 M $(CH_3)_2CDCH_2MgBr$ + 0.05 M »	4.55
0.02 M » + 0.25 M »	8.40
0.02 M $(CH_3)_2CHCH_2MgBr$ + 0.25 M »	21.4
0.02 M » + 1.50 M »	22

isobutylmagnesium bromide for a very small amount of benzophenone was shown by mass spectroscopic analysis to give a ratio of benzhydrol to α-deuteriobenzhydrol of 2.4. The lack of correlation between the values of the deuterium isotope effects found directly by rate measurements or indirectly by product analysis requires in some way a separation of the rate determining step and the product determining step. It is therefore concluded that the reaction occurs partly by a SET mechanism as for example the two step mechanism Fig. 1 (II). It remains undecided whether mechanisms I and II are independent and separate mechanisms or whether a mechanism is possible which is a hybrid between I and II.

As supplementary evidence for a SET mechanism may be taken the occurrence of a magnesium benzophenone ketyl signal in the ESR and correspondingly a transient color in the reaction mixture. On the other hand there have been no reports of CIDNP effects in the reduction and addition reactions of Grignard reagents. Likewise attemps to find benzopinacol either by crystallization or thin layer chromatography were unsuccessfull.

The over all rates observed with pseudo first order concentrations of benzophenone at various concentrations of isobutylmagnesium bromide are shown in Fig. 2. Increasing concentrations of Grignard reagent lead to increasing values of k_{obs}, but the slope of the curve is steadily decreasing, and a saturation effect is observed at concentrations above *ca.* 1 M. It seems reasonable to assume that the saturation effect is connected with the formation of complexes between the reagents and substrate.[9]

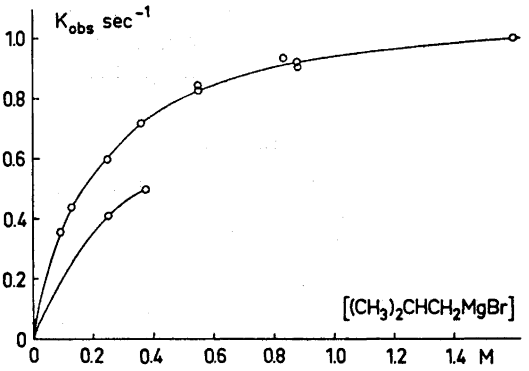

Fig. 2. Upper curve, pseudo first order rate constants k_{obs} for the reaction in diethyl ether at 20° of 0.020 M benzophenone with isobutylmagnesium bromide (9.6 % excess bromide). Lower curve, values of k_{obs} for the reaction in ether at 20° of β-deuterioisobutylmagnesium bromide (7.5 % excess bromide) with 0.02 M benzophenone.

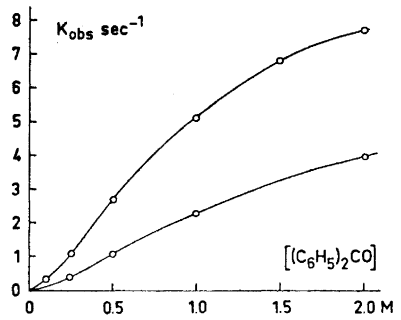

Fig. 3. Upper curve, pseudo first order rate constants k_{obs} for the reaction in diethyl ether at 20° of 0.020 M isobutylmagnesium bromide (9.6 % excess bromide) with benzophenone (see text). Lower curve, values of k_{obs} for the reaction of 0.02 M β-deuterioisobutylmagnesium bromide (7.5 % excess bromide) with benzophenone.

Rates observed with pseudo first order concentrations of Grignard reagent (0.02 M) are shown in Fig. 3. It appears from the curve that the reaction order with respect to benzophenone is above one in the concentration range up to 0.5 M benzophenone and that a saturation effect is beginning at concentrations above 1 M. Since the Grignard reagent under the reaction conditions is likely to change composition during the reaction, it is rather surprising that 40 – 60 % of the reaction followed the first order rate law. The half life of 0.02 M isobutylmagnesium bromide in 1.5 M benzophenone is *ca.* 8 times lower than the half life of 0.02 benzophenone in 1.5 M isobutylmagnesium bromide. As a tentative explanation one could suggest the formation of a highly reactive complex between one molecule of magnesium compound and two molecules of benzophenone.

The deuterium isotope effect in the case of a large excess of benzophenone was $k_H/k_D = 2.5$ and the ratio of addition to reduction was changed by the introduction of deuterium in the β-position by a factor 2.55. The agreement

between the two values in this case indicates a one step mechanism, *e.g.* the cyclic hydride transfer mechanism of Whitmore effective when isobutylmagnesium bromide reacts with excess benzophenone.

EXPERIMENTAL

Isobutyl bromide and β-deuterioisobutyl bromide [6] were fractionally distilled at 40°, 100 mmHg through a 45 cm glass helices column. The maximum impurity of *tert*-butyl bromide was found by GLC (silicone column) and NMR (Varian A 60) to be 0.4 %, comparing the 9 H singlet of *t*-butyl bromide with one absorption of the observed sextet of the β-H in isobutyl bromide. The bromide was converted to the Grignard reagent immediately after its preparation. Hexadeuterio-*t*-butylmagnesium chloride was prepared as described.[1] Dow sublimed magnesium was used and ether was freshly distilled from lithium aluminium hydride. Product distributions were determined by GLC and NMR. A 1.5 m diethyleneglycol succinate column at 195° separated benzophenone from α-isobutylbenzhydrol and benzhydrol. The areas of the peaks (flame detector) were measured with a planimeter and related to yields and concentrations by means of standard mixtures.

The rate measurements were performed at 20° by means of the thermographic method described earlier.[1] T_0 was recorded 1 – 2 msec after mixing and the final temperature was T_∞. The temperatures recorded in between (from 2 – 10 observations depending on conditions) were fitted to the first order expression

$$\ln \frac{a}{a-x} = \ln \frac{T_\infty - T_0}{T_\infty - T} = kt.$$

The disappearance of 0.02 M benzophenone in excess Grignard reagent was pseudo first order and k_{obs} for the total reaction was obtained from the first order plots. The disappearance of 0.02 M isobutylmagnesium bromide in excess benzophenone was analysed in the same way and first order rate constants were obtained from the linear part of k_{obs} *versus* time. The plot was linear for the first 40 – 65 % of the reaction.

Concentrations of isobutylmagnesium bromide above 0.8 M were obtained by mixing in the flowing stream apparatus 20 volumes of reagent with 1 volume of 0.42 M benzophenone solution.

REFERENCES

1. Holm, T. and Crossland, I. *Acta Chem. Scand.* **25** (1971) 59.
2. Blomberg, C. and Mosher, H. S. *J. Organomet. Chem.* **13** (1968) 519.
3. Maruyama, K. *Bull. Chem. Soc. Japan* **37** (1964) 897.
4. Blicke, F. F. and Powers, L. D. *J. Am. Chem. Soc.* **51** (1929) 3378.
5. Holm, T. *Acta Chem. Scand.* **21** (1967) 2753.
6. Holm, T. *J. Organomet. Chem.* **29** (1971) C 45.
7. Whitmore, F. C., as quoted by Mosher, H. S. and LaCombe, E. *J. Am. Chem. Soc.* **72** (1950) 3994.
8. Dunn, G. E. and Warkentin, J. *Can. J. Chem.* **34** (1956) 75.
9. Holm, T. *Acta Chem. Scand.* **23** (1969) 579.

Received November 22, 1972.

ACTA CHEMICA SCANDINAVICA 27 (1973) 1557–1564

Oxidation of Carbohydrate Derivatives with Silver Carbonate on Celite.

VI. 2-Ketoses

SVEIN MORGENLIE

Department of Chemistry, Agricultural University, N-1432 Ås-NLH, Norway

D-Fructose is oxidized by silver carbonate on Celite in methanol to give a glycolic ester of D-erythrose. Derivatives of D-glyceraldehyde and D-erythronic acid are also formed by further oxidation of the primary product.

The five other 2-ketoses examined are also oxidized. The products after hydrolysis and removal of acidic compounds were the aldoses resulting from cleavage of the ketoses between C-2 and C-3, and varying amounts of the aldoses produced by one further step of degradation.

D-*manno*-Heptulose and D-*glycero*-D-*manno*-octulose are found to be oxidized with greater difficulty than the hexuloses and D-*altro*-heptulose.

Silver carbonate on Celite, the oxidant introduced by Fetizon and co-workers,[1] has shown similarities to periodate and lead tetraacetate in its ability to cleave the diol group between C-1 and C-2 in reducing aldose derivatives.[2,3] Lead tetraacetate is known to cleave fructose and other 2-ketoses in furanose form between C-2 and C-3.[4,5] From D-fructose is formed 3-*O*-glycolyl-D-erythrose, which in turn is rapidly degraded to 3-*O*-formyl-2-*O*-glycolyl-D-glyceraldehyde. Acid hydrolysis liberates D-glyceraldehyde from this compound, and the method thus offers a convenient way to the triose. In addition to its synthetic applicability, this reaction has been widely used in identification of heptuloses, octuloses, and nonuloses isolated from plants.[6,7] Periodate has been reported to give a more complex oxidation pattern in the case of 2-ketoses because of its greater tendency to cause cleavage between C-1 and C-2.[8,9]

An investigation of the effect of silver carbonate on Celite on 2-ketoses seemed in light of these facts to be of interest, and has now been undertaken. In a previous paper in this series, the application of the oxidant in the synthesis of L-threose from L-sorbose has already been described.[10]

RESULTS AND DISCUSSIONS

D-Fructose (I) gave in analogy to L-sorbose on oxidation in methanol as major product a glycolic ester of D-erythrose (II) from which the tetrose (III) was liberated on acid hydrolysis. D-Erythrose (III) was characterized by

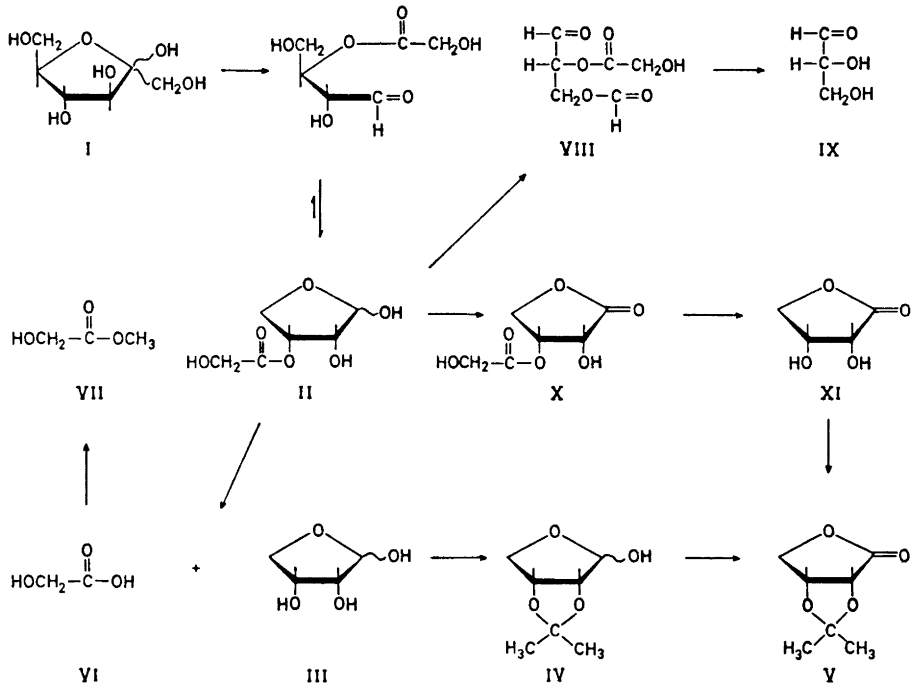

acetonation to 2,3-*O*-isopropylidene-D-erythrose (IV), which was subsequently oxidized to 2,3-*O*-isopropylidene-D-erythrono-1,4-lactone (V) by silver carbonate on Celite in benzene.

Glycolic acid (VI), formed on hydrolysis of the primary oxidation product, was isolated after conversion to its methyl ester (VII). The methyl ester was identified by chromatography and infrared spectroscopy.

The primary oxidation product, the glycolic ester of D-erythrose (II), shows that the oxidation occurs in cyclic form (or forms) of fructose. In order to obtain information about the ring form, the glycolic ester was subjected to oxidation with lead tetraacetate. The main product resulting from this treatment was a derivative (VIII) of D-glyceraldehyde with chromatographic mobility corresponding to that of 3-*O*-formyl-2-*O*-glycolyl-D-glyceraldehyde. This compound was also formed on prolonged oxidation of D-fructose with an excess silver carbonate on Celite. D-Glyceraldehyde (IX) was formed from this derivative on acid hydrolysis. The formation of a diester of glyceraldehyde from fructose by two steps of degradation, as well as with lead tetraacetate from the primary degradation product, is consistent with an initial oxidation of fructose mainly in furanose form.

Infrared spectroscopy of the reaction mixture after oxidation of D-fructose indicated the presence of small amounts of a γ-lactone. This was confirmed by the isolation of D-erythrono-1,4-lactone (XI) after acid hydrolysis. The 3-*O*-glycolyl derivative (X) is presumably the precursor of this compound, and its formation is in agreement with the assumption that D-fructose initially is cleaved between C-2 and C-3 in furanose form. It is in this connection worth to mention that the formation of aldonolactones has been observed in this laboratory to be a competing reaction to degradation when aldopentoses are treated with silver carbonate on Celite in methanol,[11] and recently the formation of D-galactono-1,4-lactone and D-lyxose was reported by Fetizon and Moreau when D-galactose was oxidized with the same oxidant in ethanol.[12]

One octulose, two heptuloses, and two hexuloses, in addition to D-fructose, have also been oxidized. The main products obtained after hydrolysis and removal of acidic compounds were the aldoses resulting from glycol cleavage between C-2 and C-3 of the ketoses, as shown by chromatography and electrophoresis. Varying amounts of the aldoses, formed by one subsequent degradation, were also detected (Table 1).

Table 1. Products obtained from the ketoses with silver carbonate on Celite in methanol after hydrolysis and removal of acidic compounds, detected by electrophoresis and chromatography.

2-Ketose	Major product	Minor product
D-Tagatose	Threose	Glyceraldehyde
D-Psicose	Erythrose	Glyceraldehyde
D-*altro*-Heptulose	Ribose	Erythrose
D-*manno*-Heptulose	Arabinose	Erythrose
D-*glycero*-D-*manno*-Octulose	Altrose	Ribose [a]

[a] The yield of the minor product in this case was relatively high.

The product mixture after oxidation of the hexuloses did not contain detectable amounts of pentonolactones. Since the pentonolactones seem to be relatively stable to the oxidant under the reaction conditions employed,[11] the possibility of significant initial cleavage between C-1 and C-2 is excluded. The oxidant thus seems to be nearer related to lead tetraacetate than to periodate in degradation of ketoses. In the case of *manno*-heptulose, however, traces of a compound with chromatographic behaviour corresponding to that of mannonolactone were detected. This compound is the product expected after initial cleavage of the heptulose between C-1 and C-2.

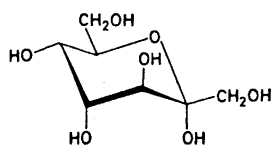

XII

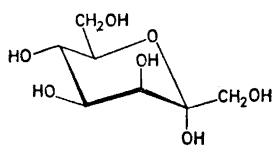

XIII

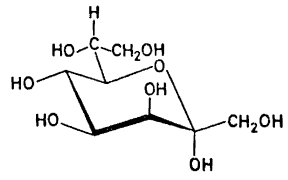

XIV

The approximate minimum reaction temperatures at which detectable degradation of the ketoses occurred within 15 min are shown in Table 2. It is seen that three of the hexuloses and D-*altro*-heptulose (XII) are oxidized at about 20°C, whereas D-*manno*-heptulose (XIII) and its homomorphous sugar D-*glycero*-D-*manno*-octulose (XIV) need considerably higher temperatures.

Table 2. Approximate temperatures below which no degradation product could be detected within 15 min on treatment of the ketoses with silver carbonate on Celite in methanol.

2-Ketose	Approximate minimum reaction temperature (°C)	Initial cleavage between C-2 and C-3 with periodate [9] (%)
D-Fructose	20	53
L-Sorbose	22	31
D-Tagatose	20	20
D-Psicose	27	–
D-*altro*-Heptulose	22	–
D-*manno*-Heptulose	35	0
D-*glycero*-D-*manno*-Octulose	40	–

D-Tagatose [13] and especially D-fructose are known to exist in solution as a mixture of different forms, and L-sorbose has been reported to exhibit small, complex mutarotation.[14] D-*manno*-Heptulose, however, does not show mutarotation,[9] and it is assumed to be very stable in α-pyranose form in the *C1* (D) conformation having the two hydroxy-methyl groups, as well as two of the secondary hydroxyl groups, equatorially attached. The *trans* diaxial arrangement of the hydroxyl groups at C-2 and C-3 is a favorable situation as a result of the anomeric and the *Δ*2 effect. The same must be supposed for the homomorphous sugar D-*glycero*-D-*manno*-octulose (XIV). For D-*altro*-heptulose (XII) on the other hand, the steric situation is less favorable in the pyranose form, because of the diaxial interaction between the hydroxyl groups at C-2 and C-4.

The explanation of the low reactivity to the oxidant of the sugars with *manno*-configuration is possibly that relatively much energy is required to bring these sugars from their stable form into a ring form and conformation suitable for cleavage between C-2 and C-3. It is in this connection worth to recognize that initial cleavage with periodate does not occur between C-2 and C-3 in the heptuloses and octuloses which on steric grounds must be assumed to be most stable in chair conformation in pyranose form, notably those with *manno*- and *gluco*-configurations, and their homomorphous sugars. D-Fructose, L-sorbose, and D-tagatose, on the other hand, are cleaved initially also between C-2 and C-3 by this reagent [9] (Table 2). It seems by inspection of the table that some correlation exists between the degree of initial C-2 – C-3 cleavage with periodate and the reactivity with silver carbonate on Celite for three of the ketoses investigated with both oxidants. D-Tagatose, however, is oxidized at a lower temperature than L-sorbose with silver carbonate on Celite, whereas the degree of cleavage between C-2 and C-3 of this sugar with periodate is less

than for L-sorbose. It seemed desirable to examine nearer the rate of oxidation of the hexuloses with silver carbonate on Celite, and the oxidation of these sugars at 30°C was followed using a colorimetric method. The results (Fig. 1) support the observation that D-tagatose is easily oxidized. At this temperature, D-tagatose is oxidized with the highest initial rate of the hexuloses.

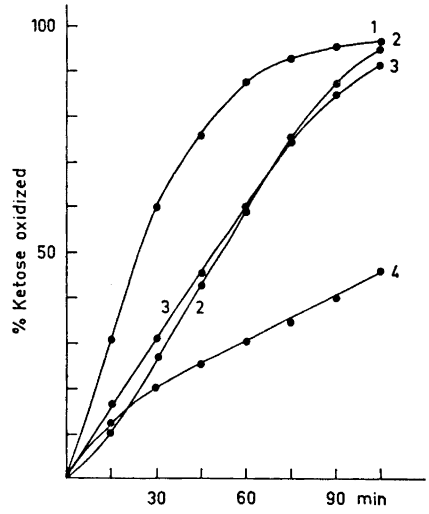

Fig. 1. Oxidation of the hexuloses at 30°C with silver carbonate on Celite in methanol. 1, D-Tagatose; 2, D-fructose; 3, L-sorbose; 4, D-psicose.

In addition to its applicability in synthesis of L-threose from L-sorbose,[10] silver carbonate on Celite may be an alternative to lead tetraacetate in identification of heptuloses and octuloses. The latter oxidant seems to cleave the primary degradation product more rapidly than it reacts with the ketoses. Silver carbonate on Celite, on the other hand, gives mainly one degradation under the conditions employed. Information about the configuration at one carbon atom more (C-4 of the ketoses) is thus obtained with this oxidant.

EXPERIMENTAL

Paper chromatography was performed on Whatman No. 1 and 3 MM papers in the solvent systems (v/v): (A) butanol-pyridine-water 5:3:2, (B) butanol-ethanol-water 40:11:19, and (C) butanone-acetone-formic acid-water 40:2:1:6. Thin-layer chromatography (TLC) was run on Silica gel G in (D) benzene-ethanol 3:1, (E) benzene-ethanol 5:1, (F) chloroform-methanol 15:1, and (G) chloroform-methanol 30:1. Paper electrophoresis was performed on Whatman No. 1 paper in borate buffer, pH 10. As spray reagents were used hydroxylamine-ferric chloride [15] for esters and lactones, diphenylamine-aniline-phosphoric acid [16] and aniline hydrogenphthalate for reducing sugars, and sulphanilamide-β-naphthol-sodium nitrite [17] for acids.

Oxidation of D-*fructose (I).* D-Fructose (I) (500 mg) in methanol (100 ml) was stirred with silver carbonate on Celite [18] (11 g) at 35°C for 35 min. The solution was filtered and the solvent evaporated under reduced pressure. The syrupy residue showed strong infrared absorption at 1735 cm^{-1} and a shoulder at 1770 − 1780 cm^{-1}. The syryp contained as major component a compound which was detectable with hydroxylamine-ferric chloride as well as with diphenylamine-aniline-phosphoric acid after TLC (solvent D). At least

three faster moving compounds were also present in small amounts. The syrup was treated with sulphuric acid, 0.2 M, for 48 h at room temperature, the solution was then neutralized with Dowex 1 (bicarbonate) ion exchanger, filtered and the solvent evaporated. The resulting syrup (192 mg) contained as major component a compound with electrophoretic, paper- (solvent A), and thin-layer (solvent D) chromatographic mobilities corresponding to those of erythrose. TLC and electrophoresis showed in addition the presence of a compound with mobilities and colours after spraying corresponding to those of glyceraldehyde. Traces of two compounds with higher mobility (TLC) were also present.

2,3-O-Isopropylidene-D-erythrose (IV). The syrup obtained as described above was shaken with acetone (20 ml) containing sulphuric acid (0.15 ml) for 3 h. The solution was then neutralized with solid sodium bicarbonate, filtered and the solvent evaporated. The residue was dissolved in benzene (50 ml), the benzene solution extracted with water (3 × 20 ml) and the water evaporated to give syrupy 2,3-*O*-isopropylidene-D-erythrose (IV); the yield was 165 mg (37 % based on fructose). The product was indistinguishable from authentic 2,3-*O*-isopropylidene-L-erythrose [3] by TLC (solvent F), $[\alpha]_D$ −72° (*c* 1, water) {lit.[19] −78°}.

2,3-O-Isopropylidene-D-erythrono-1,4-lactone (V). 2,3-*O*-Isopropylidene-D-erythrose (IV), obtained as described above, (125 mg) in benzene (30 ml), was refluxed with silver carbonate on Celite (3.5 g) for 2 h. The solution was filtered and the solvent evaporated. Crystallization of the residue from petroleum ether (b.p. 40 − 65°C) afforded 2,3-*O*-isopropylidene-D-erythrono-1,4-lactone (V), 101 mg (82 %). After recrystallization from the same solvent it had m.p. 67 − 69°C (lit.[20] 65 − 67.5°C), and $[\alpha]_D$ −114° (*c* 1, water) {lit.[20] −116°}. The compound was indistinguishable by TLC (solvent G) from a sample of the L-enantiomeric compound.[3]

Identification of glycolic acid (VI). D-Fructose (I) (500 mg) was oxidized as described above, and the product mixture was hydrolyzed in trifluoroacetic acid, 0.2 M, at 75°C overnight. The solvent was evaporated, and the residue stirred with Dowex 50 W (H^+ form) ion exchanger in methanol (50 ml) for 4 h. After filtration and evaporation of the solvent, the residue was extracted with benzene (5 × 15 ml). The benzene extracts were combined, and the solvent removed to give a syrup (67 mg), containing mainly methyl glycolate (VII). The chromatographic mobility (TLC solvents E and F) corresponded to that of authentic methyl glycolate, and the infrared spectrum was identical with that of the authentic sample, except for one small additional absorption band, presumably resulting from impurity.

The syrup was hydrolyzed overnight in 0.5 M trifluoroacetic acid (5 ml) at 60°C. The trifluoroacetic acid and the water were removed under reduced pressure, and the residue subjected to paper chromatography (solvent C). The major component was indistinguishable from glycolic acid; small amounts of a compound with lower mobility were also present.

Prolonged oxidation of D-fructose (I), identification of D-glyceraldehyde (IX). D-Fructose (I) (250 mg) was stirred at 35°C with silver carbonate on Celite (10 g) in methanol (80 ml) for 50 min. After filtration of the solution, a few drops of acetic acid were added (to prevent cleavage of formic ester during work up), and the solvent was removed under reduced pressure. The residue contained a major component with chromatographic mobility (TLC solvent E) corresponding to that of 3-*O*-glycolyl-2-*O*-formyl-D-glyceraldehyde, prepared from D-fructose by oxidation with lead tetraacetate.[21] The residue was hydrolyzed in 0.2 M sulphuric acid (5 ml) for 48 h at room temperature. The solution was neutralized with Dowex 1 (bicarbonate) ion exchanger, and the water removed under reduced pressure to give a syrupy residue (54 mg). The syrup contained mainly a compound with chromatographic (TLC solvent D) and electrophoretic mobilities corresponding to those of glyceraldehyde. The compound was purified by preparative TLC (solvent D), the resulting product (34 mg) gave a dimedone derivative (3 mg after recrystallization from ethanol-water) m.p. 194 − 198°C, (lit.[21] 196 − 198°), $[\alpha]_D$ +175° ± 25° (*c* 0.2 ethanol) {lit.[21] +210°}.

Identification of D-erythrono-1,4-lactone (XI). D-Fructose (I) (250 mg) was oxidized with silver carbonate on Celite (6 g) in methanol (50 ml) at 38 − 39°C for 40 min. After filtration of the solution, the solvent was removed and the residue hydrolyzed in trifluoroacetic acid, 0.5 M (5 ml), overnight at 60°C. After removal of water and trifluoroacetic acid under reduced pressure, the resulting residue was subjected to preparative paper chromatography (solvent A). The fraction with mobility corresponding to that of

erythrono-1,4-lactone was purified further by TLC (solvent D), affording D-erythrono-1,4-lactone (XI) as a chromatographically homogeneous syrup (18 mg). Treatment of the syrup with acetone-anhydrous cupric sulphate overnight, filtration and evaporation of the solvent gave a partially crystalline residue. Extraction of the residue with petroleum ether (b.p. 40 – 65°), evaporation of the solvent and recrystallization from the same solvent afforded 2,3-*O*-isopropylidene-D-erythrono-1,4-lactone (V) (2 – 3 mg), m.p. 68°C (lit.[20] 65 – 67.5°), $[\alpha]_D$ $-90° \pm 15°$ (*c* 0.2, water) {lit.[20] $-116°$}. The compound was chromatographically indistinguishable (TLC solvent G) from authentic 2,3-*O*-isopropylidene-D-erythrono-1,4-lactone.

Oxidation of the primary oxidation product from D-*fructose with lead tetraacetate.* D-Fructose (I) (250 mg) was oxidized at 35°C with silver carbonate on Celite in methanol (50 ml) for 35 min. The solution was filtered and the solvent evaporated after addition of a few drops of acetic acid. The reaction mixture did not contain any unreacted fructose as shown by TLC (solvent D). The residue was dissolved in acetic acid (12 ml) and stirred with lead tetraacetate (1 g) for 10 min at 16 – 18°C and further 10 min at room temperature. A solution of anhydrous oxalic acid (0.2 g) in acetic acid (2 ml) was then added, the solution was filtered and the solvent evaporated. The residue was by TLC (solvent E) shown to contain as main component a compound with mobility corresponding to that of 3-*O*-formyl-2-*O*-glycolyl-D-glyceraldehyde. The residue was hydrolyzed in 0.2 M sulphuric acid at room temperature for 48 h, the solution was then neutralized with Dowex 1 (bicarbonate) resin. Electrophoresis of the solution indicated the presence of exclusively one component, TLC (solvent D) showed the presence of a major product; the mobilities corresponded to those of glyceraldehyde. The colours with the spray reagent were identical with those given by authentic glyceraldehyde. TLC showed in addition the presence of minor amounts of a faster moving component.

Oxidation of the other 2-ketoses. The ketoses were oxidized in the same manner as described for D-fructose. The temperatures employed were from 35 to 45°C. After hydrolysis in 0.2 M sulphuric acid at room temperature for 48 h and neutralization with Dowex 1 (bicarbonate) resin, the products were detected by electrophoresis, paper chromatography (solvent A) and in part by TLC (solvent D); the results are shown in Table 1.

For determination of the approximate minimum reaction temperatures, TLC was used to detect the presence of degradation products. The results are shown in Table 2.

Oxidation rate of the hexuloses. The hexuloses (50 mg) in methanol (10 ml) were oxidized after completion of mutarotation with silver carbonate on Celite (1.2 g) at 30°C. Aliquots (10 µl) were withdrawn at intervals, diluted with water (to 1 ml) and the amount of unreacted hexulose present determined colorimetrically with the thiobarbituric acid reagent.[22] The results are shown in Fig. 1.

Acknowledgements. The author is indebted to Cand. pharm. Guri Haustveit for a gift of D-*altro*-heptulose and D-*glycero*-D-*manno*-octulose, and to Miss Astrid Fosdahl for valuable technical assistance.

REFERENCES

1. Fetizon, M. and Golfier, M. *C. R. H. Acad. Sci. Ser. C* **267** (1968) 900.
2. Morgenlie, S. *Acta Chem. Scand.* **25** (1971) 2773.
3. Morgenlie, S. *Acta Chem. Scand.* **26** (1972) 1709.
4. Perlin, A. S. and Brice, C. *Can. J. Chem.* **34** (1956) 541.
5. Perlin, A. S. and Brice, C. *Can. J. Chem.* **34** (1956) 85.
6. Haustveit, G. and Wold, J. K. *Acta Chem. Scand.* **24** (1970) 3059.
7. Begbie, R. and Richtmyer, N. K. *Carbohyd. Res.* **2** (1966) 272.
8. Sprinson, D. B. and Chargaff, E. *J. Biol. Chem.* **164** (1946) 433.
9. Sarfati, S. R. and Szabo, P. *Carbohyd. Res.* **13** (1970) 441.
10. Morgenlie, S. *Acta Chem. Scand.* **26** (1972) 2146.
11. Morgenlie, S. *Acta Chem. Scand. To be published.*
12. Fetizon, M. and Moreau, N. *C. R. H. Acad. Sci. Ser. C* **275** (1972) 621.
13. Jochimo, J. C., Taigel, G., Sediger, A., Lutz, P. and Driesen, H. E. *Tetrahedron Lett.* **1967** 4363.
14. Pigman, W. W. and Isbell, H. S. *J. Res. Natl. Bur. Std.* **19** (1937) 443.

15. Abdel-Akher, M. and Smith, F. *J. Am. Chem. Soc.* **73** (1951) 5859.
16. Schwimmer, S. and Bevenue, A. *Science* **123** (1956) 543.
17. Schmidt, G. C., Fischer, C., and McOwen, J. M. *J. Pharm. Sci.* **52** (1963) 468.
18. Balogh, V., Fetizon, M., and Golfier, M. *Angew. Chem.* **81** (1969) 423.
19. Ballou, C. E. *J. Am. Chem. Soc.* **79** (1957) 165.
20. Schaffer, R. *J. Res. Natl. Bur. Std.* **A 65** (1961) 507.
21. Perlin, A. S. *Methods Carbohyd. Chem.* **1** (1962) 61.
22. Percheron, F. *C. R. H. Acad. Sci.* **255** (1962) 2521.

Received December 7, 1972.

ACTA CHEMICA SCANDINAVICA 27 (1973) 1565–1572

Broadband Microwave Investigations on Monobromostyrenes

W. RALOWSKI, G. WETTERMARK and S. LJUNGGREN

Department of Physical Chemistry, Royal Institute of Technology, S-100 44 Stockholm 70, Sweden

Broadband microwave spectra of *p*-bromostyrene, *trans*-β-bromostyrene and *m*-bromostyrene are recorded and the sum of the rotational constants $(B+C)$ are calculated. From the results obtained, the $C_b-C=C$ angle in *p*-bromostyrene and *cis*-*m*-bromostyrene is $127\pm4°$.

High-resolution microwave spectroscopy cannot at present be successfully applied to the study of large molecules. Apart from the fact that the absorption intensities are rapidly diminished with increasing molecular weight, the spectra are usually complicated by the presence of a large number of low-lying vibrational satellites. A high-resolution spectrum often presents such an abundance of weak lines that the assignment becomes a problem of unwieldy complexity.

When the spectrum of a near-symmetric top molecule is scanned at a high sweep rate and detector time constant, a band spectrum is obtained, in which each band consists of the superposition of a large number of unresolved high K lines belonging to a particular $J\rightarrow J+1$ transition.

Neglecting the usually insignificant systematic errors, a band spectrum can be described by formula (1):

$$\nu = (B + C)(J + 1) \tag{1}$$

The constant $(B+C)$ can thus be determined from the distances between the bands and their positions.

This work is one of the first attempts to obtain significant structural information from broadband microwave studies. In this paper, investigations of three monobromostyrenes are reported, *p*-bromostyrene, *m*-bromostyrene, and *trans*-β-bromostyrene. They have all high $|\varkappa|$-values * large dipole moments along the *a* principal axis and possess no constituent at sterically hindering positions. Their vapour pressure at room temperature is

* *Cf., e.g.*, C. H. Townes and A. L. Schawlow, *Microwave Spectroscopy*, McGraw, New York 1955.

sufficiently high for microwave studies to be possible. There appears to be no reliable data available at present on the molecular geometry of styrene. The structure of only one styrene derivative has been studied experimentally so far, *trans*-β-bromostyrene, by electron diffraction.[1] Styrene is usually described as a planar molecule where π-electrons belonging to the vinyl group and the benzene ring conjugate. It is, however, conceivable that the vinyl group may rotate more or less freely or that a twisted conformation is the most stable one by analogy with biphenyl [2] and *N*-benzylideneaniline.[3] *p*- and *trans*-β-Bromostyrene are near-symmetric rotors with κ-values around −0.98. *m*-Bromostyrene, on the other hand, is less symmetric, although a band structure is still observed. The broadband microwave spectra of the three bromostyrenes are shown in Fig. 1. The natural abundances of the two bromine isotopes,[79] Br and [81]Br, are approximately equal. The spectra thus consist of two superimposed sets of bands. Although this fact provides some possibility to check on different structural assumptions, it also complicates the assignment of the spectra to a considerable degree.

EXPERIMENTAL

Commercial samples of bromostyrenes were used. The sample of *m*-bromostyrene had to be purified by vacuum distillation, whereas *p*- and *β-trans*-bromostyrene were found to be sufficiently pure for our purpose. Microwave spectra in the frequency range 26 500 to 40 000 MHz (Mc/sec) were recorded at room temperature on a Hewlett-Packard 8460A spectrometer.

RESULTS

The frequencies of the band centres are listed in Tables 1 – 3. All frequencies are given in MHz. The position of any band is calculated as the average value of the frequencies obtained from two sweeps in opposite directions.

Table 1. p-Bromostyrene.

J	Observed frequencies ^{79}Br	^{81}Br
29	26 915	26 665
30	27 802	27 545
31	28 698	28 420
32	29 597	29 310
33	30 500	30 205
34	31 393	31 098
35	32 295	31 988
36	33 195	32 873
37	34 090	33 765
38	34 990	34 645
39	35 888	35 528
40	36 785	36 417
41	37 680	37 308
42	38 580	38 202
43	39 480	39 093
44	–	39 980

Table 2. trans-β-Bromostyrene.

J	Observed frequencies ^{79}Br	^{81}Br
36	27 090	26 802
37	27 808	27 518
38	28 550	28 250
39	29 285	28 985
40	30 010	29 700
41	30 737	30 422
42	31 472	31 145
43	32 208	31 880
44	32 938	32 600
45	33 673	33 315
46	34 405	34 045
47	35 130	34 770
48	35 853	35 493
49	36 595	36 210
50	37 320	36 940
51	38 065	37 660
52	38 790	38 385
53	39 505	39 105
54	–	39 825

Table 3. m-Bromostyrene.[a]

J	Observed frequencies ^{79}Br	^{81}Br
23	27 360	27 100
24	28 510	28 230
25	29 660	29 390
26	30 785	30 500
27	31 925	31 630
28	33 070	32 730
29	34 190	33 895
30	35 345	34 995
31	36 495	36 125
32	37 640	37 295
33	38 770	38 380
34	39 905	39 505

[a] There are also strong bands at 27 580, 31 400, 33 410, 34 450, 34 740, 36 800 and 37 850 MHz. The band corresponding to the transition $J = 27 \leftarrow 26$ is weak.

Values of $(B+C)$ were obtained by a least-squares method based on eqn. (1). The obtained values of $(B+C)$ are listed in Table 4. The error in the values of $(B+C)$ was estimated to be ± 2 MHz.

Table 4.

Molecule	Bromine isotope	$(B+C)$
p-Bromostyrene	79	897.1
	81	888.4
m-Bromostyrene	79	1141.0
	81	1130.0
trans-β-Bromostyrene	79	731.9
	81	724.3

DISCUSSION

The structure of each molecule was analyzed in the following way.

(*i*) An initial structure was assumed.

(*ii*) The parameters with the largest influence on $(B+C)$ were found.

(*iii*) Agreement with experimental data could be achieved by reasonable changes of the parameters.

(*iv*) The refined structure was finally checked by computing the value of $(B+C)$ for the other isotopic isomer and comparing it with the experimental data. The initial structure was based upon the assumption of hexagonal symmetry of the benzene ring and the following bond lengths (see Fig. 2): $r_b =$

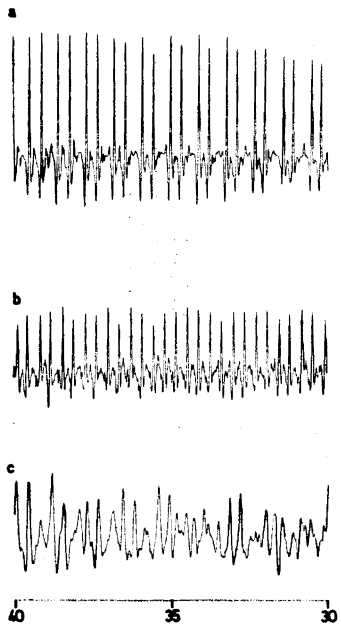

Fig. 1. Broadband microwave spectra of *p*-bromostyrene (a), *trans*-β-bromostyrene (b) and *m*-bromostyrene (c) in the frequency range 30–40 GHz.

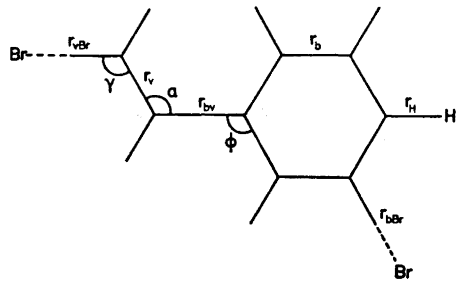

Fig. 2. Structural parameters of bromostyrene type molecules.

1.40 Å, $r_v = 1.34$ Å, $r_{bv} = 1.48$ Å, all $r_H = 1.08$ Å, $r_{bBr} = 1.87$ Å, $r_{vBr} = 1.89$ Å, and all the angles 120°.

Point (*ii*) above requires some comments. All the parameters were varied in calculations for the three molecules in order to determine their relative effects on the value of $(B+C)$. It was thus shown that the positions of the hydrogen atoms had no significant effect on $(B+C)$. The r_b, r_b, r_{Br} and r_{bv} bond lengths were far more important, but reasonable changes in these parameters did not lead to agreement with experiment. The values of r_b, r_v and r_{Br} were thus taken to be the same as those from many different investigations on similar systems.[4] The error caused by this assumption was assumed to be negligible.

The bond length r_{bv} was taken from the one existing experimental work on a styrene derivative, *trans*-β-bromostyrene.[1] The effect of the choice of r_{bv} will be discussed in connection with *p*-bromostyrene.

In addition to the bond length, r_{bv}, the following angles were the most essential parameters:

α: the $C_b - C = C$ angle.
γ: the $Br - C = C$ angle.
θ: the dihedral angle between the benzene ring and the plane of the vinyl group.
ϕ: the $C_b - C_b' - C$ angle.

Keeping the α and γ angles equal to 120°, the ϕ angle was varied in calculations for *p*-bromostyrene and *m*-bromostyrene. The experimental values of $(B+C)$ could only be reproduced for $\phi = 124°$ in *p*-bromostyrene and $\phi = 132°$ in *m*-bromostyrene. The very different values obtained for the two isomers appear quite unreasonable. Thus, in the subsequent calculations, the angle a is taken as 120° in agreement with the first assumed structure.

In the cases of *p*-bromostyrene and *m*-bromostyrene the possible influence of a deformation of the benzene ring was studied by carrying out parallel calculations for the hexagonally symmetric ring and the bromine-distorted ring structure. As a result of the above assumptions the only remaining parameters to be considered are the angles α, θ and γ.

p-*Bromostyrene*. The molecule is very nearly symmetric with $\varkappa \approx -0.98$. If r_{bBr} is assumed to be 1.87 Å, α and r_{bv} are the two remaining parameters with the largest influence on the value of $(B+C)$. If we assumed that $\alpha = 120°$ and $(B+C) = 888.4$ MHz, the bond length r_{bv} would have to be 1.546 Å.

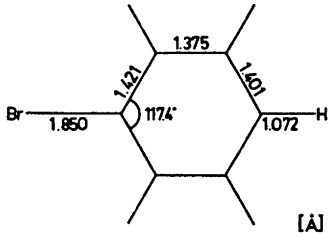

Fig. 3. Distorted structure of bromobenzene.

This value appears unreasonable, since even the single C – C bond in ethane is shorter than this. Igarashi *et al.*[1] determined r_{bv} in *trans*-β-bromostyrene as 1.48 Å. For this bond length the calculated value of α would be 126.3°. Unfortunately, these two parameters appear to be correlated and cannot be separated. This implies that for each pair of parameters which gives $(B+C)=$ 888.4 MHz, the value of $(B+C)$ for the isotopic isomer $C_6H_4{}^{79}Br-CH=CH_2$ is equal to the experimental value 897.1 MHz. A rotation of the benzene ring has only a small effect on the value of $(B+C)$. Thus, when the benzene ring is twisted from the planar to the perpendicular conformation, the value of $(B+C)$ decreases by no more than 0.7 MHz. This corresponds to a decrease of α or r_{bv} by 0.4° and 0.004 Å, respectively.

Parallel calculations were made in order to estimate the effect of the deformation of the benzene ring on the value of $(B+C)$. Bromobenzene has previously been investigated by high resolution microwave spectroscopy.[5] Rotational constants for several isotopic species have been obtained. The complete r_s structure was not reported, but a structure consistent with the experimental data has been proposed and is reproduced with minor modifications in Fig. 3.

The three rotational constants belonging to this structure are reproduced in Table 5.

Table 5.

	Measured [a]	Calculated [b]
$C_6{}^{79}H_5Br$		
A	5667.47 ± 1.05	5668.19
B	994.894 ± 0.006	994.87
C	846.250 ± 0.006	846.33
$C_6H_5{}^{81}Br$		
A	5668.87 ± 1.18	5668.19
B	984.704 ± 0.006	984.69
C	838.858 ± 0.006	838.95

[a] From Ref. 5. [b] *Cf.* Fig. 3.

The rotational constant A should be equal for both isotopic isomers and can be estimated as an average of the two measured constants. It seems reasonable to assume that the bromine atom will cause a stronger deformation of the benzene ring than the vinyl group. Hence, if we let the structure above represent the true ring structure of *p*-bromostyrene, the results are approximately the same as above, *i.e.* $\alpha = 126.9°$. A CNDO/2 calculation [6] on styrene gave an energy minimum for $\alpha = 130°$. The corresponding angle in butadiene has been experimentally determined to be 123°.[7]

trans-*β-Bromostyrene. trans-β*-Bromostyrene is the only styrene derivative whose structure has so far been experimentally investigated.[1] The molecule was found to have a planar configuration with the r_{bv} bond length equal to 1.48 ± 0.03 Å. Using the parameters suggested by Igarashi *et al.*, the value of $(B+C)$ was calculated to 739.8 MHz, which is about 15 MHz larger than the $(B+C)$ value obtained from the band spectrum.

The molecule is very nearly symmetric with $\varkappa \approx -0.99$. The two most important parameters are the angles α and γ. For example, changing the angle α by 1° causes a change of 2.5 MHz in $(B+C)$. In contrast, a rotation of the benzene ring by 90° from the planar conformation increases the value of $(B+C)$ by merely 0.2 MHz. Unfortunately, the influences of the two angles could not be separated and, in consequence, it can only be concluded that $\alpha = 120°$ corresponds to $\gamma = 128.2°$, and $\alpha = 124.5°$ to $\gamma = 120°$. The value $\alpha = 126.3°$, which was obtained for *p*-bromostyrene, gives $\gamma = 118.1°$. Igarashi *et al.* state that the γ angle is $119 \pm 2°$.

m-*Bromostyrene. m*-Bromostyrene is the only bromostyrene which can be expected to exist in two stable conformations. For the planar molecule these are *trans-* and *cis-m*-bromostyrene. The difference in the calculated value of $(B+C)$ between the *trans* ($\theta = 0°$) and the *cis* ($\theta = 180°$) form is 130 MHz (as compared to 0.2 MHz for *trans-β*-bromostyrene). The *cis* isomer should have a slightly lower energy according to our calculations using a modified CNDO-method.[8] The *trans* isomer is more symmetric than the *cis* isomer. The $|\varkappa|$-values are -0.93 and -0.80, respectively. A simulated spectrum for a model of *cis-m*-bromostyrene shows that a band structure can be obtained even for such low values of $\varkappa$. The spectrum, however, becomes more complicated, the bands broaden and may become split. Even a quasi-band structure may arise. If all the parameters are assumed equal in *p*- and *m*-bromostyrene, the resulting values of $(B+C)$ obtained for the bromine distorted structure are listed in Table 6.

Table 6. m-Bromostyrene.

Bromine isotope θ	$(B+C)$ ^{79}Br	^{81}Br	
0°	1010.2	1000.6	(*trans*)
90°	1073.7	1063.5	
180°	1144.4	1133.4	(*cis*)

The spectrum consists of two series of bands with $(B+C)_{81}=1130.0$ MHz and $(B+C)_{79}=1141.0$ MHz. Most probably, these values may be assigned to the *cis* isomer. It should be observed that $\Delta(B+C)_{180}=1144.4-1133.4=11.0$ MHz is equal to the difference between the values obtained from the measurements, *cf.* Table 4. For $\theta=180°$, $(B+C)$ becomes equal to 1130.0 and 1141.0, respectively, when $\alpha=127.8°$.

For the bromine distorted structure, $\alpha=128.0°$ is obtained. Attempts to localize the two remaining series of bands were unsuccessful, even when recording the spectra at other Stark voltages and sweep rates.

In order to establish whether it is possible to neglect the *trans* isomer signals in such a complicated spectrum, the band spectra of mixtures of *p*- and *trans*-β-bromostyrene in different concentrations were recorded. It was often found to be extremely difficult to identify the four band series, even though the exact band positions were known in advance. The Stark lobes are very strong and completely mask many of the bands. The discrepancy between the observed and expected pattern being very large, *trans*-β-bromostyrene was easily detected only in those mixtures where its relative concentration was high. It was even difficult to observe all of the bands of *p*-bromostyrene in mixtures with *m*-bromostyrene. It appears that especially the more closely lying bands are easily concealed.

The results of this study neither confirm nor exclude the existence of two conformers of *m*-bromostyrene – a conclusion similar to the results of one of the recent IR-investigations on this molecule.[9] The hypothesis about the two conformers can probably be verified if a microwave band spectrum of *m*-bromostyrene, including only one of the two bromine isotopes, is studied.

Conclusions. The $C_b-C=C$ angle (α) in the molecules *cis*-*m*-bromostyrene and *p*-bromostyrene was found to be $127\pm4°$. The uncertainty in the angle α is rather large because of the inherent assumptions in its calculation. This value $\alpha=127\pm4°$ is consistent with the $(B+C)$ value of *trans*-β-bromostyrene.

Acknowledgments. We thank Dipl. ing. J. Lewandowska for helping to purify the sample of *m*-bromostyrene and Miss A.-C. Blom for typing the manuscript.

REFERENCES

1. Igarashi, M., Cho, S. and Someno, K. *Nippon Kagaku Zasshi* **81** (1960) 23.
2. Bastiansen, O. and Smedvid, L. *Acta Chem. Scand.* **8** (1954) 1539.
3. Trætteberg, M. *Private communication.*
4. *Tables of Interatomic Distances and Configurations in Molecules and Ions, Chem. Soc. Spec. Publ.* **1965** No. 18.
5. Rosenthal, E. and Dailey, B. P. *J. Chem. Phys.* **43** (1965) 2093.
6. Hamer, G. K. and Reynolds, W. F. *Chem. Commun.* **19** (1971) 1218.
7. Haugen, W. and Trætteberg, M. *Selected Topics in Structure Chemistry*, Universitetsforlaget, Oslo 1967.
8. Höjer, G. *Diss.*, University of Stockholm 1971.
9. Fatelay, W. G., Carlson, G. L. and Dickson, F. E. *Appl. Spectry.* **22** (1968) 650.

Received December 2, 1972.

ACTA CHEMICA SCANDINAVICA 27 (1973) 1573–1578

Fungal Extractives

III.* Two Sesquiterpene Lactones from *Lactarius*

GÖRAN MAGNUSSON and SVANTE THORÉN

Organic Chemistry 2, Chemical Center, the Lund Institute of Technology, Box 740, S-220 07 Lund 7, Sweden

Two sesquiterpene lactones, isolated from *Lactarius vellereus* and *L. pergamenus*, have been shown to possess structures *1* and *2*.

In a recent publication[2] we reported the structure of a sesquiterpene dialdehyde ("isovelleral") and the isolation of two other C_{15}-aldehydes and lactones from *Lactarius vellereus* and *L. pergamenus* (Russulaceae). These terpenoids were obtained from fresh fungus extract by repeated column chromatography on silica gel. We have now shown that the two lactones have structures *1* and *2*, respectively (Fig. 1).

^{13}C-NMR spectroscopy (C-15; H-20) in combination with mass spectrometry (M^+ 232) gave the same molecular formula $C_{15}H_{20}O_2$ for both lactones, and a close structural relationship was shown by the similarity of their mass spectra and by conversion of lactone *1* to lactone *2* on heating.

In lactone *1* the IR band at 1772 cm^{-1} suggested the presence of a γ-lactone and bands at 1675 and 1652 cm^{-1} indicated one or more double bonds. The ^{13}C-NMR showed signals from a carbonyl carbon, from two disubstituted and two monosubstituted vinyl carbons and from a methylene carbon attached to oxygen (Table 1). The UV absorption maximum at 282 nm (ε 4300) required the double bonds and the carbonyl group to be in the same conjugated system, and this was further supported by the ^{1}H-NMR spectrum which showed low-field signals at 6.99 and 5.61 ppm from two olefinic protons. The signal at 6.99 ppm appeared as a broadened doublet ($J = 7$ Hz) reflecting a vicinal interaction with a secondary allylic proton and a long-range coupling. The two protons of the $-O-CH_2-$ group almost coincided at 4.72 ppm (outer AB signals negligible) and were both split by allylic coupling ($J = 3$ Hz) with the proton at 5.61 ppm (broad singlet). A methyl doublet appeared at 1.12 ppm ($J = 7$ Hz).

The IR spectrum of lactone *2* had bands at 1760 cm^{-1} and at 1670 and 1650 (C=C) cm^{-1}. The ^{13}C-NMR spectrum of *2* had signals for carbonyl carbon

* Part II, see Ref. 1.

and for methylene carbon attached to oxygen and showed three disubstituted and one monosubstituted vinyl carbon atom signals (Table 1). The ^{1}H-NMR spectrum of *2* showed, correspondingly, only one olefinic proton (5.98 ppm, broad singlet). The $-O-CH_2-$ group appeared as a broad singlet (4.68 ppm) and the methyl group was situated on a double bond (broadened singlet at 1.94 ppm). The UV spectrum had a maximum at 270 nm (ε 6100), characteristic for α,β-γ,δ-unsaturated butyrolactones [3] though the intensity was rather low.

The spectral data above suggested the partial structures *1a* and *2a*.

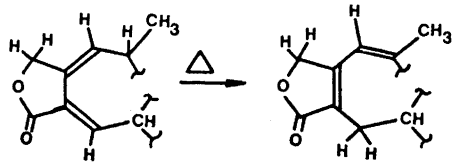

1a 2a

The molecular formulae gave an unsaturation number of six. The partial structures *1a* and *2a* both contained all three double bonds (^{13}C-NMR) and one ring, which left two rings to be accounted for. The ^{13}C-NMR spectrum of lactone *1* showed, in addition to the functional group carbons discussed above, a further nine carbon atoms – three methyl, two methylene, three methine, and one quaternary (Table 1).

Two methyl singlets at 1.02 and 0.98 ppm in the ^{1}H-NMR and a doublet at 1380 cm^{-1} in the IR spectrum established a quaternary *gem*-dimethyl group. The spectral findings and analogies with known sesquiterpenoids from basidiomycetes suggested structure *1* for this compound. The three one-proton multiplets at 3.01, 2.61, and 2.13 ppm could then be assigned to the allylic and homoallylic bridgehead protons, respectively.

Analogous interpretation of the spectral data (see Table 1 and Experimental) combined with sesquiterpenoid analogies suggested structure *2* for the second lactone.

The best analogy on which these structures can be based is "isovelleral" [2] (*9*) from the same species, but other sesquiterpenoids that have been found in basidiomycetes, *e.g.* marasmic acid,[4] the illudins,[5] hirsutic acid,[6] and fomannosin,[7] all have a 3,3-disubstituted cyclopentane ring. In two sesquiterpenoids recently isolated from *Fomitopsis* [8] (*e.g. 10*) the entire carbon skeleton has been found to be the same as is suggested here for lactones *1* and *2*. It also appears that the lactarorufins A and B found by Daniewski and Kocór in *L. rufus* [9] may well have closely related structures.*

To establish the aliphatic portion of the molecule and the position of the double bonds, lactone *1* was ozonized in methanol solution. Reductive work-up of the hydroperoxides with dimethyl sulphide [10] gave the dialdehyde *3* which was precipitated as the *bis*-dinitrophenylhydrazone *4*. Ring closure and aromatisation of the crude *bis*-DNP was effected in boiling acetic acid-conc. hydro-

* *Added in proof.* For the structure of lactarorufin A, see Barauowska, E. and Daniewski, W. M. *Bull. Acad. Pol. Sci. Ser. Chim.* **20** (1972) 313 and references cited therein.

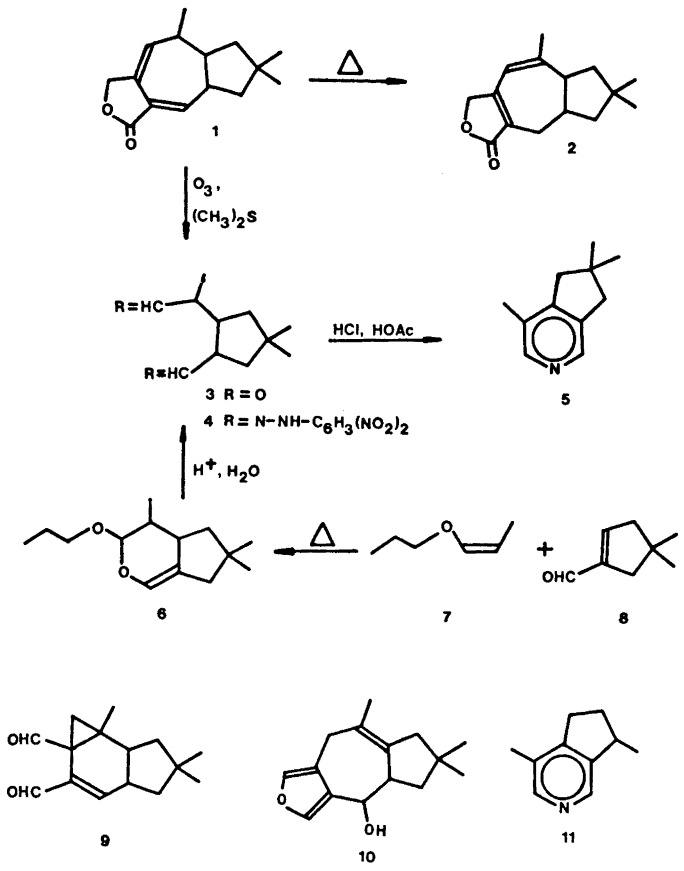

Fig. 1.

chloric acid according to the method used by Cavill and Ford in their preparation of actinidine (*11*) from iridodial.[11] The solution was made alkaline and steam-distilled. This gave the pyridine *5* in low yield. The structure of compound *5* was unequivocally ascertained by synthesis in the following way. *cis*-Propenyl propyl ether[12] (*7*) was reacted with the cyclopentenecarboxaldehyde *8*, prepared from dimedone by a newly developed procedure.[13] The Diels-Alder adduct[14] obtained (*6*) was hydrolysed and the product was reacted with dinitrophenylhydrazine. The *bis*-DNP mixture (*4*) was apparently a mixture of isomers not identical with that obtained from ozonisation (TLC). The ^{1}H-NMR spectrum of the pyridine obtained on treatment of the crude bis-DNP as above was identical with that obtained from lactone *1*. The two pyridines gave identical picrates (m.p. and mixed m.p.). The structure of the pyridine was further confirmed by elemental analysis of the picrate and by IR (ν_{max} C=N 1590 cm^{-1}), ^{1}H-NMR and UV [λ_{max} (EtOH) 261 nm (ε 3200) and 269 nm (ε 2970)]; [*cf.* Refs. 11 and 15 for the closely related alkaloid acti-

nidine *11*: λ_{max} (EtOH) 262 nm (ε 2590), 270 nm (ε 2310) and λ_{max} (EtOH) 262 nm (ε 2400), respectively].

The chemical degradation of lactone *1* together with the interrelation with lactone *2* and the spectroscopic data firmly established the structures given for the two compounds.

Work on the stereochemistry of the lactones is in progress.

Table 1. ^{13}C-NMR data for lactones *1* and *2* ($CDCl_3$/TMS).

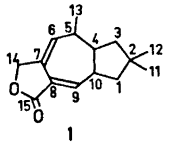

1

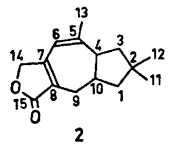

2

Chemical shifts ppm	Assignment carbon atom number	Chemical shifts ppm	Assignment carbon atom number
171.2	15	173.5	15
144.8	6,9	158.2	5,8
131.1		146.6	
127.8	7,8	122.9	7
123.4		112.7	6
69.0	14	71.2	14
47.2	1 or 3	50.5	4
46.4	4 or 10	48.6	1,3
44.6	1 or 3	47.7	
42.8	4 or 10	37.5	10
35.1	2	34.4	2
34.6	5	32.2	11,12
32.5	11,12	31.1	
31.7		30.9	9
19.4	13	26.4	13

EXPERIMENTAL

Melting points are uncorrected. The NMR spectra were recorded on a Varian XL-100 and a Varian T-60 spectrometer. Mass spectra were recorded on an LKB 1100 instrument and on a high resolution AEI MS902 instrument equipped with a AEI DS30 data system. (Dr. G. Hvistendahl, Kjemisk Institutt, University of Oslo, Norway.)

Isolation of lactones 1 *and* 2. Freshly collected fungi (*Lactarius vellereus* or *L. pergamenus*, Russulaceae) were ground with hexane and the mixture was pressed in a fruit press (Hafico). The hexane phase was separated, dried and evaporated and the residue crystallized from hexane to remove *stearic acid*. The mother liquor was partitioned between hexane and aqueous methanol (90 %). The methanol phase was diluted with water to 50 % and repeatedly extracted with chloroform. The residue from the chloroform phase was chromatographed on a silica gel column with ether (10 %) in benzene which gave "isovelleral",[2] another C_{15}-dialdehyde* and a mixture of the lactones *1* and *2* (0.015 % of the fresh fungus). The lactone fraction was rechromatographed on silica gel with methylene chloride.

* Magnusson, G., Thorén, S. and Drakenberg, T. *Tetrahedron* **29** (1973) 1621 (*added in proof*).

Lactone 1. The compound, a bright yellow oil, had $[\alpha]_D^{25}$ +364° (*c* 1.9); λ_{max} (EtOH) 282 nm (ε 4300); ν_{max} (neat) 1772 (strong) (C=O), 1730 (weak), 1675 1652 (C=C), 1385 1368 (*gem*-dimethyl), 1220 1200 1180 (ester bands), 1035 (C–O), 755 cm^{-1}; ^{1}H-NMR: δ_{TMS} ($CDCl_3$) 6.99 (1H, d J=7.0 Hz; –OCO–C=C*H*–CH–), 5.61 (1H, s broad; –O–CH_2–C=C*H*–CHCH_3–), 4.72 (2H, pair of d J=3.0 Hz; –O–CH_2–C=CH–), 3.01 2.61 2.16 (1H each, m; allylic and homoallylic protons), 1.12 (3H, d J=7.0 Hz; CH_3–CH–), 1.02 0.98 (3H each, s; –CH_3–CH_3) ppm. ^{13}C-NMR data, see Table 1. MS (70 eV): *m/e* 232 (M^+ 95 %; $C_{15}H_{20}O_2$), 217 (80 %), 122 (100 %), 91 (80 %). (Found: M. wt. 232.1465. Calc. for $C_{15}H_{20}O_2$: M. wt. 232.1463.)

Lactone 2. The compound was obtained as an oil which crystallized slowly from benzene-hexane, m.p. 41–44°; $[\alpha]_D^{25}$ –73° (*c* 0.9); λ_{max} (EtOH) 270 nm (ε 6100); ν_{max} (neat) 1760 (C=O), 1670 1650 (C=C), 1380 1370 (*gem*-dimethyl), 1118 1035 (C–O), 772 cm^{-1}; ^{1}H-NMR: δ_{TMS} ($CDCl_3$) 5.98 (1H, s broad; –C=C*H*–C=C–COO–), 4.68 (2H, s; =C–CH_2–OCO–), 2.92–2.17 (4H, m; allylic and homoallylic protons), 1.94 (3H, s broad; CH_3–C=CH–C=C–), 1.13 1.08 (3H each, s; –CH_3–CH_3) ppm. ^{13}C-NMR data, see Table 1. MS (70 eV): *m/e* 232 (M^+ 100 %; $C_{15}H_{20}O_2$), 217 (58 %, 187 (37 %), 122 (79 %). (Found: C 77.3; H 8.7. Calc. for $C_{15}H_{20}O_2$: C 77.5; H 8.7.)

Isomerization of lactone 1 *to lactone* 2. Lactone *1* was heated at 140° for 1 h under partial vacuum and then distilled, $b.p._{0.05}$ 125°. The distillate consisted of almost pure lactone *2*, identified by IR and NMR spectroscopy. It had $[\alpha]_D^{25}$ –53° (*c* 2.6).

Ozonisation of lactone 1. Lactone *1* (458 mg) was ozonized in methanol (6 ml) at –70°. The yellow colour of the solution had disappeared after 3.5 h and the ozonisation was continued for another 4 h. Dimethyl sulphide [10] (0.4 ml) was then added. The solution was stirred at –10° for 1 h, at 0° for 1 h, and finally at room temp. for 1 h. The solvents were evaporated under reduced pressure and the remaining oil was dissolved in ethanol (0.5 ml) and added to a solution of dinitrophenylhydrazine (1800 mg) in conc. sulphuric acid (3.5 ml) and ethanol (25 ml). The reaction mixture was stirred at room temp. for 1 h, and then water (75 ml) was added to complete the precipitation. The bis-dinitrophenylhydrazones were extracted with ethyl acetate-hexane (9:1) (4 × 50 ml) and the residue from the organic phase was dissolved in boiling benzene and filtered hot. The filtrate was evaporated and chromatographed on silica gel (100 g). Elution with ethyl acetate-ligroin (1:2) gave crude dinitrophenylhydrazones of *4* (408 mg) [TLC silica gel, ethyl acetate-ligroin (1:2) visualized by 0.2 % $K_3Fe(CN)_6$ in 2 M hydrochloric acid [16]]. The crude product was refluxed with conc. hydrochloric acid (2 ml) in acetic acid (10 ml) for 2 h,[11] cooled, and the pH of the solution was adjusted to 9 with 6 M sodium hydroxide and steam-distilled. The distillate (250 ml) was extracted with chloroform (3 × 25 ml), the organic phase was dried (Na_2SO_4) and the solvent was distilled through a 30 cm Vigreux column in a slow stream of dry nitrogen, the last traces of chloroform being distilled away by adding dry ether. The residue (22 mg) consisted of almost pure *2',2',5-trimethyl-3,4-cyclopentanopyridine* (*5*). The ^{1}H-NMR spectrum of *5* was superimposable on that of a synthetic sample (*vide infra*). The *picrate* was recrystallized from ethanol and had m.p. 145.5–147.0° (*cf.* synthetic sample, m.p. and mixed m.p. 145.5–147.0°). (Found: N 13.9. $C_{17}H_{18}N_4O_7$ requires: N 14.3.)

3-Propyloxy-4,6,6-trimethyl-3,4,4a,5,7-pentahydro-cyclopenta[c]pyran (6). 4,4-Dimethylcyclopentenecarboxaldehyde (*8*) [12] (3.10 g; 0.025 mol) was heated in a sealed tube under nitrogen at 170° for 65 h with the *cis*-propenyl ether *7* [12] (3.00 g; 0.03 mol) and some crystals of hydroquinone. The *cis*-olefin was contaminated by smaller amounts of the *trans* isomer. After cooling, the reaction mixture was distilled, which gave a fore-run of unreacted aldehyde, $b.p._{11}$ 57–58° (1.35 g), and as main fraction an isomer mixture (^{1}H-NMR) of *pyranyl ethers* (*6*) (63 % yield calculated on reacted aldehyde), $b.p._{10}$ 118–123°; n_D^{23} 1.4638; ν_{max} (neat) 3080, 1685 (C=C), 1380, 1370 (*gem*-dimethyl), 1125, 1085 (C–O) cm^{-1}; ^{1}H-NMR: δ_{TMS} ($CDCl_3$) 6.20 (1H; –O–C*H*=C), 4.54 (1H; –O–C*H*–O–), 3.66 (2H; –O–CH_2–CH_2–) ppm; MS (70 eV): *m/e* 224 (M^+; $C_{14}H_{24}O_2$). (Found: C 74.9; H 10.7. $C_{14}H_{24}O_2$ requires: C 74.9; H 10.8.)

2',2',5-Trimethyl-3,4-cyclopentanopyridine (5). The pyranyl ether mixture (*6*) (448 mg) was converted to *bis*-dinitrophenylhydrazones *4* by adding it to a solution of dinitrophenylhydrazine (900 mg) in conc. sulphuric acid (2 ml), ethanol (12 ml) and water (2 ml) at room temp. After 1 h, water (15 ml) was added and the crystals were filtered off, giving a quantitative yield of isomeric *bis*-hydrazones (TLC, see above). The hydrazone mixture (400 mg) was refluxed for 2 h in conc. hydrochloric acid (2 ml) and acetic

acid (10 ml) [11] and processed as described above. The brown odorous residue from evaporation of the chloroform was distilled under reduced pressure to give the *pyridine 5* in 60 % yield (71 mg). B.p.$_{12}$ 112°; n_D^{22} 1.5114; λ_{max} (EtOH) 261 nm (ε 3200), 269 nm (ε 2970); ν_{max} (neat) 3030, 1600, 1590, 1390 1370 (*gem*-dimethyl), 840, 720 cm^{-1}; ^{1}H-NMR: δ_{TMS} ($CDCl_3$) 8.27 8.22 (1H each, s broad; pyridine protons), 2.75 2.67 (2H each, s; pyr$-CH_2-$), 2.22 (3H, s; pyr-CH_3), 1.15 (6H, s; $-CH_3-CH_3$) ppm. *Picrate*: M.p. 145.5 – 147.0°. (Found: C 52.3; H 4.7; N 14.2. $C_{17}H_{18}N_4O_7$ requires: C 52.3; H 4.7; N 14.3.)

Acknowledgements. We thank Professor Börje Wickberg for stimulating discussions, Dr. Torbjörn Drakenberg for recording the ^{13}C-NMR spectra, and Dr. Brian Thomas for helpful linguistic criticism. This work was in part supported by the *Swedish Natural Science Research Council.*

REFERENCES

1. Lindberg, P. L. and Wickberg, B. *To be published.*
2. Magnusson, G., Thorén, S. and Wickberg, B. *Tetrahedron Letters* **1972** 1105.
3. Dorfman, L. *Chem. Rev.* **53** (1953) 47.
4. Dugan, J. J., deMayo, P., Nisbet, M., Robinson, J. R. and Anchel, M. *J. Am. Chem. Soc.* **88** (1966) 2838.
5. McMorris, T. C., Nair, M. S. R., Singh, P. and Anchel, M. *Phytochemistry* **10** (1971) 3341.
6. Comer, F. W., McCapra, F., Qureshi, I. H., Trotter, J. and Scott, A. I. *Chem. Commun.* **1965** 310.
7. Kepler, J. A., Wall, M. E., Mason, J. E., Basset, C., McPhail, A. T. and Sim, G. A. *J. Am. Chem. Soc.* **89** (1967) 1260.
8. Nozoe, S., Matsumoto, H. and Urano, S. *Tetrahedron Letters* **1971** 3125.
9. Daniewski, W. M. and Kocor, M. *Bull. Acad. Pol. Sci. Ser. Chim.* **18** (1970) 585.
10. Pappas, J. J., Keaveney, W. P., Gancher, E. and Berger, M. *Tetrahedron Letters* **1966** 4273.
11. Cavill, G. W. K. and Ford, D. L. *Australian J. Chem.* **13** (1960) 296.
12. Ger. Patents 952,805 (1965) and 953,973 (1965).
13. Magnusson, G. and Thorén, S. *J. Org. Chem.* **38** (1973) 1380.
14. Korte, F., Büchel, K. H. and Zschocke, A. *Chem. Ber.* **94** (1961) 1952.
15. Sakan, T., Fujino, A., Murai, F., Batsugan, Y. and Suzui, A. *Bull. Chem. Soc. Japan* **32** (1959) 315.
16. Stahl, E. *Dünnschichtchromatographie*, 2nd Ed., Springer-Verlag, Berlin, Heidelberg, New York 1967, p. 221.

Received November 29, 1972.

ACTA CHEMICA SCANDINAVICA 27 (1973) 1579–1585

Lanthanide-induced Shifts in Proton Magnetic Resonance; Studies on the Conformations of Thujane Derivatives

TORBJÖRN NORIN*, STURE STRÖMBERG and MICHAEL WEBER*

Swedish Forest Products Research Laboratory, Box 5604, S-114 86 Stockholm, Sweden

Dedicated to Professor *František Šorm* on his 60th birthday

The conformations of (+)-3-thujanol (*1*), (−)-3-neoisothujanol (*2*), (+)-*trans*-sabinol (*3*), and (−)-*cis*-sabinol (*4*) have been studied by NMR-spectroscopy. The observed coupling constants as well as europium-induced chemical shifts provide evidence for boat-like conformations in these thujane derivatives. A method is described which compensates for experimental errors in shift reagent work.

NMR-studies of the thujyl alcohols and of the thujones have shown that these compounds possess a boat-like conformation.[1] This postulation appears to be universal for all derivatives of the bicyclo[3,1,0]hexane series.[2–11] Recently, however, Hach *et al.*[12] have reported some IR data which they interpret as evidence against boat-like conformations in (+)-3-thujanol (*1*) and (−)-3-neoisothujanol (*2*).**

A correct assignment of the conformation of bicyclo[3,1,0]hexane derivatives is important for the interpretation of kinetic data in rearrangement reactions [4] and also of ORD and CD data associated with conjugated cyclopropyl chromophores [13] in these systems. We therefore decided to reinvestigate the conformations of (+)-3-thujanol (*1*) and of (−)-3-neoisothujanol (*2*). This study also includes NMR investigations of (+)-*trans*-sabinol (*3*) and (−)-*cis*-sabinol (*4*).[14,15]

The NMR-spectra of (+)-3-thujanol (*1*), (−)-3-neoisothujanol (*2*), (+)-*trans*-sabinol (*3*) and (−)-*cis*-sabinol (*4*) have previously, been studied.[1,15] The relationships between the thujanols, thujones, and sabinols are given in Fig. 1. The NMR data obtained in the present investigation are presented in Tables 1, 2 and 3 in which the assignments of the various signals and signal patterns in principle are consistent with previous investigations.

* Present address: Department of Organic Chemistry, Royal Institute of Technology, P.O.B., S-100 44 Stockholm 70, Sweden.

** Revised nomenclature according to Ref. 9.

Table 1. Chemical shifts of protons in sabinols and thujanols (τ-values, TMS internal standard).

	C(2α)-H	C(2β)-H	C(3)-H	C(4)-H	C(5)-H	C(6α)-H	C(6β)-H	C(7)-H	C(8)-H_3	C(9)-H_3	C(10)-$H_{2,3}$
(+)-3-Thujanol (*1*)											
CCl_4	8.04[a]	8.44[g]	6.82[c]	8.11	[e]	9.82	9.85	8.68[e]	9.07[b]	9.15[b]	9.00[b]
(−)-3-Neoisothujanol (*2*)											
CCl_4	8.17[a]	8.53[g]	6.20[c]	7.96	9.19[d,e]	9.7	9.8	[e]	9.03[b]	9.13[b]	9.14[b]
(+)-*trans*-Sabinol (*3*)											
CCl_4	8.34[a]	8.05[c]	5.68[f]	—	8.46[a]	8.93[d]	9.25[h]	[e]	9.05[b]	9.10[b]	5.15[h] 5.17[h]
$CDCl_3$	8.31[a]	7.98[c]	5.67[f]	—	8.36[e]	8.93[d]	[e]	[e]	9.07[b]	9.12[b]	5.02[h] 5.07[h]
(−)-*cis*-Sabinol (*4*)											
CCl_4	7.88[a]	8.48[a]	5.94[c]	—	8.40[d,e]	9.45	9.45	8.65[e]	9.06[b]	9.12[b]	5.16[b] 5.21[b]
$CDCl_3$	7.77[a]	8.46[a]	5.82[c]	—	8.33[a,e]	9.2 — 9.6		8.69[e]	9.06[b]	9.09[b]	5.05[b] 5.15[b]

[a] Quartet. [b] Doublet. [c] Multiplet. [d] Triplet. [e] Uncertain due to overlapping signals. [f] Broadened doublet. [g] Broadened quartet. [h] Broadened singlet.

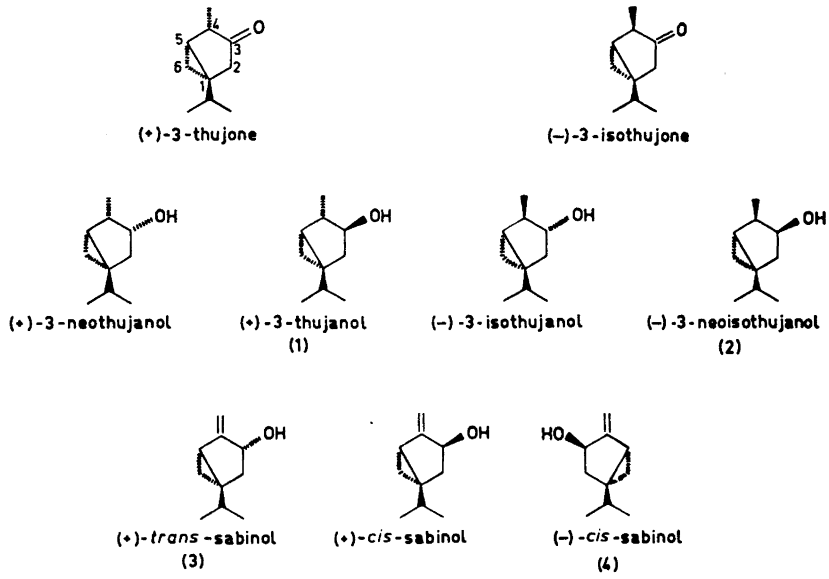

Fig. 1. Steric relationship of thujyl alcohols and related compounds.

Table 2. Apparent coupling constants (Hz) in sabinols and in thujanols.

	$J_{2\alpha,2\beta}$	$J_{2\alpha,3}$	$J_{2\beta,3}$	$J_{3,4}$	$J_{4,5}$	$J_{4,10}$	$J_{5,6\beta}$	$J_{5,6\alpha}$	$J_{6\alpha,6\beta}$	$J_{2\beta,6\beta}$	$J_{3,10}$
(+)-3-Thujanol (*1*)											
$Eu(dpm)_3$-CCl_4	12.1	6.6[b]	8.5[b]	8.2	3.8	6.2	8.0	4.0	4.9		–
(−)-3-Neoisothujanol (*2*)											
CCl_4	12.0	7.4[b]	9.3[b]	6.5	~0	7.0	8.5	4.0	~5	0.5	–
$Eu(dpm)_3$-CCl_4	12.0	7.3	9.3		~0	7.2	8.4	3.8	5.0		–
(+)-*trans*-Sabinol (*3*)											
CCl_4	13.3	1.5	6.7	–	–	–	~8	3.3	~4	~2	~0
$CDCl_3$	13.6	1.3	6.6	–	–	–	~8	~4	~4	1.6	~0
$Eu(dpm)_3$-CCl_4	13.5	~0	7.0	–	–	–	~8	3.2	~4	~2	~0
(−)-*cis*-Sabinol (*4*)											
CCl_4	12.0	7.8	8.2	–	–	–		11[a]		~0	~2
C_5D_5N	11.9	7.7	8.6	–	–	–	7.3	~4			~2
C_6D_6	~12	~8	~8	–	–	–		11.2[a]			~2
$CDCl_3$	12.0	7.7	8.2	–	–	–	~7	~4			~2
$Eu(dpm)_3$-CCl_4	12.0	7.5	~8	–	–	–	8.3	3.3	~4		~2

[a] Sum of $J_{5,6\beta}$ and $J_{5,6\alpha}$. [b] Previous values of H-C(2)-C(3)-H vicinal coupling constants ($J_{2,3}$) in (+)-3-thujanol (*1*) and in (−)-3-neoisothujanol (2) have been interchanged (*cf.* Table 3 in Ref. 1).

Table 3. Absolute values of observed and predicted $Eu(dpm)_3$-induced shifts, $|\Delta_{Eu}|$, assuming a linear dependence of log $|\Delta_{Eu}|$ upon log R, where R is the distance between oxygen and hydrogen atoms.

		(+)-3-Thujanol (*1*)		(−)-3-Neoisothujanol (*2*)		(+)-*trans*-Sabinol (*3*)		(−)-*cis*-Sabinol (*4*)	
		boat[a]	chair	boat[a]	chair	boat[a]	chair	boat[a]	chair
C(2α)-H	obs	12.71	–	12.5	–	20.78	–	11.50	–
	pred	13.84	9.92	12.40	9.14	19.55	18.49	13.52	10.46
C(2β)-H	obs	20.76	–	19.4	–	10.07	–	20.09	–
	pred	21.21	18.14	18.68	17.43	10.67	13.24	19.83	18.86
C(3)-H	obs	29.40	–	26.6	–	29.28	–	25.57	–
	pred[b]	–	–	–	–	–	–	–	–
C(4α)-H	obs	–	–	12.6	–	–	–	–	–
	pred	–	–	12.40	9.14	–	–	–	–
C(4β)-H	obs	21.31	–	–	–	–	–	–	–
	pred	21.21	18.14	–	–	–	–	–	–
C(5)-H	obs	6.80	–	5.8	–	8.09	–	6.83	–
	pred	5.21	7.43	4.85	6.71	6.20	5.94	5.63	7.89
C(6α)-H	obs	6.74	–	5.13	–	20.98	–	5.76	–
	pred	7.59	5.07	8.46	4.45	26.55	8.64	7.35	5.43
C(6β)-H	obs	4.25	–	3.46	–	7.76	–	4.28	–
	pred	3.68	3.47	3.47	2.97	7.98	4.84	4.11	3.76
C(7)-H	obs	[c]	–	[c]	–	4.43	–	4.63	–
	pred	–	–	–	–	–	–	–	–
C(8)-H_3	obs	3.32	–	3.46	–	2.74	–	3.88	–
	pred	3.68	9.66	3.47	8.88	3.24	4.99	4.33	10.20
C(9)-H_3	obs	2.25	–	2.63	–	2.50	–	2.73	–
	pred	2.68	3.35	2.57	2.86	3.09	4.02	2.76	3.89
C(10)-H_A	obs	–	–	–	–	11.17	–	19.65	–
	pred	–	–	–	–	9.82	16.86	17.84	9.64
C(10)-H_B	obs	–	–	–	–	7.73	–	9.07	–
	pred	–	–	–	–	6.07	7.95	7.54	6.04
C(10)-H_3	obs	10.18	–	13.9	–	–	–	–	–
	pred	9.34	6.03	13.23	12.17	–	–	–	–

[a] Conformations with "flap angles" of 25°. Staggered conformations of the isopropyl group were assumed. [b] Not included in the calculations (*cf.* Ref. 17). [c] Obscured by other signals.

Dihedral angles were estimated from a Dreiding model where the "flap angle" (angle between the C(1),C(2),C(4),C(5) plane and the C(2),C(3),C(4) plane) of the five membered ring was 20 – 30°. The observed spin-spin splittings of the compounds (*1*), (*2*), (*3*), and (*4*) satisfy the Karplus equation only if the molecules exist mainly in boat-like conformations with coupling constants between the C(2) and C(3) protons as indicated in Fig. 2.

Allylic coupling is observed in (−)-*cis*-sabinol but not in (+)-*trans*-sabinol. Estimated from a Dreiding model in a boat-like conformation, the

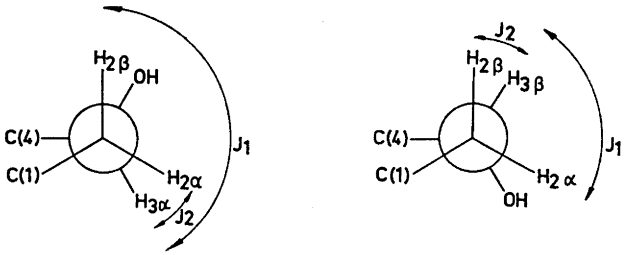

	J_1	J_2
(+)-*cis*-sabinol	8.2 Hz	7.8 Hz *
(+)-3-thujanol	8.5 Hz	6.6 Hz
(−)-3-neoisothujanol	9.3 Hz	7.4 Hz

	J_1	J_2
(+)-*trans*-sabinol	1.5 Hz	6.7 Hz

Fig. 2. Newman projection of C(2)-C(3) in boat-like conformation with observed coupling constants C(2)-H − C(3)-H (* the coupling constants were determined on the enantiomer (−)-*cis*-sabinol).

C(3)-H bond in (+)-*trans*-sabinol is only *ca.* 30° out of the allylic plane. This bond in (−)-*cis*-sabinol is almost perpendicular to the allylic plane in the boat-like conformation and should therefore give rise to a significant allylic coupling (*cf.* Ref. 15).

Europium-induced chemical shifts * for the protons of (+)-3-thujanol, (−)-3-neoisothujanol, (+)-*trans*-sabinol and (−)-*cis*-sabinol are given in Table 3. The induced paramagnetic shift is largest for protons near the coordination site in the direction of the Eu − O bond.[17–19] The europium complex induced a large paramagnetic shift of the 6-endo proton signal in (+)-*trans*-sabinol but not in (−)-*cis*-sabinol, (+)-3-thujanol and (−)-3-neoisothujanol. Furthermore, vicinal protons *cis* to the hydroxyl groups are more shifted than vicinal protons in the *trans*-positions. These induced shifts confirm previous configurational assignments of the sabinols and of the thujanols.

The observed coupling constants in the NMR-spectra of the various compounds were practically (± 0.5 Hz) not affected by the addition of europium complex (see Table 2). Thus the addition of the complex apparently has no significant influence on the conformations of the molecules. The paramagnetic induced chemical shifts, Δ_{Eu}, defined as $\tau_{Eu(dpm)_3}{}^{n=1} - \tau_{Eu(dpm)_3}{}^{n=0}$ were obtained from the slope of the plot of chemical shift ($\tau_{Eu(dpm)_3}$) against the molar ratio (n), shift reagent/substrate.[17]

Log $|\Delta_{Eu}|$ was then plotted against log R, where R is the distance between the oxygen atom of the hydroxyl group and the proton in question. A good linear correlation is observed only for boat-like conformations. Observed and predicted Δ_{Eu} -values are given in Table 3 and correlation coefficients in Table 4. The flap angles, *i.e.* the angles between the C(1),C(2),C(4),C(5)- and the C(2),C(3),C(4)-planes in boat and chair conformations were assigned to be 25°. Distances were measured in Dreiding models.

* Paramagnetic shift reagent, $Eu(dpm)_3$, tris(dipivalomethanato)europium(III).

Table 4. Correlation coefficients and slopes from the plot log $|\Delta_{Eu}|$ against log R.

Compound	Conformation	Corr. coefficient	Slope
(+)-3-Thujanol (*1*)	boat	0.983	−2.44
	chair	0.797	−2.28
(−)-3-Neoisothujanol (*2*)	boat	0.984	−2.34
	chair	0.849	−2.44
(+)-*trans*-Sabinol (*3*)	boat	0.968	−2.29
	chair	0.752	−1.91
(−)-*cis*-Sabinol (*4*)	boat	0.977	−2.19
	chair	0.741	−2.23

The precision in molar ratio (n) was as high (0.5 − 5 %) as the precision of the τ-values, if aliquots of the substrate solution were added to a solution of shift reagent and substrate. If, however, the spectrum was shifted downfield by adding small amounts of shift reagent to the substrate solution, errors were larger. In such cases, it is convenient to determine a concentration independent parameter by plotting the $\tau_{Eu(dpm)_3}{}^{n=x}$-values of a proton for arbitrary molar ratios against the corresponding $\tau_{Eu(dpm)_3}{}^{n=x}$-value for a second proton ("reference proton"), the chemical shift of which can be determined with high precision, *e.g.* the carbinyl proton, C(3) − H.

The least-square derived slope (k) of such a plot is linearly correlated to the Δ_{Eu}-value: $k = \Delta_{Eu}[\Delta_{Eu,\ \text{reference proton}}]^{-1} = \Delta_{Eu}$ const. Therefore, k-values may be used instead of Δ_{Eu}-values in the pseudocontact shift equation.[17] After the completion of this work, Kelsey [20] reported a similar method of using internal proton standards in shift reagent work. These procedures are apparently alternatives to the method of compensating for experimental errors in shift reagent work described by ApSimon and Beierbeck.[21]

It is of interest to note that such a simple approximation,[17] which does not take into account the true geometric factors,[18,19] is nontheless sufficiently accurate to predict the conformations. A refined calculation using a computer program has also been used for this problem.[22] The geometric factor $(3\cos^2\theta - 1)r^{-3}$ has been determined. Such calculations could only with slightly higher accuracy confirm the results of the more simple and approximate method presented in this paper.

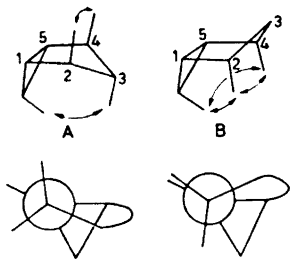

Fig. 3. Steric interactions in the bicyclo[3,1,0]hexane system. Newman projections of C(2)-C(1).

An approximate conformational analysis of the bicyclo[3,1,0]hexane system shows that the strong 1,3-interactions of the chair-like conformer (B) are relieved in favor of only one 1,4-interaction of similar magnitude by forcing the molecule into a boat-like conformation (A). Furthermore, the chair-like conformer (B) exhibits eclipsed C(1)–C(2) and C(4)–C(5) conformations (*cf.* Newman projection Fig. 3). The boat-like structure (A) is in the more favoured staggered conformation.

EXPERIMENTAL

NMR spectra were recorded on a 60 Mc/s Perkin-Elmer R-12 instrument. Chemical shifts are given in τ-units, ppm relative to tetramethylsilane (TMS).

(−)-*cis*-Sabinol was a gift from Dr. E. Klein (Dragoco) and exhibited, after recrystallisation from light petroleum (b.p. 30–40°), m.p. 45–46°, $[\alpha]_D$ −131° (*c* 1.0 $CHCl_3$) (*cf.* Ref. 14).

(+)-*trans*-Sabinol was obtained from (+)-sabinylacetate previously described.[23] (+)-*trans*-Sabinol had $[\alpha]_D$ +21.7° (*c* 2.1 $CHCl_3$). (−)-3-Neoisothujanol (*cf.* Ref. 1) had m.p. 66–68°, $[\alpha]_D$ −24° (*c* 2.0 in EtOH). (+)-3-Thujanol (*cf.* Ref. 1) had $[\alpha]_D$ +106° (*c* 1.5 $CHCl_3$).

Acknowledgement. We thank Dr. E. Klein (Dragoco) for a generous gift of crude (−)-*cis*-sabinol.

REFERENCES

1. Bergqvist, M. S. and Norin, T. *Arkiv Kemi* **22** (1964) 137.
2. Tori, K. *Chem. Pharm. Bull. Tokyo* **12** (1964) 1439.
3. Freeman, P. K., Raymond, F. A. and Grostic, M. F. *J. Org. Chem.* **30** (1965) 771.
4. Winstein, S., Friedrich, E. C., Baker, R. and Lin Yang-I. *Tetrahedron Suppl. 8 Part II* (1966) 621.
5. Smith, H. E., Brand, J. C. D., Massey, E. H. and Durham, L. J. *J. Org. Chem.* **31** (1966) 690.
6. Dieffenbacher, A. and von Philipsborn, W. *Helv. Chim. Acta* **49** (1966) 897.
7. Dauben, W. G. and Wipke, W. T. *J. Org. Chem.* **32** (1967) 2977.
8. Gray, R. T. and Smith, H. E. *Tetrahedron* **23** (1967) 4229.
9. Acharya, S. P., Brown, H. C., Suzuki, A., Nozawa, S. and Itoh, M. *J. Org. Chem.* **34** (1969) 3015.
10. Doering, W. von E. and Smith, E. K. G. *Tetrahedron* **27** (1971) 2005.
11. Herbstein, F. H. and Regev, H. *J. Chem. Soc.* **B 1971** 1696.
12. Hach, V., Raimondo, R. F., Cartlidge, D. M. and McDonald, E. C. *Tetrahedron Letters* **1970** 3175.
13. Djerassi, C., Klyne, T., Norin, T., Ohloff, G. and Klein, E. *Tetrahedron* **21** (1965) 163; Kuriyama, K., Tada, H., Sawa, Y. K., Ito, S. and Itoh, I. *Tetrahedron Letters* **1968** 2539; Ito, S., Klyne, W. and Norin, T. *Unpublished results.*
14. Klein, E. and Rojahn, W. *Chem. Ber.* **98** (1965) 3045.
15. Ohloff, G., Uhde, G., Thomas, A. F. and szKováts, E. *Tetrahedron* **22** (1966) 309.
16. Bhacca, M. S. and Williams, D. H. *Applications of NMR Spectroscopy in Organic Chemistry.* Holden-Day, San Francisco 1966, p. 108.
17. Demarco, P. V., Elzey, T. K., Lewis, R. B. and Wenkert, E. *J. Am. Chem. Soc.* **92** (1970) 5734.
18. Briggs, J., Hart, F. A. and Moss, G. P. *Chem. Commun.* **1970**, 1506.
19. Farid, S., Ateya, A. and Maggio, M. *Chem. Commun.* **1971**, 1285.
20. Kelsey, D. R. *J. Am. Chem. Soc.* **94** (1972) 1764.
21. ApSimon, J. W., Beierbeck, H. *Chem. Commun.* **1972**, 172.
22. Almin, K. E., Norin, T., Strömberg, S. and Weber, M. *Unpublished results.*
23. Norin, T. *Acta Chem. Scand.* **16** (1962) 640.

Received December 7, 1972

ACTA CHEMICA SCANDINAVICA 27 (1973) 1586–1594

The Synthesis of Fat and Water Soluble Arseno Organic Compounds in Marine and Limnetic Algae

GULBRAND LUNDE

Central Institute for Industrial Research, Oslo 3, Norway

Two green algae (*Chlorella ovalis* and *Chlorella pyrenoidosa*), one blue green (*Oscillatoria rubescence*) and two diatoms (*Phaeodactylum tricornutum* and *Skeletonema costatum*) were cultivated in fresh and/or salt water media containing radioactive arsenic ions. The incorporation of arsenic into various lipid and water soluble fractions was studied by chromatographic separation and radioactivity measurements. All the algae were found to synthesise both lipid and water soluble arseno organic compounds. Acid treatment converted different arsenolipids into a water soluble product which seemed to be identical to an arseno organic compound isolated from fat free algal material under mild conditions.

Growth of the two algae, *Phaeodactylum tricornutum* and *Chlorella ovalis*, was not influenced by the presence in the medium of 10 – 30 ppm and 1 – 3 ppm of arsenic salts having a 1:1 ratio of tri to pentavalent arsenic ions. Enrichment of arsenic (as arseno organic compounds) in the algae corresponded to 200 – 3000 times the concentration in the medium. Algae seem to be an important source of the arseno organic compounds found in higher marine organisms.

Earlier work has shown that there is a significant difference in the level of arsenic in marine plants and animals as compared with that found in terrestrial plants and animals.[1,2] It has also been established that in marine animals the arsenic both in the lipid and the non lipid phase is present as arseno organic compounds.[3–5] Other results indicate that at least lipid soluble arseno organic compounds are present in marine algae.[6] Arsenic has not been detected in the lipid phase in either plants or animals of terrestrial origin, indicating that these do not synthesise arseno organic compounds corresponding to those found in marine organisms.[3]

Little is known about the structure and chemistry of the arseno organic compounds present in marine organisms. Earlier results indicate that they are biologically very stable, as they are not broken down to inorganic arsenic when they are taken in orally by mammals.[7] These results also imply that the arseno organic compounds which are found in marine samples are less toxic than inorganic arsenic, especially arsenite.

The presence of both lipid soluble and water soluble arseno organic compounds in fish and other marine animals suggest [6] that marine algae may serve as a source of the arseno organic compounds found in organisms higher in the food chain. Previous results indicate that fish (*Salmo gardneri*) is able to synthesise lipid and water soluble arseno organic compounds from arsenite/arsenate mixed into the feed. The amount of arseno organic compounds present in the fish from this source is, however, shown to be small compared to that derived from lower stages in the marine food chain.[8]

In view of these findings it is of interest to study the uptake of arsenic in algae and to characterise the lipid soluble (and eventually the water soluble) arseno organic compounds synthesised by the algae in more detail. An investigation of this type may be carried out under laboratory conditions by adding radioactive arsenic to algal cultures and subsequently analysing for the radioactive compounds synthesised.

EXPERIMENTAL

Growth experiments. The algae were grown in 2 l spherical flasks at the Norwegian Institute for Water Research as previously described [6,9] in nutrient enriched media [10] based on uncontaminated sea water for *Chlorella ovalis* Butcher, *Phaeodactylum tricornutum* Bohlin and *Skeletonema costatum* (Grev.) Cleve. The green algae *Chlorella pyrenoidosa* Chick as well as *Phaeodactylum tricornutum* and *Oscillatoria rubescens* (D. C.) were grown in a fresh water medium based on distilled water with nutrients added. When the growth of the algae was well under way (approx. one week), half of the algal solution was filtered off each day, and new culture medium was added from the stock solution. The filters were stored in chloroform prior to analysis.

For each culture experiment 10 l of medium were prepared and between 0.01 and 0.1 mCi of arsenic tracer (As-74, AJS.1, Amersham) was added. At the time of addition the radioactive arsenic tracer consisted of a mixture of arsenite and arsenate (3/2).

In a second series of experiments *Chlorella ovalis* and *Phaeodactylum tricornutum* were grown with inactive arsenite/arsenate (1/1) added to the radioactive arsenic in the following amounts: 3, 30, 3×10^2, 10^3, 3×10^3, 10^4, and 3×10^4 μg/l.

To compare arsenite and arsenate in the absorption process, two identical cultures of the alga *Phaeodactylum tricornutum* were started. To one culture was added 30 ppb As^{3+} together with 0.04 mCi As^{3+} tracer, and to the other 30 ppb As^{5+} with the corresponding amount of As^{5+} tracer. Half a liter of the culture was filtered after 1 d, 2 d, 4 d, and 8 d, respectively. The amount of As^{3+} and As^{5+} in the filtered medium, after the experiments were finished, was determined by molecular gel filtration.* Samples were stored at -20°C prior to analysis.

Separation of organic and inorganic arsenic. Lipids were extracted from the algal material with chloroform/methanol/water (4/2/1). Following separation from the aqueous-methanolic phase, the chloroform phase was washed twice with distilled water to which inactive arsenite-arsenate had been added in order to dilute any inorganic radioactive arsenic ions present in the chloroform. The algal material was subsequently boiled in water for 20 min to produce an aqueous extract. The pH of this was adjusted to 7 – 8 by NH_3, and the solution was run through a column of anion exchange resin (Dowex 2 × 8, 200 – 400 mesh) previously equilibrated with 0.2 N HCl and washed with water. Inorganic arsenic ions are adsorbed on the resin under these conditions, while organic bound arsenic is eluted.[5]

Inorganic radioactive arsenic was also removed as volatile $AsCl_3$ by distilling it off from a solution adjusted to 6.6 N HCl. During this treatment the As^{5+} present will be reduced to As^{3+}. $AsCl_3$ will distil at 100°C; to prevent decomposition of arseno organic

* The two valencies of arsenic will be separated on a 1 m column loaded with Sephadex G 25 Fine (Pharmacia Fine Chemicals, Sweden), using 0.05 M NH_3 as eluting agent (unpublished results).

compounds, the temperature should be kept at 100 – 105°C, particularly towards the end of the process. The degree of separation obtained was estimated on thin layer chromatography by autoradiography.

All measurements of radioactivity were performed with a 2 × 2″ NaI "welltype" scintillation detector.

Thin layer chromatography (TLC). Adsorbent layers of about 1 mm thickness were used for the analyses performed by TLC, in order to obtain sufficient amounts of the synthesised radioactive arsenic compounds to allow the autoradiographic measurements. The use of 1 mm adsorbent layers resulted, however, in a reduction of both the separation and reproducibility usually obtained with TLC.

A portion from the aqueous extracts produced by boiling of defatted algal material was chromatographed in a system of chloroform/methanol/ammonia (2/2/1) (system 1) with cellulose powder (MN 300, Macherey, Nagel & Co., Düsen, GFR) as adsorbent.[11] The plate dimension was 20 by 20 cm. Some fractions from separation of the water extracts by molecular gel-filtration were characterised in a two-dimensional TLC procedure, in which the solvent system described above was used in the first direction, and methanol/water/pyridine (10/5/1) in the second (system 2).

The lipids extracted from the algal material were investigated using two different techniques. A sample of 10 – 20 mg of oil was dissolved in chloroform and polar lipids separated from the non-polar ones on a silica gel column (SiO_2, 0.2 – 0.5 mm, for chromatography, E. Merck AG, Darmstadt, West Germany). The non-polar lipids were eluted with chloroform, and the polar lipids subsequently with 90 % methanol in chloroform. As more than 98 % of the radioactivity followed the polar fraction, the latter was characterised further by "Kieselgel" (7731, E. Merck AG, Darmstadt, West Germany) using chloroform/methanol/water (65/25/4) for the development [12] (system 3).

The algal lipids were also analysed directly by TLC in the system used for the water extract (system 1, described above). The lipid soluble arseno organic compounds followed the solvent front. They were detected by autoradiography, scraped out and refluxed in hydrochloric acid (6.6 N) for 2 h. The hydrolysate was concentrated by evaporation and the residue extracted with ethanol. Samples of the ethanol solution were subsequently analysed by TLC on system 1. All plates were sprayed with ninhydrin reagent in order to detect amino acids or other compounds containing amino groups.

To see whether inorganic arsenic ions could be complexed by algal material and move in the TLC systems employed, radioactive arsenite-arsenate was added to inactive aqueous algal extracts and subjected to analysis by TLC in system 1.

Molecular gel-filtration. Aqueous algal extracts were subjected to molecular gel filtration on a dextrane resin (Sephadex G 25 Fine, Pharmacia Fine Chemicals, Sweden). A column with a diameter of 15 mm and a height of 25 cm (K 15/25, Pharmacia Fine Chemicals, Sweden) was used, and absorbance at 254 nm in the eluate monitered by a Uvicord spectrophotometer (LKB, Sweden). A 0.005 N (pH 7 – 8) ammonia solution was used as eluting agent. The eluate was collected in 10 ml fractions and the activity of each was measured. The fraction with the highest radioactivity was analysed by TLC in system 1. Aliquots from each fraction were tested for ninhydrin-positive compounds by application to filter paper, drying and spraying with ninhydrin reagent in the conventional manner.

Autoradiography. Radioactive arsenic compounds separated on TLC were detected by autoradiography. The TLC plates were dried thoroughly and placed in contact with sensitive X-ray emulsion (Ilford Industry G film). Exposure time was 1 – 14 days, depending on the amount of activity present. The film was subsequently developed as ordinary X-ray emulsion.

RESULTS AND DISCUSSION

TLC analyses of the extracts from the defatted algae all show a basic spot with an R_F value of about 0.30 (A, Figs. 1 and 2). The thickness of the adsorbent layer and poor reproducibility in preparing the plates resulted in considerable variations of this R_F value. This spot (A) is present in all the aqueous extracts produced from different algal species investigated. Despite the

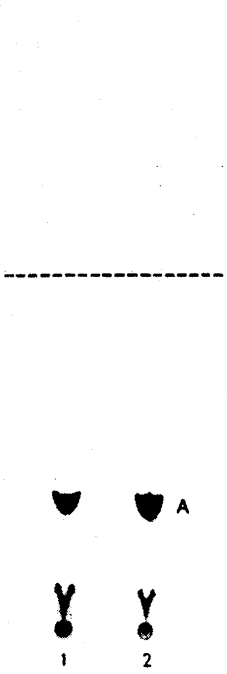

Fig. 1. Autoradiograph of TLC plate of aqueous extracts produced from *Phaeodactylum tricornutum* (1) and *Chlorella ovalis* (2). The exposed area (dark) shows the presence of radioactive arseno organic compounds. The main compound is marked A. More detail is shown on the original film. Analytical condition: Cellulose substrate (1 mm); developing solvent, chloroform/methanol/ammonia, 2/2/1 (system 1).

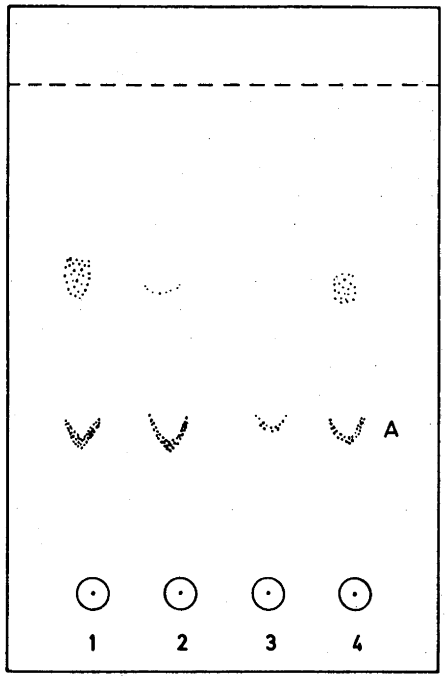

Fig. 2. Reproduction of an autoradiograph of TLC plate of aqueous extracts from *Phaeodactylum tricornutum* cultured in salt water (1) and in fresh water (2), and *Chlorella ovalis* in salt water (3) and *Chlorella pyrenoidosa* in fresh water (4). The main radioactive arseno organic compound present is compound A. Analytical conditions as described in Fig. 1.

lack of a rigid proof, the spot is supposedly caused by a single compound, namely compound A. Its presence is independent of the means used to remove the inorganic radioactive arsenic ions. There are also some weaker and more diffusely exposed areas corresponding to compounds with higher and lower R_F values. This is particularly so for the chromatograms where the aqueous extracts were treated by the ion exchange process. The amount of these compounds, in particular those with an R_F value greater than 0.30, are reduced in extracts subjected to treatment by 6.6 N hydrochloric acid. Compounds with R_F values less than 0.30, which are more polar than A, are present in all the water extracts.

A slight exposure at the spots of application on TLC plates is seen mainly for the extracts treated with hydrochloric acid. This should be compared

with results obtained when radioactive arsenite-arsenate was added to an inactive algal solution, demonstrating that the inorganic arsenic ions are stationary or moving only slightly under the TLC conditions used. Stationary radioactive arsenic compounds in the aqueous algal extract thus probably consist of arsenite-arsenate or other types of arsenic ions.

The ion exchange process is the preferred method for removal of inorganic radioactive arsenic from the aqueous algal extracts. The method is less drastic than the treatment with hydrochloric acid and seems not to cause changes in the chemical status of the arsenic. Some of the arseno organic compounds may, however, be irreversibly absorbed to the ion exchange resin. Changes, or decomposition of arseno organic compounds, may also take place in the preparation of the aqueous extracts, particularly during the boiling step. Formation of compound A is the most likely reaction.

TLC of the aqueous extracts from the algal clones of *Phaeodactylum tricornutum*, cultured both in fresh and salt water, and the two species, *Chlorella ovalis* and *Chlorella pyrenoidosa*, cultured in salt and fresh water, respectively, indicates that the concentration of compounds A is somewhat higher in the algae grown in salt water (Fig. 2).

The radioactivity in the non-polar and in the polar fractions of the algal oil, after these had been separated on the silica gel column, shows that nearly all the radioactivity (> 98 %), *i.e.* all the lipid soluble arseno organic compounds synthesised by the algae, follow the polar fraction. These results are in accordance with previous results reported for the lipid soluble arseno organic compounds present in fish oils.[13,14]

TLC-separation of the polar lipids made visible by autoradiography (Fig. 3) indicates the presence of lipid soluble arseno organic compounds different from those detected in the aqueous extracts. Moreover, the pattern of arsenic containing compounds varies with the various algae studied (*Chlor-*

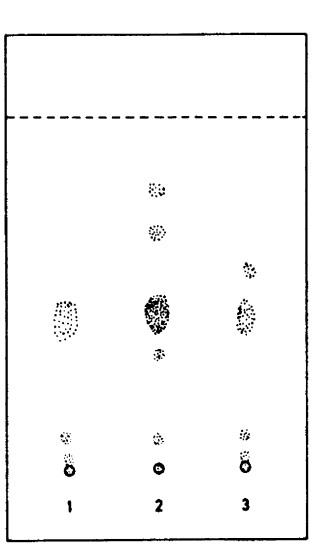

Fig. 3. Reproduction of an autoradiograph of TLC plate of the polar lipids from *Sceletonema costatum* (1). *Phaeodactylum tricornutum* (2) *and Chlorella ovalis* (3). Analytical conditions: Kieselgel G substrate (1 mm); chloroform/methanol/water, 65/25/4 (system 3).

ella ovalis, *Oscillatoria rubescens*, and *Phaeodactylum tricornutum*). A similar difference has been reported for lipid soluble arseno organic compounds in invertebrates.[15] This observation could be of significance, but new lipid soluble arseno organic compounds may be created as a result of the experimental conditions when extracting and fractionating the algal lipids.

TLC of algal lipids in system 1 shows the lipid soluble arseno organic compounds to move with the solvent front, as do the other algal lipids. In some of the samples, however, a well defined spot with an R_F value of *ca.* 0.30 was found. Presumably this is traces of compound A found in the aqueous extract.

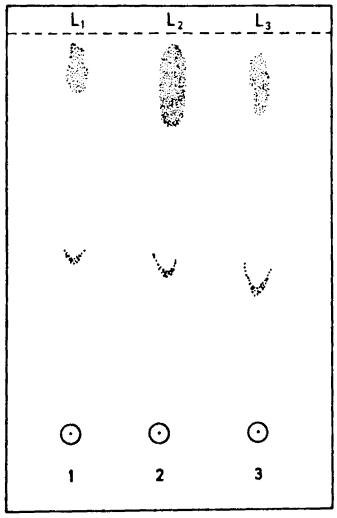

Fig. 4a. Reproduction of autoradiographs of TLC plates of the total amount of lipids extracted from *Oscillatoria rubescens* (1), *Phaeodactylum tricornutum* (2), and *Chlorella ovalis* (3). The lipids (L^{1-3}) will have R_F values close to 1 in system 1.

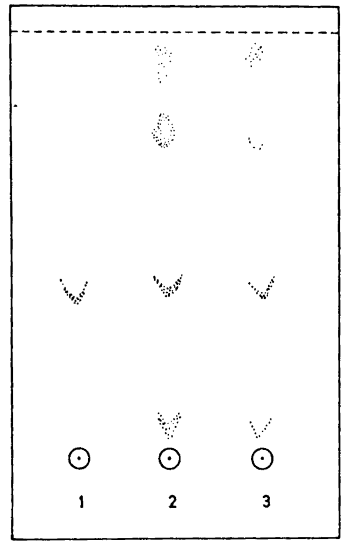

Fig. 4b. The lipids (L^{1-3}) shown in Fig. 4a were scraped out, treated with HCl and extracted with ethanol (see text). These extracts were analysed under the same conditions as described in Fig. 4a (see text).

Scraping out the lipid soluble compounds as detected by autoradiography and refluxing with hydrochloric acid (6.6 N) again produced a well defined spot at R_F 0.30 on repeated TLC-separation in system 1. Apparently compound A from the aqueous extract is also produced from the lipid soluble compounds on treatment with hydrochloric acid. A positive ninhydrin reaction is always associated with this compound. This fact becomes especially relevant when the positive reaction was obtained with compound A prepared from lipid soluble arseno organic compounds isolated by TLC, since this operation will remove most foreign ninhydrin positive material. Two-dimensional TLC of

the most radioactive fraction from the molecular gel-filtration gave coincidence between radioactivity and ninhydrin reaction.

Figs. 5 a-b show how the production of lipid and water soluble arseno organic compounds varies, as the concentration of inorganic arsenic ions is

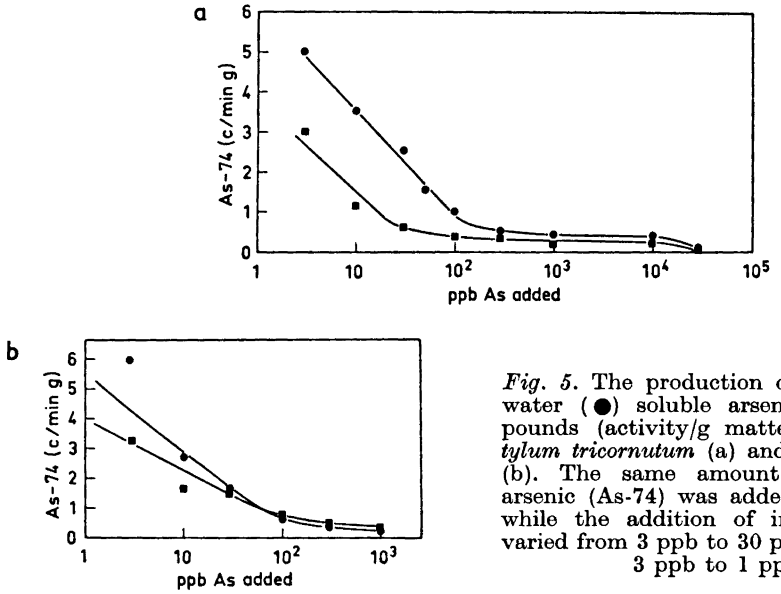

Fig. 5. The production of lipid (■) and water (●) soluble arseno organic compounds (activity/g matter) in *Phaeodactylum tricornutum* (a) and *Chlorella ovalis* (b). The same amount of radioactive arsenic (As-74) was added in each batch while the addition of inorganic arsenic varied from 3 ppb to 30 ppm (a) and from 3 ppb to 1 ppm (b).

increased in the medium under otherwise identical conditions. The ordinate is activity (counts/min) divided by weight of lipids and of dehydrated aqueous extracts, respectively. Both *Phaeodactylum tricornutum* and *Chlorella ovalis* show the same behaviour, which indicates two different patterns of uptake. One applies to media containing up to about 100 ppb of inactive arsenic ions added, and represent an active absorption of the arsenic. The percentage amount of arsenic converted to arseno organic compounds depends on the concentration of arsenic ions in the medium. The other applies to concentrations of arsenic from 100 ppb up to 10 – 30 ppm As for *Phaeodactylum tricornutum* and at least to 1 ppm As for *Chlorella ovalis*, and shows that an approximately constant fraction of the arsenic in the medium is absorbed. In the latter case an equilibrium between the arsenic absorbed and the arsenic present in solution seems to be established up to the concentration where the toxic effect of the arsenic begins to limit the alga's growth (and finally causes its death at around 30 ppm arsenic added (*Phaeodactylum tricornutum*)).

The results of the experiments where arsenite and arsenate were added independently and with radioactive arsenic tracer of the same valency show that more lipid soluble arseno organic compounds are synthesised by the culture with As^{5+} added. This is especially so in the first samples taken after one day. Gel filtration of the media shows that the arsenic in the two solutions

of As^{5+} and As^{3+}, respectively, will tend to reach an equilibrium between As^{3+} and As^{5+}. Although preliminary and not conclusive, the results indicate that the arsenate is used or preferred for the synthesis of arseno organic compounds in the algae.

Some results for the accumulation of arsenic in the algae compared to the concentration of arsenic in the culture media were obtained. The measurement of the radioactivity of the lipid and aqueous phase (counts As/g), produced from the various algae, was compared with corresponding measurements of the radioactivity of the medium. These results are shown in Table 1. They indicate

Table 1. Accumulation of arsenic [a] in algae as arseno organic compounds in the lipid phase and in the aqueous phase, respectively.

	Culturing media			
	Salt water		Fresh water	
	Lipid phase	Aqueous phase	Lipid phase	Aqueous phase
Phaeodactylum tricornutum	2900	2000	2800	1800
Chlorella ovalis	1600	1300		
Chlorella pyrenoidosa			400	190
Oscillatoria rubescens			540	240
Skeletonema costatum	1100	710		

[a] The calculation is based on the ratio between organic bound As-74 in the lipid phase and inorganic As-74 in the medium, and correspondingly in the aqueous phase and in the medium.

an accumulation factor of 250 – 3000 in the algae. It should be noted that the arsenic is somewhat more enriched in the lipid phase. From Figs. 5 a – b it must also be assumed that the accumulation is dependent upon the amount of arsenic present in the culture medium. Here the degree of accumulation will decrease with increasing arsenic concentration in the culture solution up to about 100 ppb (*Phaeodlactylum tricornutum* and *Chlorella ovalis*),

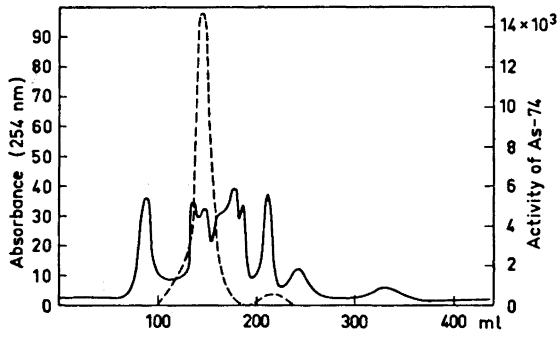

Fig. 6. UV absorbance (–) at 254 nm of molecular gel-filtrated aqueous extract from *Phaeodactylum tricornutum*. The radioactivity (– – –) of the eluate was measured in fractions of 10 ml.

and then be constant until at least a concentration of about 1 – 10 ppm arsenic in the solution is reached. The accumulation in this region is a factor 15 – 20 below the values found with no inactive arsenic added to the medium.

The results of the molecular gel filtration analysis of the water extracts are presented in Fig. 6. They show that the radioactive arseno organic compounds are eluted in two regions, one of smaller and one of larger molecular weight. The larger lies in the region where the majority of the water soluble arseno organic compounds from fish glue water are eluted. [4] This indicate that the main water soluble organic arsenic compounds in algae and fish are of similar molecular weight. By testing the fractions with ninhydrin reagent it is shown that these compounds are eluted before the amino acids. The two-dimensional TLC analyses of this fraction and subsequent autoradiography of the plate showed that no other radioactive arseno organic compounds could be detected and furthermore that the fraction shows a positive ninhydrin reaction.

CONCLUSIONS

On the basis of the results obtained in this work it is concluded that unicellular algae of limnetic as well as of marine origin are able to synthesise both fat soluble and water soluble arseno organic compounds from inorganic arsenic ions. The lipid soluble compounds are relatively unstable and may by a suitable treatment be converted to a water soluble arseno organic compound which cannot be distinguished from that which is most abundant in aqueous extracts. This main compound is present in all the algal species studied regardless of whether they are cultivated in salt or in fresh water. The results suggest that the arseno organic compounds present in the algae may be one important source for corresponding compounds found in marine organisms at higher stages in the marine food chain.

Acknowledgement. The author is indebted to the *Norwegian Institute for Water Research* and to Mr. O. Skulberg for help with the algal cultivation experiments and for valuable discussions.

REFERENCES

1. Bowen, H. J. M. *Trace Elements in Biochemistry*, Academic, London and New York 1966, p. 174.
2. Lunde, G. *J. Sci. Food Agr.* **19** (1968) 432.
3. Lunde, G. *J. Am. Oil Chemists' Soc.* **49** (1972) 44.
4. Lunde, G. *J. Sci. Food Agr.* **21** (1970) 242.
5. Lunde, G. *Nature* **224** (1969) 186.
6. Lunde, G. *Acta Chem. Scand. In press.*
7. Coulsen, E. J. *J. Nutr.* **10** (1935) 255.
8. Lunde, G. *Fiskeridir. Skr. Ser. Tekn. Undersøk.* **12** (1973) 1.
9. Skulberg, O. M. *Int. Conf. Wat. Pollut. Res., 3, Munich*, Water Pollution Control Federation, Washington 1967, 1, pp. 113 – 127.
10. Gautier, A. C. R. *Acad. Sci., Paris* **135** (1902) 833.
11. Bondivenne, R. and Busch, N. *J. Chromatog.* **29** (1967) 349.
12. Stahl, E. *Dünnschichtchromatographie*, Springer, Berlin 1962, p. 168.
13. Lunde, G. *J. Am. Oil Chemists' Soc.* **45** (1968) 331.
14. Lunde, G. *J. Am. Oil Chemists' Soc.* **48** (1971) 517.
15. Vaskovsky, V. E., Korotchenko, O. D., Kosheleva, L. P. and Levin, V. S. *Comp. Biochem. Physiol.* **41b** (1972) 777.

Received November 28, 1972.

ACTA CHEMICA SCANDINAVICA 27 (1973) 1595–1600

1-*O*-β-D-Galactopyranosyl-D-ribitol from *Xanthoria parietina**

PER J. GAREGG, BENGT LINDBERG, KARIN NILSSON and CARL-GUNNAR SWAHN

Institutionen för organisk kemi, Stockholms universitet, Sandåsgatan 2, S-113 27 Stockholm, Sweden

Dedicated to Professor *František Šorm* on his 60th birthday

O-α-D-Galactopyranosyl-(1→6)-*O*-β-D-galactopyranosyl-(1→1)-D-glyceritol and 1-*O*-β-D-galactopyranosyl-D-ribitol have been isolated from the lichen *Xanthoria parietina*. The latter substance, and the corresponding L-ribitol derivative, were synthesized in order to determine the configuration of the ribitol moiety in the natural product.

Low molecular weight carbohydrates, such as alditols, alditol glycosides, and disaccharides have been isolated from various lichens.[2a] In the present communication, studies on the low molecular weight carbohydrates in *Xanthoria parietina* are reported. The water soluble part of a methanol extract of the lichen was fractionated by carbon column chromatography followed by chromatography on paper and on Sephadex G-25. In addition to *myo*-inositol, D-arabinitol, ribitol, D-mannitol, sucrose, and α,α-trehalose, two components not previously found in lichens were obtained.

One component, m.p. 190 – 193°, $[\alpha]_{578}$ +89° in water, on acid hydrolysis yielded D-galactose and glyceritol in the molar ratio 2:1. It was indistinguishable (m.p., mixed m.p., IR) from an authentic sample of *O*-α-D-galactopyranosyl-(1→6)-*O*-β-D-galactopyranosyl-(1→1)-D-glyceritol, a common component in glycolipids.[2b] The non-acylated compound has also been isolated from a red alga.[3]

The second component (I), $[\alpha]_{578}$ −3° (in water), which did not crystallize, on acid hydrolysis yielded equimolar quantities of D-galactose and ribitol. The rate of acid hydrolysis indicated the presence of a pyranosidic linkage. The low optical rotation indicated that the component was a β-D-galactopyranoside. In accordance with these findings, it was hydrolyzed, although

* Part 29 in *Studies on the Chemistry of Lichens*. Part 28, Ref. 1.

at a low rate, by the action of β-D-galactosidase. In the NMR spectrum (D_2O) the anomeric proton gave a signal at 4.4 ppm (d), $J_{1,2}$ 8 Hz, confirming *trans*-geometry of H-1 and H-2 in the galactopyranosyl residue and thereby the presence of a β-D-galactopyranoside. On periodate oxidation, 5.3 mol reagent were consumed, with the simultaneous release of 1.08 mol formaldehyde and 2.81 mol formic acid. These findings are consistent with I being 1-*O*-β-D-galactopyranosyl-D- or -L-ribitol. In order to distinguish between these alternatives, the two substances were synthesized and compared with the natural product.

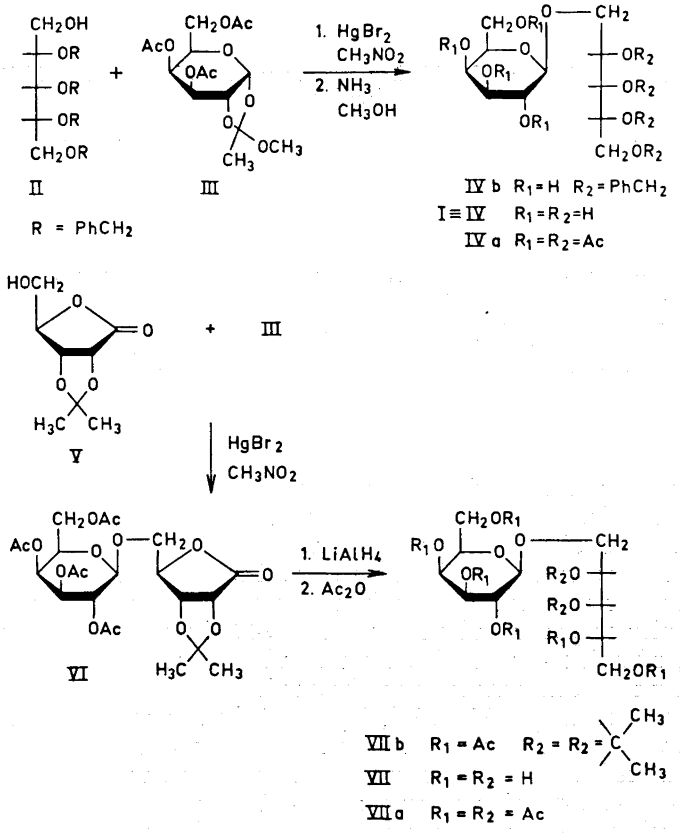

2,3,4,5-Tetra-*O*-benzyl-D-ribitol (II) was prepared from D-ribose diethyl dithioacetal[4] by benzylation, hydrolysis in the presence of mercuric chloride and mercuric oxide, and finally reduction with sodium borohydride. Condensation of II with 3,4,6-tri-*O*-acetyl-1,2-methylorthoacetyl-α-D-galactopyranose (III) in nitromethane using mercuric bromide as catalyst and the general conditions devised by Kochetkov and co-workers,[5] followed by deacetylation, yielded the β-D-galactopyranoside IVb. Removal of benzyl groups by catalytic hydrogenation

yielded 1-*O*-*β*-D-galactopyranosyl-D-ribitol (IV), which was purified as its octaacetate (IVa).

A similar orthoester synthesis, using the orthoester III and 2,3-*O*-isopropylidene-1,4-D-ribonolactone, but with a mixture of *p*-toluenesulphonic acid and mercuric bromide as catalyst, yielded crude VI. Reduction of VI with lithium aluminium hydride yielded the ribitol *β*-D-galactopyranoside derivative VIIb, which, however, was contaminated with the corresponding α-galactoside. Another example of low stereoselectivity in the orthoester glycoside synthesis has recently been described.[6] On both occasions recourse had to be taken to more strongly acidic conditions than those generally used, in order to obtain condensation. The isopropylidene group in VIIb was removed by hydrolysis in trifluoroacetic acid. The product was fully acetylated and then separated from the α-anomer VIII by chromatography on dimethyl sulphoxide-impregnated silica gel.[7] The faster-moving component, VIII, had $[\alpha]_D$ +73° in chloroform and the slower-moving one, VIIa, $[\alpha]_D$ +13° indicating that they were the α- and *β*-D-galactopyranosides, respectively. Both glycosides (VII and VIII) were converted into their octamethyl ethers, which could be separated by GLC, but gave identical mass spectra (MS) except for minor variations attributable to stereoisomerism. The MS were also identical to those of the fully methylated IV and the fully methylated natural product I, demonstrating that they were all 1-*O*-D-galactopyranosyl-ribitols. The fully methylated I, IV, and VII could not be separated on GLC. The fully trimethylsilylated I and IV were also inseparable, but had a different retention time to that of the corresponding derivative of VII. The negative rotations of the octaacetates Ia and IVa, $[\alpha]_D$ −7° and −11°, respectively, in contradistinction to the positive value for VIIa, +13°, lends further support to the identity of I and IV. Deacetylation of IVa and VIIa afforded 1-*O*-*β*-D-galactopyranosyl-D- and -L-ribitol, $[\alpha]_D$ −7° and +30°, respectively; $[\alpha]_{578}$ for I was −3°. The natural product therefore is 1-*O*-*β*-D-galactopyranosyl-D-ribitol.

Sugar alcohols have low optical rotations, but high values are observed for their molybdate complexes. Pyranosides, on the other hand, do not complex with molybdate.[8] It is therefore expected that the main contributions to the optical rotations of IV and VII should come from the 1-substituted D- and L-ribitol moieties, respectively, and have different signs, but approximately the same magnitude. In agreement with this, IV and VII, in 0.037 M sodium molybdate buffered to pH 5.5, showed $[\alpha]_{589}$ −78°, +75°, $[\alpha]_{578}$ −81°, +89°, $[\alpha]_{546}$ −95°, +92°, $[\alpha]_{436}$ −202°, +180°, and $[\alpha]_{365}$ −455°, +357°, respectively.

EXPERIMENTAL

General methods. Melting points are corrected. Concentrations were performed at reduced pressure and a bath temperature not exceeding 40°, unless otherwise stated. Optical rotations were recorded at room temperature, at *c* 0.05−0.5, using a Perkin-Elmer 141 instrument. UV and visible spectra were measured using Beckman DK2 and Beckman DB instruments, respectively. NMR spectra were recorded with a Varian A60-A instrument, using tetramethylsilane as internal standard. The NMR spectra, determined for all new compounds, were in agreement with the postulated structures. TLC was performed on silica gel F_{254} (Merck) plates. When necessary, sulphuric acid was used as spray reagent. Silica gel column chromatography was performed using Mallinck-

rodt 100 mesh silicic acid. Whatman No. 1 and 3MM papers were used for analytica and preparative paper chromatography, respectively. Solvent systems: *A*. Ethyl acetate, acetic acid, water, 3:1:1. *B*. Ethyl acetate, pyridine, water, 8:2:1. *C*. Same solvent, but 2:1:1. Silver acetate-sodium hydroxide in ethanol and *p*-anisidine hydrochloride in ethanol were used as spray reagents. GLC and GLC-MS were performed using Perkin-Elmer 900 and Perkin-Elmer 270 instruments, respectively (manifold temperature 200°, ionization potential 70 eV, ionization current 80 μA, temperature at the ion source chamber 80°). A column of XE-60 (3 %) on Gas Chrom Q (100 – 120 mesh) was used for the disaccharide derivatives.

Extraction and fractionations of lichen components. Dry, ground *Xanthoria parietina*, collected at Fiskebäckskil, Bohuslän, Sweden, (400 g), was extracted in a continuous extractor, first with diethyl ether for one week and then with methanol for one week. The methanol extract was concentrated, partitioned between chloroform and water, and the aqueous phase deionized with Dowex 50 (H^+) and Dowex 3 (free base) and then concentrated to a syrup (29 g). D-Mannitol (7 g) was obtained from the syrup by crystallization from ethanol. The remainder of the syrup, in water (40 ml) was added to the top of a carbon-Celite column (5.3 × 47 cm) which was irrigated, first with water (3.5 l) and then with aqueous ethanol (8 l 0→20 %, linear gradient). The fractionation was monitored by paper chromatography. The substances were eluted in the following order: *myo*-inositol, D-arabinitol, ribitol, D-mannitol, α,α-trehalose, sucrose, galactosylribitol and galactosylgalactosylglyceritol. No components were obtained pure, but had to be further purified by preparative paper chromatography, giving the following: *Myo*-inositol, m.p. 216 – 222°. D-Arabinitol, m.p. 102 – 104°, $[\alpha]_{578}$ +11° (saturated aqueous sodium tetraborate). Ribitol, m.p. 102 – 104°. D-Mannitol, m.p. 163 – 164°, $[\alpha]_{578}$ +33° (saturated aqueous sodium tetraborate). α,α-Trehalose dihydrate, m.p. 91 – 93°, $[\alpha]_{578}$ +175° (water). The various compounds were indistinguishable from authentic samples (m.p., IR).

O-α-D-*Galactopyranosyl-(1→6)*-O-β-D-*galactopyranosyl-(1→1)*-D-*glyceritol.* The fraction (300 mg) containing the title compound was purified by paper chromatography (solvent *A*) followed by chromatography on a Sephadex G-25 (superfine) column (1.6 × 175 cm). The pure compound (53 mg) crystallized from aqueous ethanol, m.p. 190 – 193°, $[\alpha]_{578}$ +89° (water). It was indistinguishable from an authentic sample of the title compound [3] (m.p., IR).

1-O-β-D-*Galactopyranosyl*-D-*ribitol (I).* The combined fractions containing the title compound were purified by paper chromatography (solvent *C*), followed by chromatography on the Sephadex G-25 column. The product (I, 50 mg), which gave a single spot on paper chromatography, showed $[\alpha]_{578}$ −3° (water) and did not crystallize. The hydrolysis of I in 0.05 M aqueous sulphuric acid at 80° was followed polarimetrically and reached a constant, positive value (indicating D-galactose) after 35 h. 2-*O*-β-D-Galactofuranosyl-D-arabinitol (umbilicin) was completely hydrolysed in 2 h. Paper chromatography of the hydrolysate showed the presence of galactose and ribitol. Analysis, by GLC, of the product obtained after borohydride reduction and acetylation showed, in addition to galactitol and ribitol acetates, smaller amounts (less than 2 % of each) of the acetylated arabinitol, mannitol, and glucitol. I was oxidized with 0.03 M aqueous sodium metaperiodate. The consumption of oxidant was followed spectrophotometrically,[9] the formation of formaldehyde by the reaction with chromotropic acid,[10] and the formation of formic acid by treatment with ethylene glycol followed by titration with 0.01 M sodium hydroxide.

2,3,4,5-Tetra-O-*benzyl*-D-*ribose diethyl dithioacetal.* D-Ribose diethyl dithioacetal [4] (2.5 g) was benzylated by the procedure devised by Brimacombe and Ching.[11] Part of the product was purified by TLC ($CHCl_3$) $[\alpha]_D$ +20° (chloroform). (Found: C 72.1; H 7.07; O 10.5. $C_{37}H_{44}O_4S_2$ requires: C 72.0; H 7.19; O 10.4.) Most of the product (6.0 g) was used, without purification, in the next step.

2,3,4,5-Tetra-O-*benzyl*-D-*ribitol (II).* The above compound (6.0 g) in acetone (55 ml) and water (3.5 ml) was transformed into the aldehyde by treatment with mercuric chloride (4.0 g) and yellow mercuric oxide, and worked up as described for analogous syntheses.[12] Part of the crude product was purified by TLC (toluene), yielding syrupy 2,3,4,5-tetra-*O*-benzyl-D-ribose, $[\alpha]_D$ +13° (chloroform). The remainder (5.0 g), in methanol (50 ml) containing sodium methoxide (from 50 mg sodium), was treated with sodium borohydride (2.3 g) at room temperature overnight. The product was acidified and partitioned between water and chloroform, and the chloroform phase (II) purified

by chromatography on a silica gel column (5 × 30 cm) (chloroform). Pure II (2.1 g) showed $[\alpha]_D$ −14° (chloroform). (Found: C 77.2; H 7.10; O 15.7. $C_{33}H_{36}O_5$ requires: C 77.3, H 7.08; O 15.6.)

3,4,6-Tri-O-*acetyl-1,2*-O-*methylorthoacetyl*-α-D-*galactopyranose (III)* was prepared from 2,3,4,6-tetra-*O*-acetyl-α-D-galactopyranosyl bromide as described by Kochetkov and co-workers for the corresponding ethyl orthoacetate,[5] and purified by chromatography on silica gel (diethyl ether). The yield of pure product, $[\alpha]_D$ +122° (chloroform), was 61 %.

2,3,4,5-Tetra-O-*benzyl-1*-O-(β-D-*galactopyranosyl*)-D-*ribitol* (*IVb*). The orthoester III (1.3 g) and II (1.3 g) were dissolved in nitromethane (15 ml). Solvent was distilled off at constant volume for 4 h, by the continuous addition of nitromethane. Mercuric bromide (50 mg) was added and the distillation at constant volume continued for 2 h. The mixture was filtered, concentrated, and deacetylated in methanol (120 ml) containing 1.67 % ammonia at room temperature overnight. The product was concentrated, dissolved in acetone, insoluble material removed by filtration, and the filtrate concentrated. The product (1.87 g) was separated on a silica gel column (ethyl acetate, methanol, and water 80:15:5). The main component (1.25 g) was almost pure according to TLC. Part of it was further purified by TLC in the above solvent yielding chromatographically homogeneous, amorphous IVb, $[\alpha]_D$ −6° (chloroform).

1-O-β-D-*Galactopyranosyl*-D-*ribitol octaacetate (IVa)*. Catalytic hydrogenation of IVb (1.25 g), using 5 % palladium on carbon, followed by treatment with acetic anhydride in pyridine yielded crude IVa. This was purified by chromatography on silica gel (chloroform, diethyl ether, 8:2). The amorphous product (0.99 g) showed $[\alpha]_D$ −11° (chloroform). (Found: C 50.0; H 5.71; O 44.1. $C_{27}H_{38}O_{18}$ requires: C 49.8; H 5.89; O 44.3.)

5-O-(*2,3,4,6-Tetra*-O-*acetyl*-β-D-*galactopyranosyl*)-*2,3*-O-*isopropylidene-1,4*-D-*ribonolactone* (*VI*). A solution of the orthoester III (6.5 g), *p*-toluenesulphonic acid (2 mg) and 2,3-*O*-isopropylidene-1,4-D-ribonolactone (V, 4.0 g) in nitromethane (50 ml) was distilled at constant volume for 2 h, when according to TLC all of III had reacted. Mercuric bromide (250 mg) was added and the mixture refluxed for 1 h. After dilution with chloroform, the solution was shaken with aqueous sodium hydrogen carbonate and water, dried ($MgSO_4$) and concentrated to a syrup (9.0 g). Fractionation of this syrup on a silica gel column (diethyl ether) afforded VI (3.7 g), contaminated with about 8 % of V. This material was used in the next step.

4,5-Di-O-*acetyl-1*-O-(*2,3,4,6-tetra*-O-*acetyl*-β-D-*galactopyranosyl*)-*2,3*-O-*isopropylidene*-L-*ribitol* (*VIIb*). A solution of VI (3.7 g) and lithium aluminium hydride (1.4 g) in tetrahydrofuran (50 ml) was refluxed overnight. The product was worked up as usual and acetylated with acetic anhydride in pyridine. Purification of the product by silica gel chromatography (chloroform, acetone 9:1) yielded VIIb (1.65 g), $[\alpha]_D$ +33° (chloroform). This material was contaminated with the corresponding α-form (see below). (Found: C 51.6; H 6.34. $C_{26}H_{38}O_{16}$ requires: C 51.5; H 6.31.)

1-O-β-D-*Galactopyranosyl*-L-*ribitol octaacetate* (*VIIa*). The isopropylidene derivative VIIb (1.6 g) was treated with 90 % aqueous trifluoroacetic acid (10 ml) for 10 min at room temperature. The product was concentrated to a syrup, dried by repeated concentrations with toluene, acetylated with acetic anhydride in pyridine and purified by TLC (chloroform, acetone 9:1). Chromatography on dimethyl sulphoxide impregnated paper (diisopropyl ether), as devised by Wickberg,[7] revealed the presence of two components, the slower of which (β-anomer) predominated. Separation on dimethyl sulphoxide impregnated silica gel (diisopropyl ether) yielded the two components. The α-form (180 mg) showed $[\alpha]_D$ +73° (chloroform). (Found: C 50.1; H 5.82. $C_{27}H_{38}O_{18}$ requires: C 49.9; H 5.89.) The β-form (250 mg) showed $[\alpha]_D$ +13° (chloroform). (Found: C 50.0; H 6.01).

The octamethyl ethers prepared from VIIb and its α-anomer, and also those for I and IV, gave indistinguishable mass spectra, except for minor differences in intensities. The following spectrum, from methylated IV, is typical (relative intensities in brackets): 40 (5), 41 (13), 43 (13), 44 (34), 45 (54), 53 (5), 55 (10), 57 (9), 58 (6), 59 (16), 69 (6), 71 (85), 72 (7), 73 (11), 75 (21), 83 (5), 85 (5), 88 (100), 89 (27), 95 (5), 97 (5), 101 (21), 102 (9), 103 (6), 111 (6), 115 (6), 127 (10), 133 (5), 159 (6), 187 (10), 191 (10), 192 (5), 251 (4). On GLC (XE-60)fully methylated I, IV, and VII were indistinguishable, but the methylated α-anomer of VII had a shorter retention time.

I, IV, and VII were also converted into their fully trimethylsilylated derivatives. Those of I and IV were indistinguishable on GLC (XE-60, 170 − 190°) but that of VII had a different retention time ("mixed" chromatography).

Deacetylation of IVa and VIIa afforded 1-*O*-β-D-galactopyranosyl-D- and -L-ribitol, $[\alpha]_D$ −7° and +30° (water), respectively.

Acknowledgements. The authors are indebted to Dr. C. A. Wachtmeister for the lichen material, to Professor B. Wickberg for reference material, and to *Statens Naturvetenskapliga Forskningsråd* for financial support.

REFERENCES

1. Åkermark, B. *Acta Chem. Scand.* **24** (1970) 1456.
2. a. Brimacombe, J. S. and Webber, J. M. In Pigman, W. and Horton, P., Eds., *The Carbohydrates*, Academic, New York 1972, Vol. IA; b. McKibbin, J. M., *Ibid.*, Vol. IIB.
3. Wickberg, B. *Acta Chem. Scand.* **12** (1958) 1183.
4. Zinner, H. *Chem. Ber.* **86** (1953) 495.
5. Kochetkov, N. K., Khorlin, A. J. and Bochkov, A. F. *Tetrahedron* **23** (1967) 693.
6. a. Alfredsson, G., Borén, H. B. and Garegg, P. J. *Acta Chem. Scand.* **26** (1972) 2531, 3431; b. Borén, H. B. *University of Stockholm Chem. Commun.* **1972** No. 1 (April 28).
7. Wickberg, B. *Methods Carbohyd. Chem.* **1** (1962) 31.
8. Voelter, W., Bayer, E., Records, R., Bunnenberg, E. and Djerassi, C. *Ann.* **718** (1968) 238.
9. Guthrie, R. D. *Methods Carbohyd. Chem.* **1** (1962) 435.
10. Speck, J. C. *Methods Carbohyd. Chem.* **1** (1962) 441.
11. Brimacombe, J. S. and Ching, O. A. *Carbohyd. Res.* **8** (1968) 82.
12. Zinner, H. *Chem. Ber.* **86** (1953) 496.

Received December 5, 1972.

ACTA CHEMICA SCANDINAVICA 27 (1973) 1601–1612

Permanganate Oxidation of Methylated and Unmethylated Fulvic Acid, Humic Acid, and Humin Isolated from Raw Humus

GUNNAR OGNER

The Forest Soil Fertilization Research Group, The Norwegian Forest Research Institute, N-1432 AS-NLH, Norway

Methylated and non-methylated raw humus and its fractions humin, humic acid, and fulvic acid have been oxidized by potassium permanganate at pH 9–10. After methylation with diazomethane and separation by preparative thin-layer and gas chromatography, the oxidation products found were 8 benzenecarboxylic acid methyl esters, 13 methoxy-benzenecarboxylic acid methyl esters, 7 1,2-dimethoxy-benzenecarboxylic acid methyl esters, 11 dicarboxylic acid dimethyl esters, and 2 dimethoxy-carbomethoxy-diazines. Qualitatively no major differences were found between the various humic fractions even though these fractions represent materials with large differences in solubility and molecular weights. The differences found between methylated and non-methylated samples were greater than the difference between the various humic fractions. In general, a higher yield of benzenecarboxylic acids was found from non-methylated material, and the higher homologs of the dicarboxylic acids ($C_{11}-C_{14}$) were found in this material only. 1,2-Dimethoxy-benzenecarboxylic acid methyl esters were detected among the oxidation products of methylated fractions only. A small amount of 4 different methoxy-benzenecarboxylic acids was found from unmethylated fractions, whereas methylation prior to oxidation sharply increased the total yield of this group of compounds. The dimethoxy-carbomethoxy-diazines were found from methylated material only and believed to be an artefact from the methylation with diazomethane.

For methylated material, the most pronounced difference between the various humic fractions was the decrease of the total amount of dimethoxy-benzenecarboxylic acids and the increase in the amount of dicarboxylic acids in the order humin, humic acid, and fulvic acid. The increase in the amount of dicarboxylic acids was mainly due to an increase in the amount of the lower homologs. For all humic samples, condensed aromatic structures are evidently of importance. One such structure is exemplified, based on the finding that 1,2,3,5-benzenetetracarboxylic acid is an oxidation product of non-methylated materials only. The methoxyl content (2 %) of humic materials is due to a limited number of structures, mainly those giving 2-methoxy-1,4-benzenedicarboxylic acid and 6-methoxy-1,2,4-benzenetricarboxylic acid by oxidation. Structures with 1,2-dimethoxy

substitution on the benzene ring are not present. The possibility of small amounts of 1-methoxy-2-hydroxy substituted structures cannot be excluded. 1,2-Dihydroxy substituted aromatic entities contribute significantly to the humic structure (30 – 50 % of the oxidation products) and are twice as abundant as the hydroxy substituted structures. The phenolic entities are linked together by aliphatic chains or attached to cycloaliphatic rings, the most prominent chain length is 6 – 8 CH_2 units. The aliphatic part of the humic material amounts to 17 – 44 % of the oxidation products from methylated materials.

The classical method of fractionating soil organic matter involves extraction with bases to give fractions like fulvic acids, humic acids, and humin. This method and the further separation into subfrations are reviewed by Kononowa.[1] Very little is known about the detailed chemical structure of these fractions.

From a naturally occurring fulvic acid, small amounts of 21 different phenolic and benzenecarboxylic acids were detected by chromatographic separations.[2] Recently, permanganate oxidation of methylated fulvic and humic acids and humin was shown to give a mixture of 63 – 76 % benzenecarboxylic, 32 – 20 % phenolic and 5 – 4 % aliphatic carboxylic acids.[3] A comparison has been performed between the yields of the different oxidation products resulting from permanganate oxidation of methylated and non-methylated acid resistant humic residue.[4] The results demonstrated that more structural information was obtained by this method than by oxidation of methylated samples alone.

The purpose of this work has been to investigate the composition of different humic fractions by oxidation of both methylated and non-methylated samples.

A comparison has been made between original raw humus (sample A) and its fractions: the alkali insoluble humic residue, humin, (sample B); the alkali extracted, acid insoluble humic acid (sample C), and the alkali extracted, acid soluble fulvic acid. The last mentioned material was separated into two fractions, the high molecular weight matter (fraction D) and the material able to pass through the dialysis bag used for purification (fraction E). Part of each fraction was methylated with diazomethane to give fractions AM, BM. a.s.o.

The yield of the different fractions was humin (B) 61 %, humic acid (C) 12 %, fulvic acid (D) 11 %, and low molecular weight fulvic acid (E) 9 %. The analytical data, Table 1, show that humic acid contains more C, N, and methoxyl than the two fulvic acids. After methylation, both fraction C and E have higher methoxyl contents than fraction D. Since the O content (calculated by difference) in fractions D and E is higher than in fraction C, the data indicate that fraction D contains more oxygen-containing functional groups which fail to react with diazomethane in methanol than do fractions C and E. This is verified by the carbohydrate analysis which demonstrates that twice as much carbohydrate (43 %) is present in fraction D as in fractions C and E.

Table 1. Elementary composition, methoxyl, carbohydrate, and ash contents of raw humus (A), humin (B), humic acid (C), fulvic acid (D), and low molecular weight fulvic acid (E).

Element or group	A	B	C	D	E
C	36.6	34.3	49.6	40.5	40.7
H	4.76	4.37	5.97	5.78	6.06
N	1.25	0.83	2.98	1.72	1.80
OCH_3	2.1	2.0	2.3	1.8	
Carbohydrate	22.8	20.0	17.3	42.7	21.7
Ash	31.0	31.0	5.8	6.3	7.7
OCH_3 after methylation	11.0	10.6	20.2	14.1	24.2

Prior to oxidation the water soluble fulvic acids, samples D and E, were investigated by gel separation. Sephadex G25 was used with water as eluent. According to the chromatogram. Fig. 1, sample D consisted of high molecular weight compounds. The difference in the two samples seemed obvious, al-

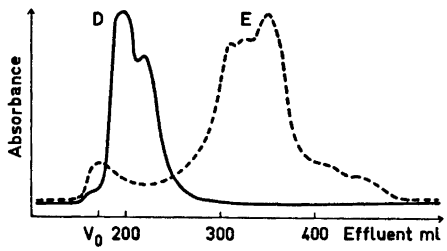

Fig. 1. Separation of high (D) and low (E) molecular weight fulvic acids on Sephadex G25.

though, because of the possibility of adsorption of humic compounds to the dextran gel, as shown by Lindquist,[5] the E sample might not necessarily contain low molecular weight compounds only. By gel separation of the methylated sample E, (sample EM) only 6 % of the fraction was eluted as low molecular weight material, *i.e.* at the same elution volume as methylbenzoate. Sephadex LH20 was used with methanol as eluent. Only trace amounts of the lower molecular weight fraction, and nothing of the other fractions isolated by separation on Sephadex LH20, was eluted from a gas chromatographic column programmed from 150° to 300°C. The results demonstrate that the major part of sample E also consists of relatively high molecular weight or nonvolatile compounds, even after methylation with diazomethane.

The original raw humus and its fractions, both methylated and non-methylated, were oxidized with potassium permanganate at 90°C at pH 9–10. The oxidation products were extracted, methylated, and separated by preparative thin-layer chromatography, followed by preparative gas chromatography.

Table 2. Yields of compounds isolated from methylated and non-methylated humic fractions after oxidation. A, raw humus; B, humin; C, humic acid; D, fulvic acid; and E, low molecular weight fulvic acid. Methylated fractions are marked with M. Yields refer to 100 g samples.

Component No	Compounds	AM mg	BM mg	CM mg	DM mg	EM mg	A mg	B mg	C mg	D mg
1	1,2-Benzenedicarboxylic acid dimethyl ester			13	18			2		
2	1,2,3-Benzenetricarboxylic acid trimethyl ester			17	17	27	28	25	6	14
3	1,2,4-Benzenetricarboxylic acid trimethyl ester	46	40	79	68	35	70	60	110	110
4	1,2,3,4-Benzenetetracarboxylic acid tetramethyl ester	59	40	69	66	43	150	62	100	68
5	1,2,3,5-Benzenetetracarboxylic acid tetramethyl ester					12	75	47	93	68
6	1,2,4,5-Benzenetetracarbozylic acid tetramethyl ester	29		23	42	17	37	31	56	40
7	Benzenepentacarboxylic acid pentamethyl ester	24		26	33	45	61	33	97	36
8	Benzenehexacarboxylic acid hexamethyl ester					17	12		8	
9	4-Methoxy-benzoic acid methyl ester	150	250	450	270	210				
10	3-Methoxy-1,2-benzenedicarboxylic acid dimethyl ester	130	120	100	49	50				
11	4-Methoxy-1,3-benzenedicarboxylic acid dimethyl ester	130	110	250	140	120				
12	2-Methoxy-1,4-benzenedicarboxylic acid dimethyl ester	29			38	5	7	7	15	23
13	4-Methoxy-1,2,3-benzenetricarboxylic acid trimethyl ester	250	170	160	79	15				
14	3-Methoxy-1,2,4-benzenetricarboxylic acid trimethyl ester	110	95	72	52	43				
15	5-Methoxy-1,2,4-benzenetricarboxylic acid trimethyl ester			81						
16	6-Methoxy-1,2,4-benzenetricarboxylic acid trimethyl ester	87	10	81	55	46	15	25	51	27
17	2-Methoxy-1,3,5-benzenetricarboxylic acid trimethyl ester			22	17	32				1
18	5-Methoxy-1,2,3,4-benzenetetracarboxylic acid tetramethyl ester	52	23	32	30	40				
19	4-Methoxy-1,2,3,5-benzenetetracarboxylic acid tetramethyl ester	120	84	110	65	75		3		4
20	3-Methoxy-1,2,4,5-benzenetetracarboxylic acid tetramethyl ester		6	20	24	18				
21	Methoxy-benzenepentacarboxylic acid pentamethyl ester	8			7	20				
22	3,4-Dimethoxy-benzoic acid methyl ester	330	600	960	510	460				
23	3,4-Dimethoxy-1,2-benzenedicarboxylic acid dimethyl ester	96	90	69	36	26				
24	4,5-Dimethoxy-1,2-benzenedicarboxylic acid dimethyl ester	390	260	650	210	330				
25	4,5-Dimethoxy-1,3-benzenedicarboxylic acid dimethyl ester	210	390	710	540	220				
26	4,5-Dimethoxy-1,2,3-benzenetricarboxylic acid trimethyl ester	310	280	240	150	81				
27	Dimethoxy-benzenetricarboxylic acid trimethyl ester	140	110							
28	Dimethoxy-benzenetetracarboxylic acid tetramethyl ester	17	17		13	13				
29	Chloro-3,4-dimethoxy-benzoic acid methyl ester	140	240	60	120	32				
30	Dichloro-3,4-dimethoxy-benzoic acid methyl ester				2	3				
31	Succinic acid dimethyl ester	19	5	42	170	260			18	
32	Glutaric acid dimethyl ester	60	15	73	110	310	6	4	61	

Table 2. Continued.

33	Adipic acid dimethyl ester	180	87	180	230	390	65	44	200	
34	Pimelic acid dimethyl ester	190	160	390	160	370	150	130	240	
35	Suberic acid dimethyl ester	160	170	410	95	230	200	170	370	33
36	Azelaic acid dimethyl ester	160	170	420	110	170	190	120	310	54
37	Sebacic acid dimethyl ester						50	30	110	22
38	Hendecaneidioic acid dimethyl ester						26	21	61	17
39	Dodecanedioic acid dimethyl ester						23	22	34	12
40	Tridecaneidioic acid dimethyl ester						8	14	11	7
41	Tetradecanedioic acid dimethyl ester						3	8	5	6
42	Dimethoxy-carbomethoxy-diazine I	200	140	37	36	120				
43	Dimethoxy-carbomethoxy-diazine II	130			23	130				

Table 3. Groups of compounds isolated from methylated and non-methylated humic fractions after oxidation. Yields refer to 100 g samples. The contribution of each group relative to the total amount of identified compounds is given in per cent.

Compounds		Fraction								
		AM	BM	CM	DM	EM	A	B	C	D
Benzenepolycarboxylic acid polymethvl esters	g	0.16	0.08	0.23	0.24	0.20	0.43	0.26	0.47	0.34
	%	4	2	4	7	5	37	31	24	63
Methoxy-benzenepolycarboxylic acid poly-methyl esters	g	1.07	0.87	1.38	0.83	0.67	0.02	0.03	0.07	0.05
	%	27	23	23	23	17	2	3	4	9
Dimethoxy-benzenepolycarboxylic acid poly-methyl esters	g	1.63	1.99	2.69	1.58	1.17				
	%	41	54	46	44	30				
Dicarboxylic acid dimethyl esters	g	0.77	0.62	1.52	0.88	1.73	0.72	0.56	1.42	0.15
	%	20	17	26	24	44	61	66	72	28
Dimethoxy-carbomethoxy-diazines	g	0.33	0.14	0.04	0.06	0.15				
	%	8	4	1	2	4				
Total	g	3.96	3.70	5.85	3.59	3.92	1.17	0.85	1.96	0.54
	%	100	100	100	100	100	100	100	100	100

The chemical structure and yield of all components identified are shown in Table 2. The results refer to 100 g samples where fractions A and B contain 31 % ash, and fractions C, D, and E show ash contents of 5.8 – 7.7 %. The identity of each compound was established by comparing thin-layer and gas chromatographic retention data, IR and mass spectra with those of known standards. No standards were available for compounds 18, 27 – 30, and 38 – 43. In these cases identification was tentatively based on the spectra obtained.

The infrared spectra of compounds 18 and 27 – 30 indicate that they all are aromatic esters. The molecular ion is easily recognized in all the mass spectra and the base peak is at M – 31. The fragmentation pattern of compound 18 is similar to that of compounds 19 and 20. The same relation is found between the mass spectra of compounds 26 and 27. Compounds 29 and 30 also show the characteristic "doublet" of the molecular ion and the base peak (M – 31), and with intensities indicating a mono- and dichloro substituted compound, respectively.

Compounds 28 – 41 give the infrared spectra typical of dicarboxylic acid dimethyl esters. The base peak in the mass spectra is as M – 31, and the molecular ion is of low intensity. In all spectra, a strong peak at *m/e* 74 is found; this is due to γ-hydrogen rearrangement of the methyl ester. Gas chromatographic retention data support the identity of compounds 38 – 41.

By mass spectroscopy the molecular formula of compounds 42 and 43 are determined to $C_8H_{10}N_2O_4$(M.W. 198). According to NMR spectra both compounds contain two methoxyl and one carbomethoxy group. The carboxyl absorption is verified by their IR spectra (1720 cm^{-1}). The last proton resonates at $\tau = 2.17$ ppm and $\tau = 2.57$ ppm for compounds 42 and 43, respectively. The results therefore indicate a substituted diazine structure, although the position of the two nitrogen atoms in the ring is uncertain.

The components isolated can be classified as benzenecarboxylic acid methyl esters (compounds 1 – 8), methoxy-benzenecarboxylic acid methyl esters (compound 9 – 21), dimethoxy-benzenecarboxylic acid methyl esters (compounds 22 – 30), aliphatic dicarboxylic acid dimethyl esters (compound 31 – 41), and dimethoxy-carbomethoxy-diazines (compounds 42 – 43). The results have been summarized in Table 3.

DISCUSSION

For all the isolated fractions the most prominent benzenecarboxylic acid methyl esters are compounds 4 and 3, followed by the methyl ester of benzenepentacarbozylic acid. These structures are schematically represented by I, II, and III in Fig. 2. The only exception is the methylated humin fraction (BM) where compounds 6 and 7 are not present in detectable amounts. The same is the case with compound 2. Disregarding these exceptions, the differences found between the humic fractions isolated were smaller than the differences introduced between methylated and non-methylated fractions. Especially noteworthy is the absence of compound 5 in methylated fractions (except for the small amount found in fulvic acid (EM)). This indicates the presence of condensed structures such as IV of Fig. 2. Depending on whether this structure has been methylated or not prior to oxidation, the products

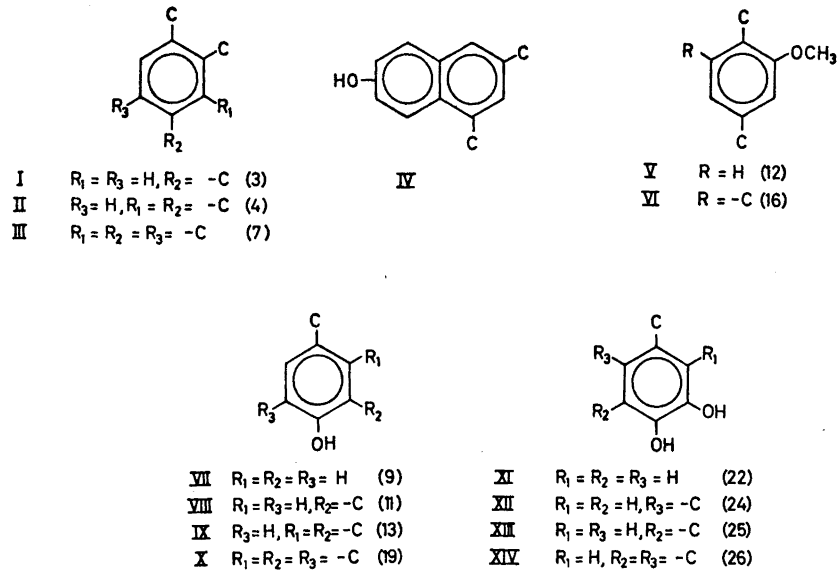

Fig. 2. Some of the major structural units in humus and humic fractions. The symbol —C denotes carboxyl or a group giving carboxyl by oxidation. The number in brackets gives the compound formed by oxidation and refers to Table 2.

will be a methoxy-benzenecarboxylic acid or 1,2,3,5-benzenetetracarboxylic acid. Different substitution and/or different ring systems might yield the oxidation products identified depending on whether the phenolic structure is methylated or not. The importance of these condensed systems, also possibly similar to those believed to be present in lignin,[6,7] is shown by the fact that the yields of benzenecarboxylic acids in general are higher for the unmethylated samples relative to the methylated samples (Tables 2 and 3).

Methoxy-benzenecarboxylic acid methyl esters are found in significant amounts among the products from oxidation of methylated samples only. Since the only methoxy derivatives found for the non-methylated samples are compounds 12,16, 17, and 19, at least part of the methoxyl content of the humic fractions (Table 1) is present in structures giving these four methoxy-benzenecarboxylic acids by oxidation. Whether the humic fractions are methylated or not prior to oxidation, the yields of compounds 12 and 16 remain fairly constant, this in contrast to the yields of the other methoxy-benzenecarboxylic acid methyl esters isolated (Table 2). This indicates that nearly all the methoxy substituted structures identified are originating from humic phenols (VII—XIV, Fig. 2). It follows, further, that the methoxyl content in humic fractions is due to a limited number of structures only, mainly those (V, VI of Fig. 2) giving compounds 12 and 16, respectively, by oxidation. Of course, also structures containing 1-methoxy-2-hydroxy substitution on the benzene ring may contribute to the methoxyl content of humus, but the data given here fail to clarify this particular question. Di-

methoxy substitution on benzene rings in humus is definitely ruled out by the absence of dimethoxy-benzenecarboxylic acids among the oxidation products from non-methylated fractions.

For all the isolated fractions, compound 9 is the most prominent among the methoxy-benzenepolycarboxylic acid polymethyl esters, followed by compounds 11, 13, 10, and 19. According to Table 3 the total yield of this group of compounds is remarkably constant for the humic fractions BM, CM, and DM (fraction EM is somewhat lower) with regard to their different chemical properties.

From Table 3 it is evident that structures with 1,2 dihydroxy (or possibly 1-methoxy-2-hydroxy) substitution on the benzene ring are contributing significantly to the structure of the raw humus used in this study, yielding 30 – 54 % of the oxidation products. The different aromatic acids isolated have different stability to alkaline permanganate oxidation;[7] their contribution to the humic structure is, therefore, not necessarily reflected by their yields.

Two main features are evident from Table 3, namely the increasing contribution of dimethoxy derivatives for fractions BM, CM, and DM relative to AM, and the decreasing relative amount from fraction BM to fraction EM (from 54 – 30 %). The oxidation of the different fractions is performed under the same condition, and thus believed to give comparable results, even though the possibility exists that the oxidation is influenced by the different solubilities of the humic fractions. The observed yields of samples AM and BM indicate that the alkali treatment of raw humus introduces free phenolic groups available for later methylation. The relative contributions of compounds 22 and 25 both increase from sample AM to BM (from 8.3 to 15.8 % and from 5.3 to 10.5 % of the total yield, respectively). The compounds 23, 24, and 26 show no significant increase. The results, therefore, indicate that structures producing compounds 22 and 25 by oxidation partly exist as 1,2 dihydroxy (1-methoxy-2-hydroxy) substituted entities and partly as structures where the one phenolic group is bound for example in an ester linkage. The other oxidation products in this group probably exist as *o*-diphenols in humus. Therefore, compound 27 most probably is 5,6-dimethoxy-1,2,4-benzenetricarboxylic acid trimethyl ester, and compound 28 5,6-dimethoxy-1,2,3,4-benzenetetracarboxylic acid tetramethyl ester.

Compounds 29 and 30 have previously been found among the oxidation products from a raw humus, hydrolyzed with hydrochloric acid,[4] and were therefore believed to be an artefact from that treatment. However, if 3,4-dimethoxy-benzoic acid and manganese dioxide in water are treated according to the procedure for oxidation mixtures in this work, both compounds 29 and 30 are synthetized if the reaction mixture gets too acidic.[8] Both components are therefore artefacts from the isolation procedure, and should correctly be calculated as component 22, which is the most prominent of all the oxidation products found.

As seen from Table 3 the percentage of dimethoxy-benzenecarboxylic acid methyl esters decrease from fraction BM to EM. With few exceptions this decrease is reflected among all compounds 22 – 26. Thus, as for the methoxy substituted components, neither does the dimethoxy derivatives show any

definite difference between the various humic fractions based on the relative amount of the different dimethoxy-benzenecarboxylic acid methyl esters.

The percentage of dicarboxylic acid dimethyl esters increases from fraction BM to EM with a possible exception for fraction DM. This indicates that the more soluble humic fractions, *i.e.* the fulvic acids, contain more aliphatic units than the less soluble humic acids and humin. By urea adduct formation, only straight chain dicarboxylic acids were shown to be present among the oxidation products from the same humic material after acid hydrolysis.[4] The stability of sebacic acid when oxidized at the same conditions as in this study resulted in a recovery of 43 % material, which, after methylation, consisted of 90 % sebacic acid dimethyl ester and 3.6 % suberic acid dimethyl ester together with decreasing amounts of the lower homologs down to succinic acid dimethyl ester.[4] The actual contribution of the aliphatic part found here is, therefore, definitely larger than indicated by the yields and must also include the different chain lengths.

The accuracy of the yields for compound 31, and also to some degree compound 32, should not be overemphasised as, unavoidably, some losses by evaporation occurred during the isolation procedure. Except for these two components, there is a general shift in yields towards shorter chain lengths from fraction BM to EM (compounds 36 – 33 in Table 2). The increase in the aliphatic part of the more soluble humic fractions is thus mainly due to an increase of shorter chain lengths, this at the expense of the content of 1,2-dihydroxy substituted entities.

The long chain dicarboxylic acid dimethyl esters compounds 37 – 41, are products of unmethylated material only. This is in accordance with earlier findings, and supports the assumption of phenolic components in humus being linked together by aliphatic chains or, to a smaller extent, cycloaliphatic rings attached to one phenolic structure.[4] Oxidation of the phenolic structure will first break down the benzene ring thus giving an aliphatic carboxylic acid only. Methylation of the phenolic structure, followed by oxidation, will, due to the greater stability of the methyl ether, more easily break the aliphatic C – C bonds. If the bond between the α and β carbon atom is oxidized, the products will be one methoxybenzene carboxylic acid plus one aliphatic carboxylic acid, at least two CH_2 units shorter than the oxidation product from the non-methylated structure. If the aliphatic chain links two penolic structures together, the effect of methylation is doubled. According to the data given in Table 2 the most prominent chain lengths consist of 6 – 8 CH_2 units with predominance of shorter chains in the more soluble humic fraction. Still, the explanation fails to comply well with the complete absence of compounds 31 – 34 for fraction D and its low yield of dicarboxylic acid (Table 3).

Compounds 42 and 43 are found among the oxidation products of methylated materials only. The question arises whether these compounds are artefacts due to isolation procedure. In general, 70 – 80 % of the nitrogen in soil organic matter can be accounted for, mainly as amino acids, amino sugars and ammonia after acid hydrolysis. The chemistry of the residual nitrogen is not known, although several teories have been forwarded.

If the diazine ring is part of the humic structure, one would expect it to appear also with other methylation agents, for instance dimethyl sulphate.

This is not the case, as repeated methylations of humin by dimethyl sulphate failed to give compounds 42 and 43 among the methylated oxidation products. Diazomethane is known to increase the nitrogen content of humic materials,[4,9] even if the increase for the fractions used in this study was too small to be significant (except for fraction DM). Diazomethane adds to double bonds to give five-membered rings with nitrogen in neighbouring position.[10] These components are usually labile at higher temperatures. Diazomethane might add to some specific structures in humus with, for example, subsequent rearrangements to six membered rings during oxidation or in the gas chromatograph. Whether this is the case or not is hard to decide from the present information. This point will probably be better understood when more structural information is available about the position of the nitrogen atoms in the diazine ring.

Low in methoxyl content (Table 1), fraction D was repeatedly treated with diazomethane in order to increase the methoxyl content. This fraction was also the only one responding with significant increase in the nitrogen content (8 %) to methylation. In spite of this fact, the yield of compound 42 and 43 is relatively low for fractions DM. The origin of the dimethoxy-carbomethoxy-diazines is, therefore, still a matter of conjecture, although, most probably, they are artefacts from the diazomethane treatment.

The results given here clearly demonstrate the complexity of humic materials, and also the relatively slight differences between the various humic fractions.

EXPERIMENTAL

Material. The ether and ethanol extracted raw humus, investigated earlier,[11] was also used in this study, sample A.

A sample of the humus (150 g) was percolated at room temperature with 0.5 N sodium hydroxide until an almost colorless eluate was obtained (2.5 l for 4 days). In order to reduce oxygen absorption and condensation reactions,[1] the whole extraction unit was kept under nitrogen, and 9 N sulphuric acid was continuously added to the eluate to maintain a pH of 3 – 4. The residue was repeatedly suspended in dilute sulphuric acid at pH 2 – 3 and filtrated to exchange sodium ions, and then thoroughly washed with distilled water and dried. Sample B, yield 91 g.

To isolate the humic acids, the extract was adjusted to pH 1.5 with sulphuric acid and centrifuged. The precipitate was stirred with water and then again centrifuged. Finally, the precipitated humic acid, suspended in water, was dialyzed against distilled water until free of sulphate ions. Yield of dry matter, sample C, 18 g.

The filtrate from humic acid precipitation was concentrated to 500 ml and dialyzed against distilled water (Kalle dialysis bag) until the dialyzate was negative on sulphate ions. The desalted material gave the higher molecular weight part of fulvic acid after drying, sample D. Yield 16 g.

The fulvic acid dialysate was evaporated to 50 ml at 30°C, 12 mmHg, and adjusted to pH 2 – 3 by adding sodium bicarbonate. The mixture was treated with 200 ml of methanol, and the precipitate, mainly sodium sulphate, was filtered off. The filtrate was concentrated and again treated with methanol (200 ml) and filtered. The process was repeated several times, and gave a methanol solution of fulvic acid sample E. This sample could not be completely dried without destructions taking place. It was therefore methylated with diazomethane before drying. Yield sample EM 14 g.

Methylation. The dried and ground samples (5 – 10 g) were suspended in 250 ml of methanol and exhaustively treated with diazomethane in ether at 5°C until maximum methoxyl content (1 – 3 days). The methylation gave no significant rise in nitrogen content (less than 5 %) except for fraction D, where the increase was 7.5 %.

To sample B (10 g), suspended in 250 ml dioxane + 150 ml water at 65°C, was added droppwise 33 ml dimethyl sulphate and a solution of 20 g sodium hydroxide in 80 ml water under stirring. After 2 h the humic sample was filtered off, rinsed with water, and again methylated as above.

Carbohydrate analysis. The samples (50 mg) were subjected to hydrolysis in 10 ml 0.5 N hydrochloric acid for 5 h. After filtration the solution was diluted to 250 ml. The hydrolysis dissolves a major part of the soil carbohydrates and also almost eliminates interfering background from humic substances. Aliquots (1 ml) of the diluted filtrate were analysed for carbohydrate according to the phenol-sulphuric acid method (Table 1).

Each hydrolysate was concentrated to 1 ml at 12 mmHg and 40°C. 1 and 10 μl aliquots were spotted on Whatman No. 1 paper and developed by the descending technique in ethyl acetate : acetic acid : water (3:3:1) for 24 h. After drying, the spots were developed by spraying with aniline phthalate reagent and drying at 105°C. For fractions A, B, C, and D the chromatograms appeared identical. Arabinose, galactose, glucose, mannose, rhamnose, and xylose were identified and estimated to be present in approximately equal amounts. Smaller amounts of fucose and ribose were also present together with higher molecular weight carbohydrate material, as demonstrated earlier.[11] Fraction E contained the same carbohydrates as mentioned above but obviously in smaller amounts.

Oxidation. The sample (5 – 10) g was suspended in 250 – 500 ml of water containing 5 – 10 g of sodium carbonate, to which was added dropwise a solution of 5 % potassium permanganate under stirring at 90°C, until no more reagent was consumed (6 – 8 h). The reaction mixture was acidified with hydrochloric acid and sodium bisulfite added to reduce manganese dioxide. The warm solution was filtered and the oxidation residue dried and weighed. The filtrate (250 – 500 ml) was extracted 4 times with 200 ml of chloroform : acetone (1:1) and 4 times with 200 ml of ethyl acetate. Each extract was dried with sodium sulphate, evaporated to dryness, and the yield recorded. The extracted acids were dissolved in methanol and methylated with diazomethane. Avoiding high temperatures, the ester mixture was taken to dryness and the yield recorded.

Yields: 10.0 g of fraction AM: 0.93 g acids, 0.85 g esters, and 4.5 g oxidation residue; 10.0 g BM: 0.86 g acids, 0.85 g esters, 4.7 g residue; 10.0 g CM: 1.14 g acids, 1.05 g esters, 0.4 g residue; 10.0 g DM: 0.66 acids, 0.67 g esters, 0.01 g residue; 8.9 g EM: 1.02 g acids, 0.83 g esters, 0.01 g residue; 10.0 g A: 0.61 g acids, 0.36 g esters 3.6 g residue; 10.0 g B: 0.31 g acids, 0.24 g esters, 4.3 g residue; 6.1 g C: 0.48 g acids, 0.41 g esters, 0.02 g residue; 5.0 g D: 0.18 g acids, 0.13 g esters, and 0.01 residue.

Chromatographic techniques. Gel fractionation of samples D and E was carried out on a 2.5 × 85 cm column with Sephadex G25. Water was used as eluent at a flow rate of 12 ml/h (Fig. 1). Sample EM was investigated on a column of Sephadex LH 20 (2.5 × 90 cm) in methanol, flow rate 16 ml/h. The eluates were continuously monitored at 254 mμ.

The ester mixtures obtained by methylation of the extracted oxidation products were separated by preparative TLC on aluminum oxide (activated at 150°C for 20 h, thickness of coating absorbent 0.5 mm). The solvent system used was toluene : ethylacetate (3:1). After separation, each plate was inspected under a UV lamp and a number of fractions were marked out (3 – 5), scraped off the plate and extracted with ethyl acetate.

Each subfraction was further separated by preparative gas chromatography (Aerograph model 1520 B_1 TC detector, 300 × 0.4 mm s.s. column packed with 4 % OV-17 on Chromosorb W HMDS, 60/80 mesh, programmed from 150 to 300°C at a rate of 10°C per min, helium being used as carrier gas). The material eluted from the column, according to recorder response, was collected in glass tubes, and analyzed by IR as micro KBr pellets on a Unicam SP 200 spectrophotometer equipped with a beam condenser, and by mass spectrometry on a Perkin Elmer Hitachi RMU-6N mass spectrometer equipped with a heated direct inlet probe.

Quantitative estimates of each major compound were made by measuring peak areas on the gas chromatogram by triangulation, and by comparing these with the peak area of reference compounds injected in known amounts. The origins of the reference compounds were identical to those described previously.[2,4]

Acknowledgments. This work was supported by the *Agricultural Research Council of Norway*. Thanks are due to Ing. W. Sørensen and Mr. W. George for technical assistance, and to cand. real. N. Gjøs, Sentralinstitutt for Industriell forskning, Oslo, for mass spectrometric analyses. Cand. real. P. Kolsaker, Kjemisk Inst., Universitetet i Oslo, is

greatly acknowledged for the NMR spectra and their interpretation, and for the high resolution mass spectra.

REFERENCES

1. Kononova, M. M. In *Soil Organic Matter*, Pergamon, Oxford 1966, p. 14.
2. Ogner, G. and Schnitzer, M. *Can. J. Chem.* **49** (1971) 1053.
3. Khan, S. U. and Schnitzer, M. *Can. J. Soil Sci.* **52** (1972) 43.
4. Ogner, G. *Soil Sci.* (1973). *In press.*
5. Lindquist, I. *Acta Chem. Scand.* **21** (1967) 2567.
6. Lai, Y. Z. and Sarkanen, K. V. In Sarkanen, K. V. and Ludwig, C. H., Eds., *Lignins; Occurrence, Formation, Structure and Reactions*, Wiley-Interscience, New York 1971, p. 165.
7. Chang, H.-M. and Allan, G. G. In Sarkanen, K. V. and Ludwig, C. H., Eds., *Lignins; Occurrence, Formation, Structure and Reactions*, Wiley-Interscience, New York 1971, p. 433.
8. Ogner, G. *Unpublished results.*
9. Barton, D. H. R. and Schnitzer, M. *Nature* **198** (1963) 417.
10. Huisgen, R., Grashey, R. and Sauer, J. In Patai, S., Ed., *Chemistry of Alkenes*, Interscience, London 1964, p. 826.
11. Ogner, G. *Soil Sci.* **110** (1970) 86.

Received January 8, 1973.

ACTA CHEMICA SCANDINAVICA 27 (1973) 1613–1621

Volatile Constituents of the *Liatris* Species, *L. spicata*, *L. elegans* and *L. gracilis*

KERSTIN KARLSSON, INGER WAHLBERG and CURT R. ENZELL

Research Department, Swedish Tobacco Company, P.O. Box 17 007, S-104 62 Stockholm, Sweden

The volatile fractions obtained from the leaves of *Liatris spicata*, *L. elegans*, and *L. gracilis* have been examined. In all, ninety-three compounds were identified using combined gas chromatography-mass spectrometry. They include mono- and sesquiterpenoids, norisoprenoids, α, β-unsaturated straight-chain aldehydes and ketones, and fatty acids; the majority of them are common to all three species. A chemical comparison with three previously examined *Carphephorus* species is made and the chemotaxonomic significance of the results is discussed.

Previous studies in this laboratory of various plant materials used as tobacco additives [1–3] have included the volatile fractions obtained from dried leaves of *Carphephorus odoratissimus* (deer tongue), a coumarin-containing plant possessing attractive flavour properties.[4] This study, which was performed on a small scale, resulted in the identification of a large number of components, of which many proved important from a flavour point of view. Subsequent studies primarily directed towards acquiring information on the flavour components of two additional, virtually coumarin-free, *Carphephorus* species have comprised the volatile fractions of *C. corymbosus* and *C. paniculatus*.[5] These, like that of *C. odoratissimus*, were found to be complex and, in all, more than one hundred and thirty constituents were identified.

With this considerable chemical information at hand, which was readily obtained by GLC-MS, it became of obvious interest to evaluate the possible chemotaxonomic significance of these volatile trace components. This was notably so because two of the *Carphephorus* species, *C. odoratissimus* and *C. paniculatus*, had recently been transferred from the genus *Trilisa*, which in turn had previously been generated by division of the genus *Liatris*.[6]

As reported earlier the comparison revealed that the compositions of the volatile fractions derived from these three species were very similar, indicating a close relationship between the plants. However, in view of the limited

information available on volatile trace components present in other plants, definitive conclusions from this isolated study were not considered justified.[5] In order to obtain further data both on the contents of volatiles and on their chemotaxonomic validity, we have now examined three members of the genus *Liatris*, *L. spicata* var. *spicata*, *L. elegans* (Walter) Michaux, and *L. gracilis* Pursh.

RESULTS

In agreement with the findings for the *Carphephorus* species, low-pressure distillation of the acetone extracts of dried leaves of *L. spicata*, *L. elegans*, and *L. gracilis* yielded only small amounts of volatiles having typical "green-leaf" aromas. The distillates were initially partitioned between pentane and water, and the pentane-soluble portions were subsequently divided into neutral and acidic components.

Neutrals. As expected, the neutral volatile fractions derived from the three *Liatris* species proved to be very complex. They were therefore further separated by chromatography on silica gel into two subfractions containing hydrocarbons and oxygenated constituents, respectively, prior to detailed GLC and GLC-MS analyses. Since the present examination was performed on a very small scale, the identifications of the compounds listed in Table 1 are based solely on comparisons of mass spectra and, when possible, retention times with those of authentic samples.

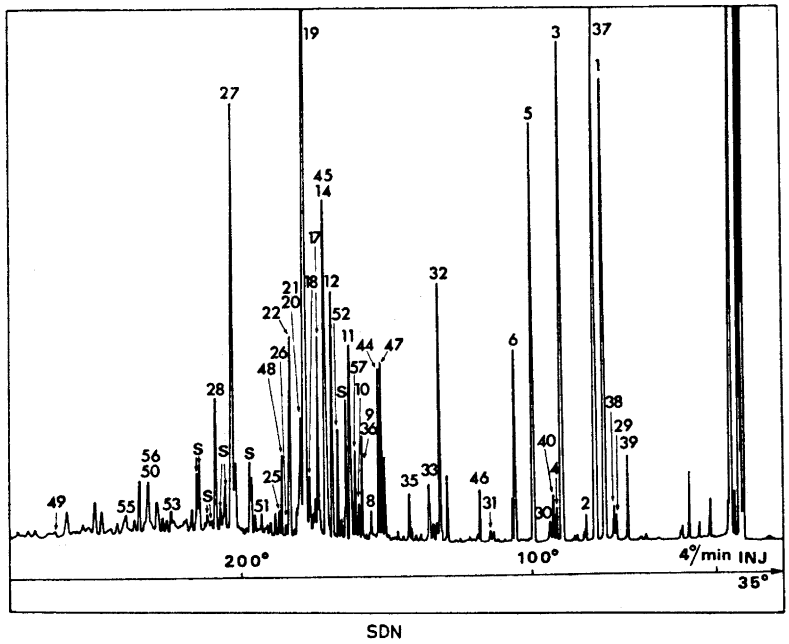

Fig. 1. Gas chromatogram of the neutral fraction from *L. spicata*. Column: HB 2000, 50 m × 0.35 mm.

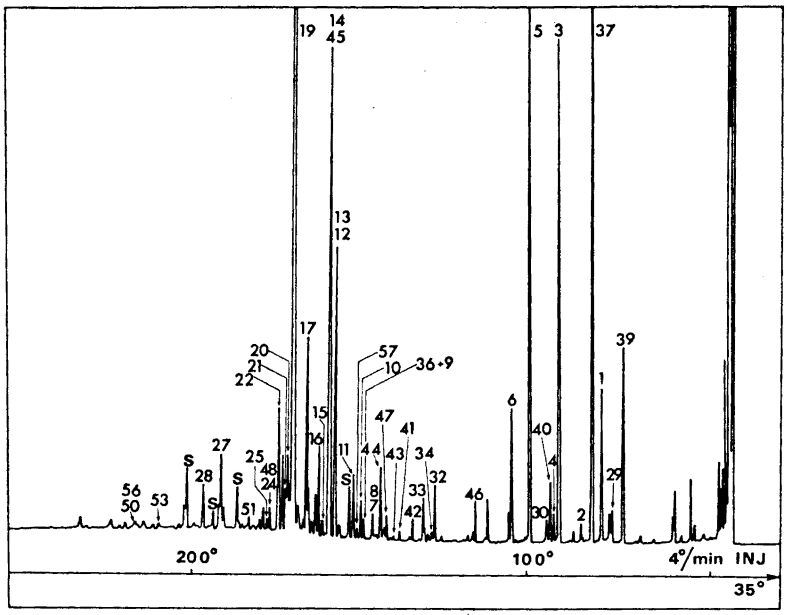

EDN

Fig. 2. Gas chromatogram of the neutral fraction from *L. elegans*. Column: HB 2000, 50 m × 0.35 mm.

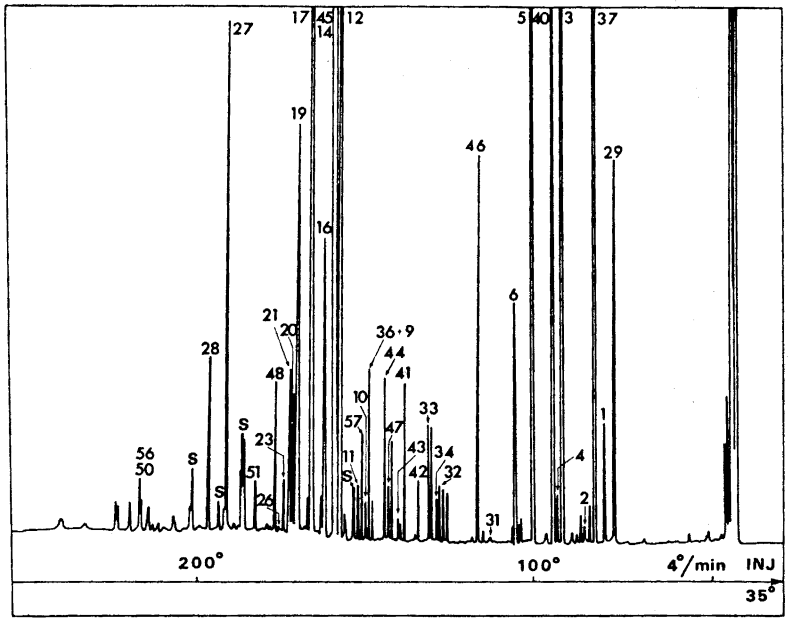

GDN

Fig. 3. Gas chromatogram of the neutral fraction from *L. gracilis*. Column: HB 2000, 50 m × 0.35 mm.

Table 1. Neutral constituents.

Peak No.	Compound	Method of identification			Ref.
		L. spicata	*L. elegans*	*L. gracilis*	
	Hydrocarbons				
	Naphthalene	MS, GLC	MS, GLC	MS, GLC	[a]
1	α-Pinene	MS, GLC	MS, GLC	MS, GLC	26
2	Camphene	MS, GLC	MS, GLC	MS, GLC	26
3	β-Pinene	MS, GLC	MS, GLC	MS, GLC	26
4	Sabinene	MS, GLC	MS, GLC	MS, GLC	26
5	Myrcene	MS, GLC	MS, GLC	MS, GLC	26
6	Limonene	MS, GLC	MS, GLC	MS, GLC	26
	p-Cymene	MS, GLC	MS, GLC	MS, GLC	26
7	α-Cubebene		MS		27
8	δ-Elemene	MS	MS		27
9	α-Ylangene	MS, GLC	MS, GLC	MS, GLC	28
10	α-Copaene	MS, GLC	MS, GLC	MS, GLC	27
11	β-Bourbonene	MS, GLC	MS, GLC	MS, GLC	27
12	β-Elemene	MS, GLC	MS, GLC	MS, GLC	27
13	β-Ylangene		MS, GLC		[a]
14	Caryophyllene	MS, GLC	MS, GLC	MS, GLC	29
15	β-Copaene	MS, GLC	MS, GLC		[a]
16	γ-Elemene		MS	MS	27
17	α-Humulene	MS, GLC	MS, GLC	MS, GLC	27
18	γ-Murolene	MS, GLC			27
19	Germacrene D	MS, GLC	MS, GLC	MS, GLC	[a]
20	α-Muurolene	MS, GLC	MS, GLC	MS, GLC	27
21	β-Bisabolene	MS	MS	MS	27
22	δ-Cadinene	MS, GLC	MS, GLC		27
23	γ-Cadinene			MS, GLC	27
24	4,10-Dimethyl-7-isopropyl-bicyclo[4.4.0]-1,4-decadiene		MS, GLC		27
25	Calamenene	MS, GLC	MS, GLC		[a]
	α-Calacorene	MS	MS		[a]
	Ethers				
26	Thymohydroquinone dimethyl ether	MS, GLC		MS, GLC	[a]
27	β-Caryophyllene epoxide	MS, GLC	MS, GLC	MS, GLC	[a]
28	Humulene epoxide II	MS, GLC	MS, GLC	MS, GLC	[a]
	Aldehydes				
29	Hexanal	MS, GLC	MS, GLC	MS, GLC	[a]
	Heptanal			MS, GLC	[a]
	3-Pentenal	MS		MS	30
30	2-Hexenal	MS, GLC	MS, GLC		[a]
31	2-Heptenal	MS, GLC		MS, GLC	31
32	2,4-Heptadienal	MS	MS	MS	[a]
33	2,4-Heptadienal	MS	MS	MS	[a]
	2,4-Decadienal	MS			32
34	Benzaldehyde		MS, GLC	MS, GLC	[a]
	3-Phenylpropanal	MS, GLC			33
35	α-Campholene aldehyde	MS, GLC			34
36	Myrtenal	MS	MS	MS	35
	Ketones				
	Pentan-2-one	MS	MS	MS	30
	2-Methyl-3,6-heptadione	MS			[a]

Table 1. Continued.

37	Mesityloxide	MS, GLC	MS, GLC	MS, GLC	*a,b*
38	Pent-*trans*-3-en-2-one	MS			36
39	4-Methylpent-4-en-2-one	MS	MS	MS	Tentative
40	Hex-3-en-2-one	MS	MS	MS	Tentative
	Hept-3-en-2-one			MS	37
	Oct-3-en-2-one			MS	37
41	Non-3-en-2-one		MS	MS	37
42	Octa-3,5-dien-2-one		MS	MS	17
43	Octa-3,5-dien-2-one		MS	MS	17
	5-Methylhex-3-en-2-one			MS	37
44	3,5-Dimethylcyclohex-2-enone	MS	MS	MS	Tentative
45	2,2,6-Trimethylcyclohex-5-enone	MS	MS	MS	38
	6-Methylheptanone	MS, GLC	MS, GLC	MS, GLC	*a*
46	6-Methylhept-5-en-2-one	MS, GLC	MS, GLC	MS, GLC	37
47	6-Methylhepta-3-*trans*-5-*trans*-dien-2-one	MS, GLC	MS, GLC	MS, GLC	*a*
48	Geranylacetone	MS, GLC	MS, GLC	MS, GLC	39
49	Farnesylacetone	MS, GLC	MS, GLC		*a*
50	Hexahydrofarnesylacetone	MS, GLC	MS, GLC	MS, GLC	*a*
51	β-Ionone	MS, GLC	MS, GLC	MS, GLC	*a*
52	Verbenone	MS			35
	1-Phenylpropan-2-one			MS	Tentative
	4-Phenyl-but-3-en-2-one	MS			40
	Esters and lactones				
53	Isopropyl myristate	MS, GLC	MS, GLC		*a,b*
54	Benzyl benzoate			MS, GLC	*a*
55	Coumarin	MS, GLC			*a*
56	Dihydroactinidiolide	MS, GLC	MS, GLC	MS, GLC	41
	Alcohols				
57	*trans*-Pinocarveol	MS	MS	MS	27
	2-Phenylethanol	MS			*a*

[a] Mass spectrum of an authentic sample. [b] Probably an artefact formed from the acetone used in the extraction.

A comparison of the gas chromatograms shown in Figs. 1 – 3 reveals immediately that the neutral fractions from the three *Liatris* species are indeed very similar. They contained predominantly mono- and sesquiterpene hydrocarbons, while oxygenated compounds of terpenoid and non-terpenoid origin were present in fairly low concentrations. The main differences between the fractions were encountered as differences in the relative concentrations of certain constituents as indicated below.

The macrocyclic and labile germacrene D, postulated as an important intermediate in the biogenesis of the sesquiterpenoids,[7] was the major neutral constituent of the distillates from *L. spicata* and *L. elegans*. In harmony with this, the majority of the sesquiterpenes encountered in these two species proved to belong to the germacrane class, *e.g.* β- and δ-elemene, δ-cadinene, α- and γ-muurolene, calamenene, α-calacorene, β-bourbonene, α-ylangene, α- and β-copaene were identified in *L. spicata*. Germacrene D was less pre-

ponderant in the volatile neutral fraction from *L. gracilis*. However, many of the sesquiterpene components were still of germacrene type. In fact, β-elemene was a major constituent of this plant in addition to α-humulene and caryophyllene, both of which belong to the humulane class. The latter two compounds were also present, although in comparatively lower concentrations, in *L. spicata* and *L. elegans*.

β-Caryophyllene oxide and humulene epoxide II proved to be constituents of all three species. The mass spectral results indicated the presence of additional epoxides of the caryophyllane and humulane types as well as a bourbonene epoxide. Since, however, no reference material was available, it has not been possible to characterize them fully at the present stage. The same also applies to the sesquiterpene ketones and alcohols denoted by S in Figs. 1 – 3.

The majority of the monoterpenoids identified were common to all three plants, *i.e.* α- and β-pinene, camphene, sabinene, myrcene, limonene, myrtenal, verbenone and *trans*-pinocarveol. Of these, α- and β-pinene and myrcene were major neutral volatiles of *L. spicata*, whereas only the latter two were of a similarly high concentration in *L. elegans* and *L. gracilis*. The remaining monoterpenoids were present in small amounts only. The aromatic thymohydroquinone dimethyl ether, often encountered in members of the *Compositae*, was found in *L. spicata* and *L. gracilis*.

In accordance with the results for the *Carphephorus species*,[4,5] compounds falling within the groups of nor-isoprenoids, saturated aldehydes, α,β-unsaturated and α,β,γ,δ-diunsaturated aldehydes and ketones were present in all three *Liatris* species, although generally in modest quantities only. The nor-isoprenoids encountered, which in all probability are formed *via* degradation of carotenoids and higher isoprenoids,[8–10] were represented by 6-methylheptanone, 6-methylhept-5-en-2-one, 6-methylhepta-3,5-dien-2-one, geranylacetone, farnesylacetone, hexahydrofarnesylacetone, β-ionone, dihydroactinidiolide, 3,5-dimethylcyclohex-2-enone and 2,2,6-trimethylcyclohex-5-enone. Most or all of these have proved to be constituents of other thoroughly examined plant materials such as tea,[11–13] tomato,[10,14] tobacco,[15] and various essential oils.[16] Similarly, the *Liatris* straight-chain oxo derivatives *trans*-2-hexenal, different stereoisomers of 2,4-heptadienal, 2,4-decadienal, and 3,5-octadienone also occur in tea.[11,17,18] Of these compounds, *trans*-2-hexenal has recently been shown to be derived from linolenic acid in Ginkgo leaves [19] and in black tea,[20] and it hence seems likely that the others may arise in a similar fashion. Since many of these nor-compounds also have aroma properties, it is reasonable to assume that an important portion of the "green-leaf" aroma originates from them.

Acids. The acidic fractions, of which that from *L. elegans* was minute, were examined after methylation using diazomethane. They contained predominantly fatty acids; hexanoic and palmitic acids being the major constituents (*cf.* Table 2). Coumarin was present in a fairly high concentration in the acidic fraction from *L. spicata*.

Concluding remarks. It follows from Tables 1 and 2 and the results presented above that the majority of the compounds are common to all three plants, and that the main differences lie in their relative concentrations. Even if the compari-

Table 2. Acidic constituents.

Compound	Method of identification			Ref.
	L. spicata	*L. elegans*	*L. gracilis*	
Pentanoic acid	MS, GLC		MS, GLC	[a]
Hexanoic acid	MS, GLC	MS, GLC	MS, GLC	[a]
Heptanoic acid	MS, GLC		MS, GLC	[a]
Octanoic acid	MS, GLC	MS, GLC	MS, GLC	[a]
Nonanoic acid	MS, GLC	MS, GLC	MS, GLC	[a]
Decanoic acid	MS, GLC		MS, GLC	[a]
Undecanoic acid	MS, GLC			[a]
Dodecanoic acid	MS, GLC	MS, GLC	MS, GLC	[a]
Tridecanoic acid	MS, GLC			[a]
Tetradecanoic acid	MS, GLC	MS, GLC	MS, GLC	[a]
Pentadecanoic acid	MS, GLC	MS, GLC	MS, GLC	[a]
Hexadecanoic acid	MS, GLC	MS, GLC	MS, GLC	[a]
Heptadecanoic acid	MS, GLC	MS, GLC	MS, GLC	[a]
3-Hexenoic acid	MS			36
Oleic acid	MS, GLC		MS, GLC	[a]
Linoleic acid	MS, GLC	MS, GLC	MS, GLC	[a]
Linolenic acid	MS, GLC	MS, GLC	MS, GLC	[a]
Benzoic acid			MS, GLC	[a]
Thymol	MS			[a]
Coumarin	MS, GLC			[a]

[a] Mass spectrum of an authentic sample.

son is extended to the *Carphephorus* species the similarities prevail, which would indicate that *Carphephorus* and *Liatris* are indeed closely related. However, it may also be that the present set of compounds are not suited for distinguishing between the species investigated. This would mean that neither the enzyme systems involved in the biogeneses of the mono- and sesquiterpene hydrocarbons, nor those associated with the production of the nor-compounds are specific to any of the species.[10,17,18] Although admittedly, little is still known about the occurrence of nor-compounds in nature; the present results and those mentioned above for other thoroughly examined plants seem to indicate that these compounds are in fact widely distributed and accordingly of limited value for chemotaxonomic purposes.

The required differentiation and hence evidence in favour of or against the above arguments might be obtained from a comparison of the polar compounds present in these plants. Thus, current studies have demonstrated that various *Liatris* species including *L. spicata* contain large amounts of sesquiterpene lactones of the germacranolide and guaianolide types.[21–23] These compounds possess the elaborate oxygenation pattern probably necessary for differentiation of the species.

However, it should be emphasized that the sesquiterpene lactones were isolated from extracts of the entire above-ground parts of the *Liatris* species. In contrast, the extracts of the leaves of the three *Liatris* species and *C. corymbosus* and *C. paniculatus* on TLC analysis showed major spots corresponding to non-polar constituents, while only minor spots were ascribed to

sesquiterpene lactones. This is consistent with our previous examination of non-volatiles from the leaves of *C. odoratissimus*, which revealed that relatively non-polar triterpenoids and lignans were the major constituents.[24,25] An investigation of the entire above-ground parts of the *Carphephorus* species is therefore highly desirable, since it might provide the complementary chemical data.

EXPERIMENTAL

Experimental apparatus and techniques have been described previously.[5]

Extraction and separation. Crushed dried leaves of *L. spicata*, *L. elegans*, and *L. gracilis* were extracted with acetone in a Soxhlet apparatus for 24 h ultimately affording green gummy concentrates (*cf.* Table 3). These were distilled separately at reduced pressure (90°, 0.1 mmHg), using carbon dioxide as a carrier gas. The distillates, containing residual acetone, were diluted with pentane (1000 ml) and subsequently extracted with water (3 × 200 ml). The pentane-soluble portions from the three distillates were separated into acidic and neutral constituents. No bases were present.

Table 3. Extraction of dry leaves of three *Liatris* species and separation of concentrates.

	Dried leaves g	Acetone extract g	Distillate g	Neutral fraction g	Acidic fraction g
L. spicata	165	25	2.2	0.7	0.5
L. elegans	188	27	1.6	1.0	0.1
L. gracilis	228	45	2.6	0.5	0.5

The neutral fractions from the three plants were initially chromatographed on silica gel (pentane-ether) to give two subfractions containing hydrocarbons and oxygenated constituents, respectively, which were studied by GLC and GLC-MS.

The acidic fractions were reacted with excess ethereal diazomethane overnight and subsequently examined by GLC and GLC-MS.

Acknowledgements. We are grateful to Miss Pia Nyberg for skilled technical assistance, to Mr. Johan Roeraade for providing capillary columns, and to Mr. Robert Lazor, Department of Biological Science, Florida State University, USA, for the collection and botanical classification of the plants. Generous gifts of reference material were received from Dr. N. P. Damodaran, Central Food Technological Research Institute, Mysore, India, and Dr. K. Morikawa, the Institute of Food Chemistry, Osaka, Japan.

REFERENCES

1. Wahlberg, I. and Enzell, C. R. *Acta Chem. Scand.* **25** (1971) 70.
2. Wahlberg, I. and Enzell, C. R. *Acta Chem. Scand.* **25** (1971) 352.
3. Wahlberg, I., Hjelte, M.-B., Karlsson, K. and Enzell, C. R. *Acta Chem. Scand.* **25** (1971) 3285.
4. Karlsson, K., Wahlberg, I. and Enzell, C. R. *Acta Chem. Scand.* **26** (1972) 2837.
5. Karlsson, K., Wahlberg, I. and Enzell, C. R. *Acta Chem. Scand.* **26** (1972) 3839.
6. Hebert, H. J. C. *Rhodora* **70** (1968) 474, and references therein.
7. Herout, V. In Goodwin, T. W., Ed., *Aspects of Terpenoid Chemistry and Biochemistry*, Academic, London and New York 1971, p. 52.

8. Isoe, S., Hyeon, S. B. and Sakan, T. *Tetrahedron Letters* **1969** 279.
9. Taylor, H. F. and Burden, R. S. *Phytochemistry* **9** (1970) 2217.
10. Stevens, M. A. *J. Amer. Soc. Hort. Sci.* **95** (1970) 461.
11. Bricout, J., Viani, R., Müggler-Chavan, F., Marion, J. P., Reymond, D. and Egli, R. H. *Helv. Chim. Acta* **50** (1967) 1517.
12. Müggler-Chavan, F., Viani, R., Bricout, J., Marion, J. P., Mechtler, H., Reymond, D. and Egli, R. H. *Helv. Chim. Acta* **52** (1969) 549.
13. Nose, M., Nakatani, Y. and Yamanishi, T. *Agr. Biol. Chem. (Tokyo)* **35** (1971) 261.
14. Viani, R., Bricout, J., Marion, J. P., Müggler-Chavan, F., Reymond, D. and Egli, R. H. *Helv. Chim. Acta* **52** (1969) 887.
15. Kimland, B., Appleton, R. A., Aasen, A. J., Roeraade, J. and Enzell, C. R. *Phytochemistry* **11** (1972) 309.
16. Gildemeister, E. and Hoffmann, F. *Die ätherischen Öle*, Vol. IIIc, Akademie-Verlag, Berlin 1963.
17. Yamanishi, T., Nose, M. and Nakatani, Y. *Agr. Biol. Chem. (Tokyo)* **34** (1970) 599.
18. Sato, S., Sasakura, S., Kobayashi, A., Nakatani, Y. and Yamanishi, T. *Agr. Biol. Chem. (Tokyo)* **34** (1970) 1355.
19. Major, R. T. and Thomas, M. *Phytochemistry* **11** (1972) 611.
20. Gonzalez, J. G., Coggon, P. and Sanderson, G. W. *J. Food Sci.* **37** (1972) 797.
21. Kupchan, S. M., Davies, V. H., Fujita, T., Cox, M. R. and Bryan, R. F. *J. Am. Chem. Soc.* **93** (1971) 4916.
22. Herz, W. and Wahlberg, I. *Phytochemistry* **12** (1973) 1421 and *J. Org. Chem.* **38** (1973) 2485.
23. Herz, W. and Wahlberg, I. *Unpublished results.*
24. Appleton, R. A. and Enzell, C. R. *Phytochemistry* **10** (1971) 447.
25. Wahlberg, I., Karlsson, K. and Enzell, C. R. *Acta Chem. Scand.* **26** (1972) 1383.
26. Ryhage, R. and von Sydow, E. *Acta Chem. Scand.* **17** (1963) 2025.
27. von Sydow, E., Anjou, K. and Karlsson, G. *Arch. Mass Spectral Data*, Heyden et Son, London 1966.
28. Hunter, G. L. K. *J. Org. Chem.* **29** (1964) 2100.
29. Moshanas, M. G. and Lund, E. D. *The Flavour Industry* **1** (1970) 375.
30. Kochman, H.-J. *Gaschromatographisch-massenspektrometrische Analyse leichtflüchtiger Verbindungen der Tomate, Thesis*, Technical University of Berlin, Berlin 1969, p. 65.
31. Schormüller, J. and Kochmann, H.-J. *Z. Lebensm. Untersuch. Forsch.* **141** (1969) 1.
32. McFadden, W. H. and Buttery, R. G. In Burlingame, A. L., Ed., *Topics in Organic Mass Spectrometry*, Wiley-Interscience, New York 1970, Vol. 8, p. 327.
33. Smouse, T. and Chang, S. *J. Am. Oil Chemists' Soc.* **44** (1967) 509.
34. Spectra obtained from the Swedish Institute for Food Preservation Research, Göteborg, Sweden.
35. von Bünau, G., Schade, G. and Gollnick, K. *Z. anal. Chem.* **227** (1967) 173.
36. Bandarowich, H. A., Giammarino, A. S., Renner, J. A., Shephard, F. W., Shingler, A. J. and Gianturco, M. A. *J. Agr. Food Chem.* **15** (1967) 36.
37. Sheikh, Y. M., Duffield, A. M. and Djerassi, C. *Org. Mass Spectrom.* **4** (1970) 273.
38. Schulte-Elte, K. H., Müller, B. L. and Ohloff, G. *Helv. Chim. Acta* **54** (1971) 1899.
39. Popjak, G. In Goodwin, T. W., Ed., *Natural Substances Formed Biologically from Mevalonic Acid*, Academic, London 1970, p. 30.
40. *Eight Peak Index of Mass Spectra*, Mass Spectrometry Data Centre, Awre, Aldermaston, Great Britain.
41. Chen, P. H., Kuhn, W. F., Will, F. and Ikeda, R. M. *Org. Mass Spectrom.* **3** (1970) 199.

Received January 4, 1973.

ACTA CHEMICA SCANDINAVICA 27 (1973) 1622–1628

Transformations of Steroids by Cell-free Preparations of *Penicillium lilacinum* NRRL 895. III. Metabolism of Progesterone during Esterase Inhibition with Clomiphene Citrate

KJELL CARLSTRÖM

Department on Pure and Applied Biochemistry, Royal Institute of Technology, and the Department of Obstetrics and Gynaecology, Sabbatsberg Hospital, Karolinska Institutet, S-113 82 Stockholm, Sweden*

The steroid esterase activity in cell-free preparations from *P. lilacinum* was completely inhibited by 3×10^{-3} M clomiphene citrate. During esterase inhibition with this compound progesterone was directly transformed into testosterone acetate, thus indicating the "biochemical Baeyer-Villiger oxidation" as the C_{17-20}-lyase mechanism in this microbe. Clomiphene citrate partially inhibited the lyase and the 20-reductase activities, the latter mainly by suppression of the formation of the 20α-epimer.

Testosterone acetate or its 1-dehydro analog is the first intermediate formed in the side chain degradation of progesterone in a number of microorganisms.[1–7] The isolation and identification of this important metabolite is often complicated by a rapid hydrolysis catalyzed by esterases. Thus, it was necessary to separate the C_{17-20}-lyase and the esterase activities by chromatography on DEAE-cellulose before the formation of testosterone acetate from progesterone could be demonstrated in cell free extracts from *Cylindrocarpon radicicola*.[2] In progesterone fermentations with *Aspergillus flavus* and *Septomyxa affinis*, significant amounts of the 17β-acetate could be detected only after selective esterase inhibition with 2.15×10^{-3} M DFP.[4,7] In similar experiments with *Penicillium lilacinum*, formation of testosterone acetate could not be demonstrated in the presence of 2.15×10^{-3} M DFP[4] and this was later shown to be due to the insensitivity of the esterase activity of this fungus to DFP.[8] During the continued studies of the mechanism of the side chain degradation of progesterone by *P. lilacinum*, clomiphene citrate was found to be an efficient in-

* Present address.

hibitor of the esterase activity. The present communication describes the identification of testosterone acetate isolated after incubation of progesterone with cell-free preparations of *P. lilacinum* in the presence of clomiphene citrate.

MATERIALS AND METHODS

Abbreviations and trivial names. DFP: diisopropyl-fluorophosphate: GLC: gas liquid chromatography; GC-MS: gas chromatography-mass spectrometry; dimethyl-POPOP: 1,4-bis[2-(4-methyl-5-phenyl-oxazolyl)]benzene; PPO: 2,5-diphenyloxazole; TLC: thin layer chromatography; UV: ultraviolet. Clomiphene citrate: 1-(*p*-2-diethylaminoethoxyphenyl)-1,2-diphenyl-2-chloroethylene dihydrogen citrate; progesterone: 4-pregnene-3,20-dione; testosterone: 17β-hydroxy-4-androsten-3-one; testololactone: 17a-oxa-4-androstene-3,17-dione; testolic acid: 13-hydroxy-3-oxo-13,17-*seco*-4-androsten-17-oic acid.

Radioactive steroids. [7-^{3}H]Progesterone (specific activity 16 Ci/mmol), [21-^{14}C]progesterone (specific activity 0.0556 Ci/mmol) and [7-^{3}H]testosterone (specific activity 25 Ci/mmol) were obtained from New England Nuclear Corp., Boston, Mass. They were purified by TLC before use. In the substrate solutions they were diluted with non radioactive steroids to give a final radioactivity corresponding to 18 000 – 100 000 cpm per 10 μl solution.

Non radioactive steroids. Progesterone, 20α-hydroxy-4-pregnene-3-one and 20β-hydroxy-4-pregnene-3-one were purchased from Ikapharm Ltd., Ramat – Gan, Israel, and 5α-cholestane, testosterone, testosterone acetate, and 4-androstene-3,17-dione from Sigma Chemical Co., St. Louis, Mo. All steroids were tested for purity by TLC and GLC.

Clomiphene citrate. Two batches of clomiphene dihydrogen citrate were used, kindly donated by Star OY, Tampere, Finland, and by Draco AB, Lund, Sweden, respectively. The preparations contained 60 % of the *cis* and 40 % of the *trans* epimer. Both batches had the same effect on the steroid transformations studied.

Other chemicals. DFP was obtained from the Research Laboratory of National Defence (FOA), Ursvik, Sweden. Other reagents were from commercial sources and were of analytical grade. Solvents were redistilled.[9]

Chromatographic systems. TLC on Silica gel GF_{254} (system I), GLC on OV-17 and GC – MS were carried out as previously described.[9]

Growth of organism and preparation of cell-free extracts. The following media and inducers were used:

Experiment	Medium	Inducer
1	Czapek-Dox with the addition of 5 mg $ZnSO_4.7H_2O$, 5 mg $MnSO_4.3H_2O$ and 0.5 mg $CuSO_4.5H_2O$ per litre.[10]	Progesterone or 4-androstene-3,17-dione (50 mg in 1.5 ml dimethylformamide per 200 ml culture).
2.3.5	Czapek-Dox (50 g glucose, 2 g $NaNO_3$, 1 g KH_2PO_4, 0.5 g $MgSO_4.7H_2O$, 0.5 g KCl, and 0.01 g $FeSO_4.7H_2O$ per litre).	Progesterone (70 mg in 2 ml dimethylformamide per 300 ml culture.
4	Czapek-Dox with the addition of 5 mg $ZnSO_4.7H_2O$ per litre.	As in 2, 3, 5.

The procedures for cultivation of the organism and preparation of cell-free extracts (in 0.06 M Tris-HCl, pH 7.2) have been described previously.[9]

Incubation of steroids with cell-free extracts. The procedure was basically the same as that described previously, using 1.0 ml aliquots of the 100 000 *g* supernatant.[9] DFP was added as a freshly prepared 10 % (v/v) solution in ethanol and the samples were preincubated with that inhibitor for 30 min. Clomiphene citrate was added in Tris buffer. The addition of clomiphene citrate caused the formation of a light, white-greyish pre-

cipitate which was not removed. After the addition of the inhibitors, NADPH was added in 0.1 ml of Tris buffer. Steroids were added in 10 µl of ethanol and the final volume was adjusted with Tris buffer to 1.4 ml. The final concentrations of inhibitors, cofactor, and steroids are given in Tables 1 and 2.

Table 1. Effect of inducers and of DFP on the transformation of progesterone by cell-free homogenates of *P. lilacinum*.

Experiment [a]	DFP added	Steroid composition of the reaction mixture (mol %) Progesterone	20(α + β)-Hydroxy-4-pregnen-3-one	Testosterone	4-androstene-3,17-dione	Testololactone [b]
1 P	None	49.6	5.8	19.9	24.7	N. d.
1 P	1×10^{-3} M	65.9	8.1	8.1	17.9	N. d.
1 P	1×10^{-2} M	72.0	17.9	4.5	5.6	N. d.
1 A	None	71.9	5.1	6.5	10.9	5.6
1 A	1×10^{-3} M	89.1	5.0	0.9	5.0	N. d.
1 A	1×10^{-2} M	74.7	19.5	1.6	4.2	N. d.

[a] [21-^{14}C] Progesterone was incubated with homogenates from cells induced with progesterone (1 P) and with 4-androstene-3,17-dione (1 A). The protein concentration of the homogenates were 1.37 mg/ml (1 P) and 1.62 mg/ml (1 A). The initial concentration of progesterone was 2.28×10^{-4} M and of NADPH 9.7×10^{-4} M. Quantitative steroid analysis was made by GLC. [b] Tentatively identified from TLC behaviour and mass spectrum.[9]

After incubation for 60 min at 26° the reaction was terminated by addition of 0.1 ml 1 M HCl and 1.0 ml 30 % (w/v) $(NH_4)_2SO_4$. The steroids were extracted with two 4 ml portions of chloroform. The chloroform phase was dried over Na_2SO_4 and was evaporated to dryness. The residue was dissolved in 100 µl of acetone.

Steroid analysis. From each sample 10 – 30 µl were subjected to TLC in system I. The chromatoplates were examined in UV light. When the samples contained radioactive steroids the steroid zones were scraped off and were eluted with two 1.0 ml portions of ethanol. To the eluates 15 ml of a solution containing 50 mg of dimethyl-POPOP and 4 g of PPO in 1 litre of toluene was added. Radioactivity was measured in a Packard Tri-Carb model 3375 liquid scintillation spectrometer. The percentage distribution of radioactivity (^{3}H) in the different metabolites was calculated. No significant radioactivity was found in UV-positive zones not corresponding to the steroids (from fungal pigments and from clomiphene citrate) and in the UV-negative zones.

When a mixture of progesterone labelled with ^{3}H at C-7 and with ^{14}C at C-21 is used as substrate, the ^{3}H/^{14}C ratio will reflect the relative amount of steroids without the side chain. This facilitates the identification of the metabolites and therefore [7-^{3}H, 21-^{14}C]-progesterone was used as substrate in experiments 2 – 5. The ^{3}H/^{14}C ratio was calculated for all metabolites in these experiments.

Quantitative GLC was carried out using OV-17 as stationary phase.[9] The samples from experiment 1 were acetylated prior to GLC, other samples were not derivatized.

Protein assays were made by the biuret method.[11]

Identification of steroids. The testosterone acetate formed from progesterone was isolated by TLC from the samples containing 3×10^{-3} M clomiphene citrate in experiments 2 and 3. It was subjected to GLC on OV-17 and to GC-MS analysis. One half of the testosterone acetate fraction was heated with 1 M KOH in methanol at 60° for 60 min and the resulting testosterone was isolated by TLC, converted into its trimethyl silyl ether and subjected to GLC on OV-17 and to GC-MS analysis.

The identification of other progesterone metabolites has been described previously.[9] As an additional criterion of identity, the ^{3}H/^{14}C ratios of the metabolites of [7-^{3}H, 21-^{14}C] progesterone was used.

Table 2. Effect of clomiphene citrate on the transformation of progesterone and the hydrolysis of testosterone acetate by cell-free homogenates of *P. lilacinum*.

Experiment [a]	Protein mg/ml	Substrate	Clomiphene citrate added	Steroid composition of the reaction mixture, (mol %) Progesterone	20(α+β)-Hydroxy-4-pregnen-3-one	Testosterone acetate	Testosterone	4-Androstene-3,17-dione	Testololactone [b]
2	0.910	[7-^{3}H,21-^{14}C] Progesterone	None	58.3	10.6	0.4[c]	23.9	5.6	1.2
2	0.910	»	3×10^{-3} M	84.3	5.5	7.1	1.4[d]	1.5[d]	0.2[d]
3	0.665	»	None	78.3	7.4	0.3[c]	10.6	2.5	0.9
3	0.665	»	1×10^{-3} M	86.8	4.5	0.3[c]	6.8	0.9	0.7
3	0.665	»	2×10^{-3} M	87.9	4.7	0.3[c]	5.5	0.9[d]	0.7
3	0.665	»	3×10^{-3} M	90.0	5.0	3.3	0.3[d]	1.2[d]	0.2[d]
3	0.665	Testosterone acetate	None	—	—	3.6	96.4	N.d.	N.d.
3	0.665	»	1×10^{-3} M	—	—	3.6	96.4	N.d.	N.d.
3	0.665	»	2×10^{-3} M	—	—	12.1	87.9	N.d.	N.d.
3	0.665	»	3×10^{-3} M	—	—	> 99	Trace	N.d.	N.d.
4	1.165	[7-^{3}H,21-^{14}C]-Progesterone	None	62.5	22.0	0.2c	5.3	8.1	1.9
4	1.165	»	3×10^{-3} M	85.9	7.8	2.7	1.5	1.2[d]	0.9
4	1.165	Testosterone acetate	None	—	—	Trace	> 99	N.d.	N.d.
4	1.165	»	3×10^{-3} M	—	—	> 99	Trace	N.d.	N.d.
5	0.729	[7-^{3}H,21-^{14}C]-Progesterone	3×10^{-3} M	90.0	4.3	3.7	0.6[d]	1.1[d]	0.3[d]

[a] The initial concentration of progesterone was 2.28×10^{-4} M, of testosterone acetate 2.16×10^{-4} M, and of NADPH 9.7×10^{-4} M. With [7-^{3}H, 21-^{14}C] progesterone as substrate the quantitative analysis was made by TLC and liquid scintillation counting, in other cases by GLC. In experiment 5, parallel incubations were also made with unlabelled progesterone+a tracer amount of [7-^{3}H]testosterone (see text). [b] Tentatively identified from TLC behaviour and mass spectrum.[9] [c] Probably insignificant, not detected by TLC. [d] Insignificant, ^{3}H/^{14}C ratio not exceeding that of the C_{21} steroids.

RESULTS

Effect of inducers and of DFP on the enzyme activity. As seen in Table 1 progesterone was the best inducer of the C_{17-20}-lyase activity. In separate experiments this was found to be true also for the esterase activity. Extracts from non induced cells had none of these activities. However, independently of the inducer used, the extracts contained very strong esterase activity. It was not possible to detect any formation of testosterone acetate even after treatment with 1×10^{-2} M DFP. The C_{17-20}-lyase was sensitive to DFP and a concentration of 1×10^{-3} M caused an inhibition of 42 % in the extract from progesterone induced cells. Thus, the attempts to bring about selective suppression of the esterase activity by selective induction and by treatment with DFP proved unsuccessful.

Effect of clomiphene citrate on the enzyme activity. Addition of 3×10^{-3} M clomiphene citrate completely inhibited the esterase activity whereas 30 – 40 % of the C_{17-20}-lyase activity was still present (Table 2). Thus, formation of testosterone acetate could be demonstrated in four independent experiments. Incubation of [7-^{3}H, 21-^{14}C] progesterone with boiled extracts in the presence of 3×10^{-3} M clomiphene citrate did not yield significant amounts of progesterone metabolites.

Since microbial acetylation of testosterone has been reported,[12,13] it was necessary to establish that the testosterone acetate was directly formed from progesterone and not by acetylation of testosterone, formed from progesterone *via* an alternative pathway. The fact that the ^{3}H/^{14}C ratio of the testosterone acetate never exceeded that of the substrate progesterone speaks against the the latter possibility. Furthermore, when unlabelled progesterone was incubated in the presence of a trace amount of [7-^{3}H] testosterone, only 0.5 % of the radioactivity could be found in the testosterone acetate which represented 2 – 4 % of the total steroids in the reaction mixture (experiment 5). More than 95 % of the radioactivity remained in the TLC fraction corresponding to testosterone, but no testosterone was formed from progesterone.

The identity of the testosterone acetate was established by its chromatographic behaviour and mass spectrometric properties before and after hydrolysis. Mass spectra of authentic testosterone acetate and of testosterone acetate isolated from the reaction mixture were identical. This was also true for the spectra of the trimethyl silyl ethers of authentic testosterone and of the product formed by hydrolysis of the testosterone acetate from the reaction mixture.

The reduction of the 20-oxo group of progesterone was partially inhibited by clomiphene citrate at all concentrations used (Table 2). TLC and GC-MS analyses revealed that the formation of the 20α-alcohol was greatly suppressed by clomiphene citrate. Thus, the 20α-hydroxysteroid represented only about 15 % of the mixture of epimers compared to about 50 % in the mixtures isolated from the control incubations.

Effect of Zn^{2+} on the enzyme activity. In experiments 1 and 4, the Czapek-Dox substrate was fortified with Zn^{2+}.[10] This resulted in an increased yield of biomass and a deeper lilaceous colour of the cells. When extracts from such cells were incubated with progesterone, 4-androstene-3,17-dione was the main C_{19} metabolite, whereas extracts from cells grown on a zinc-deficient medium yielded testosterone as the major product (Tables 1 and 2).

DISCUSSION

The formation of testosterone acetate from progesterone under the conditions described in this paper strongly supports the "biochemical Baeyer-Villiger oxidation" as the mechanism of the pregnane side chain cleavage by *P. lilacinum*.[14] The sequence of the degradation of progesterone by this fungus may therefore be outlined as follows: Progesterone ⟶ testosterone acetate ⇌ testosterone ⇌ 4-androstene-3,17-dione ⟶ testololactone ⇌ testolic acid.[10] Hitherto the "biochemical Baeyer-Villiger oxidation" seems to be the only clearly established pathway for the microbial degradation of the pregnane side chain.[1–7] The lactonization of ring D in 17-ketosteroids proceeds *via* an analogous mechanism and is carried out in several fungi, including *P. lilacinum*.[1] The lactonizing enzyme in this fungus is induced by its substrate, 4-androstene-3,17-dione.[10] As shown in this paper the latter steroid also induced the C_{17-20}-lyase, although less efficiently than progesterone. Similar observations have been made by Miller concerning the induction of the lactonizing enzyme in *Septomyxa affinis*.[7] The progesterone metabolism of this fungus parallels that of *P. lilacinum*, except that 1-dehydro derivatives are formed. Miller found progesterone to be a better inducer than 1,4-androstadiene-3,17-dione and suggested that the two "biochemical Baeyer-Villiger oxidations" are carried out by the same enzyme. The fact that 4-androsten-3,17-dione induces the side chain splitting enzyme activity in *P. lilacinum* may also be taken as a support for this suggestion.

Previous studies have shown 4-androstene-3,17-dione to be the first and major metabolite appearing in progesterone fermentations with whole cells of *P. lilacinum*.[4,7,15] On this basis it was suggested that 4-androstene-3,17-dione might be the primary C_{19} steroid metabolite of progesterone.[4,15] The cells used in those studies were grown on beer wort and on a medium fortified with Zn^{2+} to a final concentration of 2.1×10^{-6} M. In beer wort, Zn^{2+} levels of $0.8 - 8.3 \times 10^{-6}$ M have been reported.[16] The present paper shows that when the cells are grown on media fortified with Zn^{2+}, the 17-ketone/17β-alcohol ratio increases drastically. This might be due to increased levels of 17β-hydroxysteroid dehydrogenase in the cells since it is well known that many NAD-linked dehydrogenases contain zinc.[17] This might also explain the high levels of 4-androstene-3,17-dione found in the whole cell experiments. A possible role of 4-androstene-3,17-dione as the primary C_{19} steroid metabolite of progesterone is ruled out by the results given in the present communication.

Acknowledgements. The GC-MS analysis was carried out at the Department of Chemistry I, Karolinska Institutet, Stockholm, Sweden.

REFERENCES

1. Charney, W. and Herzog, H. L. *Microbial Transformations of Steroids, A Handbook*, Academic, New York and London 1967.
2. Rahim, M. A. and Sih, C. J. *J. Biol. Chem.* **241** (1966) 3615.
3. Carlström, K. *Acta Chem. Scand.* **20** (1966) 2620.
4. Carlström, K. *Acta Chem. Scand.* **21** (1967) 1297.
5. Singh, K. and Rakhit, S. *Biochim. Biophys. Acta* **144** (1967) 139.
6. Cox, P. H. and Sewell, B. A. *J. Soc. Cosmetic Chemists* **19** (1968) 461.

7. Miller, T. L. *Biochim. Biophys. Acta* **270** (1972) 167.
8. Carlström, K. and Krook, K. *Acta Chem. Scand.* **27** (1973) 1240.
9. Carlström, K. *Acta Chem. Scand.* **26** (1972) 1718.
10. Prairie, R. L. and Talalay, P. *Biochemistry* **2** (1963) 203.
11. Lowry, O. H., Rosebrough, N. J., Forr, A. L. and Randall, R. J. *J. Biol. Chem.* **193** (1951) 265.
12. McGuire, J. S., Maxwell, E. S. and Tomkins, G. M. *Biochim. Biophys. Acta* **45** (1960) 392.
13. Capek, A., Tadra, M. and Tuma, J. *Folia Microbiol. (Prague)* **9** (1964) 380.
14. Fried, J., Thoma, R. W. and Klingsberg, A. *J. Am. Chem. Soc.* **75** (1953) 5764.
15. Carlström, K. *Acta Chem. Scand.* **24** (1970) 1759.
16. Mac William, I. C. *J. Inst. Brewing* **74** (1968) 38.
17. Mildvan, A. S. *Metals in Enzyme Catalysis* (Review). In Boyer, P. D., Ed., *The Enzymes*, 3rd Ed., Academic, New York and London 1970, Vol. 2, p. 525.

Received December 23, 1972.

ACTA CHEMICA SCANDINAVICA 27 (1973) 1629–1636

Acid Catalyzed Reactions of α-Allenic and α-Acetylenic Tertiary Alcohols*

LARS-INGE OLSSON, ALF CLAESSON and CONNY BOGENTOFT

Department of Organic Chemistry, Faculty of Pharmacy, University of Uppsala, Box 6804, S-113 86 Stockholm, Sweden

The acid catalyzed rearrangements of some isomeric α-allenic and α-acetylenic tertiary alcohols have been investigated with respect to the products formed and the reaction mechanisms. The allenic alcohols react to give α,β-unsaturated ketones in acidic aqueous solutions, allenyl ethers in methanol and dienol acetates in acetic acid. The reactions are proposed to proceed *via* an allenyl-vinyl cation. The formation of α,β-unsaturated ketones implies a 1,3-hydroxy shift, a reaction analogous to the Meyer-Schuster rearrangement of α-acetylenic alcohols. It is found that α-acetylenic tertiary alcohols having α-hydrogens can rearrange according to two different mechanisms. The course of the reaction depends on the chemical character of the substrate.

It is well known that the acid catalyzed rearrangement of α-acetylenic tertiary alcohols leads to α,β-unsaturated carbonyl compounds.[1] The reaction can proceed through a 1,2- or 1,3-hydroxy shift, depending on the structure of the starting acetylenic alcohol.

Only scant information is available in the literature about the behaviour of α-allenic alcohols towards acids.[2] During the course of the present study, a systematic investigation on the acid catalyzed rearrangements of different types of α-allenic alcohols was published,[3] though only one tertiary derivative was included in that work.

α-Allenic tertiary alcohols occur in nature, *e.g.* among the carotenoids,[4] and recently several 17α-propadienyl-17β-hydroxy steroids [5] and aliphatic alcohols [6] have been prepared for pharmacological evaluations.

The aim of our study was to investigate the acid catalyzed isomerization of some allenic tertiary alcohols with respect to the products formed and the reaction mechanisms involved. As suitable substrates we chose the dimethyl and the cyclohexyl derivatives II and IV (*cf.* Table 1). These com-

* Allenes and Acetylenes II. Part I: Ref. 10.

Table 1. Acid catalyzed reactions of α-allenic and α-acetylenic tertiary alcohols.

Substrate	Catalyst	Temp. °C	Reaction time	Products	Yield [a] % GLC
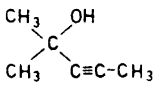 I[9]	5 % H_2SO_4 50 % HOAc	80	10 h	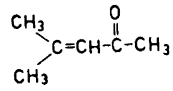 VI	75
	5 % H_2SO_4 50 % HOAc	40	2 min	VI	95
	1 % H_2SO_4 CH_3OH	20	15 min	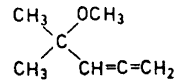 VII	75
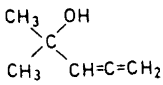 II[3]				+ VI	14
	80 % HOAc	20	8 h	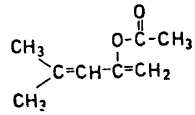 VIII	17
				+ VI	13
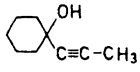 III[9]	5 % H_2SO_4 50 % HOAc	80	5 h	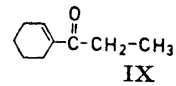 IX	95
	5 % H_2SO_4 50 % HOAc	80	2 min	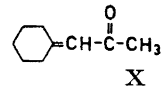 X	80
				+ 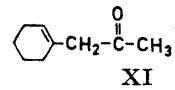 XI	5
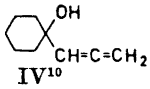 IV[10]	1 % H_2SO_4 CH_3OH	20	15 min	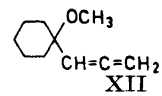 XII	70
				+ XI	13
				+ X	2

Table 1. Continued.

	80 % HOAc	20	24 h	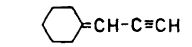 XIII	20
				+ 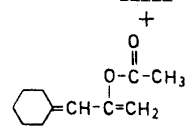 XIV	20
				+ X	30
				+ XI	3
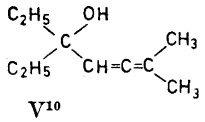 V[10]	5 % H_2SO_4 50 % HOAc	80	2 min	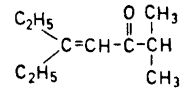 XV	70

[a] The remaining part up to 100 % consists of unreacted substrates.

pounds can be considered to represent extreme cases with respect to the expulsion of protons from their carbonium ions, and we therefore suspected that they could react according to different reaction mechanisms. In the study we also included compound V which does not have a terminal allenic function.

There has been some controversy [1] regarding the mechanism of acid catalyzed rearrangement of α-acetylenic *t*-alcohols. We therefore considered it worthwhile to elucidate the isomerization of the acetylenic derivatives I and III. To our knowledge, this is the first comparative study concerning the reaction pathways of isomeric α-allenic and α-acetylenic alcohols in acidic media.

RESULTS

Many different acidic materials are known to act as useful catalysts for the rearrangement of α-acetylenic alcohols to α,β-unsaturated ketones. In the present study we mainly used 50 % acetic acid containing 5 % H_2SO_4, and in some experiments 80 % acetic acid or 1 % H_2SO_4 in methanol were also employed.

The experiments were run at different temperatures, the products being identified by GLC-MS or by preparative GLC and subsequent structure elucidation by spectroscopic methods (*cf.* Table 2). Representative results under conditions providing good yields of different products are summarized in Table 1.

The acetylenic alcohols I and III afforded different types of compounds in acidic aqueous solutions. The cyclohexyl derivative III, as expected, reacted solely according to a 1,2-hydroxy shift (Rupe rearrangement).[1] As indicated by

GLC-MS, 1-(1-propynyl) cyclohexene-1 (XVII) was rapidly formed (5 min) as an intermediate in 60 % yield at 80°C, whereafter it was transformed into the α,β-unsaturated ketone IX. In 80 % acetic acid, the enyne XVII was the only product formed, even at elevated temperature (80°C). 2-Methylpent-3-yn-2-ol (I) did not undergo the Rupe rearrangement, but reacted exclusively *via* a 1,3-hydroxy shift (Meyer-Schuster[1] rearrangement) to afford mesityl oxide (VI). During the experiments concerning the isomerization of compound I, 2-methylpent-1-en-3-one[7] (XVIII) was used as a reference compound, but this product could not be detected in the reaction mixture (*cf.* Scheme 2).

The allenic alcohols II and IV rearranged rapidly through a 1,3-hydroxy shift producing the corresponding α,β-unsaturated ketones VI and X, respectively. This latter compound (X) isomerized further to the β,γ-unsaturated ketone XI at prolonged reaction times, and an equilibrium mixture of the two ketones was obtained after 1 h with a final composition of X:XI = 1:3.5. Compound V behaved in an analogous manner. After 2 min at 80°C the α,β-unsaturated ketone XV was formed in 70 % yield. An equilibrium was obtained after 2 – 3 h with approximately equal amounts of XV and the isomer XVI (5-ethyl-2-methyl-5-hepten-3-one) (*cf.* Scheme 1).

It is important to note the marked difference in reaction rate between the allenic and the acetylenic isomers II and I. While the conversion of II into mesityl oxide was rapid even at 0°C, compound I isomerized at a much slower rate. In the latter case, no reaction occurred at 0°C and some of the substrate still remained unchanged after 10 h at 80°C.

The allenic alcohols II and IV afforded good yields of the corresponding ethers VII and XII, respectively, when the reaction was performed in acidic methanol. This seems to be a useful synthetic procedure for allenic ethers from tertiary allenic alcohols.

Analysis of the reaction mixture obtained after treating IV with 80 % acetic acid revealed an unexpected product which was formed in 20 % yield. The IR (C=O: 1760 cm^{-1}) and NMR [(5.55 – 5.36 (m,1H), 4.80 – 4.57 (m,2H), 2.05 (s,3H)] spectra strongly suggest that this compound is represented by the unsaturated vinyl acetate structure XIV. MS-analysis at 10 eV with the ion source at 100°C gave an accurate molecular ion at *m/e* 180 supporting the structure deduced from IR and NMR data. Further evidence for the proposed structure XIV was obtained by hydrolysis in 10 % H_2SO_4 solution which yielded the ketone X. Analogous results were obtained with compound II. Compound XIV was formed in 50 % yield (GLC), when the reaction was carried out in 100 % acetic acid containing $MgSO_4$ at 80°C for ½ h.

DISCUSSION

Acetylenic tert. *alcohols.* The results obtained show that α-acetylenic tertiary alcohols having α-hydrogens can rearrange according to two different mechanisms (*cf.* compounds I and III in Table 1). The course of the reaction seems to depend on the chemical character of the substrate. The detection of the enyne XVII as an intermediate in the transformation of III to IX supports earlier findings[1] that the Rupe rearrangement involves such a

compound. The reason why the dimethyl analogue I does not react (Scheme 2) in the same manner may be the low tendency of a carbonium ion to expel a proton to form a terminal double bond.

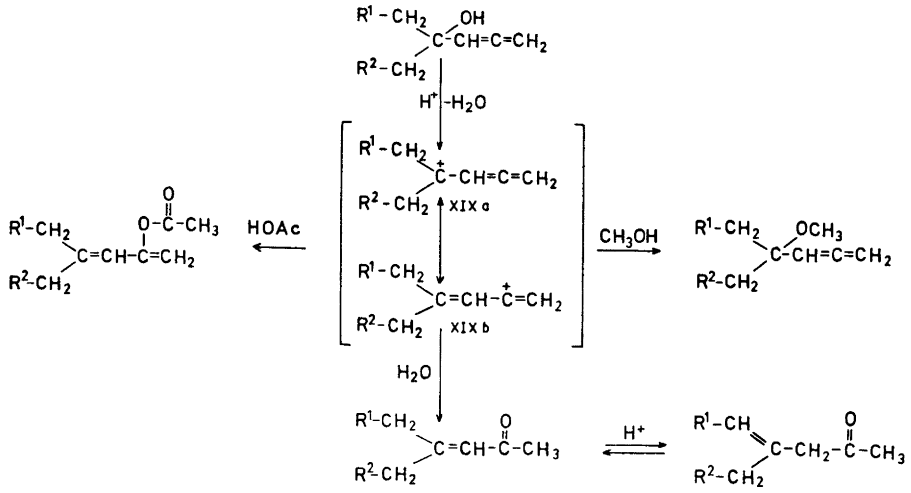

Scheme 1.

Allenic tert. *alcohols.* Our study indicates that compounds of this type react in acidic aqueous solutions according to a uniform mechanism involving a mesomeric allenyl-vinyl cation XIXa – XIXb, as outlined in Scheme 1. This isomerization implies a 1,3-hydroxy shift in analogy to the Meyer-Schuster [1] rearrangement. The proposed mechanism is supported by the formation of the allenic ethers VII and XII. Also the formation of the vinyl acetates VIII and XIV in acetic acid can be explained by this mechanism through the reaction of the carbonium ion involved with acetic acid.

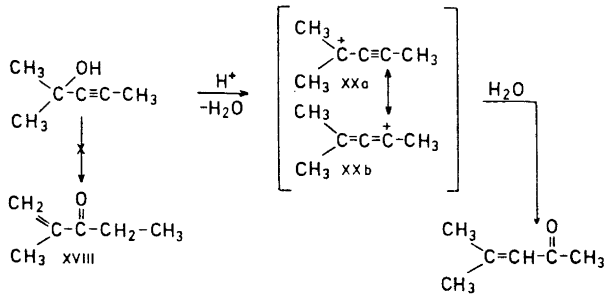

Scheme 2.

Conclusion. We propose that the very pronounced difference in reaction rate between I and II may be explained on the basis of the mesomeric cations XIX and XX. To account for this assumption, we propose that the acetylenic cation is mainly represented by the mesomeric form XXa, while the allenyl-vinyl cation is advantageously represented by both mesomeric forms XIXa – XIXb, and the reaction pathway with nucleophiles depends on kinetic factors and the thermodynamic properties of the product. This type of cation has been found to be involved in the solvolysis of some 2-bromo-4-methyl-1,3-pentadiene derivatives.[8] These compounds were solvolyzed with unexpected ease in dilute ethanol, the reaction being of first order. It was also shown that these bromodienes, which deviate from coplanarity already in the ground state, attain a conformation in the generated cation where the double bonds are perpendicular to each other (*cf.* XIXb, Scheme 1), allowing the positive charge to be delocalized over three carbon atoms. This favourable arrangement of the atoms is already present in the allenic alcohols, which constitutes a feasable explanation for their great reactivity.

EXPERIMENTAL

General. IR-spectra were run on a Perkin-Elmer Infracord 337 spectrophotometer using liquid film on NaCl discs. NMR spectra were obtained in $CDCl_3$, using a Varian A 60 spectrometer and tetramethylsilane as internal standard. Mass spectra were run on an AEI MS-30 mass spectrometer connected to a Pye 104 gas chromatograph. Column: 1.5 m glass column packed with 3 % Carbovax 20 M on Chromosorb W (60 – 80 mesh). The ionizing energy was maintained at 70 eV, the accelerating energy at 4 kV, and the temperature of the source at 200°C.

GLC analyses were run on a Perkin-Elmer F 11 or a Varian 1700 instrument equipped with flame ionization detectors. Columns: 1.5 m columns packed with 5 % Carbowax 20 M. The preparative columns were of aluminium, $\varnothing = 3.8''$, 3 m long and packed with 20 % Carbowax 20 M or 20 % OV-25 on Cromosorb W (60 – 80 mesh).

Acid catalyzed rearrangements. General procedures. Method 1. One part of alcohol was allowed to react under stirring with 10 parts of an acid mixture (50 % HOAc + 5 % H_2SO_4 + 45 % H_2O) in a flask fitted with an efficient condenser. The flask was heated in an oil-bath, the temperature being controlled with a thermostat. Samples were withdrawn periodically and the reaction was stopped by cooling in ice and adding 5 M NaOH to slightly alkaline reaction. The solution was extracted with a known volume of ether, the extract was washed with water and dried with Na_2SO_4. Samples of the dry ether extract were analyzed by GLC or GLC-MS. Preparative GLC or vacuum distillation was performed to isolate the products when necessary.

Method 2. One part of alcohol was allowed to react with ten parts of absolute methanol containing two parts of $MgSO_4$ and 1 % H_2SO_4. The reaction was carried out in a sealed flask under magnetic stirring. Samples were withdrawn at intervals. The reaction was stopped by pouring the solution into a suspension of K_2CO_3 in light petroleum. After filtering, the samples were dried and analyzed as described in Method 1.

Method 3. One part of alcohol was treated with ten parts of 80 % acetic acid. Samples were withdrawn periodically. The reaction was stopped by neutralization in an ice bath with 5 M NaOH. The products were extracted with ether and analyzed as described in Method 1.

Acknowledgement. We are indebted to Professor Bengt Danielsson for his kind interest in this work and for valuable discussions. This work has been supported financially by the *Swedish Natural Science Research Council.*

Table 2. Physical data of compounds VII–XVII.

Compound	IR[a] (cm^{-1})	NMR (δ)	MS[b] [m/e (%)]
VII	1950	5.14–4.58 (m,3H)	112(0.1), 97(3), 83(6), 81(5) 79(5), 73(100), 67(6), 65(5),
		3.12 (s,3H)	55(28), 53(12), 45(6), 43(37)
		1.26 (s,6H)	41(32), 39(30)
VIII[11]	1760	5.58–5.42 (m,1H)	140(30), 99(7), 98(96), 84(9),
	1660	4.75–4.57 (m,2H)	83(100), 82(9), 79(5), 60(5)
	1645	2.00 (s,3H)	56(7), 55(13), 44(7), 43(24),
	1605	1.84–1.67 (m,6H	42(5), 41(6)
IX[12]	1660	6.90–6.65 (m,1H)	138(14), 110(7), 109(100),
		2.80–2.37 (q,2H)	
	1620	2.37–2.00 (m,4H)	82(6), 81(93), 79(30), 77(9),
		1.80–1.32 (m,4H)	57(9),
		1.20–0.85 (t,3H)	53(16), 45(7), 41(10), 39(7)
X[13]	1680	5.94–5.80 (m,1H)	139(7), 138(53), 123(33),
	1610	2.95–2.50 (m,2H)	110(9), 109(13), 95(56), 93(7),
		2.27–1.90 (m,2H)	91(8), 81(18), 80(50), 79(21),
		2.05 (s,3H)	77(10), 67(48), 66(7), 65(8)
		1.75–1.33 (m,6H)	55(25), 53(15), 51(8), 43(100), 41(28), 39(31)
XI[14]	1710	5.48–5.27 (m,1H)	138(18), 123(6), 96(15), 95(100),
	1610	2.94–2.78 (m,2H)	94(14), 93(10), 91(7), 81(27),
		2.18–1.70 (m,4H)	80(59), 79(27), 77(15), 73(8),
		2.05 (s,3H)	68(7), 67(63), 66(7), 65(11),
		1.70–1.33 (m,4H)	55(27), 53(22), 52(7), 51(12), 45(15), 44(7), 43(68), 41(57), 40(7), 39(51)
XII	1945	5.00–4.53 (m,3H)	152(1), 137(5), 114(8), 113(100),
		3.05 (s,3H)	109(11), 91(8), 81(50), 79(15),
		1.70–1.25 (m,10H)	77(9), 71(5), 67(6), 55(5), 53(7), 45(10), 41(10), 39(10)
XIII[14]	3310	5.20–5.07 (m,1H)	121(7), 120(55), 119(7), 105(42),
	2090	2.94–2.80 (d,1H)	103(7), 92(63), 91(100), 81(55),
	1630	2.55–1.90 (m,4H)	80(8), 79(55), 78(32), 77(37),
		1.90–1.35 (m,6H)	73(17), 68(22), 67(22), 66(15), 65(38), 63(20), 59(7), 55(17), 53(25), 52(24), 51(37), 50(16), 45(43), 43(12), 41(37), 39(72)
XIV	1760	5.55–5.36 (m,1H	180(6), 139(8), 138(100), 137(5), 123(17),
	1655	4.80–4.57 (m,2H)	122(7), 120(13), 110(7), 109(6), 105(7),
	1640	2.47–1.80 (m,4H)	98(6), 96(14), 95(35), 94(10), 92(17),
		2.05 (s,3H)	91(10), 85(10), 84(5), 83(7), 82(8),
		1.80–1.32 (m,6H)	81(48), 80(85), 79(10), 78(8) 69(6), 67(12), 60(7), 59(8), 58(6), 55(8), 53(8), 44(13), 43(40), 42(12), 41(8)

Table 2. Continued.

XV	1685	6.05 – 5.93 (m,1H), 2.80 – 1.90 (m,5H)	154(7), 112(5), 111(100), 69(12),
	1615	1.20 – 0.80 (m,12H)	55(28), 53(6), 43(17), 41(25), 39(12)
XVI	1710	5.40 – 5.00 (m,1H) 3.17 – 3.00	154(10), 111(25), 83(19), 71(100),
	1620	(m,2H), 2.20 – 1.80 (m,3H)	70(6), 69(9), 67(10), 55(43),
		1.70 – 1.45 (m,3H) 1.20 – 0.70 (m,9H)	53(9), 43(12), 42(7), 41(43)
			39(22)
XVII[16]	2230	5.90 – 5.64 (m,1H) 2.20 – 1.78 (m,4H)	121(7), 120(100), 119(12),
	1675	1.82 (s,3H) 1.67 – 1.30 (m,4H)	106(9), 105(95), 103(12),
	1630		92(37), 91(91), 79(28), 78(12), 77(40), 65(9), 63(9), 51(9), 41(6), 39(12)

[a] Only important bonds of diagnostic value are listed.
[b] Only peaks with a rel. int. >5 % of the base peak are listed.

REFERENCES

1. Swaminathan, S. and Narayanan, K. V. *Chem. Rev.* **71** (1971) 429.
2. Bertrand, M. and Le Gras, J. *C. R. Acad. Sci. Paris* **261** (1965) 762.
3. Gelin, R., Gelin, S. and Albrand, M. *Bull. Soc. Chim. France* **1972** 720.
4. Weedon, B. C. L. *Rev. Pure Appl. Chem.* **20** (1970) 51.
5. Biollaz, M., Landeros, R. M., Cuéllar, L., Crabbé, P., Rooks, W., Edwards, J. A. and Fried, J. H. *J. Med. Chem.* **14** (1971) 1190.
6. Claesson, A., Bogentoft, C., Danielsson, B. and Paalzow, L. *To be published.*
7. Hays, J. T., Hager, G. F., Engelmann, H. M. and Spurlin, H. M. *J. Am. Chem. Soc.* **73** (1951) 5369.
8. Grob, C. A. and Spaar, R. *Tetrahedron Letters* **1969** 1439.
9. Fleck, B. R. and Kmiecik, J. E. *J. Org. Chem.* **22** (1957) 90.
10. Claesson, A. and Bogentoft, C. *Acta Chem. Scand.* **26** (1972) 2540.
11. Gwynn, B. H. and Degering, E. D. F. *J. Am. Chem. Soc.* **64** (1942) 2216.
12. Favorskaya, I. A. and Auvinen, E. M. *Zh. Org. Khim.* **1** (1965) 486.
13. Dickins, A. H., Hugh, W. E. and Kon, G. A. R. *J. Chem. Soc.* **1928** 1630.
14. Kon, G. A. R. and Narayana, B. T. *J. Chem. Soc.* **1927** 1546.
15. Montijn, P. P., Schmidt, H. M., van Boom, J. H., Bos, H. J. T., Brandsma, L. and Arens, J. F. *Rec. Trav. Chim.* **84** (1965) 271.
16. Mousseron, M. *C. R. Acad. Sci. Paris* **217** (1943) 155.

Received December 19, 1972.

ACTA CHEMICA SCANDINAVICA 27 (1973) 1637–1644

Outer-sphere Complex Formation between the Hexaamminecobalt(III) Ion and Iodide Ion in Aqueous Solution

LARS JOHANSSON

Division of Inorganic Chemstry 1, Chemical Center, University of Lund, P.O.B. 740, S-220 07 Lund 7, Sweden

The complex formation between $Co(NH_3)_6^{3+}$ and I^- has been studied at 25°C and at the constant ionic strengths ($NaClO_4$) $I = 1$ M, 2 M, and 4 M, by solubility measurements. The 1:1 complex is formed at all ionic strengths. At 2 M and 4 M ionic strength, the formation of the 1:2 complex has been clearly demonstrated. This complex is probably of some importance also when $I = 1$ M. The formation of even higher complexes, at high iodide concentration, is indicated.

Possible medium effects and perchlorate association have been discussed. While activity coefficient changes probably are of minor importance, perchlorate association probably occurs to some degree. The qualitative interpretation of the data is not changed by this possibility.

The data are consistent with the following constants (errors within parentheses):

$I = 1$ M: $\beta_1 = 0.4(1)$ M^{-1}, $\beta_2 = 0.04(4)$ M^{-2}
$I = 2$ M: $\beta_1 = 0.5(1)$ M^{-1}, $\beta_2 = 0.15(5)$ M^{-2}
$I = 4$ M: $\beta_1 = 0.4(2)$ M^{-1}, $\beta_2 = 0.2(1)$ M^{-2}

In an earlier paper,[1] the results from a study of $Coen_3^{3+} - I^-$ outer-sphere complexes were reported. It was found that besides the 1:1 complex the 1:3 complex was formed as well at high iodide concentration. The 1:2 complex could not be detected.

The aim of the present study has been to study the system $Co(NH_3)_6^{3+} - I^-$, especially at high ligand concentration, to show whether or not higher complexes than the well-established 1:1 complex are formed also in this system. In view of the results on the ethylenediamine system just mentioned, particular attention has been paid to the relative strengths of the complexes formed. The hexaamminecobalt iodide system has been studied earlier by several authors.[3–11] Their interest has invariably been focussed on the 1:1 complex. A discussion of the results is given on p. 1643.

Compared to $Coen_3^{3+} - I^-$, the hexaamminecobalt iodide system is less suited for experimental study. The solubilities of $Co(NH_3)_6I_3$(s) and $Co(NH_3)_6(ClO_4)_3$(s) are low, making spectrophotometric measurements [1,2] impracticable

and solubility measurements difficult, especially at high ionic strengths. The hexaamminecobalt ion is also less stable kinetically than the ethylenediaminecobalt ion (see Experimental).

The solubility of $Co(NH_3)_6I_3(s)$ has been studied at the ionic strengths 1, 2, and 4 M, $NaClO_4$ being used as supporting electrolyte. Attempts to study the solubility of $Co(NH_3)_6(ClO_4)_3(s)$ were not successful (see Experimental).

EXPERIMENTAL

Chemicals. Analytical grade chemicals were used, when available.

Cobalt salts. $Co(NH_3)_6Cl_3$ was prepared according to Bjerrum's [12] method. Samples of the salt were analyzed for Co spectrophotometrically, using the thiocyanate method, after boiling with NaOH and subsequent acidifying with HCl. Found 21.90 % Co, calculated for $Co(NH_3)_6Cl_3$ 22.05 % Cl. From the chloride, $Co(NH_3)_6(ClO_4)_3$ and $Co(NH_3)_6I_3$ were precipitated by $HClO_4$ and NaI, respectively, and recrystallized several times. A spectrum of the perchlorate dissolved in water was recorded. The following peak values were obtained: 56.6 M^{-1} cm^{-1} (475 nm) and 45.4 M^{-1} cm^{-1} (340 nm). Heck[13] reported 56.4 and 45.5 M^{-1} cm^{-1}, respectively. The iodide content of the hexaamminecobalt iodide was found to be 70.2 % (calculated 70.26 %).

Solubility measurements. (Notation, see Refs. 1 and 2.) Solutions, composed of C_L M NaI and $(I - C_L)$ M $NaClO_4$ (I = 1, 2, or 4 M) were equilibrated with $Co(NH_3)_6I_3(s)$ at 25°C in a solubility column, as described earlier.[14,15] Black tape wound around the column protected the solid and the solutions from light. It was checked frequently that equilibrium was really reached. At least two samples of each solution were equilibrated, with results normally in agreement within 1 %(I = 1 M) or 2 % (2 M and 4 M). At the highest [L], when I = 4 M, the reproducibility was poorer. On the other hand, several samples were equilibrated here, in order to improve the precision of the averages.

The equilibrated solutions were analyzed spectrophotometrically on a Zeiss PMQ II spectrophotometer. The cell compartment was carefully thermostated to 25°C with water, and the spectrophotometer was placed in a room maintained at 25°C. The solutions were allowed to attain this temperature before the cells were filled. For calibration purposes, the absorbances of solutions of known C_M and varying C_L were determined. As the solubilities were low, long cells (4 cm) had to be used, and special care had to be taken in order to assure reproducible results. Thus, to avoid the oxidation of I^- to I_3^-, all solutions were treated with nitrogen. Minute amounts of sodium thiosulfate were added to the solutions before measurement.[1] At first, high and not very reproducible absorbances were obtained for $NaClO_4$ – NaI mixtures, and consequently also for the calibration solutions. This was probably due, at least in part, to iodide complexes of metals present in the solutions as trace impurities, originating from the stock chemicals, and/or from dust particles. Satisfactory results were obtained when the following measures were taken. Stock solutions were prepared avoiding dust as much as possible. The sodium perchlorate solutions, prepared as described earlier,[15] were percolated through a cation exchanger, in the sodium form. A different brand of NaI (Merck *p.a.* or Suprapur) was used. At short wavelengths, large spreads were nevertheless obtained when I = 2 or 4 M. As the cobalt absorption increased with decreasing wavelength, a compromise had to be reached. As an optimal wavelength, 320 nm was chosen when I = 2 and 4 M. When I = 1 M, 320 and 300 nm gave consistent solubilities.

The hexaamminecobalt ion is rather sensitive to light. It was found that in a solution with $C_M = 0.2 \times 10^{-3}$ M, C_L = 1 M, when exposed to daylight for a few hours, most of the cobalt had precipitated as hydroxide. On the other hand, if the same solution was completely protected from light, the absorbance changed less than 1 % in 4 h. The solutions were consequently always handled so as to minimize their exposure to light.

Samples of $Co(NH_3)_6I_3(s)$, treated with various solutions, were analyzed for I as described earlier [1] (Table 1). The time of contact between the solid and the solution was about equal to or somewhat longer than the normal contact time in the saturator. When I = 4 M, the salt was apparently stable down to C_L = 1.0 M, which seemed to be relatively low, compared to the corresponding values when I = 1 M and 2 M. It was also found

Table 1. Iodide content in $Co(NH_3)_6I_3(s)$ treated with solutions of various compositions (calculated value 70.26 %).

C_L M	% I	C_L M	% I
$I = 1$ M		$I = 4$ M	
0.48	70.2	1.4	70.2
0.42	Trace	1.3	70.3
		1.2	70.4
$I = 2$ M		1.1	69.9
1.0	70.3	1.1[a]	55
0.9	70.0	1.0	70.3
0.8	70.0	0.9	Trace
0.7	Trace		

[a] Extended contact time; see text.

with one of the solutions ($I = 4$ M, $C_L = 1.1$ M) that a considerably longer contact time resulted in a lower I content in the solid (Table 1). Since the solid did not change during the normal contact time and the solubility in this range does not behave abnormally (Table 2), it may be concluded that $Co(NH_3)_6I_3(s)$ is metastable, probably in the range $1.0 \lesssim C_L \lesssim 1.3$ M, when $I = 4$ M.

At low iodide concentrations, $Co(NH_3)_6(ClO_4)_3(s)$ is the stable salt. Its low solubility, in conjunction with the low absorption coefficients at these low iodide concentrations, made it impossible to obtain reproducible solubilities of the perchlorate with the present technique. Moreover, the values obtained, however uncertain, were such that they could not be easily interpreted in terms of complex formation. The composition of the solid phase was constant. In view of their low precision, these measurements have been disregarded.

RESULTS, CALCULATIONS

The same notation is used as in Refs. 1 and 2. Table 2 shows the observed solubility, S_o, as a function of the solution composition. Stability constants have been calculated from these solubilities. Assuming activity factors to be constant and polynuclear complexes or complexes involving the inert salt to be absent (*cf.* Discussion on p. 1642), the following equation is valid:

$$S = \sum_{n=0}^{N} [ML_n] = \sum_{n=0}^{N} K_s \beta_n [L]^{n-3} \quad (1)$$

When [L], the free ligand concentration in the saturated solutions, differs appreciably from the initial ligand concentration, C_L, it can be calculated by the equation

$$[L] = C_L + (3 - \bar{n})S \quad (2)$$

Since S is always much smaller than C_L, only rough estimates of the ligand number $\bar{n}$ are needed. S and [L] being known, $S[L]^3$ was computed (eqn. (1)) and treated graphically according to standard procedures, to yield K_s and the various β_n.

Table 2. Solubility of $Co(NH_3)_6I_3(s)$. S_o is experimentally determined, S_c is calculated from the constants given in the text.

C_I M	[L] M	$S_o \times 10^4$ M	$S_c \times 10^4$ M	Dev. %	$C_L = [L]$ M	$S_o \times 10^4$ M	$S_c \times 10^4$ M	Dev. %
		$I = 1$ M				$I = 2$ M, ctd.		
0.484	0.486	8.07	8.09	−0.3	1.400	0.738	0.744	−0.8
0.520	0.5215	6.70	6.64	+0.9	1.500	0.632	0.634	−0.3
0.544	0.545	5.81	5.87	−1.0	1.600	0.552	0.546	+1.0
0.605	0.606	4.37	4.366	+0.1	1.700	0.475	0.476	−0.3
0.665	0.666	3.36	3.364	−0.1	1.800	0.433	(0.419)	
0.720	0.721	2.708	2.707	0.0	1.900	0.384	(0.373)	
0.800	0.8005	2.047	2.037	+0.5	2.000	0.351	(0.334)	
0.880	0.880	1.577	1.579	−0.2				
1.000	1.000	1.125	1.125	0.0		$I = 4$ M		
					1.100	0.835	0.842	−0.9
		$I = 2$ M			1.400	0.474	0.470	+0.8
0.800	0.801	2.969	2.968	0.0	1.700	0.309	0.302	+2.3
0.900	0.901	2.194	2.194	0.0	2.000	0.208	0.2125	−2.0
1.000	1.000	1.677	1.684	−0.4	2.500	0.135	0.1352	−0.3
1.100	1.100	1.347	1.329	+1.4	3.000	0.097	0.096	+1
1.200	1.200	1.069	1.075	−0.5	3.500	0.083	(0.073)	
1.300	1.300	0.893	0.887	+0.7	4.000	0.073	(0.058)	

For $I = 1$ M, the function $S[L]^3$ *vs.* [L] is shown in Fig. 1. The values follow closely a linear relationship, and it may be concluded that the free central ion and the first complex ML suffice to explain the data, *i.e.* $S[L]^3 = K_s + K_s\beta_1[L]$; $K_s = 7.41 \times 10^{-5}$ M^4 and $K_s\beta_1 = 3.82 \times 10^{-5}$ M^3 fit the line.

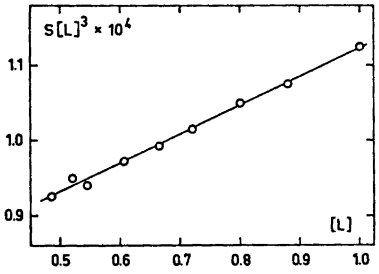

Fig. 1. 1 M ionic strength: $S[L]^3$ *vs.* [L] Straight line of best fit drawn (see text).

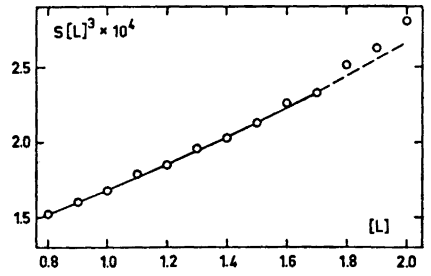

Fig. 2. 2 M ionic strength: $S[L]^3$ *vs.* [L]. The function is curved. The curve drawn is calculated from the constants given in the text.

However, the data at $I = 2$ and 4 M (below) show that also the second complex ML_2 is formed, at higher [L]. It is then natural to check whether the formation of ML_2 is consistent with the data at $I = 1$ as well. It was indeed found that an increase of the ratio β_2/β_1 from 0 to ≈ 0.25 did not affect the fit (error square sum assuming constant relative errors) significantly. The

ratio $\beta_2/\beta_1 = 0.3$ (*cf.* values at $I = 2$ M) gave a slightly poorer fit. The values S_c in Table 2 are calculated assuming the constants to be $K_s = 7.72 \times 10^{-5}$, $K_s\beta_1 = 2.94 \times 10^{-5}$, and $K_s\beta_2 = 0.59 \times 10^{-5}$, *i.e.*, $\beta_2/\beta_1 = 0.2$. It is obvious, however, that the data at $I = 1$ M alone do not permit us to conclude whether only ML or both ML and some higher complex(es) are formed. This, of course, is due to the fact that $[ML_2]$ amounts to at most about 5 % of the total concentration of M. The important fact to notice, is, however, that β_1 is altered quite significantly, from 0.52 to 0.38, when β_2 is changed from its minimum to its maximum permissible value.

When $I = 2$ (Fig. 2) and 4 M, the function $S[L]^3$ *vs.* [L] is curved, and it may safely be concluded that complexes higher than the first are formed. In both cases a good fit is obtained except at the highest [L], when it is assumed that ML and ML_2 are formed. At the highest [L], the solubilities tend to higher values, thus indicating the formation of one or more complexes beyond ML_2. Since the data at high [L] (= low solubilities) are not very reliable, no attempts have been made to estimate the compositions or stabilities of these complexes. S_c of Table 2 are calculated assuming

$K_s = 10 \times 10^{-5}$ M^4, $K_s\beta_1 = 5.3 \times 10^{-5}$ M^3, $K_s\beta_2 = 1.5 \times 10^{-5}$ M^2 ($I = 2$ M), and
$K_s = 7.0 \times 10^{-5}$ M^4, $K_s\beta_1 = 2.4 \times 10^{-5}$ M^3, $K_s\beta_2 = 1.3 \times 10^{-5}$ M^2 ($I = 4$ M).

It should be noted, though, that since ML_3, *etc.*, have been neglected in the calculations at $I = 2$ and 4 M, in an analogous manner as ML_2 was neglected at $I = 1$ M (above), the β_2 values probably come out somewhat high.

That complexes higher than the first are formed can be inferred also from the spectrophotometric calibration data (not given). When such data are plotted according to eqn. (3) of Ref. 2, straight lines with slope $-\beta_1$ should result if no higher complexes are formed. In the present case, the slopes were very small, positive or negative, and varied erratically with the wavelength. As is elucidated in Ref. 2, this is a strong indication of the formation of complexes higher than ML.

An attempt to exclude ML_2, *i.e.* to fit the data ($I = 2$ M) with M, ML, and ML_3 only (and possibly higher complexes; *cf.* the $Coen_3^{3+} - I^-$ system [1]), did not give an acceptable fit.

Table 3. Constants obtained from the solubility data. The estimated error in the last digit is given within parentheses.

I M	$K_s \times 10^5$ M^4	β_1 M^{-1}	β_2 M^{-2}	Higher complexes
1	7.6(3)	0.4(1)	0.04(4)	
2	10(1)	0.5(1)	0.15(5)	Evidence
4	7(1)	0.4(2)	0.2(1)	Evidence

DISCUSSION

The study of such weak complexes as are encountered here is subject to several limitations. In the first place, in order to get any complex formation,

it is necessary to change the medium, in this case from I M $NaClO_4$ to I M NaI. It is well known [16-18] that activity coefficients may then change despite the constant ionic strength.

In the present system, it may thus, perhaps, be asked if such medium effects alone are responsible for the solubility changes, or, as a milder alternative, if only the first complex is formed, the higher ones being artefacts due to the medium effects. It can be checked, firstly, if the experimental data are at all compatible with these hypotheses, secondly, if the required medium effects are of a reasonable magnitude.

When an electrolyte, ML, is substituted for another at constant ionic strength, activity coefficients usually follow [16] the (empirical) equation

$$\log y_{\pm} = \log y_{\pm}^{0} + \alpha[\mathrm{L}] \qquad (3)$$

where $y_{\pm}$ and $y_{\pm}^{0}$ are the mean activity coefficients at the given [L], and at [L] = 0, respectively, and α is a constant. Assuming (a) no complexes are formed and (b) only the first complex is formed, in the $Co(NH_3)_6^{3+} - I^-$ system, we find:

1. The data of Table 2 are at least roughly compatible with both hypotheses.

2. The following approximate α values for the variation in the mean activity coefficient of $Co(NH_3)_6I_3$ are required: (a) -0.045 ($I = 1$ M), -0.05 ($I = 4$ M); (b) -0.03 ($I = 4$ M). Making the somewhat bold assumption that mean activity coefficients for different electrolytes vary approximately in the same way, we compare the given values with literature values.

Ginstrup [17] studied how $y_{\pm}$ for HCl varied when the composition of the background electrolyte was changed. *E.g.*, when $NaClO_4$ was exchanged for NaCl, $\alpha = -0.022$ was found. The α values are largely independent of the ionic strength. On the other hand, they are highly dependent on the nature of the exchanging electrolytes. For various halides, this is perhaps best illustrated by the data of Nilsson.[19] From the variation in solubility product of the thallium(I) halides, the following α values for $y_{\pm}$(TlL) may be computed: -0.018 ($NaClO_4 - NaCl$), -0.008 ($NaClO_4 - NaBr$) and $|\alpha| < 0.002$ ($NaClO_4 - NaI$; the solubility product of TlI(s) did not change significantly between 4 M $NaClO_4$ and 4 M NaI). The chloride value [19] (for TlCl) is in good agreement with Ginstrup's [17] value (for HCl). The trend towards decreasing medium effect in the halide series is found also in other studies.[17,20-23] Therefore it seems safe to conclude that in the present study, medium effects, if present at all, are much smaller than those required by the above hypotheses.

Secondly, the study of weak complexes may be affected by *perchlorate ion association*. As has been briefly outlined earlier,[1] the basic equation (eqn. (1), p. 1639) is then still valid, but instead of the "true" constants β_n, composite constants are obtained. If only one perchlorate complex $MClO_4^{2+}$ is formed, its stability constant being γ_1, the composite constants $(\beta_1 - \gamma_1)/(1 + \gamma_1 I)$, $\beta_2/(1 + \gamma_1 I)$, *etc.* result. When, as in the present case, positive constants are obtained, it can be immediately concluded that even if $\gamma_1 > 0$, the corresponding β_n must also be > 0. In other words, the qualitative interpretation of the M – L system is still correct. It is also clear that it cannot be judged from the present data whether perchlorate complexes are formed or not. However, in the ethylene-

diaminecobalt iodide system,[1] data indicated a perchlorate association with $\gamma_1/\beta_1 \approx 0.2$. Heck [10,11,13] has studied various hexaamminecobalt systems spectrophotometrically; from his data at low ionic strengths a ratio γ_1/β_1 in the range 0.3 to 1.0 can be estimated. The higher limit is of course inconsistent with the data in the present investigation. However, it is most likely that $Co(NH_3)_6^{3+}$ and ClO_4^- do form associates to a significant degree. The "true" β_n are somewhat higher than those given in Table 3.

The perchlorate association is a medium effect, although of a different kind than the activity coefficient variation discussed above. As it is necessary sometimes to employ high ionic strengths, such medium effects are unavoidable. At first sight it may seem to be merely a matter of taste whether the apparent constants in the specific medium are reported or if "true" constants are sought. However, when only weak complexes are involved, different methods of study do not necessarily give the same composite constants.[1] This, on the one hand, provides a means of evaluating γ_1 and β_n independently. On the other hand, it makes it obvious that a constant cannot be reported as *the* constant, in the medium used; at least the method should also be specified.

Table 4. Earlier studies on the $Co(NH_3)_6^{3+} - I^-$ system at 25°C.

Reference	Method	I M	β_1 M^{-1}
Bjerrum [24,7]	Theory	0	66
Linhard [3]	Spectr.	Var.; ≤ 0.06	38[a]
Nancollas *et al.*[4,25]	»	0.054	17
»	»	$\rightarrow 0$	90
Kubota [5]	»	Var.; ≤ 0.1	16
Tanaka *et al.*[6]	»	0.07	0.7
»	»	$\rightarrow 0$	3
Katayama *et al.*[7]	Cond.	0	24
Mironov *et al.*[8]	Soly.	~ 0.2	0.5
»	»	$\rightarrow 0$	60
Yokoyama *et al.*[9]	Spectr.	0.06	9
Heck [11]	»	0.012	32
»	»	$\rightarrow 0$	60

[a] 17–22°C

Several authors have studied the hexaamminecobalt iodide system (Table 4). The ionic strength has been kept low in all studies. Consequently, only the first complex has been subject to study. Disregarding the results[6] obtained by the unreliable L-method,[2] the β_1 values are in fair, though not good, agreement. The strong decrease of β_1 with increasing ionic strength is noticeable.

In the present investigation attention has primarily been paid to the higher complexes. Therefore, high ionic strengths have been employed, and a closer comparison with the earlier studies is not possible. However, the present results, in conjunction with the earlier ones, give a fairly complete picture of the system.

To sum up, the present investigation adds the new information that, in the $Co(NH_3)_6^{3+} - I^-$ system, besides ML, also ML_2 and very probably some higher complex(es) are formed. The order of complex strength is more regular than in the $Coen_3^{3+} - I^-$ system.[1] Possible medium effects, probably of minor importance, or perchlorate association, probably more prominent, cannot invalidate these qualitative conclusions.

This work was supported by a grant from the *Swedish Natural Science Research Council*. The author is grateful to Mrs. Agneta Nilsson and Mr. Bengt Falk for their skilful technical assistance.

REFERENCES

1. Johansson, L. *Acta Chem. Scand.* **25** (1971) 3752.
2. Johansson, L. *Acta Chem. Scand.* **25** (1971) 3569.
3. Linhard, M. *Z. Elektrochem.* **50** (1944) 224.
4. Evans, M. G. and Nancollas, G. H. *Trans. Faraday Soc.* **49** (1953) 363.
5. Kubota, T. *Nippon Kagaku Zasshi* **75** (1954) 552.
6. Tanaka, N., Kobayashi, Y. and Kamada, M. *Bull. Chem. Soc. Japan* **40** (1967) 2839.
7. Katayama, S. and Tamamushi, R. *Bull Chem. Soc. Japan* **41** (1968) 606.
8. Mironov, V. E., Lyubomirova, K. N. and Ragulin, G. K. *Zh. Fiz. Khim.* **44** (1970) 416.
9. Yokoyama, H. and Yamatera, H. *Bull Chem. Soc. Japan* **44** (1971) 1725.
10. Heck, L. *Inorg. Nucl. Chem. Lett.* **7** (1971) 709.
11. Heck, L. *Habilitationsschrift*, Saarbrücken 1972.
12. Bjerrum, J. *Metal Ammine Formation in Aqueous Solution, Diss.*, Copenhagen 1941.
13. Heck, L. *Inorg. Nucl. Chem. Lett.* **7** (1971) 701.
14. Johansson, L. *Coord. Chem. Rev.* **3** (1968) 293.
15. Johansson, L. *Acta Chem. Scand.* **23** (1969) 548.
16. Harned, H. S. and Owen, B. B. *Physical Chemistry of Electrolytic Solutions*, 3rd Ed., Reinhold, New York 1967.
17. Ginstrup, O. *Acta Chem. Scand.* **24** (1970) 875; and references given therein.
18. Ahrland, S. and Johansson, L. *Acta Chem. Scand.* **18** (1964) 2125.
19. Nilsson, R. O. *Arkiv Kemi* **19** (1957) 363.
20. Haight, Jr., G. P. and Johansson, L. *Acta Chem. Scand.* **22** (1968) 961.
21. Leden, I. *Sv. Kem. Tidskr.* **64** (1952) 249.
22. Berne, E. and Leden, I. *Z. Naturforsch.* **8a** (1953) 719.
23. Leden, I. *Acta Chem. Scand.* **10** (1956) 540.
24. Bjerrum, N. *Kgl. Danske Videnskab. Selskab, Mat.-Fys. Medd.* **7** (1926) No. 9.
25. Nancollas, G. H. *J. Chem. Soc.* **1955** 1458.

Received December 14, 1972.

ACTA CHEMICA SCANDINAVICA 27 (1973) 1645–1652

Tautomerism of Mono- and Dinitrophenylazo-alkylphenols

PAUL JUVVIK and BJØRN SUNDBY*

Chemical Institute, The University of Bergen, N-5000 Bergen, Norway

The tautomerism between azophenolic and hydrazonic structures of 4-(2′,4′-dinitrophenylazo)-alkylphenols in tetrachloroethylene solution has been studied by infrared spectroscopy. The tautomeric composition varies between 0 and 100 % hydrazone according to the alkyl substitution. The alkyl groups increase the hydrazone proportion apparently by inductive effects. Large groups in both *meta* positions to hydroxyl sterically prevent formation of the hydrazone and destabilise the azo form. The corresponding 4-(2′-nitrophenylazo)-alkylphenols parallel the dinitro series, but with slightly lower contents of hydrazone. 4-(Phenylazo)- and 4-(4′-nitrophenylazo)-alkylphenols are all pure azo, except 4-(4′-nitrophenylazo)-2,6-di-*tert*-butylphenol (4 % hydrazone). The main conditions for stabilising the hydrazone form appear to be, the presence of a 2′-nitro group, and the presence of one or better two alkyl groups *ortho* to hydroxyl. Appreciable amounts of hydrazone are not formed unless both conditions are fulfilled.

Through the years the tautomerism between *p*-arylazophenols (I) and *p*-quinone arylhydrazones (II) has been investigated extensively on compounds derived from phenols, anthranols, and particularly naphthols. The work has been dealt with in a number of reviews.[1–6] On basis of the early work [7–10] compounds from the phenol series were long assumed to exist in the azo form only.[1,2,11,12]

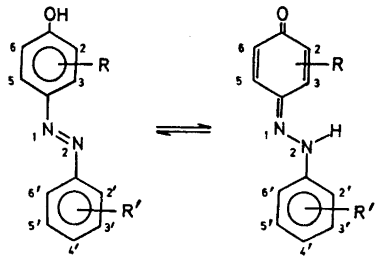

I II

* Present address: Division of Chemical Oceanography, Bedford Institute of Oceanography, Dartmouth, Nova Scotia, Canada.

Later studies by proton magnetic resonance (PMR)[13,14] have shown that substitution by nitro on the phenyl ring of 4-phenylazophenols results in the appearence of the hydrazone form. Similar effects have been found in azoanthranols[15] and azonaphthols.[9,16] A recent PMR study of phenylazophenols[17] indicates that the hydrazone form is favoured by a "push-pull" substitution of electron-donating groups on the phenol ring and withdrawing ones on the other ring: for the first time the existence of 100 % hydrazonic compounds in the phenylazophenol series was reported.

The tautomerism of 4-(2′,4′-dinitrophenylazo)-alkylphenols and mononitro analogs has now been studied in tetrachloroethylene solution, and the tautomer composition was found to vary strongly with the substitution pattern of alkyl. The slight solubility of many of the compounds in this solvent precluded recording of the PMR spectra, but most of the compounds are sufficiently soluble to give good quality infrared spectra in the OH and NH stretch region, provided long-path cells are used.

EXPERIMENTAL

Compounds. Most of the compounds were prepared by diazo-coupling of the corresponding phenols. Compounds 1, 20, 27 – 33, 35 – 37, 39 – 41, 47, and 48 were prepared from the quinone and the appropriate hydrazine in aqueous ethanol containing a little hydrochloric acid. The crude products usually contained numerous impurities in small amounts, which could not be removed by recrystallisation. All compounds were purified by repeated preparative layer chromatography on 1 – 1.5 mm layers of Merck Kieselgel PF_{254}, using chloroform or dichloromethane, or mixtures of petrol ethers or toluene with acetone, dioxane, esters, ethers, *etc.*, as solvents. The 3,5-dialkyl compounds partially decomposed on the layer; the extent of decomposition increased with increasing size of alkyl. 3,5-Di-*tert*-butylphenol coupled quantitatively to the *ortho* product.

Spectra. Infrared spectra were recorded with Unicam SP 100 and SP 200G instruments. Solutions in tetrachloroethylene were measured at 25° in 8.3 mm cells at $2-4\times10^{-3}$ M concentration to obtain the C=O band, and in 41 mm cells at $2-6\times10^{-4}$ M concentration to obtain the OH and NH bands. Spectra of the least soluble compounds (Nos. 1, 6, 7, 11, 12, 17, 18, 32, 33) were recorded with saturated solutions ($1-2\times10^{-4}$ M) up to 100° in electrically heated 41 mm cells. The intensities of the NH and OH stretching bands are given in Table 1 as *apparent* molar absorptivities ε_{app} calculated from the total concentration.

CALCULATIONS

The percentage of hydrazone tautomer (% NH) in tetrachloroethylene solution was estimated from the 3300 cm^{-1} NH and 3600 cm^{-1} OH stretching bands using eqn. (1).

$$\% \text{ NH} = 100A_{NH}/(A_{NH} + \alpha_{av}A_{OH}) \quad (1)$$

A_{NH} and A_{OH} are the band absorbances, and $\alpha_{av} = \varepsilon_{NH\,av}/\varepsilon_{OH\,av}$ is the ratio between the average molar band absorptivities of selected reference compounds with a 100 % hydrazone (Nos. 28 – 31 and 37) or azo (Nos. 38 – 40) structure. With the reference compounds mentioned, $\varepsilon_{NH\,av} = 121$; $\varepsilon_{OH\,av} = 298$; and $\alpha_{av} = 0.406$. This method was chosen because it to some extent corrects for casual impurities; this is not attained when one tautomer is determined by difference.

Table 1. Infrared spectral data and tautomer composition of 4-(substituted phenyl)-azophenols and related compounds in tetrachloroethylene solution.

No.	R in I ⇌ II,[a] or hydrazone	C=O[b] cm^{-1}	NH cm^{-1}	NH ε_{app}	OH cm^{-1}	OH ε_{app}	% NH	4-Nitroso-R-phenol: % oxime in $CDCl_3$ (Ref.)
	R′ = 2′,4′-dinitro							
1	H	0	3292	11	3590	310	8	83[18]
2	2-Me	1619	3301	72	3598	119	60	97.9[18]
3	2-Et		3301	70	3596	96	64	98.7[18]
4	2-Pr		3301	79	3595	91	68	98.8[18]
5	2-Bu	1620	3301	85	3590	40	84	99.4[18]
6	2-Ph		3298	6	3539	315	4	
7	3-Me		3300	29	3592	218	25	97[22]
8	3-Et		3300	27	3593	182	27	
9	3-Pr		3297	24	3589	252	19	
10	3-Bu	1616sh	3299	25	3589	246	20	99[22]
11	3-Ph		3295	8	3591	252	7	
12	3,5-Me_2		3328	31	3587	264	22	94[22]
13	3-Me-5-Et		3333	19	3593	262	15	
14	3-Me-5-Pr	1617sh	3331	17	3592	268	14	
15	3-Me-5-Bu		3332	18	3591	274	14	
16	3,5-Pr_2[c]		0		3608	(254)	0	
17	2,3-Me_2	1619	3302	93	3597	58	80	
18	2,5-Me_2		3303	104	3597	29	90	
19	2-Me-5-Pr	1618	3302	93	3594	30	89	
20	2-Pr-5-Me	1616	3302	93	3594	14	94	> 99.8[22]
21	2-Bu-5-Me	1620	3301	95	3605	22	91	> 99.8[22]
22	2,5-Pr_2		3300	92	3589	18	93	
23	2,5-Bu_2	1620	3300	94	3591	7	97	
24	2,3,5-Me_3	1618	3333	124	3593	73	81	
25	2,6-Me_2	1622	3301	99	3605	12	95	> 99.9[18]
26	2-Me-6-Bu	1618	3301	93	3613	6	98	
27	2,6-Pr_2	1616	3298	120	3601	5	98	
28	3-Cl-2,6-Pr_2	1616	3297	115	0		100	
29	2,6-Bu_2	1615	3300	109	0		100	> 99.94[18]
30	2,3,6-Me_3		3303	114	0		100	> 99.8[22]
31	2,3,5,6-Me_4	1625	3332	132	0		100	
32	1,4-Naphthoquinone DNPH		3302	135[d]	0		100[d]	
33	2-Me-1,4-naphthoquinone		3306	83[d]	0			
	4-DNPH		3366	36[d]	0		100[d]	
	R′ = 2′-nitro							
34	3-Et		3296	9	3587	213	10	
35	2-Pr-5-Me		3297	102	3587	57	82	
36	2,6-Pr_2	1612	3297	99	3602	18	93	
37	2,6-Bu_2	1616	3304	133	0		100	
	R′ = 4′-nitro							
38	3-Et		0		3563	322	0	
39	2-Pr-5-Me		0		3592	282	0	
40	2,6-Pr_2		0		3602	291	0	
41	2,6-Bu_2		3352	8	3628	429	4	

Table 1. Continued.

	Miscellaneous					
42	4-Ph-azophenol		0	3596	328	0
43	4-Ph-azo-2,6-Pr_2-phenol			3607	224	0
44	4-Ph-azo-2,6-Bu_2-phenol		0	3632	326	0
45	4-(2′-Tolylazo)-2,6-Bu_2-phenol		0	3635	336	0
46	4-(3′-nitro-Ph-azo)-2,6-Bu_2-phenol		0	3630	497	0
47	Thymoquinone 4-(*N*-Me-DNPH)	1643				
48	2,6-Bu_2-quinone 4-(*N*-Me-DNPH)	1654				

[a] Me = methyl; Et = ethyl; Pr = isopropyl; Bu = *tert*-butyl; Ph = phenyl; Cl = chloro. [b] sh = shoulder. [c] Unstable. [d] At 100°C.

This procedure involves at least two factors of uncertainty: α_{av} may change if the range of reference compounds is changed; and the true α of a given tautomeric compound may be different from α_{av}. However, similar uncertainties are inherent also with other methods employing reference standards.[12,15,18] It is assumed that for the present purpose the % NH obtained is sufficiently accurate. Owing to the crudeness of the method the simple molar absorptivity was found to be a satisfactory measure of peak intensity, instead of the more accurate but also more cumbersome, triangular area[1] or similar integrated expressions. The results parallel those of Hofer and Uffmann[17] in deuteriochloroform solution as far as the compounds are in common (Nos. 2, 25, 41, 44); this confirms the applicability of the method as a supplement to PMR. The method can be used only with a fixed 2′-substituent since ε_{NH} is strongly influenced by variations in the strength of the hydrogen bond N – H···2′-group.

RESULTS AND DISCUSSION

Solution spectra. The molar absorptivity of the OH band of the pure azo compounds (Nos. 38 – 40; *cf.* also No. 41) varies considerably with the substitution on the phenol ring, and the same was found with the NH band of the pure hydrazonic compounds (Nos. 28 – 34 and 37; *cf.* also Nos. 18, 24, 26, 27, 35). It was not possible, however, to detect any correlation between absorptivity and type, number, or position of alkyl. Similarly no general trends are apparent in the frequencies of the OH or NH bands *vs.* alkyl substitution pattern or tautomeric equilibrium position.

Solution spectra in the carbonyl region 1800 – 1600 cm^{-1} were investigated only for selected compounds. In most cases there is a triple band in the region 1646 – 1597 cm^{-1}. The intensity of the second of these peaks (1625 – 1612 cm^{-1}) follows that of the NH band, and it is therefore assigned to the C = O stretching vibration. As expected the position of this band in quinone dinitrophenylhydrazones is somewhat lower than in less negatively substituted quinone phenyl-

hydrazones.[1] *N*-Methylation (Nos. 47, 48) raises the C=O frequency, as expected.

The sharp, medium intensity band found at 3100 cm^{-1} in dinitrophenylhydrazones and attributed to the dinitrophenyl C–H stretching band,[19] is discussed elsewhere.[20]

In the 2′-nitro series the C=O band seems to overlap completely with a band at 1612–1616 cm^{-1} representing other double bond vibrations, since the presence of this band is not dependent on the NH band. In the 4′-nitro series it is not possible to determine the C=O band position owing to the almost complete lack of hydrazone tautomer in these compounds.

Tautomerism in low-polar solution. Early investigators [7–10] did not find spectral evidence for the existence of the hydrazone form in simple phenylazophenols, and the parent 4-phenylazophenol even does not react with carbonyl reagents or diene components.[21] Introduction of 2′,4′-dinitro substituents onto the phenyl ring of 4-phenylazophenol develops the ability to react with these reagents.[21,22] It was not surprising, therefore, to find a noticeable equilibrium amount (*ca.* 8 %) of hydrazone tautomer in this compound (No. 1, Table 1). Further substitution of alkyl on the phenol ring in the dinitro series raises the percentage of hydrazone relative to No. 1, but to different degrees depending on the type, number, and position of alkyl (*cf.* Table 1).

(1) 2-Alkylation of compound No. 1 results in a significant increase of the hydrazone proportion, and the proportion increases even more upon 2,6-dialkylation.

(2) 3-Alkylation of compound No. 1 results in a moderate increase of the content of hydrazone; this is reduced upon 3,5-dialkylation.

(3) With mixed alkylation 2-alkyl dominates over 3- or 3,5-alkyl, *i.e.*, there is always a high proportion of hydrazone.

(4) Increasing size of 2- or 2,6-alkyl rapidly increases the content of hydrazone.

(5) Increasing size of 3- or 3,5-alkyl has little effect upon or reduces the hydrazone proportion.

(6) Introduction of phenyl in 2- or 3-position has little effect upon or slightly reduces the content of hydrazone, relative to No. 1.

Although only a small number of sample compounds were investigated in the two mononitro and other series, the results seem to bear out the following trends.

(7) In the 2′-nitro series the effects of alkyl closely follow those observed in the 2′,4′-dinitro series, but with a slightly lower content of hydrazone. Only the 2,6-di-*tert*-butyl derivative (No. 37) was found to be 100 % hydrazonic.

(8) In the 4′-nitro series the hydrazone form could not be detected, except in the 2,6-di-*tert*-butyl derivative (No. 41).

(9) In the non-nitro series (Nos. 42, 43, 46), 3′-nitro series (No. 48), and 2′-methyl series (No. 51) no hydrazone was detected.

Results published by Hofer and Uffmann,[17] but not stated explicitly by them, substantiate observations (1), (4), (7), and (8).

Steric hindrance by alkyl in 2- or 2,6-position toward formation and solvent stabilisation of the phenolic group at C_1 could at first glance explain observa-

tions (1) and (4). However, the 96 % azophenolic character of No. 41 shows that these factors are not important in low-polar solvents. Instead, inductive effects must be considered (see below). In more polar solution steric effects seem to be more important.[17]

4-Nitroso-3-alkylphenols are known to exist in the *anti* configuration,[23] and the same is to be expected when dinitrophenylazo is substituted for nitroso (Nos. 7 – 10). The steric conditions at the nitrogen bridge in these compounds therefore should closely correspond to those in No. 1, and their slightly higher content of hydrazone must be ascribed to the inductive effect of the 3-alkyl group.

The steric effect of two alkyl groups in 3,5-position should be more pronounced. Space-filling models show that a *syn*-methyl substituent (Nos. 12 – 15) forces the amino hydrogen of the hydrazone form some 30° out of plane. However, even this steric destabilisation of the hydrazone structure cannot be serious, since the hydrazone content of Nos. 12 – 15 is still higher than that of No. 1.

With increasing size of both 3,5-substituents the steric hindrance at the 4′-position more than counteracts the inductive effect: the 3,5-diisopropyl derivate No. 16 shows no tendency to hydrazone formation. The increasing instability with increasing size of alkyl in the series Nos. 12 – 16 also indicates a strong interaction between the alkyl groups and the lone pair electrons on the nitrogens. This interaction is carried to the extreme with 3,5-di-*tert*-butyl: the *para*-coupling product is non-existent.

Observations (8) and (9) indicate that the inductive and mesomeric effects are not important in the formation of hydrazone; of the two effects the mesomeric is probably the stronger one. It probably acts by reducing the electron density on the hydroxyl oxygen whereby the relative density on nitrogen 2 is increased; this facilitates overlap between the two ring electron systems, increases the tendency of the nitrogen to hybridise, and increases the ability of the nitrogen to capture a hydrogen. Since the effect is weak (obs. 8), however, the higher hydrazone content in the 2′-nitro and dinitro series, relative to the 3′- and 4′-nitro series, probably is due mainly to stabilisation of the hydrazone form by chelation of the NH hydrogen with the 2′-nitro group. The importance of this presumed bonding of NH has been noted previously in 4-arylazo-l-naphthols with 2′-nitro, -methoxy, and -chloro substituents,[1] and it is further discussed in a subsequent paper.[24]

The hydrazone-promoting effect of 2-alkyl *vs.* 3-alkyl is striking. As noted previously this is not usually due to differences in steric requirements, and hence mainly inductive effects must be responsible. Since the inductive property is independent of the position to which the group is attached, the different effect in the two positions must be due to a different ability of the ring to accept the influence of the group. Although a good explanation of this is difficult to conceive, it may be pointed out that when acting from the 2-position a positive inductive effect can better contribute to an increase of electron density on nitrogen 2 than when acting from the 3-position; this increase of charge may facilitate hybridisation of the nitrogen, *etc.* Similar positional differences have been observed with various conjugated systems: it is inferred from published data [18,23] that 2- or 2,6-alkylated 4-nitrosophenols show a

greater tendency to exist in the quinone oxime form than the corresponding 3- or 3,5-analogs (*cf.* Table 1). *p*-Substituents in the β-phenyl groups of tetracyclones influence the infrared stretching frequency of the carbonyl group, whereas *p*-substituents in the α-phenyl groups do not.[25] In the 4-(4′-nitrophenylazo)-phenol series anions of 2-alkylated members absorb at higher wave lengths than 3-alkylated in basic medium, as judged from the colours formed with diethylamine on TLC plates.[26]

Comparison of Nos. 37 *vs.* 44 and 36 *vs.* 43 demonstrates that in the absence of the stabilising NH···nitro bonding, the effect from the alkyl groups is too weak to create any hydrazone. *Vice versa*, in the absence of alkyl, particularly 2- or 2,6-alkyl (*e.g.*, Nos. 25 – 29 *vs.* 1), the NH···nitro stabilisation loses much of its significance. In a "push-pull" cooperation, however, the two effects are able to displace the tautomeric equilibrium to the hydrazone side.

Only two compounds from the naphthol series were investigated (Nos. 32 and 33). The latter was exceedingly difficult to chromatograph, and its purity can be questioned. Due to low solubility in tetrachloroethylene the infrared spectra were obtained at 100°C. Both compounds seem to be 100 % hydrazonic, as expected from the general trend, naphthol series > phenol series.

Comparison of the tendencies of 4-(dinitrophenylazo)-alkylphenols and 4-nitroso-alkylphenols to assume the quinonoid structure (Table 1) indicates that the effect of the dinitrophenylhydrazono group is weaker than that of the oximo group.

REFERENCES

1. Morgan, K. J. *J. Chem. Soc.* **1961** 2151.
2. Zollinger, H., *Diazo and Azo Chemistry. Aliphatic and Aromatic Compounds*, Interscience, New York 1961, p. 322.
3. Schündehütte, K. H. In Müller, E., Ed., *Houben-Weyl's Methoden der organischen Chemie*, Georg Thieme, Stuttgart 1965, Vol. 10/3, p. 213.
4. Ershov, V. V. and Nikiforov, G. A. *Russ. Chem. Rev.* **35** (1966) 817.
5. Kitaev, Yu. P., Buzykin, B. I. and Troepol'skaya, T. V. *Russ. Chem. Rev.* **39** (1970) 441.
6. Bershtein, I. Ya. and Ginzburg, O. F. *Russ. Chem. Rev.* **44** (1972) 97.
7. Kuhn, R. and Bär, F. *Ann.* **516** (1935) 143.
8. Brode, W. R. and Herdle, L. E. *J. Org. Chem.* **6** (1941) 713; *Chem. Abstr.* **35** (1941) 7828.
9. Ospenson, J. N. *Acta Chem. Scand.* **4** (1950) 1351; **5** (1951) 491.
10. Burawoy, A. and Chamberlain, J. T. *J. Chem. Soc.* **1952** 3734.
11. Hadži, D. *J. Chem. Soc.* **1956** 2143.
12. Bekárek, V., Dobás, J., Socha J., Vetešník, P. and Večeřa, M. *Coll. Czech. Chem. Commun.* **35** (1970) 1406.
13. El-Dakhakhny, M. *Ann.* **685** (1965) 134.
14. Kaul, B. L., Nair, P. M., Rao, A.V.R. and Venkataraman, K. *Tetrahedron Letters* **1966** 3897.
15. Bansho, Y., Saito, I., and Miyamae, T. *Kogyo Kagaku Zasshi* **67** (1964) 177; *Chem. Abstr.* **61** (1964) 5817.
16. Burawoy, A., Salem, A. G. and Thompson, A. R. *J. Chem. Soc.* **1952** 4793.
17. Hofer, E. and Uffmann, H. *Tetrahedron Letters* **1971** (35) 3241.
18. Norris, R. K. and Sternhell, S. *Austral. J. Chem.* **22** (1969) 935.
19. Jones, L. A., Holmes, J. C. and Seligman, R. B. *Anal. Chem.* **28** (1956) 191.
20. Juvvik, P. *To be published.*
21. Lauer, W. M. and Miller, S. E. *J. Am. Chem. Soc.* **57** (1935) 520.

22. Borsche, W., Müller, W. and Bodenstein, C. A. *Ann.* **472** (1929) 201; *Chem. Abstr.* **23** (1929) 4679.
23. Uffmann, H. *Z. Naturforsch.* **22b** (1967) 491.
24. Juvvik, P. *To be published.*
25. Jones, R. N., Sandorfy, C. and Tucker, D. E. *J. Phys. Radium* **15** (1954) 320.
26. Juvvik, P. and Sundby, B. *J. Chromatogr.* **76** (1973) 467.

Received November 16, 1972.

ACTA CHEMICA SCANDINAVICA 27 (1973) 1653–1666

The Crystal Structure of Barium Telluropentathionate Trihydrate

KARL GJERRESTAD and KJARTAN MARØY

Chemical Institute, University of Bergen, N-5000 Bergen, Norway

The crystal structure of barium telluropentathionate trihydrate, $BaTe(S_2O_3)_2.3H_2O$, has been determined by X-ray methods. The salt crystallizes in the monoclinic space group $P2_1/c$ (No. 14) with four formula units in a unit cell of dimensions $a = 11.139(3)$ Å, $b = 5.243(2)$ Å, $c = 21.306(6)$ Å, $\beta = 106.94(4)°$. The refinement was carried out by a full-matrix least squares program using 2389 non-zero reflections, recorded by means of a single-crystal diffractometer. The R value was 0.024.

The telluropentathionate ion has the *trans* form, the sulphonate groups being rotated out of the plane of the three middle atoms to different sides of the plane. The dimensions of the S–S–Te–S–S chain, from one end of the chain to the other, are S(1)–S(2) = 2.102(2) Å, S(2)–Te = 2.384(2) Å, Te–S(4) = 2.392(2) Å, S(4)–S(5) = 2.090(2) Å, ∠S(1)–S(2)–Te = 103.08(5)°, ∠S(2)–Te–S(4) = 96.02(4)°, ∠Te–S(4)–S(5) = 102.59(5)°. The SSTe/STeS dihedral angles are 87.7° and 98.7°.

The crystal structures of two barium pentathionate dihydrates,[1,2] of barium selenopentathionate dihydrate [3,4] and trihydrate,[5] and of barium telluropentathionate dihydrate [6,7] and trihydrate [8] have been reported. The latter structure was solved and refined by means of film data. The results of the refinement were not quite satisfactory, the standard deviations being high, compared to those of the barium selenopentathionate hydrates.[4,5] The present work is a more detailed description of this structure analysis, including least squares refinement of diffractometer data.

The pentathionate, selenopentathionate, and telluropentathionate ions have been found to occur in two rotational-isomeric forms, and crystallize in the *cis* form in all of their barium salts, except in barium telluropentathionate trihydrate. The telluropentathionate ion has the *trans* form in the trihydrate, the sulphonate groups being located on opposite sides of the plane through the three middle atoms. The *trans* form of this ion was also found in the crystals of ammonium telluropentathionate [9] and rubidium telluropentathionate hemitrihydrate.[10]

EXPERIMENTAL

Barium telluropentathionate trihydrate, $BaTe(S_2O_3)_2.3H_2O$, was obtained by crystallization of crude barium telluropentathionate from dilute hydrochloric acid.[11] The crystals are light yellowish-green, flat prisms.

The intensity data used for the solution and first refinement of the structure were collected by the multiple-film technique. Integrated zero-layer and equi-inclination Weissenberg photographs were taken with Cu$K\alpha$ radiation (Ni-filtered) for the $h0l$, $h1l$, $h2l$, and $0kl$ reflections. The intensities of the 1106 independent, observed reflections were measured visually.

The intensity data used for a more accurate refinement of the structure were measured on a Siemens automatic single-crystal diffractometer using Mo$K\alpha$ radiation (Nb-filtered) and a scintillation counter.

The crystal was mounted with the b axis approximately parallel to the ϕ axis of the diffractometer, and the orientation of the crystal and preliminary unit cell dimensions were determined from the θ, χ, and ϕ angles of 10 non-coplanar reciprocal vectors.

The $\theta-2\theta$ scan technique and five-value procedure were used. The scan width was 0.70° for all reflections, and the maximum scan time per degree was 24 sec. For strong reflections the diffractometer automatically selects higher scan speed, and inserts a proper attenuation filter into the primary beam, if needed to avoid counting losses.

Two reflections, 700 and 0010, were used as reference, and measured two times each at intervals of 50 reflections. The intensities of the reference reflections decreased by 7 % during the data collection, and were used to bring the net intensities to a common scale.

Out of 2877 reflections attainable within $\theta = 28°$, 488 were found to have net intensities below three times its standard deviation. These reflections were assigned an intensity equal to this limit, and labelled as unobserved.

Lorentz and polarization corrections were applied, and absorption corrections were carried out using a modified version of the Gaussian integration method described by Coppens *et al.*[12] The linear absorption coefficients for Cu$K\alpha$ and Mo$K\alpha$ radiations are 526 cm^{-1} and 66.2 cm^{-1}, respectively. The crystals used were prisms extended along the b axes and bounded by (100) and (001). The distances between the (100), between the (010), and between the (001) boundary faces were 0.036, 0.102, and 0.066 mm, respectively, for the crystal used to collect the $h0l-h2l$ film data, 0.014, 0.080, and 0.072 mm, respectively, for the crystal used to collect the $0kl$ film data, and 0.033, 0.167, and 0.110 mm, respectively, for the crystal used to collect the diffractometer data.

The film data were eventually also corrected for secondary extinction, using the formula $F_{corr} = KF_o(1+\beta CI_o)$.[13] Here $\beta = 2(1+\cos^4 2\theta)/(1+\cos^2 2\theta)^2$, and C was calculated to 1.34×10^{-7}.

The scattering factor curves used were those given in *International Tables for X-Ray Crystallography*,[14] Table 3.3 1B for tellurium, Table 3.3. 1A for sulphur and oxygen, and the one given by Thomas and Umeda [15] for barium ion. The curves for barium, tellurium and sulphur were corrected for anomalous dispersion using the $\Delta f'$ and $\Delta f''$ values given by Cromer,[16] and taking the amplitude of f as the corrected value.

Least squares refinement was carried out with a program minimizing the function

$$r = \sum W(|F_o| - K|F_c|)^2$$

For the film data $W = [(3K)^2 + (2F_o)^2/4W_o + (0.07\ F_o)^6]^{-1}$, where W_o is a weight factor based on the estimated reliability of the individual intensities. For the diffractometer data $W = 4(I_t - I_b)^2/F_o^2[I_t + I_b + k^2(I_t - I_b)^2]$ where I_t is the total intensity of a reflection, I_b is the background intensity, and k is the relative standard deviation in the scaling curve based on the reference reflections. Unobserved reflections were included with $|F_o|$ equal to the observable limit when $|F_c|$ exceeded this limit.

The programs used for calculations of setting angles and preparation of input tape data for the diffractometer, conversion of diffractometer output tape data to the computer, calculation of atomic distances and angles, and for secondary extinction corrections of the film data are written by K. Maartmann-Moe of this institute. The programs used for calculation of unit cell dimensions, film data processing, absorption corrections, two-dimensional Fourier summations, and least squares refinement were made available

by the Chemical Department of X-Ray Crystallography, Weizmann Institute of Science, Rehovoth, Israel. The programs used for diffractometer data processing and three-dimensional Fourier summations are written by K. Åse of this institute. The program used for drawing of illustrations is written by C. K. Johnson, Oak Ridge National Laboratory, Oak Ridge, Tennessee, USA. The calculations were carried out on an IBM 360/50H computer.

The unit cell dimensions, calculated by means of a least squares program using the θ angles ($\theta = 18-22°$) of 10 reflections measured on the diffractometer are, $a = 11.139(3)$ Å, $b = 5.243(2)$ Å, $c = 21.306(6)$ Å, $\beta = 106.94(4)°$. The space group is $P2_1/c$ (No. 14) with four $BaTe(S_2O_3)_2.3H_2O$ formula units per unit cell.[11]

THE STRUCTURE ANALYSIS

Two-dimensional Patterson maps, calculated on the basis of the *h*0*l* and 0*kl* film data, revealed the positions of the two heavy atoms. The subsequent electron density maps allowed the location of the four sulphur atoms, and since two sulphur atoms are coordinated to the tellurium atom, it was possible to distinguish the tellurium atom from the barium ion. The sulphonate and water oxygen atoms were located in additional electron density maps.

Least squares refinement based on the 1106 independent, observed *h*0*l*, *h*1*l*, *h*2*l* and 0*kl* reflections was then carried out. With individual isotropic thermal parameters for all atoms the R value ($\sum||F_o| - |F_c||/\sum|F_o|$) converged at 0.120. Introduction of anisotropic thermal parameters for barium, tellurium and sulphur, followed by secondary extiction corrections, reduced the R value to 0.106 only.

None of the thermal parameters were unusually high, and the atomic distances and angles were not much different from those found in the rubidium salt of telluropentathionic acid.[10] However, the standard deviations were rather high, the agreements between $|F_o|$ and $|F_o|$ for many of the strong

Table 1. Atomic coordinates for barium telluropentathionate trihydrate. Origin at a centre of symmetry. Standard deviations are given in parentheses.

	x	y	z
Ba	0.86098(2)	0.83134(6)	0.09725(1)
S(1)	0.16922(9)	0.62221(21)	0.04248(5)
S(2)	0.32916(10)	0.80347(23)	0.10351(5)
Te	0.40372(2)	0.50579(6)	0.19076(1)
S(4)	0.53083(10)	0.26496(23)	0.13903(5)
S(5)	0.70999(9)	0.41366(21)	0.18220(5)
O(1)	0.07601(31)	0.62342(91)	0.07634(18)
O(2)	0.13999(41)	0.77857(93)	−0.01489(18)
O(3)	0.20295(39)	0.36689(81)	0.03066(21)
O(4)	0.74671(29)	0.33338(69)	0.25033(14)
O(5)	0.78286(30)	0.29377(73)	0.14358(16)
O(6)	0.70578(31)	0.68819(64)	0.17507(16)
$H_2O(1)$	0.07150(32)	0.13818(69)	0.14962(17)
$H_2O(2)$	0.01078(33)	0.59785(79)	0.21127(17)
$H_2O(3)$	0.59990(38)	0.80036(106)	0.03228(19)

reflectrons were not good, and two-dimensional difference election density maps showed unexpected high peaks.

The new set of data, recorded by means of a single-crystal diffractometer, was used for the further refinement of the structure. With atomic coordinates and thermal parameters as derived from the film data, the R value was 0.079. Refinement of the same parameters as in the film data set reduced the reliability index to 0.036, and by using anisotropic thermal parameters for all atoms, the refinement converged at $R = 0.024$. Unobserved reflections are included when $|F_o|$ exceeds the observable limit. The final maximum shift of a parameter was about one fifth of its standard deviation.

A three-dimensional difference electron density map showed no peaks higher than 0.6 e/Å^3. The regions of positive electron density near the water oxygen atoms were too diffuse for location of the hydrogen atoms.

Tables 1 and 2 give the final atomic parameters with standard deviations from least squares. The structure factors, calculated on the basis of these parameters, and the observed ones, from the diffractometer data, are given in Table 3.

Table 2. Thermal parameters expressed in the form $\exp[-2\pi^2(h^2a^{-2}U_{11} + \cdots + 2hka^{-1}b^{-1}U_{12} + \cdots)]$. All values have been multiplied by 10^4. Standard deviations are given in parentheses.

	U_{11}	U_{22}	U_{33}	U_{12}	U_{23}	U_{13}
Ba	247(1)	287(1)	302(1)	26(1)	64(1)	113(1)
S(1)	179(5)	201(5)	184(5)	−13(4)	0(4)	41(4)
S(2)	221(5)	240(6)	314(6)	−62(5)	18(5)	6(4)
Te	180(1)	308(2)	224(1)	3(1)	−28(1)	49(1)
S(4)	167(5)	295(6)	261(5)	−13(4)	−92(4)	43(4)
S(5)	152(5)	225(5)	206(4)	−10(4)	2(4)	58(4)
O(1)	262(19)	824(33)	467(22)	−159(21)	−225(22)	197(17)
O(2)	663(30)	755(33)	394(22)	−380(26)	376(23)	−207(20)
O(3)	523(27)	394(25)	740(30)	149(21)	−337(22)	−139(23)
O(4)	264(17)	400(20)	235(16)	−59(17)	70(15)	−7(13)
O(5)	252(17)	442(22)	447(20)	0(17)	−135(17)	180(16)
O(6)	355(20)	241(18)	443(20)	0(16)	39(16)	154(16)
$H_2O(1)$	362(20)	285(20)	458(21)	23(17)	58(17)	55(16)
$H_2O(2)$	345(21)	504(25)	397(20)	−82(18)	23(18)	58(16)
$H_2O(3)$	419(24)	1039(40)	417(23)	72(27)	60(25)	50(19)

RESULTS

The dimensions of the telluropentathionate ion, calculated from the atomic coordinates of Table 1, are listed in Table 4. The standard deviations given include estimated uncertainties in unit cell dimensions.

Fig. 1 is a view of the ion, as seen along a line through Te and the coordinate midpoint of S(2) and S(4), with principal bond lengths and angles. The largest differences between these values and those arrived at by the refinement based

Table 3. Observed and calculated structure factors (× 10) for barium telluropentathionate trihydrate. A minus sign on $F(O)$ indicates an unobserved reflection.

H	K	L	F(O)	F(C)	H	K	L	F(O)	F(C)	H	K	L	F(O)	F(C)	H	K	L	F(O)	F(C)	H	K	L	F(O)	F(C)
0	0	2	501	-461	4	0-22	447	-443	8	0-26	321	-303	12	0	4	416	-422	1	1 19	1009	-1003			
0	0	4	1755	-1758	4	0-20	416	-414	8	0-24	738	-722	12	0	6	591	591	1	1 20	533	-520			
0	0	6	251	211	4	0-18	407	-411	8	0-22	359	375	12	0	8	-132	-104	1	1 21	805	818			
0	0	8	1210	-1226	4	0-16	817	814	8	0-20	-111	-96	13	0-19		499	-486	1	1 22	-121	46			
0	0	10	2115	2165	4	0-14	2623	2631	8	0-18	315	318	13	0-16		547	-535	1	1 23	169	-159			
0	0	12	-167	138	4	0-12	1173	-1166	8	0-16	376	317	13	0-14		-124	-123	1	1 24	425	421			
0	0	14	1736	-1746	4	0-10	1599	-1621	8	0-14	1766	-1796	13	0-12		1393	1415	1	1 25	311	-314			
0	0	16	240	-108	4	0 -8	-159	67	8	0-12	-99	-27	13	0-10		523	-524	1	1 26	227	213			
0	0	18	1111	-1111	4	0 -6	1439	-1415	8	0-10	1021	1023	13	0 -8		652	-654	2	1-27	522	535			
0	0	20	1127	1154	4	0 -4	2591	2602	8	0 -8	1226	1191	13	0 -6		347	359	2	1-26	478	480			
0	0	22	591	574	4	0 -2	441	-450	8	0 -6	242	228	13	0 -4		567	-578	2	1-25	642	-627			
0	0	24	626	-657	4	0 0	2254	-2379	8	0 -4	1737	-1788	13	0 -2		1276	1264	2	1-24	632	649			
0	0	26	-158	-21	4	0 2	1267	-1200	8	0 -2	-111	-93	13	0 0		467	474	2	1-23	332	308			
1	0	0	386	-349	4	0 4	731	-712	8	0 0	560	498	13	0 2		1082	-1039	2	1-22	222	-208			
1	0	24	207	-205	4	0 6	2728	2710	8	0 2	-113	-37	13	0 4		-119	14	2	1-21	117	-113			
1	0	22	-124	-66	4	0 8	1495	1463	8	0 4	1038	1044	14	0-16		637	-681	2	1-20	872	-861			
1	0	20	130	126	4	0 10	2624	-2600	8	0 6	1378	-1406	14	0-14		255	257	2	1-19	195	-195			
1	0	18	1065	1074	4	0 12	484	467	8	0 8	421	-397	14	0-12		-130	113	2	1-18	352	-352			
1	0	16	1282	-1265	4	0 14	-109	25	8	0 10	610	601	14	0-10		753	753	2	1-17	1489	1496			
1	0	14	1114	-1118	4	0 16	187	173	8	0 12	518	516	14	0 -8		158	151	2	1-16	632	625			
1	0	12	413	415	4	0 18	809	801	8	0 14	923	922	14	0 -6		815	-797	2	1-15	895	-909			
1	0	10	149	165	4	0 20	1149	-1167	8	0 16	634	-640	14	0 -4		315	303	2	1-14	753	752			
1	0	-8	1627	1716	4	0 22	342	-326	8	0 18	368	-370	14	0 -2		-131	71	2	1-13	441	-446			
1	0	-6	619	-556	5	0-28	708	-704	9	0-26	312	-299	14	0 0		-159	52	2	1-12	674	-689			
1	0	-4	811	-795	5	0-26	829	811	9	0-24	167	-148	0	1 1		646	-633	2	1-11	197	-125			
1	0	-2	1101	1143	5	0-24	137	148	9	0-22	1333	-1332	0	1 2		1606	1553	2	1-10	1438	-1446			
1	0	0	126	-169	5	0-22	400	383	9	0-20	709	720	0	1 3		1625	1592	2	1 -9	1184	-1160			
1	0	2	2586	2677	5	0-20	159	154	9	0-18	1216	1195	0	1 4		1996	1975	2	1 -8	633	-618			
1	0	4	137	56	5	0-18	1349	-1346	9	0-16	829	-845	0	1 5		3113	-3193	2	1 -7	2358	2329			
1	0	6	3363	-3443	5	0-16	815	824	9	0-14	470	448	0	1 6		-91	-9	2	1 -6	639	673			
1	0	8	440	437	5	0-14	875	886	9	0-12	565	-955	0	1 7		982	916	2	1 -5	858	-823			
1	0	10	275	-261	5	0-12	105	-84	9	0-10	-105	56	0	1 8		2222	-2183	2	1 -4	2349	2369			
1	0	12	693	690	5	0-10	3158	-3330	9	0 -8	2141	2194	0	1 9		1295	1287	2	1 -3	1436	-1439			
1	0	14	1336	1329	5	0 -8	2962	-2938	9	0 -6	434	-407	0	1 10		462	-458	2	1 -2	867	820			
1	0	16	1547	-1569	5	0 -6	819	775	9	0 -4	632	-631	0	1 11		419	-451	2	1 -1	700	664			
1	0	18	543	547	5	0 -4	2159	2132	9	0 -2	1285	-1234	0	1 12		1465	1465	2	1 0	1413	-1340			
1	0	20	207	258	5	0 -2	153	145	9	0 0	351	-340	0	1 13		1396	1384	2	1 1	570	-549			
1	0	22	-111	-83	5	0 0	455	505	9	0 2	1908	1931	0	1 14		743	713	2	1 2	564	-579			
1	0	24	1058	1063	5	0 2	1369	-1447	9	0 4	189	-196	0	1 15		1090	-1114	2	1 3	2329	2301			
1	0	26	509	-601	5	0 4	667	616	9	0 6	751	-762	0	1 16		907	-921	2	1 4	1815	1720			
2	0	28	409	419	5	0 6	1265	1235	9	0 8	232	243	0	1 17		329	-333	2	1 5	853	825			
2	0	26	293	-304	5	0 8	-103	101	9	0 10	234	-241	0	1 18		1138	-1146	2	1 6	2158	2070			
2	0	22	1461	-1481	5	0 10	604	558	9	0 12	834	862	0	1 19		1011	1015	2	1 7	957	-995			
2	0	20	458	446	5	0 12	1617	-1611	9	0 14	416	398	0	1 20		-139	-55	2	1 8	354	-328			
2	0	18	-101	89	5	0 14	854	-838	9	0 16	230	-247	0	1 21		451	-464	2	1 9	144	140			
2	0	16	290	301	5	0 16	556	545	10	0-24	458	-462	0	1 22		283	265	2	1 10	1455	-1470			
2	0	14	844	828	5	0 18	286	-291	10	0-22	-113	-37	0	1 23		179	186	2	1 11	517	-503			
2	0	12	3113	-3173	5	0 20	135	79	10	0-20	461	-448	0	1 24		243	222	2	1 12	550	-571			
2	0	10	557	551	5	0 22	338	-326	10	0-18	-116	125	0	1 25		248	-264	2	1 13	652	646			
3	0	-8	2494	2552	6	0-26	587	-575	10	0-16	1557	1531	0	1 26		-123	43	2	1 14	496	483			
3	0	-6	1111	1108	6	0-24	865	880	10	0-14	623	-635	1	1-27		159	-139	2	1 15	253	247			
3	0	-4	348	344	6	0-22	1110	554	10	0-12	472	-478	1	1-26		276	303	2	1 16	710	718			
3	0	-2	2812	-2552	6	0-20	466	-472	10	0-10	175	183	1	1-25		-114	-12	2	1 17	1038	-1030			
3	0	0	519	-632	6	0-18	627	615	10	0 -8	1009	-1025	1	1-24		308	-297	2	1 18	321	304			
3	0	2	1613	1650	6	0-16	1625	-1621	10	0 -6	1550	1562	1	1-23		675	-684	2	1 19	121	143			
3	0	4	565	-569	6	0-14	-55	5	10	0 -4	307	-338	1	1-22		332	-292	2	1 20	475	-474			
3	0	6	-53	-14	6	0-12	1530	1563	10	0 -2	1126	-1137	1	1-21		711	712	2	1 21	179	-179			
3	0	8	2716	-2742	6	0-10	688	-685	10	0 0	-190	276	1	1-20		153	159	2	1 22	437	-454			
3	0	10	698	-703	6	0 -8	313	296	10	0 2	850	-860	1	1-19		253	267	2	1 23	175	185			
3	0	12	1223	1218	6	0 -6	1196	-1237	10	0 4	1279	1257	1	1-18		444	424	2	1 24	251	269			
3	0	14	1265	1260	6	0 -4	1118	-1129	10	0 6	1357	1341	1	1-17		-131	11	2	1 25	498	484			
3	0	16	346	317	6	0 -2	3450	3740	10	0 8	1128	-1142	1	1-16		696	689	3	1-27	151	-163			
3	0	18	777	-715	6	0 0	-140	-42	10	0 10	250	295	1	1-15		495	474	3	1-26	291	305			
3	0	20	467	-446	6	0 2	714	-711	10	0 12	332	-309	1	1-14		-43	27	3	1-25	804	820			
3	0	22	1059	1084	6	0 4	364	-372	10	0 14	171	181	1	1-13		1087	-1101	3	1-24	399	393			
3	0	24	-112	6	6	0 6	1251	-1252	11	0-24	571	549	1	1-12		534	-532	3	1-23	434	-442			
3	0	26	361	324	6	0 8	1568	1585	11	0-22	-151	-120	1	1-11		557	563	3	1-22	-134	46			
3	0	28	267	261	6	0 10	412	404	11	0-20	681	-677	1	1-10		796	-784	3	1-21	394	-390			
3	0	24	617	-565	6	0 12	1102	-1106	11	0-18	376	367	1	1 -9		815	831	3	1-20	718	-736			
3	0	22	186	-179	6	0 14	182	-188	11	0-16	262	310	1	1 -8		1118	1089	3	1-19	705	746			
3	0	20	1283	-1288	6	0 16	1069	-1051	11	0-14	695	758	1	1 -7		751	-762	3	1-18	636	-629			
3	0	18	1135	1136	6	0 18	756	751	11	0-12	-112	-8	1	1 -6		1207	1251	3	1-17	838	-828			
3	0	16	1572	1618	6	0 20	737	719	11	0-10	1654	-1679	1	1 -5		132	195	3	1-16	-59	-91			
3	0	14	1317	-1256	7	0-26	-115	-106	11	0 -8	-111	-52	1	1 -4		225	151	3	1-15	1034	993			
3	0	12	411	415	7	0-24	270	-253	11	0 -6	535	538	1	1 -3		2581	-2593	3	1-14	1022	1032			
3	0	10	1359	-1365	7	0-22	273	253	11	0 -4	522	506	1	1 -2		1645	-1679	3	1-13	456	-495			
3	0	-8	746	-706	7	0-20	1299	1290	11	0 -2	150	-133	1	1 -1		-97	-19	3	1-12	438	432			
3	0	-6	2757	2848	7	0-18	1074	-1055	11	0 0	1265	-1256	1	1 0		-116	6	3	1-11	2018	-2025			
3	0	-4	2234	-2204	7	0-16	1044	-1047	11	0 2	533	513	1	1 1		1479	1428	3	1-10	950	-949			
3	0	-2	1678	-1653	7	0-14	503	-457	11	0 4	604	592	1	1 2		738	728	3	1 -9	1471	1457			
3	0	0	1166	-1225	7	0-12	-68	77	11	0 6	-118	60	1	1 3		1093	-1163	3	1 -8	1396	-1360			
3	0	2	2685	-2659	7	0-10	2599	2625	11	0 8	620	632	1	1 4		1198	1173	3	1 -7	339	-353			
3	0	4	3500	3556	7	0 -8	986	-964	11	0 10	944	-985	1	1 5		1304	1304	3	1 -6	621	630			
3	0	6	449	-411	7	0 -6	873	-885	12	0-22	263	-285	1	1 6		-92	104	3	1 -5	149	204			
3	0	8	1234	-1223	7	0 -4	1429	1424	12	0-20	201	213	1	1 7		-89	-15	3	1 -4	1431	1415			
3	0	10	1344	1312	7	0 -2	666	-660	12	0-18	858	-884	1	1 8		765	-778	3	1 -3	1631	1569			
3	0	12	624	-612	7	0 0	1960	1934	12	0-16	-126	101	1	1 9		780	-770	3	1 -2	331	376			
3	0	14	1255	1245	7	0 2	118	172	12	0-14	728	729	1	1 10		947	-960	3	1 -1	2490	-2566			
3	0	16	434	421	7	0 4	1563	-2602	12	0-12	547	-553	1	1 11		2122	2095	3	1 0	933	-906			
3	0	18	665	-658	7	0 6	149	132	12	0-10	353	366	1	1 12		310	-296	3	1 1	1811	1824			
3	0	20	-114	2	7	0 8	553	-540	12	0 -8	712	-701	1	1 13		653	-627	3	1 2	292	-315			
3	0	22	731	-716	7	0 10	726	706	12	0 -6	733	-722	1	1 14		358	367	3	1 3	729	704			
3	0	24	241	240	7	0 12	457	485	12	0 -4	1408	1386	1	1 15		149	139	3	1 4	447	-406			
4	0	28	228	-235	7	0 14	1459	-1472	12	0 -2	137	171	1	1 16		723	711	3	1 5	403	-367			
4	0	26	146	-174	7	0 16	456	531	12	0 0	-160	115	1	1 17		-101	3	3	1 6	605	625			
4	0	24	854	864	7	0 18	338	380	12	0 2	332	-309	1	1 18		452	-469	3	1 7	1441	1419			

Table 3. Continued.

H	K	L	F(O)	F(C)	H	K	L	F(O)	F(C)	H	K	L	F(O)	F(C)	H	K	L	F(O)	F(C)	H	K	L	F(O)	F(C)
3	1	8	657	675	5	1	9	148	-155	7	1	15	-115	-28	10	1-12	517	497	13	1	-6	693	-684
3	1	9	1566	-1586	5	1	10	660	655	7	1	16	312	-341	10	1-11	1338	-1339	13	1	-5	-123	81
3	1	10	238	188	5	1	11	615	-595	7	1	17	729	-751	10	1-10	322	-301	13	1	-4	694	-684
3	1	11	355	-335	5	1	12	145	148	7	1	18	554	-543	10	1 -9	455	451	13	1	-3	530	513
3	1	12	685	-677	5	1	13	514	511	7	1	19	532	545	10	1 -8	579	-593	13	1	-2	181	194
3	1	13	684	689	5	1	14	358	-352	8	1-26		481	494	10	1 -7	591	617	13	1	-1	536	-536
3	1	14	165	154	5	1	15	265	-269	8	1-25		214	214	10	1 -6	-113	33	13	1	0	718	694
3	1	15	345	-357	5	1	16	128	-106	8	1-24		-111	-6	10	1 -5	354	-354	13	1	1	529	522
3	1	16	772	795	5	1	17	523	521	8	1-23		277	-284	10	1 -4	752	749	13	1	2	242	221
3	1	17	735	722	5	1	18	121	-72	8	1-22		517	-504	10	1 -3	1156	1152	13	1	3	442	-454
3	1	18	510	467	5	1	19	392	373	8	1-21		-104	36	10	1 -2	353	337	13	1	4	176	-192
3	1	19	434	-495	5	1	20	153	106	8	1-20		273	-264	10	1 -1	1039	-1026	14	1-15		332	-340
3	1	20	-110	-52	5	1	21	523	-545	8	1-19		950	941	10	1 0	594	-574	14	1-14		431	-444
3	1	21	260	-255	5	1	22	140	123	8	1-18		566	586	10	1 1	181	-185	14	1-13		-126	-82
3	1	22	187	-161	6	1-27		-118	-106	8	1-17		336	-356	10	1 2	690	-689	14	1-12		181	-191
3	1	23	564	551	6	1-26		253	-276	8	1-16		614	618	10	1 3	892	879	14	1-11		480	494
3	1	24	147	-131	6	1-25		158	162	8	1-15		-101	13	10	1 4	161	-156	14	1-10		-126	106
4	1-27		485	454	6	1-24		339	-319	8	1-14		456	-438	10	1 5	778	-815	14	1 -9		453	-431
4	1-26		360	-375	6	1-23		579	-564	8	1-13		228	-217	10	1 6	354	354	14	1 -8		346	334
4	1-25		-112	67	6	1-22		133	-116	8	1-12		764	-754	10	1 7	424	449	14	1 -7		-122	108
4	1-24		287	275	6	1-21		944	953	8	1-11		534	-527	10	1 8	453	463	14	1 -6		242	230
4	1-23		170	157	6	1-20		596	603	8	1-10		353	-390	10	1 9	306	-324	14	1 -5		235	-225
4	1-22		424	413	6	1-19		452	-453	8	1 -9		578	570	10	1 10	-131	149	14	1 -4		239	-167
4	1-21		166	151	6	1-18		935	947	8	1 -8		-104	71	10	1 11	637	-643	14	1 -3		348	-363
4	1-20		427	-434	6	1-17		302	-301	8	1 -7		572	-630	10	1 12	351	-325	14	1 -2		293	-186
4	1-19		1185	-1232	6	1-16		229	-225	8	1 -6		942	944	10	1 13	720	733	14	1 -1		674	671
4	1-18		654	-655	6	1-15		1067	1056	8	1 -5		357	-310	11	1-23	373	-377	0	2	0	667	-611
4	1-17		531	497	6	1-14		841	-839	8	1 -4		568	891	11	1-22	630	627	0	2	1	895	923
4	1-16		572	-573	6	1-13		577	-571	8	1 -3		-108	81	11	1-21	-115	-52	0	2	2	1714	-1678
4	1-15		-35	70	6	1-12		-56	-5	8	1 -2		753	-726	11	1-20	193	-185	0	2	3	1203	1214
4	1-14		-52	-31	6	1-11		1251	1304	8	1 -1		558	-619	11	1-19	446	-451	0	2	4	1216	1246
4	1-13		124	-146	6	1-10		955	985	8	1 0		866	-849	11	1-18	663	-663	0	2	5	-93	-123
4	1-12		1221	1248	6	1 -9		591	573	8	1 1		1451	1476	11	1-17	-115	-39	0	2	6	1383	1404
4	1-11		763	762	6	1 -8		638	668	8	1 2		256	303	11	1-16	179	-177	0	2	7	1503	-1534
4	1-10		1148	1132	6	1 -7		2134	-2115	8	1 3		156	176	11	1-15	786	777	0	2	8	2043	-1982
4	1 -9		1662	-1702	6	1 -6		722	-736	8	1 4		1154	1167	11	1-14	755	749	0	2	9	668	-665
4	1 -8		564	-555	6	1 -5		659	643	8	1 5		553	-548	11	1-13	387	-378	0	2	10	635	626
4	1 -7		654	664	6	1 -4		1226	-1238	8	1 6		252	264	11	1-12	705	724	0	2	11	607	608
4	1 -6		1580	-2005	6	1 -3		344	-337	8	1 7		274	278	11	1-11	-111	45	0	2	12	529	-533
4	1 -5		1180	1220	6	1 -2		672	-668	8	1 8		647	-658	11	1-10	-115	-86	0	2	13	1314	1320
4	1 -4		527	670	6	1 -1		154	-85	8	1 9		646	-641	11	1 -9	271	-253	0	2	14	226	-229
4	1 -3		406	-432	6	1 0		549	547	8	1 10		465	-468	11	1 -8	643	-642	0	2	15	-130	-16
4	1 -2		2258	2343	6	1 1		1078	1065	8	1 11		703	719	11	1 -7	-117	-107	0	2	16	1386	1384
4	1 -1		1123	1171	6	1 2		984	993	8	1 12		-119	73	11	1 -6	328	-311	0	2	17	344	-347
4	1 0		320	335	6	1 3		1186	-1188	8	1 13		-113	27	11	1 -5	1079	1073	0	2	18	476	-479
4	1 1		1554	-1564	6	1 4		201	-181	8	1 14		252	231	11	1 -4	-114	15	0	2	19	368	-376
4	1 2		1476	-1498	6	1 5		234	217	8	1 15		559	-511	11	1 -3	336	-291	0	2	20	253	-218
4	1 3		425	-423	6	1 6		1214	-1195	8	1 16		328	325	11	1 -2	574	568	0	2	21	196	196
4	1 4		1358	-1350	6	1 7		553	549	8	1 17		181	183	11	1 -1	328	-319	0	2	22	-108	-91
4	1 5		1574	1560	6	1 8		649	-650	9	1-26		380	363	11	1 0	-113	82	0	2	23	560	555
4	1 6		165	-169	6	1 9		162	-165	9	1-25		320	-355	11	1 1	-119	-113	0	2	24	232	-220
4	1 7		1339	-1293	6	1 10		658	652	9	1-24		227	222	11	1 2	917	-937	0	2	25	-129	53
4	1 8		656	670	6	1 11		1259	1241	9	1-23		288	-287	11	1 3	663	-679	1	2-26		293	-268
4	1 9		130	124	6	1 12		759	757	9	1-22		430	-441	11	1 4	551	-545	1	2-25		180	192
4	1 10		580	591	6	1 13		677	-685	9	1-21		460	487	11	1 5	772	775	1	2-24		434	403
4	1 11		528	-520	6	1 14		121	-115	9	1-20		658	-675	11	1 6	586	633	1	2-23		520	-515
4	1 12		276	-252	6	1 15		191	-191	9	1-19		455	-507	11	1 7	-123	-122	1	2-22		190	213
4	1 13		1332	-1315	6	1 16		832	-838	9	1-18		254	-241	11	1 8	542	536	1	2-21		719	-736
4	1 14		830	-675	6	1 17		571	572	9	1-17		1047	1047	11	1 9	340	-337	1	2-20		847	-834
4	1 15		1331	1387	6	1 18		303	-339	9	1-16		706	734	11	1 10	-129	91	1	2-19		149	135
4	1 16		-109	8	6	1 19		322	-311	9	1-15		270	-280	11	1 11	296	311	1	2-18		363	366
4	1 17		-105	-56	6	1 20		264	275	9	1-14		1166	1188	12	1-21	293	-285	1	2-17		498	514
4	1 18		154	147	7	1-27		158	-164	9	1-13		1275	-1261	12	1-20	476	479	1	2-16		135	-120
4	1 19		-114	23	7	1-26		-116	-71	9	1-12		761	-772	12	1-19	473	-467	1	2-15		496	500
4	1 20		528	503	7	1-25		680	-667	9	1-11		729	725	12	1-18	-115	-41	1	2-14		603	604
4	1 21		283	284	7	1-24		523	-531	9	1-10		1313	-1329	12	1-17	528	515	1	2-13		376	-387
4	1 22		353	-377	7	1-23		579	583	9	1 -9		506	-505	12	1-16	534	-532	1	2-12		504	503
4	1 23		632	-620	7	1-22		112	-56	9	1 -8		641	624	12	1-15	335	-396	1	2-11		748	-759
5	1-27		256	-320	7	1-21		-107	-24	9	1 -7		465	462	12	1-14	152	-144	1	2-10		1643	-1639
5	1-26		457	-516	7	1-20		554	570	9	1 -6		1152	1155	12	1-13	727	725	1	2 -9		551	563
5	1-25		-112	83	7	1-19		159	154	9	1 -5		660	662	12	1-12	448	458	1	2 -8		1011	998
5	1-24		268	-214	7	1-18		854	897	9	1 -4		776	787	12	1-11	212	222	1	2 -7		1390	1343
5	1-23		754	761	7	1-17		388	367	9	1 -3		1265	-1271	12	1-10	394	385	1	2 -6		165	153
5	1-22		628	568	7	1-16		162	-171	9	1 -2		367	-354	12	1 -9	838	-841	1	2 -5		768	779
5	1-21		833	-822	7	1-15		1133	-1119	9	1 -1		749	724	12	1 -8	399	-405	1	2 -4		642	-622
5	1-20		645	649	7	1-14		763	-755	9	1 0		536	-527	12	1 -7	593	582	1	2 -3		-92	58
5	1-19		238	-245	7	1-13		966	952	9	1 1		234	217	12	1 -6	639	-632	1	2 -2		1854	1851
5	1-18		650	-656	7	1-12		855	-841	9	1 2		256	-264	12	1 -5	236	-234	1	2 -1		1147	-1184
5	1-17		200	-193	7	1-11		582	571	9	1 3		-111	52	12	1 -4	-120	-92	1	2 0		1175	-1248
5	1-16		662	-661	7	1-10		-57	33	9	1 4		353	378	12	1 -3	-117	83	1	2 1		1249	-1207
5	1-15		425	-429	7	1 -9		549	-521	9	1 5		575	575	12	1 -2	125	-3	1	2 2		532	-520
5	1-14		333	324	7	1 -8		844	826	9	1 6		494	496	12	1 -1	324	341	1	2 3		987	985
5	1-13		1559	1583	7	1 -7		728	705	9	1 7		1005	-1037	12	1 0	338	321	1	2 4		372	352
5	1-12		582	1005	7	1 -6		449	429	9	1 8		145	-144	12	1 1	846	-850	1	2 5		548	548
5	1-11		585	-585	7	1 -5		2141	-2147	9	1 9		-119	-78	12	1 2	301	324	1	2 6		651	-673
5	1-10		447	463	7	1 -4		1057	-1053	9	1 10		821	-842	12	1 3	148	121	1	2 7		269	-276
5	1 -9		124	-134	7	1 -3		440	432	9	1 11		336	315	12	1 4	212	-211	1	2 8		1368	1397
5	1 -8		405	-405	7	1 -2		776	-782	9	1 12		-121	-91	12	1 5	-118	-15	1	2 9		613	-630
5	1 -7		272	284	7	1 -1		1221	1192	9	1 13		335	-343	12	1 6	237	-244	1	2 10		1002	-976
5	1 -6		1551	-1617	7	1 0		757	781	9	1 14		463	483	12	1 7	-120	67	1	2 11		243	-253
5	1 -5		834	-831	7	1 1		856	-925	9	1 15		358	392	12	1 8	197	185	1	2 12		825	-844
5	1 -4		565	-586	7	1 2		1427	1404	10	1-25		318	302	13	1-19	266	282	1	2 13		951	972
5	1 -3		1670	1726	7	1 3		944	923	10	1-24		314	308	13	1-18	174	165	1	2 14		713	709
5	1 -2		178	203	7	1 4		-111	-18	10	1-23		-112	33	13	1-17	738	-744	1	2 15		552	544
5	1 -1		427	-397	7	1 5		673	-677	10	1-22		-116	-138	13	1-16	318	-329	1	2 16		757	-765
5	1 0		1135	1184	7	1 6		508	-505	10	1-21		829	-813	13	1-15	539	525	1	2 17		-102	3
5	1 1		1257	-1267	7	1 7		374	-364	10	1-20		358	-404	13	1-14	533	-552	1	2 18		521	512
5	1 2		477	-466	7	1 8		318	-331	10	1-19		508	522	13	1-13	204	193	1	2 19		251	-289
5	1 3		283	286	7	1 9		1464	1490	10	1-18		259	-279	13	1-12	-125	-133	1	2 20		152	152
5	1 4		1358	-1414	7	1 10		-112	51	10	1-17		148	-139	13	1-11	-131	-134	1	2 21		431	-414
5	1 5		1007	-990	7	1 11		573	-559	10	1-16		-105	-53	13	1-10	565	554	1	2 22		536	-537
5	1 6		382	-361	7	1 12		-112	9	10	1-15		118	-113	13	1 -9	530	538	1	2 23		-112	57
5	1 7		553	548	7	1 13		233	214	10	1-14		561	576	13	1 -8	472	468	1	2 24		295	310
5	1 8		916	887	7	1 14		247	249	10	1-13		459	470	13	1 -7	1074	-1078	1	2 25		238	229

Table 3. Continued.

H	K	L	F(O)	F(C)
2	2-24	211	204
2	2-25	158	135
2	2-24	331	352
2	2-23	-112	103
2	2-22	235	-252
2	2-21	481	-474
2	2-20	763	777
2	2-19	725	-740
2	2-18	776	-779
2	2-17	640	636
2	2-16	393	-403
2	2-15	1019	1019
2	2-14	935	926
2	2-13	458	-456
2	2-12	-63	-57
2	2-11	536	-511
2	2-10	1151	1066
2	2-9	1065	-1064
2	2-8	1214	-1214
2	2-7	338	347
2	2-6	1537	-1564
2	2-5	1754	1748
2	2-4	2037	2089
2	2-3	427	428
2	2-2	435	-367
2	2-1	537	-563
2	2 0	560	514
2	2 1	2311	-2263
2	2 2	337	-339
2	2 3	372	327
2	2 4	1730	-1781
2	2 5	1744	1733
2	2 6	1224	1159
2	2 7	610	643
2	2 8	331	327
2	2 9	356	-345
2	2 10	215	196
2	2 11	592	-567
2	2 12	249	260
2	2 13	317	-288
2	2 14	1567	-1584
2	2 15	635	672
2	2 16	434	501
2	2 17	351	359
2	2 18	505	521
2	2 19	468	-501
2	2 20	263	-254
2	2 21	572	-562
2	2 22	-115	107
2	2 23	205	-164
2	2 24	458	-503
2	2-26	310	-325
3	2-25	273	266
3	2-24	257	-276
3	2-23	347	341
3	2-22	1783	1672
3	2-21	-139	16
3	2-20	58	-58
3	2-19	476	-467
3	2-18	390	-367
3	2-17	-136	52
3	2-16	247	224
3	2-15	1525	1523
3	2-14	436	-464
3	2-13	507	517
3	2-12	1458	1459
3	2-11	-62	-56
3	2-10	111	-55
3	2-9	550	-584
3	2-8	547	-561
3	2-7	628	-629
3	2-6	1041	1016
3	2-5	531	523
3	2-4	1471	-1488
3	2-3	697	651
3	2-2	1257	1323
3	2-1	333	-287
3	2 1	1416	-1429
3	2 2	1528	-1528
3	2 3	436	-454
3	2 4	561	548
3	2 5	676	655
3	2 6	758	-755
3	2 7	1277	1259
3	2 8	234	215
3	2 9	205	217
3	2 10	399	367
3	2 11	430	-405
3	2 12	1504	-1555
3	2 13	442	-454
3	2 14	605	595
3	2 15	158	-156
3	2 16	295	-277
3	2 17	450	464
3	2 18	576	-571
3	2 19	-113	33
3	2 20	861	857
3	2 21	269	-325
3	2 22	223	-217
3	2 23	128	-142
4	2-26	254	-252
4	2-25	115	111
4	2-24	197	158
4	2-23	438	461
4	2-22	632	-632
4	2-21	634	653
4	2-20	666	651
4	2-19	-105	19
4	2-18	646	657
4	2-17	967	-980
4	2-16	1343	-1355
4	2-15	-132	-76
4	2-14	176	181
4	2-13	374	376
4	2-12	374	-378
4	2-11	612	625
4	2-10	572	558
4	2-9	563	-564
4	2-8	1022	1119
4	2-7	1369	-1375
4	2-6	1464	-1438
4	2-5	612	-608
4	2-4	365	375
4	2-3	1168	1178
4	2-2	231	-214
4	2-1	671	658
4	2 0	328	-316
4	2 1	170	157
4	2 2	2533	2556
4	2 3	386	-381
4	2 4	502	-494
4	2 5	596	-584
4	2 6	849	-835
4	2 7	908	905
4	2 8	457	435
4	2 9	1022	1123
4	2 10	-132	-13
4	2 11	478	-476
4	2 12	1156	1185
4	2 13	851	-838
4	2 14	466	-469
4	2 15	722	-716
4	2 16	715	-699
4	2 17	443	446
4	2 18	544	551
4	2 19	459	459
4	2 20	442	-465
4	2 21	-117	32
4	2 22	461	443
5	2-26	153	158
5	2-25	128	-129
5	2-24	728	-698
5	2-23	500	510
5	2-22	205	222
5	2-21	480	477
5	2-20	453	446
5	2-19	186	174
5	2-18	363	-367
5	2-17	642	-654
5	2-16	819	758
5	2-15	1269	-1269
5	2-14	572	-574
5	2-13	-59	45
5	2-12	642	-628
5	2-11	911	907
5	2-10	1427	1399
5	2-9	138	-116
5	2-8	341	-364
5	2-7	746	-745
5	2-6	431	435
5	2-5	951	-957
5	2-4	901	-901
5	2-3	463	494
5	2-2	851	-926
5	2-1	1209	1311
5	2 0	1581	1561
5	2 1	412	395
5	2 2	751	-752
5	2 3	-105	-18
5	2 4	277	295
5	2 5	745	-754
5	2 6	442	429
5	2 7	289	-273
5	2 8	1154	-1132
5	2 9	758	907
5	2 10	714	721
5	2 11	-110	41
5	2 12	134	175
5	2 13	512	-500
5	2 14	-110	82
5	2 15	312	-301
5	2 16	328	324
5	2 17	132	-78
5	2 18	644	-646
5	2 19	422	436
5	2 20	371	385
5	2 21	377	384
6	2-26	255	-279
6	2-25	348	-341
6	2-24	160	166
6	2-23	301	-305
6	2-22	296	-293
6	2-21	281	292
6	2-20	541	-501
6	2-19	214	206
6	2-18	1064	1045
6	2-17	-102	-73
6	2-16	317	-341
6	2-15	932	-940
6	2-14	143	-141
6	2-13	868	-841
6	2-12	326	300
6	2-11	689	686
6	2-10	1574	-1564
6	2 -9	1231	1215
6	2 -8	1054	1059
6	2 -7	375	365
6	2 -6	601	597
6	2 -5	320	-315
6	2 -4	441	-420
6	2 -3	1911	-1038
6	2 -2	263	241
6	2 -1	393	384
6	2 0	1508	-1521
6	2 1	561	958
6	2 2	722	697
6	2 3	327	353
6	2 4	1258	1255
6	2 5	1009	-1020
6	2 6	582	-567
6	2 7	550	-538
6	2 8	466	430
6	2 9	175	-166
6	2 10	752	-720
6	2 11	742	749
6	2 12	244	-212
6	2 13	213	234
6	2 14	930	913
6	2 15	200	-210
6	2 16	274	-274
6	2 17	162	-174
6	2 18	-161	92
6	2 19	-116	17
6	2 20	234	-227
7	2-26	531	516
7	2-25	256	-251
7	2-24	-116	61
7	2-23	726	-748
7	2-22	560	-577
7	2-21	113	-55
7	2-20	244	242
7	2-19	451	442
7	2-18	411	-431
7	2-17	321	314
7	2-16	358	351
7	2-15	274	-274
7	2-14	575	585
7	2-13	869	-895
7	2-12	1615	-1631
7	2-11	343	344
7	2-10	385	377
7	2 -9	1167	1172
7	2 -8	-102	-56
7	2 -7	763	772
7	2 -6	-101	18
7	2 -5	222	-228
7	2 -4	637	842
7	2 -3	1042	-1149
7	2 -2	1358	-1393
7	2 -1	512	-517
7	2 0	158	140
7	2 1	638	635
7	2 2	-110	-44
7	2 3	475	510
7	2 4	402	-389
7	2 5	428	-434
7	2 6	1346	1352
7	2 7	658	-658
7	2 8	860	-861
7	2 9	351	-348
7	2 10	521	-518
7	2 11	455	453
7	2 12	923	620
7	2 13	621	625
7	2 14	388	-346
7	2 15	-115	-74
7	2 16	463	429
7	2 17	166	-184
7	2 18	-127	-96
8	2-25	-118	92
8	2-24	182	-202
8	2-23	303	-317
8	2-22	415	423
8	2-21	570	-577
8	2-20	535	-533
8	2-19	256	295
8	2-18	-105	-38
8	2-17	550	566
8	2-16	166	177
8	2-15	558	595
8	2-14	176	-161
8	2-13	-103	70
8	2-12	1127	1134
8	2-11	599	-586
8	2-10	743	-740
8	2 -9	-103	-53
8	2 -8	936	-916
8	2 -7	937	965
8	2 -6	1100	1109
8	2 -5	-112	24
8	2 -4	301	-297
8	2 -3	550	-587
8	2 -2	605	595
8	2 -1	1123	-1117
8	2 0	220	-194
8	2 1	374	-381
8	2 2	908	-909
8	2 3	694	719
8	2 4	481	473
8	2 5	372	394
8	2 6	391	-396
8	2 7	-114	-39
8	2 8	459	464
8	2 9	215	-225
8	2 10	330	332
8	2 11	377	-392
8	2 12	1148	-1156
8	2 13	624	593
8	2 14	271	289
8	2 15	453	459
8	2 16	190	183
9	2-24	886	893
9	2-23	-115	1
9	2-22	259	-267
9	2-21	406	-396
9	2-20	146	-127
9	2-19	256	-262
9	2-18	130	-122
9	2-17	690	653
9	2-16	557	-549
9	2-15	723	715
9	2-14	1048	1045
9	2-13	136	134
9	2-12	154	-155
9	2-11	525	-541
9	2-10	193	-181
9	2 -9	945	-959
9	2 -8	211	214
9	2 -7	276	266
9	2 -6	1158	-1213
9	2 -5	741	739
9	2 -4	1031	1025
9	2 -3	313	-302
9	2 -2	723	723
9	2 -1	636	-577
9	2 0	796	-768
9	2 1	430	-439
9	2 2	230	203
9	2 3	452	455
9	2 4	531	-546
9	2 5	878	877
9	2 6	435	427
9	2 7	146	179
9	2 8	529	533
9	2 9	320	-344
9	2 10	665	-689
9	2 11	226	-222
9	2 12	328	335
9	2 13	-123	-11
9	2 14	219	-223
10	2-23	352	364
10	2-22	539	543
10	2-21	-115	102
10	2-20	319	395
10	2-19	491	-493
10	2-18	657	-649
10	2-17	124	-91
10	2-16	351	349
10	2-15	351	404
10	2-14	449	-444
10	2-13	299	305
10	2-12	410	425
10	2-11	238	-219
10	2-10	677	684
10	2 -9	856	-859
10	2 -8	895	-872
10	2 -7	530	-594
10	2 -6	421	435
10	2 -5	443	426
10	2 -4	350	-364
10	2 -3	578	494
10	2 -2	366	-375
10	2 -1	347	336
10	2 0	1237	1215
10	2 1	215	-195
10	2 2	543	-559
10	2 3	227	-233
10	2 4	140	-107
10	2 5	297	283
10	2 6	-123	-101
10	2 7	624	652
10	2 8	317	-349
10	2 9	-120	-42
10	2 10	892	891
10	2 11	347	-343
10	2 12	213	-233
11	2-22	222	233
11	2-21	204	201
11	2-20	-115	-73
11	2-19	289	-295
11	2-18	518	503
11	2-17	840	-925
11	2-16	659	-663
11	2-15	-114	17
11	2-14	231	-303
11	2-13	550	541
11	2-12	405	405
11	2-11	172	159
11	2-10	-112	19
11	2 -9	351	-366
11	2 -8	695	714
11	2 -7	637	-658
11	2 -6	767	-773
11	2 -5	-116	58
11	2 -4	590	-588
11	2 -3	1054	1060
11	2 -2	964	970
11	2 -1	499	488
11	2 0	195	-187
11	2 1	180	-187
11	2 2	311	287
11	2 3	406	-412
11	2 4	-117	-10
11	2 5	281	-278
11	2 6	596	-593
11	2 7	370	392
11	2 8	411	440
11	2 9	152	122
11	2 10	-124	-91
12	2-20	755	747
12	2-19	167	-153
12	2-18	297	-306
12	2-17	425	-410
12	2-16	-118	-70
12	2-15	421	-425
12	2-14	244	242
12	2-13	174	176
12	2-12	710	-688
12	2-11	508	510
12	2-10	454	456
12	2 -9	-123	80
12	2 -8	-117	-16
12	2 -7	-112	46
12	2 -6	-118	23
12	2 -5	380	-391
12	2 -4	263	245
12	2 -3	156	147
12	2 -2	911	-914
12	2 -1	668	687
12	2 0	417	410
12	2 1	-117	27
12	2 2	455	468
12	2 3	434	-404
12	2 4	414	-425
12	2 5	374	-384
12	2 6	351	353
13	2-17	-122	-50
13	2-16	391	386
13	2-15	416	-404
13	2-14	776	-799
13	2-13	-126	-137
13	2-12	186	205
13	2-11	545	557
13	2-10	225	-223
13	2 -9	538	513
13	2 -8	202	170
13	2 -7	-116	29
13	2 -6	631	636
13	2 -5	446	-431
13	2 -4	630	-631
13	2 -3	439	-436
13	2 -2	141	130
13	2 -1	209	230
13	2 0	233	-203
13	2 1	285	289
13	2 2	152	-178
14	2-11	-126	-13
14	2-10	249	-240
14	2 -9	421	441
14	2 -8	342	343
14	2 -7	-121	65
14	2 -6	219	-228
14	2 -5	184	-186
0	3 1	1128	-1123
0	3 2	115	126
0	3 3	1412	1412
0	3 4	114	117
0	3 5	433	433
0	3 6	-95	41
0	3 7	931	949
0	3 8	268	271
0	3 9	991	-983
0	3 10	495	458
0	3 11	1960	-1957
0	3 12	495	-490
0	3 13	787	793
0	3 14	242	-235
0	3 15	390	367
0	3 16	234	235
0	3 17	347	343
0	3 18	170	-179
0	3 19	-112	-119
0	3 20	-117	-83
0	3 21	949	-988
0	3 22	-110	21
0	3 23	534	540
0	3 24	-117	-26
1	3-24	235	183
1	3-23	228	-221
1	3-22	424	413

Table 3. Continued.

H	K	L	F(O)	F(C)	H	K	L	F(O)	F(C)	H	K	L	F(O)	F(C)	H	K	L	F(O)	F(C)	H	K	L	F(O)	F(C)
1	3-21	-108	51	3	3-14	-104	-116	5	3 -4	535	533	7	3 12	-115	-72	10	3 5	827	-844
1	3-20	319	-322	3	3-13	937	935	5	3 -3	-109	33	7	3 13	323	325	10	3 6	-119	-9
1	3-19	685	-674	3	3-12	117	106	5	3 -2	431	-444	7	3 14	-127	-135	10	3 7	444	464
1	3-18	-104	-2	3	3-11	485	490	5	3 -1	670	-674	7	3 15	615	591	10	3 8	-122	-38
1	3-17	639	-641	3	3-10	227	215	5	3 0	156	-152	7	3 16	-122	-67	10	3 9	436	403
1	3-16	466	464	3	3 -9	1156	1150	5	3 1	1031	986	8	3-23	-115	9	10	3 10	-130	-110
1	3-15	1227	1247	3	3 -8	380	395	5	3 2	194	203	8	3-22	284	290	11	3-19	249	228
1	3-14	349	-378	3	3 -7	1744	-1758	5	3 3	1556	1578	8	3-21	374	-379	11	3-18	290	312
1	3-13	430	-415	3	3 -6	347	-337	5	3 4	232	-251	8	3-20	-110	-13	11	3-17	377	-379
1	3-12	214	-227	3	3 -5	460	-470	5	3 5	1142	-1134	8	3-19	219	-213	11	3-16	-119	113
1	3-11	153	156	3	3 -4	179	187	5	3 6	274	259	8	3-16	314	-333	11	3-15	171	-174
1	3-10	-96	-12	3	3 -3	673	673	5	3 7	124	-128	8	3-17	801	-795	11	3-14	273	-282
1	3 -5	556	-565	3	3 -2	829	801	5	3 8	-110	-79	8	3-16	128	95	11	3-13	687	-679
1	3 -8	511	-513	3	3 -1	171	-173	5	3 9	138	147	8	3-15	1013	1023	11	3-12	311	311
1	3 -7	1288	-1284	3	3 0	-114	-131	5	3 10	135	129	8	3-14	231	-224	11	3-11	831	835
1	3 -6	252	-264	3	3 1	761	766	5	3 11	255	-232	8	3-13	443	483	11	3-10	173	152
1	3 -5	2307	2303	3	3 2	451	-465	5	3 12	466	444	8	3-12	296	-273	11	3 -9	646	626
1	3 -4	-95	-66	3	3 3	1346	-1045	5	3 13	1017	1014	8	3-11	620	-613	11	3 -8	209	-192
1	3 -3	960	956	3	3 4	209	186	5	3 14	315	-313	8	3-10	-106	-35	11	3 -7	833	-842
1	3 -2	113	-95	3	3 5	1372	-1374	5	3 15	614	-643	8	3 -9	258	269	11	3 -6	147	143
1	3 -1	644	-631	3	3 6	173	-147	5	3 16	135	-151	8	3 -8	-112	-97	11	3 -5	-123	-82
1	3 0	266	295	3	3 7	1049	1030	5	3 17	423	-432	8	3 -7	869	-861	11	3 -4	192	-187
1	3 1	354	327	3	3 8	443	-439	5	3 18	221	219	8	3 -6	346	349	11	3 -3	643	-664
1	3 2	261	-258	3	3 9	-109	69	6	3 17	-117	65	8	3 -5	639	651	11	3 -2	332	-295
1	3 3	1726	-1742	3	3 10	-104	-15	6	3-25	424	422	8	3 -4	-114	-20	11	3 -1	579	581
1	3 4	442	418	3	3 11	1065	1052	6	3-24	-119	-25	8	3 -3	1197	1202	11	3 0	-120	9
1	3 5	659	664	3	3 12	124	-70	6	3-23	771	-754	8	3 -2	270	-257	11	3 1	1045	1033
1	3 6	558	565	3	3 13	-103	-43	6	3-22	-118	12	8	3 -1	911	-995	11	3 2	143	-103
1	3 7	404	421	3	3 14	167	165	6	3-21	-108	11	8	3 0	825	821	11	3 3	534	-500
1	3 8	645	-658	3	3 15	952	-943	6	3-20	166	158	8	3 1	303	-311	11	3 4	222	228
1	3 9	706	-706	3	3 16	-112	72	6	3-19	-106	46	8	3 2	-117	5	11	3 5	-124	-109
1	3 10	-99	11	3	3 17	537	545	6	3-18	135	119	8	3 3	954	-979	11	3 6	-116	34
1	3 11	-100	-73	3	3 18	-115	14	6	3-17	328	326	8	3 4	443	-453	11	3 7	243	-212
1	3 12	271	282	3	3 19	-113	71	6	3-16	-105	-53	8	3 5	-116	33	12	3-17	405	392
1	3 13	1155	-1153	3	3 20	200	190	6	3-15	750	744	8	3 6	166	173	12	3-16	-133	165
1	3 14	391	-377	3	3 21	-121	23	6	3-14	428	424	8	3 7	1217	1239	12	3-15	780	-789
1	3 15	185	182	3	3 22	206	-191	6	3-13	1418	-1401	8	3 8	152	-153	12	3-14	232	213
1	3 16	-107	-73	4	3-25	736	-732	6	3-12	-106	-44	8	3 9	597	-583	12	3-13	291	-218
1	3 17	1073	1064	4	3-24	156	-102	6	3-11	688	-678	8	3 10	-122	-55	12	3-12	331	-335
1	3 18	154	-147	4	3-23	248	-248	6	3-10	470	-468	8	3 11	225	-249	12	3-11	-123	-27
1	3 19	238	-211	4	3-22	-153	21	6	3 -9	192	172	8	3 12	-120	33	12	3-10	-119	73
1	3 20	122	76	4	3-21	659	660	6	3 -8	-104	-48	8	3 13	-123	56	12	3 -9	-129	113
1	3 21	183	185	4	3-20	221	-232	6	3 -7	362	368	8	3 14	146	-136	12	3 -8	-124	30
1	3 22	225	217	4	3-19	119	27	6	3 -6	349	-346	9	3-22	186	-174	12	3 -7	716	725
1	3 23	491	-350	4	3-18	-104	64	6	3 -5	1676	1686	9	3-21	451	435	12	3 -6	307	-323
2	3-25	269	-302	4	3-17	600	610	6	3 -4	-117	-105	9	3-20	-119	81	12	3 -5	695	-673
2	3-24	-114	25	4	3-16	-100	-46	6	3 -3	1019	-1040	9	3-19	587	-593	12	3 -4	-120	27
2	3-23	849	865	4	3-15	660	-616	6	3 -2	132	138	9	3-18	-114	-53	12	3 -3	175	-173
2	3-22	-107	47	4	3-14	139	99	6	3 -1	825	-818	9	3-17	264	-253	12	3 -2	-120	-43
2	3-21	-117	33	4	3-13	1146	-1159	6	3 0	-116	-57	9	3-16	352	-373	12	3 -1	293	277
2	3-20	346	343	4	3-12	541	547	6	3 1	736	712	9	3-15	324	309	12	3 0	-126	115
2	3-19	715	-706	4	3-11	1479	1470	6	3 2	-117	108	9	3-14	-110	46	12	3 1	149	-148
2	3-18	810	-154	4	3-10	239	-246	6	3 3	-123	65	9	3-13	592	589	12	3 2	-122	9
2	3-17	163	-184	4	3 -9	243	256	6	3 4	-116	-41	9	3-12	-114	83	12	3 3	814	819
2	3-16	412	-389	4	3 -8	126	171	6	3 5	1302	1293	9	3-11	912	916	13	3-12	-125	-56
2	3-15	767	-746	4	3 -7	-99	74	6	3 6	163	106	9	3-10	206	214	13	3-11	691	-688
2	3-14	162	176	4	3 -6	777	778	6	3 7	493	-485	9	3 -9	1267	-1247	13	3-10	228	-230
2	3-13	1455	1457	4	3 -5	683	-680	6	3 8	669	652	9	3 -8	-116	62	13	3 -9	697	708
2	3-12	366	-352	4	3 -4	141	-153	6	3 9	1610	-1593	9	3 -7	336	-333	13	3 -8	-125	-82
2	3-11	1117	1114	4	3 -3	2158	-2144	6	3 10	-117	95	9	3 -6	157	-180	13	3 -7	329	306
2	3-10	-95	32	4	3 -2	405	-416	6	3 11	262	267	9	3 -5	318	318	13	3 -6	-119	9
2	3 -9	1112	-1107	4	3 -1	1431	1334	6	3 12	414	-435	9	3 -4	505	503	13	3 -5	236	267
2	3 -8	221	216	4	3 0	192	161	6	3 13	-114	-54	9	3 -3	-118	17	13	3 -4	165	164
2	3 -7	211	-222	4	3 1	1169	1156	6	3 14	-119	113	9	3 -2	-117	56	13	3 -3	174	-193
2	3 -6	535	-523	4	3 2	209	-205	6	3 15	586	555	9	3 -1	856	855	0	4 0	-115	79
2	3 -5	864	-850	4	3 3	187	-185	6	3 16	-114	-49	9	3 0	349	-367	0	4 1	716	-725
2	3 -4	200	236	4	3 4	-104	-65	6	3 17	-120	5	9	3 1	913	-912	0	4 2	894	-886
2	3 -3	1345	1345	4	3 5	-130	60	6	3 18	157	-126	9	3 2	-125	133	0	4 3	1126	-1110
2	3 -2	247	-231	4	3 6	-104	-15	7	3-24	331	362	9	3 3	844	-885	0	4 4	-120	49
2	3 -1	1752	1814	4	3 7	1243	-1234	7	3-23	227	227	9	3 4	173	-181	0	4 5	218	-210
2	3 0	-110	19	4	3 8	125	-121	7	3-22	-115	-67	9	3 5	650	663	0	4 6	873	862
2	3 1	2022	-2026	4	3 9	947	945	7	3-21	765	-784	9	3 6	278	-296	0	4 7	1124	1127
2	3 2	846	826	4	3 10	184	182	7	3-20	245	-222	9	3 7	-119	7	0	4 8	479	-486
2	3 3	759	-760	4	3 11	1137	1138	7	3-19	452	-468	9	3 8	-121	40	0	4 9	418	397
2	3 4	625	-620	4	3 12	152	-175	7	3-18	379	387	9	3 9	736	751	0	4 10	343	339
2	3 5	683	-675	4	3 13	207	-177	7	3-17	1065	1045	9	3 10	-122	-73	0	4 11	460	-455
2	3 6	526	-513	4	3 14	281	276	7	3-16	-106	-24	9	3 11	147	-207	0	4 12	177	-186
2	3 7	120	157	4	3 15	-155	-16	7	3-15	189	-221	9	3 12	-125	2	0	4 13	548	-547
2	3 8	-112	44	4	3 16	396	407	7	3-14	167	-150	10	3-21	-114	-36	0	4 14	285	297
2	3 9	2117	2099	4	3 17	1092	-1060	7	3-13	165	166	10	3-20	-110	-88	0	4 15	156	-171
2	3 10	304	-285	4	3 18	313	-308	7	3-12	-103	-42	10	3-19	481	481	0	4 16	775	759
2	3 11	187	-176	4	3 19	-113	-27	7	3-11	630	-627	10	3-18	-109	-15	0	4 17	448	401
2	3 12	-104	62	4	3 20	201	-183	7	3-10	434	-433	10	3-17	471	-459	0	4 18	695	-689
2	3 13	684	-675	5	3-25	404	-392	7	3 -9	1075	-1053	10	3-16	-115	-75	0	4 19	629	599
2	3 14	-103	41	5	3-24	230	-239	7	3 -8	213	-212	10	3-15	538	-525	0	4 20	-116	-35
2	3 15	277	285	5	3-23	142	-138	7	3 -7	1548	1541	10	3-14	292	303	0	4 21	-124	-158
2	3 16	155	-133	5	3-22	249	-244	7	3 -6	-116	-123	10	3-13	887	932	0	4 22	-114	-13
2	3 17	-104	32	5	3-21	284	-281	7	3 -5	626	633	10	3-12	-114	19	1	4-22	-120	137
2	3 18	164	202	5	3-20	-129	45	7	3 -4	-114	68	10	3-11	116	65	1	4-21	208	207
2	3 19	1053	1044	5	3-19	1417	1415	7	3 -3	189	-187	10	3-10	-114	-82	1	4-20	571	-563
2	3 20	-113	19	5	3-18	132	141	7	3 -2	270	261	10	3 -9	403	392	1	4-19	-108	0
2	3 21	254	-254	5	3-17	139	137	7	3 -1	288	-288	10	3 -8	424	456	1	4-18	588	583
2	3 22	-125	138	5	3-16	411	403	7	3 0	176	-169	10	3 -7	376	-367	1	4-17	757	-775
2	3-25	178	161	5	3-15	893	-909	7	3 1	1409	-1368	10	3 -6	-130	164	1	4-16	182	-219
2	3-24	179	200	5	3-14	-102	-65	7	3 2	-113	-39	10	3 -5	1174	-1197	1	4-15	-107	-80
2	3-23	-109	3	5	3-13	-93	-40	7	3 3	1010	1033	10	3 -4	195	-183	1	4-14	-107	106
2	3-22	-106	16	5	3-12	128	-146	7	3 4	508	507	10	3 -3	601	593	1	4-13	628	630
2	3-21	258	248	5	3-11	816	-819	7	3 5	466	439	10	3 -2	-119	-76	1	4-12	1064	1052
2	3-20	165	-158	5	3-10	802	811	7	3 6	-116	-26	10	3 -1	222	241	1	4-11	136	142
2	3-19	525	507	5	3 -9	548	542	7	3 7	417	-423	10	3 0	192	-179	1	4-10	1017	-1018
2	3-18	-104	-55	5	3 -8	118	-57	7	3 8	211	-222	10	3 1	143	132	1	4 -9	-102	30
2	3-17	1147	-1140	5	3 -7	947	941	7	3 9	-114	-70	10	3 2	175	-189	1	4 -8	225	-217
2	3-16	315	-310	5	3 -6	448	-441	7	3 10	203	216	10	3 3	-119	104	1	4 -7	501	-516
2	3-15	-106	-25	5	3 -5	1527	-1529	7	3 11	844	-834	10	3 4	-113	-12	1	4 -6	248	-261

Table 3. Continued.

H	K	L	F(O)	F(C)	H	K	L	F(O)	F(C)	H	K	L	F(O)	F(C)	H	K	L	F(O)	F(C)	H	K	L	F(O)	F(C)
1	4	-5	613	-623	3	4	12	646	-684	6	4	-8	566	590	9	4	-8	-117	-16	1	5	3	619	-595
1	4	-4	249	-265	3	4	14	334	306	6	4	-7	221	-222	9	4	-7	322	-324	1	5	4	784	-768
1	4	-3	427	425	3	4	14	152	-157	6	4	-6	-108	-25	9	4	-6	506	-573	1	5	5	130	122
1	4	-2	519	508	3	4	15	207	-227	6	4	-5	742	757	9	4	-5	611	-529	1	5	6	186	-182
1	4	-1	462	466	3	4	16	169	-178	6	4	-4	625	-637	9	4	-4	695	690	1	5	7	172	-154
1	4	0	1439	-1520	3	4	17	217	-192	6	4	-3	559	614	9	4	-3	261	-262	1	5	8	436	404
1	4	1	-111	72	3	4	18	-113	63	6	4	-2	161	171	9	4	-2	210	218	1	5	9	633	-685
1	4	2	161	-153	3	4	19	214	-203	6	4	-1	208	-118	9	4	-1	767	744	1	5	10	601	610
1	4	3	264	-222	4	4	-23	479	-482	6	4	0	783	-782	9	4	0	-125	-92	1	5	11	531	514
1	4	4	674	657	4	4	-22	211	-232	6	4	1	579	-596	9	4	1	371	359	1	5	12	224	-229
1	4	5	831	-692	4	4	-21	179	-171	6	4	2	301	310	9	4	2	469	457	1	5	13	-117	-91
1	4	6	226	-233	4	4	-20	222	222	6	4	3	567	-571	9	4	3	412	-416	1	5	14	360	-349
1	4	7	231	248	4	4	-19	274	283	6	4	4	293	289	9	4	4	690	-711	1	5	15	-118	85
1	4	8	1134	1123	4	4	-18	200	215	6	4	5	655	649	9	4	5	239	-277	1	5	16	-115	35
1	4	9	795	783	4	4	-17	415	483	6	4	6	400	-401	9	4	6	184	187	1	5	17	123	162
1	4	10	-106	3	4	4	-16	871	-873	6	4	7	667	672	9	4	7	-134	-125	1	5	18	-125	129
1	4	11	-105	-11	4	4	-15	299	335	6	4	8	457	436	9	4	8	363	381	2	5	-19	-115	45
1	4	12	499	-506	4	4	-14	273	304	6	4	9	185	-173	9	4	9	231	267	2	5	-18	124	134
1	4	13	-105	-91	4	4	-13	699	-708	6	4	10	416	-413	10	4	-17	131	127	2	5	-17	508	528
1	4	14	361	407	4	4	-12	353	-368	6	4	11	401	-384	10	4	-16	164	181	2	5	-16	275	-273
1	4	15	340	-368	4	4	-11	747	-754	6	4	12	350	417	10	4	-15	253	-249	2	5	-15	493	-491
1	4	16	141	-159	4	4	-10	-112	58	6	4	13	233	-232	10	4	-14	413	-401	2	5	-14	238	-244
1	4	17	139	-139	4	4	-9	523	531	6	4	14	662	637	10	4	-13	479	-471	2	5	-13	-107	37
1	4	18	313	300	4	4	-8	1241	1236	6	4	15	-109	109	10	4	-12	-116	24	2	5	-12	-107	18
1	4	19	365	376	4	4	-7	493	500	7	4	-21	-123	131	10	4	-11	157	179	2	5	-11	-115	-124
1	4	20	222	-233	4	4	-6	758	-755	7	4	-20	325	344	10	4	-10	561	552	2	5	-10	675	675
1	4	21	153	144	4	4	-5	330	378	7	4	-19	619	-623	10	4	-9	317	317	2	5	-9	166	-144
2	4	-22	-114	110	4	4	-4	-112	3	7	4	-18	256	-246	10	4	-8	433	-465	2	5	-8	419	410
2	4	-21	271	267	4	4	-3	411	-421	7	4	-17	373	-364	10	4	-7	225	215	2	5	-7	1203	1216
2	4	-20	581	575	4	4	-2	514	510	7	4	-16	239	246	10	4	-6	-124	42	2	5	-6	728	-708
2	4	-19	341	379	4	4	-1	1196	-1113	7	4	-15	577	583	10	4	-5	-125	-117	2	5	-5	198	-172
2	4	-18	409	-425	4	4	0	152	-158	7	4	-14	759	761	10	4	-4	131	133	2	5	-4	459	-451
2	4	-17	-110	51	4	4	1	-119	15	7	4	-13	504	495	10	4	-3	400	-419	2	5	-3	432	-421
2	4	-16	-109	63	4	4	2	814	815	7	4	-12	511	-511	10	4	-2	179	192	2	5	-2	144	104
2	4	-15	813	-804	4	4	3	1103	1088	7	4	-11	132	88	10	4	-1	138	-162	2	5	-1	-119	-66
2	4	-14	437	422	4	4	4	1137	-1026	7	4	-10	-108	21	10	4	0	531	534	2	5	0	354	358
2	4	-13	322	-305	4	4	5	371	360	7	4	-9	563	-563	10	4	1	418	411	2	5	1	698	-679
2	4	-12	564	-583	4	4	6	421	-424	7	4	-8	318	-309	10	4	2	661	-659	2	5	2	351	347
2	4	-11	934	954	4	4	7	315	-311	7	4	-7	553	-556	10	4	3	291	265	2	5	3	942	964
2	4	-10	354	402	4	4	8	217	205	7	4	-6	-115	-96	10	4	4	149	-142	2	5	4	447	-451
2	4	-9	367	376	4	4	9	552	-936	7	4	-5	462	467	10	4	5	146	-87	2	5	5	-111	-94
2	4	-8	724	-702	4	4	10	692	-657	7	4	-4	746	763	10	4	6	-133	145	2	5	6	435	-411
2	4	-7	-105	57	4	4	11	-113	-55	7	4	-3	573	574	11	4	-15	-127	77	2	5	7	935	-947
2	4	-6	612	-661	4	4	12	445	431	7	4	-2	917	-912	11	4	-14	-123	-43	2	5	8	191	206
2	4	-5	1040	-1063	4	4	13	735	741	7	4	-1	-121	-11	11	4	-13	457	-473	2	5	9	193	183
2	4	-4	831	823	4	4	14	-115	-34	7	4	0	209	-180	11	4	-12	439	443	2	5	10	338	339
2	4	-3	944	-936	4	4	15	241	225	7	4	1	332	-352	11	4	-11	475	-472	2	5	11	331	-367
2	4	-2	538	-524	4	4	16	359	-373	7	4	2	447	454	11	4	-10	373	-315	2	5	12	473	474
2	4	-1	595	624	4	4	17	277	-287	7	4	3	494	-535	11	4	-9	555	553	2	5	13	608	624
2	4	0	714	715	4	4	18	423	424	7	4	4	160	-119	11	4	-8	638	659	2	5	14	192	-144
2	4	1	763	758	5	4	-22	148	-133	7	4	5	-122	26	11	4	-7	475	486	2	5	15	499	493
2	4	2	232	230	5	4	-21	523	-534	7	4	6	769	774	11	4	-6	-127	-69	2	5	16	588	-594
2	4	3	303	-292	5	4	-20	-117	126	7	4	7	622	618	11	4	-5	-125	-103	2	5	17	529	-525
2	4	4	341	-329	5	4	-19	-109	20	7	4	8	138	-122	11	4	-4	435	-454	3	5	-19	344	358
2	4	5	560	-567	5	4	-18	171	-182	7	4	9	155	141	11	4	-3	341	-327	3	5	-18	329	329
2	4	6	1284	1288	5	4	-17	559	567	7	4	10	-124	-119	11	4	-2	445	433	3	5	-17	-112	-51
2	4	7	910	-941	5	4	-16	473	489	7	4	11	271	-256	11	4	-1	413	-423	3	5	-16	-119	-38
2	4	8	137	158	5	4	-15	227	230	7	4	12	251	251	11	4	0	329	-329	3	5	-15	367	360
2	4	9	575	546	5	4	-14	713	-727	7	4	13	199	-203	11	4	1	338	334	3	5	-14	334	-344
2	4	10	293	-285	5	4	-13	-105	-66	7	4	14	278	-240	11	4	2	189	232	3	5	-13	134	-148
2	4	11	886	882	5	4	-12	131	116	8	4	-21	610	-613	12	4	-8	-127	27	3	5	-12	144	-146
2	4	12	222	215	5	4	-11	769	-781	8	4	-19	148	156	12	4	-7	389	349	3	5	-11	515	-520
2	4	13	-112	-81	5	4	-10	795	797	8	4	-18	-114	82	12	4	-6	240	-229	3	5	-10	-113	113
2	4	14	514	-518	5	4	-9	251	-271	8	4	-17	469	-453	12	4	-5	311	329	3	5	-9	547	559
2	4	15	462	-462	5	4	-8	347	-357	8	4	-16	468	492	0	5	1	422	441	3	5	-8	425	422
2	4	16	364	373	5	4	-7	1157	1180	8	4	-15	442	-428	0	5	2	751	-751	3	5	-7	-102	-25
2	4	17	419	-400	5	4	-6	1159	1051	8	4	-14	259	-238	0	5	3	534	559	3	5	-6	-126	73
2	4	18	-112	-2	5	4	-5	343	314	8	4	-13	575	575	0	5	4	457	-467	3	5	-5	118	99
2	4	19	-112	23	5	4	-4	253	-254	8	4	-12	417	408	0	5	5	893	-891	3	5	-4	675	-689
2	4	20	329	-319	5	4	-3	206	-201	8	4	-11	327	298	0	5	6	398	391	3	5	-3	-116	-97
3	4	-22	580	573	5	4	-2	1113	-1130	8	4	-10	767	-796	0	5	7	135	-125	3	5	-2	629	-627
3	4	-21	324	333	5	4	-1	243	-232	8	4	-9	154	156	0	5	8	384	377	3	5	-1	851	-875
3	4	-20	-106	21	5	4	0	771	786	8	4	-8	457	-449	0	5	9	331	349	3	5	0	450	484
3	4	-19	452	433	5	4	1	512	-528	8	4	-7	483	-436	0	5	10	-113	-57	3	5	1	336	329
3	4	-18	129	93	5	4	2	274	-255	8	4	-6	494	493	0	5	11	134	93	3	5	2	532	565
3	4	-17	-107	73	5	4	3	566	560	8	4	-5	714	-721	0	5	12	327	-335	3	5	3	235	-220
3	4	-16	213	-225	5	4	4	-112	-16	8	4	-4	555	-585	0	5	13	213	223	3	5	4	-110	58
3	4	-15	463	-444	5	4	5	539	526	8	4	-3	443	459	0	5	14	264	-267	3	5	5	-119	-37
3	4	-14	1011	-1022	5	4	6	251	-241	8	4	-2	718	731	0	5	15	745	-772	3	5	6	427	-414
3	4	-13	540	-523	5	4	7	287	-300	8	4	-1	590	577	0	5	16	239	189	3	5	7	518	491
3	4	-12	747	757	5	4	8	995	-1006	8	4	0	-117	12	0	5	17	152	-143	3	5	8	163	-116
3	4	-11	297	306	5	4	9	219	-157	8	4	1	-124	-79	0	5	18	398	391	3	5	9	392	-399
3	4	-10	-111	81	5	4	10	811	781	8	4	2	666	-686	1	5	-19	-113	-25	3	5	10	239	264
3	4	-9	527	526	5	4	11	414	-383	8	4	3	-122	-8	1	5	-18	224	-209	3	5	11	123	135
3	4	-8	626	-633	5	4	12	143	134	8	4	4	895	923	1	5	-17	488	-474	3	5	12	255	262
3	4	-7	-106	113	5	4	13	-113	74	8	4	5	613	-627	1	5	-16	453	-454	3	5	13	218	227
3	4	-6	177	182	5	4	14	-117	-79	8	4	6	-129	149	1	5	-15	258	269	3	5	14	-117	49
3	4	-5	312	-311	5	4	15	513	514	8	4	7	-123	-16	1	5	-14	133	-87	3	5	15	-115	-21
3	4	-4	526	-544	5	4	16	511	525	8	4	8	-122	-68	1	5	-13	623	-633	3	5	16	174	-167
3	4	-3	772	-767	5	4	17	-124	-38	8	4	9	591	599	1	5	-12	712	731	4	5	-19	498	-476
3	4	-2	615	667	6	4	-22	161	-183	8	4	10	-128	94	1	5	-11	218	229	4	5	-18	539	517
3	4	-1	-120	-80	6	4	-21	157	-216	8	4	11	165	174	1	5	-10	397	364	4	5	-17	304	328
3	4	0	518	522	6	4	-20	514	-500	8	4	12	511	-541	1	5	-9	710	719	4	5	-16	316	313
3	4	1	661	682	6	4	-19	442	-436	9	4	-19	-116	72	1	5	-8	452	-444	4	5	-15	402	411
3	4	2	230	-172	6	4	-18	528	540	9	4	-18	156	-175	1	5	-7	565	-557	4	5	-14	376	-330
3	4	3	357	362	6	4	-17	-113	-21	9	4	-17	229	-219	1	5	-6	117	-79	4	5	-13	120	-105
3	4	4	430	466	6	4	-16	-112	116	9	4	-16	631	-623	1	5	-5	525	512	4	5	-12	472	-482
3	4	5	448	-439	6	4	-15	503	506	9	4	-15	535	-526	1	5	-4	168	-153	4	5	-11	412	421
3	4	6	515	-485	6	4	-14	-110	102	9	4	-14	533	525	1	5	-3	311	-315	4	5	-10	279	-261
3	4	7	373	-362	6	4	-13	302	290	9	4	-13	-115	-93	1	5	-2	286	274	4	5	-9	943	-945
3	4	8	150	163	6	4	-12	153	182	9	4	-12	-118	-85	1	5	-1	-111	39	4	5	-8	352	359
3	4	9	216	-212	6	4	-11	-102	-1	9	4	-11	660	664	1	5	0	549	568	4	5	-7	275	-283
3	4	10	623	624	6	4	-10	549	-536	9	4	-10	280	-311	1	5	1	887	864	4	5	-6	353	340
3	4	11	264	282	6	4	-9	784	-778	9	4	-9	184	193	1	5	2	282	-250	4	5	-5	826	822

Table 3. Continued.

H	K	L	F(O)	F(C)
4	5	-4	313	-335
4	5	-3	376	-356
4	5	-2	337	-345
4	5	-1	-121	80
4	5	0	167	-209
4	5	1	618	-624
4	5	2	323	259
4	5	3	342	-374
4	5	4	740	743
4	5	5	534	534
4	5	6	-116	-29
4	5	7	-116	17
4	5	8	582	-581
4	5	9	277	274
4	5	10	-122	-154
4	5	11	-121	-112
4	5	12	254	255
4	5	13	572	-559
4	5	14	246	241
5	5	15	173	146
5	5	16	130	-115
5	5	17	-112	-41
5	5	16	335	322
5	5	15	147	129
5	5	14	296	283
5	5	13	640	644
5	5	12	554	-624
5	5	11	751	-809
5	5	10	491	-476
5	5	9	-115	-115
5	5	8	-106	35
5	5	7	-112	-29
5	5	6	644	642
5	5	5	398	-389
5	5	4	377	339
5	5	3	666	682
5	5	2	478	-511
5	5	1	242	-222
5	5	0	281	-267
5	5	1	398	-352
5	5	2	254	239
5	5	3	462	479
5	5	4	-125	136
5	5	5	333	-336
5	5	6	420	412
5	5	7	646	654
5	5	8	240	-257
5	5	9	-125	89
5	5	10	578	-561
5	5	11	533	-557
5	5	12	-124	-121
5	5	13	256	278
6	5	16	155	-153
6	5	17	376	-381
6	5	16	134	131
6	5	15	149	136
6	5	14	248	239
6	5	13	217	-204
6	5	12	-114	76
6	5	11	352	414
6	5	10	324	-324
6	5	9	-111	12
6	5	8	212	-158
6	5	7	670	-666
6	5	-6	242	236
6	5	-5	239	258
6	5	-4	574	568
6	5	-3	138	-130
6	5	-2	362	326
6	5	-1	534	539
6	5	0	515	-526
6	5	1	505	533
6	5	2	504	-468
6	5	3	666	-665
6	5	4	296	309
6	5	5	-129	42
6	5	6	223	250
6	5	7	144	-143
6	5	8	-121	-55
6	5	9	-139	121
6	5	10	237	-250
6	5	11	421	416
7	5	-17	-116	12
7	5	-16	153	-162
7	5	-15	533	-559
7	5	-14	527	543
7	5	-13	191	215
7	5	-12	424	453
7	5	-11	461	462
7	5	-10	214	-215
7	5	-9	235	-235
7	5	-8	176	-165
7	5	-7	326	301
7	5	-6	-121	-72
7	5	-5	417	-428
7	5	-4	257	252
7	5	-3	-131	100
7	5	-2	403	385
7	5	-1	809	801
7	5	0	-139	-53
7	5	1	339	-301
7	5	2	539	-567
7	5	3	-126	-56
7	5	4	238	-280
7	5	5	231	-236
7	5	6	269	232
7	5	7	304	-258
7	5	8	451	425
7	5	9	349	354
8	5	-16	-122	-84
8	5	-15	156	144
8	5	-14	-142	-45
8	5	-13	136	-125
8	5	-12	470	466
8	5	-11	252	-248
8	5	-10	505	523
8	5	-9	812	805
8	5	-8	456	-444
8	5	-7	129	-136
8	5	-6	353	-404
8	5	-5	-131	106
8	5	-4	-129	48
8	5	-3	-126	-51
8	5	-2	205	210
8	5	-1	708	-710
8	5	0	202	190
8	5	1	712	700
8	5	2	318	-285
8	5	3	-128	75
8	5	4	283	-266
8	5	5	419	-414
8	5	6	-129	62
8	5	7	-131	92
9	5	-13	434	-421
9	5	-12	-124	65
9	5	-11	351	385
9	5	-10	292	288
9	5	-9	-121	75
9	5	-8	161	166
9	5	-7	416	346
9	5	-6	514	-516
9	5	-5	-130	-79
9	5	-4	527	-519
9	5	-3	723	-715
9	5	-2	223	222
9	5	-1	361	378
9	5	0	348	357
9	5	1	163	-185
9	5	2	158	175
9	5	3	171	156
10	5	-2	-124	-44
10	5	-8	139	130
10	5	-7	206	212
10	5	-6	193	-205
10	5	-5	173	-184
10	5	-4	267	-210
10	5	-3	178	200
10	5	-2	-125	-133
0	6	0	816	824
0	6	1	-120	138
0	6	2	-112	-55
0	6	3	351	360
0	6	4	316	-305
0	6	5	152	116
0	6	6	362	-371
0	6	7	150	-157
0	6	8	176	-212
0	6	9	126	150
0	6	10	766	758
0	6	11	-119	-5
0	6	12	-124	141
0	6	13	-117	-95
1	6	-13	173	-174
1	6	-12	211	240
1	6	-11	-114	3
1	6	-10	234	-215
1	6	-9	-118	94
1	6	-8	739	732
1	6	-7	215	-229
1	6	-6	-109	19
1	6	-5	153	-145
1	6	-4	945	-905
1	6	-3	-114	97
1	6	-2	274	289
1	6	-1	-120	81
1	6	0	-134	69
1	6	1	236	221
1	6	2	355	382
1	6	3	-113	17
1	6	4	227	207
1	6	5	-111	14
1	6	6	769	-752
1	6	7	208	194
1	6	8	-115	95
1	6	9	-118	-101
1	6	10	-114	33
1	6	11	135	-137
1	6	12	145	152
2	6	-14	-121	-94
2	6	-13	130	-98
2	6	-12	738	-744
2	6	-11	121	-135
2	6	-10	308	403
2	6	-9	215	-232
2	6	-8	218	204
2	6	-7	-111	29
2	6	-6	254	226
2	6	-5	312	324
2	6	-4	291	274
2	6	-3	137	115
2	6	-2	1010	-1010
2	6	-1	-127	67
2	6	0	-134	4
2	6	1	-126	54
2	6	2	714	693
2	6	3	-120	-63
2	6	4	-117	31
2	6	5	-119	64
2	6	6	244	289
2	6	7	-115	41
2	6	8	939	-937
2	6	9	-122	-104
2	6	11	-124	-123
2	6	11	138	-233
3	6	-14	177	-153
3	6	-13	-113	-15
3	6	-12	229	-213
3	6	-11	219	-225
3	6	-10	439	-441
3	6	-9	152	137
3	6	-8	212	209
3	6	-7	279	312
3	6	-6	702	717
3	6	-5	-110	5
3	6	-4	237	-293
3	6	-3	135	154
3	6	-2	-134	-113
3	6	-1	-132	34
3	6	0	254	-261
3	6	1	-121	-92
3	6	2	294	-173
3	6	3	-123	51
3	6	4	723	703
3	6	5	166	-155
3	6	6	-118	33
3	6	7	160	-155
3	6	8	214	-197
3	6	9	-122	-33
3	6	10	275	-261
4	6	-13	-121	123
4	6	-12	-115	-32
4	6	-11	151	189
4	6	-10	657	-654
4	6	-9	-119	81
4	6	-8	-116	71
4	6	-7	-114	39
4	6	-6	144	-142
4	6	-5	-119	64
4	6	-4	717	743
4	6	-3	198	-147
4	6	-2	189	157
4	6	-1	-136	82
4	6	0	859	-877
4	6	1	161	139
4	6	2	-128	78
4	6	3	385	-392
4	6	4	-124	76
4	6	5	633	-635
4	6	6	298	276
4	6	7	-123	58
4	6	8	378	364
4	6	9	137	133
5	6	-12	156	137
5	6	-11	158	187
5	6	-10	118	24
5	6	-9	159	-131
5	6	-8	816	-796
5	6	-7	-123	-117
5	6	-6	248	277
5	6	-5	-123	-72
5	6	-4	255	272
5	6	-3	-124	-10
5	6	-2	-138	97
5	6	-1	-136	-107
5	6	0	327	307
5	6	1	245	-246
5	6	2	851	-892
5	6	3	-129	-31
5	6	4	-127	-20
5	6	5	136	131
5	6	6	596	618
5	6	7	-128	23
6	6	-11	188	-212
6	6	-10	-122	-81
6	6	-9	-119	86
6	6	-8	128	-114
6	6	-7	-121	-63
6	6	-6	472	-456
6	6	-5	193	-211
6	6	-4	-126	-46
6	6	-3	193	-159
6	6	-2	675	645
6	6	-1	183	-198
6	6	0	-141	-150
6	6	1	165	171
6	6	2	-132	63
6	6	3	139	207
6	6	4	378	-386
7	6	-8	-127	37
7	6	-7	134	-123
7	6	-6	771	-734
7	6	-5	144	-124
7	6	-4	-130	43
7	6	-3	-131	-19
7	6	-2	-129	71
7	6	-1	225	250
7	6	0	442	433

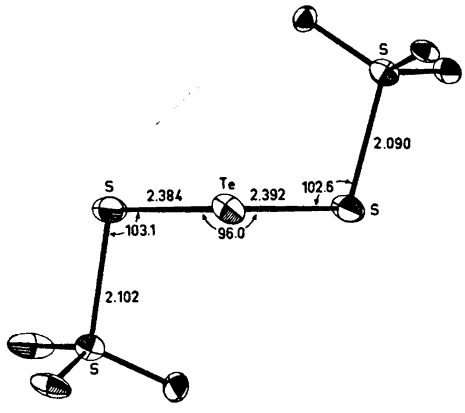

Fig. 1. The *trans* form of the telluropentathionate ion in $BaTe(S_2O_3)_2.3H_2O$ as seen along the *b* axis. The ellipsoids represent 50 % probability; the thermal parameters of the oxygen atoms are halved in size relative to those of the tellurium and sulphur atoms.

Table 4. Dimensions of the telluropentathionate ion. Standard deviations, including estimated uncertainties in unit cell dimensions, are given in parentheses.

Bond lengths and angles	
S(1) – S(2) = 2.1020(16) Å	S(4) – S(5) = 2.0898(16) Å
S(2) – Te = 2.3835(15)	Te – S(4) = 2.3924(16)
∠S(1) – S(2) – Te = 103.08(5)°	∠Te – S(4) – S(5) = 102.59(5)°
∠S(2) – Te – S(4) = 96.02(4)°	
S(1) – O(1) = 1.427(4) Å	S(5) – O(4) = 1.451(3) Å
S(1) – O(2) = 1.428(4)	S(5) – O(5) = 1.456(4)
S(1) – O(3) = 1.432(4)	S(5) – O(6) = 1.447(4)
∠S(2) – S(1) – O(1) = 107.2(2)°	∠S(4) – S(5) – O(4) = 106.7(2)°
∠S(2) – S(1) – O(2) = 102.2(2)°	∠S(4) – S(5) – O(5) = 102.0(2)°
∠S(2) – S(1) – O(3) = 108.2(2)°	∠S(4) – S(5) – O(6) = 109.1(2)°
∠O(1) – S(1) – O(2) = 114.3(3)°	∠O(4) – S(5) – O(4) = 113.5(2)°
∠O(1) – S(1) – O(3) = 111.1(3)°	∠O(4) – S(5) – O(6) = 112.5(2)°
∠O(2) – S(1) – O(3) = 113.1(3)°	∠O(5) – S(6) – O(6) = 112.1(2)°
Dihedral angles	
S(1)S(2)Te/S(2)TeS(4) = 87.7°	S(2)TeS(4)/TeS(4)S(5) = 98.7°
TeS(2)S(1)/S(2)S(1)O(1) = 70.0°	TeS(4)S(5)/S(4)S(5)O(4) = 68.8°
TeS(2)S(1)/S(2)S(1)O(2) = 169.5°	TeS(4)S(5)/S(4)S(5)O(5) = 171.9°
TeS(2)S(1)/S(2)S(1)O(3) = 50.0°	TeS(4)S(5)/S(4)S(5)O(6) = 53.1°
S(2)S(1)O(1)/S(2)S(1)O(2) = 120.5°	S(4)S(5)O(4)/S(4)S(5)O(5) = 119.3°
S(2)S(1)O(1)/S(2)S(1)O(3) = 119.9°	S(4)S(5)O(4)/S(4)S(5)O(6) = 121.9°
S(2)S(1)O(2)/S(2)S(1)O(3) = 119.6°	S(4)S(5)O(5)/S(4)S(5)O(6) = 118.8°
Non-bonded distances	
S(1) – Te = 3.5168(17) Å	Te – S(5) = 3.5028(18) Å
S(1) – S(4) = 4.3747(22)	S(2) – S(5) = 4.5652(23)
S(2) – S(4) = 3.5497(21)	S(1) – S(5) = 5.9914(27)

on film data [8] are about 1.5 times the standard deviations estimated for the film data values.

The non-planar S – S – Te – S – S chain in the *trans* form possesses the symmetry of a twofold axis, when the two halves of the chain are identical. This is the case in the crystals of tellurium dibenzenethiosulphonate,[17] where a twofold axis is crystallographically required.

In the present salt the crystal symmetry does not impose a twofold axis, but the dimensions are, except for the dihedral angles, nearly the same in the two halves of the telluropentathionate ion. The S – S and S – Te bond lengths, and the S – S – Te bond angles differ by only 0.0122 Å, 0.0089 Å, and 0.49°, respectively, and thus correspond nearly to the symmetry of a twofold axis. The dihedral angles between the S – S – Te and S – Te – S planes, however, differ by 11.0°. This difference in the degrees of rotation about the S – Te bonds is also seen from the non-bonded S(1) – S(4) and S(2) – S(5) distances which differ by 0.1905 Å. The dimensions of the two distorted tetrahedrally shaped thiosulphate groups are also nearly the same, and as seen from the

dihedral angles of Table 4, there is only a small difference in the degrees of rotation of the sulphonate groups about the S – S bonds.

The oxygen atoms are numbered in the same order as in the description of the structure of barium telluropentathionate dihydrate.[7] The dihedral angles thus show that the degrees of rotation of the sulphonate groups about the S – S bonds are different by about 21° in the two structures.

Table 5 gives the dimensions of the *trans* form of the S – S – Te – S – S chain in three compounds. The greatest variations are again found in the

Table 5. Bond lengths (Å), bond angles (°) and dihedral angles (°) of the S – S – Te – S – S chain in the *trans* form. Standard deviations are given in parentheses.

	$BaTe(S_2O_3)_2.3H_2O$	$Rb_2Te(S_2O_3)_2.1\frac{1}{2}H_2O$[10]	$Te(S_2O_2C_6H_5)_2$[17]
S – S	2.102(2), 2.090(2)	2.116(11), 2.126(9)	2.080(2)
S – Te	2.384(2), 2.392(2)	2.364(9), 2.370(7)	2.380(2)
∠S – S – Te	103.08(5), 102.59(5)	103.3(4), 102.8(3)	103.46(7)
∠S – Te – S	96.02(4)	100.1(3)	97.71(6)
∠SSTe/STeS	87.7, 98.7	77.7, 89.2	97.4

SSTe/STeS diredral angles. In each of the two salts, the two angles within a chain differ by about 11°, and the average values in the two salts differ by about 10°. The larger dihedral angles in tellurium dibenzenethiosulphonate might be due to the space requirement of the benzenesulphonate groups. The variations in the two salts, however, show that the dihedral angles are also influenced by the cation-oxygen coordination or by other packing effects. The variations in S – S and S – Te bond lengths, and in S – S – Te bond angles are small, though significant. The S – Te – S bond angles differ from 96.02(4)° in the barium salt to 100.1(3)° in the rubidium salt.

Among the barium salts of penta-, selenopenta- and telluropentathionic acids, $BaTe(S_2O_3).3H_2O$ is the only example where the anion occurs in the *trans* form. In the crystals where the *cis* form is found, each barium ion is in close contact with nine oxygen atoms, of which three are from the water molecules and the remaining six are from the anions. Two of the latter contacts are from different sulphonate groups of the same anion. All the oxygen atoms, except that of one of the water molecules in $BaSe(S_2O_3)_2.3H_2O$,[5] are involved in the Ba – O coordination. The Ba – O distances are in the range 2.75 – 2.94 Å.[4,5,7]

In the present structure the barium ions are each surrounded by eight oxygen atoms in the range 2.69 – 2.85 Å. All the water and sulphonate oxygen atoms, except O(4), take part once in these approaches. In addition there is one Ba – O distance of 3.19 Å, this oxygen atom being from the same sulphonate group as one of those involved in the closer contacts. The individual distances and related angles are listed in Table 6. Fig. 2 is a stereoscopic view as seen normal to the *b* crystal plane, showing the content of two

Table 6. Distances (Å), and angles (°) between directions, from barium ion to oxygen atoms. Standard deviations of the distances and angles are 0.003–0.005 Å and 0.1°, respectively.

				I	II	III	IV	V	VI	VII	VIII
I	$H_2O(1)$	$(1+x,1+y,z)$	2.794								
II	$H_2O(2)$	$(1+x,y,z)$	2.797	71.7							
III	$H_2O(3)$	(x,y,z)	2.838	148.1	131.7						
IV	O(1)	$(1+x,y,z)$	2.783	68.1	69.2	135.0					
V	O(2)	$(1-x,2-y,\bar{z})$	2.693	70.5	141.9	85.2	91.9				
VI	O(3)	$(1-x,1-y,\bar{z})$	2.808	123.1	126.8	64.6	71.7	72.4			
VII	O(5)	(x,y,z)	3.190	131.1	59.5	76.5	91.6	157.4	87.6		
VIII	O(5)	$(x,1+y,z)$	2.848	71.2	103.7	81.1	138.9	68.6	129.4	120.4	
IX	O(6)	(x,y,z)	2.824	120.3	71.7	63.6	133.8	134.2	116.5	46.7	73.8

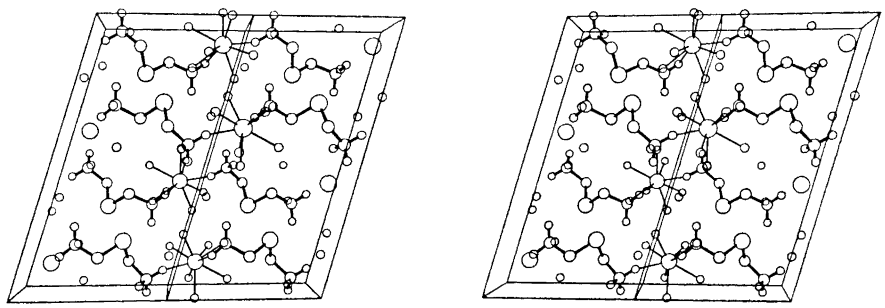

Fig. 2. A stereoscopic view as seen normal to the *b* crystal plane. The Ba–O coordination is indicated by the thin lines.

unit cells along the *a* axis. The Ba–O contacts are indicated by thin lines, whereas the bonds within the telluropentathionate ions are indicated by thick lines. The sulphonate oxygen atoms coordinated to the two barium ions in the middle of the figure are from the four nearest telluropentathionate ions shown, or from ions generated from the latter by addition or substraction of whole *b* units. The Ba–O coordination thus forms layers parallel to the *c* crystal plane, with thickness half the *c* spacing. The relation between neighbour layers is through twofold screw axes at $z=\frac{1}{4}$ and $\frac{3}{4}$. There are no Ba–O coordination contacts across the interfaces between the layers. This is very similar to the situation found for $BaTe(S_2O_3)_2.2H_2O$,[7] and the other barium salts with anions in the *cis* form, and where the crystals show perfect cleavage along the *c* crystal planes.[18] There is no such tendency of cleavage in the present crystals, and this might be due to the closer packing of the layers, to hydrogen bonds or other interionic contacts between the layers.

The most probable hydrogen bonds are; from $H_2O(1)$ to O(1) at (x,y,z) and $(x,y-1,z)$ with distances 2.993(6) Å and 3.126(6) Å and angle 117.9(2)°, from $H_2O(2)$ to $H_2O(1)$ at (x,y,z) and O(4) at $(1-x,\frac{1}{2}+y,\frac{1}{2}-z)$ with distances

2.917(6) Å and 2.864(5) Å and angle 99.3(2)°, and from $H_2O(3)$ to O(6) at (x,y,z) and O(3) at $(1-x,1-y,z)$ with distances 2.984(5) Å and 3.018(7) Å and angle 105.9(2)°. Only one of these assumed hydrogen bonds, $H_2O(2)-O(4)$, is across the interface between barium-oxygen coordination layers.

The closest interionic Te···Te approaches are between the tellurium atom at (x,y,z) and those at $(1-x,\frac{1}{2}+y,\frac{1}{2}-z)$ and $(1-x,-\frac{1}{2}+y,\frac{1}{2}-z)$. The distances are 3.833(1) Å and the Te···Te···Te angle is 86.31(3)°. The oxygen atom O(4), not involved in the Ba – O coordination, at $(1-x,\frac{1}{2}+y,\frac{1}{2}-z)$, is at a distance of 2.926(4) Å from tellurium. This oxygen atom and the tellurium at $(1-x,-\frac{1}{2}+y,\frac{1}{2}-z)$ are located only 0.11 Å and 0.40 Å, respectively, out of the S(2) – Te – S(4) plane. The angles between directions from tellurium to its four neighbours in this plane are: $\angle S(2)-Te-S(4)=96.02(4)°$, $\angle S(4)-Te\cdots Te=69.49(4)°$, $\angle Te\cdots Te\cdots O(4)=113.55(6)°$, $\angle O(4)\cdots Te-S(2)=80.63(7)°$, $\angle S(2)-Te\cdots Te=164.25(4)°$, and $\angle S(4)-Te\cdots O(4)=175.86(8)°$. There are thus two approximately linear systems, S(2) – Te···Te and S(4) – Te···O(4), at nearly right angles. The Te···Te and Te···O approaches are 0.29 Å and 0.65 Å, respectively, shorter than the sum of the van der Waals radii of the atoms involved.[19] The Te···Te and Te···O contacts are across the interfaces between the layers mentioned earlier.

REFERENCES

1. Foss, O. and Zachariasen, H. *Acta Chem. Scand.* **8** (1954) 473.
2. Foss, O. and Tjomsland, O. *Acta Chem. Scand.* **10** (1956) 288.
3. Foss, O. and Tjomsland, O. *Acta Chem. Scand.* **8** (1954) 1701.
4. Marøy, K. *Acta Chem. Scand.* **26** (1972) 36.
5. Marøy, K. *Acta Chem. Scand.* **26** (1972) 45.
6. Foss, O. and Tjomsland, O. *Acta Chem. Scand.* **12** (1958) 52.
7. Marøy, K. *Acta Chem. Scand.* **27** (1973) 1695.
8. Gjerrestad, K. and Marøy, K. *Acta Chem. Scand.* **24** (1970) 3402.
9. Foss, O. and Larssen, P. A. *Acta Chem. Scand.* **8** (1954) 1042.
10. Marøy, K. *Acta Chem. Scand.* **25** (1971) 2557.
11. Foss, O. and Tjomsland, O. *Acta Chem. Scand.* **10** (1956) 416.
12. Coppens, P., Leiserowitz, L. and Rabinovich, D. *Acta Cryst.* **18** (1965) 1035.
13. Zachariasen, W. H. *Acta Cryst.* **16** (1963) 1139.
14. *International Tables for X-Ray Crystallography*, Kynoch Press, Birmingham 1962, Vol. III.
15. Thomas, L. H. and Umeda, K. *J. Phys. Chem.* **26** (1957) 293.
16. Cromer, D. T. *Acta Cryst.* **18** (1965) 17.
17. Åse, K. *Acta Chem. Scand.* **25** (1971) 838.
18. Foss, O. *Advan. Inorg. Chem. Radiochem.* **2** (1960) 237.
19. Bondi, A. *J. Phys. Chem.* **68** (1964) 441.

Received December 27, 1972.

ACTA CHEMICA SCANDINAVICA 27 (1973) 1667–1672

Counter-ion Dependent Water and Amphiphile Orientation and Deuteron Exchange in Lyotropic Mesophases

NILS-OLA PERSSON, HÅKAN WENNERSTRÖM and BJÖRN LINDMAN

Division of Physical Chemistry 2, The Lund Institute of Technology, Chemical Center, P.O.B. 740, S-220 07 Lund, Sweden

Lamellar mesophase samples composed of alkali octanoate, decanol and heavy water were studied by means of deuteron magnetic resonance. The variations of the quadrupole splitting and of the spectral shape with pH and temperature are ascribed to chemical exchange of deuterons between decanol hydroxyl groups and water.

A method for treating chemical exchange phenomena in the presence of static quadrupolar effects is proposed and it is found that the quadrupole splitted NMR signals may give otherwise not easily accessible kinetic information. Comparison between computer-simulated and experimental spectra permits the estimation of deuteron exchange rates. It is found that the exchange rate depends markedly on the counter-ion present. Water orientation changes strongly as the counter-ion is changed whereas amphiphile orientation is almost independent of which alkali ion is present.

It has previously been observed that deuteron NMR spectra of amphiphilic liquid crystals containing heavy water are affected by three processes, *i.e.* the degree of water orientation, the degree of amphiphile orientation, and the rate of exchange of deuterons between water and amphiphile.[1–3] Since all these factors contain pertinent information on mesophase structure and/or motional processes it would be desirable to have a method for quantitatively separating the different contributions to the NMR spectral shape. It is the object of this communication to propose such a method. In this context also preliminary information on the dependence of water and amphiphile orientation and deuteron exchange rates on sample composition will be given.

EXPERIMENTAL

Heavy water was purchased from Norsk Hydro, Norway and had an isotopic enrichment of 99.8 %. Decanol and sodium octanoate were obtained from the British Drug Houses Ltd., Poole, England and the purity was better than 98 %. The lithium and potassium octanoates were prepared from metal ethanolate and octanoic acid by exact

neutralization in ethanol and the purity of the salts filtered off after washing with ethanol and drying were checked by titration in glacial acetic acid with crystal violet as an indicator. The rubidium and cesium octanoates were prepared by neutralization of alkali hydroxide with octanoic acid and their purities were checked as above. The molar weights obtained were for lithium octanoate 150.5 (calculated 150.2), for potassium octanoate 181.8 (182.3) for rubidium octanoate 225.1 (228.7) and for cesium octanoate 277.2 (276.1). Samples mostly of 1 g were prepared by weight in ampoules which were then immediately sealed off. The error in sample preparation was ± 0.002 g. The lamellar phase samples were prepared by heating the samples to a temperature above the transition point to isotropic solution and samples were then shaken and cooled.

The NMR measurements were performed on a Varian V-4200 wide line spectrometer with a 12 inch V-3603 magnet. The magnetic field was regulated with a Varian Mark II Fieldial unit and the sample temperature was controlled by means of a Varian V-4540 temperature controller. Sample temperatures were checked before and after each measurement with a copper-constantan thermocouple. The accuracy was within ± 2°C. For signal intensity reasons it was necessary to use samples of 4 g, which did not fit in the temperature controller to obtain the signals from the decanol hydroxyl deuterons (see below). These spectra were recorded at probe temperature (27 ± 3°C).

Deuteron spectra were recorded at a magnetic field of 1.403 T*, and a radio-frequency field of 9.1786 MHz. The intensities of the rf field and the modulation field were kept low enough not to affect the line-shape. For intensity reasons a slight saturation and over-modulation was necessary in the case of the decanol hydroxyl spectra.

RESULTS AND DISCUSSION

If, for a nucleus with spin quantum number I greater than one half, the motion is anisotropic on a sufficiently long time-scale then the interactions between the nuclear electric quadrupole moment and the electric field gradient lead to a splitting of the NMR signal into $2I$ components. For a deuteron ($I = 1$) this results in two major absorption maxima separated by

$$\Delta = \tfrac{1}{2} |\nu_Q S| \tag{1}$$

and

$$\Delta(\Omega) = \tfrac{1}{2} |(3\cos^2 \Omega - 1)\nu_Q S| \tag{2}$$

for powder and oriented samples, respectively.

Here $\nu_Q = \frac{3}{2}(e^2qQ/h)$, where eq is the largest component of the electric field gradient tensor in the principal axes system and eQ is the quadrupole moment. Ω is the angle between the magnetic field and the director.[4]

Recently, from the theory given by Luckhurst,[4] Lindblom [5] derived the order parameter S to be given by

$$S = \overline{D_{00}^{(2)}} + 1/\sqrt{6}\eta \, (\overline{D_{02}^{(2)}} + \overline{D_{0-2}^{(2)}}) \tag{3}$$

The $\overline{D^{(2)}}$'s are the second rank Wigner rotation matrix elements averaged over the molecular motion and η is the asymmetry parameter for the electiric field gradient tensor. The fact that the asymmetry parameter only affects the magnitude of the splitting and not the line shape (except for relaxation) has not always been recognized previously.

We have recorded deuteron NMR spectra for lamellar mesophase samples composed of heavy water, alkali octanoates and decanol.[6] As exemplified in Fig. 1 the spectra taken at room temperature consist of two signals, each split

* 1 T (tesla) = 10 000 Gauss.

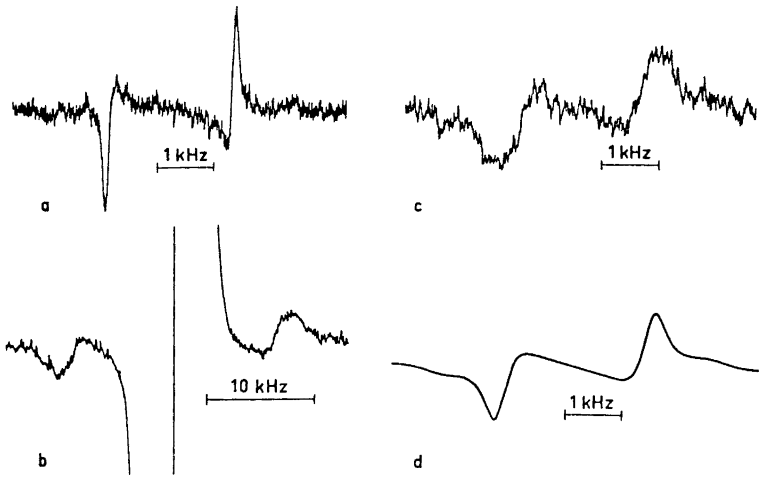

Fig. 1. Deuteron NMR spectra for a sample with the molar ratio D_2O:lithium octanoate: decanol being 83.0:6.8:10.2. a) Water deuteron spectrum at 27 ± 2°C. b) Spectrum for the decanol OD-group at 27 ± 2°C. c) Experimental spectrum at 40°C showing deuteron exchange effects. d) Corresponding computer simulated spectrum (*cf.* text) with intermediate exchange rate ($\tau = 23$ μs)

into two components. The signal of high intensity and small splitting is caused by the water deuterons, whereas the signal from the decanol deuterons gives a splitting one order of magnitude larger.

The distances between the intense peaks in the spectra are given in Fig. 2 as a function of temperature. As may be seen the splitting at first increases and then decreases with increasing temperature. Furthermore, at intermediate temperatures the NMR-signals are considerably broadened (*cf.* Fig. 2). Only

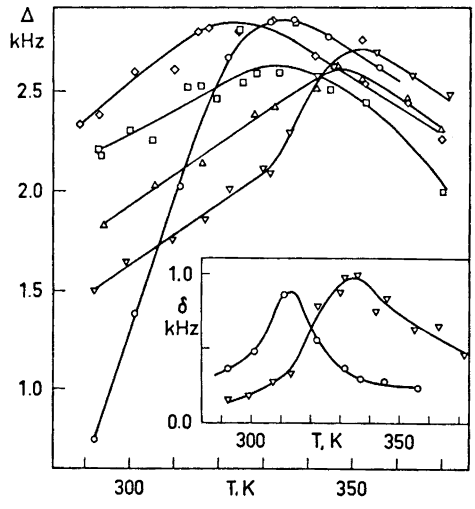

Fig. 2. Temperature dependence of the splitting corresponding to the intense deuteron signal (*cf.* text) and, inserted, the temperature dependence of the width at half height above the baseline of the inner peaks in the derivative of the NMR absorption spectrum. Samples investigated were (with molar ratios D_2O:soap:decanol given in parentheses). □ D_2O:lithium octanoate:decanol (83.0:6.8:10.2). ○ D_2O: sodium octanoate:decanol (77.5:10.8:11.7). ▽ D_2O:potassium octanoate:decanol (77.5: 10.8:11.7). △ D_2O:rubidium octanoate: decanol (77.5:10.8:11.7). ◇ D_2O:cesium octanoate:decanol (77.5:10.8:11.7).

one split signal can be detected at high temperatures in contrast to the room temperature spectra. All these facts strongly indicate that an exchange of deuterons between water and decanol takes place at a rate comparable to the splitting difference between the two sites. Such an exchange is base-catalyzed [7] and, as expected, additions of alkali hydroxide to the samples produce qualitatively the same changes as a temperature increase.

The effect of chemical exchange on the NMR spectrum of quadrupole split signals has, to the authors' knowledge, not previously been treated quantitatively. Lynden-Bell [8] has shown that if one neglects those terms in the quadrupole spin hamiltonian that do not commute with I_z, *i.e.* the secular approximation, then the transitions $m = 1 \rightarrow m = 0$ and $m = 0 \rightarrow m = -1$ are independent at low intensity radio frequency fields. (m is the magnetic quantum number.) If this is the case the problem is reduced to calculate the lineshape for each transition separately and then simply superimpose them to get the total lineshape. For each of these transitions the well known exchange equations from proton magnetic resonance [9] can be used. The shape of the deuteron signal is obtained by first solving the exchange equations for a given orientation of the microcrystallite. Then the average over all equally probable orientations is taken followed by adding the intensities from the two independent transitions. The formal expression for the lineshape $L(\nu)$ in the presence of exchange is (*cf.* Ref. 9. eqns. 13 – 15 where also symbols are defined)

$$L(\nu) = \int_{-1}^{1} (G(\nu) + G(-\nu))\, \mathrm{d}(\cos \Omega) \tag{4}$$

$$G(\nu) = \frac{\mathrm{i}\tau[2p_A p_B - \tau(p_A\alpha_B + p_B\alpha_A)]}{p_A p_B - \tau^2\alpha_A\alpha_B} \tag{5}$$

$$\alpha_{A,B} = -[\mathrm{i}2\pi((\Delta(\Omega))_{A,B}/2 - \nu) + 1/T_2 + p_{B,A}/\tau] \tag{6}$$

$$\tau = p_B/k_{A\rightarrow B} = p_A/k_{B\rightarrow A} \tag{7}$$

$\nu = 0$ corresponds to the resonance frequency without splitting. A computer simulated spectrum using the lineshape equation (4) is included in Fig. 1. Eqn. (4) gives an approximate rationalization of the variation of lineshape with temperature. It does not, however, reproduce the experimental spectra quantitatively. This is probably due to either the neglect of the non-secular terms in the hamiltonian or to the use of an intense radio frequency field.

The procedure outlined above for handling deuteron exchange has been utilized to determine exchange rates and the quadrupole splittings of water deuterons and of amphiphile hydroxylic deuterons and in particular how these quantities depend on the counter-ion.

As may be inferred from Fig. 2 the "coalescence temperature" depends significantly on which alkali ion is present. It is interesting to note for example that the deuteron exchange proceeds at a markedly higher rate with sodium as counter-ion than with potassium. Detailed calculations which are in progress are hoped to yield the activation parameters for the different cases.

Water deuteron splittings can be obtained from the signals observed at low temperatures by correcting for the effect of exchange. This was accomlished by comparing the increase in splitting obtained on hydroxide addition with the

Table 1. Water deuteron splittings for samples with molar composition 83.0 %, 6.8 % and 10.2 % of water, alkali octanoate and decanol respectively.

Counter-ion	Li^+	Na^+	K^+	Rb^+
Δ, kHz	2.21	1.14	1.50	1.46

splitting for the amphiphilic deuterons. As shown in Table 1 the water orientation depends markedly on the counter-ion present and is largest with lithium. The relation between the other counterions depends on sample composition. Besides lithium the water orientation increases with increasing atomic number of the counter-ion at least at the lowest water contents. The difference between the effect of potassium, rubidium and cesium on water orientation is small at low amphiphile concentrations.

In contrast to these observations, the degree of amphiphile orientation depends very little on the counter-ion present (Table 2). On the other hand, amphiphile splitting increases drastically with decreasing water content as well as with increasing molar ratio between soap and decanol.

Table 2. Decanol-OD deuteron splittings for samples with molar composition 83.0 %, 7.6 % and 9.5 % of water, alkali octanoate and decanol respectively.

Counter-ion	Li^+	Na^+	K^+	Rb^+
Δ, kHz	20.6	23.7	21.9	21.8

It may be concluded from this preliminary account that if deuteron exchange is not too rapid, information on both water and amphiphile orientation may be obtained from deuteron NMR studies on heavy water containing lyotropic mesophase samples. Furthermore, the rate of deuteron exchange may be estimated. Detailed studies of this type on a large number of systems, including model membrane systems, are in progress and will be presented at a later date.

An interesting aspect on studying chemical exchange in the presence of static quadrupolar interactions is the possibility of continuously varying the splitting difference in the case of macroscopically oriented samples by varying Ω (*cf.* eq. 2). Thus for oriented samples the range of exchange rates possible to investigate may be quite large.

We are indebted to Göran Lindblom and Åke Johansson for discussions and to Tom E. Bull for improving the language.

REFERENCES

1. Johansson, Å. and Drakenberg, T. *Mol. Cryst. Liquid Cryst.* **14** (1971) 23.
2. Persson, N.-O. and Johansson, Å. *Acta Chem. Scand.* **25**(1971) 2118.
3. Johansson, Å. and Lindman, B. In Gray G. W. and Winsor, P. A., Eds., *Liquid Crystals and Plastic Crystals*, Ellis Horwood Publishers, Chichester, Vol. 2, Chapter 8. *In press.*
4. Luckhurst, G. R. In Gray, G. W. and Winsor, P. A., Eds., *Liquid Crystals and Plastic Crystals*, Ellis Horwood Publishers, Chichester, Vol. 2, Chapter 7. *In press.*

5. Lindblom, G. *Acta Chem. Scand.* **26** (1972) 1745.
6. For phase diagrams see Ekwall, P., Mandell, L. and Fontell, K. *Mol. Cryst. Liquid Cryst.* **8** (1969) 157.
7. Luz, Z. and Meiboom, S. *J. Chem. Phys.* **30** (1959) 1540.
8. Lynden-Bell, R. M. *Mol. Phys.* **22** (1971) 837.
9. Binsch, G. In Eliel, E. L. and Allinger, N. L., Eds., *Topics in Stereochemistry*, John Wiley & Sons, New York 1968, Vol. 3, p. 106.

Received December 13, 1972.

ACTA CHEMICA SCANDINAVICA 27 (1973) 1673–1678

Zur Struktur des Lignins des Druckholzes von *Pinus mugo*

MAGNUS ERICKSON, SAM LARSSON und GERHARD E. MIKSCHE

Institutionen för organisk kemi, Chalmers Tekniska Högskola och Göteborgs Universitet, Fack, S-402 20 Göteborg 5, Schweden

Aus Druckholz und «normalem« Holz von *Pinus mugo* Turra. gewonnene Sulfatlignine wurden methyliert und oxydativ abgebaut. Aus dem Druckholzlignin entstanden die sich ganz oder zum Teil von *p*-Hydroxyphenylpropaneinheiten ableitenden Abbausäuren *1*, *4*, *8*, *10* und *11* in erheblich höherer Menge wie aus dem Lignin des Normalholzes. Dies zeigt, dass das Druckholzlignin von *Pinus mugo* ein Dehydrierungspolymerisat von Coniferylalkohol und *p*-Cumaralkohol darstellt. Die sich ebenfalls ganz oder zum Teil von *p*-Hydroxyphenylpropaneinheiten ableitenden Abbausäuren *13–17* wurden neu aufgefunden.

An der Unterseite von einseitig belasteten Stämmen oder Ästen von Coniferen wird Druckholz gebildet. Es weicht morphologisch – so durch die starke Lignifizierung der S2-Schicht der Sekundärwand von Längstracheiden (siehe z.B. Lit. 1a und 1b für das Druckholz von *Pinus taeda* bzw. *Pseudotsuga menzesii*) – vom «normalen« Holz der jeweiligen Pflanze ab. Charakteristisch ist der hohe Ligningehalt des Druckholzes;[2,3] Druckholzlignin enthält weniger Methoxyl als das Lignin des Normalholzes.[2,4] Dies wurde auf einen erhöhten Anteil von *p*-Hydroxyphenylpropaneinheiten am Aufbau des Druckholzlignins zurückgeführt, der auch durch vergleichsweise höhere Ausbeuten von *p*-Hydroxybenzaldehyd bei der Nitrobenzoloxydation [2,4] und von Äthanolyseprodukten [4] vom *p*-Hydroxyphenylpropantyp angezeigt wird. Die IR- und UV-Spektren von Druckholzligninen und den entsprechenden Normalligninen unterscheiden sich jedoch – im Gegensatz zur Erwartung beim Vorliegen eines höheren Anteils der *p*-Hydroxyphenylpropankomponente in den ersteren – nur unwesentlich.[5] Zwei neuere Arbeiten über das Druckholzlignin von *Abies sachalinensis* haben nicht zur weiteren Klärung des Problems der Struktur von Druckholzligninen beigetragen.[6]

Eine eingehendere Charakterisierung eines Druckholzlignins erschien daher wünschenswert. In der vorliegenden Arbeit wurden mit Hilfe eines zweistufigen

* IX. Mitteilung in der Reihe: Gaschromatographische Analyse von Ligninoxydationsprodukten. VIII. Mitteilung siehe Lit. 7b.

Abbaus[7a] das Druckholzlignin und das Normalholzlignin der Bergkiefer (*Pinus mugo* Turra. = *P. montana* Mill.) miteinander verglichen.

Die feingemahlenen, vorextrahierten Holzmehle wurden durch Erhitzen mit natriumsulfidhaltiger Natronlauge aufgeschlossen und die so erhaltenen löslichen Sulfatlignine nach Methylierung oxydativ ($KMnO_4 + NaJO_4$ in verd. Natronlauge, enthaltend *tert.*-Butanol; H_2O_2 bei pH 9 – 10) abgebaut. Die Gemische der aromatischen Abbausäuren wurden mit Diazomethan methyliert und die mengenmässig wichtigsten Abbausäuren (*1 – 4, 6 – 12*) als Methylester gaschromatographisch bestimmt (Tab. 1).

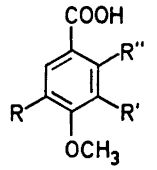

1 R, R', R'' = H
2 R = OCH_3; R', R'' = H
3 R, R' = OCH_3; R'' = H
4 R = COOH; R', R'' = H
5 R, R' = H; R'' = COOH
6 R = OCH_3; R' = COOH; R'' = H
7 R = OCH_3; R' = H; R'' = COOH

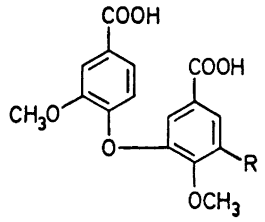

8 R = H
9 R = OCH_3

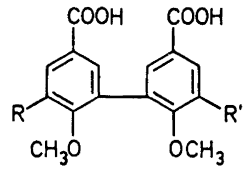

10 R, R' = H
11 R = OCH_3; R' = H
12 R, R' = OCH_3

Tab. 1. Ausbeuten an Methylestern (in mg/g Holzmehl) beim oxydativen Abbau von Sulfatligninen von *Pinus mugo* Turra.

	Methylester der Abbausäuren										
	1	*2*	*3*[a]	*4*	*6*	*7*	*8*	*9*	*10*	*11*	*12*
«Normales« Lignin	3,1	62,8	1,0	–	16,9	3,0	0,7	5,2	< 0,2	0,75	13,0
Druckholzlignin	16,5	58,8	0,85	2,9	15,7	3,2	1,55	4,8	0,45	2,5	11,9

[a] Einschliesslich des Methylesters von *5*.

Der gegenüber dem Normallignin stark erhöhte Anteil von Anissäure (*1*) und 4-Methoxy-isophthalsäure (*4*) sowie der zweikernigen Abbausäuren *8*, *10* und *11*, die sich ganz oder teilweise von *p*-Hydroxyphenylpropanstrukturen ableiten, zeigt die Bedeutung dieses Strukturtyps für den Aufbau den Druckholzlignins der Bergföhre. Demnach ist etwa jede fünfte Phenylpropaneinheit dieses Lignins vom *p*-Hydroxyphenylpropantyp. Das Hervortreten der von «gekreuzten« Kopplungsstrukturen herrührenden Abbausäuren *8* und *11* ist besonders kennzeichnend, da sie einen direkten Nachweis der Copolymerisation der Guajacyl- und *p*-Hydroxyphenylpropankomponente liefern.

Unter den Spurenkomponenten des oxydativen Abbaus von methyliertem Björkman-Lignin von Fichte [8a] (*Picea abies;* das Lignin dieser Art ist aufgrund der Ergebnisse des oxydativen Abbaus dem von Normalholz von *Pinus mugo* weitgehend ähnlich)[7b] ist eine grössere Anzahl von Abbausäuren aufgefunden worden, die sich ganz oder teilweise von *p*-Hydroxyphenylpropaneinheiten ableiten. Diese Abbausäuren treten in dem aus Druckholz von *Pinus mugo* erhaltenen Säurengemisch stärker hervor. Weiters entstand im letzteren Fall eine Anzahl zweikerniger Abbausäuren unbekannter Konstitution, von denen fünf (*13–17*) durch massenspektrometrischen Vergleich der Methylester mit den entsprechenden, synthetisch gewonnenen Estern identifiziert werden konnten.

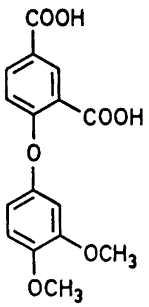

13

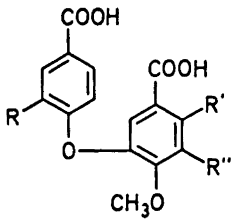

14 R, R', R'' = H

15 R = COOH; R' = H; R'' = OCH_3

16 R = OCH_3; R' = COOH; R'' = H

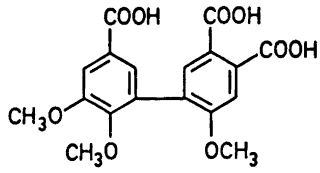

17

Die Abbausäure *13* leitet sich von einer durch (O_c,4)-Kopplung * zweier Phenoxylradikale (vom *p*-Hydroxyphenylpropantyp bzw. vom Guajacylpropantyp) gebildeten Diarylätherstruktur ab. Die den Abbausäuren *14*, *15* und *16* zugrundeliegenden Diarylätherstrukturen sind offenbar auf folgende Weise gebildet worden: (O_c,2_c)-, (O_c,6)- bzw. (O,2_c)-Kopplung. Bei den Vorstufen der Abbausäuren *13*, *15* und *16* war die *p*-Hydroxyphenylpropankomponente in einer der ursprünglich freien Kernpositionen C-kondensiert. Die Abbausäure *17* stammt von einer durch (2_c,6)-Kopplung entstandenen Biphenylstruktur ab, in welcher der Kern vom *p*-Hydroxyphenylpropantyp ebenfalls einen zusätzlichen C-Kernsubstituenten trug.

Da keiner der Vorläufer der Abbausäuren *13–17* beim Sulfataufschluss durch eine etwaige Lederer-Manasse-Reaktion oder durch C-Addition eines Phenolations an ein Chinonmethid entstanden sein kann, ist deren Vorkommen im Druckholzlignin der Bergkiefer als erwiesen anzusehen. Die Frequenz der diesen Spurenkomponenten entsprechenden Substrukturen des Lignins ist gering. Ihr Nachweis bedeutet nichtsdestoweniger eine weitere Stütze der bereits aus den quantitativen Ergebnissen (Tab. 1) gewonnenen Ansicht, dass das Lignin des Druckholzes von *Pinus mugo* ein echtes Misch-Dehydrierungspolymerisat von Coniferylalkohol und *p*-Cumaralkohol darstellt. Es bleibt natürlich noch zu untersuchen, inwiefern es hinsichtlich der Zusammensetzung

* Zur Bezeichnungsweise siehe Lit. 8b.

des Lignins Übergänge zwischen dem hier bearbeiteten, sehr deutlich ausgeprägten Druckholz und dem Normalholz dieser und anderer Coniferen gibt.

Mit der in der vorliegenden Arbeit verwendeten Methode des oxydativen Abbaus haben wir eine grössere Anzahl von Ligninen von Vertretern verschiedener Familien der Angiospermen und Gymnospermen, sowie der Bryophyten und Pteridophyten untersucht.[9] Bei diesen Untersuchungen wurden bisher keine Normallignine mit einem ähnlich hohen Anteil von *p*-Hydroxyphenylpropaneinheiten wie im Druckholzlignin von *Pinus mugo* aufgefunden. Die Ansicht, dass im Lignin primitiver Pflanzen die *p*-Hydroxyphenylpropankomponente überwiegt,[10] ist somit nicht zutreffend. Dass die Lignine von Gramineen, die beim oxydativen Abbau wechselnde Mengen von Anissäure (*1*) liefern, nur bedingt als Guajacyl-Syringyl-*p*-Hydroxyphenyl-Lignine anzusehen sind, ist bereits von Higuchi *et al.* festgestellt worden;[11] dies geht auch klar aus den Ergebnissen des oxydativen Abbaus einiger Vertreter dieser Familie hervor.[9]

EXPERIMENTELLER TEIL

Pflanzenmaterial. Aus einem Stamm eines etwa 50-jährigen, sehr krumm gewachsenen Exemplars von *Pinus mugo* Turra. (Halland, Südschweden) wurden Holzmehle (40 mesh) aus dem sehr deutlich abgesetzten Druckholz sowie aus dem Normalholz hergestellt. Sie wurden extrahiert [7a] und über P_2O_5 bei 100° im Vakuum getrocknet.

Sulfatkochung. Methylierung und oxydativer Abbau. Gaschromatographische Bestimmung der wichtigsten Abbausäuren. Siehe Lit. 7a. Nachweis der Abbausäuren *13* – *17*. Das Gemisch der Methylester der Abbausäuren (aus 500 mg Holzmehl von Druckholz) wurde auf Dünnschichtplatten (5 × entwickelt) chromatographiert. Die durch Eluieren mit Aceton gewonnenen Fraktionen wurden gaschromatographisch untersucht. Von den in Kapillaren aufgefangenen Komponenten wurden Massenspektren aufgenommen und mit den Spektren synthetisch erhaltener Präparate verglichen.

Die Methylester der Tricarbonsäuren *15*, *16* und *17* liefen im Chromatogramm langsamer als die Methylester sämtlicher «wichtiger« Abbausäuren. Der Dimethylester von *13* wurde in der selben Fraktion wie *12*-Dimethylester aufgefunden, während der im Dünnschichtchromatogramm schnellaufende Dimethylester von *14* bereits im nicht vorgetrennten Estergemisch aufgefunden worden war.

Retentionszeiten (relativ zum Dimethylester von *12*, $T = 240°$):[8b] *13*, 0,63; *14*, 0,48; *15*, 1,37; *16*, 1,42; *17*, 1,74.

Massenspektren. Wurden teils mit einem MS 902, teils mit einem MS 20 Gerät der Fa. AEI, Manchester, aufgenommen.

Protonenresonanzspektren. 60 MHz; Tetramethylsilan als innerer Standard; in $CDCl_3$; δ-Werte.

Dünnschichtchromatographie. Kieselgel HF_{254}, Merck; Benzol.

Synthesen

3',4'-Dimethoxy-diphenyläther-2,4-dicarbonsäure (13). Durch Umsetzung von 6,5 g 4-Bromveratrol und 4,0 g des Kaliumsalzes von 2,4-Dimethylphenol in Gegenwart von 1,4 g Cu-Bronze (200°, 5 Stunden) wurde der 3',4'-Dimethoxy-2,4-dimethyl-diphenyläther erhalten; Kp. (Kugelrohr) 130 – 150°/0,01 Torr. Das Rohprodukt wurde mit $KMnO_4$ in 1-proz. wässriger Sodalösung, enthaltend 25 % *tert.*-Butanol, oxydiert. Als Reaktionsprodukt wurde ein Gemisch von *13* und einer Monocarbonsäure, wahrscheinlich der 3',4'-Dimethoxy-2-methyl-diphenyläther-4-carbonsäure (Massenspektrum des Methylesters), erhalten. Die Ester (Diazomethan) wurden dünnschichtchromatographisch getrennt.

Der langsamer laufende Dimethylester von *13* fiel als farbloses, zähes Öl and. (Exakte Massenbestimmung am Molekülion. Gef.: M = 346,1035. Ber. für $C_{18}H_{18}O_7$: M = 346,1052.) NMR (5 %): 3,83 (3) s, OCH_3; 3,87 (3) s, OCH_3; 3,90 (6) s, 2 OCH_3; 6,60 (1) m, H_5'; 6,63 (1) m, H_2'; 6,80 (1) m, H_6'; 6,82 (1) d, H_6; 8,00 (1) dd, H_5; 8,61 (1) d, H_3. $J_{3,5} = 2{,}2$ Hz; $J_{5,6} = 8{,}6$ Hz. $J_{2',6'} \simeq 2$ Hz; $J_{5',6'} \simeq 8$ Hz (ABC-Spektrum).

Säure *13*; aus dem Dimethylester mit methanolischer KOH. Schmp. 258 – 260° (wässr. Methanol). (Gef.: C 60,31; H 4,40. Ber. für $C_{16}H_{14}O_7$ (318,29): C 60,38; H 4,43.)

6-Methoxy-diphenyläther-3,4'-dicarbonsäure (14). Der Methylester von *14* wurde aus dem K-Salz von *p*-Hydroxybenzoesäure-methylester und 3-Brom-anissäure-methylester in Gegenwart von Cu-Bronze bei 240° (3 Stunden) erhalten. Er wurde zur Säure *14* verseift. Schmp. 309 – 313°; Lit.[13a] Schmp. 313 – 314°.

Der Dimethylester von *14* zeigte einen Schmp. von 77 – 78° (Essigester-Hexan) bzw. 77° (Methanol-H_2O). Die in der Literatur für diesen Ester angegebenen Schmp. liegen durchwegs über 90° (90 – 92°;[13b] 94°;[13c] 94 – 96°;[13d] 97 – 98° [13a]). Das Massensprektrum sowie das Protonenresonanzspektrum stehen im Einklang mit der Struktur des Dimethylesters von *14*. NMR (5 %): 3,83 (3) s, OCH_3; 3,85 (3) s, OCH_3; 3,87 (3) s, OCH_3; 6,89 (2) m, H_2' und H_6'; 7,02 (1) d, H_5; 7,72 (1) d, H_2; 7,89 (1) dd, H_4; 7,94 (2) m, H_3' und H_5'. $J_{2,4} = 2{,}0$ Hz, $J_{4,5} = 8{,}5$ Hz. Die Protonen am disubstituierten Ring zeigen ein AA'XX'-Spektrum.

5,6-Dimethoxy-2',4'-dimethyl-diphenyläther-3-carbonsäure. Entstand durch Umsetzung von 5-Brom-veratrumsäure-methylester[12] (5,5 g) und dem K-Salz von 2,4-Dimethyl-phenol (3,2 g) in Gegenwart von Cu-Bronze (1,3 g); 1-stünd. Erhitzen auf 180 – 220°. Die bei 180°/0,01 Torr übergehende Fraktion des Reaktionsproduktes bestand aus fast reinem Methylester der obigen Säure (0,84 g). NMR (15 %): 2,24 (3) s, Ar-CH_3; 2,28 (3) s, Ar-CH_3; 3,79 (3) s, OCH_3; 3,89 (3) s, OCH_3; 3,94 (3) s, OCH_3; 6,73 (1) m, H_6'; 6,90 (1) m, H_5'; 7,02 (1) m, H_3'; 7,10 (1) d, H_2; 7,35 (1) d, H_4. $J_{2,4} = 2{,}0$ Hz. $J_{3',5'} \simeq 2$ Hz; $J_{5',6'} \simeq 8$ Hz. (ABC-Spektrum).

Die freie Monocarbonsäure zeigte einem Schmp. von 148 – 150° (wässr. Methanol). (Gef.: C 67,56; H 5,90. Ber. für $C_{17}H_{18}O_5$ (302,33): C 67,54; H 6,00.)

5',6'-Dimethoxy-diphenyläther-2,3',4-tricarbonsäure (15). Aus der voranstehend beschriebenen Monocarbonsäure mit $KMnO_4$ in siedender 1-proz. Na_2CO_3. Es entstand ein aus *15* und einer Dicarbonsäure, wahrscheinlich der 5,6-Dimethoxy-2'-methyl-diphenyläther-3,4'-dicarbonsäure (Massenspektrum des Dimethylesters) bestehendes Gemisch. Dünnschichtchromatographische Trennung der Methylester (Diazomethan) führte zum reinen, langsamer laufenden Trimethylester von *15*. Prismen aus Essigester-Hexan; Schmp. 112°. (Gef.: C 59,36; H 5,01. Ber. für $C_{20}H_{20}O_9$ (404,38): C 59,40; H 4,99.) NMR (10 %): 3,87 (6) s, 2 OCH_3; 3,91 (6) s, 2 OCH_3; 3,95 (3) s, OCH_3; 6,77 (1) d, H_6; 7,35 (1) d, H_2' oder H_4'; 7,46 (1) d, H_2' oder H_4'; 8,01 (1) dd, H_5; 8,68 (1) d, H_3. $J_{3,5} = 2{,}2$ Hz; $J_{5,6} = 8{,}6$ Hz. $J_{2',4'} = 2{,}0$ Hz.

Die freie Säure *15* schmilzt bei 265 – 268° (Nadeln aus wässr. Methanol). (Gef.: C 56,35; H 3,86. Ber. für $C_{17}H_{14}O_9$ (362,30): C 56,36; H 3,89.)

2,2'-Dimethoxy-4',5'-dimethyl-diphenyläther-4-carbonsäure. Der Methylester dieser Säure entstand durch Ullmann-Kopplung von 2-Brom-4,5-dimethyl-anisol[14] (4,3 g) mit dem K-Salz von Vanillinsäure-methylester (4,2 g) in Gegenwart von Cu-Bronze (1,3 g) bei 225 – 230° (4 Stunden). Die bei 150 – 190°/0,01 Torr übergehende Fraktion (2,1 g) der Kugelrohrdestillation des Reaktionsproduktes wurde verseift. Schmp. 180 – 182° (wässr. Methanol; 1,36 g). (Gef.: C 67,42; H 5,97. Ber. für $C_{17}H_{18}O_5$ (302,33): C 67,54; H 6,00.)

2',6-Dimethoxy-diphenyläther-3,4,4'-tricarbonsäure (16). Aus der voranstehend beschriebenen Monocarbonsäure (1,0 g) mit $KMnO_4$ in siedender 1-proz. Na_2CO_3. Farblose Kristalle (0,43 g) aus wässr. Methanol; Schmp. 234 – 238°, Umwandlung bei ca. 210°. (Gef.: C 55,91; H 3,89. Ber. für $C_{17}H_{14}O_9$ (362,30): C 56,36; H 3,89.)

Trimethylester von *16*. Farbloses, zähes Öl. (Exakte Massenbestimmung am Molekülion. Gef.: M = 404,1092. Ber. für $C_{20}H_{20}O_9$: M = 404,1107.) NMR (15 %): 3,78 (3) s, OCH_3; 3,86 (12) s, 4 OCH_3; 6,83 (1) m, H_2'; 7,17 (1) s, H_2 oder H_5; 7,23 (1) s, H_2 oder H_5; 7,56 (1) m, H_3'; 7,64 (1) m, H_5'. $J_{2',3'} \simeq 8$ Hz; $J_{3',5'} \simeq 2$ Hz (ABX-Spektrum).

2',5,6-Trimethoxy-4',5'-dimethyl-biphenyl-3-carbonsäure. Ein Gemisch, bestehend aus 3,2 g 5-Jod-veratrumsäure-methylester,[15] 5,2 g 2-Jod-4,5-dimethyl-anisol[16] und 7,9 g Cu-Bronze wurde 30 Min auf 230° erhitzt. Die bei der Kugelrohrdestillation des Reaktionsprodukts bei 130 – 185°/0,01 Torr übergehende Fraktion (3,7 g) wurde verseift. Nach

Abtrennung der 5,5'-Dehydro-diveratrumsäure (Aceton) kristallisierten 1,05 g der Monocarbonsäure aus wässrigem Methanol; Schmp. 163–165°. (Gef.: C 68,59; H 6,36. Ber. für $C_{18}H_{20}O_5$ (316,36): C 68,34; H 6,37.)

5',6,6'-Trimethoxy-biphenyl-3,3',4-tricarbonsäure (17). Aus voranstehender Monocarbonsäure (1,0 g) mit $KMnO_4$ in 1-proz. Na_2CO_3 bei 100°. Kristalle (0,72 g) aus Methanol-H_2O; Schmp. 274°, Umwandlung bei ca. 230°. (Gef.: C 57,37; H 4,44. Ber. für $C_{18}H_{16}O_9$ (376,33): C 57,45; H 4,29.)

Trimethylester von *17*. Kristalle aus Essigester-Hexan; Schmp. 126–127°. NMR (5 %): 3,69 (3) s, OCH_3; 3,84 (3) s, OCH_3; 3,86 (3) s, OCH_3; 3,89 (3) s, OCH_3; 3,95 (6) s, 2 OCH_3; 7,12 (1) s, H_2; 7,51 (1) d, H_4'; 7,60 (1) d, H_2'; 7,69 (1) s, H_5. Signale von H_2 und H_2' verbreitert im Vergleich zu den von H_5 bzw. H_4'. $J_{2',4'} = 2{,}0$ Hz. (Gef. :C 60,43; H 5,34. Ber. für $C_{21}H_{22}O_9$ (418,41): C 60,28; H 5,30.)

Die Elementaranalysen wurden unter Leitung von Dr. J. Zak am Mikroanalytischen Laboratorium am Inst. für physik. Chemie der Univ. Wien ausgeführt.

Herrn Prof. Dr. Adler danken wir für wertvolle Diskussionen. Diese Arbeit wurde durch ein Stipendium (G. E. M.) von *Cellulosaindustriens Stiftelse för teknisk och skoglig forskning samt utbildning* unterstützt.

LITERATUR

1. a. Parham, R. A. und Coté, W. A. *Wood Sci. Technol.* **5** (1971) 49.
   b. Wood, J. R. und Goring, D. A. I. *Pulp Paper Mag. Can.* **72** [3] (1971) 61.
2. Bland, D. E. *Holzforschung* **15** (1961) 102.
3. Coté, W. A., Simon, B. W. und Timell, T. E. *Svensk Papperstid.* **69** (1966) 547; Coté, W. A., Timell, T. E. und Zabel, R. A. *Holz Roh-Werkstoff* **24** (1966) 432; Coté, W. A., Pickard, P. A. und Timell, T. E. *Tappi* **50** (1967) 350.
4. Latif, A. M. Diss., Univ. of Washington, Seattle 1968. Zitiert von Sarkanen, K. V. und Hergert, H. L., in Sarkanen, K. V. und Ludwig, C. H. *Lignins*, Wiley-Interscience, New York 1971, S. 60.
5. Lee, V. P. F. Diss, Univ. of Washington, Seattle 1968. Zitiert wie Lit. 4, S. 60.
6. Morohoshi, N. und Sakakibara, A. *J. Japan Wood Res. Soc.* **17** (1971) 393, 400.
7. a. Erickson, M., Larsson, S. und Miksche, G. E. *Acta Chem. Scand.* **27** (1973) 127.
   b. *Ibid.* **27** (1973) 903.
8. a. Larsson, S. und Miksche, G. E. *Acta Chem. Scand.* **23** (1969) 3337. b. *Ibid.* **23** (1969) 917.
9. Erickson, M., Miksche, G. E. und Somfai, I. *Holzforschung* **27** (1973) 113.
10. Freudenberg, K. In Freudenberg, K. und Neish, A. C. *Constitution and Biosynthesis of Lignin*, Springer, Berlin 1968, S. 112–114.
11. Higuchi, T., Ito, Y. und Kawamura, I. *Tappi* **54** (1971) 72.
12. Whaley, W. M., Starker, L. und Meadow, M. *J. Org. Chem.* **18** (1955) 833.
13. a. Späth, E. und Pikl, J. *Ber.* **62** (1929) 2251. b. Tomita, M. und Kugo, T. *Yakugaku Zasshi* **77** (1957) 1057; zitiert in *Chem. Abstr.* **52** (1958) 5249. c. Knabe, J. *Chem. Ber.* **91** (1958) 1612. d. Grundon, M. F. und McGarvey, J. E. B. *J. Chem. Soc.* **1960** 2739. e. Yamasaki, T. und Higuchi, T. *J. Japan Wood Res. Soc.* **17** (1971) 117.
14. Tomita, M. *J. Pharm. Soc. Japan* **56** (1936) 814; zitiert in *Chem. Abstr.* **32** (1938) 8426.
15. Erdtman, H. *Svensk Kem. Tidskr.* **47** (1935) 223.
16. Carruthers, W. und Douglas, A. G. *J. Chem. Soc.* **1959** 2813.

Eingegangen am 22. Dezember 1972.

ACTA CHEMICA SCANDINAVICA 27 (1973) 1679–1683

Electrolysis in Non-nucleophilic Media

Part VI.[1] Anodic Coupling of Aromatic Hydrocarbons in Methylene Chloride in the Presence of Strong Acids

LENNART EBERSON, KLAS NYBERG, and HANS STERNERUP

Division of Organic Chemistry, University of Lund, Chemical Center, P.O. Box 740, S-220 07 Lund, Sweden

The use of strong acids, such as trifluoroacetic acid, methanesulphonic acid, and trifluoromethanesulphonic acid, in methylene chloride prevents the reductive formation of chloride ion during electrolysis. Anodic coupling of aromatic hydrocarbons in methylene chloride containing any of these acids is, however, affected. In general, the yield of biaryl products is decreased and the yield of diphenylmethanes is increased.

Anodic coupling of aromatic hydrocarbons in methylene chloride is affected adversely by the reductive formation of chloride ion at the cathode.[2] Chloride ion is oxidized at the anode simultaneously with the aromatic hydrocarbon, producing chlorine that reacts with the hydrocarbon in a homogeneous chlorination process. This side-reaction not only decreases the current yield of the desired product (dehydrodimer) but also makes its isolation difficult. Since methylene chloride is an excellent solvent for anodic reactions in other respects, we have investigated anodic coupling in methylene chloride containing strong acids, in the hope that proton reduction at the cathode would prevent reduction of methylene chloride. Strong acids have been used earlier for the anodic oxidation of alkanes in fluorosulphonic acid [3] and for voltammetric experiments in trifluoroacetic acid.[4]

RESULTS AND DISCUSSION

It is obvious that the number of suitable acids is rather limited. The acid should be soluble in methylene chloride and should not react with the aromatic hydrocarbon, except possibly for protonation to form a σ-complex. Therefore, trifluoroacetic acid, methanesulphonic acid, and trifluoromethanesulphonic acid were chosen as potentially useful acids. The first two are of comparable acidity while the last one is one of the strongest organic acids known. Tri-

fluoroacetic acid was used as a 10 % solution, methanesulphonic acid as a 0.4 M solution, and trifluoromethanesulphonic acid as a 0.2 M solution unless otherwise stated. Chlorosulphonic and fluorosulphonic acids were also tried, but could not be used since they rapidly sulphonate the aromatic hydrocarbons.

All anodic oxidations were carried out between two platinum electrodes on solutions containing hydrocarbon, tetrabutylammonium tetrafluoroborate (0.1 M), acid, and methylene chloride, using the saturated calomel electrode as a reference electrode. Analysis of the products was made by GLC, after 0.2 *F* per mol of hydrocarbon had been passed through the electrolyte.

Anodic oxidation of naphthalene in methylene chloride containing trifluoroacetic acid gave 1,1′-binaphthyl in an 8 % current yield. No chlorinated products were formed. However, the yield of binaphthyl is lower than that obtained in methylene chloride containing acetic acid or in acetonitrile containing acetic acid (14 and 28 %, respectively).[5]

Similar results were obtained from the anodic oxidation of mesitylene, as shown in Table 1. The yields of dimeric products are generally lower in the

Table. 1. Products from the anodic oxidation of mesitylene (1.0 M).

Acid	Current yields I[a]	II	III	Anode potential (V)
–	5[b]	30	16	1.8
CF_3COOH	–	18	5	1.4
CH_3SO_3H (0.2 M)	7	6	2	1.4
» (0.6 M)	1	11	3	1.4
CF_3SO_3H	–	37	7[c]	1.2

[a] 2-Chloromesitylene. [b] Data from Ref. 2. [c] 3 % of a tetramer was also formed.

presence of acids than in their absence, with the exception of trifluoromethanesulphonic acid. In all experiments, bimesityl (II) and termesityl (III) were formed, whereas in the presence of trifluoromethanesulphonic acid, a tetrameric product was also observed. Chloride ion formation can be successfully blocked in these experiments as seen from Table 1. It is also worth mentioning that the anode potential is significantly lower when acids are present in the electrolyte (approximately the same current density is used in all experiments).

Anodic coupling of naphthalene or mesitylene represent cases where only biaryls are produced. The yields are generally lower in the presence of acids than in their absence.

Anodic coupling of *p*-xylene (IV) gives 2,5,4′-trimethyldiphenylmethane (V) and 2,5,2′,5′,4″-pentamethyltriphenylmethane (VI), depending on the reaction conditions (Table 2). In the presence of acids, strong effects on the product distribution as well as the anode potential are again observed. The total yields of V and VI are considerably higher in the presence of acids than in their absence. This is opposite to the effect observed in the oxidation of

Table 2. Products from the anodic oxidation of *p*-xylene (2.0 M).

Acid	Current yields IV	V	VI	Anode potential (V)
–	–	10	–	2.0
CF_3COOH[b]	5[a]	22	4	1.4
CH_3SO_3H	–	17	4	1.5
CF_3SO_3H	–	6	18	1.3

[a] Data from Ref. 2. [b] 5–10 % yield of *p*-methylbenzyl trifluoroacetate was also obtained.

naphthalene or mesitylene. Oxidation of *p*-xylene in the presence of trifluoroacetic acid produced yet another compound, *p*-methylbenzyl trifluoroacetate.

The highest yields of dehydrodimers were obtained in the oxidation of durene in the presence of acids (Table 3). 3-Chlorodurene (VII) was almost absent in these experiments. The highest yield of 2,3,5,6,2′,4′,5′-heptamethyldi-

Table 3. Products from the anodic oxidation of durene.

Durene conc. (M)	Acid	Current yields VII	VIII	Anode potential (V)
0.2[a]	–	14	14	1.4
1.0[a]	–	12	29	1.4
0.2	CF_3COOH	–	65	1.3
1.0	»	–	77	1.3
0.2	CH_3SO_3H	1	29	1.1
1.0	»	2	54	1.1
1.0	CF_3SO_3H	–	85	1.2

[a] Data from Ref. 2.

phenylmethane (VIII) is remarkably high. Besides VIII, a trimeric product, accounting for 5–10 % of the product mixture, was formed in most reactions. In contrast to the case of *p*-xylene there was no indication of the formation of a side-chain trifluoroacetate.

Anodic oxidation of pentamethylbenzene in methylene chloride produces chloropentamethylbenzene, a small amount of decamethylbiphenyl and a nonamethyldiphenylmethane.[6] In the presence of acids, oxidation of pentamethylbenzene gave the same hydrocarbons, no significant difference in the yields being observed. In some experiments, two isomeric nonamethyldiphenylmethanes were observed. In the presence of trifluoromethanesulphonic acid, hexamethylbenzene and tetramethylbenzenes were formed in about 20 % yield. The same compounds were observed in a control experiment when no current was passed through the electrolysis mixture.

We also investigated the anodic oxidation of toluene in methylene chloride containing trifluoroacetic acid. No volatile products were formed, the anode being rapidly coated with polymers. The anode potential was also in this case significantly lower than in the absence of the acid.

In all experiments reported, the presence of acids has the effect of decreasing the amount of chlorinated products thus fulfilling our expectations. On the other hand, it influenced the yield of products and the product distribution in a way that is difficult to explain. Biaryl products were generally formed in lower yields in the presence of acid, while diphenylmethane products were formed in higher yields.

From a synthetic point of view the results show that it should be an advantage to use acids in preparing diphenylmethanes. Therefore, some large-scale oxidations were carried out using a newly developed cell construction permitting high currents.[7] Oxidation of *p*-xylene in the presence of trifluoroacetic acid produced V in a current yield of 16 % together with 10 % of *p*-methylbenzyl trifluoroacetate. Oxidation of durene in the presence of trifluoroacetic acid and methanesulphonic acid gave VIII in 39 and 23 % current yield, respectively.

EXPERIMENTAL

The apparatus and procedure for small-scale electrolysis was the same as previously described.[5] GLC analysis was carried out on a 2 m × 0.3 cm 3 % OV − 17 on Chromosorb W column using an internal standard (Perkin-Elmer 880 gas chromatograph). The following hydrocarbon products were identified on the basis of their mass spectral fragmentation pattern: VI, the tetrameric compound from oxidation of mesitylene, and the trimeric compound from oxidation of durene. All other products have been characterized or isolated in earlier work. Large-scale oxidations were carried out between a carbon anode (surface area 580 cm^2) and a steel cathode in the cell described previously.[7]

Oxidation of p-*xylene.* A solution containing *p*-xylene (4.0 mol), tetrabutylammonium tetrafluoroborate (0.04 mol), trifluoroacetic acid (200 ml), and methylene chloride (1800 ml) was electrolyzed at a constant current of 15 A, an applied voltage of 48 V, and a temperature of 32° until 0.5 *F* per mol of *p*-xylene had passed. Solvent and *p*-xylene were removed by distillation at atmospheric pressure. Further distillation gave a fraction, b.p. 83 − 85°/12 mm, identified as *p*-methylbenzyl trifluoroacetate by NMR (in $CDCl_3$, TMS internal standard, $\delta = 2.33$ ppm, 5.28 ppm, 7.23 ppm, integrated area ratio 3:2:4) and MS (*m/e* 218). The yield was 21.3 g (current yield 10 %) and the purity by GLC about 98 %. The residue was treated with pentane and the pentane soluble material run through an alumina column to remove polymeric material. After removing the solvent, further distillation afforded 2,5,4′-trimethyldiphenylmethane, b.p. 130 − 135°/1.5 mm (34.6 g, current yield 16 %). The purity was 95 %.

Oxidation of durene. A solution containing durene (1.0 mol), tetrabutylammonium tetrafluoroborate (0.01 mol), trifluoroacetic acid (50 ml), and methylene chloride (450 ml) was electrolyzed at a constant current of 10 A, an applied voltage of 31 V, and a temperature of 25° until 0.5 *F* per mol of durene had passed. The solvent was removed by distillation and durene removed from the residue by steam distillation. The residual organic material was extracted into methylene chloride. After removing the solvent, the residue was treated twice with 250 ml boiling pentane. The combined pentane solutions were run through an alumina column. From the eluate, VIII was obtained (26 g, current yield 39 %), contaminated with 7 % of the trimeric hydrocarbon.

The oxidation of durene was repeated using 0.2 mol of methanesulphonic acid instead of trifluoroacetic acid under identical conditions. The yield of VIII was 23 %.

Acknowledgements. Financial support from the *Swedish Natural Science Research Council, Kungliga Fysiografiska Sällskapet i Lund,* and *Karl Tryggers Stiftelse* is gratefully acknowledged.

REFERENCES

1. Part V, see Nyberg, K. *Acta Chem. Scand.* **27** (1973) 503.
2. Nyberg, K. *Acta Chem. Scand.* **24** (1970) 1609.
3. Bertram, J., Fleischmann, M. and Pletcher, D. *Tetrahedron Letters* **1971** 349.
4. Hammerich, O., Moe, N. and Parker, V. D. *Chem. Commun.* **1972** 156.
5. Nyberg, K. *Acta Chem. Scand.* **25** (1971) 3770.
6. Nyberg, K. *Acta Chem. Scand.* **25** (1971) 2499.
7. Eberson, L., Nyberg, K. and Sternerup, H. *Chemica Scripta* **3** (1973) 12.

Received December 16, 1972.

ACTA CHEMICA SCANDINAVICA 27 (1973) 1684–1694

Refinement of the Crystal Structure of Potassium Barium Hexathionate

KJARTAN MARØY

Chemical Institute, University of Bergen, N-5000 Bergen, Norway

The crystal structure of potassium barium hexathionate, $K_2Ba(S_6O_6)_2$, has been refined by full-matrix least squares for 2375 independent non-zero reflections. The data were collected by means of a single-crystal diffractometer using Mo$K\alpha$ radiation (Nb-filtered). The refinement converged at a conventional R value of 0.020.

The space group is $P2/c$ (No. 13) with two formula units in a unit cell of dimensions $a = 11.591(4)$ Å, $b = 10.835(5)$ Å, $c = 9.145(3)$ Å, $\beta = 111.93(4)°$.

The six-membered sulphur chain of the hexathionate anion has the *cis-cis* rotational isomeric form. The bond lengths and angles, from one end of the chain to the other, are 2.119(1), 2.042(2), 2.056(2), 2.039(2), 2.110(1) Å, and 101.25(5)°, 110.20(5)°, 108.99(5)°, 99.95(5)°. The SSS/SSS dihedral angles are 109.4°, 89.0°, and 106.3°.

The crystal struetures of two salts of hexathionic acid have been published, both in 1965. In one of these salts, $K_2Ba(S_6O_6)_2$,[1] the anion occurs in the *cis-cis* rotational isomeric form, whereas in the other one, $[Co(en)_2Cl_2]_2S_6O_6 .H_2O$,[2] the anion has the *trans-trans* form. In the latter structure there was a tendency of variation in the lengths of the three middle S – S bonds, although the differences might not have been significant. Mainly to decide this point new sets of data have been recorded on a single-crystal diffractometer and refined by a full-matrix least squares program. The refinements and results are described in the present and a following paper.[3]

EXPERIMENTAL

The measurements were carried out on a Siemens automatic single-crystal diffractometer using Mo$K\alpha$ radiation (Nb-filtered) and a scintillation counter.

The crystals of $K_2Ba(S_6O_6)_2$ were prepared by Foss and Palmork.[4] The sample used had been kept for thirteen years in a refrigerator, and showed no signs of decomposition. The crystal used for measurements of unit cell dimensions and intensities was a prism along the c axis, bounded by (100), (110), and (1$\bar{1}$0), and terminated by ($\bar{1}$11). It was mounted with the c axis approximately parallel to the ϕ axis of the diffractometer, and oriented by measurements of θ,χ, and ϕ angles of six non-coplanar reciprocal vectors.

The five-value procedure and $\theta - 2\theta$ scan technique, with scan width of 0.70°, were used. The maximum scan time per degree was 24 sec.

Two reflections, 12 0 0 and 0 10 0, were measured two times each at intervals of 50 reflections. The intensities of these reflections decreased by 6 % during the data collection, and were used to bring the net intensities to a common scale.

Reflections were measured up to $\theta = 28°$, and only 215 of the 2590 independent reflections within this region were found to have net intensities below three times its standard deviation. These reflections were assigned an intensity equal to this limit, and labelled as unobserved.

Beside Lorentz and polarization corrections, the intensities were also corrected for absorption. The linear absorption coefficient for Mo$K\alpha$ is 34.7 cm^{-1}. The crystal used had a length along c of 0.330 mm, and the distances between the (100), between the (110), and between the (1$\bar{1}$0) boundary faces were 0.087, 0.130, and 0.130 mm, respectively. The number of Gaussian grid points used along the a, b, and c axes were 6, 6, and 12, respectively. The absorption factors, by which the intensities were multiplied, varied from 1.29 to 1.51.

The scattering factor curves used where those listed in *International Tables for X-Ray Crystallography*,[5] except for barium ion, for which the curve given by Thomas and Umeda[6] was used. The curves for barium, potassium, and sulphur were corrected for anomalous dispersion using the values given by Cromer,[7] and taking the amplitude as the corrected value.

The refinement was carried out with a full-matrix least squares program minimizing the function

$$r = \sum W(|F_o| - K|F_c|)^2$$

The intensity data were eventually corrected for secondary extinction with a program written by K. Åse of this Institute.

For further details concerning the data collection and the programs used, see Ref. 8.

The unit cell dimensions, calculated by means of a least squares program using the θ angles ($\theta = 21 - 28°$) of 15 reflections measured on the diffractometer, are $a = 11.591(4)$ Å, $b = 10.835(5)$ Å, $c = 9.145(3)$ Å, $\beta = 111.93(4)°$.

The space group is $P2/c$ (No. 13) with two $K_2Ba(S_6O_6)_2$ units per unit cell.[4]

REFINEMENT

The least squares refinement was started using the positional parameters given by Foss and Johnsen,[1] and individual isotropic thermal parameters that were the averaged values of those given for the two projections. Refinement on scale factor, positional parameters, and isotropic thermal parameters resulted in an R value ($\sum||F_o| - |F_c||/\sum|F_o|$) of 0.095. On using anisotropic thermal parameters for barium, potassium, and sulphur the R value was reduced to 0.031, and with anisotropic, thermal parameters also for the oxygen atoms, the refinement converged at $R = 0.022$.

For the reflections with highest intensities, the observed structure factors were considerable lower than the calculated ones. Secondary extinction corrections were therefore carried out. The expression given by Zachariasen [9] was used. With the absorption term equal to one, C was found to be 6.0×10^{-7}. The observed values of the structure factors now corresponded well to the calculated ones also for the strongest reflections.

The final R value was 0.020, with unobserved reflections included when $|F_c|$ is greater than the observable limit. There were no shifts of the parameters in the last refinement cycle.

A final difference electron density map showed no peaks higher than 0.4 e/Å^3.

Table 1. Atomic coordinates for potassium barium hexathionate. Origin at a centre of symmetry. Standard deviations are given in parentheses.

	x	y	z
Ba	0	0.01396(2)	¼
K(1)	½	0	½
K(2)	0	0.44987(8)	¼
S(1)	0.13933(6)	0.27403(5)	0.04470(7)
S(2)	0.33447(7)	0.28355(8)	0.16708(10)
S(3)	0.34815(9)	0.42062(8)	0.32588(9)
S(4)	0.40178(8)	0.34854(8)	0.54946(9)
S(5)	0.24695(8)	0.30389(7)	0.59363(10)
S(6)	0.25238(5)	0.10984(6)	0.57818(7)
O(1)	0.10136(21)	0.39894(17)	−0.00500(25)
O(2)	0.13175(21)	0.18877(19)	−0.07952(24)
O(3)	0.08578(18)	0.22999(17)	0.15501(23)
O(4)	0.36031(19)	0.06818(23)	0.70720(24)
O(5)	0.13276(16)	0.07734(17)	0.58622(20)
O(6)	0.25668(16)	0.07982(17)	0.42586(21)

Table 2. Thermal parameters expressed in the form exp $[-2\pi^2(h^2a^{-2}U_{11}+\cdots+2hka^{-1}b^{-1}U_{12}+\cdots)]$. All values have been multiplied by 10^4. Standard deviations are given in parentheses.

	U_{11}	U_{22}	U_{33}	U_{12}	U_{23}	U_{13}
Ba	196(1)	202(1)	182(1)	0	0	77(1)
K(1)	284(5)	1270(12)	402(6)	169(6)	−366(7)	5(5)
K(2)	575(6)	254(4)	331(5)	0	0	156(4)
S(1)	300(3)	200(3)	274(3)	−33(3)	7(2)	88(3)
S(2)	302(4)	574(5)	549(5)	−72(4)	−40(4)	153(4)
S(3)	647(6)	387(4)	423(5)	−270(4)	39(4)	41(4)
S(4)	521(5)	554(5)	416(5)	−327(4)	56(4)	−15(4)
S(5)	653(6)	303(4)	574(5)	−119(4)	−124(4)	285(5)
S(6)	197(3)	279(3)	223(3)	−30(2)	32(2)	57(2)
O(1)	621(16)	250(10)	480(14)	56(10)	127(10)	145(12)
O(2)	560(15)	395(11)	446(14)	−124(11)	−172(10)	231(12)
O(3)	374(12)	302(9)	392(12)	−47(8)	38(8)	180(10)
O(4)	306(12)	676(15)	359(13)	2(11)	193(11)	−18(10)
O(5)	230(9)	369(10)	324(11)	−61(8)	7(8)	139(9)
O(6)	326(11)	335(10)	297(10)	−19(8)	−21(8)	167(9)

Tables 1 and 2 give the final atomic parameters with standard deviations from least squares. The oxygen atoms are numbered in an order different from that published earlier,[1] and have now numbers in accordance with those in the telluropentathionates described in Refs. 8 and 10.

As seen from Table 2 there is an extremely high value of U_{22} for K(1) compared to all other thermal parameters. This agrees with what was found by the refinement of the two-dimensional film data through difference maps. In the $hk0$ zone the value of B in Å^2 was $2.5+10.0\cos^2\phi$ for K(1), where ϕ is the angle between the normal of the reflecting plane and the direction of maximum vibration of the atom; this direction being parallel to the b axis.[1]

The observed structure factors and those calculated from the final atomic parameters are listed in Table 3.

Table 3. Observed and calculated structure factors ($\times 10$) for potassium barium hexathionate. A minus sign on $F(O)$ indicates an unobserved reflection.

H	K	L	F(O)	F(C)	H	K	L	F(O)	F(C)	H	K	L	F(O)	F(C)	H	K	L	F(O)	F(C)	H	K	L	F(O)	F(C)
3	0	0	1361	1367	-9	0	8	185	190	5	1	2	654	-679	-8	1	6	799	-822	-11	1	11	187	201
4	0	0	246	274	-8	0	8	369	366	6	1	2	274	-272	-7	1	6	506	-522	-10	1	11	-57	25
5	0	0	286	321	-7	0	8	620	628	7	1	2	575	-585	-6	1	6	235	-253	-9	1	11	137	-137
6	0	0	710	739	-6	0	8	513	529	8	1	2	93	-87	-5	1	6	416	-415	-8	1	11	102	-102
7	0	0	725	641	-5	0	8	152	164	9	1	2	633	-632	-4	1	6	136	-139	-7	1	11	72	71
8	0	0	1835	1781	-4	0	8	889	875	10	1	2	419	-431	-3	1	6	856	-865	-6	1	11	228	222
9	0	0	760	749	-3	0	8	849	849	11	1	2	262	-266	-2	1	6	81	-86	-5	1	11	-54	-13
10	0	0	-120	4	-2	0	8	1109	1143	12	1	2	223	-207	-1	1	6	621	-625	-4	1	11	-55	-6
11	0	0	130	156	-1	0	8	566	580	13	1	2	364	-361	0	1	6	924	-937	-3	1	11	272	262
12	0	0	887	878	0	0	8	-75	-11	-15	1	3	-59	54	1	1	6	620	-634	-2	1	11	98	-105
13	0	0	215	181	1	0	8	673	681	-14	1	3	115	-110	2	1	6	61	40	-1	1	11	114	-125
14	0	0	296	282	2	0	8	740	739	-13	1	3	249	-254	3	1	6	542	-535	0	1	11	-51	54
-14	0	2	461	-451	3	0	8	-55	-25	-12	1	3	228	223	4	1	6	380	-382	-7	1	12	346	350
-13	0	2	158	-159	4	0	8	689	703	-11	1	3	141	142	5	1	6	292	-289	-6	1	12	158	152
-12	0	2	533	-534	5	0	8	461	460	-10	1	3	52	-57	6	1	6	264	-262	-5	1	12	149	148
-11	0	2	1219	-1213	6	0	8	536	535	-9	1	3	438	448	7	1	6	417	-418	0	2	0	443	403
-10	0	2	360	-368	-12	0	10	308	-304	-8	1	3	592	594	8	1	6	248	-246	1	2	0	535	511
-9	0	2	753	-754	-11	0	10	172	-169	-7	1	3	-44	-18	9	1	6	474	-468	2	2	0	1698	1650
-8	0	2	61	25	-10	0	10	454	-451	-6	1	3	697	-693	-14	1	7	-56	-28	3	2	0	1206	1214
-7	0	2	693	-707	-9	0	10	446	-467	-5	1	3	137	158	-13	1	7	326	333	4	2	0	1575	1603
-6	0	2	1793	-1683	-8	0	10	251	-254	-4	1	3	213	223	-12	1	7	-54	-10	5	2	0	933	939
-5	0	2	1036	-1035	-7	0	10	506	-502	-3	1	3	123	149	-11	1	7	-54	-10	6	2	0	1008	1020
-4	0	2	747	-780	-6	0	10	532	-530	-2	1	3	244	236	-10	1	7	396	404	7	2	0	349	355
-3	0	2	2660	-2815	-5	0	10	776	-771	-1	1	3	74	-84	-9	1	7	96	-88	8	2	0	762	772
-2	0	2	1188	-1213	-4	0	10	169	-177	0	1	3	896	905	-8	1	7	330	-340	9	2	0	318	328
-1	0	2	522	516	-3	0	10	294	-299	1	1	3	-42	-44	-7	1	7	231	-223	10	2	0	692	701
0	0	2	206	204	-2	0	10	511	-528	2	1	3	691	-701	-6	1	7	-47	-8	11	2	0	653	643
1	0	2	2130	-2158	-1	0	10	560	-568	3	1	3	261	269	-5	1	7	761	751	12	2	0	353	350
2	0	2	1215	-1247	0	0	10	467	-482	4	1	3	590	589	-4	1	7	372	374	13	2	0	217	224
3	0	2	2233	-2238	1	0	10	353	-366	5	1	3	438	429	-3	1	7	-44	-17	14	2	0	323	317
4	0	2	727	-711	2	0	10	363	-366	6	1	3	230	-239	-2	1	7	248	241	-14	2	1	-56	18
5	0	2	1218	-1237	3	0	10	511	-506	7	1	3	140	140	-1	1	7	299	301	-13	2	1	168	-171
6	0	2	1163	-1166	-7	0	12	239	222	8	1	3	152	152	0	1	7	458	-469	-12	2	1	94	-89
7	0	2	199	184	-6	0	12	245	238	9	1	3	226	-221	1	1	7	413	-415	-11	2	1	199	195
8	0	2	59	-77	-5	0	12	251	253	10	1	3	-57	65	2	1	7	520	531	-10	2	1	354	-357
9	0	2	1056	-1071	-4	0	12	568	553	11	1	3	155	-27	3	1	7	206	211	-9	2	1	168	-162
10	0	2	553	-537	1	1	0	942	849	12	1	3	182	191	4	1	7	76	75	-8	2	1	185	182
11	0	2	528	-507	2	1	0	537	526	-15	1	4	87	80	5	1	7	61	67	-7	2	1	67	-61
12	0	2	132	-141	3	1	0	111	-91	-14	1	4	370	381	6	1	7	205	-203	-6	2	1	873	858
13	0	2	474	-465	4	1	0	1464	1525	-13	1	4	330	334	7	1	7	217	203	-5	2	1	344	-349
-15	0	4	149	132	5	1	0	214	227	-12	1	4	410	407	8	1	7	-58	-40	-4	2	1	876	-864
-14	0	4	527	515	6	1	0	482	480	-11	1	4	282	300	-14	1	8	431	430	-3	2	1	973	965
-13	0	4	396	400	7	1	0	566	574	-10	1	4	540	549	-13	1	8	273	275	-2	2	1	1157	-1120
-12	0	4	89	81	8	1	0	913	929	-9	1	4	377	377	-12	1	8	328	339	-1	2	1	593	-553
-11	0	4	308	315	9	1	0	193	193	-8	1	4	526	533	-11	1	8	234	243	0	2	1	847	800
-10	0	4	1078	1080	10	1	0	273	271	-7	1	4	184	187	-10	1	8	481	483	1	2	1	169	150
-9	0	4	863	866	11	1	0	361	353	-6	1	4	680	688	-9	1	8	245	246	2	2	1	470	462
-8	0	4	1171	1179	12	1	0	436	427	-5	1	4	806	835	-8	1	8	179	182	3	2	1	74	-85
-7	0	4	226	236	13	1	0	199	199	-4	1	4	778	786	-7	1	8	328	329	4	2	1	174	-171
-6	0	4	1114	1150	14	1	0	272	265	-3	1	4	388	372	-6	1	8	739	744	5	2	1	63	-23
-5	0	4	1118	1127	-14	1	1	118	-107	-2	1	4	1361	1348	-5	1	8	447	454	6	2	1	-43	-15
-4	0	4	194	209	-13	1	1	220	-225	-1	1	4	317	-285	-4	1	8	329	332	7	2	1	304	-304
-3	0	4	501	505	-12	1	1	208	-213	0	1	4	566	577	-3	1	8	404	406	8	2	1	-48	24
-2	0	4	1529	1897	-11	1	1	-52	42	1	1	4	409	428	-2	1	8	614	618	9	2	1	413	418
-1	0	4	1481	1564	-10	1	1	144	136	2	1	4	207	220	-1	1	8	58	54	10	2	1	268	-268
0	0	4	745	763	-9	1	1	369	-368	3	1	4	852	872	0	1	8	415	416	11	2	1	182	-198
1	0	4	123	126	-8	1	1	56	55	4	1	4	680	681	1	1	8	222	228	12	2	1	96	98
2	0	4	1560	1571	-7	1	1	695	696	5	1	4	108	93	2	1	8	535	547	13	2	1	82	-80
3	0	4	487	497	-6	1	1	1159	-1181	6	1	4	942	955	3	1	8	350	350	-14	2	2	341	-328
4	0	4	980	987	-5	1	1	782	-787	7	1	4	148	150	4	1	8	148	141	-13	2	2	632	-641
5	0	4	578	579	-4	1	1	699	724	8	1	4	334	324	5	1	8	305	310	-12	2	2	194	-203
6	0	4	848	856	-3	1	1	273	266	9	1	4	253	248	6	1	8	430	427	-11	2	2	146	-146
7	0	4	1017	1008	-2	1	1	899	878	10	1	4	315	322	-13	1	9	-58	-35	-10	2	2	468	-469
8	0	4	237	224	-1	1	1	532	-503	11	1	4	279	274	-12	1	9	-57	-26	9	2	2	730	-724
9	0	4	64	-60	0	1	1	491	-461	-15	1	5	104	-97	-11	1	9	177	176	-8	2	2	542	-554
10	0	4	560	553	1	1	1	180	187	-14	1	5	294	-292	-10	1	9	-54	27	-7	2	2	1187	-1194
11	0	4	315	309	2	1	1	1452	-1469	-13	1	5	82	79	-9	1	9	208	-219	-6	2	2	806	-834
-15	0	6	347	-335	3	1	1	1416	-1444	-12	1	5	213	229	-8	1	9	269	-274	-5	2	2	1386	-1356
-14	0	6	222	-226	4	1	1	61	43	-11	1	5	236	-243	-7	1	9	264	-266	-4	2	2	860	-835
-13	0	6	618	-616	5	1	1	1063	1083	-10	1	5	68	61	-6	1	9	218	210	-3	2	2	980	-982
-12	0	6	570	-568	6	1	1	148	-120	-9	1	5	331	343	-5	1	9	229	239	-2	2	2	497	-496
-11	0	6	381	-400	7	1	1	334	-343	-8	1	5	241	-244	-4	1	9	213	-211	-1	2	2	2340	-2421
-10	0	6	82	-59	8	1	1	323	327	-7	1	5	793	-802	-3	1	9	122	124	0	2	2	1347	-1351
-9	0	6	241	-252	9	1	1	243	-243	-6	1	5	475	-468	-2	1	9	73	-82	1	2	2	456	-467
-8	0	6	961	-984	10	1	1	175	-171	-5	1	5	334	342	-1	1	9	338	-343	2	2	2	1041	-1052
-7	0	6	1451	-1487	11	1	1	118	-115	-4	1	5	181	-178	0	1	9	334	-347	3	2	2	1022	-1009
-6	0	6	85	65	12	1	1	60	-43	-3	1	5	-42	21	1	1	9	100	-89	4	2	2	-43	-41
-5	0	6	1449	-1463	13	1	1	207	203	-2	1	5	86	-89	2	1	9	275	274	5	2	2	1139	-1165
-4	0	6	1637	-1673	-14	1	2	295	-295	-1	1	5	63	44	3	1	9	-58	60	6	2	2	625	-630
-3	0	6	-82	-9	-13	1	2	478	-473	0	1	5	503	494	4	1	9	-58	-34	7	2	2	933	-933
-2	0	6	231	-238	-12	1	2	-55	-62	1	1	5	926	-933	5	1	9	97	-88	8	2	2	796	-791
-1	0	6	868	-890	-11	1	2	577	-587	2	1	5	296	-299	-12	1	10	264	-267	9	2	2	494	-490
0	0	6	876	-873	-10	1	2	596	-593	3	1	5	686	695	-11	1	10	295	-298	10	2	2	136	-133
1	0	6	1261	-1252	-9	1	2	293	-295	4	1	5	210	-216	-10	1	10	306	-305	11	2	2	544	-542
2	0	6	146	-116	-8	1	2	439	-453	5	1	5	240	-238	-9	1	10	485	-481	12	2	2	220	-210
3	0	6	634	-633	-7	1	2	627	-649	6	1	5	167	-157	-8	1	10	192	-200	-15	2	3	109	101
4	0	6	748	-762	-6	1	2	242	-246	7	1	5	118	-118	-7	1	10	274	-271	-14	2	3	-56	-35
5	0	6	566	-560	-5	1	2	1296	-1298	8	1	5	85	-87	-6	1	10	238	-236	-13	2	3	76	75
6	0	6	131	121	-4	1	2	314	300	9	1	5	100	-102	-5	1	10	325	-320	-12	2	3	64	-73
7	0	6	671	-681	-3	1	2	763	-790	10	1	5	-57	-40	-4	1	10	399	-397	-11	2	3	54	43
8	0	6	844	-829	-2	1	2	975	-984	-15	1	6	400	-408	-3	1	10	290	-299	-10	2	3	157	-159
9	0	6	336	-323	-1	1	2	664	-663	-14	1	6	146	-135	-2	1	10	215	-215	-9	2	3	-47	0
-14	0	8	345	351	0	1	2	333	-325	-13	1	6	249	-256	-1	1	10	554	-549	-8	2	3	356	353
-13	0	8	317	324	1	1	2	1183	-1204	-12	1	6	334	-333	0	1	10	111	-111	-7	2	3	450	451
-12	0	8	209	195	2	1	2	709	-718	-11	1	6	537	-532	1	1	10	265	-260	-6	2	3	324	314
-11	0	8	609	626	3	1	2	846	-832	-10	1	6	65	-74	2	1	10	254	-249	-5	2	3	375	-366
-10	0	8	966	986	4	1	2	186	-207	-9	1	6	535	-544	3	1	10	301	-313	-4	2	3	286	-256

Table 3. Continued.

H	K	L	F(O)	F(C)	H	K	L	F(O)	F(C)	H	K	L	F(O)	F(C)	H	K	L	F(O)	F(C)	H	K	L	F(O)	F(C)
-3	2	3	498	-479	-2	2	7	137	-155	0	3	1	-41	3	-2	3	5	65	48	-4	3	10	161	-162
-2	2	3	578	-566	-1	2	7	221	221	1	3	1	1019	1007	-1	3	5	279	-295	-3	3	10	400	-400
-1	2	3	355	357	0	2	7	90	84	2	3	1	364	-379	0	3	5	63	52	-2	3	10	281	-282
0	2	3	116	-114	1	2	7	165	-161	3	3	1	361	-353	1	3	5	229	-231	-1	3	10	310	-302
1	2	3	750	767	2	2	7	149	-149	4	3	1	572	-565	2	3	5	873	-874	0	3	10	331	-335
2	2	3	220	217	3	2	7	420	423	5	3	1	876	-870	3	3	5	243	-248	1	3	10	277	-279
3	2	3	403	-396	4	2	7	77	-81	6	3	1	429	-433	4	3	5	318	-333	2	3	10	256	-251
4	2	3	289	283	5	2	7	187	-182	7	3	1	452	-447	5	3	5	432	-430	-10	3	11	129	133
5	2	3	301	-312	6	2	7	269	268	8	3	1	82	-58	6	3	5	-51	38	-9	3	11	84	83
6	2	3	-47	11	7	2	7	-57	26	9	3	1	316	312	7	3	5	217	214	-8	3	11	171	163
7	2	3	188	184	8	2	7	-56	15	10	3	1	110	-108	8	3	5	-53	-12	-7	3	11	129	135
8	2	3	-51	34	-14	2	8	500	503	11	3	1	417	-422	9	3	5	209	-205	-6	3	11	159	150
9	2	3	237	234	-13	2	8	402	405	12	3	1	112	-127	10	3	5	251	-243	-5	3	11	146	135
10	2	3	206	-199	-12	2	8	458	466	13	3	1	66	-78	-14	3	6	330	-327	-4	3	11	62	-48
11	2	3	-55	-41	-11	2	8	289	281	-14	3	2	266	-277	-13	3	6	475	-469	-3	3	11	240	270
12	2	3	140	134	-10	2	8	360	360	-13	3	2	293	-296	-12	3	6	344	-344	-2	3	11	309	314
-15	2	4	214	219	-9	2	8	412	412	-12	3	2	424	-416	-11	3	6	370	-373	-1	3	11	-61	73
-14	2	4	253	248	-8	2	8	612	615	-11	3	2	638	-638	-10	3	6	346	-335	0	4	0	752	758
-13	2	4	454	454	-7	2	8	502	507	-10	3	2	-51	30	-9	3	6	443	-449	1	4	0	1144	1139
-12	2	4	793	753	-6	2	8	909	900	-9	3	2	581	-579	-8	3	6	212	-202	2	4	0	1281	1253
-11	2	4	438	444	-5	2	8	912	897	-8	3	2	287	-285	-7	3	6	622	-630	3	4	0	423	426
-10	2	4	694	714	-4	2	8	367	362	-7	3	2	542	-550	-6	3	6	220	-211	4	4	0	661	648
-9	2	4	442	447	-3	2	8	-48	9	-6	3	2	743	-740	-5	3	6	949	-931	5	4	0	170	180
-8	2	4	328	327	-2	2	8	656	657	-5	3	2	914	-901	-4	3	6	658	-669	6	4	0	1349	1346
-7	2	4	664	669	-1	2	8	291	287	-4	3	2	724	-718	-3	3	6	219	-218	7	4	0	552	554
-6	2	4	841	856	0	2	8	694	698	-3	3	2	928	-909	-2	3	6	478	-479	8	4	0	300	298
-5	2	4	238	258	1	2	8	728	746	-2	3	2	551	-550	-1	3	6	445	-452	9	4	0	584	582
-4	2	4	1774	1746	2	2	8	642	646	-1	3	2	293	-285	0	3	6	296	-304	10	4	0	461	455
-3	2	4	1172	1154	3	2	8	486	480	0	3	2	71	-78	1	3	6	701	-703	11	4	0	188	176
-2	2	4	856	832	4	2	8	407	406	1	3	2	1616	-1603	2	3	6	297	-300	12	4	0	328	317
-1	2	4	778	767	5	2	8	73	48	2	3	2	101	-108	3	3	6	748	-743	13	4	0	263	268
0	2	4	1390	1354	6	2	8	356	361	3	3	2	1077	-1080	4	3	6	213	-214	-14	4	1	-58	-45
1	2	4	719	723	-13	2	9	-59	70	4	3	2	544	-543	5	3	6	411	-415	-13	4	1	211	-211
2	2	4	1112	1132	-12	2	9	113	-114	5	3	2	274	-282	6	3	6	193	-190	-12	4	1	97	-99
3	2	4	713	710	-11	2	9	145	-140	6	3	2	541	-553	7	3	6	314	-315	-11	4	1	92	89
4	2	4	557	556	-10	2	9	100	75	7	3	2	424	-418	8	3	6	299	-304	-10	4	1	166	-160
5	2	4	571	579	-9	2	9	97	92	8	3	2	301	-298	9	3	6	247	-242	-9	4	1	192	-180
6	2	4	540	544	-8	2	9	164	-163	9	3	2	579	-591	-14	3	7	-58	43	-8	4	1	82	-75
7	2	4	-30	16	-7	2	9	-52	0	10	3	2	322	-320	-13	3	7	214	211	-7	4	1	390	390
8	2	4	794	759	-6	2	9	100	-95	11	3	2	474	-468	-12	3	7	149	142	-6	4	1	197	-206
9	2	4	487	480	-5	2	9	156	163	12	3	2	145	-136	-11	3	7	-54	-31	-5	4	1	563	-560
10	2	4	456	435	-4	2	9	-51	31	-14	3	3	-55	35	-10	3	7	112	83	-4	4	1	56	53
11	2	4	377	369	-3	2	9	313	-319	-13	3	3	304	314	-9	3	7	575	591	-3	4	1	349	348
-15	2	5	133	-119	-2	2	9	190	192	-12	3	3	342	339	-8	3	7	428	425	-2	4	1	524	-506
-14	2	5	75	-89	-1	2	9	-52	1	-11	3	3	140	-148	-7	3	7	-48	2	-1	4	1	992	-954
-13	2	5	62	71	0	2	9	270	-270	-10	3	3	-51	57	-6	3	7	51	30	0	4	1	520	505
-12	2	5	60	-84	1	2	9	67	61	-9	3	3	87	100	-5	3	7	266	259	1	4	1	477	449
-11	2	5	133	-139	2	2	9	124	-113	-8	3	3	192	-188	-4	3	7	-47	-12	2	4	1	72	52
-10	2	5	266	-263	3	2	9	153	158	-7	3	3	801	797	-3	3	7	-45	13	3	4	1	-41	1
-9	2	5	160	164	4	2	9	-57	-37	-6	3	3	579	573	-2	3	7	313	314	4	4	1	352	-339
-8	2	5	221	219	5	2	9	124	-110	-5	3	3	141	-147	-1	3	7	770	772	5	4	1	636	631
-7	2	5	102	108	-12	2	10	271	-258	-4	3	3	690	692	0	3	7	408	407	6	4	1	285	-292
-6	2	5	178	-113	-11	2	10	549	-559	-3	3	3	550	541	1	3	7	-50	48	7	4	1	837	-843
-5	2	5	110	-119	-10	2	10	363	-371	-2	3	3	134	-163	2	3	7	-50	47	8	4	1	259	257
-4	2	5	140	145	-9	2	10	469	-456	-1	3	3	1254	1228	3	3	7	151	150	9	4	1	88	-63
-3	2	5	707	-655	-8	2	10	502	-507	0	3	3	787	786	4	3	7	90	102	10	4	1	190	-194
-2	2	5	231	-243	-7	2	10	298	-304	1	3	3	197	195	5	3	7	-54	49	11	4	1	-54	-26
-1	2	5	637	617	-6	2	10	180	-173	2	3	3	813	813	6	3	7	204	201	12	4	1	-56	-33
0	2	5	247	-252	-5	2	10	550	-579	3	3	3	273	-253	7	3	7	451	454	13	4	1	-56	22
1	2	5	311	315	-4	2	10	535	-533	4	3	3	527	-525	-14	3	8	174	168	-14	4	2	62	-46
2	2	5	-46	-16	-3	2	10	604	-605	5	3	3	505	513	-13	3	8	280	277	-13	4	2	442	-441
3	2	5	169	-171	-2	2	10	505	-500	6	3	3	-48	11	-12	3	8	334	331	-12	4	2	470	-474
4	2	5	190	185	-1	2	10	351	-351	7	3	3	210	213	-11	3	8	311	309	-11	4	2	593	-604
5	2	5	322	-324	0	2	10	161	-150	8	3	3	833	838	-10	3	8	415	420	-10	4	2	419	-426
6	2	5	74	-66	1	2	10	412	-412	9	3	3	160	171	-9	3	8	318	319	-9	4	2	603	-612
7	2	5	188	185	2	2	10	139	-129	10	3	3	-54	-10	-8	3	8	528	535	-8	4	2	710	-711
8	2	5	-53	28	3	2	10	406	-406	11	3	3	121	106	-7	3	8	387	388	-7	4	2	291	-289
9	2	5	149	-147	-10	2	11	138	131	12	3	3	71	-31	-6	3	8	423	429	-6	4	2	158	-168
10	2	5	135	-149	-9	2	11	-58	11	-14	3	4	392	381	-5	3	8	105	99	-5	4	2	1284	-1272
-15	2	6	511	-497	-8	2	11	116	-121	-13	3	4	160	162	-4	3	8	672	661	-4	4	2	422	-428
-14	2	6	176	-187	-7	2	11	153	153	-12	3	4	210	208	-3	3	8	372	371	-3	4	2	993	-982
-13	2	6	285	-282	-6	2	11	-56	45	-11	3	4	454	449	-2	3	8	262	265	-2	4	2	471	-469
-12	2	6	351	-352	-5	2	11	-56	-37	-10	3	4	629	632	-1	3	8	495	499	-1	4	2	733	-713
-11	2	6	548	-559	-4	2	11	-54	-19	-9	3	4	306	310	0	3	8	335	342	0	4	2	1098	-1095
-10	2	6	606	-615	-3	2	11	-55	34	-8	3	4	939	936	1	3	8	292	296	1	4	2	1053	-1016
-9	2	6	823	-830	-2	2	11	140	126	-7	3	4	184	158	2	3	8	472	469	2	4	2	631	-636
-8	2	6	568	-578	-1	2	11	-56	-35	-6	3	4	536	546	3	3	8	152	156	3	4	2	1348	-1338
-7	2	6	713	-705	0	2	11	94	-94	-5	3	4	395	403	4	3	8	532	532	4	4	2	931	-929
-6	2	6	438	-440	0	3	0	2075	2005	-4	3	4	59	56	5	3	8	191	183	5	4	2	397	-405
-5	2	6	418	-421	1	3	0	103	-59	-3	3	4	686	691	6	3	8	311	309	6	4	2	-68	-23
-4	2	6	393	-395	2	3	0	773	782	-2	3	4	1253	1240	-13	3	9	-56	37	7	4	2	748	-753
-3	2	6	1215	-1219	3	3	0	732	725	-1	3	4	752	757	-12	3	9	190	-188	8	4	2	213	-210
-2	2	6	834	-834	4	3	0	529	533	0	3	4	884	877	-11	3	9	308	-304	9	4	2	467	-469
-1	2	6	1021	-1014	5	3	0	698	713	1	3	4	289	292	-10	3	9	59	-54	10	4	2	441	-439
0	2	6	592	-599	6	3	0	644	644	2	3	4	675	680	-9	3	9	84	65	11	4	2	375	-380
1	2	6	678	-685	7	3	0	396	407	3	3	4	90	-64	-8	3	9	299	-301	12	4	2	426	-416
2	2	6	379	-378	8	3	0	661	665	4	3	4	733	743	-7	3	9	225	-233	-14	4	3	66	60
3	2	6	607	-616	9	3	0	343	336	5	3	4	363	356	-6	3	9	203	-198	-13	4	3	-57	-60
4	2	6	560	-564	10	3	0	504	505	6	3	4	463	471	-5	3	9	336	-330	-12	4	3	159	156
5	2	6	667	-678	11	3	0	81	78	7	3	4	591	594	-4	3	9	234	-231	-11	4	3	186	194
6	2	6	529	-529	12	3	0	432	428	8	3	4	245	242	-3	3	9	150	-141	-10	4	3	92	-89
7	2	6	477	-464	13	3	0	241	229	9	3	4	235	232	-2	3	9	158	-154	-9	4	3	198	196
8	2	6	104	-101	-14	3	1	-55	-1	10	3	4	351	359	-1	3	9	279	284	-8	4	3	340	337
9	2	6	351	-353	-13	3	1	117	-101	11	3	4	90	67	0	3	9	162	-154	-7	4	3	84	-78
-14	2	7	-55	32	-12	3	1	-55	25	-14	3	5	85	-75	1	3	9	416	-428	-6	4	3	523	-519
-13	2	7	75	72	-11	3	1	-52	38	-13	3	5	-54	6	2	3	9	83	-87	-5	4	3	499	513
-12	2	7	132	129	-10	3	1	364	-369	-12	3	5	333	-333	3	3	9	190	-186	-4	4	3	175	174
-11	2	7	128	-115	-9	3	1	652	-647	-11	3	5	210	-215	4	3	9	327	-338	-3	4	3	-42	11
-10	2	7	249	-259	-8	3	1	338	-340	-10	3	5	435	-435	-12	3	10	192	-196	-2	4	3	456	444
-9	2	7	513	511	-7	3	1	-46	-26	-9	3	5	258	-253	-11	3	10	234	-228	-1	4	3	372	-363
-8	2	7	-51	34	-6	3	1	85	-102	-8	3	5	368	369	-10	3	10	356	-344	0	4	3	179	198
-7	2	7	271	-271	-5	3	1	70	-70	-7	3	5	315	-325	-9	3	10	282	-285	1	4	3	286	282
-6	2	7	226	222	-4	3	1	875	-859	-6	3	5	534	-541	-8	3	10	217	-208	2	4	3	628	-626
-5	2	7	111	118	-3	3	1	546	-544	-5	3	5	244	240	-7	3	10	551	-549	3	4	3	159	157
-4	2	7	-47	50	-2	3	1	462	-453	-4	3	5	817	-808	-6	3	10	305	-309	4	4	3	594	603
-3	2	7	115	-110	-1	3	1	1613	-1584	-3	3	5	581	-574	-5	3	10	331	-321	5	4	3	66	53

Table 3. Continued.

H	K	L	F(O)	F(C)	H	K	L	F(O)	F(C)	H	K	L	F(O)	F(C)	H	K	L	F(O)	F(C)	H	K	L	F(O)	F(C)
6	4	2	185	-188	-7	4	8	271	270	-2	5	2	-42	-38	2	5	6	590	-593	-3	6	1	455	-439
7	4	3	228	237	-6	4	8	131	129	-1	5	2	1938	-1922	3	5	6	343	-342	-2	6	1	104	94
8	4	3	-53	-44	-5	4	8	435	424	0	5	2	962	-950	4	5	6	125	-126	-1	6	1	117	-133
9	4	3	-53	-16	-4	4	8	840	837	1	5	2	252	220	5	5	6	556	-561	0	6	1	-43	-43
10	4	3	211	208	-3	4	8	524	536	2	5	2	273	-285	6	5	6	642	-636	1	6	1	499	-499
11	4	3	97	-76	-2	4	8	567	565	3	5	2	762	-766	7	5	6	395	-375	2	6	1	262	-262
-14	4	4	421	424	-1	4	8	513	504	4	5	2	570	-574	8	5	6	64	61	3	6	1	509	509
-13	4	4	-56	30	0	4	8	635	635	5	5	2	823	-818	-13	5	7	154	157	4	6	1	743	-744
-12	4	4	284	284	1	4	8	60	-59	6	5	2	282	-297	-12	5	7	198	195	5	6	1	867	-862
-11	4	4	414	419	2	4	8	217	216	7	5	2	851	-856	-11	5	7	388	381	6	6	1	327	325
-10	4	4	422	420	3	4	8	425	413	8	5	2	655	-653	-10	5	7	215	208	7	6	1	66	68
-9	4	4	352	354	4	4	8	457	444	9	5	2	-53	17	-9	5	7	225	219	8	6	1	141	-133
-8	4	4	908	952	5	4	8	409	419	10	5	2	136	135	-8	5	7	94	84	9	6	1	62	-59
-7	4	4	905	855	6	4	8	251	244	11	5	2	531	-533	-7	5	7	300	296	10	6	1	65	-46
-6	4	4	526	512	-12	4	9	87	-97	12	5	2	270	-268	-6	5	7	84	96	11	6	1	97	-96
-5	4	4	501	492	-11	4	9	96	86	-14	5	3	138	132	-5	5	7	334	334	12	6	1	262	-262
-4	4	4	793	751	-10	4	9	58	-37	-13	5	3	74	82	-4	5	7	781	777	-13	6	2	260	-261
-3	4	4	375	379	-9	4	9	240	-240	-12	5	3	-52	7	-3	5	7	376	380	-12	6	2	147	-139
-2	4	4	1294	1292	-8	4	9	129	-115	-11	5	3	389	385	-2	5	7	353	358	-11	6	2	312	-311
-1	4	4	181	183	-7	4	9	141	-129	-10	5	3	376	371	-1	5	7	325	326	-10	6	2	207	-204
0	4	4	710	730	-6	4	9	70	-79	-9	5	3	562	564	0	5	7	145	-143	-9	6	2	492	-496
1	4	4	519	536	-5	4	9	228	236	-8	5	3	229	236	1	5	7	409	399	-8	6	2	544	-535
2	4	4	123	117	-4	4	9	248	-255	-7	5	3	212	217	2	5	7	180	186	-7	6	2	763	-754
3	4	4	337	354	-3	4	9	-52	-45	-6	5	3	634	630	3	5	7	228	235	-6	6	2	-47	-17
4	4	4	929	924	-2	4	9	99	93	-5	5	3	72	64	4	5	7	398	395	-5	6	2	131	-127
5	4	4	601	582	-1	4	9	216	-217	-4	5	3	355	350	5	5	7	277	276	-4	6	2	647	-641
6	4	4	849	847	0	4	9	251	-258	-3	5	3	702	700	6	5	7	121	117	-3	6	2	343	-351
7	4	4	259	264	1	4	9	110	118	-2	5	3	397	409	7	5	7	-59	48	-2	6	2	882	-870
8	4	4	444	458	2	4	9	-54	19	-1	5	3	859	869	-13	5	8	294	283	-1	6	2	1147	-1111
9	4	4	270	261	3	4	9	-56	-24	0	5	3	171	-171	-12	5	8	473	470	0	6	2	318	-323
10	4	4	134	188	4	4	9	-56	33	1	5	3	335	341	-11	5	8	178	165	1	6	2	1063	-1058
-14	4	5	319	-329	-11	4	10	337	-337	2	5	3	763	759	-10	5	8	153	154	2	6	2	222	210
-13	4	5	-52	-1	-10	4	10	182	-170	3	5	3	321	315	-9	5	8	466	469	3	6	2	79	-75
-12	4	5	-54	-9	-9	4	10	317	-315	4	5	3	617	624	-8	5	8	580	574	4	6	2	526	-522
-11	4	5	362	-364	-8	4	10	244	-253	5	5	3	402	401	-7	5	8	141	141	5	6	2	352	-357
-10	4	5	140	133	-7	4	10	614	-614	6	5	3	473	470	-6	5	8	305	289	6	6	2	524	-523
-9	4	5	341	339	-6	4	10	471	-468	7	5	3	257	251	-5	5	8	579	574	7	6	2	651	-653
-8	4	5	264	-263	-5	4	10	117	-104	8	5	3	88	-80	-4	5	8	530	536	8	6	2	347	-353
-7	4	5	277	-281	-4	4	10	307	-295	9	5	3	192	197	-3	5	8	-50	3	9	6	2	234	-220
-6	4	5	415	-411	-3	4	10	425	-424	10	5	3	201	185	-2	5	8	412	411	10	6	2	145	-139
-5	4	5	232	236	-2	4	10	140	-139	11	5	3	214	223	-1	5	8	518	522	11	6	2	283	-285
-4	4	5	118	123	-1	4	10	443	-439	-14	5	4	141	143	0	5	8	645	648	-13	6	3	283	278
-3	4	5	195	-193	0	4	10	385	-380	-13	5	4	210	209	1	5	8	302	307	-12	6	3	-64	-54
-2	4	5	70	-67	1	4	10	556	-563	-12	5	4	677	675	2	5	8	186	184	-11	6	3	71	-73
-1	4	5	297	300	2	4	10	295	-303	-11	5	4	387	382	3	5	8	351	343	-10	6	3	377	379
0	4	5	145	-136	-9	4	11	84	-89	-10	5	4	253	242	4	5	8	447	450	-9	6	3	105	95
1	4	5	820	-817	-8	4	11	-57	-39	-9	5	4	183	179	5	5	8	-56	-52	-8	6	3	214	-201
2	4	5	107	-107	-7	4	11	238	225	-8	5	4	389	380	-12	5	9	-56	-17	-7	6	3	572	566
3	4	5	330	326	-6	4	11	218	212	-7	5	4	887	890	-11	5	9	106	-91	-6	6	3	669	663
4	4	5	-49	-18	-5	4	11	-55	23	-6	5	4	805	797	-10	5	9	295	-303	-5	6	3	127	117
5	4	5	72	59	-4	4	11	86	67	-5	5	4	71	-66	-9	5	9	165	-167	-4	6	3	473	-463
6	4	5	158	-155	-3	4	11	176	172	-4	5	4	1382	1374	-8	5	9	336	-326	-3	6	3	82	-70
7	4	5	-52	21	-2	4	11	185	-195	-3	5	4	717	700	-7	5	9	187	-181	-2	6	3	307	309
8	4	5	118	-124	-1	4	11	-59	-23	-2	5	4	435	-414	-6	5	9	323	-322	-1	6	3	286	284
9	4	5	237	-233	0	5	0	-82	-39	-1	5	4	187	203	-5	5	9	136	-137	0	6	3	-67	15
-14	4	6	416	-416	1	5	0	711	700	0	5	4	969	963	-4	5	9	-51	10	1	6	3	315	312
-13	4	6	559	-561	2	5	0	1843	1826	1	5	4	745	743	-3	5	9	292	-292	2	6	3	801	811
-12	4	6	109	-113	3	5	0	592	554	2	5	4	1021	1028	-2	5	9	398	-402	3	6	3	68	59
-11	4	6	516	-509	4	5	0	63	74	3	5	4	302	306	-1	5	9	377	-367	4	6	3	637	-642
-10	4	6	469	-428	5	5	0	481	484	4	5	4	552	555	0	5	9	295	-296	5	6	3	208	211
-9	4	6	327	-326	6	5	0	914	909	5	5	4	648	644	1	5	9	109	-107	6	6	3	375	378
-8	4	6	277	-279	7	5	0	93	86	6	5	4	449	-7	2	5	9	292	-293	7	6	3	151	144
-7	4	6	487	-456	8	5	0	181	177	7	5	4	91	-74	3	5	9	-54	14	8	6	3	223	216
-6	4	6	890	-893	9	5	0	257	271	8	5	4	687	697	-11	5	10	512	-510	9	6	3	110	112
-5	4	6	1012	-1009	10	5	0	878	880	9	5	4	430	433	-10	5	10	173	-164	10	6	3	250	254
-4	4	6	313	-312	11	5	0	511	506	10	5	4	344	336	-9	5	10	129	-120	11	6	3	-59	46
-3	4	6	547	-547	12	5	0	81	75	-14	5	5	214	-215	-8	5	10	398	-392	-13	6	4	311	313
-2	4	6	425	-420	13	5	0	278	275	-13	5	5	275	-267	-7	5	10	328	-320	-12	6	4	412	412
-1	4	6	706	-703	-13	5	1	69	-54	-12	5	5	203	-209	-6	5	10	121	-113	-11	6	4	323	332
0	4	6	113	-124	-12	5	1	533	-527	-11	5	5	55	27	-5	5	10	391	-384	-10	6	4	304	308
1	4	6	711	-705	-11	5	1	149	-153	-10	5	5	242	-234	-4	5	10	389	-376	-9	6	4	-52	-44
2	4	6	920	-928	-10	5	1	117	-111	-9	5	5	-53	-47	-3	5	10	539	-528	-8	6	4	397	401
3	4	6	518	-500	-9	5	1	361	-374	-8	5	5	509	-506	-2	5	10	270	-264	-7	6	4	213	209
4	4	6	205	-204	-8	5	1	159	-154	-7	5	5	648	-645	-1	5	10	81	-95	-6	6	4	701	699
5	4	6	311	-303	-7	5	1	483	-473	-6	5	5	343	-333	0	5	10	232	-216	-5	6	4	838	819
6	4	6	279	-281	-6	5	1	375	-377	-5	5	5	623	-624	1	5	10	444	-445	-4	6	4	504	506
7	4	6	501	-497	-5	5	1	304	-299	-4	5	5	433	-424	-8	5	11	102	97	-3	6	4	504	509
8	4	6	141	-144	-4	5	1	593	-586	-3	5	5	-44	15	-7	5	11	183	174	-2	6	4	264	268
-14	4	7	-38	-28	-3	5	1	361	-368	-2	5	5	200	-198	-6	5	11	173	179	-1	6	4	135	127
-13	4	7	155	152	-2	5	1	456	-443	-1	5	5	417	-402	-5	5	11	337	331	0	6	4	626	624
-12	4	7	-55	38	-1	5	1	213	-194	0	5	5	680	-685	-4	5	11	202	200	1	6	4	393	383
-11	4	7	77	64	0	5	1	1153	-1155	1	5	5	289	-296	-3	5	11	132	131	2	6	4	755	748
-10	4	7	290	301	1	5	1	805	-800	2	5	5	519	-521	-2	5	11	76	67	3	6	4	443	449
-9	4	7	316	320	2	5	1	344	-343	3	5	5	127	-126	0	6	0	255	-238	4	6	4	526	532
-8	4	7	99	-95	3	5	1	938	-945	4	5	5	190	-194	1	6	0	201	205	5	6	4	52	43
-7	4	7	209	-206	4	5	1	108	-117	5	5	5	389	-401	2	6	0	1004	997	6	6	4	180	180
-6	4	7	64	49	5	5	1	315	-318	6	5	5	-53	46	3	6	0	244	243	7	6	4	302	298
-5	4	7	310	309	6	5	1	386	-392	7	5	5	467	-462	4	6	0	936	933	8	6	4	286	286
-4	4	7	100	-104	7	5	1	53	-49	8	5	5	442	-437	5	6	0	826	833	9	6	4	432	444
-3	4	7	124	116	8	5	1	436	-436	9	5	5	-57	14	6	6	0	266	270	10	6	4	282	291
-2	4	7	59	42	9	5	1	357	-354	-14	5	6	290	-286	7	6	0	483	486	-13	6	5	81	-81
-1	4	7	281	289	10	5	1	202	-204	-13	5	6	265	-269	8	6	0	144	138	-12	6	5	398	-399
0	4	7	-50	-39	11	5	1	116	-121	-12	5	6	103	-82	9	6	0	163	150	-11	6	5	-56	45
1	4	7	446	-445	12	5	1	156	-142	-11	5	6	221	-219	10	6	0	733	746	-10	6	5	56	-66
2	4	7	345	351	-14	5	2	98	-87	-10	5	6	687	-676	11	6	0	94	97	-9	6	5	620	-608
3	4	7	375	370	-13	5	2	413	-415	-9	5	6	605	-600	12	6	0	248	251	-8	6	5	-50	-22
4	4	7	93	-75	-12	5	2	346	-335	-8	5	6	84	79	-13	6	1	-56	37	-7	6	5	331	315
5	4	7	1139	148	-11	5	2	-56	-16	-7	5	6	565	-554	-12	6	1	-57	-19	-6	6	5	245	-244
6	4	7	-53	1	-10	5	2	310	-308	-6	5	6	821	-820	-11	6	1	422	-416	-5	6	5	248	-246
7	4	7	95	75	-9	5	2	939	-938	-5	5	6	389	-392	-10	6	1	220	-222	-4	6	5	642	-634
-13	4	8	257	259	-8	5	2	582	-582	-4	5	6	64	-67	-9	6	1	69	71	-3	6	5	136	-130
-12	4	8	432	445	-7	5	2	627	-616	-3	5	6	858	-845	-8	6	1	490	-492	-2	6	5	151	152
-11	4	8	217	212	-6	5	2	96	-87	-2	5	6	918	-902	-7	6	1	424	-433	-1	6	5	311	-324
-10	4	8	452	458	-5	5	2	606	-601	-1	5	6	645	-650	-6	6	1	295	291	0	6	5	107	-111
-9	4	8	442	442	-4	5	2	916	-909	0	5	6	167	160	-5	6	1	465	444	1	6	5	474	470
-8	4	8	552	544	-3	5	2	382	-381	1	5	6	310	-317	-4	6	1	581	-576	2	6	5	-49	-4

Table 3. Continued.

H	K	L	F(O)	F(C)	H	K	L	F(O)	F(C)	H	K	L	F(O)	F(C)	H	K	L	F(O)	F(C)	H	K	L	F(O)	F(C)
3	6	5	616	-626	-11	7	1	236	-241	-2	7	5	520	-517	-5	8	1	393	-386	-9	8	6	135	-136
4	6	5	474	-469	-10	7	1	424	-418	-1	7	5	488	-485	-4	8	1	115	-106	-8	8	6	84	-65
5	6	5	-54	58	-9	7	1	62	-58	0	7	5	405	-395	-3	8	1	304	-300	-7	8	6	276	-264
6	6	5	134	-137	-8	7	1	300	-309	1	7	5	166	-158	-2	8	1	60	-15	-6	8	6	344	-354
7	6	5	123	-129	-7	7	1	479	-472	2	7	5	183	-176	-1	8	1	436	425	-5	8	6	361	-359
8	6	5	-57	-32	-6	7	1	322	-326	3	7	5	456	-459	0	8	1	682	-674	-4	8	6	244	-239
9	6	5	-56	-37	-5	7	1	296	-292	4	7	5	397	-391	1	8	1	562	-557	-3	8	6	531	-537
-13	6	6	205	-187	-4	7	1	600	-594	5	7	5	188	-183	2	8	1	310	-315	-2	8	6	142	-135
-12	6	6	215	-221	-3	7	1	777	-761	6	7	5	296	-293	3	8	1	616	-632	-1	8	6	-49	1
-11	6	6	316	-321	-2	7	1	627	-622	7	7	5	143	-145	4	8	1	169	162	0	8	6	198	-193
-10	6	6	353	-357	-1	7	1	511	-506	8	7	5	251	-259	5	8	1	180	-169	1	8	6	241	-241
-9	6	6	739	-745	0	7	1	267	-264	-13	7	6	519	-503	6	8	1	232	-231	2	8	6	194	-176
-8	6	6	190	-187	1	7	1	455	-465	-12	7	6	270	-271	7	8	1	57	45	3	8	6	354	-357
-7	6	6	216	-226	2	7	1	291	-298	-11	7	6	428	-425	8	8	1	488	-482	4	8	6	158	-171
-6	6	6	334	-329	3	7	1	131	-144	-10	7	6	277	-279	9	8	1	425	-423	5	8	6	206	-195
-5	6	6	296	-296	4	7	1	686	-690	-9	7	6	166	-161	10	8	1	167	-185	6	8	6	186	-182
-4	6	6	58	-52	5	7	1	437	-437	-8	7	6	317	-310	11	8	1	-57	-43	-11	8	7	396	384
-3	6	6	582	-573	6	7	1	379	-373	-7	7	6	421	-421	-12	8	2	134	-129	-10	8	7	305	308
-2	6	6	657	-657	7	7	1	340	-339	-6	7	6	347	-336	-11	8	2	290	-291	-9	8	7	-55	33
-1	6	6	418	-433	8	7	1	249	-252	-5	7	6	676	-674	-10	8	2	301	-296	-8	8	7	69	-63
0	6	6	436	-448	9	7	1	415	-424	-4	7	6	718	-709	-9	8	2	225	-215	-7	8	7	391	378
1	6	6	309	-314	10	7	1	130	-123	-3	7	6	242	-244	-8	8	2	147	-155	-6	8	7	99	107
2	6	6	159	-160	11	7	1	170	-164	-2	7	6	55	-65	-7	8	2	402	-405	-5	8	7	120	96
3	6	6	625	-614	-13	7	2	153	-147	-1	7	6	685	-674	-6	8	2	161	-147	-4	8	7	467	458
4	6	6	-54	-15	-12	7	2	371	-367	0	7	6	119	-111	-5	8	2	430	-432	-3	8	7	209	203
5	6	6	453	-460	-11	7	2	507	-497	1	7	6	568	-568	-4	8	2	305	-300	-2	8	7	218	230
6	6	6	419	-426	-10	7	2	268	-276	2	7	6	740	-734	-3	8	2	129	-133	-1	8	7	97	109
7	6	6	105	-100	-9	7	2	260	-259	3	7	6	217	-219	-2	8	2	316	-319	0	8	7	171	-170
-13	6	7	-60	-7	-8	7	2	253	-240	4	7	6	513	-510	-1	8	2	284	-293	1	8	7	489	487
-12	6	7	176	173	-7	7	2	390	-395	5	7	6	324	-315	0	8	2	110	-107	2	8	7	257	253
-11	6	7	168	154	-6	7	2	650	-656	6	7	6	100	107	1	8	2	553	-568	3	8	7	110	108
-10	6	7	166	-160	-5	7	2	527	-526	7	7	6	396	-390	2	8	2	276	-276	4	8	7	281	272
-9	6	7	96	81	-4	7	2	436	-438	-12	7	7	114	123	3	8	2	266	-257	5	8	7	193	192
-8	6	7	328	327	-3	7	2	1448	-1454	-11	7	7	315	310	4	8	2	466	-464	-10	8	8	235	233
-7	6	7	284	286	-2	7	2	333	-333	-10	7	7	195	197	5	8	2	217	-223	-9	8	8	306	295
-6	6	7	119	123	-1	7	2	124	-120	-9	7	7	153	153	6	8	2	99	-108	-8	8	8	135	137
-5	6	7	131	-103	0	7	2	625	-627	-8	7	7	323	330	7	8	2	287	-291	-7	8	8	167	167
-4	6	7	-50	23	1	7	2	513	-505	-7	7	7	541	551	8	8	2	118	-119	-6	8	8	353	348
-3	6	7	579	573	2	7	2	650	-654	-6	7	7	377	378	9	8	2	322	-326	-5	8	8	-53	23
-2	6	7	58	-87	3	7	2	547	-542	-5	7	7	259	265	10	8	2	178	-178	-4	8	8	211	205
-1	6	7	-51	0	4	7	2	395	-403	-4	7	7	-51	6	-12	8	3	111	126	-3	8	8	274	260
0	6	7	536	531	5	7	2	762	-776	-3	7	7	416	404	-11	8	3	422	417	-2	8	8	244	254
1	6	7	241	237	6	7	2	207	-203	-2	7	7	232	230	-10	8	3	163	157	-1	8	8	248	233
2	6	7	149	-155	7	7	2	298	-296	-1	7	7	158	150	-9	8	3	383	369	0	8	8	239	233
3	6	7	81	-79	8	7	2	243	-241	0	7	7	447	454	-8	8	3	139	143	1	8	8	75	88
4	6	7	-55	45	9	7	2	491	-492	1	7	7	432	433	-7	8	3	282	-297	2	8	8	236	231
5	6	7	252	257	10	7	2	424	-419	2	7	7	317	321	-6	8	3	207	217	3	8	8	145	125
6	6	7	100	100	11	7	2	169	-165	3	7	7	197	193	-5	8	3	210	205	-9	8	9	216	-207
-12	6	8	375	374	-13	7	3	311	302	4	7	7	150	158	-4	8	3	377	376	-8	8	9	301	-303
-11	6	8	296	259	-12	7	3	140	151	5	7	7	356	349	-3	8	3	762	769	-7	8	9	178	-168
-10	6	8	68	96	-11	7	3	79	78	-11	7	8	317	315	-2	8	3	445	441	-6	8	9	157	-150
-9	6	8	282	282	-10	7	3	235	242	-10	7	8	564	556	-1	8	3	517	520	-5	8	9	150	-168
-8	6	8	506	506	-9	7	3	344	340	-9	7	8	207	206	0	8	3	57	-51	-4	8	9	57	56
-7	6	8	219	216	-8	7	3	171	175	-8	7	8	450	439	1	8	3	83	-72	-3	8	9	57	-42
-6	6	8	535	532	-7	7	3	558	557	-7	7	8	502	498	2	8	3	81	73	-2	8	9	254	-248
-5	6	8	146	144	-6	7	3	469	469	-6	7	8	-55	31	3	8	3	176	170	-1	8	9	303	-301
-4	6	8	402	358	-5	7	3	616	620	-5	7	8	152	144	4	8	3	471	487	0	8	9	151	-148
-3	6	8	424	428	-4	7	3	309	315	-4	7	8	491	500	5	8	3	227	230	-5	8	10	249	-247
-2	6	8	-52	10	-3	7	3	99	94	-3	7	8	415	418	6	8	3	311	304	-4	8	10	145	-141
-1	6	8	311	302	-2	7	3	465	467	-2	7	8	556	552	7	8	3	234	226	0	9	0	385	381
0	6	8	514	515	-1	7	3	463	464	-1	7	8	225	227	8	8	3	-57	-47	1	9	0	277	271
1	6	8	295	291	0	7	3	1571	564	0	7	8	332	329	9	8	3	112	112	2	9	0	455	461
2	6	8	341	340	1	7	3	612	613	1	7	8	267	265	-12	8	4	158	155	3	9	0	543	537
3	6	8	224	230	2	7	3	503	503	2	7	8	257	255	-11	8	4	133	126	4	9	0	915	910
4	6	8	287	291	3	7	3	419	414	3	7	8	167	173	-10	8	4	113	116	5	9	0	532	529
5	6	8	144	149	4	7	3	110	108	4	7	8	364	363	-9	8	4	400	399	6	9	0	-67	-35
-11	6	9	138	-136	5	7	3	270	275	-10	7	9	241	-238	-8	8	4	531	537	7	9	0	237	235
-10	6	9	221	-227	6	7	3	320	334	-9	7	9	302	-304	-7	8	4	99	110	8	9	0	252	252
-9	6	9	-67	-3	7	7	3	336	344	-8	7	9	158	-159	-6	8	4	326	324	9	9	0	223	218
-8	6	9	96	97	8	7	3	229	221	-7	7	9	-57	-50	-5	8	4	171	167	10	9	0	354	359
-7	6	9	89	-80	9	7	3	270	267	-6	7	9	402	-407	-4	8	4	177	191	11	9	0	245	255
-6	6	9	360	-359	10	7	3	282	298	-5	7	9	309	-308	-3	8	4	182	180	-11	9	1	343	-350
-5	6	9	214	-208	-13	7	4	175	171	-4	7	9	260	-261	-2	8	4	263	259	-10	9	1	220	-231
-4	6	9	-52	6	-12	7	4	253	253	-3	7	9	169	-169	-1	8	4	356	362	-9	9	1	-58	-13
-3	6	9	-58	-52	-11	7	4	110	105	-2	7	9	289	-293	0	8	4	499	501	-8	9	1	398	-400
-2	6	9	335	-329	-10	7	4	434	420	-1	7	9	238	-227	1	8	4	191	189	-7	9	1	450	-449
-1	6	9	114	101	-9	7	4	611	615	0	7	9	201	-182	2	8	4	177	177	-6	9	1	245	-228
0	6	9	65	57	-8	7	4	414	415	1	7	9	143	-151	3	8	4	218	214	-5	9	1	156	-163
1	6	9	231	-158	-7	7	4	452	447	2	7	9	292	-304	4	8	4	290	286	-4	9	1	477	-475
2	6	9	274	-278	-6	7	4	391	388	-8	7	10	241	-246	5	8	4	178	163	-3	9	1	426	-427
3	6	9	181	-176	-5	7	4	311	303	-7	7	10	394	-378	6	8	4	312	303	-2	9	1	307	-315
-10	6	10	264	-265	-4	7	4	499	500	-6	7	10	491	-489	7	8	4	338	332	-1	9	1	326	-337
-9	6	10	278	-290	-3	7	4	-47	-7	-5	7	10	323	-333	8	8	4	131	130	0	9	1	392	-385
-8	6	10	170	-157	-2	7	4	1033	1026	-4	7	10	124	-108	-12	8	5	203	-192	1	9	1	836	-824
-7	6	10	329	-329	-1	7	4	1083	1074	-3	7	10	149	-146	-11	8	5	-55	29	2	9	1	427	-422
-6	6	10	233	-240	0	7	4	476	476	-2	7	10	208	-200	-10	8	5	181	-174	3	9	1	131	133
-5	6	10	256	-257	1	7	4	443	445	-1	7	10	358	-359	-9	8	5	137	-142	4	9	1	498	-505
-4	6	10	227	-222	2	7	4	450	457	0	8	0	134	116	-8	8	5	454	-457	5	9	1	410	-412
-3	6	10	360	-359	3	7	4	236	236	1	8	0	396	384	-7	8	5	425	-415	6	9	1	124	-111
-2	6	10	185	-177	4	7	4	290	293	2	8	0	556	558	-6	8	5	73	-64	7	9	1	352	-356
-1	6	10	228	-221	5	7	4	293	293	3	8	0	151	144	-5	8	5	297	-295	8	9	1	248	-256
0	6	10	298	-264	6	7	4	500	500	4	8	0	326	336	-4	8	5	115	-112	9	9	1	390	-395
0	7	0	1032	1027	7	7	4	457	461	5	8	0	289	294	-3	8	5	180	177	10	9	1	225	-219
1	7	0	531	536	8	7	4	414	410	6	8	0	173	165	-2	8	5	214	-219	-11	9	2	207	-224
2	7	0	271	271	9	7	4	-58	-6	7	8	0	256	251	-1	8	5	395	-396	-10	9	2	376	-367
3	7	0	663	669	-13	7	5	293	-215	8	8	0	331	328	0	8	5	519	-520	-9	9	2	380	-384
4	7	0	620	616	-12	7	5	323	-317	9	8	0	-54	3	1	8	5	301	-316	-8	9	2	284	-288
5	7	0	210	159	-11	7	5	345	-357	10	8	0	294	305	2	8	5	318	-317	-7	9	2	805	-894
6	7	0	949	962	-10	7	5	262	-260	11	8	0	219	224	3	8	5	-51	-13	-6	9	2	447	-434
7	7	0	321	322	-9	7	5	305	-305	-12	8	1	343	-344	4	8	5	135	-136	-5	9	2	203	198
8	7	0	451	446	-8	7	5	462	-455	-11	8	1	185	-167	5	8	5	149	-165	-4	9	2	249	-253
9	7	0	614	609	-7	7	5	75	75	-10	8	1	118	116	6	8	5	65	54	-3	9	2	320	-310
10	7	0	-55	8	-6	7	5	104	-112	-9	8	1	143	-138	7	8	5	416	-419	-2	9	2	471	-466
11	7	0	163	158	-5	7	5	332	-323	-8	8	1	128	-114	-12	8	6	311	-306	-1	9	2	837	-836
12	7	0	387	391	-4	7	5	595	-598	-7	8	1	368	-381	-11	8	6	278	-276	0	9	2	465	-468
-12	7	1	158	-164	-3	7	5	600	-598	-6	8	1	711	-714	-10	8	6	143	-135	1	9	2	764	-773

Table 3. Continued.

H	K	L	F(O)	F(C)	H	K	L	F(O)	F(C)	H	K	L	F(O)	F(C)	H	K	L	F(O)	F(C)	H	K	L	F(O)	F(C)
2	9	2	519	-514	-6	9	8	592	595	7	10	4	205	201	-3	11	3	369	365	-3	12	3	469	476
3	9	2	95	-108	-5	9	8	312	305	-10	10	5	421	-413	-2	11	3	100	101	-2	12	3	471	467
4	9	2	-50	-33	-4	9	8	85	87	-9	10	5	215	-212	-1	11	3	261	256	-1	12	3	242	251
5	9	2	581	-581	-3	9	8	330	334	-8	10	5	136	-126	0	11	3	478	480	0	12	3	308	319
6	9	2	566	-559	-2	9	8	332	338	-7	10	5	235	-230	1	11	3	363	358	1	12	3	189	189
7	9	2	184	-189	-1	9	8	149	146	-6	10	5	335	-325	2	11	3	135	-135	2	12	3	150	158
8	9	2	323	-336	0	9	8	266	266	-5	10	5	133	-123	3	11	3	232	231	3	12	3	421	419
9	9	2	243	-245	1	9	8	440	433	-4	10	5	400	-396	4	11	3	599	621	4	12	3	346	347
-11	9	3	292	285	2	9	8	352	358	-3	10	5	514	-506	5	11	3	-57	41	5	12	3	350	351
-10	9	3	426	436	-7	9	9	200	-194	-2	10	5	366	-355	6	11	3	81	68	-8	12	4	-59	42
-9	9	3	128	130	-6	9	9	265	-259	-1	10	5	232	-235	7	11	3	278	289	-7	12	4	226	219
-8	9	3	254	260	-5	9	9	162	-171	0	10	5	-69	-2	-9	11	4	162	169	-6	12	4	-59	64
-7	9	3	344	344	-4	9	9	280	-276	1	10	5	136	-140	-8	11	4	462	461	-5	12	4	80	-80
-6	9	3	176	179	-3	9	9	264	-256	2	10	5	418	-415	-7	11	4	141	141	-4	12	4	217	225
-5	9	3	565	564	-2	9	9	307	-305	3	10	5	237	-249	-6	11	4	110	111	-3	12	4	265	260
-4	9	3	177	151	-1	9	9	174	-183	4	10	5	209	-210	-5	11	4	212	207	-2	12	4	92	-90
-3	9	3	396	402	0	10	0	560	554	5	10	5	385	-392	-4	11	4	167	173	-1	12	4	74	59
-2	9	3	674	667	1	10	0	262	260	-10	10	6	-57	44	-3	11	4	362	359	0	12	4	174	184
-1	9	3	68	49	2	10	0	176	-177	-9	10	6	147	-142	-2	11	4	481	489	1	12	4	88	79
0	9	3	175	170	3	10	0	161	161	-8	10	6	328	-335	-1	11	4	294	290	2	12	4	158	150
1	9	3	370	368	4	10	0	436	440	-7	10	6	144	-144	0	11	4	349	355	3	12	4	-57	-36
2	9	3	332	335	5	10	0	-69	-29	-6	10	6	-53	16	1	11	4	275	274	4	12	4	111	126
3	9	3	609	613	6	10	0	-51	10	-5	10	6	112	-115	2	11	4	-55	54	-7	12	5	353	-334
4	9	3	309	310	7	10	0	79	83	-4	10	6	362	-353	3	11	4	89	88	-6	12	5	302	-311
5	9	3	314	310	8	10	0	398	411	-3	10	6	170	-173	4	11	4	258	255	-5	12	5	211	-211
6	9	3	383	389	9	10	0	249	238	-2	10	6	179	179	5	11	4	287	289	-4	12	5	202	-192
7	9	3	99	108	10	10	0	82	-76	-1	10	6	299	-303	-9	11	5	96	-90	-3	12	5	118	-126
8	9	3	86	87	-10	10	1	454	-441	0	10	6	271	-266	-8	11	5	234	-239	-2	12	5	423	-426
9	9	3	165	166	-9	10	1	383	-381	1	10	6	121	-113	-7	11	5	336	-347	-1	12	5	453	-459
-11	9	4	-55	28	-8	10	1	259	-258	2	10	6	-54	-8	-6	11	5	272	-270	0	12	5	306	-309
-10	9	4	393	396	-7	10	1	167	-160	3	10	6	-57	-36	-5	11	5	153	-158	1	12	5	413	-425
-9	9	4	229	224	-6	10	1	270	-262	4	10	6	344	-342	-4	11	5	-53	-10	2	12	5	257	-255
-8	9	4	136	135	-5	10	1	149	-143	-9	10	7	255	252	-3	11	5	417	-418	-6	12	6	136	-121
-7	9	4	257	264	-4	10	1	103	-87	-8	10	7	254	253	-2	11	5	471	-477	-5	12	6	-55	17
-6	9	4	676	658	-3	10	1	425	-428	-7	10	7	367	368	-1	11	5	-54	35	-4	12	6	86	-75
-5	9	4	698	705	-2	10	1	511	-514	-6	10	7	247	243	0	11	5	242	-248	-3	12	6	96	-90
-4	9	4	554	554	-1	10	1	627	-628	-5	10	7	315	326	1	11	5	391	-397	-2	12	6	160	-167
-3	9	4	263	265	0	10	1	356	-362	-4	10	7	59	58	2	11	5	252	-254	-1	12	6	122	-107
-2	9	4	78	85	1	10	1	-50	-23	-3	10	7	89	65	3	11	5	77	-79	0	12	6	-60	2
-1	9	4	427	428	2	10	1	345	-356	-2	10	7	386	391	4	11	5	134	-132	0	13	0	-83	-33
0	9	4	286	286	3	10	1	404	-404	-1	10	7	413	404	-8	11	6	235	-234	1	13	0	217	218
1	9	4	-51	4	4	10	1	220	-218	0	10	7	267	269	-7	11	6	300	-307	2	13	0	201	203
2	9	4	771	784	5	10	1	384	-389	1	10	7	239	243	-6	11	6	216	-215	3	13	0	141	149
3	9	4	631	631	6	10	1	434	-438	2	10	7	112	108	-5	11	6	342	-343	4	13	0	351	355
4	9	4	295	312	7	10	1	172	-160	-7	10	8	289	297	-4	11	6	121	-103	5	13	0	120	116
5	9	4	178	175	8	10	1	195	-191	-6	10	8	117	117	-3	11	6	135	-141	6	13	0	-57	17
6	9	4	239	240	9	10	1	-65	-73	-5	10	8	-55	-18	-2	11	6	186	-177	-6	13	1	129	-118
7	9	4	273	274	-10	10	2	151	-153	-4	10	8	82	81	-1	11	6	140	-143	-5	13	1	255	-258
8	9	4	239	244	-9	10	2	-54	36	-3	10	8	182	173	0	11	6	-54	-357	-4	13	1	174	-176
-11	9	5	136	-139	-8	10	2	126	-102	-2	10	8	251	244	1	11	6	409	-409	-3	13	1	195	-193
-10	9	5	117	-128	-7	10	2	236	-241	-1	10	8	-55	-24	2	11	6	297	-291	-2	13	1	241	-244
-9	9	5	420	-429	-6	10	2	366	-362	0	10	8	128	114	-7	11	7	106	108	-1	13	1	239	-248
-8	9	5	349	-360	-5	10	2	113	-115	0	11	0	502	499	-6	11	7	342	349	0	13	1	193	-188
-7	9	5	94	-97	-4	10	2	119	120	1	11	0	376	371	-5	11	7	292	279	1	13	1	152	-144
-6	9	5	428	-430	-3	10	2	659	-662	2	11	0	226	239	-4	11	7	163	170	2	13	1	225	-227
-5	9	5	448	-452	-2	10	2	283	-281	3	11	0	160	153	-3	11	7	111	103	3	13	1	226	-226
-4	9	5	256	-241	-1	10	2	173	176	4	11	0	112	125	-2	11	7	266	264	4	13	1	209	-221
-3	9	5	239	-235	0	10	2	-56	-55	5	11	0	199	198	-1	11	7	346	345	5	13	1	248	-249
-2	9	5	369	-366	1	10	2	223	-227	6	11	0	397	398	0	11	7	93	92	-6	13	2	-57	-56
-1	9	5	422	-429	2	10	2	310	-306	7	11	0	474	479	0	12	0	-87	95	-5	13	2	185	-208
0	9	5	454	-448	3	10	2	103	103	8	11	0	340	347	1	12	0	-53	34	-4	13	2	-53	16
1	9	5	224	-215	4	10	2	-54	-47	9	11	0	120	105	2	12	0	224	235	-3	13	2	-53	-14
2	9	5	510	-507	5	10	2	523	-534	-9	11	1	332	-339	3	12	0	137	126	-2	13	2	187	-192
3	9	5	431	-433	6	10	2	166	-165	-8	11	1	148	-145	4	12	0	-68	-42	-1	13	2	224	-226
4	9	5	246	-249	7	10	2	120	-114	-7	11	1	170	-160	5	12	0	159	159	0	13	2	245	-254
5	9	5	-55	12	8	10	2	-53	-4	-6	11	1	394	-397	6	12	0	158	155	1	13	2	209	-220
6	9	5	425	-429	-11	10	3	118	96	-5	11	1	561	-570	7	12	0	68	65	2	13	2	145	-148
7	9	5	277	-275	-10	10	3	-56	41	-4	11	1	110	-105	-8	12	1	183	-182	3	13	2	-57	-59
-11	9	6	288	-279	-9	10	3	303	295	-3	11	1	103	92	-7	12	1	181	-183	4	13	2	117	-126
-10	9	6	132	-164	-8	10	3	194	195	-2	11	1	509	-509	-6	12	1	552	-554	-6	13	3	253	245
-9	9	6	454	-465	-7	10	3	513	511	-1	11	1	325	-312	-5	12	1	463	-462	-5	13	3	103	111
-8	9	6	384	-390	-6	10	3	335	339	0	11	1	143	-149	-4	12	1	383	-384	-4	13	3	224	222
-7	9	6	353	-355	-5	10	3	222	229	1	11	1	237	-231	-3	12	1	342	-346	-3	13	3	223	223
-6	9	6	70	-72	-4	10	3	586	599	2	11	1	398	-404	-2	12	1	94	-94	-2	13	3	137	142
-5	9	6	160	-161	-3	10	3	175	164	3	11	1	575	-582	-1	12	1	268	-264	-1	13	3	253	249
-4	9	6	470	-472	-2	10	3	253	-253	4	11	1	136	-119	0	12	1	408	-399	0	13	3	264	265
-3	9	6	554	-553	-1	10	3	359	356	5	11	1	64	-53	1	12	1	386	-386	1	13	3	221	224
-2	9	6	362	-361	0	10	3	582	587	6	11	1	290	-294	2	12	1	459	-467	2	13	3	225	221
-1	9	6	342	-341	1	10	3	297	300	7	11	1	350	-356	3	12	1	352	-358	3	13	3	80	84
0	9	6	477	-484	2	10	3	445	441	8	11	1	149	-130	4	12	1	168	-171	-5	13	4	180	187
1	9	6	240	-249	3	10	3	331	326	-9	11	2	189	-180	5	12	1	94	-87	-4	13	4	155	157
2	9	6	-53	19	4	10	3	213	212	-8	11	2	-55	5	6	12	1	285	-303	-3	13	4	161	161
3	9	6	317	-306	5	10	3	371	370	-7	11	2	111	-106	7	12	1	320	-331	-2	13	4	160	172
4	9	6	343	-337	6	10	3	-53	12	-6	11	2	179	-186	-8	12	2	104	-95	-1	13	4	76	-89
5	9	6	472	-477	7	10	3	175	171	-5	11	2	550	-551	-7	12	2	-55	21	0	13	4	88	87
-10	9	7	116	121	8	10	3	469	460	-4	11	2	458	-463	-6	12	2	167	-167	1	13	4	252	269
-9	9	7	204	189	-10	10	4	167	165	-3	11	2	265	-273	-5	12	2	112	-109	-3	13	5	271	-269
-8	9	7	358	353	-9	10	4	366	369	-2	11	2	429	-426	-4	12	2	173	-180	-2	13	5	164	-163
-7	9	7	255	259	-8	10	4	57	-37	-1	11	2	157	-162	-3	12	2	57	2	0	14	0	177	166
-6	9	7	287	287	-7	10	4	-54	-55	0	11	2	89	-76	-2	12	2	71	77	1	14	0	-57	23
-5	9	7	234	227	-6	10	4	292	305	1	11	2	352	-350	-1	12	2	344	-350	2	14	0	85	90
-4	9	7	159	166	-5	10	4	300	288	2	11	2	214	-210	0	12	2	146	-142	3	14	0	146	136
-3	9	7	573	558	-4	10	4	96	105	3	11	2	489	-484	1	12	2	113	120	-3	14	1	230	-234
-2	9	7	109	111	-3	10	4	131	-137	4	11	2	470	-459	2	12	2	162	-164	-2	14	1	502	-515
-1	9	7	74	78	-2	10	4	395	401	5	11	2	-54	-21	3	12	2	266	-278	-1	14	1	472	-465
0	9	7	464	457	-1	10	4	347	344	6	11	2	166	-165	4	12	2	-55	20	0	14	1	230	-234
1	9	7	269	270	0	10	4	-52	-4	7	11	2	136	-140	5	12	2	114	-90	1	14	1	178	-181
2	9	7	191	183	1	10	4	84	80	-9	11	3	159	157	6	12	2	72	-74	2	14	1	186	-183
3	9	7	253	244	2	10	4	290	289	-8	11	3	526	541	-8	12	3	288	285	-3	14	2	-54	4
4	9	7	154	153	3	10	4	329	325	-7	11	3	-57	31	-7	12	3	295	305	-2	14	2	78	50
-9	9	8	-57	30	4	10	4	-54	34	-6	11	3	-54	18	-6	12	3	-58	41	-1	14	2	84	-82
-8	9	8	270	272	5	10	4	84	-80	-5	11	3	382	382	-5	12	3	290	274	0	14	2	123	-122
-7	9	8	267	266	6	10	4	197	187	-4	11	3	448	451	-4	12	3	384	386	1	14	2	-56	-14

RESULTS

Fig. 1. is a stereoscopic view of the hexathionate ion as seen along an approximate twofold axis, and Fig. 2 is a view normal to this axis, with principal bond lengths and angles as calculated from the atomic coordinates of Table 1.

Fig. 1. The *cis-cis* form of the hexathionate ion in $K_2Ba(S_6O_6)_2$ as seen along an approximate twofold axis. The ellipsoids represent 50 % probability.

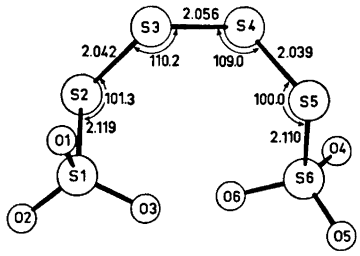

Fig. 2. The hexathionate ion as seen normal to an approximate twofold axis.

The differences between the dimensions of the hexathionate ion listed in Table 4, and those arrived at by the refinement based on two-dimensional film data,[1] are within the errors estimated for the latter. The standard deviations given in parentheses in Table 4 are about one tenth of those estimated for the film data.

The terminal S – S bonds, 2.119 and 2.110 Å, are between sulphonate sulphur atoms and divalent sulphur atoms, and are considerably longer than the three middle S – S bonds, 2.041, 2.056 and 2.039 Å, which are all between two divalent sulphur atoms. Of these three middle bonds the central one is 0.015 – 0.017 Å longer than the two others.

The dimensions of the hexathionate ion in the *cis-cis* form in the present salt will be further discussed in the next paper[3] and there compared to those of the hexathionate ion in the *trans-trans* form.

The packing in the crystal has been described in detail earlier,[1] and only a few aspects will be repeated here in order to present the redetermined dimensions.

Each barium ion, situated on a twofold axis, has ten oxygen neighbours within 2.960 Å. Eight of these are in a distorted square antiprism arrangement with Ba-O distances of 2.704(2) – 2.894(2) Å. The O – O edges of the square faces are in the range 3.243(3) – 4.117(3) Å, and the O – O edges between the square faces are in the range 3.007(2) – 3.455(3) Å. The O – O – O angles of

Table 4. Dimensions of the *cis-cis* form of the hexathionate ion. Standard deviations, given in parentheses, include estimated uncertainties in unit cell dimensions.

Bond lengths and angles

S(1)–S(2) = 2.1186(11) Å	∠S(1)–S(2)–S(3) = 101.25(5)°
S(2)–S(3) = 2.0415(14)	∠S(2)–S(3)–S(4) = 110.20(5)°
S(3)–S(4) = 2.0561(13)	∠S(3)–S(4)–S(5) = 108.99(5)°
S(4)–S(5) = 2.0394(16)	∠S(4)–S(5)–S(6) = 99.95(5)°
S(5)–S(6) = 2.1098(11)	
S(1)–O(1) = 1.443(2) Å	S(6)–O(4) = 1.435(2) Å
S(1)–O(2) = 1.441(2)	S(6)–O(5) = 1.459(2)
S(1)–O(3) = 1.448(3)	S(6)–O(6) = 1.449(2)
∠S(2)–S(1)–O(1) = 105.1(1)°	∠S(5)–S(6)–O(4) = 107.3(1)°
∠S(2)–S(1)–O(2) = 100.7(1)°	∠S(5)–S(6)–O(5) = 100.6(1)°
∠S(2)–S(1)–O(3) = 107.4(1)°	∠S(5)–S(6)–O(6) = 107.5(1)°
∠O(1)–S(1)–O(2) = 115.5(2)°	∠O(4)–S(6)–O(5) = 115.8(2)°
∠O(1)–S(1)–O(3) = 111.6(2)°	∠O(4)–S(6)–O(6) = 112.8(2)°
∠O(2)–S(1)–O(3) = 115.0(2)°	∠O(5)–S(6)–O(6) = 111.6(2)°

Dihedral angles

S(1)S(2)S(3)/S(2)S(3)S(4) = 109.4°	S(3)S(4)S(5)/S(4)S(5)S(6) = 106.3°
S(2)S(3)S(4)/S(3)S(4)S(5) = 89.0°	
S(3)S(2)S(1)/S(2)S(1)O(1) = 52.6°	S(4)S(5)S(6)/S(5)S(6)O(4) = 66.5°
S(3)S(2)S(1)/S(2)S(1)O(2) = 173.0°	S(4)S(5)S(6)/S(5)S(6)O(5) = 172.0°
S(3)S(2)S(1)/S(2)S(1)O(3) = 66.4°	S(4)S(5)S(6)/S(5)S(6)O(6) = 55.1°
S(2)S(1)O(1)/S(2)S(1)O(2) = 120.4°	S(5)S(6)O(4)/S(5)S(6)O(5) = 121.5°
S(2)S(1)O(1)/S(2)S(1)O(3) = 119.0°	S(5)S(6)O(4)/S(5)S(6)O(6) = 121.6°
S(2)S(1)O(2)/S(2)S(1)O(3) = 120.6°	S(5)S(6)O(5)/S(5)S(6)O(6) = 116.9°

Non-bonded distances

S(1)–S(4) = 4.5525(11)Å	S(2)–S(5) = 4.3872(16)Å	S(3)–S(6) = 4.4505(13) Å
S(1)–S(5) = 4.7099(13)	S(1)–S(6) = 4.8895(11)	S(2)–S(6) = 4.6100(14)

the faces are 78.05(6)°, 87.51(7)°, 94.53(8)°, and 98.52(7)°. The two oxygen atoms not involved in the antiprism arrangement are at 2.960(2) Å from barium, and lie outside the square faces with distances to the corners in the range 2.406(3) – 3.338(2) Å. Fig. 3 is a stereoscopic view of the Ba – O coordination.

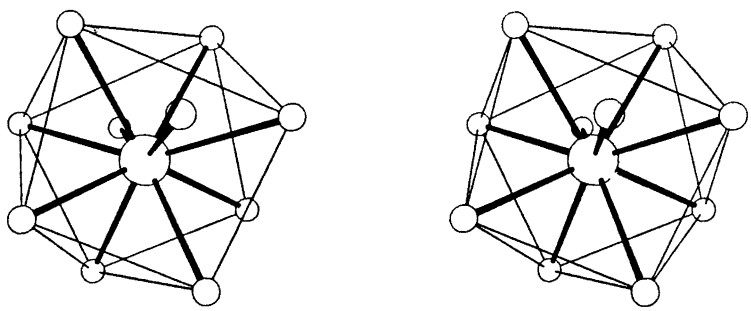

Fig. 3. A stereoscopic view where the barium-oxygen coordination is indicated by the thick lines, and the thin lines are between the oxygen atoms of the square antiprism.

Each potassium ion is surrounded by six oxygen atoms in much distorted octahedral arrangements. The distances from K(1), situated in a symmetry centre, to the oxygen atoms are 2.664(2), 2.781(2), and 3.008(3) Å. The *trans* O – K(1) – O angles are 180.0° and the *cis* O – K(1) – O angles are in the range 48.8(1)° – 131.2(1)°. The distances from K(2), situated on a twofold axis, to the oxygen atoms are 2.668(2), 2.840(2), and 3.028(3) Å. The *trans* O – K(2) – O angles are in the range 132.6(1)° – 159.0(1)° and the *cis* O – K(2) – O angles are in the range 48.0(1)° – 125.6(1)°.

REFERENCES

1. Foss, O. and Johnsen, K. *Acta Chem. Scand.* **19** (1965) 2207.
2. Foss, O. and Marøy, K. *Acta Chem. Scand.* **19** (1965) 2219.
3. Marøy, K. *Acta Chem. Scand* **27** (1973) 1705.
4. Foss, O. and Palmork, K. H. *Acta Chem. Scand.* **12** (1958) 1337.
5. *International Tables for X-Ray Crystallography*, Kynoch Press, Birmingham 1972, Vol. III.
6. Thomas, L. H. and Umeda, K. *J. Phys. Chem.* **26** (1957) 293.
7. Cromer, D. T. *Acta Cryst.* **18** (1965) 17.
8. Gjerrestad, K. and Marøy, K. *Acta Chem. Scand.* **27** (1973) 1653.
9. Zachariasen, W. H. *Acta Cryst.* **16** (1963) 1139.
10. Marøy, K. *Acta Chem. Scand.* **27** (1973) 1695.

Received December 27, 1972.

ACTA CHEMICA SCANDINAVICA 27 (1973) 1695–1704

Refinement of the Crystal Structure of Monoclinic Barium Telluropentathionate Dihydrate

KJARTAN MARØY

Chemical Institute, University of Bergen, N-5000 Bergen, Norway

The crystal structure of the monoclinic dimorph of barium telluropentathionate dihydrate, $BaTe(S_2O_3)_2.2H_2O$, has been refined by full-matrix least squares for 1306 non-zero reflections, collected by means of a single-crystal diffractometer, to a conventional R value of 0.031. The space group is $A2/m$ with four formula units per unit cell, and $a = 5.003(2)$ Å, $b = 10.588(3)$ Å, $c = 23.635(7)$ Å, $\beta = 98.61(5)°$.

Mirror plane symmetry is crystallographically required for the telluropentathionate ion, and the ion thus occurs in the *cis* form. The dimensions of the S–S–Te–S–S chain are: S(1)–S(2) = 2.104(3) Å, S(2)–Te = 2.377(3) Å, ∠S(1)–S(2)–Te = 103.79(9)°, ∠S(2)–Te–S(2′) = 100.29(8)°. The SSTe/STeS dihedral angles are 103.8°.

Barium telluropentathionate dihydrate, $BaTe(S_2O_3)_2.2H_2O$, occurs in a triclinic form when crystallized from aqueous methanol, and in a monoclinic form when crystallized from aqueous acetone, whereas a monoclinic trihydrate, $BaTe(S_2O_3)_2.3H_2O$, occurs on crystallization from water.[1]

The crystal structure of the monoclinic dihydrate was determined by Foss and Tjomsland,[2] using *0kl* and *h0l* Weissenberg photographs, taken with Cu$K\alpha$ radiation. No correction for absorption was made ($\mu = 531$ cm^{-1}), but reflections likely to be most heavily influenced by absorption were omitted from the refinement, which was carried out by difference electron density syntheses. Estimated standard deviations were 0.02 Å for S–S and S–T distances, and 1° for angles involving these atoms.

In connection with the crystal structure analyses of the trihydrate[3] and of barium selenopentathionate hydrates,[4,5] carried out with the aid of more modern facilities, it was thought of interest to refine the structure of the monoclinic dihydrate using the same methods.

EXPERIMENTAL

The crystals of monoclinic barium telluropentathionate dihydrate, $BaTe(S_2O_3)_2.2H_2O$, were obtained on addition of acetone to a solution of barium telluropentathionate in dilute perchloric acid.[1]

The crystal used for data collection was a prism along the a axis, bounded by (001), (011) and (0$\bar{1}$1), and terminated by (110) and (1$\bar{1}$0). The distance between the (001) boundary faces was 0.055 mm, and the maximum extensions along the a and b axes were 0.187 and 0.112 mm, respectively.

The intensity data were collected by means of a Siemens automatic single-crystal diffractometer using Mo$K\alpha$ radiation (Nb-filtered) and a scintillation counter.

The crystal was mounted with the a axis approximately parallel to the ϕ axis of the diffractometer, and the unit cell dimensions and setting angles for all reflections were calculated from the θ,χ and ϕ angles of 8 non-coplanar reciprocal vectors.

The procedure followed was similar to that described in a preceding paper.[3]

The net intensities of the two reference reflections, 080 and 008, decreased by about 5 % during the data collection.

Out of 1588 independent reflections attainable within $\theta = 28°$, 282 were found to have net intensities below three times its standard deviation. These reflections were assigned an intensity equal to this limit, and labelled as unobserved.

The net intensities were scaled by means of the reference reflections, and Lorentz and polarization corrections were applied. The linear absorption coefficient for Mo$K\alpha$ radiation is 63.5 cm^{-1}, and corrections were carried out using the Gaussian integration method.[6]

The scattering factor curves used for the structure factor calculations, and the computer programs used during the data collection, data processing, refinement, and drawing of illustrations are the same as in a preceding paper.[3]

The unit cell dimensions, calculated by means of a least squares program using the θ angles of 12 reflections ($\theta = 17 - 24°$) measured on the diffractometer, are $a = 5.003(2)$ Å, $b = 10.588(3)$ Å, $c = 23.635(7)$ Å, $\beta = 98.61(5)°$. The space group is $A2/m$ with four $BaTe(S_2O_3)_2.2H_2O$ formula units per unit cell.[1]

REFINEMENT

The first structure factor calculations were based on the atomic coordinates derived from the two-dimensional film data,[2] and an overall isotropic thermal factor, $\exp[-8\pi^2 U(\sin^2\theta/\lambda^2)]$ with $U = 0.040$ Å^2, was used. The resulting R value ($\sum||F_o| - |F_c||/\sum|F_o|$) was 0.154.

Refinement by least squares was then started, using a full-matrix least squares program minimizing the function

$$r = \sum W(|F_o| - K|F_c|)^2$$

Here $W = 4(I_t - I_b)^2/F_o^2[I_t + I_b + k^2(I_t - I_b)^2]$, where I_t is the total intensity of a reflection, I_b is the background intensity, and k is the relative standard deviation in the scaling curve based on the reference reflections. Non-observed reflections for which $|F_c|$ is greater than the observable limit, are included in the refinement with $|F_o|$ equal to this limit.

With individual isotropic thermal parameters for all atoms the R value converged at 0.104. The values of U were in the region $0.027 - 0.047$ Å^2 for all atoms except the $H_2O(2)$ oxygen atom, for which U was 0.184 Å^2. On refinement of the occupancy factor for the $H_2O(2)$ oxygen atom this factor was reduced from 0.500 to 0.264. An attempt to use anisotropic refinement for this oxygen atom resulted in steadily increasing thermal parameters and decreasing x and z coordinates. The refinement converged at $U = 0.109$ Å^2 when an isotropic thermal parameter for $H_2O(2)$ was used.

With anisotropic thermal parameters for all atoms, except $H_2O(2)$, the final R value was 0.031. Unobserved reflections are included when $|F_c|$ is

greater than the observable limit. The maximum shift of a parameter in the last refinement cycle was about one tenth of its standard deviation.

A final difference electron density map showed no peaks higher than 0.7 e/Å^3. The water hydrogen atoms were not located.

Tables 1 and 2 give the final atomic parameters with standard deviations from least squares. The observed structure factors, and those calculated from the final parameters, are listed in Table 3.

Table 1. Atomic coordinates for barium telluropentathionate dihydrate. Origin at a centre of symmetry. Standard deviation are given in parentheses.

	x	y	z
Ba	0.19877(11)	0	0.20457(3)
S(1)	0.36898(32)	0.23827(15)	0.33787(7)
S(2)	0.40906(48)	0.17231(19)	0.42270(8)
Te	0.71446(14)	0	0.42420(3)
O(1)	0.6382(10)	0.2527(6)	0.3234(2)
O(2)	0.2325(11)	0.3578(5)	0.3437(2)
O(3)	0.2097(10)	0.1478(5)	0.3016(2)
$H_2O(1)$	0.7293(13)	0	0.2658(3)
$H_2O(2)$	0.1778(54)	0	0.0822(11)

Table 2. Thermal parameters expressed in the form exp $[-2\pi^2(h^2a^{-2}U_{11}+\cdots+2hka^{-1}b^{-1}U_{12}+\cdots)]$. All values have been multiplied by 10^4, and standard deviations are given in parentheses.

	U_{11}	U_{22}	U_{33}	U_{12}	U_{23}	U_{13}
Ba	255(3)	219(3)	391(3)	0	0	12(2)
S(1)	275(8)	208(7)	321(8)	−11(6)	43(6)	20(6)
S(2)	784(15)	316(9)	285(9)	109(10)	−3(8)	95(9)
Te	460(4)	327(4)	354(4)	0	0	−112(3)
O(1)	280(26)	598(37)	653(38)	−82(25)	182(31)	97(24)
O(2)	595(36)	244(26)	654(38)	166(38)	−3(25)	−69(29)
O(3)	366(26)	406(29)	395(27)	−61(23)	−105(23)	14(21)
$H_2O(1)$	234(33)	469(42)	299(36)	0	0	21(28)
$H_2O(2)$[a]	1087(79)					

[a] Occupancy factor for $H_2O(2)$ oxygen atom, 0.264 instead of 0.500, and the thermal parameter is expressed in the form exp $[-8\pi^2 U(\sin\theta/\lambda^2)]$.

RESULTS

Fig. 1. gives a view of the telluropentathionate ion as seen along the *a* axis, with principal bond lengths and angles. These values are nearly the same as those given by Foss and Tjomsland,[2] the greatest difference being that of 0.04 Å for the S–Te bond length. The ion possesses mirror plane symmetry, and the non-planar S–S–Te–S–S chain thus occurs in the *cis*

Table 3. Observed and calculated structure factors (× 10) for barium telluropentathionate dihydrate. A minus sign on $F(O)$ indicates an unobserved reflection.

H	K	L	F(O)	F(C)	H	K	L	F(O)	F(C)	H	K	L	F(O)	F(C)	H	K	L	F(O)	F(C)	H	K	L	F(O)	F(C)
0	0	2	1746	-1752	0	6	16	271	305	1	0	2	1595	-1694	1	3	13	276	311	1	7-25	454	457
0	0	4	818	-1076	0	6	18	1343	-1274	1	0	4	737	692	1	3	15	653	712	1	7-23	-153	-53
0	0	6	480	-402	0	6	20	175	-215	1	0	6	1711	-1744	1	3	17	744	755	1	7-21	505	524
0	0	8	3725	-3637	0	6	22	658	-660	1	0	8	3218	3145	1	3	19	1015	976	1	7-19	774	-753
0	0	10	1178	1057	0	6	24	506	451	1	0	10	960	917	1	3	21	925	-933	1	7-17	353	-339
0	0	12	1234	1237	0	6	26	390	393	1	0	12	1520	-1534	1	3	23	313	-322	1	7-15	210	196
0	0	14	2156	2166	0	7	1	433	-462	1	0	14	535	557	1	3	25	603	-598	1	7-13	765	-778
0	0	16	353	-293	0	7	3	1338	-1360	1	0	16	1386	-1329	1	3	27	-157	111	1	7-11	1930	1946
0	0	18	573	-525	0	7	5	1090	1661	1	0	18	245	-251	1	3	29	534	520	1	7 -9	310	-312
0	0	20	-228	-387	0	7	7	487	488	1	0	20	727	728	1	4-23	-154	33		1	7 -7	178	-181
0	0	22	1392	-1405	0	7	9	538	509	1	0	22	502	460	1	4-20	-159	97		1	7 -5	-130	-62
0	0	24	1656	1659	0	7	11	433	-428	1	0	24	245	183	1	4-24	595	-609		1	7 -3	1610	-1646
0	0	26	645	638	0	7	13	591	-592	1	0	26	415	-405	1	4-22	325	-303		1	7 -1	757	749
0	0	28	-186	51	0	7	15	-139	-43	1	0	28	-164	83	1	4-20	181	192		1	7 1	-129	-114
0	0	30	199	234	0	7	17	537	-505	1	1	-31	-156	-69	1	4-18	334	-309		1	7 3	1577	1552
0	1	1	1314	-1535	0	7	19	1207	1199	1	1	-29	240	-221	1	4-16	1862	1907		1	7 5	164	143
0	1	3	1551	-1769	0	7	21	-172	55	1	1	-27	-151	-136	1	4-14	320	-312		1	7 7	1117	-1115
0	1	5	3219	3104	0	7	23	-152	-72	1	1	-25	876	862	1	4-12	942	-917		1	7 9	615	606
0	1	7	1056	924	0	7	25	-152	18	1	1	-23	-154	-207	1	4-10	144	-117		1	7 11	1820	-1822
0	1	9	1286	1250	0	8	0	2514	2514	1	1	-21	573	628	1	4 -8	2117	-2092		1	7 13	811	827
0	1	11	779	-839	0	8	2	577	-1004	1	1	-19	975	-913	1	4 -6	1613	1541		1	7 15	669	683
0	1	13	1575	-2013	0	8	4	-132	-22	1	1	-17	825	-790	1	4 -4	236	263		1	7 17	-166	-92
0	1	15	-135	145	0	8	6	203	200	1	1	-15	268	266	1	4 -2	2398	2434		1	7 19	559	566
0	1	17	771	-715	0	8	8	1226	-1231	1	1	-13	572	-641	1	4 0	479	-408		1	7 21	732	-719
0	1	19	1613	1643	0	8	10	541	533	1	1	-11	2782	2826	1	4 2	2476	-2397		1	7 23	-153	-72
0	1	21	408	404	0	8	12	-138	-35	1	1	-9	750	-730	1	4 4	757	795		1	7 25	271	-269
0	1	23	-148	-102	0	8	14	740	755	1	1	-7	-134	-15	1	4 6	2652	-2630		1	8-24	280	-290
0	1	25	172	-156	0	8	16	174	-217	1	1	-5	648	-676	1	4 8	2181	2187		1	8-22	380	-380
0	1	27	818	-818	0	8	18	216	-183	1	1	-3	2719	-2847	1	4 10	1422	1399		1	8-20	-151	67
0	1	29	182	168	0	8	20	-155	150	1	1	-1	2112	1942	1	4 12	642	-592		1	8-18	249	-215
0	2	0	2035	1725	0	8	22	734	-729	1	1	1	200	0	1	4 14	749	784		1	8-16	1257	1287
0	2	2	-122	-147	0	8	24	441	442	1	1	3	2226	2151	1	4 16	1725	-1674		1	8-14	175	-162
0	2	4	1591	1412	0	9	1	202	-189	1	1	5	709	660	1	4 18	393	-361		1	8-12	451	-472
0	2	6	2548	-2553	0	9	3	501	-520	1	1	7	2059	-2150	1	4 20	223	244		1	8-10	-140	111
0	2	8	1124	-1153	0	9	5	1078	1067	1	1	9	626	532	1	4 22	411	384		1	8 -8	1665	-1701
0	2	10	1646	1788	0	9	7	437	-645	1	1	11	2245	-2302	1	4 24	671	665		1	8 -6	939	922
0	2	12	1211	-1227	0	9	9	828	824	1	1	13	1232	1268	1	4 26	266	-271		1	8 -4	577	541
0	2	14	1666	1679	0	9	11	153	-133	1	1	15	754	814	1	4 28	-162	84		1	8 -2	994	957
0	2	16	231	359	0	9	13	867	-850	1	1	17	156	147	1	5-29	263	-199		1	8 0	-133	71
0	2	18	1143	-1074	0	9	15	646	630	1	1	19	686	693	1	5-27	-157	-78		1	8 2	1047	-1075
0	2	20	-142	117	0	9	17	653	-710	1	1	21	1199	-1224	1	5-25	834	841		1	8 4	-133	-11
0	2	22	532	-541	0	9	19	449	433	1	1	23	-149	25	1	5-23	256	-299		1	8 6	1595	-1603
0	2	24	336	287	0	9	21	182	123	1	1	25	256	-307	1	5-21	458	468		1	8 8	1426	1413
0	2	26	-151	66	0	9	23	-157	-48	1	1	27	220	191	1	5-19	659	-634		1	8 10	860	847
0	2	28	296	257	0	10	0	910	910	1	1	29	533	512	1	5-17	903	-887		1	8 12	334	-312
0	2	30	-137	100	0	10	2	-139	-114	1	2	-30	467	485	1	5-15	381	414		1	8 14	660	638
0	3	1	-125	-44	0	10	4	433	437	1	2	-28	202	-228	1	5-13	319	-283		1	8 16	1098	-1096
0	3	3	1499	-1558	0	10	6	514	-909	1	2	-26	541	533	1	5-11	1828	1843		1	8 18	402	-394
0	3	5	2415	2444	0	10	8	667	-687	1	2	-24	603	-620	1	5 -9	396	-359		1	8 20	-154	109
0	3	7	1300	-1214	0	10	10	849	857	1	2	-22	516	-899	1	5 -7	-124	33		1	9 22	363	337
0	3	9	1139	1152	0	10	12	480	-475	1	2	-20	560	615	1	5 -5	803	-759		1	8 24	425	434
0	3	11	189	89	0	10	14	751	765	1	2	-18	244	-195	1	5 -3	2090	-2086		1	9-23	-162	-131
0	3	13	1573	-1557	0	10	16	203	197	1	2	-16	1422	1450	1	5 -1	1778	1786		1	9-21	610	597
0	3	15	829	861	0	10	18	522	-523	1	2	-14	222	195	1	5 1	-125	-149		1	9-19	-154	-59
0	3	17	1011	-977	0	10	20	-159	-26	1	2	-12	521	-543	1	5 3	1239	1269		1	9-17	678	-684
0	3	19	672	627	0	11	1	351	-361	1	2	-10	946	-923	1	5 5	828	873		1	9-15	156	-134
0	3	21	-146	31	0	11	3	636	-829	1	2	-8	2682	-2631	1	5 7	1781	-1755		1	9-13	532	-519
0	3	23	-144	-76	0	11	5	1342	1334	1	2	-6	2823	2856	1	5 9	-127	35		1	9-11	1071	1046
0	3	25	332	263	0	11	7	-147	115	1	2	-4	538	-550	1	5 11	1323	-1293		1	9 -9	147	152
0	3	27	563	-552	0	11	9	380	429	1	2	-2	2432	2350	1	5 13	966	969		1	9 -7	632	606
0	3	29	201	201	0	11	11	-176	-206	1	2	0	1732	1649	1	5 15	397	446		1	9 -5	212	-239
0	4	0	3698	3736	0	11	13	650	-840	1	2	2	3973	-3994	1	5 17	291	288		1	9 -3	1732	-1708
0	4	2	1046	-1054	0	11	15	-152	45	1	2	4	-130	-48	1	5 19	470	468		1	9 -1	614	604
0	4	4	-151	66	0	11	17	287	-282	1	2	6	1251	-1226	1	5 21	1137	-1114		1	9 1	458	-466
0	4	6	498	-446	0	11	19	794	772	1	2	8	1243	1192	1	5 23	-155	126		1	9 3	947	927
0	4	8	1667	-1682	0	12	0	1545	1540	1	2	10	1268	1247	1	5 25	213	-213		1	9 5	1174	1159
0	4	10	739	793	0	12	2	290	-283	1	2	12	863	843	1	5 27	-162	131		1	9 7	744	-743
0	4	12	277	217	0	12	4	-147	-44	1	2	14	-138	-60	1	6-28	393	-435		1	9 -141		-114
0	4	14	1665	1119	0	12	6	318	-346	1	2	16	2089	-2133	1	6-26	-151	137		1	9 11	1140	-1129
0	4	16	252	-219	0	12	8	876	-876	1	2	18	363	351	1	6-24	429	-434		1	9 13	262	225
0	4	18	303	-245	0	12	10	433	437	1	2	20	343	-338	1	6-22	462	-459		1	9 15	223	230
0	4	20	155	-132	0	12	12	-170	118	1	2	22	318	280	1	6-20	935	959		1	9 17	483	500
0	4	22	928	-916	0	12	14	666	708	1	2	24	1289	1278	1	6-18	-143	52		1	9 19	621	611
0	4	24	763	704	0	13	1	266	-269	1	2	26	538	-519	1	6-16	621	641		1	9 21	740	-716
0	4	26	-153	121	0	13	3	255	-252	1	2	28	-156	-71	1	6-14	457	-431		1	10-20	397	425
0	4	28	-155	13	0	13	5	643	648	1	3	-29	254	-274	1	6-12	778	-769		1	10-18	209	-180
0	5	1	1278	-1280	0	13	7	-157	-173	1	3	-27	478	-477	1	6-10	274	-262		1	10-16	714	696
0	5	3	1046	-1039	0	13	9	517	518	1	3	-25	536	531	1	6 -8	1071	-1091		1	10-14	-149	-40
0	5	5	2470	2481	0	13	11	157	-202	1	3	-23	-148	39	1	6 -6	2402	2397		1	10-12	276	-298
0	5	7	178	190	0	14	0	555	601	1	3	-21	1015	1110	1	6 -4	189	-173		1	10-10	365	-352
0	5	9	1372	1379	1	0	-30	566	576	1	3	-19	421	-397	1	6 -2	330	332		1	10 -8	846	-840
0	5	11	646	-633	1	0	-28	263	-272	1	3	-17	1135	-1089	1	6 0	349	330		1	10 -6	1220	1206
0	5	13	1596	-2016	1	0	-26	302	-315	1	3	-15	-136	-54	1	6 2	2353	-2373		1	10 -4	371	-375
0	5	15	369	379	1	0	-24	459	-457	1	3	-13	1349	-1338	1	6 4	388	403		1	10 -2	888	901
0	5	17	637	-580	1	0	-22	213	-166	1	3	-11	1908	1975	1	6 6	-126	-55		1	10 0	378	353
0	5	19	1238	1254	1	0	-20	698	748	1	3	-9	568	995	1	6 8	1057	1074		1	10 2	1569	-1604
0	5	21	505	452	1	0	-18	-139	107	1	3	-7	580	599	1	6 10	459	469		1	10 4	393	378
0	5	23	-152	-129	1	0	-16	1461	1443	1	3	-5	566	-527	1	6 12	-138	-104		1	10 6	553	563
0	5	25	247	-237	1	0	-14	580	-590	1	3	-3	2776	-2812	1	6 14	284	-237		1	10 8	552	560
0	5	27	692	-693	1	0	-12	1659	-1672	1	3	-1	-129	166	1	6 16	1257	-1232		1	10 10	529	530
0	6	4	419	404	1	0	-10	704	679	1	3	1	491	-494	1	6 18	601	609		1	10 12	-149	138
0	6	6	2052	-2048	1	0	-8	1882	-1891	1	3	3	1990	2077	1	6 20	-146	63		1	10 14	-148	52
0	6	8	1720	-1750	1	0	-6	2601	2486	1	3	5	2122	2137	1	6 22	186	147		1	10 16	996	-996
0	6	10	1489	1484	1	0	-4	1837	1662	1	3	7	1316	-1301	1	6 24	628	632		1	10 18	305	310
0	6	12	298	-316	1	0	-2	357	161	1	3	9	201	-190	1	6 26	576	-565		1	10 20	-159	-123
0	6	14	1817	1851	1	0	0	1404	-1565	1	3	11	2289	-2295	1	7-27	-160	-95		1	11-19	543	-527

Table 3. Continued.

H	K	L	F(O)	F(C)	H	K	L	F(O)	F(C)	H	K	L	F(O)	F(C)	H	K	L	F(O)	F(C)	H	K	L	F(O)	F(C)
1	11	-17	315	-295	2	2	-28	429	-463	2	5	11	363	-338	2	9	19	496	-479	3	1	9	-145	-69
1	11	-15	391	354	2	2	-26	206	-210	2	5	13	1635	1679	2	10	-20	-158	-4	3	1	11	1144	1174
1	11	-13	455	-432	2	2	-24	-158	-154	2	5	15	517	-509	2	10	-18	-153	33	3	1	13	684	-662
1	11	-11	595	582	2	2	-22	952	988	2	5	17	-148	131	2	10	-16	-158	163	3	1	15	1170	-1164
1	11	-9	-145	-24	2	2	-20	-147	84	2	5	19	561	-543	2	10	-14	1056	-1054	3	1	17	165	145
1	11	-7	353	-353	2	2	-18	203	205	2	5	21	385	-412	2	10	-12	521	522	3	1	19	439	-441
1	11	-5	179	-147	2	2	-16	157	142	2	5	23	309	290	2	10	-10	-145	-87	3	1	21	940	954
1	11	-3	724	-722	2	2	-14	2448	-2492	2	5	25	-156	11	2	10	-8	258	219	3	1	23	322	285
1	11	-1	574	564	2	2	-12	917	924	2	6	-26	-152	-54	2	10	-6	897	911	3	1	25	-158	-57
1	11	1	-139	-66	2	2	-10	-131	14	2	6	-24	280	-271	2	10	-4	743	-731	3	2	-28	324	336
1	11	3	782	777	2	2	-8	807	804	2	6	-22	437	459	2	10	-2	-142	51	3	2	-26	178	209
1	11	5	-146	58	2	2	-6	2309	2317	2	6	-20	346	-317	2	10	0	894	-897	3	2	-24	238	-230
1	11	7	757	-771	2	2	-4	1753	-1698	2	6	-18	350	346	2	10	2	390	387	3	2	-22	440	467
1	11	9	287	288	2	2	-2	204	-223	2	6	-16	561	573	2	10	4	381	372	3	2	-20	522	-515
1	11	11	794	-790	2	2	0	2587	-2594	2	6	-14	1455	-1479	2	10	6	-145	75	3	2	-18	181	-192
1	11	13	433	499	2	2	2	769	785	2	6	-12	722	714	2	10	8	889	913	3	2	-16	290	-322
1	11	15	391	371	2	2	4	1097	1131	2	6	-10	518	-515	2	10	10	923	-914	3	2	-14	479	464
1	11	17	-156	-69	2	2	6	534	517	2	6	-8	148	134	2	10	12	208	-212	3	2	-12	607	581
1	12	-14	368	-386	2	2	8	1955	1956	2	6	-6	1181	1197	2	10	14	-150	-55	3	2	-10	469	-533
1	12	-12	383	-387	2	2	10	1994	-1960	2	6	-4	517	-518	2	10	16	245	-222	3	2	-8	1558	1571
1	12	-10	172	179	2	2	12	899	-851	2	6	-2	605	607	2	10	18	598	573	3	2	-6	2199	-2203
1	12	-8	545	-551	2	2	14	257	-216	2	6	0	1900	-1899	2	11	-17	172	159	3	2	-4	-128	-113
1	12	-6	730	767	2	2	16	320	-267	2	6	2	622	584	2	11	-15	-159	-96	3	2	-2	742	732
1	12	-4	-144	55	2	2	18	1248	1242	2	6	4	-135	93	2	11	-13	358	367	3	2	0	1030	-980
1	12	-2	259	227	2	2	20	338	313	2	6	6	176	-157	2	11	-11	156	122	3	2	2	2113	2112
1	12	0	224	-194	2	2	22	261	227	2	6	8	1784	1795	2	11	-9	615	-609	3	2	4	274	-280
1	12	2	726	-717	2	2	24	771	-758	2	6	10	1113	-1089	2	11	-7	573	553	3	2	6	260	-253
1	12	4	444	412	2	2	26	326	-330	2	6	12	191	-177	2	11	-5	832	-832	3	2	8	750	-718
1	12	6	525	-527	2	3	-29	-161	-5	2	6	14	284	-283	2	11	-3	222	219	3	2	10	693	-677
1	12	8	745	750	2	3	-27	734	712	2	6	16	490	-475	2	11	-1	732	732	3	2	12	617	647
1	12	10	293	280	2	3	-25	-156	76	2	6	18	657	669	2	11	1	434	-441	3	2	14	244	-224
1	12	12	475	-443	2	3	-23	639	-646	2	6	20	-151	86	2	11	3	578	574	3	2	16	1198	1187
1	12	14	227	239	2	3	-21	293	-248	2	6	22	485	486	2	11	5	638	-615	3	2	18	-155	-143
1	13	-11	621	606	2	3	-19	1067	-1033	2	6	24	427	-425	2	11	7	-150	-103	3	2	20	676	-694
1	13	-9	238	-241	2	3	-17	1021	1042	2	7	-25	-160	133	2	11	9	-154	-127	3	2	22	157	175
1	13	-7	228	260	2	3	-15	434	419	2	7	-23	339	-369	2	11	11	-149	27	3	2	24	579	-573
1	13	-5	-154	-55	2	3	-13	1302	1296	2	7	-21	251	234	2	11	13	650	671	3	3	-27	185	172
1	13	-3	906	-878	2	3	-11	-133	-6	2	7	-19	811	-903	2	11	15	418	-396	3	3	-25	550	-546
1	13	-1	662	655	2	3	-9	2398	-2415	2	7	-17	429	441	2	12	-14	410	-406	3	3	-23	428	446
1	13	1	331	-266	2	3	-7	227	247	2	7	-15	147	155	2	12	-12	291	193	3	3	-21	-155	-88
1	13	3	367	373	2	3	-5	1567	-1505	2	7	-13	420	412	2	12	-10	411	-394	3	3	-19	-148	88
1	13	5	423	408	2	3	-3	1619	1615	2	7	-11	483	463	2	12	-8	347	328	3	3	-17	823	819
1	13	7	538	-484	2	3	-1	2473	2434	2	7	-9	1088	-1109	2	12	-6	460	449	3	3	-15	1079	-1112
1	13	9	-153	58	2	3	1	578	-527	2	7	-7	286	246	2	12	-4	495	-501	3	3	-13	436	432
2	0	-30	-162	-155	2	3	3	344	422	2	7	-5	1106	-1104	2	12	-2	542	551	3	3	-11	661	-685
2	0	-28	-154	-130	2	3	5	2830	-2810	2	7	-3	582	575	2	12	0	738	-751	3	3	-9	272	-263
2	0	-26	389	364	2	3	7	235	-180	2	7	-1	1377	1363	2	12	2	-151	-49	3	3	-7	1082	1077
2	0	-24	784	-780	2	3	9	144	166	2	7	1	637	-645	2	12	4	260	259	3	3	-5	255	-253
2	0	-22	466	467	2	3	11	613	648	2	7	3	986	968	2	12	6	-151	-29	3	3	-3	1213	1207
2	0	-20	286	315	2	3	13	2092	2067	2	7	5	1278	-1268	2	12	8	550	549	3	3	-1	1212	-1194
2	0	-18	200	-155	2	3	15	1091	-1176	2	7	7	600	-632	2	12	10	400	-390	3	3	1	281	-281
2	0	-16	531	521	2	3	17	-146	-15	2	7	9	159	192	2	13	-7	-156	-29	3	3	3	-134	17
2	0	-14	965	-991	2	3	19	1034	-1044	2	7	11	200	171	2	13	-5	230	-219	3	3	5	1099	-1098
2	0	-12	-137	109	2	3	21	402	-411	2	7	13	1051	1042	2	13	-3	207	202	3	3	7	1852	1891
2	0	-10	1019	-1011	2	3	23	809	789	2	7	15	356	-376	2	13	-1	349	312	3	3	9	379	-373
2	0	-8	1395	1388	2	3	25	186	136	2	7	17	251	272	2	13	1	-154	-15	3	3	11	379	406
2	0	-6	831	826	2	3	27	562	537	2	7	19	720	-709	2	13	3	436	428	3	3	13	216	-200
2	0	-4	572	-594	2	4	-28	462	-466	2	7	21	358	-391	2	13	5	837	-851	3	3	15	873	-863
2	0	-2	2162	2061	2	4	-26	318	329	2	7	23	474	469	3	0	-28	-159	-4	3	3	17	239	230
2	0	0	3273	-3405	2	4	-24	627	-591	2	8	-24	415	-400	3	0	-26	-159	3	3	3	19	282	-255
2	0	2	526	376	2	4	-22	700	711	2	8	-22	625	628	3	0	-24	476	487	3	3	21	677	669
2	0	4	729	730	2	4	-20	745	737	2	8	-20	466	454	3	0	-22	704	721	3	3	23	-159	86
2	0	6	-135	-30	2	4	-18	451	-447	2	8	-18	205	-227	3	0	-20	1007	-1029	3	4	-28	-160	99
2	0	8	1691	1674	2	4	-16	-139	1	2	8	-16	-145	-41	3	0	-18	320	288	3	4	-26	-154	-48
2	0	10	582	-581	2	4	-14	1276	-1250	2	8	-14	567	-1002	3	0	-16	993	-979	3	4	-24	246	299
2	0	12	-141	135	2	4	-12	226	253	2	8	-12	171	145	3	0	-14	593	-628	3	4	-22	267	243
2	0	14	1269	-1248	2	4	-10	318	-326	2	8	-10	147	-170	3	0	-12	2254	2217	3	4	-20	847	-857
2	0	16	271	-263	2	4	-8	1405	1402	2	8	-8	1206	1191	3	0	-10	479	-453	3	4	-18	565	577
2	0	18	1352	1315	2	4	-6	1598	1615	2	8	-6	764	776	3	0	-8	1210	1151	3	4	-16	563	-595
2	0	20	534	-532	2	4	-4	2003	-1971	2	8	-4	1157	-1157	3	0	-6	1025	-1057	3	4	-14	318	-337
2	0	22	684	639	2	4	-2	568	581	2	8	-2	454	481	3	0	-4	1493	-1469	3	4	-12	1532	1533
2	0	24	267	-268	2	4	0	2060	-2027	2	8	0	1748	-1792	3	0	-2	248	-292	3	4	-10	592	-597
2	0	26	651	-654	2	4	2	199	-122	2	8	2	244	208	3	0	0	-152	115	3	4	-8	440	456
2	0	28	-165	123	2	4	4	1404	1416	2	8	4	1128	1112	3	0	2	2388	2373	3	4	-6	707	-719
2	1	-25	186	-215	2	4	6	695	684	2	8	6	253	244	3	0	4	383	-364	3	4	-4	290	-259
2	1	-27	446	426	2	4	8	968	956	2	8	8	773	788	3	0	6	522	459	3	4	-2	558	-567
2	1	-25	-151	76	2	4	10	1380	-1331	2	8	10	588	-578	3	0	8	1091	-1062	3	4	0	275	264
2	1	-23	522	-251	2	4	12	335	-252	2	8	12	237	-238	3	0	10	1924	-1902	3	4	2	1839	1879
2	1	-21	254	264	2	4	14	876	-822	2	8	14	669	-664	3	0	12	1093	1099	3	4	4	1169	-1153
2	1	-19	1258	-1245	2	4	16	-145	-55	2	8	16	-154	73	3	0	14	194	188	3	4	6	637	662
2	1	-17	885	905	2	4	18	1469	1440	2	8	18	1094	1100	3	0	16	935	919	3	4	8	614	-592
2	1	-15	-140	36	2	4	20	237	-244	2	8	20	264	-280	3	0	18	392	390	3	4	10	1369	-1326
2	1	-13	427	410	2	4	22	386	341	2	8	22	343	324	3	0	20	611	-643	3	4	12	939	962
2	1	-11	990	991	2	4	24	341	-352	2	9	-23	156	-219	3	0	22	442	-425	3	4	14	-145	-5
2	1	-9	1651	-1702	2	4	26	591	-622	2	9	-21	-160	-141	3	0	24	583	-591	3	4	16	654	676
2	1	-7	-132	60	2	5	-27	309	258	2	9	-19	756	-787	3	1	-29	-158	0	3	4	18	-150	19
2	1	-5	1142	-1208	2	5	-25	-153	-2	2	9	-17	859	868	3	1	-27	280	275	3	4	20	345	-341
2	1	-3	743	714	2	5	-23	-156	-116	2	9	-15	-151	172	3	1	-25	690	-705	3	4	22	-165	-167
2	1	-1	1803	1760	2	5	-21	-152	192	2	9	-13	366	338	3	1	-23	-151	40	3	4	24	496	-545
2	1	1	515	-561	2	5	-19	587	-978	2	9	-11	459	441	3	1	-21	208	-212	3	5	-27	313	317
2	1	3	1470	1488	2	5	-17	829	818	2	9	-9	1337	-1361	3	1	-19	324	326	3	5	-25	623	-625
2	1	5	2233	-2241	2	5	-15	221	-209	2	9	-7	-142	-96	3	1	-17	982	973	3	5	-23	-154	-2
2	1	7	653	-630	2	5	-13	345	359	2	9	-5	472	-454	3	1	-15	433	-459	3	5	-21	182	-183
2	1	9	232	269	2	5	-11	854	855	2	9	-3	776	763	3	1	-13	351	332	3	5	-19	172	214
2	1	11	-139	-107	2	5	-9	1429	-1423	2	9	-1	912	918	3	1	-11	1593	-1627	3	5	-17	871	870
2	1	13	1758	1767	2	5	-7	269	270	2	9	1	150	-114	3	1	-9	229	-235	3	5	-15	358	-373
2	1	15	454	-464	2	5	-5	917	-914	2	9	3	385	378	3	1	-7	937	903	3	5	-13	395	362
2	1	17	192	185	2	5	-3	422	437	2	9	5	1700	-1709	3	1	-5	-133	8	3	5	-11	1334	-1341
2	1	19	825	-833	2	5	-1	1089	1100	2	9	7	-145	76	3	1	-3	2120	2085	3	5	-9	280	-308
2	1	21	473	-450	2	5	1	224	-158	2	9	9	213	227	3	1	-1	1012	-1013	3	5	-7	767	768
2	1	23	471	439	2	5	3	1089	1109	2	9	11	-144	68	3	1	1	858	-823	3	5	-5	156	-129
2	1	25	-154	38	2	5	5	1958	-1945	2	9	13	1258	1260	3	1	3	719	-726	3	5	-3	1853	1842
2	1	27	568	555	2	5	7	-131	5	2	9	15	525	-525	3	1	5	958	-951	3	5	-1	801	-793
2	2	-30	-156	-8	2	5	9	-133	-7	2	9	17	202	-180	3	1	7	1869	1874	3	5	1	782	-750

Table 3. Continued.

H	K	L	F(O)	F(C)	H	K	L	F(O)	F(C)	H	K	L	F(O)	F(C)	H	K	L	F(O)	F(C)	H	K	L	F(O)	F(C)
3	5	3	431	-465	3	10	-8	750	737	4	2	20	-159	-13	4	7	7	394	286	5	2	0	-147	-16
3	5	5	587	-564	3	10	-6	895	-895	4	3	-25	291	-282	4	7	9	596	-599	5	2	2	710	-705
3	5	7	1440	1443	3	10	-4	-145	-78	4	3	-23	342	346	4	7	11	-153	127	5	2	4	-158	184
3	5	9	-143	142	3	10	-2	179	184	4	3	-21	175	-166	4	7	13	719	-750	5	2	6	246	215
3	5	11	855	889	3	10	0	434	-450	4	3	-19	538	549	4	7	15	383	428	5	2	8	313	321
3	5	13	540	-538	3	10	2	1016	1023	4	3	-17	214	-243	4	8	-18	174	128	5	2	10	705	700
3	5	15	523	-515	3	10	4	180	-200	4	3	-15	255	-274	4	8	-16	215	-203	5	2	12	866	-915
3	5	17	-152	90	3	10	6	-148	45	4	3	-13	-149	-125	4	8	-14	651	651	5	2	14	-165	34
3	5	19	438	-441	3	10	8	333	-238	4	3	-11	591	-590	4	8	-12	339	-345	5	2	16	178	-232
3	5	21	776	839	3	10	10	411	-422	4	3	-9	1135	1125	4	8	-10	-147	31	5	3	-21	229	-180
3	5	23	311	258	3	10	12	337	338	4	3	-7	-140	-77	4	8	-8	-163	111	5	3	-19	-161	73
3	6	-26	-169	160	3	10	14	181	-184	4	3	-5	301	281	4	8	-6	961	-984	5	3	-17	697	-695
3	6	-24	-156	-18	3	11	-15	418	-421	4	3	-3	177	95	4	8	-4	862	859	5	3	-15	570	557
3	6	-22	674	709	3	11	-13	277	244	4	3	-1	1481	-1454	4	8	-2	-146	-83	5	3	-13	-154	95
3	6	-20	421	-436	3	11	-11	391	-411	4	3	1	463	487	4	8	0	286	273	5	3	-11	192	233
3	6	-18	355	-368	3	11	-9	390	-423	4	3	3	320	-311	4	8	2	244	252	5	3	-9	397	408
3	6	-16	565	-557	3	11	-7	345	349	4	3	5	579	967	4	8	4	584	-612	5	3	-7	962	-957
3	6	-14	173	142	3	11	-5	-155	137	4	3	7	404	391	4	8	6	-149	-48	5	3	-5	209	174
3	6	-12	776	749	3	11	-3	712	716	4	3	9	418	-403	4	8	8	435	-446	5	3	-3	646	-668
3	6	-10	-139	-66	3	11	-1	488	-482	4	3	11	-149	57	4	8	10	614	615	5	3	-1	537	536
3	6	-8	1527	1518	3	11	1	-149	-11	4	3	13	1190	-1183	4	8	12	-163	153	5	3	1	740	741
3	6	-6	1778	-1783	3	11	3	349	-356	4	3	15	499	503	4	8	14	-157	-9	5	3	3	368	-375
3	6	-4	713	-712	3	11	5	652	-644	4	3	17	206	207	4	9	-17	179	-172	5	3	5	614	635
3	6	-2	517	488	3	11	7	579	954	4	3	19	242	254	4	9	-15	314	-313	5	3	7	1168	-1169
3	6	0	809	-839	3	11	9	-159	-91	4	4	-24	-162	124	4	9	-13	-156	136	5	3	9	-157	-77
3	6	2	1857	1917	3	12	-8	381	368	4	4	-22	-155	-96	4	9	-11	394	-405	5	3	11	199	156
3	6	4	312	276	3	12	-6	484	-439	4	4	-20	354	-388	4	9	-9	520	525	5	3	13	-165	66
3	6	6	262	-240	3	12	-4	252	-279	4	4	-18	211	235	4	9	-7	-148	54	5	3	15	616	727
3	6	8	872	-752	3	12	-2	164	-121	4	4	-16	191	-197	4	9	-5	232	233	5	4	-20	539	537
3	6	10	675	-669	3	12	0	-159	-69	4	4	-14	1023	1021	4	9	-3	-149	-122	5	4	-18	-160	30
3	6	12	485	483	3	12	2	896	915	4	4	-12	611	-630	4	9	-1	764	-759	5	4	-16	218	-219
3	6	14	-150	-81	3	12	4	281	-295	4	4	-10	-141	-11	4	9	1	484	467	5	4	-14	324	322
3	6	16	1141	1153	4	0	-26	297	-271	4	4	-8	211	206	4	9	3	465	-458	5	4	-12	802	-777
3	6	18	-158	90	4	0	-24	172	-145	4	4	-6	1679	-1668	4	9	5	623	635	5	4	-10	245	227
3	6	20	658	-703	4	0	-22	167	-159	4	4	-4	1524	1519	4	9	7	403	397	5	4	-8	-148	-76
3	6	22	-161	-3	4	0	-20	274	-230	4	4	-2	-139	87	4	9	9	463	-486	5	4	-6	553	552
3	7	-23	-152	144	4	0	-18	404	400	4	4	0	-141	109	4	9	11	-160	136	5	4	-4	253	239
3	7	-21	221	-225	4	0	-16	-171	45	4	4	2	476	487	4	10	-12	-154	-47	5	4	-2	458	-454
3	7	-19	242	225	4	0	-14	1016	1016	4	4	4	574	-939	4	10	-10	273	-272	5	4	0	335	350
3	7	-17	757	757	4	0	-12	902	-923	4	4	6	307	-290	4	10	-8	-151	-33	5	4	2	1113	-1104
3	7	-15	518	-511	4	0	-10	281	-319	4	4	8	486	-466	4	10	-6	472	-469	5	4	4	264	259
3	7	-13	242	221	4	0	-8	-156	104	4	4	10	538	959	4	10	-4	592	599	5	4	6	606	621
3	7	-11	866	-854	4	0	-6	1249	-1248	4	4	12	255	249	4	10	-2	186	-190	5	4	8	-166	-179
3	7	-9	223	-225	4	0	-4	1773	1479	4	4	14	-150	-83	4	10	0	518	535	5	4	10	556	601
3	7	-7	611	551	4	0	-2	185	159	4	4	16	448	442	4	10	2	-151	21	5	4	12	361	-404
3	7	-5	-140	103	4	0	0	211	220	4	4	18	579	-1101	4	10	4	750	-787	5	4	14	212	-312
3	7	-3	1228	1183	4	0	2	-156	-130	4	4	20	-167	59	4	10	6	322	349	5	5	-19	-162	89
3	7	-1	805	-819	4	0	4	1029	-1114	4	5	-23	455	491	4	10	8	463	-462	5	5	-17	377	-379
3	7	1	239	-249	4	0	6	173	-177	4	5	-21	255	-239	4	11	-7	247	-238	5	5	-15	422	437
3	7	3	563	-582	4	0	8	328	-307	4	5	-19	444	459	4	11	-5	-152	-79	5	5	-13	-158	-168
3	7	5	623	-622	4	0	10	1211	1229	4	5	-17	503	-512	4	11	-3	171	84	5	5	-11	166	177
3	7	7	1442	1447	4	0	12	169	163	4	5	-15	455	-473	4	11	-1	715	-714	5	5	-9	380	349
3	7	9	244	-259	4	0	14	165	-123	4	5	-13	296	279	4	11	1	356	375	5	5	-7	805	-803
3	7	11	711	722	4	0	16	225	209	4	5	-11	325	-320	5	0	-22	471	-466	5	5	-5	376	395
3	7	13	327	-321	4	0	18	1163	-1169	4	5	-9	1072	1080	5	0	-20	513	545	5	5	-3	482	-462
3	7	15	868	-863	4	0	20	251	264	4	5	-7	-140	-66	5	0	-18	-162	-113	5	5	-1	203	205
3	7	17	-154	115	4	1	-27	-168	-149	4	5	-5	-140	-71	5	0	-16	252	-262	5	5	1	570	569
3	7	19	249	-213	4	1	-25	-159	-77	4	5	-3	254	-270	5	0	-14	543	492	5	5	3	286	-297
3	8	-22	234	188	4	1	-23	563	567	4	5	-1	1168	-1161	5	0	-12	779	-761	5	5	5	426	429
3	8	-20	670	-675	4	1	-21	288	-290	4	5	1	877	873	5	0	-10	432	439	5	5	7	792	-792
3	8	-18	408	414	4	1	-19	541	551	4	5	3	308	-299	5	0	-8	362	-369	5	5	9	-156	89
3	8	-16	331	-326	4	1	-17	595	-608	4	5	5	557	968	5	0	-6	543	539	5	5	11	-157	-44
3	8	-14	-149	-123	4	1	-15	504	-503	4	5	7	299	321	5	0	-4	323	303	5	5	13	-159	36
3	8	-12	1050	1036	4	1	-13	353	351	4	5	9	878	-886	5	0	-2	666	-700	5	6	-18	-156	-51
3	8	-10	568	-636	4	1	-11	475	-504	4	5	11	-152	142	5	0	0	754	743	5	6	-16	-159	33
3	8	-8	432	425	4	1	-9	1352	1336	4	5	13	758	-830	5	0	2	1176	-1139	5	6	-14	237	152
3	8	-6	561	-564	4	1	-7	-142	-61	4	5	15	380	447	5	0	4	-162	133	5	6	-12	144	-135
3	8	-4	259	-253	4	1	-5	146	-146	4	5	17	318	342	5	0	6	665	679	5	6	-10	595	621
3	8	-2	-140	60	4	1	-3	170	-172	4	5	19	194	208	5	0	8	364	-343	5	6	-8	456	-452
3	8	0	-140	3	4	1	-1	1514	-1487	4	6	-22	380	-413	5	0	10	738	705	5	6	-6	204	208
3	8	2	1139	1120	4	1	1	1054	1053	4	6	-20	171	-170	5	0	12	435	-428	5	6	-4	591	579
3	8	4	658	-702	4	1	3	335	-349	4	6	-18	653	663	5	0	14	-172	-227	5	6	-2	599	-612
3	8	6	269	306	4	1	5	1076	1051	4	6	-16	320	-335	5	0	16	238	-231	5	6	0	291	266
3	8	8	315	-350	4	1	7	496	493	4	6	-14	657	669	5	1	-23	-159	-32	5	6	2	481	-498
3	8	10	829	-841	4	1	9	1356	-1346	4	6	-12	155	-179	5	1	-21	174	-145	5	6	4	-151	103
3	8	12	760	782	4	1	11	-154	146	4	6	-10	622	-621	5	1	-19	200	138	5	6	6	-157	125
3	8	14	-151	-79	4	1	13	569	-965	4	6	-8	144	-135	5	1	-17	487	-485	5	6	8	-156	96
3	8	16	404	376	4	1	15	499	501	4	6	-6	251	-258	5	1	-15	417	416	5	6	10	548	571
3	8	18	-155	54	4	1	17	417	364	4	6	-4	848	866	5	1	-13	-158	-69	5	7	-15	268	262
3	9	-21	-159	68	4	1	19	204	220	4	6	-2	242	-247	5	1	-11	220	211	5	7	-13	-157	77
3	9	-19	-155	28	4	1	21	255	280	4	6	0	910	923	5	1	-9	367	352	5	7	-11	-150	77
3	9	-17	271	288	4	2	-26	-165	-132	4	6	2	438	-452	5	1	-7	826	-832	5	7	-9	245	226
3	9	-15	418	-444	4	2	-24	372	363	4	6	4	1162	-1174	5	1	-5	335	347	5	7	-7	457	-461
3	9	-13	364	332	4	2	-22	419	-358	4	6	6	676	665	5	1	-3	601	-590	5	7	-5	174	179
3	9	-11	655	-668	4	2	-20	404	-385	4	6	8	606	-596	5	1	-1	306	302	5	7	-3	524	-518
3	9	-9	-152	128	4	2	-18	639	644	4	6	10	556	590	5	1	1	678	676	5	7	-1	334	341
3	9	-7	611	615	4	2	-16	643	-662	4	6	12	663	686	5	1	3	309	-303	5	7	1	399	433
3	9	-5	523	-529	4	2	-14	945	897	4	6	14	268	-324	5	1	5	503	493	5	7	3	290	-280
3	9	-3	551	944	4	2	-12	-147	99	4	6	16	-158	-82	5	1	7	959	-938	5	7	5	468	474
3	9	-1	600	-604	4	2	-10	523	-495	4	6	18	515	-545	5	1	9	-163	55	5	7	7	641	-695
3	9	1	257	-243	4	2	-8	188	-170	4	7	-21	190	-192	5	1	11	-160	-72	5	7	9	-158	-40
3	9	3	-146	128	4	2	-6	728	-722	4	7	-19	319	329	5	1	13	-163	106	5	8	-12	598	-621
3	9	5	450	-455	4	2	-4	542	938	4	7	-17	410	-396	5	1	15	639	700	5	8	-10	238	208
3	9	7	791	766	4	2	-2	464	-476	4	7	-15	185	-220	5	2	-22	214	-186	5	8	-8	227	-152
3	9	9	158	-200	4	2	0	1373	1358	4	7	-13	193	213	5	2	-20	284	291	5	8	-6	414	419
3	9	11	420	436	4	2	2	-144	-100	4	7	-11	465	-476	5	2	-18	-166	103	5	8	-4	269	296
3	9	13	342	-326	4	2	4	1493	-1462	4	7	-9	1048	1034	5	2	-16	-161	99	5	8	-2	413	-436
3	9	15	436	-446	4	2	6	709	703	4	7	-7	201	-188	5	2	-14	-158	41	5	8	0	323	319
3	9	17	238	257	4	2	8	1001	-988	4	7	-5	-146	-124	5	2	-12	953	-954	5	8	2	770	-800
3	10	-18	-155	-7	4	2	10	563	549	4	7	-3	146	106	5	2	-10	650	637	5	8	4	-159	119
3	10	-16	264	-251	4	2	12	589	993	4	7	-1	1067	-1081	5	2	-8	367	-374	5	8	6	446	462
3	10	-14	181	120	4	2	14	236	-279	4	7	1	689	671	5	2	-6	397	409	5	9	-7	725	-743
3	10	-12	342	326	4	2	16	-156	57	4	7	3	197	-177	5	2	-4	825	808	5	9	-5	236	253
3	10	-10	216	-223	4	2	18	686	-706	4	7	5	618	619	5	2	-2	710	-670	5	9	-3	297	-321

Table 3. Continued.

H	K	L	F(O)	F(C)	H	K	L	F(O)	F(C)	H	K	L	F(C)	F(C)	H	K	L	F(O)	F(C)	H	K	L	F(O)	F(C)
6	9	-1	-163	150	6	1	-17	-165	47	6	2	-14	-164	-55	6	3	-11	267	234	6	4	-6	597	602
6	0	-16	209	201	6	1	-15	424	385	6	2	-12	-168	-91	6	3	-9	344	-353	6	4	-4	483	-494
6	0	-14	495	-511	6	1	-13	327	-328	6	2	-10	375	372	6	3	-7	-155	-77	6	4	-2	222	-216
6	0	-12	-170	129	6	1	-11	309	276	6	2	-8	-159	-119	6	3	-5	445	449	6	4	0	200	205
6	0	-10	566	523	6	1	-9	458	-459	6	2	-6	314	315	6	3	-3	279	-263	6	4	2	180	-136
6	0	-8	445	-443	6	1	-7	-161	-161	6	2	-4	646	-662	6	3	-1	545	556	6	4	4	480	527
6	0	-6	627	612	6	1	-5	386	364	6	2	-2	-155	130	6	3	1	403	-419	6	5	-11	173	168
6	0	-4	417	-412	6	1	-3	249	-236	6	2	0	-157	41	6	3	3	-161	-101	6	5	-9	367	-356
6	0	-2	441	-372	6	1	-1	771	762	6	2	2	342	-300	6	3	5	-162	-197	6	5	-7	-159	-41
6	0	0	-174	100	6	1	1	494	-526	6	2	4	853	858	6	3	7	222	-203	6	5	-5	230	225
6	0	2	-177	-46	6	1	3	-165	-22	6	2	6	256	-284	6	4	-12	203	211	6	5	-3	185	-199
6	0	4	575	553	6	1	5	-170	-148	6	2	8	-166	-74	6	4	-10	414	413	6	5	-1	679	688
6	0	6	-177	-157	6	1	7	384	-384	6	3	-15	303	292	6	4	-8	519	-509	6	5	1	458	-462
6	0	8	262	260	6	2	-16	185	189	6	3	-13	369	-383										

form, the two terminal sulphur atoms being located on the same side of the plane through the three middle atoms.

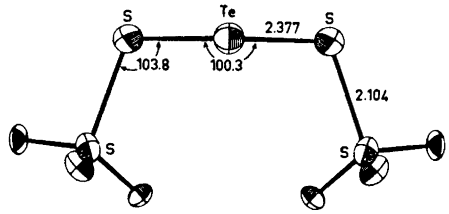

Fig. 1. The *cis* form of the telluropentathionate ion in $BaTe(S_2O_3)_2.2H_2O$ as seen along the *a* axis. The ellipsoids represent 50 % probability; the thermal parameters of the oxygen atoms are halved in size relative to those of the tellurium and sulphur atoms.

Table 4. Dimensions of the *cis* form of the telluro- and selenopentathionate ions in the dihydrates of the barium salts. For the left column X = Te, and for the right column X = Se. A prime denotes an atom generated by the mirror plane through X. Standard deviations are given in parentheses.

	$BaTe(S_2O_3)_2.2H_2O$	$BaSe(S_2O_3)_2.2H_2O$[4]
S(1) – S(2)	2.104(3) Å	2.096(3) Å
S(2) – X	2.377(3)	2.180(3)
∠S(1) – S(2) – X	103.79(9)°	103.96(11)°
∠S(2) – X – S(2′)	100.29(8)°	103.06(11)°
∠S(1)S(2)X/S(2)XS(2′)	103.8°	106.0°
S(1) – O(1)	1.446(6) Å	1.432(5) Å
S(1) – O(2)	1.447(5)	1.441(6)
S(1) – O(3)	1.443(5)	1.444(6)
∠S(2) – S(1) – O(1)	107.5(2)°	107.1(3)°
∠S(2) – S(1) – O(2)	100.3(3)°	99.1(3)°
∠S(2) – S(1) – O(3)	108.1(2)°	108.6(3)°
∠O(1) – S(1) – O(2)	113.0(3)°	113.1(3)°
∠O(1) – S(1) – O(3)	112.4(3)°	112.9(3)°
∠O(2) – S(1) – O(3)	114.5(3)°	114.7(3)°
∠XS(2)S(1)/S(2)S(1)O(1)	49.1°	50.6°
∠XS(2)S(1)/S(2)S(1)O(2)	167.3°	168.3°
∠XS(2)S(1)/S(2)S(1)O(3)	72.5°	71.7°
∠S(2)S(1)O(1)/S(2)S(1)O(2)	118.2°	117.7°
∠S(2)S(1)O(1)/S(2)S(1)O(3)	121.6°	122.3°
∠S(2)S(1)O(2)/S(2)S(1)O(3)	120.2°	120.0°

The dimensions of the ion calculated from the atomic coordinates of Table 1 are listed in the left column of Table 4. The standard deviations given include estimated uncertainties in unit cell dimensions. The non-bonded distances in the S(1) – S(2) – Te – S(2′) – S(1′) chain are: S(1) – Te = 3.530(2) Å, S(1) – (2′) = 4.779(3) Å, S(2) – S(2′) = 3.631(3) Å, S(1) – S(1′) = 5.003(3) Å.

Crystal structure determinations of barium selenopentathionate dihydrate [4,7] and trihydrate [5] have shown that the dimensions of the selenopentathionate ions are very nearly the same in these two hydrates. The ions have the same rotational isomeric form as the telluropentathionate ion in the present salt. For comparison, the dimensions of the selenopentathionate ion in the dihydrate of its barium salt are listed in the right column of Table 4.

The only significant difference in the dimensions of the two ions, except the S – X bond length and the S – X – S bond angle, is in the dihedral angles between the S – S – X and S – X – S planes. Variations in the degrees of rotation about S – X bonds are also found in the two halves of a S – S – X – S – S chain when symmetry is not crystallographically required.[3,8–10]

The difference between the S – Te and S – Se bond lengths is in accordance with the difference in the single covalent bond radii for tellurium, 1.37 Å, and selenium, 1.17 Å.[11] The bond lengths are in both cases 0.03 Å shorter than the sum of the single covalent bond radii for the atoms involved.

The S – Te – S bond angle is about 3° smaller than the S – Se – S bond angle which is again about 3° smaller than the middle S – S – S bond angle in barium pentathionates.[12] The same tendency of decreasing bond angles for the middle atom is found in the isomorphous series of penta-, selenopenta-, and telluropentathionate ions in the *trans* form.[8–10]

The bond lengths and angles of the sulphonate groups are in good agreement with those of the selenopentathionate ion and, as seen from the dihedral angles listed, there is no difference in the orientation of the S – O bonds relative to the X – S – S planes.

Each barium ion is surrounded by nine oxygen atoms, with Ba – O distances ranging from 2.747 Å to 2.938 Å. Three of the oxygen atoms coordinated to

Table 5. Distances (Å), and angles (°) between directions, from barium ion to oxygen atoms. Standard deviations of the distances and angles are 0.005 – 0.007 Å and 0.1 – 0.2°, respectively, except for the distance and angles involving $H_2O(2)$, which have standard deviations of 0.026 Å and 0.7°.

			I	II	III	IV	V	VI	VII	VIII
I	$H_2O(1)$	(x,y,z)	2.827							
II	$H_2O(1)$	$((x-1,y,z)$	2.938	120.4						
III	$H_2O(2)$	(x,y,z)	2.878	113.9	125.7					
IV	O(3)	(x,y,z)	2.770	71.1	60.7	145.6				
V	O(3)	$(x,\bar{y},z)$	2.770	71.1	60.7	145.6	68.8			
VI	O(1)	$(1-x,\frac{1}{2}-y,\frac{1}{2}-z)$	2.849	80.8	113.1	74.7	72.7	137.8		
VII	O(1)	$(1-x,-\frac{1}{2}+y,\frac{1}{2}-z)$	2.849	80.8	113.1	74.7	137.8	72.7	133.5	
VIII	O(2)	$(\bar{x},\frac{1}{2}-y,\frac{1}{2}-z)$	2.747	146.7	64.2	71.0	87.2	124.8	68.6	130.0
IX	O(2)	$(\bar{x},-\frac{1}{2}+y,\frac{1}{2}-z)$	2.747	146.7	64.2	71.0	124.8	87.2	130.0	68.6 66.5

one barium ion are from water molecules and the remaining six are from five different telluropentathionate ions. The distances and angles of the Ba – O coordination are listed in Table 5. Again there are only small deviations between these values and those given for the barium selenopentathionate hydrates.[4,5]

Fig. 2, which is a stereoscopic view as seen normal to the *a* crystal plane, shows the formation of layers through Ba – O coordination. The layers are

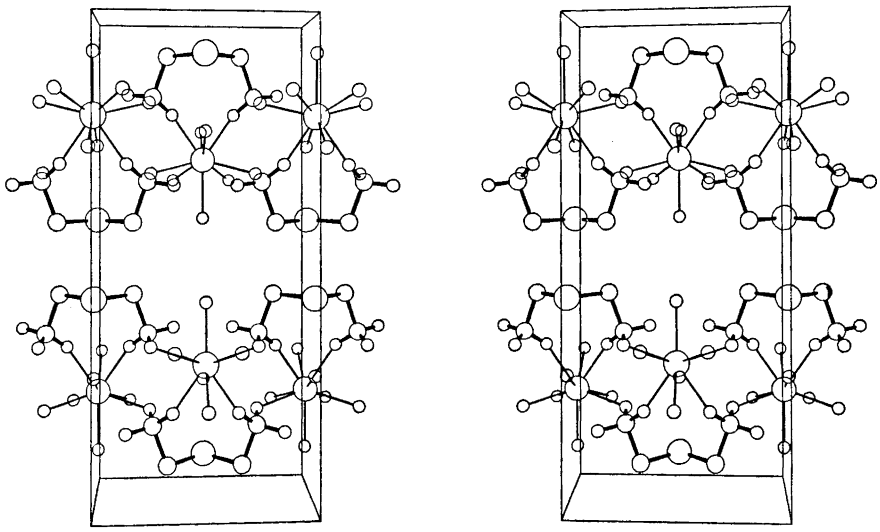

Fig. 2. A stereoscopic view of the cell packing in $BaTe(S_2O_3)_2.2H_2O$ as seen normal to the *a* crystal plane. The Ba – O coordination is indicated by the thin lines.

parallel to the *c* crystal plane and are the reason for the pronounced tendency of cleavage along this plane.[2] The relation between neighbour layers is through twofold rotation axes in the interfaces. Similar layers in barium selenopentathionate dihydrate and trihydrate are related through glide planes, and twofold screw axes, respectively.

The water molecule $H_2O(1)$ is coordinated to two barium ions and probably forms hydrogen bonds to O(1) and the image of O(1) across the mirror plane in which the water oxygen atom is located. The O – O distances are 3.067(7) Å, and the O – O – O angle is 121.5(2)°. The water molecule $H_2O(2)$ is coordinated to one barium ion, and does not seem to form any hydrogen bonds. The reason for the low occupancy factors and high termal parameters in the least squares refinement for the $H_2O(2)$ oxygen atoms in the present crystals and in the crystals of $BaSe(S_2O_3)_2.2H_2O$ [4] is probably that these water molecules are not so firmly held in the lattice. This is also shown by the fact that these water molecules are replaced by organic molecules when solvates are formed.[13]

Table 6 give the principal dimensions of the telluropentathionate ions as found in the crystals of $BaTe(S_2O_3)_2.2H_2O$ and $BaTe(S_2O_3)_2.3H_2O$.[3] The main

Table 6. Dimensions of the S – S – Te – S – S chain in the crystals of barium telluropentathionate dihydrate (*cis*) and trihydrate (*trans*). Standard deviations are given in parentheses.

	$BaTe(S_2O_3)_2.2H_2O$	$BaTe(S_2O_3)_2.3H_2O$[3]
S – S	2.104(3) Å	2.102(2) Å, 2.090(2) Å
S – Te	2.377(3) Å	2.384(2) Å, 2.392(2) Å
∠S – S – Te	103.79(9)°	103.08(5)°, 102.59(5)°
∠S – Te – S	100.29(8)°	96.02(4)°
∠SSTe/STeS	103.8°	87.7°, 98.7°

difference is the rotational isomerism: The rotations of the S – S bonds 87.7° and 98.7° to different sides of the plane through the three middle atoms in the trihydrate, and the rotations of the S – S bonds 103.8° to the same side of the plane in the dihydrate. The S – Te – S bond angles differ by 4.27°, whereas the remaining dimensions do not differ more from one ion to the other than they differ within the ion of the trihydrate, where symmetry is not crystallographically required. The larger dihedral angles and S – Te – S bond angle in the *cis* form might be due to space requirements of the sulphonate groups.

The closest interionic Te – Te, Te – S, and S – S approaches are 4.235(1) Å, 3.930(2) Å, and 3.631(3) Å, respectively.

REFERENCES

1. Foss, O. and Tjomsland, O. *Acta Chem. Scand.* **10** (1956) 416.
2. Foss, O. and Tjomsland, O. *Acta Chem. Scand.* **12** (1958) 52.
3. Gjerrestad, K. and Marøy, K. *Acta Chem. Scand.* **27** (1973) 1653.
4. Marøy, K. *Acta Chem. Scand.* **26** (1972) 36.
5. Marøy, K. *Acta Chem. Scand.* **26** (1972) 45.
6. Coppens, P., Leiserowitz, L. and Rabinovich, D. *Acta Cryst.* **18** (1965) 1035.
7. Foss, O. and Tjomsland, O. *Acta Chem. Scand.* **8** (1954) 1701.
8. Marøy, K. *Acta Chem. Scand.* **25** (1971) 2557.
9. Bøyum, K. and Marøy, K. *Acta Chem. Scand.* **25** (1971) 2569.
10. Marøy, K. *Acta Chem. Scand.* **25** (1971) 2580.
11. Pauling, L. *The Nature of the Chemical Bond*, 3rd. Ed., Cornell University Press, Ithaca 1960.
12. Foss, O. and Tjomsland, O. *Acta Chem. Scand.* **12** (1958) 44.
13. Foss, O. *Advan. Inorg. Chem. Radiochem.* **2** (1960) 237.

Received December 27, 1972.

ACTA CHEMICA SCANDINAVICA 27 (1973) 1705–1716

Refinement of the Crystal Structure of *trans*-Dichlorobis-(ethylenediamine)cobalt(III) Hexathionate Monohydrate

KJARTAN MARØY

Chemical Institute, University of Bergen, N-5000 Bergen, Norway

The crystal structure of *trans*-dichlorobis(ethylenediamine)-cobalt(III) hexathionate monohydrate, $[Co(en)_2Cl_2]_2S_6O_6.H_2O$, has been refined by a full-matrix least squares program using 1994 independent non-zero reflections. The data were collected by means of a single-crystal diffractometer using Mo$K\alpha$ radiation (Nb-filtered). The final conventional R value was 0.037.

The space group is $Pba2$ (No. 32) with two formula units per unit cell, and $a = 12.084(5)$ Å, $b = 19.160(8)$ Å, $c = 6.421(3)$ Å.

The six-membered sulphur chain of the hexathionate ion has the *trans-trans* rotational isomeric form. A twofold symmetry axis passes between the two middle sulphur atoms normal to the bond between these atoms. The dimensions of the chain are: S(1)–S(2) = 2.132(2) Å, S(2)–S(3) = 2.018(3) Å, S(3)–S(3′) = 2.069(3) Å, ∠S(1)–S(2)–S(3) = 105.08(11)°, S(2)–S(3)–S(3′) = 107.35(11)°. The three middle bonds, between divalent sulphur atoms, thus have alternating lengths, the central one being 0.05 Å longer than the two others. The SSS/SSS dihedral angle associated with the shorter bond is 85.7°, compared to 71.4° for the longer bond.

The cation is octahedral with Co–Cl = 2.299(2) and 2.261(2) Å, Co–N = 1.958(4) – 1.974(4) Å, ∠Cl–Co–Cl = 179.4(1)°, ∠Cl–Co–N = 88.8(2)° – 91.2(2)°, ∠N–Co–N = 85.9(2)° and 87.2(2)° for nitrogens from the same ethylenediamine group, and ∠N–Co–N = 92.4(2)° and 94.5(2)° for nitrogens from different ethylenediamine groups.

The hexathionate ion has a six-membered sulphur chain, where the two terminal sulphur atoms are each bonded to three oxygen atoms and form sulphonate groups. The remaining four sulphur atoms are divalent. In the crystal structure of $[Co(en)_2Cl_2]_2S_6O_6.H_2O$, determined on the basis of X-ray film data,[1] there was a small difference in the lengths of two independent divalent sulphur-divalent sulphur bonds. Mainly to decide whether this difference is significant, a refinement based on diffractometer data has been undertaken.

EXPERIMENTAL

The intensity data, and angles for unit cell dimensions, were measured on a Siemens automatic single-crystal diffractometer using Mo$K\alpha$ radiation (Nb-filtered) and a scintillation counter.

The crystal of $[Co(en)_2Cl_2]_2S_6O_6.H_2O$ used for the measurements was of a sample [2] that had been kept for thirteen years in a refrigerator, without showing any signs of decomposition. It was a well developed prism extended along the c axis. The distances between the (110) and between the ($\bar{1}\bar{1}0$) boundary faces were 0.173 and 0.193 mm, respectively, and the length of the crystal was reduced to 0.431 mm by cutting.

The crystal was mounted with the c axis approximately parallel to the ϕ axis of the diffractometer, and setting angles for all reflections were calculated from the θ, χ and ϕ angles of seven non-coplanar reciprocal vectors.

The five-value procedure and $\theta - 2\theta$ scan technique were used. The scan width was 0.70° for all reflections and maximum scan time per degree was 24 sec.

Two reflections of medium strength, 800 and 0 10 0, were measured two times each at intervals of 50 reflections. The net intensities were brought to a common scale by means of these reflections; the scale factors varied from 1.00 to 1.05.

Out of 2149 independent reflections attainable within $\theta = 29°$, only 155 were found to have net intensities below three times its standard deviation. These reflections were assigned an intensity equal to this limit and labelled as unobserved.

The linear absorption coefficient for Mo$K\alpha$ radiation is 19.6 cm^{-1}, and absorption corrections were carried out in addition to Lorentz and polarization corrections. The number of Gaussian grid points used for the absorption corrections were 8, 8, and 12 along the a, b, and c axes, respectively. The absorption factors by which the intensities were multiplied varied from 1.32 to 1.54.

The scattering factor curves used were those listed in *International Tables for X-Ray Crystallography*.[3] The curves for cobalt, chlorine, and sulphur were corrected for anomalous dispersion using the values given by Cromer,[4] and taking the amplitude as the corrected value.

The refinement was carried out with a full-matrix least squares program minimizing the function

$$r = \sum W(|F_o| - K|F_c|)^2$$

The intensity data were eventually corrected for secondary extinction with a program written by K. Åse of this Institute.

For further details concerning the data collection and the programs used, see Ref. 5.

The unit cell dimensions, calculated by means of a least squares program using the θ angles ($\theta = 22 - 28°$) of 11 reflections measured on the diffractometer, are $a = 12.084(5)$ Å, $b = 19.160(8)$ Å, $c = 6.421(3)$ Å.

The space group is $Pba2$ (No. 32) with two $[Co(en)_2Cl_2]_2S_6O_6.H_2O$ formula units per unit cell.[2]

REFINEMENT

Structure factor calculations were carried out using the positional and thermal parameters arrived at by the refinement of the film data,[1] except that isotropic thermal parameters were used for all atoms. On refinement of these parameters, the R value ($\sum||F_o| - |F_c||/\sum|F_o|$) converged at 0.093. Since only relative z coordinates are required for this space group, the z coordinate for cobalt was put equal to zero and was not included in the refinement.

Anisotropic thermal parameters were then introduced for the cobalt, chlorine, and sulphur atoms, whereby the reliability index was reduced to 0.053. The thermal parameters for two of the sulphonate oxygen atoms, the water oxygen atom, and the two carbon atoms of one ethylenediamine group were high compared to those of the other atoms. This is in accordance with the result of the refinement based on the film data.[1] When anisotropic thermal

parameters were used also for the lighter atoms, the R value was reduced to 0.040.

Secondary extinction corrections were then carried out according to Zachariasen.[6] The absorption term in the expression for F_{corr} was put equal to

Table 1. Atomic coordinates for *trans*-dichlorobis(ethylenediamine)cobalt(III) hexathionate monohydrate. Origin on a twofold axis. Standard deviations are given in parentheses.

	x	y	z
S(1)	0.25429(10)	0.09166(6)	0.50648(38)
S(2)	0.16421(13)	0.00393(8)	0.39242(34)
S(3)	0.07232(14)	−0.02888(9)	0.63589(38)
O(1)	0.33544(46)	0.06433(28)	0.64130(139)
O(2)	0.30101(51)	0.11618(28)	0.31087(105)
O(3)	0.17218(34)	0.13776(22)	0.59417(81)
Co	0.04158(5)	0.27620(3)	0
Cl(1)	0.16913(11)	0.29738(9)	0.24271(30)
Cl(2)	−0.08830(11)	0.25590(9)	−0.24602(29)
N(1)	0.08213(34)	0.17649(21)	−0.00163(97)
N(2)	−0.06717(35)	0.25312(27)	0.21536(72)
N(3)	0.00305(36)	0.37630(21)	−0.00721(99)
N(4)	0.14760(38)	0.29820(29)	−0.22361(87)
C(1)	−0.01291(54)	0.13735(28)	0.09967(109)
C(2)	−0.04811(47)	0.17955(30)	0.28668(96)
C(3)	0.08721(67)	0.41443(41)	−0.12442(192)
C(4)	0.14053(90)	0.37272(42)	−0.27471(175)
H_2O	½	0	0.31219(133)

Table 2. Thermal parameters expressed in the form $\exp[-2\pi^2(h^2a^{-2}U_{11}+\cdots 2hka^{-1}b^{-1}U_{12}+\cdots)]$. All values have been multiplied by 10^4. Standard deviations are given in parentheses.

	U_{11}	U_{22}	U_{33}	U_{12}	U_{23}	U_{13}
S(1)	288(5)	298(5)	653(9)	6(4)	11(9)	27(9)
S(2)	418(8)	378(7)	634(11)	−12(6)	−73(8)	−26(8)
S(3)	507(8)	413(8)	753(13)	−121(7)	174(9)	−70(10)
O(1)	705(35)	510(28)	1719(72)	11(26)	71(40)	−781(45)
O(2)	1047(47)	562(31)	1006(53)	−181(32)	−139(32)	627(44)
O(3)	392(22)	490(23)	555(28)	40(18)	−140(22)	72(22)
Co	198(2)	292(3)	236(3)	26(2)	−9(3)	−4(3)
Cl(1)	257(5)	550(8)	336(7)	−5(6)	−28(7)	−67(6)
Cl(2)	305(6)	481(8)	284(6)	−22(6)	13(7)	−68(6)
N(1)	395(21)	315(19)	384(23)	92(17)	−51(27)	9(30)
N(2)	232(18)	343(21)	266(26)	23(17)	24(20)	27(18)
N(3)	366(20)	298(19)	434(24)	19(16)	7(27)	25(32)
N(4)	249(20)	503(28)	326(29)	3(21)	9(24)	64(21)
C(1)	488(33)	306(26)	437(33)	25(24)	18(26)	−19(30)
C(2)	412(28)	359(27)	367(33)	9(23)	70(24)	6(26)
C(3)	682(49)	490(40)	1415(91)	68(37)	355(53)	493(62)
C(4)	1261(83)	498(42)	1069(80)	−147(47)	70(50)	763(72)
H_2O	752(47)	819(54)	607(52)	294(43)	0	0

Table 3. Observed and calculated structure amplitudes (× 10) for *trans*-dichlorobis-(ethylenediamine)cobalt(III) hexathionate monohydrate. A minus sign on $F(O)$ indicates an unobserved reflection.

H	K	L	F(O)	F(C)	H	K	L	F(O)	F(C)	H	K	L	F(O)	F(C)	H	K	L	F(O)	F(C)	H	K	L	F(O)	F(C)
0	4	0	1137	1244	4	9	0	608	587	8	8	0	75	78	13	4	0	140	136	2	16	1	261	263
0	6	0	565	567	4	10	0	158	176	8	9	0	271	267	13	5	0	286	279	2	17	1	262	255
0	8	0	1055	1036	4	11	0	164	147	8	10	0	143	133	13	6	0	-41	22	2	18	1	237	238
0	10	0	546	537	4	12	0	56	44	8	11	0	262	290	13	7	0	52	44	2	19	1	130	143
0	12	0	-37	27	4	13	0	336	356	8	12	0	153	137	13	8	0	82	75	2	20	1	121	128
0	14	0	212	225	4	14	0	89	67	8	13	0	95	88	13	9	0	199	193	2	21	1	232	234
0	16	0	92	89	4	15	0	236	237	8	14	0	-36	19	13	10	0	-52	29	2	22	1	363	357
0	18	0	54	34	4	16	0	417	421	8	15	0	155	155	13	11	0	230	213	2	23	1	58	64
0	20	0	93	93	4	17	0	554	556	8	16	0	-55	7	13	12	0	-39	4	2	24	1	47	40
0	22	0	256	247	4	18	0	114	121	8	17	0	79	70	13	13	0	168	169	2	25	1	87	91
0	24	0	93	77	4	19	0	447	453	8	18	0	83	82	13	14	0	233	221	3	1	1	344	337
0	26	0	52	44	4	20	0	231	154	8	19	0	-40	15	13	15	0	123	134	3	2	1	477	448
1	2	0	474	482	4	21	0	267	265	8	20	0	64	103	13	16	0	-45	46	3	3	1	1101	1110
1	3	0	1014	1059	4	22	0	256	241	8	21	0	-40	15	14	0	0	292	295	3	4	1	671	678
1	4	0	1127	1113	4	23	0	216	212	8	22	0	88	86	14	1	0	118	106	3	5	1	164	147
1	5	0	-40	59	4	24	0	92	91	9	1	0	256	306	14	2	0	225	214	3	6	1	417	392
1	6	0	1022	1048	4	25	0	54	54	9	2	0	-34	41	14	3	0	84	59	3	7	1	939	954
1	7	0	1550	1569	5	1	0	411	380	9	3	0	536	540	14	4	0	70	69	3	8	1	495	493
1	8	0	35	8	5	2	0	-27	6	9	4	0	965	963	14	5	0	196	213	3	9	1	291	268
1	9	0	1205	1123	5	3	0	405	162	9	5	0	275	281	14	6	0	173	177	3	10	1	466	462
1	10	0	305	355	5	4	0	79	53	9	6	0	203	206	14	7	0	238	235	3	11	1	518	543
1	11	0	748	736	5	5	0	243	264	9	7	0	867	917	14	8	0	49	39	3	12	1	674	687
1	12	0	-30	7	5	6	0	471	455	9	8	0	213	212	14	9	0	137	134	3	13	1	326	314
1	13	0	426	413	5	7	0	305	317	9	9	0	115	96	14	10	0	193	194	3	14	1	45	49
1	14	0	320	315	5	8	0	288	266	9	10	0	341	344	14	11	0	127	139	3	15	1	381	374
1	15	0	127	109	5	9	0	74	79	9	11	0	373	376	14	12	0	-40	9	3	16	1	204	195
1	16	0	108	109	5	10	0	744	758	9	12	0	430	424	14	13	0	-40	14	3	17	1	206	196
1	17	0	210	203	5	11	0	79	66	9	13	0	-36	0	15	1	0	48	51	3	18	1	186	185
1	18	0	113	109	5	12	0	405	407	9	14	0	-36	21	15	2	0	-41	43	3	19	1	135	103
1	19	0	50	57	5	13	0	349	351	9	15	0	-42	16	15	3	0	167	165	3	20	1	185	190
1	20	0	58	56	5	14	0	313	323	9	16	0	217	211	15	4	0	236	227	3	21	1	191	191
1	21	0	-40	41	5	15	0	54	114	9	17	0	115	125	15	5	0	150	159	3	22	1	78	85
1	22	0	147	147	5	16	0	111	155	9	18	0	253	243	15	6	0	187	184	3	23	1	-38	23
1	23	0	-40	9	5	17	0	131	52	9	19	0	68	69	15	7	0	319	321	3	24	1	-35	24
1	24	0	136	127	5	18	0	265	300	9	20	0	74	63	15	8	0	102	83	3	25	1	105	102
1	25	0	-41	15	5	19	0	-35	7	9	21	0	71	70	15	9	0	118	113	4	0	1	801	781
1	26	0	135	97	5	20	0	147	152	10	0	0	670	670	15	10	0	140	129	4	1	1	865	877
2	0	0	1081	895	-5	21	0	207	195	10	1	0	120	123	16	0	0	101	122	4	2	1	319	316
2	1	0	795	675	5	22	0	110	111	10	2	0	171	163	16	1	0	280	279	4	3	1	514	515
2	2	0	1214	1205	5	23	0	-41	20	10	3	0	265	263	16	2	0	196	197	4	4	1	416	447
2	3	0	327	337	5	24	0	90	55	10	4	0	310	288	16	3	0	253	257	4	5	1	399	389
2	4	0	1152	1228	6	0	0	123	111	10	5	0	543	537	16	4	0	238	226	4	6	1	308	339
2	5	0	679	689	6	1	0	432	406	10	6	0	132	95	16	5	0	191	182	4	7	1	340	309
2	6	0	78	91	6	2	0	167	172	10	7	0	415	407	16	6	0	-43	6	4	8	1	517	506
2	7	0	347	316	6	3	0	721	721	10	8	0	135	116	0	0	1	146	139	4	9	1	742	732
2	8	0	935	914	6	4	0	159	159	10	9	0	426	419	0	4	1	266	322	4	10	1	376	396
2	9	0	802	772	6	5	0	427	470	10	10	0	431	415	0	6	1	548	518	4	11	1	238	232
2	10	0	691	701	6	6	0	883	904	10	11	0	140	141	0	8	1	123	117	4	12	1	354	401
2	11	0	605	596	6	7	0	281	217	10	12	0	-38	19	0	10	1	838	819	4	13	1	189	203
2	12	0	201	212	6	8	0	-35	22	10	13	0	125	131	0	12	1	487	486	4	14	1	337	334
2	13	0	555	553	6	9	0	-35	16	10	14	0	251	269	0	14	1	359	358	4	15	1	346	346
2	14	0	127	107	6	10	0	492	471	10	15	0	44	56	0	16	1	201	212	4	16	1	134	149
2	15	0	443	425	6	11	0	45	54	10	16	0	258	293	0	18	1	437	435	4	17	1	220	213
2	16	0	148	137	6	12	0	486	516	10	17	0	84	78	0	20	1	421	431	4	18	1	268	274
2	17	0	156	142	6	13	0	316	318	10	18	0	155	140	0	22	1	108	104	4	19	1	243	249
2	18	0	155	163	6	14	0	761	757	10	19	0	87	81	0	24	1	139	141	4	20	1	177	181
2	19	0	232	207	6	15	0	283	277	10	20	0	-46	58	1	1	1	665	686	4	21	1	259	254
2	20	0	444	455	6	16	0	393	355	11	1	0	137	128	1	2	1	918	923	4	22	1	-39	20
2	21	0	75	75	6	17	0	338	334	11	2	0	145	132	1	3	1	453	416	4	23	1	125	130
2	22	0	-35	24	6	18	0	304	302	11	3	0	66	66	1	4	1	562	574	4	24	1	44	47
2	23	0	137	133	6	19	0	231	234	11	4	0	155	170	1	5	1	763	777	4	25	1	91	95
2	24	0	141	138	6	20	0	96	96	11	5	0	164	176	1	6	1	422	446	5	1	1	34	11
2	25	0	90	93	6	21	0	156	154	11	6	0	226	229	1	7	1	590	588	5	2	1	306	297
3	1	0	50	55	6	22	0	-39	4	11	7	0	149	142	1	8	1	682	709	5	3	1	597	591
3	2	0	1161	1159	6	23	0	132	127	11	8	0	180	174	1	9	1	922	949	5	4	1	301	264
3	3	0	821	788	6	24	0	-44	10	11	9	0	248	232	1	10	1	264	236	5	5	1	271	265
3	4	0	545	466	7	1	0	165	154	11	10	0	76	65	1	11	1	596	614	5	6	1	351	360
3	5	0	372	376	7	2	0	523	513	11	11	0	232	221	1	12	1	249	243	5	7	1	222	232
3	6	0	351	383	7	3	0	-39	37	11	12	0	135	143	1	13	1	412	439	5	8	1	1022	1060
3	7	0	614	613	7	4	0	650	652	11	13	0	211	210	1	14	1	280	286	5	9	1	341	331
3	8	0	492	533	7	5	0	231	235	11	14	0	222	233	1	15	1	259	260	5	10	1	320	311
3	9	0	718	738	7	6	0	722	733	11	15	0	146	138	1	16	1	130	124	5	11	1	72	64
3	10	0	526	538	7	7	0	-64	1	11	16	0	52	83	1	17	1	257	258	5	12	1	376	378
3	11	0	234	224	7	8	0	933	924	11	17	0	-35	5	1	18	1	105	101	5	13	1	122	126
3	12	0	128	132	7	9	0	335	336	11	18	0	56	64	1	19	1	49	44	5	14	1	415	413
3	13	0	721	726	7	10	0	328	333	11	19	0	-41	27	1	20	1	76	69	5	15	1	88	82
3	14	0	351	403	7	11	0	39	46	12	0	0	485	506	1	21	1	165	161	5	16	1	198	201
3	15	0	154	159	7	12	0	144	147	12	1	0	45	25	1	22	1	80	77	5	17	1	222	218
3	16	0	114	111	7	13	0	451	462	12	2	0	256	278	1	23	1	121	125	5	18	1	170	175
3	17	0	324	345	7	14	0	352	349	12	3	0	110	98	1	24	1	161	159	5	19	1	55	33
3	18	0	216	209	7	15	0	-41	22	12	4	0	56	47	1	25	1	44	46	5	20	1	90	92
3	19	0	86	74	7	16	0	54	58	12	5	0	70	68	2	0	1	2010	2110	5	21	1	47	43
3	20	0	92	91	7	17	0	165	160	12	6	0	66	65	2	1	1	736	765	5	22	1	87	88
3	21	0	72	65	7	18	0	77	71	12	7	0	-35	30	2	2	1	623	635	5	23	1	76	77
3	22	0	155	167	7	19	0	78	80	12	8	0	70	76	2	3	1	513	530	5	24	1	195	193
3	23	0	219	210	7	20	0	112	116	12	9	0	51	22	2	4	1	483	458	6	0	1	935	868
3	24	0	156	157	7	21	0	171	174	12	10	0	144	136	2	5	1	1062	1094	6	1	1	715	735
3	25	0	46	23	7	22	0	-44	44	12	11	0	33	34	2	6	1	720	719	6	2	1	51	46
4	0	0	255	118	7	23	0	62	61	12	12	0	218	214	2	7	1	376	336	6	3	1	548	536
4	1	0	458	373	8	0	0	723	654	12	13	0	90	100	2	8	1	503	471	6	4	1	761	774
4	2	0	109	69	8	1	0	1045	1067	12	14	0	132	135	2	9	1	272	264	6	5	1	490	460
4	3	0	357	324	8	2	0	434	436	12	15	0	-41	33	2	10	1	347	375	6	6	1	442	435
4	4	0	731	665	8	3	0	746	782	12	16	0	185	193	2	11	1	115	121	6	7	1	288	297
4	5	0	61	77	8	4	0	776	778	12	17	0	-42	11	2	12	1	125	120	6	8	1	262	273
4	6	0	452	434	8	5	0	625	641	13	1	0	85	96	2	13	1	153	162	6	9	1	103	95
4	7	0	436	456	8	6	0	154	156	13	2	0	121	125	2	14	1	393	381	6	10	1	226	236
4	8	0	159	164	8	7	0	318	320	13	3	0	68	73	2	15	1	128	115	6	11	1	259	268

Table 3. Continued.

H	K	L	F(O)	F(C)	H	K	L	F(O)	F(C)	H	K	L	F(O)	F(C)	H	K	L	F(O)	F(C)	H	K	L	F(O)	F(C)
6	12	1	210	206	11	6	1	150	148	1	17	2	276	264	5	22	2	81	75	10	13	2	308	310
6	13	1	140	131	11	7	1	334	321	1	18	2	257	245	5	23	2	-40	31	10	14	2	105	105
6	14	1	226	236	11	8	1	211	205	1	19	2	168	166	5	24	2	77	75	10	15	2	154	156
6	15	1	313	307	11	9	1	220	215	1	20	2	96	97	6	0	2	313	359	10	16	2	240	247
6	16	1	234	224	11	10	1	201	202	1	21	2	185	195	6	1	2	608	791	10	17	2	136	140
6	17	1	236	275	11	11	1	149	143	1	22	2	-40	17	6	2	2	492	445	10	18	2	132	131
6	18	1	243	259	11	12	1	105	103	1	23	2	146	141	6	3	2	528	520	10	19	2	99	94
6	19	1	236	242	11	13	1	251	251	1	24	2	89	76	6	4	2	675	672	11	1	2	173	175
6	20	1	135	129	11	14	1	135	131	1	25	2	165	173	6	5	2	336	337	11	2	2	352	350
6	21	1	154	152	11	15	1	159	158	2	0	2	580	564	6	6	2	366	346	11	3	2	272	271
6	22	1	-40	43	11	16	1	93	92	2	1	2	642	646	6	7	2	159	161	11	4	2	113	121
6	23	1	115	117	11	17	1	146	144	2	2	2	905	907	6	8	2	766	783	11	5	2	402	395
6	24	1	72	61	11	18	1	90	89	2	3	2	615	598	6	9	2	152	166	11	6	2	187	192
7	1	1	634	641	11	19	1	-42	44	2	4	2	301	336	6	10	2	699	703	11	7	2	402	420
7	2	1	320	333	12	0	1	567	561	2	5	2	657	645	6	11	2	136	149	11	8	2	294	284
7	3	1	212	229	12	1	1	167	171	2	6	2	208	235	6	12	2	211	207	11	9	2	313	301
7	4	1	634	631	12	2	1	99	81	2	7	2	605	618	6	13	2	227	228	11	10	2	90	90
7	5	1	111	122	12	3	1	218	210	2	8	2	323	315	6	14	2	183	186	11	11	2	207	197
7	6	1	542	511	12	4	1	323	310	2	9	2	591	599	6	15	2	166	171	11	12	2	151	146
7	7	1	346	336	12	5	1	85	74	2	10	2	66	68	6	16	2	288	287	11	13	2	228	238
7	8	1	153	155	12	6	1	329	309	2	11	2	507	491	6	17	2	207	217	11	14	2	114	107
7	9	1	-45	52	12	7	1	86	83	2	12	2	786	775	6	18	2	55	65	11	15	2	163	166
7	10	1	634	641	12	8	1	169	174	2	13	2	370	394	6	19	2	281	277	11	16	2	51	70
7	11	1	255	269	12	9	1	49	43	2	14	2	421	408	6	20	2	54	55	11	17	2	68	68
7	12	1	451	447	12	10	1	319	323	2	15	2	144	159	6	21	2	167	164	11	18	2	66	69
7	13	1	31	51	12	11	1	64	70	2	16	2	55	108	6	22	2	71	82	12	0	2	344	386
7	14	1	220	225	12	12	1	96	103	2	17	2	65	69	6	23	2	91	97	12	1	2	85	97
7	15	1	140	132	12	13	1	45	26	2	18	2	351	373	7	1	2	362	356	12	2	2	614	618
7	16	1	156	167	12	14	1	256	263	2	19	2	170	172	7	2	2	212	239	12	3	2	42	44
7	17	1	137	147	12	15	1	94	94	2	20	2	334	322	7	3	2	362	380	12	4	2	604	596
7	18	1	205	209	12	16	1	255	246	2	21	2	116	124	7	4	2	171	169	12	5	2	98	93
7	19	1	71	67	12	17	1	-41	31	2	22	2	-36	35	7	5	2	383	363	12	6	2	237	225
7	20	1	111	113	13	1	1	-43	13	2	23	2	81	79	7	6	2	62	79	12	7	2	97	84
7	21	1	175	91	13	2	1	217	211	2	24	2	90	96	7	7	2	177	183	12	8	2	142	126
7	22	1	95	83	13	3	1	245	235	2	25	2	-35	28	7	8	2	505	502	12	9	2	65	68
7	23	1	46	42	13	4	1	207	205	3	1	2	768	782	7	9	2	176	177	12	10	2	147	157
8	0	1	232	243	13	5	1	134	126	3	2	2	209	213	7	10	2	232	227	12	11	2	49	57
8	1	1	367	361	13	6	1	180	195	3	3	2	1162	1146	7	11	2	50	63	12	12	2	195	204
8	2	1	474	482	13	7	1	323	324	3	4	2	163	193	7	12	2	273	269	12	13	2	56	53
8	3	1	530	583	13	8	1	96	109	3	5	2	865	863	7	13	2	-36	23	12	14	2	161	159
8	4	1	74	75	13	9	1	160	173	3	6	2	367	391	7	14	2	419	421	12	15	2	-40	10
8	5	1	241	256	13	10	1	118	116	3	7	2	660	633	7	15	2	117	129	12	16	2	92	89
8	6	1	451	458	13	11	1	152	158	3	8	2	926	947	7	16	2	203	192	13	1	2	43	48
8	7	1	309	307	13	12	1	101	96	3	9	2	701	711	7	17	2	166	172	13	2	2	189	174
8	8	1	215	209	13	13	1	213	205	3	10	2	522	505	7	18	2	-39	21	13	3	2	196	202
8	9	1	340	339	13	14	1	74	77	3	11	2	435	441	7	19	2	96	93	13	4	2	78	92
8	10	1	316	305	13	15	1	139	144	3	12	2	443	442	7	20	2	53	53	13	5	2	378	363
8	11	1	236	216	14	0	1	174	169	3	13	2	440	434	7	21	2	43	45	13	6	2	102	101
8	12	1	165	167	14	1	1	245	248	3	14	2	502	495	7	22	2	105	106	13	7	2	254	257
8	13	1	306	296	14	2	1	226	215	3	15	2	418	415	8	0	2	347	357	13	8	2	206	204
8	14	1	80	70	14	3	1	226	234	3	16	2	115	127	8	1	2	84	94	13	9	2	213	224
8	15	1	260	261	14	4	1	334	319	3	17	2	121	112	8	2	2	103	123	13	10	2	-39	4
8	16	1	277	262	14	5	1	142	157	3	18	2	92	94	8	3	2	49	50	13	11	2	187	197
8	17	1	220	217	14	6	1	79	91	3	19	2	65	66	8	4	2	269	283	13	12	2	96	83
8	18	1	111	107	14	7	1	69	48	3	20	2	164	166	8	5	2	58	65	13	13	2	177	176
8	19	1	236	240	14	8	1	94	88	3	21	2	89	89	8	6	2	241	235	13	14	2	-40	25
8	20	1	81	90	14	9	1	96	83	3	22	2	55	46	8	7	2	102	103	14	0	2	267	272
8	21	1	104	107	14	10	1	135	141	3	23	2	76	71	8	8	2	41	31	14	1	2	134	135
8	22	1	132	137	14	11	1	55	52	3	24	2	91	88	8	9	2	-33	23	14	2	2	142	146
9	1	1	306	313	14	12	1	153	162	3	25	2	-39	26	8	10	2	172	169	14	3	2	59	60
9	2	1	395	390	14	13	1	111	105	4	0	2	1174	1214	8	11	2	49	47	14	4	2	176	171
9	3	1	255	255	15	1	1	57	53	4	1	2	1433	1441	8	12	2	182	185	14	5	2	-40	17
9	4	1	175	201	15	2	1	151	153	4	2	2	757	759	8	13	2	151	151	14	6	2	250	244
9	5	1	442	455	15	3	1	176	175	4	3	2	1357	1365	8	14	2	208	211	14	7	2	80	77
9	6	1	310	317	15	4	1	68	50	4	4	2	197	198	8	15	2	288	291	14	8	2	123	135
9	7	1	238	218	15	5	1	190	188	4	5	2	733	750	8	16	2	115	113	14	9	2	169	175
9	8	1	308	270	15	6	1	142	135	4	6	2	709	743	8	17	2	317	327	14	10	2	-40	31
9	9	1	421	421	15	7	1	129	123	4	7	2	185	190	8	18	2	269	274	14	11	2	161	172
9	10	1	211	213	15	8	1	179	187	4	8	2	250	255	8	19	2	258	259	14	12	2	76	74
9	11	1	211	202	15	9	1	144	146	4	9	2	322	325	8	20	2	165	157	15	1	2	117	108
9	12	1	125	137	15	10	1	85	84	4	10	2	257	246	8	21	2	240	239	15	2	2	63	55
9	13	1	234	242	16	0	1	159	155	4	11	2	194	206	8	22	2	86	96	15	3	2	92	98
9	14	1	308	306	16	1	1	173	177	4	12	2	187	171	9	1	2	145	165	15	4	2	143	135
9	15	1	61	64	16	2	1	145	150	4	13	2	68	59	9	2	2	113	120	15	5	2	96	88
9	16	1	100	93	16	3	1	136	137	4	14	2	127	123	9	3	2	143	133	15	6	2	155	142
9	17	1	177	176	16	4	1	81	60	4	15	2	108	110	9	4	2	347	349	15	7	2	94	94
9	18	1	-40	49	16	5	1	115	113	4	16	2	213	219	9	5	2	173	182	15	8	2	66	62
9	19	1	67	69	0	0	2	412	415	4	17	2	76	64	9	6	2	294	293	15	9	2	81	84
9	20	1	90	90	0	2	2	463	482	4	18	2	82	86	9	7	2	119	108	16	0	2	103	99
9	21	1	47	48	0	4	2	677	667	4	19	2	151	147	9	8	2	70	61	16	1	2	64	54
10	0	1	241	213	0	6	2	338	307	4	20	2	94	78	9	9	2	152	150	16	2	2	-40	27
10	1	1	380	367	0	8	2	151	162	4	21	2	114	116	9	10	2	259	256	C	0	3	1177	1197
10	2	1	562	560	0	10	2	661	673	4	22	2	112	103	9	11	2	283	296	0	2	3	240	230
10	3	1	240	247	0	12	2	402	414	4	23	2	95	93	9	12	2	250	231	0	4	3	762	800
10	4	1	470	475	0	14	2	455	454	4	24	2	41	32	9	13	2	273	271	0	6	3	374	345
10	5	1	214	224	0	16	2	669	664	5	1	2	191	196	9	14	2	-38	19	0	8	3	681	704
10	6	1	140	137	0	18	2	516	538	5	2	2	256	241	9	15	2	272	283	0	10	3	127	126
10	7	1	285	290	0	20	2	380	381	5	3	2	477	455	9	16	2	69	76	0	12	3	595	572
10	8	1	131	91	0	22	2	488	487	5	4	2	903	914	9	17	2	207	203	C	14	3	228	217
10	9	1	43	13	0	24	2	158	152	5	5	2	266	262	9	18	2	65	72	0	16	3	263	264
10	10	1	166	173	1	1	2	427	408	5	6	2	756	765	9	19	2	105	102	0	18	3	418	416
10	11	1	157	161	1	3	2	734	728	5	7	2	208	196	9	20	2	105	107	C	20	3	446	449
10	12	1	269	307	1	3	2	73	83	5	8	2	576	577	9	21	2	87	95	0	22	3	106	100
10	13	1	82	79	1	4	2	258	216	5	9	2	113	122	10	0	2	466	451	C	24	3	123	134
10	14	1	148	149	1	5	2	134	136	5	10	2	605	806	10	1	2	139	119	1	1	3	115	106
10	15	1	124	121	1	6	2	170	173	5	11	2	222	220	10	2	2	200	204	1	2	3	116	120
10	16	1	167	171	1	7	2	357	432	5	12	2	552	559	10	3	2	171	167	1	3	3	406	421
10	17	1	118	109	1	8	2	240	243	5	13	2	151	151	10	4	2	275	303	1	4	3	247	234
10	18	1	211	205	1	9	2	420	426	5	14	2	108	113	10	5	2	207	220	1	5	3	71	65
10	19	1	93	86	1	10	2	409	413	5	15	2	300	291	10	6	2	498	503	1	6	3	500	499
10	20	1	165	163	1	11	2	529	545	5	16	2	47	52	10	7	2	165	164	1	7	3	472	464
11	1	1	96	94	1	12	2	457	455	5	17	2	195	195	10	8	2	241	242	1	8	3	280	280
11	2	1	123	120	1	13	2	340	335	5	18	2	73	72	10	9	2	229	230	1	9	3	639	641
11	3	1	252	264	1	14	2	97	106	5	19	2	132	131	10	10	2	74	67	1	10	3	81	90
11	4	1	237	229	1	15	2	320	313	5	20	2	124	128	10	11	2	276	277	1	11	3	637	628
11	5	1	352	356	1	16	2	253	257	5	21	2	42	41	10	12	2	155	164	1	12	3	123	122

Table 3. Continued.

H	K	L	F(O)	F(C)	H	K	L	F(C)	F(C)	H	K	L	F(C)	F(C)	H	K	L	F(O)	F(C)	H	K	L	F(O)	F(C)
1	12	3	367	379	5	22	3	72	71	11	1	3	57	49	2	8	4	405	388	7	3	4	157	187
1	14	3	322	310	5	23	3	-40	20	11	2	3	77	81	2	9	4	331	329	7	4	4	323	318
1	15	3	256	260	6	0	3	254	315	11	3	3	142	151	2	10	4	229	229	7	5	4	142	139
1	16	3	54	52	6	1	3	489	496	11	4	3	205	198	2	11	4	441	447	7	6	4	472	461
1	17	3	173	171	6	2	3	674	665	11	5	3	336	344	2	12	4	48	47	7	7	4	170	168
1	18	3	133	125	6	3	3	513	526	11	6	3	145	158	2	13	4	324	327	7	8	4	563	558
1	19	3	158	165	6	4	3	183	151	11	7	3	248	242	2	14	4	158	151	7	9	4	50	23
1	20	3	137	138	6	5	3	341	349	11	8	3	-38	20	2	15	4	196	203	7	10	4	313	318
1	21	3	67	59	6	6	3	465	469	11	9	3	226	230	2	16	4	112	113	7	11	4	210	209
1	22	3	54	55	6	7	3	261	276	11	10	3	103	87	2	17	4	222	219	7	12	4	145	144
1	23	3	123	119	6	8	3	251	265	11	11	3	261	255	2	18	4	339	342	7	13	4	72	87
1	24	3	85	76	6	9	3	72	73	11	12	3	153	155	2	19	4	90	97	7	14	4	239	228
2	0	3	1126	1115	6	10	3	218	214	11	13	3	176	175	2	20	4	175	180	7	15	4	250	254
2	1	3	541	548	6	11	3	63	62	11	14	3	59	61	2	21	4	132	133	7	16	4	53	49
2	2	3	567	557	6	12	3	268	255	11	15	3	155	170	2	22	4	102	103	7	17	4	53	58
2	3	3	666	661	6	13	3	241	251	11	16	3	73	70	2	23	4	-41	8	7	18	4	-40	40
2	4	3	411	396	6	14	3	112	105	11	17	3	55	63	3	1	4	145	148	7	19	4	85	86
2	5	3	115	94	6	15	3	243	245	12	0	3	310	305	3	2	4	223	193	7	20	4	57	53
2	6	3	340	356	6	16	3	76	67	12	1	3	192	195	3	3	4	58	63	8	0	4	148	149
2	7	3	421	387	6	17	3	255	255	12	2	3	332	339	3	4	4	129	146	8	1	4	704	706
2	8	3	-30	29	6	18	3	103	107	12	3	3	54	45	3	5	4	239	228	8	2	4	580	559
2	9	3	73	77	6	19	3	163	155	12	4	3	155	173	3	6	4	55	44	8	3	4	508	516
2	10	3	276	264	6	20	3	126	125	12	5	3	92	85	3	7	4	231	221	8	4	4	325	336
2	11	3	171	174	6	21	3	144	149	12	6	3	310	310	3	8	4	578	579	8	5	4	391	389
2	12	3	150	154	6	22	3	157	156	12	7	3	64	65	3	9	4	110	116	8	6	4	81	72
2	13	3	63	55	7	1	3	333	320	12	8	3	242	238	3	10	4	90	84	8	7	4	367	363
2	14	3	86	80	7	2	3	131	126	12	9	3	99	93	3	11	4	452	450	8	8	4	74	62
2	15	3	79	85	7	3	3	167	166	12	10	3	136	136	3	12	4	157	160	8	9	4	39	28
2	16	3	412	411	7	4	3	491	515	12	11	3	-40	29	3	13	4	180	172	8	10	4	103	109
2	17	3	134	132	7	5	3	275	265	12	12	3	221	221	3	14	4	126	123	8	11	4	-37	11
2	18	3	144	149	7	6	3	459	472	12	13	3	-41	24	3	15	4	323	324	8	12	4	89	89
2	19	3	205	206	7	7	3	146	156	12	14	3	124	114	3	16	4	-35	41	8	13	4	153	156
2	20	3	236	240	7	8	3	251	210	12	15	3	-42	11	3	17	4	112	114	8	14	4	82	84
2	21	3	103	103	7	9	3	141	137	13	1	3	133	137	3	18	4	102	104	8	15	4	95	87
2	22	3	136	147	7	10	3	361	363	13	2	3	57	54	3	19	4	124	123	8	16	4	-43	28
2	23	3	111	117	7	11	3	76	76	13	3	3	76	86	3	20	4	78	78	8	17	4	73	69
2	24	3	76	74	7	12	3	356	353	13	4	3	166	159	3	21	4	105	105	8	18	4	106	107
3	1	3	303	298	7	13	3	124	122	13	5	3	195	191	3	22	4	-42	42	8	19	4	-41	28
3	2	3	158	161	7	14	3	148	155	13	6	3	194	206	4	0	4	364	350	9	1	4	161	168
3	3	3	346	330	7	15	3	64	72	13	7	3	210	205	4	1	4	-32	34	9	2	4	73	78
3	4	3	339	315	7	16	3	193	206	13	8	3	136	140	4	2	4	322	329	9	3	4	108	121
3	5	3	717	720	7	17	3	48	59	13	9	3	203	209	4	3	4	119	111	9	4	4	220	235
3	6	3	554	548	7	18	3	134	131	13	10	3	110	96	4	4	4	59	69	9	5	4	511	511
3	7	3	228	237	7	19	3	123	124	13	11	3	148	146	4	5	4	127	134	9	6	4	379	363
3	8	3	44	40	7	20	3	121	123	13	12	3	46	48	4	6	4	179	179	9	7	4	227	210
3	9	3	558	558	7	21	3	60	51	13	13	3	138	142	4	7	4	131	144	9	8	4	75	81
3	10	3	729	712	8	0	3	562	576	14	0	3	80	97	4	8	4	131	144	9	9	4	326	329
3	11	3	416	420	8	1	3	293	269	14	1	3	230	219	4	9	4	200	208	9	10	4	270	290
3	12	3	305	300	8	2	3	178	183	14	2	3	255	254	4	10	4	201	215	9	11	4	98	105
3	13	3	275	272	8	3	3	305	300	14	3	3	207	203	4	11	4	238	229	9	12	4	184	179
3	14	3	160	157	8	4	3	144	127	14	4	3	204	195	4	12	4	82	79	9	13	4	112	104
3	15	3	118	118	8	5	3	344	348	14	5	3	107	104	4	13	4	115	129	9	14	4	98	102
3	16	3	132	130	8	6	3	167	166	14	6	3	62	69	4	14	4	124	125	9	15	4	58	54
3	17	3	95	98	8	7	3	224	232	14	7	3	101	78	4	15	4	313	326	9	16	4	151	154
3	18	3	152	152	8	8	3	115	112	14	8	3	52	85	4	16	4	224	227	9	17	4	56	47
3	19	3	154	154	8	9	3	237	233	14	9	3	47	34	4	17	4	275	269	9	18	4	134	131
3	20	3	142	140	8	10	3	153	141	14	10	3	82	91	4	18	4	164	159	10	0	4	292	293
3	21	3	-41	23	8	11	3	252	266	15	1	3	65	86	4	19	4	276	283	10	1	4	126	133
3	22	3	37	81	8	12	3	211	203	15	2	3	123	110	4	20	4	122	117	10	2	4	265	260
3	23	3	111	112	8	13	3	235	244	15	3	3	-42	27	4	21	4	252	263	10	3	4	243	239
3	24	3	62	69	8	14	3	-36	28	15	4	3	84	79	4	22	4	173	180	10	4	4	78	76
4	0	3	426	442	8	15	3	225	233	15	5	3	155	172	5	1	4	190	177	10	5	4	139	149
4	1	3	742	705	8	16	3	260	257	15	6	3	66	85	5	2	4	343	347	10	6	4	154	164
4	2	3	525	515	8	17	3	190	188	0	0	4	1150	1207	5	3	4	308	314	10	7	4	314	308
4	3	3	646	637	8	18	3	113	109	0	2	4	1600	1602	5	4	4	301	295	10	8	4	197	193
4	4	3	446	432	8	19	3	170	173	0	4	4	525	519	5	5	4	106	103	10	9	4	236	234
4	5	3	258	276	8	20	3	85	88	0	6	4	836	840	5	6	4	123	139	10	10	4	184	188
4	6	3	54	53	8	21	3	135	125	0	8	4	80	96	5	7	4	63	49	10	11	4	153	149
4	7	3	484	513	9	1	3	149	127	0	10	4	152	136	5	8	4	213	204	10	12	4	127	146
4	8	3	358	355	9	2	3	337	348	0	12	4	58	85	5	9	4	191	189	10	13	4	-40	33
4	9	3	205	193	9	3	3	172	173	0	14	4	37	41	5	10	4	240	219	10	14	4	132	143
4	11	3	124	127	9	4	3	143	125	C	16	4	165	160	5	11	4	82	86	10	15	4	-40	9
4	11	3	270	256	9	5	3	305	326	0	18	4	88	82	5	12	4	445	451	10	16	4	270	267
4	12	3	349	345	9	6	3	170	156	0	20	4	73	71	5	13	4	56	43	10	17	4	48	37
4	13	3	335	340	9	7	3	427	419	0	22	4	52	95	5	14	4	139	134	11	1	4	40	34
4	14	3	155	152	9	8	3	443	437	1	1	4	451	465	5	15	4	191	181	11	2	4	-37	24
4	15	3	73	71	9	9	3	139	206	1	2	4	174	161	5	16	4	258	269	11	3	4	86	94
4	16	3	133	135	9	10	3	112	104	1	3	4	356	333	5	17	4	47	57	11	4	4	143	152
4	17	3	231	237	9	11	3	227	234	1	4	4	458	482	5	18	4	99	90	11	5	4	54	57
4	18	3	166	154	9	12	3	118	124	1	5	4	641	641	5	19	4	66	72	11	6	4	-39	29
4	19	3	216	217	9	13	3	158	158	1	6	4	317	314	5	20	4	101	97	11	7	4	227	223
4	20	3	156	147	9	14	3	190	193	1	7	4	346	360	5	21	4	-41	8	11	8	4	43	61
4	21	3	112	106	9	15	3	157	151	1	8	4	80	82	6	0	4	289	286	11	9	4	148	150
4	22	3	-39	29	9	16	3	54	52	1	9	4	751	767	6	1	4	398	406	11	10	4	-40	26
4	23	3	87	89	9	17	3	-41	43	1	10	4	219	227	6	2	4	50	61	11	11	4	96	104
5	1	3	379	374	9	18	3	-40	3	1	11	4	550	598	6	3	4	417	406	11	12	4	-40	11
5	2	3	531	525	9	19	3	113	116	1	12	4	115	111	6	4	4	73	78	11	13	4	138	141
5	3	3	95	96	10	0	3	225	221	1	13	4	248	246	6	5	4	248	359	11	14	4	194	198
5	4	3	141	152	10	1	3	366	365	1	14	4	242	248	6	6	4	296	252	11	15	4	136	134
5	5	3	325	326	10	2	3	367	359	1	15	4	122	121	6	7	4	137	141	12	0	4	50	54
5	6	3	560	570	10	3	3	206	152	1	16	4	145	148	6	8	4	388	387	12	1	4	83	82
5	7	3	57	67	10	4	3	425	426	1	17	4	-37	25	6	9	4	180	173	12	2	4	81	77
5	8	3	535	556	10	5	3	202	208	1	18	4	-38	34	6	10	4	151	164	12	3	4	74	73
5	9	3	245	244	10	6	3	178	176	1	19	4	84	81	6	11	4	125	124	12	4	4	168	179
5	10	3	450	465	10	7	3	108	96	1	20	4	170	179	6	12	4	539	547	12	5	4	73	60
5	11	3	183	173	10	8	3	52	67	1	21	4	-39	18	6	13	4	138	137	12	6	4	81	80
5	12	3	148	134	10	9	3	126	118	1	22	4	-38	13	6	14	4	62	64	12	7	4	75	55
5	13	3	-35	31	10	10	3	179	173	1	23	4	-40	39	6	15	4	236	226	12	8	4	81	82
5	14	3	356	403	10	11	3	117	115	2	0	4	392	405	6	16	4	143	143	12	9	4	-40	49
5	15	3	134	134	10	12	3	116	112	2	1	4	326	328	6	17	4	194	192	12	10	4	54	38
5	16	3	98	100	10	13	3	85	68	2	2	4	650	639	6	18	4	73	75	12	11	4	-40	29
5	17	3	67	69	10	14	3	200	197	2	3	4	79	88	6	19	4	172	180	12	12	4	98	100
5	18	3	60	52	10	15	3	128	134	2	4	4	567	565	6	20	4	124	113	12	13	4	-40	18
5	19	3	85	92	10	16	3	102	95	2	5	4	53	54	6	21	4	145	138	13	1	4	94	96
5	20	3	75	73	10	17	3	91	100	2	6	4	203	206	7	1	4	-37	29	13	2	4	44	42
5	21	3	91	89	10	18	3	156	151	2	7	4	417	412	7	2	4	515	511	13	3	4	93	93

Table 3. Continued.

H	K	L	F(O)	F(C)	H	K	L	F(O)	F(C)	H	K	L	F(O)	F(C)	H	K	L	F(O)	F(C)	H	K	L	F(O)	F(C)
13	4	4	78	78	4	17	5	209	208	10	11	5	-40	19	4	8	6	137	131	0	0	7	100	130
13	5	4	89	91	4	18	5	124	128	10	12	5	103	106	4	9	6	-39	28	0	2	7	251	247
13	6	4	52	45	4	19	5	209	212	10	13	5	42	41	4	10	6	98	97	0	4	7	84	100
13	7	4	171	175	4	20	5	157	151	10	14	5	174	180	4	11	6	-39	33	0	6	7	197	192
13	8	4	106	103	5	1	5	91	66	11	1	5	73	75	4	12	6	-39	22	0	8	7	107	127
13	9	4	76	76	5	2	5	227	211	11	2	5	83	79	4	13	6	87	96	0	10	7	245	239
13	10	4	-41	25	5	3	5	183	178	11	3	5	73	86	4	14	6	68	70	0	12	7	137	120
14	0	4	228	232	5	4	5	165	159	11	4	5	86	85	4	15	6	44	47	0	14	7	193	199
14	1	4	82	85	5	5	5	234	211	11	5	5	235	225	4	16	6	67	66	1	1	7	80	75
14	2	4	124	124	5	6	5	174	183	11	6	5	101	107	4	17	6	72	76	1	3	7	82	61
14	3	4	87	97	5	7	5	162	155	11	7	5	164	171	5	1	6	143	136	1	3	7	67	56
14	4	4	128	127	5	8	5	367	361	11	8	5	-41	26	5	2	6	102	112	1	4	7	130	133
14	5	4	141	150	5	9	5	70	57	11	9	5	132	135	5	3	6	111	110	1	5	7	107	107
14	6	4	123	123	5	10	5	344	333	11	10	5	78	76	5	4	6	325	321	1	6	7	71	69
14	7	4	163	173	5	11	5	134	141	11	11	5	133	142	5	5	6	-39	20	1	7	7	148	153
0	0	5	732	719	5	12	5	217	215	11	12	5	58	105	5	6	6	400	400	1	8	7	127	124
0	2	5	525	523	5	13	5	58	59	12	0	5	67	93	5	7	6	87	71	1	9	7	252	250
0	4	5	691	681	5	14	5	234	235	12	1	5	85	100	5	8	6	280	290	1	10	7	48	49
0	6	5	244	237	5	15	5	53	52	12	2	5	175	176	5	9	6	120	111	1	11	7	246	239
0	8	5	350	360	5	16	5	52	86	12	3	5	54	59	5	10	6	319	330	1	12	7	70	56
0	10	5	192	191	5	17	5	-40	23	12	4	5	104	98	5	11	6	83	93	1	13	7	160	160
0	12	5	265	263	5	18	5	33	55	12	5	5	56	50	5	12	6	180	173	1	14	7	112	112
0	14	5	203	198	5	19	5	70	66	12	6	5	248	244	5	13	6	117	120	1	15	7	98	93
0	16	5	120	122	6	0	5	268	279	12	7	5	-41	11	5	14	6	42	47	2	0	7	339	339
0	18	5	232	230	6	1	5	478	460	12	8	5	168	164	5	15	6	78	83	2	1	7	262	257
0	20	5	133	135	6	2	5	404	401	12	9	5	74	71	5	16	6	-41	33	2	2	7	236	235
1	1	5	106	102	6	3	5	235	247	13	1	5	66	71	5	17	6	99	104	2	3	7	204	205
1	2	5	210	206	6	4	5	172	184	13	2	5	52	65	6	0	6	175	175	2	4	7	177	177
1	3	5	404	424	6	5	5	154	178	13	3	5	56	58	6	1	6	272	276	2	5	7	205	202
1	4	5	101	112	6	6	5	218	210	13	4	5	107	118	6	2	6	127	124	2	6	7	111	123
1	5	5	228	223	6	7	5	161	161	13	5	5	178	178	6	3	6	256	250	2	7	7	92	104
1	6	5	237	248	6	8	5	61	69	13	6	5	69	83	6	4	6	167	159	2	8	7	-40	25
1	7	5	443	446	6	9	5	54	67	0	0	6	82	74	6	5	6	161	153	2	9	7	128	124
1	8	5	302	303	6	10	5	253	258	0	2	6	-34	35	6	6	6	227	235	2	10	7	126	125
1	9	5	348	353	6	11	5	77	72	0	4	6	76	90	6	7	6	135	125	2	11	7	-41	37
1	10	5	106	95	6	12	5	72	71	0	6	6	130	153	6	8	6	204	190	2	12	7	60	71
1	11	5	363	369	6	13	5	154	152	0	8	6	70	76	6	9	6	52	54	2	13	7	-41	47
1	12	5	73	86	6	14	5	127	122	0	10	6	117	132	6	10	6	283	289	2	14	7	98	95
1	13	5	153	161	6	15	5	139	143	0	12	6	147	152	6	11	6	84	84	2	15	7	63	64
1	14	5	72	79	6	16	5	73	61	0	14	6	99	99	6	12	6	102	93	3	1	7	82	86
1	15	5	130	133	6	17	5	145	154	0	16	6	308	314	6	13	6	116	125	3	2	7	-40	13
1	16	5	54	55	6	18	5	56	57	0	18	6	220	220	6	14	6	141	140	3	3	7	199	200
1	17	5	69	75	6	19	5	102	101	1	1	6	70	92	6	15	6	118	125	3	4	7	178	170
1	18	5	121	125	7	1	5	127	98	1	2	6	125	142	6	16	6	99	93	3	5	7	162	166
1	19	5	105	103	7	2	5	66	67	1	3	6	88	99	7	1	6	117	109	3	6	7	119	123
1	20	5	44	39	7	3	5	88	86	1	4	6	-36	48	7	2	6	94	77	3	7	7	196	191
1	21	5	44	51	7	4	5	324	332	1	5	6	83	63	7	3	6	115	102	3	8	7	165	167
2	0	5	459	469	7	5	5	182	196	1	6	6	68	62	7	4	6	-39	8	3	9	7	188	193
2	1	5	436	428	7	6	5	323	341	1	7	6	94	92	7	5	6	112	119	3	10	7	169	159
2	2	5	450	430	7	7	5	57	36	1	8	6	101	102	7	6	6	68	73	3	11	7	165	154
2	3	5	378	354	7	8	5	278	273	1	9	6	279	274	7	7	6	171	176	3	12	7	190	182
2	4	5	169	174	7	9	5	127	123	1	10	6	152	152	7	8	6	176	173	3	13	7	104	94
2	5	5	128	127	7	10	5	275	271	1	11	6	264	246	7	9	6	43	29	3	14	7	48	65
2	6	5	477	454	7	11	5	-39	30	1	12	6	183	182	7	10	6	133	128	3	15	7	-42	42
2	7	5	232	215	7	12	5	259	251	1	13	6	210	205	7	11	6	-40	33	4	0	7	165	159
2	8	5	41	13	7	13	5	137	145	1	14	6	107	110	7	12	6	130	136	4	1	7	316	311
2	9	5	120	123	7	14	5	93	101	1	15	6	78	77	7	13	6	-41	34	4	2	7	184	187
2	10	5	-38	15	7	15	5	53	55	1	16	6	65	68	7	14	6	206	205	4	3	7	251	245
2	11	5	170	159	7	16	5	146	149	1	17	6	90	80	7	15	6	-41	19	4	4	7	166	164
2	12	5	72	71	7	17	5	58	62	1	18	6	102	102	8	0	6	63	55	4	5	7	224	229
2	13	5	110	102	7	18	5	67	69	1	19	6	80	81	8	1	6	51	45	4	6	7	122	124
2	14	5	39	36	8	0	5	435	413	2	0	6	341	338	8	2	6	92	93	4	7	7	128	131
2	15	5	158	158	8	1	5	360	364	2	1	6	192	187	8	3	6	-39	14	4	8	7	89	90
2	16	5	281	266	8	2	5	52	101	2	2	6	268	268	8	4	6	105	109	4	9	7	154	150
2	17	5	78	66	8	3	5	287	289	2	3	6	267	266	8	5	6	50	54	4	10	7	118	118
2	18	5	116	120	8	4	5	117	131	2	4	6	266	259	8	6	6	-40	36	4	11	7	141	154
2	19	5	157	164	8	5	5	234	225	2	5	6	245	240	8	7	6	69	47	4	12	7	86	85
2	20	5	167	163	8	6	5	102	106	2	6	6	123	141	8	8	6	50	39	4	13	7	87	84
2	21	5	75	83	8	7	5	186	200	2	7	6	255	253	8	9	6	-41	20	4	14	7	67	70
3	1	5	282	267	8	8	5	110	114	2	8	6	-37	22	8	10	6	-41	36	5	1	7	-41	17
3	2	5	131	133	8	9	5	166	160	2	9	6	190	196	8	11	6	63	46	5	2	7	155	155
3	3	5	136	143	8	10	5	113	115	2	10	6	135	135	8	12	6	80	78	5	3	7	108	104
3	4	5	174	171	8	11	5	156	153	2	11	6	212	225	8	13	6	88	87	5	4	7	187	188
3	5	5	272	271	8	12	5	84	78	2	12	6	217	222	8	14	6	61	63	5	5	7	46	50
3	6	5	322	315	8	13	5	157	161	2	13	6	105	117	9	1	6	-40	12	5	6	7	198	197
3	7	5	93	81	8	14	5	69	79	2	14	6	206	202	9	2	6	43	45	5	7	7	110	109
3	8	5	124	125	8	15	5	146	135	2	15	6	84	62	9	3	6	63	69	5	8	7	285	286
3	9	5	374	367	8	16	5	135	138	2	16	6	98	95	9	4	6	147	140	5	9	7	77	66
3	10	5	372	370	8	17	5	99	91	2	17	6	68	71	9	5	6	52	49	5	10	7	125	124
3	11	5	209	206	9	1	5	48	52	2	18	6	179	178	9	6	6	118	123	5	11	7	64	62
3	12	5	254	252	9	2	5	114	125	3	1	6	102	90	9	7	6	61	63	5	12	7	132	138
3	13	5	251	250	9	3	5	206	208	3	2	6	146	144	9	8	6	92	86	5	13	7	65	55
3	14	5	96	98	9	4	5	105	110	3	3	6	316	325	9	9	6	98	100	6	0	7	278	255
3	15	5	90	97	9	5	5	147	169	3	4	6	90	42	9	10	6	94	96	6	1	7	192	199
3	16	5	81	75	9	6	5	156	147	3	5	6	270	280	9	11	6	107	112	6	2	7	157	159
3	17	5	156	155	9	7	5	335	346	3	6	6	208	213	9	12	6	100	99	6	3	7	190	176
3	18	5	81	76	9	8	5	271	266	3	7	6	355	356	10	0	6	204	198	6	4	7	191	204
3	19	5	-41	35	9	9	5	134	122	3	8	6	311	326	10	1	6	110	116	6	5	7	178	170
3	20	5	88	84	9	10	5	111	116	3	9	6	227	230	10	2	6	166	184	6	6	7	116	102
4	0	5	154	166	9	11	5	100	99	3	10	6	264	262	10	3	6	50	54	6	7	7	74	87
4	1	5	230	227	9	12	5	105	102	3	11	6	214	219	10	4	6	160	168	6	8	7	135	130
4	2	5	288	284	9	13	5	50	44	3	12	6	157	156	10	5	6	46	28	6	9	7	-43	53
4	3	5	320	322	9	14	5	185	181	3	13	6	45	54	10	6	6	231	236	6	10	7	56	57
4	4	5	153	139	9	15	5	129	133	3	14	6	221	233	10	7	6	104	105	6	11	7	-44	55
4	5	5	124	114	9	16	5	69	66	3	15	6	43	21	10	8	6	145	139	6	12	7	59	59
4	6	5	128	143	10	0	5	239	233	3	16	6	157	158	10	9	6	62	69	7	1	7	-43	39
4	7	5	254	263	10	1	5	201	211	3	17	6	55	43	10	10	6	62	72	7	2	7	74	80
4	8	5	153	148	10	2	5	204	205	3	18	6	-40	21	11	1	6	-41	17	7	3	7	72	69
4	9	5	152	178	10	3	5	207	202	4	0	6	486	488	11	2	6	100	99	7	4	7	137	136
4	10	5	182	178	10	4	5	276	267	4	1	6	632	646	11	3	6	135	131	7	5	7	74	70
4	11	5	266	268	10	5	5	173	156	4	2	6	235	242	11	4	6	77	77	7	6	7	158	153
4	12	5	206	214	10	6	5	78	73	4	3	6	462	444	11	5	6	184	203	7	7	7	90	87
4	13	5	128	129	10	7	5	131	129	4	4	6	206	218	11	6	6	107	97	7	8	7	101	106
4	14	5	52	65	10	8	5	109	103	4	5	6	244	247	11	7	6	244	244	7	9	7	54	55
4	15	5	146	150	10	9	5	66	66	4	6	6	235	235	12	0	6	289	296	7	10	7	146	150
4	16	5	160	176	10	10	5	65	62	4	7	6	186	191	12	1	6	81	89	7	11	7	64	49

Table 3. Continued.

H	K	L	F(O)	F(C)	H	K	L	F(O)	F(C)	H	K	L	F(O)	F(C)	H	K	L	F(O)	F(C)	H	K	L	F(O)	F(C)
6	0	7	66	71	5	5	7	62	63	1	8	8	-43	56	3	2	8	57	62	4	7	8	48	43
6	1	7	64	102	5	6	7	56	124	1	9	8	208	212	3	3	8	-42	29	4	8	8	-44	33
6	2	7	83	65	0	0	8	505	505	1	10	8	64	60	3	4	8	-41	16	5	1	8	-43	27
6	3	7	98	103	0	2	8	312	330	2	0	8	144	163	3	5	8	-42	29	5	2	8	-42	17
6	4	7	52	52	0	4	8	278	275	2	1	8	101	112	3	6	8	93	84	5	3	8	59	64
6	5	7	136	131	0	6	8	181	171	2	2	8	155	170	3	7	8	-41	31	5	4	8	-42	31
6	6	7	70	65	0	8	8	86	68	2	3	8	70	55	3	8	8	112	107	5	5	8	53	63
6	7	7	152	152	0	10	8	64	57	2	4	8	145	147	3	9	8	117	101	5	6	8	81	86
6	8	7	72	71	1	1	8	-44	39	2	5	8	-42	33	4	0	8	45	35	5	7	8	75	62
6	9	7	158	152	1	2	8	-41	26	2	6	8	106	114	4	1	8	-42	39	6	0	8	-44	47
6	1	7	-41	5	1	3	8	157	163	2	7	8	71	78	4	2	8	-40	13	6	1	8	185	186
6	2	7	114	107	1	4	8	105	103	2	8	8	117	111	4	3	8	46	44	6	2	8	-43	25
6	3	7	135	126	1	5	8	154	155	2	9	8	137	132	4	4	8	64	62	6	3	8	157	163
6	4	7	57	67	1	6	8	106	104	2	10	8	131	15	4	5	8	-41	5	6	4	8	58	67
					1	7	8	225	225	3	1	8	-41	24	4	6	8	60	53	6	5	8	126	116

one, and C was found to be 1.2×10^{-6}. Additional refinement cycles were then carried out, and the final R value was 0.037, with unobserved reflections included when $|F_c|$ exceeds the observable limit. In the last refinement cycle, all parameter shifts were less than 10 % of its standard deviation. The atomic coordinates of Table 1 and the thermal parameters of Table 2 are from the last of these refinement cycles.

The atoms O(1), O(2), C(3), and C(4) have the highest and most anisotropic thermal parameters. An electron density map showed considerably lower and more extended positive regions for these atoms than for the other atoms of the same kind.

A structure factor calculation, not including C(3) and C(4), was carried out ($R = 0.066$), followed by a difference electron density map. From this map the carbon atoms were located very close to the positions arrived at by the least squares refinement. The regions of positive electron density were extended approximately normal to the plane through cobalt and the four nitrogen atoms, but there was no tendency of splitting of the peaks.

A difference electron density map based on the structure factors calculated from the parameters of Tables 1 and 2 allowed the location of the hydrogen atoms, except those of C(3) and C(4). With these atoms included in the structure factor calculations, the R value was 0.033. An attempt to include the hydrogen atoms in the refinement was, however, not successful, as some of them were shifted to pisitions giving unreasonable bond lengths and angles. The hydrogen atoms are therefore not included in the final structure factor calculations listed in Table 3.

RESULTS

The hexathionate ion has the extended *trans-trans* form in this salt, and is thus different from the *cis-cis* form found in the potassium barium salt.[7,8] The difference between the two rotational isomeric forms is a rotation of approximately 180° about the middle S – S bond, or a rotation of approximately 180° about the S(2) – S(3) and S(4) – S(5) bonds.

The dimensions of the hexathionate ion in the *trans-trans* form are listed in Table 4. The standard deviations given in parentheses include estimated uncertainties in unit cell dimensions. A twofold symmetry axis passes between the two middle sulphur atoms normal to the bond between these atoms, and a prime denotes the equivalent of an atom across this axis. Fig. 1 is a stereo-

Table 4. Dimensions of the *trans-trans* form of the hexathionate ion. Standard deviations are given in parentheses.

Bond lengths and angles	
S(1) – S(2) = 2.1323(21) Å	∠S(1) – S(2) – S(3) = 105.08(11)°
S(2) – S(3) = 2.0184(29)	∠S(2) – S(3) – S(3′) = 107.35(11)°
S(3) – S(3′) = 2.0687(34)	
S(1) – O(1) = 1.410(7)	∠S(2) – S(1) – O(1) = 105.9(2)°
S(1) – O(2) = 1.455(7)	∠S(2) – S(1) – O(2) = 99.0(3)°
S(1) – O(3) = 1.443(5)	∠S(2) – S(1) – O(3) = 105.4(2)°
	∠O(1) – S(1) – O(2) = 112.4(4)°
	∠O(1) – S(1) – O(3) = 117.8(4)°
	∠O(2) – S(1) – O(3) = 114.9(3)°
Dihedral angles	
S(1)S(2)S(3)/S(2)S(3)S(3′) = 85.7°	S(2)S(3)S(3′)/S(3)S(3′)S(2′) = 71.4°
S(3)S(2)S(1)/S(2)S(1)O(1) = 72.3°	S(2)S(1)O(1)/S(2)S(1)O(2) = 116.5°
S(3)S(2)S(1)/S(2)S(1)O(2) = 171.1°	S(2)S(1)O(1)/S(2)S(1)O(3) = 125.5°
S(3)S(2)S(1)/S(2)S(1)O(3) = 53.1°	S(2)S(1)O(2)/S(2)S(1)O(3) = 118.0°
Non-bonded distances	
S(1) – S(3′) = 4.2089(22) Å	S(2) – S(2′) = 3.9715(31) Å
S(1) – S(2′) = 5.4282(20)	S(1) – S(1′) = 7.0786(28)

scopic view of the ion as seen along the twofold axis, and Fig. 2, with principal. bond lengths and angles, gives a view normal to this axis.

The differences between the present, refined dimensions of the hexathionate ion, and those arrived at on basis of the film data,[1] are within the errors estimated for the latter. The three independent bonds of the sulphur chain are thus of significantly different lengths.

The terminal S – S bonds are 2.132(2) Å, compared to 2.119(1) and 2.110(1) Å in the potassium barium salt, 2.124(6) and 2.110(6) Å in potassium pen-

Fig. 1. The *trans-trans* form of the hexathionate ion in $[Co(en)_2Cl_2]_2S_6O_6.H_2O$ as seen along the twofold axis. The ellipsoids represent 50 % probability.

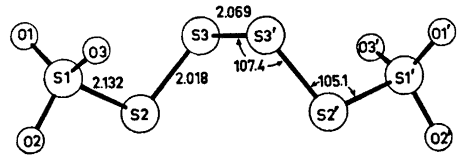

Fig. 2. The hexathionate ion as seen normal to the twofold axis.

tathionate hemitrihydrate,[9] and an average value of 2.12(2) Å in the barium pentathionates.[10] In all cases, these are the longer bonds of the sulphur chain.

The three divalent sulphur-divalent sulphur bonds are 2.018(3) Å, 2.069(3) Å, and 2.018(3) Å. They probably possess some double-bond character, arising from overlap of the $p\pi$ electron pair of one divalent sulphur atom with available 3*d* orbitals of a bond partner.[10] If it is assumed that in the sulphonate sulphur-divalent sulphur bond there is little double-bond character, the S(II) atom next to the sulphonate group has its $p\pi$ electron pair available for π-bond formation with one bond partner only, whereas each of the two central S(II) atoms has to share its $p\pi$ electron pair between two neighbours. One might therefore assume that the S(II) – S(II) bonds next to the sulphonate groups should be shorter than the central one.

When the dihedral angle associated with a sulphur-sulphur bond of this kind deviates much from 90°, there seems to be an increase in the bond length, probably caused by increase in the repulsion between the $p\pi$ electron pairs or by less favourable conditions for π-bonding.[11] The bond lengths, with associated dihedral angles given in parentheses, are 2.018 Å (85.7°), 2.069 Å (71.4°), and 2.018 Å (85.7°) in the present salt, and 2.042 Å (109.4°), 2.056 Å (89.0°), and 2.039 Å (106.3°) in the potassium barium salt. Assuming that the S(II) – S(II) bonds next to the sulphonate groups should be shorter than the central one, the differences between the bond lengths in the two salts might be correlated with the differences in dihedral angles. The small dihedral angle, 71.4°, in the present salt causes a lengthening of the central S(II) – S(II) bond and thus increases the difference between this bond and the terminal ones, which have dihedral angles of 85.7°. The large dihedral angles, 109.4° and 106.3°, in the potassium barium salt cause a lengthening of the two terminal S(II) – S(II) bonds and thus decrease the difference between these bonds and the central one, which has a dihedral ongle of 89.0°.

In potassium pentathionate hemitrihydrate [9] the average value of the S(II) – S(II) bond lengths is 2.029(7) Å with an average value of the dihedral angles of 83°, compared to 2.04 Å and 108° in the barium pentathionates.[10] The sulphur chain has the *trans* form in the potassium salt and the *cis* form in the barium salts.

The S – S – S angles vary more in the *cis-cis* chain than in the *trans-trans* chain. The individual values are 101.3(1)°, 110.2(1)°, 109.0(1)°, and 100.0(1)° in the former, and 105.1(1)°, 107.4(1)°, 107.4(1)°, and 105.1(1)° in the latter.

The sulphonate groups have the usual distorted tetrahedral form, the O – S – O angles being larger and the S – S – O angles being smaller than the tetrahedral angle. The S – S – O angle, involving the oxygen atom O(2) situated near the S(1) – S(2) – S(3) plane and with the S – O bond pointing in a direction opposite to that of the S(2) – S(3) bond, is 6.7° smaller than the average value of the two others. The reason for the apparent shortness of the S(1) – O(1) bond, 1.410(7) Å, might be the large thermal motion of O(1) normal to this bond. The largest differences between the sulphonate groups in this salt and in the potassium barium salt are in the degrees of rotation about the S – S bonds which differ by approximately 16°.

The dimensions of the *trans*-dichlorobis(ethylenediamine)cobalt(III) ion are listed in Table 5. The four nitrogen atoms are coordinated to cobalt in a

Table 5. Dimensions of the *trans*-dichlorobis(ethylenediamine)cobalt(III) ion. Standard deviations are given in parentheses. The ethylenediamine groups are N(1) – C(1) – C(2) – N(2) and N(3) – C(3) – C(4) – N(4).

Co – Cl(1) = 2.229(2) Å	∠Cl(1) – Co – N(1) = 90.5(2)°	∠N(1) – Co – N(2) = 87.2(2)°
Co – Cl(2) = 2.261(2)	∠Cl(1) – Co – N(2) = 90.7(2)°	∠N(3) – Co – N(4) = 85.9(2)°
Co – N(1) = 1.972(4)	∠Cl(1) – Co – N(3) = 90.2(2)°	∠N(1) – Co – N(4) = 92.4(2)°
Co – N(2) = 1.958(4)	∠Cl(1) – Co – N(4) = 91.2(2)°	∠N(2) – Co – N(3) = 94.5(2)°
Co – N(3) = 1.974(4)	∠Cl(2) – Co – N(1) = 90.1(2)°	∠Co – N(1) – C(1) = 106.8(3)°
Co – N(4) = 1.970(5)	∠Cl(2) – Co – N(2) = 89.4(2)°	∠Co – N(2) – C(2) = 109.0(3)°
N(1) – C(1) = 1.518(8)	∠Cl(2) – Co – N(3) = 89.3(2)°	∠Co – N(3) – C(3) = 109.5(4)°
N(2) – C(2) = 1.500(8)	∠Cl(2) – Co – N(4) = 88.8(2)°	∠Co – N(4) – C(4) = 109.5(5)°
N(3) – C(3) = 1.461(11)	∠Cl(1) – Co – Cl(2) = 179.4(1)°	∠N(1) – C(1) – C(2) = 106.8(4)°
N(4) – C(4) = 1.467(10)	∠N(1) – Co – N(3) = 178.2(2)°	∠N(2) – C(2) – C(1) = 107.7(4)°
C(1) – C(2) = 1.509(9)	∠N(2) – Co – N(4) = 178.1(2)°	∠N(3) – C(3) – C(4) = 112.8(7)°
C(3) – C(4) = 1.409(14)		∠N(4) – C(4) – C(3) = 115.2(7)°

planar arrangement, the maximum deviation of an atom from a least squares plane being 0.025 Å. The distances of the carbon atoms from this plane are: – 0.48 Å for C(1), 0.20 Å for C(2), 0.31 Å for C(3), and – 0.06 Å for C(4).The carbon atoms of one ethylenediamine group, C(3) and C(4), are thus closer to the cobalt-nitrogen plane than are the two other carbon atoms, and they form shorter C – N and C – C bonds, 1.46 and 1.41 Å, respectively, compared to 1.51 and 1.51 Å. C(3) and C(4) have large thermal motions nearly normal to the cobalt-nitrogen plane, and this is probably the reason for the short lengths and short distances from the plane. Similar effects of high thermal motions are found in the structure of $Cu_3(en)_2(CN)_4.H_2O$,[12] where disorder of the ethylenediamine groups or a dynamic flipping of the carbon atoms across the copper-nitrogen plane is suggested.

Hydrogen bonds are probably formed from the water molecule to O(3) and its image across the twofold axis on which the water oxygen atom is situated. The $H_2O – O$ distance is 3.153(9) Å, and the $O – H_2O – O$ angle is

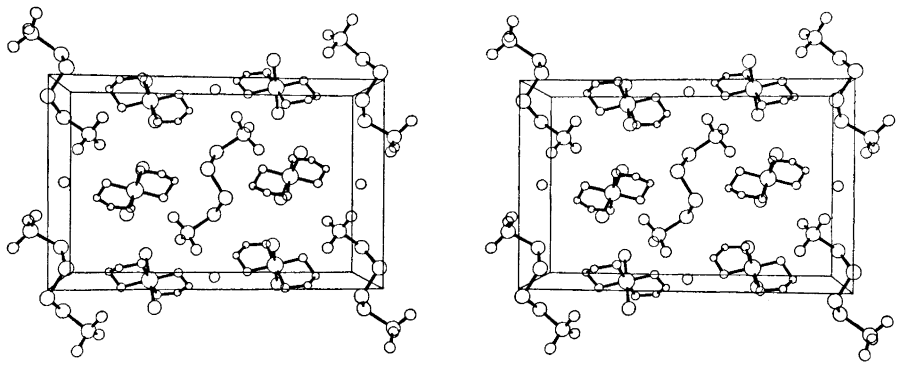

Fig. 3. A stereoscopic view of the cell packing in $[Co(en)_2Cl_2]_2S_6O_6.H_2O$ as seen normal to the *c* crystal plane.

95.8(3)°. N(1) probably forms a hydrogen bond to O(1) at $x,y,z-1$, the N–O distance being 2.910(7) Å. The hydrogen atoms located in the difference electron density map are in accordance with such hydrogen bonds.

REFERENCES

1. Foss, O. and Marøy, K. *Acta Chem. Scand.* **19** (1965) 2219.
2. Foss, O. and Palmork, K. H. *Acta Chem. Scand.* **12** (1958) 1337.
3. *International Tables for X-Ray Crystallography*, Kynoch Press, Birmingham 1962, Vol. III.
4. Cromer, D. T. *Acta Cryst.* **18** (1965) 17.
5. Gjerrestad, K. and Marøy, K. *Acta Chem. Scand.* **27** (1973) 1653.
6. Zachariasen, W. H. *Acta Cryst.* **16** (1963) 1139.
7. Foss, O. and Johnsen, K. *Acta Chem. Scand.* **19** (1965) 2207.
8. Marøy, K. *Acta Chem. Scand.* **27** (1973) 1684.
9. Marøy, K. *Acta Chem. Scand.* **25** (1971) 2580.
10. Foss, O. and Tjomsland, O. *Acta Chem. Scand.* **12** (1958) 44.
11. Hordvik, A. *Acta Chem. Scand.* **20** (1966) 1885.
12. Williams, R. J., Larson, A. C. and Cromer, D. T. *Acta Cryst.* **B 28** (1972) 858.

Received December 27, 1972.

ACTA CHEMICA SCANDINAVICA 27 (1973) 1717–1724

A Kinetic Study of the Reaction between Iron(III) and Hydroxylamine in Strongly Acid Perchlorate Solutions

GÖSTA BENGTSSON

Division of Inorganic Chemistry 1, Chemical Center, University of Lund, S-220 07 Lund 7, Sweden

The kinetics of the uncatalysed and copper ion catalysed reaction between iron(III) and hydroxylamine has been studied in strongly acid perchlorate solutions. The experimental rate laws have been found to be complicated, yielding little information about the detailed mechanisms of the reactions. The numerators have a common appearance with [Cu(II)] replacing one [Fe(III)] in the rate law of the catalysed reaction as compared with the uncatalysed reaction. This indicates that copper replaces iron in the rate-determining steps of the catalysed reaction. The first steps of both reactions seem to be the rapid formation of hydroxylamine complexes with Cu(II) and Fe(III), followed by the formation of a binuclear intermediate, or activated complex, containing two hydroxylamine bridges.

The reaction

$$4Fe^{3+} + 2NH_3OH^+ \rightarrow 4Fe^{2+} + N_2O + 6H^+ + H_2O$$

has long been used for the quantitative determination of hydroxylamine.[1–4] The method consists of boiling the solution to be analysed with an excess of iron(III) solution for a few minutes and then titrating the cooled solution with potassium permanganate. The most serious source of error by this method seems to be the incompleteness of the reaction above before the titration is performed. For this reason it was considered necessary to have iron(III) present in large excess to increase the rate of reaction. Copper(II) catalyses the reaction and has been used with success at the analysis.[5] The present paper is devoted to a study of the kinetics of the reaction both with and without copper(II) as a catalyst. Any previous studies of this topic do not seem to have been carried out, although it seems desirable to know the factors that influence the reaction rate of this reaction.

SYMBOLS AND NOTATIONS

[Fe(III)] over-all concentration of iron(III).
[Fe(II)] over-all concentration of iron(II).
[Cu(II)] over-all concentration of copper(II).
[NH_2OH] over-all concentration of hydroxylamine (=[NH_3OH^+])
A absorbance.
a linear absorption coefficient ($a = A/l$; l = path length).
λ wave length.

Index $_0$ denotes quantities at a moment immediately after mixing the reactant solutions, *i.e.* at the time $t = 0$.

A,B, ... G, A′,B′, ...S′ empirical constants containing rate constants together with constant concentration terms. The meaning of these constants will be explained further in connection with the equations in which they are used.

k_i rate constants.

EXPERIMENTAL

All the chemicals used were of analytical grade. The metal salts used were the perchlorates. The metal ion concentrations of the stock solutions were determined by standard methods: iron titrimetrically with permanganate (Fe(III) after quantitative reduction in a column of finely grained cadmium), copper gravimetrically. The stock solutions of Fe(II) contained 5 – 10 % Fe(III) and were slowly oxidized by dissolved oxygen. The values of [Fe(III)] given in this paper represent the total concentration of Fe(III), *i.e.* also the amount contributed by the Fe(II) solution.

Hydroxylamine stock solutions were prepared and the purity of the preparations used was checked in the manner described in Ref. 6. A few measurements were performed with hydroxylamine solutions prepared from $(NH_3OH)_2SO_4$ and with SO_4^{2-} removed by the addition of an equivalent amount of $Ba(ClO_4)_2.3H_2O$, filtering off the barium sulphate formed. The results of these measurements agreed within narrow limits with those obtained with $NH_2OH.HCl$.

The temperature was 25.00 ± 0.05°C; ionic strength 1.0 – 1.3 M; $[H^+] = 0.100$ M for those measurements where the effect of $[H^+]$ was not especially studied. The reaction rate was not sensitive to a change of the ionic strength from 1.0 M to 1.3 M, as was found by addition of the proper amounts of sodium perchlorate to the solutions.

The kinetic measurements were carried out spectrophotometrically by a Zeiss PMQ II Spectralphotometer at the wave length 300 nm. This wave length is at the base of the strong absorption band of iron(III) in the ultraviolet region of the spectrum. The

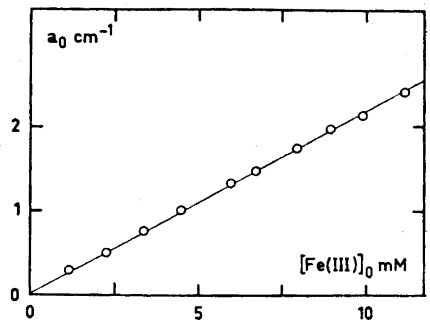

Fig. 1. Uncatalysed reaction. a_0 *versus* [Fe(III)]$_0$. [Fe(II)]$_0$ = 0.46 mM; [NH_2OH]$_0$ = 20.00 mM; λ = 300 nm.

absorbing species are Fe^{3+}, $FeOH^{2+}$, and $FeCl^{2+}$. Despite the fact that the absorbance is the sum of three terms, Lambert-Beer's law is obeyed, as can be seen from Fig. 1 which shows the initial absorbances obtained for different values of $[Fe(III)]_0$, while $[NH_2OH]_0$, $[Cl^-]$, and $[H^+]$ are kept constant. The rate laws were determined by the method of initial rates. By systematically changing the concentrations of all the relevant components it was possible to determine the complicated rate laws with a high degree of reliability. The reaction rates were evaluated graphically.

MEASUREMENTS AND RESULTS

Stoichiometry. The stoichiometry of the reaction seems to be well established by the use of the reaction for analytical purposes. The demand that Fe(III) should be in at least 3-fold excess at the analysis seems to be due to the fact that under these conditions the reaction between Fe(III) and NH_2OH is sufficiently rapid to be complete before the titration with permanganate. Thus, there is no reason to believe that the stoichiometry would be other than $\Delta[Fe(III)]/\Delta[NH_2OH] = 2/1$.

Rate laws. Preliminary measurements indicated that both the uncatalysed and the copper-catalysed reactions were inhibited by Fe(II). Therefore, the measurements were generally carried out in the presence of added Fe(II). The inhibition was strongest in the uncatalysed reaction, making the precision of the initial rates very poor in the absence of added Fe(II). Even with Fe(II)

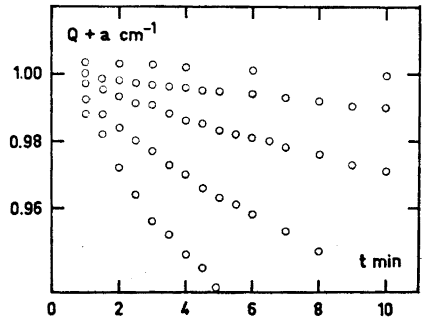

Fig. 2. Uncatalysed reaction. A few kinetic runs with $[Fe(II)]_0 = 0.46$ mM; $[NH_2OH]_0 = 20.00$ mM, while $[Fe(III)]_0$ from top to bottom is 1.14, 2.25, 4.44, 6.66, and 8.88 mM. Q is an arbitrary constant used to obtain roughly equal initial absorbances.

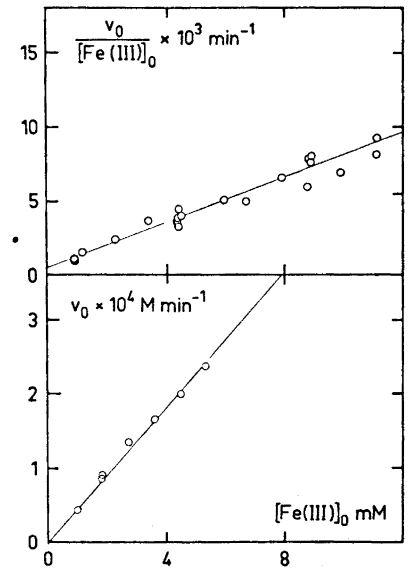

Fig. 3. Dependence of the initial rate on $[Fe(III)]_0$. Top: Uncatalysed reaction; $[Fe(II)]_0 = 0.46$ mM; $[NH_2OH]_0 = 20.00$ mM. Bottom: Catalysed reaction; $[Fe(II)]_0 = 1.80$ mM; $[Cu(II)] = 1.91$ mM; $[NH_2OH]_0 = 20.00$ mM.

added, the reproducibility was poor. The studies of the copper-catalysed reaction were carried out at so high [Cu(II)] ([Cu(II)] > 0.5 mM) that the uncatalysed reaction was negligible.

By determining the initial rates at concentrations of the components which were systematically changed, the following relationships were obtained.

Uncatalysed reaction:

$$-\left(\frac{\Delta[\mathrm{Fe(III)}]}{\Delta t}\right) = v = \mathrm{A[Fe(III)]^2}, \ ([\mathrm{NH_2OH}], \ [\mathrm{Fe(II)}] = \text{constant}) \quad (1)$$

$$1/v = \mathrm{B} + \mathrm{C[Fe(II)]^2}, \ ([\mathrm{Fe(III)}], \ [\mathrm{NH_2OH}] = \text{constant}) \quad (2)$$

$$\frac{[\mathrm{NH_2OH}]}{v} = \mathrm{D} + \frac{\mathrm{E}}{[\mathrm{NH_2OH}]}, \ ([\mathrm{Fe(III)}], \ [\mathrm{Fe(II)}] = \text{constant}) \quad (3)$$

$$\mathrm{D} = \text{constant} \ ([\mathrm{Fe(III)}] = \text{constant}) \quad (4)$$

$$\mathrm{E} = \mathrm{F[Fe(II)]^2} \ ([\mathrm{Fe(III)}] = \text{constant}) \quad (5)$$

$$v = \frac{\mathrm{G}}{[\mathrm{H^+}]^2} \ ([\mathrm{Fe(III)}], \ [\mathrm{Fe(II)}], \ [\mathrm{NH_2OH}] = \text{constant}) \quad (6)$$

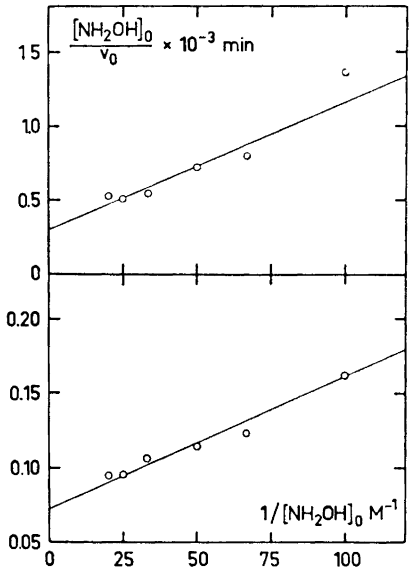

Fig. 4. $[\mathrm{NH_2OH}]_0/v_0$ *versus* $1/[\mathrm{NH_2OH}]_0$. Top: Uncatalysed reaction; $[\mathrm{Fe(III)}]_0 = 4.34$ mM; $[\mathrm{Fe(II)}]_0 = 0.261$ mM. Bottom: Catalysed reaction; $[\mathrm{Fe(III)}]_0 = 4.58$ mM; $[\mathrm{Fe(II)}]_0 = 2.66$ mM; $[\mathrm{Cu(II)}] = 1.90$ mM.

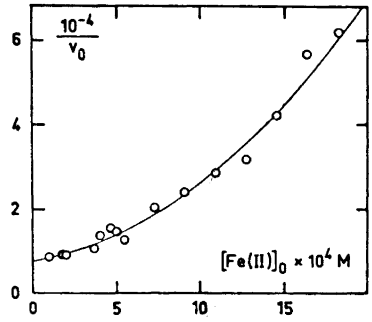

Fig. 5. Uncatalysed reaction. $1/v_0$ *versus* $[\mathrm{Fe(II)}]_0$. $[\mathrm{Fe(III)}]_0 = 8.88$ mM; $[\mathrm{NH_2OH}]_0 = 20.00$ mM.

The constants A, B, C, D, E, F, and G are empirical constants. The constants D and E represent, *e.g.*, the intercept and the slope, respectively, of the straight lines obtained, when $[\mathrm{NH_2OH}]/v$ was plotted *versus* $1/[\mathrm{NH_2OH}]$ at constant

values of [Fe(III)] and [Fe(II)]. Eqn. (4) shows that D is independent of [Fe(II)], whereas eqn. (5) shows that E is proportional to $[Fe(II)]^2$. The corresponding graphs are shown in Figs. 2 – 5. The quantities D and E are shown in Table 1. Eqn. (2) might include a term in [Fe(II)] but the experimental error

Table 1. Experimental values of the quantities D and E. $[Fe(III)]_0 = 4.34 \pm 0.02$ mM.

$[Fe(II)]_0$ mM	D	E
0.087	337 ± 63	0.29 ± 0.66
0.174	440 ± 150	2.52 ± 1.65
0.261	309 ± 194	8.50 ± 2.22
0.348	393 ± 315	13.74 ± 3.42
0.443	517 ± 333	16.20 ± 3.61

is much higher than the value of the coefficient. The value of D might likewise increase somewhat with [Fe(II)]. The precision is, however, too poor to permit any sure decision as to whether this increase is significant. The equations above can be summarized in the experimental rate law (disregarding the dependence on $[H^+]$).

$$v = \frac{k_1[Fe(III)]^2[NH_2OH]^2}{[NH_2OH] + k_2[Fe(II)]^2} \quad (7)$$

The meaning of the empirical constants A, B ... can be realised by a comparison of eqns. (1) – (6) with eqn. (7). It is seen that the empirical constants throughout represent combinations of rate constants and constant concentration terms.

Copper catalysed reaction:

$$v = A'[Fe(III)], \ ([Fe(II)], \ [Cu(II)], \ [NH_2OH] = \text{constant}) \quad (8)$$

$$\frac{[Cu(II)]}{v} = B' + C'[Cu(II)], \ ([Fe(III)], \ [Fe(II)], \ [NH_2OH] = \text{constant}) \quad (9)$$

$$B' = D'/[NH_2OH] + E'/[NH_2OH]^2, \ ([Fe(III)], \ [Fe(II)] = \text{constant}) \quad (10)$$

$$B' = F' + G'[Fe(II)], \ ([Fe(III)], \ [NH_2OH] = \text{constant}) \quad (11)$$

$$\frac{[NH_2OH]}{v} = M' + \frac{N'}{[NH_2OH]}, \ ([Fe(III)], \ [Fe(II)], \ [Cu(II)] = \text{constant}) \quad (12)$$

$$M' = P' + Q'[Fe(II)], \ ([Fe(III)], \ [Cu(II)] = \text{constant}) \quad (13)$$

$$N' = R'[Fe(II)], \ ([Fe(III)], \ [Cu(II)] = \text{constant}) \quad (14)$$

$$v = \frac{S'}{[H^+]^2} \ ([Fe(III)], \ [Fe(II)], \ [Cu(II)], \ [NH_2OH] = \text{constant}) \quad (15)$$

The graphs corresponding to some of these equations are shown in Figs. 3, 4, 6, and 7. The quantities B', C', M', and N' are shown in Tables 2 and 3. These equations can be summarized in the experimental rate law (disregarding the dependence on $[H^+]$)

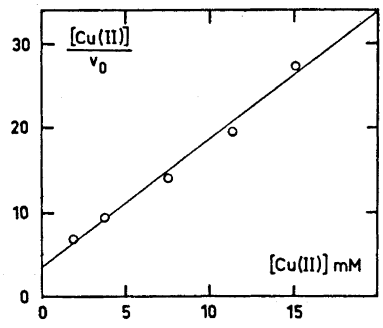

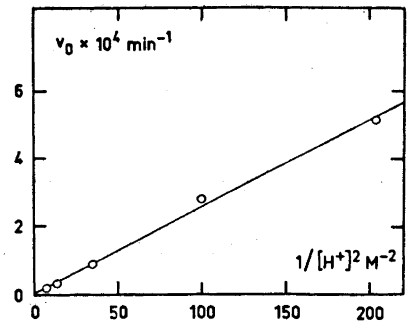

Fig. 6. Catalysed reaction. $[Cu(II)]/v_0$ *versus* $[Cu(II)]$. $[Fe(III)]_0 = 4.64$ mM; $[Fe(II)]_0 = 1.73$ mM; $[NH_2OH]_0 = 20.00$ mM.

Fig. 7. Catalysed reaction. v_0 *versus* $1/[H^+]^2$. $[Fe(III)]_0 = 4.56$ mM; $[Fe(II)]_0 = 1.69$ mM; $[Cu(II)] = 1.90$ mM; $[NH_2OH]_0 = 20.00$ mM.

Table 2. Experimental values of the quantities B′ and C′. $[Fe(III)]_0 = 4.61 \pm 0.14$ mM.

$[NH_2OH]_0$ mM	$[Fe(II)]_0$ mM	B′	C′
5.00	1.73	55.9 ± 14.1	4.90 ± 1.51
7.50		23.4 ± 3.3	3.30 ± 0.65
10.00		11.9 ± 7.6	2.62 ± 0.78
12.50		11.3 ± 3.8	1.86 ± 0.40
15.00		5.28 ± 2.98	2.02 ± 0.32
17.50		4.68 ± 4.94	1.83 ± 0.52
20.00		3.47 ± 1.69	1.51 ± 0.18
	0.85	3.31 ± 0.42	1.22 ± 0.03
	1.69	3.98 ± 2.49	1.45 ± 0.21
	2.69	7.12 ± 2.31	1.28 ± 0.18
	3.59	8.53 ± 3.92	1.38 ± 0.30
	4.46	12.68 ± 2.66	1.20 ± 0.21

Table 3. Experimental values of the quantities M′ and N′. $[Fe(III)]_0 = 4.64 \pm 0.12$ mM.

$[Fe(II)]_0$ mM	$[Cu(II)]_0$ mM	M′	N′
1.73	1.90	52.9 ± 11.1	0.491 ± 0.120
	3.80	34.1 ± 8.7	0.337 ± 0.081
	7.60	26.4 ± 4.5	0.185 ± 0.041
	11.40	27.9 ± 3.5	0.087 ± 0.029
	15.10	25.9 ± 6.2	0.087 ± 0.045
0.87	1.90	47.6 ± 8.9	0.429 ± 0.084
1.74		64.1 ± 20.5	0.78 ± 0.22
2.66		72.3 ± 10.1	0.89 ± 0.12
3.54		79.4 ± 11.9	1.37 ± 0.15
4.43		89.3 ± 25.5	1.85 ± 0.45
5.59		106 ± 41	2.52 ± 0.45
7.45		127 ± 15	3.14 ± 0.19
9.32		141 ± 67	3.83 ± 1.19

$$v = \frac{k_3[\mathrm{Fe(III)}][\mathrm{Cu(II)}][\mathrm{NH_2OH}]^2}{[\mathrm{Fe(II)}][\mathrm{NH_2OH}] + k_4[\mathrm{Cu(II)}][\mathrm{NH_2OH}] + k_5[\mathrm{Fe(II)}]} \quad (16)$$

The meaning of the empirical constants A', B' ... is evident from a comparison of eqns. (8) – (15) with eqn. (16). The following values of the constants or quotients between constants were calculated from the experimental values of B, C, D, E, B', C', M', and N': $k_1 = 126 \pm 52\ \mathrm{M^{-2}\ min^{-1}}$; $k_2/k_1 = 1800 \pm 600$ M min, $k_3 = 10.9 \pm 3.8\ \mathrm{M^{-1}\ min^{-1}}$; $k_4/k_3 = 0.125 \pm 0.040$ M min; $k_5/k_3 = (3.69 \pm \pm 0.23) \times 10^{-3}\ \mathrm{M^2}$ min. The error limits represent three standard deviations.

DISCUSSION

The experimentally determined rate laws of both the reactions are very complicated. It therefore seems difficult to draw any reliable conclusions concerning the mechanisms from either of them.

The numerators of both rate laws have a common appearance, where the rate law of the catalysed reaction contains [Cu(II)] instead of one [Fe(III)] in the rate law of the uncatalysed reaction. This indicates that Cu(II) replaces Fe(III) in the rate-determining step(s) of the catalysed reaction. The first step of both reactions seems to be the rapid formation of complexes between Cu(II) and Fe(III), respectively, and hydroxylamine, followed by the formation of a binuclear intermediate, or activated complex, containing two hydroxylamine bridges. The catalytic effect of Cu(II) can then be explained by the greater strength of the Cu(II) – NH_2OH complexes. The existence of rather strong copper complexes with hydroxylamine has been reported by Szilard,[7] whereas the corresponding iron(III) complexes are unknown (and probably very weak). The concentrations of the hydroxylamine comlexes of Cu(II), Fe(III), and Fe(II) are, however, also very small because the concentration of free NH_2OH is exceedingly small at the hydrogen ion concentrations applied in the study ($[H^+] > 0.050$ M), the dominating hydroxylamine species being NH_3OH^+.

The strong $[H^+]$-dependence can be explained by a loss of two protons from two NH_3OH^+ ions in the formation of the two complexes mentioned above.

The existence of a term in $[\mathrm{Fe(II)}]^2$ in the denominator of eqn. (7) makes it uncertain whether this equation represents the "true" rate law. An experimental rate law of this kind could be obtained from a "true" rate law of the form

$$v = \frac{P}{[\mathrm{Fe(II)}] + Q[\mathrm{NH_2OH}]} + \frac{R}{1 + S[\mathrm{Fe(II)}]} \quad (17)$$

which can be transformed to

$$v = \frac{P + (PS + R)[\mathrm{Fe(II)}] + QR[\mathrm{NH_2OH}]}{Q[\mathrm{NH_2OH}] + [\mathrm{Fe(II)}] + QS[\mathrm{Fe(II)}][\mathrm{NH_2OH}] + [\mathrm{Fe(II)}]^2} \quad (18)$$

The quantities P and R do not represent true constants but probably have the form $k_i[\mathrm{Fe(III)}]^2[\mathrm{NH_2OH}]^2$. By neglecting the proper terms, eqn. (18) can be made analogous to eqn. (7). A corresponding situation might be the case for the catalysed reaction.

From the analytical point of view it might be noted that the inhibition by the product Fe(II) is more marked with the uncatalysed reaction. With the catalysed reaction it can be made negligible by having Cu(II) in large excess.

The author is indebted to Professor Sture Fronæus for stimulating discussions, to Mrs. Christina Oskarsson for skilful assistance in the experimental parts of this work, and to Dr. Peter Sellers for linguistic revision of the manuscript.

The investigation forms part of a research program on the kinetics of redox reactions, financially supported by the *Swedish Natural Science Research Council*.

REFERENCES

1. Meyerling, W. *Ber.* **10** (1877) 1940.
2. Raschig, F. *Ann.* **241** (1887) 191.
3. Langhaus, A. *Z. anal. Chem.* **57** (1918) 401.
4. Bray, W. C., Simpson, M. E., and McKenzie, A. A. *J. Am. Chem. Soc.* **41** (1919) 1363.
5. Bhankara Rao, K. and Gopala Rao, G. *Z. anal Chem.* **157** (1957) 100.
6. Bengtsson, G. *Acta Chem. Scand.* **26** (1972) 2494.
7. Szilard, I. *Acta Chem. Scand.* **17** (1963) 2674.

Received December 12, 1972.

ACTA CHEMICA SCANDINAVICA 27 (1973) 1725–1734

Normal Coordinate Analysis of Azulene

O. GEBHARDT

Institutt for medisinsk biologi, Universitetet i Tromsø, Postboks 977, 9001 Tromsø, Norway

A normal coordinate analysis was performed for azulene. A harmonic force field, potential energy distribution, and calculated mean amplitudes of vibration are reported. The results agree reasonably well with previously given electron diffraction mean amplitude values. The mean amplitudes of vibration are shortly discussed in relation to the partial aromatic character of azulene.

Several structural and spectral investigations on cyclic hydrocarbons have been reported in the last years. Davis and Muecke [1] have reported an electron diffraction study of cyclopentene, and Adams *et al.* [2] have performed similar work on cyclopentane. An investigation of spiropentane has been reported by Dallinga *et al.*[3] Electron diffraction works on the six-membered ring molecules cyclohexene, 1,3-cyclohexadiene, and 1,4-cyclohexadiene are reported by various authors.[4–8] Recently published spectral data and normal coordinate analysis for these three molecules are also available.[9–12] Hagen in his thesis [13] has thoroughly treated the structural aspects of 1,3-cycloheptadiene, bicyclo[4.1.0]-2-heptene and bicyclopropyl on the basis of gas electron diffraction works. Structural and spectroscopic data for 1,3-cycloheptadiene are also available.[14–15] Among the other cyclic hydrocarbons treated by electron diffraction are bicyclo[1.1.1]pentane,[16–18] bicyclo[2.1.0]pentane,[19] 1,3,5,7-cyclooctatetraene,[20–23] 1,3-cyclooctadiene,[24] and perylene.[25–26] Almenningen *et al.*[27] have reported an electron diffraction study on the aromatic molecules naphthalene, anthracene, and coronene. Spectroscopic calculations of mean amplitudes have been performed for benzene,[28] naphthalene,[29] and anthracene.[29] For benzene some earlier electron diffraction analyses are available.[20,30,31]

The azulene molecule has been investigated several times, both structurally[32] and spectroscopically.[33–36] In the present work a normal coordinate analysis is carried out for this molecule, and mean amplitudes of vibration are calculated. Some comments are finally given on the interesting correlation between the aromatic character of the molecule and the mean amplitudes of vibration.

SYMMETRY COORDINATES

According to Bastiansen and Derrisen [32] azulene possesses C_{2v} symmetry. Fig. 1 shows the molecular model. The following set of symmetry coordinates were constructed by the method described by Wilson *et al.*[37]

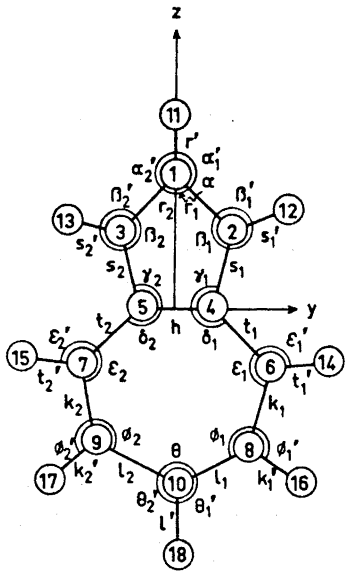

Fig. 1. Molecular model of azulene. In-plane valence coordinates are indicated. The out-of-plane coordinates (not indicated on the figure) are specified below in terms of the respective atom numbers. (i) Torsions: τ_{r1}(3-1-2-4), τ_{r2}(2-1-3-5), τ_{k1}(10-8-6-4), τ_{k2}(10-9-7-5), τ_{l1}(9-10-8-6), τ_{l2} (8-10-9-7); (ii) out-of-plane bendings: ξ_1(7,3-5-4), ξ_2(6,2-4-5), β_1''(4,1-2-12), β_2''(5,1-3-13), ε_1''(8,4-6-14), ε_2''(9,5-7-15), ϕ_1''(10,6-8-16), ϕ_2''(10,7-9-17), α''(2,3-1-11), θ''(8,9-10-18). The capital letters R, S, R', S', *etc.*, are used to designate the appropriate equilibrium distances.

Species A_1:

$$S_1 = 2^{-\frac{1}{2}}(r_1 + r_2),\quad S_2 = 2^{-\frac{1}{2}}(s_1 + s_2),\quad S_3 = 2^{-\frac{1}{2}}(t_1 + t_2)$$

$$S_4 = h,\quad S_5 = 2^{-\frac{1}{2}}(k_1 + k_2),\quad S_6 = 2^{-\frac{1}{2}}(l_1 + l_2)$$

$$S_7 = (RS/2)^{\frac{1}{2}}(\beta_1 + \beta_2),\quad S_8 = (\mathrm{HT}/2)^{\frac{1}{2}}(\delta_1 + \delta_2),\quad S_9 = (TK/2)^{\frac{1}{2}}(\varepsilon_1 + \varepsilon_2)$$

$$S_{10} = r',\quad S_{11} = 2^{-\frac{1}{2}}(s_1' + s_2'),\quad S_{12} = 2^{-\frac{1}{2}}(t_1' + t_2')$$

$$S_{13} = 2^{-\frac{1}{2}}(k_1' + k_2'),\quad S_{14} = l',\quad S_{15} = (RS/2)^{\frac{1}{2}}(\beta_1' + \beta_2')$$

$$S_{16} = (TT'/2)^{\frac{1}{2}}(\varepsilon_1' + \varepsilon_2'),\quad S_{17} = (KK'/2)^{\frac{1}{2}}(\phi_1' + \phi_2')$$

Species A_2:

$$S_1 = (RS/2)^{\frac{1}{2}}(\tau_{r1} + \tau_{r2}),\quad S_2 = (LT/2)^{\frac{1}{2}}(\tau_{k1} + \tau_{k2})$$

$$S_3 = (KL/2)^{\frac{1}{2}}(\tau_{l1} + \tau_{l2}),\quad S_4 = [(RS)^{\frac{1}{2}}S'/2]^{\frac{1}{2}}(\beta_1'' + \beta_2'')$$

$$S_5 = [(KT)^{\frac{1}{2}}K'/2]^{\frac{1}{2}}(\varepsilon_1'' + \varepsilon_2''),\quad S_6 = [(LK)^{\frac{1}{2}}K'/2]^{\frac{1}{2}}(\phi_1'' + \phi_2'')$$

Species B_1:

$$S_1 = [(ST)^{\frac{1}{2}}H/2]^{\frac{1}{2}}(\xi_1 - \xi_2),\quad S_2 = (RS/2)^{\frac{1}{2}}(\tau_{r1} - \tau_{r2})$$

$$S_3 = (LT/2)^{\frac{1}{2}}(\tau_{k1} - \tau_{k2}),\quad S_4 = (KL/2)^{\frac{1}{2}}(\tau_{l1} - \tau_{l2})$$

$S_5=[(RS)^{\frac{1}{2}}S'/2]^{\frac{1}{2}}(\beta_1''-\beta_2'')$, $S_6=[(KT)^{\frac{1}{2}}T'/2]^{\frac{1}{2}}(\varepsilon_1''-\varepsilon_2'')$
$S_7=[(LK)^{\frac{1}{2}}K'/2]^{\frac{1}{2}}(\phi_1''-\phi_2'')$, $S_8=S=(RR')^{\frac{1}{2}}\alpha''$
$S_9=(LL')^{\frac{1}{2}}\theta''$

Species B_2:

$S_1=2^{-\frac{1}{2}}(r_1-r_2)$, $S_2=2^{-\frac{1}{2}}(s_1-s_2)$, $S_3=2^{-\frac{1}{2}}(t_1-t_2)$
$S_4=2^{-\frac{1}{2}}(k_1-k_2)$, $S_5=2^{-\frac{1}{2}}(l_1-l_2)$, $S_6=(RS/2)^{\frac{1}{2}}(\beta_1-\beta_2)$
$S_7=(HT/2)^{\frac{1}{2}}(\delta_1-\delta_2)$, $S_8=(Tk/2)^{\frac{1}{2}}(\varepsilon_1-\varepsilon_2)$, $S_9=2^{-\frac{1}{2}}(s_1'-s_2')$
$S_{10}=2^{-\frac{1}{2}}(t_1'-t_2')$, $S_{11}=2^{-\frac{1}{2}}(k_1'-k_2')$, $S_{12}=(RS'/2)^{\frac{1}{2}}(\beta_1'-\beta_2')$
$S_{13}=(TT'/2)^{\frac{1}{2}}(\varepsilon_1'-\varepsilon_2')$, $S_{14}=(KK'/2)^{\frac{1}{2}}(\phi_1'-\phi_2')$
$S_{15}=(RR'/2)^{\frac{1}{2}}(\alpha_1'-\alpha_2')$, $S_{16}=(LL'/2)^{\frac{1}{2}}(\theta_1'-\theta_2')$

Table 1. Experimental frequencies of vibration (cm^{-1}) for azulene used in the present calculations.

A_1[a]	C–H stretching	3091	B_1[b]	C–H op[c] bend	1000
		3074			960
		3059			946
		3024			764
		3002			721
	C–C stretching (arom.)	1638		Ring op[c] deformation	664
		1580			492
		1443			311
		1392			165
	CCH ip[c] bend	1294			
		1117	B_2[a]	C–H stretching	3083
		1054			3044
					3007
	C–C stretching (single bond)	899		C–C stretching (arom.)	1694
					1580
	CCC ring bend	671			1479
		559			1453
		492			
		403		CCH ip[c] bend	1301
					1205
A_2[b]	C–H op[c] bend	1000			1151
		908			1007
		795			970
	Ring op[c] deformation			CCC ring bend	721
		531			593
		323[d]			559
		163[d]			478

[a] From Ref. 34. [b] From Ref. 33. [c] ip = in plane, op = out of plane. [d] Calculated in Ref. 33.

STRUCTURAL AND SPECTRAL DATA

Bastiansen and Derrisen [32] report structural data for azulene, obtained by electron diffraction. Vibrational frequencies are given by Steele,[33,35] Hunt and Ross,[36] and van Tets and Günthard.[34] There are some small discrepancies between these works, and Table 1 shows the frequencies we have adopted for the computations in the present work. The in-plane vibrational frequencies, species A_1 and B_2, are taken from van Tets and Günthard,[34] taking into consideration the assignment of Steele.[35] All out-of-plane frequencies are from Ref. 33.

FORCE FIELD AND POTENTIAL ENERGY DISTRIBUTION

The harmonic force field for azulene was arrived at through several iterations. In Table 2 the final force constants are given which reproduce the vibrational frequencies exactly. Some of the force constants in Table 2 might seem astonishingly great. However, they are understandable in wiew of the theory of redundant symmetry coordinates described by Cyvin and Cyvin.[38] Table 3 gives the approximate description of the normal modes according to the calculated potential energy distribution terms. Compared to the experimental assignment of frequencies (Table 1) there are a few discrepancies.

Table 2. Symmetry force constants (in mdyne/Å) for azulene.

1	7.320							Species A_1	
2	0.207	6.613							
3	−0.359	−0.529	7.828						
4	−0.440	−0.543	2.393	7.507					
5	−0.078	−0.315	−1.045	−1.670	7.055				
6	0.010	0.147	−3.905	−4.844	2.037	12.031			
7	−0.227	−0.059	−0.059	−0.174	0.118	0.115	0.641		
8	−0.242	−0.977	6.825	8.581	−3.415	−11.358	−0.364	23.102	
9	−0.114	−0.451	4.135	4.956	−1.813	−6.716	−0.139	13.225	8.313
10	−0.121	0.0531	−0.043	−0.006	0.006	0.009	−0.035	−0.052	−0.023
11	−0.050	−0.084	−0.027	−0.019	−0.041	−0.004	0.048	−0.012	−0.007
12	−0.020	−0.045	−0.101	0.037	−0.119	−0.006	−0.001	0.071	0.074
13	−0.014	−0.048	−0.063	−0.122	−0.012	0.070	−0.003	−0.213	−0.144
14	0	0.010	0.035	0.024	0.025	−0.092	0.005	0.126	0.087
15	−0.015	−0.075	0.085	0.074	0.029	0.013	−0.031	0.036	0.030
16	−0.035	−0.092	0.012	−0.021	−0.067	0.004	0.018	−0.094	−0.046
17	−0.042	−0.053	0.131	0.007	0.018	−0.177	−0.004	0.187	0.126
10	5.086							Species A_1	
11	0.041	5.115						(continued)	
12	−0.007	0.002	5.070						
13	0	−0.003	−0.055	4.973					
14	0	−0.001	0.018	−0.029	4.912				
15	0.013	−0.011	0.002	0.005	0.001	0.582			
16	0	−0.012	−0.016	−0.004	0.001	0.004	0.599		
17	−0.005	−0.003	0.018	−0.006	−0.010	0.012	0.032	0.595	

Table 2. Continued.

1	0.773				Species A_2				
2	−0.117	1.001							
3	−0.154	1.673	3.177						
4	−0.015	−0.046	−0.085	0.219					
5	0.020	0.009	−0.002	−0.010	0.192				
6	0.024	−0.016	−0.004	0.006	0.013	0.208			
1	0.320				Species B_1				
2	0.005	0.130							
3	−0.035	−0.018	0.195						
4	−0.041	−0.005	0.027	0.157					
5	0.031	−0.023	0.008	−0.006	0.223				
6	0.035	−0.011	0.043	−0.026	0.009	0.244			
7	−0.016	0.004	−0.043	0.053	−0.003	−0.009	0.220		
8	−0.003	0.018	−0.006	−0.002	0.005	0.003	0.004	0.217	
9	−0.020	0.002	−0.027	0.053	−0.009	0.001	0.009	0.001	0.227
1	8.482					Species B_2			
2	3.619	11.463							
3	1.050	1.583	8.241						
4	0.450	0.528	1.163	7.217					
5	0.112	0.094	0.182	0.701	6.297				
6	2.421	3.566	1.057	0.580	0.099	2.964			
7	−0.744	−1.438	0.394	0.008	−0.128	−0.668	1.466		
8	−0.040	−0.444	1.103	0.645	0.005	0.059	0.877	1.603	
9	−0.151	−0.102	0.001	−0.034	−0.006	0.006	−0.013	−0.026	
10	0.005	0.040	−0.043	−0.050	0.073	0.003	−0.026	−0.003	
11	0.014	−0.020	0.087	−0.019	−0.108	0.255	0.020	0.030	
12	−0.083	−0.107	0.042	0.080	0.005	−0.095	0.055	0.061	
13	0.068	0.137	0.217	0.135	0.044	0.059	−0.006	0.015	
14	0.022	0.041	−0.028	−0.036	−0.097	0.225	−0.066	−0.034	
15	0.216	0.096	0.008	0.020	0.012	0.026	−0.020	−0.014	
16	0.020	0.033	0.015	0.033	0.144	0.021	−0.006	0.007	
9	5.125					Species B_2 (continued)			
10	0.068	5.008							
11	−0.003	−0.040	4.925						
12	−0.001	−0.003	0.007	0.360					
13	−0.001	0.003	0.009	−0.033	0.336				
14	0	0.004	−0.010	0.007	0.038	0.374			
15	0.023	0.002	0.001	0.006	0.004	0.001	0.347		
16	0.001	0	0.013	0.007	0.014	−0.005	−0.003	0.352	

Table 3. Approximate description of normal modes and potential energy distribution for azulene.

Symm	Fre., cm^{-1}.		
A_1	3091	C−H stretching	$(31r' + 66s')$
	3074	C−H stretching	$(77t' + 16k')$
	3059	C−H stretching	$(65r' + 31s')$
	3024	C−H stretching	$(19t' + 66k' + 14l')$
	3002	C−H stretching	$(16k' + 83l')$
	1638	C−C stretching	$(20s + 44t + 33k + 34\delta + 11\varepsilon')$
	1580	C−C stretching	$(16r + 29s + 18k + 24\beta')$

Table 3. Continued.

	1443	CCC bend	$(33t+51h+19l+92\delta+102\varepsilon+19\phi')$
	1392	C–C stretching, CCC bend	$(15r+19h+18l+57\delta+10\beta'+21\varepsilon'+23\phi')$
	1294	C–C stretching, CCC bend	$(17r+23s+10\varepsilon'+17\phi')$
	1117	C–C stretching, CCC bend	$(11r+11k+10l+32\varepsilon'+19\phi')$
	1054	CCH ip [a] bend	$(33r+12\delta+43\beta')$
	899	C–C stretching	$(13k+98l+60\delta)$
	671	CCC bend	$(128\delta+466\varepsilon)$
	559	C–C stretching, CCC bend	$(35t+71h+18l+15\beta+20\delta)$
	492	CCC bend	$(12t+74\beta+106\delta+52\varepsilon)$
	403	CCC bend	$(739\delta+514\varepsilon)$
A_2	1000	Ring torsion, CCH op [a] bend	$(172\tau_k+108\tau_l+49\varepsilon''+35\phi'')$
	908	CCH op [a] bend	$(13\tau_l+58\beta''+21\phi'')$
	795	CCH op [a] bend	$(27\beta''+28\varepsilon''+39\phi'')$
	531	Ring torsion, CCH op [a] bend	$(22\tau_r+30\tau_k+14\beta''+21\varepsilon'')$
	323	Ring torsion	$(653\tau_k+701\tau_l)$
	163	Ring torsion	$(65\tau_r+27\tau_l)$
B_1	1000	Ring op [a] deformation, CCH op [a] bend	$(42\tau_k+63\tau_l+22\varepsilon''+58\phi''+42\theta'')$
	960	CCH op [a] bend	$(18\tau_r+53\beta''+40\alpha'')$
	946	CCH op [a] bend	$(64\varepsilon''+26\theta'')$
	764	CCH op [a] bend	$(35\beta''+47\alpha'')$
	721	CCH op [a] bend	$(14\varepsilon''+46\phi''+32\theta'')$
	664	Ring op [a] deformation	$(11\xi+24\tau_k+23\tau_l)$
	492	Ring op [a] deformation	$(48\xi+18\tau_r+24\tau_l)$
	311	Ring op [a] deformation	$(20\xi+65\tau_r+11\tau_k)$
	165	Ring op [a] deformation	$(13\xi+47\tau_k+14\tau_l)$
B_2	3083	C–H stretching	$(98s')$
	3044	C–H stretching	$(84t'+14k')$
	3007	C–H stretching	$(15t'+84k')$
	1694	C–C stretching	$(41s+37t+23k+17l+23\delta)$
	1580	C–C stretching	$(25s+59l+11\theta')$
	1479	C–C stretching	$(86r+21\beta+35\alpha')$
	1453	C–C stretching	$(39s+34k+21\theta')$
	1301	C–C stretching, CCH ip [a] bend	$(11s+28t+37\theta')$
	1205	Ring ip [a] bend, CCH ip [a] bend	$(25r+11s+18\beta+12\delta+47\alpha')$
	1151	Ring ip [a] bend, CCH ip [a] bend	$(12t+14k+13l+18\varepsilon'+22\theta')$
	1007	CCH ip [a] bend	$(16\delta+12\varepsilon+58\beta'+12\phi')$
	970	CCH ip [a] bend	$(18\varepsilon'+56\phi')$
	721	CCH ip [a] bend, ring ip [a] bend	$(13s+18k+12\beta+22\beta'+56\varepsilon'+16\phi')$
	593	Ring ip [a] bend	$(25s+81\beta+71\delta+92\varepsilon)$
	559	Ring ip [a] bend	$(24\beta+38\varepsilon)$
	478	Ring ip [a] bend	(42δ)

[a] ip = in plane, op = out of plane.

Table 4. Mean amplitudes of vibration, u, (Å units), for azulene.

Distance type $(i-j)^a$		(Equil. dist. in Å)	u spectr. 0 K	u spectr. 298 K	u electr. diff. Ref. 29
C–H	(1–11)	(1.085)	0.0770	0.0770	
C–H	(2–12)	(1.085)	0.0769	0.0769	
C–H	(6–14)	(1.085)	0.0772	0.0772	0.090
C–H	(8–16)	(1.085)	0.0776	0.0776	
C–H	(10–18)	(1.085)	0.0777	0.0777	
C–C	(1–2)	(1.399)	0.0447	0.0448	0.0486
C–C	(2–4)	(1.418)	0.0442	0.0445	
C–C	(4–5)	(1.501)	0.0488	0.0497	
C–C	(4–6)	(1.383)	0.0446	0.0451	
C–C	(6–8)	(1.406)	0.0445	0.0448	
C–C	(8–10)	(1.403)	0.0451	0.0454	
C···C	(1–4)	(2.290)	0.0569	0.0603	
C···C	(1–6)	(3.624)	0.0608	0.0652	
C···C	(1–8)	(4.780)	0.0648	0.0705	
C···C	(1–10)	(5.203)	0.0670	0.0741	
C···C	(2–6)	(2.487)	0.0553	0.0584	
C···C	(2–8)	(3.808)	0.0598	0.0639	
C···C	(2–10)	(4.548)	0.0636	0.0694	
C···C	(2–9)	(4.509)	0.0618	0.0657	
C···C	(2–7)	(3.685)	0.0594	0.0623	
C···C	(2–5)	(2.335)	0.0551	0.0572	
C···C	(2–3)	(2.292)	0.0575	0.0604	0.054
C···C	(4–8)	(2.499)	0.0542	0.0567	
C···C	(4–10)	(3.130)	0.0608	0.0658	0.078
C···C	(4–9)	(3.172)	0.0601	0.0637	
C···C	(4–7)	(2.599)	0.0571	0.0596	
C···C	(6–10)	(2.537)	0.0554	0.0571	0.057
C···C	(6–9)	(3.190)	0.0641	0.0687	
C···C	(6–7)	(3.227)	0.0664	0.0723	
C···C	(8–9)	(2.542)	0.0584	0.0614	
C···H	(1–12)	(2.212)	0.1007	0.1033	
C···H	(1–14)	(4.029)	0.1334	0.1379	
C···H	(1–16)	(5.703)	0.1080	0.1116	
C···H	(1–18)	(6.288)	0.0989	0.1040	
C···H	(2–11)	(2.208)	0.0975	0.0981	
C···H	(2–14)	(2.688)	0.1373	0.1420	
C···H	(2–16)	(4.598)	0.1127	0.1155	
C···H	(2–18)	(5.604)	0.0984	0.1024	
C···H	(2–17)	(5.550)	0.0979	0.1003	
C···H	(2–15)	(4.414)	0.1179	0.1207	
C···H	(2–13)	(3.335)	0.0934	0.0947	
C···H	(4–11)	(3.335)	0.0942	0.0966	
C···H	(4–12)	(2.231)	0.1055	0.1074	
C···H	(4–13)	(3.390)	0.0955	0.0976	
C···H	(4–14)	(2.103)	0.1048	0.1057	
C···H	(4–16)	(3.416)	0.0998	0.1010	
C···H	(4–18)	(4.192)	0.0961	0.0995	
C···H	(4–17)	(4.242)	0.0948	0.0970	
C···H	(4–15)	(3.528)	0.1015	0.1030	
C···H	(6–16)	(2.113)	0.1051	0.1059	
C···H	(6–18)	(3.444)	0.0998	0.1008	
C···H	(6–17)	(4.250)	0.0997	0.1032	
C···H	(6–15)	(4.293)	0.0987	0.1025	

Table 4. Continued.

C···H	(6 – 13)	(4.708)	0.1019	0.1049
C···H	(6 – 11)	(4.621)	0.0996	0.1029
C···H	(6 – 12)	(2.858)	0.1345	0.1394
C···H	(8 – 18)	(2.106)	0.1013	0.1017
C···H	(8 – 17)	(3.448)	0.1085	0.1111
C···H	(8 – 15)	(4.254)	0.0997	0.1035
C···H	(8 – 13)	(5.403)	0.1136	0.1178
C···H	(8 – 11)	(5.834)	0.0991	0.1032
C···H	(8 – 12)	(4.263)	0.1360	0.1414
C···H	(8 – 14)	(2.123)	0.1118	0.1140
C···H	(10 – 11)	(6.288)	0.0987	0.1038
C···H	(10 – 12)	(5.232)	0.1281	0.1340
C···H	(10 – 14)	(3.455)	0.1068	0.1091
C···H	(10 – 16)	(2.110)	0.1107	0.1126
H···H	(11 – 12)	(2.653)	0.1597	0.1616
H···H	(11 – 14)	(4.894)	0.1644	0.1692
H···H	(11 – 16)	(6.723)	0.1351	0.1384
H···H	(11 – 18)	(7.373)	0.1226	0.1268
H···H	(12 – 14)	(2.622)	0.1952	0.2024
H···H	(12 – 16)	(4.858)	0.1790	0.1843
H···H	(12 – 18)	(6.236)	0.1538	0.1593
H···H	(12 – 17)	(6.472)	0.1340	0.1374
H···H	(12 – 15)	(5.484)	0.1392	0.1420
H···H	(12 – 13)	(4.339)	0.1219	0.1224
H···H	(14 – 16)	(2.353)	0.1852	0.1901
H···H	(14 – 18)	(4.227)	0.1487	0.1510
H···H	(14 – 17)	(5.299)	0.1286	0.1321
H···H	(14 – 15)	(5.347)	0.1230	0.1257
H···H	(16 – 18)	(2.328)	0.1693	0.1715
H···H	(16 – 17)	(4.215)	0.1519	0.1549

MEAN AMPLITUDES OF VIBRATION

Table 4 shows the calculated mean amplitudes of vibration (u) at absolute zero and 298 K, along with the observed values from electron diffraction. No serious discrepancies between observed and calculated u values are found.

Table 5. Bond lengths, r, and mean amplitudes of vibration, u, (Å units) of bonded carbon-carbon atom pairs in some cyclic hydrocarbons at 298 K.

Molecule	C=C double bond		CC aromatic		C–C single bond	
	r	u	r	u	r	u
Benzene[a]			1.397	0.0461		
1,4-Cyclohexadiene[b]	1.334	0.0419			1.496	0.0475
1,3-Cyclohexadiene[b]	1.348	0.0427			1.465	0.0484
					1.519	0.0478
					1.538	0.0482
Azulene			1.383	0.0451	1.501	0.0497
			1.399	0.0448		
			1.403	0.0454		
			1.406	0.0448		
			1.418	0.0445		

[a] From Ref. 28. [b] From Ref. 12.

Carbon-carbon bond lengths and corresponding u values for some cyclic hydrocarbons are shown in Table 5. It is seen that a clear correlation exists between the bond length, mean amplitude of vibration, and the type of carbon-carbon bond (*e.g.* double bond, aromatic bond, single bond). Single-bond u values lie around 0.048 – 0.050 Å, double-bond values around 0.042 Å, whereas aromatic carbon-carbon u values lie in between these limits, around 0.045 – 0.046 Å. The bond 4 – 5 (Fig. 1) of azulene has typical single-bond values of r and u, and all the other carbon-carbon bond lengths and mean amplitudes are typical for aromatic molecules.

Acknowledgement. The author is indebted to Professor S. J. Cyvin for valuable discussions.

REFERENCES

1. Davis, M. I. and Muecke, T. W. *J. Phys. Chem.* **74** (1970) 1104.
2. Adams, W. J., Geise, H. J. and Bartell, L. S. *J. Am. Chem. Soc.* **92** (1970) 5013.
3. Dallinga, G., Van der Draai, R. K. and Toneman, L. H. *Rec. Trav. Chim.* **87** (1968) 897.
4. Chiang, J. F. and Bauer, S. H. *J. Am. Chem. Soc.* **91** (1969) 1898.
5. Trætteberg, M. *Acta Chem. Scand.* **22** (1968) 2305.
6. Oberhammer, H. and Bauer, S. H. *J. Am. Chem. Soc.* **91** (1969) 10.
7. Dallinga, G. and Toneman, L. H. *J. Mol. Struct.* **1** (1967) 11.
8. Dallinga, G. and Toneman, L. H. *J. Mol. Struct.* **1** (1967) 117.
9. Neto, N., Di Lauro, C., Castellucci, E. and Califano, S. *Spectrochim. Acta* **A 23** (1967) 1763.
10. Di Lauro, C., Neto. N. and Califano, S. *J. Mol. Struct.* **3** (1969) 219.
11. Stidham, H. D. *Spectrochim. Acta* **21** (1965) 23.
12. Gebhardt, O. *Thesis*, Trondheim NTH 1971.
13. Hagen, K. *Thesis*, Trondheim NLHT 1970.
14. Chiang, J. F. and Bauer, S. H. *J. Am. Chem. Soc.* **88** (1966) 420.
15. Hagen, G. *Private communication.*
16. Cyvin, S. J., Elvebredd, I., Hagen, G. and Andersen, B. *Chem. Phys. Lett.* **2** (1968) 556.
17. Chiang, J. F. and Bauer, S. H. *J. Am. Chem. Soc.* **92** (1970) 1614.
18. Almenningen, A., Andersen, B. and Nyhus, B. A. *Acta Chem. Scand.* **25** (1971) 1217.
19. Bohn, R. K. and Tai, Y.-H. *J. Am. Chem. Soc.* **92** (1970) 6447.
20. Karle, I. L. *J. Chem. Phys.* **20** (1952) 65.
21. Bastiansen, O., Hedberg, L. and Hedberg, K. *J. Chem. Phys.* **27** (1957) 1311; Erratum: *Ibid.* **28** (1958) 512.
22. Trætteberg, M. *Acta Chem. Scand.* **20** (1966) 1724.
23. Haugen, W. and Trætteberg, M. In Andersen, P., Bastiansen, O. and Furberg, S., Eds., *Selected Topics in Structure Chemistry*, Universitetsforlaget, Oslo 1967, p. 113.
24. Trætteberg, M. *Acta Chem. Scand.* **24** (1970) 2285.
25. Trætteberg, M. *Proc. Roy. Soc. (London) Ser. A* **283** (1965) 557.
26. Dallinga, G., Toneman, L. H. and Trætteberg, M. *Rec. Trav. Chim.* **86** (1967) 795.
27. Almenningen, A., Bastiansen, O. and Dyvik, F. *Acta Cryst.* **14** (1961) 1056.
28. Cyvin, S. J. *Molecular Vibrations and Mean Square Amplitudes*, Universitetsforlaget, Oslo 1968.
29. Cyvin, B. N. and Cyvin, S. J. *J. Phys. Chem.* **73** (1969) 1430.
30. Almenningen, A., Bastiansen, O. and Fernholt, L. *Kgl. Norske Videnskab. Selskabs Skrifter* **1958** No. 3.
31. Kimura, K. and Kubo, M. *J. Chem. Phys.* **32** (1960) 1776.
32. Bastiansen, O. and Derrisen, J. L. *Acta Chem. Scand.* **20** (1966) 1319.
33. Steele, D. *J. Mol. Spectry.* **15** (1965) 333.
34. Van Tets, A. and Günthard, H. H. *Spectrochim. Acta* **19** (1963) 1495.

35. Steele, D. *Spectrochim. Acta* **22** (1966) 1275.
36. Hunt, G. R. and Ross, I. G. *J. Mol. Spectry.* **3** (1959) 604.
37. Wilson, E. B., Jr., Decius, J. C. and Cross, P. C. *Molecular Vibrations*, McGraw, New York 1955, 117–125.
38. Cyvin, B. N. and Cyvin, S. J. *Acta Chem. Scand.* **23** (1969) 3139.

Received December 27, 1972.

ACTA CHEMICA SCANDINAVICA 27 (1973) 1735–1739

The Molecular Structure of Hexachlorofulvene

ANNE SKANCKE

Department of Chemistry, University of Oslo, Oslo 3, Norway

The molecular structure of hexachlorofulvene has been determined by means of the electron diffraction method. This overcrowded molecule is planar and the structure of the carbon skeleton is strongly alternating. The main conclusions from the electron diffraction investigation are verified by an SCF-MO calculation using the PPP approximation. The results are compared to recent experimental investigations of fulvene.

This work on the hexachlorofulvene molecule is part of an investigation of the aromatic character of some $sp^2\pi$ hybridized ring systems.

Previously, a PPP calculation on the hydrocarbon fulvene and the isomer 3,4-dimethylenecyclobutene has been carried out,[1] and subsequently the calculated geometry of the latter molecule was confirmed by an electron diffraction investigation.[2]

Due to its instability, the fulvene molecule is difficult to investigate by means of electron diffraction. An early investigation has been carried out,[3] but gives by no means an unambiguous solution as to the geometry of the molecule.

In this work, the effect of a substituent, chlorine, on the geometric stability of the ring system is investigated. A valuable supplement to the present studies was given by the completion of a microwave study of fulvene by Brown and coworkers.[4] The main conclusions reached in the present electron diffraction studies have been confirmed by semi-empirical studies of the same type as those applied to the hydrocarbon series.

A sample of the molecule was kindly put at my disposal by Dr. I. Agranat and Professor E. D. Bergmann at the Hebrew University of Jerusalem.

EXPERIMENTAL

The electron diffraction diagrams were taken at the Oslo diffraction unit.[5] Recordings were taken at two nozzle to plate distances, about 48 cm and about 19 cm. The nozzle temperature was about 150°C. Three plates from the longer distance and four from the shorter were used, and their optical densities measured at $\Delta s = 0.125$ Å^{-1} and $\Delta s = 0.25$ Å^{-1}, respectively. A total intensity range from $s = 1.375$ Å^{-1} to $s = 23$ Å^{-1} was covered, the range from $s = 6.75$ Å^{-1} to $s = 19.75$ Å^{-1} being the overlap region.

Recorded data beyond 23 $Å^{-1}$ on the 19 cm curves were found to be too inaccurate to be included in the work. The data were processed at a CDC 6600 computer at the University of Texas at Austin, applying computer programs described elsewere.[6]

The various peaks of the radial distribution curve, shown in Fig. 1, could readily be interpreted in terms of internuclear distances.

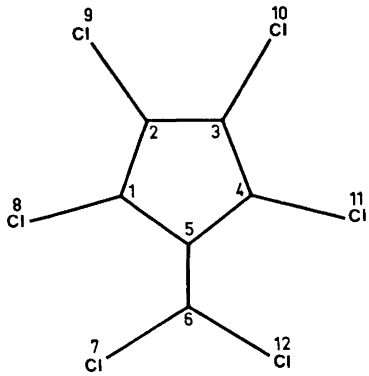

Fig. 1. Hexachlorofulvene. Numbering of atoms.

The first peak at about 1.4 Å has contributions from all C–C bond distances. The next, large peak at about 1.7 Å is composed of the six C–Cl bond distances, and at about 2.3 Å is a small peak due to the next-to-neighbours C···C distances. The peak with maximum at about 6.65 Å gives the longest Cl–Cl distance, and gives immediately an indication of the planarity of the chlorine atoms 8, 9, 11 and 12. For labelling of atoms, see Fig. 2. All other peaks are rather complex and have contributions from several

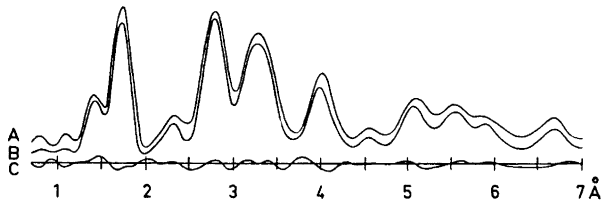

Fig. 2. Radial distribution curve. A. Experimental. B. Theoretical. C. B–A.

distances. Because of the relatively large contribution to the scattering pattern from the chlorine atoms, the radial distribution curve is highly sensitive to even small changes in parameters involving the chlorine atoms.

Little information about the C–C bond distances can be deduced directly from the corresponding peak. This is because there are four different bond distances and the peak is influenced by the large and dominating contribution from the C–Cl bond distances. The C–C bond distances were therefore estimated from the shape of the peak at about 2.3 Å and a general fit of the experimental and theoretical curves. These estimates were refined by the least squares method, but the corresponding amplitudes of vibration were not possible to refine.

Several non-planar models were tested, but none of these fits the experimental data better than the planar model given by the parameters in Table 1.

The standard deviations given in parenthesis are the results from using a diagonal weight matrix only, and may be somewhat too small. The results are compared to existing information of the related compound fulvene.

MO CALCULATIONS

A molecular orbital calculation has been carried out on the system, using the PPP scheme in the ZDO approximation. The parameters for the chlorine atoms are taken from a work by Grabe.[7] That paper also gives a complete list of references pertaining to the method of calculation applied here. The bond distances obtained in the calculation are given in Table 1, which also

Table 1. Bond distances. In Å units. Numbers in parenthesis give the standard deviation corrected for error in wave length.

Distance	Fulvene SCF-MO[a]	Fulvene M.W.[b]	Present work perchlorofulvene SCF-MO	Present work perchlorofulvene E.D.
1 – 2	1.357	1.355	1.362	1.358 (0.005) $u = 0.043$
2 – 3	1.450	1.476	1.447	1.424 (0.005) $u = 0.045$
4 – 5	1.466	1.470	1.460	1.478 (0.002) $u = 0.045$
5 – 6	1.355	1.349	1.360	1.369 (0.012) $u = 0.043$
1 – 7			1.695	1.7070 (0.0021) $u = 0.048$
2 – 8				
6 – 12			1.687	1.6960 (0.0021) $u = 0.048$

[a] Ref. 1. [b] Ref. 4.

gives the results for the hydrocarbon. As is seen from the table, the results of the SCF calculation give nearly identical carbon skeletons for the substituted and unsubstituted molecule. Comparing the SCF results of perchlorofulvene data, the general agreement is good, but there seems to be a slight effect of "smearing out" of bond distances in the perchlorinated molecule. Comparing the SCF results with those from the electron diffraction, the general agreement is good for the two double bonds. Both the calculation and the experimental results give larger double bond distances in the perchlorinated molecule than in fulvene itself. As for the single bonds, the picture is more complicated. A striking difference is seen for the values of bond 2 – 3, where the experimental result is about 0.02 Å shorter than predicted by the SCF calculation. Looking at the atomic charges in Table 2, it is seen that the ring has an increase in

Table 2. Atomic charges.

Atom	Fulvene Theor.	Hexachlorofulvene
1	1.025	1.0537
2	1.028	1.0483
5	0.870	1.0489
6	1.030	0.8714
7		1.9825
8		1.9829
11		1.9725

charge of about 0.3 electrons in going from the hydrocarbon to the perchlorinated molecule. Atoms 5 and 6 have a net positive and negative charge, respectively, in the hydrocarbon, while the reverse is true for the perchlorinated species. This is consistent with the less pronounced single bond-double bond character predicted by the SCF calculation, but the experimentally found difference in the two C – C single bonds cannot be explained in terms of the applied π-electron theory.

A possible explanation may be found by considering the electronic distribution given by the configuration generated by a double excitation from the highest filled to the lowest vacant molecular orbital. This configuration leads to a drastic increase of the mobile bond order for the bond 2 – 3. By an improvement of the molecular ground state through mixing with this configuration, a shortening of the bond 2 – 3 would occur.

The molecular spectrum for hexachlorofulvene has been calculated and compared to the experimentally recorded values.[8] The latter are measured in two solvents, ethanol and benzene, an excellent correspondence is found between the two experimental series.

Table 3. Molecular spectrum for hexachlorofulvene in the UV region. In cm^{-1}. Numbers in parenthesis give the extinction coefficients for the experimental data and the *f*-values for the calculation.

Experimental		Calculated
in EtOH	in C_6H_6	
23.000 (450)	22.500 (420)	26.900 (0.06)
31.100 (10.700)	30.700 (10.000)	
32.300 (18.300)	31.800 (15.400)	
		39.100 (0.67)
33.400 (19.000)	33.000 (15.600)	
34.480 (14.600)	34.000 (13.300)	
		52.400 (0.076)
		58.200 (0.9)
		58.200 (0.2)

The low-lying weak transition predicted at 26 900 cm^{-1} has its experimental counterpart at about 4000 cm^{-1} lower values but this discrepancy may be partly due to solvent effects for this very polar molecule. Experimentally, a series of four close-lying transitions follows, all spaced by about 1200 cm^{-1}. The calculation gives only one electronic transition in this energy range. Since a normal value for the C – Cl vibrational frequency in aromatic molecules is about 1500 cm^{-1}, it is tempting to assume that the experimental sequence is due to vibrational C – Cl transitions rather than to electronic transitions. The center of gravity of the band at about 32 500 cm^{-1} is, however, considerably lower than the calculated band at 39 100 cm^{-1}.

In addition to the above mentioned solvent shift as a possible explanation of the discrepancies between predicted and measured transition energies, it may also be appropriate to include the fact that this molecule is a strained one.

During an electronic excitation such a molecule will most likely undergo drastic deformations leading to electronic distributions deviating significantly from those for which the applied semi-empirical parameters are appropriate.

The dipole moments of the y and z directions vanish by symmetry, and the total, calculated dipole moment is along the x axis. This is calculated as 2.3 D, compared to the experimental value of 1.0 D. This indicates that the sigma core is strongly polarized.

The experimental spectrum has not been recorded in the energy range where the strongest absorptions are predicted to occur.

Acknowledgement. The author is indebted to Cand. real. A. Almenningen and Siv. ing. Birgit Andersen at the University of Oslo for help with the electron diffraction recordings. This work was in part carried out during a stay at the University of Texas at Austin, and thanks are due to Dr. D. Kohl and Dr. J. E. Boggs at that institution for placing facilities at my disposal, and for stimulating discussions. This work has been partially supported by the Robert A. Welch Foundation.

REFERENCES

1. Skancke, A. and Skancke, P. N. *Acta Chem. Scand.* **22** (1968) 175.
2. Skancke, A. *Acta Chem. Scand.* **22** (1968) 3239.
3. Rouault, M. and Waziutynska, Z. L. *Acta Cryst.* **10** (1957) 804.
4. Brown, R. D. *Private communication.*
5. Bastiansen, O., Hassel, O. and Risberg, F. *Acta Chem. Scand.* **9** (1955) 232.
6. Bartell, L. S., Kohl, D. A. Carrol, B. L. and Gavin, R. M., Jr. *J. Chem. Phys.* **42** (1965) 3079.
7. Grabe, B., *Acta Chem. Scand.* **22** (1968) 2237.
8. Agranat, I. *Private communication.*

Received December 4, 1972.

ACTA CHEMICA SCANDINAVICA 27 (1973) 1740–1748

Substituted Propanes

Part X. 2,2-Dicyano-, 2,2-Difluoro-, and 2,2-Diiodopropane

B. N. CYVIN and S. J. CYVIN

Institutt for teoretisk kjemi, Norges tekniske høgskole, N-7034 Trondheim, Norway

Harmonic force fields are given for 2,2-dicyanopropane and 2,2-difluoropropane. They are presented as F matrices in terms of thoroughly specified symmetry coordinates. For the cyano compound the analysis was based on experimental data not published previously. The similar analysis was performed tentatively for 2,2-diiodopropane, for which the available spectral data are incomplete. A set of predicted vibrational frequencies is proposed. The developed force fields were used to calculate mean amplitudes of vibration and perpendicular amplitude correction coefficients.

This work is a continuation of the systematic studies of spectra and structures of substituted propanes. It deals with 2,2-dicyano-, 2,2-difluoro-, and 2,2-diiodopropane. The related molecules 2,2-dichloro- and 2,2-dibromopropane were studied extensively before.[1,2] Also the monosubstituted molecules 2-chloro-, 2-bromo-, 2-iodo-, and 2-cyanopropane [3,4] are of relevance to the present work.

A normal coordinate analysis was performed for 2,2-dicyanopropane using recent spectral data not published previously. The developed harmonic force field was used to calculate the mean amplitudes of vibration [5] and perpendicular amplitude correction coefficients.[5] These quantities are of great interest in modern gas electron diffraction investigations (see, *e.g.*, Ref. 6). The corresponding analysis was also performed for 2,2-difluoropropane using spectral data from recent literature.[7,8] For 2,2-diiodopropane the available spectral data are very incomplete. From the present analysis we have tentatively produced a set of predicted vibrational frequencies for this molecule.

A precise definition of the applied symmetry coordinates is given. This seems to be well justified because a set of independent internal coordinates for the molecular vibrations is very important as the basis of the force field documentations.

MOLECULAR MODELS

The molecular symmetry of propane (C_{2v}) is maintained under the 2,2-disubstitutions. Fig. 1 shows the 2,2-dicyanopropane model. The same model is applicable to propane type molecules on neglecting the atoms number 12 and 13.

VALENCE COORDINATES

The notation for valence coordinates was adopted from the analysis of the propane molecular model by Vizi and Cyvin [9] and supplemented with the new coordinate types pertaining to the cyano groups. The former set is briefly summarized below.

(i) Two CX stretchings d. (ii) Two CC stretchings r. (iii) Two CH stretchings s in the skeleton plane. (iv) Four CH stretchings t involving H atoms outside the skeleton plane. (v) The CCC bending α. (vi) Four CCX bendings β. (vii) Four HCH bendings γ, where one of the H atoms lies in the skeleton plane and the other is outside. (viii) Four CCH bendings δ, where the H atom is outside the skeleton plane. (ix) Two CCH bendings ε, where H lies in the skeleton plane. (x) Two CCCH torsions, τ, where H lies in the skeleton plane.

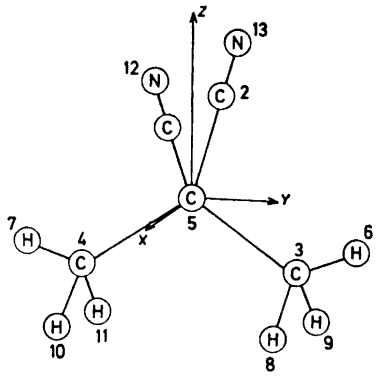

Fig. 1. The 2,2-dicyanopropane molecule model.

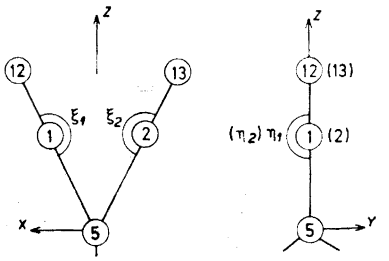

Fig. 2. Definition of the linear bending coordinates in the 2,2-dicyanopropane molecule model.

When dealing with the 2,2-dicyanopropane model the X atoms become carbon atoms of the cyano groups. The following valence coordinates are defined in addition to those summarized above.

(xi) Two CN stretchings: p_1, p_2 for the atoms 1 – 12 and 1 – 13, respectively.

(xii) Two linear bendings CCN in the XCX plane: ξ_1, ξ_2 for the atoms 5 – 1 – 12 and 5 – 2 – 13, respectively (see Fig. 2).

(xiii) Two linear bendings CCN perpendicular to the XCX plane: η_1 (5 – 1 – 12) and η_2 (5 – 2 – 13) (see Fig. 2).

SYMMETRY COORDINATES

The valence coordinates were used to construct a complete set of independent symmetry coordinates. For the 2,2-dicyanopropane type molecules, the normal modes are distributed according to

$$\Gamma_{\text{vib}}(2,2\text{-dicyanopropane}) = 11A_1 + 6A_2 + 8B_1 + 8B_2$$

The present scheme of symmetry coordinates (see below) is also applicable to propane type molecules. We have namely chosen the sequence of symmetry coordinates in such a way that the particular ones pertaining to the 2,2-dicyanopropane model within each species are added at the end. For propane type molecules, one only has to apply the appropriate number of symmetry coordinates belonging to the different species in accord with the symmetric structure:

$$\Gamma_{\text{vib}}(\text{propane}) = 9A_1 + 5A_2 + 6B_1 + 7B_2$$

Species A_1:

$$S_1(A_1) = 2^{-\frac{1}{2}}(d_1 + d_2)$$
$$S_2(A_1) = 2^{-\frac{1}{2}}(r_1 + r_2)$$
$$S_3(A_1) = 2^{-\frac{1}{2}}(s_1 + s_2)$$
$$S_4(A_1) = \tfrac{1}{2}(t_1 + t_2 + t_3 + t_4)$$
$$S_5(A_1) = R\alpha$$
$$S_6(A_1) = \tfrac{1}{2}(RD)^{\frac{1}{2}}(\beta_1 + \beta_2 + \beta_3 + \beta_4)$$
$$S_7(A_1) = \tfrac{1}{2}(ST)^{\frac{1}{2}}(\gamma_1 + \gamma_2 + \gamma_3 + \gamma_4)$$
$$S_8(A_1) = \tfrac{1}{2}(RT)^{\frac{1}{2}}(\delta_1 + \delta_2 + \delta_3 + \delta_4)$$
$$S_9(A_1) = (RS/2)^{\frac{1}{2}}(\varepsilon_1 + \varepsilon_2)$$
$$S_{10}(A_1) = 2^{-\frac{1}{2}}(p_1 + p_2)$$
$$S_{11}(A_1) = (DP/2)^{\frac{1}{2}}(\xi_1 + \xi_2)$$

Species A_2:

$$S_1(A_2) = \tfrac{1}{2}(t_1 - t_2 - t_3 + t_4)$$
$$S_2(A_2) = \tfrac{1}{2}(RD)^{\frac{1}{2}}(\beta_1 - \beta_2 - \beta_3 + \beta_4)$$
$$S_3(A_2) = \tfrac{1}{2}(ST)^{\frac{1}{2}}(\gamma_1 - \gamma_2 - \gamma_3 + \gamma_4)$$
$$S_4(A_2) = \tfrac{1}{2}(RT)^{\frac{1}{2}}(\delta_1 - \delta_2 - \delta_3 + \delta_4)$$
$$S_5(A_2) = (RS/2)^{\frac{1}{2}}(\tau_1 + \tau_2)$$
$$S_6(A_2) = (DP/2)^{\frac{1}{2}}(\eta_1 - \eta_2)$$

Species B_1:

$$S_1(B_1) = 2^{-\frac{1}{2}}(d_1 - d_2)$$
$$S_2(B_1) = \tfrac{1}{2}(t_1 - t_2 + t_3 - t_4)$$
$$S_3(B_1) = \tfrac{1}{2}(RD)^{\frac{1}{2}}(\beta_1 - \beta_2 + \beta_3 - \beta_4)$$
$$S_4(B_1) = \tfrac{1}{2}(ST)^{\frac{1}{2}}(\gamma_1 - \gamma_2 + \gamma_3 - \gamma_4)$$
$$S_5(B_1) = \tfrac{1}{2}(RT)^{\frac{1}{2}}(\delta_1 - \delta_2 + \delta_3 - \delta_4)$$
$$S_6(B_1) = (RS/2)^{\frac{1}{2}}(\tau_1 - \tau_2)$$
$$S_7(B_1) = 2^{-\frac{1}{2}}(p_1 - p_2)$$
$$S_8(B_1) = (DP/2)^{\frac{1}{2}}(\xi_1 - \xi_2)$$

Species B_2:

$$S_1(B_2) = 2^{-\frac{1}{2}}(r_1 - r_2)$$
$$S_2(B_2) = 2^{-\frac{1}{2}}(s_1 - s_2)$$
$$S_3(B_2) = \tfrac{1}{2}(t_1 + t_2 - t_3 - t_4)$$
$$S_4(B_2) = \tfrac{1}{2}(RD)^{\frac{1}{2}}(\beta_1 + \beta_2 - \beta_3 - \beta_4)$$
$$S_5(B_2) = \tfrac{1}{2}(ST)^{\frac{1}{2}}(\gamma_1 + \gamma_2 - \gamma_3 - \gamma_4)$$
$$S_6(B_2) = \tfrac{1}{2}(RT)^{\frac{1}{2}}(\delta_1 + \delta_2 - \delta_3 - \delta_4)$$
$$S_7(B_2) = (RS/2)^{\frac{1}{2}}(\varepsilon_1 - \varepsilon_2)$$
$$S_8(B_2) = (DP/2)^{\frac{1}{2}}(\eta_1 + \eta_2)$$

Here the capital letters R, D, S, T, and P are used in scaling factors and designate the equilibrium distances of C–C(methyl), C–C(cyano), C–H (in skeleton plane), C–H (out of skeleton plane) and C≡N, respectively.

The symmetry coordinate set for the propane model, which is a part of the above set, is identical to the symmetry coordinate set given elsewhere.[9] It was used previously as the basis of symmetry force constants for propane,[2,10] 2,2-dichloropropane,[2] and 2,2-dibromopropane.[2]

2,2-DICYANOPROPANE (DIMETHYLMALONITRILE)

The $(CH_3)_2C(CN)_2$ and $(CD_3)_2C(CN)_2$ molecules were investigated by infrared and Raman spectroscopy [11] as a part of systematic studies of substituted malonitriles. A report of the experimental part is to be published elsewhere. That work was performed parallel with the present analysis, and initial force constant calculations were used as an aid in the assignment of the experimental frequencies.

An initial force field was constructed by transferring the force constants from related molecules.[2,4] It seems not to be of interest to report any details of the different steps of iteration in the refinements of the force field. The final force constants (see Table 1) were adjusted so as to fit accurately the experimental frequencies for $(CH_3)_2C(CN)_2$. They are (in cm^{-1}): (A_1) 3004, 2951, 2252, 1443, 1397, 1197, 951, 665, 580, 510, and 150; (A_2) 3004, 1459, 1020, 351, 236 and 204; (B_1) 3004, 2252, 1472, 1224, 1128, 468, 320, and 282; (B_2) 3004, 2951, 1459, 1376, 1224, 951, 390, and 195. The calculated frequencies for $(CD_3)_2C(CN)_2$ from the final force field are: (A_1) 2270, 2242, 2128, 1136, 1078, 1030, 785, 622, 508, 490, and 149; (A_2) 2247, 1042, 798, 339, 187, and 167; (B_1) 2277, 2230, 1356, 931, 876, 444, 281, and 221; (B_2) 2245, 2128, 1229, 1066, 984, 743, 372, and 185. The frequencies for the deuterated compound were found to be generally in satisfactory agreement with the observed values.[11] A detailed discussion of the assignment of the experimental frequencies is postponed to the coming publication.

The final force field is given in Table 1 in terms of the symmetry F matrix blocks. It was used to calculate the mean amplitudes of vibration (u) and perpendicular amplitude correction coefficients (K).[5,6,12] The results for all the twenty-eight interatomic distance types in $(CH_3)_2C(CN)_2$ at the temper-

Table 1. Symmetry force constants (mdyn/Å) for 2,2-dicyanopropane.

Species A_1								
1	6.24							
2	0.48	3.83						
3	−0.03	−0.03	4.82					
4	0.04	−0.03	0.12	4.91				
5	−0.41	0.29	−0.05	0.03	1.19			
6	−0.11	0.05	−0.01	0.01	0.18	1.80		
7	0.07	0.01	−0.04	0.03	−0.04	0.03	1.27	
8	0.08	0.26	0.02	0.03	0.05	0.01	0.72	1.06
9	0.13	0.20	−0.03	0.05	−0.09	−0.02	0.52	0.40
10	−0.51	0.36	−0.06	0.05	−0.46	−0.05	0.03	0.11
11	−0.03	0.08	0.01	−0.00	0.04	−0.08	−0.02	0.01
Species A_1 (continued)								
9	0.73							
10	0.04	16.16						
11	−0.02	−0.02	0.22					
Species A_2								
1	4.77							
2	0.01	0.33						
3	−0.03	−0.04	0.42					
4	−0.04	−0.07	−0.04	0.42				
5	0.00	−0.01	0.02	0.01	0.06			
6	0.01	−0.06	−0.01	−0.03	0.01	0.15		
Species B_1								
1	5.05							
2	−0.02	4.75						
3	−0.12	0.04	1.08					
4	−0.14	−0.05	0.12	0.40				
5	−0.24	−0.04	0.09	0.04	0.58			
6	0.05	−0.00	0.09	0.06	0.02	0.11		
7	−1.16	0.03	−0.02	−0.14	−0.12	0.03	15.32	
8	−0.07	0.00	−0.08	−0.03	−0.01	−0.04	−0.03	0.17
Species B_2								
1	2.30							
2	−0.02	4.85						
3	−0.10	0.11	4.92					
4	−0.19	−0.00	−0.01	0.39				
5	−0.05	−0.04	0.03	−0.02	1.18			
6	0.13	0.02	0.02	−0.02	0.64	1.04		
7	0.09	−0.02	0.05	−0.03	0.46	0.37	0.65	
8	−0.21	−0.00	−0.01	0.02	−0.01	−0.02	−0.03	0.19

atures of absolute zero and 298 K are given in Table 2. The table includes the calculated interatomic separations (in Å), which implicitly give information about the structural parameters applied in the present analysis. The corresponding calculations for $(CD_3)_2C(CN)_2$ revealed no substantial secondary isotope effects on the mean amplitudes ($< 0.0003_2$ Å at 298 K). It seems therefore unnecessary to report the complete list of the mean amplitudes for

Table 2. Mean amplitudes of vibration (u) and perpendicular amplitude correction coefficients (K) for 2,2-dicyanopropane; Å units.

Distance type	(Equil. dist.)	Atom pair	$u(0)$	$u(298)$	$K(0)$	$K(298)$
$C_1-H_1^\circ$	(1.090)	3 – 6	0.0780	0.0780	0.0212	0.0289
C_1-H_1	(1.090)	3 – 8	0.0780	0.0780	0.0215	0.0300
C_1-C_2	(1.540)	3 – 5	0.0548	0.0573	0.0024	0.0037
C_2-C_2'	(1.470)	1 – 5	0.0447	0.0456	0.0029	0.0040
$C_2'\equiv N$	(1.170)	1 – 12	0.0353	0.0354	0.0073	0.0138
$C_1\cdots C_3$	(2.515)	3 – 4	0.0611	0.0646	0.0025	0.0048
$C_1\cdots C_2'$	(2.458)	1 – 3	0.0686	0.0796	0.0021	0.0034
$C_2'\cdots C_2''$	(2.401)	1 – 2	0.0641	0.0766	0.0025	0.0036
$C_2\cdots H_1^\circ$	(2.163)	5 – 6	0.1090	0.1106	0.0111	0.0167
$C_2\cdots H_1$	(2.163)	5 – 8	0.1075	0.1090	0.0113	0.0169
$C_1\cdots H_3^\circ$	(3.462)	3 – 7	0.1018	0.1035	0.0081	0.0132
$C_1\cdots H_3$	(2.741)	3 – 10	0.1390	0.1539	0.0086	0.0138
$C_2'\cdots H_1^\circ$	(2.698)	1 – 6	0.1483	0.1694	0.0081	0.0123
$C_2'\cdots H_1$	(2.698)	1 – 8	0.1458	0.1663	0.0082	0.0123
$C_2'\cdots H_1'$	(3.399)	1 – 9	0.1016	0.1058	0.0077	0.0115
$C_1\cdots N$	(3.472)	3 – 12	0.0760	0.1000	0.0015	0.0033
$C_2\cdots N$	(2.640)	5 – 12	0.0499	0.0512	0.0025	0.0058
$C_2'\cdots N'$	(3.423)	1 – 13	0.0760	0.1044	0.0016	0.0033
$H_1\cdots H_1^\circ$	(1.780)	6 – 8	0.1290	0.1292	0.0285	0.0429
$H_1\cdots H_1'$	(1.780)	8 – 9	0.1283	0.1285	0.0293	0.0448
$H_1^\circ\cdots H_3^\circ$	(4.295)	6 – 7	0.1395	0.1406	0.0119	0.0201
$H_1\cdots H_3^\circ$	(3.737)	6 – 10	0.1557	0.1642	0.0120	0.0185
$H_1\cdots H_3$	(2.515)	8 – 10	0.1953	0.2132	0.0166	0.0271
$H_1\cdots H_3'$	(3.081)	8 – 11	0.2139	0.2632	0.0115	0.0164
$H_1^\circ\cdots N$	(3.527)	6 – 12	0.1669	0.2079	0.0056	0.0090
$H_1\cdots N$	(3.527)	8 – 12	0.1647	0.2036	0.0055	0.0087
$H_1\cdots N'$	(4.485)	8 – 13	0.1034	0.1152	0.0056	0.0090
$N\cdots N'$	(4.311)	12 – 13	0.0932	0.1506	0.0009	0.0016

Table 3. Mean amplitudes of vibration (u in Å units) for the distances in 2,2-dicyanopropane-d_6 which involve deuterium.

Distance type	(Equil. dist.)	Atom pair	$u(0)$	u(298)
$C_1-D_1^\circ$	(1.090)	3 – 6	0.0667	0.0668
C_1-D_1	(1.090)	3 – 8	0.0668	0.0668
$C_2\cdots D_1^\circ$	(2.163)	5 – 6	0.0943	0.0972
$C_2\cdots D_1$	(2.163)	5 – 8	0.0930	0.0957
$C_1\cdots D_3^\circ$	(3.462)	3 – 7	0.0894	0.0920
$C_1\cdots D_3$	(2.741)	3 – 10	0.1197	0.1412
$C_2'\cdots D_1^\circ$	(2.698)	1 – 6	0.1294	0.1576
$C_2'\cdots D_1$	(2.698)	1 – 8	0.1270	0.1546
$C_2'\cdots D_1'$	(3.399)	1 – 9	0.0895	0.0948
$D_1\cdots D_1^\circ$	(1.780)	6 – 8	0.1087	0.1096
$D_1\cdots D_1'$	(1.780)	8 – 9	0.1082	0.1089
$D_1^\circ\cdots D_3^\circ$	(4.295)	6 – 7	0.1185	0.1210
$D_1\cdots D_3^\circ$	(3.737)	6 – 10	0.1323	0.1456
$D_1\cdots D_3$	(2.515)	8 – 10	0.1654	0.1929
$D_1\cdots D_3'$	(3.081)	8 – 11	0.1808	0.2480
$D_1^\circ\cdots N$	(3.527)	6 – 12	0.1458	0.1973
$D_1\cdots N$	(3.527)	8 – 12	0.1437	0.1931
$D_1\cdots N'$	(4.485)	8 – 13	0.0923	0.1059

the deuterated compound. Table 3 shows the calculated mean amplitudes only for the distances in $(CD_3)_2C(CN)_2$ which involve a deuterium atom. Complete lists of mean amplitudes and K values also for this molecule are available on request to the authors.

2,2-DIFLUOROPROPANE

The vibrational spectra of 2,2-difluoropropane have been investigated by Crowder and Jackson.[8] They recorded the gas and liquid infrared spectra along with the Raman spectrum of the solid. They also performed a normal coordinate analysis.

We have developed a harmonic force field for 2,2-difluoropropane, which is given in Table 4 in terms of the specified symmetry coordinates. An initial force field was constructed by transferring the force constants from propane [2] except for the C–F stretching, for which the value of 4.28_8 mdyn/Å was taken.[8]

Table 4. Symmetry force constants (mdyn/Å) for 2,2-difluoropropane.

Species A_1									
1	5.36								
2	0.87	4.50							
3	−0.00	−0.03	4.87						
4	0.06	0.01	0.09	4.94					
5	−0.49	0.30	−0.03	0.02	1.40				
6	0.56	0.93	−0.01	0.03	1.22	2.62			
7	0.06	0.08	−0.04	0.03	−0.01	0.07	1.29		
8	0.02	0.34	0.01	0.03	0.01	0.06	0.79	1.14	
9	0.17	0.30	−0.03	0.06	−0.04	0.06	0.50	0.43	0.68
Species A_2									
1	4.82								
2	0.01	0.48							
3	−0.04	−0.01	0.42						
4	−0.05	−0.03	−0.04	0.41					
5	0.00	−0.01	0.03	0.02	0.12				
Species B_1									
1	4.54								
2	−0.05	4.82							
3	0.81	0.02	0.44						
4	0.03	−0.03	−0.01	0.42					
5	−0.04	−0.02	−0.06	0.01	0.52				
6	0.05	−0.00	0.02	0.00	−0.00	0.084			
Species B_2									
1	3.61								
2	0.01	4.89							
3	−0.05	0.08	4.95						
4	0.21	0.01	−0.01	0.44					
5	0.04	−0.02	0.02	−0.01	1.31				
6	0.26	0.02	0.02	−0.01	0.68	1.08			
7	0.25	0.01	0.03	−0.03	0.59	0.40	0.85		

The final force constants (Table 4) are adjusted so as to fit exactly the assignment of experimental frequencies from Ref. 8. In this assignment the lowest frequency of species B_1 (designated b_2 in Ref. 8) is unobserved. Crowder *et al.*[8] have calculated the value 317 cm^{-1}. We preferred to use 242.1 cm^{-1} taken from a far-infrared investigation of Moeller *et al.*,[7] who have reported the torsional frequencies of ~ 232 cm^{-1} and 242.1 cm^{-1}, but pointed out that these observations are uncertain because of a complicated pattern.

The developed force field (Table 4) was used to calculate the mean amplitudes of vibration (u) and perpendicular amplitude correction coefficients (K). The results are given in Table 5.

Table 5. Mean amplitudes of vibration (u) and perpendicular amplitude correction coefficients (K) for 2,2-difluoropropane; Å units.

Distance type	(Equil. dist.)	Atom pair	$u(0)$	$u(298)$	$K(0)$	$K(298)$
$C_1-H_1^\circ$	(1.091)	3 – 6	0.0779	0.0779	0.0190	0.0241
C_1-H_1	(1.091)	3 – 8	0.0779	0.0779	0.0213	0.0291
C_2-F	(1.360)	1 – 5	0.0489	0.0502	0.0024	0.0030
C_1-C_2	(1.526)	3 – 5	0.0519	0.0526	0.0022	0.0027
$C_1\cdots C_2$	(2.536)	3 – 4	0.0653	0.0714	0.0011	0.0013
$C_2\cdots H_1^\circ$	(2.173)	5 – 6	0.1054	0.1060	0.0095	0.0123
$C_2\cdots H_1$	(2.173)	5 – 8	0.1053	0.1061	0.0112	0.0160
$C_1\cdots H_3^\circ$	(3.486)	3 – 7	0.1023	0.1049	0.0058	0.0077
$C_1\cdots H_3$	(2.801)	3 – 10	0.1384	0.1513	0.0071	0.0101
$C_1\cdots F$	(2.348)	1 – 3	0.0615	0.0682	0.0011	0.0015
$H_1\cdots H_1^\circ$	(1.762)	6 – 8	0.1282	0.1286	0.0268	0.0386
$H_1\cdots H_1'$	(1.761)	8 – 9	0.1293	0.1294	0.0291	0.0429
$H_1^\circ\cdots H_3^\circ$	(4.324)	6 – 7	0.1408	0.1420	0.0079	0.0101
$H_1\cdots H_3^\circ$	(3.802)	6 – 10	0.1561	0.1661	0.0101	0.0143
$H_1\cdots H_3$	(2.625)	8 – 10	0.2029	0.2261	0.0128	0.0168
$H_1\cdots H_3'$	(3.161)	8 – 11	0.2014	0.2279	0.0109	0.0155
$F\cdots F'$	(2.221)	1 – 2	0.0619	0.0715	0.0011	0.0016
$H_1^\circ\cdots F$	(2.631)	1 – 6	0.1365	0.1488	0.0067	0.0090
$H_1\cdots F$	(2.638)	1 – 8	0.1446	0.1667	0.0073	0.0103
$H_1\cdots F'$	(3.297)	1 – 9	0.0986	0.1007	0.0066	0.0092

2,2-DIIODOPROPANE

The available experimental data of vibrational frequencies for 2,2-diiodopropane are rather incomplete. The spectroscopic measurements are very difficult in this case because of the light-sensitivity of the compound. Tobin[13] has proposed tentative vibrational assignments for 2,2-dichloro-, 2,2-dibromo-, and 2,2-diiodopropane on the basis of literature data. For the iodine compound he utilized the old and incomplete Raman data from Kahovec and Wagner.[14]

We have calculated the vibrational frequencies for 2,2-diiodopropane in the following way. The equilibrium C – I distance was assumed to be 2.106 Å; otherwise the structural parameters were adopted from propane. All force constants were transferred from 2,2-dibromopropane[2] except those of C – I stretchings, which were assumed to be $F_{11}(A_1) = 2.1$ mdyn/Å and $F_{11}(B_1) =$

1.8 mdyn/Å. The calculated frequencies are: (A_1) 3010, 2939, 1444, 1393, 1146, 900, 487, 279, and 126; (A_2) 2908, 1430, 1189, 407, and 253; (B_1) 2895, 1464, 1058, 518, 302, and 184; (B_2) 2979, 2938, 1456, 1382, 1111, 952, and 284; all values in cm^{-1}. These frequencies are roughly comparable to those of Tobin's [13] assignment except for the low frequencies of species A_2. We believe that the present assignment as a whole is the more reliable one.

The mean amplitudes of vibration were also calculated for 2,2-diiodopropane. They are naturally not so reliable because of the lack of complete

Table 6. Mean amplitudes of vibration (u in Å units) at 298 K for the distances in 2,2-diiodopropane which involve iodine.

Distance type	Atom pair	u(298)
C_2-I	1 – 5	0.060
$C_1\cdots I$	1 – 3	0.076
$I\cdots I'$	1 – 2	0.083
$H_1{}^{\circ}\cdots I$	1 – 6	0.178
$H_1\cdots I$	1 – 8	0.210
$H_1\cdots I'$	1 – 9	0.108

experimental spectral data. We therefore only give the results at 298 K for some selected distances. Table 6 shows the mean amplitudes for those distances which involve an iodine atom. The values of u(298) for the C – I and I···I distances in 2,2-diiodopropane (see Table 6) are comparable with the corresponding ones in CI_4, *viz.*[5,15] 0.0628 Å and 0.0850 Å, respectively.

Acknowledgment. Financial support from *Norges almenvitenskapelige forskningsråd* is gratefully acknowledged.

REFERENCES

1. Klæboe, P. *Spectrochim. Acta* **A 26** (1970) 977.
2. Andresen, I.-L., Cyvin, S. J., Larsen, B. and Tørset, O. *Acta Chem. Scand.* **25** (1971) 473.
3. Klæboe, P. *Spectrochim. Acta* **A 26** (1970) 87.
4. Cyvin, B. N. and Cyvin, S. J. *Acta Chem. Scand. In press.*
5. Cyvin, S. J. *Molecular Vibrations and Mean Square Amplitudes*, Universitetsforlaget, Oslo, and Elsevier, Amsterdam 1968.
6. Cyvin, S. J., Ed., *Molecular Structures and Vibrations*, Elsevier, Amsterdam 1972.
7. Moeller, K. D., de Meo, A. R., Smith, D. R. and London, L. H. *J. Chem. Phys.* **47** (1967) 2609.
8. Crowder, G. A. and Jackson, D. *Spectrochim. Acta* **A 27** (1971) 2505.
9. Vizi, B. and Cyvin, S. J. *Acta Chim. Hung.* **64** (1970) 351.
10. Cyvin, S. J. and Vizi, B. *Acta Chim. Hung.* **64** (1970) 357.
11. Augdahl, E. (University of Oslo) *Private communication.*
12. Stølevik, R., Seip, H. M. and Cyvin, S. J. *Chem. Phys. Letters* **15** (1972) 263.
13. Tobin, M. C. *J. Am. Chem. Soc.* **75** (1953) 1788.
14. Kahovec, L. and Wagner, J. *Z. physik. Chem.* **B 47** (1940) 48.
15. Cyvin, S. J., Brunvoll, J., Cyvin, B. N. and Meisingseth, E. *Bull. Soc. Chim. Belg.* **73** (1964) 5.

Received December 11, 1972.

ACTA CHEMICA SCANDINAVICA 27 (1973) 1749–1755

N-Quaternary Compounds

Part XXXII. Michael Addition of Pyrid-2-thiones to α-Bromo-α,β-unsaturated Acids

KJELL UNDHEIM and REIDAR LIE

Department of Chemistry, University of Oslo, Oslo 3, Norway

In the reaction between the isomeric α-bromocrotonic acids and pyrid-2-thiones only the dihydrothiazolo[3,2-a]pyridinium derivative with 2,3-*trans* configuration was formed. The Michael adduct appears formed by *cis* addition. Hydrogen bonding to sulphur from *ortho*-phenolic hydrogen greatly reduced the reaction rate.

In Michael type additions the reaction rate depends on the properties of the nucleophile as well as on the nature of substituents attached to the electrophilic double bond.[2] In a previous work with a sulphur nucleophile the effect of double bond substituents was briefly discussed.[3] Our systems, however, involve a concurrent cyclisation step which may complicate interpretation of the experimental results. In most cases, however, the cyclisation is so rapid that the Michael addition is the rate determining step in the overall reaction.

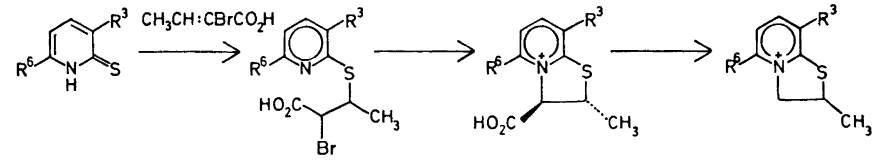

I II III IV V

a) $R^3 = R^6 = H$
b) $R^3 = H$, $R^6 = CH_3$
c) $R^3 = OH$, $R^6 = H$
d) $R^3 = OH$, $R^6 = CH_3$
e) $R^3 = OC_2H_5$, $R^6 = CH_3$

a) $R^3 = R^6 = H$
b) $R^3 = H$, $R^6 = CH_3$
c) $R^3 = OH$, $R^6 = H$
d) $R^3 = OH$, $R^6 = CH_3$
e) $R^3 = OC_2H_5$, $R^6 = CH_3$

Scheme 1.

Reactions were tried in several solvents. The most homogeneous products were obtained in acetone and ethyl acetate. The cyclisation product (IV) as HBr salt is precipitated as formed in these solvents. The quaternary acid (IV) is readily decarboxylated due to the activating effect of the annular nitrogen. To avoid decarboxylation in the stereochemical studies the reactions were run in the cold (20°C). With the exception of Ie the reaction requires a long time and was stopped and the product isolated before the reaction had gone to completion. Based on the percent yield divided by the time in days some qualitative information on relative rates of the reaction between the isomeric 2-bromocrotonic acids and the pyrid-2-thiones (I) was obtained

Table 1. Reaction rate expressed as percent yield of IV formed per day.[a]

	IVa	IVb	IVc	IVd	IVe
trans	2.3	2.1	0.2	0.4	5.10
cis	1.0	1.2	0.1	0.3	3.60

[a] Acetone was the solvent in the syntheses of IVc and IVd due to low solubility of the 3-hydroxypyrid-2-thione in ethyl acetate which was used in the case of IVa, IVb, and IVe.

(Table 1). The rate of adduct formation will depend on the electron density on the sulphur. Thus the 6-methyl derivative (Ib) reacts slightly faster than the parent pyrid-2-thione. The *ortho*-hydroxyl group in Ic might be expected to promote the reaction by its electron releasing properties. Instead a very marked rate reduction was observed. The 6-methyl group in Id again increases the rate relative to Ic but the rate is way below that of the parent pyrid-2-thione. On the other hand the 3-ethoxy derivative Ie reacts much faster than Id and faster than Ib. The electron releasing properties of the ethoxy group are therefore far more important than any steric interaction from the *ortho*-ethoxy group in the formation of the Michael adduct. The relatively low reaction rates for the hydroxy compounds are therefore attributed to hydrogen bonding with sulphur as the hydrogen acceptor. In a comparative study of hydrogen bonding ability of pyrid-2-thione and pyrid-2-one it was concluded that the former has a lower ability to form dimers through intermolecular hydrogen bonding than the oxygen analogue.[5] The otherwise weak hydrogen bonding to sulphur,[5] however, shows considerable strength in intramolecular phenolic hydrogen bonding to the sulphur in an *ortho*-thioether group.[6,7] The above discussion leads to the postulation of a relatively strong hydrogen bonding between the phenolic hydrogen and the sulphur of the thione group. Intramolecular hydrogen bonding would be stabilised through a pseudo-5-membered ring (Scheme 2).

The β-methyl group in crotonic acid, due to both steric and electronic effects, strongly reduces the reaction rate relative to acrylic acid.[3] The same was found for β-phenyl derivatives. Thus the two stereoisomeric cinnamic acids did not react to any degree with 6-methylpyrid-2-thione in the cold. The reaction required heating for several days and led only to decarboxylated

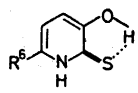

VI

Scheme 2.

material. A *para*-nitro group in the cinnamic acid should promote the reaction by its electron withdrawing properties and have no steric influence. The electronic effect of the nitro group, however, was not sufficient for making the reaction go in the cold. Heating led only to decarboxylated material. These experiments showed no difference in reaction rates between the *cis*- and *trans*-cinnamic acids.

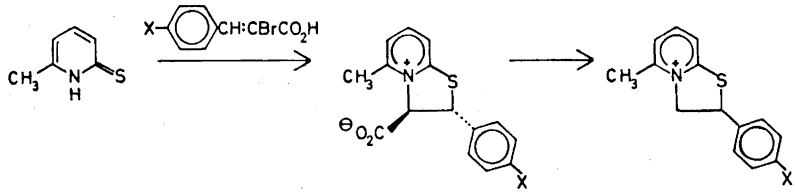

Ib VII a) X=H b) X=NO_2 VIII IX a) X=H b) X=NO_2

Scheme 3.

The low reactivity in the cinnamic acid series led us to restrict the stereochemical studies to the stereoisomeric crotonic acids. Experimentally both *cis*- and *trans*-α-bromocrotonic acid gave the *trans*-product (IVa) with pyrid-2-thione. The structural assignment follows from the NMR spectrum recorded in trifluoroacetic acid (TFA). The Karplus relationship [8] between dihedral angle and coupling constant is affected by electronegative substituents and their configuration.[9] Despite the uncertainties introduced by the electronegative substituents as to the exact value of the dihedral angle the experimentally observed coupling constant between the vicinal 2,3-methine protons, $J_{2,3}=1.0$ cps, is so small that *trans* assignment must be concluded. This assignment is also in agreement with X-ray data for a closely related compound.[10]

Since both the *cis*- and *trans*-crotonic acids give a cyclic product IV with *trans* stereochemistry, isomerisation must have occurred. A different addition mechanism for the isomeric acids seems unlikely. Isomerisation could occur in one of the acids prior to reaction, in the Michael adduct (III) or in the cyclic product first formed (Scheme 4). The reaction of Ib was therefore carried out in deuteriated acetone and the reaction progress studied by NMR. In this way it was found that the *cis*-acid was isomerised to the *trans*-acid before any

addition product was seen by NMR. The *trans*-acid was not isomerised. The isomerisation was readily demonstrated to be HBr catalysed. The intermediate Michael adduct was not observed spectroscopically or by chromatography. This confirms the rate limiting step in the overall reaction to be adduct formation. Very rapid isomerisation in the highly reactive Michael adduct seems unlikely since an optically active analogue of the adduct has been cyclised with high optical yield.[1]

Rapid epimerisation at C-3 in an initially formed *cis*-cyclisation product has not been experimentally excluded. 8-Hydroxy-5-methyldihydrothiazolo-[3,2-a]pyridinium-3-carboxylate, however, is optically stable under these conditions, although the C-3 methine proton is readily exchangeable.[11] Since the reaction of 3-hydroxy-6-methylpyrid-2-thione (Id) with both *cis*- and *trans*-crotonic acid gave the same *trans-cyclic* product, rapid isomerisation at this stage seems less likely. It should be pointed out, however, that the effect of a *cis*-methyl group on the rate of epimerisation at C-3 remains to be tried. So far such a compound has not been available. It does not seem unreasonable, however, to assume that the non-bonded interaction between the 2-methyl group and the 3-carboxy group in a *cis*-product is not sufficient to cause immediate epimerisation at C-3.

The HBr generated in the cyclisation would almost certainly exclude a free radical mechanism in the adduct formation. Support for this view follows from separate experiments carried out in the presence of hydroquinone, or benzoyl peroxide or without any external agent, which showed no detectable rate differences or different product composition.

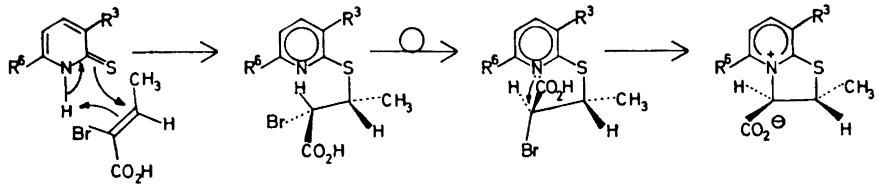

Scheme 4.

Cyclisation of the α-bromo-acid has been found to proceed by inversion of the configuration.[1] It therefore follows from the above discussions that adduct formation proceeds by a *cis* mechanism rather than the usual *trans* pathway observed in acid catalysed thiol addition and base induced thioxide additions. Free radical additions are less stereospesific.[12,13] *trans*-Addition was originally suggested, however, working with *cis*-α-bromocrotonic acid since isomerisation to the *trans*-acid had not been realised.

Pyrid-2-thione exists almost entirely in this form rather than as the tautomeric 2-mercaptopyridine.[14] The substituted derivatives should behave similarly. If these molecules are assumed to react as thiones the *cis* addition can be explained by a concerted reaction involving 6-atoms in the transition state as indicated in Scheme 4 (X).

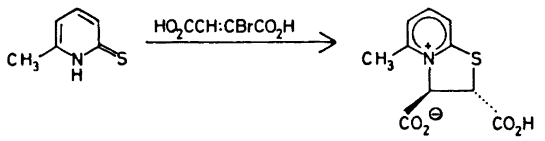

Ib XII XIII

Scheme 5.

To increase the reactivity of the α,β-unsaturated acid an electron attracting substituent was introduced onto the β-carbon, the compounds studied being bromomaleic and bromofumaric acid, respectively. Additions of the pyrid-2-thione (Ib) to these acids in cold ethyl acetate immediately led to precipitation of a product identified as the hydrobromide of the pyrid-2-thione. After two further days the pyrid-2-thione was fully converted into the cyclic product XIII (Scheme 5). The HBr arises through rapid elimination and generation of acetylenedicarboxylic acid. The pyrid-2-thione then adds to the triple bond followed by cyclisation of the resultant vinyl ether. The reason for HBr elimination lies in high activation of the vinyl proton.

The cyclic product XIII was assigned a *trans* configuration since the coupling constant between the vicinal 2,3-methine protons was close to zero. The configurational assignment has also been confirmed by X-ray work.[15] The X-ray studies show that the dihydrothiazolo ring in the solid state has an envelope conformation with the 1- and 3-atoms nearly coplanar with the pyridine ring and the C-2 carbon 0.5 Å out of the plane. The angle between the 2,3-substituents was 160° corresponding to a dihedral angle between the two vicinal hydrogens of about 80° explaining the small coupling constant in NMR. The zwitterions form infinite chains through intermolecular hydrogen bonding between the 2- and 3'-carboxyl groups in adjacent molecules. The O to H distance is larger in the 3-carboxyl group than in the 2-carboxyl group. The 3-carboxyl group has therefore a larger degree of carboxylate character as would be expected on electronic grounds.

EXPERIMENTAL

The NMR data were recorded on a Varian A-60A instrument and the UV data on a Perkin-Elmer 137-UV instrument.

trans-*2-Methyldihydrothiazolo[3,2-a]pyridinium-3-carboxylate (IVa)*. A solution of α-bromocrotonic acid (*cis* [16] and *trans* [17]) (1.65 g, 0.01 mol) and pyrid-2-thione (1.11 g, 0.01 mol) in ethyl acetate (90 ml) was left in the cold. The hydrobromide of the title compound was slowly precipitated. The yield from *trans*-acid after 22 days was 1.38 g (50 %); from *cis*-acid 0.55 g (20 %), m.p. 180–185°C (decomp.).

The zwitterion was generated by passage of an aqueous solution of the hydrobromide through a column of Amberlite IR-45(OH) followed by eluation with water. Any co-precipitated pyrid-2-thione remained on the column. The eluates were freeze-dried and the solid residue crystallised as white needles from aqueous acetone; m.p. 138°C (decomp.). (Found: C 55.43; H 4.94; N 7.43. Calc. for $C_9H_9NO_2S$: C 55.39; H 4.65; N 7.21.) UV in 0.1 N NaOH: 353 nm (log ε 3.95), 277 nm (4.04), 222 nm (4.08); in 0.1 N HCl: 325 nm (log ε 3.84), 250 nm (3.96), 212 nm (4.01). NMR in TFA: 8.18 τ (2-CH_3, doublet, $J = 7.0$ cps), 5.23 τ (2-H, octet, $J_{2,3} = 1.0$ cps), 3.84 τ (3-H, doublet), 1.1–2.3 τ (pyridyl-H).

trans-*2,5-Dimethyldihydrothiazolo[3,2-a]pyridinium-3-carboxylate (IVb)*. The hydrobromide was prepared as above from 6-methylpyrid-2-thione in 32 % yield from *trans*-acid after 15 days and 24 % yield from *cis*-acid after 20 days. The zwitterion, generated over Amberlite IR-45(OH) as above, was slightly contaminated with decarboxylated material (Vb). Elemental analysis was obtained for Vb. UV in 0.1 N NaOH: 355 nm (log ε 3.86), 275 nm (3.81), 222 nm (3.88); in 0.1 N HCl: 329 nm (logε 4.08), 242 nm (4.04), 210 nm (4.10). NMR in TFA: 8.20 τ (2-CH_3, doublet, $J_{2\text{-}CH_3}=7.0$ cps), 5.27 τ (2-H, quartet, $J_{2,3}<1$ cps), 3.92 τ (3-H, singlet), 7.10 τ (5-CH_3), 1.4 – 2.8 τ (pyridyl-H).

trans-*2-Methyl-8-hydroxydihydrothiazolo[3,2-a]pyridinium-3-carboxylate (IVc)* was prepared from 3-hydroxypyrid-2-thione in acetone. The yield of HBr salt from *trans*-acid after 40 days was 9 %; from *cis*-acid 6 %.

The HBr salt, m.p. 175 – 180°C (decomp.), was converted to the zwitterion over Amberlite IR-45(OH) as above. It was partly decarboxylated (Vc). The elemental analysis was carried out on Vc. UV in 0.1 N NaOH: 355 nm (log ε 4.04), 250 nm (3.99), 224 nm (3.86). NMR in TFA: 8.20 τ (2-CH_3, doublet, $J=7.0$), 5.28 τ (2-H, octet), 4.11 τ (3-H, doublet, $J_{2,3}=1.0$ cps), 1.6 – 2.5 τ (pyridyl-H).

trans-*2,5-Dimethyl-8-hydroxydihydrothiazolo[3,2-a]pyridinium-3-carboxylate (IVd)*. The HBr salt was prepared from 3-hydroxy-6-methylpyrid-2-thione in acetone. The yield of HBr salt from *trans*-acid was 15 % after 40 days; from the *cis*-acid 12 %. The title compound has previously been described.[3] UV in 0.1 N NaOH: 364 nm (log ε 4.06), 250 nm (4.00), 224 nm (3.92); in 0.1 N HCl: 346 nm (log ε 3.93), 240 nm (3.77), 216 nm (4.00). NMR in TFA: 8.20 τ (2-CH_3, doublet, $J=7.0$ cps), 5.27 τ (2-H, quartet), 3.95 τ (3-H, singlet, $J_{2,3}<1$ cps), 7.20 τ (5-CH_3), 2.1 – 2.6 τ (pyridyl-H).

trans-*2,5-Dimethyl-8-ethoxydihydrothiazolo[3,2-a]pyridinium-3-carboxylate (IVe)* was prepared from 3-ethoxy-6-methylpyrid-2-thione[18] in ethyl acetate. The yield of HBr salt after 4 h was 85 % from the *trans*-acid and 60 % from the *cis*-acid, m.p. 180 – 183°C (decomp.).

The zwitterion, liberated on an Amberlite IR-45(OH) column as above, was recrystallised from aqueous acetone, m.p. 93°C (decomp.) (Found: C 52.96; H 6.38; N 5.01 Calc. $C_{12}H_{15}NO_3S.H_2O$: C 53.11; H 6.32; N 5.16.) UV in 0.1 N NaOH: 357 nm (log ε 3.86), 242 nm (3.72), 220 nm (3.73); in 0.1 N HCl: 346 nm (log ε 3.90), 243 nm (3.81), 215 nm (3.89). NMR in TFA: 8.24 τ (2-CH_3, doublet, $J=7.0$ cps), 5.30 τ (2-H, quartet), 3.95 τ (3-H, singlet, $J_{2,3}=0$ cps), 7.20 τ (5-CH_3), 2.4 – 2.5 τ (pyridyl-H), 8.44 and 5.62 τ (OC_2H_5).

2-Methyldihydrothiazolo[3,2-a]pyridinium-8-oxide (Vc). A solution of 3-hydroxypyrid-2-thione (3.81 g, 0.03 mol) and *trans*-α-bromocrotonic acid (4.85 g, 0.03 mol) in ethyl acetate (80 ml) was heated under reflux for 6 days. The title compound was precipitated as hydrobromide; yield 0.74 g (9 %), m.p. 142 – 151°C (decomp.).

The betaine was generated by passage of an aqueous solution through a column of Amberlite IR-45(OH) and evaporation of the eluates. Recrystallisation from acetone gave white needles, m.p. 84 – 85°C (decomp.) (Found: C 51.62; H 6.00; N 7.71. Calc. for $C_8H_9NOS.H_2O$: C 51.85; H 5.99; N 7.56.) UV in 0.1 N NaOH: 353 nm (log ε 3.98), 263 nm (3.85), 246 nm (3.86), 221 nm (3.53); in 0.1 N HCl: 336 nm (log ε 3.93), ~245 sh. nm, 234 nm (3.71), 212 nm (4.14). NMR in TFA: 8.30 τ (2-CH_3, doublet, $J=7.0$ cps), 5.5 τ (2-H, multiplet), 4.9 τ (3-H, multiplet), 1.7 – 2.6 τ (pyridyl-H).

2,5-Dimethyldihydrothiazolo[3,2-a]pyridinium bromide (Vb). The title compound was prepared in 35 % yield by heating 6-methylpyrid-2-thione in ethyl acetate with *trans*-α-bromocrotonic acid for 20 h. The product was recrystallised from acetone, containing a drop of HBr, in white needles; m.p. 199 – 200°C. (Found: C 43.60; H 4.96; N 5.67. Calc. for $C_9H_{12}BrNS$: C 43.91; H 4.92; N 5.69.) UV in 0.1 N NaOH: 327 nm (log ε 3.88), 252 nm (3.88), ~225 sh. nm; in 0.1 N HCl: 327 nm (log ε 3.99), 252 nm (3.88), 210 nm (4.13). NMR in TFA: 8.30 τ (2-CH_3, doublet, $J=6.5$ cps), 5.5 τ (2-H, multiplet), 5.0 τ (2H, multiplet), 7.22 τ (5-CH_3), 1.8 – 2.6 τ (pyridyl-H).

5-Methyl-2-phenyldihydrothiazolo[3,2-a]pyridinium bromide (IXa). 6-Methylpyrid-2-thione (1.25 g, 0.01 mol) and α-bromocinnamic acid (*cis*[19] and *trans*[19]) (2.27 g, 0.01 mol) in ethyl acetate solution (80 ml) was heated under reflux for 1 day. The yield of precipitated material from the *trans*-acid was 0.70 g (23 %) and 0.61 g (20 %) from the *cis*-acid. After 7 days the yield was 53 %. Recrystallisation from ethanol containing a drop of HBr gave a whitish material, m.p. 201°C (decomp.) (Found: C 54,46; H 4.73; N 4.75, Calc. for $C_{14}H_{14}BrNS$: C 54.53; H 4.56; N 4.52.) UV in 0.1 N NaOH: 330 nm (log ε 3.99),

249 nm (4.08), 224 nm (3.74); in 0.1 N HCl: 330 nm (log ε 3.90), 249 nm (3.97), 209 nm (4.30). NMR in TFA: 2.37 τ (2-C_6H_5, singlet), 4.1 – 4.9 τ (2-H, 3H multiplet), 7.13 τ (5-CH_3), 1.7 – 2.7 τ (pyridyl-H).

*5-Methyl-2-*p*-nitrophenyldihydrothiazolo[3,2-a]pyridinium bromide (IXb).* 6-Methylpyrid-2-thione (1.25 g, 0.01 mol) and α-bromo-*p*-nitrocinnamic acid (*cis*[20] and *trans*[20]) (2.72 g, 0.01 mol) in ethyl acetate solution (90 ml) was heated under reflux for 1 day. The yield of precipitated material from the *trans*-acid was 1.30 g (37 %); from the *cis*-acid 1.12 g (31 %). Recrystallisation from ethanol containing a drop of HBr gave whitish material, m.p. 252°C (decomp.). (Found: C 47.33; H 3.64; N 7.96. Calc. for $C_{14}H_{13}BrN_2OS$: C 47.61; H 3.54; N 7.93.) UV in 0.1 N NaOH: 460 nm (log ε 3.41), 322 nm (4.18), 270 nm (4.02), 223 nm (4.13); in 0.1 N HCl: 328 nm (log ε 4.08), ~270 sh. nm, 253 nm (4.19), 208 nm (4.33). NMR in TFA: 1.59 and 2.12 τ (AB quartet of $C_6H_4NO_2$), 4.1 – 5.0 τ (2H, 3H-multiplet), 7.10 τ (5-CH_3), 1.6 – 2.5 τ (pyridyl-H).

trans-*2-Carboxy-5-methyldihydrothiazolo[3,2-a]pyridinium-3-carboxylate (XIII).* Bromomaleic acid [21] and bromofumaric acid,[22] respectively, (0.1 mol) in ethyl acetate (20 ml) was added to a solution of 6-methylpyrid-2-thione (1.25 g, 0.01 mol) in ethyl acetate (70 ml). The hydrobromide of the pyrid-2-thione was immediately precipitated. After stirring in the cold for 2 days chromatography showed that the initially formed material had gradually been dissolved with precipitation of the new cyclic product.

The zwitterion was obtained by crystallisation from its HBr salt in water, m.p. 180°C (decomp.). (Found: C 50.05; H 3.70; N 5.88. Calc. for $C_{10}H_9NO_4S$: C 50.20; H 3.79; N 5.85.) UV in 0.1 N NaOH: 337 nm (log ε 3.80), 242 nm (3.86), 227 nm (3.86); in formic acid: 330 nm (log ε 3.87), 262 nm (3.08). NMR in TFA: 4.65 τ (2-H, singlet), 3.28 τ (3-H, singlet, $J_{2,3} < 1$ cps), 7.02 τ (5-CH_3), 1.5 – 2.3 τ (pyridyl-H).

REFERENCES

1. Part XXXI. Undheim, K. and Ulsaker, G. A. *Acta Chem. Scand.* **27** (1973) 1390.
2. Bergmann, E. D., Ginsburg, D. and Pappo, R. *Org. React.* **10** (1959) 179.
3. Undheim, K. and Borka, L. *Acta Chem. Scand.* **23** (1969) 1715.
4. Tichy, M. *Adv. Org. Chem.* **5** (1965) 115.
5. Krackov, M. H., Lee, C. M., and Mautner, H. G. *J. Am. Chem. Soc.* **87** (1965) 892.
6. Baker, A. W. and Schulgin, A. T. *J. Am. Chem. Soc.* **80** (1958) 5358.
7. Binder, J. L., Ambelang, J. C. and Webb, F. J. *J. Am. Chem. Soc.* **81** (1959) 3608.
8. Karplus, M. *J. Am. Chem. Soc.* **85** (1963) 2870.
9. Booth, H. *Tetrahedron Letters* **1965** 411.
10. Thorup, N. *Acta Chem. Scand.* **25** (1971) 1353.
11. Undheim, K. and Greibrokk, T. *Acta Chem. Scand.* **23** (1969) 2502.
12. Pryor, W. A. *Mechanism of Sulphur Reactions*, McGraw, New York 1962, p. 71.
13. Truce, W. E. In Kharasch, N., Ed., *Organic Sulphur Compounds*, Pergamon 1961, Vol. 1, p. 121.
14. Jones, R. A. and Katritzky, A. R. *J. Chem. Soc.* **1958** 3610.
15. Groth, P. *Acta Chem. Scand.* **25** (1971) 118.
16. Pfeiffer, P. *Ber.* **48** (1915) 1048.
17. Prostenik, M., Salzman, N. P. and Carter, H. E. *J. Am. Chem. Soc.* **77** (1955) 1856.
18. Undheim, K. and Wiik, T. *Unpublished.*
19. Plisov, A. K. and Zhuravleva, I. *Zh. Obshch Khim.* **34** (1964) 3102.
20. Reich, S. and Chang, N. Y. *Helv. Chim. Acta* **3** (1925) 235.
21. Elving, P. J., Rosenthal, I., Hayes, J. R. and Martin, A. J. *Anal. Chem.* **33** (1961) 330.
22. Boudrowski, E. *Ber.* **15** (1882) 2697.

Received September 19, 1972.

ACTA CHEMICA SCANDINAVICA 27 (1973) 1756–1762

N-Quaternary Compounds

Part XXXIII. Reactions between Pyrid-2-thiones and Activated Acetylenes

REIDAR LIE and KJELL UNDHEIM

Department of Chemistry, University of Oslo, Oslo 3, Norway

Pyrid-2-thiones with acetylenedicarboxylic acid gave *trans*-2,3-dicarboxydihydrothiazolo[3,2-a]pyridinium derivatives. Vinyl thioethers were the products from the reactions with propiolic and phenylpropiolic acids. Stereochemical assignments are based on NMR data. Bromination of the vinyl thioethers is a convenient method for the preparation of the thiazolo[3,2-a]pyridinium system.

The initial reaction between pyrid-2-thiones and bromofumaric or bromomaleic acid was found to involve HBr elimination. The pyrid-2-thione would then add to the generated acetylene.[1] This observation led us to extend Michael type addition studies of sulphur nucleophiles from electron deficient double bonds into triple bonds. With acetylenedicarboxylic acid in cold chloroform the reaction was rapid with formation of the bicyclic pyridinium derivative (III). The NMR coupling constant for the vicinal 2,3-protons was in the region 0 – 1 cps and *trans* configuration could therefore be assigned to the products.[1] NMR experiments using pyrid-2-thione showed that the same product was obtained in deuterium oxide. In trifluoroacetic acid (TFA), however, a singlet signal appeared at 5τ which, once it had reached a maximum, decreased very slowly with time. The signal may be ascribed to a vinyl proton such as in the vinyl thioether II (Scheme 1). Acid catalysis in the adduct formation seems likely, even in chloroform, since acetylenedicarboxylic acid is a relatively strong acid (pK_a 1.74).[2] This would lead to a *trans*-addition product (II) as is usually found for thiol additions to triple bonds.[3,4] A further argument in favour of this configuration (II) is the *trans* configuration of the cyclised product III. The formation of the latter from the initial adduct involves nucleophilic attack from the annular nitrogen onto the double bond (Scheme 1). The *cis*-isomer, with respect to the carboxy groups, would have to be isomerised during the cyclisation or the cyclisation product rapidly epimerised to the *trans*-isomer.

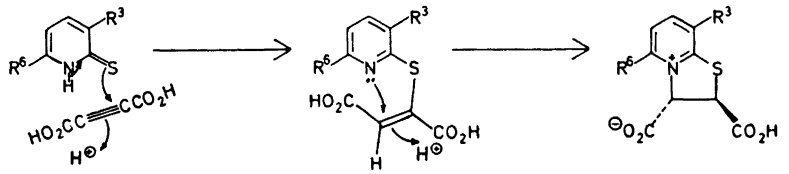

I II III

a) $R^3 = R^6 = H$

b) $R^3 = H$, $R^6 = CH_3$

c) $R^3 = OH$, $R^6 = H$

d) $R^3 = OH$, $R^6 = CH_3$

e) $R^3 = OC_2H_5$, $R^6 = CH_3$

Scheme 1.

Propiolic acid is less active towards nucleophiles than acetylenedicarboxylic acid. Even so it reacted readily with pyrid-2-thiones in cold chloroform. The phenolic pyrid-2-thiones (1c, d) were found less reactive, due to intramolecular hydrogen bonding between the phenolic-OH group and the sulphur,[1] but the reaction for all pyrid-2-thiones was complete after 1 day without heating. Two products were formed in each case and were shown by NMR and MS to be the stereoisomeric vinyl ethers IV (Scheme 2). In no case did the vinyl thioether cyclise to the dihydrothiazolo[3,2-a]pyridinium system as was the case in the acetylenedicarboxylic acid series. The NMR spectra (TFA) contain the two vinyl protons in two AB patterns in the 3.2 to 3.8 τ and 1.7 to 2.5 τ regions, the vicinal coupling constant being 10.0 cps and 15.5 – 15.9 cps, respectively. The magnetic and stereochemical relationships around the double bond in the above series should be very similar to those in β-phenylthioacrylic acid. For the latter the coupling constants were 15.3 and 10.0 cps, the former being assigned to the *trans*-isomer and the latter to the *cis*-isomer.[5] The isomer IV with the higher coupling constants, in its IR spectrum shows out of plane deformation at 960 cm^{-1} for its olefin hydrogen pair compared to 680 cm^{-1} for the other isomer. These data correlate well with the values 965 cm^{-1} and 675 – 730 cm^{-1} quoted for *trans*- and *cis*-olefins, respectively.[6] For structural assignments by NMR, however, it is important to have the stereochemistry of one member of an analogues series determined by an absolute method. Therefore the isomer of IVb with the larger coupling constant was subjected to X-ray analysis and the structure found to be *trans*.[7] The *cis*/*trans*-isomer ratio was variable but the *trans*-isomer was the major component.

The stereoisomeric mixture (IV) can arise either by two competing reaction pathways or by isomerisation of the first formed isomer. NMR studies of the reaction between 6-methylpyrid-2-thione and propiolic acid in deuteriated chloroform showed the product *cis*/*trans* ratio (1:8) to be independent of time. The *trans*-isomer would on stereochemical grounds be expected to be thermodynamically the more stable isomer as has been established in equilibration studies in the analogous β-phenylthioacrylic acid series.[8,9] Epimerisation

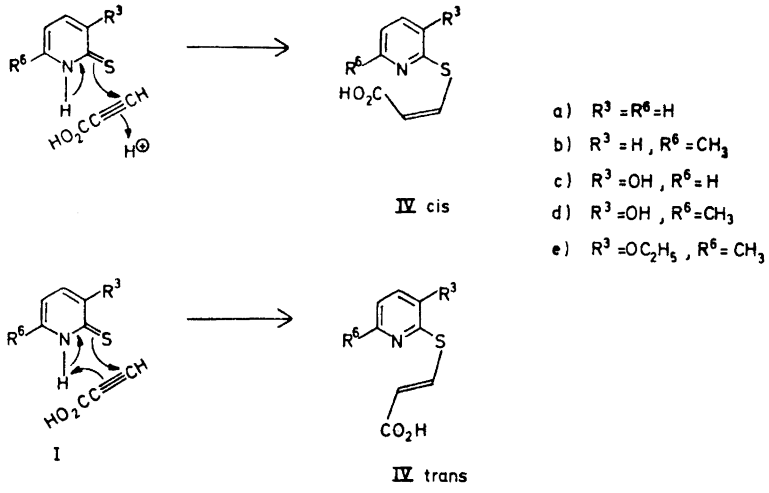

Scheme 2.

studies of IV in various solvents and conditions did not change the isomer ratio. Isomerisation to an equilibrium mixture under the mild reaction conditions is therefore excluded.

This leaves two competing reaction pathways to be considered. The acid strength of propiolic acid (pK_a 1.85)[10] is of the same order as that of acetylenedicarboxylic acid. A similar *trans*-addition mechanism is therefore reasonable to assume (Scheme 2). A reasonable explanation for the competitive formation of the *trans* product is suggested by a favourable set up for *cis*-addition if the sulphur nucleophile can be assumed to react as the thione tautomer (Scheme 2) which is by far the more important tautomeric form.

Phenylpropiolic acid showed reduced reactivity towards pyrid-2-thiones. After 10 days in cold chloroform the reaction between phenylpropiolic acid and the most reactive nucleophile (Ie) was only half completed, which is to be compared with the reaction between propiolic acid and Ie which was over in less than one day. Qualitatively the relative rates of addition for the pyrid-2-thiones to phenylpropiolic acid were established from the reaction in 0.1 M solutions in cold deuteriochloroform in tubes used for NMR recordings. The relative rates were found to follow the previously established pattern Ie > Ib > Ia > Id > Ic.[1]

NMR spectra of the addition product show the latter to consist almost entirely of one stereoisomer, the vinyl proton signal in NMR (TFA) appearing in the 3.4 – 3.5 τ region. A weak signal from the vinyl proton of the minor isomer may be seen at some 0.2 τ lower field. The second signal was strongest for Va, in which case integration of the spectrum indicated 5 – 10 % of the minor stereoisomer, while only one vinyl proton signal was seen for Vd. The configurational assignment in this case is more uncertain. The acid strength relatively to propiolic acid is decreased (pK_a 2.23).[10] The above results indicate that any correlation between the pK_a of the acetylenecarboxylic acid, because

of difference in acidity or as a measure for the reactivity of the conjugated triple bond, and the reaction mixtures would indicate an even higher proportion of product formed by *cis*-addition than in the case of propiolic acid. The suggested *cis* configuration (Scheme 3) for the major product would appear to be supported from calculations of the chemical shifts for the vinyl protons in the stereoisomers V through the use of additive shielding parameters for olefinic protons.[11] The calculations for a *trans* structure gave the value 387 cps, for a *cis* structure 343 cps. The experimental values for the two vinyl protons recorded in $CDCl_3$ were 370 – 385 cps in the minor product and 360 – 370 cps in the major product.

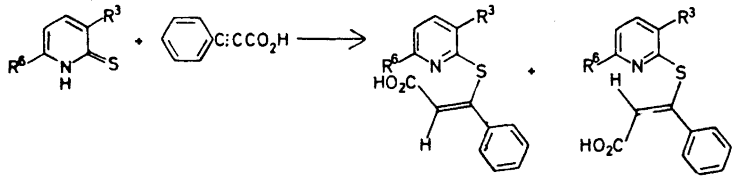

I V trans V cis

a) $R^3 = R^6 = H$
b) $R^3 = H$, $R^6 = CH_3$
c) $R^3 = OH$, $R^6 = H$
d) $R^3 = OH$, $R^6 = CH_3$
e) $R^3 = OC_2H_5$, $R^6 = CH_3$

Scheme 3.

The double bond in the vinyl thioethers prepared is activated towards electrophiles. By the reaction with bromine a very convenient synthesis to the thiazolo[3,2-a]pyridinium system is available (Scheme 4) as distinct from proton addition which led to the dihydrothiazolo[3,2-a]pyridinium system (Scheme 1). Thus bromine addition to a cold chloroform solution of the vinyl thioether gave immediate precipitation of a product which on isolation was found to be a thiazolo[3,2-a]pyridinium derivative (X). Thus the NMR spectra for the products from the phenylvinyl thioethers contained only aromatic protons, the structures assigned therefore being Xd and Xe. The products without a 2-substituent have a proton signal at low field (1.4 τ) as previously reported for such derivatives.[12]

The reaction to the bicyclic product IX may go *via* two different paths. The initial attack by bromine may be followed by back-side attack by the pyridine nitrogen (VIII) with direct formation of the dihydrothiazole (IX). Alternatively IX is formed *via* the dibromide VII. Presumably both pathways would be operative depending on substituent effects. In the present case, however, the absence of VII in the reaction product would appear to favour direct addition of the pyridine nitrogen as indicated in VIII (Scheme 4). Irrespective of the original stereochemistry in IX the HBr elimination would be expected to occur very readily because of the activation of the 3-methine

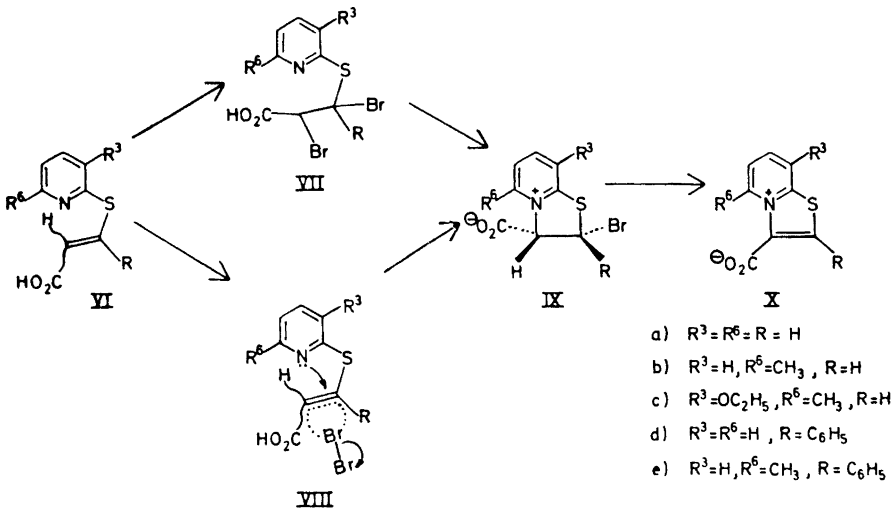

Scheme 4.

proton by both the carboxy and the ammonium groups. The same groups will stabilise the corresponding carbanion whereby the correct stereochemistry for E2 elimination can be introduced. Perhaps even more likely in this case, however, would be the two-step E1cB elimination which involves a carbanion intermediate.

EXPERIMENTAL

The NMR data were recorded on a Varian A-60A instrument.

trans-*2-Carboxydihydrothiazolo[3,2-a]pyridinium-3-carboxylates (III).* Acetylenedicarboxylic acid (1.14 g, 0.01 mol) dissolved in anhydrous ethyl acetate (20 ml) was added dropwise to a solution of a pyrid-2-thione (I) (0.01 mol) in anhydrous ethyl acetate (70 ml). A yellowish-white solid was rapidly precipitated. The crude product of the 5-desmethyl analogues was sensitive to moisture, the 5-methyl analogues insensitive.

The 5-desmethyl analogues were absorbed onto charcoal in boiling ethanol (100 ml) from which they were desorbed in formic acid (50 ml). The formic acid on standing precipitated the zwitterionic material. This could be recrystallised by dissolution in a minimum volume of formic acid and addition of some water when the material slowly crystallised out. The crude product from the 5-methyl analogues could be recrystallised directly from dilute formic acid. Physical data are given in Table 1.

Table 1.

III	M.p. °C (Decomp.)	Yield %	React. time	Empirical formulae	Found C	Found H	Found N	Calc. C	Calc. H	Calc. N
a	190	35	20 min	$C_9H_7NO_4S$	48.29	3.17	6.32	48.00	3.13	6.22
b	180	80	1 d	$C_{10}H_9NO_4S$	50.05	3.70	5.88	50.20	3.79	5.85
c	180	30	30 min	$C_9H_7NO_5S.H_2O$	41.69	3.77	5.70	41.70	3.50	5.40
d	187	86	1 d	$C_{10}H_9NO_5S.H_2O$	43.68	4.01	5.35	43.93	4.07	5.15
e	157	88	1 d	$C_{12}H_{13}NO_5S$	50.76	4.43	5.24	50.77	4.60	4.93

NMR in TFA: a; 4.55 τ (2H, $J_{2,3}=1.0$), 3.27 (3H). b; 4.65 τ (2H, $J_{2,3}<1$), 3.28 (3H), 7.02 (5-CH_3). c; 4.62 τ (2H, $J_{2,3}=1.2$), 3.30 (3H), d; 4.70 τ (2H, $J_{2,3}<1$), 3.33 (3H), 7.15 (5-CH_3). e; 4.65 τ (2H, $J_{2,3}<1$), 3.27 (3H), 7.15 (5-CH_3).

β-2-Pyridylthiopropenic acids (IV). Propiolic acid (0.70 g, 0.01 mol) in chloroform (30 ml) was added to a pyrid-2-thione (0.01 mol) dissolved in chloroform (40 ml). The phenolic derivatives came out of solution, the others were soluble. After one day at room temperature the chloroform was distilled off and the residual material crystallised from dilute ethanol. Physical data are given in Table 2. In one case (IVb) the *trans* isomer was selectively precipitated on crystallisation of the *cis/trans* mixture from dilute ethanol. This was the sample subjected to X-ray analysis.[7]

NMR in TFA: The chemical shift for the pyridyl hydrogens or the pyridyl methyl group is not affected by the double bond stereochemistry. The vinyl protons appear in two AB patterns due to *cis/trans* isomerism. The chemical shifts are (a): 3.17, 2.37 τ ($J=10.0$); 3.48, 1.87 ($J=15.3$). (b): 3.52, 2.38 τ ($J=10.0$); 3.57, 1.72 ($J=15.5$). (c): 3.27, 2.47 τ ($J=10.0$); 3.70, 1.91 ($J=15.5$). (d): 3.65, 2.55 τ ($J=10.0$); 3.87, 2.00 ($J=15.9$). (e): 3.65, 2.50 τ ($J=10$); 3.77, 1.90 ($J=15.5$).

Table 2.

IV	M.p. °C	Yield %	React. time	Emp. form.	Found C	Found H	Found N	Calc. C	Calc. H	Calc. N
a	152–153	94	1 d	$C_8H_7NO_2S$	52.83	3.84	7.48	53.03	3.89	7.73
b	125	99	»	$C_9H_9NO_2S$	55.34	4.55	7.17	55.37	4.65	7.18
c	153–154	86	»	$C_8H_7NO_3S.\frac{1}{2}H_2O$	46.89	4.03	6.98	46.60	3.91	6.79
d	174–175	95	»	$C_9H_9NO_3S$	50.98	4.40	6.66	51.16	4.29	6.63
e	189–190	93	»	$C_{11}H_{13}NO_3S$	55.50	5.29	5.81	55.21	5.48	5.85

β-2-Pyridylthiocinnamic acids (V). Phenylpropiolic acid (1.46 g, 0.01 mol) in chloroform (40 ml) was added dropwise to a pyrid-2-thione (0.01 mol) in chloroform (50 ml). In some cases the product formed was slowly precipitated. After 10 days in the cold the chloroform was distilled off and the residual material crystallised from ethanol, or in the case of Ve from dilute methanol. Physical data are given in Table 3.

NMR in TFA: The vinyl proton appears as a singlet at 3.28 τ (a), 3.40 (b), 3.47 (c), 3.50 (d), 3.52 (e). The phenyl group falls in the 2.65–2.60 τ region, the 6-methyl group 7.45–7.35 τ.

Table 3.

V	M.p. °C	Yield %	Emp. form.	Found C	Found H	Found N	Calc. C	Calc. H	Calc. N
a	169	46	$C_{14}H_{11}NO_2S$	65.24	4.51	5.58	65.34	4.31	5.45
b	141–142	57	$C_{15}H_{13}NO_2S$	66.64	5.04	5.28	66.42	4.83	5.18
c	188	32	$C_{14}H_{11}NO_3S$	61.61	4.17	4.84	61.53	4.06	5.13
d	198	40	$C_{15}H_{13}NO_3S$	62.50	4.83	4.79	62.72	4.56	4.88
e	189	30	$C_{17}H_{17}NO_3S$	64.19	5.55		64.59	5.43	

Thiazolo[3,2-a]pyridinium-3-carboxylates (X) as HBr salts. Bromine (0.005 mol) in chloroform (10 ml) was added dropwise to a solution of the β-2-pyridylthiocinnamic or -propenic acid (0.05 mol) in chloroform (40 ml). The hydrobromides were precipitated at once as a crystalline material or as an oil which solidified with time. After one day the chloroform was distilled off and the residual material recrystallised from dilute ethanol, methanol, or acetone to which had been added 1–2 drops of HBr. Physical data are given in Table 4.

Table 4.

X	M.p. °C (decomp.)	Yield %	Emp. form.	Found C	Found H	Found N	Calc. C	Calc. H	Calc. N
a	297	63	$C_8H_5NO_2S.HBr$	37.17	2.61	5.45	36.91	2.33	5.41
b	188	73	$C_9H_7NO_2S.HBr$	39.83	3.17	5.33	39.43	2.94	5.11
c	271	49	$C_{11}H_{11}NO_3S.HBr$	41.89	4.10	4.56	41.52	3.80	4.40
d	185	75	$C_{14}H_9NO_3S.HBr$	49.73	2.97	4.19	50.00	3.00	4.17
e	210	63	$C_{15}H_{11}NO_2S.HBr$	51.82	3.30	3.67	51.46	3.46	4.02

NMR in TFA: a; 1.37 τ (2H), 1.1 – 2.1 (Pyr.-H). b; 1.40 τ (2H), 1.32 – 2.2 (Pyr.-H), 7.05 (CH_3). c; 1.37 τ (2H), 1.9 – 2.2 (Pyr.-H), 7.12 (CH_3). d; 2.65 τ (2-Phenyl), 1.1 – 2.1 (Pyr.-H). e; 2.63 τ (2-Phenyl), 1.8 – 2.6 (Pyr.-H), 3.25 (CH_3).

REFERENCES

1. Part XXXII. Undheim, K. and Lie, R. *Acta Chem. Scand.* **27** (1973) 1749.
2. Ashton, H. W. and Partington, J. R. *Trans. Faraday Soc.* **30** (1934) 598.
3. Winterfeldt, E. *Angew. Chem.* **79** (1967) 389.
4. Winterfeldt, E. In Viehe, H. G., Ed., *Chemistry of Acetylenes*, Marcel Decker 1969, p. 279.
5. Truce, W. E. and Groten, B. *J. Org. Chem.* **27** (1968) 128.
6. Potts, W. J. and Nyquist, R. A. *Spectrochim. Acta* **1959** 679.
7. Groth, P., Davidkov, K. and Aasen, A. *Acta Chem. Scand.* **26** (1972) 1141.
8. Truce, W. E., Goldhamer, D. L. and Kruse, R. B. *J. Am. Chem. Soc.* **81** (1959) 4931.
9. Truce, W. E. and Heine, R. F. *J. Am. Chem. Soc.* **79** (1957) 5311.
10. Johnson, A. W. *The Chemistry of the Acetylenic Compounds*, Edward Arnold 1950, Vol. 2, p. 35.
11. Matter, U. E., Pascual, C., Pretsch, E., Pross, A., Simon, W. and Sternhell, S. *Tetrahedron* **25** (1969) 691.
12. Undheim, K. and Reistad, K. R. *Acta Chem. Scand.* **24** (1970) 2956.

Received December 20, 1972

ACTA CHEMICA SCANDINAVICA 27 (1973) 1763–1770

N-Quaternary Compounds

Part XXXV.[1] Solvolysis of Thiazolo[3,2-a]pyridinium-3-oxides

PER EINAR FJELDSTAD and KJELL UNDHEIM

Department of Chemistry, University of Oslo, Oslo 3, Norway

2-Arylthiazolo[3,2-a]pyridinium-3-oxides in acid and alkaline solutions have been investigated. Steric repulsion between 3- and 5-substituents accelerates the hydrolysis. In acid solution the hydrolysis rates increase with electron donating substituents. Most compounds are more resistant to hydrolysis in alkaline solution. Light absorption data and rate constants for nitro-pyridines and a pyrimidine are interpreted to mean that the hydrolysis in alkaline solution takes place after initial pseudo-base formation.

2-Alkylthiazolo[3,2-a]pyridinium-3-oxides are rapidly hydrolysed in aqueous media while 2-phenyl analogues are less reactive because of resonance stabilisation from the phenyl ring.[2] The preparation of an additional series of 2-aryl derivatives is described in this report and their properties in acid and alkaline solutions have been studied.

The thiazolo[3,2-a]pyridinium-3-oxides were synthesised by condensation of a pyrid-2-thione and an α-halocarboxylic acid followed by cyclisation of the intermediate α-2-pyridylthioalcanoic acid. Cyclisation of the thioalcanoic acids is apparent by the highly coloured products being formed. The reaction was run in a solution of acetic anhydride and pyridine. Without base catalysis the reaction was slow. A mixed anhydride intermediate (III) seems most likely. The formation of the latter from acetic anhydride is favoured by base induced dissociation of the thioalcanoic acid. A base will also promote the tautomerism of the lactam V to the aromatic thiazole I (Scheme 1). Mixed anhydride formation with ethyl chloroformate in pyridine and the related carboxyl activation by dicyclohexylcarbodiimide in pyridine also gave the cyclic product (I). When the pyridine carried no 6-substituent and was activated by another electron releasing group, cyclisation was achieved by heating in toluene alone. For comparative purposes other heterocyclic systems were included in this study. α-2-Benzoxazolylthiophenylacetic acid was not cyclised to VI under the usual conditions while a quinoline (VII) and a pyrimidine (VIII) were readily formed.

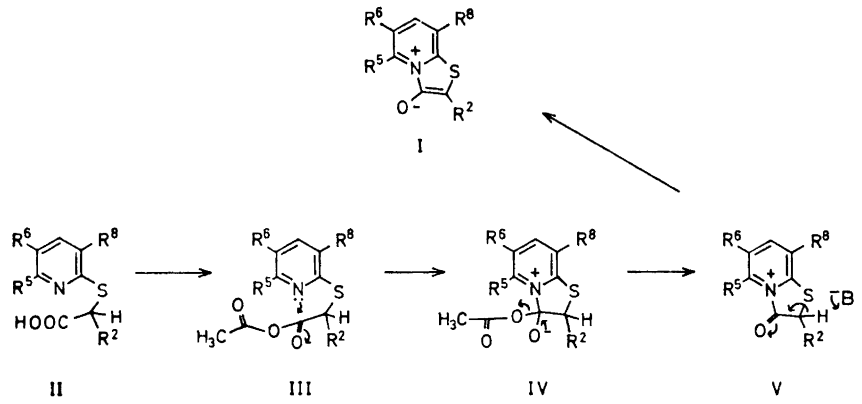

Scheme 1.

The 3-hydroxypyridines on cyclisation form an acetate. The ester formation could take place either on the 3- or the 8-phenolic oxygen. This question was settled by selective hydrolysis of a 5-methyl derivative at 20°C in 0.1

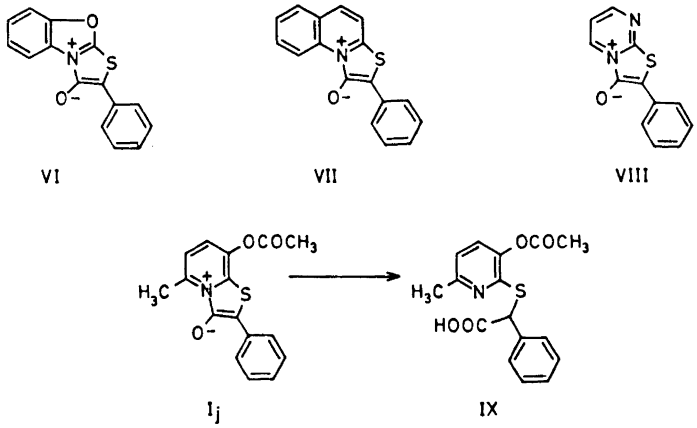

Scheme 2.

N HCl in dilute acetone (1 : 1). The choice of a 5-methyl derivative was directed by the accelerating effect exerted by a 5-substituent on the hydrolysis of the ring (see below). The resultant product was identified as the acetate IX. The original acetate is therefore the 8-acetoxy derivative I_j as had previously been suggested from spectroscopic studies.[2]

Some light absorption characteristics of the prepared thiazoles in acid and alkaline solution are given in Table 1. Hydrolysis rates as discussed below, however, show that some of the compounds will be partly hydrolysed before

Table 1. Absorption spectra in 0.1 N HCl and 0.1 N NaOH in aqueous dioxan (1 : 1).

Comp.	Substituents				0.1 N HCl in aq. dioxan (1 : 1)						0.1 N NaOH in aq. dioxan (1 : 1)					
	R^5	R^6	R^8	R	λ nm	log ε	λ nm	log ε	λ nm	log ε	λ nm	log ε	λ nm	log ε	λ nm	log ε
I a	H	H	H	H	432	4.1	283	3.8	235	4.1	436	4.2	283	3.9	238	4.1
b	H	H	NO_2	H	436	3.9	338	3.8	248	3.8	494	3.9	328	3.9	255[a]	3.7
											382	3.8	305[a]	3.8	230	3.9
c	H	NO_2	H	H	455	4.0	285	4.1	254	3.9	532[a]	3.7	357	3.9	232	4.0
											455	3.9	296	3.8		
											428					
d	H	H	CH_3	H	432	4.1	283	3.8	233	4.1	432	4.1	283	3.9	235	4.1
e	H	H	OAc	H	432	4.0	283	3.7	238	4.1	410	4.2	302[a]	3.7	258	4.1
													283[a]	3.7		
f	H	H	H	OCH_3	443	4.1	355[a]	3.6	275[a]	3.9	444	4.2	285	3.9	242	4.2
							285	3.9	242	4.1			275	3.9		
g	H	H	H	NO_2	472	4.1	290[a]	3.9	227	4.0	472	4.1	290	3.8	250[a]	3.9
							253	3.8							227	4.0
h	CH_3	H	H	H	448	—	—	—	—	—	455	4.1	290	3.9	237	4.1
i	CH_3	H	OC_2H_5	H	448	—	—	—	—	—	450	4.1	290	3.8	242	4.0
															225[a]	3.9
j	CH_3	H	OAc	H	465	—	—	—	—	—	430	4.0	317	3.6	258	3.9
													290[a]	3.5	223	3.9
k	CH_3	H	H	NO_2	494	—	302	—	256	—	494	4.4	303	3.7	256	4.1
									230[a]						227	4.1
VII					488	4.1	307	4.0	269	3.8	488	4.3	307	3.9	269	3.8
									238	4.4					238	4.4
VIII					475	3.9	288	3.9	238	4.0	449	—	347	—	222	—
													300			

[a] Shoulder.

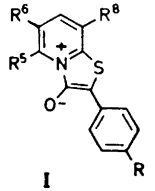

I

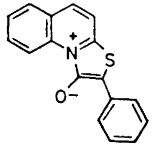

VII

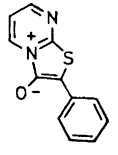

VIII

a spectrum could be recorded. The logarithms of the extinction coefficients are therefore only given with the first decimal figure or are omitted in specially reactive compounds. With the exception of compounds Ib, Ic, and VIII the positional maxima are little affected by 0.1 N HCl and 0.1 N NaOH. This strongly indicates that the phenolic group is also largely dissociated in 0.1 N HCl. In stronger acidic solutions hypsochromic shifts were seen with much increased hydrolysis rates. The isomeric nitro-pyridines Ib and Ic undergo bathochromic shifts for the highest wavelength band of 60 and 80 nm, respectively, from acid to alkaline pH. The absorption maxima in acid solution are in the region observed for the other analogues. The anomalously high wavelength maxima at alkaline pH require a molecular change. The most likely explanation is pseudo-base formation [3] caused by the additional activation of the electron deficient pyridinium system by the nitro group. By analogy[4] to other simple pyridinium derivatives the hydroxyl anion is assumed to add to the unsubstituted 5-position as indicated in Scheme 3. The reaction is reversible if acid is added after a short time. The pyrimidinium derivative VIII, on the other hand, undergoes a hypsochromic shift (25 nm) with increase in pH. The electron deficiency in the pyrimidine should be similar to that in the nitro-pyridines and therefore lead to pseudo-base formation by hydroxyl addition to the 5- or the 7-position.

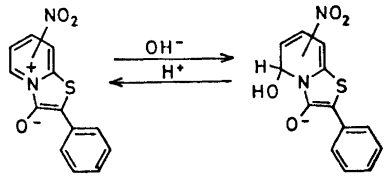

Ib,Ic X

Scheme 3.

Some of the compounds investigated were found to undergo rapid reaction in aqueous solution. Solutions of the compounds were therefore made up in dioxan. These solutions were mixed with equal volumes of 0.2 N acid or base immediately before commencement of the measurements. The dioxan also keeps in solution the less water soluble compounds. The hydrolysis was followed by the decrease in absorption in the 430 – 490 nm region where the acids (II) formed are transparent. The results are shown in Table 2. The expected first-order kinetics for the hydrolysis was observed in acid solution.

Table 2. Rate constants for the hydrolysis at 20°C in 0.1 N HCl (dioxan : water = 1 : 1) measured by the change in light absorption at the highest wavelength absorption maxima (Table 1).

	I											VII	VIII
	a	b	c	d	e	f	g	h	i	j	k		
$k \times 10^4$ sec^{-1}	2.03	0.24	0.15	1.93	1.50	7.97	0.15	88.85	41.45	46.20	2.41	3.50	0.83

From Table 2 it is seen that the 5-methyl analogues Ih – Ik fall into a series with a much higher rate constant than the respective members of the desmethyl series Ia – Ig. The methyl group in the 8-isomer (Id) in contrast to the 5-isomer (Ih), however, hardly affects the rate constant relative to the parent desmethyl compound. The higher hydrolysis rates in the 5-methyl series are therefore ascribed to steric repulsion between the 3- and 5-substituents. The closeness of these groups in the planar aromatic structure increases the energy of the system with decrease in activation energy for hydrolysis. A calculation based on the increase in the rate constant shows the 5-methyl group to decrease the activation energy by 1.8 kcal/mol. In the quinoline VII *peri*-interaction seems a likely explanation for the observed increase in the rate constant relative to the parent pyridine Ia.

The series Ia, If, and Ig only differ in the nature of the 4-substituent in the phenyl ring. The methoxy substituent (If) increases the hydrolysis rate, whereas the nitro substituent (Ig) decreases the rate relative to the unsubstituted compound (Ia). The hydrolysis rate therefore increases with an electron releasing substituent. From Table 2 it is also evident that variations in the nature of the 6- and 8-substituents affect the rate constants in such a way that electron donating substituents increase the rate constant while electron attracting substituents have the opposite effect. In both these cases the transmitted electronic effect will affect the tautomeric ratio between the one-form of the lactam and its enol. In the absence of increased steric interaction electron donating substituents would be expected to stabilise the one-form of the molecule relative to the enol. In the one-form, the molecule is present in the reactive acylpyridinium form. Any substituent, therefore, which will increase the concentration of the latter tautomer, will promote hydrolysis.

Increase in acid concentration increases the hydrolysis rates as verified for the 8-methyl derivative Id. The half life in 0.02 N HCl, 0.1 N HCl, and 0.5 N HCl was 170 min, 60 min, and 17 min, respectively.

In alkaline solution the compounds will exist as betaines presumably with partial delocalisation of the negative charge from the phenolate oxygen over the thiazolo ring. Attack by hydroxyl ions is less favourable and most compounds were resistant to hydrolysis in 0.1 N NaOH in dilute dioxan (1 : 1) at 20°C. The pyrimidine VIII and the 8-nitropyridine Ib, however, were rapidly hydrolysed (Table 3). The 6-nitropyridine Ic and the nitrophenyl derivative Ig reacted more slowly. The 5-methyl homologue Ik was even less reactive than Ig. First-order kinetics was observed.

Table 3. Rate constants for the hydrolysis at 20°C in 0.1 N NaOH (dioxan : water = 1 : 1) measured by the change in light absorption at the highest wavelength absorption maxima (Table 1).

	I			VIII
	b	c	g	
$k \times 10^4$ sec^{-1}	1.54	0.17	0.26	25.67

From Table 3 it is seen that the rate constant for the 8-nitro derivative (Ib) is almost ten times that of the 6-nitro derivative (Ic) and is further increased by a factor of about seventeen in the case of the pyrimidine (VIII). The electron withdrawing or localisation effects, however, should be similar in these analogues. The light absorption data (Table 1), however, show that these compounds (Ib, Ic, and VIII) are present as pseudo-bases in alkaline solution. The observed rate differences are therefore attributed to hydrolysis of the respective pseudo-bases. The intermediate in the base hydrolysis is formed by OH^- addition to the carbonyl group to form a tetrahedral carbon.

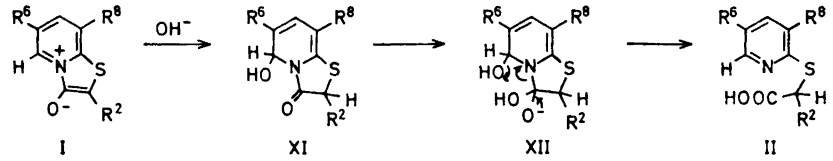

Scheme 4.

Assuming a nearly planar 5-pseudo-base (XII) intermediate the 3- and 5-substituents will be eclipsed. In contrast to the 8-substituent a bulky 6-substituent will by its non-bonded interaction with the 5-substituent increase the 3,5-steric repulsion and thereby increase the activation energy. Pseudo-base formation by addition to the 5-position might also be expected to be less favourable for the 6-isomer than for the 8-isomer while there is little steric difference in formation of a 7-adduct. The rate data therefore are consistent with formation of the 5-pseudo-base. The pyrimidine VIII carries no 6-substituent and has a higher rate constant than the 8-nitro-pyridine isomer (Ib) which suggests that the pseudo-base formation at least in part occurs in the 7-position.

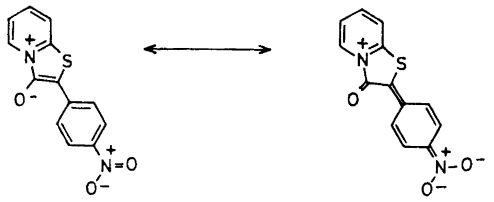

Scheme 5.

The absorption spectrum of the *para*-nitrophenyl derivative Ig shows little shift with pH within the limits studied (Table 1). This would appear to exclude the pseudo-base as a dominant species in the solution studied. The ready hydrolysis in alkaline solution is best explained by the conjugative effect of

the nitro group. The negative charge from the phenolate oxygen is thereby to a large degree delocalised over the nitrophenyl system and thus the 3-carbon is more susceptible for nucleophilic attack.

EXPERIMENTAL

The light absorption measurements were done on a CARY-14 instrument.

Kinetic measurements. The hydrolysis rates were studied at 20°C in 0.1 N NaOH and 0.1 N HCl in dioxan:water (1 : 1 v/v). The solutions were made up immediately before measurements by mixing equal volumes of a dioxan solution of the compound under investigation with aqueous 0.2 N base or acid. The rate of hydrolysis was determined by measuring the decrease in the long wave-length absorption band (Table 1). Concentrations were $1-3\times10^{-4}$ M. Rate constants were determined from log-plots of concentration against time.

Thiazolo[3,2-a]pyridinium-3-oxides (*I*). The pyrid-2-thione (0.01 mol), the α-bromophenylacetic acid (0.01 mol), and sodium bicarbonate (0.04 mol) were dissolved in water (25 ml) and the solution stirred at 50°C until the evolution of carbon dioxide had ceased (about 2 h). The solution was then acidified with acetic acid, extracted with chloroform or ethyl acetate, the extracts washed, dried and evaporated. The α-(2-pyridylthio)phenylacetic acids (II) were thus obtained as an oily material. In some cases the acids were purified and crystallised. In most cases, however, the crude products were reacted further.

For cyclisation the acid was dissolved in 10 – 20 ml of pyridine, depending on the solubility, followed by addition of an equal volume of acetic anhydride. The solution became rapidly deeply coloured due to the cyclic product. The solutions were generally left overnight at 5°C and the crystalline precipitate collected. In some cases the material was pure enough for elemental analysis but was usually recrystallised from an organic solvent. Details are given in Table 4.

Table 4.

Comp.[a]	Yield %	Solv. recryst.	Appearance	M.p. °C	Molecular formula	Found			Calc.		
						C	H	N	C	H	N
I b	80	–	Dark green	270–273	$C_{13}H_8N_2O_3S$	57.11	2.88	10.07	57.35	2.96	10.29
c	52	–	Dark red	284–290	»	57.47	3.08	10.13	»	»	»
d	50	EtOAc	Red	190–191	$C_{14}H_{11}NOS$	69.36	4.48	5.60	69.68	4.59	5.80
f	53	Toluene	Red	191–193	$C_{14}H_{11}NO_2S$	65.43	4.15	5.74	65.35	4.31	5.44
g	91	HCO_2H	Dark red	350	$C_{13}H_8N_2O_3S$	57.28	3.34	10.34	57.35	2.96	10.29
h	50	EtOAc	Red	166–167	$C_{14}H_{11}NOS$	69.59	4.54	5.86	69.68	4.59	5.80
i	59	EtOAc	Red	178–180	$C_{16}H_{15}NO_2S$	67.41	5.29	4.91	67.34	5.30	4.91
k	67	Pyridine	Dark red	318–320	$C_{14}H_{10}N_2O_3S$	58.75	3.53	9.89	58.73	3.52	9.78

[a] Data for compounds I a, I e and I j have previously been reported.[2]

α-(2-Benzoxazolylthio)phenylacetic acid. Attempted synthesis of thiazolo[3,2-b]benzoxazolium-3-oxide (*VI*). The title acid was prepared as the pyridine II from 2-mercaptobenzoxazole in 53 % yield, m.p. 140 – 142°C (dilute ethanol). (Found: C 62.91; H 4.12; N 4.69. Calc. for $C_{15}H_{11}NO_3S$: 63.14; H 3.89; N 4.91).

The acid was not cyclised in pyridine-acetic acid under the conditions described above for the formation of I.

2-Phenylthiazolo[3,2-a]quinolinium-3-oxide (*VII*) was prepared as above from quinoline-2-thione and α-bromophenylacetic acid in 94 % yield. The red crystalline material, after recrystallisation from toluene, had m.p. 198 – 199°C. (Found: C 73.46; H 3.92; N 5.10. Calc. for $C_{17}H_{11}NOS$: C 73.62; H 4.00; N 5.06).

2-Phenylthiazolo[3,2-a]pyrimidinium-3-oxide (*VIII*). Condensation between pyrimid-2-thione and α-bromophenylacetic acid as described for the pyridines yielded *α-(2-pyrimidylthio)phenylacetic acid* in 90 % yield; m.p. 143 – 145°C (decomp.) (dilute ethanol). (Found: C 58.31; H 3.33; N 11.42. Calc. for $C_{12}H_{10}N_2O_2S$: C 58.52; H 4.09; N 11.37).

The acid thus prepared (1.0 g, 0.004 mol) was dissolved in pyridine (5 ml) and acetic anhydride (5 ml) added. The reddish solution was left at 5°C for 24 h. The red crystalline precipitate, yield 0.9 g (98 %), recrystallised from ethyl acetate had m.p. 218 – 220°C (Found: C 63.07; H 34.49; N 12.18. Calc. for $C_{12}H_8N_2OS$: C 63.14; H 3.53; N 12.27).

REFERENCES

1. Part XXXIV. Lie, R. and Undheim, K. *J. Chem. Soc. Perkin Trans. 1* **1973**. *In press.*
2. Undheim, K. and Tveita, P. O. *Acta Chem. Scand.* **25** (1971) 5.
3. Albert, A. *Advan. Heterocycl. Chem.* **1** (1963) 167.
4. Schofield, K. *Hetero-aromatic Nitrogen Compounds. Pyrroles and Pyridines*, Butterworths, London 1967, p. 236.

Received December 20, 1972.

ACTA CHEMICA SCANDINAVICA 27 (1973) 1771–1780

Chlorophylls

IV. Preparation and Purification of Some Derivatives of Chlorophylls *a* and *b*

PAAVO H. HYNNINEN

Department of Biochemistry, University of Helsinki, SF-00170 Helsinki 17, Finland

The reactions of pheophorbides *a* and *b* in methanolic potassium hydroxide were studied as functions of alkali and oxygen concentration. The derivatives formed as products of these reactions were separated utilizing the aqueous formic acid-chloroform-dimethylformamide (AFCD) solvent system. In the presence of atmospheric oxygen, boiling 30 % methanolic potassium hydroxide reacted upon pheophorbide *a* to yield purpurin 18 as the principal product, while chlorin e_6 was formed to a lesser extent. Under similar conditions, a 0.5 % methanolic solution of the alkali reacted upon pheophorbide *a* to yield a product which was spectroscopically identical to chlorin e_6. Partition fractionation revealed this product to be actually a mixture of various chlorin e_6 methyl esters. Hydrolysis of the ester mixture in 30 % methanolic potassium hydroxide under an argon atmosphere yielded nearly pure chlorin e_6, which was further purified utilizing the AFCD solvent system. Beginning with pheophorbide *b*, relatively good yields of rhodin g_7 were analogously (*i.e.* through methyl esters of rhodin g_7) prepared. These results indicate that, in dilute methanolic alkali solutions, solvolysis of the pheophorbide ring V is the principal reaction, even in the presence of oxygen. Conversely, concentrated methanolic alkali solutions result in the oxidative splitting of ring V as the predominant reaction in the presence of oxygen. A mechanism for the solvolysis of ring V is proposed and discussed.

The effects of solvent and temperature upon the saponification of methylpheophorbide *a* were studied by Conant and Moyer.[1] These authors reported that the formation of chlorin e_6 was completely suppressed when saponification was performed with an alcoholic solution of potassium hydroxide in which ethyl or propyl rather than methyl alcohol was employed as solvent. The same result was also claimed when methanolic potassium hydroxide was utilized, provided that saponification was carried out at a temperature of -10°C. Chlorin e_6 was reportedly the chief product when saponification was effected by means of boiling alcoholic potassium hydroxide in pyridine solution

(Willstätter's procedure [2]); no unstable chlorins were formed under these conditions.

Alkali concentration has since appeared to be of the utmost importance among the factors that determine the saponification products of the chlorophylls or derivatives thereof possessing an intact isocyclic ring V. Oster *et al.*[3] effected the saponification of chlorophyll *a* utilizing dilute methanolic potassium hydroxide (1 ml of 7 % potassium hydroxide in methanol was added to 50 ml of chlorophyll *a* solution). Employing partition chromatography as their analytical method, they found their product to consist of only one component, chlorophyllin *a* (Mg-chlorin e_6). Holt [4] reported that treatment of methylchlorophyllide *a* with 0.5 % methanolic potassium hydroxide in the presence of atmospheric oxygen results principally in the formation of Mg-chlorin e_6 trimethyl ester. When more concentrated (5 – 30 %) methanolic potassium hydroxide solutions were utilized, Mg-chlorin e_6 products were formed only if oxygen was excluded from the reaction mixture. These results were interpreted by Holt as signifying that, in dilute methanolic potassium hydroxide, the concentration of the phase test intermediate was so low that even under aerobic conditions methanolysis could proceed at a more rapid rate than oxidation.

In the present investigation, the author has compared the products formed from pheophorbide *a* as a result of two different saponification procedures. In one procedure, drastic conditions resembling those employed by Willstätter[2] were used, while in the other, the mild conditions of Holt [4] were utilized. It will be demonstrated that, in the former procedure, oxidative splitting [5] of ring V is the primary reaction, while in the latter, solvolysis of ring V occurs almost exclusively. As a result of the present study, methods will be described for the preparation, beginning with pheophorbides *a* and *b*, of chlorin e_6 and rhodin g_7 in relatively high yields. It will further be shown that the liquid-liquid partition technique, which has been previously [6,7] adapted to the separation of dicarboxylic porphyrins and hemins, may also be successfully applied to the fractionation of magnesium-free chlorophyll derivatives.

EXPERIMENTAL

Chlorophylls a and b were isolated from frozen soybean leaves using the liquid-liquid partition method previously [8] described.

Pheophorbides a and b were prepared from chlorophylls *a* and *b*, respectively, by shaking an ethereal solution of the chlorophyll with 30 % (w/w) hydrochloric acid for 5 min. The pheophorbide thus formed was transferred into the ether phase by diluting the acidic phase. The ether solution was then washed three times with distilled water. The spectroscopic properties of these pheophorbides are presented in Table 1, a and i.

Unstable chlorin 7 was produced from pheophorbide *a* by treating an ethereal solution of the pigment for 2 min with 25 % potassium hydroxide in 1-propanol [1,9] (Table 1, e).

Purpurin 7-lactone-methyl ether (Table 1, f) was prepared by shaking an ethereal solution of Mg-purpurin 7-lactone-methyl ether-methylphytyl ester [5] with 30 % (w/w) hydrochloric acid for 5 min. The magnesium-free pigment was transferred into diethyl ether by dilution of the acidic phase. The ether solution was then washed three times with distilled water.

Purpurin 18 was isolated from the saponification products of pheophorbide *a* by means of the partition fractionation described below (Table 1, g).

Table 1. Spectroscopic properties of some chlorophyll derivatives in ethyl ether.

Compound	Peak positions (nm) and peak ratios (R)													
	I		II		III		IV		V		VI		Soret	
	nm	R	nm	R	nm	R	nm	R	nm	R	nm	R	nm	R
a. Pheophorbide *a*	667.0	2.07	609.5	13.9	560.0	39.1	532.5	10.9	504.0	8.91	467.0	22.5	408.0	1.00
b. Chlorin e_6 (1A, 3A) [a]	666.0	2.82	610.5	29.2	560.0	76.5	530.0	30.1	500.0	11.3			400.0	1.00
c. Chlorin e_6 ester mixture	666.0	2.62	609.5	20.9	559.5	43.8	530.0	19.9	500.0	10.0			400.0	1.00
d. Chlorin k (?) (1B)	665.5	3.04	610.5	28.6	(557) [b]	(48.2)	529.0	25.3	499.0	10.8			399.5	1.00
e. Unstable chlorin 7(-monomethyl ester)	668.5	2.63	611.0	18.6	560.0	42.8	529.5	15.9	499.5	10.7	(470)	(28.4)	399.0	1.00
f. Purpurin 7-lactone-methyl ether (-monomethyl ester)	668.5	2.50	611.0	18.7	561.0	47.8	528.0	14.9	498.5	10.0	(467)	(27.1)	399.0	1.00
g. Purpurin 18 (1C)	695.0	2.25	638.0	14.7	587.0	48.7	540.0	5.48	503.0	15.1	475.0	24.5	406.0	1.00
h. Chlorin p_6	670.0	2.80	615.0	24.8	565.0	63.2	529.0	21.5	498.0	11.7			399.0	1.00
i. Pheophorbide *b*	655.0	4.56	599.0	12.5	555.0	12.2	525.0	9.30					433.0	1.00
j. Rhodin g_7	652.0	6.92	597.5	25.7	560.0	20.3	524.0	15.5					427.0	1.00
k. Rhodin g_7 ester mixture	652.0	6.48	597.0	26.5	558.0	20.9	522.0	14.5					426.0	1.00

[a] Number in parentheses refers to figure number, while capital letter refers to component in that figure.
[b] Peak positions and ratios stated in parentheses are approximate.
R = quotient of absorbance at Soret band divided by absorbance at wavelength indicated.

Chlorin p_6 (Table 1, h) was produced by shaking an ethereal solution of purpurin 18 with 25 % methanolic potassium hydroxide for 10 min. [9] The pigments thus formed were transferred into the diethyl ether phase by neutralization with dilute hydrochloric acid. Chlorin p_6 was then extracted from the ether solution with 6 % hydrochloric acid. The derivative was transferred into fresh diethyl ether by diluting the acidic phase, and the ether solution was then washed three times with distilled water.

Saponification of pheophorbide a with boiling 30 % methanolic potassium hydroxide. An ethyl ether solution of pheophorbide *a*, containing about 10 mg of the pigment, was evaporated to dryness at reduced pressure. Eighty milliliters of boiling 30 % (w/w) methanolic potassium hydroxide were then added to the residue, thereby causing the yellow-brown colour of the phase test intermediate to appear. After 1 min, the solution was poured into a separatory funnel containing 200 ml of diethyl ether and 700 ml of distilled water. The pigments were then transferred into the ether phase by neutralization with hydrochloric acid. The phases were separated and the lower phase was extracted twice with 100 ml of diethyl ether. The combined ether extracts were then washed three times with distilled water. A visible absorption spectrum indicated that the product consisted of several components.

Saponification of pheophorbide a with 0.5 % methanolic potassium hydroxide. One hundred milliliters of 0.5 % (w/w) methanolic potassium hydroxide were added, in the presence of atmospheric oxygen and at room temperature, to a solution of 10 mg pheophorbide *a* in 50 ml ethyl ether. The characteristic colour of the phase test intermediate appeared within a second following the addition of the alkali solution. After 10 min, 500 ml of distilled water were added to the reaction mixture and the derivatives were then transferred into the diethyl ether phase by neutralizing with hydrochloric acid. The separated ether layer was washed three times with distilled water. The visible absorption spectrum of the ethereal solution closely resembled that of chlorin e_6 (Table 1, c). A partition fractionation, described below, indicated that the product consisted of various methyl esters of chlorin e_6.

Preparation of free chlorin e_6. The methyl esters obtained from the saponification of pheophorbide *a* with 0.5 % methanolic potassium hydroxide were transferred into 70 ml of ethyl ether. The solution was then treated for 1 h with 80 ml of 30 % (w/w) methanolic potassium hydroxide at room temperature and under an argon atmosphere. The reaction was stopped by adding 700 ml of distilled water to the mixture, and the derivatives were then transferred into diethyl ether by neutralization with hydrochloric acid. The ether solution of the saponification products exhibited an absorption spectrum which was very similar to that of chlorin e_6.

Preparation of free rhodin g_7. Pheophorbide *b* (5 mg) was first treated with dilute (0.5 %) methanolic potassium hydroxide in a manner similar to that described above for pheophorbide *a*. The absorption spectrum of the products of this saponification closely resembled that of rhodin g_7 (Table 1, k). The methyl esters were then treated with 30 % methanolic potassium hydroxide in a way analogous to that described above for the preparation of free chlorin e_6. An absorption spectrum of the saponification products indicated slight contamination by at least one impurity.

Fractionation by multiple liquid-liquid partition. Partition fractionations were performed utilizing the Hietala apparatus [10] and the aqueous formic acid-chloroform-dimethylformamide (AFCD) [7] solvent system. A phase ratio of about 0.3 was employed; in other respects, however, experimental conditions were similar to those previously used. [7] In order to effect more rapid separation, advantage was taken of stepwise pH-gradient elution.[6]

Spectroscopic data. The absorption spectra of the derivatives were recorded utilizing a Cary Model 15 spectrophotometer. Single absorbances were measured by means of a Beckman DU spectrophotometer.

RESULTS

Fig. 1 presents the results of the separation of the products formed on treating pheophorbide *a* briefly with boiling 30 % methanolic potassium hydroxide in the presence of atmospheric oxygen. Component A, which was

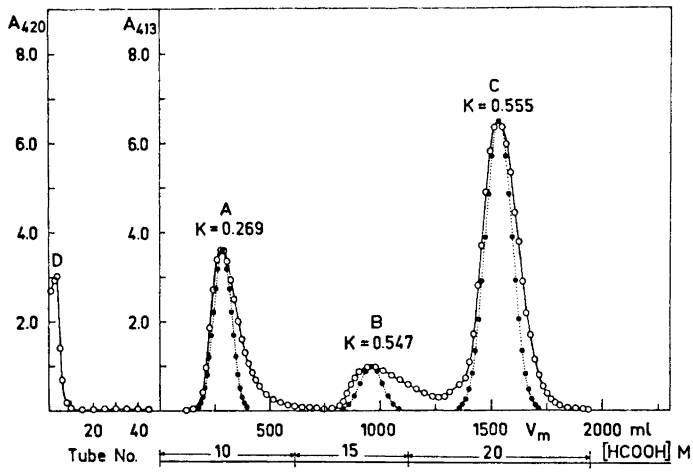

Fig. 1. Separation of chlorophyll *a* derivatives. Solvent system: HCOOH (of varied molarity)/$CHCl_3$(25) – DMF(1). The ether solution of the products formed upon the saponification of pheophorbide *a* with boiling 30 % methanolic potassium hydroxide was evaporated to dryness at reduced pressure. The residue was dissolved in 2 ml of dimethylformamide (DMF), to which were then added 50 ml of $CHCl_3$ + 8 ml of H_2O + 5 ml of HCOOH. The mixture was sampled into tubes r = 0, ...,4. Number of tubes used in the fractionation = N = 50. Average volume of mobile phase (acid) in a partition unit = v_m = 3.00 ml; average volume of stationary phase ($CHCl_3$ – DMF) in a partition unit = v_s = 10.50 ml. Total volume of effluent eluted from the apparatus = V_m = 1940 ml; flow rate = 1.5 ml/min. Theoretical (●) and experimental (○) values, the latter obtained by measuring $A_{413\,nm}$ of the effluent fractions and $A_{420\,nm}$ of the lower phases in the tubes. A = chlorin e_6, B = chlorin k (?), C = purpurin 18, and D = 10-methoxy-pheophorbide *a* (?).

eluted from the apparatus with 10 M formic acid, was characterized as chlorin e_6 upon the basis of its spectroscopic properties (Table 1, b) [11] and low hydrochloric acid number (SZ = 3).[9] The next component, B, was eluted with 15 M formic acid and possessed the following characteristics: (1) spectroscopic properties (Table 1, d) similar to those of chlorin e_6 but distinctly different from those of unstable chlorin 7 and purpurin 7-lactone-methyl ether (Table 1, e and f); (2) a hydrochloric acid number of 12; (3) neither treatment with diazomethane [12] nor standing in methanol saturated with hydrochloric acid resulted in the formation of purpurin 7-trimethyl ester or purpurin 5-dimethyl ester, thus excluding the possibility of component B representing one of the "unstable" chlorins (chlorin 7 and chlorin 5) [9,13,14] or their methyl esters; (4) after standing for 6 days in methanolic hydrochloric acid in the presence of atmospheric oxygen, the pigment was partially converted into a porphyrin exhibiting absorption maxima, in diethyl ether, at 630, 580 and 550 nm (these values are in accord with the spectroscopic properties of rhodoporphyrin-γ-hydroxymethyl-lactone-methyl ester [9,15]); (5) standing in concentrated hydrochloric acid for 5 min did not alter the spectroscopic properties of the pigment; and (6) hydrolysis with boiling 25 % methanolic potassium hydroxide for 10 min converted part of the pigment into purpurin 18, as evidenced by ab-

sorption maxima, in diethyl ether, at 695, 637, and 540 nm. Upon the basis of these properties, it is likely that fraction B eluted within the range 830 – 1180 ml consisted of chlorin k, *i.e.* rhodochlorin-γ-hydroxymethyl-lactone, which is known to be spectroscopically very similar to chlorin e_6.[16]

The principal component, C, was eluted from the apparatus with 20 M formic acid and was identified as purpurin 18 upon the basis of the following properties: (1) a visible absorption spectrum very similar to that of purpurin 18 (Table 1, g);[9] (2) a hydrochloric acid number of 18;[1] (3) shaking of a diethyl ether solution of the pigment with 25 % methanolic potassium hydroxide for 10 min resulted in the formation of chlorin p_6 (chlorin a; Table 1, h); and (4) heating with pyridine-sodium carbonate for 10 min partially converted the pigment into rhodoporphyrin-γ-carbonic acid anhydride,[17] as indicated by absorption maxima, in diethyl ether, at 655, 597 (broad band), and 550 nm.

The material (D) that remained at the sampling end of the apparatus primarily exhibited absorption peaks, in diethyl ether, at 668, 610, 535, 505, and 408 nm. These values are rather similar to the spectroscopic properties of pyropheophorbide *a* monomethyl ester.[11] However, since the hydrochloric acid number of component D must have been greater than that of purpurin 18, it appears likely that the material consisted principally of either 10-methoxy-pheophorbide *a* or 10-methoxy-pyropheophorbide *a*. The slight absorption peaks observed, in diethyl ether, at 632, 577, and 555 nm, suggest that the material contained a small quantity of chloroporphyrin e_7-lactone-methyl ester.[9]

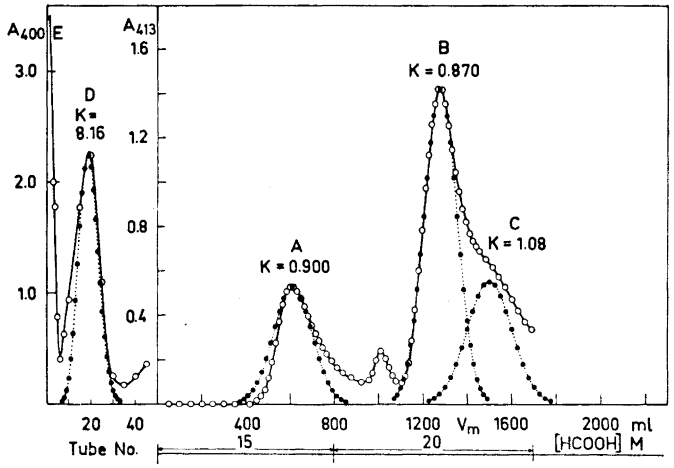

Fig. 2. Separation of chlorin e_6-methyl esters. Solvent system: HCOOH (varied molarity)/$CHCl_3$(25) – DMF(1). The ether solution of the products formed upon the saponification of pheophorbide *a* with 0.5 % methanolic potassium hydroxide was evaporated to dryness at reduced pressure. The residue was dissolved in 2 ml of DMF, to which were then added 50 ml of $CHCl_3$ + 6 ml of H_2O + 8 ml of HCOOH. The mixture was sampled into tubes r = 0,...,4. N = 50. v_m = 3.04 ml; v_s = 10.46 ml. V_m = 1680 ml; flow rate = 1.5 ml/min. Theoretical (●) and experimental (○) values, the latter obtained by measuring $A_{413\ nm}$ of the effluent fractions and $A_{400\ nm}$ of the lower phases in the tubes. A – E = various methyl esters of chlorin e_6.

The saponification of pheophorbide *a* with 0.5 % methanolic potassium hydroxide in the presence of atmospheric oxygen resulted in the formation of a product which spectroscopically appeared to be homogeneous and very similar to chlorin e_6 (Table 1, c). However, when the material was subjected to partition fractionation (Fig. 2), it was revealed to consist of a complex mixture of several components (A – E), all of which were spectroscopically identical. Fraction A is believed to consist of monomethyl ester(s), while fractions B – D are thought to be various dimethyl esters of this compound (there are three possibilities). The last component, E, is presumably chlorin e_6 trimethyl ester. The slight peak apparent between fractions A and B is probably due to a premature molarity change which has caused crowding of the tail of fraction A.

The methyl esters of the fractionation presented in Fig. 2 were combined and saponified with 30 % methanolic potassium hydroxide while carefully avoiding exposure of the reaction mixture to oxygen (refer to experimental). The fractionation of the resulting saponification products is presented in Fig. 3. Free chlorin e_6 was obtained in good yield (> 90 %), thus demonstrating in a convincing manner that the components of Fig. 2 indeed were various methyl esters of chlorin e_6.

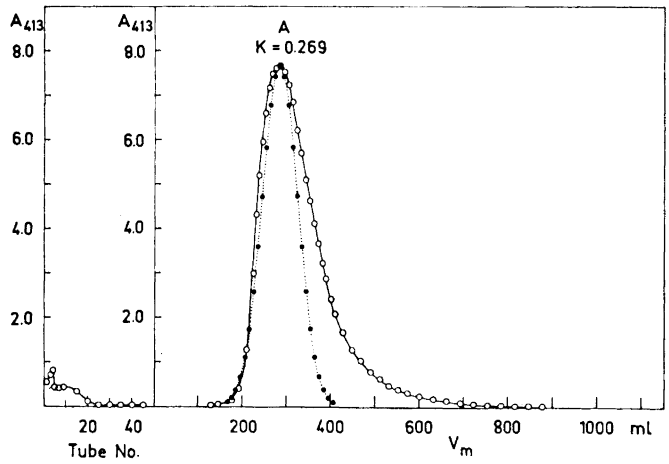

Fig. 3. Isolation of free chlorin e_6. Solvent system: HCOOH(10 M)/$CHCl_3$(25) – DMF(1). The ether solution of the products formed upon the saponification of the chlorin e_6-methyl esters of Fig. 2 was evaporated to dryness at reduced pressure. The residue was dissolved and sampled into the apparatus as described in Fig. 1. N = 50. v_m = 3.00 ml; v_s = 10.50 ml. V_m = 888 ml; flow rate = 1.5 ml/min. Theoretical (●) and experimental (○) values, the latter obtained by measuring $A_{413\ nm}$ of the effluent fractions and of the lower phases in the tubes. A = chlorin e_6.

Fig. 4 presents the isolation of rhodin g_7 (component A). The yield in this case was not as high as in the isolation of chlorin e_6. The spectroscopic properties of fraction A (Table 1, j) closely resembled those previously described for rhodin g_7 trimethyl ester.[9,18] The material that remained at the sampling end

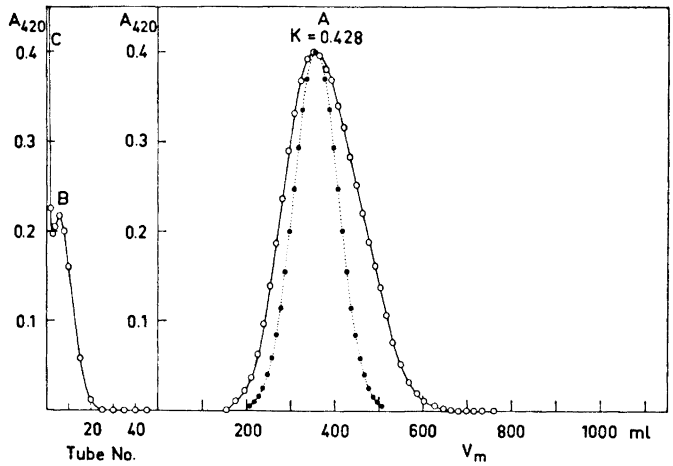

Fig. 4. Isolation of free rhodin g_7. Solvent system: HCOOH(13 M)/$CHCl_3$(25) – DMF(1). The ether solution of the products formed upon the saponification of rhodin g_7-methyl esters was evaporated to dryness at reduced pressure. The residue was dissolved in 2 ml of DMF, to which were then added 50 ml of $CHCl_3$ + 7 ml of H_2O + 7 ml of HCOOH. The mixture was sampled into tubes r = 0, ... ,4. N = 50. v_m = 2.89 ml; v_s = 10.61 ml. V_m = 760 ml; flow rate = 1.5 ml/min. Theoretical (●) and experimental (○) values, the latter obtained by measuring $A_{420\,nm}$ of the effluent fractions and of the lower phases in the tubes. A = rhodin g_7, B = a second rhodin, and C = b-purpurin 18.

of the apparatus appeared to consist of two components (B and C). Fraction B resembled rhodin g_7 regarding its visible absorption spectrum and is probably a second rhodin. Fraction C exhibited absorption maxima, in ethyl ether, at 671.5, 620, 557, 518, and 431 nm. These values are in accord with the spectroscopic properties of *b*-purpurin 18.[9]

DISCUSSION

The fact that purpurin 18 was the primary product when pheophorbide *a* was saponified with a boiling concentrated solution of methanolic potassium hydroxide indicates that, in this case, oxidative splitting of ring V[5] is the principal reaction in the presence of oxygen. The results of Fig. 2 confirm the argument presented by Holt[4] that saponification with dilute methanolic potassium hydroxide causes the solvolysis of ring V as the predominant reaction, even in the presence of oxygen.

The mechanism of this solvolysis (methanolysis, hydrolysis, or aminolysis) has not as yet been elucidated in detail. An important consideration is whether or not the methanolysis of ring V occurs through a mechanism similar to that proposed by Weller and Livingston[19] for the aminolysis of this ring. These investigators did not observe the characteristic colour of the phase test intermediate during the course of the amine reaction and they therefore concluded that this reaction differs in many respects from that of the phase test. They proposed a mechanism whereby the amine attacks carbon-9 of the all-keto form of the chlorophyll, thus resulting, through a transition state possessing

an onium-structure, in a carbanion with a free electron pair at carbon-10. The carbanion was then assumed to react rapidly with the solvent (amine) to yield a chlorin 6-carboxamide.

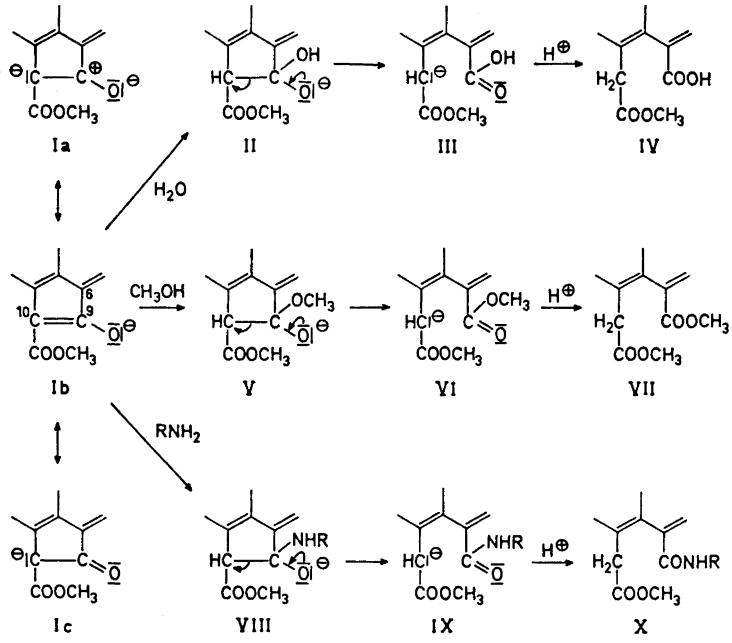

Fig. 5. Proposed mechanism for the solvolysis of ring V of the chlorophylls and their derivatives.

The present author now proposes a general mechanism, shown in Fig. 5, for the solvolysis of ring V. According to the reaction scheme, the enolate ion (I) is the key intermediate of this solvolysis.[5] The solvent (water, methanol or amine) presumably reacts with the enolate ion, through addition across the carbons-9 and -10 double bond, to yield the unstable intermediate (II, V or VIII, respectively). Such addition may be understood upon assuming that the enolate ion is a resonance hybrid to which form Ia makes a considerable contribution. The unstable intermediate is converted by rearrangement to the respective carbanion (III, VI or IX), which then reacts rapidly with the solvent to give either chlorin e_6 monomethyl ester (IV), chlorin e_6 dimethyl ester (VII) or chlorin 6-carboxamide (X). The following evidence supports the mechanism illustrated in Fig. 5:

1. Shortly after the addition of dilute methanolic potassium hydroxide to pheophorbide *a*, a brown colour was clearly observed. It is therefore probable that solvolysis proceeds *via* the phase test intermediate.

2. Fischer and Riedmair [20] concluded that methanolysis requires an activated hydrogen at the C-10 postition, since pyropheophorbide did not undergo this reaction.

3. The investigations of Fischer and Oestreicher [21] concerning phorbin synthesis (a reversed reaction to that of methanolysis) suggest the C-10 carbanion as a probable intermediate. The required presence of a strong base in the synthesis of phorbin is understandable when it is assumed that the base initiates the reaction by extracting a C-10 proton from compound VII.

4. The lack of drastic colour change during aminolysis is no proof that the reaction does not proceed through the phase test intermediate (enolate ion). If the intermediate is consumed as rapidly as it is formed, then no impressive colour change is to be expected. This situation is analogous to that of the allomerization reaction.[4,5]

5. The investigations of Pennington and co-workers [22] support the concept of aminolysis proceeding through the phase test intermediate. These researchers followed the amine reaction by means of NMR spectra in tetrahydrofuran-d_8 and observed that the C-10 proton was eliminated during the course of the reaction and that a new resonance, associated with two protons, appeared upfield. They interpreted this as confirming the deduction that ring V had been opened and that a chlorin 6-carboxamide had been formed. They also observed that a comparable amine reaction did not occur with pyropheophorbide *a* and interpreted this to signify that the β-keto ester system is essential for the cleavage of ring V.

REFERENCES

1. Conant, J. B. and Moyer, W. W. *J. Am. Chem. Soc.* **52** (1930) 3013.
2. Willstätter, R. and Stoll, A. *Untersuchungen über Chlorophyll*, Springer, Berlin 1913.
3. Oster, G., Broyde, S. B. and Bellin, J. S. *J. Am. Chem. Soc.* **86** (1964) 1309.
4. Holt, A. S. *Can. J. Biochem. Physiol.* **36** (1958) 439.
5. Hynninen, P. H. and Assandri, S. *Acta Chem. Scand.* **27** (1973) 1478.
6. Ellfolk, N., Hynninen, P. H. and Sievers, G. *Acta Chem. Scand.* **23** (1969) 846.
7. Hynninen, P. H. and Ellfolk, N. *Acta Chem. Scand.* **27** (1973) 1795.
8. Hynninen, P. H. and Ellfolk, N. *Acta Chem. Scand.* **27** (1973) 1463.
9. Fischer, H. and Orth, H. *Die Chemie des Pyrrols*, Bd. II/2, Akademische Verlagsgesellschaft, Leipzig 1940.
10. Hietala, P. *Ann. Acad. Sci. Fennicae Ser. A II* **100** (1960).
11. Stern, A. and Wenderlein, H. *Z. physik. Chem.* **A 174** (1935) 81.
12. Eistert, B. In *Newer Methods of Preparative Organic Chemistry*, Interscience, New York 1948, p. 53.
13. Woodward, R. B., Ayer, W. A., Beaton, J. M., Bickelhaupt, F., Bonnett, R., Buchschachter, P., Closs, G. L., Dutler, H., Hannah, J., Hauck, F. P., Ito, S., Langemann, A., Le Goff, E., Leimgruber, W., Lwowski, W., Sauer, J., Valenta, Z. and Volz, H. *J. Am. Chem. Soc.* **82** (1960) 3800.
14. Woodward, R. B. *Angew. Chem.* **72** (1960) 651.
15. Fischer, H., Heckmaier, J. and Hagert, W. *Ann. Chem.* **505** (1933) 209.
16. Stern, A. and Pruckner, F. *Z. physik. Chem.* **A 180** (1937) 321.
17. Fischer, H. and Orth, H. *Die Chemie des Pyrrols*, Bd. II/1, Akademische Verlagsgesellschaft, Leipzig 1937.
18. Fischer, H., Hendschel, A. and Nüssler, L. *Ann. Chem.* **506** (1933) 83.
19. Weller, A. and Livingston, R. *J. Am. Chem. Soc.* **76** (1954) 1575.
20. Fischer, H. and Riedmair, J. *Ann. Chem.* **506** (1933) 107.
21. Fischer, H. and Oestreicher, A. *Ann. Chem.* **546** (1941) 49.
22. Pennington, F. C., Boyd, S. D., Horton, H., Taylor, S. W., Wulf, G. D., Katz, J. J. and Strain, H. H. *J. Am. Chem. Soc.* **89** (1967) 3871.

Received January 4, 1973.

ACTA CHEMICA SCANDINAVICA 27 (1973) 1781–1794

The Extraction of Water, Nitric and Perchloric Acids by Nitrobenzene

ERIK HÖGFELDT,[a] FOLKE FREDLUND,[a] LARS ÖDBERG[b] and GABOR MERENYI[b]

[a] *Department of Inorganic Chemistry and* [b] *Department of Physical Chemistry, Royal Institute of Technology (KTH), S-100 44 Stockholm 70, Sweden*

The extraction of water, nitric and perchloric acids by nitrobenzene has been studied at 25°C using partition, NMR, and conductivity methods. The results can be described by the following set of complexes, equilibrium constants, chemical shifts (relative to $H_2O(l)$) and equivalent conductivities.

$H^+ + NO_3^- + 2H_2O \rightleftharpoons HNO_3(H_2O)_2(org)$ $\log K_{1,2} = -2.60 \pm 0.10$; $\delta_{1,2} = -1.45 \pm 0.11$ ppm

$2H^+ + 2NO_3^- + 2H_2O \rightleftharpoons (HNO_3.H_2O)_2(org)$ $\log K_{2,2} = -5.37 \pm 0.24$; $\delta_{2,2} = -7.59 \pm 0.73$ ppm

$[H^+ + ClO_4^- + 8H_2O \rightleftharpoons H(H_2O)_{n+}{}^+(org) + ClO_4^-(H_2O)_n(org)]$, $n_+ + n_- = 8$ $\log K_{1,8} = -6.46$ (-5.36); $\lambda_{1,8} = 16.56 \pm 0.19$; $\delta_{1,8} = 0.15 \pm 0.51$ ppm

$H^+ + ClO_4^- + 2H_2O \rightleftharpoons H(H_2O)_{n+}{}^+(org) + ClO_4^-(H_2O)_{n-}(org)$, $n_+ + n_- = 2$ $\log K_{1,2} = -7.74 \pm 0.03$; $\lambda_{1,2} = 6.80 \pm 0.08$; $\delta_{1,2} = -4.24 \pm 0.19$ ppm

$3H^+ + 3ClO_4^- + 6H_2O \rightleftharpoons (HClO_4)_3(H_2O)_6(org)$ $\log K_{3,6} = -17.94 \pm 0.07$; $\delta_{3,6} = -3.71 \pm 1.27$ ppm

In the reaction put within brackets there is a large uncertainty in the number of water molecules involved in the reaction.

From the chemical shifts some indications of the structure of the complexes are obtained.

In our first paper on the extraction of water and acids by aromatic hydrocarbons, the extraction of water and nitric acid by nitrobenzene from aqueous solutions of the acid was also included.[1] Although the data indicated formation of mixed nitric acid-water complexes, measurements at high acidities showed some inconsistencies. For that reason no attempts were made to evaluate the composition of the species present in the organic phase. In the present study

we have reexamined the extraction of nitric acid and also included perchloric acid. In addition to the titrimetric analysis, NMR and conductivity methods have been used.

EXPERIMENTAL

Chemicals and solutions. The nitrobenzene from AB Kebo was found to be at least 99.9 % pure by gaschromatography. The nitric (100 %) and perchloric (70 %) acids were of Merck *p.a.* quality and used as such. Various mixtures of nitric acid and water were prepared in the range 0 – 12 M and of perchloric acid and water in the range 0 – 10 M (mol l^{-1}) They were standardized against standard sodium hydroxide using methyl red as indicator. The chemicals and solutions prepared for the Karl Fischer titrations have been reported elsewhere.[1]

Experiments. Samples containing 15 ml nitrobenzene and 10 ml acid-water mixture were shaken in glass-stoppered bottles either overnight or for at least 1 h in a room kept at 25.0 ± 0.3°C. It was checked that 1 h was sufficient time for equilibrium to be reached. At least two samples were prepared for each concentration of acid. Actually, many extraction experiments have been performed in this laboratory by several investigators during the past ten years and an acceptable agreement has been obtained between the various studies. After equilibration the samples were centrifuged at 3500 rpm for 5 – 10 min. Aliquot portions were drawn from both phases for determination of their acid concentration. For the organic phase, water concentration, conductivity, NMR chemical shift, and viscosity ($HClO_4$ system) were also determined.

The acid concentration in both phases was determined by titrating with standard alkali using methyl red as indicator. Water in the organic phase was determined by a modification of the Karl Fischer method.[1]

The conductivity measurements on the organic phase were carried out in a paraffin oil thermostat kept in a constant temperature room. The equipment used was a commercial WTW bridge type LBR and a standard conductivity cell. The temperature in the oil thermostat was kept at 25.00 ± 0.02°C. The cell constant was determined by measuring the resistance of 0.0100 M KCl. The reproducibility of the conductance measurements was about ± 0.1 %. The NMR measurements were carried out on a Varian A-60A apparatus equipped with a Varian variable temperature controller V-6040. The chemical shifts were determined by means of the side-band technique using a Hewlett-Packard 202 A audio oscillator and a Hewlett Packard 5512 A frequency counter. The temperature was checked with a standard methanol sample (Varian 943346-06). The temperature was always well within ± 1°C of 25°C. The shift determination was made 3 – 5 times for each sample, resulting in a standard deviation of ± 0.1 – 0.2 c/s. Benzene was used as an external standard. All shifts reported in this paper are relative to water as external reference with positive shifts upfield from the reference. The chemical shift between water and benzene was determined in a separate experiment. The susceptibility of the nitrobenzene changes slightly when water and acid are dissolved. This effect is, however, well below 1 Hz and is negligible compared to the very large shift changes reported here.

The viscosity measurements (perchloric acid only) were made with a capillary viscosimeter, Ostwald No. 5253. Two samples were prepared for each acid concentration and about 10 determinations were made for each sample.

Selection of thermodynamic data

In order to evaluate the composition of the various complexes present, the activities of water and acid are required.

Nitric acid. Densities of HNO_3 solutions at 25°C have been taken from the International Critical Tables.[2a] For the activities we have in all studies including this one used the data given by Redlich in Landolt-Börnstein.[3] However, in recent years new data have appeared.[4–7] These data were tested for thermodynamic consistency by Redlich *et al.*[8] They also compiled a set of best values. The data we have been using [1,3] are found to agree with the nitric acid activities reported by Redlich *et al.*[8] while the water activities

used by us are about 0.06 logarithmic units larger than their values in the concentration range used, *i.e.* < 7 M HNO_3. This difference will only influence the values of equilibrium constants, but not the description given in this paper. It will be shown below, that the data by Redlich *et al.*[8] are consistent with our model. We have therefore not found it necessary to recalculate our data.

Perchloric acid. Densities of $HClO_4$ solutions at 25°C have been taken from Markham [9] for high concentrations and from the International Critical Tables for low concentrations.[2b] This acid was also discussed by Redlich *et al.*[8] Using the data of Robinson and Baker,[10] Dücker,[11] and Mascherpa,[12] they compiled a set of best values. We have used the data by Robinson and Baker,[10] which are in good agreement with those given by Redlich *et al.*[8]

RESULTS

The system $C_6H_5NO_2 - HNO_3 - H_2O$

This system has previously been studied by Högfeldt and Bolander.[1] We have redetermined the system and obtained results in agreement with those obtained nearly 10 years ago by other workers in our laboratory. In Fig. 1 are given both acid (●) and water (○) concentration in M (mol l^{-1}) as a function of the stoichiometric molarity of HNO_3 in the aqueous phase at equilibrium, C_{HNO_3}. At high concentrations the curves for water and acid approach each other, and one can expect the main complex to have the composition $HNO_3.H_2O$. However, at high concentrations of water and acid in the organic phase, the assumption of constant activity coefficients in this phase may not be justified. For this reason we have restricted the treatment of data to the range $C_{HNO_3} < 7$ M.

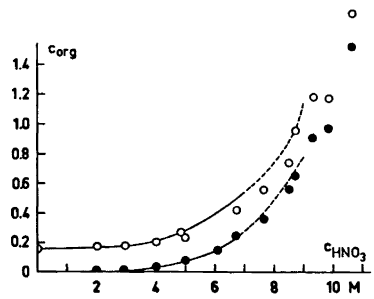

Fig. 1. The concentrations of water (○) and nitric acid (●) in nitrobenzene *versus* acid concentration in the aqueous phase for some representative points. The full-drawn curve has been calculated using the constants given in the abstract. The dashed part is an extension of the calculations above the concentration range used in the determination of the equilibrium constants.

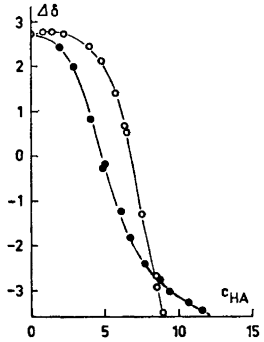

Fig. 2. The chemical shift of the water and acid protons in nitrobenzene for HNO_3(●) and $HClO_4$(○) *versus* acid concentration in the aqueous phase. The full-drawn curves have been calculated using the equilibrium constants and shifts given in the abstract.

The conductivity of this system was found to be so small that ionic species can certainly be neglected. In the NMR spectrum water and acid protons give rise to one signal only. The chemical shift is given in Fig. 2 (●) together with the same data for $HClO_4$ (○). The shifts are given in ppm with water as reference.

Treatment of data. Complexes present. The basic assumption is that the activity coefficients of the various species are constant in the organic phase.[14] For the aqueous phase the solubility of nitrobenzene can be expected to be negligible in the acidity range used for calculations [15] and we can use the activities of water and acid known from the binary system $HNO_3 - H_2O$. In the calculations the dimerization equilibrium of water in nitrobenzene has to be taken into account.[16]

For the reactions (where H^+ stands for H^+ in the aqueous phase *etc.*)

$$pH^+ + pA^- + qH_2O \rightleftharpoons (HA)_p(H_2O)_q(org) \quad (1)$$

we have the following material balances in the organic phase:

$$[H_2O]_{org} = \sum_{p_i,q_i} q_i[(HA)_{p_i}(H_2O)_{q_i}] \quad (2a)$$

$$[HA]_{org} = \sum_{p_i,q_i} p_i[(HA)_{p_i}(H_2O)_{q_i}] \quad (2b)$$

where HA in this case stands for HNO_3.

If constant activity coefficients in the organic phase are assumed and included in the equilibrium constants, eqns. (2a) and (2b) can be rewritten:

$$[H_2O]_{org} = \sum_{p_i,q_i} q_i K_{p_i,q_i}\{H^+\}^{p_i}\{A^-\}^{p_i}\{H_2O\}^{q_i} \quad (3)$$

$$[HA]_{org} = \sum_{p_i,q_i} p_i K_{p_i,q_i}\{H^+\}^{p_i}\{A^-\}^{p_i}\{H_2O\}^{q_i} \quad (4)$$

[ ] denotes concentration and { } activity.

The constants $K_{0,1}$ and $K_{0,2}$ are known from previous work.[16] As in previous papers [14,16] we have used the version of the computer program LETAGROP suitable for the treatment of NMR and extraction data.[17,18] A natural start was to try to fit our data with the extraction of $HNO_3.H_2O$ besides H_2O and $(H_2O)_2$. However, the fit was bad and when minimizing either on $[H_2O]_{tot}$ or $[HNO_3]_{tot}$ the equilibrium constant $K_{1,1}$ differed by about 50 % and it was obvious that $HNO_3.H_2O$ could not be the only species present. The next step was to try $HNO_3.H_2O$ together with other complexes, but in no case a good fit was obtained. After systematically trying various combinations of complexes the following two equilibria:

$$H^+ + NO_3^- + 2H_2O \rightleftharpoons HNO_3(H_2O)_2(org) \quad (5)$$

and

$$2H^+ + 2NO_3^- + 2H_2O \rightleftharpoons (HNO_3.H_2O)_2(org) \quad (6)$$

gave a consistent picture as illustrated in Fig. 3, where the quantity Y defined by

$$Y = \frac{[HNO_3]_{org}}{\{H^+\}\{NO_3^-\}\{H_2O\}^2} \times 10^3$$

is plotted against $\{H^+\}\{NO_3^-\}$. A straight line is obtained both when our activities and those of Redlich *et al.*[8] are used. The latter data are used in Fig. 3 giving $K_{1,2}=2.7\times10^{-3}$ and $K_{2,2}=2.4\times10^{-6}$. These values were used as input values for the computer calculations. The results of the computer calculations are given in Table 1.

Table 1. Results of computer calculations on the system $C_6H_5NO_2-HNO_3-H_2O$; $t=25°C$.

Choice	$K_{1,s}$	$\log K_{1,s}$	$K_{2,s}$	$\log K_{2,s}$*	$\sigma(y)$	U
2	$(2.27\pm0.14)\times10^{-3}$	-2.64 ± 0.08	$(1.55\pm1.13)\times10^{-6}$	$-5.81(-5.31)$	0.013	3.02×10^{-3}
3	$(2.53\pm0.19)\times10^{-3}$	-2.60 ± 0.10	$(4.30\pm0.80)\times10^{-6}$	-5.37 ± 0.24	0.008	1.31×10^{-3}

* Here $\log(K+3\sigma(K))$ is given within parentheses.

In Table 1, choice 2 means that we have minimized on $[H_2O]_{tot}$ and choice 3 that the minimization has been carried out on $[HNO_3]_{tot}$. $\sigma(y)$ is the standard deviation in $[H_2O]_{tot}$ and $[HNO_3]_{tot}$, respectively, and U is the error squares sum $\sum([H_2O]_{tot}-[H_2O]_{calc})^2$ or $\sum([HNO_3]_{tot}-[HNO_3]_{calc})^2$, the summation taken over all experimental points. The spread in $\log K$ is $\pm3\sigma(\log K)$.

When evaluating the constants $K_{1,2}$ and $K_{2,2}$ the following constants for the distribution and association of water in nitrobenzene were used:[16]

$$H_2O(aq) \rightleftharpoons H_2O(org) \qquad K_{0,1} = 1.24\times10^{-1} \quad M^{-1} \qquad (7a,b)$$

$$2H_2O(aq) \rightleftharpoons (H_2O)_2(org) \qquad K_{0,2} = 1.85\times10^{-2} \quad M^{-1}$$

As seen in Table 1 the values obtained graphically are in good agreement with the values obtained in the computer calculations. Both sets of activity data thus support the same model.

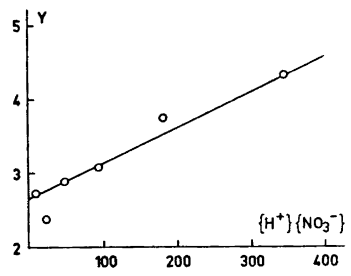

Fig. 3. The quantity $\frac{[HNO_3]_{org}}{\{H^+\}\{NO_3^-\}\{H_2O\}^2}\times$ $\times10^3$ plotted against $\{H^+\}\{NO_3^-\}$ using the activity data given by Redlich *et al.*[8]

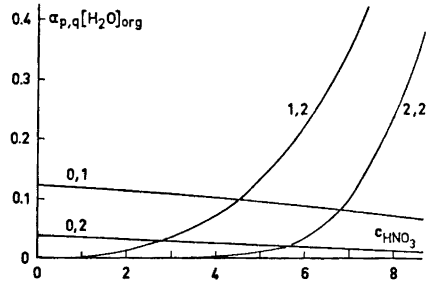

Fig. 4. The contribution from each species ($\alpha_{p,q}[H_2O]_{org}$) to the total amount of water present in the organic phase. $\alpha_{p,q}$ is the fraction of all water present in the species $_{p,q}$. The water monomer is denoted 0,1, the dimer 0,2 *etc.*

From Table 1 it is evident that there is a good agreement between the values of $K_{1,2}$ obtained when minimizing on acid or water. The relative contribution from $(HNO_3.H_2O)_2$ to the total amount of water extracted is in the interval investigated very small and hence we get a very great uncertainty in $K_{2,2}$ as determined from choice 2 and can only expect a rough agreement obtained with $K_{2,2}$ from choice 3. The fit to the acid data is somewhat better than to the water data. This is expected since the water data have to be corrected for the water extracted as H_2O and $(H_2O)_2$.

As mentioned before attempts were made to incorporate $HNO_3.H_2O$ in the calculations, but the equilibrium constant came out as zero and does not need to be taken into account. Some other complexes with more water or acid were tried, but they all gave higher error square sums or larger discrepancies between choices 2 and 3. The values selected are those from choice 3. They are given in the abstract.

Fig. 4 gives the contribution from each species ($\alpha_{p,q}[H_2O]_{org}$) to the total amount of water in the organic phase. The water monomer is denoted 0,1, the dimer 0,2, *etc.* $\alpha_{p,q}$ is the fraction of all water present in the complex p,q.

Chemical shifts. The water and acid protons in the organic phase give rise to one resonance line only, *i.e.* the proton exchange between the various kinds of sites is too rapid for giving rise to several lines. In such a case the observed resonance frequency is given by:[13b]

$$\delta_{obs} = \sum \delta_{p_i,q_i} P_{p_i,q_i} \tag{8}$$

where δ_{p_i,q_i} is an average value of the resonance frequency of the various proton sites in the species $(HNO_3)_{p_i}(H_2O)_{q_i}$ relative to the chosen reference frequency and P_{p_i,q_i} is the proton fraction for that species, *i.e.*

$$P_{p_i,q_i} = \frac{(p_i + 2q_i)K_{p_i,q_i}\{H^+\}^{p_i}\{A^-\}^{p_i}\{H_2O\}^{q_i}}{\sum_{p_i,q_i}(p_i + 2q_i)K_{p_i,q_i}\{H^+\}^{p_i}\{A^-\}^{p_i}\{H_2O\}^{q_i}} \tag{9}$$

Using the same computer program, eqn. (8) has been used but now minimizing on $\sum(\delta_{obs} - \delta_{calc})^2$. In these calculations the complexes and K-values given for choice 3 in Table 1 have been used. For the species H_2O and $(H_2O)_2$ the following δ-values have been used:[16]

$$\delta_{0,1} = 2.94 \text{ ppm}; \quad \delta_{0,2} = 2.18 \text{ ppm} \tag{10a,b}$$

The following results were obtained:

$$\delta_{1,2} = -1.45 \pm 0.11 \text{ ppm}; \quad \delta_{2,2} = -7.59 \pm 0.73 \text{ ppm} \tag{11a,b}$$

The δ-values used in this paper are related to the ν-values given elsewhere [14,16] by $\delta = (\nu - \nu_{ref})/60 \times 10^6$ where $\nu_{ref} = \nu_{H_2O(l)}$.

The system $C_6H_5NO_2 - HClO_4 - H_2O$

This system has been studied by different workers in our laboratory by titrimetric analysis. They have all obtained consistent results. Fig. 5. gives the equilibrium molarity of H_2O in the organic phase, $[H_2O]_{org}$ (the open

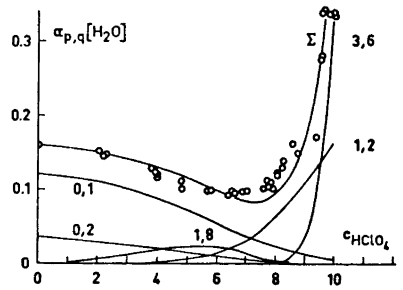

Fig. 5. The concentration of water in nitrobenzene *versus* concentration of $HClO_4$ in the aqueous phase for some representative points. The curve marked $\sum$ is the total concentration as calculated using the constants given in the abstract. Curves for (0,1), (0,2), (1,8), (1,2) and (3,6) are also drawn.

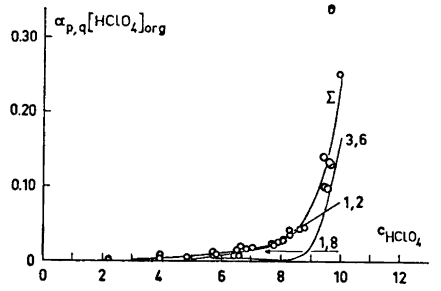

Fig. 6. The concentration of perchloric acid in nitrobenzene *versus* acid concentration in the aqueous phase for some representative points. The curve marked $\sum$ is the total concentration as calculated using the constants given in the abstracts. Curves for (1,8, (1,2) and (3,6) are also drawn.

circles) plotted against the stoichiometric molarity of $HClO_4$ in the aqueous phase, C_{HClO_4}, and Fig. 6 the equilibrium molarity of perchloric acid $[HClO_4]_{org}$ (the open circles) in the same phase also plotted against C_{HClO_4}. From these figures it is evident that at about 8 M $HClO_4$ an appreciable amount of acid is extracted. At the same time the water extraction increases, and acid-water complexes are obviously formed in the organic phase. In order to get an idea about the number of water molecules coextracted with $HClO_4$ the

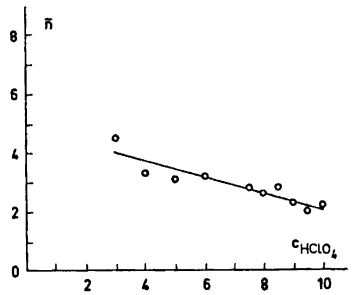

Fig. 7. The quantity $\bar{n}$ (eqn. 12) *versus* perchloric acid concentration in the aqueous phase.

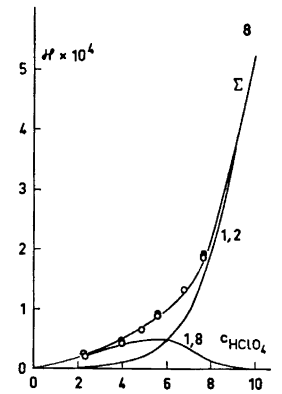

Fig. 8. The conductivity of the nitrobenzene phase *versus* the concentration of perchloric acid in the aqueous phase. Calculated values are denoted by the curve marked $\sum$. Curves for 1,8 and 1,2 are also marked out.

number of water molecules, $\bar{n}$, per acid molecule is plotted against C_{HClO_4} in Fig. 7. The quantity $\bar{n}$ is defined by

$$\bar{n} = ([H_2O]_{org} - [H_2O]_{\phi_{NO_2}})/[HClO_4]_{org} \quad (12)$$

$[H_2O]_{\phi_{NO_2}}$ is computed with the aid of eqn. (7). From Fig. 7 it is seen that $\bar{n}$ decreases from 4 and seems to approach 2 at high acidities, *i.e.* the composition $HClO_4.(H_2O)_2$. In order to check the possibility of extensive ionic dissociation, the conductivity ($\varkappa$) was measured in some representative solutions and the results are given in Fig. 8 where $\varkappa \times 10^4$ is plotted against C_{HClO_4}. Furthermore the viscosity (η) was also measured at various compositions. The results are given in Table 2. The chemical shift of the water and acid protons is plotted against C_{HClO_4} in Fig. 2 (○).

Treatment of data. Complexes present. (a). Conducting species. We begin by considering the following conducting species:

$$uH^+ + uClO_4^- + nH_2O \rightleftharpoons H_u(ClO_4)_{u-1}(H_2O)_{n+}{}^+(org) + ClO_4(H_2O)_{n-}{}^-(org) \quad (13)$$

For the sake of simplicity only one multiple cation is indicated in eqn. (13) out of all possible species.

Application of the law of mass action to (13) gives under the assumption of ideal behavior in the organic phase

$$\log [H_u(ClO_4)_{u-1}(H_2O)_{n+}{}^+][ClO_4(H_2O)_{n-}{}^-] = \log K_{u,n} + u \log \{H^+\}\{ClO_4^-\} + n \log \{H_2O\} \quad (14)$$

where $n = n_+ + n_-$.

The requirement of electroneutrality in the organic phase gives

$$[H_u(ClO_4)_{u-1}(H_2O)_{n+}{}^+] = [ClO_4(H_2O)_{n-}{}^-] = C_{u,n} \quad (15)$$

$C_{u,n}$ is the molarity in the organic phase of the completely dissociated complex containing n water molecules. Thus

$$\log C_{u,n} = \tfrac{1}{2} \log K_{u,n} + \frac{u}{2} \log \{H^+\}\{ClO_4^-\} + \frac{n}{2} \log \{H_2O\} \quad (16)$$

Between $C_{u,n}$ and the conductivity ($\varkappa$) the following relation holds

$$\varkappa = 10^{-3} C_{u,n} \lambda_{u,n} \quad (17)$$

Table 2. Viscosities in nitrobenzene-perchloric acid-water mixtures at 25°C.

C_{HClO_4}	η_{25} cP	Number of determinations
(Dry nitrobenzene)	1.3438	17
0	1.3223	9
0	1.3220	11
3.948	1.3240	11
3.939	1.3243	11
6.387	1.3372	10
6.391	1.3382	8
8.079	1.3523	11
8.075	1.3530	11
9.589	1.3943	10
9.571	1.3939	11

where $\lambda_{u,n}$ is the equivalent conductivity of the ion pair under consideration (u,n). From Table 2 it is seen that η varies only a few per cent in the concentration range of interest while $\varkappa$ has a fiftyfold variation. We now make the assumption that $\lambda_{u,n}$ is constant in the range where (u,n) makes a noticeable contribution to $\varkappa$.

By combining (16) and (17) we get

$$\log \varkappa - \frac{u}{2} \log \{H^+\}\{ClO_4^-\} = -3.00 + \tfrac{1}{2} \log K_{u,n} + \log \lambda_{u,n} + \frac{n}{2} \log \{H_2O\} \quad (18)$$

Setting $u = 1$ in (18) implies that simple ions predominate in the system while $n = 2$ means that triple ions containing cation, anion, and water predominate as conducting species. Triple ions are not unknown in either aqueous or organic solutions.[19–21]

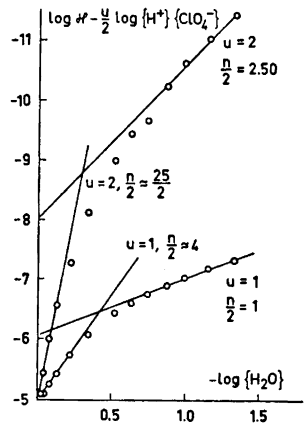

Fig. 9. $\log \varkappa - \frac{u}{2} \log \{H^+\}\{ClO_4^-\}$ (eqn. 18) *versus* the negative logarithm of the water activity for $u = 1$ and $u = 2$. Two linear asymptotes have been fitted to each curve.

In Fig 9, $\log \varkappa - \frac{u}{2} \log \{H^+\}\{ClO_4^-\}$ is plotted against $\log \{H_2O\}$ for $u = 1$ (simple ions) and $u = 2$ (triple ions). In both cases two linear asymptotes can be fitted to the data. The slopes of these lines give, according to (18), the number of water molecules belonging to the conducting species. The results are given in Table 3.

Table 3. Determination of n in eqn. (18)

u	n_1	n_2
1	8	2
2	25	5

For $u = 1$ we find that at high acidities the conducting pair of ions has $n = \bar{n} = 2$ in agreement with Fig. 7. For $u = 2$ we get much higher values for $\bar{n}$, from $25 - 5$. The value of 25 is unreasonably high and multiple ions can hardly be expected

to predominate at low acidities. At high acidities triple ions cannot be excluded. However, the agreement between the limiting value in Fig. 7 and Table 3 makes it very tempting to assume simple ions only.

We first determine approximate equilibrium constants by simple calculations. The constants obtained are then refined by the computer program LETAGROP.

From Fig. 9 it is seen that in the range where the data can be approximated by the asymptote with a slope of unity the complex 1,2 predominates in the system. In order to obtain an approximate value for $K_{1,2}$ in (16) we make the following approximation:

$$C_{1,2} \approx [HClO_4]_{org} \tag{19}$$

Using eqns. (16) and (19) with $u = 1$, $n = 2$, $K_{1,2}$ was found to be approximately constant in the range 7 – 8.5 M $HClO_4$ as shown in Table 4.

Table 4. Evaluation of $K_{1,2}$ from eqns. (16) and (19).

C_{HClO_4}	$[HClO_4]_{org}$ interpolated	$\log [HClO_4]_{org}$	$\log \{H^+\}\{ClO_4^-\}$	$\log \{H_2O\}$	$\frac{1}{2} \log K_{1,2}$
7	0.016	−1.80	5.14	−0.52	−3.85
7.5	0.021	−1.68	5.66	−0.63	−3.88
8	0.030	−1.52	6.19	−0.74	−3.88
8.5	0.041	−1.39	6.70	−0.87	−3.87
				Average:	-3.87 ± 0.02

With knowledge of $K_{1,2}$ it is possible to determine $\lambda_{1,2}$. From (18) and Fig. 9 we have with $u = 1$ and $n = 2$

$$\lim_{\log\{H_2O\}\to 0} (\log \varkappa - \tfrac{1}{2} \log \{H^+\}\{ClO_4^-\}) = -3.00 + \tfrac{1}{2} \log K_{1,2} + \log \lambda_{1,2} = -6.06$$

With $\frac{1}{2} \log K_{1,2} = -3.87$ we find:

$$\lambda_{1,2} = 6.5 \text{ cm}^2 \text{ ohm}^{-1} \text{ mol}^{-1} \tag{20}$$

From Fig. 9 it is seen that at least one more conducting ion pair carrying about 8 water molecules is needed to account for the conductivity data. We assume that all acid in the organic phase below 7 M $HClO_4$ is due to (1,2)

Table 5. Evaluation of $K_{1,8}$ from eqn. (16).

C_{HClO_4} M	$[HClO_4]_{org}$ interpolated	$C_{1,2}$	$C_{1,8}$	$\log C_{1,8}$	$\log \{H^+\}\{ClO_4^-\}$	$\log \{H_2O\}$	$\frac{1}{2} \log K_{1,8}$
4	0.003_8	0.0014	0.0024	−2.62	2.30	−0.13	−3.25
5	0.006_2	0.0030	0.0032	−2.49	3.13	−0.22	−3.18
6	0.010_0	0.0072	0.0028	−2.55	4.13	−0.34	−3.26
						Average:	-3.23 ± 0.05

and (1,8) and compute the contribution from (1,2) from (16) with $u=1$ and $n=2$ and $\frac{1}{2}\log K_{1,2} = -3.87$. This amount is subtracted from $[HClO_4]_{org}$ and the difference is attributed to (1,8). $\frac{1}{2}\log K_{1,8}$ is now computed from (16) with $u=1$ and $n=8$. The results are given in Table 5.

With knowledge of $K_{1,8}$ we can compute $\lambda_{1,8}$ from (18) and find from Fig. 9:

$$\lim_{\log\{H_2O\}\to 0}[\varkappa - \tfrac{1}{2}\log\{H^+\}\{ClO_4^-\}] = -3.00 + \tfrac{1}{2}\log K_{1,8} + \log\lambda_{1,8} = -5.00 \quad (21)$$

$$\lambda_{1,8} = 17 \text{ cm}^2\text{ohm}^{-1}\text{mol}^{-1} \quad (22)$$

(*b*). *The nonconducting species.* At concentrations above 9 M $HClO_4$ in the aqueous phase the material balances indicate further species in addition to the conducting ones. $C_{1,2}$ and $C_{1,8}$ are computed and subtracted from $[HClO_4]_{org}$ in the range $9 \le C_{HClO_4} \le 10$. We also employ the results of Fig. 7, and assume that we have two water molecules per acid in the complex. We assume the reaction to be the following:

$$uH^+ + uClO_4 + 2uH_2O \rightleftharpoons (HClO_4(H_2O)_2)_u(org) \quad (23)$$

$$\log[(HClO_4(H_2O)_2)_u] = \log K_{u,2u} + u\log\{H^+\}\{ClO_4\} + 2u\log\{H_2O\} \quad (24)$$

In Table 6 $\log K_{u,2u}$ has been computed for $u=2$ and 3.

Table 6. Evaluation of $K_{u,2u}$ from eqn. (24).

C_{HClO_4}	$[HClO_4]_{u,2u}$	$\log[HClO_4]_{u,2u}$	$\log\{H^+\}\{ClO_4^-\}$	$\log\{H_2O\}$	$\log K_{2,4}$	$\log K_{3,6}$
9.0	0.019	−1.72	7.20	−0.99	−12.46	−17.86
9.5	0.056	−1.25	7.71	−1.15	−12.37	−17.96
10	0.149	−0.83	8.22	−1.33	−12.25	−17.99
				Average:	-12.36 ± 0.12	-17.94 ± 0.08

From Table 6 it is seen that a trimer seems to fit the data better than a dimer.

As with nitric acid we have made a computer refinement with LETAGROP which has been extended to encompass also conductivity data. As starting values for the complexes the values given by Tables 4 – 6 have been used. The results are collected in Table 7 together with the results obtained in Tables 4 – 6. In the column for $\log\lambda$ the values given within parentheses have been obtained by computer and using the constants given in Tables 4 – 6. The agreement with the values obtained by extrapolation in Fig. 9 is satisfactory.

For the water equilibria the constants given by (7) have been used. As for the nitric acid case, the equilibrium constants determined from the water analysis (choice 2) are rather uncertain compared to choice 3 (acid analyses) since most of the water is involved in the equilibria (7). The agreement must, however, be regarded as rather satisfactory.

Table 7.

Choice	Complex	log K Tables 4–6	log K LETAGROP	log λ graphical	log λ computer	$\sigma(y)$	U
	[1,8	−6.46	−6.77(−6.38)*	1.23 (1.22±0.15)	0.99±0.15]		
2	1,2	−7.74	−7.52±0.10	0.81 (0.83±0.02)	0.47±0.02	0.007	4.81×10^{-4}
	3,6	−17.94	−17.99 Not varied	–	–		
	[1,8	−6.46	−5.36±0.28	1.23 (1.22±0.15)	0.88±0.15]		
3	1,2	−7.74	−7.76±0.03	0.81 (0.83±0.02)	0.54±0.02	0.0005	1.84×10^{-4}
	3,6	−17.94	−17.94±0.07	–	–		

* Here log $(K+3\sigma(K))$ is given. In other cases log $K\pm3\sigma(\log K)$.

Table 8.

Equilibrium constants	$\delta_{1,8}$	$\delta_{1,2}$	$\delta_{3,6}$	$\sigma(y)$	U
Tables 4–6	0.15±0.51	−4.24±0.19	−3.71±1.17	0.18	0.97×10^{3}
Choice 3	0.26±0.50	−4.33±0.20	−3.47±1.27	0.20	1.16×10^{3}

A dimer (2,4) instead of a trimer gives an error squares sum 50 times larger than that in Table 7 and can thus be excluded. Besides 1,2 many different complexes (1,3) (1,4) (1,5), *etc.*, up to (1,18) were tried but the best fit was found with (1,8). However, this complex is very uncertain, and can only be taken to indicate the presence of hydrated ions with more than two water molecules per acid. For that reason this species is put within brackets in Table 7.

Chemical shifts. Finally the chemical shifts have been computed with LETAGROP employing eqns. (8) and (9) and the constants given in Tables 4–6 as well as for choice 3. The results given in Table 8 were obtained.

For the two water species the shifts given by (10) have been used. As seen in Tables 7 and 8 both equivalent conductivities as well as the shifts values are somewhat dependent on the equilibrium constants used; these quantities might thus change with an improved set of equilibrium constants.

As seen in Table 7 the values obtained in Tables 4–6 agree well with the values obtained by computer for 1,2 and 3,6, while the obtained value for 1,8 in Table 5 falls between the values from choices 2 and 3. For that reason we have given the values from Tables 4–6 in the abstract with limits found by comparing data in Table 7. The fit to the data in the water extraction could be improved by introducing further species, *cf.* Fig. 6. However, we do not feel that the present data permit more than a minimum description, fairly well satisfying all three kinds of experimental data used.

DISCUSSION

$C_6H_5NO_2 - HNO_3 - H_2O$. The reason that in the previous study [1] no definite water acid complexes were reported for the organic phase was that we were not fully convinced of the reliability of the Karl Fischer method for this system. In the present study we have used the possibility to integrate the NMR signal from acid and water in the organic phase. The concentration determined from NMR agrees to within 10 % with the analytically determined one, which is as good as can be expected considering the low intensity of the NMR signal. We thus have little reason to doubt the correctness of the water analysis in the concentration range used in our calculations.

The chemical shifts determined for the species in the interval 0 – 7 M are $\delta_{HNO_3(H_2O)_2} = -1.45$ ppm and $\delta_{(HNO_3H_2O)_2} = -7.59$ ppm. In the system $C_6H_6 - HNO_3 - H_2O$ [14] we found evidence for the complexes $HNO_3.H_2O$ and $(HNO_3)_2.H_2O$. The chemical shifts for these species are close to that of the water reference, *i.e.* ≈ 0 ppm. The water resonance in nitrobenzene is ≈ 2 ppm shifted towards negative values as compared to water in benzene. It can thus be seen that the shift for $HNO_3(H_2O)_2$ in nitrobenzene is in agreement with the shifts determined for similar complexes in benzene. The shift for $(HNO_3.H_2O)_2$ is on the other hand much more removed towards lower values. It is in fact so much shifted that one is tempted to compare it with the shift of H_3O^+ (– 11 ppm in aqueous solutions).[18a] We can thus not exclude the possibility that $(HNO_3.H_2O)_2$ is better represented by $(H_3O^+NO_3^-)_2$.

At higher acid activities (> 8 M) the chemical shifts measured have a tendency to level off and not to approach the low negative value given above. The reason for this is that at these higher concentrations the dissociation of nitric acid in the aqueous phase is no longer complete. This will favour the extraction of further non ionic species into the organic phase and since these species have considerably more positive shifts the leveling off is easily rationalized.

$C_6H_5NO_2 - HClO_4 - H_2O$. The chemical shifts for this system are $\delta_{HClO_4(H_2O)_2} = 0.2$ ppm, $\delta_{HClO_4(H_2O)_2} = -4.2$ ppm and $\delta_{(HClO_4)_3(H_2O)_6} = -3.7$ ppm. We can make some approximate estimates to investigate whether these shifts are reasonable. Assume that the 1,8 complex "consists of" $H^+(-33$ ppm) and $(H_2O)_8$. Take for the shift of $(H_2O)_8$ the mean of the monomer H_2O and liquid H_2O

$$\delta_{HClO_4(H_2O)_8} = \tfrac{16}{17} \times \frac{2.94 + 0}{2} + \tfrac{1}{17}(-33) = -0.6 \text{ ppm} \qquad (25)$$

The 1,2 complex "consists of" $(H_2O)_2$ and H^+ giving

$$\delta_{HClO_4(H_2O)_2} = \tfrac{4}{5} \times 2.18 + \tfrac{1}{5}(-33) = -4.9 \text{ ppm} \qquad (26)$$

It is thus seen that these estimates can account approximately for the chemical shifts observed, and are in agreement with the observation of dissociated species in the organic phase. The shift of the trimer is rather close to that of the 1,2 complex of the same composition. This leads one to suspect that the trimer should rather be written $(H(H_2O)_2^+ClO_4^-)_3$.

The equivalent conductivity in nitrobenzene of the 1,8 complex is found to be larger than of the 1,2 complex. This might at first sight seem surprising.

It must, however, be emphasized that we have not considered the interaction between the complexes and the nitrobenzene. It might very well be so that the 1,2 ions interact more strongly with the nitrobenzene and hence exhibit a lower mobility. Finally, it should once again be emphasized that the minimum number of complexes needed to fit the three kinds of experimental data have been used. We feel that at present no complexes can be added with a reasonable significance.

Added in proof. According to recent measurements by Walter the solubility of nitrobenzene in $HClO_4 - H_2O$ is larger than we expected making the distinction between dimers, trimers *etc.* less certain, because of unknown influence on the activity coefficients.

Acknowledgements. This work has been financially supported by the *Swedish Natural Science Research Council* (NFR). The English has been revised by Dr. Kelvin Roberts.

REFERENCES

1. Högfeldt, E. and Bolander, B. *Arkiv Kemi* **21** (1963) 161.
2. *International Critical Tables*, Washburn, E. W., Ed., McGraw, New York 1928, Vol. 3. a. pp. 58 – 59; b. p. 54.
3. Landolt-Börnstein, *Physikalisch-chemische Tabellen*, Springer, Berlin 1936, EgIIIc 2145 (1936).
4. Potier, A. *Ann. Fac. Sci. Univ. Toulouse* **20** (1956) 1.
5. Vandoni, R. and Laudy, M. *J. Chim. Phys.* **49** (1952) 99.
6. Davis, W. and de Bruin, A. J. *J. Inorg. Nucl. Chem.* **26** (1964) 1069.
7. Küppers, H. A. *Diss.*, Techn. Hochschule, Aachen, 1964.
8. Redlich, O., Gargrave, W. E. and Krostek W. D. *Ind. Eng. Chem. Fundamentals* **7** (1968) 211.
9. Markham, A. E. *J. Am. Chem. Soc.* **63** (1941) 874.
10. Robinson, R. A. and Baker O. J. *Proc. Roy, Soc. New Zealand* **76** (1946) 250, as reported in *Chem. Abstr.* **41** (1947) 5000d.
11. Dücker, K. H. *Diss.* Techn. Hochschule, Aachen 1964.
12. Mascherpa, G. *Rev. Chim. Miner.* **2** (1965) 379.
13. Pople, J. A., Schneider, W. G. and Bernstein, H. J. *High Resolution Nuclear Magnetic Resonance*, McGraw, New York 1959, a. p. 443; *b.* p. 221.
14. Eriksson, J. C., Ödberg, L. and Högfeldt, E. *Acta Chem. Scand.* **21** (1967) 1925.
15. Högfeldt, E. and Leifer, L. *Arkiv Kemi* **21** (1963) 285.
16. Ödberg, L. and Högfeldt, E. *Acta Chem. Scand.* **23** (1969) 1330.
17. Ingri, N. and Sillén, L. G. *Arkiv Kemi* **23** (1964) 97.
18. Warnqvist, B. *Personal communication.*
19. Fuoss, R. M. and Accasina, F. *Electrolytic Conductance*, Interscience, New York 1959, p. 249.
20. Widmer, H. M. *J. Phys. Chem* **74** (1970) 3618.
21. Widmer, H. M. In Gregory, J. G., Evans, B. and Weston, P. C., Eds., *Solvent extraction*, Society of Chemical Industry, London 1971, p. 37.

Received December 5, 1972.

ACTA CHEMICA SCANDINAVICA 27 (1973) 1795–1806

Use of the Aqueous Formic Acid-Chloroform-Dimethylformamide Solvent System for the Purification of Porphyrins and Hemins

PAAVO H. HYNNINEN and NILS ELLFOLK

Department of Biochemistry, University of Helsinki, SF-00170 Helsinki, Finland

The purification of proto-, meso-, deutero- and hematoporphyrin preparations utilizing the aqueous formic acid-chloroform-dimethylformamide (AFCD) solvent system was investigated. Although the selectivity of this solvent system was lower than that of the aqueous formic acid-chloroform (AFC) system, it was none the less found to be more suitable for preparatory purposes owing to its higher dissolving capacity. A probable reason for the difficulties encountered in purifying hematoporphyrin is its strong tendency to form aggregates. The flexibility of the AFCD system was indicated by application to the further purification of protohemin. The isolation method of Labbe and Nishida yielded protohemin containing probably less than 1 % of impurities, as demonstrated by fractionation employing the AFCD system. This protohemin also resulted in proto- and mesoporphyrins having a high degree of purity. Conversely, a commercial preparation of protohemin yielded protoporphyrin containing 10 – 20 % of a compound thought to be a deuteroporphyrin having RCO-groups at positions 2 and 4.

The use of the aqueous formic acid-chloroform (AFC) solvent system in the separation of free dicarboxylic porphyrins has been previously described.[1] The AFC system was found to be suitable for small-scale separations of the porphyrins since it possessed high selectivity and did not exhibit the disadvantages associated with the ethyl ether-hydrochloric acid system.[2] On the preparatory level, however, the AFC system was rather unsatisfactory due to its low dissolving capacity. Attention was therefore focused upon the tendency of the porphyrins to form aggregates, which appeared to be the principal reason for the difficulties encountered in their purification, especially that of protoporphyrin IX.

In order to eliminate aggregation, a fourth component, dimethylformamide (DMF), was added to the solvent system. This component is reportedly an excellent solvent for porphyrins.[3] As is elucidated in the present article, aqueous formic acid-chloroform-dimethylformamide (AFCD) forms a valuable

solvent system for the purification of dicarboxylic porphyrins and hemins. Utilizing this improved system it was possible to study the partition behaviour of hematoporphyrin IX in greater detail. The method of multiple partition in the purification of protoporphyrin IX was also re-evaluated.

MATERIALS AND METHODS

Protohemin IX. Preparation *1* of the protohemin was isolated from bovine blood according to the method of Labbe and Nishida.[4] The ratio of the volume of blood to that of the extraction solvent was 1:10. From 400 ml of blood, 1.546 g of crystalline protohemin IX were obtained. Preparation *2* of the protohemin was a commercial product of the Sigma Chemical Co.

Protoporphyrin IX. The preparation of protoporphyrin IX from protohemin followed the ferrous sulfate method of Morell and co-workers.[5] Upon the basis of its spectroscopic properties (Table 1, e), the protoporphyrin obtained from protohemin preparation *1* appeared to have a high degree of purity. Protohemin preparation *2*, on the contrary, yielded a product exhibiting absorption maxima, in chloroform, at 632, 606, 577, 543, 508, and 408 nm. These values are slightly larger than the values reported for pure protoporphyrin IX.[6-8]

Mesoporphyrin IX was prepared according to the procedure developed by Baker and co-workers.[9] Protohemin preparation *1*, further purified by means of the partition method described below, was employed as starting material. Spectroscopy was not able to reveal any impurities in the resultant mesoporphyrin preparation.

Deuteroporphyrin IX. Protohemin (preparation *1*) was heated with resorcinol at 190 – 200°C for 15 min.[10] After cooling to room temperature, the reaction mixture was dissolved in 15 ml of concentrated sulphuric acid. Fifty grams of ice and 85 ml of water were then added to the sulphuric acid solution, which was subsequently filtered and diluted with 150 ml of water. Deuteroporphyrin precipitated from the solution upon neutralization with sodium acetate to pH 5. The product was recovered by filtration, washed with water and dried at 50°C for 2 h. No impurities were spectroscopically revealed in the preparation.

Hematoporphyrin IX. A commercial preparation of hematoporphyrin dihydrochloride (Koch-Light & Co.) was utilized. This preparation appeared to be spectroscopically pure.

Solvents. The solvents employed were of analytical grade. Chloroform was washed three times with distilled water immediately prior to use. Diethyl ether was first treated with a concentrated solution of ferrous sulfate and then washed, dried and distilled. Dimethylformamide was further purified by distillation at reduced pressure.

Fractionation by multiple liquid-liquid partition. Partition separations were performed utilizing the Hietala apparatus.[11] Porphyrins were fractionated by means of the aqueous formic acid (of varied molarity)/chloroform(25)-dimethylformamide(1), while, in the separation of hemins, the upper phase consisted of 22.5 M formic acid and the lower phase of chloroform(10)-dimethylformamide(1). The upper phase was employed as mobile solvent in all of the fractionations described in the present article. The phase ratio varied from 0.2 to 0.3 among the different fractionations. A shaking frequency of 22 cycles/min, an amplitude of $\pm 45°$ and a flow rate of 1 – 2 ml/min were utilized. Theoretical distribution curves and partition coefficients were calculated by methods previously described.[1] When considered advantageous, elution upon the basis of a stepwise pH gradient was applied.

Spectroscopy. The absorption spectra of the porphyrins were recorded by means of a Cary Model 15 spectrophotometer, while single absorbances were measured employing a Beckman DU spectrophotometer.

pH values. A Radiometer PHM 4c pH meter was utilized in measuring hydrogen ion concentrations (20°C). The pH meter was calibrated using phthalate buffer.

Table 1. Spectroscopic properties of porphyrins.

Compound	Solvent	Peak positions (nm) and peak ratios (R) I nm	R	Ia nm	R	II nm	R	III nm	R	IV nm	R	S nm
a. Hematoporphyrin IX	Py	622.0	0.200	596.0	0.100	569.0	0.447	532.0	0.595	499.0	1.000	403.0
»	Ee	623.0	0.257	596.0	0.138	569.0	0.457	529.0	0.608	497.5	1.000	397.0
b. 2(4)-Vinyl-4(2)-hydroxyethyl-deuteroporphyrin IX	Ee	627.0	0.280	602.0	0.140	573.0	0.430	532.5	0.720	500.0	1.000	400.5
»	Chl	626.0	0.310	601.0	0.184	572.5	0.526	537.5	0.724	502.5	1.000	405.0
»	Py	626.5	0.312	601.0	0.149	572.5	0.508	537.5	0.762	502.0	1.000	405.5
c. Deuteroporphyrin IX	Ee	620.5	0.317	595.5	0.087	566.5	0.415	523.0	0.585	492.0	1.000	393.5
»	Chl	619.0	0.258	—	—	565.5	0.428	529.0	0.563	496.0	1.000	398.0
d. Mesoporphyrin IX	Ee	622.0	0.412	595.0	0.105	567.5	0.456	525.5	0.725	495.0	1.000	394.0
»	Chl	620.0	0.335	594.0	0.103	566.5	0.473	531.0	0.696	498.0	1.000	398.5
e. Protoporphyrin IX (from hemin)	Ee	631.5	0.408	605.0	0.093	576.0	0.447	535.0	0.781	502.0	1.000	403.0
f. »	Ee	631.5	0.440	605.0	0.097	576.0	0.445	535.0	0.785	502.0	1.000	403.5
»	Chl	629.0	0.349	603.0	0.148	575.0	0.563	539.5	0.850	504.0	1.000	406.0
g. Porphyrin 638	Ee	638.0	0.146	—	—	582.5	0.385	539.0	0.430	506.0	1.000	408.0
»	Chl	638.0	0.114	—	—	583.0	0.371	545.0	0.372	510.5	1.000	412.0

S = Soret band, Py = pyridine, Ee = ethyl ether, and Chl = chloroform.

RESULTS

Purification of hematoporphyrin IX. No impurities had been previously [1] noted in the commercial hematoporphyrin dihydrochloride preparation (Koch-Light & Co.). However, low amounts of other porphyrins may have been present in this preparation, since rather small quantities of feeding material were employed in the partition fractionations. Moreover, the behavi-

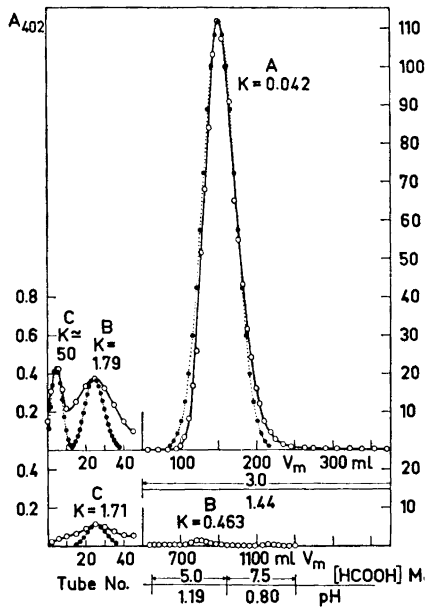

Fig. 1. Purification of the hematoporphyrin IX preparation. Solvent system: HCOOH(3.0, 5.0, and 7.5 M)/$CHCl_3$(25)-DMF(1). Ten milligrams of hematoporphyrin dihydrochloride were dissolved in 1.2 ml of DMF, and to the resulting solution were added 30 ml of $CHCl_3$ + 0.38 ml of HCOOH + 10 ml of H_2O. The mixture was then sampled into tubes $r = 0,1,2$. Number of tubes utilized = $N = 50$. Average volume of mobile phase (HCOOH) in a partition unit = $v_m = 2.64$ ml; average volume stationary phase ($CHCl_3$ – DMF) in a partition unit = $v_s = 10.86$ ml. Total volume of effluent eluted from the apparatus = $V_m = 1300$ ml; flow rate = 1 ml/min. Theoretical (●) and experimental (○) values, the latter obtained by measuring A_{402} of the effluent fractions and of the lower phases in the tubes. A = hematoporphyrin IX (96 %), B = 2(4)-vinyl-4(2)-hydroxyethyldeuteroporphyrin IX (3 %), and C = protoporphyrin IX (1 %).

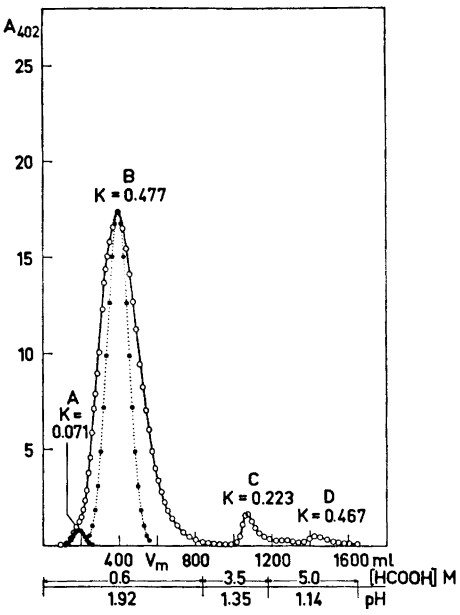

Fig. 2. Refractionation of component A (hematoporphyrin IX) in Fig. 1. Solvent system: HCOOH(0.6, 3.5, and 5.0 M)/$CHCl_3$(25)-DMF(1). The component eluted within the range 100 – 250 ml was dissolved in 20 ml of 0.6 M HCOOH, which was then sampled into tubes $r = 0,...,6$, each containing 10 ml of the lower phase. $N = 50$. $v_m = 3.14$ ml; $v_s = 10.36$ ml. $V_m = 1650$ ml; flow rate = 1 ml/min. Theoretical (●) and experimental (○) values, the latter obtained by measuring A_{402} of the effluent fractions. A, C, and D = various molecular forms of hematoporphyrin, and B = hematoporphyrin dication (70 %).

our of the hematoporphyrin had not been extensively investigated as a function of the pH of the upper phase.

The hematoporphyrin preparation was therefore, in the present study, subjected to careful examination, since Schwartz *et al.*[12] have reported that commercial preparations were found to contain 30 % or more of other porphyrins. According to the above authors, nine distinct fractions can be obtained by countercurrent distribution (CCD), while many more are apparent using column chromatography.

Fig. 1 presents the results of a fractionation which began with 3.0 M formic acid (pH 1.44). The upper portion of the figure discloses the situation at an eluted volume of 550 ml. The absorption spectrum of component A in the effluent appeared to be identical with the di-cation spectrum of hematoporhyrin IX (λ_{max}: 590, 547, and 400 nm). Moreover, the absorption spectrum of the neutral form of component A closely matched the spectroscopic properties of hematoporphyrin IX (Table 1, a). Two further components remained in the apparatus at this stage of elution: component B, having the spectroscopic properties of 2(4)-vinyl-4(2)-hydroxyethyldeuteroporphyrin IX (Table 1, b), and component C, having those of protoporphyrin IX (Table 1, f). The lower portion of the figure reveals the outcome of continued fractionation, first by eluting with 400 ml of 5.0 M formic acid and then with about 350 ml of 7.5 M formic acid. Component B, in this part of the figure, shows the approximate amount (3 %) of 2(4)-vinyl-4(2)-hydroxyethyldeuteroporphyrin eluted. The amount of protoporphyrin (C) is estimated to be 1 %.

Fig. 2 presents the results of the refractionation of component A in Fig. 1. Fractionation was begun, in this case, with 0.6 M formic acid (pH 1.92). Four separate components (A – D) were detected in the effluent, while one additional component (E, not indicated in the figure), having a diffuse concentration zone, remained in the apparatus. Components A and B exhibited normal di-cation spectra when measured in the effluent. When the absorption spectra of components C and D were measured in the effluent, however, an additional peak at 370 nm was revealed (Fig. 3, Part A). A small amount of concentrated formic acid, when added to this effluent, yielded a normal di-cation spectrum (Fig. 3, Part B). The spectra of the neutral forms of components A to E were identical with the spectrum of the neutral form of hematoporphyrin IX. The absorption spectrum of the hematoporphyrin in distilled water is presented in Fig. 4. This spectrum contains a Soret band at 370 nm and differs also in other regards from the spectroscopic properties reported for the various forms of hematoporphyrin. The spectrum in Fig. 4 is typical of hematoporphyrin in an aggregated state.

The above experimental facts indicate that components A, C, and D in Fig. 2 are different forms of aggregated hematoporphyrin. Component A was ascertained as a separate molecular form of hematoporphyrin by initiating its fractionation with 0.5 M formic acid (pH 2.00). The component was then completely separated from the principal hematoporphyrin zone (B). The possibility of component A being either 2,4-hydroxymethyldeuteroporphyrin or some other hydrophilic porphyrin was excluded by an additional refractionation, in which the feeding material consisted of the pure hematoporphyrin

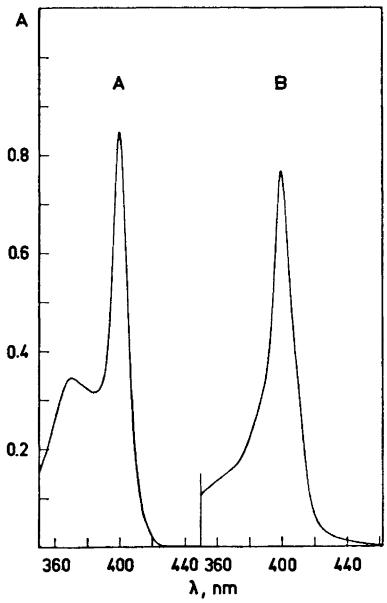

Fig. 3. Visible absorption spectrum of hematoporphyrin IX in the region of the Soret band. Part A: the spectrum of component C (Fig. 2) measured immediately following its elution (at 1105 ml) from the apparatus; part B: the same after the addition of conc. HCOOH (1.0 ml of HCOOH was added to 15 ml of the effluent eluted at 1105 ml).

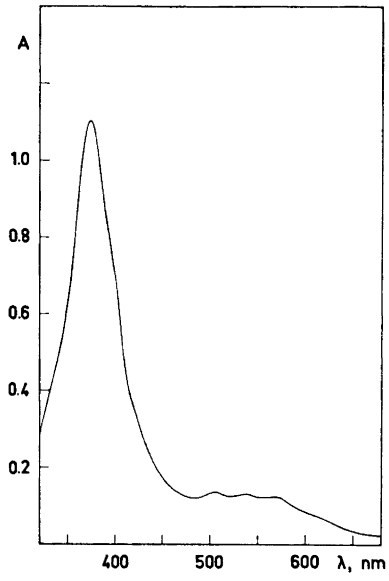

Fig. 4. Visible absorption spectrum of hematoporphyrin IX in distilled water.

fraction (B). In this case, a new fraction A was separated from the primary hematoporphyrin zone.

Purification of protohemin IX. The purification of protohemin preparation *1* utilizing the AFCD solvent system is presented in Fig. 5. Only traces (apparently less than 1 %) of two other hemins, A and B, were separated from the principal protohemin zone C. Presumably, component A represents hematohemin IX, while B is 2(4)-vinyl-4(2)-hydroxyethyldeuterohemin IX. The solvent system employed appears to be useful for the fractionation of hemins. As observed in Fig. 5, deviations from the theoretical values are negligible in the case of protohemin IX. Amounts as great as 200 mg have been purified in a single fractionation according to this method. As described below, protohemin purified by this procedure yields mesoporphyrin having a high degree of purity, when the method of Baker *et al.*[9] is utilized in preparing the latter compound.

Purification of protoporphyrin IX. Fig. 6 presents the results of a fractionation performed upon the protoporphyrin IX obtained from protohemin preparation *1*. A small amount of rapidly migrating material (component A)

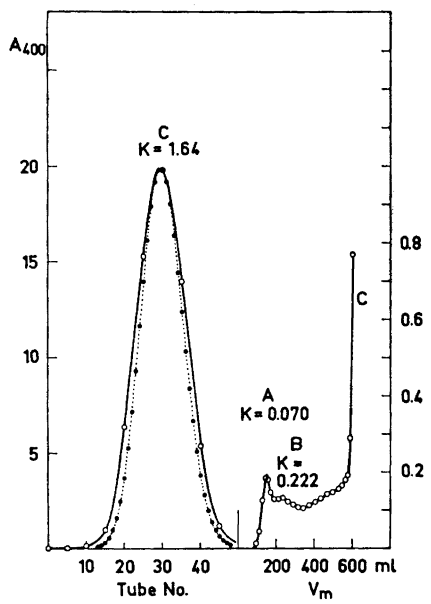

Fig. 5. Purification of protohemin IX preparation *1*. Solvent system: HCOOH-(22.5 M)/$CHCl_3$(10)-DMF(1). Twenty milligrams of the protohemin preparation were dissolved in 5.0 ml of DMF, and to the resulting solution were added 50 ml of $CHCl_3$ + 18 ml of HCOOH + 3.0 ml of H_2O. The mixture was then sampled into tubes $r = 0,...,5$. $N = 50$. $v_m = 2.28$ ml; $v_s = 11.22$ ml. $V_m = 620$ ml; flow rate = 1.5 ml/min. Theoretical (●) and experimental (○) values, the latter obtained by measuring $A_{400\,nm}$ of the effluent fractions and of the lower phases in the tubes. A = hematohemin IX, B = 2(4)-vinyl-4(2)-hydroxyethyldeuterohemin IX, and C = protohemin IX.

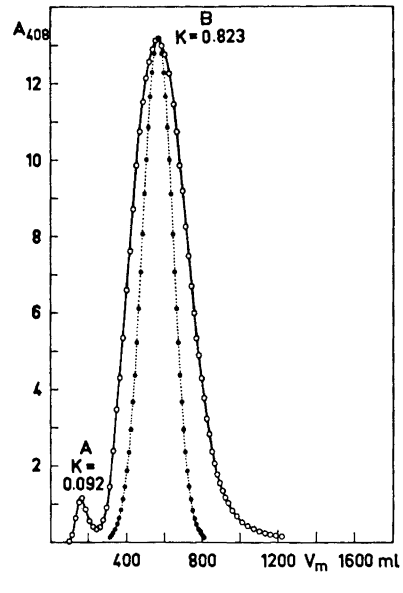

Fig. 6. Purification of protoporphyrin IX obtained from protohemin preparation *1*. Solvent system: HCOOH(8.0 M)/$CHCl_3$(25)-DMF(1). Eleven milligrams of the protoporphyrin preparation were dissolved in 2.0 ml of DMF and to the resulting solution were added 50 ml of $CHCl_3$ + 4.6 ml of HCOOH + 10.4 ml of H_2O. The mixture was then sampled into tubes $r = 0,...,4$. $N = 50$. $v_m = 3.14$ ml; $v_s = 10.36$ ml. $V_m = 1222$ ml; flow rate = 1.5 ml/min. Theoretical (●) and experimental (○) values, the latter obtained by measuring A_{408} of the effluent fractions. A = 2(4)-vinyl-4(2)-hydroxyethyldeuteroporphyrin IX (1 – 2 %) and B = protoporphyrin IX (98 – 99 %).

separated from the principal porphyrin zone (component B). Spectroscopically, fraction A appeared to consist primarily of 2(4)-vinyl-4(2)-hydroxyethyldeuteroporphyrin IX. When the protoporphyrin obtained from fraction B was refractionated utilizing the same solvent system, additional quantities of hydrophilic porphyrins appeared. The indication is that the vinyl groups of the protoporphyrin slowly become hydrated under the prevailing acidic conditions. This result is in accord with the investigations of Falk and coworkers.[7]

When protoporphyrin IX obtained from protohemin preparation *2* was subjected to partition fractionation, the result presented in Fig. 7 was achieved. Small amounts of hydrophilic porphyrins (components A and B) were also

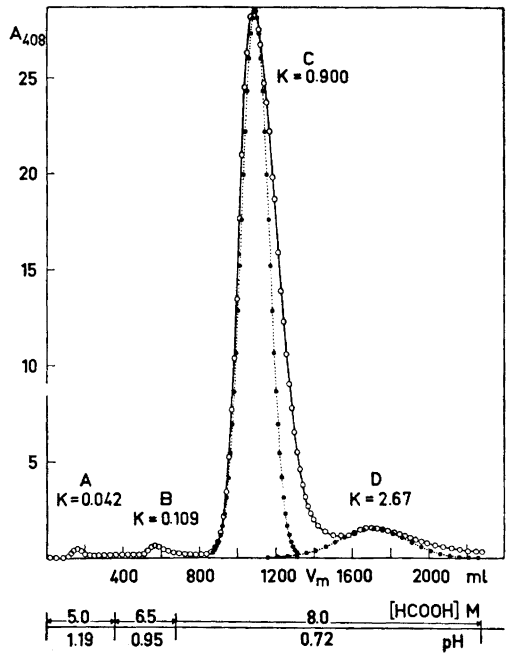

Fig. 7. Purification of protoporphyrin IX obtained from protohemin preparation *2*. Solvent system: HCOOH(5.0, 6.5, and 8.0 M)/$CHCl_3$(25)-DMF(1). Eighteen milligrams of the protoporphyrin preparation were dissolved in 4.0 ml of DMF and to the resulting solution were added 100 ml of $CHCl_3$ + 5.7 ml of HCOOH + 24.3 ml of H_2O. The mixture was then sampled into tubes $r = 0,...,9$. $N = 50$. $v_m = 2.88$ ml; $v_s = 10.62$ ml. $V_m = 2280$ ml; flow rate = 1.5 ml/min. Theoretical (●) and experimental (○) values, the latter obtained by measuring $A_{408\ nm}$ of the effluent fractions. A = hematoporphyrin IX + 2(4)-vinyl-4(2)-hydroxyethyldeuteroporphyrin IX, B = 2(4)-vinyl-4(2)-hydroxyethyldeuteroporphyrin IX, C = protoporphyrin IX (≃80 %), and D = "porphyrin 638" (≃15 %).

observed in this separation. Spectroscopically, fraction A appeared to be a mixture of hematoporphyrin IX and 2(4)-vinyl-4(2)-hydroxyethyldeuteroporphyrin IX, while fraction B consisted predominantly of the latter porphyrin. However, the principal impurity in this case was a porphyrin (component D) which differed distinctly from protoporphyrin according to its visible absorption spectrum (Table 1, g). Evidently, component D is identical to the compound previously observed (Fig. 6 in Ref. 1) as being an impurity in protoporphyrin prepared from the same commercial protohemin. The spectroscopic properties of component D, hereafter denoted as "porphyrin 638", are most similar to those of 2,4-methoxycarbonyldeuteroporphyrin IX, although the properties of 2,4-acetyl- and 2,4-propionyldeuteroporphyrin IX also fit rather well.[8] The di-cation spectrum of "porphyrin 638" exhibited absorption maxima at 607, 564, and 418 nm. These values closely approximate those reported for the di-cation of 2,4-acetyldeuteroporphyrin IX.[13] "Porphyrin 638" appeared to be stable in the employed solvent system. When the frac-

tions eluted within the range 1400 – 2250 ml were refractionated, the amounts of protoporphyrin IX and "porphyrin 638" within these fractions remained unchanged (Fig. 8). These characteristics suggest that "porphyrin 638" is a deuteroporphyrin having RCO-groups at positions 2 and 4, where R may be either the methyl, ethyl, methoxy, or ethoxy radical.

The possibility that "porphyrin 638" was formed from photoprotoporphyrin under the acidic conditions prevalent during fractionation was eliminated in the following manner: 10 mg of protoporphyrin IX, obtained from protohemin

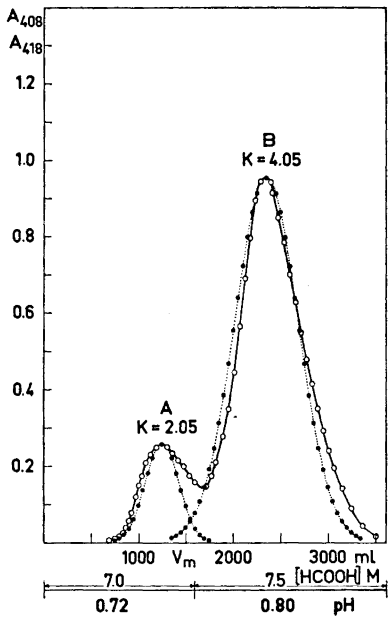

Fig. 8. Refractionation of component D ("porphyrin 638") in Fig. 7. Solvent system: HCOOH(7.0 and 7.5 M)/$CHCl_3$(25)-DMF(1). The component (eluted within the range 1400 – 2250 ml) was dissolved and sampled into the apparatus as in Fig. 6. $N = 50$. $v_m = 2.28$ ml; $v_s = 11.22$ ml. $V_m = 3500$ ml; flow rate = 2 ml/min. Theoretical (●) and experimental (○) values, the latter obtained by measuring A_{408} of the effluent fractions up to a total volume of 1600 ml and A_{418} of the effluent fractions eluted thereafter. A = protoporphyrin IX (20 %) and B = "porphyrin 638" (80 %).

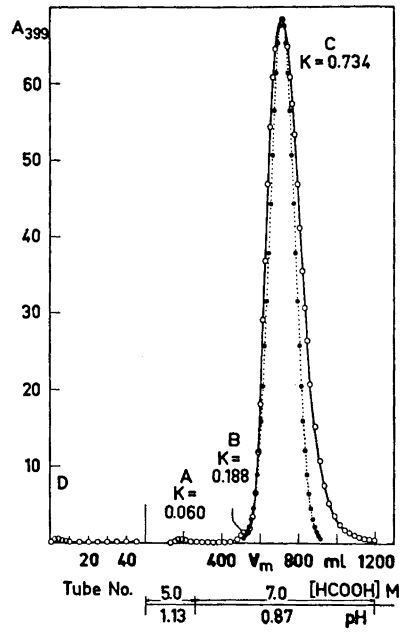

Fig. 9. Purification of mesoporphyrin IX obtained from further purified protohemin preparation *I*. Solvent system: HCOOH(5.0 and 7.0 M)/$CHCl_3$(25)-DMF(1). Twenty milligrams of mesoporphyrin, prepared according to the method of Baker *et al.*, were dissolved in 2.0 ml of DMF and to the resulting solution were added 50 ml of $CHCl_3$ + 2.85 ml of HCOOH + 12.2 ml of H_2O. The mixture was then sampled into tubes $r = 0,...,5$. $N = 50$. $v_m = 3.04$ ml; $v_s = 10.46$ ml. $V_m = 1195$ ml; flow rate 1.5 ml/min. Theoretical (●) and experimental (○) values, the latter obtained by measuring A_{399} of the effluent fractions and of the lower phases in the tubes. A = hematoporphyrin IX, B = formyldeuteroporphyrin IX (?), C = mesoporphyrin IX (99 %), and D = unknown porphyrin(s).

preparation *1* and dissolved in a neutral solvent (ethyl ether), were exposed to daylight and atmospheric oxygen. The appearance of an absorption peak at 669 nm indicated the formation of photoprotoporphyrin.[14,15] This protoporphyrin preparation, contaminated by a small amount of photoprotoporphyrin, was then subjected to partition fractionation. The result was visually similar to that of Fig. 6, with the exception that fraction A now contained, in addition to 2(4)-vinyl-4(2)-hydroxyethyldeuteroporphyrin IX, a second hydrophilic porphyrin which exhibited, in ethyl ether, an absorption peak at 650 nm. This serves as an indication that the alteration product of photoprotoporphyrin in aqueous acidic solution is probably other than "porphyrin 638".

Purification of meso- and deuteroporphyrin IX. The mesoporphyrin, obtained from protohemin preparation *1* which had been further purified by partition fractionation, contained only traces of other porphyrins, as shown by the results presented in Fig. 9. Spectroscopically, fraction A appeared to consist of hematoporphyrin IX, while fraction B possessed a Soret band at 421 nm and may be a formyldeuteroporphyrin. A small quantity of an unknown porphyrin(s) (fraction D) remained at the sampling end of the apparatus. The spectroscopic properties of fraction C eluted within the range 600 – 1000 ml closely resembled those of mesoporphyrin IX (Table 1, d).

Fig. 10 presents the results of further purification of the deuteroporphyrin IX preparation. Fraction A consisted of negligible amounts of two porphyrins exhibiting red absorption peaks, in diethyl ether, at 623 and 641 nm, respectively. A small quantity of unknown prophyrin material (fraction C) remained at the sampling end of the apparatus after this fractionation as well. The principal fraction (B) yielded deuteroporphyrin IX having the spectroscopic properties presented in Table 1, c.

DISCUSSION

Flexibility is a valuable property of the AFCD solvent system. The ratios of the solvent components may be varied. Thus, if larger amounts of porphyrins than those stated in the present work need to be purified, then the volume fraction of dimethylformamide may be increased. The fact that the AFCD system can be applied to the fractionation of hemins is an indication of its flexibility.

The selectivity of the AFCD system employed for fractionation of the porphyrins appears in Fig. 11. The slope of lines B and E, referring to 2(4)-vinyl-4(2)-hydroxyethyldeuteroporphyrin and protoporphyrin, respectively, is estimated as 2.6, while the slope of lines A, C, and D, representing hemato-, deutero-, and mesoporphyrin, respectively, is 2.2. The corresponding values for the AFC solvent system are 3.2 and 2.7.[1] The selectivity of the AFCD system is therefore less than that of the AFC system. The separation factor ($\beta = (k_1/k_2) \geq 1$) for the AFCD system is 3.0 between proto- and mesoporphyrins (pH 1.0), 3.6 between meso- and deuteroporphyrins, and 75 between deutero- and hematoporphyrins. The corresponding values for the AFC system were reported as 4.5, 6.8 – 7.4, and 75 – 80.[1]

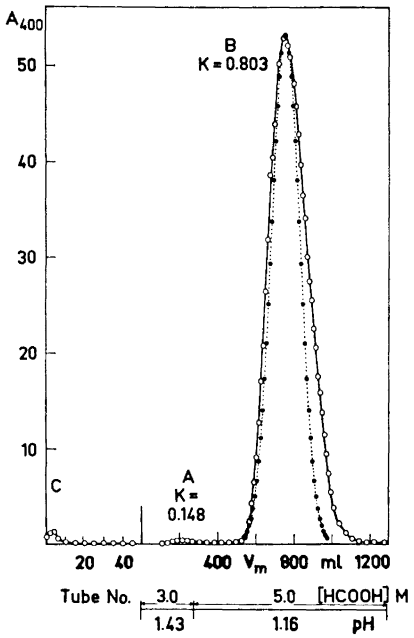

Fig. 10. Purification of deuteroporphyrin IX obtained from protohemin preparation *1*. Solvent system: HCOOH(3.0 and 5.0 M/$CHCl_3$(25)-DMF(1). Twentythree milligrams of the deuteroporphyrin preparation were dissolved in 2.0 ml of DMF and to the resulting solution were added 50 ml of $CHCl_3$ + 2.5 ml of HCOOH + 16.2 ml of H_2O. The mixture was then sampled into tubes $r = 0,...,5$. $N = 50$. $v_m = 2.44$ ml; $v_s = 11.06$ ml. $V_m = 1278$ ml; flow rate = 1.5 ml/min. Theoretical (●) and experimental (○) values, the latter obtained by measuring A_{400} of the effluent fractions and of the lower phases in the tubes. A = hematoporphyrin IX + unknown porphyrin, B = deuteroporphyrin IX (99 %), and C = unknown porphyrin(s).

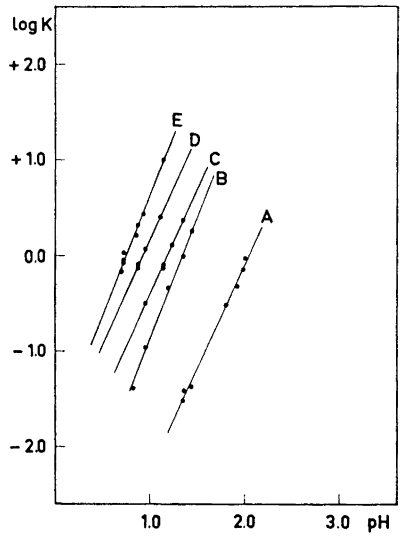

Fig. 11. Log K as a function of upper phase pH. A = hematoporphyrin, B = 2(4)-vinyl-4(2)-hydroxyethyldeuteroporphyrin, C = deuteroporphyrin, D = mesoporphyrin, and E = protoporphyrin.

For small-scale fractionations, the AFC system may be a better choice, owing to its high selectivity. However, a compromise must be achieved between the selectivity and the dissolving capacity of the solvent system when it is to be employed on the preparatory level. Otherwise, aggregation may seriously restrict the method and may lead to considerable confusion and misinterpretation of the results. This was clearly indicated by the present investigation into the behavior of hematoporphyrin. It now appears obvious that aggregation is at least one probable reason for the difficulties encountered

in the purification of this porphyrin.[12,16,17] Evidently, the high percentage of impurities observed to be present in six commercial preparations is due to the strong tendency of hematoporphyrin to from aggregates.

In light of the investigations herein described, the utilization of the multiple liquid-liquid partition technique for purifying protoporphyrin must be revaluated. This method is undoubtedly useful for the purification of crude protoporphyrin preparations. However, since hydration of the vinyl groups occurs readily under the acidic conditions employed, the technique never yields protoporphyrin of a high degree of purity. Protoporphyrin purified in this manner will always be contaminated by small quantities of 2(4)-vinyl-4(2)-hydroxyethyldeuteroporphyrin. Therefore, it would appear of greater advantage to first carefully purify the protohemin, since the vinyl groups of this compound seem to be more resistant towards hydration than those of the protoporphyrin. Highly-purified protohemin yields protoporphyrin having a comparable degree of purity, provided that the method of Morell and co-workers [5] is utilized for the removal of iron. Protoporphyrin preparations contaminated by 2(4)-vinyl-4(2)-hydroxyethyldeuteroporphyrin may be purified in the following manner. The preparation is first dissolved in a sufficient volume of chloroform(25)-dimethylformamide(1) (aggregation must be avoided). The resulting solution is rapidly extracted in a separatory funnel with successive volumes of 5.0 M aqueous formic acid, washed several times with distilled water and finally evaporated to dryness at reduced pressure.

REFERENCES

1. Ellfolk, N., Hynninen, P. and Sievers, G. *Acta Chem. Scand.* **23** (1969) 846.
2. Ellis, J., Jackson, A. H., Jain, A. C. and Kenner, G. W. *J. Chem. Soc.* **1964** 1935.
3. Scheler, W. *Biochem. Z.* **332** (1960) 344.
4. Labbe, R. F. and Nishida, G. *Biochim. Biophys. Acta* **26** (1957) 273.
5. Morell, D. B., Barrett, J. and Clezy, P. S. *Biochem. J.* **78** (1961) 793.
6. Stern, A. and Wenderlein, H. *Z. physik. Chem.* **A 170** (1934) 337.
7. Falk, J. E., Dresel, E. I. B., Benson, A. and Knight, B. C. *Biochem. J.* **63** (1955) 87.
8. Caughey, W. S., Fujimoto, W. Y. and Johnson, B. P. *Biochemistry* **5** (1966) 3830.
9. Baker, E. W., Ruccia, M. and Corwin, A. H. *Anal. Biochem.* **8** (1964) 512.
10. Chu, T. C. and Chu, E. J. *J. Am. Chem. Soc.* **74** (1952) 6276.
11. Hietala, P. *Ann. Acad. Sci. Fennicae* **A II, 100** (1960).
12. Schwartz, S., Berg, M. H., Bossenmaier, I. and Dinsmore, H. In Glick, D., Ed., *Methods of Biochemical Analysis* **8** (1960) 273.
13. Falk, J. E. *Porphyrins and Metalloporphyrins*, Elsevier, Amsterdam 1964, p. 236.
14. Inhoffen, H. H., Bliesener, C. and Brockmann, H., Jr. *Tetrahedron Letters* **1966** 3779.
15. Inhoffen, H. H., Brockmann, H., Jr. and Bliesener, K.-M. *Ann. Chem.* **730** (1969) 173.
16. Falk, J. E. *Porphyrins and Metalloporphyrins*, Elsevier, Amsterdam 1964, p. 175.
17. Granick, S., Bogorad, L. and Jaffe, H. *J. Biol. Chem.* **202** (1953) 801.

Received December 19, 1972.

ACTA CHEMICA SCANDINAVICA 27 (1973) 1807–1815

The Association of 3-Bromo-5-sulphosalicylic Acid in Aqueous Solution

YING-HUA LEE

Department of Inorganic Chemistry, University of Göteborg and Chalmers University of Technology, P.O. Box, S-402 20 Göteborg 5, Sweden

The pH equilibria of 3-bromo-5-sulphosalicylic acid have been studied, at 25°C, in acidic solution and 3 M sodium (perchlorate) medium, using a glass electrode. The total concentration, B, of disodium 3-bromo-5-sulphosalicylate, Na_2B, ranged from 0.0050 M to 0.2000 M. The data are best explained by the following equilibria and corresponding formation constants (given with 3σ, where σ is the standard deviation):

$B^{2-} + H^+ \rightleftharpoons HB^-$ $\quad \log \beta_{11} = 2.028 \pm 0.007$

$2B^{2-} + H^+ \rightleftharpoons HB_2^{3-}$ $\quad \log \beta_{12} = 2.537 \pm 0.017$

$2B^{2-} + 2H^+ \rightleftharpoons H_2B_2^{2-}$ $\quad \log \beta_{22} = 4.739 \pm 0.019$

$2HB^- \rightleftharpoons H_2B_2^{2-}$ $\quad \log K_D = 0.683 \pm 0.033$

The preliminary constants were obtained by Sillén's "curve-fitting" method and refined using the generalized least squares program LETAGROP, both E_0 for the electrode and the analytical concentrations H and B being adjusted.

The equilibrium constants of dimerization, K_{12} and K_D, and the proton association constants, K_{11} and K_{22}, are critically compared with those of salicylic acid.

The association of salicylic acid in aqueous solution has been investigated previously.[1] The dimers H_2B_2 and HB_2^- were found to coexist with salicylic acid, HB, in aqueous solution, when the total concentration of salicylate ion, B, was greater than 0.01 M. Due to the slight solubility of salicylic acid, the dimers H_2B_2 and HB_2^- exist only in minor amounts in aqueous solution. It is, therefore, difficult to obtain further information about their structures in solution by X-ray or spectroscopic methods.

A derivative of salicylic acid, 3-bromo-5-sulphosalicylic acid, was chosen for the present investigation. The larger solubility (compared with salicylic acid) of its monosalt in water and the rather high atomic number of Br, ought to make further investigations on the structures of the dimers in aqueous solution possible. In the present work only their compositions and formation constants have been investigated. Experiments on the diffraction of X-rays by the equilibrium solution of the disodium and monosodium salts of 3-bromo-

5-sulphosalicylic acid are, however, in progress. Relatively definite information concerning the structures of the dimers in solution is expected and will be reported in the future.

The experiments and calculations in the present work are similar to those in the previous paper.[1] The most important symbols are listed below for reference:

B	total concentration of disodium 3-bromo-5-sulphosalicylate, Na_2B.
b	concentration of free B^{2-} ion.
$[HB^-]$	concentration of monosodium 3-bromo-5-sulphosalicylate
$[HB_2^{3-}]$	concentration of the dimer HB_2^{3-}.
$[H_2B_2^{2-}]$	concentration of the dimer $H_2B_2^{2-}$.
β_{pq}	equilibrium constant for the reaction $pH^+ + qB^{2-} \rightleftharpoons H_pB_q^{(p-2q)}$.
Z	average number of H^+ bound per B^{2-}.
E	emf in mV.

EXPERIMENTAL

Chemicals. Sodium perchlorate and *perchloric acid* solutions were prepared and analysed as described in a previous paper.[1]

Disodium 3-bromo-5-sulphosalicylate, Na_2B, was prepared from the corresponding monosodium salt in the following way. The monosodium salt * was recrystallized three times from hot distilled water and neutralized to the disodium salt by adding sodium carbonate A. R. in hot solution. The sodium ion concentration was determined by an ion exchange technique.[2] The concentration of Na_2B was then calculated as one half of the value obtained for the sodium ion concentration.

Emf measurements. The experiments were carried out as a number of potentiometric titrations in which V_0 ml of an initial solution containing B M Na_2B and H_0 M $HClO_4$ in $(3-2B)$ M $NaClO_4$ was titrated with equal volumes, V_T ml, of an H_T M $HClO_4$ solution and a $2B$ M Na_2B solution, in $(3-H_T)$ M and $(3-4B)$ M $NaClO_4$, respectively. In each titration, the total hydrogen ion concentration, H, was varied under constant B by the addition of $HClO_4$. As Na_2B becomes insoluble in 3 M $Na(ClO_4)$ when $2B > 0.5$ M, the values of B used were chosen to be 0.0050, 0.0100, 0.0250, 0.0500, 0.1000, 0.1500 and 0.2000 M. A summary of the titrations is given in Table 1.

Table 1. Summary of the titrations.

Titn.	H_0 mM	B^a M	$H_{T(1)}$ M	$H_{T(2)}$ M
1	−0.074	0.0050	0.03985	0.09985
2	−0.074	0.0100	0.03985	0.09985
3	−0.074	0.0250	0.03985	0.09985
4	−0.074	0.0500	0.09985	0.3244
5	−0.070	0.0998	0.09992	0.3244
6	−0.068	0.1500	0.09992	0.3245
7	−0.065	0.2000	0.09992	0.3245

[a] B was obtained from the analytical composition of the solution, as the phenolic group in B^{2-} is practically undissociated in acidic solution.

* The author is indebted to Mr. Jan Nilsson, B. Sc., for preparing the salt and determining the amount of dibrominated sulphosalicylic acid impurity, which was less than 0.5 mol %, as estimated by NMR methods.

During the course of a titration, h was measured by means of the following cell:

+ RE | equilibrium solution | GE −

where GE denotes a glass electrode, and RE a reference half-cell of the composition

3 M $NaClO_4$ | 0.01 M $AgClO_4$ + 2.99 M $NaClO_4$ | Ag, AgCl

The titration vessel and the "Wilhelm bridge" used were kept in an oil bath thermostatically maintained at 25.00 ± 0.05°C in a room of temperature 25 ± 2°C. The emf of the cell was determined with a Radiometer valve potentiometer (PHM 4C) to an accuracy of ± 0.2 mV.

From the measured emf, h was calculated using the relation:

$$E = E_0 + 59.15 \log h + E_j$$

where E_0 is a constant for the glass electrode and E_j is the liquid junction potential between the equilibrium solution and 3 M $NaClO_4$. E_j can be expressed as a function of h, namely $E_j = jh$, where j is a constant. Both E_0 and j were determined by performing a separate acid titration of 3 M $NaClO_4$ and calculated from the emf by the procedure described by Biedermann and Sillén.[3]

As the quantities, h, B, H_0, and H_T were known, it was then possible to calculate Z, where Z is the average number of H^+ bound per B^-, by using the relation

$$BZ = (H_0V_0 + H_TV_T)/(V_0 + 2V_T) - h = H - h$$

In the preliminary calculations the analytical hydrogen ion concentration in the 3 M $Na(ClO_4)$ medium was taken to be H_0. As the stock solution of Na_2B was prepared by weighing an equivalent amount of Na_2CO_3 to neutralize the NaHB solution, and the concentration of Na_2B was determined as one half of the analytical value of the sodium ion concentration, any inaccuracy in the quantity of Na_2CO_3 will cause not only error in B but also in H_0. Refined values of H_0 and B were later obtained by the LETAGROP treatment.

RESULTS AND CALCULATIONS

The experimental data obtained in the titrations are shown in Fig. 1, where Z has been plotted against $-\log h$ for various B values. The error bars indicated for the titration points correspond to an error in the measured emf of ± 0.1 mV. Within the experimental error of the measured emf these curves, $Z(-\log h)_B$, do not coincide for various B values. With decreasing B they approach a limiting curve. This indicates the formation of one or several polynuclear complexes when $B > ca.$ 0.005 M.

To find the composition of these complexes and to determine the relevant formation constants, the "curve-fitting" and least squares methods were used. The most probable polynuclear complexes coexisting with HB^- were assumed to be HB_2^{3-} and $H_2B_2^{2-}$. Because of the moderate concentrations of B used, the highest being only 0.2 M, the further association of dimers is less probable. The relevant reactions and equilibrium constants can thus be written:

$$H^+ + B^{2-} \rightleftharpoons HB^- \qquad \beta_{11} = [HB^-]/hb$$
$$H^+ + 2B^{2-} \rightleftharpoons HB_2^{3-} \qquad \beta_{12} = [HB_2^{3-}]/hb^2$$
$$2H^+ + 2B^{2-} \rightleftharpoons H_2B_2^{2-} \qquad \beta_{22} = [H_2B_2^{2-}]/h^2b^2$$

The normalized function [4]

$$\mathbf{B} = \frac{[u - (1+u)Z][u(1-2\alpha) - 1]}{u[2Z(1+\alpha u) - (1+2\alpha u)]^2}$$

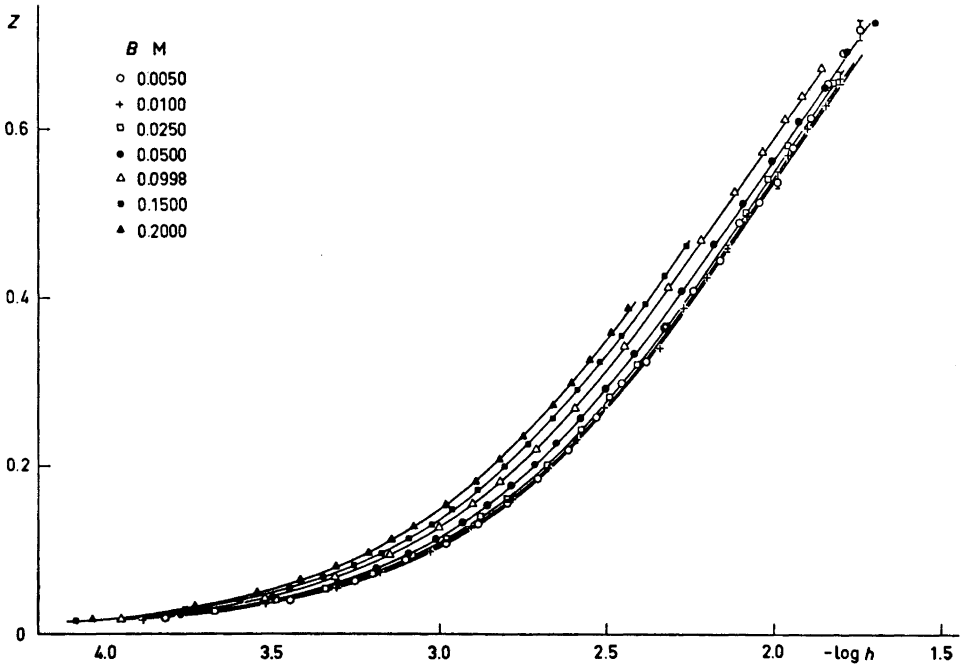

Fig. 1. Experimental data $Z(-\log h)_B$. Z is the average number of H^+ bound per B^{2-}. The error bars correspond to an error of ± 0.1 mV in the measured emf.

where $\log \alpha = \log \beta_{22} - \log \beta_{11} - \log \beta_{12}$, was then used in the "curve-fitting" method. The theoretical $\log \mathbf{B} = f(\log u)_{Z,\alpha}$ curves were calculated from the above equation and then compared with the experimental $\log B(\log h)_z$ curves

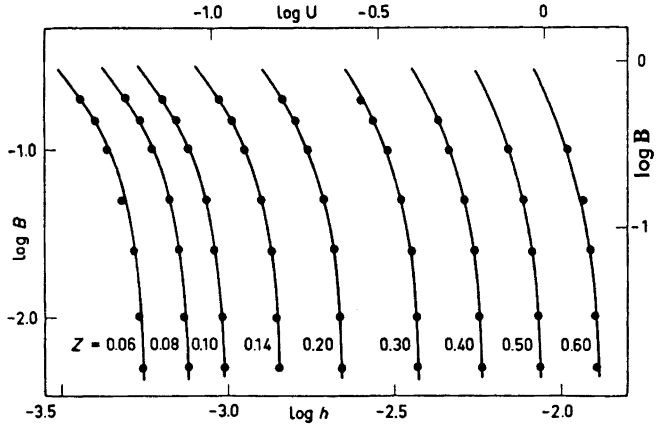

Fig. 2. Data for $\log B = f(\log h)_Z$ for the titrations of B^{2-} in 3 M $Na(ClO_4)$. The continuous curves are $\log \mathbf{B} = f(\log u)_{Z,\alpha}$ in the position of best fit for $\alpha = 1.4$.

obtained from Fig. 1. In Fig. 2, they are shown in the position of best fit, for which $\alpha = 1.4$. The equilibrium constants, β_{11} and β_{12}, were then calculated from the differences in intercept of the experimental and calculated graphs along the coordinate axes in Fig. 2, according to the following relations:

$$\log u = \log \beta_{11} + \log h, \quad \log \mathbf{B} - \log B = \log \beta_{12} - \log \beta_{11}.$$

The corresponding value of β_{22} was calculated from

$$\log \alpha = \log \beta_{22} - \log \beta_{11} - \log \beta_{12}.$$

The constants thus obtained were $\log \beta_{11} = 2.05$, $\log \beta_{12} = 2.52$ and $\log \beta_{22} = 4.72$.

These constants were then refined using the generalized least squares program LETAGROP.[5,6] In this program, the computer searches for the "best" set of equilibrium constants, β_{pq}, which give the minimum value for the error squares sum $U = \sum(H_{calc} - H_{tot})^2$. In the computer calculations, the following equations were used:

$$E = E_0 + 59.156 \log h + jh$$
$$B_{tot} = Bf_B = b + \sum q\beta_{pq} h^p b^q$$
$$H_{tot} = V_0(H_0 + \delta H_0)/(V_0 + 2V_T) + V_T(H_T + \delta H_T)/(V_0 + 2V_T)$$
$$H_{cal} = h + \sum p\beta_{pq} h^p b^q$$
$$Z = (H_{tot} - h)/B_{tot}$$

where δH_0 and δH_T correspond to the analytical errors in H in the original titration vessel and the buret solution, respectively, and $f_B = B_{tot}/B$ is the analytical error factor for B. These parameters, δH_0, δH_T, f_B, and E_0, were thus treated as an unknown group of constants to be determined and adjusted alternatively with the equilibrium constants β_{pq}. The input information comprised the estimated values of β_{pq} and $j = -11$ mV/M (common for all data), E_0, B, V_0, and H_T (for each titration), V_T and E (for each point in the titration).

The calculations were performed under five different conditions. In each calculation, a number of group constants were adjusted alternatively with β_{pq}. The resulting "best" set of values for U_{min}, β_{pq}, δH_0, δH_T, E_0, and f_B, obtained in each calculations, is given in Tables 2 and 3.

Table 2. Equilibrium constants for the reactions $pH^+ + qB^{2-} \rightleftharpoons H_pB_q^{p-2q}$ calculated by LETAGROP. 25°C, 3 M $Na(ClO_4)$, 144 points, $U = \sum(H_{calc} - H_{tot})^2$.

Calculation	$10^6 U_{min}$	$\log(\beta_{11} \pm 3\sigma)$	$\log(\beta_{12} \pm 3\sigma)$	$\log(\beta_{22} \pm 3\sigma)$	Group constants adjusted with β_{pq}
1	2.099	2.025 ± 0.009	2.566 ± 0.019	4.779 ± 0.022	δH_0
2	1.235	2.028 ± 0.016	2.548 ± 0.048	4.770 ± 0.046	δH_0, δH_T
3	1.096	2.021 ± 0.0001	2.536 ± 0.012	4.740 ± 0.001	δH_0, E_0
4	1.072	2.028 ± 0.007	2.537 ± 0.017	4.739 ± 0.019	δH_0, f_B
5	0.785	2.027 ± 0.004	2.541 ± 0.010	4.734 ± 0.011	δH_0, E_0, f_B

Table 3. E_0, f_B, δH_0, and δH_T calculated by LETAGROP for "best fit" for the calculation listed.

B M	$\delta H_0 \pm 3\sigma$ mM	$\delta H_T \pm 3\sigma$ mM	$E_0 \pm 3\sigma$ mV	$f_B \pm 3\sigma$
		Calculation 1		
0.005	-0.097 ± 0.072		47.59	1.000
0.010	-0.136 ± 0.066		48.33	1.000
0.025	-0.168 ± 0.089		48.14	1.000
0.050	-0.226 ± 0.108		47.91	1.000
0.100	-0.192 ± 0.121		47.12	1.000
0.150	-0.107 ± 0.178		47.90	1.000
0.200	-0.246 ± 0.251		48.04	1.000
		Calculation 2		
0.005	$+0.001 \pm 0.052$	-0.299 ± 0.118	47.59	1.000
0.010	-0.043 ± 0.037	-0.248 ± 0.077	48.33	1.000
0.025	-0.076 ± 0.080	-0.197 ± 0.133	48.14	1.000
0.050	-0.185 ± 0.151	-0.085 ± 0.284	47.91	1.000
0.100	-0.312 ± 0.187	$+0.165 \pm 0.261$	47.12	1.000
0.150	-0.371 ± 0.186	$+0.257 \pm 0.257$	47.90	1.000
0.200	-0.133 ± 0.282	-0.549 ± 0.306	48.04	1.000
		Calculation 3		
0.005	-0.024 ± 0.040		47.30 ± 0.08	1.000
0.010	-0.074 ± 0.039		48.04 ± 0.08	1.000
0.025	-0.114 ± 0.073		47.80 ± 0.11	1.000
0.050	-0.246 ± 0.127		47.66 ± 0.12	1.000
0.100	-0.334 ± 0.192		46.78 ± 0.12	1.000
0.150	-0.334 ± 0.172		47.48 ± 0.11	1.000
0.200	-0.144 ± 0.241		47.25 ± 0.11	1.000
		Calculation 4		
0.005	$-0.001 + 0.053$		47.59	0.9508 ± 0.0201
0.010	-0.050 ± 0.036		48.33	0.9775 ± 0.0071
0.025	-0.086 ± 0.076		48.14	0.9861 ± 0.0046
0.050	-0.199 ± 0.133		47.91	0.9956 ± 0.0042
0.100	-0.318 ± 0.161		47.12	0.9965 ± 0.0025
0.150	-0.333 ± 0.157		47.90	0.9951 ± 0.0024
0.200	-0.178 ± 0.210		48.04	0.9862 ± 0.0024
		Calculation 5		
0.005	-0.036 ± 0.052		47.10 ± 0.39	1.046 ± 0.081
0.010	-0.052 ± 0.042		48.31 ± 0.48	0.978 ± 0.048
0.025	-0.095 ± 0.075		47.49 ± 1.38	1.018 ± 0.063
0.050	-0.164 ± 0.081		46.28 ± 0.66	1.045 ± 0.022
0.100	-0.201 ± 0.169		46.51 ± 0.75	1.007 ± 0.017
0.150	-0.291 ± 0.198		47.86 ± 0.96	0.994 ± 0.022
0.200	-0.223 ± 0.246		48.90 ± 1.14	0.996 ± 0.029

DISCUSSION

It can be seen from Tables 2 and 3 that a marked improvement in the fit was obtained in Calculations 3 and 4, where the values of U are much lower and the values for β_{pq} are more certain than those in 1 and 2. The adjustment

of δH_0 and f_B in Calculation 4 indicated in Table 3 seems to be reasonable, considering the experimental conditions. The values of f_B indicate that the error in the determination of B is less than 1.4 % for all titrations except for those where the concentrations of B are low, namely 0.0100 and 0.0050 M (where the error is about 2 % and 5 %, respectively). The value of δH_0 increases with increasing B and the ratio of δH_0 to B is always less than 0.5 %.

The standard deviations found for the E_0 in Calculation 3 are reasonable, considering the reading uncertainty in measuring the emf of the electrodes.

It is obvious from Table 3, that the results of Calculation 5 had not been improved by adjusting the parameters δH_0, E_0, and f_B together with β_{pq}. The rather high standard deviations found for E_0 and f_B (up to 1.6 mV and 0.08, respectively) are not feasible in view of the uncertainty in the measurement of the emf and the analytical errors in B. Thus the preferred "best" set of equilibrium constants, β_{pq}, is that of Calculation 4 (given together with 3σ, where σ is the standard deviation), *i.e.*

$$\log \beta_{11} = 2.028 \pm 0.007$$
$$\log \beta_{12} = 2.537 \pm 0.017$$
$$\log \beta_{22} = 4.739 \pm 0.019$$

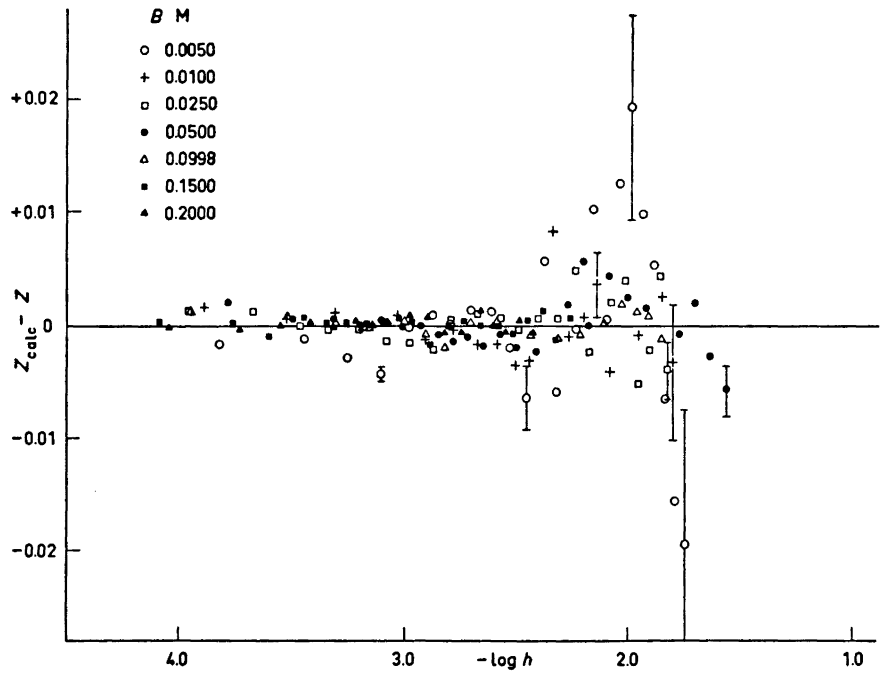

Fig. 3. $(Z_{calc} - Z)$ as a function of log h, plotted for the same titrations as in Fig. 1. The error bars correspond to an error of ± 0.1 mV in the measured emf.

Using the values of β_{11}, β_{12}, β_{22}, δH_0, and B found in Calculation 4, the differences $(Z_{calc} - Z)$, have been plotted in Fig. 3, as a function of log h, for the same titrations as shown in Fig. 1. It can be seen that the differences are randomly distributed and small, namely < 0.005 (with the exception of the 0.0050 M titration). The error bars represent the possible error in Z due to an error in the measurement of the emf E of $\pm$ 0.1 mV. It can also be seen that the possible errors become very large as Z and log h increase, especially for low concentrations of B.

The proton association constants, K_{11} and K_{22}, and the equilibrium constants of dimerization, K_{12} and K_D, corresponding to the following reactions, were calculated:

$$H^+ + B^{2-} \rightleftharpoons HB^- \qquad K_{11} = [HB^-]/hb$$
$$HB^- + B^{2-} \rightleftharpoons HB_2^{3-} \qquad K_{12} = [HB_2^{3-}]/[HB^-]b$$
$$HB_2^{3-} + H^+ \rightleftharpoons H_2B_2^{2-} \qquad K_{22} = [H_2B_2^{2-}]/[HB_2^{3-}]h$$
$$2HB^- \rightleftharpoons H_2B_2^{2-} \qquad K_D = [H_2B_2^{2-}]/[HB^-]^2$$

They are related to the values of β_{11}, β_{12}, and β_{22} by the following equations:

$$\beta_{11} = K_{11},\ \beta_{12} = K_{11}K_{12},\ \beta_{22} = K_{11}K_{12}K_{22},\ \beta_{22}/\beta_{11}^2 = K_D$$

so that log $K_{11} = 2.028 \pm 0.007$, log $K_{12} = 0.509 \pm 0.024$, log $K_{22} = 2.202 \pm 0.036$, and log $K_D = 0.683 \pm 0.033$. By comparing the values of these constants for 3-bromo-5-sulphosalicylic acid with those for salicylic acid,[1] namely log $K_{11} = 3.173 \pm 0.001$, log $K_{12} = 0.173 \pm 0.020$, log $K_{22} = 3.359 \pm 0.048$, and log $K_D = 0.359 \pm 0.031$, we see that the values of K_{11} and K_{22} of 3-bromo-5-sulphosalicylic acid are about 14 times smaller than those of salicylic acid, while the values of K_{12} and K_D are only slightly larger.

The higher acid strength of HB^- and $H_2B_2^{2-}$ for 3-bromo-5-sulphosalicylic acid, compared with that of salicylic acid, can be attributed to the $-I$ inductive effect of the substituents $-Br$ and $-SO_3^-$. The electron-attracting $-I$ effect of $-Br$ and $-SO_3^-$ causes a displacement of the bonding electron pair between the C and S, and C and Br atoms, in the direction of S and Br, respectively. This produces a succession of electron displacements along the chain towards the carboxyl group, thus increasing the tendency to dissociation of the acidic group by stabilizing the carboxylate anion.

The rather small variation in K_{12} and K_D between salicylic acid and 3-bromo-5-sulphosalicylic acid is quite understandable. It has been observed that in certain solvents, such as benzene, CCl_4, *etc.*, the equilibrium constants of dimerization are not particularly sensitive to a change in the enthalpy change, ΔH, of hydrogen bond formation,[7,8] as both ΔH and the entropy change, ΔS, affect K_D according to the equation $-RT \ln K_D = \Delta H - T\Delta S$. An increase in both ΔH and ΔS will thus to a certain extent balance each other. In aqueous solution the acids associate with the water molecules rather than with their own species. Thus not only the degree of dimerization for carboxylic acids is extremely decreased but also the variation in K_{12} and K_D is much less than that in the benzene or CCl_4 solvents.

Acknowledgements. The author is indebted to Professor Georg Lundgren for valuable discussions and support, to Dr. Arne Brändström and his colleagues for preparing the sodium salt of 3-bromo-5-sulphosalicylic acid, and to Dr. Susan Jagner for revising the English text.

The investigation was supported by a grant from the *Swedish Natural Science Research Council* (Contract No. 2318).

REFERENCES

1. Lee, Y.-H. and Lundgren, G. In Högfelt, E., Ed., *Contributions to Coordination Chemistry*, NFR, Stockholm 1972.
2. Vogel, A. I. *A Text-Book of Quantitative Inorganic Analysis Including Elementary Instrumental Analysis*, Longmans, London 1961, p. 722.
3. Biedermann, G. and Sillén, L. G. *Arkiv Kemi* **5** (1953) 425.
4. Rossotti, F. J. C. and Rossotti, H. *The Determination of Stability Constants*, McGraw, New York 1961, p. 376.
5. Ingri, N. and Sillén, L. G. *Arkiv Kemi* **23** (1964) 97.
6. Brauner, P., Sillén, L. G. and Whiteker, R. *Arkiv Kemi* **31** (1968) 365.
7. Pimentel, G. C. and McClellan, A. L. *The Hydrogen Bond*, Freeman, London 1960, p. 220.
8. Allen, G. and Caldin, E. F. *Quart. Rev. (London)* **7** (1953) 273.

Received December 14, 1972.

ACTA CHEMICA SCANDINAVICA 27 (1973) 1816–1843

Short Communications

On the Electrochemical Reduction of 1,2-(α-Ketotetramethylene)-ferrocene Oxime

STIG ALLENMARK [a] and BERTIL HELGÉE [b]

[a] *Department of Organic Chemistry, University of Uppsala, P.O. Box 531, S-751 21 Uppsala, Sweden.* [b] *Department of Organic Chemistry, University of Lund, P.O. Box 740, S-220 07 Lund, Sweden*

The stereoselective sodium-ethanol reduction of 1,2-(α-ketotetramethylene)-ferrocene oxime (I) to *endo*-1,2-(α-aminotetramethylene)-ferrocene (IIa) was recently reported.[1] The results obtained by Fry,[2,3] who found dissolving metal reduction and electrochemical reduction of bicyclic oximes to occur with quite opposite stereochemistry, thus prompted us to apply the latter method on I.

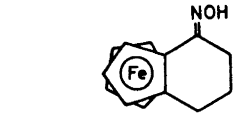

I

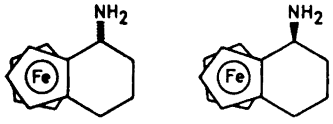

IIa IIb

The results from the reductions of I are summarized in Table 1. Completely α-deuteriated II was obtained, as shown by PMR, when the electrolysis was carried out in ethanol-d_1/D_2O.

Table 1. Stereochemical results and yields in reductions of I.

Reducing agent	Total yield [a] (%) of II	Relative amounts % IIa	% IIb
Na-EtOH	40–55	>97	< 3
Hg-cathode	65–76	~80	~20

[a] The possible recovery of starting material (I) has not been taken into account here.

The better yield obtained on electrolysis is clearly accompanied by a decrease in stereoselectivity. With both methods, however, the *endo*-isomer IIa is the predominant product, a result which is in marked contrast to those reported earlier.[2]

There are good reasons for believing that the stereochemistry of the dissolving metal reduction is kinetically controlled by protonation of the initially formed anion-radical by the solvent from the (least hindered) *exo*-side, thus yielding almost exclusively IIa. No *exo-endo*-equilibration occurs under the conditions used, which excludes thermodynamic control. The electrochemical result is more difficult to interpret, especially since the detailed mechanism of oxime electrolysis [4] is not yet known. The observed stereochemistry is, however, similar to that found for the bicyclic system in so far as the electrode attack and protonation steps involved [2] occur preferentially from the least hindered side in both cases.

The main difference, it may be noted, thus lies in the sodium-ethanol reduction of I and of the bicyclic oximes, respectively. The reason why the thermodynamically more stable amines are formed from camphor oxime and norcamphor oxime is still a matter of question.

Experimental. The preparation of I and its reduction with sodium-ethanol has been described earlier.[1] The electrolyses were carried out at a mercury pool cathode in a cell of conventional design equipped with a ceramic cup for separation of anode and cathode compartments. The anolyte was 0.1 M tetrabutylammonium tetrafluoroborate in ethanol/water solution (9/1 by volume). The catholyte contained 2 mmol (538 mg) of the oxime I in 50 ml of the same solvent-supporting electrolyte system as the anolyte. The electrolyses were run at a constant current of 0.25 A until 6 *F*/mol of substrate had passed. On work-up the catholyte was made weakly acidic with dilute hydrochloric acid and the solvent evaporated. The residue was diluted with a sodium hydrogen carbonate solution and repeatedly extracted with ether. Drying and evaporation of the ether solution yielded the crude amine II. This could be purified by extraction of the amines from the ether solution with 0.1 M hydrochloric acid, precipitation with dilute alkali and isolation of the product by extraction with ether, drying and evaporation.

The *endo*/*exo*-ratios (IIa/IIb) were determined either directly from the PMR-spectrum of the product II by integration of the peak-areas corresponding to the α-methine proton and cyclopentadienyl ring proton resonance signals, or by means of a chromatographic separation of IIa and IIb.[5]

Acknowledgements. The authors are indebted to Professor Lennart Eberson for valuable discussions and for the facilities placed at our disposal. A grant from the *Swedish Natural Science Research Council* (to S.A.) is gratefully acknowledged.

1. Allenmark, S. *Tetrahedron Letters* **1972** 2285.
2. Fry, A. J. and Newman, J. H. *J. Am. Chem. Soc.* **89** (1967) 6374.
3. Fry, A. J. *Fortschr. Chem. Forsch.* **34** (1972) 1.
4. Lund, H. (a) *Acta Chem. Scand.* **14** (1959) 249; (b) *Ibid.* **18** (1964) 563; (c) *Tetrahedron Letters* **1968** 3651.
5. Allenmark, S. and Grundström, A. *Chemica Scripta* **4** (1973) 69.

Received May 4, 1973

5-Amino-2-formylimidazo [1,2-a]pyridine

OLOF CEDER, KENNETH ROSÉN and JOHN F. WITTE

Department of Organic Chemistry, University of Göteborg and Chalmers Institute of Technology, Fack S-402 20 Göteborg 5, Sweden

In an attempt to synthesize 1,4-diazacycl[3.2.2]azine, *7*, in a "one-step" reaction (*cf.* Chart 1), 2,6-diaminopyridine, *1*, was condensed with bromomalondialdehyde, *2* (X = Br). A yellow solid with the composition $C_8H_7N_3O$ was obtained in 17 % yield. Its IR spectrum shows aldehydic C–H absorption at 3730 and 2820 cm^{-1}

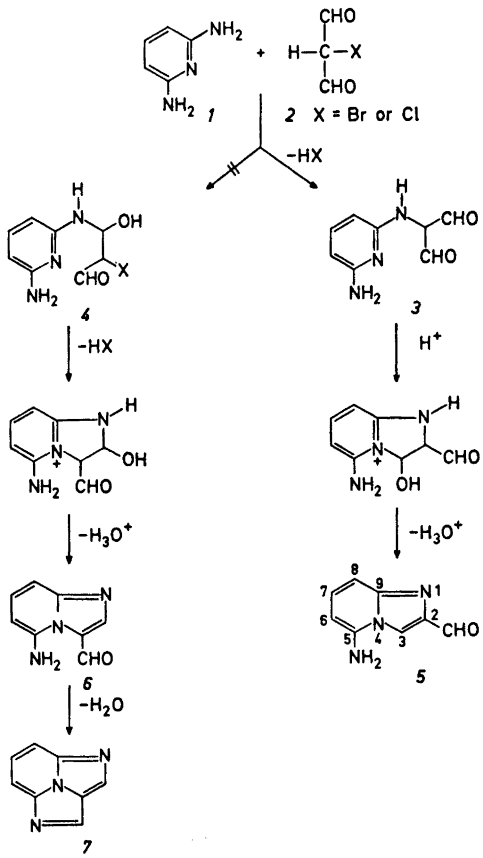

Chart 1.

Experimental. The preparation of I and its reduction with sodium-ethanol has been described earlier.[1] The electrolyses were carried out at a mercury pool cathode in a cell of conventional design equipped with a ceramic cup for separation of anode and cathode compartments. The anolyte was 0.1 M tetrabutylammonium tetrafluoroborate in ethanol/water solution (9/1 by volume). The catholyte contained 2 mmol (538 mg) of the oxime I in 50 ml of the same solvent-supporting electrolyte system as the anolyte. The electrolyses were run at a constant current of 0.25 A until 6 *F*/mol of substrate had passed. On work-up the catholyte was made weakly acidic with dilute hydrochloric acid and the solvent evaporated. The residue was diluted with a sodium hydrogen carbonate solution and repeatedly extracted with ether. Drying and evaporation of the ether solution yielded the crude amine II. This could be purified by extraction of the amines from the ether solution with 0.1 M hydrochloric acid, precipitation with dilute alkali and isolation of the product by extraction with ether, drying and evaporation.

The *endo*/*exo*-ratios (IIa/IIb) were determined either directly from the PMR-spectrum of the product II by integration of the peak-areas corresponding to the α-methine proton and cyclopentadienyl ring proton resonance signals, or by means of a chromatographic separation of IIa and IIb.[5]

Acknowledgements. The authors are indebted to Professor Lennart Eberson for valuable discussions and for the facilities placed at our disposal. A grant from the *Swedish Natural Science Research Council* (to S.A.) is gratefully acknowledged.

1. Allenmark, S. *Tetrahedron Letters* **1972** 2285.
2. Fry, A. J. and Newman, J. H. *J. Am. Chem. Soc.* **89** (1967) 6374.
3. Fry, A. J. *Fortschr. Chem. Forsch.* **34** (1972) 1.
4. Lund, H. (a) *Acta Chem. Scand.* **14** (1959) 249; (b) *Ibid.* **18** (1964) 563; (c) *Tetrahedron Letters* **1968** 3651.
5. Allenmark, S. and Grundström, A. *Chemica Scripta* **4** (1973) 69.

Received May 4, 1973

5-Amino-2-formylimidazo [1,2-a]pyridine

OLOF CEDER, KENNETH ROSÉN and JOHN F. WITTE

Department of Organic Chemistry, University of Göteborg and Chalmers Institute of Technology, Fack S-402 20 Göteborg 5, Sweden

In an attempt to synthesize 1,4-diazacycl[3.2.2]azine, *7*, in a "one-step" reaction (*cf.* Chart 1), 2,6-diaminopyridine, *1*, was condensed with bromomalondialdehyde, *2* (X = Br). A yellow solid with the composition $C_8H_7N_3O$ was obtained in 17 % yield. Its IR spectrum shows aldehydic C–H absorption at 3730 and 2820 cm^{-1}

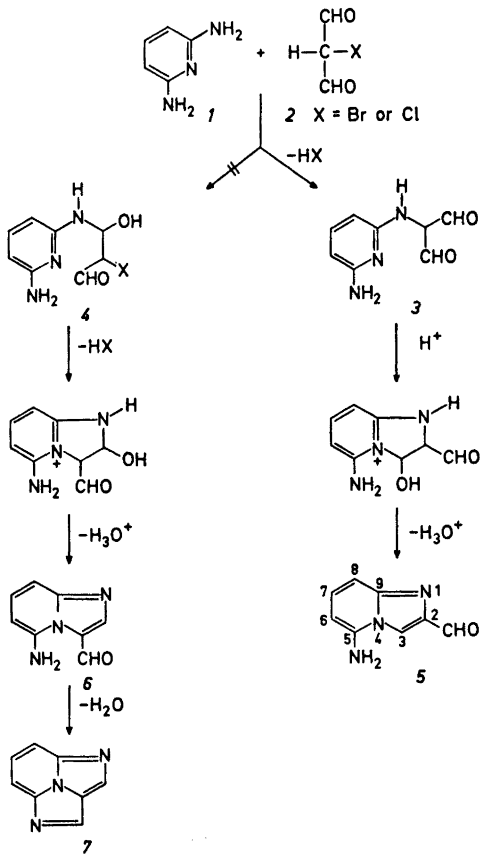

Chart 1.

and a carbonyl band at 1650 cm^{-1}; the NMR spectrum contains an unsplit aldehyde signal at 9.21 ppm and a broad NH_2 absorption at 8.30 ppm, which vanished on addition of deuterium oxide. The aromatic region displays a one-proton singlet at 8.42 ppm and an ABX pattern between 6.27 and 7.48 ppm (*cf.* Experimental). These observations indicate that the reaction product has structure *5* or *6*. The chemical-shift values for the aromatic proton singlets, H-2 in *6* and H-3 in *5*, are probably too close to allow a distinction between the two isomers. Infrared dilution studies on the yellow product demonstrated the presence of inter- but no intramolecular hydrogen bonds, which is in support of structure *5*. Recently [1] compound *6* was obtained by acid hydrolysis of *7* and was proved to have properties different from our product, which therefore possesses structure *5*.

In *2*, C-2 is thus more susceptible to nucleophilic attack than are the carbonyl-carbon atoms. Attempts to reverse this order of reactivity by substituting bromomalondialdehyde (*2*:X = Br) for its chloro-analog (*2*:X = Cl) also led to *5* and not to the desired compound *6*. Similarly, *5* was obtained in less than 10 % yield from *1* and 2,3-dibromopropionaldehyde, *8*,[2] in dilute hydrochloric acid solution. The title compound probably arose from aerial oxidation of the intermediate *9* (*cf.* Chart 2).

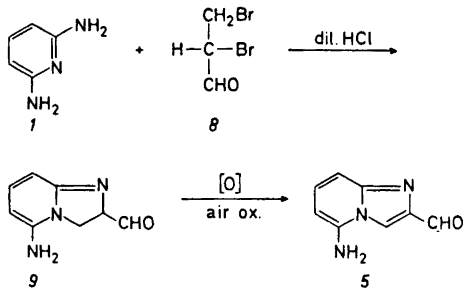

Chart 2.

The chemical-shift values for the ring protons in *5* were assigned by using the shift-change suffered by an aromatic proton on acetylation of an adjacent amino group.[3–5] Treatment of *5* with acetic anhydride in *p*-xylene yielded an *N*-acetyl derivative. In its NMR spectrum the one-proton doublet, which appeared at 6.27 ppm in *5*, was shifted 115 Hz to 8.19 ppm. These resonances are thus assigned to H-6, and in the spectrum of *5*, the triplet at 7.48 ppm to H-7, and the doublet at 6.81 ppm to H-8. Paudler *et al.*[1] have made shift assignments which are in agreement with our results, but they have not given any basis for their choice.

Experimental. Nuclear magnetic resonance (NMR) spectra were recorded with a Varian Model A-60 spectrometer, using tetramethylsilane as internal standard. Mass spectra were determined with a GEC-AEI MS 902 instrument at the Department of Medical Biochemistry, University of Göteborg. Thin-layer chromatography (TLC) was performed on Silica Gel GF_{254} (Merck) according to Stahl and the spots were visualized by means of short-wave ultraviolet light. For column chromatography, silica gel (0.05–0.2 mm; Merck) was used. Elemental analyses were carried out at Mikroanalytisches Laboratorium, Institut für Physikalische Chemie, Universität Wien.

5-Amino-2-formylimidazo[1,2-a]pyridine, 5, from bromomalondialdehyde. To a solution of 1.1 g (0.01 mol) of 2,6-diaminopyridine, *1*, in 50 ml of 1,2-dimethoxyethane was added 1.5 g (0.01 mol) of bromomalondialdehyde (*2*:X = Br), whereupon a solid precipitated. The suspension was heated at 50° for 12 h and then poured into 25 ml of a saturated aqueous sodium bicarbonate solution. All volatile materials were removed *in vacuo* and the residue was extracted with chloroform. The chloroform extracts were dried ($MgSO_4$) and evaporated under reduced pressure. The brown residue was chromatographed on 30 g of silica gel with chloroform-methanol (9:1), giving 300 mg (17 %) of a bright yellow solid, m.p. 198°. MS: $M^+ = 161$. NMR (dimethyl sulfoxide-d_6): aldehyde singlet at 9.21 (1H), broad NH_2 at 8.30 (2H), aromatic singlet at 8.42 (1H, H-3), triplet ($J = 8$ Hz) at 7.48 (1H, H-7), doublet ($J = 8$ Hz) at 6.81 (1H, H-8), doublet ($J = 8$ Hz) at 6.27 (1H, H-6) ppm; IR (KBr): 3200–3400 (NH), 3730 and 2820 (aldehydic C-H) 1650 cm^{-1} (C=O). (Found: C 59.52; H 4.42; N 25.95. Calc. for $C_8H_7N_3O$: C 59.62; H 4.38; N 26.07).

5-Amino-2-formylimidazo[1,2-a]pyridine, 5, from chlomalondialdehyde.[6] The reaction conditions were the same as those described above, except that the solution was stirred for 15 h at 65–70°. The yield was 173 mg (9 %).

Acetylation of 5 to 5-acetamido-2-formylimidazo[1,2-]pyridine. To a solution of 26 mg of *5* in 5 ml of *p*-xylene was added 0.7 ml of freshly distilled acetic anhydride. The mixture

was heated to reflux for 96 h. The solvent was evaporated under reduced pressure and the residue was chromatographed on a silica gel column, eluted with chloroform-ethyl acetate (3:1). Yield: 25 mg (77 %). MS: $M^+ = 203$; NMR (dimethyl sulfoxide-d_6): broad NH at 13.07 (1H), aldehyde singlet at 9.42 (1H), aromatic singlet at 8.36 (1H, H-3), doublet ($J = 7$ Hz) at 8.19 (1H, H-6), triplet ($J = 7$ Hz) at 7.75 (1H, H-7), doublet ($J = 7$ Hz) at 7.40 (1H, H-8), and singlet at 2.35 (3H, CH_3) ppm.

Acknowledgements. We are indebted to the *Swedish Natural Science Research Council* for financial support, to *Stiftelsen Bengt Lundqvists Minne* for a fellowship (to K.R.), and to Miss Gun Myrne for technical assistance.

1. Paudler, W. W., VanDahm, R. A. and Park, Y. N. *J. Heterocycl. Chem.* **9** (1972) 81.
2. Ward, J. P. and Van Dorp, D. A. *Rec. Trav. Chim.* **85** (2) (1966) 117.
3. Ceder, O. and Witte, J. F. *Acta Chem. Scand.* **26** (1972) 635.
4. Ceder, O., Andersson, J. E. and Johansson, L. E. *Acta Chem. Scand.* **26** (1972) 624.
5. Ceder, O. and Rosén, K. *Acta Chem. Scand.* **27** (1973). *In press.*
6. Houben-Weyl: *Methoden der organischen Chemie*, 4. Aufl. Band 7/1, S. 119. Georg Thieme Verlag, Stuttgart.

Received May 11, 1973.

Methylation Studies on Levans

BENGT LINDBERG, JÖRGEN LÖNNGREN and JAMES L. THOMPSON*

Institutionen för organisk kemi, Stockholms Universitet, S-113 27 Stockholm, Sweden

Levan, which is an essentially (2→6)-linked β-fructan, is antigenic in man and is precipitated by some myeloma proteins.[1] Different preparations show variations in their immunochemical behaviour[1,2] which must be due to structural differences. We now report methylation studies on some levan preparations of different origins.

Qualitative and quantitative analysis of the methylated sugars obtained on hydrolysis of a methylated polysaccharide is preferably performed by GLC-MS of the derived alditol acetates.[3,4] Some difficulties might be expected in working with ketoses since reduction of each partially methylated ketose should give rise to two alditol derivatives. None of the pairs of D-glucitol and D-mannitol derivatives obtained from 1,3,4,6-tetra-*O*-methyl-, 1,3,4-tri-*O*-methyl-, or 3,4-di-*O*-methyl-D-fructose separated, however, on the chromatographic columns used. Another possible source of difficulty is that the alditols derived from the 1,3,4- and 3,4,6-isomers of tri-*O*-methyl-D-fructose might not be distinguishable. When the conversion to

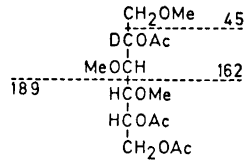

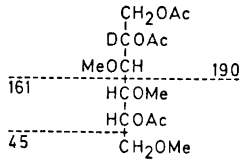

alditols is carried out with sodium borodeuteride, however, these substances give different mass spectra. The origin of some pertinent primary fragments is indicated above for the D-glucitol derivatives. When this method is used, a small proportion of 3,4,6-tri-*O*-methyl-D-fructose in the 1,3,4-tri-*O*-methyl-D-fructose might be overlooked. Therefore GLC was used to compare the acetates of the free sugars obtained on hydrolysis of methylated inulin with those obtained from the methylated levans B512 PP2, "Coryne", "Hestrin", and "Rye grass". The 1,3,4- and 3,4,6-tri-*O*-methyl-D-fructose acetates gave only one peak each on GLC and these were well separated (retention times relative to 1,5-di-*O*-acetyl-2,3,4,6-tetra-

* Present address: Collège militaire royal de Saint-Jean, Québec, Canada.

was heated to reflux for 96 h. The solvent was evaporated under reduced pressure and the residue was chromatographed on a silica gel column, eluted with chloroform-ethyl acetate (3:1). Yield: 25 mg (77 %). MS: $M^+ = 203$; NMR (dimethyl sulfoxide-d_6): broad NH at 13.07 (1H), aldehyde singlet at 9.42 (1H), aromatic singlet at 8.36 (1H, H-3), doublet ($J = 7$ Hz) at 8.19 (1H, H-6), triplet ($J = 7$ Hz) at 7.75 (1H, H-7), doublet ($J = 7$ Hz) at 7.40 (1H, H-8), and singlet at 2.35 (3H, CH_3) ppm.

Acknowledgements. We are indebted to the *Swedish Natural Science Research Council* for financial support, to *Stiftelsen Bengt Lundqvists Minne* for a fellowship (to K.R.), and to Miss Gun Myrne for technical assistance.

1. Paudler, W. W., VanDahm, R. A. and Park, Y. N. *J. Heterocycl. Chem.* **9** (1972) 81.
2. Ward, J. P. and Van Dorp, D. A. *Rec. Trav. Chim.* **85** (2) (1966) 117.
3. Ceder, O. and Witte, J. F. *Acta Chem. Scand.* **26** (1972) 635.
4. Ceder, O., Andersson, J. E. and Johansson, L. E. *Acta Chem. Scand.* **26** (1972) 624.
5. Ceder, O. and Rosén, K. *Acta Chem. Scand.* **27** (1973). *In press.*
6. Houben-Weyl: *Methoden der organischen Chemie*, 4. Aufl. Band 7/1, S. 119. Georg Thieme Verlag, Stuttgart.

Received May 11, 1973.

Methylation Studies on Levans

BENGT LINDBERG, JÖRGEN LÖNNGREN and JAMES L. THOMPSON*

Institutionen för organisk kemi, Stockholms Universitet, S-113 27 Stockholm, Sweden

Levan, which is an essentially (2→6)-linked β-fructan, is antigenic in man and is precipitated by some myeloma proteins.[1] Different preparations show variations in their immunochemical behaviour[1,2] which must be due to structural differences. We now report methylation studies on some levan preparations of different origins.

Qualitative and quantitative analysis of the methylated sugars obtained on hydrolysis of a methylated polysaccharide is preferably performed by GLC-MS of the derived alditol acetates.[3,4] Some difficulties might be expected in working with ketoses since reduction of each partially methylated ketose should give rise to two alditol derivatives. None of the pairs of D-glucitol and D-mannitol derivatives obtained from 1,3,4,6-tetra-*O*-methyl-, 1,3,4-tri-*O*-methyl-, or 3,4-di-*O*-methyl-D-fructose separated, however, on the chromatographic columns used. Another possible source of difficulty is that the alditols derived from the 1,3,4- and 3,4,6-isomers of tri-*O*-methyl-D-fructose might not be distinguishable. When the conversion to

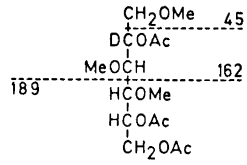

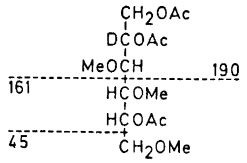

alditols is carried out with sodium borodeuteride, however, these substances give different mass spectra. The origin of some pertinent primary fragments is indicated above for the D-glucitol derivatives. When this method is used, a small proportion of 3,4,6-tri-*O*-methyl-D-fructose in the 1,3,4-tri-*O*-methyl-D-fructose might be overlooked. Therefore GLC was used to compare the acetates of the free sugars obtained on hydrolysis of methylated inulin with those obtained from the methylated levans B512 PP2, "Coryne", "Hestrin", and "Rye grass". The 1,3,4- and 3,4,6-tri-*O*-methyl-D-fructose acetates gave only one peak each on GLC and these were well separated (retention times relative to 1,5-di-*O*-acetyl-2,3,4,6-tetra-

* Present address: Collège militaire royal de Saint-Jean, Québec, Canada.

Table 1. Methylation analysis of levans.

Polysaccharide	Methylated sugar, % 1,3,4,6-Fru[a] $T^b=0.82$	2,3,4,6-Glu $T=1.00$	1,3,4-Fru $T=1.82$	3,4,6-Fru $T=1.82$	3,4-Fru $T=4.31$
Inulin	4	3	–	92	1
P6	4	1	85	–	10
B512 E	10	–	68	–	22
B512 PP2	11	–	68	–	21
Coryne	3	–	91	–	6
Hestrin	16	–	66	–	18
Rye grass	7	–	87	–	6

[a] 1,3,4,6-Fru= 1,3,4,6-tetra-*O*-methyl-D-fructose, *etc.*
[b] Retention times of the corresponding alditol acetates relative to 1,5-di-*O*-acetyl-2,3,4,6-tetra-*O*-methyl-D-glucitol on an OV-225 column.

O-methyl-D-glucitol 1.07 and 1.16, respectively). Only the 1,3,4-derivative was obtained from the levans investigated. The results of the methylation analyses of inulin and the different levans are summarized in Table 1.

According to previous results the levans are essentially (2→6)-linked, with some branches in the 1-position,[5] in contradistinction to inulin which is essentially (2→1)-linked. The mode of biosynthesis of these polysaccharides indicates that each molecule should contain a sucrose residue with D-glucose as the non-reducing end-group.

The results in the table show that all the levans have the expected structure (although the non-reducing D-glucose end-group is found only in the analysis of levan P6), a chain of (2→6)-linked D-fructose residues with some branching in the 1-positions. Since all the polysaccharides have strong negative rotations, the linkages must have the β-configuration. The degree of branching is proportional to the percentage of 3,4-di-*O*-methyl-D-fructose. For polysaccharides of high molecular weight the percentage of branch points should be equal to that of fructose non-reducing end-groups. The agreement between these figures is good for inulin and the rye grass levan, but not for the five bacterial levans. Losses of volatile 1,3,4,6-tetra-*O*-methyl-D-fructose and derivatives may partially explain this discrepancy which is, however, larger than expected. Therefore it is possible that these levans contain some minor structural feature which has been overlooked in these studies. Phosphate groups are excluded as levans B512 PP2, B512E, P6, „Hestrin", and "Rye grass" contained no phosphate.

These studies give information on the degree of branching of the different samples but not on the lengths of the side chains which, from the immunochemical point of view, may be of equal or greater importance.

Experimental. General methods. Concentrations were carried out under diminished pressure at bath temperatures which did not exceed 40°. For gas chromatography a Perkin-Elmer 990 instrument fitted with a flame-ionization detector was used. Separations were carried out on glass-columns 180 × 0.15 cm containing (a) 3 % OV-225 on Gas Chrom Q (100/120 mesh) at 170° (partially methylated alditol acetates) or (b) 3 % ECNSS-M on Gas Chrom Q (100/120 mesh) at 160° (partially methylated monosaccharide acetates). For mass spectrometry a Perkin-Elmer 270 GLC-MS instrument fitted with an OV-225 S.C.O.T. column (15 m × 0.5 mm) used at 190° was employed. Mass spectra were recorded at an ionization potential of 70 eV, an ionization current of 80 μA and an ion source temperature of 80°.

Materials. Five of the levans investigated were the same as preparations used by Allen and Kabat.[1] P6 is produced by an unidentified microorganism, B512 PP2 and B512 E by strains of *Leuconostoc mesenteroides*, and "Hestrin" by *Aerobacter levanicum*. "Rye grass" is a perennial rye grass levan. "Coryne" is produced by a *Corynebacterium* species.[6] The inulin investigated was a commercial sample.

Methylation analyses. The polysaccharide (2 mg) was methylated by Hakomori's method[3,7] and recovered by dialysis against running tap-water and concentration to dryness. The product was then treated on the steam-bath with 90 % formic acid (1 ml) for 30 min, diluted with 10 volumes of water, and returned to the steam-bath for 3,5 h. The solution was then concentrated to a small volume and the remaining formic acid was removed by co-distillation with additional water (3 × 5 ml). Finally the product was either reduced with sodium borodeuteride and acetylated or part of it was treated in this way, and the remainder was acetylated without reduction as described below. For acetylation pyridine (1 ml) and acetic anhydride (1 ml) were added to the dry product and after 10 min at room temperature the flask was moved to the steam-bath for 20 min. The acetylating agents were then removed by co-distillation with toluene (3 × 5 ml) and the product was examined by GLC.

Acknowledgements. The authors are indebted to Professor Elvin A. Kabat, New York, for supplying the different levans. This work was supported by grants from the *Swedish Natural Science Research Council*, from the *Swedish Medical Research Council* (B72-40X-2522-04), from *Harald Jeanssons Stiftelse*, and from *Stiftelsen Sigurd och Elsa Goljes Minne.*

1. Allen, P. Z. and Kabat, E. A. *J. Exp. Med.* **105** (1957) 383.
2. Lundblad, A., Steller, R., Kabat, E. A., Hirst, J. W., Weigert, M. G. and Cohn, M. *Immunochemistry* **9** (1972) 535.
3. Björndal, H., Hellerqvist, C. G., Lindberg, B. and Svensson, S. *Angew. Chem. Int. Ed.* **9** (1970) 610.
4. Lönngren, J. and Pilotti, Å. *Acta Chem. Scand.* **25** (1971) 1144.
5. Stacey, M. and Barker, S. A. *Polysaccharides of Microorganisms*, Oxford University Press, 1960.
6. Avigad, G. and Feingold, D. S. *Arch. Biochem. Biophys.* **70** (1957) 178.
7. Hakomori, S. *J. Biochem.* (Tokyo) **55** (1964) 205.

Received May 16, 1973.

The Molecular Structure of Trichlorotrimethylamine-aluminium, $Cl_3AlN(CH_3)_3$ by Gas Phase Electron Diffraction

A. ALMENNINGEN, A. HAALAND, T. HAUGEN and D. P. NOVAK

Department of Chemistry, University of Oslo, Blindern, Oslo 3, Norway

Recently we have determined the molecular structures of the complexes Me_3AlNMe_3[1] (Me = CH_3) and H_3AlNMe_3[2] by means of gas phase electron diffraction. We now report the results of a similar study of Cl_3AlNMe_3. This complex has previously been studied by X-ray crystallography,[3] but we hoped to improve on the accuracy.

The electron scattering pattern from gaseous Cl_3AlNMe_3 was recorded on the Oslo electron diffraction unit [4] with a nozzle temperature of about 330°C. Exposures were made with a nozzle-to-photographic-plate distance of about 48 cm. The intensity data thus obtained extended from $s = 1.50$ Å^{-1} to $s = 18.00$ Å^{-1}. A radial distribution (RD) curve obtained by Fourier inversion of the modified molecular intensity curve [5] is shown in Fig. 1. A.

The molecular structure was refined under the assumption that the molecular symmetry is C_{3v} with the Cl atoms of the acceptor and the Me groups of the donor staggered with respect to rotation about the Al – N bond (as they are in the crystal). The Me groups were assumed to have C_{3v} symmetry and to be oriented in such a way that the C – H bonds are staggered with respect to the bonds radiating from the N atom. The molecular structure is then determined by seven independent parameters, *e.g.* the Al – Cl, Al – N, N – C, and C – H bond distances and the ∠N – Al – Cl, ∠Al – N – C, and ∠N – C – H valance angles. The latter was fixed at 109.8°, the angle found in free NMe_3.[6] Since it was anticipated that large amplitude libration about the Al – N bond might lead to an average value of the Cl···C(*trans*) distance that was significantly smaller than that calculated for the equilibrium geometry, the shrinkage of this distance was included in the refinement as an additional independent parameter. The vibrational amplitude of the Al – N bond distance was fixed at the value found

Methylation analyses. The polysaccharide (2 mg) was methylated by Hakomori's method[3,7] and recovered by dialysis against running tap-water and concentration to dryness. The product was then treated on the steam-bath with 90 % formic acid (1 ml) for 30 min, diluted with 10 volumes of water, and returned to the steam-bath for 3,5 h. The solution was then concentrated to a small volume and the remaining formic acid was removed by co-distillation with additional water (3 × 5 ml). Finally the product was either reduced with sodium borodeuteride and acetylated or part of it was treated in this way, and the remainder was acetylated without reduction as described below. For acetylation pyridine (1 ml) and acetic anhydride (1 ml) were added to the dry product and after 10 min at room temperature the flask was moved to the steam-bath for 20 min. The acetylating agents were then removed by co-distillation with toluene (3 × 5 ml) and the product was examined by GLC.

Acknowledgements. The authors are indebted to Professor Elvin A. Kabat, New York, for supplying the different levans. This work was supported by grants from the *Swedish Natural Science Research Council*, from the *Swedish Medical Research Council* (B72-40X-2522-04), from *Harald Jeanssons Stiftelse*, and from *Stiftelsen Sigurd och Elsa Goljes Minne.*

1. Allen, P. Z. and Kabat, E. A. *J. Exp. Med.* **105** (1957) 383.
2. Lundblad, A., Steller, R., Kabat, E. A., Hirst, J. W., Weigert, M. G. and Cohn, M. *Immunochemistry* **9** (1972) 535.
3. Björndal, H., Hellerqvist, C. G., Lindberg, B. and Svensson, S. *Angew. Chem. Int. Ed.* **9** (1970) 610.
4. Lönngren, J. and Pilotti, Å. *Acta Chem. Scand.* **25** (1971) 1144.
5. Stacey, M. and Barker, S. A. *Polysaccharides of Microorganisms*, Oxford University Press, 1960.
6. Avigad, G. and Feingold, D. S. *Arch. Biochem. Biophys.* **70** (1957) 178.
7. Hakomori, S. *J. Biochem.* (Tokyo) **55** (1964) 205.

Received May 16, 1973.

The Molecular Structure of Trichlorotrimethylamine-aluminium, $Cl_3AlN(CH_3)_3$ by Gas Phase Electron Diffraction

A. ALMENNINGEN, A. HAALAND, T. HAUGEN and D. P. NOVAK

Department of Chemistry, University of Oslo, Blindern, Oslo 3, Norway

Recently we have determined the molecular structures of the complexes Me_3AlNMe_3[1] (Me = CH_3) and H_3AlNMe_3[2] by means of gas phase electron diffraction. We now report the results of a similar study of Cl_3AlNMe_3. This complex has previously been studied by X-ray crystallography,[3] but we hoped to improve on the accuracy.

The electron scattering pattern from gaseous Cl_3AlNMe_3 was recorded on the Oslo electron diffraction unit [4] with a nozzle temperature of about 330°C. Exposures were made with a nozzle-to-photographic-plate distance of about 48 cm. The intensity data thus obtained extended from $s = 1.50$ Å^{-1} to $s = 18.00$ Å^{-1}. A radial distribution (RD) curve obtained by Fourier inversion of the modified molecular intensity curve [5] is shown in Fig. 1. A.

The molecular structure was refined under the assumption that the molecular symmetry is C_{3v} with the Cl atoms of the acceptor and the Me groups of the donor staggered with respect to rotation about the Al – N bond (as they are in the crystal). The Me groups were assumed to have C_{3v} symmetry and to be oriented in such a way that the C – H bonds are staggered with respect to the bonds radiating from the N atom. The molecular structure is then determined by seven independent parameters, *e.g.* the Al – Cl, Al – N, N – C, and C – H bond distances and the ∠N – Al – Cl, ∠Al – N – C, and ∠N – C – H valance angles. The latter was fixed at 109.8°, the angle found in free NMe_3.[6] Since it was anticipated that large amplitude libration about the Al – N bond might lead to an average value of the Cl···C(*trans*) distance that was significantly smaller than that calculated for the equilibrium geometry, the shrinkage of this distance was included in the refinement as an additional independent parameter. The vibrational amplitude of the Al – N bond distance was fixed at the value found

in H_3AlNMe_3, $l(Al-N)=0.084$ Å. Vibrational amplitudes between the atoms in the donor were fixed at the values found in free NMe_3.

Simultaneous least-squares refinement of the six structure parameters, the shrinkage of the Cl···C(*trans*) distance, and the six most important vibrational amplitudes with a non-diagonal weight matrix [7] converged to the values listes in Table 1.

Table 1. Bond distances, valence angles and root-mean-square vibrational amplitudes of $Cl_3AlN(CH_3)_3$.

	R (Å)	l (Å)
C–H	1.121(25)	0.081[a]
N–C	1.516(12)	0.045[a]
Al–N	1.945(35)	0.084[a]
Al–Cl	1.121(4)	0.055(10)
∠N–Al–Cl	104.9(0.7)°	
∠Al–N–C	112.6(1.5)°	
∠N–C–H	109.8°[a]	
Cl···Cl	3.55(2)	0.14(1)
Cl···N	3.23(2)	0.07(1)
Cl···C (*gauche*)	3.57(3)	0.30(9)
Cl···C (*trans*)	4.51(6)	0.18(5)
Al···C	2.89(2)	0.11(2)

[a] Assumed value, see text.

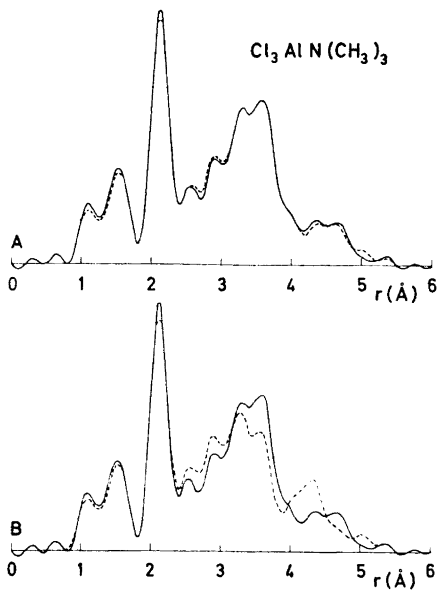

Fig. 1. A. Full line: Experimental radial distribution curve for Cl_3AlNMe_3. Stipled line: Theoretical radial distribution curve calculated for model in which the Cl atoms of the acceptor and Me groups of the donor are *staggered* with respect to rotation about the Al–N bond. B. Full line: Experimental radial distribution curve. Stipled line: Theoretical radial distribution curve calculated for model in which the Cl atoms of the acceptor and Me groups of the donor are *eclipsed* with respect to rotation about the Al–N bond. Artificial damping constant, $b=0.0025$ Å^2.

A theoretical RD-curve calculated for the best model is shown in Fig. 1 A. The good agreement between experimental and theoretical curves shows that the degree of dissociation of the complex in the gas jet must have been negligible.

Shown in Fig. 1 B is a theoretical RD-curve calculated for a model in which the Cl atoms of the acceptor eclipses the Me groups of the donor. This curve shows serious disagreement with the experimental curve in the region of the Cl···C distances and may confidently be ruled out.

The value obtained for the Al–N bond distance is in agreement with, but is considerably less accurate than the Al–N bond distance determined by X-ray crystallography, 1.96(1) Å. This bond is significantly shorter than the Al–N bond in H_3AlNMe_3, 2.06 Å, which in turn is significantly shorter than the Al–N bond in Me_3AlNMe_3, 2.10 Å. This variation probably reflects the increasing stability of these complexes with increasingly electronegative substituents in the Al atom.

With the exception of the Al–N bond distance, the structure parameters obtained in this study are more accurate than those obtained by X-ray crystallography.

The N–C bonds in the complexes X_3AlNMe_3 are longer than the N–C bond in free trimethylamine, and appears to increase in length with increasing stability of the complexes: The N–C bond in Cl_3AlNMe_3 is significantly longer than the N–C bonds in H_3AlNMe_3 and Me_3AlNMe_3, 1.476(3) Å and 1.474(3) Å, respectively, and these bonds in turn are significantly

longer than the N–C bond in free NMe_3, 1.454(2) Å.

The ∠Al–N–C angle in Cl_3AlNMe_3 is larger than the corresponding angles in H_3AlNMe_3 and Me_3AlNMe_3, 109.0(0.3)° and 109.3(0.4)°, respectively, although the difference is of marginal statistical significance. Such a difference might easily be explained as the result of encreased steric interaction between donor and acceptor due to the shortening of the Al–N bond.

The Al–Cl bond distance is in excellent agreement with the mean Al–Cl bond distance found in the crystal, 2.123 Å. Just as the N–C bond distances in the complexes X_3AlNMe_3 are longer than in free NMe_3 and appear to increase in length with increasing acceptor strength of X_3Al, so the Al–Cl bond distances in complexes of the type $Cl_3Al–L$ are longer than the Al–Cl bond in free $AlCl_3$ and appear to increase with increasing donor strength of the base L: The Al–Cl bond in Cl_3AlNMe_3 is significantly longer than the mean Al–Cl bond distance in the complex of $AlCl_3$ with propionyl chloride,[8] 2.093(3) Å, which in turn is significantly longer than the Al–Cl bond in free $AlCl_3$, 2.06 ± 0.01 Å.[9]

The shrinkage of the Cl···C(*trans*) distance was found to be 0.12(6) Å.

Acknowledgements. We are grateful to professor I. R. Beattie for a sample of Cl_3AlNMe_3 and to the *Norwegian Research Council for Science and Technology* for financial support.

1. Andersen, G. A., Forgaard, F. R. and Haaland, A. *Acta Chem. Scand.* **26** (1972) 1947.
2. Almenningen, A., Gundersen, G., Haugen, T. and Haaland, A. *Acta Chem. Scand.* **26** (1972) 3928.
3. Grant, D. F., Killean, R. C. G. and Lawrence, J. L. *Acta Cryst.* **B 25** (1969) 377.
4. Bastiansen, O., Hassel, O. and Risberg, E. *Acta Chem. Scand.* **9** (1955) 232.
5. Andersen, B., Seip, H. M., Strand, T. G. and Stölevik, R. *Acta Chem. Scand.* **23** (1969) 3224.
6. Beagley, B. and Hewitt, T. G. *Trans. Faraday Soc.* **64** (1968) 2561.
7. Seip, H. M., Strand, T. G. and Stölevik, R. *Chem. Phys. Letters* **3** (1969) 617.
8. Le Carpentier, J.-M. and Weiss, R. *Acta Cryst.* **B 28** (1972) 1437.
9. Zasorin, E. Z. and Rambidi, N. S. *J. Structural Chem.* **8** (1967) 347.

Received May 21, 1973.

Preparations of *trans*-Bis(2-picolylamine) Complexes of Chromium(III)

KIRSTEN MICHELSEN

Chemistry Department I (Inorganic Chemistry), University of Copenhagen, The H.C. Ørsted Institute, Universitetsparken 5, DK-2100 Copenhagen Ø, Denmark

In a recent paper,[1] two series of octahedral *cis*-bis(2-picolylamine) complexes of chromium were described (2-picolylamine = 2-aminomethylpyridine). The ligands in the *cis*-positions were Cl^-, Br^-, and H_2O. This paper reports the preparation of a series of the corresponding *trans*-complexes.

Only one type of geometrical isomer occurs, probably a *trans,trans,trans* isomer (Fig. 1. a). It is likely that the other imaginable isomer, the *trans,cis,cis* (Fig. 1 b), does not exist because of sterical hindrance.

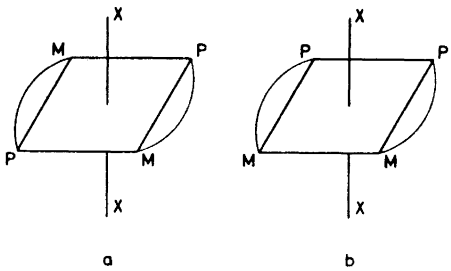

Fig. 1. The geometrical isomers of the *trans*-$[Cr(C_6H_8N_2)_2X_2]^{n+}$ ion. P symbolizes the pyridine nitrogens, M, the methylamine nitrogens. a. The *trans,trans,trans* isomer. b. The *trans,cis,cis* isomer.

The preparations are based upon the reaction between the so-called α-*cis*-$[Cr(C_6H_8N_2)_2Cl_2]Cl$[1] and moist silver oxide. The resulting solution apparently contains both *trans*- and α-*cis*-$[Cr(C_6H_8N_2)_2OH_2O]^{2+}$. By means of conc. nitric acid *trans*-$[Cr(C_6H_8N_2)_2(H_2O)_2](NO_3)_3$ is isolated from the reaction mixture and used as an initial material for *trans*-$[Cr(C_6H_8N_2)_2Cl_2]Cl$ and *trans*-$[Cr(C_6H_8N_2)_2Br_2]Br$.

The assignment of geometric configuration is based entirely upon the colours of

longer than the N–C bond in free NMe_3, 1.454(2) Å.

The ∠Al–N–C angle in Cl_3AlNMe_3 is larger than the corresponding angles in H_3AlNMe_3 and Me_3AlNMe_3, 109.0(0.3)° and 109.3(0.4)°, respectively, although the difference is of marginal statistical significance. Such a difference might easily be explained as the result of encreased steric interaction between donor and acceptor due to the shortening of the Al–N bond.

The Al–Cl bond distance is in excellent agreement with the mean Al–Cl bond distance found in the crystal, 2.123 Å. Just as the N–C bond distances in the complexes X_3AlNMe_3 are longer than in free NMe_3 and appear to increase in length with increasing acceptor strength of X_3Al, so the Al–Cl bond distances in complexes of the type $Cl_3Al–L$ are longer than the Al–Cl bond in free $AlCl_3$ and appear to increase with increasing donor strength of the base L: The Al–Cl bond in Cl_3AlNMe_3 is significantly longer than the mean Al–Cl bond distance in the complex of $AlCl_3$ with propionyl chloride,[8] 2.093(3) Å, which in turn is significantly longer than the Al–Cl bond in free $AlCl_3$, 2.06 ± 0.01 Å.[9]

The shrinkage of the Cl···C(*trans*) distance was found to be 0.12(6) Å.

Acknowledgements. We are grateful to professor I. R. Beattie for a sample of Cl_3AlNMe_3 and to the *Norwegian Research Council for Science and Technology* for financial support.

1. Andersen, G. A., Forgaard, F. R. and Haaland, A. *Acta Chem. Scand.* **26** (1972) 1947.
2. Almenningen, A., Gundersen, G., Haugen, T. and Haaland, A. *Acta Chem. Scand.* **26** (1972) 3928.
3. Grant, D. F., Killean, R. C. G. and Lawrence, J. L. *Acta Cryst.* **B 25** (1969) 377.
4. Bastiansen, O., Hassel, O. and Risberg, E. *Acta Chem. Scand.* **9** (1955) 232.
5. Andersen, B., Seip, H. M., Strand, T. G. and Stölevik, R. *Acta Chem. Scand.* **23** (1969) 3224.
6. Beagley, B. and Hewitt, T. G. *Trans. Faraday Soc.* **64** (1968) 2561.
7. Seip, H. M., Strand, T. G. and Stölevik, R. *Chem. Phys. Letters* **3** (1969) 617.
8. Le Carpentier, J.-M. and Weiss, R. *Acta Cryst.* **B 28** (1972) 1437.
9. Zasorin, E. Z. and Rambidi, N. S. *J. Structural Chem.* **8** (1967) 347.

Received May 21, 1973.

Preparations of *trans*-Bis(2-picolylamine) Complexes of Chromium(III)

KIRSTEN MICHELSEN

Chemistry Department I (Inorganic Chemistry), University of Copenhagen, The H.C. Ørsted Institute, Universitetsparken 5, DK-2100 Copenhagen Ø, Denmark

In a recent paper,[1] two series of octahedral *cis*-bis(2-picolylamine) complexes of chromium were described (2-picolylamine = 2-aminomethylpyridine). The ligands in the *cis*-positions were Cl^-, Br^-, and H_2O. This paper reports the preparation of a series of the corresponding *trans*-complexes.

Only one type of geometrical isomer occurs, probably a *trans,trans,trans* isomer (Fig. 1. a). It is likely that the other imaginable isomer, the *trans,cis,cis* (Fig. 1 b), does not exist because of sterical hindrance.

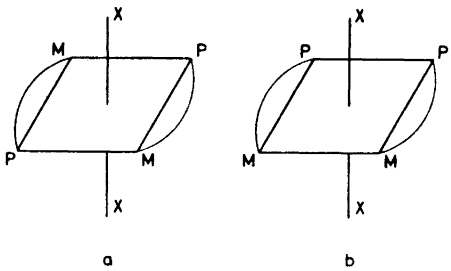

Fig. 1. The geometrical isomers of the *trans*-$[Cr(C_6H_8N_2)_2X_2]^{n+}$ ion. P symbolizes the pyridine nitrogens, M, the methylamine nitrogens. a. The *trans,trans,trans* isomer. b. The *trans,cis,cis* isomer.

The preparations are based upon the reaction between the so-called α-*cis*-$[Cr(C_6H_8N_2)_2Cl_2]Cl$[1] and moist silver oxide. The resulting solution apparently contains both *trans*- and α-*cis*-$[Cr(C_6H_8N_2)_2OH_2O]^{2+}$. By means of conc. nitric acid *trans*-$[Cr(C_6H_8N_2)_2(H_2O)_2](NO_3)_3$ is isolated from the reaction mixture and used as an initial material for *trans*-$[Cr(C_6H_8N_2)_2Cl_2]Cl$ and *trans*-$[Cr(C_6H_8N_2)_2Br_2]Br$.

The assignment of geometric configuration is based entirely upon the colours of

Table 1. Spectral data of *trans*-$[Cr\ en_2X_2]^{n+}$ and *trans*-$[Cr(C_6H_8N_2)_2X_2]^{n+}$.

X–X	Amine	$\lambda_{max}(1)$	$\varepsilon(1)$	$\lambda_{max}(2)$	$\varepsilon(2)$	$\lambda_{max}(3)$	$\varepsilon(3)$	Ref.
H_2O	en	508	22.5	442.5	29.3	361	39.2	2
H_2O	$C_6H_8N_2$	~510	~18	443.5	28.1	~360	~34	
Cl	en	578	24.5	453	22.8	396	34.0	3
Cl	$C_6H_8N_2$	578	27.1	445	24.6	393	42.1	
Br	en	607	34.9	~460	~24	406	30.7	4
Br	$C_6H_8N_2$	605	43.3	~465	~23	405	50.2	

the compounds and a comparison of their visible absorption spectra with those of known bis (ethylendiamine) analogous (Table 1).[2,3,4]

Experimental. α-*cis*-$[Cr(C_6H_8N_2)_2Cl_2]Cl.H_2O$ was prepared as described before.[1] All other reagents were reagent grade and used without further purification.

trans-*Diaquabis (2-picolylamine) chromium (III) nitrate*, $[Cr(C_6H_8N_2)_2(H_2O)_2](NO_3)_3$. 1.40 g α-*cis*$[Cr(C_6H_8N_2)_2Cl_2]Cl.H_2O$ (3.57 mmol) was added to moist silver oxide, freshly prepared from 3.0 g silver nitrate (18 mmol). After 5 min the violet solution was filtered and acidified with conc. nitric acid. During stirring and ice-cooling 250 ml ethanol (99 %) was added slowly to precipitate yellow-orange crystals of presumed *trans*-$[Cr(C_6H_8N_2)_2(H_2O)_2](NO_3)_3$. They were filtered and washed with ethanol and acetone. 0.78 g. The recrystallization was performed by dissolving the crystals in 5–6 ml boiling water, filtering and cooling on ice after the addition of 1 ml conc. nitric acid. Yield: 0.65 g (36 %) of filtered needles. (Found: Cr 10.24; C 28.3; N 19.4; H 4.40. Calc. for $[Cr(C_6H_8N_2)_2(H_2O)_2](NO_3)_3.H_2O$: Cr 10.23; C 28.4; N 19.3; H 4.36).

trans-*Dichlorobis (2-picolylamine) chromium (III) chloride*, $[Cr(C_6H_8N_2)_2Cl_2]Cl$. 1.40 g *trans*-$[Cr(C_6H_8N_2)_2(H_2O)_2](NO_3)_3.H_2O$ (2.75 mmol) was heated on a water-bath (100°) with 6–7 ml conc. hydrochloric acid. A violet solution soon formed and grey-green, shining crystals separated. After cooling on ice, they were filtered and washed with conc. hydrochloric acid and acetone. 0.65 g. The compound was recrystallized from 30 ml boiling 6 M hydrochloric acid. Washing as above. Yield: 0.54 g (47 %). (Found: Cr 12.69; C 34.6; N 13.5; Cl 25.5. Calc. for $[Cr(C_6H_8N_2)_2Cl_2]Cl.2.25H_2O$: Cr 12.52; C 34.7; N 13.5; Cl 25.6). The hydrogen analyses for this and the following compound failed to come out reproducibly).

trans-*Dibromobis (2-picolylamine) chromium (III) bromide*, $[Cr(C_6H_8N_2)_2Br_2]Br$. 1.00 g *trans*-$[Cr(C_6H_8N_2)_2(H_2O)_2](NO_3)_3.H_2O$ (1.97 mmol) was heated on a water-bath (100°) with 10 ml hydrobromic acid (48 %). A grass-green precipitate, probably *trans*-$(Cr(C_6H_8N_2)_2Br_2]Br.Br_2$ soon formed. Approx. 300 mg ascorbic acid was added and the heating continued, until the tribromide had been transformed to the more soluble, darkgreen bromide. After cooling on ice the compound was filtered and washed with ice-water and acetone. Yield 0.54 g (52 %). Recrystallization was not necessary. (Found: Cr 9.82; C 27.5; N 10.6; Br 45.7. Calc. for $[Cr(C_6H_8N_2)_2Br_2]Br.H_2O$: Cr 9.88; C 27.4; N 10.7; Br 45.6).

Electronic absorption spectra were recorded on a Cary Model 14 spectrophotometer. Data for the maxima are given in Table 1 as (λ,ε), the wavelength λ in mμ, the molar extinction coefficient ε in l mol^{-1} cm^{-1}. Medium 0.1 M hydrochloric acid.

1. Michelsen, K. *Acta Chem. Scand.* **26** (1972) 1517.
2. Woldbye, F. *Acta Chem. Scand.* **12** (1958) 1079.
3. MacDonald, D. J. and Garner, C. S. *J. Am. Chem. Soc.* **83** (1961) 4152.
4. Quinn, L. P. and Garner, C. S. *Inorg. Chem.* **3** (1964) 1348.

Received May 17, 1973.

On the Biosynthesis of Tenuazonic Acid in *Alternaria tenuis*

STEN GATENBECK and
JULIAN SIERANKIEWICZ

Department of Pure and Applied Biochemistry, The Royal Institute of Technology, S-100 44 Stockholm 70, Sweden

Tenuazonic acid (Fig. 1) was first isolated by Rosett *et al.*[1] from *Alternaria tenuis*. Its structure was established by Stickings who also showed that it is biosynthetically derived from L-isoleucine and acetate.[2,3] In an earlier publication [4] we were able to demonstrate the formation of the corresponding tetramic acids from L-valine and L-leucine after feeding the organism with the respective amino acid. Under similar conditions L-phenylalanine did not give rise to a tenuazonic acid analogue.

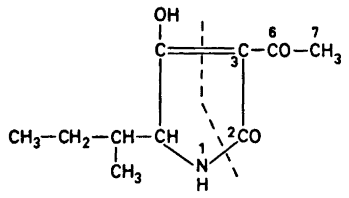

Fig. 1. Tenuazonic acid.

Very few natural tetramic acids have so far been found. One example, however, is erythroskyrine [5] isolated from *Penicillium islandicum*. This compound is derived from L-valine and acetate. In this case acetate participates in the formation of the complex side chain.

A group of substances formed according to the same biosynthetic principle as tenuazonic acid is the tetronic acids produced by *Penicillium charlesii*. In the biosynthesis of these acids the amino acids occurring in the formation of the tetramic acids are substituted with a C_4-dicarboxylic acid, presumably malate. Recently Bentley *et al.*[6] showed that the condensation partner of the C_4-acid is formed from acetate-malonate in the regular way of fatty acid synthesis.

The participation of malonate in the biosynthesis of tenuazonic acid and the possible formation of an initially long side chain which has been oxidatively degraded by the organism to the acetyl group will be considered in this publication.

There are two theoretical alternatives for the sequence of condensations between the active forms of L-isoleucine, and the appropiate β-keto acid. In one of them the carboxyl group of isoleucine first condenses with the α-methylene group of the β-keto acid and then follows the ring closure by the amide formation between the α-amino group of isoleucine and the carboxyl group of the β-keto acid. In the other alternative the amide formation precedes the reaction between the isoleucine carboxyl group and the α-methylene group of the β-keto acid which now completes the tetramic acid structure. Experiments that support the first alternative will be presented.

Experimental. The fermentation of *Alternaria tenuis* CMI 89343 was carried out in modified Czapek-Dox medium as described earlier.[4]

Incorporation of malonate-1-^{14}C. To each of two flasks 40 mg of L-isoleucine was added 68 h after incubation of the organism. After another 3 h 10 mg of L-isoleucine and 25 μCi of sodium malonate-1-^{14}C in trace amounts were added. The organism was exposed to the radioactive precursor for 24 h before the tenuazonic acid was isolated as the copper salt. The labeled product was diluted with 220 mg cold carrier by recrystallization to constant specific radioactivity from methanol/water. Yield 160 mg. Specific radioactivity of Cu-tenuazonate 2.1×10^5 dpm/mmol; Incorporation 0.2 %.

Incorporation of acetate-1-^{14}C and butyrate-1-^{14}C. Samples of radioactive tenuazonic acid were prepared as described above from 25 μCi of sodium acetate-1-^{14}C and 50 μCi of sodium butyrate-1-^{14}C, respectively.

Degradation of labeled tenuazonic acid. Specific radioactivities of the acids were determined on $BaCO_3$ obtained by trapping in $Ba(OH)_2$ the CO_2 evolved on wet-combustion according to van Slyke and Folch.[7] The radioactivities were measured in a liquid scintillation spectrometer (Packard model 3375) in toluene solution of PPO and POPOP after suspending the $BaCO_3$ with the aid of Cabosil gel. The labeled acids were hydrolysed by refluxing in M H_2SO_4 for 5 h as described by Stickings.[3] The CO_2 obtained from position 2 was trapped in $Ba(OH)_2$. The acetic acid derived from C-6 and C-7 was isolated by steam distillation and neutralization with NaOH. By decarboxylation of the sodium acetate in the Schmidt reaction [8] and transferring the CO_2 into $BaCO_3$ the

Table 1. Distribution of radioactivity in labeled samples of tenuazonic acid.

Labeled precursor	Tenuazonic acid	Dpm/mmol C-2	C-6	C-6/C-2
Malonate-1-^{14}C	10.4×10^4	5.1×10^4	4.8×10^4	0.94
Acetate		2.2×10^5	2.0×10^5	0.91
Butyrate-1-^{14}C		9.3×10^6	2.5×10^6	0.27
Butyrate-1-^{14}C		2.3×10^6	0.5×10^6	0.22

radioactivity of the C-6 position was determined. The specific radioactivities of the tenuazonic acid samples actually used for degradation, and the various degradation products, are shown in Table 1.

Trapping of radioactive N-*acetoacetyl-*L-*isoleucine.* To each of two fermentation flasks 40 mg of L-isoleucine and 100 μCi of aqueous sodium acetate were added. After 8 h exposure to the radioactive precursor the mycelium was separated from the culture medium by filtration. Acidification and subsequent extraction of the filtrate with ether yielded a radioactive solution which was dried over anhydrous Na_2SO_4 and then evaporated to dryness. The mycelium was ground with sand in acetone. The acetone solution was evaporated to dryness and the residue pooled with the extract from the culture medium. This mixture together with 100 mg of *N*-acetoacetyl-L-isoleucine (synthesized as described by Harris *et al.*[9]) were dissolved in hot benzene, treated with active carbon and filtered while still hot. The *N*-acetoacetyl derivative was recrystallized to constant specific radioactivity (3220 dpm/mg). The incorporation of radioactivity into isolated *N*-acetoacetyl-L-isoleucine was 0.07 %.

The described experiment was repeated with *N*-acetyl-L-isoleucine, instead of *N*-acetoacetyl-L-isoleucine. In this case the radioactivity was rapidly lost on recrystallizations.

Results and discussion. If the carbon atoms in positions 2 and 3 were derived from malonate and those in positions 6 and 7 from acetate an uneven labelling would be expected in positions 6 and 2 when malonate-1-^{14}C is fed to the organism. From Table 1 is seen that the specific radioactivities in these positions are almost equal which indicates that malonate as such is not involved in the biosynthesis of tenuazonic acid unless a very active malonate decarboxylase system is present in the organism. The slightly lower radioactivity in C-6 compared to C-2 depends on the experimental conditions in the degradation procedure as it is also observed in tenuazonic acid obtained from labeled acetate.

The incorporation of the intact butyric acid molecule into tenuazonic acid confirms the conclusion that malonate is not involved in the biosynthesis as well as it indicates that the acetyl group at 3 position has not been part of a longer side chain. Acetoacetyl-coenzyme A formed in the thiolase reaction is the suggested origin of the positions C-2, C-3, C-6, and C-7 of the tenuazonic acid. It is surprising that the added butyric acid appears without cleavage to the observed extent in the tenuazonic acid structure. The localizations of the involved reactions inside the cell become an intriguing question.

The demonstration of the occurrence of *N*-acetoacetyl-L-isoleucine in the organism indicates that the initial step in the biosynthesis of tenuazonic acid is *N*-acetoacetylation of L-isoleucine followed by formation of the five-membered ring.

This investigation was supported by a research grant from *The Swedish Natural Science Research Council.*

1. Rosett, T., Sankhala, R. H., Stickings, C. E., Taylor, M. E. U. and Thomas, R. *Biochem. J.* **67** (1957) 390.
2. Stickings, C. E. *Biochem. J.* **72** (1959) 332.
3. Stickings, C. E. and Towsend, R. J. *Biochem. J.* **78** (1961) 412.
4. Gatenbeck, S. and Sierankiewicz, J. *Antimicrob. Agents Chemother.* **3** (1973) 308.
5. Shibata, S., Sankawa, U., Taguchi, H. and Yamasaki, K. *Chem. Pharm. Bull.* **14** (5) (1966) 474.

6. Bentley, R., Bhate, D. S. and Keil, J. G. *J. Biol. Chem.* **237** (1962) 859.
7. Van Slyke, D. D. and Folch, J. *J. Biol. Chem.* **136** (1940) 509.
8. Phares, E. F. *Arch. Biochem. Biophys.* **33** (1951) 173.
9. Harris, S. A., Fisher, L. V. and Folkers, K. *J. Med. Chem.* **8** (1965) 478.

Received May 18, 1973.

Crystallographic and Structural Data of Three Thallium(I) Compounds

STEINAR ESPERÅS and STEINAR HUSEBYE

Chemical Institute, University of Bergen, 5000 Bergen, Norway

The crystal structures of diethylthioselenophosphinatothallium(I), [Tl(Et_2PSeS)], and diethyldithiophosphinatothallium(I), [Tl(Et_2PS_2)], have been determined by three-dimensional X-ray methods. Space group and unit cell have further been determined for diethyldiselenophosphinatothallium(I), [Tl(Et_2PSe_2)].

The crystals of [Tl(Et_2PSeS)] (I) are colourless prisms elongated along the *c* axis. The structure is monoclinic with cell dimensions $a = 10.342(3)$ Å, $b = 9.116(3)$ Å, $c = 10.154(2)$ Å, $\beta = 101.98(2)°$, and $Z = 4$. Possible space groups were $C2$, Cm, and $C2/m$.

The intensity data of 997 reflections greater than background were recorded by means of a Siemens AED-1 single crystal diffractometer, using Mo$K\alpha$-radiation. The crystal structure was solved by a three-dimensional Patterson synthesis. The map could only be interpreted in terms of a dimeric complex. In the centric space group, $C2/m$, which was the first choice and which proved to be the correct one, the dimers occupy special twofold positions with the Tl atoms on a twofold axis parallel to *b* and the Se, S, and P atoms lying in a mirror plane halfway between the two Tl atoms at right angles to *b*. The structure was refined by full-matrix least squares methods to an *R*-value of 0.088. Attempts to refine the structure in the non-centric alternative space groups were not successful.

The crystals of [Tl(Et_2PS_2)] (II) are thin colourless plates with $a = 9.026(3)$ Å, $b = 12.134(2)$ Å, $c = 8.468(3)$ Å, and $Z = 4$. The crystals are orthorhombic with the space group $Pcca$, which requires that the molecules occupy fourfold special positions.

Intensities were estimated visually from Weissenberg photographs taken with Ni-filtered Cu$K\alpha$-radiation using the multiple film technique. 376 out of 507 independent reflections from the five layers $hk0 - hk3$ and $0kl$ were observed and measured. The structure was solved by three-dimensional Patterson and Fourier syntheses. The Tl and P atoms lie on a twofold axis. The atomic parameters were refined by least squares methods to an *R*-value of 0.094.

The crystals of [Tl(Et_2PSe_2)] form extremely thin colourless monoclinic prisms extended along the *b* axis, with $a = 11.731(7)$ Å, $b = 6.741(3)$ Å, $c = 13.091(4)$ Å, $\beta = 111.71(3)°$, and $Z = 4$. The space group is $P2_1/c$. During exposure to X-rays, the crystal surface became gradually covered by a yellow powder. This happened also to the two former complexes, but to a lesser degree. This effect together with the crystal size made a structure solution difficult.

Thallium (I) compounds have a tendency to occur as polymers in the solid state.

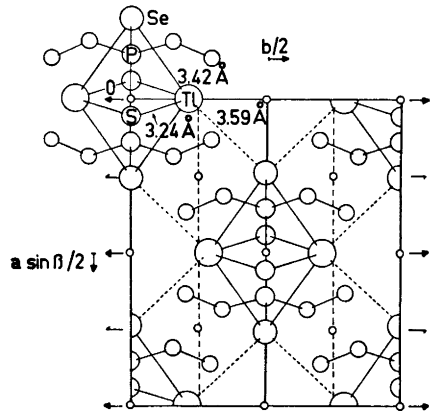

Fig. 1. The arrangement of the [Tl(Et_2PSeS)]$_2$ dimers in the unit cell as seen along the *c* axis.

6. Bentley, R., Bhate, D. S. and Keil, J. G. *J. Biol. Chem.* **237** (1962) 859.
7. Van Slyke, D. D. and Folch, J. *J. Biol. Chem.* **136** (1940) 509.
8. Phares, E. F. *Arch. Biochem. Biophys.* **33** (1951) 173.
9. Harris, S. A., Fisher, L. V. and Folkers, K. *J. Med. Chem.* **8** (1965) 478.

Received May 18, 1973.

Crystallographic and Structural Data of Three Thallium(I) Compounds

STEINAR ESPERÅS and STEINAR HUSEBYE

Chemical Institute, University of Bergen, 5000 Bergen, Norway

The crystal structures of diethylthioselenophosphinatothallium(I), [Tl(Et_2PSeS)], and diethyldithiophosphinatothallium(I), [Tl(Et_2PS_2)], have been determined by three-dimensional X-ray methods. Space group and unit cell have further been determined for diethyldiselenophosphinatothallium(I), [Tl(Et_2PSe_2)].

The crystals of [Tl(Et_2PSeS)] (I) are colourless prisms elongated along the *c* axis. The structure is monoclinic with cell dimensions $a = 10.342(3)$ Å, $b = 9.116(3)$ Å, $c = 10.154(2)$ Å, $\beta = 101.98(2)°$, and $Z = 4$. Possible space groups were $C2$, Cm, and $C2/m$.

The intensity data of 997 reflections greater than background were recorded by means of a Siemens AED-1 single crystal diffractometer, using Mo$K\alpha$-radiation. The crystal structure was solved by a three-dimensional Patterson synthesis. The map could only be interpreted in terms of a dimeric complex. In the centric space group, $C2/m$, which was the first choice and which proved to be the correct one, the dimers occupy special twofold positions with the Tl atoms on a twofold axis parallel to *b* and the Se, S, and P atoms lying in a mirror plane halfway between the two Tl atoms at right angles to *b*. The structure was refined by full-matrix least squares methods to an *R*-value of 0.088. Attempts to refine the structure in the non-centric alternative space groups were not successful.

The crystals of [Tl(Et_2PS_2)] (II) are thin colourless plates with $a = 9.026(3)$ Å, $b = 12.134(2)$ Å, $c = 8.468(3)$ Å, and $Z = 4$. The crystals are orthorhombic with the space group $Pcca$, which requires that the molecules occupy fourfold special positions.

Intensities were estimated visually from Weissenberg photographs taken with Ni-filtered Cu$K\alpha$-radiation using the multiple film technique. 376 out of 507 independent reflections from the five layers $hk0 - hk3$ and $0kl$ were observed and measured. The structure was solved by three-dimensional Patterson and Fourier syntheses. The Tl and P atoms lie on a twofold axis. The atomic parameters were refined by least squares methods to an *R*-value of 0.094.

The crystals of [Tl(Et_2PSe_2)] form extremely thin colourless monoclinic prisms extended along the *b* axis, with $a = 11.731(7)$ Å, $b = 6.741(3)$ Å, $c = 13.091(4)$ Å, $\beta = 111.71(3)°$, and $Z = 4$. The space group is $P2_1/c$. During exposure to X-rays, the crystal surface became gradually covered by a yellow powder. This happened also to the two former complexes, but to a lesser degree. This effect together with the crystal size made a structure solution difficult.

Thallium (I) compounds have a tendency to occur as polymers in the solid state.

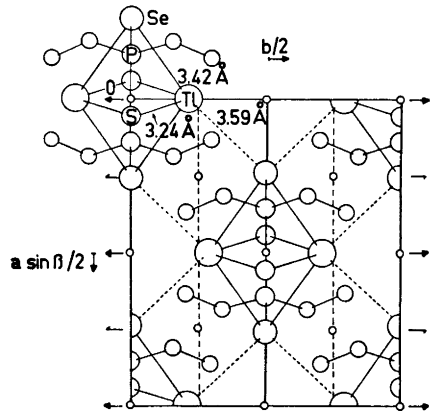

Fig. 1. The arrangement of the [Tl(Et_2PSeS)]$_2$ dimers in the unit cell as seen along the *c* axis.

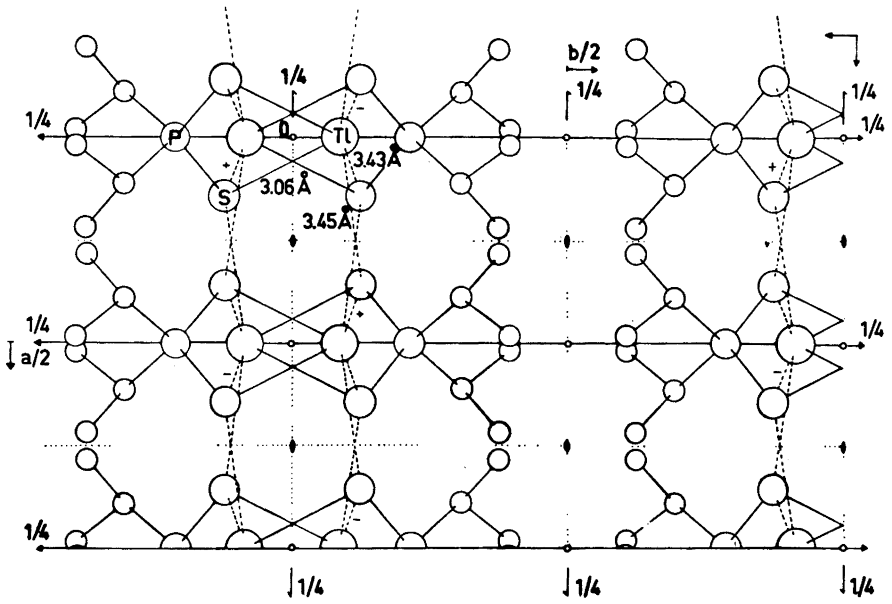

Fig. 2. The arrangement of the $[Tl(Et_2PS_2)]$ molecules in the unit cell as seen along the *c* axis. Tl—S bonds labelled plus or minus represent bonds to sulphur atoms one unit cell above or beneath the original one, respectively.

From Fig. 1 it is seen that complex I can be regarded as built up from dimeric units, $[Tl(Et_2PSeS)]_2$. In this dimer, both ligands are shared equally between the two thallium atoms, so that each sulphur and selenium atom in addition to being bonded to phosphorus also is bonded to both metal atoms. The resulting planar Tl_2S_2 and Tl_2Se_2 parallelograms are nearly at right angles to each other. The dimers are knit together into two-dimensional layers parallel to the *ab*-plane, through weak intermolecular Tl—Se bonds.

Each thallium atom is bonded to two sulphur and two selenium atoms in the dimer and to two more distant selenium atoms belonging to different neighbour dimers. The coordination is best described as a distorted trigonal prism. Analogous configurations are found in dipropyldithiocarbamatothallium(I) [1] and in dibutyldithiocarbamatocaesium(I).[2]

A schematic view of the crystal structure of $[Tl(Et_2PS_2)]$ is shown in Fig. 2. The structure is best described as monomers linked together in two-dimensional polymeric layers parallel to the *ac*-plane. Each metal atom is coordinated by six sulphur atoms situated at the corners of a distorted trigonal prism. Two of these sulphur atoms belong to the molecule proper, the remaining four more distant ones belong to four different adjacent molecules.

A general feature of the two complexes is the large Tl—S and Tl—Se bond lengths. This is not surprising in view of the bridging nature of the sulphur and selenium atoms, and the largely ionic bonding.[1,3] The intramolecular Tl—S bond lengths of 3.237(5) Å and 3.056(7) Å found in I and II, respectively, and the weak intermolecular Tl—S bonds of 3.429(10) Å and 3.453(7) Å found in II are of the same order of magnitude as those found in other complex Tl(I) compounds.[1,3-7] The Tl—Se bond in I of 3.424(4) Å is relatively weaker than Tl—S bond in I, as the difference in bond length is larger than the difference in the selenium and sulphur covalent radii. This is not unexpected as only selenium atoms are engaged in dimer-dimer interactions. The weak intermolecular Te-Se bond is found to be 3.594(3) Å.

Coordinates with standard deviations in

parentheses for the atoms in the asymmetric unit for complex I and II are listed in Table 1.

Table 1. Atomic coordinates.

	I		
	x	*y*	*z*
Tl	0.0	0.2117(2)	0.0
Se	−0.2578(4)	0.0	0.0533(5)
S	0.0551(6)	0.0	0.2616(7)
P	−0.1441(8)	0.0	0.2521(9)
C_1	−0.188(3)	0.157(4)	0.351(3)
C_2	−0.135(4)	0.298(4)	0.317(4)

	II		
	x	*y*	*z*
Tl	0.0	0.0858	0.25
S	0.1407(7)	−0.1251(5)	0.1219(12)
P	0.0	−0.2132(6)	0.25
C_1	0.111(3)	−0.306(2)	0.386(4)
C_{21}[a]	0.216(7)	−0.375(5)	0.323(10)
C_{22}[a]	0.019(7)	−0.395(5)	0.461(12)

[a] Methyl carbon positions in the disordered ethyl group.

Acknowledgement. The authors thank Dr. Wilhelm Kuchen, Institut für Anorganische Chemie der Universität Düsseldorf, for samples of crystals.

1. Nilson, L. and Hesse, R. *Acta Chem. Scand.* **23** (1969) 1951.
2. Aava, U. and Hesse, R. *Arkiv Kemi* **30** (1969) 149.
3. Boeyens, J. C. A. and Herbstein, F. H. *Inorg. Chem.* **4** (1967) 1408.
4. Verhoef, L. H. W. and Boyens, J. C. A. *Acta Cryst.* **B 24** (1968) 1262.
5. Verhoef, L. H. W. and Boeyens, J. C. A. *Acta Cryst.* **B 25** (1969) 607.
6. Hahn, H. and Klinger, W. *Z. Anorg. Allgem. Chem.* **260** (1949) 110.
7. Ohmasa, M. and Nowacki, W. *Z. Krist.* **134** (1971) 360.

Received May 23, 1973.

Bicyclic Enamines

VII. Attempted Thermal Rearrangement of 3-Methoxycarbonylbicyclo[2,2,2]oct-2-ene*

MAHDI M. AL HOLLY,** KARL-HENRIK HASSELGREN and J. LARS G. NILSSON

Faculty of Pharmacy, University of Uppsala, Uppsala, Sweden

Recently we reported that unsaturated quinuclidine-3-carboxylic acid esters[1,2] were rearranged to lactones of type *2* when heated for a few seconds at about 150°. Similarly, we observed that amides corresponding to *1* under such conditions gave imino lactones.[3] To study if similar

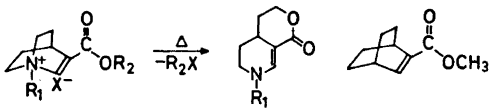

1 2 3

rearrangements also occurred in other bicyclic systems, we have now synthesized the bicyclo[2,2,2]oct-2-ene carboxylate *3* and heated this compound to 200° for 15 h. We found that *3* was stable under these conditions.

The rearrangement of *1* to *2* was originally interpreted as a sigmatropic rearrangement.[2] However, the thermal stability of *3* may indicate that other mechanisms are involved in the formation of the lactone *2*, since sigmatropic rearrangements are likely to occur in both compounds *1* and *3*.

Experimental. General comment. Melting points were determined with calibrated Anschütz thermometers in an electrically heated metal block. IR-spectra were recorded using a Perkin-Elmer 457 spectrophotometer and the NMR-spectra were measured with a Varian A 60 instrument using $CDCl_3$ solutions.

* Part VI of this series: Dolby, J., Hasselgren, K.-H., Castensson, S. and Nilsson, J. L. G. *Acta Chem. Scand.* **26** (1972) 2469.

** Present address: Chemistry Department, University of Baghdad, Science College, Athamia, Baghdad, Iraq.

Chemical shifts are expressed in δ ppm relative to tetramethylsilane. Mass spectra were obtained using an AEI 30 instrument at 70 eV.

2-Cyano-2-hydroxybicyclo[2,2,2]octane. To a solution of bicyclo[2,2,2]octane-2-one [4] (7 g; 56 mmol) in ether (30 ml) and saturated aqueous solution of potassium cyanide (3.9 g; 56 mmol), 1 N HCl solution (80 ml) was added dropwise with stirring at room temperature. The reaction mixture was then stirred for 60 min. The ether layer was separated, and the aqueous solution was extracted with ether (3 × 20 ml). The combined ethereal solution was washed with water, dried ($MgSO_4$) and evaporated under reduced pressure. The white solid residue had m.p. 145–146° (from hexane), 8.3 g; 99 % yield. ν_{max} (KBr) 3250 cm^{-1} (OH), 2225 cm^{-1} (CN). (Found: C 71.4; H 8.4; N 9.2. Calc. for $C_9H_{13}NO$: C 71.4; H 8.4; N 9.2.)

2-Carbamoyl-2-hydroxybicyclo[2,2,2]octane. The above cyanohydrin (8.3 g; 55 mmol) was mixed with conc. HCl (100 ml) and kept for 17 h at room temperature. The white solid formed was filtered off and more product was obtained by ether extraction of the filtrate. The product (10 g; 75 % yield) had m.p. 147–148° (from methanol). ν_{max} (KBr) 3360 cm^{-1} (OH), 3275 and 3195 cm^{-1} (NH_2) and 1650 and 1600 cm^{-1} (CO). Mass spectrum showed a molecular ion peak at *m/e* 169. (Found: C 63.4; H 9.1; N 8.3. Calc. for $C_9H_{15}NO_2$: C 63.9; H 8.9; N 8.3.)

2-Hydroxy-2-methoxycarbonylbicyclo[2,2,2]-octane. A mixture of the above amide (10 g; 58 mmol), methanol (25 ml) and conc. HCl (10 ml) was refluxed for 4 h. The cooled reaction mixture was evaporated under vacuum and the residue (oil) was distilled to give a colorless liquid, b.p. 61–68°/0.05 mmHg. (9 g; 90 % yield). ν_{max} (film) 3400 cm^{-1} (OH), 1715 cm^{-1} (CO) and 1225 cm^{-1} (–COC–). Mass spectrum showed a molecular ion peak at *m/e* 184. (Found: C 65.2; H 8.7. Calc. for $C_{10}H_{16}O_3$: C 65.2; H 8.8.)

2-Methoxycarbonyl-bicyclo[2,2,2]oct-2-ene. A solution of the above hydroxy ester (1 g; 6 mmol) in purified thionyl chloride (15 ml) was refluxed for 15 h. The excess thionyl chloride was evaporated under vacuum at room temperature and the oily residue was purified by thick layer chromatography (silica gel plates in light petroleum/ether; 9:1) which gave a colorless liquid (625 mg; 72 % yield). ν_{max} (film) 3020 (C=C–H), 1710 cm^{-1} (C=O), 1615 (C=C), and 1220 cm^{-1} (COC). Mass spectrum showed a molecular ion peak at *m/e* 166. (Found: C 72.0; H 8.5. Calc. for $C_{10}H_{14}O_2$: C 72.3; H 8.5.) NMR δ = 7.1 and 7.2 (d, together 1H, C=C–H, $J \sim 2$ cps) 3.63 ppm (s, 3H, O–CH_3), and 1.15–1.64 ppm (m, 10 H, aliphatic protons).

Heating of 3-methoxycarbonyl-bicyclo[2,2,2]-oct-2-ene. The unsaturated ester *3* was heated without solvent, in a sealed tube (under N_2 gas), at 200° (oil bath) for 15 h. Samples were taken out periodically and checked by TLC, IR, and NMR. The compound showed a thermal stability under these conditions.

Acknowledgement. A fellowship to M. M. Al Holly from the International Seminar in Physic and Chemistry at Uppsala University is greatly acknowledged. This work has also been supported by the *Swedish Natural Science Research Council.*

1. Dolby, J., Dahlbom, R., Hasselgren, K.-H. and Nilsson, J. L. G. *Acta Chem. Scand.* **25** (1971) 735.
2. Hasselgren, K.-H., Dolby, J. and Nilsson, J. L. G. *Tetrahedron Letters* **1971** 2917.
3. Dolby, J., Hasselgren, K.-H. and Nilsson, J. L. G. *Heterocycl. Chem.* **8**, (1971) 663.
4. Kruas, W. *Chem. Ber.* **97** (1964) 2726.

Received June 15, 1973.

Correction to "Mass Spectrometry of Onium Compounds. Part XIII."*

REIDAR LIE and KJELL UNDHEIM

Department of Chemistry University of Oslo, Oslo 3, Norway

In the structural formulas for compounds XIV a,b–XVII a,b R^5 and R^8 must be interchanged.

Received May 21, 1973.

* *Acta Chem. Scand.* **26** (1972) 3459.

The Phase Diagram of the System Cs_3AlF_6-Li_3AlF_6

M. AMORASIT,* B. JENSSEN HOLM and J. L. HOLM

Institute of Inorganic Chemistry, The University of Trondheim, N-7034 Trondheim-NTH, Norway

This work is a part of the phase investigations in binary systems of the type $M_3^IAlF_6 - M_3^{II}AlF_6$ (M = alkali metal), which were started by Holm [1] (1963) and later carried on by Holm and Jenssen Holm [2] (1970).

In the series $M_3AlF_6 - Li_3AlF_6$ we have earlier examined the systems $Na_3AlF_6 - Li_3AlF_6$,[2] $K_3AlF_6 - Li_3AlF_6$, and $Rb_3AlF_6 - Li_3AlF_6$.[3] This series is now concluded with an examination of the system $Cs_3AlF_6 - Li_3AlF_6$.

Experimental. Materials. AlF_3; aluminium fluoride, anhydrous (Mac Kay, USA) was sublimated twice in a vacuum furnace at 910°C. The method used has been described by Henry and Dreisbach.[4] Pure crystals were picked out from the product and used for these experiments. CsF; anhydrous CsF, 99.9 %, (Schuchardt, München, Germany), and LiF; anhydrous LiF (Baker Analyzed reagent, Deventer, Holland) were purified by melting in a platinum crucible under nitrogen atmosphere, and pure crystals were selected for the preparation of cesium and lithium cryolites. All handling of CsF was done in a dry box. For the preparation of Li_3AlF_6 and Cs_3AlF_6, stoichiometric amounts of the alkali fluoride and aluminium fluoride were mixed in the dry box and melted in a platinum crucible under nitrogen atmosphere at a temperature of 790°C for Li_3AlF_6 and 820°C for Cs_3AlF_6.

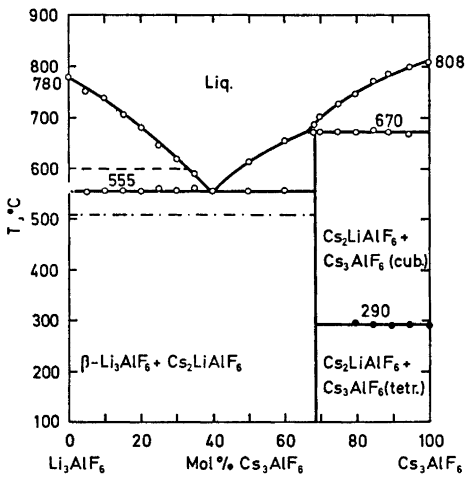

Fig. 1. The phase diagram of the system, $Cs_3AlF_6 - Li_3AlF_6$. ○, liquid-solid transitions; ●, Cs_3AlF_6(tetr) ⇌ Cs_3AlF_6(cubic); dotted line, Li_3AlF_6(tetr) → Li_3AlF_6(cubic);[6] dash-dotted line, Li_3AlF_6(orthorhombic) → Li_3AlF_6(tetr).[6]

* Present address: Department of Chemistry, Faculty of Science, Chulalongkorn University, Bangkok, Thailand.

Table 1. X-Ray data for the compound Cs_2LiAlF_6 at 25°C.

h k l	Int.	$\sin^2\theta_{obs.} \times 10^4$	$\sin^2\theta_{calc.} \times 10^4$	$d(hkl)_{obs.}$
1 1 0	w	203	206	5.40
1 1 1	vs	439	444	3.67
2 0 0	s	614	616	3.11
2 2 0	m	819	823	2.691
0 0 2	s	949	954	2.501
2 2 1	s	1057	1061	2.370
1 1 2	w	1155	1160	2.256
3 1 0	w	1434	1438	2.034
2 0 2	w	1565	1571	1.947
3 1 1	m	1672	1677	1.883
2 2 2	vw	1773	1777	1.829
3 3 0	s	1853	1854	1.789

vs = very strong, s = strong, m = medium, w = weak, and vw = very weak

The composition was checked by DTA, and adjusted by addition of AlF_3 if necessary.

The experimental methods and equipment used during the investigation (DTA, X-ray and density measurements) were the same as described previously.[2,3,5]

Results and discussion. The phase diagram is presented in Fig. 1. The experimental points were obtained from DTA cooling curves. The phase diagram of this system is similar to the two systems $Li_3AlF_6-K_3AlF_6$ and $Li_3AlF_6-Rb_3AlF_6$.[3] The system contains one incongruently melting compound, $2Cs_3AlF_6.Li_3AlF_6$, corresponding to Cs_2LiAlF_6. A peritectic point was found at 670°C and 85.5 mol % Cs_3AlF_6 while a eutectic point was established at 555°C and 40 mol % Cs_3AlF_6.

A preliminary investigation of the structure of the compound Cs_2LiAlF_6 was carried out. The X-ray data for the compound Cs_2LiAlF_6 are given in Table 1. Single crystal X-ray diffraction analysis indicated that the compound has an orthorhombic structure with a C-centered lattice and the cell constants $a=6.21\pm0.04$ Å; $b=10.72\pm0.03$ Å; $c=4.99\pm0.01$ Å. This gives a calculated density of 4.14 g cm^{-3} (2 formula units in the cell) compared to a measured value at 25°C of 4.04 g cm^{-3}.

Acknowledgements. One of the authors (M.A.) was supported during his stay in Norway by a fellowship from NORAD. The *Royal Norwegian Council for Scientific and Industrial Research* is thanked for financial support.

1. Holm, J. L. *Undersøkelser av struktur og faseforhold for en del systemer med tilknytning til aluminiumelektrolysen*, Lic. Thesis, Institute of Inorganic Chemistry, NTH, Trondheim 1963.
2. Holm, J. L. and Jenssen Holm, B. *Acta Chem. Scand* **24** (1970) 2535.
3. Grjotheim, K., Holm, J. L., Malinovský, M. and Mikhaiel, S. A. *Acta Chem. Scand.* **25** (1971) 1695.
4. Henry, J. L. and Dreisbach, S. H. *J. Am. Chem. Soc.* **81** (1959) 5274.
5. Holm, J. L. and Jenssen Holm, B. *Thermochim. Acta* **5** (1973) 273.
6. Holm, J. L. and Jenssen Holm, B. *Acta Chem. Scand.* **23** (1969) 1065.

Received May 8, 1973.

Perchlorate and Fluoride Complexes of Thallium(I) in Aqueous Solution

LARS JOHANSSON

Division of Inorganic Chemistry 1, Chemical Center, P.O. Box 740, S-220 07 Lund 7, Sweden

When weak complex systems are investigated in perchlorate media, different experimental methods may give different apparent stability constants, if the perchlorate ion is not completely inert but forms a complex with the central ion.[1] Central ion measurements, in a wide sense, give lower values of the stability constants than do ligand measurements. In the extreme case, when the perchlorate complex is stronger than that of the ligand studied, central ion measurements may give negative apparent constants. The Tl^+-F^- system appears to behave in this manner. The system has been previously studied with potentiometric and polarographic methods.[2-4] As the effects observed are small, it might be argued that they are caused mainly or in part by changes, at constant ionic strength, in liquid junction potentials and activity coefficients. Such changes are, however, not likely to be the same for different methods. Therefore, in the present work, the system has been studied with other methods than those used earlier, *viz.* two solubility methods, the first being, in effect, a central ion measurement, the second a ligand measurement. The measurements have been carried out at 25°C in a $NaClO_4$ medium of $I=0.5$, where

$$I=[L]+[A] \quad (1)$$

L and A denote fluoride and perchlorate ion, respectively.

Solubility of $TlIO_3(s)$. Solutions in the range $0\leq[L]\leq 0.5$ M were saturated in a column with $TlIO_3(s)$, and analyzed for IO_3^- by the thiosulphate method.[5] The solubilities could be reproduced within 1%.

In a separate experiment, IO_3^- but no F^- was added. The solubility, S, then was inversely proportional to $[IO_3^-]$. Thus, no

Table 1. Solubility of $TlIO_3(s)$: [L]/M, $S\times10^3$/M; 0.000, 3.289; 0.100, 3.245; 0.200, 3.219; 0.300, 3.159; 0.400, 3.107; 0.500, 3.057.

The composition was checked by DTA, and adjusted by addition of AlF_3 if necessary.

The experimental methods and equipment used during the investigation (DTA, X-ray and density measurements) were the same as described previously.[2,3,5]

Results and discussion. The phase diagram is presented in Fig. 1. The experimental points were obtained from DTA cooling curves. The phase diagram of this system is similar to the two systems $Li_3AlF_6-K_3AlF_6$ and $Li_3AlF_6-Rb_3AlF_6$.[3] The system contains one incongruently melting compound, $2Cs_3AlF_6.Li_3AlF_6$, corresponding to Cs_2LiAlF_6. A peritectic point was found at 670°C and 85.5 mol % Cs_3AlF_6 while a eutectic point was established at 555°C and 40 mol % Cs_3AlF_6.

A preliminary investigation of the structure of the compound Cs_2LiAlF_6 was carried out. The X-ray data for the compound Cs_2LiAlF_6 are given in Table 1. Single crystal X-ray diffraction analysis indicated that the compound has an orthorhombic structure with a C-centered lattice and the cell constants $a=6.21\pm0.04$ Å; $b=10.72\pm0.03$ Å; $c=4.99\pm0.01$ Å. This gives a calculated density of 4.14 g cm^{-3} (2 formula units in the cell) compared to a measured value at 25°C of 4.04 g cm^{-3}.

Acknowledgements. One of the authors (M.A.) was supported during his stay in Norway by a fellowship from NORAD. The *Royal Norwegian Council for Scientific and Industrial Research* is thanked for financial support.

1. Holm, J. L. *Undersøkelser av struktur og faseforhold for en del systemer med tilknytning til aluminiumelektrolysen*, Lic. Thesis, Institute of Inorganic Chemistry, NTH, Trondheim 1963.
2. Holm, J. L. and Jenssen Holm, B. *Acta Chem. Scand* **24** (1970) 2535.
3. Grjotheim, K., Holm, J. L., Malinovský, M. and Mikhaiel, S. A. *Acta Chem. Scand.* **25** (1971) 1695.
4. Henry, J. L. and Dreisbach, S. H. *J. Am. Chem. Soc.* **81** (1959) 5274.
5. Holm, J. L. and Jenssen Holm, B. *Thermochim. Acta* **5** (1973) 273.
6. Holm, J. L. and Jenssen Holm, B. *Acta Chem. Scand.* **23** (1969) 1065.

Received May 8, 1973.

Perchlorate and Fluoride Complexes of Thallium(I) in Aqueous Solution

LARS JOHANSSON

Division of Inorganic Chemistry 1, Chemical Center, P.O. Box 740, S-220 07 Lund 7, Sweden

When weak complex systems are investigated in perchlorate media, different experimental methods may give different apparent stability constants, if the perchlorate ion is not completely inert but forms a complex with the central ion.[1] Central ion measurements, in a wide sense, give lower values of the stability constants than do ligand measurements. In the extreme case, when the perchlorate complex is stronger than that of the ligand studied, central ion measurements may give negative apparent constants. The Tl^+-F^- system appears to behave in this manner. The system has been previously studied with potentiometric and polarographic methods.[2-4] As the effects observed are small, it might be argued that they are caused mainly or in part by changes, at constant ionic strength, in liquid junction potentials and activity coefficients. Such changes are, however, not likely to be the same for different methods. Therefore, in the present work, the system has been studied with other methods than those used earlier, *viz.* two solubility methods, the first being, in effect, a central ion measurement, the second a ligand measurement. The measurements have been carried out at 25°C in a $NaClO_4$ medium of $I=0.5$, where

$$I=[L]+[A] \quad (1)$$

L and A denote fluoride and perchlorate ion, respectively.

Solubility of $TlIO_3(s)$. Solutions in the range $0\leq[L]\leq 0.5$ M were saturated in a column with $TlIO_3(s)$, and analyzed for IO_3^- by the thiosulphate method.[5] The solubilities could be reproduced within 1%.

In a separate experiment, IO_3^- but no F^- was added. The solubility, S, then was inversely proportional to $[IO_3^-]$. Thus, no

Table 1. Solubility of $TlIO_3(s)$: [L]/M, $S\times10^3$/M; 0.000, 3.289; 0.100, 3.245; 0.200, 3.219; 0.300, 3.159; 0.400, 3.107; 0.500, 3.057.

complexes containing IO_3^- are likely to be formed. It is assumed that the only complexes formed are ML and MA (stability constants β_1 and γ_1, respectively). Thus

$$S = [IO_3^-] = [M] + [ML] + [MA] \quad (2)$$

and the following equation applies

$$(S/S_0)^2 = 1 + \beta_1(1)[L] \quad (3)$$

where S_0 is the solubility when $[L] = 0$, and

$$\beta_1(1) = \frac{\beta_1 - \gamma_1}{1 + \gamma_1 I} \quad (4)$$

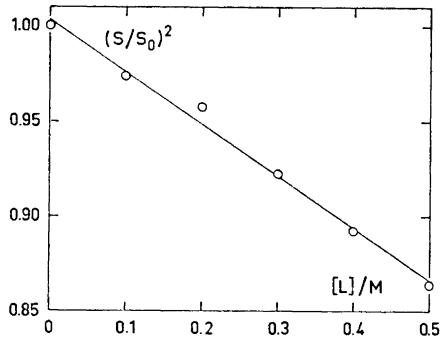

Fig. 1. Solubility of $TlIO_3$(s): $(S/S_0)^2$ *vs.* [L].

As shown in Fig. 1, $(S/S_0)^2$ decreases linearly with increasing [L]. Giving the points equal weight

$$\beta_1(1) = -0.27 \pm 0.03 \text{ M}^{-1}$$

is obtained. Errors refer to the 99 % confidence level.

Solubility of BaF_2(s). Solutions with $0 \leq C_L' \leq 0.040$ M and $0 \leq C_M \leq 0.100$ M were saturated with BaF_2(s). The initial concentration of L is denoted by C_L'. At equilibrium, the total concentration is $C_L = C_L' + 2S$. The column technique proved to be too tedious, so solution and solid samples were shaken to equilibrium in a thermostat. The shaking time was four weeks, although equilibrium was shown to be reached in about half that time. The saturated solutions were analyzed for Ba^{2+} by adding an excess of EDTA and titrating the excess with Mg^{2+}. Thallium, which interfered, was precipitated and removed as TlI(s). The reproducibility was relatively poor, within 5 % with few exceptions.

In investigations of this kind, S is normally [1,6] plotted *vs.* C_L, for different constant C_M values, the curves then being cut at constant S, giving C_L as a function of C_M:

$$C_L = [L] + \bar{n}_{Ba} S + \bar{n} C_M \quad (5)$$

where $\bar{n}_{Ba}$ refers to the $Ba^{2+} - F^-$ system, and $\bar{n}$ to the $Tl^+ - F^-$ system:

$$\bar{n} = \frac{\beta_1[L]}{(1 + \gamma_1 I) + (\beta_1 - \gamma_1)[L]} \quad (6)$$

Thus, $\bar{n}$ may be obtained as a function of [L]. The present measurements as well as literature data [7] indicate $Ba^{2+} - F^-$ complex formation to be negligible in the range studied. Moreover, for constant C_L, the solubility appeared to be roughly independent of C_M, implying that $\bar{n}$ and also β_1 are close to zero. It was therefore possible to treat the data in the following way, which is rational from a statistical point of view.

For each C_L, the average solubility, S_{av}, and the quotient S/S_{av} were computed. As S is a function of C_L and C_M, generally

$$\left(\frac{\partial S}{\partial C_M}\right)_{C_L} = -\left(\frac{\partial S}{\partial C_L}\right)_{C_M}\left(\frac{\partial C_L}{\partial C_M}\right)_S \quad (7)$$

Further, from eqns. (5) and (6), approximately

$$\left(\frac{\partial C_L}{\partial C_M}\right)_S = \bar{n} = \beta_1(2) C_L \quad (8)$$

where

$$\beta_1(2) = \frac{\beta_1}{1 + \gamma_1 I} \quad (9)$$

Eqns. (7) and (8) give, approximately

$$\left(\frac{\partial (S/S_{av})}{\partial C_M}\right)_{C_L} = -\left(\frac{\partial \log S}{\partial \log C_L}\right)_{C_M} \beta_1(2) = 2\beta_1(2) \quad (10)$$

The slope of a plot of S/S_{av} *vs.* C_M is thus independent of C_L.

Table 2. Solubility of BaF_2(s): $C_M \times 10^3$/M, *weight* (= number of points), average of S/S_{av}: 0, *20*, 1.0017; 25, *18*, 1.0042; 50, *16*, 0.9845; 75, *16*, 1.0078; 100, *9*, 1.0022.

If the individual points are given equal weight, the present data (79 points, Table 2) give the slope $(6 \pm 90) \times 10^{-3}$, and thus

$$\beta_1(2) = 0.00 \pm 0.05 \text{ M}^{-1}$$

Conclusions. The difference observed here between $\beta_1(1)$ and $\beta_1(2)$ is small, and medium effects cannot be excluded

as the major cause of the difference. However, the present results compare favourably with literature data. Thus, $\beta_1(1) = -0.20 \pm 0.02$ may be estimated from Nilsson's potentiometric data [2] in 1 M $NaClO_4$. Bond,[3] studying the formation of $TlClO_4$ in 1 M NaF with a type of central ion measurement, obtained the constant 0.32 ± 0.04. A ligand measurement method gave [3,4] for the formation of TlF $\beta_1(2) = 0 \pm 0.4$, in 1 M $NaClO_4$ as well as in 1 M $NaNO_3$. From the good agreement with the present results (activity coefficients are probably not very different in 0.5 M and 1 M media), one tends to conclude that medium effects are small. Assuming these to be negligible, the present data yield the following values of the individual constants (eqns. (4) and (9))

$$\beta_1 = 0.00 \pm 0.06 \ M^{-1}$$
$$\gamma_1 = 0.32 \pm 0.07 \ M^{-1}$$

As discussed in more detail elsewhere,[1] there is also more direct evidence of $Tl^+ - ClO_4^-$ association, *e.g.* from studies of Raman spectra.[8] For $Tl^+ - F^-$, Bell and George [5] estimated a value of β_1 at $I = 0$, but according to the authors [5] no importance should be attached to this value.

This work has been supported financially by the *Swedish Natural Science Research Council.*

1. Johansson, L. *Coord. Chem. Rev.* **11** (1973). *Submitted for publication.*
2. Nilsson, R. O. *Arkiv Kemi* **10** (1957) 363.
3. Bond, A. M. *J. Phys. Chem.* **74** (1970) 331.
4. Bond, A. M. and O'Donnell, T. A. *J. Electroanal. Chem.* **26** (1970) 137.
5. Bell, R. P. and George, J. H. B. *Trans. Faraday Soc.* **49** (1953) 619.
6. Johansson, L. *Coord. Chem. Rev.* **3** (1968) 293.
7. Connick, R. E. and Tsao, M. S. *J. Amer. Chem. Soc.* **76** (1954) 5311.
8. Jones, M. M., Jones, E. A., Harmon, D. F. and Semmes, R. T. *J. Amer. Chem. Soc.* **83** (1961) 2038.

Received May 30, 1973.

Corrections to: Synthesis of Methyl 3-*O*-(3,6-Dideoxy-α-D-*ribo*-hexopyranosyl)-α-D-manno-pyranoside *

GUNNEL ALFREDSSON and PER J. GAREGG

Institutionen för organisk kemi, Stockholms universitet, S-104 05 Stockholm 50, Sweden

Formulae V, VI, and VII are in error. The correct formulae are depicted below.

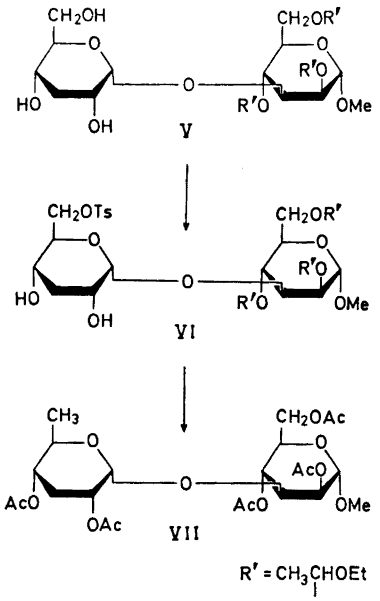

Received June 15, 1973.

* *Acta Chem. Scand.* **27** (1973) 556.

as the major cause of the difference. However, the present results compare favourably with literature data. Thus, $\beta_1(1) = -0.20 \pm 0.02$ may be estimated from Nilsson's potentiometric data [2] in 1 M $NaClO_4$. Bond,[3] studying the formation of $TlClO_4$ in 1 M NaF with a type of central ion measurement, obtained the constant 0.32 ± 0.04. A ligand measurement method gave [3,4] for the formation of TlF $\beta_1(2) = 0 \pm 0.4$, in 1 M $NaClO_4$ as well as in 1 M $NaNO_3$. From the good agreement with the present results (activity coefficients are probably not very different in 0.5 M and 1 M media), one tends to conclude that medium effects are small. Assuming these to be negligible, the present data yield the following values of the individual constants (eqns. (4) and (9))

$$\beta_1 = 0.00 \pm 0.06 \ M^{-1}$$
$$\gamma_1 = 0.32 \pm 0.07 \ M^{-1}$$

As discussed in more detail elsewhere,[1] there is also more direct evidence of $Tl^+ - ClO_4^-$ association, *e.g.* from studies of Raman spectra.[8] For $Tl^+ - F^-$, Bell and George [5] estimated a value of β_1 at $I = 0$, but according to the authors [5] no importance should be attached to this value.

This work has been supported financially by the *Swedish Natural Science Research Council.*

1. Johansson, L. *Coord. Chem. Rev.* **11** (1973). *Submitted for publication.*
2. Nilsson, R. O. *Arkiv Kemi* **10** (1957) 363.
3. Bond, A. M. *J. Phys. Chem.* **74** (1970) 331.
4. Bond, A. M. and O'Donnell, T. A. *J. Electroanal. Chem.* **26** (1970) 137.
5. Bell, R. P. and George, J. H. B. *Trans. Faraday Soc.* **49** (1953) 619.
6. Johansson, L. *Coord. Chem. Rev.* **3** (1968) 293.
7. Connick, R. E. and Tsao, M. S. *J. Amer. Chem. Soc.* **76** (1954) 5311.
8. Jones, M. M., Jones, E. A., Harmon, D. F. and Semmes, R. T. *J. Amer. Chem. Soc.* **83** (1961) 2038.

Received May 30, 1973.

Corrections to: Synthesis of Methyl 3-*O*-(3,6-Dideoxy-α-D-*ribo*-hexopyranosyl)-α-D-manno-pyranoside *

GUNNEL ALFREDSSON and PER J. GAREGG

Institutionen för organisk kemi, Stockholms universitet, S-104 05 Stockholm 50, Sweden

Formulae V, VI, and VII are in error. The correct formulae are depicted below.

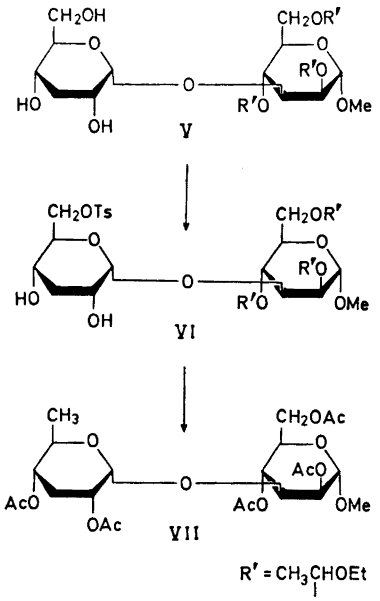

Received June 15, 1973.

* *Acta Chem. Scand.* **27** (1973) 556.

Hydrothermal Preparation and Magnetic Properties of $Dy_2O_2CO_3$, $Ho_2O_2CO_3$, $Er_2O_2CO_3$, and $Yb_2O_2CO_3$

A. NØRLUND CHRISTENSEN

Department of Inorganic Chemistry, University of Aarhus, DK-8000 Aarhus C, Denmark

Rare earth oxide hydroxides [1] and rare earth oxide carbonates [2] have been prepared hydrothermally and the magnetic properties of some rare earth oxide hydroxides have been investigated.[3] Little is known about the magnetic properties of rare earth oxide carbonates. Hydrothermal preparation of the compounds $Dy_2O_2CO_3$, $Ho_2O_2CO_3$, $Er_2O_2CO_3$, and $Yb_2O_2CO_3$ and in investigation of the magnetic properties over the temperature range 77 to 300 K is reported below.

The rare earth carbonates were precipitated with a 1 M $KHCO_3$ solution from dilute solutions of rare earth nitrate, prepared by dissolving the oxides in nitric acid. The freshly precipitated carbonates were washed with water, placed in pressure vessels lined with pure gold and kept at the experimental conditions listed in Table 1. The products were washed with water and dried in air at room temperature. X-Ray powder patterns were obtained with a Guinier camera using Cu$K\alpha_1$ radiation ($\lambda = 1.54051$ Å) and NaCl was used as internal standard ($a_{NaCl} = 5.6389$ Å). The intensities of the powder lines were measured using a Joyce double beam recording microdensitometer. The powder patterns are listed in Table 2. The powder patterns are similar to that of $Nd_2O_2CO_3$, and they can be indexed using hexagonal unit cells with dimensions close to the dimensions of the unit cell for $Nd_2O_2CO_3$. It is assumed that the structure of the four compounds is of the same type as that of $Nd_2O_2CO_3$.

The magnetization of the rare earth oxide carbonates was investigated at temperatures from 77 K to 294 K using the Faraday method. Temperatures below room temperature were obtained in a cryostate containing liquid nitrogen or

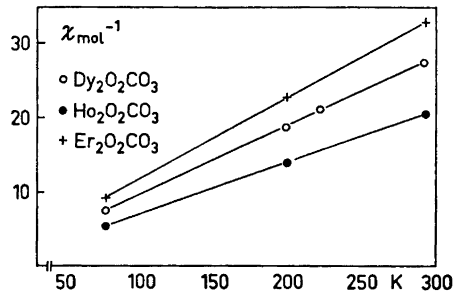

Fig. 1. Inverse molar susceptibility *vs.* temperature for $Dy_2O_2CO_3$, $Ho_2O_2CO_3$, $Er_2O_2CO_3$.

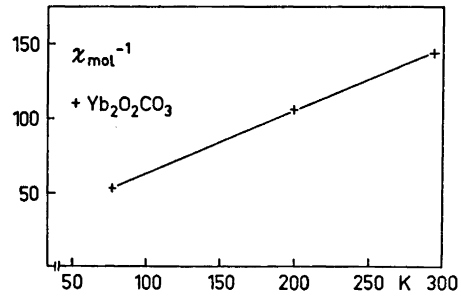

Fig. 2. Inverse molar susceptibility *vs.* temperature for $Yb_2O_2CO_3$.

Table 1. Experimental conditions for hydrothermal preparation of some rare earth oxide carbonates.

Exp. No.	Initial conditions: Freshly precipitated	Temp. (°C)	Pressure (atm)	Time (h)	Product
1	Dysprosium carbonate	575	1400	64	$Dy_2O_2CO_3$
2	Holmium carbonate	490	2000	30	$Ho_2O_2CO_3$
3	Erbium varbonate	570	1700	64	$Er_2O_2CO_3$
4	Ytterbium carbonate	540	3400	64	$Yb_2O_2CO_3$

Table 2. X-Ray powder patterns of some rare earth oxide carbonates.

$Dy_2O_2CO_3$, a = 3.868(3) Å, c = 15.156(9) Å.

h	k	ℓ	d_{obs}(Å)	d_{calc}(Å)	I
0	0	2	7.618	7.578	17
0	0	4	3.793	3.789	17
1	0	0	3.364	3.350	33
1	0	1	3.279	3.271	74
1	0	2	3.071	3.064	26
1	0	3	2.800	2.792	100
0	0	6	2.529	2.526	16
1	0	4	2.512	2.510	20
1	0	6	2.018	2.017	15
1	1	0	1.936	1.934	43
1	1	2	1.876	1.874	6
1	0	7	1.819	1.818	15
1	1	4	1.724	1.723	29
2	0	0	1.674	1.675	5
2	0	1	1.667	1.665	5
2	0	2	1.639	1.636	2
2	0	3	1.590	1.590	19
1	1	6	1.536	1.536	21
0	0	10	1.514	1.516	5
1	0	9	1.504	1.505	13
2	0	6	1.395	1.396	8
2	0	7	1.325	1.325	15
2	1	0	1.265	1.266	5
1	2	1	1.261	1.262	10
2	1	3	1.227	1.228	10

$Ho_2O_2CO_3$, a = 3.845(3) Å, c = 15.111(9) Å.

h	k	ℓ	d_{obs}(Å)	d_{calc}(Å)	I
0	0	2	7.575	7.555	16
0	0	4	3.775	3.778	18
1	0	0	3.338	3.330	52
1	0	1	3.258	3.252	96
1	0	2	3.051	3.047	55
1	0	3	2.781	2.778	100
0	0	6	2.513	2.518	23
1	0	4	2.500	2.498	22
1	0	6	2.009	2.009	31
1	1	0	1.924	1.923	92
1	1	2	1.865	1.863	22
1	0	7	1.810	1.811	31
1	1	4	1.714	1.713	26
2	0	0	1.667	1.665	9
2	0	1	1.657	1.655	16
2	0	2	1.627	1.625	6
2	0	3	1.581	1.581	26
1	1	6	1.529	1.528	19
1	0	9	1.496	1.499	5
2	0	6	1.389	1.389	5
2	0	7	1.318	1.318	12
2	1	0	1.258	1.259	5
1	2	1	1.254	1.254	10
2	1	2	1.240	1.241	5
2	1	3	1.219	1.221	15
1	1	10	1.190	1.188	5
2	0	9	1.183	1.182	5

$Er_2O_2CO_3$, a = 3.827(3) Å, c = 15.034(9) Å.

h	k	ℓ	d_{obs}(Å)	d_{calc}(Å)	I
0	0	2	7.521	7.517	28
0	0	4	3.764	3.759	30
1	0	0	3.321	3.314	43
1	0	1	3.241	3.236	82
1	0	2	3.039	3.032	39
1	0	3	2.771	2.764	100
0	0	6	2.509	2.506	33
1	0	4	2.489	2.486	24
1	0	6	2.001	1.999	35
1	1	0	1.915	1.913	67
1	1	2	1.856	1.854	16
1	0	7	1.803	1.802	44
1	1	4	1.707	1.705	35
2	0	0	1.659	1.657	10
2	0	1	1.649	1.647	10
2	0	2	1.619	1.618	6
2	0	3	1.574	1.573	35
1	1	6	1.522	1.521	34
1	0	9	1.491	1.492	14
2	0	6	1.381	1.382	11
1	0	10	1.368	1.369	6
2	0	7	1.312	1.312	13
2	1	0	1.251	1.253	10
1	2	1	1.248	1.248	10
2	1	3	1.213	1.215	5

$Yb_2O_2CO_3$, a = 3.723(5) Å, c = 15.39(2) Å

h	k	ℓ	d_{obs}(Å)	d_{calc}(Å)	I
0	0	2	7.700	7.695	45
0	0	4	3.852	3.848	29
1	0	0	3.241	3.224	38
1	0	1	3.168	3.156	63
1	0	2	2.985	2.974	31
1	0	3	2.736	2.730	100
0	0	6	2.562	2.565	30
1	0	4	2.475	2.471	20
1	0	6	2.007	2.007	26
1	1	0	1.865	1.861	47
1	0	7	1.817	1.817	32
1	1	4	1.678	1.676	16
2	0	0	1.616	1.612	6
2	0	1	1.605	1.603	7
0	0	10		1.539	
			1.540		17
2	0	3		1.538	
1	1	6	1.508	1.507	37
1	0	10	1.387	1.389	6
2	0	6	1.365	1.365	7
2	0	7	1.300	1.300	10
2	1	0	1.218	1.219	5
1	2	1	1.214	1.215	5
2	1	3	1.181	1.186	10

Table 3. Magnetic data for some rare earth oxide carbonates.

Compound	$\theta_{P(K)}$	Molar Curie constant C_M		Magnetic moments (in μB)	
		Exptl.	Calc.	Exptl.	Calc.
$Dy_2O_2CO_3$	− 3	10.74	14.17	9.3	10.6
$Ho_2O_2CO_3$	0	14.28	14.08	10.7	10.6
$Er_2O_2CO_3$	− 6	9.08	11.50	8.5	9.6
$Yb_2O_2CO_3$	−47	2.36	2.58	4.3	4.5

mixtures of solid carbon dioxide and methyl alcohol. The magnetic parameters obtained from the measurements on the four components are listed in Table 3. The inverse molar susceptibilities of $Dy_2O_2CO_3$, $Ho_2O_2CO_3$, and $Er_2O_2CO_3$ are shown in Fig. 1, and that of $Yb_2O_2CO_3$ in Fig. 2. The compounds have no magnetically ordered state at 77 K and $1/\chi_{mol}$ *vs.* temperature follows the Curie-Weiss law from 77 K to room temperature. In this paramagnetic temperature range all four oxide carbonates have molar Curie constants close to the values expected for the free ions. Further investigation of the magnetic properties of the compounds over the temperature range 4.2 K to 77 K is planned.

Acknowledgement. I am indebted to Dr. S. J. Jensen, Department of Technology, the Royal Dental College, Aarhus, C, for use of the recording microdensitometer.

1. Christensen, A. N. *Acta Chem. Scand.* **20** (1966) 896.
2. Christensen, A. N. *Les Éléments des Terres Rares*, Colloques Internationaux du Centre National de la Recherche Scientifique No. 180. Edited by: Centre National de la Recherche Scientifique, Paris 1970, Vol. I, p. 279.
3. Christensen, A. N. *J. Solid State Chem.* **4** (1972) 46.

Received June 13, 1973.

Crystallographic Computer Programs for CYBER-74

P. GROTH

Department of Chemistry, University of Oslo Oslo 3, Norway

The series of crystallographic CDC-3300 programs at the University of Oslo [1] has been modified for CYBER-74.

Among the few changes made in the file structures may be mentioned the addition of the raw intensity of each reflection, and an extra record containing estimated standard deviations of atomic parameters.

The file concept of the 6000-computers is somewhat different from that of the 3000-series, and a number of file handling routines have been added to the program system.

Data reduction programs were not adapted to the CYBER-computer since these calculations more conveniently are carried out at CDC-3300.

A new feature in the structure determination programs based upon direct methods is the possibility of changing sign or phase for all reflections of one specified parity group. Peaks from scanned Fourier synthesis may be plotted on line printer.

The program for translation of all (or a part of) the atoms through desired areas of the cell, calculating the R-value for each step, has been rewritten. In the new version, which is more than 10 times faster than the old one, trigonometric calculations are carried out only for the first step.

The maximum number of parameters that can be refined simultaneously by the modified full-matrix least squares refinement program is 300.

The system contains some new routines preparing tables suitable for publication of atomic parameters, observed and calculated structure factors, bond distances and angles *etc.*

1. Dahl, T., Gram. F., Groth, P., Klewe, B. and Rømming, Chr. *Acta Chem. Scand.* **24** (1970) 2232.

Received June 27, 1973.

Table 3. Magnetic data for some rare earth oxide carbonates.

Compound	$\theta_{P(K)}$	Molar Curie constant C_M		Magnetic moments (in μB)	
		Exptl.	Calc.	Exptl.	Calc.
$Dy_2O_2CO_3$	− 3	10.74	14.17	9.3	10.6
$Ho_2O_2CO_3$	0	14.28	14.08	10.7	10.6
$Er_2O_2CO_3$	− 6	9.08	11.50	8.5	9.6
$Yb_2O_2CO_3$	−47	2.36	2.58	4.3	4.5

mixtures of solid carbon dioxide and methyl alcohol. The magnetic parameters obtained from the measurements on the four components are listed in Table 3. The inverse molar susceptibilities of $Dy_2O_2CO_3$, $Ho_2O_2CO_3$, and $Er_2O_2CO_3$ are shown in Fig. 1, and that of $Yb_2O_2CO_3$ in Fig. 2. The compounds have no magnetically ordered state at 77 K and $1/\chi_{mol}$ *vs.* temperature follows the Curie-Weiss law from 77 K to room temperature. In this paramagnetic temperature range all four oxide carbonates have molar Curie constants close to the values expected for the free ions. Further investigation of the magnetic properties of the compounds over the temperature range 4.2 K to 77 K is planned.

Acknowledgement. I am indebted to Dr. S. J. Jensen, Department of Technology, the Royal Dental College, Aarhus, C, for use of the recording microdensitometer.

1. Christensen, A. N. *Acta Chem. Scand.* **20** (1966) 896.
2. Christensen, A. N. *Les Éléments des Terres Rares*, Colloques Internationaux du Centre National de la Recherche Scientifique No. 180. Edited by: Centre National de la Recherche Scientifique, Paris 1970, Vol. I, p. 279.
3. Christensen, A. N. *J. Solid State Chem.* **4** (1972) 46.

Received June 13, 1973.

Crystallographic Computer Programs for CYBER-74

P. GROTH

Department of Chemistry, University of Oslo Oslo 3, Norway

The series of crystallographic CDC-3300 programs at the University of Oslo [1] has been modified for CYBER-74.

Among the few changes made in the file structures may be mentioned the addition of the raw intensity of each reflection, and an extra record containing estimated standard deviations of atomic parameters.

The file concept of the 6000-computers is somewhat different from that of the 3000-series, and a number of file handling routines have been added to the program system.

Data reduction programs were not adapted to the CYBER-computer since these calculations more conveniently are carried out at CDC-3300.

A new feature in the structure determination programs based upon direct methods is the possibility of changing sign or phase for all reflections of one specified parity group. Peaks from scanned Fourier synthesis may be plotted on line printer.

The program for translation of all (or a part of) the atoms through desired areas of the cell, calculating the R-value for each step, has been rewritten. In the new version, which is more than 10 times faster than the old one, trigonometric calculations are carried out only for the first step.

The maximum number of parameters that can be refined simultaneously by the modified full-matrix least squares refinement program is 300.

The system contains some new routines preparing tables suitable for publication of atomic parameters, observed and calculated structure factors, bond distances and angles *etc.*

1. Dahl, T., Gram. F., Groth, P., Klewe, B. and Rømming, Chr. *Acta Chem. Scand.* **24** (1970) 2232.

Received June 27, 1973.

Exchange Reactions of *trans*-1,2-Diaminocyclohexanetetraacetate Complexes of Alkaline Earth Ions in the pH Range 8.5—10.5

ARNE JENSEN and NIELS RHOD LARSEN

The Royal Danish School of Pharmacy, Chemical Laboratory A, DK-2100 Copenhagen Ø, Denmark

The exchange reactions between the alkaline earth complexes of *trans*-1,2-diaminocyclohexane-*N*,*N*,*N*′,*N*′-tetraacetate (CDTA) and Cu(II) or Pb(II) have been studied by Margerum *et al.*[1] and Pausch and Margerum.[2] The reaction rate was shown to be independent of the Cu(II) and Pb(II) concentrations. Furthermore, a linear relation was found between the reaction rate constant and the hydrogen ion concentration. The pH range investigated was 5.5 – 7.6 for Mg-, Ca- and SrCDTA and 7.0 – 7.6 for BaCDTA.

The present communication describes the exchange reaction between the alkaline earth complexes of CDTA and Cu(II) in the pH range 8.5 – 10.5. The overall reaction is shown in (1). The rate of reaction was measured at 380 or 800 nm on a Durrum-Gibson stopped flow spectrophotometer for $M = Ba^{2+}$ or Sr^{2+} and on a Beckman DK-2 spectrophotometer for $M = Ca^{2+}$ or Mg^{2+}. The initial concentration of $MCDTA^{2-}$ was 10^{-3} M, and the ionic strength and pH were adjusted using NH_4NO_3 and NH_3.

$$MCDTA^{2-} + Cu(NH_3)_n^{2+} \xrightarrow{k_d} CuCDTA^{2-} + M^{2+} + nNH_3 \quad (1)$$

The rate of reaction (1) is independent of the concentration of $Cu(NH_3)_n^{2+}$ when Cu^{2+} is used in an excess of 50 – 100. Reaction (1) is accordingly pseudo first order at constant pH with the rate constant k_d.

A plot of k_d *versus* $[H^+]$ for $M = Ca^{2+}$ (*cf.* Fig. 1) indicates in the investigated pH range a linear relationship between k_d and $[H^+]$ which agrees with eqns. (2) and (3) as stated by Margerum *et al.*[1] and Pausch and Margerum.[2] Furthermore, titration curves of $MCDTA^{2-}$ ($M = Mg^{2+}$, Ca^{2+}, Sr^{2+} or Ba^{2+}) show that $MHCDTA^-$ and $M(OH)CDTA^{3-}$ are not found in the solutions used in the present investigation where the hydrogen ion concentration is low.

$$\frac{d[CuCDTA^{2-}]}{dt} = k_d[MCDTA^{2-}] = k^{MCDTA}[MCDTA^{2-}] + k_H^{MCDTA}[H^+][MCDTA^{2-}] \quad (2)$$

$$k_d = k^{MCDTA} + k_H^{MCDTA}[H^+] \quad (3)$$

Figs. 2, 3, and 4 show plots of k_d *versus* $[H^+]$ for $M = Mg^{2+}$, Sr^{2+}, and Ba^{2+}, respectively. From these plots it is seen that eqn. (2) is quantitatively correct only in the pH range 8.5 – 9.2.

k^{MCDTA} and k_H^{MCDTA} in Table 1 have been calculated from Figs. 1, 2, 3, and 4 using the relationship given in eqn. (3). The calculation for $M = Mg^{2+}$, Sr^{2+}, and Ba^{2+} has been carried out in the pH range mentioned above where the linear

Table 1. Rate constants for the dissociation of $MCDTA^{2-}$ complexes.[a]

M^{2+}	k^{MCDTA} sec^{-1}	k_H^{MCDTA} M^{-1} sec^{-1}	pH range
Mg	5.2×10^{-4}	3.8×10^4	8.5 – 9.2
	(0)[b]	(6.33×10^4)[b]	(5.5 – 7.6)[b]
Ca	2.1×10^{-4}	4.2×10^5	8.5 – 10.5
	(0)[b]	(4.14×10^5)[b]	(5.5 – 7.6)[b]
Sr	1.4×10^{-2}	6.7×10^6	8.5 – 9.2
	(3.0×10^{-2})[b]	(6.06×10^6)[b]	(5.5 – 7.6)[b]
Ba	1.2	1.1×10^8	8.5 – 9.2
	(4.4)[b]	(1.05×10^8)[b]	(7.0 – 7.6)[b]

[a] Calculated from eqn. (3) by a least squares method; for the calculation of k^{MCDTA} see text; initial $[MCDTA^{2-}] = 10^{-3}$ M; $(Cu(NH_3)_n^{2+}] = 10^{-1}$ M; NH_4^+/NH_3 buffer; $\mu = 0.5$; 25.0°C.
[b] From Ref. 2; $\mu = 0.5$; 25.0°C.

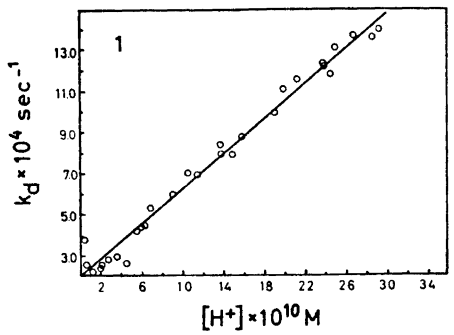

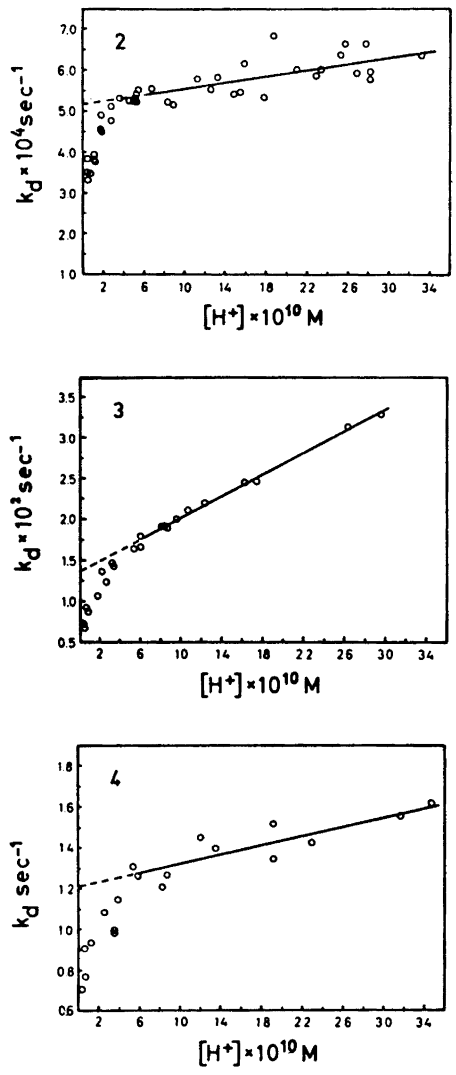

Figs. 1—4. Hydrogen ion dependence on the observed first-order rate constants k_d for, respectively, $CaCDTA^{2-}$, $MgCDTA^{2-}$, $SrCDTA^{2-}$, and $BaCDTA^{2-}$.

relation between k_d and $[H^+]$ exists. These two rate constants have also been determined by Pausch and Margerum.[2] Satisfactory agreement was found between their values and the constants calculated in the present work (Table 1).

Figs. 2, 3, and 4 also show that the plots of k_d *versus* $[H^+]$ deviate from the straight line in the pH range 9.2 – 10.5 for $M = Mg^{2+}$, Sr^{2+} or Ba^{2+}. Eqn. (3) is therefore not correct. k^{MCDTA}, when interpreted as the rate constant for the direct dissociation of the CDTA complex, is accordingly smaller than stated in Table 1.

From the observed $[H^+]$ profile, it is reasonable to conclude that k_H^{MCDTA} is probably a complex function of the hydrogen ion concentration. The $[H^+]$ dependence of k_H^{MCDTA} is negligible for pH < 9.2; *cf.* Table 1.

Nyssen and Margerum [3] have studied the kinetics of both dissociation and formation of $LaCDTA^-$ in the pH range 4.2 – 6.0. Eqn. (3) was found to be valid for the dissociation. These authors [3] have shown that the rate-determining step for the formation of $LaCDTA^-$ had to be placed after a fast formation of a reaction intermediate. The rate-determining step of formation of $LaCDTA^-$, as well as of the alkaline earth complexes of CDTA,[2] is not the characteristic water exchange rate of the hydrated metal ion. Furthermore, the rate of formation of $LaCDTA^-$ was found to increase with decreasing $[H^+]$.[3]

The $[H^+]$ profile in Figs. 2, 3, and 4 may possibly be explained by assuming the same kinetics of formation for $LaCDTA^-$ and for $MCDTA^{2-}$ ($M^{2+} = Mg^{2+}$, Sr^{2+} or Ba^{2+}). The complexity of k_H^{MCDTA} in this investigation may then be rendered more comprehensible by using a "Steady State" approximation for the reaction intermediate similar to that described for $LaCDTA^-$.

Parallel studies [4] on the rate of dissociation of these complexes are being carried out in this laboratory using the exchange of optically active CDTA instead of metal ion exchange. The studies confirm the $[H^+]$ profile of these reactions for $M^{2+} = Mg^{2+}$, Ca^{2+}, Sr^{2+} or Ba^{2+}.

1. Margerum, D. W., Menardi, P. J. and Janes, D. L. *Inorg. Chem.* **6** (1967) 283.
2. Pausch, J. B. and Margerum, D. W. *Anal. Chem.* **41** (1969) 226.
3. Nyssen, G. A. and Margerum, D. W. *Inorg. Chem.* **9** (1970) 1814.
4. Larsen, N. R. and Jensen, A. *To be published.*

Received May 14, 1973.

gem-Dimethyl-substituted Cyclic Anhydrides

GERD BORGEN

Kjemisk Institutt, Universitetet i Oslo, Oslo 3, Norway

Because of their instability few medium ring cyclic anhydrides are known. Hill and Carothers have described the synthesis of cyclic anhydrides from suberic and azelaic acid.[1] The corresponding cyclic anhydrides with two *gem*-dimethyl groups have now been prepared for conformational studies. Treatment of the tetramethyl-substituted dicarboxylic acids with acetic anhydride gave a mixture of polymeric anhydrides which by distillation were transformed into the cyclic monomer, dimer, and higher cyclic homologs. From 3,3,6,6-tetramethyl suberic acid the 9- and 18-membered ring anhydrides were prepared, and from 3,3,7,7-tetramethyl azelaic acid the 10-membered ring anhydride was synthesized.

The course of the reaction as well as the properties of the products are strikingly different when *gem*-dimethyl substituted suberic and azelaic acids are used compared with the unsubstituted dicarboxylic acids. The anhydrides which Hill and Carothers obtained by the action of acetic anhydride on the unsubstituted dicarboxylic acids were linear, solid polymers. From these linear polymeric anhydrides they got the cyclic anhydrides by slow sublimation under high vacuum.

With *gem*-dimethyl substituted dicarboxylic acids the primary reaction products seem to be cyclic anhydrides, and the monomers can be distilled off. The residues, after distillation up to 200°, are liquids and probably consist of cyclic anhydrides of moderate molecular weight; no solid, linear high polymers are isolated.

The chemical stabilities of tetramethyl-substituted and unsubstituted cyclic monomers are also very different. Hill and Carothers found no cyclic monomer from suberic acid, and with azelaic acid the cyclic monomer polymerized so rapidly even at very low temperatures (liquid air in the condenser), that a special technique was needed to demonstrate its temporary existence.

With *gem*-dimethyl substituted suberic and azelaic acid, however, the 9- and 10-membered ring anhydrides are formed in reasonable yields; they are crystalline and stable at room temperature when not contaminated. They polymerize slowly to higher cyclic homologs in chloroform solution an by melting.

The increased tendency to cyclization when *gem*-dimethyl groups are present in the chain of dicarboxylic acids represent examples of a positive *gem*-dimethyl effect.[2] The dimethyl groups increase the probability of *gauche* bonds and cause a bending of the chain whereby the chances for cyclization are increased. In addition they also seem to stabilize the cyclic anhydrides formed against polymerization.

In a previous paper,[3] differences in yields with *gem*-dimethyl groups in 1,4 and 1,5 positions by Dieckmann cyclizations have been reported. No such tendency could be observed by the cyclization to anhydrides.

The physical properties of the cyclic anhydrides and the conformational problems will be the subject of a later publication.

Experimental. 3,3,6,6-Tetramethyl suberic anhydride. 3,3,6,6-Tetramethyl suberic acid (25 g)[4] was dissolved in acetic acid anhydride (200 ml) and refluxed for 6 h. Acetic acid and acetic anhydride were distilled off at atmospheric pressure until 142°. The rest was refluxed for 2 h with acetic anhydride (200 ml) followed by distillation to 142°. The rest was vacuum distilled. The fraction b.p. 75–140°/0.05 mm was partly crystalline. The crystals were separated and sublimed at 35°/0.1 mm to give monomeric 3,3,6,6-tetramethyl suberic anhydride (1 g=4 %), m.p. 71°. (Found: C 67.89; H 9.39; mol.wt. 212 (by osmometry in chloroform). Calc. for $C_{12}H_{20}O_3$: C 67.89; H 9.50; mol wt. 216). Mass spectrometry: mol.ion+1= 213. IR anhydride group absorptions in CCl_4: 1758 and 1790 cm^{-1}. ^1H chemical shifts: 1.0, 1.4, 2.4 ppm.

The non-crystalline part of the fraction b.p. 75–140°/0.05 mm was extracted with pentane. The pentane was evaporated partly until precipitation of an oil which was shown by IR and NMR spectroscopy to be a cyclic anhydride and by osmometry in chloroform to be the *dimeric 3,3,6,6-tetramethyl suberic anhydride.* Mol.wt: Calc. 424. Found: 405 (osmometry).
IR absorptions in CCl_4: 1735 and 1810 cm^{-1}. ^1H chemical shifts: 1.0, 1.3, 2.3 ppm. The pentane solution was found by NMR spectroscopy to contain at least three other cyclic anhydrides. The residue after vacuum distillation to 200°/0.05 mm consisted of cyclic

anhydrides of molecular weight 854 (by osmometry).

3,3,7,7-Tetramethyl azelaic anhydride. 3,3,7,7-Tetramethyl azelaic acid was treated as described above. Vacuum distillation gave a partly crystalline fraction, b.p. 70–160°/0.05 mm. The crystals were dried on filter paper and sublimed at 40–42°/0.05 mm to give *monomeric 3,3,7,7-tetramethyl azelaic anhydride* (1.5 g=3.5 %), m.p. 59°. (Found: C 68.69; H 9.79. Mol.wt. 221 (by osmometry in chloroform). Calc. for $C_{13}H_{22}O_3$: C 68.99; H 9.80. Mol.wt. 226). IR absorptions in CCl_4: 1745 and 1790 cm^{-1}. ^1H chemical shifts: 1.0, 2.4 ppm (methyl and α-methylene). Neither the dimer nor other cyclic anhydrides from tetramethyl azelaic acid were found in the fraction.

1. Hill, J. W. and Carothers, W. H. *J. Am. Chem. Soc.* **55** (1933) 5023.
2. Eliel, E. L., Allinger, N. L., Angyal, S. J. and Morrison, G. A. *Conformational Analysis*, Wiley-Interscience, New York 1965, p. 191.
3. Borgen, G. and Dale, J. *Acta Chem. Scand.* **26** (1972) 952.
4. Birch, S. F., Grippe, V. E., McAllan, D. T. and Nathan, W. S. *J. Chem. Soc.* **1952** 1363.
5. Blomquist, A. T. and Miller, G. A. *J. Am. Chem. Soc.* **83** (1961) 243.

Received June 8, 1973.

Kinetics of the Hydrolysis of α-Chlorobenzyl Esters

NILS J. CLEVE and ERKKI K. EURANTO

Department of Chemistry, University of Turku, 20500 Turku 50, Finland

The uncatalysed hydrolysis of α-haloalkyl carboxylates has been investigated previously. It was found to proceed either by the mechanism of the neutral ester hydrolysis (*e.g.* chloromethyl formate,[1] chloromethyl chloroacetate,[2] and chloromethyl dichloroacetate [3]), by the S_N1 mechanism (*e.g.* α-chloroethyl acetate,[1] α,β-dichloro-*sec.*-propyl acetate,[4] and α-chloro-*sec.*-propyl acetate [5]), or by the $S_N1,2$ mechanism (*e.g.* chloromethyl acetate [1] and chloromethyl benzoate [6]). These reactions may also occur concurrently, as was found to be the case in the hydrolysis of bromomethyl chloroacetate.[7] The aim of this work was to enlarge the knowledge of the hydrolysis of the α-haloalkyl esters of carboxylic acids so as to embrace also those esters in which the α-carbon carries a phenyl or a hexachlorocyclohexyl group.

Materials. The α-chlorobenzyl esters of formic, acetic, trichloroacetic, and trifluoroacetic acids as well as hexachlorocyclohexylchloromethyl trifluoroacetate were prepared by chlorinating the corresponding benzyl esters.[8] When solvent mixtures were prepared, acetone (E. Merck A. G., guaranteed reagent) was used as received but dioxane (BDH) was purified using the method described by Hess and Frahm.[9] The symbol *p* vol. "%" employed in the following denotes 100 ml of the solvent mixture containing (100−*p*) g of water.

Determination of rate coefficients. The rate coefficients of the hydrolysis of the α-chlorobenzyl and of the hexachlorocyclohexylchloromethyl trifluoroacetate were determined by a conductometric method employing a Philips PR 9501 conductometer. The dependence of conductance on concentration was not linear, and was therefore determined experimentally. The fraction of α-chlorobenzyl acetate used in the kinetic experiments contained benzoyl chloride as an active impurity.[8] The rates of hydrolysis of this impurity were determined separately under the same experimental conditions and taken into account when calculating the rate coefficients for α-chlorobenzyl acetate. The low hydrolysis rates of benzyl trifluoroacetate were determined by a gas chromatographic method. The rate coefficients for the hydrolysis of these esters and the derived activation parameters are collected in Tables 1 and 2.

The values of the thermodynamic functions of activation presented in Table 1 show that in the hydrolysis of the α-chlorobenzyl esters of trifluoro- and trichloroacetic acids the enthalpy of activation is about 10 kcal mol^{-1} and the entropy of activation 30–40 cal $mol^{-1}K^{-1}$ lower than the corresponding values for the hydrolysis of the α-chlorobenzyl esters of formic and acetic acids. It is evident that the reaction of the former esters proceeds by the mechanism of a neutral ester

anhydrides of molecular weight 854 (by osmometry).

3,3,7,7-Tetramethyl azelaic anhydride. 3,3,7,7-Tetramethyl azelaic acid was treated as described above. Vacuum distillation gave a partly crystalline fraction, b.p. 70–160°/0.05 mm. The crystals were dried on filter paper and sublimed at 40–42°/0.05 mm to give *monomeric 3,3,7,7-tetramethyl azelaic anhydride* (1.5 g=3.5 %), m.p. 59°. (Found: C 68.69; H 9.79. Mol.wt. 221 (by osmometry in chloroform). Calc. for $C_{13}H_{22}O_3$: C 68.99; H 9.80. Mol.wt. 226). IR absorptions in CCl_4: 1745 and 1790 cm^{-1}. ^1H chemical shifts: 1.0, 2.4 ppm (methyl and α-methylene). Neither the dimer nor other cyclic anhydrides from tetramethyl azelaic acid were found in the fraction.

1. Hill, J. W. and Carothers, W. H. *J. Am. Chem. Soc.* **55** (1933) 5023.
2. Eliel, E. L., Allinger, N. L., Angyal, S. J. and Morrison, G. A. *Conformational Analysis*, Wiley-Interscience, New York 1965, p. 191.
3. Borgen, G. and Dale, J. *Acta Chem. Scand.* **26** (1972) 952.
4. Birch, S. F., Grippe, V. E., McAllan, D. T. and Nathan, W. S. *J. Chem. Soc.* **1952** 1363.
5. Blomquist, A. T. and Miller, G. A. *J. Am. Chem. Soc.* **83** (1961) 243.

Received June 8, 1973.

Kinetics of the Hydrolysis of α-Chlorobenzyl Esters

NILS J. CLEVE and ERKKI K. EURANTO

Department of Chemistry, University of Turku, 20500 Turku 50, Finland

The uncatalysed hydrolysis of α-haloalkyl carboxylates has been investigated previously. It was found to proceed either by the mechanism of the neutral ester hydrolysis (*e.g.* chloromethyl formate,[1] chloromethyl chloroacetate,[2] and chloromethyl dichloroacetate [3]), by the S_N1 mechanism (*e.g.* α-chloroethyl acetate,[1] α,β-dichloro-*sec.*-propyl acetate,[4] and α-chloro-*sec.*-propyl acetate [5]), or by the $S_N1,2$ mechanism (*e.g.* chloromethyl acetate [1] and chloromethyl benzoate [6]). These reactions may also occur concurrently, as was found to be the case in the hydrolysis of bromomethyl chloroacetate.[7] The aim of this work was to enlarge the knowledge of the hydrolysis of the α-haloalkyl esters of carboxylic acids so as to embrace also those esters in which the α-carbon carries a phenyl or a hexachlorocyclohexyl group.

Materials. The α-chlorobenzyl esters of formic, acetic, trichloroacetic, and trifluoroacetic acids as well as hexachlorocyclohexylchloromethyl trifluoroacetate were prepared by chlorinating the corresponding benzyl esters.[8] When solvent mixtures were prepared, acetone (E. Merck A. G., guaranteed reagent) was used as received but dioxane (BDH) was purified using the method described by Hess and Frahm.[9] The symbol *p* vol. "%" employed in the following denotes 100 ml of the solvent mixture containing (100−*p*) g of water.

Determination of rate coefficients. The rate coefficients of the hydrolysis of the α-chlorobenzyl and of the hexachlorocyclohexylchloromethyl trifluoroacetate were determined by a conductometric method employing a Philips PR 9501 conductometer. The dependence of conductance on concentration was not linear, and was therefore determined experimentally. The fraction of α-chlorobenzyl acetate used in the kinetic experiments contained benzoyl chloride as an active impurity.[8] The rates of hydrolysis of this impurity were determined separately under the same experimental conditions and taken into account when calculating the rate coefficients for α-chlorobenzyl acetate. The low hydrolysis rates of benzyl trifluoroacetate were determined by a gas chromatographic method. The rate coefficients for the hydrolysis of these esters and the derived activation parameters are collected in Tables 1 and 2.

The values of the thermodynamic functions of activation presented in Table 1 show that in the hydrolysis of the α-chlorobenzyl esters of trifluoro- and trichloroacetic acids the enthalpy of activation is about 10 kcal mol^{-1} and the entropy of activation 30–40 cal $mol^{-1}K^{-1}$ lower than the corresponding values for the hydrolysis of the α-chlorobenzyl esters of formic and acetic acids. It is evident that the reaction of the former esters proceeds by the mechanism of a neutral ester

Table 1. Kinetic data for the hydrolysis of α-chlorobenzyl esters RCOOCHCl(C_6H_5).

R	Solvent	10^3k (s^{-1}) 25°C	35°C	45°C	$\Delta H^{\neq}$ kcal mol^{-1}	$-\Delta S^{\neq}$ cal mol^{-1} K^{-1}
CH_3	60 % D[a]		84.4 ± 0.45			
	70 »		34.9 ± 0.35			
			35.2 ± 0.26			
			36.5 ± 0.25			
			33.4 ± 0.42			
	75 »	5.42 ± 0.018	14.4 ± 0.20	33.9 ± 0.12	16.77 ± 0.12	12.7 ± 0.4
		5.28 ± 0.022	13.6 ± 0.09	33.6 ± 0.16		
	80 "%" A[b]	3.55 ± 0.028	8.74 ± 0.053	20.2 ± 0.08	15.90 ± 0.19	16.4 ± 0.6
		3.52 ± 0.014	8.41 ± 0.045	20.5 ± 0.08		
	85 »			6.58 ± 0.032		
				7.18 ± 0.061		
	90 »			1.70 ± 0.022		
				1.66 ± 0.012		
H	60 »	8.17 ± 0.056	20.5 ± 0.20	51.0 ± 0.21		
		8.06 ± 0.063	20.4 ± 0.08	47.2 ± 0.38	16.39 ± 0.07	13.1 ± 0.2
				49.5 ± 0.49		
	70 »			14.1 ± 0.08		
				15.3 ± 0.18		
	80 »			3.34 ± 0.022		
				3.10 ± 0.028		
CF_3	90 »	34.4 ± 0.17	43.0 ± 0.68	()[c]	4.82 ± 0.29	49.2 ± 1.0
		34.3 ± 0.15	42.8 ± 0.58			
	95 »	6.72 ± 0.10				
		6.64 ± 0.11				
	98 »	0.53 ± 0.04				
CCl_3	90 »	1.18 ± 0.010	1.92 ± 0.024		7.12	48.1
			1.69 ± 0.014			
			1.78 ± 0.014			

[a]60 wt. % dioxane-water mixture. [b]80 vol. "%" acetone-water mixture. [c]$k = (16.6 \pm 0.11) \times 10^{-3}$ s^{-1} at 4.52°C, $k = (23.5 \pm 0.18) \times 10^{-3}$ s^{-1}, and $k = (23.8 \pm 0.18) \times 10^{-3}$ s^{-1} at 15.09°C.

hydrolysis ($B_{AC}3$), as is usual for the hydrolysis of trihalocarboxylic esters,[5] and the hydrolysis of the latter takes place by the nucleophilic displacement of the α-halogen atom of the alkyl component. In the latter case the carbonium ion formed is stabilized by resonance involving the phenyl group. Because the hydrolysis of α-chloroethyl acetate[1] has been found to take place by the S_N1 mechanism, it is to be expected that the hydrolysis of these esters also occurs by this mechanism. The hydrolysis of chloromethyl formate[1] has been found to take place by the mechanism of the neutral ester hydrolysis. The rate coefficient for the hydrolysis of α-chlorobenzyl formate proceeding by the $B_{AC}3$ mechanism can be estimated as about 10^{-7} s^{-1}, and so would not affect the experimentally determined rate coefficient (8.1×10^{-3} s^{-1}). When the estimation was made, it was assumed that the rate coefficients of the hydrolysis of chloromethyl formate[1] and chloromethyl dichloroacetate[3] are similarly dependent on the composition of the solvent mixture, and further, that when the hydrogen in the methyl group was substituted by a phenyl group the effect is the same in both α-chlorobenzyl formate and trifluoroacetate.

In the hydrolysis of α-chlorobenzyl formate and acetate, the retarding effect of the organic solvent component on the reaction rate is of the same order of magnitude as in the hydrolysis of α-chloroalkyl acetates (S_N1) in acetone-water mixtures.[1,4,5] In the hydrolysis of the α-chlorobenzyl and benzyl esters of trifluoroacetic acid,

Table 2. Kinetic data for the hydrolysis of benzyl trifluoroacetate and hexachlorocyclohexylchloromethyl trifluoroacetate CF_3COOR' in P vol. "%" acetone-water mixtures.

R'	P vol. "%"	°C	10^3k (s^{-1})
$CH_2(C_6H_5)$	80	25	0.0128 ± 0.00055
	85	25	0.0060 ± 0.00010
	90	25	0.0017 ± 0.00004
$CHCl(C_6H_5Cl_6)$	98	25	43 – 33
		35	49 – 42

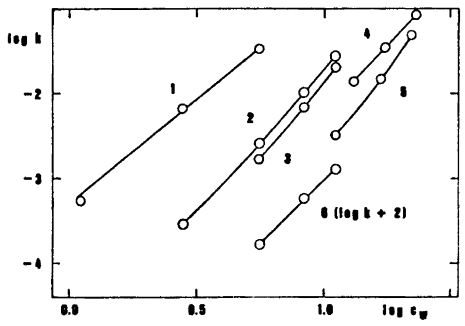

Fig. 1. Plots of log k *versus* log c_w (c_w is the molarity of water in the solvent mixture) for the hydrolyses of the following esters in acetone-water mixtures. 1. α-Chlorobenzyl trifluoroacetate. 2. α-Chloro-*sec.*-propyl acetate.[5] 3. α-Chlorobenzyl acetate. 5. α-Chlorobenzyl formate. 6. Benzyl trifluoroacetate. 4. α-Chlorobenzyl acetate in dioxane-water mixtures.

however, this effect is somewhat smaller (Fig. 1), and is measured at a different temperature. The variation may be due to different reaction mechanisms.

The rate coefficients calculated for the hydrolysis of hexachlorocyclohexylchloromethyl trifluoroacetate decrease in value as the reaction proceeds, even though the nonlinear relationship between the conductance and the concentration has been taken into account (Table 2). The decreasing value of the rate coefficient may be the consequence of several hydrolyses proceeding at different rates. The reacting ester is a mixture of several isomers and conformers. [8] The small effect of the temperature on the hydrolysis rate implies that the reaction takes place by the neutral ester hydrolysis ($B_{AC}3$) mechanism. This is in agreement with the rate coefficient for the hydrolysis of hexachlorocyclohexylchloromethyl trifluoroacetate being one hundred times greater than that for the hydrolysis of α-chlorobenzyl trifluoroacetate.

When the rate coefficients of the hydrolysis of α-chlorobenzyl and benzyl trifluoroacetates are compared, it is seen that the chlorine at the α-position increases the rate of reaction 2×10^4-fold in a 90 % acetone-water mixture, which is, when expressed with this accuracy, the same ratio as is found for aliphatic esters of trifluoroacetic acid.[10,11]

Acknowledgement. The authors wish to thank the *National Research Council for Sciences (Valtion luonnontieteellinen toimikunta)* for financial aid.

1. Euranto, E. *Ann. Univ. Turku. Ser. A I* (1959) No. 31.
2. Euranto, E. K. and Cleve, N. J. *Acta Chem. Scand.* **17** (1963) 1584.
3. Cleve, N. J. *Suomen Kemistilehti* **B 45** (1972) 235.
4. Euranto, E. *Suomen Kemistilehti* **B 35** (1962) 18.
5. Euranto, E. K. *Acta Chem. Scand.* **21** (1967) 721.
6. Euranto, E. K. and Yrjänä, T. *Suomen Kemistilehti* **B 38** (1965) 214.
7. Cleve, N. J. *Acta Chem. Scand.* **26** (1972) 1326.
8. Euranto, E. K. and Hautoniemi, L. M. *Acta Chem. Scand.* **24** (1970) 50.
9. Hess, K. and Frahm, H. *Ber.* **B 71** (1938) 2627.
10. Cleve, N. J. *Ann. Acad. Sci. Fennicae, Ser. A II* (1972) No. 167.
11. Euranto, E. K. and Cleve, N. J. *To be published.*

Received May 3, 1973.

ACTA CHEMICA SCANDINAVICA 27 (1973) 1845–1854

The Structure of Pyrazole, $C_3H_4N_2$, at 295 K and 108 K as determined by X-Ray Diffraction

TROELS LA COUR* and SVEND ERIK RASMUSSEN

Department of Inorganic Chemistry, University of Aarhus, DK-8000 Aarhus C, Denmark

The structure of pyrazole has been re-investigated using X-ray diffractometry and Mo$K\alpha$-radiation. One set of data was collected at room temperature using a four-circle diffractometer. Another set was collected also at room temperature using an equi-inclination diffractometer. The latter was employed for collecting data at 108 K as well. The three sets of data were refined independently using various constrained and unconstrained models. The refinements show that the atomic vibrations are not approximated well using a model assuming the molecules to move as rigid bodies. The two sets of room temperature data are in stronger disagreement with the rigid body model than the low temperature data. The least squares matrices show that corresponding parameters of the two crystallographically independent molecules are strongly correlated. The geometry of the pyrazole molecule indicates a high degree of de-localized π-bonding.

The crystal structure of pyrazole was determined by Ehrlich [1] in 1960 from photographically recorded X-ray diffraction data of the three pinacoid projections. An X-ray re-determination by Berthou *et al.*[2] and a neutron diffraction study by Larsen *et al.*[3] were published in 1970. The molecular formula of pyrazole with the numbering of the atoms is shown in Fig. 1. This

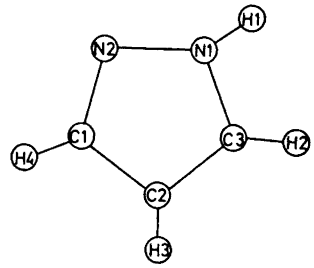

Fig. 1. The molecular formula of pyrazole with the numbering of atoms as used in the text.

* Present address: Texas A & M University, College of Science Department of Chemistry, College Station, 77843 Texas, U.S.A.

X-ray work was carried out for comparing X-ray and neutron diffraction results and for comparing bond lengths obtained by crystal diffraction with those obtained from microwave studies by Nygaard *et al.*[4]

EXPERIMENTAL

Clear oblong prismatic crystals of pyrazole of analytical grade were formed by sublimation. Five prism faces parallel to the *c*-axis were observed.

Two sets of data, one at 108 K and one at 295 K, were collected using a Buerger-Supper equi-inclination diffractometer automated by a Pace control unit. The crystals used were shaped as cylinders, using a small lathe and a diamond tool. One crystal was ground to a diameter of 0.45 mm and was used for collection of data at room temperature. The length of the crystal exceeded the diameter of the X-ray beam. The crystal used in the low temperature experiment was of diameter 0.25 mm, and it was short enough to be completely bathed in the X-ray beam.

Another room temperature data set was collected using a Picker automatic four-circle diffractometer controlled by a PDP-8 computer. The crystal used in this experiment was nearly cylindrical with a diameter of 0.3 mm and was also completely bathed in the X-ray beam. All crystals were encapsuled in sealed Lindemann glass capillaries. Intensity measurements were carried out using Mo$K\alpha$ radiation selected by monochromators designed and built in this department.[5] The counting chain included a scintillation counter and a pulse-height analyzer. The dead-time of the counting chain of the Supper-Pace instrument was determined as 2.7 μs using a method described by Chipman.[6] The results are depicted in Fig. 2. Data were obtained from a crystal cooled to 108 K by

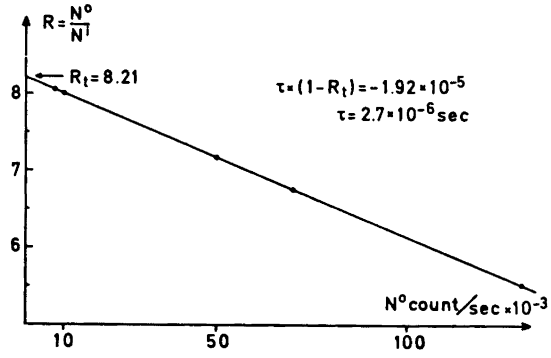

Fig. 2. Absorption coefficient of a zirconium foil measured at various count rates. N^0 is the count rate of the peak of a strong reflection measured without the zirconium foil and N^i is the count rate of the attenuated reflections. N^0 was varied by measuring different reflections.

blowing a stream of cold nitrogen on to the crystal. A stream of dry nitrogen at room temperature surrounded the cold stream coaxially. Ice formation of the crystal was not completely eliminated but was not large enough to influence the results. A thermo couple (iron-constantan) was placed 3 mm from the crystal. No temperature difference was measurable by moving the thermo couple in a region of 10 mm from this position. The temperature was recorded continuously and showed fluctuations of 2 – 3°C. Weissenberg and precession photographs of the principal zones were recorded at 108 K as well. The photographs showed no indication of change in space group upon cooling.

At room temperature four symmetry related reflections were measured in general. At 108 K only two symmetry related reflections were recorded. In the Supper-Pace data

collection, a standard reflection was measured every twenty reflections as an internal standard. A best straight line was estimated for the internal standards on each layer line and the reflections were scaled accordingly. The layer lines were scaled together using the 0,10,0 reflection as an overall standard reflection. The strongest reflections were corrected for lost counts in the following way. The integrated intensity is defined as the counting rate integrated over the time of measurement, $P = \int N(t)\mathrm{d}t$. The corrected counting rate N_c is related to the observed counting rate N by the expression $N_c = N/(1-\tau N)$ where τ is the dead-time of the counting chain. The corrected integrated intensity P_c is related to the observed intensity by means of the expression $P_c = P + \tau \int N^2 \mathrm{d}t$ to a first order approximation. The integration is performed using the assumption that the intensity distribution $N(t)$ around the Bragg-position is Gaussian-shaped with a width at half peak height maximum of $\alpha°$. The following expression for the corrected integrated intensity is consequently:

$$P_c = \mathrm{P}(1 + P \cdot \tau \cdot \mathrm{scanrate}/\alpha\sqrt{2})$$

In the data processing program the widths at half peak height maximum for each reflection were estimated using an experimentally determined relation between α and $\sin\theta/\lambda$. The 1,2,1 reflection in the room temperature set was removed because of the very high correction (25 %); the corrections needed were in all other cases in the range 0 – 10 %. The intensities from the large crystal were corrected for changes in irradiated volume caused by changes in inclination angles.

Intensities were measured on the Picker diffractometer with the $\theta - 2\theta$ scan technique. Three standard reflections were measured every 20 reflections thus scaling the previous 20 reflections on the common scale. Averages were taken over symmetry related Lp-corrected reflections, and in general the data showed a good internal consistensy. Table 1 summarizes selected characteristics of the three data sets.

Table 1. The first two columns show the number of independent observations before and after removal of reflections where $F^2 < 3\sigma(F^2)_{\mathrm{count}}$. Column three gives a measure of the internal consistency of the data.

$$R = \left(\sum_{hkl} \left(\sum_{\substack{\text{symmetry}\\ \text{related}}} |\langle F^2\rangle - F^2|\right)\right) / \sum_{hkl} \langle F^2\rangle .$$

	Number of reflections	Number of significant reflec.	R-value	$\sin\theta_{\max}$	Extinction parameter
Supper Pace 108 K	2051	957	0.054	0.63	
Supper Pace 295 K	2385	852	0.037	0.61	3.1×10^{-4}
Picker 295 K	950	535	0.025	0.42	3.2×10^{-5}

CRYSTAL DATA

The space group is $P2_1cn$ at both temperatures, and the unit cell dimensions at 108 K are $a = 8.190$ Å, $b = 12.588$ Å, $c = 6.773$ Å, while at 295 K $a = 8.232$ Å, $b = 12.840$ Å, and $c = 7.054$ Å. Linear absorption coefficient for Mo$K\alpha$ is 1 cm^{-1}.

Table 2. Observed and calculated structure factor amplitudes for the low temperature data. The scale is ten times the absolute scale.

REFINEMENT

The three sets of data were refined by the methods of least squares employing a program written by G. S. Pawley. The weights used were $W = 1/(\mu F)^2$ where $\mu F = (\sigma(F^2)_{\text{count}} + 1.02 \times F^2)^{\frac{1}{2}} - F$ and $\sigma(F^2)_{\text{count}}$ is the standard deviation of an observation based on counting statistics. Furthermore a routine for isotropic extinction correction based upon Zachariasen's 1967 paper [8] and used as described by Larson [9] was included in the least squares program. Only the two room temperature data sets were refined with respect to extinction as no indication of extinction effects were found in the low temperature set. The atomic scattering factors used for carbon and nitrogen are those of Cromer and Mann.[10] For hydrogen we used the values given by Stewart *et al.*[11] Constrained refinements were carried out for different models with the three data sets. The constrained refinement procedure described by Pawley [7] was used. Three different models were finally selected as being the more chemically reasonable. In the first model the two crystallographically independent molecules were assumed to be identical and the temperature movements of the atoms were treated as if the molecules moved as rigid bodies (IR). In the second model (INR), the two molecules were assumed to be geometrically identical, but all nitrogen and carbon atoms were allowed independent and anisotropic movements, and the hydrogen atoms were allowed independent and isotropic vibrations. The third model (NINR) was a conventional least squares refinement with nine parameters per heavy atom and four parameters per hydrogen atom. A fourth model could make use of the expected planarity of the molecules. Because of singularity problems in the least squares matrix, it was necessary to keep the z-coordinates of the two nitrogen atoms and of one carbon atom fixed with respect to a plane defined by the inertia axis of the molecules. A further constraint to planarity would only decrease the parameter space with two dimensions. This was considered too small a change for making valid statistical conclusions.

Table 2 shows the observed structure factors multiplied by 10 for the low temperature data set together with the calculated structure factors based on the INR model.

DISCUSSION

Table 3 shows results from the different refinements together with percentage points of the statistical distribution of $\mathcal{R}$ defined by Hamilton [12] and calculated by the approximation given by Pawley.[13] It is seen that one can reject the hypothesis that the molecules move as rigid bodies for all three sets of data at 0.1 % significance level. The improvements in R-values when the constraint of rigid body movement is released is much more pronounced for the room temperature data sets than for the low temperature data set. An important feature in the rigid body constraint is the instability of the least squares system as pointed out by Johnson [14] and Pawley,[15] because the molecules approximate circles in shape. This instability is clearly shown if one makes a Schomaker and Trueblood [16] least squares refinement on the u_{ij}

Table 3. Results of refinements on three different models: the two crystallographically independent molecules assumed to be identical in geometry and moving as rigid bodies (IR), the rigid body constraint released (INR) and, finally, a conventional least squares model (NINR). The R-factor ratios show a significant improvement for all three sets of data by releasing the rigid body constraint, whereas the improvement obtained by releasing the identity constraint appears to be statistically significant only for the two room-temperature sets of data.

	Data set	IR	INR	NINR	$\frac{R_w(\text{IR})}{R_w(\text{INR})}$	$\mathcal{R}_{28,\text{m},0.001}$	$\frac{R_w(\text{INR})}{R_w(\text{NINR})}$	$\mathcal{R}_{21,\text{m},z}$	z
$R_w=$	Low temp.	50.892	47.749	47.223	1.066	1.033	1.011	1.012	0.50
$[\sum w(F_o-F_c)^2]^{\frac{1}{2}}$	Room temp.	77.910	59.917	58.224	1.300	1.040	1.029	1.028	0.005
	Picker	45.287	33.764	30.116	1.344	1.066	1.121	1.057	0.001
$R_w=$	Low temp.	0.065	0.061	0.060	1.066		1.017		
$[\sum w(F_o-F_c)^2/$	Room temp.	0.063	0.048	0.047	1.313		1.021		
$\sum w(F_o)^2]^{\frac{1}{2}}$	Picker	0.046	0.034	0.030	1.353		1.133		
Number of	Low temp.	73	101	122					
parameters	Room temp.	74	102	123					
	Picker	74	102	123					

obtained from one of the models refined. If the **U** tensor of the hydrogens is changed from

$$\begin{bmatrix} .02 & 0 & 0 \\ 0 & .02 & 0 \\ 0 & 0 & .02 \end{bmatrix} \text{ to } \begin{bmatrix} .015 & 0 & 0 \\ 0 & .015 & 0 \\ 0 & 0 & .02 \end{bmatrix}$$

the principal axes of L change from (7.90, 3.25, .13)Å^2 to (4.62, 02, −1.38)Å^2. This is physically impossible.

There is also a statistically significant improvement in R-values by removing the identity constraint in the case of the room temperature data sets, whereas for the low temperature data the identity hypothesis cannot be rejected. Although the extra parameters, used in allowing for small differences between the two crystallographically independent molecules, seem to carry a statistical significance, the surroundings of the two molecules differ so little that differences in crystalline fields cannot support an assumption of inequality of the two molecules. Furthermore the surroundings around the molecules are not much different at 108 K where the two molecules seem to be identical.

The apparent disagreement between the physically and chemically plausible results and the statistical indication may be explained as follows. The two sets of atoms in the crystallographically independent molecules are approximately related via a pseudo-two-fold b-axis at $Z=\frac{1}{2}$. The pseudo-symmetry relation gives rise to large correlation coefficients between related parameters in the conventional least squares refinement where the molecules are treated as being independent entities. Correlation coefficients as large as 0.8 are found, *e.g.* between x-parameters of pseudo-symmetry related atoms. The difference in effective number of degrees of freedom between the constrained (identical molecules) and the unconstrained (independent molecules) models is difficult

to define with highly correlated parameters. The R-ratio test may be seriously affected by departures from the assumed conditions of normally distributed random errors in the observations. Because of the pseudo symmetry, certain classes of reflections like $0kl$ are systematically weak and are therefore subject to fairly large statistical errors. The R-ratio test may therefore not be strictly applicable. We propose that the constrained refinements assuming the two crystallographically independent molecules to be geometrically identical lead to the "best" results for the geometry of the pyrazole molecule employing the available data. Since librational corrections are difficult to apply, we propose that the data measured at 108 K lead to a structure in which the bond lengths are less subject to corrections than the structures obtained from the room temperature data.

The crystal structure of pyrazole is described in detail elsewhere (Ehrlich,[1] and Larsen *et al.*[3]). In Tables 4 and 5 are listed coordinates and temperature factors for the two data sets collected on the Supper-Pace diffractometer. It must be remembered by comparing coordinates at the different temperatures that cell edges differ up to 4 %. Figs. 3, 4, and 5 show bond lengths and bond angles for the INR model based on the three data sets. The standard deviations are dubious as they are calculated from marginal standard deviations on the position parameters not taking into account the special problems the constraints impose on the least squares moment matrix. The sum of the angles in the ring indicates that the molecule is planar. A calculation of distances

Table 4. Atomic positions in Å units. Least squares standard deviations are in the range 0.003 – 0.008 Å for heavy atoms and 0.02 Å for hydrogen atoms.

Molecule 1				Molecule 2		
x	y	z		x	y	z
			108 K			
7.0383	1.2357	7.7162	N(1)	1.2755	2.3205	3.3719
7.1500	2.2790	6.8630	N(2)	1.2126	1.2420	2.5584
5.9530	2.3484	6.2911	C(1)	2.4421	0.7410	2.6032
5.0876	1.3805	6.7852	C(2)	3.2683	1.4741	3.4455
5.8269	0.6714	7.6967	C(3)	2.4835	2.4952	3.9164
7.7178	1.0840	8.2990	H(1)	0.5016	2.7491	3.5760
5.6045	−0.0650	8.3974	H(2)	2.6051	3.2289	4.6443
4.1922	1.2855	6.5340	H(3)	4.1590	1.2641	3.6364
5.7683	3.0164	5.7200	H(4)	2.6272	−0.0284	2.1785
			295 K			
7.0194	1.2985	8.0661	N(1)	1.2262	2.3854	3.5197
7.1361	2.3028	7.1819	N(2)	1.1581	1.3209	2.7035
5.9568	2.3358	6.5847	C(1)	2.3723	0.8005	2.7619
5.1063	1.3751	7.0631	C(2)	3.2027	1.5132	3.5850
5.8149	0.7251	8.0260	C(3)	2.4343	2.5266	4.0690
7.7190	1.1062	8.5473	H(1)	0.5127	2.8787	3.5937
5.6103	−0.0390	8.5857	H(2)	2.6311	3.2780	4.6484
4.2048	1.2118	6.7650	H(3)	4.1293	1.3208	3.7657
5.8404	2.9822	5.9417	H(4)	2.5172	0.0403	2.2662

Table 5. The anisotropic temperature factors in Å² scaled by 10^3 in the crystal orthogonal coordinate system. Isotropic B's for hydrogen have units $Å^2/8\pi^2$.

Molecule 1							Molecule 2					
u_{11}	u_{22}	u_{33}	u_{12}	u_{13}	u_{23}	108 K	u_{11}	u_{22}	u_{33}	u_{12}	u_{13}	u_{23}
11	14	23	−2	−3	−3	N(1)	15	16	17	4	3	4
11	18	24	0	−3	4	N(2)	13	20	21	−4	−2	−3
19	15	17	4	−2	1	C(1)	18	13	22	−2	−1	0
14	17	25	−6	0	0	C(2)	11	15	14	−4	−5	3
12	12	24	−3	0	0	C(3)	11	16	20	1	1	−3
		0.50				H(1)			0.68			
		3.71				H(2)			2.76			
		1.04				H(3)			0.99			
		3.88				H(4)			0.18			
						295 K						
44	56	67	4	−10	−2	N(1)	40	57	63	9	4	3
48	57	73	−7	−3	2	N(2)	43	55	71	−2	−13	2
59	61	55	−3	−7	6	C(1)	52	47	63	3	−3	−2
39	63	66	−6	−10	−8	C(2)	40	62	57	3	−4	2
44	52	70	−3	−1	3	C(3)	45	59	54	−1	−4	−7
		5.28				H(1)			5.42			
		5.82				H(2)			5.08			
		4.69				H(3)			5.79			
		6.16				H(4)			4.65			

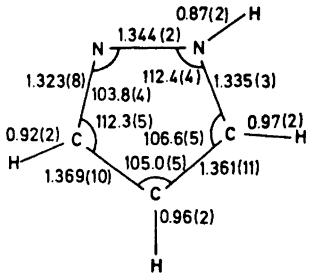

Fig. 3. Geometry of the pyrazole molecule based on the room temperature Supper data set, assuming the two molecules to be identical and non-rigid.

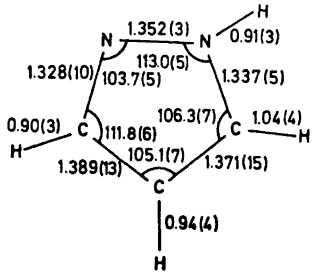

Fig. 4. Geometry of the pyrazole molecule based on the low temperature Supper data set, assuming the two molecules to be identical and non-rigid.

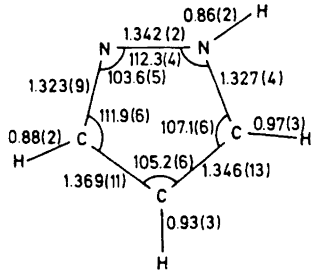

Fig. 5. Geometry of the pyrazole molecule based on the room temperature Picker data set, assuming the two molecules to be identical and non-rigid.

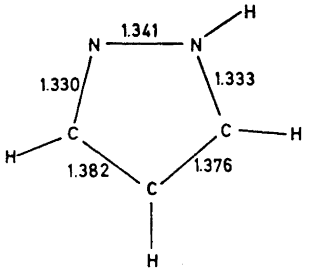

Fig. 6. Geometry of the pyrazole molecule based on the room temperature neutron data. Average over two independent molecules.

of the atoms from the best plane through the heavy atoms gives for the room temperature data sets 0.002 Å on the average, and for the low temperature data set a mean of 0.004 Å. For comparison the geometry of the pyrazole molecule as found by neutron diffraction[3] is shown in Figs. 6 and 7. Fig. 8 describes the molecular geometry which was found using microwave spectroscopy.[4]

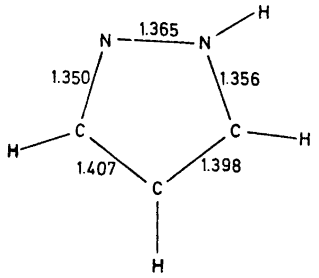

Fig. 7. Geometry of the molecule based on the room temperature neutron data as corrected for rigid body motion. Average over two independent molecules.

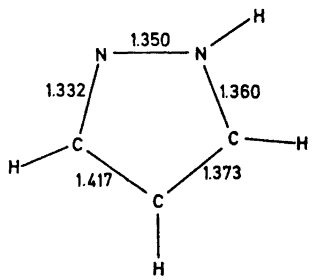

Fig. 8. Microwave substitution structure corrected to equilibrium structure.

In the crystalline state the ring atoms of the pyrazole molecule conform closely to *mm* symmetry. The differences in distances between N(2) – C(1) and N(1) – C(3), and between C(1) – C(2) and C(2) – C(3) are small in all cases. They are, however, systematic. N(2) – C(1) is in all cases found smaller than N(1) – C(3), and C(2) – C(3) is systematically smaller than C(1) – C(2). This is in accordance with the gas phase structure as determined by microwave spectroscopy.[4] Here, however, the differences are more pronounced. The following qualitative explanation is offered. The pyrazole molecule has a pronounced aromatic character. In the free state the unsymmetrical disposition of the hydrogen atoms enforces a certain degree of single bond-double bond alternation upon the distribution of bonding electrons. In the solid state the hydrogen bonding results in a slight redistribution of bonding electrons thus allowing the molecule to assume a more nearly symmetrical configuration.

The spectroscopic and the diffraction results refer to molecules in different vibrational quantum states. In neither case are the distances those of the hypothetical minimum of the potential function. Nevertheless, the experimental evidence appears to be strong enough to lead to the conclusion that the electron redistribution, which takes place upon transfer of a molecule from the gas phase to the crystalline phase, results in experimentally observable changes in bond lengths.

Acknowledgements. The *Danish State Science Foundation* is thanked for providing the Supper-Pace diffractometer. F. Krebs Larsen of this department is thanked for an active interest in this work and for helpful discussion. Rita Grønbæk Hazell and G. Stuart Pawley are thanked for use of their programs and for helpful advice on computing. We are also much indebted to Dr. Lise Nygaard for her communicating the results of the microwave investigation prior to the publication of her results.

REFERENCES

1. Ehrlich, H. W. W. *Acta Cryst.* **13** (1960) 946.
2. Berthou, J., Elguero, J. and Rérat, C. *Acta Cryst.* **B 26** (1970) 1880.
3. Larsen, F. K., Lehmann, M. S., Søtofte, I. and Rasmussen, S. E. *Acta Chem. Scand.* **24** (1970) 3248.
4. Nygaard, L., Christen, D., Tormod Nielsen, J., Pedersen, E. J., Snerling, O., Vestergaard, E. and Sørensen, G. O. *J. Mol. Struct. To be published.*
5. Rasmussen, S. E. and Henriksen, K. *J. Appl. Cryst.* **3** (1970) 100.
6. Chipman, D. R. *Acta Cryst.* **A 25** (1969) 209.
7. Pawley, G. S. *Advances in Structure Research by Diffraction Methods*, Pergamon London 1972, Vol. 4.
8. Zachariasen, W. H. *Acta Cryst.* **23** (1967) 558.
9. Larson, A. C. *Acta Cryst.* **23** (1967) 664.
10. Cromer, D. T. and Mann, J. B. *Acta Cryst.* **A 24** (1968) 321.
11. Stewart, R. F., Davidson, E. R. and Simpson, W. T. *J. Chem. Phys.* **42** (1965) 3175.
12. Hamilton, W. C. *Acta Cryst.* **18** (1965) 502.
13. Pawley, G. S. *Acta Cryst.* **A 26** (1970) 691.
14. Johnson, C. K. Paper given at the Ottawa Summer School on Crystallographic Computing. Munksgaard, Copenhagen 1970.
15. Pawley, G. S. *Acta Cryst.* **A 26** (1970) 289.
16. Schomaker, V., and Trueblood, K. N. *Acta Cryst.* **B 24** (1968) 63.

Received January 22, 1973.

ACTA CHEMICA SCANDINAVICA 27 (1973) 1855–1859

Response and Sorption Studies on Glass Electrodes in Isopropanol

BO KARLBERG and ANDERS WIKBY

Department of Analytical Chemistry, University of Umeå, S-901 87 Umeå, Sweden

Prolonged storage of hydrated glass electrodes in air and in isopropanol was shown to degrade the hydrogen ion response. On the basis of C14-labelled isopropanol experiments, it was concluded that sorption of this solvent did not influence the electrode response. Sorption effects were observed on etched glass, probably originating from solvent inclusions on the rough surface, while on the smooth hydrated glass surface no sorption could be detected. The lithium ion flux from the hydrated glass into isopropanol was about ten times less than that into water. The low lithium ion flux, as well as the slow electrode response, were explained by the dehydration of the gel-layer.

The hydrogen ion response of common glass electrodes is extremely fast.[1–3] However, prolonged storage in organic solvents may cause a sluggish response. In some instances the rapid response was shown to be restored when the electrode was immersed in water.[4,5] A certain amount of water seems to be necessary for a good electrode response in non-aqueous solutions, and therefore a dehydration of the glass surface will cause a slow response.

In an aqueous solution the hydrogen ion selective lithia glass hydrates continuously resulting in a layer in which the lithium ions are replaced by hydrogen ions.[6] The gel-layer has been described as a region located between two moving boundaries. The external boundary, solution/gel-layer, moves inwardly due to dissolution. The internal boundary, gel-layer/bulk glass, moves inwards towards the interior glass at a rate determined by the lithium-hydrogen ion exchange and the diffusional influx of water. During the first two weeks of hydration the internal boundary moves faster than the external boundary, *i.e.*, the gel-layer grows thicker.

In non-aqueous solutions the hydration process is probably retarded; inhibition has been found in isopropanol.[7] The flux of lithium ions from the glass into the solution markedly decreased when a hydrated electrode was transferred from water to isopropanol. It was also observed that the gel-layer stopped growing thicker. The reactions involved in the hydration processes

in water thus cannot proceed in isopropanol in the same way. However, other interactions with the gel-layer must not be excluded. In methanol, for instance, Folman and Yates [8–10] have studied the adsorption by interferometric and infrared spectroscopic methods. They concluded that adsorption of solvent molecules occurred on the hydroxyl groups as well as on other sites, assumed to be oxygen or silicon atoms. On amorphous silica, Lowen and Broge [11] have suggested an esterification of the hydroxyl groups by alcohols. This reaction changed the surface properties in a manner similar to dehydration.

On interpreting the delayed response behaviour of glass electrodes in non-aqueous solvents, the effect of dehydration alone has been emphasized. Solvent interactions with the gel-layer might change the electrode properties in a similar way. This study has been undertaken to investigate whether the slow response of glass electrodes is a consequence of solvent sorption.

EXPERIMENTAL

Response studies. An Ingold LoT electrode was placed in a thermostatted vessel (25°C) containing 20 ml of a 10^{-4} M picric acid isopropanol solution. 2 ml of a 10^{-2} M picric acid isopropanol solution were rapidly added from a syringe to the solution in the vessel. stirring was provided with a motor-driven glass propeller. An Ag/AgCl reference electrode was used. It was placed in a PVC tubing with a dialysis film at the bottom. The potential changes were recorded on a Mosley 680 recorder. The glass electrode pre-treatments are described below. By this procedure a step-wise change of hydrogen ion activity was produced. An ideal electrode should produce a voltage step output. The rise of the recorded voltage can be taken as a measure of electrode response rate.

Sorption studies. Semi-spherical bulbs made of Ingold LoT glass were used. Etched and hydrated bulbs were investigated. Etched glass bulbs were obtained by immersion in a 5 % hydrofluoric acid solution for 2 min. Hydrated electrodes were etched as above and then hydrated for two days in water. The bulbs were placed in isopropanol-1,3-C14 (The Radiochemical Centre, Amersham) with a specific activity of 0.05 mCi/g. After different storage times they were rinsed in four 10 ml portions of inactive isopropanol, half a minute in each portion. This rinsing procedure was shown to be satisfactory, since background activity was obtained in the last two rinsing portions. After the rinsing procedure, the bulbs were etched in 2 ml of a 5 % hydrofluoric acid solution for 1 min. An aliquot of 1 ml was taken and diluted with 10 ml of Bray's solution.[12] The samples were counted in a Packard Liquid Scintillation Spectrometer, Model 3375. The blank consisted of 1 ml hydrofluoric acid (5 %) and 10 ml Bray's solution.

Leakage studies. Semi-spherical bulbs of Ingold LoT glass, hydrated for 3 days, were stored in 10 ml inactive isopropanol during about one day and then transferred to a new 10 ml isopropanol portion for another day's storage. The samples were analysed for lithium by flame emisson spectroscopy.

RESULTS

In Fig. 1, the response of the low temperature electrode Ingold LoT is shown for different pre-treatments of the electrode surface. Curve A has been obtained after etching the electrode in a 5 % HF solution for 2 min. Such a treatment removes the entire gel-layer.[13] The response to the hydrogen ion concentration change is fast.

Curve B shows the response of a hydrated electrode, which was stored in air (about 35 % relative humidity) for 7 days. The response is obviously quite

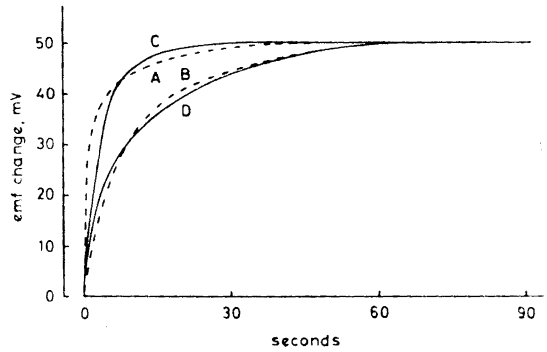

Fig. 1. Hydrogen ion response of an Ingold LoT electrode in isopropanol after different pre-treatments. The picric acid concentration was rapidly increased from 10^{-4} M to 10^{-3} M. A, etched electrode; B, air-stored hydrated electrode (7 days); C, hydrated electrode (aqueous storage); D, hydrated electrode stored in isopropanol for several months.

slow. Curve C has been obtained after immersion of the air-dried electrode in an aqueous pH 7 buffer for 2 h. It can be seen that a fast response results from this treatment. Further storage in the aqueous buffer solution did not change the response characteristics of this electrode.

Curve D illustrates the response of the hydrated Ingold LoT electrode after storage in pure isopropanol for several months. The response is retarded by this treatment.

Table 1. Amounts of isopropanol sorbed on glass bulbs at different states. Average area of the bulbs: 3 cm^2.

Glass state	Average amount of 2-PrOH (mol)	Number of observations	Rel. standard dev. (%)
Etched	2×10^{-8}	5	29
Hydrated	$< 6 \times 10^{-9}$	5	–

Table 1 shows the average amounts of isopropanol sorbed by etched and hydrated glass bulbs. The bulbs were stored for various times in isopropanol, but no significant time dependence in the region 0.5 – 144 h was found in any case. The average values have therefore been calculated from the analysis results obtained at different storage times. For hydrated glass bulbs, blank values were obtained in all cases. The detection limit of the method was 6×10^{-9} mol isopropanol when defined as the double blank value. The average area of the glass bulbs was estimated to be 3 cm^2.

Table 2 gives the amounts of lithium ions leached from hydrated Ingold LoT glass bulbs into inactive isopropanol as well as into water. As can be seen, the amount of lithium ion leakage into water is considerably higher.

Table 2. Amount of Li^+ leached into water and isopropanol from hydrated Ingold LoT glass bulbs. At zero time in the table the bulbs have been hydrated for 3 days in water.

Time period h	Amount of Li^+ (mol) leached into water	isopropanol
0 – 24	1.5×10^{-7}	9.0×10^{-9}
24 – 48	1.3×10^{-7}	8.5×10^{-9}

DISCUSSION

From Fig. 1 it can be concluded that both isopropanol and air storage of the hydrated Ingold LoT electrode caused a slow response. Both electrode pre-treatments will certainly remove water from the gel-layer. Since water molecules facilitate the transfer of hydrogen ions, the removal itself may be the cause of the response behaviour. However, an isopropanol sorption on the glass surface may influence the response in a similar manner. Absence of water might favour an adsorption of the alcohol on hydroxyl and possibly other sites analogous to that of methanol as described by Folman and Yates.[8–10]

A comparison of the results given in Fig. 1 and in Table 1 shows that no correlation between the amount of sorbed isopropanol and the response behaviour exists. On the etched glass surfaces a certain sorption was found while on hydrated surfaces no sorption could be detected. In spite of this, the response was very fast for both electrode states. It is therefore very likely that the sluggish response behaviour is caused by the desorption of water and that isopropanol sorption has no influence.

In order to explain the difference in sorption ability between etched and hydrated glasses their surface structures must be examined. By using electron scanning microscopy it has been established that pits appear on the etched glass while the hydrated glass exhibits a relatively smooth surface.[6] The detection limit of the method used corresponds to 4 – 5 monolayers of isopropanol if the surface area is 3 cm^2 and if only adsorption is accounted for. The amount of isopropanol found on etched glass was so large that effects other than adsorption (or esterification of surface sites) must be present. The main contribution to the measured sorption probably originates from solvent inclusions within porous etch-spots on the rough surface. A deeper penetration into the bulk glass is most unlikely since there is no detectable penetration into the hydrated glass surface. Penetration into a hydrated glass surface occurs more easily than into an etched surface.[13]

There are several indirect reports that the reactions between the glass network and water result in a loose gel-layer structure.[13–16] Solvent penetration into the gel-layer might thus be possible. The gel-layer thickness has been estimated to be about 1000 Å on an Ingold LoT electrode hydrated for two days.[17] The amount of isopropanol detected by the method used here corresponds to one solvent molecule per hundred ion exchange sites. Since every isopropanol analysis on the hydrated glass resulted in blank values it may be concluded that no detectable penetration of isopropanol into the gel-layer had occurred.

A high concentration of water in the external part of the gel-layer is to be expected on the hydrated Ingold LoT glass in conformity with the findings on sodium glasses.[15] As can be seen in Table 2, the amount of lithium ions leached during a certain time period in isopropanol is low compared with corresponding leakage in water. This observation is equivalent to a lower hydrogen ion flux inwards towards the glass bulk. As no isopropanol penetration was obtained, the cause of the decrease in hydrogen ion flux should be the absence of enough hydrogen ions and/or water molecules. The presence of water molecules in the gel-layer facilitates any ion transport. The water in the gel-layer will gradually be depleted due to diffusion out to the solvent and due to the continuous reaction with the dry glass. The depletion of water will slow the rate of hydrogen ion transfer which should lead to a retarded response, as observed for the electrode stored in isopropanol (curve D in Fig. 1).

Acknowledgements. The authors thank Dr. W. Ingold, Zürich, for gifts of specially made glass bulbs, Professor G. Johansson for valuable discussions and Dr. M. Sharp for linguistic revision of the manuscript.

This work was supported by grants from the *Swedish Natural Science Research Council.*

REFERENCES

1. Distèche, A. and Dubuisson, M. *Rev. Sci. Instr.* **25** (1954) 89.
2. Sirs, J. A. *Trans. Faraday Soc.* **54** (1958) 207.
3. Johansson, G. and Norberg, K. *J. Electroanal. Chem.* **18** (1968) 239.
4. Huber, W. *Titration in Nonaqueous Solvents*, Academic, New York 1967, Chapter 3.
5. Karlberg, B. *J. Electroanal. Chem.* **42** (1973) 115.
6. Wikby, A. *J. Electroanal. Chem.* **38** (1972) 429.
7. Wikby, A. *J. Electroanal. Chem.* **38** (1972) 441.
8. Folman, M. and Yates, D. J. C. *Proc. Roy. Soc.* **A 246** (1958) 32.
9. Folman, M. and Yates, D. J. C. *Trans. Faraday Soc.* **54** (1958) 429.
10. Folman, M. and Yates, D. J. C. *Trans. Faraday Soc.* **54** (1958) 1684.
11. Lowen, W. K. and Broge, E. C. *J. Phys. Chem.* **65** (1961) 16.
12. Bray, G. A. *Anal. Biochem.* **1** (1960) 279.
13. Wikby, A. *J. Electroanal. Chem.* **33** (1971) 145.
14. Karlberg, B. *Anal. Chim. Acta* **66** (1973) 93.
15. Dobos, S. *Acta Chim. Acad. Sci. Hung.* **69** (1971) 43.
16. Dobos, S. *Acta Chim. Sci. Hung.* **69** (1971) 49.
17. Wikby, A. *Unpublished results.*

Received January 11, 1973.

ACTA CHEMICA SCANDINAVICA 27 (1973) 1860–1874

Semi-empirical Parameters in π-Electron Systems

XIII. Parameters for the Lone Pair Electrons in the Carbonyl Group

GERMUND HÖJER, SARA MEZA and MARÍA ESTHER RUIZ

División de Estudios Superiores de la Facultad de Química, Universidad Nacional Autónoma de México, Ciudad Universitaria México, 20 D.F.

Parameters for the sigma lone pair electrons of the carbonyl group have been determined in a modified Pariser-Parr-Pople method. Calculated lone pair ionization potentials and n-π^* transitions are compared with experimental data whenever possible.

I. INTRODUCTION

In a series of papers,[1–12] the semi-empirical parameters in the PPP-approximation were reported for different types of molecules. Sundbom [11] determined also the appropriate parameters for taking into account the sigma lone pair electrons in azines, that is, the loosest bound sigma electrons in such compounds. Jensen and Skancke [5] (abbreviated JS in the present paper) determined the π-electron parameters for the carbonyl group, but generally, the highest occupied orbital in this type of molecules is found to be a sigma orbital of n character. Thus it is important to include these lone pair electrons in the study of the electronic structure of such molecules.

Using the JS π-parameters, we have determined the lone pair parameters by a least squares fit to the experimental data for the ionization potential of the n-orbital and the first singlet $n-\pi^*$ transition in a few standard molecules. The obtained parameters have then been tested on some other carbonyl compounds. Considering the crude approximations involved, the results are very good.

II. METHOD

Roos and Skancke introduced a modified Pariser-Parr-Pople method for π-electron systems in a paper on pure hydrocarbons.[1] In the following papers[2–12] it was extended to heteroatomic systems. We will not repeat here the basic formulas and parameters obtained for the π-electron systems. Our calculations were performed on a Burroughs B6700 at CIMASS, Universidad

Nacional Autónoma de México, with the program SCF-OPSZDO written by Roos and Sundbom.

Inclusion of the lone pair orbitals. For the π-part we used the results of JS. Their calculations gave very big net charges in the carbonyl group. Grabe and Skancke [13] studied the possibility of making the carbonyl π-parameters charge dependent. We decided to use the JS parameters as they gave good results and we were only studying neutral molecules in which the calculated net charges in the carbonyl group are fairly similar from one molecule to another. However, in the discussion of the results we will return to the problem of charge dependence of the parameters.

In a molecular orbital calculation the concept of lone pair orbitals is generally not strictly valid. The amount of delocalization depends on the method used and can vary within a class of similar molecules. For example, in an *ab initio* calculation on formaldehyde by Winter *et al.*,[14] the gross atomic populations in the n-orbital were: oxygen 1.266, carbon 0.138, and hydrogen 0.298. As comparison, we obtained in a CNDO type calculation 1.038, 0.270, and 0.346.[15] In glyoxal and *p*-benzoquinone the CNDO populations in the two highest-lying sigma orbitals were as illustrated in Fig. 1.

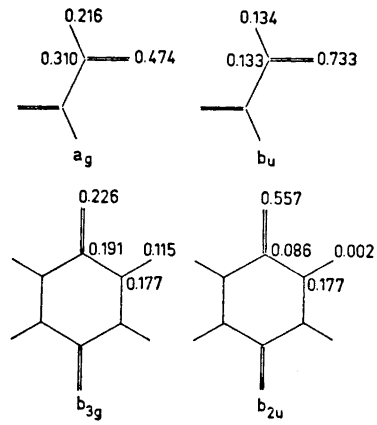

Fig. 1. The lone pair orbital populations in glyoxal and *p*-benzoquinone obtained from a CNDO calculation. [15] The orbital symmetries are given in the figure.

Turner *et al.*[16] found the splittings between the adiabatic ionization potentials of the lone pair orbitals in glyoxal and *p*-benzoquinone to be 1.6 eV and 0.3 eV, respectively. To account for these splittings, the lone pair orbitals must be considered to be partly delocalized in the MO picture. When these orbitals are included in a PPP calculation, as a first approximation they are considered to be completely localized on their respective atom and interacting with the π-system through the coulomb integrals $\gamma_{n\pi}$ and the one-center exchange integrals $K_{n\pi}$.[17] The splitting between the two n-orbitals in glyoxal, for example, is obtained by introducing a resonance integral $\beta_{nn'}$, which is not formally compatible with the approximations for the π-system as n and n' are not nearest neighbours.

Accepting this localized model for the n-orbitals, the question is which type of atomic orbital one should assume for an n-orbital. In formaldehyde, hybridization is forbidden by symmetry and the n-orbital must be a pure $2p$-orbital perpendicular to the CO-bond. In molecules in which hybridization is not forbidden by symmetry, our CNDO calculations showed that the n-orbital in benzaldehyde had 0.6 % oxygen $2s$ and 30.6 % oxygen $2p$ character.[15] In glyoxal, the $2s$ contribution to the n-orbitals was even less. In an *ab initio* calculation on formamide by Christensen *et al.*,[18] the lone pair orbital was strongly localized on the oxygen atom (70 %) and it had no $2s$ character. Our assumption has thus been, that the oxygen lone pair orbital is a pure $2p$ orbital centered on the oxygen atom and perpendicular to the π-orbital and the CO-bond.

When the n-orbitals are included in the PPP-method, one makes a small deviation from the ZDO approximation, as the one-center exchange integral $K_{n\pi}$ is kept. The modified core- and Fock-matrix elements are:

$$H_{\mu\mu}{}^{\pi} = \alpha_{\mu}{}^{\pi} = W_{\mu}{}^{\pi} - \sum_{\nu}(n_{\nu} - \delta_{\mu\nu})\gamma_{\mu\nu} + K_{n\pi}$$

$$H_{\mu\mu}{}^{n} = \alpha_{\mu}{}^{n} = W_{\mu}{}^{n} - \sum_{\nu}(n_{\nu} - \delta_{\mu\nu})\gamma_{\mu\nu} + \tfrac{1}{2}K_{n\pi}$$

$$H_{\mu\nu}{}^{n\pi} = \beta_{n\nu} = 0$$

$$F_{\mu\mu}{}^{\pi} = \alpha_{\mu}{}^{\pi} - \tfrac{1}{2}P_{\mu\mu}\gamma_{\mu\mu} + \sum_{\nu}P_{\nu\nu}\gamma_{\mu\nu} - K_{n\pi}$$

$$F_{\mu\mu}{}^{n} = \alpha_{\mu}{}^{n} - \gamma_{nn} + \sum_{\nu}P_{\nu\nu} - \tfrac{1}{2}K_{n\pi}$$

$$F_{\mu\nu}{}^{\pi\pi} = \beta_{\mu\nu}{}^{\pi\pi} - \tfrac{1}{2}P_{\mu\nu}\gamma_{\mu\nu} \qquad \mu \neq \nu$$

$$F_{\mu\nu}{}^{nn} = \beta_{\mu\nu}{}^{nn} \qquad \mu \neq \nu.$$

$$F_{\mu\nu}{}^{n\pi} = 0$$

In these formulas, $K_{n\pi} = 0$, unless the atomic orbital μ belongs to an atom with a σ lone pair, and n_{ν} is the number of electrons in the orbital ν.

In order to determine the symmetry of the lone pair orbitals in glyoxal, for example, we adopted the following convention: the phase of the n-orbital is chosen such that the CO-bond (in the direction C→O), the n-orbital and the π-orbital (on oxygen) form a right-hand system. From our CNDO calculations we determined the order of the lone pair orbitals in glyoxal, p-benzoquinone, o-benzoquinone, and maleic anhydride. The sign of $\beta_{nn'}$ was chosen such that with the above mentioned convention, the calculated orbital order in this method agreed with the CNDO results. In the cases of glyoxal and p-benzoquinone, Turner's results [16] made it possible to obtain the magnitude of $\beta_{nn'}$. In the other molecules with more than one carbonyl group, we wanted, of course, an empirical expression for $\beta_{nn'}$ to be able to estimate the splittings between the n-orbitals. Generally such expressions give β as proportional to the overlap. If the overlap integral is calculated with Slater $2p$-orbitals centered on the oxygen atoms, the obtained value decreases very rapidly with the oxygen-oxygen distance. With the convention given above for the phase, the values are: glyoxal $+10^{-4}$, p-benzoquinone -10^{-6}, o-benzoquinone -10^{-2}, and maleic anhydride -10^{-5}. As we expect the n-orbitals to be partly delocal-

ized in the molecules, the values should be bigger and possibly not fall off so rapidly with the O – O distance. The experimental splittings for the IP's in glyoxal and *p*-benzoquinone gave two β values. They were fitted to expressions of the forms

$$\beta = kS + a$$

and

$$\beta = \pm k\sqrt{|S|} + a.$$

The β's obtained from these formulas for maleic anhydride and *o*-benzoquinone were unrealistic. The formula

$$\beta = \pm \frac{k}{R_{OO'}} + a, \quad k = 50.5 \times 10^{-3}, \text{ and } a = 15 \times 10^{-3}$$

was more successful. The sign factors above were chosen to agree with the signs of the overlap integrals. This formula should partly take the delocalization into account. However, it suggests that two carbonyl groups, very far apart in a large molecule, should interact appreciably due to the constant a. Perhaps that constant should be adjusted when the O – O distance is much longer than in the cases considered here. Putting $\beta_{nn'} = 0$, of course, makes the n-orbitals degenerate, but the calculations will anyhow give the ranges where the n ionization potentials and the n-π^* transitions should be expected.

The one-center integrals $K_{n\pi}$, γ_{nn} and $\gamma_{n\pi}$ were taken from atomic spectral data.[19,20] The two-center integral $\gamma_{C(\pi)O(n)}$ and $W_{O(n)}$ were determined by a least squares fit to some experimental data as described below. The remaining Coulomb integrals were calculated by means of a charged spheres approximation. The diameters of the lone pair spheres were 1.04 Å. The experimental data used were the lone pair ionization potentials in formaldehyde, acrolein, glyoxal, and the first singlet n-π^* transitions in these molecules, plus benzaldehyde. It is now a couple of years ago since JS determined the π-parameters. Though some new data have been published on these molecules, we decided to use the corresponding lone pair data, if possible.

Table 1. Semi-empirical parameters for the carbonyl group. In atomic units.

$\gamma_{O_1(n)O_1(n)}$	0.6946	$\gamma_{O_1(\pi)O_1(\pi)}$ [a]	0.6946
$\gamma_{O_1(n)O_1(\pi)}$	0.6196	$\gamma_{C(\pi)O(\pi)}$ [a]	0.3429
$K_{O_1(n)O_1(\pi)}$	0.037485	$\beta_{C(\pi)O(\pi)}$ [a]	−0.0904
$\gamma_{O(n)C(\pi)}$	0.1980	$W_{O(\pi)}$ [a]	−0.7203
$W_{O(n)}$	−0.5950	$\Delta W_{C(\pi)(O)}$ [a]	−0.0261
$\beta_{nn'}$	$\left(\pm\frac{0.505}{R_{nn'}} + 0.15\right) \times 10^{-1}$ [b]		

[a] Parameter determined by Jensen and Skancke.[5]
[b] Sign convention explained in the text. $R_{nn'}$ in Å.

The resulting parameter set is given in Table 1. As can be seen from that table, the obtained parameters are not quite consistent. One would have expected the Coulomb integrals $\gamma_{C(\pi)O(\pi)}$ and $\gamma_{C(\pi)O(n)}$ to have similar values. The discrepancy must be due to the method.

III. RESULTS AND DISCUSSION

Geometries and charge densities. The bond lengths were estimated from the bond orders p by the formulas

$$R_{CC} = 1.517 - 0.18p$$
$$R_{CO} = 1.365 - 0.18p \text{ carbonyl}$$
$$R_{CO} = 1.430 - 0.214p \text{ ether}$$

In Table 2, only those molecules not calculated by JS are listed, since the inclusion of the n-orbitals does not affect the geometries. The numbering of the bonds is defined in Fig. 2. The bond orders are listed together with the

Table 2. Assumed, calculated and observed bond lengths. All values in Å.

Molecule	Bond	R_{ass}	R_{calc}	R_{obs}
Acetophenone	1–2	1.22	1.228	
	2–3	1.48	1.470	
	3–4	1.40	1.402	
	4–5	1.40	1.396	
	5–6	1.40	1.398	
	6–7	1.40	1.397	
	7–8	1.40	1.397	
	3–8	1.40	1.401	
	2–9	1.52		
Formic acid	1–2	1.220	1.220	1.217[a]
	1–3	1.339	1.338	1.361[a]
Acetic acid	1–2	1.497		1.497[b]
	2–3	1.227	1.227	
	2–4	1.344	1.343	
Maleic anhydride	1–4	1.344	1.343	
	4–5	1.472	1.473	
	5–6	1.349	1.349	
	2–4	1.228	1.229	

[a] Ref. 26. [b] Ref. 27.

π-electron densities in Table 3. We did not find the structures of maleic anhydride, acetophenone and acetic acid in the literature. The experimental geometry of formic acid was used as a trial geometry for acetic acid. In maleic anhydride and acetophenone we tried to guess reasonable structures. The first results showed large differences between assumed and calculated structures in maleic anhydride and the acids. Thus new geometries were assumed for these molecules. Table 2 refers to these last calculations. The results show that

Table 3. Calculated π-electron densities and bond orders for the molecules not calculated by Jensen and Skancke.[5] The numbering of atoms is given in Fig. 2.

Molecule	Atom	π-Electron density [a]	Bond	Bond order
Acetophenone	1	1.608	1–2	0.760
	2	0.484	2–3	0.264
	3	0.924	3–4	0.639
	4	1.056	4–5	0.671
	5	0.990	5–6	0.664
	6	0.994	6–7	0.665
	7	0.984	7–8	0.669
	8	0.994	8–3	0.642
	9	1.965	2–9	0.228
Formic acid	1	0.589	1–2	0.805
	2	1.541	1–3	0.428
	3	1.870		
Acetic acid	1	1.965	1–2	0.224
	2	0.558	2–3	0.769
	3	1.590	2–4	0.405
	4	1.886		
Maleic anhydride	1	1.752	1–4	0.406
	2	1.570	4–5	0.247
	4	0.594	5–6	0.933
	5	0.959	2–4	0.758

[a] The lone pair orbitals are, of course, occupied by 2.0 electrons.

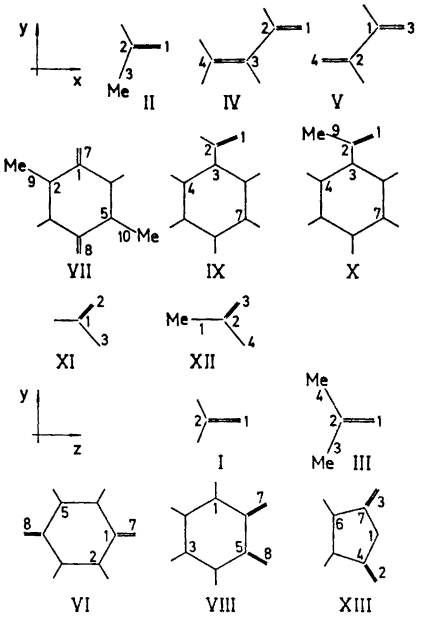

Fig. 2. Coordinate system and notation for the molecules: I formaldehyde (C_{2v}), II acetaldehyde (C_s), III acetone (C_{2v}), IV acrolein (C_s), V glyoxal (C_{2h}), VI *p*-benzoquinone (D_{2h}), VII 2,5-dimethyl-*p*-benzoquinone (C_{2h}), VIII *o*-benzoquinone (C_{2v}), IX bezaldehyde (C_s), X acetophenone (C_s), XI formic acid (C_s), XII acetic acid (C_s), XIII maleic anhydride (C_{2v}).

the calculations are almost self-consistent in the geometries when the bond angles are neglected. The other calculated properties were insensitive to these geometry variations.

The π-electron densities are obtained under the assumption that the σ cores are non-polarizable, which the *ab initio* and all-valence electron calculations have shown not to be the case. Specially in the present case, the carbonyl group, there seem to be large redistributions of both π- and σ-electrons. We have only used the charge densities to discuss the validity of our parameters but have not tried to interpret the charge distributions from a chemical point of view.

Ionization potentials. The calculated and the experimental ionization potentials are reported in Table 4. The values marked + have been used in the determination of the parameters.

The calculated IP's correspond to the vertical potentials. When the present program [1–12] was started, there were very few vertical IP's reported in the literature. Thus the adiabatic values were used instead. This means that the param-

Table 4. Calculated and observed ionization potentials. Values in eV. Previously published π ionization potentials[a] are included to allow comparison with experimental data.

Molecule	IP_{calc}	Symmetry	IP_{obs}	
Formaldehyde	10.96	$b_2(n)$	10.88[b]	10.87[c]+
	13.99	$b_1(\pi)$	14.09[b]	13.99[c]
Acetaldehyde	10.28	$a'(n)$	10.23[c]	10.20[d]
	12.14	$a''(\pi)$	12.75[c]	12.71[d]
	13.85	$a''(\pi)$	13.90[c]	13.97[d]
Acetone	9.69	$b_2(n)$	9.67[c]	9.68[d]
	11.89	$b_1(\pi)$	12.16[c]	12.16[d]
	12.28	$a_2(\pi)$		
	13.82	$b_1(\pi)$	14.15[c]	13.94[d]
			15.55[c]	15.47[d]
Acrolein	10.31	$a'(n)$	10.11[b]	9.99[c]+
	10.75	$a''(\pi)$	10.93[b]	10.82[c]
	13.75	$a''(\pi)$		13.19[c]
Glyoxal	10.18	$a_g(n)$	10.59[b]+	
	11.78	$b_u(n)$	12.19[b]	
	13.78	$b_g(\pi)$	13.85[b]	
	14.87	$a_u(\pi)$		
p-Benzoquinone	10.21	$b_{3g}(n)$	10.11[b]	9.95[d]
	10.51	$b_{2u}(n)$	10.41[b]	
	11.03	$b_{3u}(\pi)$	11.06[b]	10.88[d]
	11.12	$b_{1g}(\pi)$	11.25[b]	
	13.72	$b_{2g}(\pi)$	13.43[b]	13.26[d]
	14.53	$b_{3u}(\pi)$		14.05[d]
2,5-Dimethyl-	10.07	$a_g(n)$		
-*p*-benzoquinone	10.35	$b_g(\pi)$		
	10.37	$b_u(n)$		
	10.48	$a_u(\pi)$		
	12.88	$a_u(\pi)$		
	13.11	$b_g(\pi)$		
	13.63	$b_g(\pi)$		
	14.49	$a_u(\pi)$		

Table 4. Continued.

o-Benzoquinone	10.09	$a_2(\pi)$		
	10.10	$a_1(n)$		
	10.30	$b_2(n)$		
	12.35	$b_1(\pi)$		
	13.18	$a_2(\pi)$		
	14.45	$b_1(\pi)$		
Benzaldehyde	9.44	$a''(\pi)$	9.46[c]	9.51[e]
	9.71	$a''(\pi)$		
	10.10	$a'(n)$		
	12.50	$a''(\pi)$	11.48[c]	
	13.63	$a''(\pi)$		
Acetophenone	9.41	$a''(\pi)$		
	9.57	$a'(n)$		
	9.69	$a''(\pi)$		
	11.95	$a''(\pi)$		
	12.53	$a''(\pi)$		
	13.67	$a''(\pi)$		
Formic acid	10.38	$a'(n)$	11.33[b]	
	10.61	$a''(\pi)$	12.36[b]	
	13.67	$a''(\pi)$	~ 14.20[b]	
Acetic acid	9.82	$a'(n)$		
	10.46	$a''(\pi)$		
	11.98	$a''(\pi)$		
	13.71	$a''(\pi)$		
Maleic anhydride	10.14	$b_1(\pi)$		
	10.74	$b_2(n)$		
	10.94	$a_1(n)$		
	11.17	$b_1(\pi)$		
	13.89	$a_2(\pi)$		
	14.77	$b_1(\pi)$		

[a] Ref. 5. [b] Ref. 16, adiabatic photoionization potentials. [c] Ref. 28, adiabatic photoionization potentials. [d] Ref. 29, adiabatic photoionization potentials. [e] Ref. 30, adiabatic. [+] Experimental value used for the parametrization.

eters have been obtained by systematically fitting to slightly too low experimental values. Though vertical IP's are reported to-day in some cases, we used the adiabatic values. Furthermore, we tried to use the IP(n)'s corresponding to the IP(π)'s used by JS.

The original idea was to use the same standard molecules as JS. They based their parametrization on the assumption, that the first ionization potential in both formaldehyde and acrolein is due to the loss of a lone pair electron. The benzaldehyde spectrum [16] shows a high broad band in the region 9 to 11 eV, a second band from 11.5 to 13.5 eV, and a third one from 13.5 to 16.5 eV. A small peak at 9.46 eV was interpreted by them as the highest lying π-orbital. Their calculations were then in good agreement with the experiments when they assumed the first IP in both acetaldehyde and acetone to be due to a lone pair electron. They did not have any data for glyoxal and the quinones at the time they made their calculations. Since then, Turner [16] has reported the photoionization spectra for both glyoxal and *p*-benzoquinone. Turner has also identified the n and π IP's. In Table 4 it can be seen that the JS values are in very good agreement with the experimental data for these molecules, too.

In the preliminary parametrization we used the lone pair orbital of benzaldehyde, assuming it to be in the same energy range as the π-orbital, instead of the glyoxal n-orbital at 10.59 eV. That meant that the n-orbital in benzaldehyde should have a significantly lower ionization potential than the n-orbital in acetaldehyde. These preliminary parameters gave the correct results in glyoxal, acetaldehyde, acetone, and p-benzoquinone, besides reproducing the data on the standard molecules with one exception; the lone pair orbital in benzaldehyde had a larger orbital energy than we had assumed. Thus we decided not to try to make any interpretation of the benzaldehyde spectrum and to use for the parametrization the first IP in glyoxal instead. The final parameters obtained were in the same range as the preliminary ones. The new data on formaldehyde and acrolein [16] would not have changed neither the π nor the n parametrization to any significant degree.

Table 4 shows that our calculations reproduce the experimental ionization potentials for the lone pair orbitals in the standard molecules and in acetaldehyde, acetone, and p-benzoquinone very well. If the n-orbital is supposed to be mainly localized in the carbonyl group, then our calculated IP(n) at 10.10 eV in benzaldehyde is very reasonable when compared with acetaldehyde. The experimental spectrum [16] does not contradict this interpretation either. As a matter of fact, our three first IP's correspond very well to the experimental band in the region 9 to 11 eV, and the last two calculated IP's fall in the range of the second broad band. The π-orbitals at 9.44 and 9.71 eV are strongly localized to the ring and correspond to the degenerate e_{1g} orbitals at 9.25 eV in benzene. They are naturally split by the presence of the aldehyde perturbation. In acetophenone, there are no experimental data to compare with, but looking at acetaldehyde, acetone, and benzaldehyde, the results look very well justified. The n-orbital in acetone is destabilized by about 0.5 eV as compared to the n-orbital in acetaldehyde, and the corresponding value for acetophenone-benzaldehyde is 0.53 eV. The π-levels originating from the benzene e_{1g} level show the same behaviour as in benzaldehyde. There are no experimental data for 2,5-dimethyl-p-benzoquinone and o-benzoquinone. The partly localized character of the n-orbitals leads one to expect them not to be greatly affected by the methyl groups in the first molecule, as compared to p-benzoquinone. The calculations support such a guess.

In formic acid and acetic acid, the carbonyl oxygen [5] and the ether oxygen [6] parameters are combined in the COOH group. In the case of formic acid where there are experimental data, it can be seen that neither spacing nor absolute values for the orbital energies agree very well with Turner's [16] adiabatic photoionization potentials. One can expect the same deviations from the experimental values to be valid in acetic acid, too. Chemically, the carboxyl group is a well-defined group, which quite probably requires special parametrization. The calculated π-charges in the carbonyl part of these molecules are very close to what was obtained in the other molecules. However, this means that the ether oxygen is attached to a very positive carbon, around +0.5 units of charge. The ether oxygen parameters were determined in molecules in which the carbon atom bonded to the oxygen atom was almost neutral.[6] Thus we have a completely different situation here. Grabe and Skancke [13] obtained a little better results for the π-system in formic acid by making the

parameters charge dependent. In maleic anhydride there are no experimental data on the IP's as far as we could see in the literature. But probably we have the same problem here with the charges and the parameters as in the acids, and thus the results are not as good as in the standard molecules and the first set of test molecules. The calculated π-charge on the carbon bonded to the oxygens is $+0.41$ while in furan it is -0.08. The CNDO calculations show the same pattern in the charge distributions in these two molecules, though less pronounced. The CNDO results also indicate that the polarization of the sigma core is of greater importance in the carbonyl compounds than in molecules with ether-type oxygen only. The results for the carbon bonded to the oxygens in maleic anhydride were: $+0.17$ (π) and $+0.12$ (σ), while in furan the numbers were: -0.05 (π) and $+0.03$ (σ). The conclusion is that it is not advisable to combine the ether and the carbonyl oxygen parameters in the PPP scheme without taking the charges into account.

Electronic spectra. The calculated spectra should be compared with the experimental vertical transitions, that is ν_{max}. The experimental ν_{00} transitions have lower energies, which should be kept in mind when only ν_{00} is reported. The transitions have been calculated by mixing all singly excited states. The parametrization has been made for the singlet states. The results for such states are listed in Table 5. Experience has shown, that the triplet

Table 5. Calculated and observed singlet $n-\pi^*$ and $\pi-\pi^*$[a] transitions. Transition energies in eV.

Molecule Point group	Symmetry[b]		Calculations ν	f		Observations ν	
Formaldehyde	$^1A_2$	$n-\pi^*$	4.04	0.0		4.20	$f=2.4\times10^{-4}$ [c,+], 4.28[d]
C_{2v}	$^1A_1$	$\pi-\pi^*$	7.96	0.40		7.95[d]	
Acetaldehyde	$^1A''$	$n-\pi^*$	4.33	0.0	A	4.28	log $\varepsilon=1$[e]
C_s	$^1A'$	$\pi-\pi^*$	7.63	0.38		7.52	$f=0.13$[d,f,g]
	$^1A'$	$\pi-\pi^*$	9.09	0.07			
Acetone	$^1A_2$	$n-\pi^*$	4.63	0.0		4.43	log $\varepsilon=1.05$[e]
C_{2v}	$^1A_1$	$\pi-\pi^*$	7.66	0.38		8.05[d]	
	$^1B_2$	$\pi-\pi^*$	9.05	0.12			
Acrolein	$^1A''$	$n-\pi^*$	3.70	0.0	A	3.76[d,h,+]	
C_s	$^1A'$	$\pi-\pi^*$	6.24	0.70		6.41[d,h], 5.96	$\varepsilon=13\,000$[i]
	$^1A'$	$\pi-\pi^*$	7.61	0.09			
Glyoxal	^1A_u	$n-\pi^*$	2.81	0.0	A	2.7[j,k]	
C_{2h}	^1B_g	$n-\pi^*$	4.23	0.0		4.5[l]	
	^1B_g	$n-\pi^*$	7.30	0.0			
	^1B_u	$\pi-\pi^*$	7.48	0.70		7.44[d]	
	^1A_g	$\pi-\pi^*$	7.60	0.0			
	^1A_u	$n-\pi^*$	8.73	0.0	A		
	^1A_g	$\pi-\pi^*$	10.33	0.0			
p-Benzoquinone	$^1B_{1g}$	$n-\pi^*$	2.79	0.0		2.71	$\varepsilon=20$[m]
D_{2h}	^1A_u	$n-\pi^*$	3.04	0.0			
	$^1B_{3g}$	$\pi-\pi^*$	4.21	0.0		4.28	$f=0.008$[n], 4.49[o]
	$^1B_{1u}$	$\pi-\pi^*$	5.37	0.70		5.17	$f=0.15$[n], 5.17°
	$^1B_{3u}$	$n-\pi^*$	6.46	0.0	A		
	$^1B_{2g}$	$n-\pi^*$	6.76	0.0			
	$^1B_{3g}$	$\pi-\pi^*$	7.14	0.0			

Table 5. Continued.

	^1A_g	$\pi-\pi^*$	7.17	0.0			
	$^1B_{1u}$	$\pi-\pi^*$	7.25	0.001			
	^1A_u	$n-\pi^*$	7.45	0.0			
	$^1B_{1g}$	$n-\pi^*$	7.57	0.0			
	$^1B_{1u}$	$\pi-\pi^*$	7.93	1.35			
2,5-Dimethyl-*p*-benzoquinone C_{2h}	^1B_g	$n-\pi^*$	2.94	0.0			
	^1A_u	$n-\pi^*$	3.19	0.0	A		
	^1A_g	$\pi-\pi^*$	3.84	0.0		4.07[o]	
	^1B_u	$\pi-\pi^*$	5.16	0.70		4.98[o]	
	^1B_u	$\pi-\pi^*$	6.75	0.05			
	^1A_u	$n-\pi^*$	6.78	0.0	A		
	^1A_g	$\pi-\pi^*$	7.04	0.0			
	^1B_g	$n-\pi^*$	7.08	0.0			
	^1A_g	$\pi-\pi^*$	7.16	0.0			
	^1A_u	$n-\pi^*$	7.54	0.0	A		
	^1A_g	$\pi-\pi^*$	7.63	0.0			
	^1B_g	$n-\pi^*$	7.67	0.0			
	^1B_u	$\pi-\pi^*$	7.67	0.84			
o-Benzoquinone C_{2v}	$^1B_1$	$n-\pi^*$	2.43	0.0	A	2.07[p]	
	$^1A_2$	$n-\pi^*$	2.62	0.0			
	$^1B_2$	$\pi-\pi^*$	3.94	0.18		3.3 – 3.4	$f=0.66$[p]
	$^1A_1$	$\pi-\pi^*$	6.08	0.11		4.9	$f=0.26$[p]
	$^1B_2$	$\pi-\pi^*$	6.44	0.03			
	$^1B_1$	$n-\pi^*$	6.67	0.0	A		
	$^1A_2$	$n-\pi^*$	6.85	0.0			
	$^1A_2$	$n-\pi^*$	7.11	0.0			
	$^1A_1$	$\pi-\pi^*$	7.15	1.16		6.2 strong[p]	
	$^1B_2$	$\pi-\pi^*$	7.19	0.35			
Benzaldehyde C_s	$^1A''$	$n-\pi^*$	3.89	0.0	A	3.77	$\varepsilon=53$[q,+], 3.41[r]
	$^1A'$	$\pi-\pi^*$	4.62	0.01		4.52	$f=0.02$[s]
	$^1A'$	$\pi-\pi^*$	5.47	0.39		5.35	$f=0.26$[s]
	$^1A'$	$\pi-\pi^*$	6.37	0.56		6.35	
	$^1A'$	$\pi-\pi^*$	6.62	0.89		6.68	
	$^1A'$	$\pi-\pi^*$	7.50	0.31		6.97	$f=1.7$[s]
	$^1A''$	$n-\pi^*$	7.58	0.0	A		
	$^1A'$	$\pi-\pi^*$	7.68	0.05		7.58	
	$^1A'$	$\pi-\pi^*$	7.89	0.50			
Acetophenone C_s	$^1A''$	$n-\pi^*$	4.03	0.0	A	3.87	$\varepsilon=41$[t]
	$^1A'$	$\pi-\pi^*$	4.67	0.01			
	$^1A'$	$\pi-\pi^*$	5.66	0.33		5.20	$\varepsilon=12\,600$[t]
	$^1A'$	$\pi-\pi^*$	6.48	0.60			
	$^1A'$	$\pi-\pi^*$	6.67	1.01			
	$^1A''$	$n-\pi^*$	7.10	0.0	A		
	$^1A'$	$\pi-\pi^*$	7.49	0.44			
	$^1A'$	$\pi-\pi^*$	7.68	0.11			
	$^1A''$	$n-\pi^*$	7.69	0.0	A		
	$^1A'$	$\pi-\pi^*$	7.97	0.26			
Formic acid C_s	$^1A''$	$n-\pi^*$	4.38	0.0	A	4.8[u]	
	$^1A'$	$\pi-\pi^*$	6.78	0.36		8.0[u], 7.80	$\varepsilon=2500$[v]
	$^1A'$	$\pi-\pi^*$	8.62	0.15			
Acetic acid C_s	$^1A''$	$n-\pi^*$	4.65	0.0	A		
	$^1A'$	$\pi-\pi^*$	7.00	0.35		7.75	$\varepsilon=4200$[v]
	$^1A'$	$\pi-\pi^*$	8.22	0.19			
	$^1A'$	$\pi-\pi^*$	9.77	0.01			
Maleic anhydride C_{2v}	$^1B_2$	$\pi-\pi^*$	3.13	0.01			
	$^1B_1$	$n-\pi^*$	3.44	0.0	A	3.7 – 4.3 weak[w]	
	$^1A_2$	$n-\pi^*$	3.59	0.0		4.3 – 5.7 weak[w]	
	$^1B_2$	$\pi-\pi^*$	5.44	0.60		5.7 – 6.7 strong[w]	

Table 5. Continued.

$^1A_1$	$\pi-\pi^*$	7.06	0.01	
$^1B_2$	$\pi-\pi^*$	7.31	0.45	
$^1A_2$	$n-\pi^*$	7.34	0.0	
$^1B_1$	$n-\pi^*$	7.38	0.0	A
$^1B_2$	$\pi-\pi^*$	7.58	0.15	
$^1A_1$	$\pi-\pi^*$	7.86	0.31	

A. Dipole allowed though $f_{calc}=0.0$. + Experimental value used for the parametrization. [a] Ref. 5. [b] The symmetries refer to the choice of coordinate systems defined in Fig. 2. [c] Ref. 21, page 430, vapour ν_{max}. [d] Ref. 31, vapour. [e] Ref. 21, page 432, vapour ν_{max}. [f] Ref. 32, vapour. [g] Ref. 33, vapour. [h] Ref. 34, vapour. [i] Ref. 21, page 438. [j] Ref. 23, vapour. [k] Ref. 35, vapour. [l] Ref. 36, vapour. [m] Ref. 37, heptane. [n] Ref. 38, vapour. [o] Ref. 39, heptane ν_{max}. [p] Ref. 40, vapour ν_{max}. [q] Ref. 41, heptane ν_{max}. [r] Ref. 42, crystal. [s] Ref. 43, vapour ν_{max}. [t] Ref. 44, heptane ν_{max}. [u] Ref. 45. [v] Ref. 46, vapour ν_{max}. [w] Ref. 25, EPA.

states have not been well described by the parameters obtained in this way. Generally, the triplet $\pi-\pi^*$ transitions have been calculated around 1 eV too low. In the few cases we have experimental triplet $n-\pi^*$ transitions for the molecules considered in this paper, the calculated values seem to be better than that. The formula for the triplet transition energy is:

$$E(\text{triplet } n-\pi^*)=e_{\pi^*}-e_n-J_{n\pi^*}$$

As the n-orbital is completely localized in our model, the Coulomb integral may be too small and the calculated transition energy thus too high. The result is that in most cases the calculations predict the triplet $\pi-\pi^*$ transition to have the lowest energy. The values are given in Table 6 for comparison.

Another point to remember in the case of the singlet transitions is that the method always gives an f-value = 0 for the $n-\pi^*$ transitions though they may be dipole-allowed. We have indicated in Table 5 if an excitation is allowed though $f_{calc}=0$. Furthermore, to simplify the evaluation of the results, we have included the $\pi-\pi^*$ transitions obtained by JS. The values we give for the $\pi-\pi^*$ excitations differ sometimes in the second decimal from those published by JS due to using slightly different geometries or rounding off errors when converting units.

There seems to be no ambiguity in the assignments of the transitions in the standard molecules. The calculations reproduce very well the experimental data on these molecules. The observed shift in the $n-\pi^*$ transitions when attaching methyl groups to the carbonyl, see formaldehyde-acetaldehyde-acetone and benzaldehyde-acetophenone, is reproduced in the calculations. The explanation of this shift has been thought to be the raising of the π^*-orbital by both inductive and hyperconjugative effects, while the n-orbital was assumed to be unaffected.[21] But as can be seen from Table 4, the energy of the n-orbital is strongly affected by the methyl substitution in agreement with the experimental ionization potentials. However, the calculations also show the predicted shift of the π^*-orbital. As a matter of fact, the difference in orbital energy between π^* and n is almost constant, so it is the change in $(-J_{n\pi^*}+2K_{n\pi^*})$ which gives the observed shift in the $n-\pi^*$ transition.

Table 6. Calculated and observed triplet $n-\pi^*$ and $\pi-\pi^*$ transitions. Transition energies in eV.

Molecule	Symmetry		Calculations ν	Observations ν
Formaldehyde	$^3A_1$	$\pi-\pi^*$	3.24	3.14[a]
	$^3A_2$	$n-\pi^*$	3.51	
Acetaldehyde	$^3A'$	$\pi-\pi^*$	3.59	
	$^3A''$	$n-\pi^*$	3.86	
Acetone	$^3A_1$	$\pi-\pi^*$	3.97	
	$^3A_2$	$n-\pi^*$	4.22	
Acrolein	$^3A'$	$\pi-\pi^*$	2.31	
	$^3A''$	$n-\pi^*$	3.29	
Glyoxal	^3A_u	$n-\pi^*$	2.44	2.42[b]
	^3B_u	$\pi-\pi^*$	3.31	
p-Benzoquinone	$^3B_{1u}$	$\pi-\pi^*$	1.96	
	$^3B_{3g}$	$\pi-\pi^*$	2.23	
	$^3B_{1g}$	$n-\pi^*$	2.47	
	^3A_u	$n-\pi^*$	2.72	
2,5-Dimethyl-	^3B_u	$\pi-\pi^*$	1.97	
p-benzoquinone	^3A_g	$\pi-\pi^*$	2.14	
	^3B_g	$n-\pi^*$	2.62	
	^3A_u	$n-\pi^*$	2.86	
o-Benzoquinone	$^3B_2$	$\pi-\pi^*$	1.54	
	$^3B_1$	$n-\pi^*$	2.10	
	$^3A_2$	$n-\pi^*$	2.28	
	$^3A_1$	$\pi-\pi^*$	2.95	
Benzaldehyde	$^3A'$	$\pi-\pi^*$	2.61	
	$^3A''$	$n-\pi^*$	3.48	3.17[c]
Acetophenone	$^3A'$	$\pi-\pi^*$	2.69	
	$^3A''$	$n-\pi^*$	3.68	3.28[c]
	$^3A'$	$\pi-\pi^*$	3.76	
Formic acid	$^3A'$	$\pi-\pi^*$	3.27	
	$^3A''$	$n-\pi^*$	3.91	
Acetic acid	$^3A'$	$\pi-\pi^*$	3.69	
	$^3A''$	$n-\pi^*$	4.23	
Maleic anhydride	$^3B_2$	$\pi-\pi^*$	1.95	
	$^3B_2$	$\pi-\pi^*$	2.32	
	$^3B_1$	$n-\pi^*$	3.08	
	$^3A_2$	$n-\pi^*$	3.23	

[a] Ref. 47 0–0 band. [b] Ref. 23. 0–0 band. [c] Ref. 42.

As far as there exist experimental data to compare with, the calculated $n-\pi^*$ transitions in glyoxal and the quinones seem to be quite good. One important point here is that we have taken the interaction between the *n*-orbitals into account. As mentioned before, Turner [16] observed a large splitting of the *n*-orbitals in glyoxal and a smaller splitting in *p*-benzoquinone. Earlier it had been believed that the *n*-orbitals interact very weakly. Suzuki [21] gives the splitting to less than 100 cm^{-1} in the planar *trans*-configuration of dicarbonyls. Our results lead to a change in the MO-interpretation of the spectra of these molecules. In glyoxal, our calculated orbital order is $a_u b_g b_u a_g a_u b_g$, with the first four orbitals occupied in the ground state. The earlier inter-

pretation was that the observed $n-\pi^*$ transitions at 2.7 and 4.5 eV were due to excitations from the almost degenerate "$b_u a_g$ level" to a_u and b_g, respectively.[17,20,22] However, in our case, the b_u and a_g orbitals are well separated and the experimental transitions are calculated to be mainly excitations from the a_g to the a_u orbital, and from the b_u to the a_u orbital, respectively. We also calculate a second set of $n-\pi^*$ transitions corresponding to excitations to the b_g orbital. Studies of the polarization of the 2.7 eV transition confirm the assignment ^1A_u.[23,24]

Our calculated spectra in both formic acid and acetic acid predict too low transition energies. This is true for both the $n-\pi^*$ and the $\pi-\pi^*$ transitions. The experimental spectra were taken under such conditions that they must refer to the monomers. The reason for the poor agreement between our calculations and the experimental data on these molecules was discussed in the section on the ionization potentials.

The spectra of maleic anhydride has been studied both experimentally and theoretically by Seliskar and McGlynn.[25] Their measurements indicated that the first three bands are with increasing energy: $n-\pi^*$, $n-\pi^*$, and $\pi-\pi^*$. Their calculations with the program CNDO/s-CI by Del Bene and Jaffé supported this interpretation and allowed them to make assignments with respect to the symmetry of the transitions. Their results seem to us very convincing. Our results disagree with theirs. We get a π-orbital as the highest occupied orbital. It is strongly localized on the ring oxygen and probably due to the use of the uncorrected ether oxygen parameters. This leads in turn to our first transition being of the $\pi-\pi^*$ type.

Final remarks. This work has demonstrated the usefulness of the present method in the study of simple carbonyl compounds. It has also given a slightly different MO-interpretation of some of the observed data on these compounds as compared to what has been given in some of the earlier literature. Finally, it has pointed out some of the limitations in combining the parameters in this scheme.[1-12]

Acknowledgements. We thank Professor Inga Fischer-Hjalmars and Dr. Marianne Sundbom, University of Stockholm, for their great interest in and many helpful comments on this work. We also thank Professor Per Njål Skancke and Dr. Harald Jensen, University of Oslo, for being able to use their material and for many helpful discussions.

REFERENCES

1. Roos, B. and Skancke, P. N. *Acta Chem. Scand.* **21** (1967) 233.
2. Roos, B. *Acta Chem. Scand.* **21** (1967) 2318.
3. Fischer-Hjalmars, I. and Sundbom, M. *Acta Chem. Scand.* **22** (1968) 607.
4. Grabe, B. *Acta Chem. Scand.* **22** (1968) 2237.
5. Jensen, H. and Skancke, P. N. *Acta Chem. Scand.* **22** (1968) 2899.
6. Höjer, G. *Acta Chem. Scand.* **23** (1969) 2589.
7. Skancke, A. and Skancke, P. N. *Acta Chem. Scand.* **24** (1970) 23.
8. Seybold, P. G. and Fischer-Hjalmars, I. *Acta Chem. Scand.* **24** (1970) 1373.
9. Gropen, O. and Skancke, P. N. *Acta Chem. Scand.* **23** (1969) 2685.
10. Gropen, O. and Skancke, P. N. *Acta Chem. Scand.* **24** (1970) 1768.
11. Sundbom, M. *Acta Chem. Scand.* **25** (1971) 487.
12. Fischer-Hjalmars, I. and Meza, S. *Acta Chem. Scand.* **26** (1972) 2991.
13. Grabe, B. and Skancke, P. N. *Acta Chem. Scand.* **26** (1972) 468.

14. Winter, N. W., Dunning, T. H. and Letcher, J. H. *J. Chem. Phys.* **49** (1968) 1871.
15. Unpublished results. Method and parametrization in: Höjer, G. and Meza, S. *Acta Chem. Scand.* **26** (1972) 3723.
16. Turner, D. W., Baker, A. D., Baker, C. and Brundle, C. R. *Molecular Photoelectron Spectroscopy*, Wiley-Interscience, London 1970.
17. Sidman, J. W. *J. Chem. Phys.* **27** (1957) 429.
18. Christensen, D. H., Kortzeborn, R. N., Bak, B. and Led. J. J. *J. Chem. Phys.* **53** (1970) 3912.
19. Fischer-Hjalmars, I. In Löwdin, P.-O. and Pullman, B., Eds., *Molecular Orbitals in Chemistry, Physics and Biology*, Academic, New York 1964, p. 361.
20. Roos, B. *Acta Chem. Scand.* **20** (1966) 1673.
21. Suzuki, H. *Electronic Absorption Spectra and Geometry of Organic Molecules*, Academic, New York 1967, Ch. 21.
22. Edwards, T. G. and Grinter, R. *Mol. Phys.* **15** (1968) 357.
23. Brand, J. C. D. *Trans. Faraday Soc.* **50** (1954) 431.
24. King, G. W. *J. Chem. Soc.* **1957** 5054.
25. Seliskar, C. J. and McGlynn, S. P. *J. Chem. Phys.* **56** (1972) 275, 1417.
26. Almenningen, A., Bastiansen, O. and Motzfeldt, T. *Acta Chem. Scand.* **23** (1969) 2848.
27. Tabor, W. J. *J. Chem. Phys.* **27** (1957) 974.
28. Turner, D. W. *Advan. Phys. Org. Chem.* **4** (1966) 31.
29. Dewar, M. J. S. and Worley, S. D. *J. Chem. Phys.* **50** (1969) 654.
30. Watanabe, K. *J. Chem. Phys.* **26** (1957) 542.
31. Walsh, A. D. *Trans. Faraday Soc.* **42** (1946) 66.
32. Walsh, A. D. *Proc. Royal Soc.* **A 185** (1946) 176.
33. Lake, J. S. and Harrison, A. J. *J. Chem. Phys.* **30** (1959) 361.
34. Walsh, A. D. *Trans. Faraday Soc.* **41** (1945) 498.
35. Paldus, J. and Ramsay, D. A. *Can. J. Phys.* **45** (1967) 1389.
36. McMurry, H. L. *J. Chem. Phys.* **9** (1941) 231, 241.
37. Kuboyama, A. *Bull. Chem. Soc. Japan* **33** (1960) 1027.
38. Merkel, E. *Z. Electrochem.* **63** (1959) 373.
39. Flaig, W., Salfeld, J.-C. and Baume, E. *Ann.* **618** (1958) 117.
40. Goldschmidt, S. and Graef, F. *Ber.* **61** (1928) 1858.
41. Braude, E. A. and Sondheimer, F. *J. Chem. Soc.* **1955** 3754.
42. Kearns, D. R. and Case, W. A. *J. Am. Chem. Soc.* **88** (1966) 5087.
43. Kimura, K. and Nagakura, S. *Theor. Chim. Acta* **3** (1965) 164.
44. Tanaka, J., Nagakura, S. and Kobayashi, M. *J. Chem. Phys.* **24** (1956) 311.
45. Herzberg, G. *Molecular Spectra and Molecular Structure*, Van Nostrand, New York 1966.
46. Nagakura, S., Kaya, K. and Tsubomura, H. *J. Mol. Spectry.* **13** (1964) 1.
47. Robinson, G. W. *Can. J. Phys.* **34** (1956) 699.

Received January 3, 1973.

ACTA CHEMICA SCANDINAVICA 27 (1973) 1875–1882

NMR Studies of Conjugated Linear Trienes

II.* Hexatriene and 1,6-Dimethylhexatriene

P. ALBRIKTSEN[a] and R. K. HARRIS[b]

[a]*Chemical Institute, University of Bergen, N-5000 Bergen, Norway, and* [b]*School of Chemical Sciences, University of East Anglia, Norwich, NOR 88C, England*

The 100 MHz NMR spectra of *cis*-1,3,5-hexatriene, *trans*-1,3,5-hexatriene, and 1,6-dimethyl-1,3,5-hexatriene have been analysed. The assignment of configuration and conformation of the *cis*-triene is discussed in relation to buta- and pentadiene NMR parameters and to published electron diffraction data on dienes and trienes. The NMR data for *cis*-1,3,5-hexatriene is not inconsistent with slight non-planarity. The existence of long range coupling constants, $^6J \sim -0.14$ Hz and $^7J \sim +0.1$ Hz, are shown.

An investigation of 1,3,5-hexatrienes by NMR is of interest both from the theoretical aspect of comparing the coupling constants with those obtained for penta- and buta-dienes [1] and from the stereochemical point of view. Apart from some cases of heavily substituted hexatrienes [2,3] no detailed NMR analyses of conjugated trienes have been reported. The simplest conjugated triene, 1,3,5-hexatriene, has been studied by electron diffraction [4,5] and by infrared and Raman spectroscopy.[6,7] The infrared spectra of *cis*- and *trans*-1,3,5-hexatriene [6,7] have been analysed under the assumption that the isomers have C_{2v} and C_{2h} symmetry, respectively. Contributions from non-planar or s-*cis* structures could not be entirely ruled out by infrared and Raman spectroscopic evidence. Trætteberg *et al.*[4,5] suggested from electron diffraction studies that *trans*-1,3,5-hexatriene has an all-s-*trans* conformation, whereas the *cis*-isomer is non-planar. The present NMR investigation was undertaken to obtain more information on the structure of hexatrienes, and on long-range (H,H) coupling in conjugated systems. The spectra of three compounds have been analysed: *cis*-1,3,5-hexatriene (I), *trans*-1,3,5-hexatriene (II), and 1,6-dimethyl-1,3,5-hexatriene (III).

* Part I: Ref. 2.

EXPERIMENTAL

The *cis*- and *trans*-1,3,5-hexatrienes were obtained from a commercially available isomer mixture by the method of Hwa *et al.*[8] The *cis* isomer was obtained pure, but the *trans* isomer contained about 5 % of the *cis*-triene. The NMR spectra were used as evidence of purity.

The all-*trans* 1,6-dimethyl-hexatriene was prepared by dehydration of 2,4-octadien-6-ol with *p*-toluene sulphonic acid: b.p. 44 – 45°/12 mmHg. The triene was recrystallized from methanol at −30°C. 2,4-Octadien-6-ol was obtained from sorbaldehyde and ethylbromide by a Grignard reaction: b.p. 85 – 86°/13 mmHg.

The materials were introduced into 5 mm o.d. sample tubes; a small quantity of TMS was added to serve as NMR reference and locking substance. For double resonance experiments benzene was also added to serve as locking substance in preference to TMS. The samples were degassed by freezing and thawing under vacuum and the tubes were sealed in the evacuated condition. The spectra of *trans*-hexatriene were recorded for the neat liquid whereas the spectra of *cis*-hexatriene and 1,6-dimethylhexatriene were obtained for samples dissolved in CCl_4 (about 50 % v/v).

The spectra were recorded using a Varian Associates HA 100 spectrometer operating at 100 MHz in the field/frequency lock mode, at ambient temperature (*ca.* 35°C) with frequency sweep. Spectra of the two 1,3,5-hexatriene isomers for detailed measurement were recorded at 50 Hz sweep width at scan rate 0.02 Hz s^{-1}, calibrated every 5 Hz using a Hewlett-Packard 5212A frequency counter. The methyl decoupled spectra of *trans*-1,6-dimethyl-hexatriene were recorded at 100 Hz sweep width.

The computations were carried out using the IBM 360/50 computer at the University of Bergen and the Atlas computer at the Science Research Council Atlas Laboratory, Chilton, Didcot, England. The results were plotted with a Calcomp Plotter.

SPECTRAL ANALYSIS

The spectrum of *cis*-1,3,5-hexatriene (Fig. 1) consists of three bands at $\delta \sim 5.1$, ~ 5.9 and ~ 6.7. The separations between the bands are considerably greater than any coupling constants. This enables initial assignments and estimates of some NMR parameters to be made on a quasi first-order basis, but second-order effects are observable (in addition to those caused by symmetry). The spectrum was therefore analysed on the basis of an $[ABCD]_2$ spin system. The total spectrum is complex, but the low frequency band ($\delta \sim 5.1$) is clearly assignable to the geminal protons with major structure due to splittings by ^3J_c and ^3J_t. The main pattern within the band at $\delta \sim 5.9$ can be explained as the D part of an $[ABCD]_2$ spin system with $J_{AD} \simeq J_{A'D}$ and $J_{BD} \simeq J_{B'D}$ small, but J_{CD} large. The total spectrum was analysed using the iterative computer program LACX.[9] This procedure gave reasonably accurate values for the triene coupling constants and chemical shifts. The final RMS error of fitting observed to calculated transitions was 0.14 when all 20 parameters were allowed to vary. The computed probable errors on the coupling constants are 0.01 to 0.02 Hz when 800 computed transitions were fitted to 135 observed lines. The errors in the parameters are probably greater than those computed and it might also be possible to iterate onto another solution. However, we believe that our solution is correct, taking into account the number of transitions fitted and the analogous values of NMR parameters obtained for buta-, penta-, and hexa-dienes,[1,10,11] and trienes.[2]

The spectrum of *trans*-1,3,5-hexatriene (Fig. 2) consists of two bands at $\delta \sim 5.1$ and ~ 6.2, respectively. The band at $\delta \sim 5.1$ was assignable to the geminal protons split by ^3J_c and ^3J_t. The band at $\delta \sim 6.2$ was very complex

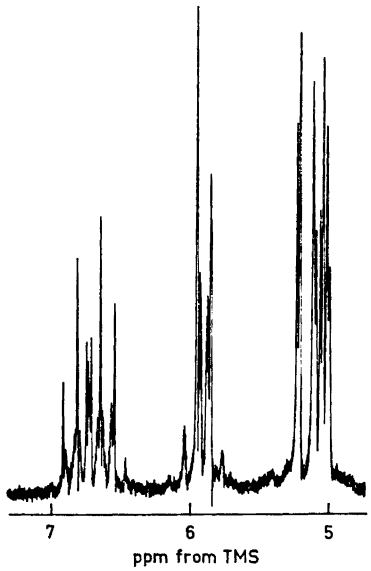

Fig. 1. 100 MHz spectrum of *cis*-1,3,5-hexatriene.

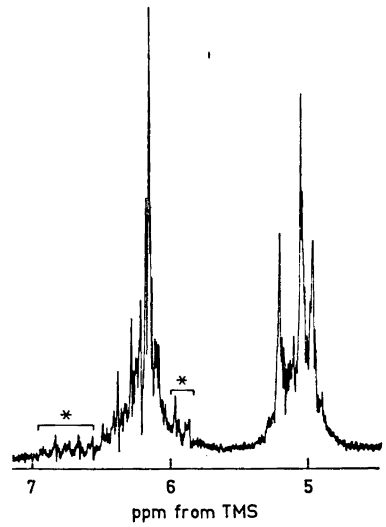

Fig. 2. 100 MHz spectrum of *trans*-1,3,5-hexatriene. Signals due to the *cis*-isomer (see text) are marked by asterisks.

due to the small chemical shift difference between the two pairs of inner protons compared to the coupling constants involved. The spectrum was simulated by computer and the parameters involved were adjusted to give a resonable fit without any iterative procedure.

The spectrum of all-*trans*-1,6-dimethyl-1,3,5-hexatriene was very complex. Even the methyl decoupled spectrum gave too little resolved fine structure to make an iterative calculation feasible. The spectrum calculated with the parameters in Table 1 gave a reasonable correlation with the observed spectra. The parameters in Table 1 were taken from values obtained for butadienes [1] and trienes [2,3] as model compounds, and the coupling constants are assumed to be correct to *ca.* 0.3 Hz.

RESULTS AND DISCUSSION

The data for the coupling constants in the trienes are in the range of analogous values for penta- and hexa-dienes,[1] and it may be assumed that the trienes have the configurations shown in Fig. 3, and are in planar or nearly planar conformations. The NMR parameters for 1,6-dimethyl-1,3,5-hexatriene suggest an all-*trans* planar or nearly planar structure. Lippincott *et al.*[6,7] studied *cis*- and *trans*-1,3,5-hexatriene by IR and Raman spectroscopy, and they assumed the structures I and II.

Table 1. Coupling constants (in Hz) for trienes and related compounds.[a]

Compound	^2J	^3J_s	^3J_c	^3J_t	^4J_c	^4J_t	$^5J_{cc}$	$^5J_{ct}$	$^5J_{tt}$
cis-Hexatriene (I)	1.91	11.14	10.77(3,4) 10.15(1′,2)	16.77	−0.71	−0.77(1′,3) −1.04(2,4)	—	0.56	1.36
trans-Hexatriene (II)[b]	1.9	10.5	9.5[c]	16.2(3,4) 15.2(1,2)[c]	−0.8(1.3) −0.8(2,4)	−0.8	0.7	0.7	—
all-*trans*-1,6-Dimethyl-hexatriene (III)[b]	—	10.8	—	16.2(3,4) 15.6(1,2)	−0.6(1,3) −0.9(2,4)	—	0.8	—	—
cis-Allo-ocimene[d]	—	11.16	—	15.20	−1.04(2,4) −0.94(4,6)	—	—	0.79	—
trans-Allo-ocimene[d]	—	11.01	—	15.28	−0.91	−0.82	0.55	—	—
Methyl 2,7-dimethyloctatrienoate-*trans*-2,*cis*-4,*trans*-6[e]	—	12.5	10.7	—	—	−1.0	—	—	—
all-*trans*-Octatrienoate[e]	—	11.5	—	14.6	−0.6	—	—	—	—
Butadiene[f]	1.74	10.41	10.17	17.05	−0.83	−0.86	0.69	0.60	1.30
trans-Pentadiene[g]	1.89	10.30	10.22	16.93(1,2) 15.06(2,4)	−0.79 −0.78	−0.81	0.74	0.61	—
all-*trans*-Hexadiene[g]	—	10.30	—	15.01	—	−0.84	0.68	—	—
cis-Pentadiene[g]	2.12	10.95	10.24(1′,2) 10.86(3,4′)	16.89	−0.85	−0.81(1′,3) −1.14(2,4′)	—	0.81	1.53
cis-2-Butene[h]	—	—	10.88	—	—	—	—	—	—
Ethylene[i]	2.08	—	10.02	16.81	—	—	—	—	—

Compound	$^5J_{scs}$	$^5J_{sts}$	$^6J_{cc}$	$^6J_{ct}$	$^6J_{tt}$	$^7J_{ccc}$	$^7J_{cct}$	$^7J_{tct}$	$^7J_{ctc}$	$^7J_{ttt}$
I	0.21	—	−0.14	−0.14	—	0.09	0.10	0.09	—	—
II[b]	—	0.25	—	−0.2	−0.2	—	—	—	0.15	0.15
III[b]	—	0.25	—	−0.2	—	—	—	—	0.15	—
cis-Allo-ocimene[d]	—	—	—	—	−0.13	—	—	—	—	—
trans-Allo-ocimene[d]	—	—	−0.09	—	—	—	—	—	—	—
Methyl 2,7-dimethyl-octatrienoate-*trans*-2, *cis*-4, *trans*-δ[e]	±0.2	—	—	—	—	—	—	—	—	—
all-*trans*-Octatrienoate[e]	—	±0.3	—	—	—	—	—	—	—	—

[a] The signs are chosen to be consistent with published values on dienes.[1] [b] The errors in the parameters for compounds II and III are *ca.* 0.3 Hz. These results were not derived from iterative spectral analysis (see text). [c] These values appears to be unreasonably low, but computations using higher values gave poorer agreement with the experimental spectrum. We suspect the errors in these parameters are, however, substantial. One of the difficulties in obtaining more accurate parameters for II is the small amount of *cis*-isomer also present in the sample. [d] Ref. 2. The *cis* and *trans* isomers are those assumed by Cunliffe *et al.*[2] [e] Ref. 3. [f] Ref. 10. [g] Position notation according to Ref. 1. [h] Ref. 14. [i] Ref. 19.

Since planarity is required for resonance it is expected that these structures should be the most stable as compared to other possible isomers. It is, however, not possible to rule out any s-*cis* structures from IR and Raman evidence

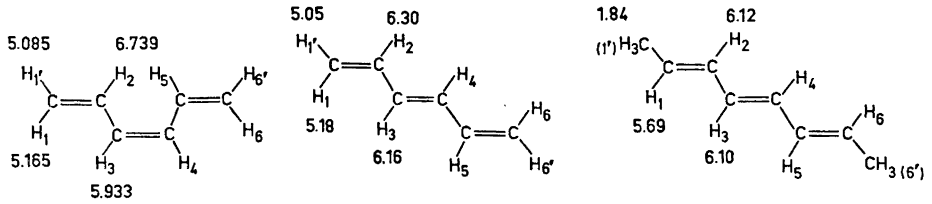

I II III

Fig. 3. Notation and chemical shifts (ppm from TMS) for the hexatrienes studied.

alone.[6,7] The *cis*-1,3,5-hexatriene is strained because of steric interaction between the central C–H groups in a similar manner to that discussed for *cis*-pentadiene.[1,12] For a planar conformation, with normal valence angles, the distance between H_2 and H_5 will be close to the sum of the van der Waals radii. Similar strain is not expected for the all-*trans*-1,3,5-hexatrienes.

Some of the coupling constants obtained for the *cis*-hexatriene (I) show significant deviations from the butadiene[10] and propene[13] values. They are, however, close to the values reported for *cis*-pentadiene.[1,11] The value of ^3J_c for the vinyl groups in the *cis*-triene, 10.15 Hz, is similar to the values obtained for butadiene,[10] 10.17 Hz, *cis*-pentadiene,[1] 10.24 Hz, and *trans*-pentadiene,[1] 10.22 Hz. It seems clear that the vinyl group angles in the triene are close to those of the dienes. This assumption is also supported by electron diffraction measurements [4,5] which show that the $C_1C_2C_3$ angle in the *cis*-triene (122.1°) is close to the butadiene value (122.8°). Moreover, ^3J_c for the protons at the disubstituted double bond, 10.77 Hz, parallels the values obtained for *cis*-pentadiene,[1] 10.86 Hz, *cis*-2-butene,[14] 10.88 Hz, and methyl 2,7-dimethylocta-2,4,6-trienoate,[3] 10.7 Hz. The $C_2C_3C_4$ angle in the *cis*-triene, 125.9°, is, however, significantly different from the butadiene value.[4,5] This angle distortion, *ca.* 4°, is comparable to the distortion of *ca.* 5° suggested for the *cis*-butene due to steric interaction between the methyl groups.[15] An "in-plane-deformation" of *cis*-1,3,5-hexatriene is also supported by observations on *cis*-pentadiene.[1] The values of ^3J_c show no significant variation due to the differences between methyl or vinyl groups substituted *cis* into ethylene, but any substituent effects might be obscured by effects arising from distortion. The proposed in-plane-distortion in *cis*-pentadiene has been treated theoretically by Bacon and Maciel.[12] They showed that all of the pertinent couplings are increased in magnitude by this deformation. Such a deformation may therefore have a significant effect on the observed coupling constants for *cis*-1,3,5-hexatriene. The value of ^3J_t for the *cis*-triene, 16.77 Hz, is slightly smaller than that for butadiene (17.05 Hz) but it is nearer to the values observed for the vinyl groups of *cis*- and *trans*-pentadiene,[1] 16.89 Hz and 16.93 Hz, respectively.

The value of ^3J_s for *trans*-1,6-dimethyl-1,3,5-hexatriene is increased by *ca.* 0.5 Hz compared to *trans*-penta- and hexa-diene.[1] This could be an effect due to extended conjugation rather than any difference in population of rotamers. Dodziuk [16] has pointed out from theoretical calculations that the torsional barrier height for the methyl group of *cis*-pentadiene is substantially higher than that for *trans*-pentadiene, a fact which is consistent with the steric in-

teractions deduced from NMR experiments on penta- and hexa-dienes.[1] Segre *et al.*[11] found a variation in ^3J_s *ca.* 0.2 Hz for *trans*-pentadiene and *ca.* 0.05 Hz for *cis*-pentadiene over a temperature range of *ca.* 75°C. The increase in ^3J_s for *cis*-1,3,5-hexatriene relative to butadiene [10,11] could be due to deformations of the triene. Barber *et al.*[3] report a value of 12.5 Hz for ^3J_s in methyl 2,7-dimethylocta-*trans*-2,*cis*-4,*trans*-6-trienoate. The increase in ^3J_s relative to *cis*-1,3,5-hexatriene could be explained by a substituent effect similar to that proposed for butadiene,[1] where ^3J_s increases by *ca.* 0.55 Hz for each *cis* methyl group present. The value of ^3J_s in butadiene is also increased by the presence of ester groups. The effect of two *trans* ester groups [17] is an increase of 1.0 Hz. Calculations [12] of ^3J_s in butadiene show that this coupling is increased substantially by out-of-plane deformations about the double bond.* Substitution of *trans* terminal methyl groups into butadiene has only a minor effect on ^3J_s whereas *cis* substitution increases this coupling significantly (in-plane deformation does not affect ^3J_s significantly [12]). This suggests that the observed *cis*-methyl effect is due to an out-of-plane distortion.

The values of ^4J are essentially the same as observed for *cis*-pentadiene.[1] The variations of ^4J in a *cis*-triene caused by in-plane-deformation and out-of-plane twist are expected to be of the same magnitude and sign, for similar degree of distortion, as suggested for *cis*-pentadiene.[12] Out-of-plane distortion about the central C=C double bond in *cis*-1,3,5-hexatriene, however, affects conjugation to a different extent from that of the analogous distortion for *cis*-pentadiene. It is difficult to distinguish between the in-plane and out-of-plane distortions for hexatriene by measurements of ^4J. Electron diffraction measurements [5] suggest that the angle of distortion for *cis*-hexatriene about the central double bond (out-of-plane twist) is *ca.* 10°. A similar suggestion is made by Hecht and Victor [15] for *cis*-2-butene, where the assumed angle is *ca.* 14°.

The value of $^5J_{tt}$ (1.36 Hz) lies between those for butadiene (1.30 Hz) and *cis*-pentadiene (1.53 Hz). The high value for *cis*-pentadiene may be connected with a proposed in-plane distortion.[1,12] Theoretical work [12] shows that $^5J_{tt}$ should drop if an out-of-plane twist occurs, and the value for *cis*-hexatriene (compared to that for *cis*-pentadiene) might indicate the presence of such a twist. The values of $^5J_{ct}$ show similar effects (0.56 Hz for *cis*-hexatriene, 0.60 Hz for butadiene, and 0.81 Hz for *cis*-pentadiene).

Table 2. Calculated and observed coupling constants (in Hz) for *cis*-hexatriene.

	$^5J_{ct}$	$^5J_{scs}$	^6J	^7J
Calculated FP [a]	0.92	0.17	−0.29	0.50
Calculated MK/CI [a]	0.81	0.09	−0.23	0.62
Observed	0.56	0.21	−0.14	0.10

[a] π contributions (see Ref. 18).

* Haugen and Trætteberg [4] do not discuss out-of-plane distortions arising from internal rotation about formal single bonds of the polyenes.

It is anticipated that the values of ^5J (except $^5J_{tt}$), ^6J, and ^7J will be π-dominated,[1,12] since σ-contributions to J attenuate rapidly with the number of bonds separating the nuclei. In Table 2 the observed values are compared to those calculated by Cunliffe *et al.*[18] The five-bond coupling constant through two formal single bonds, designated $^5J_{scs}$, is slightly greater than predicted. The only previous report of such a coupling is by Barber *et al.*[3], who list ± 0.2 Hz for $^5J_{scs}$ and ± 0.3 Hz for $^5J_{sts}$ in heavily substituted trienes. Our results for ^6J, on the other hand, are smaller by a factor of two than that calculated, though the deviation is not greatly outside experimental error. However, similar values have been reported [2] for allo-ocimene. The experimental values for ^7J in *cis*-hexatriene are a factor of five smaller than the predicted magnitude, the difference being well outside experimental uncertainty. No measurements of ^7J in a triene system have been reported previously. The assumed domination of ^6J and ^7J by the π-contribution leads to the conclusion that any out-of-plane distortion will reduce their magnitude. Our observations are therefore consistent with some out-of-plane twisting. It should be noted that the signs of the experimental six- and seven-bond coupling constants agree with those calculated.[18] Also as predicted, the values of ^6J and ^7J do not depend on configuration.

The uncertainty in the coupling constants reported here for compounds II and III argues against any detailed discussion beyond the comment that the results support the configurations illustrated.

The chemical shifts in dienes [1] are affected by the substituents. For the trienes, however, quantitative conclusions cannot be made from the available data, but certain trends are apparent. However, it should be noted that the shifts we report are for varying solvent conditions, and none of the values are extrapolated to infinite dilution. The shifts of the terminal vinyl protons in 1,3,5-hexatriene are hardly affected by the relative position of the two vinyl groups, *i.e.* the chemical shifts are nearly the same in the *cis* and *trans*-isomers. A terminal methyl group in the triene causes a high frequency shift of H_1, $+0.54$ ppm, compared to the unsubstituted compound. This shift is similar to those between butadiene [10] and *cis*- and *trans*-pentadiene,[1] and to the shift between ethylene [19] and propene.[13] Protons attached to carbon atoms at a distant C=C double bond are apparently very little affected (by < 0.1 ppm).

The shift of H_2 in *cis*-hexatriene is $+0.44$ ppm to high frequency compared to that for the *trans* isomer. This observation parallels that made for *cis*-pentadiene [1] compared to butadiene. A *cis* substituent at C_4, whether it is a methyl group or a vinyl group, causes a high frequency shift of H_2 by *ca.* 0.4 ppm. This effect is probably caused by steric influences [20,21] and this provides further evidence for a deformation due to the interaction between *cis* C–C bonds. The methyl group in *cis*-pentadiene does not show any steric shift,[1] probably due to the effect of internal rotation. The very small increase, *ca.* 0.1 ppm, of the shift for H_2 in *cis*-hexatriene compared to *cis*- penta-diene might be attributed to the different shielding effect caused by a vinyl group compared to a methyl group.

Acknowledgements. We thank A. V. Cunliffe, who performed some preliminary experiments on the hexatriene isomers, and C. W. Haigh, who provided us with a listing of the computer program LACX. One of us (P.A.) is indebted to the *Royal Norwegian Council for Scientific and Industrial Research* for a Research Fellowship and would like to acknowledge support from the *L. Meltzers Høyskolefond.*

REFERENCES

1. Albriktsen, P., Cunliffe, A. V. and Harris, R. K. *J. Magn. Resonance* **2** (1970) 150.
2. Cunliffe, A. V., Grinter, R. and Harris, R. K. *J. Magn. Resonance* **2** (1970) 200.
3. Barber, M. S., Hardisson, A., Jackman, L. M. and Weedon, B. C. L. *J. Chem. Soc.* **1961** 1625.
4. Haugen, W. and Trætteberg, M. *Acta. Chem. Scand.* **20** (1966) 1726.
5. Trætteberg, M. *Acta. Chem. Scand.* **22** (1968) 628, 2294.
6. Lippincott, E. R., White, C. E. and Sibilia, P. *J. Am. Chem. Soc.* **80** (1958) 2926.
7. Lippincott, E. R. and Kenney, T. E. *J. Am. Chem. Soc.* **84** (1962) 3641.
8. Hwa, J. C. H., de Benneville, P. L. and Sims, H. J. *J. Am. Chem. Soc.* **82** (1960) 2537.
9. a. Haigh, C. W. *Unpublished work.* b. Harris, R. K. and Stokes, J. *A Library of Computer Programs for NMR Spectroscopy*, Science Research Council, (Atlas Computer Laboratory), 1971.
10. Hobgood, R. T. and Goldstein, J. H. *J. Mol. Spectry.* **12** (1964) 76.
11. Segre, A. L., Zetta, L. and Di Corato, A. *J. Mol. Spectry.* **32** (1969) 296.
12. Bacon, M. and Maciel, G. E. *Mol. Phys.* **21** (1971) 257.
13. Bothner-By, A. A. and Naar-Colin, C. *J. Am. Chem. Soc.* **83** (1961) 231.
14. Harris, R. K. and Howes, B. R. *J. Mol. Spectry.* **28** (1968) 191.
15. Hecht, H. G. and Victor, B. L. *J. Am. Chem. Soc.* **90** (1968) 3333.
16. Dodziuk, H., *J. Mol. Struct.* **10** (1971) 275.
17. Elvidge, J. A. and Ralph, P. D. *J. Chem. Soc.* **C 1966** 387.
18. Cunliffe, A. V., Grinter, R. and Harris, R. K. *J. Magn. Resonance* **3** (1970) 299.
19. Lynden-Bell, R. M. and Sheppard, N. *Proc. Roy. Soc. Ser. A* **269** (1962) 385.
20. Gil, V. M. S. and Gibbons, W. A. *Mol. Phys.* **8** (1964) 199.
21. Gibbons, W. A. and Gil, V. M. S. *Mol. Phys.* **9** (1965) 167.

Received December 5, 1972.

ACTA CHEMICA SCANDINAVICA 27 (1973) 1883–1890

Aluminium-Oxygen Containing Species in Fluoride Melts

TORMOD FØRLAND and SIGNE KJELSTRUP RATKJE

Institute of Physical Chemistry, The University of Trondheim, Norwegian Institute of Technology, Trondheim, Norway

Cryoscopic measurements on the sodium fluoride rich side in the reciprocal salt system $NaF-AlF_3-Na_2O-Al_2O_3$ are presented. The amounts of cryolite and oxide added to NaF are so small that ideal behaviour of the solution can be expected. The results indicate complex formation, with the $Al_2OF_x^{4-x}$ complex as a dominating species when the ionic ratio Al^{3+}/O^{2-} is larger than five.

The aluminium-oxygen containing species in molten mixtures of aluminium oxide and cryolite have been of great interest over a long period of time, mainly because of the industrial importance of this kind of systems in connection with aluminium production. Grjotheim *et al.*[1] have made a list of some of the suggestions of structural entities in the melt. Summarizing some of the latest works,[1–3] one finds that the following points seem to be accepted.

1. In the dilute range, the number of oxygen atoms per complex is one. This is based on the cryoscopic measurements by Holm [2] in cryolite systems. Al_2O_3 creates three and $NaAlO_2$ two foreign particles at infinite dilution in cryolite.

2. From entropy considerations the number of aluminium atoms per complex is assumed to be one in the dilute range.[3] No measurements give this number explicitely.

3. In the more concentrated range it seems to be difficult to fit experimental data to theoretical models. Suggestions like AlO_2^-, $Al_2OF_x^{4-x}$, $Al_2O_2F_y^{2-y}$, $Al_3O_2F_z^{5-z}$ are made.

A possible way of testing these theories is to work in a ternary system where both cryolite (Na_3AlF_6) and oxide (Al_2O_3, $NaAlO_2$) are solutes. Cryoscopic measurements in these systems will give an average value of the number of aluminium- and oxygen-atoms in the complex in the ranges where ideal behaviour of the melt can be expected. Structural informations of oxygen-aluminium-containing complexes in melts with small content of cryolite, may contribute to the understanding of melts with higher cryolite content.

When sodium fluoride is used as a solvent, this component will form the first solid phase in the region of high sodium fluoride content.[5] Solid solubility of the other components in sodium fluoride is extremely small.[2,4] In the system

$NaF-Na_3AlF_6$ ideal Temkin behaviour of the melt can be expected for $x_{Na_3AlF_6} \leq 0.07$ [4]. When we neglect the differences in specific heat of solid and liquid phaces, the liquids-line of the system is given by:

$$\Delta\bar{S}_{NaF} = \Delta H_f\left(\frac{1}{T} - \frac{1}{T_f}\right) + \frac{\Delta\bar{H}_{NaF}}{T} \quad (1)$$

Calculations of the partial differential heat of mixing, $\Delta\bar{H}_{NaF}$, using data from Holm [6] will give a contribution of -0.03 e.u. with $x_{Na_3AlF_6} = 0.05$. The error limits of the measured heats of mixing are, however, so large (giving ± 0.2 e.u. at this point) that no definite conclusions can be drawn from the calculation. Since the two anions of the mixture have different charge and size, one may expect deviations from the ideal Temkin entropy of mixing. A rough estimate of the partial entropy of mixing $\Delta\bar{S}_{NaF}$ may be obtained using the equation derived by Flory for the entropy of mixing for an athermal solution of polymers and monomers. This was done for the mixture of the anions AlF_6^{3-} and F^- for the composition $x_{NA_3AlF_6} = 0.05$. In this calculation it is assumed that threevalent anions will occupy three sites, and the monovalent anion will occupy one site. The partial entropy of mixing for sodium fluoride calculated on this base from Flory's equation is 10 % higher than the value obtained from the simpler Temkin model for an ideal ionic mixture. We therefore find it unnecessary to use the Flory equation or other refined method for the calculation of the partial entropy of mixing for sodium fluoride and we will use the simple equation $\Delta\bar{S}_{NaF} = -R \ln X_{F^-}$. Neglecting the small partial heat of mixing and using the Temkin model in the entropy calculation, one obtains

$$-R \ln X_{F^-} \simeq \Delta H_f\left(\frac{T_f - T}{T_f T}\right)$$

and finally the well known cryoscopic relation:

$$\Delta T \simeq Kx \quad (2)$$

where $\Delta T = T_f - T$ and x is the fraction of anions different from F^-. Na^+ is the only cation present in the system.

Once the cryoscopic constant K is known the fraction of anions different from F^- can be found from measurements. In this case the K-value taken from experiments with Na_3AlF_6 in NaF is (430 ± 10) deg.

It is reasonable to assume that the deviation from ideal behaviour due to interaction between anions is not very different for systems containing the AlF_6^{3-} complex and systems where oxygen containing complexes are present, as long as the solutions are dilute.

Oxygen ions can be introduced into melts of $NaF-Na_3AlF_6$ by adding Na_2CO_3 to the system. The carbonate will decompose completely to oxide which is built into a complex ion. The complete decomposition of the carbonate can be verified by introducing the oxygen ions by addition of $NaAlO_2$ instead of carbonate. The addition of oxygen in the form of carbonate is chosen for reasons of convenience. The carbonate is easily obtained in high purity and it dissolves quickly. As will be shown later, addition of oxygen in the form of carbonate also gives better accuracy in the determination of solubility limits.

When a small amount of Na_3AlF_6 is added to fused NaF, the freezing point of NaF is depressed according to the fraction of anions different from F^-, the fraction of foreign particles as given by eqn. (2). If one then adds carbonate (or oxygen ions) to this mixture, one can imagine that the freezing point may continue depressing, remain constant, or be elevated. If the oxygen ions did not combine with the AlF_6^{3-} anions, the fraction of foreign particles would increase giving a depression in the freezing point. If the oxygen ions combined with AlF_6^{3-} in such a way that all complexes continued containing one aluminium, the fraction of foreign particles would not change significantly. The freezing point would be practically unaltered. Finally, if the oxygen ions formed complexes with AlF_6^{3-} containing more than one aluminium, the fraction of foreign particles would decrease and thus the freezing point would be elevated by the carbonate addition.

Theoretically we can expect the following dependence of the freezing point depression, ΔT, on the oxide addition, depending on the complex formed.

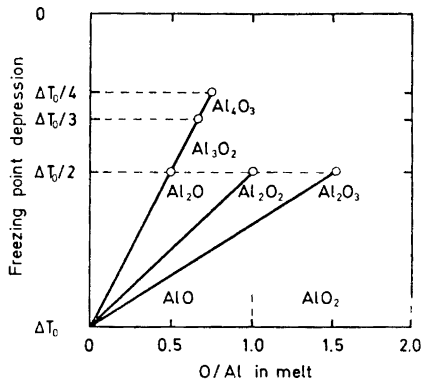

Fig. 1. Expected variation in the freezing point depression of NaF as a function of the O/Al-ratio (keeping the Al-content constant) for different structural entities in the melt. The number of fluoride ions in the complex is not considered. Dashed lines indicate theoretical limits of complex formation.

Fig. 1 illustrates that:

1. Formation of complexes of the type $AlO_kF_l^{3-k-l}$ should give no change in the number of foreign particles in the melt, irrespective of the values of k and l. The ΔT provided by the cryolite anions before adding oxide should remain constant up to the point where the solubility limit is reached.

2. Formation of complex ions with more than one Al per complex should give an increase in the freezing point of the $NaF-Na_3AlF_6$ mixture. ΔT at the solubility limit will indicate the kind of complex present if many types are possible.

If $NaAlO_2$ or Al_2O_3 are used as oxide sources instead of Na_2CO_3, the picture will be the same except for rotation of the curves around the ΔT_0-point, due to the simultaneous addition of Al.

EXPERIMENTAL

The equipment used was similar to that used by Grjotheim.[4] Temperature gradients over the system were less than 0.1°C/cm. Accuracy in temperature measurements was ±0.2°C. The Pt/Pt 10 % Rh thermocouple was annealed and calibrated before use.

To avoid undercooling, which is common in cryolite systems, stirring and addition of seeding crystals were essential. The seeding crystals were weighed to reduce uncertainty in composition.

Optimum cooling rate was 1 – 1.5°C/min. The chemicals used were: Na_2CO_3 and NaF, *p.a.* Merck, Darmstadt, and Na_3AlF_6, handpicked cryolite from Ivigtut, Greenland. Before use the $NaCO_3$ was melted in a platinum crucible.

RESULTS

The results are given graphically in Figures 2, 3, 4, 5 and in Table 1. This table gives experimental data from Figs. 2, 4, and 5.

Table 1.

Mol fraction Na_3AlF_6 before adding Na_2CO_3	0.0300	0.0529	0.0700
$\Delta T/\Delta T_0$ at solubility limit	0.55 ± 0.03	0.55 ± 0.03	0.51 ± 0.03
Ratio O/Al in melt solubility limit	0.83 ± 0.05	0.80 ± 0.05	0.80 ± 0.05
Average ratio Al:O in complex, highest and lowest value	1.70→1.50	1.80→1.55	2.00→1.60

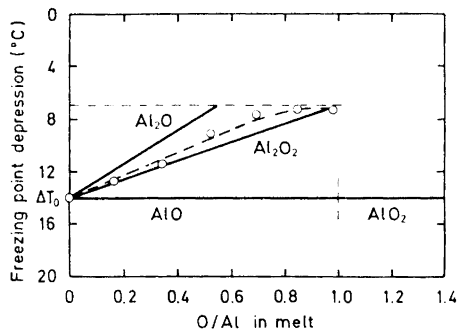

Fig. 2. Observed variation in the freezing point of NaF with addition of Na_2CO_3 to a NaF-$NaAlF_6$ mixture with $X_{Na_3AlF_6} = 0.0300$. Theoretical lines for different kinds of complex formation are indicated. Thin dashed lines show theoretical limits of complex formation.

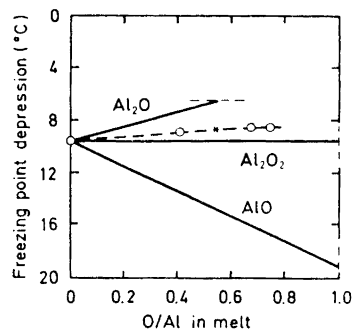

Fig. 3. Observed variation in the freezing point of NaF with addition of $NaAlO_2$ to a mixture of NaF-Na_3AlF_6. The experimental point marked * corresponds to a mixture with mol fraction of Al-atoms equal to 0.0300. Theoretical lines for different kinds of complex formation are indicated. Thin dashed lines show theoretical limits of complex formation.

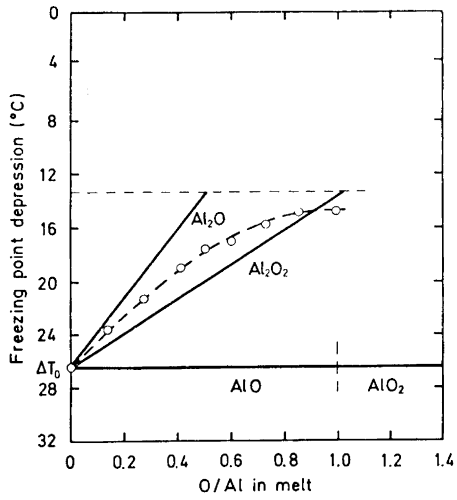

Fig. 4. Observed variation in the freezing point of NaF with addition of Na_2CO_3 to a NaF-Na_3AlF_6 mixture with $X_{Na_3AlF_6} = 0.0529$. Theoretical lines for different kinds of complex formation are indicated. Thin dashed lines show theoretical limits of complex formation.

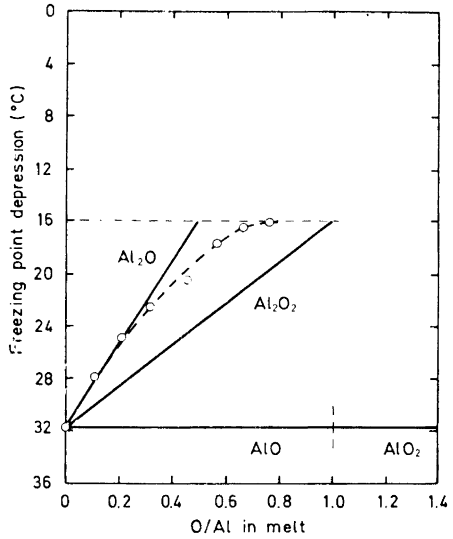

Fig. 5. Observed variation in the freezing point of NaF with addition of Na_2CO_3 to a NaF-Na_3AlF_6 mixture with $X_{Na_3AlF_6} = 0.0700$. Theoretical lines for different kinds of complex formation are indicated. Thin dashed lines show theoretical limits of complex formation.

As can be seen from Figs. 2, 4, 5 the freezing point depression, ΔT, varies with both the ratio O/Al in the melt and with the amount of cryolite initially present. Because of this, results from $NaAlO_2$ addition are not easily compared with the ones from Na_2CO_3-addition. Only one point from the curves on Figs. 2 and 3 should coincide. This is the point marked with a star on Fig. 3 and the point corresponding to the same O/Al-ratio on Fig. 2. Within experimental errors they give complete agreement for the average ratio Al:O in complexes formed in the melt, as calculated from material balance.

It is now obvious why addition of Na_2CO_3 is chosen instead of $NaAlO_2$. The relative decrease in ΔT is smaller when $NaAlO_2$ is used, and this makes the determination of solubility limits more difficult.

DISCUSSION

The following conclusions can be drawn by comparison of theoretical and experimental data:

1. More than one type of aluminium-oxygen containing species is present in the melt over the investigated interval of oxygen addition to the melt. This is concluded from the observation that the experimental curve for ΔT as a function of the O/Al-ratio does not fit any of the theoretical curves.

2. The maximum number of aluminium atoms per complex is probably two, though relatively small quantities of complexes with higher aluminium content cannot be excluded. The reason for this are the two facts: (a) ΔT at the solubility limit is more than half the starting value ΔT_0 before adding Na_2CO_3, (b) The solubility limit is given by a relatively high ratio O/Al ($\simeq 0.8$) in the melt.

Longer chains of Al – O-complexes should reduce the solubility limit and decrease the value of $\Delta T/\Delta T_0$. If these were energetically stable they should have the largest probability at high O^{2-} (in complex) concentration, that is at the solubility limit, and therefore markedly affect the values mentioned. The experimental data therefore indicate that complexs containing three aluminium are unlikely in the concentration range investigated.

3. Complexes with one aluminium cannot be dominating in the melt. Complexes of this kind will not affect the freezing point obtained for the $NaF-Na_3AlF_6$ solution. The rise in temperature is due to the formation of complexes with two Al only (if three Al per complex is excluded). From this fact and from material balances, the ratio between species with one and two Al can be calculated to have a value not higher than 1/4.

4. The existence of a complex with structure Al – O – Al is the only reasonable explanation for a line, steeper than the theoretical line for the Al_2O_2-type complex. This complex should from the above considerations be of importance.

A mixture of the following Al – O-structures is now possible:

1. Al – O
2. O – Al – O
3. Al – O – Al
4. $Al\langle{}^{O}_{O}\rangle Al$
5. Al – O – Al – O
6. O – Al – O – Al – O

As for the species No. 6, this is the neutral molecule Al_2O_3 (possibly with F-ions attached), and previous data [3] seem to exclude this kind of particles.

It should be stated that this method does not differentiate between complexes 4 and 5. But as 5 gives two oxide ions bound in different ways, No. 4 is considered as the most stable of these. In the following, a complex with structure 5 is therefore excluded.

The presence of a complex of the type O – Al – O also seems unlikely. This complex would give no change in ΔT by oxide addition. To explain the experimental results it could therefore be present only in minor quantities. Since it contains two oxygen ions it should be favoured at higher oxide additions. But then one would expect the formation of this complex to extend the solubility limit beyond the observed O/Al ratio. Energetically the complex would not be favourable as it gives a low number of Al – O bonds in the system. From entropy consideration it would also be unfavourable to have the two oxygen combined with the aluminium in a system having an excess of aluminium. If we should consider complexes where the oxygen ion has only one aluminium neighbour, the complex Al – O is more likely.

The mixture of oxygen containing species will therefore be considered most likely to be a mixture of Al – O, Al – O – Al, and Al$\langle{}^{O}_{O}\rangle$Al complex types.

To check whether the structure Al$\langle{}^{O}_{O}\rangle$Al was necessary or not for the description of the experimental lines, the following equilibrium reaction, symbolically written, was considered:

$$\mathrm{Al} + \mathrm{Al}-\mathrm{O} \rightleftharpoons \mathrm{Al}-\mathrm{O}-\mathrm{Al}$$

The only complex present giving the rise in T then would be the Al – O – Al type. If n_1 is the initial number of mol of cryolite in the system, n_2 is the number of moles of Na_2CO_3, and n_3 is the number of moles of foreign particles in the melt (calculated from ΔT and K) we will have:

Mol	Al – O – Al :	$n_1 - n_3$	
Mol	Al – O :	$n_2 - (n_1 - n_3)$	(oxygen balance)
Mol	Al (cryolite anions) :	$n_3 - n_2$	(aluminium balance)

The results of these calculations give an "equilibrium constant" varying with concentration and a wrong solubility limit. The bending of the ΔT *versus* O/Al curve cannot be understood. So the conclusion must be: The set of complexes in the above equation is not sufficient to explain the observations.

Now let us assume that the complete picture can be described by the equilibria:

(1)	$\mathrm{Al} + \mathrm{O} \rightarrow \mathrm{Al}-\mathrm{O}$	(completely)
(2)	$\mathrm{Al}-\mathrm{O} + \mathrm{Al} \rightleftharpoons \mathrm{Al}-\mathrm{O}-\mathrm{Al}$	
(3)	$2\,\mathrm{Al}-\mathrm{O} \rightleftharpoons \mathrm{Al}\langle{}^{O}_{O}\rangle\,\mathrm{Al}$	

When the Al/O ratio is large, reaction (2) is dominating. This is demonstrated by the fact that the experimental line approaches the theoretical line for Al_2O-configuration as the starting value of cryolite is increased from mol fraction 0.030 to 0.070.

As the amounts of Na_2CO_3 (O^{2-} in the complex) increases, reaction (3) will give Al$\langle{}^{O}_{O}\rangle$Al configurations because of excess Al – O formed. This will explain the curving of the experimental line.

Since previous measurements give no information about the number of aluminium atoms in oxygen containing species in cryolite, the results from this investigation may be of importance for the understanding of the structure of these species. The present results are not in contradiction to Holm's cryoscopic measurements in pure cryolite mentioned earlier, but they indicate that the number of aluminium atoms in the one-oxygen containing complex is more likely to be two than one at infinite dilution. The results also show that the stability of the AlO_2^- ion in NaF-rich melts are probably not so high as suggested by Foster.[5]

To give more definite statements, further investigations are needed over the whole range of concentrations. It may be valuable to combine the cryoscopic measurements with spectroscopic measurements. Such measurements are in progress.

SUMMARY

1. Oxygen ions form several kinds of stable complexes in sodium fluoride-cryolite mixtures.

2. The number of aluminium atoms in these complexes is probably not higher than two.

3. When the number ratio of cryolite to sodium oxide is larger than five, the dominating part of the complexes are of the type Al – O – Al.

4. With decreasing ratio cryolite/sodium oxide, the average ratio Al:O in complex will decrease, but it is still larger than one at the solubility limit.

REFERENCES

1. Grjotheim, K., Holm, J., Krohn, C. and Matiasovsky, K., *Svensk Kem. Tidsskr.* **78** (1966) 547.
2. Holm, J. *Undersøkelser av struktur og faseforhold for en del systemer med tilknytning til aluminiumelektrolysen*, Lic. techn. thesis 56, Institute of Inorganic Chemistry, The Technical University of Norway, Trondheim 1963.
3. Brynestad, J., Grjotheim, K., Grønvold, F., Holm, J. and Urnes, S. *Disc. Faraday Soc.* **32** (1962) 90.
4. Grjotheim, K. Contribution to the theory of aluminium electrolysis, *Det Kgl. Norske Videnskabers Selskabs Skrifter*, No. 5, (1956).
5. Foster, P. Jr. *J. Am. Ceram. Soc.* **45** (1962) 145.
6. Holm, J. Thermodynamic properties of molten cryolite and other fluoride mixtures, Dr. techn. thesis, Institute of Inorganic Chemistry, The Technical University of Norway, Trondheim 1971.

Received December 18, 1972.

ACTA CHEMICA SCANDINAVICA 27 (1973) 1891–1899

Synthesis and Mechanism of Formation of 2,3-Dialkyl-1,2,3,4-tetrahydrophthalazine-1,4-diones by Utilizing an O—N Rearrangement of 1-Alkoxy-3-alkyl-3,4-dihydrophthalazin-4-ones

BRIAN G. PRING and CARL-GUNNAR SWAHN*

Research and Development Laboratories, Astra Läkemedel AB, S-151 85 Södertälje, Sweden

The reaction of 1-(2′-hydroxyethoxy)-3-methyl-3,4-dihydrophthalazin-4-one (VII) with thionyl chloride in refluxing chloroform results in formation of 2-(2′-chloroethyl)-3-methyl-1,2,3,4-tetrahydrophthalazine-1,4-dione (III). The mechanism of the reaction has been investigated and is discussed.

Recently, we wished to prepare 2-(2′-chloroethyl)-3-methyl-1,2,3,4-tetrahydrophthalazine-1,4-dione (III), the starting material for a series of amino-derivatives required for pharmacological testing. The two most direct methods for preparing this compound appeared to be *via* *N*-alkylation of 1-hydroxy-3-methyl-3,4-dihydrophthalazin-4-one (I) (the compound is best represented by this tautomer [1]), or condensation of phthalic anhydride with an *N*-ethyl-*N*′-methylhydrazine appropriately substituted in the ethyl group. The former method proved to be unsuitable since *O*-alkylation prevailed, this being in agreement with previous findings.[2] The latter method, which is successful with simpler hydrazines,[3,4] also worked here. The hydrazine used in the condensation step, *N*-(2-hydroxyethyl)-*N*′-methylhydrazine, was prepared according to a literature method for preparing symmetrically substituted hydrazines.[5] The starting material, *N*-(2-hydroxyethyl)hydrazine, was dibenzoylated with benzoyl chloride in the presence of aqueous sodium hydroxide to give *N*-(2-hydroxyethyl)-*N*,*N*′-dibenzoylhydrazine. This compound was methylated with dimethyl sulphate and alkali, and the benzoyl groups were subsequently removed by hydrolysis with hydrochloric acid giving *N*-(2-hydroxyethyl)-*N*′-methylhydrazine as its dihydrochloride in an overall yield of 36 %. The condensation of the hydrazine dihydrochloride with phthalic anhydride was carried out in aqueous acetate buffer, resulting in a 40 % yield

* Present address: Institute of Organic Chemistry, University of Stockholm, S-104 05 Stockholm, Sweden.

of 2-(2′-hydroxyethyl)-3-methyl-1,2,3,4-tetrahydrophthalazine-1,4-dione (VI). This compound could then be converted to the required compound III by refluxing with thionyl chloride in chloroform. However, the synthetic procedure is rather tedious and the overall yield from *N*-(2-hydroxyethyl)-hydrazine is only *ca.* 10 %.

Fortunately, the synthetic path was simplified and improved by the timely discovery that compound III could be prepared in a two step synthesis involving an O – N rearrangement from the readily available 1-hydroxy-3-methyl-3,4-dihydrophthalazin-4-one (I). The sodium salt of compound I was *O*-alkylated (*cf.* Ref. 2) with 2-chloroethanol in dimethylformamide affording 1-(2′-hydroxyethoxy)-3-methyl-3,4-dihydrophthalazin-4-one (VII) in 70 % yield. On reacting compound VII with thionyl chloride in refluxing chloroform, the product was not the expected 1-(2′-chloroethoxy)-3-methyl-3,4-dihydrophthalazin-4-one (II), but compound III, identical with that obtained in the unambiguous method described above. The yield was 88 % and the structure of the product was confirmed by spectral data (see Table 1). The UV absorption curve of the tetrahydrophthalazinedione system differs from that of the dihydrophthalazinone system [1] and the aromatic protons of the former give two distinct two-proton multiplets in the NMR spectrum whereas those of the latter give a one-proton and a three-proton multiplet.

A similar rearrangement reaction in the aliphatic series is that of imino-2-chloroethyl ethers to *N*-2-chloroethylcarboxamides involving an oxazoline intermediate.[6] More recently, O – N rearrangements of certain *O*-acyl [7] and *O*-alkanesulphonyl [8] derivatives of phthalhydrazide have been reported by Le Berre *et al.*

In order to investigate the mechanism of the rearrangement reaction, we first wished to find if the unrearranged chloro-compound, *i.e.* compound II, was an intermediate. This compound was prepared in good yield by alkylating the sodium salt of compound I with 1-bromo-2-chloroethane in DMF at room temperature for 72 h. Interestingly, when this reaction was carried out at 100° for 1 h, compound II could not be isolated from the reaction mixture. Instead two isomeric compounds were formed, which were separable by fractional crystallization. These compounds gave practically identical mass spectra. The molecular ion appeared at *m/e* 378 and the base peak at *m/e* 203. The minor product (IV) gave a UV spectrum (Table 1) characteristic of a 3,4-dihydrophthalazin-4-one.[1] The intensity of the absorption maxima suggest the presence of two such ring systems, and the NMR spectrum (Table 1) indicates a symmetrical structure. The major product (V) gave a UV spectrum (Table 1) rather more in agreement with a 1,2,3,4-tetrahydrophthalazine-1,4-dione.[1] However, the NMR spectrum (Table 1) indicates an unsymmetrical structure. The designated structures are given in Fig. 1. The similarity of the mass spectra may be attributed to the formation of a common base ion (*m/e* 203). This is formed from compound IV by cleavage of a C – O bond β to a ring, and from compound V by cleavage of the C – O bond β to the ring or the bond attaching the ring nitrogen to the central chain. The structure of this base ion is probably a resonance stabilized oxazolinium ion (VIII in Fig. 2).

Table 1. Spectral data.

Compound	IR ν_{max}(KBr) cm^{-1}	UV λ_{max}(CH_3OH) nm	ε_{max}	NMR τ ($CDCl_3$) Aromatic H	*N*-Methyl H
II	1653	252	3840	1.4 – 1.7 (m, 1H)	6.26 (s, 3H)
	1625	261.5	4050	1.8 – 2.4 (m, 3H)	
	1600	297	5990		
III	1645	297	5700	1.5 – 1.8 (m, 2H)	6.28 (s, 3H)
	1608			2.0 – 2.3 (m, 2H)	
IV [a]	1650	253.5	7400	1.4 – 1.7 (m, 2H)	6.25 (s, 6H)
	1608	263.5	8030	1.8 – 2.4 (m, 6H)	
	1583	301.5	12820		
V	1640	261.5	5770	1.5 – 1.9 (m, 3H)	6.20 (s, 3H)
	1585	298.5	9360	2.0 – 2.4 (m, 5H)	6.25 (s, 3H)
VI	3340	303	4290	1.8 – 2.1 (m, 2H)	6.21 (s, 3H)
	1649			2.2 – 2.5 (m, 2H)	
	1620				
	1604				
VII	3350	252.5	3350	1.4 – 1.7 (m, 1H)	6.31 (s, 3H)
	1635	262	3780	1.9 – 2.4 (m, 3H)	
	1585	297.5	5870		

[a] UV spectrum taken in chloroform solution.

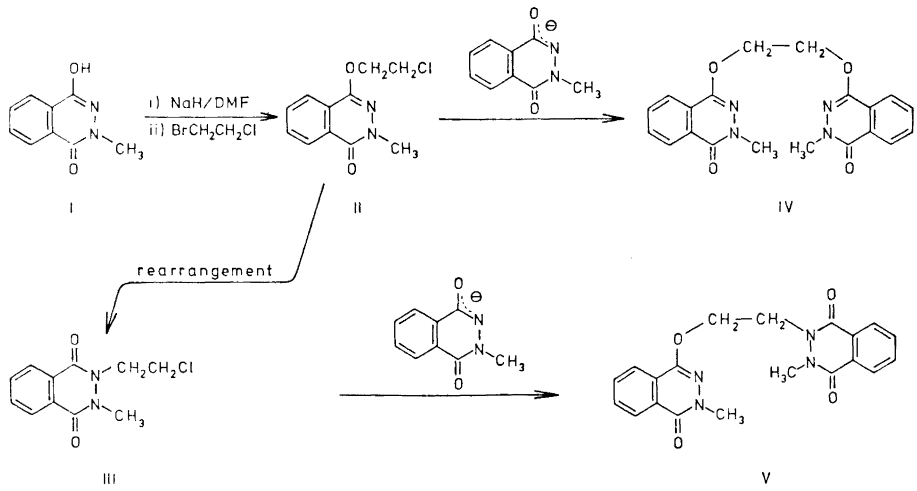

Fig. 1. Formation of compounds IV and V.

The formation of V suggests that the initial product of the alkylation reaction, compound II, can rearrange to compound III which then *O*-alkylates the anion of compound I. This anion may also be alkylated by compound II, in which case compound IV is formed. These reaction paths are illustrated in Fig. 1. The possibility of direct *N*-alkylation may be ruled out on the basis of previous findings.[2]

It was then attempted to isomerize compound II to III. After refluxing compound II in dimethylformamide for 4 h, 85 % of the material had been isomerized. Conversely, refluxing III in dimethylformamide led to the formation of some II. We suggest that this equilibrium, which favours the formation of compound III, proceeds *via* an oxazolinium ion, *i.e.* structure VIII (Fig. 2). It is known that the reaction of 2-hydroxyalkylamides with thionyl chloride leads to the formation of oxazolines.[9,10] From bond energies, it is calculated that III is thermodynamically more stable than II by *ca.* 8 kcal mol^{-1}. Evidence for the stability of ion VIII in the gas phase is provided by the mass spectra of compounds IV and V.

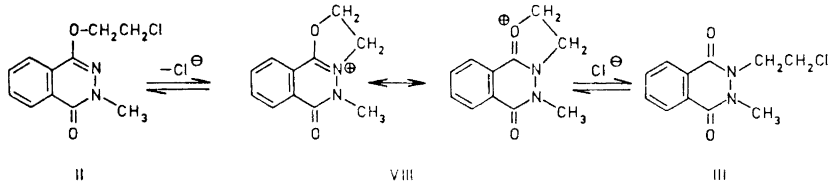

Fig. 2. Isomerization of compound II *via* an oxazolinium ion (VIII).

However, refluxing compound II in chloroform gave no isomerization product. This suggests that II is not an intermediate in the formation of III from VII with thionyl chloride in refluxing chloroform. In order to verify this, we followed the reaction by means of TLC on silica with ethyl acetate as moving phase. After only 10 min, the spot due to compound VII (R_F 0.42) had disappeared completely, and only one spot was observable (in UV), which was due to compound III (R_F 0.58). A spot due to the unrearranged chloride (II) (R_F 0.73) could not be detected. The reaction of compound VI with thionyl chloride in refluxing chloroform was followed in the same way. After only 2 min, the reaction was complete. The product was compound III, no other spot being observable. The rapidity of these two reactions suggests participation of a neighbouring group, and the reaction mechanisms outlined in Fig. 3 are proposed.

Here also, it is suggested that the oxazolinium ion VIII is an intermediate. It can be formed from the chlorosulphite of alcohol VII by the nucleophilic attack of the 2-nitrogen on the 2′-carbon and from the chlorosulphite of alcohol VI by the nucleophilic attack of the oxygen of the 1-carbonyl group on the 2′-carbon. The intermediacy of a chlorosulphite in the formation of oxazolines from 2-hydroxyalkylamides and thionyl chloride has been advocated previously.[10] The S_Ni mechanism,[11] which would lead to the formation of the chloro-

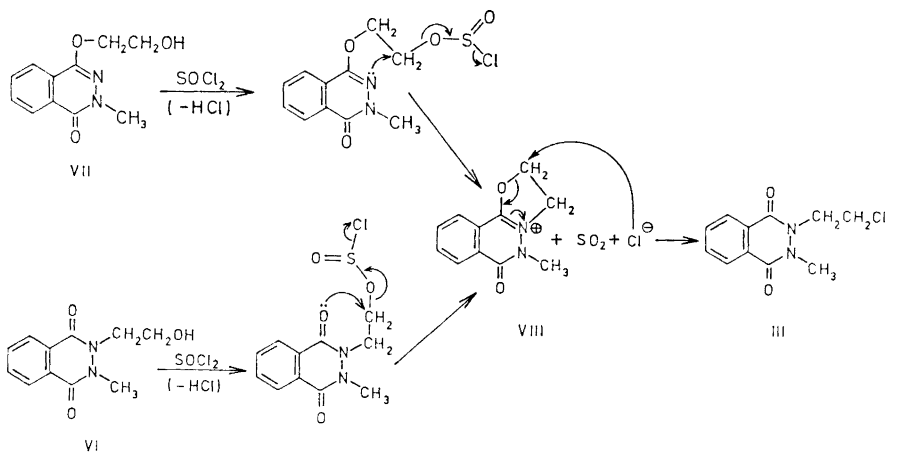

Fig. 3. Proposed mechanism of formation of compound III from compounds VI and VII.

compound II from the chlorosulphite of alcohol VII, is apparently completely suppressed. The reason for the exclusive product of the nucleophilic attack of the chloride ion on the oxazolinium ion VIII being compound III is probably that the activation energy from VIII to the transition state for formation of II is prohibitively high under the reaction conditions.

When the reaction of compound VII with thionyl chloride was carried out in the presence of an equimolar amount of pyridine at 0°C, only 20 % of the rearranged chloro-compound III was formed. The main product was chloro-compound II (yield 60 %). Here nucleophilic chloride ion is present in the reaction mixture [11] and attacks the 2'-carbon of the chlorosulphite competing successfully with the nucleophilic attack of the neighbouring nitrogen atom. When the reaction was carried out in refluxing chloroform in the presence of a catalytic amount of dimethylformamide, the main product (over 80 %) was chloro-compound III. However, thin layer chromatography revealed that some chloro-compound II was formed. Here, the chloride ion concentration of the reaction solution is lower, but there is still some S_N2 attack on the 2'-carbon of the chlorosulphite intermediate by chloride ion from the dimethylformamide-thionyl chloride adduct.[12] Thus a clean rearrangement reaction is observed only when alcohol VII is reacted with thionyl chloride in the absence of pyridine or dimethylformamide as catalyst.

EXPERIMENTAL

All melting points are uncorrected. IR spectra were recorded on a Unicam SP 200 spectrophotometer and UV spectra on a Beckman DK-2A instrument. NMR spectra were measured on a Varian A-60 spectrometer operating at 60 Mc/s with TMS as internal standard. Mass spectra were recorded on an LKB 9000 mass spectrometer operating at 70 eV. Microanalyses were carried out by Dr. A. Bernhardt, Elbach, West Germany, or at our analytical laboratories.

N,N′-*Dibenzoyl*-N-*(2-hydroxyethyl)hydrazine.* A solution of sodium hydroxide (44.0 g 1.10 mol) in 120 ml water and benzoyl chloride (147.6 g, 1.05 mol) were added simultaneously from separate dropping funnels to an ice-cold stirred solution of 2-hydroxyethylhydrazine (38.05 g, 0.50 mol) in 100 ml water, the aqueous alkali being added at a slightly faster rate. When addition was complete, after 1.5 h, the reaction mixture was stirred for a further 2 h. When necessary, 2 N sodium hydroxide was added to maintain alkalinity in the aqueous phase. The reaction mixture was then saturated with carbon dioxide, and extracted with ethyl acetate. The organic phase was washed with aqueous sodium bicarbonate and water, then dried over magnesium sulphate. Removal of the solvent left a viscous syrup, which began to crystallize after standing some time under ethyl acetate. The crystals (79.7 g, m.p. 106 – 110°) were recrystallized from ethyl acetate giving 65.4 g, m.p. 109 – 111°. A further recrystallization from ethyl acetate gave 52.0 g, m.p. 110 – 111.5°. Yield 37 %. (Found: N 9.68. Calc.: N 9.85.) IR (KBr): ν_{OH} 3450 (s), ν_{NH} 3320 (s), $\nu_{C=O}$ 1660 (s, sh), 1530 (s) cm^{-1}. NMR ($CDCl_3$): τ 6.21 (broad s, 4H), 5.59 (broad s, 1H, removed with D_2O), 2.3 – 3.0 (m, 10H), 0.06 (broad s, 1H, removed with D_2O).

N,N′-*Dibenzoyl*-N-*(2-hydroxyethyl)*-N′-*methylhydrazine.* A solution of sodium hydroxide (4.20 g, 0.105 mol) in 10 ml water and dimethyl sulphate (13.20 g, 0.105 mol) were added simultaneously from separate dropping funnels to a stirred solution of *N,N′*-dibenzoyl-*N*-(2-hydroxymethyl)hydrazine (25.85 g, 0.091 mol) in a minimum amount of ethanol. A quarter of the total amounts of each were added, and after 1 h, a further quarter was added, and so on. When addition was complete, 250 ml water was added to the stirred mixture. The oily product was extracted with chloroform, dried over sodium sulphate and the solvent removed, leaving 26.8 g viscous oil, which could not be induced to crystallize. IR (liquid film): ν_{OH} 3450 (s), $\nu_{C=O}$ 1660 (s, sh) cm^{-1}. NMR ($CDCl_3$): τ 6.88 (s, 3H), 5.8 – 6.5 (m, 5H, 1H removed with D_2O), 2.3 – 3.1 (m, 10H).

N-*(2-Hydroxyethyl)*-N′-*methylhydrazine dihydrochloride.* The crude *N,N′*-dibenzoyl-*N*-(2-hydroxyethyl)-*N′*-methylhydrazine (26.8 g) was stirred at 100° with 134 g concentrated hydrochloric acid for 2 h. The solution was then cooled, and the precipitated benzoic acid removed by filtration and washed with water. The filtrate and washings were combined and concentrated under reduced pressure. The residue (14.62 g) crystallized, but was very hygroscopic and could not be recrystallized. (Yield of crude product based on *N,N′*-dibenzoyl-*N*-(2-hydroxyethyl)-hydrazine, 98.5 %.) NMR (D_2O): τ 7.12 (s, 3H), 6.6 – 6.9 (m, 2H, one half of A_2B_2 system), 6.0 – 6.3 (m, 2H, other half of A_2B_2 system).

2-(2′-Hydroxyethyl)-3-methyl-1,2,3,4-tetrahydrophthalazine-1,4-dione (VI). Phthalic anhydride (0.91 g, 6.1 mmol) was added to a solution of *N*-(2-hydroxyethyl)-*N′*-methylhydrazine dihydrochloride (1.00 g, 6.1 mmol) and sodium acetate trihydrate (0.83 g, 6.1 mmol) in 11 ml 40 % aqueous acetic acid. The mixture was heated under reflux under argon for 4 h. After evaporation of the solution to dryness, the residue was triturated several times with boiling isopropyl ether until no more dissolved. On cooling the isopropyl ether solution, 644 mg crystalline product was obtained. Recrystallization from isopropyl ether gave 542 mg, m.p. 124 – 126°. Yield 40 %. (Found: C 60.13; H 5.53; N 12.85. Calc. for $C_{11}H_{12}N_2O_3$: C 59.99; H 5.49; N 12.72.)

1-(2′-Hydroxyethoxy)-3-methyl-3,4-dihydrophthalazin-4-one (VII). 1-Hydroxy-3-methyl-3,4-dihydrophthalazin-4-one [1] (I) (26.5 g, 0.150 mol) was added portionwise to a stirred suspension of sodium hydride (4.32 g, 0.180 mol) in 180 ml dry dimethylformamide under argon. When evolution of gas had ceased, 2-chloroethanol (16.9 g, 0.210 mol) in 100 ml dry dimethylformamide was added during 30 min. The mixture was heated under reflux for 1.5 h. Most of the solvent was removed under reduced pressure, then 200 ml water added. The mixture was extracted with chloroform, the chloroform solution dried over magnesium sulphate and the solvent removed, leaving a residue which was recrystallized from methanol affording 23.2 g, m.p. 147 – 148°. Yield 70 %. (Found: C 60.06; H 5.56; N 12.85. Calc. for $C_{11}H_{12}N_2O_3$: C 59.99; H 5.49; N 12.72.)

2-(2′-Chloroethyl)-3-methyl-1,2,3,4-tetrahydrophthalazine-1,4-dione (III). Method A (from compound VI). Compound VI (0.44 g, 0.002 mol) was heated under reflux with thionyl chloride (0.71 g, 0.006 mol) in 10 ml dry chloroform for 16 h. The solvent was removed under reduced pressure, the last traces of thionyl chloride being removed azeotropically with benzene. The residue was recrystallized from methanol giving 0.36 g, m.p. 118 – 119.5°. Yield 75 %. (Found: C 55.40; H 4.75; Cl 14.92; N 11.89. Calc. for $C_{11}H_{11}ClN_2O_2$: C 55.35; H 4.65; Cl 14.85; N 11.74.)

Method B (from compound VII). Compound VII (5.28 g, 0.024 mol) was heated under reflux with thionyl chloride (8.54 g, 0.072 mol) in 60 ml dry chloroform for 24 h. After removal of the solvent *in vacuo*, the last traces of thionyl chloride being removed azeotropically with benzene, the residue was recrystallized from methanol, giving 4.99 g, m.p. 118.5 – 120°C. Yield 88 %. A mixed m.p. with the product from method A showed no depression.

1-(2'-Chloroethoxy)-3-methyl-3,4-dihydrophthalazin-4-one (II). 1-Hydroxy-3-methyl-3,4-dihydrophthalazin-4-one [1] (I) (13.2 g, 0.075 mol) was added portionwise to a stirred suspension of sodium hydride (2.16 g, 0.090 mol) in 150 ml dry dimethylformamide under argon. When evolution of gas was complete, this suspension was added to a stirred solution of 1-bromo-2-chloroethane (75 g, 0.525 mol) in 60 ml dry dimethylformamide under argon during 30 min, the mixture being cooled in an ice-bath. The mixture was then stirred for 72 h at room temperature. Most of the solvent and excess 1-bromo-2-chloroethane were removed under reduced pressure, 200 ml water added and the mixture extracted with chloroform. The chloroform solution was dried over magnesium sulphate, the solvent removed and the residue recrystallized from methanol giving 12.8 g, m.p. 109 – 110°. Yield 71 %. (Found: C 55.61; H 4.59; Cl 15.04; N 11.62. Calc. for $C_{11}H_{11}ClN_2O_2$: C 55.35; H 4.65; Cl 14.86; N 11.74.)

1,2-Bis-(3'-methyl-3',4'-dihydrophthalazin-4'-on-1'-yloxy)ethane (IV) and 1-(3'-methyl-3',4'-dihydrophthalazin-4'-on-1'-yloxy)-2-(3'-methyl-1',2',3',4'-tetrahydrophthalazine-1',4'-dion-2'-yl)ethane (V). 1-Hydroxy-3-methyl-3,4-dihydrophthalazin-4-one [1] (I) (4.41 g, 0.025 mol) was added portionwise to a stirred suspension of sodium hydride (0.72 g, 0.03 mol) in 50 ml dry dimethylformamide. When evolution of hydrogen had ceased, the suspension was added to a stirred solution of 1-bromo-2-chloroethane (5.0 g, 0.035 mol) in 20 ml dry dimethylformamide under argon during 30 min. The reaction mixture was heated up to 100° during 1 h, kept at this temperature for 1 h, then allowed to cool to room temperature. Next day, the solvent was removed under reduced pressure and 50 ml water added. The mixture was extracted with chloroform and the organic phase dried over magnesium sulphate. On allowing a warm methylene chloride solution of the residue to cool, 0.3 g crystalline material was obtained which was recrystallized from 1,2-dichloroethane, giving compound IV (0.18 g, m.p. 259.5 – 261°). MS: M^+, *m/e* 378 (6 %), 203 (100 %), 162 (4 %), 133 (4 %), 130 (11 %), 104 (12 %), 76 (6 %). (Found: C 63.30; H 4.91; N 14.72. Calc. for $C_{20}H_{18}N_4O_4$: C 63.47; H 4.71; N 14.80.) The filtrate from the methylene chloride solution was evaporated and recrystallized twice from methanol giving compound V (0.86 g, m.p. 220 – 220.5°). MS: M^+, *m/e* 378 (6 %), 203 (100 %), 162 (5 %), 130 (8 %), 104 (12 %), 76 (8 %). (Found: C 63.46; H 4.91; N 14.69. Calc. for $C_{20}H_{18}N_4O_4$: C 63.47; H 4.79; N 14.80.)

Isomerization experiments

The reactions of chloro-compounds II and III in refluxing dimethylformamide (bath temperature 170°) and that of chloro-compound II in refluxing chloroform were followed by means of thin layer chromatography (Merck Kieselgel F_{254}, 20 × 20 cm plates) with ethyl acetate as moving phase. 10 µl samples were removed at various intervals (5, 15, 30 min, 1, 2, 4, 6 h) and diluted with 0.8 ml ether, then 10 µl of each solution chromatographed. The plates were observed under a short-wave ultraviolet lamp.

1-(2'-Chloroethoxy)-3-methyl-3,4-dihydrophthalazin-4-one (II) in refluxing DMF. 500 mg of compound II were dissolved in 6 ml DMF and heated under reflux for 6 h. A spot corresponding to compound III (R_F 0.60) appeared within 5 min. After 2 h, the ratio of the intensities of the spot at R_F 0.60 to that of starting compound II (R_F 0.73) appeared to remain constant. However, a third spot, having the same R_F value as hydroxy-compound VI appeared after 30 min and increased in intensity.

After 6 h, the DMF was removed under reduced pressure and the residue chromatographed on 20 g Merck 0.05 – 0.20 mm Kieselgel using isopropyl ether-isopropanol (4:1) as eluent. Three compounds were isolated: compound II (40 mg, m.p. 105 – 107°), compound III (190 mg, m.p. 117 – 118°), and compound VI (45 mg, m.p. 124 – 126°). None of the compounds gave a depression in m.p. on admixture with authentic specimens. The formation of compound VI may be ascribed to the presence of moisture in the solvent.

2-(2'-Chloroethyl)-3-methyl-1,2,3,4-tetrahydrophthalazine-1,4-dione (III) in refluxing DMF. 240 mg of compound III were dissolved in 3 ml DMF and heated under reflux for 8 h. A spot corresponding to compound II (R_F 0.73) appeared within 5 min. The ratio of the intensity of the new spot to that of the starting material (R_F 0.60) appeared to remain constant after 2 h, the starting material giving the more intense spot. After 30 min, a third spot having the same R_F value as compound VI appeared.

1-(2'-Chloroethoxy)-3-methyl-3,4-dihydrophthalazin-4-one (II) in refluxing chloroform. A solution of 55 mg of compound II in 1.5 ml chloroform was heated under reflux for 24 h. Only one spot, that due to the starting material (R_F 0.72) was observed, no other spot appearing.

Reaction of 1-(2'-hydroxyethoxy)-3-methyl-3,4-dihydrophthalazin-4-one (VII) with thionyl chloride in the presence of catalysts

Pyridine as catalyst. Compound VII (6.0 g, 0.027 mol) was mixed with dry pyridine (2.15 g, 0.027 mol) and 25 ml dry ether added. Thionyl chloride (6.4 g, 0.054 mol) was then added dropwise to the stirred mixture which was cooled in an ice-bath. The mixture was allowed to stand overnight, then heated under reflux for 30 min. After cooling, water was added and the precipitate removed by filtration, washed with water and dried. The filtrate was extracted with ether and the ether phase dried over $MgSO_4$ and the solvent removed. The residue was combined with the dried precipitate and 1 g of this material was chromatographed on 50 g Kieselgel (Merck, 0.05 – 0.20 mm). Elution was performed using isopropyl ether. Two compounds were obtained, the first eluted (0.60 g) having m.p. 107 – 110° being identical with compound II, and the second (0.19 g, m.p. 111 – 115°) being identical with compound III.

DMF as catalyst. Compound VII (11.0 g, 0.050 mol) was dissolved in 85 ml dry chloroform and 0.8 ml dry DMF was added. Then thionyl chloride (17.8 g, 0.150 mol) was added dropwise to the stirred solution which was subsequently heated under reflux for 7 h. The solvent and excess thionyl chloride were removed under reduced pressure, the last traces of the latter being removed azeotropically with benzene. The residue was recrystallized from methanol affording 9.70 g, m.p. 116 – 118°. This material was identical with 2-(2'-chloroethyl)-3-methyl-1,2,3,4-tetrahydrophthalazine-1,4-dione (III). Yield 82 %.

Investigation of the course of the reactions of compounds VI and VII with thionyl chloride

General procedure. The compounds were heated under reflux with thionyl chloride in dry chloroform for 4 h at a bath temperature of 70 – 72°. Samples (10 µl) were removed at various intervals (2, 5, 10, 15, 30 min, 1, 2, 4 h), immediately shaken with 1 ml water and the mixture was extracted with 0.4 ml ether. 10 µl of each ether phase was applied to a TLC plate (Merck Kieselgel F_{254}, 20 × 20 cm) and the chromatograms developed using ethyl acetate as the moving phase. The plates were observed under a short-wave ultraviolet lamp.

Reaction of compound VI with thionyl chloride in chloroform. Compound VI (55 mg, 0.25 mmol) and thionyl chloride (90 mg, 0.75 mmol) were heated under reflux in 1 ml chloroform. Within only 2 min, the reaction was complete, the product having the same R_F value as compound III (0.61). No other spots were observed after this time.

Reaction of compound VII with thionyl chloride in chloroform. Compound VII (220 mg, 1.0 mmol) and thionyl chloride (360 mg, 3.0 mmol) were heated under reflux in 3 ml chloroform. After 5 min, 4 spots were observable, R_F 0.34, 0.42 (identical with compound VII), 0.58 (identical with compound III) and 0.68. After 10 min, only one spot was observable, R_F 0.58. A spot corresponding to chloro-compound II (R_F 0.73) was never observed.

Reaction of compound VII with thionyl chloride in chloroform with DMF as catalyst. Compound VII (220 mg, 1.0 mmol), thionyl chloride (357 mg, 3.0 mmol) and 0.02 ml dry

DMF were heated under reflux in 3 ml chloroform. After 5 min, 4 spots were observable, R_F 0.35, 0.40 (identical with compound VII), 0.55 (identical with compound III) and 0.67. After 10 min, there were still 4 spots, those with R_F 0.35 and 0.40 being less intense, and that at R_F 0.55 being more intense than in the previous sample. The fourth spot, R_F 0.70, was less intense than that at R_F 0.55. It had the same R_F value as compound II. The spot at R_F 0.67 was no longer observable. After 15 min, only 2 spots were observable, R_F 0.55 and 0.70. Their intensities relative to each other in subsequent samples remained unchanged, the spot at R_F 0.55 being more intense.

Acknowledgement. The authors wish to thank Docent Nils E. Stjernström for reading the manuscript.

REFERENCES

1. Elvidge, J. A. and Redman, A. P. *J. Chem. Soc.* **1960** 1710.
2. Buu-Hoi, Ng. Ph., Le Bihan, H. and Binon, F. *Rec. Trav. Chim.* **70** (1951) 1099.
3. Rowe, F. M. and Peters, A. T. *J. Chem. Soc.* **1933** 1331.
4. Drew, H. D. K., Hatt, H. H. and Hobart, F. A. *J. Chem. Soc.* **1937** 33.
5. Ramsperger, H. C. *J. Am. Chem. Soc.* **51** (1929) 918.
6. Wislicenus, W. and Körber, H. *Ber.* **35** (1902) 164.
7. Dormoy, M., Godin, J. and Le Berre, A. *Bull. Soc. Chim. France* **1968** 4222.
8. Le Berre, A. and Dumaitre, B. *Bull. Soc. Chim. France* **1970** 4376.
9. Frump, J. A. *Chem. Revs.* **71** (1971) 483.
10. Fry, E. M. *J. Org. Chem.* **14** (1949) 887.
11. Gould, E. S. *Mechanism and Structure in Organic Chemistry*, Holt, Rinehart and Winston, New York 1959, pp. 294–295.
12. Ferré, G. and Palomo, A. L. *Ann. Quim.* **65** (1969) 163.

Received January 25, 1973.

ACTA CHEMICA SCANDINAVICA 27 (1973) 1900–1906

Paper Electrophoresis of Carbohydrates in Glycerol-Boric Acid Buffer

BIRGITTA PETTERSSON and OLOF THEANDER*

Chemistry Department, Swedish Forest Products Research Laboratory, Box 5604, S-114 86 Stockholm, Sweden

The paper electrophoretic mobilities of various monosaccharides and methyl ethers, disaccharides, furanosides, uronic and hexulosonic acids in glycerol-boric acid buffer, pH 6.8, have been examined and have been compared with those in borate, pH 10 and sulphonated phenylboronic acid, pH 6.5. The mobilities in the new buffer for most of the carbohydrates parallel those obtained in the sulphonated phenylboronic acid buffer. Advantages of the new procedure include more available chemicals used, higher absolute mobilities and sharper spots obtained.

Paper electrophoresis involves the migration of charged substances in a conducting solution under the influence of an applied electrical field with filter paper as support for the electrolyte. In order to make neutral carbohydrates migrate it is necessary to ionise them by using a solution of high pH or to complex them with some charged ionic species.

The reaction of polyhydroxy compounds with boric acid and borate ion has long been known and thoroughly studied.[1,2] Borate buffer of pH 10 has been used in paper electrophoresis of carbohydrates.[3,4] The complexes involved can be formulated as follows:

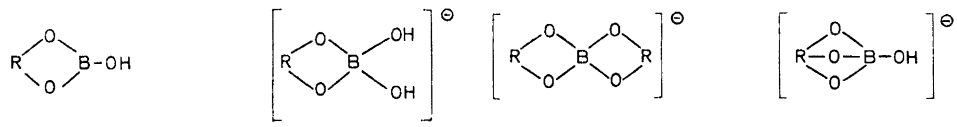

I II III IV

The ionic species II – IV migrate during electrophoresis. Of these, the tridentate complex (IV) is formed only under favourable steric conditions. These charged tetragonal boron complexes occur in low concentrations in

* Present address: Department of Chemistry, Div II, Agricultural College of Sweden, S-750 07 Uppsala, Sweden.

aqueous boric acid. At higher pH their concentration is increased which results in increased electrophoretic mobilities of various carbohydrates.[3,5] The maximum mobilities of carbohydrates are generally in the region 9 – 10, a pH range which has been used much for paper electrophoresis. It is also important, however, that the relative mobilities of certain pairs of carbohydrates are dependent on pH. Thus, for instance, at pH 9 – 10 D-glucose has a mobility greater than that of D-fructose, but at pH 7 – 8 the reverse relationship is obtained. Both sugars, however, have considerably lower migrations at pH 7 – 8 than in alkaline borate. The migration of various types of carbohydrates in alkaline borate and its dependence on the spatial disposition of the hydroxyl groups have been discussed in detail in reviews.[3,4]

Thus, *cis*-1,2-diols of the five-membered ring compounds complex more readily with borate than the corresponding *trans* compounds, which is reflected by greater electrophoretic mobilities. In the zig-zag conformations of acyclic 1,2-diols the *trans* isomer, however, seems to react more strongly with borate than the *cis* isomer. In glucopyranosides the mobilities are attributed to borate complexes between the C-4 and C-6 hydroxyls.

No significant increase in the rate of mobility of sugars at pH 7 was found by using phenylboronic acid instead of boric acid.[6,7] Sulfonated phenylboronic acid at neutral pH-values, however, increased the mobilities for a number of carbohydrates and gave much more selective reactions than borate at pH 10. The new buffer was also more suitable for alkali-labile carbohydrates. The sulphonic group is believed to decrease the ionisation of the boronic acid group, thus leading to trigonal boronic esters (I) rather than tetragonal complexes. These migrate during paper electrophoresis due to the ionisation of the sulphonic acid group. With reducing sugars and glycosides, the largest contribution to the mobilities was found to arise from *cis*-1,2-diols of five-membered rings, but none from *cis*-1,2-diols of six-membered ring compounds or from such a diol group as that on C-4 and C-6 in D-glucopyranose. Important complex formation in this electrolyte occurs across a *cis*-1,3-diol grouping of axially disposed hydroxyl groups.[6,8]

More recently, paper electrophoresis of various carbohydrates in diphenylborinate at pH 10 was studied [9] and the electrophoretic mobilities were compared with those in borate. Only one type of charged complex, analogous to type II, can be formed with diphenylborinate. Nevertheless, the mobilities for the various polyols in this buffer closely parallel those obtained in borate at pH 10.

Various other complexes of inorganic ions are known to be formed with carbohydrates and their behaviour in electrophoresis has been studied.[4] Thus, at this laboratory, paper electrophoresis of sugars and carbonyl derivatives of carbohydrates in hydrogen sulphite buffers has been examined.[10]

Sugars can be separated chromatographically on an ion exchange resin as borate complexes and by elution with alkaline borate.[11,12] Earlier a modification was developed, which allowed separation of borate complexes of neutral sugars at neutral pH and elevated temperature, using a glycerol-boric acid buffer adjusted to pH 6.8 by addition of sodium hydroxide.[13] This system gave a higher degree of resolution of various sugars and higher recoveries than with the alkaline borate buffer.

In the present investigation the use of a similar buffer in paper electrophoresis has been studied. One would expect that the high content of glycerol in the electrolyte would favour a high concentration of a glycerol complex of type II, which is considerably more acidic than boric acid. The ionic strength will thus be increased and higher buffer capacity will be possible than with a boric acid-phosphate buffer.

As discussed above, electrophoresis at neutral pH-values has previously shown interesting differences compared to alkaline borate.[5,6] The high concentration of glycerol-type II complex will favour the formation of a complex of type III in the glycerol-boric acid buffer. Opposite to that, the type I complex is formed when the sulphonated phenylboronic acid is used.[6] One could therefore expect some differences between the two buffer systems because of structural reasons but similarities because of the pH.

In a preliminary experiment D-glucose and its monomethyl ethers in four different buffers based on glycerol, boric acid, and the requisite amount of sodium hydroxide for the desired pH were tested (Table 1). As a comparison,

Table 1. Glucose and its methyl ethers in different buffers.

$$M_G = \frac{\text{true distance of migration of the substance}}{\text{true distance of migration of glucose}}$$

Substance	Buffer A M_G	Buffer B M_G	Buffer C M_G	Buffer D M_G	Buffer E M_G
D-Glucose	1.00 (9.9 cm)	1.00 (10.5 cm)	1.00 (10.3 cm)	1.00 (17.9 cm)	1.00 (8.5 cm)
2-*O*-Methyl-D-glucose	0	0.04	0.07	0.14	–
3-*O*-Methyl-D-glucose	1.18	1.21	1.34	1.03	1.34
4-*O*-Methyl-D-glucose	0	0.10	0.29	0.19	0.12
6-*O*-Methyl-D-glucose	0.68	0.79	0.80	0.83	0.82

a related buffer containing mannitol was examined. The electrophoresis was run at 40° and 1500 V (about 30 V/cm) for 1.5 h. The spread of mobilities in the four glycerol-boric acid buffers was found to be greater than in borate and of similar order as in sulphonated phenylboronic acid,[6] but the absolute mobilities were higher than those reported for the latter.

Buffer B, pH 6.8, was chosen for further studies. Buffer A did not give as distinct spots as B and when buffer C, with the highest glycerol content, was used, the paper sometimes burned off outside the cooling area. Buffer D of pH 7.4 did not give as good a separation pattern as B, although the mobilities were higher. Buffer E containing mannitol, gave similar M_G-values as the glycerol buffers, but was not studied further.

The paper electrophoretic mobilities in buffer B, pH 6.8, sulphonated phenyl boronic acid, pH 6.5 and borate, pH 10.0, of some monosaccharides and their monomethyl ethers, oligosaccharides, and furanosides are shown in Tables 2–5. Electrophoretic mobilities of hexuronic and hexulosonic acids in buffer B, borate pH 10.0, and hydrogen sulphite pH 4.7 are given in Table 6.

Table 2. Monosaccharides.

Substance	Buffer B M_G	Sulphonated phenylboronic acid [6] pH 6.5, M_G	Borate pH 10 M_G
D-Xylose	1.60	1.8	1.00 [6]
D-Lyxose	1.24	2.3	0.71 [6]
L-Arabinose	1.28	2.4	0.96 [6]
D-Ribose	1.74	4.7	0.77 [6]
D-Glucose	1.00	1.00	1.00 [6]
D-Mannose	0.87	1.1	0.72 [6]
D-Galactose	1.06	1.8	0.93 [6]
D-Gulose	1.60	–	0.82 [17]
D-Idose	1.84	–	1.02 [17]
D-Talose	1.85	–	0.87 [17]
D-Allose	1.28	–	0.83 [17]
D-Altrose	1.64	5.8	0.97 [6]
D-Fructose	1.74	9.3	0.90 [6]
L-Sorbose	2.00	8.5	0.95 [6]
D-Tagatose	1.93	8.6	0.95 [6]
D-Allulose	1.99	–	0.79
D-Xylulose	2.12	–	0.67
D-Ribulose	2.32	–	0.80
D-*glycero*-D-*gulo*-Heptose	1.49	–	0.89
D-*glycero*-D-*ido*-Heptose	2.37	–	0.91
D-*glycero*-L-*gluco*-Heptose	1.72	–	0.98
D-*glycero*-L-*manno*-Heptose	1.00	–	0.73
D-*glycero*-D-*galacto*-Heptose	0.89	–	0.73
D-*glycero*-D-*talo*-Heptose	1.48	–	0.62

Table 3. Methyl ethers of xylose, glucose, and galactose.

Substance	Buffer B M_G	Sulphonated phenylboronic acid [6] pH 6.5, M_G	Borate pH 10 M_G
D-Xylose	1.60	1.8	1.00 [6]
2-*O*-Methyl-D-xylose	0.04	0	0.39 [6]
3-*O*-Methyl-D-xylose	1.49	2.9	0.66 [6]
D-Glucose	1.00	1.0	1.00 [6]
2-*O*-Methyl-D-glucose	0.04	0	0.23 [6]
3-*O*-Methyl-D-glucose	1.21	1.3	0.80 [6]
4-*O*-Methyl-D-glucose	0.10	0	0.24 [6]
6-*O*-Methyl-D-glucose	0.79	0.5	0.80 [6]
D-Galactose	1.06	1.8	0.93 [6]
2-*O*-Methyl-D-galactose	0.23	–	0.43 [18]
3-*O*-Methyl-D-galactose	0.86	–	0.63 [18]
4-*O*-Methyl-D-galactose	0.08	–	0.30 [18]

Table 4. Disaccharides.

Substance	Buffer B M_G	Borate pH 10 M_G
Sucrose, α-G-(1↔2)-β-Fru	0.08	0.10 [19]
Kojibiose, α-G-(1→2)-G	0.10	0.32 [20]
Sophorose, β-G-(1→2)-G	0.08	0.24 [21]
Laminaribiose, β-G-(1→3)-G	1.16	0.69 [21]
Maltose, α-G-(1→4)-G	0.26	0.32 [21]
Mannobiose, β-Man-(1→4)-Man	0.36	0.54
Cellobiose, β-G-(1→4)-G	0.29	0.23 [21]
Xylobiose, β-Xyl-(1→4)-Xyl	0.12	0.20
Lactose, β-Gal-(1→4)-G	0.31	0.38 [21]
Gentiobiose, β-G-(1→6)-G	0.74	0.75 [21]
Melibiose, α-Gal-(1→6)-G	0.91	0.76

Table 5. Furanosides.

Substance	Buffer B M_G	Sulphonated phenylboronic acid pH 6.5, M_G	Borate pH 10 M_G
1,2-*O*-Isopropylidene-α-D-glucofuranose	1.14	3.4 [8]	0.66 [6]
1,2-*O*-Isopropylidene-α-D-*ribo*-hexofuranos-3-ulose	0.94	0	0.39
1,2-*O*-Isopropylidene-α-D-*xylo*-pentodialdo-1,4-furanose	0.78	0.88	0.57
1,2-*O*-Isopropylidene-α-D-*gluco*-hexodialdo-1,4-furanose	0.98	2.21	0.65
Methyl α-D-mannofuranoside	1.81	16.0 [6]	0.79

In spite of the fact that two different types of complexes, discussed above, are expected to predominate using buffer B and sulphonated phenylboronic acid, respectively, many similarities between the mobilities in the two systems were found and they were rather different from those in borate pH 10. On the other hand the mobilities for various carbohydrates in borate pH 10 closely paralleled those obtained in diphenylborinate [9] pH 10, in spite of the much more restricted complexing possibility in the latter buffer. This indicates that the pH of the boric acid-borate buffers may be the most important factor for most of the compounds studied. Advantages of the glycerol-boric acid buffer over the one based on sulphonated phenylboronic acid are the availability of the chemicals used in the former and the higher absolute mobilities and sharper spots obtained. A disadvantage is the impossibility, because of the glycerol present, to use the common silver and periodate-detecting reagents.

Table 6. Uronic and hexulosonic acids.

Substance	Buffer B [15] M_G	Borate pH 10 M_G	Hydrogen sulphite [15] pH 4.7 $M_{vanillin}$
D-Glucuronic acid	2.10; 2.88	1.19	0.91; 1.24
D-Galacturonic acid	2.50	1.16	1.33
D-Mannuronic acid	2.71	1.12	1.06; 1.45
L-Guluronic acid	2.70	1.02	1.41
L-Iduronic acid	3.07	1.04	1.05; 1.59
D-Altruronic acid	2.91	–	1.37; 1.49
D-Alluronic acid	3.22	–	1.35
D-*xylo*-5-Hexulosonic acid (5-Keto-D-gluconic acid)	3.22	–	1.29
D-*lyxo*-5-Hexulosonic acid (5-Keto-D-mannonic or 5-Keto-L-gulonic acid)	3.11	–	1.25
L-*ribo*-5-Hexulosonic acid (5-Keto-D-talonic or 5-Keto-L-allonic acid)	3.33	–	1.32
D-*arabino*-Hexulosonic acid (2-Keto-D-gluconic acid)	3.04	–	1.65
L-*xylo*-Hexulosonic acid (2-Keto-L-gulonic acid)	2.96	–	1.60

As shown in Table 2, buffer B is useful for the separation of the pentoses, hexoses, and heptoses. The differences in the mobilities between the ketoses and aldoses are not so great in buffer B as in sulphonated phenylboronic acid. For the sugar monomethyl ethers (Table 3) studied, buffer B seems to be the most useful of the three buffers. The same is true for oligosaccharides (Table 4). The limited results with furanosides (Table 5) indicate similarities between buffer B and sulphonated phenylboronic acid and that the former is a useful complement to the hydrogen sulphite buffer [10] for dicarbonyl sugar derivatives. The lack of migration of the 3-keto compound in the sulphonated phenylboronic acid is notable and is probably caused by a strong predominance of the hemiketal form of the compound.[14] Mobilities of various dialdoses and their corresponding monomethyl glycosides will be published elsewhere.

In the characterisation of hexuronic and hexulosonic acids, paper electrophoresis in buffer B has been useful and a good complement to the hydrogen sulphite buffer.[15] Both these buffers give more selectivity than borate pH 10 (Table 6) and often yields characteristic spots corresponding to both the lactone and the free acid form in the former systems.

EXPERIMENTAL

Substances. The substances used were available at this laboratory.
Composition of the buffers:

Buffer A: 0.4 M H_3BO_3, 0.6 M Glycerol, 0.060 M NaOH, pH = 6.8
B: 0.4 M H_3BO_3, 1.0 M Glycerol, 0.096 M NaOH, pH = 6.8
C: 0.4 M H_3BO_3, 1.4 M Glycerol, 0.134 M NaOH, pH = 6.8
D: 0.4 M H_3BO_3, 1.0 M Glycerol, 0.172 M NaOH, pH = 7.4
E: 0.4 M H_3BO_3, 0.5 M Mannitol, 0.290 M NaOH, pH = 6.8

Electrophoresis. The apparatus and technique of the paper electrophoresis are the same as described before by Foster.[16] The electrophoresis was run at 40° and the temperature was maintained with thermostated water circulating through the condensing block. The electrophoresis was run at 1500 V for 90 min. Hydroxymethylfurfural was used to indicate the endosmotic effect and glucose was the standard reference substance. The compounds were located by the anisidine hydrochloride spraying reagent. Also the non-reducing furanosides could be detected with this reagent after examination of the heated paper in UV-light (366 nm).

REFERENCES

1. Böeseken, J. *Advan. Carbohyd. Chem.* **4** (1949) 189.
2. Isbell, H. S., Brewster, J. F., Holt, N. B. and Frush, H. L. *J. Res. Natl. Bur. Std.* **40** (1948) 129.
3. Foster, A. B. *Advan. Carbohyd. Chem.* **12** (1957) 81.
4. Weigel, H. *Advan. Carbohyd. Chem.* **18** (1963) 61.
5. Consden, R. and Stanier, W. M. *Nature* **169** (1952) 783.
6. Garegg, P. J. and Lindberg, B. *Acta Chem. Scand.* **15** (1961) 1913.
7. Garegg, P. J. *Svensk Kem. Tidskr.* **77** (1965) 28.
8. Theander, O. *Acta Chem. Scand.* **18** (1964) 1297.
9. Garegg, P. J. and Lindström, K. *Acta Chem. Scand.* **25** (1971) 1559.
10. Theander, O. *Acta Chem. Scand.* **11** (1957) 717.
11. Khym, J. X. and Zill, L. P. *J. Am. Chem. Soc.* **73** (1951) 2399; **74** (1952) 2090.
12. Hallén, A. *Acta Chem. Scand.* **14** (1960) 2249.
13. Walborg, Jr., E. F., Christensson, L. and Gardell, S. *Anal. Biochem.* **13** (1965) 177.
14. Theander, O. *Acta Chem. Scand.* **17** (1963) 1751.
15. Carlsson, B., Samuelson, O., Popoff, T. and Theander, O. *Acta Chem. Scand.* **23** (1969) 261.
16. Foster, A. B. *Chem. Ind. London* **1952** 1050.
17. Frahn, J. L. and Mills, J. A. *Austral. J. Chem.* **12** (1959) 65.
18. Lindberg, B. and Swan, B. *Acta Chem. Scand.* **14** (1960) 1043.
19. Bourne, E. J., Hutson, D. H. and Weigel, H. *Chem. Ind. London* **1960** 1111.
20. Haq, S. and Whelan, W. J. *Nature* **178** (1956) 1221.
21. Foster, A. B. *J. Chem. Soc.* **1953** 982.

Received February 7, 1973.

ACTA CHEMICA SCANDINAVICA 27 (1973) 1907–1913

Studies on Orchidaceae Alkaloids

XXXII.* Crepidine, Crepidamine and Dendrocrepine, Three Alkaloids from *Dendrobium crepidatum* Lindl.

MAGNUS ELANDER, KURT LEANDER, JAN ROSENBLOM and ENE RUUSA

Department of Organic Chemistry, University of Stockholm, Sandåsgatan 2, S-113 27 Stockholm, Sweden

Dedicated to Professor *František Šorm* on his 60th birthday

Three alkaloids, crepidine (I), crepidamine (IV), and dendrocrepine (VII), have been isolated from *Dendrobium crepidatum* Lindl. Their structures have been determined by physical methods. Two substances, isocrepidamine (V) and isodendrocrepine (VIII), previously believed to be present in the plant, have been shown to be artefacts formed during the isolation process.

The relative[2,3] and absolute[3] configurations of crepidine (I), an alkaloid found in *Dendrobium crepidatum* Lindl., have been determined by X-ray diffraction studies of the corresponding methiodide (II). In the present communication the isolation and characterisation of crepidine (I) and two additional alkaloids, crepidamine (IV) and dendrocrepine (VII), are reported. Two further substances, isocrepidamine (V) and isodendrocrepine (VIII), were previously believed to be present in the plant.[2,3] Since, however, they were not found in an acidic fresh plant extract, it is now concluded that they are artefacts formed during the isolation process.

Crepidine. From the results of the X-ray diffraction studies of crepidine methiodide (II) it follows that crepidine has the structure I.

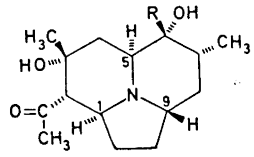

I R = phenyl

* For number XXXI of this series, see Ref. 1.

The IR spectrum of crepidine (I) shows a strong band at 1675 cm^{-1} (KBr), the low wave-number of which indicates hydrogen bonding between the carbonyl group and the 3-hydroxyl group. In dilute solution (CCl_4, 0.004 M) crepidine (I) shows only one band in the hydroxyl stretching region (3510 cm^{-1}), which indicates that in addition to the 3-hydroxyl-carbonyl hydrogen bond, the hydrogen in the 6-hydroxyl group is intramolecularly bonded to the nitrogen atom.

Treatment of crepidine methiodide (II) with sodium hydroxide (2 M, 30 min) at room temperature afforded an optically active amorphous base (III), exhibiting IR bands (CCl_4) at 1632 and 1685 cm^{-1} (α,β-unsaturated ketone), 1705 and 1725 cm^{-1} (saturated ketone, *vide infra*). The molecular formula for III, $C_{22}H_{31}NO_3$, was determined from the integral of its NMR spectrum and by mass spectrometry. The proposed structure for III, in accordance with the NMR spectrum, is shown in Fig. 1. The signal at τ 8.33 (s, 3 H) is attributed to the C(1) hydrogens, which are strongly shielded by the phenyl ring.

As mentioned above, the absorptions at 1705 and 1725 cm^{-1} are assigned to the C(2) carbonyl group. The hydrochloride of III (in KBr) shows the same pattern in the carbonyl region and hence the doublet nature cannot be due to interference of the carbonyl group with the nitrogen atom. The splitting of the C(2) carbonyl band may possibly arise from Fermi resonance between the C(2) carbonyl stretching mode, and an overtone or combination band.[4]

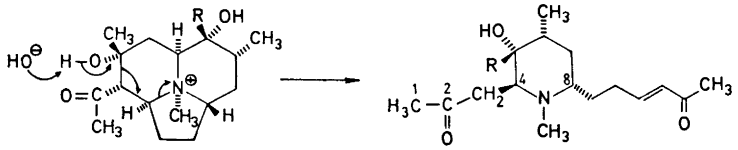

II R = phenyl III

Fig. 1. Alkaline degradation of crepidine methiodide (II).

Crepidamine. Crepidamine (IV), which is optically inactive, was shown by elemental analysis and high resolution mass spectrometry to have the empirical formula $C_{18}H_{25}NO_2$. On spectral evidence discussed below, the structure IV

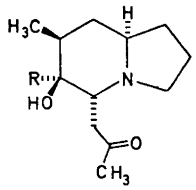

IV* R = phenyl

* In the following, all compounds depicted, except lobeline, are racemic, but only one enantiomer is shown.

is proposed for crepidamine. Its NMR spectrum is similar to that of III except for signals due to the α,β-unsaturated ketone system and the *N*-methyl group. This indicates that the structural differences between III and IV are to be found at the nitrogen atom and at C(8). The IR and NMR spectra of crepidamine (IV) show no alkene bands or olefinic protons. The remaining atoms to be accounted for, C_3H_6, must accordingly be members of an additional ring, suggesting that crepidamine has the structure IV.

The IR spectrum of crepidamine (IV) (0.005 M solution in carbon tetrachloride) shows only one band (3470 cm^{-1}) in the hydroxyl stretching region, which indicates an intramolecular OH···N bonding. This evidence implies that the predominant conformation of crepidamine (IV) in carbon tetrachloride solution should be that depicted in Fig. 2. The *trans*-fusion of the rings in the octahydroindolizine system is supported by weak Bohlmann bands (2720 and 2820 cm^{-1}).[5-7]

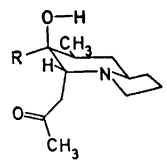

Fig. 2. The predominant conformation of crepidamine (IV) dissolved in carbon tetrachloride.

R = phenyl

Crepidamine (IV) was easily isomerised to isocrepidamine (V) by boiling in ethanol or, more slowly, by chromatography on neutral alumina. Compounds with the $N-CH-CH_2-C=O$ system, *e.g.* hygrine,[8] pelletierine [9] (= isopelletierine [10]), and lobeline,[11] are known to isomerise in alkaline solution. The reaction is considered to involve an intermediate α,β-unsaturated ketone,[8-9] which then preferably recyclisises to the thermodynamically most stable product.

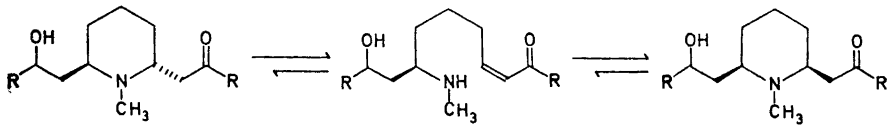

Fig. 3. Isomerisation of lobeline.

An analogous reaction of crepidamine (IV) would result in a product with the structure VI. The IR spectrum of isocrepidamine (V) shows, however, a hydroxyl band but no absorption in the carbonyl stretching region. This indicates that the hydroxyketone VI, initially formed, has cyclisised to the corresponding hemiketal.

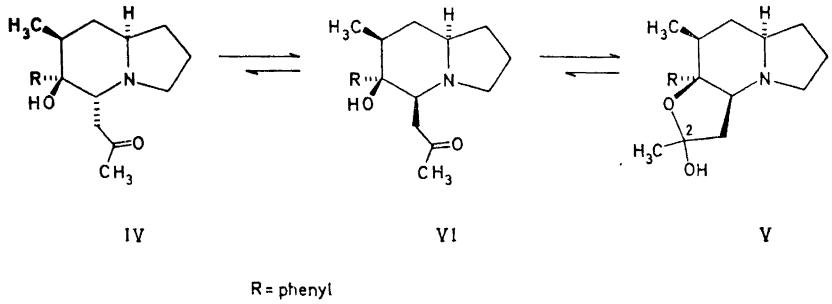

Fig. 4. Isomerisation of crepidamine (IV) to isocrepidamine (V).

The configuration at C(2) was determined by hydrogen bonding studies. A dilute solution of isocrepidamine (V) in carbon tetrachloride (0.005 M) shows only one band (3290 cm^{-1}) in the hydroxyl stretching region, the low wave-number indicating a strong intramolecular OH···N bonding. This evidence implies that the predominant configuration and conformation of isocrepidamine (V) in carbon tetrachloride should be that depicted in Fig. 5. As expected, isocrepidamine (V) shows stronger Bohlmann bands than crepidamine (IV).[5–7]

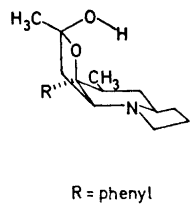

Fig. 5. The predominant configuration and conformation of isocrepidamine (V) dissolved in carbon tetrachloride.

Dendrocrepine. Dendrocrepine (VII), which is optically inactive, was shown by molecular weight determinations and elemental analysis to have the empirical formula $C_{33}H_{44}N_2O_3$. From its NMR spectrum, which is similar to that of crepidamine (IV), and from its mass spectral fragmentation, the structure VII was indicated.

To elucidate whether dendrocrepine (VII) is a racemic or meso compound, it was reduced with lithium aluminium hydride. As only one reduction product could be detected, the alkaloid was considered to be a racemate. Attempts to resolve dendrocrepine (VII) into its antipodes were, however, unsuccessful. The dihydrobromide of dendrocrepine (VII) was therefore subjected to an X-ray diffraction analysis, which established that dendrocrepine (VII) is indeed a racemic compound.[12]

Dendrocrepine (VII) was easily isomerised to isodendrocrepine (VIII) by boiling in ethanol or by chromatography on neutral alumina. A dilute solution of isodendrocrepine (VIII) in carbon tetrachloride (0.005 M) shows two bands in the hydroxyl stretching region at 3420 cm^{-1} and 3260 cm^{-1}, respectively.

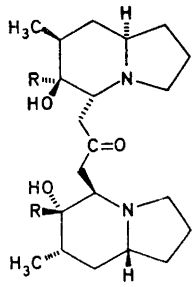

VII

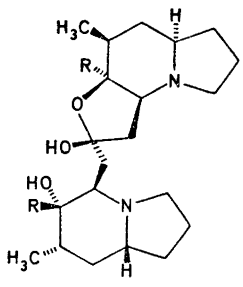

R = phenyl VIII

In the NMR spectrum of dendrocrepine (VII) and dihydrodendrocrepine (IX), the methyl groups appear as one doublet at τ 9.18 and τ 9,20, respectively. Reduction of isodendrocrepine (VIII) with lithium aluminium hydride gave two dihydro compounds (X and XI), the methyl groups of which appear as two doublets at τ 9.22, 9.48 and 9.17, 9.47, respectively. This indicates that the isomerisation of dendrocrepine (VII) to isodendrocrepine (VIII) has involved only one centre in the molecule. On the basis of this evidence, structure VIII is proposed for isodendrocrepine.

EXPERIMENTAL

All melting points are corrected. Mass spectra were measured on an LKB 9000 spectrometer (ionisation energy 70 eV), and the optical rotations on a Perkin-Elmer 141 polarimeter. The IR spectra were recorded on a Perkin-Elmer 257 instrument, the NMR spectra on a Varian A-60A spectrometer, and the ORD spectra on a Cary 60 spectropolarimeter.

Isolation of the alkaloids. Fresh plants of *Dendrobium crepidatum* Lindl. (8.6 kg) were extracted with methanol (20 l). The extract was concentrated to 2 l, acidified and washed with ether (5 × 0.4 l). One fourth of the aqueous solution was made alkaline with small portions of sodium hydroxide and extracted with ether (0.1 l) after each addition of alkali. The ether solution was extracted with aqueous hydrochloric acid (2 %) and the extraction procedure above was repeated twice. The resulting ether extract was dried (Na_2SO_4) and evaporated to dryness. The residue (4.3 g) was chromatographed on silica gel (5 × 65 cm) using chloroform-methanol (19:1) as eluent. The first fraction (fraction A, 1.41 g), contained dendrocrepine (VII) and crepidamine (IV), and the second fraction (fraction B, 0.47 g) contained crepidine (I) and a small amount of crepidamine (IV).

The components in fraction A were chromatographed on silica gel (5 × 60 cm) using ether as eluent. The material in the first fractions (1 – 40, 0.52 g) was recrystallised from ether at – 20°, giving dendrocrepine (VII, 0.25 g). The components in the combined fractions 51 – 70 were chromatographed on neutral alumina (2.6 × 25 cm) using ether as eluent. The material in the first fraction was recrystallised from ether at – 20°, giving crepidamine (IV, 0.08 g).

The components in fraction B were chromatographed on neutral alumina (2.6 × 18 cm) using ether as eluent. The first fraction contained crepidamine (IV). The material in the second fraction was recrystallised from ethanol giving crepidine (I, 0.20 g).

Characterisation of crepidine (I). Crystallisation of I from ethanol gave needles, m.p. 221 – 222°; $[\alpha]_D^{24}$ – 82° (*c* 0.43, methanol); $[\alpha]_D^{24}$ – 78° (*c* 0.50, chloroform). ORD (*c* 0.041, ethanol), $[\Phi]_{255}^{27}$ – 12 500°. (Found: C 73.5; H 8.30; N 4.19; O 14.1. Calc. for $C_{21}H_{29}NO_3$: C 73.4; H 8.50; N 4.08; O 14.0.) IR spectrum: σ_{max} (KBr) 1675(s), 3475(m), 3505(m) cm^{-1}; σ_{max} ($CHCl_3$) 1690(s), 3490(m) (broad) cm^{-1}; σ_{max} (0.004 M, solution, CCl_4) 3510(s) cm^{-1}. UV spectrum, nm (ε): λ_{max} (ethanol) 294 (190), 208 (22 000), $\lambda_{shoulder}$ 264

(740), 257 (1100), 240 (1900); λ_{max} (hexane) 295 (140), 240 (3000), $\lambda_{shoulder}$ 264 (900), 257 (1500), 252 (2000). NMR spectrum (pyridine-d_5) τ: 2.18 – 2.85 (m, 5 H), 4.65 (s, 1 H, exchangeable in D_2O), 5.48 (s, 1 H, exchangeable in D_2O), 5.85 – 6.34 (m, 2 H), 6.8 – 7.4 (m, 1 H), 7.46 (d, 1 H, J = 11 Hz), 7.74 (s, 3 H), 8.80 (s, 3 H), 9.14 (d, 3 H, J = 6.5 Hz), 7.7 – 9.0 (9 H). Pertinent mass spectral peaks m/e (rel. intensity): M^+ 343 (71), 342 (18), 328 (35), 326 (24), 300 (13), 286 (38), 285 (18), 282 (23), 267 (16), 243 (59), 242 (80), 209 (59), 196 (88), 166 (25), 152 (17), 151 (10), 139 (16), 138 (23), 134 (16), 133 (16), 109 (100), 108 (35), 105 (55), 97 (71), 96 (66), 95 (24), 94 (25), 91 (19), 82 (16), 80 (10), 77 (28), 69 (26), 68 (24), 67 (13), 64 (12), 58 (21), 55 (17), 54 (13), 43 (83), 41 (25).

Crepidine methiodide (II). A solution of I (138 mg) in methyl iodide (1 ml) and acetone (2 ml) was heated in a sealed tube at 60° for 2 h. After cooling, the crystalline methiodide was collected in a 90 % yield, m.p. 240 – 242° (dec.); $[\alpha]_D^{24}$ −17° (*c* 1.04, methanol). (Found: I 26.2. Calc. for $C_{22}H_{32}INO_3$: I 26.2.) IR spectrum: σ_{max} (KBr) 1705(s) cm^{-1}. UV spectrum, nm (ε): λ_{max} (ethanol) 288 (30), 265 (180), 258 (240), 219 (19 000), 215 (20 000), 211 (19 000), $\lambda_{shoulder}$ 268 (110), 252 (260). NMR spectrum (pyridine-d_5) τ: 6.30 (s, 3 H), 7.50 (s, 3 H), 8.60 (s, 3 H), 8.99 (d, 3 H, J = 6.5 Hz).

Alkaline degradation of crepidine methiodide (II). II was dissolved in aqueous sodium hydroxide (2 M, 25°) and the solution was extracted continuously with ether for 30 min. The extract was dried (Na_2SO_4) and concentrated, leaving III as a viscous oil, $[\alpha]_D^{22}$ −22° (*c* 0.36, methanol). IR spectrum: σ_{max} (CCl_4) 1632(m), 1685(s), 1705(m), 1725(m) cm^{-1}. NMR spectrum (pyridine-d_5) τ: 2.2 – 2.9 (m, 5 H), 3.14(B) and 3.82(A) (2 H, ABX_2 pattern, J_{AB} = 16 Hz, J_{AX_2} = 1.1 Hz, J_{BX_2} = 6 Hz), 5.38 (s, 1 H, exchangeable in D_2O), 6.48 (t, 1 H, J = 5 Hz), 7.55 (d, 2 H, J = 5 Hz), 7.77 (s, 3 H), 7.82 (s, 3 H), 8.33 (s, 3 H), 9.10 (d, 3 H, J = 6 Hz). Pertinent mass spectral peaks m/e (rel. intensity): M^+ 357 (7), 300 (19), 260 (88), 242 (28), 223 (10), 210 (100), 202 (10), 185 (9), 180 (15), 166 (9), 153 (7), 152 (13), 140 (17), 134 (14), 133 (18), 105 (34), 100 (53), 96 (7), 91 (27), 84 (9), 83 (8), 82 (13), 81 (8), 77 (18), 69 (7), 58 (24), 57 (14), 56 (13), 55 (14).

On standing, III was transformed into several other products, which were not further investigated.

Characterisation of crepidamine (IV). Crystallisation of IV from ether at −20° gave needles, m.p. 107.5 – 109°; $[\Phi]_{200-600}^{25}$ 0° (*c* 0.026, methanol). (Found: N 5.03, M^+ 287.186. Calc. for $C_{18}H_{25}NO_2$: N 4.88, M^+ 287.1885. ^{12}C = 12.00000.) IR spectrum: σ_{max} (KBr) 1712(s), 2720(w), 2820(m), 3395(m); σ_{max} (0.005 M solution, CCl_4) 3470 cm^{-1}. UV spectrum, nm (ε): λ_{max} (ethanol) 264 (270), 258 (380), 209 (11 000), $\lambda_{shoulder}$ 268 (160), 251 (460). NMR spectrum ($CDCl_3$) τ: 2.35 – 2.87 (m, 5 H), 5.6 – 6.1 (1 H, exchangeable in D_2O), 6.47 (t, 1 H, J = 5 Hz), 6.90 – 7.30 (m, 1 H), 7.61 (d, 2 H, J = 5 Hz), 8.35 (s, 3 H), 9.12 (d, 3 H, J = 6.5 Hz), 7.5 – 9.0 (9 H). Pertinent mass spectral peaks m/e (rel. intensity): M^+287 (13), 244 (15), 230 (21), 182 (6), 154 (28), 153 (35), 152 (10), 140 (100), 139 (10), 138 (17), 133 (7), 124 (5), 112 (6), 110 (13), 105 (18), 96 (27), 91 (5), 83 (6), 82 (6), 77 (10), 70 (12), 56 (13), 55 (7).

Isomerisation of crepidamine (IV) to isocrepidamine (V). A solution of IV (26 mg) in ethanol was refluxed for 3 h. The solution was evaporated to dryness and the residue was chromatographed on silica gel (1.4 × 25 cm) using chloroform-methanol (19:1) as eluent. The first fraction contained isocrepidamine (V). Evaporation of the solvent and recrystallisation of the residue (20 mg) from ether at −20° afforded isocrepidamine (V) (7 mg) as needles, m.p. 102 – 105°; $[\alpha]_D^{23}$ 0° (*c* 0.29, methanol). (Found: C 75.0; H 8.83; N 5.04. Calc for $C_{18}H_{25}NO_2$: C 75.2; H 8.77; N 4.87.) IR spectrum: σ_{max} (CCl_4) 2720(w), 2810(s), 3280(m) (broad); σ_{max} (0.005 M solution, CCl_4) 3290 cm^{-1}. UV spectrum, nm (ε): λ_{max} (ethanol) 267 (110), 263 (180), 260 (170), 257 (240), 251 (180), 247 (130), 242 (97), 209 (9600). NMR spectrum ($CDCl_3$) τ: 2.4 – 2.9 (m, 5 H), 3.1 – 3.7 (1 H, exchangeable in D_2O), 6.6 – 6.9 (m, 1 H), 6.90 (q, 1 H, J_1 = 0.8 Hz, J_2 = 3.4 Hz), 8.43 (s, 3 H), 9.23 (d, 3 H, J = 6 Hz). Pertinent mass spectral peaks m/e (rel. intensity): M^+ 287 (28), 286 (15), 269 (11), 268 (10), 244 (26), 230 (11), 226 (10), 212 (57), 182 (9), 154 (24), 153 (31), 152 (11), 140 (100), 139 (9), 138 (12), 124 (10), 112 (8), 110 (16), 105 (21), 96 (28), 83 (10), 77 (12), 70 (25), 56 (12), 55 (8).

Characterisation of dendrocrepine (VII). Crystallisation of VII from ether at −20° gave needles, m.p. 158 – 163° (dec., gives isodendrocrepine (VIII), *vide infra*); $[\Phi]_{200-600}^{20}$ 0° (*c* 0.13, methanol). (Found: C 76.7; H 8.44; N 5.51; O 9.58. Calc. for $C_{33}H_{44}N_2O_3$: C 76.7; H 8.58; N 5.42; O 9.29). Molecular weight determination: 516 (mass spectrometry), 508 (osmometry). IR spectrum: σ_{max} (KBr) 1720(s), 2720(w), 2800(m), 3408(s) cm^{-1}. UV

spectrum, nm (ε): λ_{max} (ethanol) 264 (560), 258 (770), $\lambda_{shoulder}$ 252 (920). NMR spectrum ($CDCl_3$) τ: 2.4 – 2.9 (m, 10 H), 5.8 – 6.3 (2H, exchangeable in D_2O), 6.77 (t, 2 H, $J = 5$ Hz), 7.2 – 7.6 (m, 2 H), 7.6 – 9.0 (20 H), 9.18 (d, 6 H, $J = 6$ Hz). Pertinent mass spectral peaks *m/e* (rel. intensity): M^+ 516 (3), 383 (65), 365 (13), 269 (10), 268 (22), 230 (100), 213 (31), 212 (34), 198 (16), 159 (23), 158 (11), 140 (17), 138 (10), 124 (17), 110 (13), 105 (20), 96 (20), 91 (10), 77 (10), 70 (17), 55 (10).

Isomerisation of dendrocrepine (VII) to isodendrocrepine (VIII). A solution of VII (100 mg) in ethanol was refluxed for 3 h. The solution was evaporated to dryness and the residue was recrystallised three times from chloroform-ethanol giving isodendrocrepine (VIII, 30 mg) as plates, m.p. 162 – 166°; $[\alpha]_D^{23}$ 0° (*c* 0.87, methanol). (Found: C 76.9; H 8.64; N 5.38; O 9.17. Calc. for $C_{33}H_{44}N_2O_3$: C 76.7; H 8.58; N 5.42; O. 9.29.) IR spectrum: σ_{max} (KBr) 2710(w), 2800(m), 3260(m), 3430(m) cm^{-1}. UV spectrum, nm(ε): λ_{max} (ethanol) 267 (220), 264 (350), 258 (480), 252 (500). NMR spectrum ($CDCl_3$) τ: 2.35 – 3.70 (11 H), 6.55 – 9.07 (26 H), 9.07 – 9.60 (7 H) Pertinent mass spectral peaks *m/e* (rel. intensity): M^+ 516 (4), 383 (100), 365 (16), 268 (20), 244 (14), 230 (92), 213 (22), 212 (22), 201 (11), 198 (11), 159 (21), 158 (14), 153 (11), 140 (34), 138 (12), 131 (12), 124 (20), 110 (16), 105 (32), 104 (16), 96 (36), 91 (17), 84 (11), 83 (21), 82 (19), 77 (40), 70 (44), 56 (10).

Dihydrodendrocrepine (IX). Dendrocrepine (VII) was reduced with lithium aluminium hydride in ether, giving dihydrodendrocrepine (IX) as a chromatographically pure (TLC) amorphous solid. NMR spectrum ($CDCl_3$) τ: 9.20 (d, 6 H, $J = 6$ Hz). Pertinent mass spectral peaks *m/e* (rel. intensity): M^+ 518 (1), 385 (24), 367 (12), 274 (22), 272 (6), 256 (5), 251 (5), 230 (100), 188 (7), 140 (5) 124 (6), 110 (5), 105 (15), 98 (5), 97 (5), 96 (9), 84 (7), 83 (5), 77 (5), 70 (10), 56 (5), 55 (5).

Dihydroisodendrocrepine (X and XI). Isodendrocrepine (VIII, 200 mg) was reduced with lithium aluminium hydride in ether. According to TLC two products were formed, which were separated by preparative TLC on neutral alumina using ether as eluent. The main product (130 mg) was recrystallised from methanol-chloroform giving X, m.p. 168 – 169°. (Found: C 74.8; H 8.59. Calc. for $C_{33}H_{46}N_2O_3$. H_2O: C 74.4; H 8.96.) NMR spectrum ($CDCl_3$) τ: 9.22 (d, 3 H, $J = 6$ Hz), 9.48 (d, 3 H, $J = 6$ Hz). Pertinent mass spectral peaks *m/e* (rel. intensity): M^+ 518 (1), 385 (35), 367 (16), 274 (30), 272 (6), 256 (10), 251 (8), 230 (100), 188 (5), 140 (6), 124 (5), 112 (7), 110 (5), 105 (15), 98 (5), 97 (6), 96 (10), 84 (7), 83 (6), 77 (5), 70 (10), 56 (5).

The minor product (XI, 30 mg) was obtained as a chromatographically pure (TLC) amorphous solid. NMR spectrum ($CDCl_3$) τ: 9.17 (d, 3 H, $J = 6$ Hz), 9.47 (d, 3 H, $J = 6$ Hz). The mass spectrum of XI is similar to that of X except for differences in the intensity of some of the peaks.

Acknowledgements. We are indebted to Dr. Björn Lüning for his interest in this work, to Dr. Rolf Håkansson and Mr. Jan Glans (Kemicentrum, Lund) for measuring the optical rotatory dispersion curves, and to Dr. Ragnar Ryhage for measuring the mass spectra. We thank *Stiftelsen Bengt Lundqvists Minne* for a fellowship to one of us (K. L.), and the *Swedish Natural Science Research Council* for financial support.

REFERENCES

1. Brandänge, S., Lüning, B. and Lundin, C. *Acta Chem. Scand.* **27** (1973) 433.
2. Kierkegaard, P., Leander, K. and Pilotti, A.-M. *Acta Chem. Scand.* **24** (1970) 3757.
3. Pilotti, A.-M. *Acta Cryst.* **B 27** (1971) 887.
4. Wilson, E. B., Jr., Decius, J. C. and Cross, P. C. *Molecular Vibrations, McGraw*, New York 1955, p. 1.
5. Bohlmann, F. *Chem. Ber.* **91** (1958) 2157.
6. Rader, C., Young, R. and Aaron, H. *J. Org. Chem.* **30** (1965) 1536.
7. Chen, C. and LeFèvre, R. *Tetrahedron Letters* **1965** 1611.
8. Galinovsky, F. and Zuber, H. *Monatsh.* **84** (1953) 798.
9. Galinovsky, F., Bianchetti, G. and Vogl, O. *Monatsh.* **84** (1953) 1221.
10. Galinovsky, F. and Höllinger, R. *Monatsh.* **85** (1954) 1012.
11. Ebnöther, A. *Helv. Chim. Acta* **41** (1958) 386.
12. Pilotti, A.-M. and Wiehager, A.-C. *Acta Cryst.* **B 29** (1973) 1563.

Received January 9, 1973.

ACTA CHEMICA SCANDINAVICA 27 (1973) 1914–1922

On the Synthesis and Structure of 2-Methylenethiazolidin-4-ones.* Carbalkoxy Derivatives and Isolation of Geometrical Isomers

OLOF CEDER,[a] URBAN STENHEDE,[a] KJELL-IVAR DAHLQUIST,[b] JACQUES M. WAISVISZ[c] and MARCEL G. van der HOEVEN[c]

[a] *Department of Organic Chemistry, University of Göteborg and Chalmers Institute of Technology, Fack, S-402 20 Göteborg 5, Sweden,* [b] *Department of Physical Chemistry, Royal Institute of Technology, S-100 44 Stockholm 70, Sweden and* [c] *Gist-Brocades N.V., Delft, the Netherlands*

An alternative synthesis of 2-carbalkoxymethylenethiazolidin-4-ones ** and the separation of the two geometrical isomers in pure form from the reaction mixture by fractional crystallization is described. Attempts to assign configuration to the two isomers based on NMR data are also discussed.

In connection with investigations on the pharmacological activity of certain thiazolines, which have been the subject of much synthetic effort since it was recognized that penicillin contains such a moiety, it was of interest to prepare 2-methylenethiazolidin-4-ones of type *1*, having an exocyclic double bond in the 2 position.

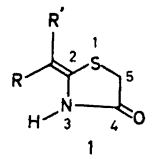

1

R′ = H, R = COOEt or COOMe

R′ = COOEt or COOMe, R = H

At the time our work was initiated, compounds of this type had not been described. Since then reports concerning this system have been published by

* Presented in part at "Organikerdagarna", Göteborg, June 14–16, 1967; *cf. Svensk Kem. Tidskr.* **79** (1967) 578.

** According to the IUPAC recommendations [1] these compounds should be named alkyl 4-thiazolidone-$\Delta^{2,\alpha}$-acetates. We have chosen to retain the nomenclature used by Satzinger [2] and by Taylor [3] since this enables direct comparisons to be made.

Satzinger [2] and by Taylor.[3] The purpose of the present and the following [4] communication is to describe a different and probably general synthesis for compounds of type *1*, to verify the observations by Taylor [3] that they exist in two forms, both containing an exocyclic double bond, to confirm that they are geometrical isomers, which are readily interconvertible, and to propose a mechanism for the interconversions, based on deuterium-exchange experiments.

Our synthesis was based on the following observations. Condensation of the hydrochlorides of imidic esters with esters of 2-amino-3-mercaptocarboxylic acids have been reported to yield Δ^2-thiazolidines [5–7] of type *2* (R = alkyl or aryl).

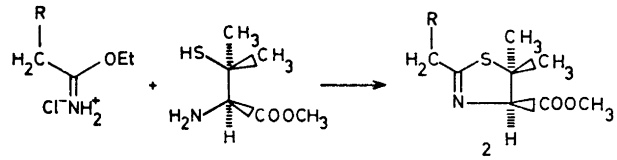

It is well-known that heterocyclic compounds of the general type *3*, with X = NH, O, or S, often exist in the tautomeric form *4*.[8]

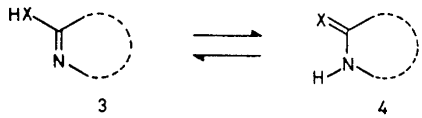

Consequently we reacted mercaptoacetamide with the hydrochlorides of different imidic esters, expecting to obtain *5a*, which would then tautomerize to *5b*.

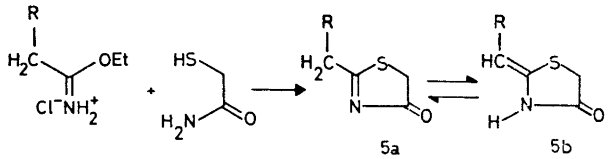

We have carried out condensations with R = COOEt, COOMe, and CN,[4] and in all cases compounds of type *5b* have been isolated. When R = H no reaction took place. The reaction product of mercaptoacetamide and carbethoxyacetimidic ethyl ester hydrochloride (R = COOEt) yielded, when isolated and purified by fractional crystallization, the two isomeric compounds *6* and *7*.[3]

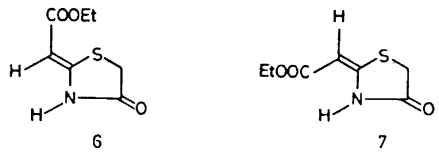

The lower melting, here called "L", and the higher melting, here called "H", carbethoxy compounds gave very similar elemental analysis values and molecular weights (182 and 186, respectively) by the Rast method. Mass spectrometry proved them to be isomers with a molecular ion at $m/e = 187$ and an M+2 isotope peak of 5.4 %, which corresponds to the molecular formula $C_7H_9NO_3S$. The mass spectra of "L" and of "H", discussed in an accompanying communication,[4] displayed almost identical fragmentation patterns, which is often characteristic of stereoisomers.[9]

The spectral data for *6* and *7* (*cf.* Experimental) are the same as those reported [3] for the compounds Taylor refers to as the "stable" and "metastable" isomers.

Since internally hydrogen-bonded protons suffer a paramagnetic shift,[10–12] and since a lowering of the ester C=O and NH infrared-absorption frequences in dilute solution are characteristic of intramolecular hydrogen bonding, we believe that "L" should be represented by structure *8* and "H" by *9*.

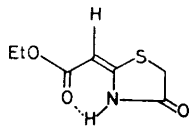

8

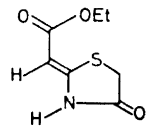

9

Simon *et al.*[13] have published a semi-empirical rule for the calculation of the chemical shifts of olefinic protons, which, when applied to these compounds, leads to close agreement with the observed values and also supports the conclusion that the hydrogen-bonded formula *8* represents "L" (*cf.* Table

Table 1. Observed (in chloroform-*d*) and calculated [13] values for the chemcal shifts of the olefinic proton in the methyl and ethyl ester compounds.

Compound	Observed Isomer	Observed δ, ppm	Calculated Isomer	Calculated δ, ppm	Difference δ, ppm
2-Carbethoxymethylene-thiazolidin-4-one	"H"	5.54	*Z*	5.33	0.21
	"L"	5.07	*E*	5.02	0.05
2-Carbomethoxymethylene-thiazolidin-4-one	"H"	5.58	*Z*	5.33	0.25
	"L"	5.13	*E*	5.02	0.11

1). These proposals will later be supported by additional observations. When carbomethoxyacetimidic ethyl ester hydrochloride is condensed with mercaptoacetamide a corresponding pair of high- and low-melting methyl esters is obtained. The structures of these two isomers were determined in the way described for the ethyl esters. Pertinent data can be found in Experimental and in Table 1.

While our work was in progress, Satzinger [2] described the synthesis of the same compounds by the following different route.

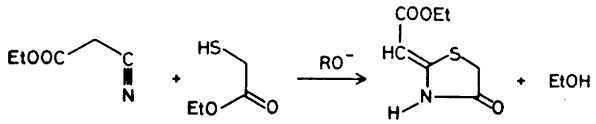

He did not notice the presence of two forms, probably because a different isolation and condensation procedure was used. We have repeated the Satzinger synthesis and have found that the products are identical with those obtained by our procedure. Satzinger's method is probably more convenient than ours. Taylor [3] has since proposed what can be regarded as a modification of the Satzinger method, using ethyl cyanoacetate and mercaptoacetic acid in acid toluene solution.[14]

Investigations on a thiazolidine system similar to *1* (or *5*) have also been reported by Cook, Elvidge, Graham, and Harris.[15–17] They describe two compounds, having identical UV spectra ($\lambda_{max} = 290$ nm), which they first assumed to have structure *10a* (R = H and CH_3) but since attempts to nitrosate one of them (R = CH_3) in the side chain failed, they proposed that these compounds were instead the 2-methylene tautomers of type *10b*.

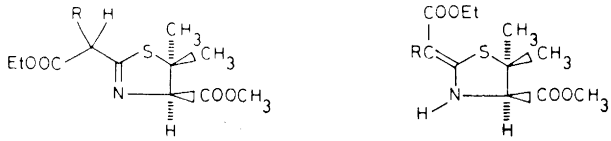

10a 10b

The same authors also report [15] two isomeric compounds, displaying almost identical UV spectra, which they propose to be the *cis* and *trans* isomers *11* and *12*.

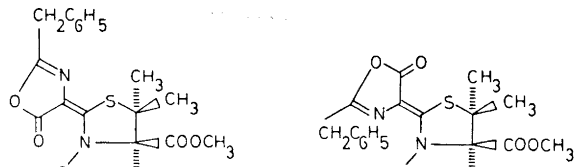

11 12

The true character of these thiazolines has not been established with modern spectroscopic methods.[17]

With the gross structures of "L" and "H" ethyl esters verified we wish to discuss briefly some details in their NMR spectra and the change in their UV spectra on addition of base.

In an NMR spectrum (*cf.* Fig. 1) at 100 MHz of a sample containing both "L" and "H" the CH_2S resonance signals are very close, $\delta = 3.69$ and 3.65, respectively. Expansion of this region revealed that the band in "L" was a doublet ($J = 0.4$ Hz), while the same absorption in "H" was a singlet within the experimental accuracy. Since this CH_2 group has no adjacent protons

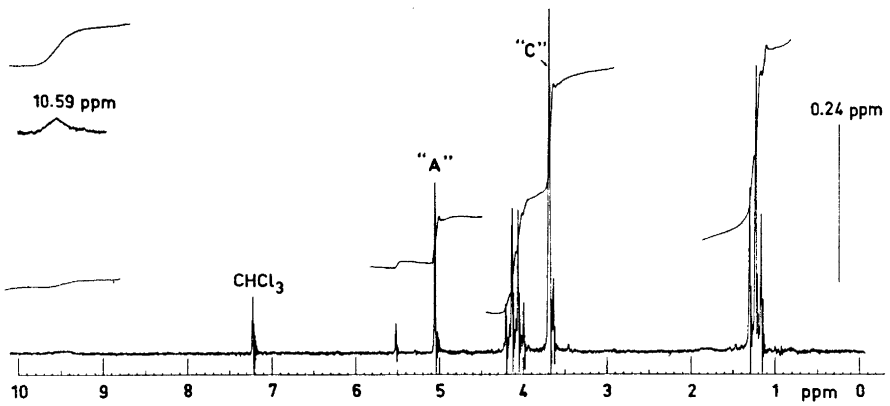

Fig. 1. NMR spectrum (100 MHz, $CDCl_3$) of a mixture (*ca.* 85:15) of *8* and *9*.

and the five-membered ring probably is planar, long-range coupling is likely to exist with either the olefinic or the amide protons. After addition of heavy water to the solution, the amide proton had exchanged, but the resonance from the CH_2S protons remained a doublet. Expansion of the olefinic proton region showed that the olefinic proton in "L" appeared as a triplet ($\delta = 5.07$, $J = 0.4$ Hz), while the same proton in "H" ($\delta = 5.54$) was a singlet with a bandwidth of 0.5 Hz. No change in the appearance of the signals from these protons took place on addition of heavy water. Irradiation of the olefinic proton signal "A" (*cf.* Fig. 1) reduced the CH_2S signal "C" to a singlet, and this shows that long-range coupling exists between these protons in "L". Identical measurements on "H" showed that the coupling constant between the same protons is less than 0.05 Hz. These findings are in agreement with the proposal that "L" is the hydrogen-bonded form where all protons are held in a more rigid position, resulting in a shorter distance between the olefinic and methylene protons. The methyl esters (*5b*, R = COOMe) were prepared with the hope that their NMR spectra would be simpler to analyze than those of the ethyl esters. This, however, did not materialize since the chemical shifts of the CH_3 and CH_2S protons are almost the same (*cf.* Experimental), giving rise to overlapping signals. The long-range coupling ($J = 0.4$ Hz) between the methylene protons and the olefinic proton was also present in the low-melting methyl ester, but not in the corresponding high-melting isomer.

The dissociation constants for "L" and "H", which are very close (pK_a ("L") = 10.7 and pK_a("H") = 10.1, in methanol-water, 9:1)* do not allow a definite conclusion to be drawn as to which isomer contains an intramolecular bond, since "L" and "H" both form the same anion.

As was pointed out earlier, the UV spectra of "L" and "H" are virtually identical and of a type expected for the proposed chromophore.[15,16] The spectra of "L" and "H" in ethanol solution both remained unchanged on addition of acid. If, instead, base was added to a neutral ethanol solution, new maxima

* Taylor [3] reports 9.80 and 8.60 respectively, in 60 % aqueous methanol.

developed at 308 nm ($\varepsilon = 30\,000$) for both "L" and "H". When the basic solutions were acidified with an excess of hydrochloric acid, the original maximum at 283 nm reappeared. This reversible process can be pictured in terms of the following transformation:

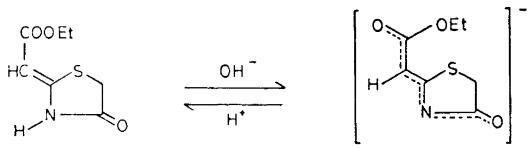

When the experiment was carried out on a preparative scale, it was discovered that pure "H" was isolated when a solution of "L" was first treated with base and then neutralized with acid. The ionization-reprotonation process of the amide system was therefore accompanied by a *cis-trans* isomerization of the exocyclic double bond.

In order to illuminate this process, the NMR spectra of the two isomers were recorded in different media. The transformations reported below were followed by means of the olefinic proton signal at $\delta = 5.23$ (pyridine-d_5) and 5.07 (chloroform-d) for the E isomer,[18] *8*, and at $\delta = 5.82$ (pyridine-d_5) and at 5.54 (chloroform-d) for the Z izomer,[18] *9*.

The present NMR studies were carried out under conditions slightly different from those of Taylor,[3] but the results and conclusions are essentially identical with his.

Addition of a few drops of trifluoroacetic acid to a chloroform solution of the synthetic product, which contained a 60:40 mixture of the two isomers, caused an immediate rearrangement to a 25:75 mixture of the Z and E isomers, respectively. Addition of excess pyridine-d_5 to the same trifluoroacetic acid-containing solution caused a change in the Z:E ratio to 70:30. It was also observed that the dissolution rate was increased considerably when a drop of trifluoroacetic acid was added. The reason for this behavior is a fast rearrangement of Z into the more soluble low-melting isomer. The positions of the NMR signals of the two isomers were not changed by the above additions. This fact excludes the formation of appreciable quantities of charged species.

Similar experiments with the two isomerically pure (melting point and infrared studies) Z and E isomers gave the following results. The Z isomer, dissolved in chloroform which was allowed to evaporate slowly, was completely converted to the E isomer after 24 h. If, however, the Z isomer was dissolved in chloroform and kept in a closed vessel at room temperature for 72 h, an NMR spectrum showed that 75 % had rearranged to the E isomer. When this mixture was left for a longer period of time in the same solvent, no further change in the isomer ratio could be detected. If pure E was dissolved in pyridine, an NMR spectrum, recorded immediately, showed the presence of 90 % of Z (and 10 % of E). When pure E was dissolved in dimethyl sulfoxide and an NMR spectrum was recorded immediately, only signals from the Z isomer could be detected. It was also observed that the NMR spectra of the pyridine and dimethyl sulfoxide solutions had not changed after 48 h. These results are summarized in Chart 1.

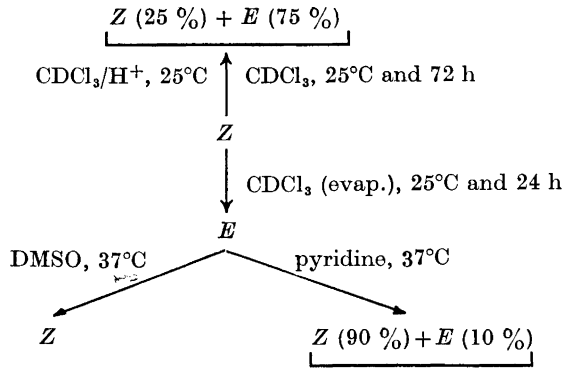

Chart 1.

EXPERIMENTAL

IR spectra were determined in chloroform solution (*ca.* 2 %), when not otherwise stated, with a Beckman model IR-9 spectrophotometer. NMR spectra were obtained with a Varian A-60 and a Varian HA-100 spectrometer. The chemical shifts are reported in δ-values, using tetramethylsilane as internal standard. UV spectra were measured in ethanol with a Beckman DB spectrophotometer and dissociation constants with an automatic titrator, model Titrigraph TTT1. Mass spectra were recorded with an LKB 9000 instrument. Melting points were determined with a Reichert melting-point microscope. Thin-layer chromatography was carried out on Silica Gel GF_{254} (Merck) according to Stahl.

Preparation of 2-carbethoxymethylenethiazolidin-4-one. In a 1 l three-necked flask, equipped with a reflux condenser, a gas inlet tube and a mechanical stirrer, 600 ml of chloroform, 56 g (0.62 mol) of mercaptoacetamide and 123 g (0.62 mol) of carbethoxyacetimidic ethyl ester hydrochloride were introduced. The suspension was stirred and refluxed under dry carbon dioxide for 6 h. The reactants had then dissolved and ammonium chloride had precipitated. The reaction mixture was cooled to room temperature, and the solid was removed by filtration and washed with chloroform. The filtrates were concentrated under reduced pressure to a volume of *ca.* 65 ml. After the solution had been cooled in ice water, 27.0 g of ester mixture (m.p. 161 – 162°C, dried at room temperature at 2 torr) was removed by filtration and washed with chloroform. Concentration of the mother liquor yielded another 23.6 g, m.p. 145 – 148°C. The two fractions were combined and pure "H" and "L" were obtained by fractional crystallizations from ethanol and ethyl acetate at different temperatures.

Solvent (ethanol) Volume ml	Temp. °C	Yield g	M.p. °C	
80	35	21.8	164 – 166	(a)
80	25	7.4	109 and 161 – 162	(b)
80	15	2.2	109 and 162	(c)
80	5	1.2	110 and 160	(d)
40	5	1.2	110 and 163	(e)
20	5	0.6	110 and 156	(f)
5	5	1.2	163 – 165	(g)

Fractions (a) and (g) were then combined and recrystallized from ethanol, yielding 16.9 g of "H", m.p. 164–166°C. A final recrystallization from ethanol-ether (1:1) gave 10.0 g of "H", m.p. 163–165°C.

Fractions (b)–(f) were then combined and fractionated from ethanol: yield, m.p., (fraction); 8.0 g, 109–159°C, (a'); 3.0 g, 109–159°C, (b'); 0.5 g, 158–160°C, (c').

Fractions (a') and (b') were then combined and recrystallized from ethyl acetate: yield, m.p., (fraction); 2.8 g, 138–159°C, (a''); 2.3 g, 152–158°C, (b''); 5.1 g, 108–111 and 155°C, (c'').

Of these, fraction (c'') was recrystallized from ethyl acetate: yield, m.p., (fraction); 2.5 g, 108 and 155°C, (a'''); 0.9 g, 108°C, (b'''). Recrystallization of (b''') from ethyl acetate gave 0.46 g of "L", m.p. 105–108°C.

When the melting point of already melted and solidified "L" was retaken, it had changed to 155–160°C. Consequently "L" is partially converted to "H" at this high temperature.

The following properties were recorded for the *high-melting* isomer. IR: 3420 (NH), 1714 (amide C=O), 1682 (ester C=O), and 1595 cm^{-1} (C=C). UV: λ_{max} = 283 nm (ε = 21 500). NMR ($CDCl_3$): triplet (J = 7.0 Hz) at 1.21 (3H, CH_3), singlet at 3.56 (2H, SCH_2), quartet (J = 7.0 Hz) at 4.10 (2H, OCH_2), singlet at 5.54 (1H, =CH), and broad NH absorption at 9.48 ppm. *Anal.* (Found: C 45.01; H 4.91; N 7.53; S 17.15. Calc. for $C_7H_9NO_3S$: C 44.92; H 4.85; N 7.48; S 17.10.) MS: M^+ = 187. For the *low-melting* isomer the following properties were recorded. IR: 3290 (NH), 1732 (amide C=O), 1668 (ester C=O), and 1602 cm^{-1} (C=C). UV: λ_{max} = 283 nm (ε = 21 500). NMR ($CDCl_3$): triplet (J = 7.0 Hz) at 1.21 (3H, CH_3), doublet (J = 0.4 Hz) at 3.69 (2H, SCH_2), quartet (J = 7.0 Hz) at 4.10 (2H, OCH_2), triplet (J = 0.4 Hz) at 5.07 (1H, =CH), and broad NH absorption at 10.59 ppm. *Anal.* (Found: C 44.98; H 4.82; N 7.55; S 17.16. Calc. for $C_7H_9NO_3S$: C 44.92; H 4.85; N 7.48; S 17.10.) MS: M^+ = 187.

2-Carbomethoxymethylenethiazolidin-4-one was obtained from carbomethoxyacetimidic ethyl ester hydrochloride and mercaptoacetamide according to the procedure described above. Fractional crystallization of the crude mixture in the way described for the ethyl ester mixture, but instead with acetone-methanol-petroleum ether (60–80°), 10:1:10, as the solvent, eventually yielded two isomeric methyl esters. The following properties were recorded for the *high-melting* isomer. M.p. 182–186°C. IR: 3430 (NH), 1718 (amide C=O), 1680 (ester C=O), and 1600 cm^{-1} (C=C). UV: λ_{max} = 283 nm (ε = 19 940). NMR (pyridine-d_5): singlet at 3.70 (3H, OCH_3), singlet at 3.85 (2H, SCH_2), singlet at 5.80 (1H, =CH), and NH absorption at 10.58 ppm. *Anal.* (Found: C 41.68; H 4.13; N 8.07; S 18.60. Calc. for $C_6H_7NO_3S$: C 41.61; H 4.05; N 8.09; S 18.50.) MS: M^+ = 173. For the *low-melting* isomer the following properties were recorded. M.p. 146–148°C. IR: 3260 (NH), 1730 (amide C=O), 1668 (ester C=O), and 1605 cm^{-1} (C=C). UV: λ_{max} = 283 nm (ε = 21 020), NMR (pyridine-d_5): singlet at 3.62 (3H, OCH_3), doublet (J = 0.4 Hz) at 3.89 (2H, SCH_2), and triplet (J = 0.4 Hz) at 5.25 ppm (1H, =CH), the NH proton absorption could not be found. *Anal.* (Found: C 41.61; H 4.09; N 8.14; S 18.60. Calc. for $C_6H_7NO_3S$: C 41.62; H 4.05; N 8.09; S 18.50.) MS: M^+ = 173.

The rule of Simon *et al.*,[13] applied to the chemical shifts for the olefinic protons, predicts (*cf.* Table 1) the low-melting methyl ester to be the *E* isomer and the high-melting methyl ester to be the *Z* isomer, as was the case with the ethyl ester isomers.

Acknowledgements. We are indebted to Dr. R. Ryhage, Karolinska Institutet, Stockholm, for mass spectra and to Professor Lars Melander for valuable criticism of the manuscript. This work has been supported by grants from the *Swedish Natural Science Research Council.*

REFERENCES

1. *IUPAC Nomenclature of Organic Chemistry. Sections A, B and C*, Butterworths, London 1969, pp. 122 and 173.
2. Satzinger, G. *Ann. Chem.* **665** (1963) 150.
3. Taylor, P. J. *Spectrochim. Acta* **A 26** (1970) 153.
4. Ceder, O. and Stenhede, U. *Acta Chem. Scand.* **27** (1973) 1923.

5. Cook, A. H., Elvidge, J. A., Graham, A. R. and Harris, G. *J. Chem. Soc.* **1949** 3220 and 3232.
6. Sheehan, J. C., Hill, Jr., H. W. and Buhle, E. L. *J. Am. Chem. Soc.* **73** (1951) 4373.
7. Smith, H. A. *J. Org. Chem.* **26** (1961) 820.
8. Katritzky, A. R. and Lagowski, J. M. *Advan. Heterocyclic Chem.* **1** (1963) 311.
9. Meyerson, S. and Weitcamp, A. W. *Org. Mass Spectrom.* **1** (1968) 659.
10. Dudek, G. O. and Holm, R. H. *J. Am. Chem. Soc.* **83** (1961) 2099.
11. Dudek, G. O. and Volpp, G. P. *J. Am. Chem. Soc.* **85** (1963) 2697.
12. Dudek, G. O. and Holm, R. H. *J. Am. Chem. Soc.* **84** (1962) 2691.
13. Matter, U. E., Pasqual, C., Pretsch, E., Pross, A., Simon, W. and Sternhell, S. *Tetrahedron* **25** (1969) 691.
14. Clarkson, R., Hull, R. and Newbould, B. B. U.K. Pat. 971.176 (1961) and Belg. Pat. 624.576 (1963) [*Chem. Abstr.* **60** (1964) 1451f].
15. Bentley, R., Cook, A. H. and Elvidge, J. A. *J. Chem. Soc.* **1949** 3216.
16. Cook, A. H., Elvidge, J. A., Graham, A. R. and Harris, G. *J. Chem. Soc.* **1949** 3220.
17. Personal communication from Professor Elvidge.
18. IUPAC Tentative Rules for the Nomenclature of Organic Chemistry, Section E, Fundamental Stereochemistry. *J. Org. Chem.* **35** (1970) 2849.

Received January 11, 1973.

ACTA CHEMICA SCANDINAVICA 27 (1973) 1923–1938

On the Structure of 2-Methylenethiazolidin-4-ones

Cyano and *N*-Methyl Derivatives and Assignment of Geometrical Configuration

OLOF CEDER and URBAN STENHEDE

Department of Organic Chemistry, University of Göteborg and Chalmers Institute of Technology, Fack, S-402 20 Göteborg 5, Sweden

The isolation and configurational assignments (NMR) of the geometrical isomers *2a* and *2b* of 2-cyanomethylene-3-methylthiazolidin-4-one are reported and the exchange of the olefinic and methylene protons in the same system has been investigated by NMR. The mass spectrometrical fragmentation processes for the 2-cyano-, 2-carbethoxy-, and 2-carbomethoxymethylenethiazolidin-4-ones and for their *N*-methyl derivatives are discussed.

In the preceding paper[1] we described the isolation of two geometrical isomers of both 2-carbethoxy- and 2-carbomethoxymethylenethiazolidin-4-one, made preliminary assignments of geometrical configurations, which agreed with the findings of Taylor,[2] and discussed the interconversion. The present communication reports similar results on 2-cyanomethylenethiazolidin-4-one, its *N*-methyl derivative, and the *N*-methyl-carbalkoxy-analog. NMR studies on the same compounds, which strengthen the earlier assignments of geometrical configuration, and a mechanism for the interconversion, based on deuterium-exchange experiments, are also discussed.

Condensation of malononitrile with ethyl mercaptoacetate, following the procedure of Satzinger,[3] gave 2-cyanomethylenethiazolidin-4-one, *1*, with the same properties as reported earlier.[2,3]

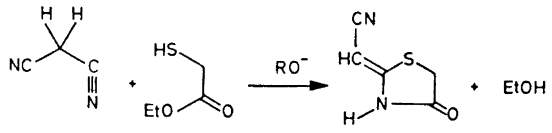

1

The existence of *cis* and *trans* carbalkoxy derivatives led us to expect the same kind of isomers of *1*, as was discussed by Taylor.[2] All attempts to isolate two forms by fractional crystallization failed, however, and crystalline *1* showed a very sharp melting point, indicating a pure compound. The NMR spectrum (in dimethyl sulfoxide-d_6), containing two dominating, sharp bands at 4.03 (CH_2S) and 4.95 (=CH) ppm and a broad amide-proton signal at 11.87 ppm, is in exact agreement with the expected structure. The resonance signals of the methylene and olefinic protons appear at slightly higher field than those of the carbethoxy compounds. Expansion of the signals in the spectrum of *1* did not reveal any fine structure and therefore no coupling is likely to exist among the protons in *1*. The mass spectrometrical fragmentation pattern will be discussed later.

There seems to be no obvious reason why the cyano compound should not form geometrical isomers, as does the carbethoxy compound, and Taylor,[4] in fact, reports chemical shift values for the *cis* and *trans* forms of *1*. It is not clear, however, whether he tried to isolate them or whether he attempted a closer study of the interconversion. We suspected that the failure to isolate the isomers by fractional crystallization was due to a lower energy barrier for the isomerization. A freshly sublimed sample of *1* was dissolved in dimethyl sulfoxide and recording of a series of NMR spectra was started immediately. After 2 min, four peaks at 4.95, 4.82, 4.03, and 3.99 ppm were present, but after 20 min, two of them (4.95 and 4.03 ppm) dominated. This series of spectra clearly shows that in the crystalline state one form predominates and that in dimethyl sulfoxide solution a rearrangement to the other geometrical isomer takes place with a half life of *ca.* 4 min, assuming a first or pseudo-first order reaction. The conversion also occurs in dimethylformamide and in pyridine at approximately the same rate. In these solvents the carbethoxy compound isomerizes much faster than the cyano analog.[1] The assignments of geometrical configurations will be described in connection with the discussion of the *N*-methyl compounds (*vide infra*).

Methylation studies. Satzinger reported [3] that 2-cyanomethylenethiazolidin-4-one, *1*, on methylation with dimethyl sulfate formed the *N*-methyl derivative *2* and that treatment of *1* with diazomethane in dimethylformamide-ether gave the *O*-methyl derivative, *3*. He also showed that dilute sodium hydroxide

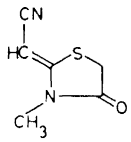

2

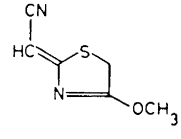

3

rearranged the alleged enolic isomer *3* into *2*. Since such a process is difficult to visualize in basic medium, and since Satzinger's proposals were not supported by detailed spectral studies and, moreover, since there seemed to be no particular reason why *O*-methylation should occur in dimethylformamide with diazomethane in ether solution, we suspected that the two compounds isolated were instead the geometrical isomers *2a* and *2b*.[5]

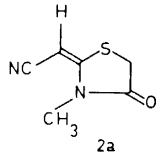

2a

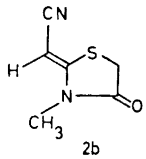

2b

Treatment of *1* with dimethyl sulfate gave a methyl derivative, *2b*, with a molecular weight of 154 (mass spectrometry) and an M + 2 isotope peak of 5.3 %, in agreement with the molecular formula $C_6H_6N_2OS$. The UV spectrum ($\lambda_{max}=272$ nm; $\varepsilon=18\,780$) was almost identical with that of the starting material. Therefore, it seemed that no change of the chromophoric system had taken place. Addition of base to a solution of the compound caused no change in position or intensity of this absorption maximum, which shows that the NH group is absent. The IR spectrum displayed an amide band at 1725 cm^{-1} and the NMR spectrum (chloroform-*d*) contained a new methyl singlet at 3.15 ppm in addition to the bands expected from the other protons in structure *2*. Treatment of *1* with diazomethane in dimethylformamide yielded two compounds, one of which was identical with the dimethyl sulfate product discussed above. The ratio between the two products varied with the temperature at which the reaction was performed and the time between dissolution of *1* and addition of diazomethane. Room temperature and slow addition of diazomethane favored the formation of *2b*, while low temperature, 0°C, and an immediate, rapid addition of diazomethane favored the formation of the other product, *2a*. This is to be expected since *1* isomerizes to the other geometrical isomer on dissolution in dimethylformamide. This reaction is rather slow ($t_{1/2}=30$ min at -5.5°C) compared to the reaction between *1* and diazomethane. The new compound, *2a*, on treatment with dilute sodium hydroxide followed by dilute hydrochloric acid, rearranged to the other *N*-methyl compound, *2b*. Treatment of *2a* with dilute sodium hydroxide only did not, however, cause the same rearrangement. The molecular weight (mass spectrometry) and M + 2 isotope peak of the diazomethane product, *2a*, corresponded to the molecular formula $C_6H_6N_2OS$. The UV spectrum ($\lambda_{max}=272$ nm; $\varepsilon=18\,450$), which remained unchanged on addition of base, was almost identical with that of the starting material. The IR spectrum displayed bands at 2208 (conjugated CN), 1735 (C=O), and 1600 cm^{-1} (C=C). The NMR spectrum (chloroform-*d*) contained the methyl singlet now at 3.56 ppm and the bands expected from the other protons in structure *2* (*cf.* Experimental). These observations leave no doubt that both the diazomethane and the dimethyl sulfate products are the *N*-methyl derivatives of *1*, and that they are geometrical isomers represented by structures *2a* and *2b*.

The most striking dissimilarity between the NMR spectra of the isomers is the considerable difference in the chemical shifts of the *N*-methyl protons. The change seems to be too large to be caused only by opposite configurations. Molecular models (Dreiding) show that in *2a* the *N*-methyl group is located in the negative region of the anisotropic cone caused by the triple bond in the cyano group (*cf.* Fig. 1). This circumstance could be responsible for the unusual

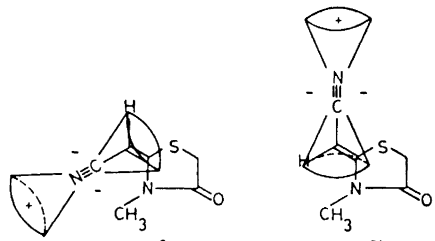

Fig. 1. Anisotropic regions in *2a* and *2b* induced by the C≡N group.

difference in the chemical shifts observed.[6] In *2b* the methyl group lies outside the above-mentioned region (*cf.* Fig. 1). Based on these observations, we propose, that the *Z* isomer [7] (*2b*) should represent the dimethyl sulfate product and the *E* isomer [7] (*2a*) the diazomethane product which dominates at low reaction temperature. The application of the rule of Simon *et al.*[8] gives the values 4.51 and 4.82 ppm for the chemical shifts of the olefinic protons in *2a* and *2b*, respectively. These are in agreement with the observed ones (4.55 and 4.78 ppm, respectively), but the differences between the calculated values and the observed ones are probably too small to allow a definitive assignment.

At room temperature, in a polar solvent like dimethyl sulfoxide, the pure *E* isomer *2a* rearranged slowly to the *Z* isomer *2b*, as was the case with the *N*-norcompounds. At elevated temperatures (180°C) a less polar solvent like *o*-dichlorobenzene effected the same conversion. Addition of a drop of trifluoroacetic acid at room temperature to a chloroform or an *o*-dichlorobenzene solution of the *E* isomer *2a* immediately resulted in solutions containing 100 % of the *Z* isomer *2b*. The purity of *2a* and also the isomer ratio were determined from the olefinic proton signals at 4.55 and 4.78 ppm, respectively. The results are summarized in Chart 1.

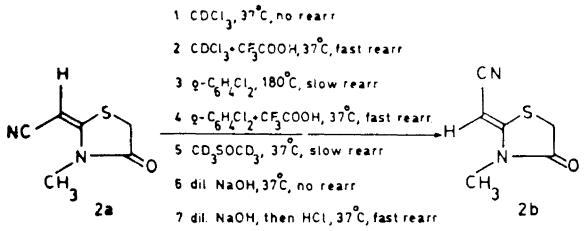

Chart 1.

Alkylation of the *Z* and of the *E* ethyl esters [1] with dimethyl sulfate in ethanol-sodium carbonate gave one and the same product, which is expected, since the *E* isomer rearranges to the *Z* isomer in basic medium. Spectral properties proved the alkylation product to be the *N*-methyl derivative, and its properties agreed with those of the *N*-methyl compound reported by Satzinger [3] and by Taylor.[2] Alkylation of the *E* and *Z* isomers with diazomethane

in dimethylformamide yielded only one compound, which was identical with the one obtained from the dimethyl sulfate treatment. In no case could a second methylated isomer be detected. The *N*-methylated ethyl ester showed a molecular weight of 201 (mass spectrometry) corresponding to the molecular formula $C_8H_{11}NO_3S$. The UV spectrum ($\lambda_{max} = 281$ nm; $\varepsilon = 21\,100$) was almost identical with that of the starting material and therefore no change in the chromophore seemed to have occurred. On addition of base, the spectrum remained unchanged. The IR spectrum displayed carbonyl absorption at 1710 and 1660 cm^{-1}. These observations definitely exclude the possibility of an *O*-methyl structure. The NMR spectrum contained a new methyl singlet at 3.17 ppm and the NH signal had vanished. The chemical shift of the vinylic proton had been slightly shifted to 5.47 from 5.51 ppm in the norcompound *4*, for which *Z* configuration has been proposed. Since treatment of the *E* isomer with base always yields 100 % of the *Z* isomer, it is reasonable to assume that the *N*-methyl derivative of *4* has the geometry pictured in *5*. The rule of Simon *et al.* predicts the value 5.33 for the olefinic proton in the *Z* isomer *5*. This is in good agreement with the observed value of 5.47 ppm. On the basis of steric considerations, using molecular models (Dreiding), it is unlikely that the carbethoxy and the *N*-methyl groups could be accommodated on the same side of the double bond without disturbing the planarity of the chromophoric system. Since the UV spectra of *4*, ($\lambda_{max} = 283$ nm; $\varepsilon = 21\,500$) and of *5* ($\lambda_{max} = 281$ nm; $\varepsilon = 21\,100$) are virtually identical, one may assume that both compounds possess the same degree of planarity.

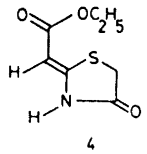

4

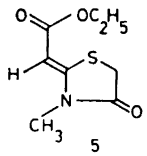

5

Exchange studies. To clarify the mechanism of the *cis-trans* isomerization, exchange experiments using $CDCl_3/D_2O$, $CDCl_3/TFA/D_2O$, and $CDCl_3/base/D_2O$ were performed with the cyano and the *N*-methyl cyano compounds and with the ethyl ester and the *N*-methyl ethyl ester. The fast exchange of the NH and also of the CH_2S protons was expected since a number of cases have been reported where the methylene protons in thiazolidinones exchange easily in basic media and also condense with, *e.g.*, benzaldehyde under the same conditions.[9] It was further found that, in basic media such as pyridine/D_2O or $CDCl_3$/triethylamine/D_2O, the olefinic proton exchanged rapidly in the NH-containing compounds *1* and *4*. The *N*-methylated compounds *2a*, *2b*, and *5*, however, did not exchange the olefinic proton under the same conditions. Therefore, in basic media, the NH group must be involved in the exchange reaction, outlined below.

In the acidic medium $CDCl_3/TFA/D_2O$, the olefinic proton in the non-methylated compound *4* exchanged rapidly. Due to low solubility in this solvent system, compound *1* could not be studied. The methylated compounds *2b* and *5* also exchanged the olefinic proton under the same conditions. The

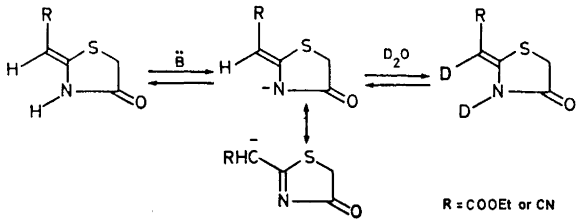

Z isomers *2b* and *5* did not exchange the olefinic proton in dimethyl sulfoxide/D_2O, while the *N*-norcompounds *1* and *4* rapidly exchanged this proton in the same solvent.

The isomerization of the *E* isomer *2a* to the *Z* isomer *2b* was studied in the same solvent systems. Under basic conditions ($CDCl_3$/triethylamine/D_2O, pyridine/D_2O, or pyridine/D_2O/NaOD) *2a*, which lacks the amide proton, did not isomerize. Satzinger [3] claimed that base rearranges *2a* (which he pictures as the *O*-methyl derivative) to *2b*, but we believe that the isomerization occurs when the reaction mixture is treated with acid (*vide infra*).

Under the acidic condition, $CDCl_3$/TFA/D_2O, *2a* isomerizes to *2b* within a few seconds. The same conversion was effected by dimethyl sulfoxide/D_2O, although at a much lower rate (50 % in 24 h).

At least two possible mechanisms under acidic conditions can lead to isomerization of the *N*-methyl compounds.

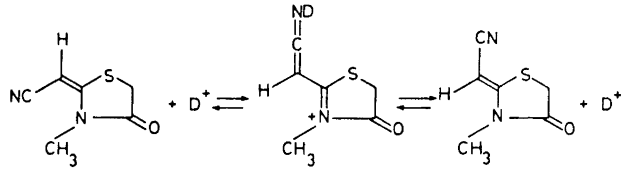

I

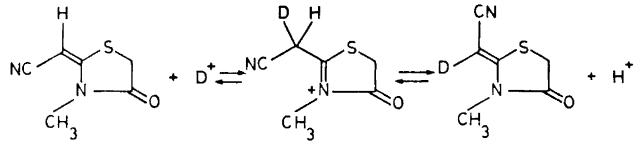

II

If mechanism I is the only one operating, no exchange of the olefinic proton with deuterium should occur during the isomerization. If, instead, mechanism II is correct, deuterium should be found in *2b*. In both $CDCl_3$/TFA/D_2O and in dimethyl sulfoxide/D_2O, 98 % of deuterium was present in the *2b* formed. This atom of deuterium could be due to exchange in *2b* after it has been formed from *2a*. We have, however, already reported above that in the solvent system dimethyl sulfoxide/D_2O the olefinic proton in *2b* was not substituted by deuterium, and from Table 1 it is evident that the rate of proton exchange is much lower than that of the formation of *2b* in

Table 1. Exchange studies.

Compound	Conditions: $CDCl_3/TFA/D_2O$ =CH	$CDCl_3/TFA/D_2O$ SCH_2	$DMSO/D_2O$ =CH	$DMSO/D_2O$ SCH_2	$CDCl_3/Et_3N/D_2O$ =CH	$CDCl_3/Et_3N/D_2O$ SCH_2	Pyridine/D_2O =CH	Pyridine/D_2O SCH_2
1	---	---	50 % exchange after 1/2 h	45 % exchange after 20 h	---	---	61 % exchange after 24 h	53 % exchange after 24 h
2a	22 % isomerization to *2b* in 20 s Exchange was found only in formed *2b* 24 % after 20 s	0 % after 20 s	48 % isomerization to *2b* in 24 h Exchange was found only in formed *2b* 46 % after 24 h	20 % after 24 h	0 %	50 % exchange after 7 h	0 %	40 % exchange after 24 h
2b	50 % exchange after 10 min	15 % exchange after 72 h	0 %	21 % exchange after 24 h	0 %	50 % exchange after 7 h	0 %	40 % exchange after 24 h
4	82 % exchange after 3 h	27 % exchange after 3 h	50 % exchange after 1/2 h	50 % exchange after 24 h	50 % exchange after 1 h	50 % exchange after 16 h	80 % exchange after 24 h	20 % exchange after 24 h
5	56 % exchange after 10 min	12 % exchange after 3 h	0 %	20 % exchange after 24 h	0 %	50 % exchange after 16 h	0 %	18 % exchange after 24 h

$CDCl_3$/TFA/D_2O. These observations lead us to believe that the isomerization and exchange proceed according to mechanism II, at least with the *N*-methylated cyano compound *2a*. Taylor [2] has proposed a mechanism similar to I for the isomerization of the potassium salt of 2-carbethoxymethylenethiazolidin-4-one. Our results are summarized in Table 1 where more detailed information about conditions, *etc.*, can be found.

Mass spectrometrical studies. We now wish to discuss the mass spectrometrical fragmentation patterns of the compounds described in this and the preceding communication.[1] The spectra with assignments are reproduced

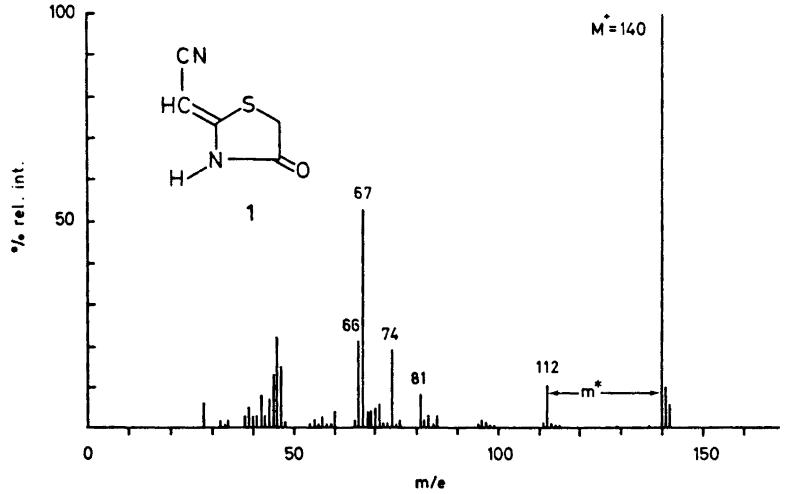

Fig. 2. Mass spectrum of *1* ($m^* = 89.5$).

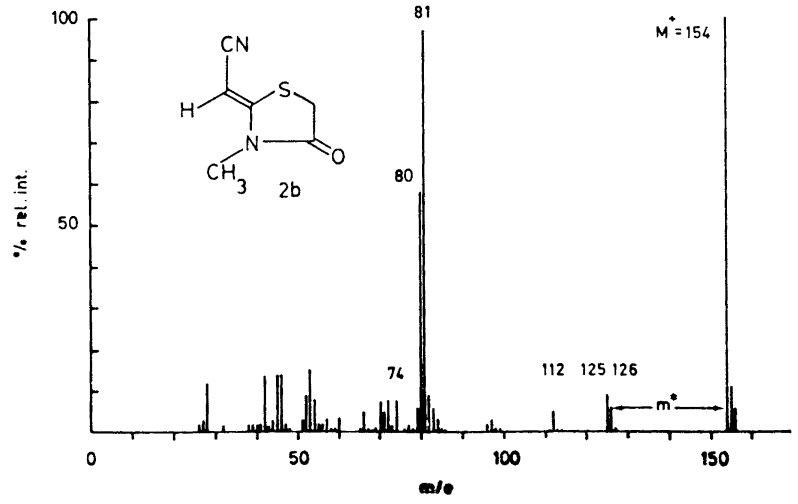

Fig. 3. Mass spectrum of *2b* ($m^* = 103.2$).

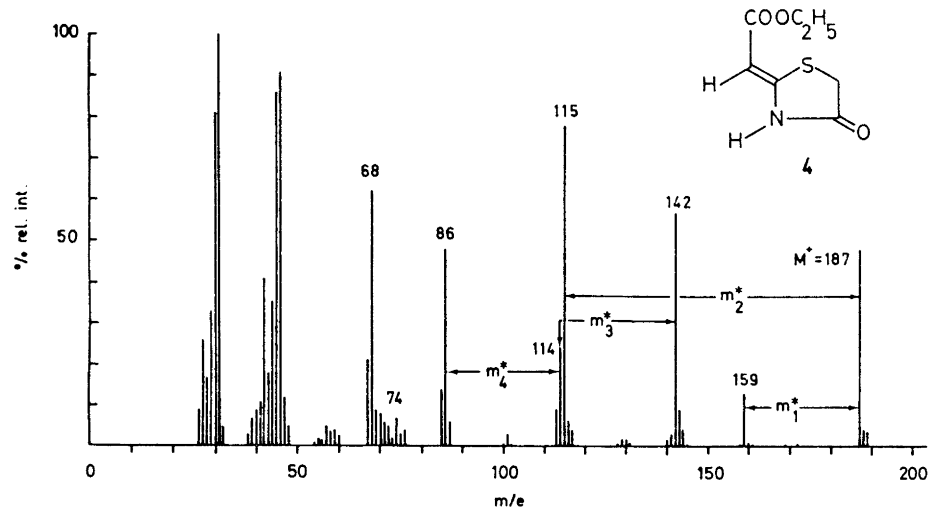

Fig. 4. Mass spectrum of *4* ($m_1^* = 135.2$, $m_2^* = 70.7$, $m_3^* = 91.5$, and $m_4^* = 64.9$).

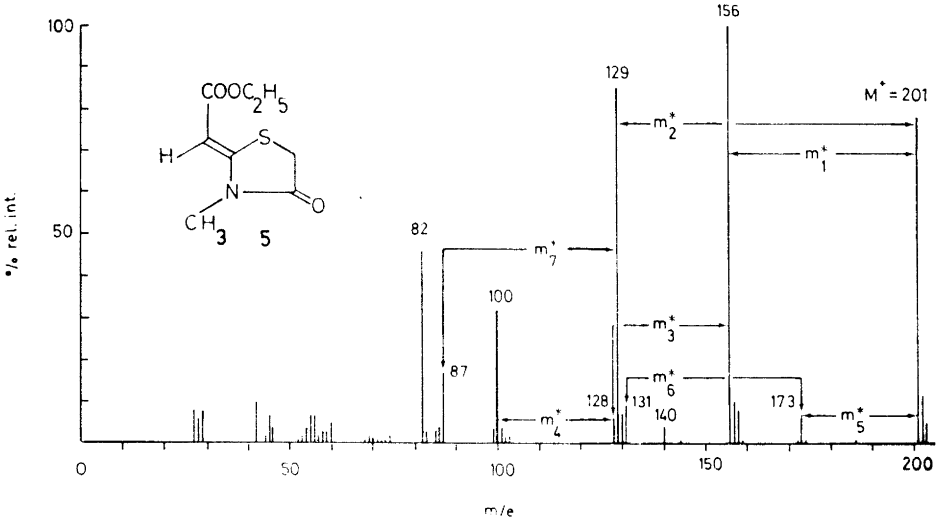

Fig. 5. Mass spectrum of *5* ($m_1^* = 121.1$, $m_2^* = 82.8$, $m_3^* = 105.0$, $m_4^* = 78.1$, $m_5^* = 148.9$, $m_6^* = 99.2$, and $m_7^* = 58.7$).

in Figs. 2 – 7. Determination of exact masses confirmed the assignments of the molecular compositions of some of the individual fragments proposed in Charts 2 – 8 and in the text below. A number of fragmentation paths, supported by the presence of metastable ions, are indicated in the spectra and in the charts. As expected,[10] the two geometrical isomers give identical mass spectra.

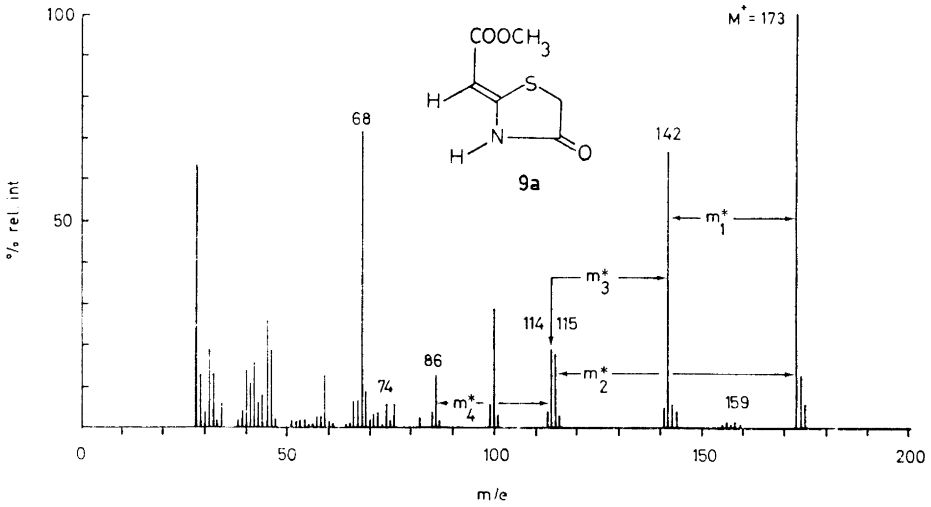

Fig. 6. Mass spectrum of *9a* ($m_1^* = 116.6$, $m_2^* = 76.5$, $m_3^* = 91.5$, and $m_4^* = 64.9$).

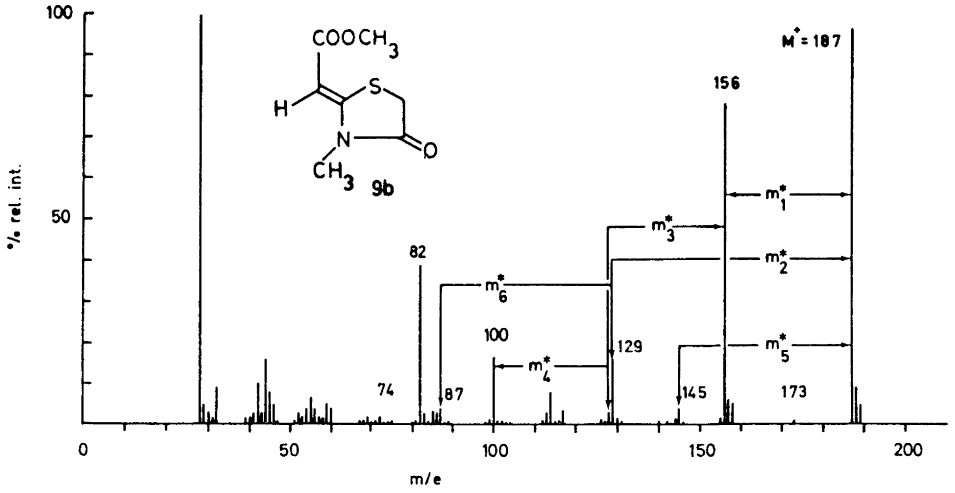

Fig. 7. Mass spectrum of *9b* ($m_1^* = 130.1$, $m_2^* = 89.0$, $m_3^* = 105.0$, $m_4^* = 78.1$, $m_5^* = 112.4$, and $m_6^* = 58.7$).

All compounds show large molecular ion peaks, which in the cyano compounds are the base peaks. The *N*-methyl compounds give fragmentation patterns almost identical with those of the norcompounds, but displaced by 14 mass units.

The major fragmentation processes for the ethyl ester and its *N*-methyl homolog, *5*, seem to be the ones usually found for ethyl esters, and loss of 45 and 72 mass units to form *6* and *7*, respectively, is observed. These peaks

are of high intensity (base peaks in the spectra of *4* and *5*). They also lose 28 mu, proved to be C_2H_4, to give *8*. The methyl ester, *9*, analogously loses 31, 58, and 14 mu to form the ions *6*, *7*, and *8*, respectively. These reactions are outlined in Chart 2.

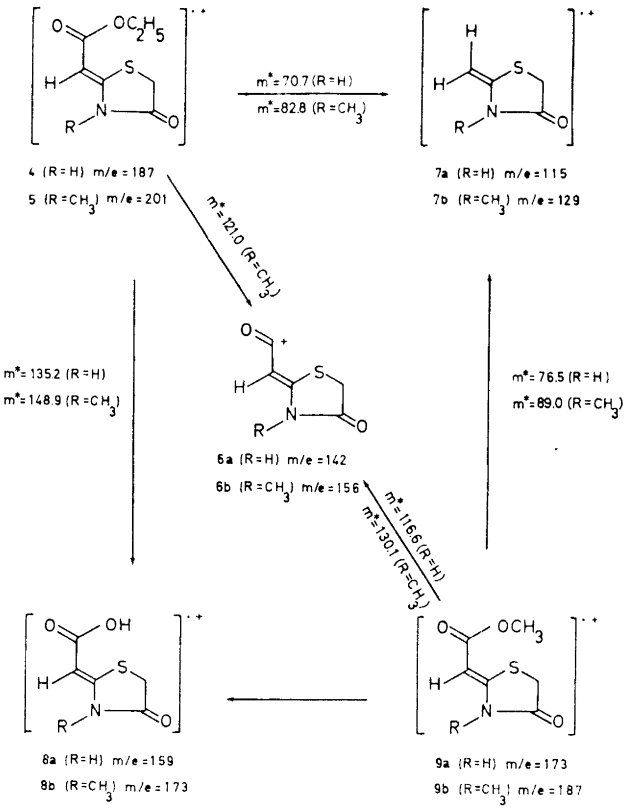

Chart 2.

Corresponding fragmentation in the cyano compounds, *1* and *2*, are prevented by the stability of the cyano group. The first ions formed are instead of type *10* (M – 28), *11* (M – 29), and *12* (M – 42), as outlined in Chart 3. Their compositions are supported by exact mass measurements.

The ease of fragmentation in the ethyl ester group probably explains why no ion due to loss of the amide CO group can be detected, which was observed in the spectra of the cyano compounds (*vide infra*). The ion *6*, however, loses 28 mu to yield *13*, which in turn again loses 28 mu to form a fragment

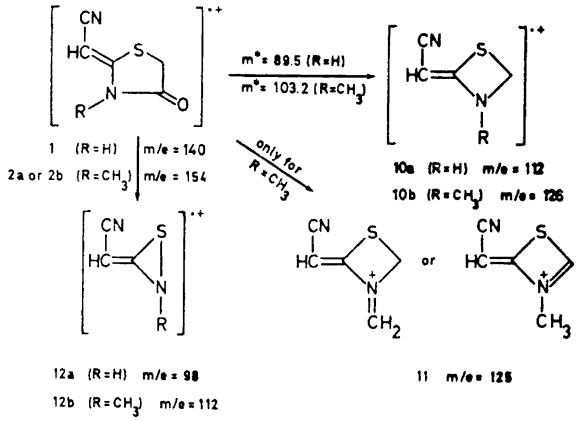

Chart 3.

for which we would like to propose the structure *14*. These transformations, which are supported by metastable ions, are outlined in Chart 4. The elimination of the two CO groups could possibly take place in the reverse order.

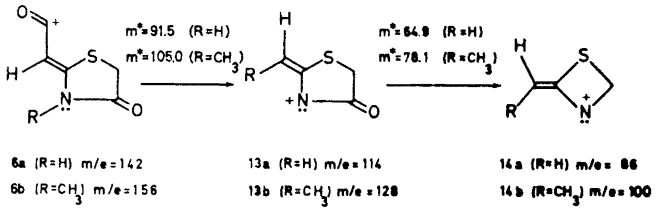

Chart 4.

In the spectrum of the *N*-methyl compound *5*, metastable peaks are present at $m^* = 58.7$ and 99.2, respectively, corresponding to the formation of the fragments *15* and *16* from *7b* and *8b*, respectively. The metastable ion at $m^* = 58.7$ is also present in the spectrum of the *N*-methyl compound *9b*, but an ion at $m^* = 99.2$ was not observed, probably because of the difficulty of generating ion *8b* from the *N*-methyl methyl ester *9b*. These transformations are outlined in Chart 5. In the spectrum of *9b*, a metastable ion is also present at $m^* = 112.4$, corresponding to the formation of the fragment *17* with the composition $C_5H_7NO_2S$. The latter fragmentation process, outlined in Chart 5, is analogous to the one that gave $m^* = 99.2$ in the spectrum of the ethyl ester compound *5*. In the ethyl ester it seems to be easier to first lose C_2H_4 to give *8b*, and then CH_2CO to give *16*, but in the *N*-methyl methyl ester, *9b*, a direct loss of CH_2CO to give *17* is observed.

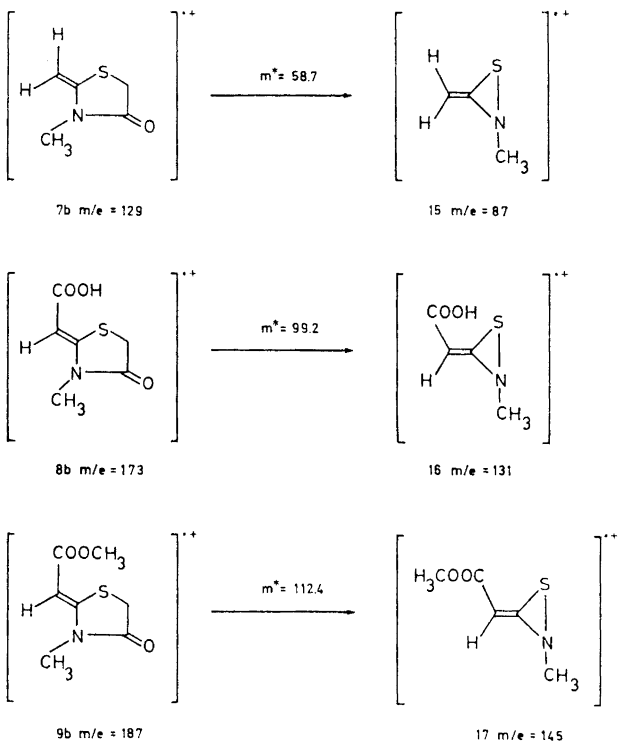

Chart 5.

The peaks at M − 73 in the spectrum of the cyano compounds are the second highest ones (55 − 98 % of the base peaks). In the spectra of *1*, *2a*, and *2b* these peaks have the compositions $C_3H_3N_2$, $C_4H_5N_2$, and $C_4H_5N_2$ respectively. For these we propose structures *18a* and *18b*. In addition, the M − 73 peaks in the spectran of *2a* and *2b* contain an ion with the composition C_4H_3NO. In the spectra of *1*, *2a*, and *2b* ions are also present at M − 74 with the compositions $C_3H_2N_2$, $C_4H_4N_2$, and $C_4H_4N_2$. These fragments may have the structures *20a* and *20b* as indicated in Chart 6.

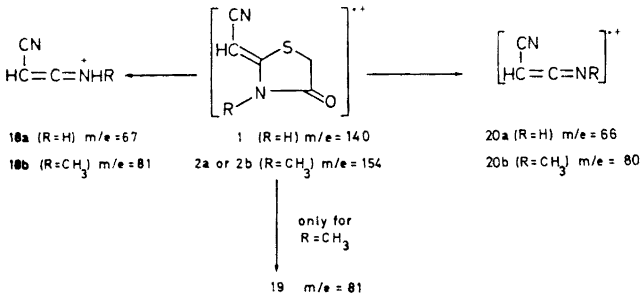

Chart 6.

The spectra of *4*, *5*, *9a*, *9b*, *1*, and *2a* or *2b* contain an ion at $m/e = 74$ with the composition C_2H_2OS for which structure *21* is proposed. This transformation is outlined in Chart 7.

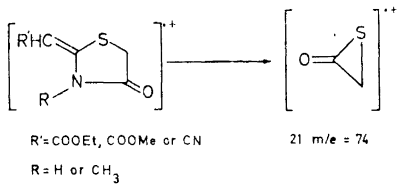

Chart 7.

Compounds *4* and *9a* give rise to a peak at $m/e = 68$ which has the composition C_3H_2NO. The corresponding ion in the spectra of *5* and *9b* appears at $m/e = 82$ and has the composition C_4H_4NO. These fragments are probably formed by the loss of CH_2S from the ions *13a* and *13b*, as outlined in Chart 8.

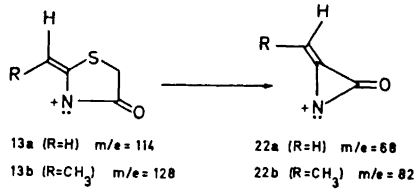

Chart 8.

The fragment at $m/e = 140$ in the spectrum of *5* has the composition C_6H_6NOS. The fragment at $m/e = 81$ with the composition C_4H_3NO in the spectrum of *1* is formed by the loss of HCNS from the molecular ion (*cf.* Fig. 2). We cannot propose any reasonable structures for these fragments.

EXPERIMENTAL

IR spectra were determined in KBr with a Beckman IR 9 spectrophotometer and UV spectra in ethanol with a Cary Model 15 spectrophotometer. The NMR spectra have been recorded with a Varian Model A – 60 spectrometer with tetramethylsilane as internal reference. The chemical shifts are reported in δ-values. Mass spectra were recorded with a GEC – AEI 902 instrument at the Department of Medical Biochemistry, University of Göteborg. Melting points were determined with a Reichert melting-point microscope. Thin layer chromatography was carried out on Silica Gel GF_{254} (Merck) according to Stahl.

Exchange experiments. The exchange experiments were generally performed in the following way. Two drops (*ca.* 0.05 ml) of deuterium oxide were added to an NMR tube containing 0.30 ml of a 0.50 M solution of the compound in question in the solvent system used in each case. When chloroform was used, two drops of triethylamine or trifluoroacetic acid were added immediately before the addition of the deuterium oxide. The solutions were then shaken for 5 min and NMR spectra were recorded at different times until possible exchange was observed. If no exchange could be detected after 72 h,

the experiments were discontinued. In order to determine the rate of exchange in 2-cyanomethylenethiazolidin-4-one, *1*, which contains only exchangeable protons, a weighed amount of sodium 2,2,3,3-tetradeuterio-3-trimethylsilylpropionate (TSP) was added to the NMR tube. The integral of the TSP signal ($\delta = 0.00$ ppm), which remained constant during the experiment, was used as a reference for the proton intensities. The results of these measurements are summarized in Table 1.

2-Cyanomethylenethiazolidin-4-one, *1*, was prepared and isolated as described by Satzinger.[3] Sublimation of recrystallized *1* yielded material (m.p. 185–187°C, dec.) showing only one spot on thin layer chromatography (chloroform-ethyl acetate, 3:1; $R_F = 0.22$). IR: 3110 (NH), 3070 (=CH), 2220 (CN), 1720 (C=O), and 1610 cm^{-1} (C=C). UV: $\lambda_{max} = 272$ nm ($\varepsilon = 18\ 970$). NMR (dimethyl sulfoxide-d_6): singlet at 4.03 (2H, SCH_2), singlet at 4.95 (1H, =CH), and NH absorption at 11.87 ppm. MS, *cf.* Fig. 2.

Z-2-Cyanomethylene-3-methylthiazolidin-4-one, *2b*, was prepared from *1* and dimethyl sulfate and isolated as described by Satzinger.[3] Recrystallized product, m.p. 138–140°C, showed only one spot on thin layer chromatography (chloroform-ethyl acetate, 3:1; $R_F = 0.41$). IR: 3085 (=CH), 2206 (CN), 1725 (C=O), and 1580 cm^{-1} (C=C). UV: $\lambda_{max} = 272$ nm ($\varepsilon = 18\ 780$). NMR (chloroform-*d*): singlet at 3.15 (3H, NCH_3), singlet at 3.94 (2H, SCH_2), and a singlet at 4.78 (1H, =CH). MS, *cf.* Fig. 3.

E-2-Cyanomethylene-3-methylthiazolidin-4-one, *2a*, was prepared and isolated according to a somewhat modified version of the method described by Satzinger.[3,*] His procedure was followed with the exception that ethereal diazomethane solution was added until an excess was present in the reaction solution. Thin layer chromatography (chloroform-ethyl acetate, 3:1) showed the presence of two components, $R_F = 0.48$ and 0.41. Two-dimensional thin layer chromatography in the same solvent system indicated that the compound which had $R_F = 0.48$ rearranged on the chromatographic plate. If chloroform-ethyl acetate (3:1) containing 1 % acetic acid was used as eluent, no rearrangement took place. The two products were separated using preparative thin layer chromatography in the last-mentioned solvent system. When 200 mg of crude product was chromatographed, 60 mg (30 %) of each component was obtained. The slower-moving product was shown (NMR, TLC, and IR) to be identical with *Z*-2-cyanomethylene-3-methylthiazolidin-4-one, *2b*, and the faster-moving component was found to be *E*-2-cyanomethylene-3-methylthiazolidin-4-one, *2a*. The following data were recorded for *2a*. M.p. 105–106°C. IR: 3060 (=CH), 2208 (CN), 1735 (C=O), and 1600 cm^{-1} (C=C). UV: $\lambda_{max} = 272$ nm ($\varepsilon = 18\ 450$). NMR (chloroform-*d*): singlet at 3.56 (3H, NCH_3), singlet at 3.87 (2H, SCH_2), and singlet at 4.55 ppm (1H, =CH). MS, *cf.* Fig. 3.

2-Carbomethoxymethylene-3-methylthiazolidin-4-one, *9b*, was prepared from 2-carbomethoxymethylenethiazolidin-4-one, *9a*,[1] and diazomethane, as described for *2a*. The desired product, *9b*, could also be obtained from *9a* and dimethyl sulfate, as described for *2b*. White crystals, m.p. 159–161°C, were obtained by recrystallization from ethanol. Thin layer chromatography (chloroform-ethyl acetate, 3:1) showed only one component ($R_F = 0.44$). IR: 3070 (=CH), 1715 (amide C=O), 1690 (ester C=O), and 1595 cm^{-1} (C=C). UV: $\lambda_{max} = 282$ nm ($\varepsilon = 19\ 950$). NMR (chloroform-*d*): singlet at 3.15 (3H, NCH_3), singlet at 3.73 (2H, SCH_2), singlet at 3.75 (3H, OCH_3), and singlet at 5.58 ppm (1H, =CH). MS, *cf.* Fig. 7.

2-Carbethoxymethylene-3-methylthiazolidin-4-one, *5*, was prepared and isolated in the same way as was *9b*. Both methods gave only one component (thin layer chromatography; chloroform-ethyl acetate, 3:1; $R_F = 0.55$). M.p. 96–97°C. IR: 3080 (=CH), 1715 (amide C=O), 1680 (ester C=O), and 1575 cm^{-1} (C=C). UV: $\lambda_{max} = 281$ nm ($\varepsilon = 21\ 100$). NMR (chloroform-*d*): triplet ($J = 7.0$ Hz) at 1.28 (3H, CH_3), singlet at 3.17 (3H, CCH_3), singlet at 3.73 (2H, SCH_2), quartet ($J = 7.0$ Hz) at 4.19 (2H, OCH_2), and singlet at 5.47 ppm (1H, =CH). MS, *cf.* Fig. 5.

Acknowledgments. Financial support from the *Swedish Natural Science Research Council* and from the grant *Främjande av ogradueradе forskares vetenskapliga verksamhet* to the University of Göteborg is gratefully acknowledged. We thank Mrs. Inger Nilson for technical assistance.

* Satzinger claims that this compound is the *O*-methyl ether, *3*.

REFERENCES

1. Ceder, O., Stenhede, U., Dahlquist, K.-I., Waisvisz, J. M. and van der Hoeven, M. G. *Acta Chem. Scand.* **27** (1973) 1914.
2. Taylor, P. J. *Spectrochim. Acta* **A 26** (1970) 153.
3. Satzinger, G. *Ann. Chem.* **665** (1963) 150.
4. *Cf.* p. 159 in Ref. 2.
5. *Cf.* p. 160 in Ref. 2.
6. Mathieson, D. W. *Nuclear Magnetic Resonance for Organic Chemists*, Academic, London 1967, p. 38.
7. IUPAC Tentative Rules for the Nomenclature of Organic Chemistry, Section E, Fundamental Stereochemistry; *J. Org. Chem.* **35** (1970) 2849.
8. Matter, U. E., Pasqual, C., Pretsch, E., Pross, A., Simon, W. and Sternhell, S. *Tetrahedron* **25** (1969) 691.
9. Elderfield, R. C. *Heterocyclic Compounds*, Wiley, New York 1957, Vol. 5, p.714.
10. Meyerson, S. and Weitcamp, A. W. *Org. Mass Spectrom.* **1** (1968) 659.

Received January 11, 1973.

ACTA CHEMICA SCANDINAVICA 27 (1973) 1939–1949

The Adduct between Triphenyl Phosphine and Triphenyl Phosphine Telluride. A Tellurium(0) Compound

TOR AUSTAD,[a] TERJE RØD,[a] KJELL ÅSE,[a] JON SONGSTAD[a] and A. HUGH NORBURY[b]

[a] *Chemical Institute, University of Bergen, N-5000 Bergen, Norway and* [b] *Department of Chemistry, Loughborough University of Technology, Loughborough LE 11 3TU, England*

Tetraphenylarsonium tellurocyanate reacts with excess triphenyl phosphine in acetonitrile in the presence of lithium perchlorate to form a bright yellow compound in high yield. This compound, which is very stable in the solid state, is shown to be the adduct between triphenyl phosphine and triphenyl phosphine telluride.

An X-ray structure determination of the adduct reveals that all tellurium atoms and phosphorus atoms lie on threefold axes and each formula unit contains a linear P–Te–P configuration. The results show that in the linear P–Te–P configuration there is a "normal" bond between tellurium and one of the phosphorus atoms, while the interaction between tellurium and the other phosphorus atom is rather weak. IR and Raman spectra of the adduct are presented and complement the X-ray studies regarding the general shape of the molecule.

It is concluded that the adduct may be regarded as a tellurium(0) compound and the structural similarity with isoelectronic species like the trihalide anions is discussed.

The reactions of tervalent phosphorus compounds with oxygen, sulfur, and selenium and the products from these reactions have been investigated in great detail for over a century. The reaction of phosphines and related compounds with tellurium and the corresponding phosphine tellurides appear to be far less known.

The first known organophosphorus compound with a phosphorus-tellurium bond was made by Foss.[1] He noted that finely divided tellurium dissolved on gentle heating in an ethanol solution of potassium diethyl phosphite to give the corresponding tellurophosphate. The colourless hygroscopic needles, rapidly darkening in moist air, were found to be less stable than the corresponding thio and seleno salts.[2]

Gryszkiewicz-Trochimowski and co-workers[3] found similarly that tellurium dissolved in a benzene solution of diethyl ethylphosphonite to give a red solution. The product, however, decomposed readily on attempted purifica-

tion by distillation. Allyl diethylphosphonite, on the other hand, is known to give a distillable tellurophosphonate.[4]

In recent years, Zingaro and co-workers have made a number of phosphine tellurides from the corresponding phosphines and finely divided tellurium.[5–7] Several of the phosphine tellurides have been found to be sufficiently stable to allow elemental analysis and IR studies to be performed.[7,8] Likewise, tris-dimethylamino phosphine [9,10] and *N*-diphenylphosphino triphenylphosphazene [11] have been found to react readily with tellurium to give crystalline products. The dipole moment of trioctyl phosphine telluride [12] has been determined and found to be of the same order of magnitude as that of the corresponding sulfide and selenide. A review on phosphorus chalcogenides has recently been published.[13]

According to Zingaro,[6] tellurium dissolves in toluene solutions of trialkyl phosphines, aryldialkyl phosphines and, although to a very limited extent, in alkyldiaryl phosphines. No alkyl diaryl phosphine tellurides appear to have been reported. Elemental tellurium was found not to dissolve in solutions of triphenyl phosphine. Interestingly, a similar reactivity pattern of these phosphines is observed in their reaction with carbon disulfide; trialkyl phosphines and aryldialkyl phosphines form adducts easily with this substrate, while the other two members in this series do not.[14] The smooth increase in hydrogen basicity from triphenyl phosphine to trialkyl phosphine [15] suggests that the hydrogen basicities of the various tervalent phosphorus compounds are a poor measure of the ability of these compounds to form adducts with very polarizable Lewis acids. This view is supported by the facile formation of tellurophosphonates from the weakly basic dialkyl alkylphosphonites and tellurium.[3,4]

The differing and mainly negative temperature coefficients of the solubility of tellurium in the various phosphines [6] indicate that the formation of phosphine tellurides is thermodynamically controlled. The formation of phosphine tellurides may not be directly connected with the generally accepted nucleophilicities of the phosphorus compounds, as has been suggested.[6,13]

As an equilibrium mixture is obtained from the reaction between tellurium and tervalent phosphorus compounds,[6] an improvement to the synthesis of phosphine tellurides would be to use a reagent containing tellurium, but with a leaving group of lower tellurium basicity. Potassium selenocyanate has been used successfully in the facile synthesis of triaryl phosphine selenides,[16] suggesting the cyanide ion to be a poorer selenium base than is a triaryl phosphine. Similarly, from the unstable nature of the tellurocyanate ion,[18] the tellurium basicity of the cyanide ion appears to be low and a salt of the tellurocyanate ion was therefore tried as a reagent toward triphenyl phosphine.

When a four- or fivefold excess of triphenyl phosphine was added to a solution of tetraphenylarsonium tellurocyanate in purified acetonitrile, a very slight increase of the yellow colour of the solution was observed. The IR of the solution, however, showed that the amount of ionic tellurocyanate was unchanged and no products could be detected after work-up of the solution. Increasing the reaction time, up to several hours, even at 40°C, did not cause any reaction, except that the solution turned slightly brownish, presumably due to traces of elemental tellurium. Using unpurified acetonitrile, the solution turned rapidly cream yellow and on evaporation of the solvent, a yellow product crystallized among unreacted reactants.

Previously [17] it has been shown that tetraphenylarsonium and tetramethylammonium selenocyanate react with triphenyl phosphine in purified acetonitrile to give a quantitative yield of triphenyl phosphine selenide provided traces of hard Lewis acids, like acetic acid or lithium perchlorate, were present.[17] On adding a small amount of lithium perchlorate to an acetonitrile solution of ionic tellurocyanate with triphenyl phosphine in excess, the solution turned instantaneously cream yellow and a yellow crystalline compound could be isolated.

Contrary to the reaction with an ionic selenocyanate and triphenyl phosphine where a quantitative yield of triphenyl phosphine selenide is obtained with only minute quantities of lithium perchlorate present, the reaction between ionic tellurocyanate and triphenyl phosphine was found not to be quantitative, as an IR of the reaction mixture still showed a peak due to ionic tellurocyanate at 2081 cm^{-1} even after prolonged periods.

The dependence upon the amount of lithium perchlorate was examined by slowly adding various amounts of lithium perchlorate to 20 ml solution, containing 1 g tetraphenylarsonium tellurocyanate, 1.86 mmol, and 2 g triphenyl phosphine, 7.64 mmol, and measuring the amount of unreacted ionic tellurocyanate. As each drop of lithium perchlorate entered the reaction mixture, a greyish colour was formed which disappeared immediately upon stirring. Addition of lithium perchlorate to an acetonitrile solution of tetraphenylarsonium tellurocyanate, without triphenyl phosphine being present, causes an immediate precipitation of elemental tellurium. The results are listed in Table 1.

Table 1. Amount of unreacted ionic tellurocyanate after the addition of various amounts of lithium perchlorate to a solution of tetraphenylarsonium tellurocyanate and triphenyl phosphine.

$[Ph_3P]$	$[LiClO_4]$	$[TeCN^-]$
0.382	0	0.093
0.35	0.00454	0.068
0.32	0.00833	0.060
0.30	0.0462	0.039
0.28	0.0789	0.013[a]
0.26	0.107	0.008[a]

[a]These values are approximate as the product started to separate.

The results indicate clearly that even in an excess of lithium perchlorate, some ionic tellurocyanate is unaffected by triphenyl phosphine.

Elemental analysis showed the yellow product to consist of one molecule of triphenyl phosphine telluride together with one molecule of triphenyl phosphine, and not to be triphenyl phosphine telluride itself. The compound decomposed immediately with the formation of elemental tellurium when dissolved in acetonitrile, benzene, acetone, or diethyl ether. When these solvents contained a large amount of triphenyl phosphine, the compound could

be crystallized without any trace of decomposition. Acetone was found to be the most suitable solvent since it allowed a considerable amount of the product to crystallize prior to the precipitation of triphenyl phosphine. Even in this solvent great care was necessary during the recrystallization, as the low stability of the compound in warm acetone containing triphenyl phosphine in various amounts precluded the use of heat to dissolve the product in a small amount of solvent. The solid product was very stable, and could be stored for long periods in sun-light or moist air without any visible signs of formation of elemental tellurium. The temperature of decomposition was found to be slightly above that of the melting point of triphenyl phosphine.

When excess tetraphenylarsonium cyanide was added to a solution of the compound in acetonitrile containing excess triphenyl phosphine, the colour disappeared immediately, and the required amount of ionic tellurocyanate was formed. These results indicate that the following equilibrium is displaced completely to the left when pure acetonitrile is employed as solvent:

$$NCTe^- + 2Ph_3P \rightleftharpoons (Ph_3P)_2Te + CN^-$$

The yellow crystalline compound appeared as hexagonal prisms. The space group, from oscillation and Weissenberg photographs, was found to be either $P3$ (No. 143) or $P\bar{3}$ (No. 147). Using Mo$K\alpha_1$ radiation ($\alpha = 0.70926$ Å), the unit cell dimensions, with standard deviations in parenthesis, were found to be, $a = 14.455(8)$ Å, $c = 12.714(10)$ Å. With three formula units in the unit cell, the calculated density was 1.412 g cm^{-3}. The observed density was 1.40 ± 0.02 g cm^{-3}, determined by flotation in a mixture of 1,4-dibromobutane and a fairly concentrated solution of triphenyl phosphine in benzene. Due to the viscosity of this mixture and the solubility of the adduct, the accuracy in the observed density is somewhat limited.

Pseudo extinctions in $hk0$ for $h-k \neq 3n$ indicate that all tellurium and phosphorus atoms lie on threefold axes, and thus that each formula unit (associated with a threefold axis) contains a linear P – Te – P configuration. A full X-ray structure determination has been carried out. The results have shown that in the linear P – Te – P configuration there is a "normal" bond between tellurium and one of the phosphorus atoms, while the interaction between tellurium and the other phosphorus atom is rather weak. Because of disorder in the structure, with alternating positions for the tellurium atoms, six crystallographically independent "normal" Te – P bond lengths have been observed, instead of three bond lengths, as would be observed for an ordered structure. In Table 2 are listed the observed bond lengths, where the tellurium atoms marked with a prime refer to the tellurium atoms of smallest occupancy. Full details of the structure will be reported later.

Due to the disorder in the structure it appears difficult to compare the long P – Te interactions and the short P – Te bonds with the sum of the van der Waals radii, 3.86 Å,[19] and the covalent single bond radii, 2.42 Å,[19] respectively. As no structure determinations of organophosphorus tellurides appear to have been performed, one cannot say whether the observed short P – Te bond lengths are longer or shorter than in pure phosphine tellurides.

The infrared spectra of triphenyl phosphine, Ph_3P, and the adduct between triphenyl phosphine and triphenyl phosphine telluride, $(Ph_3P)_2Te$, were,

Table 2. Tellurium-phosphorus distances in the adduct between triphenyl phosphine and triphenyl phosphine telluride. Standard deviations in parentheses.

Short distances (Å)	Long distances (Å)
Te(1) – P(1) = 2.388(11)	Te(1) – P(2) = 3.412(11)
Te(1′) – P(2) = 2.424(17)	Te(1′) – P(1) = 3.376(18)
Te(2) – P(3) = 2.381(9)	Te(2) – P(4) = 3.413(11)
Te(2′) – P(4) = 2.270(18)	Te(2′) – P(3) = 3.523(17)
Te(3) – P(5) = 2.278(14)	Te(3) – P(6) = 3.948(12)
Te(3′) – P(6) = 2.373(12)	Te(3′) – P(5) = 3.853(14)

as would be expected, very similar in many respects. Vibrations due to phenyl groups are identical in both cases, and are not repeated here. The X-sensitive vibrations of Ph_3P and their counterparts in $(Ph_3P)_2Te$ are recorded in Table 3 together with the appropriate assignments. It is seen that the two sets of data are very similar in each case, but that there are slight differences indicating the effects of heavy tellurium atoms co-ordinated to the Ph_3P moieties. The observed shift to higher frequencies of the *q* and *t* modes in co-ordination of Ph_3P is in accordance with the findings by Deacon and Green.[20] The X-sensitive peaks arising from $(Ph_3P)_2Te$ are slightly broader than those from Ph_3P which may suggest some small amount of dissociation, even though this is not apparent from an inspection of the disc.

Table 3. X-Sensitive bands (cm^{-1}).

Ph_3P[a]	Ph_3P[b]	$(Ph_3P)_2Te$[b]	Assignment
1089	1090	1096	*q*
512	514	513	
497	500	500	*y*
489	491	491	
433	431	441	
423	420	431	*t*
	254	249	*u*
	248		
	215	208	
	197	196	*x*
	186	183	

[a]Ref. 21. [b]This work.

There are, however, three peaks in $(Ph_3P)_2Te$ which are not observed in Ph_3P; these are at 528 (s), 318 (b) and 226 (m) cm^{-1}. Since they cannot be due to either the C_6H_5 or C_3P fragments they presumably arise from the P_2Te part of the molecule.

The Raman spectrum of $(Ph_3P)_2Te$ shows much primary scattering, presumably due to the heavy Te atoms. Nevertheless it is in general agreement with the above and, in particular, confirms the presence of a peak at 530 cm^{-1}

not observed in Ph_3P. It was not possible to measure the Raman spectrum of $(Ph_3P)_2Te$ below 400 cm^{-1}.

If we regard this P_2Te skeleton as a triatomic molecule then we would expect three fundamental vibrations if it were either angular or linear (although one of these vibrations would be doubly degenerate in the latter case). However, as a linear molecule the formula seems to imply that P_2Te would be centrosymmetric, whereas the coincidence of a peak (at 528 cm^{-1}) in the infrared and Raman spectra excludes such a possibility; further, only two fundamental vibrations would be active in the infrared region for a P_2Te micro-symmetry of $D_{\infty h}$.

Nevertheless we can assume that the three vibrations observed arise from the P_2Te skeleton alone or in conjunction with the associated phenyl groups, and indeed it is difficult to suggest an alternative origin for the peaks. They are relatively strong peaks and it is not easy to account for them as combination bands or overtones. In any case we conclude that these are fundamental vibrations, and, in view of the above, the framework of the molecule is presumably angular or, if linear, not centro-symmetric. This latter case, although not established unequivocally by these infrared data, complements the X-ray studies regarding the general shape of the molecule. Similar coincidences between infrared and Raman spectra have been observed in the spectra of the linear trihalide ions, XY_2^-, which might also have been assumed to be centrosymmetric.[22]

The P=O stretching frequency occurs at 1195 cm^{-1} in triphenylphosphine oxide,[23] and Chittenden and Thomas [24] have assigned peaks in the ranges 769–685 and 596–532 cm^{-1} to P=S frequencies, and 577–517 and 535–473 cm^{-1} to P=Se frequencies. It is possible, therefore, that the peak at 528 cm^{-1} in the present compound is essentially a P=Te stretching frequency, in which case the other peaks correspond to adduct vibrations or to Te–P–Te modes. Adams [25] quotes M–P stretching frequencies in the range 460–180 cm^{-1} for various phosphine complexes. In Table 4 are collected some representative stretching frequencies of some phosphorus chalcogenides.

Table 4. ν(P–X) stretching frequencies (cm^{-1}), R_3PX[a].

R_3PX	X=O	X=S	X=Se	X=Te
Ph_3PX	1195[b]	637[c]	562[c,d]	528[e]
$(Me_2N)_3PX$	1210[f]	565[f]	530[f]	519[f]
$(CH_3)_3PX$	1176	570	441	
$(n\text{-}C_3H_7)_3PX$	1172	596, 583	496	445, 400
$(n\text{-}C_4H_9)_3PX$	1169	596	511	462, 400
$(n\text{-}C_5H_{11})_3PX$		599, 588	507	467, 404
$(c\text{-}C_6H_{11})_3PX$	1143	619	543	518
$(c\text{-}C_3H_5)_3PX$		727[g]	685[g]	
$CH_3P(X)Cl_2$	1270[h]	670[h]	553[h]	
$CH_3P(X)(OC_2H_5)_2$	1250[h]	591[h]	505[h]	

[a]From Ref. 8, unless otherwise stated. [b]Ref. 23. [c]Ref. 16. [d]Ref. 26. [e]Stretching frequency for P–Te in $(Ph_3P)_2Te$, this work. [f]Ref. 10. [g]Ref. 27. [h]Ref. 28.

Generally organophosphorus chalcogenides can be represented by the following two resonance structures, the dipolar form (I) or as (II) in which there is $d_\pi - p_\pi$ bonding between the phosphorus atom and the chalcogen atom (X = O, S, Se, and Te).

$$R_3P^+ - X^- \qquad R_3P = X$$
(I) (II)

Stretching frequencies of phosphorus chalcogenides are known to be a poor measure for the electronic distribution and hybridization in the P – X bond. As pointed out by Goubeau,[29] from an extensive study on the phosphorus-sulfur bond, differences in P – S force constants in phosphorus sulfur compounds may be traced to several factors which have been demonstrated separately in different examples. The increase in calculated force constant for the P – X bond in tris-dimethylamino phosphine chalcogenides from the sulfide to the telluride has suggested that the Siebert rule [30] may not at all be valid when comparing the different chalcogenides.[10] Furthermore, the view of the bonding between the phosphorus and the chalcogen atom arrived at from studies of stretching frequencies, may be at variance with results obtained from X-ray crystallographic studies.[27] ESCA has likewise been shown to be a method of limited usefulness when examining the P – O, P – S, and P – Se bonds.[31] Recently, McFarlane and Rycroft [32] have developed a heteronuclear triple resonance technique to obtain ^{77}Se chemical shift in organophosphorus selenides, and this appears to be a valuable method for the investigation of the factors determining the charge distribution in such compounds. The amount of negative charge on selenium in phosphorus selenides appears to be dependent upon not only $p_\pi - d_\pi$ bonding between selenium and phosphorus and the electronegativity of the substituents, but also the ability of the p orbitals of the substituents, such as in trimethyl selenophosphate,[32] to compete with those of the selenium atom.

Due to their dipolar nature, most phosphorus chalcogenides act as powerful donors to a series of acceptors, the phosphorus selenides making their most stable adducts with soft Lewis acids, while the oxides generally make their most stable adducts with hard ones.[33]

Rather few structure determinations of these adducts have been performed, but generally when the phosphorus chalcogenides are donors, the formed adducts may formally be regarded O(II), S(II), and Se(II) compounds, and as such they are bent.[34] In the 2:3 adduct between triphenyl phosphine sulfide and iodine, the P–S–I angle is 106°,[35] in the bridged adduct between triphenyl phosphine selenide and mercuric chloride, the P – Se – Hg angle is 98°.[36] In tellurium bis(dimethyldithiophosphate),[37] bis(diethylthiophosphoryl) diselenide,[37] tellurium bis(diethylthioselenophosphinate),[38] and selenium bis-(diethyldiselenophosphinate)[39] the P–X–M angles lie in the 103 – 106° range.

The linear configuration of the P – Te – P skeleton in the present adduct suggests that the phosphine telluride is not the donor, although a tervalent phosphorus compound may well behave as an acceptor.[40] However, the total number of valency electrons in the P – Te – P skeleton is 22. Walsh [41] has given a correlation diagram for the orbitals of linear and non-linear triatomic molecules in their ground states. Using this diagram it is seen that the apex

angle reaches a minimum for molecules with 20 electrons, but that molecules with 22 electrons are linear. (The fact that other groups could contribute electrons to orbitals of a triatomic skeleton, as the phenyl groups are required to do in the above, was recognised by Walsh when he compared the ground states of allene and ketene with that of CO_2.) Thus, the linear structure of $Ph_3PTePPh_3$ is in accord with previous theoretical ideas, and accordingly is similar in structure to other systems containing 22 valence electrons such as the triiodide ion I_3^-,[42] and, similarly, the tribromide ion, Br_3^-.[43] No iso-electronic species from the fifth main group appear to have been synthesized. The bis(triphenylphosphine)iminium cation,[44] $(Ph_3P)_2N^+$, and the chlorite ion,[45] ClO_2^-, both iso-electronic with tellurium(II) compounds, are angular, as are the examples of 20-electron systems originally listed by Walsh.

Whilst the above gives a satisfactory overall view of the bonding in the adduct, it is interesting to speculate in a little more detail on the changes in the orbitals which occur as the adduct is formed. Taking a naive view point, if tellurium acts as donor to phosphorus, the lone pair electrons on phosphorus are superfluous, or alternatively, if phosphorus acts as donor to tellurium, the lone pair on tellurium is. Whichever its origin, this pair of electrons may be compared with the pair discussed by Walsh in going from a 20- to a 22-electron system. Thus, if tellurium acts as donor, an angular system is observed with a stereochemically significant lone pair in an orbital localized on the central atom.

An alternative description of the formation of the bond between triphenyl phosphine and triphenyl phosphine telluride is analogous to the one suggested by Pimentel [46] and Rundle [47] for the formation of the triiodide ion, I_3^-, from iodine and iodide. In this description, the three-center four-electron bond system, the extra two electron pairs, one from each donor, are combined with the $5p_z$ orbital of the central atom without employing outer d-orbitals.

With regard to the weak tellurium-phosphorus bond, this bond may be regarded as formed by an interaction between the lone pair of the phosphorus atom and the σ^* orbital of the normal phosphorus-tellurium bond, what is termed a "secondary bond" by Alcock.[48] Fundamentally, this "secondary bond" and the "normal" bond is the same as an unsymmetrical three-center four-electron system with a tellurium atom of zero charge as central atom.

It is not clear why the P–Te bond lengths should be dissimilar within a given molecule, nor why they should vary from one molecule to another within the unit cell (see Table 2). It seems likely that lattice effects and electrostatic effects may be exerting a significant influence on bond lengths in three-center four-electron bond systems, as has been shown for the triiodide ion.[42]

A possible explanation for the non-existence of triphenyl phosphine telluride and the stability of the present adduct is to consider triphenyl phosphine telluride to be polarized in the following way in view of the low electronegativity of tellurium relative to phosphorus in triphenyl phosphine:

$$\overset{\delta-}{Ph_3P}-\overset{\delta+}{Te}$$

This implies that triphenyl phosphine telluride is the acceptor in the interaction with triphenyl phosphine. When forming the adduct with triphenyl phos-

phine, the electron demand of the tellurium atom will be satisfied by the electron pair of the incoming phosphine. In this connection it is worth noticing that phosphine tellurides with weakly electronegative substituents bonded to phosphorus are rather stable compounds and show no ability to form adducts with an extra tervalent phosphorus compound.[13]

Undoubtedly the large polarizability of the tellurium atom and the drop, albeit slight, in electronegativity from selenium to tellurium, combined with the electronegative nature of the phenyl groups, should make the above-mentioned resonance structure possible in the case of the unstable triphenyl phosphine telluride.

The exceptional behaviour of organophosphorus tellurides appears to have been noted once in the literature. Trinuclear iron carbonyls containing tellurium were found to add tributyl phosphine without displacing one molecule of carbon monoxide, contrary to what was found for the similar sulfur and selenium compounds.[49] No definite proof, however, was given for the suggested structure of the addition compound, or for the occurrence or involvement of organophosphorus tellurides.

EXPERIMENTAL

Tetraphenylarsonium tellurocyanate, tetraphenylarsonium cyanide, triphenyl phosphine, and acetonitrile were purified as reported.[18] Lithium perchlorate (Fluka *purum*, Wasserfrei) and acetone, "Baker Analyzed" reagent, were used without further purification.

The adduct between triphenyl phosphine telluride and triphenyl phosphine: To 1 g tetraphenylarsonium tellurocyanate, 1.86 mmol, dissolved in 20 ml purified acetonitrile, carefully flushed with dry nitrogen, was added 2 g triphenyl phosphine, 7.64 mmol. A slight increase of the yellow colour could be observed. A total amount of 0.34 g lithium perchlorate, 3.2 mmol, in 10 ml acetonitrile, was then added very slowly. After addition of the first drop of this solution, the colour changed immediately to cream yellow; the colour increased in intensity as more lithium perchlorate was added.

After half the lithium perchlorate had been added, a yellow crystalline compound started to separate. On further addition, tetraphenylarsonium perchlorate and lithium isocyanide started to precipitate as well. After stirring for some minutes at room temperature, 2 g of triphenyl phosphine in 15 ml acetonitrile was added, making a total volume of 45 ml. The reaction mixture was then stirred at 35°C until the white precipitates had dissolved. The yellow, microcrystalline product was filtered from the reaction mixture and dried. Yield 0.71 g, 59 %. Evaporation of the solvent in vacuum left more yellow crystals among the otherwise white products and reactants. No blackening due to deposited tellurium was observed during the evaporation. A manual separation of the yellow product from the white residue proved tedious and not satisfactory.

The adduct was dissolved in 20 ml acetone containing 3 g triphenylphosphine, traces of tellurium dioxide and elemental tellurium were filtered off, and the clear solution was left at 0°C for a couple of hours until the first crystals of triphenyl phosphine appeared. The product was rapidly filtered, washed with some ice-cold acetone containing triphenyl phosphine, and dried. The final, overall yield of pure compound was never found to be higher than 30 %, as a considerable amount of the product was left in the mother liquor. The decomposition temperature of the adduct was 83 – 85°C, slightly above that of the melting point of triphenyl phosphine, 80 – 81°C. (Found: C 66.85; H 5.04; N negative: Calc. for $C_{36}H_{30}P_2Te$: C 66.25, H 4.65.)

The reaction between tetraphenylarsonium tellurocyanate and triphenyl phosphine in the presence of lithium perchlorate was followed by measuring the peak height at 2081 cm^{-1} using IR liquid cells.[18] The measurements were performed with a Unicam SP 200 G Infrared Spectrophotometer (see Table 1).

The spectra (4000 – 250 cm^{-1}) were measured on KBr discs using a Perkin-Elmer 457 spectrophotometer: no blackening was observed in the disc and the peaks were in the same positions as in the less well-resolved nujol spectrum. From 400 – 40 cm^{-1} the spectra were measured by the Physico-Chemical Measurements Unit at Harwell as pressed polythene discs. Raman spectra were recorded at the Nottingham University.

Acknowledgement. The authors are indebted to Dr. O. Foss for valuable comments.

REFERENCES

1. Foss, O. *Acta Chem. Scand.* **4** (1950) 1241.
2. Foss, O. *Acta Chem. Scand.* **1** (1947) 8.
3. Gryszkiewicz-Trochimowski, E., Quinchon, J. and Gryszkiewicz-Trochimowski, O. *Bull. Soc. Chim. France* **1960** 1794.
4. Razumov, A. I., Liorber, B. G., Gazizov, M. B. and Khammatova, Z. M. *J. Russ. Gen. Chem.* **34** (1964) 1851.
5. Zingaro, R. A. *J. Organometal Chem.* **1** (1963) 200.
6. Zingaro, R. A., Steeves, B. H. and Irgolic, K. *J. Organometal Chem.* **4** (1965) 320.
7. Chremos, G. N. and Zingaro, R. A. *J. Organometal Chem.* **22** (1970) 637.
8. Chremos, G. N. and Zingaro, R. A. *J. Organometal Chem.* **22** (1970) 647.
9. Grechkin, N. P., Nuretdinov, I. A. and Buina, N. A. *Izv. Akad. Nauk SSSR, Ser Khim.* **1969** 168 and 169.
10. Räuchle, F., Pohl, W., Blaich, B. and Goubeau J. *Ber. Bunsenges. Phys. Chem.* **75** (1971) 67.
11. Mardersteig, H. G. and Nöth, H. *Z. anorg. allgem. Chem.* **375** (1970) 272.
12. Borovikov, Y. Y., Raltsev, E. V., Boldeshul, I. E., Feschenko, N. G., Makovetskij, Y. P. and Egorov, Y. P. *J. Russ. Gen. Chem.* **40** (1970) 1957.
13. Zingaro, R. A. *Ann. N. Y. Acad. Sci.* **192** (1972) 72.
14. Issleib, K. and Brack, A. *Z. anorg. allgem. Chem.* **277** (1954) 271.
15. Henderson, W. A., Jr., and Streuli, C. A. *J. Am. Chem. Soc.* **82** (1960) 5791.
16. Nicpon, P. and Meek, D. W. *Inorg. Chem.* **5** (1966) 1297.
17. Songstad, J. and Stangeland, L. J. *Acta Chem. Scand.* **24** (1970) 804.
18. Austad, T., Songstad, J. and Åse, K. *Acta Chem. Scand.* **25** (1971) 331.
19. Bondi, A. *J. Phys. Chem.* **68** (1964) 441.
20. Deacon, G. B. and Green, J. H. S. *Spectrochim. Acta* **A 24** (1968) 845.
21. Norbury, A. H. *Spectrochim. Acta* **A 26** (1970) 1635.
22. Maki, A. G. and Forneris, R. *Spectrochim. Acta* **A 23** (1967) 867.
23. Cotton, F. A., Barnes, R. D. and Bannister, E. *J. Chem. Soc.* **1960** 2199.
24. Chittenden, R. A. and Thomas, L. C. *Spectrochim. Acta* **20** (1964) 1679.
25. Adams, D. M. *Metal-Ligand and Related Vibrations*, Arnold, London 1967.
26. King, M. G. and McQuillan, G. P. *J. Chem. Soc.* **A 1967** 898.
27. Cowley, A. H. and Mills, J. L. *J. Am. Chem. Soc.* **91** (1969) 2915.
28. Quinchon, J., Le Sech, M. and Gryszkiewicz-Trochimowski, E. *Bull. Soc. Chim. France* **1961** 735 and 739.
29. Goubeau, J. *Angew. Chem. Intern. Ed. Engl.* **8** (1969) 328.
30. Siebert, H. *Z. anorg. allgem. Chem.* **273** (1953) 170.
31. Morgan, W. E., Stec, W. J., Albridge, R. G. and Van Wazer, J. R. *Inorg. Chem.* **10** (1971) 926.
32. McFarlane, W. and Rycroft, D. S. *Chem. Commun.* **1972** 902.
33. Karayannis, N. M., Mikulski, C. M. and Pytlewski, L. L. *Inorg. Chim. Acta Rev.* **5** (1971) 69.
34. Bagnall, K. W. *The Chemistry of Selenium, Tellurium and Polonium*, Elsevier, New York 1966.
35. Schweikert, W. W. and Meyers, E. A. *J. Phys. Chem.* **72** (1968) 1561.
36. Dent Glasser, L. S., Ingram, L., King, M. G. and McQuillan, G. P. *J. Chem. Soc.* **A 1969** 2503.
37. Husebye, S. *Acta Chem. Scand.* **20** (1966) 24 and 51.
38. Husebye, S. *Acta Chem. Scand.* **23** (1969) 1389.

39. Husebye, S. and Helland-Madsen, G. *Acta Chem. Scand.* **23** (1969) 1398.
40. Amonoo-Neizer, E. H., Ray, S. K., Shaw, R. A. and Smith, B. C. *J. Chem. Soc.* **1965** 4296.
41. Walsh, A. D. *J. Chem. Soc.* **1953** 2266.
42. Runsink, J., Swen-Walstra, S. and Migchelsen, T. *Acta Cryst.* **B 28** (1972) 1331.
43. Willett, R. D. and Breneman, G. L. *Acta Cryst.* **B 25** (1969) 1073.
44. Handy, L. B., Ruff, J. K. and Dahl, L. F. *J. Am. Chem. Soc.* **92** (1970) 7327.
45. Gillespie, R. B., Sparks, R. A. and Trueblood, K. N. *Acta Cryst.* **12** (1959) 867.
46. Pimentel, G. *J. Chem. Phys.* **19** (1951) 446.
47. Rundle, R. E., *Record Chem. Progr. (Kresge-Hooker Sci. Lib.)* **23** (1962) 195.
48. Alcock, N. W. *Advan. Inorg. Chem. Radiochem. In press.*
49. Cetini, G., Stanghellini, P. L., Rossetti, R. and Gambino, O. *J. Organomet. Chem.* **15** (1968) 373.

Received January 5, 1973.

ACTA CHEMICA SCANDINAVICA 27 (1973) 1950–1956

An Electron Diffraction Investigation of the Molecular Structure in *anti-cis,cis*-2,2′-Dibromobiscyclopropyl in the Vapour Phase

G. SCHRUMPF and R. STØLEVIK

Organisch-Chemisches Institut der Universität Göttingen, B.R. Deutschland, and Department of Chemistry, University of Oslo, Blindern, Oslo 3, Norway

The experimental intensities obtained for the title compound are best reproduced by assuming a nearly s-*trans* conformation for the molecule. There is no indication from the experimental data of a second conformer.

The following values were found for the bond lengths: $r(C-Br) = 1.926(5)$ Å, $r(C-C, \text{ring}) = 1.527(3)$ Å, $r(C-C, \text{central}) = 1.470(7)$ Å, and $r(C-H) = 1.094(9)$ Å. Values in parentheses are estimated standard deviations, and bond distances are r_a-values.

Bond angles and mean amplitudes of vibration are found in Table 1.

According to well established theoretical interpretations of the nature of bonding in the cyclopropane molecule,[1,2] the exocyclic carbon orbitals involved in the C–H bonds of cyclopropane are nearly sp^2 hybridized. Those sp^2 hybrid orbitals constitute the σ bond framework of a large variety of organic molecules like conjugated olefins and aromatic compounds. However, extensive conjugation obscures the properties of the pure $sp^2 - sp^2$ bond between carbon atoms. Apart from a small unknown amount of conjugation, the C–C bond between two cyclopropane rings is expected to be a pure σ bond of the $sp^2 - sp^2$ type, and its properties may be studied in these models unaffected by large conjugative interactions.

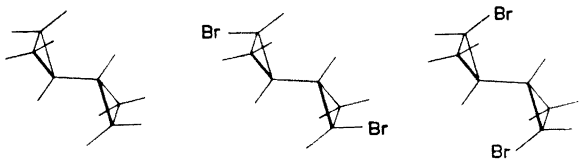

Fig. 1.

In order to investigate the structure and the conformational equilibrium of biscyclopropyl *1* (Fig. 1) an electron diffraction study of this molecule in the vapour phase had been undertaken previously.[3] Most of the structural parameters had been obtained. The experimental data indicated the presence of a *trans-gauche* rotational equilibrium, the two conformations being approximately equally populated. However, the equilibrium angle of the *gauche* form and the torsional amplitude of both rotational isomers had not been determined accurately, because the information about the torsion dependent parameters had to be extracted from a region of the radial distribution curve where many distances overlap extensively. In order to overcome this difficulty, the two derivatives *anti-trans,trans-* and the *anti-cis,cis*-2,2'- dibromobiscyclopropyl (*2* and *3*, respectively, Fig. 1) were synthesized.[4] In both compounds the conformation dependent Br···Br distances are well outside the range of all other distances in the two molecules. Besides, their scattering intensity is a large fraction of the total molecular intensity, a fact that facilitates the quantitative treatment of the conformational problem.

Only one of these dibromobiscyclopropyls can actually be compared to biscyclopropyl, because only in *2* the environments of the central C–C bond are essentially the same as in the hydrocarbon *1*. One may expect that the same potential energy function describes internal rotation in the two molecules *1* and *2*. On the other hand, one may anticipate a completely different conformational behaviour of *3*. The particular spacial relationship between the C–Br bond and the neighbouring cyclopropane ring leads to an extraordinary steric strain in most conformations. This will probably lead to a conformationally pure compound with an s-*trans* structure, because in that rotamer steric repulsion will be a minimum as judged from a molecular model.

In the present paper we report the results of our electron diffraction investigation of the *cis,cis* isomer, whereas our study of the *trans,trans* isomer will be published in a separate paper.[5]

EXPERIMENTAL AND CALCULATION PROCEDURE

The compound was synthesized and purified as described elsewhere.[4] The purity as determined by VLP chromatography was better than 98 %.

Diffraction photographs were obtained in the usual way with the Oslo apparatus.[6] The nozzle temperature was approximately 80°C. The electron wave length was determined from a gold foil diffraction pattern. Plates from three different nozzle-to-plate distances of about 130, 48, and 19 cm were obtained. Four plates from each camera distance were photometered and the intensity data treated in the usual way.[7] The 130 cm data cover the s-range between 0.500 and 7.375 Å^{-1} with $\Delta s = 0.125$ Å^{-1}, the 48 cm data extend from $s = 1.25$ to 20.50 Å^{-1}, and the 19 cm data from $s = 6.75$ to 46.50 Å^{-1} both in intervals of $\Delta s = 0.25$ Å^{-1}. Nonrelativistic atomic scattering factors for 35 kV electrons were computed using the partial wave method.[8] The calculations for hydrogen and carbon were based on Hartree Fock potentials, those for bromine on a TFD potential.[9] The resulting average intensity curve modified [7] by $s/|f_C||f_{Br}|$ is shown in Fig. 2, Curve A.

STRUCTURAL ANALYSIS

Preliminary values for the bond distances and bond angles were obtained from the experimental radial distribution curve (Fig. 3, Curve A). The peak at

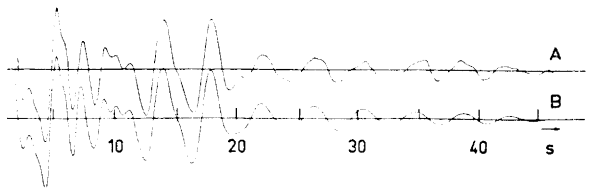

Fig. 2. Reduced molecular intensity curve of *anti-cis,cis*-2,2′-dibromo biscyclopropyl. A. Experimental curve. B. Theoretical curve calculated from the structural parameters listed in Table 1. The inner part of the intensity curves has been omitted.

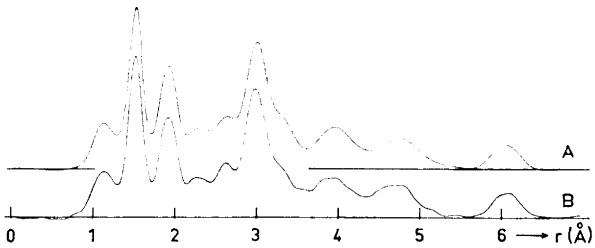

Fig. 3. RD curve of *3* calculated from the corresponding intensity curve by a Fourier inversion. A. Theoretical curve calculated from the intensity of Fig. 2. B. Experimental curve; damping constant in both calculations, $k = 0.0015$ Å^2.

1.1 Å corresponds to the eight C–H, that at about 1.5 Å to the five C–C, and the maximum at 1.9 Å to the two C–Br bond distances. Nonbonded C···C distances over one angle are found at 2.6 Å. The peak between 2.8 and 3.8 Å contains contributions from the two types of conformation independent nonbonded C···Br distances. The two complex peaks with maxima at about 3.8 and 4.8 Å originate from the various conformation dependent C···Br and C···C distances, and the isolated peak at 6.1 Å corresponds to the Br···Br distance.

A. *Least squares calculations using a rigid s*-trans *model.* In order to reduce the number of parameters to be refined to a practical limit, the following assumptions about the molecular geometry have been made at the initial stage of the analysis. The numbering of the atoms is shown in Fig. 4.

(1) All C–C bonds in the rings are equal, which implies an equilateral triangle for the cyclopropane ring.

(2) The substituents on each ring, *i.e.* hydrogen, bromine, and the central C–C bond, are oriented in a plane which is perpendicular to the plane of the three-membered ring and which contains the bisector of the inner angles of the three-membered ring. This means that we ignore a possible repulsive interaction between the two substituent atoms Br and C on the same cyclopropane ring.

(3) The position of the hydrogen atoms is the same as determined for the cyclopropane molecule,[10] where $r_{CH} = 1.089$ Å and the angle HCH = 115.1°.

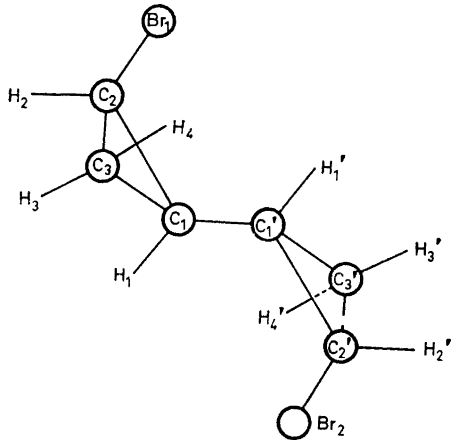

Fig. 4. Numbering of atoms of *3*.

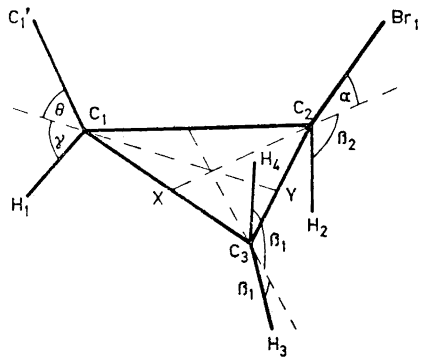

Fig. 5. Definition of angles of the cyclopropane moiety of *3*. The bisector of the inner ring angles are indicated by dashed lines.

(4) The molecule exists in a rigid s-*trans* conformation. Rotamers of *gauche* or even *cis* structure are highly improbable and are not considered hereafter.

In order to aid the analysis of the ED data in the initial stage of the investigation, the space group of the crystals was determined by X-ray diffraction to be $P2_1/a$ with two molecules in the unit cell. This is interpreted to mean centrosymmetric molecules, which must, therefore, exist in the s-*trans* conformation in the solid state at room temperature.

Initially the calculations were carried out taking into account the structure of the molecular framework of the heavy atoms carbon and bromine only. The contribution of all distances involving hydrogen atoms to the total intensity was treated as a constant. It was calculated from an assumed model and subtracted from the total intensity. This process was repeated after a series of calculations when a more refined model of the framework had been obtained. Keeping the *u*-values of the conformation dependent C···C and C···Br distances over the rings constant, the framework parameters refined to reasonable values, but the agreement between the experimental and the theoretical intensity curve was not very satisfactory. In the region between 3.5 and 5.0 Å containing nearly all the distances over the central C – C bond, considerable deviation from the experimental radial distribution curve was observed. Besides, the Br···Br distance calculated from this rigid s-*trans* model is larger than the experimental one as obtained from the RD-curve.

A more refined model was tried by admitting the bromine atoms to leave the bisector plane of the cyclopropane ring. A series of calculations with different values for the angle of deviation from that plane led to improved fit in the region between 3.5 to 5.0 Å, but yielded Br···Br distances too short by 0.2 to 0.5 Å. We therefore dropped this distorted model.

B. *Least squares calculations with a rigid non s*-trans *model.* Considerable improvement in the fit of the intensity curves could be achieved by varying the angle of torsion ϕ about the central C – C bond. While the s-*trans* conformation possesses C_i symmetry, other rotamers are without any symmetry element. Rotation about the $C_1 - C_1'$ bond leads to a splitting of three pairs of heavy atom distances into a longer and a shorter distance $C_2 \cdots C_3'/C_3 \cdots C_2'$, $C_2 \cdots Br_2/C_2' \cdots Br_1$, and $C_3' \cdots Br_1/C_3 \cdots Br_2$. Although there is no symmerty element in these conformations, it can be shown that rotation about the central C – C bond by an angle of $+\phi$ and $-\phi$, respectively, leads to molecules, which are mirror images of each other. This means that the potential energy as a function of the angle of torsion is symmetric about the s-*trans* form. A converging fit could be obtained by simultaneously varying all distances and *u*-values involving carbon and bromine. Only the *u*-values of the two long distance pairs $C_2 \cdots C_3'/C_3 \cdots C_2'$, and $C_2 \cdots Br_2/C_2' \cdots Br_1$ have been coupled together in the calculation by giving them the same shift in the least squares procedure.

C. *Least squares calculations including hydrogen atom geometry and differences in the C – C bond lengths.* In the next stage of the structural analysis the average length of the C – H bonds as well as their angle of inclination towards the ring plane have been included in the refinement process. Convergence was achieved only when one of these angles was refined at a time. By a mapping procedure, estimates of the three types of angles and the average bond length were obtained.

Finally differences between the average endocyclic and the central exocyclic C – C bond length were introduced. Because of the strong coupling between these bond distances and their *u*-values, we were unable to refine them simultaneously. Assuming a *u*-value of 0.045 Å for the central C – C bond, least squares calculations were performed for several values of this bond differing by an increment of 0.005 Å. The agreement between the experimental and the theoretical intensity curve improved noticeably. This additional degree of freedom allows an adjustment of all distances over the central bond while at the same time keeping the distances within the cyclopropane moiety constant. The best value for the central C – C bond length was found to be 1.470 Å and the average C – C bond length within the ring 1.527 Å. This result does not change much when the *u*-value of the central C – C bond is increased to 0.050 Å or decreased to 0.040 Å. The computations done during this final stage of the refinement involved strongly damped iterations using 0.5 times the calculated shift of the current iteration cycle and 0.2 times the shift of the previous cycle.

The intensity data show a large noise in the *s*-region above *ca.* 30 $Å^{-1}$. Therefore, the data between 30 and 46.5 $Å^{-1}$ have been weighted down in the least squares calculation. The effect of using limited parts of the molecular intensity data for the iterative refinement process was studied by changing the weighting scheme of the experimental intensity. The resulting changes of the geometry are negligibly small, whereas the *u*-values are more strongly affected.

RESULTS

The intensity curve is best reproduced by assuming an angle of torsion about the central C–C bond of 18° relative to the s-*trans* conformation. This deviation from a rigid s-*trans* form may be interpreted as a real non-s-*trans* equilibrium structure, or it may be an indication of a sizable shrinkage effect.[11] There is no indication from the experimental data of the presence of a second conformer.

Table 1. The values in parentheses are estimated standard deviations, and (–) means assumed parameter. The bond lengths (r) are r_a-values, and u is the root mean square amplitude of a distance.

	r(Å)	u(Å)
C–Br	1.926(5)	0.043(7)
C_1-C_2	1.527(3)	0.045(4)
C_1-C_1'	1.470(7)	0.045(–)
C–H	1.094(9)	0.083(9)
$Br_1\cdots Br_2$	6.063(8)	0.179(8)
$Br_1\cdots C_1$	2.991(4)	0.074(5)
$Br_1\cdots C_1'$	3.315(7)	0.127(8)
$Br_1\cdots C_3'$	3.957(20)	0.165(43)
$Br_2\cdots C_3$	4.508(20)	0.132(29)
$Br_1\cdots C_2'$	4.798(8)	0.145(16)
$Br_2\cdots C_2$	4.783(8)	0.145(16)
$C_2\cdots C_1'$	2.637(6)	0.085(8)
$C_2\cdots C_3'$	3.609(9)	0.160(–)
$C_3\cdots C_2'$	3.878(9)	0.140(–)
$C_2\cdots C_2'$	4.040(8)	0.184(78)

$\theta = 50.7\ (0.6)°$	$\gamma = 59.6\ (3.0)°$	$C_1'C_1C_2 = 123.3°$
$\alpha = 55.2\ (0.4)°$	$\beta_1 = 57.9°(-)$	$C_1C_2Br_1 = 119.6°$
$\phi = 18.8\ (2.0)°$	$\beta_2 = 53.5°(-)$	

The structural parameters are listed in Table 1 together with estimates of their standard deviations. An uncertainty in the wavelength (0.14 %) is included in the standard deviations for distances, and corrections for the effect of correlation [12] between the intensity data are included in all estimates of standard deviations.

The assumption (2) and that of an equilateral triangle for the cyclopropane ring, which were retained in the final model, fit the data well, as indicated by the small standard deviation of the C–C and C–Br bond distances and those over one and two angles. The structural data of the present compound are discussed together with those of the *trans,trans* isomer in the next paper.[5]

Acknowledgements. The authors thank Cand. Real. A. Almenningen for having taken the diffraction photographs, and Cand. Real. B. Klewe for determining the space group of the crystals. Professor W. Lüttke we acknowledge for his continuing support in connection with this work. Financial support from *Norges Almenvitenskapelige Forskningsråd*, and from *Deutsche Forschungsgemeinschaft*, Bad Godesberg, is gratefully acknowledged.

REFERENCES

1. Coulson, C. A. and Moffitt, W. E. *Phil. Mag.* **40** (1949) 1; Coulson, C. A. and Goodwin, T. H. *J. Chem. Soc.* **1962** 2851; **1963** 3161.
2. Walsh, A. D. *Trans. Faraday Soc.* **45** (1948) 179.
3. Bastiansen, O. and de Meijere, A. *Acta Chem. Scand.* **20** (1966) 516.
4. Schrumf, G. and Lüttke, W. *Liebigs Ann. Chem.* **730** (1969) 100.
5. *Acta Chem. Scand. To be published.*
6. Almenningen, A., Bastiansen, O., Haaland, A. and Seip, H. M. *Angew. Chem.* **77** (1965) 877.
7. Andersen, B., Seip, H. M., Strand, T. G. and Stölevik, R. *Acta Chem. Scand.* **23** (1969) 3224.
8. Peacher, J. L. and Wills, J. G. *J. Chem. Phys.* **46** (1967) 4809.
9. Bonham, R. A. and Strand, T. G. *J. Chem. Phys.* **39** (1963) 2200.
10. Bastiansen, O., Fritsch, F. N. and Hedberg, K. *Acta Cryst.* **17** (1964) 538.
11. Almenningen, A., Bastiansen, O. and Münthe-Kaas, T. *Acta Chem. Scand.* **10** (1956) 261; Morino, Y. *Acta Cryst.* **13** (1960) 1107; Cyvin, S. J. *Molecular Vibrations and Mean Square Amplitudes*, Universitetsforlaget, Oslo, and Elsevier, Amsterdam 1968.
12. Seip, H. M. and Stölevik, R. In Cyvin, S. J., Ed., *Molecular Structures and Vibrations*, Elsevier, Amsterdam 1972.

Received January 17, 1973.

ACTA CHEMICA SCANDINAVICA 27 (1973) 1957–1962

A Further Illustration of Nearest-neighbour Auto-inhibitory Effects in the Oxidation of Alginate by Periodate Ion

TERENCE PAINTER and BJØRN LARSEN

Institute of Marine Biochemistry, N-7034 Trondheim-NTH, Norway

Samples of sodium alginate from *Laminaria digitata* were treated separately with dilute, aqueous sodium metaperiodate until 5 %, 10 %, 20 %, and 30 %, respectively, of the hexuronic-acid residues had been oxidised. The products were then reduced with sodium borohydride, and oxidised again with an excess of periodate under conditions that suppress overoxidation. In each case, the additional consumption of periodate was 0.42 ± 0.02 mol per 198 g.

It was shown theoretically that this result is to be expected, on the assumption that both aldehyde groups of oxidised hexuronic-acid residues spontaneously form highly stable, intramolecular hemiacetals with the secondary hydroxyl groups on unoxidised residues adjacent to them in the chains.

When sodium alginate is oxidised in dilute, aqueous sodium metaperiodate under conditions that suppress depolymerisation and overoxidation, reaction ceases when only 44 % of the hexuronic-acid residues have been oxidised.[1] This oxidation-limit corresponds closely to that calculated on the assumption that only one residue in a given chain is oxidised at a time, and that oxidised residues, once formed, spontaneously protect the two adjacent, unoxidised residues in the chain from subsequent oxidation.[1,2]

The protective mechanism consists in the spontaneous formation of six-membered hemiacetal rings between the aldehyde groups of the oxidised residue and the closest hydroxyl groups on the two adjacent, unoxidised residues, thus removing their vicinal-diol functions.[1] When the hemiacetal rings are cleaved by treatment of the limit-oxidised alginate with sodium borohydride, the vicinal-diol groups in the remaining, unoxidised hexuronic-acid residues are again exposed.[1]

The molecule then consumes further periodate until a second oxidation-limit, corresponding to the oxidation of a total of about 88 % of the original hexuronic-acid residues, is reached. A second reduction with borohydride then permits oxidation of the remaining 12 % of intact hexuronic-acid residues.[1]

Although further evidence in support of these deductions is perhaps not needed, it was of interest to enquire how much additional periodate a sample of alginate would consume, if reduction with borohydride was carried out before the first oxidation-limit of 44 % had been reached. The results, which are now reported, are pleasingly simple, and provide a further illustration of the operation of the nearest-neighbour, auto-inhibitory mechanism.

THEORY

After oxidation to its first limit, the remaining, unoxidised hexuronic-acid residues in alginate exist in the chains either as "singlets", with oxidised residues in both neighbouring positions, or as "doublets", in which each member has only one oxidised residue in a neighbouring position.[1] The ratio of singlets to doublets is 2.35:1. Reduction with borohydride and further treatment with periodate result in complete oxidation of all the singlets, but of only one member in each doublet. This implies that the second oxidation-limit should be exactly twice the first, and the experimental result agrees well with this.[1]

When oxidation has been stopped before the first limit has been reached, the remaining, unoxidised residues must exist in the chains not only as singlets and doublets, but also as triplets, quadruplets, *etc.* All these groups must be isolated from one another by an oxidised residue, so that, after reduction of the oxidised residues, they must undergo further oxidation independently of one another. The total population of chains can therefore be regarded, for purposes of calculation, as consisting of a fraction, x_1, of chains containing singlets only, a fraction, x_2, containing doublets only, a fraction, x_3, containing triplets only, and so on.

The hypothetical group of chains containing singlets only will, upon reduction and re-oxidation, consume 1 mol of periodate for every unoxidised residue, corresponding to 0.5 mol, based upon the weight of the starting-material. Those containing doublets only will consume only 1 mol of periodate for every doublet, corresponding to 0.33 mol, based upon the starting material. The behaviour of those containing larger groups can be readily calculated from published data,[2] as follows.

For a group of N contiguous, oxidisable units, the oxidation-limit, D_N, expressed as a fraction of these units, is known.[2] For every such group, there is one unit that was oxidised in the first treatment with periodate, and then reduced. Therefore, the fraction of the total number of units in the chains that are oxidised in the second treatment with periodate is $ND_N/(N+1)$. The results for various values of N are shown in Table 1.

Formally, it is now necessary to evaluate x_1, x_2, x_3, *etc.*, but it is seen from Table 1 that, for values of N greater than 2, the results for each group are approximately the same. It is clearly necessary to evaluate x_1 and x_2. This can be done by considering the two groups together, as follows.

At very low degrees of oxidation, singlets and doublets must be generated with equal frequency, because, on the assumption of random attack, the probability of the nearest neighbour of a singly-protected unit being attacked

Table 1. Calculation of the periodate consumed by hypothetical alginate molecules containing groups of N contiguous, oxidisable hexuronic-acid residues, each being separated by a single residue which has previously been oxidised by periodate and reduced by borohydride. D_N is the oxidation-limit of each group, and $ND_N/(N+1)$ expresses it as a fraction of all the units in the chain.

N	D_N	$ND_N/(N+1)$
1	1.000	0.500
2	0.500	0.333
3	0.556	0.417
4	0.500	0.400
5	0.493	0.411
6	0.481	0.412
7	0.475	0.416
8	0.469	0.417
10	0.462	0.420
15	0.452	0.424
20	0.447	0.426
40	0.440	0.429

must be identical with the probability of its next-nearest neighbour being attacked. Initially, then, $x_1 = x_2$, and the average, limiting degree of oxidation of the two groups will be $(0.5x_1 + 0.333x_2)/(x_1 + x_2) = 0.416$.

As the degree of oxidation increases, the probability that an oxidisable unit will lie next to a singly-protected unit will increase until, at the first oxidation-limit, $x_1/x_2 = 2.35$, giving a value for the limit of 0.44 as previously shown.[1,2] It is therefore safe to conclude that, regardless of the degree of oxidation at which reduction with borohydride is carried out, the additional units oxidised in the second treatment with periodate will always be 42 $\pm$ 2 % of the total number of units in the original sample of alginate.

EXPERIMENTAL

Materials. Sample of 5 %, 10 %, 20 %, and 30 % periodate-oxidised alginates were isolated as their sodium salts as described by Smidsrød and Painter.[3] Their intrinsic viscosities in 0.01 M sodium chloride at 20° were 8.10, 5.75, 4.15, and 3.95 dl/g, respectively. They were reduced by adding the freeze-dried solids directly to freshly-prepared, 20 % w/v aqueous sodium borohydride at room temperature, and stirring until solution was complete (*ca.* 1 h). The solutions were then brought to pH 6 with acetic acid, dialysed exhaustively against water, centrifuged, and freeze-dried. The intrinsic viscosities of the products in 0.01 M sodium chloride at 20° were 5.90, 3.85, 3.30, and 2.03 dl/g, respectively.

Periodate oxidation. A solution of each sample (200 mg) in a mixture of 0.2 M sodium acetate-acetic acid buffer (pH 5.0, 40 ml) and 1-propanol (5 ml) was cooled to 0° in an ice-bath, and reaction was initiated by addition of 0.25 M sodium metaperiodate (5 ml), previously cooled to 0°. At intervals, portions (5 ml) of reaction mixture were added to a mixture of ice-cold, 0.5 M sodium phosphate buffer (pH 7.0, 25 ml) and aqueous potassium iodide (30 % w/v, 4 ml), and the liberated iodine was rapidly titrated with 0.01 M sodium thiosulphate.

Measurement of the rate of reduction of limit-oxidised alginate with sodium borohydride. Portions (5 ml) of aqueous (4 % w/v) limit-oxidised alginate [1] at 20° were mixed rapidly

with aqueous sodium borohydride (5 ml, variable concentration) at the same temperature. After the required interval of time, a few drops of 1-butanol were added to break foam, and then an amount of glacial acetic acid, calculated to bring the pH to about 6, was added quickly while shaking. After the effervescence had subsided, the volume of the mixture was made up to 25 ml with water, and the optical rotation was measured.

From the result, and the known specific rotations of the unreduced and fully reduced materials (+102° and −36°, respectively), the extent of reaction was calculated. With the large excess of borohydride, the reactions were approximately pseudo-first order, and the times of half-change were calculated.

RESULTS

Suppression of depolymerisation and overoxidation. To avoid complications arising from end-group effects, it was essential to keep the molecular weights of the samples as high as possible during the initial oxidation with periodate [3] and the subsequent reduction with borohydride.

It was known from earlier work [1] that depolymerisation occurs during the initial oxidation with periodate, apparently by a free-radical mechanism which is mediated by impurities. By including 1-propanol in the reaction mixture to serve as a radical-scavenger, and by working with very pure alginate, it was possible to suppress depolymerisation and consequent end-group effects to such an extent that the first oxidation limit could be measured reproducibly with an accuracy of ±1 %.

Propanol was therefore used in the initial preparation [3] of the partially-oxidised alginates for the present work, and it was also included in the second oxidation with periodate. However, poor reproducibility (about ±5 %) was still obtained in the second oxidation, until it was recognised that considerable depolymerisation was also occurring during reduction with borohydride.

It was logical to assume that this kind of depolymerisation was occurring by the well-known β-alkoxycarbonyl elimination [4] under the alkaline conditions of the reduction. Although this elimination is general-base catalysed,[5] it seemed likely that hydroxyl ions would be the major catalytic species under the conditions of the reduction. Sodium borohydride is a buffer, and the pH of a freshly-prepared solution varies very little with concentration (see Table 2). On the other hand, the rate of reduction of an aldehyde or hemiacetal should

Table 2. Effect of the concentration of sodium borohydride upon the pH of an aqueous solution, and upon the rate of reduction of limit-oxidised alginate, expressed as the time of half-change ($t_{½}$).

$NaBH_4$ (% w/v)	pH of an aqueous solution at the following times (in h) after preparation:					$t_{½}$ (min)
	0	1	2	3	4	
2	9.6	10.1	10.2	10.4	10.4	3.8
4	9.5	10.2	10.3	10.3	10.5	2.3
10	9.4	10.3	10.4	10.6	10.6	1.1
20	9.3	10.4	10.4	10.6	10.6	0.4

be directly proportional to the concentration of borohydride ions. It should therefore be possible to increase the rate of reduction relative to the rate of alkaline depolymerisation by increasing the concentration of sodium borohydride in the reaction mixture.

Pertinent experimental data are given in Table 2. The hydroxyl-ion activity apparently decreases slightly with increasing concentration of borohydride in freshly-prepared solutions, but increases as the solutions age, and the borohydride ions undergo hydrolysis to give borate ions. As expected, the rate of reduction of limit-oxidised alginate is approximately proportional to the concentration of borohydride. A freshly-prepared, concentrated solution of sodium borohydride was therefore indicated as the best means of minimising alkaline depolymerisation during reduction.

Confirmation of these ideas was provided by measurements of intrinsic viscosity. Thus, when the 5 % oxidised sample of alginate was reduced with 2 % w/v aqueous sodium borohydride as described in the earlier work,[1] its intrinsic viscosity in 0.01 M sodium chloride at 20° dropped from 8.10 to 1.35 dl/g, but when it was reduced with 20 % borohydride as described in the present paper, the intrinsic viscosity fell only to 5.90 dl/g. Similarly, 2 % borohydride decreased the intrinsic viscosity of 10 % oxidised alginate from 5.75 to 0.59 dl/g, while 20 % borohydride lowered it only to 3.85 dl/g.

Measurement of the additional periodate consumed by the borohydride-reduced samples. The second oxidation of each of the four samples was carried out at 0° to suppress overoxidation in the accepted manner. Good reproducibility was obtained in parallel experiments, and, as shown in Fig. 1, the reaction

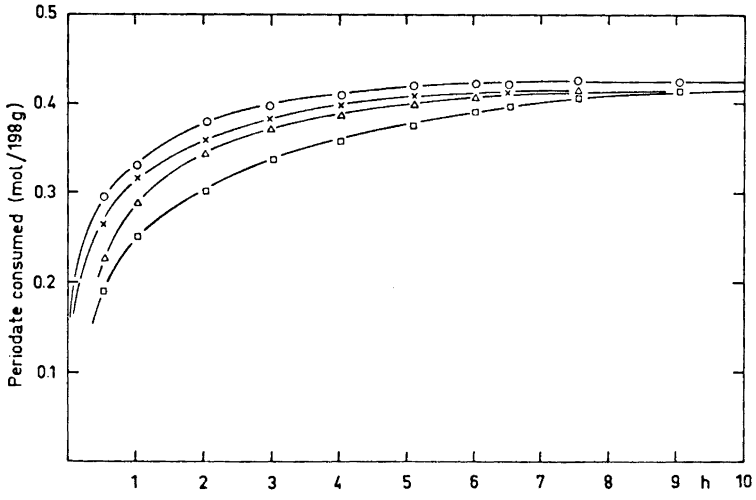

Fig. 1. Oxidation at pH 5.0 and 0° in 25 mM sodium metaperiodate of 5 % (○), 10 % (×), 20 % (△), and 30 % (□) periodate-oxidised alginates, after they had been reduced with sodium borohydride. The consumption of periodate is expressed as mol per 198 g of material; that is, for every hexuronate residue present in the original sample of unoxidised alginate.

in each case became very slow after the consumption of about 0.425 mol of periodate per 198 g of material. The different initial rates of oxidation are, of course, due to the different amounts of oxidisable hexuronic-acid residues initially present, and in accordance with this, the ratio of the initial slopes is about 95:90:80:70 for the 5 %, 10 %, 20 %, and 30 % oxidised samples, respectively.

DISCUSSION

The status of periodate oxidation as a tool in structural polysaccharide chemistry rests upon the assumption that it measures the total proportion of vicinal diol functions in the substrate. The recognition that the formation of inter-residue hemiacetals sometimes prevents it from doing this, led the authors, in an earlier paper,[1] to propose that reduction of the product obtained after the initial treatment with periodate, followed by a second oxidation step, should always be carried out to determine whether or not the true, Malapradian oxidation-limit has been reached. It was also suggested that this procedure should be repeated, until no further periodate is consumed.[1]

In principle, this proposal is sound, but if depolymerisation occurs during the oxidation steps, and again in the reduction steps, new end-groups will constantly be exposed, and the material will continue to consume periodate indefinitely.

Apart from its theoretical interest, the present project provided an opportunity of determining how accurately a second oxidation-limit can be measured. It is concluded that the use of 1-propanol to minimise free-radical depolymerisation in the oxidation steps, and concentrated aqueous sodium borohydride for the reduction steps, allows accurate results to be obtained. These conditions are now used routinely in this laboratory.

The authors are indebted to Kjersti Andresen for skilful technical assistance, to Dr. Olav Smidsrød for the measurements of intrinsic viscosity, and to Prof. N. A. Sørensen for his continued interest.

REFERENCES

1. Painter, T. and Larsen, B. *Acta Chem. Scand.* **24** (1970) 813.
2. Painter, T. and Larsen, B. *Acta Chem. Scand.* **24** (1970) 2366.
3. Smidsrød, O. and Painter, T. *Carbohyd. Res.* **26** (1973) 125.
4. Whistler, R. L. and BeMiller, J. N. *Advan. Carbohyd. Chem.* **13** (1958) 289.
5. Haug, A., Larsen, B. and Smidsrød, O. *Acta Chem. Scand.* **21** (1967) 2859.

Received February 14, 1973.

ACTA CHEMICA SCANDINAVICA 27 (1973) 1963–1970

Lattice Energies of Some Univalent Nitrate Phases

J. H. FERMOR and A. KJEKSHUS

Kjemisk Institutt, Universitetet i Oslo, Blindern, Oslo 3, Norway

The lattice bonding energies of univalent nitrates in calcite-like modifications are calculated using a method in which dispersion and multipolar forces are implicitly accounted for. The results accord well with experimental data. It is deduced from the temperature dependences of the energies that there are significant departures from the calcite type structure at higher temperatures in $LiNO_3$, $NaNO_3$, and KNO_3. The nature and extent of the deviations are discussed.

The evaluation of crystal lattice energies can be approached from both theoretical and experimental points of view, permitting tests regarding the nature of the bonding forces in the compounds. The results also have implications in connection with many bulk and defect properties of the crystals, and their behaviour on being dissolved, or transformed to the vapour state.

The lattice energy of a crystal may be defined relative to that of the constituent atoms at infinite dispersion *in vacuo* at absolute zero temperature, but for ionic crystals, the usual procedure is to employ as reference level the energy of the fully ionized atoms and groups of atoms at infinite dispersion. This is evidently realistic when the internal bonding forces of an ionic group are large compared with the external interionic forces, so that the group behaves as a discrete entity, and physical characteristics such as interionic separations and charge distribution are little affected by the state of aggregation. The infrared frequencies of internal and lattice oscillations provide a convenient indication of whether this condition is fulfilled, as it is in the nitrates, where the frequency ratio approaches 10:1.

The chief contribution to the lattice energy of an ionic crystal is the classical electrostatic (Coulomb) energy, which for an ion labelled i in an aggregate of ions, each having a spherically symmetric distribution of charge, is given by

$$U_i = q_i \sum_j q_j r_{ij}^{-1} \qquad (1)$$

where r_{ij} is the separation of the charges q_i and q_j. For one mol of a binary crystal, the total electrostatic energy may be written in the form

$$U_E = -NMz^2e^2r_0^{-1} \quad (2)$$

where N is Avogadro's number, M is the Madelung constant for the crystal structure, ze is the ionic charge, and r_0 the separation of adjacent anion and cation in the lattice. More difficult to calculate are the attractive forces arising between the fixed dipoles which are mutually induced on the ions as a result of their individual polarizabilities; and the dispersion (van der Waals) forces, arising from the fluctuations of charge about their mean positions. Where a non-uniform distribution of charge exists on an ionic group, as, *e.g.*, in NO_3^-, there is an opportunity for allowing (to some extent) for the multipolar and dispersion forces, since these may be included in eqn. 2 by means of a suitable adjustment of a hypothetical charge distribution for the group.

U_E is a negative quantity, whereas the repulsive energy U_R originating from the overlap of electrons between ions of both like and opposite charge is positive, and usually of the order of $-0.1U_E$. Exponential and inverse power laws of force have been used in calculating the energy due to these short range forces. A discussion of repulsive, multipolar, dispersion, and zero point energies has been given by Waddington [1] for alkali nitrates and other crystals.

Using an effective radius of 1.89 Å for the nitrate group, Yatsimirsky [2] derived values for the lattice energies of $NaNO_3$, KNO_3, $RbNO_3$, and $CsNO_3$ from a modified empirical equation due to Kapustinsky, and values based on the use of lyotropic numbers have been published by Morris.[3] Other experimentally based data have been presented by Ladd and Lee,[4] who utilized the Born-Haber cycle and direct calculation. All of these data relate to room temperature, where $LiNO_3$ and $NaNO_3$ alone have the calcite type structure;[5,6] the latter compounds retaining trigonal symmetries up to the melting points (253.1 [7] and 404°C,[8] respectively). KNO_3 has a closely related phase I structure over the range from 128.5°C [9] to the melting point (338°C [10]),[11] and $RbNO_3$ is rhombohedral in phase II (219 – 281°C [12]),[13] and this is also the case for phase I $AgNO_3$ [5] from ~159°C [14] to the melting point 209.6°C.[15]

CALCULATION OF LATTICE ENERGIES

Calculations of the electrostatic energy of crystals with the calcite type structure, from a point charge approximation for both anion and cation, were performed by Højendahl [16] and Evjen,[17] both authors obtaining values of the Madelung constant from rapidly converging series. In two earlier articles, Chapman *et al.*[18] and Topping and Chapman [19] considered the stability of the calcite type structure using a model which allows for the non-spherical charge distribution of the anion. Their method will be discussed in some detail, as it is used in modified form to calculate the lattice bonding energies of univalent nitrates with calcite-like structures. A numerical treatment of complex ions was recently described by Jenkins and Waddington.[20]

The rhombohedral, calcite type structure of $LiNO_3$, is shown in Fig. 1. The nitrogen atoms are situated at the centres of equilateral triangles defined by the oxygen atoms, and are indicated in the diagram by lattice points only. The layer-like nature of the structure is shown in Fig. 1b, where the first

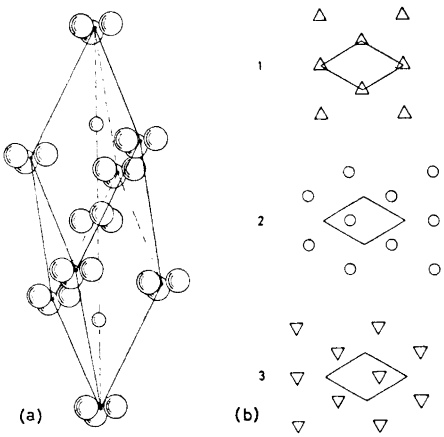

Fig. 1. (a) Calcite type structure of $LiNO_3$, (b) three strata of ions perpendicular to the hexagonal *c*-axis.

three of twelve strata occurring along the diagonal of the rhombohedron are shown. Also shown in Fig. 1b are the projections of the alternative, hexagonal unit cell, the *c*-axis of which coincides with the diagonal of the rhombohedral cell, and is of the length shown in Fig. 1a. The nitrate group is thought to be planar, or practically so, and for present purposes the charge distribution is arbitrarily regarded as $+5e$ at the centre of the nitrogen atom, and three charges of $-2e$ each, at a distance l (Chapman *et al.* used the notation b for this dimension) from the centre of the nitrogen atom, in the directions of the oxygen atoms. l is regarded here as an empirical quantity, adjustable for each compound so that the model has the same stable configuration and unit cell dimensions as are found in the crystal. In this way, multipolar and dispersion forces are implicitly incorporated in the model for each compound, whereas Topping and Chapman considered l to be constant for the group. The restriction of dipoles to the plane of the group is consistent with their greater polarizability in the plane than perpendicular to it.

Chapman *et al.* introduced the parameters $t=\pi a/3\sqrt{3}d$ and $\lambda=l/a$ where a is the hexagonal unit cell dimension, and d $(=c/12)$ is the separation of ionic planes perpendicular to the *c*-axis. The relationship between λ and t was then plotted for a constant size of the anion group, and constant separation between oxygen atom and adjacent cation (configuration curves); these being superimposed on curves of constant electrostatic potential. The locus of points of contact between these curves defines possible structural configurations, as shown in Fig. 2, where the inset diagram shows how the locus is related to the configuration curve C and equipotential curve P. The points marked on the curve refer to $LiNO_3$ at 20 and 251.4°C, and $NaNO_3$ at 25 and 300°C, according to structural data from Refs. 5 and 6.

From a comparison of the experimental and theoretical values of the rhombohedral angle (of a unit cell other than that of Fig. 1), Chapman *et al.* obtained good agreement for five carbonates using the appropriate λ *versus* t curve, and a constant value of 0.92 Å for l. At that time, the results could be applied to only a single nitrate compound, *viz.* $NaNO_3$, for which they found

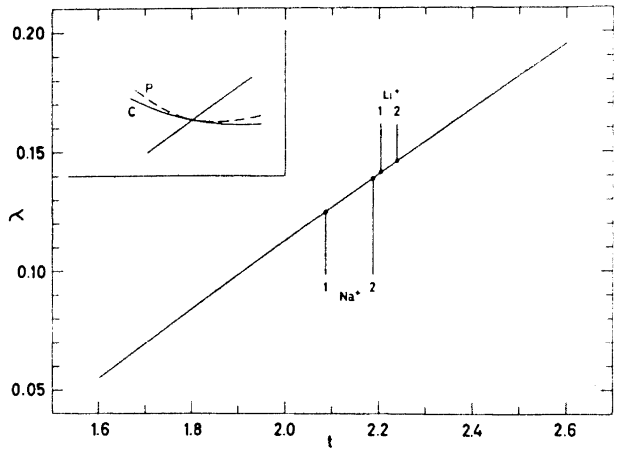

Fig. 2. λ *versus* t for univalent crystals with the calcite type structure according to the results of Chapman *et al.*[18] The inset diagram shows how the curve is derived as the locus of points of contact of configuration curves C and equipotential curves P.

$l = 0.72$ Å. These values of l were modified slightly on dealing differently with the repulsive energy, but this is of no consequence here.

The values of λ and t for a given compound determine the Madelung constant, the actual expression used being

$$U_E = -\frac{96e^2NF(\lambda,t)}{lJ} \tag{3}$$

where J is the mechanical equivalent of heat. As the values of $F(\lambda,t)$ are not readily obtained from the original work, they are plotted in Fig. 3 for both

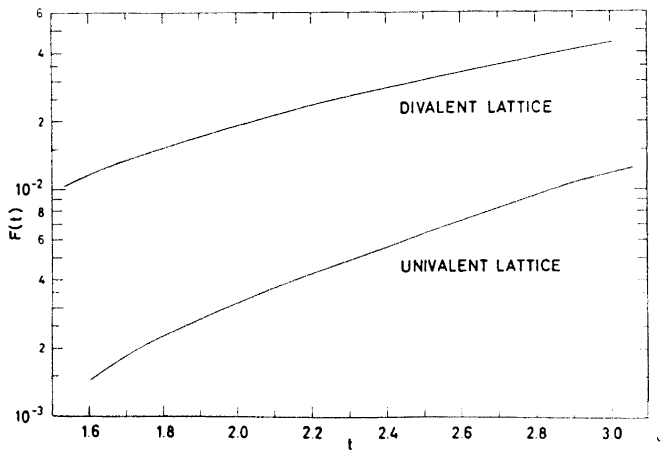

Fig. 3. $F(t)$ derived from the results of Chapman *et al.*[18] for univalent (nitrate) and divalent (carbonate) lattices.

univalent (nitrate) and divalent (carbonate) lattices. The curves are seen to have an approximately logarithmic dependence on t.

Information is now available on the variation of unit cell dimensions of $LiNO_3$, $NaNO_3$, KNO_3, $RbNO_3$, and $AgNO_3$ with temperature, and the modified method may be used to determine the corresponding values of electrostatic energy on the assumption that the crystal structures are of the calcite or orientationally disordered calcite types over certain ranges of temperature. Besides yielding values of the electrostatic energies of the compounds, the results also reflect the influence of temperature upon the structures.

NUMERICAL RESULTS

The calculated values of l and U_E at selected temperatures are presented in Table 1, together with the structural data on which they are based. It is seen that l varies considerably between the various compounds. Topping and

Table 1. Values of the adjustable parameter l and lattice bonding energy U_E for univalent nitrates in rhombohedral modifications.

Compound	Temp. (°C)	Phase	Unit cell dimensions a (Å)	c (Å)	Ref.	l (Å)	$-U_E$ (kcal/mol)
$LiNO_3$	Rm.temp.	I	4.693	15.224	21	0.687	208
$NaNO_3$	25	II	5.0694	16.8200	6	0.703	191
KNO_3	128	I	5.423	19.277	5	0.640	170
$RbNO_3$	250	II	5.48_3	21.41_0	5	0.526	162
$AgNO_3$	210	I	5.174	17.018	5	0.730	187

Chapman show how the repulsive energy may be calculated from an inverse eleventh power law for the repulsive force. The values of U_R for $NaNO_3$ and KNO_3 corresponding to the data of Table 1 are $NaNO_3$, 22 kcal/mol, and KNO_3, 11.3 kcal/mol. These results are not of high precision owing to the fact that the positions of the centres of repulsion of the oxygen atoms are not well defined. For both $NaNO_3$ and KNO_3, approximately equal contributions to the repulsive energy derive from cation-oxygen and oxygen-oxygen interactions, while cation-cation contact is negligible. A lack of suitable coefficients prevented a similar calculation for $LiNO_3$.

The present data are shown together with literature values in Table 2. There is seen to be good consistency between the present results and those published earlier. $AgNO_3$ has an anomalously high value of lattice energy, as may be seen from the results of Ladd and Lee plotted in Fig. 4; the dependence of U upon ionic separation (the crystal structure being of secondary importance), has been observed by Kapustinsky.[22] It seems likely that the high value of U for $AgNO_3$ results from the exceptionally large electronic polarizability of Ag^+.[23]

Table 2. Lattice energy U and electrostatic energy U_E for univalent nitrates. [a] indicates use of the Born-Haber cycle, [b] semi-empirical data, the remaining results being calculated.

Author(s) and year	Energy (kcal/mol)	$LiNO_3$	$NaNO_3$	KNO_3	$RbNO_3$	$CsNO_3$	NH_4NO_3	$AgNO_3$	$TlNO_3$
Topping and Chapman[19] (1927)	$-U$		178						
Højendahl [16] (1938)	$-U_E$		180						
Yatsimirsky [2] (1956)	$-U$		181.1[b]	164.2[b]	157.6[b]	151.1[b]			
Morris [3] (1958)	$-U$	198.8[b]	177.6[b]	162.5[b]	155.8[b]	149.7[b]	158.2[b]	195.6[b]	164.6[b]
Ladd and Lee [4] (1960)	$-U$	193[a]	172[a]	156[a]	147	143	143	189[a]	158[a]
Present work	$-U_E$	208	191	170	162			187	
	$-U$		169	159					

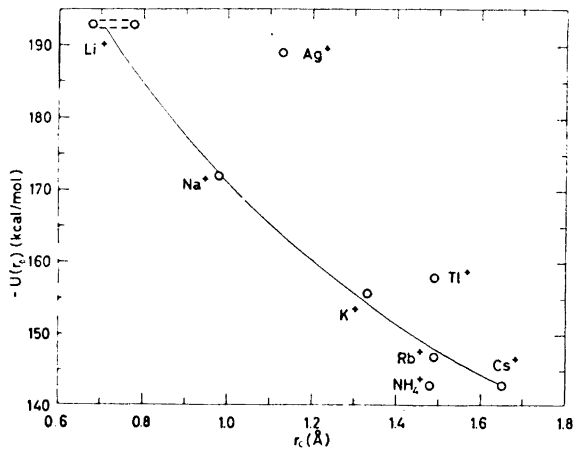

Fig. 4. Lattice energies $-U$ for univalent nitrates *versus* cation radius r_c. Values of $-U$ from Ladd and Lee.[4]

INFLUENCE OF TEMPERATURE INCREASE ON BONDING ENERGIES

With increasing temperature and distortion of the average unit cell due to anharmonicity of thermal vibration, there is in general an increase in the electrostatic contribution to the lattice energy (*i.e.* it becomes less negative). Since the attractive and repulsive forces are virtually in equilibrium at all stages of the expansion, the increase in lattice energy depends on the far smaller force constants which are, for example, reflected in lattice mode frequencies. Even where a sharp polymorphic phase transformation occurs, the enthalpy increment of the crystal may in most cases be largely accounted for by the effects of positional or orientational disorder of the ions,[24] without the necessity of introducing terms expressing increments in bonding energies. The effects of alterations in the lattice bonding forces over the continuous phase II to I transformation in $NaNO_3$ have, however, been considered in relation to changes in the Debye temperature and entropy of the compound.[25]

Although the change in U_R due to this transformation is difficult to calculate, the increment in U_E may be derived from the expansion properties of the lattice as determined by X-ray diffraction.[5] The amount calculated according to the present method is $\Delta U_E = 10.7$ kcal/mol over the temperature interval 25 to 300°C. This is a considerable change in energy, especially when compared with the repulsive energy at 25°C, $U_R = 22$ kcal/mol, or the experimentally determined enthalpy increment of ~ 9 kcal/mol over the same temperature interval.[10] Thus it seems that the only way in which ΔU may be of the correct order of magnitude (*i.e.* negligible compared with these amounts) is for there to be a significant departure from the assumed calcite type structure in $NaNO_3$ I. This interpretation is consistent with the findings of Strømme,[26] from X-ray diffraction data, of the displacement of a proportion of the nitrate groups parallel to the *c*-axis in the phase. It also seems probable that some groups undergo metastable angular displacements about axes perpendicular to the threefold axis, the overall effect being to expand the thickness of the planar distribution of negative charge associated with the anions. Such a mechanism is consistent with the relative constancy of the *a*-axis of $NaNO_3$ over the temperature interval.[5]

The apparent increase in U_E with temperature may be used as a measure of the distortion from the ideal structure, and a comparison of values obtained for the various compounds is complementary to (and at present a substitute for) complete structure determinations. There is no direct information on lattice changes in $LiNO_3$ above room temperature, but anomalies have been detected in the range 120 to 230°C by means of UV [27] and electrical measurements.[28] The increment ΔU_E for $LiNO_3$ over the range 20 to 251.4°C is 4.6 kcal/mol, which may be taken as a measure of the corresponding lattice distortion. The corresponding value for KNO_3 I over the temperature interval 128 to 335°C is 8.9 kcal/mol.

It would be of interest to extend the present approach to the calculation of lattice energies to other compounds, *e.g.* the remaining nitrates, and to examine in detail the problem of repulsive energies. The barrier separating alternative metastable positions of the anion might then be determinable on the assumption (which was also used here) that the cation sublattice remains virtually undisturbed.

Acknowledgement. This work was made possible by the financial support of *Nansenfondet.*

REFERENCES

1. Waddington, T. C. *Advan. Inorg. Chem. Radiochem.* **1** (1959) 157.
2. Yatsimirsky, K. B. *J. Gen. Chem. USSR* **26** (1956) 2655.
3. Morris, D. F. C. *J. Inorg. Nucl. Chem.* **6** (1958) 295.
4. Ladd, M. F. C. and Lee, W. H. *J. Inorg. Nucl. Chem.* **13** (1960) 218.
5. Fischmeister, H. F. *J. Inorg. Nucl. Chem.* **3** (1956) 182.
6. Rao, K. V. K. and Murthy, K. S. *J. Phys. Chem. Solids* **31** (1970) 887.
7. Doucet, Y. and Vallet, C. *Compt. Rend.* **259** (1964) 1517.
8. Bizouard, M., Cerisier, P. and Pantaloni, J. *Compt. Rend.* **264** (1967) 144.
9. Fermor, J. H. and Kjekshus, A. *Acta Chem. Scand.* **21** (1967) 1265.
10. Kelley, K. K. *U. S. Bur. Mines Bull.* **584** (1960).

11. Strømme, K. O. *Acta Chem. Scand.* **23** (1969) 1625.
12. Fermor, J. H. and Kjekshus, A. *Acta Chem. Scand.* **26** (1972) 2645.
13. Strømme, K. O. *Acta Chem. Scand.* **25** (1971) 211.
14. Arell, A. *Ann. Acad. Sci. Fennicæ Ser. A VI* **1962** No. 100.
15. Janz, G. J., James, D. W. and Goodkin, J. *J. Phys. Chem.* **64** (1960) 937.
16. Højendahl, K. *Kgl. Danske Videnskab. Selskab Mat. Fys. Medd.* **16** (1938) No. 2.
17. Evjen, H. M. *Phys. Rev.* **39** (1932) 680.
18. Chapman, S., Topping, J. and Morrall, J. *Proc. Roy. Soc.* **A 111** (1926) 25.
19. Topping, J. and Chapman, S. *Proc. Roy. Soc. (London)* **A 113** (1927) 658.
20. Jenkins, H. D. B. and Waddington, T. C. *Nature Phys. Sci.* **232** (1971) 5.
21. Felty, E. J. *Dissertation*, Ohio State University, 1963.
22. Kapustinsky, A. F. *J. Gen. Chem. USSR* **13** (1943) 497.
23. Tessman, J. R. and Kahn, A. H. *Phys. Rev.* **92** (1953) 890.
24. Newns, D. M. and Staveley, L. A. K. *Chem. Rev.* **66** (1966) 267.
25. Fermor, J. H. and Kjekshus, A. *Acta Chem. Scand.* **26** (1972) 2039.
26. Strømme, K. O. *Acta Chem. Scand.* **23** (1969) 1616.
27. Rhodes, E. and Ubbelohde, A. R. *Proc. Roy. Soc.* **A 251** (1959) 156.
28. Fermor, J. H. and Kjekshus, A. *Acta Chem. Scand.* **23** (1969) 1581.

Received January 18, 1973.

ACTA CHEMICA SCANDINAVICA 27 (1973) 1971–1981

Autolysis of β-Trypsin

Influence of Calcium Ions and Heat

DETLEF GABEL and VOLKER KASCHE

Institute of Biochemistry and the Gustav Werner Institute, University of Uppsala, Box 531, S-751 21 Uppsala 1, Sweden

The effect of calcium ions and heat on the autolysis of β-trypsin has been investigated. A considerable decrease in the rate constant of autolysis was observed in the presence of calcium. Below 40°, 0.02 M $CaCl_2$ reduced the velocity of autolysis by a factor of 100, as compared to the velocity recorded in the absence of Ca^{2+}. At about 40° a change in the apparent activation energy for the reaction was found both in the presence and absence of calcium. This has been attributed to reversible cooperative transitions in β-trypsin and the β-trypsin-calcium complex. Conformational transitions in the different trypsins were also manifested by changes in the activity towards *N*-*p*-tosyl-L-arginine methyl ester, but not towards *N*-benzoyl-L-arginine ethyl ester. β-Trypsin immobilized on Sephadex was more heat stable than β-trypsin bound to agarose.

The kinetics of activation of trypsinogen has been investigated to a considerable extent.[1–3] It has been shown that the velocity of activation as well as the amount of inactive material formed depend on the concentration of calcium ions present.[1,2] Two highly active forms of trypsin, α-trypsin and β-trypsin, are formed during the activation,[4] besides a less active form, ψ-trypsin.[5] These enzyme species, together with inactive material, are found in commercial enzyme preparations.[4]

A conformational change between different active forms at about 45° has been shown to occur in commercial enzyme preparations in the presence of Ca^{2+} (Refs. 6, 7). This change was attributed to the formation of a stable Ca-trypsin complex, as no similar conformational change was observed in the absence of Ca^{2+} (Ref. 7). Recently, reversible cooperative transitions between enzymatically active conformations have been observed in pure preparations of free and immobilized α- and β-trypsin in the absence of Ca^{2+} (Ref. 8). It is considered that the discrepancy between these findings may be partly due to autolysis and the use of heterogeneous enzyme preparations.

Although it has been known for a long time that trypsin solutions are stabilized by calcium ions, presumably by a reduction of the rate of autol-

ysis,[9-11,32-34] no extensive quantitative investigations on this phenomenon on pure enzyme preparations have been made. In the present study we found a considerable stabilization of pure β-trypsin towards autolysis at all temperatures up to 65°, indicating the existence of Ca-trypsin complexes. These complexes could not be isolated by gel chromatography.

MATERIALS AND METHODS

Bovine trypsin was a gift from Novo A/S, Copenhagen. It was separated into α- and β-trypsin by chromatography on SE-Sephadex [4] and the components were recovered by lyophilization after dialysis against 0.001 M HCl. The β-trypsin sample was found to contain ≃10 % α-trypsin and ≃10 % inactive material, as determined by analytical bioaffinity chromatography on soy bean trypsin inhibitor agarose (STI-agarose).[12] As rechromatography of the β-trypsin peak on the same column gave similar results, it was concluded that some autolysis during the bioaffinity chromatography procedure is unavoidable (as observed for α-chymotrypsin [13]) and that the original sample contained less α-trypsin and inactive trypsin. The α-trypsin sample contained more (≃40 %) inactive trypsin. STI-Sepharose 4B, α- and β-trypsin-Sephadex G-200, and β-trypsin-Sepharose 2B were prepared using the cyanogen bromide method.[13-15] *N*-Tosyl-L-arginine methyl ester (TAME) and *N*-benzoyl-L-arginine ethyl ester (BAEE) were purchased from Sigma, Cleveland, Ohio, and used without further purification. Casein (Hammarsten quality) was from Merck and Co., Darmstadt, Germany.

Determination of esterase activity. (a) *Free enzyme.* Stock solutions of the enzyme in 0.001 M HCl were prepared the day they were used and stored on ice. Activity measurements were performed under nitrogen in the thermostatted titration vessel of a Radiometer pH-stat. A correction for nonenzymatic alkali uptake was applied. The temperature of the assay solution was determined with a calibrated thermistor; the precision was ±0.2°. 50μl of the enzyme stock solution was added either to 2.0 ml 0.1 M NaCl, 0.01 M BAEE and the activity at pH 8.0 recorded immediately, or added to 1.9 ml 0.11 M NaCl adjusted to pH 8.0 After 30 sec, 0.1 ml of a prethermostatted 0.2 M BAEE solution (giving a final concentration of 0.01 M) was added and the activity recorded immediately. The activity in the presence of calcium ions (the assay solution then contained 0.02 M $CaCl_2$ and 0.04 M NaCl) was independent of the order of addition. (*b*) *Conjugated enzyme.* The procedure described elsewhere [8] was adapted. When BAEE was the substrate, a final concentration of 0.03 M was used; with TAME the final concentration was 0.05 M.

Determination of catalytic constants. The activity assay was carried out at 25.0° in a pH-stat in a total volume of 10 ml. β-Trypsin was added to the assay solution containing Tris-HCl ($I = 0.0025$), 0.25 M NaCl and TAME in the concentration range 0.04 to 15 mM. The activity was recorded at pH 8.0. K_M and k_{cat} were determined from an Eadie-Hofstee plot, using the activity values at substrate concentrations below 4 mM. Above that concentration, substrate activation was observed.[16]

Determination of protease activity. A procedure described elsewhere (Gabel and von Hofsten [22]) was followed, with the modification that 0.1 M $NaBO_3$-HCl buffer, pH 8.1, was used.

Autolysis of β-trypsin. A β-trypsin solution of suitable concentration in 0.01 M $NaBO_3$-HCl buffer, 0.02 M $CaCl_2$, 0.04 M NaCl, pH 8.1, was incubated at the desired temperature in a water bath. Samples were withdrawn at regular time intervals and tested for their activity as described above, or introduced into a STI-agarose column (1.4 × 10 cm) equilibrated with 0.05 M sodium acetate buffer, pH 5.0, containing 0.5 M NaCl. After washing, a linear gradient of the initial buffer and 0.05 M glycine-HCl buffer, pH 2.7, containing 0.5 M NaCl (100 ml of each) was applied. From the chromatograms obtained the relative amounts of inactive, α- and β-trypsin were determined. Apparent second order rate constants k_{EE} were determined from the obtained residual activity or the amount of β-trypsin.[8]

Calcium dependence of autolysis. The calcium dependence at 50° of the rate constant of autolysis was determined in 0.01 M $NaBO_3$-HCl buffer, pH 8.1, containing 10^{-6} to 10^{-2} M $CaCl_2$ and NaCl to give an ionic strength of 0.1. 100 μl of a suitable β-trypsin solution

was added to 10 ml of the prethermostatted buffer. Samples were withdrawn at time intervals and tested for their activity as described above. The apparent second order rate constants were plotted against the logarithm of the calcium concentration for determination of the binding constant.

Measurements of tryptophan fluorescence were performed in a Turner Spectro 210 spectrofluorometer (Palo Alto, California). The excitation bandwidth was 10 nm, the excitation wavelength 280 nm. The emission bandwidth was 2.5 nm. The reproducibility of the spectra was estimated to ±1 nm. All measurements were done in 0.01 M $NaBO_3$-HCl buffer, pH 8.1, containing either 0.1 M NaCl or 0.04 M NaCl and 0.02 M $CaCl_2$. In some cases the buffer contained 0.01 M BAEE in addition to the salts. 100 µl of the enzyme solution (approximately 1 mg/ml in 0.001 M HCl) were added to 1.9 ml of the prethermostatted buffer, and the fluorescence spectrum was recorded after 1 min. The wavelength of maximum emission was reached after about 5 min. The temperature inside the cuvette was monitored after each run with a thermistor.

Binding of $^{45}Ca^{2+}$ to β-trypsin. 10 mg β-trypsin (this special preparation contained ≃20 % α-trypsin) was incubated at 50° for 2 min in 1 ml 0.1 M $NaBO_3$-HCl buffer, pH 8.0, containing 0.02 M $CaCl_2$ with 10^7 dpm $^{45}Ca^{2+}$ (Radiochemicals, Amersham). The solution was cooled immediately in an ice bath and applied to a Sephadex G-25 column (dimensions 1.4 × 50 cm) equilibrated with the same buffer. The effluent was collected in 4.5 ml fractions. Enzymatic activity was measured as described above. 1 ml of each fraction was added to 10 ml scintillation fluid (70 % (v/v) toluene, 30 % (v/v) Triton X-100 with 7 g 2,5-diphenyloxazole and 0.35 g dimethyl-1,4-di[2-(5-phenyloxazolyl)]benzene per liter solution) and radioactivity measured with a Mark II Liquid Scintillation Counter (Nuclear Chicago). The counting efficiency was 50 %.

RESULTS

Dependence of activity on calcium. The recorded activity of β-trypsin-Sephadex towards BAEE as substrate was not dependent on the presence of calcium ions at all temperatures. The activity increased up to 70° with a constant value of the activation energy, and then decreased rapidly with increasing temperature; but incubation at 95° for 15 min did not lead to an irreversible inactivation, as complete recovery of activity was observed after cooling to room temperature.

The activity of free β-trypsin towards BAEE had a similar temperature dependence as observed for β-trypsin-Sephadex up to 70°, when calcium was present in the assay solution (Fig. 1). When no calcium was present, the recorded specific activity at temperatures above 50° depended on the order of addition of enzyme and substrate, as well as on the amount of enzyme added. When the enzyme was added to the thermostatted salt solution prior to the substrate, a considerably lower activity was recorded than when the order of addition was reversed. This is shown in Fig. 1. From the concentration of BAEE present (0.01 M) and the K_M value for trypsin-BAEE (10^{-5} M)[35] it can be calculated that about 0.1 % of the total trypsin is not in complex with BAEE under these conditions and thus has an unoccupied active site. Therefore the rate of autolysis may be expected to be considerably lower. When relatively high amounts of trypsin were assayed in the absence of calcium, a progressive inactivation was observed even during the activity measurement at temperatures above about 50°. Increased amounts of β-trypsin in calcium solutions above 65° showed a similar behaviour.

The esterolytic activity of α-trypsin in free and Sephadex-bound form decreased at temperatures above 55° both in the presence and absence of

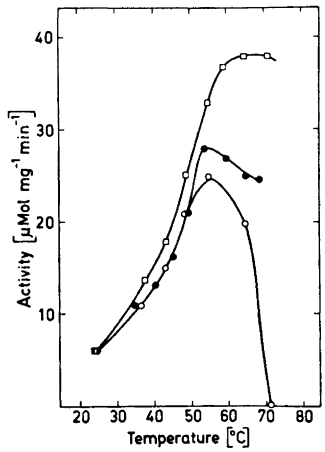

Fig. 1. Dependence of activity towards BAEE on temperature for β-trypsin. The initial activity at the temperatures indicated was measured at pH 8.0 in the presence of 0.1 M NaCl (●, ○) or 0.02 M $CaCl_2$ and 0.04 M NaCl (□). The closed circles represent values obtained when the enzyme stock solution was added after the substrate. For the open circles, the substrate stock solution was added to the salt solution 30 sec after the addition of the enzyme. In the presence of calcium the order of addition was of no importance for the recorded activity.

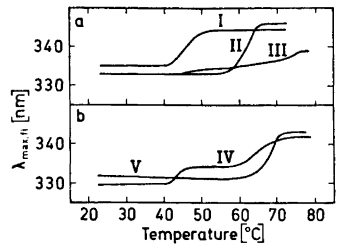

Fig. 2. Fluorescence of β-trypsin at different temperatures. Part a shows values obtained at pH 8.1 in 0.1 M NaCl (curve I) or in 0.02 M $CaCl_2$ and 0.04 M NaCl (curve II) for free β-trypsin (final concentration 2 μM) after 5 min. Curve III shows the curve for β-trypsin-Sephadex in 0.1 M NaCl. Part b shows values obtained at pH 8.1 in the presence of 0.01 M BAEE in 0.1 M NaCl (curve IV) or 0.02 M $CaCl_2$ and. 0.04 M NaCl (curve V). All measurements were made in 0.01 M $NaBO_3$-HCl buffer.

calcium. The peptide bond cleavage leading to the formation of α- from β-trypsin,[4] which has no influence on the rate of urea denaturation,[15] seems to decrease the heat stability when compared to β-trypsin.

Dependence of fluorescence on calcium. Fig. 2 shows the influence of temperature on the tryptophan fluorescence of trypsin. A considerable shift of the maximum of fluorescence emission to longer wavelengths occurred in the presence of calcium at 60°. A similar shift occurred at 40° when only sodium chloride was present. (In the temperature range of 50 – 60° and in the absence of calcium, precipitation was sometimes observed.) In the presence of BAEE (Fig. 2b) this shift did not occur until the temperature was raised to 65°. In this case, the spectrum below 40° was slightly shifted to shorter wavelengths as compared to the spectra measured without BAEE. Changes in the exposure of tyrosyl and tryptophyl residues in β-trypsin due to competitive inhibitors have been described recently.[17] Above 45° a slight but significant shift to longer wavelengths was observed, so that the wavelengths of maximum intensity was identical to that in the presence of $CaCl_2$, but in the absence of substrate. This may reflect a minor opening of the protein structure, as observed for β-trypsin-Sephadex.[8] The curve for the insoluble enzyme is also included in Fig. 2.

The results depicted in Figs. 1 and 2 can be caused by autolysis, as can be shown from the rates of autolysis published.[8] The concentration of trypsin in the fluorescence measurements was about 2 μM. At 50° and in the absence of calcium and substrate the rate constant of autolysis is $\simeq 2 \times 10^3$ $sec^{-1}M^{-1}$. The half life for β-trypsin is then ≃200 sec. The maximum of the fluorescence spectrum was, however, not reached until after 300 sec. Considerable autolysis has thus occurred during the measurement. The same may be true for the measurements over 60° in the presence of calcium or in the presence of substrate only, and over 70° in the presence of both calcium and substrate.

Autolysis of β-trypsin. The effect of temperature on the apparent bimolecular rate constant for the autolysis of β-trypsin in the presence of

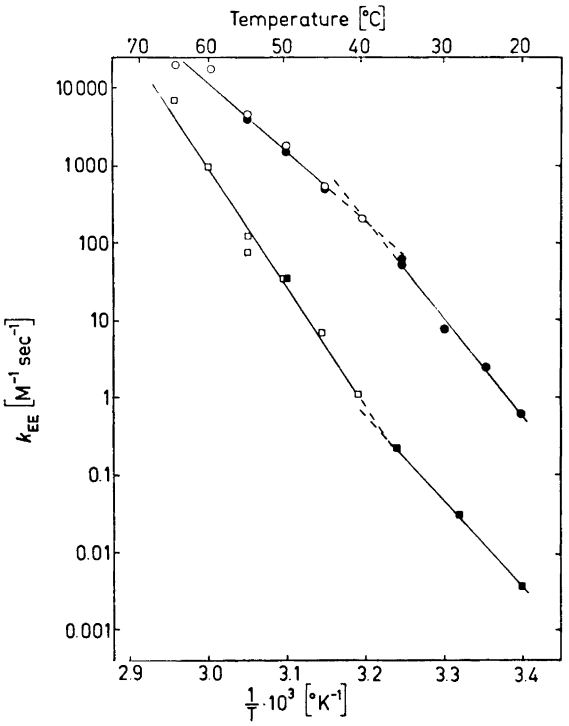

Fig. 3. Influence of calcium ions and temperature on the autolysis of β-trypsin. The logarithm of the apparent rate of autolysis of β-trypsin k_{EE} as determined by activity assay (open) or bioaffinity chromatography (filled symbols) is plotted against the reciprocal of the absolute temperature. The measurements were made in 0.01 M $NaBO_3$-HCl buffer, pH 8.1, containing either 0.1 M NaCl (circles) or 0.02 M $CaCl_2$ and 0.04 M NaCl (squares).

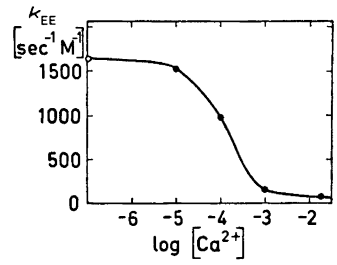

Fig. 4. Influence of calcium ions on the rate of inactivation at 50°. The inactivation rate as measured by activity assay was determined in 0.01 M $NaBO_3$ buffer, pH 8.1, containing the indicated amount of calcium ions and sodium chloride to give an ionic strength of 0.1. The open circle represents the rate measured in the absence of Ca^{2+}.

sodium chloride has been described before.[8] Fig. 3 compares these results with the autolysis in the presence of calcium chloride. Good agreement was found between the rate constants based on activity measurements and those obtained by bioaffinity chromatography. Bioaffinity chromatography was used to determine the relative amounts of α-, β-, and inactive trypsin present. Below 45° a steady state concentration of α-trypsin, amounting to about 10 % of the originally present β-trypsin, was found until about half of the β-trypsin had been degraded, whereafter even the concentration of α-trypsin decreased. Above 45°, negligible amounts of α-trypsin were observed. A markedly reduced rate of autolysis in the presence of calcium was found at all temperatures up to 65°, the highest temperature investigated. Whereas at temperatures below 40° the activation energy for the reaction was not influenced by calcium as compared to the value obtained with sodium chloride, both being around 60 kcal/mol, the presence of calcium ions above this temperature resulted in a considerable increase in the activation energy observed in the absence of calcium, from 40 to 80 kcal/mol. The apparent rate constant of autolysis at 50° was influenced by calcium as expected for the presence of a single metal ion binding site. The dissociation constant determined from the rate constants was 10^{-4} M (Fig. 4). At this temperature the ratio of the rate constants in the presence and absence of Ca^{2+} was much larger than the ratio of free β-trypsin to the total enzyme content. Therefore the observed temperature dependence of k_{EE} cannot be due to autolysis of free β- or β′-trypsin and a temperature dependent dissociation of the enzyme-calcium complex.

As pointed out previously,[8] "breaks" in the Arrhenius plot for k_{EE} do not alone provide sufficient evidence for the existence of conformational transitions. Additional evidence is provided by the temperature dependence of the rate constant for TAME hydrolysis.[6-8] We therefore concluded that the "break" in the Arrhenius plot for k_{EE} in the presence of Ca^{2+} is due to a conformational change in the calcium-trypsin complex similar to that observed in the absence of Ca^{2+}.[8]

Calcium-trypsin complex. The calcium-trypsin complex formed above 45° has been proposed to be so stable that it can be separated from other trypsin forms by chromatography.[7] We therefore attempted to isolate a β-trypsin-calcium complex by gel filtration. Fig. 5 shows the chromatogram obtained, after β-trypsin had been incubated at 50° for 2 min in the presence of $^{45}Ca^{2+}$. The specific enzyme activity (enzyme activity was found only in fractions 6 and 7) of the blank was slightly higher than that of the heated sample, probably due to some autolysis during the heating period. A small amount of radioactivity emerged before the total column volume (which corresponded to fraction 18) in both the blank and the heated sample, but no radioactivity was associated with the protein peak. A 1:1 complex of trypsin and calcium would have had a radioactivity of about 5×10^4 dpm, considerably more than that observed in all fractions before the total volume.

The complex of β-trypsin and calcium therefore has a life time considerably shorter than one hour, the time needed for the experiment shown in Fig.5. One can also exclude that the α-trypsin-calcium complex is stable enough to allow a chromatographic separation, as the preparation used contained about

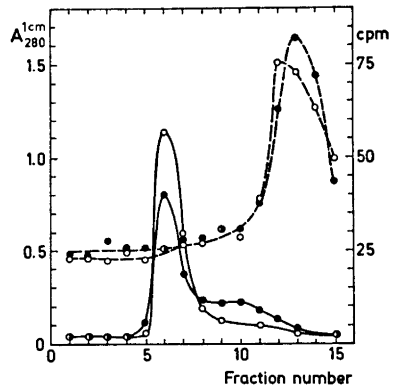

Fig. 5. Binding of $^{45}Ca^{2+}$ to β-trypsin. 10 mg β-trypsin in 1 ml 0.1 M $NaBO_3$-HCl buffer, pH 8.0, containing 0.02 M $CaCl_2$ with 10^7 dpm $^{45}Ca^{2+}$ were incubated at 50° for 2 min and gel filtered on a Sephadex G-25 column in 0.1 M $NaBO_3$-HCl buffer 0.02 M $CaCl_2$, pH 8.0 (●). A blank run on the same column, where the heating step has been omitted, is shown by open circles. The fractions were analysed for A_{280} and radioactivity (– – –). The total volume of the column emerged at fraction 18. Enzyme activity was found only in fractions 6 and 7.

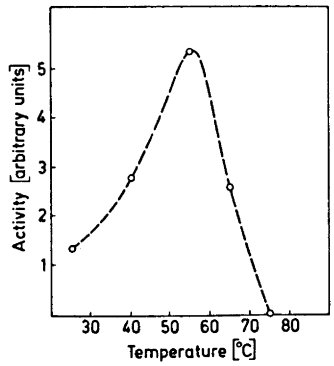

Fig. 6. Activity of β-trypsin-Sephadex against casein at different temperatures. A 1 % solution of casein in 0.1 M $NABO_3$-HCl buffer, pH 8.0, was digested with the immobilized enzyme and analysed for trichloroacetic acid soluble material.

20 % of this enzyme species. This behaviour is expected on the basis of published binding constants [3] and rates for protein-ligand reactions.[18] Our results are supported by the observation that a specific calcium complex has not been found in the X-ray crystallographic study of this enzyme.[19] A very stable complex of the type found in thermolysin,[20,21] where the calcium ion is deeply buried in the inner part of the molecule, is therefore not formed in the present case.

Proteolysis of casein at elevated temperatures. The temperature dependence of the activity of β-trypsin-Sephadex towards casein as substrate differed from that towards esters at higher temperatures. An apparent hydrolysis maximum was found at 55°, and the activity decreased again at higher temperatures, as shown in Fig. 6. This is probably due to a conformational change of the substrate, leading to its exclusion from the relatively tight gel. Conformational changes in the substrate other than expansion, making it a less good substrate, or conformational changes in the enzyme in addition to the one observed at 45° could also account for the observed phenomenon. Although more permeable matrices such as agarose gels should allow a further investigation of the different possible explanations, the properties of the conjugate described below disqualified these gels for the purpose.

Esterolytic activity of β-trypsin-agarose at elevated temperatures. β-Trypsin covalently bound to agarose exhibited below 50° a catalytic behaviour compar-

able to that of free and Sephadex-bound β-trypsin, when BAEE or TAME were used as substrates. The cooperative transition observed at 40° with TAME as substrate [8] was found also with the agarose-bound enzyme (Fig. 7). At temperatures above 55°, however, irreversible inactivation occurred, and after heating to 75° for 15 min the conjugate showed only very little activity at room temperature, in contrast to the Sephadex-bound enzyme. Although the treatment with cyanogen bromide at alkaline pH renders the gel stable towards melting even at 100°, presumably by cross-linking,[22] minor changes in the conformation of the supercoiled agarose chains [23] may directly or indirectly impair the function of the enzyme.

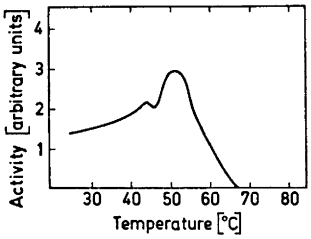

Fig. 7. Dependence of the activity of β-trypsin-agarose against TAME on temperature. The activity at pH 9.3 was measured in 0.1 M NaCl against 0.05 M TAME after preincubation of the enzyme for 15 min at the desired temperature.

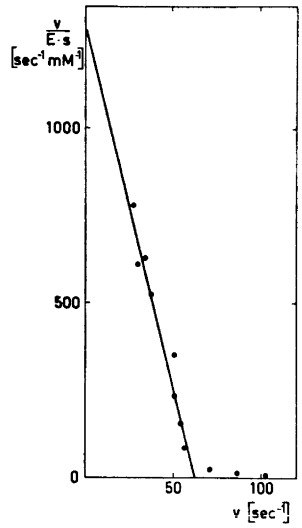

Fig. 8. Eadie-Hofstee plot of β-trypsin/TAME. The activity was measured at pH 0.8 in 0.0025 M Tris-HCl, 0.25 M NaCl at 25° in a pH-stat. The concentration of TAME varied between 0.04 and 15 mM. The enzyme concentration was 0.50×10^{-8} M.

Catalytic constants of β-trypsin. The constants for hydrolysis of TAME by the β-trypsin used here were determined at 25° from an Eadie-Hofstee plot (Fig. 8) and were: $K_M = 0.05$ mM, and $k_{cat} = 62$ sec^{-1}. If a correction was applied for the possible presence of 20 % impurities (10 % α-trypsin and 10 % inactive material, as determined by bioaffinity chromatography and discussed in Materials and Methods), a value for k_{cat} of 77 sec^{-1} was obtained. The corresponding constants for β-trypsin prepared by us from Worthington trypsin were: $K_M = 0.12$ mM, and $k_{cat} = 88$ sec^{-1}.[24] The differences in K_M are considered to be significant as they are much larger than the experimental error, estimated to be ≃20 % from the Eadie-Hofstee plot.

DISCUSSION

The transitions between the different molecular forms of the proteins derived from trypsinogen are shown in Fig. 9. Reversible temperature-induced transitions are indicated by double arrows, autolytic inactivations by arrows pointing backwards. Those reactions, for which no direct experimental evidence could be found, are indicated by dashed arrows. The subscript of rate constants refers to the corresponding reactions in Fig. 9.

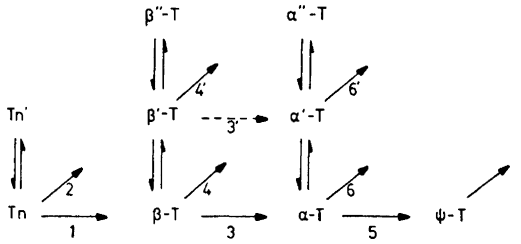

Fig. 9. Arrangement of the proteins derived from trypsinogen. For a description of this scheme, see Discussion. Tn designates trypsinogen, T trypsin.

The reversible transition from native trypsinogen to a more unordered structure at low pH has been described by Pohl.[25] The corresponding reactions leading to β′-trypsin and α′-trypsin have been described in a previous paper [8] as well as the reactions 3,4,4′,6, and 6′. There is no experimental evidence for reaction 3′; this will be discussed below.

The temperature-induced transitions leading to the doubleprimed forms of α- and β-trypsin have been observed only in the immobilized derivatives of these enzyme. These forms seem to have negligible enzyme activity. Investigation of the soluble derivatives is obscured by the rapid autolysis, and it could not be unambiguously established whether this reaction in the free enzyme leads to a reversibly inactivated form.

The most striking effect of calcium on β-trypsin is the great stabilization towards autolysis. The addition of calcium reduces the observed velocity of autolysis at room temperature by a factor of 100. This means that it is advisable for practical purposes to add calcium to the incubation mixtures which are to be digested by the enzyme, as has been observed before.[9–11] When pure β-trypsin is used, there is little risk of "parasitic splitting" which is observed with the commercial enzyme preparations.[26,27] Complete avoidance of the type of cleavage apparently caused by ψ-trypsin can be achieved by the immobilization of β-trypsin.

It has been shown before that calcium ions reduce the apparent rate constant k_2 (Ref. 1) (Fig. 9) and increase the constant k_1 (Ref. 3). In the present work it is established that calcium also decreases the rate constants k_4 and k_6. k_3 seems equally to be decreased, as a steady state concentration of α-trypsin is observed both in the presence and absence of calcium ions. The apparent constant k_4' is also decreased, whereas the experiments conduc-

ted here do not allow a similar conclusion for k_6'. As, however, no steady state concentration of α-trypsin is observed in the presence of calcium at higher temperatures, k_6' should be considerably larger than k_3'.

The calcium-trypsin complex which seems to be formed at temperatures both below and above 40° (as deduced from the altered rate of autolysis) is not sufficiently stable to allow isolation by chromatographic procedures. This is in contrast to previous results.[7] The critical dependence of the separation on SE-Sephadex on ionic strength, temperature, and concentration of the protein applied may have caused the observed phenomenon. The two peaks observed by Sipos and Merkel [7] could probably be α- and β-trypsin.

The results obtained here and elsewhere permit the following conclusions about the nature of the β-trypsin-calcium complex. Fluorescence measurements (presented here), difference spectra and optical rotatory measurements (described by Sipos and Merkel [7]) suggest that the trypsin molecule acquires a more compact structure upon binding of calcium. Below 40° the presence of BAEE in the absence of calcium causes, however, a more pronounced shift of the fluorescence spectrum to shorter wavelengths than calcium does. Above that temperature, a more open structure is found. Owing to the interference of autolysis with the fluorescence measurements nothing can be said about the fluorescence properties of trypsin in the absence of both calcium and substrate. Fluorescence measurements as well as the temperature dependence of the autolysis rate of free β-trypsin indicate a more loose structure above 40° (Ref. 8).

The cooperative transitions described here and in a previous paper [8] cannot always be inferred from activity measurements alone. Only with TAME as substrate was a "break" in the Arrhenius plot and a minimum in the curve activity *vs.* temperature observed. BAEE did not yield such results. The importance of a constant conformation of the substrate throughout the interval of conditions investigated is stressed by the fact that casein is not hydrolyzed by the Sephadex-bound enzyme above 60°, which may be ascribed to an extension of the molecular dimensions of casein at higher temperatures, hindering the penetration of the molecule into the gel. Therefore the temperature dependence of several molecular properties must be studied to establish the possible existence of a reversible cooperative transition.[8]

Intermolecular reactions as those observed with free enzymes are unlikely to occur in immobilized proteins. In a number of cases, however, the immobilized products have properties which are not found in the free proteins, and which have not been expected by exclusion of intermolecular reactions.[15,28–31] In the present investigation, the properties of the matrix are found to be transferred to the protein. Melting of agarose at higher temperatures is prevented by the reaction with cyanogen bromide.[22] This reaction apparently does not restrict the mobility of the matrix chains completely, and some changes in its structure seem still to occur. Similar effects will have to be considered when the molecular properties of immobilized proteins are to be elucidated.

The enzyme kinetic characteristics k_{cat} and K_M found in this work for β-trypsin obtained from Novo differed significantly from those found for β-trypsin from Worthington.[24] The reason can be genetic differences between

these two β-trypsins. Similar differences in k_{cat} and K_M have been found for π-chymotrypsin from different mice strains (H. Amnéus and V. Kasche, manuscript in preparation). We therefore suggest that minor differences, presumably in the primary sequence, exist between these two trypsin preparations.

Acknowledgements. This study has been financially supported by the *Swedish Natural Science Research Council* (D. G.) and the *Swedish Atomic Research Council* (V. K.).

REFERENCES

1. McDonald, M. R. and Kunitz, M. *J. Gen. Physiol.* **25** (1941) 53.
2. Delaage, M. and Lazdunski, M. *Biochem. Biophys. Res. Commun.* **28** (1967) 390.
3. Abita, J. P., Delaage, M., Lazdunski, M. and Savrda, J. *Eur. J. Biochem.* **8** (1969) 314.
4. Schroeder, D. D. and Shaw, E. *J. Biol. Chem.* **243** (1968) 2943.
5. Smith, R. and Shaw, E. *J. Biol. Chem.* **244** (1969) 4704.
6. Sipos, T. and Merkel, J. R. *Biochem. Biophys. Res. Commun.* **31** (1968) 522.
7. Sipos, T. and Merkel, J. R. *Biochemistry* **9** (1970) 2766.
8. Gabel, D. and Kasche, V. *Biochem. Biophys. Res. Commun.* **48** (1972) 1011.
9. Gorini, L. *Biochim. Biophys. Acta* **7** (1951) 318.
10. Bier, M. and Nord, F. F. *Arch. Biochem. Biophys.* **33** (1951) 320.
11. Nord. F. F., Bier, M. and Terminiello, L. *Arch. Biochem. Biophys.* **65** (1956) 120.
12. Kasche, V. *Biochem. Biophys. Res. Commun.* **38** (1970) 875.
13. Kasche, V. *Acta Universitatis Upsaliensis* **2** (1971).
14. Axén, R. and Ernback, S. *Eur. J. Biochem.* **18** (1971) 351.
15. Gabel, D. *Eur. J. Biochem.* **33** (1973) 348.
16. Trowbridge, C. G., Krehbiel, A. and Laskowski, M. *Biochemistry* **2** (1963) 843.
17. Villanueva, G. B. and Herskovits, T. T. *Biochemistry* **10** (1971) 4589.
18. Eigen, M. and Hammes, G. G. *Advan. Enzymol.* **25** (1963) 1.
19. Stroud, R. M., Kay, L. M. and Dickerson, R. E. *Cold Spring Harbour Symp.* **36** (1972) 125.
20. Matthews, B. W., Colman, P. M., Jansonius, J. N., Titani, K., Walsh, K. A. and Neurath, H. *Nature New Biol.* **238** (1972) 41.
21. Matthews, B. W., Jansonius, J. N., Colman, P. M., Schoenborn, B. P. and Duporcque, D. *Nature New Biol.* **238** (1972) 37.
22. Gabel, D. and von Hofsten, B. *Eur. J. Biochem.* **15** (1970) 410.
23. Rees, D. A. *Biochem. J.* **136** (1972) 257.
24. Kasche, V. Abstract, *Swedish Biochemical Society Meeting*, Lund, June 11–12, 1971.
25. Pohl, F. M. *FEBS Lett.* **3** (1969) 60.
26. Keil-Dlouhá, V., Zylber, N., Imhoff, J. M., Tong, N.-T. and Keil, B. *FEBS Lett.* **16** (1971) 291.
27. Keil-Dlouhá, V., Zylber, N., Tong, N.-T. and Keil, B. *FEBS Lett.* **16** (1971) 287.
28. Wilson, R. J. H., Kay, G. and Lilly, M. D. *Biochem. J.* **108** (1968) 845.
29. Erlanger, B. F., Isambert, M. F. and Michelson, A. M. *Biochem. Biophys. Res. Commun.* **40** (1970) 70.
30. Gabel, D., Vretblad, P., Axén, R. and Porath, J. *Biochim. Biophys. Acta* **214** (1970) 561.
31. Gabel, D., Steinberg, I. Z. and Katchalski, E. *Biochemistry* **10** (1971) 4661.
32. Buck, F. F., Vithayathil, A. J., Bier, M. and Nord, F. F. *Arch. Biochem. Biophys.* **97** (1962) 417.
33. Gorini, L. and Felix, F. *Biochim. Biophys. Acta* **11** (1953) 535.
34. Yon, J. *Biochim. Biophys. Acta* **31** (1959) 75.
35. Carlsson, J., Gabel, D. and Axén, R. *Hoppe-Seylers Z. Physiol. Chem.* **353** (1972) 1850.

Received December 8, 1972.

ACTA CHEMICA SCANDINAVICA 27 (1973) 1982–1986

Studies on Orchidaceae Alkaloids

XXXIII.* Two New Alkaloids, *N-cis-* and *N-trans*-Cinnamoylnorcuskhygrine from *Dendrobium chrysanthum* Wall.

ULF EKEVÅG, MAGNUS ELANDER, LARS GAWELL, KURT LEANDER and BJÖRN LÜNING

Department of Organic Chemistry, University of Stockholm, Sandåsgatan 2, S-113 27 Stockholm, Sweden

Dedicated to Professor *František Šorm* on his 60th birthday

Two new alkaloids, *cis-* and *trans*-dendrochrysine (I and II), have been isolated from *Dendrobium chrysanthum* Wall. Their structures have been determined by physical methods and confirmed by the synthesis of racemic II. The absolute configuration at the *N*-cinnamoylpyrrolidinyl group has been established by comparing the CD curve of I with those of *N-cis*-cinnamoyl-L-prolinol (VIII) and *N-cis*-cinnamoyl-L-2-methylpyrrolidine (X).

The occurrence of hygrine in *Dendrobium chrysanthum* Wall. has been reported earlier.[2] Two further alkaloids, *cis-* and *trans*-dendrochrysine (I and II), have now been isolated from this species. The alkaloids I and II have the same empirical formula, $C_{21}H_{28}N_2O_2$, as shown by high resolution mass spectrometry. From the IR, UV, and NMR spectra it is evident that I contains a *cis*-cinnamoylamide and II a *trans*-cinnamoylamide grouping.[3] The occurrence in both I and II of a keto group, an *N*-methyl group and two tertiary nitrogen atoms is also indicated. The base peak (*m/e* 84) in the mass spectra of I and II indicates the presence of an *N*-methylpyrrolidin-2-yl group,

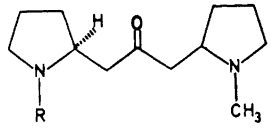

I: R = *cis*-cinnamoyl

II: R = *trans*-cinnamoyl

Fig. 1.

* For number XXXII of this series, see Ref. 1.

and the peaks at *m/e* 140 and 126 show the position of the keto group. On the basis of the evidence presented above, the structures of I and II shown in Fig. 1 have been deduced.

The structures of I and II were confirmed by the synthesis of racemic II. An equimolar mixture of *N*-methylpyrrolidin-2-one and *N*-benzylpyrrolidin-2-one was reduced with sodium dihydro-bis(2-methoxyethoxy)aluminate, and the resulting mixture of the corresponding carbinolamines was condensed with 3-oxopentanedioic acid at pH 8 in aqueous solution (*cf.* the synthesis of cuskhygrine[4]). The condensation product was decarboxylated (pH 2) giving *N*-benzyl-norcuskhygrine (III). Hydrogenation of III in glacial acetic acid (PtO_2, 70°, 3.5 atm.) followed by reaction with *trans*-cinnamoyl chloride produced, according to TLC and MS, two isomers of *N-trans*-cinnamoyl-dihydronorcuskhygrine (V). Upon oxidation with chromic acid, the two isomers of V gave the same *N-trans*-cinnamoyl-norcuskhygrine which was indistinguishable from II (UV, IR, NMR, MS, and TLC).

Hydrogenation of *cis*- and *trans*-dendrochrysine (I and II) gave the same dihydroderivative (VI), showing that the alkaloids have the same absolute configuration. The absolute configuration at the *N*-cinnamoylpyrrolidinyl group has been established by comparing the CD curve of I with those of *N-cis*-cinnamoyl-L-prolinol (VIII) and *N-cis*-cinnamoyl-L-2-methylpyrrolidine (X). It follows from the similarity of the CD curves (Fig. 2) that these compounds

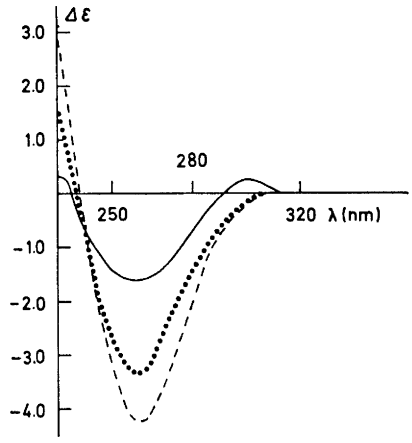

Fig. 2. CD curves of *cis*-dendrochrysine (I, —), *N-cis*-cinnamoyl-L-prolinol (VIII, ···), and *N-cis*-cinnamoyl-L-2-methylpyrrolidine (X, - - -). Methanol was used as solvent.

have the same absolute configuration, and hence that I and II possess the absolute configuration depicted in Fig. 1. Since compounds containing the $N-CH-CH_2-C=O$ system are easily isomerised in alkaline solution, the isolation procedure used would produce the thermodynamically most stable configuration at the *N*-methylpyrrolidinyl group (*cf.* Ref. 1). The absolute configuration at this centre remains to be determined.

In the synthesis of VIII and X, L-prolinol[5] and L-2-methylpyrrolidine were reacted with phenylpropiolyl chloride[6] and the amides (VII and IX) formed were hydrogenated over a palladium catalyst poisoned with quinoline.[7]

EXPERIMENTAL

All melting points are corrected. Mass spectra were measured on an LKB 9000 spectrometer (ionization energy 70 eV) and on an Atlas SM 1 spectrograph, the optical rotations on a Perkin-Elmer 141 polarimeter, and the circular dichroism spectra on a Cary 60 spectropolarimeter. The IR spectra were recorded on a Perkin-Elmer 257 instrument, the UV spectra on a Beckmann DK 2 instrument, and the NMR spectra on a Varian A-60A spectrometer.

Isolation of the alkaloids. Fresh plants of *Dendrobium chrysanthum* Wall. (10 kg) were extracted with methanol (40 l). The extract was concentrated to 1 l, acidified with hydrochloric acid and washed with carbon tetrachloride (5 × 0.4 l). The aqueous solution was made alkaline with sodium hydroxide and extracted with chloroform (5 × 0.4 l). The combined chloroform solutions were dried (Na_2SO_4) and concentrated, leaving the crude alkaloid mixture (13 g). The alkaloids were separated by preparative thin layer chromatography on neutral alumina. The plates were developed twice with chloroform. From 180 mg of the crude alkaloid mixture were isolated 30 mg of I, 30 mg of II, and 60 mg of hygrine.

Characterization of I. The base was obtained as a viscous oil, $[\alpha]_D^{22}$ −19°(*c* 1.92, chloroform). CD curve, see Fig. 2. IR spectrum: σ_{max} (CCl_4) 1719 (s), 1647 (s), 1620 (s) cm^{-1}. UV spectrum, nm (log ε): λ_{max} (ethanol) 253 (4.06), 210 (4.24). NMR spectrum ($CDCl_3$) τ: 2.4 − 2.9. (m, 5 H), 3.37 (d, 1 H, J = 12.5 Hz) and 3.98 (d, 1 H, J = 12.5 Hz) AB spectrum, 7.71 (s, 3 H). Pertinent mass spectral peaks *m/e* (rel. intensity): M^+ 340 (3), 140 (12), 131 (25), 126 (5), 103 (13), 97 (10), 84 (100), 83 (11), 82 (8), 77 (8), 70 (7), 42 (11).

Characterization of II. The base was obtained as a viscous oil, $[\alpha]_D^{22}$ −11° (*c* 0.81, chloroform). (Found: Mol weight 340.211. Calc. for $C_{21}H_{28}N_2O_2$: 340.215. ^{12}C = 12.0000.) IR spectrum: σ_{max} (CCl_4) 1713 (s), 1655 (s), 1611 (s) cm^{-1}. UV spectrum, nm (log ε): λ_{max} (ethanol) 281 (4.31), 224 (4.05), 218 (4.14). NMR spectrum ($CDCl_3$) τ: 2.33 (d, 1 H, J = 16 Hz) and 3.27 (d, 1 H, J = 16 Hz) AB spectrum, 2.5 − 2.9 (m, 5 H), 7.72 (s, 3 H). Pertinent mass spectral peaks *m/e* (rel. intensity): M^+ 340 (3), 140 (16), 131 (34), 126 (8), 103 (16), 97 (15), 84 (100), 83 (16), 82 (13), 77 (9), 70 (9), 42 (13).

N-*Benzyl-norcuskhygrine* (*III*). To a solution of *N*-methylpyrrolidin-2-one (17.5 g) and *N*-benzylpyrrolidin-2-one (31.0 g) in dry ether (500 ml), sodium dihydro-bis(2-methoxyethoxy)aluminate (56.5 g of a 70 % solution in benzene) was added with stirring at room temperature. After refluxing for 30 min, the reaction mixture was cooled to room temperature and a solution of 3-oxopentanedioic acid (25.0 g) and sodium hydroxide (6.85 g) in water (1500 ml) was added with cooling. The pH was adjusted to 8 with sodium dihydrogen phosphate (65.0 g, containing 2 mol of water of crystallisation) and the mixture was diluted with water to 4 l and left at room temperature for 60 h. The reaction mixture was acidified (pH 2) and heated until the evolution of carbon dioxide ceased, cooled and washed with chloroform (6 × 50 ml). The reaction mixture was made alkaline (pH 13) and extracted with chloroform (20 × 100 ml). The combined chloroform solutions were dried and the solvent evaporated, leaving a dark brown oil (46.4 g). After distillation (0.02 torr, bath temperature 145 − 155°), III (9.0 g) was obtained as a pale yellow oil. IR spectrum: σ_{max} ($CHCl_3$) 1710 (s). NMR spectrum ($CDCl_3$) τ: 2.55 − 2.95 (m, 5 H), 6.13 (d, 1 H, J = 13.0 Hz) and 6.76 (d, 1 H, J = 13.0 Hz) AB spectrum, 7.80 (s, 3 H), 6.76 − 8.90 (18 H). Pertinent mass spectral peaks *m/e* (rel. intensity): M^+ 300 (1), 216 (3), 209 (13), 160 (39), 159 (21), 91 (65), 84 (100), 42 (11).

Dihydronorcuskhygrine (*IV*). A solution of III (1.93 g) in glacial acetic acid (200 ml) was hydrogenated over Adams catalyst (100 mg) at 70° and 3.5 atm. After 5 h the catalyst was filtered off and the solution concentrated, diluted with water and washed with ether. The aqueous solution was made alkaline (pH 13, volume 100 ml) and extracted with ether (4 × 50 ml) followed by chloroform (3 × 50 ml). The combined chloroform solutions were dried (Na_2SO_4) and the solvent evaporated leaving IV (0.41 g) as an oil. NMR spectrum ($CDCl_3$) τ: 5.42 (s, 1 H) 5.7 − 6.4 (m, 1 H), 6.45 − 7.60 (6 H), 7.63 (s, 3 H), 7.70 − 9.10 (13 H). Pertinent mass spectral peaks *m/e* (rel. intensity): M^+ 212 (3), 110 (3), 98 (4), 85 (6), 84 (100), 83 (5), 82 (3), 70 (19), 44 (4), 43 (3), 42 (6), 41 (3).

N-trans-*Cinnamoyl-dihydronorcuskhygrine* (*V*). To a solution of IV (0.24 g) in sodium hydroxide (1 M, 10 ml), *trans*-cinnamoyl chloride (0.19 g) dissolved in tetrahydrofuran (30 ml) was added dropwise under stirring at room temperature. The reaction mixture

was then extracted with chloroform (4 × 15 ml), the combined chloroform solutions dried (Na_2SO_4) and the solvent evaporated. The residue was chromatographed on neutral alumina (3 × 15 cm) using chloroform as eluent. The second fraction consisted of two products (0.13 g, 1:1), which were separated by preparative thin layer chromatography using the same system as above. The plates were developed eight times. The mass spectra of the two components are indistinguishable which indicates that they are isomers. IR spectrum (on the mixture): σ_{max} (CCl_4) 3350 (m), 1650 (s), 1605 (s) cm^{-1}. Pertinent mass spectral peaks *m/e* (rel. intensity): M^+ 342 (3), 211 (3), 142 (4), 131 (13), 128 (3), 124 (3), 103 (6), 98 (3), 85 (6), 84 (100), 77 (3), 70 (5), 42 (5).

Oxidation of V. The two isomers of V were oxidised separately with Jones' reagent [8] (0°, 3 h), giving the same compound indistinguishable from II (IR, MS, TLC).

Hydrogenation of I and II. Solutions of I (8 mg) and II (13 mg) in methanol (5 ml) were hydrogenated over palladium supported on carbon (10 %, 20 mg) at room temperature and atmospheric pressure. After 20 min the catalyst was filtered off and the solvent evaporated to give the dihydro derivative VI, $[\alpha]_{578}^{24}$ −13° (*c* 0.70, chloroform). IR spectrum: σ_{max} (CCl_4) 1714 (s), 1642 (s) cm^{-1}. Pertinent mass spectral peaks *m/e* (rel. intensity): M^+ 342 (3), 140 (15), 126 (10), 105 (3), 98 (5), 91 (6), 85 (6), 84 (100), 83 (7), 82 (4), 70 (21), 42 (5).

L-*Prolinol*, $[\alpha]_D^{22}$ +2.6° (*c* 0.75, methanol) (lit. [9] $[\alpha]_D$ + ≃ 1°), was synthesized according to the procedure of Gassman and Fentiman.[5]

N-*Phenylpropiolyl*-L-*prolinol* (*VII*). To a solution of L-prolinol (0.47 g) in ether (15 ml), phenylpropiolyl chloride [6] (0.38 g) dissolved in ether (5 ml) was added dropwise under stirring over a period of 15 min. After the addition, the stirring was continued for 30 min at room temperature. The reaction mixture was washed successively with hydrochloric acid (4 M, 20 ml) and sodium hydroxide (2 M, 15 ml), dried (Na_2SO_4) and the solvent evaporated. The residue was chromatographed on neutral alumina (2.5 × 15 cm) using chloroform as eluent. The first fraction contained, according to its IR spectrum, the phenylpropiolyl ester of VII. After evaporation of the solvent, the second fraction gave VII (0.23 g) as a viscous oil, $[\alpha]_D^{23}$ −61° (*c* 0.32, methanol). IR spectrum: σ_{max} ($CHCl_3$) 3380 (m), 2220 (m), 1608 (s) cm^{-1}. NMR spectrum ($CDCl_3$) τ: 2.12 − 2.60 (m, 5 H), 5.69 (m, 1 H), 5.74 (s, 1 H), 6.00 − 6.50 (m, 4 H), 7.58 − 8.35 (m, 4 H). Pertinent mass spectral peaks *m/e* (rel. intensity): M^+ 229 (2), 198 (31), 129 (100), 102 (4), 101 (5), 85 (13), 83 (19), 77 (4), 75 (7), 70 (4), 51 (5).

N- cis-*Cinnamoyl*-L-*prolinol* (*VIII*). A solution of VII (230 mg) in methanol (9 ml) was hydrogenated over 5 % palladium supported on barium sulphate (60 mg) poisoned with quinoline [7] (60 mg) at room temperature and atmospheric pressure. When one molar equivalent of hydrogen had been consumed (18 min) the catalyst was filtered off and the solvent evaporated. The residue was chromatographed on neutral alumina (2.5 × 15 cm) using chloroform as eluent, giving VIII (150 mg) as an oil, $[\alpha]_D^{25}$ −52.5° (*c* 0.55, methanol). CD curve of VIII, see Fig. 2. UV spectrum, nm (log ε): λ_{max} (methanol) 253 (4.08). IR spectrum: σ_{max} ($CHCl_3$) 3350 (m), 1640 (m), 1605 (s), 1595 (s) cm^{-1}. NMR spectrum ($CDCl_3$) τ: 2.30 − 2.70 (m, 5 H), 3.20 (d, 1 H, J = 12.5 Hz) and 3.82 (d, 1 H, J = 12.5 Hz) AB spectrum, 5.69 (s, 1 H), 5.72 (m, 1 H), 6.10 − 7.13 (m, 4 H), 7.85 − 8.55 (m, 4 H). Pertinent mass spectral peaks *m/e* (rel. intensity): M^+ 231 (2), 200 (22), 132 (11), 131 (100), 103 (30), 77 (20), 70 (28), 51 (7).

N-*p*-Toluenesulphonyl-L-prolinol-*p*-toluenesulphonate, m.p. 99°, $[\alpha]_D^{23}$ −119° (*c* 0.62, methanol) and *N*-*p*-toluenesulphonyl-L-2-methylpyrrolidine, m.p. 70 − 71°, $[\alpha]_D^{23}$ −69° (*c* 0.45, ethanol), were prepared according to Karrer and Ehrhardt [10] who reported m.p. 104 − 105°, $[\alpha]_D^{16}$ −129.5° and m.p. 68 − 69°, $[\alpha]_D^{18}$ −61.1° (ethanol), respectively.

L-*2-Methylpyrrolidine*. A mixture of *N*-*p*-toluenesulphonyl-L-2-methylpyrrolidine [10] (20 g), phenol (1.9 g), hydrobromic acid (48 %, 20 ml) and propionic acid (3 ml) was refluxed for 2 h under nitrogen (*cf.* the preparation of dihydroisoindole [11]). The reaction mixture was cooled to room temperature, washed with ether (4 × 25 ml), made alkaline (pH 13) with sodium hydroxide pellets and extracted with ether (8 × 25 ml). The combined ether solutions were dried (Na_2SO_4) and concentrated. From the residue, L-2-methylpyrrolidine, $[\alpha]_{578}^{25}$ −13° (*c* 0.45, water) was isolated by preparative GLC (column: 5 % SE-52 on Chromosorb AW DMCS, 60 − 80 mesh; 3 mm × 2.0 m; retention time 3 min at 80°, gas flow rate 80 ml/min). Karrer and Ehrhardt [10] have reported $[\alpha]_D^{22}$ −11.97° (water) for L-2-methylpyrrolidine.

N-*Phenylpropiolyl*-L-*2-methylpyrrolidine* (*IX*). L-2-Methylpyrrolidine (0.20 g) in ether (5 ml) and sodium hydroxide (1 M, 15 ml) was reacted with phenylpropiolyl chloride [6] (0.80 g) at room temperature. After stirring for 1 h, IX (0.23 g) was isolated as a viscous oil, $[\alpha]_D^{24}$ −38° (*c* 1.29, methanol). IR spectrum: σ_{max} ($CHCl_3$) 2220 (m), 1612 (s) cm^{-1}. NMR spectrum ($CDCl_3$) τ: 2.18 – 2.70 (m, 5 H), 5.43 – 5.87 (m, 1 H), 6.03 – 6.55 (m, 2 H), 7.68 – 8.35 (m, 4 H), 8.62 and 8.73 (2 d, 1:1, 3 H, $J = 6$ Hz). Pertinent mass spectral peaks *m/e* (rel. intensity): M^+ 213 (18), 198 (17), 130 (10), 129 (100), 116 (5), 102 (8), 101 (5), 77 (2), 75 (6), 51 (5).

N-cis-*Cinnamoyl*-L-*2-methylpyrrolidine* (*X*). IX (0.20 g) was hydrogenated in the same way as described for VIII. The reaction mixture was concentrated and chromatographed on neutral alumina (1 × 15 cm) using ether as eluent, giving X as an oil, $[\alpha]_D^{25}$ −21° (*c* 1.12, methanol). CD curve of X, see Fig. 2. UV spectrum, nm (log ε): λ_{max} (methanol) 252.5 (4.11). IR spectrum: σ_{max} ($CHCl_3$) 1640 (m), 1608 (s), 1600 (s) cm^{-1}. NMR spectrum ($CDCl_3$) τ: 2.30 – 2.80 (m, 5 H), 3.30 (d, 1 H, $J = 12.5$ Hz) and 3.84 (d, 1 H, $J = 12.5$ Hz) AB spectrum, 5.50 – 7.20 (m, 3 H), 7.83 – 8.64 (m, 4 H), 8.65 – 9.05 (m, 3 H). Pertinent mass spectral peaks *m/e* (rel. intensity): M^+ 215 (31), 132 (13), 131 (100), 103 (35), 84 (29), 77 (23), 70 (22).

Acknowledgements. We are indebted to Dr. Rolf Håkansson and Mr. Jan Glans (Kemicentrum, Lund) for measuring the circular dichroism spectra and to Dr. Ragnar Ryhage for measuring the mass spectra. We thank *Stiftelsen Bengt Lundqvists Minne* for a fellowship to one of us (K.L.), and the *Swedish Natural Science Research Council* for financial support.

REFERENCES

1. Elander, M., Leander, K., Rosenblom, J. and Ruusa, E. *Acta Chem. Scand.* **27** (1973) 1907.
2. Lüning, B. and Leander, K. *Acta Chem. Scand.* **19** (1965) 1607.
3. Lloyd, H. A. *Tetrahedron Letters* **1965** 4537.
4. Galinovsky, F., Wagner, A. and Weiser, R. *Monatsh.* **82** (1951) 551.
5. Gassman, P. G. and Fentiman, A. *J. Org. Chem.* **32** (1967) 2388.
6. Wotiz, J. H. and Buco, S. N. *J. Org. Chem.* **20** (1955) 210.
7. Cram, D. J. and Allinger, N. L. *J. Am. Chem. Soc.* **78** (1956) 2518.
8. Bowers, A., Halsall, T. G., Jones, E. R. H. and Lemin, A. J. *J. Chem. Soc.* **1953** 2555.
9. Karrer, P., Portmann, P. and Suter, M. *Helv. Chim. Acta* **31** (1948) 1617.
10. Karrer, P. and Ehrhardt, K. *Helv. Chim. Acta* **34** (1951) 2202.
11. Bornstein, J., Sherman, L. C. and Boisselle, A. P. *J. Org. Chem.* **22** (1957) 1255.

Received January 9, 1973.

ACTA CHEMICA SCANDINAVICA 27 (1973) 1987–2000

Formation of 5-Hydroxy-Δ^2-1,2,3-triazolines, 1,2,3-Triazoles, and Ketohydrazones in Base-catalyzed Reactions of Organic Azides with Methyl Ketones

CARL ERIK OLSEN

*Department of Organic Chemistry, Technical University of Denmark, DK-2800 Lyngby, Denmark and Organic Chemical Laboratory, Royal Veterinary and Agricultural University, Thorvaldsenvej 40, DK-1871 Copenhagen, Denmark**

Under the influence of potassium *tert*-butoxide (PTB) organic azides, *e.g.* benzyl and phenyl azide, react with methyl ketones, *e.g.* acetone, pinacolone, and acetophenone, to give 5-hydroxy-Δ^2-1,2,3-triazolines, which under these reaction conditions normally react further, either by eliminating water under the formation of 1,2,3-triazoles (IX) or, after ring-opening, by reacting with one further molecule of azide to give bis-triazeno ketones (XI). XI may ring-close and eliminate water under formation of a triazenotriazole (XIII) or eliminate an amine under formation of an aliphatic diazo compound (XV), which is in a position to couple with an additional molecule of methyl ketone to give ketoazo compounds (XVII). In solution XVII is shown to be present in the NH tautomeric form (ketohydrazone) with the possibility of either a *cis* (chelated) or a *trans* configuration about the C=N bond. The position of the equilibrium between these two forms depends on substituents and solvent.

As reported previously [1,2] organic azides react with various ketones under the influence of potassium *tert*-butoxide (PTB) to give 5-hydroxy-Δ^2-1,2,3-triazolines. The reason that the reactions of methyl ketones have been singled out is that the triazolines formed here (those formed from methyl ethyl ketone being exceptions [1,2]) normally react further to give more complex compounds. The reactions of three methyl ketones with benzyl azide and phenyl azide have been investigated. They are summarized in Scheme 1 and may be rationalized in terms of reactivity of the azide and position of the always existing [1,2] equilibrium between the initially formed triazene VII and its ring-chain tautomer, the hydroxytriazoline VIII.

* Present address.

REACTIONS OF METHYL KETONES WITH BENZYL AZIDE (R^1 = benzyl)

The reaction (Scheme 1) of benzyl azide with acetone (R^2 = methyl) in the presence of PTB produced 1-benzyl-5-methyl-1,2,3-triazole (IXa), formed by dehydration of VIIIa, and 1-benzyl-4-isopropenyl-5-methyl-1,2,3-triazole

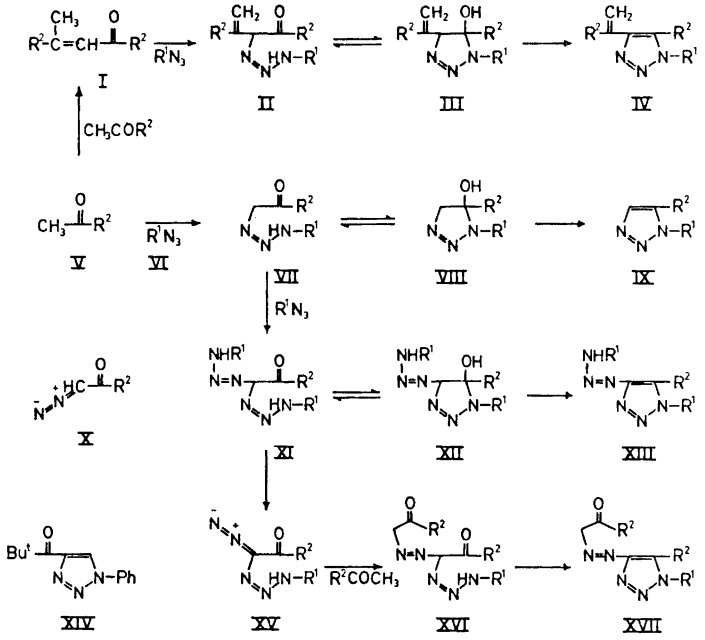

Yields

	R^1	R^2	IV	VIII	IX	XII	XIII	XVII
a	$PhCH_2$	Me	40		37			
b	$PhCH_2$	But			34	24		
c	$PhCH_2$	Ph		24	31			
d	Ph	Me	1.3		0.9		1.6	74
e	Ph	But						31
f	Ph	Ph		13				11

Scheme 1.

(IVa), identified by comparison with the corresponding 1-phenyl compound (IVd, *vide infra*). IVa is presumably formed from the triazene IIa by ring-closure and dehydration (IIa→IIIa→IVa). IIa might be produced either by reaction of preformed mesityl oxide (Ia) with benzyl azide or by reaction of VIIa (which is in equilibrium with VIIIa) with a second molecule of acetone. The latter possibility could be excluded, however, since treatment of VIIIa

(prepared in a 7 % yield from acetone and benzyl azide, using short reaction time) with acetone in the presence of PTB gave IXa and not IVa. Although the self-condensation of acetone in basic media often stops at the stage of the β-hydroxyketone,[3] dehydration to mesityl oxide may well take place in the presence of the very strong base PTB. In support of this interpretation NMR analysis of the mixture resulting from the PTB-catalyzed reaction of mesityl oxide with benzyl azide demonstrated a high yield of IVa.

The reaction of benzyl azide with pinacolone ($R^2 = Bu^t$) gave a mixture of 1-benzyl-5-*tert*-butyl-1,2,3-triazole (IXb) and the benzyltriazeno hydroxytriazoline XIIb. As expected, no IVb was formed, the self-condensation V→I being highly retarded by the bulky *tert*-butyl groups. XIIb, a tautomer of the bis-triazene XIb, must be formed from VIIb by reaction with an additional molecule of azide. This is quite conceivable, since a *tert*-butyl group at the 5-position of a 5-hydroxy-Δ^2-1,2,3-triazoline is known to retard the dehydration to triazole,[4] thus giving the benzyl azide a better chance to attack VIIb. No VIIIb is, however, accumulated in the reaction mixture, as demonstrated by NMR spectra of samples taken at intervals. The reactions VIIIb→IXb and VIIb→XIb must therefore proceed with comparable rates and much faster than the initial step, V + VI→VII (the equilibration VII⇌VIII is considered to be relatively fast). The compounds IXb and XIIb were formed in almost exactly the same ratio when a threefold excess of pinacolone was used in place of an equimolecular amount.

The reaction of benzyl azide with acetophenone ($R^2 = Ph$) yielded a mixture of 1-benzyl-5-phenyl-5-hydroxy-Δ^2-1,2,3-triazoline (VIIIc) and its dehydration product, 1-benzyl-5-phenyl-1,2,3-triazole (IXc); but the NMR spectrum of the product mixture showed no signs of XIIc, significant signals within the range 5.6 – 6.8 ppm being absent (the H-4 proton of XIIb lies at 5.54 ppm). Obviously the dehydration of VIIIc is relatively slow, and it is surprising that VIIc does not react with more azide to form XI (or its tautomer XII), as was the case with VIIb. However, it may be explained by the general reluctance of 5-phenyl-5-hydroxy-Δ^2-1,2,3-triazolines toward ring-opening [1,2] in combination with a relatively high reactivity of acetophenone, resulting in a rather short reaction time (2.5 h as compared with 5 days for pinacolone). As reported elsewhere [4] bulky groups at the 5-position seem to retard the dehydration of 5-hydroxy triazolines, and this may be the reason why VIIIc is not fully converted into IXc.

REACTIONS OF METHYL KETONES WITH PHENYL AZIDE (R^1 = phenyl)

The reaction of phenyl azide with acetone yielded four products: 1-phenyl-5-methyl-1,2,3-triazole (IXd) (0.9 %), 1-phenyl-4-isopropenyl-5-methyl-1,2,3-triazole (IVd) (1.3 %), 1-phenyl-4-phenyltriazeno-5-methyl-1,2,3-triazole (XIIId) (1.6 %), and the main product XVIId (74 %), the structure of which shall be discussed later. The presumed intermediate VIIId (in equilibrium with VIId) could not be isolated, but its presence was demonstrated by NMR analysis of the product mixture resulting from the reaction, when it was carried out in dilute solution (ether) and interrupted after one minute. The protons

at the 4-position showed up as a characteristic AB pattern centered at 4.3 ppm ($J_{AB} = 18$ cps).

The structure of IVd was established by NMR spectroscopy and by oxidation with potassium permanganate to give 1-phenyl-4-acetyl-5-methyl-1,2,3-triazole, identical with a sample prepared from ethyl 1-phenyl-5-methyl-1,2,3-triazole-4-carboxylate by aldol condensation with ethyl acetate and subsequent hydrolysis. Furthermore, IVd was produced in a high yield (91 %) from mesityl oxide and phenyl azide.

The structure of XIIId, determined by IR and NMR spectroscopy, was confirmed by an independent synthesis. Curtius transformation of the azide of 1-phenyl-5-methyl-1,2,3-triazole-4-carboxylic acid gave 1-phenyl-4-amino-5-methyl-1,2,3-triazole, which by coupling with benzenediazonium chloride yielded XIIId.

The low yield of IVd shows that the reaction V + VI → VII goes much faster than the self-condensation of acetone (V + V → I). IXd is probably formed in small amounts for two reasons. First, the equilibrium VII ⇌ VIII is shifted considerably more to the left side for R^1 = phenyl than for R^1 = benzyl [1,2] thus making more VII available for reaction with phenyl azide. Second, the reaction VII + VI → XI proceeds much faster for R^1 = phenyl than for R^1 = benzyl. XIIId must be formed *via* XId and XIId, and the low yield shows that the elimination reaction XId → XVd (*vide infra*) is relatively fast.

Phenyl azide and pinacolone reacted to give a 31 % yield of XVIIe along with a compound $C_{13}H_{15}N_3O$, which is possibly 1-phenyl-4-pivaloyl-1,2,3-triazole (XIVe). The formation of XIVe is rather obscure; it must presumably be ascribed to an impurity in the pinacolone, although none such was detectable by NMR.

With acetophenone phenyl azide reacted to give XVIIf (11 %) and the triazoline VIIIf (13 %). As in case c the accumulation of VIII may be explained by a shift to the right of the equilibrium VII ⇌ VIII and by a retarded dehydration of VIII caused by the phenyl group (R^2), and also by a short reaction time.

The formation of XVIIf in a base-catalyzed reaction of phenyl azide with acetophenone has been observed previously by Dimroth *et al.*[5] Using sodium ethoxide as the base they obtained XVIIf in a 20 % yield. The structure was firmly established by independent synthesis and by reductive cleavage into 1,5-diphenyl-4-amino-1,2,3-triazole by zink powder in ethanolic ammonia. Similarly we have converted XVIId into 1-phenyl-4-amino-5-methyl-1,2,3-triazole in a yield of 71 % by catalytic hydrogenation (*cf.* Ref. 6).

The route V → VII → XI → XVII for formation of XVII was proposed by the above authors,[5] but on somewhat weak evidence.[7] Undoubtedly the bis-triazene XI is an intermediate. The existence of such bis-triazeno ketones, respectively their ring-chain tautomers (XII), has just been demonstrated for R^1 = benzyl (XIIb), and evidence for the occurrence of XId in the reaction mixture of phenyl azide and acetone was provided by the isolation of the dehydration product of XIId, the 4-phenyltriazeno triazole XIIId (1,5-diphenyl-1,2,3-triazole (IXf) did not react with phenyl azide to give XIIIf in the presence of PTB). In addition the potential intermediacy of X (VII → X → XV → XVI → XVII) is rendered improbable by the fact that only a trace,

perhaps nothing at all, of pyruvaldehyde 1,5-diphenyl-4-1,2,3-triazolyl hydrazone (an analogue to XVII, *vide infra*) was obtained on successive treatment of diazoacetophenone (X, R^2 = phenyl) with phenyl azide and acetone in the presence of PTB. The compound XVIId was the main product.

Having established the intermediacy of XI, three routes for the conversion of it into XVII lend themselves to discussion. The route XI→XII→XIII→XVII may be excluded by the fact that XIIId failed to react with acetone in the presence of PTB. Then there remain the two pathways XI→XVI→XVII and XI→XV→XVI→XVII. The presence of a strong diazo band at 2130 cm^{-1} in the IR spectrum of the product mixture from phenyl azide and acetophenone is possibly caused by diazoacetophenone, since a weak signal at 5.90 ppm was present in the NMR spectrum. This suggests that diazo group transfer from phenyl azide, analogous to that from tosyl azide,[8] is well possible, even to singly activated $-CH_2-$ groups as the one in acetone. However, diazo group transfer to VII (VII→XI→XV) should be even more feasible, the methylene group of VII being flanked by both a keto group and an azo group. Actually, VII must be just as activated as malonic ester, to which the possibility of diazo group transfer from phenyl azide has been suggested by others.[9] This in conjunction with the fact that the central nitrogen atom of a triazene chain is an unlikely site for the attack of a carbanion, particularly when the reaction should be intermolecular (V + XI→XVI), suggests that XV is an intermediate between XI and XVI. It is well known that carbanions attack diazo compounds at the extreme nitrogen atom (XV→XVI).[10] The reason that no XVII is formed when R^1 is an alkyl group is now easy to understand: the leaving ability of an aliphatic amine is too poor for the step XI→XV to take place.

COMMENTS ON THE STRUCTURE OF COMPOUNDS XVIId–f

For clarity the compounds XVIId–f were formulated as ketoazo compounds in Scheme 1. Actually this is a misrepresentation of facts, since the NMR spectra do not exhibit signals from $-CH_2-$ groups. This indicates that XVII, at least in solution, adopt other tautomeric forms. Two others are possible: an NH (ketohydrazone) and an OH (enolazo) form (*cf.* Scheme 2). The NH form may exist as two geometrical isomers with respect to the C=N double bond, the NH_{cis} and NH_{trans} forms. Leaving out the possibility of a, presumably unstable,[11] *cis* geometry about the N=N double bond, the OH form may analogously exist as two geometrical isomers with respect to the C=C double bond, the OH_{cis} and OH_{trans} forms. Seemingly the NH_{cis} and OH_{cis} forms both have the possibility of forming intramolecular hydrogen bonds, as illustrated in Scheme 2; but it seems to be an established fact that an NH···O=C grouping is much more stable than an N···HO grouping,[12–16] at least if the oxygen atom is not attached to a potential aromatic system [15,17,18] (the postulated enolazo structure of some cyclohexane derivatives [19] does not seem to be well founded). In particular an N=N···HO grouping is relatively very unstable.[20] Therefore it can probably be assumed that an eventual OH_{cis} form would not form an intramolecular hydrogen bond, as opposed to the NH_{cis} form.

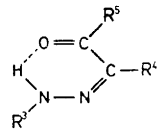

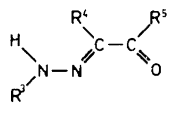

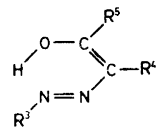

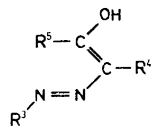

	R^3	R^4	R^5
XVIId	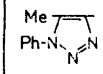	H	Me
XVIIe	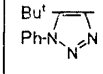	H	Bu
XVIIf	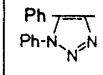	H	Ph
XVIII	Ph	H	Me
XIX	Ph	H	Ph
XX	Ph	Me	Me

Scheme 2.

The problem of differentiating between the four structures in question is a very subtle one, even after the advent of NMR spectroscopy. IR spectra are certainly considered in the following, but since they are difficult to interpret, the emphasis has been placed on the proton NMR spectra. With the purpose of enlarging the experimental basis, the compounds XVIII – XX (*cf.* Scheme 2) have been included in the discussion. The spectra (IR and NMR) of XVIII and XIX were recorded by us, while those of XX and its *N*-methylated derivative are described in the literature.[14] All available NMR data are collected in Table 1. Some compounds (XVIId and XVIII in $CDCl_3$ and XVIIe in DMSO) appear two times for the same solvent. This is because an equilibration, which may easily be followed by NMR spectroscopy, takes place between two of the structures shown in Scheme 2 when these substances are dissolved. On basis of the position of the exchangeable NH or OH proton, the so-called acidic proton, the species present in chloroform solution could be classified in two groups. One group has the acidic proton at very low field (13.7 – 14.4 ppm), the position being insensitive to variations in the concentration. This is just what is to be expected for an intramolecularly hydrogen bonded (chelated) proton,[14] and the group is therefore assumed to represent the NH_{cis} form. The other group has its acidic proton at higher field (8.0 – 10.1 ppm), the position this time being somewhat dependent on the concentration. All members of this group have R^5 = methyl, and the constant chemical shift of this methyl group (2.46 – 2.51 ppm) suggests that the group contains only one of the forms shown in Scheme 2. Based solely on the position of the acidic proton this form could be either one of the OH forms, or it could be the NH_{trans} form. However, the fact that the position of the NMR signal of neither R^4 nor R^5 differs much between XX and its *N*-methylated derivative makes it plausible that their structures are very much alike. The OH forms may therefore be excluded as possible structures, and since an unchelated NH_{cis} form is hard to imagine, the group must be identified with the NH_{trans} form. This conclusion is supported by the appearance of a characteristic [14] conjugated carbonyl

Table 1. NMR data (magnet temperature) of the compounds shown in Scheme 2. δ-Values of the acidic protons are in parenthesis when dependent on concentration. The position of $R^4=H$ (situated in the aromatic region) in XVIId–f in $CDCl_3$ was confirmed by running the spectra at both 60 and 100 Mc.

	Compound	3 % w/v in $CDCl_3$ (XX 0.8 M) R^3	R^4	R^5	NH	Other signals
NH_{trans}	XVIId	2.38(s,5-Me) 7.55("s", 1-Ph)	7.35(d, 1H)	2.51(s, 3H)	(10.1)	
	XVIII	6.8–7.6(m)		2.46(s, 3H)	(8.5)	
	XX[14]		1.98(3H)	2.49(3H)	(8.0)	
	XX(N-Me)[14]		2.04(3H)	2.48(3H)		4.49(3H,N-Me)
NH_{cis}	XVIId	2.43(s, 5-Me)	7.04(s, 1H)	2.29(s, 3H)	(13.7)	
	XVIII	6.8–7.6(m)		2.28(s, 3H)	13.9	
	XVIIe	1.29(s, 9H, 5-Bu) 7.2–7.7(m, 5H)	7.39(s, 1H)	1.29(s, 9H)	13.7	
	XVIIf	7.1–8.1(m)	7.83(s, 1H)	7.1–8.1(m)	14.4	
	XIX	6.8–8.2(m)	7.74(s, 1H)	6.8–8.2(m)	14.4	
		6 % w/v in DMSO-d_6				
NH_{trans}	XVIId	2.28(s, 3H, 5-Me) 7.64(s, 5H)	7.35(s, 1H)	2.42(s, 3H)	11.3	
	XVIII	6.7–7.6(m, 5H)		2.34(s, 3H)	11.2	
unknown	XVIIe	1.18 or 1.26(s, 9H) 7.62(s, 5H)	7.34(s, 1H)	1.26 or 1.18 (s, 9H)	10.15	
	XVIIf	7.0–7.8(m)	7.76(s)	7.0–7.8(m)	11.3	
	XIX	6.7–8.2(m)	7.80(s)	6.7–8.2(m)	11.6	
NH_{cis}	XVIIe	1.24 or 1.20(s)	7.49?	1.20 or 1.24 (s)	13.4	

band at 1665 cm^{-1} in the IR spectra of XVIId and XVIII in freshly prepared chloroform solutions as well as in KBr. Yagi[21] also arrived at the NH_{trans} configuration for compound XVIII in CCl_4 solution and in the crystalline phase, and so did Elguero *et al.* for XX in chloroform solution.[14]

According to the above authors,[14] the carbonyl band of those compounds which in chloroform solution are present in the NH_{cis} form occurs at an unexpected low frequency (1628 cm^{-1} for XVIIe and below 1630 cm^{-1} for XVIIf and XIX in $CHCl_3$ as well as in KBr). Thus the chelate hydrogen bond must be stronger than usual,[14] as is also indicated by the very high δ-value of the acidic proton, there being a linear relationship between the C=O stretching frequency and the chemical shift of the proton in the grouping NH···O=C in closely related compounds.[22]

In dimethyl sulfoxide XVIId and XVIII are in the NH_{trans} form, showing carbonyl bands at 1650 cm^{-1}. XVIIe is present in two forms at equilibrium, one with the acidic proton at 13.4 ppm, presumably the chelated NH_{cis} form,

and another form with the acidic proton at 10.15 ppm. We are unable to identify this latter form with certainty, but the NH_{trans} form may possibly be excluded, since an eventual C=O absorption must occur below 1630 cm^{-1}, which is very low for an unchelated C=O group. XVIIf and XIX cannot be in the NH_{cis} form, since the acidic proton is unchelated as judged from its position in the NMR spectrum; but we are not in a position to tell which of the remaining three forms is the correct one. No C=O absorption occurred above 1620 cm^{-1} and 1625 cm^{-1}, respectively.

As expected, coupling was not observed between R^4=H and R^5=Me (compounds XVIId and XVIII), but this fact alone would certainly not have been sufficient evidence for excluding the OH forms, since an allylic coupling may sometimes vanish.[23] In chelated β-thioketothiolesters [24] the corresponding coupling is 1.1 cps. In the NH_{trans} form of XVIId (in $CDCl_3$) the protons R^4=H and NH surprisingly couple with a coupling constant of 1 cps. The doublet at 7.35 ppm collapses to a singlet on treatment of the $CDCl_3$ solution with deuterium oxide or on irradiation of the proton at 10.1 ppm with a strong secondary field. The coupling is missing in the chelated NH_{cis} form, but whether this is owing to an unfavorable conformation or to a reduced bond order of the N–H bond is not known. The coupling is also absent in DMSO solution.

Table 2. Equilibrium content (%) of the NH_{cis} form in solution.

Solvent	XVIId	XVIII	XVIIe	XVIIf	XIX
$CDCl_3$	20 [a]	42 [b]	100	100	100
DMSO-d_6	0	0	15	0	0

[a] Equilibration time: approx. 10 min. [b] Equilibration time: a few hours.

The equilibrium content of the NH_{cis} form in solution is given in Table 2. Obviously it is lower in DMSO solution than in chloroform solution. This is quite conceivable in view of the capability of DMSO to act as a proton acceptor, those structures that are in a position to form intermolecular hydrogen bonds being stabilized relative to the NH_{cis} form. The effect is, however, surprisingly dramatic in that it results in complete reversal of the equilibrium position for two compounds, namely XVIIf and XIX. The difference between XVIId and XVIII on one hand and XVIIe, XVIIf, and XIX on the other is also striking. In chloroform solution the last three compounds are entirely in the NH_{cis} form, whereas the first two are only present partly in this form (20 % and 42 %, respectively). The explanation must probably be sought in the R^5 substituent, and since XVIIe (R^5 aliphatic) falls in the same group as XVIIf and XIX (R^5 aromatic), it is probably for steric rather than for electronic reasons that this group prefers the chelated NH_{cis} form. This is in line with the enhanced chelation in β-diketones containing bulky substituents, and the reason is possibly that steric repulsion between R^4 and R^5 results in a

reduction of the distance between the NH and C=O groups, thus making the hydrogen bond stronger.[25,26]

The ketoazo tautomer cannot be an intermediate in the equilibration $NH_{trans} \rightleftharpoons NH_{cis}$, since $R^4 = H$ is not exchanged with deuterium on treatment of the chloroform solutions of XVIId–f with deuterium oxide (*cf.* Refs. 15 and 27). However, this does not necessarily imply the OH tautomers as intermediates, since phenylhydrazones are able to equilibrate spontaneously between *cis* and *trans* forms.[27,28]

EXPERIMENTAL

Melting points are uncorrected. NMR spectra were recorded on a Varian A-60 or HA-100 instrument. Unless otherwise stated the solvent was $CDCl_3$ with TMS as an internal standard. Chemical shifts are given as δ-values. Analyses of NMR spectra were done on a first order basis, except for AB systems which were treated on a second order basis. IR spectra were recorded on a Perkin-Elmer model 421 instrument, using NaCl cells for measuring in chloroform solution and BaF_2 cells for dimethyl sulfoxide. Preparative thin-layer chromatography (TLC) was carried out using Merck Kieselgel PF_{254}.

A stock solution of PTB in *tert*-butyl alcohol was prepared by dissolving 19.6 g of potassium in 400 ml of *tert*-butyl alcohol (Fluka, *puriss.* grade) at reflux temperature. When needed an appropriate amount of this solution was pipetted off. The stock solution kept for months.

Pyruvaldehyde monophenylhydrazone (XVIII) and phenylglyoxal monophenylhydrazone (XIX) were prepared by coupling phenyl diazonium chloride with acetoacetic acid and benzoylacetic acid, respectively.[29]

Reaction of benzyl azide with acetone. Benzyl azide (1.24 ml, 0.01 mol) and acetone (2.2 ml, 0.03 mol) were added to 20 ml of PTB solution. The color immediately turned yellow and gradually shifted to reddish brown. A slight evolution of heat was observed after approx. 10 min, and cooling was necessary to keep the temperature below 30°C. No evolution of nitrogen occurred. TLC did not show the presence of any azide after 2 h of reaction, and after 3.5 h the mixture was poured into 200 ml of ice-water. Extraction with ether, drying over Na_2SO_4, and removal of the solvent gave 2.37 g of an orange oil. Preparative TLC of 383 mg of this oil, using ethyl acetate-pentane (1:3) as eluent, gave two main fractions. *Fraction 1* (fastest running) consisted of 136 mg (40 %) of 1-benzyl-4-isopropenyl-5-methyl-1,2,3-triazole (IVa) as a yellow syrup. Low-temperature crystallization from ether-pentane gave an almost colorless product with m.p. 35–36°C. (Found: C 73.04; H 7.21; N 19.85. Calc. for $C_{13}H_{15}N_3$: C 73.20; H 7.09; N 19.70), NMR data: 2.26 (s,3H), 2.26 (t, $J = 1.2$ cps, 3H), 5.18 (q, $J = 1.2$ cps, 2H) (this signal collapsed to a singlet on irradiation at 2.26 ppm), 5.51 (s,2H), and 7.0–7.5 ppm (m,5H). *Fraction 2* contained 104 mg (37 %) of 1-benzyl-5-methyl-1,2,3-triazole (IXa) as a yellow syrup. Several recrystallizations from ethyl acetate-pentane gave a white, crystalline product with m.p. 80–81°C (reported [30] 84°C). NMR data: 2.19 (*d*, $J = 0.8$ cps, 3H), 7.48 (broad s, 1H), 5.51 (broad s, 2H), and 7.0–7.5 ppm (m, 5H). The ratio IXa:IVa = 37:40 = 0.92 was also found by integration of the NMR spectrum of the crude product mixture.

Carrying out the reaction in the following manner the intermediate hydroxytriazoline could be isolated. Acetone (1.5 ml) was added to 2.48 ml of benzyl azide in 20 ml of PTB solution. After 10 min the reaction mixture was poured into 150 ml of ice-water, and the product was extracted with methylene chloride (2 × 100 ml). Drying and evaporation resulted in an orange, thin oil mainly consisting of benzyl azide. This was removed at 0.01 mmHg/40–60°C, and from the residue 278 mg (7 %) of 1-benzyl-5-methyl-5-hydroxy-Δ^2-1,2,3-triazoline (VIIIa) was obtained by low temperature crystallization from ether. Two recrystallizations from ethyl acetate-pentane gave a white product with m.p. 90–91°C. (Found: C 62.80; H 6.87; N 22.17. Calc. for $C_{10}H_{13}N_3O$: C 62.81; H 6.85; N 21.98). NMR data: 1.43 (s, 3H, $C-CH_3$), 7.36 ("s", 5H, aromatic protons), calc. δ-values for the benzylic protons: 4.70 and 4.98 ppm ($J_{AB} = 16$), and calc. δ-values for the protons at the 4-position: 4.26 and 3.78 ppm ($J_{AB} = 17.5$ cps).

Treatment of VIIIa with acetone in the presence of PTB. Acetone (0.11 ml, 1.5 mmol) and VIIIa (86 mg, 0.5 mmol) were added to 5 ml of PTB solution, and the mixture was let stand for 7 h at room temperature. The mixture was then poured into 40 ml of ice-water and extracted with ether. Drying (Na_2SO_4) and removal of the solvent gave an oily crystal mixture, which mainly consisted of 1-benzyl-5-methyl-1,2,3-triazole as apparent from the NMR spectrum. No 1-benzyl-4-isopropenyl-5-methyl-1,2,3-triazole (IVa) was detectable by NMR. Treatment with activated carbon in water followed by recrystallization from the same solvent gave 60 mg (77 %) of 1-benzyl-5-methyl-1,2,3-triazole (IXa) (m.p. 77 – 79°C).

Reaction of benzyl azide with pinacolone. Benzyl azide (1.24 ml, 0.01 mol) and pinacolone (1.25 ml, 0.01 mol) were added to 20 ml of PTB solution. The mixture was allowed to stand at room temperature for 5 days, during which time the color changed from yellow to orange. All azide was consumed (NMR). Only negligible nitrogen evolution occurred. The reaction mixture was poured into 75 ml of ice-water, and the separating oil was extracted with ether. The ether and *tert*-butyl alcohol were removed *in vacuo*, and the residue was dissolved in 20 ml of methylene chloride and dried over Na_2SO_4. Filtration and removal of the solvent gave 2.25 g of an orange oil. This oil (0.428 g) was subjected to preparative TLC using ether-benzene (1:2) as eluent. Two main fractions were obtained. *Fraction 1* (fastest running) consisted of 80 mg (24 %) of 1-benzyl-4-benzyltriazeno-5-*tert*-butyl-5-hydroxy-Δ^2-1,2,3-triazoline (XIIb) as a light yellow syrup. Crystallization from ether-pentane gave a white product with m.p. 106 – 107°C (nitrogen evolution). (Found: C 65.68; H 7.12; N 23.00. Calc. for $C_{20}H_{26}N_6O$: C 65.54; H 7.15; N 22.93). IR data (KBr): 3390 cm^{-1} (sharp and strong, presumably NH), 3220 cm^{-1} (broadened but strong, presumably OH). No C=O band was present neither in $CHCl_3$ solution nor in KBr. NMR data (4 % w/v, $CDCl_3$, 100 Mc): 8.4 (broad, 1H), 4.1 (broad, 1H), 0.90 (s,9H), 5.54 (broad s, 1H, nonexchangeable with deuterium on treatment with D_2O, identified as the proton at the 4-position), and 7.0 – 7.6 ppm (multiplet, 10H, aromatic protons). The CH_2 group of the triazene side chain is a broad singlet at 4.64 ppm, and that attached to the triazoline ring constitutes an AB system with $\delta_A = 4.70$ ppm, $\delta_B = 4.82$ ppm, and $J_{AB} = 16$ cps, indicating that the equilibration XIb⇌XIIb [1] is not fast enough to render the two benzyl groups equivalent. *Fraction 2* consisted of 139 mg (34 %) of 1-benzyl-5-*tert*-butyl-1,2,3-triazole (IXb) as a yellow syrup. Low temperature crystallization from ether gave a light yellow compound with m.p. 38 – 39°C. (Found: C 72.36; H 7.89; N 19.65. Calc. for $C_{13}H_{17}N_3$: C 72.52; H 7.96; N 19.52). NMR data: 1.28 (s,9H), 5,71 (s,2H), 7.50 (s,1H), and 6.8 – 7.6 ppm (m, 5H).

Using a threefold excess of pinacolone almost the same ratio between IXb and XIIb was obtained (2.9 instead of 3.2), as apparent from the NMR spectrum of the crude product mixture.

Reaction of benzyl azide with acetophenone. Benzyl azide (1.24 ml, 0.01 mol) and acetophenone (1.17 ml, 0.01 mol) were added to 20 ml of PTB solution. A yellow color immediately developed, and this had changed to deep reddish brown after 2.5 h, at which time the mixture was poured into 200 ml of ice-water. The product was extracted with ether (100 + 3 × 50 ml), and after removal of the solvent (ultimately using 1 mmHg/40°C) a mixture of oil and crystals remained. The crystals were washed with a few ml of methylene chloride at 0°C and with water. 1-Benzyl-5-phenyl-5-hydroxy-Δ^2-1,2,3-triazoline (VIIIc) (0.61 g, 24 %) with m.p. 119 – 123°C (decomp.) resulted. Recrystallization from ethyl acetate raised the m.p. to 127 – 128°C (N_2-evolution). (Found: C 71.34; H 5.94; N 16.78. Calc. for $C_{15}H_{15}N_3O$: C 71.13; H 5.97; N 16.59). NMR data: 4.63 (s,2H, $-CH_2Ph$) and 7.1 – 7.7 ppm with a sharp peak at 7.26 ppm (aromatic protons). The two protons at the 4-position appeared as an AB system with calculated δ-values of 4.08 and 4.49 ppm ($J_{AB} = 18$ cps).

The methylene chloride phase was dried over Na_2SO_4, and removal of the solvent resulted in a thick, orange oil. Preparative TLC (ethyl acetate:pentane, 1:3) of 285 mg gave several fractions, one of which consisted of 129 mg (31 %) of 1-benzyl-5-phenyl-1,2,3-triazole (IXc) as a thick oil. Repeated recrystallization from ethyl acetate-pentane gave a product with m.p. 69 – 70°C (reported [31] 69 – 70°C).

Reaction of phenyl azide with acetone. In the course of 10 min 4.4 ml (0.06 mol) of acetone was added with stirring to a solution of 5.5 ml (0.05 mol) of phenyl azide in 100 ml of PTB solution. Frequent cooling was necessary to keep the temperature within the range 20 – 30°C. Stirring was continued for half an hour at room temperature, and the

brown mixture was poured into 50 ml of ice. Ether (200 ml) was added, and after shaking and separation, the ether phase was treated with approx. 10 ml of diluted KOH. The solvent was removed from the ether phase on a rotary evaporator (using 1 mmHg/40°C in the last stage). The remaining syrup was treated with 50 ml of 10 % KOH and 200 ml of ether, and the two phases were separated. A voluminous precipitate (XVIId) was formed on acidification of the combined aqueous phases (three in total) with 4 N HCl while cooling in ice-water. Washing with water and drying gave 4.50 g (74 %) of a light brown compound with m.p. 170 – 177°C (gas evolution). Recrystallizations from methanol and ethyl acetate raised the m.p. to 186 – 187°C. (Found: C 59.40; H 5.47; N 28.97. Calc. for $C_{12}H_{13}N_5O$: C 59.24; H 5.38; N 28.78).

The solvent was removed from the ether phase, and the bulk of aniline (1.12 g) was distilled off at 1 mmHg at 25 – 40°C. The components of the residue were separated by TLC using ethyl acetate-benzene (1:2) as eluent. Several spots showed up, but only three main fractions were isolated. *Fraction 1* (fastest running) contained a compound that was shown by IR, NMR, and TLC to be identical with otherwise prepared 1-phenyl-4-isopropenyl-5-methyl-1,2,3-triazole (IVd). Yield 1.3 %. NMR data: 7.52 ("s", 5H, aromatic protons), 2.40 (s,3H,Me at the 5-position), 2.33 (dd ($J_1 = 1.0$ cps, $J_2 = 1.6$ cps), 3H, Me of the isopropenyl group), and 5.2 – 5.4 ppm (two poorly resolved quartets, 2H, $=CH_2$). *Fraction 2* consisted of 1-phenyl-4-phenyltriazeno-5-methyl-1,2,3-triazole (XIIId) as red crystals with m.p. 152 – 155°C (gas evolution). Recrystallization from ethyl acetate raised the m.p. to 162 – 163°C (gas evolution). Yield 1.6 %. IR showed the identity with an otherwise prepared sample. (Found: C 64.80; H 5.16; N 30.33. Calc. for $C_{15}H_{14}N_6$: C 64.73; H 5.07; N 30.20). NMR: data: 2.54 (s,3H), 7.62 (s, 5H, presumably ring-phenyl), 7.2 – 7.6 (m, 5H), and 9.9 ppm (broad s, 1H). *Fraction 3* was shown by IR and NMR to contain 1-phenyl-5-methyl-1,2,3-triazole [32] (IXd), but one further TLC separation (ethyl acetate) was necessary to obtain a pure product. Yield 0.9 %.

XVIId was acetylated by boiling 371 mg of the crude product for 13 h with 10 ml of acetic anhydride. Excess solvent was removed, leaving a brown crystallizing syrup. Recrystallization from methanol gave 228 mg (53 %) of a brown product with m.p. 156 – 157°C, and recrystallization from ethyl acetate-ether gave a white product with m.p. 157 – 158°C. (Found: C 59.06; H 5.41; N 24.77. Calc. for $C_{14}H_{15}N_5O_2$: C 58.94; H 5.30; N 24.55). NMR data: 2.20 (s, 3H), 2.49 (s,3H), 2.66 (s, 3H), 6.94 (s, 1H), and 7.58 ppm (s, 5H). IR data: the following absorptions were present within the range 1500 – 2000 cm^{-1}: 1715, 1690, and 1580 cm^{-1}, all strong bands.

XVIId was hydrogenated in the following way. Crude XVIId (481 mg) and 5 mg of PtO_2 catalyst were dispersed in a mixture of 1 ml of conc. HCl and 15 ml of methanol. Hydrogenation was continued for 18 h at a hydrogen pressure of 1 atm., whereby 95 ml of hydrogen was absorbed. Platinum and solvent were removed, and 5 ml of water was added. After neutralization with saturated $NaHCO_3$, the product was extracted with methylene chloride. Drying and evaporation gave a brownish syrup, which was purified by treatment with activated carbon in water. Extraction of the aqueous phase with methylene chloride yielded 246 mg (71 %) of weakly miscolored crystals of m.p. 93 – 95°C. Recrystallization from ethyl acetate-cyclohexane raised the m.p. to 102 – 103°C. IR, NMR, and mixed m.p. showed the identity with otherwise prepared 1-phenyl-4-amino-5-methyl-1,2,3-triazole.

Reaction of phenyl azide with mesityl oxide. In the course of 5 min a total of 5.7 ml (0.05 mol) of mesityl oxide was added with stirring to a solution of 5.5 ml (0.05 mol) of phenyl azide in 50 ml of PTB solution. The mixture was cooled continuously in an ice-water bath. The reddish brown reaction mixture stayed in the cooling bath for 10 min, and it was then allowed to stand at room temperature for 30 min before being poured into 300 ml of ice-water. Extraction with ether and evaporation (1 mmHg/40°C in the last stage) left 9.05 g (91 %) of a brown crystal cake. Recrystallization from pentane gave a product (IVd) with m.p. 65 – 66°C, identical with the product obtained from phenyl azide and acetone. (Found: C 72.41; H 6.71; N 21.31. Calc. for $C_{12}H_{13}N_3$: C 72.35; H 6.57; N 21.10).

IVd was converted into 1-phenyl-4-acetyl-5-methyl-1,2,3-triazole in the following manner. To 0.524 g of the above IVd, dissolved in 20 ml of 50 % acetic acid, was added, while stirring, 5 g of $KMnO_4$ at such a rate that the temperature remained in the range 35 – 40°C. Stirring was continued for half an hour, and a mixture of 50 ml of water and 10 ml of conc. hydrochloric acid was then added. While cooling in ice-water, Na_2SO_3

(approx. 10 g) was added slowly until all MnO_2 had dissolved, and the mixture was then neutralized with solid $NaHCO_3$. Extraction with methylene chloride, drying over $MgSO_4$, and evaporation gave 0.304 g (58 %) of a crystallizing oil. After recrystallization from pentane the m.p. was 99 – 100°C as reported.[33] Mixed m.p., IR, and NMR showed the identity with the 1-phenyl-4-acetyl-5-methyl-1,2,3-triazole prepared from 1-phenyl-5-methyl-4-1,2,3-triazole-carboxylic acid (see below).

Preparation of 1-phenyl-4-acetyl-4-methyl-1,2,3-triazole. Ethyl 1-phenyl-5-methyl-4-1,2,3-triazole-carboxylate [33] (1.15 g), 2 ml of ethyl acetate, and 0.2 g of sodium powder (prepared in xylene) were refluxed in 10 ml of benzene for 8 h. An oil separated when the solution, obtained by evaporation and dissolution in 20 ml of water, was acidified with acetic acid. The oil was extracted with methylene chloride. The NMR spectrum showed that it consisted of ethyl 3-oxo-3-(1-phenyl-5-methyl-4-1,2,3-triazolyl)-propionate rather than the expected 4-acetyl triazole.[33] Column chromatography (ethyl acetate: pentane, 1:3, silica) gave 0.61 g (45 %) of a pure compound, which was crystallized from ether-pentane at −76°C. M.p. 48 – 49°C. (Found: C 61.36; H 5.65; N 15.32. Calc. for $C_{14}H_{15}N_3O_3$: C 61.52; H 5.53; N 15.37). NMR data: 1.32 (t, 3H), 2.63 (s, 3H), 4.27 (s,2H), 4.30 (q, 2H), and 7.3 – 7.9 ppm (m, 5H).

The ethyl ester (0.146 g) was refluxed with 8 ml of 2 % NaOH for one h. 1-Phenyl-4-acetyl-5-methyl-1,2,3-triazole precipitated from the reaction mixture on cooling. The product was filtered off, washed with water, and dried. Yield 71 mg (66 %), m.p. 98°C.

Preparation of 1-phenyl-4-phenyltriazeno-5-methyl-1,2,3-triazole. 1-Phenyl-5-methyl-4-1,2,3-triazole-carboxylic acid [32] (6.8 g, 0.03 mol) was melted together with 6.8 g (0.03 mol) of phosphorus pentachloride. A vigorous reaction took place, and 5 min later the reaction was complete. Phosphorus oxychloride was distilled off *in vacuo* on a water bath, and the residue was dissolved in 80 ml of acetone. Sodium azide (5.8 g), dissolved in 25 ml of water, was added during 5 min, and the mixture was let stand at room temperature for one h. Concentration to half volume and addition of 150 ml of water caused the azide to crystallize. Washing with water and drying gave 6.99 g of a product with m.p. 90 – 91°C (decomp.). Refluxing with 100 ml of abs. ethanol for 24 h resulted in the urethane, m.p. 97 – 100°C, (102 – 103°C after recrystallization of a sample from ethanol-pentane), which on boiling for 4 h with 50 ml of 2 N NaOH gave the wanted 1-phenyl-4-amino-5-methyl-1,2,3-triazole, separating as colorless crystals on cooling. Recrystallization from water gave 4.15 g (79 % based on carboxylic acid), m.p. 99 – 100°C. Repeated recrystallization raised the m.p. to 104 – 105°C. (Found: C 61.94; H 5.98; N 32.30. Calc. for $C_9H_{10}N_4$: C 62.05; H 5.78; N 32.16). The compound has been prepared in a different way by others.[34] NMR data: 2.24 (s, 3H) and 7.54 ppm (s, 5H).

The aminotriazole was converted into 1-phenyl-4-phenyltriazeno-5-methyl-1,2,3-triazole in the following manner. Aniline (0.31 g), dissolved in 10 ml of 4 N HCl, was diazotized with $NaNO_2$, until iodine-starch paper gave a positive reaction (approx. 0.2 g of $NaNO_2$ was required). This solution was added to 0.58 g of 1-phenyl-4-amino-5-methyl-1,2,3-triazole, dissolved in 50 ml of 1 N NaOH. The temperature was kept at *ca.* 20°C by cooling in ice-water. A yellow precipitate formed in a few minutes, and after one h it was filtered off, washed with water, and dried. Yield 0.65 g (70 %) of a light brown product. Recrystallization from ethyl acetate raised the m.p. to 158°C (gas evolution). The IR spectrum proved the identity with XIIId.

Treatment of XIIId with acetone and PTB. XIIId (31 mg, isolated from the reaction mixture of phenyl azide with acetone) was dissolved in 5 ml of PTB solution, and 0.3 ml of acetone was added. After 30 min the mixture was poured into 30 ml of water and 0.5 ml of acetic acid. Extraction (methylene chloride), drying (Na_2SO_4), and evaporation gave an oil, from which 24 mg of crystalline starting material (m.p. 160 – 162°C) was recovered by treatment with 5 ml of ether at 0°C. TLC and NMR showed that no XVIId was present in the mother liquor.

Reaction of phenyl azide with pinacolone. Pinacolone (1.25 ml, 0.01 mol) was added to a solution of 1.1 ml (0.01 mol) of phenyl azide in 20 ml of PTB solution. The reaction mixture rapidly turned reddish brown, and a slight evolution of nitrogen occurred. After 40 min the mixture was poured into 150 ml of ice-water and extracted with ether. Drying over Na_2SO_4 and evaporation of the solvent, using 0.5 mmHg/30°C in the last stage, resulted in 1.47 g of a thick, orange oil. The aniline was distilled off at 0.01 mmHg (heating on a 50°C water bath), and from the residue, which was dissolved in 10 ml of ether, 181 mg of XVIIe crystallized. The compounds in the mother liquor were separated by TLC,

using ether-pentane (1:2) as eluent. Two fractions were isolated. *Fraction 1* (fastest running) consisted of 79 mg (3.5 %) of a yellowish oil, presumably 1-phenyl-4-pivaloyl-1,2,3-triazole (XIVe). Low temperature crystallization from ether gave a white, crystalline product melting at 106°C. (Found: C 68.31; H 6.77; N 18.06. Calc. for $C_{13}H_{15}N_3O$: C 68.09; H 6.59; N 18.33). NMR data: 1.50 (s, 9H), 7.4 – 8.0 (multiplet, 5H), and 8.49 ppm (s, 1H, nonexchangeable on treatment with D_2O). IR data: 1680 cm^{-1} (strong, C=O), 3130 cm^{-1} (strong and sharp). The latter band is characteristic of 1,4-disubstituted 1,2,3-triazoles and excludes the possibility of a 1,5-disubstituted 1,2,3-triazole.[35] Mass spectrum: The molecular ion was present at *m/e* 229. The most conspicuous feature was a large peak at *m/e* 144, representing a cleavage between the pivaloyl group and the triazole nucleus. A metastable peak, which could be accounted for by loss of nitrogen from this ion, was present at *m/e* 93.5. *Fraction 2* consisted of 331 mg of XVIIe as a red syrup, which crystallized on inoculation. Total yield of XVIIe: 0.512 g (31 %). Recrystallization from ethyl acetate-pentane gave yellow crystals, which melted at 130 – 131°C. (Found: C 66.14; H 7.61; N 21.21. Calc. for $C_{18}H_{25}N_5O$: C 66.03; H 7.70; N 21.39).

Reaction of phenyl azide with acetophenone. Acetophenone (2.33 ml, 0.02 mol) was added, while stirring and cooling (ice-water), to a solution of 2.2 ml (0.02 mol) of phenyl azide in 20 ml of PTB solution. The mixture immediately became dark, and considerable nitrogen evolution occurred. After one min the mixture was poured into 150 ml of ice-water and 10 ml of 4 N HCl. The product was extracted with ether. Drying over Na_2SO_4 and evaporation gave a dark red oil, from whose ethereal solution 0.64 g (13 %) of 1,5-diphenyl-5-hydroxy-Δ^2-1,2,3-triazoline (VIIIf) crystallized on standing. Several recrystallizations from ethyl acetate raised the m.p. (140 – 142°C) to 159 – 160°C (decomp.). (Found: C 70.04; H 5.60; N 17.44. Calc. for $C_{14}H_{13}N_3O$: C 70.26; H 5.47; N 17.56). NMR data: The compound was too sparingly soluble in $CDCl_3$ to allow an NMR spectrum to be recorded in this solvent. In pyridine (4 %) the two hydrogens at the 4-position appeared as an AB system with $\delta_A = 4.57$ ppm, $\delta_B = 5.09$ ppm, and $J_{AB} = 18$ cps.

On washing the Na_2SO_4 used for drying above with water 0.39 g (11 %) of phenylglyoxal 1,5-diphenyl-4-1,2,3-triazolylhydrazone (XVIIf) was left. Mixed m.p., IR, and NMR proved the identity with a sample prepared according to Dimroth *et al.*[5]

Treatment of 1,5-diphenyl-1,2,3-triazole with phenyl azide and PTB. Phenyl azide (1.1 ml, 0.01 mol), 1,5-diphenyl-1,2,3-triazole [36] (1.11 g, 0.01 mol), and tetrahydrofurane (10 ml, distilled over copper(I) chloride and dried over drierite) were added to 15 ml of PTB solution. After 5 months the mixture was poured into 150 ml of water. When the separating oil had crystallized, it was filtered off, washed with water and pentane, leaving 0.97 g of unchanged 1,5-diphenyl-1,2,3-triazole. Considerable amounts of phenyl azide were present in the mother liquor (TLC).

Successive treatment of diazoacetophenone with phenyl azide and acetone in the presence of PTB. Diazoacetophenone [37] (292 mg) was added to a mixture of 0.22 ml of phenyl azide, 5 ml of ether (sodium dried), and 5 ml of ice-cold PTB solution. The mixture immediately became dark, but no nitrogen evolution took place. After two h at 0°C, 0.29 ml of acetone was added, and after an additional period of 0.5 h the mixture was poured into 50 ml of water and 0.5 ml of acetic acid. Extraction (ether), drying (Na_2SO_4), and evaporation gave an oily crystal mixture. The NMR spectrum of this mixture exhibited a weak signal at 2.6 ppm, which could possibly be ascribed to pyruvaldehyde 1,5-diphenyl-4-1,2,3-triazolylhydrazone. However, the signals corresponding to XVIId (Table 1) were approx. ten times stronger.

Acknowledgements. The author thanks Professor C. Pedersen for advice and inspiration. Likewise the constructive criticism by Professor P. Olesen-Larsen is much appreciated.

Microanalyses were performed by Dr. A. Bernhardt.

REFERENCES

1. Olsen, C. E. and Pedersen, C. *Acta Chem. Scand.* **27** (1973). *In press.*
2. Olsen, C. E., Thesis, Technical University of Denmark, DK-2800 Lyngby, Denmark, 1969 (in English).
3. Hine, J. *Physical Organic Chemistry*, McGraw, New York 1962, p. 259.

4. Olsen, C. E. *To be published.*
5. Dimroth, O., Frisoni, E. and Marshall, J. *Ber.* **39** (1906) 3920.
6. Regitz, M. and Stadler, D. *Ann.* **687** (1965) 214.
7. Boyer, J. H. In *Heterocyclic Compounds*, Wiley, New York 1961, Vol. 7, p. 389.
8. Regitz, M. *Angew. Chem.* **79** (1967) 786.
9. Begtrup, M., Larsen, P. S. and Pedersen, C. *Acta Chem. Scand.* **22** (1968) 2476.
10. Regitz, M., Liedhegener, A. and Stadler, D. *Ann.* **713** (1968) 101.
11. Buckingham, J. and Guthrie, R. D. *Chem. Commun.* **1967** 1241.
12. Bose, A. K. and Kugajevsky, I. *Tetrahedron* **23** (1967) 1489.
13. Blanchard, M.-L., Strzelecka, H., Martin, G. J., Simalty, M. and Fugnitto, R. *Bull. Soc. Chim. Fr.* **1967** 2677.
14. Elguero, J., Jacquier, R. and Tarrago, G. *Bull. Soc. Chim. Fr.* **1966** 2981.
15. Brown, N. M. D. and Nonhebel, D. C. *Tetrahedron* **24** (1968) 5655.
16. Jones, R., Ryan, A. J., Sternhell, S. and Wright, S. E. *Tetrahedron* **19** (1963) 1497.
17. Snavely, F. A. and Yoder, C. H. *J. Org. Chem.* **33** (1968) 513.
18. Zollinger, H. *Azo and Diazo Chemistry*, Interscience, New York 1961, Section 13.2.
19. Altiparmakian, R. H. and Braithwaite, R. S. W. *J. Chem. Soc.* **C 1967** 1973.
20. Brealey, G. J. and Kasha, M. *J. Am. Chem. Soc.* **77** (1955) 4462.
21. Yagi, Y. *Bull. Chem. Soc. Jap.* **36** (1963) 487.
22. Dudek, G. O. *J. Org. Chem.* **30** (1965) 548.
23. Newsoroff, G. P. and Sternhell, S. *Tetrahedron Lett.* **1968** 6117.
24. Duus, F., Jacobsen, P. and Lawesson, S.-O. *Tetrahedron* **24** (1968) 5323.
25. Nonhebel, D. C. *Tetrahedron* **24** (1968) 1869.
26. Musso, H. and Bantel, K.-H. *Chem. Ber.* **102** (1969) 686.
27. Bellamy, A. J. and Guthrie, R. D. *J. Chem. Soc.* **C 1968** 2090.
28. Karabatsos, G. J. and Taller, R. A. *J. Am. Chem. Soc.* **85** (1963) 3624.
29. *Organic Syntheses*, Wiley, New York 1952, Vol. 32, p. 84.
30. Wolff, L. and Krüche, R. *Ann.* **394** (1912) 56.
31. Moulin, F. *Helv. Chim. Acta* **35** (1952) 177.
32. Dimroth, O. *Ber.* **35** (1902) 1029.
33. Borsche, W., Hahn, H. and Wagner-Roemmick, M. *Ann.* **554** (1943) 21.
34. Pocar, D., Maiorana, S. and Croce, P. D. *Gazz. Chim. Ital.* **98** (1968) 949.
35. Begtrup, M. *Unpublished results.*
36. Dimroth, O. *Ber.* **35** (1902) 4041.
37. Regitz, M. and Menz, F. *Chem. Ber.* **101** (1968) 2622.

Received January 22, 1973.